Laboratory Directed Research and Development

Los Alamos National Laboratory
FY11 Annual Progress Report

90
Th

Cl(4)
Cl(3)
O(2)
O(4)
Th(1)
O(1)
O(3)
Cl(2)
Cl(1)

INNOVATION
for our NATION

Los Alamos
NATIONAL LABORATORY
— EST.1943 —
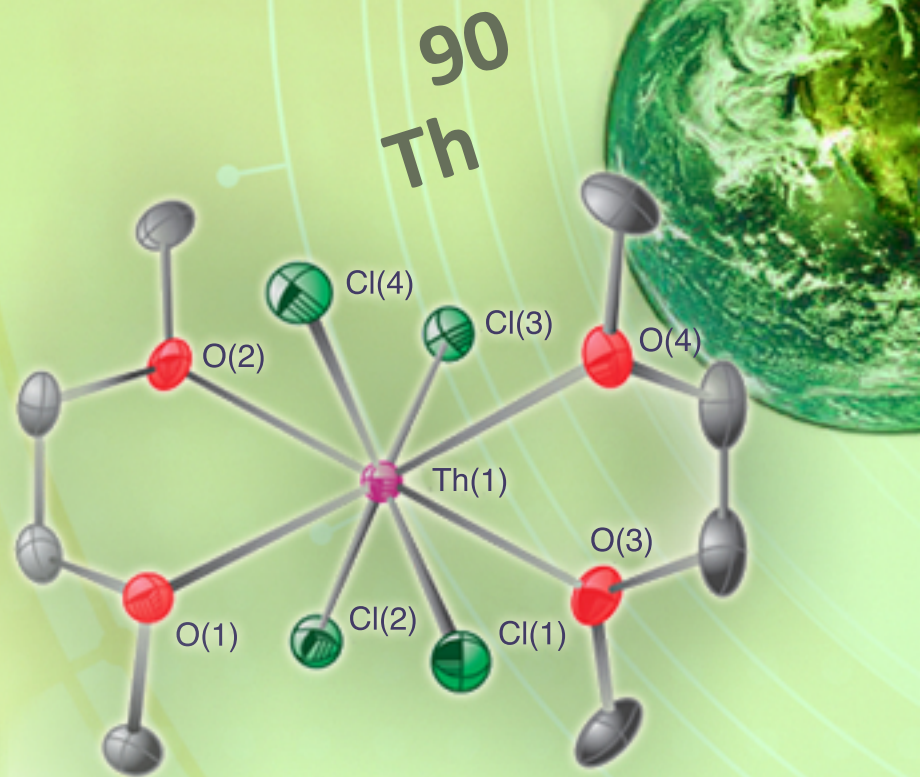
About the Cover

Th-ING was developed by LDRD researchers Jaqueline Kiplinger and Thibault Cantat as a straightforward, cost-effective, and safe method to produce thorium. Thorium is an element discovered in 1828 that is capable of producing more energy than both uranium and coal using significantly lower quantities. This element is only slightly radioactive, making it an excellent candidate for a future sustainable energy source. Before Th-ING, thorium could only be produced in hazardous settings at unreasonably high prices. This new method involves reacting thorium nitrate with aqueous hydrochloric acid under mild conditions, which can be performed using conventional glassware in a traditional laboratory setting. Then, a novel combination of anhydrous hydrochloric acid and trimethylsilyl chloride is used to remove coordinated water molecules, replacing them with dimethoxyethane to make the new thorium chloride reagent. The process cuts costs of production from $5,000 per kilogram to a mere $30 per kilogram and is "green"—as it does not produce wasteful solvent ring-opening/polymerization or waste thorium (95 percent production yields). With Th-ING, thorium becomes a practical and reliable source of energy for the future. This technology won a 2011 R&D 100 award.

Structure of this Report

In accordance with U.S. Department of Energy Order (DOE) 413.2B, the Laboratory Directed Research and Development (LDRD) annual report for fiscal year 2011 (FY11) provides summaries of each LDRD-funded project for the fiscal year, as well as full final reports on completed projects. The report is organized as follows:

Overview: An introduction to the LDRD Program at Los Alamos National Laboratory (LANL), the program's structure and strategic value, the LDRD portfolio management process, and highlights of outstanding accomplishments by LDRD researchers.

Project Summaries: The project summaries are organized first by science and technology categories: Physics, Chemistry and Material Sciences, Environmental and Biological Sciences, Information Science and Technology, and Technology. Within each category, summaries are organized by LDRD component: Directed Research (DR) projects first, Exploratory Research (ER) second, and Postdoctoral Research and Development (PRD) projects last. Full final reports are included at the end of each section.

Projects are listed in numerical order according to their project identification number, which consists of three parts. The first is the fiscal year in which the project began; the second is a unique numerical identifier; and the third identifies the project component.

Table of Contents

Environmental and Biological Sciences

Physics

by William Priedhorsky, LDRD Program Manager

R&D is one of the best investments a country can make. As quoted in *Rising Above the Gathering Storm, Revisited*, "Robert Solow received a Nobel Prize in economics in part for his work that indicated that well over half of the growth in United States output per hour during the first half of the twentieth century could be attributed to advancements in knowledge, particularly technology." The impact of research and development (R&D) has only continued to grow in the half century since.

America competes with the world not only economically, but also in the hard currency of national security. A small but critical fraction of the nation's investment in national security – less than 10% – is R&D. Indeed, science and technology are arguably the nation's best option for advantage against our adversaries.

Los Alamos National Laboratory has contributed to national security since 1943. Our mission is to develop and apply science and technology to

- ensure the safety and reliability of U.S. the nuclear deterrent,
- reduce the threat of weapons of mass destruction, proliferation, and terrorism, and
- solve national problems in defense, energy, environment, and infrastructure.

These missions demand that we *anticipate, innovate, and deliver* to solve the unsolved and know the unknown. We seek innovation that can drive breakthroughs in mission performance, whether that mission demands prediction of weapons aging, the remediation of legacy contamination, or the mitigation of transnational terrorism.

At Los Alamos, LDRD is an open market for ideas, inspired by mission. We succeed because of the diversity of our investments, which mix applied and fundamental research. Although no single project can guarantee results, the aggregate results of LDRD investment drive the Laboratory forward. Margaret Thatcher spoke in 1988 about the powerful but unpredictable benefits of R&D: "...although basic science can have colossal economic rewards, they are totally unpredictable. And therefore the rewards cannot be judged by immediate results. Nevertheless, the value of Faraday's work today must be higher than the capitalization of all shares on the stock exchange... . The greatest economic benefits of scientific research have always resulted from advances in fundamental knowledge rather than the search for specific applications ... transistors were not discovered by the entertainment industry ... but by people working on wave mechanics and solid state physics. [Nuclear energy] was not discovered by oil companies with large budgets seeking alternative forms of energy, but by scientists like Einstein and Rutherford..."

Our missions require breadth and depth in science and technology. Their complexity demands a span of excellence that crosses nearly every discipline in science. For example, the core nuclear weapons program demands prediction and control of materials in extreme conditions, computing at the petascale and soon the exascale, the understanding of turbulent fluid flow, miniaturized smart sensors, and advances in nuclear and high-energy density physics.

By investing in LDRD, Los Alamos builds its vision: to be the National Security Science Laboratory of choice, ready to take on whatever complex issue the nation asks of us.

> "The study committee recommends that Congress and NNSA maintain strong support of the LDRD program as it is an essential component of enabling the long-term viability of the Laboratories."

Laboratory Directed Research and Development is the most prestigious source of research and development funding at the Los Alamos National Laboratory. It follows a strategic guidance derived from the missions of the U.S. Department of Energy, the National Nuclear Security Administration, and the Laboratory. To execute that strategy, the Los Alamos LDRD program creates a free market for ideas that draws upon the bottom-up creativity of the Laboratory's best and brightest researchers. The combination of strategic guidance and free-market competition provides a continual stream of capabilities that position the Laboratory to accomplish its missions.

The LDRD program provides the Laboratory Director with the opportunity to strategically invest in forward-thinking, potentially high-payoff research that strengthens the Laboratory's capabilities for national problems. Funded in FY11 with approximately 6% of the Laboratory's overall budget, the LDRD program makes it possible for researchers to pursue cutting-edge research and development. This in turn enables the Laboratory to anticipate, innovate, and deliver world-class science, technology, and engineering.

Program Structure

The LDRD program is organized into three program components with distinct institutional objectives: Directed Research (DR), flagship investments in mission solutions; Exploratory Research (ER), smaller projects that invest in people and skills that underpin key Laboratory capabilities; and Postdoctoral Research and Development (PRD), recruiting bright, qualified, early-career scientists and engineers. In FY11, the LDRD program funded 291 projects with total costs of $139.7 million. These projects were selected through a rigorous and highly competitive peer-review process and are reviewed formally and informally throughout the fiscal year.

Directed Research

The DR component makes long-range investments in multidisciplinary scientific projects in key competency or

technology-development areas vital to LDRD's long-term ability to execute Laboratory missions. In FY11, LDRD funded 50 DR projects, which represents approximately 55% of the program's research funds. Directed Research projects are typically funded up to a maximum of $1.7M per year for three years.

The DR component is guided by the LDRD Strategic Investment Plan, which is in turn guided by eight Grand Challenges that define the advances in science and technology that are needed to address Los Alamos missions. These challenges were originally set out in the Los Alamos National Security LLC contract and refined in a Laboratory-wide workshop. The Grand Challenges have evolved in their four years in response to an ever-changing world. Figure 1 shows how the Grand Challenges align with the Laboratory's three "Science that Matters" thrusts.
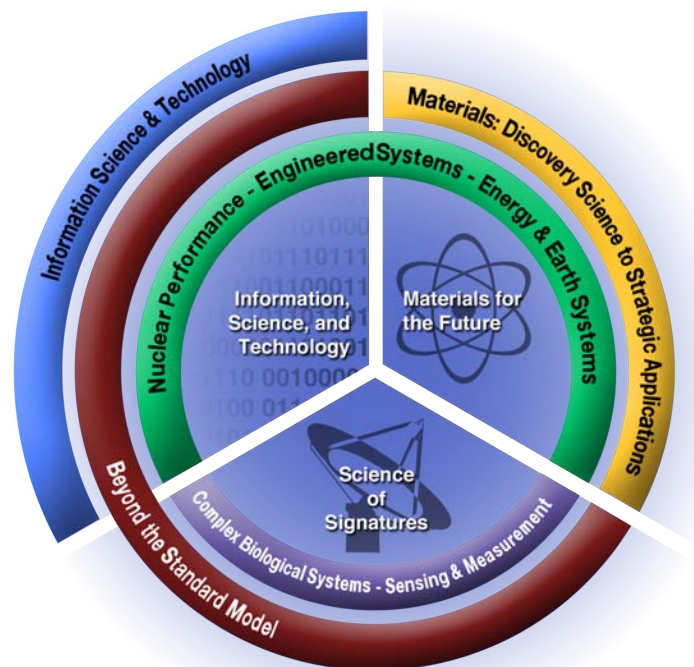
Figure 1: Grand Challenges guide LDRD investments in Directed Research.

Exploratory Research

The ER component is focused on developing and maintaining technical staff competencies in key strategic disciplines that form the foundation of the Laboratory's readiness for future national missions. Largely focused on a single discipline, ER projects explore highly innovative ideas that underpin Laboratory programs. In FY11, LDRD funded 138 ER projects, which represents approximately 33% of the program's research funds. Exploratory Research projects are typically funded up to a maximum of $375K per year for three years.

Unlike DR proposals, division endorsements are not required for ER proposals; instead, this component of the LDRD program is operated as an open and competitive path for every staff member to pursue funding for his/her great idea. The ER component is a critical channel for purely bottom-up creativity at the Laboratory. Nonetheless, it is strongly driven by mission needs via the definition of the 12 ER research categories, and the assignment of investment between them.

First Z bosons ever produced and reconstructed in heavy ion collisions

The Z boson is an electrically neutral subatomic particle that mediates the weak nuclear force. It has a mass 182,000 times that of the electron. Unlike the other weak force mediator (the W boson), the Z boson does not change particles it interacts with into other types of particles.

During the lead-lead collisions at the unprecedented energy of 2.76 GeV (a factor 14 higher than at the Relativistic Heavy Ion Collider) at the Large Hadron Collider at CERN in November, Los Alamos researchers participated in data collection at the Compact Muon Solenoid (CMS) experiment and began data analysis. Their goal is to understand the quark gluon plasma on a quantitative level.

On November 9, the CMS heavy ion dilepton group, convened by Subatomic Physics (P-25) postdoctoral researcher Catherine Silvestre, found the first Z boson ever produced and reconstructed in heavy ion collisions. The Los Alamos team was responsible for including the Z^0 measurements in the CMS heavy ion Technical Design Report enabled by LDRD funding that began in 2006. Preparation for the current dilepton analysis was made possible by a second LDRD project started in 2009. Part of the funding supports theoretical predictions of Z^0 and hadronic jet productions. A CERN seminar on the first results from heavy ion collisions was held on December 2, 2011. The CMS talk featured a preliminary dimuon mass spectrum with 27 identified Z bosons. The manuscript in preparation, "First Unambiguous Measurement of Jet Fragmentation and Energy Loss in the Quark Gluon Plasma," was led by principal investigator Gerd Kunde.

CMS Experiment at LHC, CERN
Data recorded: Tue Nov 9 23:51:56 2010 CEST
Run/Event: 150590 / 776435
Lumi section: 183

Muon 0, pt: 29.7 GeV

Muon 1, pt: 33.8 GeV
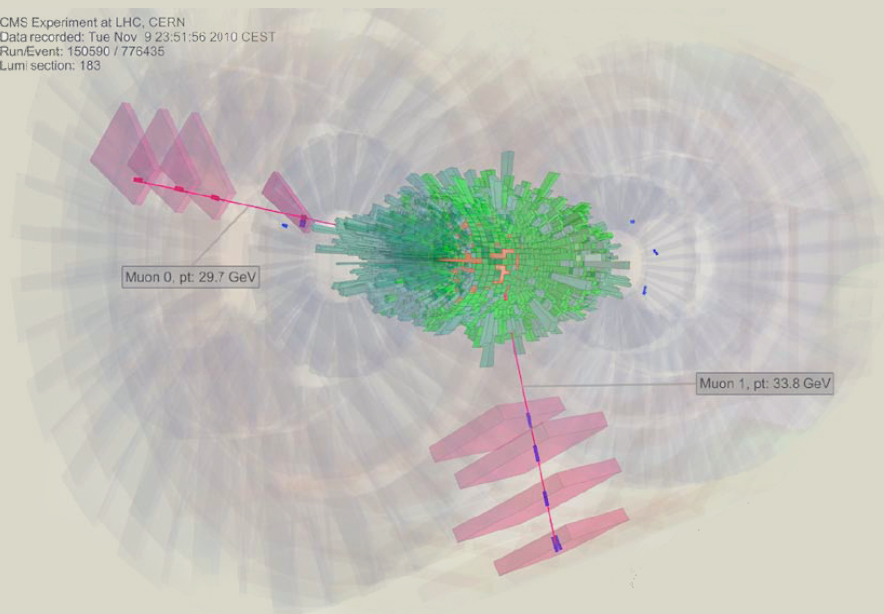
The first Z boson candidate reconstructed in heavy ion collisions. The figure shows the calorimetric and charged particle tracking response to a lead-lead collision in the CMS detector plus the two muon tracks from the Z^0 decay.

Directed Research Grand Challenges	Mission Impact
Beyond the Standard Model	Sensitive instrumentation and tools to manipulate massive data volumes, in support of national security missions
Materials: Discovery Science to Strategic Applications	Energy sources, efficiency and storage; sensing for threat reduction; materials underpinnings of stockpile security
Complex Biological Systems	Energy, national security, health and the environment
Information Science and Technology	Overarching capability supporting all Laboratory missions
Earth and Energy Systems	Energy and climate security
Nuclear Performance	Stockpile safety, surety and reliability
Sensing and Measurement Science for Global Security	Nuclear weapons of mass destruction, space situational awareness, global environmental treaty monitoring and emerging threats
Engineered Systems	Systems-level solutions for all missions

Exploratory Research Technical Categories	Laboratory Capability
Nuclear Physics, Particle Physics, Astrophysics and Cosmology	Nuclear physics, astrophysics and cosmology
Materials Science	Materials
Earth and Environmental Sciences and Space Physics	Earth and space sciences
Chemistry and Chemical Sciences	Chemical sciences
Engineering Applications	Weapons science and engineering, advanced manufacturing, sensors, remote sensing and sensor systems
Computational Physics, Applied Math and Knowledge Sciences	Information and knowledge sciences, computer and computational sciences
High-Energy Density, Plasma and Fluid Physics	High-energy density plasmas and fluids
Biological Science, Biosecurity and Cognitive Sciences	Biosciences
Quantum and Optical Sciences	Fundamental interactions and excitations in atomic, optical, and molecular systems
Energy Sciences, Technology and Engineering	Energy sciences, technology and engineering
Computational Co-Design	Stockpile stewardship, molecular dynamics and materials in extreme environments
Emergent Phenomena in Materials Functionality	Theoretical, computation and modeling, and experimental methods to understand basic phenomena of materials

Postdoc Research and Development

The PRD component of the program ensures the vitality of the Laboratory by recruiting early-career researchers. Through this investment, the LDRD program funds postdoctoral fellows to work for two years under the mentorship of PIs on high-quality projects. The primary criterion for selection of LDRD-supported postdocs is the raw scientific and technical talent and performance of the candidate, with the exact specialty of the candidate a secondary factor. In FY11, LDRD funded 77 PRD projects, which represents 6% of the program's research funds. Postdoctoral Research and Development researchers are supported full-time for two years.

In addition to approximately 63 "Director's Postdocs," the LDRD program supported 15 distinguished postdoctoral fellows at a higher salary and for a three-year term. Distinguished postdoctoral fellow candidates typically show evidence of solving a major problem or providing a new approach or insight to a major problem; in other words, they show evidence of having a major impact in their research field. To recognize their role as future science and technology leaders, these appointments are named after some of the greatest leaders of the Laboratory's past.

Even more LDRD-funded postdocs are hired through DR and ER projects than directly through PRD appointments. Counting both avenues, the LDRD program supported 57% of the Laboratory's 580 postdocs in FY11. Among the DOE labs, the LANL postdoc population is exceeded only by Lawrence Berkeley National Laboratory, which has a special relationship with the neighboring University of California campus.

As the principal pipeline for new technical staff, the health of the postdoctoral program is of vital interest to the Laboratory. A 2011 analysis revealed strong evidence that the postdoctoral program is excelling:

- Acceptance rate for Laboratory offers of postdoc appointments remains high, at 89%

- 68% of US citizen distinguished postdocs selected since 1999 were still at the Laboratory as staff

- The quality of postdocs hired at Los Alamos reveals a clear upward trend, evidenced by the high numbers of publications and citations at the time of their hire

Postdocs Supported by Individual LDRD (PRD) Projects
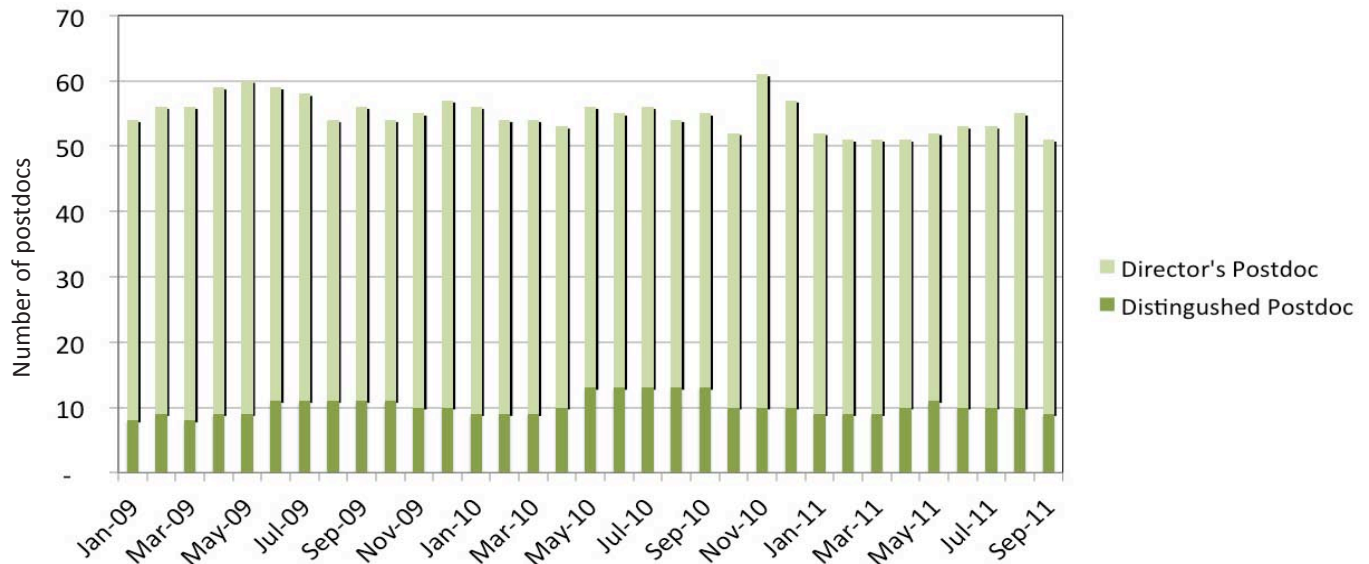
LDRD Investment in a promising postdoc pays off

Eric Bauer of Condensed Matter and Magnetic Science, is the recipient of a Presidential Early Career (PECASE) Award for Scientists and Engineers. The award is the highest honor the U.S. government bestows to outstanding scientists early in their careers. Bauer was honored for his pioneering research in condensed matter physics through the discovery and synthesis of new materials, especially strongly correlated and f-electron systems, and clarifying their novel physical properties. The award also recognizes Bauer's involvement in outreach activities with students and the scientific community. He is one of 13 DOE researchers honored with the award.

Bauer has published more than 200 papers that have been cited more than 2,500 times, including 24 in *Physical Review Letters*, two in *Science*, and three in *Nature*. Bauer is principal investigator of an LDRD project on "Understanding and Controlling Complex States of Matter in New Iron-Arsenide Superconductors through Strain and Disorder." Bauer joined the Laboratory in 2002 as a Director's Postdoctoral Fellow, funded by the LDRD program.

Two of the world's leading intermetallic synthesis experts, Eric Bauer (left) and Yuri Green from the Max Planck Institute for Chemical Physics, Dresden, discuss their views on the challenges of material design.

Project Budgets

Number of projects (y-axis, 0–100)

Project budget ($K) (x-axis: 0–50, 50–100, 100–150, 150–200, 200–300, 300–400, 400–500, 500–600, 600–800, 800–1000, 1000–1200, 1200–1400, 1400–1600, 1600–1800, 1800–2000, 2000–2200, 2200–2400, 2400–2600)

Legend: FY11 BOY, FY12 BOY
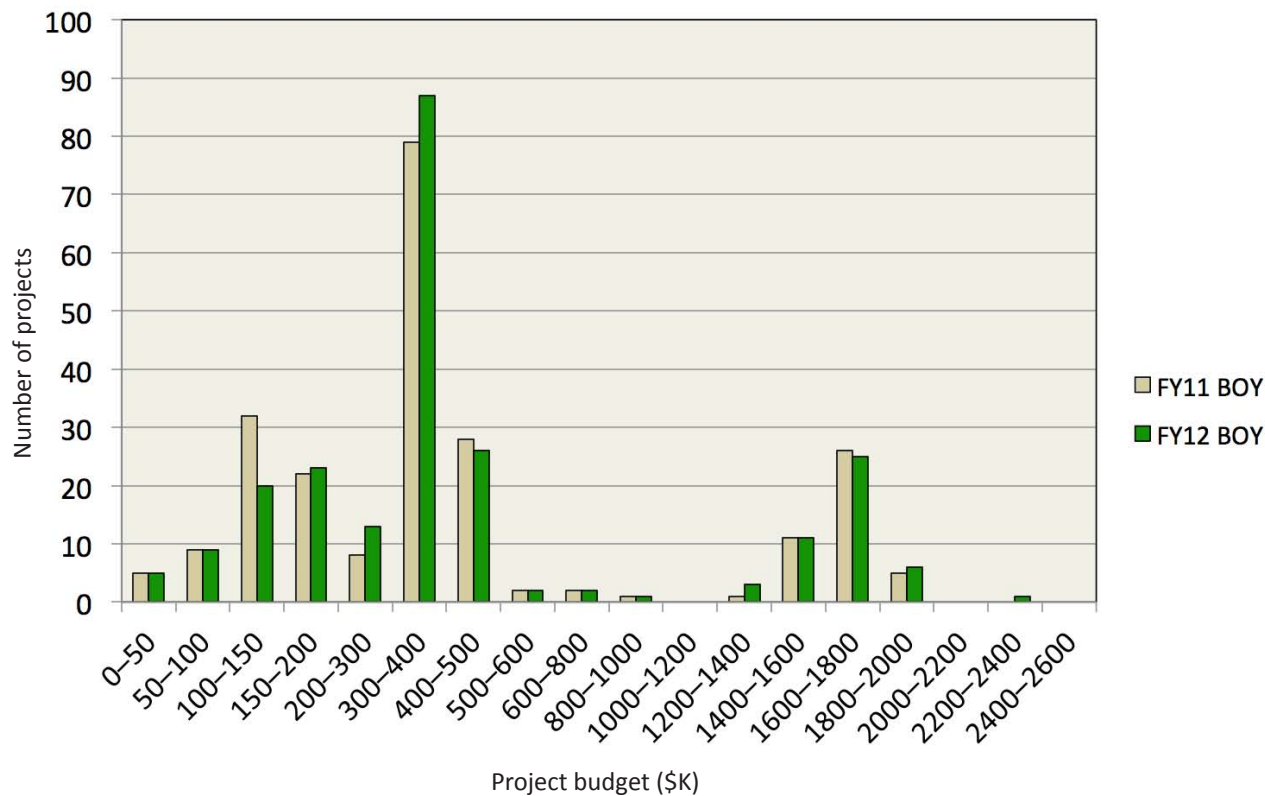
LDRD project sizes have changed little in recent years, except for modest adjustments for inflation. Projects in the range of $300-$500K annum are single-PI Exploratory Research projects; $1200-$2400K multi-disciplinary Directed Research projects; and smaller projects are reserve or postdoctoral R&D projects. Project sizes are reviewed annually by senior management with the goal of keeping projects as small as possible in order to keep their numbers up and accomplish our diverse strategic objectives.

Program Reserve

Most LDRD investments are selected in a rigorous, multi-step peer-review process during the nine months preceding the new fiscal year. However, in a fast-changing world, there are needs that cannot wait until the next cycle of competition. The LDRD Program Office holds a reserve each year for these needs. This reserve is small on a program basis, but allows the opportunity to make modest investments that address new opportunities. In FY11, the beginning-of-year reserve budget was approximately $6M, about half of which was held for incoming postdoc and early career projects.

Reserve decisions are guided by strategic priorities articulated by Division Leaders, Associate Directors, and more senior management. They are also informed by the just-concluded competitive cycle, in which selection panels sometimes identify ideas that are exciting but just not mature enough for a full-scale investment. Reserve is held foremost to exploit opportunity, rather than fix problems, and the expectation is that reserve projects will be the first step in a chain that leads to bigger things.

In FY11 LDRD supported 34 new reserve projects, an unusually high number unique to that fiscal year, thanks to an additional $7M reserve in the second quarter of the fiscal year. The additional reserve added mid-year was used to target mission areas in sustainable energy, science of signatures, and materials in extreme conditions.

One project in particular exemplifies how early LDRD investment enables spectacular results: Andrew Bradbury's work to unravel the secrets of how human genes function. Bradbury and colleagues are developing an automated pipeline to generate antibodies against human gene products, without using animals. Their work was partially supported by a 2011 LDRD reserve project, and has resulted in more than $4 million in funding from the National Institutes of Health. Bradbury's related ER project was named "Most Marketable Technology" at LDRD Day 2011.

Antibodies in the Fast Lane

A National Institutes of Health (NIH) grant to LDRD researcher Andrew Bradbury of Los Alamos National Laboratory's Bioscience Division could help unravel the gnarly secrets of how many human genes function.

Originally enumerated by the Human Genome Project, the approximately 20,000 genes of the human body have been slow to give up their exact roles. And one of the best tools for exposing a gene's function is to take the protein it produces and generate specific antibodies, usually by vaccinating mice or rabbits. Antibodies are specialized proteins the immune system deploys to block the actions of potentially harmful bacteria and viruses.

By looking at antibodies, researchers can identify where, in a cell, genes are active and under what conditions they increase or decrease their expression. Antibodies are also one of the fastest growing classes of new therapeutics, with sales of about $40 billion in 2010.

With the new NIH Common Fund grant of more than $4 million, researchers led by Andrew Bradbury aim to develop an automated pipeline to generate antibodies against human gene products, without using animals.
Bradbury's team will use "antibody libraries" expressed in bacteria and bakers yeast. These libraries are enormous, comprising billions of different antibodies, and the ultimate goal is to identify antibodies in the libraries that recognize each human protein. The broad availability of antibodies against all human proteins will facilitate the understanding of human disease and provide likely targets for therapeutic intervention, with the antibodies themselves potentially becoming therapeutic leads.

This project will leverage technology developed over the years at LANL, including flow cytometry, antibody libraries and fluorescent protein technology, and has the potential to create a set of tools applicable to many different problems of interest to stakeholders beyond NIH, including the U.S. Department of Energy and Department of Defense.

The Los Alamos LDRD portfolio reflects diversity at all levels, from innovative projects that span the DOE missions, to a diverse pool of researchers that range from early career to senior scientist.

LDRD Researchers Across Divisions and Directorates

LDRD Supports Researchers at All Career Stages

Project Selection

The Los Alamos LDRD program operates as a free market for ideas driven by Laboratory strategy: Senior Laboratory leadership set science and technology priorities, then open an LDRD competition for ideas across the breadth of the Laboratory. Panels formed from the Laboratory's intellectual leaders rigorously review proposals. Conflict of interest is carefully regulated. Evaluation criteria include innovation and creativity, potential scientific impact, viability of the research approach, qualifications of the team and leadership, and potential impact on Laboratory missions. The selection processes are modeled on best practices established by the National Science Foundation (NSF) and National Institutes of Health (NIH).

OUTSTANDING (5)
Work leads its technical field; outstanding ratio of results to investment; potential for revolutionary impact on Los Alamos Missions; results of project have spurred follow-on research.

GOOD (3)
Identifiable impact on mission or field; results mixed; success would have a distinct impact on Lab programs; identifiable early signs of external recognition

DEFICIENT (1)
Quality of research does not meet national and Laboratory standards; serious problems with project execution; anticipated minimal impact on Lab mission and science; minimal evidence of external recognition.

EXCELLENT (4)
Clear differentiation from previous work; team is making very good progress; potential for important impact on mission and technical field; follow-ons visible within Laboratory.

FAIR (2)
Largely incremental, marginal impact on mission or field; identifiable lack of progress; notional connections to National Security missions; minimal evidence of external recognition.

Analysis of FY11 DR project appraisals showed an average score of 4.2, which is between excellent and outstanding. This average reflects 22 appraisals.

To guarantee fairness and transparency, and to ensure that the strongest proposals are funded, the selection panels include managers and technical staff drawn from the full range of technical divisions. Serving on an LDRD selection panel, such as the DR Strategy Team, is often a starting point on the path to leadership roles in the scientific community. Past LDRD panelists have gone on to be Laboratory fellows, division leaders, program directors, association fellows, and chief scientists, while others have transitioned from the Laboratory to become leaders in academia.

Independent project appraisals validate mission relevance

In FY11, the LDRD Program Office conducted an appraisal of every ongoing project it intended to fund in the next fiscal year. The primary objective is to assess progress and provide peer input to help PIs maintain the highest quality of work. The appraisals also help the LDRD Program Office monitor and manage the program portfolio. In addition to formal project appraisals, which are conducted annually, the LDRD Program Director and Deputy Program Director meet informally with PIs in their labs at least once a year to discuss their projects. The purpose of these one-on-one meetings is to give PIs individualized assistance and to determine what the LDRD Program Office can do to positively impact the success of the project. Each DR project has also been assigned a Program Development Mentor to assist the transition of LDRD successes to mission. Any weak-

nesses are actively addressed. The project leader is asked to respond to the report with a revised project plan.

Continuing DR projects are appraised every year of the life of the project, with at least one of the reviews including external reviewers. The internal-external review is open to all Laboratory staff and leaders. Four project appraisers – two internal and two external – are nominated by the PI and approved by the LDRD Program Director. When possible, the appraisal is held as part of a broader workshop hosted by the Laboratory.

Written appraisals, held in the LDRD archives, address: (1) Brief summary of accomplishments; (2) Assessment of quality of science and technology, relevance to Laboratory and national missions, progress toward goals and milestones, project leadership, and the degree to which the project may establish or sustain a position of scientific leadership for the Laboratory; and (3) Recommendations by the committee for changes in the scope or approach of the project. The criteria for the most important point – number (2) above – are derived from criteria developed by the National Academy of Science to assess all federally sponsored research.

Continuing ER projects are appraised in their first and

second years. The LDRD Deputy Program Director collaborates with the technical divisions to conduct project appraisals. Like DRs, the projects are appraised according to the Federal criteria of quality, performance, leadership, and relevance.

LDRD service provides benefit to all

The mission of the Laboratory is to solve the nation's most difficult national security problems. By their nature, these problems lack a well-defined path to solution. In fact, the path is often completely unknown. It is rare that such creative work is done alone; the ideas and results from many colleagues are needed, often drawn out in conferences, hallway conversations, journals, seminars. LDRD is an internal arena in which Laboratory staff serve as peer reviewers and play a key role of interaction in the scientific process. Proposal selection panelists are chosen for their subject-matter expertise, and the discussions in which they engage are not only critical to the LDRD process, but they also provide an opportunity for panelists to educate themselves on the latest results and practices, and expose themselves to opportunities for collaboration. As noted in an evaluation of peer review conducted by the UK House of Commons, "Peer review is regarded as an integral part of a researcher's professional activity; it helps them become part of the research community."

The idea that LDRD service benefits both the volunteer and the Laboratory is supported in a recent statement by DOE LDRD Program Director John Labarge. "Being on these review committees is a critical part of being a scientist at a DOE National Laboratory, and a benefit to both the laboratory and the employee," he noted. "The Laboratories encourage all researchers to stay current with the latest research advances, and this is a good way for them to keep fresh and thinking in new ways about their research for DOE."

In FY11, the Los Alamos LDRD Program Office conducted a survey of current-year DR and ER panelists to evaluate the benefit, if any, they received from their LDRD service. The feedback that resulted from the evaluation was markedly positive:

"In leading the IST SAP, I was able to better understand the portfolio of research capabilities in the IST arena and to identify scientific researchers who could contribute to new scientific directions in CNLS. An example of note is that I learned the importance of understanding and quantifying the human-machine interface as an integral part of machine learning development."

"Insight into these newest concepts and ideas in a variety of fields has enabled me to facilitate the formation of new, broad teams to attack such problems. Service on these panels is both critical and unique for this type of activity…. Without a doubt, my expertise in peer review proposals has primarily grown through service on LDRD review panels."

"Certainly, I agree that it helped to expand my research network connections at the lab, but that doesn't directly translate into more stable funding for myself… However, I learned tremendously about leadership skills on how to manage a team of unique members with diverse view points and form consensus."

"I think that the main benefit has been that LDRD service, especially for DR, has forced me to broaden my knowledge of the Lab's key technologies, to include not just how the technologies work but also to the R&D challenges that exist as we try to advance them."

"As a member of the ASC Alliance Strategy Team, helping theNNSA HQ ASC program manage their university alliances, my service as a SAP chair was useful in identifying commonalities and possible links between LANL LDRD research and academic research."

"I became aware of some new collaboration possibilities, and gained some new insights into where my work could play a role in areas that I hadn't previously considered."

"I learned a great deal of about the frontier areas in science, many of which are relevant to, but loosely connected to my own area of specialty."

"My sense is that there are a relatively few people who 'know everybody' around the lab (and thus are valuable in making connections) … and the correlation between that cohort and those who serve LDRD is near [100%]….I honestly believe I'm more qualified and capable for my job as Office of Science Program Director as a result of my service on the DR strategy team."

"My knowledge of physics has been broadened, particularly in areas outside [but] close to my areas of responsibility. This has made me a more valuable manager for LANL."

"Cross organizational teaming and understanding the work of other disciplines is certainly a much better recipe for innovation, which in turn benefits the programs that have historically paid my salary…I learn, I synthesize new ideas, I potentially identify beneficial interactions/ collaborations."

Mission Relevance

The LDRD Program Office treats mission relevance as one of the most important criteria in the evaluation of a potential LDRD project. Mission impact is considered carefully in project selection. Later, the mission impact of funded projects is tracked annually through the data sheet process. Because of the basic science and engineering nature of most LDRD projects, the work often proves to be relevant to numerous missions and agencies. In the chart below, the sum of the total LDRD investment in DOE missions is significantly greater than the annual LDRD budget because LDRD investment in a single project is often relevant to more than one mission area.

Ultra-low field nuclear magnetic resonance technology developed at Los Alamos with support from LDRD provides compelling examples of research that has broad-reaching relevance across many mission areas and sponsor interests. In addition to the climate applications highlighted next, the same technology is relevant to neuroscience and the detection of liquid explosives.

Investigating Tree Mortality with Ultra-Low Field Nuclear Magnetic Resonance

Los Alamos researchers have observed, for the first time, that water content can be monitored non-invasively and unobtrusively in intact trees via ultra-low-field/nuclear magnetic resonance (ULF NMR). The researchers have seen evidence of both changes in water content for day versus night in an aspen tree, as well as the overall decline in water content as the tree is dying. The work represents a first in application of the ULF NMR method to the study of plant function and mortality. Additional validation with traditionally accepted environmental methods is underway. If validated, the work appears to represent a first non-invasive look at how water movement changes inside an aspen tree over time; for example, during the onset of mortality.

The work was accomplished using LDRD Science of Signatures reserve funding. The effort demonstrates that the combination of Los Alamos's unique abilities in ultra-low field magnetic resonance imaging with climate-driven vegetation mortality research can provide insight into basic questions of plant function and mortality.

FY11 LDRD Funding to DOE Missions ($M)

Legend:
- Project directly addresses identified mission challenge
- Project builds underlying science, technology, or engineering
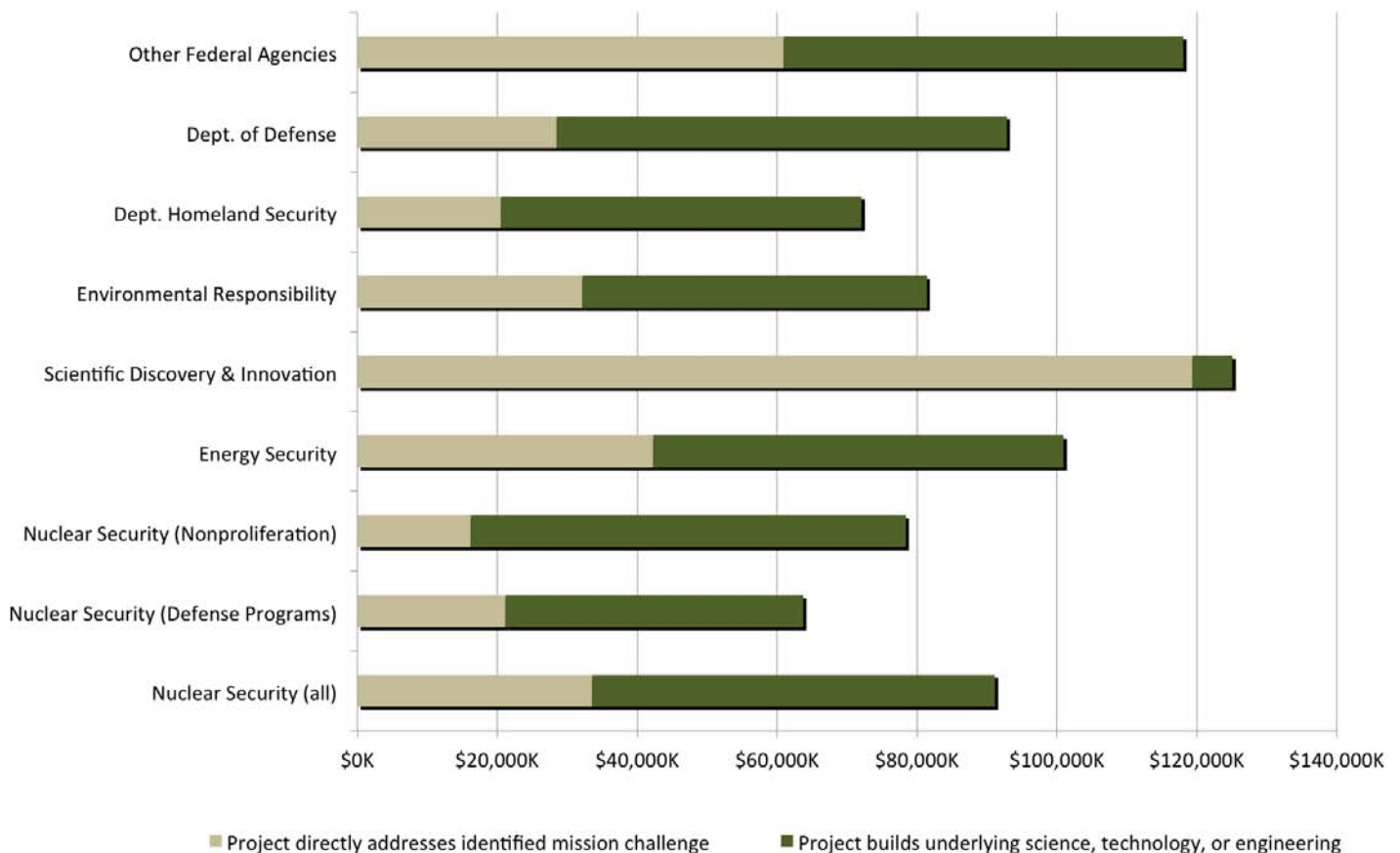
Their ultimate aim is to provide basic insights into questions such as how plants die, especially during drought. While the question of plant mortality is easy to conceptualize, it is difficult to study because of the spatial and temporal variation of processes over the plant. Understanding these mechanisms of mortality, especially the tipping points, will provide critical input to forecasts of future climate because presently models cannot simulate vegetation change and related climate effects. The work here represents a first step towards fieldable, non-invasive monitoring to answer these fundamental questions.

Researchers include M. Espy (P-21), N. McDowell (Earth System Observations, EES-14), J. Resnick (P-21) I. Savukov (P-21), and S. Sevanto (EES-14).

Calibration data showing correlation between weight and ULF NMR signal in a dying branch.

Top row: Two photos of the tree in the ULF NMR system. The NMR system is located inside the silver magnetic shield. The photo at left was taken approximately seven days before the photo at right, and significant decline in leaves is noted. Bottom row: Left shows close up of leaves infected with parasite. Right shows close up of NMR system around tree trunk.

ULF NMR signal from aspen tree over three days. A daily cycle associated with the NMR signal (water content) is present, as is a downward trend that appears to correlate with overall decline of the tree's health.

Investment in Information Science and Technology
Benefits Multiple Capabilities

Energy and Earth Systems

Signatures and Sensing

Multi-Perspective Network-Scale Modeling & Detection for Cyber Systems

Algorithmic Co-Design: Paradigms for Unstructured Problems on Accelerated Architectures

Optimization Principles for Co-Design applied to Molecular Dynamics

Hierarchical Sparse Models for Robust Analysis of Video Data.

Information Science and Technology: Metagenomics

The Physics of Algorithms

Statistical Physics of Networks, Information

Uncertainty Quantification for Networks

Robust Unsupervised Operation Under Uncertainty Through Information Theoretic Optimization of Complex Systems.

InfoFusion: "Connecting the Dots" Using Cyberspace Information Models

New and Enhan... in Quantum... Pro...

...nd Dynamics ...on Science

Detecting and Defending Against Viral Threats in Cyberspace

Efficient Interdiction

Combinatorial Approaches To Graphical Models: Theory & Applications

Information Science and Technology

Computational Complexity and Quantum Entanglement

Complex Biological Systems

Synthetic Cognition through Peta-Scale Models of the Primate Visual Cortex

Engineering

New Mathematical Tools for the Quantum Dynamics of a Bose-Einstein Condensate

Nuclear Performance

Materials: Discovery Science to Strategic Applications

Beyond the Standard Model

Sharp characterization of minimizers (typically) involving interfaces in images

Statistical Models for Natural Graphs

Network-Centric Quantum Communications

CoCoMANS: Computational Co-design for Multi-scale Applications in the Natural Sciences

Information Science and Technology: Streaming Data

Neyman-Pearson Learning

New Approach to Bayesian Inference Under Modeling Uncertainty

...rated Scientific ...ation Capabilities in Large Scale Data Environments Via Application of Advanced Hybrid Computing Technologies

...ce for ... Quantum M...

Designing Communication Methods for Bottom-Up Self-Assembled Nanowire Networks of Emerging Computer Architectures

RADIUS: Rapid Automated Decomposition of Images for Ubiquitous Sensing

Investment in projects that fall within the Information Science and Technology Grand Challenge and/or ER Category provide benefit to mission areas across the Laboratory. This map illustrates how IS&T projects connect to other grand challenges and help build capabilities in a wide range of areas beyond IS&T.

Mission Impact

LDRD delivers capabilities and explores solutions for all Los Alamos missions: Nuclear Security, Global Security, Energy Security, and Scientific Discovery. In some cases these lead to clearly identified follow-on projects. In part, this can be attributed to the program development mentors who help transition these projects from LDRD to external funding.

Putting a quantitative metric on mission impact is difficult. The obvious metric (follow-on funding) omits other benefits like new ideas and approaches that feed into ongoing work. Counting dollars is also imperfect because, although LDRD is part of what enables new mission solutions, the Laboratory brings other assets to bear, including facilities, ideas, and personnel from a range of programs. Nonetheless, admittedly rough numbers show that projects active in FY11 played an important part on the path to $67M of externally funded R&D.

The path from LDRD to mission is clearly demonstrated by follow-on projects from sponsors that range, inside DOE, from the nuclear weapons program to nonproliferation programs, applied energy programs, and the Office of Science, and more broadly, across a range of sponsors that include DoD (DARPA, ONR, and DTRA), DHS and DNDO, NIH and CDC, classified agencies, and a suite of industrial partners. The capabilities sustained by these external sponsors feed back once again to enable the Laboratory's execution of NNSA missions.

Here we highlight just a few successful projects transitioned from LDRD to external funding in FY11:

The Department of Homeland Security Science and Technology (S&T) Directorate is funding basic research within LANL's Shock and Detonation Physics group aimed at understanding the effects of addition of inerts to liquid explosives on the explosive's sensitivity and performance. Under the extreme conditions reached by shock compression, chemical reactions may occur between an explosive and "inert" additive at the leading edge of the shock/detonation wave, altering the explosive's bulk initiation and/or detonation behaviors, e. g. the inert additive may not be inert under these conditions. The work capitalizes on capabilities and expertise gained through an LDRD DR project focused on understanding shock-induced chemical reactions over decades in length and time scales behind the shock front.

A project focused on developing a multi-source energy harvesting solution designed to provide reliable power for embedded sensing systems resulted in external funding from Samitaur Medical Technologies. The goal of the spin-off project is to develop a compact energy source that can power a neurological implant device used to treat patients with motor control disorders such as epilepsy and Parkinson's disease. The system of interest would harvest kinetic energy from the patient's movement and couple this with energy scavenged from the ambient background environment emitted by standard WiFi systems and cellular telephones. The device developed for this project relies on a single electromagnetic transducer to harvest both kinetic and wireless energy sources. A prototype transducer has been designed and tested to prove the feasibility of this concept. Follow-on efforts are in discussion to develop power conditioning electronics to collectively harvest both kinetic and wireless energy simultaneously and provide extended battery life for the embedded power source. The benefit of this device is that it would reduce the number of surgeries a patient must undergo in the initial procedure, while also providing a long term power solution that can be recharged from ambient energy sources, or powered directly using a wireless energy transmission scheme.

In 2009, LDRD researchers set out to identify host proteins that are targeted by Y. pestis during infection using RNA interference (RNAi), a powerful tool for analyzing gene function by silencing, or inactivating, target genes through the specific destruction of their mRNAs. They performed high-throughput genome-wide screens and more directed automated confocal microscopy studies to select for genes that, when silenced, lead to inhibition of Y. pestis infection. In FY11 their notable results led to funding from the Defense Threat Reduction Agency to generate a high-throughput research capability for functional gene discovery that can be applied to multiple complex biological problems, such as development of innate immunity and differential host response. The expected result is a robust methodology by which to ascribe function to previously uncharacterized genes, a major challenge in biomedical research given that approximately half of all predicted human genes have no known function.

Metrics of Excellence

The LDRD program is a key resource for addressing the long-term science and technology goals of the Laboratory, as well as for enhancing the scientific capabilities of Laboratory staff. Through careful investment of LDRD funds, the Laboratory builds its reputation, recruits and retains excellent scientists and engineers, and prepares to meet evolving national needs. The impacts of the LDRD program are particularly evident in the number of publications and citations resulting from LDRD-funded research, the number of postdoctoral candidates supported by the program, and the number of awards LDRD researchers received.

Publications

LDRD produces a large volume of high-quality scientific contributions relative to its portion of the Laboratory's budget. The numerous publications made possible with LDRD funding help the Laboratory maintain a strong presence and scientific reputation in the broader scientific community. In FY11, LDRD researchers generated 452 peer-reviewed publications, accounting for 22% of the Laboratory's total. The quality of these publications is evidenced by the number of times they were cited. LDRD publications published in FY11 were cited 987 times, accounting for 29% of the Laboratory's citations, as well as four of the Laboratory's top 10 cited publications. With increased efforts to collect post-project performance metrics, LDRD publication and citation counts increase year-to-year. Recent analysis of 2008 citations reveals that all ten of the Laboratory's top cited publications in FY08 are linked to LDRD work.

Peer-Reviewed Publications				
	FY08	**FY09**	**FY10**	**FY11**
LANL Pubs	1800	1713	1741	2079
LDRD Supported	444	398	408	452
% due to LDRD	25%	23%	23%	22%

Citations				
	FY08	**FY09**	**FY10**	**FY11**
LANL Citations	21879	16755	10413	3400
LDRD Supported	7383	5545	2871	987
% due to LDRD	34%	28%	28%	29%
Top 10 Most Highly Cited Publications				
LDRD Supported	10	4	4	4

Patents and Disclosures

Another indication of the cutting-edge nature of the research funded by LDRD is the contribution the program makes to the intellectual property of the Laboratory. In FY11, LDRD-supported research resulted in 15 patents, 25% of the Laboratory's total, and 28 disclosures, 22% of the Laboratory's total.

Postdoctoral Support

LDRD remains an important vehicle for recruiting the brightest researchers to the Laboratory, where they become innovators and scientific leaders.   In FY11, LDRD supported 330 postdocs, accounting for 57% of the Laboratory's total.

Patents				
	FY08	**FY09**	**FY10**	**FY11**
LANL Patents	28	52	61	59
LDRD Supported	8	12	15	15
% due to LDRD	29%	23%	25%	25%

Disclosures				
	FY08	**FY09**	**FY10**	**FY11**
LANL Disclosures	116	110	116	129
LDRD Supported	36	38	16	28
% due to LDRD	31%	38%	21%	22%

Postdoc Support				
	FY08	**FY09**	**FY10**	**FY11**
LANL Postdocs	477	470	547	580
LDRD Supported	274	291	325	330
% due to LDRD	61%	62%	59%	57%

Postdoc Conversions				
	FY08	**FY09**	**FY10**	**FY11**
LANL Conversions	39	37	53	208
LDRD Supported	21	14	33	107
% due to LDRD	54%	38%	62%	51%

FY11 LDRD Collaborators in the USA

Collaborator Distribution Key (logarithmic scale)

1   25   40

FY11 LDRD Collaborators Worldwide

Collaborator Distribution Key (logarithmic scale)

1   25   650
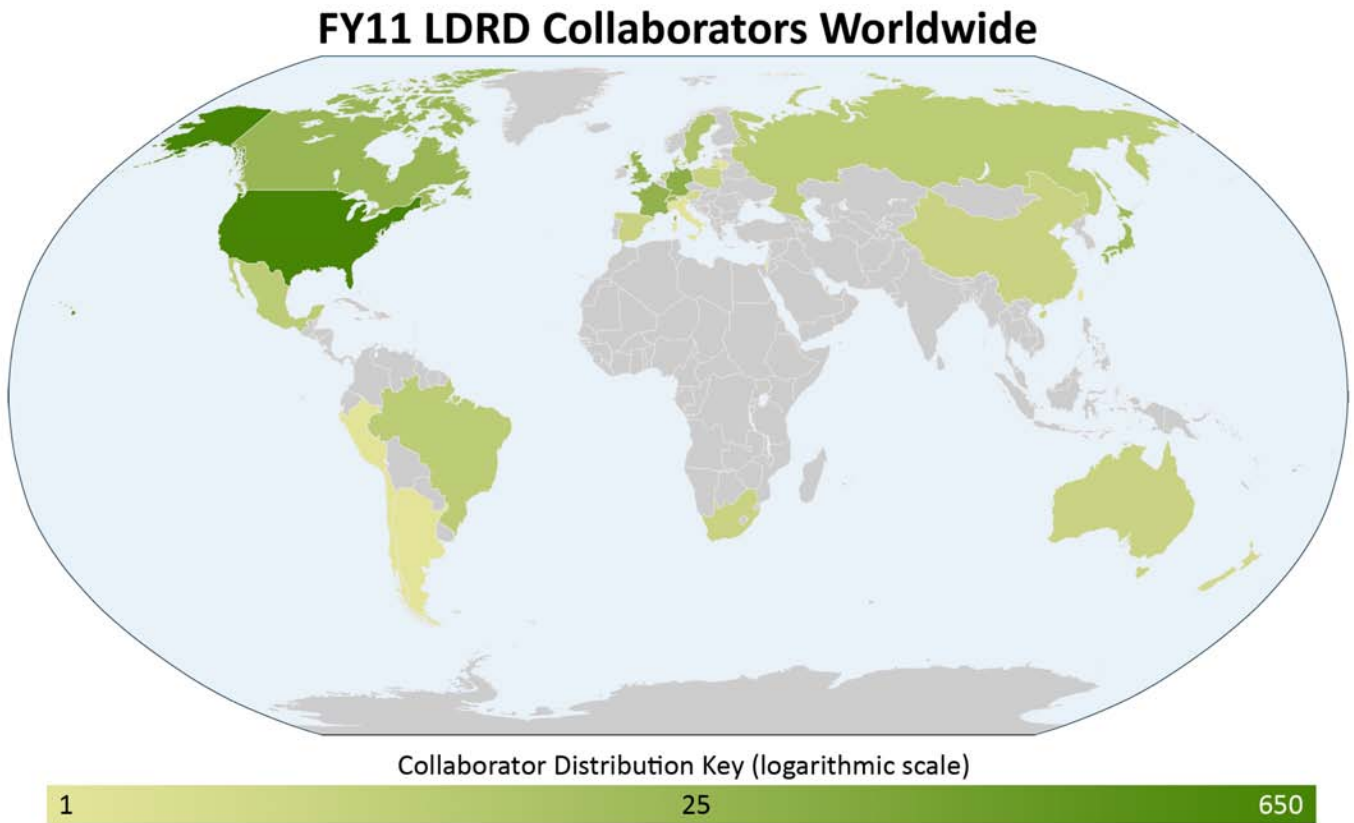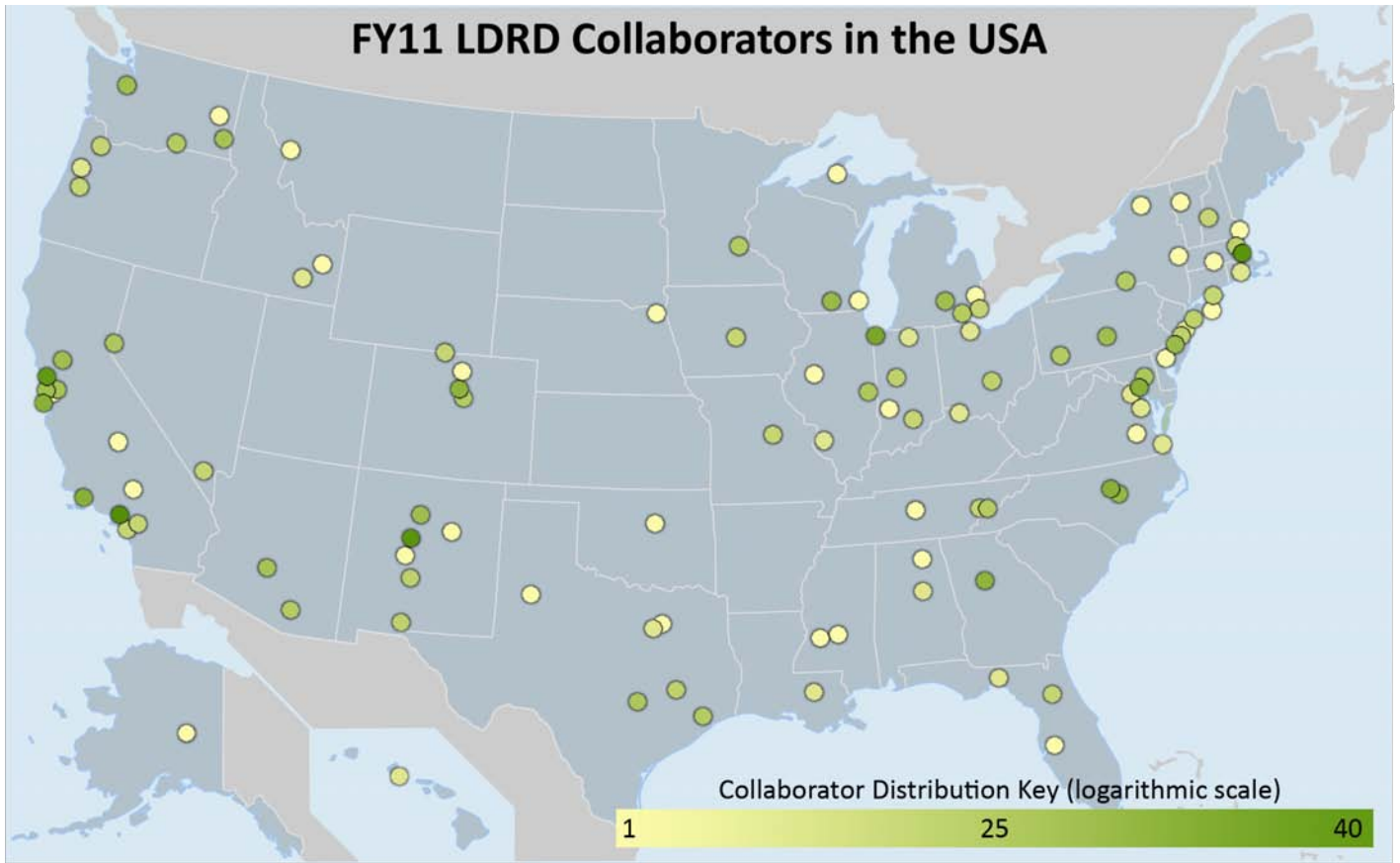
External collaborations are often critical to a successful LDRD project. Formal collaborations between LDRD PIs and researchers at other national laboratories, academia, and industry enable access to world-leading facilities and knowledge. Such collaborations enable LDRD researchers to be active and prominent members of the broad scientific community. The figures above illustrate the far-reaching collaborations established by LDRD researchers in FY11.

FY11 LDRD Metrics Summary

Metric	Evidence
LDRD work is of high technical quality and impact	● Peer-reviewed publications remain a large fraction of Laboratory output (25%) **- LDRD supports approximately 23% (4-year average)** ● Patents and disclosures remain a large fraction of Laboratory output (25%) **- LDRD supports approximately 25% and 28%, respectively (4-year average)** ● Top-cited papers are dominated by LDRD work **- LDRD supports more than 50% (4-year average)** ● Quantitative appraisal scores for ongoing projects show a pattern of excellence **- Independent project appraisal scores average outstanding to excellent** ● Citation counts show that LDRD makes a major contribution to Laboratory technical output **- LDRD supports 30% of the Laboratory's total (4-year average)**
LDRD is essential to the Laboratory's ability to deliver mission solutions	● Success stories show clear path from LDRD investment to major mission impacts ● Funded follow-on projects show LDRD prepares the Laboratory to meet national needs **- Active projects resulted in approximately $67M in external funding** ● Proposals and briefings tracked by the program development mentor program show sponsor engagement - Engaging with weapons and global security program management to reinforce program development mentor process
LDRD builds the Laboratory's human capital	● Number of postdocs supported by LDRD provides a strong pool for future Laboratory needs **- LDRD supports approximately 60% of Laboratory postdocs (4-year average)** ● LDRD supports researchers at all career stages, from postdocs to senior staff **- Analysis of PI career stages revealed LDRD is supporting a desirable cross section of the Laboratory population** ● LDRD supports numerous and substantive national and international collaborations that reinforce internal capabilities **- LDRD researchers established 871 collaborations worldwide**
LDRD is a major factor behind the Laboratory's technical reputation	● LDRD work contributes significantly to awards such as R&D 100, Lab and Society Fellows, and others ● Journal covers based on LDRD work show a prominent national impact

● **Excellent**   ● **Satisfactory**   ● **Improvement sought**

The strategy and outcomes of the LDRD program are tracked by these metrics. The results show that LDRD is on track to meet the challenging goals we have set for ourselves.

> "LDRD is critical for attracting and retaining high quality technical staff and thus for assuring long-term viability of the Laboratories and their ability to carry out their mission in the future."

The LDRD program supports some of the Laboratory's most accomplished researchers, as well as many of its most promising young scientists and engineers. In FY11, LDRD researchers received more than 75 awards and recognitions, including R&D 100 Awards; fellowships from the American Physical Society, American Ceramic Society, Materials Research Society, and American Association for the Advancement of Science; the Presidential Early Career Award for Science and Engineering, and many others. Here we highlight only a few:

Awards and Recognitions

Muon tomography, a Los Alamos invention that uses cosmic ray muons to image cargo and vehicles for threat materials such as uranium or plutonium, has been named one of the 100 best inventions of the year by *Popular Science* magazine. The technology is incorporated into the Multi-Mode Passive Detection System, which will be installed at specific U.S. and international ports this year through a Cooperative Research and Development Agreement (CRADA) between Los Alamos and the California security company Decision Sciences International Corporation.

LDRD funded the initial research through a 2002 ER project and a 2004 DR project.
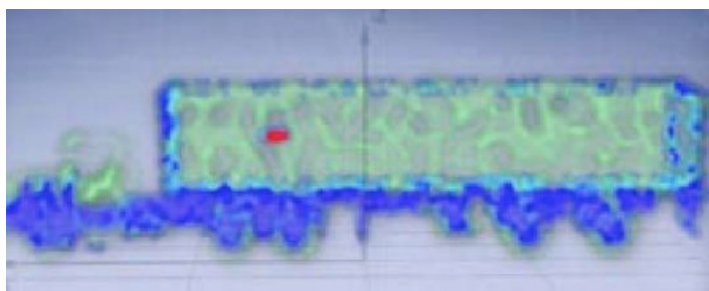
A tomograph analysis of a truck showing a "hotspot" depicted in red) of radioactivity. Image courtesy of Decision Sciences International Corporation.

John Welsh, a post-masters student in the Bioenergy and Environmental Science Group, received a scholarship for his international poster presentation at the Keystone Symposia on Molecular and Cellular Biology. Welsh's research was one of two presentations selected for this honor among a very competitive peer group. The Keystone Symposia on Molecular and Cellular Biology are a series of meetings targeting researchers focused in the biomedical and life sciences. The Symposium, held in Singapore, featured internationally recognized scientists that are at the forefront of their respective fields to address the worldwide energy crisis. The meeting provided a unique opportunity to foster new relationships with Singaporean officials and scientists while showcasing U.S. state-of-the-art research.

Welsh is conducting research at LANL before beginning the doctorate program at the University of Pennsylvania. He is examining bioengineering of both heterotrophic (*E. coli*) and phototrophic (bluegreen algae) organisms for commodity chemical production. He is instrumental in LANL's efforts for microbial production of catechol and catecholate-type derivates that are derived exclusively from glucose or carbon dioxide and light. Welsh employed the National Flow Cytometry Resource (also developed with LDRD support) in Bioscience Division to develop a rapid method for selecting blue-green algae with both altered phenoand genotypes. Claire Sanders (Advanced Measurement Science, B-9), the key technologist within the flow resource, provided all the necessary technical expertise to pursue and advance the research team.

The combined effort of this research culminated in an invited poster presentation to the Keystone Biofuels Symposium and a $1500 scholarship for Welsh. Andrew Koppisch and David Fox (B-8) are co-Principal Investigators on the LDRD project that funded the research, which supports the Laboratory's Energy Security mission area and the Materials for the Future and Science of Signatures capabilities.

Leonid Gurvits, a mathematician in Information Sciences, completed fundamental work on the algebraic construct of the permanent, "the ugly twin" of the mathematically well-behaved and better-known determinant. His original work came from a 2007 LDRD ER project "Hyperbolic Polynomials Approach to Approximate Counting and Lower/Upper Bounds in Combinatorics, Statistical Physics and Computational Geometry." He published this research in the highly competitive ACM (Association for Computing Machinery) Symposium on the Theory of Computing conference. The title of the paper is "Hyperbolic Polynomials Approach to Van der Waerden/Schrijver-Valiant Like Conjectures: Sharper Bounds, Simpler Proofs and Algorithmic Applications."

The "Proof of Permanents" achievement is receiving significant attention in the global mathematics and computer science community. Lex Schrijver, the well-known mathematician and Von Neuman Theory prize-winner, studied Gurvits's novel proof technique. Schrijver subsequently published an article on the subject in the *American Mathematical Monthly* journal, which is the most widely read mathematics journal in the world. Don Knuth, Professor Emeritus of The Art of Computer Programming at Stanford University, is one of the founders of computer science as a discipline. He has been given many awards, including the Turing award and the John Von Neumann Medal. Most LANL scientists are using Knuth's work every time they use the LaTeX type setting system that Knuth developed. Knuth has become fascinated by Gurvits's work. He gave a talk, "Leonid's Breakthrough about Lower Bounds for the Permanent," at the Stanford University theory seminar series.

Improving on Existing Molecular Beacons

NanoCluster Beacons are collections of silver atoms maneuvered to illuminate when bound to specific nucleic acids, such as the DNA of particular pathogens. Created by Hsin-Chih (Tim) Yeh, James Werner, Jaswinder Sharma, and Jennifer Martinez, these beacons can be used to probe for diseases that threaten humans by identifying the nucleic acid targets that represent a person's full genome, and allow for personalized medication. They also can be used in quantitative biology applications, such as counting individual molecules inside a cell.

Once bound with a specific target, a NanoCluster Beacon lights up, emitting fluorescence approximately 200 times greater than in the unbound state and easily viewed by the naked eye under ultraviolet light. The beacons come in an array of colors for multiplexed analyses, are more photostable than beacons used today, and can be turned on and off reversibly. Inexpensive, easy to use, and reversible, NanoCluster Beacons are superior molecular probes for detecting specific targets, human oncogene (cancer) sequences, and molecular disease sequences (such as sickle cell anemia).

LDRD was the sole supporter of this work, funded though a 2009 DR project titled, "Predictive Design of Nobel Metal Nanoclusters."

Hsin-Chih (Tim) Yeh, James Werner, Jennifer Martinez and Jaswinder Sharma

Th-ING: Thorium Is Now Green

Th-ING was developed by Jaqueline Kiplinger and Thibault Cantat as a straightforward, cost-effective, and safe method to produce thorium. Thorium is an element discovered in 1828 that is capable of producing more energy than both uranium and coal using significantly lower quantities. This element is only slightly radioactive, making it an excellent candidate for a future sustainable energy source. The work was supported in-part by the Los Alamos LDRD program.

Before Th-ING, thorium could only be produced in hazardous settings at unreasonably high prices. This new method involves reacting thorium nitrate with aqueous hydrochloric acid under mild conditions, which can be performed using conventional glassware in a traditional laboratory setting. Then, a novel combination of anhydrous hydrochloric acid and trimethylsilyl chloride is used to remove

coordinated water molecules, replacing them with dimethoxyethane to make the new thorium chloride reagent. The process cuts costs of production from \$5,000 per kilogram to a mere \$30 per kilogram and is "green"—as it does not produce wasteful solvent ring-opening/polymerization or waste thorium (95 percent production yields). With Th-ING, thorium becomes a practical and reliable source of energy for the future.

Approximately 20,000 drums (3,200 metric tons) of thorium nitrate await disposal. However, such waste is ideal as a starting material for producing the $ThCl_4(DME)_2$ reagent that in turn would lead to the use of such stockpiled nuclear waste as fuel for thorium-based nuclear reactors.

Showcasing results to stakeholders

The Laboratory Directed Research and Development Program at Los Alamos National Laboratory hosted its third-annual LDRD Day on September 13, 2011, at Buffalo Thunder Resort in Pojoaque, New Mexico. The event attracted more than 250 participants, including LANL employees, congressional staffers, elected officials, venture capitalists, and students. Keynote presentations by Clinton Bybee, co-founder and managing director of ARCH Venture Partners, and John Chavez, president of the New Mexico Angels, focused on the important role the National Laboratories play in generating innovative technologies that can eventually be developed in the private sector and positively impact the national economy. More than 40 posters were displayed at LDRD Day, showcasing the Laboratory's investment in research related to energy security, nuclear security, global security, and scientific discovery. The poster titled "Discovering How the Brain Sees," presented by Luis Bettencourt and colleagues, snagged the "Best Poster" award, which was determined by votes cast by LDRD Day participants. Andrew Bradbury and colleagues won the "Best Market Potential" award for their poster, "Stabilizing Cellulases Using an Evolutionary Approach."
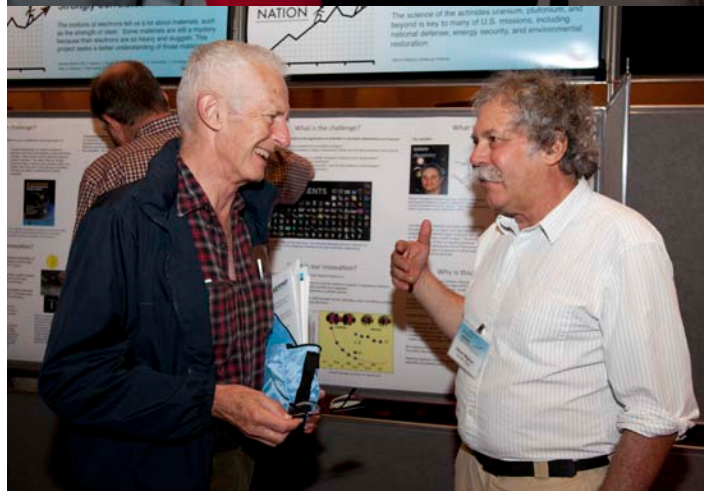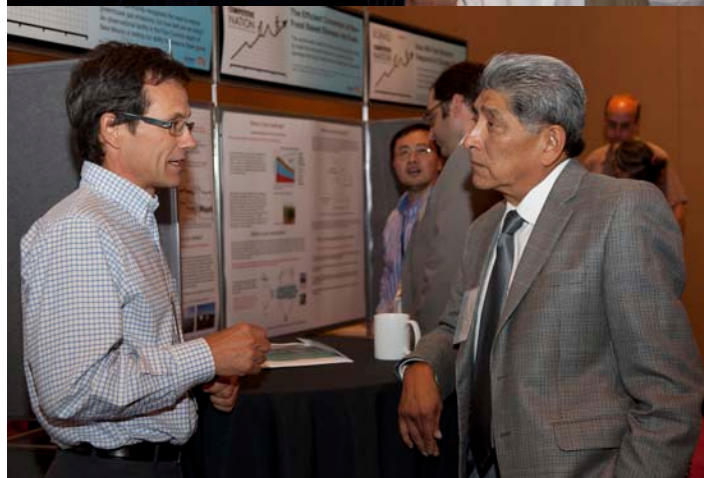
External Reviews

As noted elsewhere in this report, independent assessments of individual LDRD projects range from excellent to outstanding. At the broader program level, our self-assessment is that the Los Alamos LDRD program is succeeding at producing excellent science with high mission impact. However, it is useful to validate our assessment with independent external analysis. In FY11, two external reviews were held in assessment of the LDRD program.

Program Effectiveness

The independent Functional Management Review (FMR) of Los Alamos LDRD Program Effectiveness was held on August 16-19, 2011.   The review was not of specific LDRD projects, but rather an assessment across the full program to understand what it delivers to the Los Alamos National Laboratory and the nation in the way of technical capability and mission solutions. The Committee members who assessed the program included Raymond Jeanloz (Chair), University of California, Berkeley; William Goldstein, Lawrence Livermore National Laboratory; Kim Budil, Lawrence Livermore National Laboratory; Everet Beckner, Independent Consultant; Samuel Kaplan, University of Texas Medical School; Ethan Miller, University of California, Santa Cruz; John Bercaw, California Institute of Technology; Anthony Rollett, Carnegie Mellon University; and Michael Turner, University of Chicago. The main objective of the Committee was to validate that LDRD investments effectively and efficiently meet the goals of the program.

The review consisted of a combination of poster sessions and interviews with mission stakeholders, associate directors, division management, and panelists from DRs and ERs selection process. The Committee found that "the LDRD Program at LANL is critical to maintaining cutting-edge science and engineering capability and a world-class workforce." Most notable was the peer review process which offers benefits in quality, transparency, avoiding conflict of interest, informing staff of capabilities and developments, and continuing education of staff of technical disciplines. The Committee identified opportunities for improvement (not deficiencies), in the context of processes and outcomes that are currently of high quality.

Peer Review Process

Regarding LDRD's peer review processes, the Committee noted that proposal review "...incorporates best practices from the peer review systems used by NSF, NASA and NIH, has safeguards against conflicts-of-interest, and relies upon both internal reviewers and reviewers from outside LANL."

A recommendation to incorporate external reviews into the ER proposal process was driven by the potential for projects to vary in quality due to the highly bottom-up nature of the ER component. The Committee noted that external reviews are helpful in maintaining the quality of the ER component and justifying its impact. The Committee also recommended considering using more flexibility in assigning category quotas.

The Committee noted ndications of risk aversion in LDRD peer review processes, which could result in missed opportunities to support innovative and high-impact work. The recommendation was to consider, on an experimental basis, a few small-scale projects (approximately one year) that do not go through the full formal review. If successful, projects funded under this mechanism would be in a stronger position to compete for full LDRD funding. Additional recommendations included establishing metrics to assess the risk level of projects.

Mission Relevance

The Committee acknowledged that LDRD "has made substantive and measurable impacts on LANL's national security missions" and that "Program leaders in weapons and global security indicated LDRD was relevant to their mission areas." The Committee specifically noted that the Grand Challenges serve to focus the DR portfolio on the strategic directions identified by the Laboratory. To strengthen the LDRD program in this area, the Committee recommended establishing a process for periodically updating and articulating the Grand Challenges to support the Laboratory strategy. While there is indeed a review of the individual Grand Challenges every fall, benefit could be gained from reviewing them in their entirety.

Bolstering Capabilities in Engineering

The Laboratory has identified engineering as a critical capability to support its missions. As noted by the Committee, LDRD is seeking ways to foster engineering innovations across the program, especially in the DR component. The Committee recommended tracking engineering investment made through science-centric projects; modifying proposal review criteria to be more encompassing of engineering; and improving the articulation of the engineering Grand Challenge. A new engineering strategy has since been developed, and revised proposal review criteria has been implemented.

The Committee concluded their review by stating that the LDRD program "plays a key role in sustaining the intellectual health of the Laboratory" and that it is "important for staff morale and retention in the sense of providing a crucial outlet for creativity and innovation."

Business Processes

The Los Alamos LDRD program, in conjunction with the Chief Financial Officer (CFO), requested a Parent Organization Functional Management Review of LDRD Business Practices. The review was performed from March 15 – 17, 2011. The review encompassed a risk-based analysis of LDRD compliance with DOE order regarding mission relevance, augmentation, project duration, and direct relevance of LDRD expenditures to project R&D goals.

The independent panel was chaired by John Birely, Consultant to the University of California Office of the President, and included Todd Hansen, LBNL LDRD Program Director; Paul Rosenkoetter, Director, Prime Contract Management Office and Manager; and Ross Thomas, Chief Technical Officer for Babcock & Wilcox.

The panel's primary objective was to determine whether LANL has developed a management approach to the stewardship of LDRD moneys, thus achieving the objectives of applicable legislation and DOE Order 413.2B. The review panel conducted interviews, and held discussions with personnel and representatives of: LANL LDRD Program Office; LANL CFO personnel; LASO, NNSA Headquarters & Albuquerque Service Center; LANL Ethics & Audit Division; LANL Contractor Assurance Office; LANL LDRD Principal Investigators; and LANL Group and Division Managers.

The review panel reported that the LDRD Program is vital to the health and future of the Laboratory. The LDRD Program has been responsive to issues raised in audits and reviews of LDRD business practices.   More specifically, the review panel found a very robust tie between the LDRD Program and the Laboratory, DOE Missions, and a strong postdoctoral component. It also noted that an effective management system, PI training, CFO time-charging practices training, and deployed financial personnel to line organization all prove to be beneficial to LDRD business management.

The review panel also identified opportunities for improvement (not deficiencies) in their report. The review panel identified the need for a consistent policy for reporting time and effort for bid and proposals. LANL has implemented a lab-wide guidance of this new policy, which was transmitted to all employees on March 30, 2011.   The review panel recommended an opportunity for continuous improvement of LDRD business management metrics. The LDRD Program Office has since established a project management schedule and has put calendar management controls in place when setting performance expectations and goals for business processes. Lastly, the panel recommended an "improved" application of risk management, balancing management effort with actual business process gains. An example of improvement in this area is LANL's effort to track post-project costs to ensure these costs remain below 1%.

The panel summed up their final report by stating that "We can give reasonable assurance that the Laboratory's LDRD business systems are based on good management practice," and concluded that "LANL has developed a management approach to the stewardship of LDRD resources that achieves the objectives of applicable legislation and DOE Order 413.2B."

CHEMISTRY AND MATERIAL SCIENCES

Isolating the Influence of Kinetic and Spatial Effects on Dynamic Damage Evolution

Darcie Dennis-Koller
20100026DR

Introduction

This project studies the effectsof dynamic shock loading on the material microstructure, such as defect distributions, to understand how material damage starts and evolves. To this end, macro-scale and meso-scale models have been utilized to design dynamic experiments that sample known volumes of microstructure. Then, post shock specimen characterization has been employed to interrogate the influence of these experiments on damage evolution. Specifically, we believe that both time and length scale of a dynamic event are critically important to the development of damage. In the first year of this project, we successfully showed the role of microstructural length scales on dynamic damage. In the second year of this work, we have performed experiments to isolate the effect of kinetics, interrogate its unique contribution to damage response, and incorporate this physical understanding into predictive models.

Benefit to National Security Missions

The incorporation of the physics of small length-scale, dynamic damage evolution into predictive models has important implications for many programs. Currently, accurate prediction of damage in metals is critical to the nuclear weapons, nuclear energy, insensitive munitions, transportation, and infrastructure maintenance programs supported by DOE, DoD, DHS, and NASA. Additionally, understanding the critical materials design parameters for damage evolution is necessary as we consider the design of next generation metals to meet future energy demands.

Progress

For the first time, plate impact experiments have been modeled and designed to examine the influence of pulse duration (time under peak compressive load), peak tensile stress, and the rate at which that peak tensile stress is achieved (release rate) on damage evolution in copper. Copper microstructures were tailored for these experiments to keep the number density of defects sampled in all tests the same. This means that differing grain size specimens were examined, but in all cases, the

modeled zone of tension contained similar densities of defects. This was done because the findings of year one of this same project indicated that this was a critically important parameter to control in terms of damage evolution [1,2]. The experimental configuration for plate impact experiments used in this work permitted real-time measurements of the sample free surface velocity histories, soft-recovery, and post-impact examination of the incipiently damaged microstructure. Free surface velocity measurements wereused to calculate spall strength values and have already been shown to be independent of grain size.

The quantitative metallographic analyses of recovered samples, via optical metallography and electron back scattered diffraction (EBSD), show that both release rate and the pulse duration significantly influence damage evolution during shock loading conditions. Experiments conducted with release rates of both 17 and 24 GPa/us and then again 29 and 39GPa/us, with similar pulse duration respectively, show that lower release rates led to fewer but larger voids as compared to smaller but more voids at higher release rates. This suggests that damage at the lower release rates is growth controlled whereas the damage at the higher release rates is nucleation dominated. Moreover, pulse duration appears to play a role in nucleation of damage, as smaller pulse durations appear to have fewer voids than longer pulse durations. This is likely linked to differences in substructural evolution or shock processing of the microstructure under compression. Such processing can change the development of stress concentrations in the microstructure under tensile load and thereby alter damage evolution [3].

In addition, two new capabilities have become available in the past year. As a product of this LDRD project and to further examine release rate effects, a new test platform has been acquired. A low-velocity, gas gun has been designed and installed in MST-8. The purpose of this gun is to fill a gap in capability at Los Alamos for firing plate impact experiments at velocities between 50 and 200m/s. This velocity regime was of interest as this project aims to interrogate the early stage of

damage nucleation and growth. Current experiments have been fired at velocities of ~130m/s allowing us to examine early stage growth and coalescence. New experiments conducted on this low velocity gas gun will be fired between 40 and 80m/s to allow for examination of late stage nucleation. In addition to this, a characterization platform has become available: a nano-computed tomography capability. This capability, which can characterize voids at the nano-scale, will be crucial as we transition to study the early stage of damage nucleation and growth as opposed to early stages of growth and coalescence.

Continuum and meso-scale level simulations have been ongoing and underlying developments are being implemented. Specifically, analysis of copper experimental results revealed that damage transitions from nucleation dominated to growth and coalescence dominated behavior under specific loading profiles. Predictions of response using a current, continuum-based, ductile-damage model shows that especially for the nucleation dominated regime, the model inadequately represents the material response. Experimental results demonstrate a variable damage field with the primary mechanism of failure being void nucleation at grain boundaries. Present nucleation models do not represent this damage response. These results strongly point to the need for physically based models for the failure of grain boundaries for these loading regimes.

Further continuum level work, simulated several LDRD experiments using a recently modified, single crystal plasticity model for high rate loading in FLAG hydro code with macroscopic models to reveal the adequacies of current models in predicting damage. Some low-pressure incipient spallation experiments were simulated very well, however in the cases where the damage was not simulated well, frequently it was because the damage evolution at grain boundaries was not well represented. Specifically, single crystal plasticity modeling showed the strength of twin type grain boundaries, which experienced high local calculated stresses but did not fracture experimentally. The simulation was a proof of capability for a large 3D hydro code simulation.

To address problems observed in continuum level simulations, an entirely new single crystal model for the high rate deformation response of cubic materials has been developed. This model has been formulated with average dislocation density as the primary materials state variable in place of the traditional slip system deformation resistance to facilitate improved predictability. The model features equations representing both the thermally activated glide and dislocation drag response of dislocations. The generation, annihilation, and interaction of populations of mobile dislocations, immobile dislocations and debris are represented. This is a significant advance over other models, which generally represent these dislocation interactions through a single scalar value enhancing hardening. This model treats this interaction through a tensoral representation.   Several results were produced for copper and compare favorably to experimental data. This model will eventually be used to represent the meso-scale shock response of Cu.

Additionally, this year we have continued the development and implementation of a computational framework capable for predicting the initiation and evolution of strain localization in metals. This framework consists of a sub-grid finite element technique, coupled with appropriate material models. The finite element formulation (including a material stability analysis which predicts localization nucleation) was generalized to enable the treatment of finite-deformation problems. An isotropic, hypo-elastic-plastic, constitutive model with linear, isotropic hardening was implemented. To include rate and temperature effects, an elasto-viscoplastic constitutive model based on the Mechanical Threshold Stress (MTS) flow stress theory was also incorporated into the framework. The current focus of our work is on verifying the computational implementation and improving its robustness.

Finally, this year, we have developed two different constitutive models for polycrystalline aggregates with intergranular cavities: one mean-field approach based on second-order homogenization and one full-field approach based on Fast Fourier Transforms (FFT). Both models are relevant to model our Cu spallation experiments, in which the dilatational effects associated with the presence of cavities must be accounted for, and standard polycrystalline models for incompressible plasticity were not appropriate. Then, using our newly developed FFT-based method [4,5], we have analyzed microstructural effects on void growth and compared with post-mortem EBSD measurements on our shocked copper. We found that the interaction between neighbor voids, leading to growth and coalesce, is affected by the crystallographic orientation of the crystals surrounding the voids. This effect was first predicted by the model and then confirmed by the experiments.

Future Work

Modeling and experiments will continue to address the role of peak tensile stress on dynamic damage and transition to investigating the role of a new defect distribution, inclusions. This work is aimed at understanding the way in which spatial distributions of defects in a less ideal material (not a high purity metal) couple with loading profile to evolve damage. Such an understanding underlies the meso-scale interpretation of damage evolution in the extreme environment of shock loading and can be utilized to derive the mathematical representations required to capture damage nucleation. This work will rely on tailored, model-driven-design of wave shape experiments; an approach developed in year two of the project, along with post mortem materials

characterization. It will utilize both new platforms described above: the low velocity launcher and the nano-computed tomography.

Conclusion

To date, this research has three important results: (1) classification of deterministic versus stochastic features of damage evolution, (2) a newly formulated high-rate, single crystal plasticity model, and (3) a novel approach for plate-impact experiment design that controls features of the tensile release. Each result has implications for the weapons and energy programs as current structural materials are pushed to new design requirement expectations. These results will also be critical for transportation and energy industries as future applications will call for design of next generation metals requiring an understanding of the behavior of materials in extreme environments such as dynamic loading.

References

1. Escobedo, J P., D. D. Koller, E. K. Cerreta, B. P. Patterson, C. A. Bronkhorst, B. L. Hansen, D. Tonks, and R. A. Lebensohn. Effects of Grain Size and Boundary Structure on the Dynamic Tensile Response of Copper. 2011. *Journal of Applied Physics.* **110**: 033513.

2. Patterson, B. P., J. P. Escobedo, D. D. Koller, and E. K. Cerreta. Dimensional Quantification of Embedded Voids or Objects in Three Dimensions Using X-ray Tomography. To appear in *Microscopy and Microanalysis.*

3. Perez-Bergquist, A. G., E. K. Cerreta, C. P. Trujillo, F. Cao, and G. T. Gray III. Orientation Dependence of Void Formation and Substructure Deformation in a Spalled Copper Bicrystal. To appear in *Scripta Materialia.*

4. Lebensohn, R. A., M. I. Idiart, P. Ponte-Castaneda, and P. G. Vincent. Dilatational Viscoplasticity of Polycrystalline Solids with Intergranular Cavities. 2011. *Philosophical Magazine* . **91**: 3038.

5. Lebensohn, R. A., A. D. Rollett, and P. Suquet. Fast Fourier Transform-Based Modeling for Determination of Micromechanical Fields in Polycrystals. 2011. *Journal of Minerals, Metals and Materials.* **63**: 13.

Publications

Abeele, K. Van Den, T. J. Ulrich, P. Le Bas, M. Griffa, B. Anderson, and R. Guyer. Vector Component Focusing in Elastic Solids using a Scalar Source in Three Component Time Reversal. 2010. In *International Congress on Ultrasonics ; 20090111 - 20090117 ; Univ Santiago Chile, Santiago, CHILE.* Vol. 3, 1 Edition, p. 685.

Barton, N. R., J. V. Bernier, J. Knapp, A. J. Sunwoo, E. K. Cerreta, and T. J. Turner. A Call to Arms for Task Parallelism in Multi-scale Materials Modeling. 2011. *International Journal for numerical Methods in Engineering.* **86**: 744.

Bronkhorst, C. A., A. R. Ross, B. L. Hansen, E. K. Cerreta, and J. F. Bingert. Modeling and Characterization of Grain Scale Strain Distribution in Polycrystalline Tantalum . 2010. *Computers, Materials, and Continua.* **17**: 149.

Bronkhorst, C. A., P. J. Maudlin, G. T. Gray III, E. K. Cerreta, E. N. Harstad, and F. L. Addessio. Accounting for Microstructure in large Deformation Models of Polycrystalline Metallic Materials. 2010. In *Computational Methods for Microstructure-Property Relationships.* Edited by Ghosh, S., and D. Dimiduk. Vol. 1, First Edition, p. -. Norwell: Springer.

Bronkhorst, C. A., S. R. Kalidindi, and S. R. Zavaliangos. Editorial - Special Issue in Honor of Lallit Anand. 2010. *International Journal of Plasticity.* **26**: 1071.

Cao, F., I. J. Beyerlein, F. L. Addessio, B. H. Sencer, C. P. Trujillo, E. K. Cerreta, and G. T. Gray III. Orientation Dependence of Shock Induced Twinning and Substructures in a Copper Bi-Crystal. 2010. *Acta Materialia.* **59**: 549.

Dennis-Koller, D., E. Cerreta, J. Escobedo-Diaz, and C. Bronkhorst. "Controlled Shock Loading Conditions for Microstructural Correlation of Dynamic Damage Behavior" . To appear in *17th Biennial International Conference of the American Physical Society Topical Group on Shock Compression in Condensed Matter.* (Chicago, Ill, June 26 - July 1, 2011).

Escobedo, J. P., D. D. Koller, E. K. Cerreta, B. M. Patterson, C. A. Bronkhorst, B. L. Hansen, D. Tonks, and R. A. Lebensohn. Effects of Grain Size and Boundary Structure on the Dynamic Tensile Response of Copper. 2011. *Journal of Applied Physics.* **110** (3): 033513.

Escobedo-Diaz, J., D. Dennis-Koller, E. Cerreta, B. Patterson, and C. Bronkhorst. Effects of Grain Size and Boundary Structure on the Dynamic Tensile Response of Copper. To appear in *17th Biennial International Conference of the American Physical Society Topical Group on Shock Compression in Condensed Matter.* (Chicago, IL, June 26 - July 1, 2011).

Hansen, B. L., C. A. Bronkhorst, and M. Ortiz. Dislocation Subgrain Structures and Modelingthe Plastic Hardening of Metallic Single Crystals. 2010. *Modelling and Simulation Materials Science and Engineering.* **18**: 055001.

Lebensohn, R. A., A. D. Rollett, and P. Suquet. Fast Fourier Transform Based Modeling for the Determination of Micro-mechanical Fields in Polycrystals. 2011. *Journal*

of Minerals, Metals and Materials Society. **63**: 13.

Lebensohn, R. A., M. I. Idiart, P. Ponte Castaneda, and P. G. Vincent. Dilatational Visco-plasticity of Polycrystalline Solids with Intergranular Cavities. 2011. *Philospohical Magazine.* **91**: 3038.

Lebensohn, R., C. Hartley, C. Tome, and O. Castelnau. Modeling the mechanical response of polycrystals deforming by climb and glide. 2010. *PHILOSOPHICAL MAGAZINE.* **90** (5): 567.

Luscher, D. J., D. L. McDowell, and C. A. Bronkhorst. A Second Gradient Theoretical Framework for Hierarchical Multi-scale Modeling of Materials. 2010. *International Journal of Plasticity.* **26**: 1248.

Patterson, B. M., J. Campbell, and G. J. Havrilla. Integrating 3D Images Using Laboratory-based micro x-ray computed tomography and confocal x-ray fluorescence techniques. 2010. *X-ray Spectrometry.* **39** (3): 184.

Patterson, B. M., and C. E. Hamilton. Dimensional Standard for Micro-CT for the Quantification of 3D Voids Structures. 2010. *Analytical Chemistry.* **82** (20): 8537.

Patterson, B. P., J. P. Escobedo-Diaz, D. D. Koller, and E. K. Cerreta. Dimensional Quantification of Embedded Voids of Objects in Three Dimensions Using X-Ray Tomography. To appear in *Microscopy and Microanalysis.*

Perez-Bergquist, A. G., E. K. Cerreta, C. P. Trujillo, and F. Cao. Orientation Dependence of Void Formation and Substructure Deformation in a Spalled Copper Bicrystal. To appear in *Scripta Materialia.*

Preston, D. L., V. I. Levitas, and D. W. Lee. Interface Propagation and Microstructure Evolution in Phase Field Models of Stress-Induced Martensitic Phase Transformations. 2010. *International Journal of Plasticity.* **26**: 395.

Rollett, A. D., R. A. Lebensohn, M. Groeber, Y. Choi, J. Li, and G. S. Rohrer. Stress hot spots in viscoplastic deformation of polycrystals. 2010. *Modelling and Simulation in Materials Science and Engineering.* **18** (7): 074005 (16 pp.).

Tonks, D. L., and J. Bingert. Mesoscale Polycrystal Calculations of Damage in Shock Loaded Copper. 2010. *European Physics Journal, Web of Conference.* **10**: 6.

Understanding and Controlling Complex States Emerging from Frustration

Vivien Zapf
20100043DR

Introduction

Much of our national security relies on capabilities made possible by magnetism, in particular the ability to compute and store huge bodies of information as well as to move things and sense the world. Most of these technologies exploit ferromagnetism, i.e. the global parallel alignment of magnetic spins as seen in a bar magnet. Recent advances in computing technologies, such as spintronics and MRAM, take advantage of antiferromagnetism where the magnetic spins alternate from one to the next. In certain crystal structures, however, the spins take on even more complex arrangements. These are often created by frustration, where the interactions between spins cannot be satisfied locally or globally within the material resulting in complex and often non-coplanar spin textures. In layman's terms, a frustrated system lacks a straightforward arrangement because no one arrangement can satisfy all the forces in play. As with people, it is sometimes impossible to make everyone happy at the same time. Frustration in materials can lead to the close proximity of many different magnetic states, letting us jump from one to the other with small perturbations in magnetic field, temperature, and/or pressure. It is this tunability that makes frustrated systems both scientifically interesting and desirable for applications.

We move beyond frustration in insulators to itinerant systems, where the interaction between mobile electrons and the non-coplanar magnetic states lead to quantum magneto-electric amplification. Here a small external field is amplified by many orders of magnitude by non-coplanar frustrated states. This greatly enhances their sensitivity and opens broader fields for applications. Our objective is to pioneer a new direction for condensed matter science at the Laboratory as well as for international community by discovering, understanding and controlling states that emerge from the coupling of itinerant charges to frustrated spin textures.

Benefit to National Security Missions

This project directly addresses frustration, a topic called out in "Directing Matter and Energy: Five Challenges for Science and the Imagination". The novel mechanism for magnetoelectric coupling operates both in insulators and metals. Potential applications include: ultra-sensitive magnetic sensors; strong coupling of magnetization and electrical polarization in insulators with the ability to switch magnetization by an electric field or electrical polarization by a magnetic field; electrical control of optical properties; and new concepts for binary magnetic storage. These rich possibilities can be used to create entirely new classes of devices as well as improve the energy efficiency of existing ones.

Progress

A pre-requisite for understanding how magnetic frustration can couple to the electric properties of a material is to first understand the magnetic frustration by itself. We have investigated how frustration can create complex spin textures, novel quantum mechanical effects, spin liquids, and even superconductivity.

We have studied several insulating systems where magnetic frustration and quantum mechanics combine to create complex spin textures. In these systems, the magnetism can be treated as a quantum condensation of integer-spin (boson) excitations in a lattice, so-called Bose Einstein condensation (BEC). In $Ba_3Mn_2O_8$ we explore the role of geometrical frustration on the magnetic BEC theoretically and experimentally. [1-3] In another magnetic BEC compound, $NiCl_2$-$4SC(NH_2)_2$ we explore the role of quantum fluctuations at the phase transition [4]. We completed a related theoretical work on magnetic frustration in body-centered tetragonal systems that has important consequences not only for this compound but other frustrated materials with similar geometries, such as the iron pnictides [5]. We introduce further frustration in $NiCl_2$-$4SC(NH_2)_2$ by doping Br on the Cl site [6]. We find the long sought-after experimental evidence for a crossover from Bose-Einstein Condensation to a Bose Glass. This crossover can be thought of as the bosonic equivalent of a metal-

to-insulator transition in fermions.

In metals we have explored how complex magnetic states can be created as a direct consequence of interactions between local moments and itinerant electrons [7] For two-dimensional systems we have demonstrated that the magnetic moments of itinerant electrons will line up into a non-coplanar pattern in which the chirality (or "handedness") of moments varies spatially. We are also investigating several compounds, $CeGaCu_4$, $DyInO_3$, $TbInO_3$, and $EtMe_3Sb[Pd(dmit)_2]_2$, in which the magnetic frustration is so severe that long-range magnetic order is suppressed altogether despite strong interactions between magnetic ions. The mysterious spin liquid or strongly correlated spin state that results is a current unsolved mystery.

Moving on to how frustration affects electrical properties, we have studied how magnetic frustration can be used as a tool to create coupling of complex magnetic textures to electrical resistance, Hall effect, ferro-electricity, and superconductivity. We explore three categories of materials: metals, insulators with local itinerant electrons, and finally materials at the boundary between metals and insulators where we can maximize the coupling between magnetic and electrical properties.

In metals we show how the phenomenon of quantum magneto-electric amplification allows magnetic fields to have out-sized effects on the electrical resistance [8-10]. We have identified UCu_5 as a promising material in which we can explore these effects experimentally. Here the U ions occupy corner-sharing tetrahedral, leading to frustration and non-coplanar magnetic order. We found that the itinerant charges acquire a quantum mechanical (Berry) phase as they traverse the underlying non-coplanar spin texture, and this in turn leads to strong effects on the electrical resistance and Hall effect (Figure 1) [11]. We are currently investigating the effects of chemical disorder on this unusual state in $U_{1-x}Lu_xCu_5$ and $UCu_{5-x}Ni_x$.

In insulators we used our first year's theoretical efforts to guide the discovery of new compounds where frustration leads to complex spin textures and in turn coupling to ferroelectricity. This is key for applications such as new ultra-sensitive and smart sensors and circuit devices where magnetic fields can tune the ferroelectricity and electric fields can tune the magnetism. We have completed a joint experimental and theoretical study of Lu_2MnCoO_6 [12] where frustration leads to an up-up-down-down arrangement of spins (Figure 2). These spins, while collinear, nevertheless form a low symmetry state that creates an electric polarization. In organic materials, we studied how their soft crystal lattice enhances magneto-electric coupling when the magnetic spins strain the lattice. Work on $CuCl_2$-$2SO(CH_3)_2$ [13] and $NiCl_2$-$4SC(NH_2)_2$ [14] has been completed and a detailed theoretical model developed for the latter that closely matches the experimental results. Large magneto-electric couplings are also found in the highly frustrated material $CoCl_2$-$2SC(NH_2)_2$ via electric polarization measurements in high magnetic fields. Theoretical calculations of coupling mechanisms between magnetic order in triangular systems and electric polarization are in progress. Finally, we have developed a theory of how frustration can have the maximum effect on the electrical properties, namely to cause a Mott insulator to become superconducting [15].
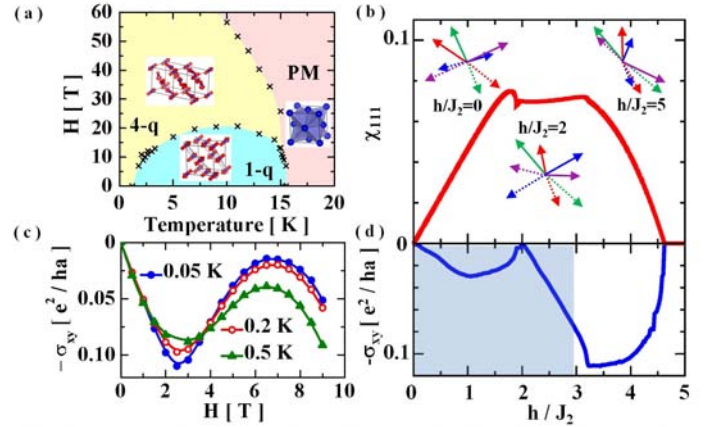
Figure 1. Experimental and theoretical results of UCu_5. (a) Experimental phase diagram showing different non-coplanar structures, namely the 4-q (four wave vectors on four sublattices) and 1-q (one wave vector) phases, and the paramagnetic (PM) phase with no spins shown. (b) The calculated chirality _111 of the spins as a function of magnetic field with spins on different sublattices for the 4-q structure shown in different colors. c) The experimental Hall conductivity versus field at various temperatures. (d) The calculated zero temperature Hall conductivity vs normalized magnetic field.
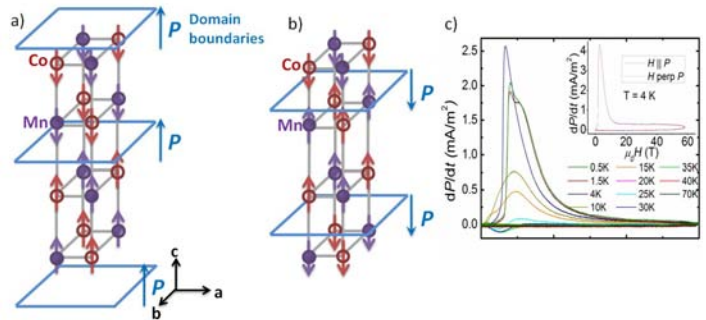
Figure 2. a) and b) Two configurations of experimentally determined up-up-down-down spin configuration for Lu2MnCoO6 along Co and Mn chains resulting from magnetic frustration, and the proposed electric polarization resulting from magnetostriction at the boundaries between up-up and down-down regions of spins . c) Measured electric polarization derivative with respect to time dP/dt as a function of magnetic field H.

In materials at the interface between metallic and insulating behavior, frustration can lead to greatly enhanced magneto-electric effects. While crossover

between band insulators and electrical conductors leads to semiconducting behavior and their myriad applications, the crossover between Mott insulators and conductors is poorly explored. In materials residing at this Mott insulating/conducting crossover, charge order and strong spin-lattice couplings can occur, which can lead to new physics and enhanced magneto-electric effects with practical implications. We have predicted [16] and measured very large magnetoresistances and Hall effect in $Na_{0.5}CoO_2$ and we are exploring the possibility of noncoplanar magnetic order. We are also studying CdV_2O_4, a Mott insulator where the distance between V ions lies on the border of conductivity and direct exchange. Magnetic frustration can drive this crossover, leading to large fluctuations in both the magnetism and the structure and to coupling of the magnetic and electric polarizations. Studies of the magnetic and electric polarization in magnetic fields are being conducted to understand the details of the fascinating behavior of this compound.

Future Work

Frustration provides great flexibility and tunability to configure complex magnetic structures and interactions between magnetism and electrical properties of materials. Even a small perturbation in parameters, such as composition, pressure, or temperature, can lead to a phase transformation with dramatic consequences for thermal and transport properties. This tunability makes frustrated systems highly desirable for applications.

The range of emergent phenomena resulting from the coupling of electrons to frustrated magnetic states has been barely tapped. Most of the magnetic compounds that have been studied by others have simple structures that do not generate quantum magnetoelectric amplification. Moreover, the desirable non-coplanar magnetic states are difficult to identify experimentally and can be often confused with their simpler cousins – coplanar (e.g., spiral or helical) or even collinear (e.g., simple antiferromagnetic) states. A suite of experimental techniques combined with theory and modeling is needed to unambiguously identify, understand, and exploit these unusual and promising states of matter. In our final year we continue to develop the fundamental understanding of the interplay between frustrated magnetism and charge degrees of freedom. We will focus on the following four objectives:

- Identification of the unconventional broken symmetry (low-temperature) states and phase transitions

- Understanding of the "normal" (high-temperature disordered) state

- Determination of the necessary conditions for large magneto-transport responses in magnetically-frustrated metals

- Enhancement of magneto-electric effects in materials at the border of insulating and metallic behavior.

We are achieving these objectives by a coordinated approach combining theory, including both analytical and numerical approaches, and a wide range of experimental techniques, including neutron scattering, nuclear magnetic resonance (NMR), magnetization, transport, thermodynamic, de Haas-van Alphen, electron spin resonance (ESR), and electric polarization measurements.

Conclusion

Materials with complex magnetic properties resulting from frustration could produce revolutionary new functionalities due to the interplay between electric and magnetic properties at the quantum level. This work provides the basic understanding that will open a new field of applications ranging from energy storage to computing to novel magnetic sensors.

References

1. Samulon, E. C., K. A. Al-Hassanieh, Y. -J. Jo, M. C. Shapiro, L. Balicas, C. D. Batista, and I. R. Fisher. Anisotropic phase diagram of the frustrated spin dimer compound Ba3Mn2O8. 2010. *PHYSICAL REVIEW B.* **81** (10): 104421.

2. Stone, M. B., M. D. Lumsden, S. Chang, E. C. Samulon, C. D. Batista, and I. R. Fisher. Singlet-Triplet Dispersion Reveals Additional Frustration in the Triangular-Lattice Dimer Compound Ba3Mn2O8 (vol 100, 237201, 2008). 2010. *PHYSICAL REVIEW LETTERS.* **105** (16): 169901.

3. Suh, S., Al-Hassanieh, K. A., Samulon, E. C., Fisher, I. R., Brown, S. E., and Batista, C. D.. Nonuniversal magnetization at the BEC critical field: Application to the spin dimer compound Ba3Mn2O8. 2011. *Phys. Rev. B.* **84**: 054413.

4. Kamiya, Y., N. Kawashima, and C. D. Batista. Crossover behavior from decoupled criticality. 2010. *PHYSICAL REVIEW B.* **82** (5): 054426.

5. Kohama, Y., A. V. Sologubenko, N. R. Dilley, V. S. Zapf, M. Jaime, J. A. Mydosh, A. Paduan-Filho, K. A. Al-Hassanieh, P. Sengupta, S. Gangadharaiah, A. L. Chernyshev, and C. D. Batista. Thermal transport and strong mass renormalization in NiCl2-4SC(NH2)2. 2011. *Physical Review Letters.* **106** (3): 037203.

6. Yu, R., L. Yin, N. S. Sullivan, J. S. Xia, C. Huan, A. Paduan-Filho, N. F. Oliveira Jr., S. Haas, A. Steppke, C. F. Miclea, F. Weickert, R. Movshovich, E. D. Mun, V. S. Zapf, and T. Roscilde. Bose glass and Mott glass of quasiparticles in a doped quantum magnet. *Science.*

7. Solenov, D., D. Mozyrsky, and I. Martin. Chirality waves in two-dimensional magnets. *Physical Review Letters.*

8. Chern, G. W., and C. D. Batista. Spin superstructure and noncoplanar ordering in metallic pyrochlore magnets with degenerate orbitals. To appear in *Physical Review*

Letters.

9. Kato, , Martin, Ivar, and Batista, C. D.. Stability of the Spontaneous Quantum Hall State in the Triangular Kondo-Lattice Model. 2010. *Phys. Rev. Lett..* **105**: 266405.

10. Zenker, B., Fehske, H., and Batista, C. D.. Competing chiral and multipolar electric phases in the extended Falicov-Kimball model. 2010. *Phys. Rev. B.* **82**: 165110.

11. Ueland, B. G., C. F. Miclea, Y. Kato, O. Ayala-Valenzuela, R. D. McDonald, R. Okazaki, P. H. Tobash, M. A. Torrez, F. Ronning, R. Movshovich, Z. Fisk, E. D. Bauer, I. Martin, and J. D. Thompson. Geometrical Hall effect in a magnetically frustrated metal. *Nature Materials.*

12. Yanez-Vilar, S., E. D. Mun, V. S. Zapf, B. G. Ueland, J. S. Gardner, J. D. Thompson, J. Singleton, M. Sanchez-Andujar, J. Mira, N. Biskup, M. A. Senaris-Rodriguez, and C. D. Batista. Multiferroic behavior in the double-perovskite Lu2MnCoO6. To appear in *Physical Review B.*

13. Zapf, V. S., M. Kenzelmann, F. Wolff-Fabris, F. Balakirev, and Y. Chen. Magnetically induced electric polarization in an organometallic magnet. 2010. *PHYSICAL REVIEW B.* **82** (6): 060402.

14. Zapf, V. S., P. Sengupta, Batista, C. D., Nasreen, F., Wolff-Fabris, F., and Paduan-Filho, A.. Magnetoelectric effects in an organometallic quantum magnet. 2011. *Phys. Rev. B.* **83**: 140405.

15. Isaev, L., Ortiz, G., and Batista, C. D.. Superconductivity in Strongly Repulsive Fermions: The Role of Kinetic-Energy Frustration. 2010. *Phys. Rev. Lett..* **105**: 187002.

16. Martin, I., and C. D. Batista. Itinerant Electron-Driven Chiral Magnetic Ordering and Spontaneous Quantum Hall Effect in Triangular Lattice Models. 2008. *Physical Review Letters.* **101**: 156402.

Publications

Al-Hassanieh, K. A., C. D. Batista, G. Ortiz, and L. N. Bulaevskii. Field-Induced Orbital Antiferromagnetism in Mott Insulators. 2009. *PHYSICAL REVIEW LETTERS.* **103** (21): 216402.

Al-Hassanieh, K. A., C. D. Batista, P. Sengupta, and A. E. Feiguin. Robust pairing mechanism from repulsive interactions. 2009. *PHYSICAL REVIEW B.* **80** (11): 115116.

Al-Hassanieh, K. A., Y. Yang, I. Martin, and C. D. Batista. Effective Low-Energy Model for f-Electron Delocalization. 2010. *PHYSICAL REVIEW LETTERS.* **105** (8): 086402.

Batista, C. D.. Canted spiral: An exact ground state of XXZ zigzag spin ladders. 2009. *PHYSICAL REVIEW B.* **80** (18): 180406.

Chern, G. W., and C. D. Batista. Spin superstructure and noncoplanar ordering in metallic pyrochlore magnets with degenerate orbitals. To appear in *Physical Review Letters.*

Isaev, L., Ortiz, G., and Batista, C. D.. Superconductivity in Strongly Repulsive Fermions: The Role of Kinetic-Energy Frustration. 2010. *Phys. Rev. Lett..* **105**: 187002.

Kamiya, Y., N. Kawashima, and C. Batista. Finite-Temperature Transition in the Spin-Dimer Antiferromagnet BaCuSi2O6. 2009. *JOURNAL OF THE PHYSICAL SOCIETY OF JAPAN.* **78** (9): 094008.

Kamiya, Y., N. Kawashima, and C. D. Batista. Crossover behavior from decoupled criticality. 2010. *PHYSICAL REVIEW B.* **82** (5): 054426.

Kamiya, Y., N. Kawashima, and C. D. Batista. Dimensional crossover in the quasi-two-dimensional Ising O(3) model . 2011. *Journal of Physics: Conference Series.* **320**: 012023.

Kato, , Martin, Ivar, and Batista, C. D.. Stability of the Spontaneous Quantum Hall State in the Triangular Kondo-Lattice Model. 2010. *Phys. Rev. Lett..* **105**: 266405.

Kohama, Y., A. V. Sologubenko, N. R. Dilley, V. S. Zapf, M. Jaime, J. A. Mydosh, A. Paduan-Filho, K. A. Al-Hassanieh, P. Sengupta, S. Gangadharaiah, A. L. Chernyshev, and C. D. Batista. Thermal transport and strong mass renormalization in NiCl2-4SC(NH2)2. 2011. *Physical Review Letters.* **106** (3): 037203.

Samulon, E. C., K. A. Al-Hassanieh, Y. -J. Jo, M. C. Shapiro, L. Balicas, C. D. Batista, and I. R. Fisher. Anisotropic phase diagram of the frustrated spin dimer compound Ba3Mn2O8. 2010. *PHYSICAL REVIEW B.* **81** (10): 104421.

Seo, J. W., W. Prellier, P. Padhan, P. Boullay, J. -. Kim, H. Lee, C. D. Batista, I. Martin, E. M. Chia, T. Wu, B. Cho, and C. Panagopoulos. Tunable Magnetic Interaction at the Atomic Scale in Oxide Heterostructures. 2010. *PHYSICAL REVIEW LETTERS.* **105** (16): 167206.

Solenov, D., D. Mozyrsky, and I. Martin. Chirality waves in two-dimensional magnets. *Physical Review Letters.*

Stone, M. B., M. D. Lumsden, S. Chang, E. C. Samulon, C. D. Batista, and I. R. Fisher. Singlet-Triplet Dispersion Reveals Additional Frustration in the Triangular-Lattice Dimer Compound Ba3Mn2O8 (vol 100, 237201, 2008). 2010. *PHYSICAL REVIEW LETTERS.* **105** (16): 169901.

Suh, S., Al-Hassanieh, K. A., Samulon, E. C., Fisher, I.

R., Brown, S. E., and Batista, C. D.. Nonuniversal magnetization at the BEC critical field: Application to the spin dimer compound Ba3Mn2O8. 2011. *Phys. Rev. B.* **84**: 054413.

Ueland, B. G., C. F. Miclea, Y. Kato, O. Ayala-Valenzuela, R. D. McDonald, R. Okazaki, P. H. Tobash, M. A. Torrez, F. Ronning, R. Movshovich, Z. Fisk, E. D. Bauer, I. Martin, and J. D. Thompson. Geometrical Hall effect in a magnetically frustrated metal. *Nature Materials.*

Yanez-Vilar, S., E. D. Mun, V. S. Zapf, B. G. Ueland, J. S. Gardner, J. D. Thompson, J. Singleton, M. Sanchez-Andujar, J. Mira, N. Biskup, M. A. Senaris-Rodriguez, and C. D. Batista. Multiferroic behavior in the double-perovskite Lu2MnCoO6. To appear in *Physical Review B.*

Yu, R., L. Yin, N. S. Sullivan, J. S. Xia, C. Huan, A. Paduan-Filho, N. F. Oliveira Jr., S. Haas, A. Steppke, C. F. Miclea, F. Weickert, R. Movshovich, E. D. Mun, V. S. Zapf, and T. Roscilde. Bose glass and Mott glass of quasiparticles in a doped quantum magnet. *Science.*

Zapf, V. S., F. Wolff-Fabris, M. Kenzelmann, F. Nasreen, F. Balakirev, Y. Chen, and A. Paduan-Filho. Multiferroic behavior in organo-metallics. 2011. *Journal of Physics: Conference Series.* **273**: 012132.

Zapf, V. S., M. Kenzelmann, F. Wolff-Fabris, F. Balakirev, and Y. Chen. Magnetically induced electric polarization in an organometallic magnet. 2010. *PHYSICAL REVIEW B.* **82** (6): 060402.

Zapf, V. S., P. Sengupta, Batista, C. D., Nasreen, F., Wolff-Fabris, F., and Paduan-Filho, A.. Magnetoelectric effects in an organometallic quantum magnet. 2011. *Phys. Rev. B.* **83**: 140405.

Zenker, B., Fehske, H., and Batista, C. D.. Competing chiral and multipolar electric phases in the extended Falicov-Kimball model. 2010. *Phys. Rev. B.* **82**: 165110.

First Principles Predictive Capabilities for Transuranic Materials: Mott Insulators to Correlated Metals

Richard L. Martin
20100044DR

Introduction

We combine experiment and theory in an effort to develop a computational tool which is predictive for 'strongly correlated' materials. These materials lie at the heart of many technologically important applications, and a predictive theory is critically needed to be able to predict, control and manipulate their properties. Unfortunately, no such tool currently exists, nor is it precisely clear exactly what it should contain. This is therefore a basic research effort, and carries with it the associated risk. Breakthroughs in theory over the past year, however, suggest a path forward. We approach the problem by examining materials where these effects are paramount: the carbides, nitrides and oxides of uranium, neptunium, and plutonium. These materials are important in nuclear weapons (Pu), as advanced nuclear energy fuels (UC), and in nuclear reactor waste forms (PuO2). Advances in synthesis and spectroscopy over the past year now allow us to make extremely high quality samples which can be probed with state-of-the-art experimental measurements. These measurements will confront the theory, critically test its predictions, and stimulate refinements. In this manner, we hope to produce a predictive tool for 'strongly correlated' materials.

Benefit to National Security Missions

The development and experimental validation of a first principles predictive capability for transuranic materials principally addresses the area of scientific discovery and innovation. These materials currently defy quantitative theoretical treatments, but have direct implications to DOE/NNSA and DOE/BES in the areas of nuclear security (Pu metal), nuclear energy (advanced actinide carbide fuels), and environmental remediation (PuO_2). A successful theory will also have ramifications for more general (non-actinide) materials which share the feature of 'strong correlations' with the transuranics studied here. The most important applications in this regard involve renewable energy.

Progress

Our major accomplishments during the past year include:

Characterization of the three phases of U_3O_8 synthesized in the previous report has progressed. This includes a new electron energy loss spectroscopy (EELS) study of the unoccupied states , as well as photoemission work on the occupied bands. This EELS capability was generated in collaboration with our colleagues from Livermore, and allows for core-level studies of light elements in 'hot' samples to be done. A separate paper reporting hybrid DFT results on all three phases has also been prepared.

The UC2 high temperature cubic phase prepared in the past review period has been characterized by photoemission, and XAS experiments will be conducted this fall. The optical band gaps have also been determined. A manuscript is in preparation, as is a separate theory paper.

The UO_2, NpO_2, and PuO_2 work has been written up and will soon be submitted. The synthesis paper has been sent to Nature Materials. A longer paper describing its properties from the point of view of DFT has also been prepared and will be submitted shortly. Importantly, new band gaps for this important series have been measured, which are of much higher quality than previous measurements. This new data has allowed us to distinguish among the leading many-body approximations as to which are predictive, and which are not. Hybrid DFT stands as the only consistent predictor of the lattice constants, the magnitude of the band gap, and its origin (Mott vs. charge-transfer).

Our collaborators have made significant progress. With Lubos Mitsas and his group at North Carolina State University, we had performed the first diffusion Quantum Monte Carlo calculations on an actinide complex, Cp_2ThCl_2, last year. We have extended this work to ThX4, X=Cl, Br, I, in the current period. In addition, a new approach that allows spin-orbit operators to be included in DQMC has been implemented and tested (successfully) on the Pb atom. The first DQMC studies of an actinide solid, ThO_2, have been performed and gaps determined from the calculation agree well with experiment.

At Rice, continued progress on new many-body approximations appropriate for description of both Mott insulators and correlated metals is being made. An extremely promising new approach based on breaking and restoring various symmetries of the Hamiltonian has proven quite successful for molecular species. It is of a sufficiently simple form to allow implementation for solids, if the proper manner of extending it to the thermodynamic limit can be found. At Los Alamos we have begun studies of the metal-insulator transition in hydrogen lattices.

At Colorado State University, another approach to the strong correlation problem has been implemented and tested in small atoms and molecules. It allows simple pair approximations to be examined and multiplets to be addressed within the context of DFT.

We have presented our work in several conferences through plenary, invited and contributed talks. In the current review period, we have been asked to write a review for the journal Chemical Reviews, on theory studies of actinide dioxides, which we will do in the coming period. We are still working on the invited review article for Actinide Quarterly Review. A total of 14 papers have been published during the first two years, four are currently being reviewed, and 12 are in preparation.

Future Work

This work will combine synthesis, spectroscopy and theory in an effort to develop a first principles predictive tool for strongly correlated transuranic materials. We will focus on the series AnC, AnN, and AnO2, An=(U, Np, Pu). These span behavior from strongly correlated metals (AnC, AnN) to Mott insulators (AnO2), and thereby provide a systematic evolution of the transition from strongly correlated metals to Mott insulators as a function of ligand. Our approach combines several facilities unique to LANL which now allow the properties of these materials to be studied with single-crystal quality samples, a requirement for the angle-resolved photoemission measurements we propose. Specifically we will:

- Synthesize, via the polymer assisted deposition (PAD) technique developed at LANL, quality thin films. The AnC and AnC_2 species will be the prominent target in the next review period.

- As they become available, the samples will be characterized with X-ray crystallography, IR and optical spectroscopy.

- Energy and angle-resolved photoemission experiments will be undertaken on the thin films to determine their electronic structure.

- Ligand K-edge X-ray absorption and EELS spectroscopy experiments will determine the character and metal-ligand interactions in the unoccupied levels.

- Screened hybrid density functional theory (DFT) calculations will be performed for all members of the series in order to see where, and in what manner, the current state-of-the-art fails.

- The projected quasi-particle theory developed at Rice will continue development. Applications of this method at LANL will continue.

- Applications of QMC to actinide molecules and solids will continue.

- These steps will be thoroughly integrated and support one another. The structure, band gaps, photoemission spectra and x-ray absorption spectra computed will be compared with experiments (2,3,4).

Conclusion

Many materials which lie at the heart of many technologically important applications currently cannot be described by predictive theories. In this effort, we combine experiment and theory in order to develop a computational tool applicable to these 'strongly correlated' materials. This is a basic research effort; no such tool currently exists. It is critically needed, however, in order to be able to predict, control and manipulate the properties of materials of importance in nuclear weapons (Pu), advanced nuclear energy fuels (UC), and in nuclear reactor waste forms (PuO_2).

Publications

An, Y. Q., A. J. Taylor, T. Durakiewicz, and G. Rodriguez. Pump-probe reflectivity study of ultrafast dynamics of strongly correlated 5f electrons in UO_2. 2011. In *International Conference on Strongly Correlated Electron Systems (SCES 2010) ; 27 June-2 July 2010 ; Santa Fe, NM, USA.* Vol. 273, p. 012144 (4 pp.).

An, Y., A. Taylor, S. Conradson, S. Trugman, T. Durakiewicz, and G. Rodriguez. Ultrafast Hopping Dynamics of 5f Electrons in the Mott Insulator UO2 Studied by Femtosecond Pump-Probe Spectroscopy. 2011. *PHYSICAL REVIEW LETTERS.* **106** (20): 207402.

Durakiewicz, T., J. J. Joyce, Y. Li, P. S. Riseborough, P. M. Oppeneer, E. D. Bauer, and K. S. Graham. Band renormalization effects in correlated f-electron systems. 2011. In *International Conference on Strongly Correlated Electron Systems (SCES 2010) ; 20100627 - 20100702 ; Santa Fe, NM.* Vol. 273, p. 012029.

Ellis, J., C. Jimenez-Hoyos, T. Henderson, T. Tsuchimochi, and G. Scuseri. Constrained-pairing mean-field theory. V. Triplet pairing formalism. 2011. *JOURNAL OF CHEMICAL PHYSICS.* **135** (3): 034112.

Henderson, T. M., J. Paier, and G. E. Scuseria. Accurate treatment of solids with the HSE screened hybrid.

2011. *Physica Status Solidi B.* **248** (4): 767.

Joyce, J. J., T. Durakiewicz, K. S. Graham, E. D. Bauer, D. P. Moore, J. N. Mitchell, J. A. Kennison, R. L. Martin, L. E. Roy, and G. E. Scuseria. Pu Electronic Structure and Photoelectron Spectroscopy. 2011. In *International Conference on Strongly Correlated Electron Systems (SCES 2010) ; 20100627 - 20100702 ; Santa Fe, NM.* Vol. 273, p. 012023.

Joyce, J. J., T. Durakiewicz, K. S. Graham, E. D. Bauer, D. P. Moore, J. N. Mitchell, J. A. Kennison, R. L. Martin, L. E. Roy, and G. E. Scuseria. Pu Electronic Structure and Photoelectron Spectroscopy. 2011. In *International Conference on Strongly Correlated Electron Systems (SCES 2010) ; 27 June-2 July 2010 ; Santa Fe, NM, USA.* Vol. 273, p. 012023 (5 pp.).

Joyce, J., T. Durakiewicz, K. Graham, E. Bauer, D. Moore, J. Mitchell, J. Kennison, T. Mark. McCleskey, Q. Jia, A. Burrell, E. Bauer, R. Martin, L. Roy, and G. Scuseria. 5f electronic structure and fermiology of Pu materials. 2010. In *2010 MRS Spring Meeting ; 20100405 - 20100409 ; San Francisco, CA, United States.* Vol. 1264, p. 93.

Kolorenc, J., S. Hu, and L. Mitas. Wave functions for quantum Monte Carlo calculations in solids: Orbitals from density functional theory with hybrid exchange-correlation functionals. 2010. *PHYSICAL REVIEW B.* **82** (11): 115108.

Kolorenc, J., and L. Mitas. Applications of quantum Monte Carlo methods in condensed systems. 2011. *REPORTS ON PROGRESS IN PHYSICS.* **74** (2): 026502.

Scuseria, G., C. JimeÃÅnez-Hoyos, T. Henderson, K. Samanta, and J. Ellis. Projected quasiparticle theory for molecular electronic structure. 2011. *Journal of Chemical Physics.* **135** (12): 124108.

Tsuchimochi, T., G. Scuseria, and A. Savin. Constrained-pairing mean-field theory. III. Inclusion of density functional exchange and correlation effects via alternative densities. 2010. *JOURNAL OF CHEMICAL PHYSICS.* **132** (2): 024111.

Tsuchimochi, T., T. Henderson, G. Scuseria, and A. Savin. Constrained-pairing mean-field theory. IV. Inclusion of corresponding pair constraints and connection to unrestricted Hartree-Fock theory. 2010. *JOURNAL OF CHEMICAL PHYSICS.* **133** (13): 134108.

Tsuchimochi, T., and G. Scuseria. Constrained active space unrestricted mean-field methods for controlling spin-contamination. 2011. *JOURNAL OF CHEMICAL PHYSICS.* **134** (6): 064101.

Molecular Forensic Science of Nuclear Materials

Marianne P. Wilkerson
20100048DR

Introduction

We proposed that application of state-of-the-art techniques to characterize chemical speciation could transform forensics analyses of nuclear materials, provided that the fundamental science required to interpret the signatures is understood. Current forensics methods rely upon physical, isotopic, and elemental analyses. With this approach, potentially useful chemical information is unrecognized, and chemical heterogeneity in samples may not be detectable in a bulk measurement. The need for innovative approaches to address challenges particular to forensics has been recognized by the Joint Working Group of the AAAS and APS in a report, "Nuclear Forensics Role, State of the Art, and Program Needs" [1]. We are addressing these issues by exploiting newly developed tools to provide the ability to couple chemical speciation with isotopic, elemental and morphological signatures, providing an unprecedented ability to assess sample origin, intended use, and history prior to or after loss of control.

Benefit to National Security Missions

A revolutionary approach to nuclear particle analysis has direct benefit to three national security challenges: forensic characterization of illicit material handling and trafficking; location of clandestine facilities producing, processing, and weaponizing nuclear material; and detection of undeclared operations within nuclear facilities under IAEA safeguards.

Progress

We are developing an understanding of forensics-critical molecular signatures carried by actinide materials ranging from bulk to the micron scale. Key accomplishments include: 1) measurements and analyses of environmental samples containing actinide materials and products of actinide process chemistry, 2) development of capabilities to manipulate particles, 3) characterization of oxidized uranium (U) and plutonium (Pu) particles following aging under controlled conditions. We are training students and post-doctoral scientists under this program to attract a new generation of scientists to the field of forensic science, and we

are revitalizing UF6 chemistry and microanalysis at the National Laboratories by training researchers new to this field.

In support of 1): We have explored the use of synchrotron-based micro-X-Ray absorption techniques developed at the Stanford Synchrotron Radiation Lightsource (SSRL) Beam Line 2-3 to image elemental compositions and chemical speciation of environmental samples containing actinides. These samples were collected from soil contaminated by a fire at McGuire Air Force Base in 1960, sediments surrounding containment cribs at the Z-Plant complex at the Hanford site, soils contaminated by the smoke plume generated from the Chernobyl Nuclear Power Plant accident, and soils collected from the Mayak nuclear facility. Following elemental imaging of the samples to identify particles of interest, lattice constants were measured with micro X-ray Diffraction Analysis (micro-XRD), determination of U oxidation state was measured with micro Extended X-ray Absorption Near-Edge Structure (micro-EXANES) and characterization of chemical speciation was measured with micro X-ray Absorption Fine Structure (micro-EXAFS).

Particles containing Pu were identified and isolated from environmental samples collected from an environmental remediation site in New Jersey. Elemental maps of two particles reveal the presence of Pu, U, gallium, iron, and titanium, spatially arranged in a heterogeneous fashion. Although an oxidized U chemical species is predicted based upon the exposure of the material to heat and moisture in the environment, the chemical species of the U and Pu is fluorite AnO_2 (An – U, Pu).

Analyses of environmental samples collected from the soil rim surrounding Hanford Z-19 trench at Hanford Sit reveal blocks of material composed of light elements, likely from the process chemistry. A significant fraction of Pu is attached to these blocks, but the Pu does not correlate spatially with any other elements present in Hanford soils.

Alpha track analyses were first employed to locate

particles in soil sediments collected from a waste reservoir at Mayak. Analyses of these samples reveal that, while the U may consist of a particular chemical species, the species may engage in different spatial associations within the environmental matrix (Figure 1). In one example, one particle of U_3O_8 is sitting next to an environmental mineral, while another U_3O_8 particle is correlated with a calcium-based material in close proximity to an environmental mineral.
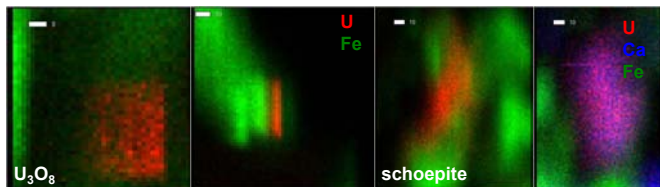
Figure 1. Micro-XRF images and micro-EXAFS spectra of actinide particles in Mayak waste reservoir sediments reveal the presence of U_3O_8 and schoepite chemical species, each characterized by different spatial associations within the sediment matrix.

Uranium hexafluoride (UF_6) is a ubiquitous material in the nuclear enterprise. Our goal is to identify clear forensic characteristics of UF_6 hydrolysis products that can be used to accurately determine the history and origin of the U particles. It has been reported that UF_6 hydrolyzes rapidly in air to a series of hydrated UO_2F_2 and $UO_2(OH)_2$ complexes, depending on humidity, temperature, and environmental chemistry (pH, oxidizing potential, etc.) [2,3]. Other recent reports on the generation and characterization of uranium containing particles by atmospheric hydrolysis reveal interesting information about the isotopic and morphologic properties of UF_6 reaction products [4,5]. We have assembled a reaction chamber in which UF_6 will react with a humidified atmosphere at a predetermined humidity and temperatures (Figure 2). The resulting uranium containing particles are allowed to gravimetrically settle onto the surface of sample collectors on the bottom of the reaction vessel. The sample collectors have been designed to facilitate transport and analyses of particles by SEM, micro-Raman, XRD and other methods on-site with minimum physical manipulation of products. The ability to analyze these samples soon after generation, as well as to age and store them under controlled and closely monitored conditions, ensures that analytical results can be accurately attributed to known chemogenic conditions.

In support of 2): We installed particle probe and gripper manipulators from DCG Systems that interface with our Field Emission Environmental Scanning Electron Microscope. In a test measurement, we located a particle estimated to be a few micrograms from an approximately 80 gram soil sample, and isolated it from the surrounding bulk material, placing it on a registered location. We installed a confocal optical imaging microscope for

imaging U particles 120 nm laterally and 50 nm axially with hyperspectral fluorescence and Raman microscopy for bench-top characterization. Installation of both a custom-designed Class 1000-10,000 rated Clean Laboratory and the Cameca IMS 1280 was completed. This activity required facility modifications (fire detection/suppression systems, HVAC installation and an electrical remodel), and on-site installation by four factory engineers over five months to complete physical installation, alignment, tuning, acceptance testing, and training.

$$UF_6 + H_2O \rightarrow UOF_4$$
$$UOF_4 + H_2O \xrightarrow{rapid} UO_2F_2 \quad \approx \left([UO_2]^{2+} 2F^G\right)$$
$$UO_2F_2 + H_2O \xrightarrow{slower} UO_2F_2 \cdot nH_2O$$
$$UO_2F_2 \cdot nH_2O \xrightarrow{slow} UO_3 \cdot HF, H_2O$$
$$UO_3 \cdot HF, H_2O \rightarrow UO_3 \cdot nH_2O + HF \uparrow$$
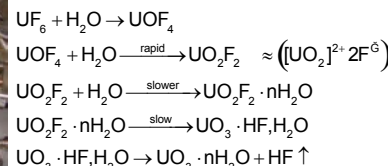
Figure 2. (a) The reaction chamber, shown above, is used to allow UF_6 to react with a humidified atmosphere under controlled temperature and relative humidity. (b) Depending on the amount of moisture present, UF_6 hydrolyses through a number of compounds. All of these intermediates – with the exception of UOF_4 – may coexist.

In support of 3): Theoretical modeling was carried out to understand the initial steps of UO_2 oxidation by studying how oxygen atoms add to UO_2 (111) surfaces, and to characterize the complete bulk oxidation process from UO_2 to U_3O_8 including formation of U_4O_9 and U_3O_7 compounds. Oxidation was simulated using DFT by adding oxygen atoms to a UO_2 crystal described by a 2x2x2 supercell expansion of the fluorite unit cell. Clustering was investigated by creating different local oxygen configurations based on earlier results from the preferred local cluster geometries and by performing DFT based molecular dynamics simulations that try to achieve simulated annealing of the starting configurations. In order to complement studies of the oxidation of fluorite UO_{2+x}, we performed simulations of U_3O_8 reduction using a similar supercell approach. The results show that fluorite UO_{2+x} is stable up to U_3O_7, after which the U_3O_8 phase is preferred. Both U_4O_9 and U_3O_7 emerge as stable phases, in good agreement with experiments; however, our simulations propose new structure models for these compounds. We are currently analyzing experimental structure data for U_3O_7 and U_4O_9 in terms of the new structure models to determine if they offer an advantage over existing models in the literature (Figure 3).

We are pursuing measurements at the Los Alamos Neutron Science Center to measure the kinetics of the formation of uranium-oxygen phases UO_2, UO_{2+x}, beta-U4O9 and alpha-U_3O_7, the diffusivity of the oxygen in different media-defect structures, and the micro-structural changes during oxygen defect formation and migration. We are also initiating measurements to perform in situ neutron diffraction

of UO_2 to probe the complete circle of oxidation and reduction conditions, the atomic-scale changes in micro-structure, the mechanism of oxygen defect formation and subsequent clustering, the anisotropic oxygen diffusion pathway, and phase transformations for the complex oxidation processes of UO_2 and UO_{2+x}.

We have three Post-doctoral Research Associates, two Graduate Research Assistants and one undergraduate student working on this project, and we are bringing in a fourth Post-doctoral Research Associate to contribute to the project in January 2012.
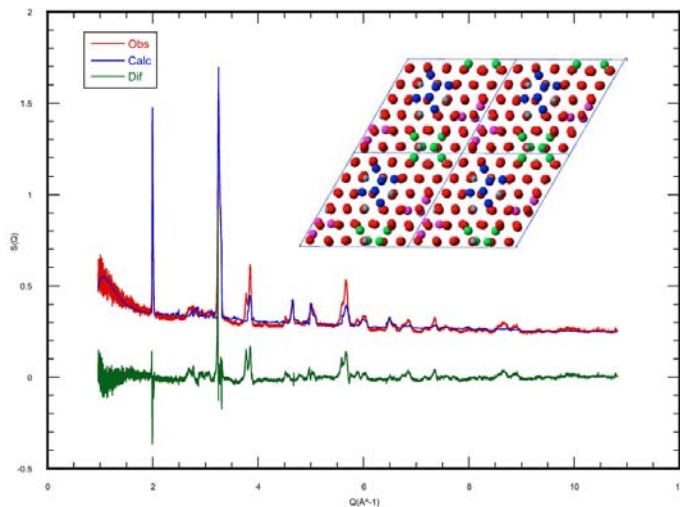
Figure 3. This graph is a comparison of fit (background, lattice parameters, and profile functions) of the proposed U_3O_7 structure to neutron diffraction data. The inset shows the new U_3O_7 structure model derived from DFT calculations with the oxygen cluster ions highlighted.

Future Work

Our research plan is designed to answer fundamental scientific questions required to exploit both new and "traditional" forensic signatures. Current techniques employed for forensics analysis cannot exploit the full range of information potentially available from nuclear materials, particularly process and age information that could be measured from speciation changes. More crucial is a lack of understanding of the fundamental reaction processes that drive changes in various chemical and isotopic signatures, how the rates of these processes are impacted by changes in the simplest parameters found in an industrial setting, and if/how these scale as a function of material size. Our research plan in the final year of this project is to complete analyses of synchrotron-based measurements for publication in peer-reviewed journals, to characterize complete modeling studies of oxidation of uranium oxides, and to accomplish the spatial registration of a particle and measurements in order to characterize the chemical speciation, image morphology, and determine isotopic composition of the sample.

Conclusion

Experiments carried out on particles reveal that signatures of their origin and chemical history are quite strong, including details of other materials which were in close physical proximity or accumulating elements from structures that they contacted. In agreement with reports to study environmental transport and fate of actinides [6], it is apparent that materials produced from waste streams are relatively small and homogeneous, while materials released from more extreme conditions, such as heat or pressure, are larger and elementally inhomogeneous.

References

1. Nuclear Forensics Role, State of the Art, and Program Needs. 2008. *Joint Working Groups of the American Physical Society and the American Association for the Advancement of Science.*

2. Bacher, W., and J. Eberhard. Uranium Hexafluoride. 1986. In *Handbook on the Physics and Chemistry of the Actinides.* Edited by Freeman, A. J., and C. Keller. , p. 1. New York: Elsevier.

3. Katz, J. J., and E. Rabinowitch. The Chemistry of Uranium. 1951.

4. Kips, R., A. J. Pidduck, M. R. Houlton, A. Leenaers, J. D. Mace, O. Marie, F. Pointurier, E. A. Stefaniak, P. D. P. Taylor, S. Van den Berghe, P. Van Espen, R. Van Grieken, and R. Wellum. Determination of fluorine in uranium oxyfluoride particles as an indicator of particle age. 2009. *Spectrochimica Acta B.* **64**: 199.

5. Pickrell, P.. Characterization of the solid, airborne materials created when UF6 reacts with moist air flowing in single-pass mode. 1985. *ORNL Report K/PS-1134.*

6. Salbu, B., O. C. Lind, and L. Skipperud. Radionuclide speciation and its relevance in environmental impact assessments. 2004. *Journal of Environmental Radioactivity.* **74**: 233.

Publications

Andersson, D. A., D. R. Conradson, F. J. Espinosa-Faller, and S. D. Conradson. Oxidation of UO2 from density functional theory calculations: evolution of U4O9, U3O7 and U3O8. 2011. *Manuscript in preparation.*

Andersson, D. A., F. J. Espinosa-Faller, B. P. Uberuaga, and S. D. Conradson. Configurational stability and migration of large oxygen clusters in UO2+x: density functional theory calculations. 2011. *Manuscript in preparation.*

Batuk, O. N., I. E. Vlasova, A. L. Costello, S. N. Kalmykov, S. D. Conradson, M. P. Wilkerson, and D. L. Clark. Characterization of U and Pu oxide particles formed during the accident at the Chernobyl NPP by various spectroscopic and microscopic techniques. 2010. In

Plutonium Futures - The Science 2010. (Keystone, CO, 19-23 September 2010). , p. 89. LaGrange Park, Illinois: American Nuclear Society.

Bowen, J. M., W. Kinman, M. Smith, S. Glover, and H. Spitz. Method for identifying and isolating residual particles of plutonium in soil. 2011. *Manuscript in preparation.*

Bowen, J. M., W. Kinman, and M. P. Wilkerson. Nanomanipulation - a tool for analysis of trace nuclear forensic evidence. 2011. *Manuscript in preparation.*

Conradson, S. D., A. L. Costello, F. J. Espinosa-Faller, D. E. Hobart, J. N. Mitchell, and P. T. Martinez. Atomic scale mechanism of plutonium corrosion. 2010. In *Plutonium Futures - The Science 2010.* (Keystone, CO, 19-23 September 2010). , p. 232. LaGrange Park, IL: American Nuclear Society.

Conradson, S. D., Y. An, A. D. Andersson, K. S. Boland, J. A. Bradley, D. L. Clark, D. R. Conradson, L. L. Conradson, A. E. Costello, F. J. Espinosa-Faller, N. J. Hess, S. A. Kozimor, J. L. Pacheco, A. Llobett, R. L. Martin, J. Mustre de Leon, T. E. Proffen, G. Rodriguez, D. Schwartz, G. T. Seidler, A. J. Taylor, and S. A. Trugman. Dynamical charge-lattice instabilities in hypervalent urania: a complex correlated material. 2011. *Manuscript in preparation.*

Felmy, A. R., K. J. Cantrell, and S. D. Conradson. Plutonium contamination issues in Hanford soils and sediments: discharges from the Z-Plant (PFP) complex. 2010. *Physics and Chemistry of the Earth.* **35** (6-8): 292.

Hobart, D. E., D. S. Peterson, S. A. Kozimor, K. S. Boland, M. P. Wilkerson, and J. N. Mitchell. Diffuse reflectance spectroscopy of plutonium metal, alloys, and compounds. 2010. In *Plutonium Futures - The Science 2010.* (Keystone, CO, 19-23 September 2010). , p. 61. LaGrange, IL: American Nuclear Society.

Hobart, D. E., and K. S. Boland. Diffuse reflectance spectroscopy of plutonium solids. 2011. *Actinide Research Quarterly.* : 1.

Reilly, D. D., O. Batuk, S. Conradson, A. Costello, K. Czerwinski, R. Gostic, and M. P. Wilkerson. Element maps and chemical speciation in plutonium particles. 2011. *Manuscript in preparation.*

Wilkerson, M. P., A. D. Andersson, J. M. Berg, K. S. Boland, C. J. Burns, D. L. Clark, S. D. Conradson, A. L. Costello, D. E. Hobart, P. K. Kennedy, S. A. Kozimor, P. T. Martinez, J. Mitchell, K. D. Rector, D. Reilly, L. R. Riciputi, L. Tandon, and G. L. Wagner. Application of chemical structure and bonding of actinide oxide materials for forensic science. 2010. In *Institute of Nuclear Materials Management 51st Annual Meeting.* (Baltimore, MD, 11-15 July 2010). , p. 10. Deerfield, IL: INMM.

Understanding, Exploiting, and Controlling Competing Interactions in Complex Oxides

Quanxi Jia
20100073DR

Introduction

Epitaxial nanocomposites, in which emergent behaviors can be achieved through interfacing different strongly correlated materials at the nanoscale, provide a new design paradigm to produce enhanced and/or novel properties that cannot be obtained in the individual constituents. Several recent experimental results have shown that new functionalities and emergent behaviors in complex metal-oxides can be obtained through constituent interactions on micro-, meso-, and macro-scopic scales. However, empirical rules are currently used to guide research on such materials, and the state of the art remains at the "observation/validation" stage. We cannot yet fully control or predict their properties. We proposed an innovative approach to control emergent behavior in hybrid complex oxide nanostructures. More specifically, our goal is to manipulate the competing interactions by designing and synthesizing complex oxide nanocomposites using ferroelectric, ferromagnetic, and high-temperature superconducting materials as the functional components. We pursue a conceptually new approach to design new architectures with entirely new or significantly improved functionalities, by understanding the emergent physics that evolves over multiple length and time scales in these systems. Our ultimate objective is to develop a framework for understanding and controlling the states that emerge from strong electronic correlations. The impact of this project is expected to reach well beyond these particular materials as this study will enable the transition from "observation and validation" to "prediction and control."

Benefit to National Security Missions

This research strongly supports the LDRD Materials Grand Challenge, specifically, "Strategies exploring and developing the ability to control emergent phenomena." It underpins three of the five Scientific Grand Challenges identified in the DOE-BES Report, "Directing Matter and Energy: Five Challenges for Science and the Imagination." This research will result in materials with tunable and/or improved or novel functionalities such as enhanced magnetoelectric effects, which will enable next-generation devices for sensing, information storage, advanced detection, or spintronics of interest to DOE, DOD, IC, and industry. Finally, this work exploits the capabilities at MPA-CINT of Los Alamos National Laboratory, a DOE National User Facility.

Progress

In the past year, we made tremendous progress for this project. This can be testified by our many refereed journal articles published in 2011. In the following, we summarize the key technical accomplishments.

We have used both conventional pulsed laser deposition and laser molecular beam epitaxy to grow vertically aligned epitaxial nanocomposites and multilayered structures needed for this project. We have successfully prepared fully strained much thicker $BaTiO_3$:Sm_2O_3 vertically aligned epitaxial nanocomposites. In more detail, we have grown self-assembled nanoscale composites of $BaTiO_3$ (BST) and Sm_2O_3 (SmO) up to 1.25 _m thick that exhibit tetragonality up to at least 800°C and strong remnant polarization to at least 330°C (potential for ferroelectricity up to 800°C). The enhanced Curie temperature is a consequence of uniform, vertical strain coupling between stiff 10 nm regular interspersed nanocolumns of SmO and a surrounding BTO nanomatrix, preventing the onset of the tetragonal to cubic phase transition. The nanocomposite structure improved BTO crystalline quality and reduced the leakage current (please see our article published in Nature Nanotechnology, 2011 for more details). We have also synthesized single layer and multilayer films for scanning tunneling microscopy (STM) and ultrafast optical spectroscopy studies central to the project. In particular, we have deposited high quality superlattices of $[(La_{0.7}Sr_{0.3}MnO_3)_n/(BiFeO_3)_n]_m$ (n = 1, 2, 4, 8, and m = 48, 24, 12, 6) on $SrTiO_3$ (STO) substrates by laser molecular beam epitaxy. These superlattices were fully characterized by polarized neutron reflectivity.

We have made significant progress in applying ultrafast optical spectroscopy to the study of quasiparticle dynamics in different complex oxides and oxide

heterostructures. We have performed some of the first ultrafast optical experiments on multiferroic $BiFeO_3$ (BFO) which exhibits both antiferromagnetic (AFM) and ferroélectric (FE) ordering at room temperature. Optical pump-probe spectroscopy reveals rapid destruction of the FE polarization within ~1 picosecond (ps), followed by electron-phonon coupling and radiative recombination (observed in BFO for the first time) on a timescale of tens of ps. We have also examined superlattices of BFO and the half-metallic ferromagnetic (FM) manganite $La_{0.7}Sr_{0.3}MnO_3$ (LSMO), revealing large oscillations in the signal that may be due to photoinduced strain wave propagation. We are currently performing static and time-resolved second harmonic generation (SHG) experiments on BFO to more directly access the AFM and FE order parameters.

Optical pump-probe and time-resolved Kerr rotation spectroscopy experiments on the AFM and FE ordered multiferroic manganite $TbMnO_3$ (TMO) revealed a coexisting weak FM phase in TMO at low temperatures, which dominates the measured dynamics on intermediate time scales. We have also examined heterostructures composed of TMO and the canonical high-temperature superconductor $YBa_2Cu_3O_7$ (YBCO), which show that the superconducting state strongly influences quasiparticle dynamics in TMO. Finally, we have performed optical pump-probe and optical-pump, terahertz (THz)-probe spectroscopy on YBCO/LSMO heterostructures. Our data indicates that the magnetism in LSMO breaks Cooper pairs in YBCO, reducing the superconducting gap. We are currently preparing publications on our BFO, TMO, and YBCO/LSMO results.

We used scanning tunneling microscopy/spectroscopy (STM/STS) and magnetic force microscopy (MFM) to discover unusual electronic and magnetic behavior of ferromagnetic/superconducting heterostructures. Usually, complex material functionalities disappear below certain threshold film thickness due to strain effects. Indeed, our spatially- and energy-resolved STM studies of very thin ferromagnetic LSMO films on insulating STO substrate revealed that LSMO becomes insulating below 4 nm thickness due to presence of the residual stress, while above this threshold thickness LSMO behaves like a bulk material with a well-defined Curie transition temperature. However, we have shown that metallic and magnetic response of a LSMO deadlayer can actually be restored and enhanced by interfacing with superconducting $EuBa_2Cu_3O_7$ (EBCO) film - even 2 nm LSMO films exhibited finite conductivity and ferromagnetic domain structure when interfaced with EBCO. Moreover, the extent of functional enhancement can be controlled by oxygen content in the superconducting layer. We have attributed this behavior to doping of the LSMO films by means of hole transfer from EBCO layer. When films are exposed to different environments (ultra-high vacuum or ambient) one can observe slow (~days) transition of electronic response of LSMO/EBCO heterostructures from metallic

to semiconducting. This agrees well with hole-doping explanation when oxygen depletion from EBCO layer causes doping decrease of LSMO films. Theoretical simulations confirmed hole transfer across the interface from the superconducting EBCO to ferromagnetic LSMO and provided characteristic depth of the doping process of ~ 5 nm, in good agreement with experimentally determined 4 nm value. These results demonstrate that degradation of material properties (i.e. conductivity and magnetism) caused by reduced dimensionality can be overcome by proper interface choice, and are directly relevant to applications of deadlayers for future device miniaturization.

As one part of understanding the interaction between magnetism and superconductivity, we have identified the effect of the ferromagnetism in a mangnite, to which a high temperature superconducting cuprate is in contact, being of classical field or electronic nature. As such, we have been calculating the optical conductivity response in the superconductor in the presence of a macroscopic magnetic field, which generates magnetic vortices, and to an exchange field. The former effect is revealed through the change of Drude peak width due to the generation of low-energy quasiparticles while the latter effect can be related to the spin splitting. We have finished the study of the former effect and the study of the latter effect is in progress. The contrast between two effects can be used to compare with the experimental measurement of THz optical conductivity in the LSMO/YBCO interfacial structure.

Theoretically, we have developed a theory of ferroelectric (FE) transition induction by superconductor (SC) correlations in the interfacial film. We examined the effect of an electric potential on the carrier densities and on transition temperature (Tc) of the conducting $LaAlO_3$/STO interfaces. We find that the electron density and superconducting temperature can be significantly modified by an external electric field. There have been experimental observations that have explored the relationship between an applied potential on STO heterostructures and the increased carrier density or capacitance. Here, we take this relationship one step further: we assume it is the field effect that through nonlinear capacitance changes carrier density. That in turn affects the superconducting coupling and ultimately Tc. We present a simple mechanism of such a phenomenon assuming a conventional pairing state at the interface. This mechanism shows a possible route to tunable materials properties and suggests an exciting perspective on the way to tunable superconductivity.

Future Work
Interfaces and surfaces have played a critical role in determining the physical properties of a broad range of electronic materials. One of the most important goals of modern materials physics and nanoscience is to control materials and their interfaces to atomic dimensions.

We use the broken symmetry at controlled interfaces in complex oxide heterostructures to perturb the subtle balance between competing physical phenomena. Specifically, we will synthesize and investigate epitaxial ferroelectric/ferromagnetic and ferromagnetic/superconductor nanocomposites of different geometries and controlled dimensions using laser molecular beam epitaxy. We explore two architectures: the layered laminar-like and the vertically aligned pillar-like nanocomposites. A fundamental understanding of these material systems necessitates the use of advanced characterization techniques to study their physics. We use ultrafast temperature-dependent optical spectroscopy from THz through UV frequencies to probe electronic, lattice, and spin dynamics in these materials. We also employ scanning tunneling microscopy to characterize electronic phase inhomogeneities as well as magnetic force microscopy and magnetic resonance force microscopy to characterize the magnetic properties on a nanometer scale. The emergent behaviors (such as the magnetoelectric effect, proximity-induced metal-insulator transition, and giant superconductivity-induced modulation of the ferromagnetic magnetization) and enhanced functionalities (such as magnetic-domain-induced flux pinning in superconductors) of the materials enable us to understand the coupling between these components. In a coupled synthesis, characterization and theory effort, we further use ultrafast optical spectroscopy and nanoscale scanning probes to investigate, and ultimately control, the character of competing electronic, magnetic, and lattice interactions as a function of structure and material composition.

More specifically, we will expand our effort to synthesize layered structures consisting of $Ba_{0.1}Sr_{0.9}TiO_3$ (BST)/LCMO bilayers and other superlattices consisting of different functional materials. This, for example, will allow us to examine the interplay between FE order in BST and FM order more directly, since the transition temperatures are T_{FE}~100 K and T_C~250 K, well within our experimentally accessible range. This will also allow us to examine the effect of "turning on" FE order on dynamics in the FM phase by tuning the temperature below T_{FE}. We will also continue to examine TMO/YBCO heterostructures, as well as $SrMnO_3$ (SMO)/YBCO heterostructures. Since SMO does not exhibit FE order but does exhibit AFM order, this will allow us to examine the effect of the proximal SC order on quasiparticle dynamics in TMO and SMO. By comparing these materials systems, we can discern the separate effects of FE order. Further, our initial data on YBCO/LSMO heterostructures indicates that the LSMO layer may also influence the pseudogap state in YBCO; we will thus perform additional experiments and data analysis to explore this exciting possibility.

We will continue MFM studies to investigate the presence of inhomogeneous ferromagnetic ordering of thin (<4 nm) LSMO films deposited on both STO and EBCO. The goal is to determine if the film thickness can be used to control the magnetic properties of the nanocomposites. We have already designed new sample holder for a cross-sectional STM studies. We will use this technique to gain direct access to electronic/magnetic properties variation in the vicinity of the interface in all future studies of interfaces. In particular, this approach will allow deeper understanding of the charge transfer effect through unambiguous obsevration of characetristic doping scales and electronic signatures of FM/SC orders competition.

Conclusion

We expect to develop a conceptually new approach to understand the emergent physics that evolves over multiple length and time scales in order to design new materials with new or significantly improved functionalities. The proposed integration of nanoscale synthesis and coherent control, guided by forefront condensed matter theory, is poised to forge a new paradigm in the design of novel functionality through both intrinsic and extrinsic control of competing interactions. This research will result in materials with tunable, enhanced or novel functionality, which will enable next-generation devices for sensing, information storage, advanced detection, or spintronics.

Publications

Balatsky, A. V., D. N. Basov, and J. X. Zhu. Induction of charge density waves by spin density waves in iron-based superconductors. 2010. *Phys. Rev. B.* **82**: 144522.

Bi, Z., A. Chen, H. Wang, E. Weal, J. L. MacManus-Driscoll, H. Luo, and Q. X. Jia. Microstructure and magnetic properties of (La0.7Sr0.3MnO3)0.7:(Mn3O4)0.3 nanocomposite thin films. 2011. *J. Appl. Phys. .* **109**: 054302.

Bi, Z., O. Anderoglu, X. Zhang, J. L. MacManus-Driscoll, H. Yng, Q. X. Jia, and H. Wang. Nanoporous thin films with controlable nanopores processed from vertically aligned nanocomposites. 2010. *Nanotechnology.* **21**: 285606.

Bi, Z., O. Anderoglu, X. Zhang, J. MacManus-Driscoll, Q. X. Jia, and H. Wang. Nanoporous thin films with controllable nanopores processed from BiFeO3:Sm2O3 vertically aligned nanocomposites. Presented at *2010 MRS Spring Meeting.* (San Francisco, CA, April 5 – 9, 2010).

Chen, A., Z. Bi, C. F. Tsai, J. H. Lee, Q. Su, X. Zhang, Q. X. Jia, J. L. MacManus-Driscoll, and H. Wang. Tunable low-field magnetoresistance in (La0.7Sr0.3MnO3):(ZnO)0.5 self-assembled vertically aligned nanocomposite thin films. 2011. *Adv. Funct. Mater..* **21**: 2423.

Chen, A., Z. Bi, H. Hazariwala, X. Zhang, Q. Su, L. Chen, Q. X. Jia, J. L. MacManus-Driscoll, and H.

Wang. Microstructure, magnetic, and low-field magnetotransport properties of self-assembled (La0.7Sr0.3MnO3)0.5:(CeO2)0.5 vertically aligned nanocomposite thin films. 2011. *Nanotechnology.* **22**: 315712.

Choi, E. M., S. Patnaik, E. Weal, S. L. Sahonta, H. Wang, Z. Bi, J. Xiong, M. G. Blamire, Q. X. Jia, and J. L. MacManus-Driscoll. Strong room temperature magnetism in highly resistive strained thin films of BiFe0.5Mn0.5O3. 2011. *Appl. Phys. Lett. .* **98**: 012509.

Haraldsen, J. T., S. A. Trugman, and A. V. Balatsky. Induced polarization at a paraelectric/superconducting interface. 2011. *Phys. Rev. B .* **84**: 020103(R).

Harrington, S. A., J. Zhai, S. Denev, V. Gopalan, H. Wang, Z. Bi, S. A. Redfern, S. H. Baek, C. W. Bark, C. B. Eom, Q. X. Jia, M. E. Vickers, and J. L. MacManus-Driscoll. Thick lead-free ferroelectric films with high Curie temperatures through nanocomposite-induced strain. 2011. *Nature Nanotechnology .* **6**: 491.

Jia, Q. X.. Synthesis and characterization of nanocomposite films. Invited presentation at *2010 MRS Spring Meeting, San Francisco.* (San Francisco, CA, April 5-9, 2010).

Jia, Q. X.. Control of lattice strain and electrical properties of epitaxial nanocomposite films. Invited presentation at *Control of lattice strain and electrical properties of epitaxial nanocomposite films.* (Lake Buena Vista, FL, Jan. 20 - 22, 2010).

Kang, B. S., L. Stan, I. O. Usov, J. K. Lee, T. A. Harriman, D. A. Lucca, R. F. DePaula, P. N. Arendt, M. Nastasi, J. L. MacManus-Driscoll, B. H. Park, and Q. X. Jia. Strain mismatch induced titled heteroepitaxial (000l) hexagonal ZnO films on (001) cubic substrates. To appear in *Adv. Eng. Mater..*

Liu, Y. H., J. Xiong, J. Haraldsen, A. V. Balasky, Q. X. Jia, A. J. Taylor, and D. Yarotski. Charge transfer at the interface between ferromagnetic La0.7Sr0.3MnO3} and superconducting EuBa2Cu3O7. *Science.*

Liu, Y. H., J. Xiong, Q. X. Jia, A. J. Taylor, and D. Yarotski. Vacuum-aging effect on electronic structure of YBa2Cu3O6+x thin film: an STM/STS study. Presented at *APS March Meeting.* (Dallas, 21-25 March 2011).

MacManus-Driscoll, J. L., S. Harrington, L. Jew, E. Weal, H. Wang, H. Yang, Z. Bi, and Q. X. Jia. Vertical nanocomposites for multiferroics and enhanced single phase functionality. Invited presentation at *Electronic Materials and Applications 2010.* (Lake Buena Vista, FL, Jan. 20 - 22, 2010).

Park, B. H., Y. R. Li, J. Xiong, and Q. X. Jia. Dielectric properties of epitaxial Ba1-xSrxTiO3 films on MgO substrates. 2011. *Functional Mater. Lett. .* **4**: 41.

Prasankumar, R. P.. Understanding the Interplay between Electrons, Spins, and Phonons in Multiferroic Oxides. Invited presentation at *IEEE Photonics Society seminar.* (New Mexico, 2011).

Qi, J., S. Trugman, J. X. Zhu, A. J. Taylor, Q. X. Jia, and R. P. Prasankumar. Multiferroic properties of epitaxial TbMnO3 films using ultrafast pump-probe spectroscopy. *Phys. Rev. Lett..*

She, J. H., J. Zaanen, and A. R. Bishop. Stability of quantum critical points in the presence of competing orders. 2010. *Phys. Rev. B.* **82**: 165128.

Sheng, G., Y. L. Li, J. X. Zhang, S. Choudhury, Q. X. Jia, V. Gopalan, D. G. Schlom, Z. K. Liu, and L. Q. Chen. A modified Landau-Devonshire thermodynamic potential for strontium titanate. 2010. *Appl. Phys. Lett..* **96**: 232902.

Sheng, G., Y. L. Li, J. X. Zheng, S. Choudhury, Q. X. Jia, V. Gopalan, D. G. Schlom, Z. K. Liu, and L. Q. Chen. Phase transitions and domain stabilities in biaxially strained (001) SrTiO3 epitaxial thin films. 2010. *J. Appl. Phys..* **108**: 084113.

Su, Q., J. H. Lee, Z. Bi, B. Zhu, K. K. Shung, Q. Zhou, S. Takeuchi, B. H. Park, Q. X. Jia, and H. Wang. Self-separated PZT thick films with bulk-like piezoelectric and electromechanical properties. 2011. *J. Mater. Res. .* **26**: 1431.

Talbayev, D., A. D. LaForge, N. Hur, T. Kimura, S. A. Trugman, A. V. Balatsky, D. N. Basov, A. J. Taylor, and R. D. Averitt. Dynamic investigations of multiferroics: terahertz and beyond. 2009. *J. Phys: Conf. Series.* **148**: 01203.

Talbayev, D., K. S. Burch, E. E. M. Chia, S. A. Trugman, J. X. Zhu, E. D. Bauer, J. A. Kennison, J. N. Mitchell, J. D. Thompson, and J. L. Sarrao. Hybridization and superconducting gaps in heavy-fermion superconductor PuCoGa5 probed via the dynamics of photoinduced quasiparticles. 2010. *Phys. Rev. Lett.* **104**: 227002.

Talbayev, D., S. A. Trugman, S. Lee, H. T. Yi, S. W. Cheong, and A. J. Taylor. Long wavelength magnetic and magnetoelectric excitations in the ferroelectric antiferromagnet BiFeO3. 2011. *Phys. Rev. B .* **83**: 094403.

Vidmar, L., J. Bonca, M. Mierzejewski, P. Prelovsek, and S. A. Trugman. Nonequilibrium dynamics of the Holstein polaron driven by an external electric field. 2011. *Phys. Rev. B .* **83**: 134301.

Wimbush, S. C., J. H. Durrell, C. F. Tsai, H. Wang, Q. X.

Upgrading Renewable and Sustainable Carbohydrates for Production of High Energy Density Fuels.

John C. Gordon
20100089DR

Introduction

We are executing a transformational strategy to obtain high-density hydrocarbon fuels from (non-food derived) carbohydrates. To transform sugars to diesel and gasoline, we need to get the oxygen out and hydrogen in, and do so efficiently and environmentally soundly. The development of effective biomass conversion technology that integrates with existing fuel production and distribution infrastructure would permit a shift away from our dependence on foreign petroleum imports. In fact, efficient conversion of renewable biomass can account for 100% of current U.S. petroleum imports, which add $250-450B per year to the country's trade imbalance. Even a 5% contribution from biofuels eliminates approximately 375 million tons of carbon dioxide per year. This area of transformational research directly addresses important national security transportation issues (tanks, jets and helicopters) and can meet the mission needs of a wide range of sponsors.

Initially, we will extend the carbon skeletons of biomass-derived carbohydrates through a class of environmentally friendly, carbon-chain extension reactions with other naturally occurring polyalcohols. Inexpensive, water soluble metal catalysts will then be developed for efficient deoxygenation and hydrogenation of the resulting extended chain polyalcohols, allowing facile separation of the resulting chain-extended hydrocarbons. An essential element of our strategy is the development of highly functional catalysts that operate at low temperatures, thus enabling dramatically higher conversion efficiencies and selectivities than current methods. Successful execution of the proposed work will provide transformational science (especially in aqueous phase homogeneous catalysis) required to obtain useful fuels from cellulose-derived feedstocks without wasting energy or carbon.

Benefit to National Security Missions

This area of transformational research directly addresses National security transportation issues and represents significant opportunities to address nationally-significant WFO missions. For example, the DOD, the largest consumer of petroleum in the world, has significant interest in the future development of domestically sourced biologically derived fuels. DOE's OBP has seen a dramatic increase in mission priority. With the successful demonstration of the novel energy efficient conversion of carbohydrates to high energy density fuels proposed herein, LANL will demonstrate its capabilities for the OBP mission and be successful in fostering a biomass-related research and development program dedicated to energy security.

Progress

Significant progress has been made across several key areas:

We have further increased the scope of catalysts and substrates in the carbon chain elongation chemistries that utilize sugars or sugar derived molecules. This gives us access to a wide range of potential fuels precursors of varying carbon chain lengths.

We have investigated the mechanism of acid catalyzed ring opening chemistry using furfural based systems derived from eight and nine carbon atoms. This has provided us with a greater understanding as to the mechanistic aspects of the reactions using biomass derived substrates

We have investigated the use of multi-component catalytic systems and have demonstrated their utility in preparing alkanes in a single reactor system

In collaboration with our theory colleagues, we have investigated mechanistic aspects of several of the transformations required to convert the chain extended polyols into hydrocarbons. These include; (a) mechanistic aspects of the organocatalyzed aldol chemistries, and in particular the role of amine based catalysts in determining reaction pathways and transition state geometries; (b) the role of Bronsted acids in ring opening chemistries; (c) the role of metal based catalysts in deoxygenation chemistries.

We and our collaborators are also developing earth

abundant metal catalysts (based on iron and copper) for the hydrogenation of various pertinent substrates.

We have investigated the applicability of deoxygenation chemistries using the so-called Barton-McCombie chemistry with our biomass derived substrates

A provisional patent related to the production of hydrocarbons was filed in the US patent office on 9/14/11.

Two of the PIs (Gordon and Silks) were symposium organizers at the ACS National Meeting, Denver CO, Aug 2011. The symposium was entitled "Recycling Carbon: Catalyzed Conversion of Non-Food Based Biomass to Fuels and Chemicals".

Future Work

Lignocellulose-derived polyalcohols constitute the most abundant renewable organic carbon source on the planet. In contrast to hydrocarbons, these polyalcohols are characterized by an abundance of oxygen and typically possess C3-6 chain lengths. Therefore, we seek to perfect the chemical and engineering methods required to selectively extend the carbon chain length and remove the oxygen content of the starting material, while minimizing energy input and loss of carbon (in the form of CO_2). Maintaining a focus toward large-scale industrial viability, it is critical to develop thermally efficient (e.g. < 100 deg C) and "atom economical" processes for these transformations. With appropriately designed catalysts, the slight driving force required for these reactions could be harnessed from industrial waste heat that is presently discarded. The use of waste heat as an energy source for fuel upgrading removes the need to drive a high temperature process using a (sizable) portion of the feed stock as the fuel. In addition, direct use of waste heat in biomass conversion obviates the need for cooling towers (where huge amounts of useful potable water are consumed by evaporation). However, before this can be realized, the required fundamental molecular science must be perfected. The objective of this project is to develop the transformational science needed to enable the high yield, energy-efficient production of hydrocarbon fuels from biomass-derived polyalcohols.

Conclusion

Within the next 30 years, world energy consumption is projected to double. With decreasing global production of crude oil, it is essential to our National security that renewable alternatives to petrochemical feedstocks for hydrocarbon fuels are developed. A constant, reliable supply of these fuels would ensure that the transportation of food, medicine, and consumer goods about the country remains uninterrupted, regardless of sociopolitical conflict. This project will integrate expertise in catalysis, stable isotope chemistry, reaction engineering and theory/modeling to forge a unique technical approach for energy-efficient, carbon-neutral conversion of biomass-derived polyalcohols to high energy density fuels.

Publications

Keith, J. M., J. K. Kim, L. Alexander, R. Wu, R. L. Martin, E. R. Batista, R. Michalczyk, B. L. Scott, S. K. Hanson, A. D. Sutton, L. A. Silks, and J. C. Gordon. Aqueous Organocatalysis Applicable to the Carbon Chain Extension of Carbohydrate Derivatives: Application to the Production of Transportation Fuels. *Green Chemistry.*

Waidmann, C. R., A. W. Pierpont, E. R. Batista, J. C. Gordon, R. L. Martin, L. A. "Pete" Silks, Ryan M. West, and R. Wu. Catalytic Ring Opening of Furan Rings Within Biomass Derived Substrates: An Experimental and Theoretical Study. *Green Chemistry.*

Radioparagenesis: Robust Nuclear Waste Form Design and Novel Materials Discovery

Christopher R. Stanek
20110009DR

Introduction

Nuclear waste disposal is a significant technological issue, and the solution of this problem (or lack thereof) will ultimately determine whether nuclear energy is deemed environmentally friendly, despite significantly lower carbon emissions than fossil fuel energy sources. A critical component of any waste disposal strategy is the development of a waste form that prevents radionuclides from entering the environment. The design of robust nuclear waste forms requires consideration of several criteria, including tolerance to radiation damage and leaching, geological interaction, and chemical durability; all of these criteria ensure that the radionuclides do not escape. Over the past 30 years, there have been numerous and thorough studies of candidate waste forms driven by these criteria. However, most of these efforts have focused on the performance of the candidate waste form at $t = 0$, with far less attention paid to the phase stability, and subsequent durability, of candidate waste forms during the course of daughter product formation; that is, the aging of the material as its chemistry changes. Systematic understanding of phase evolution as a function of chemistry is important for predictions of waste form performance as well as informing waste form design. In this LDRD project, we attack the research challenges associated with understanding waste form stability, systematically studying the effects of dynamic composition variation due to in situ radionuclide daughter production formation.

The initial goal of this project was to validate and verify the new concept of "radioparagenesis" discovered by members of our team. Radioparagenesis is the formation of unconventional crystal structures (e.g. a rocksalt structure not seen in nature for BaCl) for compounds formed during the chemical transmutation that occurs during radioactive decay. In order to develop a predictive capability to design radiation tolerant and chemically robust nuclear waste forms (and in the process, remove a significant obstacle limiting the expansion of nuclear energy), we must first address a fundament materials science question: *What is the impact of daughter product formation on the stability of solids comprised of radioactive isotopes?* To answer this question, we are pursuing a multidisciplinary approach aimed at accelerating the chemical aging process, by integrating first principles modeling with the synthesis and characterization of small, highly radioactive surrogate samples. Improved and systematic understanding of chemical aging will allow us to markedly improve the predictability of nuclear waste form performance, letting us backward design robust waste forms. In addition to providing a potential innovative solution to the nuclear waste problem, radioparagenetic phases may also exhibit interesting materials properties for non-nuclear applications.

It is worth noting that the nuclear weapons and geophysics communities are faced with a similar problem, namely the inability to directly obtain information regarding aging of components due to radiation damage and the composition of the Earth's core-mantle boundary, respectively. Their problems are similar to our accelerated aging approach for the study of compositional variation in nuclear waste forms. Thus, we elected to embed our project appraisal in to a workshop, which we have titled, "Formation of Novel Phases Under Extreme Conditions." The purpose of this workshop was to explore potential relationships between research activities that are similar in their aim to discover novel materials, but differ by synthesis routes (e.g. high pressure, radioactive transmutation, radiation damage and dimensional constraint). The workshop took place December 8, 2012, at Los Alamos, and attendees are recognized international leaders in their respective fields.

Benefit to National Security Missions

A critical problem for DOE-NE is providing a solution for nuclear waste disposal. In fact, the Administration's description of the Fuel Cycle R&D program states that the focus of this problem is "on long-term, science-based R&D of technologies with the potential to produce beneficial changes to the manner in which the nuclear fuel cycle and nuclear waste is managed." This project directly fits this description. This project also addresses issues of fundamental materials science, using

computer simulation to design materials with engineered functionality.

Progress

Significant and exciting progress has been made in relatively short time. This is especially true for the experimental component of our project, which involves the synthesis and characterization of very small and very radioactive samples. Our first sample was ^{109}CdS, produced in hot cells at the Isotope Production Facility (IPF). ^{109}Cd decays to ^{109}Ag, with different chemical properties. We produced ^{109}Cd by irradiating an indium target for a week, producing 1.34 Curies of ^{109}Cd, or approximately 0.5 mg. After the main sample was prepared on filter paper, a smaller specimen was broken off and a suspension made from it, which could be drop-cast onto TEM sample grids at different points during the decay process. XRD has shown that the nature of the sample at time zero is somewhat uncertain, with a few unknown peaks appearing, but showing no peaks attributable to the Greenockite or Hawleyite polymorphs of CdS. A group of four sulfur (S8) peaks was observed early in the decay, after ~ 6 months. Five months later, two small peaks consistent with elemental silver could be seen. TEM (now possible in the MSL after a significant safety basis effort) of the sample showed a significant amount of impurities, including some silicon as well as what appear to be amorphous silver nanoparticles. Our experiments continue, seeking to understand the nature of the chemical evolution. Also, we have expanded our sample inventory by considering other isotopes. ^{7}Be, which decays to ^{7}Li significantly faster than the others (53 day halflife), has been obtained as a byproduct of RbCl targets that were irradiated to produce ^{82}Sr. We are also considering compounds of ^{65}Zn, which will be crystallized as the oxide or the sulfide. It will be made on a smaller scale (several μg) because of the higher gamma activity of this isotope. ^{65}Zn decays to ^{65}Cu and is obtained in several hundred mCi quantities as a byproduct of the production of ^{68}Ge from gallium metal, where it is left behind after the desired ^{68}Ge has been extracted. Finally, we are also pursuing ^{55}Fe and ^{177}Lu.

Other activities within our project have also been successful. Our first principles calculations has predicted interesting bonding behavior for our experimental materials, suggesting the potential for non-intuitive materials property variation as a function of daughter product formation. Further first principles calculations provide pore-scale modeling parameters as inputs to leaching calculations. We enhanced our pore-scale model by accounting for strongly coupled ion transport, species mass transfer, electrolyte hydrodynamics, as well as homogenous and heterogeneous electrochemical reactions. Numerically, the model is constructed using more advanced finite difference discretization techniques. This numerical modification enables the model to be freely implemented on non-uniform grids, which is particularly useful for describing the dynamic detail in the thin interfacial electric double layer. The model is being used to explore the interplay of ion transport, electrolyte hydrodynamics, and electrode kinetics under different electrochemical conditions. Next, the model will be applied to investigate subsurface flow coupled with surface complexation, which may be important for geologic storage of nuclear waste. Regarding the applied nuclear waste aspects of this project, wadeite (of the type $Cs_2ZrSi_3O_9$) and hollandite phases have been examined as phases that may have the chemical "flexibility" to accommodate the formation of Ba daughter products. Specifically, Hollandite-type compounds, $A_xB_8O_{16}$ (A = Cs^{1+}, Ba^{2+}, etc.; B = Ti^{3+}, Al^{3+}, Fe^{3+}, etc.), possess a framework structure of $[BO_6]$ octahedra via edge- and corner-sharing with A cations occupying the tunnel sites. This group of materials is of considerable interest as potential waste forms for radioactive ^{137}Cs and its beta-decayed ^{137}Ba. To assess the suitability of their use for Cs/Ba immobilization, it is essential to determine their phase stability at extreme temperature, pressure, and radiation conditions.

Future Work

This project consists of three tasks that correspond to each of the following goals: develop a new branch of physics and chemistry associated with our recent discovery of radioparagenesis, utilize the insights gained to design robust nuclear waste forms, and discover and characterize heretofore unobserved materials with potentially interesting properties. In the first year of this project, we have established the capabilities to achieve these goals (e.g. theoretical approaches have been confirmed, experimental procedures for samples synthesis and characterization have been established). Thus, we will continue to pursue these goals via the approach described in the project.

Conclusion

To conclude, modern theoretical methods along with new experimental facilities offer a new opportunity to understand the chemistry that occurs upon transmutation and thus provide insight into the chemical aging of crystalline waste forms. By combining first principles calculations with accelerated aging experiments, new insight into the chemical evolution of these materials - critical for predicting stability within a geologic repository - can be gained. In particular, thermodynamic studies can elucidate the propensity for phase decomposition, while accounting for kinetics will give insight into the rates at which this phase decomposition might occur within the geological setting. Nevertheless, insight is expected from chemical aging studies, providing new avenues for waste form design.

References

1. Jiang, C., C. Stanek, N. Marks, K. Sickafus, and B. Uberuaga. Radioparagenesis: The formation of novel compounds and crystalline structures via radioactive

decay. 2010. *PHILOSOPHICAL MAGAZINE LETTERS.* **90** (6): 435.

2. Jiang, C., C. R. Stanek, N. A. Marks, K. E. Sickafus, and B. P. Uberuaga. Predicting from first principles the chemical evolution of crystalline compounds due to radioactive decay: The case of the transformation of CsCl to BaCl. 2009. *PHYSICAL REVIEW B.* **79** (13): 132110.

3. Uberuaga, B. P., C. Jiang, C. R. Stanek, K. E. Sickafus, N. A. Marks, D. J. Carter, and A. L. Rohl. Implications of transmutation on the defect chemistry in crystalline waste forms. 2010. *NUCLEAR INSTRUMENTS & METHODS IN PHYSICS RESEARCH SECTION B-BEAM INTERACTIONS WITH MATERIALS AND ATOMS.* **268** (19): 3261.

Publications

Jiang, C., B. P. Uberuaga, K. E. Sickafus, F. M. Nortier, J. J. Kitten, N. A. Marks, and C. R. Stanek. Using "radioparagenesis‚Äô‚Äô to design robust nuclear waste forms. 2010. *ENERGY & ENVIRONMENTAL SCIENCE.* **3** (1): 130.

Jiang, C., C. R. Stanek, N. A. Marks, K. E. Sickafus, and B. P. Uberuaga. Predicting from first principles the chemical evolution of crystalline compounds due to radioactive decay: The case of the transformation of CsCl to BaCl. 2009. *PHYSICAL REVIEW B.* **79** (13): 132110.

Jiang, C., C. Stanek, N. Marks, K. Sickafus, and B. Uberuaga. Radioparagenesis: The formation of novel compounds and crystalline structures via radioactive decay. 2010. *PHILOSOPHICAL MAGAZINE LETTERS.* **90** (6): 435.

Uberuaga, B. P., C. Jiang, C. R. Stanek, K. E. Sickafus, N. A. Marks, D. J. Carter, and A. L. Rohl. Implications of transmutation on the defect chemistry in crystalline waste forms. 2010. *NUCLEAR INSTRUMENTS & METHODS IN PHYSICS RESEARCH SECTION B-BEAM INTERACTIONS WITH MATERIALS AND ATOMS.* **268** (19): 3261.

Hydrogen Effects in Delta-Stabilized Pu Alloys: Fundamental Thermodynamics and Interactions at Reduced Dimensionality

Daniel S. Schwartz
20110011DR

Introduction

We made significant strides in the first year of our LDRD program investigating the behavior of hydrogen in Pu-Ga alloys. These include both administrative successes in Pu research authorizations and meaningful steps in our understanding of the H-Pu-Ga system.

Benefit to National Security Missions

LANL has a critical role in assessing and maintaining the nation's nuclear stockpile. A key LANL mission is to understand the current state of the nuclear stockpile and what will happen to it as it ages. In addition, LANL is tasked with sustaining the capability to manufacture Pu-containing parts for the stockpile. Since hydrogen is a widespread impurity in our plutonium metal supply, a comprehensive study of hydrogen effects will support our ability to understand and predict the behavior of the plutonium during manufacture and storage.

Progress

Experiments in FY11 focused on Pu-2 at.% Ga alloys. The solubility of hydrogen in Pu-2Ga at 400°C was measured at low concentrations (up to ~0.1 at. % H). This is a first for the project; accurate solubility measurements below ~0.04% hydrogen have never before been made. The solubility is plotted in Figure 1 as a function of H-content, and it can be seen that the solubility increases significantly with relatively small increases in H concentration in the low hydrogen regime. This novel result supports the idea that H is a vacancy creating and stabilizing impurity: as H makes its way into the Pu alloy lattice, it stabilizes, or creates, vacancies which in turn serve as sites for trapping more H. This self-trapping mechanism results in an increasing solubility vs. concentration curve. If no such mechanism was active, we would expect solubility to remain low and constant in this dilute regime.

In conjunction with these solubility measurements, x-ray diffraction was used to determine the effect of hydrogen content on the lattice parameter of Pu-2 at. % Ga. A 3-step XRD measurement was conducted: 1) pure Pu-2Ga was measured, 2) the same specimen was then charged with ~1 at. % H (just below the level of hydrogen that would cause the precipitation of PuH_2), and the measurement repeated, and finally 3) the hydrogen was removed from the specimen by vacuum annealing at elevated temperature and a final XRD scan was performed. The results showed a decrease in lattice parameter of ~0.14% after hydrogen-charging. This is an important finding. It may be evidence for a vacancy-multiplying effect due to the presence of hydrogen, as vacancies would be expected to contract the Pu-2Ga lattice. However, we are reluctant to commit to this conclusion yet, because the results are complicated by the presence of a surface layer of Pu-oxycarbide which reduces the accuracy of the XRD lattice parameter measurements. We must determine if this layer is connected to the hydrogen charging process, as well as develop a method for removing it from our specimens.
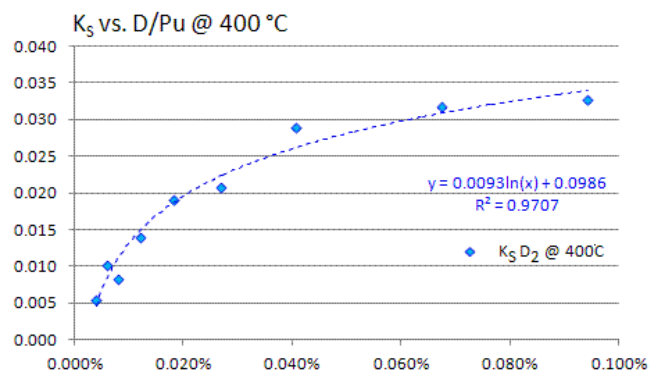
Figure 1. Solubility (Ks) as a function of hydrogen concentration at 400°C, in the dilute regime.

A set of specimens from the same batch of Pu-2Ga alloys was prepared for examination at the Stanford Synchrotron Light Source (Beamline 10-2). Both diffraction and EXAFS (Extended x-ray absorption fine structure) data were collected and are undergoing analysis. Like the XRD data, the synchrotron diffraction data clearly shows the presence of a significant Pu-oxycarbide layer. EXAFS data will give us information

about local bonding, e.g. bond lengths for H-Pu and Ga-Pu bonds; this analysis is underway.

One goal of this program is to engage LANL's Pu facility and Pu manufacturing program as an active research partner. A major step was taken in this direction by a collaborative effort to cast a multi-kilogram lot of high-purity Pu-7 at. % Ga alloy, accomplished in August 2011 (Figure 2). This was the first time in many years that a high-Ga casting was made in the Pu Facility. A portion of the Pu-7Ga alloy will be used as a master alloy, which will be enriched with Pu to make a series of Pu-Ga alloys, so that thermodynamic measurements can be made on a meaningful portion of the Pu-Ga-H compositional space.

Figure 2. Freshly cast Pu-7 at.% Ga rods, shortly after breaking out of the mold.

Photoemission Spectroscopy (PES) was performed on highly pure Pu-2Ga specimens. These specimens underwent a special repeated de-hydrogenating process to push the hydrogen content below detection limits. The PES measurements were performed at the lowest temperature (9 K) and with the highest resolution (12 meV) to-date. These high resolution measurements give direct information about the electronic structure of the alloys. The measurements of hydrogen-free Pu-2Ga are critical baseline data for understanding how the electronic structure of Pu-Ga-H alloys is modified by the presence of H.

We are measuring magnetic susceptibility on a variety of Pu-Ga alloys as a function of hydrogen content to seek transitional states between the non-magnetic Pu state and the strongly magnetic Pu-hydride state. In FY11, we measured the susceptibility of high purity, hydrogen-free Pu-2Ga at LANL's National High Magnetic Field Laboratory.

As expected, no magnetic signature was observed; this material will serve as the baseline for comparison to H-charged Pu-2Ga, currently being prepared.

Positron Annihilation Lifetime Spectroscopy (PALS) will be used by the project to detect the presence and measure the volume of vacancy-hydrogen defects in Pu-Ga alloys. In FY11, MST-7's PALS system was successfully brought from a storage state to full functionality, including all work authorizations. Zr specimens were successfully measured on the system as a readiness test. Unexpected complications arose in FY11 regarding bringing Pu specimens into the PALS location. Through the concerted efforts of several project members, these have been resolved, and PALS measurements will be made on Pu specimens in FY12.

The interpretation of PALS data is complex. We decided that a surrogate system should be used to develop our understanding of PALS with respect to the detection and quantification of vacancies *prior* to making measurements on Pu-Ga-H alloys. PdIn was selected as a surrogate due to its well-characterized and potentially very high vacancy concentrations and its high solubility for hydrogen. A series of alloys $Pd_{(50-x)}In_{(50+x)}$ alloys, with $0<x<4$, were synthesized and characterized. Based on density measurements the vacancy concentration could be as high as 8% in the $Pd_{46}In_{54}$ specimen, so the PALS signal should be quite high. The PALS measurements on the PdIn specimens will be made in early FY12. In parallel with this experimental effort, density functional theory (DFT) methods are being used to model the Pd-In system. A modification of basic DFT methodology, involving adding a second density for positrons in addition to the standard density for electrons, allows the calculation of positron lifetimes. Calculating lifetimes for a catalog of possible atomic defects in PdIn provided a set of plausible lifetimes for comparison to experimental PALS measurements. In addition, standard DFT methods were used to examine structural properties of Pd-In alloys. Using a relationship between the relative locations of vacancies in the palladium lattice in PdIn and the crystal structure of the indium-rich phase Pd_2In_3 we were able to calculate the lattice parameter of PdIn as a function of stoichiometry. Excellent agreement was found with experimental results (Figure 3), giving confidence to the connection between the theoretical calculations and the actual defect structure in these materials.

DFT calculations were also performed to explore Pu-H interactions, both at Pu surfaces and in the bulk. A variety of methods were considered, each of which have strengths and weaknesses. Ultimately, it was found that treating the Pu metal as a quasi-random disordered antiferromagnetic system suitably reproduced known Pu material and chemical properties. Using this methodology, the energetics of the entire hydriding process was calculated: 1) hydrogen dissociation and adsorption onto Pu surfaces , 2) hydrogen absorption into the Pu lattice, and finally 3)

the formation of PuH_2 hydride. Analysis of the electronic structure of hydrogen in the Pu lattice indicated that it has a partially anionic character. This observation emphasized the need for the development of improved methods for inclusion of ionic bonding into our atomistic modeling efforts. Atomistic modeling using the modified embedded atom (MEAM) formalism is extremely useful, in that it allows us to model complex systems with a large number of atoms. However, it is based purely on covalent electronic interactions. Work is underway to develop methods for extending MEAM to include ionic bonding aspects, which will be a significant enhancement of the method. This improvement will be particularly valuable for systems that have strong ionic or mixed ionic/covalent character, which we believe to be the case for the Pu-H system.
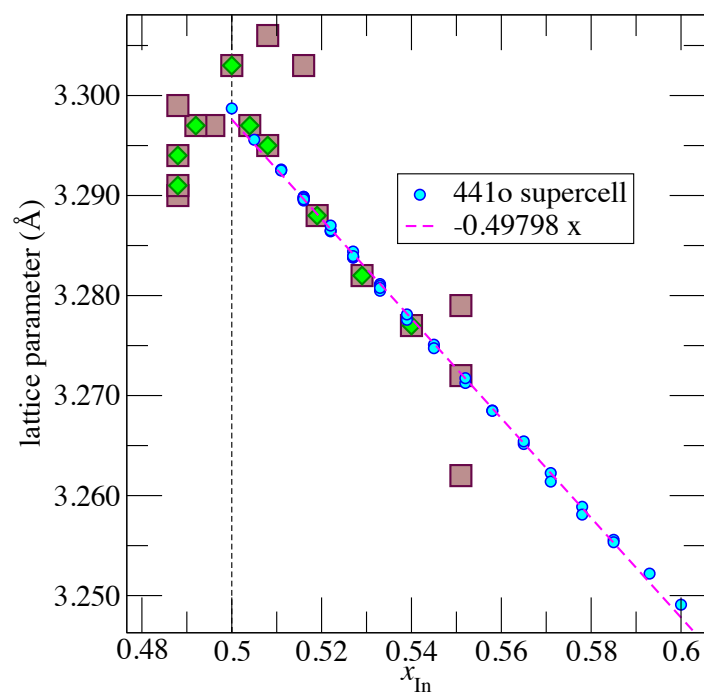
Figure 3. Lattice parameter of PdIn as a function of indium content (xIn). The square and diamond shaped data points are experimentally measured by XRD, and the circular points and dotted line are calculated using DFT.

Future Work

In FY12, we will expand our analyses to include alloys with higher Ga content, in order to develop our understanding of the Pu-Ga-H ternary phase diagram. We will perform PALS experiments on H-free and H-charged Pu alloys, as a direct determination of the H-induced defect structure. The methodologies developed for determining positron lifetimes in Pd-In alloys will be extended to Pu alloys. We will initiate surface analyses, and develop an understanding of the means by which hydrogen moves through the Pu-oxide and Pu-oxycarbide surface layers on Pu alloys as it enters the bulk.

Conclusion

In FY11, hydrogen solubility and XRD experiments showed evidence of anomalous behavior for Pu-2Ga when charged with hydrogen. We demonstrated the functionality of PALS for detecting atomic-scale defects and laid the authorization groundwork for working with Pu in the PALS facility. We will be able to use these results to make strong progress in FY12.

Publications

Joyce, J. J., T. Durakiewicz, K. S. Graham, E. D. Bauer, D. P. Moore, J. N. Mitchell, J. A. Kennison, R. L. Martin, L. E. Roy, and G. E. Scuseria. Pu Electronic Structure and Photoelectron Spectroscopy. 2011. In *International Conference on Strongly Correlated Electron Systems (SCES 2010) ; 27 June-2 July 2010 ; Santa Fe, NM, USA.* Vol. 273, p. 012023 (5 pp.).

Taylor, C.. Surface segregation and adsorption effects of iron-technetium alloys from first-principles. 2011. *Journal of Nuclear Materials.* **408** (2): 183.

Valone, S.. Quantum Mechanical Origins of the Iczkowski-Margrave Model of Chemical Potential. 2011. *JOURNAL OF CHEMICAL THEORY AND COMPUTATION.* **7** (7): 2253.

First Reactions: Simple Molecule Chemistry Behind the Shock Front

Dana M. Dattelbaum
20110012DR

Introduction

Shock compression creates extreme conditions on a rapid (ps) timescale, invoking multiple effects on local chemical structures, including drastic molecular compaction, unique steric and electronic structures, adiabatic heating, and transient non-equilibrium partitioning of kinetic energy behind the front. As a result, reaction mechanisms, their kinetics, and final products can be quite different than under any other conditions (thermal, catalytic, etc.). If the first chemical reactions were better understood, our predictive capabilities for the dynamic response of materials would be dramatically improved, and further, shock-driven reactivity could be "designed" into new molecules for functional use under these conditions. However, there remain significant challenges to understanding and predicting chemical reactivity under these conditions; most notably the harsh conditions, fleeting existence of reactants and intermediates, and one-shot nature of shock experimentation. Here a synergistic experimental-theoretical program is aimed at interrogating and interpreting chemical reactivity under shock conditions, with a focus on establishing guiding principles for simple, relevant chemical functional groups.

Benefit to National Security Missions

Predicting the evolution of chemical reactions in extreme environments underpins our ability to perform weapons assessments through predicting how materials behave under dynamic compression, and the development of realistic reactive models that capture chemistry in both "inert" materials (such as polymers, etc.) and explosives under shock conditions. An improved fundamental knowledge is the only means of enabling the design of new materials (beyond trial-and-error) either for operation under shock loading, or produced by the action of shock compression. The themes of this project are directly aligned with Stockpile Stewardship and related National Security missions, and LANL's Materials Strategy (materials discovery, extreme environments).

Progress

We have chosen to investigate three classes of simple molecules containing C, N, O, and H, selected for isolating key features of bond reactivity in relevant chemical functional groups: high-oxygen molecules, unsaturated structures, and ring compounds. Molecules studied to date include simple high-oxygen structures, including hydrogen peroxide and formic acid, carbon-carbon single, double and triple bond structures (substituted acetylenes, and olefin-containing structures such as cyclohexenes, benzene, and acrylonitrile), and C-N nitrile compounds (acetonitrile). We have established an order of reactivity for C-C, C=C, C C, C=N, N-N, and C=O bonding under both shock compression and static high pressure/temperature conditions.[1] The ordering of reactivity has been established through in-situ measurements of shock wave structures capturing the reaction "cusp" condition on the principal Hugoniot, and the temporal evolution of reactive flow behind the first shock front. For example, molecules with carbon-carbon double and triple bonds have been found to react at modest shock input thresholds (near 4-7 GPa), while aromaticity in benzene appears to stabilize the molecule, pushing reactivity to ~14 GPa. Nitrile groups react near 8 GPa, and C-C single bonds are stable to much higher pressures (>20 GPa). We have observed that shock-induced reactions near the incipient reaction threshold occur over tens-to-hundreds of nanoseconds behind the shock front.   Figure 1 shows particle velocity wave profiles from acrylonitrile, with an initial shock input condition at 7.7 GPa. The initial shock wave (black curve) evolves into a multiple wave structure indicative of chemical reaction transforming acrylonitrile to a higher density intermediate and product. From the evolution of the 2nd and 3rd waves, we can estimate the global reaction kinetics for the two steps. At P_{input} = 7.7 GPa, the first step occurs over ~ 75 ns, and the second step over ~ 50 ns.

Furthermore, the reaction kinetics has been found to be dramatically accelerated by increasing the shock input pressure relative to the reaction threshold "cusp." Figure 1 (right) shows the transformation times (global
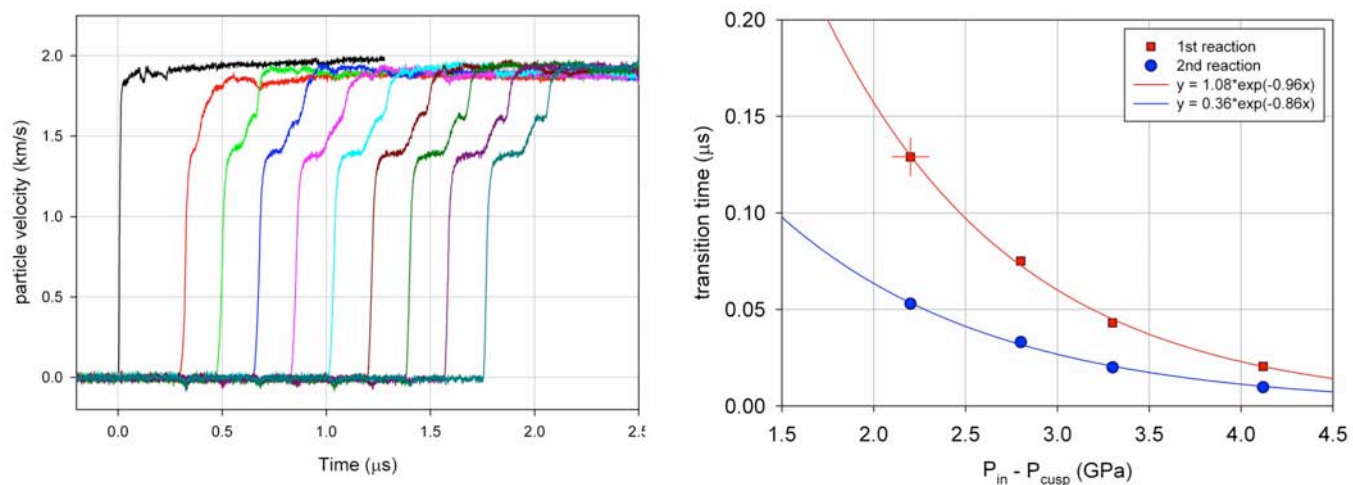
Figure 1. (left) Particle velocity profiles at ten Lagrangian positions in acrylonitrile shocked to 7.7 GPa. The evolution of the input shock wave into a multiple wave structure is indicative of chemical reaction and the formation of a higher density intermediate and product. (right) Transformation (reaction) time as a function of shock input pressure above the threshold condition. The reactions are found to be very state sensitive and easily accelerated with increasing shock input pressures.
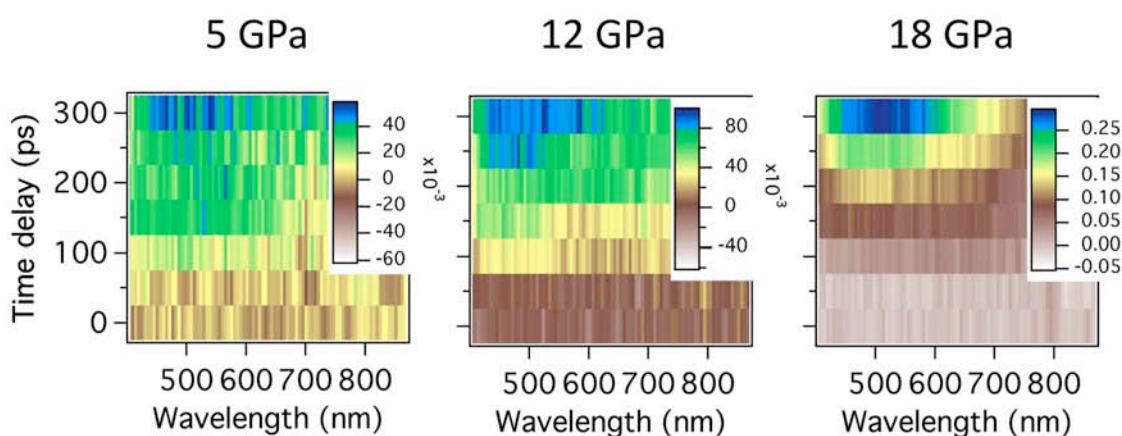
Figure 2. Transient absorption spectra (wavelength vs. time behind the shock input) of phenylacetylene shocked to 5, 12, and 18 GPa. An absorption in the red portion of the visible spectrum is observed following a temporal delay behind the shock front. The pronounced absorption at 18 GPa is believed to be due to chemical reaction.

kinetics) of the two reactions in acrylonitrile as a function of the shock input pressure above the threshold condition. The reactions are highly state sensitive, speeding up a 5-fold rate acceleration when the pressure doubles. The temperature rise over this range of shock pressures is 200K. This sensitivity is similar to that observed in the initiation of liquid explosives. Overdriving the reactions is also allowing us to make comparisons between gas gun-driven and laser-driven shock experiments, linking the timescales between them (>1 ns for gas gun experiments, < 300 ps for laser experiments). Concurrent ultrafast laser-driven shock compression experiments coupled to transient absorption diagnostics in the first half-nanosecond have shown red-shifts in molecular absorption bands under shock compression that are indicative of band gap collapse. Ultrafast transient absorption

measurements under shock compression have been performed for cyclohexene, benzene, phenylacetylene and other structures. Dramatic dynamic band gap collapse was observed for phenylacetylene and benzene at moderate shock pressures, Figure 2 [2]. A strong absorption appears in the red portion of the visible spectrum for phenylacetylene, following a temporal delay behind the shock. The absorption is most pronounced at a shock input condition of 18 GPa, Figure 2. Saturation of the transient absorption feature for phenylacetylene may indicate the first evidence of chemical reactions at early times following shock compression. At 18 GPa, the reaction is overdriven by ~ 14 GPa compared with the reaction threshold determined by gas gun-driven experiments and nanosecond-timescale diagnostics. We are comparing gas gun-driven reactive threshold pressures
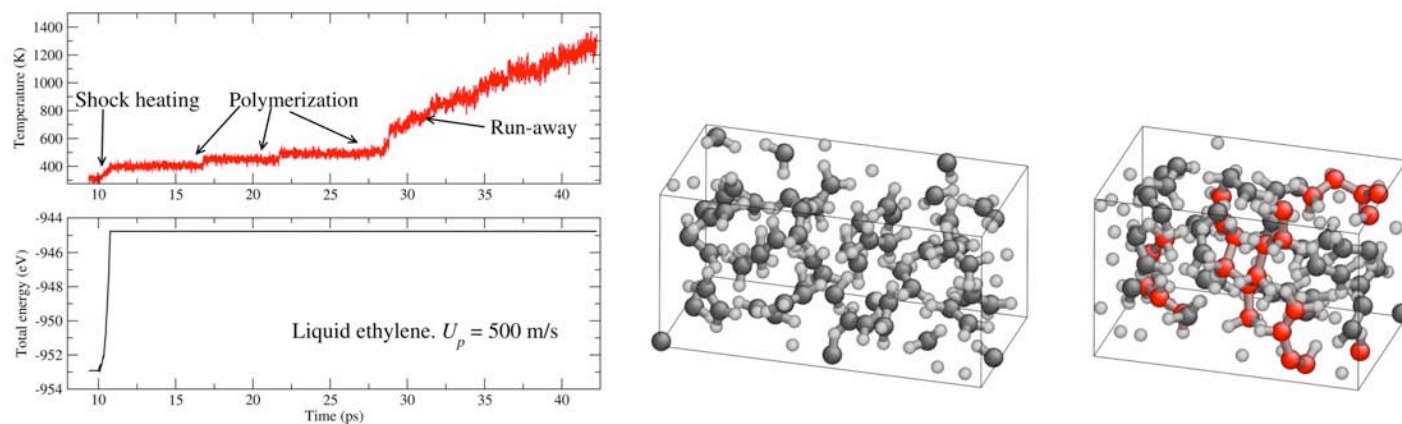
Figure 3. (Left) Results of LATTE simulation of shocked liquid ethylene showing a polymerization reaction initiating after shock heating occurs. (Right) Liquid ethylene molecules before (at left) and during (at right) an intermediate stage in the shock-induced reaction. C atoms in polymerized chains are depicted in red.

and laser-driven spectral changes to link the two time scales, and to identify electronic changes leading to chemical reaction.

Comparisons between static high pressure/temperature and shock-induced reaction thresholds indicate that reactions often occur at 3-4 GPa lower pressures under shock conditions than in static high pressure experiments. High pressure reactions have been followed using both Raman and IR spectroscopy at the National Synchrotron Light Source, and high pressure angle dispersive x-ray diffraction at the Advanced Photon Source. In two systems studied to date, tert-butylacetylene and ethynyl trimethylacetylene, raising the temperature at static high pressure was found to reduce the reaction pressure threshold for polymerization reactions to those closer to shock thresholds. From these experiments, polymer products, synthesized only with high pressure conditions, have been recovered, and characterization of reaction kinetics and product structures is on-going [3].

The development of a new theoretical reactive molecular dynamics code, LATTE, has allowed for computation of reaction pathways under simulated shock conditions for an unprecedented number of atoms, and exciting progress has been made in the first computations of spectral features (specifically Raman-active modes) under these environments [4,5]. For example, by improvements in energy conservation in LATTE, early exothermic bond-making reactions have been computed in the polymerization of ethylene under high P/T conditions, Figure 3.

The number of atoms that can be simulated has been significantly increased by using sparse matrix or GPU (graphical processor) implementations of novel computational algorithms. We have also developed a novel approach for the explicit simulation of the non-equilibrium processes unique to shock compression that is made

possible only because of our unique ability to precisely conserve the total energy during self-consistent MD.

Future Work

The interrogation of shock-induced chemical reactions in simple organic structures using a suite of dynamic (shock) drives, advanced diagnostics, quantum molecular dynamics simulations, and static high pressure/ temperature investigations offers the best approach for understanding the first reactions behind a shock front. Our efforts will continue to focus on studying the same chemical species using all of the methods available to the team, including laser- and gas gun-driven platforms, advanced velocimetric and spectroscopic diagnostics, and in-situ probes of static reactions using synchrotron x-rays, and infrared spectroscopies. A focus in year 2 will be implementation and application of time-resolved spectroscopic probes to identifying bonding changes under shock driven reactions, as well as measurement of slower timescale kinetics observed under static high pressure conditions. MD simulations of reactive chemistry will provide feedback to the experiments via computed species and their spectral signatures. We believe this integration of experiment and simulation, matched in time scale and diagnostic output, will define a new paradigm in shock compression science.

Conclusion

Understanding chemistry under extreme conditions has implications in space and planetary science, materials performance in extremes, and weapons materials response. Breakthroughs in establishing new chemical reactivity paradigms under extreme conditions hold tremendous potential for the discovery of enhanced functional materials, and the design of more robust materials for use in extremes. Not only would our predictive capabilities of materials response to shock conditions be substantially improved, this understanding

could lead to the use of shock waves for preparing new materials or tailoring response under shock compression.

References

1. Dattelbaum, D. M., and S. A. Sheffield. Shock-induced chemical reactions in simple organic molecules. (Chicago, IL, 26 June - 01 July 2011).

2. McGrane, S. D., N. Dang, V. Whitley, C. Bolme, and D. Moore. Shocked reactions: the first half nanosecond. (Chicago, IL, 26 June-01 July, 2011).

3. Chellappa, R. S., D. M. Dattelbaum, S. A. Sheffield, and D. L. Robbins. Pressure-induced polymerization in substituted acetylenes. (Chicago, IL, 26 June-01 July, 2011).

4. Cawkwell, M. J., E. J. Sanville, S. M. Mniszewski, and A. M. N. Niklasson. Self-Consistent Tight-binding Molecular Dynamics Simulations of Shock-Induced Reactions in Hydrocarbons. (Chicago, IL, 26 June-01 July 2011).

5. Cawkwell, M. J., and A. M. N. Niklasson. Energy Conserving, Linear Scaling Born-Oppenheimer Molecular Dynamics. *Phys. Rev. Lett..*

Publications

Cawkwell, M. J., E. J. Sanville, S. M. Mniszewski, and A. M. N. Niklasson. Self-Consistent Tight-binding Molecular Dynamics Simulations of Shock-Induced Reactions in Hydrocarbons. To appear in *American Physical Society Shock Compression of Condensed Matter Topical Group Meeting.* (Chicago, IL, 26 June-01 July 2011).

Cawkwell, M. J., and A. M. N. Niklasson. Energy Conserving, Linear Scaling Born-Oppenheimer Molecular Dynamics. *Phys. Rev. Lett..*

Chellappa, R. S., D. M. Dattelbaum, S. A. Sheffield, and D. L. Robbins. Pressure-induced polymerization in substituted acetylenes. To appear in *American Physical Society Shock Compression of Condensed Matter Topical Group meeting.* (Chicago, IL, 26 June-01 July, 2011).

Dattelbaum, D. M., and S. A. Sheffield. Shock-induced chemical reactions in simple organic molecules. To appear in *American Physical Society Shock Compression of Condensed Matter Topical Group meeting.* (Chicago, IL, 26 June - 01 July 2011).

Davidson, A., R. Chellappa, D. M. Dattelbaum, and C. S. Yoo. Pressure-induced isostructural metastable phase transition of ammonium nitrate. To appear in *J. Phys. Chem. .*

Davidson, A., R. Dias, C. S. Yoo, and D. M. Dattelbaum. "Stubborn" Triaminotrinitrobenzene (TATB): Unusually High Chemical Stability of a Molecular Solid to 150 GPa . To appear in *J. Chem. Phys..*

Manner, V. W., S. A. Sheffield, D. M. Dattelbaum, and D. B. Stahl. Shock compression of formic acid. To appear in *American Physical Society Shock Compression of Condensed Matter Topical Group meeting.* (Chicago, IL, 26 June - 01 July, 2011).

McGrane, S. D., N. Dang, V. Whitley, C. Bolme, and D. Moore. Shocked reactions: the first half nanosecond. Invited presentation at *American Physical Society Shock Compression of Condensed Matter Topical Group Meeting.* (Chicago, IL, 26 June-01 July, 2011).

Innovative and Validated Sub-micron to Meso-scale Modeling of the Evolution of Interface Structure and Properties under Extreme Strains

Irene J. Beyerlein
20110029DR

Introduction

We propose to radically transform materials modeling and processing into a new regime of interface dominance by developing and validating a new Meso, Multi-Scale (M2S) model. In bulk multi-phase composite metals containing an unusually high density of heterophase interfaces, the bi-metal interface controls all defect-related processes. Quite unconventionally, the constituent phases play only a secondary role. With the 'right' characteristics, these bi-material interfaces can possess significantly enhanced abilities to absorb and eliminate defects. Through their unparalleled ability to mitigate damage accumulation induced under severe loading and/or severe environments, they will provide their parent composite with a highly effective healing mechanism and consequently an unrivaled robustness not possible in existing advanced structural materials. Today's bulk synthesis techniques and materials models, however, are unprepared to treat materials that are dominated by bi-metal interfaces. Consequently we cannot fabricate interface-dominant composites with the needed interfacial properties. We plan to solve this problem via the predictive and experimentally validated M2S model. It will hold the unique capability to predict the evolution of the interfacial structure and behavior during bulk large strain deformation. To succeed in this pioneering effort, we will spearhead new and creative ways to overcome the areas in which current methodologies are the weakest—in linking length scales over the so-called 'micron gap' and accounting for the special roles of bi-metal interfaces. This innovative multi-scale predictive capability will for the first time offer a tool to address materials falling within the new paradigm of interface dominance and to predict the synthesis routes needed for a targeted set of desired interfacial properties.

Benefit to National Security Missions

This project addresses two themes of our Materials Grand Challenge. 1) Defects and Interfaces: the model we propose to develop can be used to control interface behavior through its structure and crystallography across sub-micron to meso length scales. 2) Extreme environments: we will exploit very large strain deformation to evolve interfaces with desired properties. For the past decade, LANL scientists have advanced our understanding of the atomic-scale processes responsible for the extraordinary behavior of bi-metal interfaces [1-2]. Our DR will integrate this knowledge into higher-order length scale models in order to synthesize structural materials with radically extended lifetimes for next generation applications. New classes of robust materials benefit missions as diverse as military aircraft and armor, nuclear reactors, and nuclear weapons.

Progress

The goal of this project is to develop a predictive and experimentally validated model that holds the unique capability to predict the evolution of the interfacial structure and behavior during bulk large strain deformation. This innovation will for the first time offer a tool to predict the synthesis routes needed for a targeted set of desired interfacial properties. Our efforts in the first year have been focused on developing new and creative ways to overcome the two key areas in which current methodologies are the weakest: 1) linking length scales over the so-called 'micron gap' and 2) accounting for the special roles of bi-metal interfaces. We have also succeeded in making some first-time observations of interface evolution during bulk processing.

A crystal plasticity finite element method (CPFEM) model of the multi-layered composite assembly has been developed. Most FEM based models generate a mesh that has no connection to the microstructure of the actual material (Figures 1-2). Uniquely, we developed a method to take discretized experimental maps of the actual initial microstructure of the material and transform them into discretized numerical maps for simulation. We have also constructed dislocation density based models for copper and niobium, the two constituent metals in our experimental composites that account for large-strain deformation (Figure 1). These two accomplishments enabled us to predict

crystallographic and morphological grain development during large strain rolling (Figures 2b,c). The next step is to incorporate interface/dislocation interactions.
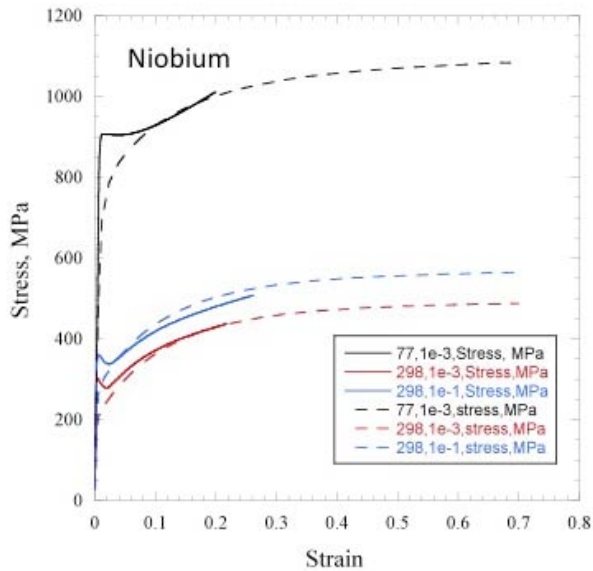
Figure 1. Characterization of the dislocation density model for Niobium via experimental data from Chen and Gray. This material model is used in the crystal plasticity finite element calculations shown in Figure 2.
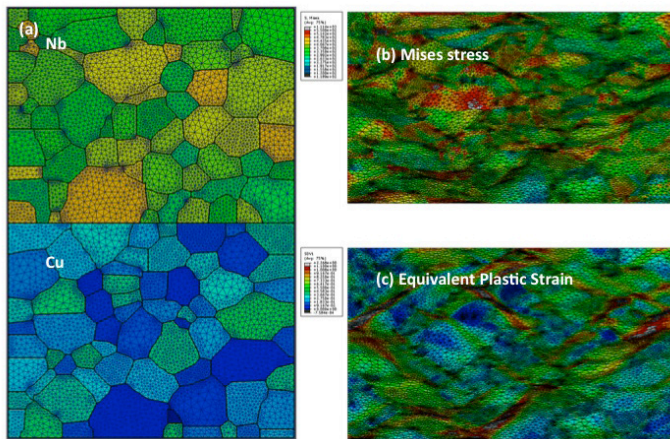
Figure 2. Predictions of the crystal plasticity finite element model (a) Initial structure, (b) Von Mises stress, and (c) Equivalent plastic strain.

Important interface/dislocation processes regulated by the interface include: 1) annihilation (sink), 2) nucleation (source), 3) blocking (barrier), and 4) absorption (storage) of lattice dislocations. Currently no interface model exists that captures these phenomena. In our DR program, we propose to develop an original analytical interface model (AIM). To date, we have completed our first version of AIM, which is a simplified form suitable for initial incorporation into CPFEM.

In order to incorporate AIM into CPFEM we identified

the need to develop a novel flux-based interface model. This new methodology essentially provides a vehicle for incorporating AIM for interfacial response into the bi-metal interface elements in the CPFEM code. Its formulation has been completed and at present, programming has begun. In its current form, it couples a standard crystal plasticity framework to a model of dislocation transport through a well-known kinematic relationship. Nonlocality is incorporated via the long-range internal stress fields that arise due to the accumulation of like-signed dislocations. Detailed modeling of dislocation/interface interactions is possible through the application of flux boundary conditions for the transport equations at the interfaces between neighboring grains.

We utilize Accumulative Roll-Bonding (ARB) to successfully synthesize bulk Cu-Nb nanolamellar composites from 1 mm thick high-purity polycrystalline sheet into finer composites with layer thicknesses in the range of 2 microns to 10 nm. Through extensive analysis using neutron diffraction, electron back scatter diffraction, transmission electron microscopy (TEM), and high resolution TEM, we found that the interface crystallography transforms from one type to another. This transition and its influence on microstructural evolution, such as texture, begins in the submicron range (around 800 nm). This result suggests that the interface evolves to a stable state during synthesis and its new state has a strong control on slip activity. Significantly, it also proves one of the hypotheses put forth in our DR proposal. Two papers are currently in preparation for submission into Acta Materialia.

Prior studies on multilayered composites fabricated by a bottom-up approach, physical vapor deposition, and subsequently rolled or shocked indicate that the interface can alter slip activity via confined layer slip or deformation twinning, respectively. In contrast, in our work, TEM analysis of the deformation mechanisms in ARB multilayered composites finds that confined layer slip initiates at layer thicknesses in the range of 40-90 nm and deformation twins appear at 18 nm and 10 nm. These mechanisms, therefore, operate at layer thickness far below the critical value of 800 nm at which the interface begins to alter slip activity. Consequently, we are seeking alternative explanations for the role the interface plays in microstructural evolution. As a first attempt, the geometry of slip across the different interfaces encountered during the ARB process is being analyzed (Figure 3).
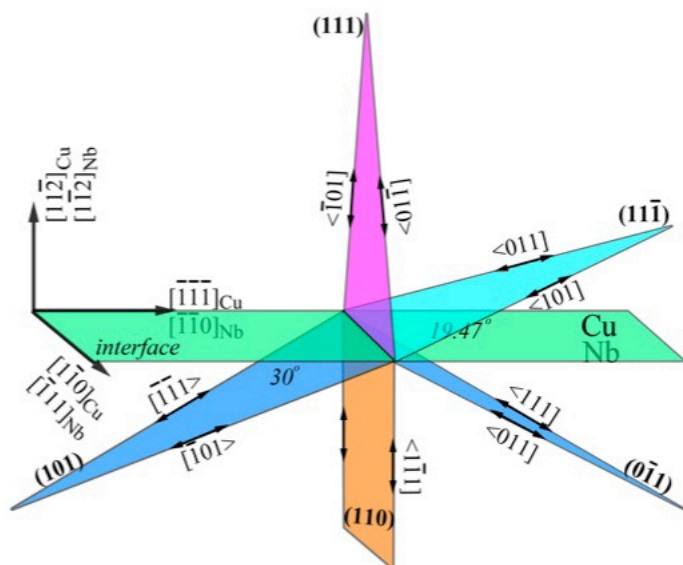
Figure 3. Analysis of the geometric relationship between the copper and niobium slip systems across the bi-metal interface observed in the copper-niobium samples made by accumulative roll bonding.

Future Work

The breakthroughs achieved in this project are realized through the ways in which we bridge interface physics across the length scales Linkages between different modeling methodologies will be created in two ways: indirectly by passing information and directly by embedding one model in another. Our DR will exclusively focus on bridging scales over the micron gap, where methodologies suffer the most, as opposed to attempting to span the entire length scale range from atomistics to continua. Our experimental component will guide and validate the various components of the model at complementary length scales and then ultimately the full-scale, polycrystal model, M2S. The AIM is our key modeling component that is wholly unique and innovative. To communicate interface physics, we will creatively extend well recognized and sophisticated LANL model capabilities, including phase field modeling (PFM), single-interface (SIM), and crystal plasticity finite element modeling (CPFEM). We will take full advantage of the processing, modeling, and nano-scale characterization expertise and capabilities unique to LANL and this project team.

Conclusion

This DR pioneers a multi-scale materials model incorporating bi-metal interfacial character. It contains groundbreaking ways to 1) link atomic-scale interface physics to the polycrystal level and 2) close the micron gap that limits current methods. Such exceptional capabilities can revolutionize the way we approach multi-scale modeling for a wide variety of advanced materials. It will for the first time navigate within the paradigm of interface dominance and advance a new basic understanding of interfaces in microstructural evolution. This fundamental ability will provide for a radically new set of processing design principles for orders of magnitude leaps in damage tolerance.

References

1. Wang, J., R. Hoagland, J. P. Hirth, and A. Misra. Atomistic modeling of the interaction of glide dislocations with ''weak'' interfaces . 2008. *Acta Materialia.* **56** (19): 5685.

2. Demkowicz, M. J., R. Hoagland, and J. P. Hirth. Interface structure and radiation damage resistance in Cu-Nb multilayer nanocomposites . 2008. *Physical Review Letters.* **100** (13): 136102.

Publications

Al-Maharbi, M., I. Karaman, I. J. Beyerlein, D. Foley, K. T. Hartwig, L. J. Kecskes, and S. N. Mathaudhu. Microstructure, crystallographic texture, and plastic anisotropy evolution in an Mg alloy during equal channel angular extrusion processing. 2011. *Materials Science and Engineering A.* **528** (25-26): 7616.

Chen, X., I. J. Beyerlein, and L. C. Brinson. Bridged crack models for the toughness of composites reinforced with curved nanotubes. 2011. *Journal of the Mechanics and Physics of Solids.* **59** (9): 1938.

Chu, H. J., E. Pan, J. Wang, and I. J. Beyerlein. Three-dimensional elastic fields due to a dislocation loop in an anisotropic bi-material . To appear in *Journal of Applied Mechanics.*

Chu, H. J., E. Pan, J. Wang, and I. J. Beyerlein. Three-dimensional elastic displacements induced by a dislocation of polygonal shape in anisotropic elastic crystals . 2011. *International Journal of Soilds and Structures.* **48**: 1164.

Chu, H. J., J. Wang, C. Zhou, and I. J. Beyerlein. Self-energy of elliptical dislocation loops in anisotropic crystals and its application for defect-free core/shell nanowires. 2011. *Acta Materialia.* **59**: 7114–7124.

Hunter, A., I. J. Beyerlein, T. C. Germann, and M. Koslowski. Influence of the stacking fault energy surface on extended partials with a 3D phase field dislocations model. To appear in *Physical Review B.*

Wang, J., I. J. Beyerlein, N. A. Mara, and D. Bhattacharyya. Interface-facilitated deformation twinning in copper within submicron Ag-Cu multilayered composites. 2011. *Scripta Materialia.* **64**: 1083.

Xu, X. F., K. Hu, I. J. Beyerlein, and G. Deodatis. Statistical strength of hierarchical carbon nanotube composites. To appear in *International Journal for Uncertainty*

Quantification.

Zhou, C., I. J. Beyerlein, and R. LeSar. Plastic deformation mechanisms of FCC single crystals at small scales. To appear in *Acta Materialia.*

Next Generation Ionic Liquids for Plutonium Science, Separation, and Production

George S. Goff
20110083DR

Introduction

Ionic Liquids (ILs) offer a wide range of tunable physical properties which can be used to stabilize unusual *f*-elements oxidation states and unique structural motifs and could be utilized in virtually every separations technique relevant to the nuclear industry, including solvent extraction, ion exchange, dissolution, crystallization, and electrorefining. Ionic liquids are low-melting salts, often containing an asymmetrical organic cation (such as a quaternary ammonium or substituted imidazolium) and an organic or inorganic anion. The ultimate goal of this project is to develop a fundamental understanding of the chemistry of plutonium and other actinides in ILs needed to develop advanced separation technologies for manufacturing applications and advanced nuclear fuel cycles. The behavior of plutonium and actinides in non-conventional media such as ionic liquids is currently not understood, but studies of these systems offer great opportunities for scientific discovery with the potential to revolutionize or augment current separations and production technologies. We will seek to understand the fundamental chemical and physical phenomena such as solvation, solubility, electronic structure of *f*-element complexes, and electrochemical reduction and plating processes. Specifically, this project will focus on identifying ionic liquids suitable for electrochemically separating Pu from the other light actinides (Th, U, Np, Am, Cm) as well as the light actinides from the lanthanides.

Benefit to National Security Missions

This project addresses LANL's weapons and energy security missions. Understanding actinide behavior in non-conventional solvents can lead to revolutionary nuclear material processing technologies that can reduce costs, proliferation risks, and environmental impacts, and eventually contribute to a sustainable nuclear energy portfolio. Expanding the scientific understanding of Pu and actinide chemistry is central to LANL's leadership in Pu science and its function as the NNSA Plutonium Center of Excellence. Developing advanced separation technologies for used fuel, other nuclear materials, or high-value isotopes such as Pu-242

supports LANL's Plutonium Science and Research Strategy, and is of interest to NNSA and several DOE Offices. The scientific challenge of understanding the radiation-induced degradation of ionic liquids in extreme radiation environments as found in used nuclear fuel reprocessing is of great important to the MaRIE mission. Training a new generation of actinide chemists as postdocs is a critical aspect identified across the DOE complex.

Progress

We have been taking a multi-faceted approach to study the structural, thermodynamic, and kinetic behavior of Pu in ILs in order to demonstrate the feasibility of using ILs for advanced Pu separations. We have made significant progress in exploring the chemistry of actinides in both conventional and task-specific ILs (TSILs), which are functionalized with coordinating ligands to incorporate the actinides into the cation of the ionic liquid. For our project we have identified 1-ethyl-3-methylimidazolium bis(fluorosulfonyl)imide, $[C_2MIM][Tf_2N]$, as our baseline conventional IL and *N,N,N*-trimethylglycine bis(fluorosulfonyl)imide, also known as betaine bis(fluorosulfonyl)imide or [Hbet][Tf_2N], as our baseline TSIL. A white paper has been developed in completion of our first project milestone, examining the potential application of ionic liquids to defense applications of nuclear materials processing. The guidelines developed in this white paper will be used to evaluate the ionic liquids developed in this project. Several highlights from the first year are presented below.

Prediction of Electrochemical Stability of Ionic Liquids

Currently, computational methods exist to predict certain physical properties of ionic liquids, but there are no methods to predict the electrochemical stability of ILs. The electrochemical window corresponds to the range of voltages that can be applied to an ionic liquid before the cation will reduce and the anion will oxidize. Having a predictive capability to accurately describe the redox behavior of a new ionic liquid is key to being able to identify and screen potential ILs with

an electrochemical window wide enough to allow the electroplating of Pu. Modeling ionic liquid systems proved to be more challenging than standard polarizable solvents (such as water), which can be adequately described with a polarizable continuum model. Due to the low dielectric constants and the ionized nature of ILs, the response due to a change in oxidation state is the rearrangement of the solvent environment rather than a change in polarization. Our methodology for predicting the electrochemical window uses a combination of quantum-mechanics and molecular mechanics (QM/MM) approaches in order to be able to explicitly simulate a large region of the solvent. A single anion-cation pair is simulated using QM and the surrounding environment is modeled with MM, for which force-fields have been developed previously by other authors. With this approach we have successfully calculated electrochemical windows in good agreement with experimental data for C_2MIM^+-BF_4^-, C_4MIM^+-BF_4^-, C_2MIM^+-Tf_2N^-. A manuscript is in preparation for the computational methodology development with a follow-up manuscript on the stability of these ILs at the edge of the electrochemical windows.

Dissolution Mechanism of Uranium Oxides in Betaine Bis(fluorosulfonyl)imide

One of the drawbacks of conventional ionic liquids is the low solubility of metals in the ILs. In order to overcome this, TSILs have been developed which have been designed to bind with the metal ions to increase their solubility. Previously, Nockemann and co-workers [1] showed that the hydrophilic IL betaine bis(fluorosulfonyl)imide has significantly higher solubility for U by incorporating it into the cation of the IL. We have undertaken a systematic study to understand the dissolution mechanism of UO_3 and to quantify the role of water during dissolution. Our dissolution studies have shown that dissolution rates increase at higher temperatures and at higher water concentrations. Solution studies indicate that the uranium is being dissolved as the UO_2^{2+} moiety and is forming a strong complex with betaine. Only one solution species has been observed over a range of U, water, and betaine concentrations. Yellow crystals were isolated from both the aqueous and ionic liquid phases, single-crystal X-ray diffraction studies show a structure of $[(UO_2)_2(bet)_6(H_2O)_2][Tf_2N]_4 \cdot 2H_2O$. Characterizing the undissolved solids by powder X-ray diffraction showed that over time (days to weeks), undissolved UO_3 left in contact with the $[Hbet][Tf_2N]$ is being reduced to U_3O_8. Figure 1 shows the diffusion controlled dissolution of UO_3 into a water-saturated $[Hbet][Tf_2N]$ solution. Over the course of 36 hours, the UO_3 dissolves into the bottom IL layer, which turns yellow, and the red _-UO_3 turns to the dark gray U_3O_8. Because the IL appears to be a reducing environment, UO_2 has significantly slower dissolution rates than UO_3 and the UDS remain unchanged.

0 hours   *12 hours*   *36 hours*
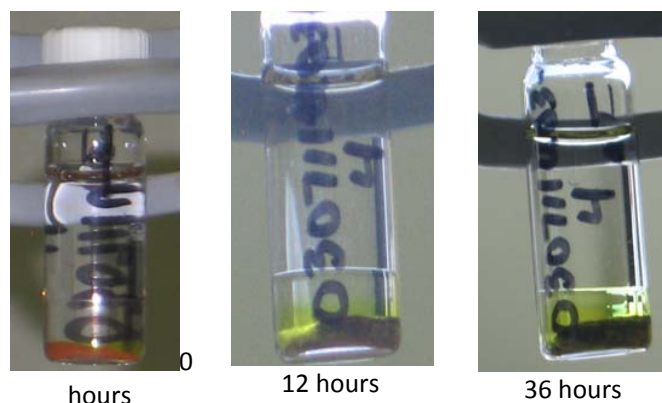
Figure 1. Diffusion controlled dissolution of -UO_3 into the task-specific ionic liquid betaine bis(fluorosulfonyl)imide which is saturated with water. Over the course of 36 hours, the UO_3 dissolves into the bottom IL layer, which turns yellow, and the red -UO_3 turns to the dark gray U3O8.

Solution Chemistry of Neptunium and Plutonium in Betaine Bis(fluorosulfonyl)imide

The dissolution studies for UO_3 into $[Hbet][Tf_2N]$ indicated that the IL is a reducing environment. This has been confirmed by observing the solution behavior of both Np and Pu in the same IL. Unlike U, which is primarily stable as U(VI), Np and Pu have rich chemistries and can be stabilized in multiple oxidation states. For the betaine system, we have observed Pu in the +IV, V, and VI oxidation states and Pu in the III and IV oxidation states. For example, starting with a Np(V) solution, the NpO_2^+ slowly reacts with betaine to form a complex. At the same time the Np(V) is reduced to Np(IV), which can then also react with betaine to form a solution complex. We have observed changes in both the oxidation state and complexation of Np with betaine over the course of months, and Pu exhibits similar behavior with slow reaction rates. Our future work will continue to identify and characterize the dominant solution species and oxidation states for both Np and Pu in $[Hbet][Tf_2N]$.

Future Work

Our project future research efforts are divided into the following thrust: Synthesis and Characterization of Ionic Liquids (**I**), Characterization of Actinide Complexes in Ionic Liquids (**II**), and Radiation and Chemical Stability Studies (**III**), and Engineering Feasibility Analysis (**IV**). **I** will identify synthesis routes for desired ILs that is not commercially available. Purity and water content will be determined along with key physical properties (viscosity, density, electrochemical window, etc). Structure-function relationships will be evaluated with modeling and simulation, which will aid in screening and identifying ILs for experimental studies. **II** will examine the coordination chemistry, solvation, solubility, and molecular interactions of actinides and lanthanides with

ILs. Dissolution rates of actinide metals, oxides, and select salts (such as Pu oxalates) will be studied. Electroplating of Pu will be studied by varying a range of conditions including temperature, electrode material, and current density. Modeling and simulation will provide insight into the molecular interactions of ILs with *f*-elements, and will guide experiments by identifying potential TSILs which form stable complexes with Pu. **III** will encompass short-term, high-dose irradiation studies as well as long-term contact studies to examine stability of a few select ILs. Decomposition temperatures and electrochemical stabilities will also be examined. Identifying an IL system with the potential for future process development will depend on the evaluations against technical targets developed in our white paper examining the potential application of ionic liquids to defense applications of nuclear materials processing.

Conclusion

This project is developing the detailed knowledge of the behavior of plutonium and other actinides in conventional and task-specific ionic liquids. This knowledge will be used to develop advanced separation technologies for manufacturing applications and advanced nuclear fuel cycles. For example, if the electrochemical separation of Pu can be demonstrated, this new technology can have revolutionary impact on future separations strategies. The results to date have been promising and we continue to extend the knowledge-base of actinide chemistry in ionic liquids.

References

1. Nockemann, P., R. Van Deun, B. Thijs, D. Huys, E. Vanecht, K. Van Hecke, L. Van Meervelt, and K. Binnemans. Uranyl Complexes of Carboxyl-Functionalized Ionic Liquids. 2010. *INORGANIC CHEMISTRY.* **49** (7): 3351.

Publications

Joyce, E. L., and L. D. Schulte. Plutonium reprocessing requirements and considerations for ionic liquid development . 2011. *Los Alamos National Laboratory Report, LA-CP 11-01479.*

Long, K. M., G. S. Goff, and W. H. Runde. Exploring the chemistry of transuranic elements in ionic liquids. Presented at *242nd ACS National Meeting & Exposition.* (Denver, CO, United States, August 28-September 1, 2).

Predictive Design of Noble Metal Nanoclusters

Jennifer Martinez
20090017DR

Abstract

Few-atom metal nanoclusters are collections of small numbers of gold or silver atoms with strong fluorescence emission. Nanoclusters are ideal for use in mission-relevant applications including the imaging of complex biological systems, the detection of biothreat agents, and the development of nanoscale materials for the harvesting and manipulation of solar energy. Toward these goals, we have explored bio-inspired and traditional methods of cluster synthesis; characterized cluster morphology and photophysical properties; correlated these experimental measurements with theoretical studies; and demonstrated the utility of the clusters for applications in biological sensing and imaging.

Background and Research Objectives

The next revolution in materials science will be the first principles design and "atom-by-atom" assembly of nanoarchitectures having specific properties. Recent advances in the synthesis of fluorescent noble metal nanoclusters, for example, suggest that they will likely permit the manipulation of light at the molecular scale, if only their size and structure can be controlled at the atomic level. Fluorescent nanoclusters are collections of silver or gold atoms (2-31 atoms). They are small and brightly fluorescent.

Biological systems make materials with precise structure and controlled function. In nature, the design of materials is encoded by DNA. From this genetic blueprint, protein and peptide templates are produced. These templates control the assembly of inorganic atoms. These blueprints lead to materials with controlled structure and properties that span many length scales. However, nature's materials fabrication is not perfect. Most materials nature makes are: structural (i.e. the foundation of the house) and neither electronic nor optical. A major opportunity in materials science is to develop methods to create inorganic optical nanomaterials using atom-by-atom assembly approaches inspired by and derived from Nature.

We are mimicking biology to develop fluorescent nano-clusters with exquisite synthetic precision. We are using state-of-the-art experimental and theoretical tools to develop an understanding of the electronic structure and remarkable photophysical properties of these materials.

Scientific Approach and Accomplishments

While fluorescent clusters have tremendous potential for use as fluorescent probes, there are a number of fundamental challenges that prevent their widespread use:

- Nanoclusters are difficult to make
- Nanoclusters are difficult to characterize
- There is little detailed chemical, physical, or theoretical understanding of their neither size nor photophysics
- Nanoclusters are difficult to use for bioimaging and sensing.

Toward solving these problems, we have: utilized small molecules and biological templates to produce nanoclusters and used those clusters to detection protein and DNA; developed methods to characterize cluster photophysics and size; and characterized their charge state and ligand environment.

Toward production of clusters in stable templates that allow ease in biolabeling, we have reported the synthesis and photophysical properties of silver-nanoclusters templated on DNA. We have produced a suite of clusters with distinct excitation and emission wavelengths, tuned to common laser lines [1]. These clusters are very bright fluorophores (quantum yield up to ~60%) Utilizing these clusters for multiplex protein detection, we have developed an intrinsically fluorescent recognition ligand that combines the strong fluorescence of oligonucleotide templated AgNCs with the specificity and strong binding affinity of DNA aptamers for their target proteins, to develop a new strategy for detection of specific proteins (Figure 1)[2]. This new recognition ligand and detection scheme is simple, inexpensive, and a sensitive method for protein detection. When mixed with target protein, the nanocluster looses fluorescence. When mixed with nontarget protein(s), the nanocluster remains fluorescent. In related work, we have developed

a AgNC that is dark. We find that this nanocluster can turn-on the fluorescence, by 500 fold, when placed in proximity to guanine-rich DNA sequences[3-5]. Beyond red fluorescence, caused by guanine-rich DNA, we have created a limited palette of colors by changing the nature of the proximity sequence. Based upon this newly observed phenomenon, we have designed a DNA detection probe (NanoCluster Beacon, NCB) that "lights up" upon target binding (Figure 2).
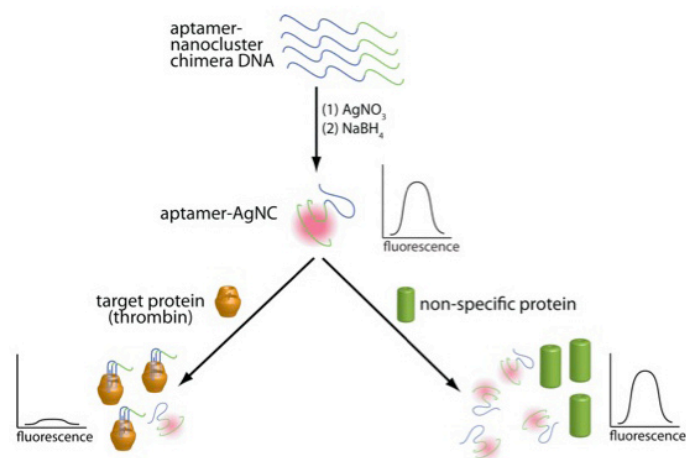
Figure 1. AgNC that contains a protein recognizing aptamer and fluorescent Ag nanocluster. The fluorescence of the AgNC is only quenched when the aptamer binds its specific protein target.
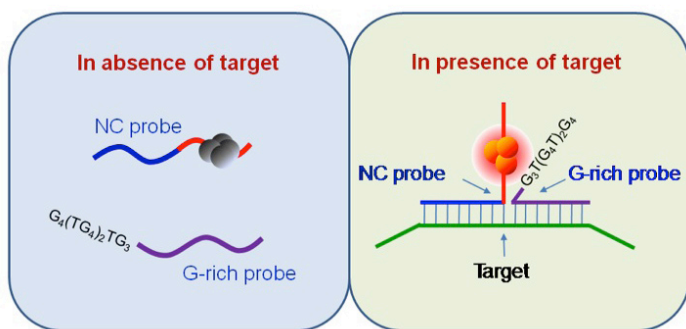
Figure 2. NanoCluster Beacons turn a dark AgNC into a fluorescent AgNC when, and only when, they bind a specific DNA target.

In a separation-free assay, a signal-to-background ratio of 76 was demonstrated for the detection of a human cancer target (Braf) and 175 for flu (H1N1) detection. In addition to eliminating the need to purify DNA nanocluster probes that do not bind targets, there is no need to remove the silver nanocluster precursors used during nanocluster formation. Since the observed fluorescence enhancement is caused by intrinsic nucleobases, our detection technique is simple, inexpensive, and compatible with commercial DNA synthesizers. This new material has been awarded an R&D100 award for 2011. More recently we have developed "chameleon" NanoCluster Beacons [6]. Like the reptile, these chameleons change their color, in addition to turning-on, based on subtle differences in their environment. We have used these chameleons to detect single nucleotide polymorphisms (SNPS). SNPS are important in human disease.

While other investigators have studied AgNCs, they have had little definitive proof that these materials were collections of Ag atoms (true clusters) and little information about their ligand environment. For the first time in fluorescent nanocluster science we have proven by EXAFS analysis:

- AgNCs are clusters and have Ag-Ag bonds
- AgNCs have Ag-DNA bonds.
- The AgNC size is between 4-18 atoms (EXAFS: extended x-ray absorption fine structure, Figure 3)[7].
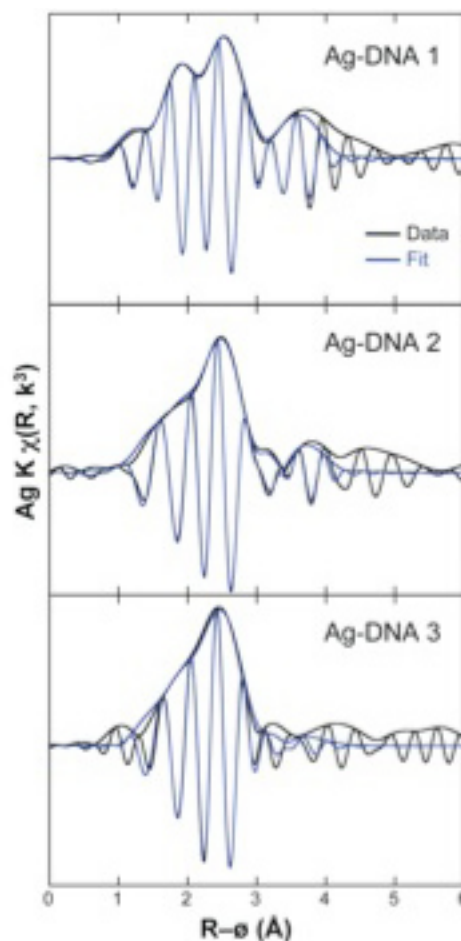
Figure 3. EXAFS was used to characterize three different AgNC. Each had a different size and ligand environment, showing that there is DNA sequence specificity.

Cluster neutrality and template selection

The small size of few-atom fluorescent metal clusters, intrinsic biocompatibility, and tunability of their optical properties make them promising candidates for imaging and sensing techniques via detection of their light emission.

However, before our work, no significant evidence of cluster's neutrality has been presented. Since it was believed that conventional approaches for the synthesis of Au or Ag nanoclusters would require large and complex stabilizing ligands, such as dendrimers, peptides or DNA, no mechanistic studies of the cluster formation have been carried out in detail. We have demonstrated that the use of simpler molecules, namely, primary and secondary amines could lead to the formation of the luminescent species from many types of gold and silver precursors. We find that the first step in the formation of the light-emitting species is through the formation of small metal nanoparticles, followed by a digestion of the formed nanoparticle with amine leading to the formation of small luminescent metal (Au or Ag) clusters. We have characterized these clusters and for the first time in cluster research we show that the luminescent species is from neutral Au.

Photophysics: Cluster geometry, size and ligand environment

From our theoretical studies we have determined the effect of cluster geometry and ligand environment. We find that while a simple "jellium" model can describe isolated clusters, it poorly describes clusters with attached ligands. Further, while dogma posits that the nanocluster fluorescence depends mostly on cluster size, our computational results suggest that the cluster geometry, ligand functionality, and ligand number are the critical factors for determination of fluorescence properties. Further, we show that strong binding ligands (i.e. phosphine or thiol) will not produce fluorescent species, while poor binding ligands (i.e. amine or carboxylate) do. We have experimentally validated the predictions in two recently accepted papers and in a mechanistic study. For this work, we have developed a Density-Functional-Theory-(DFT)-based model to treat the ligand effects and applied this model to the calculations of the absorption and emission energy and oscillator strength of the ligated clusters. The calculations have clearly demonstrated how the ligands influence the fluorescence properties (by shifting the oscillator strength towards or away from the lowest band edge state) and also suggested what type of ligands can be used to produce the nanoclusters with the high quantum yield [8-11].

Traditionally, nanoclusters have been synthesized using soft ligands, such as phosphines or thiols that form strong bonds with gold, and, with the exception of a mixed-ligand protected cluster, tend to exhibit low fluorescence quantum yields. Supporting the theoretical studies, we have instead produced fluorescent metallic gold nanoclusters stabilized by small molecule amine ligands (hard ligands). The morpholine and piperazine backbones of Good's buffers were used to template fluorescent clusters, through a process of etching of nanoparticles first formed in the reaction (Figure 4)[12,13]. The clusters are found to be subnanometer sized, with nanosecond fluorescence lifetimes and as bright, or brighter, than the commercial dye norharmane.

Another aspect of the theoretical work is to study the energy migration (FRET) in collections of fluorescent nanoclusters. In other words, study how energy moves from one cluster to the other. This work has important implications in biological labeling and solar energy harvesting. To address this problem, we have developed a general theoretical approach to treat FRET dynamics from first principles. This approach allows us to express the FRET rate using transition densities available from the DFT calculations performed as a part of the electronic structure characterization in small Au nanoclusters. Our primary result is fine-tuning the ability to predict deviations from well-known R^{-6} FRET scaling regime, where R is a nanocluster radius. Provided, we have an ensemble of NCs, e.g. in a dendrimer pocket, FRET dynamics becomes an energy hopping problem in a disordered system. In this case, a distribution of the FRET characteristic times carries information on the bio-molecule dynamics. To address this problem, we have developed and currently implemented into a computational tool, a multiple scale hopping algorithm on a graph. The approach has been applied to simulate the energy transfer in Au-cluster assemblies.
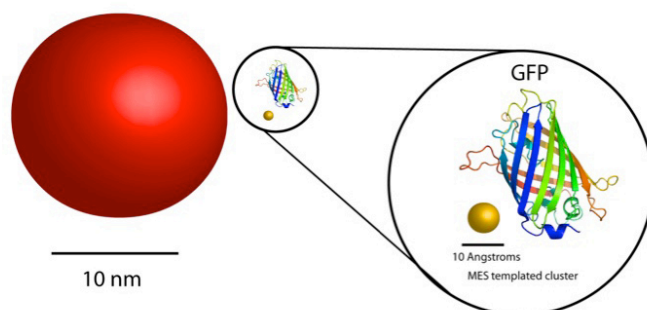
Figure 4. Small molecule templated Au nanoclusters are highly fluorescent and small (smaller than dendrimer templated nanoclusters and quantum dots).

Impact on National Missions
This project supports the DOE mission in Threat Reduction by enhancing our understanding of the design and synthesis of materials with defined properties for application in chem/biothreat reduction, imaging, and the biosciences missions of the DOE Office of Science. This work has brought a brand-new capability, generation of fluorescent nanoclusters, to the laboratory. Further, we have shown their use in biodetection and are working with program managers to develop new proposals and funding opportunities. This project has resulted in attracting and permanently hiring one theoretician.

References
1. Sharma, J., H. Yeh, H. Yoo, J. Werner, and J. Martinez. A complementary palette of fluorescent silver nanoclusters. 2010. *CHEMICAL COMMUNICATIONS.* **46** (19): 3280.

2. Sharma, J., H. Yeh, H. Yoo, J. Werner, and J. Martinez.

Silver nanocluster aptamers: in situ generation of intrinsically fluorescent recognition ligands for protein detection. 2011. *CHEMICAL COMMUNICATIONS.* **47** (8): 2294.

3. Yeh, H., J. Sharma, J. Han, J. Martinez, and J. Werner. A DNA-Silver Nanocluster Probe That Fluoresces upon Hybridization. 2010. *NANO LETTERS.* **10** (8): 3106.

4. Yeh, H., J. Sharma, H. Yoo, J. Martinez, and J. Werner. Photophysical characterization of fluorescent metal nanoclusters synthesized using oligonucleotides, proteins and small molecule ligands. 2010. In *Conference on Reporters, Markers, Dyes, Nanoparticles, and Molecular Probes for Biomedical Applications II ; 20100125 - 20100127 ; San Francisco, CA.* Vol. 7576, p. 75760N.

5. Yeh, H. C., J. Sharma, J. S. Martinez, and J. H. Werner. NanoCluster beacon- a new molecular probe for homogeneous detection of nucleic acid targets. 20. *IEEE Nanotechnology Magazine.* **5**: 28.

6. Yeh, H. C., J. Sharma, I. M. Shih, D. M. Vu, J. S. Martinez, and J. H. Werner. Colorimetric detection of single nucleotide variations using silver nanoclusters. *Proceedings of the National Academy of Sciences, USA.*

7. Neidig, M., J. Sharma, H. Yeh, J. Martinez, S. Conradson, and A. Shreve. Ag K-Edge EXAFS Analysis of DNA-Templated Fluorescent Silver Nanoclusters: Insight into the Structural Origins of Emission Tuning by DNA Sequence Variations. 2011. *JOURNAL OF THE AMERICAN CHEMICAL SOCIETY.* **133** (31): 11837.

8. Ivanov, S., I. Arachchige, and C. Aikens. Density functional analysis of geometries and electronic structures of gold-phosphine clusters. the case of au$_4$(pr$_3$) $_4$$^{2+}$ and au$_4$(Œº$_2$-i) $_2$(pr$_3$)$_4$. 2011. *Journal of Physical Chemistry A.* **115** (27): 8017.

9. Guzei, I., I. Arachchige, and S. Ivanov. Two polymorphs of chlorido(cyclo-hexyl-diphenylphosphine)gold(I). 2010. *Acta Crystallographica Section C: Crystal Structure Communications.* **66** (3): m55.

10. Goel, S., K. A. Velizhanin, A. Pyrintinski, S. A. Ivanov, and S. Tretiak. Ligand effects on optical properties of small gold clusters: A TDDFT study. *Journal of Physical Chemistry C.*

11. Goel, S., K A. Velizhanin, A. Piryatinski, S. Tretiak, and S. A. Ivanov. DFT study of ligand binding to small gold clusters. 2010. *Journal of Physical Chemistry Letters.* : 1927.

12. Bao, Y., H. Yeh, C. Zhong, S. Ivanov, J. Sharma, M. Nei-

dig, D. Vu, A. Shreve, R. Brian. Dyer, J. Werner, and J. Martinez. Formation and Stabilization of Fluorescent Gold Nanoclusters Using Small Molecules. 2010. *JOURNAL OF PHYSICAL CHEMISTRY C.* **114** (38): 15879.

13. Arachchige, I., R. Soriano, C. Malliakas, S. Ivanov, and M. Kanatzidis. Amorphous and crystalline GeTe nanocrystals. 2011. *Advanced Functional Materials.* **21** (14): 2737.

Publications

Arachchige, I., R. Soriano, C. Malliakas, S. Ivanov, and M. Kanatzidis. Amorphous and crystalline GeTe nanocrystals. 2011. *Advanced Functional Materials.* **21** (14): 2737.

Bao, Y., H. Yeh, C. Zhong, S. Ivanov, J. Sharma, M. Neidig, D. Vu, A. Shreve, R. Brian. Dyer, J. Werner, and J. Martinez. Formation and stabilization of fluorescent gold nanoclusters using small molecules. 2010. *Journal of Physical Chemistry C.* **114** (38): 15879.

Goel, S., K. A. Verlizhanin, A. Piryatinski, S. A. Ivanov, and S. Tretiak. Ligand effects on optical properties of small gold clusters: a TDDFT study. *Journal of Physical Chemistry C.*

Goel, S., K. A.Velizhanin, A. Piryatinski, S. Tretiak, and S. Ivanov. DFT study of ligand binding to small gold clusters satyende. 2010. *Journal of Physical Chemistry Letters.* **1** (6): 927.

Guzei, I., I. Arachchige, and S. Ivanov. Two polymorphs of chlorido(cyclo-hexyl-diphenylphosphine)gold(I). 2010. *Acta Crystallographica Section C: Crystal Structure Communications.* **66** (3): m55.

Ivanov, S., I. Arachchige, and C. Aikens. Density functional analysis of geometries and electronic structures of gold-phosphine clusters. the case of au$_4$(pr$_3$) $_4$$^{2+}$ and au$_4$(Œº$_2$-i) $_2$(pr$_3$)$_4$. 2011. *Journal of Physical Chemistry A.* **115** (27): 8017.

Neidig, M., J. Sharma, H. Yeh, J. Martinez, S. Conradson, and A. Shreve. Ag K-edge EXAFS analysis of DNA-templated fluorescent silver nanoclusters: Insight into the structural origins of emission tuning by DNA sequence variations. 2011. *Journal of the American Chemical Society.* **133** (31): 11837.

Sharma, J., H. C. Yeh, H. Yoo, J. H. Werner, and J. S. Martinez. Silver nanocluster aptamers: in situ generation of intrinsically fluorescent recognition ligands for protein detection. 2011. *Chemical Communications.* **47** (8): 2294.

Sharma, J., H. Yeh, H. Yoo, J. Werner, and J. Martinez. A

complementary palette of fluorescent silver nanoclusters. 2010. *CHEMICAL COMMUNICATIONS.* **46** (19): 3280.

Yeh, H. C., J. Sharma, I. M. Shih, D. M. Vu, J. S. Martinez, and J. H. Werner. Colorimetric detection of single nucleotide variations using silver nanoclusters. *Proceedings of the National Academy of Sciences, USA.*

Yeh, H., J. Sharma, H. Yoo, J. Martinez, and J. Werner. Photophysical characterization of fluorescent metal nanoclusters synthesized using oligonucleotides, proteins and small molecule ligands. 2010. In *Reporters, Markers, Dyes, Nanoparticles, and Molecular Probes for Biomedical Applications II ; 20100125 - 20100127 ; San Francisco, CA, United States.* Vol. 7576, p. var.pagings.

Yeh, H., J. Sharma, J. Han, J. Martinez, and J. Werner. A DNA-silver nanocluster probe that fluoresces upon hybridization. 2010. *Nano Letters.* **10** (8): 3106.

Yeh, H., J. Sharma, Y. Bao, J. Martinez, and J. Werner. Photophysical characterization of fluorescent metal nanoclusters synthesized using oligonucleotides, proteins, and small reagent molecules. Presented at *2010 BiOS SPIE Photonics West.* (San Francisco, January 23-28, 2010).

Yeh, Hsin-Chih, J. Sharma, J. J. Han, J. S. Martinez, and J. H. Werner. A Beacon of Light. 2011. *IEEE Nanotechnology Magazine.* **5** (2): 28.

Understanding Anisotropy to Develop Superconductors by Design

Filip Ronning
20090022DR

Abstract

Condensed matter physics is entering an exciting age where our emerging ability to control materials properties holds tremendous promise for addressing the world's most basic needs. Superconductivity, the perfect flow of electricity resulting from quantum mechanics on a macroscopic scale, will be critical for meeting the energy demands of the future. Unconventional superconductors, with their inherent strong electronic correlations of d- or f-electrons allowing the flow of current without loss at temperatures nearly half that of room temperature, provide the best opportunity for meeting these energy needs. To date, the inability to design superconducting materials from basic principles has plagued the international scientific community and represents one of its greatest challenges. Recent experimental discoveries reveal materials-specific anisotropic characteristics of these complex electronic oxides and metals that enhance their superconducting properties, but their microscopic origins are completely unknown. Our scientific objective was to utilize a novel approach to discover the fundamental atomic-scale, structure-property materials' characteristics that generate this unconventional superconductivity employing a comprehensive suite of experimental probes and state-of- the-art theoretical tools.

Background and Research Objectives

In conventional superconductors phonons (lattice vibrations) can actually create an attractive interaction between two electrons, which results in a superconducting state. Unconventional superconductors take advantage of strong magnetic interactions to create an attractive interaction between electrons. Exactly how this is done is still not clear, but if we assume an analogy to the conventional phonon mechanism then the superconducting transition temperature, T_c, is determined by the expression $T_c = T_{SF} \exp(-1/N\_)$ where T_{SF} describes the magnitude of the magnetic fluctuations, N is the density of states at the Fermi level (which is just another way to say how many electrons are available to go superconducting) and _ is a term that describes how strongly the magnetic fluctuations are coupled to the electrons. In this description the devil is in the details of _. Phenom-

enologically, it is clear that more layered structures lead to higher superconducting transition temperatures. The basic reason is that when either the magnetic fluctuations or the charge excitations become more anisotropic _ becomes bigger which allows for higher transition temperatures T_c (assuming N and T_{SF} are the same). Our research objective was to help develop a set of empirical rules that converted crystal chemistry information (ie. bond angles and bond distances) to physical observables that correlate with the superconducting transition temperature.

Scientific Approach and Accomplishments

The fact that cuprates, pnictides, organics, and heavy fermions share common phase diagrams, and that T_c scales with the neutron resonance energy suggests that the origin of superconductivity is common to all these systems. Our approach looked to exploit the so-called "115" family of cerium and plutonium based heavy fermion superconductors (see Figure 1). There exist different advantages for studying different classes of superconductors depending of the approach to be taken. For our approach we have chosen to focus on heavy fermions for five reasons:

- 12 known superconductors exist in this family, which allows us to see how changes in crystal chemistry influence physical properties.

- The very small energy scales allow stoichiometric materials to be easily tuned with modest amounts of pressure and/or magnetic field, in contrast to cuprates, which are not easily tuned with "clean" parameters.

- The mean free path has been shown to exceed 1 _m in the 115's, which allows for more detailed studies of the intrinsic electronic behavior. Contrast this with inhomogeneity in cuprates and pnictides, which is so prevalent that one is forced to consider whether it is a necessary ingredient for superconductivity.

- T_c varies by two orders of magnitude from 0.2 K in $CeIn_3$ to 20 K in $PuCoGa_5$!

- Finally, aside from the many observations, which tie the physics of heavy fermions directly to that of the cuprates, one should keep in mind that *heavy fermions are high temperature superconductors in their own right.* Compared to the characteristic energy scale of the electrons (T_F) the 115's have T_c/T_F = 2.3 K/41 K = 0.056 which is even greater than the high T_c cuprates T_c/T_F = 95/2400 = 0.040.

Consequently, by understanding how the variation in crystal chemistry of these materials leads to differences in their physical properties, we hope to unlock some of the mysteries to design future superconductors. This family is built out of alternately stacked layers of $CeIn_3$ (Cerium-indium) and MIn_2, where M represents a transition metal (Figure 1). The more layered the material, the more anisotropic the physical properties become which should be good for superconductivity on both theoretical and phenomenological grounds.

A major accomplishment of this projected was the directed search and discovery of superconductivity in a more layered version of $CeRhIn_5$ (Cerium-rhodium-indium). $CePt_2In_7$ (Cerium-platinum-indium; see (Figure 1) is a magnet at ambient pressure, an antiferromagnet to be precise where the spins of the cerium atoms point in opposite directions for neighboring sites. By applying pressure we could suppress the tendency for magnetism and superconductivity emerged with a maximum transition temperature of 2.1 K. However, this superconducting transition temperature is not higher than $CeRhIn_5$ which has a maximum superconducting transition temperature of 2.3 K. Why not?
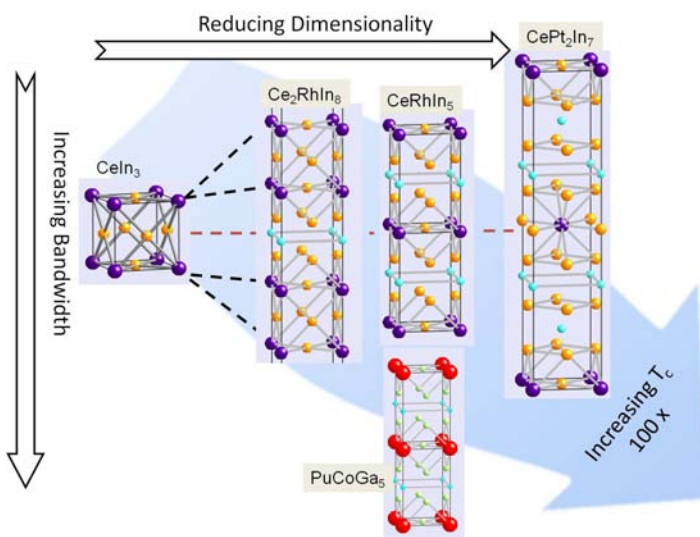
Figure 1. The "115" family. CeIn3 is a cubic material shown on the left. By inserting a MIn2 (M=transition metal) layer one arrives at either the bilayer 218 structure or the single layer 115 structure. An additional MIn2 layer can be inserted resulting in the even more layered 127 structure. Finally, replacing the cerium atoms (purple) with plutonium atoms (red) one sees that the plutonium superconductors have the same structure as the cerium based superconductors.

While the structure of $CePt_2In_7$ is certainly more layered than the 115's we needed to determine if the charge and spin degrees of freedom in the material actually were more anisotropic. This was accomplished first by growing single crystals of the material, which allows for their anisotropy to be measured. This was an incredibly challenging task requiring over 200 different synthesis attempts to achieve a successful growth recipe. The anisotropy of the charge degrees of freedom were subsequently measured experimentally at the National High Magnetic Field Laboratory. They confirmed our theoretical prediction that the charge anisotropy is indeed greater in $CePt_2In_7$ than it is in $CeRhIn_5$. Thus, all else being equal _ should be larger in $CePt_2In_7$ and consequently so should Tc.

However, we now believe that all else is not equal. Our theoretical work suggests that the magnitude of the magnetic fluctuations (T_{SF}) is likely weaker in $CePt_2In_7$ than in $CeRhIn_5$, and another possibility is that the magnetic anisotropy has changed. Our studies of the spin degrees of freedom using nuclear magnetic resonance has shown that T_c is enhanced in the 115's as the tendency for the magnetic spins to lie flat in the plane is increased. It still needs to be determined how strong this tendency is in $CePt_2In_7$.

With the discovery of $CePt_2In_7$ single crystals, came the knowledge of how additional materials with a similar structure could be synthesized. We have been able to exploit this knowledge to discover several related plutonium compounds. $PuCoIn_5$ (plutonium-cobalt-indium) is a new compound we have succeeded to grow with this newfound information, and it is the third known plutonium based material to exhibit superconductivity, in this case at 2.3 K. During the course of our studies of the magnetic degrees of freedom we discovered that the cubic material $PuIn_3$ is an antiferromagnet at 14 K. The fact that $CeIn_3$ (Cerium-indium) is an antiferromagnet at 10K and $CeCoIn_5$ (Cerium-cobalt-indium) is a superconductor at 2.3 K at ambient pressure, makes for a striking similarity between the plutonium and cerium based compounds. This perfect analogy is however broken with our results that show that the plutonium analog of $CePt_2In_7$ (namely PuPt2In7 – Plutonium-platinum-indium) is neither magnetic nor superconducting down to 2 K. Thus, it becase imperative to understand theoretically the similarities and differences of the cerium and plutonium based 115s.

This was a difficult task because it is not easy to capture the strong electronic correlations, which are present in these materials in today's state of the art electronic structure codes. To do so, we made several upgrades to the "solver" for our dynamical mean field theory calculations, which gave us the energy and temperature resolution to see what is happening to the charge degrees of freedom. We found that for plutonium the behavior as a function of pressure is the same as that in the cerium compounds. The calculations also indicate that while the structure of $PuPt_2In_7$ is the same as $CePt_2In_7$ it may have different be-

havior because it is significantly more strongly bonding than $PuCoIn_5$. This leads to a new interpretation for the 20 K superconductor $PuCoGa_5$ (Plutonium-cobalt-gallium) that was discovered at LANL eight years ago. It suggests that the high transition temperature in that material is not due to magnetic fluctuations, but rather to fluctuations in the valence (charge) degrees of freedom.

The work we have done support a set of phenomenological rules that suggest layered structures in the proximity of magnetism are good for superconductivity. We have exploited our ideas of using common building blocks to the new pnictide superconductors as well, and have discovered several new Ni-based superconductors. In addition, we have established that the Nickel-based systems are likely to be conventional superconductors. Surprisingly, the superconducting transition temperature scales in the Nickel compounds in a similar way to the Iron compounds, which suggests that coupling to the lattice is more important than, originally thought for producing the relatively high transition temperatures. We have also performed measurements of the charge degrees of freedom and theoretical modeling work to understand the interplay of magnetism with the anisotropic pairing potential, which generates superconductivity. NMR measurements have shown that the magnetism coexists microscopically with the superconductivity. As promised, we have also synthesized new systems with actinides and the iron-arsenide compounds, discovering a new Uranium-Iron-Arsenide material. This material is magnetic. As in other iron arsenide compounds, it may require pressure or doping to generate superconductivity.

To help identify whether additional compounds with promising structural features could be stabilized experimentally we also investigated the structural stability of hypothetical compounds using brute force theoretical calculations coupled with chemical intuition provided by our chemists. This approach predicted several new compounds. Although we did not expect that they had the correct microscopic elements for superconductivity, we confirmed the validity of this approach by synthesizing one of these predicted compounds ($CeIr_4In$ – a cerium-iridium-indium compound).

Additional theoretical work has demonstrated how we can interpret point contact tunneling and field angle specific heat experiments. In addition, we have developed a large-N equation-of-motion impurity solver, and are also developed the NRG algorithm for two-impurity models. This is an important step for trying to understand the Coulomb interaction between two different f-element atoms. Specifically, this permitted us to explicitly look for effects due to magnetism and Kondo coherence and be able to predict superconducting transition temperatures in the vicinity of magnetism.

We also finished refurbishing a zone refinement setup and built our own electro-refining setup, which can remove strain and magnetic impurities from crystals, respectively. Higher quality crystals result in much better signal to noise ratios in our measurements. This helped allowed us to observe the physics that is responsible for superconductivity, and future material studies will certainly benefit from this new capability.

Impact on National Missions

This project supported the DOE mission in nuclear weapons by enhancing our understanding of actinide materials in general, and helping to sustain the LANL plutonium capability, in particular with respect to growth of plutonium containing compounds. In addition, we directly supported the DOE mission in energy security by enhancing our understanding of superconductors, and our ability to discover new ones.

Publications

Albers, R.C., N.E. Christensen, and A. Svane. Hubbard-U band-structure methods. 2009. *Journal of Physics Condensed Matter.* **21**: 343201.

Altarawneh, M. M., N. Harrison, L. Balicas, P. H. Tobash, J. D. Thompson, F. Ronning, and E. D. Bauer. Superconducting pairs with extreme uniaxial anisotropy in URu2Si2. *Physical Review Letters.*

Altarawneh, M. M., N. Harrison, R. D. McDonald, F. F. Balakirev, C. H. Mielke, P. H. Tobash, J. -X. Zhu, J. D. Thompson, F. Ronning, and E. D. Bauer. Fermi surface of CePt2In7: A two-dimensional analog of CeIn3. 2011. *PHYSICAL REVIEW B.* **83** (8): 081103.

Altarawneh, M. M., N. Harrison, S. E. Sebastian, L. Balicas, P. H. Tobash, J. D. Thompson, F. Ronning, and E. D. Bauer. Sequential Spin Polarization of the Fermi Surface Pockets in URu2Si2 and Its Implications for the Hidden Order. 2011. *PHYSICAL REVIEW LETTERS.* **106** (14): 146403.

Baek, S. -H., H. Sakai, E. D. Bauer, J. N. Mitchell, J. A. Kennison, F. Ronning, and J. D. Thompson. Anisotropic spin fluctuations and superconductivity in "115" heavy fermion compounds: Co59 NMR study in PuCoGa₅. 2010. *Physical Review Letters.* **105** (21): 217002.

Baek, S.-H., H. Lee, S. E. Brown, N. J. Curro, E. D. Bauer, F. Ronning, T. Park, and J. D. Thompson. NMR Investigation of Superconductivity and Antiferromagnetism in CaFe[sub 2]As[sub 2] under Pressure. 2009. *Physical Review Letters.* **102** (22): 227601.

Bauer, E. D., H. O. Lee, V. A. Sidorov, N. Kurita, K. Gofryk, J. -X. Zhu, F. Ronning, R. Movshovich, J. D. Thompson, and T. Park. Pressure-induced superconducting state and effective mass enhancement near the antiferromagnetic quantum critical point of CePt2In7. 2010. *PHYSICAL REVIEW B.* **81** (18): 180507.

Bauer, E. D., P. H. Tobash, J. N. Mitchell, J. A. Kennison, F. Ronning, B. L. Scott, and J. D. Thompson. Magnetic order in $Pu_2M_3Si_5$ (M = Co, Ni). 2011. *JOURNAL OF PHYSICS-CONDENSED MATTER.* **23** (9, SI): 094223.

Bauer, E. D., T. Park, R. D. McDonald, M. J. Graf, L. N. Boulaevskii, J. N. Mitchell, J. D. Thompson, and J. L. Sarrao. Possible two-band superconductivity in $PuRhGa_5$ and $CeRhIn_5$. 2009. *Journal of Alloys and Compounds.* **488** (2): 554.

Bauer, E. D., V. A. Sidorov, H. Lee, N. Kurita, F. Ronning, R. Movshovich, and J. D. Thompson. Coexistence of Antiferromagnetism and Superconductivity in CePt2In7. 2010. *Journal of Physics: Conference Series.* **200**: 20110.

Beaux, M. F., T. Durakiewicz, J. J. Joyce, E. D. Bauer, J. L. Sarrao, L. Moreschini, M. Grioni, F. Offi, M. T. Butterfield, G. Monaco, G. Panaccione, and E. Guziewicz. U HAXPES- hard X-Ray and angle-resolved photoelectron spectroscopy of single crystal UPd3, UGe2, and USb2. *J. Electr. Spectr. Rel. Phenom. .*

Bobev, S., S. Q. Xia, E. D. Bauer, F. Ronning, J. D. Thompson, and J. L. Sarrao. Nickel deficiency in RENi2-xP2 (RE = La, Ce, Pr). Combined crystallographic and physical property studies. 2009. *Journal of Solid State Chemistry.* **182** (6): 1473.

Booth, C. H., Bauer, E. D., Bianchi, A. D., Ronning, F., Thompson, J. D., Sarrao, J. L., Cho, Jung Young, Chan, Julia Y., Capan, C., and Fisk, Z.. Local structure and site occupancy of Cd and Hg substitutions in CeTIn_5 (T=Co, Rh, and Ir). 2009. *Phys. Rev. B.* **79**: 144519.

Booth, C. H., T. Durakiewicz, C. Capan, D. Hurt, A. D. Bianchi, J. J. Joyce, and Z. Fisk. Electronic structure and f-orbital occupancy in Yb-substituted CeCoIn5. 2011. *PHYSICAL REVIEW B.* **83**: 235117.

Curro, N., B. Young, R. Urbano, and M. Graf. Hyperfine Fields and Magnetic Structure in the B Phase of CeCoIn5. 2009. *JOURNAL OF LOW TEMPERATURE PHYSICS.* **158** (3-4): 635.

Curro, Nicholas J., Ben-Li Young, Ricardo R. Urbano, and Matthias J. Graf. NMR studies of field induced magnetism in $CeCoIn_5$. 2010. *Physica C.* **470**: S521.

Dai, J. H., J. X. Zhu, and Q. M. Si. f-spin physics of rare-earth iron pnictides: Influence of d-electron antiferromagnetic order on the heavy-fermion phase diagram. 2009. *Physical Review B.* **80** (2): 020505.

Dai, J. H., Q. M. Si, J. X. Zhu, and E. Abrahams. Iron pnictides as a new setting for quantum criticality. 2009. *Proceedings of the National Academy of Sciences of the United States of America.* **106** (11): 4118.

Das, T., J. -X. Zhu, and M. J. Graf. Spin-fluctuations and the peak-dip-hump feature in the photoemission spectrum of actinides. *Physical Review Letters.*

Das, T., J. Zhu, and M. J. Graf. Local suppression of the superfluid density of PuCoGa5 in the swiss cheese model. *Physical Review B.*

Durakiewicz, T., J. J. Joyce, Y. Li, P. S. Riseborough, P. M. Oppeneer, E. D. Bauer, and K. S. Graham. Band renormalization effects in correlated f-electron systems. 2011. In *International Conference on Strongly Correlated Electron Systems (SCES 2010) ; 20100627 - 20100702 ; Santa Fe, NM.* Vol. 273, p. 012029.

Fogelstrom, M., W. K. Park, L. H. Greene, G. Goll, and M. Graf. Point-contact spectroscopy in heavy-fermion superconductors. 2010. *PHYSICAL REVIEW B.* **82** (1): 014527.

Fredeman, D. J., P. H. Tobash, M. A. Torrez, J. D. Thompson, E. D. Bauer, F. Ronning, W. W. Tipton, S. P. Rudin, and R. G. Hennig. Computationally driven experimental discovery of the $CeIr_4$In compound. 2011. *Physical Review B (Condensed Matter and Materials Physics).* **83** (22): 224102 (6 pp.).

Harrison, N., R. D. McDonald, C. H. Mielke, E. D. Bauer, F. Ronning, and J. D. Thompson. Quantum oscillations in antiferromagnetic CaFe/sub 2/As/sub 2/ on the brink of superconductivity. 2009. *Journal of Physics: Condensed Matter.* **21** (32): 322202 (4 pp.).

Hu, X., C. S. Ting, and J. X. Zhu. Vortex core states in a minimal two-band model for iron-based superconductors. 2009. *Physical Review B.* **80** (1): 014523.

Joyce, J. J., T. Durakiewicz, K. S. Graham, E. D. Bauer, D. P. Moore, J. N. Mitchell, J. A. Kennison, R. L. Martin, L. E. Roy, and G. E. Scuseria. Pu Electronic Structure and Photoelectron Spectroscopy. 2011. In *International Conference on Strongly Correlated Electron Systems (SCES 2010) ; 20100627 - 20100702 ; Santa Fe, NM.* Vol. 273, p. 012023.

Joyce, John J., Tomasz Durakiewicz, Kevin S. Graham, Eric D. Bauer, David P. Moore, Jeremy N. Mitchell, John A. Kennison, T. Mark McCleskey, Quanxi Jia, Anthony K. Burrell, Eve Bauer, Richard L. Martin, Lindsay E. Roy, and Gustavo E. Scuseria. 5f electronic structure and fermiology of Pu materials. 2010. In *Materials Research Society Symposium Proceedings.* Vol. 1264, p. 93. Materials Research Society.

Klimczuk, T., T. M. McQueen, A. J. Williams, Q. Huang, F. Ronning, E. D. Bauer, J. D. Thompson, M. A. Green, and R. J. Cava. Superconductivity at 2.2 K in the layered

oxypnictide La[sub 3]Ni[sub 4]P[sub 4]O[sub 2]. 2009. *Physical Review B (Condensed Matter and Materials Physics).* **79** (1): 012505.

Kothapalli, K., F. Ronning, E.D. Bauer, A.J. Schultz, and H. Nakotte. Single-crystal neutron diffraction studies on Ni-based metal-pnictide superconductor BaNi₂As₂. 2010. In *Journal of Physics: Conference Series.* Vol. 251, p. var.pagings. Institute of Physics Publishing.

Kurita, , Ronning, Filip, Miclea, Corneliu F., Bauer, Eric D., Gofryk, Krzysztof, Thompson, J. D., and Movshovich, Roman. Fully gapped superconductivity in SrNi${}_{2}$P${}_{2}$. 2011. *Phys. Rev. B.* **83**: 094527.

Kurita, N., F. Ronning, C. F. Miclea, E. D. Thompson, A. S. Sefat, M. A. McGuire, B. C. Sales, D. Mandrus, and R. Movshovich. Low-temperature thermal conductivity of BaFe[sub 2]As[sub 2]: A parent compound of iron arsenide superconductors. 2009. *Physical Review B (Condensed Matter and Materials Physics).* **79** (21): 214439.

Kurita, N., F. Ronning, C. F. Miclea, E. D. Bauer, K. Gofryk, J. D. Thompson, and R. Movshovich. Fully gapped superconductivity in SrNi2P2. 2011. *Physical Review B.* **83**: 094527.

Kurita, N., F. Ronning, Y. Tokiwa, E. D. Bauer, A. Subedi, D. J. Singh, J. D. Thompson, and R. Movshovich. Low-Temperature Magnetothermal Transport Investigation of a Ni-Based Superconductor BaNi[sub 2]As[sub 2]: Evidence for Fully Gapped Superconductivity. 2009. *Physical Review Letters.* **102** (14): 147004.

Lu, X., F. Ronning, P. H. Tobash, K. Gofryk, E. D. Bauer, and J. D. Thompson. Pressure-tuned point-contact spectroscopy of URu$_2$Si$_2$ from hidden order to the antiferromagnetic state: similarity of the fermi surface gapping. *Physical Review Letters.*

Park, W. K., E. D. Bauer, J. L. Sarrao, P. H. Tobash, F. Ronning, J. D. Thompson, and L. Greene. Observation of the hybridization gap and Fano resonance in the Kondo lattice URu2Si2. *Physical Review Letters.*

Qi, Y. N., J. X. Zhu, and C. S. Ting. Validity of the equation-of-motion approach to the Kondo problem in the large-N limit. 2009. *Physical Review B.* **79** (20): 205110.

Ronning, F., E. D. Bauer, T. Park, N. Kurita, T. Klimczuk, R. Movshovich, A. S. Sefat, D. Mandrus, and J. D. Thompson. Ni2X2 (X = pnictide, chalcogenide, or B) based superconductors. 2009. *Physica C-Superconductivity and Its Applications.* **469** (9-12): 396.

Ronning, F., E. D. Bauer, T. Park, S.-H. Baek, H. Sakai, and J. D. Thompson. Superconductivity and the effects of

pressure and structure in single-crystalline SrNi[sub 2]P[sub 2]. 2009. *Physical Review B (Condensed Matter and Materials Physics).* **79** (13): 134507.

Sakai, H., S. -H. Baek, E. D. Bauer, F. Ronning, and J. D. Thompson. 29Si-NMR study of magnetic anisotropy and hyperfine interactions in the uranium-based ferromagnet UNiSi2. 2010. *IOP Conference Series: Materials Science and Engineering.* **9**: 012097 (7 pp.).

Sakai, H., S. E. Brown, S. -H. Baek, F. Ronning, E. D. Bauer, and J. D. Thompson. Magnetic-Field-Induced Enhancements of Nuclear Spin-Lattice Relaxation Rates in the Heavy-Fermion Superconductor CeCoIn_5 Using 59Co Nuclear Magnetic Resonance. 2011. *Phys. Rev. Lett..* **107**: 137001.

Sakai, H., S. Kambe, Y. Tokunaga, Y. Haga, S. -H. Baek, F. Ronning, E. D. Bauer, and J. D. Thompson. Anisotropy of antiferromagnetic spin fluctuations in the heavy fermion superconductors of CeMIn5 and PuMGa5 (M=Co, Rh). To appear in *MRS Proceedings.* (,).

Sakai, H., Y. Tokunaga, S. Kambe, H. -O. Lee, V. A. Sidorov, P. H. Tobash, F. Ronning, E. D. Bauer, and J. D. Thompson. Stabilization of commensurate antiferromagnetism in CePt2In7 by pressure up to 2.4 GPa: In-115 NMR and NQR under zero field. 2011. *PHYSICAL REVIEW B.* **83** (14): 140408.

Sefat, A. S., D. J. Singh, R. Y. Jin, M. A. McGuire, B. C. Sales, F. Ronning, and D. Mandrus. BaT2As2 single crystals (T = Fe, Co, Ni) and superconductivity upon Co-doping. 2009. *Physica C-Superconductivity and Its Applications.* **469** (9-12): 350.

Sefat, Athena S., Michael A. McGuire, Brian C. Sales, and E. D. Bauer. Structure and anisotropic properties of BaFe[sub 2 - x]Ni[sub x]As[sub 2] (x = 0, 1, and 2) single crystals. 2009. *Physical Review B (Condensed Matter and Materials Physics).* **79** (9): 094508.

Si, Q. M., E. Abrahams, J. H. Dai, and J. X. Zhu. Correlation effects in the iron pnictides. 2009. *New Journal of Physics.* **11**: 045001.

Spehling, J., R. H. Heffner, J. E. Sonier, N. Curro, C. H. Wang, B. Hitti, G. Morris, E. D. Bauer, J. L. Sarrao, F. J. Litterst, and H. -H. Klauss. Field-Induced Coupled Superconductivity and Spin Density Wave Order in the Heavy Fermion Compound CeCoIn5. 2009. *PHYSICAL REVIEW LETTERS.* **103** (23): 237003.

Stock, C., D. Sokolov, P. Bourges, E. D. Bauer, F. Ronning, K. Gofryk, K. C. Rule, and A. D. Huxley. Anisotropic critical magnetic fluctuations in the ferromagnetic superconductor UCoGe. To appear in *Physical Review Letters.*

Talbayev, D., K. S. Burch, E. M. Chia, S. A. Trugman, J. -X.

Zhu, E. D. Bauer, J. A. Kennison, J. N. Mitchell, J. D. Thompson, J. L. Sarrao, and A. J. Taylor. Hybridization and superconducting gaps in the heavy-fermion superconductor PuCoGa5 probed via the dynamics of photo-induced quasiparticles. 2010. *Physical Review Letters.* **104** (22): 227002.

Tobash, P. H., B. L. Scott, V. A. Sidorov, F. Ronning, K. Gofryk, J. D. Thompson, R. C. Albers, J. -. Zhu, M. D. Jones, and E. D. Bauer. Heavy Fermion Behavior in the New Antiferromagnetic Compound UIr4Al15. 2011. In *International Conference on Strongly Correlated Electron Systems (SCES 2010) ; 20100627 - 20100702 ; Santa Fe, NM.* Vol. 273, p. 012061.

Tobash, P. H., F. Ronning, J. D. Thompson, B. L. Scott, P. Moll, B. Batlogg, and E. D. Bauer. Physical properties on single crystals of CePt2In7: a heavy fermion superconductor. *New Journal of Physics.*

Tobash, P. H., Y. Jiang, F. Ronning, C. H. Booth, J. D. Thompson, B. L. Scott, and E. D. Bauer. Synthesis, structure and physical properties of YbNi3Al9.23. 2011. *JOURNAL OF PHYSICS-CONDENSED MATTER.* **23** (8): 086002.

Tobash, P., F. Ronning, J. D. Thompson, S. Bobev, and E. Bauer. Magnetic order and heavy fermion behavior in CePd$_{1+x}$Al$_{6-x}$: Synthesis, structure, and physical properties. 2010. *Journal of Solid State Chemistry.* **183** (3): 707.

Tokiwa, Y., R. Movshovich, F. Ronning, E. D. Bauer, A. D. Bianchi, Z. Fisk, and J. D. Thompson. Anomalous effect of doping on the superconducting state of CeCoIn5 in high magnetic fields. 2010. *PHYSICAL REVIEW B.* **82**: 220502.

Wang, C. H., J. M. Lawrence, E. D. Bauer, F. Ronning, K. Gofryk, J. D. Thompson, and F. Trouw. UMn2Al20: small itinerant moment or induced local moment ferromagnetism?. To appear in *Rare Earth Research Conference.* (,).

White, J S, P Das, M R Eskildsen, L DeBeer-Schmitt, E M Forgan, A D Bianchi, M Kenzelmann, M Zolliker, S Gerber, J L Gavilano, J Mesot, R Movshovich, E D Bauer, J L Sarrao, and C Petrovic. Observations of Pauli paramagnetic effects on the flux line lattice in CeCoIn$_5$. 2010. *New Journal of Physics.* **12**: 023026 (11 pp.).

Yu, R., J. -X. Zhu, and Q. Si. Mott transition in modulated lattices and parent insulator of (K,Tl)FexSe2 superconductors. 2011. *Physical Review Letters.* **106**: 186401.

Zhou, T., H. Huang, Y. Gao, J. -X. Zhu, and C. S. Ting. Quasiparticle states around a nonmagnetic impurity in electron-doped iron-based superconductors with spin-density-wave order. 2011. *Physical Review B.* **83**: 214502.

Zhu, , and Zhu, Jian-Xin. Coherence scale of coupled Anderson impurities. 2011. *Phys. Rev. B.* **83**: 195103.

Zhu, J. -X., P. H. Tobash, E. D. Bauer, F. Ronning, B. L. Scott, K. Haule, G. Kotliar, R. C. Albers, and J. M. Wills. Electronic Structure and Correlation Effects in PuCoIn5 as compared to PuCoGa5. To appear in *Physical Review B.*

Zhu, J. -X., R. Yu, A. V. Balatsky, and Q. Si. Local electronic structure of a single nonmagnetic impurity as a test of the pairing symmetry of electrons in (K,Tl)FexSe2 superconductors. To appear in *Physical Review Letters.*

Zhu, J., R. Yu, H. Wang, L. Zhao, M. D. Jones, J. Dai, E. Abrahams, E. Morosan, M. Fang, and Q. Si. Band narrowing and mott localization in iron oxychalcogenides La2O2Fe2O(Se,S)2. 2010. *Physical Review Letters.* **104** (21): 216405.

Zhu, L., and J. -X. Zhu. Magnetic-field-induced quantum phase transitions in the two-impurity Anderson model. 2011. *Physical Review B.* **83**: 245110.

Zhu, L., and J. Zhu. Superconducting pairing of interacting electrons: implications from the two-impurity Anderson model. 2011. In *International Conference on Strongly Correlated Electron Systems (SCES 2010) ; 20100627 - 20100702 ; Santa Fe, NM.* Vol. 273, p. 012068.

Spatial-temporal Frontiers of Atomistic Simulations in the Petaflop Computational World

Timothy C. Germann
20090035DR

Abstract

We have developed and demonstrated accurate techniques for combining the power of both accelerated and large-scale molecular dynamics (MD) methods, enabling for the first time atomistic simulations with both large size and long time scales – tens of millions of atoms for microseconds rather than the previous nanoseconds. These techniques have been used to study two fundamental materials science problems: (1) the nucleation, growth, and coalescence of voids leading to failure in metals; and (2) the interaction of a dislocation pileup forced against a grain boundary (GB), a fundamental issue controlling material strength. During this three-year project, we have made a significant advancement in hybrid accelerated/large-scale MD methods, and improved our understanding of the fundamental physics underlying our two targeted problems; however, much work remains to be done before hybrid accelerated/large-scale MD methods can be applied to a wider class of problems. In this final report, we focus on the progress made in five areas: (a) Local-bias hyperdynamics algorithm development and implementation; (b) Dislocation pileup – grain boundary interactions; (c) Void nucleation and the ultimate strength of materials; (d) Void growth dynamics and system embedding; and (e) tantalum potential development and applications, to enable subsequent study of body centered cubic (bcc) metals.

Background and Research Objectives

In recent years the field of atomistic-scale simulations of materials behavior has seen two exciting developments. First, the continuing advances in high-performance computing, in particular the maturation of massively parallel supercomputers consisting of hundreds, to hundreds of thousands, of processors working in concert, have enabled the study of complex phenomena in fluids and solids by the direct atom-by-atom ("molecular dynamics" (MD)) modeling of systems containing millions to billions of atoms. Secondly, "accelerated MD" algorithms, developed at Los Alamos over the past decade, are enabling the modeling of thermally activated, rare event processes that take place on timescales of seconds or longer, far beyond the nanoseconds (billionths of a sec-

ond) that traditional MD simulations have been able to reach (Figure 1). However, such accelerated simulations have thus far been limited to several hundred to a few thousand atoms at most. This project has developed and demonstrated accurate techniques for combining the power of both accelerated and large-scale MD methods, enabling for the first time atomistic simulations with both large size and long time scales, that will in certain cases directly overlap those of ultrafast, high-resolution experimental measurements. We have pursued two distinct approaches for achieving this integration, while studying two specific materials science problems: (1) the nucleation, growth, and coalescence of voids under tension, which can lead to "spall" failure of ductile metals following shock impact; and (2) the interaction of a dislocation pileup forced against a grain boundary (GB), a fundamental process which often determines the strength of materials. These two phenomena are representative of a large class of problems that have until now been tantalizingly just out-of-reach of current simulation techniques: requiring timescales of microseconds to milliseconds that have eluded direct MD, and sample dimensions as large as a micrometer that accelerated MD techniques have not been able to reach.
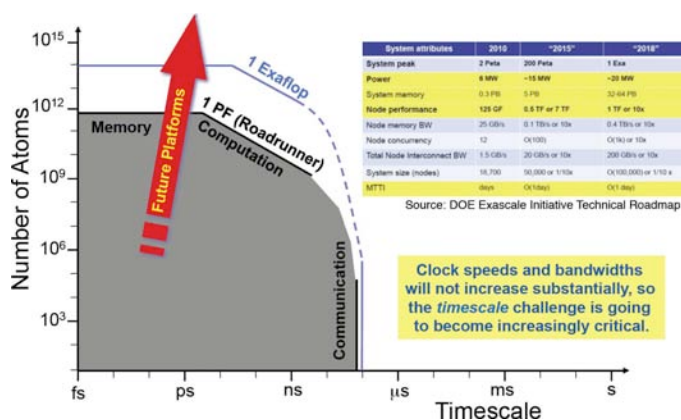
Figure 1. Spatio-temporal scales directly accessible by molecular dynamics simulations on current (petascale) leadership-class supercomputers and projections for future (~2020) exascale-class supercomputers. Due to the increasingly communication-bound nature of massively par-

allel applications, brute computer performance alone is not enough to model processes occurring on timescales of microseconds, milliseconds, or longer - the invention of intelligent algorithms are required, which is the focus of this project.

Scientific Approach and Accomplishments

In this final report, we will focus on five key technical accomplishments, starting with the algorithm development and moving on to the chosen materials science problems. Acting on advice from our external review committee midway through this three-year project, we also added a small effort to study body centered cubic (bcc) metals, in particular tantalum, due to important differences between bcc metals and face centered cubic (fcc) ones such as copper and aluminum. We will conclude with this as our fifth key technical accomplishment.

Local-bias hyperdynamics: algorithm development and implementation

The goal of this effort was to develop a rigorous *local* formulation of hyperdynamics that can give good boost (computational acceleration)on arbitrarily large systems. The key concept of hyperdynamics is to modify the potential energy surface by adding a "bias potential" which causes a trajectory to make state-to-state transitions more frequently, but with correct relative escape probabilities. To do this requires that the bias potential must vanish at all dividing surfaces between such state-to-state transitions; however as the system is made very large, there is a transition or near-transition somewhere in the system virtually all the time, so the bias potential is nearly always shut down. As a consequence, previous hyperdynamics simulations have been limited to systems containing a few hundred to a few thousand atoms, at most. In the local bond-boost hyperdynamics method which we have developed, we replace the concept of a *global* bias potential with a *bond-based* bias, and rather than apply a bias force to the bond with the lowest bias energy in the entire *system* (as done in previous bond-based hyperdynamics approaches), only apply the bias force to the bond with the lowest bias energy in its local domain (Figure 2). Unlike global hyperdynamics, the overlapping domains mean that more than one bond might have a force within a domain, but we can show that these appear in a way that gives self-cancelling errors in a time average. We have implemented this local-bias hyperdynamics method in the large-scale SPaSM code, demonstrated that correct state-to-state rates are obtained, and in a 24-hour simulation run on 256 processors, modeled the evolution of a 10 million atom copper sample with 200 vacancies (missing Cu lattice atoms) for 10 microseconds, a boost factor of 20,000. As seen in Figure 1, this combination of time and length scales is far beyond what is accessible by direct MD, demonstrating the potential of our approach. The next step remains to apply it not to such simplified model systems, but to real-world problems where additional complications may (and in general, do) arise.
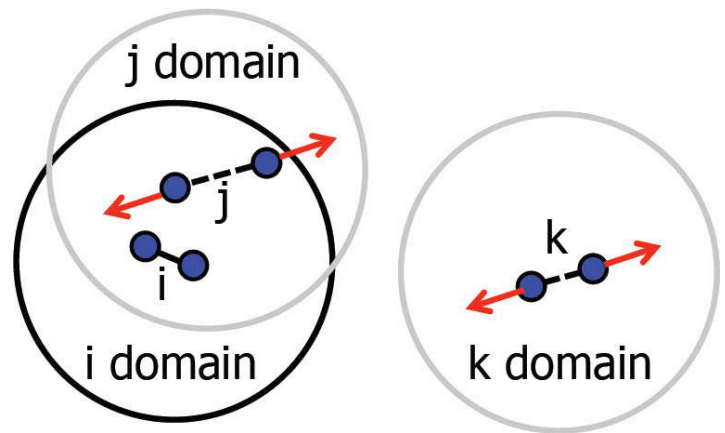
Figure 2. Schematic of the local bond-boost hyperdynamics approach. Each bond has its own instantaneous boost factor that is based upon the bond with the lower bond-based bias energy in its domain, i.e. a true hyperdynamics in that domain. Unlike global hyperdynamics, the overlapping domains mean that more than one bond might have a force within a domain, but these lead to self-cancelling errors over time.

Dislocation pileup – grain boundary interactions

We have focused on a "typical" asymmetric GB in aluminum, applying dislocation pileup theory to introduce the leading few (3-5) dislocations which are atomistically represented, and the elastic strain field due to the remaining, more distant, dislocations in the pileup. An alternate method in which dislocations are introduced one at a time, allowing the system to relax at each step, has also been developed and will enable us to study scenarios in which the loading is gradually increased at a constant strain rate. The configuration created by either technique is then imported into SPaSM, which applies the appropriate shear boundary conditions as implemented on both the Roadrunner and conventional code versions. We have studied a variety of GBs, using conventional MD simulations at high-applied stresses so that dislocation absorption, reflection, and/or transmission occur at the ps-to-ns timescales accessible without acceleration. As shown in Figure 3, this has given insight into the processes that may occur. We have also carved out a small active site near the GB, both before and after introducing the dislocation pileup, to accelerate using ParRep. One of our main concerns was that a GB could rapidly hop between a very large number of detailed atomistic configurations and limit the potential boost (acceleration). In some cases, this fear was realized; while in others, even after introducing the dislocation pileup (and more disorder) near the GB, only a few dozen distinguishable states have been found. However, this still requires advanced "superbasin" techniques, in which these few dozen states are recognized and only transitions to *new* states are accelerated. Such developments are underway as part of a related DOE Basic Energy Sciences project in accelerated MD algorithm development, and the dislocation pileup-grain boundary studies carried out under this program provide an early target application.
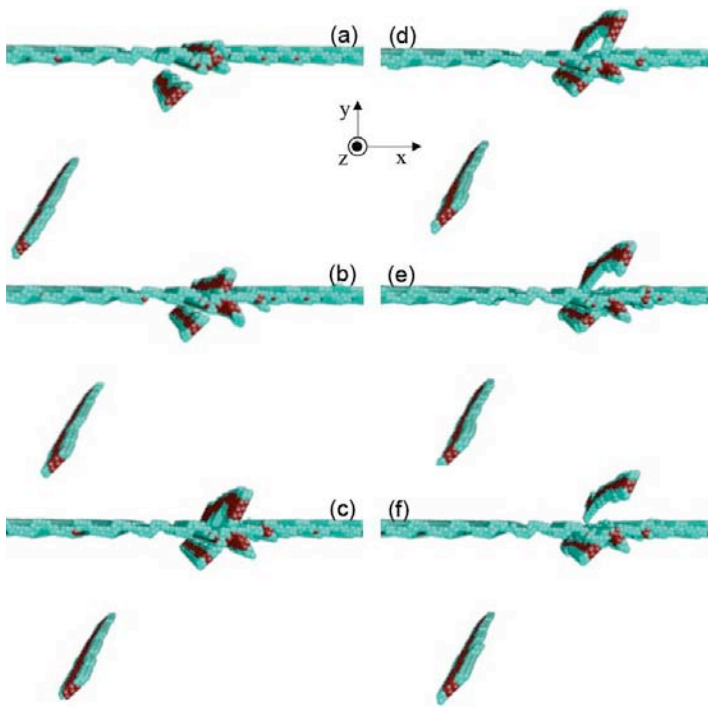
Figure 3. Detailed mechanisms leading to the transmission of a dislocation pileup across a general grain boundary. (a) The leading 1-2 dislocations in a pileup react with the grain boundary and cause shear and local rearrangements. (b) A three-fold dislocation structure is formed, which leads to (c) the nucleation of multiple partial dislocations in the transmitted grain. (d,e) Partial dislocation loops grow and coalesce, before (f) eventually detaching from the grain boundary and completing the transmission process.

Void nucleation: ultimate strength of materials

During the first year of this project, we utilized separate large scale and accelerated MD studies to probe different aspects of the spall failure of materials (specifically copper) under shock loading and release. This work, which included several production simulations on Roadrunner during its "Open Science" period, has provided insight about how voids nucleate (primarily at dislocation intersections or GBs), grow (once they reach a critical void size), and coalesce. Of particular note, we have demonstrated a competition between heterogeneous nucleation of voids at GBs, which leads to spall failure along such boundaries at slower strain rates, and the homogeneous void nucleation inside crystalline grains at higher strain rates. This latter process has also been studied by accelerated MD simulations (temperature accelerated dynamics, or TAD), in order to determine the time to failure and failure mode of a defect-free macroscopic region of crystal at a given temperature and applied strain. While mechanisms of homogeneous nucleation had been postulated but never rigorously validated, our work revealed the basic unit processes, which produce Frenkel pairs (a lattice atom moving into an interstitial position, leaving behind a vacancy), dislocation loops, or other defects under an applied stress or

strain. In the case of uniaxial stress/strain, our results suggest that the dislocation mode dominates at high strains (>9%), while the Frenkel pair formation mechanism dominates at lower strains. We have discovered a remarkable property of such simulations due to their high degree of symmetry that enables us to make conclusions about the spontaneous defect formation timescales in macroscopic samples. However, we have also found that the dislocation loop nucleation rate is strongly anharmonic, due to the strong dependence of vibrational properties on the strain state. As a consequence, the TAD method (which relies on harmonic transition state theory assumptions) requires generalization before it can be further applied to this problem.

Void growth dynamics: system embedding

Direct MD and ParRep accelerated molecular dynamics simulations have been used to study the growth of a pre-existing void in copper at tensile strain rates between 10^5/s (matching typical shock experiments on microsecond timescales, which would have been impossible with direct MD) and 10^{11}/s. For a microscopic 13-atom void, we find that the critical tensile stress ("spall strength") required for the void to grow and induce material failure is fairly independent, around 15 GPa, in contrast with experiments which exhibit a spall strength that increases with strain rate. The reason for this is found in a "strain rate paradox": once the void begins to grow by emitting dislocation loops, it grows very rapidly with an effective *local* strain rate that is ~10^{11}/s regardless of the applied *bulk* strain rate. This indicates that the size distribution of pre-existing voids plays a strong role in a material's spall strength: tiny voids such as this require an enormous critical stress to be applied before triggering this explosive void growth, while larger voids have smaller critical stresses, and thus smaller *local* strain rates once plastic deformation begins. To study the later stages of this explosive growth process, as well as the coalescence of neighboring voids, which leads to material failure, we have developed an embedding scheme. Initially the ParRep accelerated MD algorithm is used, with a number of processors each modeling independent replicas of a small (~10 thousand atom crystal with a 13-atom void) being slowly strained until one of the replicas exhibits a state-to-state transition (dislocation emission in this case). As previously mentioned, this allows us to model tensile strain rates down to 10^5/s, a regime heretofore inaccessible by MD. As soon as this transition occurs, we embed the small system in a larger (~10 to 100 million atom) lattice, which has been thermally equilibrated and matched. As shown in Figure 4, this allows us to study the subsequent dislocation emission and interaction processes, which allow the void to grow by plastic deformation, without artificially constraining the size scale. This hybrid scheme utilizes a parallel computer (or emerging many-core processor) in a natural way, with each core initially exploring escape pathways in a small system independently to accelerate *time*, and then all cores working

concurrently to model the subsequent evolution of a larger *spatial* domain of the sample.
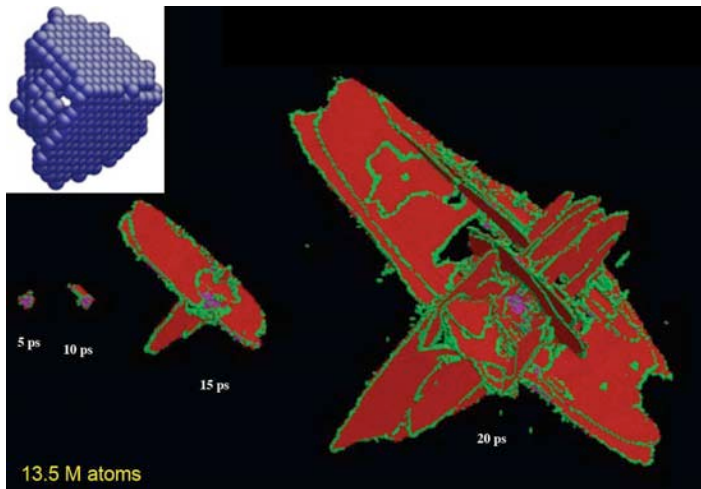
Figure 4. Demonstration of the hybrid accelerated/large-scale molecular dynamics embedding scheme developed under this project. A pre-existing void (13-atom vacancy) in a copper sample is slowly strained at experimental strain rates using parallel replica dynamics until dislocation emission is induced (upper left). At this time the ~13 thousand atom sample is embedded into a ~13 million atom large-scale MD simulation, allowing the explosive growth of the void to proceed by the proliferation of dislocation loops (lower snapshots at 5, 10, 15, and 20 ps).

Toward bcc metals: Ta potential development and applications

Finally, at the suggestion of our mid-project review panel we dedicated a small effort towards modeling bcc metals, which in general have a stronger rate dependence than fcc metals due to differences in how dislocations move within the crystal. However, for the extreme strains and strain rates of interest for spall failure, we quickly discovered that most existing interatomic potentials were inadequate for modeling, either with fundamental flaws in their physics, or impractical computational costs for this exploratory research phase. For instance, for tantalum (a material chosen for its interest in the NNSA community, with active experimental programs studying its spall behavior) all of the existing embedded atom method (EAM) potentials predicted a phase transformation from the bcc structure to a hexagonal close packed (hcp) one under compression, at pressures of 35-85 GPa. Since (a) no such transition has been experimentally observed, and (b) this is exactly the pressure range at which deformation slip and twinning is activated, we needed to develop a new interatomic potential before proceeding. The potential that we have developed (and which has been eagerly greeted by the external research community) predicts a stable bcc structure up to nearly 500 GPa (5 Mbar), in accord with experiments and high-quality theory. We fit to experimental and density function theory (DFT) data for compressing up to 50% (500

GPa), including activation energies for various deformation pathways, and demonstrated that the resulting potential accurately reproduces experimental shock Hugoniot measurements, as well as reveal the microscopic competition between slip and twinning processes in single crystals shocked in various crystal directions, as well as nanocrystalline samples with varying grain sizes.

Impact on National Missions

Atomistic-scale simulations are playing an increasing role in fundamental and applied materials science. Los Alamos has two distinct internationally recognized capabilities in this area: large-scale molecular dynamics (MD) simulations, specifically the SPaSM (*Scalable Parallel Short-range Molecular dynamics*) code supported primarily by the weapons program (ASC), and accelerated molecular dynamics algorithm development and implementation under the auspices of LDRD and Basic Energy Sciences (BES). This project has developed and demonstrated the coupling of these two capabilities to address heretofore-inaccessible problems in materials science. The resulting transformational capability is expected to have immediate benefits to DOE missions in the Office of Science and Nuclear Weapons (NNSA Advanced Simulation and Computing) programs, by providing new computational tools and enhancing our understanding of the fundamental dynamics of materials, in particular under extreme loading conditions that are difficult to probe experimentally. The methods demonstrated here should have applications beyond these initial materials science issues that we will focus on, for instance in studying the resistance of materials to other extreme conditions including radiation and corrosive environments; similarly, the materials science questions addressed here have impacts in nuclear and non-nuclear energy (e.g. turbine blade design), DOD programs (e.g. armor/anti-armor), and beyond. The unique capability that we are developing may be used to investigate fundamental materials science questions that have eluded direct study for a half-century or longer. Through this effort, we will help maintain America's leadership role in advanced high-performance computing, materials science, and nanotechnology, directly addressing needs cited in the June 2011 *Materials Genome Initiative for Global Competitiveness* which was issued by the White House Office of Science and Technology Policy (OSTP).

Publications

An, Q., R. Ravelo, T. C. Germann, W. Z. Han, S. N. Luo, D. L. Tonks, and W. A. Goddard III. Shock compression and spallation of single crystal tantalum. To appear in *Shock Compression of Condensed Matter - 2011.* (Chicago, IL, 26 June - 1 July 2011).

Arman, B., C. Brandl, S. N. Luo, T. C. Germann, A. Misra, and T. Cagin. Plasticity in Cu(111)/Cu46Zr54 glass nanolaminates under uniaxial compression. 2011. *JOURNAL OF APPLIED PHYSICS.* **110** (4): 043539.

Arman, B., S. Luo, T. Germann, and T. Cagin. Dynamic response of Cu46Zr54 metallic glass to high-strain-rate shock loading: Plasticity, spall, and atomic-level structures. 2010. *PHYSICAL REVIEW B.* **81** (14): 144201.

Du, S., T. Germann, J. Francisco, K. Peterson, H. Yu, and J. Lyons. The kinetics study of the S + S-2 -> S-3 reaction by the chaperone mechanism. 2011. *JOURNAL OF CHEMICAL PHYSICS.* **134** (15): 154508.

Germann, T.. LARGE-SCALE CLASSICAL MOLECULAR DYNAMICS SIMULATIONS OF SHOCK-INDUCED PLASTICITY IN BCC NIOBIUM. 2009. In *16th Conference of the American-Physical-Society-Topical-Group on Shock Compression of Condensed Matter ; 20090628 - 20090703 ; Nashville, TN.* Vol. 1195, p. 761.

Germann, T., and K. Kadau. LARGE-SCALE MOLECULAR DYNAMICS SIMULATIONS OF THE FCC-FCC VOLUME COLLAPSE TRANSITION IN SHOCKED CESIUM. 2009. In *16th Conference of the American-Physical-Society-Topical-Group on Shock Compression of Condensed Matter ; 20090628 - 20090703 ; Nashville, TN.* Vol. 1195, p. 1209.

Hammerberg, J. E., B. L. Holian, T. C. Germann, and R. Ravelo. HIGH VELOCITY PROPERTIES OF THE DYNAMIC FRICTIONAL FORCE BETWEEN DUCTILE METALS. 2009. In *16th Conference of the American-Physical-Society-Topical-Group on Shock Compression of Condensed Matter ; 20090628 - 20090703 ; Nashville, TN.* Vol. 1195, p. 777.

Han, L., Q. An, R. Fu, L. Zheng, and S. Luo. Local and bulk melting of Cu at grain boundaries. 2010. *PHYSICA B-CONDENSED MATTER.* **405** (2): 748.

Han, L., Q. An, R. Fu, L. Zheng, and S. Luo. Melting of defective Cu with stacking faults. 2009. *JOURNAL OF CHEMICAL PHYSICS.* **130** (2): 024508.

Han, L., Q. An, S. Luo, and T. Germann. THE EFFECTS OF DEFECTS ON MELTING OF COPPER. 2009. In *16th Conference of the American-Physical-Society-Topical-Group on Shock Compression of Condensed Matter ; 20090628 - 20090703 ; Nashville, TN.* Vol. 1195, p. 1187.

Han, W. Z., Q. An, S. N. Luo, T. C. Germann, D. L. Tonks, and W. A. Goddard III. Deformation and spallation of shocked Cu bicrystals with Σ3 coherent and symmetric incoherent twin boundaries. To appear in *Acta Materialia.*

Han, W. Z., Q. An, S. N. Luo, T. C. Germann, D. L. Tonks, and W. A. Goddard III. Left-right loading dependence of shock response of (111)//(112) Cu bicrystals: deformation and spallation. *Journal of Applied Physics.*

Holian, B. L.. A History of constitutive modeling via molecular dynamics: Shock waves in fluids and gases. 2010. In *Conference on New Models and Hydrocodes for Shock Wave Processes in Condensed Matter ; 20100524 - 20100528 ; Paris, FRANCE.* Vol. 10, p. 00002.

Holian, B. L., M. Mareschal, and R. Ravelo. Burnett-Cattaneo continuum theory for shock waves. 2011. *PHYSICAL REVIEW E.* **83** (2, 2): 026703.

Holian, B. L., M. Mareschal, and R. Ravelo. Burnett-Cattaneo continuum theory for shock waves (vol 83, 026703, 2011). 2011. *PHYSICAL REVIEW E.* **83** (2, 2): 029902.

Holian, B. L., M. Mareschal, and R. Ravelo. Test of a new heat-flow equation for dense-fluid shock waves. 2010. *JOURNAL OF CHEMICAL PHYSICS.* **133** (11): 114502.

Holian, B. L., and M. Mareschal. Heat-flow equation motivated by the ideal-gas shock wave. 2010. *PHYSICAL REVIEW E.* **82** (2, 2): 026707.

Hunter, A., I. J. Beyerlein, T. C. Germann, and M. Koslowski. Influence of the stacking fault energy surface on extended partials in fcc metals with a 3D phase field dislocation dynamics model. To appear in *Physical Review B.*

Luo, S., Q. An, T. Germann, and L. Han. Shock-induced spall in solid and liquid Cu at extreme strain rates. 2009. *JOURNAL OF APPLIED PHYSICS.* **106** (1): 013502.

Luo, S., T. Germann, D. Tonks, and Q. An. Shock wave loading and spallation of copper bicrystals with asymmetric Sigma 3 < 110 > tilt grain boundaries. 2010. *JOURNAL OF APPLIED PHYSICS.* **108** (9): 093526.

Luo, S., T. Germann, Q. An, and L. Han. SHOCK-INDUCED SPALL IN COPPER: THE EFFECTS OF ANISOTROPY, TEMPERATURE, DEFECTS AND LOADING PULSE. 2009. In *16th Conference of the American-Physical-Society-Topical-Group on Shock Compression of Condensed Matter ; 20090628 - 20090703 ; Nashville, TN.* Vol. 1195, p. 1015.

Luo, S., T. Germann, T. Desai, D. Tonks, and Q. An. Anisotropic shock response of columnar nanocrystalline Cu. 2010. *JOURNAL OF APPLIED PHYSICS.* **107** (12): 123507.

Luo, S., T. Germann, T. Desai, D. Tonks, and Q. An. Anisotropic shock response of columnar nanocrystalline Cu. 2010. *JOURNAL OF APPLIED PHYSICS.* **107** (12): 123507.

Luo, S., T. Germann, and D. Tonks. Spall damage of copper under supported and decaying shock loading. 2009. *JOURNAL OF APPLIED PHYSICS.* **106** (12): 123518.

Enhance Radiation Damage Resistance via Manipulation of the Properties of Nanoscale Materials

Michael A. Nastasi
20090061DR

Abstract

Our work focuses on the concept that interfaces in materials can act as "super sinks" for point defects in an irradiation environment, which if full understood allows to develop highly radiation tolerant nanocomposite materials. The main emphasis of this work has been to explore how defects associated with energetic He injection are influenced by interface structure. We have shown that such interfaces stabilize material microstructure and efficiently heal radiation damage by attracting, absorbing, and catalyzing the annihilation of radiation-induced point defects. Our objectives in this work have been: 1) develop a *generalized* description, applicable to any interface in any material, of the properties that make an interface a "super sink" for radiation-induced defects; 2) explore the irradiation stability of nano-composites over a broad spectrum of extreme environments (high irradiation dose, long time, high temperature, and corrosion to simulate real reactor environments conditions); and 3) explore the effect of irradiation (particularly at high doses) on mechanical properties such as strength and ductility. Our approach integrates theory, modeling, and experiments to formulate, validate, and test the limits of strategies for enhancing radiation damage resistance of materials by maximizing their content of super sink interfaces.

Background and Research Objectives

The design of future nuclear power reactors, including advanced fuel cycles, Gen IV and fusion reactors places high demands on reactor cladding and structural materials. These extreme operating conditions include extremely high irradiation doses, and higher operating temperatures with minimal change in mechanical properties. At present, the best-engineered materials for high dose nuclear applications reach their structural limit at relatively low irradiation dose. Their elevated temperature mechanical integrity at even lower irradiation doses. Thus, the transformative research in materials development is required to meet the needs of future nuclear reactors.

The reason why materials fail under irradiation can be traced at the most fundamental level to the accumulation of the defects produced during the irradiation process. Left unbridled such processes lead to swelling, and chemical changes that compromise the material's mechanical and corrosion resistant properties. Therefore, the principal challenge in the development of materials with radically extended performance limits in extreme radiation environments is to increase the recovery efficiency of radiation-induced defects.

Our first objective is to develop a *generalized* description, applicable to any interface in any material, of the properties that make an interface a "super sink" for radiation-induced defects.

Our second objective is to explore the irradiation stability of nano-composites over a broad spectrum of extreme conditions. By extreme, we mean a combination of high irradiation dose, long time, high temperature, and corrosion to simulate real reactor environments. This objective will explore the ultimate failure limits of nanocomposites under nuclear reactor environments.

Our third objective is to explore the effect of irradiation (particularly at high doses) on mechanical properties such as strength and ductility. This addresses the issue of retention of the unusually high strengths and ductility of nanocomposites after irradiation.

We propose to enhance the radiation resistance of materials by manipulating their properties at the nanoscale to directly affect the evolution of damage cascades. Our approach in addressing this problem will be to develop materials that will contain special internal features, i.e., interfaces, that can be designed at the atomic-scale to attract, absorb and annihilate radiation-induced defects, thereby allowing design of nanostructured materials for radiation damage tolerance. This builds on previous scientific breakthroughs at LANL that presented a new paradigm in designing materials with the specific property of radiation damage tolerance. The central idea of this proposal is atomic-scale design of stable internal interfaces that impart radiation tolerance to materials by attracting, absorbing, and annihilating point defects.

Scientific Approach and Accomplishments

Our purpose is to enhance the radiation resistance of materials by manipulating their properties at the nanoscale to directly affect the evolution of damage cascades. Our approach will be to develop materials that will contain special internal features, i.e., interfaces, that can be designed at the atomic-scale to attract, absorb and annihilate radiation-induced defects, thereby allowing design of nanostructured materials for radiation damage tolerance. This builds on past scientific breakthroughs at LANL that presents a new paradigm in designing materials with the specific property of radiation damage tolerance.

As part of this work we have examined three different aspects of defect-boundary interactions, using Cu as a model system: 1) thermodynamics of defects interacting with boundaries, 2) kinetics of vacancies near boundaries, and 3) the incorporation of He at boundaries. We examined the role that grain boundaries play in radiation. We focused on two timescales: ps, over which defects are created, and the longer timescales over which those defects evolve. During the damage production stage, boundaries absorb large numbers of interstitials and vacancy-interstitial recombination is suppressed. This implies that when thermally activated processes are not possible, nanocrystalline materials are less tolerant than polycrystalline materials. However, on long timescales, interstitials absorbed at the boundary can be reemitted to annihilate with vacancies in the bulk. This *interstitial emission* mechanism (Figure 1.) occurs with relatively small barriers, leading to enhanced radiation tolerance at temperatures where vacancies are essentially immobile. This work was published in *Science* **327**, 1631 (2010).
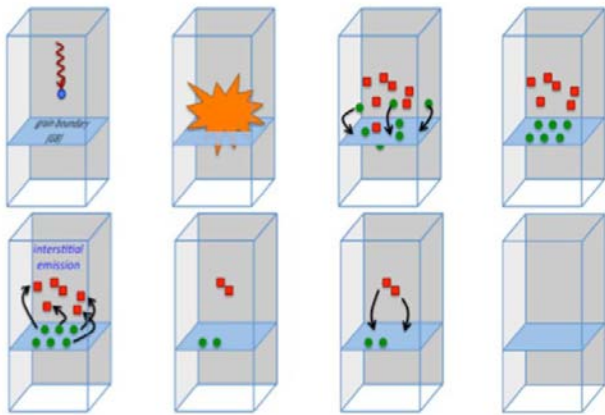
Figure 1. Schematic showing the evolution of a nanocrystalline material under irradiation. An energetic particle hits an atom, creating interstitials (green circle) and vacancies (red square), which are absorbed unequally by the boundary. Via interstitial emission and enhanced vacancy diffusion, the material recovers.

We also used modeling to examine how He is incorporated into grain boundaries in Cu. Here, we focused solely on twist boundaries with small twist angles, between 3 and 8 degrees. The structure of these boundaries is characterized by a set of screw dislocations at the boundary plane that criss-cross, creating dislocation intersections, or nodes, in the network. We found that He atoms feel a strong attraction to the nodes. This correlates with experimental studies of He implantation near twist boundaries in Au, which observed preferential He bubble nucleation at the intersections of the screw dislocation network.

Finally, we examined how the screw dislocation network changes as a function of angle, from perfect screw dislocations (large angles) to split partial dislocations (small angles). Vacancies in the higher angled twist boundaries strongly prefer the dislocation intersections. However, in the smaller angled boundaries, while the nodes are still preferred, this preference is only slightly more than at other places within the dislocation structure. For 5 degree twist boundaries, where there is a crossover in the dislocation structure, the corresponding atomic structures of the nodes become very complex. Not all nodes are equivalent, and some interact only very weakly with vacancies. This suggests that the He bubble network that forms in would depend on the twist angle.

Our work has shown that interfaces can be used to "manage" implanted He. Therefore, it is crucial to understand the impact that trapped He nano-bubbles may have on strength and deformability. We used nanoscale metallic multilayers as model systems for this aspect of our work since the interface atomic structure and the interface spacing may be independently varied, via choice of constituent layers and deposition parameters, respectively.

Using ion implantation, a uniform distribution of He bubbles approximately 2 nm in diameter, see Figure 2, and was produced over 1 micrometer depth in multilayered films. Nanoindentation was used to measure hardness and stress-strain curves via compression of focused ion beam milled micro-pillar specimens. Significant findings are summarized below:

- As the interface spacing was reduced, the hardening due to bubbles decreased significantly, and was negligible when the interface spacing was on the order of or less than the average bubbles spacing. Both interface boundaries and helium bubbles are obstacles to dislocation motion and cause hardening. At relatively large (tens to hundreds of nanometers) interface spacing, the bubble hardening is additive to interface hardening. But when interfaces are more closely spaced than the bubbles, there is insignificant bubble hardening relative to interface spacing.

- At layer thickness of a few nanometers, the critical unit mechanism that determines the strength of a multilayer is the stress needed to transmit a single dislocation across interfaces. In the helium-implanted samples, helium nano-bubbles preferentially nucleate at the misfit dislocation intersections forming a two-dimen-

sional bubble lattice at the interface. Atomistic modeling showed that the equation-of-state (and hence, pressure) of He bubbles at interfaces is different from that in the bulk. Thus, the nano-bubbles at interfaces may interact more weakly with glide dislocations than those in the bulk.

This work has shown that specific interfaces that have a high number density of misfit dislocation intersection points can be used to trap a high concentration of helium in the form of stable nano-meter scale bubbles that interact weakly with glide dislocations and do not cause hardening (and embrittlement) as in bulk materials without interfaces.
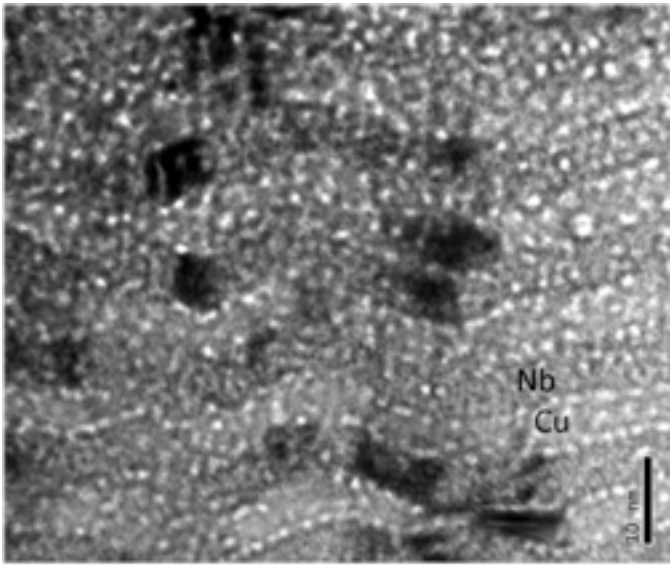
Figure 2. Under-focused bright field transmission electron microscopy (TEM) image of helium implanted 5 nm Cu – 5 nm Nb multilayers. Helium nano-bubbles are visible as white dots decorating the interfaces.

As part of this project we studied He bubble formation in bulk and at interfaces formed by dislocation networks (pure twist boundaries) in pure fcc and bcc metals and in several alloys. We aimed at interpreting experimental results available for the He-Au system, and to contribute to the computational study of He at interfaces in.

Our study of He bubbles had two avenues, one was the thermodynamics of heterogeneous He precipitation, which focuses on the determination of preferential location for He bubbles on a given microstructure, and the form He bubbles adopt. Simulations are done with a parallel Metropolis Monte Carlo code under the assumption of He/vacancy ratio equal to 1, a sensible assumption for He implantation occurring simultaneously with some dpa damage. For fcc metals, it has been shown experimentally within this LDRD project that pure twist Au grain boundaries, formed by a square array of screw dislocations, show dislocation intersection as preferential sites for He precipitation. Our simulations are done for an equivalent fcc ma-

terial, Cu, which fully confirm this result, Figure 3. Moreover, simulations show the decomposition of initial perfect screw dislocation into partials that leave the (100) plane of the interface creating a constriction between the nodes. This new result was confirmed by dislocation dynamics energy calculations.
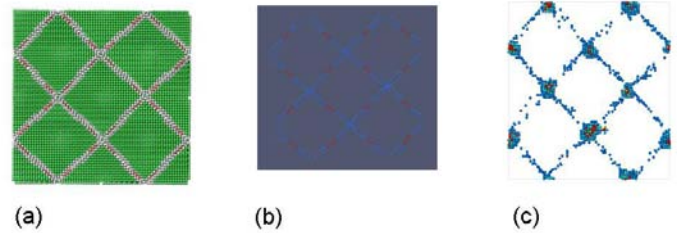
Figure 3. (a) atomic scale view of a slice containing the grain boundary plane showing the network of initially perfect l // <110>, b // <110> dislocations, with l the dislocation segment and b the Burger vector. (b) These dislocations decompose into partials with l//<110>, b1 // <-1 -1 2>, and b2 // <-12-1>. These two partials are contained in (111) planes instead of the original (100) plane. (c) He (red atoms) shows precipitation at the nodes of the network.

The second avenue was the study of bubble growth via the incorporation of He into an existing bubble and monitoring the mechanisms by which these bubbles grow. In bulk we observed that the mechanism is the emission of <111> dislocation loops with diameter equal to the bubble size. In interface dislocations this mechanism is more complex.

Both these avenues gave us the elements to construct an equation of state for He bubbles in bulk and another for bubbles at interfaces. We observed that bubbles at interfaces have less pressure that those in bulk, and that this pressure depends on the nature of the interface.

We additionally studied the influence of the interface between a nanoscale precipitate and a matrix for the cases when these precipitates have different crystalline structure than the matrix. We observed that regardless of the thermodynamic driving force to direct He towards the metal with less solution energy, He prefers always the incoherent interface, due to the existence of sites with larger volume

In addition, this project enabled us to perform the first ever quantitative measurements of critical He concentrations necessary to nucleate bubbles observable in transmission electron microscopy at heterophase interfaces. These studies, first conducted on Cu-Nb interfaces, were subsequently also done on Cu-V and Cu-Mo interfaces and have provided a clear criterion for predicting heterophase interface resistance to He bubble formation: misfit dislocation intersections at interfaces are trapping sites for He. Thus, the more such intersections an interface has, the more resistant it is to implanted He. Conversely, if an interface has few or no misfit dislocation intersections, its response to implanted He is indistinguishable from that of a perfect single crystal.

To understand these phenomena in greater detail, we undertook to study interface interactions with He in greater detail. Using density functional theory calculations, we constructed a predictive Cu-Nb-He potential. With this potential, we quantified He binding energies at Cu-Nb interface (Figure 4) and confirmed the critical role of misfit dislocation intersections in He trapping. This potential also opened the door for us to undertake detailed studies of He cluster and bubble growth as well as the effect of He on interface mechanical properties.
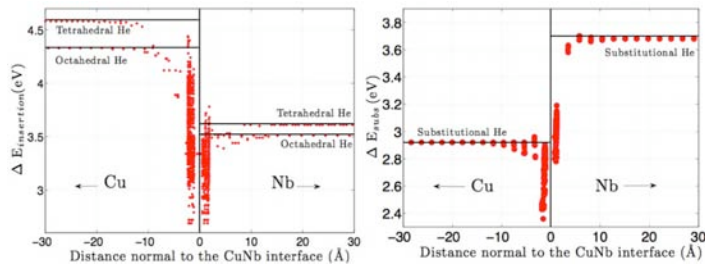
Figure 4. Formation energies of He interstitials (left) and substitutionals (right) at a Cu-Nb interface. The interface is a sink for He arriving from both of the neighboring crystalline layers.

Impact on National Missions
This work supports the mission of the DOE Office of Science, explicitly the BES-stated Basic Research Needs for Advanced Nuclear Energy Systems, included a priority research direction on Nanoscale Design of Materials and Interfaces that Radically Extend Performance Limits in Extreme Radiation Environments.

Publications
Bai, X. M., A. F. Voter, R. G. Hoagland, M. Nastasi, and B. P. Uberuaga. Efficient annealing of radiation damage near grain boundaries via interstitial emission. 2010. *Science.* **327**: 1631.

Demkowicz, M. J., D. Bhattacharyya, I. Usov, A. Misra, Y. Q. Wang, and M. Nastasi. The Role of the atomic structure of the Cu-Nb interface on helium bubble formation at interfaces. 210. *Applied Physics Letters.* **97**: 161903.

Kashinath, A., and M. J. Demkowicz. A predictive interatomic potential for He in Cu and Nb. 2011. *Modeling and Simulation in Materials Science and Engineering .* **19**: 3507.

Li, N., E. G. Fu, H. Wang, J. J. Carter, L. Shao, S. A. Maloy, A. Misra, and X. Zhang. He ion irradiation damage in Fe/W nanolayer films. 2009. In *Symposium on Particle Beam Induced Radiation Effects in Materials held at the Annual Meeting of the Mineral-Metals-and-Materials-Society ; 20080310 - 20080312 ; New Orleans, LA.* Vol. 389, 2 Edition, p. 233.

Li, N., J. J. Carter, A. Misra, L. Shao, and X. Zhang. The influ-

ence of interfaces on the formation of bubbles in He ion irradiated Cu/Mo multilayers. 2011. *Philosophical Magazine Letters.* **91**: 19.

Li, N., N. A. Mara, Y. Q. Wang, M. Nastasi, and A. Misra. Compressive flow behavior of Cu thin films and Cu/Nb multilayers containing nanometer-scale helium bubbles. 2011. *Scripta Materialia.* **64** (10): 974.

Li, N., N. A. Mara, Y. Q. Wang, M. Nastasi, and A. Misra. Compressive flow behavior of Cu thin films and Cu/Nb multilayers containing nanometer-scale helium bubbles. 2011. *Scripta Materialia.* **64** (10): 974.

Li, Nan, M. S. Martin, O. Anderoglu, A. Misra, L. Shao, H. Wang, and X. Zhang. He ion irradiation damage in Al/Nb multilayers. 2009. *Journal of Applied Physics.* **105** (12): 123522 (8 pp.).

Liu, X. -Y., R. G. Hoagland, J. Wang, T. C. Germann, and A. Misra. The influence of dilute heats of mixing on the atomic structures, defect energetics and mechanical properties of fcc-bcc interfaces. 2010. *ACTA MATERIALIA.* **58** (13): 4549.

Liu, X. -Y., R. G. Hoagland, J. Wang, T. C. Germann, and A. Misra. The influence of dilute heats of mixing on the atomic structures, defect energetics and mechanical properties of fcc-bcc interfaces. 2010. *ACTA MATERIALIA.* **58** (13): 4549.

Wei, Q. M., N. Li, N. Mara, M. Nastasi, and A. Misra. Suppression of irradiation hardening in nanoscale V/Ag multilayers. 2011. *Acta Materialia.* **59** (16): 6331.

Wei, Q. M., Y. Q. Wang, M. Nastasi, and A. Misra. Nucleation and growth of bubbles in He ion implanted V/Ag multilayers. 2011. *Philosophical Magazine.* **91**: 553.

Wei, Q. M., Y. Q. Wang, M. Nastasi, and A. Misra. Nucleation and growth of bubbles in He ion-implanted V/Ag multilayers. 2011. *PHILOSOPHICAL MAGAZINE.* **91** (4): 553.

Wei, Q. M., Y. Q. Wang, M. Nastasi, and A. Misra. Nucleation and growth of bubbles in He ion-implanted V/Ag multilayers. 2011. *Philosophical Magazine.* **91** (4): 553.

Zhang, X., E. G. Fu, A. Misra , and M. J. Demkowicz. Interface-enabled defect reduction in He ion irradiated metallic multilayers. 2011. *Journal of Materials.* **62**: 75.

Zhernenkov, M., M. Jablin, A. Misra, M. Nastasi, Y. Wang, M. Demkowicz, J. Baldwin, and J. Majewski. Trapping of implanted He at Cu/Nb interfaces measured by neutron reflectometry. 2011. *APPLIED PHYSICS LETTERS.* **98** (24): 241913.

Seaborg Institute Fellows

Albert Migliori
20090475DR

Abstract

The Seaborg Institute Postdoctoral and Student Fellows enhances LANL's capabilities in advanced actinide chemistry, actinide materials science, and actinide theory. Knowledge of actinide science continues to be essential to the U.S. and central to the mission of the NNSA, including national defense, energy security, nuclear nonproliferation, environmental restoration, and radioactive waste management. Seaborg Institute Postdoctoral and Student Fellows are supported to perform experimental, theoretical, or modeling research that underlies missions in stockpile stewardship, nuclear energy and safeguards, nonproliferation and forensics, environmental restoration and transport, biological interactions, and radioactive waste management. These areas are strategic for the Laboratory and include supporting the LANL "plutonium center of excellence" and the Plutonium Science and Research Strategy.

Postdoctoral Fellows are funded primarily halftime, must be approved by LANL Postdoctoral program, and must choose a project that connects directly with actinide science. Student Fellows are funded primarily full-time for 10-12 weeks during the summer. The program is administered by the G. T. Seaborg Institute for Transactinium Science. A brief description of each funded postdoctoral Fellow's research topic is provided in the technical description of the project and is amended as postdocs arrive and exit the program.

Background and Research Objectives

The tasks in this LDRD project were dedicated to addressing important gaps in our current level of understanding of actinides, promoting a creative and expert core actinide workforce, and to scientific excellence in the many important scientific problems in the field. LDRD resources were used to build capabilities, address outstanding scientific problems, advance new scientific concepts via initial support to seed research elements of feasibility studies, and cutting-edge scientific research that addresses critical scientific questions.

Scientific Approach and Accomplishments

Because of the breadth of the science supported by this project, there is only room in this report to touch briefly on selected topics. In all cases, peer-reviewed publications can be accessed to understand the work in depth. The work supported by this project has produced important advances including the first complete set of elastic moduli at high precision of alpha, beta, and gamma plutonium over their entire range of stability that is crucial for all dynamic testing and is now being used to analyze programmatic studies of plutonium; ground-breaking work in the production of important uranium-nitride complexes; studies of grain boundaries and heat transport in nuclear fuels; actinide catalysts for cleaning dirty fossil energy feedstocks; fundamental discoveries in f-electron physics, chemistry, and materials science and more.

Theoretical Modeling of Nanoscale Heterogeneity in Actinide Alloys and Oxides

Uranium dioxide, UO_2, is the major constituent of nuclear fuels. In this task we explored the physics and chemistry of hyperstoichiometric uranium, neptunium and plutonium dioxides that are derived from the parent fluorite lattice, i.e. $AnO_{2\pm x}$ and An_4O_9 (An=U, Np and Pu). Using density functional theory (DFT) techniques, we identified the underlying physics that governs trends in oxidation thermodynamics along the actinide series and recognized the crucial role of hydrogen in forming hyperstoichiometric compounds of PuO_2.

Photoemission Spectroscopy (PES) of Actinides

Using PES measurement techniques, we have obtained information on the electronic structures of a number of actinide materials including USb_2, UGe_2, UPd_3, [1] UC_2 and delta plutonium. UC_2 is of particular interest as a potential next generation fuel for nuclear energy, and our PES measurements suggest UC_2 is metallic, important for heat transport in nuclear reactor fuel.

QSGW Electronic Structure of Neptunium

A critical problem in actinide physics is to understand the effect of electron-electron correlation effects. Two methods, first-principles electronic band-structure or local-density-functional (LDA) methods have been applied in the weakly correlated limit and dynamical mean-field theory (DMFT) methods have been employed in the strongly correlated limit. The key goal of this task was to reconcile these methodologies using quasi-particle GW (QSGW) theory [2] for delta-plutonium. We found that that the single-particle band structure obtained differs from the LDA in two significant ways: (1) The 5f electron energy dispersion is flatter and (2) the crystal field splitting between 5f states is significantly smaller. We have now done similar calculations on Np. [3]. We have discovered that our current code, and in fact no other available GW code, adequately and correctly treats the spin-orbit interaction. Our revised code, in progress, will represent a substantial and important scientific advance.

Development of a two-dimensional system for mapping gamma-emitting radionuclides in support of forensic examination

In conducting a nuclear forensic examination of a sealed container, an external gamma spectrometer is used. To provide more information about the identity and location of the gamma-emitting nuclides within a sealed container, a two-dimensional gamma mapping system was built using high-atomic-number shielding, a two-dimensional linear stage, and a high-purity germanium (HPGe) detector. Programming and the testing of the system with standard sealed radioactive sources are in progress.

Spectroscopic Analysis of Actinyl Systems

Previous studies on actinyl heteropolyoxotungstates (POMs) have shown that tri-lacunary POMs readily coordinate to the actinyls ($An^{VI}O_2^{2+}$ and $An^VO_2^+$, An = U, Np, Pu, Am) forming a range of structurally diverse complexes. These systems have relevance in environmental remediation, nuclear waste management and nuclear fuel separation technologies. The goal of this research was to increase our understanding of the electronic structure and bonding properties of the actinyls through polyoxometalate coordination. One of many results from single crystal X-ray structural analysis revealed a complex with two full and one partial occupancy $[UO_2]^{2+}$ cations sandwiched between two $[A-\alpha-GeW_9O_{34}]^{10-}$ anions.

Another task used synchrotron techniques to develop an in-situ hydrogenation capability that combined synchrotron EXAFS and XRD. The in situ-hydrogenation capability was successfully developed and tested on the palladium–hydrogen system. Our effort to understand the chemical processes associated with the corrosion of plutonium and plutonium metal alloys containing ~1.8 atomic % Ga indicated this process was more complex than previously considered.

Proliferation-resistant separation technologies

A significant challenge for creating proliferation-resistant separation technologies for spent nuclear fuel is developing methods to efficiently partition trivalent actinides from lanthanide ions. This task has focused on elucidating favorable electronic structure-function relationships in dithiophosphinates using sulfur K-edge X-ray absorption spectroscopy (XAS) to identify electronic properties that may account for the high selectivity for extraction of actinides over lanthanides observed using $HS_2P(o$-$CF_3C_6H_4)_2$ and related compounds. This work resulted in the synthesis and characterization of 15 previously unreported compounds.

Elastic moduli of alpha, beta, gamma and gallium-stabilized delta plutonium

Accurate elastic moduli in all the phases of plutonium are of central importance in assessing both applications for and theory of Pu. The resonant ultrasound spectroscopy measurements performed for this complete the set of the temperature dependence of elastic moduli of polycrystalline pure Pu from 18 K to 616 K, and alloyed delta phase from 9 K to 496 K (Figure 1) [4,5,6]. In addition, we have shown that where pure and Ga stabilized delta co-exist, they are nearly identical elastically, an important calibration datum for theory and modeling.
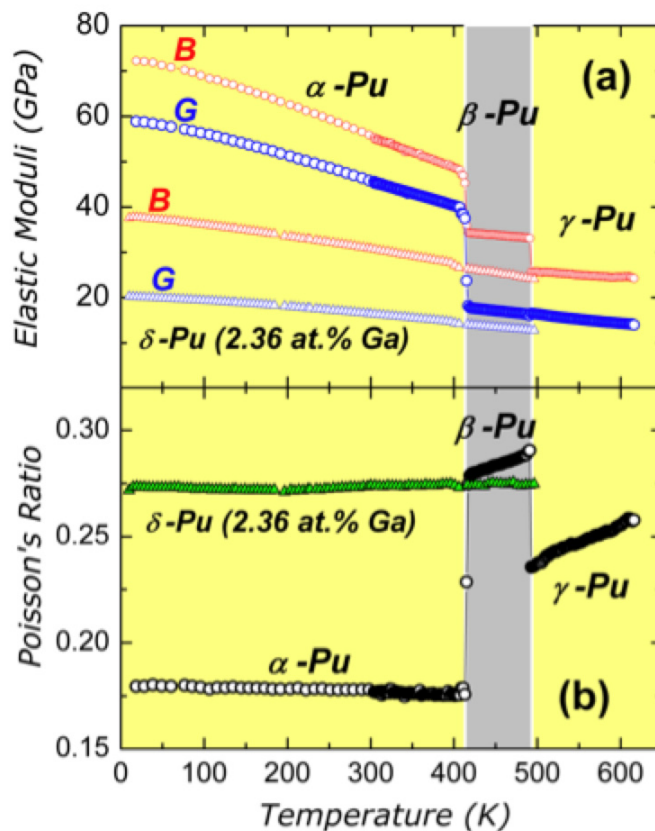
Figure 1. Temperature dependence of the bulk and shear moduli for pure plutonium and 2.36% gallium stabilized delta plutonium.

Peroxide Enhanced Partitioning of Spent Nuclear Fuel in Alkaline Solutions

A separations approach based on the different speciation and solubilities of U, fission products (FPs) and actinides in oxidative alkaline solutions would provide a revolutionary alternative to the PUREX-type processes. Our approach processes spent nuclear fuel (SNF) in alkaline media utilizing peroxide (H_2O_2) to enhance the dissolution of the uranium oxide matrix of spent nuclear fuel (SNF) and provide novel routes for selectively partitioning the actinides and FPs. Results include the determination of several important aspects of the chemistry.

Synthetic Routes to Pentavalent Uranium Organometallic Complexes

Alkyl-, alkenyl-, aryl-, alkynyl-gold(I) complexes are easily derivatized, and are safe to handle. We showed that phosphane-gold(I) complexes are excellent reagents for the oxidative functionalization of uranium, demonstrating a new class of reaction for gold. Heavy chalcogen (Se/Te) soft donor ligands have traditionally been exploited to investigate trivalent actinide/lanthanide separation technologies and to address questions regarding covalency in hard-soft interactions. Indeed, oxidation of $(C_5Me_5)_2U(=N-2,6-^iPr_2-C_6H_3)$ (THF) with PhE-EPh yields corresponding U^V-chalcogenate complexes). This work resulted in an invited review on the synthesis and characterization of pentavalent uranium complexes.

Transformation pathways and energetics in multiphase materials: Pu as a prototype

The mechanism for phase transformation between the fcc delta phase and the monoclinic phase of plutonium is an outstanding problem. This task searched for the subgroups that are common to both fcc and monoclinic symmetry and their energies using density functional theory (DFT) and (LDA) and modified embedded atom methods (MEAM). The effects of defects on mechanical, electrical and magnetic properties were explored via Landau theory that incorporates Kröner's continuum theory of dislocations. We found that the inability of MEAM to capture simultaneously the internal degrees of freedom in a low-symmetry a phase and its energetics makes the current parametrization of this potential unsuitable for our further studies.

Synthesis and Characterization of Novel Uranium IV, V, and VI Imido Complexes

Imido complexes of the actinide elements continue to generate great interest. Our niche has been the exploration of uranium imido chemistry. We discovered a conproportionation reaction between a bis-imido uranium (V) dimer, $[U(N^tBu)_2I(^tBu_2bipy)]_2$, and $UI_3(THF)_4$.

Spectroscopic tests of actinide theories

Cutting-edge spectroscopic techniques were employed to address limitations in theories of actinide (An) electronic structure. Preliminary findings suggest that trends in covalency are more complex than often assumed (three complete manuscripts and several more that are in preparation).

Theoretical modeling of fission product behavior in oxide nuclear fuels

Fission products that are formed during the burning of the nuclear fuel strongly influence the in-core performance and the long-term storage of the fuel. Understanding these interactions would lead to the development of advanced fuel forms. This work has focused on the two critical components that affect fuel performance – microstructure (Figure 2) and composition – and how fission products interact with them. We have discovered that electrostatic dipoles can be created. These results may lead to new possibilities for engineering nanostructured ceramics.
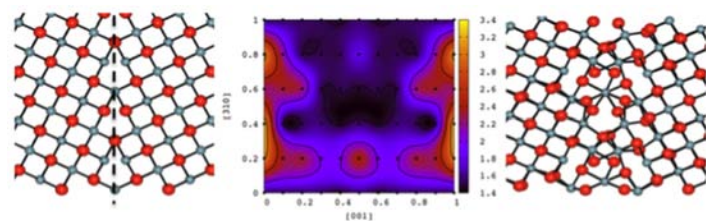
Figure 2. Structure of the S5 tilt boundary in UO2: (a) idealized (b) g-surface plot and (c) translated and relaxed. The relaxed structure exhibits an electric field strong enough to influence thermal and mass transport properties.

U and Th complexes as catalysts for hydrodenitrogenation and hydrodesulfurization

Homogenous U and Th complexes can be used as catalysts for hydrodenitrogenation (HDN) and hydrodesulfurization (HDS), which entail removal of nitrogen and sulfur impurities, respectively, from crude oil contaminants. Computational methods were used to find U complexes more reactive than Th as HDN/HDS catalysts and that a Th complex catalyzes a novel thiophene ring opening/dimerization reaction. We have computed a mechanism for this reaction and are currently studying the electronic structure of the product.

Mechanisms and applications of natural [238]U/[235]U fractionation

[238]U/[235]U ratios vary by ~1.5‰ (deviations per 1000) across near-surface (low temperature) environments. Theory suggests that this is a result of differences in the ability of individual uranium nuclei to undergo reduction. The difficulty reproducing this fractionation in the laboratory necessitates examination of modern variability in natural settings to resolve fractionation mechanisms. Water samples strongly support the assertion that this fractionation is

controlled by redox conditions.

Bis(imido) Uranium(V)/(VI) Complexes

This effort is focused on exploring reactivity, structure, and bonding to develop a more complete understanding of high oxidation state actinide science. We found striking differences in reactivity in $[U(NR)_2]^{2+}$ complexes. For uranium(VI) chalcogenate chemistry (chalcogenate = O, S, Se, Te donors), we found that the coordination of "soft" donor ligands such as thiolates, selenolates, and tellurolates can be achieved with the $[U(NR)_2]^{2+}$ ion. Our studies extended to organoactinide complexes and their catalytic potential. We also found that the a dimeric uranium(V) bis(imido) complex could be synthesized by the addition of 2 equiv of $Na(C_5Me_5)$ to $U(N^tBu)_2(I)_2(bpy^{bu})$ (bpy^{bu} = 4,4'-di-tert-butyl-2,2'-bipyridyl) [7]. This discovery represents an important finding that demonstrates f-electron communication between actinide metal centers.

Modeling uranium hydriding

To improve the modeling of uranium-hydrogen interactions a new interatomic potential has been developed to accurately capture the properties of uranium and uranium-hydrogen interactions. Five manuscripts have been prepared and published on these and related topics, as well as four talks, including an invited presentation at the Gordon Research Conference in Aqueous Corrosion.

Growth and measurements of new intermetallic compounds

This task succeeded in growing many novel samples. Details for each compound have been published. Ultimately, we examined several new structures to better understand structure/property relationships. The discovery of new intermetallic compounds required techniques and capabilities developments as well including a unique capability for the purification of these large single crystals through electro-refinement.

Neutral and tricationic lanthanide complexes

We prepared several neutral and tricationic lanthanide complexes, which have been characterized using a suite of spectroscopic techniques. The successful application of these new ligand frameworks to lanthanide coordination chemistry has resulted in exploration of the ability of these complexes to catalyze organic transformations.

Geometrical Hall effect in UCu$_5$ and current results for UAuPt$_4$

Geometric magnetic frustration occurs when localized magnetic moments (spins) can not satisfy all of their nearest neighbor magnetic interactions. We have found that a large geometrical Hall effect occurs in UCu$_5$ below $T = 1$ K, and developed a theoretical treatment for it.

Development of cerium(III)halide nanoparticles for gamma-ray detection

This task involved fabrication of CeBr$_3$-containing materials for application as novel gamma-ray detecting species via single crystalline CeBr$_3$. We achieved an order of magnitude yield increase. Further extension of the use of the ionic liquid to CeBr$_3$(THF)$_4$ has resulted in access to the hitherto unknown polydentate oxygen donor solvates.

Comparison of the structures, electronic and optical properties of actinide dioxides

A systematic comparison of the lattice structures, electronic and optical properties of actinide dioxides, AnO$_2$ (An=U, Np and Pu), predicted by density functional theory + U (DFT+U) and the Heyd-Scuseria-Ernzerhof screened hybrid density functional (HSE06) found that the lattice constant, partial density of states, f-band dispersion and associated covalency, are all in significant error when compared to experiment (Figure 3). The current work provides important information to benchmark next-generation theory.
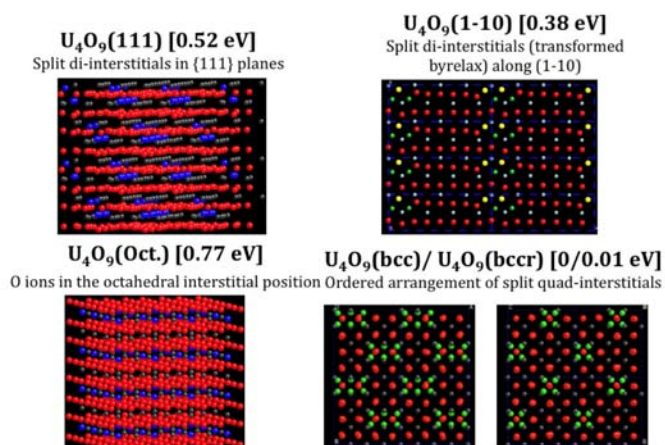
Figure 3. Ordering and relative stability of different U$_4$O$_9$ compounds.

Actinide based f-electron systems

The f-electron compounds of plutonium, uranium, and cerium exhibit critical phenomena with changes in temperature, pressure and magnetic field [9-11]. URu$_2$Si$_2$ (Ru: Ruthenium and Si: Silicon) has a transition at 17.5 K [8] whose origin is "hidden" [8]. This task supplied important clues to this long-standing mystery by mapping out the Fermi [12] surface using world-record 45T magnetic fields at the National High Magnetic Field Laboratory. In another actinide material, PuCoGa$_5$ a superconductor below 18.5K [13], the careful mapping of the upper critical field at the National High Magnetic Field Laboratory will lead to a better understanding of the superconducting mechanism.

Impact on National Missions
This project is strongly related to the broader mission of the Seaborg Institute, advancing actinide chemistry,

actinide materials science, and actinide simulation and modeling to position LANL for excellence in an area that is crucial to the missions of energy security, stockpile stewardship, and nuclear safeguards and forensics. This work has also supported the LANL Institutional Plutonium Science and Research Strategy implementation plan. Seven postdocs from this project became LANL staff, one became a Director's fellow, and six were hired into academia during the three years of this LDRD-DR project.

References

1. Beaux, M. F., T. Durakiewicz, L. Moreschini, M. Grioni, F. Offi, G. Monaco, G. Panaccione, J. J. Joyce, E. D. Bauer, J. L. Sarrao, M. T. Butterfield, and E. Guziewicz. Electronic structure of single crystal UPd3, UGe2, and USb2 from hard X-ray and angle-resolved photoelectron spectroscopy . To appear in *Journal of Electron Spectroscopy and Related Phenomena.*

2. Chantis, A. N., R. C. Albers, M. D. Jones, M. van Schilfgaarde, and T. Kotani. Many-body electronic structure for metallic uranium. 2008. *Physical Review B.* **78**: 081101.

3. Chantis, A. N., R. C. Albers, A. Svane, and N. E. Christensen. GW correlation effects on plutonium quasiparticle energies: changes in crystal-field splitting. 2009. *Philosophical Magazine.* **89**: 1801.

4. Migliori, A., C. Pantea, H. Ledbetter, I. Stroe, J. B. Betts, J. N. Mitchell, M. Ramos, F. Freibert, D. Dooley, S. Harrington, and C. H. Mielke. Alpha-plutonium's polycrystalline elastic moduli over its full temperature range . 2007. *Journal of the Acoustical Society of America.* **122** (4): 1994.

5. Stroe, I., J. B. Betts, A. Trugman, C. H. Mielke, J. N. Mitchell, M. Ramos, F. J. Freibert, H. Ledbetter, and A. Migliori. Polycrystalline gamma-plutonium's elastic moduli versus temperature . 2010. *Journal of the Acoustical Society of America.* **127** (2): 741.

6. Soderlind, P., A. Landa, J. E. Klepeis, Y. Suzuki, and A. Migliori. Elastic properties of Pu metal and Pu-Ga alloys . 2010. *Physical Review B.* **81** (22): 224110.

7. Spencer, L., P. Yang, R. Gdula, B. Scott, J. Thompson, E. Batista, and J. Boncella. Cation-Cation interactions, magnetic communication, and reactivity of the pentavalent uranium ion [U(NtBu2] +. 2009. *Angewandte Chemie - Internation Edition.* **48** (21): 3795.

8. Kim, K. H., N. Harrison, M. Jaime, G. S. Boebinger, and J. A. Mydosh. Magnetic-field-induced quantum critical point and competing order parameters in URu2Si2. 2003. *Physical Review Letters.* **91** (25): 256401.

9. Fisk, Z., D. W. Hess, C. J. Pethick, D. Pines, J. L. Smith, J. D. Thompson, and J. O. Willis. Heavy-electron metals: New highly correlated states of matter. 1988. *Science.* **239** (4835): 33.

10. Lander, G. H., E. S. Fisher, and S. D. Bader. The solid-state properties of uranium: a historical perspective and review . 1994. *Advances in Physics.* **43** (1): 1.

11. Soderlind, P.. Ambient pressure phase diagram of plutonium: A unified theory for alpha-Pu and delta-Pu. 2001. *Europhysics Letters.* **55** (4): 525.

12. Jo, Y. J., L. Balicas, C. Capan, K. Behnia, P. Lejay, J. Flouquet, J. A. Mydosh, and P. Schlottmann. Field-induced fermi surface reconstruction and adiabatic continuity between antiferromagnetism and the hidden-order state in URu2Si2. 2007. *Physical Review Letters.* **98**: 166404.

13. Curro, N. J., T. Caldwell, E. D. Bauer, L. A. Morales, M. J. Graf, Y. Bang, A. V. Balatsky, J. D. Thompson, and J. L. Sarrao. Unconventional superconductivity in PuCoGa5. 200. *Nature.* **434**: 622.

Publications

Andersson, D. A., J. Lezama, B. P. Uberuaga, C. Deo, and S. D. Conradson. Cooperativity among defect sites in AO2+x and A4O9 (A=U,Np,Pu): Density functional calculations. 2009. *Physical Review B.* **79**: 024110.

Andersson, D. A., J. Lezama, B. P. Uberuaga, and S. D. Conradson. Electronic origin of co-operativity among defect sites in AnO2+x (An = U, Np or Pu). 2009. *Physical Review B.* **79**: 024110.

Andersson, D. A., L. Casillas, M. I. Baskes, J. S. Lezama, and S. D. Conradson. Modeling of the phase evolution in Mg1-x AlxB2 (0 < x < 0.5) and its experimentalsignatures. 2009. *The Journal of Physical Chemistry B.* **113**: 11965.

Andersson, D. A., T. W. Watanabe, C. Deo, and B. P. Uberuaga. Role of di-interstitial clusters in oxygen transport in UO2+x from first principles. 2009. *Physical Review B.* **80**: 060101.

Bauer, E. D., P. H. Tobash, J. N. Mitchell, J. A. Kennison, F. Ronning, B. L. Scott, and J. D. Thompson. Magnetic order in Pu2Ni3Si5. To appear in *Condensed Matter Physics Conference Proceedings.*

Bauer, E. D., P. H. Tobash, J. N. Mitchell, J. A. Kennison, J. J. Joyce, T. Durakiewicz, B. L. Scott, J. L. Sarrao, L. A. Morales, and J. D. Thompson. Complex magnetic order in PuSb2 single crystals. 10. In *Plutonium Futures - The Science 2010.* (Keystone, 19-23 Sept 2010). , p. 315. Illinois: American Nuclear Society.

Berg, J., A. L. Costello, A. J. Gaunt, I. May, S. D. Reilly, B. L. Scott, and M. P. Wilkerson. Neptunyl(VI) interac-

tion with A-type tri-lacunary heteropolyoxotungstate anions – distinctive spectroscopic features and subtle structural variations. *Inorganic Chemistry.*

Chantis, A. N., R. C. Albers, A. Svane, and N. E. Christensen. GW correlation effects on plutonium quasiparticle energies: changes in crystal-field splitting. 2009. *Philosophical Magazine.* **89**: 1801.

Daly, S. R., K. S. Boland, J. R. Klaehn, S. A. Kozimor, D. R. Peterman, and B. L. Scott. NMR spectroscopy and structural characterization of dithiophosphinates relevant to minor actinide extraction processes. *Dalton Transactions.*

Graves, C. R., and J. L. Kiplinger. Pentavalent uranium chemistry - synthetic pursuit of a rare oxidation state. 2009. *Chemical Communications.* **26**: 3831.

Graves, C., B. Scott, D. Morris, and J. Kiplinger. Selenate and tellurate complexes of pentavalent uranium. 2009. *Chemical Communications.* **2009**: 776.

Groger, R., T. Lookman, and A. Saxena. Atomistic studies of transformation pathways and energetics in plutonium. 2009. *Philosophical Magazine.* **89**: 1779.

Jilek, R. E., L. P. Spencer, D. L. Kuiper, B. L. Scott, U. J. Williams, J. M. Kikkawa, E. J. Shelter, and J. M. Boncella. A general and modular synthesis of monoimido uranium(IV) dihalides. *Journal of the American Chemical Society.*

Kraft, S. J., U. J. Williams, S. R. Daly, E. Schelter, S. A. Kozimor, K. S. Boland, J. M. Kikkawa, W. P. Forrest, C. N. Christensen, D. E. Schwarz, P. E. Fanwick, D. L. Clark, S. D. Conradson, and S. C. Bart. The synthesis, characterization, and multi-electron reduction chemistry of uranium supported by redox-active α-diimine ligands. 2011. *Inorganic Chemistry.* **epub** (7/15/11): 1.

Nerikar, P. V., K. Rudman, T. G. Desai, D. Byler, C. Unal, K. J. McClellan, S. R. Phillpot, S. B. Sinnot, P. Peralta, B. P. Uberuaga, and C. R. Stanek. Intrinsic electrostatic effects in nanostructured ceramics. 2010. *Physical Review B.* **81**: 064111.

Nerikar, P. V., K. Rudman, T. G. Desai, D. Byler, C. Unal, K. J. McClellan, S. R. Phillpot, S. B. Sinnott, P. Peralta, B. P. Uberuaga, and C. R. Stanek. Grain boundaries in uranium dioxide: scanning electron microscopy experiments and atomistic simulations. 2011. *Journal of the American Ceramic Society.* **94** (6): 1893.

Placzek, C. J., J. Quade, and P. J. Patchett. Isotopic tracers of paleohydrologic change in large lakes of the Bolivian Altiplano . 2011. *Quaternary Research.* **75** (1): 231.

Schelter, E. J., R. Wu, J. M. Veauthier, E. D. Bauer, C. H. Booth, R. K. Thompson, C. R. Graves, K. D. John, B. L.

Scott, J. D. Thompson, D. E. Morris, and J. L. Kiplinger. Comparative study of f-element electronic structure across a series of multimetallic actinide and lanthanoid-actinide complexes possessing redox-active bridging ligands. 2010. *Inorganic Chemistry.* **49** (4): 1995.

Soderlind, P., A. Landa, J. E. Klepeis, Y. Suzuki, and A. Migliori. Elastic properties of Pu metal and Pu-Ga alloys . 2010. *Physical Review B.* **81** (22): 224110.

Spencer, L. P., P. Yang, B. L. Scott, E. R. Batista, and J. M. Boncella. Uranium(VI) bis(imido) disulfonamide and dihalide complexes: Synthesis density functional theory analysis . 2010. *Comptes Rendus Chimie.* **13** (6-7): 758.

Spencer, L. P., S. A. Kozimor, P. Yang, R. E. Jilek, T. W. Hayton, R. L. Gdula, B. L. Scott, E. R. Batista, and J. M. Boncella. Tetrahalide complexes of the [U(NR)2]2+ ion: sythesis, theoretical, and Cl K-edge x-ray absorption spectroscopic analysis. *Journal of the American Chemical Society.*

Spencer, L., B. L. Scott, E. Batista, and J. Boncella. Oxidative addition to U(V)-U(V) dimers: facile routes to uranium(VI) bis(imido) complexes. 2009. *Inorganic Chemistry.* **48** (24): 11615.

Spencer, L., B. Scott, E. Batista, and J. Boncella. Uranium(VI) bis(imido) chalcogenate complexes: synthesis and density functional theory analysis . 2009. *Inorganic Chemistry.* **48** (6): 2693.

Spencer, L., P. Yang, R. Gdula, B. Scott, J. Thompson, E. Batista, and J. Boncella. Cation-Cation interactions, magnetic communication, and reactivity of the pentavalent uranium ion [U(NtBu2) +. 2009. *Angewandte Chemie - Internation Edition.* **48** (21): 3795.

Stroe, I., J. Betts, A. Trugman, C. H. Mielke, J. N. Mitchell, M. Ramos, A. Migliori, and H. Ledbetter. Polycrystalline gamma-plutonium's elastic moduli versus temperature. 2010. *Journal of the Acoustical Society of America.* **127**: 741.

Suzuki, Y., V. F. Betts, F. J. Freibert, C. H. Mielke, J. N. Mitchell, M. R. Mitchell, T. A. Saleh, and A. Migliori. Temperature dependence of elastic moduli of polycrystalline beta-plutonium. 2011. *Physical Review B.* **84** (6): 064105.

Swartz, D. L., L. P. Spencer, B. L. Scott, A. L. Odom, and J. M. Boncella. Exploring the coordination modes of pyrrolyl ligands in bis(imido) uranium(VI) complexes . 2010. *Dalton Transactions.* **39** (29): 6841.

Taylor, C. D.. Periodic trends governing the interactions between impurity atoms [H-Ar] and α-U. 2009. *Philosophical Magazine.* **89**: 465.

Taylor, C. D.. Connections between the energy functional

and interaction potentials for materials simulations. 2009. *Physical Review B.* **80**: 24104.

Taylor, C. D., T. Lookman, and R. S. Lillard. Ab initio calculations of the uranium-hydrogen system: Thermodynamics, hydrogen saturation of α-U and phase-transformation to UH$_3$. 200. *Acta Materialia.* **58** (3): 1045.

Taylor, C. D., and R. S. Lillard. Ab-initio calculations of the hydrogen-uranium system: Surface phenomena, absorption, transport and trapping. 2009. *Acta Materialia.* **57** (16): 4707.

Thompson, R. K.. Noble reactions for the actinides: safe gold-based access to organouranium and azido complexes. 2009. *European Journal Inorganic Chemistry.* **11**: 1451.

Thomson, R. K. G., C. R. Graves, B. L. Scott, and J. L. Kiplinger. Synthesis and molecular structure of (C5Me5)2U(OtBu)(SePh): a mixed-ligand selenide-alkoxide Uranium(IV) metallocene complex resulting from tert-butoxy-trimethylsilane elimination. 2011. *Journal of Chemical Crystallography.* **41** (8): 1241.

Thomson, R. K. G., R. Christopher, B. L. Scott, and J. L. Kiplinger. Uncovering alternate reaction pathways to access uranium(IV) mixed-ligand aryloxide–chloride and alkoxide–chloride metallocene complexes: Synthesis and molecular structures of (C5Me5)2U(O-2,6-iPr2C6H3)(Cl) and (C5Me5)2U(O–tBu)(Cl). 2011. *Inorganica Chimica Acta.* **369** (1): 270.

Thomson, R. K., B. L. Scott, D. E. Morris, and J. L. Kiplinger. Synthesis, structure, spectroscopy and redox energetics of a series of uranium(IV) mixed-ligand metallocene complexes. 2010. *Comptes Rendus Chimie.* **13** (6-7): 790.

Thomson, R. K., T. Cantat, B. L. Scott, D. E. Morris, E. R. Batista, and J. L. Kiplinger. Uranium azide photolysis results in C-H bond activation and provides evidence for a terminal uranium nitride. 2010. *Nature Chemistry.* **2** (9): 723.

Thomson, R., C. Graves, B. Scott, and J. Kiplinger. Organometallic uranium(IV) fluoride complexes: Preparation using protonolysis chemistry and reactivity with trimethylsilyl reagents. 2010. *Dalton Transactions.* **39** (29): 6826.

Tobash, P. H., E. D. Bauer, F. Ronning, J. N. Mitchell, J. A. Kennison, B. L. Scott, and J. D. Thompson. Physical properties of the new intermetallic compound Pu-2Ni3Si5". 20. In *Plutonium Futures - The Science 2010.* (Keystone, CO, 9- Sept 2010). , p. 317. LaGrange Park, IL: American Nuclear Society.

Tobash, P. H., F. Ronning, J. D. Thompson, S. Bobev, and E. D. Bauer. Magnetic order and heavy fermion behavior in CePd1+xAl6-x: synthesis, structure, and physical properties. 2010. *Journal of Solid State Chemistry.* **183** (3): 707.

Tobash, P. H., V. A. Sidorov, F. Ronning, K. Gofryk, J. D. Thompson, R. C. Albers, J. -X. Zhu, M. D. Jones, and E. D. Bauer. Heavy fermion behavior in the new antiferromagnetic compound UIr4Al15. 2010. *Journal of Physics Conference Series.* **273**: 012061.

Vasudevan, K. V., N. A. Smith, B. L. Scott, E. A. McKigney, J. C. Gordon, and R. E. Muenchausen. An ionic liquid-mediated route to cerium(III) bromide solvates. 2011. *Inorganic Chemistry.* **50**: 4627.

Vasudevan, K. V., N. A. Smith, M. W. Blair, B. L. Scott, E. A. McKigney, and J. C. Gordon. Facile routes to novel cerium(III) bromide solvates. To appear in *Inorganic Chemistry.*

Wen, X. D., S. P. Rudin, E. R. Batista, G. E. Scuseria, and R. L. Martin. First-principles comparison of PBE+U and HSE06 predictions for the electronic, optical properties of the actinide dioxides UO2, NpO2 and PuO2. *Journal of Chemical Physics.*

Wen, X. D., S. P. Rudin, E. R. Batista, G. E. Scuseria, and R. L. Martin. Hybrid DFT and DFT+U studies of the electronic, optical properties of U3O8. *Journal of Physical Chemistry C.*

Accelerating Materials Certification

John L. Sarrao
20110734DR

Abstract

The goal of this six-month project was to make specific near-term progress against the grand challenge goal of "materials by design." We initiated a series of four thrusts, each of which is compelling in its own right; however, taken together, the whole is greater than the sum of its parts. We pursued i) the co-design of micro-mechanical models to improve the predictive capability of engineering analyses into the regimes of high-pressures and strain rates, ii) utilization of ion beam irradiation as a means of accelerating materials damage with the goal of realizing improved certification models of relevance to nuclear energy, iii) ultrafast in-situ, transient measurement approaches to separate coupled degrees of freedom essential to predicting materials functionality, and iv) synthesis strategies for tailoring materials properties based on near-real-time diagnostic feedback. While a comprehensive strategy to accelerating materials certification likely includes simultaneous in situ measurements (iii) in relevant environments (ii) yielding directed synthesis (iv) through theory (i), progress was made by pursuing thrusts i) – iv) in parallel in a single overarching project in which the project leadership's principal responsibility was fostering integration and collaboration among these thrusts.

Background and Research Objectives

This project was a focused attempt to accelerate progress towards realizing the decadal vision shared by LANL's materials strategy - "controlled functionality" - and the Laboratory's vision for MaRIE - "revolutionizing materials in extremes through a focus on the micron frontier." A number of community workshops, including some led by LANL, have concluded that multiple simultaneous in situ measurements on real materials (i.e., those with microstructures and defects) in relevant environments coupled to directed synthesis through theory is a key strategy for realizing this vision. It is also clear that full success in realizing this vision is a decadal (or beyond) challenge requiring experimental and theoretical capabilities not yet available. In the near term we believe a more segmented, staged approach is required for partial success.

Specifically, in this project our approach was based on a series of smaller thrusts and integration among these teams, exploiting technical synergies among them. We believe that these small steps yielded tangible benefits in the near term and laid the foundation for greater progress in the longer term.

Scientific Approach and Accomplishments

Thrust I

Microstructure can have a significant impact on the mechanical response of metallic polycrystalline materials directly affecting performance. The microstructure of the material evolves with deformation history. Predictive models that capture the salient physics of the evolution of microstructure are lacking. This is especially true for dynamic loading conditions and phenomena, which are driven by the extremes in the statistically distributed response of the material. The objective of this thrust was to develop the theoretical capability required to quantitatively understand the relevant phenomena that are inherent to the shock loading of materials. The specific focus of our effort was a study of the alpha-omega transition in zirconium. A multi-disciplinary, multi-scale approach for improving the predictive capability of modeling phase transformations under the conditions of shock loading was developed. The coupled elements of theory, experiment, coarse graining, and statistical analysis were included in this investigation, and future experiments to provide new insights into our understanding of retained phases in zirconium were defined.

Thrust II

The focus here was on exploiting ion beam irradiation as an accelerated source of radiation damage to provide key insights to multi-scale modeling, with a focus on microstructure-scale phenomena. We established a capability for simultaneous irradiation and corrosion environments at the Ion Beam Materials Laboratory (IBML) at LANL. The capability enables testing the combined effect of radiation, high temperature, and corrosive media on samples of solid metal in a chemically controlled envi-

ronment. We also partially established a dual-ion beam irradiation capability, including simulations of the calculated depth profile of displacement damage and He deposition in specimens under test (5 MeV Fe ion, 150 KeV He, using the TRIM code). A 100 keV H+ beam was used to test the beam transport efficiency from Varian chamber into the dual-beam chamber. 200 uA beam on sapphire target was achieved (70% efficiency) and the scanned beam produced a 20 mm diameter uniform blue circle as expected.

Thrust III

In this thrust, two small scale capability development projects were undertaken. The first focused on x-ray approaches to separate coupled degrees of freedom essential to predicting materials functionality in complex materials, and the second aimed at fostering collaborative experiments that leverages the Linac Coherent Light Source (LCLS) XFEL facilities for development of diagnostic techniques utilizing ultrafast coherent ultrafast x-rays for probes of transient states. For the first effort, we developed an ultrafast time-resolved soft x-ray dichroism spectroscopic station for measuring magnetic ordering in complex correlated electron materials (CEM). A plasma spectroscopy experiment was chosen for the LCLS XFEL experiment. We participated in an experiment in the soft x-ray hutch of the LCLS, in which non-local thermal equilibrium plasma kinetics were investigated by selectively pumping specific electronic transitions in an optical laser generated plasma.

Thrust IV

This thrust proposed and explored a new step in reducing the effort in finding stable compounds with desired functionality. Researchers aiming to synthesize new materials often rely on a homologous conjecture (HC): more often than not, chemically similar materials show similar physical properties. This HC has led to many discoveries and serves as the foundation of attempts at moving from a fortuitous approach to a predictive strategy for materials discovery. Modern density functional theory (DFT) methods allow the computational exploration of an array of chemically similar materials to probe them for desired physical properties. This allows a rapid down-selection of candidates suggested by the HC, so synthesis can be attempted on a smaller number of systems. Especially for materials with costly synthesis, this reduction in plausible systems lessens the cost significantly. Rather than requiring a reasonably complete description of every phase diagram in which the sought-after compounds sit, the idea is to computationally explore a small array of structures --- stable, metastable, and unstable --- at the exact stoichiometry of the desired compound in the array of chemistries. The down-selection then relies on correlations extracted from the many-dimensional space of chemistries, structures, calculated properties, and measured properties of previously-known compounds.

Each of the project's thrusts made significant progress in accomplishing its goals given the limited six-month execution period. Further, collaborative bridges were built between and among each thrust enabling significant strides towards the ultimate grand challenge goal of simultaneous in situ measurements (iii) in relevant environments (ii) yielding directed synthesis (iv) through theory (i).

Impact on National Missions

The need to predict and control materials in extremes spans the full range of DOE missions from weapons performance to energy security. Further, successful nuclear weapons program approaches to certification of materials performance (and the associated quantification of performance margins and uncertainty) have not e.g., been translated to nuclear energy materials certification challenges. In this project, we made important strides to both address specific process-aware materials performance challenges in our enduring nuclear weapons stockpile (e.g., zirconium phase transition studies) and work to develop a paradigm for accelerated materials certification for fusion energy (e.g., accelerated radiation damage with ion beams). Finally, BES mission drivers in the area of materials by design were advanced by our exploration of advanced ultrafast spectroscopies and innovative theoretical approaches for materials design.

Publications

Niezgoda, S., Y. Yabansu, and S. Kalidindi. Understanding and visualizing microstructure and microstructure variance as a stochastic process. 2011. *Acta Materialia.* **59** (16): 6387.

Earth Tremor, Time Reversal and Earthquake Forecasting

Paul A. Johnson
20100141ER

Introduction

Along tectonic plate boundaries, two plates move relative to each other. Under circumstances not well understood, portions of the plates become locked due to friction. As a result, the locked portions accumulate stress while the surrounding rock continues to deform. When the locked region reaches a critical state and releases catastrophically, an earthquake occurs. It is this scenario that has produced the largest and most devastating earthquakes in history, and the details of which we must ultimately understand if earthquake forecasting is to become a reality. A recent phenomena has been discovered that could have a profound impact on forecasting large earthquakes: an Earth rumbling called non-volcanic tremor comprised of long seismic signals with no discrete beginning or end. Tremor has been observed in an increasing number of active tectonic environments, including subduction zones and transform faults such as the San Andreas. Tremor, if it is located on the plate interface, may be the manifestation of slip on a series of faults, that may organize and accelerate before reaching a critical size where the system destabilizes catastrophically and an earthquake occurs. However, we cannot be certain tremor originates at the plate interface because tremor cannot be located applying classical seismic means. A number of tremor location schemes are in development that are based on unproven assumptions; the tremor locations resulting from these procedures are literally all over the map. Until tremor is definitely located, we have no hope of taking the next step and testing it as an earthquake precursor. We know how to locate tremor using our unique expertise in seismology and time reversal. That is the goal of our work.

Benefit to National Security Missions

In addition to impacting the national security by enabling earthquake prediction, there are numerous other problems of interest to DOE where location of long-duration sources would have direct application, such as locating underground structures that broadcast long duration signals from machinery located within. Other pertinent problems include locating moving vehicles (aircraft, ships, submarines), as well as swimmers. The techniques we develop for large natural structures can be, and have been, applied to testing components important to the weapons program.

Progress

We have made much progress on our project as evidenced by our publications. We have published three papers on this topic in the past year, one a selected for the first issue of *Parity*, the new Japanese journal published by *Physics Today*. We also have one manuscript in review and two manuscripts in preparation. Our modeling work has focused on locating tremor in California, triggered by the August, 2009 Mexicali earthquake several hundred km south of the tremor location. We have for the first time successfully located tremor and a manuscript is in preparation. This is a major milestone. The problem has been difficult because time reversal requires a very good numerical velocity model of Earth and high quality seismic stations close to the region of tremor. We did not appreciate how important these issues were when we began our work. The tremor is located in the deep crust at 22 km. This is the region of plastic behavior, well below where earthquakes occur. The results are in line with other location methods that are in development. We have also conducted a number of laboratory experiments exploring tremor in support of the seismic field studies, and an outcome of that are two papers on application of time reversal to laboratory samples. A paper is also in review that describes the association of tremor and slow slip in the laboratory. This is another major milestone because it demonstrates that tremor is associated with slip on faults. Our model results suggest the same result, and a paper describing this was just published in the journal European Physics Letters. Our collaborators include individuals at ETH in Zurich, UC Santa Cruz, Pennsylvania State University and the USGS.

Future Work

Our approach will be comprised of: (a) laboratory experiments, (b) modeling of synthetic tremor, leading to (c) location of actual tremor, described as follows.

Laboratory studies. Since tremor frequently appears to move rapidly spatially-temporally, we will conduct laboratory studies of moving sources to gain insight into the Earth problem under controlled conditions. This will be followed by experiments of a moving tremor source, since in the Earth, tremor appears to move in time and space in some cases. In this manner we will (a) study the limits of resolution of the time windows vs. frequencies and velocities of the lab sample; (b) scale them to Earth; and (c) uncover unforeseen problems. These experiments will guide the numerical and Earth tremor studies.

Model studies. We will proceed by identifying the best candidate region for TR location of tremor. Clearly, we require previous observation of tremor. Key ingredients to success are (1), a high density of seismic stations and (2), a high quality velocity model for back-propagation. Top candidates are Japan and Cascadia because both regions exhibit tremor and these are two of the best-instrumented regions in the world, with highly developed velocity models. We cannot overstate the importance of high instrument density (the N2 dependence) and the velocity model, based on our previous studies.

Tremor location in Earth. At this point we will locate real tremor, having developed all of the necessary tools as described above. We will select actual seismic data, window it appropriately, and backpropagate it in the appropriate velocity model.

Conclusion

At the end of three years we will have definitively answered the question of where tremor originates in the San Andreas Fault—whether it is from the deep crust or mid crust in transform faults. By doing so, we will resolve whether or not tremor can be tested in the framework of a new earthquake forecasting tool. We will create a new goal at LANL in locating noisy underground structures, swimmers/divers with nefarious intent, location of moving vehicles, and aircraft, all difficult problems at present for the same reason as tremor: no discrete wave arrivals.

References

1. Anderson, B., M. Griffa, P. L. Bas, T. Ulrich, and P. Johnson. Experimental implementation of reverse time migration for nondestructive evaluation applications. 2011. *Journal of the Acoustical Society of America.* **129** (1): EL8.

2. Bas, P. Le, T. J. Ulrich, R. A. Guyer, and P. A. Johnson. Time reversal reconstruction of finite sized sources in elastic media. 2011. *Journal of the Acoustical Society of America Express Letters .* **130**: 219.

3. Griffa, M., E. Daub, R. Guyer, P. Johnson, C. Marone, and J. Carmeliet. Vibration-induced unjamming of sheared granular layers and the micromechanics of dynamic earthquake triggering. 2011. *European Physical Review Letters.* **96**: 14001.

4. Larmat, C., R. A. Guyer, and P. A. Johnson. Time reversal in Seismology. 2011. *Parity.* **63**: 19.

Publications

Anderson, B., M. Griffa, T. J. Ulrich, and P. A. Johnson. Time reversal reconstruction of finite sized sources in elastic media. 2011. *Journal of the Acoustical Society of America Express Letters.* **130**: 219.

Anderson, B., M. Griffa, T. J. Ulrich, and P. A. Johnson. Time reversal reconstruction of finite sized sources in elastic media. 2011. *Journal of the Acoustical Society of America Express Letters.* **130**: 219.

Bas, P. Y. Le, T. J. Ulrich, R. A. Guyer, and P. A. Johnson. Probing the interior of a solid volume with time reversal and nonlinear elastic wave spectroscopy,. 2011. *Journal of the Acoustical Society of America Express Letters.* **130**: 2263.

Griffa, M., E. Daub, R. A. Guyer, and P. A. Johnsn. Vibration-induced unjamming of sheared granular layers and the micromechanics of dynamic earthquake triggering. 2011. *European Physics Letters.* **96**: 1401405.

Larmat, C., R. Guyer, and P. A. Johnson. Tremor source location using Time Reversal: selecting the appropriate imaging field. 2009. *GEOPHYSICAL RESEARCH LETTERS.* **36**: L22304.

Larmat, C., R. Guyer, and P. Johnson. Time-reversal methods in geophysics. 2010. *PHYSICS TODAY.* **63** (8): 31.

Larmat, C., and R. Guyer. Time reversal in Seismology. 2011. *Parity.* **63**: 19.

New Generation "Giant" Nanocrystal Quantum Dots for   Transformational Breakthrough in Solid State Lighting

Han Htoon
20100144ER

Introduction

Since their initial discovery, nanocrystal quantum dots (NQDs) have been considered as a key candidate material for solid state lighting (SSL) because they not only exhibit robust optical characteristics ideally suited for the SSL application but also can be synthesized and processed into LED devices in very cost efficient ways. However, NQD-based Light Emitting Diodes (NQD LEDs) reported to date suffer from low efficiency (external quantum efficiency, EQE < 2%) and short device lifetimes (<300 h). The relatively poor EQEs and stabilities of NQD-LEDs originate primarily from two deficiencies of the NQD active layer: (1) a strong dependency of NQD optical properties on molecular organic surface ligands and (2) the existence of various non-radiative recombination processes including multi-carrier Auger recombination. Previous work in our team has demonstrated that g-NQDs are far less susceptible to these "inherent" NQD properties, exhibiting suppressed blinking and ligand-related photobleaching [1,2] and suppressed Auger recombination [3,4]. G-NQD therefore holds great promise for LED application. However, there are also several potential issues that could make g-NQDs unsuitable for LED applications, e.g., relatively lower quantum yields, a large size that reduces the number of emitters per NQD layer, and a thick shell that could hinder charge injection compared to thin-shell NQDs.

To investigate these issues, we have set the following as the research objectives for this research:

1. Demonstrate superiority of g-NQDs over standard NQDs in LED applications

2. Develop novel active layer for the LED by integrating g-NQDs into a semiconducting solid-state matrix.

3. Develop the first, all-solid-state NQD-LED for a paradigm shift in efficiency and stability

Benefit to National Security Missions

The proposed g-NQD based, low-cost, all-solid-state LED architecture has the potential to become the key enabling technology for energy-efficient SSL applications.

Furthermore, it could also pave the way for electrically pumped NQD lasers and single-photon sources that have applications in defense and intelligence programs. Our project, therefore, directly addresses the main mission of DOE "Discovering the solution to power and secure America's future" through strategic themes of "energy security" and "scientific discovery and innovation."

Progress

Demonstrating the superiority of g-NQDs over standard NQDs in LED application

To demonstrate this point, we integrate our g-NQDs and conventional thinner shell NQDs into a very simple "test-bed" LED device architecture and compare their device performances. The "test-bed" LED architecture used in our studies comprises (CdSe)CdS NQD films sandwiched between a PEDOT:PSS hole-injecting anode and a LiF/Al cathode (Figure 1a). Despite the simplicity of the device, we obtain a maximum external electroluminescence quantum efficiency (EQE) of ~0.17% and maximum luminance of 2000 Cd/m^2 (Figure 1b). This performance represents a nearly two order-of-magnitude improvement compared to a similar device utilizing conventional NQDs as the emitting layer. Furthermore it is also on par with recently reported all-inorganic, red-emitting LEDs based on more complex device architectures but using conventional NQDs (~0.09% and 2000 Cd/m^2: [5]; ~0.2% [6].

To clarify the role of shell thickness on LED performance, we directly compare CdSe/CdS core/shell NQDs of increasing shell thicknesses, ranging from 4 to 16 CdS monolayers. Our results show that EQE and maximum luminance improve dramatically for thicker shell systems, even though both solution-phase emission efficiencies and the number of g-NQDs in the emitting films actually decline for thicker shell NQDs (Figure 1c-d). Furthermore we also observed that electroluminescence turn-on voltage does not change with shell thickness, showing that the thick shell does not impede charge injection Figure 1e).
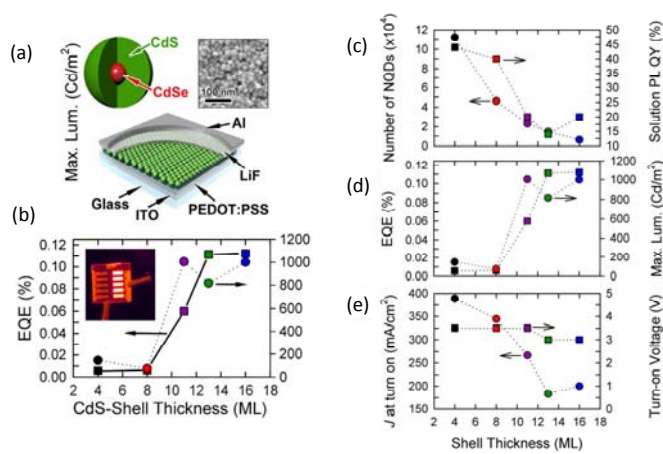
Figure 1. (a) Schematic representation of a g-NQD-based LED showing the ITO-coated glass substrate, the PEDOT:PSS hole injecting layer, the active NQD monolayer film and the LiF/Al cathode. Schematic of g-NQD and a scanning electron microscopy images (250 nm × 250 nm) of the active layer are shown as insets. (b) External quantum efficiency of the LED plotted as a function of current density. Inset: Photograph of a working LED at driving voltage of 9V (J = 450 mA/cm2) showing uniform EL emission from several LEDs on the same substrate. (c) Shell thickness dependence of device parameters: a) Number of NQDs per cm2 in the LED active layer (circles) and solution PL quantum yield (squares); d) maximum EQE (squares) and maximum light output (circles); e) EL turn-on voltage (squares) and current density at turn-on (circles) as a function of shell thickness.

Our results clearly reveal that g-NQDs provide unique and potentially transformative advantages (e.g., suppressed Auger recombination, insensitivity to surface ligands) for LED applications, while retaining other signature characteristics of NQDs, such as high quantum yields, narrow emission, and the ability to be processed using low-cost, solution-based methods. A manuscript reporting this work: "'Giant' CdSe/CdS core/shell nanocrystal quantum dots as efficient electroluminescent materials: Strong influence of shell thickness on light-emitting diode performance," is currently under review at Nano Letters.

Evaluating the potential of g-NQDs as a red phosphor for white light LEDs

We fabricated optical down-conversion LEDs as simple platforms for comparing g-NQDs with conventional thin-shell NQDs with respect to (1) operational stability and (2) self-reabsorption. These devices comprised an indium-tin-oxide (ITO)-coated glass substrate onto which a commercially available, electroluminescent, copper-doped ZnS powder-phosphor (ELmax = 445 nm) dispersed in a transparent insulating binder was deposited. Copper tape adhered onto the EL phosphor layer was utilized as a top contact. g- NQD dispersed in a polymer was utilized to create a uniform film on the glass slide (opposite to the ITO side) as the active down-conversion nano-phosphor material (Figure

2a-b). We prepared devices using core-only CdSe NQDs, as well as 4-shell, 11-shell and 16-shell CdSe/CdS NQDs. We probed the long-term operational stability of these devices under continuous AC bias voltage for more than 50 hours by following the change in the down-converted PL intensity of the NQD films (Figure 2c). The study reveals that while the thick shell device can retain more than 80% of their emission after 50 hours of operation, PL of core only and 4 shell devices are reduced by more than 60%.
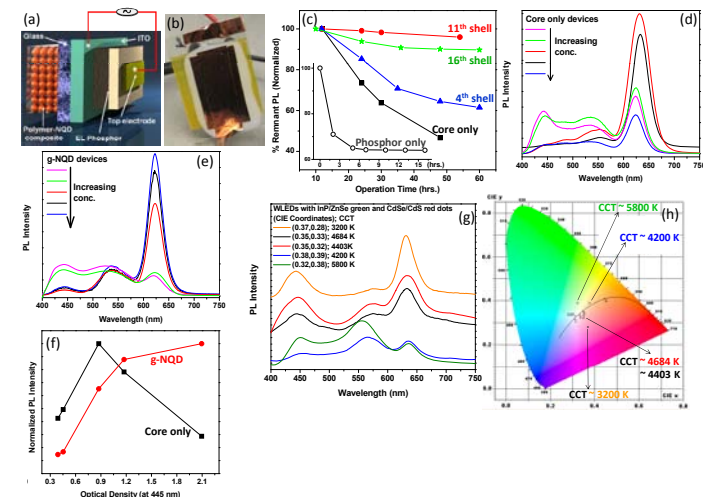
Figure 2. (a-b) Schematic of down-conversion device geometry and fabricated device, (c) device temporal stability as a function of shell thickness, (d-f) comparison of self-reabsorption effect for g-NQDs and core only devices, and (g-h) down-conversion WLEDs and their CCTs on the 1931 CIE color space.

SSL devices typically utilize high concentration of active NQDs that can result in lower device efficiency because of self reabsorption issues (self PL quenching at high NQD concentrations). In order to study the self reabsorption effect, we have compared the device PL for g-NQDs and core only NQDs (Figure 2d-f). We find that our g-NQD devices exhibit significantly less self- reabsorption effects as compared to core only devices. Furthermore, unlike conventional NQDs, minimal unwanted yellow/green absorption is also observed for g-NQDs. More recently, we have integrated green emitting InP/ZnS core/shell NQDs into our device structure consisting of red g-NQDs and blue EL phosphor to demonstrate down-conversion white light LEDs (WLEDs). We have successfully fabricated WLEDs with tunable CCT ranging from 3200 to 5800 K representing warm to cool white light shade interval while maintaining the chromaticity point in the white region of the CIE color space (Figure 2g-h).

These results clearly demonstrate the superiority of g-NQDs over conventional NQDs as stable and efficient nano-phosphors for down-conversion LED applications with minimal self reabsorption. g-NQDs can also be easily integrated into WLED platforms to create white light

source within a tunable CCT range. A manuscript reporting this work: "Giant Nanocrystal Quantum Dots (g-NQDs) as Stable and Efficient Down-Conversion Phosphors for Applications in Light-Emitting Diodes" is under preparation.

Encapsulation of g-NQD into Semiconductor Matrix

In integration of the g-NQDs with polymer-assisted deposition (PAD) grown GaN film, we have identified that the quenching of the PL of g-NQD film under the chemical environment and annealing temperature required for the PAD process as the key road blocks. We have further observed that g-NQD can survive up to 350 °C if annealing is performed under high vacuum. Based on this observation, we are currently exploring the way to grow amorphous GaN at low temperature and at the same time improving temperature endurance level of our g-NQDs. In parallel with this effort, we are investigating alternative thin film deposition approaches including pulsed laser deposition (PLD) which has been demonstrated to grow high quality metal oxide films (ZnO, NiO and CuO) in UHV environment without requiring high temperature treatments [7]. Preliminary study show that g-NQDs encapsulated with PLD grown ZnO layer can retain its PL emission (Figure 3a). We are also pursuing a solution chemistry approach. This approach will employ co-deposition of ultra-small nanocrystals of the intended semiconductor matrix composition with the g-NQDs, where deposition will afford an intimate mixture of these two species. Subsequent ligand exchange followed by mild annealing to facilitate melting of the ultra-small nanocrystals will result in an effectively melt-sintered composite film. We have recently performed a proof of the principle experiment for this approach and the findings are summarized in Figure 3b.
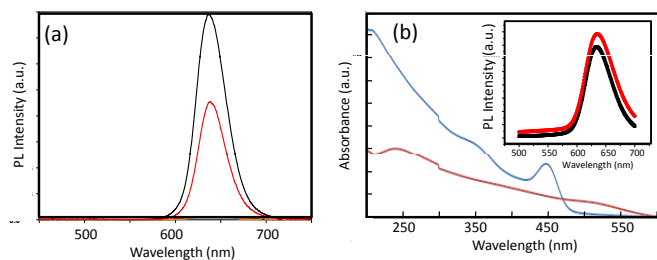
Figure 3. (a) PL spectra of g-NQD film before (black line) and after (red line) the deposition of ZnO film by PLD. (b) Absorbance spectra of 2nm diameter CdS film before (blue) and after (red) the annealing at 350 _C under UHV. Disappearance of the NQD absorption peak after the annealing indicated that the small diameter NQD has complete melted. Inset: PL spectra of g-NQD before (red) and after (black) the annealing at the same temperature and pressure show that the PL of the g-NAD film is unaffected by the annealing.

Future Work

Integration of g-NQDs into a semiconducting matrix and fabrication of LEDs

We will perform cross-sectional TEM study on the g-NQD/PLD-grown-ZnO film to investigate the quality of encapsulation. We will further integrate a g-NQD/ZnO active layer into our test-bed LED device structure. In addition we will explore another solution chemistry approach for encapsulation of g-NQDs into a semiconducting matrix. Here we will utilize literature approaches [8] for inorganic ligand exchange and subsequent thermally induced reaction of the inorganic ligands to form a composite film comprising NQDs and a continuous semiconductor film.

Evaluating the potential of g-NQD as red phosphor for down conversion LEDs

We will integrate our polymer-NQD composite film with GaN blue LED and test its performance in actual device geometry. We will systematically study the effect of heating on quantum yield and stability of our g-NQD phosphor. Furthermore we will also integrate metallic nanostructures into our g-NQD polymer composite film and investigate the way to further enhance the performance of the LED via plasmonic effect.

Fundamental study on charge and energy transfer processes

We will also investigate the transfer of charge and energy from the g-NQDs to the electron-hole transport layers and semiconducting matrices. This study will give us the guideline for development of semiconducting matrices and device design. In parallel, we will also investigate charge/energy transfer among the NQDs emitting at different wavelengths. The finding of this study will help us design better white light emitting phosphors.

Conclusion

This project will enable a transformational breakthrough in NQD-LED technology and establish our g-NQD based all solid-state LED as a viable "third technology" toward achieving the ultimate goal of SSL. Since general lighting applications consumed 20% of U.S. electricity use, even if 50% efficient SSL were achieved and replaced current white-lighting technologies, electricity use for lighting will be cut by 62% and in the U.S. alone, consumers would save around $42 billion each year in electricity cost by 2025. Our project therefore has great potential to make tremendous economical and ecological impacts through energy conservation.

References

1. Chen, Y., J. Vela, H. Htoon, J. Casson, D. Werder, D. Bussian, V. Klimov, and J. Hollingsworth. "Giant" multishell CdSe nanocrystal quantum dots with suppressed blinking. 2008. *JOURNAL OF THE AMERICAN CHEMICAL SO-*

CIETY. **130** (15): 5026.

2. Vela, J., H. Htoon, Y. Chen, Y. Park, Y. Ghosh, P. Goodwin, J. Werner, N. Wells, J. Casson, and J. Hollingsworth. Effect of shell thickness and composition on blinking suppression and the blinking mechanism in 'giant' CdSe/CdS nanocrystal quantum dots. 2010. *Journal of Biophotonics.* **3** (10-11): 706.

3. Garcia-Santamaria, F., S. Brovelli, R. Viswanatha, J. Hollingsworth, H. Htoon, S. Crooker, and V. Klimov. Breakdown of Volume Scaling in Auger Recombination in CdSe/CdS Heteronanocrystals: The Role of the Core-Shell Interface. 2011. *NANO LETTERS.* **11** (2): 687.

4. Htoon, H., A. V. Malko, D. Bussian, J. Vela, Y. Chen, J. A. Hollingsworth, and V. I. Klimov. Highly Emissive Multiexcitons in Steady-State Photoluminescence of Individual "Giant" CdSe/CdS Core/Shell Nanocrystals. 2010. *NANO LETTERS.* **10** (7): 2401.

5. Caruge, J. M., J. E. Halpert, V. Wood, V. Bulovic, and M. G. Bawendi. Colloidal quantum-dot light-emitting diodes with metal-oxide charge transport layers. 2008. *NATURE PHOTONICS.* **2** (4): 247.

6. Wood, V., M. J. Panzer, J. Caruge, J. E. Halpert, M. G. Bawendi, and Bulovic&acute. Air-Stable Operation of Transparent, Colloidal Quantum Dot Based LEDs with a Unipolar Device Architecture. 2010. *ACS Nano Letters.* **10** (1): 24.

7. Lee, S. Y., Y. Li, J. S. Lee, J. K. Lee, M. Nastasi, S. A. Crooker, Q. X. Jia, H. S. Kang, and J. S. Kang. Effects of chemical composition on the optical properties of Znl(1-x)Cd(x)O thin films. 2004. *APPLIED PHYSICS LETTERS.* **85** (2): 218.

8. Mitzi, D. B., L. L. Kosbar, C. E. Murray, M. Copel, and A. Afzali. High-mobility ultrathin semiconducting films prepared by spin coating. 2004. *NATURE.* **428** (6980): 299.

Publications

Hollingsworth, J. A.. "'Giant' Nanocrystal Quantum Dots: A New Class of Optical Nanomaterials for Light Emission Applications". Invited presentation at *CINT/SSLS EFRC Joint Conference.* (Albuquerque, 14, Sept. 2011).

Hollingsworth, J. A., Y. Ghosh, A. Dennis, J. Kundu, S. Brovelli, A. V. Malko, V. I. Klimov, and H. Htoon. 'Giant' nanocrystal quantum dots: a new class of active emitters for photonics applications. Invited presentation at *SPIE Optic + Photonic 2011.* (San Diago , 21-15 Aug, 2011).

Hollingsworth, J. A., Y. Ghosh, A. M. Dennis, J. Kundu, B. D. Mangum, B. N. Pal, Y. S. Park, and H. Htoon. Nanocrystal quantum dot architectures and assemblies for light emission applications. Invited presentation at *American Chemical Society, Fall Meeting, 2011.* (Denver, Co, 08/26/11- 09/01/11).

Htoon, H.. New type of nanocrystal quantum dots for light emitting applications: From solid state lighting to single photon sources. Invited presentation at *National Academics Quantum dots and Technology Surprise; National Security Implication Workshops.* (WashinTon , DC, 08/28/2011).

Pal, B. N., S. Brovelli, Y. Ghosh, V. I. Klimov, J. A. Hollingsworth, and H. Htoon. New type of core-shell nanocrystal quantum dots for applications in light emitting diodes . Presented at *MRS 2011 Spring Meeting.* (San Francisco, April 25-29).

Pal, B. N., Y. Ghosh, S. Brovelli, R. Laocharoensuk, V. I. Klimov, J. A. Hollingsworth, and H. Htoon. 'Giant' CdSe/ CdS core/shell nanocrystal quantum dots as efficient electroluminescent materials: Strong influence of shell thickness on light-emitting diode performance. *Nano Letters.*

Pal, B. N., Y. Ghosh, S. Brovelli, V. I. Klimov, and J. A. Hollingsworth. New Type of Core-Shell Nanocrystal Quantum Dots for Applications in Light Emitting Diodes (LEDs . Presented at *American Physical Society, March Meeting, 2011, .* (Dallas, March 21-25).

New Catalytic Methods for Selective C-C Bond Cleavage in Lignin: Towards Sustainable and Renewable Chemicals and Fuels

Louis A. Silks III
20100160ER

Introduction

We proposed to develop new catalysts for the selective unraveling and monomer unit extraction of the natural polymer lignin. Lignin is a non-food biomass that makes up the woody component of lignocellulose. The DOE estimates that the US could produce as much as 1.3 billion tons/y of lignocellulosic biomass, enough to replace 30% of the current US petroleum consumption. Efficient transformation of lignocellulose into usable chemicals and fuels remains a major challenge, particularly due to the difficulties associated with lignin breakdown. Lignin is resistant to natural decomposition processes, and has been considered a nuisance or roadblock in the conversion of biomass to fuels. Methods to depolymerize lignin would therefore potentially be a key breakthrough towards the production of bioderived fuels and chemicals. Our catalytic oxidation of lignin is targeted to convert lignin into smaller, soluble, more useful components using less energy and generating less waste than current methods. Such a process will have dual usage: it would provide a way to improve biofuels processing by removing lignin, as well as provide a new route to valuable aromatic compounds necessary for jet fuels (DOD applications) and industrial applications (Industry has expressed a strong interest in our lignin depolymerization program for their aromatic chemical feedstock needs).

Benefit to National Security Missions

The proposed work will significantly contribute to the development of alternative and renewable sources of energy, facilitate reduction of CO2 emissions, and contribute new technologies to enable us to live in a more sustainable fashion. Catalysts currently used with great success in the petroleum industry are not compatible with the highly functionalized compounds derived from biomass, and thus, new catalytic approaches are fundamentally required for the unraveling of complex organic molecules of biological origin. Moreover, this project directly impacts the sustainable and renewable energy needs the US.

Progress

Efficient transformation of lignocellulose into more valu-able products remains a major challenge, particularly due to the difficulties associated with breakdown of lignin. New methods to depolymerize lignin would represent a major breakthrough towards the production of bio-derived chemicals and fuels. An aerobic oxidation could be an inexpensive, environmentally friendly approach to convert lignin into smaller, soluble components. As described below, we have developed several vanadium catalysts capable of aerobic oxidation under mild conditions and have carried out studies to understand the mechanisms of these reactions and explore the substrate scope and selectivity. A greater understanding of the mechanism of vanadium-mediated oxidations could enable the development of more effective vanadium catalysts, and could elucidate factors underlying the overall reaction selectivity. Detailed investigations of the mechanism of alcohol oxidation by dipicolinate vanadium(V) have been carried out. The role of the pyridine in the reaction has been studied. Kinetic studies of the alcohol oxidation suggest a pathway where the rate-limiting step is a bimolecular reaction involving attack of pyridine on the C-H bond of the isopropoxide ligand. The oxidations of mechanistic probes cyclobutanol and t-butylbenzylalcohol support a two-electron pathway proceeding through a vanadium(III) intermediate. The alcohol oxidation reaction is promoted by more basic pyridines and facilitated by electron-withdrawing substituents on the dipicolinate ligand. The involvement of the base in the elementary alcohol oxidation step determined for dipicolinate vanadium(V) is a substantial departure from what has been previously proposed and may provide a new handle for controlling selectivity in vanadium-mediated lignin oxidations. This work was published (Hanson, S. K., Baker, T. R., Gordon, J. C., Scott, B. L., Silks, L. A., Thorn, D. L. "Mechanism of Alcohol Oxidation by Dipicolinate Vanadium (V): Unexpected Role of Pyridine" J. Am. Chem. Soc. 2010, 132, 17804).

Based on the results of the mechanistic study described above, a new catalytic system was discovered capable of aerobic oxidation under very mild conditions. A number of different additives, solvents, and vanadium catalysts were tested, and it was found that the combination of

the complex (HQ)2VV(O)OiPr (HQ = 8-quinolinate) and NEt3 is a highly active catalyst for aerobic alcohol oxidation. Conversion is significantly diminished in the absence of triethylamine. The substrate scope was also investigated; benzylic, allylic, and propargylic alcohols were readily oxidized to the corresponding aldehydes while aliphatic and sterically hindered alcohols showed little or no conversion. This catalytic system is advantageous in that it features an inexpensive base metal catalyst, uses air as the co-oxidant, produces water as the by-product of oxidation, and provides a significant improvement in atom economy over traditional stoichiometric oxidants. This work has both been published (Hanson, S. K., Wu, R., Silks, L. A. "Mild and Selective Vanadium-Catalyzed Oxidation of Benzylic, Allylic, and Propargylic Alcohols Using Air" Org. Lett. 2011, 13(8), 1908), and is undergoing patenting (doc # S121573/L2011037). In addition, our catalyst systems have been compared to copper catalysts for the oxidation of lignin model systems (see Comparison of Copper and Vanadium Homogeneous Catalysts for Aerobic Oxidation of Lignin Models. Baburam Sedai, Christian Díaz-Urrutia, R. Tom Baker, Ruilian Wu,L. A. "Pete" Silks, and Susan K. Hanson Catalysis, 2011, Special Issue, Victor S. Y. Lin Memorial Issue, 1, 794.). The oxidations of several lignin model complexes are currently being tested using the optimized catalytic system. The model systems have been constructed and are stable isotope labeled in strategic positions to provide mechanistic insight. Very recently, we found that the 8-quinolinate vanadium catalyst mediates a unique C-C bond cleavage reaction in our lignin dimer model system. Surprisingly, an acrolein derivative was formed, resulting from a highly unusual alkyl-phenyl bond cleavage reaction. Vanadium complexes have been reported to oxidatively break the C-C bonds between vicinal diols, α-hydroxyketones, and α-hydroxyethers, as well as mediate the decarboxylation of 1,2- and 1,3-hydroxycarboxylic acids, but vanadium-mediated cleavage of a benzylic carbon-carbon bond has never previously been observed. A manuscript describing this work has been submitted. (Hanson, S. K., Wu, R., Silks, L. A. P. "C-C or C-O Bond Cleavage in a Phenolic Lignin Model Compound: Selectivity Depends on Vanadium Catalyst," Angew. Chem. 2011, in review)

Future Work

Preparation of V and Mn complexes and the investigation of their stoichiometric and catalytic reactivity with lignin models and air are in progress. Future work will involve investigating several new vanadium catalysts, synthesizing new types of lignin model compounds and testing their reactivity with vanadium catalysts, and evaluating the reactivity of the vanadium catalysts in ionic liquid solvents.

Conclusion

This work has the goals; (a) The synthesis and characterization these complexes, investigation of catalytic reactivity with lignin model compounds; (b) Elucidation of the mechanism of the reaction allow us to develop more effective and selective catalysts; (c) Upon selection of the best performing catalyst(s) begin study with commercially available lignins such as organosolv and kraft lignin. This project then, would provide sustainable and renewable sources of these important industrial compounds.

Publications

Hanson, S., R. Tom. Baker, J. Gordon, B. Scott, L. A. Silks, and D. Thorn. Mechanism of Alcohol Oxidation by Dipicolinate Vanadium(V): Unexpected Role of Pyridine. 2010. *JOURNAL OF THE AMERICAN CHEMICAL SOCIETY.* **132** (50): 17804.

Hanson, S., R. Tom. Baker, J. Gordon, B. Scott, L. A. Silks, and D. Thorn. Mechanism of alcohol oxidation by dipicolinate vanadium(V): Unexpected role of pyridine. 2010. *Journal of the American Chemical Society.* **132** (50): 17804.

Hanson, S., R. Wu, and L. A. Silks. Mild and Selective Vanadium-Catalyzed Oxidation of Benzylic, Allylic, and Propargylic Alcohols Using Air. 2011. *ORGANIC LETTERS.* **13** (8): 1908.

Sedai, B., C. DiÃÅaz-Urrutia, R. Tom. Baker, R. Wu, L. A. Silks, and S. Hanson. Comparison of copper and vanadium homogeneous catalysts for aerobic oxidation of lignin models. 2011. *ACS Catalysis.* **1** (7): 794.

Probing the Structure of Superconducting States with Rotating Magnetic Field

Roman Movshovich
20100172ER

Introduction

Superconducting materials may have a significant impact on the energy use and requirements of the future. Superconductors provide means for loss-less energy transmission and energy storage among other important applications. The symmetry of the superconducting gap is one of the most important properties of a superconductor that might reveal its underlying microscopic mechanism. It is commonly the first question posed after the discovery of a new superconductor. Thermal transport and specific heat often provide important clues into the structure of the superconducting gap. For a fully gapped Fermi surface, both low temperature electronic specific heat and thermal conductivity in the superconducting state decay exponentially as a function of temperature, while the presence of nodes, where the super-conducting gap goes to zero, manifests itself in a power-law temperature dependence of these quantities. For example, thermal conductivity of $CeCoIn5$ in a magnetic field rotating within the a-b plane displayed four-fold oscillations, which was attributed to the presence of nodes in the superconducting gap that are located along the [110] direction, suggesting symmetry of the superconducting order parameter. Specific heat measurements also revealed four-fold oscillations in a field rotated within the a-b plane. With recent theoretical advances, a combination of ARCK tools (Angle-Resolved specific heat C and magneto-thermal conductivity κ) has the potential of becoming a powerful probe of the symmetry of the superconducting order parameter. We will validate the general correctness of our present theoretical understanding by performing ARCK on $CeCoIn5$ down to 20 mK and fields up to $Hc2 \approx 12$ T. By combining both thermal conductivity and specific heat measurement capabilities at a single facility, together with the underpinning theoretical support required for this project, we will take the lead in this emerging field of ultralow-energy quasiparticle spectroscopy.

Benefit to National Security Missions

Superconductivity was the first examples of a macroscopic phase that arose from fundamentally quantum interactions. Since its discovery, superconductivity remains a foremost field of research, both basic as applied. Basic research in superconductivity these days is focusing on unconventional superconductivity, where novel phenomena and novel states of matter are discovered at great pace. This field of superconductivity is also directly related to applications, since most of the recently discovered high temperature superconductors belong to this class of materials. DOE/SC and NSF are therefore primary agencies. Basic Understanding of Materials is the primary mission relevance of this project.

Progress

We have completed the conversion of the dilution refrigerator/superconducting magnet system in 32/128 from 9 Tesla to 14 Tesla magnet with a new high holding capacity dewar. This now allows us to conduct preliminary investigations/selection of unconventional superconductors for the field-rotated studies in the same field range, as well as perform ground work, such as thermometer calibration, up to 14 T.

We have established collaboration with Prof. Bill Halperin of the Northwestern University to investigate high purity UPt3 samples prepared in his laboratory, and obtained two UPt_3 samples for specific heat measurements in rotating field - the highest quality UPt3 samples. These samples were thoroughly characterized via poor resistivity and magnetization measurements. These two samples have different orientation of the long axis, that will allow rotation of the magnetic field both in the equatorial *a-b* plane (azimuthal angle ϕ) and *a-c* plane (polar angle Θ). The *a-b* sample is mounted and the experiment is being assembled for cooldown. The specific heat cell for the rotator probe has been assembled, with calibrated thermometer, the sample mounted, and the first experimental investigations are being conducted.

Papers on non-centrosymmetric (NCS) superconductors $LaRhSi_3$ and $La_3Bi_4Pt_3$ are being prepared. NCS SC are expected to have tendency toward mixed singlet and triplet SC components, and therefore potentially possess nodes in the SC order parameter. ARCK should be a useful tool in probing such complex order parameter. Thermal conductivity and specific heat measurements

were finished on LaRhSi$_3$, which turned out to be a Type I superconductor. Expectations of thermal conductivity for Type I superconductor, both in zero and applied magnetic field, are being explored by our theory collaborators (Ilya Vekhter from LSU).

Within the theoretical component of the project, we carried out the first realistic thermodynamic and thermal transport calculations to study the ab-initio band-structure effect on the magnetic-field orientation dependence of the superconducting gap function in various families of high-temperature and heavy-fermion superconductors. When a magnetic field is applied along a particular direction to the sample, it excites electrons locally inside and outside the vortex core. As a feedback effect, the relevant thermodynamic properties acquire a characteristic field-angle dependence which has been used earlier as a direct manifestation of the underlying superconducting anisotropy. For the first time our theoretical study shows that the anisotropy of the underlying electronic state itself plays a crucial role in the oscillations of the thermal properties so that a direct map between the maxima/minima of oscillations and the superconducting anisotropy can not always be made. We used realistic Fermi surfaces and electronic dispersions, and calculated the angle-resolved oscillations of the specific heat and thermal conductivity in a rotating in-plane magnetic field for FeSe and CeCoIn$_5$, using realistic tight-binding Fermi surfaces.

For FeSe our calculations show sign reversals in the amplitude of specific heat and thermal conductivity oscillations (Figure 1) as a function of temperature and fixed field for all gap symmetries investigated!!! These results can be tested in the FeSe$_{0.45}$Te$_{0.55}$ compound and emphasize the importance of Fermi surface anisotropies for the identification of gap structures. These results (authors are Das, Vorontsov, Vekhter, Graf) will be submitted to Physical Review Letters; the manuscript is in preparation.

In the case of CeCoIn$_5$, also a multiband superconductor, we find that an electron pocket at the M point and a hole pocket at the Gamma point of the Brillouin zone, yield sufficiently large Fermi surface anisotropies to produce large oscillations even for isotropic s-wave pairing. Our calculations show sign reversals in the amplitude of specific heat and thermal conductivity oscillations as a function of temperature and fixed field **for all gap symmetries** investigated (Figure 2 and Figure 3). These results can be tested in CeCoIn$_5$ and emphasize the importance of Fermi surface anisotropies for the identification of gap structures and gap symmetries. These results (authors are Das, Vorontsov, Vekhter, Graf) will be submitted to PRB; the draft is in preparation.

These theoretical results were completely unexpected, and took the community by surprise. They will lead to re-examination of old experimental results on identification of the order parameter symmetry in unconventional superconductors, as well as design of the future experiments. Combining thermal conductivity and specific heat may be absolutely necessary to gleam the order parameter symmetry form these type of measurements.
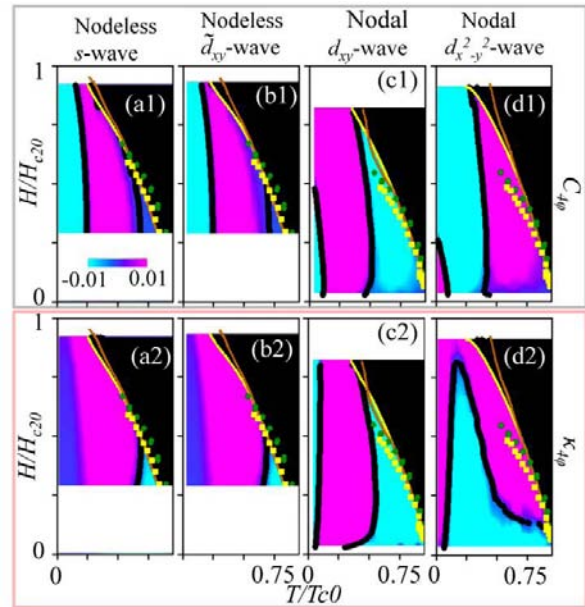
Figure 1. Field-temperature phase diagram of the oscillations minima/maxima in specific heat (top four panels, a1 through d1) and thermal conductivity (bottom four panels, a2 through d2) of FeSe. Both s-wave and three considered d-wave order parameters result in switching of maxima and minima (color change) of oscillations.
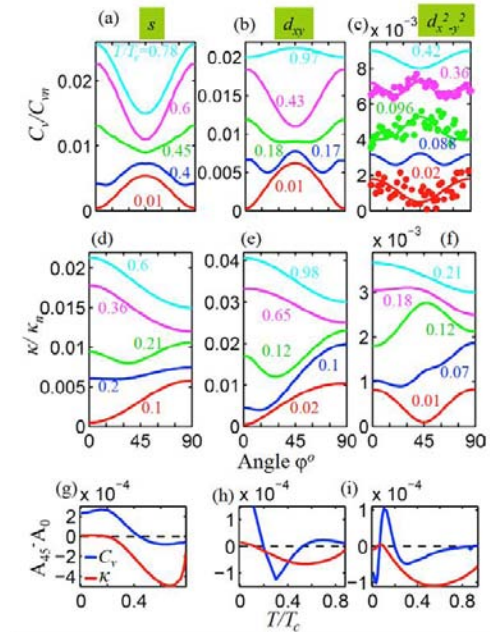
Figure 2. Specific heat (a-c) and thermal conductivity (d-f) of CeCoIn$_5$ for three possible symmetries of the order parameter (s, d_xy and d_x2y2) as a function of the direction of magnetic field within the equatorial a-b plane, for several values of reduced temperature T/Tc. Both s-wave and d-wave order parameters result in switching of maxima and minima of oscillations as a function of reduced temperature, shown in panels g-i.
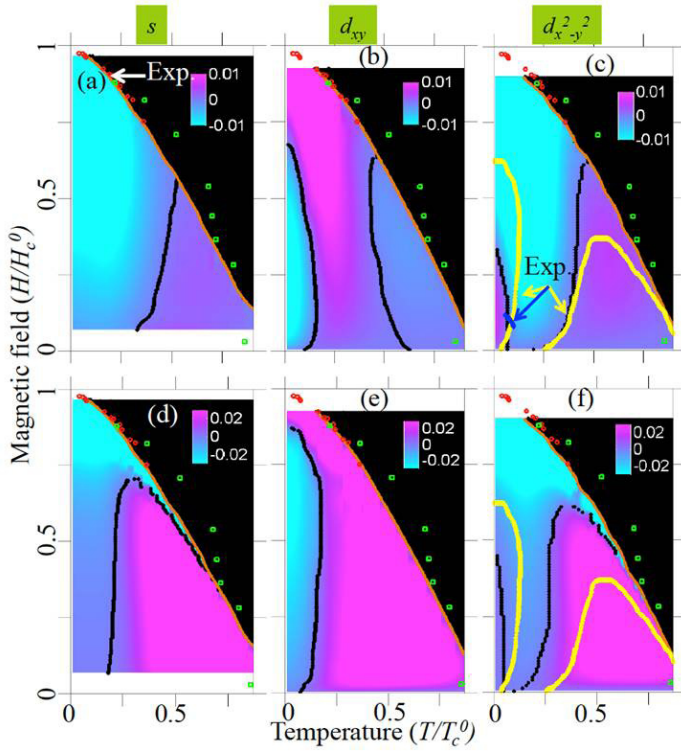
Figure 3. Field-temperature phase diagram of the oscillations minima/maxima in specific heat (top three panels, a through c) and thermal conductivity (bottom four panels, d through f) of CeCoIn$_5$. Both s-wave and two considered d-wave order parameters result in switching of maxima and minima (color change) of oscillations in both specific heat and thermal conductivity, however at different positions in the H-T plane.

Future Work

We are turning our immediate attention to investigation of superconducting order parameter symmetry in UPt$_3$, both due to our acquiring the highest quality samples from Pr. Halperin group in Northwestern University, and due to resurgent interest in this question. New experimental results on thermal conductivity in rotating magnetic field from Machida et al. in Japan point to the need for complimentary specific heat measurements, and we will perform specific heat measurements on UPt$_3$ in a rotating magnetic field first.

We will then turn our attention to CeCoIn$_5$. Thermal conductivity measurements under a rotating magnetic field are proving to be a powerful probe of the structure of the superconducting energy gap and location of its nodes. CeCoIn$_5$, originally discovered at LANL with Tc=2.3 K, was shown to be unconventional, with lines of nodes, via specific heat and thermal conductivity in zero magnetic field, based on the zero-temperature universal thermal conductivity and a power-law temperature dependence of the thermal conductivity. CeCoIn5 was the first HFS where thermal conductivity in a magnetic field rotated in the (a,b) plane displayed four-fold oscillations, which was attributed to the presence of nodes in the superconducting gap that

are located along the [110] direction, suggesting symmetry of the superconducting order parameter. Similar thermal conductivity studies were subsequently used by the same group for the identification of the superconducting gap structure in a number of different superconductors, including organic, and a Pr-based (possibly electric quadrupolar origin) HFS. However, the need for a deeper understanding of the thermodynamic and transport phenomena under rotating magnetic fields was exposed by the subsequent specific heat measurements. These measurements too revealed four-fold oscillations in a field rotated within the a-b plane, where the experimentally observed minima in the specific heat, under a rotating magnetic field, would place the nodes along the [100] and [010] directions, suggesting symmetry, in clear contradiction with the interpretation of the thermal conductivity measurements. This controversy pushed the development of more complicated theories of specific heat and thermal conductivity for nodal superconductors in rotating fields, which predicted that the positions of maxima and minima with rotating field, for both specific heat and thermal conductivity, should switch in the H-T plane, compared to the T=0 K expectations. We will look for this switching, thereby validating our understanding of Abrikosov vortex physics.

Conclusion

Our ARCK measurements, over a broad range of field (from zero to Hc2 = 12 T) and temperature (from Tc down to 20 mK), will validate the available theoretical model, which reconciled the initially contradictory results in the higher temperature regime. A detailed comparison between experimental results and theory will necessitate further refinement of theoretical models and shed light on the appropriateness of the approximations made in the model calculations. Using ARCK as the new ultralow-energy quasi-particle spectroscopy tool, we will establish the symmetry and structure of superconducting order parameters in a number of systems of current high interest.

Biocatalysts: A Green Chemistry Approach to Industrially Relevant Compounds

Andrew T. Koppisch
20100182ER

Introduction

Catechol and catechol-derived products are globally consumed commodities of importance to a wide range of industrial applications, including textile and pharmaceutical synthesis, pesticide production and the specialty chemical industry [1]. Catechol, like the majority of all phenol derivatives, is currently produced on an industrial scale (global consumption >20,000 metric tons per year) via distilling of thermally cracked crude oil, or by oxidation of benzene. Not only are these processes environmentally harmful, production costs are dictated by the price of crude oil. The main goal of this project is to develop a photosynthetic, environmentally friendly route to production of these important industrial products. This will be undertaken by metabolically engineering a cyanobacterial species, Syenchocystis PCC 6803, with a unique enzyme discovered by our team which will afford it a means to produce the catechol precursor, 3,4-dihydroxybenzoic acid. Further metabolic engineering processes will be pursued to provide a means to yield adipic acid, which is the primary component of nylon.

Benefit to National Security Missions

This work aims to produce commodity chemicals independent of the petroleum industry, and to do so via an approach that itself mediates environmental greenhouse gasses. This is directly in line with stated DOE-EERE missions in renewable energy and materials, and environmental stewardship. It also provides fundamental biological and engineering studies in algae, which is of interest to other governmental agencies such as NIH or NSF.

Progress

Multiple poster and oral presentations, both on domestic and international stages, were showcased to a diverse range of audiences. In addition, this work has led to a successfully submitted patent application that is currently on the USPTO docket for approval as a formally issued U.S. patent [2]. We have met our ongoing milestones outlined in our proposal for years 1 and 2 and are ahead of schedule for year 3. We were able to contribute to the recent review highlighting biofuels research as part of a joint effort between LANSCE-PCS, the University of Wisconsin-Madison, and the University of New Mexico [3].

Thus far, we have identified and verified all of the catalytic competency of the enzymes necessary to produce all four commodity chemicals of listed in our proposal 3,4-DHB, catechol, cis, cis-muconic acid, and b-carboxy-cis, cis-muconic acid. The last compound was not specifically called out as a targeted milestone in the proposal but is an integral component of expanding our substrate repertoire in both hetero- and phototrophic microbes. The above mentioned compounds were all produced and secreted into the extracellular matrix when expressed in E. coli and grown in minimal media containing glucose. Importantly, we did not see an accumulation of intermediates when multiple steps in the shunt pathway were introduced, which is an important feature in order to ensure minimal purification schemes when isolating the final product. The produced chemicals also exhibited virtually undetectable toxicity to the host. This early work was presented at Virginia Tech University (Figure 1).
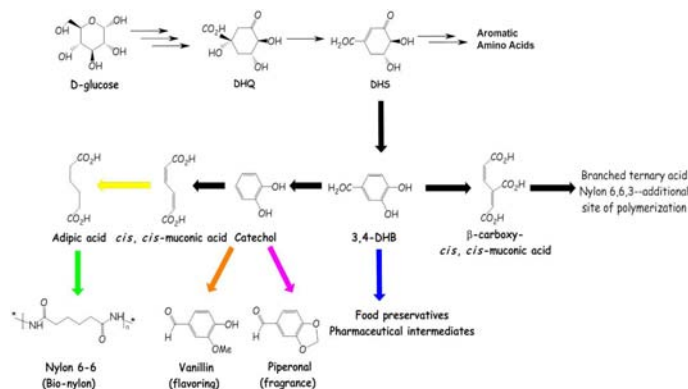
Figure 1. The metabolic pathway toward amino acid biosynthesis is being exploited for production of our desired commodity chemical. We have identified four different classes of enzymes for our bioengineering studies.

Concomitant to the work in E. coli, we have clearly established optimal growth conditions for Synechocystis PCC6803 ranging from 5 mL up to 15 L. During this time frame John identified an interesting growth pattern for PCC6803 using by flow cytometry. Within a single mon-

oculture, two very discrete populations were observed that had clearly differentiated phenotypes that corresponded to different growth rates (in the same shake flask!). This phenomenon is being explored to a greater extent but we feel that the results from this study may lead to new insights into identifying optimal growth conditions for isolating a PCC6803 population that is more amenable to our bioengineering platforms. We expect a peer-reviewed publication to be communicated from these exciting studies during the final year of this project. Importantly, this work received an award for best poster presentation at the internationally recognized Keystone Biofuels Symposium in Singapore [5]. This work was showcased as a PADSTE highlight in April and was well received amongst the LANL biofuel community [6].

Figure 2. Cartoon sketch for the theoretical conversion of CO_2 and light toward our bioengineered shunt pathway in phototrophic microbes.

The final, and arguably the most difficult, task of this project is to move our genes encoding the identical enzymes for our heterotroph into PCC6803 via a double homologous recombination event. This task is further complicated due to the fact that PCC6803 has multiple (>100) genomic copies. Statistically, complete integration of our gene(s) in a single transformation is highly unlikely and, we found, requires multiple rounds of transformation and screening for transformants against our selection marker. We developed a protocol that utilizes both a positive (kanamycin resistance) and negative (sucrose sensitivity) selection marker in order to generate a homogenous PCC6803 population harboring complete insertion of our genes of interest. Our early stage experiments have revealed partial integration as judged by PCR and weak resistance to kanamycin. We received invaluable input on how to overcome these bioengineering barriers at the ASM meeting in New Orleans where the culmination of all our work was presented [7]. Continued studies towards this end will continue for the duration of this project. Ultimately, we anticipate having

an established bioengineering protocol in place specific for PCC6803 within the next 6 months. However, we recognize bioengineering into this organism may prove an insurmountable task. Therefore, we have recently acquired a related cyanobacterium, *Synechococcus elongatus* PCC7942, for our bioengineering studies. Through personal communications, we believe this organism may be more suitable for our genetic engineering studies. The balance of the project will be dedicated towards moving our genes of interest, beginning with AsbF, into the genome with the expectation the first step in the shunt pathway (3,4-DHB production) will be clearly demonstrated (Figure 2).

This work was presented at the LANL Biosciences Capability Review {8} and elsewhere [9].

Future Work

The specific aims of this work are threefold. First, we will engineer a photosynthetic cyanobacterium, Synechocystis PCC 6803 or Synechococcus PCC7942, to produce the catechol precursor, 3,4 dihydroxybenzoate (DHB).

Second, further engineering of the recombinant DHB producing cyanobacteria will be undertaken to afford a strain which can produce cis, cis muconate (nylon precursor). Third, we will optimize growth and maintenance conditions of both PCC 6803 *S. elongates* PCC7942 for enhancement of DHB and cis, cis muconate production, and to conduct advanced structural studies on our key enzyme, asbF.

In order to address the first goal, we will transform the cyanobacteria cells with *asbF*, which is a novel enzyme discovered by our team. We have observed that integration of *asbF* into other bacteria outfits them with a means to make 3,4-DHB. Various reports document protocols for introduction of exogenous plasmids into Synechocystis and a number of promoters will be tested to effect optimum DHB production. Accomplishment of goal one is observable upon isolation of DHB from culture extracts of the recombinant strain. Note: We are extending our studies into another cyanobacterium, *Synechococcus elongatus*, due to some technical difficulties we have encountered in PCC6803. Vector design and assembly will be slightly altered as a result.

Further engineering of the strain in aim 1, by introducing a second construct to the strain with genes encoding DHB decarboxylase and catechol 1,2-dioxygenase. This process will enable the bioengineered organism a facile means to produce cis, cis-muconate, which is the penultimate intermediate to adipic acid, the Nylon 6,6 precursor. Adipic acid is readily produced through chemical reduction of the double bonds in cis, cis-muconate via hydrogenation. Quantification of adipic acid production will also be undertaken.

Third, we will conduct studies to optimize the production of both aforementioned products in the recombinant host.

The effect of various environmental variables on chemical production, such as light intensity, media nutrients and CO_2 concentration will be explored to optimize production.

Conclusion

We aim to equip the cyanobacteria *Synechocystis* PCC 6803 and *Synechococcus elongates* PCC7942 with a means to produce a number of industrially important commodity chemicals, including catechol and adipic acid precursors, via metabolic engineering. Tens of thousands of tons of these commodities are consumed annually across the globe, and currently they are almost exclusively produced from petroleates. Our work provides a renewable, petroleum-independent route to these commodities. Furthermore, since Synechocystis only requires light and carbon dioxide for growth, our approach also provides a means to mitigate environmental greenhouse gases in this process.

References

1. Langan, P., S. Gnanakaran, K. Rector, N. Pawley, D. Fox, D. W. Cho, and K. Hammel. Exploring new strategies for cellulosic biofuels production. 2011. *Energy and Environmental Science.* **4** (10): 3820.

2. Welsh, J. D., L. McClellan, E. Schmidt, C. Sanders, A. T. Koppisch, K. Hotta, and G. Montano. Commodity chemical production through metabolic engineering of hetero-, photo-, and mixotrophs. 2011. *Presented at the Bioscience Division Seminar. July 14, 2011.*

3. Welsh, J. D., L. M. McClellan, K. Hotta, A. T. Koppisch, and D. T. Fox. Interdisciplinary methods to characterize bioengineered microbes. Invited presentation at *LANL Bioscience Capability Review.* (Santa Fe, NM, 13 Jun. 2011).

4. Welsh, J. D., E. N. Schmidt, K. Hotta, L. M. McClellan, A. T. Koppisch, and D. T. Fox. Commodity chemical production through metabolic engineering of microbes. Invited presentation at *American Society of Microbiology.* (New Orleans, LA, 20-24 May, 2011).

5. Hadley, D. A., A. T. Koppisch, and D. T. Fox. Engineered bacteria for specialty chemical production. 2011. *Summary of work to be uploaded onto LANL web by TT..*

6. Fox, D. T., J. D. Welsh, A. T. Koppisch, G. Montano, and C. Sanders. John Welsh Awarded Scholarship for International Keystone Biofuels Symposium Presentation. 2011. *PADSTE Highlight. April 13, 2011.*

7. Fox, D. T., A. T. Koppisch, K. Hotta, J. D. Welsh, and C. Sanders. Tunable microbes: Commodity chemical production in hetero-, photo-, and mixotrophs. 2011. In *Keystone Biofuels Symposium.* (Singapore, Singapore, 1-6 Mar. 2011). , p. 1. Singapore: Keystone Symposia.

8. Hotta, K., J. D. Welsh, A. T. Koppisch, and D. T. Fox. Production of industrially relevant compounds in prokaryotic organisms. 2011. *Patent application, Jan. 31, 2011, S-116,316.*

9. Welsh, J. D., M. J. Waltman, D. Edlin, K. Hotta, A. T. Koppisch, and D. T. Fox. Metabolic engineering of hetero- and phototropic microbes . 2010. *Presented at the Sigma Xi Annual Meeting, Virginia Tech, Nov. 2010 .*

Ultrafast Cathodoluminescence for Improved Gamma-Ray Scintillators

Jeffrey M. Pietryga
20100183ER

Introduction

Energy resolving gamma-ray detectors are crucial to national security, nonproliferation, and basic research. Principally, there is a need to identify radioactive materials (such as fissile material) and detect their movement. When gamma-rays interact with matter, much of the energy is converted into energetic electrons that cascade into showers of lower and lower energy electrons. In single-crystal scintillators, the electrons produce visible photons in a relatively well-understood manner. Energy resolution is simply a matter of counting the number of photons produced by a gamma-ray absorption event: the more photons produced, the higher the energy of the gamma ray that caused them.

Semiconductor nanocrystals are of significant interest as scintillators because of their high gamma-stopping power, high emission quantum yields, solution processibility and low cost in comparison to large single crystals. While nanomaterials will convert incident gamma-rays into energetic electrons the same as other materials, the transduction of those electrons into photons is poorly understood, as it is made more complex in nanomaterials because of their unique optical properties, and the influences of interfaces throughout the very heterogeneous composite material. While ultrafast lasers and detectors have allowed us to achieve amazing insight into how optically excited nanocrystals relax to emit photons, similar experiments are not possible with a gamma-ray source, since its spontaneous emission cannot be synchronized to a detector. However, an ultrafast, short-pulse electron gun can act as a synchronizable surrogate for a gamma-ray source, allowing the type of time-resolved measurements needed to understand how electrons are converted into photons. In this work, we build just such an electron gun, and use it to perform transient cathodoluminescence experiments that will elucidate both favorable and undesirable relaxation pathways during electron-to-photon conversion in nanomaterials. Further, this insight will provide feedback to synthetic efforts aimed at producing high performance energy-resolving gamma-ray scintillators that are operable at room temperature.

Benefit to National Security Missions

Energy resolving gamma-ray detectors are vital to nuclear nonproliferation and security as these devices impair material diversion and movement/smuggling of fissile materials. Semiconductor nanocrystals are recognized candidates for application as highly fieldable, high-energy resolution, scalable scintillators. This project aims to determine the extent of their utility for this purpose and thereby aid in threat reduction. Low-cost detectors may also contribute to managing nuclear materials in the weapons complex.

Progress

As described in the technical description, this project consists of three main tasks: 1) establish a transient cathodoluminescence capability with adequate time resolution (on order 10 picoseconds) and reproducible operation at controllable pulse intensities (i.e. current) and voltages; 2) perform studies of known nanocrystal materials, such as cadmium selenide/zinc sulfide core/shell nanocrystals, to produce a database of spectral signatures corresponding to known excitation states of semiconductor nanocrystals and inform the design of enhanced materials; and 3) development of new nanocrystals and/or composites with enhanced cathodoluminescence efficiency, applying continuous feedback from ongoing cathodoluminescence studies. A simplistic summation of our schedule expectations would roughly be that each task would take approximately one year of the three year project lifetime. Thus, at the end of year two, we should expect to have established the instrumental capability, performed a baseline survey of CdSe/ZnS nanocrystals of a range of sizes, and to have developed the mathematical analysis techniques required to turn the raw data into conclusions regarding the relaxation process in these nanocrystals that we will soon use to identify the next candidate material system for study. As will be described in more detail below, this is exactly the case.

In the first quarter of FY11, we designed and constructed a new electron gun, featuring nested electron optics for full exclusion of stray external fields (Figure 1a). It

was successfully mounted in the instrument chamber, was fired up, and was shown to work extremely well, capable of producing a tightly focused beam of electron pulses (~1 mm spot size, Figure 1b) controllable in intensity from 5-150 picoamps, and at voltages from ~8 to 21 kilovolts. In the second quarter of FY11, we focused on optimization of the luminescence collection pathway, using a simple drop-cast film of cadmium selenide/zinc sulfide core/shell nano-crystals to produce enough cathodoluminescence signal to couple the instrument to a Hamamatsu streak camera for collection of time- and spectrally-resolved emission. The optimization of the collection pathway and synchroniza-tion were far from trivial, but as of March, the instrument has been reliably producing beautiful streak camera traces of nanocrystal emission produced by electrons. Further analysis has brought to our attention a number of subtle yet extremely important details about the operation of this streak camera, including how to avoid saturation effects from the instrumental gain, and how to account for the ef-fect of the reverse sweep of the oscillating streak bias.
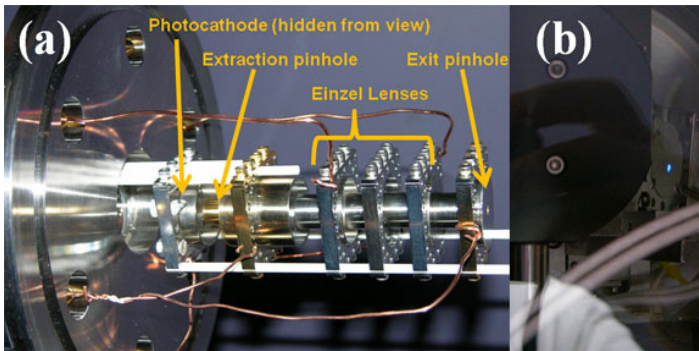
Figure 1. (a) The newly constructed electron gun, featuring nested optics for elimination of stray fields. A ~50 fs pulse of 266 nm light excites the photocathode from the back, and the resulting electrons are accelerated, collimated and directed onto the sample in the main chamber. (b) The elec-tron beam makes a bright blue spot on a phosphor screen in the sample holder. The view is partially blocked by newly installed emission collection optics.

While our appreciation of the complexities of the instru-ment was still evolving, the third quarter of FY11 was de-voted to collection of a database of cathodoluminescence traces from a size-diverse series of cadmium selenide/zinc sulfide (CdSe/ZnS) core/shell nanocrystals. In paral-lel, we collected time-resolved photoluminescence on the same exact samples, which provide a vital starting point for analysis of features found in the more complex cathod-oluminescence traces. A comparison of the two is shown in Figure 2. At this point, we can confidently say that the quality of the data between the two experiments is com-pletely equivalent, which is a significant achievement in its own right. As of now, we have full data sets for four differ-ent sizes of CdSe/ZnS nanocrystals, emitting from 530 to 665 nm.
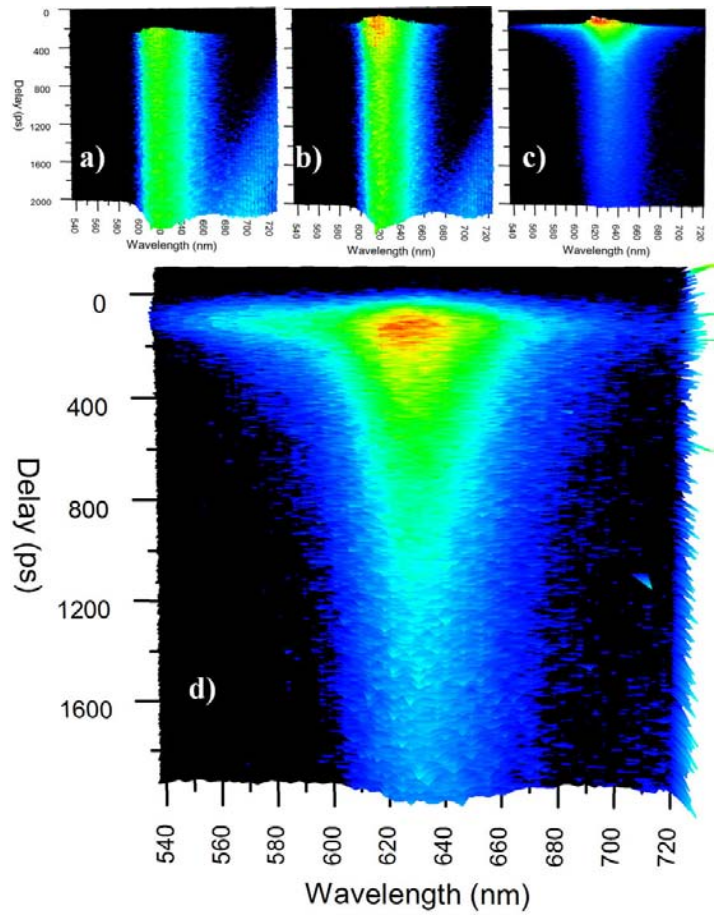
Figure 2. (a-c) Time-resolved photoluminescence for a sample of CdSe/ZnS nanocrystals emitting at 630 nm. In (a), only single-exciton dynamics are observed. As power is increased (b), a faster biexciton peak emerges at the same energy. Finally, at very high powers (c), a very fast triexci-ton peak is seen at shorter wavelengths. (d) A cathodolu-minescence trace of the same sample shows strong contri-butions from the multiexciton states. When these contribu-tions are deconvolved, hints of charged "trion" emission emerge.

Through careful analysis over the final quarter of FY11, we have both fully characterized the time resolution of our instrument, and developed the methodology for identify-ing and deconvolving the contributions of several types of excited states to the cathodoluminescence decay traces. A side-by-side comparison of traces recorded at several beam currents revealed that decay lifetimes associated with a given size of nanocrystal showed no dependence on the beam current, as expected (Figure 3a). However, the apparent rise-time of the signal depended strongly on the current, but not at all on the size of the nanocrystals. Effec-tive pulse widths were extracted from the rise times mea-sured for a range of currents and sizes. When plotted to-gether, the dependence of the pulse widths on current be-comes clear (Figure 3b). Extrapolating to 0 current, we see that our nominal response time for cathodoluminescence is 9 ps, which compares favorably to the measurements using the streak camera with laser excitation (~6 ps). We

believe that the additional rise stems from a combination of Coulombic pulse spread and possible bulk charging effects within the film itself during measurements. Ongoing experiments are aimed at minimizing the importance of these effects.
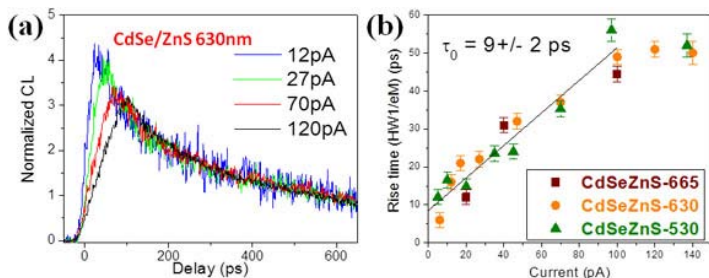
Figure 3. (a) Although rise time slows with increasing current, the decay lifetimes of a single nanocrystal sample do not vary, and are superimposable at later times. (b) An analysis of the effect of current on lifetime for several nanocrystal sizes reveals a consistent trend that implies an instrument response time of only 9 ps, which is further broadened by pulse effects that can be processed out after the measurement.

At the present time, we are using the rise-time measurements and laser-based photoluminescence experiments to deconvolve the chief features in our cathodluminescence traces. Preliminarily, we report contributions from a range of excited states, including single exciton, biexciton and tri- and higher multi-exciton states (these last states being indistinguishable by our method). In addition, we have evidence of a substantial signal from charged nanocrystal states, i.e., excited states with an imbalance in electrons and holes resulting in a net charge on the nanocrystal, the simplest being a "trion" (two electrons and one hole). Currently, we are refining a model for inferring the fraction of charged nanocrystals in the whole population.

Future Work
The exact fraction of nanocrystals that are charged by the initial high-energy excitation is the subject of current analysis. However, it is fairly clear that it is significant. Since multiple states with a charge imbalance decay by radiative recombination (slow) and non-radiative Auger recombination (fast) to eventually produce non-emissive ground-state charged nanocrystals, this result yields a possible reason why nanocrystal-based scintillators have underperformed. This suggests two new immediate goals. The first is to show that the electron excitation method we employ does not preferentially result in more charged nanocrystals than would be produced by a gamma-ray of similar energy. This will be the subject of near term studies based on varying the sample form factor, by which we hope to modify the ability of potentially excess charges to be captured by or flow out of the sample. The second is to study nanocrystals or composites that should exhibit modified charging probability (that is, materials that are easier or harder to ionize). Intentional manipulation of the fraction of charged

nanocrystals would be the first step towards true optimization of the gamma-to-photon transduction process.

Conclusion
Now that we have optimized and benchmarked the performance of our cathodoluminescence instrument, we have been able to collect the first substantial set of decay traces on a size series of CdSe/ZnS NCs, which is the material system most studied for gamma scintillation. In conjunction with photoluminescence studies, we have been able to identify the contributions of a number of familiar excited states to the decay dynamics. Most surprising so far is the not-insignificant presence of charged nanocrystals. While more complete and quantitative analysis is under way, this observation already suggests the next logical steps for our studies, which will focus on the determining the source and possibly manipulating the fraction of charged states. If this turns out to be the dominant factor in the performance of semiconductor nanocrystals as gamma scintillators, our study will be the first ever to suggest an active pathway toward realizing the latent potential of these materials. This could very well reinvigorate worldwide efforts in developing cheap, rugged replacements for single-crystal scintillators based on this fascinating class of materials.

Understanding and Controlling Complex States of Matter in New Iron-arsenide Superconductors through Strain and Disorder

Eric D. Bauer
20100210ER

Introduction

Superconductivity is an important technology for a variety of applications including energy transmission, energy storage, and sensor design. The discovery of superconductivity in the iron-arsenide materials roughly one year ago has set off a flurry of international activity. These superconductors are more metallic and isotropic than their cuprate counterparts and show great promise for future energy applications. In addition, the similarity of the phase diagrams of the iron-arsenides and the high temperature cuprates, in which an antiferromagnetic state in the parent compound is suppressed with charged doping giving rise to a dome of superconductivity, suggests that these new superconductors may help finally unlock the secret pairing mechanism for generating such high transition temperatures (e.g Tc=55 K in SmFeAs(O,F)).

However, some striking differences between the phase diagrams are now emerging. Isoelectronic substitutions and pressure studies on the iron-arsenides demonstrate that strain and disorder are also equally effective at suppressing the antiferromagnetic state and inducing superconductivity. In the cuprates, pure disorder (without changing carrier concentration) is always detrimental for superconductivity. This then begs the question as to what is the interplay between local structure, magnetism, and superconductivity that allows disorder and strain to promote superconductivity in the iron-arsenides. Our novel approach, which combines the materials synthesis capabilities in MPA-10 in bulk single crystals and thin films in MPA-STC, will determine how strain and disorder affects the local atomic structure in the iron-arsenide planes to suppress the antiferromagnetic order and induce superconductivity in this new family of superconductors.

Benefit to National Security Missions

The understanding of the role of disorder and strain in generating superconductivity in the new iron-arsenide superconductors ties directly into the central theme of LANL's Materials Grand Challenge of emergent phenomena. The novel approach described herein for inducing disorder and strain into these superconductors in a precisely controlled manner may lead to new ways to enhance their superconducting properties. Furthermore, since these three-dimensional superconductors show promise for superior energy-transmission performance over their anisotropic cuprate counterparts, the knowledge (and subsequent possible control) gained through the success of this project ties in well with the Lab's long-term energy security strategy.

Progress

We have made progress on two main tasks in our project aimed at understanding how strain and disorder affect the properties of the new iron-pnictide superconductors that lead to superconductivity, and to probe the nature of the superconducting state. This progress is evidenced by the consistently large number of publications in peer-reviewed journals, including the eight submitted or published this year, and the large number of citations (46) over a span of 15 months. The nature of superconductivity in these iron-pnictide materials including the pairing mechanism and the symmetry of the superconducting order parameter—both fundamentally important quantities for understanding any new superconductor--remains unclear despite intense experimental and theoretical efforts. We have made an exciting discovery in the compound $CaFe_2As_2$ that describes in detail the interactions that contribute to superconductivity in these new iron-pnictide materials. We used angle resolved photoemission spectroscopy to make direct measurements of the electronic structure and Fermi surface of the untwinned uniaxial state of $CaFe_2As_2$, which undergoes a simultaneous structural phase transition from a tetragonal to an orthorhombic structure, and a magnetic transition to an antiferromagnetic state. In collaboration with Daniel Dessau (University of Colorado, Boulder), we observe differences in the Fermi surface geometries along the orthogonal Fe-Fe bond directions, consistent with the development of an exotic type of charge order, indicating that there are a number of competing interactions (e.g., magnetic, structural, charge order that influence superconductivity in the iron-pnictide materials. Furthermore, the doping dependence of this order extrapolates to a possible quantum critical point of the

disappearance of this order at doping levels corresponding to the heavily overdoped regime of these materials, where superconductivity exists in the absence of magnetic/charge ordering. Thus, our results provide information about subtle structural and electronic effects that may cause the superconductivity. The results have been submitted for publication in the Proceedings of the National Academy of Sciences [1].

We address the nature of superconductivity through investigation of the low-temperature heat capacity. By analyzing the temperature dependence of this physical quantity, we gain information about the symmetry of the superconducting order parameter, which allows us to speculate on the origin of superconductivity in these exciting materials. We have measured the superconducting properties of annealed Ba(Fe1-xCox)2As2 samples and find that annealing significantly improves some superconducting characteristics. We found that annealing Ba(Fe1-xCox)2As2 increases Tc by up to 20% [2,3] and we are currently investigating the origin of this increase in collaboration with Dr. Sefat at Oak Ridge National Laboratory, which may be related to subtle local structure changes in the FeAs plane. The higher purity annealed samples allows for a more conclusive determination of the superconducting gap symmetry of Ba(Fe1-xCox)2As2 and in collaboration with I. Vekhter at University of Louisiana, we find fully gapped behavior for optimally doped Ba(Fe1-xCox)2As2 and a possible nodal gap for under and optimally-doped materials [4,5]. The difference of sample quality offers a natural explanation for the variation in low-temperature power laws observed by many techniques. We also made heat capacity measurements on Ba(Fe1-xCox)2As2 in very high magnetic fields to determine the pairing symmetry of the superconducting state [6]. This work shows that the measured behavior of the specific heat as a function of field up to the upper critical field Hc2=30 T obeys $C/T = H^{0.7}$, similar to the Volovik effect for nodal superconductors. This indicates that there are two superconducting bands, one with line nodes and one fully gapped in these materials.   In addition, we investigated the superconducting order parameter symmetry in SrNi2P2 [7], and BaNi2P2 [8]. These results allow us to conclude that fully gapped superconductivity is likely to be a universal feature of Ni-based pnictide superconductors.

We have grown thin films of Ba(Fe1-xCox)2As2 in collaboration with Professor Xiaoxing Xi at Temple University. These Ba(Fe1-xCox)2As2 films have planar defects within the ab-plane of the tetragonal structure (Figure 1). This result may provide clues as to the type of disorder (and strain) that may be beneficial to superconductivity in these iron-pnictide materials. Furthermore, experiments are planned to probe the critical current density of the Ba(Fe1-xCox)2As2 films grown on different substrates to see if planar defects and different amounts of disorder may enhance the superconducting properties, which may be favorable for future energy applications. For example, Ba(Fe1-xCox)2As2 epitaxial thin films fabricated on a piezo-

electric PMN-PT substrate allow direct investigation of the effects of strain in the iron-arsenic layer on superconductivity.
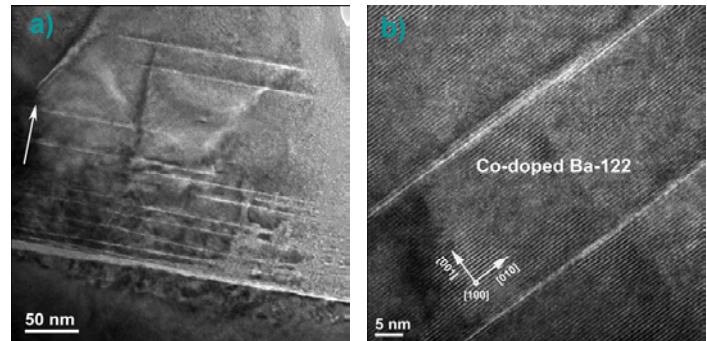
Figure 1. Thin film growth of superconducting Ba(Fe0.91Co0.09)2As2 in collaboration with Prof. Xi at Temple University showing planar defects within the tetragonal crystal structure of this material.

Future Work
Our novel approach, which combines materials synthesis capabilities in bulk single crystals and thin films, will determine how strain and disorder affects the local atomic structure in the iron-arsenide planes to suppress the antiferromagnetic order and induce superconductivity in this new family of superconductors. This approach demands that we accurately control both the applied strain, which we will accomplish through the synthesis of epitaxial thin films of the iron-arsenide materials on both lattice mis-matched substrates and on appropriate piezo-electric "substrates", and the induced disorder, which we will achieve through isoelectronic substitution in single-crystalline AFe2As2 (A=Ca, Sr, Ba), such as replacing ruthenium for iron in CaFe2As2. Carefully selected measurements on these bulk and thin film samples will provide essential information about the symmetry of the superconducting order parameter—currently one of the most outstanding issues in these materials. The combination of charge-sensitive, x-ray absorption spectroscopy and spin-sensitive nuclear magnetic resonance local structure probes will delineate how the induced changes in the local Fe or As environment alter the spin density wave order and accompanying superconductivity that will be a critical test of existing and future theories. In addition, the synthesis of these materials will enable several studies of the superconducting order parameter in real and momentum space, which are critical guides for determining the mechanism of superconductivity for any material.

Conclusion
Our discoveries will uncover synthetic design principles that offer new routes to enhancing the already high transition temperatures in the new iron-arsenide superconductors and make them even more attractive for energy applications. At this crucial time when the scientific community is intensely exploring these materials, this novel

approach provides an exceptional opportunity to make a large impact that would propel LANL to the top of this ever-growing field.

References

1. Wang, Q.. Symmetry-broken electronic structure and uniaxial Fermi surface nesting of untwined CaFe2As2. *Proc. Nat. Acad. Sci.*.

2. Gofryk, K.. Physical Review B. *Physical Review B.* **83** (6): 064513.

3. Gofryk, K.. Effect of annealing on the specific heat of optimally doped Ba(Fe0.92Co0.08)2As2. 2011. *J. Phys. Condensed Matt Conf Series.* **273**: 012094.

4. Gofryk, K.. Physical Review B. *Physical Review B.* **81** (18): 184518.

5. Jang, D.. Calorimetric evidence for nodes in the over-doped Ba(Fe0.9Co0.1)2As2. 2011. *New J. Phys.* **13**: 023036.

6. Kim, J. S.. Specific Heat To Hc2: Evidence for Nodes or Deep Minima in the Superconducting Gap of Under- and Overdoped BaFe2-xCoxAs2. *Phys. Rev. B.*

7. Kurita, N.. Physical Review B. *Physical Review B.* **83** (9): 094527.

8. Kurita, N.. Fully gapped superconductivity in Ni-pnictide superconductors BaNi2As2 and SrNi2P2. 2011. *J. Phys Condensed Matt Conf Series.* **273**: 012097.

Publications

Gofryk, K., A. B. Vorontsov, I. Vekhter, A. S. Sefat, T. Imai, E. D. Bauer, J. D. Thompson, and F. Ronning. Effect of annealing on the specific heat of Ba(Fe_{1-x}Co_x)₂As₂. 2011. *Physical Review B (Condensed Matter and Materials Physics).* **83** (6): 064513 (8 pp.).

Gofryk, K., A. S. Sefat, E. D. Bauer, M. A. McGuire, B. C. Sales, D. Mandrus, J. D. Thompson, and F. Ronning. Gap structure in the electron-doped iron-arsenide superconductor Ba(Fe0.92Co0.08)(2)As-2: low-temperature specific heat study. 2010. *NEW JOURNAL OF PHYSICS.* **12**: 023006.

Gofryk, K., A. S. Sefat, M. A. McGuire, B. C. Sales, D. Mandrus, J. D. Thompson, E. D. Bauer, and F. Ronning. Doping-dependent specific heat study of the superconducting gap in Ba(Fe(1-x)Cox)(2)As-2. 2010. *PHYSICAL REVIEW B.* **81** (18): 184518.

Gofryk, K., A. S. Sefat, M. A. McGuire, B. C. Sales, D. Mandrus, T. Imai, J. D. Thompson, E. D. Bauer, and F. Ronning. Effect of Annealing on the Specific heat of Optimally Doped Ba(fe_{0.92}Co_{0.08})₂As₂. 2011. In *International Conference on Strongly Correlated Electron Systems (SCES 2010) ; 27 June-2 July 2010 ; Santa Fe, NM, USA.* Vol. 273, p. 012094 (5 pp.).

Gofryk, K., A. S. Sefat, M. A. McGuire, B. C. Sales, D. Mandrus, T. Imai, J. D. Thompson, E. D. Bauer, and F. Ronning. Effect of annealing on the specific heat of optimally doped Ba(Fe0.92Co0.08)(2)As-2. 2011. In *International Conference on Strongly Correlated Electron Systems (SCES 2010) ; 20100627 - 20100702 ; Santa Fe, NM.* Vol. 273, p. 012094.

Kurita, N., F. Ronning, C. F. Miclea, E. D. Bauer, K. Gofryk, J. D. Thompson, and R. Movshovich. Fully gapped superconductivity in SrNi₂P₂. 2011. *Physical Review B (Condensed Matter and Materials Physics).* **83** (9): 094527 (7 pp.).

Kurita, N., F. Ronning, C. F. Miclea, Y. Tokiwa, E. D. Bauer, A. Subedi, D. J. Singh, H. Sakai, J. D. Thompson, and R. Movshovich. Fully gapped superconductivity in Ni-pnictide superconductors BaNi₂As₂ and SrNi₂P₂. 2011. In *International Conference on Strongly Correlated Electron Systems (SCES 2010) ; 27 June-2 July 2010 ; Santa Fe, NM, USA.* Vol. 273, p. 012097 (5 pp.).

Kurita, N., F. Ronning, C. F. Miclea, Y. Tokiwa, E. D. Bauer, A. Subedi, D. J. Singh, H. Sakai, J. D. Thompson, and R. Movshovich. Fully gapped superconductivity in Ni-pnictide superconductors BaNi2As2 and SrNi2P2. 2011. In *International Conference on Strongly Correlated Electron Systems (SCES 2010) ; 20100627 - 20100702 ; Santa Fe, NM.* Vol. 273, p. 012097.

Kurita, N., F. Ronning, C. Miclea, E. Bauer, K. Gofryk, J. D. Thompson, and R. Movshovich. Fully gapped superconductivity in SrNi2P2. 2011. *PHYSICAL REVIEW B.* **83** (9): 094527.

Developing Actinide Catalysis for Cleaning Dirty Fossil Feedstocks

Jaqueline L. Kiplinger
20100228ER

Introduction

This project outlines innovative directions in actinide chemistry that support the Lab's mission in Energy Security. The primary focus is to determine whether actinides can be used to efficiently catalyze the breakdown of petroleum into more useful component materials. In addition, this work will provide basic understanding of the chemistry of these reactions that may lead to ever improved approaches to efficient transformation of raw carbon-rich materials into starting materials for fuel and polymer synthesis. Results from our group demonstrate that thorium and uranium alkyl and aryl complexes show extraordinary behavior towards aromatic N-heterocycles, which are some of the most recalcitrant contaminants in fossil fuel feedstocks. The current effort takes advantage of the ability of actinides to engage in C-N cleavage and dearomatization chemistry with multiple N-heterocycle substrates per metal. These transformations represent new reactivity behavior for pyridine ring systems which have not been observed for transition metal or lanthanide complexes. This project will not only improve our fundamental understanding of key steps in hydrodenitrogenation (HDN) processes (such as C-N bond cleavage and dearomatization) but will also assess whether milder conditions than those currently used are viable. If the actinide compounds examined in this work prove to be catalysts for this industrially important process, patent applications will be pursued. This technology capitalizes on LANL's core capability in actinide science and offers to provide much needed insight into directions for the development of new HDN catalysts, which is a technological and cost-prohibitive gap that is currently limiting the U.S. from exploring the use of lower-quality petroleum feedstocks while transitioning from energy derived from fossil fuels.

Benefit to National Security Missions

These proposed studies relate directly to the Lab's mission in Energy Security by providing much-needed insight into directions for the development of new hydrodenitrogenation (HDN) catalysts. What is learned from HDN studies will be, by extension, applicable to HDO (oxygen removal) and HDS (sulfur removal) process-es. Furthermore, understanding the chemistry between actinides and N-heterocycles finds application in the country's nuclear energy future as well as nonproliferation issues since poly(vinylpyridine)-based Reillex-HPQ resin is used in separation columns for actinide processing at TA-55 and elsewhere in the world.

Progress

Over the past year, we have explored both theoretically and experimentally the ability of the thorium and uranium benzyne complexes, $(C_5Me_5)_2Th(C_6H_4)$ (**3**) and $(C_5Me_5)_2U(C_6H_4)$ (**4**), respectively, to cleave strong C-N, C-S and C-O bonds in substrates that are commonly found in crude petroleum and are the most difficult to process (i.e. break apart and remove during the refining process).

As shown in Scheme 1, the thorium and uranium benzyne complexes $(C_5Me_5)_2An(C_6H_4)$ (An = Th (**3**), U (**4**)) are prepared from benzene (C_6H_6) elimination from their diphenyl precursors $(C_5Me_5)_2An(C_6H_5)_2$ (An = Th (**1**), U (**2**)). For uranium, this reaction takes place at room temperature, but for thorium significantly higher temperatures are required (~110 °C). Initially, we spent time focusing on the nitrogen-containing heterocycles since the theoretical calculations for the reaction chemistry gave promising results, with C-N cleavage being thermodynamically favorable to give the actinide ketimido complexes **5** and **6**. However, experimentally we discovered that both of the actinide benzyne complexes react preferentially with the C-H bonds on pyridine compounds to give the η^2-pyridyl complexes $(C_5Me_5)_2An(C_6H_5)(NC_5H_4)$ (An = Th (**3**), U (**4**)); no C-N cleavage is observed.

A completely different story was encountered with sulfur-containing compounds. We discovered distinct and unprecedented reaction chemistry between the thorium benzyne complex $(C_5Me_5)_2Th(C_6H_4)$ (**3**) and thiophene. As illustrated in Figure 1, we proposed that the reaction between the thorium and uranium benzyne complexes $(C_5Me_5)_2An(C_6H_4)$ (An = Th (**3**), U (**4**)) and thiophene

would result in C-S cleavage to yield the thorium and uranium thiolate complex **9** and **10**, respectively. However, our experimental results determined that this pathway is not favored. Instead, reaction with the thorium benzyne complex **3** at 110 °C gives a deep red colored solution, which is unusual since thorium complexes are typically colorless. Workup yields the remarkable thorium bimetallic complex **11** in which two thiophene molecules have undergone C-S cleavage and subsequent C-C coupling. There are no examples of this type of chemistry with either the transition metals or the lanthanide metals. We think the same chemistry is taking place with uranium at room temperature, but we need to obtain a crystal structure to be certain.

Also, during this past year, the thorium chemistry that we developed last year to convert waste thorium nitrate to useful thorium tetrachloride was acknowledged by a 2011 LANL Pollution Prevention Award (Making Peace with Thorium) and was selected by TT to be a 2011 LANL R&D 100 Award submission (ThING - Thorium is Now Green).
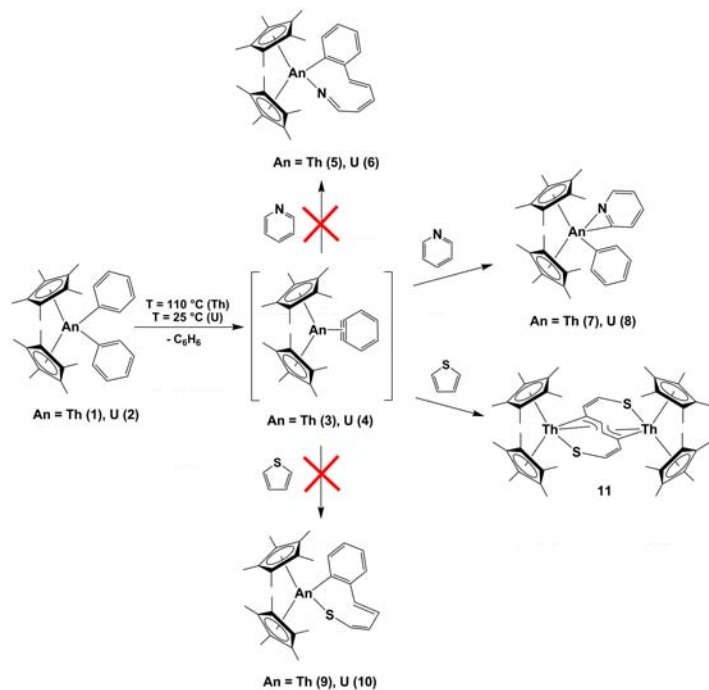
Figure 1. Synthetic scheme illustrating the reaction chemistry of thorium and uranium benzyne complexes $(C_5Me_5)2An(C_6H_4)$ (An = Th (3), U (4)) with pyridine and thiophene

Future Work
In general, the chemistry between actinides and sulfur-containing compounds is poorly developed. This is primarily due to the belief that little chemistry will be observed because sulfur is a "soft" donor and actinides are "hard" metals. Clearly, our current results will change the way the field thinks about hydrodesulurization (HDS) technology and will open up a new area of actinide science. Moreover, the sulfur chemistry we discovered this past

year provides a new model for desulfurization and HDS. It would be interesting to see if we can make this chemistry catalytic, by placing the dimer complex **11** under an atmosphere of hydrogen. This would cleave the Th-S bonds and replace them with Th-H bonds. Since hydrides are masked alkyl complexes, they should display similar behavior with thiophene and give a catalytic cycle. Of course, in this final year, we will also write up and publish our results.

Conclusion
This effort offers to provide much needed insight into directions for the development of new HDN catalysts, which is a technological and cost-prohibitive gap that is currently limiting the U.S. from exploring the use of lower-quality petroleum feedstocks while transitioning from energy derived from fossil fuels.*.*

Publications
Cantat, T., B. L. Scott, and J. L. Kiplinger. Convenient access to the anhydrous thorium tetrachloride complexes ThCl4(DME)2, ThCl4(dioxane)4 and ThCl4(THF)3.5 using commercially available and inexpensive starting materials. 2010. *Chemical Comunications.* **46**: 919.

Kiplinger, J. L., and O. Ramos, Jr.. IIt's an environmental ThING…. 2011. *Los Alamos National Laboratory-National Security Science (LALP-11-015).*

Monreal, M. J., R. K. Thomson, N. E. Travia, T. Cantat, B. L. Scott, and J. L. Kiplinger. Convenient and Safe Access to Next Generation Thorium and Uranium Halide Starting Materials. Presented at *26th Rare Earth Research Conference* . (Santa Fe, NM, June 19-24, 2011).

Monreal, M. J., R. K. Thomson, T. Cantat, N. E. Travia, B. L. Scott, and J. L. Kiplinger. UI4(dioxane)2, [UCl4(dioxane)]2, and UI3(dioxane)1.5: Stable and versatile starting materials for low- and high-valent uranium chemistry," . 2011. *Organometallics* . **30**: 201.

Pierpont, A. W., R. L. Martin, E. R. Batista, J. L. Kiplinger, and N. E. Travia. DFT study of Cp2Th and Cp2U catalysts for hydrodenitrogenation (HDN), hydrodesulfurization (HDS) and hydrodeoxygenation(HDO) (INOR-784). Presented at *241st ACS National Meeting & Exposition* . (Anaheim, CA, March 27-31, 2011).

Pierpont, A. W., R. L. Martin, E. R. Batista, J. L. Kiplinger, and N. E. Travia. DFT study of Cp2Th and Cp2U catalysts for hydrodenitrogenation (HDN) and hydrodesulfurization (HDS) (INOR-251). Presented at *242nd ACS National Meeting.* (Denver, CO, Aug 28-Sept 1, 2011).

Pierpont, A. W., R. L. Martin, E. R. Batista, and J. L. Kiplinger. DFT Study of Cp2Th and Cp2U Catalysts for pyridine hydrodenitrogenation. 2011. *Theory, Simulation, and Computation Directorate Science-Highlights (LA-UR-11-01084).*

Travia, N. E., M. J. Monreal, B. L. Scott, P. L. Diaconescu, and J. L. Kiplinger. Snapshots of thorium-mediated THF ring-opening reactions using bis(pentamethylcyclopentadienyl) and ferrocene-diamide ligand frameworks. Invited presentation at *Gordon Research Conference on Inorganic Reaction Mechanisms* . (Galveston, TX, March 6-11, 2011).

Travia, N. E., M. J. Monreal, B. L. Scott, P. L. Diaconescu, and J. L. Kiplinger. Thorium-mediated THF ring-opening reactions: bis(pentamethylcyclopentadienyl) versus ferrocene-diamide ligand frameworks. Presented at *26th Rare Earth Research Conference* . (Santa Fe, NM, June 19-24).

Travia, N. E., M. J. Monreal, B. L. Scott, P. L. Diaconescu, and J. L. Kiplinger. Snapshots of thorium-mediated THF ring-opening reactions using bis(pentamethylcyclopentadienyl) and ferrocene-diamide ligand frameworks. Presented at *Los Alamos National Laboratory Annual Postdoc Research Day.* (Los Alamos, NM, June 16, 2011).

Travia, N. E., R. K. Thomson, M. J. Monreal, T. Cantat, B. L. Scott, and J. L. Kiplinger. Convenient and safe access to next generation thorium and uranium halide starting materials. Invited presentation at *Gordon Research Conference on Inorganic Reaction Mechanisms* . (Galveston, TX, March 6-11, 2011).

Planetary Analog Geochemical Explorations with Laser-Induced Breakdown and Raman Spectroscopies

Roger C. Wiens
20100230ER

Introduction

The ability to quantitatively characterize and interpret both mineralogical and chemical compositions from complex geological samples is an enormous challenge for planetary exploration. The most informative distinctions between terrestrial, lunar, Martian, Venusian, and asteroidal geochemistry are extracted from subtle differences and require sophisticated analysis. Remote Raman and Laser Induced Breakdown Spectroscopy (LIBS) developed at Los Alamos National Laboratory (LANL) for NASA are exciting new geochemistry tools which were R&D100 prize winners in 2003. Raman spectroscopy is fundamentally sensitive to molecular structure while LIBS primarily determines elemental compositions. We have demonstrated that one can use an integrated remote Raman-LIBS instrument for planetary geological exploration.

Recently, seminal work demonstrated new data calibration techniques that extract greatly improved chemical and mineral accuracies from these two analytical techniques. In this project, combined LIBS-Raman analysis of planetary analog samples are providing new understanding of surface chemistry of lunar samples and small-scale analyses of carbon-rich asteroidal materials. We are also synthesizing planetary analog samples of ice-bearing lunar polar deposits and analog Venusian rocks. The current critical need is to explore geological analogs for Venus, lunar, and asteroidal samples and identify the relevant geochemical parameters detected from a Raman-LIBS instrument. This entails investigating volatile elements such as hydrogen, carbon, nitrogen, and oxygen, which are highly important to planetary science, but which more traditional planetary instruments are not capable of analyzing.

Benefit to National Security Missions

The LIBS and Raman spectroscopy techniques being extensively used and tested in this project have very wide applicability to many of the lab's and DOE's missions. They are used for nuclear detection (i.e., uranium isotopes), explosives detection, chem-bio detection, detection of environmental hazards such as Pb or Be in soils, carbon sequestration studies, production of silicon wafers for solar arrays, as well as for NASA space exploration. Techniques for determining detection limits and quantitative elemental compositions in this LDRD study can be directly applied to the LIBS and Raman core programs at LANL.

Progress

So far we have studied both lunar and Venusian analog samples. The third area, astroidal materials, will be the subject of work in the coming year.

Lunar studies: Lunar simulant JSC-1 has been analyzed by LIBS in vacuum to understand the accuracies, precisions, and detection limits for a number of elements of interest to lunar exploration. We measured for the first time the absolute irradiances of a number of LIBS emission lines under vacuum and studied the detection limits using three different typical methods. Major elements (Si, Al, Fe, Ca, Na, K, Ti, O) have relative errors of ~20% or below. The following minor and trace elements were observed: Li, K, Co, Ni, Sr, Ba, and Zr, with negative detection for F, P, S, Cl, V, Cr, Zn, Rb, La, Ce, Th, U. The ability to distinguish between different types of lunar soils was investigated. Differentiation between lunar feldspathic highlands samples and mare basalts can easily be done on the basis of Al and Fe compositions, while Mg can be used to identify Mg-rich lunar samples. The alkalis can be used to identify KREEP (K, Rare-Earth Enriched, and Phosphorous) provenances. Additionally, Ni can distinguish meteoritic material from lunar soils.

To investigate the advantages of LIBS for volatile elements we mixed JSC-1 simulant with water ice and studied the detection of hydrogen in vacuum, showing for the first time that water is very easily seen. This is particularly important in light of recent detection of hydrogen from orbit at high lunar latitude but outside of permanently shadowed craters. This opens up a broad range of possible lunar reservoirs for H, OH, and H2O.

We presented results at two conferences and in May we submitted a full paper to the Journal of Geophysical Research, Planets. The paper is now accepted, pending

two minor revisions [3]. We hope to revisit and refine our understanding of LIBS capabilities for volatiles (H, C, Zn, V, Pb, and cold-trapped volatile compounds) next year after installing a replica of the ChemCam instrument, which has significantly higher sensitivity.

Venus studies: A concentrated effort was dedicated to studying Venus analog materials using both LIBS and Raman spectroscopy under Venus pressure (92 bars) and temperature (740 K), with some studies also done at Venus pressure but at 423 K. The latter conditions are at significantly higher gas density than on Venus, resulting in some sense in a more stringent environment for LIBS, for which temperature has essentially no effect. Much of the experimental work was done at LANL and the U. HI, while the highest-temperature experiments were done at JPL to take advantage of their Venus temperature and pressure (VTP) facility. This is the first instance of either Raman spectroscopy or LIBS analyses at VTP. In a nutshell, remote pulsed-laser Raman spectroscopy is unaffected by the pressure and is largely unaffected by the temperature except as it alters mineral phases (e.g., dehydration, and alteration of some low-temperature phases). LIBS is clearly feasible at VTP. The high pressure results in strong Bremstrahlung backgrounds which can be overcome through time-gating of the emission to 1 microsecond or shorter, some broadening of the peaks, and more frequent self-adsorption. Other effects were studied: suspension of LIBS-generated dust above the samples and atmospheric turbulence. Neither of these are expected to pose a risk to performing analyses on Venus. Samples studied include basalt and andesite standards, olivine minette, carbonatite, granite, and mixtures in which anhydrite, labradorite, quartz, and olivine were incorporated as small fractions in a glass matrix to test detection limits. For most of these, Raman detection was demonstrated down to 1 vol%. For LIBS a calibration model was produced using sixteen standards and the following RMS accuracies were demonstrated: SiO_2 ±6%, Fe_2O_3 ±3.5%, CaO ±3%, MgO ±2.4%, Al_2O_3 ±1.7%. These are compared to typical basalt abundances of 45% SiO_2 and roughly 10% each of Fe_2O_3, CaO, MgO, and Al_2O_3. These results confirm for the first time that measurements made on Venus with a similar instrument would provide vast improvements in accuracy over the previous Venusian measurements and would be able to distinguish between different potential types of volcanism on our sister planet.

Two papers have been published on the Raman spectroscopy results under Venus conditions [1,2]. We are currently preparing to submit a full paper for publication on the LIBS results under Venus conditions.

Future Work

In the final year of this project we plan to perform LIBS analyses of various meteorites to learn more about LIBS capabilities both as a tool for analyzing meteorites on Earth and also to understand the capabilities of a LIBS instrument on a future mission to explore an asteroid. To

that end, we have obtained, on loan from the University of New Mexico, samples of the following meteorite classes: H, L, and LL ordinary chondrite, enstatite chondrite, carbonaceous chondrite, eucrite, aubrite, mesosiderite, pallasite, octahedrite, and a shergottite. The samples we obtained have both interior surfaces and also surfaces with weathering and with fusion crusts, so that we can study the chemical weathering of these different classes of meteorites. We plan to use the ChemCam laboratory body unit for these measurements, as it is far more sensitive than the commercial spectrometers used previously. We will analyze them with laboratory standards to enable quantitative elemental analyses.

As a lower priority we will investigate obtaining pyroclastic lunar glasses in order to study their volatiles. The ChemCam lab unit should enable good detection limits for these elements. Finally, the Venus analogue samples may be revisited with the ChemCam lab unit as well.

We are optimistic that this investment will position LANL to lead the first US experiment to study the composition of the Venus surface materials, and will lead to additional opportunities to deploy LIBS in other parts of the solar system. This work should also provide significant benefits to core LANL programs that use LIBS and Raman spectroscopies in other areas.

Conclusion

In terms of space instrumentation, the power and importance of remote analytical capability for both mineralogy and chemistry provided by a combined LIBS-Raman instrument cannot be overstated; competing methods that require drill or scoop sampling with ingestion into a rover analytical module are fraught with high complexity, cost, and risk. The scientific results from these studies are very important in their own right, but they will also position LANL to provide our LIBS-Raman technology for missions to the Moon and to Venus.

References

1. Sharma, S., A. Misra, S. Clegg, J. Barefield, R. Wiens, T. Acosta, and D. Bates. Remote-Raman spectroscopic study of minerals under supercritical CO $_2$ relevant to Venus exploration. 2011. *Spectrochimica Acta - Part A: Molecular and Biomolecular Spectroscopy.* **80** (1): 75.

2. Sharma, S., A. Misra, S. Clegg, J. Barefield, R. Wiens, and T. Acosta. Time-resolved remote Raman study of minerals under supercritical CO2 and high temperatures relevant to Venus exploration. 2010. *PHILOSOPHICAL TRANSACTIONS OF THE ROYAL SOCIETY A-MATHEMATICAL PHYSICAL AND ENGINEERING SCIENCES.* **368** (1922): 3167.

3. Lasue, J., R. C. Wiens, S. M. Clegg, D. T. Vaniman, K. H. Joy, S. Humphries, A. Mezzacappa, N. Melikechi, R. E. McInroy, and S. Bender. Laser induced breakdown spectroscopy (LIBS) for lunar exploration. To appear in *Journal of Geophysical Research, Planets.*

Publications

Anderson, R. B., J. F. Bell III, R. C. Wiens, R. V. Morris, and S. M. Clegg. Clustering training set selection methods for improving the accuracy of quantitative laser induced breakdown spectroscopy. *Spectrochimica Acta B.*

Anderson, R. B., R. V. Morris, S. M. Clegg, J. F. Bell III, R. C. Wiens, S. D. Humphries, and S. A. Mertzman. Remote quantitative chemical composition of rocks using laser induced breakdown spectroscopy with partial least squares and artificial neural network methods. To appear in *Icarus.*

Lasue, J., R. C. Wiens, S. M. Clegg, D. T. Vaniman, K. H. Joy, S. Humphries, A. Mezzacappa, N. Melikechi, R. E. McInroy, and S. Bender. Laser induced breakdown spectroscopy (LIBS) for lunar exploration. To appear in *Journal of Geophysical Research, Planets.*

Sharma, S., A. Misra, S. Clegg, J. Barefield, R. Wiens, T. Acosta, and D. Bates. Remote-Raman spectroscopic study of minerals under supercritical CO_2 relevant to Venus exploration. 2011. *Spectrochimica Acta - Part A: Molecular and Biomolecular Spectroscopy.* **80** (1): 75.

Sharma, S., A. Misra, S. Clegg, J. Barefield, R. Wiens, and T. Acosta. Time-resolved remote Raman study of minerals under supercritical CO_2 and high temperatures relevant to Venus exploration. 2010. *PHILOSOPHICAL TRANSACTIONS OF THE ROYAL SOCIETY A-MATHEMATICAL PHYSICAL AND ENGINEERING SCIENCES.* **368** (1922): 3167.

One-Dimensional Nanomaterials for Enhanced Solar Conversion

Samuel T. Picraux
20100237ER

Introduction

To meet the earth's future energy needs, the efficiency of solar energy harvesting must be increased and the cost decreased. This requires new approaches which go beyond simply re-engineering currently established methods. One of the greatest, but least-explored, opportunities for enhancing the light-to-electric conversion process is to exploit energy transfer concepts made possible by nanoscale materials design. The objective of this project is to discover and determine the underlying scientific issues required to implement an enhanced light harvesting approach for electrical energy generation based on composite one dimensional nanowire structures. Nanoscale materials offer opportunities to achieve materials properties not possible in bulk materials. The project will use a new approach to solar cell design using one-dimensional materials, where the light absorption and charge collection constraints are decoupled. Vertical nanowire arrays provide strong diffuse scattering, resulting in nearly 100% light absorption in the vertical direction within a shallow depth over a broad wavelength region. This enables highly efficient charge carrier generation in the semiconducting wires. Radial p-i-n junctions in the nanowires provide strong local electric fields for highly efficient carrier separation in the lateral direction. Contacts to the nanowire core and shell then provide carrier collection from the wires. The key concept derives from the one-dimensional design of these structures—in essence light absorption is controlled by the vertical direction and charge separation by the lateral direction. In addition, and of critical importance, these nanoscale materials are produced by low cost chemical vapor deposition techniques that are suitable for large scale manufacturing and do not require single crystal silicon substrates.

Benefit to National Security Missions

This project addresses fundamental challenges in implementing low-cost solar cell concepts and is directly relevant to the DOE energy security mission. The objective is to achieve crystalline solar cell efficiencies at the low cost of thin film approaches. The proposed transformational science will develop composite nanoscale materials concepts that will enable decoupling of photon and electron collection. This coupling currently limits silicon solar cell design. These concepts are also important to the remote sensing and threat reduction areas, for example in developing new approaches to highly sensitive, near infrared sensing.

Progress

Our key achievements in this project are: (i) development of top down processes for the fabrication of vertically-aligned Si nanowires over large areas on thin (for optical absorption measurements) and thick (for device fabrication) Si substrates; (ii) the observation of remarkably enhanced optical absorption in Si nanopillar arrays compared to planar bulk Si and its dependence on nanopillar dimensions and spacing, (iii) the epitaxial growth of single crystalline doped Si shells for radial nanowire solar cell and measuring its preliminary electrical characteristics, and (iv)   performing scanning photocurrent microscopy (SPCM) to measure effective minority carrier diffusion lengths in single nanowire devices.

For a rigorous understanding of the optical properties and electronic characteristics of nanowire solar cells, we performed systematic experiments in each of the areas cited above. Our approach was to fabricate large nanowire arrays as model structures for in-depth synthesis, optical and device physics studies. We have used deep inductive coupled plasma (ICP) etching in a process known as Bosch etch to obtain precisely controlled arrays of nanowires with diameters in the range of 200 nm – 1000 nm and lengths of 2 – 10 micrometers. To eliminate the effect of the underlying Si substrate on the optical properties, we developed a fabrication process to etch these structures on thin (50 micrometer starting thickness) Si substrates and performed optical absorption measurements on nanowires with different diameters, lengths and spacings. Nanowires with ~ 500 nm diameter, 10 micrometers length, and 750 nm to 1 micrometer spacing showed the best results with an enhanced optical absorption compared to bulk Si throughout the solar spectrum of up to 60% at the longest wave wavelengths (1100 nm), validating that the optical thick-

ness of the material required for full absorption of light is much lower with Si nanowires compared to bulk Si.

We have developed processes for the radial growth of doped Si to achieve radial p-n junction nanowires for solar cell studies. By using a sequence of oxidation/etching of the damaged etched nanopillar surface, we were able to smooth the nanowires and achieve epitaxial-growth-ready surfaces. We then developed methods to grow doped and undoped shells with controlled interfaces and doping densities. These results contrast to popular approaches in the literature which mostly rely on thermally diffusing dopants into the nanowires to obtain radial junctions, and which because of their graded junctions are of inferior quality as well as difficult to control. Subsequently, these radial p-n junction structures were used to fabricate solar cells by depositing metal electrodes around the nanopillar array for contacting the top most deposited layer and on the back of the substrate for contacting the substrate and extracting carriers from nanowire cores. Initial electrical measurements have demonstrated rectifying behavior. We have further found that the formation of a thin oxide layer at the base of the nanowires significantly reduces leakage currents in these structures, which appears to be due to blocking defects in the region around the base of the Si nanowires. We are currently optimizing the design of mesa structures for detailed studies of the optoelectric response of both arrays of nanowires and of single nanowires. These model structures will enable the study of the charge collection in radial nanowire structures for the first time and allow us to decouple the optical and electrical effects in the overall solar cell performance.

On the single nanowire level, we have performed controlled growth of axial in-situ doped nanowire p-n junctions and used these structures to fabricate two- and four-terminal devices where ohmic behavior was observed on individual n- and p- segments of the wire and rectifying behavior was observed in between the p-n junction. Scanning probe current microscopy measurements using a laser microscope show an exponential decrease in the photocurrent as the laser light is scanned away from the depleted region on either side of the metallurgical p-n junction. This behavior was modeled and shown to provide the effective minority electron and hole diffusion lengths, which were found to be on the order of ~ 1 micrometer for electrons and 700 micrometers for holes (for an 80 nm diameter nanowire), with the expected temperature and bias dependences. This is in contrast to bulk Si where minority carrier diffusion lengths are strongly dependent on the doping level, and highlights the importance of surface recombination in nanowires which have large surface area to volume ratios. These effective minority carrier diffusion lengths show among the highest figure of merit (diffusion length/ nanowire diameter) reported in the literature for nanowires to date, and demonstrate the high quality of our synthesized Si nanowire materials. Current efforts in this area concentrate on further surface passivation techniques and

characterization of surface and diameter effects to further understand and enhance these effective carrier diffusion lengths.

Future Work

The scientific issue we will address is to understand and control photovoltaic performance in nanostructured materials with nanoscale variations in material composition and electronic doping. To achieve these goals we must understand one dimensional (1D) nanostructured materials design for strong, broad-band collection of light; understand charge generation in 1D structures with unprecedented electric field gradients; understand rapid charge separation and recombination control under such nanoscale separation conditions; and determine the feasibility of efficient radial single crystal nanowire solar cells. The fundamental science to be developed will not only be relevant to energy harvesting, but also to a wide range of 1D nanomaterials electrical and optical applications. Such materials have attracted great attention, but have received little scientific study to understand how to extend and exploit these benefits beyond this specific empirical example. Our plan for the next year is to design and measure the electro-optic properties of prototype cells consisting of single nanowire vertical Si radial junction devices as well as nanowire array devices. These studies, together with our modeling work, will enable the decoupling of optical absorption and carrier collection contributions to the efficiency of these novel solar cells. As a result we will achieve fundamental understanding of how to optimize the nanoscale architecture for this new approach to solar energy collection.

Conclusion

This project will develop new understanding and control of the photovoltaic performance in nanostructured materials through variations in material composition and electronic doping. Using silicon nanowires as our model system, we will: 1) understand one dimensional nanostructured materials design for strong, broad-band absorption of light; 2) understand rapid charge separation and recombination processes in nanoscale structures with large electric field gradients; and 3) fabricate prototype solar cells to determine the feasibility of this approach for low cost, efficient solar cells.

Publications

Dayeh, S. A., J. Wang, N. Li, J. Y. Huang, A. V. Gin, and S. T. Picraux. Growth, defect formation, and morpholog control of germanium-silicon semiconductor nanowire heterostructures. To appear in *Nano Letters.*

Dayeh, S. A., N. H. Mack, J. Y. Huang, and S. T. Picraux. Advanced core/multishell germanium/silicon nanowire heterostructures: the Au-diffusion bottleneck. 2011. *Applied Physics Letters.* **99**: 023102.

Dayeh, S. A., R. M. Dickerson, and S. T. Picraux. Axial Bandgap engineering in gemanium-silicon heterostructured

nanowires. 2011. *Applied Physics Letters.* **99**: 113105.

Dayeh, S., A. Gin, and S. T. Picraux. Advanced core/multi-shell germanium/silicon nanowire heterostructures: Morphology and transport. 2011. *Applied Physics Letters.* **98**: 163112.

Dayeh, S., J. Huang, A. Gin, and S. T. Picraux. Synthesis, Fabrication, and Characterization of Ge/Si Axial Nanowire Heterostructure Tunnel FETs. 2010. In *IEEE Nano 2010 .* (Seoul, Korea, 17-20 Aug. 2010). , p. 85. Seoul: IEEE.

Dayeh, S., J. Huang, A. Gin, and S. T. Picraux. Elimination of Gold Diffusion in the Heterostructure Core/Shell growth of High Performance Ge/Si Nanowire HFETs. 2010. In *IEEE Nano 2010 International Conference.* (Seoul, Korea, 17-20 Aug. 2010). , p. 95. Seoul: IEEE.

Dayeh, S., and S. T. Picraux. Axial Ge/Si Nanowire Heterostructure Tunnel FETs. 2010. In *SiGe, Ge, and Related Compounds 4: Materials, Processing, and Devices.* (Las Vegas, NV, 12-14 Oct. 2010). Vol. 33, p. 22. New Jersey: Electrochemical Society.

Jung, Y., A. Vacic, D. E. Perea, S. T. Picraux, and M. A. Reed. Minority carrier lifetimes and surface effects in VLS-Grown axial pn junction silicon nanowires. 2011. *Advanced Materials.* **23**: 4306.

Kar, A., P. Upadhya, S. Dayeh, S. T. Picraux, A. J. Taylor, and R. P. Prasankumar. Probing ultrafast carrier dynamics in silicon nanowires (Invited). 2011. *Journal Selected Topics in Quantum Electronics.* **17**: 889.

Le, S. T., P. Jannaty, A. Zaslavsky, S. Dayeh, and S. T. Picraux. Growth, electrical rectification, and gate control in axial in situ doped p-n junction germanium nanowires. 2010. *Applied Physics Letters.* **96**: 262102.

Le, S. T., S. Dayeh, S. T. Picraux, and A. Zaslavsky. Growth and electrical rectification in axial in-situ doped p-n junction germanium nanowires. 0920. In *The Second International Workshop on Nanotechnology and Application – IWNA 2009.* (Vietnam National University, Ho Chi Minh City, 16 Sept. 2009). , p. 40. Ho Chi Minh City: --.

Picraux, S. T., J. Yoo, I. H. Campbell, S. A. Dayeh, and D. E. Perea. Semiconductor nanowires for solar cells. To appear in *Semiconductor nanostructures for optoelectronic devices.* Edited by Yi, G. C..

Picraux, S. T., S. A. Dayeh, P. Manandhar, D. E. Perea, and S. G. Choi. Silicon and Germanium Nanowires: Growth, Properties and Integration (Invited Overview). 2010. *Journal of Materials.* **62** (4): 35.

Seo, M. A., S. A. Dayeh, P. C. Upadhya, J. Martinez, B. S. Swartzentruber, S. T. Picraux, and A. J. Taylor. Understanding ultrafast carrier dynamics in single quasi-one-dimensional Si nanowires. *Nano Letters.*

Sierra-Sastre, Y., S. Dayeh, S. T. Picraux, and C. Batt. Epitaxy of Ge Nanowires from Biotemplated Au Nanoparticle Catalysts. 1209. *ACS Nano.* **4**: 2010.

Electron Spin Injection, Transport and Detection in Semiconductor Nanowires

Samuel T. Picraux
20100261ER

Introduction

Today's electronics industry is based on electron charge transport in bulk (3D) or planar (2D) semiconductors. However, there is a belief that by further exploiting the fact that electrons have spin, semiconductor devices can be made energy efficient (low power), smaller and thus faster with versatile functionality, and this is the focus of the rapidly growing field of "semiconductor spintronics." Concurrently, there is great interest in electronic devices based on 1D nanowires, which hold promise for unconventional device architectures allowed by their unique dimensionality. Both fields—semiconductor spintronics and 1D nanowires—are now sufficiently mature to marry these ideas. Therefore this project will investigate electron spin injection, transport, and detection in semiconductor nanowires. This area holds great promise for new advances in materials physics science and for a new generation of low power and high speed electronics, quantum information processing systems, and single electron spintronic devices. This team is uniquely suited to pursue this new direction and, to the best of our knowledge, no spin injection, transport, and detection measurements or analyses has been performed at the time of the initiation of this project with semiconductor nanowires.

Benefit to National Security Missions

This project is central to LANL's materials mission and leadership in the subcategory of emergent phenomena, which specifies the need for exploitation of nanostructures, quantum confinement and crystalline interfaces to produce new properties and new functionalities in designed materials. By manipulating electron spin in a semiconductor, low power devices may be realized with compact size for multi-functionality, and with high speed and performance. Silicon nanowires will enable significant advances through long mean free paths and coherence times. Demonstration of spin electronics in Si nanowires will generate worldwide attention and form a robust platform for a nanoscale spintronics program at LANL.

Progress

We have optimized material synthesis, device fabrication, measurement instrumentation improvements and noise reduction, and have started collecting spin transport data. To study the physics of spin injection, transport, and detection in semiconductor nanowires, we have pursued two approaches in forming the tunnel barriers for spin filtering. The first approach utilizes an atomic-layer deposited Aluminum Oxide barrier layer whose thickness has been finely tuned between 6 – 10 Angstroms. This layer is applied to n-doped Si nanowires grown by the vapor-liquid-solid growth technique in our labs or to uniform and conformal n-doped Ge shells on an undoped Ge nanowires. The second approach for barrier formation is a new concept in spin devices developed here at Los Alamos, in which a thin p-doped shell layer deposited on the n-doped nanowire form a depletion region (space charge region) and forms a tunneling barrier whose width and height can be controlled by the doping and thickness of the deposited p-layer. This approach will eliminate any associated surface state problems that may arise in conventional oxide-barrier/semiconductor interfaces.

Two-probe and four-probe measurements are used to characterize the electrical doping, contact specific resistivities to adjust the conductivity mismatch between the nanowire and the metal lead for spin injection. Controlling these parameters is known from bulk materials studies to be of critical importance to spin injection. In our controlled doped core-shell approach, the conductivity is dominated by the uniformly doped shell leading to uniform resistivity throughout the nanowire length, which is in contrast to what is typically published in the literature where only a small segment of the nanowire is used as the active device due to variation of doping throughout the nanowire length. From transmission line measurements, where the channel length is systematically varied in order to extrapolate the device resistance to zero channel length, we find a contact resistance of ~ 5 Kohm for n-doped Ge shells, and ~ 2 Kohm for p-doped Ge shells when contacted by a ferromagnetic cobalt contact. We then infer an n-doping resistivity of ~ 1E-3 ohm-cm2

and specific contact resistivity of ~ 1E-6 ohm-cm. As such, the contact specific resistivity needs to be increased by 100-1000 times in order to match that of the semiconductor and allow efficient spin filtering. Using thin doped Ge shells, our initial efforts have led to an increase of 10X in contact resistivity and further increase in the p-layer shell thickness is expected to solve the conductivity mismatch problem. On the other hand, for Al_2O_3 barrier layers on Si nanowire, initial electrical measurements have shown that the specific contact resistivity has increased by ~ 50 – 100 times, which is suitable for spin filtering.

Our measurement setup consists of a low temperature electrical transport system for which the normal magnetic field can be changed in order to perform Hanle and spin-valve type measurements. We have built up a low temperature spin transport measurement system, the measurement sensitivity of which was demonstrated to be high enough to resolve the spin signal in a standard Fe/GaAs thin film device. Devices are being characterized at 4K for the Hanle effect and this key measurement capability is an area of current focused effort. Specifically our signal to noise ratio is being further optimized in order to have the sensitivity to resolve detailed spin effects in our nanowire devices. Gaining high sensitivity in nanoscale systems has proven to be a major challenge in the project due to noise signals associated with these structures and we have made significant progress in this area over the past year. We have measured a large number of Si and Ge devices to establish the appropriate device parameters that give rise to spin injection in semiconductor nanowires. We currently have our first working devices as discussed below. Further improvements in the stability of these devices and reduction in noise background are currently underway.

We have performed two-terminal and four- terminal measurements on silicon nanowire devices with 0.5 nm Al_2O_3 barrier layers. Our preliminary results suggest spin-valve-like effect in our devices. Figure 1 (a) shows a typical four-terminal Si nanowire device. The contacts are 200 nm cobalt capped with 30 nm gold. In the non-local spin-valve measurement, the spin-polarized electrons are injected into the nanowire from contact 3, diffuse towards contact 2 and are then sensed by a voltage drop, V_{4T}, between contact 1 and 2. A magnetic field is applied in parallel with the cobalt electrodes. As shown in Figure 1 (b), when the magnetic field is at ~ -1000 G, both contacts 2 and 3 are magnetized toward the negative direction. When the magnetic field is increased to about 200 G, the magnetic moment in contact 2 switches to positive direction, and hence is anti-parallel to contact 3 and the electron spins in the silicon channel, which gives rise to a sudden change of voltage ($\_V_{4T}$). Further increasing the field to ~ 400 G and above, both contacts 2 and 3 are now magnetized toward the positive direction, and V_{4T} changes back to the initial value. When the field is swept back from 1000 G to -1000G, a similar change of V_{4T} as a function of magnetic field is observed. We are currently making and measuring new Si and

Ge nanowire devices to reproduce this spin-valve signal. By studying the dependence of $\_V_{4T}$ on the distance between contacts 2 and 3, we will be able to extract the electron spin diffusion length. We will also perform Hanle-type of measurements to investigate the electron spin dynamics in nanowires, and obtain the spin relaxation time which is an important parameter for spintronic applications. With these advances we anticipate submitting a number of resulting publications on doping control, contact resistance optimization for spin injection, as well characteristic spin transport parameters in semiconductor nanowires.
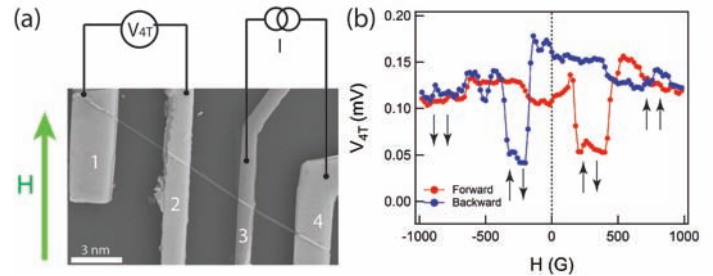
Figure 1. (a) a scanning electron microscopy (SEM) image of a four-terminal silicon nanowire device; (b) the non-local spin-valve signal (V4T) as a function of magnetic field. The two arrows denote the magnetic moments of contacst 2 and 3.

Future Work
The scientific challenge we will address is to understand the injection, transport, and detection of electron spins in semiconducting nanowires. A silicon nanowire contacted with ferromagnetic metal contacts with a thin insulator in between will allow tunneling to occur primarily for those electrons in the ferromagnetic contact with the majority spin. This approach will permit a spin polarized current to flow into the nanowire. The spin current will be detected by another ferromagnetic contact. By application of magnetic fields parallel and perpendicular to the plane of the ferromagnetic contacts, the device resistance can be varied, allowing representation of "on" and "off" states by electron spins, rather than by the large currents typically employed in semiconductors logic devices. This method allows us to unambiguously detect spins and analyze spin transport in semiconducting nanowires for the first time. Our proposed work aims to: 1) investigate electron spin injection, transport and detection in silicon or gernanium nanowires as a function of temperature, electrical and magnetic fields ; 2) establish the influence of nanowire diameter, doping, and surface passivation on electron spin dynamics; and 3) study spin transport in radial and axial nanowire Si/Ge heterostructures and the new physics resulting from strain, and band-structure modifications. Both theoretical and experimental techniques will be employed in this project.

Conclusion
This project will use experiment and theory to study the

manipulation of spins in silicon nanowires grown by our chemical vapor deposition method. Electron spin injection and transport will be detected and quantified by magneto-impedance, spin valve and Hanle effect techniques. The influence of temperature, and electric and magnetic fields will be measured. Effects of surface passivation and diameter on spin transport in nanowires will be determined. In addition, we will exploit our ability to synthesize Si/Ge nanowire heterostructures to explore spin transport across hetero-interfaces and to examine the effects of strain on spin transport in radial heterostructures.

Publications

Dayeh, S. A., N. H. Mack, J. Y. Huang, and S. T. Picraux. Advanced core/multishell germanium/silicon nanowire heterostructures: the Au-diffusion bottleneck. 2011. *Applied Physics Letters.* **99**: 023102.

Dayeh, S., A. Gin, and S. T. Picraux. Advanced core/multi-shell germanium/silicon nanowire heterostructures: Morphology and transport. 2011. *Applied Physics Letters.* **98**: 163112.

Dayeh, S., J. Huang, A. Gin, and S. T. Picraux. Elimination of Gold Diffusion in the Heterostructure Core/Shell growth of High Performance Ge/Si Nanowire HFETs. 2010. In *IEEE Nano 2010 International Conference.* (Seoul, Korea, 17-20 Aug. 2010). , p. 95. Seoul: IEEE.

Dayeh, S., and S. T. Picraux. Ge/Si Core/Multi-shell Heterostructure FETs. 2010. In *Electrochemical Society: SiGe, Ge, and Related Compounds 4: Materials, Processing, and Devices.* (Las Vegas, NV, 11-14 Oct. 2010). , p. 56. Las Vegas: Electrochemical Society.

Dayeh, S., and S. T. Picraux. Direct Observation of Nanoscale Size Effects in Ge Semiconductor Nanowire Growth. 2010. *Nano Letters.* **10**: 4032.

Le, S. T., P. Jannaty, A. Zaslavsky, S. Dayeh, and S. T. Picraux. Growth, electrical rectification, and gate control in axial in situ doped p-n junction germanium nanowires. 2010. *Applied Physics Letters.* **96**: 262102.

Picraux, S. T., S. Dayeh, P. Manandhar, D. E. Perea, and S. G. Choi. Silicon and Germanium Nanowires: Growth, Properties and Integration (Invited Overview). 2010. *Journal of Materials.* **62** (4): 35.

Transformational Approach for the Fabrication of Semiconductor Nanowires: "Flow" Solution-Liquid-Solid Growth

Jennifer A. Hollingsworth
20100285ER

Introduction

Semiconductor nanowires (SC-NWs) constitute "next-generation" nanoscale building blocks for a range of applications from nanoelectronics and photonics to energy-harvesting. SC-NWs can be fabricated using solution-phase methods that offer simplified processing and scale-up, as well as almost unlimited choice of materials systems from Group III-V to Groups IV, II-VI, IV-VI, and I-III-VI2 semiconductors. The solution-phase methods, however, suffer from two fundamental flaws: (1) lack of examples of patterned, vertical SC-NW growth at surfaces and (2) limitations to growing complex axial heterostructures. Overcoming these drawbacks would move the field of solution-phase SC-NW fabrication forward to the point that this approach could be realistically considered for real-world applications. Therefore, our overall research goal is to develop a novel solution-phase SC-NW growth method that aims to address these limitations. We call this new approach Flow-Solution-Liquid-Solid (FSLS) growth.

Like conventional SLS, FSLS entails thermally decomposing chemical precursors in the presence of molten metal nanoparticle "catalysts" that promote the nucleation and growth of the SC-NWs. Unlike SLS, FSLS will allow us to introduce precursors into a reaction vessel by way of a continuously supplied flow of carrier solution, rather than all at once in a single injection. In this way, unreacted precursor and by-products will be constantly removed, approximately steady-state precursor concentrations will be maintained, and different precursors will be able to be supplied in an alternating fashion. Further, rather than utilizing "free-standing" metal nanoparticle catalysts, FSLS will employ nanoparticles adhered to solid substrates. The coupled ability to flow precursors past bound catalyst particles will enable us to synthesize complex axial heterostructures and fabricate SC-NW arrays.

Benefit to National Security Missions

The proposed work addresses two key LANL Materials: Discovery Science to Strategic Applications Grand Challenge FY10 Priorities: Develop (1) the underlying materials science, physics and chemistry to support materials needs in energy efficiency and (2) intrinsic techniques to control functionality with novel architectures resulting from new synthesis, fabrication and processing concepts. Further, it supports the Energy and Earth Systems Grand Challenge FY10 Priority to develop transformational science and technology that enables clean, efficient power generation, addressing energy efficiency and security mission areas.

Progress

Progress has been remarkable over the last 12 months of the project. Having previously modified a commercial microfluidic reactor for FSLS, we have now advanced this novel technique to realize several of our original technical objectives, as well as to reveal new fundamental mechanistic understanding of solution-phase SC-NW growth. During recent months, we have moved far beyond our initial successful efforts to establish and demonstrate FSLS as a new, controlled approach to solution-phase SC-NW growth. Specifically, we have (1) achieved our targeted synthesis of complex axial heterostructures and (2) shown for the first time that SLS growth follows the Gibbs-Thomson effect as previously described for Vapor-Liquid-Solid grown SC-NWs.

Axially heterostructured growth

We have now shown that complex structures are enabled by our new approach. Here, we have fabricated CdSe/ZnSe nanowires comprising up to 8 alternating segments (Figure 1). Previous literature efforts were limited to 2-3 segments and required tedious purification steps in between addition of each segment. In contrast, FSLS allows sequential addition of precursors, where earlier supplied precursors are naturally flushed from the system that is under continuous flow. Depending on growth conditions, segments are either pure-phase CdSe or ZnSe, or CdZnSe alloys. Before extending to segmented SC-NW growth, we conducted systematic, system-specific studies of the effects of precursor concentration, flow-rate, anion-to-cation ratio, reaction temperature, and bismuth film thickness (Bi films separate into nano-droplets upon heating). Optimized conditions were then used in the studies of axial heterostructuring, where reaction

temperature and Bi film thickness were again varied. It was found that higher temperatures, longer growth times and/or thinner Bi films facilitated complete transition from one composition to another, while lower temperatures, shorter growth times, and/or thicker Bi films resulted in incomplete compositional transitions. Both abrupt and alloyed interfaces were thus observed.
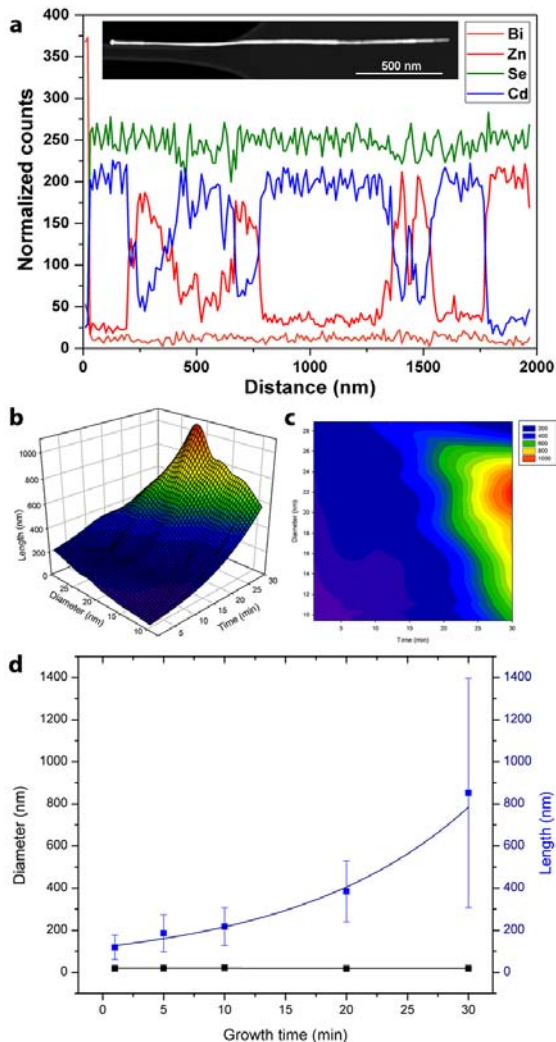
Figure 1. a. STEM image (inset) of complex heterostructured NW comprise 8 segments of CdSe/ZnSe. EDX line scan profile of the total length of NW showing the compositional changes switching between ZnSe and CdSe segments. The compositional fluctuation of ZnSe segment could be caused by the relatively slower growth rate of ZnSe, hence competitive growth of CdSe during growth of ZnSe segment. b-d. Dependence of CdSe nanowire (NW) length on the growth time. NWs were synthesized from 5 nm Bi layer at 300 °C and constant flow rate of 0.2 mL/min. A 3D plot (b) and contour map (c) of NW length as a function of NW diameter and growth time. Gradient spectral color from magenta to red represents the NW length scale. (d) Line graph demonstrate an exponential increase of average NW length as a function of growth time from 1-30 min. Average NW diameter are constant at different growth time. Error bars represent standard deviation value.

New mechanistic understanding

We have shown for the first time that SLS growth follows the Gibbs-Thomson relation between catalyst droplet size and growth rate, where decreasing catalyst diameter leads to a progressive reduction in supersaturation (ultimately to zero) and suppression of growth (Figure 1b-d). Thus, smaller Bi particles (here, thinner Bi films) should result in slower SC-NW growth. Indeed, we obtained temperature-dependent growth rates that were 0.40 nm/sec (300 C) or 0.75 nm/sec (330 C) for NW diameters >20 nm compared to 0.25 nm/sec (300 C) or 0.50 nm/sec (330 C) for diameters <20 nm. Interestingly, each of these growth rates is considerably slower than one-pot SLS, which ranges from 5-70 nm/sec. Likely for this reason, we also observed purely wurtzite growth in the case of our CdSe flow-SLS NWs as opposed to the more common mixed wurtzite/zinc-blende or purely zinc-blende NWs obtained by SLS, where wurtzite is the thermodynamically preferred phase.

We have also made significant progress toward demonstrating utility of our SC-NWs for applications in energy harvesting by establishing approaches for integration of the materials into device structures and for electrical characterization. First, we attempted to incorporate free-standing SLS SC-NWs into hybrid inorganic-organic photovoltaic device architectures used previously for quantum dots. However, we were not able to prepare NW-based films of sufficient uniformity/optical quality to use this platform as the desired "device test best." Therefore, we are currently pursuing alternative approaches to infiltrating NW films with conducting polymers or using all-inorganic constructs. To this end, we have recently successfully grown NWs from an ITO-coated glass substrate for subsequent infiltration by conducting polymer. We have also addressed the issues that previously prevented us from casting high-quality NW-polymer blend films from solutions of free-standing NWs and polymer.

In addition, we are establishing a new capability for correlated electrical/optical characterization – see summary of progress-to-date in Future Work.

Lastly, we demonstrated *in situ* fabrication of SC-NW/metal contacts by chemically adhering SC-NW bismuth catalysts to metal nanorods (gold and silver) and subsequently initiating SLS growth of the SC-NW (Figure 2). To date, attempts to electrically characterize these hybrid nanostructures have been hindered by the persistent presence of a polymer coating that was used to adhere the catalyst nanoparticles to the metal rods. Recently, we made a breakthrough in our synthetic approach that has allowed us to avoid the use of the insulating/chemically persistent polymer (Figure 2b) that should permit electrical properties characterization in the third year of the project.
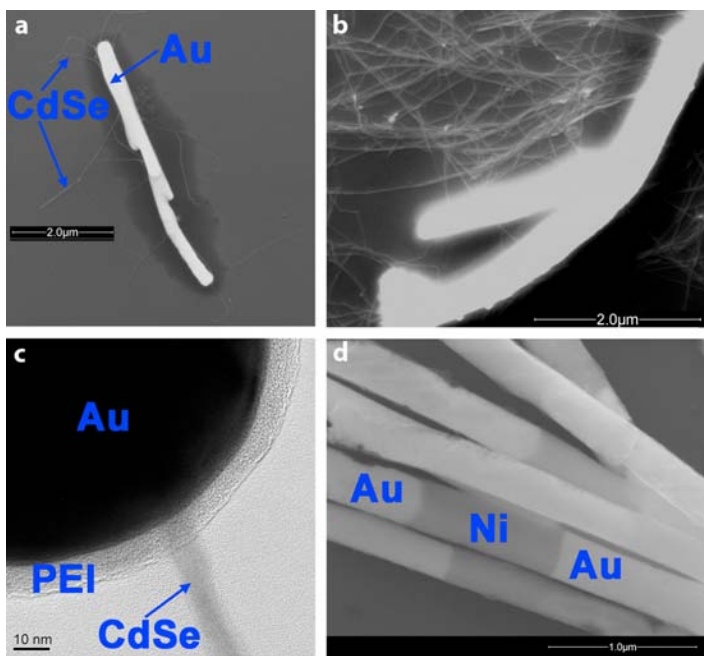
Figure 2. a.Scanning electron microscopy (SEM) image of cadmium selenide (CdSe) nanowires grown from gold (Au) rods, for which a polymer was used to adhere the metal catalyst particles to the rod. b. SEM image of CdSe nanowires grown from Au rods, for which bismuth (Bi) nanoparticle adhesion was achieved using bifunctional biphenyl-4,4'-dithiol. c. High-resolution transmission electron microscopy (HR-TEM) image of the CdSe-Au interface. d. SEM image of Au rods into which a nickel (Ni) segment was incorporated to facilitate magnetic separation of the rods from non-adhered Bi and free-standing (unattached) SC-NWs.

Future Work
Transform SLS into FSLS for Advanced Solution Growth of SC-NWs

Work for this Task has largely been completed. Future work will entail extension of the FSLS method to more energy-relevant materials systems, e.g., CdTe, CuInSe$_2$ and Pb-chalcogenide SC-NWs.

Assess Utility of FSLS Method for Energy Harvesting Applications

Photovoltaic example: At the level of device proof-of-concept, we will significantly advance the state-of-the-art in hybrid inorganic/polymer solar cells by fabricating NW-based devices wherein vertically aligned SC-NWs and/or non-aligned SC-NW mats will provide substantially improved charge transport compared to quantum-dot-based devices by changing the mechanism of charge transport from charge hopping (quantum dot case) to more efficient direct transport (SC-NW case).

At the level of fundamental understanding, we will apply simultaneous optical/electrical characterization. We have successfully integrated the single nanowire electrical transport and photocurrent measurement capability into our single-nanowire optical spectroscopy capabilities (Raman, PL, TR-PL) to perform correlated electrical/optical measurements on single-nanowire devices. Scanning photocurrent microscopy performed on a VLS-grown single Si nanowire device (Figure 3) affords a demonstration of this new capability. In order to apply this technique to SLS-grown single nanowires (CdTe, CdSe, InP, etc.), we are currently optimizing the single-nanowire device fabrication process. Although such processes are well established for VLS-grown, large diameter SC-NWs (d>100 nm), they are not directly applicable to the small-diameter/organic-ligand-coated SLS SC-NWs. The devices we have fabricated so far show very low conductivity, where poor ohmic contacting likely results from the presence of the organic ligands. In addition, where we have achieved higher conductivities, SEM analysis reveals that the "single" SC-NWs are really bundles (Figure 3c). We are currently exploring multiple approaches including Ar plasma cleaning and ligand exchange, and hi-vacuum annealing to remove these ligands. In parallel, we are also optimizing the dispersion process to achieve single NWs devices (Figure 3d).
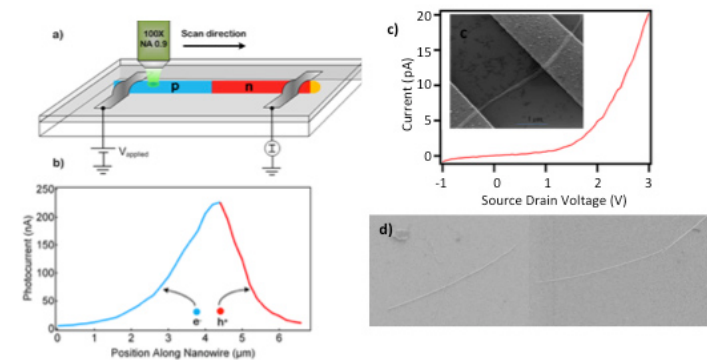
Figure 3. a. Schematic of scanning photocurrent microscopy set up. b. Photocurrent measured across the p-n junction of a single Si SC-NW showing the peak at the junction. The exponential decay of the current on each side of the decay gives electron and hole minority carrier diffusion lengths. c. I-V curve and SEM image (inset) of the device made from a SC-NW bundle. d. SEM image of single SC-NW dispersed onto a substrate.

If successful, this novel capability will allow us to directly correlate the photocurrent generation efficiency of individual SC-NWs with their optical characteristics, such as PL emission efficiency and lifetime. A systematic analysis of such correlated data will shed new light on the competing processes of charge separation and carrier recombination that play critical roles in defining photovoltaic performance.

Thermoelectric example: We will use FSLS to demonstrate for the first time nanoscale axial heterostructuring in solution-grown SC-NWs and to provide experimental support for theoretical predictions that such structures will enable

ultra-high efficiency thermoelectrics. We have now done this, but for a non-thermoelectrics system, i.e., CdSe/ZnSe, as this system was more easily adapted to flow-SLS growth. In our third year, we will attempt to growth thermoelectric-relevant PbSe/PbTe hetero-SC-NWs by flow-SLS.

We will submit at least three manuscripts to high-level journals (2 in preparation: (1) Flow-SLS from new mechanistic understanding to unprecedented axial heterostructuring and (2) *In situ* fabrication of semiconductor-metal contacts).

Conclusion
We have enabled for the first time the solution-phase synthesis of complex axially heterostructured semiconductor nanowires (SC-NWs). Demonstration of patterned, vertical SC-NW arrays by this method remains to be demonstrated. These new capabilities will address the factors that are currently limiting the utility of solution-phase-grown SC-NWs for key applications in energy harvesting -- SC-NW-based photovoltaics and thermoelectrics. In addition to developing new functional nanomaterials synthesis and fabrication capabilities, we will provide a proof-of-concept demonstration of enabled photovoltaic and thermoelectric devices.

Publications
Hollingsworth, J. A.. Novel functional semiconductor nanocrystal quantum dots and nanowires for applications involving energy conversion. Invited presentation at *2010 Materials Research Society Spring Meeting.* (San Francisco, April 5-9).

Laocharoensuk, R., N. Smith, J. Baldwin, A. Gin, and J. A. Hollingsworth. Versatile Solution-Phase Approach for Fabrication of Metal-Semiconductor Heterostructured Nanowires. Presented at *2010 Materials Research Society Spring Meeting.* (San Francisco, 5-9 April 2010).

Laocharoensuk, R., N. Smith, K. Palaniappan, J. K. Baldwin, and J. A. Hollingsworth. Integration and Development of Solution-Phase Techniques for Fabrication of Novel Heterostructured Nanowires. Presented at *2010 Materials Research Society Fall Meeting.* (Boston, Nov. 29-Dec. 3 2010).

Palaniappan, K., R. Laocharoensuk, N. Smith, R. Dickerson, J. L. Casson, J. K. Baldwin, and J. A. Hollingsworth. Flow-solution-liquid-solid growth: novel solution-phase technique for fabrication of axially heterostructured semiconductor nanowires. Presented at *CINT User Conference.* (Albuquerque, NM, 14-16 Sept. 2011).

Unraveling Electron-Boson Interactions in High-Tc Superconductors With Ultrafast Infrared Spectroscopy

Rohit P. Prasankumar
20100298ER

Introduction

The first high-T_c superconductor (HTSC) was discovered over 20 years ago, yet the mechanism underlying this unique phenomenon remains poorly understood. In particular, an understanding of whether electrons in these materials form pairs known as Cooper pairs through electron-boson interactions or through strong electronic correlations alone is lacking. The DOE Office of Science has made understanding superconductivity a priority research direction, signified by the workshop on "Basic Research Needs for Superconductivity" that was held in 2006. Advances in understanding the coupling between electrons and bosons in HTSCs will require the application of novel experimental and theoretical methods proposed here.

The goal of this project is to couple the new experimental technique of ultrafast infrared spectroscopy (UIS) with novel theoretical models to investigate electron-boson interaction dynamics in HTSCs, understand the coupling between different degrees of freedom, and determine their relevance to Cooper pairing. UIS will enable us to directly photoexcite low energy excitations in complex materials and dynamically probe the resulting changes in the complex conductivity. This stands to significantly impact our understanding of HTSCs, since we will be able to probe electron-boson coupling by photoexciting relevant bosonic modes and temporally resolving the resulting changes in optical conductivity, $\sigma(\omega, t)$. This experiment alone should answer the important question of whether bosons are the pairing glue in HTSCs. Analysis of the data using novel theoretical models for the photoinduced changes in $\sigma(\omega, t)$ could then be used to uncover the specific bosonic mode that serves as the pairing glue between electrons. In short, the use of ultrafast infrared spectroscopy to examine the dynamics of low energy excitations in HTSCs, coupled with advanced theoretical models, is an innovative approach for exploring electron-boson interactions in HTSCs, with the potential to finally uncover the pairing glue in these extensively studied systems.

Benefit to National Security Missions

The DOE Office of Science, in particular Basic Energy Sciences, has made understanding superconductivity a priority research direction, signified by the workshop on "Basic Research Needs for Superconductivity" that was held in 2006. The research described in this proposal directly addresses many of the issues identified in the report from this workshop, along with the Basic Understanding of Materials grand challenge at LANL, and will thus be very relevant to these areas.

Progress

In the second year of this project, our experimental progress towards the proposed ultrafast infrared spectroscopy system, which would allow us to perform mid-infrared pump, terahertz (THz)-probe (MPTP) measurements on the high-T_c superconductor YBCO, was hindered due to unanticipated difficulties with our ultrafast infrared spectroscopy (UIS) system. Our initial MPTP experiments on YBCO, undertaken near the beginning of the year, were unsuccessful due to high reflections of the pump beam at the cryostat windows. We were able to devise a solution by designing a novel dual cryostat window that allows us to simultaneously propagate both mid-IR and THz pulses to the sample. However, after successfully implementing and testing the validity of this approach, our optical parametric amplifier (OPA) that generates mid-IR pulses failed due to a burnt power supply. We have since fixed this problem and are currently realigning the system, after which we plan to resume our MPTP experiments on YBCO. We will also perform optical-pump, THz-probe (OPTP) experiments on YBCO while varying the pump fluence; these experiments can be done using any of the several OPTP systems in our laboratories, offering us more flexibility in case any single system has problems. The resulting data from these experiments, as well as that from optical-pump, mid-IR probe (OPMP) experiments to be done on our UIS system, can be directly compared to our theoretical models for the photoinduced optical conductivity in a high-T_c superconductor, as described below.

Due to these difficulties with our MPTP experiments, we used other femtosecond laser systems in our laboratories

to pursue related directions. In the first year of this project, we had performed MPTP experiments on graphene, arguably the "hottest" material in current condensed matter physics research and subject of the 2010 Nobel Prize in Physics. However, these experiments were relatively difficult to interpret, and therefore we performed near-IR pump, visible-probe experiments to obtain a better understanding of carrier dynamics in graphene. These experiments were surprisingly fruitful, as we were able to directly demonstrate the relativistic nature of a photogenerated electro-hole plasma in graphene as early as 100 femtoseconds (fs) after photoexcitation. A publication on this work has been submitted to Physical Review Letters, and this work was selected for an invited talk at the Nonlinear Optics conference in July 2011.

In addition, we were able to perform OPTP experiments (using another laser system) on FeAs films that were deposited on LAO substrates. FeAs is a pnictide superconductor with T_c~12 K (in our samples); this class of superconductors was first discovered in 2008 and has attracted much attention since they are the only noncuprate superconductors with T_c>50 K (for optimized samples). To date, no OPTP experiments have been done on these superconductors. We were able to perform the first experiments of this kind on our FeAs/LAO samples (Figure 1), which were quite difficult since the signals were extremely small and required >2 hours of averaging for each trace. These measurements revealed that the superconducting condensate recovers on a relatively slow time scale (~30 ps) after pump excitation, while quasiparticles recover much more rapidly (~10 ps) above T_c.
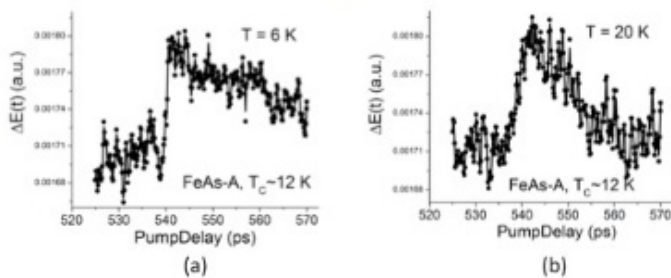
Figure 1. Optical-pump, THz-probe measurements on FeAs/LAO samples at (a) 6 K and (b) 20 K.

Finally, before our MPTP system went down, we completed our experiments on type-II InAs/GaSb strained layer semiconductor superlattices (SLS), which were begun in the first year of this project. This work was presented at the Optical Terahertz Science and Technology conference in 2011, and we are currently preparing a manuscript describing our results.

On the theoretical side, we have laid down the framework of time-resolved phenomena for high-temperature superconductors based on an effective-temperature model (J. Tao and J.-X. Zhu, Phys. Rev. B 81, 224506 (2010)). In this framework, (i) we divide the system into three subsystems: electrons, hot phonons that are strongly coupled to electrons, and cold lattice, and assume that the energy transfer within each subsystem is much faster than that between different subsystems so that a local equilibrium within each subsystem can be reached; (ii) according to the energy conservation law, we develop a three-temperature model to simulate the time evolution of the temperatures of electrons, hot phonons, and cold lattice. The framework is valid for both normal and superconducting states. Within this framework, all time-resolved quasiparticle dynamical quantities can be calculated seamlessly.

Our preliminary results have shown the potential to reveal the nature of the bosonic mode that is most strongly coupled to electrons. For the past year, we have been formulating a theory for time-resolved optical conductivity and Raman scattering of HTSCs (J. Tao, R. P. Prasankumar, E. E. M. Chia, A. J. Taylor, and J.-X. Zhu, Phys. Rev. B (to be submitted)). Our results show that, in the superconducting state, the dynamical conductivity exhibits a second peak at higher (mid-IR) frequencies, in addition to the peak due to the Drude response at zero frequency. This higher-frequency peak disappears when the system evolves into the normal state, suggesting the significant effect of the superconducting gap upon the time-resolved optical properties of HTSC, and the ultimate importance of electronic coupling to bosonic modes. A similar structure has also been revealed in our simulations of time-resolved Raman spectroscopy.

Simultaneously, we have also started with the formulation of a fully quantum mechanical simulation of time-resolved optical conductivity. This new theory goes beyond the effective model, as explained above. Our initial results have enabled us to track the time-evolution of photoexcited quasiparticles, and we expect to make more progress in this direction during the next year of the project.

Future Work

Our initial goal in the last year of this project is to get our UIS system working; we are currently working on this and expect it to happen early in the year. Once this system is working and its performance is optimized, we have several experiments planned. We will first use UIS to temporally resolve changes in the complex conductivity σ(ω, t) after direct photoexcitation of specific bosonic modes in YBCO. We will use THz probe pulses to measure the effect of photoexcitation on the superconducting condensate fraction f_s and quasiparticle fraction f_n as a function of temperature. Any observed decrease in f_s (and corresponding increase in f_n) upon photoexcitation would provide strong evidence that the given mode is linked to Cooper pairing in YBCO. Pump wavelength and doping dependent experiments will give further insight into these phenomena.

We will also perform optical-pump, mid-IR probe experiments on YBCO and Bi-2212 samples early in the next year to compare to our theoretical predictions of a mid-IR peak

in the dynamical conductivity in the superconducting state. OPTP experiments will also be performed on FeAs and other pnictide superconductors, especially after we obtain samples optimized for these experiments (ideally thicker FeAs films on another substrate such as MgO). Finally, we will finish our manuscript describing our MPTP experiments on the type-II SLS.

Our theoretical studies will be pursued in parallel with the experimental efforts. We will continue to develop rate equations for the electron and bosonic mode temperatures as part of a microscopic two-temperature model. We will then calculate the time evolution of σ(ω, t) and compare it with experiments to understand its origin. Finally, we will develop a non-equilibrium optical conductivity model within a density-matrix theory and compare the calculated and experimentally measured σ(ω, t). This powerful theoretical and experimental combination is an innovative approach for exploring electron-boson interactions, with the potential to finally uncover the pairing glue in HTSCs.

Conclusion

We expect that in the last year of this project, we will make substantial progress towards accomplishing the goals of this project, particularly in coupling our experimental applications of ultrafast infrared spectroscopy to cuprate and pnictide superconductors with our novel theoretical models. This will allow us to investigate electron-boson interaction dynamics in high-temperature superconductors, understand the coupling between different degrees of freedom, and determine their relevance to Cooper pairing. Overall, this novel approach has the potential to finally uncover the pairing mechanism in high-T_c superconductors, which could lead to room temperature superconductivity and will certainly enable many new applications of HTSCs in areas such as power transmission and magnetic resonance imaging.

Publications

Dani, K. M., J. F. O'Hara, Q. McCulloch, F. Chen, A. K. Azad, G. Dakovski, S. A. Crooker, A. J. Taylor, and R. P. Prasankumar. Ultrafast broadband mid-infrared pump, terahertz probe spectroscopy. Presented at *Conference on Lasers and Electro-Optics.* (San Jose, CA, 2010).

Dani, K. M., J. Lee, A. D. Mohite, C. M. Galande, P. M. Ajayan, A. M. Dattelbaum, H. Htoon, A. J. Taylor, and R. P. Prasankumar. Observation of the ultrafast relativistic response of a non-equilibrium electron-hole plasma in graphene. *Physical Review Letters.*

Dani, K. M., J. Lee, R. Sharma, A. D. Mohite, C. M. Galande, P. M. Ajayan, A. M. Dattelbaum, H. Htoon, A. J. Taylor, and R. P. Prasankumar. Observation of the relativistic response of an electron-hole plasma in graphene on femtosecond timescales. Invited presentation at *Nonlinear Optics 2011.* (Lihue, HI, 17-22 July 2011).

Dani, K. M., J. Lee, R. Sharma, A. D. Mohite, C. M. Galande, P. M. Ajayan, A. M. Dattelbaum, H. Htoon, A. J. Taylor, and R. P. Prasankumar. Observation of the relativistic response of an electron-hole plasma in graphene on femtosecond timescales. Presented at *Conference on Lasers and Electro-Optics.* (Baltimore, MD, 2011).

Lee, J., K. M. Dani, A. D. Mohite, R. Sharma, A. J. Taylor, and R. P. Prasankumar. Probing intraband conductivity dynamics in graphene. 2011. In *17th International Conference on Ultrafast Phenomena.* (Aspen, CO, 18-23 July 2010). , p. 308. London: Oxford University Press.

Lee, J., K. M. Dani, R. Sharma, A. D. Mohite, C. M. Galande, P. M. Ajayan, A. M. Dattelbaum, H. Htoon, A. J. Taylor, and R. P. Prasankumar. Ultrafast relativistic response of photo-excited carriers in graphene. Presented at *March Meeting of the American Physical Society.* (Dallas, TX, 2011).

Tao, J., and J. X. Zhu. Theory of the time-resolved spectral function of high-temperature superconductors with bosonic modes. 2010. *Physical Review B.* **81**: 224506.

Upadhya, P. C., K. M. Dani, S. D. Mukherjee, N. Gautam, A. Gin, M. Cich, J. Kim, S. Krishna, A. J. Taylor, and R. P. Prasankumar. Time-resolved mid-infrared pump, terahertz-probe spectroscopy of type-II strained layer superlattices. Presented at *Optical Terahertz Science and Technology 2011.* (Santa Barbara, CA, 2011).

GO FISH, A Smart Capture and Detection Strategy for Intact and Viable Pathogens

Harshini Mukundan
20100308ER

Introduction

Current methods of biodetection use carbohydrates and antibodies, binding either a single or a few sites on the target. These methods, therefore, do not discriminate viable pathogens from dead. It is critical that the interrogation of a pathogen include a measure of viability for accurate determination of threat, for only intact organisms are infective and of concern. For example, bacterial signatures and debris are likely after a decontamination process has been performed on a contaminated site. PCR-based identification, which is most often used for evaluation of decontamination procedures assays for nucleic acid signatures, does not discriminate between live and dead organisms either. However, assessment of presence of viable bacteria is the only true measurement required to confirm the efficacy of the countermeasures. This is currently achieved by confirmatory culture, a process that can take days to weeks depending on the pathogen. The same situation presents itself in evaluating potentially contaminated food products such as dairy or meat. Having a rapid method to inform on the presence of viable pathogens of concern can significantly enhance current bio-detection methods.

The current project aims to achieve a rapid, specific and sensitive method for the selective capture of viable bacteria in a complex background by exploiting a highly sensitive iron sequestration system evolved by the pathogen. As suggested by the proposal title, Go Fish, we will use a novel capture process that occurs only with the active participation of a viable pathogen. In this work, we use a 'bait' to hook a pathogen onto a tether with an active internalization process that is conducted only by an intact viable pathogen (Figure 1).

Iron is a sparse element that is critical for life and hence, all pathogens have evolved siderophores to bind and sequester iron with incredible affinity. Once iron-bound, the siderophores return to the bacterium (targeting) and deliver the iron through one of two different transport systems. Our project exploits this naturally occurring, universal, high affinity phenomena to capture viable pathogens in a complex matrix. Since iron uptake is a requisite of only living cells and actively performed by the organism, dead bacteria and debris do not cross-react with this binding reaction. By virtue of this biochemical feature, our approach can be used for the selective capture of only live, viable agents.
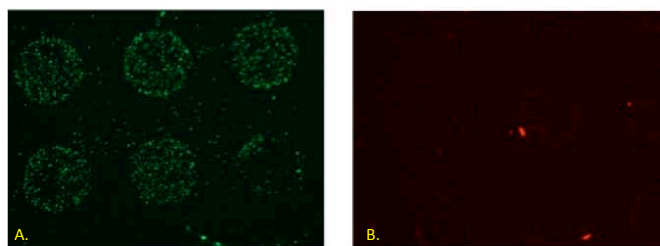
Figure 1. Selective capture of live (green) E. coli on glass slides functionalized with silane-based monolayers, and patterened with desferrioxamine (circles). Relatively poor capture of dead (red, B) bacteria using the same approach. 10X magnification.

Benefit to National Security Missions

The work is a strategy to specifically detect viable pathogens, and is universally applicable to several classes of pathogens of interest to the food safety (DoD, DARPA, DHS), biosecurity (NIH, DoD, DHS, DARPA, DTRA) and medical community (NIH). Also, the project will offer valuable information on siderophore synthesis and capture, of great interest to the basic research community (DOE:SC). We are currently working on submitting a phase 2 proposal to the USDA to address the issue of potential contamination of dairy (esp. milk) with viable mycobacteria. We are also submitting a white paper to DTRA. This work will be presented at the annual DTRA CBD conference in November by Dr. Mark Wolfenden.

Progress

Contaminated food and resulting infection of consumers is of increasing concern. The pathogens that are mostly and increasingly affiliated with food poisoning in the United States include, but are not limited to, Escherichia coli, Salmonella species and Listeria Species. E. coli has been a pathogen of growing concern primarily
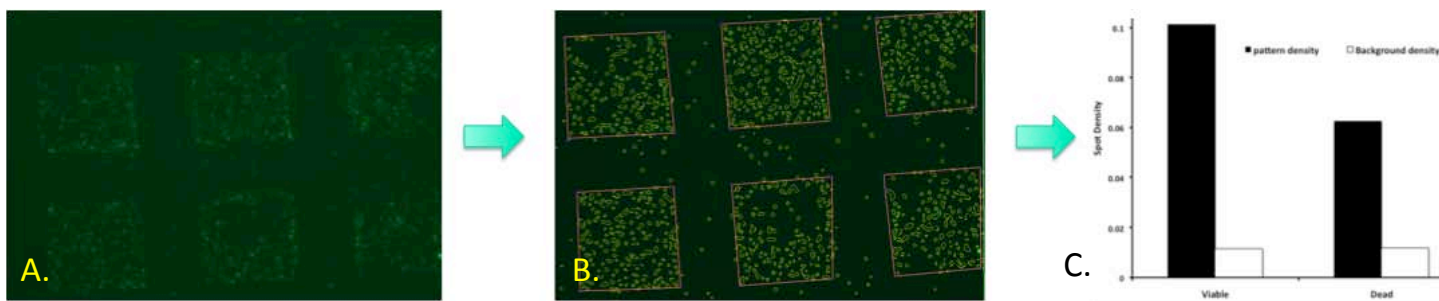
Figure 2. Preliminary quantitative extrapolation of the microscopy data. Panel A demonstrates the selective capture of viable E. coli in the patterned glass slides. Panel B demonstrates the edge selection of the intensity spots within the patterned area using the software algorithm. C shows the quantitation of the density of the spots in B, and also in a slide stained for the dead organisms. Currently, the software does not correct for staining intensity, time of exposure or differing extinction co-efficients of the red vs. green dyes.

because of the evolution of highly pathogenic strains (e.g. 0157) and sharing of genetic material with other enteric bacteria (e.g. Shiga Toxin carrying E. coli, E. coli with the NDM-1 drug resistance gene and others). With these novel mutants, responsiveness of routine health practices to coliform infection is weakening. Early and rapid detection of contamination with viable E. coli can allow for a rapid and more effective intervention.

We used E. coli as a model system for the preliminary demonstration of our approach (Figure 1). For this, we have demonstrated the sensitive and discriminatory capture of intact, viable E. coli cells using surface-bound desferrioxamine (Figure 2). To achieve this, patterned, silane-based, PEG-modified thin-films were prepared. Briefly, 3'-amino-propylmethyldiethoxysilane (APMDES) was vapor deposited onto a cleaned microscope slide. The resulting surface amines were modified with a mixture of mono-disperse, defined polyethylene glycol (PEG) chains, one with a methoxy group for non-specific binding resistance, and one with an Fmoc-protected amine for functionality. The Fmoc-groups were removed and the resulting amine was reacted with biotin. Irradiation of the slides with UV/O3 through a chrome photomask (500 μm, feature size) removed the thin film in exposed areas while leaving the biotinylated film in the masked areas. The cleaned areas were reacted with another portion of APMDES and the methoxy-terminated PEG chain to afford patterned surfaces with discrete capture patches.

We used the patterned thin-films to build in a negative control in the non-biotinylated regions. To these surfaces was added streptavidin, which reacted only with the portions of the thin film that contained biotin. This streptavidin surface was treated in one of two solutions. First, biotinyl-desferrioxamine (BD), which was prepared by reacting commercially available desferrioxamine with NHS-PEG-biotin , was attached to the streptavidin molecules. Second, BD was pre-incubated with E. coli (see preparation below) then added to the streptavidin-coated thin-films. Desferrioxamine was chosen because of the relative ease of modification.

We have demonstrated the capture of E. coli that were prepared using a BacLite kit. This kit differentially stains live and dead bacterial cells; using this method, viable cells are dyed green and dead cells are dyed red. The treated E. coli cells were either added to desferrioxamine coated slides, or pre-incubated with the capturing agent and used as described above. These treatments were imaged using fluorescence microscopy. Both methods were able to capture intact, viable pathogens, but pre-incubation of the bacteria with the siderophore seemed to give less non-specific binding. Very few dead cells, only those still intact in morphology, were bound from a 50% mixture of dead and living cells. We may suggest that the "dead" cells captured were those dying but still intact enough to perform the active uptake of iron.

Most recently, we have worked with Dr. L. Prasad (ISR-3) to adapt his MatLab statistical analysis software program, originally developed to enhance satellite images, for the quantitative extrapolation of the microscopy results (Figure 3) and shown that the staining intensity with 'green (viable)' agents is significantly higher than that associated with the 'red (dead)' pathogens. The statistical analysis, however, does not currently correct for difference in exposure times and the difference in extinction co-efficient between the two dyes. Dr. Prasad is working on adapting these features to the program. We are working on developing threshold intensity for live agents that can be corrected in any statistical analysis, resulting in the easy and accurate quantitation of the data available. Adaptation of this program, with the addition of the requisite algorithms mentioned, will facilitate simple and rapid analysis of microscopy data, a process that currently requires long hours of manual effort.

We have also completed preliminary evaluation of the pathogen count (CFU/mL) to determine the sensitivity of the assay platform. We are also confident, based on preliminary data, that rigorous washing with buffer containing tween 20 (detergent) will allow for further decrease in the intensity of the background staining in non-patterned areas, thereby enhancing sensitivity.

A communication is under preparation and will be submitted to JACS in November 2011.
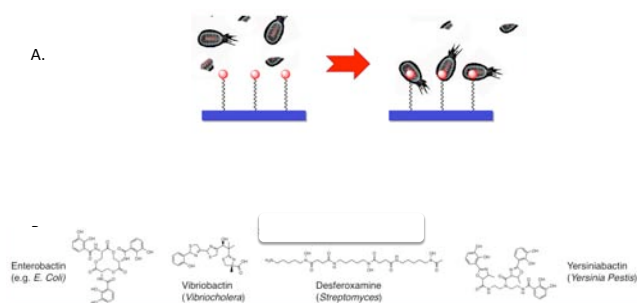
Figure 3. Representative processing of a fluorescence microscopy image using edge detection. Panel A shows the fluorescence mi-croscope image of specific staining for live bacteria using desf B capture. Panel B demonstrates edge detection of the image using a Canny edge detector, resulting in the identification of edge pixels around each site. Panel C demonstrates the conversion of the measured pixel intensity to spot density. Black bars indicate the quantitative spot density for the patterned areas when the slides were stained for viable (green) and dead (red) bacteria. Clear bars indicate background staining under the same conditions.

Future Work

Our future objectives are: 1) design and synthesize tethered SDP-fluorophore markers for solution detection, 2) adapt this technology to the detection of carboxy-myco-bactin, a siderophore for *M. tuberculosis*, 3) refine the statistical analysis algorithm to better reflect the observed data, and 4) refine this technology to distinguish among species and strains (potential multiplex detection).

We have established collaboration with Dr. Toby Dickerson at Scripps Institute, through whom we have obtained mycobactin and are expecting to receive some carboxy-mycobactin, the siderophore for tuberculosis infections. We have developed a membrane insertion (direct detection) assay for mycobactin as a joint effort between the current ER and a LDRD DR led by Korber and Swanson (ended October 2011). We are initiating experiments to tether the carboxy mycobactin to glass slides, to allow for the selective capture of mycobacteria in infected samples. This is of special interest to the USDA and we were invited to submit an AFRI Proposal on the adaptation of this technology to detection of viable mycobacteria in infected milk. We are currently exploring both commercial IP interest and sources of follow on funding for this unique technology, and have submitted a provisional patent application.

Conclusion

The research will lead to capture agents tethered to surfaces or soluble fluorescent reporters that complement our detection tools for pathogens. While traditional recognition is unable to distinguish viable from dead cells, we have demonstrated selectivity to viable agents only. Species selective capture, and likely strain preferences will be demonstrated, increasing our capability to respond effectively to a biosecurity or food safety threat, or improve medical diagnostic strategies.

Ultra-Fast DFT-Quality Forces for Molecular Dynamics Simulations of Materials

Arthur F. Voter
20100366ER

Introduction

The molecular dynamics (MD) simulation method, in which atoms are evolved in time according to the classical equations of motion, has become a standard and powerful tool in materials science. If the underlying model for the forces between the atoms is accurate, high-quality predictions of molecular and material behavior can be made, helping researchers interpret experiments, develop new models, and generally understand how materials behave in full microscopic detail. Electronic structure methods, such as density functional theory (DFT), can be used to provide very accurate forces on the atoms, but the computational cost of DFT is extremely high, typically limiting MD simulations to at most picoseconds (trillionths of a second) for relatively small systems of a few hundred atoms. In contrast, MD simulations using empirical interatomic potentials, although not as accurate, can reach much longer times, up to roughly a microsecond. Moreover, using accelerated molecular dynamics methods, we can push to times of milliseconds and sometimes beyond. In this project, we are trying to develop a totally new approach for calculating interatomic forces, aimed at achieving roughly the accuracy of DFT with a speed close to that of empirical potentials. We are developing a self-adaptive data-mining approach, in which force and local geometry information from every DFT evaluation is saved in a database for future use. During a simulation, the force on each atom is obtained by selecting, from the database, clusters of atoms that are similar to the cluster comprised of the atom of interest and its neighbors, and then applying a novel physics-based interpolation to approximate the force on the central atom. If no good match exists in the database, this new cluster geometry is added to the database, along with the DFT force on its central atom. This high-risk, high-payoff project requires method development in a number of areas: determination of an accurate electronic-structure force from only a cluster; fast approximation for the distance between two clusters; fast retrieval of closely matching clusters from the database; fitting a highly accurate local potential to a set of clusters; and parallelization of the final algorithm.

Benefit to National Security Missions

This project is aimed at developing a capability for very fast, very accurate force calculations for molecular dynamics simulations of materials, so that unprecedented time scales can be achieved with good accuracy. This capability will be valuable in many areas, such as designing advanced materials for nuclear reactors and nuclear waste storage, designing alloys for aerospace and energy applications, designing catalysts for fuel cells, and improving processing steps for growth of solar cells or superconducting films.

Progress

As sketched above, we are developing a novel molecular dynamics approach in which the force on each atom is determined by retrieving geometrically similar clusters from a database, where for each of these stored clusters the force on the central atom has been determined accurately using electronic structure theory. Our prototype system for development and testing is silicon (e.g., a block of 216 or 1000 Si atoms with one or more defects in it), chosen because it offers enough complexity and because we have a high quality Si tight binding potential that can act as a less-expensive surrogate for DFT.

Early this year, our investigations showed the benefits of making the domain belonging to each cluster larger than we had originally planned. This prevents exponential runaway in the number of clusters in the database, as shown in Figure 1. However, this puts a greater burden on the quality of the potential function representing the force on the central atom of the cluster. This potential must accurately describe this force as the cluster is distorted over a larger range.

To address this, we have redesigned our force approximation procedure. Rather than performing a potential fit on the fly for each atom after closely matching clusters are extracted from the database, we now fit an interatomic potential in advance for each database cluster and store it with the cluster. To perform this fit, we generate auxiliary clusters in its neighborhood to use in the fit, rather than using other clusters existing in

the database (whose positions are history dependent, and hence biased). This eliminates the computational cost of fitting the potential at run-time; it instead becomes part of the overhead when a new cluster is added to the database. This approach also allows us to perform a more comprehensive fit without significantly impacting the overall speed of the method.
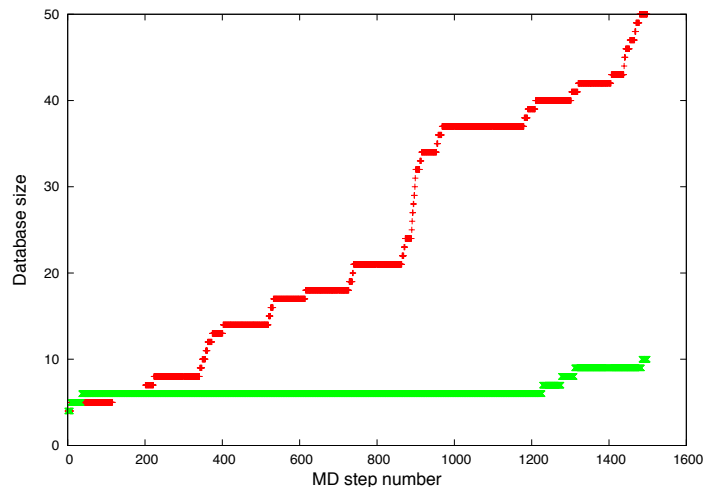
Figure 1. Database size vs. MD time for a 215-atom Si system with one vacancy. The lower curve (smaller database) is for a cluster domain-size cutoff of 1.4 Angstroms, and the upper curve is for a cutoff of 1.0 Angstroms. The smaller cutoff (tighter tolerance) leads to a larger database whose size will continue to grow at a high rate. The MD time step in these runs is 2 femtoseconds.

Unfortunately, we struggled for a large fraction of this year trying, but failing, to get good and reproducible results, until we finally realized that it was because the signature-based cluster-matching method was not working as well as we thought. (Recall that this is the fast method we developed for computing an approximate distance between two clusters, enabling rapid retrieval of the closely matching clusters from the database.) It works well for clusters that are only a small distance away, but for cluster pairs with very different geometries, such as when there is a vacancy in the first neighbor shell in one cluster and not the other, it gives an erroneously small distance. Consequently, as we made each database cluster cover a larger domain, the signature-based method was not correctly distinguishing between the case of similar clusters at a larger distance and the case of clusters that were very different, and our results became erratic.

To remedy this, we have written an exact rotation code, which rotates and renumbers atoms as necessary to find the best possible matchup between two clusters. We also wrote a second, exact rotation code based on quaternion analysis. Having two independent codes, we can verify that we are obtaining the correct distance between any two clusters. These are fast codes, but explicit rotations are much slower than the signature method, which does not

require rotation at all. Consequently, our testing is going much slower now, but all other aspects of the method can still be developed and tested in spite of this.

We now have a working overall code that performs the database lookup with perfect distance accuracy and all the necessary options for testing a wide range of different approaches for performing high-accuracy potential fits and extracting accurate electronic structure forces from finite clusters. Very briefly, we have tried: fitting to the cluster Hessian elements from electronic structure in addition to the forces; using different forms of potential (e.g., modified embedded atom method, Stillinger-Weber); varying the number of free parameters in the potential; performing downhill fits vs. global fits, varying the cluster domain size, varying the number of auxiliary clusters; varying the cluster size, passivating the truncated cluster with hydrogen-like bonds for higher force accuracy; implementing Fermi-level smearing to reduce the force discontinuity at energy level crossings; implementing a fixed Fermi level. We have more work to do, but the trends and the remaining sources of error are beginning to become clear.

A major issue in the development of this method is that the dynamical evolution does not conserve energy, because our forces, which come from a different cluster for each atom, cannot be written as derivatives of a particular total energy of the system. This nonconservation error manifests itself by overheating -- the simulated system goes to a higher temperature than is requested by the thermostat.

There are two sources of this nonconservation error: The first error arises from taking the force from a finite-size cluster. Formally, this only gives a conservative force if the cluster consists of the entire system. However, we have established that if the cluster is made large enough, the force converges to a value very close to the correct value -- i.e., the force for that atom in the entire system. If we use this electronic-structure cluster force at every time step, we achieve reasonable energy conservation, as shown in Figure 2. The second component of the nonconservation error comes from the imperfect approximation to this cluster force as the cluster geometry varies. If the cluster-specific potential is accurate enough to exactly mimic the electronic structure cluster force for any distortion of the cluster, this second error disappears. Interestingly, this second error is coupled to the more general potential fitting challenge we have. If the cluster-specific potential gives the kind of accuracy we want from this method, we automatically solve the nonconservation problem as well. Figure 3 shows an example of the temperature accuracy in a recent simulation.
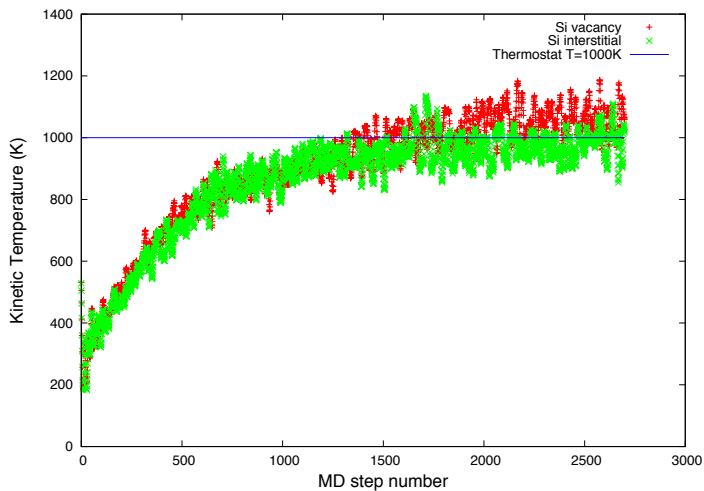
Figure 2. Kinetic temperature vs. MD time for systems in which the force on each atom is taken directly from an electronic structure calculation (tight binding in this case) on a finite cluster with a radius of 7.5 Angstroms. This demonstrates that if the cluster is large enough there is adequate energy conservation. Because in this approach we have only the forces, not the energy, we cannot examine the energy conservation directly. Instead, we examine the average kinetic temperature, verifying that it is very close to the Langevin thermostat temperature setting (T=1000 K in this case). The temperature for the interstitial case (green) is ~2.5% low and the vacancy case (red) is ~6% high. A larger cutoff would make this error even smaller.
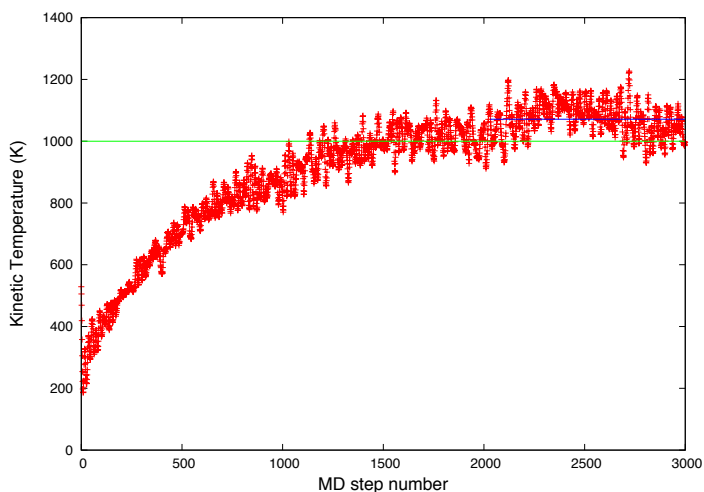
Figure 3. Kinetic temperature vs. MD time for a Si vacancy simulation, using the same 1.4-Angstrom-domain system shown in Figure 1. The average kinetic temperature of T=1071 K (blue line, averaged over the last 1000 MD steps), is somewhat higher than the value of the Langevin thermostat setting of T=1000K (green line), indicating some nonconservation error, although some of it is coming from the finite-size cluster (see Figure 2).

Future Work

Our two main tasks for the near future are 1) Improve the quality of the cluster-specific fit so that it gives very high accuracy over its entire domain; and 2) Improve the signature-based approximate distance method to give a more accurate distance when the clusters differ substantially. We also have two secondary tasks, which become important in the event we fail one or both of the first two tasks: 3) Develop ways to make the exact-rotation retrieval go as fast as possible; and 4) Investigate ways to modify the forces to directly correct for the nonconservation error.

Conclusion

Our goal is to design a procedure for calculating fast, accurate interatomic forces for molecular dynamics simulations of materials. We are making good progress, but we are not there yet. If we succeed, this approach opens the way for unprecedented predictive-quality simulations on long time scales, so that we can directly simulate processes such as fracture, plastic deformation, impurity precipitation, film growth and catalytic reactions, comparing the results directly to experiment. This capability will be valuable in designing advanced materials and understanding processes for nuclear reactors and nuclear waste storage, as well as many other energy applications.

Controlling Charge Recombination Processes in "Giant" Nanocrystal Quantum Dots Toward High-Efficiency Solid-State Lighting

Jennifer A. Hollingsworth
20100469ER

Introduction

The most widely used sources of artificial illumination remain incandescent and fluorescent lamps, but these are not optimized for efficiency or longevity. Significant economic and environmental savings—~20% of electricity is consumed in lighting—could be achieved if efficient and robust low-cost alternatives were available for general lighting purposes. The primary alternative as perceived by industry and government is so-called 'solid-state lighting' (SSL). As described in the DOE SSL Roadmap, SSL differs fundamentally from existing technologies, and its development is central to DOE's—and LANL's—mission in energy efficiency. Existing technologies, most notably nitride-based and organic or polymer-based light emitting diode (LED) technologies, have thus far fallen short of providing the desired combination of properties: high-efficiency, long-term robustness, low-cost, and facile color-tunability. An ideal "building block" for LED technologies would possess the high-efficiency and innate robustness of nitride-based technologies coupled with low-cost processibility and color tunability. Here, we aim to establish a new class of colloidal semiconductor nanocrystal quantum dot (NQD)—the "giant" NQD (g-NQD)—as the ideal building block for high-efficiency, general-use SSL through three research goals:

- Fundamental photophysics: understand charge-recombination processes toward controlling/optimizing electronic→photonic conversion pathways.

- Materials-by-design: establish general synthesis capability for engineering key physical and electronic structure parameters that influence electronic→photonic conversion processes.

- Proof-of-principle devices: fabricate g-NQD-LEDs to test hypothesis that g-NQDs provide significant performance improvements.

Benefit to National Security Missions

The proposed work addresses key LANL-identified Materials and Energy Grand Challenge FY10 Priorities: e.g., Develop (1) the underlying materials science, physics and chemistry to support materials needs in energy efficiency and (2) intrinsic techniques to control functionality with novel architectures resulting from new synthesis, fabrication and processing concepts. Thereby, the science developed here will provide the necessary fundamental understanding that will enable significant progress in SSL technology, where, according to the DOE, "No other lighting technology offers as much potential to save energy and enhance the quality of our building environments, contributing to our nation's energy and climate change solutions."

Progress

Task I: In our effort to synthesize/structurally characterize g-NQDs representing a range of physical/electronic-structure parameter space, we prepared a series of CdSe/CdS systems (electronic structure is quasi type-II) for which the core/shell interface was intentionally alloyed. Specifically, we fabricated thick-shell NQDs where the shell was either fully alloyed [CdSe/(CdSexS1-x)n, x = 0.25-0.75, n = 1-9] or where the first 1-2 monolayers were alloyed but the remainder of the shell was pure CdS [CdSe/(CdSexS1-x)n(CdS)m, x = 0.10-0.75, n = 1-2, m = 1-7]. In the case of the fully (homogeneously) alloyed systems, average radiative lifetimes were always observed to be in the range typically reported for core-only or conventional core/shell CdSe NQDs, i.e., 20-30 ns, and independent of shell thickness. Blinking was not suppressed in these systems. In the case of the compositionally graded shell systems, for which a 1-2 monolayer alloy region was grown in between the nominally compositionally pure core and CdS shell, average radiative lifetimes at 5 total shell monolayers showed little increase above that of a core-only sample, while at 9 shells, lifetimes were approximately doubled (~60 ns) without dependence on 'x.' Blinking behavior for the 9-shell system was found to be comparable to moderately shelled non-alloyed CdSe/CdS g-NQDs (e.g., 5-6 shell monolayers). More recently, we expanded our investigations into core-shell interface effects by synthesizing alloyed cores of varying degrees of core-to-shell compositional grading (as a function of synthetic method employed). Significantly, to date, neither intentional shell alloying nor core alloying has resulted in improved blinking properties of

CdSe/CdS NQDs. We have also attempted post-synthesis alloying by way of high-temperature, long-time annealing, which demonstrated that the core/shell interface is actually very stable to intermixing.

In contrast to our investigations of core-shell interface effects on blinking, which did not result in significant modifications or enhancements, we have observed that electronic structure plays a key role in tuning nonradiative/radiative carrier recombination processes and fluorescence intermittency. To investigate this aspect of core/shell nanostructures, we developed new synthesis strategies for thick-shell InP-based core/shell NQDs that, according to theoretical predictions conducted for this effort, were expected to span the full range of electronic structures from type I to quasi-type II to type II. These were InP/ZnS, InP/ZnSe, InP/CdS, InP/CdSe. Each system afforded unique challenges in achieving effective, controlled shell growth. Compared to our original CdSe-based g-NQD system, InP suffers from a greater susceptibility to surface oxidation, a poor starting core quantum yield, and a tendency to etch in the presence of standard ligands used for surface stabilization. Despite these system-specific conditions, we were able to synthesize representatives of each core/shell combination and to effect significant control over emission 'color' (green to near-infrared) and electronic structure. Electronic structures characterized by either partial (quasi-type II) or complete (type II) spatial separation of electron-hole pairs exhibited long average radiative lifetimes, e.g., InP/CdS core/shell NQDs: 500 ns at 1 shell monolayer, 686 ns at 4 shell monolayers, and 806 ns at 10 shell monoalyers. This was the predominant condition in the case of Cd-containing shells compared to Zn-containing shells that resulted in charge-localized electronic structures (type I) and shorter lifetimes comparable to InP cores (e.g., 28-73 ns). Most recently, single-NQD-level blinking studies of the InP/CdS core/shell system show suppression of blinking in these near-infrared emitters (~700-1000 µm), up to complete suppression of blinking in the case of InP/10-monolayer CdS NQDs (Figure 1). This result provides the first new "g-NQD" system to realize the unique and important single-NQD optical properties originally demonstrated by us for the prototype CdSe/CdS g-NQD system, as well as the first *near-IR* non-blinking NQD. A manuscript describing this seminal work is in preparation.

Task 2: Through advanced optical spectroscopic studies conducted at both ensemble and single nanocrystal levels, we have made significant progress in establishing a comprehensive understanding of the competition between nonradiative and radiative recombination processes in g-NQDs. Specifically, we have (a) Shed new light on the mechanism responsible for the suppression of Auger recombination (AR) processes in g-NQDs, (b) Revealed the mechanism responsible for the suppression of blinking in g-NQDs and the correlation between the AR suppression and blinking suppression, (c) Developed two single-NQD spectroscopy approaches to independently and directly

measure the quantum yield of bi-exciton states, enabling significant advances in our fundamental understanding of g-NQD optical properties, (d) Developed a novel single-NQD spectro-electrochemistry capability for controllably and reversibly injecting/extracting charges into/out of the g-NQD while simultaneously monitoring the changes in PL emission intensity and lifetime fluctuation, (e) Demonstrated that the g-NQD thick shell affords control over the electron-hole exchange interaction that define the splitting between the optically active and inactive lowest excitonic transitions. (See publication list.)

Task 3: We have demonstrated proof-of-concept light-emitting devices of two types -- direct charge injection and down-conversion, completing this task.
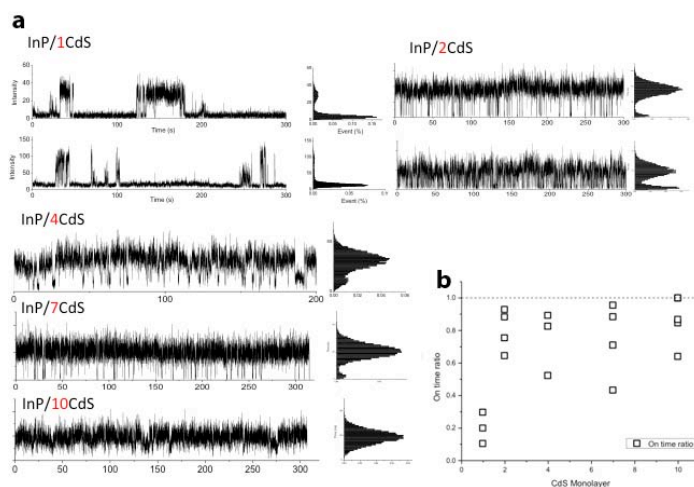
Figure 1. (a) Photoluminescence intensity traces over time for single InP/CdS core/shell nanocrystal quantum dots (NQDs) of increasing CdS shell thickness (red numbers represent number of shell monolayers) under continuous excitation at 405 nm. Single-monolayer NQDs exhibit standard blinking behavior, while for thicker-shell NQDs, shorter off-times are observed, or blinking is suppressed all-together. (b) Ratio of on-to-off times versus shell thickness (on/off ratio of 1 indicates non-blinking behavior).

Future Work

We will conduct highly correlated synthesis and advanced spectroscopy studies (Tasks 1 and 2) toward a proof-of-principle light-emitting diode demonstration (Task 3) of the utility of the novel "giant" nanocrystal quantum dot (g-NQD) structural motif for light-emission applications. Thereby, we will address scientific issues of materials-by-design and fundamental photophysics.

Task 1: Synthesize and structurally characterize g-NQDs representing a range of physical/electronic-structure parameter space: By judicious choice of core and shell compositions and sizes, we will continue to controllably engineer four classes of g-NQDs: (1) type-I electronic structure, simple-core/shell interface, (2) type-I electronic structure, energy-graded core/shell interface, (3) quasi-

type-II electronic structure, simple-core/shell interface, and (4) quasi-type-II electronic structure, energy-graded core/shell interface. This set of materials is allowing us to distinguish the effects of physical and electronic structure, as well as composition (II-VI and III-V semiconductors) and bandgap ("blue"—CdS and ZnSe—to "red"—CdSe and InP) on our ability to achieve the desired unique g-NQD properties. Further, to understand the precise structure-function relationships, we will conduct correlated single-NQD optical and transmission electron microscopy (TEM) measurements.

Task 2: We have and will continue to directly investigate the competition between radiative and non-radiative recombination pathways, especially in newly developed core/thick-shell systems by performing advanced ultrafast spectroscopic studies (low-T PL→multiexciton-state structures, PL excitation spectroscopy→fine-structure of band-edge exciton, and TR-PL→recombination rates) on both g-NQD ensembles and single g-NQDs of various size (shell thickness and core diameters) and compositions. Ensemble measurements will provide efficient comparison of different g-NQD samples, while single-NQD studies will allow us to study variations within an ensemble.

Task 3: Complete – LED proof-of-concept devices successfully demonstrated.

Conclusion

Conventional nanocrystal quantum dots (NQDs) are characterized by several basic properties that have limited their utility in light-emission applications: (1) deleterious sensitivity to surface chemistry and chemical environment, (2) the requirement for a surface layer of "protective" but electronically insulating organic molecules, and (3) efficient non-radiative Auger recombination. We recently discovered that these properties no longer apply in the case of our novel "giant" NQDs. In this effort, we are making significant progress toward generalizing these exciting results to the full range of NQD materials systems to achieve efficient, robust, and color-tunable building block for next-generation solid-state lighting.

Publications

Brovelli, S., R. D. Schaller, S. A. Crooker, F. Garcia-Santamaria, Y. Chen, R. Viswanatha, J. A. Hollingsworth, H. Htoon, and V. I. Klimov. Nano-engineered electron-hole exchange interaction controls exciton dynamics in core-shell semiconductor nanocrystals. 2011. *NATURE COMMUNICATIONS.* **2**: 280.

GarciÃÅa-SantamariÃÅa, F., S. Brovelli, R. Viswanatha, J. Hollingsworth, H. Htoon, S. Crooker, and V. Klimov. Breakdown of volume scaling in auger recombination in CdSe/CdS heteronanocrystals: The role of the core-shell interface. 2011. *Nano Letters.* **11** (2): 687.

Ghosh, Y., A. Steinbruck, A. M. Dennis, H. Htoon, and J. A.

Hollingsworth. Giant (core)shell compound semiconductor nanocrystal quantum dots: From light emission applications to bioimpact. Presented at *2011 Materials Research Society Spring Meeting.* (San Francisco, April 25-29, 2011).

Ghosh, Y., B. Mangum, Y. Park, S. Brovelli, J. Casson, H. Htoon, and J. Hollingsworth. Controlling the electronic structure in II-VI core/shell nanocrystal quantum dots toward tuned optical properties. 2011. *ABSTRACTS OF PAPERS OF THE AMERICAN CHEMICAL SOCIETY.* **241**.

Hollingsworth, J. A.. Novel functional semiconductor nanocrystal quantum dots and nanowires for applications involving energy conversion. Invited presentation at *2010 Materials Research Society Spring Meeting.* (San Francisco, April 5-9, 2010).

Hollingsworth, J. A.. Nanocrystal quantum dot architectures and assemblies for light emission applications. Invited presentation at *American Chemical Society Fall 2011 National Meeting & Exposition.* (Denver, CO, 28 Aug. - 1 Sept.).

Hollingsworth, J. A., A. Steinbruck, Y. Ghosh, and A. Dennis. Direct and indirect redox processes of semiconductor nanocrystal quantum dots: Implications for biological applications. Invited presentation at *241st American Chemical Society National Meeting & Exposition.* (Anaheim, March 27-31, 2011).

Hollingsworth, J. A., H. Htoon, B. N. Pal, J. Kundu, and Y. Ghosh. "Giant" nanocrystal quantum dots: Uniquely stable and efficient building blocks for light emitting diodes. Presented at *241st American Chemical Society National Meeting & Exposition .* (Anaheim , March 7-31, 2011).

Htoon, H., A. V. Malko, D. Bussian, J. Vela, Y. Chen, J. A. Hollingsworth, and V. I. Klimov. Highly emissive multiexcitons in steady-state photoluminescence of individual "giant" CdSe/CdS core/shell nanocrystals . 2010. *Nano Letters.* **10** (7): 2401.

Park, Y. -S., A. V. Malko, J. Vela, Y. Chen, Y. Ghosh, Garci&acute, J. A. Hollingsworth, V. I. Klimov, and H. Htoon. Near-unity Quantum Yields of Biexciton Emission from CdSe/CdS Nanocrystals Measured Using Single-particle Spectroscopy. 2011. *Physical Review Letters.* **106** (18): 187401 (4 pp.).

Vela, J., H. Htoon, Y. Chen, Y. S. Park, Y. Ghosh, P. Goodwin, J. H. Werner, N. P. Wells, J. L. Casson, and J. A. Hollingsworth. Effect of shell thickness and composition on blinking suppression and the blinking mechanism in 'giant' CdSe/CdS nanocrystal quantum dots. 2010. *Journal of Biophotonics (Special Issue on Nanobiophotonics).* **3** (10-11): 706.

Exploratory Research
Continuing Project

Superconducting Vortices in Magnetic Media

Boris A. Maiorov
20110138ER

Introduction

As electricity demand continues to rise, and environmental constraints become more relevant, it is imperative to enhance the performance of superconductors for applications oriented towards energy efficiency and storage. In most applications, the superconductors are exposed to relatively high magnetic fields (H) that penetrate the material by creating superconducting vortices. Any electric current that flows through the superconductor exerts a Lorentz force (FL) on the vortex that is proportional to the magnitude of the current. When the current density, J, reaches a critical value, Jc, FL becomes strong enough to overcome the pinning force that anchors vortices. Vortex motion leads to energy dissipation, i.e., the material acquires a finite resistivity for J>Jc. Therefore, one hopes to find mechanisms to increase Jc and/or reduce dissipation for J>Jc. The pinning force comes from material defects that create an attractive vortex potential. In particular, magnetic defects can lead to so-called magnetic pinning. In principle, magnetic pinning can significantly increase the value of Jc (in particular at high temperatures) as it can result in pinning energies larger than those achieved by non-magnetic defects (core pinning). However, the interplay between vortices and magnetic media cannot be properly exploited without a comprehensive study that includes both static and dynamical properties of the entire system. We are studying the effect of a magnetic medium on the dynamics of the vortex state.

Benefit to National Security Missions

The superconductivity research community is changing focus. After several years of tremendous success with core pinning enhancement, there is the need to go back to the drawing board and think of new ways of reducing energy dissipation in superconducting materials. The BES workshop on superconductivity highlighted research directions that we will address. With other SC efforts at LANL we could reach critical mass for big programs such as an EFRC. This work directly relates to the energy security future of our nation.

Progress

The idea is to explore the interaction between superconducting vortices and magnetism. ErB_2Ni_2C and LuB_2Ni_2C single crystals were obtained from Ames Lab, (Dr. Sergey Bud'ko,). ErNiBC has several magnetic phases that coexist with superconductivity and LuB_2Ni_2C is non magnetic. We will compare and contrast the results obtained in these single crystals. We plan to make micro bridges that will allow us to inject high current densities in these very clean crystals.

We have acquired a new Variable Temperature Insert (VTI) to be installed in our 7T (Tesla) split coil system. This insert will allow us to sweep temperature while passing substantial amount of current, something that is not possible to do in commercial systems.

Dr. Marcus Weigand was hired as post-doc starting on April. He has performed all the necessary training and is taking the lead on sample preparation of the micro bridges. We started by thinning down single crystals using polishing (generally use for TEM samples preparation). We have been able to reduce the cross section from 1mm^2 down to 0.005 mm^2, a factor of 200 improvement. A small decrease in T_c was observed, that did not affect T_N. Annealing of the samples was performed and we found that Tc can be back up. This allowed us to perform critical current measurements that are would only be possible by pulsed field technique with great advantage of DC measurement, e.g. it's possible to measure the response of the current going up and down, something not possible with pulsed current measurements.

A Center for Integrated Nanotechnologies (CINT) proposal was accepted to perform Focused Ion Beam (FIB) as part of their user facility program. The first microbridges in YBCO films (Figure 1) and initial cuts in single crystals were already performed at Sandia Nat. Lab. A critical step we are finding is to get samples thin enough to do

FIB. We are planning to use Broad Ion Beam and mechanical polishing, available at MPA-STC, to thin down the single crystals down to 10 microns.
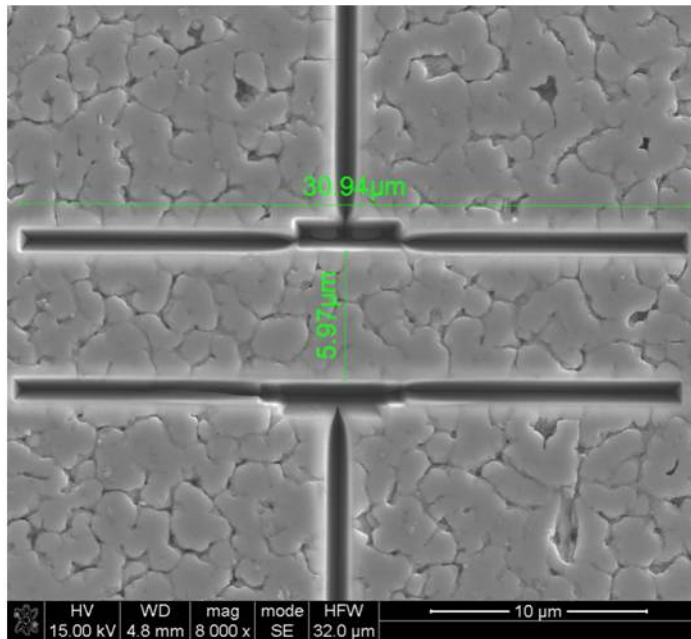
Figure 1. Micro bridge on a YBCO fim made using Focused Ion Beam (FIB).

Magnetization measurements were started in REB2Ni2C (RE=Er, Lu) to find effect of the AFM phase with T_N=6K. We have observed a clear effect on the critical current (Ic) at the phase transition T_N. We observe a clear peak in Jc at T_N, at low fields, that remind up to higher fields. We are currently working in mapping this effect and performing similar measurements by transport. We are studying also the flux creep by measuring the magnetization relaxation.

We performed measurement of electrical voltage (**V**) that indicates vortex movement, as a function of current density amplitude (**J**), which measures the force that acts on the vortices. Both DC and AC transport measurements were performed. There is a clear decrease in V as a function of increasing **J** in the associated with the AFM transition as seen in Figure 2.

Modeling is underway to understand the observation and a manuscript is being prepared with the experimental data. Simulations of the interaction of vortices and magnetic media were done. We see a clear effect of the domain boundaries in AFM phase. We find that they can interact with vortices and eventually be moved by vortices (Figure 3). This has great similarities of current DMW movement by ionized current. A manuscript is being prepared and will be sent.

We also started working in the heterostructures, and we plan to combine Nb with different AFM materials, that are being selected. We started measurements of Ic in Nb films as function of temperature, field and angle.
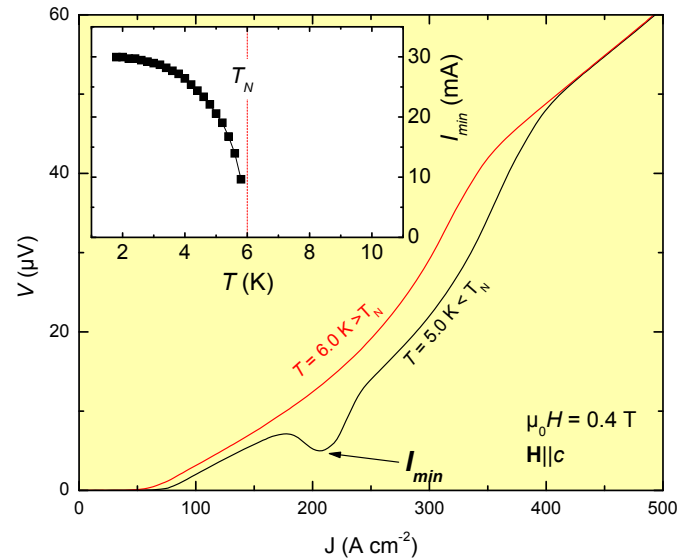
Figure 2. Voltage (V) versus applied current density (J) curves for temperatures (T) above and below Neel temerature (T_N). A decrease in V at I_min is observed indicating decreased velocity of vortices upon increasing current at I_min. Inset: I_min versus temperature for H||c=0.4T.
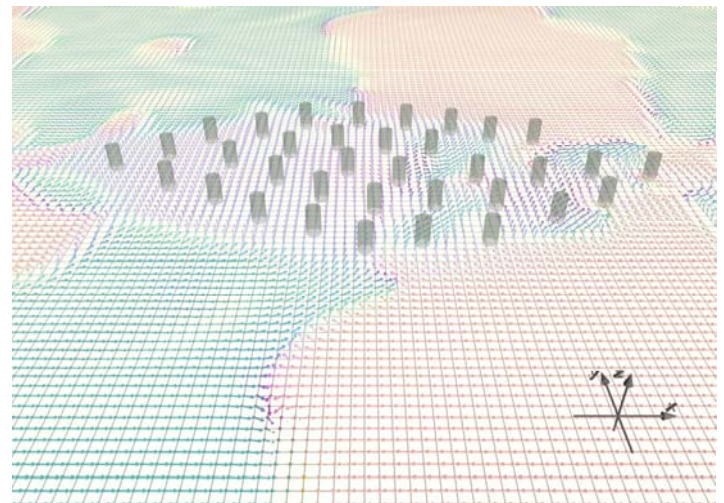
Figure 3. Simulation of magnetic moments (small arrows) in presence of superconducting vortices (grey columns) with an applied current. Different spin domain form (diffrent colors) and interact with vortices particlarly in the domain walls.

Future Work

We plan to develop new experimental and theoretical tools to understand the interplay between superconducting vortices and magnetic media. All previous experiments on magnetic pinning were only focused on achieving higher values of Jc (static effect). We plan to explore theoretically

and experimentally new aspects of the vortex dynamics by expanding our analysis to antiferromagnetic media that mostly affects the vortex dynamics. A common problem in previous studies of magnetic pinning is the inability of separating the core (local suppression of the superconducting order parameter) and magnetic contributions. To unequivocally study the effect of the magnetic medium, it is necessary to be able to induce substantial changes in the magnetic properties. For this purpose, we will study different system where the magnetic ordering transition takes place inside the superconducting phase.

We choose the Borocarbide family of superconductors as well as tunable YBCO/magnetic heterostructures to study the effect of magnetic media on the vortex dynamics. We will focus on systems that have a magnetic ordering temperature lower than the superconducting transition temperature Tc. This is useful to separate the magnetic contribution to the vortex dynamics from the non-magnetic contributions. In particular, we will calculate and measure the magnetic influence on the relevant parameters for the pinning, flux-creep and flux-flow regimes. In more detail, we will measure the change in the critical current and flux flow dynamics induced by the magnetic medium and model the mechanisms that can explain such change. We will also model the magnetic contribution to the vortex mass and viscosity in order to predict the effect of the magnetic medium on the flux creep and flux-flow regimes. These predictions will be tested against their corresponding measurements. We will also test the novel idea that AFM media can be effective in reducing vortex motion.

Conclusion

Our primary goal is to unveil new qualitative behaviors of the vortex state in the presence of a magnetic medium. For the static regime, we will look for different mechanisms to increase Jc. We will explore routes to bridge the gap between present performance and theoretical limit.

In the dynamic regime, we expect to qualitatively demonstrate the effect of magnetic media on reducing vortex motion and to calculate the effect and the threshold vortex velocity needed for the 'vortex Cherenkov' effect. We are measuring a decrease in flux-flow dissipation and finding the conditions for such improvement to occur.

Novel Anti-Perovskite Electrolytes for Superionic Lithium Transport

Luc L. Daemen
20110139ER

Introduction

Lithium ion batteries have shown great promise in terms of electric energy storage parameters such as energy density, power capacity, charge-discharge rates, and cycling lifetimes. However many fluid electrolytes consisting of lithium salts dissolved in solvents are toxic, corrosive, or flammable. They tend to work poorly with lithium anodes. Solid electrolytes with superionic conductivity can avoid those shortcomings, and can work much better with a metallic lithium anode, allowing for much higher energy densities. We propose a novel class of superionic solid electrolytes with 3D conducting pathways based on anti-perovskites of high lithium content. The new crystalline materials can form adaptable solid solutions and lend themselves to structural and chemical modifications to boost ionic transporting.   We have measured the ionic conductivities of the order of 10-2 S/m for the anti-perovskites Li_3OCl and $Li_3OCl_{0.5}Br_{0.5}$, respectively, and the high temperature measurements derive the activation energies of range 0.3-0.5 eV corresponding, well within the superionic transporting region. These initial studies demonstrate that the anti-perovskites can serve as a solid electrolyte material for superionc conduction of Li-ion battery.

Benefit to National Security Missions

It supports the Laboratory Energy & Earth Systems Grand Challenge "to develop transformative new energy technologies" as well as LDRD Materials Grand Challenge of "controlled functionality through discovery and application of fundamental materials properties". In particular, this work tackles the research priority of "electrical energy storage for transportation applications" and underpins DOE-BES scientific mission of "Directing Matter and Energy". This research will advance fundamental materials theory, develop novel materials for super-ionic electrochemistry, and enable next-generation devices with substantially enhanced energy/power properties. This ER project directly supports LANL Institutional Goal on establishment of "expertise/capability to solve national problem in energy security". Our integrated research on battery materials synthesis, modeling, and characterization for electric energy storage also represents important elements of the MaRIE strategy, and our new and unique neutron-electrochemical capabilities at LANSCE would place LANL at the forefront of clean energy researches.

Progress

Synthesis

We have developed novel synthetic techniques to produce a wide variety of Li-rich anti-perovskites. A simple method with quantitative yield is detailed presently. The first step of the synthesis of, say, Li3OCl consists in grinding together two equivalents of LiOH and one equivalent of LiCl. In a typical synthesis, 4.79 g LiOH (0.2 mol; Aldrich, > 99% purity) and 4.24 g LiCl (0.1 mol; Aldrich, > 99% purity) are ground together for several minutes with a mortar and pestle. This mixture is then placed in an alumina boat and heated to 280 oC under vacuum. The material is kept at this temperature overnight. During heating, water is actively removed with a condensation (cold ice bath or liquid nitrogen) trap and an efficient vacuum pump. At the end of the synthesis, the vacuum is removed and the apparatus is flushed with a dry inert gas (e.g., N_2 or Ar) for a few minutes. Continuous removal of water under vacuum drives the chemical equilibrium toward the formation of the product. The reaction is fast and simple and the sample production can be massive. The Li_3OCl and Li_3OBr samples can also be obtained with higher purity if the reaction temperature is increased to beyond the melting points (T > 280 °C), in which case the product is obtained as:

$$LiCl + 2LiOH \rightarrow Li_3OCl + H_2O \uparrow (360oC, vacuum) \quad [1]$$

$$LiBr + 2LiOH \rightarrow Li_3OBr + H_2O \uparrow (360oC, vacuum)$$
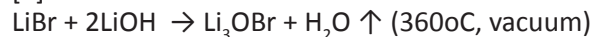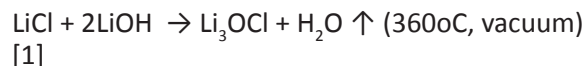
This molten material can be slowly cooled or rapidly quenched to produce a polycrystalline mass with texture and various degrees of disorder. If the reaction is incomplete, reagents contaminate the product. This is detrimental to conductivity measurements. The synthesis described here is novel to the best of our knowledge, and produces a pure Li-rich anti-perovskite material

with quantitative yield and relative ease. We have also developed a high-pressure and high-temperature synthesis route and have recovered high quality samples of anti-perovskites.

Characterization

X-ray diffraction (XRD, Rigaku Ultima III instrument) reveals that Li_3OCl and Li_3OBr have the typical perovskite crystal structure, Figure 1, albeit with distortions from the ideal cubic structure. These distortions are typical of many perovskites 25. The extra peaks in the Li_3OCl and Li_3OBr diffraction pattern are typical of tetragonal distortion and some are amplified due to texture. The mixed phase of $Li3OCl_{0.5}Br_{0.5}$ shows a good solid-solution of the two end members. The XRD patterns in Figure 1 are indexed with Miller indices corresponding to the pseudo-cubic structure. The lattice parameter is approximately 3.91 Å with one formula unit per unit cell (Z=1). The space group is P m -3 m (#221). The calculated density is 2.0 g/cm³. This compound of $Li3OCl$ is reported here for the first time. The Li_3OBr sample shows substantially the same pseudo-cubic structure as Li_3OCl. The lattice a ≈ 4.02 Å, with Z=1, and space group P m -3 m (#221). Our high-P/high-T synthesis **23** produces the similar distorted anti-perovskite structure as the high-T melting synthesis.
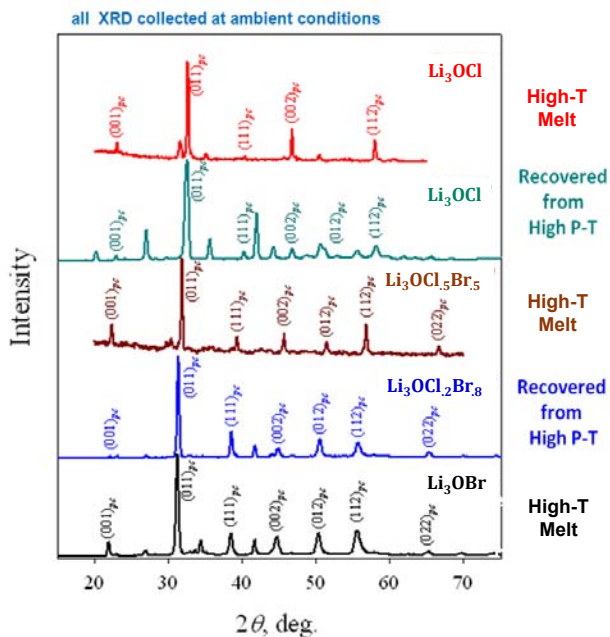
Figure 1. X-Ray diffraction data for the anti-perovskite samples.

The diffraction patterns of anti-perovskites display different degrees of superlattice peaks, indicating various degree of octahedral tilting, structural distortion, and A/A' site disorder, etc. It is not surprising given the differences in pressure and temperature conditions, in cooling and quenching rates, and in ionic size between Cl and Br, and the possibility of random occupation of the A-site by Cl and

Br.Notice from the diffraction pattern of the mixed phase that Br is indeed incorporated in the lattice and replaces Cl to form the solid solution.   The x-ray diffraction shows gradually cleaner patterns closer to the cubic perovskite structure as temperature increases, and it also shows the melting at high-T and texture formation when cooling down.

Structural changes in anti-perovskites and melting were observed with thermal analysis. We performed Differential Scanning Calorimetry (DSC, Netzsch, Jupiter 449C) measurements on the anti-perovskite samples. The results are shown in Figure 2.
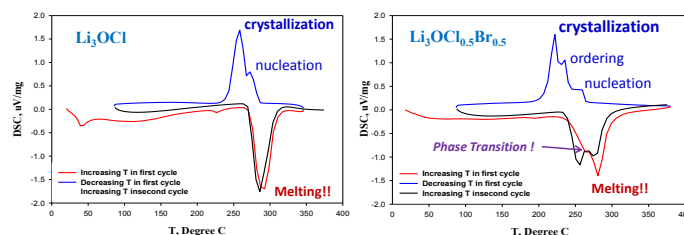
Figure 2. Differential calorimetric scanning (DSC) data collected at heating and cooling for the anti-perovskites Li_3OCl and $Li_3OCl_{0.5}Br_{0.5}$.

The last peak at high temperature heating is the melting phase transition. The mixed compound has a lower melting point than the two end member parent compounds. There is a very small endothermic peak in the Li_3OCl sample around 225 °C. In some perovskites, it is due to the loss of one order parameter, *i.e.* one octahedral tilting along one particular lattice axial direction. It corresponds to the unfolding of either the M point or the R point of the Brillouin zone in lattice dynamics. The XRD does not reveal anything remarkable below or above this peak other than slight changes in the intensity of the superlattice peaks. Melting occurs at 282 °C, but the onset of melting occurs some 10 degrees lower. The Li3OBr sample displays the same weak endothermic feature as Li_3OCl, but at 206 °C. A new endothermic peak appears at 232 °C, below the melting point of 280 °C. The mixed halogens sample $Li_3OCl_{0.5}Br_{0.5}$ inherits this new feature of Li_3OBr with a peak at 247 °C, and with a lower melting point of 270 °C. The cooling down DSC measurements of the sample $Li_3OCl_{0.5}Br_{0.5}$ shows three exothermic peaks, which corresponding to nucleation of crystallites, ordering of the mixed halogens, and crystallization to the solid state. There are only two exothermic peaks of nucleation and crystallization for the end member samples. As the halogens possess widely different ionic sizes, the substitution of halogens in the Li-rich anti-perovskites should be a very efficient method of structural manipulation, as well as decreasing the temperature of structural phase transition and melting. This will affect ionic conductivity and, possibly help achieve superionic conductivity closer to room temperature.

The ionic conductivity measurements for all three samples
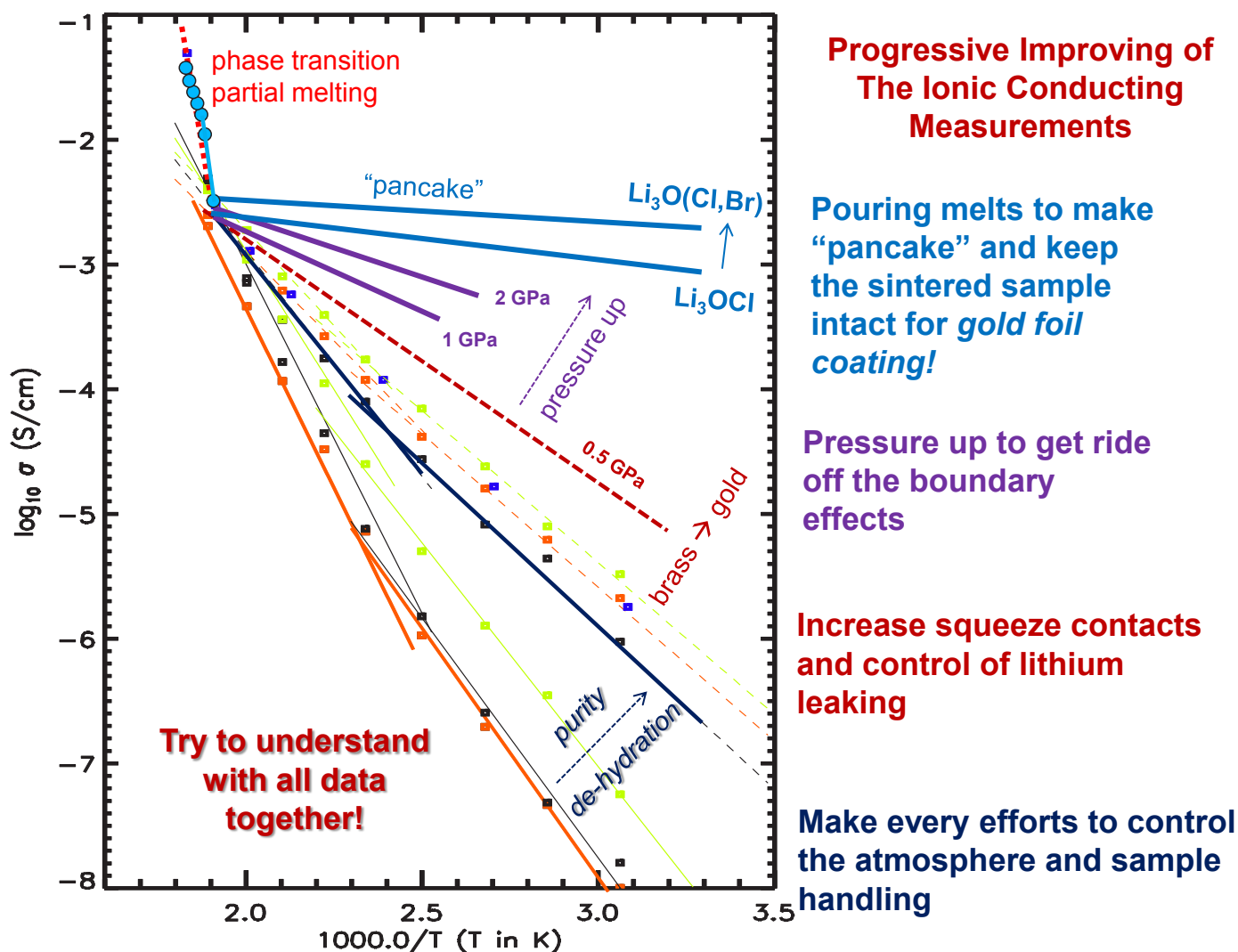
Figure 3. Ionic conductivity measurements plot as a function of invered temperature (1000/T) for the anti-perovskites.

show a very wide range of 10^{-5} -to- 10^{-2} S/m at the room temperature, Figure 3. Much speculation has been raised for the measurement techniques, sample handling, and data reductions, as shown in the side pane of the Figure 3. We intend not to report a definite result for the ionic conductivity of the anti-perovskites at the moment, rather choose to leave it as a big question mark to our self; much more works are needed to solve it.

Future Work

Important parameters for battery/capacitor materials include currents sustainability, discharge capacity, and reversibly rechargeable for long life cycles. We link the performance issues to atomic structures of the new anti-perovskite electrolytes. The concept of superionic electrochemistry to enhance battery/capacitor performances is novel and the relevant knowledge building up will be fruitful with our integrated R&D efforts of synthetic chemistry, neutron diffraction, and computational optimization. Further developments in thin film deposition of the

anti-perovskites and electron microscopy works will result in advanced solid-electrolyte applications and structural interpretations for layer structured state-of-the-art EES devices.

We consider the Li-rich anti-perovskite Li_3OA as a lithium "swamp" and it needs "trenches" to channel fast ionic transporting. The structural manipulations of mixing, doping, and depleting can effectively generate the vacancy channels in the crystal structure,thus forming "drainages" to allow easy hopping and fast transporting of the lithium ions. We will further explore different synthesis route to produce the maximized structural effect on the superionic conductivity of the anti-perovskites.

Conclusion

High P-T synthesis with chemical tuning, electrochemical and thermodynamic measurements, in situ neutron scattering, and computational modeling guidance will allow us to optimize the solid-electrolytes made of the lithium-rich

anti-perovskites for transportation EES functions. Novel solid electrolytes based on structural and electrochemical phase transitions in lithium enriched materials (anti-perovskites) will be developed to achieve enhanced electric conduction via superionic transporting. The new class of anti-perovskite electrolytes with superionic electrochemistry represents great advances in Li-rich electrolyte development and will permit further optimization of EES performance, including the use of metallic Li electrodes.

Understanding Earth's Deep Water Cycle: Neutron Diffraction and Calorimetric Studies of Hydrous Minerals

Hongwu Xu
20110190ER

Introduction

As part of the global hydrologic cycle, the Earth's deep water cycle plays a significant role in many geological processes, including arc volcanism, deep focus seismicity, and, in a larger con-text, the evolution of our planet [1]. To understand Earth's deep water cycle, it is essential to determine the stability and fate of hydrous minerals, which occur in hydrated oceanic crust, when the crust is subducted into the mantle via the mechanism of plate tectonics [2]. The aim of this research is to characterize the crystal structures, mechanical properties, thermodynamic stability and phase equilibria of a number of important hydrous minerals using neutron and synchrotron X-ray diffraction at high-pressure (P) and/or high-temperature (T) conditions [3,4] together with high-T oxide-melt calorimetry [5]. Specifically, we will examine three groups of minerals: 1) simple hydroxides; 2) oceanic crust minerals; and 3) potential hydrous mantle minerals. Since these minerals contain large amounts of light elements, especially hydrogen, neutron diffraction is particularly useful for such studies. Systematic measurements of these minerals using neutron diffraction coupled with our cutting-edge high P-T technique at the Los Alamos Neutron Scattering Center (LANSCE) will yield valuable information such as hydrogen positions and displacement parameters. In addition, high P-T synchrotron X-ray diffraction is employed to provide complementary structural and stability information (e.g., on heavy atoms in hydrous phases). Lastly, high-T calorimetric analysis will determine thermodynamic properties of these minerals, which will be used to construct related phase diagrams. The results will provide important parameters for models of Earth's deep water cycle and thus will shed light on mechanisms underlying the storage, fate, and dynamics of water in the Earth's interior.

Benefit to National Security Missions

Successful execution of this project will contribute greatly to the fundamental understanding of Earth's deep cycling of water, CO_2 and other volatiles and related geological phenomena including volcanism and seismicity. This work is also an essential part of studies of the global water cycle which integrates physical, chemical, and bio-logical processes that sustain ecosystems and influence climate, natural hazards, and related global change. The unique high P-T neutron/synchrotron and high-T calorimetric capabilities developed/utilized in this research have a wide range of applications in materials science, physics, chemistry, Earth and environmental sciences, and thus will strengthen key capabilities required for future Laboratory mission areas in plutonium science, energy security and environmental remediation. Potential future sponsors for water/volatile cycle research include NASA, DOE's Office of Science, and NSF.

Progress

We have synthesized two simple hydroxides, brucite and beta-nickel hydroxide, using hydrothermal and chemical precipitation methods, respectively, and have studied their structural and stability behavior at high T and/or high P using neutron diffraction. Though not major phases in the deep Earth, these compounds (especially brucite) are present as component units in the structures of complex hydrous minerals (such as phase-E, $Mg_{2.08}Si_{1.16}H_{3.20}O_6$), which are potential hosts for water in Earth's mantle. Thus studying their structures and stability will provide important insights into the mechanisms of water storage in the Earth's interior.

Sample synthesis: Since hydrogen has a high incoherent scattering cross section for neutrons, which causes high backgrounds in neutron diffraction patterns, we synthesized deuterated phases instead. The $Mg(OD)_2$ sample was prepared from hydrothermal reaction of high-purity MgO powders with D_2O in an autoclave at 548 K for about 20 h. For synthesis of $Ni(OD)_2$, $Ni(NO_3)_2 \cdot 6D_2O$ was first prepared by dissolving $Ni(NO_3)_2 \cdot 6H_2O$ in D_2O and dried at 313 K on a rotary evaporator. The obtained $Ni(NO_3)_2 \cdot 6D_2O$ was then dissolved in D_2O, and while being stirred, NaOD solution was added dropwise. The mixed solution was decanted and filtered under Ar atmosphere, and the obtained precipitate was dried at 473 K in a vacuum oven overnight. Transmission electron microscopy (TEM) imaging indicates that $Ni(OD)_2$ grains exhibit a layered hexagonal morphology (Figure 1). The resulted $Mg(OD)_2$ and $Ni(OD)_2$ samples were confirmed

as single-phase brucite and beta-Ni(OD)$_2$, respectively, by powder X-ray diffraction.
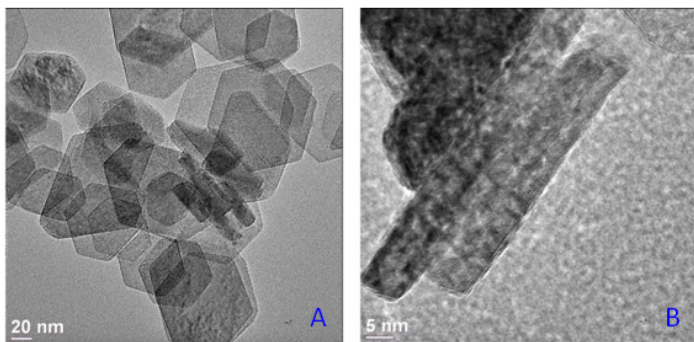
Figure 1. TEM images of Ni(OD)2 grains along (A) and perpendicular to the c-axis (B).

Neutron diffraction of Mg(OD)$_2$: Two types of time-of-flight neutron experiments were performed at the HIPPO beamline of LANSCE: 1) high-T measurements from 313 to 553 K; and 2) high-P high-T measurements up to 5 GPa and 800 K. Our high-T neutron patterns indicate that Mg(OD)$_2$ was stable from 313 to 553 K. However, the sample partially decomposed into periclase (MgO) and D$_2$O (gas) when T = 583 K. Thus the onset temperature of the dehydroxylation lies between 553 and 583 K. Rietveld analysis of the data reveals that with increasing temperature, the c-dimension expands at a rate about 5.5 times more rapidly than that for the a-dimension. This anisotropy of thermal expansion is due to rapid increase of the interlayer thickness along the c-axis with increasing T. Moreover, on heating, the hydrogen-mediated interatomic interactions within the interlayer become weakened, as reflected by increases in the interlayer D···O and D···D distances with increasing T. Correspondingly, the three equivalent sites over which D is disordered become further apart, suggesting a more disordered distribution of D at high T. For the high P-T measurements, we are currently analyzing the neutron data using the Rietveld method.

Neutron diffraction of Ni(OD)$_2$: We carried out similar neutron experiments on Ni(OD)$_2$, including high-T measurements up to 500 K and high-P high-T measurements up to 3 GPa and 600 K. The high-T neutron patterns show that Ni(OD)$_2$ started to decompose into NiO and D$_2$O (gas) at a temperature between 435 and 453 K. Rietveld analysis (Figure 2) demonstrates similar behavior to Mg(OD)$_2$ in variations of lattice constants and bonding parameters with T (Figure 3). However, the thermal expansion anisotropy of Ni(OD)$_2$ is much more dramatic than that of Mg(OD)$_2$. The coefficient of thermal expansion (CTE) of Ni(OD)$_2$ along the c-axis is about 11 times that along the a-axis, as compared with 5.5 times for Mg(OD)$_2$. High-P neutron results show that with increasing P, cell parameter c decreases much more rapidly than a, which is largely due to rapid reduction of the interlayer spacing. Fitting of the determined cell volumes to a Birch-Murnaghan equation

of state yielded a bulk modulus (K_0) of 57.3(1.0) GPa and a zero-pressure volume of 38.33(2) Å^3 with K_0' fixed at 4.7. Moreover, upon compression, the hydrogen-mediated interactions between the neighboring layers become strengthened, as reflected in decreases in interlayer D···O and D···D distances with increasing P. On heating at 3 GPa, the mean volume CTE is 6.58 × 10^{-5}/K, smaller than 8.95 × 10^{-5}/K measured at room pressure, which is apparently due to the confining effect.

Other activities: 1) We acquired a natural antigorite sample from the Smithsonian and will try to deuterate it at high P-T to obtain deuterated antigorite for neutron diffraction measurements. 2) Our Japanese collaborators are currently preparing deuterated phase A (Mg$_7$Si$_2$O$_8$(OD)$_6$) using high P-T multi-anvil techniques. We provided Mg(OD)$_2$ powders as a starting material for their synthesis. 3) We purchased a Netzsch DSC/DTA/TG thermal analyzer, which have recently been installed in the geochemistry and geomaterials laboratory (GGRL) at LANL.
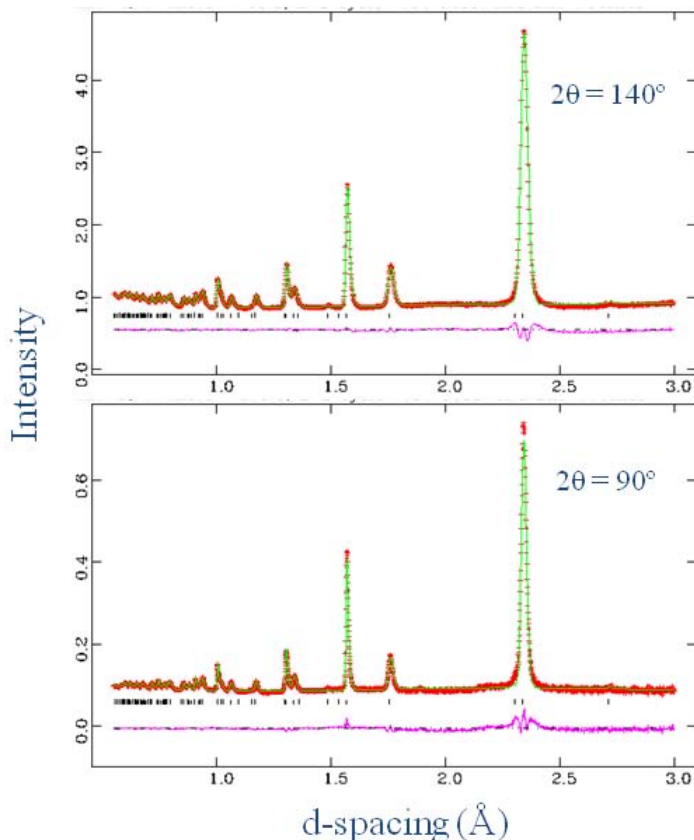
Figure 2. Fitted neutron diffraction patterns of Ni(OD)2 collected at 25 °C. Data are shown as red plus signs, and the green curve is the best fit to the data.
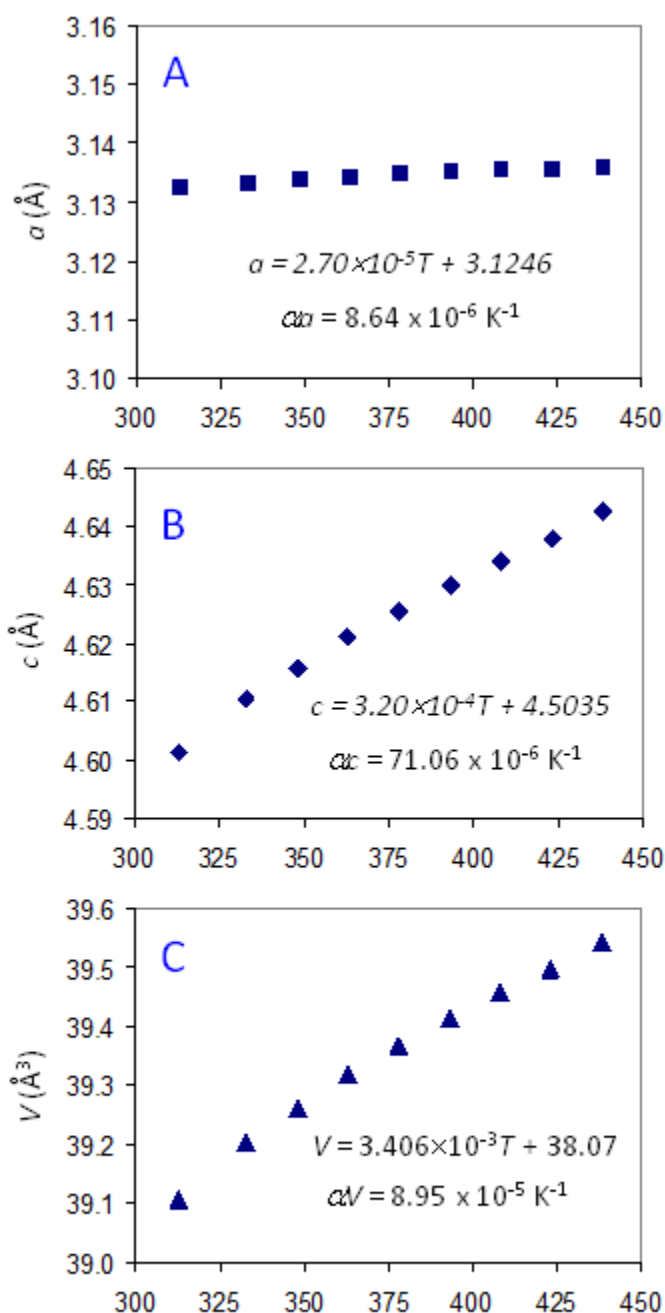
Figure 3. *Variation of unit-cell parameters a (A), c (B), and cell volume V (C) of Ni(OD)2 with temperature.*

Future Work

A major capability for this project is neutron diffraction at LANSCE to locate hydrogen positions in hydrous minerals at simultaneous high P and T. Neutron diffraction, which detects the nucleus rather than electron cloud and can sense light elements, represents a powerful tool for such measurements. With our developed high P-T capability (10 GPa and 1500 K), we have successfully conducted neutron experiments on various minerals and materials (including hydrous phases) aimed at refining their atomic positions

and thermal parameters under extreme P/T conditions. In addition, to obtain complementary crystal structural and phase stability information, we will conduct high P-T synchrotron XRD at the National Synchrotron Light Source (NSLS) and high-T calorimetric measurements at LANL.

In the remaining two years of this project, we will continue our studies on simple hydroxides (e.g., high P-T synchrotron XRD of nickel hydroxide) and will extend to studies of more complex phases including antigorite, hydromagnesite, other magnesium silicates (e.g., phase A), and/or germanate analogues (e.g., phase D) (potential hydrous mantle minerals). We expect to determine crystal structures and phase equlibria of these hydrous phases at mantle P-T conditions. These results will provide important insights into the effects of water on phase relations, physical properties and melting temperatures of mantle minerals, which are important aspects in Earth's deep volatile cycle.

Conclusion

Using neutron/synchrotron X-ray diffraction and solution calorimetry, we will determine crystal structures, elastic properties, thermodynamic stability and phase equilibria of a number of hydrous minerals at high P-T conditions. In particular, we will characterize hydrogen bonding in these minerals, which plays a key role in their thermodynamic stability, dehydration processes and phase relations. These results will help construct phase diagrams of hydrous peridotite in MgO-SiO_2-H_2O and related systems at mantle conditions and will in turn shed light on the mechanisms of volatile circulation through the mantle and the origins of the arc volcanoes and deep focus earthquakes.

References

1. Hirschmann, M.. Water, melting, and the deep Earth H2O cycle. 2006. *ANNUAL REVIEW OF EARTH AND PLANETARY SCIENCES.* **34**: 629.

2. Kerrick, D. M., and J. A. Connolly. Metamorphic devolatilization of subducted marine sediments and the transport of volatiles into the Earth's mantle. 2001. *NATURE.* **411** (6835): 293.

3. Zhao, Y., J. Zhang, H. Xu, K. Lokshin, D. He, J. Qian, C. Pantea, L. Daemen, S. Vogel, Y. Ding, and J. Xu. High-pressure neutron diffraction studies at LANSCE. 2010. *APPLIED PHYSICS A-MATERIALS SCIENCE & PROCESSING.* **99** (3, SI): 585.

4. Xu, H., Y. Zhao, J. Zhang, D. Hickmott, and L. Daemen. In situ neutron diffraction study of deuterated portlandite Ca(OD)(2) at high pressure and temperature. 2007. *PHYSICS AND CHEMISTRY OF MINERALS.* **34** (4): 223.

5. Navrotsky, A.. Progress and new directions in high temperature calorimetry revisited. 1997. *Physics and Chemistry of Minerals.* **24**: 222.

Publications

Xu, H., Y. Zhao, S. Vogel, D. Hickmott, L. Daemen, and M. Hartl. Thermal expansion and decomposition of jarosite: a high-temperature neutron diffraction study. 2010. *PHYSICS AND CHEMISTRY OF MINERALS.* **37** (2): 73.

Quasiparticle Scattering for Multiscale Modeling of Electronic Materials

Sergei Tretiak
20110212ER

Introduction

A quantitative understanding of matter at the nanoscale is a grand-challenge for theory. Over the years, electronic structure calculations, such as density functional theory (DFT), transformed theoretical chemistry, surface science and materials physics and have created a new ability to describe the electronic structure and interatomic forces in molecules with hundreds of atoms. Still, these calculations require atomistic information (electrons and orbitals). Consequently, numerical cost is high, effectively limiting the range of treatable systems by ~1000 atoms.On the other hand, design of functional nanostructures such as a photovoltaic unit or nanoscale electronic chip, requires quantum-mechanical modeling of extended systems with millions atoms in size. This challenge calls for development of multiscale approaches. Notably, any reduction of computational complexity is highly non-trivial, since we need to take advantage of complex quantum-mechanical phenomena, such as delocalized wavefunctions, quantum confinement, and coherences, to achieve new functionalities. In this project we will develop a theoretical framework based on the quasiparticle scattering concept, which will allow multiscale modeling of electronic properties on nanomaterials with limited numerical effort. Our theory bridges traditional molecular description (spatially confined wavefunctions, orbitals) with solid-state physics picture (periodic delocalized wavefunctions, quasiparticles) and directly addresses nanostructures spanning intermediate sizes. Scattering calculations include two steps: i) conventional quantum-chemical calculations and/or analysis of experimental data of simple molecular fragments (building blocks ~10-100 atoms in size) to retrieve the quasiparticle properties; and ii) applying scattering theory to large nanostructures to obtain electronic properties of interest. The resulting numerical effort scales cubically with the number of molecular building blocks (not electrons!) in the superstructure.

Benefit to National Security Missions

First and foremost our project upon completion will provide novel computational capabilities critical for understanding light-induced dynamics in many technologically relevant nanostructures. Consequently, we envision extremely broad applications of developed tools, relevant to the current and future LANL/DOE missions. Our project primarily addresses Energy and Earth Systems LANL Grand challenge by providing computational means for molecular materials suitable for clean energy (solar energy capture and energy storage). Secondly, it strongly relates to Materials: Discovery Science to Strategic Applications challenge by discovering emergent phenomena in complex systems. Consequently, proposed activities have potential for extending our program through LANL, and will place us in the excellent position to respond to incoming National Initiatives in energy and materials, particularly BES calls.

Progress

During the first year of the project our effort focused on several research directions. First of all, we have applied the Exciton Scattering (ES) approach to understand excited-state structure of donor and acceptor substituted conjugated oligomers. The extracted reflection phases, transition charge, and dipole parameters of the modified termini are used to quantify the influence of the substitution on the molecular electronic and optical spectra. In particular, intuitive relationships between the substituent's electron withdrawing or donating ability and the ES parameters have been established. A good agreement of the absorption spectra between the ES approach and the reference quantum-chemical computations demonstrates that the ES approach is qualified for such conjugated push-pull systems. This work has been recently published [1]. Secondly, we have extended the ES method to include symmetric triple and quadruple joints that connect linear segments on the basis of the phenylacetylene backbone. The obtained scattering matrices that characterize these vertices are used in application of our approach to several test structures, where we find excellent agreement with the transition energies computed by the reference quantum chemistry. We introduce topological charges, associated with the scattering matrices, which help to formulate useful relations between the number of excitations in the exciton band and the number of repeat units. The obtained fea-

tures of the scattering phases are analyzed in terms of the observed excited state electronic structure. This work has been recently published [2]. Currently we are preparing a large review article to be submitted to the Accounts of Chemical Research journal.

Finally we have applied the principles of the ES approach to study excited state dynamics in semiconductor nanostructures. Namely, we have implemented our interband exciton scattering model into a numerical code to simulate the processes of carrier multiplication (CM) (also referred in the literature as the multi-exciton generation) in narrow gap, PbSe and PbS, nanocrystal quantum dots. Using this approach we have performed a systematic study of the CM pathways in these materials [3,4]. Two fundamentally different processes of multiple-exciton photogeneration and subsequent phonon assisted cooling are investigated and their contributions to the CM quantum efficiency are determined. The analysis shows that the exciton scattering induced impact ionization dynamics is the main mechanism responsible for the CM during both the photogeneration and the population relaxation events. These results allowed us to provide interpretation of experimentally observed phenomena. Specifically, our model gives clear picture why the experimentally observed quantum efficiency in various size nanocrystals never exceeds the same quantity in bulk materials. The answer has been found in the quantum-confinement induced scaling of the carriers density of states and the Coulomb interactions contributing to the interband exciton scattering (i.e., impact ionization) processes.

Another fundamental question that has been addressed in our study is the spectroscopic signatures of the interband exciton scattering and the Coulomb correlations that lead to this process. We have used our exciton scattering theory to calculate the nonlinear coherent response to a sequence of three ultrafast optical pulses and specifically focused on the so-called double-quantum coherence technique, which is proved too sensitive to the carriers correlations [5]. The theory has been implemented into a computational code and further used to simulate the response of PbSe nanocrystals. Our simulations have determined unique nonlinear spectroscopic features in the double quantum coherence response indicating the presence of the exciton scattering dynamics of interest. This work can be considered as the guideline for further experimental studies.

Future Work
Interesting properties at nanoscale arise from the competing quantum interactions such as spin, charge, orbital, and lattice degrees of freedoms. Theoretical physics conveniently describes such electronic and vibrational excitations or degrees of freedom in materials as quasiparticles. They could undergo complex dynamics leading to many important photochemical and transport phenomena. A detailed knowledge of quasiparticle properties allows

constructing compact and accurate models for material's electronic structure and dynamics. It is, however, a highly nontrivial task to obtain such information from atomistic simulations and/or experiment. Our Exciton Scattering (ES) model is a successful example allowing us to map the results of quantum chemistry applied to molecular fragments into the scattering problem for exciton on the entire structure. Consequently we compute a static 'snapshot' of excited states of large structures. We will start this project by applying the ES technique to understand the excited states in many nanostructures featuring complex and collective excitations (Task 1). In parallel we will work on the theoretical methodology establishing scattering framework for other quasiparticles and provide a universal scattering picture for electronic dynamics in many materials allowing for multiscale modeling (Task 2). Step-by-step we will incorporate scattering of excitons on phonons, conformational defects, design polaron scattering model, and solve for coupled exciton/polaron dynamics describing decay of the exciton into charges at the defects and interfaces. This will allow us to model a complete scenario of excitation dynamics all the way from light absorption event to energy transfer to charge separation (charge transfer) to carrier transport and/or recombination. Finally we will apply developed tools to a number of important materials (Task 3).

Conclusion
Upon successful completion, the developed theoretical methodology will allow the quantum chemical techniques that have proven themselves in providing accurate and adequate results in organic/inorganic molecules of intermediate size to be extended to the world of macromolecules and superstructures. The range of treatable systems will be extended from ~1,000 atoms to at least 10,000-100,000 atoms sized nanostructures, without any substantial information loss or accuracy compromise. The proposed method will contribute to modeling and designing of new organic/inorganic materials with desired electronic properties. Close synergistic interaction with experiment at LANL and word-wide will allow us to disseminate our theoretical findings.

References
1. Li, H., C. Wu, S. Malinin, S. Tretiak, and V. Chernyak. Excited States of Donor and Acceptor Substituted Conjugated Oligomers: a Perspective from the Exciton Scattering Approach. 2010. *Journal of Physical Chemistry Letters.* **1**: 3396 .

2. Li, H., C. Wu, S. Malinin, S. Tretiak, and V. Chernyak. Exciton Scattering on Branching Centers in Conjugated Molecules. 2011. *Journal of Physical Chemistry B.* **115**: 5465 .

3. Velizhanin, K. A., and A. Piryatinski. Numerical Study of Carrier Multiplication Pathways in Nanocrystalline and Bulk Forms of PbSe. 2011. *Physical Review Letters.* **106**: 207401.

4. Velizhanin, K. A., and A. Piryatinski. An exciton scattering model for carrier multiplication in semiconductor nanocrystals: Numerical study of PbSe. *Physical Reviews B.*

5. Velizhanin, K. A., and A. Piryatinski. Probing Interband Coulomb Interactions in Semiconductor Nanostructures with 2D Double-Quantum Coherence Spectroscopy . 2011. *Journal of Physical Chemistry B.* **115**: 5372.

Publications

Li, H., C. Wu, S. Malinin, S. Tretiak, and V. Chernyak. Excited States of Donor and Acceptor Substituted Conjugated Oligomers: a Perspective from the Exciton Scattering Approach. 2010. *Journal of Physical Chemistry Letters.* **1**: 3396 .

Li, H., C. Wu, S. Malinin, S. Tretiak, and V. Chernyak. Exciton Scattering on Branching Centers in Conjugated Molecules. 2011. *Journal of Physical Chemistry B.* **115**: 5465 .

Velizhanin, K. A., and A. Piryatinski . Numerical Study of Carrier Multiplication Pathways in Nanocrystalline and Bulk Forms of PbSe. 2011. *Physical Review Letters.* **106**: 207401.

Velizhanin, K. A., and A. Piryatinski . An exciton scattering model for carrier multiplication in semiconductor nanocrystals: Numerical study of PbSe. *Physical Reviews B.*

Velizhanin, K. A., and A. Piryatinski . Probing Interband Coulomb Interactions in Semiconductor Nanostructures with 2D Double-Quantum Coherence Spectroscopy . 2011. *Journal of Physical Chemistry B.* **115**: 5372.

Solving the Active Site Conundrum in Oxygen Reduction Catalysis

Piotr Zelenay
20110236ER

Introduction

In this research, a unique multidisciplinary approach is implemented to obtain molecular-level information on the nature of transition-metal sites, Fe sites in particular, at the surface of non-precious metal oxygen reduction reaction (ORR) catalysts for the polymer electrolyte fuel cell (PEFC) cathode. NO and alkyl peroxides are used as probe molecules for ORR active-site elucidation. Metal-focused characterization techniques of analog-bound catalysts, electron paramagnetic resonance (EPR), Mößbauer and nuclear resonance vibrational spectroscopy (NRVS), are used to yield, through a differential approach, electronic and structural information for surface ORR sites. By spectroscopic characterization with DFT modeling and spectral simulations, we intend to determine surface Fe speciation, probe oxygen reduction coordinate, and evaluate novel structures as potential catalyst synthesis targets. The ultimate outcome of this research will be the first direct evaluation of ORR active sites in non-precious metal catalysts and the development of critical structure-property relationships for the advancement of Fe-based oxygen reduction catalysts for the PEFC cathode.

Benefit to National Security Missions

The research expands LANL's expertise in several areas, including ORR catalysis, surface characterization, mechanisms of surface catalytic reactions and advanced characterization of Mößbauer-active nuclei (i.e. NRVS). ORR catalysis is directly related to the fuel cell program at LANL, which directly supports the national energy security mission. The acquired capabilities and expertise in surface characterization and enhanced understanding of reaction mechanisms provide a strong platform for the application to other current and future energy and environmental related problems under investigation at LANL, including biomass conversion, CO_2 capture and/or conversion, etc. Expertise in NRVS has broad applications at the Lab to other Mößbauer-active nuclei, most notably neptunium (Np). Thus, this expertise provides a foundation for the application of NRVS to the basic science programs in actinide chemistry as well as national security related programs interested in the structures of, for example, complex Np containing materials including oxides.

Progress

Catalyst Modeling

Catalyst modeling has concentrated on the following three goals:

1. Calibration - Computationally obtain database of vibrational spectra for comparison with NRVS experiments, and hyperfine electronic spectra for comparison with the EPR experiments.

2. Exploration - Use database from (1) to compare to experiment, narrow active-site candidates, explore ORR-relevant energy surface/reaction pathways to determine rate-limiting steps.

3. Optimization - Use data from (1) and (2) along with molecular modeling to decrease ORR activation barrier and enhance active-site stability

High Performing Computing (HPC) resources at LANL were obtained by applying to the Call for Institutional Computing in January 2011. Further computational support is being sought through an Argonne National Laboratory (ANL) call for High-Impact Nanoscience & Nanotechnology User Proposal. Access to the code Gaussian 09 [1] was obtained using the site license managed by Rich Martin (T-1). Candidates were interviewed for the post-doctoral decision, and a qualified applicant was selected (Edward Holby).

Three systems have been selected for the initial screening: graphitic edge-type structures in which an iron or cobalt ion bridges two N-terminated graphitic edges (Figure 1a); porphyrinic structures; and, impurities embedded into graphene sheets (Figure 1b). For graphitic edge structures, Gaussian 09 is being employed and the Hartree-Fock method used to compute the electronic structure. A similar method has been employed for the porphyrinic systems. For the doped graphene sheets,

the *Vienna Ab-initio Simulation Package (VASP)* [2-5] is being used with density functional theory (DFT) in the generalized-gradient approximation [6-9]. A second approach for examining doped graphene sheets has been generated over the latter part of FY11 using the Metropolis Monte Carlo algorithm [10] to search for low-energy structures consisting of clusters of Fe atoms, N atoms, and graphene defects.
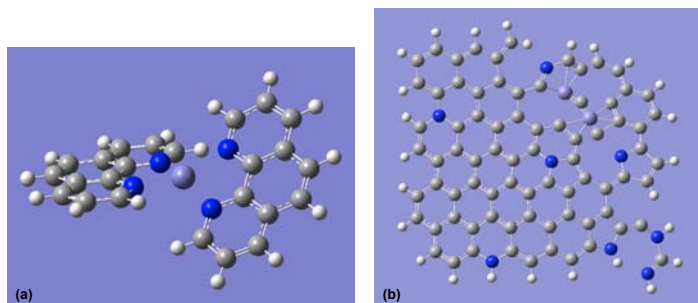
Figure 1. (a) Iron (II/III, LS/HS) bis-phenanthroline complex used as a surrogate system to model iron bridging two graphene sheets. The effects of additional ligands coming from the top and bottom are also being considered (CN-, NO, O2). (b) Defective graphene structure obtained as intermediate products in "randomized" search strategy using the Metropolis Monte Carlo algorithm for 2% Fe weight loading with 4:1 N:Fe ratios and 1:1 N:vacancy ratios in the model graphene flake.

In FY11, numerous models have been created and tested using available computational resources to provide for a comprehensive, computational-based search for the active site in this material. The strategy involves rational design based on known templates as well as global "random" search methods. The framework has been put in place for the new modeling hire to rapidly screen and validate structures against the experimental data generated by EPR and NRVS.

Synthesis of PANI-Fe and CM-Fe Catalysts

Commercial carbon blacks (Ketjenblack EC 300J, 950 $m^2 g^{-1}$ and Black Pearl 2000, 1500 $m^2 g^{-1}$;) were used as supporting materials in polyaniline (PANI-Fe) and cyanamide (CM-Fe) catalysts synthesis. In a typical approach [11-17], carbon supports were treated in hydrochloric acid solution for 24 hours to remove metal impurities and oxidized in 70% nitric acid at 80°C for 8 h for oxygen functionalization. $^{57}FeCl_3$ and $^{57}Fe(CH_3COO)_2$ were prepared as iron precursors in PANI-Fe and CM-Fe catalyst synthesis, respectively. In the case of PANI-Fe, 2.0 mL aniline was first dispersed with 0.4 g acid-treated carbon black in 0.5 M HCl solution and $FeCl_3$ added into above solution with a nominated Fe content of 10wt%. The suspension was kept below 10°C while the oxidant (ammonium peroxydisulfate, APS) was added, followed by constant mixing for 24-48 hours to allow PANI to fully polymerize and uniformly deposit onto the carbon

black particles. In the case of CM-Fe, 3.5 g CM and 0.3 g $^{57}Fe(CH_3COO)_2$ were mixed with 1.0 g oxidized carbon in reagent alcohol. The mixture was refluxed for 12 h at 80°C. In both cases, the suspensions containing carbon support, nitrogen precursors, and iron were evaporated at 80-90°C overnight to remove solvent. Subsequent heat treatment was performed at a temperature of 900-950°C in nitrogen gas for 1 hour. These heat-treated samples were then pre-leached in 0.5 M H_2SO_4 at 60-80°C for 8-12 hours to remove unstable and inactive species from the catalyst, and finally thoroughly washed with de-ionized water. In the last step, the catalyst was heat-treated for the second time in nitrogen-gas atmosphere for 1-3 hours.

EPR Characterization

Methods and Materials

EPR measurements have been performed with a Bruker EleXsys E-500 spectrometer equipped with an Oxford cryostat for temperature control down to 5K. The X-band spectrometer consists of an SHQE-W1 cavity, SuperX bridge, NMR Tesla meter, field/frequency stabilizer, and a 13 inch magnet. Data have been acquired by taking the first derivative of the absorption curve with field modulation 100 kHz, amplitude 1 mT, and a microwave power of 2 mW. A total of six EPR samples were measured. An oxidized, reduced, and NO absorbed sample were each prepared for two different catalysts.

Results

All samples show a signal at ca. g=4.3 from Fe^{3+} in a distorted octahedral symmetry (Figure 2a). The position does not shift significantly for different samples, but the NO and reduced PANI-Fe samples are more intense and have larger linewidths (Figure 2b). The significance of the intensity differences is difficult to establish since EPR intensity is directly proportional to mass, yet unknown [18]. The increased linewidth is probably caused by either increased local crystal disorder (symmetry around the Fe site) [19,20] or faster relaxation times [20-22]. Without measuring the EPR spectra as a function of temperature it is difficult to distinguish between these mechanisms. The oxidized/NO lineshapes are slightly more "Gaussian", but not enough to contribute the increased linewidth solely to inhomogeneous broadening and changes in crystal disorder. However, since reduction will decrease the number of Fe^{3+}, it may be that spin-spin relaxation processes are reduced in favor of spin-lattice relaxation processes.

Figure 2c shows the resonance near g=2. The prominent signal is likely from Fe^{3+} in axially distorted sites and the small linewidths indicate a relatively low ion population [23,24]. The reduced and NO samples of PANI-Fe again show slight differences from the other samples; these two samples had large background signals and the resonances appear to be slightly shifted with broader linewidths.
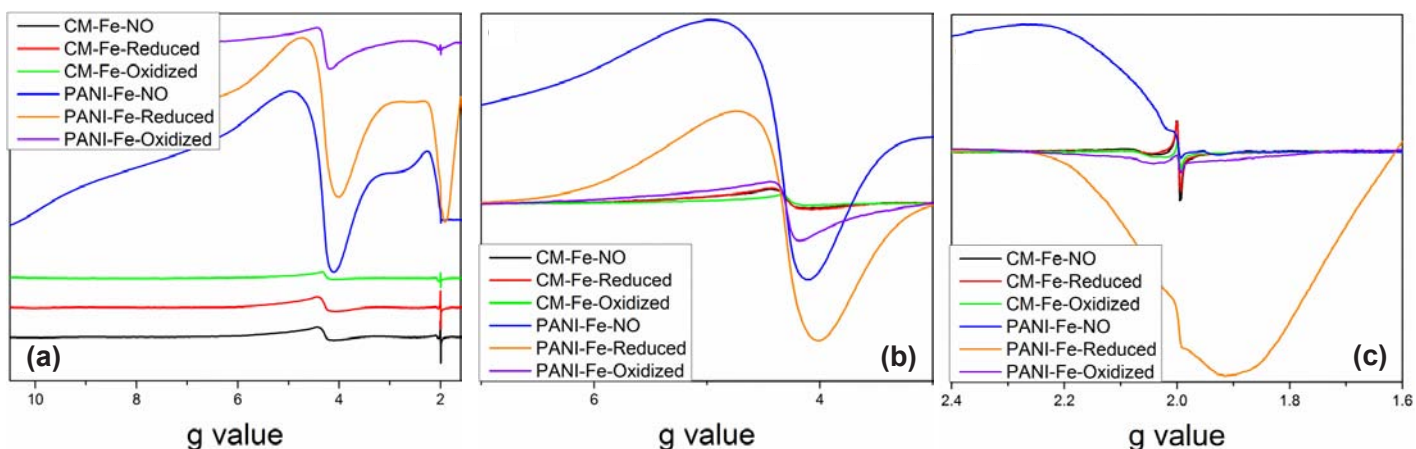
Figure 2. Spectra of all catalyst samples: (a) full scale; (b) region near g=4.3; (c) region near g=2.
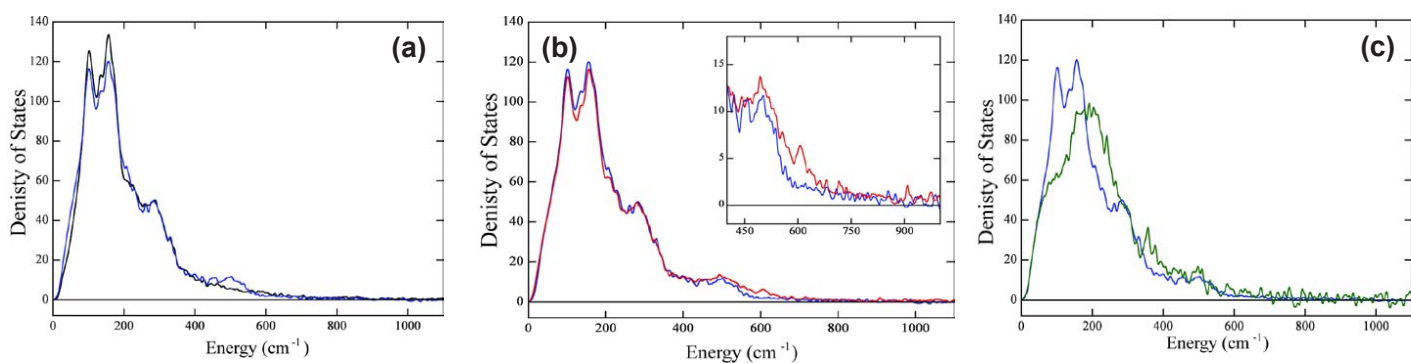
Figure 3. NRVS spectra of (a) as-prepared (black) and electrochemically reduced (blue) PANI-Fe catalyst; (b) electrochemically reduced (blue) and reduced plus NO-treated (red) PANI-Fe catalyst (inset showing an expanded view of the energy region at higher energy); (c) reduced PANI-Fe (blue) and reduced CM-Fe catalyst (green).

There was no clear evidence of NO absorption, i.e., the reduced and NO spectra have no obvious differences. One difficulty was the presence of significant Fe that results in a low Q-value or sensitivity. Such low sensitivity may have prevented the detection of NO signals.

Nuclear Resonance Vibrational Spectroscopy

In FY11, we have completed an initial set of NRVS experiments at ANL's Advanced Photon Source (APS), focusing predominately on PANI-Fe catalysts. The studies evaluated Fe-ligand vibrational bands for as-synthesized, electrochemically-reduced and reduced plus NO-treated samples, all prepared with ^{57}Fe. While the majority of the iron-ligand vibrations in NRVS spectrum ((Figure 3a) remain unchanged (unreduced bulk Fe species), several key changes are observed that can be attributed to reduced surface iron, specifically, an increase in the density of states between 425 and 575 cm^{-1}, a decrease in the low energy bands below 200 cm^{-1}, and additional perturbations between 200 and 250 cm^{-1}. These results demonstrate that NRVS is sufficiently sensitive to observe the change in metal-ligand vibrational features for surface-iron reduction. Of

greater interest is the effect of NO addition on the reduced iron samples since NO is an analog molecule for O_2 binding to Fe sites. New vibrational features observed upon NO treatment can be attributed to Fe-NO binding and likely constitute ORR sites. Figure 3b provides a comparison of NRVS spectra of the reduced and reduced plus NO-treated samples. Several new features are observed upon NO treatment, in particular, additional intensity at ca. 540-650 cm^{-1}, including a more intense feature at 606 cm^{-1}. This energy region is consistent with v(Fe-NO) for various known Fe-NO hemes [25]. The use of DFT site models, from which one can calculate Raman spectra including the v(Fe-NO) of a particular structure, will provide more definitive assignment of these features, allowing to specifically probe possible catalytic site structures in the PANI-Fe catalyst, consistent with the NRVS results. An additional higher energy feature at 908 cm^{-1} is also present in the NO-treated sample. The possibility that this may represent a bridging NO ligand, i.e. Fe-NO-Fe, is currently under investigation using modeling.

NRVS studies of CM-Fe catalyst have also been performed. Due to beam time limitation (four days total, ca. 24 hours required per sample), the only CM-Fe data obtained so far

are for the electrochemically reduced sample. However, a comparison of the reduced forms of the two catalysts provides initial experimental insight into the relative differences of the iron site structure and, hence, the iron vibrations present in PANI-Fe and CM-Fe catalysts (Figure 3c). Substantial differences in the Fe-ligand vibrations have been observed, indicating the likely presence of distinct Fe sites (surface and bulk) in these catalysts. Further CM-Fe catalyst studies, including NO-treated reduced sample, will be carried out next to elucidate the nature of possible surface Fe-site differences and their correlation to ORR activity.

Future Work

NRVS

A second round of beamtime will be utilized to complete studies initiated with the CM-Fe catalyst, including as-prepared and NO-treated samples. Time permitting the measurements will be expanded to additional catalyst formulations.

Spectroscopic Studies of NO treated catalysts

The studies will encompass both Mössbauer spectroscopy and magnetic circular dichroism. Mössbauer studies will allow for an expanded and detailed investigation of the effects of the NO treatment on surface iron electronic structure. Magnetic circular dichroism, which probes the differential absorption of left- and right-circularly-polarized light in a high magnetic field, has previously been shown to provide unprecedented insight into Fe-NO complexes (particular ligand-field and low energy charge transfer bands in the near-infrared region). This technique yields an increase by three orders of magnitude in transition from paramagnetic centers (i.e. iron) relative to the diamagnetic background (i.e. carbon support). MCD will be applied in conjunction with EPR, Mössbauer and NRVS to elucidate the structure of the surface iron sites perturbed by NO ligation.

Correlation to DFT structures

A key focus in the following year will be the development of DFT models of the iron site structure in order to correlate to spectroscopic data for NO-treated samples, exemplified by the initial NRVS results with PANI-Fe catalyst.

Conclusion

In FY11, we have successfully initiated a multidisciplinary research project that targets, for the first time, the determination of active ORR sites in fuel cell catalysts. We constructed an elaborate system that allows for treating catalysts with O_2 analogs in controlled atmosphere, and implemented methods for storing and transporting catalyst samples (e.g. from LANL to APS-ANL) in liquid nitrogen. We completed the synthesis and extensive electrochemical/ fuel cell testing of non-precious metal catalysts derived from PANI and CM. Finally, we carried out first EPR and NRVS experiments with NO used as a molecular probe of

active Fe sites for oxygen reduction. While Fe content in catalysts appeared to be too high for positive EPR verification of Fe surface sites (to be addressed via dilution in the future), NRVS experiments revealed significant differences between NO-untreated and NO-treated sample as well as differences between catalyst obtained from different precursors. Once verified in upcoming experiments and linked to DFT models these data are likely to lead to the first ever direct proof of the presence of transition-metal ORR sites on non-precious metal catalysts – an important discovery for the understanding of the ORR mechanism and for the future development of precious-metal-free fuel cell catalysts.

References

1. Frisch, M. J.. Gaussian 09, Revision C.01 (Computer Porgram). 2009. *Gaussian Inc..*

2. Kresse, G., and J. Hafner. Ab initio molecular-dynamics simulation of the liquid-metal-amorphous-semiconductor transition in germanium. 1994. *Physical Review B.* **49**.

3. Kresse, G., and J. Hafner. Ab inito molecular dynamics for liquid metals. 1993. *Physical Review B.* **47**.

4. Kresse, G., and J. Furthmüller. Efficiency of ab-initio total energy calculations for metals and semiconductors using a plane-wave basis set. 1996. *Computational Materials Science.* **6**.

5. Kresse, G., and . . Efficient iterative schemes for ab initio total-energy calculations using a plane-wave basis set. 1996. *Physical Review B.* **54**.

6. Perdew, J. P., J. A. Chevary, S. H. Vosko, K. A. Jackson, M. R. Pederson, D. J. Singh, and C. Fiolhais. Atoms, molecules, solids, and surfaces: Applications of the generalized gradient approximation for exchange and correlation . 1992. *Physical Review B.* **46**.

7. Perdew, J. P., J. A. Chevary, S. H. Vosko, K. A. Jackson, M. R. Pederson, D. J. Singh, and C. Fiolhais. Erratum: Atoms, molecules, solids, and surfaces: Applications of the generalized gradient approximation for exchange and correlation. 1993. *Physical Review B.* **48**.

8. Perdew, J. P., K. Burke, and M. Ernzerhof. Generalized gradient approximation made simple. 1996. *Physical Review Letters.* **77**.

9. Perdew, J. P., K. Burke, and M. Ernzerhof. Erratum: Generalized gradient approximation made simple. 1997. *Physical Review Letters.* **78**.

10. Metropolis, N., A. W. Rosenbluth, M. N. Rosenbluth, and A. H. Teller. Equations of State Calculations by Fast Computing Machines. 1953. *Journal of Chemical Physics.* **21** (6): 1087.

11. Chung, H. T., C. M. Johnston, F. H. Garzon, and P. Zelenay. A Non-Precious Electrocatalyst for Oxygen Reduction Based on Simple Heat-Treated Precursors. 2008. Edited by T. S. Fuller, M. M. S; Inaba, and T. L. Zawodzinski. Vol. 16, 2 Edition, p. 385.

12. Wu, G., Z. Chen, K. Artyushkova, F. H. Garzon, and P. Zelenay. Polyaniline-derived Non-Precious Catalyst for the Polymer Electrolyte Fuel Cell Cathode. 2008. Edited by T. S. Fuller, M. M. S; Inaba, and T. L. Zawodzinski. Vol. 16, 2 Edition, p. 159.

13. Chung, H. T., C. M. Johnston, K. Artyushkova, M. Ferrandon, D. J. Myers, and P. Zelenay. Cyanamide-derived non-precious metal catalyst for oxygen reduction. 2010. *Electrochemistry Communications.* **12** (12): 1792.

14. Wu, G., M. A. Nelson, N. H. Mack, S. Ma, P. Sekhar, F. H. Garzon, and P. Zelenay. Titanium dioxide-supported non-precious metal oxygen reduction electrocatalyst. 2010. *Chemical Communications.* **46** (40): 7489.

15. Jaouen, F., E. Proietti, M. Lefevre, R. Chenitz, J. Dodelet, G. Wu, H. T. Chung, C. M. Johnston, and P. Zelenay. Recent advances in non-precious metal catalysis for oxygen-reduction reaction in polymer electrolyte fuel cells. 2011. *Energy & Environmental Science.* **4** (1): 114.

16. Wu, G., C. M. Johnston, N. H. Mack, K. Artyushkova, M. Ferrandon, M. Nelson, J. S. Lezama-Pacheco, S. D. Conradson, K. L. More, D. J. Myers, and P. Zelenay. Synthesis-structure-performance correlation for polyaniline-Me-C non-precious metal cathode catalysts for oxygen reduction in fuel cells. 2011. *Journal of Materials Chemistry.* **21** (30): 11392.

17. Wu, G., K. L. More, C. M. Johnston, and P. Zelenay. High-performance electrocatalysts for oxygen reduction derived from polyaniline, iron, and cobalt. 2011. *Science.* **332**: 443.

18. Eaton, S. S., and G. R. Eaton. Signal Area Measurments in EPR. 1979. *Bulletin of Magnetic Resonance.* **1** (3): 9.

19. Pidol, L., O. Guillot-Noël, A. Kahn-Harari, B. Viana, D. Pelenc, and D. Gourier. EPR study of Ce. 2006. *Journal of Physics and Chemistry of Solids.* **67** (4): 643.

20. Abragam, A., and B. Bleaney. 1970.

21. Nash, F. R.. Size-dependent relaxation times at liquid helium temperatures. 1961. *Physical Review Letters.* **7** (2): 59.

22. Nash, F. R.. Electron spin relaxation in copper tutton salts at low temperatures. 1965. *Physical Review.* **138** (5A): A1500.

23. Ibrahim, M. M., G. Edwards, M. S. Seehra, B. Ganguly, and G. P. Huffman. Magnetism and spin dynamics of nanoscale FeOOH particles. 1994. *Journal of Applied Physics.* **75**: 5873.

24. Singh, R. Kumar, and A. Srinivasan. EPR and magnetic susceptibility studies of iron ions in ZnO–Fe2O3–SiO2–CaO–P2O5–Na2O glasses. 2010. *Journal of Magnetism and Magnetic Materials.* **322** (14): 2018.

25. Benko, B., and N. Tu. Resonance Raman studies of nitric oxide binding to ferric and ferrous hemoproteins: Detection of Fe(III)-NO stretching, Fe(III)-N-O bending, and Fe(II)-N-O bending vibrations. 1983. *Proc. Natl. Acad. Sci. USA.* **80**: 7042.

Publications

Zelenay, P.. Non-precious metal catalysts for oxygen reduction. Invited presentation at *Tongji University, State Research Center for Fuel Cell Vehicle and Powertrain System Engineering Technologies.* (Shanghai, China, September 6, 2011).

Zelenay, P.. Non-precious Metal catalysts for oxygen reduction. Invited presentation at *Nanjing University, Department of Materials Science.* (Nanjing, China, September 8, 2011).

Zelenay, P.. Non-precious metal catalysts for oxygen reduction. Invited presentation at *Dalian Institute of Chemical Physics, Chinese Academy of Science.* (Dalian, China, September 15, 2011).

Zelenay, P.. Non-PGM electrocatalysis of oxygen reduction. Invited presentation at *Tsinghua University, Institute of Nuclear and New Energy Technology.* (Beijing, China, September 19, 2011).

Zelenay, P.. Non-precious metal catalysts for oxygen reduction in fuel cells: In pursuit of platinum. Invited presentation at *Peking University, College of Engineering.* (Beijing, China, September 20, 2011).

Innovative Process for Making Ultra-thin Dielectrics

Quinn R. Marksteiner
20110246ER

Introduction

Barium Strontium Titanate ($BaSrTiO_3$) ceramics have many interesting properties, including ferroelectricity, piezoelectricity, pyroelectricity, superconductivity, high permittivity, and nonlinear dependence of permittivity on applied electric field [1]. The nonlinearity of these materials can be used to generate a nonlinear transmission line (NLTL), which is a compact device that can be used to generate high power microwave (HPM) radiation in the GHz frequency range [2].

The objective of this project is to develop a novel method for fabricating ultra-thin plates of nonlinear dielectric ceramics. These thin dielectrics have important applications in generating a practical NLTL, in addition to other high power microwave applications. This transformational technology has the potential to create a new paradigm in the field of high power microwave devices.

Two innovative approaches are proposed to overcome the extreme difficulty in making ultra thin dielectric plates. The first of these is a direct tape laminating method. This process integrates the tape casting process and the tape laminating technology. The second approach is to integrate the spin coating technique using the nonlinear dielectric slurry and the tape laminating technology.

In addition, we are fabricating thicker blocks of nonlinear dielectrics, to find the optimal chemistry for minimizing RF losses in the material and maximizing nonlinearity.

After the best approach is down-selected, a compact NLTL system will be built which produces 1 MW of peak RF power at 1 GHz, to demonstrate the usefulness of this technology.

Benefit to National Security Missions

An important aspect of warfighter support is the development of non-lethal, HPM weaponry. Currently the United States Army and Air Force are actively pursuing NLTL based HPM sources for their respective arsenals. In addition, the Joint Non-lethal Weapons Directorate of the US Marine Corps is developing a vehicle stopping system to be deployed at check points in order to counter vehicle-borne improvised explosives. The current system is based on conventional HPM sources, but they are actively pursuing an HPM NLTL source as an alternative. The common roadblock to all of these systems is the lack of an appropriate non-linear material. This project would solve this problem.

Progress

We have made several new batches of bulk ceramic blocks (not thin films), to optimize the bulk properties of the material. In particular, we have varied the amount of zirconium used as a dopant in the $BaSrTiO_3$ nonlinear material, and the temperature at which the material is baked to. After the materials were fabricated, they had to be metalized.   Dr. Chen had to spend some time developing this capability in the first three months of the project. He tested several different metals, and found silver to be the most reliable. After this, we measured the dielectric constant and loss tangent of the materials. The results indicate that zirconium is an important dopant in this nonlinear material, and that 1450 C is a good baking temperature for the ceramics. We have tested different levels of zirconium, and found an optimum level that minimizes the loss in the material.

We have focused so far on the tape casting method for fabrication of thin materials. There were some initial setbacks in the fabrication of these thin materials, because the materials tend to crack during the baking process.   These setbacks were overcome by using materials that are 200 um instead of the 100 um that is given in the original proposal. Simulations of NLTLs indicate that 200 um will be thin enough to design high impedance NLTLs in the 1 to 2 GHz range. The fabricated 200 um materials have improved mechanical properties, and will be metalized and ready for dielectric testing by November. Figure 1 shows a picture of the thin $BaSrTiO_3$ material, with the zircon laminates.

We have also designed several resonant cavities for measuring the high frequency properties of $BaSrTiO_3$, both for the bulk materials and the thin materials. These cavities are designed to measure the dielectric constant

and conductivity at the 0.5 GHz to 2 GHz range. Before constructing the cavities, we performed numerical simulations with different electromagnetic codes to optimize the design. We have now constructed 2 cavities which are currently being used to characterize the material properties of $BaSrTiO_3$ at high frequencies. A picture of one of these cavities is shown in Figure 2. The cavities that we have designed are novel, because they can be used to measure the high frequency properties of both the thin materials and the bulk ceramic. Previous resonant cavity techniques for $BaSrTiO_3$ can be used only on materials that have been machined to a specific shape and size. We are ordering a commercial material with high permittivity to test our cavities.

We have gained theoretical understanding of the potential improvement that thin materials can bring to Nonlinear Transmission Lines (NLTLs). Simulations indicate that unwanted transverse modes develop when using thick ceramics. We are developing an analytical model of this effect, and have made improvements on our ability to realistically simulate NLTLs with the Electromagnetic code Remcom.
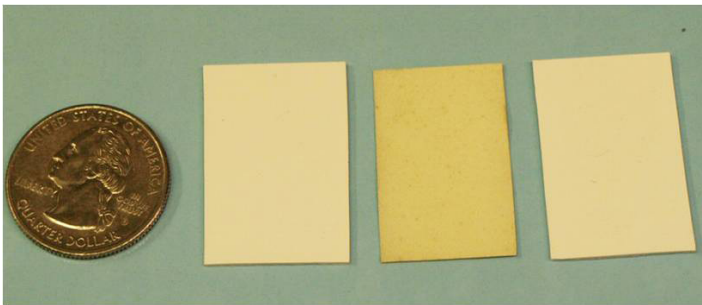
Figure 1. The thin BSTO dielectric will be sandwiched between two zircon laminates, which have low dielectric constant and are used only for mechanical support.
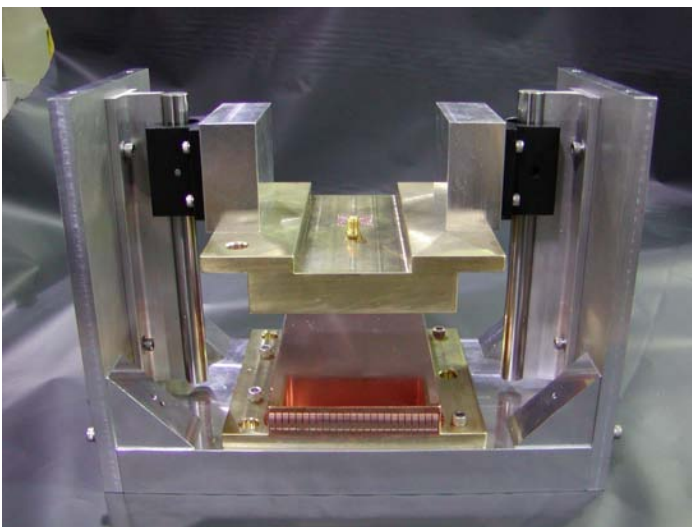
Figure 2. This is a picture of one of the resonant cavities being used to measure the high frequency (0.5 - 2 GHz) properties of BSTO.

Future Work

The objective of this project is to develop a transformational technology for the fabrication of ultra thin non-linear dielectrics. This has the potential to create a new paradigm in the production of high power microwave devices. It has long been recognized that $BaSrTiO_3$ materials could have a revolutionary impact on the field of small, tunable, high-frequency (> 1 GHz) microwave devices. However, since the minimum permittivity that will have adequate nonlinearity is 3000, a 1 GHz nonlinear transmission line with high enough impedance to function as a practical device will have dielectric components that are no more than ~0.25 mm (250 μm) thick. Conventional ceramic processing methods cannot achieve these thin plates without any significant camber or warpage. In addition, 250 μm thin plates are too fragile to withstand the handling, metallization, and bonding process. Both "thin film" and "thick film" techniques have their inherent limitations. Due to these limitations in conventional ceramic processing the progress in high power microwave generation with solitons has been limited.

What has been lacking is a novel processing method to fabricate ultra thin $BaSrTiO_3$ plates on the order of 250 μm thick with low cost, high performance, and a fast production rate. Two innovative approaches are proposed to overcome the extreme difficulty in making ultra thin dielectric plates. One of the novel ideas is a direct tape laminating method. This process integrates the tape casting process and the tape laminating technology. The other novel idea is to integrate the spin coating technique using the $BaSrTiO_3$ slurry and the tape laminating technology. The new dielectric laminates will be extensively measured to verify the performance of the laminates and to down select the better method. A short non-linear transmission line (NLTL) will be constructed to demonstrate the applicability of the laminates.

Conclusion

The goal of this project is to overcome a significant barrier in the field of nonlinear applications of $BaSrTiO_3$. In particular, this technology will revolutionize NLTL RF sources, and will open up new applications in HPM non-lethal weaponry, which all of the branches of the military have shown interest in. An HPM nonlethal weapon can be used for vehicle stopping and for the disruption of weapons and communications systems. These laminates will also have applications in a variety of RF tunable devices, including tunable filters, phase shifters, and tunable dielectric resonators.

References

1. Chen, C., D. Reagor, S. Russell, Q. Marksteiner, L. Earley, D. Dalmas, H. Volz, D. Guidry, P. Papin, and P. Yang. Sol-Gel Processing and Characterization of a Ba0.75Sr0.25Ti 0.95Zr0.05O3 Ceramic. To appear in *Journal of American Ceramics Society* .

2. Marksteiner, Q., B. Carlsten, and S. Russell. Numerical Calculations or RF Efficiency from a Soliton Generating Non-linear Transmission Line. 2009. *Journal of Applied Physics.* **11** (106): 5.

Embedding Plasmonic Nanostructures at Semiconductor Interfaces for Enhancing Photovoltaic Efficiency

Todd L. Williamson
20110290ER

Introduction

The remarkable optical properties and tunability over visible wavelengths of plasmonic nanostructures make them attractive candidates for enhancing the performance of photovoltaic (PV) devices. Measureable improvements in performance and efficiency of inorganic semiconductor-based PV devices have been observed by placing plasmonic nanostructures on either their front or back surface. Ideally, plasmonic nanostructures should be embedded into the active p-n junction in PV devices to achieve new, higher levels of efficiency. We intend to investigate new mechanisms for enhancing PV efficiency by embedding plasmonic nanoparticles at the p-n junction in InGaN-based semiconductor PV devices whose tunable bandgaps cover nearly the entire solar spectrum making them ideal materials for high efficiency hybrid PVs. In this project, we propose to merge conventional PV semiconductor device architectures with advanced metal nanoparticle (NP) synthetic techniques to produce enhanced PV devices with superior performance characteristics. Our overall target is to create the first PV devices with plasmonic NPs buried at active semiconductor p-n junction interfaces with tailored properties for higher conversion efficiencies. These PV devices will take advantage of near field interactions to manipulate their local electronic fields resulting in enhanced performance. The fundamental advances in materials science and photophysics made through this work will drive the development of novel PV device architectures that far out perform current implementations.

Benefit to National Security Missions

The planned work will directly impact LANL's emerging core missions in energy and materials science. The fundamental insights into plasmon-exciton interactions and their direct manipulation will be of broad interest to both the nanomaterials and optoelectronics communities. Applying principles from the emerging fields of plasmonics and photovoltaics based on InGaN alloys, this work is poised to have direct implications on the next generation of PV technologies that are of significant interest to energy independence, national security, and environmental missions that are ongoing at LANL and the DOE complex. Direct impact in LANL threat reduction and energy security missions via applications in sensing and improvements in semiconductor-based energy harvesting materials are expected. This project will position LANL for numerous external follow-on funding calls from various agencies.

Progress

For this project to be successful, 3 key goals have to be established and then carefully integrated together. These three areas are InGaN film growth, nanoparticle synthesis and deposition, and device fabrication and testing. During the first year of this project we have made excellent progress in these key areas so that we can begin to smoothly integrate them towards the end of this first FY, and continuing into the the second FY.

For the InGaN film growth thrust, the most important capability that needs to be demonstrated is the creation of p-n junctions for InGaN films over the range of In compositions (0% - 35%) having optical bandgap energies overlapping with the plasmon resonance energies (400 nm - 650 nm) we wish to study. To date, we have demonstrated growth of n-type and p-type InGaN films that have appropriate electrical, crystallographic, and optical properties. The most difficult aspect of this work is optimizing the appropriate electrical properties of the films. Most InGaN films grown by conventional techniques in the high end of the In composition range we require for this work (In > 30%) have residual n-type carrier concentrations that are too high both for straightforward p-type doping with Mg (a common dopant for these materials) and for the creation of good quality devices. Following the success in growing individual n- and p-type films, we have begun creating p-n junctions of these films and the first set of these structures are in the process of being micro-patterned into devices for testing.

For the nanoparticle synthesis and deposition thrust, we have successfully synthesized a variety of metal and metal oxide nanoparticle geometries. These include Au, Ag, and Au-SiO2 nanoparticles that range in size from 10nm up to 150nm in diameter. These size ranges and compositions exhibit surface plasmon resonances throughout

the visible-near IR energy ranges and overlap well with the bandgap energies of the InGaN films. We are investigating the ideal nanoparticle deposition technique. Initial attempts to deposit Ag nanoparticle solutions on InGaN films using a modified scraping technique have resulted in homogeneous submonolayer nanoparticle films that are approximately 10% surface coverage. These are ideal initial nanostructured films to begin InGaN overgroth studies. In parallel, we have set up a nanoparticle spray booth and are in the process of getting all required IWD documentation before attempting to make nanoparticle films via this method.

Device fabrication and testing has begun with initial patterning of n-type InGaN films performed to obtain the necessary processing parameters that will be required for the fabrication of test structures. Reliable protocols for lithography and plasma etching of the films have been established. While the processing required for device fabrication for this project is relatively straightforward, it is still necessary to establish and verify a reliable processing scheme. We are also acquiring a semiconductor analyzer that will allow us to evaluate our plasmonically enhanced p-n junctions. Important parameters we can measure that need to be studied to evaluate our plasmon-enhanced photo-junctions include open-cicuit voltage (Voc), short-circuit current (Isc), Max Power output (Pmax), Fill factor (FF), System efficiency (Rsh), and Quantum Efficiency (QE). Evaluating these parameters in our prototype devices will allow us to measure the enhancement in PV efficiency expected for embedded plasmonic particles at semiconductor p-n junctions, the overall goal of this project.

Overall, this project is proceeding along the expected timeline. The ground work required in each of the three thrust areas identified above has been successfully completed on schedule. We expect a rapid acceleration of work as we begin to integrate these efforts together in the coming months.

Future Work

The fundamental photophysical properties of nanostructures embedded at semiconductor interfaces are a pristine research area where significant advancements will facilitate extraordinary optoelectronic properties. The primary limiting factor of these nanostructure architectures has been the successful fusion of high-quality, low temperature thin film growth techniques with chemically synthesized, uniform, optically active nanomaterials. The work involves using a unique combination of fabrication and synthetic capabilities at LANL to produce novel PV designs. Plasmonically active NPs will be produced by colloidal synthetic techniques. The most rudimentary particle designs will involve colloidal Au and Ag that are prepared using standard wet chemical synthetic techniques allowing plasmon excitation across much of the visible spectral region (400nn to 600nm). Increasing the particle complexity using nanoshell particles will allow access to a wider range of

plasmon energies. These materials will then be deposited on a n- or p-type semiconductor surface that will subsequently be overgrown with the oppositely doped analog, creating devices with plasmonic nanostructures embedded at a p-n semiconductor junction. The targeted semiconductor system for this work will be the $In_xGa_{1-x}N$ ternary alloy system. This important semiconductor system has a tunable direct bandgap ranging from 0.7 eV (1800 nm) to 3.4 eV (365 nm), a range that encompasses nearly the entire solar spectrum. In order to take full advantage of plasmon-semiconductor interactions, the resonance frequency and the semiconductor bandgap need to be carefully chosen and optimized to yield the maximum enhancement. Our prototype plasmon-PV devices will be tested under simulated solar illumination to probe the influence of the plasmonic nanostructures on PV efficiency. Prototype devices will be tested by creating simple mesa structures that expose both the p and n regions of the device for subsequent electrical contact.

Conclusion

Our plan to place plasmonic nanostructures specifically at a semiconductor interface is largely unexplored, representing a new method for improving the performance of PV devices. While there has been growing interest over the last several years in creating enhanced PV devices with plasmonic nanostructures, there are few reports of successful embedding of plasmonic nanostructures at a semiconductor junction. Our unique ability to synthesize a wide range of plasmonic NPs and embed them at the p-n junction in InGaN semiconductors of varying bandgaps will greatly increase our fundamental understanding of the nature of embedded plasmonic NPs at semiconductor p-n junctions.

Bio-analogue Catalysts: Evolved Aptazymes for the Hydrolysis of Organophosphorous Compounds

Robert F. Williams
20110338ER

Introduction

This project is developing novel DNA based aptamers to function as catalysts to hydrolyze organophosphorus (OP) compounds such as OP nerve agents. As enzyme mimics, these catalysts are not designed to hydrolyze the phosphorous-fluorine bond of the OP agents; rather, they specifically target other phosphorous bonds, such as P-O, P-S, or P-N for breakage leading to an unstable intermediate that will rapidly decompose. Our approach allows a universal capture and breakage of bonds to phosphorous found in all chemical weapon agents (CWAs) as well as all related OP toxic industrial chemicals and materials (TICs/TIMs) such as pesticides. The development of this robust toolbox, which specifically targets bonds for catalytic breakage, has important ramifications for the chemical and pharmaceutical industries, for therapeutic applications, and for our fundamental understanding of biological catalysis. A long standing objective for bioorganic chemists has been to understand the role that molecular conformations play in enzyme catalysis and this project will advance this understanding. The current unifying picture of enzyme catalysis invokes an ensemble of coupled conformational states that are altered as ligand binding and catalysis occur through a 'catalytic network'. Thus, a multi-dimensional free-energy landscape, which requires multiple sequential intermediates, is necessary for efficient catalysis to occur. Each intermediate on the reaction pathway is associated with an ensemble of conformational states producing parallel reaction paths. The enzyme-substrate complex induces structural reorganizations as the reaction proceeds through the critical transition state to product and although this process appears intuitively reasonable, such a chronology has not yet been effectively utilized to design enzyme mimics that target specific bonds in a molecule and catalytically break the targeted bond in an efficient manner, *vide infra*, an enzyme. Our evolved aptamers are designed to produce the required structure and reorganization leading to efficient catalytic hydrolysis, just like an enzyme (enzyme mimic or aptazyme). Systematic evolution of ligands by exponential enrichment (SELEX) is an *in vitro* selection technique that utilizes combinatorial chemistry to produce nucleic acid ligands with high binding affinity and specificity toward a desired target. The attraction of nucleic acid-based combinatorial chemistry lies in its potential for amplification and directed evolution. Mimicking the process of natural selection in the laboratory setting, repeated cycles of selection for specific high-affinity binding with increasing stringency, followed by PCR (polymerase chain reaction) amplification can lead to the isolation of oligomers 'evolved' to bind tightly and selectively to a target of choice. These selected aptazymes will have a demonstrated affinity for their targets and break only specifically targeted phosphorous bonds. Nucleic acids have played a significant role in the early evolution of life with their specific abilities to make and break phosphate bonds and it is this functionality that we are enhancing. By utilizing combinatorial techniques to develop nucleic acid constructs with effective conformational structures for binding, catalytic breakage of a targeted bond that mimics an enzyme active site with its concomitant rate acceleration will be achieved. This project also addresses a critical LANL mission by developing a new technical means to reduce the global threat of existing and emerging CWAs and thwart terrorist attacks that might employ them by providing a tool to re-mediate an exposure event.

Benefit to National Security Missions

The development of technologies that allow for the rapid and specific identification/elimination of chemical threat agents in the environment and mitigation of adverse effects on exposed individuals are essential for threat reduction. A primary mission goal of the Laboratory is to develop the technical means to reduce the global threat of existing and emerging chemical and biological weapons of mass destruction and to thwart terrorist attacks that might employ them by providing the necessary science and technology. Consequently, development of effective countermeasures to CWAs, TICs, TIMs, and related compounds are critical to LANL's non-proliferation activities and mission to prevent or reduce the capability for rogue nations or terrorists to do our nation harm. The application of our systematic, iterative, computationally driven, coupled experimental approach

has the potential to provide new tools for the discovery of enzyme function, a problem at the core objective of understanding Complex Systems of biological function.

Progress

Four key accomplishments of this project have been made during this past, first year of the ER project. The first accomplishment was the design and implementation of a synthetic route to a phosphonate compound that is coupled to a polyethylene glycol linker that ends in a biotin moiety. This was required in order to select a specific phosphorous-ligand (oxygen, sulfur, or nitrogen) bond that will be selectively hydrolyzed by the DNA aptamers. The initial target molecule is a phosphonate that contains the P-O-LB bond linkage. The oxygen is connected to both the phosphorous and the polyethylene glycol linker that ends in a biotin moiety (LB). The biotin moiety is required to bind to streptavidin that is attached to a solid support and this binding will remove all of the DNA aptamers that do not hydrolyze the target P-O bond. Any aptamers that successfully hydrolyze the target P-O bond will be recovered for subsequent amplification. On the other side of the phosphorus containing molecule, the DNA aptamer library is attached to the phosphorous through another polyethylene glycol linker (PGL) through an alkyl bond to the phosphorous (PGL-C-P). The PGL-P bond is not hydrolysable.

The second key accomplishment was the synthesis of the complete phosphonate that contained polyethylene linkers on both sides of the molecule, with one ending in the biotin and the other ending in an azide functional group (N3-PGL-C-P-O-LB). Thus, the complete complex construct can now be attached to the DNA aptamer library using copper mediated click chemistry to produce DNA-Library-CCN-PGL-C-P-O-LB.

The third key accomplishment was design and synthesis of the DNA aptamer library terminating in an alkyne moiety for the click coupling to the azide terminated moiety containing the phosphorus described above. Additionally, the primer molecules for PCR amplification of the selected DNA aptamers were also designed; however, additional design work in this next year is anticipated in order to optimize the amplification of aptamers that show hydrolytic activity.

The fourth key accomplishment was a redesign of the selection strategy to take advantage of temperature as a selection stringency parameter and to eliminate the cross-linking interactions caused by high density placement of the complete complex construct (DNA-Library-CCN-PGL-C-P-O-LB) on a streptavidin-linked solid support. If the complex constructs are too close together they can interact, possibly causing an adjacent DNA aptamer to hydrolyze its neighbor phosphonate rather that the phosphonate to which it is attached. This could add aptamers that are not truly competent with correct conformations to the pool of successful aptamers. Initially, the solid support design was

going to be constructed with sufficient spacing to avoid this problem. While we are continuing with this approach, we will also use dilute solutions of the DNA aptamer library complexes first heated to ~80 deg C to denature the aptamers followed by metal addition and then cooling to allow the DNA aptamers to refold. In dilute solution they will not interact with their neighbors as they can on the solid support. Again, only the DNA aptamers that hydrolyze the P-O bond will survive and pass through a streptavidin column allowing recovery and subsequent amplification of the desired aptazyme. Additionally, this approach will allow us to shorten contact times selecting for the fastest reaction times and we will be able to use temperature to select for the most robust folding aptazymes.

Future Work

Aptamers are nucleic acid binding species capable of recognizing a wide range of target molecules and biological structures with varying conformational flexibilities and we will look at additional targets as the project progresses. Isolated from our high diversity combinatorial libraries of synthetic nucleic acids by a rapid iterative selection process, we will select aptamers for effective binding recognition as well as a designed catalytic function (enzyme mimic or aptazyme) for multiple classes of phosphorus bonds. After we have completed our first selection protocols to hydrolyze the initial target P-O bond, we will construct additional phosphorus targets with P-S and P-N bonds and select optimum aptazymes for these specific bonds. We anticipate generating three aptazyme classes that function on P-O, P-S, and P-N bonds. This represents all classes of CWAs and pesticides and we will demonstrate that the selected apatazymes are efficient catalysts to hydrolyze these compounds. To enhance aptamer capabilities, synthetic chemistries for modifying nucleotides will also be used to increase the potential of aptamers for binding, catalysis, and stability.

Conclusion

The expected results are aptazymes that show specific, rapid hydrolysis of CWAs, TICs, and TIMs and an understanding of the structure/conformation-activity relationships necessary for catalysis. The aptazyme function and structure diversity will be sequenced and the evolution of enzyme function related to mechanistic studies by NMR and computational studies. This integrative approach will yield novel insight into the mechanism of designed enzymes for organophosphorous hydrolysis, as well as structural and chemical constraints. In combination with molecular modeling the experimental results will provide an innovative means of furthering our understanding of CW aging, biological processing, and enzymatic hydrolysis.

Developing a Mild Catalytic Route for the Reduction of N2 to NH3

John C. Gordon
20110358ER

Introduction

The research outlined in this project concerns the development of catalysts capable of supporting the conversion of dinitrogen (N_2) to ammonia (NH_3) under mild conditions using the Earth-abundant metal iron (Fe). Largely due to the demands of food production, industrial generation of NH3 consumes more than 1 % of the world's energy output as a result of the energetically intense conditions employed. Enzymatic NH3 production occurs under ambient temperature and pressure, and translation of this efficiency to a synthetic system would significantly decrease energy production demands. We aim to pursue this goal through a heretofore unexplored reaction manifold designed to maximize N_2 activation and minimize the number of intermediates necessary for NH3 production. The interdependent use of experiment and theoretical calculations will be used to realize the secondary objectives of advancing scientific understanding of N_2 functionalization and probing the boundaries thereof, understanding the effect of varied electronic structure on N_2 reactivity, and exploring new Fe coordination chemistry

Benefit to National Security Missions

The energy impact of industrial NH3 production is a national and global issue. An effort to ameliorate it by using well-defined catalysts based on abundant and inexpensive metals to decrease its energy requirements intimately meshes with the Laboratory's Energy and Earth Systems Grand Challenge and missions in energy security. Results from the research contained in this proposal have the potential to lay the groundwork for future funding through the DOE as well as garner interest from corporate partners interested in continuing work on commercially applicable solutions. Advances in this area are also of significant basic scientific interest and would serve to raise the Laboratory's profile in sustainable energy research and attract talented investigators in the field to LANL.

Progress

Within the first year of this project, we have made excellent progress in the preparation and characterization of a series of iron complexes pertinent to the goals of this proposal. We have utilized molecular modeling to guide our design of tridentate phosphine (triphos and triphos') ligands capable of supporting the bridging dinitrogen complexes that we are targeting as catalytically relevant intermediates for NH3 production. We have taken the results gleaned from the predictive modeling into the laboratory and have already demonstrated success in the synthesis of targeted molecular species.

In this regard, we have isolated the divalent Fe precursors (triphos)FeX2 (X = Cl, Br) and have subsequently carried out reduction chemistry to reduce the Fe(II) to monovalent Fe complexes e.g. (triphos)FeBr$_2$. We have characterized this particular molecule via a single crystal X-ray structure.

A major target in the context of the proposed work is to be able to isolate, characterize and probe reactivity of zerovalent complexes containing Fe-N_2-Fe linkages. To this end we have studied several routes towards the synthesis of such complexes. In the hope that we could isolate such an iron complex, we investigated the use of a commercially available zerovalent Fe complex in the form of Fe(COT)2 (COT = cyclooctatetraene) and reacted this with the triphos liagnd in the presence of N_2. In this case, an N_2 adduct was not isolated, but rather an interesting zerovalent Fe complex i.e. (triphos)Fe(COT). A similar species was isolated with the related triphos' ligand, and some interesting differences in the reduction of the COT ligand within these two compounds were observed, as were those of the spin states of the iron centers

Reaction of the divalent iron compound (triphos)FeCl$_2$ with sodium tetraphenylborate (NaBPh$_4$), results in the formation of a green cationic species [(triphos)FeCl]BPh4 which can subsequently be reduced with K/C8 under N_2 to indeed yield a very interesting molecule molecule containing zerovalent iron centers and a bridging N_2 ligand, i.e. (triphos)Fe-N_2-Fe(triphos), a desired target. A single crystal X-ray structure determination of the complex reveals that the Fe-N distances within this molecule are short and the N-N distance is quite long (compared with free N2). We are currently working on gathering

other spectroscopic characterization on this molecule that will speak to the nature of the N-N interaction; however qualitatively speaking, these features that are consistent with a metal promoted weakening of the bonds between coordinated nitrogen atoms. This is a very promising observation, in that to access another of the key synthetic targets i.e. an iron nitride moiety (Fe≡N), the bridging N2 unit in such a complex has to be cleaved in half. The isolation of this complex thus represents what we believe to be a significant discovery in the context of the proposed work. There are very few examples of such molecules that have been structurally characterized, and the structural features of this particular example lead us to believe that this could represent a general class of molecules with important ramifications in developing lab scale demonstration mild catalytic routes for the reduction of N2 to NH3. The use of theory is helping us understand the electronic structure and bonding characteristics within the Fe-N-N-Fe core of this and related molecules.

We are currently investigating electrochemical methods to characterize the ability of these complexes to undergo electron transfer reactions (these will also be required to effect a catalytic cycle to convert N2 into NH3). Current work is also focused on the isolation of nitride containing species supported by such tripodal phosphine ligands, and the isolation of Fe containing intermediates that "lie between" the functionalities of bridging N2 and nitride ligands in terms of reactivity are also being targeted. We are also working on the synthesis of a number of different versions of the triphos ligand, in particular on varying the sterics within the phenyl ring of each phosphine arm. This will allow for "tailoring" of the cavity in which the N2 ligand sits and also the propensity for cleavage of the Fe-N2-Fe moiety towards Fe≡N unit formation.

Future Work

Biological and industrial N2 fixation are the processes by which one of the most inert molecules known (N2) is transformed into a bioavailable nitrogen source (NH3). NH3 is then used as the sole building block for all nitrogen-containing biomolecules, rendering this transformation essential to sustaining life on our planet. The Haber-Bosch process for NH3 synthesis is currently carried out on an enormous scale and requires pressures of approximately 200 atm. and temperatures as high as 500 °C. This brute-force, high-energy input solution to N2 fixation accounts for about 50 % of the nitrogen atoms present in all human beings and consumes more than 1 % of the world's energy output. Development of an NH3 production process at or near ambient conditions would undoubtedly help curb the negative environmental impacts of the Haber-Bosch process, which is run on the order of 108 tons per year.

If this chemistry is to be applicable on a large scale, first row transition metals will be required to carry this out. We have thus targeted iron (Fe) compounds for this purpose. Studies will commence with the ligation of soluble Fe halide precursors using tripodal N-heterocyclic carbene ligands (i.e. ligands that we believe to be suitable for supporting, N2, nitride (and intermediate fragments) on an Fe center. Reduction of the Fe halide starting materials under an atmosphere of N2 will then be investigated in order to access a bridging-N2 Fe(0) dimer, the direct formation of an Fe(III) nitride complex, or an equilibrium between the two. These are species that will have to be accessed in order for the substrate reduction chemistry to function. Characterization and identification of reaction products and intermediates and mechanistic study of their interconversion en route to N2 reduction will be achieved using a variety of physical techniques in tandem with theory.

Conclusion

Developing a process to affect the low cost reduction of N2 to NH3 under mild conditions remains a major challenge in the field of modern chemistry. Although the fundamental chemistries of this transformation have been demonstrated, an economically viable catalyst system that also exhibits reasonable turnover numbers has thus far been elusive. The research we have proposed will both advance our fundamental knowledge about the stepwise reduction of N2 at a cheap and abundant transition metal center and lay the groundwork for a less energy intensive NH3 production scheme than the current Haber-Bosch process.

Determination of Fluid Properties at Carbonate Interfaces - An Experimental and Theoretical Approach

Donald D. Hickmott
20110363ER

Introduction

Little experimental or theoretical attention has focused on solid/fluid interfaces at high pressure and temperature (P-T) because relevant experimental and theoretical techniques are not widely available and/or such techniques are difficult to implement at elevated P-T. Neutron reflectometry (NR) [1, 2] represents a powerful technique for examining fluid properties, particularly density, near interfaces at high Ps because of the ability of neutrons to penetrate high P-T cells and because of its sensitivity to hydrogen.

In NR an unpolarized neutron beam (wavelength 1.5 to 16 angstroms (Å)) is directed at a solid/fluid interface at a glancing angle and a range of momentum transfer vectors (Q_z) are measured. Such measurements provide information on changes in fluid density within a few dozen Å of a solid/liquid interface. At Los Alamos Neutron Science Center (LANSCE), the Surface Profile Analysis Reflectometer (SPEAR) beamline provides advanced NR capabilities to study solid-liquid interfaces.

Carbonate interfaces have been extensively investigated during past decades at room P-T. Such studies have included: titration investigations of zeta potentials and points-of-zero-charge [3], surface probe studies in vacuum such as atomic force microscopy (AFM) [4] and x-ray photon spectroscopy (XPS) [5] to examine kink sites and phase growth mechanisms, and synchrotron-based methods such as x-ray reflectivity [6, 7] and x-ray absorption fine structure [8] to probe surface chemistries. Surfaces are hydrated in aqueous environments, but details of the hydration layer remain controversial.

Computational chemistry studies of calcite ($CaCO_3$) interfaces at room P-T have included molecular dynamics (MD) [9] and density functional theory (DFT) simulations of processes [10]. Initial MD results suggested a calcite surface hydrated by adsorption of a monolayer [9] and with a single water molecule associated with each exposed Ca^{2+} at a distance of ~ 2.4 Å. More recent DFT and MD simulations [10] suggested surface hydration layers on calcite with water molecules at 2.2 and 3.2 Å.

Calculated orientations and positions of protons in the absorbed layer differed between theoretical studies – this question may be answered by new theory combined with neutron studies, which are sensitive to hydrogen (deuterium) on surfaces.

Benefit to National Security Missions

Processes at carbonate-fluid interfaces control a wide-range of phenomena of crucial importance in energy/environmental applications. Calcite, in particular, is important in many energy/environmental applications. Sorption on calcite is postulated as a method of contaminant/radionuclide immobilization, calcite colloids may be crucial in plutonium mobilization in repository environments, calcite buffers the pH of fluids preventing contaminant mobilization, and, most importantly, precipitation/dissolution of calcite is a key process during geologic sequestration of CO_2. Processes at calcite/fluid interfaces *control* how calcite will interact with mixed-volatile (H_2O-CO_2) subsurface fluids. These energy-related processes occur at depths in Earth's crusts up to several kilometers (Ps of up to 30,000 pounds-per-square (psi)), where Ts are high (several 100 C). At these extreme P-T, which are above the critical points of CO_2 (31 C, 1070 psi) and H_2O (374 C, 3200 psi), the physical chemistry of calcite-fluid interactions may change from room P-T, where the majority of studies have been completed. If we are ever going to be able to predict and ultimately control calcite/fluid interactions, we must develop a fundamental microscale understanding of such interactions based on both experiments and theory. Processes at mineral/fluid interfaces are also analogous to processes at material interfaces under the influence of fluids under extreme conditions; techniques developed to understand mineral interfaces at high P-T are applicable to material systems relevant to energy security.

Progress

This project has focused on three tasks: 1) P-T cell construction; 2) development and application of new NR methods; and 3) novel applications of theoretical methods to the calcite/fluid interface.

P-T Cell Development

We designed and built a high P-T cell for NR measurements from ambient conditions to 200°C and 30,000 psi (Figure 1). This cell allows experiments to be conducted at simulated crustal conditions up to 6 km depth, which are relevant to deep oil and gas fields or to geologic carbon sequestration. The cell is constructed of anodized aluminum, has a piston-based P system to allow fluid to be equilibrated with samples at extreme P-T, and contains powder wells to enable saturation of experimental fluids with phases at high P-T. Pressure is generated by a hand pump and T can be precisely controlled using conductive heating inserts and thermocouples connected to a proportional–integral–derivative T controller. We have tested the cell up to a P of 15000 psi and T of 200 C.
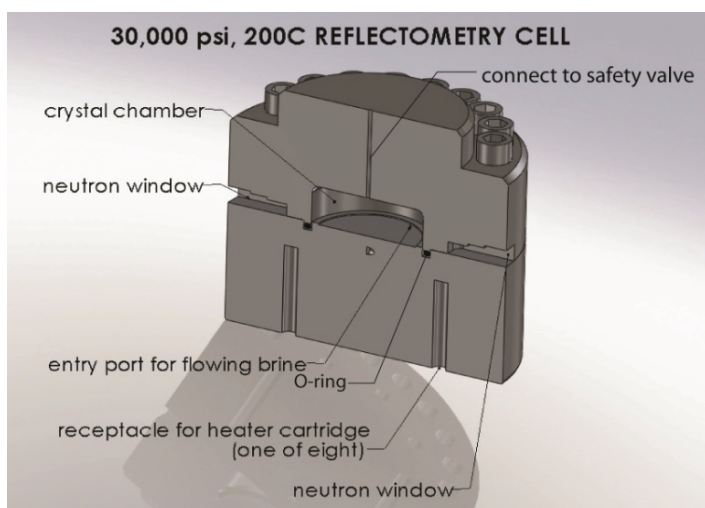
Figure 1. Cross section of NR P-T cell without powder wells. Cell diameter is 5 inches.

NR Experiments

The most significant challenge in designing NR experiments for mineral systems at high P-T is obtaining large enough (> 1 in. square), flat enough (< 10 angstrom (Å) roughness) surfaces for NR interrogation. We explored cutting and polishing natural, gem-quality crystals of calcite as well as cleaving these crystals using a custom-made cleaving device. Crystals with either adequate roughness or adequate surface area, but not both, were produced and characterized using surface profilometry, and x-ray and neutron reflectometry. An alternative method of calcite surface preparation – chemical vapor deposition (CVD) [11] – was also attempted. CVD was able to produce large (2 in. diameter), flat (~ 3 Å roughness) surfaces on amorphous silica and monocrystalline Al_2O_3 substrates.

The CVD- calcite-coated disks were analyzed using LANSCE's SPEAR instrument, a Time-Of-Flight (TOF) neutron reflectometer with a wavelength range from 4.5 Å to 16 Å. A deuterium oxide/water mixture was used to highlight density differences at the calcite interface. Figure 2 shows a NR spectrum of calcite/deuterated water at ambient conditions showing interference 'fringes' indicative of a density anomaly at the calcite interface. Preliminary fits of these data suggest a 30 Å thick anomalous density layer that is ~ 6.4% denser than bulk water. This represents the first ever observation of structured water at a mineral/fluid interface using NR.
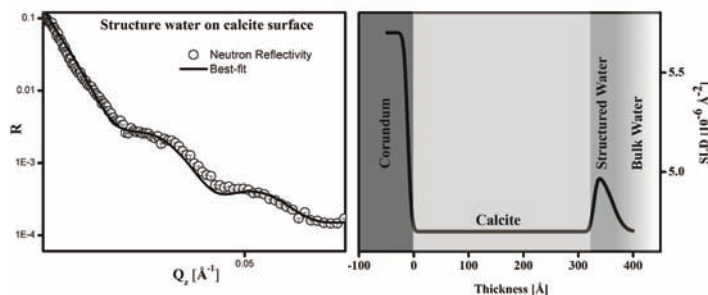
Figure 2. (Left) NR in the form of R (reflected neutron intensity/incoming neutron intensity) vs. Qz from calcite deposited on corundum in contact with a D2O/H2O mixture matched in scattering length density (SLD) to calcite. The data are represented by open circles and the solid lines represent the data fit and yield the (right) best-fit SLD profile.

Theoretical Modeling of Carbonate Interface/Fluid Processes

The theoretical investigation of the calcite/water system focuses on both static and dynamical properties of the solid/liquid interface. Since NR can probe the water density profile near the calcite surface, it would be useful to have simulation data to compare with the NR data. Initially, MD simulations were used to model the system. We adopted the empirical force field developed by Raiteri et al. [12], which provides reasonable accuracy in predicting calcite structure and the interactions between calcite and water molecules. Water oxygen and hydrogen density profiles as a function of vertical distance from the calcite (1014) surface were calculated for various P-T conditions (Figure 3). The first three peaks in the oxygen density curves (about 2.0, 3.5, 4.8 A above the surface) elucidate water structure near the interface. In the P-T range of interest, there is no significant shift in the peak positions. However, the intensity of peaks decreases with T indicating the population of ordered water molecules decreases at high T. The width and the relative intensity of those peaks also show slight changes at high T, which could imply a difference in water structure. The orientation of the water molecules near the surface was also studied. The results show that water molecules in the first three layers exhibit preferred orientations.
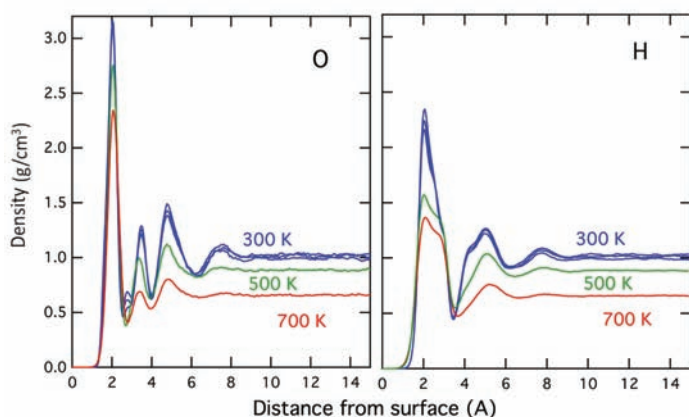
Figure 3. Densities calculated based on oxygen (left) and hydrogen (right) as a function of vertical distance from the calcite (1014) surface for different P-T conditions (blue: 300 K at 1, 500 and 1000 atm; green: 500 K at 1000 atm; red 700 K at 1000 atm). Density values are rescaled to corresponding water densities in units of g/cm3.

We are also interested in the dynamics at the calcite/water interface. Our preliminary calculations using dimer search, nudged elastic band methods, and regular MD simulations have shown that a dry calcite (1014) surface is stable at Ts to 800 K. In an aqueous environment, the surface becomes less stable due to the interactions with water molecules. We found reactions, such as dissolution and diffusion of an extra $CaCO_3$ unit deposited on the surface or penetration of water molecules into the surface (at 526 C (800 K), 14,700 psi (1000 atmospheres)), can easily occur in a regular MD simulation

Future Work

In the coming year the project will focus on: 1) *Pressure cells* – testing the new cell to higher P (30,000 psi). Investigating designs for higher T cells using different alloys. 2) *NR experiments* – extending experiments to elevated P-T and a broader range of fluid compositions. Characterizing CVD samples both prior to and after experiments. Exploration of CVD deposition methods for other carbonates. 3) *Theory* - Complex phenomena observed in experiments such as humidity-induced restructuring of the calcite surface can take place at a time scale much longer than a second. In order to simulate such slow dynamics, we need accelerated molecular dynamics (AMD) methods to bridge the time scale difference. Since the energy landscape of the system is much more complicated in the presence of water, problems such as frequent low barrier transitions will greatly reduce the efficiency of the current AMD scheme. The challenge and the next step of our work is to find a suitable method, which can handle those complex situations and to push the simulation toward longer timescales.

 The molecular modeling methods will be applied to the interpretation of NR and other data, and the resultant fundamental understanding of rate constants and mechanisms will inform larger-scale models of processes relevant to energy systems such as geologic carbon sequestration. The experimental and theoretical tasks are synergistic; each will refine hypotheses related to the other.

Conclusion

We will address hypotheses related to carbonate/fluid interfaces in need of testing based on x-ray reflectometry results, data from other surface analytical methods, and theory. We hypothesize interfacial densities will remain relatively constant as P increases for end member aqueous fluids but will increase with increased T and with decreased P for intermediate fluid compositions. Higher interfacial densities imply more hydrophilic behavior, hence lower dihedral angles and easier flow through porous media. These results will provide key insights into flow dynamics of supercritical fluids in contact with carbonates and may pave the way for controlling subsurface flow dynamics.

References

1. Doshi, D. A., P. B. Shah, S. Singh, E. D. Branson, A. P. Malanoski, E. B. Watkins, J. Majewski, F. van Swol, and C. J. Brinker. Investigating the interface of superhydrophobic surfaces in contact with water. 2005. *Langmuir.* **21** (17): 7805.

2. Doshi, D. A., E. B. Watkins, J. N. Israelachvili, and J. Majewski. Reduced water density at hydrophobic surfaces: Effect of dissolved gases. 2005. *Proceedings of the National Academy of Sciences of the USA.* **102** (27): 9458.

3. Wolthers, M., L. Charlet, and P. Van Cappellen. The surface chemistry of divalent metal carbonate minerals; A critical assessment of surface charge and potential data using the charge distribution multi-site ion complexation model . 2008. *American Journal of Science.* **308** (8): 905.

4. Astilleros, J., C. Pina, L. Fernandez-Daiz, M. Prieto, and A. Putnis. Nanoscale phenomena during the growth of solid solutions on calcite {1014} surfaces. 2006. *Chemical Geology.* **225**: 322.

5. Stipp, S.. Towards a conceptual model of the calcite surface: Hydration, hydrolysis, and surface potential. 1999. *Geochemica et Cosmochimica Acta.* **63** (19-20): 3121.

6. Chiarello, R., R. Wogelius, and N. Sturchio. In-situ synchrotron X-ray reflectivity measurements at the calcite-water interface. 1993. *Geochimica et Cosmochimica Acta.* **57**: 4103.

7. Geissbuhler, P., P. Fenter, E. DiMasi, G. Srajer, L. Sorensen, and N. Sturchio. Three-dimensional structure of the calcite-water interface by surface X-ray scattering. 2004. *Surface Science.* **573**: 191.

8. Elzinga, E. J., and R. J. Reeder. X-ray absorption spectroscopy study of Cu. 2002. *Geochimica et Cosmochimic Acta.* **66** (22): 3943.

9. Rohl, A., J. Wright, and J. Gale. Evidence from surface phonons for the (2 x1) reconstruction of the (10-14) surface of calcite from computer simulations. 2003. *American Mineralogist.* **88**: 921.

10. Keresit, S., S. Parker, and J. Harding. Atomistic simulation of the dissociative adsorption of water on calcite surfaces. 2003. *Journal of Physical Chemistry B.* **107**: 7676.

11. Nilsen, O., H. Fjellvag, and A. Kjekshus. Growth of calcium carbonate by the atomic layer chemical vapour deposition technique. 2004. *Thin Solid Films.* **450** (2): 240.

12. Raiteri, P., J. D. Gale, D. Quigley, and P. M. Rodger. Derivation of an accurate force-field for simulating the growth of calcium carbonate from aqueous solution: A new model for the calcite/water interface. 2010. *Journal of Physical Chemistry C.* **114** (13): 5997.

Publications

Hickmott, D. D., A. Lerner, P. Wang, J. Majewski, and M. Taylor. Neutron reflectometry at elevated pressures and temperatures - novel P-T cell and preliminary experiments. To appear in *American Geophysical Union Annual Meeting.* (San Francisco, 4-9 Dec. 2011).

Photo-triggerable Immolative Polymers: A New Modality for Radiation Dosimetry

Robert D. Gilbertson
20110421ER

Introduction

We plan to develop a new radiation dosimetry method with high specificity and high sensitivity for X-ray and gamma radiation that is specifically suited for personal dosimetry and long dwell time applications. This proposal may also be extended and applied to neutron dosimetry and detection. The work takes advantage of a recently developed class of functional polymers that have been called "self-immolative" polymers.   The defining feature of self-immolative polymers is that the polymer backbone, and in some cases the polymer side chains, can be completely depolymerized in a controlled manner when subjected to a single triggering event. [1,2] The depolymerization of the polymer backbone in addition to the side chains can be engineered in such a way that a large number of copies of a single "reporter" molecule are released after a triggering event.   These polymers can be constructed of masked fluorescent monomers that "turn on" once the polymer has disintegrated providing a positive signal response that is significantly amplified as a single event releases all of the monomer units in the polymer. The amplification in this system is limited only by the number of reporter units in the polymer which can vary from 10-1000 (giving a signal amplification of several orders of magnitude).

For this proposal we have designed a system in which scintillating nanoparticles are imbedded in a composite material which also contains the "masked fluorescent" immolative polymers. The depolymerization of the polymers is triggered by emission of light or electrons from the nanoparticles when the composite is exposed to radiation (see Figures 1 and 2).
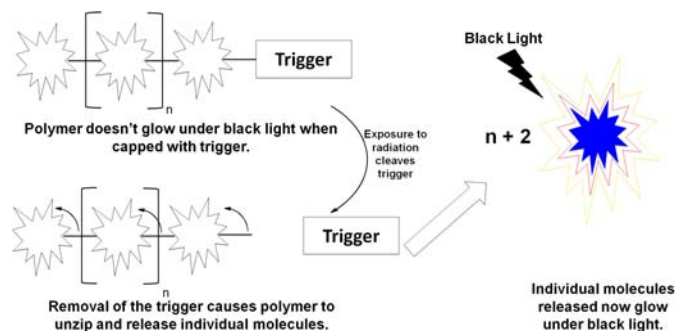
Figure 1. Schematic of immolative polymer degradation upon exposure to radiation.
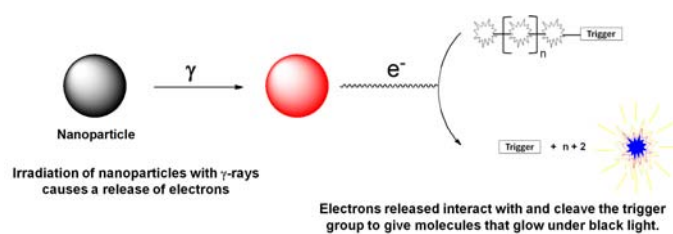
Figure 2. Schematic of nanoparticle/immolative polymer composite for radiation dosimetry.

Benefit to National Security Missions

This work will directly support existing laboratory programs in the development of new radiation detector materials, as well as provide foundation resources for the development of new radiation detector systems. Our plan is to use the LDRD funding to perform high risk research closely related to the basic science of radiation detection. Using the results from this project as a foundation, we will create several proposals in this area and market them to new and existing sponsors. Recent experience has demonstrated that sponsors including DHS, NA-22, and DTRA are interested in supporting new concepts at relatively high funding levels, but that initial results, such as those obtained through LDRD projects, are crucial in demonstrating the wisdom of a particular approach. Under this strategy, a single LDRD-ER might spawn two or three new external projects, depending on what additional development is required for individual applications.
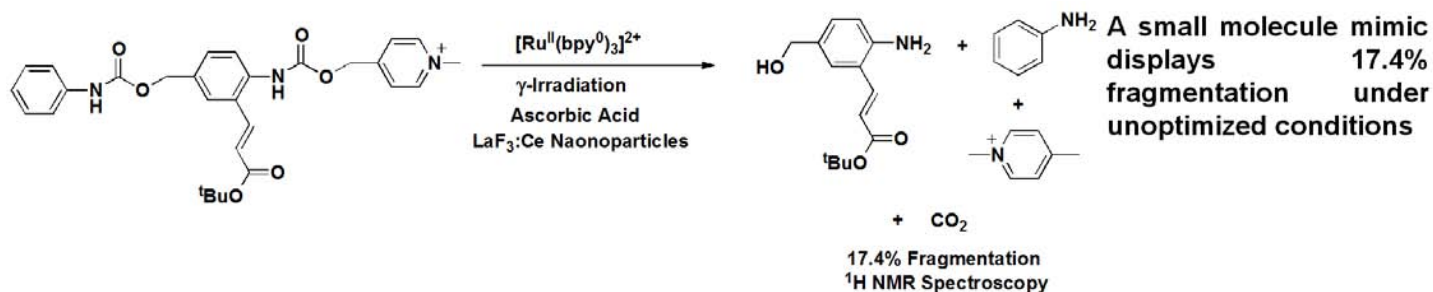
Figure 3. Proof of concept experiment. A model compound shows fragmentation when exposed to gamma-rays.

Progress

The initial phases of the project have involved a large synthetic effort for the synthesis of model compounds, immolative polymers, and scintillating nanoparticles. We first prepared a monomeric model compound in order to test the proof of concept of the project. That is, could we initiate cleavage of a polymer system (a monomer in the model case) using the response of scintillating nanoparticles to gamma-ray irradiation. To this end a monomeric immolative model compound with a picolinium trigger was synthesized. In addition to the model compound we also prepared lanthanum fluoride scintillating nanopaticles with a cerium dopant. In the proof of concept experiment a solution of the model compound and scintillating nanoparticles was exposed to gamma-ray irradiation for 30 minutes resulting in 7% fragmentation as measured by integration of proton NMR signals. An additional proof of concept experiment was carried out using a monomeric model compound with a masked fluorescent reporter. When this compound was exposed to gamma-ray irradiation in the presence of scintillating nanoparticles, 18% fragmentation was observed by NMR and a fluorescent compound was produced (see Figure 3).

With the results of two successful proof of concept experiments in hand we began the synthesis of gamma-ray triggered immolative polymers which should show signal amplification proportional to their molecular weight when cleavage of the trigger is initiated. A synthesis based on work published in the literature was developed and immolative polymers with picolinium based triggering mechanisms were prepared.[3] Polymers up to thirty repeat units in length were produced using slight modifications of the literature procedures. When a solution of this polymer was subjected to gamma-ray irradiation in the presence of scintillating nanoparticles no fragmentation was observed in the NMR spectra. We surmised that impurities present in the polymer solution (due to the difficulties of polymer purification) led the the inhibition of the cleavage and/or polymer fragmentation reactions.

In order to determine the root cause of the lack of fragmentation and have better analytical accuracy in doing so,

a plan was devised to synthesize a model polymer of 2 repeat units. To date, this model polymer has been synthesized, however it has not yet been exposed to gamma-ray irradiation. We anticipate that this experiment will be carried out and that the results will available in short order.

In addition to the LaF_3 nanoparticles, we have recently begun efforts to prepare other types of scintillating nanoparticles that may have better light yield and more appropriate emission wavelengths. For example, cerium doped yttrium-aluminum-garnet (YAG) is a well know gamma-ray scintillator. Recently, high pressure-low temperature methods have been developed to produce nanoparticles of this material.[4] We have acquired a high pressure reactor system and are currently in the process of modifying the synthesis of these particles so they can be employed in our composite materials.

Based on the initial results of this effort and the potential for signal amplification we have submitted several additional research proposals outside the laboratory including proposals using immolative polymers for latent fingerprint visualization, explosives detection, and as an aid to enhance photo-dynamic therapy in cancer treatment. We anticipate that positive results from this ER work will enhance our efforts to further develop this work and obtain support from additional funding sources outside the laboratory.

To date, work on this project has not been published in peer review journals, but some initial results were presented at the 241st National Meeting & Exposition of the American Chemical Society (Anaheim, CA, March 27-31, 2011) in a talk titled "Release of chemical signal molecules for gamma radiation detection: Electron transfer initiated fragmentation of small molecules and self-immolative polymers." The talk was presented by David Kuiper, a post-doctoral research associate who carried out the first synthetic work on the project. We anticipate the submission of a manuscript to a peer review journal within the next six months.

Future Work

We are planning the development of self-immolative polymers prepared with masked fluorescent monomers and

terminated with a trigger which can be activated by light emitted from a gamma ray or neutron scintillator upon exposure to ionizing radiation. We have proposed two examples of a polymer / trigger combination, both of which should be applicable to X-ray and gamma radiation and one of which may be useful for neutron dosimetry.

The critical component of this project is the synthesis of a self-immolative polymer(s) that fluoresces only when it separates into its constituent monomer units. Upon development of this structure and a photo-labile trigger, we will functionalize multiple trigger mechanisms (chemical trigger + scintillator) that are specific to multiple types of radiation. The resulting polymer systems will be evaluated for general radiation dosimetry properties including radiation type specificity, minimum detectable dose, linear absorbed dose response, and stability of the fluorescence signal. In order to optimize these properties and attain the overall goal of a new, highly sensitive radiation dosimetry method, we will need to understand the underlying mechanisms at each step of the process.

The task areas are 1) materials synthesis & structural characterization, 2) properties characterization and 3) dosimetry perfomance. Materials synthesis includes developing condensation polymerization approaches using monomeric chromophores, coupling that to the photo-triggerable capping group and formulating a nanocomposite with the appropriate inorganic scintillator. This may also involve functionalizing a polymerizable ligand onto the nanoparticle to facilitate homogeneous dispersion in the polymer matrix. Properties characterization focuses on assessing photo trigger efficiency, polymer degradation rate and overall fluorescence efficiency, chemical and thermal stability and reproducibility. This is in contrast to performance characterization which will assess fluorescence output as a function of dose and dose rate for pure X-ray and gamma radiation.

Conclusion

Our overarching research goal is to develop a radiation dosimetry method based on self-immolative polymers that has a high sensitivity (low minimum detectable dose) for X-ray and gamma radiation, long-term stability, and a simple readout method. Eventually we hope to extend this research to other types of radiation including neutron dosimetry. Within this framework, we also will strive to understand the energy transfer efficiency of the triggering process (radiation→light→photo trigger), the triggering mechanisms and how they can be tailored to multiple stimuli, the depolymerization process including ambient environment effects and time constraints, and the optimal readout process.

References

1. Sagi, A., R. Weinstain, N. Karton, and D. Shabat. Self-immolative polymers. 2008. *JOURNAL OF THE AMERICAN CHEMICAL SOCIETY.* **130** (16): 5434.

2. Weinstain, R., A. Sagi, N. Karton, and D. Shabat. Self-immolative comb-polymers: Multiple-release of side-reporters by a single stimulus event. 2008. *CHEMISTRY-A EUROPEAN JOURNAL.* **14** (23): 6857.

3. Esser-Kahn, A., N. Sottos, S. White, and J. Moore. Programmable microcapsules from self-immolative polymers. 2010. *Journal of the American Chemical Society.* **132** (30): 10266.

4. Asakura, R., T. Isobe, K. Kurokawa, T. Takagi, H. Aizawa, and M. Ohkubo. Effects of citric acid additive on photoluminescence properties of YAG:Ce^{3+} nanoparticles synthesized by glycothermal reaction. 2007. *Journal of Luminescence.* **127** (2): 416.

Exploiting Non-Innocent Ligands in Catalysis: New Base Metal Catalysts for the Reduction of Carbon Dioxide

Susan K. Hanson
20110537ER

Introduction

This project aims to develop new non-precious metal catalysts for the reduction of CO_2. The conversion of CO_2 into fuels or chemicals could provide a renewable source of non-petroleum fuels, but the catalytic technologies required for this type of transformation are lacking. Improved non-precious metal catalysts are needed to reduce CO_2 under mild conditions. The objective of this work is to investigate how altering the ligand framework around a non-precious metal center could result in better catalysts. Specifically, incorporating a tethered base (proton acceptor) in the metal coordination sphere could increase catalytic activity or enable new reaction modes. A "non-innocent" ligand (one that participates in the reaction) of this type could direct the flow of protons or hydrides in the catalytic reaction, causing the reaction to occur more rapidly or to produce different, more valuable types of products. The work will involve the synthesis of a new family of metal complexes having non-innocent ligands with tethered bases. The reactivity of these complexes will be studied for the hydrogenation of CO_2 and the electrochemical reduction of CO_2.

Benefit to National Security Missions

New technologies enabling more effective use of renewable carbon feedstocks and clean energy sources could have a transformative impact on domestic energy security. Recently, the Office of Basic Energy Sciences has highlighted the importance of new catalytic technologies for the reduction of CO_2 to fuels. This area is critical to ensuring energy security and directly pertains to the LANL Energy and Earth Systems Grand Challenge. Production of fuels at remote bases is a high priority for DoD, because of their need to reduce their logistics tail.

Progress

Carbon dioxide is an abundant potential renewable carbon feedstock, but the catalytic conversion of carbon dioxide to fuels or chemicals is a major challenge. Significant obstacles remain in the development of viable transition metal catalysts for the reduction of carbon dioxide, including the development of catalysts with improved activities and selectivities, with greater stability, or with inexpensive non-precious metals. New and more effective earth abundant metal catalysts are needed to convert carbon dioxide into chemicals and fuels under mild conditions.

Incorporating a pendant base functionality into the ligand scaffold of earth abundant metal catalysts could increase catalytic activity and give rise to new reaction modes. This hypothesis is based on a concept called metal-ligand cooperativity, in which the ligand and the metal center work together to carry out the catalytic reaction. Metal-ligand cooperativity could be especially beneficial for base metals, which often display reduced reactivity compared to their precious metal analogues. This work aims to explore how ligands with a pendant base could enhance the reactivity of earth-abundant metals for the catalytic reduction of carbon dioxide.

Initial experiments have targeted the synthesis of new ligands which have pendant base functionalities. Three new ligands have been prepared which have phosphine donor groups and nitrogen groups either tethered or in the metal coordination sphere. The synthesis of Fe, Co, and Ni complexes of the new ligands is underway. A number of different Fe, Co, and Ni precursors have been used for the syntheses, and several new complexes have been isolated.

New cationic and neutral nickel hydride complexes have been prepared using a bis-cyclohexyl-substituted phosphine ligand with an incorporated nitrogen base. The nickel hydride complexes have been isolated, and attempts to generate the alkyl analogues are underway. The neutral nickel hydride complex reacts with carbon dioxide and several other molecules with C=X multiple bonds, but preliminary tests suggest that this complex is not active for catalytic hydrogenation reactions. The cationic analogue has also been prepared (which has a protonated nitrogen). Evaluation and comparison of the reactivity of the neutral and cationic nickel hydride complexes is underway.

Future Work

Future work will focus on full characterization of the Ni

complexes described above, as well as preparation of the Fe and Co analogues. The reaction of the new complexes will be studied with hydrogen and formic acid, and efforts to hydrogenate substrates with carbon-oxygen double bonds will continue, including carbon dioxide.

Conclusion

This project will provide a significant advance in our understanding of how non-innocent ligands having a pendant base impact the catalytic reduction of CO_2. It is expected that the intentional incorporation of a base into the ligand framework will result in dramatic improvements in the reactivity of the metal catalysts. A successful demonstration of this concept will highlight the viability of base-metal catalysts for CO_2 reduction.

Molecular Scale Shock Response of Explosive1

Shawn D. Mcgrane
20090186ER

Abstract
Shock and detonation physics are fields central to the missions of the Department of Energy (DOE) and the Department of Defense (DoD). Huge investments have been made and continue to be made into establishing the capability to *predict* how explosives will react in any given scenario. Yet on the molecular level, very little is known about the dynamic response of these materials. This project has developed new experimental capabilities to directly observe the molecular scale shock response of explosives. We have performed the first resolved measurements of the shock-induced reaction in explosive crystals, qualitatively validating the predictions of molecular dynamic simulations. We have developed a new method of measuring temperature with very high temporal and spatial resolution and several orders of magnitude higher sensitivity than previous methods, for application to measure shock temperatures. The project has generated sufficient follow on funding to allow further use of these new capabilities to continue to pursue discoveries in the science of high explosives important to national missions.

Background and Research Objectives
The early events that occur upon shock loading explosives are crucial in determining the sensitivity of the material to accidental or intentional initiation. Various theories have been proposed regarding the chemical reaction mechanisms, but there are few experiments capable of testing them. The principle goals of this project were to develop new diagnostics to answer the questions: 1) are the predicted time scales of reactive molecular dynamics calculations of shocks reasonable, 2) are electronic excitations important in shock initiation, and 3) what is the temperature that drives shock induced reactions?

We were able to observe shock induced reactions on time scales predicted by molecular dynamics calculations, a few hundred millionths of a millionth of a second[1]. There was no evidence of electronic excitations being important to shock initiation, but a small amount of further work is required to solidify this conclusion. We had ambitious goals of measuring time dependent temperature in laser-shocked materials on very small time and length

scales and have developed the necessary tools to do so. Due to the high risk/high reward nature of the project, experiments were significantly more difficult than anticipated and required extensive time and effort developing both the theoretical foundations and the experimental capability to measure temperature at these scales. Because these measurements are crucial to shock and detonation physics, yet have remained elusive for decades, we spent most of our effort in the project pursuing this goal. In the end, we were able to measure time dependent temperatures with unprecedented time resolution and sensitivity [2,3], and will perform these measurements on shocked materials in the future.

Due to the extensive development of new experimental capabilities, most of the project's scientific journal publications occurred in the final year. Indeed, we are expecting at least two publications in the following year on the results of shocked explosive crystals and on single shot measurement of transient temperatures. The LDRD project has led to a DTRA funded project as well as follow on work occurring in Campaign 2: High Explosive Science. This follow on funding will allow us to complete the work initiated in the LDRD project and utilize the capabilities developed.

Scientific Approach and Accomplishments
The data provided in this project sought to experimentally measure molecular scale mechanisms of reactivity in shocked explosives. These data are necessary to answer even qualitative questions regarding explosive initiation. These questions must be answered to identify the correct theoretical framework to understand, predict, and simulate explosive initiation.

There are no detailed experimental shock data on time scales less than a billionth of a second that can be used to test molecular level theories of shock initiation; this project developed new diagnostics that could resolve shock induced chemical reactions on time scales one thousand times faster than this. We coupled absorption measurements across the visible and near infrared range to ultrafast laser shock loading of high explosive single crystals, as shown in Figure 1.
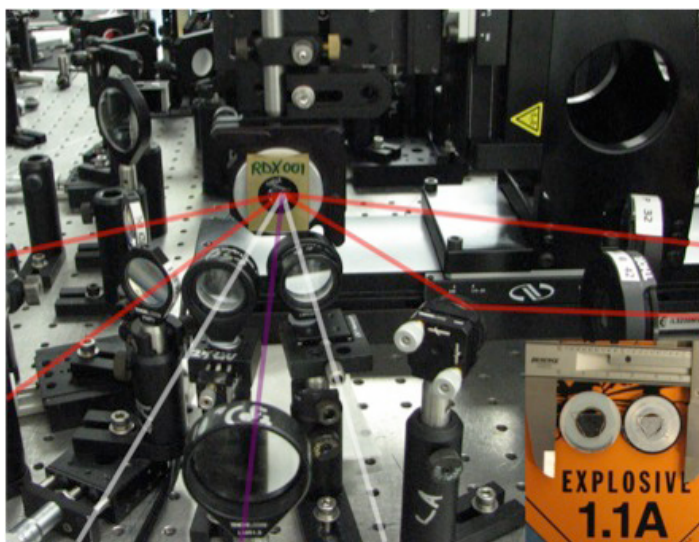
Figure 1. The tabletop experiments allow small quantities of explosives to be studied in detail with a number of advanced optical diagnostics.

While transient absorption spectroscopy is now a relatively common methodology for laser excited processes, coupling to shock loading required additional developments. We determined a method of timing the absorption to the shock on a shot by shot basis, which is important because of significant jitter in shock arrival times due to variations in thickness of the aluminum drive film and shot to shot laser energy. We found better procedures for preparing explosive crystals to a near optical polish. We studied the effect of different tamper materials to confine the laser generated plasma that drives the shock wave. Optimization of these numerous experimental parameters allowed us to observe the first evidence of shock induced reaction occurring on these time scales[1], as shown in Figure 2. The new absorption features that grow in with time following shock loading indicate that the initial explosive molecules, which are transparent in the visible and near-infrared, are transforming into products which absorb broadly in this region. Due to the broad and featureless nature of the absorptions, additional spectroscopic observations will be required to identify the product species. However, the product absorptions increase on a timescale an order of magnitude faster that many experts in the field would have assumed. The absorption measurements have been reported in conference proceeding and will lead to scientific journal publication in the near future.

We developed a completely new method of optically measuring temperature that was over 50,000 times more sensitive than the only other method that could achieve these time resolutions[2,3], illustrated in Figure 3. The technique, femtosecond stimulated Raman spectroscopy or FSRS, is widely used to perform chemical imaging microscopy and examine time dependent chemical dynamics. We have shown that it can also be used to measure temperature, by acquiring the data in a slightly different manner (looking at

energy gain and energy loss simultaneously) and analyzing the data in a new way. Performing FSRS on laser excited materials allowed us to measure temperature with time scales less than one millionth of one millionth of a second, obtaining an instantaneous snapshot of dynamic temperature on the timescales of molecular motion. Using FSRS, we can now quantitatively watch the energy from the laser or shock excitation equilibrate into molecular bonds. This was reported in a prestigious scientific journal [2] and a detailed follow on article is nearly complete. This method allows simultaneous determination of chemical reaction and temperature with no prior calibrations or intrusions into the material.
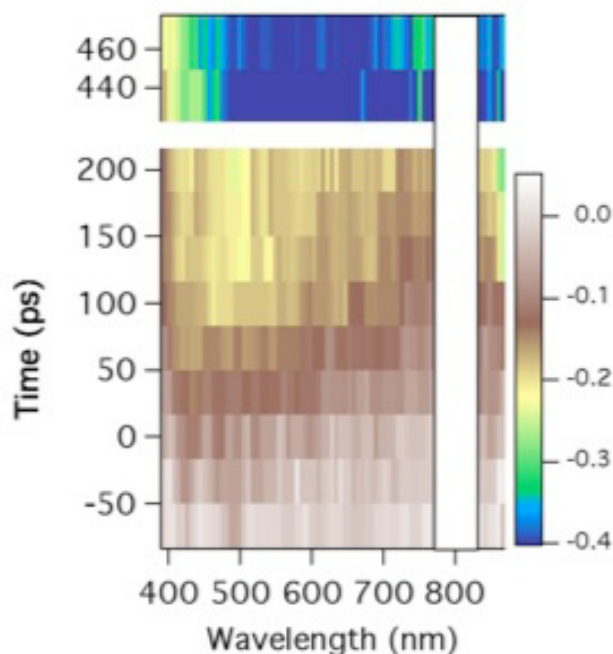
Figure 2. A single crystal of RDX, a common explosive, shocked to 230,000x atmospheric pressure shows transient absorption building on timescales of 100s of picoseconds (1 picosecond = 1 millionth of a millionth of a second). These absorptions signal product formation following chemical reaction under the elevated pressures and temperatures caused by the shock. The timescales are comparable to, but slightly longer than those observed in simulations.

We also performed auxiliary experiments regarding details of the ultrafast shock physics [4] and simple laser/explosive safety experiments [5] that led to scientific journal publications. Initial examination of explosive crystals probed with weak laser driven shocks showed a complicated structure. This structure was initially thought to be a separation of the elastic (nondamaging) and plastic (permanently deforming) response of the explosive crystal. More careful examination showed that the elastic and plastic yielding were not due to the explosive, but originated in the thin layer of aluminum used to drive the shock into the explosive. In determining the origin of this observation, we found that the

yield strength of aluminum on these time and length scales was 10 times larger than that observed in bulk materials. In fact, as we probed shorter time and length scales, the aluminum became monotonically stronger. These observations were sensitive to the initial plastic yielding events in the aluminum which were taking place on the time scale of our experiment [4]. Additionally, questions arose during the project regarding the safety of putting laser light on explosives. We had access to the appropriate lasers, explosives, and were operating under approved safety documentation for performing these types of experiments and could quickly perform a series of measurements useful in determining conditions in which personnel could be present when laser light directly illuminated explosives. These brief measurements led to a publication [5] to aid others in the determination of safe parameters, and our results are now the basis for LANL's policy for lasers on explosives.

To summarize our primary quantifiable metrics, this project has generated five conference proceedings articles, three journal publications, six invited presentations, and seven contributed presentations.
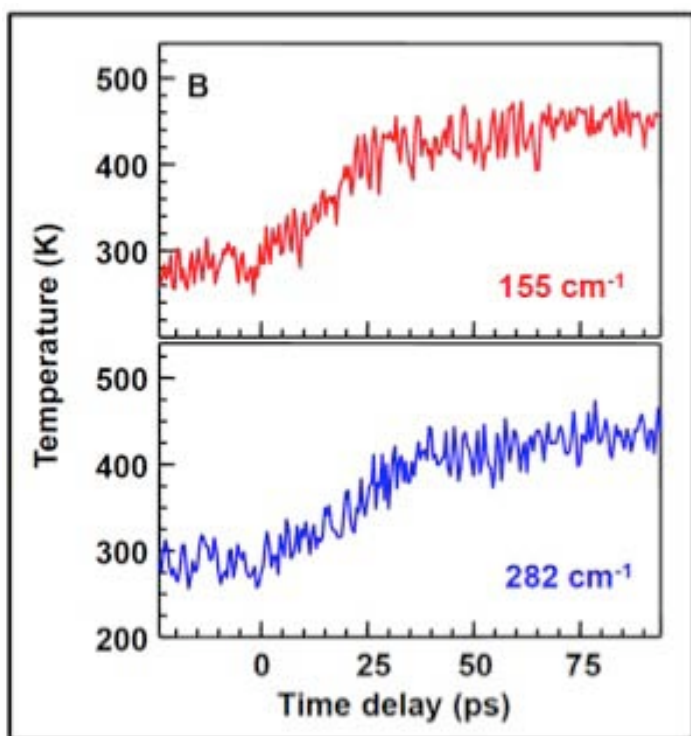
Figure 3. We have developed a technique to measure temperatures with sub-picosecond temporal resolution. The data shown are measurements for a laser flash heated crystal. This technique is over 50,000x more sensitive than the only comparable technique, and will be used in the future to measure shock temperatures.

Impact on National Missions
The application, optimization, and therefore fundamental understanding of explosives are essential to DOE and DoD missions. Initiation of explosives occurs through a chain reaction, where localized molecular insults lead to the collective emergence of the phenomena of detonation. Understanding the initial events is crucial in predicting, and tailoring, explosive material properties.

This project has developed new capabilities to observe these initial events in shocked explosives, and has made measurements of the time scale of the first chemical reactions. These reactions are occurring on time scales similar to those predicted by molecular dynamic modeling, allowing the first qualitative validation of those simulations. We have also developed methods of transient temperature measurement that will continue to address these problems, leading to new discoveries in the future. From a programmatic perspective, these results have led to follow-on support from both external and internal sources to allow the progress initiated in this LDRD project to continue to meet mission needs.

References
1. McGrane, S. D., N. C. Dang, V. H. Whitley, C. A. Bolme, and D. S. Moore. Transient absorption spectroscopy of laser shocked explosives. 2010. (Coeur d'Alene, Idaho, Apr 11-16, 2010). p. 407. Arlington, VA: Office of Naval Research.

2. Dang, N. C., C. A. Bolme, D. S. Moore, and S. D. McGrane. Femtosecond Stimulated Raman Scattering Picosecond Molecular Thermometry in Condensed Phases. 2011. *Physical Review Letters.* **107** (4): 043001 (4 pp.).

3. McGrane, S. D., N. C. Dang, C. A. Bolme, and D. S. Moore. Development of coherent Raman measurements of temperature in condensed phases. 2011. (Orlando, Fl, 4 Jan. 2011). p. AIAA2011. USA: AIAA.

4. Whitley, V. H., S. D. McGrane, D. E. Eakins, C. A. Bolme, D. S. Moore, and J. F. Bingert. The elastic-plastic response of aluminum films to ultrafast laser-generated shocks. 2011. *Journal of Applied Physics.* **109** (1): 013505 (4 pp.).

5. McGrane, S., and D. Moore. Continuous wave laser irradiation of explosives. 2011. *Propellants, Explosives, Pyrotechnics.* **36** (4): 327.

Publications
Dang, N. C., C. A. Bolme, D. S. Moore, and S. D. McGrane. Femtosecond Stimulated Raman Scattering Picosecond Molecular Thermometry in Condensed Phases. 2011. *Physical Review Letters.* **107** (4): 043001 (4 pp.).

McGrane, S. D., C. A. Bolme, V. H. Whitley, and D. S. Moore. Ultrafast Dynamic Ellipsometry And Spectroscopy Of Laser Shocked Materials. 2010. In *International Symposium on High Power Laser Ablation.* (Santa Fe, NM, Apr18-22, 2010). Vol. 1278, p. 392. USA: A.

McGrane, S. D., C. A. Bolme, V. H. Whitley, and D. S. Moore. Ultrafast dynamic ellipsometry and spectroscopies of laser shocked materials. 2010. In *Ultrafast Phenomena XVII.* (Snowmass, CO, July 1-23, 2010). , p. 332. Oxford: Oxford University Press.

McGrane, S. D., D. S. Moore, V. H. Whitley, C. A. Bolme, and D. E. Eakins. MOLECULAR SHOCK RESPONSE OF EXPLOSIVES: ELECTRONIC ABSORPTION SPECTROSCOPY. 2009. In *16th Conference of the American-Physical-Society-Topical-Group on Shock Compression of Condensed Matter ; 20090628 - 20090703 ; Nashville, TN.* Vol. 1195, p. 1301.

McGrane, S. D., N. C. Dang, C. A. Bolme, and D. S. Moore. Development of coherent Raman measurements of temperature in condensed phases. 2011. In *AIAA Aerospace Sciences Meeting.* (Orlando, Fl, 4 Jan. 2011). , p. AIAA2011. USA: AIAA.

McGrane, S. D., N. C. Dang, V. H. Whitley, C. A. Bolme, and D. S. Moore. Transient absorption spectroscopy of laser shocked explosives. 2010. In *International Detonation Symposium.* (Coeur d'Alene, Idaho, Apr 11-16, 2010). , p. 407. Arlington, VA: Office of Naval Research.

McGrane, S., and D. Moore. Continuous wave laser irradiation of explosives. 2011. *Propellants, Explosives, Pyrotechnics.* **36** (4): 327.

Whitley, V. H., S. D. McGrane, D. E. Eakins, C. A. Bolme, D. S. Moore, and J. F. Bingert. The elastic-plastic response of aluminum films to ultrafast laser-generated shocks. 2011. *Journal of Applied Physics.* **109** (1): 013505 (4 pp.).

Multifunctional Materials

James E. Gubernatis
20090187ER

Abstract

We sought to bridge the microscopic and macroscopic descriptions of multifunctional materials with a well parameterized, multiple order-parameter Landau theory. This "bridging the gap" is an outstanding challenge in materials science. Materials science typically is studied at three different scales: the macroscopic (what we see unaided), the mesocopic (what we see with conventional microscopy); and the microscopic (what we can see with sophisticated microscopy). Our understanding of materials must be consistent among the scales. Establishing this consistency however has been difficult. For a particular class of materials, the multifunctionals, we proposed to achieve consistency in a novel way by placing the Landau phenomenological theory for the free energy, typically used at the mesoscale, at the center of our analysis and fixing as many of its unspecified parameters as possible by deriving them from microscopic theory and by measuring them experimentally. The question to be answered was: With the theory parameterized better than ever, can we predict the many phase transitions exhibited by multifunctional materials and also predict the evolution of their mesoscale structure which is so important for the design of such devices as new switches, sensors, and actuators. We started by studying tin tellurium. For fifty years, this material was believed to be both ferroelastic and ferroelectric. We found however that it was actually a co-elastic metal, almost the opposite of what was believed. Our paper publishing our experimental findings in Physical Review B was designated as an "Editor's Choice." Our theoretical work confirmed our experimental measurements. To replace tin tellurium as of material of focus, we studied the structural transitions and twinning in iron mono-oxide and cerium. For cerium, we developed a Landau theory of an iso-structural phase transition and explored possible inhomogeneous phases consistent with this theory. We also studied the magnetic symmetry properties of relevant multifunctional multiferroic materials in order to study phase transitions with multiple order parameters.

Background and Research Objectives

Our main scientific task was investigating symmetry changes in phase transitions for materials possessing two or more simultaneously ordered phases. A change of symmetry accompanies a phase transition. This symmetry change is captured by an order parameter which is zero above the transition temperature (or pressure) and non-zero below it. A Landau theory is simply a specific expression for the free energy of a material in terms of its order parameters.

Multifunctional materials are those materials whose order parameters have cross-field responses between two (or more) applied fields. For example, in a piezoelectric material, electric polarization and strain both respond to a stress or to an electric field. It is this type of response that makes the materials interesting scientifically and important technologically. Typically, a Landau phenomenology lacks such responses. Our objective in co-generating a Landau theory on the mesoscopic and microscopic scales was to ensure "uploading" maximal information from the microscopics to mesoscopics. Such information included these responses. Experiment played a special role in our research. We had recently developed new unique capabilities that enable the measurement of an important class of cross-field responses, magneto-electric responses. These measurements could benchmark the theory in a way never before possible.

An important class of multifunctional materials is ferroics which are characterized by two or more orientation states. There are four primary ferroics: ferroelectrics described by an electric polarization, ferromagnets described by magnetization, ferrotoroidics described by "twisting", and ferroelastics described by elastic strain. The prefix "ferro" in these different states of matter refers to the ability, in principle, to reverse the direction, let us say, of the magnetism, with the application of an external field, which in the case of magnetism would be a magnetic field. The ability to reverse the directions of multiple ferrostates and the coupling between these states makes the material multifunctional. Materials possessing two or more ferroic properties are called multiferroics. In particular, crystals exhibiting simultaneous ferroelectricity and magnetism are called magneto-electrics. The properties of crystals of these materials

are highly susceptible to disorder. Above the phase transition temperature the disorder may be in a tweed structure whereas below the transition temperature a glassy state (a state with no macroscopic order) may result.

Of particular interest was the interplay between the parameters describing the phases. To this end, we experimentally studied other materials in addition to the semiconductors. Consequently, we prepared and characterized materials with cross-coupled order parameters, for example, coupled magnetic and electrical orders. We successfully measured four cross-coupling constants. Our successful measurements of three of these couplings accomplished one of the major experimental objectives of our proposal.

We began by studying the properties of a family of semiconductors fabricated with elements from the fourth and sixth columns of the periodic table. Many in this family show a paraelectric to ferroelectric transition (the electrical analog of a non-magnetic to magnetic transition), which is accompanied by a change in their length and shape. Most exist in the same very simple crystal structure as table salt. Additionally, the properties of all are very sensitive to the density of electrons participating in their electrical conduction. Thus, this family sports crystallographically simple representations of a system having multiple simultaneous phases, that is, states of matter with specific symmetries and different physical properties. These types of materials were the central theme of our research.

Scientific Approach and Accomplishments

We mainly studied tin-tellurium as a simple manifestation of a multifunctional material. For about fifty years, it has been widely regarded as a ferroelectric and ferroelastic material whose structural phase transition involved changes between relatively simple crystal structures. Further, when small amounts of a magnetic material, such as chromium, are added, the resulting alloy becomes ferromagnetic. From the viewpoint of individual atoms, the temperature-dependent mechanism for the structural transition associated with the length and shape changes is generally viewed as either being a change in the motion of the electrons, the vibration frequency of the atoms in the crystal, or the interaction between these two dynamical effects. We judged that the structural transitions required at least a combination of the last two mechanisms to capture published measurements. Accordingly, we focused on a microscopic (atomistic) model for these materials proposed by Sakai [1] that does this synthesis. This model also leads to a Landau theory. The Landau assumption does not give the coefficients of the expansion. These we proposed getting from the microscopic model and experiment.

In the past, the widely accepted ferroelectricity in tin-tellurium had been inferred from indirect evidence. In the first year of the project, we kept finding that tin-tellurium behaved more like a metal (a good conductor of electricity) than a semiconductor or insulator (poor or bad conduc-

tors of electricity). Ferroelectricity cannot exist in a metal. In our second project year, we executed a suite of experimental measurements, backed by theoretical calculations, to resolve this matter. We established that tin-tellurium is neither ferroelectric nor ferroelastic.

We performed the first angular-resolved photoemission spectroscopy of the electronic structure of tin-tellurium. These photoemission measurements found a Fermi surface (Figure 1), which is a signature of a metal, and both simple and state-of-the-art electronic structure calculations agreed with the principal features of the measured Fermi surface topology (Figure 1). We also performed the first piezoelectric measurements of the material. For a piezoelectric material, applying an electric field across its body changes the volume of the material and vice versa. Ferroelectricity is the spontaneous development of an electric polar state. All ferroelectrics are piezoelectric. We found no piezoelectricity.
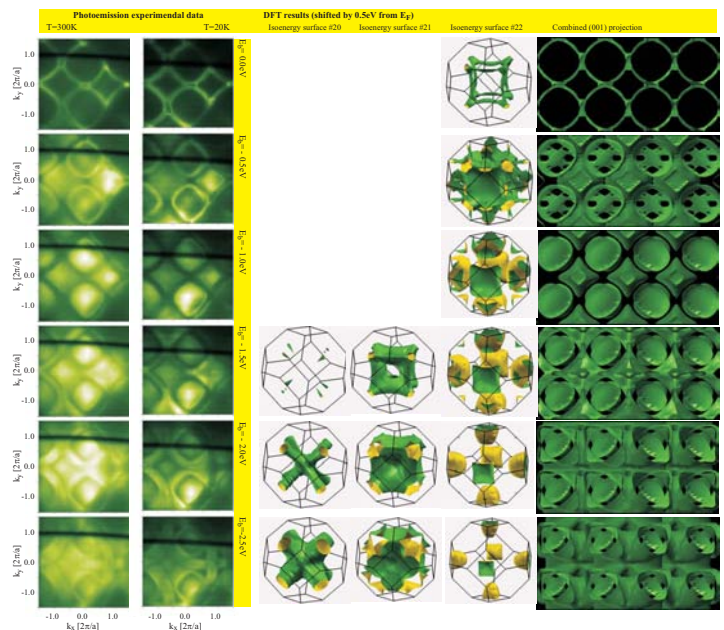
Figure 1. On the left is a two-dimensional representation of the data from the angular-resolved photoemission as a function of beam energy (going down the column). The presence of bright line at zero energy indicates the existence of a Fermi surface. On the right is our results form a density functional calculation, mincing the angular-resolved photoemission measurements. Shifting the right column down one panel places theory and experiment in better agreement. The shift corresponds to an adjustable parameter. The center is the theoretical construction of the Fermi surface.

We also performed the first resonant ultrasound spectroscopy of the elastic properties of the material. This technique measures the material's elastic constants. While we saw the structural phase transition, we were unable to confirm the previously reported and widely accepted low-temperature rhombohedral crystal structure. We found

that on transforming key elastic constants of the material, instead of jumping in value, as they should for a ferroelastic, barely changed. Barely measureable changes were also found for the expected jumps in specific heat and thermal expansion. A Landau theory for the material was constructed, several of its parameters were fitted to the experiments, and from them we inferred that material is not ferroelastic but rather co-elastic. For a co-elastic material, the directions of the elastic deformations are not reversible. The measured changes in the properties of tin-tellurium on structurally transforming are among the smallest ever reported for a co-elastic material.

Adding small amounts of chromium to tin-tellurium did result in the alloy becoming ferromagnetic. In fact, with only a few percent of chromium, a room temperature ferromagnetic resulted. A temperature this high for such small alloying is a rather surprising result. Further, measurements of the resonant ultrasound spectroscopy indicated the alloy was distinctly ferroelastic. Changing material classes is an even more surprising result. The physical mechanisms for both results are studied but unfortunately still remain unknown.

We published one paper describing our angular-resolved photoemission spectroscopy measurements and calculations [2] and a second paper reporting the results of the other measurements and calculations [3]. The editors of Physical Review B, one of the most prestigious journals in condensed matter physics, designated our second paper as an "Editors's Choice."

Concomitant with the model building and experimental work, we also explored more formal aspects of Landau theory [4]. Using group theory, the mathematics of symmetries and their relationships, we verified the Landau theory generated microscopically is the correct one for the symmetries of the crystal, the length changes, and the shape changes. To study phase transitions in materials that couple electrical and magnetic orderings, it is important to incorporate the symmetries of magnetism into group theory by augmenting the crystallographic groups with time reversal symmetry, which leads to what are called color (or black and white) groups. We enumerated the color groups in quasi-one-dimensional and quasi-two-dimensional cases and studied a representative phase transition (Figure 2). We also suggested possible chemical compositions of quasi-one-dimensional materials with coupled magnetic and electric orders and quasi-two-dimensional materials coupling electric, magnetic, and structural orders. In addition, we enumerated all classes of chemical species consistent with two-dimensional magnetic groups.

Unfortunately, our surprising finding that the properties of tin tellurium differ so essentially from what had been believed for 50 years had the consequence of it being an unsuitable multifunctional material. We ceased studying it. Fortunately, other options existed. In the third year of our

project, we followed two.

We began the third year by studying iron mono-oxide. It is the second most abundant mineral in the earth crust and an important source of iron for steel making. It has the same simple crystal structure as tin tellurium; however, its structural phase transition however occurs only under the application of an external pressure. In the absence of an external pressure, it does undergo a metal-to-insulator transition as a function of temperature, that is, a phase transition from a state that conducts electrical current well to one that conducts it poorly. Accompanying this transition is a second transition from an anti-ferromagnetic to non-magnetic phase. An anti-ferromagnetic state is an ordered magnetic state, like a ferromagnetic state, but one in which that material does not attract or repel itself from a magnet.
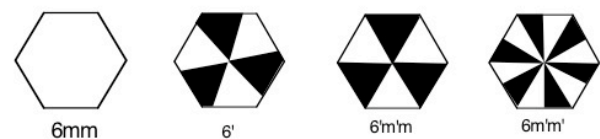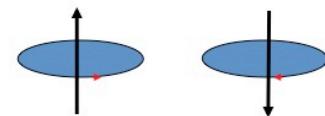
Figure 2. Upper panel: For a hexagon (with point group symmetry 6mm) three new magnetic symmetries can be created (with magnetic point groups 6', 6'm'm, 6m'm') with an equal black and white area. Some of these new magnetic symmetries can also lead to ferroelectricity. Here 6' means a 60 degree rotation followed by a color change (black to white and vice versa). Similarly m' means a mirror plane with a change of color. Lower panels: Reversing magnetization is equivalent to flipping a spin which is equivalent to changing the direction of current i in a loop, or formally time reversal.

For iron mono-oxide we assembled the theoretical capabilities needed relative to the suite of planned experiments necessary to quantify its properties. Mainly, we proposed to interplay band structure and many-electron mean-field approximations to describe the metal-to-insulator and the anti-ferromagnetic to non-magnetic transitions. Critical would be modeling the coupling of the magnetism to the structural transition. From this microscopic approach we derived a Landau phenomenology that has comparable terms as the one already derived on the mesoscopic scale.

We wanted to study the mesoscopic development and growth of the grains. The key task here would have been predicting the development and growth of twin boundaries between the grains.

Twin boundaries occur when two crystals of the same type grow with only a slight mis-orientation between them. The interface is highly symmetrical, with the atoms being shared by the two crystals at regular intervals. This specific type of interface has a lower energy than the grain boundaries that form arbitrary crystalline orientations. Experimentally, we planed to execute many of the same measurements we used to unravel the properties of tin tellurium, the core ones being angular-resolved photoemission spectroscopy, neutron scattering, and resonant ultrasound spectroscopy. The key measurement would have been that of the strength of the magneto-striction that will give us the cross-field coupling of the anti-ferromagnetic state with the transforming lattice structure. The strength of this coupling is hard to predict theoretically.

The challenge was growing the crystals needed for these measurements. We prepared reasonably pure iron mono-oxide in granular form using a novel sintering method. The problem was fusing this power into large crystals. Our approach was the victim of most other approaches in preparing large crystals of iron mono-oxide, contamination by another form of iron oxide that is ferromagnetic. This other compound is the chemically equivalent to rust. This material is ferromagnetic and its presence makes studying the anti-ferromagnetism impractical.

We terminated this project as soon as possible and moved to studying twining and stacking faults in cerium. For Cerium we had the crystals, direct observations of twinning and stacking faults, and a lot of published experimental data. Stacking faults are common in materials with a crystal structure like that of cerium. They refer to layers of atoms which should be sequenced as ABAB... instead being sequenced as ABCABAB. We succeeded in developing a Landau theory and identified some of the types of inhomogeneous phases this theory supports. Unfortunately we found that some of the published experimental data was analyzed inconsistently and thus were unable to perform cerium specific calculations. We were however able to understand from our Landau theory how twinning could develop in cerium and other materials that undergo an iso-structural phase transition. We intend to use this knowledge in future work on iso-structurally transforming materials.

Impact on National Missions
This project will support the DOE mission in the Office of Science by enhancing our understanding of multifunctional materials and establishing a theoretical paradigm for addressing their properties. In particular it supports the DOE Basic Energy Science program office mission for fundamental materials science research for energy independence.

References
1. Sakai, K.. Vibronic theory of a structural phase transition and a tricritical point in IV-VI compounds,. 6. *Physical Review B .* **34**: 8019.

2. Littlewood, P. B., B. Mihaila, R. K. Schulze, J. E. Gubernatis, A. Bostwick, E. Rotenberg, C. P. Opeil, T. Durakiewicz, J. L. Smith, and J. C. Lashley. Band structure of SnTe studied by photoemission spectroscpy. 2010. *Physical Review Letters.* **105**: 86404.

3. Salje, E. K., D. J. Safarik, J. C. Lashley, J. E. Gubernatis, K. A. Modic, J. C. Cooley, R. D. Taylor, B. Mihalia, A. Saxena, T. Lookman, J. L. Smith, R. A. Fischer, M. Pasternik, C. P. Opeil, and P. B. Littlewood. Tin telluride: a weakly co-elastic material. 2010. *Physical Review B.* **82**: 84112.

4. Saxena, A., and T. Lookman. Magnetic symmetry of low dimensional multiferroics and ferroelastics. 2011. *Phase Transitions.* **84**: 421.

Publications
Lashley, J. C., S. M. Shapiro, B. L. Winn, C. P. Opeil, M. E. Manley, A. Alatas, W. Ratcliff, T. Park, R. A. Fisher, B. Mihaila, P. Riseborough, E. K. H. Salje, and J. L. Smith. Observation of a continuous phase transition in a shape-memory alloy. 2008. *Physical Review Letters.* **101**: 135703.

Littlewood, P. B., B. Mihaila, R. K. Schulze, D. J. Safarik, J. E. Gubernatis, A. Bostwick, E. Rotenberg, C. P. Opeil, T. Durakiewicz, J. L. Smith, and J. C. Lashley. Band structure of SnTe studied by photoemission spectroscpy. 2010. *Physical Review Letters.* **105**: 86404.

Lookman, T., and P. B. Litlewood. Nanoscale heterogeneity in functional materials. 2009. *Materials Research Society Bulletin.* **34**: 822.

Porta, M., T. Lookman, and A. Saxena. Piezoelectric properties of ferroelectrics: effect of criticality and disorder. 2010. *Journal of Physics: Condensed Matter.* **22**: 345902.

Salje, E. K. H., D. J. Safarik, J. C. Lashley, J. E. Gubernatis, K. A. Modic, J. C. Cooley, R. D. Taylor, B. Mihalia, A. Saxena, T. Lookman, J. L. Smith, R. A. Fischer, M. Pasternik, C. P. Opeil, and P. B. Littlewood. Tin telluride: a weakly co-elastic material. 2010. *Physical Review B.* **82**: 184112.

Saxena, A.. Broken symmetry, ferroic phase transitions and multifunctional materials. To appear in *Integrated Ferroelastics.*

Saxena, A., and G. Aeppli. Phase transitions at the nanoscale in functional materials. 2009. *Material Research Society Bulletin.* **34**: 804.

Saxena, A., and T. Lookman. Magnetic symmetry of low dimensional multiferroics and ferroelastics. 2011. *Phase Transitions.* **84**: 421.

Yang, X. D., P. S. Riseborough, K. A. Modic, R. A. Fisher, C. P. Opeil, T. R. Finlayson, J. C. Cooley, J. L. Smith, P. A. Goddard, A. V. Silhanek, and J. C. Lashley. Influence of magnetic fields on structural martensitic transitions . 2009. *Philosophical Magazine.* **89**: 2083–2091.

Photodynamics and Photochemistry of Carbon Nanotube Materials

Sergei Tretiak
20090253ER

Abstract

This project aims to conduct systematic theoretical investigation of electronic structure and excited state dynamics in carbon nanotube materials. Our modeling uses LANL-developed quantum chemical tools, which outperform similar techniques world-wide. Time dependent semiempirical and density functional theory (TDDFT) is used as the basic quantitative framework for computing electronic structure and photoexcited trajectories and dynamics. Our research program involving the necessary expertise in quantum chemistry, condensed matter, spectroscopy, synthesis, and optical physics, provides detailed understanding of fundamental physical processes, which, in particular, govern the operation of nanotube-based electronic devices. As a result of this project we answered many currently outstanding questions in nanotube science. Namely, an interplay between excitonic and vibrational effects in photochemistry, the role of dark excitons and chemical defects in luminescence, formation of polarons and triplet states, transport, inter-tube and solvent interactions, nonlinear dynamics and localization effects have been investigated in detail. We developed synthetically viable strategies in order to improve dramatically photoluminescence and electroluminescence of carbon nanotubes. Development of novel hybrid materials such as nanotubes wrapped with polymers or DNA and tubes functionalized with intercalated dyes opens new and exciting properties and functions of these materials: notably an intriguing opportunity poised by Scanning Tunneling Microscopy (STM) sequencing of short DNA fragments and development of nanotube-based bio-sensing. The theoretical insights are implemented synthetically and experimentally tested using spectroscopic and STM facilities at LANL. This will provide guidance to worldwide efforts in development of new functional nanotube-based electronic materials and devices. This project directly addresses LANL institutional goals in Materials Sciences, Energy Security, Threat Reduction, as well as LDRD strategic priorities in Nanotechnology, Multi-Scale Materials, and Sensing.

Background and Research Objectives

Carbon nanotubes (CNT) constitute a class of the most promising technological materials for high-strength materials with desirable - and tunable - electrical properties. Our progress in understanding and manipulating nanotube's fundamental electronic properties, and subsequent practical applications has been slow due to difficulties in synthesizing sample materials. A lack of the experimental knowledge of electronic processes in carbon nanotubes has impeded advances in theory and simulations. In particular, hybrid materials involving carbon nanotubes (CNT) and deoxyribonucleic acid (DNA)/polymer/surfactant molecules promise a broad range of applications in electronics, medicine and threat reduction technologies. For example, practical implementation of CNT-based nano-devices has long been hampered by inadequacy or plain absence of reliable methods for separation of CNT according to the structural and electronic properties. Recently, an unexpected breakthrough was achieved and unsurpassed efficiency of CNT separation demonstrated by combining single-stranded DNA molecules with the nanotubes in solution. Preliminary studies revealed that the outcome of the separation process is sensitive to the sequence of DNA and ensuing DNA-CNT binding geometries. However, very little is presently known about the exact structure of the CNT-DNA complexes – an essential pre-requisite to understanding of the mechanisms responsible for enhanced separation efficiency and to further optimization of existing procedures. A detailed knowledge of the physics behind CNT-DNA interactions should also advance single-CNT device fabrication technology where DNA hydrogen bond selectivity can be exploited for bio-inspired self-assembly of three-dimensional CNT networks. In addition, combination of the unique transport/optical properties of CNT and biochemical affinity of DNA makes CNT-DNA complexes an attractive system for bio-sensing application and highly specific drug delivery. Finally, electronic structure variation of single nucleotides adsorbed onto the CNT surface might provide a basis for rapid electronic DNA sequencing method development.

Thus, we have still not achieved a quantitative under-

standing and prediction of nanotube materials properties; however, several challenges in nanotube science are expected to be overcome in the near future. Carbon nanotube and graphene based electronics are rapidly becoming today's reality given the huge R&D effort in the industry. This creates a need for modeling and simulation effort to predict physical phenomena and deliver comprehensive theoretical framework of electronic structure and dynamics in carbon nanotubes. Such theory should provide guidance and a platform for future experimental studies, and impact technology. In this project we conducted systematic theoretical and experimental investigation of electronic structure and excited state dynamics in carbon nanotube materials. Our modeling used LANL-developed quantum chemical tools, which outperform similar techniques world-wide.

We answered many outstanding questions in nanotube science. Namely, an interplay between excitonic and vibrational effects in photochemistry, the role of dark excitons and chemical defects in luminescence, formation of polarons and triplet states, transport, inter-tube and solvent interactions, nonlinear dynamics and localization effects were investigated in detail.

Scientific Approach and Accomplishments

Over the duration of this project, our theoretical studies with close synergistic interactions with experiment at LANL have focused on multiple areas related to electronic properties of carbon nanotube materials, their excited states, dynamics and modification introduced by various chemical functionalization and hybridization with other organic materials.

First of all, we have used the Scanning Tunneling Microscopy (STM) setup built at Center for Integrated Nanotechnologies (CINT) to successfully demonstrate binding geometry of single strand DNA to carbon nanotube. The STM is based on quantum tunneling of electrons through the energy barrier formed by the sharp metallic tip and the sample placed in the tip vicinity. The strong dependence of the current on the tip-sample spacing enables the mapping of the surface topography variations with sub-angstrom resolution. Previous theoretical studies suggested multiple, energetically-degenerate DNA-CNT binding geometries ranging from linear alignment of DNA molecule along the CNT axis to insertion of DNA into CNT interior. STM images revealed that ssDNA prefers to wrap around CNTs of particular (6,5) chirality with a coiling period of 3.3 nm and a stable wrapping period of DNA at ~60 degrees (Figure 1) which coincide with natural tube coordinates and agreed very well with our theoretical predictions [1,2]. We have extended our investigations by simulating CNT/DNA structures with different wrapping angles, different DNA sequences, and different CNT chiralities. We have also found that sonication of CNT-DNA hybrids leads to reduction of nanotube ends uncoated by DNA. This result suggests that the length of the CNT-DNA hybrids can be reduced in a

controlled manner by varying the length of DNA sequence adsorbed on the tube surface. To complement and help interpret STM measurements, we have performed force field simulations that provided detailed information on the geometry and energetic stability of CNT-DNA hybrids. The modeling results are in very good agreement with experimental observations. All structures we studied show DNA wrapping angles of about 50-60 degrees, independent on the tube chirality, while being very stable (with ~0.8 eV binding energy per base, see Figure 1). Such a structure and stability suggest that DNA is unlikely be detached from the CNT because of external fluctuations, such as thermal vibrations and solvent effects, that is a very reliable property for drug delivery systems [3]. This observation might be important for medical application of these materials, since shortening of functionalized CNTs reduces their toxicity to the cell. Overall, our results lead to the further elucidation of self-assembling and structure-property predictions of CNTs functionalized by DNA – a topic of general interest due to the recent focus on bio-applications of such hybrid systems, including drug delivery, cancer diagnostics and therapy.
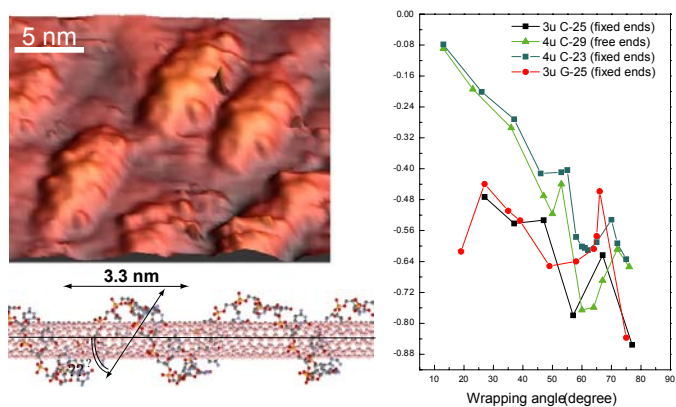
Figure 1. STM image of DNA-CNT complexes deposited on Si surface (24 x 24 nm) and results of MD simulations of the hybrid structure and binding energy as a function of wrapping angle.

We have also carried out structure-property studies on CNTs functionalized by small organic molecules and conjugated polymers. Unlike CNT/DNA hybrids, the interaction between conjugated polymers and the nanotube is relatively weak (with ~0.1-0.3 eV binding energy per base). Our simulations predict the most stable polymer wrapping angles of about 15-20 degrees, which compares well with available experimental data for these systems. Despite a weak interaction, the wrapping affects the first and second optical excitations (E11 and E22 bands) of the nanotube, slightly shifting them to the red, compared to pristine tubes. Moreover, the conformational changes in the wrapped polymer strongly affect its optical spectra, resulting in the significant blue shift of the excited energy and broader linewidth. These results have been finalized in two articles submitted for publication [4,5].

Using the time dependent density functional theory (TD-DFT), we were able to analyze the energy splitting, relative ordering, electron-hole binding, and localization properties of the optically active and forbidden excitations in nanotubes. This detailed analysis provides an explanation for the low luminescence efficiency of these materials. Our research has been finalized in the perspective feature article [6] and has been selected to represent the issue of this journal by highlighting a graphical summary of our paper on the journal's cover (Figure 2). Finally we investigated theoretically the electronic couplings and interactions in the carbon nanotube ensembles to understand properties of bulk materials [7].

Figure 2. Quantum-chemical calculations explore energetics and localization properties of optically active (bright) and forbidden (dark) states in single wall carbon nanotubes.

We have also explored theoretically and experimentally subtleties of electronic states and dynamics in carbon nanotubes in the presence of environment which is essential to tuning photophysical properties and enhancing behavior for nanotube separations and sensing applications. Experimental studies have been focused on understanding surfactant structure at the CNT interface [8], with an aim of determining the limits of tunability of that structure for optimizing photoluminescence (PL) response. We have shown that changing the electrostatic environment of sodium dodecyl sulfate (SDS) through addition of electrolyte can cause it to reorient to being perpendicular to the nanotube surface. The reorientation also causes a dense packing of the structure. In parallel an increase in photoluminescence (PL) intensity is observed during this reorganization [9]. We are currently developing a theoretical model for how the reorientation can impact exciton behavior and nonradiative decay routes to cause this behavior, and are currently putting together a draft article describing the work. The increased understanding of surfactant structure and response to environmental perturbations is allowing us to control its behavior to facilitate incorporation of nanotubes into new composite materials. In the past year, we have successfully used interfacial control to allow us

to generate highly luminescent composites of nanotubes with silica aerogels. The PL behavior indicates the nanotube environment in the aerogel is free of surfactant. This characteristic has allowed us to demonstrate novel surface adsorption behavior and has enabled new fundamental low-temperature photophysics to be observed [10]. This work is forming the basis for a white paper proposal for submission to DOE BES.

At a more detailed level, we have also investigated the 1-D surface chemistry of single dopant species on nanotubes using PL imaging (Figure 3). We demonstrate that mid-gap dopants such as gold adatoms act as localized quenching sites. In contrast we demonstrate that hole dopants are delocalized over the whole nanotube. Even single dopants of this nature will quench PL emission from the whole tube. Direct imaging of gold adatoms shows them diffusing on the surface. This work is in review at Nature Nanotechnology and we anticipate it being accepted shortly [11] (Figure 3). In parallel, our theoretical calculations have shown that the hydrogen atom adsorption on the nanotube sidewalls leads to a confinement of the spatial extent of electronically excited wavefunction to the near-vicinity of the dopant. Depending on the hydrogen position, the adsorbent perturbs and mixes the bright and dark states, frequently resulting in brightening and red shifting of the lowest-lying excitons, thus providing a guideline toward enhanced PL from CNTs using chemical functionalization [12] (Figure 4).

Finally we have conducted joint theoretical and experimental studies of Raman Spectroscopy of structurally pure nanotube samples. Probing the G-band (carbon-carbon deformations at frequencies of ~1600 cm-1) behavior of nanotubes with Raman spectroscopy can provide information on electronic structure unavailable with investigation of lower frequency phonons. To do so, however, requires working with samples consisting of a single nanotube structure or chirality. We have performed G-band Raman excitation profiling of a set of 12 different pure chiralities to test several models for the nanotube Raman response. Typical excitation profiles for such a high frequency mode will show two resolved bands for resonances with the excitation and scattered photons of the Raman process. Surprisingly, we find that the scattered resonance is significantly weaker than the excitation resonance. This is a general result for all chiralities and classes of structure. The observed behavior results from violation of the Condon approximation and originates in changes in the electronic transition dipole due to nuclear motion (non-Condon effect), as confirmed by our quantum chemical calculations. The agreement of our calculations with the experimental spectra asymmetries and observed trends in family dependence indicates the behavior is intrinsic [13].

In general, our research established a systematic and insightful understanding of photoinduced electronic dynamics in nanotube based materials, which will guide the

design of new experimental probes, and potentially lead to new nanotechnological applications. In addition, besides improving the fundamental understanding of the properties of DNA-CNT complexes, we have introduced an integrated experimental/theoretical capability, which will find a broad range of applications in the rapidly growing field of nano-bio interfaces.

Impact on National Missions

This project will make a significant contribution to our basic understanding of materials, a LANL Grand Challenge. Carbon nanotube technology is widely expected to impact many areas including energy security, threat reduction, ubiquitous sensing, among others. These are major mission areas within DOE, DHS, DOD, and other government agencies.
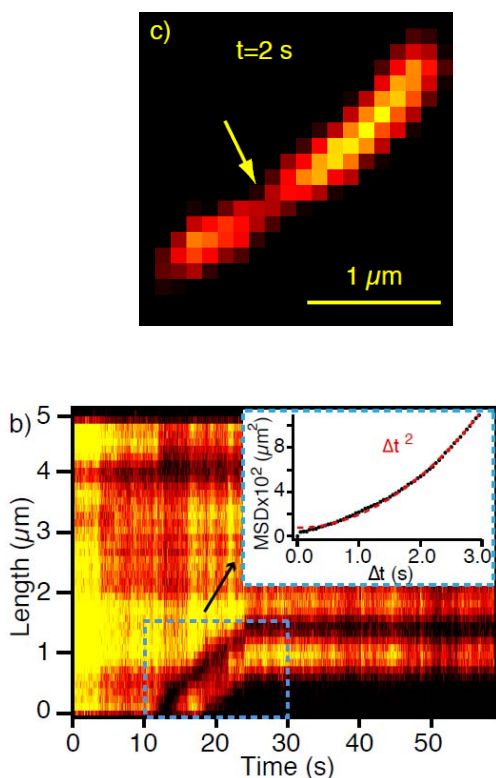
Figure 3. Confocal photoluminescence imaging of single carbon nanotubes allows us to probe surface chemistry in 1-dimension: Top) Single nanotube PL image showing single-dopant quenching site resulting from adsorption of a single gold atom. Bottom) Time-dependent imaging shows single dopant species can diffuse on the nanotube surface. Inset) Analysis of the diffusion behavior shows adatom surface motion is non-linear with time. This indicates directed motion in response to an external force. In this case it may be excess electrostatic charge at the tube ends.
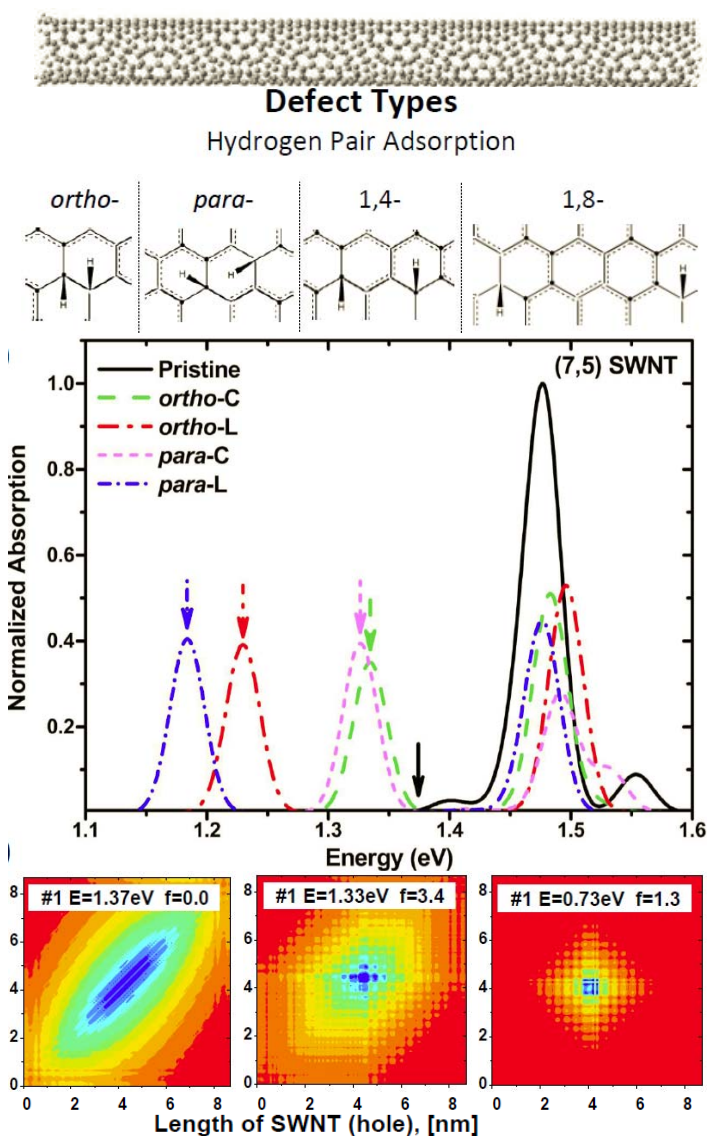
Figure 4. Theoretical calculations of hydrogenated carbon nanotubes (chemical structures are shown on the top panel) predict significant enhancement of the photoluminescence efficiency of the material, i.e. nanotube 'brightening' (middle panel). This occurs since the lowest excited state becomes moderately localized defect state slightly below the conduction band (bottom panels) gaining significant oscillator strength. The results of our theoretical modeling reproduce and explain recent experimental data on nanotube brightening via chemical functionalization at LANL and elsewhere.

References

1. Yarotski, D., A. Balatsky, S. Kilina, A. Talin, J. X. Zhu, S. Tretiak, and A. Taylor. Scanning Tunneling Microscopy of DNA-Carbon Nanotube Hybrids. 2009. *Nano Letters* . **9**: 12.

2. Structure of DNA-wrapped carbon nanotubes revealed. 2009. *PADSTE HIGHLIGHTS* .

3. Kilina, S., D. A. Yarotski, A. A. Talin, S. Tretiak, A. J. Tay-

lor, and A. V. Balatsky. Unveiling Stability Criteria of DNA-Carbon Nanotubes Constructs by Scanning Tunneling Microscopy and Computational Modeling. 2011. *Journal of Drug Delivery.* **2011**: 415621.

4. Ramirez, J., S. Kilina, and S. Tretiak. DFT Simulations of Optical Response of Carbon Nanotubes Functionalized with Diazonium Reagents. *Journal of Physical Chemistry.*

5. Furmanchuk, A., S. Tretiak, and S. Kilina. Electronic Properties of Carbon Nanotubes Wrapped in Conjugated Polymer. *Journal of Physical Chemistry C.*

6. Kilina, S., E. Badaeva, A. Piryatinski, S. Tretiak, A. Saxena, and A. Bishop. Bright and Dark Excitons in Semiconductor Carbon Nanotubes. 2009. *Physical Chemistry Chemical Physics.* **11**: 4113.

7. Wong, C. Y., C. Curutchet, S. Tretiak, and G. D. Scholes. Ideal dipole approximation fails to predict electronic coupling between semiconducting single wall carbon nanotubes. 2009. *Journal of Chemical Physics.* **130**: 081104.

8. Niyogi, S., C. G. Densmore, and S. K. Doorn. Electrolyte Tuning of Surfactant Interfacial Behavior for Enhanced Density-Based Separations of Single-Walled Carbon Nanotubes. 2009. *Journal of the American Chemical Society.* **131**: 1144.

9. Duque, J., C. Densmore, and S. Doorn. Saturation of surfactant structure at the single-walled carbon nanotube surface. 2010. *Journal of the American Chemical Society.* **132** (45): 16165.

10. Duque, J., G. Gupta, L. Cognet, B. Lounis, S. Doorn, and A. Dattelbaum. New Route to Fluorescent Single-Walled Carbon Nanotube/Silica Nanocomposites: Balancing Fluorescence Intensity and Environmental Sensitivity. 2011. *Journal of Physical Chemistry C.* **115** (31): 15147.

11. Crochet, J. J., J. G. Duque, J. H. Werner, and S. K. Doorn. Photoluminescence Imaging of Localized and Delocalized Electronic Defects in Single-Wall Carbon Nanotubes. *Nature Nanotechnology.*

12. Ramirez, J., S. Kilina, and S. Tretiak. Brightening of the Lowest Exciton in Carbon Nanotubes via Hydrogen Adsorption. *Nano Letters.*

13. Duque, J., H. Chen, A. Swan, A. Shreve, S. Kilina, S. Tretiak, X. Tu, M. Zheng, and S. Doorn. Violation of the Condon Approximation in Semiconducting Carbon Nanotubes. 2011. *ACS NANO.* **5** (6): 5233.

Publications

Structure of DNA-wrapped carbon nanotubes revealed.

2009. *PADSTE HIGHLIGHTS .*

Crochet, J. J., J. G. Duque, J. H. Werner, and S. K. Doorn. Photoluminescence Imaging of Localized and Delocalized Electronic Defects in Single-Wall Carbon Nanotubes. *Nature Nanotechnology.*

Duque, J., C. Densmore, and S. Doorn. Saturation of surfactant structure at the single-walled carbon nanotube surface. 2010. *Journal of the American Chemical Society.* **132** (45): 16165.

Duque, J., G. Gupta, L. Cognet, B. Lounis, S. Doorn, and A. Dattelbaum. New Route to Fluorescent Single-Walled Carbon Nanotube/Silica Nanocomposites: Balancing Fluorescence Intensity and Environmental Sensitivity. 2011. *Journal of Physical Chemistry C.* **115** (31): 15147.

Duque, J., H. Chen, A. Swan, A. Shreve, S. Kilina, S. Tretiak, X. Tu, M. Zheng, and S. Doorn. Violation of the Condon Approximation in Semiconducting Carbon Nanotubes. 2011. *ACS NANO.* **5** (6): 5233.

Furmanchuk, A., S. Tretiak, and S. Kilina. Electronic Properties of Carbon Nanotubes Wrapped in Conjugated Polymer. *Journal of Physical Chemistry C.*

Kilina, S., D. A. Yarotski, A. A. Talin, S. Tretiak, A. J. Taylor, and A. V. Balatsky. Unveiling Stability Criteria of DNA-Carbon Nanotubes Constructs by Scanning Tunneling Microscopy and Computational Modeling. 2011. *Journal of Drug Delivery.* **2011**: 415621.

Kilina, S., E. Badaeva, A. Piryatinski, S. Tretiak, A. Saxena, and A. Bishop. Bright and Dark Excitons in Semiconductor Carbon Nanotubes. 2009. *Physical Chemistry Chemical Physics.* **11**: 4113.

Niyogi, S., C. G. Densmore, and S. K. Doorn. Electrolyte Tuning of Surfactant Interfacial Behavior for Enhanced Density-Based Separations of Single-Walled Carbon Nanotubes. 2009. *Journal of the American Chemical Society.* **131**: 1144.

Ramirez, J., S. Kilina, and S. Tretiak. Brightening of the Lowest Exciton in Carbon Nanotubes via Hydrogen Adsorption. *Nano Letters.*

Ramirez, J., S. Kilina, and S. Tretiak. DFT Simulations of Optical Response of Carbon Nanotubes Functionalized with Diazonium Reagents. *Journal of Physical Chemistry.*

Wong, C. Y., C. Curutchet, S. Tretiak, and G. D. Scholes. Ideal dipole approximation fails to predict electronic coupling between semiconducting single wall carbon nanotubes. 2009. *Journal of Chemical Physics.* **130**: 081104.

Yarotski, D., A. Balatsky, S. Kilina, A. Talin, J. X. Zhu, S. Tre-

tiak, and A. Taylor. Scanning Tunneling Microscopy of DNA-Carbon Nanotube Hybrids. 2009. *Nano Letters* . **9**: 12.

Compositionally Graded InGaN-based High Efficiency Photovoltaic Devices

Mark A. Hoffbauer
20090260ER

Abstract

This project's goal was to explore an alternative materials system for creating photovoltaic (PV) devices, namely Indium-Gallium-Nitride ($In_xGa_{1-x}N$) thin film materials (x ranging from 0 to 1). Significant progress has been achieved towards our goal of creating a new type of PV device based on InGaN materials with tunable bandgaps covering the visible solar spectrum offering several advantages over conventional PV materials with fixed bandgaps. A unique LANL technology has demonstrated that it is the only method capable of growing high-quality InGaN over the full composition range from GaN to $In_xGa_{1-x}N$ to InN. Substantial work has set the basis for creating these challenging materials and understanding their use in PV devices. The In-rich InGaN materials grown during this project show the highest quality materials properties ever produced. Methods for routinely growing compositionally graded $In_xGa_{1-x}N$ films have also been developed. In many cases, background carrier concentrations have been shown to be sufficiently low to allow successful p-type doping of these nitride films, and p-n junctions have been grown that show rectifying photovoltaic activity. The results of this project have allowed us to solve many of the materials challenges regarding In-rich InGaN materials, paving the way for making compositionally-graded, single-junction InGaN-based PV devices with the potential to achieve record efficiencies of ~30%. These devices would be alternatives to current thin film single-junction PV devices, substantially lowering costs and making PV technology competitive with fossil fuels for producing electricity.

Background and Research Objectives

For PV technology to significantly impact our nation's energy portfolio, the cost of modules needs to be reduced from the current value of around 14¢/kWh to close to 5¢/kWh, making PV costs competitive with conventional fossil fuel energy [1]. For widespread PV deployment, modules based on single p-n junction devices are the most likely near-term candidates. Although multi-junction devices have higher efficiency (current record ~43%), their high cost and complexity make them unlikely for widespread domestic/commercial use. Currently, there are three materials systems being aggressively explored for widespread deployment: Si, CdTe, and CIGS (Cu-In-Ga-Se). Single crystal-based Si devices are currently the most efficient form of single junction PVs, with laboratory record efficiencies of 24.7%. Poly-Si based devices are cheaper than single crystal Si, but are limited to about 15% efficiency. CdTe and CIGS devices are also relatively inexpensive and are currently being promoted by the DOE for commercialization, but modules based on these materials are limited to around 11% and 18% efficiency, respectively, and there are concerns about the toxicity of components of these devices (both Cd and Se). Clearly, breakthroughs in the cost and efficiency of PVs are needed for widespread deployment.

In nearly all conventional PV devices, the material's bandgap is fixed at a single value (e.g. Si = 1.1eV), limiting device efficiency because of two basic issues. Photon energies below a material's band gap are not absorbed, and the extra photon energy above of the band gap is converted into heat without producing charge carriers (electricity). The ideal PV device would encompass two demonstrated methods for improving efficiency: fabrication from a single material system having tunable (multiple) band gaps tailored to match the full solar spectrum; and the use of PV films with high mobility charge carriers. For widespread use, PVs must be manufactured inexpensively from materials that exhibit exceptional photo, chemical, and thermal stability and are non-toxic. In addition, graded InGaN-based PV devices offer several advantages: absorption of photons over a wide spectral range directly creates more charge carriers; the polar material generates an electric field enhancing carrier transport; and the high bandgap active layer increases output power.

Our research objective was to use an alternative materials system for creating high-efficiency PV devices, namely compositionally graded InGaN, offering inexpensive, single-junction PV device efficiencies approaching 30%. These devices can combine the advantages of the high efficiency of single-crystalline Si PV devices with the low cost and simplicity of CdTe and CIGS based PV devices. Our unique device architecture uses p- and n-

type doped InGaN films with a p-i-n structure as shown in Figure 1 where a p-i-n film structure functions essentially like a single junction PV device. This device structure can be fabricated from compositionally-graded, undoped, intrinsic i-InGaN films using a unique LANL technology called ENABLE (see below) and is the basis for a LANL patent application [2]. The key difference in this device design is that charge carriers are generated in the active "i" portion of the device and are then separated and transported by the p and n regions, making contact to an external circuit to provide electric power.

This design offers several advantages over conventional PV devices. Because high-In-content InGaN has a lower bandgap than high-Ga-content InGaN, the device shown in Figure 1 will have an internal electric field directing both holes (positive charges) and electrons towards the p-i and n-i interfaces, respectively, and substantially improving carrier transport. Also, because the bandgap of $In_xGa_{1-x}N$ system is tunable from 0.7 eV (InN) to 3.4 eV (GaN), the p and n layer compositions can be designed for maximize efficiency. In addition, the bandgaps of the p and n layers could be made slightly lower than the lowest bandgap in the compositionally graded film, creating an additional electric field for enhancing carrier transport. Overall, this device is simple to produce and could eventually be grown on inexpensive glass substrates, keeping production costs low. Thus, the potential of the InGaN materials system offers a real opportunity for realizing low-cost, high-efficiency PV devices.
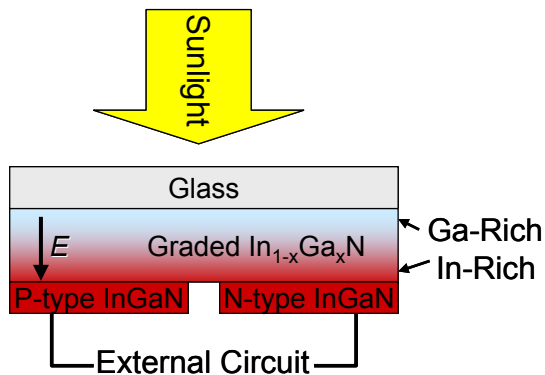
Figure 1. Compositionally graded InGaN p-i-n PV device architecture. The internal field in the graded "i" layer directs carriers toward the p and n layers, improving efficiency.

Scientific Approach and Accomplishments

Most semiconductor devices utilizing graded InGaN fall into the following categories: using graded InGaN as a buffer to alleviate strain in various InGaN based optoelectronic devices; using graded InGaN as the active layer in quantum well devices to take advantage of the bandgap bending and electric field that is generated by the grading to enhance device performance; and using graded InGaN as the active layer in photocathodes to take advantage of the

inherent electric field for increasing quantum efficiency. There are no current examples of graded InGaN PV devices in the literature, but it is well established that having carriers generated in a larger bandgap material and transported to smaller bandgap layers should improve output power. Thus, we expect to observe significant efficiency improvements for compositionally graded InGaN where the accessible bandgap range is large, from 0.7 eV to 3.4 eV.

For InGaN film growth we have utilized a unique LANL MBE-like growth capability called ENABLE (*Energetic Neutral Atom Beam Lithography & Epitaxy*) that is a lower temperature thin film growth technology ideally suited for growing high-quality InGaN films. ENABLE is a *2006 R&D 100 Award* winning technology unique to LANL that utilizes an energetic beam of neutral N atoms (kinetic energies from 1 to 5 eV) for nitride thin film growth, reducing the need for high substrate temperatures to overcome reaction barriers. The high energy and reactivity of N atoms allow lower temperature growth of high-quality, crystalline thin film materials that are difficult, if not impossible, by conventional metal organic chemical vapor deposition (MOCVD) or molecular beam epitaxy (MBE) techniques. Growth occurs in a clean MBE-type environment at exceptionally high growth rates (current InGaN growth rates exceed 3 micron/hr over a 20cm² area). The complete absence of charged species and contaminants (e.g. oxygen, carbon, or hydrogen containing species) combined with the elimination of toxic precursors or reaction products make ENABLE ideally suited for growing high-purity, single-phase, crystalline materials. This project has used ENABLE to grow high-quality GaN, InN, AlN, and $In_xGa_{1-x}N$ over the whole composition range (0 < x < 1) [3-6]. High-quality $In_xGa_{1-x}N$ films have been demonstrated with both fixed and/or graded compositions. We have also demonstrated p-type doping of In-rich InGaN that is an important result considered to be technologically very difficult. These results were all important goals of this project and represent significant progress toward demonstrating efficient InGaN-based PV devices.

A particularly significant accomplishment of this project is that isothermal growth of GaN, InN and high-In-content InGaN films are now routinely achieved [5,6]. The materials produced show excellent crystallinity and optical properties. For example, Figure 2 shows XRD data for an In-rich InGaN film ~500 nm thick grown on a sapphire substrate with a single well-defined In composition of ~36%. The InGaN film shows excellent single-phase crystal quality (~380 arcsec <0002> FWHM) resulting from careful control of the epitaxial growth on the sapphire substrate using an ~100 nm thick GaN buffer layer for improved epitaxy. Similar results across the full composition range of device quality InGaN films [8] and on other substrates (e.g. silicon) are routinely produced by ENABLE. Growing high-quality In-rich InGaN materials is a long sought goal of many other worldwide efforts, and our results are measurably better than any other reported results [7].
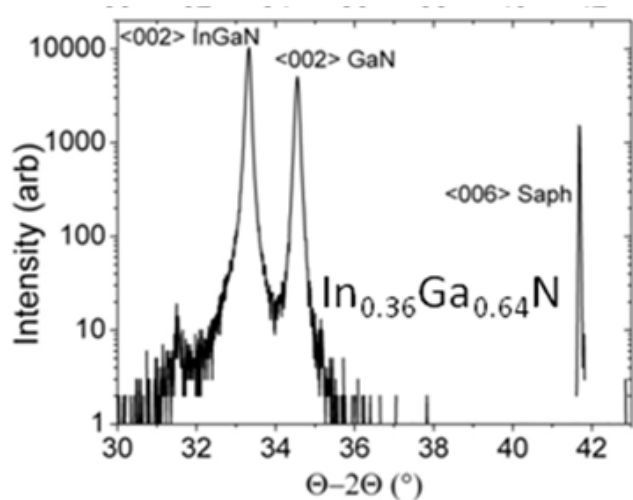
Figure 2. X-ray diffraction (XRD) scan of a ~500nm thick InGaN film grown by ENABLE showing the <0002> diffraction peak. This film had an In composition of 36% and was grown at 490°C.

Details concerning the impact of variations in the film growth temperature on the observed x-ray diffraction (XRD) and photoluminescence (PL) measurements for ~500nm thick, ~37% In-content films of InGaN grown on sapphire substrates at relatively low temperatures are shown in Figure 3. In all cases the films show excellent crystallinity and bright band edge PL. These results are critical for this project since creating graded composition structures over wide ranges requires isothermal growth at moderately low temperatures. We have also demonstrated on a routine basis: (1) the growth of graded composition films; (2) methods for forming the uniform gradients in InGaN composition needed for prototype PV devices; (3) and ways to vary the rate at which changes in the graded composition can be made to better define the graded layer thicknesses critical for making PV device structures. These necessary capabilities and flexibilities are unique to the ENABLE growth capability.

By carefully optimizing film epitaxy and controlling sources of contamination in the source gas streams and in the Ga and In evaporators, we now routinely grow semiconducting $In_xGa_{1-x}N$ films with background carrier concentration in the low $10^{17}cm^{-3}$ range. These low levels are necessary for p-type doping of the films. Intrinsic InGaN-related films show carrier mobilities in the 100 to >500 cm²/Vsec range suitable for fabricating prototype PV devices.

P-type doping of GaN with a high concentration of active Mg is now well established, and solid results indicate successful p-type doping of high-In-content InGaN films. These results are unique for high-In-content InGaN films and have not been reported in the literature. Spectrally resolved electroluminescence measurements (EL) indicate that Mg can be doped into InGaN at In contents up to ~50% yielding bright, tunable band edge EL. Electrical transport measurements have verified the formation of

our first functional p-n junctions in InGaN films. These steps are all critical for creating functional PV devices and optimizing their efficiencies, particularly since n- and p-type doped In-rich InGaN films are needed for the bottom of our PV device structure (see Figure 1).

In addition, we have designed a new ENABLE source and will be moving our ENABLE technology to a new MBE system that will allow us to routinely grow InGaN-related thin films over larger substrate areas. Over the course of this project, we have successfully transitioned our substrates from one cm² areas to 5 cm diameter substrate wafers (~20 cm² area), the standard size for research grade devices. Routine growth on much larger substrate sizes (20 cm diameter) will facilitate the low-cost fabrication of efficient PV devices.

The growth of high-quality high-In-content InGaN on crystalline and polycrystalline silicon substrates has also been demonstrated. These experiments yield highly-crystalline InGaN films. On crystalline Si, InGaN film quality is similar to that observed for growth on sapphire (see Figure 2 above). Once optimized, the ability to grow InGaN-related thin film materials on inexpensive Si substrates will significantly reduce the costs of PV devices by providing a path forward for adding value to existing Si-based PV device architectures.

This project's significant accomplishments can be summarized as follows. Our goals were to develop a new materials system, InGaN, and use this material to create a new type of high efficiency PV device. On the materials side, we have solved numerous material challenges and now grow the highest quality In-rich InGaN materials in the world. Compositional grading of InGaN is now routine and reproducible over a broad range. All of these materials have excellent crystallinity and uniform stoichiometry. The In and Ga compositions are tunable over a very broad range with either fixed and/or graded compositions, show bright band edge photoluminescence, have low carrier concentrations and reasonably high mobilities, and can be grown on sapphire and Si substrates. On the device side, we have demonstrated p-type doping of GaN and In-rich InGaN, grown p-n junctions in GaN and In-rich InGaN, shown EL from p-n junctions, and observed PV activity from a GaN p-n junction. The In-rich InGaN films still need further improvements to reduce the background (intrinsic) carrier concentrations to levels suitable for demonstrating active p-n junctions and for fabricating the full PV devices structure shown in Figure 1. We have succeeded in reducing these levels by more than an order of magnitude during the last year of this project, but an additional factor of two to three is still needed to achieve our ultimate goal of ~30% efficiency for graded composition PV devices.

Preliminary results show a clear path to making device-quality compositionally-graded InGaN materials. One of our first tasks is to further improve (reduce) the prototype

PV devices. High-quality compositionally graded InGaN will be grown over well-defined, relatively narrow composition ranges optimized for performance in single junction PV devices and these devices will be fully characterized. These graded InGaN films will also be grown on Si substrates and fabricated into working PV devices to measure their overall efficiency. Our ultimate goal is to achieve ~30% PV efficiency for these graded composition devices and explore fabricating these devices on inexpensive substrates.
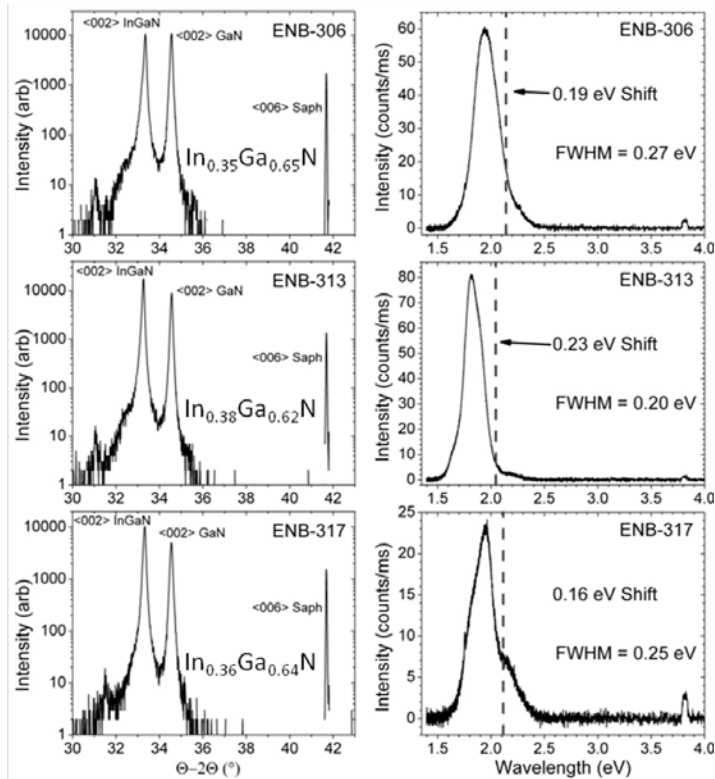
Figure 3. X-ray diffraction scans (left column) and photoluminescence spectra (right column) of a series of ~500nm thick InGaN films grown by ENABLE showing the <0002> diffraction peak (left column) and bandgap luminescence (right column). These films had In compositions of 35% to 38%. ENB-306 (top) was grown at 570°C, ENB-313 (middle) was grown at 530°C, and ENB-317 (bottom) was grown at 490°C. The dashed lines indicate energy shifts in the PL spectra (right column) from the expected position of the bandgap luminescence based on the composition determined from the XRD scans.

Impact on National Missions

The results of this research will directly support LANL and DOE core missions in national energy security and threat reduction by developing a new electronic and photonic material system. Applications for semiconducting InGaN materials range from photovoltaics with unprecedented efficiency and lower costs, to efficient LEDs for solid state lighting, and to efficient high-speed/high-power switching electronics. These areas are all key elements in several DOE programs including the Solar America Initiative, Solid State Lighting, and Innovative Manufacturing. Solving the numerous technological challenges in making and testing these new materials and devices has built a foundation for expanding this effort in to a much larger program. The results of this project will position us to compete for follow-on funding from DOE (e.g. DOE/BES, ARPA-E, and EERE initiatives) to expand this effort into a much larger program. There are also many DOD programs interested in a broad range of applications including satellite power, battlefield systems, communication systems, and sensing with potential sponsors including DARPA, DITRA, and others. This project has built an exceptionally strong capability in the general area of advance materials science including synthesis, defect control, and semiconductor properties, all of which utilize and expand upon existing capabilities at LANL. In addition to direct science and mission relevance, having the capability to make advanced materials and to design and build devices utilizing their unique properties will provide the basis for an expanded program in semiconductor sensor development. In the long term, the results of this project will have important consequences for our nation's energy security, national security, and environment.

References

1. Zweibel, K., J. Mason, and V. Fthenakis. By 2050 solar power could end US dependence on foreign oil and slash greenhouse gas emissions. 2008. *SCIENTIFIC AMERICAN.* **298** (1): 64.

2. Hoffbauer, M., and T. Williamson. Nitride-based Photovoltaic Device. 2009. *U. S. Patent Application, S112,641, Fled Dec. 21, 2009.*

3. Williamson, T. L., M. A. Hoffbauer, K. M. Yu, L. A. Reichertz, M. E. Hawkridge, R. E. Jones, N. Miller, J. W. Ager, Z. Liliental-Weber, and W. Walukiewicz. Highly luminescent In$_x$Ga$_{1-x}$N thin films grown over the entire composition range by energetic neutral atom beam lithography & epitaxy (ENABLE). 2009. *Physica Status Solidi C.* **6** (S2): S409.

4. Miller, N., R. E. Jones, E. E. Haller, null. Dept. of Materials Science and Engineering, K. M. Yu, J. W. Ager, Z. Liliental-Weber, W. [Materials Sciences Division. Walukiewicz, T. L. Williamson, and M. A. Hoffbauer. Low-temperature grown compositionally graded InGaN films. 2008. *Physica Status Solidi C.* **5** (6): 1866.

5. Williamson, T., A. Salazar, J. Williams, and M. Hoffbauer. Improvements in the compositional uniformity of In-rich In$_x$Ga$_{1-x}$N films grown at low temperatures by ENABLE. 2011. *Physica Status Solidi (C) Current Topics in Solid State Physics.* **8** (7-8): 2098.

6. Williamson, T., J. Williams, J. D. Hubbard, and M. Hoffbauer. High in content In$_x$ Ga$_{1-x}$ grown by energetic neutral atom beam lithography and epitaxy under slightly N-rich conditions. 2011.

Journal of Vacuum Science and Technology B: Micro-electronics and Nanometer Structures. **29** (3): 03C132.

7. Doolittle, W. A.. IWN Showcases the Diversity of III-Nitrides. 2010. *Compound Semiconductor, Nov/Dec, p. 46.*

Publications

Williamson, T. L., J. J. Williams, null. Hubbard, and M. A. Hoffbauer. High In content In_xGa_{1--x}N grown by energetic neutral atom beam lithography and epitaxy under slightly N-rich conditions. 2011. *Journal of Vacuum Science & Technology B (Microelectronics and Nanometer Structures).* **29** (3): 03C132 (5 pp.).

Williamson, T. L., M. A. Hoffbauer, K. M. Yu, L. A. Reichertz, M. E. Hawkridge, J. W. Ager, Z. Liliental-Weber, W. [Materials Sciences Division. Walukiewicz, R. E. Jones, N. [Materials Sciences Division. Miller, and null. Department of Materials Science and Engineer. Highly luminescent In{sub x}Ga{sub 1-x}N thin films grown over the entire composition range by energetic neutral atom beam lithography and epitaxy (ENABLE). 2009. *Physica Status Solidi C.* **6** (SUPPL.2): S409.

Williamson, T., A. Salazar, J. Williams, and M. Hoffbauer. Improvements in the compositional uniformity of In-rich In_xGa_{1-x}N films grown at low temperatures by ENABLE. 2011. *Physica Status Solidi (C) Current Topics in Solid State Physics.* **8** (7-8): 2098.

Plasmonic Bandgap Materials: Fusion of Interparticle and Particle-Photon Interactions at the Nanoscale

Stephen K. Doorn
20090325ER

Abstract

The ability to simultaneously exploit the ability for optical excitations of electrons in noble metals (plasmons) within interacting particles to generate surface enhanced Raman signals, within particle assemblies with photonic bandgap properties, has the potential to dramatically improve sensitivity and selectivity of new optical-based sensing modes. This project targeted the development of nanoparticle assemblies aimed at realizing such sensing improvements. At the same time, it would build on the goal of arriving at a better understanding of how interparticle interactions can drive enhanced optical processes. To this end, we focused on routes to generating two-dimensional (2-D) assemblies of interacting particles and structures. This involved developing new routes to synthesis of a range of plasmonic and magnetic nanoparticles and substrates. New methods for flow- and microscopy-based spectral characterization of the resultant particles were also developed. New capability for directed assembly of interacting particles was generated. The project successfully built new capability at LANL for nanoparticle synthesis, SERS substrate development, flow-based nanoparticle characterization, robust microscopic spectral imaging, electron-beam lithography, and routes to directed assembly of complex nanoparticle arrays.

Background and Research Objectives

Optical excitation of surface electrons (plasmons) within multiple interacting metal nanoparticles can result in huge amplification of associated surface enhanced Raman (SERS) responses from adsorbed molecules, providing single-molecule sensitivity. Gaining a fundamental understanding of these interparticle plasmonic interactions is essential for future exploitation of this phenomenon for next-generation sensing needs. Engineering such plasmonic nanoparticles into ordered arrays that also exhibit tunable photonic bandgap properties (with well-defined optical resonances) will present a novel system for exploring optical behaviors that will provide new modes for sensing opportunity. Our broad goal was to probe, understand, and manipulate the interparticle and particle-photon interactions required to realize a functional plasmonic/photonic material hybrid. Our proposed multi-pronged approach consisted of three interconnected focus areas:

1. Fundamental understanding of the interparticle plasmonic interactions responsible for hot spot generation would be investigated through controlled 2-D and 3-D assembly of particle aggregates.

2. Plasmonic particles would be assembled with long-range 3-D order to generate and characterize an easily manipulated dynamic photonic material that is SERS active.

3. We would incorporate elements into the dynamic plasmonic/photonic lattice to impart a chemoresponsive route to lattice manipulation and demonstrate its potential as a novel concept in SERS-based sensing.

Scientific Approach and Accomplishments

The overall goal of this proposal was to develop novel approaches to nanoparticle aggregate formation using SERS activity as a metric for successful particle geometries. This work utilized several parallel approaches for particle synthesis and manipulation. The work was organized along the lines of particle synthesis, particle characterization, and approaches to particle manipulation. Ultimately, challenges associated with goals two and three as listed above forced a re-focusing of our efforts onto goal number one.

Particle Synthesis

The primary goal was to produce multifunctional particles that match spectroscopic signatures with suitable physical traits for efficiently manipulating inter-particle interactions. Realization of self-assembled plasmonic photonic lattices requires synthesis of multilayered, multifunctional particles with complex surface chemistry. The synthetic aspect of this work therefore involved development of techniques for generating magnetic and plasmonic nanoparticles. These must be integrated in a core-shell geometry. Methods for generation of com-

plex particle geometries and surface functionalization are also necessary.

We have developed synthetic approaches for generating simple colloidal particle systems, and also the development of new particle structures that have promise in SERS applications. We have demonstrated the synthesis of solid noble metal (Au and Ag) colloidal systems as well as core-shell nanoshell geometries as effective SERS active materials. These particles would be the primary particles of interest in the 2-D and 3-D aggregate assembly experiments. Our core-shell architectures have an oxide central core (silica) that is encapsulated by a thin metallic shell (gold). Development of these nanoparticles revealed detailed light mediated reaction pathways that have not been previously reported and is the subject of a manuscript in preparation.

As an extension on this initial particle work, we have also developed several synthetic routes to magnetic plasmonically active particle architectures. In this area, significant work has gone into developing colloidal Fe_3O_4 particle systems with overall diameters on the order of 100nm. Attempts at these particles were only marginally successful, in that we generated Fe_3O_4 materials that are magnetically active. However, the particle sizes and morphologies were highly heterogeneous and not suitable for magnetic self-assembly. Additionally, in parallel, we successfully developed several alternate routes to similar superparamagnetic materials. We have been successful in creating silica core particles that have been decorated with small (~10nm) iron oxide particles that act as nucleation points for subsequent metallization (see Figure 1). We also used larger iron oxide particles (~18nm) to serve as the central core of an oxide-metal, core-shell particle system. These particles have been extensively characterized for overall homogeneity in size and morphology. In a side collaboration, the 10 nm superparamagnetic particles were critical in our ability to generate novel heterstructures with carbon nanotubes [1].
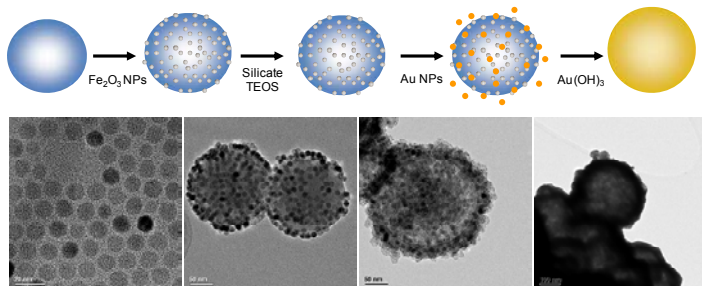
Figure 1. Depiction (top) of and SEM images of actual synthesized magnetic/gold nanoshell hybrid structures. SEM images show (from left to right) individual Fe_2O_3 nanoparticles, silica core with iron oxide particles attached, iron oxide functionalized bead with overlayer of silica shell, final gold-coated magnetic core hybrid.

As part of our efforts to generate complex multifunctional particle geometries with tailored surface functionalization, we also demonstrated the ability to combine multiple particle types into a larger assembly on support bead structures (see Figure 2) [2]. The goal in this case was to increase the range of spectral responses available with SERS-active nanoparticle spectral tags (SERS-tags). Individual tags were generated by adding a Raman-active dye label to the surface of a plasmonic nanoparticle. The tag is coated with a silica shell, which was then functionalized with a bioreceptor molecule. Three different types of tags were generated. We demonstrated the ability to generate more complex spectral signatures through controlled assembly of different ratios of the three tags at the surface of a support bead. The self-assembly was driven by strong bioreceptor interactions available with appropriate functionalization of the bead and tag surfaces.
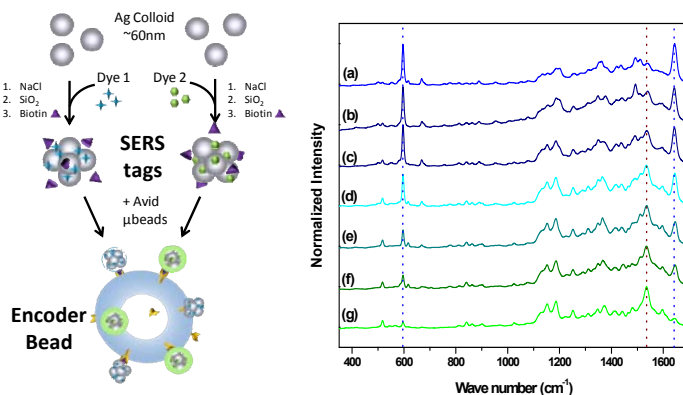
Figure 2. Left: Depiction of build-up of surface enhanced Raman spectroscopic encoder bead. Beads are assembled by first generating SERS tags from aggregated silver colloid that has been functionalized with a spectral dye. The SERS tags are then bound to silica support beads. Tags with different spectral signatures may be co-assembled in different ratios to give varying spectral signatures as shown by the examples on the right.

In addition to colloidal synthetic approaches, we have studied surface-directed growth of metallic nanoparticles in an attempt to reveal inter-particle interactions in-situ as the particles are nucleated and formed. This parallel approach has the significant advantage over colloidal solutions in that we are not required to manipulate the particles once they are formed; the surface dictates how the particles interact. These studies use conducting polymer thin films to reduce metal ions to zero valent metallic particles. The subsequent particle morphologies formed on the polymer surface are found to be highly dependent on the polymer processing conditions and solution properties of the metal ions. However, conditions producing long (10_m), thin (100nm) Ag sheets were found to produce extremely large and consistent SERS responses (Figure 3). Such features are rarely found concurrently on traditional SERS active materials. From these materials, we estimated an overall enhancement in the Raman signal to be on the order of 10^7. This ranks these materials among the best overall SERS active materials to date.
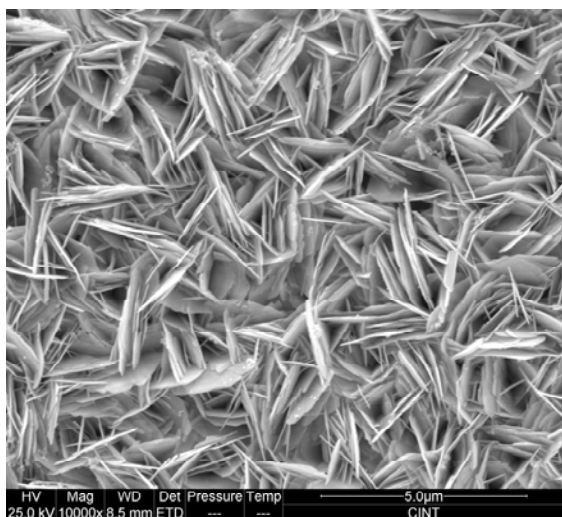
Figure 3. SEM image of SERS active Ag nanosheets formed on a polyaniline thin film.

We have published several papers on this work in FY10 and FY11 [3-6]. This technology was awarded a patent (US#7,786,037) and we are working with TT division to explore these materials as potential sensors for a variety of analyses. Additionally, these materials have received significant interest at LANL for sensing explosive residues. We are conducting proof of principal experiments for DTRA sensing needs, and will present results at an upcoming conference in November. Overall, this aspect of the project was successful in developing a SERS active material that outperforms all other materials in terms of cost, signal intensity, material design flexibility, and uniformity. We hope to transition this work into external funding opportunities over the course of FY12.

Particle Characterization

In an addition to our project scope we used recent advances in full-spectral flow-based analysis of nanoparticles to observe spectroscopic signatures of plasmonic nanoparticles at the single particle level. This newly-developed high-throughput instrumentation enables multi-parametric spectral analysis of 100s of particles per second. This enabled us to assemble particle structure-property relationships using statistically relevant particle population sizes. In many ways, this flow-based work is merely a 1-d extension of the 2-d and 3-d manipulation approaches proposed in this project. This work not only drives cutting edge instrument development, but also has resulted in a publication (as the May 5th cover article) in the Journal of the American Chemical Society, "High Resolution Analysis of Individual Surface-Enhanced Raman-Active Nanoparticle Spectral Tags in Flow" [7]. In addition to allowing probing of fundamental particle properties, the new instrumentation also promises to be a powerful new tool for advancing development of a variety of nanoparticle types.

Particle Manipulation/Directed Assembly

As an alternative to the polymer-based SERS film synthesis, we also pursued the use of directed assembly of nanoparticles into patterned wells as an approach to defining particle interaction geometries. These two converging approaches enabled us to generate metal nanostructures on a surface with varying degrees of complexity. The idea is to first generate lithographically patterned wells of specific geometries. Once the wells have been generated, the plasmonic nanoparticles of interest would be drawn into the wells. Interaction geometries would be defined by the well shapes and sizes.

Significant challenges had to be overcome to pursue this directed-assembly route. The first hurdle was to do a complete overhaul of the electron-beam patterning instrument. The instrument was made fully operational by the end of the first year. A first generation of patterned arrays were then generated with the e-beam lithography to create the desired patterns in polymer thin films. It was hoped the polymer films would be suitable as substrates, since they would allow rapid prototyping of our arrays. However, these films were found to be unstable to the nanoparticle solutions. Once a pattern was exposed to the nanoparticle solutions, many particles would irreversibly stick to the surface, making these patterns only usable for one particle deposition. To get around this limitation, we began transferring the pattern to a silicon/silicon oxide substrate via reactive ion etching. This resulted in robust patterns of silicon oxide that could be reused for different nanoparticle preparations simply by washing the bound particles with strong acids. Examples of patterned surfaces are shown in Figure 4.
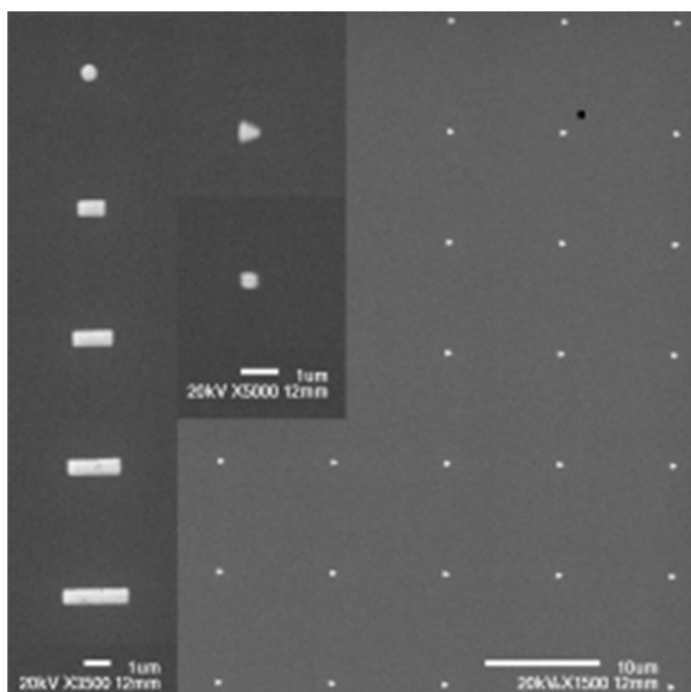
Figure 4. SEM image of various lithographically patterned well types on Si/SiO$_2$ substrate.

The final and most difficult hurdle for this project was determining a protocol for depositing the plasmonic nanoparticles onto the patterned surfaces. We initially attempted spin coating and dip coating, however, the relatively hydrophobic nature of the surface resulted in highly aggregated particles that were deposited as the solvent (water) evaporated. These aggregates did not follow the fabricated patterns on the surface. The next approach involved a custom device that would draw a blade over the patterned surface at a predefined height above the surface. When the particle solution is placed on the surface, the blade compresses the solution droplet. As the blade is drawn across the surface, the resulting meniscus is drawn out across the patterned surface and the particles get trapped in the patterns. The drawing speed, height of the blade, concentration of the particle solution, and hydrophobicity of the surface were all found to affect the resulting deposition. With proper tuning, this approach was found to work marginally well. We were able to trap particles at the surface, which reasonably followed the patterned surfaces. However, not all of the patterns were filled, and not all of the filled patterns were filled with identical nanoparticle aggregates (Figure 5). Refinements to this technique were being explored at the end of FY11, with only nominal improvements to the pattern fill rate. No SERS microscopy was performed on these patterned samples; with the observed fill rates, we expect the Raman signals to resemble metal dimer and trimer spectra that have been reported previously.
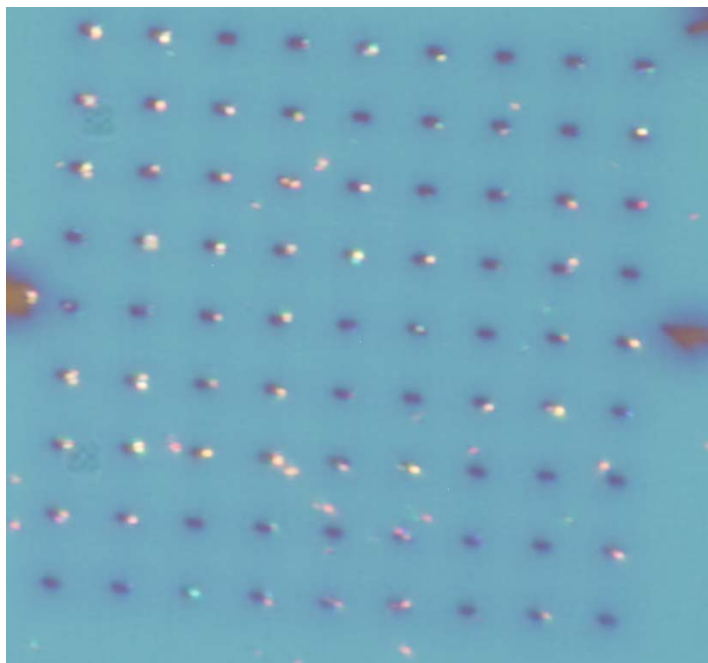
Figure 5. Polarized light micrograph of Ag nanoparticles on a patterned silicon surface.

Overall, this aspect of the project had limited SERS results. It has, however, significantly increased the fabrication capabilities at LANL. The techniques utilized for particle patterning have been demonstrated to work extremely well for micron sized particles, yet when scaled down to the nanometer regime, the deposition rules begin to break down. Most likely this is due to stabilization forces (primarily electrostatic) on the colloids tending to repel the particles from the patterned surface. In fact, much of the chemistry used to synthesize the particles is intended to keep the particles in solution in the most stable manner possible. For FY11, we were able to explore several aspects of tailored surface patterned nanoaggregates, however, the spontaneous synthesis of Ag aggregates (Figure 3) was found to be much more effective at generating usable SERS signals.

Impact on National Missions

Our goal was to address DOE's need for development of advanced functional nanomaterials. DOE is also interested in materials that function at the nano-bio interface. Our plasmonic bandgap materials were targeted at ultimately being functionalized to interact with bioanalytes at the nanoscale. These materials also could have applications relevant to mission areas in other government agencies. While ultimately we were unable to produce the targeted materials within the project, we were successful at building a number of new capabilities that will be important for advancing LANL missions. These include:

We have developed a mature capability for both plasmonic and magnetic nanoparticle synthesis. This includes generation of SERS spectral tags that may be used for multiplexed bioanalysis. This capability is also being extended into applications of interest to NN20 as authentication tags for securing strategic materials . Our magnetic nanoparticles also served as a basis for development of a magnetic carbon nanotube hybrid material. The need to evaluate SERS properties of our materials at the micron scale served to further strengthen LANL's capabilities in Raman microscopy and spectral imaging. Multi-parameter spectroscopic flow-based particle analysis arising from these efforts promises to be a powerful new tool for rapid characterization and feedback for enhancing particle synthesis. Acquisition of a spatial light modulator for 3-D particle trapping will strengthen efforts aimed at building complex composite assemblies of nanomaterials within the Center for Integrated Nanotechnologies (CINT, a DOE BES funded nanoscience research center). New lithographic patterning capability was also built within Chemistry division. Finally, as highlighted above, our polymer-based SERS substrate development is proving quite successful and is forming the basis for new external sponsorship of sensing technologies. These substrates are also enabling new work at CINT aimed at understanding plasmonic interactions with excitons and how plasmons can be use to drive new photophysical behaviors in quantum dots and carbon nanotubes.

References

1. Li, X., J. D. thompson, Y. Zhang, C. I. Brady, G. Zou, N. H. Mack, D. Williams, J. G. Duque, Q. Jia, and S. K. Doorn. Efficient syntehsis of tailored magnetic carbon nanotubes via a noncovalent chemical route. 2011. *Nano-*

scale. **3**: 668.

2. Brady, C. I., N. H. Mack, L. O. Brown, and S. K. Doorn. Self-assembly approach to multiplexed surface-enhanced Raman spectral-encoder beads. 2009. *Analytical Chemistry.* **81** (17): 71817188.

3. Xu, P., N. H. Mack, S. H. Jeon, S. K. Doorn, X. Han, and H. L. Wang. Facile fabrication of homogeneous 3D silver nanostructures on gold-supported polyaniline membranes as promising SERS substrates. 2010. *Langmuir.* **26** (11): 8882.

4. Xu, P., S. H. Jeon, N. H. Mack, S. K. Doorn, D. J. Williams, X. Han, and H. L. Wang. Field-assisted synthesis of SERS-active silver nanoparticles using conducting polymers. 2010. *Nanoscale.* **2**: 1436.

5. Xu, P., B. Zhang, N. H. Mack, S. K. Doorn, X. Han, and H. L. Wang. Synthesis of homogeneous silver nanosheet assemblies for surface enhanced Raman scattering applications. 2010. *Journal of Materials Chemistry.* **20**: 7222.

6. Mack, N. H., J. A. Bailey, S. K. Doorn, C. A. Chen, H. M. Gau, P. Xu, D. J. Williams, E. A. Akhadov, and H. L. Wang. Mechanistic study of silver nanoparticle formation on conducting polymer surfaces. 2011. *Langmuir.* **27**: 497.

7. Goddard, G., L. O. Brown, R. Habbersett, C. I. Brady, J. C. Martin, S. W. Graves, J. P. Freyer, and S. K. Doorn. High-resolution spectral analysis of individual SERS-active nanoparticles in flow. 2010. *Journal of the American Chemical Society.* **132**: 6081.

Publications

Brady, C. I., N. H. Mack, L. O. Brown, and S. K. Doorn. Self-assembly approach to multiplexed SERS encoder beads. 2009. *Analytical Chemistry.* **81**: 7181.

Goddard, G., L. Brown, R. Habbersett, C. Brady, J. Martin, S. Graves, J. Freyer, and S. Doorn. High-resolution spectral analysis of individual sers-active nanoparticles in flow. 2010. *Journal of the American Chemical Society.* **132** (17): 6081.

Li, X., J. D. Thompson, Y. Zhang, C. I. Brady, G. Zou, N. H. Mack, D. Williams, J. G. Duque, Q. Jia, and S. K. Doorn. Efficient synthesis of tailored magnetic carbon nanotubes via a noncovalent chemical route. 2011. *Nanoscale.* **3**: 668.

Mack, N. H., J. A. Bailey, S. K. Doorn, C. A. Chen, H. M. Gau, P. Xu, D. J. Williams, E. A. Akhadov, and H. L. Wang. Mechanistic study of silver nanoparticle formation on conducting polymer surfaces. 2011. *Langmuir.* **27**: 4979.

Xu, P., B. Zhang, N. MacK, S. Doorn, X. Han, and H. Wang. Synthesis of homogeneous silver nanosheet assemblies for surface enhanced Raman scattering applications. 2010. *Journal of Materials Chemistry.* **20** (34): 7222.

Xu, P., N. Mack, S. Jeon, S. Doorn, X. Han, and H. Wang. Facile Fabrication of Homogeneous 3D Silver Nanostructures on Gold-Supported Polyaniline Membranes as Promising SERS Substrates. 2010. *LANGMUIR.* **26** (11): 8882.

Xu, P., S. Jeon, N. MacK, S. Doorn, D. Williams, X. Han, and H. Wang. Field-assisted synthesis of SERS-active silver nanoparticles using conducting polymers. 2010. *Nanoscale.* **2** (8): 1436.

Probing the Origin and Consequences of Quantum Critical Fluctuations

Tuson Park
20090335ER

Abstract

The melting of ice as it is warmed is a well-known phase transition, in this case from a solid to a liquid. Transitions such as this are driven by a change in temperature and their physics is well understood. A very different type of phase transition is possible at absolute zero temperature. Because there can be no change in temperature to drive the transition, the melting of an ordered phase (analogous to ice) into a disordered phase (analogous to liquid water) is driven by principles of quantum mechanics. Though seemingly irrelevant to everyday life, these so-called quantum-phase transitions pose fundamental questions about how we understand matter and, more importantly by answering these questions, have the potential to increase significantly the rate at which energy technologies develop. The goal of this project has been to understand more fully the nature and consequences of quantum-phase transitions. Using experimental techniques unique to Los Alamos, we have discovered unexpected relationships between quantum-phase transitions and superconductivity as well as new superconductors and a new state of matter. These accomplishments respond directly to the national need to discover and understand how collective states of matter emerge from complex correlations among electrons, one of five grand challenges identified by the Department of Energy, Office of Basic Energy Sciences and a core theme of the Laboratory's materials strategy.

Background and Research Objectives

The solid to liquid transition that takes place when a material is heated arises because thermal energy supplied by the increase in temperature causes atoms in the solid to fluctuate so significantly that it becomes energetically favorable for the atoms to randomize their position in space. This example of a classical phase transition from ordered to disordered states is analogous to what happens when the temperature of a magnetic material is raised above its ordering temperature. In this case, thermal energy does not disrupt the periodic arrangement of atoms. Instead, increasing temperature causes the periodic arrangement of magnetic moments, or equivalently the periodic orientation of electron spins, to melt and become randomly oriented. These classical phase transitions are very well understood, and we know that fluctuations of the spin arrangement affect physical properties of the material only in a very narrow temperature region around the critical phase-transition temperature [1].

It also is possible for the spin arrangement in a magnetic material to melt at absolute zero temperature (T=0). In this case there is no thermal energy to induce magnetic melting. The phase boundary between magnetically ordered and magnetically disordered states in this case must be accessed by some non-thermal control parameter, such as applied pressure, magnetic field or chemical substitution, as illustrated in Figure 1. When the control parameter is adjusted toward its critical value where the magnetic-non-magnetic transition occurs, quantum-mechanically driven fluctuations become increasingly important in controlling physical properties of the material. Likewise, at the critical value of the control parameter (the quantum-critical point), decreasing temperature toward T=0 causes quantum properties of the magnetism to become increasing dominant [2]. The fundamental physical principle underlying the quantum nature of this type of T=0 phase transition is Heisenberg's uncertainty principle which states that, if we know the energy E and momentum q of the magnetic configuration to high accuracy ΔE and Δq, then the time and position of the state cannot be determined with accuracy better than $\Delta t = \hbar / \Delta E$ and $\Delta x = \hbar / \Delta q$, where $\hbar$ is Planck's constant. Consequently, at the T=0 quantum-phase transition Δt and Δx become very large and fluctuations of the magnetic state are long-lived and long-ranged.

By definition, the presence of long-ranged, long-lived fluctuations with no long range order implies the presence of a huge amount of entropy at low temperatures, and this is reflected in part by a corresponding divergence of specific heat (and an anomalous temperature dependence of other physical properties) as temperature decreases toward T=0. Remarkably, the fluctuations from this T=0 transition influence materials properties over a broad temperature range, well above T=0, which is distinctly different from the limited influence

of fluctuations near a classical phase transition. A further consequence of this huge entropy is that the system may remove part of it, and thus save energy, by undergoing another phase transition to some other long-range ordered state, possibly a new type of magnetic order, superconductivity or even an entirely new type of order. Which, if any, of these possible outcomes are realized depends on the nature of the quantum-critical state and associated spectrum of quantum fluctuations. Currently, there are two general classes of theories of quantum criticality. The conventional model is a quantum extension of the well-established theory of classical phase transitions [3]. In this model, only quantum fluctuations of the near-by magnetic order are relevant and this gives the fluctuations a particular momentum (q) dependence and, hence, a particular anisotropy in real space. More recently, several models of unconventional quantum criticality have appeared, with the common feature that they are local in nature [4]; that is, they have no momentum dependence (no real space anisotropy) and allow for quantum fluctuations of magnetic as well as electronic states of the material.

Certain classes of lanthanide (4f-electron) and actinide (5f-electron) materials have emerged as prototypes for discovering and exploring magnetic quantum-phase transitions, though evidence for quantum criticality has been found in a few transition-metal (3d-electron) materials [2]. A common feature of all these materials is that they host strong electron-electron correlations. The complexity inherent to such strong correlations makes the ordered states that they host particularly sensitive to small perturbation, and consequently, those ordered states can be tuned to a T=0 ordered-disorder transition with relatively modest pressure, magnetic field or chemical composition. Because of the strong influence of quantum fluctuations near their T=0 transition, conventional descriptions of the behavior of electrons breakdown, demanding entirely new conceptual frameworks. Despite over a decade of experimental and theoretical study, there still is no consensus on what that description should be. Nevertheless, one of the most intriguing experimental observations is that superconductivity in these strongly correlated electron materials appears almost exclusively at or near a magnetic quantum-phase transition [5]. This striking fact has led to speculation that quantum fluctuations of the magnetic order are responsible for producing the attractive interaction between electron pairs that results in superconductivity. The possibility that quantum fluctuations of magnetic order mediate superconductivity is in stark contrast to the well-established conventional theory of superconductivity in which thermally-driven fluctuations of the crystal lattice provide the attractive interaction. Whereas, the conventional mechanism of superconductivity appears to limit the maximum temperature to which superconductivity survives to of order 50 K or so, there is, so far, no apparent limit to the maximum superconducting temperature in materials where fluctuations of magnetic order create electron pairs [6]. Though the highest magnetically-mediated supercon-

ducting transition temperature T_c is about 180K, the apparent lack of an upper bound for T_c with this mechanism has strong scientific and energy-security implications.

With these opportunities in mind, we have had the goal of exploring the origin and consequence of quantum-critical fluctuations, particularly in regard to their relationship to superconductivity.
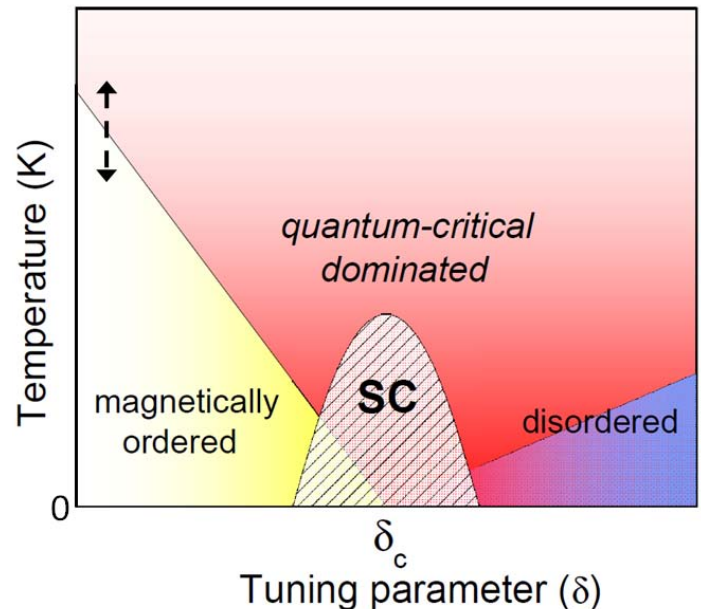
Figure 1. Schematic temperature versus tuning parameter phase diagram for a magnetic system. Crossing the magnetic phase boundary by increasing or decreasing temperature (dashed arrow) defines a classical phase transition. A quantum-critical transition between magnetically ordered and magnetically disordered states occurs at zero temperature at a critical value of the tuning parameter where the magnetic boundary reaches T=0. Fluctuations emanating from the quantum-critical point control physical properties of the material over a broad temperature range above T=0 and may be responsible for inducing a dome of superconductivity (SC) in strongly correlated electron materials. When superconductivity is present, it hides the quantum-critical point, which can be revealed in high magnetic fields.

Scientific Approach and Accomplishments

Anisotropy in physical properties, such as the electrical resistivity and specific heat, provide critical insights into the nature of the quantum-critical state as well as into the nature of possible superconductivity that appears from it. To this end, we have developed and applied a unique technique that is based on a vector-magnet in which the applied magnetic field can be rotated in any direction with respect to the axes of a crystal. This special magnet accommodates a ^{3}He refrigerator with base temperature of 0.30 K and simultaneously a pressure clamp that generates hydrostatic pressures to 3 GPa. We have used these capabilities to study strongly correlated 4f- and 3d-electron

systems that are tuned to a quantum-phase transition by applied pressure, magnetic field or chemical substitutions. The materials selected for study were chosen to display a necessary variety of possible outcomes. Three were very pure crystals of 4f-electron materials $CeRhIn_5$ (cerium-rhodium-indium5), $CePt_2In_7$ (cerium-platinum2-indium7) and $CeIrIn_5$(cerium-iridium-indium5), where the first two might exhibit unconventional quantum criticality and the third possible conventional criticality. Other materials included Cd-doped $CeCoIn_5$ (cadmium-doped cerium-colbalt-indium5), to study the effects of disorder, and a new family of 3d-electron compounds $CaFe_2As_2$ (calcium-iron2-arsenic2) and chemically doped $BaFe_2As_2$ (barium-iron2-asenic2). As discussed below, applied pressure or chemical doping induces unconventional superconductivity. On an absolute scale, the superconducting transition temperature of these systems is not high, but relative to the characteristic energy scale of electrons that form the superconducting state, theses T_c's are as high as the highest T_c's known.

An expected hallmark of unconventional criticality is a lack of anisotropy in electrical resistance and a sub-linear temperature dependence of the resistivity. We found these hallmarks in $CeRhIn_5$ at its pressure-tuned quantum-critical point P2 [7]. At atmospheric pressure, the moments of Ce's localized 4f-electrons order antiferromagnetically. With increasing pressure, the magnetic ordering temperature T_N initially increases and above 1GPa begins to decrease toward T=0 at an extrapolated critical pressure P2=2.35 GPa. Before reaching this critical pressure, superconductivity develops, first coexisting with magnetic order for P<1.75 GPa and then reaching a maximum T_c at P2. This pressure-induced superconductivity hides the QCP that is revealed in a magnetic field sufficient to completely suppress the superconductivity. Measurements of the specific heat C in the superconducting state as a magnetic field was rotated relative to crystal axes provided detailed information about the symmetry of the paired superconducting electrons. Our measurements found a four-fold oscillation of C that indicates an unconventional form of superconductivity, specifically one with $d_{x^2-y^2}$ symmetry [8]. The lack of electrical anisotropy, a sub-linear temperature dependence of resistivity and a strongly enhanced scattering rate of electrons at P2 implied that fluctuations from this unconventional quantum-critical transition are responsible for inducing unconventional superconductivity. Though theory has suggested that fluctuations from a conventional quantum-critical transition might produce unconventional electron pairs, our discovery was the first to show that fluctuations from an unconventional, local-type of quantum critically also could induce superconductivity very effectively. Further, our discovery of pressure-induced unconventional quantum criticality and unconventional superconductivity in $CePt_2In_7$ showed that $CeRhIn_5$ was not unique, a crucial step in establishing the generality of our conclusions [9].

In the pressure range below P1, where antiferromagnetic order and unconventional superconductivity coexist, we found that the T_c measured by electrical resistance was always higher than that measured by specific heat. This difference disappeared once magnetic order disappeared above P1 (in zero magnetic field). From measurements of anisotropy in the electrically measured T_c, we discovered the superconductivity was 'textured' , that is, developed a new symmetry different from that of the underlying crystal structure [10]. We further showed that this new state of matter appears to be a general consequence of coexisting orders in strongly correlated electron superconductors, a conclusion with broad and significant implications for designing new superconductors for energy applications.

At atmospheric pressure, $CeCoIn_5$ is quantum critical, with all of its properties consistent with a conventional type of criticality. Unconventional ($d_{x^2-y^2}$) superconductivity develops directly out of this critical state, but replacing a very small number of In atoms with Cd induces coexisting antiferromagnetic order, and with slightly more Cd, there is only antiferromagnetism. Compared to $CeRhIn_5$ under pressure, Cd-substitution acts in many respects as an effective negative pressure. Indeed, adding positive pressure to Cd-doped $CeCoIn_5$ antiferromagnetic samples induces superconductivity and appears to just reverse the effects of Cd substitutions. Surprisingly, though, we discovered that under these pressure conditions Cd-doped $CeCoIn_5$ does not recover the quantum-critical state of pure $CeCoIn_5$. Instead, the Cd atoms nucleate short-range antiferromagnetic order by 'stealing' entropy from the spectrum of quantum fluctuations [11]. An effect such as this also may be the clue for resolving a controversy over the relationship between quantum criticality and high-T_c superconductivity in copper-oxide materials because chemical disorder is necessary for their superconductivity.

The relationship among magnetism, quantum criticality and superconductivity in $CeIrIn_5$ has been controversial. Our field-angle specific heat measurements on $CeIrIn_5$ at high pressures showed that even at high pressures the superconductivity was unconventional, with $d_{x^2-y^2}$ symmetry [12]. Though there is no long-ranged magnetic order coexisting with this unconventional superconductivity, there is a pronounced difference between T_c measured by resistivity and specific heat, just as in $CeRhIn_5$ at P<P1. From independent measurements, we concluded that this difference arises from the coexistence of some form of 'hidden order' that coexists with superconductivity. This hidden order appears to be similar in nature to the so-called pseudogap state in the high-T_c copper oxide superconductors, and quantum fluctuations from it may play a role in producing superconductivity.

In another class of correlated electron materials, those based on the 3d-electron element iron, we discovered superconductivity in $CaFe_2As_2$ as its antiferromagnetic and structural transitions were tuned toward T=0 by applied pressure [13]. Though more complex than the 4f-electron systems discussed above, these studies, including nuclear

magnetic resonance measurements under pressure [14], are consistent with magnetic fluctuations in a phase of coexisting structures being important for superconductivity. The complication of a pressure-dependent structural change, however, made it impossible to determine the nature of the quantum-critical state in this material. Besides pressure, chemically doping the related compound $BaFe_2As_2$ also suppresses magnetic and structural transitions toward T=0 where superconductivity emerges. In a collaboration, we used time-resolved optical spectroscopy to reveal a precursor state to superconductivity [15], analogous to that found in $CeIrIn_5$, and further we showed from specific heat studies that the symmetry of superconducting electrons was unconventional [16].

Collectively, accomplishments in this project have revealed new and unexpected relationships between quantum-critical fluctuations and unconventional superconductivity in classes of complex materials as well as the emergence of new states of matter in proximity to a quantum-phase transition. These discoveries define a new framework for understanding how collective states of matter emerge from complex correlations among electrons.

Impact on National Missions
Besides making progress toward one of DOE's five grand challenges for science and the imagination, we have identified essential interactions, namely quantum fluctuations, as important for high temperature superconductivity, a DOE basic research need. Beyond critical new knowledge, these insights define a path forward to designing new materials with emergent properties that will enable technologies needed to ensure the energy security of the nation.

References

1. Wilson, K. G., and J. Kogut. Renormalization group and the epsiv expansion. 1974. *Physics Reports.* **12c**: 75.

2. vonLohneysen, H., A. Rosch, M. Vojta, and P. Wolfle. Fermi-liquid instabilities at magnetic quantum phase transitions. 2007. *Reviews of Modern Physics.* **79**: 1015.

3. Hertz, J. A.. Quantum critical phenomena. 1976. *Physical Review B.* **14**: 1165.

4. Si, Q., S. Rabello, K. Ingersent, and J. L. Smith. Locally critical quantum phase transitions in strongly correlated metals. 2001. *Nature.* **413**: 804.

5. Gegenwart, P., Q. Si, and F. Steglich. Quantum criticality in heavy-fermion metals. 2008. *Nature Physics.* **4**: 186.

6. Moriya, T., and K. Ueda. Antiferromagnetic spin fluctuation and superconductivity. 2003. *Reports on Progress in Physics.* **66**: 1299.

7. Park, T., V. A. Sidorov, H. Lee, F. Ronning, E. D. Bauer, J. L. Sarrao, and J. D. Thompson. Unconventional quantum criticality in the pressure-induced heavy-fermion superconductor CeRhIn5. 2011. *Journal of Physics: Condensed Matter.* **23**: 094218.

8. Park, T., and J. D. Thompson. Magnetism and superconductivity in strongly correlated CeRhIn5. 2009. *New Journal of Physics.* **11**: 055062.

9. Bauer, E. B., H. O. Lee, V. A. Sidorov, N. Kurita, K. Gofryk, J. X Zhu, F. Ronning, M. Movshovich, J. D. Thompson, and T. Park. Pressure-induced superconducting state and effective mass enhancement near the antiferromagnetic quantum critical point in CePt2In7. 2010. *Physical Review B.* **81**: 180507.

10. Park, T., H. O. Lee, I. Martin, X. Lu, V. A. Sidorov, F. Ronning, E. D. Bauer, and J. D. Thompson. Textured superconducting state in the heavy fermion CeRhIn5. *Physical Review Letters.*

11. Seo, S., X. Lu, T. Park, L. D. Pham, E. D. Bauer, Z. Fisk, and J. D. Thompson. Avoided quantum criticality in the slightly Cd-doped quantum critical metal CeCoIn5. *Physical Review Letters.*

12. Lu, X., H. O. Lee, T. Park, F. Ronning, E. D. Bauer, and J. D. Thompson. Probing gap nodes of the heavy-fermion superconductor CeIrIn5 deep inside its pressure-dependent superconducting dome. *Physical Review Letters.*

13. Lee, H. O., E. Park, T. Park, V. A. Sidorov, F. Ronning, E. D. Bauer, and J. D. Thompson. Pressure-induced superconducting state of antiferromagnetic CaFe2A2. 2009. *Physical Review B.* **80**: 024519.

14. Baek, S. H., H. O. Lee, S. E. Brown, N. J. Curro, E. D. Bauer, F. Ronning, T. Park, and J. D. Thompson. NMR investigation of superconductivity and antiferromagnetism in CaFe2As2 under pressure. 2009. *Physical Review Letters.* **102**: 227601.

15. Chia, E. E. M., D. Talbayev, J. X. Zhu, H. Q. Yuan, T. Park, J. D. Thompson, C. Panagopoulos, G. F. Chen, J. L. Luo, N. L. Wang, and A. J. Taylor. Ultrafast pump-probe study of phase separation and competing orders in the underdoped (Ba,K)Fe2As2 superconductor. 2010. *Physical Review Letters.* **104**: 027003.

16. Jang, D. J., A. B. Voronstov, I. Vekhter, K. Gofryk, Z. Yang, S. Ju, J. B. Hong, J. H. Han, Y. S. Kwon, F. Ronning, J. D. Thompson, and T. Park. Calorimetric evidence for nodes in the overdoped BaFe1.8Co.2As2. 2011. *New Journal of Physics.* **13**: 023036.

Publications

Baek, S. H., H. Lee, S. E. Brown, N. J. Curro, E. D. Bauer, F. Ronning, T. Park, and J. D. Thompson. NMR investigation of superconductivity and antiferromagnetism in

CaFe2As2 under pressure. 2009. *Physical Review Letters.* **104**: 227601.

Bauer, E. D., H. O. Lee, V. A. Sidorov, N. Kurita, K. Gofryk, J. X. Zhu, F. Ronning, R. Movshovich, J. D. Thompson, and T. Park. Pressure-induced superconducting state and effective mass enhancement near the antiferromagnetic quantum critical point of CePt2In7. 2010. *Physical Review B.* **81**: 1805071.

Bauer, E. D., T. Park, R. D. McDonald, M. J. Graf, L. N. Boulaevskii, J. N. Mitchell, J. D. Thompson, and J. L. Sarrao. Possible two-band superconductivity in PuRhGa5 and CeRhIn5. 2009. *Journal of Alloys and Compunds.* **488**: 554.

Chia, E. E., D. Talbayev, J. X. Zhu, H. Q. Yuan, T. Park, J. D. Thompson, C. Panagopoulos, G. F. Chen, J. L. Luo, N. L. Wang, and A. J. Taylor. Ultrafast pump-probe study of phase separation and competing orders in the underdoped (Ba, K)Fe2As2 superconductor. 2010. *Physical Review Letters.* **104**: 027003.

Jang, D. J., A. B. Voronstov, I. Vekhter, K. Gofryk, Z. Yang, S. Ju, J. B. Hong, J. H. Han, Y. S. Kwon, F. Ronning, J. D. Thompson, and T. Park. Calorimetric evidence for nodes in the overdoped BaFe1.8Co.2As2. 2011. *New Journal of Physics.* **13**: 023036.

Lee, H. O., E. Park, T. Park, V. A. Sidorov, F. Ronning, E. D. Bauer, and J. D. Thompson. Pressure-Induced Superconducting State of Antiferromagnetic CaFe2As2. 2009. *Physical Review B.* **80**: 024519.

Lu, X., H. O. Lee, T. Park, F. Ronning, E. D. Bauer, and J. D. Thompson. Probing gap nodes of the heavy-fermion superconductor CeIrIn5 deep inside its pressure-dependent superconducting dome. *Physical Review Letters.*

Park, T., H. O. Lee, I. Martin, X. Lu, V. A. Sidorov, F. Ronning, E. D. Bauer, and J. D. Thompson. Textured superconducting state in the heavy fermion CeRhIn5. *Physical Review Letters.*

Park, T., V. A. Sidorov, H. Lee, F. Ronning, E. D. Bauer, J. L. Sarrao, and J. D. Thompson. Unconventional quantum criticality in the pressure-induced heavy-fermion superconductor CeRhIn5. 2011. *Journal of Physics: Condensed Matter.* **23**: 094218.

Park, T., Y. Tokiwa, F. Ronning, H. Lee, E. D. Bauer, R. Movshovich, and J. D. Thompson. Field-induced quantum critical point in the pressure-induced superconductor CeRhIn5. 2010. *Physica Status Solidi.* **247**: 553.

Park, T., and J. D. Thompson. Magnetism and Superconductivity in Strongly Correlated CeRhIn5. 2009. *New Journal of Physics.* **11**: 055062.

Ronning, F., E. D. Bauer, T. Park, N. Kurita, T. Klimczuk, R. Movshovich, A. S. Sefat, D. Mandrus, and J. D. Thompson. Ni2X2 (X=pnictide, chalcogenide, or B) based superconductors. 2009. *Physica C.* **469**: 396.

Ronning, F., E. D. Bauer, T. Park, S. H. Baek, H. Sakai, and J. D. Thompson. Superconductivity and the effects of pressure and structure in single-crystalline SrNi2P2. 2009. *Physical Review B.* **79**: 134507.

Seo, S., X. Lu, T. Park, L. D. Pham, E. D. Bauer, Z. Fisk, and J. D. Thompson. Avoided quantum criticality in the slightly Cd-doped quantum critical metal CeCoIn5. *Physical Review Letters.*

Sidorov, V. A., P. H. Tobash, C. Wang, B. L. Scott, T. Park, E. D. Bauer, F. Ronning, J. D. Thompson, and Z. Fisk. Quenching of ferromagnetism in beta-UB2C and UNiSi2 at high pressure. 2011. *Journal of Physics: Conference Series.* **273**: 012014.

Linear Scaling Quantum-Based Interatomic Potentials for Energetic Materials

Marc J. Cawkwell
20090369ER

Abstract

Complex series of chemical reactions driven by extreme conditions are difficult to resolve experimentally. We have developed theoretical and computational methods and the supporting code 'LATTE' to provide LANL with the capability to resolve and predict reactions in organic materials over very short time scales using molecular dynamics (MD) simulations. We have implemented a semi-empirical description of interatomic bonding that is computationally tractable and which maintains the accuracy of fully quantum mechanical methods. Large-scale, long duration MD simulations require interatomic forces to be computed rapidly, preferably with a computational cost that scales linearly, O(N), with the number of atoms, N. We have developed and implemented a number of advanced algorithms that enable the rapid computation of high quality, quantum-derived forces. Heterogeneous computational architectures based on graphics processing units (GPUs) were utilized to accelerate force computations. The performance of LATTE on a single GPU was shown to exceed that measured on multiple central processing unit (CPU) cores with highly optimized codes. We have also accomplished the O(N) scaling of the force calculations using sparse matrix algebra with a numerical threshold on matrix elements. The use of the extended Lagrangian Born-Oppenheimer MD formalism eliminated the systematic drift in the total energy seen in many quantum-based MD methods and allowed us to capture accurately the effects of endo and exothermic chemistry during reactions. A number of challenging simulations of shock-induced chemistry were performed using LATTE with an accurate and transferable model that was developed for hydrocarbons. The new capabilities for theory, simulation, and hybrid computation that the development of LATTE have granted LANL have led to major new research efforts supported by the LDRD program at LANL as well as the DOE-BES.

Background and Research Objectives

The making and breaking of individual chemical bonds occurs at the atomic scale over extremely short time intervals. Thus, if a complex series of chemical reactions are driven rapidly by a violent stimulus, during, for example, the detonation of an energetic material, the sequence of events becomes extremely difficult to resolve by experiment alone. The intermediate stages through which complex reactions pass, noting that there are often many potential routes between products and reactants, are critical to understanding many aspects of the overall outcome of the process [1]. As a result, computer simulations of chemical reactions are being used increasingly to resolve and predict reaction pathways since simulations access naturally the pertinent spatial and temporal scales [2, 3].

Molecular dynamics (MD) simulations involve computing trajectories for ensembles of atoms by moving each atom according to the force acting on it incrementally over a large number of time steps, _t [4]. These forces are derived from an interatomic potential that gives the energy of the system as a function of the relative positions of all of the atoms. The ability of a MD simulation to capture with high fidelity the system of interest is determined almost entirely by the physical accuracy of the interatomic potential. The development of better, more efficient interatomic potentials for organic materials formed the central thrust of this project.

Interatomic potentials form a hierarchy in terms of their physical accuracy and the speed at which forces can be computed. Ideally, potentials that describe very accurately the details of interatomic bonding in complex materials would also enable forces to be computed rapidly such that long duration simulations with large numbers of atoms could be tackled. Unfortunately, a trade-off must always be made between accuracy and the size of the simulation. Fully quantum mechanical formalisms such as Hartree-Fock or density functional theory [5] set the gold standard in terms of accuracy, but these methods are computationally very expensive and hence not suited to large-scale simulations. Furthermore, the computational cost scales as the cube, $O(N^3)$, of the number of atoms, N, such that around ten times more computing power is required when the number of atoms doubles [6]. On the other hand, empirical potentials enable very large simulations since they are computationally cheap, exhibit an ideal linear scaling, O(N), and are well suited

to implementation on parallel supercomputers [7]. However, these methods are based on simple functional forms that are fitted to reproduce the results of experiments or quantum mechanical calculations. As a result, their accuracy is often limited outside of the scope of the data that was employed in their construction [5].

The approach taken in this project to modeling organic materials exploits the middle ground between these two extremes. We have pursued a semi-empirical description of bonding that is derived from density functional theory where we maintain the predictive capabilities associated with quantum mechanics but approximate and parameterize a number of hard-to-calculate terms [5, 8]. Approaches of this type have been shown to be around 1000 times faster than fully quantum mechanical models.

We focused our work on interatomic potentials based on the self-consistent tight-binding approximation [8]. This is the simplest explicitly quantum mechanical scheme that captures all of the most important interactions in organic materials: the making and breaking of covalent bonds, the transfer of charge between species of differing electronegativity, long-range electrostatics, and weak van der Waals interactions. Our aim was to turn this method into a practical tool for large-scale MD simulations by implementing it in a code using state-of-the-art algorithms and computational methods to overcome well-known bottlenecks and to achieve O(N) scaling. These aims were met and greatly exceeded over the duration of the project.

The principle deliverable of this project is the MD code 'LATTE' (Los Alamos Transferable Tight-binding for Energetics) [9]. This code has been made publically available under the Gnu Public License. The scope of the theoretical and computational work increased over the project to encompass the extended Lagrangian Born-Oppenheimer MD formalism that enables a precise conservation of the total energy [10, 11], the development of a simple scheme to mimic in periodic systems the effects of shock compression, the utilization of hybrid computational architectures, in particular graphics processing units (GPUs) [12], and the first example of O(N), energy conserving Born-Oppenheimer MD [13]. We also developed parameterizations for organic materials that were employed in realistic simulations of shock-induced chemistry [14].

Scientific Approach and Accomplishments
Accurate and transferable quantum-based MD employing interatomic potentials based on the self-consistent tight-binding formalism [8] have been implemented in the code LATTE [9]. This code was written from scratch over the duration of the project and has been released to the scientific community. This code serves not only as our workhorse to produce meaningful MD simulations of chemical reactions under extreme conditions, but also as a test bed for the development of new theoretical and computational tools for quantum-based MD.

Self-consistent tight-binding requires the solution of the Schrödinger equation for the density matrix with a parameterized Hamiltonian that depends on both charge transfer and the overlap between valence orbitals centered on each atom [5]. The total energy and forces can be computed rapidly once the density matrix is known, but the computation of the latter is by far the most time-consuming step in the simulation. The density matrix is typically computed by the diagonalization of the Hamiltonian matrix. This complex algorithm has undesirable $O(N^3)$ scaling and is difficult to parallelize [6, 13]. We have implemented in a LATTE a number alternative methods that are very much simpler and well-suited to acceleration via parallelism or implementation in a O(N) scheme.

The optimal scheme for calculating the density matrix was found to be the second-order spectral projection purification (SP2) algorithm [13-15]. This is based on an expansion in a recursive series of matrix-matrix multiplications. The multiplication of two matrices is an $O(N^3)$ task, but it is simplicity makes it an obvious target for optimization. One of our most notable successes, and one which has provided us with an entirely new capability, is the use of GPUs and heterogeneous computing to accelerate this step [12].

Modern general purpose GPUs offer exceptional levels of raw performance, which is amplified further when normalized by their cost and power consumption. These aspects have made them extremely attractive for use in next-generation supercomputers. However, algorithms must be rewritten to run on the new architecture. We have ported the entire SP2 algorithm from the central processing unit (CPU) to GPUs using Nvidia's CUDA language [12]. It was necessary to pursue the revolutionary approach of porting the whole algorithm rather than the evolutionary approach of calling kernels on the GPU from the CPU in order to minimize the data transfer between the two devices. We present in Figure 1 a comparison between the wall clock times required to compute the density matrix on a single GPU to that for a parallel CPU implementation running on 12 cores with highly optimized mathematics libraries. Here it is evident that the performance of the SP2 algorithm on GPUs far exceeds those measured on the CPU. These results emphasize the importance of tailoring algorithms to hardware to extract the maximum levels of performance from both.

The use of GPUs is particularly attractive when a significant fraction of the elements in the density matrix are non-zero. However, this dense matrix algebra approach leads unavoidably to undesirable $O(N^3)$ scaling of the computational cost. We have successfully implemented another approach that takes advantage of those density matrices that have a large fraction of their elements equal to zero [13]. This sparse matrix approach, where only the non-zero elements are stored and operated upon, yields an O(N) scaling of the computational time since the number of non-zero elements is proportional to N [6]. We have

taken this approach a step further where we enforce high levels of sparsity by discarding elements from the density matrix whose absolute value is smaller than a user-defined threshold at each step in the recursive SP2 algorithm. This has the effect increasing the sparsity in the density matrix and hence decreasing the computation time. We plot the wall time required to compute the density matrix for liquid methane as a function of problem size in Figure 2 using regular diagonalization, the SP2 algorithm in dense matrix form, and in sparse matrix form with three different thresholds, _. It is clear that not only does the sparse matrix implementation yield O(N) scaling, but it also yields a level of performance that exceeds the O(N³) methods by several orders of magnitude. While discarding matrix elements may seem to be a drastic step in order to speed up calculations we measure only tiny errors in the interatomic forces that drive the MD simulations.
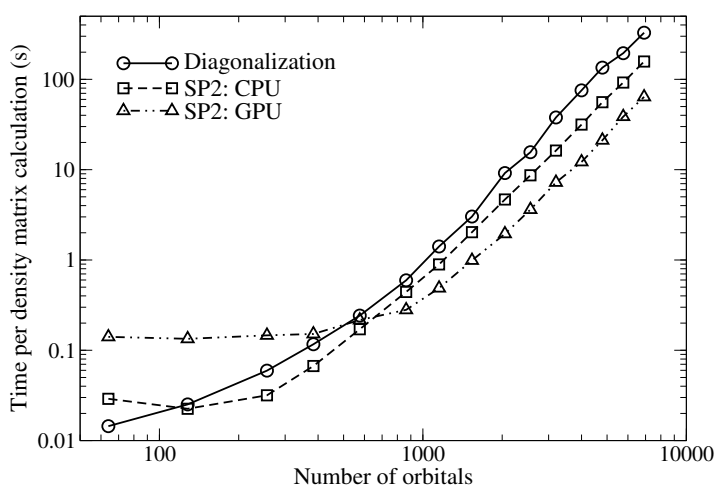
Figure 1. Wall clock time per density matrix calculation using diagonalization and the SP2 algorithm on 12 cores of a dual Xeon workstation with Intel MKL DSYEV and DGEMM and on an Nvidia C2070 with CUBLAS.
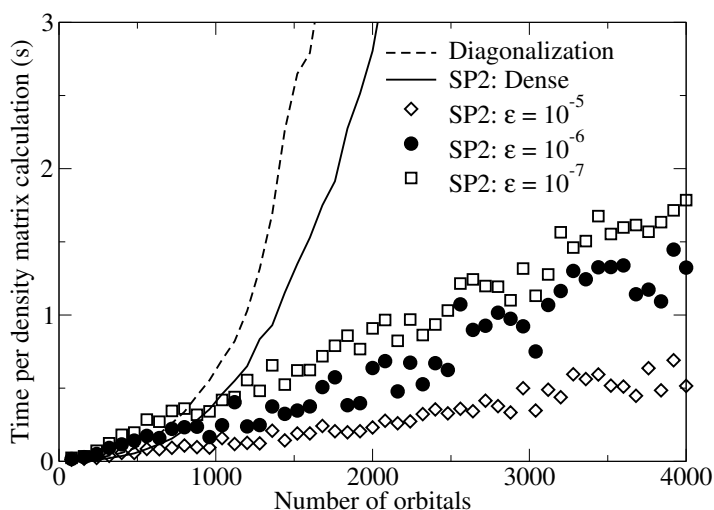
Figure 2. Time per density matrix calculation for liquid methane using diagonalization and the SP2 algorithm in dense matrix algebra and sparse matrix algebra with a numerical threshold.

An unanticipated but very profitable research direction during the project was the implementation in LATTE of the LANL-developed extended Lagrangian Born-Oppenheimer MD formalism [10-14]. Born-Oppenheimer MD [5], of which our scheme is an example, tends to exhibit systematic drifts in the total energy unless interatomic forces are computed to an impractical level of accuracy. Systematic drifts in the total energy require the addition of a thermostat to a simulation to control run-away heating, but this step would hide temperature changes caused by the endo- or exothermic reactions we aim to study. The extended Lagrangian Born-Oppenheimer MD formalism provides a solution to the systematic drift of the total energy by introducing time reversal symmetry in the propagation of the electronic degrees of freedom during a MD trajectory. In Figure 3 we present trajectories computed with and without the extended Lagrangian formalism [13]. The trajectory that employs the extended Lagrangian Born-Oppenheimer MD formalism conserves the total energy precisely when only one self-consistent field (SCF) optimization is performed during the computation of the forces per MD time step. The other trajectories show strong systematic drifts in the total energy that persist even when ten SCF cycles, at ten times the computational expense, are performed per time step. We have also demonstrated that the extended Lagrangian Born-Oppenheimer MD formalism is sufficiently robust that the total energy conserved even when approximate forces computed from the O(N) scheme are employed [13]. This result opens a new paradigm in quantum-based MD as it shows for the first time that there are no conceptual limits to the scaling of these types of simulations.
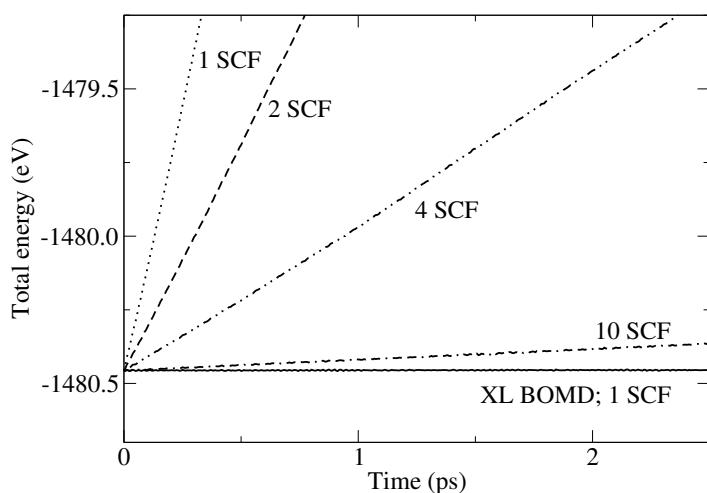
Figure 3. Conservation of the total energy during extended Largrangian Born-Oppenheimer MD (XL BOMD) with 1 SCF cycle per time step, and regular Born-Oppenheimer MD with 1, 2, 4, and 10 SCF cycles per time step.

We have developed a parameterization of our self-consistent tight-binding model for hydrocarbons – those compounds that contain only carbon and hydrogen. The small number of adjustable parameters in the model were fitted

to the results of a series of quantum mechanical calculations. We assessed the transferability of the model by testing its predictions for the energy and geometry of 45 molecules from 12 functional groups against the results of highly accurate quantum calculations. These tests revealed an average error of only 1.62 % and demonstrated our model is a very capable description of the complexities of organic chemistry [14].

Our new computational tools were applied in the study of shock-induced chemistry in two simple liquid hydrocarbons, ethane and ethene [12]. The effects of shock compression were mimicked using a technique developed during the project. These simulations showed, as expected, that the fully saturated ethane molecule is relatively inert. However, the simulations showed that at a relatively low threshold ethene undergoes a radical chain polymerization reaction. This reaction was seen to progress via a number of stochastic exothermic polymerization events that led to a run-away reaction once the temperature had reached a threshold value. These results are summarized in Figures 4 and 5, where the former shows a snap shot from a simulation of liquid ethene at an intermediate stage where about half the molecules have polymerized, and the latter shows how our simulations conserve accurately the total energy even during chemical reactions and strong exothermic temperature changes.
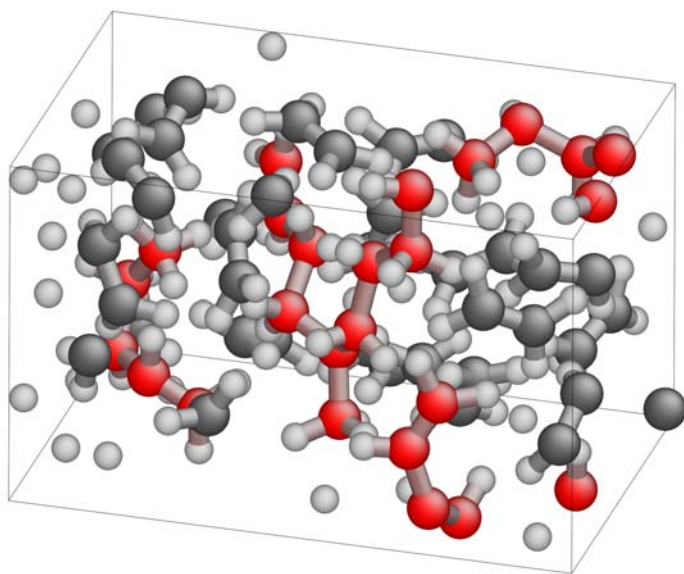
Figure 4. Snapshot from a LATTE simulation of the shock compression of liquid ethene. The black and red spheres correspond to unreacted carbon atoms and those that are part of polymer chains, respectively. The small spheres are hydrogen atoms.
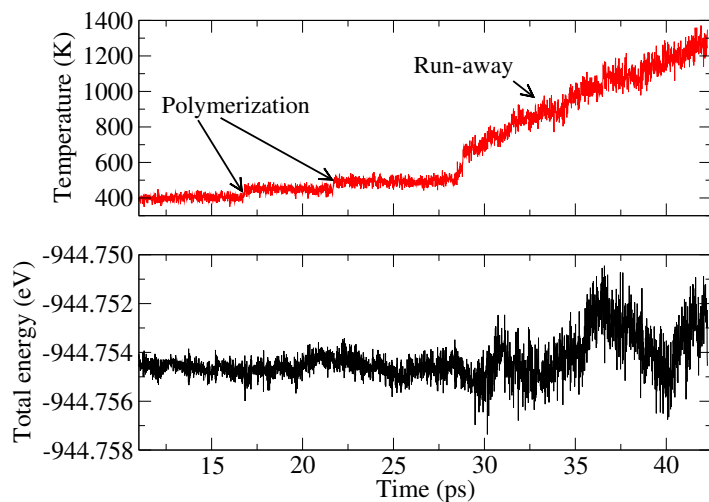
Figure 5. Temperature (a) and total energy (b) during a shock compression simulation of liquid ethene. The total energy exhibits no discontinuities or systematic drift during the evolution of exothermic chemical reactions in the liquid.

Impact on National Missions

The development of the quantum MD code LATTE and the realization of a capability for performing highly accurate simulations of organic materials under extreme conditions with O(N) expense have led already to new research programs at LANL. Simulations using LATTE comprise the main theoretical thrust of the FY11 LDRD-DR project "First Reactions: Simple Molecule Chemistry Behind the Shock Front," PI: D. Dattelbaum. Here we move beyond the code and method development stage undertaken in this project to large-scale 'production' runs. Moreover, LATTE's role as a test bed code for the development new theoretical and computational methods supported work that resulted in the project "Next Generation First Principles Molecular Dynamics," PI: A. Niklasson, that was funded by the DOE-BES. Our foresight in pursuing GPU implementations of our algorithms has made our work very relevant to a number of LANL and external efforts related to the development of computing at the exascale. Our capabilities in these areas, including the team assembled under the auspices of this project, have the potential to impact many areas of ongoing research. Our overall goal of providing LANL a tool that enables a significant improvement in the quality and predictive capabilities of simulations of organic materials under extreme conditions is of obvious benefit to LANL's core missions.

References

1. Strachan, A., A. C. van Duin, D. Chakraborty, S. Das-gupta, and W. A. Goddard. Shock waves in high-energy materials: the initial chemical events. 2003. *Physical Review Letters.* **91** (9): 098301/1.

2. Reed, E., M. Riad. Manaa, L. Fried, K. Glaesemann, and J. D. Joannopoulos. A transient semimetallic layer in

detonating nitromethane. 2008. *NATURE PHYSICS.* **4** (1): 72.

3. Manaa, M. Riad., E. Reed, L. Fried, and N. Goldman. Nitrogen-rich heterocycles as reactivity retardants in shocked insensitive explosives. 2009. *Journal of the American Chemical Society.* **131** (15): 5483.

4. Allen, M. P., and D. J. Tildesley. Computer simulation of liquids . 1989.

5. Finnis, M. W.. Interatomic forces in condensed matter. 2003.

6. Goedecker, S.. Linear scaling electronic structure methods. 1999. *Reviews of Modern Physics.* **71** (4): 1085.

7. Germann, T., and K. Kadau. TRILLION-ATOM MOLECULAR DYNAMICS BECOMES A REALITY. 2008. *INTERNATIONAL JOURNAL OF MODERN PHYSICS C.* **19** (9): 1315.

8. Elstner, M., D. Porezag, G. Jungnickel, J. Elsner, M. Haugk, T. Frauenheim, S. Suhai, and G. Seifert. Self-consistent-charge density-functional tight-binding method for. 1998. *Physical Review B (Condensed Matter).* **58** (11): 7260.

9. Sanville, E. J., N. Bock, J. D. Coe, S. M. Mniszewski, A. M. N. Niklasson, and M. J. Cawkwell. LATTE (LA-CC 10-004). 2010. .

10. Niklasson, A. N., C. J. Tymczak, and M. Challacombe. Time-reversible Born-Oppenheimer molecular dynamics. 2006. *PHYSICAL REVIEW LETTERS.* **97** (12): 123001.

11. Niklasson, A. N.. Extended Born-Oppenheimer molecular dynamics. 2008. *PHYSICAL REVIEW LETTERS.* **100** (12): 123004.

12. Cawkwell, M. J., E. J. Sanville, S. M. Mniszewski, and A. M. N. Niklasson. Self-consistent tight-binding molecular dynamics simulations of shock-induced chemistry in hydrocarbons. (Chicago, 26 June - 1 July 2011).

13. Cawkwell, M. J., and A. M. N. Niklasson. Energy Conserving, Linear Scaling Born-Oppenheimer Molecular Dynamics. *Physical Review Letters.*

14. Sanville, E. J., N. Bock, A. M. N. Niklasson, M. J. Cawkwell, T. D. Sewell, D. M. Dattelbaum, and S. A. Sheffield. Extended Lagrangian quantum molecular dynamics simulations of shock-induced chemistry in hydrocarbons. (Coeur d'Alene, 11 - 16 April 2010).

15. Niklasson, A. M.. Expansion algorithm for the density matrix. 2002. *PHYSICAL REVIEW B.* **66** (15): 155115.

Publications

Cawkwell, M. J., E. J. Sanville, S. M. Mniszewski, and A. M. N. Niklasson. Self-consistent tight-binding molecular dynamics simulations of shock-induced chemistry in hydrocarbons. To appear in *The Seventeenth Biennial International Conference of the APS Topical Group on Shock Compression of Condensed Matter.* (Chicago, 26 June - 1 July 2011).

Cawkwell, M. J., and A. M. N. Niklasson. Energy Conserving, Linear Scaling Born-Oppenheimer Molecular Dynamics. *Physical Review Letters.*

Odell, A., A. Deiin, B. Johansson, M. J. Cawkwell, and A. M. N. Niklasson. Geometric integration in Born-Oppenheimer molecular dynamics. To appear in *The Journal of Chemical Physics.*

Sanville, E. J., N. Bock, A. M. N. Niklasson, M. J. Cawkwell, T. D. Sewell, D. M. Dattelbaum, and S. A. Sheffield. Extended Lagrangian quantum molecular dynamics simulations of shock-induced chemistry in hydrocarbons. To appear in *14th International Detonation Symposium.* (Coeur d'Alene, 11 - 16 April 2010).

Transparent Organic Solar Cells

Ian H. Campbell
20090393ER

Abstract

The ideal solar cell would convert every bit of energy in photons originating from the sun into usable energy. We proposed a completely novel approach which would "milk" a small amount of energy from solar photons in a most unobtrusive fashion. We proposed to develop a new class of truly transparent solar cells using organic semiconductors. A transparent solar cell is designed to have > ~85% transmission in the visible region of the solar spectrum. Although transparency necessarily decreases the maximum possible efficiency of the cell, it enables two specialty applications: windows and stealth. A transparent solar cell for windows is designed to use window glass as the substrate for the solar cell and thus reduce costs associated with fabrication and installation. Many of the materials required for transparent solar cells are already used in high performance windows and transparent solar cells can be designed to also function as low-e window coatings. Transparent solar cells for stealth applications are designed to provide power in applications where the solar cell should be difficult to detect; for example, it can be added to an existing surface to provide power for surreptitious electronic devices.

Background and Research Objectives

The basic requirements for a transparent solar cell are relatively straight forward. To be an efficient transparent solar cell, the cell must collect photons outside the visible spectrum, either in the infrared (IR) or the ultraviolet (UV). The solar spectrum has a large amount of energy in the IR and much less in the UV. The ideal output power of a solar cell is largely determined by its short circuit current and open circuit voltage. Each photon contributes one carrier to the short circuit current and the open circuit voltage is limited by the energy gap (~ absorption threshold) of the material. There is thus a tradeoff between collecting more photons, which requires a lower energy gap, and increasing the output voltage, which requires a higher energy gap. This tradeoff leads to a theoretical maximum power efficiency of 31% for a material with an energy gap of 1.35 eV (920 nm). For transparent solar cells, we estimated the maximum theoretical power efficiency of an IR solar cell which has an absorption band from 1350 nm to 700 nm to be about 20%. In contrast, the maximum theoretical efficiency of a UV solar cell with an absorption band starting at 400 nm is only about 3%. The 20% IR theoretical efficiency compares well to the maximum theoretical efficiency of 31% for the entire solar spectrum.

The goals of this work were to demonstrate, for the first time, a truly transparent solar cell by exploiting the unique electronic structure of organic semiconductors, and to understand and optimize the electronic structure of these materials for this application. Technologically, organic semiconductors are of increasing importance for large area low cost applications such as displays, solid state lighting, large area electronics, and solar cells. From a scientific perspective, organic semiconductors offer a model system for studying multiscale physics involving, for example, the properties of individual molecules and their solid state intermolecular interactions.

Scientific Approach and Accomplishments

We used a closely coupled fabrication/measurement/theory approach to demonstrate and optimize transparent organic solar cells. We fabricated specialized material test structures and prototype solar cells to understand the semiconductor and device parameters that control the cell performance. Simultaneously, the electronic structure and optical properties of these organic semiconductors were calculated and the results used to interpret the test structure and device performance and, most importantly, to guide materials design modifications needed to maximize device performance. We used our established relationships with organic chemical companies to obtain new, specialized organic semiconductors. The project naturally divided into work focusing on two tasks: 1) understanding the relevant properties of the organic semiconductors and 2) designing and fabricating solar cells made from these materials.

The organic semiconductors we worked with are naphthalocyanine compounds that are transparent in the visible spectrum and absorb strongly in the near infrared. We explored two major types of naphtalocyanine compouds: those that can be solution processed and

those that can be thermally evaporated in vacuum. Solution processing is a very low cost method of producing thin films and electronic devices but the chemical purity of the materials can be difficult to control. Thermal evaporation in vacuum is also a low cost technique for device fabrication and it has the advantage that the materials used may be purified by a variety of sublimation techniques. The solution processed materials are part of the family of octabutoxy naphthalocyanines (OctNc). We made chemical substitutions to the base OctNc molecule by adding a central metal atom or varying the ligands attached to the naphthalocyanine core to control the molecule's absorption in the infrared. The vacuum processed materials are part of the family of naphthalocyanines (Nc) where we again made chemical substitutions to control the molecular optical properties. These two classes of molecules are very similar as they share the naphthalocyanine core. In addition to their processing and purity differences, the two molecular families have very different intermolecular interactions in the solid state. In the solid state, the absorption of the smaller, vacuum evaporated molecules can red shift by ~ 100 nm, significantly improving their infrared response. In contrast, the absorption properties of the solution processed molecules are essentially unchanged in the solid state. We performed theoretical calculations of the electronic structure of these molecules to understand them and design new molecules with improved properties.

We fabricated and tested transparent, organic solar cells using these naphthalocyanine compounds as the critical, infrared absorbing layer. Indium tin oxide (ITO) was used as a transparent electrode. When combined with special surface layers, ITO can function as either an electron or hole injecting material. This is critical to retain the high transparency required in these devices. We used very thin layers of C60 to dissociate excitons produced in the Nc layer and we have also explored large energy gap organic semiconductors such as bathocuproine to serve as an exciton blocking layer. The device results are very encouraging. We made structures that are > 80% transparent throughout the visible spectrum and have strong absorption in the infrared (IR). These devices have near ideal IR quantum efficiency, i.e. every photon absorbed produces one electron of photocurrent. This work has now been published in four Applied Physics Letters articles, one Journal of Physical Chemistry A paper, and widely disseminated in the trade journal Laser Focus World.

Impact on National Missions
This work contributed to enhancing national energy security, a key DOE mission area. The ability to incorporate solar cells into conventional windows, using many of the materials and coatings already used in high performance windows, could provide an economic method to deploy solar cells.

Publications
Campbell, I.. Low-cost organic photodiodes reach into the infrared. 2010. *LASER FOCUS WORLD.* **46** (3): 45.

Campbell, I. H.. Transparent organic photodiodes with high quantum efficiency in the near infrared. 2010. *APPLIED PHYSICS LETTERS.* **97** (3): 033303.

Campbell, I. H.. Improving the Spectral Response of Amorphous Se Photodetectors Using Organic Semiconductors. 2011. *Applied Physics Letters.* **99** (6): 63303.

Campbell, I. H., and B. K. Crone. A near infrared organic photodiode with gain at low bias voltage. 2009. *APPLIED PHYSICS LETTERS.* **95** (26): 263302.

Jakubikova, E., I. H. Campbell, and R. L. Martin. Effects of Peripheral and Axial Substitutions on Electronic Transitions of Tin Naphthalocyanines. 2011. *Journal of Physical Chemistry A.* **115** (33): 9265.

Liu, F., P. P. Ruden, I. H. Campbell, and D. L. Smith. Exciplex Current Mechanism for Ambipolar Bilayer Organic Light Emitting Diodes. To appear in *Applied Physics Letters.*

Uranium Imido Complexes as Catalysts for the Reduction of Carbon Dioxide

James M. Boncella
20090397ER

Abstract

The main focus of this project has been the study of the reduction of carbon dioxide or carbon dioxide surrogates using new uranium complexes as catalysts. The reaction and conversion of acid to hydrogen using similar uranium compounds has also been examined. These are both examples of difficult, multielectron chemical reactions that have the potential to generate usable fuel materials from renewable resources. Success in either of these endeavors will teach us how to perform some of the most difficult chemical reactions that have been proposed as the foundation of a carbon neutral fuel cycle. Using actinide chemistry to solve these types of problems has never been demonstrated and is only conceivable now because of the new and unusual types of compounds that have been synthesized and studied. The synthesis of a series of uranium compounds that span the 4+, 5+ and 6+ oxidation states has been achieved and represents a significant advance in fundamental uranium chemistry. These compounds have allowed us to begin to explore the use of uranium compounds in multielectron transfer reactions. This work will be used to predict what structures will be more efficient catalysts and it will provide a better understanding of how these reactions occur. The principles that we uncover with this work will be applicable to the broader subject of how to perform chemical reactions that proceed only with the input of more external energy than is possible with simple heating.

Background and Research Objectives

The chemistry of uranium is dominated by the chemistry of uranyl compounds (Figure 1). These uranium 6+ compounds have been known for over 100 years and their chemistry is crucial to obtain the material necessary for many of the industrial uses for uranium. These processes include: the extraction of uranium from its ore, the processing of nuclear fuel and the disposition of spent fuel and waste from nuclear reactors. Relative to uranyl compounds, much less is known about the chemistry of the other oxidation states of uranium; U^{3+}, U^{4+} and U^{5+}. This project has been focused on developing the chemistry of uranium in these less studied oxidation states.
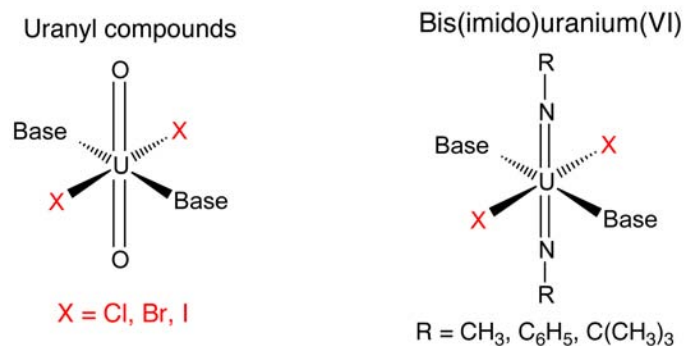
Figure 1. Structures of uranyl and bis(imido)uranium(VI) compounds.

The multi-electron transfer reactivity of uranium (eg. from lower to higher oxidation states) is poorly understood because a series of uranium compounds having the same ancillary groups bound to uranium in a range of oxidation states does not exist. One objective of this project was to synthesize a series of compounds with common structures that would enable us to investigate transformations between oxidation states without concurrent structural changes in the molecules. With a family of lower valent uranium compounds, we could study multi-electron transfer reactions with simple substrate molecules to understand the fundamental reactivity of uranium.   Thus, investigating the use of lower valent uranium complexes (U^{3+}, U^{4+} and U^{5+}) to effect the reduction of carbon dioxide or of acid to hydrogen is a good vehicle to understand the redox chemistry of uranium while also investigating a problem that is of national and global concern.

We believed that we could synthesize the necessary family of uranium compounds by using the bis(imido) U(VI) compounds in Figure 1 [1] as starting materials. These compounds are the nitrogen analogues of uranyl compounds but differ significantly because they possess the attractive property of having different and interchangeable NR groups.   Changing the group bound to nitrogen allows the synthetic chemist to change the redox properties of uranium (electronic effects) as well as the size of the group bound to uranium (steric effects).

By making these changes the range of possible reactivities can be determined and controlled. With the uranyl ion, such changes are not possible since there is no way to vary the electronic or steric properties of the oxygen atoms. It was our fundamental premise that changing the identity of the NR group would result in the synthesis of compounds that can exist in the multiple oxidation states that are necessary to investigate the use of uranium as a redox catalyst.

Scientific Approach and Accomplishments

Early on in this project, we were able to synthesize and characterize a series of new uranium bis (imido) complexes whose reactivity we investigated. The successful synthesis of this series of U(V)-U(V) dimer complexes (Figure 2) has allowed us to investigate their reactivity with carbon dioxide and hydrogen as a function of ligand. During this work, computational analysis of these dimers suggested that the single f electron on each U metal should interact with one another via a spin pairing interaction (antiferromagnetic coupling). This was demonstrated experimentally and is only the second molecular actinide complex that shows such electronic interactions and resulted in a publication in *Angew. Chem. Int. Edn.* [2]. The synthesis of the series of derivatives including iodide, bromide, chloride and aryl sulfide compounds has allowed us to learn how the nature of the ligands affect the ability of the U atoms in these compounds to undergo electronic communication.
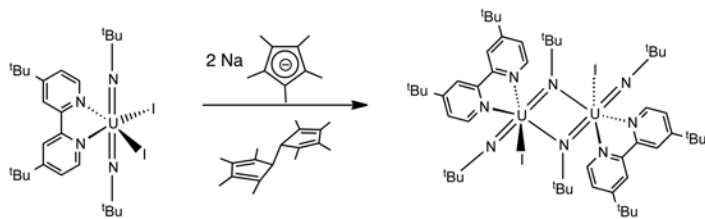
Figure 2. Synthesis of U(V)-U(V) dimer.

We have also investigated the reactivity of the U(V)-U(V) dimers with respect to their ability to be oxidized to U(VI) complexes. These compounds react with weak oxidants such as silver salts and elemental sulfur and selenium. The products are generally not accessible via other synthetic techniques and include the first examples of U(VI) atoms that are bridged by sulfur or selenium atoms. Controlling the stoichiometry of the reactions determines whether single atom or multi-atom bridges are formed [3].

We have also begun to investigate the use of polydentate mono- or di- anionic ligands with the bis(imido)U(VI) metal framework. The intention was to design a ligand set which facilitates the reduction of U(VI) to mononuclear U(V) or U(IV) complexes whose reactivity with hydrogen or carbon dioxide could then be investigated. [4] Electrochemical studies of these compounds did not demonstrate reversible reduction of the U(VI) halide complexes, though reduction obviously occurs. Furthermore, reaction of the halide compounds with chemical reductants results in the formation of the dimers or intractable, reduced materials. The

focus of the project then turned to generating mononuclear, uranium(IV) and uranium(V) imido complexes to be able to investigate, understand and control the chemistry of these unusual molecules.

Investigating the reaction chemistry of the bimetallic, U(V)-U(V) complexes has led to the synthesis of U(IV) mono imido complexes through a very unusual conproportionation reaction with U(III) complexes as shown in Figure 3, Equation 1 [5]. This revealed that simple U(IV) mono imido complexes are in fact stable and has led us to discover facile, high yielding syntheses of a family of U(IV) mono imido complexes, Figure 3, Equation 2 that originate from readily available U(IV) starting materials and which are formed in very high yields. The reaction chemistry of these new molecules demonstrates that the compounds readily undergo multi-electron transfer chemistry forming U(VI) complexes rather easily. One example of this is the reaction with oxygen to generate the U(VI) (oxo)(imido) complex; a compound that is effectively a hybrid of the uranyl and the U(VI) bis(imido) complexes. It appears that the formation of the U(VI) compounds provides a significant driving force for the reaction thereby facilitating the multi-electron transfer reactivity of these species.
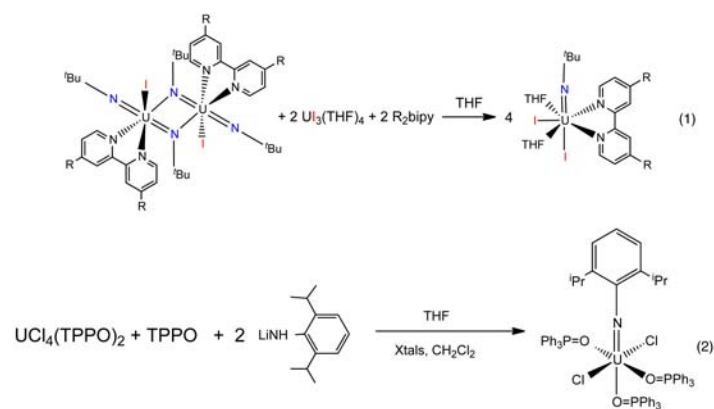
Figure 3. Synthesis of U(IV) mono(imido) complexes.

We have also been able to generate a U(IV) bis-imido complex that is extremely reactive. While this compound has not been isolated, its reaction chemistry is consistent with our hypothesis that it is (or at least reacts as) a bis(imido) U(IV) material. This compound is a molecular analogue of uranium dioxide. This compound is an extremely rare example of a molecular species that is effectively a solublized chunk of an extended, ionic solid. This complex readily forms the mono-nuclear U(VI) bis(imido) complexes through the reaction of halogenated organic compounds via halide abstraction, Figure 4, Equation 1. It also reacts with the N-H bonds of amines to give oxidized, U(VI), products, Figure 4, Equation 2. The most likely reduced species in this reaction system are the protons of the amine. This reaction suggests that U(IV) imido complexes are capable of reducing protons (acid) to hydrogen gas. Unfortunately, we have not yet been able to obtain irrefutable evidence for the formation of hydrogen gas in this reaction.
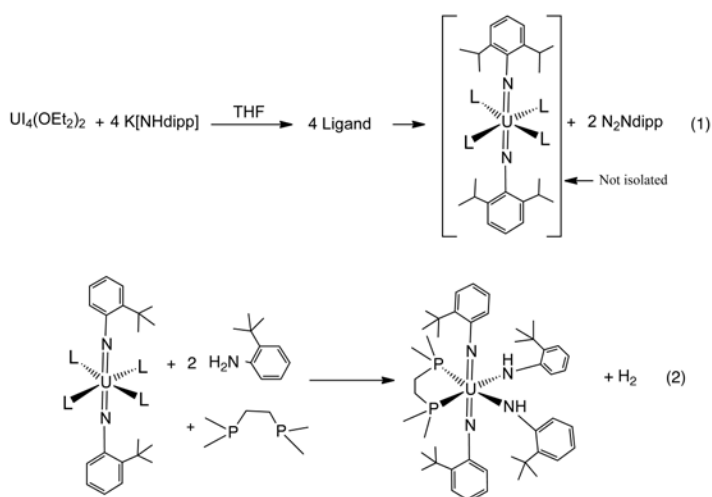
Figure 4. Synthesis and reactivity of U(IV) bis(imido) complexes.

Most recently, we have discovered that the reaction between the U(IV) bis(imido) species and a stoichiometric amount of organic halide gives novel U(V)bis(imido) complexes in high yield, Figure 5, Equation 1 [6]. These compounds have provided us with an opportunity to investigate the simple one electron oxidation to the U(VI) bis(imido) complexes. We have also been able to observe reversible electrochemistry between the U(V) and U(VI) complexes from which we have learned a great deal about the differences in the U=O and U=NR bonds.
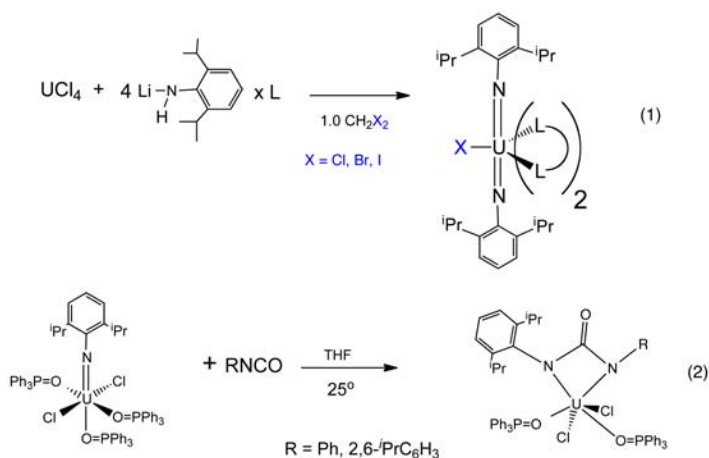
Figure 5. Synthesis of U(V) bis(imido) and reactivity of U(IV) mono(imido) complexes.

Finally, we have discovered that the U(IV) mono(imido) complexes react rapidly with isocyanates or carbon dioxide through electrphilic attack on the imido nitrogen atom, Figure 5, Equation 2. These addition complexes demonstrate that there is significantly more negative charge on the nitrogen of the imido group in the U(IV) compounds than the U(VI) compounds. While the products of the reaction between carbon dioxide and the U(IV) compounds are not clean, the formation of uranyl complexes as one product

of this reaction shows that reduction of the carbon dioxide has occurred. This demonstrates the reactivity potential of lower valent uranium species with even rather unreactive molecules such as carbon dioxide and confirms the possibility of using uranium species as redox catalysts for carbon dioxide.

The difference in the reaction chemistry of the U(IV) vs U(VI) imido species is caused by significant differences in the properties of the U=N bond in these compounds. This contradicts the long-held belief that the bonding in actinide compounds is primarily ionic in nature and relatively invariant with oxidation state. These results provide significant experimental proof of the variability of the reaction chemistry of uranium as a function of oxidation state and suggest that other chemistries can be developed that take advantage of these differences. Such fundamental information could be used to design new schemes for actinide separation processes in which changing the chemistry by changing the oxidation state could be used as the crucial factor that controls the separation.

In summary, during the course of this project several families of new uranium compounds in the +4, +5 and +6 oxidation states have been synthesized. These compounds have been demonstrated to undergo reactions in which acid and carbon dioxide have been reduced. While no new catalysts for hydrogen production or carbon dioxide reduction have been discovered, the fundamental reactivity that is necessary for these types of processes has been observed. Furthermore, the new compounds have provided fundamental insight into the nuances of bonding in uranium and actinide complexes in general. Qualitatively, the observed extreme reactivity of some of these compounds demonstrates that the simple theories of actinide bonding and reactivity are clearly incorrect. The ability of these molecules to undergo oxidation reactions has allowed us to begin to understand the redox reactivity of uranium. Surprisingly, this reaction chemistry is not well developed despite the fact that uranium has 4 stable oxidation states. It is likely that the standard ligand systems that have been used throughout the historical development of uranium chemistry have not allowed this redox chemistry to occur. It is the combination of the imido ligand with the other ancillary ligands that we have used that has allowed us to investigate this chemistry and exploit it for potentially interesting reaction chemistry.

Impact on National Missions
This project supports the U.S. drive for energy security and to maintain a safe nuclear stockpile by enhancing our understanding of actinide coordination and organometallic chemistry. The work supports DOE energy security and nuclear weapons missions.

References

1. Hayton, T. W., J. M. Boncella, B. L. Scott, P. D. Palmer, E. R. Batista, and P. J. Hay. Synthesis of imido analogs of the uranyl ion. 2005. *Science.* **310** (5756): 1941.

2. Spencer, L., E. Schelter, P. Yang, R. Gdula, B. Scott, J. Thompson, J. Kiplinger, E. Batista, and J. Boncella. Cation-Cation Interactions, Magnetic Communication, and Reactivity of the Pentavalent Uranium Ion [U(NtBu)(2)](+). 2009. *Angewandte Chemie-International Edition.* **48** (21): 3795.

3. Spencer, L., P. Yang, B. Scott, E. Batista, and J. Boncella. Oxidative Addition to U(V)-U(V) Dimers: Facile Routes to Uranium(VI) Bis(imido) Complexes. 2009. *Inorganic Chemistry.* **48** (24): 11615.

4. Spencer, L., P. Yang, B. Scott, E. Batista, and J. Boncella. Uranium(VI) bis(imido) disulfonamide and dihalide complexes: Synthesis density functional theory analysis. 2010. *Comptes Rendus Chimie.* **13** (6-7, SI): 758.

5. Jilek, R. E., L. Spencer, D. Kuiper, B. Scott, U. Williams, J. Kikkawa, E. Schelter, and J. Boncella. A General and Modular Synthesis of Monoimidouranium(IV) Dihalides. 2011. *Inorganic Chemistry.* **50** (10): 4235.

6. Jilek, R. E., L. P. Spencer, R. A. Lewis, B. L. Scott, T. W. Hayton, and J. M. Boncella. A Direct Route to Bisimido Uranium(V) Halides via Metathesis of Uranium Tetrachloride: Evidence for in situ Formation of Bis(imido) Uranium(IV). *Journal of the American Chemical Society.*

Publications

II, D. Swartz, L. Spencer, B. Scott, A. Odom, and J. Boncella. Exploring the coordination modes of pyrrolyl ligands in bis(imido) uranium(VI) complexes. 2010. *Dalton Transactions.* **39** (29): 6841.

Jilek, R. E., L. Spencer, D. Kuiper, B. Scott, U. Williams, J. Kikkawa, E. Schelter, and J. Boncella. A General and Modular Synthesis of Monoimidouranium(IV) Dihalides. 2011. *Inorganic Chemistry.* **50** (10): 4235.

Spencer, L., E. Schelter, P. Yang, R. Gdula, B. Scott, J. Thompson, J. Kiplinger, E. Batista, and J. Boncella. Cation-Cation interactions, magnetic communication, and reactivity of the pentavalent uranium ion [U(NtBu)₂]⁺. 2009. *Angewandte Chemie - International Edition.* **48** (21): 3795.

Spencer, L., P. Yang, B. Scott, E. Batista, and J. Boncella. Uranium(VI) bis(imido) disulfonamide and dihalide complexes: Synthesis density functional theory analysis. 2010. *Comptes Rendus Chemie.* **13** (6-7, SI): 758.

Spencer, L., P. Yang, B. Scott, E. Batista, and J. Boncella. Uranium(VI) Bis(imido) Chalcogenate Complexes: Synthesis and Density Functional Theory Analysis. 2009. *Inorganic Chemistry.* **48** (6): 2693.

Spencer, L., R. Gdula, T. Hayton, B. Scott, and J. Boncella. Synthesis and reactivity of bis(imido) uranium(VI) cyclopentadienyl complexes. 2008. *Chemical Communications.* (40): 4986.

Modeling Molecular Scale Natural Abundance Isotope Signatures For Chemical, Biochemical, and Nuclear (CBN) Threat Attribution

Toti E. Larson
20110510ER

Abstract

Natural abundance Isotope Ratio Mass Spectrometry (IRMS) has the ability to answer many of the requirements for chemical, biochemical, and nuclear (CBN) threat attribution. Recent approaches using IRMS techniques have focused on measuring the relatively large Primary Kinetic Isotope Effect (PKIE) that occurs during chemical bond cleavage and formation in simple low carbon number molecules; however, it was recognized that the global carbon isotope value (*i.e.,* the average isotope ratio of all carbons ($^{13}C/^{12}C$) in a molecule as measured by IRMS) is not unique. It is affected by at least three variables: the PKIE related to C-N bond cleavage/formation, incomplete reaction (starting materials, intermediates, and products), and the initial global IRMS carbon isotope value of the starting materials. This demonstrates the inherent limitation of using a single global IRMS ratio measurement when attempting to attribute multistep, multivariate, and complex processes typically used to process (synthesize, isolate, and purify) chemical, biochemical, and nuclear materials. The key requirement for accurate forensics attribution lies in the ability to differentiate subtle differences in processing techniques while simultaneously identifying signatures for the overall batch production pathways employed. We have demonstrated that a new signature measurement capability, **S**ite-specific **N**atural abundance **I**sotope **F**ractionation **N**uclear **M**agnetic **R**esonance spectroscopy (SNIF-NMR) has the requisite precision for the quantitative measurement of natural abundance carbon isotope variations at the molecular site-specific level (*i.e.* isotopic substitution at specific sites within the molecules). Using this advanced capability we have measured and identified Non-Covalent Isotope effects (NCIE) (*i.e.,* isotope effects that do not involve covalent bond breakage or formation) in several systems such as distillation, chromatography, and extraction. Furthermore, we have shown that the inter- and intra-molecular interactions that occur during processing techniques are responsible for these unique NCIE signatures. Unfortunately, our preliminary work demonstrated that our theoretical understanding of this phenomenon is lacking. Consequently, development of preliminary approaches to link computational models to theory and experiment are necessary. While this reserve project did not accomplish our overall scientific goal of developing a fundamental understanding of the physical organic principles that influence and/or control the "communication effects in isotopic fractionation" resulting in NCIE, we believe that our preliminary efforts have moved in the correct direction and support our contention site-specific signatures will address many forensics capability needs.

Background and Research Objectives

The goal of this research was to begin to interpret and understand *how molecular-scale natural abundance isotopic distributions* in molecules, subject to chemical, biochemical, or nuclear processing techniques, are altered by the processes they experience and what signatures they produce. Our initial efforts focused on measuring natural abundance carbon isotope variations ($^{13}C/^{12}C$ ratios) at the molecular site-specific level (*i.e.* isotopic substitution at specific carbon sites within the molecules) and establishing a framework to begin to understand what influences the natural abundance isotopic distributions so they can be used as signatures. We now have the requisite precision to measure, at the molecular site-specific level, natural abundance isotope substitutions by coupling LANL's unique site-specific quantitative Nuclear Magnetic Resonance (SNIF-NMR) and Isotope Ratio Mass Spectrometry (IRMS) capabilities. We have demonstrated that these small, yet measurable differences in stable isotope substitutions (which may include carbon, nitrogen, oxygen, sulfur, and hydrogen), can be correlated with specific processing techniques and environmental interactions. Experimentally, this was extremely successful and generated significant enthusiasm related to site-specific isotopic analysis that will result in submission of a note to Langmuir. However, much less data is available to develop the underpinnings required to fully connect the observed measurements with theory and demonstrate a viable computational approach. Consequently, this research attempts to define and delineate such a computational approach. By initially employing simple models, we will establish that the requisite precision can be obtained to computationally predict, suc-

cessfully and robustly, the magnitude and direction of the observed site-specific carbon isotope variations. Accurate measurement and interpretation of unique stable isotope signatures at specific molecular sites can address many forensics capability needs by uniquely tracking and reporting the molecule's environmental history. Our overarching hypothesis is that *an understanding of the theoretical basis that causes atomical isotopic fractionation will provide a predictive forensic tool to attribute threats by identifying unique molecular fingerprints imposed by the processes of synthesizing, isolating, compounding, and/or purifying.*

Scientific Approach and Accomplishments

This research focused on defining a computational and experimental approach required to accurately predict, successfully and robustly, the magnitude and direction of observed site-specific isotope variations in molecules subject to NCIE. We have successfully demonstrated that IRMS global measurements, coupled to SNIF-NMR measurements produce site-specific $^{13}C/^{12}C$ ratios that have the requisite precision (< 1 per mil) for differentiation between states and identification of unique isotope patterns. A SNIF-NMR/IRMS study of tri-butylphosphate [P(=O) (O-C_1-C_2-C_3-C_4)$_3$] from multiple manufacturers and production lots (ten separate samples) clearly demonstrated that each carbon in the butyl chain had a different $^{13}C/^{12}C$ ratio that was lot and sample dependent (Figure 1). While carbon site-specific values (C_1, C_2, and C_4 of the butyl group) showed $\Delta^{13}C/^{12}C$ of ~3 to 4 per mil over this entire series of ten samples, the global IRMS values differed by only < 0.4 per mil. This result reinforces our observations regarding global IRMS values for attribution and signature development in that they are not reliable for many materials. While additional experimentation is necessary, preliminary analysis indicates that one carbon, C_3, is relatively invariant compared to the other three and could be used as an internal standard for comparative quantitation.

In order to establish if the oft-used, but phenomenological, Rayleigh equation is capable of describing the increasingly complex site-specific isotopic fractionation processes we have observed in our previous separations using distillation or extraction; we attempted to fit distillation curves using a classical Rayleigh approach. Figure 2 shows a plot of the acetone component of an azeotropic distillation of a ternery mixture of acetone, methanol, and chloroform where SNIF-NMR of the acetone component successfully measured the site-specific $^{13}C/^{12}C$ ratios of the methyl and carbonyl groups. Distilled sample fractions of the constant boiling mixture are not expected to show the changes in isotopic fractionation in the isotopologues that are actually observed in Figure 1. No α values could be identified that would allow the classical Rayleigh equation to reproduce the acquired data. Thus, a more sophisticated approach is required.

Site-Specific $^{13}C/^{12}C$ Ratios In TBP (Tri − n-butyl phosphate) Samples

Compound	Lot #	-C_1-O-P	-C_2-	-C_3-	-C_4-	Global IRMS
TBP (97%, Aldrich)	04913EU	-27.32	-29.74	-27.01	-30.05	-28.53
TBP (99%, Acros)	A0292647	-25.65	-27.95	-28.24	-33.72	-28.89
TBP (99%, Acros)	A0291450	-28.50	-25.85	-26.73	-32.90	-28.50
Maximum Difference, Δ ‰		-2.85	-3.89	-1.51	-3.67	-0.39

Internal Standard
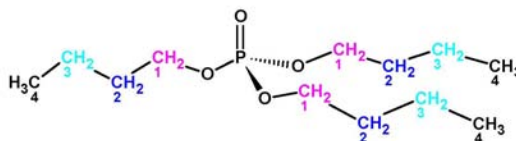
Figure 1. Selected site-specipic carbon isotope ratios in tri-n-butylphosphate samples from different manufacturers and lots.
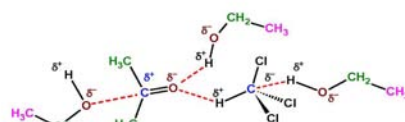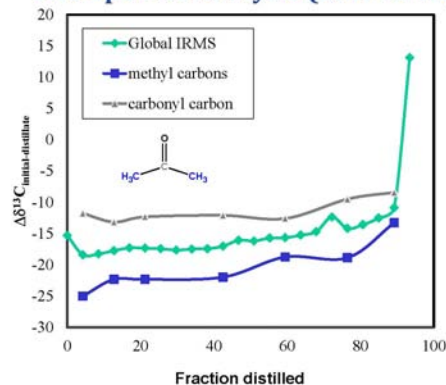
Figure 2. Change in carbon fractionation for acetone in a ternary azeotrope upon distillation and removal of equal volume fractions. Fractionation of the methyl (blue) or carbonyl (gray) of acetone is not modeled successful by the Rayleigh equation.

Traditional views of isotopologue thermodynamics (*e.g.* fractionation between phases) are often based on the notion that isotopic substitution leads to changes in (primarily) the zero point vibrational energies, which in turn, control the thermodynamic properties. It is often assumed that the intermolecular potentials (electronic configurations) are unaffected by the isotopic substitutions. We examined this assumption with regard to site-specific isotopic substitution wherein small changes in intermolecular potentials could contribute to the subtle changes in properties observed upon substitution. Furthermore, it is

not absolutely clear that changes in vibrational states are absolutely required in order to cause some observed behavior, such as fractionation between fluid phases. These questions were explored using a very simple fluid model. Specifically, vapor-liquid of a square well fluid was calculated. The square well fluid has a hard sphere intermolecular potential combined with an attractive well and is the simplest intermolecular potential with both an attractive and repulsive contributions. The well depth was varied to represent an isotopic substitution while conventional Lorentz-Bethalot mixing rules were used for interactions between the distinct isotopologues. Simulations that kept the size of the hard sphere core constant, while varying the depth of the attractive well, suggest that behavior such as fractionation can result from non-vibrational changes within molecules. We envision a short paper based on these results in the near future.

Consequently, an alternative approach, firmly grounded in theory, needs to be developed to explain the theoretical basis for our observation. One approach is to determine if a proper blending of isotope-specific intermolecular potentials can predict the fractionation observed in a simple gas-solid adsorption system (Figure 3). While this is the simplest system that we can probe, we were unable to complete simulations with the available software by the termination of the reserve project. Density functional theory (Amsterdam Density Functional) was used as our starting point and trial versions of the software were used to evaluate the software for purchase. Our preliminary calculations were done with this software without modification even though the intermolecular potentials are not specifically designed to account for isotopic substitutions. Nevertheless, our preliminary calculations uphold our supposition that we can do these calculations with sufficient precision to calculate the small isotopic differences observed.
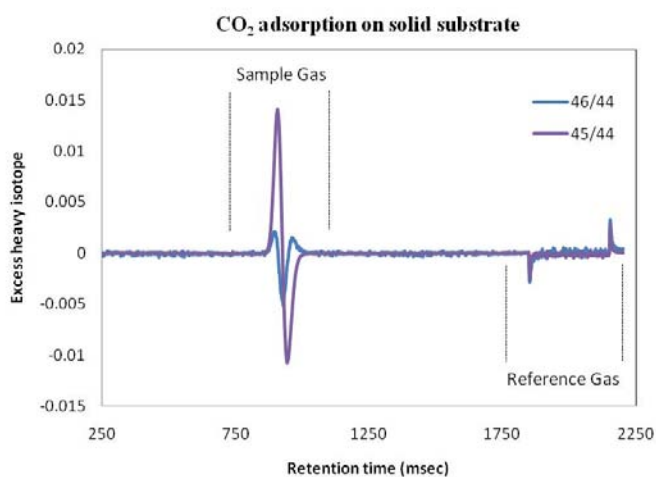
Figure 3. Fractionation of carbon dioxide gas on a solid support.

While our theoretical understanding of equilibrium isotope fractionation is well founded, development of a compre-

hensive theoretical understanding of NCIE, requires a new paradigm. These effects are controlled not only by molecular zero point energy differences, but also by subtle changes in the electron densities caused by hydrophobic and hydrophilic molecular interactions (hydrogen bonding; van der Waals interactions). Thus, the sign and magnitude of NCIE in condensed phases are closely related to the nature of the intermolecular forces in liquids and solutions. According to Born-Oppenheimer, electronic structures are independent of the isotopic distributions of nuclear mass; however, in contrast to the potential energy surface, kinetic energy terms are mass dependent. Thus, the total energy of the system, which includes potential and kinetic parts, and therefore the associated free energy, is isotope dependent. For example, the vapor pressure of compound X in a solvent can be expressed as

$$p^X(T) = exp\left\{\frac{\mu_S^X - \mu_A^X}{kT}\right\},$$

where μ_S^X is the chemical potential of compound X in mixture S, and μ_A^X is the chemical potential of compound X in the gas phase. These chemical potentials depend on both the chemical structure of X and the solvent mixture. However, a priori calculation of these chemical potentials is problematic. It has been shown in H_2O-D_2O mixtures that the complex dielectric has components (relaxation term) that are linearly related to the mole fraction of isotope; consequently, we suggest that a dielectric continuum solvation model can be used to parameterize the chemical potential. While similar models (**CO**ductor-like **S**creening **MO**del – **COSMO**) have been employed routinely to approximate solvation effects, they use only a primary and secondary polarization charge density term. Isotope effects arising from zero-point vibrations and thermal, vibrational, and rotational excitations, as well as the translational and rotational energy of the entire molecule, which also must contribute to the free energy, are usually ignored. These contributions can be calculated using a quantum mechanical (QM) approach and we decided to examine a generalization of the COSMO-RS model (**R**eal **S**olvent), re-parameterized with multiple descriptors fitted from *ab initio* QM calculations to provide a refined expression of molecular interactions related to isotope effects. The ADF software includes an implementation of the COSMO-RS program which was an additional reason we were evaluating the software.

We applied COSMO-RS to analyze the isotopomers of the compounds we used in our distillation and extraction experiments that showed site-specific fractionation. Our objective was to discern whether a dielectric continuum approach would be sensitive and precise enough to lend support to our contention that by re-parameterizing COSMO-RS we would be able to generate models that would estimate and ultimately predict the NCIE that we experimentally observe in site-specific fractionation. Similar re-parameterization of COSMO to COSMO-SAC (segment ac-

tivity coefficient) produced an alternative thermodynamic model similar to COSMO-RS. Consequently, using the ADF version of COSMO-RS we performed multiple quantum mechanical (QM) calculations on isotopomers of ethanol, acetone, chloroform, methanol, *etc.* and generated isotope specific sigma profiles by choosing all isotopomers for a given compound. From a high level QM calculation a sigma profile is generated. The sigma profile is a histogram of the surface charge density which is molecule specific and unique. Figure 4 shows the sigma profile of the four ^{13}C isotopomers of ethanol (*e.g.* $^{13}CH_3$-$^{13}CH_2$-OH to $^{12}CH_3$-$^{12}CH_2$-OH) calculated using the COSMOS-RS program with standard, unoptimized parameters. While it is difficult to see all four curves, the red and yellow curves clearly show small but reproducible changes across the histogram that are only due to isotopic variation in the ethanol. Similar sigma profiles were obtained from the other compounds that we have investigated. While the most time consuming part of these calculations is the QM computation and is rigorous for each isotopomer, from our preliminary calculations, parameters such as the cavity size and calculation of screening charges appear to be isotope dependent their optimization will improve our results and more clearly differentiate between site-specific isotope fractionations.

Figure 4. Sigma profile of the four isotopomers of ethanol showing small but reproducible changes due to the isotopic variations in the ethanol

While this project did not resolve the development of a comprehensive theoretical understanding of NCIE, it successfully demonstrated that classical methods of explaining these subtle isotope effects were unsuccessful and that our proposed method of using a modified continuum solvation model to calculate site-specific isotopic fractionation was valid and deserving of additional work.

Impact on National Missions
This research directly supports many National security programs and strengthens the core mission of reducing global threats and solving emerging national security challenges through innovative science-based prediction and signature development. It is relevant to nuclear, chemical, and biological threat forensic applications. The emerging field of site-specific stable isotope signature development has the potential to be transformational since it may provide a method to attribute materials without prior knowledge of their natural abundance stable isotope patterns providing an understanding of the theoretical underpinnings of NCIE is achieved.

Delta-Pu Single Crystal Growth Capability for Advanced Electronic Structure Measurements

Jeremy N. Mitchell
20110511ER

Abstract

The many unusual properties of plutonium are direct consequences of its complex electronic structure. Although there have been significant advances in electronic structure calculations, the various theoretical tools have proven inadequate in describing the unusual behavior of Pu's 5f electrons. Direct measurement of electronic structure has been impossible due to the lack of single-crystal samples of δ-Pu and the required advanced experimental methods. In this project, we have re-established LANL's δ-Pu grain growth capabilities and are in the process of characterizing the product of these efforts. We have also exercised two new experimental tools, the proximity diode oscillator at the National High Magnetic Field Laboratory and resonant inelastic x-ray scattering at the Stanford Synchrotron Radiation Laboratory, that have produced exciting new results on the electronic structure of plutonium and plutonium compounds.

Background and Research Objectives

The actinide series marks the development of the 5f electrons within the valence band, and, in particular, plutonium's 5f electrons are tenuously poised at the edge between bonding and non-bonding configurations. These nearly degenerate configurations give rise to an electronic structure that is arguably the most complex in the periodic table. This complex electronic structure leads to emergent behavior—all a direct consequence of its 5f electrons—including six allotropic phases, large volumetric changes associated with these transitions, and mechanical properties ranging from brittle α-Pu to ductile δ-Pu used in nuclear weapons. A first-principles description of Pu's electronic structure and the consequences for its equation of state (EOS) poses one of the most significant challenges to the scientific community and to the success of DOE's national security missions. Despite advances in electronic structure calculations, such as Density Functional Theory (DFT) and Dynamical Mean-Field Theory (DMFT), these methods are inadequate for explaining nearly all of the unusual behavior of plutonium's 5f electrons because they rely on approximations that have yet to be circumvented. Advancing the theoretical state-of-the-art in Pu demands new types of experiments on single crystals to set limits on which theoretical approximations might be acceptable and where others fall short. However, direct experimental verification of Pu's electronic structure is still unavailable despite 65 years of research due to a lack of a suitable δ-Pu single crystal and the necessary state-of-the-art experimental techniques.

To make progress towards this outstanding problem, we have been applying and refining δ-Pu grain growth methods that employ combinations of long-term annealing, secondary recrystallization, and critical strain. The ultimate goal of our effort is to grow large grains of high-purity δ-242Pu, which will enable new experiments on samples with comparatively little radiation damage and allows for various neutron scattering experiments. Thus, a portion of this project was devoted to evaluating LANL's holdings of this less-common isotope. Finally, we have performed several world-class experiments to (1) measure the Fermi surface of a plutonium compound and (2) provide an accurate measure of the f-occupancy in plutonium for the first time. Details on these aspects of the project are described below.

Scientific Approach and Accomplishments

Grain Growth

We undertook parallel Ga-stabilized δ-Pu grain-growth experiments in the TA-55 Plutonium Facility (PF-4) and the CMR Building. These efforts took advantage of samples that had been machined for other tests and material that had been characterized for other programs. The three experiments all involve long-term annealing in controlled atmospheres.

TA-55: The first method used samples that had been obtained for LDRD 2011011DR (D. Schwartz, PI) and were subjected to cyclic hydrogen loading and unloading at elevated temperatures following annealing for 100 hours at 450 °C. Previous work suggested that this process promotes greater than expected δ-Pu grain growth. Figure 1 is an optical photomicrograph of this sample and

highlights a 200-micrometer sized grain that grew from the ~30 micrometer grain size starting material. We are in the process of further characterizing this material using orientation imaging microscopy [1-2].
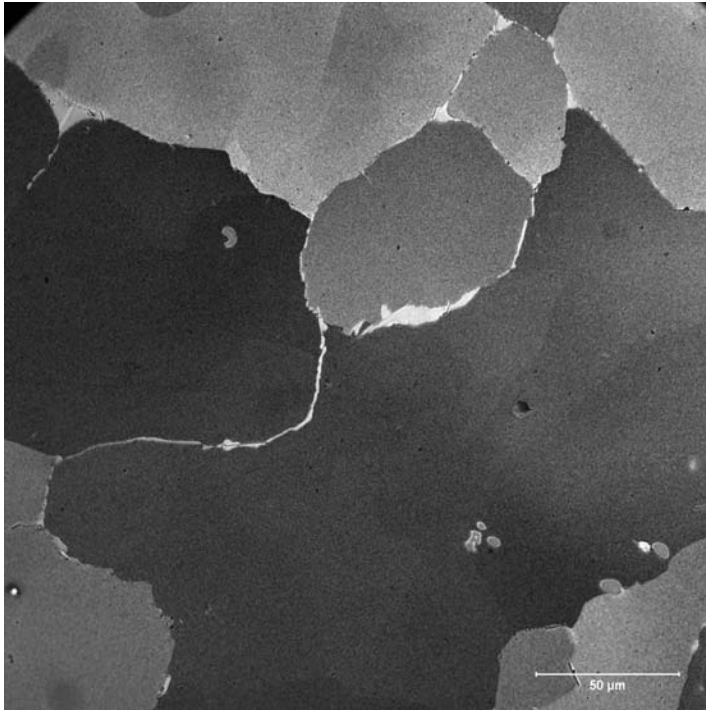
Figure 1. Optical photomicrograph of δ-Pu sample. This sample was annealed for 100 hours at 450 °C and then subjected to cyclical loading and unloading of hydrogen. The starting grain size was about 25 micrometers and this special heat treatment grew grains as large as 200 micrometers.

The critical-strain method has successfully grown large δ-Pu grains in several previous studies [3-8]. We are using a slightly different approach that includes long-term annealing (>100 hours at 450 °C) of a machined tensile-test sample, straining the sample using a mechanical testing frame, followed by additional annealing at 450 °C. To date, we have pulled the samples to strains of 2.56 and 4.08 % and will begin annealing them in early October. We are in the process of modifying a sample holder to allow for non-destructive grain size evaluation of these large specimens using orientation imaging microscopy.

CMR: We also undertook a secondary recrystallization experiment to encourage large grains to grow. We pressed the δ-Pu sample and reduced the thickness by 20%, followed by a 500-hour anneal at 450 °C. Our initial attempt at imaging the grains using a chemical etch to reveal grain boundaries followed by scanning electron microscopy analysis was unsuccessful.

Evaluation of [242]Pu Samples

An important aspect of this project was to evaluate (1) the condition of MST-16's [242]Pu samples stored in PF-4 and

(2) LANL's holdings of this material type in support of the Plutonium Science Strategy. MST-16's materials have been used in various previous experiments and have a range of compositions. These samples were in a variety of configurations, including embedded in epoxy, stored in welded sample holders, encapsulated in quartz tubes to provide a protective atmosphere, and stored in gloveboxes or safes. Our review of other material stored in PF-4 focused on material that was of high isotopic purity (>90% [242]Pu with as little [238]Pu as possible) and large enough size so that it could be prepared into large samples for neutron scattering experiments.

Our investigation of a subset of the MST-16 materials revealed that they are in surprisingly good condition given their age (some >20 years) and the surface reactivity of Pu even in an inert atmosphere.

Measurements

To position our team for a successful DR to determine the nature of the 5f electrons of plutonium, we developed a robust method for measuring the Fermi surface of Pu compounds. Our approach consisted of preparing a very small, perfect single crystal of $PuIn_3$ (Figure 2 inset) and measuring it within hours of removing it from the furnace. Ross McDonald of MPA-CMMS and the National High Magnetic Field Laboratory, along with visiting quantum oscillation expert Yoshinori Haga from the Japan Atomic Energy Agency, carried out measurements of the Fermi surface using an extremely sensitive technique, called the proximity diode oscillator (PDO) technique, developed by our team a couple years ago. This turned out to be very important, since the oscillations we observed were destroyed by the self-irradiation of [239]Pu within about two to three days. As shown in Figure 2b, the quantum oscillations are periodic in 1/H after subtraction of a background from the raw frequency shift data of the circuit (Figure 2a). There is one frequency observed at 2000 T (Figure 2c), which corresponds to a small spherical Fermi surface pocket, labeled gamma (Figure 1d and inset). These measurements extend previous experiments by Dr. Haga and his team in Japan. In particular, the effective mass of the itinerant charge carriers was determined to be of order five times the free electron mass in this new study. This is the first observation of quantum oscillations of a plutonium compound at LANL and provides a clear path forward for performing similar measurements on a delta-Pu single grain in our new DR "Pu-242: A National Resource for the Understanding the 5f Electrons of Plutonium." These results are currently being prepared for publication.
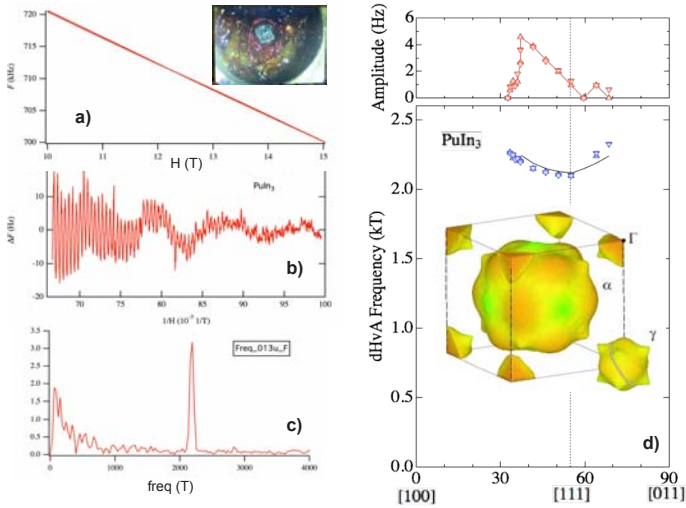
Figure 2. Fermi surface measurements of PuIn3. (A) Raw frequency shift data vs magnetic field H. (B) Quantum oscillations of PuIn3 vs 1/H. (C) Fourier Transform (FT) of the data in (B) showing the single frequency corresponding to the gamma orbit in the inset of D. (D) Angular dependence of amplitude and frequency of gamma orbit.

We have performed ultra-high resolution x-ray absorption spectroscopy measurements on α-Pu, δ-Pu, and a variety of other plutonium and uranium compounds. By employing resonant inelastic x-ray scattering (RIXS) and x-ray absorption near-edge structure (XANES) spectroscopy (not shown) and making comparisons to specific heat measurements, we demonstrate the presence of multiconfigurational f-orbital states in the actinide elements U and Pu, and in a wide range of uranium and plutonium intermetallic compounds. We collected RIXS data on α-Pu (Figure 3A-D) at the Pu $L_{\alpha1}$ emission line ($3d_{5/2} \rightarrow 2p_{3/2}$ corresponding to an emission energy E_E of about 14.2 keV. We are able to resolve three excitations from the raw spectra (Figure 3E), which remain well separated by about 4 eV in the transfer energy E_T ($E_T = E_I - E_{E'}$, the energy difference between the incident energy and the emission energy), consistent with a difference of one electron occupancy for each state. The excitations at 3783 eV, 3787 eV, and 3791 eV are assigned to f^6, f^5, and f^4 configurations, respectively. These results provide a robust experimental basis for a new framework for understanding strongly-correlated actinide materials. In particular, α- and δ-Pu are best described by partially delocalized and strongly multiconfigurational f orbitals, with partial occupancies of f^4 (17%), f^5 (38%), and f^6 (45%) fractions in δ-Pu. Indeed, qualitative agreement is obtained with DMFT calculations [9] for the configuration f^4, f^5, and f^6 fractions in δ-Pu, which indicate about 50-60% f^5 configuration, compared to about 38 ± 10% measured here. DMFT predicts a difference in the total f occupation $\Delta n_f = 0.2$ between α-Pu and δ-Pu, whereas the RIXS results give $\Delta n_f = 0.12 \pm 0.02$. Our results not only provide an accurate measure of the f occupancy in plutonium for the first time, they advance a new paradigm for understanding the light actinides based upon a 5f-electron

multiconfigurational ground state that goes far beyond a "dual nature" scenario. These results are currently being prepared for publication.
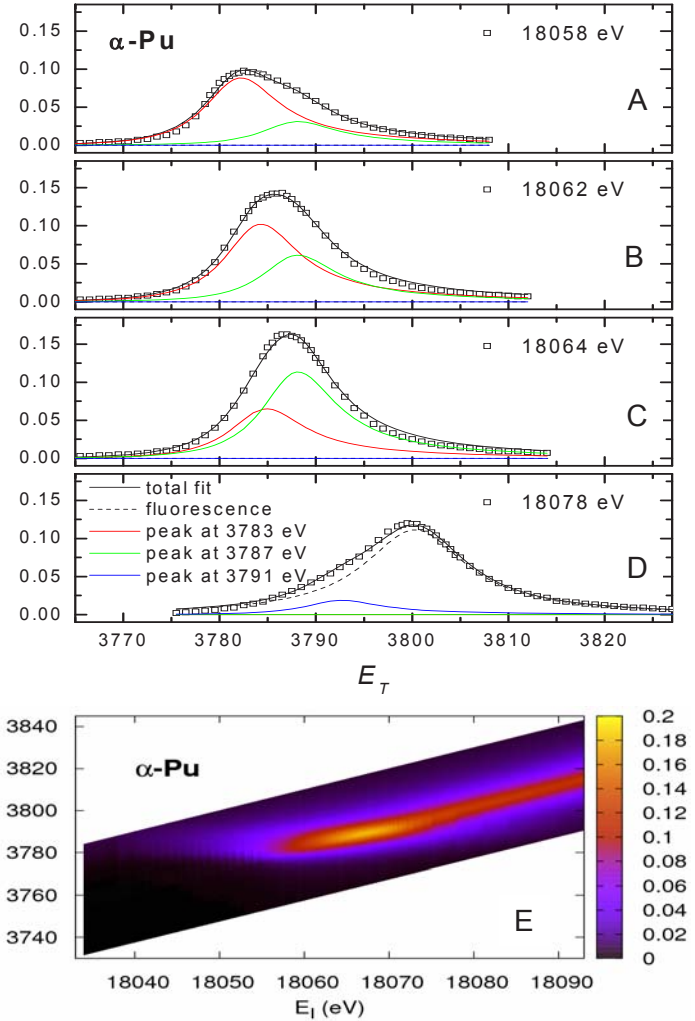
Figure 3. Resonant Inelastic X-ray Spectroscopy (RIXS) of α-Pu vs transfer energy ET at the Pu Lα1 emission line. (A-D) RIXS data at various incident energies showing the resonance features (peaks) at 3783 eV, 3787 eV, and 3791 eV, which are assigned to f6, f5, and f4 configurations, respectively. (E) Raw RIXS spectra as a function of incident and emission energy, from which horizontal cuts A-D were made.

Impact on National Missions

This project represents the re-establishment of δ-Pu grain growth capability that has been dormant for a decade. This technological absence has severely limited our ability to understand key issues relating to the materials science and condensed matter physics of plutonium and its alloys. Furthermore, our experiments described above show that fundamental electronic structure and valence measurements can be made on Pu and Pu compounds. The coupling of this grain growth capability with similar experiments will ultimately enable a clear understanding of the electronic structure of plutonium, which is essential for un-

derstanding and predicting nuclear weapons performance.

References

1. Boehlert, C. J., R. K. Schulze, J. N. Mitchell, T. G. Zocco, and R. A. Pereyra. Initial electron backscattered diffraction observations of a plutonium alloy. 2001. *SCRIPTA MATERIALIA.* **45** (9): 1107.

2. Boehlert, C. J., T. G. Zocco, R. K. Schulze, J. N. Mitchell, and R. A. Pereyra. Electron backscatter diffraction of a plutonium-gallium alloy. 2003. *JOURNAL OF NUCLEAR MATERIALS.* **312** (1): 67.

3. MOMENT, R. L.. CRITICAL STRAIN AND GROWTH OF LARGE GRAINS OF PU-1 WT DEGREES GA ALLOY. 1966. *JOURNAL OF NUCLEAR MATERIALS.* **20** (3): 341.

4. BEER, B. J., and J. E. PAVLICK. CRITICAL RECRYSTALLIZATION STRAIN OF PU-1 WT PERCENT GA. 1967. *JOURNAL OF NUCLEAR MATERIALS.* **23** (2): 236.

5. BERNDT, A. F.. GROWTH OF LARGE GRAINS IN A GALLIUM-STABILIZED DELTA-PLUTONIUM ALLOY. 1966. *JOURNAL OF THE LESS-COMMON METALS.* **10** (1): 71.

6. Lashley, J. C., M. S. Blau, K. P. Staudhammer, and R. A. Pereyra. In situ purification, alloying and casting methodology for metallic plutonium. 1999. *JOURNAL OF NUCLEAR MATERIALS.* **274** (3): 315.

7. Lashley, J. C., M. S. Blau, and R. L. Moment. Preparing single crystals of gallium-stabilzied plutonium. 2000. *Los Alamos Science* .

8. Lashley, J. C., M. G. Stout, R. A. Pereyra, M. S. Blau, and J. D. Embury. The critical recrystallization strain of delta-plutonium. 2001. *SCRIPTA MATERIALIA.* **44** (12): 2815.

9. Shim, J. H., K. Haule, and G. Kotliar. Fluctuating valence in a correlated solid and the anomalous properties of delta-plutonium. 2007. *NATURE.* **446** (7135): 513.

Developing Proton Radiography for Fundamental Solidification Experiments

Amy J. Clarke
20110512ER

Abstract

The goal of this work was to perform the first in-situ solidification experiments using 800 MeV Proton Radiography (pRad), a unique capability at the Los Alamos Neutron Science Center (LANSCE) at Los Alamos National Laboratory (LANL) used to probe dynamic material phenomena, to capture images of advancing solid-liquid interfaces and local solute segregation information in alloy melts. A furnace apparatus for directional solidification of metal alloy sections was built for insertion into pRad that, in combination with high speed cameras, allowed for in-situ monitoring of solidification. Time-resolved images were obtained during melting and solidification of 2 mm thick Sn-Bi and Al-Cu alloy samples. For pRad, the spatial resolution is approximately 65 microns for a large (approximately 44 x 44 mm^2) field of view, which allowed for the acquisition of statistically relevant data. From this work, the feasibility of using pRad to perform in-situ solidification experiments in metal alloys to study solid-liquid interfaces and to perform future process-aware solidification experiments at temperature extremes was established.

Background and Research Objectives

Understanding solidification microstructures is vital for structural materials, since the as-cast, initial microstructure affects the subsequent microstructure evolution during processing and the final microstructure of a part, which ultimately determines properties. Indirect methods, such as decanting of liquid metal after partial solidification or examination of surrogate transparent organic materials with microscopy during cooling, are commonly used to study solidification phenomena [1]. But, direct observations of metal alloy solidification are lacking. More recently, synchrotron x-ray radiography has been used to examine time-resolved solidification for a 1.4 x 1.4 mm^2 field of view in foils less than 200 microns thick in Al-Cu alloys [2,3]. Interestingly, the primary dendrite widths (~200 microns) produced during these experiments were similar to the mold thickness used, suggesting that surface artifacts, such as capillarity, may be important. The results obtained from this work highlight the importance of in-situ solidification studies for advancing our understanding of dendrite formation, growth and fragmentation, solid-liquid interface morphology, and solute segregation [2,3].

In this work, pRad was used for the first time to monitor in-situ solidification of metal alloys. Using pRad, examination of a larger field of view (44 x 44 mm^2) in millimeter thick specimens was possible, allowing for improved statistics and the reduction of artifacts. The acquisition of local solute segregation information during solidification from density contrast was also possible. To develop and demonstrate the technique, solid-liquid interface growth during melting and solidification was monitored in Sn-Bi and Al-Cu alloys and time-resolved images were obtained. The results from these initial experiments demonstrate the viability of using pRad for fundamental solidification experiments. pRad allows for direct observations of solidification phenomena, providing new experimental results and discoveries to compare with solidification theory; it will also advance casting technology.

Scientific Approach and Accomplishments

Goals of this work were to develop the technique to perform in-situ, fundamental solidification experiments at temperature extremes using pRad at the LANSCE facility at LANL and to obtain time-resolved images during melting and solidification. A furnace built at LANL that promotes directional solidification is shown in Figure 1 that was inserted into pRad for these experiments. Each graphite crucible had a machined inside pocket that contained a metal alloy sample nominally 112 mm (4.4 in) in width and 108 mm (4.25 in) in height. Two millimeter thick Sn-Bi or Al-Cu samples were examined. A window approximately 50 mm x 50 mm (2 in x 2 in) was machined into the center of the front and back of each graphite crucible to reduce the amount of material in the beam path. The crucible assembly was contained within a 305 mm x 305 mm (12 in x 12 in) Al box with front and back Al plates with machined windows. Images were obtained from the windowed region of material during heating and cooling. The top and bottom of the crucible were heated with resistive heaters. These heaters were

embedded into the graphite blocks that held the crucible in place. The adjacent copper blocks were water cooled. The entire system was under vacuum. This furnace, along with the high speed cameras at pRad, allowed for in-situ solidification monitoring. The X3 magnifier set-up at pRad was used that allowed for 65 micron resolution for a 44 x 44 mm^2 field of view.
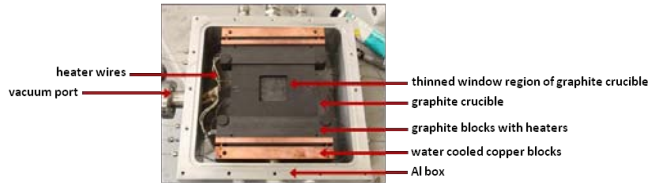
Figure 1. A furnace was designed and built in MST-6 at LANL for insertion into pRad (August, 2011). (Downstream view; the outer Al box is 305 mm x 305 mm (12 in x 12 in). The back Al plate is removed.)

Approximately three days of beam time were used in August 2011 for these initial proof-of-concept experiments. Example images obtained during the melting and solidification of a 2 mm thick Sn-Bi alloy sample are shown in Figure 2. Based upon the density contrast observed in these images, darker regions likely correspond to Bi-rich regions, whereas lighter regions likely correspond to Sn-rich regions. Some interesting features are displayed in images 1-9 (left to right) during melting in Figure 2. Beginning in image 2 and ending in image 5, an interface appears to pass from the top downward. In images 7 and 8, another interface appears to pass from the bottom upward. The sample is fully melted in image 9, while solidification begins during cooling in image 10. In image 11, bright and dark regions are clearly evident in the microstructure, and interestingly in image 12 the formation of additional bright regions occurs in regions that were dark in some instances in the previous images.
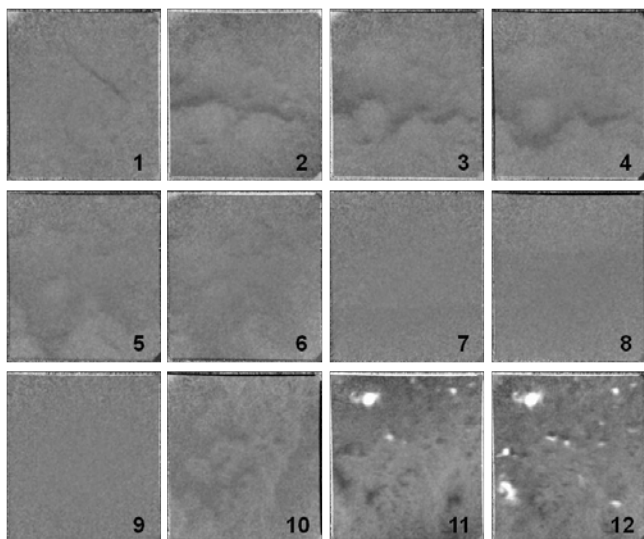
Figure 2. A 2 mm thick Sn-Bi alloy sample during melting, images 1-9, and solidification, images 10-12.

This same sample was subsequently re-heated and cooled. Example images are shown in Figure 3. During melting, an interface appears to pass in images 2 and 3, albeit from the bottom upward instead of the top downward as shown in Figure 2. Another interface then appears to pass in images 4 and 5 from the bottom upward in Figure 3, similar to the results shown in Figure 2. Solidification begins in image 7 and continues until image 12. Features that appear to resemble the formation of dendrites (branched structures) are evident in these images, along with the formation of a dark region in image 10 that becomes progressively darker as solidification continues. This dark region is speculated to be Bi-rich, based upon the observed contrast, and may correspond to the last to freeze region of the microstructure in this field of view.
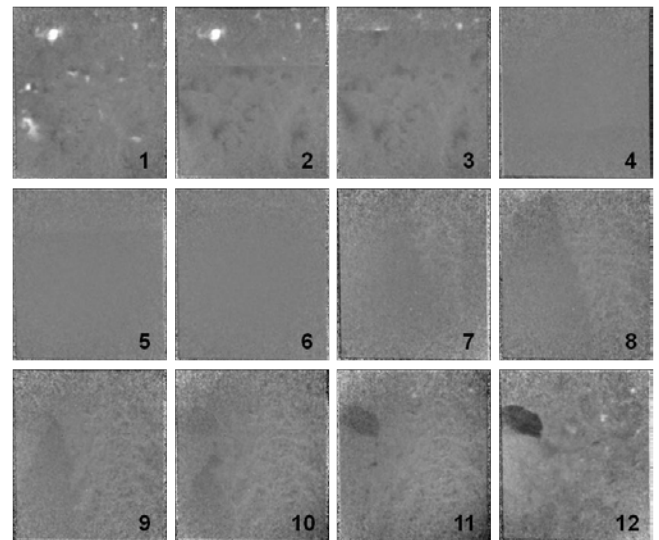
Figure 3. The 2 mm thick Sn-Bi alloy sample shown in Figure 2 during subsequent melting, images 1-6, and solidification, images 7-12.

Example images are also shown in Figure 4 for a 2 mm thick Al-Cu alloy. During melting, an interface appears to pass from the bottom upward. During solidification that begins in image 6, significant contrast develops and continues to develop until the final image. Here, the bright regions are anticipated to correspond to Cu-rich regions, whereas darker regions are anticipated to correspond to Al-rich regions. The formation of bright regions during solidification is consistent with the formation of the last to freeze interdendritic eutectic (two phase microconstituent) that contains the $CuAl_2$ intermetallic phase.

The never before seen dynamic processes that occur during melting and solidification in Figures 2-4 are complex. Future work of a follow-on LDRD project will involve pairing the time and temperature information acquired from these experiments with the images that were obtained. Post-mortem microstructure characterization will also be performed; these results, in combination with the in-situ melting and solidification results will provide a complete history of the complex microstructure evolution.
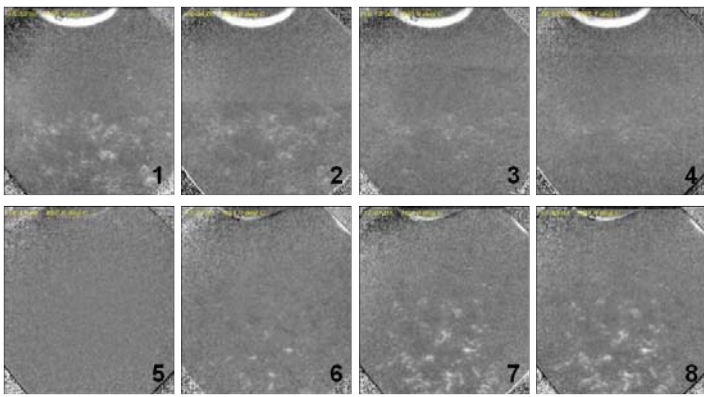
Figure 4. A 2 mm thick Al-Cu alloy sample during melting, images 1-5, and solidification, images 6-8.

Impact on National Missions

pRad is a capability that is unique to LANL. There is a scientific opportunity to further develop pRad at the LANSCE facility at LANL to perform in-situ solidification experiments at temperature extremes and future process-aware experiments, in alignment with the LDRD Defects and Interfaces in Materials topical area, the long term institutional goals of MaRIE that are identified in LANL's 2010 *Decadal Challenges for Predicting and Controlling Materials Performance in Extremes* report [4], and assessments made in the 2007 *Basic Research Needs for Materials under Extreme Environments* report by Basic Energy Sciences (BES) [5] and the 2009 *Frontiers in Crystalline Matter from Discovery to Technology* report by the National Research Council of the National Academies [6]. These preliminary results are also of potential interest within the Synthesis and Processing Science topical area of the Office of Science's BES Early Career Research program.

References

1. Flemings, M. C.. Solidification Processing. 1974.

2. Mathiesen, R. H., and L. Arnberg. X-ray Radiography Observations of Columnar Dendritic Growth and Constitutional Undercooling in an Al-30wt.% Alloy. 2005. *Acta Materialia.* **53**: 947.

3. Ruvalcaba, D., R. H. Mathiesen, D. G. Eskin, L. Arnberg, and L. Katgerman. In Situ Observations of Dendritic Fragmentation due to Local Solute-Enrichment During Directional Solidification of an Aluminum Alloy. 2007. *Acta Materialia.* **55**: 4287.

4. Decadal Challenges for Predicting and Controlling Materials Performance in Extremes. 2010. *Report of a Los Alamos National Laboratory Workshop, LA-UR 10-02959, Los Alamos National Laboratory, Los Alamos, NM.*

5. Basic Research Needs for Materials under Extreme Environments. 2007. *Report of the Basic Energy Sciences Workshop, Office of Science, U.S. Department of Energy.*

6. Frontiers in Crystalline Matter from Discovery to Technology. 2009. *National Research Council, National Academies of Science, The National Academies Press, Washington, D.C.*

Time-Resolved ARPES Studies of Strategic Materials

George Rodriguez
20110515ER

Abstract

The physics of strongly correlated electron materials were studied using the new LANL-developed photoelectron spectroscopic instrument: time-resolved angle-resolved photoemission spectroscopy (trARPES)[1]. The instrument measures the energy-, momentum-, and *time*-resolved dynamic electronic band structure of occupied and empty electronic bands in complex material. We focused on *dynamical* correlations and collective phenomena in these systems aimed at measuring quantum particle interactions at the energy and time scales necessary for understanding emergent properties. We concentrated on several systems of scientific and technological interest: hidden order phase transition in an *f*-electron heavy fermion system, *f*-electron Mott insulator charge transport, quasiparticle dynamics in a low-dimensional (2D) electronic material, and intrinsic inhomogeneities in a high-temperature cuprate superconductor.

Background and Research Objectives

Traditional ARPES is a vital technique for understanding complex correlated electron materials by providing detailed measurements of ground state electronic band structure of occupied states in static mode. In trARPES, the *dynamics* of electronic structure is revealed as time evolution of occupied (and unoccupied) states is measured stroboscopically. The significance of dynamical based measurements is the ability to directly measure time-dependent interplay between the various particle subsystems and their collective effect on emergent properties. A comprehensive set of trARPES studies of strongly correlated electron materials does not exist. There are only a very few investigations [2-3] on simple metals, semiconductors, and only one on a correlated material (1D charge density wave [4]) using an extreme ultraviolet (XUV) based trARPES instrument. This work represents the Laboratory's (and DOE's) first foray into this scientific frontier with LANL poised as the leader in a rapidly emerging field.

The merger of ARPES and ultrafast spectroscopy offers the ability to study time-dependent dynamics of photo-excited electronic processes with femtosecond time res-olution. ARPES is a well-established experimental technique for studying the electronic structure of solids. The simultaneous detection of the kinetic energy and angle of the emitted photoelectrons allows for a measure of the two-dimensional energy-momentum (E, k) map along a given direction in k-space, thus providing accurate information about the dispersion of filled electronic bands and the Fermi surface topology. The LANL trARPES instrument [1], the first of its kind in the DOE complex (and one of only a few in the world), is used to map out the dispersion of normally unoccupied bands provided that electrons are excited ("pumped") with an ultrafast optical pulse (30 fs) into unfilled bands and subsequently photoemitted ("probed") with an appropriately time-delayed ultrafast XUV pulse, tunable between 15-50 eV. The dynamics of the transient electrons is on the femto- to pico-second time scales, and the measured ARPES spectra can provide detailed information of the various relaxation pathways (electronic, lattice, spin, etc.) as determined by various near and long range ordering forces in the material. Armed with this capability, under this project we used trARPES to study several strongly correlated electron systems to elucidate our understanding of dynamical and collective phenomena in DOE relevant strategic materials.

Scientific Approach and Accomplishments

We studied several strongly correlated electron systems using trARPES, and in each case, determine the relevant quasiparticle dynamics with a goal of measuring the energy- , momentum-, and *time*-dependent spectral density function of the transient electronic structure with femtosecond time resolution. The dynamical coupling processes and their interplay were characterized, thus providing vital information for models describing ordering in normal and non-normal states. We investigated a set of four correlated electron materials systems (described below), all of significant scientific interest.

Quasiparticle dynamics at the hidden order transition in URu_2Si_2

The second-order phase transition at T_0=17.5K in URu_2Si_2

is of unknown origin, and the order parameter remains hidden. In recent years, roughly about 30 different theories have been proposed to explain the nature of this transition in the correlated *f*-electron system [5]. We already know that the largest gap structure opening at high temperatures is the hybridization gap. Knowing the size of the gap, and more specifically, its temperature evolution including possible departures from the mean-field behavior is crucial in understanding the background for the hidden order state emergence. Experiments in this project used femtosecond pump-probe trARPES to elucidate the ultrafast dynamics of the quasiparticle structure responsible for hidden order emergence. Figure 1 is an example trARPES measurement from our experiments [6]. By optically pumping the empty states above the Fermi level, we were able to identify the principal actor responsible for Fermi surface renormalization upon entering the hidden order phase. Details of these findings can be found in Reference [6].
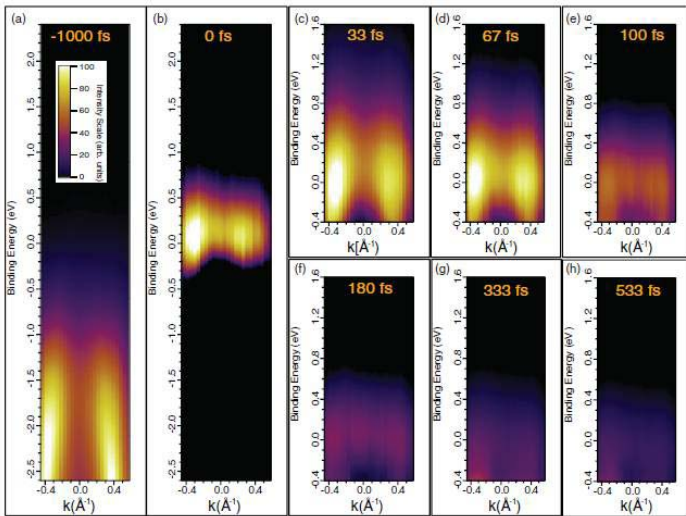
Figure 1. Time-resolved ARPES study of URu_2Si_2 in the hidden order state. (a) The case of a very long, "negative" 1-ps delay between probe and subsequent pump pulses. This spectrum is used to subtract a background from all other spectra collected for the probe pulse arriving after the pump pulse with delays between 0 and 533 fs, with (b) the "0-fs" case corresponding to the overlap of pump and probe pulses. The double structure seen above the Fermi level corresponds to the different, long-lived QPs, decaying in density between 0 and 533 fs, as shown in (b)–(h). The characteristic lifetime estimated from the decay in intensity as a function of delay is 213 ± 12 fs, corresponding to a quasiparticle peak width of 3 meV. Long-lived QPs are located right above the Fermi level and separated by the vector q<110> = 0.56 ± 0.08 Angstrom^-1. All pump-probed angle-resolved spectra shown here are taken below T=17.5 K with a variable pump-probe delay.

Tracing ultrafast separation and coalescence of carriers in graphene with time-resolved photoemission

Graphene, a recently discovered two-dimensional form of carbon, is a strong candidate for many future electronic devices [7-10]. A question of central importance

in optoelectronics, particularly high-speed applications, is how photoexcited carriers behave on ultrashort time scales. Even though time-resolved studies have provided a wealth of information, fundamental questions concerning the quantum descriptions of the transient electron-hole plasma remain [11-13]. On one hand, some descriptions of the photoexcited electrons and holes allow for phenomena, such as THz lasing or using graphene as a saturable absorber in tunable lasers [14,15]. On the other hand, the observation of phenomena such as ultrafast photoluminescence and studies of carrier multiplication in graphene [13,16], imply fundamentally different quantum descriptions of the photo excited electron hole plasma. In this project task we applied the technique of time-resolved photoemission to directly obtain the evolving quantum distributions of the electrons and holes: on an ultrashort 500 fs time scale the electron and hole populations can be described by two separate Fermi-Dirac distributions, while on longer time scales the populations coalesce to form a single Fermi-Dirac distribution at an elevated temperature. This unusual behavior is a consequence of graphene's unique band structure and has important implications for possible applications.
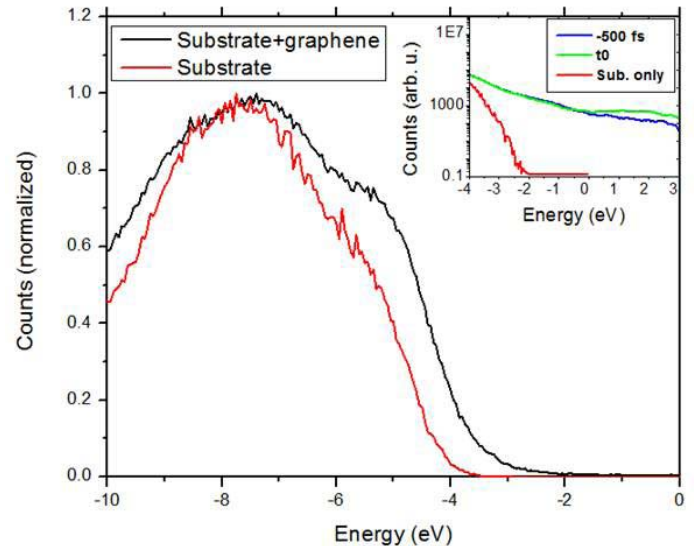
Figure 2. Plots of the static photoemission spectra for graphene on the SiO_2 substrate (black line) and the substrate alone (red line). The inset shows the photoemission spectra for a delay of -500 fs (blue line) and at time zero (green line). The spectra are plotted on a Log plot to accentuate differences in the signal near the Fermi edge. Also shown in the inset is the spectrum of the substrate-only (red line) for comparison.

Figure 2 is plot of the static photoemission data of a monolayer graphene sample on a SiO_2 substrate. Clear signature of the photoemission spectrum signal from graphene is distinguished from the graphene plus substrate case. The time-dependent photoemission signal is shown in Figure 3 for the case of photoexcitation with 1.5 eV photons. Figure 3(a) plots the time dynamics of the conduction band electron population versus kinetic energy showing an initial

electron population that relaxes over a period of approximately one picosecond. Figure 3(b) is a plot of the electron population lifetime versus the energy above the Fermi energy level for two cases: 1.5 eV and 3.0 eV pump photon energies. The trend in Figure 3(b) shows that electrons that are born high up in the conduction band relax more rapidly than those near the Fermi level and is attributed to the available phase space scatterings at higher energies than near the Fermi level. Additional details on these studies are found in Reference [17].
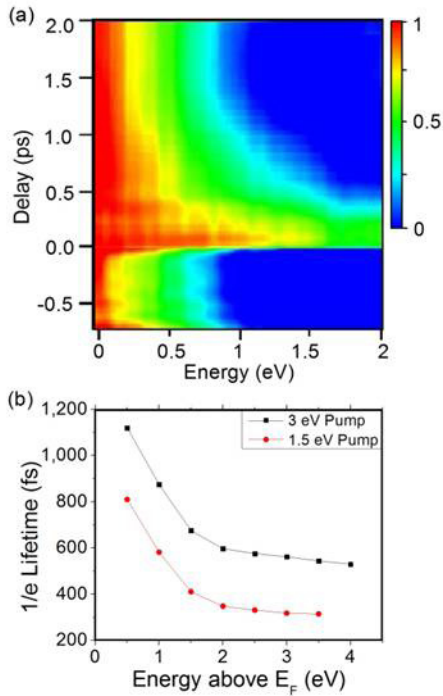
Figure 3. (a) Surface plot of the energy spectra of the electrons as a function of delay for graphene pumped with 1.5 eV photons. (b) The measured 1/e decay times of the electrons are shown for 1.5 eV (red circles) and 3 eV (black squares) pump photon energy.

Momentum-dependent ultrafast dynamics of reentrant superconductivity

The light-induced nonthermal phase transition between different phases of matter is found in a variety of systems [18-20], and continues to be a fascinating research topic. Here focused on a trARPES study of an optically triggered phase transition in a high-temperature superconductor BSCCO ($Bi_2Sr_2CaCu_2O_{8+\delta}$), T_c=95K. By strongly perturbing the system with 30 femtosecond pulses of 1.55eV photons, we observed an instantaneous collapse of the superconducting phase followed by recovery dynamics that vary distinctly between different regions of the Brillouin zone. We showed that the unexpectedly efficient electron-phonon coupling causes rapid and momentum-dependent reentrance of the superconducting condensate. Contrary to previous reports [21,22], the reentrance in the antinodal region in the presence of energetic phonons leads to

complex relaxation dynamics, absent in the nodal region where the superconducting gap vanishes. With the onset of condensation occurring after approximately 200fs, this momentum-dependent melting and reentrance of superconductivity can be captured only by using radiation with sufficient intensity, and having temporal resolution in the tens of femtoseconds range. This study clearly demonstrates the significant difference between the nodal and antinodal excitations in establishing superconductivity, and opens the possibility for investigating anisotropic ultrafast phase transitions in a variety of systems. An example set of the results from our recent publication submission [23] is shown in Figures 4 and 5.
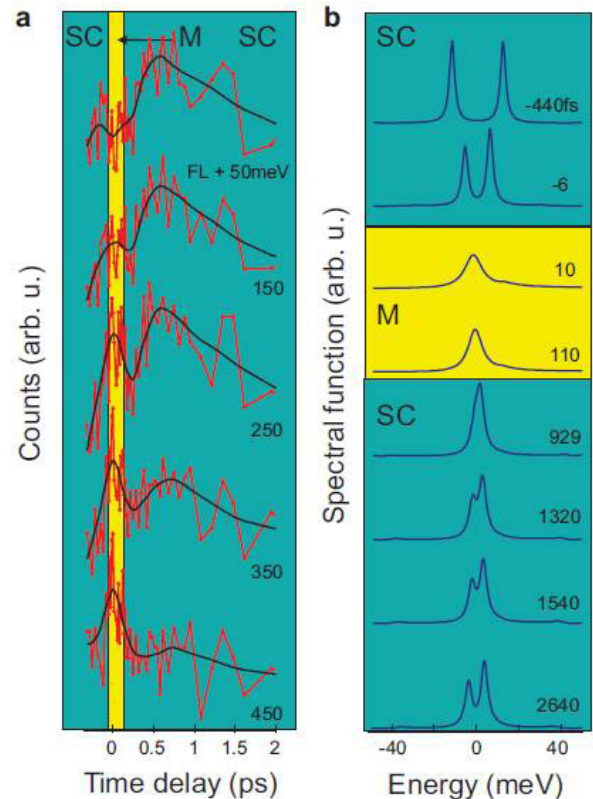
Figure 4. Dynamics of photoexcited electrons in the antinodal region. Portions colored in teal indicate the intervals of time when superconductivity (labeled SC) is either existing (before t=0) or reentering (after t=200fs), as determined from the experiment. Portions in yellow correspond to the transient light-induced metallic (labeled M) phase. (a) Temporal evolution of the quasiparticle states in the antinodal region, excited to different energies above the Fermi level. Following the ultrafast relaxation in the M phase, a well-developed delayed peak in the photoelectron signal is observed when the SC gap formation and phonon-driven electron re-excitation balances relaxation. The maximum of this peak appears ~600fs after photoexcitation. Black curves are a guide to the eye. (b) Spectral function (antinodal region) calculated at different delay times. The scale is the same for all curves. Evident around t=0 is the SMT, followed by reentrance back into the SC phase at later times.
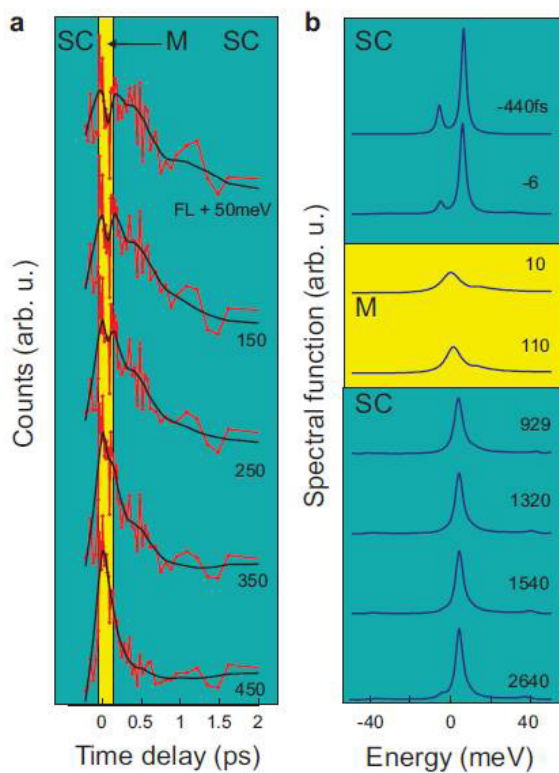
Figure 5. Dynamics of photoexcited electrons in the nodal region. Color coding is the same as in Fig. 4. (a) Temporal evolution of the quasiparticle states in the nodal region, excited to different energies above the Fermi level. The re-entrance of SC phase after the M phase does not affect appreciably the quasiparticle relaxation. A small delayed peak above the Fermi level is attributed to possibly probing regions in the Brillouin zone where the gap is non-vanishing. Black curves are a guide to the eye. (b) Spectral function calculated (nodal region) at different delay times. The scale is the same for all curves, and is the same to the one in Fig. 4b. The superconducting-to-metal transition (SMT) modifies the spectral function, though it remains gapless, leading to ultrafast monotonic relaxation.

Electron Hubbard band dynamics in the f-electron Mott insulator uranium dioxide

In this strongly correlated system, the Mott gap (~2eV) is comprised of occupied lower and empty upper Hubbard bands each with 5f-character [24]. When charge carriers are injected into this system, the question arises as to the nature of electronic transport: hopping versus polaronic behavior. Our recent results from femtosecond optical spectroscopy [25] suggests that, upon photoexcitation, two (5f^2)U^{+4} sites are converted to pairs of (5f^3)U^{+3} and (5f^1) U^{+5} excitonic states and a lattice distortion forms excitonic polarons. Corresponding time-resolved photoemission measurements under this project helped clarify our conclusions made in Ref. [25]. Using ultrafast pump-probe time-resolved photoemission we observed inter- and intra-Hubbard band dynamics by photoexcitation carriers across the gap with 4.5 eV pump photons and then probing the

transient states with 30 eV XUV photons in photoemission [26]. The photoemission results are consistent with pump fluence dependent hot-carrier relaxation and subsequent lattice coupling on the ten picosecond time scale.

In summary, progress in using trARPES to understand quasiparticle dynamics in several strongly correlated material systems is reported. Results using the trARPES approach among these systems highlight the utility of this spectroscopic approach for understanding quasiparticle dynamics in complex strongly correlated electron systems relevant to LANL's strategic materials science programs.

Impact on National Missions

The research in this project was aimed at fundamental understanding of electronic structure and behavior of complex correlated electronic materials. It supported fundamental experiments as a foundation for future energy technologies by improving our understanding of emergent phenomena for the discovery of new material properties. Hence, this project embraced the Laboratory's Materials Strategy, as well as the LDRD Grand Challenge in Materials. Broadening our knowledge about phenomena such as superconductivity, magnetism, electrical transport, and physics of low dimensional electron systems is relevant to DOE energy security mission, and ultimately National Security, by providing the scientific base for next generation energy efficient technologies. The scientific capabilities demonstrated in this project enhanced the Laboratory's portfolio in these studies for DOE Basic Energy Sciences program in Material Sciences and Engineering.

References

1. Dakovski, G. L., Y. Li, T. Durakiewicz, and G. Rodriguez. Tunable ultrafast extreme ultraviolet source for time- and angle-resolved photoemission spectroscopy. 2010. *Review of Scientific Instruments.* **81** (7): 073108 (7 pp.).

2. Mathias, S., M. Wiesenmayer, F. Deicke, A. Ruffing, L. Miaja-Avila, M. M. Murnane, H. C. Kapteyn, M. Bauer, and M. Aeschlimann. Time and angle resolved photoemission spectroscopy using femtosecond visible and high-harmonic light. 2009. In *LXIII Yamada Conference on Photo-Induced Phase Transition and Cooperative Phenomena ; 11-15 Nov.* (2008 ; Osaka, Japan). Vol. 148, p. 012042 (8 pp.).

3. Mathias, S., M. Wiesenmayer, F. Deike, A. Ruffing, L. Avila Miaja, M. M. Murnane, H. C. Kapteyn, M. Aeschlimann, and M. Bauer. Angle-resolved photoemission spectroscopy with a femtosecond high harmonic light source. 2007. *Review of Scientific Instruments.* **78**: 083105.

4. Rohwer, T., S. Hellmann, M. Wiesenmayer, C. Sohrt, A. Stange, B. Slomski, A. Carr, Y. Liu, L. M. Avila, Kalla&uml, S. Mathias, L. Kipp, K. Rossnagel, and M.

Bauer. Collapse of long-range charge order tracked by time-resolved photoemission at high momenta. 2011. *Nature.* **471** (7339): 490.

5. Oppeneer, P. M., J. Rusz, S. Elgazzar, M. -T. Suzuki, T. Durakiewicz, and J. A. Mydosh. Electronic structure theory of the hidden-order material URu$_2$Si$_2$. 2010. *Physical Review B (Condensed Matter and Materials Physics).* **82** (20): 205103 (21 pp.).

6. Dakovski, G. L., Y. Li, S. Gilbertson, G. Rodriguez, A. V. Balatsky, J. X. Zhu, K. Gofryk, E. D. Bauer, P. H. Tobash, A. J. Taylor, J. L. Sarrao, P. M. Oppeneer, P. S. Riseborough, J. A. Mydosh, and T. Durakiewicz. Anomalous femtosecond quasiparticle dynamics of hidden order state in URu2Si2. To appear in *Physical Review B Rapid Communications.*

7. Novoselov, K. S., A. K. Geim, S. V. Morozov, D. Jiang, Y. Zhang, S. V. Dubonos, I. V. Grigorieva, and A. A. Firsov. Electric field effect in atomically thin carbon films. 2004. *Science.* **306** (5696): 666.

8. Zhang, Y., Y. W. Tan, H. L. Stormer, and P. Kim. Experimental observation of the quantum Hall effect and Berry's phase in graphene. 2005. *Nature.* **438**: 201.

9. Peres, N. M., F. Guinea, and A. H. Neto. Electronic properties of disordered two-dimensional carbon. 2006. *PHYSICAL REVIEW B.* **73** (12): 125411.

10. Gusynin, V. P., and S. G. Sharapov. Unconventional integer quantum Hall effect in graphene. 2005. *Physical Review Letters.* **95** (14): 146801/1.

11. Sun, D., Z. K. Wu, C. Divin, X. Li, C. Berger, W. A. de Heer, P. N. First, and T. B. Norris. Ultrafast relaxation of excited Dirac fermions in epitaxial graphene using optical differential transmission spectroscopy. 2008. *Physical Review Letters.* **101**: 157402.

12. Breusing, M., S. Kuehn, T. Winzer, Malic&acute, F. Milde, N. Severin, J. P. Rabe, C. Ropers, A. Knorr, and T. Elsaesser. Ultrafast nonequilibrium carrier dynamics in a single graphene layer. 2011. *Physical Review B (Condensed Matter and Materials Physics).* **83** (15): 153410 (4 pp.).

13. Lui, Chun Hung, Kin Fai Mak, Jie Shan, and T. F. Heinz. Ultrafast Photoluminescence from Graphene. 2010. *Physical Review Letters.* **105** (12): 127404 (4 pp.).

14. Sun, Z., D. Popa, T. Hasan, F. Torrisi, F. Wang, E. J. R. Kelleher, J. C. Travers, V. Nicolosi, and A. C. Ferrari. A stable, wideband tunable, near transform-limited, graphene-mode-locked, ultrafast laser. 2010. *Nano Research.* **3**: 653.

15. Ryzhii, V., M. Ryzhii, A. Satou, T. Otsuji, A. A. Dubinov, and V. Ya. Aleshkin. Feasibility of terahertz lasing in optically pumped epitaxial multiple graphene layer structures. 2009. *Journal of Applied Physics.* **106** (8): 084507 (6 pp.).

16. Winzer, T., A. Knorr, and E. Malic. Carrier multiplication in graphene. 2010. *Nano Letters.* **10** (12): 4839.

17. Gilbertson, S., G. L. Dakovski, T. Durakiewicz, J. X. Zhu, K. M. Dani, A. D. Mohite, A. Dattlebaum, and G. Rodriguez. Tracing ultrafast separation and coalescence of carriers in graphene. *Physical Review Letters.*

18. Fiebig, M., K. Miyano, Y. Tomoika, and Y. Tokura. Visualization of the local insulator-metal transition in Pr0.7Ca0.3MnO3. 1998. *Science.* **280**: 1925.

19. Yusupov, R., T. Mertelj, V. V. Kabanov, S. Brazovskii, P. Kusar, Jiun-Haw Chu, I. R. Fisher, and D. Mihailovic. Coherent dynamics of macroscopic electronic order through a symmetry breaking transition. 2010. *Nature Physics.* **6** (9): 651.

20. Coslovich, G., C. Giannetti, F. Cilento, S. Dal Conte, G. Ferrini, P. Galinetto, M. Greven, H. Eisaki, M. Raichle, R. Liang, A. Damascelli, and F. Parmigiani. Evidence for a photoinduced nonthermal superconducting-to-normal-state phase transition in overdoped Bi2Sr2Ca0.92Y0.08Cu2O8+delta. 2011. *Physical Review B (Condensed Matter and Materials Physics).* **83** (6): 064519 (9 pp.).

21. Cortes, R., L. Rettig, Y. Yoshida, H. Eisaki, M. Wolf, and U. Bovensiepen. Momentum-resolved ultrafast electron dynamics in superconducting Bi2Sr2CaCu2O8+delta. 2011. *Physical Review Letters.* **107**: 097002.

22. Graf, J., C. Jozwiak, C. L. Smallwood, H. Eisaki, R. A. Kaindl, D. H. Lee, and A. Lanzara. Nodal quasiparticle meltdown in ultrahigh-resolution pump-probe angle-resolved photoemission. 2011. *Nature Physics.* **7**: 806.

23. Dakovski, G. L., T. Durakiewicz, J. X. Zhu, P. S. Riseborough, G. Gu, S. Gilbertson, and G. Rodriguez. Momentum-dependent dynamics of reentrant superconductivity . *Nature Physics.*

24. Roy, L. E., T. Durakiewicz, R. L. Martin, J. E. Peralta, G. E. Scuseria, C. G. Olson, J. J. Joyce, and E. Guziewicz. Dispersion in the Mott Insulator UO$_2$: a comparison of photoemission spectroscopy and screened hybrid density functional theory. 2008. *Journal of Computational Chemistry.* **29** (13): 2288.

25. An, Y. Q., A. J. Taylor, S. D. Conradson, S. A. Trugman, T. Durakiewicz, and G. Rodriguez. Ultrafast Hopping Dynamics of 5f Electrons in the Mott Insulator UO$_2$ Studied by Femtosecond Pump-

Probe Spectroscopy. 2011. *Physical Review Letters.* **106** (20): 207402 (4 pp.).

26. Gilbertson, S. M., G. L. Dakovski, Y. Li, M. T. Paffett, S. D. Conradson, J. X. Zhu, T. Durakiewicz, and G. Rodriguez. Ultrafast electron band dynamics in the 5f Mott insulator UO2. *Physical Review Letters.*

Publications

An, Y. Q., A. J. Taylor, T. Durakiewicz, and G. Rodriguez. Pump-probe reflectivity study of ultrafast dynamics of strongly correlated 5f electrons in UO2. 2011. *Journal of Physics Conference Series.* **273**: 121440.

An, Y., A. Taylor, S. Conradson, S. Trugman, T. Durakiewicz, and G. Rodriguez. Ultrafast hopping dynamics of 5f electrons in the Mott insulator UO2 studied by femtosecond pump-probe spectroscopy. 2011. *Physical Review Letters.* **106** (20): 207402.

Dakovski, G. L., S. M. Gilbertson, T. Durakiewicz, and G. Rodriguez. Tracing transient electronic states with femtosecond time-resolved ARPES . Presented at *Gordon Research Conference: X-Ray Science.* (Waterville, ME, 7-12 Aug. 2011).

Dakovski, G. L., T. Durakiewicz, J. X. Zhu, P. S. Riseborough, G. Gu, S. Gilbertson, and G. Rodriguez. Momentum-dependent dynamics of reentrant superconductivity . *Nature Physics.*

Dakovski, G. L., Y. Li, S. Gilbertson, G. Rodriguez, A. V. Balatsky, J. X. Zhu, K. Gofryk, E. D. Bauer, P. H. Tobash, A. J. Taylor, J. L. Sarrao, P. M. Oppeneer, P. S. Riseborough, J. A. Mydosh, and T. Durakiewicz. Anomalous femtosecond quasiparticle dynamics of hidden order state in URu2Si2. To appear in *Physical Review B Rapid Communications.*

Durakiewicz, T., G. L. Dakovski, Y. Li, G. Rodriguez, J. J. Joyce, E. D. Bauer, P. H. Tobash, P. M. Oppeneer, and P. S. Riseborough. Band renormalization at the hidden order transition in URu2Si2. Presented at *American Physical Society March Meeting.* (Dallas, TX, 21-25 Mar. 2011).

Durakiewicz, T., G. L. Dakovski, Y. Li, S. M. Gilbertson, G. Rodriguez, A. V. Balatsky, J. X. Zhu, K. Gofryk, E. D. Bauer, P. H. Tobash, A. J. Taylor, J. L. Sarrao, P. M. Oppeneer, P. S. Riseborough, and J. A. Mydosh. Anomalous quasiparticle dynamics in the hidden order phase of URu2Si2. Invited presentation at *American Vacuum Society International Symposium.* (Nashville, TN, 30 Oct. - 4 Nov. 2011).

Durakiewicz, T., J. J. Joyce, G. Rodriguez, and J. D. Thompson. From kinky physics to transuranics: f-electron angle resolved photoemission spectroscopy at Los Alamos National Laboratory. Presented at *Abstracts of the X-Ray Scattering Contractors Meeting.* (Warrenton, VA, 14-17 Nov. 2010).

Gilbertson, S. M., G. L. Dakovski, Y. Li, M. T. Paffett, S. D. Conradson, J. X. Zhu, T. Durakiewicz, and G. Rodriguez. Ultrafast electron band dynamics in the 5f Mott insulator UO2. *Physical Review Letters.*

Gilbertson, S., G. L. Dakovski, T. Durakiewicz, J. X. Zhu, K. M. Dani, A. D. Mohite, A. Dattlebaum, and G. Rodriguez. Tracing ultrafast separation and coalescence of carriers in graphene. *Physical Review Letters.*

Liu, M. K., R. D. Averitt, T. Durakiewicz, E. D. Bauer, P. H. Tobash, A. J. Taylor, and D. A. Yarotski. Evidence of pseudogap hidden order state in URu2Si2 using ultrafast laser optical spectroscopy. To appear in *Physical Review B Rapid Communications.*

Liu, M., D. Yarotski, T. Durakiewicz, S. Trugman, and R. Averitt. Ultrafast quasiparticle dynamics in the hidden order state of URu2Si2. Presented at *American Physical Society March Meeting.* (Dallas, TX, 21-25 Mar. 2011).

Zhu, J. X.. Theory of ultrafast pump-probe phenomena in high-temperature superconductors. Invited presentation at *American Physical Society March Meeting.* (Dallas, TX, 21-25 Mar. 2011).

Microstructure Analysis for Extreme Events: A Stochastic Modeling Framework for Microstructure Datasets

John F. Bingert
20110602ER

Abstract

The study of microstructure-property relationships is a defining concept in the field of materials science and engineering. Despite the paramount importance of microstructure to the field a rigorous systematic framework for the description of structural variance between samples of materials with the same processing history and between different material classes has yet to be adopted. In this work we utilize the formalism of stochastic processes to develop a statistical definition of microstructure and develop measures of structural variance in terms of the measured scatter in estimators of higher order probability distributions. Principal component analysis is used to develop reduced order data representations and produce visualizations of the structure space spanned by characterized realizations. This structural variance can be correlated with property/performance variance and structure/property maps can be produced in this reduced order space. While seemingly abstract the activities undertaken in this project have large potential in the field of quality control and material standards. Additionally, having a firm understanding of material variance is critical to understanding potential error in material performance models and code and thus critical to the larger LANL mission of uncertainty quantification at the system level.

Background and Research Objectives

The concept of microstructure is central to the field of materials science and engineering. It can be argued that the birth of metallurgy and materials as a physical science was coincidental with the development of microscopy. Since the mid 1800's developments in the field have been tied to the understanding that materials are not homogeneous in nature but possesses an internal structure that spans several disparate length scales. The near simultaneous development of metallography and stereology to obtain point estimates of microstructural distribution parameters (e.g. mean grain size) highlights the significance of randomness and how deeply it permeates our understanding of materials. Despite this central role that randomness plays in material performance we have not hot yet developed tools to characterize and quantify microstructure in a manner that facilitates quantification and visualization of structural variance.

The recent revolution in characterization techniques has enabled the rapid collection of vast amounts of digital 3D structural information. As the ability to collect data increases, the development of analysis tools to synthesize raw data into useful materials knowledge must also progress in parallel. An understanding of the quality or information content of the collected data is critically lacking. For example, "How much new information is gained by the addition of new datasets, or is additional characterization redundant?" "Given an ensemble of characterized structures how accurately can the tails of the performance distribution be predicted?" or "Can accurate bounds be placed on the occurrence of extreme properties?" are questions that as a field we currently have no means of addressing.

Significant advances have been made in the quantitative description of microstructure via statistical measures and descriptors. The most common measures are the n-point correlation functions, nearest neighbor descriptors, or entropic (information content) descriptors [1-6]. This body of work is largely concerned with the average statistics of the material as a whole and limited attention is paid to the observed scatter in statistics at the level of the ensemble or individual realizations, the relationship between the variance and the observed distribution in performance, or the identification/prediction of structural outliers which are likely to exhibit performance measures far from the mean.

The need for quantification of structural variance is highlighted by the emergence of the new sub-disciplines of materials-by-design, microstructure-sensitive-design, or integrated computation materials engineering [2, 7, 8]. The above frameworks seek to optimize the microstructure and processing to obtain superior properties and predictable performance and integrate this optimization into the component level design and manufacturing process (inverse material design). For these efforts to be successful it is necessary to manipulate the microstructure as a continuous design variable. More importantly the statistically expected variation in microstructure must be

carried through the integrated design process if defect-sensitive properties, such as fatigue and fracture are to be considered. A key advantage of this approach is that it forms a natural foundation that incorporates complex higher-order effects that would be difficult to capture otherwise. As an example the potential interaction between grain size, grain boundary-character distribution, and morphology on fatigue life, which would be nearly impossible to capture explicitly would be incorporated into the microstructure statistics.

In our view the quantification of structural variance is best addressed through the formalism of stochastic processes. A stochastic process can be understood as a set of probability rules that assign a function or random field to every experimental outcome. In the case of materials each sample or micrograph is an experimental outcome and there exists a set of *rules* that assign a microstructure constituent to each infinitesimal point in the sample. Through characterization, realizations of these processes are viewed as micrographs or 3D datasets. In turn the distribution associated with the microstructure can be estimated from the collected micrographs. In this project three main ideas were explored: (1) The formalization of the microstructure concept through the language and mathematics of stochastic processes; (2) The construction of reduced order representations of higher order microstructure distributions for visualizing the microstructural variance and the microstructure space spanned by the collected material datasets; (3) The linking of structural variance in an ensemble with the measured variance in microscale properties/performance.

Scientific Approach and Accomplishments

In this work we considered each characterized material region to be the output of some stochastic process $\mathbf{m}(x, $ the microstructure function, which assigns a microstructure constituent described by the random variable $\mathbf{h} = h$ to position x in the material region. A very brief overview is described here; full details can be found in our recent publication [9]. Estimation of higher order distributions (third and higher order probability distribution functions) and moments of the microstructure function is often impractical or impossible to estimate. Instead we relied on the *n*-point correlation functions which have long history in the literature to describe the spatial statistics of heterogeneous systems [2, 6]. The 2-point correlation gives the conditional probability of finding microstructure constituent $\mathbf{h} = h_1$ at pointpoint x_1 given that constituent $\mathbf{h} = h_2$ is at point $x_2 = x_1 + r$. The two-point correlation was used as it can be rigorously linked to a broad range of mechanical and transport properties in heterogeneous media [refs]. Each material sample serves as an estimate of the microstructure statistics. Figure 1 shows that the estimates obtained from individual single realization (material samples) of the same material can vary drastically. Understanding the variance estimates of the spatial statistics from different samples are a key topic of this work.
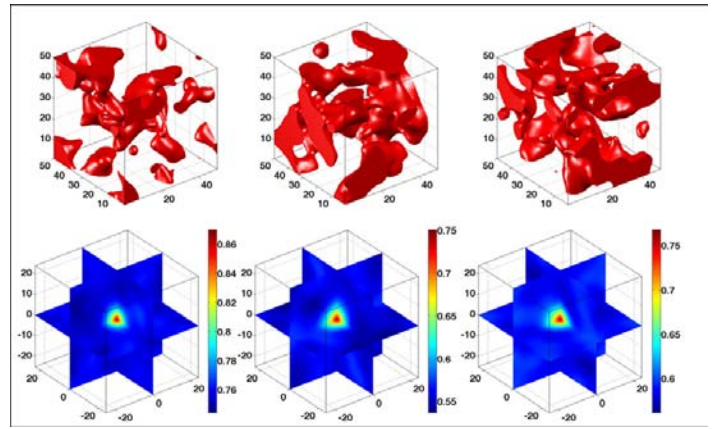
Figure 1. (top) Three microstructure realization from the same material (digitally created). For clarity the stiffer elastic phase (local state h1) is made transparent and the lower volume fraction compliant phase (local state h2) is shown in red. (bottom) The (h1,h1) two-point correlation for the realizations shown above. The variability of statistical estimates is clearly seen.

For all but the most simple material systems the space of microstructure statistics forms a very high dimensional space, not amenable to the computation and visualization of structural variance, and therefore a reduced order representation of the data is required. In this work the following features of a reduced space were identified 1) The data corresponding to microstructure realizations must be easily visualized in an intuitive manner 2)The data must be represented in a small number of parameters so that optimization problems and searches of data can be performed 3) A simple and intuitive measure of distance is required to quantify how similar/dissimilar microstructure realizations are from each other 4) The microstructural variance must be easily visualized and quantified and 5) A simple test is required to gauge the information content of new microstructure datasets. For these reason principal component analysis (PCA) was chosen to construct lower order representations of the data [9].

Figure 2 shows the projection of the microstructure realizations (three large ensembles of structures similar to those shown in Figure 1) into the PCA space and is a key result of this work. It shows at a glance the scatter in microstructure realization collected and allows the ready identification of structural outliers or realizations expected to exhibit performance or property values far from the mean. Simple visualizations of this type could have large impact on quality control and related applications. Regions of space that correspond to acceptable material could be delineated through characterization and property measurements. As new material is produced the microstructure could be projected into the space, operators would immediately be aware of any process drift and corrective action could be take before material that fails to meet specifications is produced. The mapping of property values into this space is shown in Figure 3 and could be used to make fast and accurate property estimates for line production materials

reducing the need to perform repeated qualifying mechanical testing.
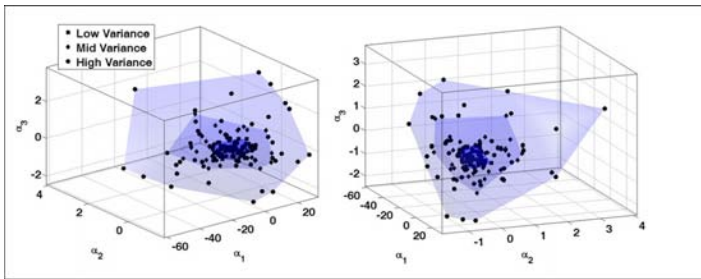
Figure 2. Projection of realizations of three different materials in the PCA space. Each material has the same average microstructure statistics but different microstructural variance. The average or representative microstructures are those close to the origin while outliers or samples that are expected to exhibit property values far from the mean are those farthest from the origin.
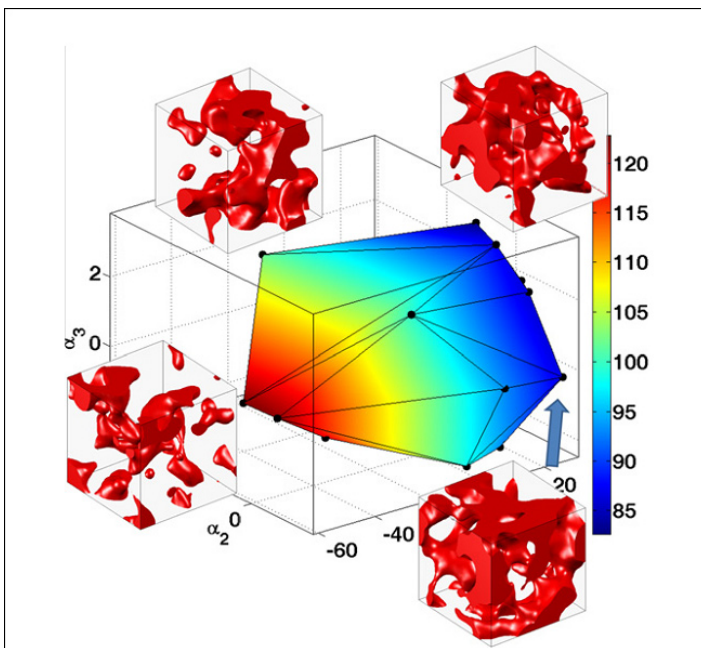
Figure 3. Map of predicted modulus values projected into the PCA space. The above figure shows that the PCA representation accurately captures the variability in property and allows for fast and accurate estimates of effective properties and property variance from microstructure observations.

While the above work describes the main focus of this project, preliminary work was undertaken on two important future endeavors, 1) the generation of digital material samples that correspond to target microstructure statistics and 2) the efficient estimation of microstructure statistics (local lattice orientation correlations) in polycrystalline materials. The generation of digital microstructures is critical to exploratory use of the reduced order space. Generative models of materials are also critical for exploring the

information captured by the statistical descriptions, for examples it is well know that second order spatial statistics do not capture long range connectivity or percolation. Often it is not possible to determine *a priori* whether certain structural features important to properties or performance are captured by a metric, and the accuracy of the model can only be determined by generating potential realizations. Even when the features of interest are adequately described by the statistics it is often useful to generate extrapolative structures outside of the structural space spanned by characterization. These extrapolative structures can be used as the inputs to property/performance models and simulations to identify regions of the PCA space to target structures of interest for further study. The generation of realizations from incomplete statistics is inherently ill posed and must be solved as an optimization problem with some sort of data regularization. In this work we have had good luck using compressed sensing techniques which seek structures that are space with respect to the l1-norm of their total variation [10]. An example of three structures generated with the same target statistics is shown in Figure 4. While the generation algorithms are still at their preliminary stages, a short manuscript is under preparation for submission to Acta Materialia describing some novel results concerning the uniqueness of statistical reconstructions and the novel mathematical framework developed under this project.

Figure 4. Example of microstructure generation model. The left image served as a target while the center and right images are example of structures that could have come from the same stochastic microstructure process as the target.

Spatial statistics of polycrystalline materials represents the next level of abstraction and complication for inclusion into the above framework. While conceptually the same, moving from a microstructure with constituents described by discrete local states (e.g. matrix/pore, ferrite/austenite, etc) to one with constituents described by a continuous matrix group (e.g. local lattice orientation at each point is described the special orthogonal group in 3-dimensions $SO3$) involves significant mathematical challenges. Historically orientation correlations have been described in terms of a generalized Fourier series using symmetrized spherical harmonics as a basis [11]. In this case the Fourier

coefficients were fit by least squares after sampling many hundreds of thousands of orientation pairs. In this work we were able to demonstrate that the coefficients can be efficiently calibrated by fast Fourier transform convolution. While complete discussion of the procedure is beyond the scope of this short technical report, a complete description is being prepared for publication in Scripta Materialia or Computational Materials Science. An example of an orientation correlation plot for highly deformed tantalum is shown in Figure 5.
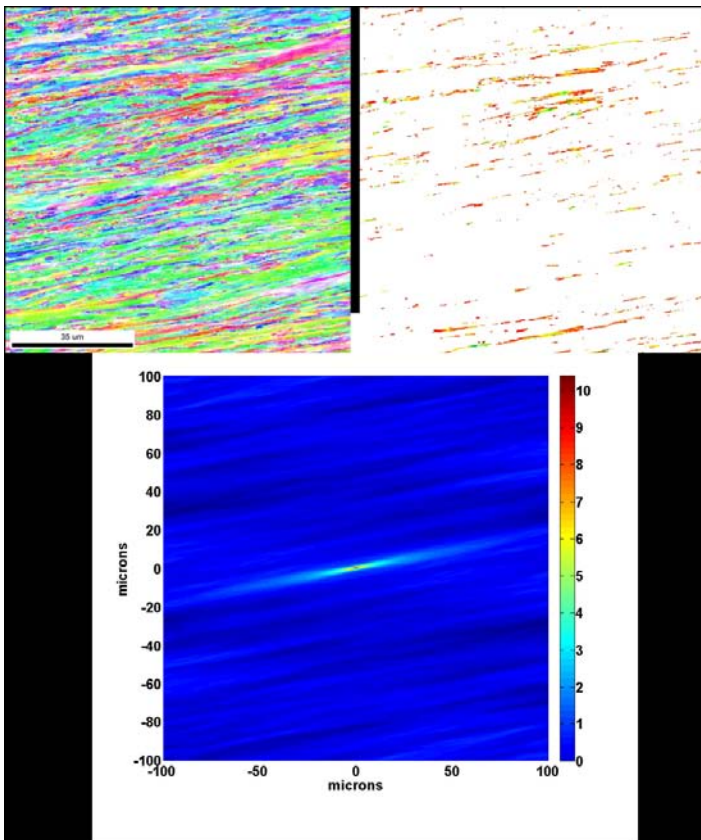
Figure 5. (top-left) Inverse pole figure map showing structure of deformed Ta plate. (top-right) points with local lattice orientation falling within 10 degrees of orientation (-1 0 0)[0 0 1]. Autocorrelation for grains with (-1 0 0)[0 0 1] orientation.

Impact on National Missions

One of LANL key materials science goals is to provide tools necessary to develop the next-generation materials. These new materials are expected to push the envelope and exhibit predictable lifetime performance in extreme environments for longer service lives than are attainable with today's materials. Future characterization facilities such as MaRIE aim to combine state of the art temporal and spatially resolved 3D characterization with the development of synthesis and characterization tools needed for advanced applications. In addition, advanced characterization tools will accumulate data at a rate that leaves current microstructural quantification and analysis tools inadequate.

Success in these endeavors requires working at the edges of the performance distribution and implies a level of microstructural control well beyond what is currently achievable. These activities were a crucial first step of a larger microstructure analysis toolbox. While still largely in their nascent stages of development many of the techniques presented have a potentially transformative potential in areas such as quality control and standards. Rigorous accounting of microstructural variance is critical to understand the uncertainty in materials model and thus should be a lab priority for inclusion into the greater uncertainty quantification framework for both weapons and civilian nuclear energy programs.

References

1. Singh, H., A. M. Gokhale, Y. Mao, and J. E. Spowart. Computer simulations of realistic microstructures of discontinuously reinforced aluminum alloy (DRA) composites. 2006. *Acta Materialia.* **54** (8): 2131.

2. Fullwood, D. T., S. R. Niezgoda, B. L. Adams, and S. R. Kalidindi. Microstructure sensitive design for performance optimization. 2010. *Progress in Materials Science.* **55** (6): 477.

3. Fullwood, D. T., S. R. Niezgoda, and S. R. Kalidindi. Microstructure reconstructions from 2-point statistics using phase-recovery algorithms. 2008. *Acta Materialia.* **56** (5): 942.

4. Lu, B., and S. Torquato. Lineal-path function for random heterogeneous materials. 1992. *Physical Review A.* **45** (2): 922.

5. Piasecki, R.. Microstructure reconstruction using entropic descriptors. 2011. *Proceedings of the Royal Society A: Mathematical, Physical and Engineering Science.* **467** (2127): 806.

6. Torquato, S.. 2002.

7. Olson, G. B.. Computational Design of Hierarchically Structured Materials. 1997. *Science.* **277** (5330): 1237.

8. Olson, G. B.. Computational Design of Hierarchically Structured Materials. 1997. *Science.* **277** (5330): 1237.

9. Niezgoda, S., Y. Yabansu, and S. Kalidindi. Understanding and visualizing microstructure and microstructure variance as a stochastic process. 2011. *Acta Materialia.* **59** (16): 6387.

10. Figueiredo, M. A., R. D. Nowak, and S. J. Wright. Gradient Projection for Sparse Reconstruction: Application to Compressed Sensing and Other Inverse Problems. 2007. *Selected Topics in Signal Processing, IEEE Journal of.* **1** (4): 586.

11. Adams, B. L., P. R. Morris, T. T. Wang, K. S. Willden, and

S. I. Wright. Description of orientation coherence in polycrystalline materials. 1987. *Acta Metallurgica.* **35** (12): 2935.

Publications

Niezgoda, S., Y. Yabansu, and S. Kalidindi. Understanding and visualizing microstructure and microstructure variance as a stochastic process. 2011. *Acta Materialia.* **59** (16): 6387.

Developing and Synthesizing Epitaxial Nanocomposites with Controlled Defect Landscapes and Desired Functionalities

Quanxi Jia
20110614ER

Abstract

Imperfections such as point, line, planar, and/or volume defects in crystals play critical roles in determining the functionalities of materials. To design materials with desired functionalities, one needs to synthesize such materials with controlled defect landscapes. Our ultimate goal is to control the defect landscapes in epitaxial nanocomposite films to achieve desired functionalities. To reach this goal, we have completed the following tasks: *i*) establishing an advanced intermediate scale synthesizing capability which has the capability to generate 2nd phase materials in the format of nanoparticles and/or clusters in an epitaxial matrixes; *ii*) demonstrating a representative epitaxial nanocomposite system (YBa$_2$Cu$_3$O$_7$ (YBCO):BaZrO$_3$) with a controlled nanoparticle size and density; and *iii*) revealing the relationship between the flux pinning property and the defect landscape in epitaxial nanocomposites.

Background and Research Objectives

Defects (such as point, line, planar, and/or volume defects) locally disturb the regular arrangement of atoms, which can significantly modify the properties of materials. In other words, the functionalities and defects in a given material are intimately related. Defects, notoriously, are considered to be detrimental to materials since they can potentially introduce complicated issues. On the other hand, the greatest breakthroughs in science and technology have been achieved through artificial introduction of preferred defects in materials. One well known example is the introduction of extrinsic defects such as impurities to semiconductors. Such point defects make it possible to change the type of conductions. This discovery itself has led to the fabrication of p-n junctions that are the workhorses of diodes used for light emitting diodes, photovoltaic devices, and transistors in computers. Similarly, it has been found that flux pinning can be significantly enhanced by engineering defects in high temperature superconductors [1]. It is well known that a wide range and variety of defects can be potentially used as pinning centers [2] as long as one can control them. Last but not least is the discovery of novel functionalities

at the interface through *interfacing* different metal-oxides at nanoscales [3, 4], where planar defects play the most important roles in determining the properties of the materials.

From a structure point of view, single crystals with high crystal perfection are usually used for the study of intrinsic properties and/or the application of high-end electronics. However, many materials are not available in single crystal forms. Bulk ceramics have been generally studied as structural materials. Issues related to *uncontrolled* grain boundaries and impurities in ceramics have limited them for a wide range of applications. Epitaxial films, on the other hand, represent sweet spots between single crystals and ceramics. For instance, they show quasi-single crystal quality with controlled microstructures. Recently, epitaxial nanocomposite films have proved to be one of the most interesting architectures to produce novel functionalities that cannot be obtained in individual constituents. Limited nanocomposite architectures such as superlattices and self-assembled nanoparticles have been synthesized using physical (or chemical) vapor and chemical solution deposition techniques.

Imperative for the fundamental understanding of materials is the control of defect landscapes and the production of desired defects so that we can enhance our capability to design, manipulate, and control their ultimate functionalities. Current synthesizing capabilities as mentioned above are not designed to control defect landscapes in complex materials. For example, the formation of volume defects such as nanoparticles or nanopillars in complex metal-oxides relies exclusively on self-assembly [1-3,5]. It is very common in the community that an observed phenomenon reported by one group cannot be replicated by another.

Our research objective is to control the defect landscapes in epitaxial nanocomposite films to achieve desired functionalities. To reach this goal, we focused on the following tasks: *i*) establishing an advanced intermediate scale synthesizing capability which has the capability to generate 2nd phase materials in the

format of nanoparticles and/or clusters in an epitaxial matrixes; *ii*) demonstrating a representative epitaxial nanocomposite system ($YBa_2Cu_3O_7$ (YBCO):$BaZrO_3$) with a controlled nanoparticle size and density; and *iii*) revealing the relationship between the flux pinning property and the defect landscape in epitaxial nanocomposites. We chose YBCO as the epitaxial matrix and $BaZrO_3$ as the defect inclusion because we have many years' experience working with these materials.

Scientific Approach and Accomplishments

Epitaxial nanocomposite films with certain degree of control of morphologies have been demonstrated recently. However, the size, the density, and the location of these nanoparticles reported in the literature were not fully controlled, which is the main limitation of the current technology. The establishment of an intermediate scale capability by integrating laser molecular beam epitaxy (or laser MBE) with a long wavelength laser to generate nanoparticles allows us to grow epitaxial nanocomposite films that have controlled volume defects such as nanoparticles *with controlled sizes and densities at desired locations*. In the following, we summarize our key technical accomplishments for this project.

Establishment of an advanced synthesizing system having the capability to generate 2nd phase materials in the format of nanoparticles and/or clusters in an epitaxial matrix: We have made good progress to setup the new deposition system which includes two laser beams, where one laser is used to generate second phase nanoparticles, and the other is used to produce the epitaxial matrix.

Control of the size and the density of epitaxial nanocomposite films through managing the processing parameters: To test our concept and to control the size and the density of the 2nd phase materials, we have designed our experiments through manipulating the processing parameters. Using high resolution x-ray diffraction and transmission electron microscopy, we, in particular, have discovered that the size and the density of the second phase materials (for example in vertically aligned nanocomposite) can be fine-tuned by the laser pulse rate: the higher the laser repetition rate during the deposition, the smaller the size of the nanopillars of the 2nd phase materials.

Effect of film thickness on the defect density of $YBa_2Cu_3O_7$:$BaZrO_3$ (YBCO:BZO) nanocomposites: It is well known that defects play a critical role in determining the current carrying capability of superconducting films in an external magnetic field. In our designed experiment, we have synthesized epitaxial nanocomposite YBCO:BZO films with different film thickness in order to study the thickness dependence of defect density in such a composite, where YBCO serves as the epitaxial matrix and BZO as the nanoparticles. We have used high-resolution x-ray diffraction analysis to extract the screw-type dislocations, and have observed that the density of screw-type dislocations increases with increasing film thickness.

Impact on National Missions

This work directly addresses the following scientific and technological questions: *i*) how do we predict and control the microstructure for designed material performance? *ii)* can we design and synthesize new materials with controlled functionalities? Our efforts directly address these issues central to DOE's missions in energy, science, and security.

References

1. MacManus-Driscoll, J. L., S. R. Foltyn, Q. X. Jia, H. Wang, A. Serquis, L. Civale, B. Maiorov, M. E. Hawley, M. P. Maley, and D. E. Peterson. Strongly enhanced flux pinning in BaZrO3-doped YBa2Cu3O7-x coated conductors. 2004. *Nature Materials.* **3**: 439.

2. Foltyn, S. R., L. Civale, J. L. MacManus-Driscoll, Q. X. Jia, B. Maiorov, H. Wang, and M. P. Maley. Materials science challenges for high-temperature superconducting wire. 2007. *Nature Materials.* **6**: 631.

3. Zheng, H., J. Wang, S. E. Lofland, Z. Ma, L. Mohaddes-Ardabili, T. Zhao, R. L. Salamanca, S. R. Shinde, S. B. Ogale, S. Bai, D. Viehland, Y. Jia, D. G. Schlom, M. Wuttig, A. Roytburd, and R. Ramesh. Multiferroic BaTiO3-CoFe2O4 nanostructures. 2004. *Science.* **303**: 661.

4. Reyren, N., S. Thiel, A. D. Caviglia, A. F. Kourkoutis, G. Hammerl, C. Richter, C. W. Schneider, T. Hopp, A. S. Ruetschi, D. Jaccard, M. Gabay, D. A. Muller, J. M. Truscone, and J. Mannhart. Superconducting interface between insulating oxides. 2007. *Science.* **317**: 1196.

5. MacManus-Driscoll, J. L., P. Zerrer, H. Wang, H. Yang, J. Yoon, S. R. Foltyn, M. G. Blamire, and Q. X. Jia. Spontaneous ordering, strain control and manipulation in vertical nancomposite heteroepitaxial films. 2008. *Nature Materials.* **7**: 314.

Publications

Bi, Z., L. Yan, N. F. Haberkorn, L. Civale, and Q. X. Jia. Effect of interfaces on the superconducting properties of YBCO films . *Supercond. Sci. Technol..*

Jia, Q. X.. Effect of interface on the transport properties of superconducting nanocomposites. Invited presentation at *Superconductivity at Oxide Interfaces.* (London, UK, 14-15 Sept. 2011).

Zhuo, M. J., B. P. Uberuaga, L. Yan, E. G. Fu, Y. Q. Wang, A. Misra, M. Nastasi, and Q. X. Jia. Microstructural evolution of epitaxial anatase TiO2/SrTiO3 films under Ne ion irradiation. *Acta Materialia.*

Three Dimensional Quantification of Metallic Microstructures in the Presence of Damage

Curt A. Bronkhorst
20110615ER

Abstract

The physical understanding of events which take place in metallic polycrystal materials during shock loading conditions is necessary for successful representation of this behavior in numerical simulations. Our ability to computationally predict the ductile damage response of metals under extreme loading condition is generally lacking and therefore new insight into this complex physical process is necessary and is the thrust of this work. In collaboration with colleagues at Carnegie Mellon University (CMU), High Energy Diffraction Microscopy (HEDM) measurements were performed at the Advanced Photon Source (APS) on a small sample of copper which had previously been shock loaded and contained small nucleated pores. HEDM measurements on a sample of this type had never before been attempted and therefore were also a development step for this emerging experimental technique. Results of these measurements produced a non-destructive three-dimensional mapping of this material containing voids. The same sample was also HEDM characterized before loading to enable detailed examination of changes to the material as a result of loading. New work to develop the tools to quantitatively examine these large three-dimensional data sets was initiated in this project. The analysis effort was concentrated on the undeformed Cu data set. Since pores generally form at grain boundaries in pure materials, the focus was on identifying particular grain boundary types. This allows the linking of pore formation to specifics of grain boundaries and microstructure. Early effort into adapting machine learning tools, such as hierarchical filtering methods was also performed.   Theory and software tools to enable the forward and reverse simulation of x-ray diffraction from a virtual metallic microstructure were also developed. The forward problem produces a diffraction image from a virtual microstructure of the material. The reverse problem reconstructs the microstructure from the diffraction image. This capability is a direct link between material theory and in-situ diffraction experiments.

Background and Research Objectives

The damage and failure process in metallic polycrystal materials during shock loading is a complex series of events which is intimately linked to the character of the material and its structure. We are unable to computationally predict the damage and failure response of these materials under extreme loading conditions.   The reason for this is that in large part we have inadequate understanding of this process and how it is linked to natural property variability within the material.

LANL has recently been collaborating with CMU to image and reconstruct 3D samples of dynamically loaded copper. This new capability has provided the opportunity to non-destructively obtain microstructural orientation information from x-ray imaging when damage is present within the sample. The opportunity of new materials characterization which HEDM offers also poses a challenge to quantitatively extract complex physics information from very large data sets. Clearly, new tools to allow the analysis of these statistical data sets are needed. The complex features inherent in the structure of materials must be identified and characterized using new and sophisticated tools which allow the information to be extracted quickly. In order to facilitate the direct linkage between materials theory and x-ray diffraction experiments, we need the capability to simulate the deformation experiments using advanced meso-scale modeling tools and also create x-ray diffraction patterns from those theoretical simulations. This linkage is critical to the enhanced interpretation of the experimental results but also will facilitate the rapid use of the experimental results to improve materials theory.

The objective of this project was to develop techniques for producing and analyzing a statistical data set representing a 3D microstructure to probe the nature of dynamic deformation. This was accomplished through a close interaction between LANL and Carnegie Mellon University to measure and reconstruct 3D HEDM results from a dynamically damaged copper sample produced at LANL. This work also advanced the capability for simulating x-ray diffraction patterns of a virtual 3D polycrystal. This allows the study and interpretation of dynamic as well as quasi-statically deforming diffraction results. This work is meant to directly address the understand-

ing gap in order to achieve computational predictability of these complex behaviors.

Scientific Approach and Accomplishments

This project was split into three activity areas. First, experimental material originating from LANL was examined using HEDM at the APS facility. This resulted in two three-dimensional data sets of the same section of material in its undeformed and deformed state. The deformed material was shock loaded and contained early stage pores. Secondly, the undeformed experimental data set was examined using an undirected graphical model in which grains and boundaries are represented by vertices and edges, respectively. This quantitative examination of HEDM data sets is critical to being able to link the formation of pores to the details of the material and its structure. Third, work was performed to advance our ability to link x-ray diffraction experiment to materials theory with the development of the theory and tools necessary to produce synthetic diffraction images from general continuum based polycrystal simulation results and also use diffraction images to construct material microstructures.

Experimental – Shock Loading and HEDM Measurements

The focus of examination of this study was the early stage ductile damage response of high purity copper. Due to size limitations of the HEDM configuration at the APS the sample dimensions were 1.2 mm diameter and 0.72 mm thick. This small size required an innovative experimental setup for shock loading the sample and therefore a customized configuration for an existing high rate test system (Taylor Anvil) was designed and constructed. Since examination of the post-test sample was required, soft recovery was necessary and therefore a sample configuration allowing for deformed sample recovery was incorporated. This same sample was then shock loaded.

The HEDM measurement process [1,2,3,4] is a new and innovative procedure for the non-destructive metallographic examination (grain mapping) of materials which are crystalline or polycrystalline in nature. It has been pioneered by R. Suter at Carnegie Mellon University and it is with him and his research group that LANL has been collaborating. Although the measurement technique is still an active area of research, it is mature enough such that in-situ examination of damage fields within the Cu material of this study can be attempted – which had heretofore never been performed.

HEDM measurements for both the copper sample in its undeformed and deformed state were successfully performed. Microstructure reconstruction of the undeformed sample is complete. Results for the deformed copper data set are still being examined and at this time there exist preliminary images of the tomographic and HEDM measurements. Results from the undeformed sample HEDM measurements and reconstruction are shown in Figure 1.
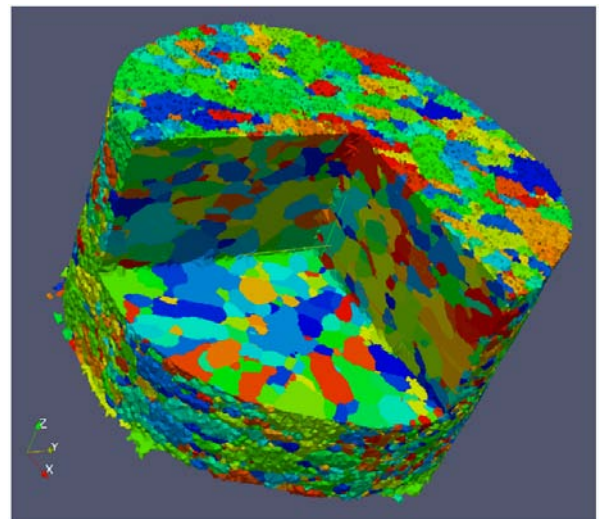
Figure 1. Image of the reconstructed microstructure of the undeformed copper sample. Each individual grain is colored differently.

This image represents a reconstruction of the full volume of the 3D data set. Each of the individually colored grains in the Cu sample are clearly distinguished. Preliminary results from the deformed sample HEDM measurements and reconstruction are shown in Figure 2. This image is taken within the damaged region of the sample. Due to greater complexity in the diffraction images due to the deformation and damage, the reconstruction contains greater uncertainty and as a result there are some missing portions of the sample cross-section. This has pointed to possible improvements to the positioning of the detectors as well as to improvements in the reconstruction algorithm used. Since measurements on voided material has never been performed before this has been a tremendous success.
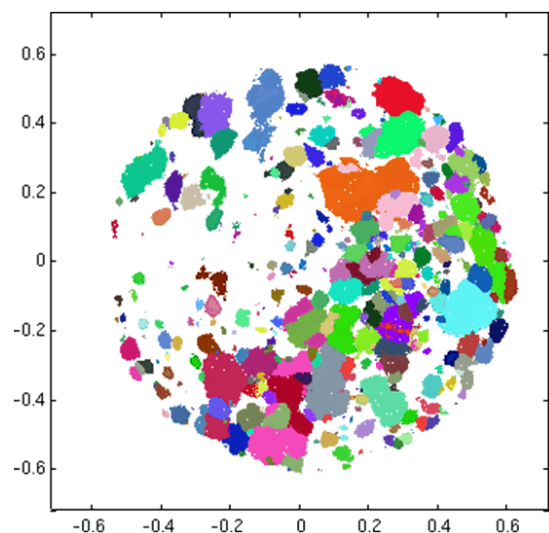
Figure 2. Preliminary reconstructed microstructure with the voided region of the deformed copper sample. The missing regions of the reconstructed image are due to uncertainty of crystal orientation determination during the reconstruction process.

Data Mining of Large Three-Dimensional Data Sets

We have begun to develop analysis techniques to mine the rich multi-dimensional experimental data sets generated by HEDM experiments in order to model the relationship between microstructural features and the environmental conditions defining the ductile damage of the polycrystalline material. Even in its undeformed state the polycrystalline copper sample has a very complex 3D structure. In order to represent the complex nature of the 3D grain microstructure we have extracted an undirected graphical model in which grains and grain boundaries are represented by vertices and edges, respectively (Figure 3). Each grain vertex was assigned a single grain-averaged orientation while each edge was assigned a full five dimensional characterization (lattice misorientation and boundary plane orientation). By identifying features such as those given in Figure 3, we can begin to identify which grain boundary types are primarily responsible for the creation of voids within the material. This is very powerful information and can lead to the motivation of new models to account for these relationships.
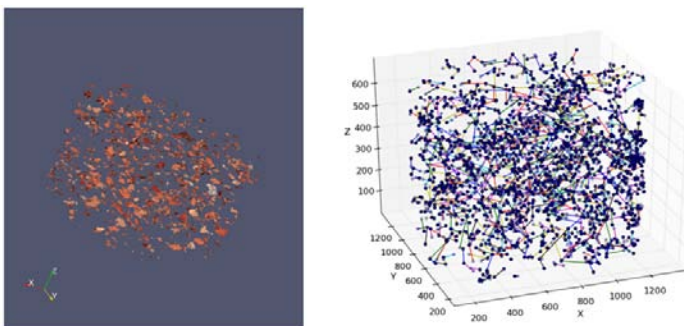
Figure 3. Grain boundary interfaces (left) and a network representation (right) of the full 3D grain boundary network characterized by Sigma 19.5 edges only. The network representation enhances the analysis by providing both local (degree distribution) and global (connectedness) characterizations of the boundary network.

We have also explored some ideas from compressed sensing and vision research in order to build *sparse, hierarchical representations* of microstructures. The goal is to learn from real-world samples a dictionary of characteristic features (basis) that can be used to achieve a sparse description of polycrystals. Learning such a dictionary can significantly improve image reconstruction algorithms – including orientation and topology reconstruction algorithms used to generate the data analyzed in this project – or statistical learning algorithms aiming at extracting relationships between damage and structure. The key insight for this approach can be strong correlations between density values in adjacent pixels to allow for sparse representation. A more powerful approach for exploiting sparsity is to express the density using only a few coefficients with respect to a previously-learned dictionary, a collection of basis vectors that can be customized to the problem. This can be done either for a large class of materials, or more specialized for a sample of a specific kind. As shown by theory, the sparser this representation, the better the reconstruction one can obtain from fewer, noisier data. Our approach to constructing a sparse dictionary is unsupervised and builds a hierarchical convolutional decomposition of images under a sparsity constraint [5].

Simulation of Coherent X-Ray Scattering from Polycrystalline Materials

Photons passing through a material sample have the capacity to elastically scatter off the electrons it contains. When, in addition, the ensemble of incident photons is produced by a coherent source, the subsequent diffraction of the scattered light generates a pattern that may be detected by a film plate or an array of CCD pixels. These patterns yield various types of data about the structure of the illuminated sample, and such experiments furnish a valuable tool in materials science applications. In particular, the indirect inference of the structural properties of a crystalline sample from its coherent scattering pattern is the basis of more than a century of theory and practice in the field of crystallography. More recently, the recovery of direct images of a two- or three-dimensional sample via post-processing of its scattering pattern has been achieved via the use of coherent x-ray diffraction imaging (CXDI) [6,7]. Nevertheless, the design and implementation of scattering experiments - which are typically performed in the soft- to hard-x-ray regime - are fraught with difficulty due to conflicting experimental requirements and uncertainties about the response of the materials involved. To aid in this process, we have developed algorithms and software for the simulation of x-ray scattering experiments, both in the context of classical crystallography and for CXDI. These tools are intended to aid both the design and interpretation of imaging experiments, as well as to assist in the analysis of material simulations.

The Forward Problem

A typical x-ray scattering experiment consists of a source, a sample, and a detector. Although the light source is sometimes a point source, in materials science applications more often it takes the form of a coherent, collimated beam with photon energy in the 100 eV to 100 keV range, as assumed in this work. The sample may be anything from a quasi-two-dimensional thin film to a fully three-dimensional dense solid. A modern detector usually consists of a rectangular array of several million CCD pixels, each of which is 5 to 100 microns in width. The forward problem of x-ray scattering simulation consists of calculating the pattern which results from a given experimental setup and sample.

This work concentrates on the critical special case of polycrystalline samples. A polycrystal consists of numerous grains, each of which may be approximated as a perfect crystal. Examples of simulated polycrystalline scattering

patterns are shown in Figure 4. For Figure 4, we have generated a model polycrystal consisting of a Voronoi lattice of randomly-positioned and -oriented grain centers. Each grain was assumed to have a simple cubic structure, with the same lattice size (2.88 Å) as iron. The crystalline periodicity of each grain was used to cast the electron number density of the model polycrystal onto a regular grid, and fast Fourier transform techniques were used for each pixel on the detector. Here we have assumed an incident photon energy of 42 keV, sample-detector distances of 4.5 cm, as well as a 1024x1024 detector of 13.5 micron pixels. To check the accuracy of our calculations, the predicted radii of several Bragg peaks are labeled for each pattern according to their Miller indices, and there is good agreement between simulation and theory.
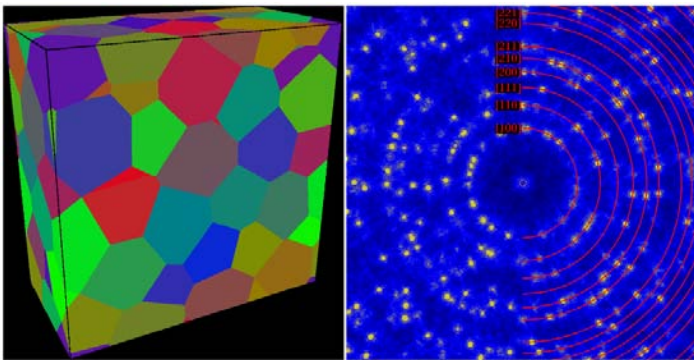
Figure 4. Left: A model cubic polycrystal based on continuum-style orientation data. Grains are color-coded according to their orientation. Right: The corresponding simulated diffraction pattern (42 keV photons), with rings of Bragg peaks labeled in red.

The Inverse Problem

Whereas classical crystallography extracts indirect structural information about a sample, the *inverse problem* of x-ray scattering seeks to generate a *direct* image of the sample from its scattering pattern alone. Although such a pattern is simply related to the Fourier transform of the sample, it preserves only the magnitude, and not phase, of the scattered field. Thus the sample cannot be retrieved via a simple inverse Fourier transform. Nevertheless, it was suggested as early as 1952 that a scattering pattern might be used to reconstruct this missing phase information, provided that the pattern is *oversampled* at a resolution greater than that corresponding to the known boundaries of the sample alone. Such a method is known as iterative phase retrieval (IPR), and the resulting imaging technique is known as coherent x-ray diffraction imaging (CXDI). CXDI was first demonstrated experimentally for two-dimensional sample in 1999 [6] and for three-dimensional samples in 2010 [7].

As an aid to the design of CXDI experiments, and for the processing of experimental data, we have built a robust suite of software tools for performing IPR from real or

simulated diffraction patterns. Figure 5 shows an example of such calculations for model polycrystalline samples. Although three-dimensional CXDI has been experimentally demonstrated in small and/or soft-matter samples [7], at the high photon energies required to penetrate a significant thickness of dense materials (e.g. iron) there is insufficient information present in a scattering pattern to allow three-dimensional reconstruction. We therefore provide examples here of simulated CXDI performed on two-dimensional slices of three-dimensional samples. Figure 5 shows a model continuum-based polycrystal, the resulting scattering pattern obtained by illuminating the sample with a 50 keV beam possessing a Gaussian profile, and the resulting image reconstruction after the computational process of IPR.
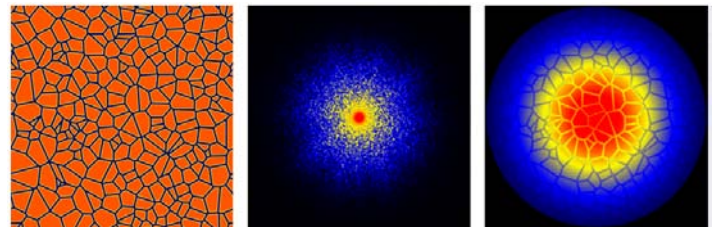
Figure 5. Simulated CXDI for a 2D slice of a model polycrystal, showing the sample (left), the scattering pattern (middle), and the iteratively-retrieved image. (Note that the rings of color evident in the reconstruction result from our assumption of a Gaussian beam profile.)

Impact on National Missions

This work is directly motivated by demonstrated needs of the nuclear weapons program. This work will impact the capability for design and assessment of the national stockpile. This work has also brought to LANL a post-doc from Carnegie Mellon University to enable us to fully engage in HEDM measurements. This work has also spawned other research activities in related areas.

References

1. Lienert, U., S. F. Li, C. M. Hefferen, J. Lind, R. M. Suter, J. V. Bernier, N. R. Barton, M. C. Brandes, M. J. Mills, M. P. Miller, B. Jakobsen, and W. Pantleon. High-energy diffraction microscopy at the Advanced Photon Source. 2011. *Journal of Metals and Materials.* (July): 70.

2. Hefferen, C. M., S. F. Li, J. Lind, and R. M. Suter. Tests of microstructure reconstruction by forward modeling of high energy x-ray diffraction microscopy data. 2010. *Powder Diffraction.* **25**: 132.

3. Suter, R. M., D. Hennessy, C. Xiao, and U. Lienert. Forward modeling method for microstructure reconstruction using x-ray diffraction microscopy: single-crystal verification. 200. *Review of Scientific Instruments.* **77**: 123905.

4. Hefferen, C. M., S. F. Li, J. Lind, U. Lienert, A. D. Rollett,

P. Wynblatt, and R. M. Suter. Statistics of high purity nickel microstructure from high energy x-ray diffraction microscopy. 2009. *Computers, Materials and Continua.* **14** (3): 209.

5. Zeiler, M. D., D. Kirshnan, G. W. Taylor, and R. Fergus. Deconvolutional networks. 2010. In *23rd IEEE Conference on Computer Vision and Pattern Recognition.* (San Francisco, 13-18 June 2010). , p. 2528. Los Alamitos, CA: IEEE Computer Society.

6. Miao, J., P. Charalambous, J. Kirz, and D. Sayre. Extending the methodology of x-ray crystallography to allow imaging of micrometer-sized non-crystalline specimens. 1999. *Nature.* **400**: 342.

7. Raines, K. S., S. Salha, R. L. Sandberg, H. Jiang, J. A. Rodriguez, B. P. Fahimian, H. C. Kapteyn, J. Du, and J. Miao. Three-dimensional structure determination from a single view. 2010. *Nature.* **463**: 214.

Fluid Flow Imaging of Alloy Melts and In-situ Fundamental Solidification Experiments at Temperature Extremes

Amy J. Clarke
20110618ER

Abstract

The goal of this work was to perform in-situ examinations of alloy melt fluid flow and fundamental solidification phenomena at temperature extremes to provide new experimental findings regarding solute segregation in the melt and solidification microstructure development. Fluid flow imaging of alloy melts with the addition of tracer particles was performed using 800 MeV Proton Radiography (pRad) at the Los Alamos Neutron Science Center (LANSCE) at Los Alamos National Laboratory (LANL). Two alloy systems (Ga-Bi and Al-In) that exhibit liquid-liquid phase separation at elevated temperatures were selected to produce a small fraction of a minor liquid phase that would have sufficient density contrast from the major liquid phase in the alloy melt. Regions of the minor liquid phase would serve as internal tracer particles in the melt for monitoring localized fluid flow on a scale suitable for the resolution of pRad (~65 microns for a 44 x 44 mm^2 field of view). These experiments, in addition to recent in-situ solidification experiments performed under LDRD Reserve Program 20110512ER, Developing Proton Radiography for Fundamental Solidification Experiments, demonstrate the usefulness of pRad, a capability that is unique to LANL, for performing process-aware solidification studies, ranging from monitoring fluid flow characteristics that are of great importance for the validation of casting mold filling and solidification simulations, to monitoring solidification behavior in-situ. Preliminary x-ray radiography and tomography work at LANL was also performed, in preparation for future complementary synchrotron x-ray radiography during solidification studies of a small field of view in foil samples at Argonne National Laboratory's (ANL) Advanced Photon Source (APS). The results obtained from this early x-ray radiography and tomography support that synchrotron x-ray radiography will be able to provide fine-scale solidification behavior details to supplement the larger field of view results obtained from thicker specimens at pRad in FY11. More importantly, this work demonstrates important aspects of the ability to perform future process-aware solidification studies with capabilities that may be integrated into a future MaRIE facility at LANL. Process-aware solidification studies will significantly advance solidification science and casting technology, which is of particular interest to LANL.

Background and Research Objectives

The filling of molten metal into a casting mold is conventionally simulated by water modeling, where water is poured into a mold to examine the filling behavior. Casting mold filling and solidification simulations can also be performed using available simulation codes or flow modeling software, such as the TRUCHAS code developed at LANL or Flow-3D®. The fluid dynamics of the molten metal during mold filling influence the overall quality of the casting, controlling factors such as macrosegregation and homogeneity, voids and shrinkage, and the resulting as-cast microstructure.

The goal of the first stage of this work was to obtain time-resolved images of fluid flow of an alloy melt that contains tracer particles using pRad at the LANSCE facility at LANL to determine if the acquisition of localized fluid flow and corresponding velocities is possible with this technique. The ability to perform localized fluid flow experiments is important for validating fluid flow predictions obtained from simulations; it also has important practical implications with respect to understanding and improving casting quality.

Understanding the influence of processing variables on the evolution of solidification microstructures is also important, since the as-cast microstructure affects subsequent microstructure and property development. In-situ observations of solidification are limited, but synchrotron x-ray radiography has been recently used to examine solidification for a 1.4 x 1.4 mm^2 field of view in foils less than 200 microns thick in Al-based alloys [1,2]. These results highlight the ability of this technique to obtain detailed information about solidification structures for a small field of view in thin specimens. For the second stage of work, preliminary x-ray radiography and tomography was performed on an Al-Cu alloy at LANL in preparation for future x-ray synchrotron radiography experiments at ANL's APS facility. It is envisioned that synchrotron x-ray radiography results will complement

the larger field of view, in-situ solidification results obtained at LANL's pRad facility on millimeter thick samples. Together, these experiments will highlight solidification processing aspects related to casting and the evolution of solidification structures at length scales of interest for a process-aware first experiment at a future MaRIE facility, where localized fluid flow monitoring, the examination of solute segregation, and the monitoring of solidification microstructure development will be possible.

Scientific Approach and Accomplishments

Time-resolved fluid flow imaging of an alloy melt containing tracer particles was performed using 800 MeV pRad at the LANSCE facility at LANL. A furnace built in MST-6 that was inserted into the beamline at pRad is shown in Figure 1(a). Graphite crucibles were machined with an inside pocket that contained a metal alloy sample nominally 112 mm (4.4 in) in width and 108 mm (4.25 in) in height. Four or 6 millimeter thick Ga-Bi or Al-In samples, respectively, were examined. A window approximately 50 mm x 50 mm (2 in x 2 in) was machined into the center of the front and back of each graphite crucible to reduce the amount of material in the beam path. The crucible assembly was contained within a 305 mm x 305 mm (12 in x 12 in) Al box with front and back Al plates with machined windows. Images were obtained from the windowed region of material during heating and cooling. The top and bottom of the crucible were heated with resistive heaters. These heaters were embedded into the graphite blocks that held the crucible in place. The adjacent copper blocks were water cooled. The entire system was under vacuum. This furnace, along with the high speed cameras at pRad, allowed for in-situ melting and solidification monitoring. The X3 magnifier set-up at pRad was used that allowed for 65 micron resolution for a 44 x 44 mm^2 field of view. TRUCHAS, a LANL developed casting simulation code, was also used to simulate the furnace heat-up. Example results are shown in Figure 1(b).

Approximately three days of beam time were used in August 2011 for the alloy melt imaging experiments at pRad. Ga-Bi and Al-In alloys were selected for the fluid flow imaging experiments, because each alloy exhibits liquid-liquid phase separation at elevated temperatures, as shown in the phase diagrams in Figure 2 [3]. The intent of these experiments was to produce a small fraction of a minor liquid phase that would be distinguishable from the major liquid phase in the alloy melt at elevated temperatures. The minor liquid phase regions served as internal tracer particles at temperatures in the liquid-liquid phase field, so that localized fluid flow could be monitored.

Example images obtained during melting and cooling of a 4 mm thick Ga-Bi alloy sample are shown in Figure 3. Images 1 through 4 (left to right) highlight the melting of this alloy. Significant phase contrast is observed in this alloy prior to full melting into the single liquid phase field (image 5). The light regions in images 1-4 are speculated to correspond to

Ga-rich regions, whereas the darker regions are thought to correspond to Bi-rich regions. During cooling, dendritic (branched structure) growth is evident from the bottom upward into the melt in images 6-8.
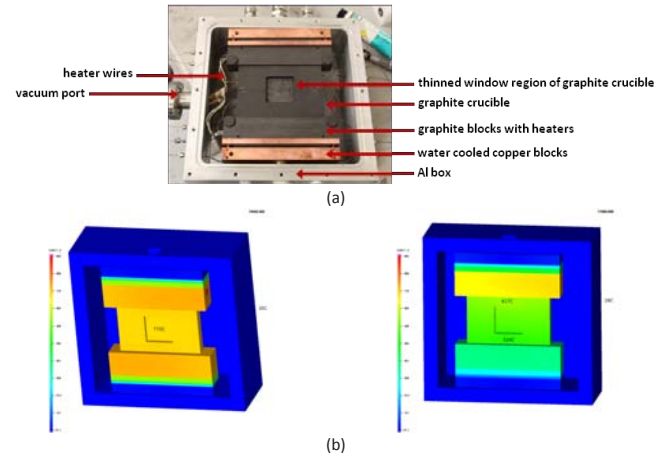
Figure 1. (a) A furnace was designed and built in MST-6 at LANL for insertion into pRad (August, 2011). (Downstream view; the outer Al box is 305 mm x 305 mm (12 in x 12 in). The back Al plate is removed.) and (b) early furnace heat-up simulations performed using TRUCHAS, a LANL developed casting simulation code.
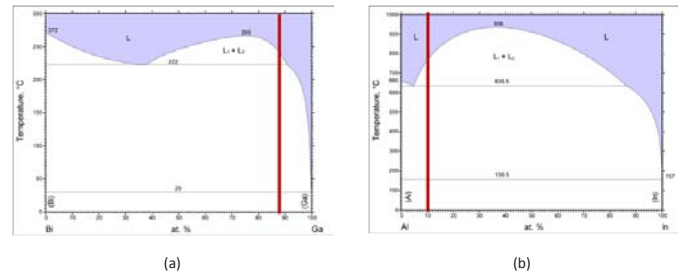
Figure 2. (a) Ga-Bi and (b) Al-In phase diagrams showing liquid-liquid (L1 +L2) phase separation, adapted from reference [3].
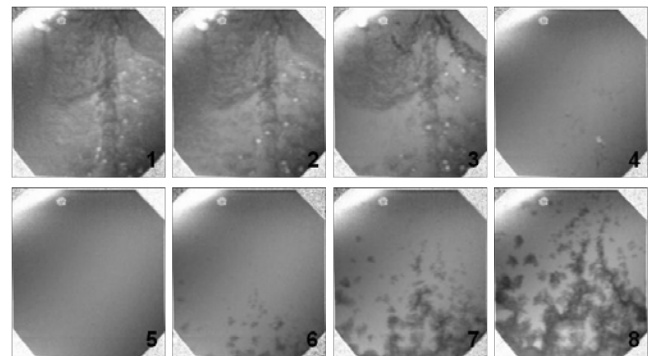
Figure 3. A 4 mm thick Ga-Bi alloy sample during melting, images 1-5, and solidification, images 6-8.

Example images are shown in Figure 4 for a 6 mm thick Al-In sample during melting and solidification. Light regions correspond to Al-rich regions and darker regions

correspond to In-rich regions. Images 1-4 obtained during melting clearly show dark, In-rich liquid and evidence of liquid-liquid phase separation, along with an interface passing from the top downward. Given the lack of contrast at the highest temperature in image 5, it is speculated that a single phase liquid was achieved. It is possible that the local alloy composition was lean, or that the phase field boundaries of the liquid-liquid region in Figure 2(b) for the Al-In binary alloy are not accurate. Solidification from the bottom upward is shown in images 6-8. Interestingly, evidence of In-rich regions in the melt just prior to the start of solidification was observed in some of the images.
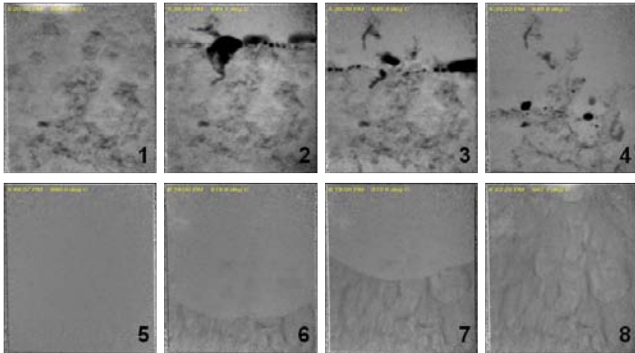
Figure 4. A 6 mm thick Al-In alloy sample during melting, images 1-5, and solidification, images 6-8.

The never before seen dynamic processes that occur during melting and solidification in Figures 3 and 4 are complex. Future work of a follow-on LDRD project will involve pairing the time and temperature information acquired from these experiments with the images that were obtained. Post-mortem microstructure characterization will also be performed; these results, in combination with the in-situ melting and solidification results will provide a complete history of the complex microstructure evolution.

Preliminary x-ray radiography and tomography were also performed at LANL to examine the solidification microstructure of an Al-Cu sample, in preparation for future synchrotron x-ray radiography and tomography experiments at APS. Example tomography results are shown in Figure 5 that highlight the wealth of information that will be obtained about the dynamic processes and solidification microstructure evolution that occurs, once tomography is added to in-situ solidification monitoring by synchrotron x-ray or proton radiography. In addition to tomography during solidification at APS, the acquisition of 2D solidification microstructure evolution details will be pursued for comparisons with pRad results in a future LDRD reserve investment project.
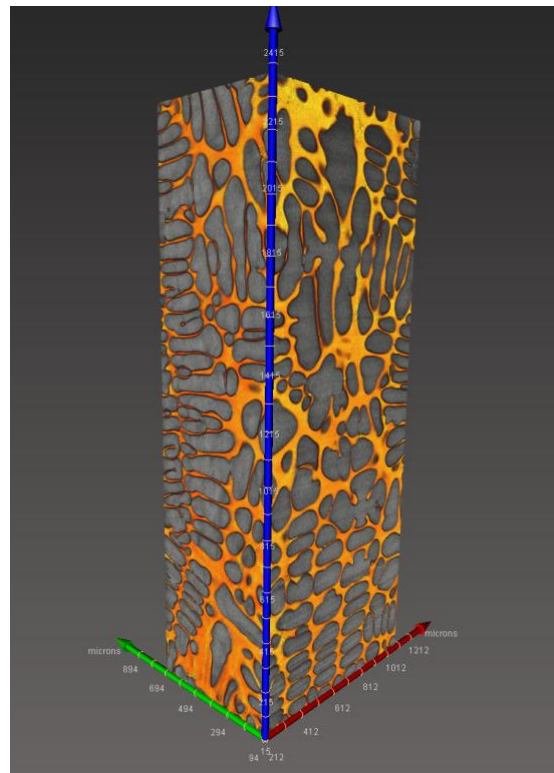
Figure 5. Example x-ray tomography results obtained from Al-15wt.%Cu at LANL. The region is approximately 0.7 x 1.2 x 2.4 mm^3. The interdendtitic eutectic regions are colored orange, and the Al-rich dendrites appear gray in color.

Impact on National Missions

This work demonstrates that there is a scientific opportunity to monitor localized fluid flow in alloy melts using pRad at LANL. The ability to better understand alloy melt fluid flow is important for improving casting quality, which is of technological significance to LANL. The results from this work also support the need for a facility where in-situ characterization of materials during processing, specifically casting, could be performed, as identified in the LANL 2010 MaRIE report *Decadal Challenges for Predicting and Controlling Materials Performance in Extremes* [4]. The National Academies' *Frontiers in Crystalline Matter from Discovery to Technology* report also addresses the critical need to support the discovery and growth of crystalline materials within the U.S. to advance our technology and design new materials for our energy needs [5], while a recent BES report highlights the need to advantageously use extreme environments for materials design and synthesis and for characterization on the scale of fundamental interactions [6]. The preliminary x-ray radiography and tomography results obtained at LANL highlight the detailed information that will be obtainable for a small field of view in foil samples. These results also highlight the importance of incorporating the micostructure evolution during solidification in 3D.

References

1. Mathiesen, R. H., and L. Arnberg. X-Ray Radiography Observations of Columnar Dendritic Growth and Constitutional Undercooling in an Al-30wt%Cu Alloy. 2005. *Acta Materialia.* **53**: 97.

2. Ruvalcaba, D., R. H. Mathiesen, D. G. Eskin, L. Arnberg, and L. Katgerman. In Situ Observations of Dendritic Fragmentation due to Local Solute-Enrichment during Directional Solidification of an Aluminum Alloy. 2007. *Acta Materialia.* **55**: 4287.

3. ASM Alloy Phase Diagrams Center. 2006.

4. Decadal Challenges for Predicting and Controlling Materials Performance in Extremes. 2010. *Report of a Los Alamos National Laboratory Workshop, Los Alamos National Laboratory, LA-UR 10-02959, Los Alamos National Laboratory, Los Alamos, NM.*

5. Frontiers in Crystalline Matter from Discovery to Technology. 2009. *National Research Council, National Academies of Science, The National Academies Press, Washington, D.C.*

6. Basic Research Needs for Materials under Extreme Environments. 2007. *Report of the Basic Energy Sciences Workshop, Office of Science, U.S. Department of Energy.*

In-Situ Probing Monitoring of Microstructure Evolution During Annealing of Radiation Damage with High Energy Synchrotron Xray Diffraction

Donald W. Brown
20110619ER

Abstract

We have completed a series of in-situ xray and neutron diffraction measurements at the Advanced Photon Source at Argonne National Lab (ANL) and the Lujan Center at LANL on HT-9 steel and Zircalloy-2. Specifically, we have performed diffraction based measurements pre- and post-irradiation, as well as in-situ during annealing and deformation, conditions that approximate those seen in service. From quantitative phase analysis, we have identified and determined the volume fraction of minor phases in the HT-9 steel as a function of irradiation conditions. Diffraction line profile analysis has allowed us to monitor the dislocation density and character of irradiated materials and relate this to the macroscopic response. Finally, pair distribution function (pdf) analysis has provided information about the local chemical ordering (irradiation induced segregation) in the microstructure.

As well as advancing the understanding of microstructural evolution during irradiation, this program has developed advanced characterization techniques that are useful to the nuclear materials field in general, and the proposed Fission-Fusion Facility (F^3) of the Matter and Radiation In Extremes (MaRIE) facility, specifically. Accurately defining F^3 requirements will require a clear understanding of the opportunity space implicit in the application of high energy photon sources to irradiated material. By making unique measurements on irradiated materials at APS and at Lujan we have developed and validated the techniques under the stringent xray energy and diffraction angle requirements of F^3 and can more effectively predict F^3 requirements in advance of the conceptual design.

Background and Research Objectives

Post irradiation examination (PIE) has long been the standard for characterizing irradiated materials. While valuable, PIE (e.g. microscopy) requires sample cutting, grinding, etc, is necessarily ex-situ, and is limited. High energy x-ray and neutron diffraction offer the opportunity to characterize materials remotely, in-situ, and with little or no sample preparation.

HT-9 steel samples which experienced different dose and temperature conditions were removed from an irradiated fuel duct for advanced characterization. These samples are of interest to the Fuel Cycle R&D program. Also, zirconium alloys samples were harvested from a pressure tube which had 6 years of service in a CANDU power reactor. Both of these materials were studied toward the following objectives.

1. Measure microstructural evolution of irradiated materials under simulated operating conditions.

2. Develop diffraction based techniques for in-situ or near in-situ probing of irradiated materials.

3. Develop protocol for experiments on irradiated materials at large facilities (e.g. APS).

4. Adapt analytical techniques for use on irradiated microstructures.

Scientific Approach and Accomplishments

HT-9 steel samples were harvested from six positions in a duct (ACO3) which was part of a six year long fuel irradiation experiment at the Fast Flux Test Facility (FFTF). The samples had seen different levels of radiation damage at different temperatures. The dose on each sample position varies from two displacements per atom (dpa) to nearly 150 dpa while the radiation temperature varies from 380 to 500C. Also, zirconium alloys (Zr-2.5%Nb) samples were harvested from a pressure tube which had seen 7 years of service in a CANDU power reactor. The location that the sample was removed from had an operating temperature of ~250°C and experienced a moderate fluence of 1.6x10^{24} n/m^{-2} fast neutrons (E>1MeV).

A series of experiments at the Lujan Center Neutron source and the APS and PETRA x-ray sources were completed. Specifically, at the Lujan Center, the HIPPO (High Pressure Preferred Orientation) instrument was used to measure the crystallographic texture of the irradiated samples and the Neutron Powder Diffractometer (NPDF) was used to measure the neutron pair distribution function as well as for diffraction line profile analysis.

Complimentary x-ray pair distribution function measurements were completed at the PETRA synchrotron x-ray source. Likewise, diffraction line profile analysis was also completed at the 1ID beamline at the APS. Finally in-situ diffraction measurements during deformation of irradiated samples were completed at the 1-ID beamline of the APS.

Results

Phase Analysis

Figure 1 shows diffraction patterns collected at the PETRA x-ray source in Germany from a control sample and samples with two dose/temperature conditions. The data is expanded to highlight the minor phases; the peaks from the major phase (bcc steel or ferrite) are off scale. The evolution of the minor phases is evident from comparison to the control material. Initially present are the ferrite and carbide phases, marked by the blue and red tick marks respectively. After 110dpa at 416C, new peaks indicative of new phases are apparent.
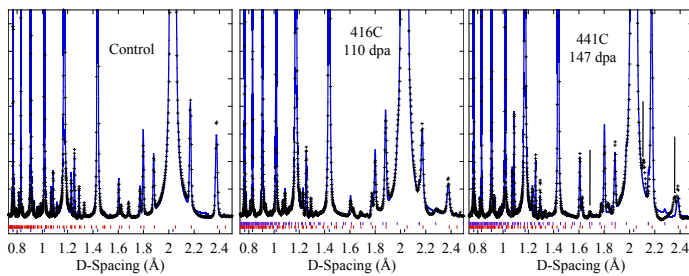
Figure 1. Diffraction pattern from control sample and 2 of the irradiated HT-9 samples.
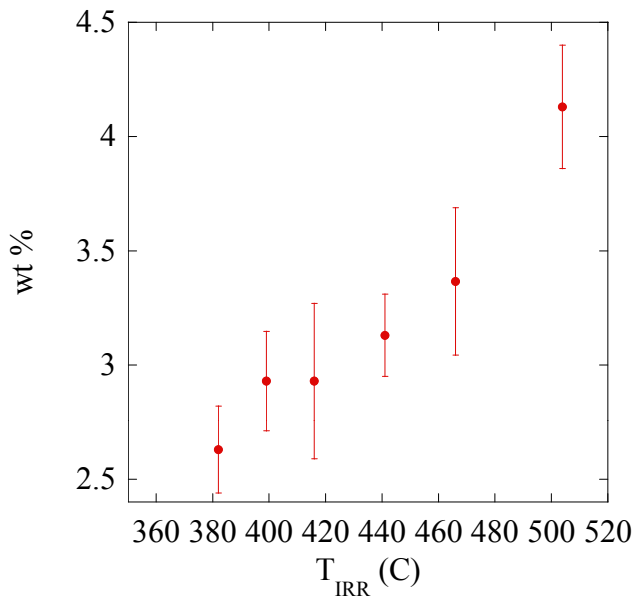
Figure 2. Weight fraction of carbide particles as a function of irradiation temperature.

These peaks are consistent with the G-phase that microscopy studies report, represented by the purple tick marks. Again, after 147dpa at 441C, new peaks are also observed, but these are not consistent with the G-phase, nor any other precipitate reported in irradiated HT-9. We are currently attempting to identify the phase associated with these peaks. It is difficult to see on this scale, but the ferrite peaks broaden considerably after irradiations.

Figure 2 shows the evolution of the carbide volume fraction as a function of irradiation temperature. The increase of carbide volume fraction indicates increased precipitation of carbides from the matrix as the sample was held at elevated temperature for extended time periods.

Microstructural evolution

We have interpreted the broadening of the ferrite peaks as in increase in dislocation density. From whole profile diffraction line profile analysis, we have quantitatively determined the dislocation densities before and after irradiation. In the Zr2.5%Nb, the dislocation density increased 4-fold during irradiation. Moreover, the analysis shows that the increase is due to an increase of only <a> type dislocations. Also, the analysis indicates that the dislocations are randomly located in the microstructure, rather than forming organized dislocation cells as they would during large scale plastic deformation. Presumably this is due to the stochastic nature of the interaction of the neutron irradiation with the atoms and the relatively low irradiation temperature. This is a high energy configuration for dislocations and may affect annealing of the dislocations at elevated temperature.

Figure 3a shows a plot of the dislocation density in the HT-9 steel as a function of the irradiation temperature. Clearly, the dislocation density is controlled by the temperature. At higher temperature, the atoms are able to diffuse and defects are annealed out, resulting in the relatively low dislocation density. In deformed materials, the dislocation density can be related to the flow strength of the material by the Taylor law, $\_=\_0+m\_G\_^{1/2}$, where $\_$ is the dislocation density. The flow strength of these materials has been measured elsewhere. Figure 3b plots the flow strength versus $\_^{1/2}$. The linear response shows that the Taylor law holds for radiation damaged material as well. This presents an interesting non-destructive evaluation method for materials with radiation damage. By measuring the dislocation density using diffraction techniques, the flow stress can be estimated, which in turn would allow one to estimate the ductility; as the flow stress increases the ductility decreases.

Figure 4 shows the pair distribution functions (PDFs) of the control HT-9 sample and the 5E1 sample irradiated to 147dpa at 441C. The pair distribution function, G(r), is related to the probability of finding an atom a distance r from the origin give an atom at the origin, and is a measure of the short range order in the material. PDF's mea-

sured with x-rays and neutrons are complimentary because different elements have different contrasts to x-rays and neutron. For example, Fe and Cr (the two primary constituents of HT-9) look very similar to x-rays (have little contrast) because they have similar numbers of electrons. In contrast, they look very different to neutrons because they have very different scattering length. Thus, the two probes give distinct looks at chemical ordering.

In the control material, the neutron and x-ray pdf's agree very well indicating a lack of chemical ordering. The pdf's evolve with irradiation, and most importantly, the x-ray and neutron pdf's no longer agree, suggesting chemical ordering. This is an important result in its own right, but also demonstrates the ability of pdf measurements to monitor irradiation enhanced chemical segregation. This would be a very important measurement on mixed oxide fuels (MOX) for example.
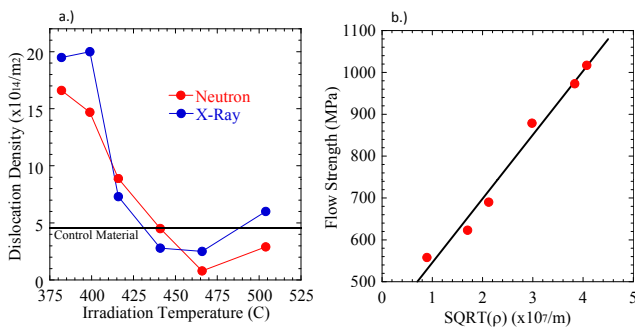
Figure 3. a. Dislocation density of HT-9 samples as a function of irradiation temperature measured with Neutron and X-ray DLPA. b.) Flow strength as a function of observed dislocation density.
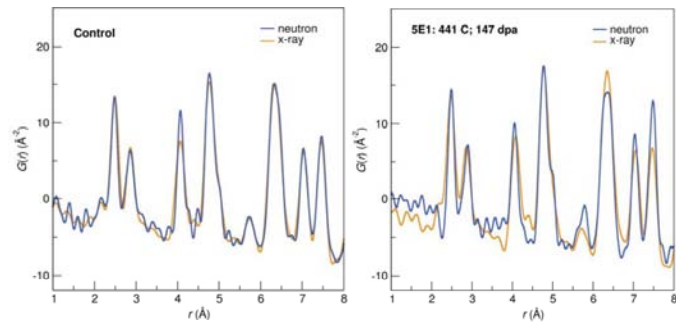
Figure 4. Neutron and X-ray pair distribution functions for control HT-9 and sample 5E1 irradiated to 147dpa at 441C.

In situ diffraction measurements during deformation

Control and irradiated HT-9 samples were deformed in-situ on the 1ID beamline at the APS. The lattice strain, ε, of both the ferrite and carbide phases was calculated from the lattice parameters of each phase, $\varepsilon=(d-d_0)/d_0$. Figure 5a shows the lattice strain of both phases as a function of applied stress. The composite nature of the material is evident from this plot. The two phases deform in a linear

elastic manner to roughly 600MPa. Beyond 600MPa, the elastic strain in the ferrite saturates indicating that the ferrite has yielded and is deforming plastically. The decrease in slope of the carbide strain indicates that the reinforcing carbide phase is supporting the load shed from the now plastic ferrite. This is precisely how a composite is designed to work and highlights the important role the carbides play in the strength of the material.

Figure 5b shows the evolution of the carbide peak widths as a function of strain. Beyond 0.07 strain, the peak width rapidly increases. Above, we have related peak width to dislocation density, but it is unlikely the carbides would accept dislocations. In this case the peak width is more likely related to a decrease in crystal size. Thus, the data suggests that the carbides are fracturing with increased strain. Further analysis will both clarify and quantify this point.
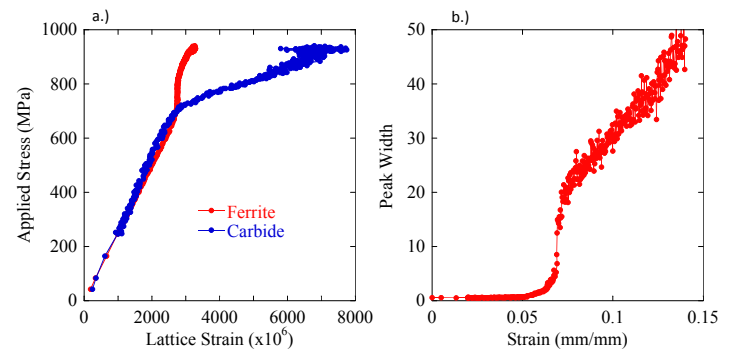
Figure 5. a). Applied stress versus lattice strain for control HT-9 material. b.) Evolution of carbide peak width with enforce strain.

Impact on National Missions

The results discussed above will have a strong impact on the Fuel Cycle Research and Development (FCR&D) program. First they provide insight that could not have been collected by other means. For instance, the quantitative measurement of dislocation densities is very difficult, if not impossible to obtain any other way. The fact that these measurements suggest a non-destructive way to infer the evolution of macroscopic properties such as flow strength and ductility could be very important for enhanced surveillance of reactor components. The relevance of this work to the FCR&D structural materials program has resulted in programmatic FY12 funding to continue the efforts on other materials of interest to the program.

Second, the results have demonstrated the value of these techniques for microstructural characterization for other materials of interest, e.g. nuclear fuels. The PDF analysis, for instance, could be used to monitor chemical ordering in mixed oxide (MOX) fuels both in the virgin state and after different levels of burn. Also, it has demonstrated that the techniques could, in large part, be viable at the proposed F^3 facility as part of MaRIE. This directly leads to better definition of the F^3 facility.

The results of this program will contribute to several papers in peer reviewed archival journals. The Zr work has been submitted to Phys. Rev. Lett. We intend a paper comparing the microstructure of the HT-9 before and after irradiation which will highlight the evolution of the carbide volume fraction and dislocation density. This paper is in the writing stage. Finally, a third paper will be written on the load sharing between the ferrite and carbide and the broadening of the carbide peaks. Some analysis is still required before writing of this paper can commence.

Learning New Things From Old Uranium Activation Data (U)

Hugh D. Selby
20110650ER

Abstract

The Science of Signatures Reserve project entitled "Learning New Things from Old Uranium Activation Data" was intended to achieve two goals: At the conceptual level, the principal objective was to probe the notion that new signatures relevant to the technical nuclear forensics (TNF) mission might be gleaned from studying old nuclear test data. Instead of asking questions from the perspective of assessing the performance of a known experiment, we wanted to see if the data were sufficiently well resolved in certain signatures that we could use these signatures to infer, with confidence, characteristics of devices of unknown design (DUDs). The LDRD supported study accomplished this first goal. The second more specific objective was to develop a technical basis for a specific signature thought to be a function of neutron fluence. The second objective was largely achieved although, as is often the case in scientific endeavors, new questions were discovered along the way. Our approach to achieving these two goals was to combine high performance computing (HPC) simulations with theoretical study of the outputs of the simulations and real debris data to parameterize and develop an analytical model of the phenomena that produce the signature. This approach has yielded a defensible technical basis for the signature and has successfully defined where the signature is of clear value and where further study is needed. Despite the short duration of the project, the development of the new signature has had immediate positive impact on the radiochemical data evaluation component of the TNF mission.

Background and Research Objectives

Recent studies have suggested that the current approach to DUD assessment could be enhanced by reconsidering certain uranium activation products in post-detonation debris data. Uranium activation product data have long been useful diagnostic tools but the development of a DUD-characteristic signature has been only partially successful to date. We surmised that the neutron fluence sensitivity of these activations might provide such a signature if the activations' production were well understood. Our objective was two-fold: 1) Using HPC simulations and theoretical modeling, develop an analytical framework that described the activation production in a subset of potential DUDs, and 2) show that this signature is evident in real data and consistent with the analytical framework. This second objective is perhaps the most significant in that it could demonstrate the concept that previously undiscovered signatures lie in the archival data but require new questions to be asked in order to reveal them.

Scientific Approach and Accomplishments

Readers are referred to the classified presentation LA-CP 11-01237 and subsequent reports for the details of the approach and accomplishments. In general, our approach was to combine the "empirical" HPC simulations with theoretical studies and compare the resultant analytical model/framework with real archival test data. Given the short term of the study, simulation and theory focused on a region of weapons physics that was specific enough to provide confidence in the relevant parameters but broad enough that extension to more general statements will be straightforward in future studies. The key parameters that underpin the signature in question were arrived at by systematically altering independent (or as close to independent as possible) variables within each simulation, affording a suite of virtual nuclear experiments. Simultaneously, the theory effort considered these results and attempted to arrive at these parameters from first principles physics considerations of nuclear explosions. Unlike early efforts by the Manhattan Project theoreticians, our study was uniquely designed to describe the *integral* data that arises from debris data. In other words, the present study did not attempt to reproduce the complex physics present in HPC simulations, but instead focused on approximating the "integral" of a subset of the appropriate physics necessary to produce the radiochemical result observed in real data. This is a tremendously difficult undertaking and remains in the developmental stage at the end of this project. Nevertheless, progress has been made in estimating neutron fluencies which compare reasonably well with simulation results. It is of note that this theoretical approach naturally leads to a framework that is

very similar to existing semi-empirical methods currently in use in radiochemistry to evaluate debris data. In all, we have found that both theory and simulation are consistent with the real data in hand. There are limits to the new signatures applicability to every scenario; with the work accomplished to date, we have developed a sufficiently strong and defensible framework for the use of the signature in a relatively broad range of DUD assessments.

Impact on National Missions

It is too early to accurately assess the impacts of the current SoS Reserve study on the greater TNF mission. However, the local radiochemical evaluation process has already begun to evolve and incorporate the signature. The theoretical efforts are still in their infancy but appear to have great potential to impact much more than the TNF mission.

Publications

Selby, H. D., M. E. Schillaci, and S. C. Frankle. Learning New Things from Old Uranium Activation Data: A Science of Signatures Study. Presented at *Nuclear Explosive Design Physics Conference.* (Los Alamos, New Mexico, 17-21 Oct. 2011).

Atomic Interface Design of Nanocomposites for Extreme Mechanical Loadings

Irene J. Beyerlein
20100596PRD1

Introduction

In recent years, there has been an increasing demand for next generation structural nanomaterials that can withstand extreme mechanical loadings, such as those generated in severe plastic deformation (SPD) and shock loadings. One material that has exhibited extraordinarily high strength, ductility, and resistance to radiation and mechanical loading is the nanostructured copper-niobium (Cu-Nb) multilayer composite made by physical vapor deposition at LANL. While LANL scientists have shown that bimetal composite nanolayers have superior damage resistance to extreme environments, only one material combination has been studied: Cu-Nb. A practical material combination for advanced structural applications has yet to be identified and hence the potential of nanolayered composites remains untapped. The problem is the inability to model, at the atomistic scale, any bi-material interface. To overcome this, Dr. Zhang proposed to develop new atomic scale theoretical methodologies and techniques that will enable for the first time study of a variety of nanocomposites. The breakthrough in his work will be the atomic scale mechanisms that distinguish one nanomaterial from another in its robustness to extreme environments, such as high temperature, radiation, and shock

Benefit to National Security Missions

Dr. Zhang's research will lead to controlled synthesis of structural-sized nano-composite metals that--by virtue of their high density of bi-metal interfaces--will be an order of magnitude more resistant to extreme mechanical conditions (shock) and environments (radiation, high temperatures) than currently available materials. These shock- and radiation-resistant bulk nanocomposites will greatly benefit nuclear power applications (longer lifetimes of structural components), weapons applications (armor and penetrator technology) and transportation, where high strength, high-temperature resistance, lightweight, and damage tolerance are critical for boosting energy efficiency. We support LANL missions in 1) solving emerging national security (energy) challenges, and 2) leading in materials and process modeling. In addition, novel nanomaterials

in bulk form will open new opportunities for material testing in MARIE, such as real-time, in-situ diagnostic of bi-metal interfaces in deformation under a wide range of strain rates and temperatures. Research in shocked materials builds underlying capability for the weapons program.

Progress

In the past year, Dr. Ruifeng Zhang concentrated his research on fcc/bcc interfaces that are minimum energy and atomistically flat, such as {111}fcc//{110} bcc Kurdjumov-Sachs (K-S) and Nishiyama-Wasserman (N-W) interfaces. They form naturally in composites of two immiscible metals fabricated by magnetron sputtering or casting [1]. Such composites exhibit extraordinary enhancements in strength, stability, and damage resistance as the spacing between interfaces is driven down to the nanoscale [2]. Dr. Zhang's MD simulations show that when deformed, K-S interfaces emit Shockley partial dislocations first into Cu [3]. His analysis proved that nucleation was governed by interface structure and not solely determined by Schmid factors. A unique aspect of [3] was the development of a method to isolate a single, two-dimensional dislocation loop via the single loop isolation method (SLIM) (Figure 1). With SLIM, he was able to determine that the activation barrier and critical resolved shear stresses for nucleation from the K-S interface are lower than that for homogeneous nucleation in the perfect fcc lattice, indicating for the first time that a flat fcc/bcc incoherent interface can act as a viable source of lattice dislocations. This important result suggests that the slip activity and hence plastic deformation near the interface will be controlled by the structure of the interface. This type of information can be transferred to higher length scale models and numerical codes. Two papers report on this work, one in press for Scripta Mater and one in preparation for Physical Review B.

Interfaces produced in the same material systems fabricated under non-equilibrium, large strain deformation conditions are not generally the same as those formed in equilibrium conditions. Despite this, like

those formed in equilibrium, these interfaces lead to ultra-high strength composites that are, at least, just as stable at high temperatures [our unpublished work]. One interface that seems to prevail in rolling and extrusion processes is the {112}fcc//{112}bcc and <110>fcc//<111>bcc interface [4]. The {112}KS interface has a distinct atomic structure from the classical {111}//{110}KS interface that predominately form in PVD foils. High-resolution TEM observes that {112}KS interfaces are ordered and faceted, wherein the terrace planes match the compact planes of Cu and Nb [5]. MD modeling predicts the faceted structure observed in HR-TEM, as well as the development of three sets of intrinsic interfacial dislocations, one of which (set 1) has a Burgers vector lying out of plane [our unpublished work]. Dr. Zhang found that this interface contains many more defects and some of the defects have a stepped structure.
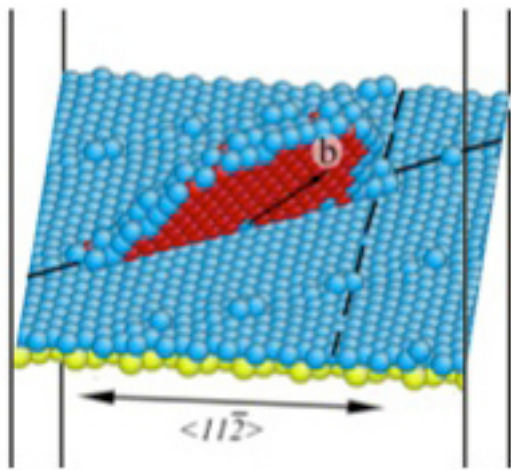
Figure 1. Nucleation of a single loop from a copper-niobium interface via the SLIM method.

In order to carry out simulation studies on shock response, it is critical that the interatomic potentials used in simulation are suitable under these extreme conditions. Dr. Zhang found that the interatomic potential currently used for niobium in simulations at LANL is inadequate for simulations at extreme conditions and leads to unphysical results. To remedy this problem, he considered five different empirical potentials, and with each, simulated the shock-induced crystalline structure in niobium single crystals. The potentials produced different results. At sufficiently large shock strength, they either formed an "fcc-like" stacking fault or deformation twins (Figure 2). To determine which was correct, he carried out ab initio density functional theory calculations of the gamma surface at various pressures and compared to them to those calculated using the five interatomic potentials. The inaccurate potentials did not produce the correct gamma surface at high pressures, an error that led to the artificial "fcc-like" stacking fault. As a result of this work, he has not only identified two interatomic potentials for niobium that should be used in future shock simulations,

but also introduced a new method for selecting suitable interatomic potentials for other metals for reliable atomic-scale shock compression simulations (and likely for other extreme loadings). The results of this work are in press in Philosphical Magazine Letters.
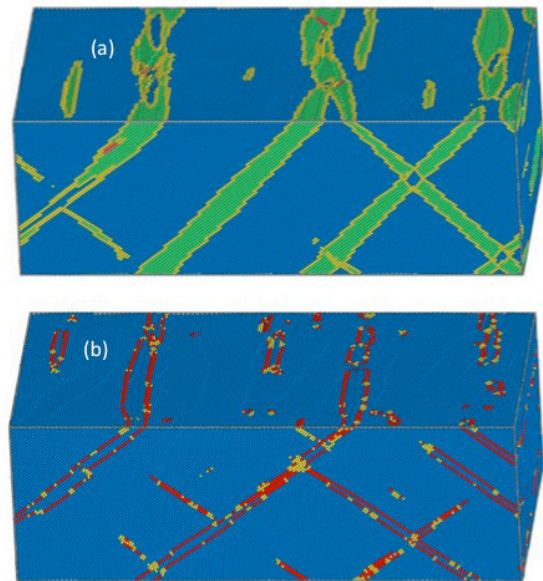
Figure 2. Shocked niobium single crystals with (a) a potential that gives the incorrect response of a phase transformation and (b) a potential gives the correct response of twinning.

He then proceeded to use these two interatomic potentials in large-scale simulations of Cu-Nb systems at high rates of strain and shock. The first step he accomplished was to develop a large-scale molecular dynamics (MD) simulation model using the LANL code, SPaSM. Once developed, he then simulated the shock response of multi-layered composites with different thicknesses. For copper/niobium multilayers with layer thickness less than 5nm, dislocations preferably nucleate at the interface (Figure 3a), and then transmit into the neighboring copper and niobium layers (Fig. 3b). In the former mechanism, he observed that the preferred nucleation sites depended strongly on the local atomic structure of the interface. In the latter event, he found that preferred sites for dislocation transmission are associated with slip systems that are well-aligned across the interface and intersection points of intrinsic interfacial misfit dislocations. A paper reporting these results is currently in preparation for Acta Materialia.

Overall, Dr. Zhang's results to date on the relationship between physical and functional properties of the interface will open the way to further improve the mechanical properties of nanocomposites via atomic design of its interface.
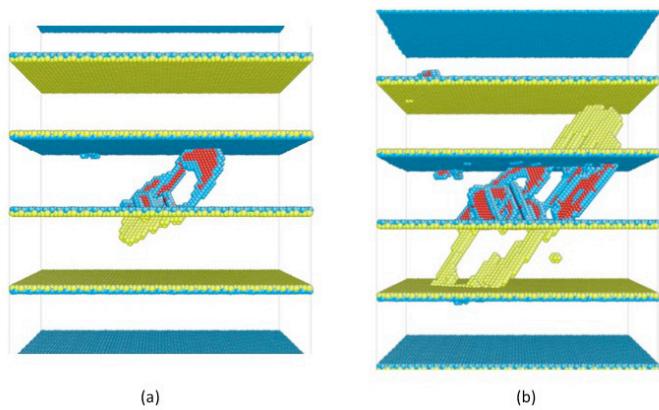
Figure 3. Atomic scale simulation of compressed copper-niobium multilayers showing (a) nucleation and (b) transmission across the interface.

Future Work

Because of their remarkably different atomic structure, the interfaces formed in composites produced by mechanical processing are not expected to nucleate dislocation by the same mechanisms as the low-energy interfaces that develop by magnetron sputtering. These interfaces are found to be significantly distinct in structure from those of flat interfaces and are much higher in energy. His working hypothesis is that the observed mechanically stable interface prevails because it is an excellent source for dislocations. Thus, in future work, Dr. Zhang will study the mechanisms of dislocation nucleation and emission from these mechanically generated interfaces. With this information, he plans to develop a mechanism map for designing interfaces based on their propensity to nucleate dislocations. He will also simulate these interfaces in shock conditions to determine their stability under this extreme environment.

Conclusion

Dr. Zhang's research results will determine which material composite systems will be robust in extreme conditions such as shock and irradiation. Stronger and more robust materials in next generation nuclear power (e.g., fuel cladding), weapons applications (armor and penetrator technology), and transportation systems (where high strength to weight ratio is critical) will be safer, more economical, and sustainable. In this way, his research supports LANL's mission to solve emerging national security (energy) challenges.

References

1. Misra, A., J. P. Hirth, and R. G. Hoagland. Length-scale-dependent deformation mechanisms in incoherent metallic multilayered composites . 2005. *Acta Materialia.* **53** (18): 4817.

2. Demkowicz, M. J., R. Hoagland, and J. P. Hirth. Interface structure and radiation damage resistance in Cu-Nb multilayer nanocomposites . 2008. *Physical Review Letters.* **100** (13): 136102.

3. Zhang, R. F., J. Wang, I. J. Beyerlein, and T. C. Germann. Disloclation nucleation mechanisms from fcc/bcc incoherent interfaces. . To appear in *Scripta Materialia.*

4. Lee, S. B., J. E. LeDonne, S. C. V. Lim, I. J. Beyerlein, and A. D. Rollett. The five-parameter heterophase interface character distributions (HICD) of physical vapor-deposited and accumulative roll-bonded Cu-Nb multilayer composites. *Acta Materialia.*

5. Han, W., J. Carpenter, J. Wang, I. J. Beyerlein, and N. A. Mara. Interface-driven deformation twinning in Accumulative Roll-Bonding Prepared Cu-Nb nanolamellar composites. *Applied Physics Letters.*

Publications

Zhang, R. F., I. J. Beyerlein, T. C. Germann, and J. Wang. Deformation twinning in bcc metals under shock loading: a challenge to empirical potentials. To appear in *Philosophical Magazine Letters.*

Zhang, R. F., J. Wang, I. J. Beyerlein, and T. C. Germann. Disloclation nucleation mechanisms from fcc/bcc incoherent interfaces. To appear in *Scripta Materialia.*

Zhang, R. F., J. Wang, X. Y. Liu, I. J. Beyerlein, and T. C. Germann. Non equilibrium molecular dynamics simulations of shock wave propagation in nanolayered Cu/Nb nanocomposites. To appear in *17th APS Topical Conference on Shock Compression of Condensed Matter.* (Dallas, Texas, 10-15 July 2011).

Multi-scale Computational Approach for Studying Radiation Resistant Nanoclustered Alloy

Blas P. Uberuaga
20100598PRD1

Introduction

This theoretical project is using atomistic and mesoscale (micrometer) simulation techniques to examine nanostructured ferritic alloys (NFAs). These are metallic materials with nanometer-sized oxide particle embedded within that have been shown to have great exceptional strength and radiation tolerance and are thus considered prime candidates for future generation nuclear energy applications. However, there is currently no fundamental understanding of how these materials obtain these exceptional properties. This work will provide the fundamental understanding of both the structure of these materials and how that structure leads to the observed properties. We performed electronic structure calculations to determine the properties of the interface between the oxide particles and the metal matrix, including the behavior of defects and alloying elements near the interface. This information will be used to develop a model at the mesoscale that can then simulate the performance and behavior of the material under irradiation. By understanding how the oxide particles improve the performance of the material, we will be able to guide the future design of new NFAs that meet the demands of extreme applications.

Benefit to National Security Missions

This work will provide the underpinning science necessary to develop future generation radiation tolerant materials, especially for cladding in nuclear fuel pin assemblies. As such, it is directly related to the missions of DOE/SC and DOE/NE, especially as regards energy security and the development of carbon-neutral energy sources. Further, it develops our basic understanding of materials such that we understand what leads to the improved radiation tolerance of these nanostructured materials in a way that allows for the design of such materials in the future.

Progress

Current understanding is that the enhanced radiation tolerance of nanostructured ferritic alloys is due to the defect recombination reaction that may occur at the oxide-metal interface under radiation. Further,

this interface helps to reduce other radiation-induced damage modes like formation of voids and bubbles. Such damage is known to severely degrade the mechanical properties of these alloys. Hence, it is essential to develop a fundamental understanding of the structure and behavior of this interface under radiation.

Experimentally it has been observed that orientation relationship between the oxide and the ferritic matrix depends strongly on the alloying elements present within the matrix. For example, if the matrix has Cr as the alloying element the orientation relationship is $[110]_{Oxide} || [110]_{FeCr}$ and $(1\text{-}1\text{-}1)_{Oxide} || (1\text{-}10)_{FeCr}$ while with Al as the alloying element within the ferritic matrix the orientation relationship is $[110]_{Oxide} || [010]_{FeAl}$ and $(100)_{Oxide} || (001)_{FeAl}$. It is to be noted that the primary constituent of the matrix is Fe while Cr and Al are alloying elements. It is interesting to observe that even minor alloying elements like Cr or Al (present in quantity less than 12wt %) can affect the interface structure between the oxide particles and the ferritic matrix. It is worthy of mention that the system chooses an orientation of the interface so as to minimize the total energy, which comprises of the elastic and the interfacial energy.

We performed electronic structure calculations and determined the structure of iron/oxide interface at the atomic scale with orientation relationship of $[110]_{Oxide} || [010]_{Fe}$ and $(100)_{Oxide} || (001)_{Fe}$ as shown in Figure 1(a). It is clear from the figure that the displacement of iron atoms at the interface is not uniform. Among the interfacial iron atoms, atoms at the middle are more displaced than the atoms at the edges. This is because unlike the Fe atoms at the edges two columns of iron atoms at the middle share electrons with one column of oxygen (indicated by solid arrows). Interface calculation further reveals that the lattice mismatch between Fe and the oxide results in the formation of a misfit dislocation at the interface (shown by the orange dotted line in Figure 1(a)). In this regard, a dislocation is a line defect (consists of an extra half plane of atoms) commonly present in materials whose density and mobility determines the strength and

other mechanical properties of materials. The misfit dislocation arises because 5 atomic rows of Fe are trying to match to 4 atomic rows of oxygen; the incompatibility is accommodated by a misfit dislocation. It is to be noted that the oxygen has higher electro-negativity than iron i.e. oxygen accepts electrons from iron. However, excess of iron compared to oxygen at the interface makes it impossible for the certain iron atoms at the interface to give up all its valence electrons to the neighboring oxygen in yttria. This results in an excess charge on certain iron atoms at the interface. The system would like to get rid of the iron atoms with excess charge on them as shown in Figure 1(b). The figure shows that vacancy will form spontaneously (with negative vacancy formation energy) at these iron sites with excess charge on them (with Bader charge greater than zero). Now the question naturally arises how many interfacial iron vacancies the system can accommodate. To determine that we systematically introduce vacancy at the interfacial Fe sites and calculates the change in energy of the system. It was found that starting with fifty-five iron atoms (in the pristine structure with no vacancy) at the interface the energy of the system decreases monotonically till the total number of vacancies within the interfacial layer is twenty nine. The energy of the system increases as further vacancies are introduced within the interfacial iron sites (Figure 1c).
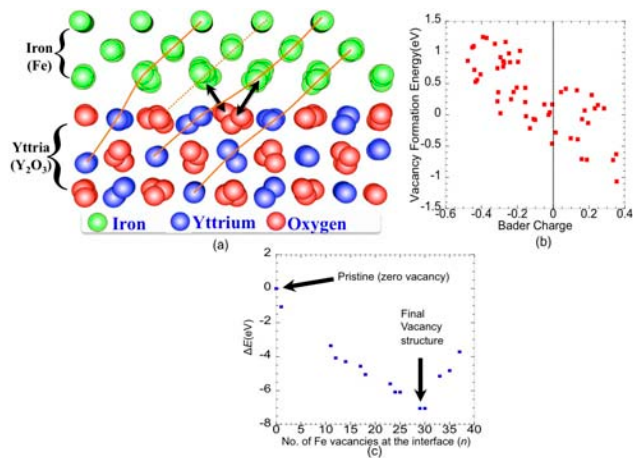
Figure 1. (a) Relaxed structure of the iron/yttria interface. The black arrows indicate that two columns of interfacial iron share one column of oxygen. The solid orange lines connect the metal atoms (yttrium and iron) while the dotted line represents the extra half plane (connecting iron and oxygen); (b) Plot of the vacancy formation energy of interfacial iron as a function of Bader charge (excess charge) on the iron; (c) Change in the energy of the system as the interfacial iron vacancies are introduced.

Later systematic calculations were performed to study the role of fifteen different alloying elements (relevant to real engineering cladding material) on the structure and properties of the oxide-metal interface. Based on the calculated segregation energy (not shown) it was observed that the alloying elements that have a body centered

cubic structure prefer to stay in the bulk Fe while alloying elements with face centered cubic structure tend to segregate to the oxide-iron interface. Alloying elements with hexagonal close packed structure show a mixed behavior. Our calculations further reveal that the behavior of alloying elements at the interface not only depends on the individual crystal structure of the alloying elements but also their charge and ionic radius. Further, our preliminary calculations provide some insights about the role of fission products like silver on the structure and electronic properties of the interface. We are currently working to gain a comprehensive understanding of the oxide-matrix interface, by performing similar study for the interface with orientation relationship as $[110]_{Oxide} || [110]_{Fe}$ and $(1\text{-}1\text{-}1)_{Oxide} || (1\text{-}10)_{Fe}$. We are also performing calculations to study the effect of radiation-induced damages on the structure and properties of the interface.

Future Work

This theoretical project will use atomistic and mesoscale (micrometer) simulation techniques to examine nanostructured ferritic alloys (NFAs). These are metallic materials with nanometer-sized oxide particles embedded within and have shown great exceptional strength and radiation tolerance and are thus considered prime candidates for future generation nuclear energy applications. However, there is currently no fundamental understanding of how these materials obtain these exceptional properties. This work will provide the fundamental understanding of both the structure of these materials and how that structure leads to the observed properties. We have already performed electronic structure calculations to determine the properties of the interface between the oxide particles and the metal matrix, including the behavior of defects near the interface. These calculations will provide the thermodynamic and kinetic quantities of defects near the metal/ceramic interface. Such information will be used to develop a model at the mesoscale -- a phase field model -- that can then simulate the performance and behavior of the material under irradiation. In particular, the phase field model will examine the ability of the nanoparticles to retain their shape under irradiation and how that ability depends on the composition and properties of the particles. By understanding how the oxide particles improve the performance of the material, we will be able to guide the future design of new NFAs that meet the demands of extreme applications.

Conclusion

Future nuclear reactors will demand even more from the materials that comprise them, in terms of mechanical strength and radiation tolerance, to extract the most energy from the fuel. This requires new materials that can withstand these extreme environments. One candidate for such applications are NFAs. While these materials hold great promise, the origins of their exceptional behavior is

unknown. Current NFAs are "designed" by an Edisonian trial-and-error approach. By studying these materials at the atomic level, we will develop the fundamental understanding that will allow for first-principles design of improved materials that will form the foundation of future reactors.

Publications

Uberuaga, B., S. Choudhury, X. Bai, and N. Benedek. Grain boundary stoichiometry and interactions with defects in SrTiO$_3$. 2012. *Scripta Materialia.* **66** (2): 105.

Unique Semiconductor Nanowire Heterostructures in Physics and Applications

Samuel T. Picraux
20100601PRD2

Introduction

Semiconductor nanowires (NWs) enable novel device concepts and emergent physics and applications, by allowing materials synthesis in three dimensions. To fully utilize their potential, a thorough understanding of and control over growth mechanisms and charge carrier transport properties are necessary. Expertise in III-V and Si/Ge NW growth, device fabrication, structural and transport characterization, and analysis, will enable implementation of new NW research ideas beyond the traditional approaches in the field. Three novel areas are being investigated in detail: 1) radial nanowire solar cells promising a new generation of photovoltaic devices with low cost and high efficiency performance; 2) spin transport in Si NWs which will enable control of both spin and charge in the technologically relevant Si materials system; and 3) radial nano-probe capacitors to enable neuronal signal detection and stimulation by this new approach.

Benefit to National Security Missions

This work aims to develop a fundamental understanding of nanoscale materials based on nanowire synthesis for application to devices not presently possible by any other means. In addition to advancing basic new understanding of materials and device science at the nanoscale this work will specifically address new approaches to energy harvesting by photovoltaics, spin and charge control in electronic devices, and neuronal probes for biomedical applications.

Progress

In this past year, we have brought to maturity our understanding of the field of heterostructure growth and devices as well as defects that arise during their growth. In addition to refining our control of the growth of Ge-Si axial nanowire heterostructures and demonstration of transistor devices with excellent switching behavior, we proposed a new model – based on our high resolution TEM imaging and molecular dynamics simulations with Jian Wang of MST-8 – that provides an atomic level understanding of defect nucleation and kinking in semiconductor nanowires. With such understanding, we were able to control and eliminate defect nucleation and kinking in nanowires.

In addition, our work has established the foundations of material synthesis, fabrication, and device design on two fronts of NW research at Los Alamos: (i) spin-based devices and (ii) radial solar cell devices. In the area of electron spin based devices, we proposed a new approach for barrier formation (spin filter) in spin devices in which a thin p-doped shell layer deposited on the n-doped nanowire forms a depletion region (space charge region) that establishes a tunneling barrier whose width and height can be controlled by the doping and thickness of the deposited p-layer. This approach eliminates any associated surface state problems that may arise in conventional oxide-barrier/semiconductor interfaces. We then fabricate devices to evaluate reference samples and test this concept. Using cobalt as the spin injecting ferromagnetic contact into Ge nanowires, we find a contact resistance of ~ 5 Kohm for n-doped Ge shells, and ~ 2 Kohm for p-doped Ge shells inferring an n-doping resistivity of ~ 1E-3 ohm-cm2 and specific contact resistivity of ~ 1E-6 ohm-cm. As such, the contact specific resistivity needs to be increased by 100-1000 times in order to match that of the semiconductor and allow efficient spin filtering. Using thin doped Ge shells, our initial efforts have led to an increase of 10X in contact resistivity and further increase in the p-layer shell thickness is expected to solve the conductivity mismatch problem. In addition, we are fabricating reference samples with Al_2O_3 tunnel barriers based on the uniform core-shell doping approach we reported last year.

In the area of nanowire solar cells, we developed a simple and intuitive model to aid in designing efficient radial nanowire solar cells based on a given set of nanowire geometry and material parameters. We then performed systematic experiments that allowed the perfection of the fabrication of large nanowire arrays using deep inductive coupled plasma (ICP) etching of nanowires with diameters in the range of 150 nm – 750 nm and lengths of 2 – 10 micrometers. This was also performed on thin Si substrates for eliminating effects

of substrate absorption and isolating the optical properties of nanowire arrays. The optical absorption measurements (performed by Ian Campbell of MPA-11) showed that nanowires with ~ 500 nm diameter, 10 micrometers length, and ~ 750 nm – 1 micrometers spacing or lower display the most enhanced optical absorption compared to bulk Si throughout the solar spectrum, reaching up to 60% at the longest wave wavelengths (1100 nm) validating that the optical thickness of the material required for full absorption of light is much lower with Si nanopillars compared to bulk Si. We then followed by developing a fabrication/growth process that allowed excellent control over the radial doping profile for achieving radial solar cell junctions. By using a sequence of oxidation/etching of the damaged etched nanopillar surface, we were able to smooth the surface to become epi-ready. We then were able to grow doped or undoped shells epitaxially with controlled interfaces and doping densities, in contrast to popular approaches in the literature which rely on thermally diffusing dopants into the nanowires to obtain radial junctions, and which are of inferior control and quality. Subsequently, these radial p-n junction structures were used to fabricate solar cells whose electrical and photovoltaic response is currently being evaluated.

Future Work

Three areas will be addressed. (a) Radial nanowire (NW) solar cells: Concentric NW p-i-n junctions allow decoupling of light absorption along NW length and field driven charge carrier separation along NW radius for enhanced solar energy conversion. This work aims at discovering and understanding material design for strong broad-band light absorption, carrier separation and recombination in this new regime of ultra-short collection times, and feasibility of efficient tandem cells in Si/Ge and III-V NWs. (b) Spin transport in Si NWs: Through collaborating with lab leaders in the area of spintronics, we will utilize the 1D nature of Si/Ge NWs to enable long spin diffusion lengths and study spin transport across semiconductor heterostructures for the first time. Further, single electron spin devices in quantum confined NWs promise high on/off switching behavior (i.e. high magneto-resistance coefficient) in spin devices. (c) Radial nano-probe capacitors for neuronal signal detection and stimulation: With the approach of controlled NW core-shell junction capacitors and the feasibility of biocompatible dielectric coatings, as demonstrated at this Laboratory, high density neuronal nanoprobe arrays that rely on capacitive sensing rather than direct current microprobe arrays are feasible. This allows safe, lower power, corrosion resistant and high resolution in-vivo measurements and stimulations.

Conclusion

These studies will allow us to gain new understanding of multifunctional material properties and novel device physics based on nanoscale materials. The results will be important to developing advanced one dimensional

devices, will enhance our ability to address national research and development needs such as in solar energy harvesting, and will enable the realization of a new generation of efficient, high performance spin, opto-electronic and bio-electronic devices, as well as new probes for brain research.

Publications

Dai, X., S. A. Dayeh, V. Veeramuthu, A. Larrue, J. Wang, H. Su, and C. Soci. Tailoring the vapor liquid solid growth toward the self-assembly of GaAs nanowire junctions. To appear in *Nano Letters.*

Dayeh, S. A.. Electron transport in indium arsenide nanowires. 2010. *Semiconductor Science and Technology.* **25** (2): 024004 (20 pp.).

Dayeh, S. A., A. V. Gin, and S. T. Picraux. Advanced core/multi-shell germanium/silicon nanowire heterostructures: Morphology and transport. 2011. *Applied Physics Letters.* **98**: 163112.

Dayeh, S. A., J. Wang, N. Li, J. Y. Huang, A. V. Gin, and S. T. Picraux. Growth, defect formation, and morpholog control of germanium-silicon semiconductor nanowire heterostructures. 2011. *Nano Letters.* **11**: 4200.

Dayeh, S. A., J. Y. Huang, A. V. Gin, and S. T. Picraux. Elimination of gold diffusion in the heterostructure core/shell growth of high performance Ge/Si nanowire HFETs. 2010. In *IEEE Nano 2010 International Conference.* (Seoul, 17-20 August 2010.). , p. 95. Seoul: IEEE.

Dayeh, S. A., N. H. Mack, J. Y. Huang, and S. T. Picraux. Advanced core/multishell germanium/silicon nanowire heterostructures: The Au-diffusion bottleneck. 2011. *Applied Physics Letters.* **99**: 023102.

Dayeh, S. A., R. M. Dickerson, and S. T. Picraux. Axial Bandgap engineering in gemanium-silicon heterostructured nanowires. 2011. *Applied Physics Letters.* **99**: 113105.

Dayeh, S., and S. T. Picraux. Direct observation of nanoscale size effects in Ge semiconductor nanowire growth. 2010. *Nano Letters.* **10** (10): 4032.

Kar, A., P. C. Upadhya, S. A. Dayeh, S. T. Picraux, A. J. Taylor, and R. P. Prasankumar. Probing ultrafast carrier dynamics in silicon nanowires. 2011. *Journal of Selected Topics in Quantum Electronics.* **17**: 889.

Le, S., P. Jannaty, A. Zaslavsky, S. A. Dayeh, and S. T. Picraux. Growth, electrical rectification, and gate control in axial in situ doped p-n junction germanium nanowires. 2010. *Applied Physics Letters.* **96** (26): 262102.

Liu, X. H., L. Q. Zhang, L. Zhong, Y. Liu, H. Zheng, J. W.

Wang, J. H. Cho, S. A. Dayeh, S. T. Picraux, J. P. Sullivan, S. X. Mao, Z. Z. Ye, and J. Y. Huang. Ultrafast electrochemical lithiation of individual Si nanowire anodes. 2011. *Nano Letters.* **11**: 2251.

Picraux, S. T., J. Yoo, I. H. Campbell, S. A. Dayeh, and D. E. Perea. Semiconductor nanowires for solar cells. To appear in *Semiconductor nanostructures for optoelectronic devices.* Edited by Yi, G. C..

Picraux, S. Tom., S. Dayeh, P. Manandhar, D. Perea, and S. Choi. Silicon and germanium nanowires: Growth, properties, and integration. 2010. *JOM.* **62** (4): 35.

Seo, M. A., S. A. Dayeh, P. C. Upadhya, J. Martinez, B. S. Swartzentruber, S. T. Picraux, A. J. Taylor, and R. P. Prasankumar. Understanding ultrafast carrier dynamics in single quasi-one-dimensional Si nanowires. *Nano Letters.*

Sierra-Sastre, Y., S. Dayeh, S. T. Picraux, and C. Batt. Epitaxy of Ge nanowires grown from biotemplated Au nanoparticle catalysts. 2010. *ACS Nano.* **4** (2): 1209.

Polymer-Coated Surfactant Micro-reactors for Applications in Chemical Sensing, Contaminant Remediation and Synthetic Biology

James M. Boncella
20100624PRD3

Introduction

This research project is directed toward the generation of a new detection system for chemicals like organophosphates, which are the chemical constituents of nerve agents and pesticides. We utilize a biotechnology approach to make a system that will specifically recognize the desired analyte (organophosphate). Upon recognition, the system will glow when exposed to ultraviolet light (blacklight). This type of detection scheme is enabled by our ability to use surfactants (soap–like molecules) to encapsulate DNA and to generate an environment that will allow a dye that glows when exposed to UV light to change the color of its fluorescence in the presence of an analyte. Because this scheme will use RNA or DNA, which is randomly generated using DNA finger printing techniques, a successful system can be "evolved" to improve the detection process. This would be a completely new way to do chemical detection with an almost unlimited potential for improvement because of the tremendous variability that is possible with DNA polymers. For example, a DNA polymer that is 30 base pairs long has more that a billion billion possibilities of unique structures that would be able to recognize small molecule analytes.

Benefit to National Security Missions

This work is ultimately intended to generate a novel method for the detection of phosphate chemicals or metabolites in solution. If successful, it will be a new way of detecting pesticide or chemical weapons residues in samples of interest. This type of detection scheme will be of interest to agencies including the Department of Homeland Security, the intelligence services, DoD, as well as those parts of DOE who have interest in detecting these type of molecules. We therefore intend to transition this program to those agencies for more permanent funding/development. Future extensions of this capability may target other trace molecules of interest to nuclear nonproliferation.

Progress

A family of 35 DNA aptamers (single stranded DNA molecules that fold into unique shapes) having 80 base sequences consisting of a 40 base variable sequence and two 20 base primer end groups have been generated. These aptamers have been shown to bind a dye that has the functionality to react with a phosphonic acid chemical weapons surrogate. The dissociation constants of the aptamer-dye complexes are in the sub-micromolar range, which demonstrates that the concept of using DNA aptamers to bind and recognize small molecules is viable for this class of analyte. The procedure for binding the aptamers involves stabilizing the aptamer with anionic surfactants so that a hydrophobic binding environment can be generated within the aptamer molecules. When the dye moledcules bind, there is a significant increase in the fluorescence intensity of the dye as well as a shift in the wavelength of fluorescence. In this way, the binding of dye is easily distinguished from background of the unbound dye.

The aptamers were selected against dye molecules that were bound to sephedex beads. While some of the aptamers bind to the analyte appended to the bead, others do not bind so strongly and were washed away from the beads using buffer solution. The bound aptamers were then cleaved from the bead and amplified using standard PCR techniques. After 8 rounds of selection, the remaining aptamer population has only those sequences that bind strongly to the dye. These aptamers were then introduced into DNA plasmids and expressed by bacteria by generating bacterial colonies that grow from only one bacterium and thus have only one aptamer sequence in their genome. The bacteria colonies were then harvested, lysed, the DNA extracted and amplified by PCR and then sequenced using standard sequencing techniques. In this fashion 21 different aptamers that bind the dye were generated.

The aptamers have been sequenced and have been analyzed to determine homologous sequences between the aptamers that display strong binding constants to the desired analytes. There appear to be two consensus sequences that are important for binding to the dye-phosphate conjugate, AGAGCGCC and ACGGTGAG. A secondary structure for one of the aptamers has been proposed as step toward understanding the mechanism

of how the aptamer binds the dye-phosphate conjugate. Comparison of the likely secondary structures for other strongly binding sequences using readily available software is giving clues as to the structure of the binding site in these complex molecules.

In order to develop an analytical test for the desired analytes, the possibility of using the phosphorylation of the bound dye by halophosphate was explored. While there were changes in the fluorescence of the aptamer-dye complex when the chlorophosphonate was added, they were not big enough to use as an effective sensor. When a cationic surfactants, eg. cetyl trimethyl ammonium bromide, CTAB, are added to DNA aptamers, an insoluble material composed of DNA aptamer surrounded by surfactant, in this case CTAB, is formed. This creates a very hydrophobic environment around the aptamer. When the dye is now complexed by this DNA-CTAB aggregate, its fluorescence becomes very sensitive to the nature of the aptamer.

The DNA-CTAB-dye aggregate was then exposed to various alkylchlorophosphonates. The results of these experiments show that the bound dye–apatamer-CTAB aggregate reacts with the alkylchlorophosphonates to give a new material that has a greatly enhanced and shifted fluorescence signal (Figure 1). Thus, the reactive binding of the analyte through phosphorylation of the aptamer-dye-surfactant complex is a "turn on" sensor for the analyte. The data shows that this "turn on" signal is very selective for a specific analyte and suggests that a selective sensor for these analytes is possible. Several of the aptamer sequences have been sent to an outside laboratory for testing with a better surrogate, specifically, diisopropyl fluorophosphates and we are currently awaiting the results of those tests.
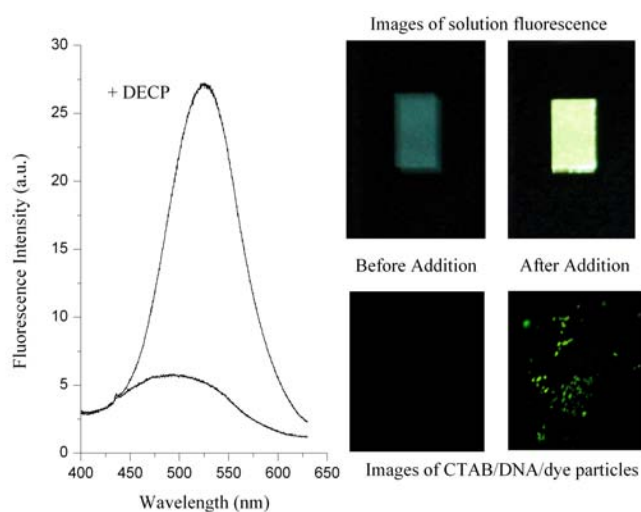
Further experiments demonstrate that rather than interacting directly with the dye molecules as originally intended, the alkylchlorophosphonates react directly with the DNA aptamer. The initial hypothesis is that the DNA bases get phosphphorylated, which causes a change in the DNA conformation, which, in turn, leads to a shifted and enhanced fluorescence from the material. When different alkylchlorophosphonates are allowed to react with the CTAB-DNA-dye particles, significantly different fluorescent responses are observe. This is interesting because it shows that the particles show a rather good specificity toward an individual analyte.

Future Work

The overall goal of the project is to generate a chemical detection scheme for organophosphates (pesticides/nerve agent residues) that will only respond to a specific, desired compound.

The tasks that will be performed are as follows:

- Understand the physico-chemical properties of the surfactant-dye-aptamer particles.

- Utilize the insoluble nature of the aptamer-CTAB-dye aggregates to created a film type sensor that is specific for various alkylchlorophosphonates.

Conclusion

The goal of this project is to produce a new way to detect/sense organo phosphate chemicals which are the constituents of pesticides and nerve agents. This technology would offer a more selective and possibly more sensitive way to monitor these agents. It could also be used to determine whether someone was manufacturing these materials in a clandestine way by examining the effluent from such a process.

Figure 1. Fluorescence spectra of DNA-CTAB-Dye (1:80:1) aggregate before and after addition of 0.5mg of diethylchlorophosphonate. To the right are photographs of the the fluorescence cuvette window (side on illumination) and fluorescence micrographs (400X)of particles of the DNA-CTAB-Dye aggregate during this addition.

Growth of Actinide-Nanocomposites using Hyperbaric Laser Chemical Vapor Deposition.

William L. Perry
20100626PRD3

Introduction

Without the ability to test nuclear weapons systems, the predicted response of each component needs to be accurately computed. Our goal is to contribute to the fuller understanding of the thermal ignition behavior of the important DOE secondary high explosive, octahydro-1,3,5,7-tetranitro-1,3,5,7-tetrazocine (HMX), in a specific parameter space that has not been well-studied. Microwave (MW) energy will be used as a heating tool to effectively and reproducibly reach a fast kinetic regime (10^{-2} s) with the unique ability to uniformly heat material at extremely high rates while maintaining a uniform temperature distribution [1]. Beginning at 160 °C, HMX undergoes a β- to δ- conformational phase transformation; the δ-form of HMX produces a second-harmonic generation (SHG) at 532 nm when irradiated with 1064 nm light [2]. Detection of the SHG intensity as a function of temperature is a useful probe for describing the HMX decomposition kinetics, and we aim to use this information to build a more complete model of HMX decomposition and better understand the role that the crystalline phases play including chemical kinetics and temperature dependence.

Benefit to National Security Missions

The highly tunable MW-assisted transformations will provide an important tool for better understanding the decomposition kinetics of HMX, adding to the foundation necessary for a quantitative understanding of the thermal behavior of explosives in nuclear weapons. Such knowledge is key to further reducing the likelihood of inadvertent nuclear detonation.

Progress

Because HMX alone is not MW-active, it must first be doped with a MW-sensitized component before rapid heating effect from MW absorption may be observed. It has been shown that addition of carbon nanotubes to a dielectric matrix significantly increases the effective electrical conductivity and dielectric loss of the resulting composite material at very low loadings (<1 wt %) compared to other common carbon additives [3]. Carbon nanotubes themselves are known to absorb MW radiation with highly efficient conversion to heat, and will act as internal "nano-heaters" when dispersed throughout a matrix material [4]. We fabricated HMX-binder nanocomposites loaded with varying weight percentages of multi-walled carbon nanotubes (MWNTs) or graphite as the MW absorber. To determine the optimal amount of MW absorbing additive (0.1 – 1 wt%) needed, we measured the dielectric properties of each sample (real and imaginary permittivities from 1 – 18 GHz, Figure 1), which are an intrinsic value that describes the expected MW-materials interaction and predicted heating response. Our ideal case will have a real permittivity value (dielectric constant) between 4 – 5 and an imaginary permittivity (loss component) ~0.1. Figure 1 shows the measured real and imaginary permittivity of four different samples (HMX with 5 wt% Estane, a polymeric binder, and 0.1 – 0.5 wt% of MWNTs or graphite). Two different measurement techniques were used to collect the data – the cavity perturbation method that measures response at discrete frequencies (in this case 2.5 GHz), and the open circuit method that measures continuously from 1 – 18 GHz. The combination of these techniques provides an accurate, wide band measurement necessary for experimental design purposes. The results show that addition of only 0.5 wt% MWNTs increases the real permittivity ~1.2x and the imaginary component ~2.6x, relative to the control material that does not contain MW absorber (HMX + Estane only). Furthermore, addition of the same amount of graphite has a less-pronounced effect, increasing the real permittivity by 1.08x and the imaginary permittivity 1.05x. This corroborates other studies that have shown the high aspect ratio tubular structure of carbon nanotubes, compared to the planar layers in graphite, supports higher electronic mobility leading to increased dielectric response of the MWNT-loaded composites [5].

In order to observe ignition timing and solid-state phase change behavior of HMX as a function of temperature, we must accurately measure the temperature of the sample as it is rapidly heated with MWs. Conventional methods for measuring temperature, such as a metal thermocouple, will not work in the presence of a MW

field. The presence of metal adversely affects the MW distribution within the system and will also absorb a portion of the incident MW energy. Infrared methods provide an alternative, and we successfully obtained dynamic temperature measurements of a similar MW-sensitized explosive composite during MW exposure using a single-point fiber-optic pyrometer. Careful calibration is the key step to achieving accuracy using an infrared sensitive fiber-optic probe. The calibration uses an external heat source (no MWs) with all other conditions identical to the actual experimental set-up. The sample geometry and fiber-optic configuration remain the same, which automatically corrects for emissivity; we also placed several thermocouples on and around the sample itself to provide more than one temperature readout for comparison with the pyrometer response.
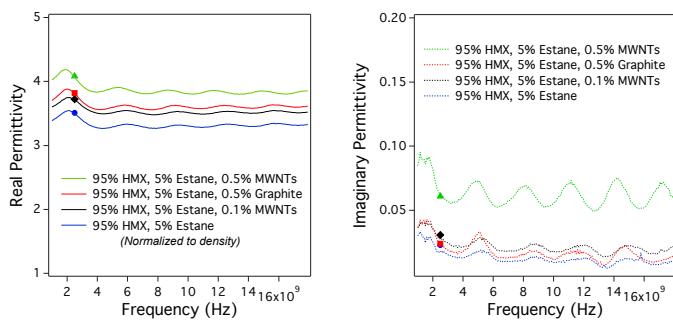
Figure 1. Measured dielectric properties (1-18 GHz) of HMX-binder nanocomposites loaded with varying wt% multi-walled carbon nanotubes or graphite. The real permittivity (left graph) was corrected for density variation using the values obtained from the cavity perturbation method at 2.5 GHz (solid symbols).

Figure 2 shows data collected from two representative MW temperature measurement experiments, both exposed to 2500 W for 150 ms; heating rates were measured to be ~300 °C/s with maximum temperatures ranging from 160 – 200 °C. The graphs to the far left compare the measured incident and reflected MW power; subtracting the two gives the total absorbed power (green trace). Time integration of the absorbed power data provides the total absorbed MW energy, and is shown on the same graph (blue trace). The middle set of graphs compare the absorbed MW power to the measured voltage response versus time recorded by the optical temperature probe. It is evident that the temperature continues to increase throughout the MW pulse, and reaches a maximum just after the pulse has ceased. The temperature then drops, but reaches a steady state that is higher than the initial observed temperature. The third set of graphs (far right) show the temperature probe output plotted as temperature versus time, calculated from the results of the calibration experiments described above. Finally, the bottom-most graph in Figure 2 overlays the difference in temperature (relative to the initial temperature) of the two

representative runs. This graph illustrates that the final steady state temperature correlates with the total amount of energy absorbed in the sample (~800 – 850 J). Due to experimental error and/or slight changes in the system configuration, we found that this may change between runs, even when the input power and pulse time are constant.
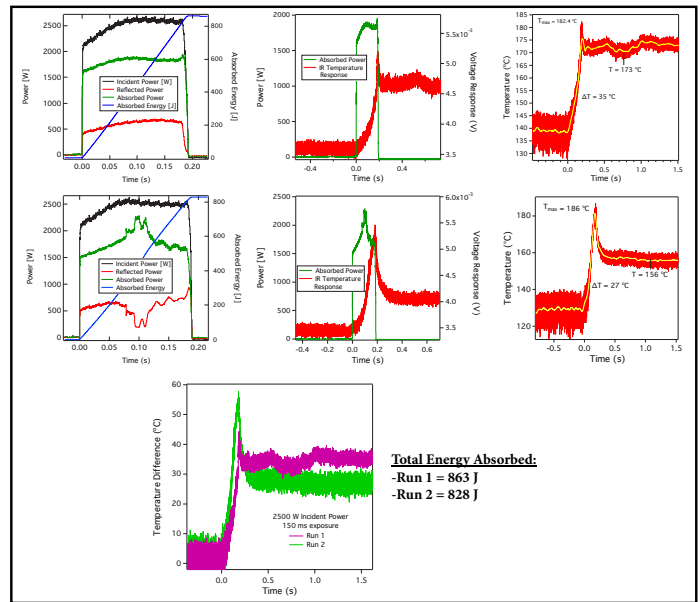
Figure 2. Two representative temperature measurement runs compared; the graphs in row 1 correspond to one run, while those in row 2 correspond to the second. The data show that observed temperature rise may be correlated to the amount of MW energy observed in the sample.

The dielectric data was used to design an appropriate microwave fixture, or applicator, suitable for experiments to observe the effects of MW exposure on the explosive material. The electromagnetic and thermal characteristics, in addition to the 4-step reversible kinetics model for HMX that include expressions for the solid-state transition, decomposition, and combustion, were modeled using electromagnetic and heat transport modeling tools (COMSOL) [6]. To predict the temperature response of the sample, the modeling parameters included applying 2.5 GHz radiation (2500 W) to a cylindrical pressed carbon-doped sample of HMX (1/4" diameter x ¾" height) contained in an aluminum resonant cavity (91 mm diameter). The top of Figure 3a shows still images of a time-lapse 2D model of the temperature increase as MWs are applied. The model images are from the perspective of a side view "slice" of the sample contained in the circular resonant fixture (illustration at the bottom of Figure 3a). It is evident that the sample heats uniformly until ignition (final frame, sample shows sharp temperature rise in the center). This is the desired outcome since the experimental temperature will be monitored at one point on the sample; thus it is necessary that the entire sample be the same temperature. Furthermore, uniform heating

is needed to extract reproducible kinetic decomposition data from the experiments. In addition to temperature predictive capabilities, COMSOL modeling may also be used to calculate the ignition time; Figure 3b shows the temperature profile of a point in the center of the sample as it is exposed to 2500 W at three different pulse lengths. The ignition time (vertical temperature rise) decreases with increasing pulse time. It can also be seen that there is a pulse time threshold that must be passed in order to observe ignition (blue trace at 100 ms does not ignite).
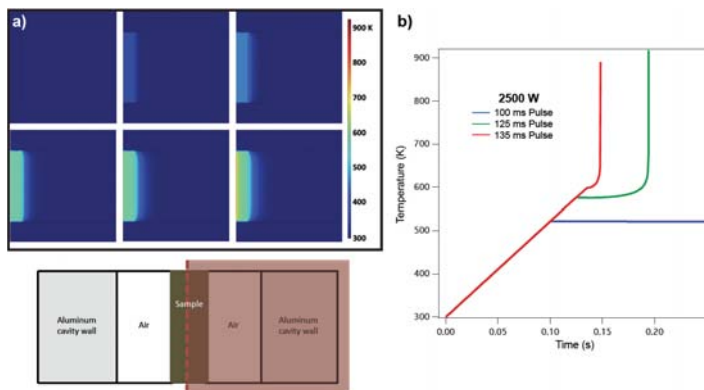
Figure 3. COMSOL modeling results for predictive temperature monitoring in carbon-doped HMX. a) 2-D representation of the temperature rise over time as the sample is exposed to MWs, and b) single point temperature profile at varying MW pulse lengths.

Future Work

A series of ignition studies that correlate MW exposure with ignition time will be conducted to corroborate the modeling results. This is necessary to determine the optimal parameters to use for SHG monitoring. The SHG monitoring experiments will require interfacing a 1064 nm laser and detection optics with the current experimental apparatus. The equipment is already in place, only minor modifications to the MW resonant cavity design will need to be made. Once the SHG timing data correlated with temperature is collected, expressions involving HMX decomposition behavior in this fast kinetic regime will be derived and related to the previous kinetic model.

Conclusion

We have shown that fiber-optic temperature measurement techniques may be effectively interfaced with a MW resonator, and may be correlated to the amount of MW energy absorbed in the sample. Reproducible surface temperature measurements of a non-HMX MW sensitized explosive were achieved upon exposure to a 200 ms pulse of 2500 W MW energy (2.45 GHz) that closely follows modeling results. Uniform, fast, and non-perturbing MW heating provides the ideal scenario for kinetic decomposition measurements. The temperature and ignition response of the HMX-based samples correlated to the length and power of MW pulses may be predicted using electromagnetic and heat transport modeling tools (COMSOL).

References

1. Henson, B. F., B. W. Asay, R. K. Sander, S. F. Son, J. M. Robinson, and P. M. Dickson. Dynamic measurement of the HMX beta-delta phase transition by second harmonic generation. 1999. *Physical Review Letters.* **82** (6): 1213.

2. Glover, B. B., and W. L. Perry. Microwave ignition of single-wall carbon nanotube loaded HMX. 2006. *Defense Research Review Journal.* **13** (3): 21.

3. Glover, B. B., and W. L. Perry. Observation of localized charge transport in isolated microscopic mats of single-wall carbon nanotubes. 2007. *Journal of Applied Physics.* **101** (6): 064309.

4. Higginbotham, A. L., P. G. Moloney, M. C. Waid, J. G. Duque, C. Kittrell, H. K. Schmidt, J. J. Stephenson, S. Arepalli, L. L. Yowell, and J. M. Tour. Carbon nanotube composite curing through absorption of microwave radiation. 2008. *Composites Science and Technology.* **68** (15-16): 3087.

5. Junhua, W. U.. Broad microwave dielectric property of single-walled carbon nanotube composites. 2008. *Journal of Materials Science & Technology.* **24** (4): 661.

Attosecond Probing of Dynamical States in Solids - Graphene

George Rodriguez
20100633PRD4

Introduction

The development of future high-speed nanoscale electronic devices will depend on understanding fundamental electronic carrier transport properties in novel materials. One such material, is the carbon-based nano-semiconductor graphene. Graphene is a flat monolayer of carbon atoms tightly packed into a two-dimensional (2D) honeycomb lattice. Graphene is quite different from most conventional three-dimensional materials. Intrinsic graphene is a semi-metal or zero-gap semiconductor with very high electron mobility. Understanding the electronic structure of graphene is the starting point for finding the band structure of graphite from which further tailoring of its electronic properties can be altered.

This project uses an advanced transient electronic spectroscopic technique called "time-resolved angle-resolved photoemission spectroscopy" (tr-ARPES) [1,2] to study the band structure of graphene. Since electronic carrier transport is intimately tied to the various ultrafast carrier scattering processes among energy bands in the material, we will use this technique to better understand carrier relaxation channels and electronic transport for improved characterization of future novel electronic materials.

Benefit to National Security Missions

Understanding the electronic carrier properties of graphene will be of most interest to DOE/SC, specifically the Office of Science where Materials for Basic Energy Sciences is concerned. Results from measurements on electronic dispersion in energy and momentum scales is of high interest, not only for graphene, but for other functional materials as well: superconductors, carbon nanotubes, actinides, topological insulators, etc. Many of these materials have emergent properties that are dynamical, where coupling between the various degrees of freedom (electronic, lattice, spin) are time dependent and can precisely be understood using the spectroscopic technique in this project: time-resolved ARPES. The project long term plan is to develop a portfolio set of novel materials experiments that demonstrate the capability in a technologically relevant material (i.e., graphene), and then to pursue others under sponsorship from DOE BES Materials.

Progress

Ultrafast time-resolved photoemission spectroscopy (trPES) of graphene mounted on silicon dioxide (SiO2) has been studied using the ultrafast femtosecond laser and ultrafast soft x-ray capabilities of the Center for Integrated Nanotechnology (CINT) in LANL's Materials Physics and Applications Division. This allowed direct carrier electron and hole dynamics in graphene to be studied with femtosecond (fs = 10^{-15} sec) time precision. Using this technique, new properties of the material, namely the behavior of the carrier dynamics in the linear momentum dispersion region (Dirac point region) of graphene, have been observed which improves our understanding for potential future optoelectronic applications of graphene. Upon femtosecond photoexcitation of electronic carriers in graphene, the ensuing carrier relaxation dynamics is probed with the technique of time-resolved photoemission (Figure 1).
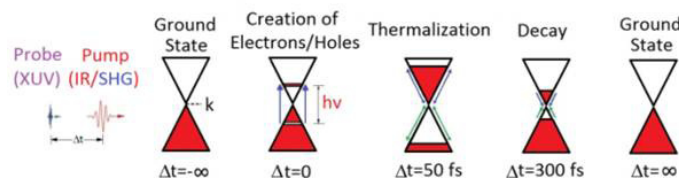
Figure 1. Illustration of graphene ultrafast carrier dynamics near the Dirac point in energy and momentum space. Ultrafast photoexcitation of carriers across the the graphene Dirac point with either a near-IR (800 nm, 1.5 eV) or blue (400 nm, 3.0 eV) pump pulse generates electrons and holes in the conduction and valence bands, respectively. Ultrafast scattering from thermalization and decay channels are then probed with a time-delayed extreme ultraviolet (XUV) ultrashort pulse using a photoelectron spectrometer. The XUV pulse photon energy is centered at 30 eV, well above the work function of graphene (4.6 eV). The kinetic energy of photoemitted electrons are then measured as a function of time pump-probe delay to map out the dynamical distribution of carriers in the valence and conduction bands.

Probing the nonequilibrium electronic states with photoemission allows for distinct monitoring of the electron and hole populations in a true single-particle manner. We observed two distinct regimes characterizing the relaxation process: on an ultrashort 500 fs time scale the electron and hole populations can be described by two separate Fermi-Dirac distributions, while on longer time scales the populations coalesce to form a single Fermi-Dirac distribution at an elevated temperature. The Fermi-Dirac distribution is given by $F_D=[1+\exp(E-u/kT]^{-1}$ where u is the chemical potential; T is the temperature, T; E is the particle energy. This dual behavior arises from the fact that upon photoexcitation, the initial resultant transient state form populations mimicked by two separate Fermi-Dirac distributions with distinctly different chemical potentials and temperatures for electrons and holes, and then after thermalization and relaxation, the resultant nature of the transient state is best described by a single Fermi-Dirac distribution with a zero chemical potential, u=0, for both electrons and holes, but with an overall raised temperature, T. Experimental results illustrating this behavior are shown in Figure 2 where ultrafast transient electron-hole distributions are plotted for two cases where graphene is pumped with either 1.5 eV or 3.0 eV photons.
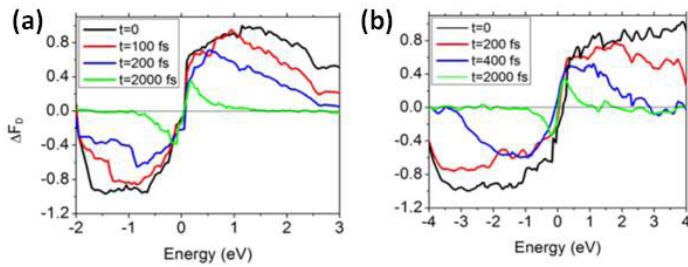
Figure 2. Plots of the Fermi function changes versus kinetic energy as measured experimentally at different pump-probe time delays for the cases of (a) 1.5 eV and (b) 3.0 eV pump photon energy. The plots distinctly show the creation of holes below the Fermi level (where E=0) and electrons above the Fermi level with energy spreads larger for the 3.0 eV case than the 1.5 eV case because of increased phase space for scattering in the 3.0 eV case. The data shown is the difference of the experimentally obtained pumped spectrum (T>12 K) and the unpumped spectrum (T=12 K) divided by the linear density of states function.

At early times (t < 500 fs) the transient electron-hole populations each have non-zero chemical potentials, but then later eventually "coalesce" into single temperature, zero chemical potential (u=0) like distribution. Simulations (Figure 3) of transient electron-hole population distributions for 1.5 eV pump photoexcitation are used to fit the data and show that best fit with the data is obtained when a time varying non-zero chemical potential _(t) is used to fit the data before t=500 fs (Figure 3(a)), and later at t=2000 fs, the zero chemical potential, but at an elevated temperature of T=1950K (Figure 3(b)) is used to best fit the data. Figure 3(c) shows the time

varying chemical potential and temperatures necessary for best fits of the data like in Figure 2 that are necessary for best description of graphene carrier dynamics. This unusual behavior is a consequence of graphene's unique band structure that allows for extremely rapid carrier thermalization via electron-electron and electron-phonon scattering resulting in electron-hole distributions spread over a larger energy range than expected. Our observations determine that electron-electron thermalization is extremely rapid and occurs on the time scale of our photoexcitation pulse (< 30 fs) timescale, while electron-phonon processes are occurring at the hundreds of femtosecond timescale. A journal manuscript describing our results and interpretation of these first trPES studies of graphene on SiO2 has been submitted to Physical Review Letters for publication [3].
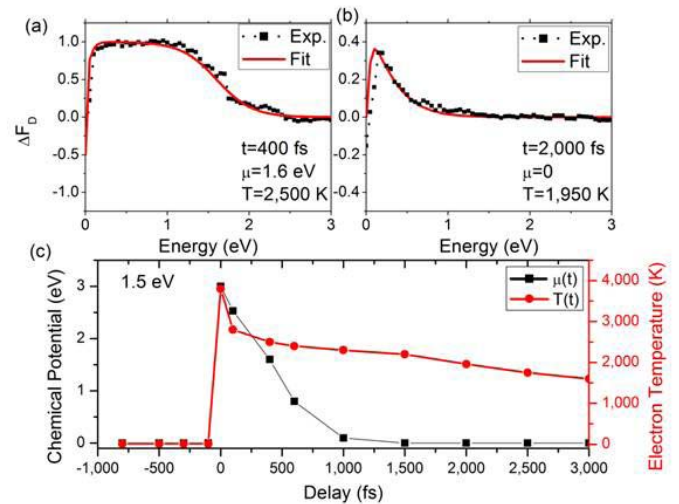
Figure 3. Fitting of the experimental data (black squares) with a model for the Fermi change (red line) for a 1.5 eV pump pulse at delays of (a) t=400 fs and (b) t=2000 fs. Only the electrons are fitted since the data does not have perfect symmetry between the electrons and holes due to p-doping of the sample. For delays closer to time zero (see (a)), the fitting cannot be accomplished without the inclusion of a non-zero chemical potential. At later delays (b), the chemical potential can be zero and still achieve fitting. The values of electron temperature (T, red circles) and chemical potential (u, black squares) for several delay values are plotted in (c).

Time- and angle-resolved photoemission spectroscopy (trARPES) on additional samples of graphene is just beginning. Due to the polycrystalline nature of graphene mounted on SiO2, the results to date are angle-integrated (non-momentum resolved) spectra. We believe that trARPES studies of graphene grown on silicon carbide (SiC) will provide angle-resolved results, and allow us to probe carriers with energy and momentum dependence. Additional experiments based on the measurement of momentum (and energy) state properties of the carriers

near the Dirac cone will allow us to construct energy and momentum based time-dependent models that include relevant quasiparticle coupling mechanisms across the energy and momentum band.   We are proceeding with trARPES measurements of graphene on SiC in the hopes of understanding the time-dependence of quasiparticle interactions about the Dirac cone region with energy- and momentum-resolved results.

Future Work

In addition to fully (momentum and energy) resolving particle time dependence about the Dirac point in graphene, other Dirac materials such the topological insulator Bi_2Se_3, will be studied with tr-ARPES. We also desire to probe faster dynamics in graphene like core-hole or hot electron thermalization dynamics, believed to occur on the femtosecond timescale, therefore requiring even shorter (attosecond) pulse than currently available with our setup. In the second year of work we will also determine feasibility and requirements for attosecond pulse generation coupled to probing solids with tr-ARPES. This would require an upgrade implementation of the double optical gating (DOG) technique to the existing femtosecond tr-ARPES setup to generate attosecond pulses. Time-resolved ARPES would directly measure the carrier spectral function dynamics of the valence and conduction bands with momentum, energy, and attosecond temporal resolution simultaneously. It is expected that temporal resolution will be fast enough as to resolve the carrier fundamental scattering time.

Conclusion

We have improved understanding of ultrafast electronic carrier transport in graphene. In the first year of work, we measured electron (and hole) population distributions, phonon induced scattering rates, and recombination times under ultrafast photoexcitation of carriers. Still, fundamental electron-electron scattering rates are faster than our current instrument can resolve. Improvement on the time resolution of our light source is necessary. Nonetheless, our results on graphene have important implications for designing high speed circuits and devices based on this material.

References

1. Dakovski, G. L., Y. Li, T. Durakiewicz, and G. Rodriguez. Tunable ultrafast extreme ultraviolet source for time- and angle-resolved photoemission spectroscopy. 2010. *Review of Scientific Instruments.* **81** (7): 073108 (7 pp.).

2. Dakovski, G. L., Y. Li, S. M. Gilbertson, G. Rodriguez, A. V. Balatsky, J. X. Zhu, K. Gofryk, E. D. Bauer, P. H. Tobash, A. J. Taylor, J. L. Sarrao, P. M. Oppeneer, P. S. Riseborough, J. A. Mydosh, and T. Durakiewicz. Anomalous femtosecond quasiparticle dynamics of hidden order state in URu2Si2. 2011. *Physical Review Letters B Rapid Communications.* **84**: 161103(R).

3. Gilbertson, S., G. L. Dakovski, T. Durakeiwicz, J. X. Zhu, K. M. Dani, A. Mohite, A. Dattelbaum, and G. Rodriguez. Tracing ultrafast separation and coalescence of carriers in graphene with time-Resolved photoemission. *Physical Review Letters.*

Publications

Gilbertson, S.. Attosecond observation and control of autoionization in helium. Invited presentation at *International Symposium on (e,2e), Double Photoionization and Related Topics & 16th International Symposium on Polarization and Correlation in Electronic and Atomic Collisions.* (Dublin, Ireland, 4-6 Aug. 2011).

Gilbertson, S., G. L. Dakovski, T. Durakeiwicz, J. X. Zhu, K. M. Dani, A. Mohite, A. Dattelbaum, and G. Rodriguez. Tracing ultrafast separation and coalescence of carriers in graphene with time-Resolved photoemission. *Physical Review Letters.*

Mechanistic Investigation of C-C Bond Forming Reactions for the Production of Long Chain Hydrocarbons

Enrique R. Batista
20110542PRD1

Introduction

Due to instabilities in the global supply of crude oil, the development of bio-fuels is a top priority. A critical step toward realization of high energy density bio-fuels is the development of organic fuels with a narrow distribution of longer hydrocarbon chains, which have higher energy density than current bio-fuels like ethanol. The key challenge in the synthesis of long hydrocarbon chains is the formation of new carbon-carbon bonds. One fundamental organic transformation ubiquitous in modern organic chemistry, the aldol condensation, is a carbon-carbon bond-forming reaction involving ketones and aldehydes (species with a C-O double bond, or carbonyl group). Our experimental collaborators have enjoyed some success with a new type of catalyst that can affect this reaction. A mechanistic understanding coud lead to new options for improvement and optimization. We are using computational tools to analyze the atomistic aspects of the reaction mechanism and exploiting this understanding to test new possibilities that will then be visited by the experimentalists for testing in the laboratory.

Benefit to National Security Missions

This project includes organic aldol catalysis for carbon-carbon chain extension. Optimization of this process will result in significant impact to the fuels and specialty chemical sectors. Because the approach to producing liquid fuels is based on bio-mass, this project will contribute to the carbon-neutral fuel cycle impacting environment and climate missions. The development of efficient catalytic mechanisms for production of biofuels has also been identified as a research need by the Office of Science BES report on "Clean and Efficient Combustion of 21st Century Transportation Fuels." Having established credibility in the areas of biomass conversion, we will be positioned to support the missions of EERE and BES

Progress

In an effort to upgrade bio-renewables to high-energy-density fuels and chemical feedstocks, we are developing a strategy to convert readily available cellulose-derived polyols (such as hydroxymethyl furfural HMF) to high-density C8-C15 hydrocarbons. This first involves chain lengthening through C-C bond forming aldol condensation followed by systematic defunctionalization involving such challenges as catalytic ring-opening of furans, removal of oxygen atoms through dehydration, and reduction and removal of the resulting unsaturation through hydrogenation.

Detailed mechanistic results derived from theory focusing on the C-C bond-forming step in this process was produced for the piperidine catalyzed aldol condensation between HMF and acetone. The catalytic aldol condensation process was determined to proceed through a six-step mechanism involving a two-step substrate activation, a C-C bond forming step, a two-step release of products/catalyst regeneration followed by an additional dehydration of the products. In order to arrive at this conclusion we had to analyze all possible reactions involving the catalyst and the two substrates as well as the involvement of the solvent molecules during each step of the reaction. This last consideration is usually treated in a very approximated fashion or ignored all together. We found that many of the steps along the reaction pathway require proton transfers, which are catalyzed by clusters of water molecules requiring inclusion of explicit solvent. In addition, this mechanism proceeds through a very reactive zwitterionic intermediate previously believed to react with itself. Our more accurate approach utilizing explicit solvent molecules was used to clarify this confusion in the literature about intermediate steps of this nature in similar reactions. Consideration of those confused intermediate structures would make one believe that a key step in the catalytic process is not possible.

This work has been further expanded to examine the C-C bond-forming step in a related aldol condensation process utilizing bio-derived ethyl levulinate in place of acetone. This procedure also requires an acetic acid co-catalyst and is performed in the absence of water. While the general mechanism has not changed, these new reaction conditions present several new problems: 1) Unlike acetone, ethyl levulinate has multiple active sites

requiring understanding of the observed regioselectivity; 2) While the general mechanism is believed to be the same, water, which was found to be critical in the previous studies, is no longer present; 3) The role of the co-catalyst is unknown. Through an examination of the possible reaction pathways we have determined that while reaction at multiple sites in ethyl levulinate leads to thermodynamically stable products, the observed product is the result of substantially lower kinetic barrier. The other two issues were found to solve each other as the acetic acid was found to act as a proton transfer catalyst in the place of water.

As for reaching the broad community, our initial work was presented at the Gordon Conference on reaction mechanisms, and at the American Chemical Society National meeting in Denver, CO. A joint experimental/ theory paper has been submitted to the peer-reviewed journal *Green Chemistry* with an exhaustive description of the whole catalytic process. In addition a new joint experimental/theory manuscript is in preparation detailing the mechanistic differences involved with substrate modification, changes in solvent and the addition of co-catalysts.

Conference presentations

- Inorganic Reaction Mechanisms Gordon Conference, March 2011, Galveston, TX, USA.
- National Meeting of the American Chemical Society, August 2011, Denver, CO, USA. **"**Catalyzed conversion of non-food biomass to fuels: Probing the mechanism of the initial C--C bond forming step" by Jason M. Keith, Enrique R. Batista, Richard L. Martin, Rulian Wu, L. Pete Silks, and John C. Gordon

Future Work
The theoretical aspect of this project will consist of developing a detailed mechanistic model that incorporates what has been discovered by our experimental collaborators, and expands on it by illuminating the facets of these reactions that cannot be discerned in the laboratory. We will use high-level quantum chemistry calculations to understand all aspects of these catalyzed chemical reactions. This will begin by mapping out the relevant stationary points on the reaction's potential energy surface (PES). This involves gaining an understanding of all of the stereo- and regioisomers, enantiomers and tautomers possibly involved at the quantum chemical level. The next step (and most complex) is the location of saddle points (transition states) connecting low-energy species on the PES. Evaluation of the reaction profile (minimum energy pathway, MEP, from reactants to products on the PES) and the rate-limiting transition state(s) (maximum point along the MEP) will provide valuable insight into the factors governing the reaction, and provide a template to evaluate possible changes to the system which can then be integrated into

the experiment. Through this recursive process, theory and experiment can work together efficiently to optimize this chemical reaction and realize previously unobtainable goals.

Conclusion
Obtaining high energy density fuels from biomass is a long-sought goal identified by the government as a key step for the country's energy security. The goal of this project is to produce narrow distributions of long hydrocarbon chains of the type need for jet fuel, starting from biomass. Catalysts to do this transformation efficiently have been elusive. Our experimental collaborators at LANL have identified a new family of catalysts to effect this transformation. Our atomistic understanding will lead to improvement and optimization of those new catalysts.

Publications
Keith, Jason M., Jin K. Kim, L. Alexander, R. Wu, R. L. Martin, E. R. Batista, R. Michalczyk, B. L. Scott, S. K. Hanson, A. D. Sutton, L. A. Pete Silks, and J. C. Gordon. Aqueous Organocatalysis Applicable to the Carbon Chain Extension of Carbohydrate Derivatives: Application to the Production of Transportation Fuels. *Green Chemistry.*

Exploiting the Fermi Surface to Understand Quantum Criticality in Complex Electronic Materials

Eric D. Bauer
20110549PRD1

Introduction

Standard models for simple metals and insulators often fail for strongly interacting electronic systems, in which correlations between d- or f-electrons and conduction electrons promote new and unexpected states of matter. An increasingly common example of emergent phenomena in these complex electronic materials (e.g., heavy fermions and high-Tc cuprates) is found when a magnetic phase transition is tuned to absolute zero temperature by an external parameter, such as doping, pressure, or magnetic field. At the resulting quantum critical point, new and distinct states are found, which cannot be understood by knowing the properties of the two parent magnetic or nonmagnetic states. This type of behavior has continued to defy a complete description after nearly 20 years and poses one of the most significant challenges to the condensed matter community. While many theories have been proposed, these models do not describe all the properties of even a single quantum critical material. A solution to this quantum criticality conundrum will come from carefully designed experiments that distinguish between existing theories and guide in the development of new ones. A crucial yet unresolved issue of quantum criticality is what happens to the Fermi surface (the surface of constant energy that dictates the motion of the valence electrons) at the quantum critical point. Ryan Baumbach, a Director's Funded postdoctoral Fellow, is working synthesize and characterize d- and f-electron compounds that exhibit quantum critical behavior, mainly involving Mn, Ce, and U, to quantitatively determine the evolution of the Fermi surface volume through direct measurements including de Haas van Alphen, Hall effect, and thermopower. This research will lay the scientific foundation for understanding quantum criticality and will play a central role in understanding and exploiting functional complex electronic materials of the 21st century.

Benefit to National Security Missions

The study of quantum criticality is one of the true frontiers in modern science. Understanding the eseential interaction among strongly correlated electron materials is a necessary step for the Laboratory and for DOE to fullfill its missions in energy security. This research will provide the scientific foundation for understanding and exploiting functional complex electronic materials of the 21st century. Fundamental research on the condensed matter physics of actinides builds underlying capability for the weapons program and nuclear energy.

Progress

Standard models for simple metals and insulators often fail for strongly interacting electronic systems in which correlations between d- or f-electrons and conduction electrons promote new and unexpected states of matter. The unusual behavior that occurs near the point where a magnetic phase transition is suppressed to zero temperature is attracting intense effort by the condensed matter community. An unresolved issue of quantum criticality is what happens to the Fermi surface (the surface of constant energy that dictates the motion of the valence electrons) at the quantum critical point. To explore what happens there, we have synthesized and characterized a number of materials to search for the best quantum critical systems as outlined below:

$CePtSi_2$ and $CeNiSi_2$ have a nearly tetragonal crystal structure, which is very similar to the well known ThCr2Si2 structure, which is the prototype for several quantum critical systems: e.g., $CePd2Si_2$. The quantum critical point is accessed by suppressing a magnetic transition to zero temperature. $CePtSi_2$ orders antiferromagnetically near 2 K and is suppressed to T = 0 by applied pressure near 1.1 GPa, where non-Fermi-liquid behavior is observed and is an indication of proximity to a QCP. On the other hand, $CeNiSi_2$ has a smaller unit cell and exhibits intermediate valence behavior of the Ce ions. Therefore, I studied the system $CePt1-xNixSi_2$ in order to (1) compare the affect of chemical pressure to that of applied pressure and (2) address the evolution of a heavy fermion antiferromagnet ($CePtSi_2$) into an intermediate valence system ($CeNiSi_2$), which has not been done before. From specific heat and electrical resistivity, we have identified that the antiferromagnetic ordering is

suppressed to T = 0 near x = 0.2. We have grown a single crystal of this composition and are currently investigating its physical properties. Above x = 0.2, the crossover into the intermediate valence state appears to be gradual, a situation that has not been considered in detail in other quantum critical systems before. Future work will include Hall effect measurements on samples near the critical point (x=0.2) to reveal changes in the Fermi surface across this quantum critical point.

We have made single crystals of $CePt_2Si_2$ for the first time in the tetragonal $ThCr_2Si_2$ structure, in which many other quantum critical systems have been found. This material orders magnetically at 10 K with properties very similar to the prototypical pressure-induced quantum critical system $CePd_2Si_2$. Measurements of our newly discovered $CePt_2Si_2$ single crystals under pressure will be conducted later this year.

We have synthesized several large single crystals of CeCoGe by the Czochralski crystal growth technique. CeCoGe crystallizes in the PbClF-type structure, which is closely related to both the $ThCr_2Si_2$ and $CeNiSi_2$-type structures. This system orders antiferromagnetically below 5.5 K and these large single crystals will be used to identify the exact magnetic structure of this interesting material. Future work will explore various substitutions to suppress the magnetic order and find the quantum critical point.

We discovered a new class of materials with the chemical formula LnT2M2X (Ln = La-Nd, T = Ru, Os; M = Al, Ga; X = B, C). These compounds crystallize in a filled variant of the $CeMg_2Si_2$–type structure and are closely related to the ubiquitous $ThCr_2Si_2$-type structure, which is associated with a large number of systems that exhibit non-Fermi-liquid behavior and quantum criticality. As such, the LnT2M2X materials provide an exciting new avenue for the study of correlated electron physics. I have focused on producing polycrystalline specimens using our mono-arc system. Coupled together with our rapid characterization capabilities, this approach has allowed us to employ a powerful feedback loop between synthesis and characterization to guide our study of this family of materials and, in particular, to search for quantum critical behavior. We have also produced high quality single crystalline samples using our Czochralski crystal pulling apparatus.

We have focused my attention on the CeT2M2X materials, as these are the most likely to exhibit quantum critical behavior. Thus far, we have produced $CeRu_2Al_2B$, $CeRu_2Ga_2B$, and $CeRu_2Ga_2C$. Contrary to what is often observed for Ce-based compounds, these three compounds show pronounced local magnetic moment behavior, resulting in ferromagnetic ordering of the Ce-ions at strikingly high temperatures: i.e., Curie temperatures Tc = 12.8 K, 16.1 K, and 16.7 K for $CeRu_2Al_2B$, CeRu2Ga2B, and $CeRu_2Ga_2C$, respectively. In addition, CeRu2Al2B undergoes antiferromagnetic ordering at a Neel temperature T_N = 14.1 K. The unit cell volumes for these three compounds decrease in the order $CeRu_2Al_2B$, $CeRu_2Ga_2B$, $CeRu_2$, commensurate with the increase in Tc. This trend suggests that the Ce 4f electrons in these materials are localized and magnetic, supporting the point of view that in order to access the quantum critical point, it is necessary to further reduce the unit cell volume. In order to accomplish this goal, I have acquired a pressure cell and am preparing to perform electrical resistivity measurements under applied pressure on these materials.

Finally, we have synthesized a series of Yb compounds, including $YbTSi_3$, where T=Co, Ni, Pd, and Pt. These materials also adopt a nearly tetragonal crystal structure and order magnetically below 10 K. Substitutional studies are under way to find a suitable doping to access the quantum critical point, such as expanding the lattice in YbNiSi3 to drive the system towards a paramagnetic ground state from an antiferromagnetic state at 5 K.

Future Work
Ryan Baumbach as a Director's Funded postdoctoral Fellow, will synthesize and characterize d- and f-electron compounds that exhibit quantum critical behavior, mainly involving Mn, Ce, and U, to quantitatively determine the evolution of the Fermi surface volume through direct measurements including de Haas van Alphen, Hall effect, and thermopower. The research in the next year will focus on three materials that can be tuned with modest amounts of pressure: 1) $Ce_2Rh_3Si_5$, 2) CeNiGa2, and 3) $U_4Ru_7Ge_6$. The application of pressure is a particularly clean way to access the quantum critical point in these antiferromagnets ($Ce_2Rh_3Si_5$ and $CeNiGa_2$) and ferromagnets ($U_4Ru_7Ge_6$) to determine the evolution of the Fermi surface in the vicinity of a quantum critical point. This research will lay the scientific foundation for understanding quantum criticality.

Conclusion
A solution to the quantum criticality conundrum will come from carefully designed experiments that distinguish between existing theories and guide in the development of new ones. Measurements will be performed on a number of quantum critical materials and will finally resolve what happens to the Fermi surface (the surface of constant energy that dictates the motion of the valence electrons) at the quantum critical point. This research will lay the scientific foundation for understanding quantum criticality and will play a central role in understanding and exploiting functional complex electronic materials of the 21st century.

Non-aqueous Organic Materials for Bio-defense

Rico E. Del Sesto
20110580PRD2

Introduction

We have developed a new general strategy for producing ionic liquid formulations of cationic pharmaceutical agents that is more robust than the current state of the art and features a simplified synthetic method. Ionic liquid formulations of medicines are useful because they circumvent crystal polymorphism purity issues by producing amorphous liquid phases of drugs, stabilize drugs to high temperature or UV irradiation, and improve bioavailability of the drug. The goals include producing orally or transdermally bioavailable forms of pharmaceuticals that must otherwise be administrated i.v. in a hospital setting, and developing unstable, finicky small molecule drugs into room temperature-tolerant, robust compositions.

Benefit to National Security Missions

The warfighter will benefit because drugs formulated as ionic liquids will be more stable at extremes of temperature and under exposure to sunlight and should therefore prove more useful for battlefield use. Other applications of this work will include defense related needs for rapid and facile delivery of antimicrobial, anti-tubercular, and other pharmaceutical agents, as well as national security applications related to administration of prophylactic agents in the case of a CBRNE attack on the general population.

Progress

In the first five months of this project, we have identified a novel, unpublished, and eminently patentable synthetic strategy for reliably synthesizing ionic liquids from pharmaceutical salts. We have synthesized and characterized 10 ionic liquids using this approach and have initiated collaboration with Northern Arizona University for investigation of the antimicrobial effects of our ionic liquids. An abstract on this work has been accepted for presentation at the American Chemical Society national meeting in March 2012 and a manuscript for submission to the peer-reviewed journal *Chemical Communications* has been prepared.

Our strategy, a novel one that has yet to be introduced to the ionic liquid and pharmaceutical formulation research communities, predictably produces ionic liquids from small molecule drugs. The formation of ionic liquids using this method has been successful for every pharmaceutical agent that we have tried, as long as the melting point of the standard pharmaceutical salt is less than 200°C. Our own initial experiments with the state-of-the-art synthesis of pharmaceutical ionic liquids revealed issues not readily revealed by published literature. The syntheses involved metathesis reactions or activation of components by ion exchange columns. The metathesis reactions inevitably produced side products, such as NaCl, which were difficult to purify from the final ionic liquid. The use of ion exchange columns also sometimes introduced impurities, either through material leaching from the columns themselves or because the organic molecules degraded in the presence of the strongly acidic and basic ion exchange resins. Our method succeeds without production of side products or impurities because of the nature of the synthesis. We also realize benefits of eliminating the use of ion exchange columns due to the extra time it takes to pass reagents through the column, the loss of a certain percentage of reagent to the stickiness of the column and the cost of the column resin.

The synthesized ionic liquids are formulations of cationic pharmaceutical agents that vary in molecular weight from 140 to 448 g/mol and have resulted in melting point decreases that range from 91 to 286°C. The ionic liquids are more stable than the standard salts and the temperatures at which they begin to decompose are increased by up to 110°C and an average of 26°C. The ionic liquid formed from procainamide shows only 3% decomposition over 4 hours at 120°C and the procainamide salt shows 50% decomposition under the same conditions, Figure 1.

The new ionic liquid formulations investigated, listed along with their uses, include those based on: benzethonium, used as an antimicrobial agent; phenoxybenzammonium, treats complex regional pain; ranitidinium, treats gastric bleeding and ulcers; procainamide, treats irregular heartbeat;

homatropinium, cocaine analog and eye dilator; choline, B vitamin; lysine, essential amino acid, experimental herpes treatment; nicardipinium, treats vascular disorders; glutamate, amino acid; ethambutol, treatment for tuberculosis, Figure 2.
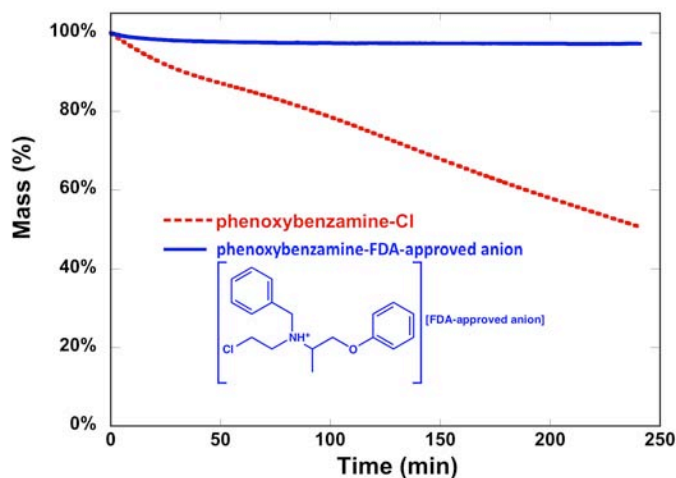
Figure 1. Thermal decomposition of the procainamide chloride salt and the procainamide ionic liquid formulation over 4 hours at 120°C as determined by thermigravimetric analysis.
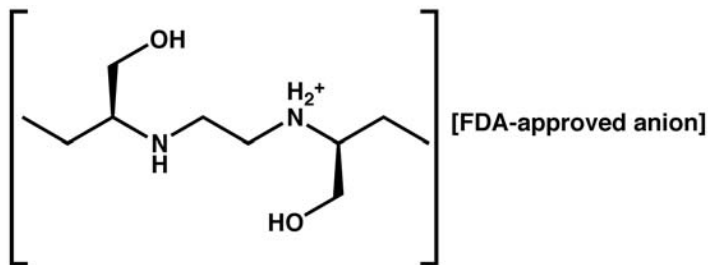
Figure 2. Ionic liquid formed from the anti-tubercular agent ethambutol and anion partner.

Attempts to produce formulations of the anti-anthrax drug ciprofloxacin using either the traditional composition or our new composition failed to produce suitably amorphous, homogenous ionic liquids. Ciprofloxacin is an extraordinarily rigid fluoroquinolone-based molecule with a melting point of over 300°C that does not easily convert to an amorphous form, which is required for ionic liquid formation. Other, less rigid, drugs that are useful in the treatment of anthrax and would be good ionic liquid candidates include erythromycin, which has a melting point of about 140°C, vancomycin, m.p. = 82°C, and the beta-lactams. Because we have had difficulties formulating other organics with high melting points as ionic liquids (ex. 9-aminoacridine, m.p. = 300°C), we propose that our strategy generally applies to cationic pharmaceuticals with melting points below ~200°C.

Completed analyses on these materials include thermal gravimetric analysis for determination of thermal stability, differential scanning calorimetry for identification of glass transitions and melting temperatures, Raman spectroscopy, infrared spectroscopy for observation of cation-anion interaction in solution, mass spectrometry for evaluation of purity and speciation, and viscosity measurements.

Future Work

We are beginning collaborations that will characterize the antibacterial and therapeutic behavior of our ionic liquids. We will prepare to make our new formulations available to others by filing a patent application. It will be useful to identify the behavior of the cations and anions in physiologically relevant solutions and on skin. We should know if the drugs contact cell membranes or the epidermal layer as overall neutral pairs of cations and anions, as hydrated and separated ions, or in some other form. Conductivity, osmotic pressure, and pH measurements can address this issue. Although initial experiments on thermal stability over time have begun, we will expand these to look at other temperatures and time periods to obtain rough estimates of shelf life.

We predict additional favorable interactions between other biologically compatible anions and cationic drugs and biomolecules based on principles of aqueous speciation chemistry. Additionally, we plan to formulate one or several of the anti-anthrax agents erythromycin, vancomycin, or a beta-lactam such as penicillin in ionic liquid form.

Conclusion

We have developed a versatile strategy for predictably converting pharmaceuticals into thermally stable ionic liquid formulations. The synthesis of amorphous ionic liquids from cationic small molecule drugs and a particular FDA-approved anion is demonstrated. Small molecules obtainable as chloride salts with melting points less than about 200°C are reliably formulated as amorphous ionic liquids using our approach. We predict additional favorable interactions between other biologically compatible FDA-approved anions and cationic drugs and biomolecules based on principles of chemistry in aqueous solutions. The new ionic liquids show indications of improved shelf life, and should also alter bioavailability, eliminate problems of crystal polymorphism, and allow pharmaceuticals to be administered in liquid form for use by the warfighter in the battlefield. The combination of two FDA-approved components to form new ionic liquids should facilitate translation of the new ionic liquids to practical use. We expect to further develop these new, biologically active materials over the project timeline, building a capability that is relevant to several missions and addressing areas where significant intellectual property can be generated.

Metal Catalysts for Oxidation of Lignocellulose and Reduction of Carbon Dioxide

Susan K. Hanson
20110581PRD2

Introduction

The goal of the project is to investigate new multi-metallic catalysts for the oxidation of lignocellulose and the catalytic reduction of carbon dioxide. In light of increasing cost and demand for energy, the development of alternative energy sources is becoming increasingly urgent. Non-food derived biomass (lignocellulose) and carbon dioxide are the only renewable carbon feedstocks that could be used to replace petroleum as a source of carbon-based fuels and chemicals. However, converting either lignocellulose or carbon dioxide to useful chemicals and fuels is a major challenge. A catalyst (a chemical which enables the desired reaction) is required to produce fuels or other industrial chemicals from lignocellulose or carbon dioxide, but the current catalytic technologies are lacking. More effective and selective catalysts are needed to fully utilize these renewable feedstocks. This project will investigate the synthesis of new catalysts for the conversion of lignocellulose and carbon dioxide to useful chemicals and fuels.

Benefit to National Security Missions

The aim of this work is to develop new, more effective catalysts for the oxidation of lignocellulose and the reduction of carbon dioxide. Several recent DOE reports have established the development of new catalysts for the reduction of carbon dioxide to fuels as a priority research direction. The office of Basic Energy Sciences has also identified a need for the elucidation of the reaction mechanisms of lignocellulose, stating "catalytic conversion of biomass derived molecules to fuel products is likely to involve a series of elementary processes… information is lacking on the reactive intermediates involved in these transformations." Thus, we expect to be highly relevant to Office of Basic Energy Sciences mission priorities. DoD relevance is driven by the fact the DoD is aggressively seeking new energy sources for its deployed operations.

Progress

The desired reactions to convert the renewable feedstocks into chemicals or fuels are complex, requiring multiple proton and electron transfers. Through careful ligand design and/or by incorporating more than one metal center into a catalyst, it may be possible to observe a beneficial "cooperative" effect, resulting in improved catalysts. Several new ligands have been synthesized which have oxygen and nitrogen donor groups designed to coordinate to vanadium. Initial coordination chemistry studies with vanadium are underway, and have resulted in the isolation of two new vanadium catalysts. The potential of these complexes to catalyze the aerobic oxidation of lignin model compounds will be evaluated. In addition, new ligands featuring P and N donor groups have been prepared and reacted with Fe and Ni precursors. Full characterization of these metal complexes is in process.

Future Work

Our work will focus on the development of new transition metal catalysts for the oxidation of lignocellulose and the reduction of carbon dioxide. More effective catalysts to transform renewable carbon feedstocks into chemicals and fuels could improve our ability to harness these petroleum alternatives. Specifically, new complexes will be prepared and their reactivity towards the oxidation of lignocellulose and the reduction of carbon dioxide will be explored. Future work will involve more detailed studies of the new vanadium complexes with lignin and cellulose model compounds, as well as reactivity studies of new iron and nickel complexes with carbon dioxide. In addition, the proposed studies will aim to determine whether or not incorporating more than one metal center into the catalyst can result in more effective catalysts for these reactions.

Conclusion

More effective use of renewable energy sources could help alleviate rising petroleum prices and demand for foreign oil. This project investigates the development of catalysts to convert carbon dioxide or non-food biomass to more useful fuels or chemicals. The development of these catalytic technologies could enable more effective use of renewable energy resources and contribute to improving domestic energy security.

Aberration-corrected Transmission Electron Microscopy Study of Interfaces in Multilayered Composites

Robert M. Dickerson
20110606PRD2

Introduction

Nano-composite materials provide the potential to design materials with unprecedented combination of properties via control of material length scales and structure of interfaces. In the bulk form, metals are soft, malleable and ductile and ceramics are hard but brittle. Likewise, metallic glasses (alloys of different metals that are amorphous or lack long range order) are hard and brittle. Recent work at LANL has shown that nanolayers of metals and ceramics (e.g., Al/TiN) or metals and metallic glass (Cu/PdSi) can achieve an unusual combination of strength approaching the theoretical limit of strength for perfect crystals, while still maintaining the high malleability of metals. These unusual properties are observed when both the metallic (Al or Cu) AND the ceramic (TiN) or glassy metal (Pd-Si) layers are nanometer-scale, typically less than approximately 10 nm thick. At these length scales, the material is interface-rich and it is the atomic structure, chemistry and properties of interfaces that determine the bulk response of nanocomposites. Transmission electron microscopy (TEM) is a critical tool in studying the defects and interfaces in materials and has been used to discover unusual atomic arrangements at interfaces. However, conventional "high-resolution" TEM provides a spatial resolution of approximately 1.7 Å. Thus, much of the finer details of the atomic structures are not revealed. For example, in magnetron sputtered Al-TiN multilayers, conventional TEM only reveals planes of Ti and Al atoms and cannot image the N atoms. Similarly, in interfaces between crystals (e.g., Cu) and metallic glasses (e.g., Pd-Si), there may be local atomic ordering in the glassy layer at the interface that is not resolved in conventional HRTEM. This project will utilize a new technique, referred to as "aberration-corrected" TEM, with better than 1 Å resolution, to precisely identify atomic positions, chemistry and defects at interfaces.

Benefit to National Security Missions

This project supports the DOE missions in defense and nuclear energy by providing fundamental understanding of atomic structures of interfaces and defect-interface interactions in ultra-high strength nanolayered composite materials. In particular, it provides the scientific underpinning of damage tolerant materials under extreme environments for defense, nuclear energy and transportation applications.

Progress

Ying Li was hired by LANL on May 31, 2011 and is working in MPA / CINT, the Center for Integrated Nanotechnologies. He has taken or is scheduled for all the courses on his training plan. He completed training to use the LANL Tecnai F30 transmission electron microscope (TEM) and is currently training on the new Titan 80-300 (scanning) transmission electron microscope. He has prepared several TEM samples from bulk nanolayered Cu metal / CuZr glass and is beginning to study the atomic-level details of the interphase interfaces, studying layer thickness effects on crystallization in the bulk, in thin foils, under TEM examination, and during mild heating. Thinner layers crystalize more easily under all the conditions stated. This is shown in Figure 1. The basic goal of this project is to determine how and why. He presented early results as a poster at the 23rd Annual Rio Grande Symposium this fall will be presenting further results at the MRS Fall Meeting in November 2011 and the TMS Annual Meeting in March 2012, with more to follow.

Future Work

For this project, LANL's new aberration-corrected TEM ("Titan 80-300") will be used to study the interface structures and chemistries in nano-layered metal-ceramic and metal-metallic glass composites. In this new generation of microscopes, the spherical aberration in the electro-magnetic lenses has been corrected to produce better than 1 Å resolution in imaging and spectroscopy. A variety of techniques such as (i) high-resolution scanning transmission electron microscopy (HR-STEM) or Z-contrast imaging, (ii) electron energy loss spectroscopy (EELS), (iii) energy filtered transmission electron microscopy (EFTEM), and (iv) simulation of images will be used. The detailed

microstructure including atomic positions, chemical valence, possible defect structures (dislocations, etc.) of the interfaces will be investigated based on the obtained experimental data. The metal-ceramic (Al-TiN) and metal-glassy metal (Cu-Pd/Si) multilayer thin films for this study will be synthesized utilizing magnetron sputtering at the Center for Integrated Nanotechnologies (CINT). The initial studies on Cu/CuZr will proceed via detailed interfacial analysis concerning crystallization sites and mechanisms and will proceed to TEM in-situ mechanical deformation mechanism effects study on crystallization and mechanical properties.
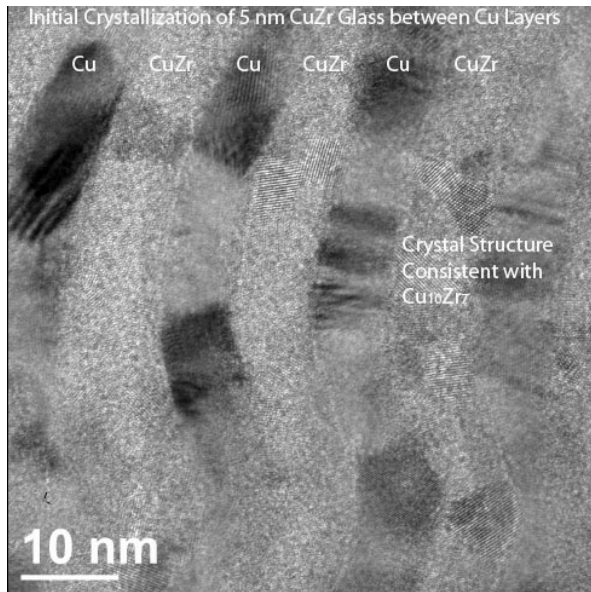
Figure 1. We are exploring the crystallization of amorphous CuZr in alternating Cu/CuZr films. When the layer thicknesses are small (5 nm in this transmission electron microscope image), the CuZr has started to crystallize and show atomic fringes in the as-grown state. Larger thicknesses require the sample to be heated before crystallization is observed.

Conclusion

The project is based on characterizing the spatial arrangement of atoms and defects at interfaces and chemical sharpness of interfaces in metal-metallic glass and metal-ceramic multilayers. A detailed characterization of the atomic structure and chemistry of interfaces is crucial in determining the mechanical properties and radiation damage tolerance of these composites.

References

1. Li, Y., R. M. Dickerson, and A. Misra. Transmission electron microscopy study on the interface of Cu/CuZr multi-layer thin films. Presented at *The 23rd Annual Rio Grande Symposium on Advanced Materials.* (Albuquerque, New Mexico, 3 Oct. 2011).

Publications

Li, Y., R. M. Dickerson, and A. Misra. Transmission electron microscopy study on the interface of Cu/CuZr multi-layer thin films. Presented at *The 23rd Annual Rio Grande Symposium on Advanced Materials.* (Albuquerque, NM, 3 Oct. 2011).

Chemical Reactivity Signatures of Uranium Fluorides

Jaqueline L. Kiplinger
20110645PRD2

Introduction

Detection of undeclared uranium conversion and enrichment activities requires new approaches and technologies that differ significantly from those used traditionally for on-site verification. To date, the primary schemes for detecting UF6 processing facilities have focused on the environmental hydrolysis of UF6 and the remnant signatures from this reaction (i.e., production of uranium oxyfluorides). In marked contrast, very little work has been done to examine the reactivity signatures of UF6 with structural or environmental materials. These UF6 reactivity signatures are the basis for a paradigm shift in detecting undeclared operations in nuclear facilities. Importantly, they would be distinct from UF6 hydrolysis signatures, they would remain after a facility has been sanitized of uranium, and their detection can be non-destructive and in many cases detectable in real time using field-portable instrumentation.

This project is designed to establish a new capability for detecting undeclared uranium conversion and enrichment activities based on fluorine incorporation into structural and environmental materials upon reaction with UF6. We intend to demonstrate that uranium fluorides react with construction and process materials to produce unique "fluorination fingerprints" in solvents, greases, plastics, phenolic resins (benchtop materials), cellulosics (wood, paper), glass and metal surfaces, and that they may be chemically incorporated into ceramics, concrete and oxides. Because of their origin, these UF6 reactivity signatures would be distinct from those of HF (or UF6 or IF7 hydrolysis) and can be used as nondestructive diagnostics of nuclear fuel cycle activities, even if uranium is no longer present in the sample

This project offers a new paradigm for characterizing the chemistry and chemical history of uranium released as UF6, which will improve the ability to detect clandestine proliferation activities. This will build an unprecedented competency in signature science of clear, long-term benefit to LANL core programs in global security.

Benefit to National Security Missions

This project offers a new paradigm for characterizing the chemistry and chemical history of uranium released as UF6, which will improve the ability to detect clandestine proliferation activities and monitor for process changes indicative of proliferation. This will build an unprecedented competency in signature science of clear, long-term benefit to LANL core programs in global security. This effort represents innovative transformational science that would support and advance monitoring of the Nuclear Non-Proliferation Treaty (NPT) and the proposed Fissile Material Cut-Off Treaty (FMCT) and would address the Sensing and Measurement Science for Global Security Grand Challenge. Likely solicitations by organizations responsible for detecting and monitoring proliferation activities including DoD-DTRA, the U.S. Intelligence Community, NA-22, NA-24 and the IAEA, will provide a venue for translating our LDRD successes to mission impact.

Progress

During the first five months of this project, access to a fluorine line has proven to be quite difficult. As such, we decided to start this project using a slightly different approach. Instead of directly starting with UF6, we have chosen to make a series of actinide (thorium and uranium) fluoride compounds and then use them as surrogates to study the reaction chemistry of uranium fluoride bonds.

Although fluoride complexes are well known for the transition metals and main group metals, they are still rare for the actinides. Progress in the field has been hampered by a lack of general synthetic routes to actinide-fluorides. In the past few months, we have developed new general entries for the preparation of actinide fluoride complexes. For example, as shown in Figure 1, reaction of $(C_5Me_5)_2ThMe_2$ (**1**) in toluene with 2 equiv of HF from $Et_3N\cdot3HF$ results in gas evolution, consistent with the generation of methane, and the

formation of a clear, colorless solution. Addition of pyridine to this solution, gives the new thorium fluoride complex $(C_5Me_5)_2ThF_2(NC_5H_5)$ (**3**) as a white solid in 60% isolated yield. Similar chemistry is observed for uranium, and reaction of $(C_5Me_5)_2UMe_2$ (**2**) in toluene with 2 equiv of HF from $Et_3N\cdot3HF$ also results in gas evolution and the generation of a yellow solution. From this solution, depending on the donor ligand added, $(C_5Me_5)_2UF_2(NC_5H_5)$ (**4**) or $(C_5Me_5)_2UF_2(O=PMe_3)$ (**5**) can be isolated as a green-brown or yellow-green solid, respectively, in 65% or 50% yield (Figure 1).

An = Th (**1**), U (**2**)

An = Th; L = NC₅H₅ (**3**)
An = U; L = NC₅H₅ (**4**)
Me₃P=O (**5**)
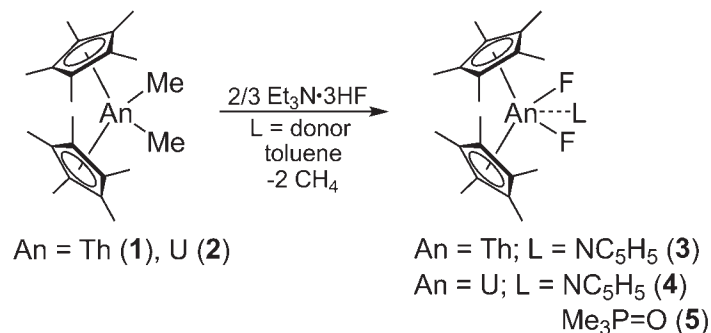
Figure 1. Scheme illustrating the synthesis of a new class of monomeric actinide fluoride complexes. Reaction of $(C_5Me_5)_2AnMe_2$ (An = Th U) in toluene with 2 equiv of HF from $Et_3N\bullet3HF$ results in the generation of methane and the formation of the corresponding difluoride complexes. Addition of pyridine or trimethylphosphine oxide stabilizes the difluoride molecules.

Complexes **3**-**5** represent a *new class* of monometallic actinide difluoride complexes that feature the $(C_5Me_5)_2An$ (An = Th, U) framework. Due to the basicity of the fluoride ligand, a characteristic feature of metal fluoride complexes is the tendency to form fluoride bridges between two or more metal atoms. Indeed, most of the structurally characterized metallocene difluoride complexes are dimeric with fluoride bridges. In the present systems, the added donor ligands, pyridine (NC_5H_5) and trimethylphosphine oxide $(Me_3P=O)$, help to sterically saturate the thorium and uranium metal centers and prevent dimer formation in both the solid-state and solution.

The ^1H NMR spectrum of complex $(C_5Me_5)_2ThF_2(NC_5H_5)$ (**3**) in C_6D_6 is shown in Figure 2. It is simple and consists of a single resonance at δ -2.08 for the C_5Me_5 protons. Consistent with reversible coordination to the uranium metal center, the three resonances for the different pyridine ligand protons are broad and appear at δ 6.56, 6.80, and 7.16. The ^{19}F NMR spectrum of $(C_5Me_5)_2ThF_2(NC_5H_5)$ (**3**) in C_6D_6 is given in Figure 3 and shows a singlet at δ 134.82 for the two fluoride ligands. ^{19}F Nuclear Magnetic Resonance spectroscopy is a very

sensitive tool for detecting the presence of fluorine in a molecule. The data we are obtaining for these new actinide fluoride complexes is very important for future databases and signatures.
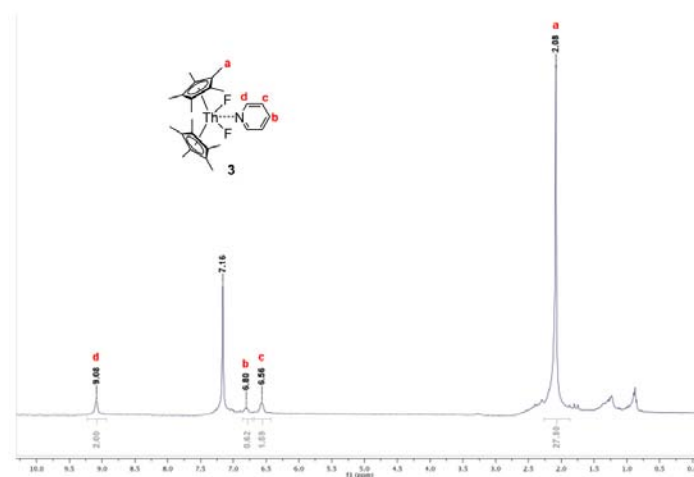
Figure 2. 1H Nuclear Magnetic Resonance spectrum for the thorium fluoride complex, $(C_5Me_5)_2ThF_2(NC_5H_5)$ (2), which consists of a single resonance at -2.08 ppm for the C_5Me_5 protons (peak a). The three resonances for the different pyridine ligand protons are broad and appear at 6.56, 6.80, and 7.16 ppm (peaks c, b, and d, respectively).
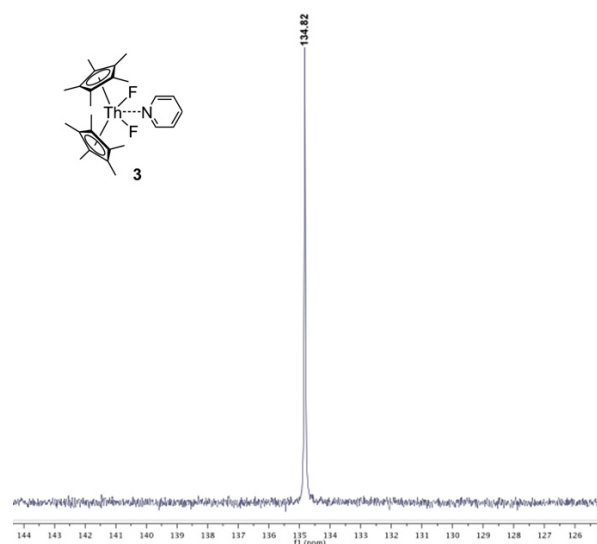
Figure 3. 19F Nuclear Magnetic Resonance spectroscopy is a very sensitive tool for detecting the presence of fluorine in a molecule. 19F NNMR spectrum for the thorium fluoride complex, $(C_5Me_5)_2ThF_2(NC_5H_5)$ (2), shows a singlet at 134.82 ppm for the two fluoride ligands.

Future Work

We will continue to explore mew methods for accessing actinide fluoride complexes. We will seek to prepare uranium fluorides in a variety of different oxidation states and study their chemistry with goal of obtaining fluorination signatures.

Conclusion

This project offers to develop a transformative detection method that capitalizes on the unique signatures left by UF6 after it reacts with structural and environmental materials. The importance of this work is clear: new techniques for the detection of undeclared uranium enrichment programs are essential (1) for a broader range of methods for safeguards applications, and (2) to fill gaps in current detection capabilities. Furthermore, there have been very few systematic laboratory studies on UF6 reactivity in the context of proliferation detection; the research proposed here will surpass previous efforts with its scope and high level of analytical capability.

Publications

Monreal, M. J., R. K. Thomson, N. E. Travia, T. Cantat, B. L. Scott, and J. L. Kiplinger. Convenient and safe access to next generation thorium and uranium halide starting materials. Presented at *26th Rare Earth Research Conference.* (Santa Fe, NM, June 19-24, 2011).

Travia, N. E., M. J. Monreal, B. L. Scott, P. L. Diaconescu, and J. L. Kiplinger. Snapshots of thorium-mediated THF ring-opening reactions using bis(pentamethylcyclope ntadienyl) and ferrocene-diamide ligand frameworks. Presented at *Los Alamos National Laboratory Annual Postdoc Research Day.* (Los Alamos, NM, June 16, 2011).

Nano-spintronics: Spin Injection, Transport and Detection in One-dimensional Semiconductor Nanowires

Samuel T. Picraux
20110733PRD2

Introduction

This project focuses on understanding how to control the spin and transport of electrical charge carriers in nanoscale structures. Adding a spin degree of freedom to conventional charge based electronics is expected to add a significantly greater degree of capability and performance of advanced electronics. For example, new capabilities in nonvolatile memories, increased data processing speeds and decreased electric power consumption may become possible in future spin-based semiconductor devices. Dramatic progress such as all-electrical spin injection, transport/modulation and detection has recently been realized in planar structures, however little attention has been paid on new one-dimension nanoscale structures. In this project we will develop methods for charge carrier (electron and hole) spin injection, transport and detection in semiconductor nanowires. We will study the fundamental properties of spin-controlled injection and transport in nanowires in order to provide a basic understanding needed for potential applications of spintronics to new nanotechnology advances. We will also explore the properties of small bandgap semiconductor topological insulators such as Bi_2Te_3 and how these properties influence charge transport. This new electronic material is expected to have novel spin properties. Owing to their unique aspects, such as reduced scale, confined dimensions, and novel transport behavior, these reduced-dimensional materials are expected to possess novel and useful physical properties for spintronics and to offer opportunities for a new generation of spin and charge based nanoscale devices.

Benefit to National Security Missions

The development of a viable spintronics technology would have revolutionary impact on ultra high speed computation, communications, and on the basic understanding of materials. This proposal seeks to develop the underlying science for this advance.

Progress

We are targeting charge transport and spin injection into two semiconductor nanomaterials: silicon nanowires and Bi_2Te_3 nanostructures. The major progress we have made includes the controlled synthesis and fundamental characterizations of these two materials. Spin injection and detection in silicon nanowires require electrons to be the majority carriers because they are expected to have much longer spin diffusion length and relaxation time than holes. Thus phosphorous doped silicon nanowires are being synthesized on silicon substrates via the metal-catalyzed vapor-liquid-solid mechanism using our cold-walled chemical vapor deposition (CVD) system. Using different sizes of Au nanoparticles as metal catalyst, we obtained nanowires with diameters of 50 nm and 100 nm, and length of 20 to 30 micrometers. Scanning electron microscopy was used to confirm the aspect ratio and surface morphology of nanowires. Methods for fabricating the nanowire devices via optical and e-beam lithography followed by metal deposition and liftoff process have been developed. Various metals (Ti, Al, Ni and Co) have been used as metal contacts for the devices. Basic electrical characterization, including current-voltage characteristics and gate response measurements, were performed to determine the nanowire conductivity and carrier type. We found that the 50 nm nanowires show p-type conductivity (i.e. holes are majority carriers), which suggests that the negative charged surface states cause hole accumulation in nanowires and compensate the electrons donated by donor (phosphorous) impurities. By increasing the nanowire diameter to 100 nm, the influence of surface states is minimized and the n-type conductivity (electrons are majority carriers) is recovered. From the four-probe current-voltage measurements, we determined the conductivity of the 100 nm nanowires and estimated the electron density to be 10^17 cm^-3 to 10^18 cm^-3, which is slightly lower than the regime where spin injection and detection were observed in bulk silicon. Most recently we have synthesized more highly doped n-type silicon nanowires, fabricated devices, and initiated low temperature spin injection measurements.

The small bandgap semiconductor Bi_2Te_3 has recently been discovered to exhibit the properties of a new type

of electronic material called topological insulators with potential applications in spintronics. The strong spin-orbit coupling and time-reversal symmetry in this material give rise to dissipation-less spin current at the surface. The goal of this part of the project is to inject spin polarized current from a ferromagnetic layer into the surface channel of Bi_2Te_3, and study the exotic physics arising from the topological protection of electrons against impurities. We have demonstrated the synthesis of epitaxial thin films of Bi_2Te_3 on Si (111) substrate at a low pulsed laser rate of 0.2 Hz. High quality epitaxial Bi_2Te_3 films have not previously been reported by pulsed laser deposition.
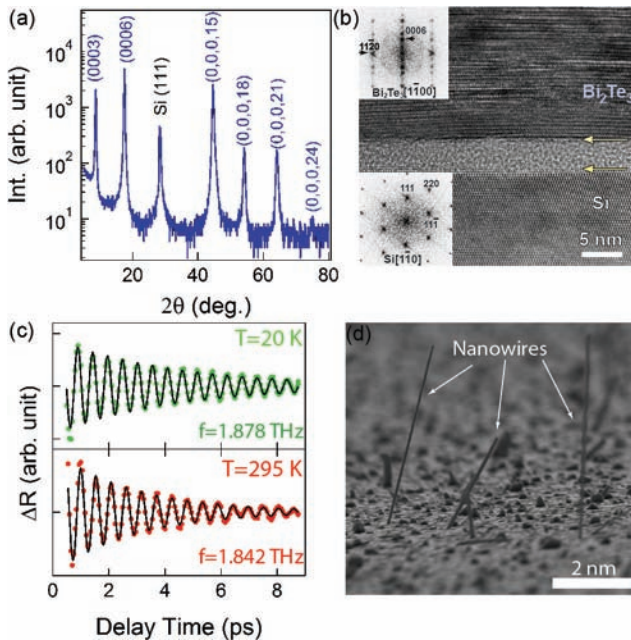
Figure 1. Nanoscale bismuth telluride materials have been fabricated and are shown to exhibit a recently-discovered type of electronic behavior referred to as a topological insulator. We grew two-dimensional Bi2Te3 films by pulsed laser deposition for the first time, and our data demonstrate high crystalline quality: (a) x-ray diffraction (J-2J scan) pattern shows expected reflections from (000l) planes; (b) high resolution transmission electron microscopy image confirms high quality epitaxial film growth; and (c) ultrafast reflectivity measurements give oscillatory signal corresponding to the expected longitudinal optical phonon mode for single crystalline Bi2Te3. One dimensional nanowires of Bi2Te3 have also been synthesized as shown here by a scanning electron microscopy image (d).

The high quality of these films was established by systematic structural characterization using x-ray diffraction (Figure 1a) and transmission electron microscopy (Figure 1b). Composition analysis by Rutherford backscattering spectrometry shows that the films are nearly stochiometry with a slight Te deficiency. We performed ultrafast time-resolved reflectivity measurements on these films and observed the A_{1g}

longitudinal optical phonon mode (f~1.842 THz at 295 K, Figure 1 (c)), consistent with what have been found in single crystal Bi_2Te_3. Temperature dependent resistivity and Hall measurements have shown an n-type metallic behavior, consistent with the Te deficiency. A 2-D weak anti-localization effect is observed by angle-dependent magneto-conductivity measurements at low temperatures, which suggests the existence of topologically protected 2-D surface states. By simply annealing the thin films at ~ 300 °C in vacuum, we have been able to obtain Bi_2Te_3 nanowires (Figure 1d). We are currently performing transmission electron microscopy, and energy-dispersive X-ray spectroscopy studies of these nanowires to confirm their single crystallinity, and determine their compositions, respectively. Recently we have also initiated additional studies on the synthesis of Se doped Bi_2Te_3 thin films and nanowires to minimize the bulk conduction and hence magnify the surface transport which is the key to achieve spintronic applications using this group of materials.

Future Work

In this work, we will combine the advances in the fields of both spintronics and nanoscience to investigate charge transport and spin physics properties in reduced-dimensional structures. Specifically we will carry out nanowire growth, device fabrication and characterization to investigate spin injection, transport and detection in germanium and silicon nanowires as a function of temperature and electrical and magnetic fields. Semiconductor nanowires and heterostructures will be synthesized based on the vapor-liquid-solid method by using a chemical vapor deposition system. We will also develop methods to fabricate topological insulator materials such as Bi_2Te_3.The device fabrication will involve e-beam lithography, tunnel barrier and electrical contact fabrication, and wire bonding in the clean room. High quality gate dielectrics and tunneling barriers will be fabricated by using a new atomic layer deposition system. The device characterization will be performed using a low temperature transport measurement system, a superconducting quantum interference device, and magneto-optical Kerr microscope. Once spin injection and detection are successfully demonstrated, we will then perform the first measurements of the influence of nanowire diameter, doping, and surface passivation on electron/hole spin dynamics. We will further study the novel electronic properties of topological insulators. This work will for the first time investigate spin transport in radial and axial nanowire heterostructures and in topological insulators where the transport is confined to surfaces or interfaces. The heterostructure-induced strain, band-structure modifications, and novel transport-controlled materials are expected to lead to new physics on spin transport not previously observed.

Conclusion

We will develop a new class of nanoscale structures that

allow us to detect and control the transport and spin of electrical charge carriers in nanoscale materials in ways not previously possible. The spin behavior in these structures will advance our understanding in electronics and nanotechnology into novel regimes. This new knowledge is anticipated to enable a new generation of high performance, low power microelectronics not currently achievable.

Publications

Zhang, S. X., L. Yan, M. Zhuo, Y. Q. Wang, B. Qi, R. P. Prazankumar, Q. X. Jia, and S. T. Picraux. Pulsed laser deposition and characterizations of epitaxial topological insulator Bi2Te3 thin films. *Applied Physics Letters.*

Probing the Structure of Superconducting States with Rotating Magnetic Fields

Roman Movshovich
20110748PRD3

Introduction

Dr. Weickert is working on a detailed study of the anisotropy of the superconducting order parameter (OP) in heavy Fermion Superconductors (HFS) by thermal conductivity and heat capacity experiments.

CeCoIn5 with unconventional d-wave symmetry is one such system of interest, where heavy quasiparticles form Cooper pairs. CeCoIn5 is one of the best investigated heavy-Fermion superconductors ever, but still, there is a big controversy whether the system belongs to the dxy or dx2-y2-class of materials, because experiments conducted in different temperature ranges support opposite interpretations. For solving this key question, we are developing new capabilities for heat capacity and thermal conductivity experiments in rotating magnetic fields (as strong as 14T) at temperatures well below (1%) the superconducting transition temperature of 2.3K in a dilution refrigerator. Our experimental work is closely partnered with internal and external theoreticians, leading to a further refinement of existing phenomenological models. Subsequent investigations are planned for CeIrIn$_5$ and UPt$_3$. CeIrIn5 is a sister compound of CeCoIn$_5$ and has a lower superconducting transition temperature of 0.4K. Recent results propose a hybrid order parameter for this system, but the final proof is still missing and angle-resolved experiments are badly required. UPt$_3$ is another HFS with two superconducting phase transitions at 0.58K and 0.53 K. The observation of multiple phases in the H-T phase diagram supports the existence of internal degrees of freedom for the Cooper pairs. Specific heat experiments can help to solve the question, if these degrees are of orbital or spin nature.

Benefit to National Security Missions

Electronic correlations in 4f-electron (rare earth) and 5f-electron (actinides) materials drive many of their exotic physical properties that are of primary importance to LANL's missions. For example, these correlations are at the core of the evolution of the crystal structure across the actinide series of elements, and manifest themselves in the most pronounced fashion in the richness of the phases exhibited by elemental Ce and Pu. Exploration of electronic correlations and resulting phenomena in f-electron compounds is therefore fundamental in building a strong scientific foundation to LANL's mission of stockpile stewardship and its leadership in materials research.

Progress

Dr. Weickert took very active part in completing the conversion of the dilution refrigerator/superconducting magnet system in 32/128 from 9 Tesla to 14 Tesla with a new high holding capacity dewar. This allows us to conduct preliminary investigations/selection of unconventional superconductors for the field-rotated studies in the same field range, as well as perform ground work, such as thermometer calibration, up to 14 T.

She has also helped to assemble the unique two-component rotator cell that will allow precise alignment of the sample with respect to the rotation axis after the sample is mounted on the specific heat platform. She was trained in operation of the Laue X-ray spectrometer (MST-11), needed for precise orienting of the sample with respect to the rotation axis. The cell has been assembled with the UPt$_3$ sample, and experiment is now in progress.

In parallel, Dr. Weickert was involved in several project at Los Alamos and follow-up projects to her postdoctoral appointment in Germany. These resulted in a number of articles published and submitted, including one submitted to Science on a doped Bose Glass system 8% Br doped DTN compound that exhibits Bose-Einstein Condensation of magnetic excitations [1]. Dr. Weickert also published an article on magnetostriction of pure DTN based on her work in Dresden [2], and a regular article on her work at Los Alamos is close to submission to PRB. Magnetization measurements in the Faraday magnetometer here at LANL produced an intriguing double phase transition, and these results are in preparation for submission to JMMM, with Dr. Weickert as first author.

Future Work

In several classes of superconductors, such as Heavy Fermion Superconductors (HFS) and High Temperature Superconductors (HTS), superconductivity is believed to be unconventional, where the symmetry of the combined spin and orbital spaces of the superconducting order parameter are lower than that of the underlying crystal lattice. For example, for most of the HTS compounds it was shown that the order parameter or superconducting gap has $d_{x^2-y^2}$ symmetry. This symmetry was identified via phase sensitive experiments based on Josephson tunneling using corner junctions Superconducting Quantum Interference Devices (SQUIDs). There are many indications that superconductivity in HFS is also unconventional. What is missing to date is the unambiguous identification of the pairing symmetry of the superconducting ground state of most heavy fermions and non-Cooper based high temperature superconductors.However, a different set of powerful tools to probe the superconducting gap structure is emerging, namely that of specific heat and thermal transport measurements in rotating magnetic fields. We will develop these capabilities in a dilution refrigerator equipped with a horizontal-axis rotator insert and a super-conducting magnet, thereby spanning the B-T phase diagram down to unprecedented 20 mK and up to 14 Tesla. Opening this phase space to experimental investigations will allow us to perform critical tests of existing theories of unconventional superconductivity in magnetic fields, which are instrumental for the interpretation of experiments (see the following section). Only by combining experiment and theory will this suite of tools be able to reach its full potential, enabling unambiguous determination of the gap structure in a variety of superconductors of current interest. We will use this apparatus to study energy gap in HFS, such as CeCoIn5 and UPt3.

We have established a collaboration with Prof. Bill Halperin of the Northwestern University to investigate high purity UPt_3 samples (the highest quality available) prepared in his laboratory, and obtained two UPt_3 samples for specific heat measurements in rotating field - UPt_3 samples. These samples were thoroughly characterized via resistivity and magnetization measurements in the past. These two samples have different orientations of the long axis that will allow rotation of the magnetic field both in the equatorial *a-b* plane (azimuthal angle ϕ) and *a-c* plane (polar angle Θ). The *a-b* sample is mounted, and the first experimental investigations are being conducted.

After UPt_3 Dr. Weickert will turn her attention to $CeCoIn_5$ with unconventional d-wave symmetry, where heavy quasiparticles form Cooper pairs, as described in introduction.

Conclusion

The development of a new experimental device to estimate angle-sensitive heat capacity and thermal conductivity at temperatures as low as 20mK and magnetic fields up to 14T will be unique in the world, complementing the experimental techniques already available at LANL. This powerful method allows us to establish the symmetry and structure of the energy-gap in any superconducting material and opens a wide door for fundamental investigations of new classes of superconductors of currently high interest and visibility, like heavy fermion superconductors, recently discovered iron-based pnictide superconductors, Sr2RuO4, etc.

References

1. Yu, R., L. Yin, N. S. Sullivan, A. Paduan-Filho , C. Miclea, F. Weickert, R. Movshovich, V. Zapf, and T. Roscilde . Bose glass and Mott glass of quasiparticles in a doped quantum magnet. To appear in *Science.*

2. Weickert, F., R. Kuchler, V. Zapf, M. Jaime, and A. Paduan-Filho. Direct measurement of spin correlations using magnetostriction (vol 77, 020404, 2008). 2011. *PHYSICAL REVIEW B.* **83** (9): 099901.

Publications

Daou, R., A. Haase, M. Doerr, M. Rotter, F. Weickert, M. Nicklas, and F. Steglich. Magnetoelastic quantum oscillations in GdSb to 55 T. 2011. In *International Conference on Strongly Correlated Electron Systems (SCES 2010) ; 27 June-2 July 2010 ; Santa Fe, NM, USA.* Vol. 273, p. 012111 (4 pp.).

Janson, O., A. A. Tsirlin, J. Sichelschmidt, Y. Skourski, F. Weickert, and H. Rosner. Long-range superexchange in Cu2A2O7 (A= P, As, V) as a key element of the microscopic magnetic model. 2011. *Physical Review B (Condensed Matter and Materials Physics).* **83** (9): 094435 (7 pp.).

Janson, O., A. A. Tsirlin, J. Sichelschmidt, Y. Skourski, F. Weickert, and H. Rosner. Long-range superexchange in Cu₂A₂O₇ (A= P, As, V) as a key element of the microscopic magnetic model. 2011. *Physical Review B (Condensed Matter and Materials Physics).* **83** (9): 094435 (7 pp.).

Tsirlin, A., I. Rousochatzakis, D. Kasinathan, O. Janson, R. Nath, F. Weickert, C. Geibel, A. Lauchli, and H. Rosner. Bridging frustrated-spin-chain and spin-ladder physics: Quasi-one-dimensional magnetism of BiCu2PO6. 2010. *PHYSICAL REVIEW B.* **82** (14): 144426.

Weickert, F., R. Kuchler, V. Zapf, M. Jaime, and A. Paduan-Filho. Direct measurement of spin correlations using magnetostriction (vol 77, 020404, 2008). 2011. *PHYSICAL REVIEW B.* **83** (9): 099901.

Local Atomic Arrangements in Phase Change Materials

Thomas E. Proffen
20080791PRD4

Abstract

Optical storage devices are nearing terabyte data storage densities, and emphasis is quickly shifting to electronic nonvolatile memory. Improvements in promising materials for this application, 'phase-change materials' (PCM), have largely been made through a trial and error process. We have pursued the use of state-of-the-art local structure studies, using neutron and synchrotron X-ray total scattering techniques, to provide a better understanding of the crystal chemistry, local structure, bonding, and properties in well-established and novel phase-change materials. Along with these studies, we have advanced scattering capabilities for disordered, complex, and amorphous materials.

Background and Research Objectives

In optical and electronic memory device technology a deposited crystalline phase is liquefied with a laser and solidified with quenching to form an amorphous one. Low intensity light or an electrical pulse ´reads' the distinct reflectivity or resistivity in the amorphized region while a longer and more intense source can render it crystalline once again, enabling re-writable media. Current phase-change materials are group 15 and 16 alloys with octahedral-like atomic arrangements in the crystalline state. Successful candidates for technological applications have large optical or electrical contrast between phases, thermal and chemical stability, fast switching speed for the phase change, and scalability. Improvements in PCM have largely been made through a trial and error process, with very little experimental insight into the distinct features that give rise to their remarkable properties. This has been largely due to the difficulties in accessing structural information for both amorphous materials and disordered thin film materials. Neutron and x-ray total scattering methods based in pair distribution function (PDF) analysis, are well-poised to provide this information. The PDF provides experimentally all atom-atom pairs probed in a scattering experiment. Local atomic structure can be modeled over small length scales (a few nanometers), and long-range structure or crystalline correlation length scale can be accessed over longer length scales.

This project was aimed at understanding the interplay between structure and property in phase-change chalcogenide alloys.   Our objectives were to prepare and characterize several classes of canonical PCM materials and explore the structural features that give rise to distinct properties across phase transitions. Along with these goals we aimed to explore the application of total scattering measurement techniques to thin films and further develop data reduction and analysis tools for finite materials.

Scientific Approach and Accomplishments

We prepared GeSb2 Te4 and Sb2Te thin films of thicknesses between 50 nm and several microns by sputtering from a stoichiometric target, at LANL's Center for Integrated Nanotechnologies. Initially we experimented with several substrates, with the goal of providing optimal samples for synchrotron and neutron studies. Samples were deposited on polyimide and on silica for synchrotron studies. For the silica deposition, half the substrate was masked during deposition, aiding in data reduction procedures. Multi-layer films were deposited on vanadium foil in order to explore neutron measurements of thin films.

At the Advanced Photon Source, Argonne National Laboratory, we explored *in situ* thermal annealing of the thin films for the first time, using a commercially available heat stage with minor modifications of the beamline. The measurements were very successful. We found data reduction was possible for films as thin as 50 nm and also for films deposited on either polyimide or silica. We collected temperature dependent data for 1 um thick samples for several heat ramping rates. There were some significant findings from these studies. (1) The amorphous (as-deposited) phase has a strongly correlated structure up to 8 Å, a length scale not accessible with complementary techniques, including EXAFS/XANES. (2) We found, as others have, that the nearest neighbor (Ge-Te, Sb-Te) coordination is shorter and sharper than in the crystalline phase, an unusual property for inorganic solids. This is in contrast to the next nearest neighbor (Te-Te) coordination, which is broader than in the crystal-

line phase. (3) For the technologically relevant metastable crystalline phase we found a disordered rocksalt crystal structure describes the average structure well, however, large atomic displacement parameters suggest a superposition of local (disordered) structural states. These measurements allowed us to extract correlation length scale, bond lengths, and chemical short range order (ordering of Ge, Sb, and vacancies) in the different states of this PCM, and we are currently preparing a manuscript summarizing these findings. We are collaborating with world-leading scientists in this field to correlate our observations to charge transport and optical reflectivity properties, and compare our results to several ab initio calculations completed for prototype phases of Ge2Sb2Te5 and Ge1Sb2Te4.

We have made significant strides with several other PCM compositions. We have completed our first measurements on thin film materials based on the Sb70Te30 eutectic (Sb2Te), where crystallization is believed to be growth controlled. This will allow important comparisons to be made with Ge-Sb-Te compositions. We have also completed measurements with amorphous and ordered GeTe nanoparticles from a collaborator at the Molecular Foundry, Lawrence Berkeley National Laboratory. We are investigating the crystal chemistry and local atomic structure in order to explore the promise of finite PCM particles for technological applications.

All of these experimental strides have been made hand in hand with several key methods advancements for determining local atomic structure of disordered crystalline, amorphous, and nanocrystalline materials. (1) The ability to distinguish separate peak contributions to pair correlation functions was previously limited. We developed a program MIXSCAT that extracts differential pair distribution functions using respective x-ray and neutron data sets. This program has been published for the wider scientific community. We have planned complementary neutron scattering experiments and anomalous x-ray scattering experiments both GeSb2Te4 and Sb2Te. If successful, this will allow us to completely separate the contribution of separate pair correlations to the total pair distribution function experimentally (without structure models). (2) Incoherent scattering contributions present a significant challenge in neutron total scattering experiments, especially for many nanomaterials. We have developed a method for correcting such contributions, and have made this routine available for use and published our procedure for the scientific community. (3) We have demonstrated that amorphous and polycrystalline thin film samples can be studied in transmission geometry at a synchrotron source by conventional x-ray total scattering methods. We found data reduction is possible for films deposited on polymer and glass substrates and films as thin as 50 nm. These methods can be adapted for a wide variety of thin film materials and sample environments where local atomic structure and behavior of thin film samples are of interest. (4) We have advanced the tools available for modeling total scattering data of finite nanoparticles, and we have submitted a paper detailing our methods and tools for the scientific community. All of these advancements are aiding in investigating how lattice distortions, vacancy concentrations, chemical short-range order, crystalline length scale, and local bonding environments affect properties in PCM, and will be valuable for investigation of many other functional materials of interest today.

Impact on National Missions

An energy efficient nonvolatile memory with fast switching speeds has the potential to revolutionize our data storage infrastructure and realize substantial leaps in computing power. This project has furthered our understanding of the interplay between structure and property in the remarkable class of existing phase-change materials and has provided direction towards the types of compounds suitable for future data storage technologies. In this sense, our work has brought the much anticipated electronic nonvolatile universal memory closer to reality.

This project has further supported the missions of the Office of Science by enhancing our understanding of complex disordered materials on the atomic level and enhancing experimental techniques to study complex materials. In the broadest sense, this work has advanced the methods of characterization available for amorphous-crystalline phase transitions in solids, bridging an important gap in solid state characterization as it is pursued today. Such advances in total scattering capabilities have the potential to broadly impact government agencies and programs.

Publications

Aksel, E., J. Forrester, J. L. Jones, P. A. Thomas, K. Page, and M. Suchomel. Monoclinic crystal structure of polycrystalline Na0.5Bi0.5TiO3. *Applied Physics Letters.*

Im, W. B., K. Page, S. P. DenBaars, and R. Seshadri. Probing local structure in the yellow phosphor LaSr2AlO5:Ce3+, by the maximum entropy method and pair distribution function analysis. 2009. *Journal of Materials Chemistry.* **19** (46): 8761.

Melot, B. C., K. Page, R. Seshadri, E. M. Stoudenmire, L. Balents, D. L. Bergman, and T. Proffen. Magnetic frustration on the diamond lattice of the A-site magnetic spinels CoAl2-xGaxO4: The role of lattice expansion and site disorder. 2009. *Physical Review B.* **80**: 104420.

Page, K., C. E. White, E. G. Estell, A. Llobet, and T. Proffen. Treatment of hydrogen background in bulk and nanocrystalline neutron total scattering experiments. To appear in *Journal of Applied Crystallography.*

Page, K., T. C. Hood, T. Proffen, and R. B. Neder. Building and refining complete nanoparticle structures with total scattering data. *Journal of Applied Crystallography.*

Page, K., T. Proffen, M. Niederberger, and R. Seshadri. Prob-

ing local dipoles and ligand structure in BaTiO3 nano-particles. 2010. *Chemistry of Materials.* **22**: 4386.

Page, K., T. Proffen, and R. B. Neder. Structure of Nanoparticles from Total Scattering. To appear in *Modern Diffraction Methods.* By Mittemeijer, E., and U. Welzel.

Page, K., and T. Proffen. tructure from Neutron Total Scattering: the Pair Distribution Function Approach. To appear in *Neutrons and Nanoscience.* By Hurd, A. J., and S. Sinha.

Wurden, C., K. Page, A. Llobet, C. E. White, and T. Proffen. Extracting differential pair distribution functions using MIXSCAT. 2010. *Journal of Applied Crystallography.* **43** (3): 635.

Effect of Charging on Carrier Relaxation Dynamics in Quantum Confined Semiconductor Nanocrystals

Milan Sykora
20080793PRD4

Abstract

Owing to their unique properties, quantum confined semiconductor nanocrystals (NCs) have potential to be source of breakthroughs needed for development of next generation of energy conversion and solid-state lighting technologies. Initial studies of NC-based photovoltaic (PV) and light emitting devices (LEDs), which rely on efficient charge transport in NC films, have however shown that one of the main obstacles in development of efficient NC-based applications is our limited understanding of how charged NCs are formed and how charging affects the radiative and nonradiative relaxation pathways of excitons formed by light absorption or electrical doping. The objective of the proposed work is to address this critical deficiency. The objective of the research performed in this project was to develop an experimental capability for controlled charging of the quantum confined semiconductor NCs and studies of their properties by steady state and time-resolved optical methods. We were able to develop a new capability for studies of charged NCs and generated important insights about the properties of the charged NCs. Our research made important progress in supporting the drive toward national energy security, a key DOE mission.

Background and Research Objectives

Due to the projected increase in the global demand for energy there has been a growing interest in harnessing solar energy in an efficient and cost-effective manner. Nanomaterials and more specifically quantum-confined semiconductor nanocrystal quantum dots (NQDs) have potential to play an important role in the next generation of technologies for conversion of solar energy into electricity (photovoltaics, PV) and chemical energy (photocatalysis). Their appealing properties include size-tunability of absorption spectra and electrochemical potentials, and the ability to generate multiple excited electron–hole pairs, or excitons, from a single photon via the process of carrier multiplication. These properties are all important for increasing the efficiency with which these materials convert sunlight into electricity. While a great deal of progress has been made on the photophysics of
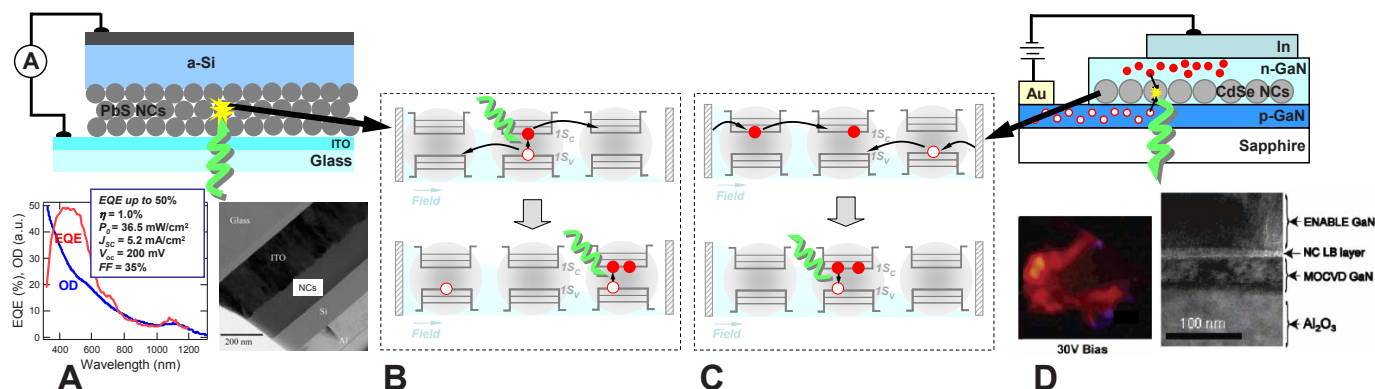
Figure 1. Formation of excitons in charged NCs in photovoltaics (PV) and light-emitting diodes (LED). (A) Schematic diagram, performance characteristics and an electron micrograph of a PV device based on PbS NCs. (B) Formation of excitons in charged NCs during operation of a PV device. Top: Following photon absorption the carriers are separated by NC-to-NC carrier hopping driven by internal field (in principle, multiple charges can be present in each NC as a result of carrier hopping). Bottom: Following absorption of a second photon an exciton is formed in a charged NC. The effects of an excess charge on exciton relaxation are currently virtually unknown. (C) Scheme showing formation of excitons in charged NCs during operation of an LED. (D) Schematic diagram of an example LED based on CdSe NCs, red electroluminescence observed during the device operation and a electron micrograph of the device.
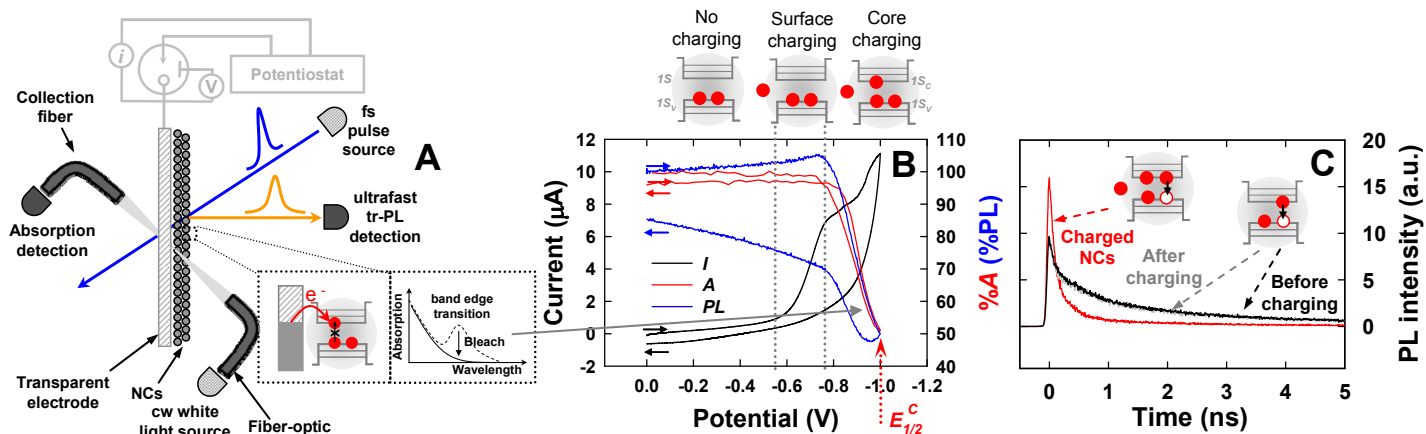
Figure 2. (A) Schematic diagram of the experimental setup for studies of optical properties of charged NCs. The inset shows absorption bleach formation upon injection of charge into NC. (B) Results showing changes in current (I), absorbance bleach (A) and photoluminescence intensity (PL) as a function of applied potential. The combination of electrochemical and optical methods allows determination of the potential needed for deposition of charges onto the NC surface and injection into the NC core. The potential at which 50% of the band edge absorption is bleached defines the absolute energy of the conduction band offset (E1/2C). (C) Results of studies of the effect of charging on the carrier relaxation dynamics. The exciton relaxation is significantly faster in charged NCs and the changes in the dynamics are reversible upon removal of excess charge.

neutral NQDs, little is known about charged NQDs. This deficiency is crucial to remedy as the operation of practical PV devices is likely to lead to the formation of significant populations of charged NQDs (Figure 1), which can dominate the carrier relaxation and recombination processes and thus dictate the device performance. In this project we will study the fundamental physics of charged NQDs with the goal to determine the potential impact of charging on the performance of PV devices based on NQDs.

Scientific Approach and Accomplishments

One of the challenges in studies of charged nanocrystal quantum dots (NQDs) is achieving a high level of control over the number of carriers introduced into the NQD. One approach that allows accurate control over the degree of charging is possible through a combination of electrochemical and optical methods. Exploiting this approach we have developed an experimental apparatus shown in Figure 2A. In the experiment the charging of a NC, deposited as thin film on transparent electrode, is achieved by a high-precision potentiostat. To avoid potential interference in charging of NCs from oxygen or water a special "air free" spectroelectrochemical cell was designed, where the portion of the cell consists of standard 1cm optical cuvette. All sample preparation steps and the filling and sealing of the electrochemical cell were performed in an argon atmosphere filled glove box. The extent of NC charging is determined optically, from the magnitude of the bleach (i.e., decrease in absorbance) of the NC band edge absorption, probed by a white-light source. The dynamics of radiative and nonradiative relaxation in charged NCs is probed using amplified femtosecond Ti-Sapphire laser and ultrafast streak camera detection (time resolution ~2 ps) of NC pho-

toluminescence (PL). This approach allows us to introduce specific numbers of charge carriers into NCs with high level of control and to study the charging process and the carrier relaxation dynamics in the charged NCs with very high temporal resolution.

Studies of CdSe NC cores

Our initial studies focused on understanding of charging of "as prepared", core CdSe NCs. The NCs were deposited as thin films on the surface of transparent electrode (ITO). We have found that the most reproducible experimental results were obtained when prior to charging the electrode with the film was rinsed with acetonitrile and soaked for ~12 hours in electrolyte solution (0.1 M tetrabutylammonium hexafluorophosphate in acetonitrile). Upon applying the charge a significant current flow was observed prior to the optical bleaching of the NC band edge transition, which indicates deposition of charge carriers onto the NC surface (potential range ~ -0.6 to -0.8 V in Figure 2 B). At more negative potentials we observed clear bleaching of the optical band edge transition (potential range ~-0.8 to -1.0 V), which indicates injection of the charge carrier into NC "core". In case of CdSe NCs a 50% bleach indicates that on average each NC "core" was injected with a single excess carrier. In studies of NCs of various sizes we found that the energy onset at which the injection of carrier occurs varies systematically with and NC size. This is a very important result as an accurate knowledge of the conduction and valence band offsets of the semiconductor materials is an important prerequisite for the construction of PV cells or LEDs. Unlike bulk semiconductors, for which the band offsets are determined by the material chemical composition, in quantum confined NCs the energies of the band offsets
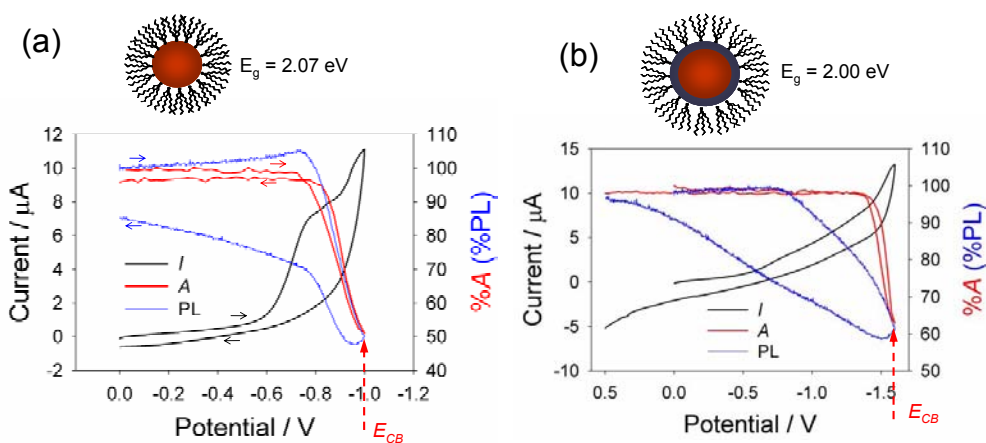
Figure 3. Results of the spectroelectrochemical studies of the CdSe NC cores (a) and CdSe/ZnS core/shell structures (b). The results show that as a result of the addition of the thin (~0.1nm) shell of ZnS over the CdSe core an additional potential of ~0.6V is needed to inject a carrier into the NC core. The slower recovery of the photoluminescence in case of core/shell structures indicates less efficient charge transport in films based on these materials.

are expected to depend on numerous other factors, such as NC size and shape (i.e, extent of quantum confinement), and type and quality of surface passivation. Our results show that the tools developed in this project allow us to develop a quantitative "map" of band offsets (as defined via parameters, such as E1/2C in Figure 2) for variety of NC materials, and their dependence on parameters, such as NC size, shape and surface properties.

Building on our understanding of how the NCs are charged in next step we performed studies of carrier relaxation dynamics in charged NCs, where the number of charges per NC was carefully controlled. As shown in Figure 2C we found that in charged NCs the exciton relaxation dynamics is significantly enhanced. The enhancement in PL intensity at picosecond time delays suggest enhancement in radiative decay, while the quenching of the PL at nanosecond time delays indicates enhancement in nonradiative decay. We found that this trend is consistent across various sizes of the NCs, however, the details of the NC relaxation dynamics vary with NC size. A careful analysis of the relaxation dynamics allowed us to determine the dynamics of the charged exciton (trion) as a function of NC size.

Studies of CdSe/ZnS core/shell structures

NC-based core-shell structures are an important group of materials studied extensively particularly in the context of lighting application, such as LEDs and lasing. In these structures the thin shell of the large band-gap material (e.g., ZnS) serves as a protection of the core (e.g., CdSe) from surface defects, which reduce the light emission efficiency (quantum yield) of the core. The techniques for preparation variety of core/shell structures have been described in literature. An important question from the practical standpoint of the light applications is what role the shell plays in our ability to inject charges into the NC core. Thus, in practical application the injection of both a positive and

negative charge simultaneously is required for generation of light from the NQD. Therefore, in next phase of our research we have investigated the effect of the shell on charging of the NC core. The sample results are shown in Figure 3. Although, the exact shell structure of the samples we used in our studies is not known, the thickness of the shell was estimated to vary between 0–2 monolayers of ZnS. We find that when the potential is applied the bleaching of the 1S absorption feature is very rapid beyond 1.2 V, eventually reaching 60% of the initial value at 1.3 V. This indicates that the conduction band is roughly 0.6 V more negative than CdSe with the core of the same size. This indicates that the shell, although extremely thin, is an effective barrier against charge injection due to the high band gap of ZnS.

We further observed that the PL intensity recovers on a significantly slower timescale than the absorption recovery, similar to the CdSe core films. However, the emission begins to decrease at roughly 0.7 V, or the same potential at which CdSe (1S at 585 nm) films become charged. The quenching thus occurs ~0.6 V before the absorption is bleached. The reason for the different dynamical responses of these two optical properties is an intriguing question. One reason for this difference may be due to surface-trapped charges ability to contribute to the nonradiative relaxation via so called Auger processes. Although the surface of the CdSe core is well-passivated by the ZnS shell, the nonuniformity of the shell and the removal of surface ligands during purification may lead to a substantial number of defect sites supporting surface electronic states. Injection of electrons into the shell may have effects on the core, as the electronic wavefunction from the core leaks partially into the shell, although this is more of an issue when shells of CdS, a material with a lower band gap, are used (see next section). Finally, additional trap sites for electrons may exist at the interface between core and

shell, and tunneling through the shell into this region could subsequently affect the carriers in the core through Auger processes or overlap with the tails of the core electronic wavefunction.

Studies of CdSe/2CdS, CdSe/4CdS and CdSe/16CdS ("giant NCs") core/shell structures

In next phase of our research we focused on systematic studies of the effect of the shell thickness on the charging properties of the NCs. This part of research was performed in collaboration with Dr. Jennifer Hollingsworth of CINT. With the help of Dr. Hollingsworth's team the core/shell structures with carefully synthesized shell thicknesses varying between 2 and 16 monolayers of CdS over the CdSe core. In these studies we have chosen to prepare shells from CdS, rather than ZnS, due to lower band gap of the material. This should allow us to inject the carriers even through relatively thick shell material.

Consistent with our studies of CdSe/ZnS structures we find that increasingly more negative potentials are required for NC charging with increasing shell thickness. At the extreme of 16CdS layers we find that the bleach of the core absorption is not detected even at potentials more negative than 1.6V, where the films start to chemically break down. Compared to the CdSe and CdSe/ZnS films discussed in previous sections, charging and discharging in CdSe/CdS is significantly slower. In addition to creating a barrier to charge injection or ejection, the thick shell also reduces the rate at which carriers can hop between NQD cores and thus lower the conductivity of the film.

 If the CdSe/4CdS film is maintained at -1.2 V, a clear change in the dynamics is observed which is reversible once the potentiostat is turned off. The increase in emission intensity near zero delay, combined with the enhanced decay rate, is a signature of trion dynamics. Multiexponential fits may be used to estimate a trion lifetime of 800 ps, which is comparable to the lifetime measured for CdSe/CdS core/shells with 1–2 monolayers of CdS. While few, if any, electrons are injected into the core at this potential, trions are clearly being produced. Injection of charges to the core/shell interface, as discussed in the previous section, is one possibility, especially considering that the penetration of the core electronic wavefunction into the shell region is greater for CdS shells. For trion dynamics to exist, however, a pathway for the excess charge to combine with the photogenerated hole must exist. This implies enough excess electron density to be present in the core to cause a 1S bleach. A crude explanation for the lack of the bleach is that the delocalization of the core electrons into the shell simply makes the bleach extremely broad and hard to detect. Consistent with the results of steady state studies, the enhanced relaxation dynamics is often observed at potentials lower than bleaching of the NQD absorption. This suggests that the exciton the core interacts with the excess charge before it is injected into the NQD core. This is an important result that is likely to have implications for development of practical applications of NCs not only in solid state lighting, but also in biological tagging. The results of our studies are now being summarized in a manuscript.

In terms of basic science the main objective of the project was to develop understanding of physics of charged NQDs. The practical objective was to determine how charging of individual nanocomponents of a LED or a PV device during its operation affects its performance and how the potential losses in the performance can be minimized. By performing the research summarized above we were able to make important progress in this direction.

Impact on National Missions
The results of this project made contributions in support of the drive toward national energy security. In particular, the research performed here enhanced our understanding of how nanoscale materials can be utilized to improve the efficiencies of solid lighting and solar energy conversion technologies.

The Kondo Lattice Problem

Joe D. Thompson
20080794PRD4

Abstract

Strong interactions among electrons force a correlated, collective response to their physical and chemical environments. Experimental and theoretical work over the past three decades to understand these correlated responses have failed to provide a microscopic or even firmly based phenomenological understanding of the complex underlying physics of such systems. A recent conceptual breakthrough from our examination of one large class of electronically correlated materials, so-called Kondo-lattice materials, has provided an entirely new phenomenological description of the complex physics. This project has had the goal of exploring the predictive consequences of this phenomenology, especially regarding the possible emergence of unconventional superconductivity from this model. Additionally, we have explored whether a more basic microscopic understanding of this phenomenology can be developed.

Background and Research Objectives

The Kondo-lattice materials can be described by a dense, periodic array of localized f-electrons coupled to a sea of 10^{23} itinerant electrons. Understanding its various exotic properties, such as unconventional superconductivity, defines the so-called Kondo-lattice problem. The building block of the problem, namely the single-impurity problem that describes a single localized electron coupled to 10^{23} itinerant electrons, has been intensively studied in 20th century and is well understood. However, a solution to the Kondo-lattice problem remains obscure despite three decades' of theoretical and experimental effort. So far, it has been generally believed that the essential physics of the problem comes from the competition between two fundamental magnetic interactions characterized by their energy scales: a Kondo energy scale T_K, that results from the local (Kondo) interaction of an individual f-spin and resembles the single-impurity Kondo problem, and an exchange energy scale T^*, that originates from the long-range (Ruderman-Kittel-Kasuya-Yosida (RKKY)) interaction of neighboring f-spins and tends to correlate f-spins into collective excitations. However, theories along this line have not been able to give a comprehensive solution to the large amount of experimental data, even though such a picture has been quite successful in interpreting the qualitative features of the low temperature phase diagram of Kondo-lattice materials. In light of this, we have been pursuing the problem from a different aspect. We base our research on experimental analysis and develop a new conceptual framework based on a phenomenological two-fluid model [1-4] in which the Kondo and RKKY interactions give rise to two interpenetrating 'fluids'—one of itinerant electrons with very heavy effective mass and the other of weakly interacting local magnetic moments . Our ultimate goal is to explore the new framework and develop it into a standard theory for the Kondo-lattice problem. We also investigate other problems raised by latest experiment.

Scientific Approach and Accomplishments

Our work is a fruitful result of close collaborations between experiment and theory. The following progress has been made from either our theoretical analysis of existing experimental data or experimental realization of our theoretical proposal.

A new conceptual framework for the Kondo-lattice problem

We have proposed a new conceptual framework based on our previous studies of the two-fluid model. Figure 1 summarizes our results and shows that the physics of the Kondo lattice can be separated into three distinct regimes depending on temperature. The two fluids, a fluid of emergent heavy electron Kondo liquid and a fluid of residual unhybridized magnetic moments, describe the gradual nature of the heavy electron emergence below T^* from the high temperature localized f-spins. In contrast to a conventional picture, the RKKY interaction is always the dominant one for most Kondo-lattice materials. This work has been accepted for publication in Journal of Physics: Conference Series and appears on-line as Y.-F. Yang et al., arXiv:1005.5184 (2010).
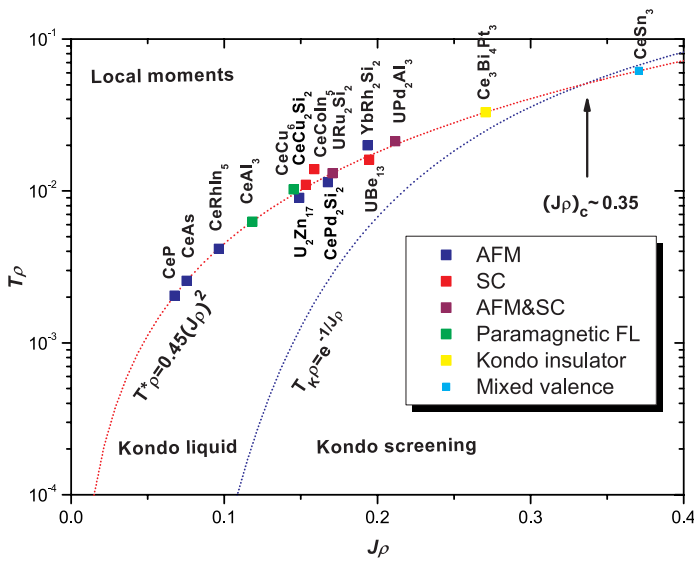
Figure 1. A general phase diagram proposed for heavy electron materials based on our new framework. The expected values of two characteristic temperature scales, the RKKY scale T* and the Kondo scale TK, are compared in the figure and all materials are placed according to their T*. J is the local Kondo coupling and rho is the conduction electron density of states. For most materials, T* is much larger than TK. The f-electrons are localized above T* and become partially itinerant forming a heavy electron Kondo liquid below T*. At very low temperatures around TK, the itinerant heavy electrons condense into some exotic states, such as unconventional superconductivity.

Theory for electron tunneling and point contact spectroscopy

Experimental point-contact spectroscopy and scanning tunneling spectroscopy studies [5] of Kondo-lattice compounds probe the energy-dependent electronic states and observe a spectral asymmetry between plus and minus voltages (energies) below T^*. Building on our new conceptual framework for the Kondo lattice, we have developed the first semi-microscopic scenario based on quantum interference between 'light' and 'heavy' electrons that accounts for these experimental observations. A comparison between experimental results and our model calculations are shown in Figure 2. The same hybridization between f-electrons and conduction electrons that leads to the emergence of the heavy electron Kondo liquid gives rise to the quantum interference of electrons and explains the asymmetry in the conductance spectra. Results of this research appeared in Y.-F. Yang, Phys. Rev. B: Rapid Communications 79, 241107 (2009).
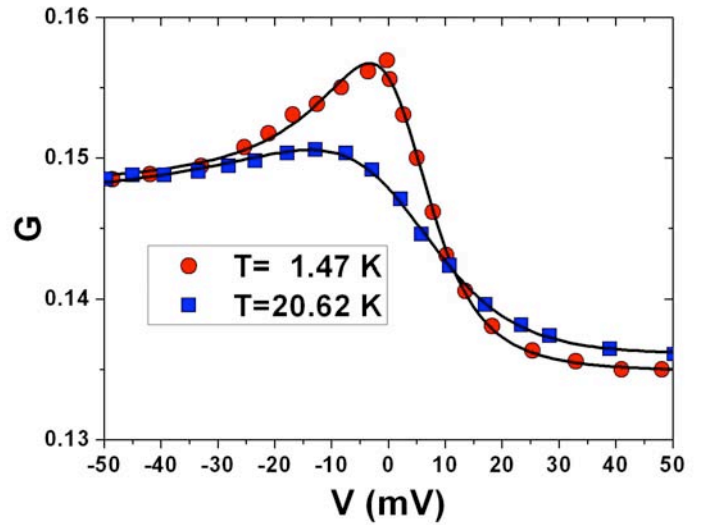
Figure 2. Comparison of experimental (symbols from [5]) and our theoretical (solid lines) point contact conductance spectra G as a function of the bias voltage at two different temperatures. The asymmetry in the spectra around zero-bias voltage results from quantum interference of two hybridized channels, the conduction-electron channel and the f-electron channel, for the electron current.

A new route to new superconductors

We have applied our phenomenology to provide a natural explanation for the evolution of the experimentally determined spin susceptibility (Knight shift) in the superconducting state of the Kondo-lattice material CeCoIn$_5$. We find that the unconventional superconductivity originates from the condensation of electronic excitations intrinsic to the Kondo liquid. Because the characteristic temperature scale T^* of the Kondo liquid is given by the magnetic interaction between the Ce ions in these materials, our analysis further concludes that the superconducting transition temperature is actually controlled by this single magnetic interaction. This conclusion, which would not have followed from conventional views of the Kondo lattice, points to a qualitatively new direction for discovering new superconductors with higher transition temperatures. See Y.-F. Yang et al., Phys. Rev. Lett. 103, 197004 (2009).

Connecting Mott and Kondo-lattice physics

Using analytical many-body and numerical techniques, we have shown that a generalization of the Kondo-lattice problem, the Anderson lattice problem, can be mapped under certain circumstances onto the so-called Mott-Hubbard model that considers the consequences of strong Coulomb repulsion on the motion of electronic charges. This is a rather important result because the Mott-Hubbard model is used commonly to describe the physics of strongly correlated d-electron materials, in particular the

high temperature superconductors based on copper-oxide. The mapping that we have discovered now provides a link between the physics of strongly correlated f-electron systems, such as Kondo-lattice systems based on Pu and related heavy-electron superconductors, and technologically important d-electron systems. Because of the extensive theoretical underpinning of the Mott-Hubbard model, the bridge that we have made now to the Anderson lattice problem opens the path to a microscopic theory of our phenomenological model of the Kondo lattice. See K. A. Al-Hassanieh et al., Phys. Rev. Lett. 105, 086402 (2010).

Superconducting Swiss cheese

Intrinsic electronic inhomogeneity is a hallmark of strongly correlated d-electron materials, such copper-oxide superconductors and certain materials that exhibit a colossal change in electrical resistivity when subjected to small magnetic fields. Electronic inhomogeneity, however, has rarely, if ever, been considered to appear in an f-electron Kondo lattice. Motivated by observations made in the course of developing our conceptual framework for the Kondo lattice, we have analyzed the superconducting properties of Kondo-lattice/heavy-electron superconductors and discovered strong evidence for electronic inhomogeneity that is revealed when small amounts of non-magnetic impurities are introduced into these systems. This inhomogeneity is hidden in the absence of foreign atoms. The picture that emerges from these studies is that foreign atoms produce an electronic 'Swiss cheese', analogous to what is found in copper-oxide superconductors that contain small amounts of certain non-magnetic impurities. Unlike the copper-oxide superconductors, however, this unexpected manifestation of electronic inhomogeneity in Kondo-lattice superconductors appears to be a generic response that is independent of the specific type of added impurity. An account of this discovery is under consideration by Nature Communications.

Impact on National Missions
Complex correlations among electrons control the physical properties of unconventional superconductors and actinide materials that are important for DOE missions for energy security and understanding materials. This work has attacked the unsolved problem of complex correlations from a completely new perspective, with the goal of understanding how they control physical properties

References
1. Nakatsuji, S., D. Pines, and Z. Fisk. Two fluid description of the Kondo lattice. 2004. *Physical Review Letters.* **92**: 016401.

2. Curro, N. J., B. L. Young, J. Schmalian, and D. Pines. Scaling in the emergent behavior of heavy-electron materials. 2004. *Physical Review B.* **70**: 235117.

3. Yang, Y. F., and D. Pines. Universal behavior in heavy-electron materials. 2008. *Physical Review Letters.* **100**: 640409.

4. Yang, Y. F., Z. Fisk, H. O. Lee, J. D. Thompson, and D. Pines. Scaling the Kondo lattice. 2008. *Nature.* **454**: 611.

5. Park, W. K., J. L. Sarrao, J. D. Thompson, and L. H. Greene. Andreev reflection in heavy-fermion superconductors and order parameter symmetry in CeCoIn5. 2008. *Physical Review Letters.* **100**: 177001.

Publications
Al-Hassanieh, K. A., Y. F. Yang, I. Martin, and C. D. Batista. Effective low-energy model for f-electron delocalization. 2010. *Physical Review Letters.* **105**: 086402.

Durakiewicz, T., P. S. Riseborough, C. D. Batista, Y. F. Yang, P. M. Oppeneer, J. Joyce, and E. D. Bauer. Quest for band renormalization and self-energy in correlated f-electron systems. 2010. *Acta Physica Polonica A.* **117**: 264.

Yang, Y. F.. The Fano effect in the point-contact spectroscopy of heavy electron materials. 2009. *Physical Review B.* **79**: 241107(R).

Yang, Y. F., N. J. Curro, Z. Fisk, D. Pines, and J. D. Thompson. A predictive standard model for heavy electron systems. To appear in *Journal of Physics: Conference Series.*

Yang, Y. F., R. Urbano, N. J. Curro, D. Pines, and E. D. Bauer. Magnetic excitations in the Kondo liquid: Superconductivity and hidden magnetic quantum critical fluctuations. 2010. *Physical Review Letters.* **103**: 197004.

Classical/quantum Mechanical Simulations of Electronic Nanomaterials

Sergei Tretiak
20080795PRD4

Abstract

In this project we used a combination of ab initio techniques, such as density functional theory (giving an accurate electronic structure of a system), with classical force field calculations (providing reasonably fast geometries, packing and dynamics for large molecules) to predict and to explain experimental results on dynamics, transport, and optical properties of several hybrid composites and nano-scaled materials. We applied our new methodologies to a variety of materials, which are promising for optoelectronics and sensing, and several bio-applications such as drug delivery, cancer diagnostics and therapy.

Background and Research Objectives

The idea of harnessing molecular building blocks to assemble nanometer-scale devices promises many fascinating applications in fields ranging from electronic to medical technologies. Unfortunately, our fundamental understanding of the underlying physics and chemistry of such complex structures lag the experimental observations; the major reason being the computationally unmanageable number of atoms in such systems. In this project we developed a new theoretical approach able to predict and to explain experimental results on dynamics, transport, and optical properties of several hybrid composites and nano-scaled materials. Our goal was to be able to compute the optical and transport properties of complex molecular composites. Our developed methodology was applied to: i) Adsorbed Deoxyribonucleic Acid (DNA) strands or other bio-molecules on metallic surfaces. Here the unique Scanning Tunneling Microscope (STM) spectra of bases promised resolution of the structure and fast sequencing of DNA. To interpret experimental results, the Postdoc simulated tunneling spectra and identifyiedthe underlying electronic features; ii) Semiconductor quantum dots to clarify the role of soft ligand layer and surface roughness on electron-electron and electron-phonon coupling important in experimentally observed efficient carrier multiplication processes. These systems are promising for harvesting of solar energy; iii) Molecular-functionalized carbon nanotubes to investigate computationally photoinduced structural relaxation and uncaging. This has a potential to make carbon nanotubes into highly luminescent materials. Many other applications are envisioned and broad dissemination of these methods is expected. Besides providing fundamental theoretical understanding of transport, and photoexcited properties of complex molecular composites, this research is envisioned for developing a fast and accurate "virtual computational nano-scale laboratory" to be used in a variety of projects with significant LANL, DOE, and NIH investments, and supports a number of experimental efforts currently carried out at LANL/CINT.

Scientific Approach and Accomplishments

This project combines two approaches: ab initio methods (giving an accurate electronic structure of a system) and force field (FF) methods (providing reasonably fast geometries, packing, and dynamics for large molecules). We proposed to: i) construct new FF potentials using quantum mechanical calculations (e.g., Density Functional Theory, DFT) to be performed on a set of representative units; ii) conduct FF simulations of the dynamics of the entire system at specific temperature, pressure, etc; iii) DFT and time-dependent DFT calculations of electronic structure of ground and excited states using selected resulting geometries (snapshots); iv) develop a computational package to allow non-adiabatic photoinduced dynamics based on correlated excited states in time-dependent DFT method. Using this approach, the ultimate goal is to predict and to explain experimental results on several nanoscale molecular composites/hybrids.

Over the project duration we investigated optical response and phonon induced dynamics in pure CdSe quantum dots (QD) and QDs functionalized by different organic molecules [1,2]. Currently, our main focus is on organic ligands that cover the QD surface. The role of ligands is expected to be crucial in the carrier multiplication processes experimentally observed in these systems and promising for the harvesting of solar energy. Surface ligands also impact phonon-assisted carrier dynamics

that competes with carrier multiplication. In contrast to the common point of view, we found that ligands strongly impact charge relaxation in QDs for high-energy excitations. No molecular orbitals of ligands appear as trap states inside or near the band gap of the QD. We found that the surface ligands introduce new electronic states which are strongly delocalized over the ligands and the dot surface and open new relaxation paths for the nonradiative charge relaxation, increasing relaxation rates [3]. These results are obtained for small $Cd_{33}Se_{33}$ clusters passivated by different organic molecules and extended to larger systems ($Cd_{111}Se_{111}$) which are comparable to the common QDs used in experiments. The main focus of these studies is the trap states inside the band gap of the QD originated from the detachment of one of the ligands from the surface. These investigations have resulted in several published articles [1-3] and other papers to be submitted soon. Our results were also presented in several conferences. We also investigate optical and transport properties in dye-functionalized metallic clusters self-assembled on the DNA template. Some of our results have been already published [4]. All these composites hold great promise in the areas of bio-inspired self-assembly of electronic circuits.

We also studied charge and energy transfer mechanisms in CdSe QDs functionalized with ruthenium Ru(II) complexes. New photovoltaic and photocatalysis applications have been recently proposed based on these hybrid systems, while the exact mechanism and direction of the charge transfer controlling their photochemistry is still under debate. As a first step, we investigated how the addition of protonated and deprotonated carboxyl groups to the Ru(II)-bipyridine changes the electronic and optical properties of the complex [5]. We also have shown that the structure of these molecules allows one to express their excitations in terms of wavefunctions localized on individual ligand via the Frenkel exciton model. This simple effective model is able to accurately explain the optical activity, localization properties, and splitting patterns of the low-energy excited states [5]. Next, we focus on how the Ru(II) complex binds to the QD and how the adsorbed complex affects the electronic structure of the QD. Our calculations predict that deprotonation of the carboxyl group favors the QD-complex interaction. This occurs via "bridging" attachment of two Cd atoms with two oxygens. The calculated vibrational modes associated with such bridging bonding are in good agreement with vibrational spectroscopy data for these systems confirming the stability of hybrids interacting via bridging attachment.

Our results on excitonic and electron-phonon couplings in semiconductor carbon nanotubes (CNTs) and quantum dots were also summarized in the book [6,7] that was published by World Scientific/Pan Stanford (a science publishing company of high reputation) this summer (Figure 1). This project was extended by studies of photocurrent and its dependence on the photoexcitation energies in CNTs.

Finally, we also investigated the conformational inter- and intra-molecular disorder and its impact on the electronic structure of amorphous conjugated polymers, which are the commonly used materials for organic optoelectronic devices. Classical molecular dynamics is used to determine probable molecular arrangements, and first-principle calculations based on DFT are used to compute the electronic structure. We also calculated the participation ratios to characterize electronic localization properties of amorphous organic polymers. We found that these quantities for polyfluorenes differ drastically from those of poly-phenylenevinylenes, because of the long side chains that prevent the close packing and interactions among molecules, which should affect transport properties of these materials [8]. These results are useful for calculations of charge mobilities in these materials.
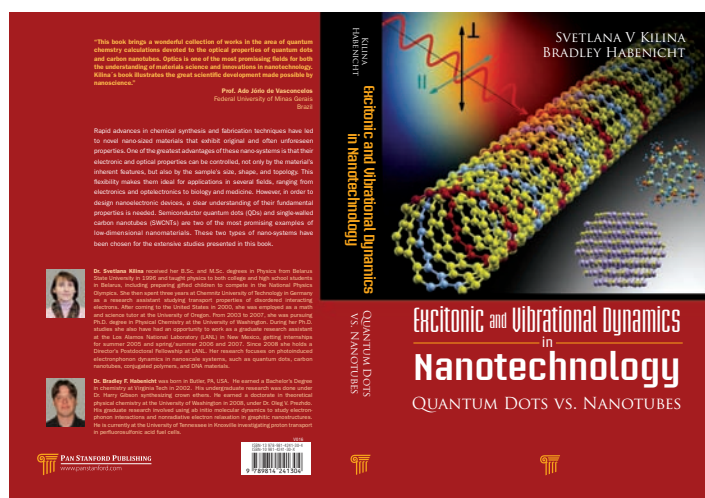
Figure 1. Cover of the published book on excitonic and electron-phonon couplings in semiconductor carbon nanotubes and quantum dots illustrated light interaction with these systems.

Impact on National Missions
This project directly addresses LANL institutional goals in basic understanding of materials, energy security, and threat reduction. Furthermore, the project strongly connects to thrusts of the DOE-funded Center for Integrated Nano-Technology (CINT) by impacting priorities in nanotechnology, multi-scale material modeling, and sensing.

References
1. Kilina, S., S. Ivanov, and S. Tretiak. Effect of Surface Ligands on Optical and Electronic Spectra of Semiconductor Nanoclusters. 2009. *Journal of the American Chemical Society* . **131**: 7717–7726.

2. Kilina, S., D. Kilin, and O. Prezhdo. Breaking the Phonon Bottleneck in PbSe and CdSe Quantum Dots: Time-Domain Density Functional Theory of Charge Carrier Relaxation. 2009. *ACS NANO.* **3** (1): 93.

3. Isborn, C., S. Kilina, X. Li, and O. Prezhdo. Generation

of Multiple Excitons in PbSe and CdSe Quantum Dots by Direct Photoexcitation: First-Principles Calculations. 2008. *Journal of Physical Chemistry C.* **112**: 18291–18294.

4. Kilin, D., K. Tsemekhman, S. Kilina, A. Balatsky, and O. Prezhdo. Photoinduced Conductivity of a Porphyrin-Gold Composite Nanowire. 2009. *Journal of Physical Chemistry C.* **113**: 4549.

5. Badaeva, E., V. Albert, S. Kilina, A. Koposov, M. Sykora, and S. Tretiak. Effect of deprotonation on absorption and emission spectra of Ru(II)-bpy complexes functionalized with carboxyl groups. 2010. *PHYSICAL CHEMISTRY CHEMICAL PHYSICS.* **12** (31): 8902.

6. Svetlana Kilina coauthors book on nanotechnology. 2009. *PADSTE HIGHLIGHTS .*

7. Habenight, B., and S. Kilina. Excitonic and Vibrational Dynamics in Nanotechnology: Quantum Dots vs Carbon Nanotubes. 2009.

8. Kilina, S., E. Batista, P. Yang, S. Tretiak, A. Saxena, R. Martin, and D. Smith. Electronic structure of self-assembled amorphous polyfluorenes. 2008. *ACS NANO.* **2** (7): 1381.

Nanoclusters. 2009. *Journal of the American Chemical Society .* **131**: 7717–7726.

Kilina, S., and O. Prezhdo. Breaking the Phonon Bottleneck in PbSe and CdSe Quantum Dots: Time-Domain Density Functional Theory of Charge Carrier Relaxa. 2009. *ACS Nano.* **3**: 93.

Publications

Svetlana Kilina coauthors book on nanotechnology. 2009. *PADSTE HIGHLIGHTS .*

Badaeva, E., V. Albert, S. Kilina, A. Koposov, M. Sykora, and S. Tretiak. Effect of deprotonation on absorption and emission spectra of Ru(II)-bpy complexes functionalized with carboxyl groups. 2010. *PHYSICAL CHEMISTRY CHEMICAL PHYSICS.* **12** (31): 8902.

Habenight, B., and S. Kilina. Excitonic and Vibrational Dynamics in Nanotechnology: Quantum Dots vs Carbon Nanotubes. 2009.

Isborn, C., S. Kilina, X. Li, and O. Prezhdo. Generation of Multiple Excitons in PbSe and CdSe Quantum Dots by Direct Photoexcitation: First-Principles Calculations. 2008. *Journal of Physical Chemistry C.* **112**: 18291–18294.

Kilin, D., K. Tsemekhman, S. Kilina, A. Balatsky, and O. Prezhdo. Photoinduced Conductivity of a Porphyrin-Gold Composite Nanowire. 2009. *Journal of Physical Chemistry C.* **113**: 4549.

Kilina, S., D. Kilin, and O. Prezhdo. Breaking the Phonon Bottleneck in PbSe and CdSe Quantum Dots: Time-Domain Density Functional Theory of Charge Carrier Relaxation. 2009. *ACS NANO.* **3** (1): 93.

Kilina, S., S. Ivanov, and S. Tretiak. Effect of Surface Ligands on Optical and Electronic Spectra of Semiconductor

Energy Transfer Processes in Type-Specific Single-Walled Carbon Nanotubes

Stephen K. Doorn
20080797PRD4

Abstract

In the past two years Juan Duque's efforts have been aimed at several aspects of understanding fundamental photophysical processes between single-walled carbon nanotubes (SWNTs) and their surroundings for energy transfer processes aimed at energy harvesting and sensing applications. With one patent application submitted, seven peer reviewed articles published in important journals like JACS and ACS Nano, two are under review (Nature), and several more are in different stages of completion. Importantly, after his director's postdoc term ends, Juan will be converted to permanent staff in the Chemistry Division, Physical Chemistry and Applied Spectroscopy (C-PCS) group.

Background and Research Objectives

Single-Walled Carbon Nanotubes (SWNT) has remarkable optical and electrical properties. These photophysical properties are heavily dependent on the sidewall purity, diameter and chirality (a property of the geometry) of the tube. While this heterogeneity offers many opportunities in sensing and electronic applications, full utilization of these properties requires the development of well defined materials. This includes controlling the energy transfer (ET) that occurs between distinct tube types and between the tube and environment. Control of ET is important because it can enhance and/or quench the detectable photophysical properties of the tubes, and allows tunability of their absorption range. Current research on bulk samples is lacking because their diverse properties (heterogeneity) inherently limits the sensitivity and reproducibility of the measurements. However, new separation techniques allow access to chirality-enriched samples and offer the possibility of engineering samples with specific bandgap and reactivity properties. We are proposing to utilize enriched chirality samples to engineer and enhance ET reactions between specific tube types and between SWNTs and molecules in ensemble systems and at the single molecular level.

Scientific Approach and Accomplishments

Some of the major accomplishments are highlighted below:

Solubility of SWNTs in solutions

We studied the solubility and dispersability of SWNTs in oleum and surfactant suspensions. We found that small diameter SWNTs disperse at higher concentrations in aqueous surfactants and dissolve at higher concentrations in oleum than do large-diameter SWNTs.   These results highlight the importance of SWNT diameter distribution in order to optimize processes dependent on solubility, since solubility and dispersability are key parameters for macroscopic SWNT processing techniques including fiber spinning, and thin-film production, as well as for fundamental research in type selective chemistry, optoelectronics, and nanophotonics. This work was accomplished in collaboration with Rice University and Bordeaux University in France. This collaborative effort resulted in a publication in ACS Nano ("Diameter Dependent Solubility of Single Walled Carbon Nanotubes" DOI: 10.1021/nn100170f). Understanding the interfacial interaction between SWNTs and the local environment and control over the dispersability of the tubes in solutions allows tunability over the energy transfer processes between different SWNT species and their local environment and has helped us further understand the mechanism of SWNT separation.

Saturation of surfactant structure at the SWNT surface

We expanded our current understanding of the interfacial interaction between surfactants and SWNTs to other anionic surfactants. Juan's results have shown that the structure, packing density, and concentration of surfactant around the SWNTs are the major components that affect the optical properties of SWNT suspensions. This work is directly relevant to our efforts in the separation of different SWNT chiralities via ultracentrifugation, and has helped us further understand and corroborate a LANL-developed model for SWNT separation. As a result, we have a manuscript explaining the effects of surfactants on the optical properties of SWNTs and their correlation to packing density in JACS ("*Saturation of Surfactant Structure at the Single-Walled Carbon Nanotubes Surface*", *J. Am. Chem. Soc.* **2010**, 132, 16165). Some of the techniques employed by Juan to obtain

these results include Ultraviolet-Visible-near-Infrared Absorbance and fluorescence spectroscopy.

Raman spectroscopy of different SWNT chiralities

Resonant Raman scattering experiments using excitation wavelengths in the visible, near infrared and ultra violet (UV) regions were performed on enriched fractions of semiconducting and metallic SWNTs. This type of work is the first of its kind in the SWNT community and aims to answer fundamental question of the exciton-phonon coupling of SWNTs and their transition energies. Raman excitation profiles for the G-band in semiconducting samples reveal a strong asymmetry in the intensities of the resonance coupling to incident and scattered photons and can be understood as a consequence of the presence of non-Condon effects. These behaviors hold significant consequence for our ability to understand and manipulate excitation and emission processes, and understanding of observed transition energies, all with important implications for envisioned energy transfer applications. This work is being conducted in collaboration with a group from NIST lead by Ming Zheng, a group in Boston University lead by Prof. Anna Swan and a group in Rice University lead by Prof. Jun Kono. As result, we have submitted a manuscript to Nature showing for the first time the break-down of the Frank-Condon approximation in SWNTs (*"Violation of the Condon Approximation in Semiconducting Carbon Nanotubes,"* submitted to *Nature,* 2010). Moreover, we are preparing several manuscripts that will be submitted to Physical Review Letters and other high impact journals.

4. Formation of SWNT gels

We have identified a new approach to obtain SWNT-silica nanocomposite silica gels, which retain SWNT emission properties upon encapsulation with silica (SiO2). By modifying the surfactant composition adsorbed on the SWNT surface, we were able to control the interactions between the tubes and their local environment and in some cases the tubes were virtually insensitive to changes in the surrounding environment. Subsequent supercritical drying of the Si-SWNT gels resulted in monolithic low-density solution-free composites with significant near-infrared emission intensity. These unique solid platforms of fluorescent SWNTs will enable ultrasensitive optical sensors for bioweapons, gases, and basic research in areas like low temperature excitonic dynamics, exciton-phonon coupling, and energy transfer for photovoltaic applications. We aim to design and engineer the functionality of nano-structured materials, specifically SWNT-aerogel nanocomposites, by controlling inter-tube and matrix interactions. Such control will allow mitigation and/or enhancement of key energy transfer processes needed for targeted energy and sensing applications. This work is in collaboration between MST-7, C-PCS and MPA-CINT. As a result, we have submitted an article to ACS Nano ("*A New Route to Fluorescent SWNT/Silica Nanocomposites: Balancing Fluorescence Intensity and Environmental Sensitivity,*" submitted to ACS Nano, 2010.) and we are working on a manuscript that will be submitted to Nature Materials (*"Fluorescent Surfactant-free Single-Walled Carbon Nanotube Silica Aerogel Nanocomposites"*)

Impact on National Missions

In summary, the goal of Juan's work here at LANL was to conduct fundamental studies of the spectroscopic energy transfer and photophysical processes between SWNTs and their surroundings both in bulk and at the single molecular level for energy harvesting applications. His results are helping us understand the optical and electronic structures of SWNTs and their strong correlation to changes in environmental conditions, and consequently will help us engineer and design new experiments and advanced materials for energy transfer and chemistry at the single tube level.

This project supports the development of advanced functional nanomaterials that support threat reduction, energy security, human health, and basic science missions in DOE and other government agencies.

Publications

Duque, J. G., C. E. Hamilton, G. Gupta, S. A. Crooker, J. J. Crochet, A. Mohite, H. Htoon, K. A. DeFriend Obrey, A. M. Dattelbaum, and S. K. Doorn. Fluorescent single-walled carbon nanotube aerogels in surfactant-free environments. 2011. *ACS Nano.* **5**: 6686.

Duque, J. G., C. G. Densmore, and S. K. Doorn. Saturation of surfactant structure at the single-walled carbon nanotube surface. 2010. *Journal of the American Chemical Society.* **132**: 16165.

Duque, J. G., G. Gupta, L. Cognet, B. Lounis, S. K. Doorn, and A. M. Dattelbaum. A new route to flourescent swnt/silica nanocomposites: balancing fluorescence intensity and environmental sensitivity. 2011. *Journal of Physical Chemistry C.* **115**: 15147.

Duque, J. G., H. Chen, A. B. Swan, E. H. Haroz, J. Kono, X. Tu, M. Zheng, and S. K. Doorn. Revealing new electronic behaviors in the Raman spectra of chirality-enriched carbon nanotube ensembles. 2010. *Physica Status Solidi B.* **247**: 2768.

Duque, J. G., H. Chen, A. K. Swan, A. P. Shreve, S. Kilina, S. Tretiak, X. Tu, M. Zheng, and S. K. Doorn. Violation of the Condon approximation in semiconducting carbon nanotubes. 2011. *ACS Nano.* **5**: 5233.

Duque, J., A. Nicholas G. Parra-Vasquez, N. Behabtu, M. Green, A. Higginbotham, B. Katherine. Price, A. Leonard, H. Schmidt, B. Lounis, J. Tour, S. Doorn, L. Cognet, and M. Pasquali. Diameter-Dependent Solubility of Single-Walled Carbon Nanotubes. 2010. *ACS NANO.* **4** (6): 3063.

Haroz, E. H., J. G. Duque, W. D. Rice, C. G. Densmore, J.

Kono, and S. K. Doorn. Resonant Raman spectroscopy of armchair carbon nanotubes: absence of broad G-minus feature. 2011. *Physical Review B.* **84**: 121403.

Kalugin, N., I. Kalichava, J. Fallt, C. D. Barga, C. Cooper, J. Duque, E. Gonzales, S. Doorn, E. Shaner, and A. Gin. The characterization of non-planar graphene nano-wires with an Œ© shape cross-section. 2010. *Carbon.* **48** (12): 3405.

In situ X-ray Microdiffraction Study of Nanomechanical Behavior

Amit Misra
20090513PRD1

Abstract

Investigations into the role of plasticity in the mechanical behavior of materials have great importance to the field of materials science, especially for nano-materials where submicron and nanoscale devices are built near the size of their microstructural features. The creation of such small components requires a thorough understanding of the mechanical properties of materials at these small length scales. Integration of nanoscale materials into bulk composite materials systems such as nanolayered copper-niobium developed at LANL opens the opportunity to develop bulk materials with ultra-high strengths. A recent DOE, BES workshop report on *Materials under Extreme Environments* has called for structural materials that are tolerant to damage under extreme mechanical stresses. The evolution of damage in nanocomposite materials remains an open question. In this work, x-ray diffraction techniques, including synchrotron white-beam x-rays, are being utilized to evaluate the defect densities in plastically deformed nanolayered composites. Synchrotron x-ray microdiffraction observation of a deformed nanopillar sample can provide insights into the dislocation hardening mechanisms that have not been possible from post mortem studies that show minimal retained defects. Our study provides the fundamental understanding crucial to the design of nanomaterials that are ultra-high strength and possess damage tolerance.

Background and Research Objectives

Studying deformation mechanisms in the nanoscale metallic multilayered composite materials has become especially important with the oncoming development of next generation nuclear energy systems. Nanoscale metallic multilayered composite materials are interesting due to their unusual mechanical properties such as very high flow strength and stable plastic flow to large strains as well as high radiation damage tolerance [1-3]. These unique mechanical properties have been proposed to result from the interface-dominated plasticity mechanisms in nanoscale composite materials. Studying how the dislocation configurations and densities evolve *during* deformation will be crucial in highlighting the yield, work hardening and recovery mechanisms in the nanolayered materials.

However, previous studies [1] on deformation of metallic multilayered composite materials have been largely done *ex situ* and using a macro-scale X-ray diffraction technique that sampled a rather large area of the material. Lacking the sensitivities needed in the deformation of such small length scale materials, these studies did not reveal much contrast in terms of dislocation density and cell structure formation within layers between before and after the deformation. *In situ* study of metallic multilayered thin films utilizing a high brilliance synchrotron source and sub-millimeter X-ray beams was used earlier [4] in the measurements of residual stress prior to deformation and elastic-plastic transition during tensile straining. However, as the deformation was tensile, the experiments were limited to multilayers with individual layer thickness greater than 30 nm, since fracture before yield was observed at lower length scales. Also, as the samples were polycrystalline – thus only monochromatic X-ray beams (single wavelength) could be used – with fine grain sizes, no significant change in the shape of the X-ray diffraction peaks could be observed and therefore, no information on the evolution of dislocation density during deformation was obtained.

In this project, we succeeded in growing nanoscale single crystal metallic multilayered composite materials thereby enabling the use of synchrotron-based Laue microdiffraction technique utilizing a focused, micrometer-scale, white (polychromatic) X-ray beam to characterize compressed micropillar samples. This approach provided us with the quantitative examination of dislocation densities and configurations, and more importantly insights on the defect evolution during the deformation in the nanoscale multilayered composite materials. Furthermore, the information obtained averages over a representative volume in the material, in contrast to *in situ* straining in a transmission electron microscope (TEM)

that is useful in studying the unit processes of dislocation nucleation, multiplication and annihilation.

Scientific Approach and Accomplishments

Using an electron beam evaporation with optimized deposition parameters, we have grown good quality and thermally stable epitaxial/quasi-single crystal Cu/Nb nanoscale multilayered composite materials with individual layer thickness of 20nm as shown in Figure 1. The film exhibits mostly continuous layers of Cu and Nb with minimum pinch-off between layers of Cu and Nb, which was a step forward from nanoscale multilayers deposited at much higher temperatures. Our observations suggest the importance of maintaining epitaxial/quasi-single crystal growth and continuity from one layer to the next in order to grow high quality epitaxial/quasi-single crystal Cu/Nb nanoscale multilayers of desired thicknesses. These quasi-single crystal Cu/Nb nanoscale multilayer samples enable us to follow closely the Laue diffraction spots from the multilayers of Cu and Nb and observe how they evolve during the deformation of the sample and thereby learn about the plasticity mechanisms that are at play in the deformation of our nanoscale multilayered materials.
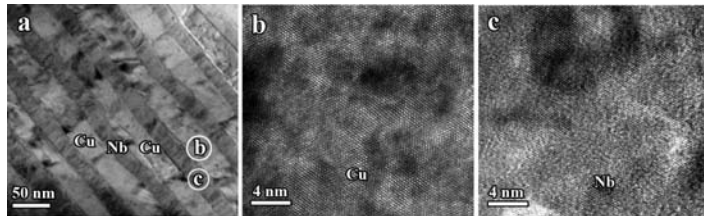
Figure 1. Cross-sectional TEM images of a epitaxial/quasi-single crystal Cu/Nb multilayered film deposited at 200 °C and at deposition rates of 0.5 nm/s for Nb and 5 nm/s for Cu: (a) a low magnification image showing the overall layer continuity of Cu and Nb, with (b) and (c) local high magnification images showing single crystals of Cu and Nb, respectively, in the specified locations as shown in (a).

Initial deformation experiments were performed as follows: nanopillar compression samples from the 20nm Cu/20nm Nb multilayer films on sapphire substrates were made via focused-ion-beam machining technique. These pillars had a nominal diameter of 1000 nm and height of 600 nm. The samples were then taken to Advanced Light Source (ALS) at Berkeley to obtain Laue microdiffraction patterns from individual pillars. Then the samples were taken to Stanford University to perform pillar compression to a plastic strain of approximately 10% and brought back to ALS beamline the same day for measurement of the Laue microdiffraction from the same pillar after deformation. The exact same Laue spot from the Cu layers were measured before and after deformation. The same process was repeated for Nb. The results are shown in Figure 2.
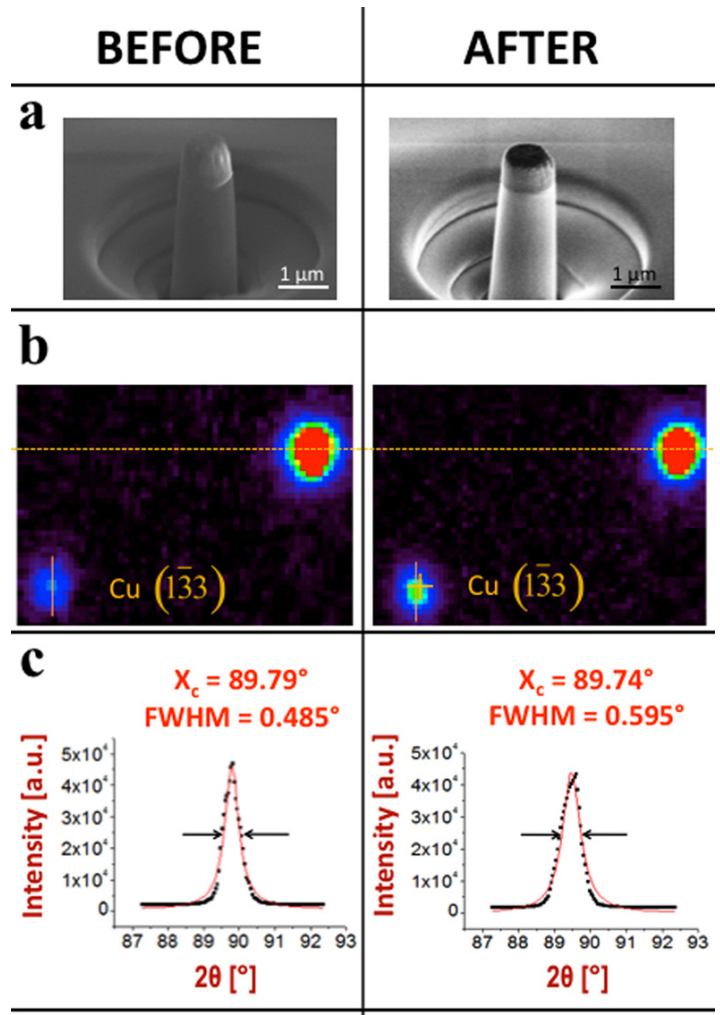
Figure 2. Quantitative data analysis of a selected Laue diffraction peak from the micron-size Cu 20 nm/Nb 20 nm single crystal multilayered materials pillar specimen as shown in (a) between before and after the uniaxial compression; The enlarged images of the Cu diffraction peak before and after the deformation is shown in (b), and the analysis of their width is shown in (c). Xc and FWHM are the location of the maximum intensity (in 2ϑ axis) and the full-width at half-maximum intensity (in 2ϑ angle) respectively .

Analysis of the measured Laue spots in Cu indicates a slightly uniform broadening as evident from Figure 2. The increase in spot size indicated a uniform increase in statistically stored dislocation density from approximately 7 x 10^14 /m^2 to 1.2 x 10^15 /m^2. The deformation in Nb is accommodated both elastically as well as plastically. There appears to be recovery in both crystals and/or interface of Cu and Nb during the deformation. For an annealed single crystal of Cu, the initial dislocation density is on the order of 10^10 /m^2. The dislocation density increase after equivalent plastic strain in annealed Cu would almost be two orders of magnitude. In the nanolayers, the initial dislocation density is very high because of the high interface area per unit volume. The interface contains a cross-grid

of misfit dislocations of an average 2 nm spacing and given the 20 nm spacing of the interfaces this amounts to a very high estimated dislocation density per unit volume in the as-synthesized materials, on the order of 10^17 /m^2. Our results show that the measured initial dislocation density in nanolayered Cu is very high as compared to annealed Cu, although less than the theoretical upper bound estimate. Furthermore, the increase in the dislocation density after deformation is marginal, when compared to the bulk annealed single crystalline metals. This is indeed the significance of this study. It provides the experimental evidence that the interfaces in the nanolayered Cu/Nb are very effective in trapping and annihilating dislocation content during mechanical deformation and this is the origin of many extraordinary mechanical properties as well as radiation damage tolerance of the nanoscale multilayered materials.

Most recently, we further studied the **evolution** of plasticity in the nanoscale Cu/Nb single crystal multilayers *during* successive uniaxial compression experiments using synchrotron-based Laue X-ray microdiffraction at Beamline 12.3.2 in the Advanced Light Source (ALS), Berkeley Lab (Figure 3). Studying how the dislocation configurations and densities evolve *during* deformation is crucial in understanding the yield, work hardening and recovery mechanisms in the nanolayered materials. Using this approach, we first characterized the initial plasticity state in the Cu and Nb nanolayers (as fabricated pillars, before any compression/deformation) at ALS, and then brought it to Stanford Nanomechanical Lab (we collaborated with Prof. Nix's group at Stanford – one of his senior Ph.D. students, Lucas Berla, was helping us with the pillar compressions) to perform the first pillar compression, and then brought it back to ALS again to characterize the plasticity state after the first compression (by observing amongst others X-ray ring width broadening, shifts as well as intensities). We subsequently did these experiments back and forth between ALS Berkeley and Stanford Lab in Bay Area for four successive pillar compressions (total strains = 1%, 2%, 10% and 20%). Through these measurements, we studied the plasticity evolution that occurred in the course of successive compressions on the nanoscale Cu/Nb multilayer pillars and found significant X-ray ring width broadening in both Cu and Nb layers (which indicates storage of statistically stored dislocations) **initially** (up to strains of about 4%) which was then followed by the saturation of the X-ray ring width broadening (up to large strains of 20%) as shown in Figure 4. This indicates that the interfaces in the nanolayered Cu/Nb are very stable and effective in trapping and annihilating dislocation content during mechanical deformation, and explains why the Cu/Nb nanolayers can be deformed to large plastic strains without any onset of plastic instabilities.
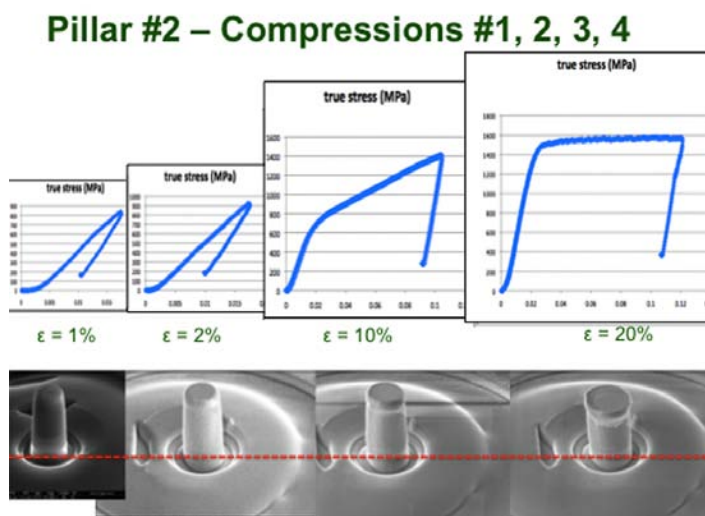
Figure 3. Successive pillar compressions from total strains = 0%, 1%, 2%, 10% and 20%. The stress-true strain curves show an initial elastic stress increase but eventually a stable deformability to large strains (up to 20%), as evident from the SEM images below.
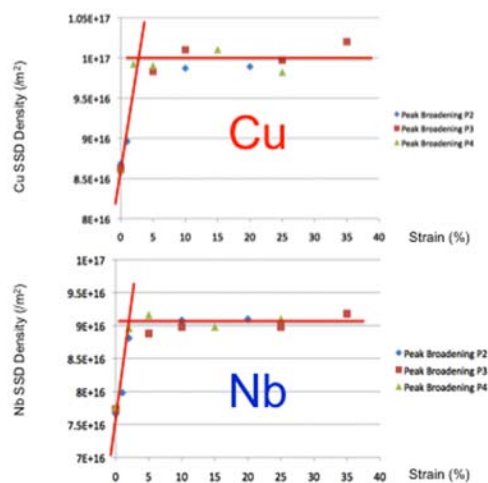
Figure 4. The evolution of dislocation density in the Cu as well as Nb nanolayers during successive pillar compressions with increasing strains up to 35% showing initial increase in dislocation density followed by an eventual saturation of dislocation density for large strains of up to 35%.

This recent work has significance in terms of our understanding of plasticity mechanisms in the nanolayers. It shows the role of the interfaces in these nanolayers in absorbing and annihilating crystal defects such that they will not accumulate to such high level that plastic instability would occur as in the bulk materials. It indeed provided the experimental evidence of the model proposed earlier by our team [1] for deformation mechanisms in nanoscale multilayer materials. The importance and significance of this work has also been recently acknowledged as an in-

vited presentation in the PLASTICITY 2011 International Conference in January this year.

Impact to National Security Missions

This project supports the missions of DOE and other agencies in areas of defense, nuclear energy, and other mission spaces by providing fundamental understanding of damage tolerance of ultra-high strength nanolayered composite materials. In particular, it provides the scientific underpinning of damage tolerant nanolayered composites for materials under extreme environments for a broad range of defense, nuclear energy, and transportation applications.

References

1. Misra, A., J. P. Hirth, and R. G. Hoagland. Length-scale-dependent deformation mechanisms in incoherent. 2005. *Acta Materialia.* **53** (18): 4817.

2. Grimes, R., R. M. Konings, and L. Edwards. Greater tolerance for nuclear materials. 2008. *NATURE MATERIALS.* **7** (9): 683.

3. Demkowicz, M. J., R. G. Hoagland, and J. P. Hirth. Interface structure and radiation damage resistance in Cu-Nb multilayer nanocomposites. 2008. *PHYSICAL REVIEW LETTERS.* **100** (13): 136102.

4. Aydiner, C. C., D. W. Brown, A. Misra, N. A. Mara, Y. -C. Wang, J. J. Wall, and J. Almer. Residual strain and texture in free-standing nanoscale Cu-Nb multilayers. 2007. *JOURNAL OF APPLIED PHYSICS.* **102** (8): 083514.

Publications

Budiman, A. S., S. M. Han, Q. Wei, P. Dickerson, N. Tamura, M. Kunz, and A. Misra. Plasticity in the Nanoscale Cu/Nb Single Crystal Multilayers as Revealed by Synchrotron Laue X-ray Microdiffraction . *Journal of Applied physics.*

Budiman, A. S., and A. Misra. Growth and structural characterization of epitaxial Cu/Nb multilayers. To appear in *Thin Solid Films.*

Novel Fabrication of Metal-Semiconductor Heterostructured Nanowires

Jennifer A. Hollingsworth
20090514PRD1

Abstract

The primary aim of this postdoctoral research project was to develop a novel method for creating nanoscale electrical contacts. We sought to couple two distinct nanowire growth techniques -- Solution-Liquid-Solid (SLS) semiconductor-nanowire (SCNW) growth and template-based metal electrodeposition. By doing so, we aimed to establish a general route to new, hybrid nanoscale structures, including technologically important (but currently impractical) high-density, vertically addressable nanowire assemblies, enhancing LANL's reputation in the growing field of nanomaterials design and integration.

Background and Research Objectives

Semiconductor nanowires (SCNWs) have tremendous potential as building blocks in the assembly of nanoscale devices and nanocircuits for optoelectronics and electronics applications. For these applications, however, electrical contacts must be made to the SCNWs. To date, electron-beam lithography is the common approach employed to define contacts for constructing, for example, single-SCNW devices. The contacts created via this approach are considerably larger than the SCNWs themselves, limiting many advantages of nanoscale systems. To address this problem, fabrication of integrated nanoscale contacts have been proposed, but only a few demonstrated: (1) the localized electroless deposition of gold on the tips of CdSe nanorods, (2) the lithographic patterning of metallic Ni on Si NWs to form NiSi/Si/NiSi metal/SC/metal NWs, and (3) the electrodepositions of Au/CdS/Au NWs. These techniques are limited by choice of metal, inadequate size control, and/or the low quality of the electrodeposited SCs. Therefore, a new and more versatile approach for fabrication of functional nanoscale metal-SCNW interfaces is required to facilitate SCNW device applications. Here, we have sought to realize controlled synthesis of nanoscale semiconductor-metal contacts toward vastly improved integration into optoelectronic and electronic devices by developing a novel approach that couples two solution-phase growth methods. Specifically, we turned to electrochemical synthesis (in porous anodic alumina templates) as the means to fabricate the metallic nanowire component and solution-liquid-solid (SLS) synthesis as the method for growing high-quality, single-crystalline SCNWs. Template-directed synthesis is ideal for metal growth, and it is a facile method for fabricating multi-segmented metal nanowires via sequential reductions of metal ions into a nanopore template. In the SLS method, low-melting metal catalysts [e.g., indium (In), bismuth (Bi), and tin (Sn)] support the growth of high-quality SC-NWs—upon supersaturation of chemical precursors in the molten catalyst, the semiconductor-nanowire nucleates and then grows with high crystallinity. The unique combination of these techniques was predicted to enable fabrication of heterostructured metal-semiconductor nanowires integrated at the nanoscale.

Scientific Approach and Accomplishments

An electrochemical workstation was setup in the first-year for electrochemical synthesis (Setup 1). This setup consisted of a potentiostat and an electrochemical deposition cell that was custom-made to support membrane electrode assemblies. It was used to synthesize Au nanowires of various lengths. The focus in the second year was on fine-tuning this synthesis to control deposition such that the Au filled the porous alumina membranes either to the top or nearly to the top of the membrane. Although we were previously able to deposit Bi solution-liquid-solid (SLS) catalyst into the porous membranes and onto the templated Au nanowires (Year 1), and subsequently to grow CdSe nanowires by the SLS mechanism, the resulting constructs were not ideal. Specifically, we observed two general problems: (1) if the CdSe nanowire grew from a Au nanowire surface, the CdSe component was short and narrower (often significantly) in diameter compared to the Au, rendering the CdSe component more rod-like than wirelike, and (2) longer CdSe nanowires grew only from Bi that had separated from the Au and resided on the top of the alumina membrane surface, with these nanowires being very long and thin and without any structural relationship to the thicker Au component. In the second year, the postdoc emphasized modifications to the fabrication of the membrane-Au-Bi system to (1) improve the SLS CdSe growth and (2) to improve the interaction between the Bi and

the Au and, thereby, the interaction between the CdSe and the Au. Specifically, thin alumina membranes (quality optimized as discussed below) were constructed that allowed the postdoc to fill, or nearly fill, the membranes with Au. Even in this case, electrodeposition of Bi exclusively into the pores proved difficult and insufficiently reproducible. Therefore, as an alternative approach, Bi was deposited by e-beam evaporation. The Bi was observed to partially enter the pores and otherwise reside on the membrane surface. A pre-synthesis anneal was used to melt the Bi and encourages it to enter the pores. Alternatively, polishing was also tried as a means to remove Bi from the top surface of the membrane and ensure its presence exclusively in the pores. The distance between the top of the Au nanowires and the top of the membrane (from 0 nm to 10's of nms) proved to be a key factor in determining our ability to limit CdSe nanowire growth to the Au interface.

Nevertheless, using this approach, the postdoc successfully synthesized Au-CdSe hybrid nanowires comprising approximately equal 500 nm segments and uniform diameter across the interface (Figure 1). This is a significant advance from the short and thin (or the detached long and ultra-thin) CdSe nanowire segments produced in the first year of the project. While chemical yield of these hybrid structures remains low, the approach is clearly on the right track toward realizing the primary goal of the project.
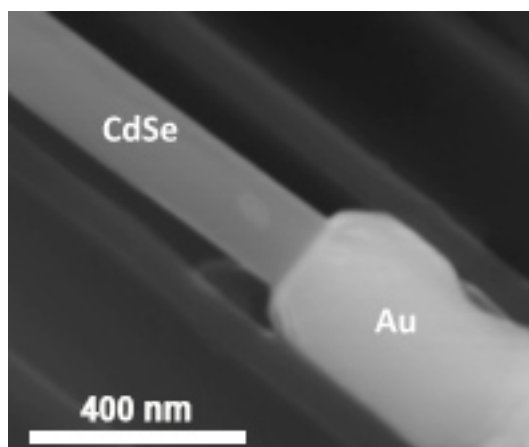
Figure 1. Scanning electron microscopy (SEM) image of Au rod / CdSe semiconductor nanowire hybrid nanostructure.

Utilizing second electrochemical setup (Setup 2), we have continued to fabricate a range of ultra-thin porous anodic alumina membranes. This setup consists of a DC voltage power supply and an anodization cell that is designed to house an anode and a cathode for anodization of metal (e.g., aluminum and titanium). This setup gives us the ability to prepare in-house Al_2O_3 and TiO_2 porous-membranes, possessing controlled thicknesses and pore diameters. In Year 2, we optimized the method and established clear materials parameter requirements for successful synthesis of uniform (laterally and vertically) porous membranes (Figure 2). Significantly, we found that high quality metal films are critical for the successful preparation of the ideal

porous membrane. We determined that to prepare the alumina membranes, controlled growth of thick (500-2000 nm) aluminum films was required. Our experience with Al films prepared during the duration of this project (using existing LANL and SNL equipment), demonstrated that conventional deposition systems (not specifically designed for thick and large-area metals deposition) resulted in non-optimal variations in thickness and grain size. These variations rendered the alumina membranes prepared from the aluminum films irregular in pore size and uncontrolled in terms of the percent of pores that access the underlying Au layer. Both of these factors inhibited our ability to grow well-defined arrays of metal nanowires and to fully optimize our approach.
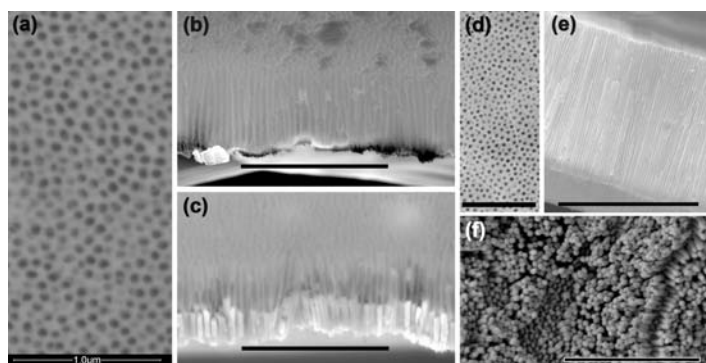
Figure 2. Optimized porous anodic alumina templates: (a)-(b) Ultrathin membranes on solid substrate support. (c) Au rods electrochemically grown within an ultrathin membrane. (d)-(e) Thick, free-standing small-diameter membranes. (f) Au nanowire vertical array formed in a freestanding membrane.

Given the challenges to our initial approach described above, we sought an alternative approach to introduce Bi catalyst to Au NWs or rods. Doing so, we were able to achieve an important breakthrough in our ability to grow SCNW-nanometal contacts. Namely, we found that we were able to modify a literature report for synthesizing heterobranched-SCNWs [1] to fabricate semiconductor-metal NW heterostructures. Specifically, we used a polymer (PEI: polyethyleneimine) to adhere Bi nanoparticles to Au nanorods, which were synthesized electrochemically but subsequently liberated from their templates. In the case of large-diameter (>200 nm) Au rods, the Au rod/Bi nanoparticle assemblies were easy to separate from any unattached Bi nanoparticles, while in the case of thinner Au rods, standard separation methods (centrifugation / sedimentation) did not adequately remove free Bi nanoparticles. Therefore, we (successfully) incorporated a magnetic segment (Ni) into the thinner Au rods via sequential (Au then Ni) electrochemical deposition to enable magnetic separation of the bound Bi from any free Bi nanoparticles. The Au/Bi constructs were then suspended in a reaction solution for subsequent SLS-based CdSe NW growth. Adhesion of Bi nanoparticles to the Au rods and growth of high-quality semiconductor NWs from their surfaces were

confirmed by SEM and TEM characterization (Figure 3). Using this general approach, we have also demonstrated versatility in choice of metal backbone (Ag, Cu) and an ability to control the density of semiconductor wires on the surface of the metal.
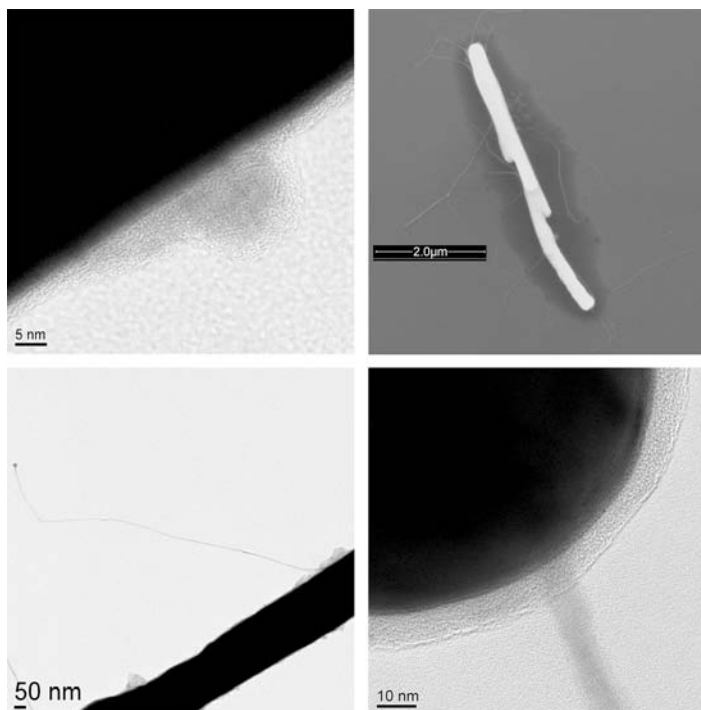
Figure 3. (top-left) Transmission electron microscopy (TEM) image of a Bi nanoparticle adhered to a Au rod and surrounded by PEI polymer. (top-right) SEM image of a Au rod with numerous CdSe nanowires growing from it. (bottom-left) TEM image of a Au rod with a CdSe nanowire growing from it. A Bi nanoparticle is evident at the end of the nanowire. (bottom-right) Higher resolution TEM image of a CdSe nanowire extending from a Au rod. The nanowire growth starts at the Au interface and projects through the PEI polymer layer.

Current status: The novel composite semiconductor-metal nanoscale structures remain to be tested for electronic and optical properties; nevertheless, the structural characterization results are compelling, and these along with the synthetic methods development are being written up for submission to *Chemistry of Materials*. The postdoc has also been instrumental this year in establishing our new flow-SLS synthesis capability (Laocharoensuk et al., in preparation). In addition, she contributed her nanomaterials characterization skills to studies of quantum dot-based light-emitting diodes (Bhola et al., submitted to *Nano Letters*).

Impact on National Missions

This project benefitted the DOE missions in Energy Security and Threat Reduction by providing critical supporting technologies that will enable the further miniaturization of functional optoelectronic devices with enhanced efficiencies. For example, the materials fabrication strategies developed will be applicable to photovoltaics and sensor technologies.

References

1. Dong, A., R. Tang, and W. E. Buhro. Solution-based growth and structural characterization of homo- and heterobranched semiconductor nanowires. 2007. *Journal of the American Chemical Society.* **129** (40): 12254.

2. Laocharoensuk, R., N. Smith, K. Palaniappan, J. K. Baldwin, and J. A. Hollingsworth. Integration and development of solution-phase techniques for fabrication of novel heterostructured nanowires. (Boston, Nov. 29-Dec. 3 2010).

3. Laocharoensuk, R., N. Smith, J. K. Baldwin, A. Gin, and J. A. Hollingsworth. Versatile Solution-Phase Approach for Fabrication of Metal-Semiconductor Heterostructured Nanowires. (San Francisco, 5-9 April 2010).

Publications

Laocharoensuk, R., N. Smith, J. K. Baldwin, A. Gin, and J. A. Hollingsworth. Versatile Solution-Phase Approach for Fabrication of Metal-Semiconductor Heterostructured Nanowires. Presented at *Materials Research Society Spring Meeting 2010.* (San Francisco, 5-9 April 2010).

Laocharoensuk, R., N. Smith, K. Palaniappan, J. K. Baldwin, and J. A. Hollingsworth. Integration and development of solution-phase techniques for fabrication of novel heterostructured nanowires. Presented at *Materials Research Society Fall Meeting 2010.* (Boston, Nov. 29-Dec. 3 2010).

Nanogenerators Driven by Both Magnetic and Mechanical Waves

Quanxi Jia
20090519PRD2

Abstract

Magnetoelectric materials, which simultaneously exhibit ferroelectricity and ferromagnetism, have attracted much attention recently due to their both scientific interest and potential technological applications. The large ME coupling at room temperature of $BiFeO_3$ (BFO) makes it the model system in the research community. We have used polymer assisted deposition (PAD) to grow high quality epitaxial $BiFeO_3$ films on different substrates. The main advantage of the PAD approach is that metal ions can bind to polymer to form very stable and homogenous precursor solutions. This, in return, leads to the growth of very high quality epitaxial metal oxide films. We show that the lattice parameters of BFO thin films could be controlled by the lattice mismatch between the BFO film and the substrates such as $LaAlO_3$, $SrTiO_3$, and $BaTiO_3$.

Background and Research Objectives

Wireless devices have found wide applications in real-time biomedical monitoring and operation, but their practical applications are limited by the short lifetime of power sources. For long-term applications, these devices should be self-powered or powered by the energy from non-contact sources such as mechanical or magnetic waves. Nowadays, the advances in nanostructured materials and technologies have dramatically reduced the size of the devices. It is indispensable that nanogenerators are developed so that they can be used to power these devices. Recently, piezoelectric nanogenerators, which could transform vibrational or mechanical energy directly to electricity to power nano-devices, have been reported [1]. However, when the wireless devices are embedded into a substance, the body may absorb and decrease the applied vibration energy. Our objective was to explore different electronic films and ceramic-like materials to develop the nanogenerators that can be driven by both magnetic and mechanical waves. Compared with mechanical sources, a magnetic source is easier to control since it can be adjusted by both the frequency and intensity of the magnetic field. Therefore, the nanogenerators can potentially function as an efficient power source that will enable the wide applications of nano wireless devices.

Scientific Approach and Accomplishment

Multiferroic magnetoelectric (ME) materials, which simultaneously exhibit ferroelectricity and ferromagnetism, have recently been extensively investigated due to their both scientific interest and technological promise for novel multifunctionalities [2]. For example, high performance devices such as magnetic sensors, microwave phase shifters, and electrical and/or magnetic tunable devices can be readily fabricated based on this class of materials. As the objective of this project is to develop innovative electronic devices using such materials in thin film form, we target to grow high quality ME thin film materials using the techniques available at Los Alamos National Laboratory.

The ME effect was first observed in single phase materials nearly 50 years ago. The largest value of ME voltage coefficient for a single phase material has been detected in Cr_2O_3 crystals, where the ME voltage coefficient is around 20mV/cm-Oe. The ME effect in single phase material, although scientifically interesting, has always shown small values of ME voltage coefficient. From a technological point of view, the appearance of such an effect at low temperatures also limits its applications. In other words, the weak ME effects at very low temperature cannot meet the requirements of practical applications. Recently, $BiFeO_3$ (BFO) thin film has attracted a lot of attention due to its large multiferroic ME coupling at room temperature [3]. Most of these films have been fabricated by physical vapor deposition such as pulsed laser deposition. Although pulsed laser deposition can deposit epitaxial BFO thin films, the deposition setup itself is complex. Chemical solution technique, on the other hand, does not need a complicated setup. However, existing methods such as the sol-gel process often yield polycrystalline BFO thin films, which show degraded properties. In the following, we highlight our efforts to achieve high performance BFO films by polymer assistant deposition (PAD), a cost effective and patented process developed at Los Alamos National Laboratory.

Polymer assisted deposition offers the advantages to grow high quality epitaxial metal oxide films [4]. To form epitaxial BFO thin films, we first prepared Bi and Fe polymeric liquid precursors. The Fe precursor solution was prepared by mixing two individual aqueous solutions of Bi and Fe bound to polymers [polyethyleneimine (PEI)]. The mixed precursor solution (Bi^{3+} : Fe^{3+}=1:1) was then spin-coated onto (001)-oriented $LaAlO_3$ (LAO), $SrTiO_3$ (STO) and $BaTiO_3$ (BTO) substrates at 5000 rpm for 25s. The films were then annealed at 700 °C in pure oxygen for 2h. We use single crystal substrates, such as LAO, STO and BTO, since they are structurally and chemically comparable to BFO.

Epitaxial BFO thin films were grown on STO, LAO, and BTO substrates. Figure 1 compares θ-2θ scan patterns around (002) BFO on different substrates examined by high-resolution XRD. Here (002) substrates have been calibrated to standard (002) LAO, BTO and STO respectively. It is clearly demonstrate that lattice parameter of BFO thin film could be controlled by lattice mismatch of BFO and substrates. For BFO thin film grown on LAO, (002) BFO peak is at 45.77°, close to unstrained BFO single crystal. While for BFO thin film deposited on STO, (002) BFO peak is at 44.82°, shifted to lower angle direction. On the contrary, for BFO thin film deposited on BTO, (002) BFO peak shifts to higher angle direction.
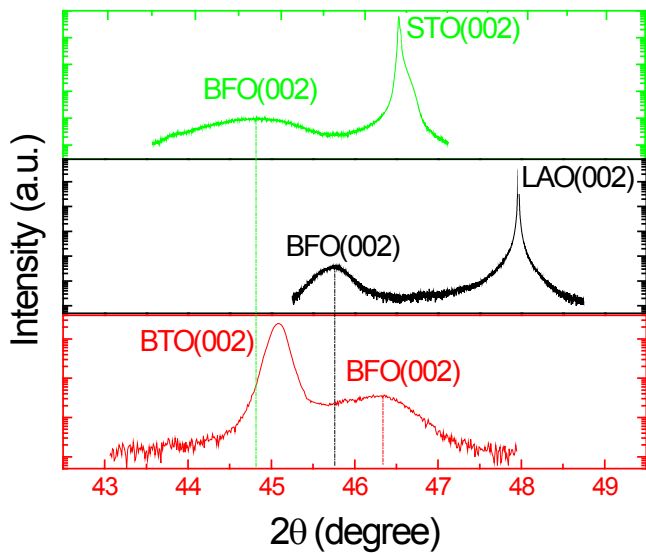
Figure 1. X-ray diffraction normal scans of BFO thin films on LAO, STO and BTO substrates.

Figure 2 shows a high resolution cross-sectional transmission electron microscopy (HRTEM) image of BFO thin film on LAO substrates. As can be seen from the image, the interface between the thin film and the substrate is quite sharp. The intermixing, if there is any at all, should be minimal. In addition, misfit dislocations are clearly observed. The distance between the adjacent dislocations is around 91 Å, which fits well with the lattice mismatch between the BFO thin film and the LAO substrate. In conjunction with

high resolution XRD result, it is clear that BFO thin film grown on LAO substrate is a fully relaxed.
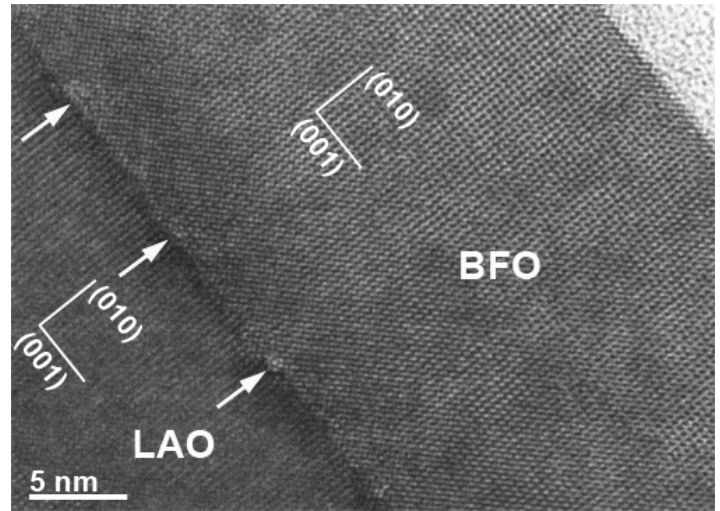
Figure 2. High resolution TEM image of BFO film on LAO substrate.

Impact on National Missions

This project supports the mission of DOE Office of Science for fundamental understanding of materials. LANL's thrusts in functional materials, nanotechnology, and sensors directly benefit from this project. Microsensors for a range of national security problems, including monitoring weapons inventories, could ultimately benefit from this work.

References

1. Wang, Z. L., and J. H. Song. Piezoelectric nanogenerators based on zinc oxide nanowire arrays. 2006. *Science.* **312**: 242.

2. Nan, C. W., M. I. Bichurin, S. Dong, D. Viehland, and G. Srinivasan. Multiferroic magnetoelectric composites: historical perspective, status, and future directions. 2008. *J. Appl. Phys..* **103**: 031101.

3. Chu, Y., L. W. Martin, M. B. Holcomb, and R. Ramesh. Controlling magnetism with multiferroics. 2007. *Mater. Today.* **10**: 16.

4. Jia, Q. X., T. M. McCleskey, A. K. Burrell, Y. Lin, G. Collis, H. Wang, A. D. Q. Li, and S. R. Foltyn. Polymer-assisted deposition of metal-oxide films. 2004. *Nat. Mater..* **3**: 529.

Publications

Harrington, S. A., J. Zhai, S. Denev, V. Gopalan, H. Wang, Z. Bi, S. A. T. Redfern, S. H. Baek, C. W. Bark, C. B. Eom, Q. X. Jia, M. E. Vickers, and J. L. MacManus-Driscoll. Green micron thick ferroelectric films with high Curie temperature using a vertical nano-scaffold. To appear in *Nat. Nanotechnology.*

Xiong, J., V. Matias, H. Wang, J. Zhai, B. Maiorov, D. Trug-

man, B. W. Tao, Y. R. Li, and Q. X. Jia. Much Simplified IBAD-TiN Template for High Performance Coated Conductors. 2010. *J. Appl. Phys..* **108**: 083903.

Zhai, J., Y. Y. Zhang, G. F. Zou, L. Yan, J. Xiong, P. Shi, and Q. X. Jia. Epitaxial multiferroic BiFeO3 thin film grown by polymer assistant deposition. Invited presentation at *MS&T'10.* (Houston, 17-21 Oct. 2010).

Zhai, J., Y. Y. Zhang, G. F. Zou, L. Yan, M. J. Zuo, J. Xiong, and Q. X. Jia. Multiferroic epitaxial BiFeO3 thin film grown by polymer assistant deposition. Presented at *MRS Spring Meeting.* (San Francisco, CA, 5-9 April 2010).

Zhai, J., Y. Y. Zhang, G. Zou, J. Xiong, L. Yan, M. Zhuo, P. Shi, and Q. X. Jia. Strain controlled epitaxial multiferroic BaFeO3 thin film deposited by polymer assisted deposition. Presented at *241st ACS National Meeting & Exposition.* (Anaheim, CA, 2-31 March, 2011).

Zhang, Y. Y., C. J. Sheehan, J. Zhai, G. F. Zou, H. M. Luo, J. Xiong, Y. T. Zhu, and Q. X. Jia. Polymer-embedded Carbon Nanotube Ribbons for Stretchable Conductors. 2010. *Adv. Mater..* **22**: 3027.

Zou, G., H. M. Luo, Y. Y. Zhang, J. Xiong, Q. Wei, M. Zhuo, J. Zhai, H. Wang, D. Williams, N. Li, E. Bauer, X. H. Zhang, T. McCleskey, Y. R. Li, and A. K. Burrell. A Chemical Solution Approach for Superconducting and Hard Epitaxial NbC Film. 2010. *ChemComm.* **46**: 7837.

Hybrid Semiconductor-metal Nanostructures for Amplification of Surface Plasmons

Jeffrey M. Pietryga
20090523PRD2

Abstract

Metal nanostructures allow versatile manipulation of light via morphology controlled resonances associated with collective electron oscillations known as surface plasmons (SPs), which are of interest for a range of emerging applications in transmitting, storing, and processing information. Practically, however, the utility of "plasmonic circuits" is restricted by strong damping of plasmons that limits the propagation length of SP polaritons to a few microns. As a possible solution to this, we sought to develop a unique hybrid material in which interactions between metal nanoparticles and nearby semiconductor nanocrystal quantum dots (QDs) produces SP amplification. This effort focused on discrete, structurally durable but dispersible hybrid nanosuperstructures comprising single nanoparticles and a layer of ~10s to 100s of QDs separated by a dielectric spacer of controlled thickness. In order to fully realize the desired effect, we developed a new synthesis method not only capable of creating the desired material, but flexible enough to be applied to combine metal and semiconductor nanoparticles of arbitrary shape, sizes and composition at a finely tunable separation distance. Spectroscopic studies have revealed some very interesting consequences of the interparticle interactions within these superstructures, including enhanced absorption and interparticle energy-transfer in the QDs that render them of interest to a lager range of applications.

Background and Research Objectives

Near the beginning of the 20th century, Einstein discovered the "photoelectric effect," in which light hitting a metal surface can cause electrons to move, and even to be ejected from the metal if the energy is high enough. Light interacts with nano-sized metal particles in a somewhat different way, by causing all the free flowing conductive electrons within the particle to slosh back and forth collectively. These motions are called "surface plasmons," and they are responsible for the intense colors of solutions of metal nanoparticles (such as in some types of stained glass). Because of their intensity, these light-absorbing transitions have tremendous potential for use in photonic circuitry (the next generation of

ultra-fast computers based on moving photons instead of electrons), as well as in enhancing the spectroscopy of nearby molecules (such as for detection of single molecules of chemical threat agents by Surface-enhanced Raman Spectroscopy). However, these plasmon excitations are hard to extract from the nanoparticles, because they are quickly dampened within a very short distance from the surface. Thus, practical application of these effects has been limited. A possible solution to this problem is the development of methods for plasmon amplification. A recent theoretical paper [1] discussed the possibility of plasmon amplification using direct stimulated emission of plasmons from a proximal system of resonant dipole emitters, such as semiconductor quantum dots (QDs). Our goal was to create a novel, processible nanomaterial that would exploit this new physical process, which is similar to that applied to make the intense, coherent light of lasers, to amplify plasmons by many orders of magnitude. In a nutshell, we set out to create discrete, dispersible hybrid superstructures in which a metal nanoparticle was surrounded with fluorescent semiconductor QDs of size and composition specifically chosen to establish the desired resonance. The 10s-100s of QDs in such a structure, when excited by a light source, would pump their energy directly into the plasmon vibrations of the metal nanoparticle, creating a non-linear increase in the spatial extent and gain lifetime of surface plasmons. Ultimately, our superstructures could finally allow plasmon-based lasers, circuitry and single-molecule chemical agent detectors.

Scientific Approach and Accomplishments

By combining earlier work from our Team with his unique abilities in metal nanoparticle synthesis, Dr. Bishnu Khanal was able to make impressive progress over the 13-month duration of his postdoctoral term. The plan was to apply methods published by a previous postdoc [2] to a much broader range of Au and Au@Ag core/shell nanoparticles and QD formulations. During his graduate studies at Rice University under Prof. Eugene Zubarev, Dr. Khanal developed a library of metal nanospheres, nanowires and nanoplatelets of exquisite quality and shape regularity that produced SP resonances

tunable over a broad energy range across the visible and well into the infrared (Figure 1A). His first task was to demonstrate the controllable coating of these particles with a dielectric shell of SiO$_2$. Via a modification and expansion of the methods in Ref. 2, he established a reliable protocol for growth of a controlled shell thickness on every type of particle within a relatively short time, despite considerable differences in surface reactivity.
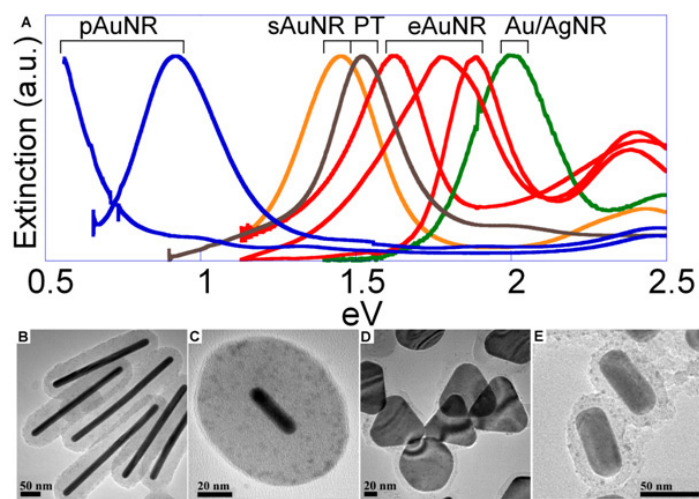
Figure 1. (A) Extinction spectra of various metal nanoparticles. From lower to higher energy: Pentahedral Au nanorods (pAuNR), single crystalline Au nanorods (sAuNR), Au nanoplatelets (PT), etched Au nanorods (eAuNR), and silver coated Au nanorods (Au/AgNR). (B-E) TEM images of various superstructures: (B) pAuNR|SiO$_2$|CdSe/ZnS, (C) sAuNR|SiO$_2$|PbS, (D) Platelet|SiO$_2$|CdSe/ZnS, (E) Au/Ag NR /Ag|SiO$_2$|CdSe/ZnS)

The next task was to attach QDs of several different compositions in a manner that allowed control over loading level (i.e. ratio of QDs to metal nanoparticle) and did not damage the surfaces of the QDs in a way that would alter their optical properties. In conjunction with fellow Director's Postdoc Anshu Pandey (who performed the spectroscopic characterization of these hybrid materials), Bishnu was able to develop methods for attaching QDs spanning the desired energy range, from the visible (CdSe/ZnS core/shell and CdS/CdSe/CdS/ZnS core/multishell QDs), through the near-infrared (CdTe/CdS and CuInS$_2$) and into the midinfrared (PbS and PbSe/CdSe) while retaining good surface quality, as evidenced by retention of QD fluorescence. A selection of these hybrid materials can be seen in Figure 1B-E.

Advanced spectroscopic studies of these materials are still ongoing, but some preliminary data proves the strong coupling between metal and semiconductor nanoparticles. In a superstructure based on Au nanorods with a longitudinal SP near 800 nm and QDs that fluoresce at ~530 nm, the QDs show strongly enhanced two-photon absorption. In this non-linear process, two photons with energies well below the band gap of the material can be absorbed simul-

taneously to excite an electron across the band gap. Ordinarily this is very weak process that requires really high intensities of excitation light to observe. However, using an excitation source in resonance with the Au nanorod SP, the attached QDs show two-photon absorption cross sections (i.e. probabilities) enhanced by over an order of magnitude, producing the highest cross sections ever observed (Figure 2). Currently, we are submitting the synthesis and characterization of these novel materials to ACS Nano, a well-recognized journal in the field of nanomaterial chemistry, physics and technological application. In addition, two other manuscripts and a patent application, all based on the new hybrid materials, are in preparation.
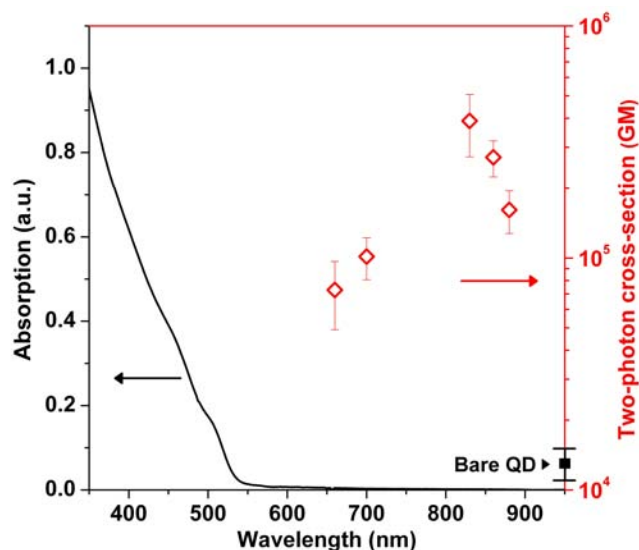
Figure 2. Two-photon absorption enhancement in a hybrid superstructure. CdS/CdSe/CdS/ZnS core/multishell QDs show no linear absorption (black trace) at 800 nm, and exhibit a modest two-photon cross section of ~10,000 Geoppert-Meyers (GM, black dot on right axis). However, when coupled to Au nanorods, two-photon absorption is increased by up to an order of magnitude as the nanorod SP is tuned closer to 800 nm (red diamonds: horizontal position corresponds to longitudinal SP position of the Au nanorods for a given superstructure sample).

Impact on National Missions

This project and the ongoing studies it engendered support the DOE mission in Threat Reduction, by enhancing our understanding of plasmon amplification, which could ultimately lead to a new class of chemical threat agent sensor with orders of magnitude higher sensitivity. This level of sensitivity may also contribute to tracking trace materials in the weapons program. We also discovered that these materials may have a significant impact on solar energy capture technologies because of the enhanced absorption and energy-transfer they display. This could be of tremendous value to LANL efforts in renewable, carbon-neutral energy sources. Follow-on work specifically in the direction of applying these nanomaterials toward efficient solar en-

References

1. Bergman, D. J., and M. I. Stockman. Surface plasmon amplification by stimulated emission of radiation:. 2003. *Physical Review Letters.* **90** (2): 027402/1.

2. Liu, N., B. Prall, and V. Klimov. Hybrid gold/silica/nano-crystal-quantum-dot superstructures: Synthesis and analysis of semiconductor-metal interactions. 2006. *JOURNAL OF THE AMERICAN CHEMICAL SOCIETY.* **128** (48): 15362.

Publications

Khanal, B. P., A. Pandey, L. Li, W. K. Bae, V. I. Klimov, and J. M. Pietryga. Generalized synthesis of hybrid metal-semiconductor nanostructures tunable from the visible to the infrared. *ACS Nano.*

New Generation of Fluorescent Probes for In-Vivo Imaging

Jennifer Martinez
20090534PRD3

Abstract

Fluorescent nanoclusters are collections of a few atoms of silver or gold (2-31 atoms; <1 nm diameter). These materials have intriguing fluorescence properties, if only their size and structure can be controlled. We have developed methods to synthesize these materials in DNA. Further we have begun to characterize their fluorescence and physical structure.

Background and Research Objectives

Selection of suitable probes for in-vivo imaging has been a challenge for decades. Noble metal nanoclusters (NCs) (made of 4-30 atoms, ≤ 1nm) have strong fluorescence and are very small. Thus, NCs may well be good candidates for biological imaging, if only they can be produced in biological materials. Recently, Martinez and colleagues developed strategies to synthesize water-soluble nanoparticle-free nanoclusters. We have created nanoclusters of defined size/fluorescence, using biological molecules (DNA, small molecules, and proteins) as templates to guide their formation. Our goals were to create: a multifunctional molecule (i.e. in DNA) that can template a nanocluster and contains a recognition unit to bind proteins; a nanocluster beacon that fluoresces on binding of DNA and does not require separation from a mixture; and templated gold nanowires and hollow triangles (for plasmonic sensing).

Scientific Approach and Accomplishments

DNA is an attractive tool for biothreat detection because of:

- Complimentary base pairing
- Rapid enzymatic means of replication
- Inexpense

 In medicine, the molecular specificity of DNA is often used to accurately confirm the presence of disease(s). The simultaneous measurement of multiple DNAs requires many different fluorophores. We are using DNA to not only template nanomaterials (NCs), but to use them for multiplex analysis of DNA or proteins. Cytosine (a DNA base) is well known for its ability to bind Ag+ ions.

Taking advantage of Ag+-base binding, other groups have developed strategies to synthesize Ag-nanoclusters. While Dickson and coworkers produced individual silver nanoclusters with distinct emissions, most of the clusters were produced under different buffer and salt conditions, limiting their practical application. Conversely, while Fygenson produced clusters under one reaction condition, the resultant clusters had broad excitation and emission profiles. Because most multiplex assays are performed under one buffer condition there is still a need for a palette of nanoclusters that each emit at different wavelengths, under the same conditions. We synthesized and photophysically characterized Ag-nanoclusters, which were templated on DNA under one reaction condition, with distinct, and narrow, excitation and emission profiles, and which were tuned to common laser lines. These bright nanoclusters were used for protein detection.

While advancements in nanocluster synthesis have been made, the use of metallic nanoclusters for biological- or chemical-sensing is still in its infancy, largely resulting from difficulty in bioconjugation of these intriguing fluorophores. Whereas one can chemically conjugate a fluorophore to a biomolecule (i.e., recognition ligand), a simpler method is to use the recognition ligand to directly template the fluorophore. We developed an intrinsically fluorescent recognition ligand, based on a DNA aptamer-templated NC for the: one pot, single step, purification free, and specific and sensitive detection of protein. This material combines the strong fluorescence of an NC with the specificity of a DNA aptamer for its target protein, to develop a new strategy for detection of specific proteins. We have also used DNA-templated nanoclusters for DNA detection.

NCs are an emerging set of fluorophores that are smaller than semiconductor quantum dots and can have better photostability and brightness than commonly used organic dyes. We found that the red fluorescence of NCs can be enhanced 500-fold when placed in proximity to guanine-rich DNA sequences. We designed a DNA detection probe (NanoCluster Beacon, NCB) that "lights up" upon target binding. These materials can easily reach

high (>100) signal-to-background ratios upon target binding. We demonstrated NCB detection of an influenza target with a S/B ratio of 175, a factor of 5 better than a conventional molecular beacon probe. Since the observed fluorescence enhancement is caused by intrinsic nucleobases, our detection technique is simple, inexpensive, and compatible with commercial DNA synthesizers. This work was submitted for a patent and is recipient of a 2011 R&D100 Award.

Finally, we have utilized surfactants to control the growth and structures of Au wires, triangular plates and hallow triangles. Au fibers with micron-scale lengths were successfully prepared *via* a solution-phase synthetic method. By controlling the composition of the solution we formed rod-shaped micelles, which directed the one-dimensional growth of Au wires. Additionally, hollow metallic nano and microsystems (i.e., cages, frames, rings, and shells) represent an area of intense research interest, because of their unique morphologies and applications ranging from diagnostics to therapeutics. By use of an Au^{n+} precursor and commercially available neutral polymeric surfactant, we have successfully generated Au rings through a single-step, one-pot synthesis, for future use in electronic devices and as oriented catalysts.

Impact on National Missions

This project is largely focused on biological threat reduction and health science as applicable for NIH and DoD/DHS agencies. Control at the nanoscale, as exercised in this project, builds underlying capability for renewable energy missions.

References

1. Sharma, J., H. Yeh, H. Yoo, J. Werner, and J. Martinez. Silver nanocluster aptamers: in situ generation of intrinsically fluorescent recognition ligands for protein detection. 2011. *CHEMICAL COMMUNICATIONS.* **47** (8): 2294.

Publications

Bao, Y., H. Yeh, C. Zhong, S. Ivanov, J. Sharma, M. Neidig, D. Vu, A. Shreve, R. Brian. Dyer, J. Werner, and J. Martinez. Formation and stabilization of fluorescent gold nanoclusters using small molecules. 2010. *Journal of Physical Chemistry C.* **114** (38): 15879.

Neidig, M., J. Sharma, H. Yeh, J. Martinez, S. Conradson, and A. Shreve. Ag K-Edge EXAFS Analysis of DNA-Templated Fluorescent Silver Nanoclusters: Insight into the Structural Origins of Emission Tuning by DNA Sequence Variations. 2011. *JOURNAL OF THE AMERICAN CHEMICAL SOCIETY.* **133** (31): 11837.

Sharma, J., H. Yeh, H. Yoo, J. Werner, and J. Martinez. A complementary palette of fluorescent silver nanoclusters. 2010. *CHEMICAL COMMUNICATIONS.* **46** (19): 3280.

Sharma, J., H. Yeh, H. Yoo, J. Werner, and J. Martinez. Silver nanocluster aptamers: in situ generation of intrinsically fluorescent recognition ligands for protein detection. 2011. *CHEMICAL COMMUNICATIONS.* **47** (8): 2294.

Yeh, H., J. Sharma, H. Yoo, J. Martinez, and J. Werner. Photophysical characterization of fluorescent metal nanoclusters synthesized using oligonucleotides, proteins and small molecule ligands. 2010. In *Reporters, Markers, Dyes, Nanoparticles, and Molecular Probes for Biomedical Applications II ; 20100125 - 20100127 ; San Francisco, CA, United States.* Vol. 7576, p. var.pagings.

Yeh, H., J. Sharma, H. Yoo, J. Martinez, and J. Werner. Photophysical characterization of fluorescent metal nanoclusters synthesized using oligonucleotides, proteins and small molecule ligands. 2010. In *Conference on Reporters, Markers, Dyes, Nanoparticles, and Molecular Probes for Biomedical Applications II ; 20100125 - 20100127 ; San Francisco, CA.* Vol. 7576, p. 75760N.

Yeh, H., J. Sharma, J. Han, J. Martinez, and J. Werner. A DNA-Silver Nanocluster Probe That Fluoresces upon Hybridization. 2010. *NANO LETTERS.* **10** (8): 3106.

Yoo, H., J. Sharma, H. Yeh, and J. Martinez. Solution-phase synthesis of Au fibers using rod-shaped micelles as shape directing agents. 2010. *CHEMICAL COMMUNICATIONS.* **46** (36): 6813.

Yoo, H., J. Sharma, J. K. Kim, A. P. Shreve, and J. S. Martinez. Tailored microcrystal growth: a facile solution-phase synthesis of gold rings. To appear in *Advanced Materials.*

Study of Chemical and Electronic Structure in Metal-Containing Nanoparticles and Nanoclusters

Andrew P. Shreve
20090539PRD4

Abstract

This document provides the final report for a Laboratory Directed Research and Development (LDRD) postdoctoral research project. Metal-containing nanoclusters consist of only a few metal atoms. These clusters have unique properties compared to larger scale materials. For example, nanoclusters comprised of gold or silver atoms are often very fluorescent, in striking contrast to bulk gold or silver metals. Thus, clusters can be used as fluorescent labels for biological imaging and sensing. Until now, very little has been known currently about the atomic-level geometry and structure of metal nanoclusters, nor how their atomic-level structure correlates to their optical properties. In the absence of structural knowledge, it is hard to design new types of clusters with desired optical properties. This research project has developed and used new methods for the study of metal clusters. Most notably, the use of x-ray absorption methods has been shown to provide important structural information about DNA-templated silver nanoclusters.

Background and Research Objectives

Many applications in the imaging or detection of biological molecules require that a fluorescent label be used. The ideal fluorescent label would be smaller than typical biological macromolecules such as proteins. It would also emit light brightly, be stable under illumination, be biologically inert, and have an emission wavelength that could be tuned through synthetic procedures. No such ideal label currently exists. However, many scientists at Los Alamos and elsewhere are exploring the study of small clusters of noble metal atoms as possible fluorescent labels.

Metal nanoclusters (<2 nm) have been studied in the past, and have interesting catalytic properties and may also respond to light in unusual ways.[1-6] More recently, unusually bright and wavelength tunable fluorescence emission has been observed from clusters of silver or gold that are prepared using ligands such as amines or carboxylates as templates.[7,8] In these cases, in addition to controlling the fluorescence properties of the cluster, the template also serves to stabilize the cluster against further growth in size.

Templates that have been used to produce fluorescent clusters include synthetic and biological polymers, as well as small molecules.[8,9] In this project, we have studied two types of clusters. One type is gold nanoclusters templated by small molecules, so-called Good's buffers. Here, we have used two-dimensional fluorescence excitation-emission maps to study whether the clusters are homogeneous, that is, whether all clusters in a solution behave identically. The other type is silver nanoclusters templated by DNA oligomers. In this case, the luminescence wavelength is controlled by the DNA sequence, making these very useful materials for biological sensing and imaging. However, nothing is known about the atomic-level structure of these clusters, so we have applied extended x-ray absorption fine structure (EXAFS) methods to verify that silver clusters are formed and to study the silver-silver and silver-DNA chemical bonding.

Scientific Approach and Accomplishments

The small molecule MES (2-(N-morpholino)ethanesulfonic acid) was used to template the growth of fluorescent gold nanoclusters.[10] In a typical procedure, nanoclusters were synthesized by mixing a gold chloride aqueous solution (0.2 wt%, 1mL) with MES (100 mM, pH 7, 5 mL) at room temperature, followed by incubated shaking for three days (37 ˚C, 250 rpm). This procedure generates solutions with gold nanoparticle precipitates, but with fluorescent supernatant. In the case of the MES template, the maximum absorption/emission wavelengths are 420 nm/485 nm, and a variety of experiments indicated that the fluorescent species is a small gold nanocluster (< 1nm in size) stabilized by MES molecules. The fluorescent lifetime of the MES-templated nanocluster was found to be 3.7 nsec. In order to explore whether sample heterogeneity influences the emission properties of the clusters, we measured a two-dimensional excitation-emission map (Figure 1). This analysis provides an unambiguous determination that a single species is generating the emission. In essence, one finds that the same emission spectrum is obtained for all excitation wavelengths that lead to fluorescence. Hence, there is

no evidence of multiple fluorescent species being present.
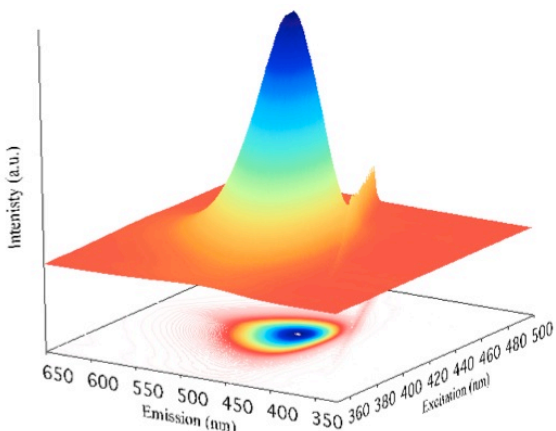
Figure 1. Fluorescence excitation-emission plot of a MES-templated gold nanocluster.

Another class of fluorescent clusters with very important applications are silver clusters templated by DNA. In this case, prior work shows that specific DNA sequences can generate clusters with different emission wavelengths.[9] In addition, various experimental protocols can lead to cases in which the emission of these clusters can be used for either protein or nucleic acid sensing.[9,11] However, further work in developing these important clusters has been limited by a lack of understanding of how their structure correlates with their light-emitting properties. In order to begin to address this important question, we have performed an extended x-ray absorption fine structure (EXAFS) study on DNA-templated silver clusters.[12]

The EXAFS technique relies on analysis of small features that appear in the x-ray absorption spectrum of, in this case, silver atoms. Basically, these small features arise from the interaction of the silver atom and its near neighbors. Thus, analysis of these features provides information on the chemical identity of near neighbors and on the geometry of surrounding atoms. An example of EXAFS data and analysis for three different DNA-templated silver clusters is shown in Figure 2.

This study provides several important results:

There is unambiguous evidence that silver clusters are present. Specifically, the EXAFS analysis indicates that silver-silver bonds exist, with bond lengths ranging from 2.74 to 2.77 Å depending on the DNA sequence. This bond length is somewhat smaller than the 2.89 Å length for silver metal. Such shortening of the bond length is also consistent with the formation of small clusters of silver.

The size of the silver clusters has been determined to be less than 30 atoms. This determination is based on an analysis of the amplitude of peaks corresponding to silver-silver interactions relative to the same peaks measured for bulk silver metal. This peak amplitude is related to the number of nearest neighbor silver atoms, a number that varies with overall cluster size. Thus, one is able to determine that cluster sizes vary from approximately 8 to 14 atoms for the smallest clusters studied (Ag2 and Ag3) to approximately 20 to 30 atoms for the largest cluster (Ag1).
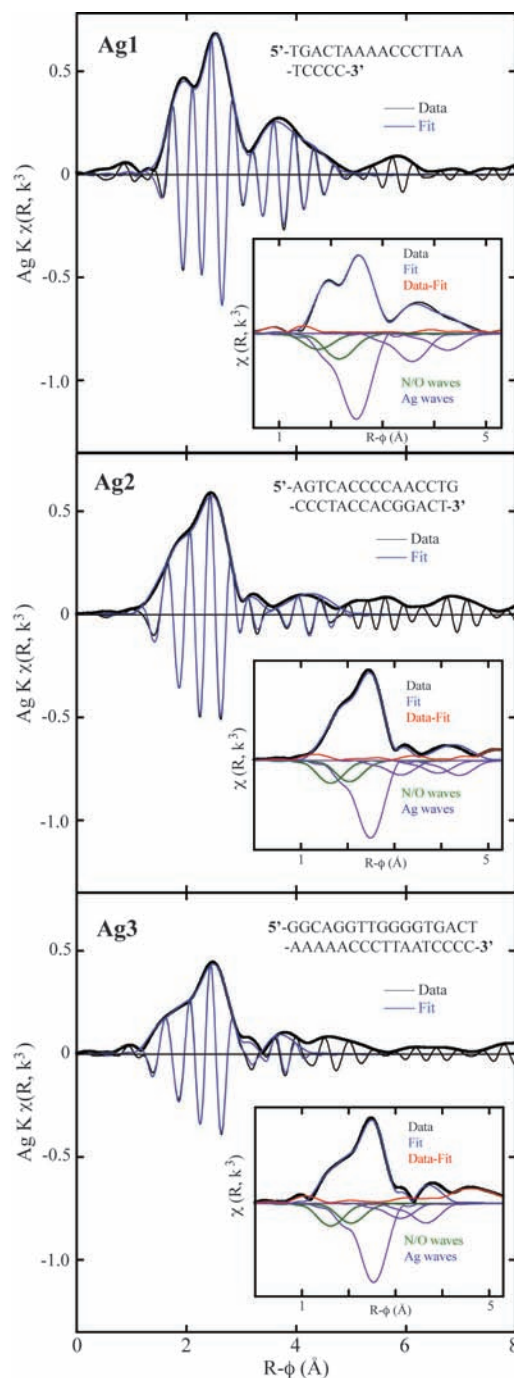
Figure 2. EXAFS data of DNA-templated silver nanoclusters. The modulus and real part of the transform of both the data and fit are shown using the same vertical scale. The insets show the spectra of the moduli of the data, fit, difference between the data and fit and the individual contributions to the fit (inverted for clarity).

There is significant interaction between silver atoms and DNA. This interaction is apparent from features in the EXAFS data that correspond to silver atoms being in close proximity to nitrogen or oxygen atoms. On average, approximately one nitrogen (or oxygen) atom is bound to each silver atom at bond lengths ranging from 2.27 Å to 2.12 Å for the different clusters studied.

There is no simple, direct correlation between the structural properties (e.g., cluster size or bonding distances) and the fluorescence emission wavelengths. This result is consistent with a model that fluorescence emission wavelengths are determined by a complex, cooperative interaction that involves both silver-DNA interaction and cluster size.

Impact on National Missions

Taken together, the results reported here demonstrate the use of advanced characterization tools to improve understanding of the structure and properties of an important class of materials. Fluorescent metal nanoclusters have the potential to improve biological sensing and imaging techniques. Such techniques are at the heart of a large number of biological detection and analysis approaches in areas ranging from biological energy production, disease diagnostics, pathogen identification, and forensics. By improving our understanding of this important class of materials, the research reported here could thus have long-term positive impact in all of these areas of national needs.

References

1. Lee, D., R. Donkers, G. Wang, A. Harper, and R. Murray. Electrochemistry and Optical Absorbance and Luminescence of Molecule-like Au₃₈ Nanoparticles. 2004. *Journal of the American Chemical Society.* **126** (19): 6193.

2. Zhu, M., C. Aikens, F. Hollander, G. Schatz, and R. Jin. Correlating the crystal structure of A thiol-protected Au-25 cluster and optical properties. 2008. *JOURNAL OF THE AMERICAN CHEMICAL SOCIETY.* **130** (18): 5883.

3. Bigioni, T. P., R. L. Whetten, and O. Dag. Near-infrared luminescence from small gold nanocrystals. 2000. *Journal of Physical Chemistry B.* **104** (30): 6983.

4. Varnavski, O., R. G. Ispasoiu, L. Balogh, D. Tomalia, and T. Goodson. Ultrafast time-resolved photoluminescence from novel. 2001. *Journal of Chemical Physics.* **114** (5): 1962.

5. Jadzinsky, P. D., G. Calero, C. J. Ackerson, D. A. Bushnell, and R. D. Kornberg. Structure of a thiol monolayer-protected gold nanoparticle at 1.1 Å resolution. 2007. *Science.* **318** (5849): 430.

6. Herzing, A. A., C. J. Kiely, A. F. Carley, P. Landon, and G. J. Hutchings. Identification of active gold nanoclusters on iron oxide supports for CO oxidation. 2008. *Science.* **321** (5894): 1331.

7. Zheng, J., J. T. Petty, and R. M. Dickson. High quantum yield blue emission from water-soluble Au-8 nanodots. 2003. *JOURNAL OF THE AMERICAN CHEMICAL SOCIETY.* **125** (26): 7780.

8. Bao, Yuping, Chang Zhong, D. M. Vu, J. P. Temirov, R. B. Dyer, and J. S. Martinez. Nanoparticle-free synthesis of fluorescent gold nanoclusters at physiological temperature. 2007. *Journal of Physical Chemistry C.* **111** (33): 12194.

9. Sharma, J., H. Yeh, H. Yoo, J. Werner, and J. Martinez. Silver nanocluster aptamers: in situ generation of intrinsically fluorescent recognition ligands for protein detection. 2011. *CHEMICAL COMMUNICATIONS.* **47** (8): 2294.

10. Bao, Y., H. Yeh, C. Zhong, S. Ivanov, J. Sharma, M. Neidig, D. Vu, A. Shreve, R. Brian. Dyer, J. Werner, and J. Martinez. Formation and stabilization of fluorescent gold nanoclusters using small molecules. 2010. *Journal of Physical Chemistry C.* **114** (38): 15879.

11. Yeh, H., J. Sharma, J. Han, J. Martinez, and J. Werner. A DNA-silver nanocluster probe that fluoresces upon hybridization. 2010. *Nano Letters.* **10** (8): 3106.

12. Neidig, M. L., J. Sharma, H. C. Yeh, J. S. Martinez, S. D. Conradson, and A. P. Shreve. Ag K-Edge EXAFS of DNA-templated fluorescent silver nanoclusters: Insight into the structural 0rigins of emission tuning by DNA sequence variations. 2011. *Journal of the American Chemical Society.* **133**: 11837.

Publications

Bao, Y., H. Yeh, C. Zhong, S. Ivanov, J. Sharma, M. Neidig, D. Vu, A. Shreve, R. Brian. Dyer, J. Werner, and J. Martinez. Formation and Stabilization of Fluorescent Gold Nanoclusters Using Small Molecules. 2010. *JOURNAL OF PHYSICAL CHEMISTRY C.* **114** (38): 15879.

Neidig, M. L., J. Sharma, H. C. Yeh, J. S. Martinez, S. D. Conradson, and A. P. Shreve. Ag K-Edge EXAFS of DNA-templated fluorescent silver nanoclusters: Insight into the structural origins of emission tuning by DNA wequence variations. 2011. *Journal of the American Chemical Society.* **133**: 11837.

Dopant Distribution and Interface Studies of Si and Ge Nanowire Heterostructures

Samuel T. Picraux
20090540PRD4

Abstract

We have learned how to create silicon-germanium nanowire heterostructures with much more precise control of composition in the vertical direction and greatly reduced kinking of the nanowires. In this new process we use *in situ* alloying of the gold growth catalyst with gallium through the introduction of trimethylgallium vapor during growth. The gallium reduces the silicon and germanium solubility in the liquid catalyst, enabling much less diffuse interfaces and much better control of the compositional abruptness of heterostructured nanowire interfaces grown via the vapor-liquid-solid growth process. Our novel approach also dramatically reduces structural kinking by stabilizing the liquid catalyst and reducing the growth rate without any sidewall contamination by gold catalyst diffusion. This work provides motivation to further explore alternative catalyst metals and metal alloys with Au in order to tailor interfacial abruptness by manipulating the semiconductor and dopant solubility in the catalyst. This same growth approach of using a low-solubility liquid can also be applied to control the junction width between electrically doped axial segments to create more abrupt junctions, as for example in a p-n junction nanowire for PV applications.

Background and Research Objectives

Both radial and axial p-n junction semiconductor nanowire heterostructures hold promise for high performance solar cells as well for low power remote sensing and high performance electronics and photonics. The formation of straight, compositionally abrupt heterointerfaces is important for the application of nanowires for energy, electronic, and photonic applications. Until now, this has been hard to achieve. Because of the importance of nanowires as a new approach to photovoltaic electricity, our work to overcome this problem is especially timely. The structure/composition and the electronic transport properties of individual nanowire heterostructures are basic enabling elements for optimizing device performance. Heterostructured nanowires hold the greatest promise for their eventual application but relatively little control or understanding of the electrical doping and composition control during synthesis

of the heterostructured interfaces and the resulting electrical properties has been possible. This has held back nanowire heterostructure applications in photovoltaic devices, tunnel field effect transistors, and thermoelectric devices. For group IV semiconductors such as Si and Ge, abrupt heterojunction formation has been a challenge due to the relatively high solute solubilities in the commonly used liquid Au catalyst during vapor-liquid-solid growth. The objectives of this project are to modify the growth catalyst through alloying in order to give increased control of the synthesis process during vapor-liquid-solid growth of nanowires. In this way the abruptness of interfaces and the perfection of the resulting nanowire growth might be greatly improved.

Scientific Approach and Accomplishments

In this project we have demonstrated significant progress in both understanding how to control compositional abruptness of heterostructured nanowire interfaces grown via the vapor-liquid-solid (VLS) growth process, as well as how our novel approach also dramatically reduces structural kinking as well stabilize the catalyst and eliminate sidewall contamination by catalyst diffusion. Specifically we have demonstrated significantly increased abruptness in the compositional transition between Si and Ge in Si/Ge nanowire axial heterostructures by in situ trimethylgallium alloying of the liquid Au catalyst with Ga. At the same time, Si/Ge heterostructure growth from a Ga-Au alloy allows for a significant decrease in structural kinks which form in a high percentage of nanowires grown from pure Au. This basic understanding is equally relevant to the formation of abrupt electrical dopant profiles during nanowire growth.

Controlling Nanowire Axial Heterojunction Abruptness and Kinking

We have taken a new approach of using a liquid Ga-Au alloy catalyst to create a sharper axial heterojunction in Ge-Si, relative to that obtained using pure Au. This novel alloy lowers the solubility of Si and Ge in the liquid, which sharpens the interface, while at the same time reducing the growth rate, thus promoting a significant

reduction in kinking. For example, considering a ~65nm diameter nanowire, for the transition from Ge to Si, the solubility of Ge is significantly decreased and the interface sharpness increases by about 4-times from a width of 45 nm to 11 nm for growth at 380 °C using a $Au_{0.67}Ga_{0.33}$ alloy, as compared to growth from pure Au. At the same time, the growth rate decreases from 170 nm/min for kinked Si segments grown from a pure Au catalyst, to 15 nm/min with a 10X increase in unkinked Ge/Si heterostructure growth from approximately 85% kinking to <10% (Figure 1). Based on the only moderately lower growth rates compared to Au-catalyzed growth rates, we determine that nanowire growth from the Ga-Au alloy proceeds via the vapor-liquid-solid growth process making it practical for heterostructure device growth. Detailed analyses demonstrate 100% Ge to Si compositional change with good morphology control.
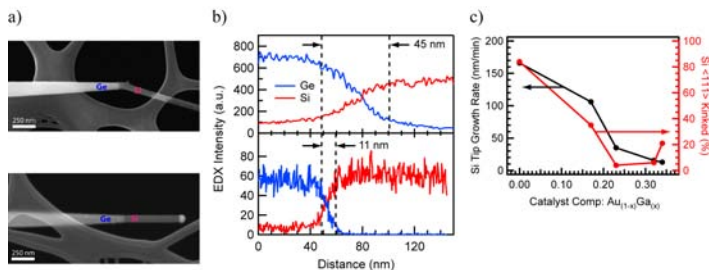
Figure 1. A high percentage of Si-Ge axial heterstructured nanowires grown from a pure 60 nm Au catalyst nanoparticle exhibit a kinked morphology (a-top panel) after the junction and have an average interfacial width of 45+/- 3 nm (b-top panel) as measured by EDAX analysis. A high percentage of nanowires grown from a Au0.67Ga0.33 catalyst alloy are straight, i.e. do not kink (a-bottom panel) and have a sharpened interface of 11+/- 4 nm (b-bottom panel). c) Correlation between nanowire growth rate and the frequency of kinking away from the initial <111> growth direction. This correlation indicates that kinking is a kinetically-driven process.

While the underlying mechanisms for kinking which drives a nanowire to change growth direction are not well understood, it is known that this effect is sensitive to the kinetics of growth (Figure 1c) and becomes a significant issue when changing the growth precursors or temperature. Most recently, we have shown that the decrease in growth rate with increasing Ga concentration in the AuGa alloy catalyst is a result of a reduction in the catalytic activity at the alloy catalyst surface.

Dopant Mapping Using Atom Probe Tomography

As a follow on to this project we plan to use the technique of atom probe tomography (APT) to quantitatively map the 3-D dopant distribution of individual Si pn-junction nanowires as well as Si-Ge pn-heterojunction nanowires. Currently, APT is the only tool to directly map the dopant distribution within a nanostructured material. The 3-D

dopant mapping will allow us to probe the limits of abrupt electrical dopant profiles within nanowires grown from the VLS growth method and further allow us to correlate with the electrostatic potential maps obtained from e-beam holography, thus providing a means to quantify the number of active and inactive dopant impurities. APT will be performed through a Center for Integrated Nanotechnologies (CINT) User Agreement with Los Alamos National Laboratory using the APT managed at the EMSL user facility at PNNL. The APT experiments will require that individual nanowires be grown atop microfabricated Si micropost substrates. The specialized micropost growth substrates were developed using the cleanroom facilities at the Core facility of CINT

Impact on National Missions

The new capability developed in this project for creating sharp interfaces along the length of Si and Ge semiconducting nanowires and eliminating kinking of the nanowires is anticipated to enable a revolutionary new approach in nanomaterials synthesis by the vapor-liquid-solid technique. The approach developed here through catalyst alloying greatly broadens capabilities for the fabrication of nanowire devices and arrays. Future uses of this approach are anticipated for such applications as low cost, high efficiency solar cells and high performance electronic devices. The knowledge learned is also anticipated to lead to new approaches for high efficiency sensing.

Publications

Jung, Y., A. Vacic, D. E. Perea, S. T. Picraux, and M. Reed. Minority carrier lifetimes and surface effects in VLS-grown axial pn junction silicon nanowires. 2011. *Advanced Materials.* **23**: 4306.

Mohite, A. D., D. E. Perea, S. Singh, S. A. Dayeh, I. H. Campbell, and S. T. Picraux. Highly efficient charge separation and collection across In situ doped axial VLS-grown Si nanowire p-n junctions. *Nano Letters.*

Perea, D. E., J. Yoo, N. Li, A. Misra, and S. T. Picraux. Altering catalytic activity in situ to suppress kinking in VLS-grown semiconductor nanowire heterostructures. *Nano Letters.*

Perea, D. E., N. Li, A. Misra, and S. T. Picraux. Controlling heterojunction abruptness in VLS-grown semiconductor nanowires via catalyst alloying. 2011. *Nano Letters.* **11**: 4306.

Perea, D. E., and S. T. Picraux. Controlling the transition region width of VLS-grown axial nanowire heterostructures by catalyst alloying. Presented at *Materials Research Society.* (Boston, 29-30 Nov. 2010).

Perea, D. E., and S. T. Picraux. Control of interface sharpness in nanowire axial heterostructures by catalyst alloying. Presented at *Los Alamos Postdoc Career Fair.*

(Los Alamos, 1 Sept. 2010).

Perea, D. E., and S. T. Picraux. Controlling heterointerface abruptness in Vapor-Liquid-Solid grown semiconductor nanowires via a Gold/Gallium alloy catalyst; . Presented at *Postdoc Research Day.* (Los Alamos, 16 June 2010).

Perea, D. E., and S. T. Picraux. Control of interface sharpness in nanowire axial heterostructures by catalyst alloying. Presented at *Center for Integrated Nanotechnologies User Conference.* (Albuquerque, 10-11 Aug. 2010).

Picraux, S. T., S. A. Dayeh, P. Manandhar, D. E. Perea, and S. G. Choi. Silicon and germanium nanowires: growth, properties, and integration. 2010. *Journal of Materials.* **62** (4): 43.

Control of Shape, Dispersion and Size of Disorder in High-Temperature Superconducting Films and its Effect on in-Field Superconducting Properties

Leonardo Civale
20090542PRD4

Abstract

The large scale introduction of high temperature super-conductors (HTS) into the electric grid would result in significant energy savings through higher efficiency, as well as enhanced power quality and reliability. The key requirement for superconducting wires is a high critical current density, J_c, which is controlled by the presence of nanoscale defects in the crystalline structure that act as "pinning centers", precluding vortex motion. The most promising HTS wires are the *coated conductors* (CCs), based on $REBa_2Cu_3O_7$ films (RE=Y or a rare earth). The main goal of this work was the exploration of vortex pinning and dynamics in REBCO films and CCs with micro-structural disorder designed and artificially engineered to produce the desired performance. A secondary topic was the study of vortex pinning and dynamics in iron-arsenide superconductors, with the purpose of learning by comparing and contrasting the behavior of both types of materials.

Background and Research Objectives

The large scale introduction of HTS into the electric grid and other power applications would result in significant energy savings through higher efficiency, as well as enhanced power quality and reliability. US industries currently produce long lengths of "second generation" HTS wires based on films of $REBa_2Cu_3O_7$ (REBCO, where RE=Y, a rare earth, or combinations of them), known as *coated conductors* (CCs). The use of CCs requires the capability to carry large electric currents without dissipation. To that end it is necessary to increase J_c, which is controlled by the presence of nanoscale disorder or "defects" in the superconductor that act as "pinning centers", precluding the motion of the superconducting vortices that would produce dissipation. The effectiveness of the pinning centers depends in a complex way on their size, shape, composition, and distribution. The overall purpose of this project is to artificially create nanoscale defects into films of $REBa_2Cu_3O_7$ to improve their pinning properties, particularly in the presence of large magnetic fields. We have large experience in this topic, and we have previously obtained HTS with record high J_c [1-3]. Those previous

studies demonstrate [3] that the best results are obtained through a combination of different types of defects, so in this project we are focusing on developing methods to engineer "mixtures" of defects in a controllable fashion and to investigate their pinning properties.

Scientific Approach and Accomplishments

The research performed by Dr. Miura at LANL can be divided in two topics. The main focus was the exploration of vortex pinning and dynamics in REBCO films and CCs with microstructural disorder (vortex pinning landscape) designed and artificially engineered to produce the desired performance. In particular, Dr. Miura focused on the understanding and optimization of landscapes where pinning is mainly produced by randomly distributed nanoparticles (NPs). Most previous studies of pinning enhancement in CCs (by us at STC-LANL and by others) had concentrated on the effects of nanorods (columnar defects) [1,3]. The realization that random nanoparticles can produce very strong pinning in CCs is relatively recent, [4,5] and was supported by earlier work by Dr. Miura [6].

The second topic was the study of vortex pinning and dynamics in iron-arsenide superconductors, particularly single crystals of $Ca_{1-x}Na_xFe_2As_2$. The purpose was to learn by comparing and contrasting the behavior of both types of materials, an approach that we are pursuing in our team as part of our BES-funded SISGR project. The complex vortex physics in the oxide HTS, which contrasts with the simpler phenomenology in conventional low T_c superconductors, arises from the strong influence of thermal fluctuations, which is a consequence of the small superconducting coherence length (x) and the large crystalline anisotropy (g). The iron-based superconductors provided a chance to "bridge the gap" by studying vortex matter in a family of materials with intermediate T_c and broad ranges of g, where the small x in some of them results in large fluctuation effects.

To perform this research Dr. Miura used several characterization techniques, including (1) electrical resistivity in DC and pulsed fields at the NHMFL to determine the upper critical field H_{c2} (where superconductivity disappears) and the irreversibility field H_{irr} (where vortex matter goes

through a solid-liquid transition and J_c vanishes), (2) J_c measurements by transport using a home-made system, and (3) magnetization in a commercial SQUID magnetometer to explore J_c and its decay with time due to thermal fluctuations (flux creep).

REBCO

Dr. Miura studied the effect of various combinations of disorder on the dependence of J_c on temperature (T) and magnetic field strength (H) and orientation (Q, the angle between H and the crystallographic c axis), on $H_{irr}(T,Q)$ up to 60 T, and on the flux creep rate (S). He used metal organic deposition (MOD) to grow films on the metal substrates used in CCs. He grew the films in Japan before his post-doctoral appointment and brought them to LANL. MOD is particularly well suited to produce NPs of second phases, which are added to the precursor material. The analysis of the pinning in these films is simplified by the fact that they do not contain nanorods, in contrast to the YBCO films with BaZrO$_3$ additions grown by pulsed laser deposition (PLD) that we had studied previously. Dr. Miura developed the capability to control independently the size and density of the NPs. To change the size of the NPs he used three different additive materials, namely BaMO$_3$ (BMO) with M=Zr, Nb, Sn. He independently varied the density of NPs by changing the second phase content (wt %), as shown in Figure 1a.
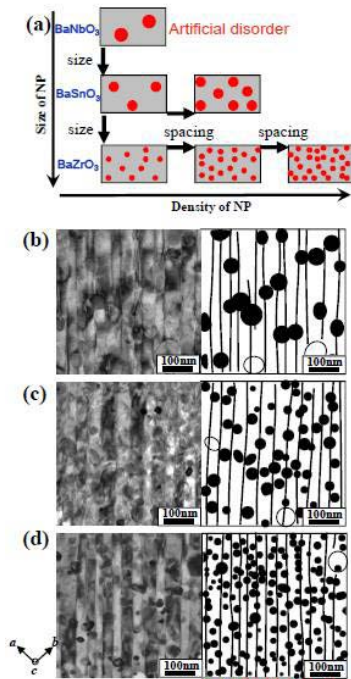
Figure 1. We insert nanoparticles into our superconducting films, allowing them to carry larger currents without dissipation. We can control both the size and density (concentration) of the nanoparticles by changing the chemical composition and the amount of the additions respectively, as sketched in (a). The electron micrographs in (b) (c) and (d) show some examples of the nanoparticle-loaded films that we have tested.

In a first study [7] we explored $J_c(T,H,Q)$ and $H_{irr}(T,Q)$ in a Y$_{0.77}$Gd$_{0.23}$Ba$_2$Cu$_3$O$_y$ film with random nanoparticles created by the addition of 1wt% content of BZO (YGdBCO+BZO). To single out the effects of the NPs we extensively compared and contrasted this system with a MOD YBa$_2$Cu$_3$O$_y$ (YBCO) film. We performed additional comparisons against two other systems without BZO NPs, MOD Y$_{0.77}$Gd$_{0.23}$Ba$_2$Cu$_3$O$_y$ (YGdBCO) and previously studied PLD YBCO films [8]. To characterize the pinning landscape Dr. Miura analyzed high-magnification planar- and cross-section TEM images of the films. He found that both the MOD YGdBCO+BZO and MOD YBCO films possessed a similar low density (~10^{20}/m^3) of large RE$_2$Cu$_2$O$_5$ precipitates with sizes (diameters) ranging from ~75 to 100 nm with an average size of ~86 nm, as well as a large density of twin boundaries (TB), which act as correlated (planar) disorder. In addition, the YGdBCO+BZO film contained a large density (3.7x10^{21}/m^3) of BZO nanoparticles, with sizes varying from ~18 to ~28 nm and average ~23 nm. Examples of RE$_2$Cu$_2$O$_5$ and BZO NPs can be seen in Figure 1.

We found that the BZO NPs improve pinning at all temperatures, but that the beneficial effects are much stronger at high temperatures ($T > 40$ K). In particular, J_c at low T is larger in the MOD YGdBCO+BZO than in the YBCO film, but they both show the same power-law dependence $J_c \propto H^{-}$ with similar exponent a~0.60 to 0.70, as well as similar S. Moreover, $J_c(Q)$ in the YGdBCO+BZO film shows a peak for **H||c** that, although less pronounced than in the YBCO film, points to the presence of correlated pinning produced by the TBs. These observations indicate that at low T the BZO NPs contribute to the pinning landscape but do not drastically modify it. On the contrary, at higher T the fractional increase in J_c due to the BZO NPs is much larger and J_c becomes almost isotropic, as expected for pinning dominated by random disorder. We also observed a decrease in S, which is beneficial for applications.

We obtained additional information by exploring $J_c(T)$. In type II superconductors, pinning results from spatial variations of the order parameter that are associated with disorder in T_c or with spatial variations in the charge carrier mean free path l near lattice defects, called dT_c" and dl" pinning, respectively. The dT_c" pinning occurs in the case of non-superconducting defects larger than x, such as NPs, while dl" pinning is observed in the case of point-like defects. In both cases $J_c(T/T_c) \propto [1-(T/T_c)^2]^m$, and for single vortex pinning m is ~ 1.2 for dT_c pinning and ~2.5 for dl pinning. As shown in Figure 2, for $T < 40$ K the MOD YGdBCO+BZO and MOD YBCO films have similar temperature dependencies, while for $T > 40$ K clear differences arise. Above 40 K the YBCO film shows m = 1.53±0.05, slightly larger than the theoretical value for dT_c pinning, and a rapid decay of J_c for $T > 83$ K. In the YGdBCO+BZO film, m = 1.24±0.04 coincides with the dT_c pinning expectation, and no rapid decrease in $J_c(T)$ occurs. We concluded that pinning in the YBCO film is consistent with the presence of the large RE$_2$Cu$_2$O$_5$ precipitates. However, as those

particles are sparse, large portions of the vortex cores are only weakly pinned by random point defects, resulting in a larger m and the rapid decrease in J_c at high T. In contrast, the large density of BZO NPs fully dominates the pinning landscape in the YGdBCO+BZO film, producing a very large J_c and retaining the strong pinning up to very close to T_c.
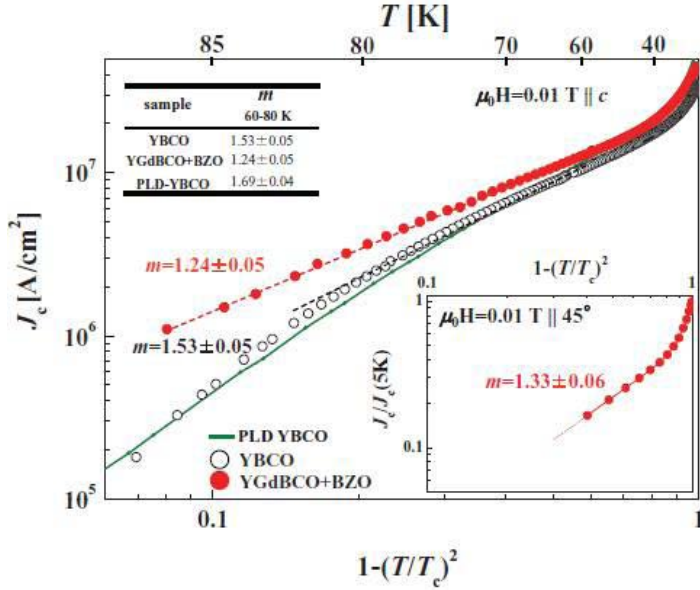
Figure 2. The maximum current that our superconducting films can carry without dissipation (the critical current density) depends on the temperature. The data for three films are shown for comparison. From the differences in the temperature dependence (particularly visible in the lower left portion of the figure) we distinguish the different vortex pinning mechanisms that operate in the various films.

Finally we investigated the H_{irr}, a key factor that determines the upper boundary of nonzero $J_c(H)$, by performing measurements in both pulsed and DC fields. We found that the addition of the BZO nanoparticles enhances H_{irr} at all temperatures, for $H||c$ and $H||45°$, the effect being more pronounced for $H||45°$, but have no measurable effect for $H||ab$. We analyzed these results in terms of changes in the exponent n when H_{irr} is plotted in the functional form $H_{irr}(T/T_c) \mu [1-(T/T_c)^2]^n$. More details can be found in the published work. [7]

The study described above highlighted the importance of both the density and size of the NPs. Although it is well known from general principles that to produce strong pinning a defect should have a size similar to the vortex core (~2x), the exact conditions for pinning optimization are not fully understood. To explore this problem Dr. Miura expanded his study to include particles of different sizes. As examples, Figures 1(b), (c) and (d) show planar-view TEM images of the (Y,Gd)BCO+2wt%BaNbO$_3$ (2BNO), 2wt%BaSnO$_3$ (2BSO), and 2wt%BaZrO$_3$ (2BZO), respectively, with average diameter and density of the NPs of 83 nm - 0.25x10^{21}/m^3; 43 nm - 2.1x10^{21}/m^3; and 23 nm - 7.1x10^{21}/m^3 respectively. In addition, all films have ~10^{20}/

m^3 of large RE$_2$Cu$_2$O$_5$ precipitates. The vortex core size for these films (at low T) is ~ 5 nm, and for $H = 1$ T the inter-vortex distance is ~50 nm, which is similar to the distance between BZO nanoparticles (~60 nm) or TBs (~34 nm). This indicates that the RE$_2$Cu$_2$O$_5$ precipitates are too big and too sparse to produce strong pinning, but in contrast the combination of TBs and high density of BMO NPs can work as an effective pinning landscape even in high H.

We investigated the effect of these mixtures of correlated and uncorrelated defects on $J_c(H, Q)$. Figures 3(a) and (b) show $J_c(1T,Q)$ at 77 K and 65 K for (Y,Gd)BCO and (Y,Gd)BCO+BMO films. The pure (Y,Gd)BCO film shows anisotropic $J_c(Q)$ and a small c-axis peak due to the TBs. Addition of increasing densities of BMO NPs progressively improve $J_c(1T, Q)$ and the films with 2 and 3 wt % BZO show a nearly isotropic $J_c(Q.)$ These results indicate that the $J_c(H, Q)$ improvement is related to the density of NPs and not just to the volume percent of dopant.
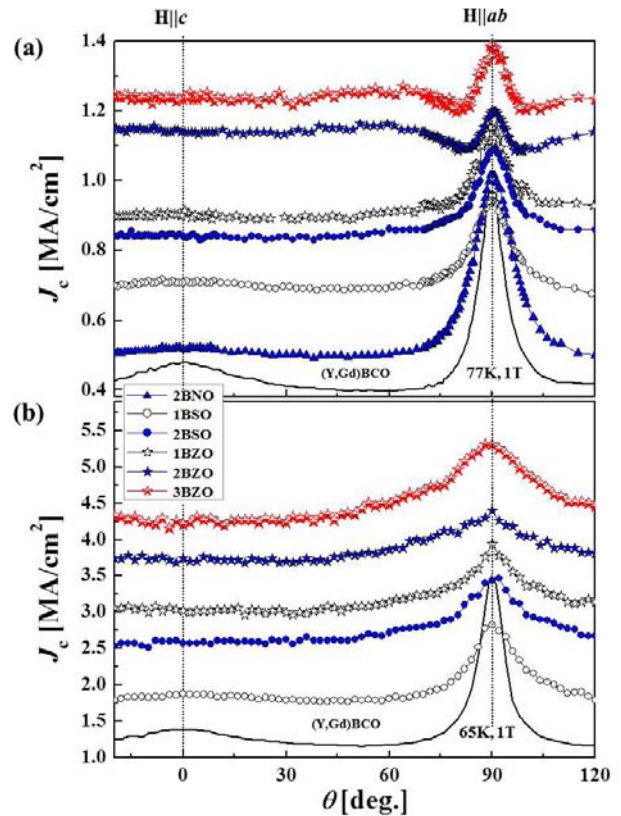
Figure 3. The maximum current that our superconducting films can carry without dissipation (the critical current density) also depends on the orientation of the applied magnetic field with respect to the crystalline axes of the films. In the figure we show the critical current density for several of our films containing nanoparticles of different size (determined by the chemical composition) and in different concentrations, as a function of the field orientation. A film without added nanoparticles is also shown for reference. All curves were measured at the same magnetic field. (a) and (b) show two different temperatures.

We measured H_{irr} up to 7T for the (Y,Gd)BCO+BMO films and the pure (Y,Gd)BCO film at three angles as shown in Figure 4. For **H**||*ab* all films have very similar H_{irr}, indicating no influence of the nanoparticles. For **H**||*c* and **H**||45°, the H_{irr} increases systematically with the NPs density as shown in Figure 5. Although the volume percent of dopants in the 2BNO, 3BZO and 2BSO films are almost the same, their H_{irr} curves are clearly different, indicating that H_{irr} is correlated with the density of NPs; in fact, the films with a similar nanoparticle density (2BSO and 1BZO) show almost the same H_{irr}. The enhancement in H_{irr}(||45°) is much prominent than that observed for **H**||*c*, due to the active role of TB along the *c*-axis, not acting for **H**||45°. A manuscript describing these results is in preparation.

Figure 5. The irreversibility field (the line above which the critical current density becomes zero, thus setting the upper limit for applications) increases with the concentration (density) of the nanoparticles, until it reaches a saturation at high concentrations. As examples, the figure shows the results for all our films at two temperatures and two field orientations.

Iron-arsenide superconductors

Besides his main focus on YBCO films, Dr. Miura has been involved in exploring vortex physics and dynamics in single crystals of $Ca_{1-x}Na_xFe_2As_2$ (iron-arsenide superconductors of the "122" phase). A strong motivation for this work was the realization that these clean single crystals have a much simpler pinning landscape where J_c arises mainly from a sparse distribution of random NPs. This gave us the opportunity to apply several of the tools, analysis techniques and pinning models previously used for the REBCO films in a different family of superconductors.

In a first study [9] we investigated the correlation between crystalline structure and superconducting properties in $Ca_{1-x}Na_xFe_2As_2$ single crystals for x = 0.5, 0.6, 0.75. We found the maximum T_c ~ 33.4 K at x ~ 0.75. The Na substitution causes the decrease of the *a-b* crystallographic axis and the increase of the *c* axis in the tetragonal phase. The H_{c2} anisotropy (near T_c) is _ = 1.85 ± 0.05, independently of the Na content. A narrow vortex liquid phase was detected in the sample with highest T_c, consistent with the expectations based on a Lindeman criterion. $J_c(H,\_)$ shows no evidence of correlated pinning and indicates that at low fields pinning by random nanoparticles dominates, with the same power-law dependence $J_c \mu H^-$ found in REBCO and similar a ~0.55.

In a related study [10] we focused on the vortex dynamics of the $Na_xCa_{1-x}Fe_2As_2$ crystals with x = 0.5 (underdoped) and 0.75 (optimally doped), T_c ~ 19.4 K and 33.4 K respectively, by performing magnetization measurements of J_c and S. We found that $J_c(T)$ is consistent with dT_c pinning (m ~ 1.2 to 1.4), associated with randomly distributed NPs, while $S(T)$ shows a crossover between glassy (elastic) and plastic

Figure 4. Temperature dependence of the irreversibility field (the line above which the critical current density becomes zero, thus setting the upper limit for applications) for several of our films with different sizes and concentrations of nanoparticles. A film without added nanoparticles is also shown for reference. Panels (a), (b) and (c) show three different orientations of the magnetic fields. The insets show the same data in logarithmic scales. From the linear slopes of those logarithmic plots we extract information about the vortex pinning mechanisms.

creep regimes. The boundary $T_{cr}(H)$ between both regimes coincides with the upper limit of the regime of strong pinning by nanoparticles. The glassy exponent (m) in the optimally doped crystal is consistent with the collective creep theory previously applied to oxide HTS, but in the under-doped sample the plateau in $S(T)$ indicates that m ~ 3 - 3.3, a value larger than existing theoretical predictions, suggesting a novel creep regime.

Impact on National Missions

This project has advanced the physics and materials science of vortex pinning in HTS, contributing to DOE goals on superconductivity. We have developed new methods to engineer the pinning landscape that allowed us unprecedented control and deeper understanding of $J_c(T,H,\_)$ and $H_{irr}(T,\_)$ in REBCO films. These results may lead to enhanced performance of HTS wires and contribute to goals of DOE/OE to improve electricity transmission and energy reliability. These materials may also contribute to electric power generation, transmission and utilization for DOD, DHS, and other agency programs. The studies on both the REBCO and the iron-arsenide superconductors have contributed to the BES goal of increasing the fundamental understanding of vortex matter in superconductors.

References

1. Macmanus-Driscoll, J. L., S. R. Foltyn, Q. X. Jia, H. Wang, A. Serquis, L. Civale, B. Maiorov, M. E. Hawley, M. P. Maley, and D. E. Peterson. Strongly enhanced current densities in superconducting coated conductors of YBa2Cu3O7-x+BaZrO3. 2004. *NATURE MATERIALS.* **3** (7): 439.

2. Foltyn, S. R., H. Wang, L. Civale, Q. X. Jia, P. N. Arendt, B. Maiorov, Y. Li, M. P. Maley, and J. L. MacManus-Driscoll. Overcoming the barrier to 1000 a/cm width superconducting coatings. 2005. *Applied Physics Letters.* **87** (16): 162505.

3. Maiorov, B., S. A. Baily, H. Zhou, O. Ugurlu, J. A. Kennison, P. C. Dowden, T. G. Holesinger, S. R. Foltyn, and L. Civale. Synergetic combination of different types of defect to optimize pinning landscape using $BaZrO_3$-doped $YBa_2Cu_3O_7$. 2009. *Nature Materials.* **8** (5): 398.

4. Gutierrez, J. Llordes., J. Gazquez, M. Gibert, N. Roma, S. Ricart, A. Pomar, F. Sandiumenge, N. Mestres, T. Puig, and X. Obradors. Strong isotropic flux pinning in solution-derived $YBa_2Cu_3O_{7-x}$ nanocomposite superconductor films. 2007. *Nature Materials.* **6** (5): 367.

5. Solovyov, V. F., H. J. Wiesmann, L. Wu, Q. Li, L. D. Cooley, M. Suenaga, B. Maiorov, and L. Civale. High critical currents by isotropic magnetic-flux-pinning centres. 2007. *Superconductor Science & Technology.* **20** (4): L20.

6. Miura, M., T. Kato, M. Yoshizumi, Y. Yamada, T. Izumi, T. Hirayama, and Y. Shiohara. Rare earth substitution effects and magnetic field dependence of critical current in $Y_{1-x}RE_xBa_2Cu_3O_y$ coated conductors with nanoparticles (RE = Sm, Gd). 2009. *Applied Physics Express.* **2** (2): 023002 (3 pp.).

7. Miura, M., B. Maiorov, S. A. Baily, N. Haberkorn, J. O. Willis, K. Marken, T. Izumi, Y. Shiohara, and L. Civale. Mixed pinning landscape in nanoparticle-introduced YGdBa2Cu3Oy films grown by metal organic deposition. 2011. *PHYSICAL REVIEW B.* **83** (18): 184519.

8. Baily, S. A., B. Maiorov, H. Zhou, F. F. Balakirev, M. Jaime, S. R. Foltyn, and L. Civale. Smectic vortex phase in optimally doped $YBa_2Cu_3O_7$ thin films. 2008. *Physical Review Letters.* **100** (2): 027004.

9. Haberkorn, N., B. Maiorov, M. Jaime, I. Usov, M. Miura, G. F. Chen, W. Yu, and L. Civale. Effect of doping on structural and superconducting properties in Ca1-xNaxFe2As2 single crystals (x=0.5, 0.6, 0.75). 2011. *PHYSICAL REVIEW B.* **84** (6): 064533.

10. Haberkorn, N., M. Miura, B. Maiorov, G. F. Chen, W. Yu, and L. Civale. Strong pinning and elastic to plastic vortex crossover in Na-doped $CaFe_2As_2$ single crystals. 2011. *Physical Review B (Condensed Matter and Materials Physics).* **84** (9): 094522 (7 pp.).

Publications

Haberkorn, N., B. Maiorov, M. Jaime, I. Usov, M. Miura, G. F. Chen, W. Yu, and L. Civale. Effect of doping on structural and superconducting properties in $Ca_{1-x}Na_xFe_2As_2$ single crystals (x=0.5, 0.6, 0.75). 2011. *Physical Review B (Condensed Matter and Materials Physics).* **84** (6): 064533 (10 pp.).

Haberkorn, N., M. Miura, B. Maiorov, G. F. Chen, W. Yu, and L. Civale. Strong pinning and elastic to plastic vortex crossover in Na-doped CaFe2As2 single crystals. 2011. *PHYSICAL REVIEW B.* **84** (9): 094522.

Miura, M., B. Maiorov, S. A. Baily, N. Haberkorn, J. O. Willis, K. Marken, T. Izumi, Y. Shiohara, and L. Civale. Mixed pinning landscape in nanoparticle-introduced YGdBa2Cu3Oy films grown by metal organic deposition. 2011. *PHYSICAL REVIEW B.* **83** (18): 184519.

ENVIRONMENTAL AND BIOLOGICAL SCIENCES

Integrated Experimentation and Hybrid Modeling for Prediction and Control of Multiphase Flow and Reaction in CO2 Injection and Storage

James W. Carey
20100025DR

Introduction

The prediction and control of multiphase flow and reaction in geologic media is one of the great challenges in the Earth and Energy Sciences. This challenge has come into even greater focus with the recognition that the environment cannot sustain the CO_2 released from oil, gas, and coal combustion. These carbon-based fuels form the backbone of the world economy and have enabled nearly all of the technological innovations of the past 100 years. As developing countries with large populations strive to attain higher standards of living, their emphasis will be on the utilization of even more inexpensive and abundant fossil fuel. A promising approach for avoiding this impending environmental crisis is the geologic sequestration of CO_2 in depleted oil reservoirs and deep saline aquifers.

As a response to global warming, geologic disposal of CO_2 represents an enormous challenge: a single 1-GW coal-fired power plant produces a volume of about 10 m x 1 km^2 of supercritical CO_2 each year. Predicting the fate of this CO_2 in the subsurface requires a fundamental under-standing of multiphase, reactive flow and transport where competing physical and chemical processes generate complex, heterogeneous flow and reaction patterns. The injection of CO_2 into a saline aquifer upsets a system that has been close to chemical equilibrium and hydrodynamic steady state for millennia. Determining the long-term mobility of the buoyant, immiscible CO_2 is essential to making this technology viable. Our project integrates the innovative, cutting-edge experimental and numerical approaches to directly observe CO_2 flow and reaction and will use these results to develop and validate predictive models of CO_2 mobility.

Benefit to National Security Missions

This proposal supports LANL's Grand Challenge goals in Energy and Earth Systems. It accomplishes this by enabling geologic sequestration of CO_2, which will allow the continued use of fossil fuels without continuing to emit dangerous quantities of CO_2 to the environment. Our proposal support's DOE's top priority of carbon sequestration as a means of mitigating the impacts of fossil fuel consumption. On a more fundamental level, the proposed research maps directly to the Basic Energy Sciences Advisory Committee's Grand Challenge to "Characterize and Control Matter Away From Equilibrium" as "crucial for energy supply and security."

Progress

We are now at the end of our second year. The project continues with two productive collaborations with Oregon State University and the University of Illinois. In addition to Los Alamos and University staff, the project supports 5 post-doctoral fellows and two graduate students.

In the following, we describe progress on each of our major scientific challenges:

Flow patterns and the dissolution of CO_2 into brine

Our experimental investigations of flow patterns are based on microfluidics experiments. These are 2-dimensional systems consisting of silicon wafers etched to produce a porous medium. In our experiments, 2D fluid distribution patterns were analyzed by identifying trapped wetting and non-wetting fluid blobs and measuring their area and interfacial contact length with the opposing fluid and the solid. From these individual measurements, we computed the residual fluid saturations, hydraulic radii distributions and fluid pattern correlations to comment on the capillary or viscous mechanisms at play at given conditions. The oil-water experiments have been illuminating and have shown predictable changes in fluid patterns as a function of the viscosity ratios of oil and water and the injection rate (Figure 1).

Additional Immiscible fluid displacement experiments were designed, conducted and analyzed. These experiments were required to address some fluid instability observations (at high capillary number and low viscosity ratio). Videos captured by a digital SLR camera with a macro lens (as opposed to steady-state images captured by a microscope) revealed a previously unobserved phenomenon of remobilization of oil blobs leading to snap-

off of invading water fingers. Now with this comprehensive physical understanding, all our data is being summarized for a publication and is in its final stage of preparation.
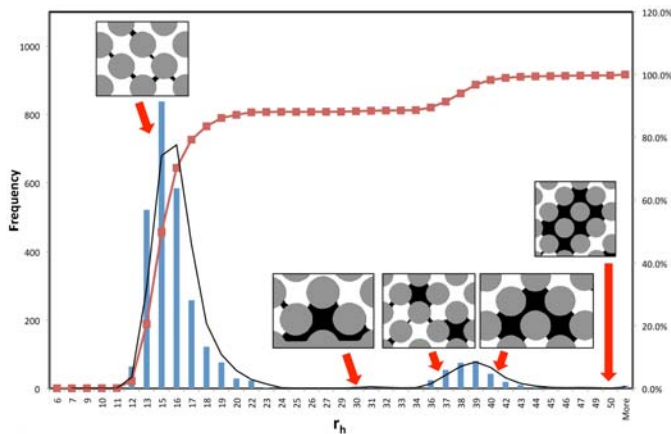
Figure 1. Measured hydraulic radius versus frequency of occurrence for the immiscible displacement of oil by water in a system with a viscosity ratio of 0.22 and an injection rate of 0.3 ml/hr. The inset figures illustrate the trapped oil pattern corresponding to the varying hydraulic radii.

Capillary trapping of CO_2

We continue to focus our efforts on investigating the effect of interfacial tension, viscosity, and fluid flow rate on CO_2 capillary trapping efficiency. Capillary trapping has several benefits: capillary forces are greater than buoyant forces, reducing the need for impervious caprock; CO_2 is immobilized in pore-scale bubbles facilitating its dissolution into the brine; and CO_2 can be distributed over a large reservoir volume allowing increased mineral dissolution and carbonate deposition.
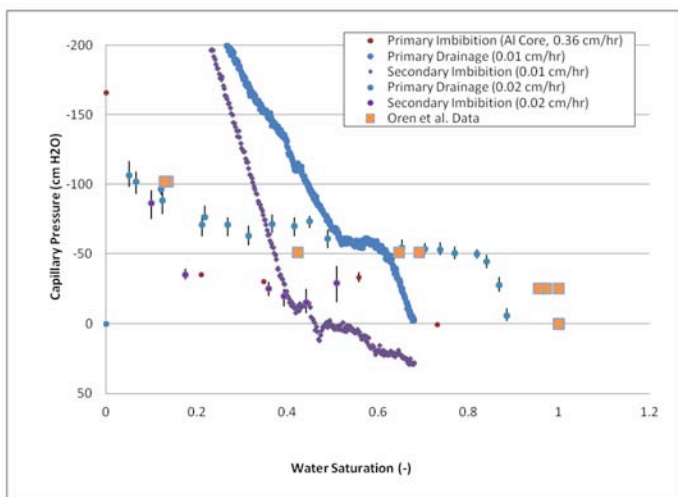
Figure 2. Capillary pressure versus saturation curves for Bentheimer sandstone under ambient conditions. The plot includes data for both static points (where equilibration is reached at each point) and containuous flow measurement, which shows that beyond 50% saturation, viscous pressure build-up starts to dominate.

We have ordered two tomography-compatible Hassler-type core-holders. With the larger unit, we have measured permeability and capillary pressure saturation curves on Bentheimer sandstone core at ambient conditions (Figure 2). We have found that capillary pressure versus saturation curves must be measured at very slow pump speeds to avoid viscous effects. We have also observed that equilibration times are rather significant. Using high-resolution x-ray tomography, we have explored the effects of interfacial tension, viscosity and flow rate on the effectiveness of capillary trapping using analog fluids in bead packs. We have begun a set of experiments on sandstone using the newly developed high-pressure, high-resolution x-ray tomography coreflood unit.

Chemical reactions of CO_2 with rock

We completed a set of experiments in which we have measured the rate of dissolution of supercritical CO_2 into porous media. The experiments were conducted at 75 °C and 200 bars CO_2 pressure and consisted of the injection of CO_2 into the headspace of a horizontal reactor and the measurement of the pressure decay as the CO_2 dissolved into water. Mass transfer into brine was slower by one order of magnitude compared with pure brine.

We used microfluidics to study the evaporation of brine, a process that is important near the injection well. Evaporation results in precipitation that may reduce injection efficiency as pores become clogged with precipitate. In the experiments, the solution was relatively dilute (without NaCl) but near saturation with calcite. This experiment showed that it is unlikely that residual brine of this composition will impact injection conditions. More concentrated brines may have a different outcome but limitations in the experimental devices limit our ability to test high-salinity brines.

Gravitational Mixing of CO_2-saturated brine

CO_2 is partially miscible in brine, and in this activity we explore processes that enhance the amount of CO_2 dissolved in water. Gravitationally driven instabilities can lead to downwelling of dense CO_2-saturated brine, increasing the amount of dissolved CO_2 by orders of magnitude. We have published a manuscript in Physical Review Letters describing the results of 2D measurements of the gravitational mixing process. This paper discusses the properties of the initial fluid instability, the transition to large-scale fingers, and the final steady-state dissolution rate. During this year, we have also extended the experimental approach by designing, building, and running 3D experiments. The data gathered in these measurements expand our results to the parameter space relevant for a large number of saline reservoirs in the U.S. and Canada. In addition, we found preliminary evidence for a new secondary instability that is crucial to understanding the steady-state dissolution rate realistic reservoirs. The data collection phase of this experiment is complete and a manuscript is in preparation.

Development of a hybrid numerical scheme to couple pore- and continuum-scale processes

Significant progress has been made toward enhancing existing modeling capabilities, developing new capabilities, and applying them to problems relevant to geologic storage of CO_2 at various scales. At the pore scale, we have developed a hybrid theory and numerical algorithm to couple the lattice Boltzmann method with conventional finite-volume approach to solve the Navier-Stokes equation for fluid flow. We have also integrated many of our existing lattice Boltzmann simulation tools into a new open source code, called *Taxila* LBM, and added numerous new enhancements into the code. Using this code, we have simulated the micromodel experiments conducted on immiscible displacement of surrogate fluids for CO_2 and brine. For pore-scale reactive transport, we have coupled *Taxila* with PFLOTRAN, with the former to solve for fluid flow and the latter for transport and reaction. We have developed a hybrid framework to couple the pore-scale LBM and continuum-scale PFLOTRAN for flow through fractured systems. At the continuum scale, PFLOTRAN has been used to simulate CO_2 dissolution experiments and density-driven fingering.

As an illustration of the algorithms we are using to combine continuum scale and pore scale simulations, we consider a problem of flow in a fractured medium. A regular porous medium is split by a fracture, and single-phase flow across this domain is calculated (Figure 3a). Within the majority of the medium, Darcy's equation is valid at the continuum scale. Within the fracture, Darcy's equation is not valid, and Navier-Stokes equations at the pore scale are solved. To solve equations over the entire domain, an overlapping set of subdomains are solved at the pore and continuum scales (Figure 3a). To test the hybrid method, we compare the hybrid solution (Figure 3b) to a solution done at the pore scale everywhere (Figure 3c), which is up-scaled to the continuum scale.
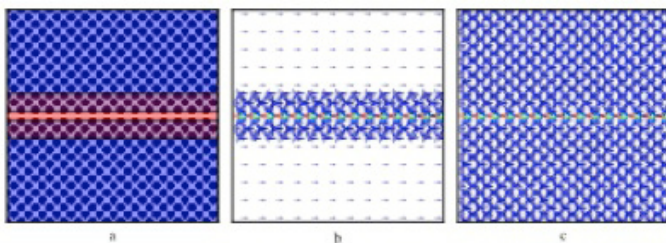
Figure 3. Solution for the fractured hybrid problem: (a) shows the background geometry, with black indicating wall and a fracture running through the center. Continuum subdomains are in blue, and pore-scale subdomains are in red (with overlap in purple); (b) demonstrates the iterated hybrid solution; and (c) the solution with the entire domain calculated at the pore scale.

Future Work

Work in the coming year will include use of our new high-pressure microfluidics cell, tomographic studies, 3-D gravitational experiments, and further developments in LBM and hybrid modeling.

Conclusion

We will make direct observations of CO_2-brine-water interactions in porous rock systems that will provide the first fundamental data on the mobility of CO_2 in the subsurface. This information is essential to evaluating the potential risk of CO_2 leakage back to the surface and will form the basis of engineering CO_2 injection projects to maximize the immobility of the CO_2. The direct observations will allow validation of predictive computer codes, which will be used to evaluate the long-term effectiveness of CO_2 sequestration as a means of mitigating greenhouse gas-induced warming.

Publications

Abdel-Fattah, A. I.. An Overview of the Colloid and Interface Science Research at {LANL} Related to Energy and Environmental Applications: Current and Future Directions. 2011. In *Presentation at the Leibniz Institute of Polymer Research Dresden, Germany, July 13, 2011.*.

Backhaus, S.. Convective Instability and Mass Transport of the Diffusion Layer in CO2 Sequestration. 2011. In *American Geophysical Union Fall Meeting, December 2011.*

Backhaus, S., K. Turitsyn, and R. E. Ecke. Convective instability and mass transport of diffusion layers in a Hele-Shaw geometry. 2010. *Physics Review Letters.* **106**: 104501.

Chen, Y., Q. Kang, Q. Cai, and D. Zhang. Lattice Boltzmann Method on Quadtree Grids. 2011. *Physics Review E.* **83**: 026707.

Coon, Ethan T., Mark L. Porter, Qinjun Kang, Peter C. Lichtner, and J. David Moulton. Coupling lattice Boltzmann and continuum equations for the solution of multiscale flow and reactive transport in porous media. 2012. In *Computational Methods in Water Resources (CMWR) XIX International Conference, Urbana-Champaign, IL, June 17-21, 2012.*

Coon, Mark L. Porter andEthan, Qinjun Kang, Peter Lichtner, David Moulton, and James W. Carey. Taxila LBM: A lattice-Boltzmann simulator single- and multi-phase flow in complex porous media. 2012. In *Computational Methods in Water Resources (CMWR) XIX International Conference, Urbana-Champaign, IL, June 17-21, 2012.*

Ecke, R. E., S. Backhaus, and K. Turitsyn. Unstable Diffusion Layers: Laboratory Experiments on Carbon Sequestra-

tion Phenomena. 2010. In *63rd Annual Meeting of the APS Division of Fluid Dynamics.* Vol. 55.

Harper, E. D., D. Wildenschild, R. T. Armstrong, and A. L. Herring. Optimization of capillary trapping for application in geological carbon dioxide sequestration. 2011. In *American Geophysical Union Fall Meeting, December 2011.*

Herring, A. L., D. Wildenschild, E. D. Harper, R. T. Armstrong, and J. W. Carey. Quantifying the effects of fluid properties and flow rates on the effectiveness of capillary trapping of CO2 in a Bentheimer sandstone. 2011. In *American Geophysical Union Fall Meeting, December 2011.*

Kang, Q., and P. C. Lichtner. Lattice Boltzmann modeling of multiphase flow and reactive transport at the pore scale and its coupling with PFLOTRAN. 2011. In *Pore Scale Modeling Challenges Workshop, DOE's Environmental Molecular Sciences Laboratory, Hanford, WA.*

Kang, Q., and P. C. Lichtner. A Lattice Boltzmann Method for Coupled Fluid Flow, Solute Transport, and Chemical Reaction. subm. In *Novel Trends in Lattice-Boltzmann Methods --- Reactive Flow, Physicochemical Transport and Fluid-Structure Interaction.* Vol. 3. Bentham Science Publishers.

Keating, E. H., A. Hakala, H. S. Viswanathan, J. W. Carey, J. E. Fessenden, and R. J. Pawar. Assessing the impact of CO2 and brine leakage on shallow groundwater quality: Results from a natural analog study in New Mexico, USA. 2011. In *American Geophysical Union Fall Meeting, December 2011.*

Lipnikov, K., J. D. Moulton, and D. Svyatskiy. Adaptive Strategies in the Multilevel Multiscale Mimetic (M3) Method for Two-Phase Flows in Porous Media. 2011. **9**: 991.

Newell, D. L., H. S. Viswanathan, P. C. Lichtner, J. W. Carey, G. Thyne, and J. P. Kaszuba. Experimental Determination of Supercritical CO2 Mass Transfer Rates into Brine. 2011. In *American Geophysical Union Fall Meeting, December 2011.*

Porter, Mark L., Ethan Coon, Qinjun Kang, Peter C. Lichtner, and James W. Carey. Hybrid modeling of CO2 sequestration processes using the lattice-Boltzmann method and PFLOTRAN. 2011. In *American Geophysical Union Fall Meeting, December 2011.*

Porter, Mark L., Ethan Coon, Qinjun Kang, Sowmitri Tarimala, and James W. Carey. Modeling of immiscible displacement experiments in a homogeneous micromodel. 2012. In *Computational Methods in Water Resources (CMWR) XIX International Conference, Urbana-Champaign, IL, June 17-21, 2012.*

Porter, Mark L., Qinjun Kang, Sowmitri Tarimala, Amr I. Abdel-Fattah, Scott Backhaus, and James W. Carey. Lattice-Boltzmann modeling of experimental fluid displacement patterns, interfacial area and capillary trapped CO2. 2010. In *Fall Meeting of the American Geophysical Union.*

Shi, Y., Q. Kang, P. C. Lichtner, and W. Tao. Hybrid modeling for fluid transport: Using lattice Boltzmann method couple with continuum Navier-Stokes equation-based numerical methods. in r. *Physics Review E.*

Striblet, Jonathan C., LeChell S. Rush, Myles J. Floyd, Mark L. Porter, and Riyadh I. Al-Raoush. Combined use of computed tomography and the lattice-Boltzmann method to investigate the influence of pore geometry of porous media on the permeability tensor. 2011. In *American Geophysical Union Fall Meeting, December 2011.*

Tarimala, S., A. Abdel-Fattah, J. W. Carey, and S. Backhaus. Distributions of Residual Fluid in Non-Wetting Invasions in Porous Media. 2011. In *American Geophysical Union Fall Meeting, December 2011.*

Werth, C. J., A. J. Valocchi, H. Yoon, K. Dehoff, and C. Zhang. Pore-scale mineral precipitation and permeability reduction. 2011. In *Pore Scale Modeling Challenges Workshop, DOE's Environmental Molecular Sciences Laboratory, Hanford, WA.*

Werth, C. J., A. J. Valocchi, H. Yoon, K. Dehoff, and C. Zhang. Evaluation of pore-scale mineral precipitation and permeability reduction of relevance to geological carbon sequestration. 2011. In *Association of Environmental Engineering and Science Professors Conference, Tampa, FL, July, 2011.*

Wildenschild, D., R. T. Armstrong, and J. W. Carey. Exploring capillary trapping efficiency as a function of interfacial tension, viscosity, and flow rate. 2010. In *Gordon Conference.*

Wildenschild, Dorthe, Ryan T. Armstrong, Anna L. Herring, Iain M. Young, and J. William Carey. Exploring capillary trapping efficiency as a function of interfacial tension, viscosity, and flow rate. 2011. *Energy Procedia.* **4**: 4945.

Yoon, H., A. J. Valocchi, C. J. Werth, and T. Dewers. Pore-scale simulation of mixing-induced calcium carbonate precipitation and dissolution in a microfluidic pore network. unde. *Water Resource Research.*

Zhang, , Dehoff, Karl, Hess, Nancy, Oostrom, Mart, Wietsma, Thomas W., Valocchi, Albert J., Fouke, Bruce W., and Werth, Charles J.. Pore-Scale Study of Transverse Mixing Induced CaCO3 Precipitation and Permeability Reduction in a Model Subsurface Sedimentary System.

2010. *Environmental Science \& Technology.* **44**: 7833.

Zhang, C., K. DeHoff, A. J. Valocchi, M. Oostrom, T. Wietsma, and C. J. Werth. Pore-scale investigation of the impacts of solution chemistry on mixing-induced mineral precipitation. 2010. In *American Chemical Society National Spring Meeting, San Francisco, CA, 2010.*

Directed Research
Continuing Project

Transformative Bioassessment of Engineered Nanomaterials: Materials by Design

Rashi S. Iyer
20100027DR

Introduction

Applications of ngineering nanomaterials (ENM) are increasing every day, along with the potential for human exposure to them. Our goal is to understand at the fundamental level the response of humans to ENM. Individual particle-by-particle testing using conventional approaches (cell®animal®human) for assessing the bio-impact of chemical agents are grossly inadequate to address the extent of the ENM problem. The overarching goal of our proposed effort was to enable predictive and high-throughput screening of the bio-impact of ENMs. Importantly, demonstrating the use of a 3-D tissue bio-platform for the rapid assessment of ENMs would immediately establish a new state-of-the-art capability for the toxicological analyses of nanomaterials. In the current study, we evaluated the tissue, cellular and molecular level responses of *in vitro* reconstructed organotypic 3-D skin and lung tissue on exposure to semiconductor nanomaterials and carbon-based nanomaterials. *By judicious choice of ENM composition and explicit control over ENM properties, we proposed to understand the specific effects of the distinct physicochemical properties of ENMs on nano-bio interactions, with the 3-D human tissue bio-platform providing a unique and highly relevant biological "test bed."*

Benefit to National Security Missions

Since 2000, LANL has pioneered R&D efforts in nanomaterials, at the time accounting for over 1% of worldwide production. Today, LANL hosts one of only five DOE Nanoscale Science Research Centers – Center of Integrated Nanotechnology (CINT). The intense interest in engineered nanomaterials (ENMs) is fueling a $1B industry and global demand is expected to reach $1 trillion by 2015. Beyond commercial considerations, ENMs provide the potential to address such national and global issues as energy security and WMD through realized and potential applications in energy harvesting, efficient lighting, biomedicine, catalysis, and sensor technologies. Given the proximity of these applications to DOE (and LANL) mission, nanotechnology has achieved tremendous prominence within the complex. CINT is a testament to this fact.

Progress

We established a 3-D skin and lung tissue bioassesment platform enabling multiplex analyses. To date, we have successfully developed and established an artificially reconstructed skin and lung tissue. The 3-D tissue cultures developed in this task correspond more stringently to human biology (anatomically, physiologically and functionally) and closely mimic human responses to environmental insults. In addition, a unique advantage offered by the tissue model is the ability to rapidly screen multiple ENMs simultaneously using a multi-well format. We performed a concurrent and replicate analysis of parameters such as penetration depth, cytotoxicity, proliferative function, ROS induction and molecular level responses (Figure 1).
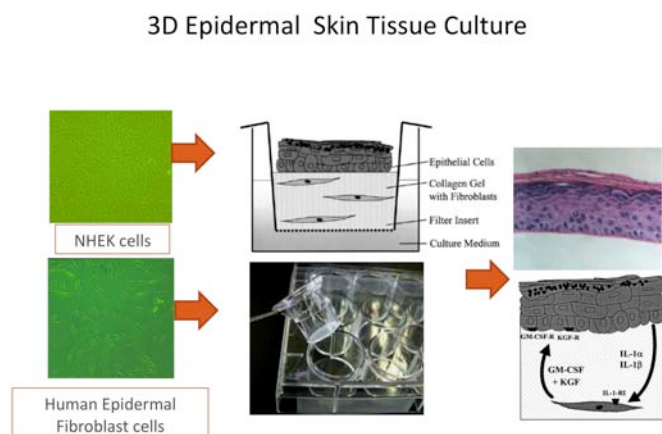
Figure 1. Development of multiwell skin tissue for HTP analysis

We synthesized ENMs with distinct chemical and physical properties. Turning modes 'on' or 'off' by judicious choice of ENM chemical, physical, and structural properties allows us to categorize ENM bio-impact in terms of ENM 'function' rather than ENM chemical identity. We have synthesized semiconductor ENMs that have the potential to interact with biological systems through one or more modes of action – 1. Metal/composition toxicity, 2. Surface chemistry effects, 3. Redox activity depen-

dent, and/or 4. Geometry—size and shape effects. ENMs synthesized thus far are cadmium selenide (CdSe), indium phosphide (InP), and titanium dioxide (TiO2), functionalized fullerenes and silver. These ENMs are of varying sizes, negatively and positively charged, and spherical nanocrystals or elongated nanowires (Figures 2).
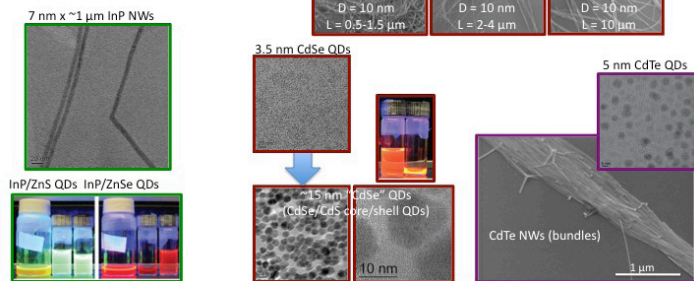
Figure 2. Synthesis of semiconductor QDs.

We correlated the physical and chemical characteristics of ENMs to biological responses. A combination of fluorescence microscopy, biochemical assays, mass spectroscopy-based proteomics and RT-PCR gene analysis were employed to evaluate tissue responses to ENMs (Figure 3). Our results indicate that positively charged ENMs elicited relatively more toxic responses than their negative counterparts both in skin/lung cells and tissues. In addition, nanowires were significantly more toxic when compared to nanospheres, suggesting that shape may impact bioresponses. In regards to composition, we observed that nano shell (CdSe core-ZnS shell) may be relatively less toxic than the nano core (CdSe), moreover InP QDs were relatively benign compared to CdSe and CdTe. Further investigations indicated that the larger the nanomaterial the less bioreactive it is. For example, the 5 nm QD are less toxic than the 3 nm QD and the 10 nm QD was the least toxic. Molecular level responses (protein and gene level) were also investigated and analyzed by employing advanced bioinformatic tools to perform data visualization and preprocessing. Processed data is being used to develop computational model(s) integrating multiple levels of biological responses to enable a comprehensive understanding of nano-bio-interactions allowing for the design of high function-low-bioimpact ENMs, targeted experimental design, and bio-marker identification.
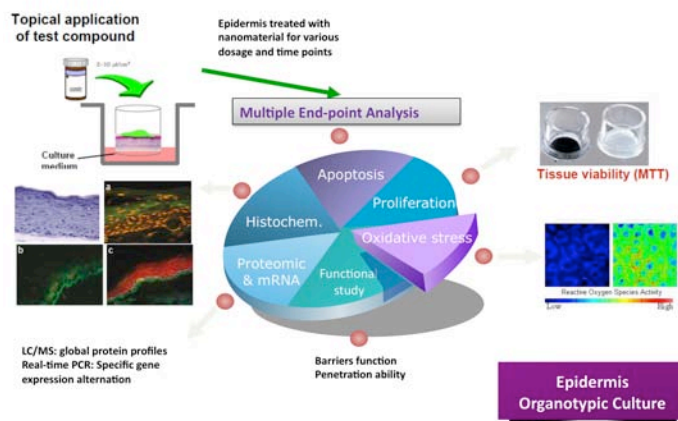
Figure 3. Multi-level Analysis of reconstructed tissue

Future Work
We will validate our tissue models and further develop them for use as in vitro model systems for rapid and accurate screening of environmental toxicants and drugs. In addition, we will develop 'control' nanomaterials that can potentially be used as standardized materials for testing of nanomaterials. In addition, to facilitate communication we will develop a website that describes the results from our studies. Initial studies suggest that composition, size, charge and shape can all impact tissue level responses to varying extents and it may be possible to guide the design of nanomaterials such that their impact on biological systems is minimized.

Conclusion
To date we have demonstrated the utility of a novel 3-dimensional human organ-tissue bioassessment platform as a valid alternative to animal testing. We have also established critical physical and chemical properties of ENMs that can potentially impact biological responses and ultimately human health. These properties are generalizable across ENMs. Instead of the conventional particle-by-particle evaluation, our approach of understanding 'properties-dependent' bioimpact of ENMs can provide for a rapid and pertinent analysis of the biological impact of ENMs. In addition, our controlled synthesis and extensive physico-chemical characterization of ENMs enables a 'properties-dependent' correlation of the biological impact of ENMs on human health. Synergizing our biological and materials expertise, our approach provides guiding principles for the design and synthesis of high-function and low-bioimpact nanomaterials.

Publications
Gao, J., H. L. Wang, A. Shreve, and R. Iyer. Fullerene derivatives induce premature senescence: A new toxicity paradigm or novel biomedical applications. 2010. *Toxicology and Applied Pharmacology.* **244** (2): 130.

Gao, J., H. L. Wang, A. Shreve, and R. Iyer. Modulation of γ-irradiation induced ROS responses by engineered fullerenes in human epidermal keratinocytes. 2008. In *2008 NSTI Nanotechnology Conference and Trade Show, NSTI Nanotech 2008 Joint Meeting, Nanotechnology 2008 ; 20080601 - 20080605 ; Quebec City, QC, United States.* Vol. 2, p. 77.

Gao, J., H. Wang, and R. Iyer. Suppression of Proinflammatory Cytokines in Functionalized Fullerene-Exposed Dermal Keratinocytes. 2010. *JOURNAL OF NANOMATERIALS.* : 416408.

Rebecca, M., W. Hsing-Lin, G. Jun, I. Srinivas, M. Gabriel, M. Jennifer, S. Andrew, Bao Yuping, W. Chun-Chih, C. Zhong, G. Yuan, and I. Rashi. Impact of physicochemical properties of engineered fullerenes on key biological responses. 2009. *Toxicology and Applied Pharmacology.* **234** (1): 58.

Terrestrial Vegetation, CO_2 Emissions, and Climate Dynamics

Nathan G. Mcdowell
20110014DR

Introduction

Vegetation mortality rates are increasing globally, appear to be driven by our changing climate, and are releasing large and sustained amounts of CO2 to the atmosphere. There is no comprehensive capability to monitor vegetation mortality and subsequent carbon emissions, thus the locations, timing and magnitudes of ecosystem CO2 emissions are unknown. The critical urgency of forecasting climate impacts and feedbacks, coupled with the rising international focus on carbon management, make understanding, quantifying, and predicting terrestrial carbon balance and subsequent climate impacts one of the greatest science challenges currently facing America. We propose to build the world's highest resolution and most accurate monitoring and predictive capability for terrestrial CO2-climate dynamics and feedbacks. We will improve remote sensing techniques to allow hypothesis tests of the patterns and climatic-dependence of vegetation mortality and its early-warning signals at regional and ultimately global scales. These observations will then be used to drive the state-of-the-art model of terrestrial carbon dynamics at unprecedented resolution, allowing us to test the critical question: how much stored carbon is lost to the atmosphere as a result of vegetation mortality? Finally, we will employ the observation-driven carbon dynamics model within a global-capacity climate simulation to test the hypotheses that vegetation mortality influences climate, resulting in a feedback loop. Our ultimate goal is to provide an unprecedented capability to simultaneously monitor and predict global vegetation dynamics and their consequences to carbon storage and climate change.

Benefit to National Security Missions

This project directly addresses the Grand Challenge to "….develop the capability to measure, model, and predict ... impacts of energy choices on climate and their cascading effects on environment and society" including the priorities of 1) next generation, high resolution climate simulation and climate impact models using novel data assimilation and fusion techniques, 2) transformational measurement techniques to monitor changes in greenhouse gases, and 3) fundamental ecological science to understand and predict complex energy impacts s. We will test fundamental carbon cycle hypotheses to provide critical guidance to both DOE's Climate and Environmental Science Division and to the United States' developing focus on a global greenhouse gas treaty information system. We aim for a radical improvement over current policy-making tools in speed, spatial resolution, temporal precision, and mechanistic accuracy. Remote sensing aspects of this project are relevant to a range of national security problems, including nuclear nonproliferation.

Progress

We have achieved great progress in the first year of our project. As of June 1, all three or our selected postdocs have now arrived and are working at LANL. Prior to their arrival, the staff members on the team have written two papers (McDowell 2011, McDowell et al. in press) and given numerous invited presentations on the subject of vegetation mortality, the carbon cycle, and climate. Our project has three main tasks: 1) to improve remote sensing of vegetation stress and mortality, 2) improve the ability of carbon cycle models to simulate the carbon consequences of vegetation mortality, and 3) improve model simulation of the climate consequences of mortality. On task 1, we have generated the full suite of 1-km MODIS (moderate resolution imaging spectrometer) global disturbance index, normalized water index, and photosynthesis and growth datasets from 2000 to present (2005 to present for disturbance), for development of a global mortality index and subsequent hypothesis testing and use as a model validation tool. The smaller scale remote sensing Discovery of Vegetation over Earth (DOVE) has moved quickly, with one manuscript in preparation describing new methods for classifying stressed and dead vegetation, and three more manuscripts in the analysis stage that describe the patterns of leaf temperature and water use of stressed vegetation prior to mortality. Further, a patent is being filed for DOVE, and we have made excellent progress with a new image co-registration program (not yet accomplished by any group). For task 2, we have developed

an independent version of the Ecosystem Demography (ED) model with tree mortality linearly or exponentially dependent on carbon starvation, which uses the photosynthesis subroutine from the National Center for Atmospheric Research's (NCAR) Community Land Model (CLM). This new model is in the testing stage, and has many novel subroutines that promise a large increase in model reality. Uncertainty analysis and testing against forest inventory and remote sensing data at plot or site level are being initiated. Much of the remote sensing and forest inventory data have now been collected and are being processed for manuscripts and for model testing. Also, the Ecosystem Demography model is currently being coupled to the Community Land Model, for eventual use against the MODIS datasets. For task 3, we have ported NCAR's Community Earth System Model to LANL's institutional computing system to allow testing. Using this system, we have conducted thousands of simulations of the potential impacts of climate extremes on vegetation mortality, and subsequent feedbacks of mortality on climate. There are clear model results showing the impact of drought on vegetation mortality and subsequent impacts on regional climate, but no apparent impacts on global climate at this time. Further, we have successfully integrated the Model for Prediction Across Scales (MPAS) into CESM and are currently evaluating the predictions.

Future Work

Fundamental carbon cycle-climate questions are the focus of our hypotheses: 1) can vegetation mortality be anticipated using remote detection of tree canopy signatures that exhibit early-warning signatures indicative of plant stress? 2) Is the recent increase in global vegetation mortality associated with climate variation? 3) Has recent vegetation mortality changed terrestrial carbon storage? 4) Does vegetation mortality influence regional or global climate? 5) Does climate-induced vegetation mortality drive a positive feedback in the climate system? We will test these hypotheses within three key tasks: 1) remote sensing detection of vegetation stress and mortality, 2) estimating carbon storage and fluxes, and 3) assessing climate consequences based on results of (1) and (2). Success of any task will represent a radical scientific jump in our understanding and capability, thus providing robustness of the project to failure. Our highest priority though, is success of the integrated product that will transform our ability to monitor, understand, and predict climate-terrestrial impacts and feedbacks. Our goal is to develop a globally comprehensive tool; however, because the computational requirements for complete global coverage are beyond the capacity of a DR, we will test our approach utilizing data sets of vegetation mortality and carbon storage, CO2 fluxes, and climate that are distributed across disparate regions. The result will be a globally distributed test with the integrated product and its components validated against independent benchmarks. Successfully answering the fundamental questions constitutes enormous scientific advances by ad-

dressing some of the largest uncertainties in the response of the Earth's ecosystems to climate change.

Conclusion

Our current knowledge of the rate, location, and mechanisms of vegetation mortality and feedbacks on CO2 storage and climate are inadequate. This lack of knowledge is disturbing given the immediate national and international need to quantify and understand these processes. If successful, this project will yield direct tests of fundamental theory, will provide the world's best quantitative tool for monitoring vegetation mortality and feedbacks, and will narrow uncertainty on the likely magnitude of terrestrial-climate impacts and feedbacks.

References

1. McDowell, N.. Mechanisms Linking Drought, Hydraulics, Carbon Metabolism, and Vegetation Mortality. 2011. *PLANT PHYSIOLOGY.* **155** (3): 1051.
2. Xu, C., C. Liang, S. Wullschleger, C. Wilson, and N. McDowell. Importance of feedback loops between soil inorganic nitrogen and microbial communities in the heterotrophic soil respiration response to global warming. 2011. *NATURE REVIEWS MICROBIOLOGY.* **9** (3).

Publications

Allen, C., A. Macalady, H. Chenchouni, D. Bachelet, N. McDowell, M. Vennetier, T. Kitzberger, A. Rigling, D. Breshears, E. H. Hogg, P. Gonzalez, R. Fensham, Z. Zhang, J. Castro, N. Demidova, J. Lim, G. Allard, S. Running, A. Semerci, and N. Cobb. A global overview of drought and heat-induced tree mortality reveals emerging climate change risks for forests. 2010. In *Conference on Adaptation of Forests and Forest Management to Changing Climate with Emphasis on Forest Health ; 20080825 - 20080828 ; Umea, SWEDEN.* Vol. 259, 4, SI Edition, p. 660.

McDowell, N.. Mechanisms Linking Drought, Hydraulics, Carbon Metabolism, and Vegetation Mortality. 2011. *PLANT PHYSIOLOGY.* **155** (3): 1051.

McDowell, N., D. Beerling, D. Breshears, R. Fisher, K. Raffa, and M. Stitt. The interdependence of mechanisms underlying climate-driven vegetation mortality. 2011. *TRENDS IN ECOLOGY & EVOLUTION.* **26** (10): 523.

Xu, C., C. Liang, S. Wullschleger, C. Wilson, and N. McDowell. Importance of feedback loops between soil inorganic nitrogen and microbial communities in the heterotrophic soil respiration response to global warming. 2011. *NATURE REVIEWS MICROBIOLOGY.* **9** (3).

Advanced Metagenomic Analysis to Understand Dynamics of Soil Microbial Community under Conditions of Climate Change

Shunsheng Han
20110034DR

Introduction

Climate change and energy production are huge challenges for humankind. Bacteria, the most ancient and abundant form of life, could help us to face these challenges if we understand them better. Bacteria survive in their environments by living in complex, closely integrated communities. Our overall scientific objective is to characterize microbial communities in arid land in terms of population structure and function, and to measure their dynamic response to changes of their environment in a manner that informs climate models. To accomplish this goal, we will develop and integrate two complementary technologies: single cell genome sequencing and a signature-based metagenomics analysis pipeline. The first is an experimental method to dissect and fully characterize the genomes of important members within microbial communities. The second is a fast and sensitive analysis tool that leverages existing sequenced genomes to classify sequencing data into functional and phylogenetic groups. The two technologies are complementary and will be integrated to study the response of microbial communities in arid lands to environmental changes. Our experimental samples will be collected from a desert field site in Moab, Utah (depending on a new development, we could use some wetland samples collected from coastal area effected by the oil spill in the Gulf), to generate two types of sequence data: First, sequences for individual genomes will be generated from single cell, with a goal of assembling genomes of key organisms in the communities that are not present in existing databases. Second, broad shotgun metagenomic sequences will be produced from environmental samples as well. To better analyze the sequencing data, we will develop a fast assembly-free analysis tool to assign phylogeny and function to individual reads that can detect small but statistically significant changes. This will produce a probabilistic breakdown of biological function and phylogeny conducive to constrain climate-modeling efforts.

Benefit to National Security Missions

The project will develop a unique capability to sequence uncultured bacterial species with very high coverage that has not been achievable by other researchers and with ability to analyze huge amount of data with incomparable speed and accuracy.

Our results are relevant to DOE OBER and NHGRI of NIH. We plan to work with them to develop a comprehensive metagenomics research program at LANL in the area of Carbon Sequestration and Energy Security. We will also work to develop applications of the technologies in the biothreat area.

This LDRD project is also engaged with the Warfighter Support Program Office. This office will help enable and facilitate transition of the work into the DOD community.

Progress

We have been working on three main tasks in the first year of this project, sequencing metagenomic DNA samples from DOE Utah field experimental site to determine the genomic composition variations at different location, improving single cell genomics with artificial polyploidy, design and improve protein signature based metagenomic data analysis pipeline.

Metagenomic DNA sequencing: a field trip was taken last fall to collect soil samples from Moab desert experimental sites. A total of 56 samples were collected at different treatment conditions from the top soil crust. To resolve special heterogeneity of soil crust, a subset of samples were collected from two different soil types that are ~50 miles apart. Three sampling sites that are meters away from each other were selected. Three soil crust samples were collected within a foot at each sample site. These samples were sequenced through Illumina HiSeq2000 and is being analyzed.

Single cell genomics, combination of methods whose goal is to decipher the genomic sequence from a single cell, has been applied mostly to organisms with smaller genomes, such as bacteria and archaea. Prior single cell studies showed that a significant portion of a genome could be obtained, but only one finished genome has resulted. Typically, breakages of genomic DNA and amplification bias have made it very challenging to acquire a complete genome with single cell genomics. Here we

show that artificial bacterial polyploidy induced by blocking cell division can significantly improve the performance of single cell genome recovery. Artificial polypoidy forces the bacteria to produce and keep multiple copies of its genetic material. This method promises a nearly complete genomic sequence from a single bacterial cell within a given environment. Our results indicate that induced artificial polyploidy will improve the performance of single cell genomics. It is already known that adding more cells to an amplification reaction results in better genome coverage. Average locus representation in DNA amplified from a single cell was shown to be approximately 30%, and increased to near 80% with 10 cells as the starting amplification template. Our own data confirm this trend. Instead of adding more cells of the same species, which one cannot do easily from a complex environmental or human associated sample, we increased the copies of genomic template within a single cell. This has achieved the same goal of better genome coverage. With millions of uncultured bacterial species in nature, this method may greatly enhance our understanding of the diversity of the bacterial world.

Protein signature-based metagenomic data analysis: Both inheritance and selection pressure result in similarity among biological sequences. Unlike selection pressure, inheritance can be independently estimated with phylogenetic tree. Here we derive a phylogeny of bacterial reference genomes and use it to organize a list of amino-acid 10-mers shared among at least two genomes. We then employ these signature peptides to classify the function and phylogeny of shotgun metagenomic reads. The sensitivity and specificity of our method is comparable to other techniques on 400 base pair reads. However, our method performs far better on shorter reads and is orders of magnitude faster. A single desktop computer could keep up with the output of a next-generation DNA sequencer. Moreover, our method can be readily scaled to larger data sets because it builds on the same technologies used in web search engines. Because tree-based signatures allow a simple and efficient way of organizing biological sequence, their utility should extend far beyond metagenomic analysis. For example, it is possible that signature peptides, especially those assigned near the root of the tree, could bind small molecules and catalyze reactions when synthesized as peptides without needing the rest of the protein, in which case they might be useful in screening for antibacterial compounds or the diagnosis of disease.

Future Work
Our goal in this project is to demonstrate tools and techniques to probe the dynamics of microbial communities. To accomplish this goal, we will develop, integrate, and systematically apply two complementary technologies to explore spatial heterogeneity and temporal response to changes in temperature and precipitation at an experimental field site in Utah and in manipulated experiments in the laboratory. Our single cell genomics efforts will generate reference genomic sequences of individual members of uncultured microbial species from the native samples. Our novel analysis technique uses 20 million signatures, each with 10 contiguous amino acids from reference genomes to reconstruct phylogenetic (who) and functional (what) profiles from the metagenomic DNA sequences. The integration of our technologies will enable us to achieve our scientific objective of characterizing arid land microbial communities in terms of population dynamics and biological processes by answering the following questions: Which microbial populations in arid lands contribute most to the C and N cycles and how do they change in response to variations in temperature and moisture that typify climate change scenarios?

There are three major tasks to accomplish our goals:

1. Soil sample collecting from field and lab experiments. The soil will be treated in field and lab conditions that is related to climate change. Total 72 samples will be collected.

2. Microbial community in the soil samples will be sequenced as a whole and as individual cells. In the second sequencing strategy, we will develop the sequencing method to cover broader regions of a genome.

3. The sequencing data will be analyzed with our state-of-the-art computational tool: amino acid signature based analysis. This method will be expanded to apply to eukaryote with better functional categories.

Conclusion
The deliverable of this project is to demonstrate tools and techniques to probe the dynamics of microbial communities. We will develop, integrate, and systematically apply two complementary technologies, single cell genomics and signature based analysis, to explore spatial heterogeneity and temporal response to changes at an experimental field site and in manipulated experiments in the laboratory.

We will sequence up to 70 controlled metagenomic samples and 100-200 hundred single cell genomes from the sample environment samples, and thereby characterize arid land microbial communities in terms of population dynamics and biological processes that typify climate change scenarios.

Publications
Berendzen, J., W. J. Bruno, J. D. Cohn, N. W. Hengartner, C. R. Kuske, B. H. McMahon, M. A. Wolinsky, and G. Xie. Accurate, sensitive, and rapid classification of short random fragments of bacterial DNA using phylogenetic signature peptide 10-mers. *BMC Genomics.*

Dichosa, A. E K, M. Fitzsimons, L. L Weston1, L. G. Preteska,

J. P. Snook, C. C. Lo, X. Zhang, W. Gu, K. McMurry, L. D. Green, P. S. Chain, J. C. Detter, and C. S. Han. Artificial polyploidy improves bacterial single cell genomics. *PLOS One.*

Dunbar, J., S. Eichorst, L. Gallegos-Graves, G. Xie, N. Hengartner, R. Evans, B. Hungate, R. Jackson, J. Megonigal, C. Schadt, R. Vilgalys, D. Zak, and C. Kuske. Common bacterial responses in six ecosystems exposed to ten years of elevated atmospheric carbon dioxide. To appear in *Environmental Microbiology.*

Scholz, Matthew B., C. C. Lo, and P. SG Chain. Next generation sequencing and bioinformatic bottlenecks: the current state of metagenomic data analysis. To appear in *Current Opinion in Biotechnology.*

Illuminating the Dark Matter of the Genome: Small RNAs as Novel Targets for Bioterrorism Countermeasures

Elizabeth Hong-Geller
20110051DR

Introduction

In this project, our primary scientific challenge is to pioneer functional discovery of small RNAs (sRNAs) in infectious disease, as a means to identify novel targets for therapeutic countermeasures. For decades, control of cellular behavior was thought to be the exclusive purview of protein-based regulators. However, the recent discovery of sRNAs as a universal class of powerful RNA-based regulatory biomolecules has the potential to revolutionize our understanding of gene regulation in practically all biological functions. (Waters and Storz, 2009; Bartel, 2004) We will specifically focus on sRNA discovery in Yersinia pestis, the causative agent of plague, which is of great interest to the biodefense community. Y. pestis is categorized as a CDC Select Agent, signifying great potential risk for adverse impact on public health and national security, and thus represents a high-value target for biodefeat strategies. We will apply our sRNA discovery pipeline to a Grand Challenge in the public health arena: development of sRNAs as potential targets for antimicrobial design against infectious disease. We posit that fundamental sRNA research applied to a biodefense envelope represents a viable research space that is well-aligned with LANL's mission of biothreat reduction.

Benefit to National Security Missions

This research project on elucidation of sRNA-mediated gene regulation in high-risk host-pathogen interactions is well-aligned with the LANL Program Offices for Warfighter Support and Weapons of Mass Effect, liasions to DHS and DoD, including DTRA and DARPA. The identification of small RNAs in both the pathogen and host can lead to development of biological signatures for virulence, infection, and pre-symptomatic disease, with potential applications in therapeutic development and bioforensics strategies. In the last year, our team has submitted multiple proposals on sRNAs as potential biological signatures and we are awaiting funding decisions on a DTRA SEED proposal on the identification of sRNAs as key regulators of bacterial persistence in antibiotic-resistance bacteria. These activities are all evidence of the broad relevance of our work.

Progress

In the first year of this project, we have made considerable progress in establishing the experimental and modeling pipelines to discover key small RNAs (sRNAs) that function in host-pathogen interactions (Figure 1).
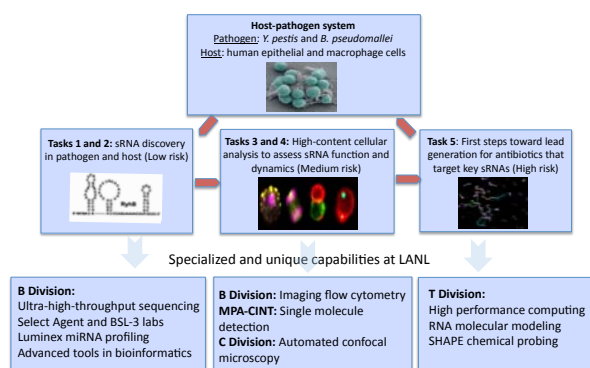
Figure 1. Overview of experimental plan.

Discovery of sRNAs in Y. pestis

We have established Yersinia pestis bacterial culturing and generated RNA fractions in Y. pestis grown at 26°C and 37°C, the growth temperatures of the flea host and human host, respectively, to simulate host infection without a requirement for host cells to be present. We have also extracted RNA from infected host macrophage cells with Y. pestis and are optimizing procedures for processing sRNA samples for ultra high throughput sequencing using the Illumina Genome Analyzer IIx platform in Biosciences Division. We are developing bioinformatics pipelines for extraction of up and down-regulated regions within intergenic spaces to identify small Y. pestis RNAs. Currently, we are analyzing sequencing data to identify putative sRNA sequences.

Host miRNA function in high-risk infection

Unlike the Select Agent pathogens for which very few sRNAs are known, there are currently ~800+ validated human sRNAs or microRNAs (miRNAs). We have es-

tablished a Y. pestis-human cell line infection model and isolated RNA fractions for analysis by miRNA microarrays (outsourced to Exiqon Corp.) to profile expression of the ~800 known miRNAs in host cells in response to *Y. enterocolitica* and *Y. pestis* infection. We are performing qPCR to validate miRNA hits from the microarray experiments and predicting host targets of the candidate miRNAs for further studies on mechanisms of host response.

High-content analysis of Y. pestis infection in host

We will knock-out expression of the identified sRNAs and miRNAs in the pathogen and host, respectively, and assess downstream physiological endpoints. We are developing the capabilities for use of the imaging flow cytomter and automated confocal microscopy to validate the role of identified sRNAs and miRNAs in host-pathogen phenotypes, such as inflammatory response, cell growth and cytoskeleton changes. Initially, we will start with known sRNAs, such as miR-146, which functions in the host innate immune response.

Single cell and single molecule analysis of miRNA targets

We are optimizing conditions for single molecule fluorescence in situ hybridization (FISH) to directly count individual messenger RNA targets of key miRNAs. We are currently using FISH to visualize gene targets of miR-146, such as TRAF6, and the inflammatory mediator IL-1a in response to lipopolysaccharide, a cell component of Gram negative bacteria and are developing programs to quantify the imaging data. We are also planning to visualize the small RNAs in *Yersinia.* The data that we acquire from the advanced spectroscopic and imaging methods to quantify cell-to-cell heterogeneity in host and pathogen will allow us to develop stochastic modeling methods of infection and host response.

First steps toward lead generation for antibiotics that target sRNAs

Finally, we will develop an integrated computational and experimental pipeline to identify small molecule compounds that bind to the sRNAs identified in our study. As we wait for candidate sRNAs from the sequencing efforts, we have started to synthesize two known Y. pestis sRNAs, gcvB and sgrS, that control metabolic functions, and determine their secondary and tertiary structures by SHAPE chemical probing. We will develop our modeling pipeline using these two sRNAs to identify small molecules that inhibit RNA folding and binding to target RNAs.

We expect that successful completion of this project will lead to several high-impact deliverables that span scientific discovery and technology development.

Future Work
Our scientific motivation for this project is sRNA discovery

and elucidation of sRNA-mediated mechanisms of gene expression in high-risk host-pathogen interactions. In the next year, we plan to begin to integrate results from our five tasks in order to leverage our capabilities towards the common objective of translating basic discovery of key sRNAs into signature development for therapeutics.

(1) We will use bioinformatics tools to analyze novel sRNAs in Y. pestis from the ultra high-throughput deep sequencing efforts and downselect unique sRNAs for pipeline analysis by cell biology, imaging studies, and molecular modeling.

(2) We will further analyze the miRNAs identified from the microarray work and perform gene knock-outs of key sRNAs (e.g. mir-146) in the host and pathogen to understand signaling function in immune response to infection.

(3) We will develop cellular assays based on cytokine release, nitric oxide production and other host responses using high throughput, high content analysis to validate the identified sRNAs in host and pathogen with the sRNA knock-outs.

(4) We will employ single cell and single molecule analysis to quantify mRNA targets of sRNAs and develop novel methods of imaging the very short 20 nucleotide sRNAs to build stochastic models to predict cellular behavior.

(5) Finally, we will apply our high-performance computing and SHAPE chemical probing pipeline to model interactions between sRNAs identified from the sequencing efforts and small molecules with antibiotic potential.

Conclusion
The innovation of our project lies in the translation of sRNA function discovery in high-risk pathogen infection into novel countermeasure strategies to target infectious disease. Since intensive efforts to develop new classes of antibiotics have proved to be elusive, there is a great mission need for novel approaches to design more effective antimicrobial therapies. We expect that successful execution of this project can increase the repertoire of potential targets to include sRNAs. Given the newly-discovered central role of sRNA in gene regulation, we are poised to deliver high-impact discoveries in molecular mechanisms of sRNA–mediated host-pathogen interactions and potentially, antimicrobial design.

References
1. Waters, L., and G. Storz. Regulatory RNAs in bacteria. 2009. *Cell.* **136**: 628.

2. Bartel, D. P.. MicroRNAs; genomics, biogenesis, mechanism, and function. 2004. *Cell.* **116**: 1.

Publications
Chain, P. S., G. Xie, S. R. Starkenburg, M. B. Scholz, N. Beck-

loff, C. C. Lo, K. W. Davenport, K. G. Reitenga, H. E. Daligault, J. C. Detter, T. A. Freitas, C. D. Gleasner, L. D. Green, C. S. Han, K. K. McMurray, L. J. Meinke, X. Shen, and A. Zeytun. Genomics for key players in the N cycle from guinea pigs to the next frontier. 2011. *Methods in Enzymology.* **496**: 318.

Hennelly, S., and K. Sanbonmatsu. Tertiary contacts control switching of the SAM-I riboswitch. 2011. *Nucleic Acids Research.* **39** (6): 2416.

Hong-Geller, E., and N. Li. miRNAs as therapeutic targets to combat diverse human diseases. To appear in *Drug Development/Book 2.* Edited by Rundfeldt, C..

Hu, B., G. Xie, C. C. Lo, S. Starkenburg, and P. S. Chain. Genomics in the Next-Generation Sequencing Era: Genome Alignments, Pangenomics and Metagenomics. To appear in *Briefings in Functional Genomics.*

Shepherd, D., N. Li, E. Hong-Geller, B. Munsky, and J. Werner. New tools for discovering the role sRNA plays in cell regulation. To appear in *SPIE Photonics West.* (San Francisco, 21-26 Jan 2012).

Zhang, M., A. S. Perelson, and C. S. Tung. RNA Structural Motifs. 2011. In *eLS.* Edited by Wiley, J.. , p. 10.1002. Chichester: John Wiley .

Multi-Scale Science Framework for Climate Treaty Verification: Attributing and Tracking Greenhouse Gas Fluxes Using Co-Emitted Signatures

Manvendra K. Dubey
20110081DR

Introduction

Climate treaty verification is a major international challenge and a growing mission for LANL. While consensus on the dangers of climate change continues to strengthen, viable strategies for verifying greenhouse gas (GHG) emissions remain lacking. The 2009 Copenhagen Accord identified this verification shortfall as the critical barrier to a viable global climate treaty. With the formidable requirement of detecting small changes in CO_2 above a large and variable natural background, current in situ CO_2 measurement approaches are grossly inadequate, and inapplicable to denied territories. Current satellites lack instrumentation for monitoring CO_2 with sufficient precision. Furthermore, no verification methodology exists to attribute observed CO_2 enhancements to individual sectors or nations. A purpose-designed satellite verification system is clearly needed, and a compelling opportunity exists in defining what it should measure. Our project seizes that opportunity with a powerful new strategy that can enable both enhanced GHG detection and rigorous source attribution (i.e., identify violators). We hypothesize that CO_2 from various natural and anthropogenic sources can be distinguished and tracked by monitoring associated "signature" gases and isotopomers, co-emitted in distinctive ratios by different fuels and combustion processes. We are testing this strategy through a unique convergence of assets: (1) An ideal experimental test-bed, in our own backyard: the Four Corners region of NM, with two major power plants of distinctively different emissions profiles in an isolated locale; (2) The new Greenhouse gas Observing SATellite (GOSAT), which we, as science team members, will point at our site; (3) LANL's state-of-the-art capabilities in atmospheric observations, multi-scale modeling, and powerful new instrumentation.

Benefit to National Security Missions

LANL's leadership in nuclear nonproliferation treaty verification has stimulated us to seek a defining role in the emerging climate treaty verification domain. Our study will guide the formulation of a climate treaty and development of verification protocols that need to go hand in hand. Our project will catalyze the expansion of our verification mission and is synergistic with our growing expertise in climate modeling, infrastructure impacts and space surveillance. In particular our science will used to strengthen the ongoing GHGIS initiative with NNSA, NASA, OSc and NOAA working together. We will strengthen climate monitoring programs where we are under-utilized and propose world-wide deployments in climate sensitive regions. In turn, the remote sensing techniques we develop build capabilities for nuclear nonproliferation.

Progress

We made significant progress in FY11 having successfully deployed our robotic laboratory with the solar Fourier Transform Spectrometer (FTS) and in situ GHG, CO and meteorological sensors at our Four Corners site. Our multi-scale observational test-bed that is located between the Four Corners and San Juan power plants has been operational continuously since early 2011 (Figure 1). We have been collecting real time data on seconds to minute resolution on point to 100km scales. A typical sunrise to sunset profile of GHGs and CO measured at our site shown in Figure 2 for March 12, 2011. Typical power-plant signals increase the FTS-measured column CO_2 by 2 to 8 ppm while our surface *in situ* signals increase by 10 to 50 ppm when the winds are favorable for power plant plume sampling at our site. *In situ* CH_4 data reveal 4-5 ppm nocturnal increases together with 0.05-0.09 ppm FTS column increase in the morning suggesting a dispersed source. A customized multi-scale model that resolves the power plants in a regional chemistry transport model has been developed to analyze our Four Corners data. Our retrieval algorithms for the FTS column GHG measurements were validated by vertical profiles taken by NCAR's HIaper Pole to Pole Observations (HIPPO) campaign above our site (Figure 3). Our calibration factors are consistent with those in the Total Column Carbon Observing Network. We have acquired collocated GOSAT measurements of CO_2 and CH_4 with our FTS for validation. We have used satellite NO_2 data over Four Corners from NASA's Ozone Monitoring Instrument to discover a declining long tem trend that is attributed to the environmental boiler upgrades at the San

Juan power plant. We are making several unanticipated discoveries such as the presence of significantly enhanced CH_4 in a semi-arid region. We are initiating attribution studies to discriminate various CO_2 sources in the region as well as the long-range transport of the Wallow fire plume that we sampled at our site. In summary, we are collecting high quality validated data at our Four Corners test-bed and developing a multi-scale model and measurement framework for the quantification, discrimination and attribution of distinct anthropogenic and natural CO_2 sources using signature pollutants.

First Solar FTS to Monitor Power Plant Operational San Juan NM

Goal: Separate CO_2 contributions fro high NOx and low NOx PPs using FTS data

https://tccon-wiki.caltech.edu/Sites/Four_Corners

Four Corners PP
High NOx/CO_2

San Juan PP
Low NOx/CO_2

Figure 1. View of our Four Corners site with instruments inside our robotic laboratory that is located between the two power plants in a semi-arid region as United States' first verification test bed.
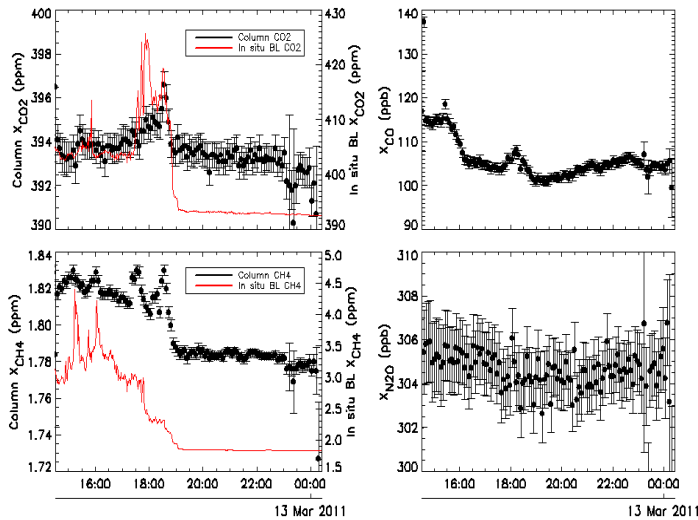
Figure 2. Columnar (black) and in situ boundary layer (red) measurements of CO_2, CH_4, CO and N_2O and on March 12, 2011 resolve CO_2 signals from power plants when meteorology is favorable and methane from unknown sources. Column data are taken every two minutes and the in situ data every second. Sunrise is on the left and sunset is on the right and the time is in UTC.
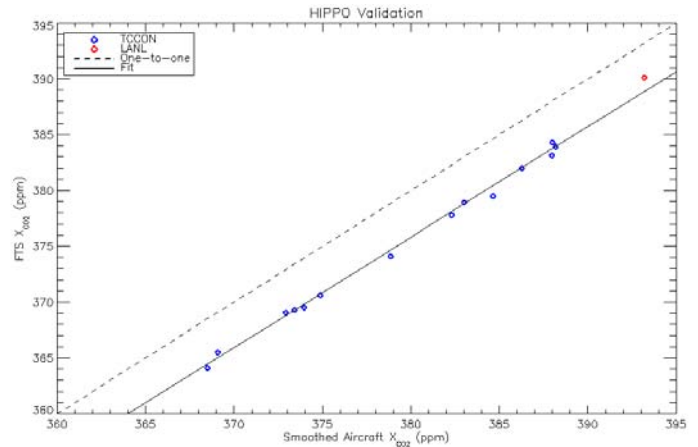
Figure 3. Calibration of our FTS retrieved CO_2 with the integrated vertical airborne in situ profile measured on June 7 over by HIPPO at our site (red) and previously at other TCCON sites (blue) world-wide. Our calibration is at the highest CO_2 level and the only semi-arid power plant site. Note the linearity over all sites and the systematic low offset from the 1:1 dashed line results from imprecise spectral data on the line shapes of trace gases, and the scale factor from the validation is used to empirically correct for this.

Specific tasks, challenges, milestones and results for our project in FY11 are described below:

Multi-Scale Observations

Our solar FTS was deployed at the Four Corners, Farmington NM site in December 2010. The system required realignment and a new laser and has been operational remotely, collecting spectra in all good weather days since March. New middle infrared detectors were also installed to monitor signature pollutants.

We have developed a protocol for routine retrieval of all greenhouse gases, and carbon monoxide a signature pollutant, from the high-resolution spectra we collect. We have analyzed over 3000 spectra and have achieved good quality.

Our data clearly shows late morning power-plant plumes with CO_2 enrichments of order 2-8 ppm. On windy days the plume is dispersed quickly without significant accumulation. This is a robust finding verified with over a month long data set. We have also measured large early morning signals from methane that are like coming from coal mining since we do not see concomitant increases in other gases.

We have installed in situ sensors to measure CO_2, CH_4, and CO at the surface site that are providing continuous real time data day and night in the surface air at about 10 m level. Also included are a meteorological station, accurate pressure sensors and celiometers to measure boundary layer heights. The systems are also operational.

On June 7, we achieved a milestone where the NCAR G-V aircraft equipped with state of the art in situ greenhouse gas sensors (as part of the HIPPO project) measured in situ GHG profiles over our site that were used to validate our FTS retrievals.

We also measured the Wallow fire plumes at our site with large enhancements of CO_2, CH_4, and CO from May 31 to June 12. This unplanned experiment has allowed us to acquire a unique data set examine methods to separate fire CO_2 emissions from power-plant CO_2 emissions.

NASA is deploying sun photometers to measure aerosol optical depth and CO_2 (less precisely) at our site to test their performance.

We have verified the drop in NO_2 over the Four Corners power plants from space and verified the environmental upgrades at the San Juan power worked.

We are now an active and integral part of the international TCCON network.

We have GOSAT data at our site and are beginning to compare it at our site. GOSAT appears to have a low bias of about 5-10ppm relative to our solar FTS observations.

Multi-Scale Models

We have performed high-resolution plume dispersion simulations of the two Four Corners power plant plumes using realistic meteorology and CO_2 and NO_2 emissions. These are the most detailed plume simulations performed anywhere to date.

We have customized a regional Weather Forecast Model with Chemistry for the Four Corners region. The model output is used to provide the boundary conditions for the high-resolution plume models and the two are coupled. Chemistry and CO_2 pollution simulations are running successfully. We are running the regional and plume models for specific days where we have FTS observations in order to quantify the emissions. Preliminary results indicate that the 2-8ppm signals we see is consistent with the emissions and meteorology.

Multi-Scale Uncertainty Quantification

An uncertainty quantification framework has been coupled to our plume model and a data driven ensemble Kalman filter approach has been used to infer CO_2 emissions from our column CO_2 observations. This is being expanded to include co-emitted pollutants like NO_2 and quantify the improved precision it provides us.

We made AGU, EGU and AMS presentations that will be published. Our research was showcased at the LANL sensors and remote sensing capability review where external experts, including NASA-JPL's David Crisp (Science lead for OCO-2) noted the rapid progress we have made. Our vis-ible science has resulted in the Japanese operators of a FTS facility in the Arctic (Poker Flats) to approach us for a partnership for long term monitoring of the carbon fluxes from the warming Arctic. We are also helping validate JPL's airborne FTS for the CARVE project at our Four Corners site. Finally, we have been approached by Chevron to help develop CH_4 monitoring and modeling analysis at their gas fields.

Updates and images of our site are at: https://tccon-wiki.caltech.edu/Sites/Four_Corners

Future Work

We will test our signature-based CO_2 attribution science using 4-Corners' rich but tractable mix of power plant, urban, and oil/gas production emissions. The most comprehensive set of cutting-edge instruments to date, including LANL's unique solar tracking Fourier Transform Spectrometer and in situ ground and airborne sensors, will be used to exhaustively measure signature pollutants and greenhouse gas distributions simultaneously over a range of scales. We will task GOSAT to stare at our site, enabling GHG retrieval validation to maximize its precision in measuring CO_2 as well as help prepare for OCO-2. Other satellites will provide additional signature data. Detailed multi-scale chemical transport models, built on LANL's renowned theory, numerical and supercomputing capabilities, will be developed and used to analyze the multi-perspective data. The robustness of signature science for GHG source attribution and flux inversion form real-world data will be examined. Uncertainty quantification will provide rigorous assessment of our verification ability. Our observation, modeling, and analysis at Four Corners will lay the foundations for signature science and enable the design of next-generation multi-species satellite sensors that will push the frontiers of GHG monitoring. The long-term value of our test-bed and expertise base is such that it will likely become a permanent site dedicated to air-quality and GHG monitoring. We anticipate agencies like DOE, NASA, NSA, NOAA and the private sector to work synergistically with us to harness our Four Corners multi-scale analysis test-bed to develop and evaluate other more precise and/or less expensive methods for verification.

In summary, our tasks include:

1. Remote sensing of CO_2 at Four Corners: Deploy FTS at a ground site, collect spectra routinely, develop and implement retrievals, calibrate satellites, establish baseline and variability for verification.

2. *In situ* and remote measurements of signatures and green house gases to discriminate the two power plant plumes and resolve the diffuse sources from urban and oil and gas exploration.

3. Develop and apply multi-scale carbon and chemistry transport models to analyze data and use them to verify in stack emissions and urban inventory.

Conclusion

Our work lays the scientific foundations where atmospheric observations of greenhouse gases and pollutants can be used to determine if industries, states and nations are accurately reporting their green house gas emissions. This will allow congress to negotiate an equitable and verifiable climate treaty internationally. It also will guide the design of a monitoring network to monitor national greenhouse gas emissions, long range transports of pollutants as well as enable early detect of potential abrupt releases of carbon stored in the Arctic as it thaws as the earth warms.

References

1. Deutscher, N. M., D. W. Griffith, G. W. Bryant, P. O. Wennberg, G. C. Toon, R. A. Washenfelder, G. Keppel-Aleks, D. Wunch, Y. Yavin, N. T. Allen, J. -F. Blavier, R. Jimenez, B. C. Daube, A. V. Bright, D. M. Matross, S. C. Wofsy, and S. Park. Total column CO2 measurements at Darwin, Australia - site description and calibration against in situ aircraft profiles. 2010. *ATMOSPHERIC MEASUREMENT TECHNIQUES.* **3** (4): 947.

2. Wunch, D., G. C. Toon, P. O. Wennberg, S. C. Wofsy, B. B. Stephens, M. L. Fischer, O. Uchino, J. B. Abshire, P. Bernath, S. C. Biraud, J. -F. Blavier, C. Boone, K. P. Bowman, E. V. Browell, T. Campos, B. J. Connor, B. C. Daube, N. M. Deutscher, M. Diao, J. W. Elkins, C. Gerbig, E. Gottlieb, D. W. Griffith, D. F. Hurst, R. Jimenez, G. Keppel-Aleks, E. A. Kort, R. Macatangay, T. Machida, H. Matsueda, F. Moore, I. Morino, S. Park, J. Robinson, C. M. Roehl, Y. Sawa, V. Sherlock, C. Sweeney, T. Tanaka, and M. A. Zondlo. Calibration of the Total Carbon Column Observing Network using aircraft profile data. 2010. *ATMOSPHERIC MEASUREMENT TECHNIQUES.* **3** (5): 1351.

3. Wunch, D., P. O. Wennberg, G. C. Toon, G. Keppel-Aleks, and Y. G. Yavin. Emissions of greenhouse gases from a North American megacity. 2009. *Geophysical Research Letters.* **36** (15): L15810 (5 pp.).

4. Schneising, O., M. Buchwitz, M. Reuter, J. Heymann, H. Bovensmann, and J. P. Burrows. Long-term analysis of carbon dioxide and methane column-averaged mole fractions retrieved from SCIAMACHY. 2011. *ATMOSPHERIC CHEMISTRY AND PHYSICS.* **11** (6): 2863.

5. Kuze, A., D. M. O,ÄôBrien, T. E. Taylor, J. Day, C. O,ÄôDell, F. Kataoka, M. Yoshida, Y. Mitomi, C. Bruegge, H. Pollock, R. Basilio, M. Helmlinger, T. Matsunaga, S. Kawakami, K. Shiomi, T. Urabe, and H. Suto. Vicarious Calibration of the GOSAT Sensors Using the Railroad Valley Desert Playa. 2011. *IEEE TRANSACTIONS ON GEOSCIENCE AND REMOTE SENSING.* **49** (5): 1781.

6. Morino, I., O. Uchino, M. Inoue, Y. Yoshida, T. Yokota, P. O. Wennberg, G. C. Toon, D. Wunch, C. M. Roehl, J. Notholt, T. Warneke, J. Messerschmidt, D. W. Griffith, N. M. Deutscher, V. Sherlock, B. Connor, J. Robinson, R. Sussmann, and M. Rettinger. Preliminary validation of column-averaged volume mixing ratios of carbon dioxide and methane retrieved from GOSAT short-wavelength infrared spectra. 2011. *ATMOSPHERIC MEASUREMENT TECHNIQUES.* **4** (6): 1061.

7. Ishida, H., T. Nakjima, T. Yokota, N. Kikuchi, and H. Watanabe. Investigation of GOSAT TANSO-CAI Cloud Screening Ability through an Intersatellite Comparison. 2011. *JOURNAL OF APPLIED METEOROLOGY AND CLIMATOLOGY.* **50** (7): 1571.

8. Butz, A., S. Guerlet, O. Hasekamp, D. Schepers, A. Galli, I. Aben, C. Frankenberg, J. -M. Hartmann, H. Tran, A. Kuze, G. Keppel-Aleks, G. Toon, D. Wunch, P. Wennberg, N. Deutscher, D. Griffith, R. MacAtangay, J. Messerschmidt, J. Notholt, and T. Warneke. Toward accurate CO_2 and CH_4 observations from GOSAT. 2011. *Geophysical Research Letters.* **38** (14): L14812.

9. Parker, R., H. Boesch, A. Cogan, A. Fraser, L. Feng, P. Palmer, J. Messerschmidt, N. Deutscher, D. T. Griffith, J. Notholt, P. Wennberg, and D. Wunch. Methane observations from the Greenhouse Gases Observing SATellite: Comparison to ground-based TCCON data and model calculations. 2011. *GEOPHYSICAL RESEARCH LETTERS.* **38**: L15807.

10. Chevallier, F., L. Feng, H. BoÃàsch, P. Palmer, and P. Rayner. On the impact of transport model errors for the estimation of CO $_2$ surface fluxes from GOSAT observations. 2010. *Geophysical Research Letters.* **37** (21): L21803.

11. Bovensmann, H., M. Buchwitz, J. P. Burrows, M. Reuter, T. Krings, K. Gerilowski, O. Schneising, J. Heymann, A. Tretner, and J. Erzinger. A remote sensing technique for global monitoring of power plant CO2 emissions from space and related applications. 2010. *ATMOSPHERIC MEASUREMENT TECHNIQUES.* **3** (4): 781.

12. Crisp, D.. Measuring CO_2 from space: The nasa Orbiting Carbon Observatory-2. 2010. In *61st International Astronautical Congress 2010, IAC 2010 ; 20100927 - 20101001 ; Prague, Czech Republic.* Vol. 7, p. 5719.

13. Kim, S. -W., A. Heckel, G. J. Frost, A. Richter, J. Gleason, J. P. Burrows, S. McKeen, E. -Y. Hsie, C. Granier, and M. Trainer. NO_2 columns in the western United States observed from space and simulated by a regional chemistry model and their implications for NO_x emissions. 2009. *Journal of Geophysical Research - Part D - Atmospheres.* **114** (D11): D11301 (29 pp.).

Publications

Costigan, K. R., M. K. Dubey, P. Chylek, S. P. Love, B. G. Henderson, B. A. Flowers, J. M. Reisner, T. Rahn, and C. R. Quick. Multi-Scale Science Framework for Attributing and Tracking Greenhouse Gas Fluxes at LANL's Four Corners New Mexico Test Bed. 2010. In *American Geophysical Union Annual Meeting.* (San Francisco, 0-13 Dec. 2010). , p. GC13D. San Francisco: AGU.

Dubey, M. K.. Solar Fourier Transform Spectrometry in mid-near infrared and visible-ultraviolet to monitor greenhouse gas and co-emitted pollutant emissions from Four Corners, NM power plants. 2011. In *European Geosciences Union General Assembly 2011.* (Vienna, 3-8 April 2011). Vol. 13, p. EGU2011. Vienna: Geophysical Research Abstracts.

Flowers, B. A., H. H. Powers, M. K. Dubey, and N. G. McDowell. Field inter-comparison of two high-accuracy fast-response spectroscopic sensors of carbon dioxide. 2011. *Atmospheric Measurement Techniques Discussions.* **4** (1): 5837.

Keeling, R., A. Manning, and M. Dubey. The atmospheric signature of carbon capture and storage. 2011. *PHILOSOPHICAL TRANSACTIONS OF THE ROYAL SOCIETY A-MATHEMATICAL PHYSICAL AND ENGINEERING SCIENCES.* **369** (1943): 2113.

Multi-scale Dynamics of Biological Systems

Robert E. Ecke
20110435DR

Introduction

Biological systems involve dynamics in a fundamental way, spanning many orders of magnitude in time with corresponding multi-scale spatial structures. We are elucidating the complex interactions of temporal and spatial degrees of freedom by using the modern tools of physical and mathematical sciences to make quantitative predictions about biological systems. Our work spans length scales from nanometers to millimeters, ranging from individual bio-molecules through complex phenomena within a single cell to the behavior of group of cells. At the molecular level, we are working to understand how the diversity of biological molecules such as DNA, RNA, or proteins arises from competing deterministic energy scales associated with chemical bonds, mechanical bending/breaking, and electrostatic interactions and stochastic thermal energy. will apply this insight to model proteins and their substrates with applications to bio-fuel production. At the cellular level, we average over parts of the complex cellular bio-chemical kinetics to produce reduced models of gene regulation, expression, and differentiation. We develop phenomenological models of cell regulatory processes that allow effective descriptions of cell functions without precise correspondence to microscopic detail. For inter-cellular interactions, we develop models of interacting neurons that form the basis for image recognition and cognitive reasoning.

Benefit to National Security Missions

Our quantitative approach to biological dynamics at the molecular, cellular and systems level may have significant impact on applications in bio-security, energy, and health by ultimately allowing for cellular engineering, i.e., the manipulation of cellular behaviors for useful purposes. In bio-security, our work may contribute to the mitigation and detection of pathomic agents and pandemic diseases. For example, such approaches may be key to the rapid development of drug therapies or vaccines against emerging bio-threats. Another area of important impact is the design of new bio-fuel processes for a sustainable energy economy. Indirect outgrowths of our work may be quantitative modeling of tumor growth and cancer treatment. Understanding biological systems at a quantitative and predictive level is the great challenge of the 21st century and our approach and research efforts will contribute substantively to that agenda in service of the LANL national security mission.

Progress

In the area of macromolecules, we focused on problems in cellulosic biofuels, protein folding and assembly, and molecular motors.

Natural cellulose often assumes a crystalline form that is difficult to process for biofuel production. Our biofuel research centered on understanding how the crystal form of cellulose is determined by the underlying molecular interactions, and how the processing rate of cellulose into simpler sugars is influenced by the crystal form. We performed *in silico* studies of crystalline cellulose and its degradation by enzymes, and performed neutron crystallographic and molecular dynamics studies of the structure of ammonia-cellulose I to understand how hydrogen bonding rearranges during the treatment of cellulose with ammonia. We studied the restructuring of the crystalline cellulose hydrogen bond network and determined its relation to enhancing the depolymerization rate. Our results complement and expand experimental findings by revealing how the main structural and thermodynamic differences between natural and ammonia-treated cellulose affect their degradation rates, and by providing new insights for more efficient cellulose degradation protocols.

For folding and aggregation, we used a minimalist computational model to investigate how polar/non-polar patterns on a surface can induce the folding of an otherwise unstructured peptide. We used coarse-grained simulations to suggest a possible explanation for the experimentally observed increase in stability of the four-helix bundles with increasing sequence length, suggesting that simple computational models can be used as a complementary tool in the design process of de novo proteins. We studied the effect of surface interactions on peptide aggregate morphology. We also applied molecular dynamics simulations to study the

conformations displayed by intrinsically disordered protein (IDP), α-synuclein, a highly studied IDP that is implicated in Parkinson's disease. We showed that the heterogeneous collapsed state of the protein might enable α-synuclein to be decomposed into fragments that can be studied independently to build up a picture of the whole protein. We also performed molecular dynamics simulations on varying sequences of the HIV envelope protein gp120 and found a rationale for the immune escape mechanisms in different sequences of the protein.

For molecular motors, we developed a numerical approach to separation of time scales in molecular dynamics simulations of molecular motor kinetics, and applied it to model the dynamics of a molecule that acts like a rotor, and also to a catenane molecule.

In the area of cellular dynamics and function, we published the proceedings of the Third and Fourth q-bio Conferences, ran the Fifth conference in August 2011, and began organizing the Sixth q-bio Conference (http://q-bio.org). This conference was initiated by CNLS and has emerged as one of the top systems biology conferences worldwide. We used computational modeling to study regulation of autophagic flux, B cell antigen receptor (BCR) signaling, the functional significance of APC mutation in cancer, and the effects of lipid rafts on IgE receptor signaling. We developed an algorithm that uses comparative genomics methods to correct errors in predicted gene maps for bacterial genomes, and implemented the algorithm in a software pipeline (http://code.google.com/p/gmv/). We wrote a manuscript describing the characterization of anomalous clustering effects on the photo-physical properties of quantum dots, which is relevant to their use to label trace particles for characterizing cellular dynamics. We wrote a review on modeling cellular variability, and developed a stochastic model of gene regulation in response to osmotic stress in yeast.

In the area of cooperative cellular interactions, we studied tissue dynamics, flocking behavior, viral evolution and spread, and human vision.

For tissue dynamics, we developed a multiscale model of the growth of new blood vessels in response to signals using data from embryonic mice. We showed that two commonly used stochastic models of lymphocyte proliferation and death are mathematically equivalent, and obtained an analytic solution that agrees with simulated and experimental data.

For flocking behavior, we studied Topotaxis, which is how to use the topology of a substrate to control the motion of self-driven particles including biologically motivated systems. We demonstrated that a ratchet effect occurs for particles on an asymmetric substrate and developed a model for flocking particles where both a ratchet effect and a reversed ratchet effect can arise. This research opens up new avenues in modeling swarms and self-driven particles on patterned substrates.

For viral evolution and spread, we modeled the influence of recombination on increased viral diversity, and used the model to simulate viral infection dynamics during drug therapy. We developed a method for detecting important evolutionary effects (hitchhiking and bottlenecks) in samples of DNA sequences. We developed an algorithm for classification of HIV subtypes and used it to determine that CRF02 of HIV-1 is a recombinant of Subtypes A and G. We determined genetic signatures in the envelope glycoproteins of HIV-1 that associate with broadly neutralizing antibodies, and determined that persistence of multiple subpopulations of HIV-1, each bearing different versions of the env gene, is consistent with neutrality during high-frequency patient sampling. Finally, we used homology modeling to show that a set of monoclonal antibodies that neutralize HIV-1 pseudoviruses each target the V1V2 region of the gp120 envelope protein.

Using LANL super-computing resources we developed the first full-scale, real-time model of visual processing in the human brain. We applied our algorithms to a wide range of imagery types, including vegetation detection with NASA satellite imagery, and man-made object detection with aerial video. We also demonstrated that our program learns color, texture and motion cues to detect multiple object categories simultaneously and used human input to accelerate training mark-up of video streams.

Future Work

We use quantitative methods of statistical physics, applied mathematics, physical chemistry, nonlinear dynamical systems, and computer simulations to develop models of biological systems at the molecular, cellular and multi-cellular level. We attempt to bridge spatial scales from molecular building blocks to full cell function using different modeling and coarse-graining methods. At the molecular level, we use numerical simulation and network models to characterize energetics, allostery, multidimensionality and intrinsic disorder in proteins. We also use molecular dynamics simulations to understand and describe protein-protein, protein-carbohydrate, and protein-membrane interactions. We consider dynamics at the cellular level from several perspectives. One approach is to understand intra-cellular processes that regulate gene expression based on phenomenological models that employ quantitative approaches from statistical physics and mathematics such as stochastic models of the nuclear pore complex or of gene expression feedback networks. Another direction is to coarse grain over the complex biochemical kinetics in the cell to yield a model to predict how the cell will behave based on a highly reduced set of control variables. At the multi-cellular level, we are interested in collective behavior of cells including the interaction of neurons to produce collective cognitive response, e.g., human vision. In our work, we have close collaborations with experimental efforts that underpin our quantitative modeling of biological dynamics.

Conclusion

Using quantitative models of biological dynamics spanning multiple time and length scales, we will provide tools for predictive analysis of biological function. At the molecular level, we will provide models of individual bio-molecules including connecting protein structure and function, describing the cooperative role of protein-protein interactions that enable cell regulatory processes, and simulating the interactions of macromolecules. At the cellular level, we will coarse-grain over microscopic degrees of freedom consisting of bio-chemical reactions to achieve cell-level models of cell regulatory processes. We will develop phenomenological models of cell function that characterize a particular cellular process rather than being microscopically accurate.

Publications

Akimov, A., and N. A. Sinitsyn. Sensitivity field for nonautonomous molecular rotor. *Journal of Chemical Physics.*

Barua, D., W. S. Hlavacek, and T. Lipniacki. A computational model for early events in B cell antigen receptor signaling: analysis of the roles of Lyn and Fyn. To appear in *Journal of Immunology.*

Bellesia, G., A. Asztalos, T. Y. Shen, P. Langan, A. Redondo, and S. Gnanakaran. In silico studies of crystalline cellulose and its degradation by enzymes. 2011. *Acta Crystallographica Section D-Biological Crystallography.* **201** (66): 1184.

Bellesia, G., A. I. Jewett, and J. E. Shea. Relative stability of de novo four-helix bundle proteins: Insights from coarse grained molecular simulations. 2011. *Protein Science.* **20** (5): 818.

Bellesia, G., S. P. Chundawat, P. Langan, B. E. Dale, and S. Gnanakaran. Probing the Early Events Associated with Liquid Ammonia Pretreatment of Native Crystalline Cellulose. 2011. *Journal of Physical Chemistry B.* **115** (32): 9782.

Chundawat, S. P., G. Bellesia, N. Uppugundla, L. D. Sousa, D. H. Gao, A. M. Cheh, U. P. Agarwal, C. M. Bianchetti, G. N. Phillips, P. Langan, V. Balan, S. Gnanakaran, and B. E. Dale. Restructuring the Crystalline Cellulose Hydrogen Bond Network Enhances Its Depolymerization Rate. 2011. *Journal of the American Chemical Society.* **133** (29): 11163.

Drocco, J., C. J. Olson, and C. Reichhardt. Fluctuation theorem in driven nonthermal systems with quenched disorder. To appear in *Europhysical Journal E.*

Drocco, J., C. J. Olson, and C. Reichhardt. Bidirectional sorting of flocking particles on asymmetric substrates. *Proceedings of the National Academy of Sciences of the USA.*

Gintautas, V., B. Kunsberg, M. Ham, S. Barr, S. Zucker, S. Brumby, L. M. Bettencourt, and G. T. Kenyon. Contours and 2D form an improved model for contour completion in V1 using learned feature correlation statisitcs. 2010. *Journal of Vision.* **10** (7): 1162.

Gintautas, V., M. Ham, B. Kunsberg, S. Barr, S. Brumby, C. Rasmussen, J. George, I. Nemenman, L. M. Bettencourt, and G. T. Kenyon. Model cortical association fields account for the time course and dependence on target complexity of human contour perception. 2011. *PLoS Computational Biology.* **7** (10): e1002162.

Gnanakaran, S., M. G. Daniels, T. Bhattacharya, A. S. Lapedes, A. Sethi, M. Li, H. L. Tang, K. Greene, H. M. Gao, B. F. Haynes, M. S. Cohen, G. M. Shaw, M. S. Seaman, A. Kumar, F. Gao, D. C. Montefiori, and B. Korber. Genetic Signatures in the Envelope Glycoproteins of HIV-1 that Associate with Broadly Neutralizing Antibodies. 2010. *PLoS Computational Biology.* **6** (10): e1000955.

Gnanakaran, S., S. Bhattacharya, M. G. Daniels, B. F. Keele, P. T. Hraber, A. S. Lapedes, T. Y. Shen, B. Gaschen, M. Krishnamoorthy, H. Li, J. M. Decker, J. F. Salazar-Gonzalez, S. Wang, C. Jiang, F. Gao, R. Swanstrom, J. A. Anderson, L. H. Ping, M. S. Cohen, M. Markowitz, P. A. Goepfert, M. S. Saag, J. J. Eron, C. B. Hicks, W. A. Blattner, G. D. Tomaras, M. Asmal, N. L. Letvin, P. B. Gilbert, A. C. Decamp, C. A. Magaret, W. R. Schief, Y. E. Ban, M. Zhang, K. A. Soderberg, J. G. Sodroski, B. F. Haynes, G. M. Shaw, B. H. Hahn, and B. Korber. Recurrent signature patterns in HIV-1 B clade envelope glycoproteins associated with either early or chronic infections. 2011. *PLoS Pathogens.* **7** (9): e1002209.

Ham, M. I., V. Gintautas, M. A. Rodriguez, R. A. Bennett, C. L. Maria, and L. M. Bettencourt. Density-dependence of functional development in spiking cortical networks grown in vitro. 2010. *Biological Cybernetics.* **102** (1): 71.

Lemons, N. W., B. Hu, and W. S. Hlavacek. Hierarchical graphs for rule-based modeling of biochemical systems. 2011. *BMC Bioinformatics.* **12**: 45.

Lynch, R. M., R. Rong, S. Boliar, A. Sethi, B. Li, J. Mulenga, S. Allen, J. E. Robinson, S. Gnanakaran, and C. A. Derdeyn. The B Cell Response Is Redundant and Highly Focused on V1V2 during Early Subtype C Infection in a Zambian Seroconverter. 2011. *Journal of Virology.* **85** (2): 905.

Morriss-Andrews, A., G. Bellesia, and J. E. Shea. Effect of surface interactions on peptide aggregate morphology. To appear in *Journal of Chemical Physics.*

Nemenman, I., J. R. Faeder, W. S. Hlavacek, Y. Jiang, M. E. Wall, and A. Zilman. Selected papers from the fourth annual q-bio conference on cellular information processing. 2011. *Physical Biology.* **8** (5): 050301.

Nemenman, I., W. S. Hlavacek, Y. Jiang, M. E. Wall, and A. Zilman. The third q-bio conference on cellular information processing. 2010. *IET Systems Biology.* **4** (6): 331.

Olson, C. J., J. Drocco, T. Mai, M. B. Wan, and C. Reichhardt. Active matter on asymmetric substrates. 2011. *Proceedings of the International Society for Optics and Photonics.* **8907**: 80970A.

Ramakhrishnan, P., G. Bellesia, S. P. Chundawat, P. Langan, B. E. Dale, and S. Gnanakaran. New insights into hydrogen bonding and stacking interactions in cellulose. To appear in *Journal of Physical Chemistry A.*

Reichhardt, C., J. Drocco, and C. J. Olson. Vortex matter with attractive interactions. To appear in *Physica C.*

Sethi, A., J. Tian, D. Vu, and S. Gnanakaran. Identification of minimally interacting modules in an intrinsically disordered protein. *Biophysical Journal.*

Skar, H., R. N. Gutenkunst, K. Wilbe, A. Alaeus, J. Albert, and T. Leitner. Persistence of multiple env subpopulations is consistend with neutrality during high-frequency sampling of a chronic HIV-1 patient. 2011. *PLoS One.* **6**: e21747.

Tian, J., A. Sethi, D. Anunciado, D. Vu, and S. Gnanakaran. A-Synuclein Interactions with Sodium Dodecyl Sulfates: A molecular dynamics study of the self-assembly system. *Journal of Chemical Physics.*

Wada, M., Y. Nishiyama, G. Bellesia, T. Forsyth, S. Gnanakaran, and P. Langan. Neutron crystallographic and molecular dynamics studies of the structure of ammonia-cellulose I: rearrangement of hydrogen bonding during the treatment of cellulose with ammonia. 2011. *Cellulose.* **18** (2): 191.

Wall, M. E.. Structure-function relations are subtle in genetic regulatory networks. 2011. *Mathematical Biosciences.* **231** (1): 61.

Wall, M. E., S. Raghavan, J. D. Cohn, and J. Dunbar. Genome majority vote improves gene predictions. To appear in *PLoS Computational Biology.*

Yang, J., X. Meng, and W. S. Hlavacek. Rule-based modelling and simulation of biochemical systems with molecular finite automata. 2010. *IET Systems Biology.* **4** (6): 453.

Yang, J., and W. S. Hlavacek. Scaffold-mediated nucleation of protein signaling complexes: Elementary principles. 2011. *Mathematical Biosciences.* **232** (2): 164.

Yang, J., and W. S. Hlavacek. Efficiency of reactant site sampling in network-free simulation of rule-based models for biochemical systems. To appear in *Physical Biology.*

Zhang, M., A. S. Perelson, and C. S. Tung. RNA Structural Motifs. 2011. *eLS.* (August): -.

Zhang, M., B. Foley, A. K. Schultz, J. P. Macke, I. Bulla, M. Stanke, B. Morgensterm, B. Korber, and T. Leitner. The role of recombination in the emergence of a complex and dynamic HIV epidemic. 2010. *Retrovirology.* **7**: 25.

Zhuang, Z. Y., A. I. Jewett, S. Kuttimalai, G. Bellesia, S. Gnanakaran, and J. E. Shea. Assisted Peptide Folding by Surface Pattern Recognition. 2011. *Biophysical Journal.* **100** (5): 1306.

Zilman, A., V. V. Ganusov, and A. S. Perelson. Stochastic Models of Lymphocyte Proliferation and Death. 2010. *PLoS One.* **5** (9): e12775.

Understanding Drug Resistance and Co-infectivity in HIV and TB Infections

Bette T. Korber
20090098DR

Abstract

We have developed methodologies that both provide better diagnostics and enable better understand the biology of two deadly pathogens, the human immuno-deficiency virus (HIV) that causes AIDS and Mycobacterium tuberculosis (*Mtb)* that causes tuberculosis. These two pathogens are linked: Drug resistant TB is spreading rapidly in areas with a high prevalence of HIV, and they are particularly lethal in combination. This project had several goals, each linked to developing tools for population surveillance and understanding acquisition of drug resistance in these pathogens. Our first objective was to improve TB biomarker detection strategies, to provide a methodology that could ultimately improve accurate diagnosis of active TB. We have developed highly sensitive biomarker assays for TB molecules in biological samples, and these methods may be extended to other pathogens. Our second objective was to better define genetic markers for emerging patterns of drug resistance in TB, and we developed the bioinformatics and analysis strategies needed to define mutational patterns associated with TB drug resistance, and both confirmed established patterns of drug resistance and identified new patterns. Finally, we developed methods to use recent advances in sequencing technology allowing the generation of tens of thousands of DNA sequences per sample to track emerging patterns of drug resistance and immune escape in HIV-infected individuals. We discovered that the speed and the extent of varied pathways associated with HIV immune escape within an individual were far greater than previously understood. Using the same methodology at the population level, we are determining if using anti-retrovirals in a prophylactic gel, which can reduce transmission rates, impacts level of anti-retroviral resistance in the population. The experimental and analytic tools we have developed in the basic research context of this project offer pathways for improved surveillance strategies for both HIV and *M.tb*, and could be extended to other pathogens.

Background and Research Objectives

Mycobacterium tuberculosis (*M.tb.),* which causes tuberculosis (TB), has ravaged mankind for thousands of years, and continues to claim over 4000 lives worldwide every day. The WHO estimates that ~2 billion people are infected, although most infected people never get active TB. Drug resistant forms of TB are on the rise [1,2]. Drug resistant TB essentially can be thought of as a new outbreak. Treatment saves lives and is critical for turning around the TB epidemic, however an inevitable consequence of widespread treatment availability is the emergence of drug resistance in some individuals who have ineffective treatment regimen.

HIV/AIDS is estimated to infect 33 million people, with over 2.1 million dying of AIDS each year. AIDS and TB each cause tremendous human suffering, and combined these two diseases have a terrible synergy. People die rapidly when co-infected, and untreatable extensively drug resistant TB (XDR-TB) is emerging most rapidly in regions of the world where the two epidemics are coincident [2]. It is likely that infection with HIV exacerbates transmission of these forms of TB, and drug resistant TB is a particularly serious public health in southern Africa, where both pathogens are highly prevalent. But the drug resistant TB that evolves in the context of the coincident infections in S. Africa is not appearing in isolation. Multidrug resistant TB (MDR-TB) and XDR-TB are gaining ground; the short time since it has been discovered and tracked, 69 countries/territories have now reported XDR-TB strains [2]. XDR-TB is a contagious air born pathogen, it is untreatable, and puts both our troops and travelers at risk. Rapid diagnostics to track, treat, and understand these diseases are urgently needed. The changing epidemic profile of drug resistance and increases the MDR-TB and XDR-TB throughout the globe is an issue that if not properly addressed may become an international public heath issue of enormous impact; thus we have a window of opportunity to develop and implement new surveillance strategies.

Diagnosis of TB and identifying drug resistant forms of TB for treatment remains a very challenge global health problem; most diagnostic methods for drug resistance require culture and can take weeks to get results, while life saving treatment can depend on rapid and correct diagnosis. We have developed novel methods to detect TB

biomarkers in different tissue samples for use in rapid diagnosis for active TB; such methods could ultimately be used as an initial screen in combination with tests for genetic markers for drug resistance. A new rapid detection system, GeneXpert [1], has recently been endorsed by the World Health Organization, and is gaining use throughout the globe. MDR-TB is defined by resistance to two drugs, isoniazid and rifampicin, and rifampicin resistance can be detected using the GeneXpert system and is a good indicator for MDR-TB. The complexity of drug resistance acquisition, however, suggests more is needed. While transmission of resistant strains is one mechanism of drug resistance, acquisition of drug resistance in an ineffective treatment course is another, and thus there are multiple pathways to the acquisition of drug resistance. While some of the characteristic genetic patterns of mutations that confer resistance to specific classes of TB drugs are defined, others are still being mapped. To date, XDR-TB genomes have only been sequenced from 2 outbreaks in S. Africa, and understanding of emergent drug resistance in the context of different lineages is limited. We have used state of the art sequencing methods and developed analysis tools to enable us to combine the globally available data and to obtain new XDR-TB and MDR-TB data to characterize the genetic diversity in TB infections and determine how it impacts resistance.

Finally, we applied new "ultradeep" sequencing methods to study HIV in early infection and at the population level as a function of treatment. When we started, the experimental methods for this kind of rapid sequencing of millions of bases from a highly variable virus sample were still in their infancy. Interpreting the sequences, which are very error prone and very data rich, was computationally challenging. Methods were relatively well worked out for large stable genomes like TB: millions of short sequence reads that start at random positions in the genome are assembled based on their overlap, and the genome is covered many times over; the consensus base at each position allows one to get a reasonable reconstruction of the full sequence with minimum error. In contrast, HIV evolves so rapidly that instead we wanted to reconstruct the full population variation over a short region of interest, and every sequence in the 5,000 to 50,000 we obtained in a sample counted distinct as a member of the population. Thus for ultradeep viral sequencing, clean up had to be conducted on each sequence independently, and then we needed to devise methods to analyze and compare such extensive datasets. We accomplished this, and have made some important biological findings the process regarding the dynamics of the human immune response and HIV escape in early infection, and we are actively writing new proposals based on this work.

Scientific Approach and Accomplishments
Pathogen biomarker detection

We have developed assays for several TB molecular markers, such as lipoarabinomannan (LAM), a major virulence factor in TB. Our assay system and its sensitivity are illustrated in Figure 1. Through this project we developed a system where biomarkers are presented in the context of a lipid membrane [3], a method mimics recognition of bacteria by our innate immune system; this advance accounts for the greatly enhanced sensitivity shown in the lower panel of Figure 1. With sufficient sensitivity, active infections can be detected before symptoms appear in easily drawn samples such as serum and urine (Figure 2), and this system has the potential to eliminate false negatives if developed as a point-of-care diagnostic or in population surveillance if deployed through testing centers. We have studied a suite of TB biomarkers (LAM, ESAT-6, Ag85C, mycobactin, PGL-1). This is essential because no single biomarker can accurately predict disease status. To this end, we have developed a multiplex biomarker detection assay [4] that can accommodate a number of molecules, and hope to continue these studies to resolve if assessment of the expression profiles of these biomarkers in combination could be used to assess disease progression, and to detect drug resistant TB. The basic strategy of multiplexing through multichannel waveguide for simultaneous detection of multiple bio-markers [4], can be readily extended to simultaneously detecting biomarkers from multiple pathogens in one sample [5], as illustrated in Figure 3.

Sandwich assays for TB biomarkers (LAM, ESAT-6, Ag85C, CFP-10)

Functionalized Waveguide with Capture antibody → Binding of the antigen To the entrapped capture antibody → Formation of a sandwich with the fluorescently labeled reporter antibody

Waveguide level of detection of LAM = 1 pM

Commercial ELISA level of detection, 200 nM
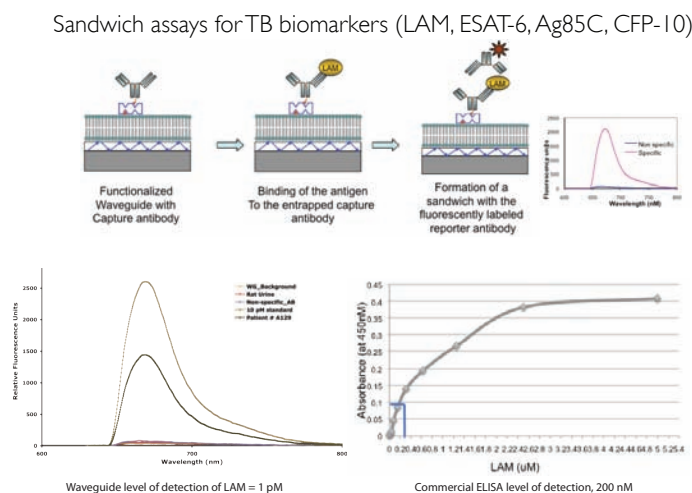
Figure 1. This figure illustrates the basic methodology of our detector. It also shows the exquisite sensitivity detection of LAM, a molecule (biomarker) produced by M.tb., in biological samples using our waveguide assay approach. It compares our method to to a currently available commercial assay called an ELISA, an enzyme-linked immunosorbent assay.
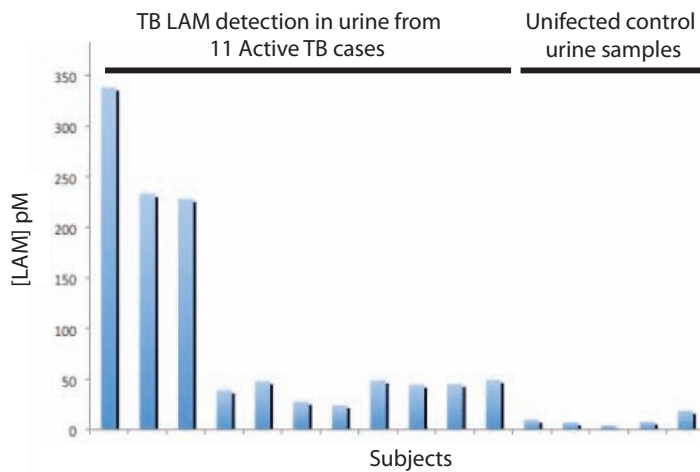
Figure 2. Our waveguide detection assay can discriminate between active TB cases and uninfected individuals by detecting the LAM biomarker in urine samples. The great sensitivity of this assay has the potential to eliminate or reduce false positive samples.
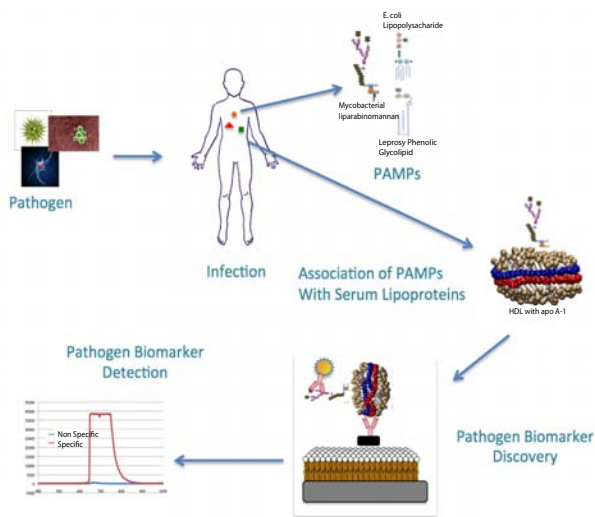
Figure 3. The strategy we employed in our waveguide detection system for detection of biomarkers associated with TB has many potential applications. As illustrated here, multiplexing using multiple PAMPS, or pathogen-associated molecular patterns, that are characteristic of different groups of pathogens could be useful for classifying an infection. Detection of PAMPS may be helpful for baseline diagnosis, or in some cases as an indicator of disease progression.

Understanding mechanisms by which LAM interacts with the host is important for gaining understanding of the pathology of tuberculosis. No three-dimensional structure of LAM was available, so we built an all-atom molecular model of LAM based on structural details assembled from the literature, consisting of 2139 atoms, with a MW of 16,100 [6]. The all atom model revealed a relatively large non-peptide glycolipid with a width of 14

nm, and we explored how LAM interacts with the membrane through structural modeling. We have modeled the chemistry of membrane interactions of these other pathogen-associated molecular patterns (PAMPs), to better understand their biology and the chemistry of carbohydrate lipid interations [6,7]. We have also been developing new antibodies that bind to these biomarkers for use in our assay system (manuscript in preparation). Other projects that were initiated through this DR include studying trafficking of PAMPs through the vascular system and determining their distribution within the body, and developing a detection platform for M. bovis to identify TB in cattle, of agricultural importance, through a NMSBA/USDA collaboration.
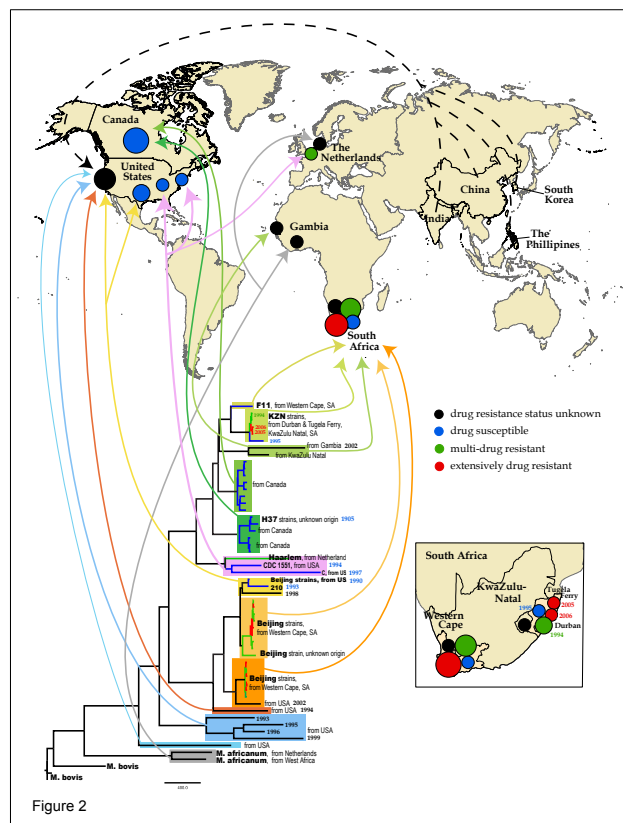
Figure 4. The phylogentic tree of all sequenced M.tb genomes as of 2011. The complete global set of all published genomes, each one over 4 million bases, was brought together for this analysis. These genomes were not fully assembled when we obtained them, nor were they annotated in the same manner, so we developed the software to align and analyze each of over 4,000 genes relative to a TB reference strain, and we developed clean up strategies to automatically remove problematic stretches of sequence. Variable sequence positions (or SNPs), where at least 1 of 55 sequences differed from other sequences, and were then extracted and used to build this phylogenetic reconstruction to define the genetic associations between isolates and their lineages. The fine genetic resolution in this tree provides a unique view into M.tb's diversity, and an essential baseline for defining resistance mutations.

Genetic markers of TB for associated with drug resistance

Before we began analysis of any new TB genomes, we fully assembled and analyzed the published globally available data. We identified 60 available full genomes and determined the drug resistance profiles of isolates either through the literature or through directly contacting primary authors. We then extracted and annotated all genes and all single nucleotide polymorphisms (SNPs) to reconstruct the phylogenetic relationships between the isolates, as shown in Figure 4. This was the first full genome phylogeny of TB utilizing the global data, based on all variable positions. We compared this phylogenetic by mapping it on current simpler TB genetic typing methods. We had a mostly consistent picture, but the full length genomes provided richer detail and we documented more extensive variation than had been previously resolved [8]. While there is extensive global diversity, there is still very limited global sampling, particularly of drug resistant strains (Figure 4) [8]. Before a complete mapping of drug resistance mutations and pathways can be resolved, more sequences need to be obtained. In this spirit, we obtained five new TB genomic sequences, using 454 sequencing technology, from 5 infected subjects from the KwaZulu Natal province of S. Africa. We combined this new data with 60 previously published TB genomes, and conducted systematic a statistical analysis which identified 15 novel proteins with mutations associated with drug resistance, and validated expected drug resistance profiles in 8 known proteins [9]. We have extended this work in an analysis with the NIH, combing new data provided by the NIH team from 27 XDR or drug sensitive strains from Korea with our global set (manuscript in preparation).

HIV evolution, emerging drug resistance and immune evasion

We used 454 ultradeep sequencing to track immune escape and drug resistance in HIV-infected people. Old sequencing methods allowed us to examine up to 100 viruses per sample, but new ultradeep sequencing technology allowed us to sequence between 10,000-50,000 viruses per sample, revealing the population complexity and enabling us to detect rare variants. Our challenge was to devise computational ways to clean up and biologically interpret such massive genetic data sets. Our first difficulty was primer design (primers are short stretches of DNA used to trigger the sequencing process), and to more fully understand the implications of mismatches in primers in real conditions we did experimental studies [10], and developed primer design code to address the sequence diversity seen in HIV samples (manuscript and website tools in preparation). In our first biological study we worked with sequences obtained by the Broad Institute and Harvard to track emerging drug resistance in chronically infected individuals, providing clean up and analysis strategies [11]. We then obtained our own sequences in collaboration with the sequencing group at LANL, and used

454 ultradeep sequencing of HIV to study viral escape from the initial immune responses in acutely infected people [12-14]. We demonstrated that: i) a single virus initiates infection, ii) the virus explores a vast array of mutations to evade the initial immune response during its first escape, and dozens of variants in an immune target region are explored in a very rapid evolutionary trajectory away from the transmitted form of the virus (Figure 5), and iii) the earliest immune responses were initiated earlier than previously thought, indicating these immune responses play a key role in the initial control of the explosive viremia that follows infection.
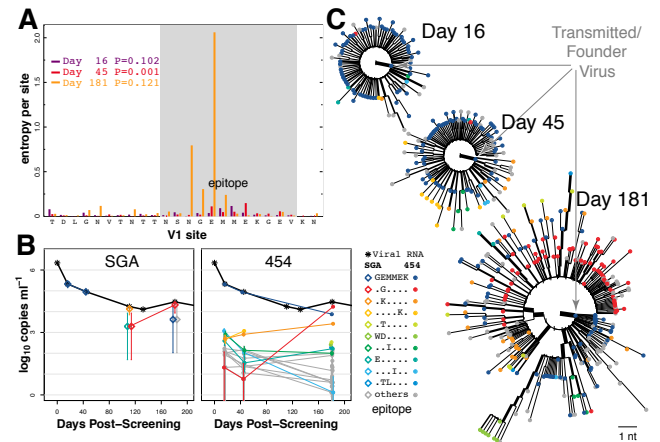
Figure 5. Evolution in the fast lane: viral immune escape in an acutely HIV-1 infected man. Evolution of a neutralizing antibody (NAb) target region in the virus is illustrated. This figure shows within-host evolution from a single founder virus evident by ultradeep 454 amplicon sequencing. (A) Comparison of amino-acid entropies (entropy is a quantitative measure of variation in an infected individual) inside (grey background) and outside (white background) the antibody-targeted region, showing that under immune pressure viral diversity in the immune target increases dramatically with time. (B) Frequency of variants (blue for the founder variant, then red, orange, yellow, etc. for common variants, and grey for other, less common variants) in the virus within and outside the antibody target region (black line). Error bars quantify uncertainty from sampling as 95% confidence intervals from the binomial distribution. Traditional sequencing can identify the most common variants, but 454 sequencing shows earlier emergence of escape variants and greater diversity than traditional sequencing. (C) Maximum-likelihood nucleotide sequence phylogenies show the distinct patterns in the antibody-recognition site as colored dots. Each line represents a base mutation that the virus has accrued, and the thickness of the line represents the number of viruses that share that form. Diversity increases massively with time and escape variants prevail by day 181, with extensive diversity in the antibody target.

Our last 454 viral study was still underway at the end of the DR funding cycle, so we obtained additional funding from the CAPRISA 004 study group for its completion (It

should be done in the winter of 2011). Vaginal micro-bicides applied before sex can reduce HIV transmission [15]. Their widespread use, however, could favor transmission of resistant viruses. LANL is partnering with the South African CAPRISA 004 [15] study group to determine if among breakthrough cases where Tenofovir gel did not block infection there is an increased prevalence of Tenovofir-resistance. Results from our pilot study indicate our methods are extremely sensitive and quantitative, and the last experiment in the series is nearing completion for analysis.

Impact on National Missions

LANL has a strong foundation in the evolutionary analysis of pathogen genetic diversity, state of the art sequencing facilities, and has the biochemical expertise needed for the development of detection assays for TB and other agents. This DR has enabled us to bring together our experimental and theoretical expertise in these areas, our expertise in HIV and TB, and develop new experimental and analysis methods. We applied these methods to biologically interesting samples that provide new insights into the biology of these two pathogens, two of the most serious public health problems of our times. The new methodologies for diagnostics and metagenomics apply to the extreme scenarios of a very rapidly evolving small virus (HIV), and a slowly evolving large bacterial genome (TB). These methods could readily be transitioned to a broad spectrum of other pathogens, addressing threat reduction, human health, and basic science missions relevant to DOE, DHS, and other government agencies. As we developed new detection methods for drug resistance and disease progression, we improved our understanding of the associated biological and evolutionary processes related to these pathogens. These methods can potentially be used to both improve patient care and to track the movement of drug resistant forms of HIV and TB pathogens globally. Furthermore, the technologies and tools we are developing to combat current real world problems of TB and HIV could be adapted and applied if infectious bio-organisms are ever used as a weapon.

References

1. Global tuberculosis control 2011. 2011. *World Health Organization.*

2. Multidrug and extensively drug-resistant TB (M/XDR-TB). 2010. *World Health Organization.*

3. Mukundan, H., H. Xie, D. Price, J. Kubicek-Sutherland, W. Grace, A. Anderson, J. Martinez, N. Hartman, and B. I. Swanson. Quantitative multiplex detection of pathogen biomarkers on multichannel waveguides. 2010. *Analytical Chemistry.* **82** (1): 136.

4. Mukundan, H., D. N. Price, M. Goertz, R. Parthasarathi, G. A. Montano, S. Kumar, M. R. Schofield, A. S. Anderson, S. Gnanakaran, S. Iyer, J. S. Schmidt, and B.

I. Swanson. Understanding the interaction of lipoarabinomannan with membrane mimetic architectures . To appear in *Tuberculosis.*

5. Sakamuri, M., T. I. Dickerson, H. Makundan, and B. I. Swanson. Detection of small molecule antigens using membrane insertion. *Journal of the American Chemical Society, Communication.*

6. Tian, J., R. Parthasarathi, B. Swanson, and S. Gnanakaran. Sugar-membrane interactions: A molecular dynamics simulations study of a virulent factor from TB. *Journal of Physical Chemistry.*

7. Parthasarathi, R., J. Tian, A. Redondo, and S. Gnanakaran. A Quantum Chemical Study of Carbohydrate-Phospholipid Interactions. To appear in *J. Phys. Chem A .*

8. Ford, C., K. Yusim, S. Feng, T. Ioerger, M. Chase, M. Green, B. Korber, and S. Fortune. Whole genome sequencing of Mycobacterium tuberculosis: Where have we been and where are we going? . *Tuberculosis.*

9. Yusim, K., S. Feng, P. Moodley, H. Shusheng, C. S. Tung, W. Sturm, and B. Korber. Five new Mycobacterium tuberculosis genomes from KwaZulu-Natal when compared to the global diversity allow definition of new drug resistance associated mutations and mixed infections. *Biomed Central Genomics.*

10. Desmarais, S. M., T. Leitner, and A. E. Barron. A novel method to probe DNA barcode dimerization risk using free-solution capillary electrophoresis. To appear in *Electrophoresis.*

11. Tsibris, A. M., B. Korber, R. Arnaout, C. Russ, C. C. Lo, T. Leitner, B. Gaschen, J. Theiler, R. Paredes, Z. Su, M. D. Huges, R. M. Gulick, W. Greaves, E. Coakley, C. Flexner, C. Nusbaum, and D. R. Kuritzkes. Quantitative deep sequencing reveals dynamic HIV-1 escape and large population shifts during CCR5 antagonist therapy in vivo. 2009. *PLoS One.* **4** (5): 5683.

12. Fischer, W., V. V. Gaunsov, E. E. Giorgi, P. T. Hraber, B. F. Keele, T. Leitner, C. S. Han, C. D. Gleasner, L. Green, C. C. Lo, A. Nag, T. C. Wallstrom, S. Wang, A. J. McMicael, B. F. Haynes, B. H. Hahn, A. S. Perelson, P. Borrow, G. M. Shaw, T. Bhattacharya, and B. T. Korber. Transmission of single HIV-1 genomes and dynamics of early immune escape revealed by ultra-deep sequencing. 2010. *PLoS One.* **5** (8): e12303.

13. Cale, E. M., P. Hraber, E. E. Giorgi, W. Fischer, T. Bhattacharya, T. Leitner, W. Yeh, C. Gleasner, L. D. Green, C. S. Han, B. Korber, and N. L. Letvin. Epitope-specific CD8+ T lymphocytes cross-recognize mutant simian immunodeficiency virus (SIV) sequences but fail to contain very early evolution and eventual fixation of

epitope escape mutations during SIV infection. . 2011. *Journal of Virology.* **85** (8): 3746.

14. Kim, E. Y., T. Bhattacharya, K. Kuntsman, P. Swantek, F. A. Koning, M. H. Malim, and S. M. Wolinsky. Diversification and accelerate adaptation to selective pressure . 210. *Journal of Virology.* **84** (19): 10402.

15. Karim, Q. A., S. S. A. Karim, J. A. Frohlich, A. C. Grobler, C. Baxter, L. E. Mansoor, A. B. Kharsany, S. Sibeko, K. P. Mlisana, Z. Omar, T. N. Gengiah, S. Maarschalk, N. Arulappan, M. Mlotshwa, L. Morris, and D. Taylor. Effectiveness and safety of tenofovir gel, an antiretroviral microbicide, for the prevention of HIV infection in women. 2010. *Science.* **329** (5996): 1168.

Publications

Cale, E. M., P. Hraber, E. E. Giorgi, W. Fischer, T. Bhattacharya, T. Leitner, W. Yeh, C. Gleasner, L. D. Green, C. S. Han, B. Korber, and N. L. Letvin. Epitope-specific CD8+ T lymphocytes cross-recognize mutant simian immunodeficiency virus (SIV) sequences but fail to contain very early evolution and eventual fixation of epitope escape mutations during SIV infection. . 2011. *Journal of Virology.* **85** (8): 3746.

Desmarais, S. M., T. Leitner, and A. E. Barron. A novel method to probe DNA barcode dimerization risk using free-solution capillary electrophoresis. To appear in *Electrophoresis.*

Fischer, W., V. V. Gaunsov, E. E. Giorgi, P. T. Hraber, B. F. Keele, T. Leitner, C. S. Han, C. D. Gleasner, L. Green, C. C. Lo, A. Nag, T. C. Wallstrom, S. Wang, A. J. McMicael, B. F. Haynes, B. H. Hahn, A. S. Perelson, P. Borrow, G. M. Shaw, T. Bhattacharya, and B. T. Korber. Transmission of single HIV-1 genomes and dynamics of early immune escape revealed by ultra-deep sequencing. 2010. *PLoS One.* **5** (8): e12303.

Ford, C., K. Yusim, S. Feng, T. Ioerger, M. Chase, M. Green, B. Korber, and S. Fortune. Whole genome sequencing of Mycobacterium tuberculosis: Where have we been and where are we going? . *Tuberculosis.*

Kim, E. Y., T. Bhattacharya, K. Kuntsman, P. Swantek, F. A. Koning, M. H. Malim, and S. M. Wolinsky. Diversification and accelerate adaptation to selective pressure . 210. *Journal of Virology.* **84** (19): 10402.

Lynch, R. M., R. Rong, B. Li, T. Shen, W. Honnen, J. Mulenga, S. Allen, S. Zolla-Pazner, A. Pinter, S. Gnanakaran, and C. A. Derdeyn. Subtype-specific conservation of Isoleucine 309 in the Env V3 domain is linked to immune evasion in subtype C HIV-1 infection. 2009. *Virology.* **404** (1): 5970.

Mukundan, H., D. N. Price, M. Goertz, R. Parthasarathi, G. A. Montano, S. Kumar, M. R. Schofield, A. S. Anderson, S. Gnanakaran, S. Iyer, J. S. Schmidt, and B. I. Swanson. Understanding the interaction of lipoarabinomannan with membrane mimetic architectures . To appear in *Tuberculosis.*

Mukundan, H., H. Xie, D. Price, J. Kubicek-Sutherland, W. Grace, A. Anderson, J. Martinez, N. Hartman, and B. I. Swanson. Quantitative multiplex detection of pathogen biomarkers on multichannel waveguides. 2010. *Analytical Chemistry.* **82** (1): 136.

Neher, R., and T. Leitner. Recombination rate and selection strength in HIV intra-patient evolution. 2010. *PLoS Computational Biology.* **6** (1): e1000660.

Parthasarathi, R., J. Tian, A. Redondo, and S. Gnanakaran. A Quantum Chemical Study of Carbohydrate-Phospholipid Interactions. To appear in *J. Phys. Chem A .*

Rebecca, M., T. Shen, S. Gnanakaran, and C. Derdeyn. Appreciating HIV-1 diversity: subtypic differences in Env. 2009. *AIDS Research and Human Retroviruses.* **25**: 237.

Sakamuri, M., T. I. Dickerson, H. Makundan, and B. I. Swanson. Detection of small molecule antigens using membrane insertion. *Journal of the American Chemical Society, Communication.*

Tian, J., R. Parthasarathi, B. Swanson, and S. Gnanakaran. Sugar-membrane interactions: A molecular dynamics simulations study of a virulent factor from TB. *Journal of Physical Chemistry.*

Tsibris, A. M., B. Korber, R. Arnaout, C. Russ, C. C. Lo, T. Leitner, B. Gaschen, J. Theiler, R. Paredes, Z. Su, M. D. Huges, R. M. Gulick, W. Greaves, E. Coakley, C. Flexner, C. Nusbaum, and D. R. Kuritzkes. Quantitative deep sequencing reveals dynamic HIV-1 escape and large population shifts during CCR5 antagonist therapy in vivo. 2009. *PLoS One.* **4** (5): 5683.

Yusim, K., S. Feng, P. Moodley, H. Shusheng, C. S. Tung, W. Sturm, and B. Korber. Five new Mycobacterium tuberculosis genomes from KwaZulu-Natal when compared to the global diversity allow definition of new drug resistance associated mutations and mixed infections. *Biomed Central Genomics.*

Distributed Metabolic Regulation: The Key to Synthetic Biology for Carbon Neutral Fuels

Pat J. Unkefer
20090117DR

Abstract

DOE's goal of harnessing biological systems for renewable energy production, carbon sequestration and environmental restoration and DOD's goal of mitigating biological risks to their personnel are frustrated by our limited understanding of cellular-level metabolic regulation. A critical limitation in achieving these goals was our lack of understanding of the effects transcription factor (TF) / metabolite effector interactions have on TF binding of their respective DNA regulatory sequences. We developed an efficient and effective set of tools and approaches to gain the needed detailed experimental data to gain this understanding of target TFs. We demonstrated our methods with four TFs. We discovered the function of three TFs with previously unknown function and as such identified genes they regulate, their metabolite effector molecules and the DNA sequences they bind and thus control expression of the genes they regulate. Of the four TRs we characterized, three of them had strong affinities for multiple small molecule metabolites, thus supporting our original hypothesis that TFs can function as signal processors of metabolic status. This function mediates their affinities for their DNA binding sites with implications for regulating gene expression. Thus we meet all of our major goals in this project. This work created the capability to address DOE's need for faster photosynthetic growth to support biofuels production and is now being employed in LANL's Algal Biofuels project. It also created the capability to target multidrug resistance mechanisms that confound modern antibiotics and create major risks for US military and civilian personnel; this application is being pursued. A new staff member was hired from the postdoctoral researchers on this project.

Background and Research Objectives

To understand and ultimately to harness living systems for practical purposes, we must a) know the functions of cell parts, b) assess the roles that the cell parts play in operational networks, and c) decipher how control processes are integrated within and between these operational networks. Much progress has been made on characterizing the functions of cell parts and their operational networks. However, we do not yet understand how their networks are integrated.

One of the least understood but critical integrating functions in the cell is the transcription factor (TF)-mediated regulation of gene expression. TF-mediated regulation allows cells to respond to environmental changes and yet control cellular metabolism to maintain homeostasis and to survive. It is this ability of cells to over-ride the disruption caused by environmental challenges that confounds our ability to truly optimize/engineer organisms for practical purposes. TFs regulate the expression of sets of genes, called regulons, which are composed of sub-groups of genes termed operons. TFs bind to specific DNA sequences upstream of the regulated gene(s) and either induce or repress gene expression. TF recognition and binding to a particular DNA sequence is modulated by the binding of a small-molecule effector to the TF [1-3].

The binding of an effector by the TF alters the TF's conformation. The conformational change alters the affinity of the TF-effector complex for the DNA sequence. This mechanism, termed allostery, is widely used by biological systems to modulate protein function; it is especially valuable in sensing/response systems because it allows a few components to respond appropriately to numerous signals [4]. The conventional view of TF-effector complexes has been that they are simple "On/Off" switches. We hypothesized that their activity is far more complex, but experimental difficulties had hindered progress in characterizing their regulatory activity. Only a few effector molecules have been identified and little quantitative information is available about their binding with TFs [5].

We chose the Burkholderia genus as our model because it contains members that carry out functions important to the Los Alamos national security mission. Some Burkholderia are high-risk pathogens important to the Department of Defense; others carry out functions utilized in DOE environmental restoration activities and most can produce fuel alcohols through fermentative pathways important for DOE's goals in biofuels production [6].

This project focused on discovering the functions of TFs of unknown function. The major objectives of the project were to develop an efficient and effective method to identify small molecule effectors of TFs and couple this with known and emerging methods for finding the DNA sequences they recognize and bind. We focused on TFs common among the Burkholderia genus. We also sought to learn if TFs could function as information processors; such a role would be possible if they are had affinity for multiple small molecule effectors. We achieved our major objectives.

Scientific Approach and Accomplishments

The identification of the small molecule effectors has been extremely challenging because of the high degree of diversity in the chemical structure, solubility and stability among the several thousand known small molecule metabolites. Furthermore, recent studies have detected hundreds of additional unidentified small molecules. Any given microbe can be expected to contain almost a thousand known and unidentified small molecules. Thus, a method of predicting a set of molecules to be screened was needed. We developed a bioinformatics approach that allowed us to capitalize upon physical conservation with the genome. We found that when searches were conducted using sequence homology as the basis, that we could often find conserved patterns within the Burkholderia genus that reflected physical conservation of the location of genes encoding a given function or metabolic pathway and that the TF would often be located near that cluster of genes. This sequence-based approach is supported by the MicrobesOnLine site and this capability provides much more accurate analysis than searches based on previous annotations which are now recognized to be replete with errors. The capability to associate a TF gene with a metabolic pathway is extremely powerful because of the known small molecule TF effectors they are usually products or intermediates of the pathway the TF is regulating. Our bioinformatics studies allowed us to postulate and test the metabolic function that the TF might be regulating for almost a hundred of the TFs of unknown function most common among in Burkholderia genus. We chose a small subset of these TFs for focused efforts to develop and demonstrate our approach.

With the capability to predict the metabolic pathway being regulated, we could assemble relatively small metabolite libraries that could be readily screened to find those that bound to the target TF. For the screen, we developed a Frontal Affinity Chromatography (FAC) system as a front end of a mass spectrometer (MS) [6.7]. In the FAC system the TF was immobilized onto the solid support in the column and a solution of the candidate effectors was continuously infused through the column. The molecules not bound by the TF eluted continuously and were detected by the MS; the molecules bound by the TF were retained in the column and were only eluted and detected after the TF molecules in column became saturated with them.

The MS detected their elution as a function of time, which reflected the TFs affinity for these molecules. We used this information to estimate dissociation constants for the TFs.

The next task was to find the specific DNA sequence recognized and bound by the TF. We used a protein-binding microarray under development by our collaborator Professor Bulyk [9]. This array contains all possible combinations of 10mrs of nucleic acids and thus allowed us to investigate a TF for its consensus DNA sequence that it can bind. TFs are known to be somewhat degenerate in the DNA sequences it can recognize and bind; the microarray detects and reveals this degeneracy; hence it finds the consensus sequence. We compared the results of this approach with those of the standard Electrophoretic Mobility Shift Assay (EMSA) method in which DNA sequences are incubated with the candidate TF and then analyzed by to separate the DNA/ TF complex. The DNA is then eluted from the gel and sequenced. This classic experimental method is time consuming but highly reliable. We found that the micro array and classic experimental results were in good agreement. We also used the EMSA assay to detect the impact of the effector on the TF-DNA complex. True effectors of TFs mediate the TF-DNA complex formation / dissociation. With two methods available to find the DNA sequence bound by a TF, we developed a fluorescence anisotrophy-based method to quantitatively assess the strength of the binding of the TF for the DNA sequence and to study further the impact of the effector on the TF-DNA complexes. These methods provide an extremely strong, comprehensive capability for discovering and characterizing the function of TFs.

For all of the methods development we used the TF metJ that regulates the biosysnthesis of the amino acid, methionine. The known effector is S-adenosyl methionine, (SAM) an intermediate in the pathway. We discovered that metJ also recognized and bound adenine and 5'-deoxy-5'-(methylthio) adenosine (MTA) (Figure 1). Neither of these two metabolites had a direct effect on metJ-DNA binding. However, the dissociation constants were such that these metabolites could be expected to compete with SAM for the effector binding site on metJ and thus interfere with formation of the metJ-DNA complex. MTA as a potential modulator of metJ function is significant because it has been implicated in regulating gene expression [10]. MTA is produced during polyamine biosynthesis and is a starting point in a major methionine salvage pathway [10]. MTA as an inhibitor of metJ and thus of methionine biosynthesis would be consistent with the cell's need to suppress methionine biosynthesis when methionine is readily available from the salvage pathway. This finding is consistent with our hypothesis that TFs can function as signal processors, taking input from more than one pathway to assess the overall need for the function that is being regulated.
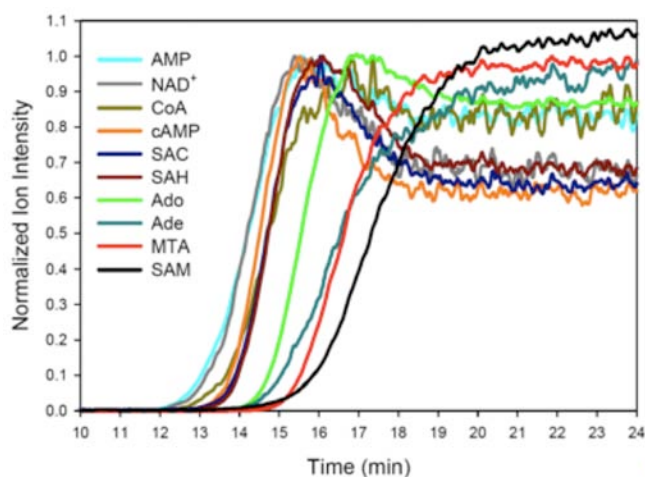
Figure 1. Screening for effectors of transcription factor (TF) metJ. The relative affinity of candidates is obtained from the elution time with the highest affinity ligands eluting last. The strongest binders in order are S-adenosyl methionine, the known effector, and methylthioadenosine and adenonine, two newly discovered effectors of metJ.

We applied these methods to discover the function, small molecule effector and DNA binding sites for three Burkholderia TFs of unknown function. The TF, Bxe A076 was associated with the oxidative tryptophan degradation pathway and we have therefore designated this TF as KynR. The TF had the greatest affinity for L-kynurenine among all other amino acids and pathway intermediates. KynR binds a set of four degenerate and palindromic sites within the inter-genomic region between the gene for itself and the N-formyl kynurenine deformylase KynB. The optimal consensus sequence was ATATTCCGAATAT. Fluorescence anisotropy experiments demonstrated that kynurenine affected KynR binding to its DNA sequence (Figure 2). Homologs of KynR were found throughout the proteobacteria, including several high-risk pathogens.
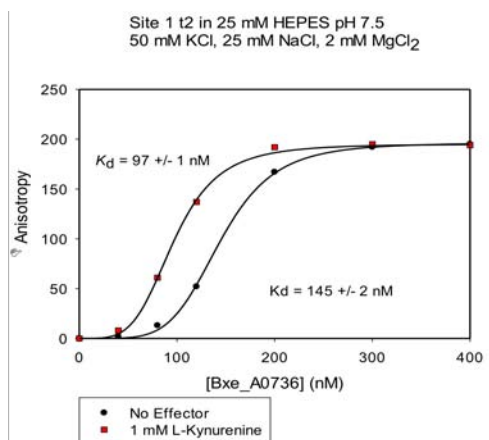
Figure 2. The presence of the effector L-kynurenine alters the binding affinity of the KynR transcription factor for its DNA sequence. Thus L-kynurenine can be expected to change gene expression of the genes encoding steps in tryptophan metabolism.

The TF Bxe B2842 was found to be an organic hydroperoxide resistance regulatory protein (ohrR) involved in regulating the expression of the gene osmC, which encodes an organic hydroperoxide resistance protein. Our FAC-MS screen indicated that 2-aminophenol binds to the protein and is a potential effector. EMSA experiments confirmed that 2-aminophenol and a general source of organic peroxide attenuate DNA binding by this TF. This is the first ohrR protein to have affinity for both oxidative and non-oxidative effectors. The consensus sequence is shown in Figure 3; it was present in repeating units upstream of the osmC gene. Our analysis of its sequence indicates that B284 is member of the MarR (multiple antibiotic resistance regulator) family of TRs; it has homologs in other key pathogens among the genus of Bacillus, Xanthomonas, Agrobacterium and Streptomyces.

Figure 3. The consensus DNA sequence for Burkholderia transcription factor Bxe B2842. This display indicates locations in which either of two nucleotides can serve and locations where only one nucleotide can serve.m.

The TF Bxe B3018 was associated with glycine, serine threonine and pyruvate metabolism. This TF bound to the pallindromic sequence CGAGGGAGAATGATCGTTCTACCCTT. Aminoacetone, N, N-dimethylaminoacetone and methylglyoxal were identified as potential effectors and each decreased the affinity of B3018 for the DNA sequence; other structurally related compounds had no effect.

Our results demonstrate that the complexity and sophistication of effector-TF interactions has been overlooked. Our work strongly suggests that TFs can act as sophisticated signal processors, not merely as "On /Off" switches because they can have affinity for multiple small molecules that can effect the TF function. As we observed, simple competition for the effector binding site between molecules of related but non identical structures can modulate the effectiveness of the TF. In addition, multiple effectors with similar binding affinities for a TF could interact with the TF and potentially generate a complex set of effector-TF complexes with potentially complex conformational changes that may generate complex influences on gene expression.

The work on each of the TFs is described in detail in at least one manuscript per TF.

Impact on National Missions
DOE's goal of harnessing biological systems for renewable energy production, carbon sequestration and environmental restoration and DOD's goal of mitigating biological

threats to their personnel are frustrated by our limited understanding of cellular-level metabolic regulation. To realize these goals we must gain a much better understanding of the critical but poorly understood roles TFs play in regulating and coordinating gene expression with the cells metabolic status. This project focused on gaining this understanding.

New Capabilities driving New Program Directions: This project developed a broadly applicable set of tools and approaches to discover and characterize TF function, effector molecules and their DNA regulatory sites. This new capability is now being employed to investigate the regulation of algal growth and lipid production for LANL's Algal Biofuels Center; it is also attracted the interest of Defense Threat Reduction Agency as providing the means to silence mechanisms that confer resistance to our modern antibiotics.

References

1. Jiang, J., and M. Levine. Binding affinities and cooperative interactions with bHLH activators delimit threshold responses to the dorsal gradient morphogen. 1993. *Cell.* **72** (5): 741.

2. Gaudet, J., and S. E. Mango. Regulation of organogenesis by the Caenorhabditis elegans FoxA protein PHA-4. 2002. *Science.* **295** (5556): 821.

3. Tanay, A.. Extensive low-affinity transcriptional interactions in the yeast genome. 2006. *Genome Research.* **16** (8): 962.

4. Changeux, J. P., and S. J. Edelstein. Allosteric mechanisms of signal transduction. 2005. *Science.* **308** (5727): 1424.

5. Wall, M. E., W. S. Hlavacek, and M. A. Savageau. Design of gene circuits: lessons from bacteria. 2004. *Nature Reviews Genetics.* **5**: 34.

6. Tringe, G., C. von Mering, A. Kobayashi, A. A. Salamov, and K. Chien. Comparative metagenomics of microbial communities. 2005. *Science.* **308** (5721): 554.

7. Marti-Arbona, R., M. Teshima, P. Anderson, P. Unkefer, and C. Unkefer. Discovery of novel transcription factor effectors for metJ. 2009. In *American Chemical Society.* (Washington, DC, 16-20 Aug. 2009). Vol. 238, p. 822. New York: American Chemical Society.

8. Slon-Usakiewicz, J. J., W. Ng, J. R. Dai, A. Pasternak, and P. R. Redden. Frontal affinity chromatography with MS detection (FAC-MS) in drug discovery. 2005. *Drug Discovery Today.* **10** (6): 409.

9. Berger, M. F., A. Phillippakis, A. M. Qureshi, F. S. He, P. W. Preston, and M. Bulyk. Compact, universal DNA microarrays to comphrensively determine transcription factor bind site specificities. 2006. *Nature Biotechnology.* **24** (11): 1429.

10. Avila, M. A., E. R. Garcia-Trevijano, S. C. Lu, F. J. Corrales, and J. M. Mato. Merthylrthioadenosine. 2004. *International Journal of Biochemistry and Cell Biology.* **36**: 2125.

Publications

Bauer, A., W. Hlavacek, P. Unkefer, and F. Mu. Using Sequence-Specific Chemical and Structural Properties of DNA to Predict Transcription Factor Binding Sites. 2010. *PLos Computational Biology.* **6** (11): e1001007.

Bauer, A., W. Hlavacek, and F. Mu. Using sequence-specific chemical and structural properties of DNA to predict transcription factor binding sites. Presented at *q-Bio-conference.* (Santa Fe, June 26-28. 2009).

Hall, R., R. Marti-Arbona, S. Hennelly, t. Maity, F. Mu, T. Nguyen, M. Teshima, J. Dunbar, C. Unkefer, and P. Unkefer. Discovery and characterization of an L-kynurenine responsive transcriptional regulator of the oxidative tryptophan degradation pathway in Burkholderia xenovorans. *Journal of Biological Chemistry.*

Maity, T., D. Close, Y. Valdez, K. Nowak-Lovato, R. Marti-Arbona, P. Unkefer, E. Hong-Geller, A. Bradbury, and J. Dunbar. Discovery of DNA operators for TetR and MarR family transcription factors from Brukholderia xenovorans. *Microbiology.*

Maity, T., D. Close, Y. Valdez, K. Nowak-Lovato, R. Marti-Arbona, T. Nguyen, P. Unkefer, E. Hong-Geller, A. Bradbury, and J. Dunbar. Discovery of DNA operators for TetR and MarR family of transcription factors from Burkholderia xenovorans. *Microbiology.*

Marti, R., R. Hall, K. Nowak-Lovato, E. Hong-Geller, T. Maity, C. Unkefer, and P. Unkefer. Characterization of Burkholderia xenovorans transcriptional regulator Bxe B3018. *Journal of Biological Chemistry.*

Marti-Arbona, R., M. Teshima, P. Anderson, P. Unkefer, and C. Unkefer. FAC-MS uncovers new effectors for old transcriptional regulators: Discovery of novel transcription factor effectors for MetJ. Presented at *Gorden Research Conferences "Enzymes, coenzymes and metabolic pathways.* (New Hampshire, 5-10 July 2009).

Marti-Arbona, R., M. Teshima, T. Maity, J. Dunbar, C. Unkefer, and P. Unkefer. Discovery of novel transcription factor effectors for metJ. . 2009. In *238 ACS national meeting.* (Washington, DC, 1-20 Aug. 2009). Vol. 238, p. 822. New York : American Chemical Society.

Marti-Arbona, R., T. Maity, J. Dunbar, C. Unkefer, and P. Unkefer. Discovery and function annotation of novel transcription factors. Presented at *Gorden Research*

Conference "Enzymes, Coenzymes and Metabolic Pathways". (New Hampshire, 18-23 July 2010).

Mu, F., A. Bauer, J. Faeder, and W. Hlavecek. Using systems biology techniques to determine metabolic fluxes and metabolic pool sizes. 2010. In *Handbook of Chemoinformatics Algorithms.* Edited by Faulon, J., and A. Bender. Vol. I, First Edition, p. 399. Boca Raton, FL: CRC Pres.

Mu, F., C. Unkefer, and P. Unkefer. Using sequence-specific chemical and structural properties of DNA to predict transcription factor binding sites. 2011. *Bioinformatics.* **27** (11): 1537.

Nguyen, T., R. Hall, R. Marti-Arbona, T. Maity, Y. Valdez, J. Dunbar, C. Unkefer, and P. Unkefer. Identification and characterization of a novel ohrR transcriptional regulator in Burkholderia xenovorans LB400. *Journal of Biological Chemistry.*

A Molecular View of Cellulase Activity: A Single-Molecule Imaging and Multi-Scale Dynamics Approach

Peter M. Goodwin
20100129ER

Introduction

The overall goal of this research is to contribute towards a carbon-neutral fuel economy based on the efficient conversion of abundant lignocellulosic biomass, the woody inedible material from plant cell walls, to biofuels such as ethanol. A crucial step in this process is the enzyme-catalyzed hydrolysis of cellulose to glucose that is then converted into fuel by fermentation. This step is a roadblock to the economical, large-scale conversion of lignocellulosic biomass to fuel. The enzyme-catalyzed hydrolysis of cellulose is complex -- it entails the cooperative (synergistic) action of three enzymes known collectively as cellulases. In contrast to homogeneous solution-phase catalysis, it is well known that the overall efficiency of this heterogeneous catalysis process depends on factors in addition to the catalytic rates of the cellulases, including: cellulase absorption, desorption and diffusion rates on the insoluble cellulose substrate, enzyme-catalyzed conversion of cellulose from its crystalline to amorphous forms, and the processivity of eznyme-catalyzed hydrolysis of individual cellulose strands. To date, due in large part to limitations of the bulk analysis methods used for its study, this heterogeneous reaction is poorly understood. The aim of this work is to use single-molecule fluorescence imaging coupled with all-atom and coarse-grained computer simulations to elucidate molecular-level details of cellulase/cellulase interactions during cellulose degradation and to develop a molecular model of the cellulase-catalyzed hydrolysis of cellulase.

Benefit to National Security Missions

Developing bioenergy is germane to both national security and the environment. A major roadblock to using biomass for energy is the cost of converting recalcitrant lignocellulosic biomass to sugars that can then be used to produce fuels. Further cost reductions and improvements in enzyme activity are necessary to make cellulosic fuel economically viable. The goal of this project, a molecular level understanding of the cellulase-catalyzed hydrolysis of cellulose, is the logical means to this end.

Progress

Experiment: We have made substantial progress towards our goal of imaging the activity of single cellulases on cellulose substrates. We entered into a collaboration with DSM, a commercial entity based in the Netherlands, that specializes in the industrial-scale production of cellulases. DSM has been working with Andrew Bradbury on the engineering of thermostable endocellulases. Through Dr. Bradbury we were able to negotiate permission from DSM to use their exocellulase (T. emersonii CBHI) in our single-molecule imaging experiments. We have also obtained another purified exocellulase (T. reesei Cel7A) from Professor Tina Jeoh (UC Davis).

Dr. Jaemyeong Jung, a postdoctoral research associate, started working full-time on the experimental (single-molecule imaging) aspects of this project in October 2010. Since then Dr. Jung has: 1) Labeled both the T. emersonii CBH1 and T. reesei Cel7A exocellulases with a fluorescent reporter dye (Cy5). 2) Verified that both Cy5-labeled exocellulases exhibit hydrolytic activity. 3) Rebuilt the dual-view optics of our total-internal reflection excited fluorescence microscope for the acquisition of simultaneous images of the cellulose substrate and single Cy5-labeled cellulases required for our experiments. 4) Optimized the imaging conditions to permit us to image individual Cy5-labeled cellulases for up to twenty minutes.

Our image data show that both the Cel7A and CBH1 exocellulases bind specifically to the cellulose substrate. Since we image the binding and movement of *single* fluorescently labeled exocellulases, we can use these data to generate super-resolution (~lambda/20) images of the binding of exocellulase to the cellulose substrate as shown in Figure 1. Moreover, since we collect our image data as a function of time, we can reconstruct time-resolved super-resolution images of cellulase binding. Figure 2 shows such a time-resolved super-resolution image of a 5 x 5 micron region. Most of the image area shows no significant binding as the exocellulases do not bind strongly to the BSA-blocked glass. Binding is readily apparent in regions occupied by

the cellulose substrate at high coverage (as determined by scattered light imaging). In this case two such high-coverage regions appear in the lower half of the image. The upper half of the image shows two linear features, one ~1000 nm long in the upper left hand corner and one ~500 nm long in the upper right hand corner. The width of these features, ~20-30 nm, is primarily due to the precision with which we localize single fluorescent exocellulase molecules in each 1 second frame. We commonly see such linear features in our images. Control experiments and atomic force microscopy (data not shown) lead us to believe that these linear features are due to binding of exocellulases to individual, crystalline cellulose microfibers. Moreover, the time-dependence of the binding of the exocellulases to these microfibers show evidence of linear motion of individual exocellulases along microfibers as well as cooperative binding of multiple exocellulases along microfibers. We find that initial binding events often appear to trigger rapid subsequent binding of exocellulases along the length of the microfiber. This is evident in the color-coded image shown in Figure 2.
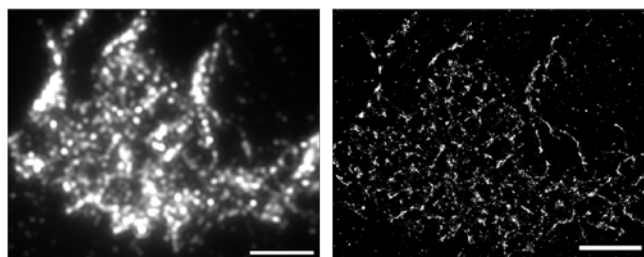
Figure 1. Conventional (left) and reconstructed super-resolution (right) images of Cy-5 labeled T. reesei Cel7A bound to cellulose from Cladophora sp. Scale bars = 5 µm.
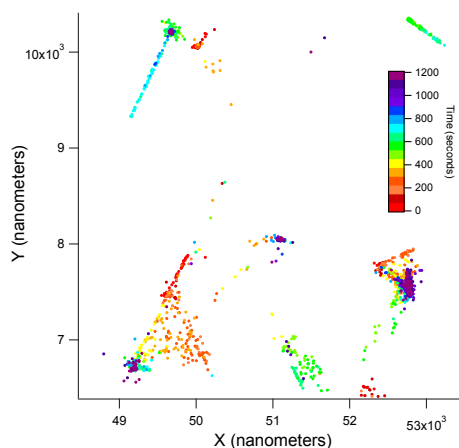
Figure 2. Time-resolved super-resolution image of Cy-5 labeled T. reesei Cel7A binding to cellulose from Cladophora sp. Image area is 5 µm × 5 µm. Time-dependence of the binding is displayed according to the inset color-scale.

The linear feature in the upper right hand corner appeared between ~600-700 s whereas the feature in the upper left hand corner appeared between ~700-800 s. The red linear feature extending from apex of the triangular area in the lower left quadrant appeared much earlier, between ~0-200 s. If the exocellulase binding were completely random one would expect that these features would be gradually built up over the entire observation time and, therefore, to appear in this color-coded image as being comprised of a larger range of colors.

Theory: In a recent paper, we join Shishir Chundawat and Bruce Dale of Michigan State University, and collaborators from the Great Lakes Bioenergy Research Center in describing a potential pretreatment method that can make plant cellulose five times more digestible by enzymes that convert it into ethanol, a useful biofuel.[1] Our theoretical modeling work and the experimental evidence confirmed, that the pretreatment reduced the strength of hydrogen bonds in the cellulosic network (Figure 3). This work was highlighted in several news stories (). Also, it was prominently featured in the September issue of Chemical Engineering Progress (CEP Magazine) – flagship magazine for the American Chemical Engineering Society.
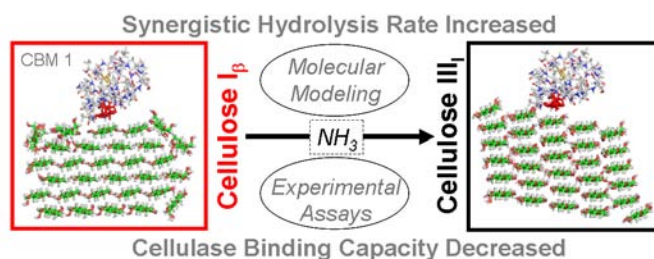
Figure 3. Conversion of lignocellulose to biofuels is partly inefficient due to the deleterious impact of cellulose crystallinity on enzymatic saccharification. We demonstrate how the synergistic activity of cellulases was enhanced by altering the hydrogen bond network within crystalline cellulose fibrils. We provide a molecular-scale explanation of these phenomena through molecular dynamics (MD) simulations and enzymatic assays. Ammonia transformed the naturally occurring crystalline allomorph I_beta to III_I, which led to a decrease in the number of cellulose intrasheet hydrogen bonds and an increase in the number of intersheet hydrogen bonds. This rearrangement of the hydrogen bond network within cellulose III_I, which increased the number of solvent-exposed glucan chain hydrogen bonds with water by 50%, was accompanied by enhanced saccharification rates by up to 5-fold (closest to amorphous cellulose) and 60–70% lower maximum surface-bound cellulase capacity. The enhancement in apparent cellulase activity was attributed to the "amorphous-like" nature of the cellulose III_I fibril surface that facilitated easier glucan chain extraction. Unrestricted substrate accessibility to active-site clefts

of certain endocellulase families further accelerated deconstruction of cellulose III_I. Structural and dynamical features of cellulose III_I, revealed by MD simulations, gave additional insights into the role of cellulose crystal structure on fibril surface hydration that influences interfacial enzyme binding. Subtle alterations within the cellulose hydrogen bond network provide an attractive way to enhance its deconstruction and offer unique insight into the nature of cellulose recalcitrance. This approach can lead to unconventional pathways for development of novel pretreatments and engineered cellulases for cost-effective biofuels production.

In a subsequent paper, we provided mechanistic details of how liquid ammonia was able to penetrate and disrupt the hydrogen bonding network in native cellulose to create cellulose III.[2] Although the experimental protocol for the ammonia-based pretreatment of cellulose is well-established, the molecular mechanism by which liquid ammonia interacts with cellulose and how it contributes to the structural change was still unknown. Our simulations reveal that early structural changes in the fibril are driven by the rapid formation of an extended hydrogen bond network between the solvent-exposed surface chains and ammonia that precedes ammonia penetration into the fibril. The emergence of this hydrogen bond network causes relative shifting of the cellulose layers within the fibril that in turn leads to the formation of channels orthogonal to the (100) and (-100) fibril surfaces. The channels allow ammonia molecules to penetrate into the cellulose fibril. These findings may have an impact on the design of new and more efficient experimental protocols directed to lower the crystalline cellulose stability and recalcitrance to enzymatic hydrolysis. In particular, cellulose chemical treatments that rely on the disruption/alteration of the internal cellulose hydrogen bond network such as the ones based on liquid ammonia and ionic liquids may be improved on the basis of our findings.

In a paper that will appear in the Journal of Physical chemistry, for the first time, we are able to quantify the relative contributions from stacking and hydrogen-bonding interactions to the different crystalline cellulose allomorphs.[3] In this quantum chemical study, we consider a model system of six pairs of cellobiose units arranged in three layers with two chains per layer to represent the cellulose crystalline core. Our calculations demonstrate that individual H-bonding interactions are stronger in cellulose I than in cellulose III_I. Surprisingly, we find significant contribution from cooperative stacking interactions to the stabilization of cellulose I.

Future Work

Experiment: The cellulose microfibers that give rise to the

linear features we see in our super-resolution cellulase binding images are too small (~1000-3000 nm long, ~100-400 nm wide, ~50 nm high) to be easily seen using optical microscopy unless they are fluorescently stained (as they are when bound with fluorescent cellulases). We are preparing cellulose substrates labeled with green-emitting fluorescein. These counter-stained cellulose substrates will permit us to simultaneously image the positions of the cellulose microfibers and binding of the fluorescent cellulases to confirm that the linear features we see in our binding images are due to binding of cellulases to the microfibers.

We are also preparing endocellulases labeled with Cy-3 a green-emitting fluorophore. We will use these along with our red-emitting Cy-5 labeled exocellulases to simultaneously monitor exo- and exoglucanase binding to cellulose substrates. These imaging experiments will allow us to directly visualize the synergistic activity of these two cellulases.

Theory: We will use large-scale Molecular Dynamics simulations and the Adaptive Biasing Force (ABF) algorithm to study cellulase binding and activity on crystalline cellulose surfaces. Our efforts will be focused on the analysis of the interaction between cellulases and different cellulose nanofibers. A detailed understanding of the interactions between catalytic enzymes (cellulases) and different crystalline cellulose substrates may lead to the design of new synthetic cellulases with enhanced specific activities for crystalline cellulose hydrolysis.

Conclusion

Our goal is a molecular-level understanding of the cellulase-catalyzed hydrolysis of cellulose. Imaging of individual cellulases interacting with the cellulose substrate will be used to obtain insight into the molecular mechanisms of cellulase synergy as well as information on cellulase kinetics. These data will be used guide and refine simulations of cellulase activity on cellulose. This molecular-level model of cellulase activity will be crucial for the rational design of improved cellulases.

References

1. Chundawat, S. S., G. Bellesia, N. Uppugundla, L. Da Costa Sousa, D. Gao, A. Cheh, U. Agarwal, C. Bianchetti, G. Phillips Jr., P. Langan, V. Balan, S. Gnanakaran, and B. Dale. Restructuring the crystalline cellulose hydrogen bond network enhances its depolymerization rate. 2011. *Journal of the American Chemical Society.* **133** (29): 11163.

2. Bellesia, G., S. S. Chundawat, P. Langan, B. Dale, and S. Gnanakaran. Probing the early events associated with liquid ammonia pretreatment of native crystalline cellulose. 2011. *Journal of Physical Chemistry B.* **115** (32): 9782.

3. Parthasarathi, R., G. Bellesia, S. P. S. Chundawat, B. E. Dale, P. Langan, and S. Gnanakaran. New insights into hydrogen bonding and stacking interactions in cellulose. To appear in *Journal of Physical Chemistry A.*

Publications

Bellesia, G., S. S. Chundawat, P. Langan, B. Dale, and S. Gnanakaran. Probing the early events associated with liquid ammonia pretreatment of native crystalline cellulose. 2011. *Journal of Physical Chemistry B.* **115** (32): 9782.

Chundawat, S. S., G. Bellesia, N. Uppugundla, L. Da Costa Sousa, D. Gao, A. Cheh, U. Agarwal, C. Bianchetti, G. Phillips Jr., P. Langan, V. Balan, S. Gnanakaran, and B. Dale. Restructuring the crystalline cellulose hydrogen bond network enhances its depolymerization rate. 2011. *Journal of the American Chemical Society.* **133** (29): 11163.

Gaiotto, T., H. B. Nguyen, J. Jung, A. M. Bradbury, S. Gnanakaran, J. G. Schmidt, G. S. Waldo, and P. M. Goodwin. A photophysical study of two fluorogen-activating proteins bound to their cognate fluorogens. Presented at *Single Molecule Spectroscopy and Imaging IV.* (San Francisco, CA, 22-27 January, 2011).

Parthasarathi, R., G. Bellesia, S. P. S. Chundawat, B. E. Dale, P. Langan, and S. Gnanakaran. New insights into hydrogen bonding and stacking interactions in cellulose. To appear in *Journal of Physical Chemistry A.*

Bacterial Invasion Reconstructed Molecule by Molecule

James H. Werner
20100215ER

Introduction

Understanding the mechanisms of host-pathogen interactions is a crucial first step to developing countermeasures to infection, whether natural or man-caused. We are developing advanced imaging methods to explore bacterial infection of human host cells with unmatched spatial and temporal resolution.   This work exploits state of the art 3D single molecule tracking technology developed in our lab to study the kinetics of bacterial virulence factors in live human host cells. We are also building a new instrumental capability for this laboratory, super-resolution optical imaging, that will be used to directly visualize the bacteria-host interface with unmatched spatial resolution.

The host-pathogen system we are working on is Salmonella Typhimurium infection of human cells. This system is ideally suited for super-resolution visualization methods as the identities of key human host receptors are already known, but the spatial organization occurs at length-scales below the wavelength of visible light. This study will be the first to reveal the spatial organization of this bacteria-host interface at near nanometer resolution, greatly increasing our knowledge of bacteria-host interactions, not only for this one bacteria-host system, but for a whole class of virulent bacteria that all employ a highly conserved type three secretion system for infection.

Benefit to National Security Missions

This work helps LANL missions in Biosecurity science and Complex Biological systems, by creating instrumentation to study bacteria-host interactions with unprecedented detail. This work should create a much better understanding of bacterial infection mechanisms on a molecular level. This work will position our team to respond aggressively and competitively to proposal calls from the NIH, DARPA, and DTRA. In addition to studying bacteria-host interactions, the super-resolution imaging techniques being supported and developed in this work can also be used to study and characterize important functional soft materials.

Progress

We have made substantial progress during the first two years of this project. From an instrument development perspective, we have built a super-resolution optical microscope and have written the software needed for instrument control/data analysis (Figure 1). We optimized protocols for staining and visualizing cellular structures (the actin cytoskeletal matrix) using this new system and obtained super-resolution images of key cellular structures important in bacterial infection. We studied the time-course of infection of bacteria and human host cells (0, 2, 5, 10 minutes post-infection) using standard and super-resolution fluorescence microscopy (Figure 2). We characterized human host cells that had key membrane receptors labeled with green fluorescent protein (GFP) variants.
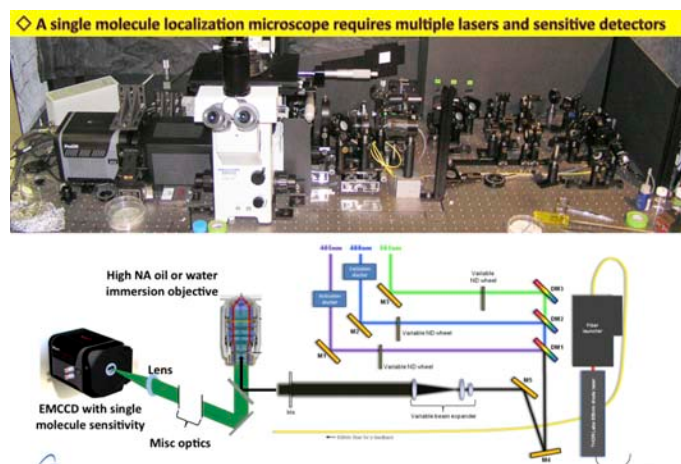
Figure 1. Top: Picture of the super-resolution optical microscope built during year 1 of the project. Bottom: A schematic of the microscope design.

In addition to developing and using new super-resolution imaging methods, we have followed the 3D motion of individual green fluorescent protein variants using unique 3D tracking instrumentation developed by our laboratory. This represents an important proof of principle experiment for visualization of bacterial proteins in human cells. This result was presented as an abstract at the 2011 Biophysical Society meeting and

is currently being written up for publication as a research article for the Biophysical Journal. Our work on 3D tracking resulted in invited talks at the American Chemical Society National Meeting, the UNM IGERT Seminar series, and the Banff International Research Station.
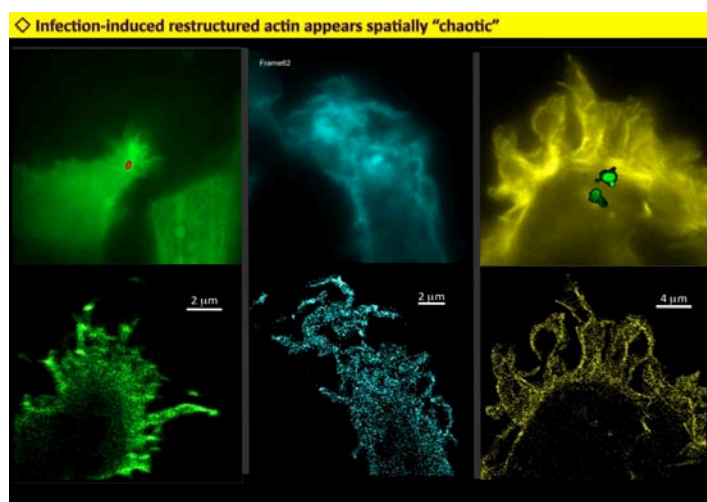
Figure 2. Images of the actin cytoskeleton of human He-La cells following bacterial infection and internalization. Top is a normal fluorescence microscope image. Bottom is images of the cells obtained using single-molecule super-resolution imaging.
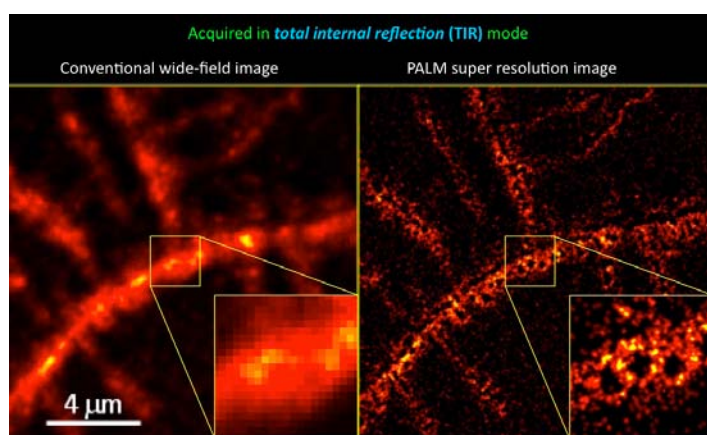
Figure 3. Fluorescence image of a diblock copolymer vapor-anneald thin film as it would be seen in conventional fluorescence microscopy (left) and using super-resolution imaging techniques (right).

While the primary goal of our project is to build and exploit new fluorescence microscopic instrumentation to study changes in human cells in response to bacterial infection, we also view this research as an opportunity to bring advanced microscopic methods developed for biological imaging into the arena of soft materials research. As such, we have continued studies using super-resolution optical imaging to explore structure and phase segregation in diblock copolymers (Figure 3). These experiments may soon result in the introduction of super-resolution imaging techniques into the soft-materials research community. As

a result of these efforts, our group was invited to submit a review/methods article for the book "Characterization of Materials" on Super-Resolution Optical Microscopy.

Future Work

We proposed to observe the initial stages of bacterial infection of a human host cell with un-matched spatial and temporal resolution. Thus far, we have observed key changes in human host cells that result from bacterial infection. In the coming year, we anticipate publishing our results concerning changes in host cell morphology that occur upon bacterial infection. We will also continue our studies on specific human host cell receptors key for bacterial adhesion/infection.

In addition to super-resolution imaging, this project has supported the continued development and use of 3D tracking instrumentation developed by our laboratory. In particular, in the coming year, we will complete some needed experiments and anticipate publishing a high-impact paper on the ability to follow individual GFPs moving at biologically relevant transport rates.

Time-permitting, in addition to these proof-of-principle measurements, we may begin to follow the exact routes key bacterial proteins (bacterial effectors) take to find their host targets in human cells. Attempts to obtain follow on funding from the NIH, DARPA, or DTRA will be of the utmost importance in the third year of this project.

Conclusion

We expect a number of key outcomes of this research. First, we have already developed a super resolution microscope that will be a valuable research tool for exploring the finer details of cellular structure. Second, we will directly test scientific hypotheses concerning bacteria-host interaction dynamics in ways only now technically feasible, due to state of the art 3D molecular tracking technology developed by our group. Finally, this work will provide mechanistic insights into conserved infection strategies used by many high-risk pathogens, and as such, will substantially increase our knowledge of the molecular basis of host-pathogen interactions.

Publications

Han, J., A. Shreve, and J. Werner. Super Resolution Optical Microscopy. *Characterization of Materials.*

Metabolic Regulation of Light-harvesting and Energy Transfer

Gabriel A. Montano
20100257ER

Introduction

The energy from sunlight that strikes the earth in one hour (4.3×10^{20}J) is more than the global yearly demand (4.1×10^{20} J). While having tremendous potential, solar energy production currently provides less than 1% of total energy consumption. This is due in part to a lack of efficient capture and conversion into a useful energy supply in either the form of biomass or by man made solar collection devices. The physical energy capture and conversion processes of photosynthesis, such as light-harvesting, are remarkably efficient and serve as a model for development of efficient solar energy systems. These photosynthetic processes are complex, highly evolved, and carefully regulated metabolically. However, the complexity of this regulation makes it difficult to ascertain how such precise and dynamic control occurs. The chlorosome antenna complexes of green bacteria combine efficiency with novel self-assembly mechanisms to create robust light-harvesters. We are investigating the metabolic regulation of synthesis, light-harvesting and energy transfer of the chlorosomes and chlorosome metabolic regulation under various environmental conditions. The project research aims to understand the role of metabolic control in developing an optimized photosynthetic light-harvesting complex, increasing our fundamental understanding of the metabolic regulation of light-harvesting complexes and advancing research in artificial photosynthetic design and other bio-energy applications.

Benefit to National Security Missions

Developing new forms of energy is fundamental to the laboratory mission. The proposed research is directly related to the LDRD grand challenges of "Enhancing the Nation's Energy Security" and "Enhancing the Nation's Fundamental Scientific Capabilities." Developing mechanisms of energy transfer from molecular scale assembly is a fundamental focus of the Center for Integrated Nanotechnologies (CINT) at Los Alamos National Laboratory. This research will lead to new program development in bioenergy and bio-inspired design within CINT and with programs within Basic Energy Sciences.

Progress

It is our goal to understand metabolic regulation of light-harvesting and energy transfer in chlorosomes on picosecond, minutes, hours, and day time scales as well as to determine levels of heterogeneity within a given population. In order to perform such a task we are using a suite of developed capabilities. Bacteria are grown anaerobically in a Coy anaerobic chamber that contains a mini-prep area capable of growing small amounts of bacteria in stringently controlled anaerobic conditions that can be adjusted accordingly. For example, it is possible to alter anaerobic and light conditions to grow bacteria under varying levels and types of stress. Bacteria have been cultured and grown under varying conditions and cells harvested at varying time points in the growth cycle.

Several studies have shown modulated bacteriochlorophyll fluorescence from anoxygenic photosynthetic bacteria. However, there has been little evidence to support a link between this variable fluorescence and a regulatory mechanism that controls the flow of energy between antenna complexes and the reaction center. Recent evidence has suggested variable fluorescence mechanisms in green sulfur bacteria could be due to a number of different mechanisms and cooperative mechanisms similar to those observed in more complex oxygenic photosystems. This indeed would be a remarkable finding, linking these archaic anaerobic systems to the significantly more complex aerobic systems. However, understanding any relation these systems have to more advanced oxygenic systems relies on the ability to decipher the mechanisms involved in regulation. It is proposed that any number of mechanisms could result in the observed variable fluorescence, including protective mechanisms against formation of radical oxidative species, and regulation by electron donors and acceptors that interact with the photosystem. As described below, we have determined that a structural mechanism may be a dominant factor in regulating the observed variable fluorescence.

We previously reported the observation that the

fluorescence quenching mechanism of the chlorosome was actually due to a complex regulation mechanism that was controlled by communication between various components of the photosystem to maintain an equilibrium of electron availability. While these observations may remain true for harvested bacteria, we observed surprising results when we attempted to verify our observations with live cells. The existing dogma for this system, and for many photosynthetic systems is that fluorescence modulation under oxygenic conditions for *C. tepidum*, is a protective mechanism, in essence a mechanism for the organism to deal with excess energy. This serves to protect the photosystem from unwanted formation of destructive photo-oxidative species. This has been a widely accepted mechanism since it makes sense from a physiological standpoint. However, recent evidence has indicated other light-induced regulatory mechanisms occur that are more comparable to oxygenic photosystems. Our research this year has led to results that make a new mechanism dependent on conformational change the likely contributor to observed light-induced variable fluorescence. Our new mechanism that we are proposing is one in which excess emissive energy is the result of a conformational change that actually decouples the light-harvesting and reaction center components. (Figure 1) This is a dogma-changing discovery that shows a structural regulatory mechanism relationship to more advanced oxygenic photosystems that are capable of a similar process. For such a mechanism to be present in an archaic photosynthetic organism is truly remarkable. It 1) highlights the importance of studying archaic systems as a means of understanding more complex photosynthetic organisms and 2) indicates a paradigm shift in our understanding of regulatory mechanisms of photosynthesis, the primary goal of this ER. We are currently writing up what we think will be a high-impact article with a high citation record.
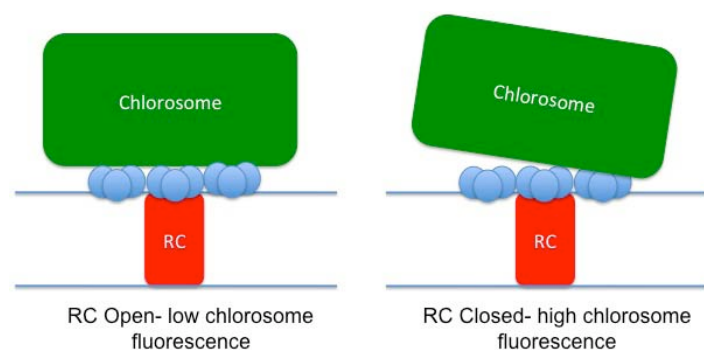
Figure 1. Proposed conformational release mechanism for decoupling of chlorosome antenna from photosystem resulting in variable fluorescence.

We decided not to publish our AFM (atomic force microscopy) effort as it stood at the end of last year due to some reconsideration on our part as to the impact we could have with further experimentation. Therefore,

we began an effort to isolate small populations of membrane fragments from carefully controlled growth conditions. This has proven more difficult than we initially anticipated however we are beginning to get results necessary. What we believe we can determine beyond relative stoichiometric variations in a given chlorosome population is actually devolve a mechanism for chlorosome biogenesis, a highly debated topic. What we have found is that there is a difference in the standard deviation of the width of chlorosomes versus the length and height. We are exploring this difference in isolated membranes with bound chlorosomes of bacteria grown under various light conditions and isolated from bacteria at different stages in the growth cycle, a labor intensive process. What we hope this effort will help us determine is the mechanism of chlorosome biogenesis by systematically investigating variations in chlorosome dimensions under varying conditions. It will also more completely help us to understand previously observed heterogeneity in chlorosome size.

We had two poster presentations, one postdoc talk (Greg Uyeda) at a photosynthetic antenna meeting, one poster presentation at the Society for the Advancement of Chicanos and Native Americans in Science (SACNAS) conference from undergraduate student Fatima Pino and three invited talks of which this research is a part.

Future Work
Having determined that the regulatory mechanism involved in variable chlorosome fluorescence is likely due to antenna decoupling, we are focusing our efforts this last year on two fundamental goals 1) determining the nature and mechanistics that lead to the decoupling and 2) regulatory mechanisms of chlorosome biogenesis and C. tepidum photosystem organization. C. tepidum photosystems contain an intermediary FMO (Fenna-Matthews-Olson) antenna complex that connects the chlorosome to the membrane. C. aurantiacus chlorosomes, however,are directly connected to the membrane. As stated above, the fluorescence quenching mechanism observed in C. tepidum is not observed in C. aurantiacus chlorosomes. We have established that the observed quenching is due to a conformational decoupling of the chlorosome from presumably the FMO complex. The lack of a FMO complex in C. aurantiacus likely plays a role in the lack of an observed quenching under varying redox conditions. However, it is still unclear as to what actually drives the decoupling. In order to address this question, we will investigate fluorescence response of live cells when varying the excitation intensity and varying the oxidative state. We hypothesize that a state exists in which reaction centers can no longer undergo light-induced cycling that is responsible for the decoupling mechanism and test this hypothesis via time-resolved fluorescence microscopy/spectroscopy. We will also try to understand the differences between the live and harvested cells and determine why such observations have not been

previously reported.

In order to determine regulatory mechanisms of chlorosome biogenesis we are using AFM, as previously described. AFM allows for a 3-dimensional determination of chlorosome dimensions. All prior determinations of chlorosome dimensions, including our own, have been from large batch cultures of cells that have, even within a single 1L culture, been exposed to large variations of environmental conditions such as light intensity. By growing small, controlled samples of solutions with relatively uniform light intensity exposure, we will isolate cells and thus membranes from single batch cultures at various time points and under varying environmental constraints. Our current hypothesis is that the chlorosome baseplate is synthesized immediately upon cell formation and sets the lower boundary for chlorosome size. As the cells mature, and dependant upon environmental conditions, the chlorosomes will grow to relatively uniform size (uniform per cell).   Our unique cellular growth and AFM characterization capabilities make us uniquely set up to complete such studies.

Conclusion

It is our goal at the end of this last year to answer regulatory mechanisms that control both biogenesis and regulatory mechanisms of light-harvesting complexes of green photosynthetic bacteria. We further plan to turn the knowledge gained into a BES program exploring regulatory mechanisms in other photosynthetic systems, including more complex systems of interest to biofuels.

Environmental and Biological Sciences

Exploratory Research
Continuing Project

Understanding Arctic Hydrologic Response to Climate Change

Joel C. Rowland
20100312ER

Introduction

The impact of global climate change is predicted to disproportionately affect arctic systems. Many of the changes in the Arctic documented over the past several decades (shrinking lakes, changes in flows and chemical loading of rivers, vegetation distributions, and thermokarst expansion) are intimately linked with the hydrology of permafrost dominated landscapes. The rate and timing of these hydrological changes will have a direct impact on the fate of the approximately 1600 Gt of carbon presently sequestered in frozen arctic soils. At present, our ability to monitor ongoing activity and predict the spatial and temporal scales over which future changes in the arctic hydrological cycle will occur is greatly limited by current modeling and remote sensing technologies. Current models of permafrost thawing focus exclusively on the thermal diffusion of temperature changes and neglect the role of hydrologic flow in transporting heat into the subsurface. Presently, there are no remote sensing technologies that can directly detect changes in permafrost. This project addresses these two fundamental challenges by combining numerical modeling of groundwater and heat flow through frozen soils with the development of novel algorithms to apply to remote sensing data that will provide new tools to infer permafrost distributions and changes.

Benefit to National Security Missions

Predicting the timing and spatial patterns of permafrost changes in response to global climate change, and associated carbon release, is of direct relevance to DOE Office of Science climate change programs. The hydrologic and geomorphic impacts of permafrost thawing are highly relevant to the energy industry and the Departments of Defense, Commerce and State in that defense bases, transportation routes, ports and energy infra-structure will be impacted these changes. The natural resource impacts have direct relevance to the USGS, USFWS, BLM and state agencies. The remote sensing technologies develop have a direct application to NNSA and DOD programs.

Progress

In FY2011 our project has made significant progress on modeling, remote sensing, and data acquisition in Alaska for validating both the modeling and remote sensing efforts. Project results have generated one published (Rowland et al., 2011) and 5 peer reviewed manuscripts in submission or preparation for submission. An additional seven conference presentations on ER work have been or will be made this FY, including two invited presentations at the annual Fall AGU meeting on the connections between hydrological and landscape changes on Arctic carbon cycles.

We have compared ARCHY to a variety of analytic and experimental data sets to confirm that the code works correctly for processes relevant to arctic permafrost systems. We have coupled the code to ED, an ecosystem demography model (Moorcroft et al 2001). This coupled model combines surface climate profiles from Global Climate Model (GCMM) simulations (temperature, precipitation, gas concentrations, solar irradiance vs time), with surface vegetation evolution, surface small-scale topography, with subsurface permafrost thawing/freezing cycles, hydrology - both vertical and horizontal flow, and microbial and greenhouse gas (GHG) dynamics, in 3D. This fully coupled model is allowing us to start simulations that couple ground surface changes and surface lakes to vegetation, subsurface permafrost and soil microbial dynamics. One series of simulations, with a manuscript in submission, quantified the influence of groundwater flow and advective heat transport on thinner permafrost and its increasing sensitivity to warming and degradation.

Remote sensing work has focused on algorithm development and change detection. We have demonstrated a new application of sparse representations over learned dictionaries for multi-spectral remote sensing. These techniques will be extended to using RADARSAT and to fused RADARSAT and WorldView2 data sources. By comparing high resolution pan-chromatic and multi-spectral imagery with lower resolution thermal data from LANDSAT we

have identified hydrological-thermal feedbacks arising from meter to decimeter scale degradation of ice-wedges not discernable in coarser resolution LANDSAT multi-spectral imagery. By using high-resolution data, typically limited in both spatial and temporal availability, to identify indicators of permafrost degradation in coarser, but widely available datasets we have the potential to find novel methods for quantifying Arctic hydrological and landscape responses to warming. Using high-resolution topographic data from light detection and ranging (LiDAR) measurements, we have developed metrics to distinguishing unique topographic signatures of permafrost landscapes and to detect varying levels of degradation in terrains with polygonal ground.

Additional modeling efforts have focused on the development and testing of a thermo-mechanical conceptual and mathematical model for thermokarst development. Thermokarst is a change in the landscape due to thawing of permafrost. When ice thaws, the resulting water volume is less than the ice volume; this change in volume and support frequently leads to a collapse of surface terrain, leading to the formation of new lakes, and is a major characteristic of arctic regions. This work has led to a conceptual model for how to "release" melting ground ice pore water from the permafrost column so it could account for volume loss due to mass loss. The next step in this work will be the incorporation of deformation in a more realistic variably saturated domain.

In order to quantify thermal responses of permafrost to thermal disturbances and to provide additional data to develop and validate both remote sensing and modeling efforts, focused field investigations have been conducted in Alaska. This work has included installation of meteorological and subsurface sensors to relate changes in soil temperature and soil moisture to air temperatures, net solar radiation and changes in precipitation.

Future Work
Incorporation of the hydrological impacts of, and feedbacks on, permafrost thawing into Global Climate Models is presently limited by a lack of understanding of what scale (temporal and spatial) changes will take place, how to parameterize these changes, and how to determine important properties from indirect and remote measurements.

Individual processes and features, such as the active layer and individual lakes and rivers, each have their own spatial scales ranging from soil pores to entire watersheds. Interactions between dominant processes occurring at different scales determine the integrated system response. The inclusion of processes occurring over the relevant range of spatial scales will allow us to quantify the relative impact of each process at each scale. This knowledge will provide a basis for parametrization into global climate models.

The inclusion of hydrologic flow will allow the determination of a range of physical time scales presently absent in strictly thermal models of permafrost. One goal of this effort will extend the LANL MAGHNUM hydrologic model to enable prediction of the dynamic interactions between permafrost thawing, changes in hydrology and land surface responses by inclusion of topography, and a geomechanics model that can simulate soil collapse and river bank erosion.

Our second goal addresses a common problem in remote sensing applications: the feature most of interest is not directly observable to the satellite. In the case of the Arctic, the permafrost is overlain with a layer of vegetation and seasonally thawed soils. Instead, estimates of permafrost extent can be built up from indirect observations of vegetation, hydrologic features (lakes, rivers) and changes in topography (collapsing frozen banks). We will leverage the existing Genie software base and results from the facility monitoring project to develop statistical relational learning algorithms that combine continuous features found using regression and classification algorithms, extracted from different sensors.

Conclusion
We will produce two new technologies: 1) the first fully coupled heat and fluid transport model with the capability to predict the interactions between permafrost thawing, changes in hydrology and land surface responses; and 2) a software platform with integrated statistical relational learning algorithms. With these two advancements, we will: 1) determine rates, timing, magnitude, and scales of hydrologic changes arising from permafrost thawing, and 2) assess the evolution of hydrologic conditions amenable to activation of biotic and geomorphic processes that will drive carbon release. Major changes in the arctic regions will impact climate, food supplies and land usage.

References
1. Moorcroft, P. R., G. C. Hurtt, and S. W. Pascala. A method for scaling vegetation dynamics: the ecosystem demography model (ED). 2001. *Ecological Monographs.* **71**: 557.

2. Rowland, J. C., B. J. Travis, and C. J. Wilson. The role of advective heat transport in talik development beneath lakes and ponds in discontinuous permafrost. 2011. *GEOPHYSICAL RESEARCH LETTERS.* **38**: L17504.

Publications
Brumby, S. P.. Image fusion for remote sensing using fast, large-scale neuroscience models. Presented at *SPIE Defense Security and Sensing 2011.* (Orland, 25-29 Apr 2001).

Rowland, J. C., B. J. Travis, and C. J. Wilson. The role of advective heat transport in talik development beneath lakes and ponds in discontinuous permafrost. 2011.

GEOPHYSICAL RESEARCH LETTERS. **38**: L17504.

Rowland, J. C., C. E. Jones, G. Altmann, R. Bryan, B. T. Crosby, G. L. Geernaert, L. D. Hinzman, D. L. Kane, D. M. Lawrence, A. Mancino, P. Marsh, J. P. McNamara, V. E. Romanovsky, H. Toniolo, B. J. Travis, and C. J. Wilson. Arctic Landscapes in Transition: Responses to Thawing Permafrost. 2010. *EOS, Transactions, American Geophysical Union.* **91** (26): 229.

Deciphering the Controlled Chaos of Intrinsically Disordered Proteins

Dung M. Vu
20100328ER

Introduction

Many cellular proteins are intrinsically disordered and undergo folding upon binding to their physiological targets. While the absence of well-defined structures and conformational flexibilities of these intrinsically disordered proteins (IDPs) enable them to bind to multiple partners and to modulate their functional pathways, this transient nature also makes them susceptible to many human diseases (cancers, neurodegenerative diseases, and cardiovascular diseases). Therefore to understand the causes of these diseases and to derive effective treatments, it is crucial to understand the correlation between the underlying structures of these IDPs to their biological functions.

Alpha-Synuclein (aSyn) is an ideal model protein to study the structural and functional characteristics of IDPs because it is relatively small (140 residues) and it possesses many of the unique characteristics of IDPs. aSyn is a protein whose function is relatively unknown but has been widely implicated as the major causative protein in numerous neurodegenerative diseases such as Parkinson's disease. The central goal of this project is to elucidate the underlying mechanisms and molecular forces that induces the binding of ligands to aSyn, the conformational changes associated with ligand binding, and the competing self-assembly process that result in the pathological formation of filamentous aggregates. Because of the intrinsic heterogeneity of aSyn, structural and functional characterizations of this protein have proven to be very challenging. To help overcome this obstacle, we propose to integrate vibrational spectroscopic techniques along with advanced computational methods to characterize the structure, function, and dynamics of aSyn. We expect the methods and approaches developed in this study to find wide application in the elucidation of the structures and functions of other IDPs that are implicated in many human diseases.

Benefit to National Security Missions

We expect the experimental, theoretical and computational methods and approaches developed in this study to find wide application in the elucidation of the structures and functions of other IDPs that are implicated in many human diseases. Understanding the structures, folding, and functions of IDPs will help advance the Laboratory's mission by developing a predictive understanding of complex biological systems and developing applications to solve health and the environmental issues that are relevant to DOE, DHHS, and other government agencies.

Progress

Simulating the structural conformations of IDPs has proven to be very challenging. This is because finding the right parameters (e.g. setting up the right force fields and defining the initial structural conformations) is not a trivial process. While others and we have been using traditional methods to simulate the structures of these IDPs, we are finding that we have to make adjustments to these methods to be able to adequately simulate these proteins. We desperately need new experimental techniques to validate these simulations. As a starting point, we have been using replica exchange molecular dynamics (REMD) simulations to try to simulate the structural conformations of aSyn.   This year, we have expanded our all-atom MD simulations of full-length aSyn in explicit water from our previous work.   This was done in response to a major criticism we received from reviewers who stated that our original 355 ns MD simulation might not be sampling enough starting conformations that would result in meaningful results. By using the LANL Institutional Computing for superconducting time, we were able to carry out a total of 100 MD simulations that were each 100 ns long. Fifty of these simulations had some partial helical character as the starting conformation and the other fifty simulations were started from random conformations generated from the random conformation generator. For all the simulations we observe that:

1. aSyn rapidly collapses into compact states within 20-50 ns (Figure 1).   These compact states had radius of gyration between 16-30 angstroms, which is much smaller than the radius of gyration expected

for a self-avoiding polypeptide chain of the same length (42 angstroms).
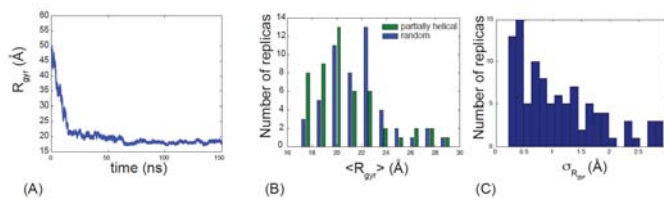
Figure 1. Early collapse of aSyn: (A) time evolution of the radius of gyration of aSyn during the MD simulations. The histogram of the (B) average and (C) standard deviation of radius of gyration displayed by the protein from 50-100 ns in the 100 replicas. The histogram of the average radius of gyration is shown for the partially helical and random simulations separately.

2. While these collapsed states are stabilized by tertiary contacts, they still comprise a heterogeneous distribution of conformations with different long-range contacts.

3. In these collapsed states, aSyn does display some secondary structure propensity that regularly forms and breaks during the simulation. The N-terminal half of the protein has a slight bias for helical structures and the C-terminal half has a bias towards transient beta-strands.

4. The network contacts of the full-length protein will behave different from that of its fragments. Our results have not changed significantly from our original long timescale MD simulation. This work is currently submitted to the Biophysical Journal. We are now in the process of using these structures to simulate amide I IR spectra and comparing them with our experimental IR spectra to help us test and refine our MD simulations.

Since aSyn has been found to interact with presynaptic vesicle membranes, we have also carried out all-atom MD simulations with aSyn in the presence of sodium dodecyl sulfate (SDS), a well-studied lipid mimetic. We focused on the early interactions of aSyn with SDS to gain a better understanding of the role that lipid binding plays in the conformational changes of aSyn. aSyn has been shown to adopt various helical conformations when interacting with SDS micelles or lipid membranes. However, the stability and flux of the helical conformations of aSyn as it interacts with lipid membranes or micelles have been shown to be complex. The result of one of our simulations is shown in Figure 2. Our MD simulations results show that: 1) aSyn interacts non-specifically with SDS monomers to form a collapsed complex followed by structural changes to form secondary structure in a microsecond timescale and 2) the helical conformations of aSyn is not stable without interaction with SDS micelles.
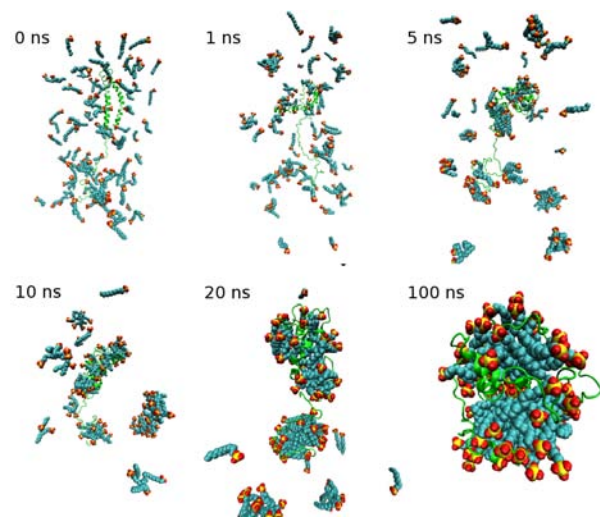
Figure 2. Snapshots of SDS micellation at 0, 1, 5, 10, 20, 100 ns from the 100 Folded System (SDS:aSyn ratio of 100:1). Only the aSyn and SDS in the final complex are shown in the snapshot for clarity. The aSyn protein is in green cartoon presentation. The SDS molecules are in space-filling representation, while the head groups are in red and yellow and the alkyl carbon tails are in cyan. SDS monomers, which are not part of the final complex, are not shown for clarity. The snapshots are made in VMD.

When interacting with SDS, aSyn showed a secondary structure formation with residues 1 to 30 having a high helical propensity and residues 31 to 100 have beta-sheet propensity. The N-terminal helix is highly stablilized due to strong interactions with micelles. These results agree well with our IR and experimental results from others. These simulations provide valuable microscopic insight into the nature of the aSyn-SDS interactions, which will be useful for future experimental designs of intrinsic disordered protein membrane systems. These results have been presented at the Biophysical Society Meeting (March 2011). This work has been submitted to the Journal of Biophysical Chemistry A.

For our experimental work, we have started to characterize the full-length protein and peptide fragments in the bound and unbound ligand forms. The results from our IR data show that while the unbound form of aSyn is dominated by random coil or disordered structures, we also observe some helical and beta-sheet structures associated with it (Figure 3). We also observe that in the presence of SDS monomers and micelles, the structure of aSyn can be modulated. We show in Figure 3 that at low concentrations of SDS (0.5 mM), aSyn has a higher propensity to form intermolecular beta-sheet that causes it to self-assembly and fibrillate. As our MD simulations suggest, this may be because SDS monomers can interact with aSyn in a non-specific way that causes the hydrophobic region of this protein to become exposed and more prone to self-assemble. As the concentration

of SDS (40 mM) is further increased to favor micellation, we observe that this protein has a higher propensity to form helical structures that protect it from self-assembly and fibrillation. This data corresponds very well to our MD simulation and other experimental work done by others.   We are currently integrating and validating our computational results with these experimental results. What we expect to get is a better model for our simulated IR spectra that will provide us with some specific details on the conformational behavior of aSyn. We are currently preparing a manuscript for this work.
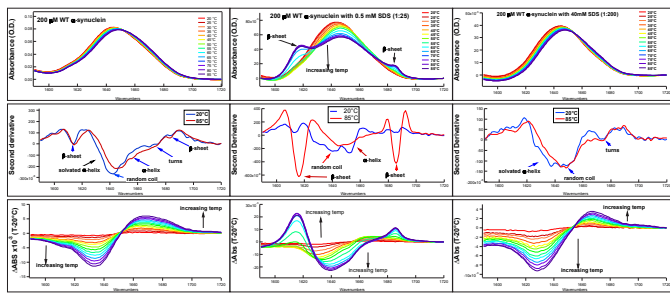
Figure 3. Infrared measurements of aSyn in the presence and absence of sodium dodecyl sulfate (SDS).

We have also done IR measurements of the C-terminal peptides in the absence and presence of dopamine. Surprisingly the C-terminal peptide is not as disordered as we thought. It appears to form beta-sheet structures, which show reversible folding and unfolding with temperature.   Because this C-terminal end is predicted to be the binding site for various ligands (including dopamine), we performed measurements in the presence of dopamine. We observe some conformational changes in the structure of the C-terminal peptides that indicates that dopamine does interact with these peptides, but these changes are minimal.

We have made significant progress on our project. We have been able to setup and carry out our IR experiments and MD simulations of aSyn. We are well on our way to being able to analyze these simulations to compare our simulated IR spectra with our IR measurements.

Future Work
1. Continue to simulate IR spectra and comparing them with our experimental IR spectra to help test and refine our MD simulations.

2. Incorporate IR labels on aSyn to follow the conformational changes of specific regions of the protein. We will incorporate these labels in regions of the proteins that have been identified by MD simulations to have some secondary structure propensity.

3. Continue to make IR measurements of aSyn in the presence of other ligands to try to understand the induced binding and folding mechanism of aSyn.

4. Identify predictive structural signatures for IDPs.

Conclusion
Understanding the molecular mechanistic details of the binding, folding and aggregation of aSyn will have a significant impact in defining the function of this protein and its role in many human diseases. By comparing the interactions and conformations of the bound and unbound states of the peptide fragments of aSyn and whole protein, we expect results that will provide us with insight on how binding induced folding dictate the various functions of this protein. In addition, by studying deviations from this folding mechanism (misfolding and aggregation) we can also begin to understand the pathogenesis of many aSyn related diseases.

Publications
Sethi, A., B. Goldstein, and S. Gnanakaran. Quantifying Intramolecular Binding in Multivalent Interactions: A Structure-Based Synergistic Study on Grb2-Sos1 Complex. 2011. *PLoS Computation Biology.* **7** (10): e1002192.

Sethi, A., J. Tian, D. M. Vu, and S. Gnanakaran. Identification of Minimally Interacting Modules in an Intrinsically Disordered Protein. *Biophysical Journal.*

Tian, J., A. Sethi, D. Anunciado, D. M. Vu, and S. Gnanakaran. Characterization of a Disordered Protein During Micellation: Alpha-Synuclein Interactions with Sodium Dodecyl Sulfates. *Journal of Physical Chemistry A.*

Algal Lipid Regulatory Networks

Scott N. Twary
20100456ER

Introduction

Algae are the leading candidates for biodiesel production due to their potential to produce 10 to 100 times more oil/ lipids than plants. Algae produce and accumulate lipids as energy dense storage compounds to survive environmental stress. Current algal lipid production systems are not cost competitive, however, due to the lack of concurrent biomass accumulation and lipid biosynthesis. It is poorly understood how the cell determines resource allocation. Developing an understanding of the factors controlling and limiting lipid biosynthesis can lead to enhanced production systems. To meet the twin goals of decreasing our dependence on petroleum-based energy production and producing environmentally friendly fuels, this project will elucidate the regulatory network controlling lipid biosynthesis allowing for optimization of algal biofuel production. This project will identify the genetic changes that occur in algal cells during nitrogen limitation induction of lipid production. The identification of coordinated changes in cellular metabolites will allow for the development of an understanding of the complex regulatory networks involved in transitioning algal cells from rapid growth to energy allocation for lipid storage. This project will modify the activity of key genetic steps to permit unrestricted allocation of resources to increase lipid production. By combining LANL's innovative capabilities in genomic characterization, metabolomics profiling, gene expression modification, automated algae culture methods, and systems analysis we can identify and optimize the key regulatory mechanisms for maximum lipid production potential.

Benefit to National Security Missions

This work directly addresses the challenges outlined by EERE and DARPA for the development of productive algal biodiesel systems. The results of this project will define the fundamental regulatory mechanisms controlling lipid biosynthesis. Regulation of the key genetic elements will result in increased lipid production and the development of an algal strains suitable for industrial production systems. These systems will provide greater energy security through decreasing dependence on petroleum based fuels and enhance environmental stewardship through CO_2 recapture into a high value product.

Progress

The objectives of this project are to identify the molecular and biochemical changes that occur in the algae Nannochloropsis salina as it transitions from rapid cell growth to lipid biofuel accumulation. Carbon is a limiting structural component of both cells and energy dense storage compounds and must be partitioned between making new cells or energy storage for later use. The cell is able to monitor its environment and identify potential growth inhibiting stresses. These stresses then elucidate a complex response in the cell shifting its metabolism from cell growth to energy storage. We utilize nitrogen depletion from the growth media as the inducer of lipid accumulation. Cell status is monitored by measuring nitrogen storage compounds, carbohydrates, lipids, key metabolites, and biomass. Genetic responses are determined by deep sequencing (RNAseq) of all the expressed genes and small regulatory RNAs throughout the transition. We have developed a bioreactor system that can monitor and regulate many growth conditions including O_2, CO_2, pH, light, and cell density. Automated sampling systems allow for extensive sample collection and preservation every four hours over a three week growth experiment. Nitrogen status of the media can be monitored daily to identify the key time points during the algal growth transition. An axenic culture of *Nannochloropsis salina* CCMP1776 was grown in the controlled bioreactor and characterized for lipid production. Samples were obtained and archived for analysis. Lipid accumulation is significantly induced in response to nitrogen depletion. The cells maintain around 12% of the biomass as neutral lipids for energy storage and metabolism. After recognizing the environmental stress of limiting nitrogen, the cells begin to accumulate neutral lipids as cell growth slows. After two weeks, cell accumulation of triacylglycerol reaches a maximum of 30% or more. We also discovered light may be severely limiting carbon assimilation. When we grew the algae under conditions limiting the cell density to about one third of maximum, lipid accumulation

increased two-fold. Genetic responses throughout the transition from growth to lipid accumulation can be classified into two groups: genes which are down-regulated and genes which are up-regulated. Over 80 genes have been identified which are down-regulated in direct response to nitrogen depletion. These are involved in cell signaling and metabolic activation such as protein kinases and transcription factors. Fatty acid modification enzymes are also suppressed as fatty acids pools are re-directed from cell membrane synthesis to energy storage. Over 220 genes are up-regulated in direct response to nitrogen depletion. These include nitrogen scavenging genes such as ammonium transporters, proteinases, nitrogen assimilating enzymes, and amino acid recycling. Primary carbon assimilation was enhanced through rubisco activase. Partitioning of resources was significantly altered through increased starch synthesis, which may compete for carbon for triacylglycerol biofuels. Altering this pathway may provide resources for additional lipid accumulation. Fatty acid biosynthesis enzymes also increased in response to nitrogen depletion providing the precursor fatty acids for triacylglycerol. Carbon recycling systems were also activated as cells became more stressed and attempted to scavenge non-essential cellular components. Protein phosphatases were activated as an opposite response to kinases, which were down-regulated. These key enzymes are involved in many environmental signaling pathways and cascade kinase/ phosphatase responses. General cell stress responses were also activated including protein protection chaperonins and nutrient transporters. Identification of all of these gene targets will now allow us to directly genetically engineer algae for greater overall lipid biofuel production. We identified a region of the genome where all of the nitrogen responsive genes were co-located. This region may play a key role in nutrient monitoring and response. Within this gene cluster were four unknown genes that were highly expressed and responsive to changes in nitrogen status. These will be key targets for genetic modification. Many of the additional differentially expressed genes have unknown function and will be targets for intense future investigations to understand their importance and roles in regulating lipid metabolism. Identifying concurrent patterns of changes in gene expression with metabolite pools will provide insight into their potential functional roles. We have begun to develop genetic transformation systems for Nannochloropsis and other algal species. Vector optimization, including heterologous and homologous promoters, selectable markers, and reporters have been explored. We have successfully transformed Nannochloropsis with a non-antibiotic selectable marker utilizing an Agrobacterium transformation system. Nannochloropsis is resistant to most antibiotics so standard selection is problematic. The novel selection system we have developed will provide a valuable molecular tool for detailed elucidation of many regulatory genes controlling lipid accumulation.

Future Work

The objective of this project is to elucidate the nitrogen sensing and signaling regulatory network coordinated with control of triacylglycerol biosynthesis in the green algae Nannochloropsis salina. Algae are leading candidates for biodiesel production because they have the potential to produce 10-100 times more oil than higher plants have. Overcoming the critical limitation to commercialization requires increasing lipid biosynthesis. Lipid production in algae is induced when the external nitrate supply is depleted. The assimilation of N is coordinately regulated with carbon assimilation because quantities of C skeletons are required for ammonia incorporation into amino acids. The interdependences of N and C metabolism create a complex regulated network of responses. Sensing and signaling are required to maintain homeostatic pools of N substrates to maintain growth and metabolism. Environmental N limitation induces numerous physiological responses and adaptations including a shift in C allocation to energy-dense storage compounds such as triacylglycerol. Optimizing lipid production for algal biodiesel production requires developing an understanding of the fundamental regulatory networks partitioning carbon and energy between growth and lipid biosynthesis.

We have now identified numerous key genes and regulatory control elements, which contribute to changes in triacylglycerol accumulation. We will build network models based on concurrent and interdependent changes in both gene expression and metabolite concentrations. These models will be utilized to identify significant pathway changes that contribute to re-directing carbon resources into desired biofuels. Genetic modification of individual and multiple genes will be performed to determine the impact on lipid accumulation. In addition, we will artificially alter the environmental response to nitrogen depletion by utilizing specific metabolic inhibitors. These inhibitors will alter specific enzyme function in the nitrogen sensing and assimilating system. This differential response will allow us to further refine the identification of critical regulatory elements affecting lipid biofuel synthesis.

Conclusion

The goal of this research is to create an algae strain with enhanced biodiesel lipid production. This will be a primary component in developing a cost effective industry. This project will identify the key regulatory processes allocating carbon and energy in algae cells between biomass and lipid production. Genetic modification of each critical step will allow for optimal lipid production. Advances in understanding the complex regulation of biosynthesis will allow for the creation of an algae biofuel crop. Algae biodiesel production will decrease our dependence on petroleum based energy and contribute to environmental sustainability through carbon neutral fuels.

Modeling the Global Circulation and Evolution of Influenza A Virus

Alan S. Perelson
20100479ER

Introduction

Each year, 5-15% of the world becomes infected with influenza, and an average of 36,000 people in the United States, and 500,000 people in the world, are estimated to die as a result. Moreover, the highly pathogenic avian influenza A-H5N1 and swine origin influenza A-H1N1 strains currently pose pandemic threats. The global patterns of influenza virus circulation and evolution remain unknown, and understanding these patterns in detail will increase our ability to respond to and prevent seasonal and pandemic influenza infections. Influenza outbreaks are strongly seasonal in temperate regions of the globe, affecting populations primarily in winter months, and follow more complicated patterns in regions closer to the equator. The central hypothesis of this proposal is that global influenza circulation patterns can be predicted by weather features. Based on this hypothesis, we are attempting to develop a mathematical model of the annual global movement and evolution of influenza A virus as a function of weather phenomena, at the scale of several geographical regions per country. We will use multiple regression analysis to determine which weather-related features, such as latitude, time of year, humidity, temperature and cloud cover, are correlated with influenza outbreaks. Given these factors, a worldwide model of influenza spread and evolution will be constructed, integrating susceptible-infected-recovered (SIR) models for each region. Viral genetic and antigenic evolution will be included in these models, together with the evolution of host susceptibility. Each region will experience its own outbreaks, which will then spread to other regions, both near and far. Precise annual geographic patterns of circulation within East and Southeast Asia, and of transmission to temperate regions of the northern and southern hemispheres, will be predicted.

Benefit to National Security Missions

This work hopes to uncover basic features determining the world-wide circulation and evolution of influenza A. It has direct application to the basic mission of NIH, CDC and other agencies, such as DARPA, DTRA, DTRA/TMT and DHHS, which are concerned about the effects of influenza pandemics. The model will both address basic science questions as well as be used for examining intervention strategies, such as vaccination and the use of antivirals, to slow the spread of influenza.

Progress

Last year we began to develop a new algorithm for global disease simulations that accounts for the entire global population. Different from other methods (e.g., EpiFast, EpiSim, etc.) this method uses a recursive hierarchical tree method to generate a scalable algorithm. In this method we begin with finely grained population data. This data is then divided, recursively, into regions of ever finer regions until some criteria is met. By recursive, we mean that each sub-region is considered as a new region, thereby avoiding, for example, resolving regions with little population, such as the oceans. The method is similar to the famous Barnes-Hut method for performing molecular dynamics of many-body systems (e.g., galaxy formation). Moreover, the method also introduces a threshold map that allows one to purposefully resolve some regions better than others. This can be used to correctly introduce boundary conditions in what would otherwise be a non-global spatial model. For example, suppose one wished to simulate New Mexico or the United States; how does one include flights from, say, Tokyo without resolving Asia? With a mask, one can place different population thresholds in different regions of the globe that informs the recursively generated tree to only resolve to the limits set by the mask. Scalability, and accuracy, of the algorithm depends upon how travel is described. In all global-scale influenza models that we are aware of travel is handled in an approximate way, which does not actually track human movement, but rather assumes that one geographical region knows what is happening in all other geographical regions instantaneously. We carried out some analysis of this assumption and it appears to be sound for most of an epidemic; however, it is completely inaccurate for short time scales. Such short time scales are crucial for describing the early stages of an epidemic, or more importantly, a pandemic. We concluded that our global model will include explicit human movement patterns.

Because short time scales are so important at the beginning of an outbreak, we are also examining whether deterministic models that do not allow for random fluctuations can describe the beginning of an outbreak, or whether stochastic models that do incorporate some randomness are required. We are examining this question also from the point of view of the emergence of drug resistance, when antiviral drug treatments are incorporated into models. Drug resistance first emerges in small numbers of people, and history has shown that many drug resistant strains are extinguished before they have a chance to spread widely. The likelihood that an evolutionarily fit drug resistant strain will propagate rather than die off can be estimated, and we can attempt to assess the relative importance of fitness vs. random chance in whether a widespread outbreak of a new strain, drug resistant or otherwise, will emerge. We have a computer code developed to examine this question and are looking at it now.

In parallel, we have begun to explore multiscale models that couple the population scale dynamics to the in-host tissue scales. In the first year, we developed a two-dimensional influenza infection model of the lung (presented at the Viral Dynamics Workshop at the Santa Fe Institute); which we have now greatly extended. Despite its use in the literature, we have found that viral transport in the lung is not likely to be described accurately by a 2D model, under any conditions. Thus, we are developing a stochastic random walker model in 3D so that we can include more realistic biophysics of virus and mucous transport caused by cilia, and we have begun to explore the velocity fields generated by ciliary action. We have also developed analytical models that correspond to the stochastic processes and which may provide more insight. Using the new 3D models, we are examining several issues, such as arrival probabilities of virions at cells that can be infected; this is important for understanding the percentage of virions that are added to the tissue (from an inhaled droplet or through budding from an already infected cell) that are available for further infection. Key to developing a multi-scale model is linking in-host dynamics to between-host dynamics. That is, given what we believe is happening at the tissue level, how would that affect our epidemiological models? In the simplest scenario, we can assume that what happens inside a particular person is not affected by the remaining population; in this case, we can use the results of several in-host solutions to "program" the infectivity into an epidemiological model. We have explored this and have settled on a McKendrick-von Foerster model, which we borrow from ecology where it is used to incorporate age structure. Numerical methods for this equation are lacking, and we are currently examining various methods.

We have also returned to very simple models of seasonality to understand how conclusions about seasonality can be affected by the model that is used. An important work on the subject noted that seasonality comes out of the equations nearly automatically by a process called stochastic resonance, without the need for external, exogenous drivers, such as weather changes, seasonal variations in vitamin D levels in the population, or school closures, among other possibilities. This now highly-cited work uses a model in which immunity falls off over time, and one can become reinfected several years later. In this model, people who recover from flu infection gradually become susceptible to infection once again. We are re-examining and refining this model so that ultimately the results can be incorporated into the global models described above.

Future Work

We will begin FY12 with an analysis of the simplest models for influenza epidemics to unravel what the most important features are. Because seasonality occurs across hemispheres and yearly time scales, some form of evolution must be added the model. We will explore the very simple model discussed above in which people that have recovered (i.e., are immune), then become susceptible to the disease again after a time associated with waning immunity. We believe that such models, which neglect the statistics of new mutations, cross immunity, and the fact that seasonality does not occur in the same way in the tropics, might include spurious correlations. More sophisticated models will be developed and compared with data. The simplest of the models we construct, consistent with our requirements, will be used as the single-patch model in the global model. We will also continue to explore the effects of drug intervention, and the emergence and spread of drug resistance.

Conclusion

The goal of this project is to develop a mathematical model of the annual global movement and evolution of influenza virus as a function of weather phenomena, such as latitude, humidity, temperature and cloud cover at the scale of several geographical regions per country. Such a model will help us understand worldwide influenza virus circulation, and substantially improve our predictive capability for vaccine strain selection and targeted antiviral drug use, in order to protect populations from both seasonal and pandemic influenza more efficiently. This project thus attempts to answer basic questions about influenza evolution and global circulation.

Publications

Hoopes, J. D., E. M. Driebe, E. Kelley, D. M. Engelthaler, P. S. Keim, A. S. Perelson, L. Rong, G. T. Went, and J. T. Nguyen. Triple combination antiviral drug (TCAD) composed of amantadine, oseltamivir and ribavirin impedes the selection of drug-resistant influenza virus. *Public Library of Science One.*

Perelson, A. S., L. Rong, and F. G. Hayden. Combination antiviral therapy for influenza infection: Predictions from modeling human infections. *Journal of Infectious Diseases.*

Grayscale Flow Cytometry - Multicoil NMR Sensors for Portable Flow Cytometry

Pulak Nath
20110166ER

Introduction

The long term research goal of this project is to build a new capability at LANL for measuring cellular and molecular information applicable to bioscience research and medical diagnostics. The measurement tool will utilize magnetic labeling, magnetic separation and magnetic detection to measure cells in flow. The underlying technology is inspired by flow cytometry – a high throughput cell analysis platform that has medical applications ranging from complete blood count to cancer diagnosis. However, it is not desired to reinvent or replace current flow cytometers, rather, to address some fundamental limitations of the existing technology. Current flow cytometry relies on optical methods that makes it difficult to miniaturize, difficult to analyze turbid samples, and sensitive to autofluorescence of cells. In this work we address such fundamental limitations by developing a miniaturized magnetic sensor based on NMR detection.

Benefit to National Security Missions

This project is directed to the development of advanced platforms for agent detection and pre-symptomatic diagnosis - one of the priorities identified by the LDRD Complex Biological Systems grand challenges. This work also fits the new themes of the National Institutes of Health (NIH) roadmap. The DOD Congressionally Directed Medical Research Programs also seeks new technologies for medical diagnostics applications.'Portable' flow cytometers requiring minimal sample processing can find applications in several LANL mission areas including environmental monitoring, bio-defense and military applications. Finally, this new capability can be the basis for seeking external funding from NIH or DOD to develop programs based on magnetic sensing for biological analysis.

Progress

Magnet Design: We have designed two types of permanent magnet systems that will be suitable for Grayscale Flow Cytometry. The first design is a Halbach array consisting of a set of hexagonal magnet pieces producing uniform magnetic fields up to 1.1 Tesla. The second design is a novel system that consists of a ring magnet with a coaxial ferromagnetic shim. This is an exciting novel design that alleviates a key limitation with the Halbach design – the need for precise alignment of individual magnets into a desired orientation. The novel design called 'Shim-a-ring' magnet will be easy to fabricate and shows field uniformity equivalent or superior to the Halbach designs. Figure 1 shows a schematic of the Shim a ring design. A magnet prototype has been fabricated and tested for NMR (nuclear magnetic resonance) relaxometry with successful measurement of FID (free induction decay) signal from $CuSO_4$ solutions. A patent application on the 'Shim-a-ring' was submitted on June 13, 2011.
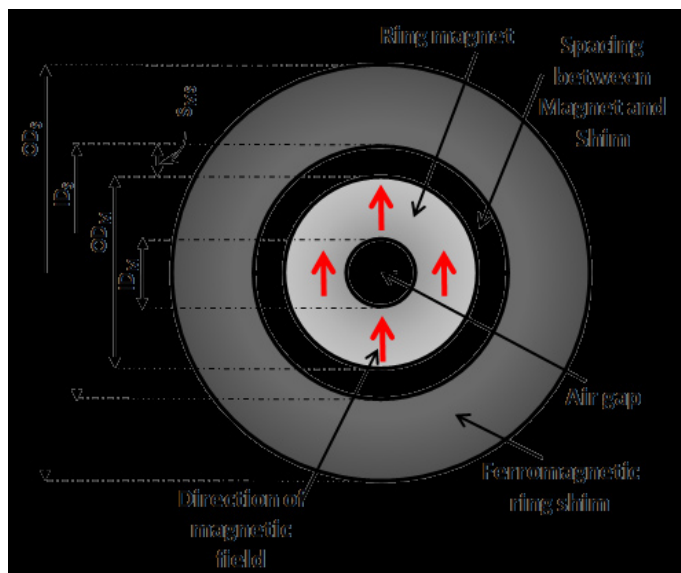
Figure 1. Schematic of the Shim a ring design.

Microfluidics and RF Coil Design: A new option has been identified to synchronously deliver samples (e.g. magnetically tagged cells) into the detection zone. Synchronous particle delivery would simplify data acquisition and analysis on the eventual microfluidic platform. To aid microfabrication and droplet generation, two parallel approaches have been pursued. An ultra fast laser cutting tool was utilized to fabricate microfluidic

channels in combination with adhesive transfer tape based microfabrication technique. Droplet generation on such a microfluidic chip has been successfully demonstrated.

This is a rapid prototyping method that allows us to fabricate microfluidic channels and develop microfluidic integration strategy for Gray Scale Flow Cytometry. However, integration of custom metallic components such as planar RF (radio frequency) coils is difficult with the rapid prototyping method. Therefore, a conventional photolithography based microfabrication method is being considered. To pursue conventional microfabrication, a user proposal to the Cneter for Integrated Nanotechnologies Albuquerque Core facility has been submitted and approved.

The work on the magnet design garnered the Best Poster Award at the 2011 LANL Postdoc Symposium.

Future Work

Fundamental limitations of flow cytometry such as the need for extensive sample preparation or noise due to cell autofluorescence will be addressed by using magnetic labels/detection. The signal from a magnetic source (e.g. magnetically tagged cells) diminishes rapidly with increasing distance from the sensing surface, making the state-of-the-art magnetic sensors inadequate to fit in the flow configurations of flow cytometry. NMR based detection measures the signal from the protons surrounding the magnetic sample, rather than the source directly. Therefore, it is possible to detect signals from a greater distance. However, conventional NMR data acquisition is too slow compared to current flow cytometers. The novel multicoil approach presented in this work can overcome such critical limitations. Furthermore, NMR based approaches are amenable to miniaturization, which can lead to portable flow cytometers. The proposed NMR sensor will be composed of 10 microfabricated RF coils in series placed on top of a microfabricated channel. Magnetically tagged cells will be passed through the channel such that one cell is present under a coil at a time. The first RF coil will be utilized for NMR excitation and the rest of the coils will be used for data acquisition. Following excitation, the protons will relax according to the total number of magnetic nanoparticles aggregated in the sample. The relaxation time will be extrapolated based on the data acquired by all the receiver coils as the sample passes through. Thus we can measure the total relaxation time without having to spend the entire relaxation period under one coil and maintain higher throughput. The platform will be composed of cells tagged with magnetic nanoparticles, planar RF coils, microfluidic channels and a permanent magnet based NMR setup.

Conclusion

This work is expected to develop a novel platform for flow cytometry using magnetic nanoparticle tags and NMR based detection. 'Proof of concept' is the key expected outcome from this research. We expect to measure beyond yes/no answers and give insight to specific properties of the cell such as antigen expression levels. We also expect to demonstrate magnetic detector flow cytometry with footprint small enough to build portable flow cytometers. Ultimately, we expect to analyze 100-1000 cells per second in a turbid sample – a throughput comparable to a commercial flow cytometer available for HIV infection diagnosis.

Biofuel from Magnetic Algae

Pulak Nath
20110168ER

Introduction

The long term goal of this project is to develop cost effective and scalable technology to harvest biofuel from algae. High production costs limit algae based biofuel from becoming a viable replacement for fossil fuels. Current technologies for algae harvesting and oil extraction are either too expensive or only feasible at a laboratory scale. In this project, we will use magnetism to transform algal harvesting and oil extraction. A key challenge in using magnetics is that the object of interest needs to contain magnetic materials. Following a recent precedent with human cells, we will introduce a single gene into algal cells enabling them to form intracellular magnetic nanoparticles from soluble iron. The presence of these nanoparticles will make them susceptible to low cost magnetic separation for harvesting and magnetic hyperthermia for oil extraction. The performance of this technology in a continuous flow system will be quantified to assess feasibility and scaling requirements for technology transfer to industry.

Benefit to National Security Missions

Although this work is directed towards advanced biofuel research, we hope to develop a new program based on intrinsic magnetism in biology. Such a program will address several medical applications in addition to the proposed biofuel research. Such a program will fit well into the biology by design mission of LANL addressing both fundamental and applied research opportunities. We will also pursue external funding from agencies such as the National Institute of Food and Agriculture and the National Institutes of Health (NIH), who has existing programs for transformative research ideas such as the one depicted in this project.

Progress

Genetic Transformation: We have investigated two genetic transformation methods to express MagA genes in Chlamydomonas reinhardtii: (i) Agrobacterium based transformation; and (ii) Bolistic gene gun based transformation. The gene sequence of MagA was optimized using codon equivalency to match the chlamydomonas GC-rich genome. Protocols have been developed to insert MagA into two different vectors: (i) pSL18 and (ii) PSAD. These transformation constructs contained the MagA sequence and a paramomycin resistance gene. The paramomycin resistance gene was inserted so that the transformed cells can be selected using their antibiotic resistance. Agrobacterium based transformation protocols were developed using the vector pSL18, where as Gene gun based transformation technique was developed using the vector PSAD.

Custom High Gradient Magnetic sorters: The magnetic properties of the transformed cells were expected to be small such that commercial bench top magnetic sorters were of insufficient magnetic strength to sort the transformed cells. A small high gradient magnetic sorter was developed which was suitable for both batch and continuous magnetic separation. The fringe field of the magnet was in the order of 1.0 Tesla near the surface of the magnet.

Magnetic properties of the transformed Algae: The magnetic properties of the transformed Chlamydomonas were tested using our custom high gradient magnetic sorter by placing the transformed algae inside a test tube positioned on the magnet within 24 hours of transformation and selection. Magnetic responses of the cells were qualitatively examined by observing the accumulation of the transformed Algae near the high gradient locations of the magnet. Wilde type algae were used as positive controls for comparison. The transformed cells were selected based on antibiotic resistance on a plate and were then grown in a liquid culture for about 24 hours. Gene transformation into the Algae was successful with both the methods. Magnetic separations of the transformed algae were demonstrated for both types of transformation. Figure 1 shows wild type algae and magnetic algae (PSAD transformation) placed in a test tube next to a permanent magnet. The wild type (left) settles to the bottom of the tube under the influence of gravity. The genetically transformed algae (right) stick to the wall due to magnetic attractions. PSAD is a known strong, constitutive promoter native to Chlamydomonas. Therefore, the Gene gun/PSAD based transformed cells

showed a stronger response to the external magnetic field. The effect of iron (Fe+2) concentration (10 micromols – 200 micromols) and the types of iron salts (Ferrous sulfate vs ferrous citrate) in the culture media was also investigated. Approximately 100 micromol of ferrous citrate was found to be optimum for the production of magnetotactic algae. The presence of MagA gene in the transformed population was confirmed by polymerase chain reactions. Positive response to magnetic fields indicated MagA gene expression/activity (i.e. magnetic nanoparticle production) in the transformed cells. In order to confirm the formation of magnetite nanoparticles inside the transformed cells we have established a collaboration with Rob Dickerson at the LANL Materials Science Lab. Protocols for high resolution imaging and elemental analysis techniques on the transformed cell population are being developed. Our IWD at TA-35 is being updated to account for the policies associated with nanoparticles use at the laboratory.

A provisional patent application on the formation of biogenic magnetic nanoparticles using genetic transformation of Algae was submitted on June 13, 2011.
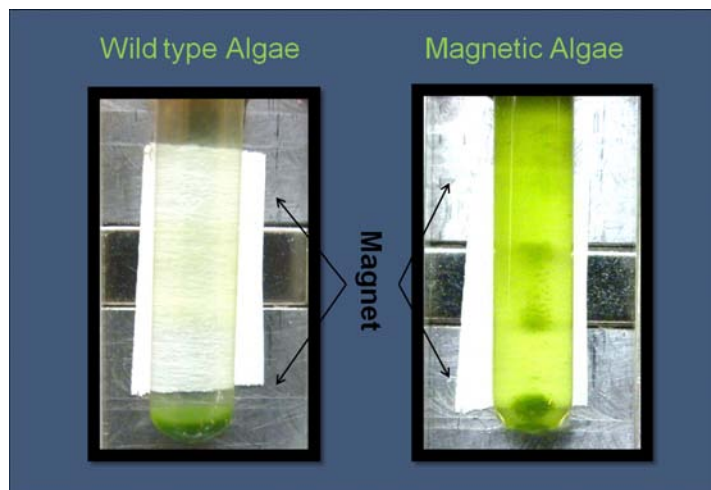
Figure 1. The photos show wild type algae and magnetic algae placed in a test tube next to a permanent magnet. The wild type (left) settles to the bottom of the tube under the influence of gravity. The genetically transformed algae (right) stick to the wall due to magnetic attractions.

Future Work
This work aims to genetically modify algae to form magnetite nanoparticles and use magnetic fields for algae harvesting and oil extraction.The bacterial gene MS-1 MagA will be transformed into the model algae, Chlamydomonas reinhardti, by using glass bead transformation or a gene gun. Transformed cells will be optimized for expression of the MagA gene to make sufficient magnetic nanoparticles inside the cells such that they can be manipulated by external magnetic fields. The ability to sort magnetic algae using magnetic separation will be carried out in a custom magnetic sorter. The magnetic sorter will be built using permanent magnets to reduce cost of separation. Based on the magnetic separation characteristics,

design and adaptation of a commercial magnetic sorter for high throughput algae harvesting will be investigated. Algal magnetite nanoparticles can also be heated by placing the algae in an alternating magnetic field to extract the oil. An experimental setup to investigate magnetic hyperthermia on magnetic algae will also be built. Magnetic hyperthermia will be evaluated for cell lysis and lipid extraction. Unlike existing methods where the total volume of the bulk slurry needs to be energized for oil extraction, magnetic hyperthermia only requires energizing the algal cells. Therefore, the cost of energy for the extraction process could be reduced significantly. Knowledge gained from this research in terms of biogenic magnetite formation and intracellular heating will have additional impacts beyond algal biofuel research such as on biomedical applications of magnetic nanoparticles.

Conclusion
This work plans to genetically modify algae to form magnetite nanoparticles and use magnetic fields for algae harvesting and oil extraction. Algae can be harvested using magnetic separation, a low cost/high throughput technique. Algal magnetite nanoparticles can also be heated by an alternating magnetic field to extract the oil. This heating technique, known as magnetic hyperthermia, heats the cells from the inside significantly reducing the cost of extraction. Knowledge gained from this research in terms of biogenic magnetite formation and intracellular heating will have additional impacts beyond algal biofuel research such as on biomedical applications of magnetic nanoparticles.

Understanding Thunderstorm Effects on the Ionosphere: A New Approach to Investigate Possible Convective and Electrical Coupling Mechanisms

Xuan-Min Shao
20110184ER

Introduction

The goal of this project is to investigate and characterize the possible mechanical and electrical coupling mechanisms from thunderstorms to the ionospheric D-layer, and to quantify the magnitude of the electron density perturbations due to the various coupling mechanisms in space and time relative to the storm, by assimilating previously archived lightning observations and model simulations. Understanding how thunderstorms affect the D-layer is important in forecasting radio frequency (RF) communication and electromagnetic pulse (EMP) detection within the earth-ionosphere waveguide for ground-base systems, and in forecasting transionospheric communication and detection for satellite systems. Various thunderstorm-ionosphere coupling mechanisms have been proposed but very limited evidence has been obtained to quantify each of the theories. The unique approach of this proposal is to use lightning-produced EMPs that had been previously captured from an array of receivers [1] to map the spatial and temporal perturbations of the D-layer electron density, and to compare the perturbations with existing and new electrical and convective models to understand the physical mechanisms.

Benefit to National Security Missions

This work will have a direct impact on LANL's new thrust area of Space Situational Awareness, which depends on understanding of space weather conditions for reliable space-ground communication and persistent and accurate global surveillance. The success of this project will form the foundation for a new LANL program supported by DOD. Through this project, our understanding on time-domain, long-distance VLF/LF (very low frequency/low frequency) propagation will be significantly improved, and this will be directly applied to a new Air Force mission that uses ground-based RF measurement for long-range nuclear explosion detection. In addition, the result of this project will be used to understand fundamental ionosphere anomalies, and will be used to improve the performance of LANL's space-based nuclear sensors.

Progress

In the area of data analysis, we confirmed that our technique provides a much higher time and spatial resolution measurement of the D-layer fluctuation as compared to previously reported frequency domain techniques. As a result, a series of new D-layer phenomena have been discovered. In papers [2,3] we reported the new techniques along with fluctuation observations from a single station measurement. It was clearly demonstrated that the apparent reflectivity and height exhibit significant variation on spatial scales of tens of kilometers and over time periods of hours. The range of the reflectivity variation was as large as 100% away from the averaged reflectivity, and the height varies by as much as 5% (4 km). The time scales and propagation velocities (50-100 m/s) of the fluctuations appear to be consistent with signatures of atmospheric gravity waves (AGW) at D-layer altitudes, and the direction of the fluctuation propagation suggests that the gravity waves were originated from the storm. In some localized ionosphere regions, we discovered some apparent splitting of the D-layer by 2 – 4 km that lasted a short time period of about 10 minutes.

Following the initial analysis, we extended the analysis to multiple-station measurement and to different storms. In the work of [4, 5] we confirmed that the AGW-like fluctuations were indeed originated from the storm, by looking at the D-layer from three different directions. For the analysis, fluctuation maps in space and time were produced, and the movement of the fluctuations was examined based on the space-time maps. As proposed, we also examined the D-layer with two radio frequency bands (<30 kHz and 30-60 kHz) by digitally filtering the original waveforms and found that the high-band signal penetrated deeper into the ionosphere by 2-4 km, and produced more detailed features of the fluctuations.

In order to understand the D-layer properties behind the measurements, we improved the full wave, ground-ionosphere VLF/LF propagation model [6, 7] by increasing the frequency and incident angular resolutions in the model computation. For the specific

purpose of this project, a new technique was developed to coherently combine the ground and ionospheric-reflected waves at the sensor locations. The output of the model predication was compared with the measurement, and some outstanding agreements on the time waveforms were obtained. In the paper [8], we showed that reliable lightning return stroke waveforms can be reproduced at different observing distances by the model simulation. Applying the model results to actual observations we found that additional and stationary ionization at the lower-boundary of the D-layer was introduced by the storm. This newly discovered phenomenon might be due to static electrical heating from the storm. We are in the process of further examining this new result.

The other new scientific result from this project in FY11 is a new understanding of the discharge physics of the lightning stroke to ground. In an attempt to obtain a "standard" return stroke time waveform from the observations for the VLF/LF propagation simulation, we found a statistically significant feature in the waveform after accumulating thousands of individual waveforms. This small but persistent feature could not be explained by any existing return strokes models. Instead, the feature can only be explained by a dispersive discharge process along the lightning channel. This new result has a fundamental impact on the understanding of the dynamics of lightning discharge, and we are in the process of submitting the result for a publication [9].

During the first ten months of this project, one paper was published in JGR, two papers were presented in the XIV International Conference on Atmospheric Electricity, two papers to GRL and JGR are in the process of submission, and one presentation was given in the AGU fall meeting, as listed below.

Future Work
Our work in the first year of this project demonstrated the great success of the proposed technique for high spatial and temporal resolution D-layer detection with the natural lightning EMP, and a series of new phenomena that related D-layer changes to thunderstorms has been discovered. To better understand these phenomena, we will first focus on comparing the observation with our VLF/LF propagation simulation and to retrieve the corresponding electron density profile due to the storm. To do this, a range of possible profiles will be considered, and a template of predicated EMP time waveforms at different distances will be established.

By post-processing the broadband data to two different frequency bands, it was confirmed that the higher frequency signals penetrate deeper into the ionosphere (by 2-4 km, [2]). In FY 12 we will study the detailed correlation (or lack of it) between the two-frequency measurements to examine any possible vertical propagation of the disturbances.

We started to examine corresponding total electron content (TEC) measurement from a network of GPS receivers that were situated in and near LASA sensors to investigate if any of the thunderstorm-produced D-layer fluctuations would propagate up to the F-layer. If the result proved to be positive, it would be substantially important to both the scientific community and the programmatic missions.

And finally, we started to look into the fundamental physical mechanisms of the ionization and attachment chemistries at the altitude of D-layer under the influence of additional external electric field to study the EM effect on the D-layer changes.

Conclusion
Time evolving 2-D maps for D-layer conditions will be produced at different temporal and spa-tial scales (seconds-hours, 10-600 km). The D-layer condition will be represented by an electron profile that is derivable from an exponential form. The upward propagation of the variation within the D-layer will be examined with LASA's broadband capability, and further upward propagation to F-layer will be examined by studying TEC measurements from GPS receiver networks. We will further validate and improve the propagation model by comparison to LASA waveforms under many different ionospheric conditions. Temporal and spatial ionospheric variability will then be used to investigate, identify, and characterize the different coupling mechanisms from the troposphere thunderstorms to the ionosphere.

References
1. Shao, X. M., M. Stanley, A. Regan, J. Harlin, M. Pongratz, and M. Stock. Total lightning observations with the new and improved Los Alamos sferic array (LASA). 2006. *JOURNAL OF ATMOSPHERIC AND OCEANIC TECHNOLOGY.* **23**: 1273.

2. Lay, E. H., and X. M. Shao. High temporal and spatial-resolution detection of D-layer fluctuations by using time-domain lightning waveforms. 2010. In *AMERICAN GEOPHYSICAL UNION 2010 FALL MEETING.* (San Francisco, CA, 13-17 Dec. 2010). , p. AE21B. San Francisco, CA: American Geophysical Union.

3. Lay, E. H., and X. M. Shao. High temporal and spatial-resolution detection of D-layer fluctuations be using time-domain lightning waveforms. 2011. *JOURNAL OF GEOPHYSICAL RESEARCH.* **116** (A01317): doi:1029/2010A016018.

4. Lay, E. H., and X. M. Shao. High temporal and spatial-resolution detection of D-layer fluctuations by using time-domain lightning waveforms. 2011. In *XIV INTERNATIONAL CONFERENCE ON ATMOSPHERIC ELECTRICITY.* (Rio de Janeiro, Brazil, 8-12 Aug. 2011). Vol. I, First Edition, p. 1. Rio de Janeiro, Brazil:

International Commision on Atmospheric Electricity.

5. Lay, E. H., and X. M. Shao. Probing thunderstorm-generated D-layer fluctuations by using time-domain lightning waveforms. *GEOPHYSICAL RESEARCH LETTER.*

6. Shao, X. M., and A. R. Jacobson. Model simulation of very sow-frequency and low-frequency lightning signal propagation over intermediate ranges. 2009. *IEEE TRANSACTIONS ON ELECTROMAGNETIC COMPATIBILITY.* **51** (3): 519.

7. Jacobson, A. R., X. M. Shao, and R. Holzworth. Full-wave reflection of lightning long-wave radio pulses from the ionospheric D-region:1. Numerical model. 2009. *JOURNAL OF GEOPHYSICAL RESEARCH.* **114** (A03303): DOI:10.1029/2008JA013642.

8. Shao, X. M., A. R. Jacobson, and E. H. Lay. Study of ionospheric D-layer fluctuation by comparing VLF/LF propagation model simulation with remotely detected lightning time waveforms. 2011. In *XIV INTERNATIONAL CONFERENCE ON ATMOSPHERIC ELECTRICITY.* (Rio de Janeiro, Brazil, 8-12 Aug. 2011). Vol. I, First Edition, p. 1. Rio de Janeiro, Brazil: International Commision on Atmospheric Electricity.

9. Shao, X. M., A. R. Jacobson, and E. H. Lay. The behavior of return stroke current derived from remote radiation electric field measurement. *JOURNAL OF GEOPHYSICAL RESEARCH.*

Publications

Lay, E. H., and X. M. Shao. High temporal and spatial-resolution detection of D-layer fluctuations be using time-domain lightning waveforms. 2011. *JOURNAL OF GEOPHYSICAL RESEARCH.* **116** (A01317): doi:1029/2010A016018.

Lay, E. H., and X. M. Shao. Probing thunderstorm-generated D-layer fluctuations by using time-domain lightning waveforms. *GEOPHYSICAL RESEARCH LETTER.*

Lay, E. H., and X. M. Shao. High temporal and spatial-resolution detection of D-layer fluctuations by using time-domain lightning waveforms. 2010. In *AMERICAN GEOPHYSICAL UNION 2010 FALL MEETING.* (San Francisco, CA, 13-17 Dec. 2010). , p. AE21B. San Francisco, CA: American Geophysical Union.

Lay, E. H., and X. M. Shao. High temporal and spatial-resolution detection of D-layer fluctuations by using time-domain lightning waveforms. 2011. In *XIV INTERNATIONAL CONFERENCE ON ATMOSPHERIC ELECTRICITY.* (Rio de Janeiro, Brazil, 8-12 Aug. 2011). , p. 1. Rio de Janeiro, Brazil: International Commision on Atmospheric Electricity.

Shao, X. M., A. R. Jacobson, and E. H. Lay. The behavior of return stroke current derived from remote radiation electric field measurement. *JOURNAL OF GEOPHYSICAL RESEARCH.*

Shao, X. M., A. R. Jacobson, and E. H. Lay. Study of ionospheric D-layer fluctuation by comparing VLF/LF propagation model simulation with remotely detected lightning time waveforms. 2011. In *XIV INTERNATIONAL CONFERENCE ON ATMOSPHERIC ELECTRICITY.* (Rio de Janeiro, Brazil, 8-12 Aug. 2011). , p. 1. Rio de Janeiro, Brazil: International Commision on Atmospheric Electricity.

High Density Neuronal Recording Using Nanowire Capacitor Sensors

Shadi Dayeh
20110264ER

Introduction

Understanding the neural basis of the processes of sensory perception, motor control, learning and memory, and even consciousness, is the final frontier of the biological sciences. This task requires us to measure and ultimately manipulate the dynamic function of large populations of individual neurons. With extensive, high density recording arrays, local neural activity across many cells (or even across different parts of a single neuron) could be electrically recorded. Basic science and biomedical applications require compact, highly sensitive, high-resolution and high density, implantable 3D probes well beyond current microprobe technology, necessitating new approaches. We propose a novel scheme for in-vivo neuronal signal detection using individually addressed semiconductor nanowire capacitor probes that operate by displacement currents, thus allowing the sensor to be completely encapsulated and eliminating problems associated with electrochemistry. In our approach, sensors can be integrated and/or co-fabricated with active microelectronic devices, greatly increasing the feasible number of channels, which can be simultaneously recorded. In the past fiscal year, we have made significant progress on developing the fabrication of these pillar arrays and their passivation with biocompatible layers, made reference physiological measurements, and installed a high-channel input neurophysiology station to test our high density sensor arrays. In the next phase of the project, we will optimize the device structure and start physiological measurements on moderate and high density pillar electrodes.

Benefit to National Security Missions

This work aims to develop a fundamental understanding of nanoscale materials based on nanowire synthesis for application to prosthetic devices not presently possible by any other means. In addition to advancing basic new understanding of materials and device science at the nanoscale, this work will specifically address new approaches to neuronal probes for biomedical applications. This technology also is relevant for new approaches to high density, sensitive detection of electrical, optical or chemical signals. Capabilities developed in this project will support new project activities for transitioning to mission-relevant work in NIH, DARPA and DOD.

Progress

The goals of this project are to demonstrate a new device concept for capacitive coupling in neural interfaces that is suitable for sensing neural signals and to implement high density neural electrodes that will enable high spatial and temporal resolution for advanced neuroscience studies. This task requires

- developing fabrication processes to form the basic material template (1D micropillars) for sensor formation;
- devising growth processes for forming radial junction capacitors;
- passivation of the semiconductor interfaces with encapsulating and biocompatible materials;
- conducting electrical and material characterization of such sensors; and
- validating their performance in physiological environments.

In the first fiscal year, we have made significant progress in the first three areas, placing us closer to realizing the complete sensor and performed initial reference experiments in the last two areas.

We have utilized thin Si substrates (50 micron thick) to realize implantable devices that can be conformably applied to the curved surfaces of the brain (Figure 1a). Using deep inductive plasma coupled etching/passivation technique, we were able to etch micropillars into the Si substrate with 500 nm wide diameter, and 5 to 10 micron length with minimal taper throughout their length. With dry etching, the resulting surface becomes rough and damaged due to physical bombardment of heavy ions that strip away the Si material. Through successive oxidation and wet etching of formed oxides, we were able to retain smooth micropillar sidewalls that

follow an RCA cleaning procedure (an industry standard) to become epi-ready for epitaxial growth of doped Si shells. TEM characterization post the oxidation/etching process validates the smooth micropillar surface and its single crystalline quality. We then performed chemical vapor deposition growth of thin doped shells and optimized the growth temperature/pressure (high T/low P) in order to obtain single crystal doped shells. Phosphine doped n-Si shells up to 10 nm thick (target is only 2 nm) were deposited and examined by TEM (transmission electron microscopy) showing single crystal core/shell structure without noticeable defects at the interface. In addition, we investigated applying conformal metal/dielectric coatings to these pillar arrays. Using two-step electron beam evaporation on arrays that are tilted at ~ 3° off-normal, we were able to deposit a conformal Au shell on the closely spaced nanopillar arrays. As the thickness of the Au layer increased, some clustering of the Au shell was observed on the nanowire surface (see Figure 1b). Such nanopillar electrodes are suitable for both physiological neural sensing as well as for Electrocorticography (ECoG – applied to external head skin) measurements. The ultimate conformal coating of these nanopillars with noble metals will be achieved by atomic-layer-deposition (ALD). We have received an ALD Pt source to perform such deposition and we are currently developing recipes to optimize this deposition approach.
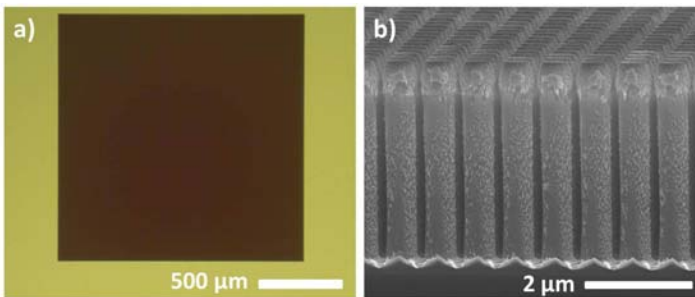
Figure 1. (a) Optical microscope image of 4 million nanopillar arrays over an area of 1.5x1.5 mm2. (b) Scanning electron microscope image of a cross-section of the pillar arrays in (a) after being coated with a gold metal film.

To sustain the physiological interface and to enable chronic implantable devices, these structures need to be encapsulated in dielectric and biocompatible layers. To avoid compromising the large capacitance provided by the increased surface area of these micropillars, dielectric layers need to be as thin as possible. We therefore carried out experiments on calibrating ALD deposited high-k dielectrics such as Al_2O_3 and HfO_2 on these micropillars and have currently control on conformal and dense layer coating from several tens of nanometers down to 6 Angstroms (target is 2 nm). The development of biocompatible coatings and assessment of stability required systematic studies on different Si and oxide surfaces. Our general strategy for biocompatible coatings

is to deposit and link self-assembled-monolayers (SAM) of long chain perfluorocarbons to the oxide dielectric layer. We have previously developed a silane-based linkage chemistry and are exploring an alternative phosphonate-based linkage that we anticipate will provide greater stability. We found no differences in deposition and stability of phosphonate-linked monolayers on different Si surfaces. On oxide surfaces, both phosphonate and silane-based SAM coatings displayed longer stability (currently two weeks) on HfO_2 surfaces compared to SiO_2 and Al_2O_3 surfaces. We plan next to study deposition and stability measures on Si micropillars coated with HfO_2 dielectrics. We are currently integrating the progress in the three areas of fabrication, growth, and passivation in order to form a test device for physiological measurements.

We have undertaken redevelopment of our capabilities for physiological measurements of neural tissue based on both electrode arrays and intrinsic optic signals. We have purchased a new data acquisition system for multi-channel electrophysiology and are integrating a new high performance camera for optical imaging. A University of New Mexico PhD student in chemical engineering has been working on deposition and characterization of coatings and will participate in physiological experiments. We have recruited two Postdocs to assist with the device fabrication work and with physiological measurements.

Future Work

We will first develop synthesis and fabrication processes that will allow the realization of radial nanowire capacitor devices and optimize these processes for achieving the desired probe resistance and capacitance. Biocompatible perfluoroalkane coating to the 3D probes will be developed, optimized, and tested for pin-hole free and resistant films. We will then test the functionality of these probes with measurements on neuronal cultures and of retinal photoresponses using conventional electrode arrays and intrinsic signal imaging techniques. We will fabricate nanowire capacitor detectors on passive electrode arrays for electrophysiological measurements in isolated retina using capacitive detection. We will then characterize retinal oscillatory responses with the new devices and compare with our existing optical platforms and perform pilot studies with implanted devices. Single cell measurements and investigation of sensing synaptic activity using our capacitive sensors will be performed.

We will etch Si pillars that will serve as templates for the growth of radial p-n junction capacitor sensors, high-k dielectric deposition, and SAM layer coating and device encapsulation. The electrical properties of these will be evaluated and optimized for high density and sensitivity. Study of neural signal propagation in cultured neurons between arrays of these vertical capacitors will be performed and evaluated. We will then investigate synchronization of retinal spiking activity in response to extended patterns of visual stimulation delivered by video,

including extended linear edges and looming stimuli. In the third year of this project, we will employ studies of neuronal cultures for hybrid sensors and cortically implanted arrays for a prosthetic control interface.

Conclusion

Development of the capacitor probe will lead to new insights on emergent electronic behavior in radial p-n junctions as well as interaction between SAM layer coatings and charged 3D structures. Physiological studies will provide a new dimensionality to current understanding of action potential propagation in neural circuits which will provide an opportunity for future projects to address treating synaptic diseases by electrical transmission rather than malfunctioned chemical neurotransmission. We will optimize device arrays that will be suitable for cortical implantation and 3D sensing of neural activity for prosthetic control interface. The results will help to treat people with neurological disorders.

Publications

Anderson, A., J. Schmidt, A. Dattelbaum, H. Mukundan, and B. Swanson. Robust silane-based, PEG-modified sensing films: A versatile bio-inorganic interface. 2011. *ABSTRACTS OF PAPERS OF THE AMERICAN CHEMICAL SOCIETY.* **241**.

Dai, X., S. A. Dayeh, V. Veeramuthu, A. Larrue, J. Wang, H. Su, and C. Soci. Tailoring the Vapor Liquid Solid Growth toward the Self-Assembly of GaAs Nanowire Junctions. 2011. *Nano Letters.* : 1.

Dayeh, S., N. MacK, J. Y. Huang, and S. T. Picraux. Advanced core/multishell germanium/silicon nanowire heterostructures: The Au-diffusion bottleneck. 2011. *Applied Physics Letters.* **99** (2): 023102.

George, J.. Casting Light on Neural Function: A Subjective History. 2010. In *Casting Light on Neural Function: A Subjective History.* , p. 1.

Restoring Neurological Function with Self-assembled Lipid Bilayers

Srinivas Iyer
20110411ER

Introduction

Myelin is a complex tissue that covers nerves and permits electrical conduction through our bodies. The role of myelin is central to all neurological functions, thus perturbations of this tissue have devastating consequences to human health. These perturbations are typically manifested as "demyelination", a condition where segments of the nerve are left uncovered which then leads to a reduction in electrical conduction through the nerve. While conditions such as injury trauma and diabetes result in this condition, it is most prominent in the debilitating disease Multiple Sclerosis. The events surrounding myelin damage and repair have remained at the forefront of neurochemical research; however, insufficient information is available due to the lack of suitable experimental systems that reproduce the complexity of the natural tissue.

The foremost goal of our effort is to generate an experimental system to investigate the role of specific structural features in myelin function. The complexity of natural myelin precludes such studies with tissue isolates; hence our assembly will enable mechanistic interrogations of structural events. The second and more long term direction is to establish self-assembly principles that will guide the ultimate development of artificial myelin tissue.

Benefit to National Security Missions

Development of biomimetic models is an example of how molecules self-assembled at the nanometer length scale can improve our understanding of complex biological systems, a major area of interest of DOE BES. Upon successful completion of this project we will have created a dynamic model system with which we can begin to understand processes critical to myelin sheath formation and degradation. This exploratory work will lay the groundwork for an increase in the scientific understanding of complicated myelin-associated diseases (Department of Health and Human Services interest). These efforts tie in with LANL's stated mission goals of being a premier materials laboratory with a focus on developing next-generation biomaterials. The health impacts fits into the Public Health mission of Bioscience Division and is of interest to certain agencies of the DoD especially in the area of treating warfighters after nerve trauma from battlefield injuries.

Progress

Thus far, we have achieved the following milestones:

We have been able to generate self-assembled bilayers of the lipid POPC on an As-doped silicon wafer. This is significant since prior efforts had been using lipids that were not physiologically relevant and we had run into problems with generating POPC constructs. To do this, we etched the Silicon surface to remove the oxide layer prior to loading vesicles. We are currently investigating to what extent etching must be done and how long the wafers are stable after the etching process.

The aforementioned construct was built in a newly developed impedance cell made by boring a hole in the bottom of a plastic disposable cuvette. This has made our measurement inexpensive, but more importantly, this now facilitates many parallel measurements so we can compare several assemblies. Our earlier methodology required extensive washing so we were only able to a single measurement every couple of days.

Using this approach, we assembled multiple POPC bilayers on HF etched silicon wafers and measured impedance across the assembly. This data is shown in Figure 1. Increase in resistance and change in capacitance is observed, indicating formation of multiple bilayers.

We have also examined an alternative approach to assemble hybrid multilayers by using chemical vapor deposition of silica on a multilamellar lipid template. This is shown in Figure 2 where a schematic and a TEM image of the assembly are shown. This approach allows us to form functional and stable architectures in a single step while controlling the thickness of the assembly (number of multilayers).

A talk titled "Mimicking the Myelin Sheath: Stable

and Fluid Multilayer Phospholipid-Silica Thin Films" was presented at AICHE 2011, Minneapolis, MN.
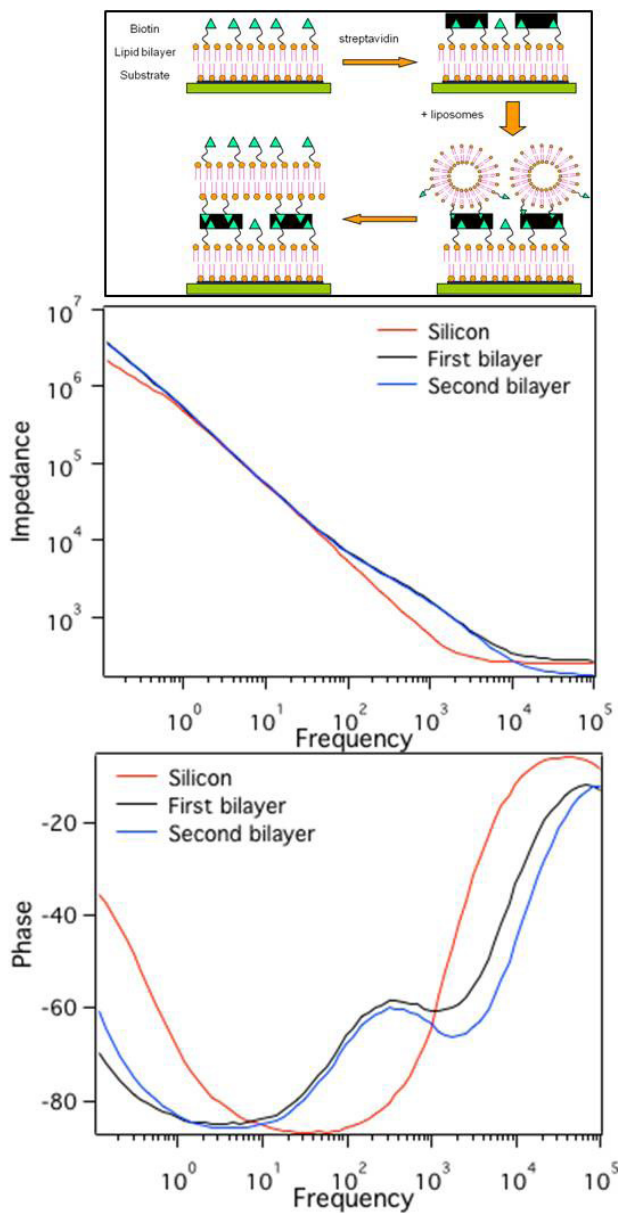
Figure 1. Top panel shows a schematic of the protein mediated assembly strategy.   Middle panel shows a plot of impedance versus frequency of POPC assemblies. Bottom panel shows phase information for the assemblies.
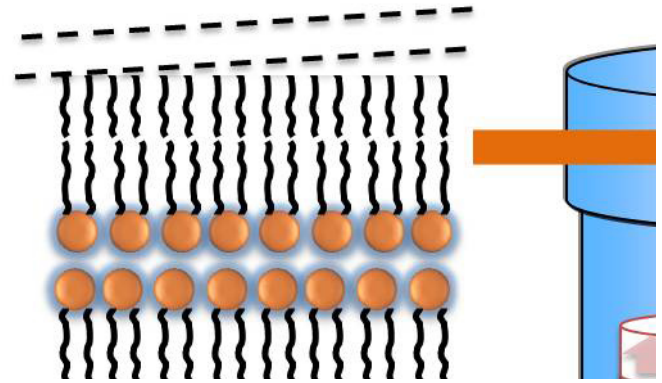
Figure 2. Schematic of multilamellar hybrid films synthesized using lipid POPC multilamellar template. A TEM micrograph also shows alternating layers of lipids and silica

Future Work

The research approach is based on the ability of lipid vesicles to self-assemble into bilayers when deposited on a suitable surface. Each bilayer will be sequentially assembled using Myelin Basic Protein to "stitch" consecutive layers. Upon successfully demonstrating this approach, we will investigate the use of the second myelin protein P0 (P-zero) to form the alternating structure seen in natural myelin. In an alternative approach, we are also examining the use of chemical vapor deposition techniques to generate multilayered structures.

Task1: Use native myelin proteins to sequentially link several lipid bilayers. Here we will work towards larger assemblies and more complex compositions incorporating cholesterol, sphingomyelin etc. in accordance with known myelin composition values. These structures will be assembled using Myelin Basic Protein and characterized to determine overall structure. In parallel, we will also generate the CVD based assemblies.

Task 2: Study size, integrity, fluidity and insulating capacity of the assembled structures. Characterization will be performed on all assemblies; thus this task is spread over the whole project period.   Assemblies will be analyzed by AFM (size), FRAP (fluidity) and electrical impedance spectroscopy (resistance and capacitance).

Task 3: Mimic known biochemical events surrounding demyelination and assess their contribution to structural perturbations. This aim will be conducted using only MBP-stitched multilayers. MBP is commercially available and both water- and lipid-soluble forms can interact with lipids. We will then explore how stoichiometry of, and modification to, the proteins affects the function of the bilayer assembly.

Conclusion

During this period of the project, we have used a nanoscale, controlled self-assembly method to create an architecture that closely mimics structural and functional aspects of the dense line of natural myelin. We have also performed electrical impedance measurements on these structures. This mimic will facilitate studies of the effect of myelin structure on its function and provide insights into hitherto unknown details of this very important tissue. These results will be used to design strategies for treating neurological disorders stemming from myelin damage.

Understanding the Mechanisms of Biological Transport for Nano-technology Applications

Sandrasegaram Gnanakaran
20110412ER

Introduction

Proper functioning of living cells requires selective molecular transport into and out of the cell, and between different cell compartments. Many such channels carry selective transport without an input of metabolic energy and without large scale structural transitions from a 'closed' to an 'open' state; the transport is based on diffusion only. Understanding the selective transport through such 'always open' channels is a fundamental biological problem, poses challenging physical questions and has potentially far-reaching technological applications. This project is about transport through one particular channel of this kind, the Nuclear Pore Complex (NPC), which gates nucleo-cytoplasmic transport in all eukaryotic cells.

The transport through the NPC involves interactions of certain transport factors with the natively unfolded proteins lining the NPC channel. Understanding the conformational dynamics of these unfolded flexible proteins is a major challenge and requires development of new hybrid coarse-grained and atomistic simulation techniques.

The principles of function of the NPC and similar biological channels can be used for novel applications in nano-technology and nano-medicine, such as design of novel vectors for delivery of materials into cell nucleus and creation of artificial bio-mimetic nano-filtering devices. Such bio-mimetic devices are currently being made and are technologically cutting-edge in the design of novel molecular sensors.

The long-term goal of the research is to provide an integrated description of how conformational changes of the NPC constituents determine the dynamics of transport through it and, in particular, its selectivity. The conceptual understanding arising from the study of the NPC will be leveraged for design of artificial nano-sorting devices based on the same principles. Currently, we are one of the very few groups in the world working on the subject. The current specific aims are 1) development of conceptual models that capture the essentials of what is known about the transport mechanism and its selectivity for the nuclear pore complex and related nano-technological devices 2) development of reliable techniques for more detailed molecular understanding of the conformational dynamics of the channel constitutes.

Benefit to National Security Missions

This project addresses basic questions about the mechanisms of intra-cellular transport as well as the technological and bio-medical applications, in an area where theoretical modeling is scarce and crucially needed. The research will provide a clear picture of the mechanisms of intracellular transport. This work supports missions of Threat Reduction by understanding the mechanisms of host -viral pathogens interactions. It also develops the connection between protein biophysics and materials science paving the way for creation of biosensors for detection of pathogens and chemical agents. We expect that successful completion of this project may provide a conceptual framework for design of bio-mimetic nano-molecular sensors. Finally, the principles of function of the NPC and similar biological channels can be used for novel applications in nano-technology and nano-medicine, such as design of novel vectors for delivery of materials into cell nucleus and creation of artificial bio-mimetic nano-filtering devices.

Progress

Progress on coarse-grained simulation and modeling of equilibrium behavior

We have focused on developing computational tools towards understanding the structure and dynamics of the unfolded proteins that fill the lumen of the NPC. This requires novel methods to describe the behavior of assemblies of unfolded proteins, because the standard state of the art molecular dynamics simulations can only probe the events on time and length scales much shorter than the relevant ones. Therefore, we have developed a coarse-grained approach based on polymer physics and statistical mechanics. In this approach, the

unfolded proteins are represented as flexible polymeric chains and the models can be treated either by analytical methods or by computer simulations. The model has been so far realized in the planar geometry where the flexible chains are grafted to a flat surface and are in equilibrium with the solution of the transport factors (Figure 1). We have done this part in collaboration with Prof. Rob Coalson and Prof. David Jasnow and the graduate student Mr. Michael Opferman from the Pittsburgh University. In parallel, we have developed simple approximate analytical models that capture the essential properties of the polymer-transport factor mixtures. Preliminary results of the models seem to explain the in vitro experiments on the nanomechanic behavior of the filaments with and without transport factors. The model has also uncovered hitherto unknown collective structural transitions in the assemblies of these polymers, induced by the presence of the transport factors. These transitions seem to explain the experimental in vitro data (hitherto unexplained) and might be important in the gating and transport mechanisms of the NPC. Two papers are currently being prepared for publication.

Increasing density
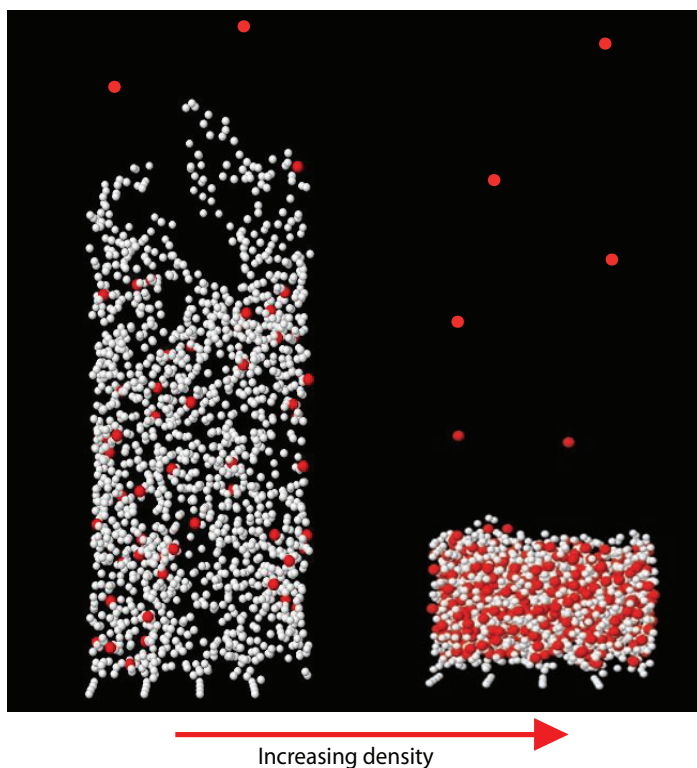
Figure 1. Snapshots of the coarse-grained simulations illustrating the collapse of the layer of flexible chains upon addition of the protein-like object that bind to the monomers of the chains, corresponding to experimental setups in vitro, investigating the effect of transport factors on the conformations of the unfolded proteins. The monomers of the flexible chains are white circles, the proteins are red circles.

Progress on coarse-grained simulation and modeling of dynamic behavior

We are in the final stages of submitting a manuscript detailing our findings from our initial coarse-grained simulation studies. In that study, we provide evidence supporting the hypothesis that the layer of flexible polymers that forms a key component of biological and artificial channels presents a selective potential through which large molecules must diffuse. From this evidence, a recipe for optimizing the choice of the chemical constituents in these devices emerges in the case where the channel serves as a gateway separating two finite sized chambers. Using theoretical arguments augmented by Brownian dynamics simulations, we demonstrate that an optimal rate of translocation across these gateways may be engineered by systematically selecting the geometry as well as the synthetic or natural components of the polymer layer. The key to this optimization lies in tuning the local interactions between all of these constituents and the targeted cargo, striking a balance between the transit times and the probability of crossing the channel. The study reveals four findings significant to future artificial molecular sorter designs. First, increasing the local binding affinity between the transport moieties and the chain segments yields a non-monotonic variation in the rate of transit across the channel. Second, the time to travel across the channel increases as the binding affinity increases. Third, in accord with gene knockout experiments, reducing the number of chains within the channel changes the magnitude of the transit rates and times, but preserves the qualitative functionality for large cargos. Fourth, one may work within the practical constraints of synthetic chemistry and still reach a maximal rate of translocation, as prescribed by a simple analytical treatment relating the effective potential to the binding strengths of a distribution of sites.

Progress on atomistic simulations

NPCs are composed of multiple copies of about 30 different proteins known as nucleoporins or Nups. The FG family of the Nups (FG Nups) contains extensive regions of FG motifs that facilitate the passage of the cargo complexes through the NPCs. However, the mechanism of the interaction of FG Nups with cargo complexes is not clear. We have done all-atom molecular dynamics simulations for two types of FG nups, non-cohesive Nsp1 (AA 377-471) and cohesive Nup116 (AA 348-458), in explicit water to study their conformational characteristics and intra-molecular interactions. Simulation results for radius of gyration and end-to-end distance of the two FG nups are consistent with experimental measurements. Furthermore, we are able to distinguish the differences between the two types of FG nups: cohesive Nup116 nup has stronger intra-molecular interaction and smaller radius of gyration compared with Nsp1 nup. Currently, we are exploring the inter-molecular interactions between

FG nups with a goal of extracting the interplay between inter- and intra- molecular interactions of FG nups in crowded in-vivo like conditions. Our simulations consider a system where a pair of extended FG nups is anchored at two ends (total of four FG nups). Several simulation runs are carried out for Nsp1 and Nup116 with four different spacing between the anchoring points (2.0, 3.0, 4.0 and 5.0 nm). The strength of inter-molecular interactions of FG nups shows a strong dependence on the spacing between anchor points. We find that the inter-molecular interaction for Nsp1 is weaker compared to that of Nup116. While most of the FG nups are mainly disordered despite inter- and intra- molecular interactions, we observe noticeable beta-sheet formation in Nup116 with 2.0 nm spacing between anchoring points (Figure 2).
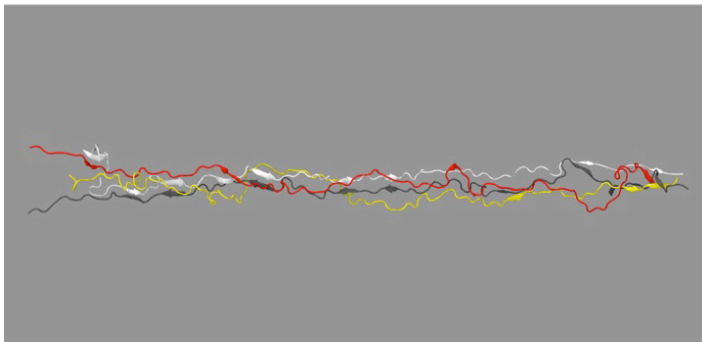
Figure 2. Snapshot from all-atom molecular dynamics simulations of FG nups indicating that Nup116 has stronger inter-molecular interactions compared to Nsp1. Also, beta strands are observed for Nup116 when anchored with 2.0 nm spacing.

Future Work

Building upon the results of this study, we will further refine the coarse-grained model to more faithfully reflect the geometry of the NPC and the sequence of the proteins. We will also explore more complex scenarios, including competition between transport cargo with different binding affinities and sizes in setups that model both the equilibrium situations in vitro as well as the dynamics in vivo. In parallel with the coarse grained Langevin dynamics simulations described above, we shall develop more realistic models of unfolded proteins. We will develop atomistic Molecular Dynamics simulation protocols for unfolded proteins, with the emphasis on realistic representation of water and hydrophobic and electrostatic interactions. The results of the atomistic simulations will be compared with the coarse-grained simulations and experiments in order to determine what features of the NPC lie at the core of the gating and selectivity mechanism. Coarse-grained models will be developed by Welch' group in collaboration with the Zilman's group at the University of Toronto. In particular, the collaboration plan includes two month summer visits by Zilman together with a student to LANL in 2012 and 2013 and corresponding visits during the year by Gnanakaran and Welch to Toronto.

Conclusion

The ultimate goal of the project is the mechanistic understanding of the biophysical dynamics of transport through the nuclear pore complex and leveraging this understanding towards design of bio-mimetic devices and sensors. We have made considerable progress in developing appropriate computational and theoretical tools and have already gained several important insights into both the equilibrium conformations of the system and its dynamic function. Three manuscripts are currently in the last stages of preparation for publication.

Publications

Jovanovic-Talisman, T., and A. Zilman. Nanobiotechnology: Building a basic nanomachine. 2011. *Nature Nanotechnology.* **6**: 397.

Opferman, M., R. Coalson, D. Jasnow, and A. Zilman. Morphology control of polymer films by nanoparticle binding. *Physical Review Letters.*

Identifying, Creating, and Controlling Functional Hotspots in DNA

Boian Alexandrov
20110516ER

Introduction

Cellular behavior is governed by the genetic code encrypted in the DNA molecule. Understanding how to control via external stimuli the transcription of this code is one of the dreams of biotechnology. In this project we study the role of DNA conformational breathing dynamics in the regulation of gene expression. In particular, we investigate the role of DNA local transient openings (DNA breathing) in the transcription initiation and transcription factors binding, as well as the possibility to control these processes via external terahertz radiation (THz). Our approach is founded on the innovative interrelation between the self-trapped breathing modes of double-stranded DNA (aka bubbles) and biological function as well as on our previous theoretical and experimental observations that these modes are connected with the location and strength of the transcription regulatory elements such as; transcription starts sites (TSS) and transcription factor binding sites (TFBS). When DNA-bubbles fall at the TSS or TFBS regions, we call them functional hotspots. The main goal of this project is to develop a predictive understanding of the role of DNA hotspots in biological function and the possibility to rationally modify them.

Benefit to National Security Missions

Los Alamos National Laboratory has a large interest in genomic studies, development of modern statistical learning computational tools, and advanced knowledge on cell biological functions in connection with bioenergy, biomaterials of the future, and for environmental and safety concerns. Our project is directly related to the Complex Biological Systems Grand Challenge and targets the gain a multiscale predictive understanding of the functionality of complex biological system – from large biomolecules, and single cell - to cellular cultures. The tools we are creating for predicting, designing, and modifications of the strength of core promoters and transcription factor binding sites, i.e. for controlling genomic functional elements, will be a timely and impactful contribution to the rapidly growing field of biotechnology and functional genomics.

Progress

This year we completed each goal we set and stated in our proposal for the first year. Our results were featured in the LANL, 2011 ADTSC Highlights, in a press release of Optical Society of America; they were highlighted in the *ScienceDaily* digital research news, and in the digital editions of *Science news*. Below we outline our results.

This year we completed each goal we set and stated in our proposal for the first year. Our results were featured in the LANL, 2011 ADTSC Highlights, in a press release of Optical Society of America; they were highlighted in the *ScienceDaily* digital research news, and in the digital editions of *Science news*. Below we outline our results.

Computational prediction of core promoters and their transcription start sites

We developed a hybrid core promoter prediction protocol that exploits structural and motif-based DNA characteristics together with breathing dynamics of the double helix. Our novel recognition algorithm used supervised and unsupervised learning techniques for core promoter recognition on genomic scale. Via our Markov Chain Monte Carlo algorithm, we performed extensive computer simulations of the DNA breathing dynamics of the following genomic sequences: 30,000 core promoters (all the human genomic promoters of the protein coding genes), 30,000 exons, and 30,000 non-promoters – a total of 10 million base pairs. We demonstrated that adding DNA breathing dynamics characteristics to currently used recognition characteristics and applying modern machine learning methods leads toward a general and more accurate genomic-scale promoter prediction in this genomic set.

Understanding the mechanisms governing affinity of the transcription factors binding

We investigated the influence of DNA breathing dynamics on the binding of the factor for inversion stimulation (Fis) protein, which is conserved between *Escherichia coli* and *Salmonella typhimurium,* and for which is known to bind at highly variable sequences.

Our simulations demonstrated that DNA dynamical activity at the vicinity of the binding site strongly correlates with the affinity of Fis–DNA binding, at several sets of *in vitro* and *in vivo* experimental data. We show that Fis binding can be suppressed by a few point mutations at the flanks of the consensus sequence – outside the direct points-of-contact between the protein and DNA, specifically designed by our computer simulations to alter DNA local breathing dynamics. To test our understanding of how Fis binding is influenced by DNA breathing we additionally designed various nucleotide modifications, such as mismatches and nucleotide methylations, in DNA segments that are known to interact (or not interact) with Fis. In each case, our intention was to make the DNA breathing dynamics either closer to or farther from the typical simulated profile of a "good" Fis binding site. For the modified DNA segments, we found that Fis-DNA binding, as assessed by gel-shift assay, was changed in accordance with our predictions. We conclude that DNA breathing dynamics, which may be regulated by genetic or epigenetic modifications, regulates Fis binding.

We studied DNA breathing dynamics of various trinucleotide repeats sequences (TRS) that represent a common type of genomic DNA motif whose expansion is associated with a large number of human diseases (e. g. Huntington disease, X-syndrome, and many others). We found a novel and notable collective breathing behavior of genomic DNA of tandem TRS, leading to a propensity for large local DNA transient openings at physiological temperature. Our computer simulations demonstrate that the patterns of openings of various TRSs depend specifically on their length. Importantly, we suggested that the collective propensity for DNA strand separation of repeated sequences could serve as a precursor for outsized intermediate bubble states independently of the repeat's G/C-content. Additionally, we reported that repeats have the potential to interfere with the binding of transcription factors to their consensus sequence by altered DNA breathing dynamics in the proximity of the binding sites. Using our computational framework, we designed a modification of the TATA-box, and investigate experimentally the binding site of the TATA-box binding protein (TBP). Our simulations revealed that the bubble spectrum of the wild type TBP-binding site is significantly altered when the flanking sequence is replaced by repeat: $(GAA.TTC)_{15}$. We demonstrated experimentally that the presence of $(GAA.TTC)_{15}$ repeats leads to inhibition of TBP-binding, although the binding motif and its direct points-of-contact were entirely preserved.

Biological effects of terahertz (THz) radiation

We evaluated cellular response of mesenchymal mouse stem cells exposed to broadband THz radiation. In particular, we successfully conduct a set of terahertz irradiations on mesenchymal stem cells in the MPA facility. After designing the experiments, we conducted the irradiations and performed: mRNA extraction, gene chip statistical survey, and quantitative real time polymerase chain reaction (Q-PCR) experiments, as well as computational analysis. We found that extended exposure to broad-spectrum terahertz radiation results in specific changes in gene expression. The differential gene expression response depended strongly on the irradiation condition and time of exposure. Our findings suggested that the applied terahertz irradiation accelerates cell differentiation (cell reprogramming) toward the adipose phenotype by activating the transcription factor peroxisome proliferator-activated receptor gamma (PPARG). Finally, our molecular dynamics computer simulations indicated that the local breathing dynamics of the PPARG promoter DNA coincides with the gene specific response to the THz radiation. Hence, we argued that THz radiation could be a potential tool for cellular reprogramming.

We evaluated the non-thermal cellular response of mesenchymal mouse stem cells exposed to THz radiation. We apply low-power radiation from both a pulsed broadband (centered at 10 THz) source and from a continues-waves (CW) laser (2.52 THz) source. Modeling, empirical characterization, and monitoring techniques were applied to minimize the impact of radiation-induced increases in temperature. Q-PCR was used to evaluate changes in the transcriptional activity of selected hyperthermic genes. We found that temperature increases were minimal, and that the differential expression of the investigated heat shock proteins (HSP105 (heat-shock protein), HSP90 (heat-shock protein), and CRP (participates in the clearance of necrotic and apoptotic cells)) was unaffected, while the expression of certain other genes (Adiponectin (protein hormone that modulates a number of metabolic processes), GLUT4 (insulin-regulated glucose transporter found in adipose tissues), and PPARG) showed clear effects of the THz irradiation after prolonged, broadband exposure. We showed that the 2 hours CW irradiation do not affect the genes that accelerates cell differentiation toward the adipose phenotype.

We investigated theoretically the physical conditions of DNA-bubble appearances in a THz field. We calculated the nonlinear response manifolds (NLRM) for the period T-solutions and the period-doubled 2T-solutions of the DNA nonlinear vibrations, were T is the period of the external THz field. We demonstrated that the period-doubled breathers (DNA bubbles) appear naturally in a THz field, even at the amplitude (A) of the external field |A|~0. We showed that these period-doubled breathers arise from the multistability overlap between various stages of the Feigenbaum period-doubling cascades in the non-linear potential of the DNA hydrogen bonds.

Future Work

We will continue the development of hybrid TSS genomic

prediction methods relying on the dynamical patterns of the functional hotspots and machine learning. We will start to develop the methodology for design of TSS and TFBS with various strengths validating our approach with experiments with DNA segments with various epigenetic modifications. In particular, we will design various mutants of well-known genomic TFBSs with rationally modified binding affinities, using methylations and nucleotide mishmashes. Finally, we plan to verify our hypothesis that THz radiation has frequency-specific effect on DNA functional hotspots by: irradiating cell cultures, establishing differential gene expression, and analyzing *in silico* the correlations between propensity for bubble creation and the THz response.

Conclusion

Based on DNA breathing dynamics we expect to develop a functional hotspot recognition protocols that significantly out-perform the available state-of-the-art TSS prediction tools, and thus help to understand how DNA performs its function. Further, we expect to develop a methodology that will enable the design of hotspots so we can try to control gene expression. Finally, we expect to validate the hypothesis that THz irradiation has a frequency-specific effect on DNA functional hotspots that can be used for gene expression control.

Publications

Alexandrov, B. S., K. O. Rasmussen, A. R. Bishop, A. Usheva, L. B. Alexandrov, S. Chong, Y. Dagon, L. G. Booshehri, C. H. Mielke, M. L. Phipps, J. S. Martinez, H. T. Chen, and G. Rodriguez. Non-thermal effects of terahertz radiation on gene expression in mouse stem cells. 2011. *Biomedical Optics Express* . **2** (9): 2679.

Alexandrov, B., V. Valtchinov, L. Alexandrov, V. Gelev, Y. Dagon, J. Bock, I. Kohane, K. Rasmussen, A. Bishop, and A. Usheva. DNA Dynamics Is Likely to Be a Factor in the Genomic Nucleotide Repeats Expansions Related to Diseases. 2011. *PLOS ONE.* **6** (5): e19800.

Bishop, A. R., K. O. Rasmussen, A. Usheva, and B. S. Alexandrov. Entropy–Driven Conformations Controlling DNA Functions. 2011. In *Disorder and Strain-Induced Complexity in Functional Materials.* Edited by Kakeshita, T., T. Fukuda, A. Saxena, and A. Planes. Vol. XV, 1 Edition, p. 273. Berlin: Springer.

Bock, J., Y. Fukuyo, S. Kang, M. Lisa. Phipps, L. Alexandrov, K. Rasmussen, A. Bishop, E. Rosen, J. Martinez, H. Chen, G. Rodriguez, B. Alexandrov, and A. Usheva. Mammalian Stem Cells Reprogramming in Response to Terahertz Radiation. 2010. *PLoS One.* **5** (12): Article No.: e15806.

Maniadis, P., B. S. Alexandrov, A. R. Bishop, and K. O. Rasmussen. Feigenbaum cascade of discrete breathers in a model of DNA. 2011. *PHYSICAL REVIEW E.* **83** (1, 1): 011904.

Mechanistic Studies Toward an Improved Carbonic Anhydrase for Biofuel Production.

Suzanne Z. Fisher
20110535ER

Introduction

Carbonic anhydrases (CAs) have great potential for industrial use in DOE mission areas of using algae for the production of renewable fuels and other value-added products. CAs are enzymes that can capture and regulate CO_2 by interconverting it with bicarbonate, thereby enhancing biofuel production. Our main goal is to characterize the structural and catalytic properties of carbonic anhydrase (CA). We will use the information to re-engineer CA so that it can be used over the broad range of process conditions involved in algae growth. The mechanistic studies of CA will require combining for the first time several different experimental techniques, some available only at LANL. We will then co-optimize and select for interdependent catalytic and pH stability properties to create a super-CA to test in culture with algae. The approach developed is generalizable and applicable to many different enzymes for pharmacology, drug design, biomedical research, and industrial applications.

Benefit to National Security Missions

This research directly supports LANL and DOE missions in renewable energy, biofuels, carbon management by providing a robust product that will enhance the production of renewable biofuels. Furthermore, the development of a new measurement capability based on combining dynamic and static information from neutrons and NMR, and a new engineering capability based on co-optimizing enzymes with complementary engineering steps, will be of broad significance for the study of a broad range of biological problems. The work is of interest to DOE-BER, EERE and OBP. We will also work to incorporate our project and products into the existing efforts of in these areas. Fuel stocks, especially deployed to the field, are essential to multiple DoD missions.

Progress

Our second neutron structure of wild type HCA II at neutron pH is now complete and the data has being presented at a national crystallographic conference in May 2011. We have also written a paper about this structure and that has been accepted to *Biochemistry* for publication. This comparative study of the two neutron structures revealed many interesting details about catalysis and we have been able to see a pH "switch" in the hydrogen bonded network in the enzyme active site (Figure 1). This is a major observation and represents the first study of its kind in the field of enzymology. We are the first to directly observe a completed hydrogen bonded network stretching from the proton donor to acceptor.
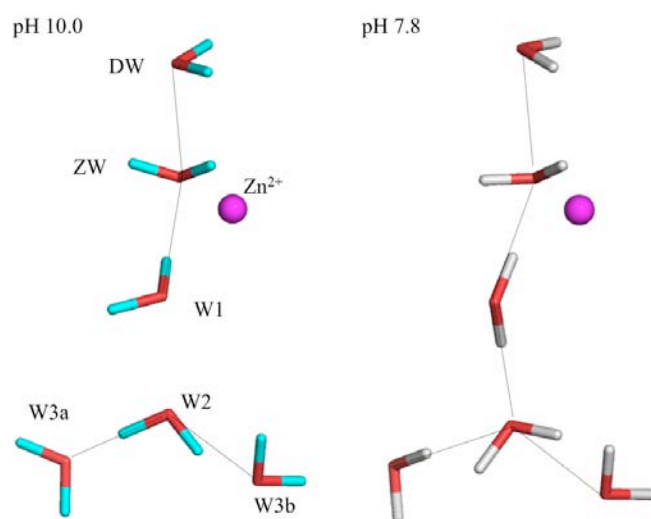
Figure 1. Comparison of the CA active site water network between pH 10 and 7.8. The high pH form is shown on the left and the neutral pH structure on the right. We observed a re-arrangement of the water network and the establishment of completed hydrogen bonded network.

We have also made a breakthrough in the sample preparation for the NMR spectroscopy portions. We were able to prepare specifically labeled CA and measured high quality initial data. We are now starting the process of titrating the pH to determine the participation of key catalytic residues in the enzyme mechanism.

We have begun to co-culture wild type unmodified

enzyme with a particular algae strain. The initial data with the unmodified enzyme looks promising and we do observe some growth boost early on. We are now planning the next set of culture conditions to test. We have also constructed several mutants of CA and have expressed and purified these.

We have also completed a detailed biophysical characterization of the mutants and all of them display enhanced thermal stability compared to wild type. The melting temperatures for the variants are 1-7 °C higher than it is for wild type. TS1 appears to be the best and we are now testing the TS1 mutant in co-culture with algae to determined growth rate enhancement. We have also completed detailed structural and kinetic analysis of the TS 1-5 mutants. These results are being written up with my collaborators at the University of Florida. We expect to submit the paper to a peer-reviewed journal in early 2012.

Future Work

We will continue detailed studies of CA to gain information for re-engineering CAs for use over a broad range of process conditions involved in algae growth (pH and temperature). The mechanistic studies of CA will require combining for the first time several different experimental techniques, some available only at LANL. Based on these results we will re-design CA and select for catalytic and pH stability properties to produce a versatile super-CA for use in enhancing algal growth.

Goal 1: Continue complementary measurements to characterize the structural properties and catalytic mechanism of CA. These techniques, applied together here for the first time include: neutron crystallography to determine the static positions of H atoms in CA, combined with dynamic H mapping through pH titrations of key active site residues with NMR spectroscopy. This produces a powerful approach for enzyme characterization unique to LANL.

Goal 2: Results obtained from Goal 1 are being used to guide re-engineering of CA to produce highly active but stable enzyme for use in algal growth applications. By co-optimizing and selecting for interdependent enzyme properties (i.e. properly folded mutants that are still highly active and resistant to extreme temperatures and pH) we provide a new and generalizable capability for enzyme engineering.

Goal 3: We are continuing to test our enhanced CA product for its ability to improve algae growth. A stable, highly active CA that is not sensitive to pH would be of enormous benefit as an additive to algae cultures, by providing either bicarbonate or CO2 for uptake, components that are rate-limiting for algal growth. This part is being done in conjunction with collaborators in Bioscience Division at LANL.

Conclusion

The expected result will be 1) a complete understanding of the carbonic anhydrase (CA) catalytic mechanism, 2) a super CA that will be used for enhanced algal growth, and 3) development of a novel approach to study enzyme mechanism through combined NMR and neutron crystallography. Results from preliminary algae cultures are extremely encouraging, but need to be expanded with all the appropriate controls and tested with different CA mutants.

Publications

Fisher, Z., A. Kovalevsky, M. Mustyakimov, D. Silverman, R. McKenna, and P. Langan. Neutron structure of human carbonic anhydrase II: A hydrogen bonded water network "switch" is observed between pH 7.8 and 10.0. 2011. *Biochemistry.* : 1.

Low-Frequency Acoustic Interferometry for Probing the Stratosphere.

Stephen J. Arrowsmith
20110556ER

Introduction

The goal of this project is to test the hypothesis that low frequency acoustic noise can be used to probe a part of the atmosphere not well recorded by current ground or satellite sensors. A new paradigm in seismic imaging has been the recent discovery that seismic noise interferometry can be used to image the Earth's crust – thus seismic images of the crust are no longer limited by the global distribution of earthquakes, which largely occur at plate boundaries. It is well known that low frequency acoustic waves (or 'infrasound'), which can travel thousands of kilometers in the atmosphere, sense temperatures and winds along path, since these parameters affect the sound speed. Recent work has investigated the use of infrasound to probe the atmosphere for temperature and wind using signals from volcanoes and rocket launches.

The goal of this project is to develop and apply a framework for atmospheric acoustic noise interferometry, exploiting a ubiquitous source of low-frequency acoustic noise from ocean storms ('microbaroms') to probe the stratosphere. It has been recently argued that knowledge of stratospheric temperatures and wind fields are critical for improving climate change models, which typically only incorporate data on the troposphere. Infrasound monitoring has unique potential for constraining temperatures and winds in the stratosphere, thus improving the fidelity of weather and climate models.

Benefit to National Security Missions

The results of this project would have clear potential to expand LANL capability in global climate monitoring and modeling (BER, GHGIS) through utilizing expertise in low-frequency acoustics that has historically been focused on nuclear explosion monitoring applications. In addition, the capability would revolutionize the use of infrasound for nuclear explosion monitoring. This R&D is a natural fit for LANL, since it is applicable to a strategic focus area. The state of the stratosphere is important to DoD missions such as air transport, and to the non-proliferation challenge of predicting long-range transport of nuclear markers such as tracer particles. More broadly, the project builds additional capability for nuclear event detection.

Progress

Significant progress has been made in two areas of this work: (1) the development of a mathematical framework for estimating temperatures and wind speeds in the stratosphere using infrasound noise, and (2) the subsequent validation and refinement of this framework using a suite of synthetic tests.

For the first progress item, I have developed a suitable mathematical representation of the atmosphere using Empirical Orthogonal Functions (EOFs) [1]. This representation allows for the representation of any temperature or wind profile with as few as 10 EOFs, significantly reducing the number of unknowns. I have coded up the Tau-P formulism [2], which allows for the efficient computation of ray paths through atmospheric models, accounting for variations in effective sound speed with height, and for horizontal advection of each ray path by wind. Finally, I have developed an inverse algorithm that is suitable for iteratively perturbing a starting wind or temperature profile by minimizing the fit between predicted and observed delay times between pairs of spatially-separated arrays.

For the second progress item, I have developed and applied a suite of different synthetic tests to validate and refine the framework. For each synthetic test, I know the true profile, which is the profile used for the forward problem (calculating travel times from a synthetic source to each receiver array). I then perturb this profile to generate a starting profile. Assuming that the starting profile represents an *a priori* estimate of the temperature or wind, the goal is then to refine this profile using the synthetic infrasonic delay times. In the ideal case, the final estimated profile should approximate the true profile. An example simulation is plotted in Figure 1, demonstrating that the estimated profile closely converges on the true profile in the lowermost 50 km of the atmosphere. In this test, no ray paths reach above 50 km elevation; therefore the profile

is unconstrained at these heights (and is set as the starting model). A sigmoid function controls the gradation from unconstrained to constrained portions of the model.
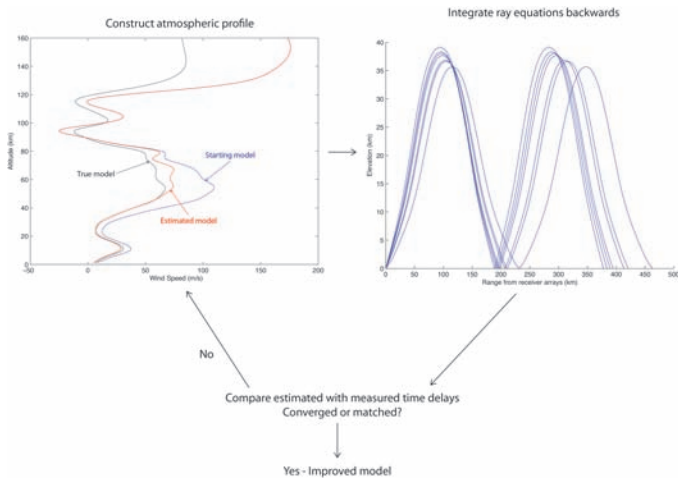
Figure 1. Illustration of the iterative process used to refine an a priori starting wind profile using infrasound constraints. The wind profile is parameterized by a set of 10 EOFs, which are iteratively perturbed using a nonlinear regression technique such that the fit between synthetic (observed) and predicted delay times between receiver arrays is minimized. In this example, the estimated model converges on the true model for the lowermost 50 km, and is fixed to the starting model for the region above 80 km (since we have no constraints above this elevation).

After experimenting with a suite of synthetic tests, it was found that the addition of adjoint constraints helps to reduce the non-uniqueness of the problem. In particular, I have implemented a dual-cost function that minimizes both the fit to infrasound observables and the difference between the estimated and starting profiles for the lowermost 15 km (a region that is already well-constrained). This damping approach effectively prevents non-physical oscillations in the profiles that also fit the data.

The development of an inverse technique has led to the realization that a network of sensor arrays is required, rather than a network of individual point sensors. Thus, the application to real data will focus on a 9-array infrasound network in Utah that has been deployed as part of an NA-22 funded project that I am involved with [3], rather than USArray (which contains only point sensors). This minor change in dataset from the proposal does not change the scope of the project, and the synthetic tests have all been calculated using the Utah network sensor array configuration.

Future Work
The next focus of this project is to apply the techniques developed and tested on synthetic data to a real dataset. As discussed in the previous section, the dataset that I will focus on comprises a 9-array network of infrasound

sensors in Utah. Applying this technique to real data will challenge the set of assumptions made in the synthetic tests. In particular, in the synthetic tests I was able to start from the premise that delay times representative of the infrasound propagation between receiver arrays can be measured from cross-correlation. However, this premise requires several conditions to be met: microbaroms from the same storm must be observed at multiple spatially separated arrays, the signals at each array must be correlated, and it is necessary that the delay-time of correlation shows consistency as a function of time. I believe that the framework developed thus far is sufficient for a peer-reviewed paper on the methodology. However, the demonstration that this technique works for real data is important for demonstrating the practical application of this research.

Conclusion
At the end of the first quarter of this Early Career project I now have a robust mathematical framework that, for synthetic tests, consistently improves upon *a priori* starting profiles for temperatures and winds in the stratosphere. The next challenge is to apply this technique to real data, which requires the demonstration that one can reliably measure delay times between pairs of sensor arrays that are representative of the infrasonic propagation paths.

References

1. Hannachi, A., I. T. Jolliffe, and D. B. Stephenson. Empirical orthogonal functions and related techniques in atmospheric science: A review. 7200. *International Journal of Climatology.* **27** (9): .

2. Drob, D. P., M. Garces, M. Hedlin, and N. Brachet. The temporal morphology of infrasound propagation. 2010. *Pure and Applied Geophysics.* **167**: 453437.

3. Arrowsmith, S., J. M. Hale, R. Burlacu, K. Pankow, B. Stump, C. Hayward, G. Randall, and S. Taylor. Infrasound signal characteristics from small earthquakes. Presented at *Monitoring Research Review 2011.* (Tucson, 13-15 Sept.).

Using Small Molecules to Control RNA Conformations

Karissa Y. Sanbonmatsu
20090163ER

Abstract
We have used biochemistry experiments and computer simulations to understand a new kind of genetic switch called a riboswitch. Biochemistry experiments were performed to understand the overall process of switching and the inner workings of the switch were simulated. Our new method and discovery have led to unprecedented insight regarding the mechanism of this molecular switc, including its tunability.

Background and Research Objectives
A riboswitch is a molecule inside a bacterium that turns genes on or off. The riboswitch is controlled by small molecules present inside the cell, such as vitamins, amino acids, and metabolites. They are exciting because they represent a new form of gene control that was only recently discovered. They have applications in the development of new antibiotics. How they work is not understood in atomic detail. If we can understand how they work, then we can design better ones.

More specifically, these switches have a normal configuration that occurs when the small molecule is not present. The normal configuration does not allow gene expression. When the small molecule is present, the switch folds into an alternative configuration that turns the gene on, allowing gene expression. Riboswitches can easily discriminate between very similar small molecules. Considering that a prototype riboswitch-based biosensor chip has been constructed, riboswitches are excellent candidates for next generation biosensors . The sensitivity to minute differences between ligands also makes the riboswitch a promising target for antibacterial drug design. So far, these switches have only been found in bacteria. Therefore, antibiotics that target riboswitches are thought to have very few side effects, since the switches have not been found in humans.

Our goal is to understand how these switches switch. We will address the questions, 1) how does the small molecule bind?, 2) how does binding result in switching?, and 3) how tunable is the switch?

Scientific Approach and Accomplishments
We made tremendous progress, including several important discoveries that will help us to design molecular switches. We were able to optimize our new technique to measure the operating characteristics of molecular switches. Our simulations agreed well with the experimental results. We discovered that salt is critical for the operation of the switch, and, that both salt and the sensed small molecule must be present for the switch to work properly.

We have used our novel 2-piece switching system to uncover part of the mechanism of switching in riboswitches. In our new method, we split the switch into two pieces. When we add the second piece to the mix, we are able to observe automatic switching from state 1 to state 2. We discovered that certain parts of the genetic switch have a large affect on the capability to switch properly. Certain alterations make the switch completely unusable. We identified the most critical parts of the switch required for switch function. The study is was accepted and is in press [1] at "Nucleic Acids Journal", which has an impact factor higher than "Physical Review Letters".

We performed biochemical experiments measuring the mobility of each piece of the riboswitch using fluorescence. These were performed for many different biochemical environments. We then performed all-atom molecular dynamics simulations of the same systems. The simulations used a simplified force field potential that has just a few free parameters. This technique is closely tied to experimental data and is also quite easily adjustable to experimental data. The first simulations showed overall similarity to experiments but differed significantly in some important parts of the riboswitch. We developed new analytical measures to enable direct comparison to experiment. We isolated those parts that differed and modified the corresponding force field potential for the parts showing differences from experiment. This is the first such agreement ever for a riboswitch system.

We did a wide range of experiments focused on determining the effect of ionic concentration and electrostatic

environment on the switch. This included experiments of the binding part of the switch. We also performed switching studies that probed the effect of magnesium ions. We found something startling – both the small molecule that triggers switching and salt are important for the operation of the riboswitch. The riboswitch is controlled by a tiny small molecule. It is an unsolved problem (for many years) regarding how such a tiny small molecule can cause a huge change in the conformation of the switch. We have evidence that the salt works together with the small molecule to cause the gigantic configurational movement of this riboswitch. Our studies are consistent with a dynamic equilibrium between two switching states that favors one state. When the small molecule and the salt are present, the equilibrium changes to the other state.

We have performed computer simulations of the effect of salt on the genetic switch. We have tuned our simulation parameters to improve the agreement between computer models and experiments. We expect to uncover how the genetic switch melts as a function of temperature. Finally, we have examined single gene switches using single molecule experiments, giving us a more detailed picture of how gene switches work.

Impact on National Missions

Because the study focuses on genetic switches that are biosensors, the project is directly related to the "Science of Signatures" grand challenge, as well as the sensing component of the "Biology of Infectious Agents" key capability. The project is also related to the "Biology of Infectious Agents" by its applications to antibiotic design. Potential sponsors include NIH, DARPA and DOE.

Publications

Hayes, R., J. N. Onuchic, and K. Y. Sanbonmatsu. Glassy state Mg2+ inside the SAM-1 riboswitch. *In Preparation for Journal of the American Chemical Society.*

Hennelly, S. P., P. M. Goodwin, and K. Y. Sanbonmatsu. Single molecule dynamics of the SAM-1 riboswitch. *In Preparation for Structure.*

Hennelly, S. P., and K. Y. Sanbonmatsu. Tertiary contacts control switching of the SAM-I riboswitch. 2011. *Nucleic Acids Research.* **39** (6): 2416.

Hennelly, S. P., and K. Y. Sanbonmatsu. Cooperativity effects between Mg2+ and ligand on the SAM-1 riboswitch. *In Preparation for Nucleic Acids Research.*

Whitford, P. C., A. Schug, J. Saunders, S. P. Hennelly, J. N. Onuchic, and K. Y. Sanbonmatsu. Nonlocal helix formation is key to understanding S-adenosylmethionine-1 riboswitch function. 2009. *Biophysical Journal.* **92** (2): L7.

Whitford, P. C., J. K. Noel, S. Gosavi, A. Schug, K. Y. Sanbonmatsu, and J. N. Onuchic. An all-atom structure-based potential for proteins: bridging minimal models with all-atom empirical forcefields. 2009. *Proteins: Structure, Function, and Genetics.* **75** (2): 430.

Functional Gene Discovery Using RNAi-based Gene Silencing

Elizabeth Hong-Geller
20090202ER

Abstract

In this study, we identified host proteins that are targeted by Yersinia bacteria during infection using Ribonucleic Acid Interference (RNAi), a powerful tool for analyzing gene function by silencing, or inactivating, target genes through the specific destruction of their messenger RNAs (mRNAs). We have performed high-throughput genome-wide screens to select for genes, that when silenced, lead to inhibition of Yersinia infection. From these functional genomics studies, we identified host proteins targeted by Yersinia and can thus exploit their associated mechanisms of pathogenicity to develop therapeutic countermeasures against Yersinia infection. We expect that development of genomic screens using our human small interfering RNA (siRNAs) library will establish a robust methodology by which to ascribe function to previously uncharacterized genes, a major challenge in biomedical research given that approximately half of all predicted human genes have no known function. This project contributes significantly to the study of host-pathogen interactions, a key strategic research capability that supports the LANL mission of biothreat reduction and protection of national security. Yersinia pestis, a potential agent of bioterrorism, is a Center for Disease Control (CDC) Category A pathogen, signifying great potential risk for adverse impact on public health. New strategies to counteract Y. pestis infection, based on increased fundamental understanding of Y. pestis virulence, can greatly impact our ability to contain potential outbreaks of plague in the population.

Background and Research Objectives

Human pathogens have evolved sophisticated mechanisms by which to attack the host immune system. Yersinia pestis, the causative agent of plague, is a CDC Category A pathogen with bioweapon potential, and thus represents a high-value target for the development of novel therapeutic strategies. Y. pestis employs multiple virulence strategies during host infection, including the type III secretion system (TTSS), a "syringe-like" needle complex that injects virulence proteins, or Yop effectors, into the host cell. To identify host proteins essential for microbial pathogenicity, we have established a platform for genome-wide loss-of-function high-throughput screens (HTS) employing RNAi, a powerful tool for loss-of-function studies used to analyze gene function by silencing target genes through the specific destruction of their mRNAs. We have focused our studies on the Yersinia species, including Y. pestis, the etiological agent of bubonic and pneumonic plague, because of its high virulence and potential threat for social devastation, and Y. enterocolitica, a causative agent of gastrointestinal disease. In the last several years, both small and large-scale RNAi screens have been applied to the discovery of host targets in response to infection by pathogens that exhibit a primarily intracellular lifestyle, including the bacterial pathogens *S. typhimurium*, *M. tuberculosis*, and *L. monocytogenes*, and the HIV, HCV, and influenza viruses. To the best of our knowledge, this is the first major RNAi effort to screen for host targets that modulate a key host signaling pathway in response to a predominantly extracellular pathogen.

Scientific Approach and Accomplishments

We have obtained two sub-family short hairpin (shRNA) libraries for Kinase genes (~760 genes, ~2000 constructs) and Druggable target genes (~7000 genes, ~20,500 constructs) cloned into a lentiviral vector pGIPZ from Open Biosystems. We have based our RNAi screen on the rescue of gene expression of the transcription factor, NF-___ following *Y. enterocolitica* infection of HEK-293 cells. NF-κB controls expression of genes involved in inflammatory response, including the cytokines TNF-α, IL-1, IL-6, IL-12, and MIP1β, and thus plays a critical role in the clearance of the bacteria by the immune response. The assay is based on TNF-_ activation of NF-kB linked to a fluorescence or luminescence reporter gene. Infection with Yersinia blocks the TNF-_ activation step, leading to decreased levels of reporter gene expression. Inhibition of Yersinia infection with shRNA constructs will restore reporter gene expression (Figure 1).
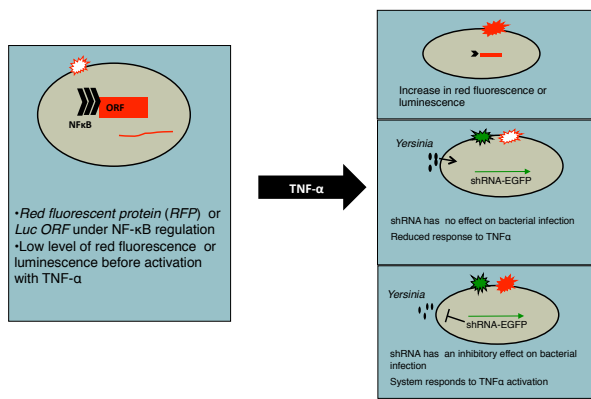
Figure 1. Assay for RNA interference screen.

We have screened the entire kinase library and a selection of heat shock proteins from the druggable target library using this assay. We have identified ~20 human genes, that when silenced, leads to decreased Yersinia infectivity (Table 1). These genes fall into multiple functional categories, including signal transduction, cell stress and apoptosis, protein folding, cell adhesion, and membrane potential. The identified genes function in different cellular processes including signaling pathways (c-KIT, MAP3K14, ERK4), ion channel activity (SGK1, WNK1), and regulation

of cell growth (CK2). We have validated a selection of the genes identified in Table 1 by creating stable cell lines that express the shRNAs and demonstrate the same phenotype of rescue of NF-kB expression (Figure 2). We also used alternative methods of gene knock-down such as siRNAs. We demonstrate that specific small molecule inhibitors of c-KIT, SGK1, and CK2 increased NF-__ gene activation and/ or pro-inflammatory cytokine release in epithelial, macrophage, and primary dendritic cells in response to either *Y. enterocolitica* or *Y. pestis* (Figure 2). These small molecule inhibitors are potential candidates for development of novel drugs for the treatment of Yersinia infection and possibly, for other infectious diseases.

We have developed a robust RNAi-based platform for HTS functional genomics and discovery of host proteins that play a role in *Yersinia* pathogenicity. Identification of these targeted host proteins during *Yersinia* infection has greatly elucidated *Yersinia* virulence mechanisms and serves as the basis for design of novel inhibitor therapeutics that block *Yersinia* infection. Furthermore, we've developed a RNAi-based high-throughput research capability that can be used to ascribe function to human genes in many complex host response processes. We expect this methodology and the shRNA reagents can be broadly applied to study

TARGET PATHWAY				
Signal Transduction	Cell stress and Apoptosis	Protein Folding	Cell Adhesion	Membrane potential
Gene Function				
•**MAP3K14**, binds TRAF and stimulates NFkB •**MAP2K1**, regulates ERK activation •**MAP3K3**, directly regulates ERK pathways by activating MEK1/2 •**LKB1/PJS**, involved in SR-BI activation of AKT •**ERK4/MAPK7**, translocates in the nucleus and activates many TFs •**CK2**, cell cycle and cell growth regulation •**PIK3R2**, regulatory subunit 2β of PI3K •**PI3-K-C2A**, class 2 α-polypeptide of PI3K family, involved in cell proliferation, survival, migration and intracellular protein trafficking; may be involved in integrin-dependent signaling •**ACTR-IIB**, activin A type II B receptor, transmembrane cell growth and differentiation factors belonging to TGFβ superfamily	•**HSP90AB1**, regulates apoptosis through AKT, BIRC5, and Apaf1 signaling, also FKBP38 direct inactivation •**HSPH1**, role in ER stress response through GSK3 •**SGK1**, has an important role in cell stress response, negative regulation of apoptosis •**MAP3K3**, directly regulates stress-activated protein kinase (SAPK) by activating SEK •**ULK2**, regulates authophagy in response to mTOR signaling •**WNK3**, binds to Casp3 and prolongs cell survival upon stress stimulus; Ca+-transport regulation •**ABL/JTK**, non-receptor Tyr kinase involved in cell differentiation, stress response, and apoptosis (activates AKT)	•**HSP90AB1,** has a key role in folding newly synthesized proteins or stabilizing the structure and promoting proper function of many signal transduction proteins •**HSPH1**, senses unfolded proteins	•**ABL/JTK**, non-receptor Tyr kinase involved in actin cytoskeleton organization •**SGK1**, has a negative regulation of microtubule polymerization •**DMRV/GNE**, a rate-limiting enzyme in the sialic acid biosynthesis pathway, thus having a crucial role in cell adhesion and signal transduction	•**WNK1**, regulates Na and Cl-ion transport, activates MAP3K3 and SGK1 •**SGK1**, activates certain K, Na, and Cl-ion channels •**SGK2**, regulates K -ion channels, has a role in epithelial ion transport •**MONaKA/PXK**, regulates both Na,K-ATPase enzymatic and ion pump activities

Table 1. Host genes identified in RNA interference screen.

host response to other pathogens or chemical agents. We are preparing manuscripts describing our experimental work and are in the process of pursuing follow-on opportunities for funding from different agencies. We have secured funding from DTRA to apply this methodology to the study of host genes targeted by another high-risk bioagent, *Burkholderia pseudomallei*. We have submitted an Invention Disclosure describing a reporter cell line for assessment of host immune response that came out of this work and a Technology Maturation proposal to obtain additional funding to validate these studies for Intellectual Property rights.
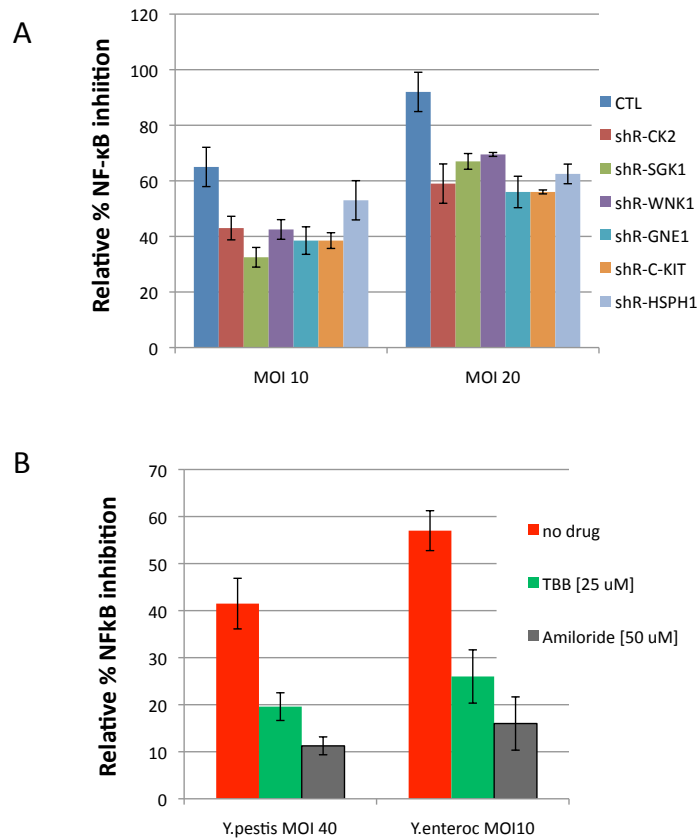
Figure 3. Validation of host genes from RNAi screen using stable cell lines and small molecule inhibitors.

Impact on National Missions

This project supports the DOE/NNSA mission in Threat Reduction by enhancing our understanding of host-pathogen interactions and biodefense capabilities. It is also relevant to goals of the Department of Homeland Security. Furthermore, identification of host genes that are targeted by different *Yersinia* species, or potentially across bacterial genuses, can enable the development of broad-spectrum therapeutics against high-risk pathogens.

Publications

Hong-Geller, E., K. Nowak-Lovato, S. Micheva-Viteva, and S. Lauer. Regulation of host chemokine response by the pathogenic Type III secretion system. 2011. In *Chemokines: Types, Functions, and Structural Characteristics.* Edited by Walker, K.. , p. 111. New York: Nova Science Publishers Inc.

Hong-Geller, E., and S. Micheva-Viteva. Functional gene discovery using RNA interference-based genomic screen to combat pathogen infectin. 2010. *Current Drug Discovery Technologies.* **7**: 94.

Micheva-Viteva, S., K. Rector, and E. Hong-Geller. Functional gene discovery in Y. pestis infection using RNAi-based gene silencing. 2009. In *2009 Chemical and Biological Defense Science and Technology Conference.* (Dallas, TX, 16-20 Nov. 2009). , p. 262. Dallas: DTRA.

Micheva-Viteva, S., K. Rector, and E. Hong-Geller. Functional gene discovery using RNAi-based gene silencing. 2010. In *2010 Chemical and Biological Defense Science and Technology Conference.* (Orlando, FL, 15-19 Nov. 2010). , p. CD. Washington DC: DTRA.

Micheva-Viteva, S., K. Rector, and E. Hong-Geller. Functional gene discovery using RNAi-based gene silencing. 2011. In *High Content Analysis.* (San Francisco, 12-14 Jan. 2011). , p. 16. San Francisco: Cambridge Healthtech.

Micheva-Viteva, S., Y. Shou, K. Nowak-Lovato, K. Rector, and E. Hong-Geller. Functional gene discovery using RNAi-mediated gene silencing in host-pathogen interactions. To appear in *2011 Chemical and Biological Defense Science and Technology Conference.* (Las Vegas, Nov. 15-18, 2011).

Micheva-Viteva, S., Y. Shou, K. Nowak-Lovato, K. Rector, and E. Hong-Geller. Functional gene discovery using RNAi-mediated gene silencing in host-pathogen interactions. To appear in *High Content Analysis 2012.* (San Francisco, .Jan. 11-13, 2012).

A Visionary New Approach to Assess Regional Climate Impacts on Vegetation Survival and Mortality

Nathan G. Mcdowell
20090305ER

Abstract

The goal of this project was to lay the foundation for a new approach to modeling vegetation mortality in relation to climate change. This has been accomplished. We have radically improved the theory and application of physiological mechanisms of mortality within land surface models. Second, we have downscaled predictions at finer resolution and better time scales for regional climate. Integration of these tasks has been accomplished and lead to large improvements in our understanding of where mortality has occurred in the past and will occur in the future.

Background and Research Objectives

Models of climate change and its impacts on ecological systems must be accurate at regional scales for predictions to be of use to policy-makers. By regional scale, we mean at the level of individual states and smaller. We proposed to dramatically improve climate change and climate impacts modeling at the regional scale through a two component, integrated project. Our first component tested cutting edge theory of plant survival and mortality with both empirical and modeling efforts to develop the first mechanistic model of vegetation dynamics in response to climate. Our second component improved downscaled predictions of climate over the 50 year timespan. By downscaled we mean taking climate predictions made at the global level and scaling them to the scale of individual states and smaller. We have integrated these two facets into an improved model of regional climate change and ecological impacts.

Scientific Approach and Accomplishments

Vegetation mortality: We investigated the potential for the observed vegetation mortality event at the Los Alamos National Environmental Research Park to inform us of the potential cause of death of the pinon trees at the site. Our analysis of the long term leaf water potential records, and our increasing understanding of pinon mortality resulting from allied LANL projects, indicated that

the three month period of static leaf water potentials was actually consistent with both hydraulic failure and carbon starvation as modes of death. This means that, given appropriate fitting of the free parameters associated with both physiological mechanisms, the model can be made to fit the observations using either set of assumptions. This result, while being a negative science result and thus not amenable to publication, has been instrumental in navigating our scientific efforts towards measurements that will likely soon yield data capable if distinguishing between the two hypotheses.

In addition we have published a study investigating the ecological consequences of the carbon starvation model for long term vegetation trends (Fisher et al. 2010). This represents the first time that this explicit mechanism has been incorporated into a dynamic vegetation model and has generated motivation to measure the relevant parameters in fieldwork studies (there are currently three funded proposals that tackle this topic directly).

This work on vegetation dynamics clearly demonstrates that vegetation mortality and regrowth, as community level processes, cannot be considered in isolation from ecosystem structure. Indeed, the same mortality model can generate vastly different results depending on how functional diversity in plant resilience, and the sharing of water resources are proscribed. This lead to discussions with National Center for Atmospheric Research (NCAR) on potential improvements to the Community Land Model (CLM) ecology representation, and the integration of a combined mortality- vegetation dynamics model into CLM. We are collaborating with our former postdoc in her new position at NCAR on this model, which is now in the testing phase, but it due to form the core of the next release of the CLM model (CLM4.5).

Further investigations of the mechanisms of vegetation mortality have focused in the methodologies for inverse parameterisation of non-structural carbohydrate stores using experimental data from a tropical forest ecosystem. This site was chosen to demonstrate this technique on account of the mature status of the observations and analyses. We have designed a technique to infer the

constraints in the distribution of NSCs in a population from ecosystem level mortality and carbon economics data. A manuscript on our findings, which suggest that trees are a factor of 2-3 times more resilient that existing parameterizations assume, is in the latter stages of preparation (Fisher, et al).

McDowell has published numerous papers regarding vegetation mortality, listed in the publications section, that were supported either directly, i.e. through work with Rosie Fisher, or indirectly, through stimulating discussions and T&E support with this ER team. He has also given numerous invited presentations, including to DOE and multiple Universities.

Regional climate

In order to test hypotheses about the effects of vegetation change on Southwest climate, Rausher and Ringler worked on customizing the regional climate model WRF (Weather Regional Forecasting model) for use over the western United States. They continued to test different configurations of WRF, including the use of different boundary conditions (NCEP(National Centers for Environmental Prediction)/NCAR Reanalysis, North American Regional Reanalysis (NARR)), different physics options (e.g., cumulus and radiation schemes), and the effects of including the CLM on the simulation. So far the biases compared to observations are still larger than preferable (precipitation should be within +/- 20% of observations and temperature biases within 1-2 degrees). Furthermore, with the addition of the new land surface model (CLM) different solutions were obtained with different numbers of processors. This challenge was solved by switching compilers from PGI to INTEL and using reduced optimization. In addition to testing, new output variables were added to WRF for diagnosis, and the code was modified so that CO_2 (carbon dioxide) can be transient (necessary for climate change simulations).

Coupled vegetation-climate regional modeling

We have compiled the driver dataset and high resolution datasets to drive the version of CLM native to WRF (3.5) and have commenced these simulations. Initial results indicate that a physiological signal of the drought is indeed manifested in the model, and further tests are necessary to determine the impact on vegetation dynamics. We are scheduled to present this work at the American Geophysical Union meeting, and as a publication in the spring. This work is novel in several respects- its high spatial resolution, the focus of the model on semi-arid systems, and the diagnosis of a mortality event.

In addition to the coupled model system (WRF-CLM), Fisher and Rauscher are currently running CLM at high resolution (~30 km) off-line with atmospheric data forcing (NARR). In this way, CLM can be validated quickly, and we can efficiently perform mortality experiments. We know have the scripts to obtain the data from the NCAR mass store system and to convert the data into the necessary format to force CLM. The data conversion process is ongoing, as it requires obtaining 60,000 files (3 hourly data for nearly 30 years) from the NCAR mass store system, and processing them.

Impact on National Missions

This project has developed fundamental understanding of climate change and of ecological impacts. Our coupled WRF-ED-CLM model is allowing regional scale predictions of climate change and its impacts, and is leading to continued knowledge gain and model improvements. Improved understanding will allow this tool to be more accurate, greatly enhancing our ability to inform policy makers of coming changes within their regions. A subsequent LDRD DR proposal was awarded that is allowing us to take this science to the global scale. In addition, DOE-BER has funded us to conduct work on Arctic modeling and vegetation dynamics, which is a direct result of this proposal. Lastly, the work achieved through this ER is of large interest to DOE-BER for extension to the Amazon and elsewhere globally.

Publications

Fisher, R., N. G. McDowell, D. Purves, P. Moorcroft, S. Sitch, P. Cox, C. Huntingford, P. Meir, and I. Woodward. Assessing uncertainties in a second-generation dynamic vegetation model due to ecological scale limitations. 2010. *New Phytologist.* **187** (3): 666.

McDowell, N. G.. Mechanisms linking drought, hydraulics, carbon metabolism, and vegetation mortality. . 2011. *Plant Physiology.* : 10.1104/pp.110170704.

McDowell, N. G., C. Allen, and L. Marshall. Growth, carbon isotope discrimination, and mortality across a ponderosa pine elevation transect. 2010. *Global Change Biology.* **16** (1): 399.

Rauscher, S. A., F. Kucharski, and D. B. Enfield. The role of regional SST warming variations in the drying of Meso-America in future climate projections. 2011. *Journal of Climate.* : 10.1175/2010JCLI3536.1.

Seth, A., S. A. Rauscher, M. Rojas, A. Giannini, and S. J. Camargo. Enhanced Spring Convective Barrier for Monsoons in a Warmer World? . 2011. *Climatic Change Letters.* : 10.1007/s10584.

Membrane Micro-chromatography: A Novel Approach to Preparative Nucleic Acid Sample Processing

Goutam Gupta
20090363ER

Abstract
Traditionally, infectious diseases are diagnosed by monitoring symptoms that include distinct changes occurring at the tissue and organ level in mammals or plants and that can be detected by simple imaging methods. Recently, detection of biomarkers has emerged as an important part of unambiguous disease diagnosis. In this LDRD-ER project, our goal has been to develop and apply a novel method that is capable of detecting infection at a stage much earlier than the occurrence of tissue damage and organ failure. This pre-symptomatic diagnosis is achieved on Lateral Flow Microarray (LFM) platform, which is designed to detect several disease-specific gene biomarkers in a multiplex format (Figure 1). The pattern of expression of these biomarkers is indicative of initiation of a given disease with the most critical aspect of disease diagnosis being the identification and validation of disease-specific gene biomarkers. Here we describe our development of a novel and sensitive method for pre-symptomatic diagnosis, which includes the discovery of both host and pathogen biomarker genes and early detection of disease on LFM.

Background and Research Objectives
This project focused on discovering and validating a set of reliable biomarkers for seasonal flu in humans and for Pierce's Disease (PD) in grapes and adapting these for optimal performance on LFM platform [1, 2]. Once designed, the LFM was tested for pre-symptomatic diagnosis of seasonal flu using both laboratory and clinical samples [3, 4]. Biomarkers for PD were also discovered and validated.

Recognition of nucleic acid signatures on LFM involves two essential objectives (Figure 1). First, the discovery and validation of pathogen and host nucleic acid signatures for a particular type of human, animal, or plant infection. Second, the detection of amplified nucleic acid signatures on LFM to include only informative "capture" and "detection" moieties.
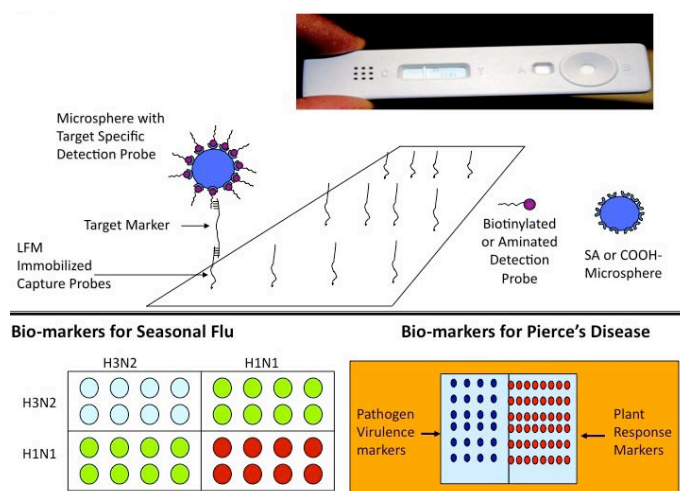
Figure 1. Architecture and design of the LFM platform for detection of nucleic acid biomarkers. (Top) Description of the device and schematics of the detection protocol. The designed capture probes are immobilized on the platform. Each probe recognizes a specific region of a target biomarker. The detection probes are attached (by amide or streptavidin-biotin linkage) to microspheres in the flow. Each detection probe binds at a site on the target gene away of the site of binding of the capture. Thus the target biomarker gene is sandwiched by the detection and capture probes and is seen colorimetrically. (Bottom) Flu bio-markers consist of host genes that determine the balance between viral growth and clearance. For two seasonal flu subtypes, i.e., H1N1 with high pathogenicity and H3N2 with low pathogenicity, we discovered markers that are common to both of them and unique to each. For PD diagnosis, we discovered genes belonging to the pathogen (Xf) life cycle and plant (grape) response genes.

Scientific Approach and Accomplishments
For the pre-symptomatic diagnosis of seasonal flu, we developed a LFM to detect host gene markers that appear in the first 24 hours of Influenza A infection and to distinguish between high pathogenic (H1N1) and low pathogenic (H3N2) Influenza A strains.
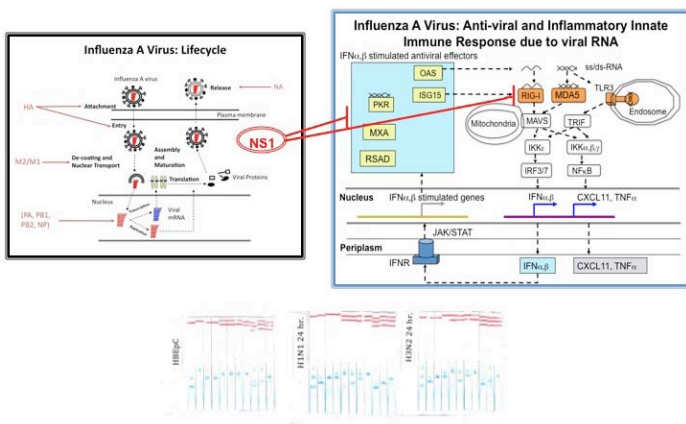
Figure 2. Discovery and utilization of human host biomarkers for pre-symptomatic diagnosis of flu. (Top Left) The viral life cycle occurs in multiple steps with involvement of different influenza proteins encoded by different gene segments. At each step, host proteins are also involved in addition to the influenza proteins. (Top Right) The primary innate immune response consists of anti-viral and inflammatory response primarily triggered by the intracellular receptors (RIG-I, MDA5, and TLR3) that recognize viral small RNA. A major component of anti-viral response is mediated by type I interferons (IFN α/β), which produce various host proteins (PKR, MXA, RSAD, etc.) that block one or more steps in the viral life cycle. Also there is feedback loop in that some of the upstream activators of the intracellular receptors (RIG-I, MDA5, and TLR3) are also induced by type I interferons. The Influenza A virus in turn tends to circumvent the anti-viral effector by NS1. While both the anti-viral effectors and the upstream activators of type I interferons are induced early by both H1N1 and H3N2 influenza subtypes, some of them induced at higher levels by low-pathogenic H3N2 than by high-pathogenic H1N1. (Bottom) The expression pattern of key anti-viral effectors and the upstream activators of type I interferons are compared in control (HBEpC), H1N1, and H3N2 after 24 hours of virus exposure. The expression pattern of these genes on lateral flow report strain specific influenza infection by either H1N1 or H3N2.

With the flu threat and other pandemics looming large, it is timely that we advance methods for detecting infections in hosts during the initial stages to facilitate better disease management. The Influenza A lifecycle consists of multiple steps (Figure 2) [5]. First, the virus attaches to the cell surface and then enters the host via a process called endocytosis. Upon entry, the influenza A virus utilizes the host machinery to complete the rest of the steps in viral lifecycle that include replication, transcription, and translation of viral RNA, packaging and assembly of viral RNA and proteins, and finally formation of viral envelop and release of mature virus particles. The host-virus interactions trigger two competing responses: one in which the host immune defense system attempts to clear the virus and the other

in which the viral machinery tries to hijack the host cellular systems to propagate its growth and establish infection [6]. Viral attachment/entry and replication/transcription/translation occur during the first 24 hours of Influenza A infection. We analyzed gene expression by whole genome microarray and validated the expression of 80 selected genes by real-time polymerase chain reaction (PCR) to inventory a small yet critical subset of human genes that define the delicate balance between the influenza A virus lifecycle and the host anti-viral innate immune defense. Indeed, we observed a substantial difference in host gene response to the high-pathogenic H1N1 and low-pathogenic H3N2 strains. The LFM detection platform contains host markers unique to H1N1 and H3N2 and common to both of them; these genes are induced relative to the negative control (Figure 2).

In addition to gene expression or level of messenger RNA, specific micro or small RNAs can also provide highly informative nucleic acid signatures of Influenza A infection. Each micro-RNA targets a specific gene and controls the level of protein produced by the gene. To take advantage of this fact, we analyzed nucleic acid samples from Lovelace Respiratory Research Institute for H5N1 (both high and low-pathogenic) infections because H5N1 represents influenza strains that jump from birds to humans whereas H1N1 and H3N2 strains can circulate in both human and swine populations concurrently. Expression analysis of human host small ribonucleic acids post exposure to H5N1 virus was accomplished using the latest bridge amplification technology in deep sequencing.

For the pre-symptomatic diagnosis of Pierce's Disease (PD), we developed a suite of nucleic acid signatures by utilizing RNA samples from transformed and non-transformed grapes. PD is caused by a gram-negative bacteria *Xylella fasitidiosa* (Xf), which is transmitted by sharpshooters to the grape xylem [7]. Xf colonization results in the clogging of the xylem and total shutdown of water transport through the grape plant. Leaf scorching appears to be the only obvious symptom of Xf-induced PD. However, visually prominent "leaf scorching" occurs 3-6 months after the initial exposure of Xf, which may be too late to protect the infected plant. We, therefore, set out to discover PD-specific biomarkers that can be monitored to predict the onset and progression of PD. For this, we chose two sets of grape plants: one (Thompson Seedless Variety) that is susceptible to Xf and the other (also Thompson Seedless, TS) that is transformed to be resistant to PD. The transgenic TS lines differ from the regular TS plants only in that they express an engineered, non-native Xf-killing protein. Previously we reported the design of this Xf-killing protein by combining both recognition and clearance functions of plant defense

(United States Patent 7432419). Several PD-susceptible and PD-resistant plants were inoculated with a million copies of Xf. Leaf scorching and xylem clogging were then monitored. The symptoms began to appear three months later. RNA samples were collected from 30 PD-susceptible plants and multiple PD-resistant lines each containing 15 plants. Real-time PCR (polymerase chain reaction) probes were designed to test the expression of 40 genes belonging to both Xf and grape genomes. By surveying literature on Xf pathogenesis and PD in grapes, we chose two classes of genes: one belonging to Xf virulence and the other corresponding to the grape pathways induced by stress and dehydration during Xf colonization. Much like using both high and low pathogenicity markers to build biomarkers on our Influenza A LFM, the use of both PD-susceptible and PD-resistant plants offered an efficient route to discovery and validation of grape biomarkers. Genes that are related to PD development should be up- or down-regulated in PD-susceptible plants. If the pattern of expression of the same set of genes were shown to reverse in the PD-resistant plants, then the trend would confirm grape biomarkers for PD. Similarly, the expression of the virulence factors in PD-susceptible plants would be higher than that in the PD-resistant plants because a significant fraction of transmitted Xf is killed in the PD-resistant plants. Figure 3 (top) shows the expression of a small subset of 6 grape biomarkers for PD. Note that the PD-susceptible and PD-resistant plants show an opposite pattern of expression. Figure 3 (bottom) shows the expression of Xf virulence genes PD-susceptible and PD-resistant plants; note that these genes are down-regulated in the PD-resistant plants. By quantifying the relative expression of candidate genes in PD-susceptible and PD-resistant plants, we selected 15 grape and 5 Xf biomarkers that are predictive of PD. The expression of these genes is independent of sampling, i.e., tissue samples from different parts of the tree show the same expression pattern. Future studies will include the design and development of a LFM to call out grape and Xf genes that present early in PD. We will then test LFM for diagnosis of PD using field samples. For this, RNA will be extracted from the leaves of grape plants suspected of being exposed to Xf via the sharpshooter vectors. The RNA collection will be performed at different time-points after the suspected exposure. The temporal pattern of the expression of both grape and Xf genes will indicate if PD will develop in the exposed grape plants. If so, one would be able to predict the time of onset. Such a diagnostic would provide a valuable tool for monitoring and managing vineyard or crop health in advance of a devastating disease outbreak.

To conclude, the successful completion of this project has resulted in the development of a crucial capability for contemporary disease management in public health, agriculture and bio-threat scenarios. It has opened numerous possibilities for collaboration with other academic institutes and industries. Currently, we are in consultation with SHARP Laboratories of America for a possible collaboration that would utilize an impedimetric test system to diagnose flu and PD using our biomarkers (Figures 2 and 3). Instead of relying on colorimetric detection as in the LFM platform, the impedimetric platform uses electrical detection in a flow device and offers some advantages over LFM.
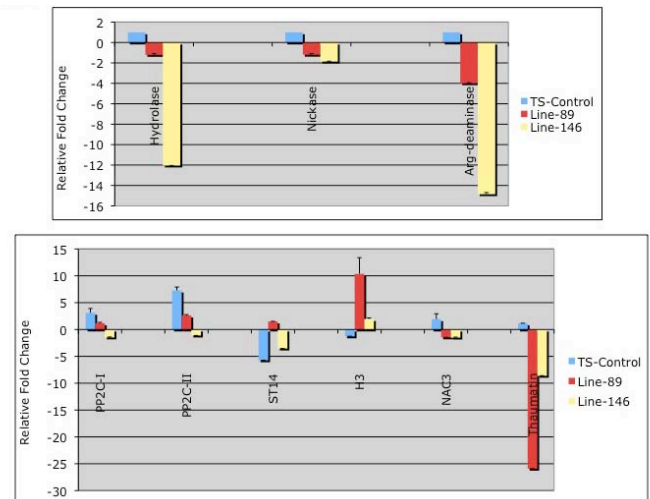
Figure 3. Discovery of key Xf and grape genes for pre-symptomatic diagnosis of PD from comparing expression patterns in susceptible and resistant (TS-89 and TS-146) grape. (Top) The prominent Xf gene regulated proteins are: hydrolase that is involved in catalysis nucleotide triphosphates into monophosphates (an essential step in DNA/RNa metabolism) and arginine deaminase involved in nitrogen cycle. Both enzymes are important in Xf life cycle. As expected, decreasing levels of Xf in resistant grapes also reduces the level of these expressed enzymes/proteins. (Bottom) The prominent grape genes are: phosphatase PP2C-II that suppresses the plant response after pathogenic infection; histone H3 that is down-regulated during apoptosis or cell death which is a PD symptom; and thaumatin (a flavor modifying protein) that is induced during infection. As expected PP2C-II is expressed at lower level in resistant grape suggesting rescue of host plant defense mechanisms whereas H3 is expressed at higher level in resistant grape suggesting decreased cell death. Also, the disease marker gene thaumatin is significantly down-regulated in resistant grape. Comparing expression patterns of Xf and grape genes in transgenic and non-transgenic plants revealed to us biomarkers that can be utilized for the pre-symptomatic diagnosis of PD.

In response to a USDA/NIFA call, we are also proposing discovery and detection of biomarkers for a citrus disease that represents a serious threat to industries across the world.

And finally, we continue the process of preparing two manuscripts for publication in peer reviewed journals:

Identification of Host Markers for Early Stages of Human Influenza A infection. Paige Pardington, Ahmet Zeytun, Anu Chaudhary, Jennifer Foster-Harris, Ruy Rebeiro, and Goutam Gupta.

Boosting of Host Innate Immunity for Protection Against Pierce's Disease in Grape. Abhaya M. Dandekar, Ana Maria Ibanez, Hossein Gouran, Federico Martinelli, Russell L. Reagan, Charles Leslie, Gale McGranahan, George Bruening, Paige Pardington, Meghan, Norvell, Anu Chaudhary, and Goutam Gupta.

Impact on National Missions

As a national security laboratory, LANL has identified Science of Signatures (SoS) as one of the thrusts relevant to redefining the lab's mission in global security. SoS develops innovative research and advanced technologies for (i) understanding the science of nuclear, chemical, and biological signatures and (ii) rapid and sensitive detection of these signatures. This project falls within the scope of SoS because it offers a proof-of-concept for identification and validation of biological signatures of infection before the appearance of disease symptoms in the host. In addition, the work carried out under this project shows how validated pre-symptomatic markers can be detected on a LFM platform. Note that, capability in pre-symptomatic diagnosis is critical to effective disease surveillance and management. Thus, the capabilities developed under this project add strength to LANL SoS while supporting LANL missions in Bio-Security Science.

References

1. Vanderhoeven, J., K. Pappaert, B. Dutta, P. Vanhummelen, G. V. Baron, and G. Desmet. Exploiting the benefits of miniaturization for the enhancement of DNA microarrays. 2004. *Electrophoresis.* **25** (21-22): 77.

2. Carter, D. J., and R. B. Cary. Lateral flow microarrays: a novel platform for rapid nucleic acid detection based on miniaturized lateral flow chromatography. 2007. *Nucleic Acids Research.* **35** (10): e74, 1.

3. Dandekar, A. M., F. Martinelli, C. E. Davis, A. Bhushan, W. Zhao, O. Fiehn, K. Skogerson, G. Wohlgemuth, R. D'Souza, R. Soumen, R. L. Reagan, D. Lin, R. B. Cary, P. Pardington, and G. Gupta. Analysis of early host responses for asymptomatic disease detection and management of speciality crops. 2010. *Critical Reviews in Immunology.* **30**: 277.

4. Zeytun, A., A. Chaudhary, P. Pardington, R. B. Cary, and G. Gupta. Induction of cytokines and chemokines by toll-like receptor signaling: strategies for control of inflammation. 2010. *Critical Reviews in Immunology.* **30**: 53.

5. Samji, T.. Influenza A: understanding the viral life cycle. 2009. *Yale Journal of Biology and Medicine.* **82** (4): 153.

6. König, R., S. Stertz, Y. Zhou, A. Inoue, H. H. Hoffmann, S. Bhattacharyya, J. G. Alamares, D. M. Tscherne, M. B. Ortigoza, Y. Liang, Q. Gao, S. E. Andrews, S. Bandyopadhyay, P. De Jesus, B. P. Tu, L. Pache, C. Shih, A. Orth, G. Bonamy, L. Miraglia, T. Ideker, A. García-Sastre, J. A. Young, P. Palese, M. L. Shaw, and S. K. Chanda. Human host factors required for influenza virus replication. 2010. *Nature.* **463** (7282): 813.

7. Redak, R. A., A. H. Purcell, J. R. Lopes, M. J. Blua, R. F. Mizell the 3rd, and P. C. Anderson. The biology of xylem fluid-feeding insect vectors of Xylella fastidiosa and their relation to disease epidemiology. 2004. *Annual Review of Entomology.* **49**: 243.

Publications

Dandekar, A. M., A. M. Ibanez, H. Gouran, F. Martinelli, R. L. Reagan, C. Leslie, G. McGranahan, G. Bruening, P. Pardington, A. Chaudhary, and G. Gupta. Boosting of host innate immunity for protection against infectious diseases. Invited presentation at *International Conference on Antimicrobial Research.* (Valladolid, Spain, 3-5 Nov. 2010).

Dandekar, A. M., F. Martinelli , C. E. Davis, A. Bhushan, W. Zhao, O. Fiehn, K. Skogerson, G. Wohlgemuth, R. D'Souza, R. Soumen, R. L. Reagan, L. Dawei, R. B. Cary, P. Pardington, and G. Gupta. Analysis of early host responses for asymptomatic disease detection and management of specialty crops. 2010. *Critical Reviews in Immunology.* **30**: 277.

Kunkel, M., M. Vuyisich, G. Gnanakaran, G. E. Bruening, A. M. Dandekar, E. Civerolo, J. J. Marchalonis, and G. Gupta. Rapid clearance of bacteria and their toxins: development of therapeutic proteins. 2007. *Critical Reviews in Immunology.* **27** (3): 233.

Pardington, P., A. Chaudhary, A. Zeytun, J. Harris, R. Ribeiro, and G. Gupta. Pre-symptomatic Influenza markers: discovery based upon early innate immune response in the human host. Invited presentation at *8th International Conference on Innate Immunity.* (Chania, Crete, Greece, 15-20 June 2011).

Pardington, P., A. Zeytun, A. Chaudhary, R. B. Cary, and G. Gupta. Early host responses due to influenza A infection. Invited presentation at *Eighth International Conference on Pathways, Networks, and Systems Medicine.* (Ixia, Rhodes, Greece, 9-14 Jul. 2010).

Pardington, P., M. Norvell, A. Chaudhary, and G. Gupta. Protection against infectious disease by boosting host innate immunity . Invited presentation at *Fifth Biological Therapeutics Research and Development .* (San Francisco, 20-22 Oct. 2010).

Zeytun, A., A. Chaudhary, P. Pardington, R. B. Cary, and G. Gupta. Induction of cytokines and chemokines by toll-like receptor signaling: strategies for control of inflammation. 2010. *Critical Reviews in Immunology.* **30**: 53.

Isotopic Tracer for Climate Relevant Secondary Organic Aerosol

Thomas A. Rahn
20090425ER

Abstract

Aerosols by definition are simply fine solid particulates or liquid droplets suspended in a gas. In Earth's atmosphere these can take many forms - from fine dust particles to clusters of inorganic molecular species to amalgams of complex organics and as a whole, they have a profound influence on Earth's radiation budget, cloud and precipitation distribution and climate. The least understood of the atmospheric aerosols are the Secondary Organic Aerosols (SOA), those aerosols that result from the oxidation and coalescence of volatile organic gaseous compounds. In this work, we have attempted to unravel some of the intricacies of the formation and evolution of these SOA by applying state of the art isotopic and ultrahigh resolution mass spectrometry techniques, as well as chemometric techniques. In particular, we have developed novel analyses of the carbon and oxygen isotopic content of SOA that have shed some insight into pathways of oxidation and details of structure that have heretofore been elusive. These techniques have been applied to SOA generated in a series of controlled experiments in our laboratory at LANL. In addition we have utilized the National High Magnetic Field Laboratory at the Woods Hole Oceanographic Institute to analyze SOA samples by ultrahigh resolution mass spectrometry, thus providing precise molecular analyses of SOA produced in these experiments. We have also collected SOA samples from several diverse environments and have secured limited follow on funding to apply our new methods and techniques toward the characterization of SOA from pristine and human influenced environments.

Background and Research Objectives

Secondary Organic Aerosols (SOA) comprise as much as 70 percent of the global carbonaceous aerosol burden by mass. Because aerosols have multiple feedback mechanisms to Earth's radiation budget, a complete understanding of the formation and fate of aerosols is imperative for understanding their influence on global climate. SOA in particular are poorly understood due to the multitude of precursors responsible for their formation and because they are a complex, heterogeneous mixture of organic species. Because the atmosphere is, in general, an oxidizing environment, the evolution from precursor organic gas species to aerosol results from reaction of biogenic and anthropogenic organic gases with various oxidizing species. The oxygen atoms that are found in SOA are derived, for the most part, from reactive oxygen species that have been shown to carry a mass independent signature in the stable isotopes of oxygen. Our research objectives were to first develop analytical methods for measurement of the stable isotopic content of SOA, specifically carbon (^{13}C:^{12}C) and oxygen (^{18}O:^{17}O:^{16}O). These methods were then to be applied to measurement of mixed carbonaceous species generated by controlled ozonolysis of biogenic volatile organic compounds (VOCs) in a laboratory setting. A third objective in our study was to perform precise molecular analyses of SOA generated in our controlled ozonolysis experiments. Our ultimate goal was then to extend these measurements to ambient atmospheric SOA samples collected in biogenic dominated regions.

Scientific Approach and Accomplishments
SOA generation

The success of our project first required the design and manufacture of a 1.5 cubic meter Teflon aerosol chamber which was installed in our laboratory space along with the requisite ozone generator as well as monitors for both inside the chamber and in the laboratory. SOA generation via ozonolysis reaction was performed with four different monoterpenes (α-pinene, β-pinene, limonene, D-carene) and one sesquiterpene (caryophyllene). This was achieved by injecting 2 ppm of the individual terpenes in to the Teflon chamber and allowing the gaseous phase terpene to react with ozone without the presence of light and OH radical scavenger under dry condition. SOA was formed right after the injection of ozone into the chamber. Particle number concentrations were recorded for this experiment. Highest particle number formation was recorded from the reaction of caryophyllene with ozone whereas ozonolysis of beta pinene yielded the list number of particles under the same condition. The produced SOA was collected on pretreated quartz fiber filters at a flow rate of 9.5 l/min

for 3 h. These filter samples were used for stable carbon isotope analysis of SOA and for detailed chemical analysis of SOA at the National High Magnetic Field Laboratory (NHMFL) using an ultra-high resolution mass spectrometer by our collaborator Lynn Mazzoleni at Michigan Technological University.

Stable isotope analysis

The stable carbon isotopic composition (_^{13}C) of total SOA was measured using an elemental analyzer (EA) coupled to an isotope ratio mass spectrometer. An example of how the ^{13}C composition of the precursor terpene material changes as a function of reaction is shown in Figure 1. In this case, limonene is reacted with ozone and small aliquots of chamber air are collected during the course of the experiment. As the limonene reacts and its concentration decreases (red symbols in Figure 1), its ^{13}C content (blue symbols in Figure 1) increases over time. From these types of measurements, the fractionation coefficient can be determined. Prior to that the _^{13}C values of the individual terpenes were measured using a bulk analysis of the liquid terpenes by EA coupled to our isotope ratio mass spectrometer, and by a gas chromatograph coupled to isotope ratio mass spectrometer via a combustion furnace (GC-IRMS). For some terpenes, up to 1‰ difference was observed between the EA and GC-IRMS measurements. We hypothesize that the reason for this difference is due to impurities in the liquid compounds used for bulk (EA) analysis. The total carbon isotope ratio (δ^{13}C) of SOA produced from ozonolysis of different terpene ranged between -32.6‰ to -28.1‰ (Figure 2). In general the δ13C value of the SOA is depleted in ^{13}C compared to their precursor material by about 1‰ with the exception of caryophyllene which is enriched by 0.9‰. Results such as these will be important for determining precursor carbon sources when interpreting analyses of true atmospheric samples.
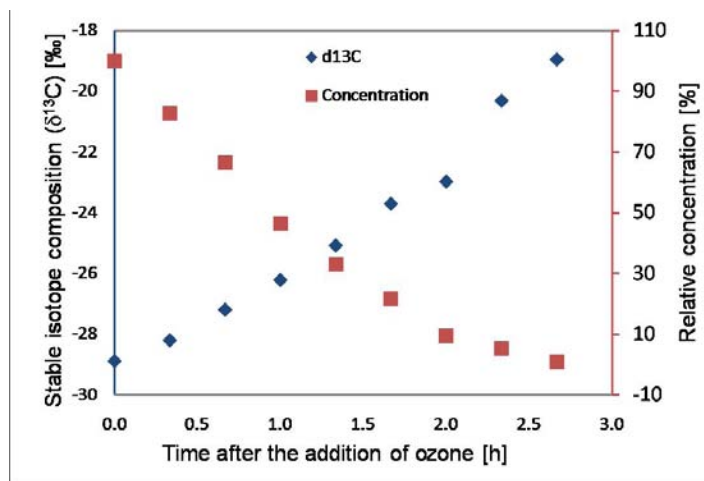
Figure 1. Example of how the 13C composition of the precursor terpene material changes as a function of time. 13C content of limonene (blue symbols) increases over time while limonene reacted with ozone decreases (red symbols).
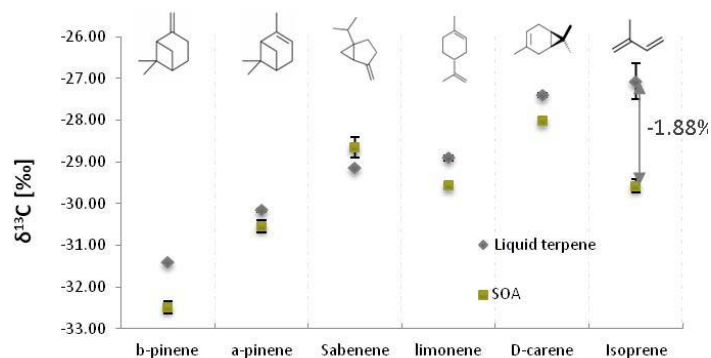
Figure 2. The total carbon isotope ratio (δ13C) of SOA produced from ozonolysis of different terpenes. Grey symbols are the precursor terpene and green symbols are the resultant SOA after reaction with ozone.

The oxygen atoms that are found in SOA are derived, for the most part, from reactive oxygen species that have been shown to carry a mass independent signature in the stable isotopes of oxygen (i.e. _^{17}O ≠0.52 _^{18}O). The ^{17}O anomaly from reactive oxygen species that is transferred to the secondary organic compound reaction products can thus serve as a quantitative signature of the pathways of SOA generation. Oxygen isotope analyses require completely different methodology in order to perform simultaneous analysis of all three O stable isotopes (^{18}O:^{17}O:^{16}O). To perform these measurements, it was necessary to develop, a new, specialized technique that first pyrolyzes (absence of O_2) SOA to form carbon monoxide (CO) which is then converted to methane (CH_4) and water vapor (H_2O) on a nickel catalyst in the presence of hydrogen (H_2) followed by conversion of the H_2O to hydrofluoric acid (HF) and molecular oxygen (O_2) by reaction with cobalt tri-fluoride (CoF_3). Given the extremely small quantities of SOA analyte that are collected in a given experiment, on the order of 100 nmol, a complex analytical technique such as that described contains many hurdles. An example of O_2 analyses performed on 5 microliter (~300 nmol) injections of reference H_2O to test the final stage of our analytical setup ($H_2O + CoF_3 \rightarrow O_2$ +HF) is shown in Figure 3. Unfortunately, we have fallen just short of completing this work within the timeframe of the ER project as the result of several time-costly delays, in particular the loss of a postdoc early in the project (to a faculty position) and time spent recruiting a replacement. In the final weeks of the project, we have also dealt with untimely down time for the mass spectrometer. Fortunately, we have secured a small amount of follow-on funding for the current postdoc to complete the analyses of archived SOA chamber based samples as well as additional environmental samples both archived, and to be collected during an upcoming field campaign.
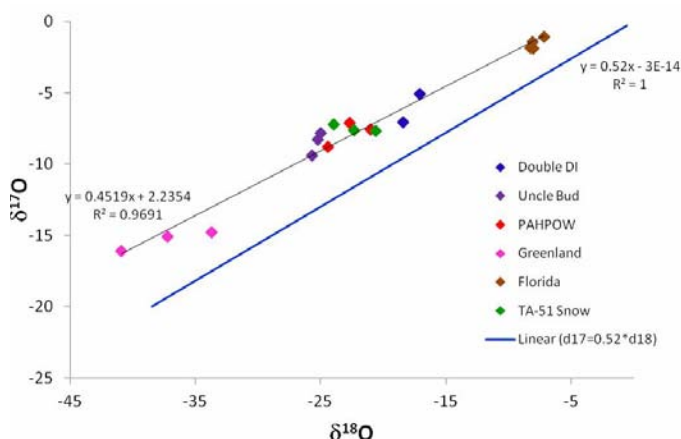
Figure 3. O_2 isotope analyses performed on 5 micor-liter (~300 nmol) injections of reference H_2O.

Ultra-high resolution mass spectrometry

We have performed a number of analyses at Michigan Technological University and at the National High Magnetic Field Laboratory at Woods Hole Oceanographic Institute. The chemical composition and formation of high molecular weight secondary organic aerosol (HMW-SOA; m/z > 300) from limonene ozonolysis was studied using electrospray ionization ultrahigh resolution Fourier transform ion cyclotron resonance (FT - ICR) mass spectrometry. Results of these analyses yield insight into the types of reactions that occur during the formation of SOA from the precursor materials. Fragmentation analysis of selected peaks (Figure 4) and the prominent DBE changes of 2 in the compound groups (Figure 5) indicate the predominance of HMW compound formation via the hydroperoxide, Criegee and hemi-acetal pathways. Most of the HMW-SOA compounds studied are composed of a few different building units. These results confirm the co-polymeric nature of HMW-SOA. Details of these analyses are in press and in review (see Dissemination, next section).
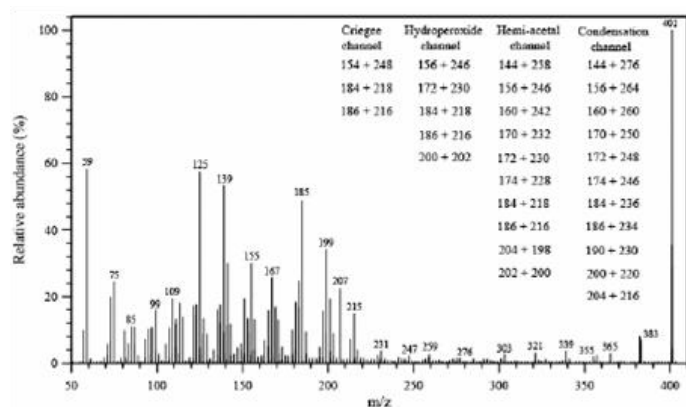
Figure 4. Fragmentation mass spectra of the most abundant peak (m/z = 401.1817) in group II. The infrared multiphoton dissociation technique (IRMPD) on the FT ICR – MS was used to fragment the selected ion. The inset shows the possible combinations of building units in each of the reaction channels that could form m/z 401. From Putman et al, in press.
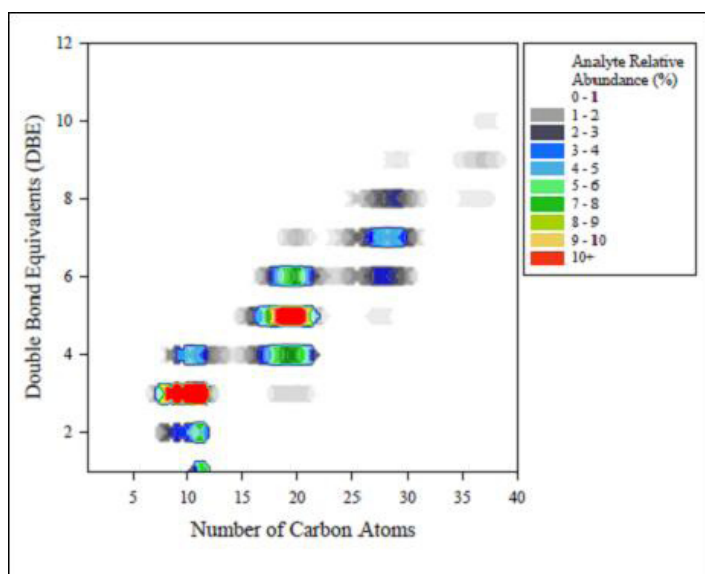
Figure 5. Double bond equivalency (DBE) as related to carbon number and ion intensity. The color gradient, with red fading through green to blue and gray, expresses the relative abundance. Only signals with ≥ 1% relative abundance are included in the plot, from Putman et al, in press.

Results

Meeting abstracts

American Geophysical Union, Fall, 2009

Aerosol Optical Properties at the Elevated Site of the Storm Peak Laboratory (3200 m a.s.l.), Colorado during Winter and Spring 2007-2008

American Geophysical Union, Fall, 2010

Molecular characterization of monoterpene ozonolysis products using ultrahigh-resolution Fourier transform ion cyclotron resonance mass spectrometry

Characterization of Secondary Organic Aerosols (SOA) from oxidation of biogenic volatile organic compounds (VOCs) using stable isotopes

Works in preparation

Derseh, Putman, Mazzoleni and Rahn, Stable isotope composition of secondary organic aerosols produced from ozonolysis of terpenes, for submission to Environmental Science and Technology.

Derseh, Putman, Larson, Mazoleni and Rahn, Triple oxygen isotope measurement in organics, for submission to Analytical Chemistry

Impact on National Missions

By identifying the production pathways of secondary organic aerosol formation, this project supports DOE's Office of Science Atmospheric Science Program's stated mission

"to develop a comprehensive understanding of the atmospheric processes that control the transport, transformation, and fate of energy related chemicals and particulate matter" and in particular the focus of "characterization of aerosol properties, and transformations". The methods and techniques developed in this project will also have applications to DOE and LANL forensic missions.

Publications

Derseh, R., A. Putman, L. Mazzoleni, and T. Rahn. Stable carbon isotope kinetic effect of the ozonolysis reaction ofLimonene and alpha pinene. *Journal of Geophysical Research.*

Derseh, R., and T. Rahn. Characterization of Secondary Organic Aerosols (SOA) from oxidation of biogenic volatile organic compounds (VOCs) using stable isotopes. Presented at *American Geophysical Union, Fall 2010.* (San Francisco, Dc., 2010).

Kundu, S., R. Derseh, A. Putman, T. Rahn, and L. Mazzoleni. High resolution mass spectrometric characterization of secondary organic aerosols from sesquiterpene ozonolysis. *Environmental Science and Tecnology.*

Mazzoleni, L., R. Derseh, A. Putman, S. Kundu, and T. Rahn. Molecular characterization of monoterpene ozonolysis products using ultrahigh-resolution Fourier transform ion cyclotron resonance mass spectrometry. Presented at *American Geophysical Union, Fall 2010.* (San Francisco, De. 2010).

Putman, A., L. Mazzoleni, S. Kundu, T. Rahn, R. Derseh, and . J. Offenberg. Ultrahigh-resolution FT-ICR mass spectrometry characterization of alpha-pinene ozonolysis SOA. To appear in *Atmospheric Environment.*

Evolving a Thermostable Cellulase by Internal Destabilization and Evolution

Andrew M. Bradbury
20090443ER

Abstract

Cellulose is the "backbone" and predominant component of all plant material. While biofuel generation has largely focused on the sugar/starch containing plant matter, these are the foundation of the global food market, whereas cellulosic materials are largely the "waste" from food production. The main research goal of this project was to create a highly thermostable cellulase that will be usable in the generation of biofuels. This would facilitate the use of cellulose as feedstock, permitting the use of otherwise marginal land and plant waste products. By carrying out this goal, we will also have carried out an important secondary goal: the demonstration of the universality of a new protein thermostabilization method we developed by its application to an important industrial enzyme. We expect success in this project to position LANL well to exploit future funding in bioenergy for which enzyme and protein thermostabilization are required.

A number of different approaches were applied to the thermostabilization of two cellulases. The most important result was the development of a new paradigm for protein thermostabilization, which will have very broad applicability (Figure 1). This involves the application of a three stage selection procedure to develop improved protein variants. In the first stage clones that are correctly folded are selected. The next step is the use of a rapid fluorescent screening assay, followed by the use of a careful functional assay. By using these three steps, we have been able to create a library of mutated cellulase clones in which a very high percentage is functional at up to 20°C higher temperature than the wild type enzyme.

By developing a new method to stabilize cellulases, this project will support the DOE mission in energy security. Cellulases are enzymes that breakdown cellulose to sugars suitable for fermentation. However, commercial cellulases tend not to be sufficiently thermostable for industrial processes, a problem we hope to solve specifically for cellulases, and generally for other enzymes involved both in biofuels and other processes.

Background and Research Objectives

In biotechnological applications, increases in protein stability lead to longer survival times, improved reaction kinetics and diminished microbial contamination. In the pharmaceutical arena, increased stability of protein therapeutics leads to longer serum half lives and more effective drugs. Proteins of increased stability are also generally more resistant to mutations than the protein from which they are derived, promoting evolvability by providing greater permissivity to mutations leading to novel functions.

A number of different methods have been developed to improve protein stability, most of which involve the creation of libraries and the identification of improved proteins by selection or screening. Conceptually, the most straightforward way has been to apply a thermal challenge to individual clones and test the remaining functionality of the clones, repeating the process if necessary to combine useful point mutations. This large scale screening method has been used to evolve a number of different proteins and enzymes esterases. A similar method, relying on selection rather than screening, involves direct selection of clones growing at elevated temperature within thermophilic bacteria, and is restricted to the natural growth temperature of the bacteria used.

As a result, considerable effort has been put into the development of alternative methods that involve selection for biophysical or biological properties that can serve as surrogates for, and are often correlated with, increased stability. An early approach was based on the discovery that second site mutations selected to overcome temperature sensitive mutations in staphylococcal nuclease conferred increased thermostability on the wild type protein. This is similar to the discovery of 'global suppressor mutations' that overcome mutations in tail spike proteins interfering with folding and assembly.

Cellulases are enzymes that breakdown cellulose, the most abundant organic material on earth. In order for cellulosic ethanol, and other biofuels based on cellulose, to become routinely used, the suite of enzymes that de-

grade cellulose to simple sugars must be improved. In particular, their themostability must be increased, and costs of production must be reduced. In this project we proposed to apply a method previously used (insertional destabilization, evolution and gene synthesis (IDEAS)) to create an extremely thermostable fluorescent protein [1] to cellulase. This involved the development of a suite of cellulase assays, and the application of IDEAS to cellulase. This proved to be more challenging than expected, but resulted in the development of a new paradigm for thermostable protein selection that will have broad applicability to other enzymes of industrial use.

Scientific Approach and Accomplishments

Establishing the system

The main research goal of this proposal is to create a highly thermostable cellulase, which would be useful in biofuel production. Before the start of this project, our laboratory had no experience whatsoever in cellulase expression or analysis. For any directed evolution project, there is need for an optimized expression system and a high-throughput screening assay. In initial experiments we cloned and expressed the genes encoding *T. reseei* celluase in E. coli, a bacterium used in research. This expression system gave measurable activity using Carboxymethyl Cellulose (CMC) as the substrate when the reaction was carried out at 50°C for 24h. We adopted two published assays for use in the laboratory, and developed a third. The first assay was Carboxy Methyl Cellulose (CMC) agar based, wherein the active clones are spread on agar plate containing CMC and the plate is stained using Congo Red dye. Haloes corresponding to CMC consumption by endoglucanase are then observed around active clones. Although we were able to successfully implement the agar assay, it was found to be too unreliable to be used routinely and was abandoned. The other assay is liquid based wherein enzyme is incubated with CMC solution and 2,4-dinitro salicylic acid (DNS) is added. Cellulase activity is seen by conversion of the color of the substrate from yellow to red. This assay was optimized for use in a high-throughput manner in 96-well microtitre plates (Figure 1). However, it proved to be relatively low throughput, with the screening of 1000 clones requiring a week. For this reason we developed a third assay, which was based on a fluorescent cellulase substrate which allowed the screening of thousands of colonies in fifteen minutes (Figure 1).

Although we were able to express *T. reseei* cellulase in bacteria, levels of expression were very low. We attempted to improve the expression in deep well plates using different bacterial host strains (such as BL21, Origami2 and RossettaBlue) and co-expression of five different chaperones (proteins that improve folding - dnaK-dnaJ-grpE-groES-groEL, groES-groEL, dnaK-dnaJ-grpE, groES-groEL-tig and tig). However, no alternative host strain or chaperone co-expression was found to improve cellulase activity or expression.
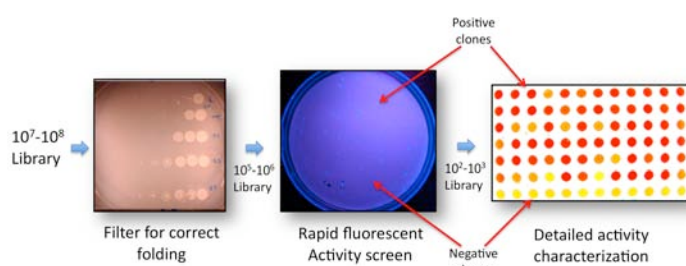
Figure 1. New screening paradigm. Large libraries of ten to one hundred million clones are first screened for correct folding, then using a rapid fluorescent enzymatic screen (center) and finally a more accurate enzymatic screen (right). Positive and negative clones are indicated in the two screens.

Improving celluase activity

The relatively low activity of this cellulase when expressed in E. coli, required us to embark upon a program to improve the cellulase activity. For this, we used a technique termed Iterative Saturation Mutagenesis at eight flexible sites within the protein. This involves identifying those amino acids that are the most mobile in the protein, and then creating small libraries in which the original amino acid is replaced with all the twenty natural amino acids. We created eight such libraries, and identified one clone Gln284Leu (I) from one of the libraries that gave improved activity. This was used as a template for a second round of saturation mutagenesis at the remaining sites followed by screening using the CMC/DNS screening method. This procedure was carried out three times, until we obtained a clone containing three mutations: Thr371Phe, Gln284Leu, Gly230Ala (III) that was able to show activity after only 30 minutes of CMC reaction (compared to 24 hours for the wild type) (Figure 2). The increased activity of this mutant allowed us to use it for the insertion of destabilizing loops.
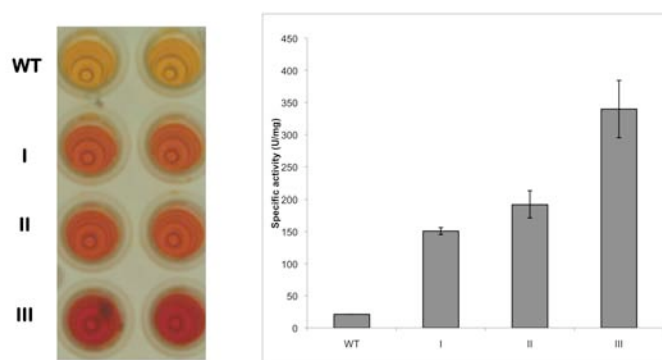
Figure 2. Improved cellulase activity created using Iterative saturation mutagenesis. I, II and III are the progressively improved forms of the wild type (wt) cellulase.

Six sites were chosen for loop insertion. The insertion of the destabilizing loops led to the expected loss of much of the activity. Mutagenesis was carried out on these six clones to recover the activity loss using a mutational tech-

nique termed error-prone PCR. Screening was carried out using the CMC-DNS based test, but after screening over 4000 clones, no mutants with improved activity as compared to the template (mutant III + loop) were observed.

This disappointing result led us to realize that an additional test prior to direct enzymatic screening was required since the mutagenesis library likely had a large population of mis-folded proteins that need to be eliminated prior to screening. For this we turned to the concept of folding reporters, of which there are many known in the literature, including ß-lactamase based filtering on ampicillin gradients, GFP-based folding reporters and yeast display. While folding reporters have been widely used to evolve proteins for improved crystallizability, they have not been used to evolve thermostability. The concept of using folding reporters in this concept is illustrated in Figure 3.
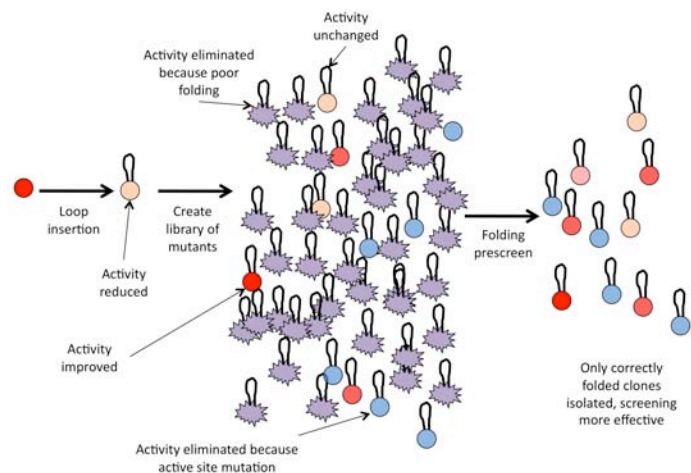
Figure 3. Depiction of the use of folding reporters to select mutants that demonstrate improved folding. By carrying out preselection for folding, the number of positive clones that are found by screening is significantly increased.

Using folding reporters

The basic idea is that the gene-of-interest is expressed along with a reporter gene and if the protein encoded by the gene of interest folds well, the reporter gene is also folded properly and gives the desired signal that can be antibiotic resistance (e.g. ß-lactamase) or fluorescence (as in the case of GFP based reporters). If the protein of interest is destabilized by the insertion of a loop, the folding reporter will select those versions of the destabilized protein that have improved folding. With the T. reesei cellulase we tested two different folding reporters: ß-lactamase and yeast display. While ß-lactamase was unfortunately ineffective for this enzyme, we were able to use yeast display. For this, the cellulase gene and the three mutants I, II and III were subcloned in a yeast display vector for expression on the yeast cell surface. We optimized the yeast display system such that the activity can be accessed directly from the cellulase displayed on yeast cells itself. We were able

to obtain good activity levels of cellulase in the yeast display system, the loop mutants were subcloned in the yeast display vector. It was observed that loop insertion reduced the enzyme activity significantly and some activity was observed in loop clones after 24h of reaction with CMC. However, attempts to evolve improved variants on the surface of yeast led to the selection of clones that had eliminated the destabilizing loops. We were able to overcome this by using an alternative destabilizing loop based on a fluorescent protein, which allowed us to directly select for those clones in which the destabilizing loop was maintained. Although we were able to demonstrate this concept in principle, the *T. reseei* enzyme continued to be difficult to work with. Consequently, we turned to another cellulase produced by *T. emersonii* that we have found more tractable.

T. emersonii cellulase

T. emersonii cellulase was expressed in E. coli and shown to be active when expressed both in the cytoplasm and periplasm as determined by the CMC/DNS test. At least six different positions were chosen for loop insertions. All the loop insertions resulted in significant decrease in activity. Like the other cellulase, we soon realized that a pre-screen was required because the CMC/DNS screen is such low throughput. However, unlike the *T. reesei* cellulase, we had been able to show in previous work that the cellulase from *T. emersonii* was active as a fusion with B-lactamase. This enabled the use of the B-lactamase screen in order to "filter" out misfolded or poorly folding clones generated in our libraries. This allowed us to select clones containing loops that had been mutated to fold better. Importantly, the use of the ß-lactamase pre-screen resulted in a 10-100 fold enrichment of our library meaning our odds of finding an improved clone were greatly enhanced (Figure 4).
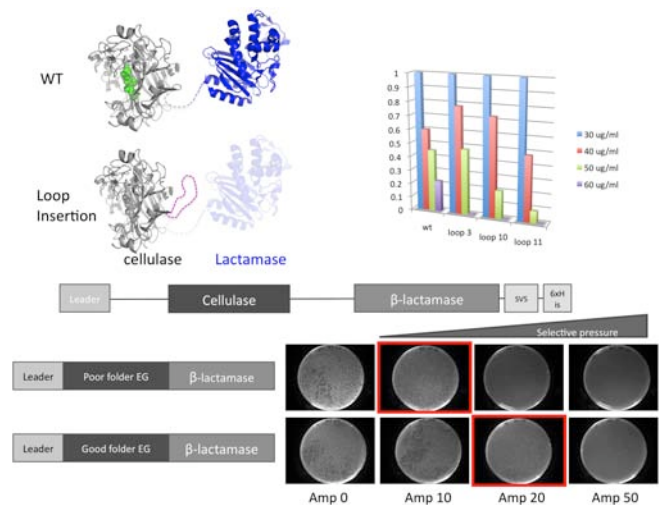
Figure 4. Depiction of the use of ß-lactamase as a folding reporter. ß-lactamase is fused to the C terminus of cellulase. Only if the cellulase folds correctly, does the ß-lactamase fold correctly, providing ampicillin resistance. The bottom panel shows that a well folding cellulase confers resistance to 20µg/ml ampicillin, while a poorly folding cellulose does so only to 10µg/ml ampicillin.

When we started to analyze *T. emersonii* within the context of this project, we had created clones that had single inserted loops with enzyme activity equivalent to the wild type enzyme. After continuing evolution with two inserted loops and ß-lactamase prescreening we have been able to carry out 6 rounds of evolution and have >30 unique clones with average activity equal to or greater than wild type activity (Figure 5).
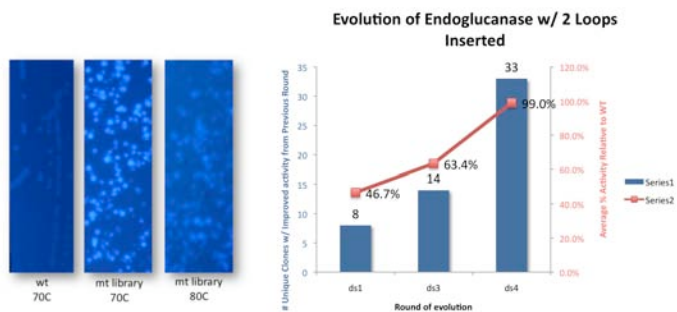
Figure 5. Comparison of the activity of wild type cellulase with a library of cellulase mutants derived after six rounds of evolution The wild type enzyme has little activity at 70°C, while the mutated library has many clones that show activity at 70°C. Some clones even show activity at 80°C. The average activity of mutated clones containing two loops increases with increasing numbers of rounds of evolution, as does the number of different mutated clones with improved activity (as determined by sequencing).

These clones contain a number of mutations that are common amongst various clones within this set and many of these mutations have been enriched from previous rounds of evolution. The mutations are found throughout the protein implying that the evolutionary process is generating mutations throughout the protein to overcome the destabilizing force of loop insertions. This implies that we are in fact evolving a gene that encodes a protein that is more robust and able to withstand the insertion of two loops, a significant amount of destabilizing force. To test if our process is working and see whether these mutations improved the stability of the protein when the loops are removed, we next made a library in which the mutations were shuffled and the destabilizing loops were removed. This new library, which contains millions of different clones, was tested for activity at increasing temperatures. We found that at least half of the clones in this library had substantially improved activity at higher temperatures relative to the wild-type cellulase. At 60°C wild type enzyme had activity comparable to many of the clones within the library, but when tested at higher temperatures, such as 70°C, the wild type clone had essentially no activity whereas the library still had a substantial number of clones with activity levels comparable to activity at 60°C. Many of the clones within this library even had activity at 80C (Figure 5). This implies that there are mutations within this library that confer a significant amount of thermostability to the cellulase. This screen was carried out using the plate based fluorescence

assay and tested protein produced in bacteria.

Future plans

To confirm our results with proteins found in bacteria, we need to isolate single clones and test the relative stability of proteins that have been purified and tested at equal concentrations. In addition, the final step of our evolution technology (IDEAS) is synthesis of genes containing consensus mutations that are enriched in our improved clones. This is a required step to truly optimize a clone containing all of the most beneficial mutations because statistically it would be nearly impossible to expect that we could pull this clone out of our library by chance. This demonstrates that even after only two loop insertions into our gene and evolution around these insertions we attain a substantially improved cellulase. Since there are at least six other sites for loop insertions in this protein, this implies that we can improve this enzyme even further.

Impact on National Missions

By developing a new method to stabilize cellulases, this project will support the DOE mission in energy security. Cellulases are enzymes that breakdown cellulose to sugars suitable for fermentation. However, commercial cellulases tend not to be sufficiently thermostable for industrial processes, a problem we hope to solve. Furthermore, this problem applies to many other industrial enzymes, including ones involved in biofuels production. By improving the thermostability of cellulases and developing a method generally applicable to other industrial enzymes, this work will impact national energy security.

References

1. Kiss, C., J. Temirov, L. Chasteen, G. Waldo, and A. M. Bradbury. Directed evolution of an extremely stable fluorescent protein. 2009. *Protein Engineering Design & Selection.* **22** (5): 313.

Staphylococcus Aureus Virulence Factor Interaction with Host Proteins (CFS)

Geoffrey S. Waldo
20110443ER

Abstract
The proposed research supports a long-term goal of understanding host-pathogen biology in order to develop effective means to: (1) prevent disease and infection (2) treat existing infection by virus or bacteria, especially those employing secreted protein factors that modify or thwart innate and adaptive immunity. Staph and many pathogens secrete effector proteins into tissue or cells to interfere with host immunity (Figure 1). The specific near-term goals of this project are to develop supporting technologies to allow study of movements of multiple pathogen effector proteins and their interactions with host proteins. To accomplish this goal well-characterized model systems of pathogen/host interactors were used where the affinity of the interactors have been independently established. This way the relative level of the fluorescent readout of the assay was correlated with the known affinity of the interacting proteins. Specific interactors as well as non-interactors are used. This supplies much-needed data regarding the ability of the assay to report on the presence or absence of interactions of pathogen proteins and host proteins. By benchmarking the protein interaction technology, it can then be used to draw inferences about the relative importance of measured interactions using the split GFP assay. We were able to construct a model system for Staph infected tissue and monitored protein secretion from cells supported in a gel matrix using our split fluorescent protein reporters. In particular, additional color variants were engineered to enable future proposals using multiplex labeling (multiple targets detected simultaneously), and optimized versions of split protein based on Corynactis california fluorescent protein were engineered that don't cross-talk with GFP. *This means scientists can now, for the first time, monitor multiple effectors using these different tags and illumination/viewing colors.* The results will be used to support program development collaborative NIH proposals directed to NIIAD.

Background and Research Objectives
The objective is to validate a set of double and triple split fluorescent proteins that can be used to label protein complexes, including optimizing a set of split GFPs for cyan and yellow colors; to use these in a protein-protein interaction assay in living cells; and to use them in an immobilized bead format to validate protein complexes, a validation and benchmark needed to study secreted proteins such as those produced by Staphylococci.
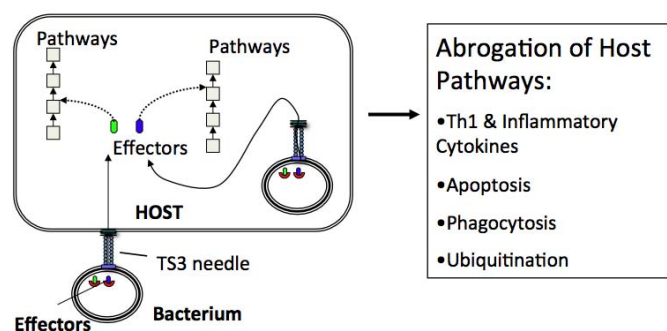
Figure 1. Depiction of secretion of virulence effectors into host cells by pathgens such as Staphylococci.

Scientific Approach and Accomplishments
Our approach for protein-protein interaction detection uses a split GFP 3-body system as depicted in Figure 2. As depicted our approach is to target virulence proteins that are secreted and label with small split fluorescent protein pieces. The effector is secreted into the milleu where the fluorescent protein tag binds to and interacts with the rest of the fluorescent split protein. 2 body GFPs of different colors can be used to detect the target and the effector (secreted protein) independently due to their unique colors. Interactions between host and effector proteins are detected using the 3 body GFP. This way the effector, host protein, and the interaction level can all be simultaneously quantify expression and interaction. Since we were not able to work with virulent Staphylococcus directly, we employed a physical model system. This is similar in approach to using tissue models for respiratory infection. In our model, E. coli cells were immobilized in a hydrogel to simulate Staph cells residing in a tissue they have invaded. Release of the S11 tagged proteins from the E. coli is used as a functional model system in which the E. coli cells act in lieu

of virulent Staph cells, and the immobilized GFP 1-10 acts as a tagged host cell protein in a tissue in which the Staph would reside.
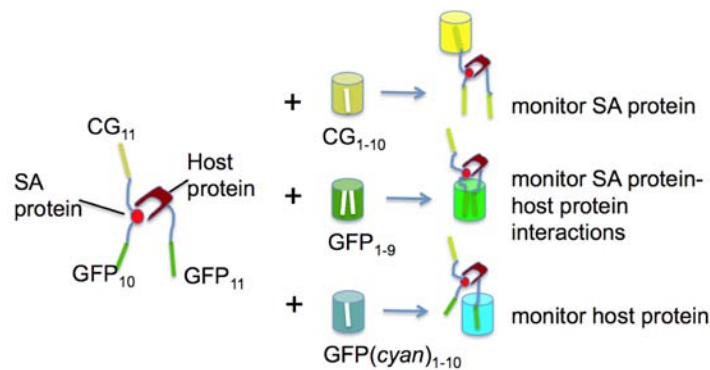
Figure 2. Use of yellow and cyan variants from non-cross talking split fluorescent proteins derived from Corynactis california (CG) and GFP to independently and simultaneously monitor concentrations of all test proteins, as well as green GFP 1-9 to monitor protein interactions.

Validating 2 body and 3 body protein detection using the new GFP 1-9 we developed during this project
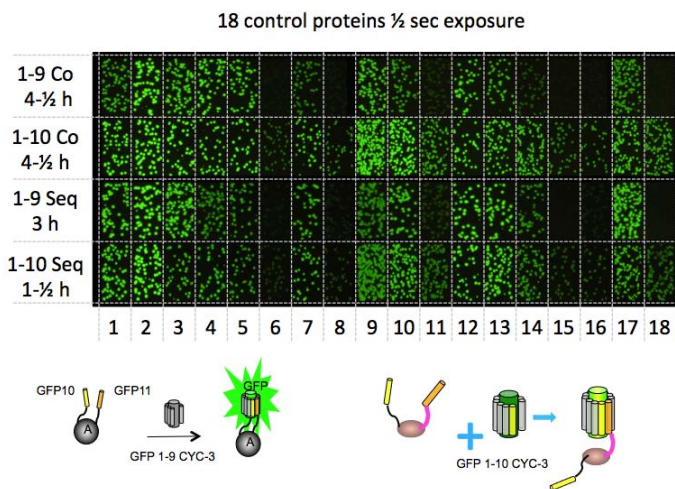
Figure 3. Test of using either GFP 1-9 or GFP 1-10 to detect proteins labeled with N-terminal GFP S10 and C-terminal GFP S11. GFP 1-9 must bind both 10 and 11 to become fluorescent. GFP 1-10 need only bind S11 (see Schema, lower inset). Simultaneous expression of tagged and detector protein (Co), transient expression of tagged protein followed by detector protein (Seq). Even at long times GFP 1-9 appears to detect only the soluble proteins, while GFP 1-10 can detect both soluble and insoluble proteins when co-expressed.

Dual plasmids were used to express the 18 control proteins from P. aerophilum and the detector proteins, labeled as S10-X-S11. We found that the three body system gave fluorescence only in the case of soluble proteins, regardless of whether the tagged protein or detector was expressed at the same time or sequentially. The GFP 1-10 gave a signal

proportional to soluble protein when sequentially expressed, or total protein when simultaneously expressed. This led us to conclude that the S10 and S11 would need to bind nearly simultaneously to the 1-9 in order to be detected. The lack of signal for insoluble proteins only for 1-9 is consistent with this model…likely the protein aggregates prior to the two strands being able to find the 1-9. In the case of the GFP 1-10, only one recognition event need happen, suggesting the binding is fast enough to occur prior to aggregation (Figure 3). *This supports the schema depicted in Figure 2, that we can set up detection that can selectively monitor 1 or both split protein tags.*

Testing the new color variants of GFP and CalGrn split GFP for multiplex labeling

We were able to individually detect GFP S11, CalGrn S11 tags in cells or in the test tube. Split cyan variant of GFP (CFP) and CalGrn split GFP are distinct spectroscopically (Figure 4). In particular GFP 1-10 is not detected when illuminated with 520nm light and viewed with 550 nm filter, and is thus 'invisible'; under the same conditions YFP 1-10 is easily detected. More importantly, illumination with 488nm light and viewing with 510 nm filter selectively visualizes proteins tagged with Corynactis S11 and detected with Corynactis strands 1-10. Under these conditions proteins labeled with YFP are 'invisible.' *This means scientists can now, for the first time, monitor multiple effectors using these different tags and illumination/viewing colors.*
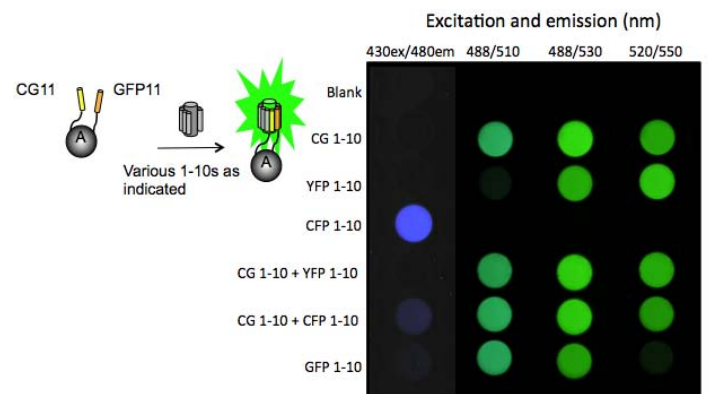
Figure 4. Demonstration of specific tag detection using various 1-10 domains (color variants, and different non-cross-reacting fluorescent proteins) (left column, indicates each row is a different experiment with 1-10s). Indicated 1-10 fragment was mixed with the CG11-Sulfite reductase-S11 GFP test protein then imaged. Columns show different excitation and emission windows. CalGrn (CG). GFP 1-10 does not recognize CalGrn S11, and CalGrn 1-10 does not recognize GFP S11. The cyan GFP 1-10 is spectroscopically distinct from GFP and CalGrn. Cyan GFP 1-10 and 'yellow' GFP 1-10 can be distinguished from each other.

Agarose microdrop bead assay for secreted proteins

We were able to clearly detect S11-tagged proteins re-leased from bacteria that were encapsulated in agarose that had bound GFP 1-10 attached to it. As the S11-tagged protein diffused from the bacteria, it was captured by the immobilized GFP 1-10 and the beads turned green fluores-cent as expected (Figure 5). Release of the S11 tagged pro-teins from the E. coli is used as a functional model system in which the E. coli cells act in lieu of virulent Staph cells, and the immobilized GFP 1-10 acts as a tagged host cell protein in a tissue in which the Staph would reside.
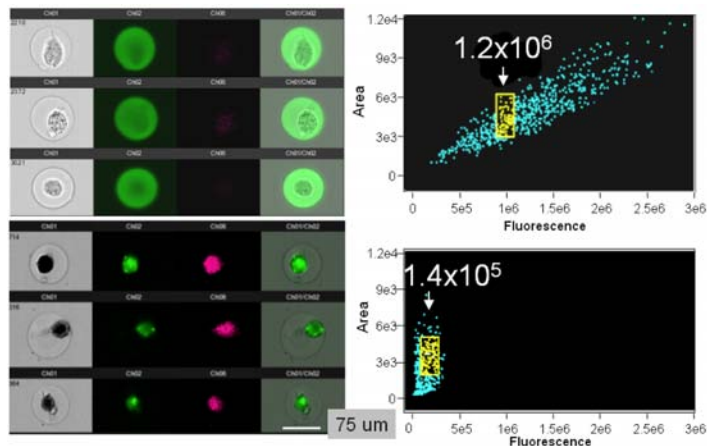
Figure 5. Feasibility of S11 protein capture in 1-10 decorat-ed gel microdrops. First part of microdrop assay (minus the RFP detection) applied to soluble purine-nucleoside phos-phorylase (top) and insoluble phosphate cyclase (bottom). Flow microscope Amnis photos (left), FACS showing ca. 10-fold difference in signal between soluble and insoluble protein (right). Note scattering from inclusion bodies (pink) in GMDs for insoluble protein. Single bacteria expressing the protein were encapsulated in 40 um diameter agarose that had been decorated with GFP 1-10 biotin.

Impact on National Missions
While the underlying technology we have developed is sophisticated enough to perform many assays in high-throughput format at low cost when fully matured. In order to gain wide¬spread acceptance the methodology must be carefully validated using experiments that are te-dious, precise, and involve living systems and considerable human and experimental resources. We achieved the goal of our small feasibility project. The preliminary data will be used to write competitive research proposals to exploit the technology for understanding host/pathogen biology. This directly supports the lab mission in human health and biosurveillance.

Publications
Lockard, M., P. Listwan, J. Pedelacq, S. Cabantous, H. Nguy-en, T. Terwilliger, and G. Waldo. A high-throughput immobilized bead screen for stable proteins and multi-protein complexes. 2011. *Protein Engineering Design & Selection.* **24** (7): 565.

Towards Rapid Development of Immunomodulatory Drugs (CFS)

William S. Hlavacek
20110446ER

Abstract

This project was focused on the development of assays for direct binding interactions of proteins that play an important role in innate immunity, such as MyD88, myeloid differentiation primary response gene. We demonstrated the usefulness of the assays by using them to study how a bacterial protein involved in the pathogenesis of Brucellosis interacts with MyD88. We anticipate that the assays developed in this project will be useful for obtaining a basic understanding of the molecular mechanisms by which the immune system detects and responds to infection. We also anticipate that the assays will be useful for screening libraries of small-molecule compounds to identify potential drugs. In addition to the experimental work, this pilot project also involved computational/theoretical work as part of an effort to develop systems biology expertise and capabilities at LANL. To complement the experimental work, we developed a theoretical framework for computational modeling of protein interactions involved in innate immunity. This pilot project successfully generated preliminary data that will support our mission in systems biology and threat reduction and be useful for competing for external funding to continue and expand research at LANL focused on innate immunity and bio-security science.

Background and Research Objectives

The main goal was to develop assays for protein-protein interactions involved in Toll-like receptor (TLR) signaling, especially interactions of the adapter protein MyD88, which is involved in 9 of the 10 TLR pathways in humans. TLR signaling pathways play an important role in innate immunity, which is our front-line defense against infection. TLRs bind to molecules that are peculiar to pathogens, such as lipopolysaccharide (a cell membrane component of gram-negative bacteria), and trigger alarm signals and inflammation. Sometimes, the inflammation triggered by TLR signaling does more harm than good, as in acute respiratory distress syndrome (ARDS), which is triggered by many viral and bacterial infections. To treat ARDS, it would be beneficial to have drugs capable of turning off TLR-mediated inflammation. Clues about how to accomplish this goal are provided by the immune evasion mechanisms of pathogens. Pathogens, such as *Brucella* bacteria (which cause Brucellosis), sometimes express proteins (e.g., the protein TcpB in *Brucella*) that bind to MyD88 and thereby interfere in TLR signaling and limit pathogen clearance by the immune system. By seeking to develop assays for direct interactions of proteins with MyD88, we sought to develop a capability to characterize the manner in which proteins such as TcpB bind to MyD88 to subvert immune responses and a capability to discover through screening protocols small-molecule drug-like compounds that bind to MyD88 similarly. Recently, it has been discovered that MyD88 is overexpressed in some forms of cancer. Thus, compounds that bind to MyD88 may be useful for treating not only ARDS but also cancer.

A secondary goal of this project was to develop preliminary computational models for TLR pathways. Signaling pathways are complex and models are needed to help us understand how molecularly targeted drugs can be used to alter signaling behavior.

Scientific Approach and Accomplishments

We developed protein-fragment complementation assays for direct binding interactions of MyD88 based on green fluorescent protein (GFP) and *Gaussia* luciferase wherein domains of MyD88 and potential binding partners of MyD88 are fused to complementary fragments of enzymes, which when brought together through an interaction produce a detectable fluorescence signal. We demonstrated the feasibility of these assays for detecting direct binding interactions by using the assays to characterize interaction of the TcpB protein with MyD88 (Chaudhary et al., submitted). We found that interaction of TcpB with MyD88 depends on the death domain in MyD88. We developed a theoretical framework for visualizing and annotating large-scale mechanistic models of signaling pathways (Chylek et al., 2011).

The manuscripts cited above and other preliminary experimental and computational results, including studies of MyD88 homodimerization and specification of a preliminary model for the TLR4 pathway, lay the groundwork for competing for external funding to build a re-

search program at LANL focused on quantitative character-ization of TLR signaling. It is anticipated that an external grant will be prepared with Dr. Chaudhary, who is now at University of Washington, once the manuscript about TcpB has been accepted for publication. This grant application will request funding for modeling work at LANL. It is also anticipated that a grant application focused solely on mod-eling work will be submitted. A number of manuscripts are currently in preparation.

Impact on National Missions

This work enhances our mission capability in science of sig-natures tied to threat reduction. Human health is an im-portantd component of our national security mission. The research studied here has impact on our understanding of the innate immune response to foreign agents.

Publications

Chaudhary, A., K. Ganguly, S. Cabantous, G. S. Waldo, S. N. Micheva-Viteva, K. Nag, W. S. Hlavacek, and C. S. Tung. The Brucella TIR-like protein TcpB interacts with the death domain of MyD88. *Biochemistry.*

Chylek, L. A., B. Hu, M. L. Blinov, T. Emonet, J. R. Faeder, B. Goldstein, R. N. Gutenkunst, J. M. Haugh, T. Lipniacki, R. G. Posner, J. Yang, and W. S. Hlavacek. Guidelines for visualizing and annotating rule-based models. 2011. *Molecular BioSystems.* **7**: 2779.

A Comprehensive Study of Host-Influenza Virus (A/B) Interactions at the Single Host Cell Level (CFS)

Kumkum Ganguly
20110449ER

Abstract

Infections, whether natural or engineered, present great threats to public health and national security. Detecting these infections in the earliest stages and designing appropriate countermeasures is a challenging task. In order to accomplish this, it is necessary to develop a thorough and quantitative understanding of key pathogen machineries that are utilized to subvert host immune defense and establish infection. Influenza type A and influenza type B viruses are the two main etiologic agents of influenza infection in humans, causing yearly seasonal epidemics. These result in high morbidity and billions of dollars of economic losses in the USA every year. Moreover, in some years most cases are due to influenza A and in others influenza B is more prevalent. Both viruses evolved from a common ancestor, but currently there is no indocation that they reassort their genomes, that is, they do not seem to exchange genetic material, as occurs among viruses of the same type. The reason for this behavior is not well understood, as it has been shown that viral particles mixing influenza A and B proteins *in vitro* are viable, and that the replication machinery of influenza A recognizes the promoter regions of influenza B. It is also known that these viruses can infect the epithelial cells in the respiratory tract at similar degree, even though the viruses' surface glycoproteins are different. In addition, it has been shown that the surface glycoproteins (neuraminidase and hemagglutinins) of influenza B can be productively used by influenza A viruses. We have studied this puzzle of influenza virus genome reassortment by studying the lifecycle of influenza A in comparison to that of influenza B, and by performing competition infection experiments at the single cell level. This has been done using imaging flow cytometry (Amnis Image Stream X) to measure important parameters in the viral lifecycle and the interaction of the viruses at the level of single host cells. Our long term goal is to understand how evolution shaped the lifecycle of these two viruses in such a way that they can no longer reassort. Moreover, this work will help elucidate the unique adaptations in pathogenicity and lifecycle of influenza B (beyond surface glycoprotein differences) that make it an exclusive human pathogen compared to influenza A,
a virus with a wide host range (human, swine, horses, bird etc). This knowledge will be instrumental in better management of yearly influenza epidemics and sporadic pandemics.

Background and Research objectives

Influenza type A and influenza type B viruses are the two main etiologic agents of influenza infection in humans, causing yearly seasonal epidemics. These result in high morbidity and billions of dollars of economic losses in the USA every year. Moreover, in some years most cases are due to influenza A and in others influenza B is more prevalent [1]. Both viruses evolved from a common ancestor, but currently do not seem to reassort their genomes, that is, they can not exchange genetic material, as occurs among viruses of the same type. The reason for this behavior is not well understood, as it has been shown that viral particles mixing influenza A and B proteins *in vitro* are viable [2], and that the replication machinery of influenza A recognizes the promoter regions of influenza B [3]. It is also known that these viruses can infect the epithelial cells in the respiratory tract at similar degree, even though their surface glycoproteins are different [4]. We proposed to study this puzzle of influenza virus genome reassortment by studying the lifecycle of influenza A in comparison to that of influenza B, and by performing competition infection experiments at the single cell level. This was be done using imaging flow cytometry to measure important parameters in the viral lifecycle and the interaction of the viruses with the host cells.

Our long term goal is to understand how evolution shaped the lifecycle of these two viruses in such a way that they can no longer reassort. This may also reveal the mechanisms of virulence of these viruses, and what are the similarities and differences. Moreover, this work will help to elucidate the unique adaptations in pathogenicity and lifecycle of influenza B (beyond surface glycoprotein differences) that make it an exclusive human

pathogen compared to influenza A, a virus with a wide host range (human, swine, horses, bird etc). This knowledge will be instrumental in better management of yearly influenza epidemics and sporadic pandemics.

Another important goal of this pilot project was to contribute towards establishing a capability for high-throughput studies of the structural and functional responses of single cells to infection by respiratory pathogens. This utilized a newly acquired imaging flow cytometer and combine expertise in experimental biology with modeling and theoretical biology. Such a study of cell systems at the single cell level needs to combine molecular and microscopic experimental techniques with modeling to understand the molecular structure and functionality of the cell system. We hypothesized that there are further differences, for example, at the replication stage that explain the lack of reassortment and correlate with the high host specificity of influenza B. Our study helped to understand these differences studying at the single cell level, thus considering the heterogeneity of the cell population. This may ultimately help establish signatures of viral respiratory diseases with possible application to identification of new emerging and engineered pathogens at a very early stage of infection.

Scientific Approach and Accomplishments

During this project, we have standardized a procedure to label influenza virus by lipid staining dyes DiD (1,1´-dioctadecyl-3,3,3´,3´-tetramethylindodicarbocyanine) and DiO (3-octadecyl-2-[3-(3-octadecyl-2(3H)-benzoxazolylidene) -1-propynyl]) (from Molecular Probes, Invitrogen). The viruses were incubated with the dyes in a carbonate buffer (pH 9.3) at R/T for 2hrs. In both cases unbound dyes were removed via buffer exchange into 50mM HEPES biffer using gel filtration columns [5]. The labeled viruses were quantified using standard plaque forming assays. We recovered 10^8-10^9 PFU/mL viable viruses .We produced labeled stocks of two influenza A viruses [A/Beijing/95 (H1N1) and A/Sydney/5 (H3N2)] and two B viruses [B/Lee and B/Herbin] for infection study. We have conducted experimental infections exposing human lung epithelial cells (A549) to influenza virus at different MOI (multiplicity of infection) 1, 2 and 4 and measured the kinetics of viral internalization and localization of the viruses at single cell level (Figures 1-3).

A: Histograms representing the internalization frequency of IAV *vs.* IBV

B: Representative images from each histogram

C: Internalization % of IAV and IBV at MOI:1

Influenza A & B viruses were stained with lipid staining dye DiD (red) (Invitrogen). Surface bound viruses were stained with primary antibody mouse anti-Influenza A or B followed by secondary goat-anti-mouse AlexaFluor 488 . Cells were scanned by Amnis Image StreamX (Amnis Inc. WA). Red dots and red graphs represent internalized viruses. Green dots and graphs represent viruses on the surface.

Figure 1. Kinetics of internalization of influenza virus in human lung epithelial cells (A549) Multiplicity of infection (MOI): 1

A: Histograms representing the internalization frequency of IAV *vs.* IBV

B: Representative images from each histogram

C: Internalization % of IAV and IBV at MOI:2

Influenza A & B viruses were stained with lipid staining dye DiD (red) (Invitrogen). Surface bound viruses were stained with primary antibody mouse anti-Influenza A or B followed by secondary goat-anti-mouse AlexaFluor 488 . Cells were scanned by Amnis Image StreamX (Amnis Inc. WA). Red dots and red graphs represent internalized viruses. Green dots and graphs represent viruses on the surface.

Figure 2. Kinetics of internalization of influenza virus in human lung epithelial cells (A549) Multiplicity of infection (MOI): 2

A: Histograms representing the internalization frequency of IAV *vs.* IBV

B: Representative images from each histogram

C: Internalization % of IAV and IBV at MOI:4

Influenza A & B viruses were stained with lipid staining dye DiD (Invitrogen). Surface bound viruses were stained with primary antibody mouse anti-Influenza A or B followed by secondary goat-anti-mouse AlexaFluor 488 . Cells were scanned by Amnis Image StreamX (Amnis Inc. WA). Red dots and red graphs represent internalized viruses. Green dots and graphs represent viruses on the surface.

Figure 3. Kinetics of internalization of influenza virus in human lung epithelial cells (A549) Multiplicity of infection (MOI): 3

For this study we have exposed the lung cells to labeled viruses [red in color] at different MOI for one hour to al-

low the viruses get adsorbed on the cell surfaces. After this one hour of exposure the unbound viruses were removed from the cell surfaces by aspiring the medium containing viruses. The cells were incubated with fresh medium at 37°C to allow the internalization of viruses. The cells were harvested at different time points and then fixed with 4% paraformaldehyde. The surface bound viruses were stained with mouse anti-influenza A and anti-influenza-B antibodies respectively. These primary antibodies were successively labeled with green fluorescence tagged anti-mouse antibodies. These cells were then scanned with Amnis imagestreamX (National Flow Cytometry Resource; NIH Grant P41-RR01315; LANL) to determine the percentages of internalized viruses in the cell population. We scanned 25000 cells per experimental conditions in a high-throughput assay and used the spot counting feature of the instrument to quantify the red spots (representing internalized viruses) *vs.* green spots (representing viruses on the cell surface). We have observed that Influenza A and B virus exhibit different percentages of internalization (40% in case of A virus *vs.* 90% in B virus at MOI 1 at 8 hrs) in human lung A549 cells (Figures 1-3). In a separate batch of experiments we have exposed A549 cells to different A viruses and also A & B viruses at MOI 1 and followed the exposure for 24 hrs to track the invasion of multiple viruses to a single cell causing 'super-infection.' Our preliminary results showed that both influenza A&B viruses can infect a single cell (Figure 4).

A: Co-infection of A/Beijing/262/95 (stained in red) and A/Sydney/5 (stained in green)

B: Co-infection of A/Beijing/262/95 (stained in red) and B/Herbin (stained in green)
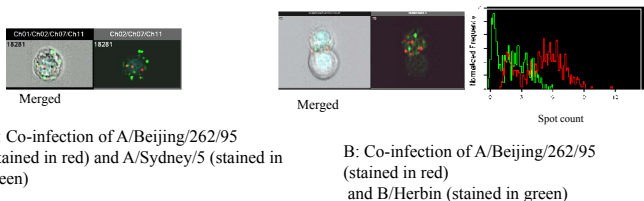
Figure 4. Identification of co-infection of different influenza viruses at single cell level.

On the modeling side, we developed and coded a preliminary model for influenza infection lifecycle (Figure 5). This model follows the transcription and translation of each of the segments of influenza virus upon cell infection. We model the transport of virion nucleoprotein and mRNA between the cytoplasm and the nucleus. We used published studies on the concentrations of different RNA types and proteins in infected cells to calibrate and validate the modeling. Our work was focused on determining the appropriate structure of the interactions among these molecular species and characterizing the parameters of the model. Preliminary fits of the data indicate that we are approaching a predictive model, but more work needws to be done to fully implement the model. We intend to use this model (Figure 5) as a resource to interpret and quantify the re-

sults of the single cell flow cytometer experiments.
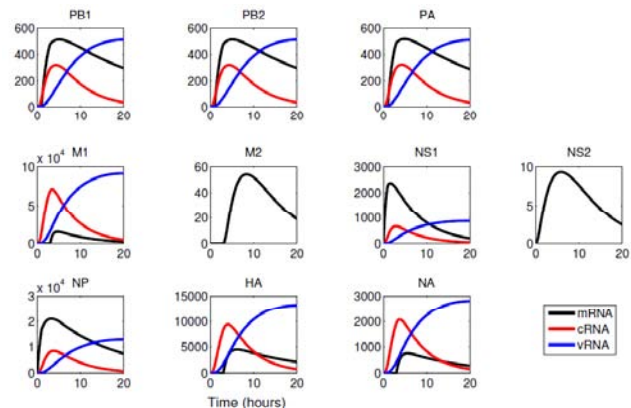
Figure 5. Influenza Replication Model Simulation

In this "Mission Incubator Feasibility Study" study we have

- established procedure to track Influenza virus at single cell level with Amnis Image Stream Cytometer

- observed that Influenza A & B viruses showed different kinetics of internalization in human lung cells.

- seen co-infection of Influenza A & B in cell culture (Human A 549 cells)

- developed a preliminary model for the influenza infection lifecycle

- established several new collaborations and the new capabilities that we have developed, including virus tracking in vitro in human cells, will position us to better contribute to the control of influenza in the U,S.

Impact on National Mission

Infections, natural or engineered, present great threats to public health and national security. Their early detection, design of countermeasures and consequence management are challenging tasks that depend on a systemic understanding of the host-pathogen interaction. This project developed the capability to characterize influenza infection by two different viruses at single cell level, by high throughput assays. The ability to make phenotypic measurement on single cells will complement the bulk measurement genomics, proteomics, and metabolomics efforts that are already established LANL strengths in the Biosciences. These capabilities will form a cornerstone of the biosecurity science, and the project provided preliminary data while demonstrating a new capability, all of which enhance external funding potential.

References

1. A, G. A. Flandorfer. Chimeric influenza A viruses with a functional influenza B virus neuraminidase or hemagglutinin. 2003. *J Virol.* **77**: 9116.

2. Lakadamyali, M., M. J. Rust, H. P. Babcock, and X. Zhuang. Visualizing infection of individual influenza viruses. 2003. *Proc Natl Acad Sci U S A.* **100** (16): 9280.

3. Manicassamy, B., S. Manicassamy, A. Belicha-Villanueva, G. Pisanelli, B. Pulendran, and A. Garcia-Sastre. Analysis of in vivo dynamics of influenza virus infection in mice using a GFP reporter virus. 2010. *Proc Natl Acad Sci U S A.* **107** (25): 11531.

4. Muster, T., E. K. Subbarao, M. Enami, B. R. Murphy, and P. Palese. An influenza A virus containing influenza B virus 5' and 3' noncoding regions on the neuraminidase gene is attenuated in mice. 1991. *Proc Natl Acad Sci U S A.* **88** (12): 5177.

5. Raj, A., P. van den Bogaard, S. A. Rifkin, A. van Oudenaarden, and S. Tyagi. Imaging individual mRNA molecules using multiple singly labeled probes. 2008. *Nat Methods.* **5** (10): 877.

Publications

Ganguly, K., J. F. Harris, and R. M. Ribeiro. A Comprehensive Study of Host-Influenza Virus (A/B) Interactions at the Single Host Cell Level . Presented at *XXVI International Congress of the International Society for Advancement of Cytometry (Cyto 2011).* (Baltimore, 21-25 May, 2011).

Neutron Reflectometry Determination of Fluid Properties at Salt Interfaces - Proof of Concept (CFS)

Donald D. Hickmott
20110452ER

Abstract
Understanding and controlling interface processes for salts, especially at moderate pressures (P) and temperatures (T), is crucial for a range of energy and environmental applications, particularly in salt repositories such as those at the Waste Isolation Pilot Project (WIPP) or at future salt-hosted high-level waste repositories. Specifically, the deformation and transport properties of NaCl/fluid aggregates are controlled by interface processes. We propose to develop a new LANL capability in experimental neutron science to address key questions concerning NaCl/fluid interface phenomena. We will develop and implement new high-T capabilities for the Surface Profile Analysis Reflectometer (SPEAR) neutron reflectometry beamline at LANSCE and study ambient T to high-T NaCl/fluid interface properties, particularly fluid densities, from ambient conditions to fluid boiling conditions. Understanding fluid/salt interfaces at a fundamental level opens up the possibility of manipulating surface structures and free energies and thereby manipulating flow in salt-dominated subsurface environments.

Background and Research Objectives
Dissolution and precipitation processes at salt (halite, sylvite, other chloride salts) interfaces in high pressure-temperature (P-T) brines control the deformation and transport behavior of salt aggregates in Earth's subsurface. Understanding elevated P-T properties of these minerals' interfaces is crucial for a range of energy and environmental applications. Salt/fluid interactions may control the success or failure of high-T salt-hosted geologic sites that may be proposed for future nuclear waste repositories. In this proof- of-concept study we attempted to use neutron reflectometry (NR) to probe halite-fluid interfacial density profiles as a function of T and fluid composition (degree of oversaturation/under-saturation).

Little experimental attention has focused on salt/fluid interfaces at high P or T because relevant surface analytical methods are difficult to implement at such conditions. NR [1,2] represents a potentially powerful technique for examining fluid properties, particularly density, near salt interfaces at high T, because of the ability of neutrons to penetrate high P-T cells [3,4] and because of their sensitivity to hydrogen (deuterium) in brines using contrast matching techniques. NR thus represents a novel method for high T interface studies – both for salt/brine systems and solid/fluid systems in general.

Halide salts (NaCl - halite, KCl - sylvite etc.) are important phases in a wide-range of energy/environmental applications. In particular, halite is a major phase at the Waste Isolation Pilot Project (WIPP) [5] and will be the key phase to understand in a salt-hosted nuclear repository. Importantly, the thermal load associated with high-level wastes may change the transport properties of salt. In addition, salt plays a key role as a caprock for some oil and gas deposits, and brine-rich fluids (at or near salt saturated) occur in some deep-saline aquifers considered for geologic carbon sequestration.

Halite interfaces have been investigated extensively at ambient conditions (room T and P) during the past two decades. Salt/fluid surface free energies control both the deformation behavior of salt and the porosity and permeability of polycrystalline halite. *In-situ* deformation studies of halite/fluid have shown that pressure solution in salt is rate-limited by diffusion through an interfacial medium [6]. These studies of pressure solution have also hypothesized the existence of a strongly adsorbed (i.e. structured) interfacial water layer present at halite interfaces during plastic deformation. However, the nature of this fluid has not been investigated using direct surface interrogation methods.

Studies of dihedral (wetting) angles between halite and aqueous and CO_2-rich fluids have elucidated the variations of fluid connectivity in polycrystalline halite as a function of P, T, and fluid composition [7,8]. These studies have indirectly constrained the surface free energies for halite/halite interfaces and for halite/fluid contacts. The H_2O-halite dihedral angle is a function of P and T and decreases monotonically with both P and T. Most importantly, the dihedral angle decreases (becomes

more hydrophilic – promoting wetting and rapid fluid flow) to below 60° at ~200 C at ambient pressure (Figure 1), suggesting fluids begin to form interconnected networks at this T, whereas at lower T, the dihedral angles suggest confinement of fluids to grain corners. This change may have important implications for fluid-flow behavior in salt repository environments, where temperature may increase above 200° C during thermal loading. This scientific problem may be the largest technological barrier to potential use of salt beds for high-level waste disposition.
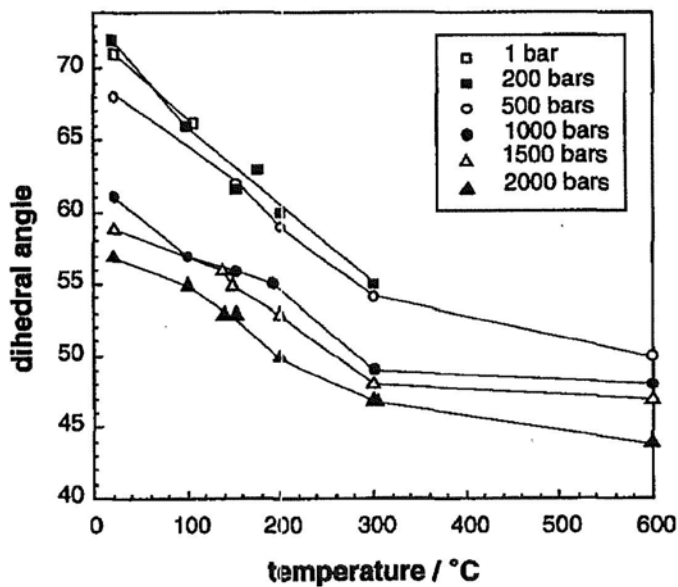
Figure 1. Dihedral angle as a function of T for H_2O-halite system at various Ps. (after Holness and Lewis (1997)).

Infrared spectroscopy has been used to interrogate the interfacial fluid structures and diffusive properties in halite aggregates at ambient T and moderate P [9]. These authors demonstrate slower diffusion in grain boundary fluid (by an order of magnitude) than in bulk fluid at similar P-T conditions. These results are in conflict with electrical impedance measurements [10], which suggest that diffusion in wet grain boundaries in polycrystalline halite is 5-6 orders of magnitude lower than in bulk water. Clearly the behavior of fluids at halite interfaces, particularly at elevated P or T, remains controversial.

This one year, proof-of-concept project focused on two interrelated objectives: 1) designing and building a high T cell for NR with capabilities to hundreds of degrees C, and 2) using existing cells coupled with the new cell to interrogate halite/brine interfaces, first at ambient conditions and then at elevated T.

Scientific Approach and Accomplishments

Temperature Cell Development

We constructed and tested a new high P-T cell capable

of NR measurements from ambient conditions up to Ts of 200°C and Ps of 30,000 pounds per square inch (psi) (Figure 2). This cell allows experiments to be conducted in simulated crustal conditions up to 6 km depth. The cell is constructed of anodized aluminum (7075 T6 alloy), has a piston-based pressure system to allow small volumes of fluid to be equilibrated with samples at high P-T, and contains powder wells to enable saturation of experimental fluids with salts at high P-T. The cell sample chamber is designed to hold sample disks up to 2 inches (in.) in diameter and 15 millimeters in thickness. Pressure is imparted by a hand pump and T can be precisely controlled using conductive heating inserts and thermocouples connected to a proportional–integral–derivative (PID) temperature controller. A stainless steel wrapped enclosure filled with KAOWOOL Moldable Mastic is used to thermally insulate the cell from the environment. Two thinned areas in the aluminum walls serve as the neutron windows, through which the neutron beam enters and exits.
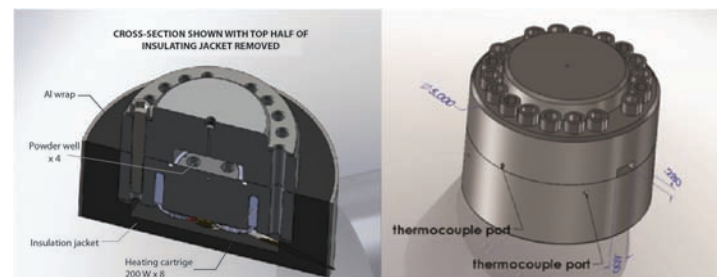
Figure 2. Left: Cross-section of the pressure-temperature cell with thermal control system embedded; Right: Thermocouple positions in the closed cell. Cell diameter = 5 in.

NR Experiments

We obtained a 2 in. diameter halite disk that was potentially suitable for NR experiments (Figure 3). We characterized this using surface profilometry, which showed that the long range surface smoothness was ~ 5 micrometers (µm) (Figure 3), making it a promising sample for neutron interrogation, although true angstrom (Å)-level smoothness must be determined through reflectometry techniques. The halite disk was analyzed using the Los Alamos Neutron Scattering Center's (LANSCE's) Surface Profile Analysis Reflectometer (SPEAR) instrument, a Time-Of-Flight (TOF) neutron reflectometer with a wavelength range from 4.5 Å to 16 Å (Figure 4). Unfortunately, the high neutron absorption associated with [35]Chlorine (Cl) in the natural salt sample attenuated the neutron signal by over 99 %, rendering it impractical for the NR experiment , with only the critical edge able to be resolved from the reflectivety data. This result was unexpected because NaCl assemblies are typically used in high P-T experiments in the TAP-98 cell at LANSCE [4].
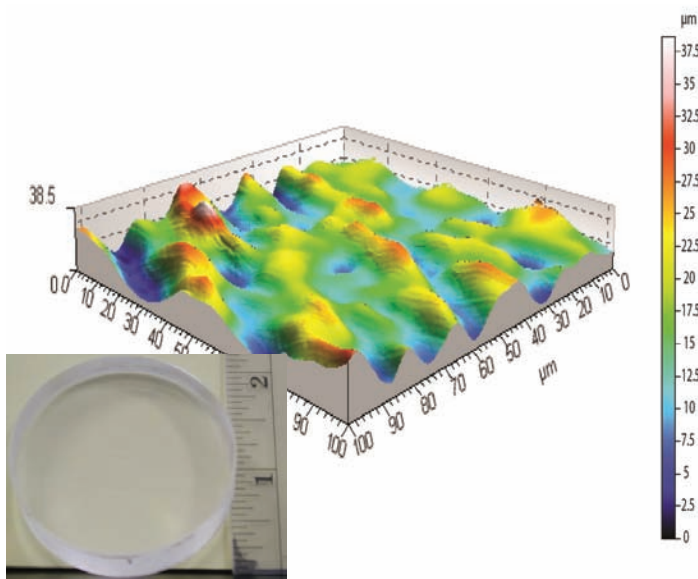
Figure 3. Optical Surface Profilometer image of 0.1 x 0.1 mm area of halite disk. RMS roughness = 5.39 um. Inset: Photo of 2 in. halite disk.
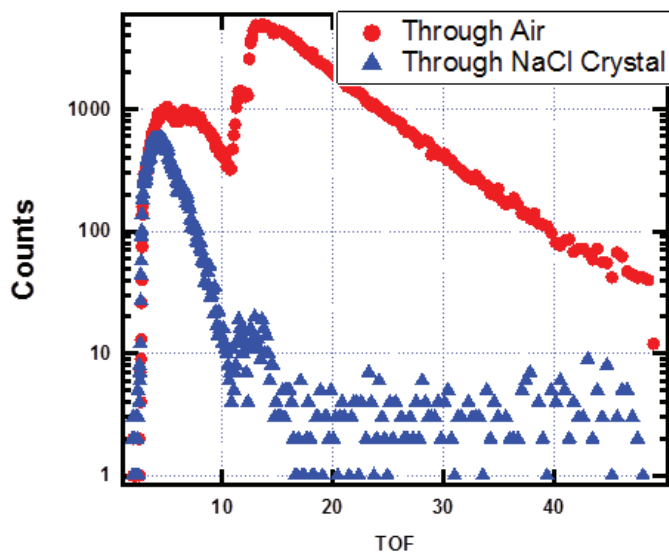
Figure 4. Neutron absorption spectrum through air vs. through NaCl single crystal showing significant neutron attenuation.

Next Steps

We envision two potential paths forward to enable NR experiments on salt-fluid interfaces to be successfully completed in the new cell: 1) interrogated salt crystals could be composed of [37]Cl-enriched material; [37]Cl has much lower neutron absorption compared to natural chlorine (0.021 cm^{-1} vs. 1.01 cm^{-1} neutron absolute cross-sections, respectively). Unfortunately, [37]Cl enriched materials are expensive (~ $30,000/gram from Oak Ridge National Laboratory), so a much more extensive project would be needed to complete these types of experiments. 2) Thin-film atomic layer deposition (ALD) techniques could be developed

that would allow [35]Cl halite films to be deposited with thicknesses of ~100 nanometers (nm), which would not significantly attenuate the neutron beam. ALD deposition of halite on germanium (Ge) (100) may potentially produce halite surfaces with acceptable flatness [11-13]. Our calculations show that depending on the smoothness of the film, a layered sample of SiO_2 wafer coated with ~20 nm of Ge, with a 200 nm halite film grown on top will enable us to resolve structured water on the halite surface. Other potential directions for this research would be to engage theorists to perform molecular dynamics calculations of halite/fluid interactions at elevated P-T.

Impact on National Missions

Understanding the behavior of mineral-fluid interfaces at Ps and Ts relevant to the Earth's subsurface is crucial for many national energy sectors. Such mineral-fluid interface interactions are important for developing geothermal resources, geologic carbon sequestration, extraction of oil and gas, and design of nuclear waste repositories – particularly salt repositories. Halite-fluid interactions at elevated Ts are particularly important if salt-hosted high-level waste repositories will be considered in our future national nuclear energy strategy. The new high P-T NR cell we have designed and built, will be widely applicable to developing a fundamental understanding of such mineral-fluid interactions, in particular for halite in the presence of heated waters. It also may be useful for broader materials corrosion processes, such as the degradation of fuel elements and cladding materials in nuclear reactor environments.

References

1. Doshi, D. A., P. B. Shah, S. Singh, E. D. Branson, A. P. Malanoski, E. B. Watkins, J. Majewski, F. van Swol, and C. J. Brinker. Investigating the interface of superhydrophobic surfaces in contact with water. 2005. *Langmuir.* **21** (17): 7805.

2. Doshi, D. A., E. B. Watkins, J. N. Israelachvili, and J. Majewski. Reduced water density at hydrophobic surfaces: Effect of dissolved gases. 2005. *Proceedings of the National Academy of Sciences of the United States of America.* **102** (27): 9458.

3. Lokshin, K. A., and Y. Zhao. Advanced setup for high-pressure and low-temperature neutron diffraction at hydrostatic conditions. 2005. *Review of Scientific Instruments.* **76** (6): 63909.

4. Zhao, Y. S., R. B. von Dreele, and J. G. Morgan. A high P-T cell assembly for neutron diffraction up to 10 GPa and 1500 K. 1999. *High Pressure Research.* **16** (3): 161.

5. Lambert, S. J.. Geochemistry of the Waste Isolation Pilot Plant (WIPP) site, southeastern New Mexico, U.S.A. 1992. *Applied Geochemistry.* **7** (6): 513.

6. Hickman, S. H., and B. Evans. Kinetics of pressure solu-

tion at halite-silica interfaces and intergranular clay films. 1995. *Journal of Geophysical Research.* **100** (B7): 13113.

7. Lewis, S., and M. Holness. Equilibrium halite-H2O dihedral angles. 1996. *Geology.* **24** (5): 431.

8. Holness, M. B., and S. Lewis. The structure of the halite-brine interface inferred from pressure and temperature variations of equilibrium dihedral angles in the halite-H2O-CO2 system. 1997. *Geochimica et Cosmochimica Acta.* **61** (4): 795.

9. Meer, S. de, C. J. Spiers, and S. Nakashima. Structure and diffusive properties of fluid-filled grain boundaries: An in-situ study using infrared (micro) spectroscopy. 2005. *Earth and Planetary Science Letters.* **232** (3-4): 403.

10. Watanabe, T., and C. J. Peach. Electrical impedance measurement of plastically deforming halite rocks at 125o C and 50 MPa. 2002. *Journal of Geophysical Research.* **107** (B1): ECV2.

11. Barjenbruch, U., S. Folsch, and M. Henzler. Surface states on epitaxial thin films of NaCl and KCl. 1989. *Surface Science.* **211/212**: 749.

12. Folsch, S., U. Barjenbruch, and M. Henzler. Atomically thin epitaxial films of NaCl on germanium. 1989. *Thin Solid Films.* **172**: 123.

13. Glocker, M., M. Sokolowski, A. Soukopp, and E. Umbach. Initial growth of insulating overlayers of NaCl on Ge 100 observed by scanning tunneling microscopy with atomic resolution. 1996. *Physical Review B (Condensed Matter).* **54**: 7705.

Publications

Hickmott, D., A. Lerner, P. Wang, J. Majewski, and M. Taylor. : Neutron reflectometry at elevated pressures and temperatures ? Novel p-t cell and preliminary experiments . To appear in *American Geophysical Union Annual Meeting.* (San Fransisco, 4-9 Dec. 2011).

Sample Receipt and Characterization of Unique Actinide Samples from LANL Environmental Sites

Robert C. Roback
20110517ER

Abstract
This LDRD project takes advantage of the unique opportunity to study actinide-bearing environmental samples from the world's oldest contaminated weapons Pu processing site at LANL's Technical Area 21. The LDRD team was able to obtain several samples from different sites at TA-21 during its remediation and to conduct characterization studies on some of these samples. Characterization was carried out at LANL and using the Scanning TEM at the University of Nevada at Las Vegas (UNLV) and the Synchrotron at Stanford University. The remainder of these samples and others, which have not yet been studied, are archived at the CMR and TA-48. Two talks were given, one at the LANL Pu-Workshop and the other as an invited presentation at the Annual Meeting of the American Chemical Society in Denver, CO. Two papers are in preparation: one summarizes results of plutonium solubility by ligands in Material Disposal Areas (MDA) -B soil, and a second describes X-ray Absorbance Spectroscopy (XAS) results from soil samples also from MDA-B

Background and Research Objectives
This project was funded through LDRD reserve and the team worked closely with LANL Environmental Programs (EP) while they conducted remediation and planning for remediation of three sites at Technical Area (TA) -21. Many sites at TA-21 are currently being investigated by LANL's Environmental Programs (EP) Directorate to assess environmental risk and to determine remediation strategies. Through these sampling efforts (for which costs will exceed $10M), our team had access to unique and otherwise unobtainable samples. Identifying the phases formed, their stability, and mechanisms for actinide release and transport is critical for environmental management. This information is vital to fulfill our goal of understanding fundamental mechanisms of actinide behavior in environmental settings.

Scientific Approach and Accomplishments

Material Disposal Area (MDA) - B is a trench, which was used for solid waste disposal in the mid -1940's. Most of the material disposed of in this trench is non-radioactive or contains very low levels of radioactivity. However; higher levels of radioactivity were encountered sporadically as excavation of the trench progressed. Working with LANL Environmental Programs (EP), we were able to obtain samples, each approximately 0.5 kg of soil, from four different locations in the trench. These samples are contaminated with Pu and Am at levels of approximately 0.1 to 1.0 mCi/g.

Samples were also obtained from the General's Tanks, which consist of 2 steel tanks, each 60' long and 12' in diameter. They were used in 1946 to store Pu- and Am-bearing precipitates derived from early Pu-purification operations. The Pu and Am reside in chemical sludges, and as crusts on the steel walls of the tanks and support structures. Some of the LDRD team participated in a LANL EP-funded project that planned and eventually sampled this material. This leveraging allowed collection of several samples from each of the tanks at no cost to this LDRD project and freed up funds to focus on characterization efforts. Several samples of sludge and crusts are now archived at CMR and TA-48 and available for further study.

No sampling was performed at MDA-T this past year, due to decisions made by EP. Rather, during 2011, LANL EP was engaged in development of a sampling plan to be implemented in 2012 or 2013. Through this LDRD project we were able to participate in planning meetings to help guide sampling needs and methods.

Most of the sample characterization performed for this project was done on samples from MDA-B. LANL EP funded extensive characterization of General's tanks sludge and sediment samples and these data provide an excellent foundation for future studies. A small amount of characterization of General's tanks samples was performed as part of this LDRD study.

MDA-B gravity settling experiments

Our initial experiments on MDA-B soils consisted of gravity-settling experiments performed to separate the different grains and aggregates of the soil according to

their size and mineralogy. The goal of performing these experiments is to determine if there is preferential association of plutonium with specific mineral phases or specific particle fractions. The experiments were performed by suspending the soil in groundwater and allowing it to equilibrate until the start of the settling experiment. Different soil fractions were collected at different settling times and their mineralogy, size distribution, and radiological content determined. We found that plutonium was most concentrated in the finest fraction of the soil (0.1 to 0.2 um), which is composed of mainly fine clay particles. We also found that plutonium is associated with the solids and that the concentration of any soluble species present is below our detection limits. Our data show that plutonium and other radionuclides associated with contaminated soils can be concentrated to up to 30 times over the concentration in the bulk soil. The different fractions collected were used for some preliminary characterization by Transmission Electron Microscopy, Energy Dispersive X-ray Spectroscopy (TEM-EDX), and bulk X-ray Absorption Fine Structure (EX-AFS). Select particles from the different fractions separated were also analyzed using micro-X-ray Fluorescence to establish plutonium distributions and elemental associations. Important findings from the settling experiment are:

- In all experiments, >50% of the total Pu was partitioned into fine fractions; most Pu is liberated in the first wash.

- Pu concentrations increase considerably in the finest fractions.

- Pu in ultracentrifuges supernatant is not detectable (using LSC) indicating very low solubility in natural groundwater.

MDA-B Synchrotron and TEM Results

Subsamples derived from the gravity-settling experiments described above from two samples were analyzed by EXAFS and micro-X-ray Fluorescence at the Stanford Synchrotron (SSRL) during two analytical sessions, one in February 2011 and the second in June 2011. We identified plutonium in 11 particles and obtained X-ray Absorption Near Edge Spectra (XANES), and EXAFS data on a bulk soil sample as well as 4 plutonium-bearing particles, 2 from one sample and 2 from a second sample. The five EXAFS analyses we obtained essentially *doubles* the number of such analyses known *worldwide* from environmental samples and reveal information that will force reevaluation of our understanding of plutonium speciation under environmental settings. This information was presented at the annual meeting of the American Chemical Society (Roback et al, 2011, invited talk) and is in preparation for publication. Results are summarized below.

Elemental concentration measurements determined using micro-X-ray Fluorescence reveal correlations and spatial

distribution of plutonium and other elements. Eleven plutonium-bearing particles from two soil samples were analyzed; the following associations were identified:

- Relatively pure Pu Particles (3 particles)

- Relatively pure Pu particles associated with Fe-bearing particles (2 particles)

- Particles of Pu+Fe admixtures associated with Fe particles (4 particles)

- Pu+Cu admixtures on Fe particles

We successfully obtained EXAFS measurements from four of the eleven particles described above and from a bulk soil sample; examples are shown in Figure 1.

The EXAFS spectra from a particle with a good correlation between Fe and Pu (top spectra in Figure 1) show well defined peaks at 2.3 Å and another at 3.8 Å. The peak at 2.3Å is modeled as the Pu-O shell and the peak at 3.8Å corresponds to the Pu-Pu shell. This spectra is typical of disordered PuO_2 In contrast, spectra from two other particles from the same sample (Figure 1, bottom spectra) do not show peaks beyond the Pu-O shell at 2.3Å. This spectra is also similar to that of the forth particle as well as the bulk sample (not shown). These spectra are interpreted to indicate that, while the plutonium is present as a $PuO_{2,}$ it is in a highly disordered state.
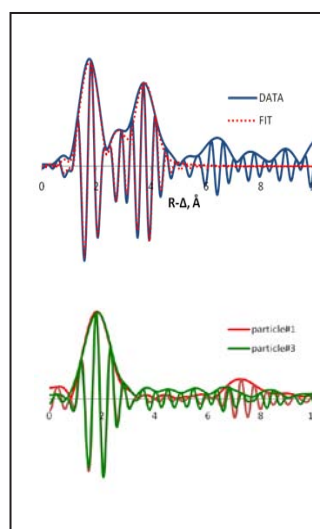
Figure 1. EXAFS spectra obtained from the analysis of pure plutonium particles associated with iron

We also analyzed subsamples from the fractions obtained by the gravity-settling experiments by TEM-EDX, performed at UNLV. The EDX data confirmed the abundance of Ti- and Fe-bearing particles along with unusually high levels of Cu and also revealed the presence of some interesting elemental concentrations such as Osmium, present at ppm levels, which is many orders above natural abun-

dance. Unfortunately, we were unable to identify any pure plutonium phases in the natural samples analyzed using the TEM (perhaps due to either insufficient measurement sensitivity or insufficient instrument time); and thus we did not obtain crystallographic information as was one of our goals.

We conducted an experiment meant to mimic a known depositional scenario for plutonium at TA-21. In this experiment we leached a sample of native Bandelier Tuff obtained from the site in 4.0 M nitric acid. We removed the supernatant, along with tuff colloidal material, spiked this solution with plutonium and then raised the pH to precipitate the Pu along with other dissolved rock constituents. Samples from this experiment were also examined by TEM at UNLV. Plutonium was identified in several occurrences associated with distinct colloidal grains as well as within amorphous mats of material. Transmission electron microscopy revealed that plutonium in both types of occurrences was present as a non-crystalline, amorphous form.

MDA-B leaching experiments

We examined plutonium mobilization from MDA-B soils by natural siderophores and synthetic ligands. Our results show that plutonium and other radionuclides associated with MDA-B soils are easily released in the presence of relatively low concentrations of natural and synthetic chelators. EDTA and NTA, which are often co-disposed with radionuclides, are the most efficient at solubilizing plutonium. Natural siderophore desferrioxamine B was also effective at solubilizing plutonium. Under our specific experimental conditions we found that the rate of plutonium solubilization is up to 1000 times faster than the rates of plutonium solubilization reported in the literature for synthetic freshly precipitated PuO_2 materials. Our data highlight the high reactivity of the plutonium forms in MDA-B soils and the ease by which Pu can be mobilized by synthetic and natural ligands. This study is in contrast with previous investigations that examined plutonium environmental speciation and that concluded that plutonium is only present as stable and uncreative oxides under environmental conditions and highlights the risks of plutonium transport in the environment as soluble solutes or in association with mobile colloids.

Impact on National Missions

Numerous unique actinide bearing samples from TA-21 were collected and are archived at the CMR or TA-48. These samples likely represent the oldest Pu-contaminated environmental samples in the world. Our initial characterization work has shown that previously held views of Pu environmental behavior will require substantial revision. Continued investigation of samples collected through this study and elsewhere at TA-21 will undoubtedly transform our understanding of the environmental behavior of plutonium and associated actinides, which is an important goal for DOE's Office of Environmental Management.

Plant Growth Technology – Increasing Our Scientific Leadership Position and Our Impact

Pat J. Unkefer
20110519ER

Abstract

Nitrogen fertilizer production for the developed nations consumes about two percent of the total energy used globally. Thus, there is great value in making more extensive use of the biological process of nitrogen fixation in which N_2 is reduced to NH_3 and subsequently used to supply this chemically reduced nitrogen to the growing plant. We focused on engineering plants to enhance the symbiotic nitrogen fixation and overall performance of a model legume. Our approach was to engineer plants to selectively manage the concentration of a plant growth regulating compound. We successfully created a gene construct with the appropriate promoter, gene sequence and antibiotic resistance gene. We used this construct to transform *Medicago truncatula*, a commonly used model and commercial legume. Several healthy transformed seedlings were produced. Additional work was done to support a licensee of a related genetic technology that provided additional data related to the concentration and role of the growth regulating compound in plant roots.

Background and Research Objectives

Nitrogen is a growth-limiting nutrient for plants and consequently must be used efficiently. As we have recently shown, plants monitor their N status and regulate their overall metabolism and growth accordingly (1). We discovered this fundamental regulatory mechanism including the N-signaling metabolite and successfully re-engineered plants to increase their CO_2 fixation, primary C and N metabolisms and growth. But managing these systems is only a part of what is required for energetically sustainable biofuels and food production. Plants are not only consumers of nitrogen, some of them--legumes such as soybean or our model *M. truncatula*--also partner symbiotically with specific bacteria to fix atmospheric N_2 into biologically useful NH_3 and, as such, contribute significantly to the global N cycle [1]. The bacterium provides the N_2 fixing machinery; the plant supplies photosynthetically derived energy. N_2 fixation is energetically expensive and consequently must be regulated by the plant. Little has been known about this regulation beyond the observation of suppression by an abundant exogenous N supply [2-4]. Our discovery of the N status signaling metabolite also revealed a fundamental insight into what governs the extent and productivity of this legume-bacterial relationship. Increased metabolite signals abundant N; in a leaf this signal triggers faster CO_2 fixation, metabolisms and growth; whereas in a legume root, it apparently triggers suppression of the unneeded and energetically expensive N_2 fixation. We are uniquely positioned to discover how this signal is used to regulate symbiotic N_2 fixation and subsequently to manipulate it for the benefit of our emerging biofuels industry.

Original objectives

We sought to understand how N metabolite-mediated suppression of symbiotic N_2 fixation operates in a representative legume, *Medicago truncatula*. We wished define the gene and metabolic response networks for the apparent N-metabolite suppressor, 2-oxoglutaramate. We sought to engineer our model legume to degrade the 2-oxoglutaramate *in vivo* to defeat the suppression and examine the effects on N_2 fixation.

One promising approach to successfully manipulating photosynthetic growth is based on our discovery of the mechanism that plants use to assess their nitrogen nutrient status and its function as a "master switch" triggering very vigorous photosynthetic growth and greater overall productivity. This switch is the cellular concentration of 2-oxoglutaramate (2-OGM), a small molecule synthesized from the amino acid glutamine that is formed when nitrogen is first assimilated into the plant's metabolism. The first generation of our technology throws this switch by managing the concentration of 2-OGM by either treating plants with 2-OGM or genetically manipulating expression of two enzymes, phenylpyruvate transaminase (GPT) and glutamine synthetase (GS), which are responsible for 2-OGM synthesis. Our genetically engineered plants have been tested in greenhouse trials at Los Alamos and at the University of Southern Maine. A total of 13 different plant species were transformed to create high-producing lines as a result of the over-production of 2-OGM in their leaves. In greenhouse trials, the engineered plants far surpassed the

performance of plants sprayed with the pure metabolite.

The transfer of the genetic engineering phase of this technology to the private sector began with licensing the portfolio to L1 Agrosciences, Inc. Their staff had been growing the plants at their facility and experiencing difficulties in achieving the differences in plant growth that LANL and University of Southern Maine scientists (and students at USM) had readily and consistently achieved. The original objectives of this work were put aside to address this immediate problem.

New Objectives

The objective of this work was to find the solution to L1 Agrosciences' problems with growing the high-performance tobacco lines. To do this, we investigated several potential causes of the problem including improper light spectrum or intensity, their use of ammonium- and urea-supplemented potting mixes and insufficient total nutrient supply.

Scientific Approach and Accomplishments

The original focus of this project was an investigation of the effects of inhibition of the 2-OGM in the roots of symbiotic nitrogen fixing model legume. Significant progress was made on the project before it was derailed to address the need described above. An appropriate gene construct was made for expression in the model legume Medicago truncatula and the crop legume Medicago sativa. The construct contained the *Arabidopsis thialana* gene encoding for ω-amidase, an enzyme capable of breaking down 2-OGM. This gene was placed under the control of a fragment of the RolD promoter to direct its expression to the root tissues. A kanamycin resistance gene was included as a selectable marker for transformed plants. Our initial attempts at transformation appeared to be successful and generated several *M. truncatula* seedlings resistant to kanamycin. The seedlings were being grown to greater size before being characterized further or inoculated with the nitrogen fixing bacterium *Sinorhizobium meliloti* to test for the effects on nodule development and N_2 fixation. Unfortunately the seedlings did not survive the shutdown of the laboratory for the forest fire this past summer. We were encouraged by the results and will continue this work at our earliest opportunity.

LANL researcher and inventor of the plant technology visited the L1 Agrosciences facility in North Carolina to learn details of the problem and how they were growing the plants. Unkefer undertook two courses of action: learn how they were growing the plants and conduct plant growth experiments under controlled conditions.

Unkefer traveled to the L1 facility and observed the L1 plant growth conditions and observed the lighting under which their plants were growing. L1 staff initially provided little information on their growth protocols and never provided data on the plant growth / performance. Unkefer

measured the light intensity of several of the racks and tables on which the plants were growing. The light intensity ranged from ~160 to 250 microE/m^2/sec for 16 hour day and 8 hour night cycles, values that could be expected to achieve good healthy plant growth. The plants were growing at room temperature in air-conditioned rooms or in temperature-controlled growth rooms in the University of North Carolina phytotron. These environmental conditions were also appropriate to support healthy plant growth. Later conversations with L1 staff provided critical insight into their growth protocols, when they revealed that they were growing with a standard commercially available Hoagland's nutrient solution and the seeds were being germinated in professional germination mix that contained supplemental nutrients including an ammonium salt and the seedlings were being transplanted into a potting mix that also contained nutrients including an exceptionally high concentration of urea, another source of ammonium. Each of these components provides significant ammonium. Ammonium is important with respect the performance of the engineered plants because they are over-expressing the 2-OGM synthesizing GPT enzyme in their roots as well as in their leaves. The response system in plants requires that the 2-OGM concentration increase in the leave tissues relative to that in the roots for the high performance to be achieved. Plants prefer nitrate as their nitrogen source because they can and do assimilate it in their leaves and roots. Ammonium is essentially not moved to the leaf and is thus primarily assimilated in the roots [5]. Because the 2-OGM concentration is positively correlated with the amount of nitrogen being assimilated in these tissues, ammonium could be expected to increase the 2-OGM concentration in the roots but not in the leaf. Thus providing ammonium to the plants could be expected to work against the up-regulation of plant metabolism, growth and overall performance. Because the L1 staff indicated that the plants were fed "every two or three days with about 1-1.5 liters per standard tray", which is a rather casual feeding regime, this was also considered a likely contributor to the under performance of the transgene plants in their hands. The tops of the solid support that their plants were growing and the tray bottoms were dry when Unkefer observed them on several occasions.

Several plant growth experiments were designed and conducted to discover the underlying cause of their failure to observe the high-performance of our engineered tobacco plants and to design a solution to the problem. Wild type and engineered tobacco plants were grown and their performance compared under different nutrient supply and composition.

A tobacco line over-expressing GPT only was tested by growing with nutrient media with and without ammonium (2 mM) at a concentration below that present in the germination and potting mixes used by L1. As predicted by our hypothesis and previous performance of our transgenic plants, the plants provided ammonium were much smaller

than those provided nitrate as their sole nitrogen source, ranging from ~40-60% of their fresh weight. Ammonia inhibited their growth. Thus an important contributor to the problem was the presence of the ammonium salts in the nutrient media and the germination and potting mixes.

The question of whether sufficient nutrient was being provided was difficult to approach quantitatively with the lack of quantitative information from L1. Thus more extensive tests were necessary to assess the potential that they were underfeeding the plants. A large set of plants including wild type and transgenes were examined and compared. Different feeding regimes were undertaken to establish regimes that would define adequate and inadequate nutrition. Observations of the plants' performance were made daily and correlated with the feeding regimes. The plants were grown in sand as the nutritionally inert solid support. The standard 10x20" trays were used to correspond directly with L1's set up. The high performance was observed only when the plants were feed daily with sufficient nutrient to maintain at least ½" of solution in the tray at its lowest daily level. This required that each tray be essentially filled daily; this required a minimum of one liter of the nutrient. A working observation emerged that was consistent with adequate nutrition and this was the development of a thick lawn of healthy dark green algae on the surface of the sand or in later tests of the peat moss/vermiculite support. Unkefer observed that a thick lawn of algae was never observed on any of the L1 grown plants. The growth tests established that the high performance could be achieved in either sand on in solid mixes that represented the potting mixes but without the nutrients they contained.

In conclusion, L1's problems with the plant growth were correlated with both inadequate nutrient supply and an inappropriate form of nitrogen in the nutrient supplied.

Impact on National Missions

This work contributed strongly and directly to the LANL priority "Energy Security-Clean Energy." It provided critically and immediately needed technical understanding required to support the transfer of LANL's Plant Growth Technology to the private sector. This effort addresses DOE/EERE's biofuels program's critical need to discover and deploy technologies to increase photosynthetic growth for plants and algae. The increased productivity is essential to realizing biofuels as cost-effective alternatives to petroleum-based transportation fuels. This work directly supported Los Alamos National Laboratory's federally mandated transfer of inventions important to the national security and economic welfare.

References

1. Schlesinger, W. H.. The global cycles of nitrogen and phosphorous. 1997. In *Biogeochemistry: An analysis of global climate change..* Edited by Schlesinger, W. H.. , Second Edition, p. 383. San Diego: Academic Press.

2. Kumar, P., M. Parry, R. Mitchell, A. Ahmad, and Y. Abrol. Photosynthesis and nitrogen-use efficiency. 2002. In *Photosynthetic nitrogen assimilation and associated carbon and respiratory metabolism..* Edited by Foyer, C., and G. Noctor. , p. 23. The Netherlands: Kluwer Academic Publishers.

3. Foyer, C., and G. Noctor. Photosynthetic nitrogen assimilation: Inter-pathway control and signalling. 2002. In *Photosynthetic nitrogen assimilation and associated carbon and respiratory metabolism.* Edited by Foyer, C., and G. Noctor. , p. 1. The Netherlands: Kluwer Academic Publishers.

4. Vidal, E., and R. Gutierrez. A systems view of nitrogen nutrient and metabolite responses in Arabidopsis. . 2008. *Current Opinion in Plant Biology.* **11**: 521.

5. Schjoerring, J., S. Hustead, G. Mack, and M. Mattsson. The regulation of ammonium translocation in plants. 2002. *Journal of Experimental Botany.* **53** (370): 883.

Mechanism of Inhibition of Acetylcholinesterase (U)

Robert F. Williams
20110532ER

Abstract

The overarching goal of this project is to examine the interaction of chemical warfare agents (CWAs) with their primary biological target; human acetylcholinesterase (hAChE; EC 3.1.1.7). Historically, AChE has been studied by classical methods, solution of innumerable crystal structures, and isolated computational studies. This body of information currently fails to produce a mechanism that explains the inhibition of AChE by the entire class of **o**rgano**p**hosphorous **a**nti**c**holin**e**sterase (OPACE) inhibitors. Moreover, effective countermeasures for the extremely toxic and persistent OPACE CWAs are not universal. However, since AChE studies have primarily used either the non-human forms of the enzyme and/or the monomeric form (*e.g.* eel), these results may not be surprising. hAChE is found in brain, muscle, and other tissues and, most importantly, is tetrameric. It contains disulfide-links between subunits and forms oligomers with (ColQ) or -containing Proline Rich Membrane Anchor (PRiMA) structures. The ColQ or PRiMA anchors serve to maintain the enzyme in intercellular junctions with the required in neuromuscular junctions and the PRiMA in synapses. Consequently, it is of critical importance to study tetrameric hAChE with its attached anchor in order to ascertain alternative mechanistic understanding and more fundamental explanations of inhibition and, therefore, countermeasure treatment. Thus, in this project, we aimed to express and purify tetrameric hAChE of the central nervous system. Since the Proline Rich Membrane Anchor (PRiMA) has been shown to be required for proper assembly and processing of the hAChE tetramer in neurological tissue, we chose a mammalian expression system and co-transfected AChE and PRiMA in order to express and purify the hAChE tetramer with its anchor. Without this critical tetrameric form of AChE, further studies are not possible.

Background and Research Objectives

In mammals, the glycoprotein AChE is encoded by a single AChE gene. Diversity in the transcribed products from the sole mammalian gene arises from alternative and associations of catalytic and structural subunits.

There are three known major forms that possess alternative C-terminal peptide sequences (R, H, or T) that define post-translational maturation, quaternary associations, and anchoring: $AChE_R$ generates soluble monomers; $AChE_H$ generates glycosylphosphatidyl inositol-anchored (GPI) homodimers; and $AChE_T$ generates an array of homo- and hetero-oligomers, including collagen-tailed molecules. $AChE_R$ has only been found in *Torpedo sp.* and mice, so far, although it is hypothesized to be present in other species. It is thought to be involved in the stress response and, possibly, inflammation. $AChE_R$ has been expressed in *N. benthamiana* plants. $AChE_H$ is found primarily in tissue but differs at the from $AChE_R$ and also contains a cleavable   with a site. It associates with through the GPI moieties, which are added post-translationally. $AChE_R$ has not been successfully expressed. $AChE_T$, found in brain, muscle, and other tissues, is the major form of acetylcholinesterase and it forms disulfide-linked oligomers with (ColQ) or -containing (PRiMA) structural subunits. In the neuromuscular junction $AChE_T$ is found in an asymmetric form that associates with the subunit. In the central nervous system it is associated with the Proline Rich Membrane Anchor (PRiMA) to form a symmetric form. In either case, the ColQ or PRiMA anchor serves to maintain the enzyme at the intercellular junction, for the neuromuscular junction and PRiMA for synapses. In both the ColQ- and PRiMA-tailed forms, the catalytic subunits of $AChE_T$ are linked in pairs by disulfide bonds through the cysteine residue located at a position 24 amino acids from the C terminus and two subunits are linked directly to each other while the other two are attached to the structural subunit. Thus, $AChE_T$ is tetrameric and is the form we are interested in expressing and investigating.

In the membrane-bound tetramers from mammalian brain the two subunits are linked to PRiMA. In collagen-tailed $AChE_T$ this arrangement is reproduced with the PRAD, the proline rich attachment domain of the ColQ subunit. PRAD not only links through disulfides to the two catalytic subunits, but also noncovalently interacts with four peptide sequences in the tetrameric cluster. When $AChE_T$ subunits are expressed alone in transfected COS cells or *Xenopus* oocytes, no $AChE_T$ appears on the

cell surface. AChE$_T$ surface expression does occur when AChE$_T$ subunits are cotransfected with a chimeric membrane-bound PRAD. In light of these findings a mammalian expression system and co-transfection of PRiMA and AChE$_T$ is clearly suggested. While such an expression system has not been published for AChE$_T$ linked to PRiMA (only for ColQ), we believe that a mammalian expression system is feasible. Alternatively, an insect cell expression can be used if glycosylation is not important or if it turns out to be similar to a mammalian expression.

Scientific Approach and Accomplishments

This goal of this reserve project was to develop, specifically, a mammalian expression system to produce both the monomeric form of hAChE and the membrane-bound tetrameric form of hAChE$_T$. All work was done under an approved IBC application for the expression and purification of tetrameric AChE$_T$. We were successful in both of these goals; however, additional work is necessary to optimize the protein yield of the tetrameric form of hAChE$_T$ and PRiMA and fully investigate the tetrameric form of the hAChE$_T$.

The co-expression of AChE$_T$ with PRiMA in human cells is required for the correct and efficient expression of functional tetrameric hAChE$_T$ on the cell surface. We first attempted to co-express the two proteins in Human Neuroblastoma cells (SK-N-SH); however, this proved unsuccessful. Consequently, HEK293 cells were used for all subsequent expressions to produce tetrameric, active hAChE$_T$. Cells were cultured in Modified Eagle's Minimum Medium containing 10% Fetal Calf Serum. All expressions were performed using standard protocols for transient transfection (*i.e.* no stable transfection, no selection for stable transformants, and generation of new cell lines). Constructs containing the hAChE$_T$ and/or human Proline rich membrane anchor 1 gene are commercially available in a mammalian expression vector pGen2.1 (GenScript) or a bicistronic vector pBICEP-CMV (Sigma). We expected the tetrameric hAChE$_T$ to be either secreted from the cell membrane or bound to PRiMA. If secreted, we anticipated purifying the AChE from the cell supernatant by chromatography; however, if the tetrameric hAChE$_T$ remained bound to PRiMA in the cell membrane, we anticipated purifying the protein complex using sucrose gradient centrifugation of the lysed cells. It was the latter case that obtained.

Three plasmids were obtained from Dr. Karl Tsim, Hong Kong University (-FLAG-AChE-pCDNA4 (rat); -AChE-pCDNA4 (human); -HA-PRIMA-pEF-Bos (mouse)) and two plasmids were made by Genscript, Inc. (-AChE-p.Gen2.1 (human); -PRIMA-pGen2.1 (human)). All five plasmids were expanded in competent *E. coli*. and single colonies/clones were picked and verified by restriction digests and sequencing (Figure 1). Glycerol stocks of verified *E. coli* clones were made and frozen at -70 °C for convenient expansion to produce plasmids for transfection. Liquid broth was inoculated with 250-300 ml of the *E. coli* clones containing the plasmids for AChE and PRiMA made by Genscript. DNA from

two clones, one for AChE and one for PRiMA, selected for transfection of HEK293 cells, were isolated by Midipreps (Qiagen). DNA concentrations of purified DNA were determined by absorbance (A230, Nanodrop) and 15 to 60 µg DNA were obtained from these preparations.

Left to right (upper)
1 kB ladder
7 = 4/1 digested Hind III
6 = 5/3 undigested
6 = 5/3 digested Hind III
5 = 5/4 undigested
5 = 5/4 digested Hind III
4 = 5/2 undigested
4 = 5/2 digested Hind III
3 = 5/1 undigested
3 = 5/1 digested Hind III
2 = 4/3 undigested
2 = 4/3 digested Hind III
1 = 4/2 undigested
1 = 4/2 digested Hind III

Left to right (lower)
1 kB ladder
Combined clones 3/1 through 3/4 undigested
Combined clones 3/1 through 3/4 digested Bgl II
8 = 4/4 undigested
8 = 4/4 digested Hind III
7 = 4/1 undigested

Figure 1. Digests of PRiMA and AChE clones PRIMA = clones 3/1 through 3/4 (Dr. Tsim) and 5/1 through 5/4 (Genscript) AChE = clones 4/1 through 4/4 (Genscript).

Three transfections of HEK293 cells, using different transfection reagents and ratios of AChE and PRIMA, were performed. Approximately 5×10^5 HEK cells at ~ 50% confluence were plated into 6-well plates and transfected with 1 or 2 µg of DNA for AChE and 1 µg of PRiMA using Trans IT 293, Trans IT LT1, or TransIT 2020 transfection reagents. Cells at 70-90% confluency were harvested after 48 hours, washed, and lysed in the presence of protease inhibitors. For the first two transfections, 0.25 ml of cell lysates from 5×10^5 cells were layered on 12.5 ml of continuous sucrose gradients (5-20%) and spun for 18 hours at 38,000 rpm in a swinging bucket rotor.[1-3] Ultracentrifugation of the cell lysates on a sucrose gradient results in a large dilution of the sample. In order to confirm that the hAChE$_T$ activity, seen in the first two transfections, was due to the expression of the hAChE$_T$, a third transfection doubled the number of transfected cells (1×10^4). Also, the cell lysates were not subjected to sucrose gradient centrifugation (avoiding the 1:50 dilution of the lysates) to ensure that sufficient amounts of hAChE$_T$ protein were produced.

Fractions obtained from the sucrose gradient were analyzed for hAChE$_T$ activity using the Amplex Red AChE assay (Molecular Probes) and protein concentrations of the positive fractions ranged from 1.7 to 5.7 µg/ml. Non-denatured gels (68 to 228 ng of protein per sample) were run and the AChE-positive fractions from the gel were blotted onto PVDF membranes in an unsuccessful attempt to directly determine the oligomerization state of hAChE$_T$ and association with PRiMA by Western Blotting. The blotted membranes were probed with either a monoclonal anti-

AChE antibody or a polyclonal anti-PRiMA antibody but no bands were detected using either these antibodies or HRP-labeled secondary anti-mouse or anti-rabbit antibodies. Detection of HRP was performed with the SuperSignal West Dura Substrate (Pierce) which is supposed to have a sensitivity in the mid femtogram range; however, this depends significantly on the quality of the antibodies used.

We also performed Dot blots with fractions collected after sucrose density centrifugation using anti-PRiMA and anti-AChE antibodies. With the polyclonal anti-PRiMA antibody we detected a positive fraction (Figure 2). The positive fraction displayed an AChE activity of ~16 U/ml and contained ~ 2 ug of protein. The dot blot results indicate that the polyclonal anti-PRiMA and secondary anti-rabbit HRP antibodies recognize PRiMA and that PRiMA is expressed. Unfortunately, the Dot blot with the anti-AChE antibody did not show positive results. The following conclusions can be drawn: (A) there is insufficient tetrameric $hAChE_T$ protein present in the samples, (B) the monoclonal anti-AChE does not recognize the expressed tetrameric $hAChE_T$, (C) the secondary antibody is inactive (HRP loses activity over time), and/or (D) the transfer from the gel to the blotting membrane is inefficient. Since B is most likely, these results need to be repeated with a polyclonal anti-AChE antibody using the same secondary HRP-labeled anti-rabbit antibody. The use of a polyclonal Anti-AChE antibody is more appropriate, in hindsight, for these verification experiments than using the available monoclonal anti-AChE antibody since the monoclonal antibody only recognizes one epitope while the polyclonal antibody can recognize many epitopes. Unfortunately, we could not acquire a suitable polyclonal Anti-AChE antibody in time to repeat these experiments.
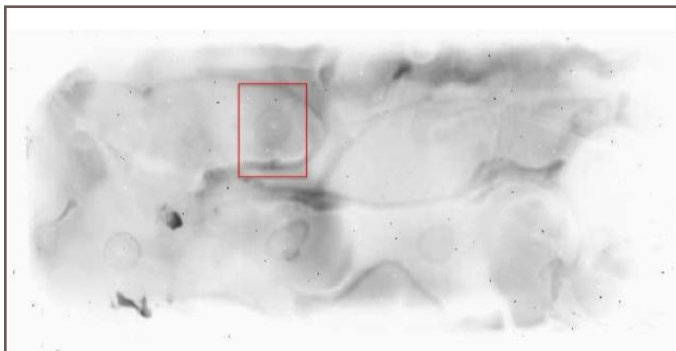
Figure 2. Dot-Blot probed with anti-PRiMA polyclonal antibody.

In order to confirm that the observed AChE activity was due to the expression of the $hAChE_T$ protein we wanted to ensure that we had sufficient amounts of $hAChE_T$ protein. Therefore, a third transfection was performed where the numbers of transected cells were doubled (1×10^4) and the cell lysates were not subjected to sucrose gradient centrifugation (to avoid dilution). The protein content in the nuclei-free supernatants (BCA protein assay) ranged between 900 and 1150 µg. This is ~40- to 100-fold higher

than the combined protein amount in all fractions from the previous transfections (corrected for the two-fold increase in cell numbers). This suggests that protein is lost during the sucrose density centrifugation or there is increased protein degradation when lysates are diluted during the sucrose density centrifugation since the protease inhibitors in the lysates are also diluted. These observations required additional experimentation in order to understand the loss of protein during the ultracentrifugation step. The two procedures needed to be compared and the loss of AChE activity determined by examining the protein content and AChE activity at each step throughout the isolation and purification procedures (Figure 3).
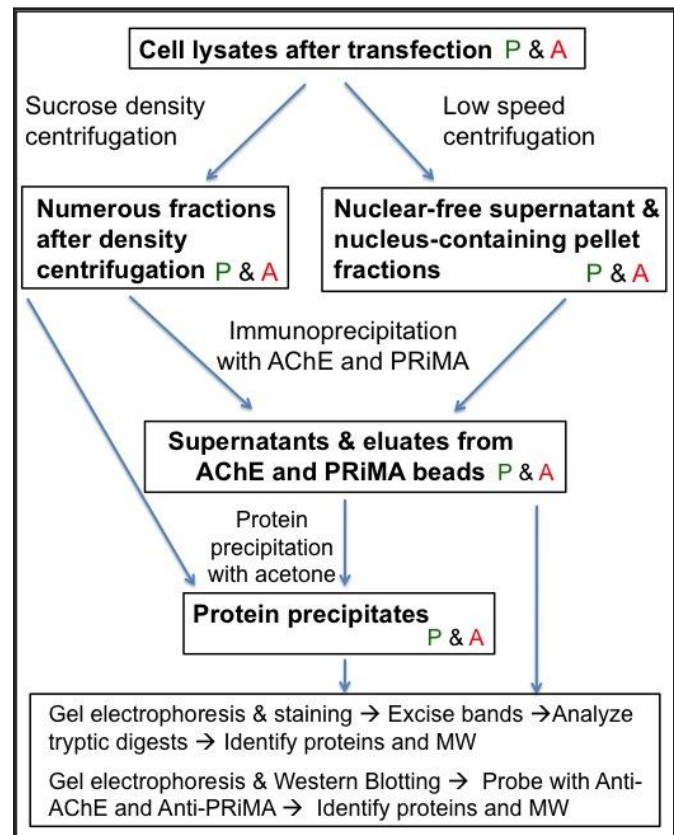
Figure 3. Flow Chart for supernatants and eluates from AChE and PRiMA beads where P & A indicates (P) Protein and (A) AChE activity measurements.

Consequently, monoclonal anti-AChE and polyclonal anti-PRiMA antibodies were bound to magnetic Protein G and anti-rabbit-antibody beads, respectively. These beads were incubated with the nuclei-free lysates from transfected cells and the lysate from non-transfected cells (control). After incubation of the anti-AChE beads with the nuclei-free lysates, the supernatants were removed from the beads (should not contain AChE or PRiMA) and the bound proteins eluted from the beads. The supernatants and eluates were analyzed by mass spectrometry (MS) and denaturing gel electrophoresis. In the MS of all four samples two prominent peaks were observed, 68 kDa and ~ 45 kDa. The size of Protein G is between 58 and 65 kDa depending on

the source, the size of an antibody heavy chain is ~50 kDa and that of an antibody light chain is ~25 kDa, whereas, the size of AChE is ~68 kDA and the size of PRiMA is ~20 kDa. The 68 kDa band is not Protein G since two incubations did not contain Protein G (anti-rabbit antibody beads incubated with anti-PRiMA antibody). However, the band could represent a modified heavy and light chain of one of the antibodies (~75 kDa) since all four incubations contained at least one antibody (anti-AChE and anti-PRiMA) or the band is tetrameric AChE (68 kDa) since AChE in the lysates could bind to the anti-PRiMA beads. To determine the identity of the 68 kDa peak, incubations of the lysates from the control cells, which were not transfected, need to be performed and the amino acid sequence determined from tryptic digests of 68 kDa band(s) excised from gels. The peak at 45 kDa, detected in all samples, likely represents an antibody heavy chain. This identification also requires sequencing the 45 kDa band(s); consequently, further work is necessary.

Denaturing gels of the acid eluates and the supernatants from the bead incubations were performed to determine whether tetrameric hAChE$_T$ also bound to the beads. One gel was stained with Coomassie and the other was transferred to a PVDF membrane for Western blotting. The Coomassie-stained gel showed multiple bands for both the supernatant and acid eluate fractions; however, some of the bands were not present in the non-transfected cells indicating transfection-specific expression. Unfortunately, the molecular weights of these bands are difficult to determine precisely without excising and tryptically digesting them for MS analysis (not yet completed). The Western Blot of the anti-AChE did exhibit a band at ~70 kDa, as desired, but this also requires additional confirmation.

In summary, the transient transfection of HEK293 cells with the isolated DNA works, as designed, since tetrameric hAChE$_T$ activity is observed. However, these results need to be repeated to produce increasing quantities of the protein. While not much difference was observed between the transfection efficiency of the three different transfection reagents employed, Trans IT-LT worked best. At the present time, which isoforms (monomer, dimer, tetramer, *etc.*) are preferentially expressed under particular transfection conditions is unclear and additional work needs to be done to determine and optimize the tetrameric form. This requires more tedious protein isolation and analytical work than this program had time to perform. Once transfection conditions have been optimized, the transfection can be scaled to isolate sufficient amounts of tetrameric hAChE$_T$ protein for subsequent use in the desired kinetic experiments.

Impact on National Missions
LANL is the only U.S. facility with world-class capabilities in structural biology, large-scale dynamic simulations, isotope-edited vibrational spectroscopy, stable isotope synthesis, bioorganic chemistry, and enzyme kinetics that

are required to solve this critical problem in a classified environment.

Affinity Maturation and Specificity Broadening of Anti-influenza Antibodies Suitable for Therapy and Prophylaxis

Andrew M. Bradbury
20110533ER

Abstract

The M2 protein of influenza is an ion-channel protein expressed on the surface of the virus. M2 is one of the most conserved influenza proteins and has been proposed as a "universal vaccine target" due to its high level of conservation. Effective vaccination leads to the development of antibodies that are able to neutralize virus. Our objective in this project was to develop the technology to be able to select antibodies against the M2 protein in its natural membrane embedded state. Success in this objective, would also be relevant to the selection of antibodies against other membrane proteins, which are the targets of most therapeutic antibodies. An additional objective was to identify and characterize single chain antibodies that recognize the M2 ectodomain. The major challenge for this project is that the M2 is a transmembrane protein, only a very small portion of which (termed the ectodomain) is available for recognition by specific antibodies. Although there are antibodies, including one we developed, that recognize the ectodomain of M2, most of them have a restricted recognition spectrum.

During the progress of this project, we have established selection and screening conditions, using ELISA (enzyme-linked immunosorbent assay) and flow cytometry, for selecting antibodies against M2, an integral membrane influenza protein using virus like particles and eukaryotic cells expressing M2 on their surface. These protocols are applicable not just to M2, but will also be applicable to any target membrane protein. Furthermore, preliminary application of the selection strategy we developed, indicates that we have selected six to eight scFvs (single-chain variable fragments) that specifically recognize M2 present on VLPs. This indicates that we have significantly advanced our capacity to select antibodies against membrane proteins, and M2, a key influenza target, in particular.

This new capability enhances LANL's ability to select antibodies against membrane bound targets, and in particular, ones on viral surfaces. Antibodies against viruses are the one of the most important host defenses, and application of this approach to other viruses of biothreat interest will have a significant impact on national security missions in biothreat.

Background and Research Objectives

The M2 protein of influenza is an ion-channel protein expressed on the surface of the virus. M2 is one of the most conserved influenza proteins. The conserved nature of this protein makes it a potential universal target for vaccines. Our project is to identify and characterize single chain antibodies that recognize the M2 ectodomain. The major challenge for this project is that the M2 is a transmembrane protein, only a very small portion of which (termed the ectodomain) is available for recognition by specific antibodies. Although there are antibodies, including one we developed, that recognize the ectodomain of M2, most of them have a restricted recognition spectrum. The goal of this LDRD reserve was to establish conditions to be able to select antibodies that recognized a broad panel of M2 from many different influenza strains. This required setting up selection and screening assays that used "authentic" M2, such as that found on the surface of the influenza virus itself.

The approach described here has general applicability to the selection of antibodies against other membrane bound proteins. In the past, this has been attempted by creating soluble versions of membrane proteins. However, such soluble forms do not necessarily mimic the folds of proteins when they are in their natural membrane context. Consequently, development of a method to select antibodies against membrane proteins in their natural contexts will have broad utility.

Scientific Approach and Accomplishments

Strategies used

- Prepare a mutagenized library of a humanized anti-M2 antibody and select high affinity binders.

- Synthesize virus like particles (VLP) that contain M2 as a transmembrane protein in its natural state and use them for selection and screening.

- Prepare eukaryotic cells that express M2 gene and use whole cells or vesicles for selection and screening.

Preparation of mutagenized h14C2 library for yeast display and sorting on M2 peptide

H14c2 is a humanized version of the murine antibody that recognizes the M2 protein. We had previously created this from a well characterized mouse antibody, 14C2. This scFv recognizes M2 expressed on eukaryotic cells and reduces the viral replication efficiency (1). The affinity of h14C2 was previously calculated to be 1nM. In order to increase the affinity, with the goal of preparing a therapeutic that would be functional at lower concentrations, a mutation library was created of h14C2 using error prone PCR (polymerase chain reaction). This library was cloned into a yeast display vector and displayed. Figure 1 shows the binding of clones in this library at a concentration of M2 peptide of 0.3nM, and indicates that a significant number are able to recognize M2 at this lower concentration. We sorted the top 5% of the peptide binders and will further analyze the clones obtained for their ability to recognize M2 in its natural form on either cell membranes or on VLPs.
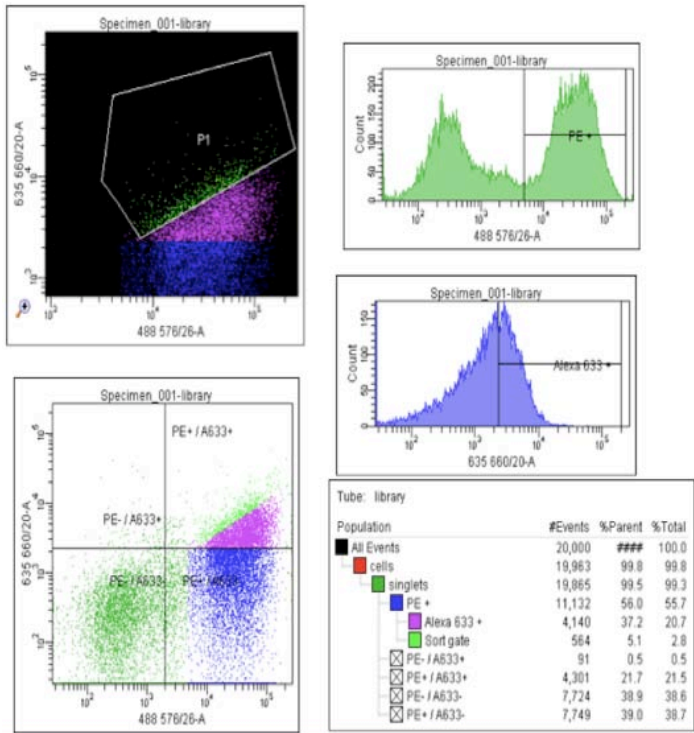
Figure 1. This figure shows the flow cytometry dot blot for analyses of mutagenized h14C2 library displayed on yeast. In this experiment the yeast were stained with 0.3nM M2-peptide. Gate P1 represents the top 5% population of yeast that has the highest scFv expression and binding for the peptide. This population was stored for further analyses.

Selection on virus like particles (VLP) that contain M2 in its natural form

One problem with the use of peptide targets for selection is that they do not necessarily resemble the ectodomain in its natural state. H14C2 is able to recognize M2 peptide as well as M2 on cell surfaces, but it is not clear whether

it can recognize M2 on virus. In order test this, and overcome this potential problem we established a collaboration with Integral Molecular Inc. This company produces virus like particles (VLPs) that contain M2 embedded in their outer membranes (as well as other VLPs with other proteins). VLPs have never been used for selection before, and in order to establish the system, we also synthesized a positive controls scFv (Z3) that has been reported to recognize M2 on virus surfaces (2). Z3 was cloned into protein expression and yeast display vectors. The data in Figure 2 shows that scFv Z3 was able to recognize the Udorn (M2 containing VLP) both as pure protein in ELISA and Figure 3 shows recognition also in the yeast displayed format.
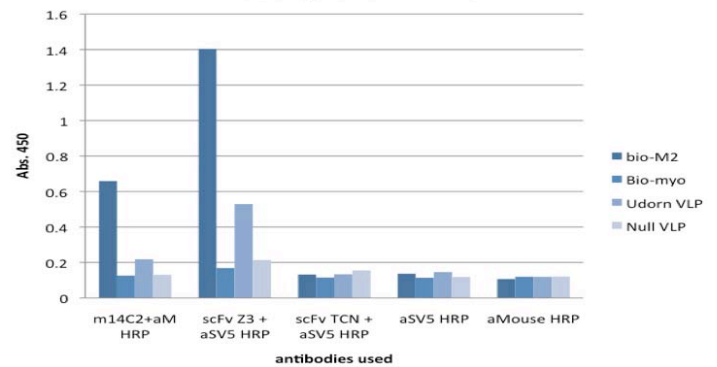
Figure 2. M2 protein on VLPs can be recognized by antibodies in an ELISA assay. Only the biotinylated M2 peptide (bio-M2) and the VLPs with M2 on their surface (Udorn VLP) provide positive signals with The antigens used are bio-M2 peptide, bio-myoglobin, Udorn VLP and null VLP. The monoclonal IgG 14C2 was used as positive control. The data shows that both m14C2 and scFv Z3 recognizes the M2 peptide and M2 VLP (Udorn) specifically. They do not give signal for negative antigens myoglobin and null VLP. The TCN scFv did not work in our hands. Signals for anti-SV5 HRP and anti-SV5 mouse are given as controls.

scFv	Udorn	Null
Z3	35.67	1.3
TCN	2.63	1.73
14C2	2.73	1.36
Y13-259	1.53	0.77
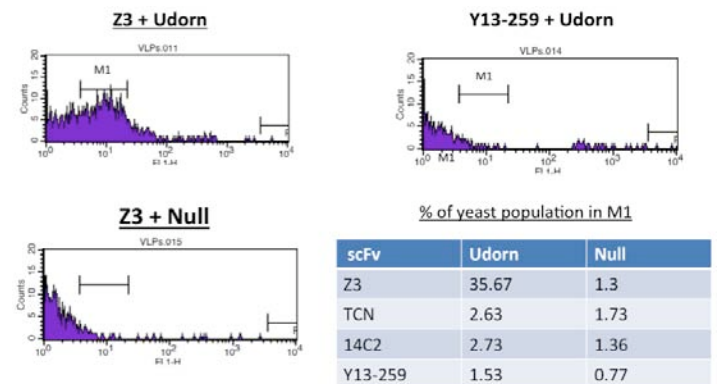
Figure 3. Z3 scFv binding to fluorescent udorn VLP. The table shows that 35 % of yeast displaying Z3 recognized the Udorn VLP in comparison to 1.3% the null VLP. The data also showed that in this format h14C2 does not recognize the Udorn VLP when displayed on yeast. scFv Y13-259 was used as negative scFv.

Furthermore h14C2 showed weak binding to Udorn VLPs. The null VLP was used as negative antigen and scFv Y13-259 was used as non-specific scFv. This is the first time VLP recognition by yeast display scFv has been demonstrated. To further analyze the interaction between VLPs and yeast displaying anti-M2 antibodies, we used the Amnis flow cytometer (Figure 4). This produces pictures of individual yeast cells as they pass through the flow cytometer. Direct interaction can be visualized when the VLPs are fluorescently labeled.
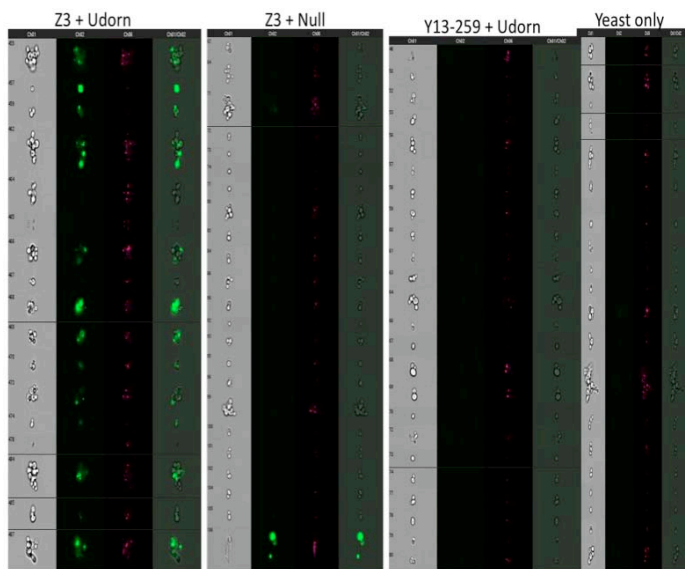
Figure 4. Pictures from the Amnis image flow cytometer. When yeast displaying Z3 scFv is incubated with fluorescent VLP containing M2 (Udorn) the pictures show the yeast binding to the VLP. The second panel shows no binding was observed with null VLP and third panel shows non-specific scFv Y13-259 do not bind to Udorn VLP. Yeast only sample is also given as control.

We also worked out conditions to sort VLP binding yeast clones using flow cytometers. Z3 displaying yeast was mixed with non-specific scFv at 1:100 ratio, after sorting we obtained 40% enrichment as shown by peptide based analyses (not shown).

After assay conditions were established using the Z3 scFv as positive control, we performed new antibody selections directly on M2 VLP (Udorn). Conditions were set up for subtractive selection and subtractive sorting in presence of null VLP. The pool of scFvs obtained after two rounds of selection and either one or two rounds of sorting was sub-cloned into protein expression vector for ELISA on VLPs. The data in Figure 5 shows that we were able to select scFvs that had higher signal for M2 containing VLP, as compared to VLPs that do not contain M2 (null). However, the two antibodies that appeared to specifically recognize M2 VLPs most strongly (3c/5b and 9h) were truncated antibodies. The other selected antibodies (2A, 3H, 6D, 8A and 10D) were all different and full length with binding signals similar to Z3, although with slightly higher background

binding levels. One problem with the use of VLPs is that we have to rely on Integral Molecular to supply VLPs, and the amounts provided tend to be very low. In order to investigate the possibility of developing our own M2 expressing membrane vesicles, we explored the possibility of using tissue culture cells expressing M2 as a potential source. HEK293 cells transformed with the M2 gene (HEK293-M2) and controls were obtained from collaborators. The cells were grown and induced for M2 production. We were able to show specific binding to M2-HEK293 using both ELISA and flow cytometry.
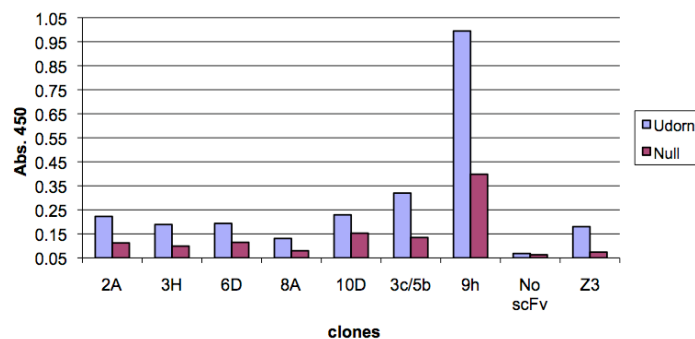
Figure 5. ELISA values for seven selected scFvs and controls are given. ELISA was performed on both Udorn and null VLP. scFv 2A, 3H, 6D, 8A and 10D were obtained after two rounds of selection on Udorn while blocking with an excess of null particles. Finger printing showed them to be different scFvs. scFv 3c/5b was obtained after one round of sorting and contains only a VL domain. scFv 9h was obtained after two rounds of sorting and contains only a VH domain. scFv Z3 was used as positive control and no scFv value is given as negative control.

Impact on National Missions

This technology developed here enhances LANL's general antibody selection capability, and in particular, the ability to select antibodies against membrane bound targets. As antibodies against viruses are one of the most important host defenses, the application of this approach to other viruses of biothreat interest will have a significant impact on national security missions in biothreat. Antibodies able to recognize biothreat targets developed using the methods described here, will have utility for biodetection, diagnosis, passive vaccination and therapeutic intervention.

References

1. Gabbard, J., N. Velappan, R. Di Niro, J. Schmidt, C. A. Jones, S. M. Tompkins, and A. R. Bradbury. A humanized anti-M2 scFv shows protective in vitro activity against influenza. 2009. *Protein Engineering Design & Selection.* **22** (3): 189.

Light Stable Isotope Signatures for Accelerator and Reactor Emissions

Claudia Mora
20110663ER

Abstract

This project examined the application of novel stable isotope measurements to common gas emissions from the LANSCE accelerator stacks in order to evaluate their utility as signatures for accelerator activity. Near real-time measurement of stable isotope compositions of CO_2 ($\_^{13}C$) and H_2O ($\_D$, $\_^{18}O$) over a three month period using cavity ring down spectrometers directly tapping the emissions stack indicate stack emissions are dominated by atmospheric gas compositions, muting any accelerator signal. Similarly, tree ring cellulose $\_^{18}O$ values near the accelerator emissions stack are dominated by an environmental signal, yet consistent with 13C-enriched CO_2 at the site. The emissions isotope time series captured evidence of unusual atmospheric vapor compositions consistent with an extraordinary hydro-climatic regime over the southwestern US in 2011, even compared to previous drought years since 1895. First-ever measurement at LANL of multiply-substituted CO_2 isotopologues in the emissions are consistent with a low temperature source of CO_2. The results of this brief study demonstrated the potential use of newly-available stable isotope science and technology in a wide range of forensic and climate signatures science.

Background and Research Objectives

Over the past 50 years, natural-abundance stable isotope studies have provided fundamental insights into a vast array of geological and biological processes. These studies have focused almost exclusively on *bulk* stable isotope compositions (i.e., the different isotopologues contributing to each mass are undifferentiated) of *batch* samples (i.e., one-time or aggregate collections). Recent advances in stable isotope science and technology support precise, high temporal resolution (approaching real-time) measurement of bulk stable isotope compositions by cavity ring-down spectrometry (CRDS), as well as the measurement of rare isotopologue abundances, such as CO_2 with mass 47 or mass 48. There are few examples yet of the application and significance of these new techniques. The present experiments were prompted by detection at TA-51 of simultaneous, significant, and compositionally unusual isotopic variations in $\_^{13}C$ of CO_2, $\_D$

and $\_^{18}O$ of water vapor, and methane concentrations concurrent with the delivery of air to our sample intake from TA-53. To test the hypothesis that these unusual compositions were related to LANSCE beam activity (i.e., effects due to beam-air interaction at leaks or target-cooling water interactions), three novel approaches were utilized to evaluate LANSCE stack emissions for anthropogenic isotope signals: (1) near real-time stable isotope monitoring of stack emissions by cavity ring-down spectrometry (CRDS) over a period of ~ 3 months, including periods when the beam was on or off, (2) a comparison of the abundances of the multiply-substituted isotopologues of carbon dioxide in the stack emissions versus the natural environment, and (3) investigation of tree-ring stable carbon isotope records prior to and during the operation of the LANSCE accelerator facilities.

Scientific Approach and Accomplishments

Isotope monitoring of stack emissions

Stable isotope compositions of carbon dioxide (C isotopes) and water vapor (H,O isotopes) emitted at the LANSCE emission stack 2 were monitored from June 6 through September 19, 2011 (Figure 1). Isotope values at the stack do not support the original hypothesis that the accelerator beam-related isotope effects can be readily detected in the stack emissions of CO_2 and water vapor. These emissions are instead dominated by isotope compositions consistent with local atmospheric conditions. Little variation is noted in the $\_^{13}C$ of carbon dioxide. Hydrogen and oxygen isotope compositions in water vapor co-vary, typical of atmospheric compositions, and, from mid-July through mid-September, have values common for local summer meteoric water vapor in the Los Alamos region. Of greatest interest, a rise in values from June through mid-July captures evidence of a regional water vapor mass that was unusually depleted in ^2H and ^{18}O. We conducted additional investigation of the hydro-climatic regime of the North American Southwestern region for spring and early summer 2011 and demonstrated that it was extraordinary in terms of atmospheric circulation and available moisture compared to other 21st and 20th century drought years. Investigation of at-

mospheric back trajectories and meteorological data indicate deep penetration and residence of a high latitude air mass over the region, with unusually low water vapor concentrations, may have predisposed the region to the extent of the Las Conchas fire in late June and early July, as well as other 2011 major fires in the southwestern region [1,2]. The apparent sensitivity of the CRDS isotope monitoring to the origin and evolution of air masses was demonstrated.
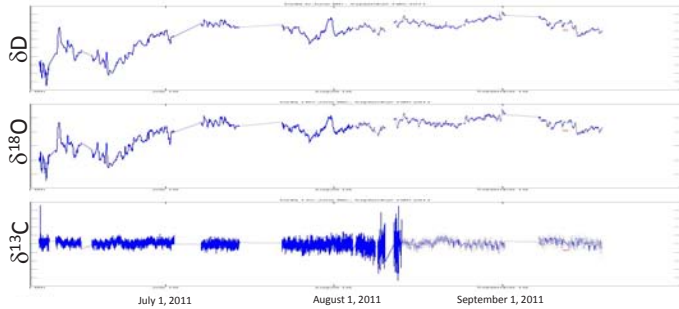
Figure 1. Isotope time series of LANSCE ES-2 emissions June 6-September 19, 2011.
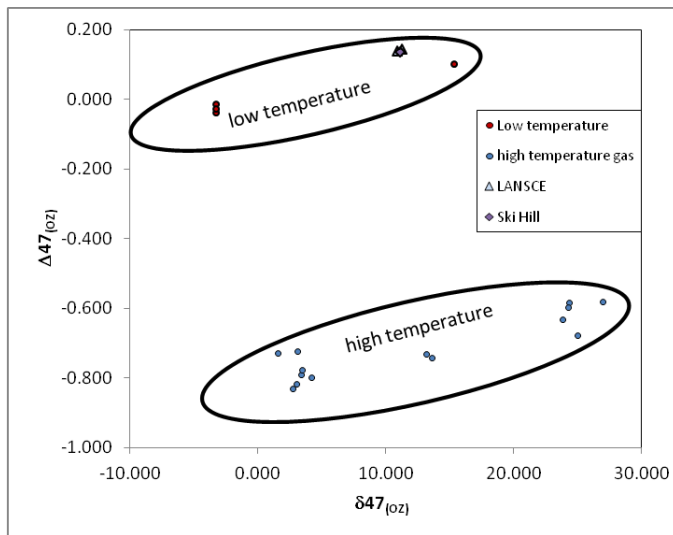
Figure 2. Multiply substituted isotopologues (mass 47) in emissions from LANS ES-2 and the ski hill preserve low temperature compositions.

Multiply-Substituted Isotopologues (MSI)

We compared an atmospheric gas sample, collected from the ski hill road at on September 12 at 12:30pm, to two samples of stack emission collected at LANSCE-ES2 on the same day, at 11am (beam off) and 4:15pm (beam on). Samples were collected in 6 liter sample vessels. CO_2 was isolated from these samples using cryogenic vacuum distillation techniques (yield ~ 90 micromoles of CO_2) and sealed in a quartz break seal tube. Purified samples of CO_2 were analyzed for $\_^{13}C$, $\_^{18}O$, $\_^{47}$ and $\_^{47}$ isotope values, as defined by Eiler, 2007 [3]. Results are shown in Figure 2. $\_^{47}$ is conventionally interpreted with respect to temperature

of equilibration. High temperatures favor more random, or stochastic, distribution of multiply-substituted isotopologues, whereas low temperature equilibration favors an increased abundance of the heavy isotopes, resulting in non-stochastic distributions in mass 47 CO_2. Our measurements are shown in Figure 2, and fall within the range of 'low temperature' equilibration, a result that is consistent with these samples being comprised predominately of atmospheric CO_2. The measured $\_^{13}C$ values (approximately -8.7‰) and $\_^{18}O$ values (approximately 41‰), are consistent with tunable diode laser data collected during the same time period at the TA-51 field station, three miles away ($\_^{13}C$=-8.3‰ and $\_^{18}O$=42.3‰).

Tree-ring isotope analysis

Living piñon trees (*Pinus edulis*) growing near the accelerator stack were sampled and the wood was dated by conventional tree-ring analysis. Cellulose was collected from individual annual rings representing the 1960s decade (prior to opening of the LANSCE facilities) and the 1990s decade (during operation of the LANSCE facilities) and was analyzed for $\_^{13}C$-cellulose. The results were compared against mean annual precipitation at the site, and to cellulose $\_^{13}C$-time series in piñon from TA-71 (collected in a previous study). The tree ring isotope variations at the LANSCE site suggest that an environmental signal dominates, with values best explained as a typical isotope response to available moisture, with higher values during periods of relative drought and lower values associated with relatively higher amounts of precipitation. The isotopic shifts are opposite what would be hypothesized if trees were significantly influenced by the significant production at the accelerator of ^{13}N (decaying to ^{13}C and incorporated into environmental CO_2) during the 1990s decade. The relatively 13-C enriched values of trees at the LANSCE site relative to the TA-71 site is nonetheless intriguing and consistent with the presence of enriched carbon in the area near LANSCE, however, the difference may also be explained by greater water availability in the TA-71 area, located off the mesa top.

Impact on National Missions
This study contributes to our understanding of how newly-available stable isotope science and technology can be developed for a wide range of forensic applications and signatures science, emphasizing stable isotope compositions in common emissions such as carbon dioxide and water vapor. This study brought new capabilities to the lab with the modification of our gas source isotope ratio mass spectrometer and development of analytical techniques to support analysis of "clumped" (i.e., multiply substituted) isotopologues of carbon dioxide, such as 13C-18O-16O. It presented a first opportunity to deploy a full suite of cavity ring-down spectrometers for rapid measurement of gas abundances and isotope ratios in the field. These capabilities have been incorporated into new and developing, funded projects in arctic climate change and atmospheric

methane detection and attribution. "Clumped" isotope science and technology may be particularly useful to distinguish the source of emitted greenhouse gases, by distinguishing high-temperature/combustion (fossil fuel) from low temperature (biological). These capabilities will immediately impact climate science programs supported by DOE- BER (e.g., Ecosystem Science, Carbon Cycle Science, NGEE) and future efforts to attribute greenhouse gases to particular sources.

References

1. Rahn, T., N. Hryniw, and A. Trugman. The Historic 2011 American Southwest Fire Season: More than a Lack of Precipitation. Presented at *American Geophysical Union Fall Meeting.* (San Francisco, ec. 2011).

2. Rahn, T., A. P. Williams, A. Trugman, N. Hryniw, N. Mc-Dowell, C. Mora, and D. Noone. The 2011 Southwest wildfires: More than a lack of precipitation. *Nature Geoscience.*

3. Eiler, J.. "Clumped-isotope" geochemistry—The study of naturally-occurring, multiply-substituted isotopologues. 2007. *Earth and Planetary Science Letters .* **262**: 309.

Soil Microbial Signatures for Large-Scale Climate Change Field Experiments

Cheryl R. Kuske
20110665ER

Abstract

Our goal in this project was to substantially improve our capability to measure microbial signatures, with a focus on signatures associated with terrestrial ecosystem responses to climate change. We exploited two unique LANL resources: 1) microbial signatures identified from high throughput DNA sequencing datasets recently obtained from DOE climate change experiments, and 2) a capability developed via DHS funding for *in silico* design of sophisticated DNA detection assays. We thoroughly benchmarked the exceptional capabilities of our assay design platform by designing and experimentally validating assays for a group of bacteria that appears to be involved in ecosystem response to elevated atmospheric CO_2 in multiple ecosystems. The results of our benchmark study are described in a manuscript submitted to Nucleic Acids Research, a biosciences journal with a high impact factor. We also revised the model at the heart of the assay design platform to improve the sensitivity of discriminating between "good" and "bad" assays. This improvement provided a 15-fold increase in the number of candidate assays in a simulated design problem. This improvement in the design platform keeps Los Alamos National Laboratory at the cutting edge of technical sophistication, allowing us to deliver the best possible solutions (i.e. assays) to support biosurveillance or to enable new discoveries and insights in climate science.

Background and Research Objectives

"Microbial signature" has several meanings. We use the phrase to refer to microbes or genes whose presence or abundance is indicative of phenomena of interest. Phenomena of interest vary depending on the application (e.g. biosecurity, public health, climate change). For a given application, one would like to measure a particular microbial signature or set of signatures in samples. The fastest and cheapest way to do this is to use an assay that amplifies DNA specifically from the signature microbe(s). Such assays are called quantitative polymerase chain reaction (qPCR) assays. The challenge is to design effective assays that specifically target the signature and avoid amplification of closely related non-signature microbes or genes.

In this project we focused on climate change as an application. Terrestrial ecosystems provide substantial feedbacks that modify climate. Microbial processes in soils are particularly important. Soil serves a huge carbon reservoir (2300 GT) and microbial respiration and decomposition of plant matter have been estimated to account for about half (60 GT) of the carbon flux in the terrestrial biosphere. The balance between carbon inputs to soil, respiration, and storage is the net soil carbon flux. The net flux determines if soils act as a sink or source for CO_2. The net flux of carbon in soils under climate change conditions over the next hundred years is uncertain. Indeed, a variety of predictive models have projected very different, and sometimes contradictory outcomes, with soils serving either as a carbon source or a carbon sink. Improving the predictive models such that we can anticipate climate change effects before they occur requires a better understanding of microbial processes and how processes respond to altered climate.

Identifying microbial signatures for key processes and using the signatures to measure dynamics in response to climate factors is a key step towards improving our understanding of climate change effects. Information on the variability among different ecosystems is needed to scale up from ecosystem to regional effects. Studies of plant community responses to climate change have demonstrated that there are some common trends across ecosystems (e.g., enhanced primary productivity), but also important species and ecosystem-specific effects (e.g., extent of carbon allocation to roots) that are critical for accurate predictive models. Similar observations are emerging for soil microbial communities.

The objective of this research effort was to improve our capability to design effective qPCR assays for microbial signatures of interest in the context of climate change.

Scientific Approach and Accomplishments

The approach to developing an improved design capability was to first benchmark the performance of an existing design capability and then to improve the mathematical model used for assay design.

The pre-existing assay design capability (developed at LANL) is, to our knowledge, the most advanced assay design capability in existence. The platform is uniquely able to handle difficult design problems. Assay design becomes difficult when a large number of DNA sequences must be used in the design process because the computational effort substantially increases. Our assay design platform was implemented on a mid-sized cluster (i.e. hundreds of cores) to distribute the computational burden and accommodate design problems at an unprecedented scale. Assay design also becomes difficult when DNA sequences in target microbes are highly similar to DNA sequences in non-target microbes. All but one published assay design algorithm requires a unique piece of DNA in the target microbe compared to non-target microbes, but this requirement cannot always be fulfilled. To overcome this obstacle, our assay design platform adopted a different approach that is computationally more demanding, but can potentially find effective assays where all other programs fail. We benchmarked these features by designing and experimentally validating assays for a large taxonomic group of microbes, called *Acidobacteria* Group 1. This group of microbes was of interest because it showed a consistent response pattern in five ecosystems exposed for a decade to elevated atmospheric CO_2 (a central factor contributing to climate change)[1].

Designing assays for *Acidobacteria* Group 1 is challenging because there is a very large number of DNA sequences and because there is a high degree of similarity between DNA sequences from this group of microbes and from close relatives outside the group. Thus, this design problem provided a good benchmark test for our pre-existing assay design platform. We used a total of nearly 34,000 DNA sequences (an exceptionally large number) for assay design. After about one week of computation, the design platform predicted 83 assays that would *collectively* detect nearly all of the microbes in *Acidobacteria* Group 1 while avoiding close relatives (Figure 1). We experimentally validated the top 3 assays and showed that the assays achieved the predicted specificity. We also verified that conventional algorithms could not have designed the assays because the assays did not fulfill the conventional requirement for a unique piece of DNA in the target microbes. The results of our benchmark study are described in a manuscript submitted to Nucleic Acids Research.

The benchmark validation was extremely important. The study confirmed the exceptional features of our assay design platform but also helped us identify several areas for improvement. For example, we identified an alternate approach computing assay coverage of the target group that is less thorough, but would substantially reduce the computational time, and would enable identification of assays that cover the largest *diversity* of target group members. More importantly, the benchmark study emphasized the need for an improved mathematical model for assay design, as described below.

Our platform used a primitive model—the same type of model used to date by all assay design algorithms. The model predicts which assays are viable based on the melting temperatures of the DNA sequences used in each assay. If the melting temperature results for DNA sequences from target and from non-target microbes are too similar, an assay will be predicted to be non-specific and will be rejected. However, this model only accounts for one of several key features of the biochemical process that occurs during the assay. Use of this type of model is extremely conservative. It therefore creates the risk of rejecting many assays that would have acceptable performance in practice. The finding that 83 assays were needed to obtain nearly 100% coverage of *Acidobacteria* Group 1 (the desired outcome was 1 or 2 assays for 100% coverage), emphasized the need for a less conservative set of computational solutions.
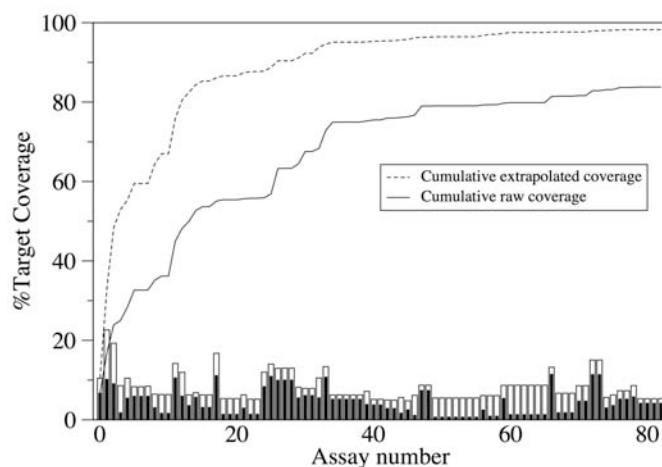
Figure 1. Candidate assays from our design platform predicted to specifically detect members of the microbial group, Acidobacteria Group 1. The 83 candidate assays produced by the design platform, in order of discovery, are shown on the x-axis. The cumulative percentage of Acidobacteria Group 1 DNA sequences predicted to be detected by the assays is shown by the dashed curve in the plot. Other details of the plot are described in the manuscript (Reference 2) submitted to Nucleic Acids Research.

After thoroughly benchmarking performance of the design platform, we focused our efforts on improving the computational model at the heart of the design algorithm. Our goal was to create a model that more accurately predicts the *end point* of the biochemical assay process, instead of merely the initial thermodynamics. The challenge was to develop an appropriate conceptual model that incorporated salient biochemical features of the process. Our expectation was such a model would provide a larger set of feasible assays because an assay that has a small differential in initial thermodynamics between target and non-target microbes may exhibit an expanding performance gap as the DNA amplification process in the assay proceeds to completion. After constructing the revised model, we performed a simulation to assess its effectiveness in pro-

viding a broader set of solutions. As shown in Figure 2, the new model increases about 15-fold the number of assays that are predicted to be effective in distinguishing target from non-target microbes. This illustrates a remarkable advance in sensitivity in discriminating "good" assays from "bad" assays. An increase in the number of possible assays to detect a given target (or set of targets) generally offers greater flexibility, which may include better assay choices in some cases and in other cases may provide a solution for a detection problem that did not previously have a solution. As we just completed this new model, applying it to *Acidobacteria* Group 1 (or other microbial signatures) and experimentally validating the predicted outcomes awaits further funding.
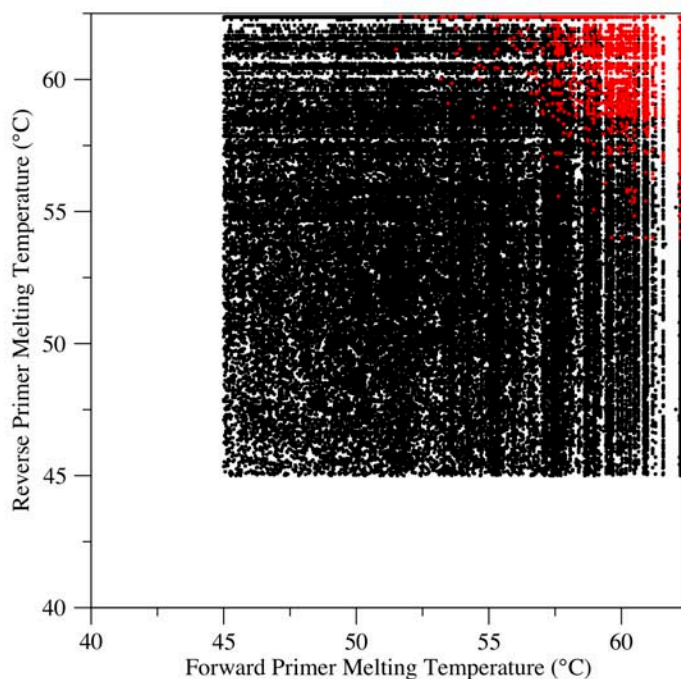
Figure 2. Comparative performance of our new versus old computational model for assay design. Each point in the graph is a candidate assay. The new model predicts all of the assays shown as black dots are valid and will specifically amplify the target DNA sequence while excluding closely related non-target sequences. The old, conservative model rejected about 93% of the assays shown as black dots and predicted that only the assays shown as red dots were suitable. Thus, the number model increased the set of candidate assays about 15-fold by providing more sensitive discrimination between good and bad assays.

Impact on National Missions
The work from this project has significant benefit to national missions in climate science and biosecurity. These missions require rapid, low-cost assays to detect and quantify microbial signatures in environmental samples. This project enabled us to demonstrate concretely the exceptional value of our assay design platform, which is uniquely able to handle design problems at an unprecedented scale and degree of complexity. In climate science and biosecu-

rity, a number of microbial signatures have been identified for which conventional assay design algorithms have failed. In many cases, even our own platform has failed to produce desired outcomes (e.g. a single assay was desired to detect all member of *Acidobacteria* Group 1, but our platform could only find a set of 83 assays that had to be used cumulatively to achieve the coverage).   Our improvement of the design platform keeps Los Alamos National Laboratory at the cutting edge of technical sophistication, allowing us to deliver the best possible solutions (i.e. assays) supporting biosurveillance or enabling new discoveries and insights in climate science.

References
1. Dunbar, J., S. A. Eichorst, L. Gallegos-Graves, S. Silva, G. Xie, N. W. Hengartner, R. D. Evans, B. A. Hungate, R. B. Jackson, J. P. Megonigal, C. W. Schadt, R. Vilgalys, D. R. Zak, and C. R. Kuske. Common bacterial responses in six ecosystems exposed to ten years of elevated atmospheric carbon dioxide . *Microbial Ecology.*

2. Gans, J. D., J. Dunbar, S. A. Eichorst, L. V. Gallegos-Graves, M. Wolinsky, and C. R. Kuske. A robust PCR primer design platform applied to the detection of Acidobacteria Group 1 in soil. *Nucleic Acids Research.*

Publications
Gans, J. D., J. Dunbar, S. A. Eichorst, L. V. Gallegos-Graves, M. Wolinsky, and C. R. Kuske. A robust PCR primer design platform applied to the detection of Acidobacteria Group 1 in soil. *Nucleic Acids Research.*

Assessing the Immunogenicity of Mosaic Hepatitis C Vaccines in a Mouse Model

Karina Yusim
20110714ER

Abstract

Immunological control of the hepatitis C virus (HCV) is mediated by host T-cell responses, but the genetic diversity of the virus poses a major challenge to successful vaccine development. HCV genetic diversity is comparable to HIV diversity at the population level. For HIV, our group created a promising novel vaccine design algorithm that creates natural-like "mosaic" proteins that optimize coverage of the genetic variability. Very encouraging results were obtained using this vaccine design in experimental studies in mice and monkeys; the vaccine is highly immunogenic and the breadth of coverage is much better than with traditional vaccines. Our HIV mosaic vaccines are currently being tested in humans.

We then applied the mosaic approach to the design HCV vaccines that maximize population coverage. To be able to advance this strategy, preliminary studies in mice are essential, and the performance of this design has been tested in mice. We worked with our colleagues at Harvard to analyze the results of a mouse study they have embarked based on our HCV paper. We designed optimal reagents for them to use in experiments that to allow a clear assessment of the potential for global cross-reactivity. The LANL team designed a comprehensive cost-effective peptide set and helped the Harvard team to design their experiments. The experimental results are being performed by the Harvard team using their own funding. While their experiments are ongoing, the first results are very encouraging, confirming that our novel HCV mosaic vaccines fold and are processed like natural proteins, are immunogenic in mice, and have increased breadth of T-cell responses compared to natural antigens.

Background and Research Objectives

Hepatitis C virus (HCV) causes chronic infections that can result in liver cirrhosis, liver failure and hepatocellular carcinoma. More than 170 million people are infected worldwide. The currently available treatments have limited success, generate toxicity and drug resistance, and require sophisticated medical management that puts them out of reach for many infected people. Develop-

ment of prophylactic and therapeutic vaccines remains paramount.

Historically, most vaccines have been based on a well-studied natural reference strain, and this strategy has been quite successful for less variable pathogens like polio, measles and rubella. Because of the genetic diversity of viruses like HIV and HCV, circulating sequences are likely to be so different from the vaccine strain that they are not recognized by the immune response generated by the vaccine, making the vaccine irrelevant. In the US, HCV has genetic diversity that is comparable to HIV, and for a global vaccine design an HCV vaccine faces even greater population diversity challenges than HIV.

In the face of these problems, our group created a ground breaking novel mosaic vaccine design method for HIV with the support of an LDRD DR (2005-2008) [1]. The method uses a genetic algorithm to design antigens consisting of sets of mosaic proteins that are in silico recombinants of real protein sequences, optimized to maximize the coverage of potential T-cell epitopes circulating in natural sequences. Mosaic vaccines have proven to be very promising for HIV.

Candidates for human vaccines have to go through a series of hurdles before they can be tested in humans. Our HIV mosaics have successfully advanced through these stages. They fold and are processed like natural proteins, are immunogenic in animal models, and they have greatly increased breadth and cross-reactivity of T-cell responses compared to natural antigens [2, 3]. The mosaics are an important component of our CHAVI NIH grant with Duke University (B.Korber, LANL PI), which brings to LANL more than 1.2 million annually; CHAVI has supported the testing of the vaccine in animal models and allowed us to very carefully analyze the vaccine responses. Preparations for a human trial of the HIV mosaic vaccine we designed are now underway, and B. Korber is a part of this study.

Based on the successful HIV model, we adopted the mosaic algorithm to Hepatitis C [4]. The purpose of this small short-term grant (April though Sep 2011) was to

perform initial experimental testing in mice of our set of mosaic proteins we designed for HCV and generate preliminary experimental data to enable future grant applications for studies in monkeys.

Scientific Approach and Accomplishments

This initial experimental testing of HCV mosaics was done using 2 HCV protein regions (NS3/NS4a and E1/E2), and placing them in 2 different adenovirus constructs (Ad35 and Ad26) to allow a heterologous prime boost. This work was done in collaboration with Dr. Barouch from Harvard University, one of our main collaborators on the HIV vaccine animal models. Dr. Barouch performed all experiments and the LANL team performed all the analysis and helped with experiment design. The main goal of this project was to immunize mice with a set of our mosaic HCV proteins and test and cross-compare immune responses on a set of peptides reflecting the HCV generic diversity, and so the work consisted of two major tasks.

Task One

The first part of the work, the design of a cost-effective test peptide set that reflects the diversity of circulating HCV sequencing, was performed by the LANL team by adopting several computational algorithms. The idea was to maximize coverage of circulating viruses with the minimal number of peptides to minimize cost.

To assess coverage of circulating sequences, the first step was to put together the best data sets for peptide design. The LANL-based HCV sequence database was a great asset in doing this work, as it allowed us to put together 1700 genotype 1 natural sequences.

The next step was to develop a peptide set that would provide the best coverage of these 1700 circulating sequences as well as 6 vaccine candidates. As peptides are very expensive ($200 to $450 per peptide), and since hundreds of peptides are required to achieve 75%-85% coverage of these 2 protein regions, it was imperative to minimize the number of required peptides. Two methods of peptide design previously used in HIV studies [2, 3] were compared: (i) Peptides designed using the algorithm which finds all 15-mer peptides among circulating natural sequences, that provide desired coverage (i.e. 85%) of all 9-mers, the potential T-cell epitopes (PTE); (ii) Overlapping 15-mer peptides covering several genetically disparate natural isolates, that provide the best coverage of all circulating viruses.

Both methods had their advantages and disadvantages. While overlapping peptides based on natural strains would have allowed us to determine the immune recognition of actual complete proteins from distinct circulating virus strains, PTE peptides were extremely cost effective and had much better coverage of common potential epitopes (9-mers) with significantly smaller number of peptides. However, both methods had a disadvantage that the vaccine strains were not 100% covered by the peptide sets.

We therefore developed a modified PTE method to include components of both approaches. We found all 15-mers among our 6 vaccine candidates that provided 100% coverage of all 9-mrs in the vaccine set, resulting in 304 NS3/NS4a peptides and 337 E1/E2 peptides. Then we checked the coverage of circulating 900 natural sequences by this peptide set. While the coverage of the more conserved NS3/NS4a region was 92%, the variable E1/E2 region was covered only at 65%. We then applied the PTE algorithm again to the E1/E2 region and found additional 50 peptides that increased E1/E2 coverage to 75%. The resulting set had 677 peptides and provided 100% coverage of the vaccine strains, 92% coverage of circulating NS3/NS4a natural sequences and 75% of circulating E1/E2 natural sequences. We then performed the extensive market research to purchase these 677 peptides with requisite quality control.

Task 2

The second task was to immunize mice with a set of our mosaic HCV proteins and test immune responses in mice to LANL-designed peptide sets. The experiments, performed at Harvard, are ongoing, but the first preliminary results are very encouraging. Our novel HCV mosaic vaccines fold and are processed like natural proteins, are immunogenic in mice, and they have increased breadth of T-cell responses compared to natural antigens. Currently responses to peptide pools are being finalized and the study of responses to individual peptides is ongoing. Once the Harvard team finishes the experiments, the results will be submitted for publication and LANL and Harvard teams will together apply for further funding for experimental testing in monkeys, using the experimental data in mice, generated through this funding, as preliminary data.

Impact on National Missions

Previous LDRD Directed Research funding allowed us to develop the mosaic concept and computational methods that have already resulted in further funding through the NIH, by making LANL a key component of the CHAVI project and in the human trial that is being prepared. In addition, the promising results have made LANL's HIV analysis work highly visible in the HIV field and beyond.

The HCV mosaic pilot study performed though this LDRD funding is analogous to the HIV mosaic vaccine study in mice, which was required before HIV mosaics could be moved to monkeys. Here we showed that HCV mosaic vaccines are immunogenic in mice; this critical data can support our next NIH application. We already submitted a small grant application with the NIH-sponsored Center for Evolutionary & Theoretical Immunology Seed Grant Program to continue this work.

Our results on HCV mosaic vaccines also open the door for further work on other variable pathogens, including several that are very important either from a biothreat (DoD, DHS) or a global public health perspective (NIH). Work has

already started to perform initial testing on a multi-species Ebola vaccine (with John Dye at USAMRIID). We have initiated a collaboration with Dr Timothy Endy (SUNY) to look at the development of a 4-serotype Dengue vaccine. The Defense Department's Threat Reduction Agency (DTRA) has informally shown interest in a more ambitious future project to design a vaccine against a whole viral genus, initially probably the Flaviviruses, since preliminary sequence analysis shows that the variability of this genus makes it a good candidate. This project will be proposed to DARPA. Our experimental results showing that mosaic vaccines are promising not for one, but two, differently variable pathogens provide a solid proof of principle for the applicability of this work to other variable pathogens.

References

1. Fischer, W., S. Perkins, J. Theiler, T. Bhattacharya, K. Yusim, R. Funkhouser, C. Kuiken, B. Haynes, N. Letvin, B. Walker, B. Hahn, and B. Korber. Polyvalent vaccines for optimal coverage of potential T-cell epitopes in global HIV-1 variants. 2007. *NATURE MEDICINE.* **13** (1): 100.

2. Kong, W., L. Wu, T. Wallstrom, W. Fischer, Z. Yang, S. Ko, N. Letvin, B. Haynes, B. Hahn, B. Korber, and G. Nabel. Expanded Breadth of the T-Cell Response to Mosaic Human Immunodeficiency Virus Type 1 Envelope DNA Vaccination. 2009. *Journal of Virology.* **83** (5): 2201.

3. Barouch, D., K. O'Brien, N. Simmons, S. King, P. Abbink, L. Maxfield, Y. Sun, A. La Porte, A. Riggs, D. Lynch, S. Clark, K. Backus, J. Perry, M. Seaman, A. Carville, K. Mansfield, J. Szinger, W. Fischer, M. Muldoon, and B. Korber. Mosaic HIV-1 vaccines expand the breadth and depth of cellular immune responses in rhesus monkeys. 2010. *Nature Medicine.* **16** (3): 319.

4. Yusim, K., W. Fischer, H. Yoon, J. Thurmond, P. Fenimore, G. Lauer, B. Korber, and C. Kuiken. Genotype 1 and global hepatitis C T-cell vaccines designed to optimize coverage of genetic diversity. 2010. *JOURNAL OF GENERAL VIROLOGY.* **91** (5): 1194.

Analysis of Protein Structure-Function Relations in Antibiotic Biosynthesis and Signal Transducing Receptors

Louis A. Silks III
20100603PRD2

Introduction

With the discovery of Penicillin in 1928 by Alexander Fleming, drugs with antibacterial properties started to transform medicine dramatically by providing efficient and rational treatments against bacterial infections that were previous too often lethal. Until 15-20 years ago, new compounds were isolated or known drugs further developed, to treat new infectious diseases and counter slowly emerging drug-resistant pathogenic bacterial strains. This pipeline of new antibiotics has dried up as pharmaceutical industry changed focus while for the last two decades an accelerated emergence of multi-drug resistance significantly reduces the availability of effective antibiotic treatment options.

Today, bacterial infections have become once again major public health threats. Gram-negative bacteria like *Acinetobacter baumannii* and *Pseudomonas aeruginosa* and gram-positive bacteria such as *Staphylococcus aureus* or *Clostridium difficile* rapidly evolve resistance against multiple treatment options. In fact, *A. baumannii, Staph. aureus* and *M. tuberculosis* are now causing untreatable infections due to the emergence of extreme resistance against all known antibiotics and last resort treatments. As a consequence, CDC and WHO rate bacterial infections as the #3 cause of death in developed countries including the United States again. Manmade bacterial threats with one or multiple modified or added genes for diverse resistance mechanisms challenging countermeasures in bio-threat response to intentional disseminated pathogens.

The vast majority of antibiotics, chemotherapeutics and fungicides, and anti-inflammatory and immunosuppressant medications are generated out of nature's reserve of secondary metabolites. Isolated natural products or their chemical variants are applied to clinical practice based on their pharmacologic profile. All secondary metabolites are biosynthesized by complex multi-enzymatic multi-domain protein clusters, which are organized in assembly line logic and can reach Mega-Dalton range. Most antibiotics are synthesized by so called Non-Ribosomal Peptide Synthetases (NRPS) and their biosynthesis usually starts as short-chain peptides without encoding DNA or transcribed RNA. All those short peptide precursors are further processed along their assembly lines with a vast variety of enzyme-driven modifications. Providing novel compounds as drug candidates for antibiotics requires search strategies and exploration methods to identify unique features in genomes, predict the encoded protein functions, the assembled product and finally to isolate the novel compounds, test and progress into potential drugs candidates. A promising path is the proteins of Non Ribosomal Peptide Synthetases (NRPS), their structures, structural complexes and their dynamic interactions. This path promises to lead to the isolation of new natural products and their chemical and biochemical characterization. Using currently available genetic information and data about the biosynthetic logic of NRPS assembly lines, we could solve the protein structure of the larges protein complex ever done by NMR spectroscopy and identified a total of nine novel NRPS assembly lines coding for nine examples of a potentially new class of natural products that not yet reported in the literature.

Our work is intended to (**1**) to further characterize the biosynthetic details of all isolated and tested natural products and structural features of the involved proteins, (**2**) to synthesize *de novo* the parent chemical structure of all compounds for structure confirmation and mode of action studies (**3**) to synthesize a variety of similar compounds to modulate the efficacy against certain bacterial pathogens, (**4**) to study potential side effects by extended toxicology assays in cell culture and in mice and rat models and (**5**) to extend our research to similar assembly lines that we have recently discovered.

Benefit to National Security Missions

A long-term benefit of this research is the exploration of novel protein assemblies, understand their structural interaction and to elucidate novel products of pathways for natural product biosynthesis. We develop a discovery process that will lead to new drug candidates for antibiotics with new chemotypes that are urgently

needed to combat bacterial resistance. The ultimate goal of our research is the ability to predict the chemical structure of secondary metabolites by understanding the biosynthetic logic and structural assembly of unknown NRPS assembly lines based on genetic and structural analyses. Our collected data demonstrate a "Genome to Proteome to Drugs" success long envisioned and rarely achieved. Pharmaceutical discovery can result from approach of deciphering genetically encoded protein functions, elucidating the protein structures and functional enzyme complexes, predicting encoded secondary metabolites, and isolating the predicted compounds. The development of antibiotics directly relate to efforts in the Biosecurity Center and the overarching mission of biothreat reduction. This research clearly has the potential to generate follow on funding for basic research and valuable intellectual property. It establishes a structural biology and protein function effort at LANL that immediately leads to new pathogen countermeasures.

Progress

Our multi-disciplinary approach deploys protocols and tools of bioinformatics, structural biology, microbiology, synthetic chemistry and analytical methods such as NMR and mass spectrometry to identify candidate producer strains of bioactive compounds, predict the produced secondary metabolite, study protein folding and structural complexes of proteins producing the compound, express, isolate and identify the natural products and finally to test the activity profile of these novel natural products.

We identified and characterized the details of the biosyntheses of three different compounds, is searching for additional examples of similar natural product assembly lines. We characterized a total of nine natural products will include *de novo* chemical synthesis to confirm the chemical structures and solved the largest ever studied protein complex by NMR spectroscopy. We are currently preparing a manuscript and will submit the results of his structural studies by the end of 2011.

We will screen genome databases with a wide variety of different bacterial strains for particular genomic markers associated with the synthesis of novel secondary metabolites and continues efficacy studies (MIC) internal as a first screening and with an outside contractor for validation of newly found natural products. Our studies include bacterial strains that have become insusceptible to standard treatments due to established antibiotic resistance (*C. difficile*, *MRSA*) or strains that develop antibiotic drug-resistant on an incredible fast rate (*Acinetobacter baumannii and Pseudomonas aeruginosa*). Our studies will extend to include pathogens that are naturally insusceptible due to highly hydrophobic cell walls (*Mycobacterium t.* and *bovis*). NCCLS standard disk diffusion and CLSI MIC liquid culture assays are used at LANL and/or at the facilities of an established outside contractor under BSL-1 to BSL-2+ conditions

(drug resistant pathogens pending BSL 3 availability at LANL or alternatively at a commercial collaborator). His current data demonstrate very promising ratios between antibacterial efficacy and toxicology in cell line and mice model for the first three isolates. The development of novel antibiotics also directly relates to efforts in Federal Government and private sector funded basic and applied research. New countermeasures for infections with human pathogenic bacteria are the focus of federal funding agencies including HHMI, NSF, NIH and DTRA (DoD), CDC and are supported by private sector funding including Venture Capital, private research foundations (e.g. Bill and Melinda Gates foundation) or funds to fight co-infections with HIV or during cancer treatments (e.g. Jimmy Fund of Dana Farber Cancer Institute or Susan Comen foundation). OUr current research has the potential to generate follow-up funding out of federal and private sector resources and he is going to pursue this pathway. We can develop valuable intellectual property, but most importantly might leads a path to drug candidates to fight re-emerging infectious diseases. Our long-term goal is to establish a structural biology and protein function effort at Los Alamos National Laboratory to study the logic for natural product biosynthesis that immediately will lead to new pathogen countermeasures and can change paradigms in the field for drug discovery.

Future Work

Our research requires (**1**) further characterization of the biosynthetic details of isolated and tested natural products, (**2**) continued work in structural biology to gain more detailed insight of structural protein complexes (**3**) synthesis of a variety of similar compounds to modulate the efficacy against certain bacterial pathogens and mode of action studies, (**4**) studying potential side effects by extended toxicology assays in cell culture and in mice and rat models and (**5**) extending our research to similar assembly lines that we have recently discovered. Identifying specific genetic markers and combinations of them will help elucidate whether a newly discovered assembly line is coding for the biosynthesis of new antibiotics, chemotherapeutic agents, immunosuppressant compounds and/or known or not yet described bacterial or fungal toxins.

Conclusion

The vast majority of available antibiotics and chemotherapeutics are natural products or chemical variants of those, which are synthesized by large multi-enzymatic protein clusters, called Non-Ribosomal Peptide Synthetases (NRPS). Non-ribosomal peptides have a variety of medicinal properties including activity as antibiotics, antitumor drugs, immunosuppressant or anti-inflammatory drugs, or toxins. Structural and biochemical information on isolated catalytic functions such of adenylation (A) to activate amino acid residues by ATP hydrolysis, condensation (C) to form a peptide bond, peptidyl carrier

(PCP) function to shuttle the growing peptide chain and thioesterase (TE) domains to hydrolyze the matured natural product off the biosynthetic assembly line was gathered over the past decade with our postdoc's help. Still, little is known about product specific functionalities of these biosynthetic systems, how NRPS clusters assemble, domain interactions and substrate recognition are accomplished. Understanding the pathways and structural assembly of involved enzymes is crucial to the discovery of novel NRPS biosynthetic clusters that include extracellular processing steps of a precursor metabolite. Realizing that natural products that are modified outside the host cell promise to be bioactive led to the isolation, characterization and testing of novel, previous unknown compounds with broad-spectrum antibiotic properties.

Quantitative Modeling of Cellular Noise

Michael E. Wall
20100604PRD2

Introduction

Dr. Munsky's research is pioneering in its ambition and achievements. As a student, he developed powerful tools to analyze discrete stochastic processes. As a postdoc, he showed that these tools are perfectly well suited to complement experimental investigations of cell-to-cell variability in biological systems. Previously, single cell behaviors were measured, but modelers only considered the mean and variance of these behaviors. Munsky showed that the full dynamical distribution provides a much greater wealth of information. He developed an integrated experimental and computational approach to identify parameters of stochastic models for biological systems. Previously, he published an article in Nature/EMBO Molecular Systems Biology (the top systems biology journal) to demonstrate that these tools work when applied to a simple synthetic genetic system. Brian has now scaled up the up the applicability of this approach and has applied it to a much broader class of biological systems and a much broader class of mechanistic models. His recent work on the systematic identification of predictive models for the mechanisms and parameters for signal activated gene regulation is already attracting attention from the best single-cell / synthetic biology labs world-wide.

Benefit to National Security Missions

The project addresses the general problem of modeling and predicting the response of stochastic systems. It seeks to validate these methods using bacterial, yeast, and mammalian gene regulation as important biological test bed applications. The results will advance all technical problems that involve attempting to understand and predict the responses of noisy or random systems, cross-cutting the needs of many agencies and missions including DOE (biothreat reduction and using microbes for biofuel production), NIH (design of therapeutics for bacterial or viral infection), and broad problems in chem-bio, materials, chemistry, bioscience, health research, and bioenergy research.

Progress

Since this project began, Dr. Munsky has made significant progress towards the project objectives. He has developed new efficient software for the identification of gene regulation based upon cell-to-cell variability, and he has extended these to make use of parallel computing capabilities. The first version of this software is currently available under LANL copyright (LA-CC-10-103) and future versions are in preparation to be copyrighted and released to the public in open source format.

Since April 2010, Dr. Munsky has applied his software and algorithms to the identification of the regulatory mechanisms of an important gene in yeast. He has recently completed a book chapter on the analysis and identification of stochastic gene regulation. He has published a paper in IET System Biology on a similar topic. Dr. Munsky has given a number of invited talks on the topic of this project, including at the Santa Fe Complex (April, 2010); the 2010 Congress of the International Society for the Advancement of Cytometry (Seattle, May, 2010); the University of Washington (May, 2010 and Feb. 2011); The University of New Mexico (Nov., 2010); the Conference on Stochastic Systems Biology (Monte Verita, Switzerland, June, 2011); and gave tutorials at the Fourth and Fifth q-Bio Conference (Santa Fe, Aug., 2010 and Aug., 2011). Dr. Munsky won the 2010 Leon Heller Postdoctoral Publication prize and presented a prestigious Physics/Theory Colloquium talk at LANL (Oct., 2010).

An important step toward identifying a useful model is being able to estimate how well the model will predict behaviors in new conditions. Models that are too simple to match important behaviors in observed conditions will not be able to predict these behaviors in new conditions. On the other hand, models that are too complicated will be extra-sensitive to measurement errors and will also perform poorly when tested at new conditions. Dr. Munsky has developed a new approach to estimate the predictive power of discrete stochastic models, when these models are fit to real experimental data. This approach, which provides a guideline to help

researchers decide when a model is too simple or too complex, was successfully applied to select a model that can accurately predict the cellular responses of yeast cells during a certain type of stress response (manuscript under revisions for resubmission to *Science*).

During this project, Dr. Munsky has been strongly involved in organizing local, national, and international events to strengthen the quantitative biology community at LANL and beyond. He is a co-organizer of the q-Bio Seminar Series at the LANL Center for Non-Linear Studies (since 2010). He was an organizer for the Fifth International q-Bio Conference on Cellular Information Processing in Santa Fe, NM (Aug. 2011), which attracted a record of over 220 participants from around the world. Dr. Munsky also organized the 3rd International Workshop on Stochasticity in Biochemical Reaction Networks, which was held in Banff, Canada in September 2011. In order to help researchers attend this workshop, Dr. Munsky applied for and won the equivalent of approximately $50,000 in lodging support from the Banff International Research Station (BIRS) and $25,000 in travel support from the Institute of Complex Adaptive Matter (ICAM). Finally, Dr. Munsky was the main organizer of the 2010 and 2011 quantitative biology summer schools at LANL (over two and a half weeks each July and August), where he taught his methods to over 80 domestic and international students.

Dr. Munsky's algorithms, approaches and expertise are currently being utilized by collaborators at the University of California at Santa Barbara (Dr. David Low), Massachusetts Institute of Technology (Drs. Alexander van Oudenaarden and Gregor Neuert), the University of California at San Francisco (Drs. Christopher Voigt and Chunbo Lou), Duke (Dr. Linchong You), the University of Washington (Dr. Eric Klavins), the Swiss Federal Institute of Technology (ETH, Dr. Mustafa Khammash), and the University of Pittsburgh (Dr. James Faeder). In addition to these, Dr. Munsky's methods have spurred new collaborations with numerous students of the 2011 q-Bio Summer School. Many of these projects are reaching fruition, and many more significant accomplishments are anticipated and will be reported on a future datasheet.

Dr. Munsky's approaches are contributing to a recently funded DR (20110051DR, Illuminating the Dark Matter of the Genome: Small RNAs as Novel Targets for Bioterrorism Counter-measures). In this project, of which Dr. Munsky is a Co-Investigator, LANL has hired a new postdoc (Dr. Doug Shepherd), who has been working with Dr. Munsky's to integrate experimental and computational approaches to the study the stochastic dynamics of small RNA molecules during bacterial infections. In the initial stages of this project, Dr. Munsky and Dr. Jim Werner (MPA-CINT) have helped to guide Dr. Shepherd's progress toward developing new protocols to label, image, and analyze the distributions of mRNA molecules in mammalian cells.

In the course of this project, Dr. Munsky recognized that the problem of identifying a predictive model is very similar to the problem of diagnosing a disease. As such, the analysis of cell-to-cell variability within a blood or fluid is expected to contain information about the underlying disease state of an organism. With this in mind, Dr. Munsky has made initial progress to extend his methods to aid the process of automated diagnostics. In initial collaborations with Cr Babetta Marone and Dr. Kumkum Ganguly, Dr. Munsky showed that the statistics of cellular responses could be used to identify influenza-infected cell populations without the need of expensive chemical labels.

Future Work
The project focuses on development of integrated computational/experimental protocols to identify predictive models of important biomedical processes, including (i) the E. coli gene (pap), which causes urinary tract infections, (ii) the Hog1 pathway, which relates to cancer growth, (iii) various genes (plac, ptet, etc...), which are used to build synthetic organisms for biofuel applications, and (iv) sRNA dynamics important during host-pathogen interactions. The research uses the National Flow Cytometry Resource's advanced equipment to measure millions of individual cells and construct detailed histograms of transient cell responses under myriad controllable inputs (temperature, nutrient levels, chemical inducers, etc...). Most researchers examine only the means and sometimes variances of such data, ignoring other aspects. However, these approaches enable capturing of the full qualitative and quantitative shapes of these non-gaussian histograms and thus extract more information from each experiment. In preliminary studies, integrated experimental/computational approaches have been used to identify and validate predictive stochastic models for gene regulation in bacteria and yeast. This project will use experiments to identify stochastic models, but then use these models to design better experiments (i.e., find more revealing experimental conditions to explore). Iterating these steps will produce more thorough quantitative characterizations of biological processes and make it easier to develop predictive models and design medical treatments.

In addition to helping to identify predictive models for biological systems, initial studies also suggest that Dr. Munsky's approaches could have significant potential to increase the precision and accuracy of medical diagnostic procedures. Dr. Munsky and colleagues have proposed extending this work to develop a semi-automated diagnostic procedure based upon the integration of information science and technology with high-throughput single-cell biological experiments (2011 LDRD-DR, unfunded). This capability will be examined in greater detail in later stages of this project.

Conclusion

This project will have many levels of impact. First, the models will improve the diagnosis, understanding and treatment of numerous biomedical problems, including (i) systems linked to bacterial infections, antibiotic resistance, and bioterrorism countermeasures, (ii) processes related to cancer, and (iii) influenza virulence. Second, the methods will improve quantitative modeling of synthetic genes being considered for biomedical research, biofuels, and biochemical sensors. The publicly-released software and experimental protocols will help other researchers to identify stochastic models for numerous applications in academia and industry. By enabling fast and precise analyses, the work will enable researchers to solve currently unapproachable problems.

Publications

Munsky, B., and M. Khammash. Identification from stochastic cell-to-cell variation: A genetic switch case study. 2010. *IET Systems Biology.* **4**: 356.

Neuert, G., B. Munsky, R. Tan, M. Khammash, and A. van Oudenaarden. Systematic Identification of Signal-Activated Stochastic Gene Regulation. To appear in *Science.*

Roles of Fungi in Terrestrial Ecosystem Carbon Cycling

Cheryl R. Kuske
20100625PRD3

Introduction

Soil fungi control the cycling of carbon in and out of soil, locally and globally. However, the impacts of climate change factors, such as elevated CO_2, on this complex group of microorganisms are poorly understood and therefore cannot be reliably included in predictive models of terrestrial ecosystem. The soil fungi that control carbon cycling are very complex and most are not culturable. This project aims to develop new metagenomic (collective genomes or DNA of the entire soil microbial community) and metatranscriptomic (collectively expressed genes that identify active processes) approaches to identify and track changes in soil fungi in response to elevated CO_2 and other climate change factors in a landscape-level field experiment and laboratory manipulation experiments. We will combine a targeted approach that detects genes that we know to be important as well as broad scale methods to comprehensively detect active fungal genes in soils under different conditions. The study uses soil samples collected over a 2 yr time course, from the DOE's pine FACE site and other FACE sites, and explores the interactive effects of soil depth, N fertilization, and elevated atmospheric CO_2 on the composition and carbon cycling activities of soil fungi.

Benefit to National Security Missions

The most direct agency relevance for this project is tied to DOE missions in carbon cycling, climate change response, genomics technology development, and understanding complex systems. The soil microbiota is a key part of the environmental response to insult, with applications to waste management in the complex.

Progress

Task 1: We successfully sequenced our first soil metatranscriptome last August from soil from the loblolly pine plantation site, generating over 96,000 sequences. About 90% of these sequences are ribosomal, allowing us to determine which fungi are active at this site. We are just beginning to mine the remaining 10% for key functional genes that may be important in carbon cycling. We are planning to write a manuscript detailing the findings of this preliminary dataset. Preliminary findings from this dataset were presented at the Mycological Society of America Conference in August 2011.

Task 2: We completed experimental testing of two reverse transcription PCR (RT-PCR) methods to determine which methods would be suitable for us to use in our functional gene expression studies. We discovered that a method called SMART-PCR, a method that is increasing in popularity in the scientific community, substantially restricts the richness and composition of the expressed genes in our dataset as compared to another RTPCR approach. A manuscript detailing these findings has been published by the *Journal of Microbiological Methods*.

We have successfully completed a second study of RT-PCR methods in which we compare the datasets resulting from two different priming methods used to generate cDNA (random hexamers and oligo(dT) primers). The two methods are abundantly used in the literature, but the performance of the two methods had not been compared previously; such a comparison is important because it was not clear which method was most suitable for our purposes or if comparisons could be made across studies in the literature using both of the methods. We were able to demonstrate that the two methods do yield comparable results with some caveats; we have prepared a manuscript detailing these findings that will be submitted to the *Journal of Microbiological Methods* by the end of October 2011.

We have successfully developed qPCR methods to examine the quantitative expression of three fungal genes involved in complex carbon degradation, which encode cellobiohydrolase, xylanase and mannosidase enzymes. Using pyrosequencing, we have generated a total of almost 350,000 fungal ribosomal large subunit (LSU) and internal transcribed (ITS) spacer sequences from four sets of soil cores from the loblolly pine plantation FACE site. These pyrotag datasets provide a high-resolution profile of fungal community composition, across depth intervals (0-2 cm, 2-5 cm,

5-10 cm and 10-15 cm) as well as CO_2 and nitrogen treatments. Data analyses of these profiles indicate that significant shifts in fungal composition across these gradients occur at the phylum level. Basidiomycota become more abundant under elevated CO_2 across all depth intervals. Ascomycota generally become more abundant in nitrogen fertilized plots. These profiles will allow us to correlate fungal community composition with quantitative expression of the functional genes described above. Further data analyses have indicated that overall fungal richness is significantly impacted by fertilization. In addition, soil chemical analyses were performed on all soil depth intervals. The highest nitrogen concentrations were found in the 0-2 cm depth; this correlates with the most dramatic community shifts being observed in this depth interval. These preliminary results were presented the Mycological Society of America Conference in August 2011, and the data is currently being incorporated into a manuscript.

Task 3: The database of cellobiohydrolase (cbhI) sequences from the FACE sites and reference taxa was successfully compiled and discussed in a recently published manuscript in *Environmental Microbiology*. This database is being put to use in a study to identify cellobiohydrolase genes that are present across five seasonal time points at the loblolly pine plantation site as well as in ongoing parallel gene expression studies. Preliminary findings show that cellobiohydrolase richness does not change substantially across seasons or treatments. However, parallel seasonal profiles based on the Fungal LSU gene show that there are significant impacts of treatment that vary across seasons. This is interesting because it shows that the cellulolytic fungal guild may be a perennial component of the soils at this site. We are in the process of using our reference database to classify the cbhI sequences and also examine the LSU profiles to determine which taxa are impacted by treatment and or season. Expression profiles of cbhI demonstrate that Basidiomycota dominate the expression profiles and it is not the prototypical cellulose degraders (e.g. *Trichoderma, Aspergillus, Chaetomium*) that are likely responsible for cellulose degradation in situ. We are currently in the process of trying to identify these potentially novel cellulose degraders. The *cbhI* database has been expanded from 114 sequences to 235 and has been used to classify *cbhI* transcripts from the Duke Forest FACE site in soils in a factorial experiment with elevated CO_2 conditions and nitrogen fertilization. The details of this study have been incorporated into a draft manuscript that we are in the process of editing.

We have completed a study in soil and litter in which we compare the composition of resident cellulolytic fungi (using DNA-based methods) and active cellulolytic fungi (using RNA-based methods). We found that the compositions of resident and active cellulolytic fungi were distinct in soil and litter, but they were more similar in litter than in soil. This finding is consistent with previous findings and suggests that compositional overlap of profiles from resident and active taxa may be a useful ecological metric to describe selection factors driving microbial community composition in soil. We have submitted a paper to *The ISME Journal*, which explores this hypothesis and the potential ecological significance of these types of datasets.

Future Work
Task 1: Continue data analysis efforts of a fungal community transcription approach based on high-coverage transcriptome sequencing of fungal messenger RNAs to identify all fungal genes that are being expressed in CO2-enriched and non-enriched sites.

Task 2: Develop and use a sensitive molecular probing technique (reverse transcriptase PCR) to examine the expression levels of key functional genes such as cellobiohydrolase (cbh) and chitinase. Submit a manuscript to Journal of Microbiological Methods detailing our findings in a comparison of cDNA generation methods. Complete analysis of sequence datasets, soil chemistry data and quantitative PCR results for incorporation into two manuscripts detailing the impacts of elevated CO2 and nitrogen fertilization on fungal communities in different soil depth intervals and across five seasonal sampling points

Task 3: Use these tools in replicated field experiments to track the response of complex groups of soil fungi to over a decade or elevated atmospheric CO2 conditions, and the influence of N fertilization and soil depth on those responses. Work with collaborators to finalize a manuscript describing our 235-sequence cbhI database and the classification of expressed fungal cbhI genes in soils exposed to four different CO2 and nitrogen regimes.

Conclusion
Globally, soil stores more carbon on Earth than plant biomass, and fungal activities in soil that control storage of this carbon, or its release back into the atmosphere, are critical to stability of global atmospheric conditions. The metagenomics and metatranscriptomics techniques we develop will provide a powerful approach to understanding the roles of fungi, a major soil component in all terrestrial soils and sediments, to complex carbon cycling in terrestrial ecosystems. Filling this knowledge gap is essential for accurate assessment of climate change impacts on natural and agricultural systems and prediction of air quality and altered weather patterns.

Publications
Weber, C., D. Zak, R. Jackson, R. Vilgalys, R. Evans, C. Schadt, J. Megonigal, and C. Kuske. Responses of soil cellulolytic fungal communities to elevated atmospheric CO2 are complex and variable across five ecosystems. 2011. *Environmental Microbiology.* **13** (10): 278.

Weber, C., and C. Kuske. Reverse transcription-PCR methods significantly impact richness and composition measures of expressed fungal cellobiohydrolase I genes in soil and litter. 2011. *JOURNAL OF MICROBIOLOGICAL METHODS.* **86** (3): 344.

Stochastic Spatially Explicit HIV Dynamic Models

Alan S. Perelson
20100627PRD3

Introduction

HIV causes a chronic infection despite a vigorous immune response against the virus. It is still a mystery why the virus persists and can not be eliminated, even with the help of potent drug therapies. New mechanistic models may help provide insights into the mechanisms of HIV persistence. These could help us attain the ultimate goals of preventing progression to a persistent infection or achieve HIV eradication. Current HIV models, while successful in predicting the chronic stage of infection, have failed in helping guide the end game of HIV infection - i.e. full eradication of the virus and hence cure. We feel that a new generation of models is needed that takes into account many features that existing models have neglected - namely that the viral infection need not be homogeneous in space (by that we mean that there may be more virus in one part of the body than others) and that certain aspects of the infection process may be random (by that we mean that if one considers what happens to an infected cell, whether it lives or dies by a certain time may be random rather than fully determined as it is in existing models). Our goal in this project is to develop models that take into consideration spatial heterogeneity, as well stochastic (i.e. random) effects. We will use these models to help interpret published data on HIV infection, the effects of therapy, and the establishment of chronic infection.

Benefit to National Security Missions

Quantitative models that can help us understand the interactions between a host and pathogens, and mitigate such interactions while they are still in an early stage of development. The work proposed here will help advance our knowledge in viral infections and the effects of drug therapy. The work could impact how new infections are treated and provide new fundamental knowledge about viral infections. This would support our mission of scientific discovery and innovation in basic health research as well as defense against biological weapons. The work is also highly relevant to various DHHS programs at NIH and CDC as well as DOD programs in DTRA (Defense Threat Reduction Agency) such as their Transformational Medical Technology (TMT) program.

Progress

The objective of this research is to better understand the mechanisms of HIV persistence despite very potent antiretroviral therapy. We are looking at the question of HIV persistence from two perspectives: a) First, we are asking what happens during the initial stages of HIV infection (i.e., primary infection) that leads to the virus establishing itself in the face of an immune response; and b) what prevents very potent antiretroviral therapy from eliminating the virus once an infection is established. We have taken the following steps to answer these questions.

We have used a model with time-dependent infectiousness to fit HIV levels measured in blood during early primary infection of a set of individuals that were sampled regularly and frequently even before infection. The concentrations of HIV and several types of immune system cells were measured from the blood samples. Acute infection was monitored in unprecedented detail, providing a unique opportunity to explore early HIV infection kinetics. For instance, the initial exponential growth of virus can be clearly tracked for most patients, and the time for the viral level to reach a peak can be determined more precisely than before. The HIV viral load data of 24 patients was quantified and these viral load data have been fitted by our model with high quality (Figure 1). The fits provide information about the parameters that characterize early infection, such as the rate at which HIV virions infects target cells, the death rate of infected cells, the strength of immune responses in reducing infectiousness, etc. These new parameter estimates are improving our understanding of early HIV infection.

We have been developing a new model of viral infection and are using it to fit the data on viral levels in blood (plasma) and CD4+ T cell levels in SIV primary infection. This is the simian model of HIV infection where it is feasible to directly inject monkeys with virus and study the kinetics of primary infection. We are collaborating with scientists at Tulane National Primate Research Center and at University of Pennsylvania. We have

fitted their data obtained during infection with different strains of SIV (SIVmac239, deltaGY, and delta nef) that lead to different persistence outcomes (Figure 2). We are currently revising the model to improve the quality of fits to the data, and are exploring the differences in immune responses to the different viral strains. Experiments are also being done using different monkey species and we are trying to understand via fits of the model to data the impact of different host species on the immune response elicited by the infection.

We are analyzing the very early processes that occur during HIV infection, with emphasis on the stochastic nature of these processes. Because early in the infection very few virus particles are involved and very few cells are infected, stochastic effects many play a role in deciding whether an infection is established or not. We have developed a branching process model of early infection and production of new virions, and are using it to evaluate the probability that a person exposed to a certain amount of virus becomes infected and what interventions could reduce this probability.

Once infection is established, the virus persists and cannot be eliminated, even with the help of potent drug therapies. Indeed, today's drug therapies are very successful at suppressing the amount of virus measured in the blood of patients to very low levels, but cannot completely cure the infection. To probe these phenomena better, we are working on the following tasks:

Follicular dendritic cells (FDC), which are found in lymph nodes, spleen and tonsils, act to help filter viruses out of blood. These cells capture viral particles (virions) on their surface and may serve as a reservoir of HIV-1 virions. We believe this physical storage of virus on FDC is impairing complete eradication of HIV-1 infection by drug therapy. However, the long-term ability for FDC to retain HIV-1 has not been fully quantified. We have developed a theoretical method to study the dynamics of FDC retention of HIV-1, and have used it to explain published data on the levels of plasma viremia in patients under long-term antiretroviral therapy. We are also using the model to explore theoretically the effects of new drug candidates to drive HIV-1 off of FDC. We have a draft manuscript that is being finalizing for submission in a scientific journal. These results have been presented in a poster "Quantifying the role of FDC as a long term reservoir of HIV-1 virus" at the "LANL Postdoc Research Day."

We are studying the effects of spatial heterogeneity and spatial spreading of HIV virus within lymphatic tissues. These models take virion diffusion and migration of infected CD4 cells into account. We believe this work will help us understand how the infection is maintained in patients, and whether there are spatial reservoirs where it is more difficult to eliminate the virus.
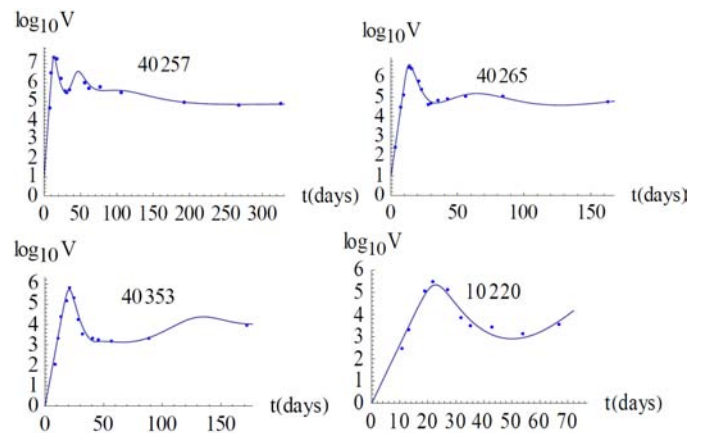
Figure 1. The fit of our mathematical model (solid line) to data on HIV viral load, V, for four representative individuals.
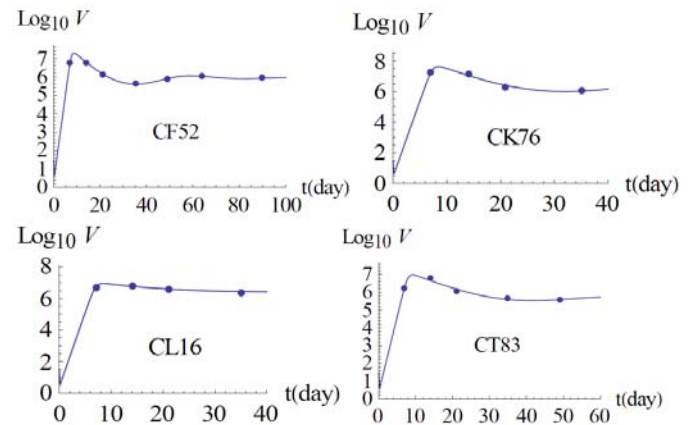
Figure 2. The fit of our mathematical model (solid line) to data on SIV viral load, V, for four representative monkeys.

Future Work

HIV is a chronic infection despite a vigorous immune response against the virus. Why the virus persists and can't be eliminated is still a mystery. Very early events in infection seem to set the stage for chronic infection, which can't be eradicated even with therapy that suppresses HIV below the limit of detection of standard assays. During treatment the viral load often remains detectable when very sensitive viral load assays are used. Further, higher levels of intermittent viremia, called viral blips, are sometimes observed. The study of early infection and the phenomenon of "viral blips" will help improve therapies for HIV infection in which one's goal is to eradicate the virus.

The theoretical methods we will use include dynamical and stochastic effects in viral replication and release. Most models of HIV population dynamics yield a steady state, where the virus population level remains stable, and which under therapy can be driven to zero. These models assume that infected cells release virus at a constant rate regardless of how long the cell has been infected. However,

there is a time-lag between infection and generation of new virus, and it is well-known that time delays can lead to oscillations. After the time-lag the viral production rate may change, with other dynamical consequences. Moreover, existing theories are deterministic, implicitly assuming infinite population sizes. We will explore whether stochastic effects in finite systems enhance fluctuations in the virus population level and give rise to "blips". Furthermore, most existing models on HIV dynamics are spatially uniform. However, spatial heterogeneity in viral load, drug concentration, immune response and cell type may also be important. If control of the virus is poor in some regions, local viral replication might occur and such virus leaking into blood might contribute for HIV persistence. Models of this type, while developed for HIV, will also be applied to other viral infections.

Conclusion

The outcome of this project will be a new set of more realistic models of HIV that take into consideration that the levels of HIV may be different in different parts of the body. These models will allow some events to be random rather than deterministic. Thus, for example whether a virus particle will be destroyed or not will be modeled as a random event with the virus lifetime given by a probability distribution. These models should help us attaining the goal of curing HIV – either by preventing progression to chronic infection or by enhancing therapy effectiveness.

Engineering of Phosphotriesterase Enzymes for Nerve Agent Degradation

Robert F. Williams
20100628PRD3

Introduction

Enzymes for *ex vivo* applications should be readily expressed in bulk quantities, possess large enzymatic activities, be stable within wide ranges of temperatures, pHs and ionic strengths in solution, show no substrate or product inhibition, and preferentially exhibit robustness with respect to organic solvents or preservative content in solution. Unfortunately, without significant bio-engineering, no natural enzymes exhibit all these desired features. One enzyme, Diisopropyl Fluorophosphatase (DFPase), important as a potential CWA countermeasure, is capable of catalyzing the hydrolysis of the highly toxic G-type nerve agents like Sarin (GB) or Soman (GD). However, the native enzyme exhibits considerably lower turnover of the most toxic stereoisomer of these G-type agents and is ineffective against the more toxic V-type agents (VX). The enzyme is isolated from squid, and its natural substrate and function is currently unknown. DFPase is structurally well-characterized with both an atomic resolution (0.85Å) X-ray crystal structure and a rare neutron diffraction structure, obtained at LANL, which identifies the orientation of water and other hydrogens in the active site allowing the proposed reaction mechanism to be confirmed. Recently, enzyme mutants of DFPase have been generated that reverse the native stereochemical preference of the enzyme so that the more toxic enantiomers of the G-type nerve agents are preferentially degraded; however, while k_{cat} was enhanced by ~10-fold, the K_m was increased resulting in unfavorable consequences for degradation at low substrate concentrations. Additionally, some mutants exhibited limited activity (low turnover) against the V-type agents. This project will extend these preliminary bio-engineering efforts with DFPase to derive designed and customized properties for the active site and overcome the current limitations of unsatisfactory binding and catalytic turnover (K_m and k_{cat}), thus producing an enzyme specific for G- and V-type agents useful in *ex vivo* and potentially *in vivo* applications.

Benefit to National Security Missions

Once the "rules" for evolving enzymes are deciphered to produce a desired catalytic activity, a highly attractive structural template is available to generate new enzymes by design. This template can be used to design new nerve agent degrading enzymes, which are better suited against V-type agents or other specific targets. This directly addresses LANL and DOE's mission of Threat Reduction and Global Security as well as supporting the decontamination, forensics, and therapeutic missions of the DoD, DHS, and NIH. The results from this study, in understanding structure-activity relationships, can reduce the threat and remediate current and future chemical and biological weapons of mass destruction.

Progress

The overall aim of the proposed work is to generate variants of the phosphotriesterase Diisopropyl Fluorophosphatase (DFPase) with enhanced activity against V-type nerve agents, especially VX. Previously recorded qualitative data revealed that a quadruple mutant of DFPase shows a small but distinct activity against three different V-agents (among them VX). This activity is not observed with the DFPase wild-type. Live agent measurements, conducted during a trip to the Bundeswehr Institute for Pharmacology and Toxicology in Munich in April 2011, have yielded the required quantitative data for this activity. Quantitative measurements were also conducted to assess the activity of DFPase against the toxic VX degradation product O,O-diethyldimethylpyrophosphonate (VX-pyro). Additionally, a number of enzyme mutants based on the original quadruple mutant were screened for VX and VX-pyro activity. This data was combined with computational docking and MD simulations to model the binding of VX and VX-pyro at the DFPase active site and structure activity relations for the additional mutants were established. This work is currently being prepared for publication.

Based on this work, DFPase residues have been identified for mutagenesis with the aim to generate a region rich in aromatic residues to stabilize the (most likely) protonated leaving-group of VX. The rational follows the stabilization that occurs in the anionic

binding site of Acetylcholinesterase. We anticipate this work to be completed in the next six to nine months. Also, additional computational work is being carried out using a suite of programs including ADF (DFT code), MD simulations, autodock (molecular ligand docking), and Rosetta to generate and test mutants *in-silico* and to model the reaction step that produces the phospho-enzyme intermediate on the enzyme.

The reaction mechanism of DFPase is proposed to involve nucleophilic attack of residue D229 on the bound organophosphorous substrate with the subsequent generation of a short lived phospho-enzyme intermediate. This mechanism was recently challenged despite data from isotopic labeling experiments showing the existence of a covalently bound intermediate. The alternative mechanism invokes activation of a metal bound water molecule with proton abstraction by D229 and subsequent attack of the hydroxyl species on the substrate. Despite in-direct evidence against this mechanism, work was carried out to establish the existence of the phospho-enzyme intermediate and support the mechanism involving nucleophilic attack of D229 on the intermediate. DFPase was reacted with diisopropylfluorophosphate and immediately precipitated to trap the phospho-enzyme intermediate. Using a published procedure known to trap similar phosphoaspartates, the protein was treated with $NaBH_4$ to reduce the phosphorylated aspartate to homoserine and then digested with trypsin. Preliminary mass spectral data of the digested peptides shows the presence of a homoserine containing peptide in about 10% yield (comparable to the yield observed in the literature for reduction of other phosphoaspartates). Unfortunately, the tryptic digest yielded a peptide that was not ideally suited for characterization by ESI-MS/MS; consequently, the experiment is being repeated using GluC. This work will help establish the correct reaction mechanism for DFPase.

In addition to the above research accomplishments and subsequent publications in preparation, M.M. Blum is currently serving as an assistant editor for a special issue of the journal "Drug Testing & Analysis" titled "Analysis of Drugs for the Therapy of Anticholinesterase Poisoning". He has also contributed three articles to this issue: One research article is titled "*In-vitro* and *in–vivo* efficacy of PEGylated Diisopropyl Fluorophosphatase (DFPase)" and describes the successful PEGylation of DFPase, subsequent characterization by ESI-TOF-MS, kinetic measurements with agents, and animal experiments (rats) that show that an evolved DFPase mutant are protective against a 3x LD50 challenge with soman. The second article is a review titled "Review on UV-spectroscopic, chromatographic and electrophoretic methods for the cholinesterase reactivating antidote pralidoxime (2-PAM)" and the third is an article titled "Historical perspective and modern applications of Attenuated Total Reflectance – Fourier Transform Infrared Spectroscopy (ATR-FTIR)". These articles were handled by the journals editor in chief and are currently either published online or at the proof state and represent work accomplished prior to coming to LANL.

Future Work

Recent computational studies have revealed that the structurally highly similar proteins, including DFPase, Drp35, Regucalcin, and SMP30, all belong to the SGL (SMP30/Glucono-lactonase/Luciferin Regenerating Enzyme) domain. Approximately 2000 protein sequences within this domain family can be found in databases such as PFAM. Homology modeling of a few test cases has revealed a very high structural similarity for other members of the domain family despite a very low sequence similarity (<20%). This opens a path towards generating new *de-novo* proteins with the same fold and specifically tailored active sites. In addition to performing further mutational studies with DFPase, we will also generate new DFPase-like enzymes based on the SGL domain and the six-fold _-propeller fold. This will also require computational chemistry using MD simulations, DFT calculations, and molecular modeling; consequently, the leading computational facilities and theoretical chemists at LANL will be highly beneficial for the success of the *in silico* part of this project.

Enzyme testing will be carried out at LANL using pesticides (e.g., Demeton-S) that are satisfactory simulants of the actual agents and at the Bundeswehr Institute for Pharmacology and Toxicology in Munich or at the Edgewood Chemical Biological Center (ECBC)/USAMRICD using live CW agents. Enzyme variants that exhibit the desired properties will be characterized kinetically and structurally. X-ray and, if feasible, neutron structures of new generated V-agent enzymes will be solved to gain further understanding of the enzyme active site and conformational structure to complement and extend the existing X-ray and neutron structures of DFPase. The state-of-the-art equipment at LANSCE (PCS) and ongoing method development efforts by the PCS staff make LANL the prime location in the world for these experiments. Successful mutants will be computationally reevaluated and mutated further to obtain more enantioselective and specific enzymes (low K_m) with rapid turnovers (high k_{cat}). The enzymes will be PEGylated and tested for CWA activity as potential in-vivo bioscavengers.

Conclusion

This project will produce a DFPase-like enzyme variant, designed and customized to overcome the limitations of unsatisfactory binding and catalytic turnover (K_m and k_{cat}) currently observed with enzymes active against the G- and V-type agents. Thus, a new, specific enzyme that will be useful in both *ex vivo* and *in vivo* applications to recognize and degrad organophosphorus CWAs will be produced. In a more general sense the results from this study will also benefit our understanding of structure-activity relationships in enzymes and, most importantly, molecular recognition. We expect this to be a major success on

the way to the directed creation (*de novo*) of enzymatic activities in proteins.

Publications

Blum, M. M., J. C. Chen, M. Mustyakimov, and B. P. Schoenborn. Neutron structure and mechanistic studies of diisopropyl fluorophosphatase (DFPase). 2010. *Acta Crystalography D.* **66** (11): 1131.

Blum, M. M., J. Gab, and H. John. Formation of pyrophosphate-like adducts from nerve agents sarin, soman and cyclosarin in phosphate buffer: Implications for analytical and toxicological investigations. 2011. *Toxicological Letters.* **200** (1-2): 4034.

Blum, M. M., M. Melzer, A. Heidenreich, F. Dorandeu, J. Gab, K. Kehe, H. Thiermann, and T. Letzel. In vitro and in vivo efficacy of PEGylated Diisopropyl Fluorophosphatase (DFPase). To appear in *Drug Testing and Analysis.*

Blum, M. M., S. Wellert, B. Tiersch, J. Koetz, A. Richardt, A. Lapp, O. Holderer, and J. Gab. The DFPase from Loligo vulgaris in sugar surfactant-based bicontinuous microemulsions: structure, dynamics, and enzyme activity. 2011. *European Biophysical Journal.* **40** (6): 761.

Blum, M. M., and H. John. Historical perspective and modern applications of Attenuated Total Reflectance – Fourier Transform Infrared Spectroscopy (ATR-FTIR). To appear in *Drug Testing and Analysis.*

Blum, M. M., and H. John. Review on UV-spectroscopic, chromatographic and electrophoretic methods for the cholinesterase reactivating antidote pralidoxime (2-PAM). To appear in *Drug Testing and Analysis.*

Modeling the Surface Mass Balance and Freshwater Runoff from the Greenland Ice Sheet in a Changing Climate

Matthew W. Hecht
20100631PRD4

Introduction

The Greenland Ice Sheet (GrIS) is the Northern Hemisphere's largest reservoir of ice and snow, storing the equivalent of 7 m of global sea level. The freshwater flux from the GrIS to the ocean could increase substantially in a warming climate because of enhanced surface melting and runoff, and warmer coastal ocean currents. Recent observations suggest that the GrIS may respond more quickly to climate perturbations than previously thought, especially at the margins. Simulations indicate, that during the last five decades runoff from Greenland has increased by approximately 30%. In order to predict global sea level it is critical to understand the impact of 21st century climate changes on Greenland freshwater fluxes, including the influence of changing freshwater fluxes on ice-sheet dynamics.

We apply SnowModel/IceHydro, a state-of-the-art modeling system, to predict local and regional changes in Greenland's surface mass balance and runoff to adjacent seas in a changing climate. The model is applied broadly to the GrIS and the entire ice-covered extend of Greenland, and at higher resolution to the key region of the Sermilik Fjord drainage. Similar methods may also be applied to simulate changes in mountain glaciers elsewhere around the globe, in order to extend upon what is known from observations of these smaller but numerous glaciers that collectively are contributing to sea level rise at a rate comparable to that of the GrIS.

We note that while the COSIM project at the Laboratory is funded to develop a dynamical model of ice sheets, Dr. Mernild's work is aimed at hydrological processes occurring on and within the ice sheet. It does not directly advance the project's mandate of producing a dynamical ice sheet for use in climate modeling applications.

Benefit to National Security Missions

This project will significantly advance our quantitative understanding of the effects of climate change on the mass balance and distribution of runoff from Greenland. Demonstration of an accurate, high-resolution, integrated hydrological model that can simulate surface mass balance, englacial and subglacial hydrology will provide a more complete estimate of 21st century sea-level rise, a point of great uncertainty in climate prediction that is of particular interest to the DOE Office of Science's climate modeling program. Sea level rise is also of interest to DoD because it can impact the future of key naval bases, like Diego Garcia, where infrastructure is vulnerable to sea level rise.

Progress

Dr. Mernild has been tremendously productive and is well on track to address the aims of the Fellowship. Over this past year he has made significant contributions to our understanding of the mass balance of Greenland -- of the net rate at which snow and ice has been lost over recent decades [1, 3], along with estimates of melting trends under climate model projections of 21st Century conditions [2].

Dr. Mernild's contributions to determination of the mass balance of the GrIS and runoff from Greenland have led to a recent request from the Lead Author to serve as a Contributing Author to the chapter on sea level rise, to appear in the Fifth Scientific Assessment Report of the Intergovernmental Panel on Climate Change (the IPCC). This will be one of the most prominent chapters in the Assessment.

He has also published a paper discussing Greenland's mass balance over the longer period of several thousand years [4], and several additional papers have either been submitted [5] or are in preparation. Two of these papers in preparation document Dr. Mernild's development, along with Dr. Glen E. Liston of Colorado State University, of a model of meltwater routing within the ice sheet itself. This extends upon the model-based work listed above, all of which involves analysis of surface runoff rather than subsurface runoff.

The work on the 20th Century cited above is based on a combination of computer modeling, analysis of available observational data and Dr. Mernild's own fieldwork from the summer of 2010. Again in the summer of

2011 Dr. Mernild has engaged in fieldwork on Greenland, and we expect his new data again to be published (parts have already been accepted for publication, and will be published in November 2011 [5]). The COSIM program, in accordance with the instructions of our program management, does not support fieldwork.

Future Work

We will undertake the following applications: (1) Simulate interannual variability in GrIS surface melt extent and compare it with satellite-derived values; (2) Simulate variability in accumulation and ablation in key regions and for the entire GrIS, and estimate the water balance components; (3) Monitor runoff from the Kangerlussuaq and Sermilik Fjord drainage areas and use the results to calibrate the model; (4) Simulate and analyze the water balance components (including surface mass balance and iceberg calving) for the entire GrIS; (5) Use SnowModel/IceHydro to validate the GrIS surface mass balance and runoff in the Community Earth System Model and to develop improved methods to extract a greater level of detail from global models; and (6) Estimate the contribution of Greenland freshwater fluxes to future sea-level rise. Dr. Mernild also intends to extend the SnowModel/IceHydro modeling system to trace meltwater flow through the interior of ice sheets, mountain glaciers and ice caps, so as to better simulate the spatial and temporal distribution of runoff and to predict changes in the basal strength, sliding rate of the ice sheet, and contribution to future sea-level rise. In collaboration with LANL ice sheet modelers, Mernild will couple the full model to CISM and CESM, providing a uniquely comprehensive estimate of Greenland's contribution to sea-level rise.

Conclusion

Expected results include significant advancement of our understanding of the fate of the Greenland Ice Sheet and glaciers and ice caps in the 21rst Century. We expect our results to be groundbreaking, even on an international scale. The questions of polar climate in the 21rst Century and implications for global sea level rise are of considerable importance to the American public.

References

1. Mernild, , Knudsen, N. T., Lipscomb, W. H., Yde, J. C., Malmros, J. K., Jakobsen, B. H., and Hasholt, B.. Record mass loss from Greenland's best-observed local glacier. 2011. *The Cryosphere Discussions.* **5**: 461.

2. Mernild, , Liston, Glen E., Hiemstra, Christopher A., Christensen, Jens H., Stendel, Martin, and Hasholt, Bent. {Surface Mass Balance and Runoff Modeling Using HIRHAM4 RCM at   Kangerlussuaq (Sondre Stromfjord), West Greenland, 1950-2080}. {201. *{JOURNAL OF CLIMATE}.* **{24}**: {609.

3. Mernild, , Mote, Thomas L., and Liston, Glen E.. {Greenland ice sheet surface melt extent and trends: 1960-2010}. {201. *{JOURNAL OF GLACIOLOGY}.* **{57}**: {621.

4. Mernild, , M.-S. Seidenkrantz, P. Chylek, and and G. E. Liston. Climate-driven fluctuations in freshwater to   {S}ermilik {F}jord, {E}ast {G}reenland. 2011. *The Holocene.* : in press.

5. Mernild, , and G. E. Liston. Greenland freshwater runoff. {P}art {II}: {D}istribution and trends, 1960–2010. 2011. *J. Climate.* : submitted.

6. Mernild, , N. T. Knudsen, and E. Hanna. Mittivakkat {G} letscher, {SE} {G}reenland. 2011. In *The Arctic Report Card, Greenland.* Edited by J. E. Box et al.. NOAA Report.

7. Mernild, , Knudsen, N. T., Lipscomb, W. H., Yde, J. C., Malmros, J. K., Hasholt, B., and Jakobsen, B. H.. Increasing mass loss from Greenland's Mittivakkat Gletscher. 2011. *The Cryosphere.* **5**: 341.

Publications

Mernild, , Knudsen, N. T., Lipscomb, W. H., Yde, J. C., Malmros, J. K., Hasholt, B., and Jakobsen, B. H.. Increasing mass loss from Greenland's Mittivakkat Gletscher. 2011. *The Cryosphere.* **5**: 341.

Mernild, , Knudsen, N. T., Lipscomb, W. H., Yde, J. C., Malmros, J. K., Jakobsen, B. H., and Hasholt, B.. Record mass loss from Greenland's best-observed local glacier. 2011. *The Cryosphere Discussions.* **5**: 461.

Mernild, , Liston, Glen E., Hiemstra, Christopher A., Christensen, Jens H., Stendel, Martin, and Hasholt, Bent. {Surface Mass Balance and Runoff Modeling Using HIRHAM4 RCM at   Kangerlussuaq (Sondre Stromfjord), West Greenland, 1950-2080}. {201. *{JOURNAL OF CLIMATE}.* **{24}**: {609.

Mernild, , M.-S. Seidenkrantz, P. Chylek, and and G. E. Liston. Climate-driven fluctuations in freshwater to   {S}ermilik {F}jord, {E}ast {G}reenland. 2011. *The Holocene.* : in press.

Mernild, , Mote, Thomas L., and Liston, Glen E.. {Greenland ice sheet surface melt extent and trends: 1960-2010}. {201. *{JOURNAL OF GLACIOLOGY}.* **{57}**: {621.

Mernild, , N. T. Knudsen, and E. Hanna. Mittivakkat {G} letscher, {SE} {G}reenland. 2011. In *The Arctic Report Card, Greenland.* Edited by J. E. Box et al.. NOAA Report.

Mernild, , and G. E. Liston. Greenland freshwater runoff. {P}art {II}: {D}istribution and trends, 1960–2010. 2011. *J. Climate.* : submitted.

Novel Laboratory and Field Observations to Model Climate Warming by Aged Absorbing Aerosols

Manvendra K. Dubey
20110751PRD3

Introduction

Climate forcing by absorbing aerosols, such as soot emitted by fossil energy consumption, fires and dust, are the most uncertain elements in our ability to assess climate change. We are applying state-of-the-art techniques to measure absorbing soot and dust in the field and the laboratory to improve their treatments in climate models. This will significantly reduce the uncertainties in climate impacts of anthropogenic activity, fossil energy and/or land use change, on climate.

Laboratory studies of soot mixed with organics co-emitted by combustion will measure both the soot mass using an ultra-sensitive (femtogram/m^3) single particle laser induced incandescence spectrometer (SP2) and the light absorption cross-section with existing multiple photoacoustic spectrometers (PASS). The SP2 is a new capability to measure soot mass on a single particle basis that complements our established expertise with the PASS. The ratios of light absorption to soot mass will provide the specific light absorption cross-sections for mixed soot and organics. This will be used to measure and quantify the effect of organic coatings on light absorption for implementation in climate models. Preliminary data collected recently during the Las Conchas fire will be analyzed as a test bed. This was followed up with a field campaign in the Colorado forest focused on measuring biogenic aerosols. In the next year we will deploy our new SP2 instrument to India as part of a much larger Indo-US DOE field campaign, to measure the impacts of the extreme brown haze (organic carbon and soot from biomass burning) on atmospheric heating and the Indian Monsoon. India is a high signal region where changes in the monsoon impact two billion people and has global implications that are prioritized by DOE for analysis. We will also analyze dust samples collected from desert regions and in the Four Corners area to determine the warming by hematite.

Benefit to National Security Missions

High sensitivity measurements of soot and dust are relevant to climate (DOE-Sc, NOAA), air quality (EPA) and forensics (DOD, DHS, intelligence).

Progress

Our project started recently, in August 2011. Measurements were made in Colorado (Pike National Forest) as a part of BEACHON-RoMBAS (Bio-hydro-atmosphere interactions of Energy, Aerosols, Carbon, H2O, Organics & Nitrogen - Rocky Mountain Biogenic Aerosol Study), an interdisciplinary campaign led by NCAR and CU-Boulder in July-August 2011. The SP2 and 3 PASS instruments were deployed with complementary aerosol equipment to measure size-distributions and denude (heat the aerosol to remove semi-volatile components) the aerosol as were used during the sampling of the Las Conchas fire. BEACHON-RoMBAS was determined to be a "semi-clean" environment being impacted by pollution transported from nearby cities (Colorado Springs, Denver, etc.). Average black carbon mass concentrations were approximately 50 ng m^{-3}, with peak periods exceeding 500 ng m^{-3}. Figure 1 shows a time series of the black carbon data and a 24-hour average size distribution, which remained relatively constant during the course of the campaign. In comparison, the Las Conchas Fire appears to have a smaller mean diameter size distribution of black carbon particles but at concentrations ranging from 150 ng m^{-3} to >12 µg m^{-3} during highly-impacted periods from the fire (concentrations two orders of magnitude higher than anything seen during BEACHON-RoMBAS).
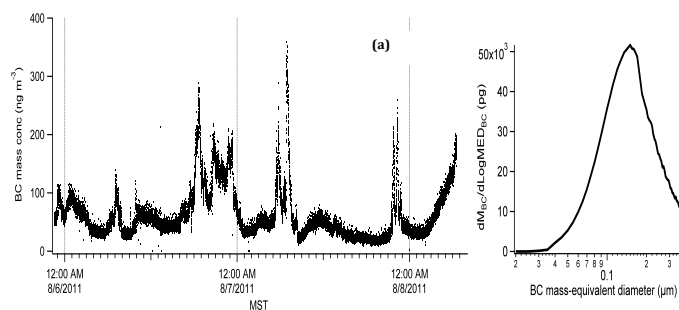
Figure 1. Black carbon (BC) is a potent global warming and ice melting agent, with efficacy much greater than greenhouse gases. Atmospheric BC occurs at low concentrations (femtograms/m3) and the particles are

extremly small (sub micron) making them a challenge to measure. Here we show sensitive size resolved measurements of BC in the field with our state-of-the-art laser based instruments. a) BC mass concentrations as a function of time and (b) 24-hour mean size distribution of BC containing aerosols measured on August 6, 2011 at the Manitou, CO forest site during a field campaign with NCAR and University of Colorado.

Future Work

The project will focus on the light absorption potency of soot and dust that warms the climate. Laboratory studies on size-selected soot and/or dust using an electrostatic classifier will be performed using ultra-sensitive laser-induced incandescence and photoacoustic spectrometers. The pure soot (or dust) particles will be coated with organics co-emitted by fires (and water present in the air), to examine the effects of coatings on the specific light-absorption cross-section of soot (or dust). Coatings are expected to amplify the model by focusing light when they are thin enough and reducing the warming when thick. Our data will be used to develop a validated model, test it in the field and provide it to climate modelers. Field experiments including the Las Conchas fire, a mixed conifer forest in Colorado, and then in India will be used to examine our light absorption models. Measurements will also be made locally and at Four Corners. Finally, our findings will be used to quantify the regional and global warming by absorbing aerosols.

Task1: Laboratory studies of size-selected observations of light absorption and scattering by soot/dust, followed by the investigation of the role of organic and water coatings on these optical properties. Use the data to develop an optical model for coated soot/dust and then test this in the field

Task2: Analysis of field data from Los Conchas fire, the Colorado forests, Ganges Valley India and Four Corners to assess the predictive power of the optical models.

Task 3: Use our optical model to reduce the uncertainties in warming effects of soot/dust in climate change.

Presentations at peer reviewed meetings and publications will be our metric of progress and success.

Conclusion

The absorption of sunlight by soot and dust warms climate, but the exact optical properties and distributions of soot and dust are the largest uncertainties in climate change globally. They are implicated in suppressing the monsoons in the Southwestern US and India. The largest impacts threaten India, the world's largest democracy and a strong US partner in trade and national security. We will provide data to better predict the impact of the aerosols on the water cycle. We will provide a scientific basis for the effects of soot on climate and health.

Multi-scale Analysis of Multi-physical Transport Processes of Electroosmosis in Porous Media

Qinjun Kang
20080727PRD2

Abstract

Electrokinetic phenomena, such as electrophoresis and electro-osmosis, were discovered nearly 200 years ago, and have had a wide range of applications in many fields since then. However, simulation and analysis of these phenomena is a great challenge because of the multi-scale and multi-physics nature of the problem. The primary objective of this project is to develop a comprehensive numerical framework to investigate electrokinetic flow in porous media. Scientific accomplishments of the project include a multi-lattice Boltzmann model framework to solve the highly coupled nonlinear partial differential equations, modeling and analysis of physiochemical transport mechanism in micro and nanoscale electro-osmosis, and analyses of electrochemomechanical energy conversion efficiency in nanofluidic channels. This project has resulted in over 10 publications.

Background and Research Objectives

Electro-osmosis is the motion of polar liquid through a porous material or a biological membrane under the influence of an applied electric field. Since its discovery, it has had growing applications in many fields. In environmental engineering, it is used to dry or decontaminate soil; in microfluidic devices, it provides an efficient way to generate fluid flows; in fuel cells, it causes protons moving through a proton exchange membrane to drag water molecules from anode to cathode; in biology, it is used as an alternative explanation for the movement of polar liquids via the phloem. Therefore, a better understanding of multi-physical transport, including hydrodynamic, thermodynamic, and electrodynamic, of electro-osmosis in porous media is critical to a wide range of fields. However, this problem is notoriously difficult because (1) the multi-physical transport processes are highly coupled; (2) the geometry of natural porous media is so complex that accurately reproducing the microstructure of porous media numerically is itself a great challenge; (3) the driving force of electro-osmosis is sensitive to distributions of inter-phase surfaces; (4) transport processes have pronounced multi-scale features in both space and time. None of the existing (macroscopic, mesoscopic, microscopic) methods can individually solve such multi-scale multi-physical transport phenomena accurately with present-day computers. Therefore it is critical to develop multi-scale modeling and analysis tools to capture the effects of microscale geometry on the macroscale multi-physical transports of electro-osmosis in porous media.

The objectives of this project are to develop a comprehensive numerical framework for modeling electro-osmosis in natural porous media, to obtain new insights into the physiochemical transport mechanism in micro- and nanoscale electro-osmosis, and to optimize designs of N/MEMS devices using the electrokinetic transport.

Scientific Approach and Accomplishments

To achieve these objectives, we have carried out the following studies:

A multi-LBM framework to solve the highly coupled nonlinear partial differential equations

At pore scale (from microns to centimeters), the Poisson-Boltzmann model is available to describe the electrokinetic transports within the electric double layer (EDL) for most slow flows; however, when the scale goes down to submicrons or even to nanometers, the Boltzmann distribution assumption may break down due to the overlap of EDLs. Another factor that may make the PB model unusable is the heterogenous charge of surfaces. The ion convection may play a more important role when the relative velocity is larger. All these factors cannot be reflected by the popular Poisson-Boltzmann model. The applicability of the Poisson-Boltzmann model is not only a fundamental problem in physics but also of significant importance for engineering applications. To investigate this problem, we introduced a more fundamental model, the Poisson-Nernst-Planck model, without any ion distribution hypothesis. In this model, the fluid flow, electric transport, ion diffusion and convection, chemical regulation and energy transports are highly coupled together. This model brings big challenges to numerical solutions, especially at micro- and nanoscales and for complex geometries.

In order to solve the coupled governing equations efficiently, we have developed a coupled LBM framework. The governing equation for each transport process is solved by a lattice Boltzmann model and the entire process is simulated through an iteration procedure, which has been shown in Figure 1. After validation, this method is used to study the applicability of the Poisson-Boltzmann model for electrokinetic flows in microchannels. The results show that for homogeneously charged long channels, the Poisson-Boltzmann model is applicable for a wide range of electric double layer thickness. For the electric potential distribution, the Poisson-Boltzmann model can provide good predictions until the electric double layers fully overlap, meaning that the thickness of the double layer equals the channel width. For the electro-osmotic velocity, the Poisson-Boltzmann model is valid even when the thickness of the double layer is ten times the channel width. For heterogeneously charged microchannels, a higher zeta potential and an enhanced velocity field may cause the Poisson-Boltzmann model to fail to provide accurate predictions. The ionic diffusion coefficients have little effect on the steady flows for either homogeneously or heterogeneously charged channels. However the ionic valence of solvent has remarkable influences on both the electric potential distribution and the flow velocity even in homogeneously charged microchannels. Both theoretical analyses and numerical results indicate that the valence and the concentration of the counter-ions dominate the Debye length, the electrical potential distribution, and the ions transport. The results may improve the understanding of the electrokinetic transport characteristics in microchannels. This study has been published in the *Journal of Computational Physics* in 2010.
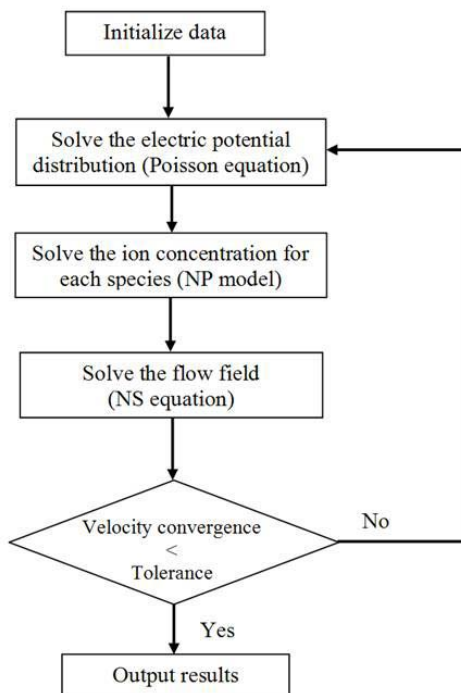
Figure 1. Flow chart of the multi-LBM framework.

Modeling and analysis of physiochemical transport mechanism in micro and nanoscale electro-osmosis

Due to the complexity, the electrokinetic transport in microchannels with random roughness has never been investigated before. We developed a numerical tool to model the electrokinetic transport in microchannels with random roughness. The three-dimensional microstructure of the rough channel is generated by a random generation-growth method with three statistical parameters to control the number density, the total volume fraction and anisotropy characteristics of roughness elements. Figure 2 (a-c) shows three generated 3D geometries of one single roughness element on a grid system of 60×60×60. Figure 2 (d-f) shows the effects of the roughness distribution probability and the roughness volume fraction on the geometries and connections in the rough microchannels. The roughness elements are assumed to be statistically isotropic.
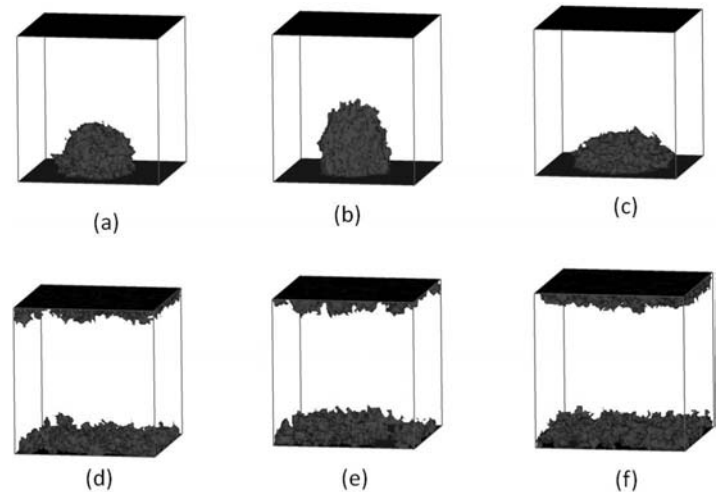
Figure 2. Generated 3D geometries for different parameters.

The governing equations for the electrokinetic transport are then solved by a high-efficiency lattice Poisson-Boltzmann method in complex geometries. The effects from the geometric characteristics of roughness on the electrokinetic transport in microchannels are therefore modeled and analyzed. For a given total roughness volume fraction, a higher number density leads to a lower fluctuation due to the random factors. The electroosmotic permeability increases with the roughness number density as a nearly logarithmic law for a given volume fraction of roughness, but decreases with the volume fraction of roughness for a given roughness number density. When both the volume fraction and the number density of roughness are given, the electroosmotic permeability is enhanced by increases of the characteristic length along the external electric field direction or decreases of the length of the cross-channel direction. For a given microstructure of rough microchannel, the electroosmotic permeability decreases with the Debye length. Compared with the corresponding flows in a smooth channel, the rough surface may enhance the electrokinetic transport when the Debye length is smaller than

the roughness characteristic height under the assumption of constant zeta potential for all surfaces. The present results may improve the understanding of the electrokinetic transport characteristics in microchannels. This work has been published in *Analytical Chemistry.*

Electro-osmosis in porous media has been studied for nearly two hundred years because of its importance in geophysical systems, and this phenomenon is also critical to electrokinetic decontamination of soils and long-term geological storage of nuclear wastes. Although there have been several theoretical studies on electro-osmotic phenomena in porous media, it is still a big challenge to predict the physicochemical transport behavior accurately and efficiently, especially in complex microporous media.

In this work, the physicochemical transport due to electro-osmosis of dilute electrolyte solutions ($<1\times10^{-3}$ mol/L) through microporous media with granular random microstructures has been modeled by our three-step numerical framework. First, the three-dimensional microstructures of porous media are reproduced by a random generation-growth method. Second, the effects of chemical adsorption and electrical dissociation at the solid-liquid interfaces are modeled to determine the electrical boundary conditions, which vary with the ionic concentration, pH, and temperature. Finally the nonlinear governing equations for electrokinetic transport are solved using a highly efficient lattice Poisson-Boltzmann algorithm.

Figure 3 illustrates typical electrical potential and velocity fields for $\varepsilon =0.14$. The electrolyte fluid is driven along the x direction. Figure 3(a) demonstrates four slices of electrical potential contours perpendicular to the flow direction. The electrical potential has distributions in pores and those dark (or blue in color version) parts denote solid grains. The velocity field is shown in Figure 3(b) where the arrows are velocity vectors (and the contours represent velocity scales in color version) of x-direction velocities. The velocity field is only plotted in pores and the solid phase is blocked, which also leads to an illustration of the geometric characteristics. The simulation indicates that the electro-osmotic permeability through the granular microporous media increases monotonically with the porosity, ionic concentration, pH, and temperature. When the surface electric potential is higher than about -50 mV, the electro-osmotic permeability exponentially increases with the electric potential. The electro-osmotic permeability increases with the bulk ionic concentration even though the surface zeta potential decreases correspondingly, which deviates from the conclusions based on the thin layer model. The electro-osmotic permeability increases exponentially with pH, and linearly with temperature. The present modeling results improve our understanding of hydrodynamic and electrokinetic transport in geophysical systems, and help guide the design of porous electrodes in micro-energy systems. This work has been published in *Journal of Geophysical Research--Solid Earth*.
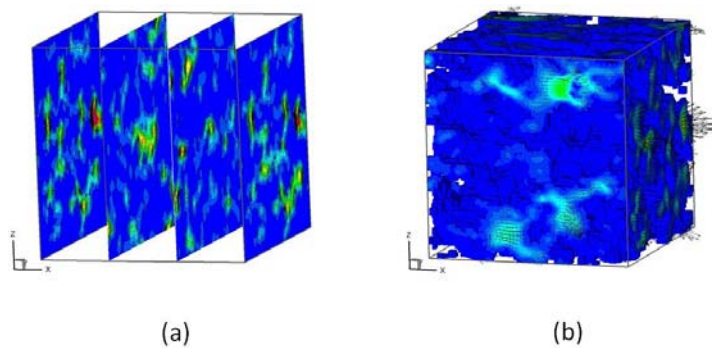
Figure 3. Schematic electrical potential and velocity fields. (a) Four slices of electrical potential contours. (b) Velocity vector field represented by arrows and the x-velocity scale contours by color. The solid phase is blocked and invisible.

Electrochemomechanical energy conversion efficiency in nanofluidic channels

When an electrolyte solution flows in a channel, the channel walls will be charged because of the physical and chemical interactions between ions and surfaces. A pressure-driven flow through a narrow channel therefore carries a net electrical charge with it, inducing both a current and a potential. These so-called streaming currents and streaming potentials can drive an external load and therefore represent a means of converting hydrostatic energy into electrical power. The scheme of energy conversion process is shown in Figure 4. Such an electrokinetic effect in energy conversion devices has received much attention in the context of microfluidic and nanofluidic devices because of its potential attractive conversion efficiency and clean process of power generation. High energy-conversion efficiency and high output power are the requirements for such a device to be practical. Physical modeling of electrokinetic energy conversion is needed to guide the design and optimization of these properties.
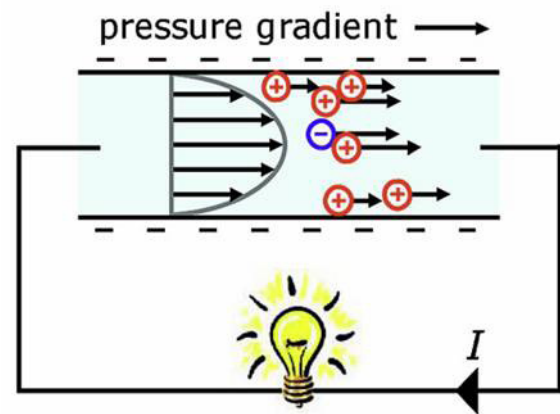
Figure 4. Electrochemomechanical energy conversion process in nanofluidic channels.

We proposed a new theoretical and numerical framework for modeling the multi-physiochemical transport in long

silica nanochannels to study the electrochemomechanical energy conversion efficiency. Both the chemical dissociation effects on surface charge boundary conditions and the bulk concentration enrichment caused by double layer interactions are considered in the framework. The results show that the energy conversion efficiency decreases monotonically with the increasing ionic concentration at pH=8. For a given ionic concentration, there is an optimal channel height for the highest efficiency. The efficiency does not increase with the pH value monotonically and there is an optimal pH value for the maximum energy conversion efficiency as the other conditions are given. The energy conversion efficiency increases with the environmental temperature. The present results may guide the design and optimization of nanofluidic devices for energy conversion. This work has been published in *Microfluidics and Nanofluidics*.

Impact on National Missions

This project supports the DOE/NNSA missions in Energy Security, Environmental Quality, and the missions of the Office of Science by enhancing our understanding of multi-physical (hydro-, thermo-, and electro-dynamic) transport of electro-osmosis in porous media. This research has direct implications in a broad spectrum of research highly relevant to LANL missions, including new energy exploitation (fuel cells and biofuels), fossil energy prospecting (oil and gas), environmental protection (decontamination of radionuclides in solids), biological applications (enzymatic analysis, DNA analysis, and proteomics), and biomedical applications (clinical pathology and bio-smoke alarm). In addition, this project has resulted in over 10 peer-reviewed publications.

Publications

Chen, Q., M. Wang, and Z. Guo. Field Synergy Principle for Energy Conservation and Applications. 2010. *Advances in Mechanical Engineering.* **2010**: 129313.

Kang, Q. J., M. Wang, P. P. Mukherjee, and P. C. Lichtner. Mesoscopic Modeling of Multiphysicochemical Transport Phenomena in Porous Media. 2010. *Advances in Mechanical Engineering.* : 142879 (11 pp.).

Mukherjee, Partha P., M. Wang, Q. Kang, and P. C. Lichtner. Pore-Scale modeling of transport in charged porous media. Presented at *Computational Methods in Water Resources XVII International Conference.* (San Francisco, CA, 6-10, July 2008).

Wang, M.. The Physical Chemistry of Materials: Energy and Environmental Applications. 2010. *Materials Today.* **13** (3): 67.

Wang, M. R., C. C. Chang, and R. J. Yang. Electroviscous effects in nanofluidic channels. 2010. *Journal of Chemical Physics.* **132** (2).

Wang, M. R., Q. Chen, Q. J. Kang, N. Pan, and E. Ben-Naim. Nonlinear effective properties of unsaturated porous materials. 2010. *International Journal of Nonlinear Sciences and Numerical Simulation.* **11** (1): 49.

Wang, M. R., and Q. J. Kang. Electrokinetic Transport in Microchannels with Random Roughness. 2009. *Analytical Chemistry.* **81** (8): 2953.

Wang, M. R., and Q. J. Kang. Modeling electrokinetic flows in microchannels using coupled lattice Boltzmann methods. 2010. *Journal of Computational Physics.* **229** (3): 728.

Wang, M. R., and Q. J. Kang. Electrochemomechanical energy conversion efficiency in silica nanochannels. 2010. *Microfluidics and Nanofluidics.* **9** (2-3): 181.

Wang, M., Q. J. Kang, H. Viswanathan, and . . Electroosmosis of Dilute Electrolyte Solutions in Microporous Media. 2010. *Mnhmt2009, Vol 1.* : 195.

Wang, M., Q. J. Kang, H. Viswanathan, and B. A. Robinson. Modeling of electro-osmosis of dilute electrolyte solutions in silica microporous media. 2010. *Journal of Geophysical Research-Solid Earth.* **115**.

Wang, M., Q. J. Kang, and E. Ben-Naim. Modeling of electrokinetic transport in silica nanofluidic channels. 2010. *Analytica Chimica Acta.* **664** (2): 158.

Wang, M., Q. J. Kang, and N. Pan. Thermal conductivity enhancement of carbon fiber composites. 2009. *Applied Thermal Engineering.* **29** (2-3): 418.

Wang, M., and A. Revil. Electrochemical charge of silica surfaces at high ionic strength in narrow channels. 2010. *Journal of Colloid and Interface Science.* **343** (1): 381.

Carbon and Oxygen Isotopic Variability in Succulent Plants and Their Spines: A New Tool for Climate and Ecosystem Studies in Desert Regions

Claudia Mora
20090526PRD2

Abstract

This project examined the environmental parameters that control the carbon and oxygen isotope variations in succulent plant water and newly grown stem and spine tissue. Growth experiments under controlled conditions provided new understanding of how to interpret isotope variations preserved in spines grown in series along the stems of long-lived cactuses. These spines are retained for decades to centuries and potentially provide the highest resolution proxy record of past environmental variability in arid regions, which typically have few other climate proxies (e.g., tree rings, lake sediments) available for study. The new climate proxy for cacti that we have created represents a major breakthough in our ability to understand the sensitivity of arid regions to past climate change, and to better predict ecosystem changes in response to future climate change. The project made use of two cutting-edge technologies available at LANL for high temporal (tunable diode laser) and spatial (laser volatilization IRMS) resolution stable isotope analysis of cactus response to environmental parameters.

Background and Research Objectives

Arid and semi-arid lands are still the "nether lands" of climate research understanding, despite representing almost 45% of global land area and some of the most sensitive and critical regions. We need new ways to quantify past, and therefore potential future, impacts of climate change on arid ecosystems. This projects goal was to provide such a tool by allowing us to utilize stable isotope ratios in cactus spines as chemical records of past environments and climate change.

Spiny succulent cactuses and euphorbs are vital to the functioning of arid and semi-arid ecosystems by providing reliable sources of water, nutrients and energy in times of drought. These iconic plants and the ecosystems they inhabit are especially vulnerable to climate change, human and natural disturbance, and exist in regions with few other high resolution, centuries-long proxy records of climate. Stable carbon and oxygen isotopic variations in spines grown by long-lived cactus species record time-series evidence of changing climate and environment over a range of timescales (days to decades), however, little is known about the relative importance of different environmental parameters on these variations. A deeper understanding of which parameters control isotopic variability in cactus spines may provide a novel proxy for environmental variability in treeless, arid regions, and allow us to better predict how future climate change or human disturbance may affect these foundation species and their ecosystems.

Scientific Approach and Accomplishments

We intensively monitored columnar cactuses and spiny succulents euphorbs grown in environmentally controlled growth chambers over 18 months time. We evaluated the impact of different parameters (e.g., light, relative humidity and temperature) on the isotopic variability of succulent water and stem tissue using (a) established IRMS analytical methodologies and (b) by developing new laser volatilization techniques for higher resolution, in situ, analysis of spine material. We then used gas exchange measurements and online isotope analysis of respired CO_2 and H_2O using a tunable diode laser system to examine real-time response by cacti to drought or rainfall. Finally, we developed a robust numeric model to (a) reconstruct past environmental variables based on stable isotopes in cactus spines, and (b) quantify the uncertainty associated with these reconstructions.

Postdoc Nathan English's key accomplishments have been the creation and operation of the Stable Isotope Preparation Laboratory at TA-51, the completion of an online discrimination and gas exchange experiment, determining the processing procedures and developing the capability to extract cellulose from tree rings for an isotopic mortality study of western US forest species, the analysis of over 5,000 carbon and oxygen isotope samples, a guest appearance as a biogeochemical expert on the National Geographic Channels television special "America Before Columbus," the co-authorship of a successful $102,000 IGPP grant for a University of Arizona graduate student and the mentoring and co-mentoring of eight undergraduate and post-baccalaureate students.

The Stable Isotope Preparation Laboratory (SIPL) at TA51 was built in previously unused space and has now processed over 5,000 unique samples for isotopic and other analyses. The development of this lab and the accompanying IWD's and WPF's has improved the safety and efficiency of all chemistry operations at TA51. Over the course of two-years, not a single injury or accident occurred in this lab, a credit to the supervision by and procedures developed by myself, Clif Meyer, Heath Powers, Nate McDowell and many others at the lab. In addition to its safety and productivity, SIPL has the capability to process a wide range of sample types for isotopic analysis, including but not limited to whole wood, cactus spines, waters, sucrose, starch, cellulose. The lab has also become a classroom for high school, post-baccalaureate, and post-masters students/mentorees working on a variety of projects at TA51 who are interested in cutting edge ecological research. At least two students (Samantha Stutz and Meghan Montoya) have decided to pursue studies in environmental sciences due in part to their work at the lab.

Using this lab, in conjunction with the MAT253 at TA48, Nathan English has determined that cellulose extracted from whole wood in live and dead conifer trees from western US forests processed using the Jayme-Wise and Standard Brendel methods yield consistently offset results from whole sapwood. This data is unique, and shows that we can proceed to analyze d13C isotopes in whole wood and oxygen isotopes using the modified Brendel method, a safer, less wasteful method. These experimental results also bolstered a proposal submitted by Alison Macalady to the IGPP program that will fund her research into the causes of drought induced mortality in Piñon/Juniper forests across the Southwestern US.

Along with continuing research and publication on spiny succulents In January, 2010, Drs. David G. Williams and Dustin Bronson from the University of Wyoming, along with Heath Powers and Nate McDowell at LANL, participated in research led by Nathan English to examine the real-time isotopic characteristics of CO_2 gas exchange of cactus over diurnal cycles. Using a combined Infra-Red Gas Analyzer/Tunable Diode Laser Trace Gas Analyzer Potted cactus from Tucson, AZ in the TA51 greenhouse. We found that three species of cactus exhibited similar patterns of diurnal CO_2 uptake and discrimination, however, we were unable to find a morning or evening pulse associated with increased levels of C3 photosynthesis. The publication of these results is being lead by Dr. Williams, and will shed light on the photosynthetic mechanisms of plants with a Crassalacean Acid Metabolism and the isotopic impact of these processes on the isotopic record produced in the spines of cactus. Sanna Sevanto is now a collaborator on this project and will help to develop numerical, process based models of oxygen isotopic variation in cactus spines using data from natural and potted cactus.

In addition to his research on succulents, Nathan English has pursued a new avenue in his academic career – the carbon and oxygen isotopic signals that dying conifer trees leave in their tree rings. This research takes advantage previous research performed by Drs. Nate McDowell Claudia Mora on carbon and oxygen isotopes in trees, and the MAT253 operated by Dr. Mora at TA48. Nathan English ran samples that were included in a successful IGPP proposal to fund Alison Macalady, and University of Arizona Ph.D. candidate to explore the same issues. This past year, Nathan English has focused his efforts on determining the proximal causes of western US forest mortality and how this is expressed in a dying trees last rings. We have now completed the bulk of carbon isotope analyses for the isotope portion of the Western Mountain Initiative. This includes, roughly, whole year $\_^{13}C$ chronologies of whole wood from 1975 onward in 3 living and 3 dead trees of seven species from seven geographically diverse sites across the Western United States (54 trees total, some sites have more than one species present). However, a partial dataset from piñon, juniper $\_^{13}C$ chronologies was presented at the annual American Geophysical Union meeting in December, 2010. In addition, samples from living and dead trees in nearby Bandelier National Park and nearby forests (prior to the Los Conchas fire) were analyzed to compare to previously published research undertaken by Drs. Nate McDowell, Craig Allen and A. Park Williams. Analysis of this data continues as Nathan English takes on a new position as Adjunct Faculty at James Cook University in Australia. He expects to submit a manuscript of these results in Spring 2012.

Finally, Nathan English spent a great deal of time mentoring students who were processing ecological samples in his laboratory. Samantha Stutz used data she developed in South American in the summer of 2009 in her Senior Honor's Project at University of Wyoming. Jamie Resnick and Kelsey Neal, already exceptional high school seniors, learned a wide variety of ecological research techniques and honed their laboratory problem solving skills and returned the following year. In collaboration with Toti Larson and colleagues at the New Mexico Institute of Mining and Technology, Nathan mentored Bob Dryja while he examined the nitrogen isotope signatures in spines. Nathan English also collaborated with Clif Meyer and Turin Hill to expand SIPL capabilities to include sugar and starch extraction from woody materials for isotopic analysis. In 2010-2011, Nathan English mentored one undergraduate (Liz Stockton) and three high school students (Meghan Montoya, Zach Brashears and Josh Bowman, all pictured at left with Natahn English). Meghan Montoya has expressed an interest in pursuing environmental science during her undergraduate work at William and Mary College, in part due to her interest in the work she undertook at LANL.

Synergistic Activities

- Biogeochemical and paleoecological expert on Chaco Canyon for the National Geographic Channel special "America Before Columbus" (Air date Nov. 22, 2009).

- Professional reviewer for Geochimica et Cosmochimica Acta, Environmental Monitoring and Assessment, Chemical Geology, Plant Cell and Environment, Climate Dynamics, Trees.

Mentorees

2010 – 2011: Meghan Montoya, Zach Breshears and Josh Bowman, Los Alamos High School; Liz Stockton, Tufts University.

2009 – 2010: Rebecca Boerigter, Rensselaer Polytechnic Institute; Samantha Stutz, University of Wyoming; Robert Dryja, New Mexico Institute of Mining and Technology; Jamie Resnick and Kelsey Neal, Los Alamos High School.

Presentations

English NB, McDowell NG, Allen CD, Das AJ, Mora CI, Stephenson NL (2010) Investigating the underlying causes of tree mortality with carbon and oxygen isotopes. Fall meeting, Abstract B21A-0291.

English NB, Bronson D, Dettman DL, Trees M, Williams DG (2009) An easy path from precipitation amount to _^{18}O values in the spines of columnar cactuses, *Carnegiea gigantea*. Geological Society of America Annual Meeting, Portland, Oregon October 18-21, 2009 T-41, 199-2.

English NB, Dettman DL, and DG Williams. Stable isotopes in the spines of columnar cactus: a new proxy for climate and ecophysiological research. University of New Mexico, Dept. of Biology Seminar Series, 2009.

Impact on National Missions

This work has directly benefited LANL through enhancing our ability to support DOE's climate impacts mission lead by the Climate and Environmental Science Division within the Office of Science. The paleo-climate record that we can now obtain from arid ecosystems is unparalleled and allows a new view into climate impacts in particularly sensitive, semi-arid systems that cover a large fraction of the world. Further, the tree ring work done by Nathan English is the first continental assessment of the signatures of tree death during drought, enabling a much broader investigation into how climate drives vegetation mortality. We anticipate significant growth in the directions that Dr. English has pioneered.

Publications

Bronson, D. R., N. B. English, D. L. Dettman, and D. G. Williams. Paradoxical patterns of seasonal photosynthetic gas exchange and water-use efficiency in a constitutive CAM plant, the giant saguaro cactus (Carnegiea gigantea). . 2011. *Oecologia.* **10.1007/s00442-011-2021-1**: 30.

English, N. B., D. L. Dettman, D. R. Sandquist, and D. G. Williams. An easy path from precipitation amount to d18O values in the spines of columnar cactuses, Carnegiea gigantea. Presented at *Geological Society of America Annual Meeting.* (Portland, OR, 18-21 Oct. 2009).

English, N. B., N. McDowell, C. I. Mora, N. L. Stephenson, A. J. Das, and C. D. Allen. Investigating the underlying causes of tree mortality with carbon and oxygen isotopes in tree-rings. . Presented at *American Geophysical Union Annual Meeting.* . (San Francisco, 11-17 Dec. 2010).

English, N., D. Dettman, D. Sandquist, and D. Williams. Daily to decadal patterns of precipitation, humidity, and photosynthetic physiology recorded in the spines of the columnar cactus, Carnegiea gigantea. 2010. *JOURNAL OF GEOPHYSICAL RESEARCH-BIOGEOSCIENCES.* **115**: G02013.

English, N., D. Dettman, and D. Williams. A 26-year stable isotope record of humidity and El Nino-enhanced precipitation in the spines of saguaro cactus, Carnegiea gigantea. 2010. *PALAEOGEOGRAPHY PALAEOCLIMATOLOGY PALAEOECOLOGY.* **293** (1-2): 108.

Placzek, C., J. Quade, J. Betancourt, P. Jonathan. Patchett, J. Rech, C. Latorre, A. Matmon, C. Holmgren, and N. English. CLIMATE IN THE DRY CENTRAL ANDES OVER GEOLOGIC, MILLENNIAL, AND INTERANNUAL TIMESCALES. 2009. *Annals of the Missouri Botanical Garden.* **96** (3): 386.

Probing Molecular Physics of Biological Nano-channels: from Viruses to Biosensors

Benjamin H. Mcmahon
20090527PRD2

Abstract

Proper functioning of living cells requires selective molecular transport into and out of the cell, and between different cell compartments. Remarkably, many channels are very selective in what they pass, without an input of metabolic energy and without large-scale structural transitions from a 'closed' to an 'open' state; the transport is based on diffusion only. Understanding the selective transport through such 'always open' channels is a fundamental biological problem, poses challenging physical questions and has potentially far-reaching technological applications. This project was specifically about transport through one particular channel of this kind, the Nuclear Pore Complex, which gates nucleo-cytoplasmic transport in all eukaryotic cells.

The project also studies another subject of high practical and fundamental interest: the mechanism of entry of viruses into to the cell nucleus. Survival of the virus depends on its ability to deliver its genetic material to the cell nucleus and replicate before the infected cell is destroyed by the immune system. This process is inherently stochastic, as it depends on the transport of a single protein-DNA complex into the nucleus and the computational modeling is crucial for further progress.

This project focused on the development of conceptual models that capture only the essentials of what is known about the transport mechanism and its selectivity for the nuclear pore, and how these transport mechanisms can be used by viruses to infect the cells.

Background and Research Objectives

One may view the nuclear pore as a tube of ~35 nm in diameter whose walls are composed of essentially fixed structural proteins. The tube is lined by unstructured unfolded polypeptide filaments that are grafted to the walls and protrude to the tube lumen. Small molecules (<6-7 nm) in size can diffuse freely through the pore. Larger molecules have to be shuttled through by special transport proteins. The major challenge is to understand how the basic kinetic mechanisms of stochastic transport interplay with other effects, related to the filament conformation and dynamics. These include:

(a) Stochastic transport models with crowding: The nuclear pore complex operates in the extremely crowded environment of the cell. Although our work provides some answers, it is still largely unknown how it achieves selective transport in both directions ('in' and 'out') in the presence of vast amount of background molecular noise.

(b) Conformation of the filaments: Accumulating experimental evidence shows that the conformation of the filament layer and its dynamic transitions during the particle passage play an important role in the transport mechanism. Its role was investigated using the methods of polymer physics and Brownian dynamic simulations.

(c) Single molecule level: Transport has to be understood. New experimental techniques allow tracking of single particles inside the channel; this motion is highly stochastic. The project developed stochastic models of the dynamics of particle passage in presence of molecular crowding.

(d) Viral entry into the nucleus: Viruses employ various strategies for delivery of their genome to the nucleus. In particular, DNA-protein complexes of many viruses are extremely big in terms of cell dimensions. For instance, HIV 'preintegration-complex' is ~56 nm in size – larger than the pore diameter. This poses a major question: how the delivery of these large objects into the nucleus is achieved?

Competing efforts are much narrower in scope, typically applying existing tools, such as molecular dynamics simulations, to examine individual components outside of the overall system context. Unfortunately, this three-year project ended with Dr. Zilman accepting a faculty position at the University of Toronto after year one, so the objectives were only partially met.

Scientific Approach and Accomplishments

We researched the biophysics of transport through the Nuclear Pore Complex (NPC), using several approaches. NPC is a biological nano-gate that regulates all the transport between cell nucleus and cytoplasm. The long-term

goal of the research was to provide an integrated description of how conformational changes of the NPC constituents determine the dynamics of transport through it and, in particular, its selectivity. The conceptual understanding arising from the study of the NPC can be leveraged for design of artificial nano-sorting devices based on the same principles. Currently, we are one of the very few groups in the world working on the subject.

We continued to develop computational tools towards understanding the structure and dynamics of the unfolded proteins that fill the lumen of the NPC. This requires novel methods to describe the behavior of assemblies of unfolded proteins, because the standard state of the art molecular dynamics simulations can only probe the events on time and length scales much shorter than the relevant ones. Therefore, we are using coarse-grained approach based on polymer physics and statistical mechanics. In this approach, the unfolded proteins are represented as flexible polymeric chains and the models can be treated either by analytical methods or by computer simulations. We have done this part in collaboration with Prof. Rob Coalson and Prof. David Jasnow and the graduate student Mr. Michael Opferman from the Pittsburgh University. Mr. Opferman has spent the summer at Los Alamos, developing a simulation code to describe these polymers in the presence of the transport factors. In parallel, we have developed simple approximate analytical models that capture the essential properties of the polymer-transport factor mixtures.

Preliminary results of the models seem to explain the in vitro experiments on the nano-mechanic behavior of the filaments with and without transport factors. The model has also uncovered hitherto unknown collective structural transitions in the assemblies of these polymers, induced by the presence of the transport factors. We believe that these transitions are important in the gating and transport mechanisms of the NPC. These findings are currently being summarized in a paper. Currently, we are working on introducing more realistic features into the model in geometries mimicking the actual NPC. We have established collaboration with Dr. Gnanakaran (T-6) and Dr. Welch (T-4) in order to supplement the coarse-grained models with direct atomistic simulations at short time and length in a more general context of studying the behavior of unfolded proteins.

We have also continued our previous work on stochastic models of transport through the NPC and related nano-channels. In one work, together with experimental collaborators at the Rockefeller University, we investigated how the competition between different species influences the transport selectivity. The works explains recent experimental results [1]. In another project, together with Dr. Golan Bel (LANL), we investigated how the crowding inside a nano-channel affects the transport times through it. Proper understanding of these phenomena is imperative for interpretation of single-molecule tracking experiments, which can follow dynamics of transport of a single fluorescently labeled transport factor with a resolution of several nanometers. The results are reported in [2].

Impact on National Missions
This project supported the DOE mission in Promoting Science by enhancing our understanding of basics biophysics involved in the nuclear-cytoplasmic particle exchange. The work also provided the foundational understanding of cell processes that enable development of strategies to combat both natural disease and bio-WMDs, as well as to understand how to probe eukaryotic biology in the general context of climate and environment. In this way, this work supports missions of Threat Reduction by understanding the mechanisms of host -- viral pathogens interactions. It also develops the connection between protein biophysics and materials science / physical chemistry, shedding insight on both.

References
1. Zilman, A., and T. Jovanovic-Talisman. Enhancement of transport selectivity through nano-channels by non-specific competition. 2010. *PLoS Computational Biology.* **6**: e1000804.

2. Zilman, A., and G. Bel. Effects of crowding on non-equilibrium transport through nano-channels. 2010. *Journal of Physics: Condensed Matter.* **22**: 454130.

Publications
Jovanovic-Talisman, T., J. Tetenbaum-Novatt, A. S. McKenney, A. Zilman, R. Peters, M. P. Rout, and B. T. Chait. Artificial nanopores that mimic the transport selectivity of the nuclear pore complex. 2009. *Nature.* : 457.

Zilman, A.. Effects of multiple occupancy and inter-particle interactions on selective transport through narrow channels: theory versus experiment . 2009. *Biophysical Journal.* **96**: 1235.

Zilman, A., J. Pearson, and G. Bel. Effects of jamming on non-equilibrium transport times through nano-channels . 2009. *Physical Review Letters.* **103**: 128103.

Zilman, A., S. Di Talia, T. Jovanovic-Talisman, B. T. Chait, and M. P. Rout. Enhancement of transport selectivity through narrow channels by non-specific competition: a novel kinetic mechanism . 2010. *PLoS Computational Biology.* **6**: e1000804.

Zilman, A., V. Ganusov, and A. Perelson. Stochastic models of lymphocyte proliferation and death. 2010. *PLoS ONE.* **5**: 125.

Zilman, A., and G. Bel. Effects of crowding on non-equilibrium transport through nano-channels. 2010. *Journal of Physics. Condensed Matter.* **22**: 454.

Theoretical Investigations of Ribosome Dynamics

Karissa Y. Sanbonmatsu
20090530PRD2

Abstract

The project has pushed the envelop of computational biology by performing the largest biomolecular simulations to date. We are the first to study spontaneous large-scale conformational changes of the ribosome in atomic detail using molecular simulation. The ribosome is the molecular machine in all living things that implements the instructions in DNA. We have produced a close connection with experimental studies of single ribosomes. Structure-based models, where the native, experimentally determined structure is the lowest energy state, have had great success in illuminating the role of entropy in protein folding, binding and function. We have applied this new technique to the ribosome. During "accommodation", the transfer ribonucleic acid (tRNA) moves from outside of the ribosome into a tight corridor and eventually moves the new amino acid into the ribosome. Similar to folding, the loss in entropy is balanced by energy contributions that stabilize the final conformation. By simulating the accommodation transition with an all-atom structure-based model we map the entropy and free energy as functions of the tRNA position, and characterize the resulting transition states. To complement the picture obtained from structure-based simulations, we perform explicit-solvent simulations, with full electrostatics, of the ribosome.

Background and Research Objectives

The stated goal of this project is to characterize the relationship between structure, function and energetics during ribosome translation. Translation is the process by which the ribosome converts genetic messages into protein sequences, and it is essential to cellular life and antibiotic action. During translation, the ribosome undergoes a sequence of large-scale internal rearrangements which results in transfer RNA molecules moving processively through a series of binding sites, which results in amino acids being added to the growing protein. These rearrangements can be generally described by the following steps: Initial selection, accommodation, hybrid-state formation, translocation and tRNA release. We have had substantial progress towards characterizing accommodation, hybrid-state formation, and rearrange-

ments related to translocation, over the past year, and they are described below.

Scientific Approach and Accomplishments

Our work on accommodation has resulted in two peer-reviewed publications that have generated substantial new physical insight into the function of ribosome, one of the most important antibiotic targets in biomedical systems. In general terms, the ribosome is a molecular machine that is critical for the survival of bacteria that are harmful to humans. Antibiotics that target the ribosome are small molecules that act like monkey wrenches and jam up the machine. Thus, to understand how antibiotics work, it is important to understand how the machine works. The machine has many moving parts that move spontaneously on different time scales. In our first publication (Whitford et al, *RNA* **16**, 1196-1204, 2010, impact factor 6.1), we used our novel simulation method (structure-based simulation) to study one of the moving parts called a transfer RNA (tRNA). Specifically, we studied how this part spontaneously moves from the outside of the ribosome to the inside of the ribosome. This movement, called "accommodation" is one of the most important movements in ribosome function. Previous computer simulations used "driven" techniques, where the tRNA is forced to move. We performed the first ever spontaneous simulations where the tRNA spontaneously moves into the ribosome. The simulations revealed that the tRNA makes many large scale attempts before moving into the ribosome. This was confirmed by single molecule fluorescence experiments performed in Cornell University. In addition, we show that a portion of the tRNA is so flexible that it has a tremendous amount of entropy. This entropy actually impedes the motion. However, the final state of the tRNA is so energetically favorable that the tRNA is still able to move into the ribosome. In summary, we found several new potential antibiotic target sites, and identified specific structural features that may govern the dynamics the tRNA.

In the second paper about accommodation (Whitford et al, *J. Amer. Chem. Soc.* **132**, 13170-13171, 2010, impact factor 9.0), we employed very large simulations (3.2 million atoms) to characterize the diffusive properties of

tRNA inside of the ribosome. This enabled us to construct a table converting kinetic rates measured by experiments (time scale information) into thermodynamic barriers (energy information). These barriers are impossible to measure experimentally. Thus, our simulations produced critical information to understand the energetics for accommodation. In other words, our simulations enable mechanistic interpretation of kinetic experiments in terms of thermodynamics.

Both of these studies represent different milestones in the field of computational biophysics. The first article was the first study that was able to observe spontaneous accommodation events through simulations. The second study is the largest (3.2 Million atoms) simulation of a biomolecular complex, and it is the most extensive sampling of any multi-million atom simulation in biophysics (2.1 microsecond, with individual trajectories ranging up to 301 nanoseconds each).

We next moved onto a more complicated type of motion in the ribosome: "translocation". The ribosome must move along the genetic message by exactly three units (nucleotides) at a time. For this to occur, many different parts of the machine have to move. To probe translocation, we developed a new integrated simulation method that allows us to obtain atomic resolution models from cryo-electron microscopy. More simply, our experimentalist colleagues in Berlin produce snapshots of the ribosome by freezing it in the act of motion at cryogenic temperatures. With this technique they are able to produce low-resolution 3-D images of the ribosome. However, because the ribosome is an extremely precise machine, we need to know the ribosome's structure at atomic resolution to gain more physical insight. We developed a new method that does just this. Our simulations and all-atom models of the ribosome caught in the act of translocation revealed that there is an addition intermediate step called "head swivel" where the "head" of the ribosome twists to help propel it along the genetic message. Our results were published in Nature magazine (Ratje et a. *Nature* **468**, 713-716, 2010, impact factor 36.1).

Impact on National Missions

The project is relevant to antibiotic design, which is important for threat reduction. Specifically, biological agents need to be treated with antibiotics capable of killing them. Our project focuses on a relevant antibiotic target (the ribosome).

Publications

Ratje, A. H., P. C. Whitford, K. Y. Sanbonmatsu, C. M. Spahn, and M. A. N. Y. Coauthors. Head swivel on the ribosome facilitates translocation by means of intra-subunit tRNA hybrid sites. 2010. *Nature.* **468** (7324): 713.

Whitford, P., J. Onuchic, and K. Sanbonmatsu. Connecting energy landscapes with experimental rates for aminoacyl-tRNA accommodation in the ribosome. 2010. *Journal of the American Chemical Society.* **132** (38): 13170.

Whitford, P., P. Geggier, R. Altman, S. Blanchard, J. Onuchic, and K. Sanbonmatsu. Accommodation of aminoacyl-tRNA into the ribosome involves reversible excursions along multiple pathways. 2010. *RNA-A PUBLICATION OF THE RNA SOCIETY.* **16** (6): 1196.

INFORMATION SCIENCE AND TECHNOLOGY

Optimization and Control Theory for Smart Grids

Michael Chertkov
20100030DR

Introduction

National interest in a broad class of problems loosely characterized as the smart grid is growing rapidly. At its core, the smart grid is the modernization of our existing electric power systems through improvements in efficiency, increased robustness and resiliency, integration of time-variable renewable generation, and reduction of environmental impacts. To date, the focus of most commercial entities has been on development of hardware such as smart meters and green technologies. However, with the exception of a handful of academic researchers, there has been limited research on optimization, control and more broadly, the information science required to effectively utilize this hardware. Our project targets development of the basic information science that will effectively bridge this gap. Using our expertise in information theory, network analysis, infrastructure analysis and power engineering, we will develop new algorithms for optimal design of the nation's next generation power transmission and distribution system that address the realities and challenges of the future grid.

We focus on three core information science challenges in Grid Design, Grid Control, and Grid Stability by considering a set of challenging problems. First, we study efficient and robust integration of geographically widespread renewable generation by solving large, cutting-edge optimization problems that incorporate difficult constraints imposed by the transmission of electrical power. Second, we consider two load balancing problems in the low-voltage distribution grid: development of robust and efficient distributed control techniques and algorithms based on queuing theory. We will also develop efficient control algorithms for maintaining an operational distribution grid via switching of redundant lines. Third, we will develop a preventive toolbox capable of detecting instabilities and failures prior to their occurrence. We will focus on estimating the probability of power outages, identifying their signatures and precursors, and developing detection algorithms for alerting the transmission grid operator.

Benefit to National Security Missions

Our smart grid effort enables the laboratory to expand its infrastructure planning and analysis programs, currently focused mainly on infrastructure security and sponsored by the Department of Homeland Security, to a broader set of programs in energy infrastructure planning and efficiency analysis with the Department of Energy as primary sponsor. The project thereby positions the lab closer to the center of mass in energy research. In a broader sense, infrastructure analysis tools like ours build the ability to understand the complicated infrastructure of the nuclear weapons complex.

Progress

The project consists of three parts, related to grid design; grid control, and grid stability. During the first two years of the project we have achieved significant results in all three areas. The results are documented in multiple papers.

Our specific achievements in the following three areas:

Grid Design

We proposed new strategies for Generation Expansion Planning and Transmission Network Expansion via Simulation Optimization Approach and in particular Discrepancy Bound Local Search (DBLS). The algorithm was verified on large realistic models of transmission systems. We investigated a randomization strategy that builds on DBLS and dramatically increases the computational efficiency of the algorithm. This approach included the incorporation of AC power flow models, optimal dispatching, renewable generation, and carbon emissions. We also designed a new Majorization-Minimization Approach to design of power transmission networks, and worked on new optimization problems for implementing vehicle-to-grid technology into smart grids.

Grid Control

We developed new control strategy for tripping overheated lines which allows extremely efficiently

mitigation of power outages. We introduced and analyzed Markov Decision Process (MDP) machines to model individual devices which are expected to participate in future demand-response markets on distribution grids. We developed a new model of Thermostatically Controlled Loads (TCL) capable to compensate for fast time-scale fluctuations in generated power.   We considered last-mile disaster recovery for power restoration, i.e., how to schedule and route a fleet of repair crews to restore the power network as fast as possible after a disaster. We showed how distributed control of reactive power can serve to regulate voltage and minimize resistive losses in a distribution circuit that includes a significant level of photovoltaic (PV) generation. We developed control algorithms based on randomized Electric Vehicle charging start times and simple one-way broadcast communication allowing for a time delay between communication events.

Grid Stability

We developed an approach to predict power grid weak points, and specifically to efficiently identify the most probable failure modes in static load distribution for a given power network. The approach was tested on realistic models of transmission. We suggested a new algorithm discovering most probable extreme stochastic events in static power grids associated with intermittent generation of wind turbines. The algorithm becomes EXACT and EFFICIENT (polynomial) in the case of the proportional (or other low parametric) control of standard generation, and log-concave probability distribution of the renewable generation, assumed known from the wind forecast. We introduced a new microscopic model of the outages in transmission power grids. This model accounts for the automatic response of the grid to load fluctuations, when the optimum power flow adjustments and load shedding controls are unavailable. We described extreme events, initiated by load fluctuations, which cause cascading failures of loads, generators and lines. In the limit where the number of consumers along a linear segment of a power system is large and spatial variations in power flows are smooth functions, we derived differential equations for the power flow. We verified phenomenon of voltage collapse in this setting, and studied the effect of disorder/irregularities in injection/consumption on the voltage profile. We studied the impact of time-delays on small-signal angle stability of power systems, introduced a power system model based on delay differential algebraic equations (DDAE) and described a general technique for computing the spectrum of DDAE, and performed time domain simulations which confirmed the results of the DDAE spectral analysis. We have shown that the effect of time delays can be interpreted as a "virtual" load increase. We also started statistical analysis of solar radiation data, which is required for reliability analysis of renewable solar generation.

Future Work

The basic structure of the electrical power grid has remained unchanged for a hundred years. It has become increasingly clear, however, that the hierarchical, centrally-controlled grid of the twentieth century is ill-suited to the needs of the twenty-first. A future grid, in which modern sensors, communication links, and computational power are used to improve efficiency, stability, and flexibility, has become known as the ``smart grid.'' Much of the hardware that will enable smart grids is in development or already exists: ``smart'' meters and appliances that respond to pricing signals, distributed wireless sensor networks, improved batteries for plug-in hybrid electric vehicles (PHEVs) that enable distributed storage, and so on. While much of the needed hardware necessary to enable the smart grid may be in place, the Information Science and Technology (IS&T) foundation for the smart grid design, operation, and risk assessment requires major development.

In the last year of the project we will continue our work on development of the basic information science that will effectively bridge this gap. Using our expertise in information theory, network analysis, infrastructure analysis and power engineering, we will develop new algorithms for optimal design of the nation's next generation power transmission and distribution system that address the realities and challenges of the future grid.

In the area of Grid Design, we will extend the approaches developed in the direction of more accurate accounting for effects of renewable, and more generally fluctuations in the grid. In Grid Control, we will continue working on both transmission and distribution systems extending into development more advanced control systems also accounting for results from grid planning and grid stability portions of the project. In Grid Stability, we will develop a toolbox capable of detecting instabilities and failures for preventing costly outages. All three problems require the development of efficient new algorithms.

Conclusion

This project is driven by emerging technologies such as renewables, storage, and meters and accordingly specifies the technical challenges in Power Grid Design, Power Grid Control and Power Grid Stability. Rather than tackle the full complexity and requirements of the grid, from security to operations to pricing, we focus on a set of problems where we have well-developed Information Science & Technology (IS&T) capabilities, and thus make a significant impact. The new IS&T challenges for smart grids require coherent advances in analysis and control, stability and reliability metrics, state estimation, data aggregation and assimilation, and communication for the grid.

Publications

Ben-Naim, E., and P. L. Krapivsky. Kinetics of ring formation. 2011. *PHYSICAL REVIEW E.* **83** (6, 1): 061102.

Bent, R., A. Berscheid, and G. Loren. Toole. Transmission network expansion planning with simulation optimization. 2010. In *24th AAAI Conference on Artificial Intelligence and the 22nd Innovative Applications of Artificial Intelligence Conference, AAAI-10 / IAAI-10 ; 20100711 - 20100715 ; Atlanta, GA, United States.* Vol. 1, p. 21.

Bent, R., and P. Van Hentenryck. Spatial, Temporal, and Hybrid Decompositions for Large-Scale Vehicle Routing with Time Windows. 2010. In *16th Annual International Conference on the Principles and Practice of Constraint Programming ; 20100906 - 20100910 ; St Andrews, SCOTLAND.* Vol. 6308, p. 99.

Chertkov, M., F. Pan, and M. Stepanov. Predicting failures in power grids: The case of static overloads. 2011. *IEEE Transactions on Smart Grid.* **2** (1): 150.

Coffrin, C., P. Van Hentenryck, and R. Bent. Strategic planning for power system restoration. 2011. In *International Conference on Vulnerability and Risk Analysis and Management, ICVRAM 2011 and the International Symposium on Uncertainty Modeling and Analysis, ISUMA 2011 ; 20110411 - 20110413 ; Hyattsville, MD, United States.* , p. 180.

Hentenryck, P. Van, R. Bent, and C. Coffrin. Strategic Planning for Disaster Recovery with Stochastic Last Mile Distribution. 2010. In *Integration of AI and OR Techniques in Constraint Programming for Cominatorial Optimization Problems.* (7th International Conference, CPAIOR 2010 ; 14-18). , p. 318.

Hentenryck, P. Van, R. Bent, and C. Coffrin. Strategic planning for disaster recovery with stochastic last mile distribution. 2010. In *7th International Conference on Integration of AI and OR Techniques in Constraint Programming for Combinatorial Optimization Problems, CPAIOR 2010 ; 20100614 - 20100618 ; Bologna, Italy.* Vol. 6140 LNCS, p. 318.

Johnson, J. K., and M. Chertkov. A majorization-minimization approach to design of power transmission networks. 2010. In *2010 49th IEEE Conference on Decision and Control (CDC 2010) ; 15-17 Dec.* (2010 ; Atlanta, GA, USA). , p. 3996.

Pan, Feng, R. Bent, A. Berscheid, and D. Izraelevitz. Locating PHEV exchange stations in V2G. 2010. In *2010 1st IEEE International Conference on Smart Grid Communications (SmartGridComm) ; 4-6 Oct.* (2010 ; Gaithersburg, MD, USA). , p. 173.

Santhi, N., and Feng Pan. Detecting and Mitigating Abnormal Events in Large Scale Networks: Budget Constrained Placement on Smart Grids. 2011. In *2011 44th Hawaii International Conference on System Sciences (HICSS 2011) ; 4-7 Jan.* (2011 ; Kauai, HI, USA). , p. 1.

Toole, G. L., M. Fair, A. Berscheid, and R. Bent. Electric Power Transmission Network Design for Wind Generation in the Western United States: Algorithms, Methodology, and Analysis. 2010. In *2010 IEEE/PES Transmission & Distribution Conference & Exposition (T&D) ; 19-22 April 2010 ; New Orleans, LA, USA.* , p. 1.

Toole, G. Loren., M. Fair, A. Berscheid, R. Bent, and IEEE. Electric Power Transmission Network Design for Wind Generation in the Western United States: Algorithms, Methodology, and Analysis. 2010. In *2010 IEEE PES Transmission and Distribution Conference and Exposition - Smar Solutions for a Changing World ; 20100419 - 20100422 ; New Orleans, LA.*

Toole, G. Loren., M. Fair, A. Berscheid, and R. Bent. Electric power transmission network design for wind generation in the Western United States: Algorithms, methodology, and analysis. 2010. In *2010 IEEE PES Transmission and Distribution Conference and Exposition: Smart Solutions for a Changing World ; 20100419 - 20100422 ; New Orleans, LA, United States.* , p. var.pagings.

Toole, G. Loren., M. Fair, A. Berscheid, and R. Bent. Electric power transmission network design for wind generation in the Western United States: Algorithms, methodology, and analysis. 2010. In *2010 IEEE PES Transmission and Distribution Conference and Exposition: Smart Solutions for a Changing World ; 20100419 - 20100422 ; New Orleans, LA, United States.* , p. var.pagings.

Turitsyn, K., N. Sinitsyn, S. Backhaus, and M. Chertkov. Robust Broadcast-Communication Control of Electric Vehicle Charging. 2010. In *2010 1st IEEE International Conference on Smart Grid Communications (SmartGridComm) ; 4-6 Oct.* (2010 ; Gaithersburg, MD, USA). , p. 203.

Turitsyn, K., N. Sinitsyn, S. Backhaus, and M. Chertkov. Robust Broadcast-Communication Control of Electric Vehicle Charging. 2010. In *2010 1st IEEE International Conference on Smart Grid Communications (SmartGridComm) ; 4-6 Oct.* (2010 ; Gaithersburg, MD, USA). , p. 203.

Turitsyn, K., P. Sulc, S. Backhaus, M. Chertkov, and IEEE. Distributed control of reactive power flow in a radial distribution circuit with high photovoltaic penetration. 2010. In *PES General Meeting ; 20100725 - 20100729 ; Minneapolis, MN.*

Turitsyn, K., P. Sulc, S. Backhaus, and M. Chertkov. Options for Control of Reactive Power by Distributed Photovoltaic Generators. 2011. *PROCEEDINGS OF THE*

IEEE. **99** (6): 1063.

Turitsyn, K., P. Sulc, S. Backhaus, and M. Chertkov. Local Control of Reactive Power by Distributed Photovoltaic Generators. 2010. In *2010 1st IEEE International Conference on Smart Grid Communications (SmartGridComm) ; 4-6 Oct.* (2010 ; Gaithersburg, MD, USA). , p. 79.

Turitsyn, K., P. Sulc, S. Backhaus, and M. Chertkov. Local Control of Reactive Power by Distributed Photovoltaic Generators. 2010. In *2010 1st IEEE International Conference on Smart Grid Communications (SmartGridComm) ; 4-6 Oct.* (2010 ; Gaithersburg, MD, USA). , p. 79.

Zdeborova&acute, , A. Decelle, and M. Chertkov. Message passing for optimization and control of a power grid: model of a distribution system with redundancy. 2009. *Physical Review E (Statistical, Nonlinear, and Soft Matter Physics).* **80** (4): 046112 (9 pp.).

Zdeborova, L., S. Backhaus, and M. Chertkov. Message Passing for Integrating and Assessing Renewable Generation in a Redundant Power Grid. 2010. In *2010 43rd Hawaii International Conference on System Sciences (HICSS-43) ; 5-8 Jan.* (2010 ; Honolulu, HI, USA). , p. 1.

Zdeborova, L., S. Backhaus, and M. Chertkov. Message Passing for Integrating and Assessing Renewable Generation in a Redundant Power Grid. 2010. In *2010 43rd Hawaii International Conference on System Sciences (HICSS-43) ; 5-8 Jan.* (2010 ; Honolulu, HI, USA). , p. 1.

Multi-Perspective Network-Scale Modeling & Detection for Cyber Systems

Michael E. Fisk
20110093DR

Introduction

We will establish a new regime of cyber security detection and defense that uses whole-network traffic modeling and detection. In contrast, existing detection techniques are myopic and unable to detect the most subtle of contemporary attacks. In our approach cyberspace activity is represented as a cohort of temporal graphs representing different observational perspectives of the same underlying events. We exploit those multiple perspectives as well as structural and temporal patterns across entire graphs and sub-graphs. To accomplish this shift requires advances in cyber sensing, temporal graph modeling & analysis, graph-theoretic detection, and data-intensive computing. We will develop data-driven models and understanding of cyber network dynamics and use that knowledge to design scalable detection algorithms.

Benefit to National Security Missions

This project will positively impact cyber security missions executed by both LANL's internal security program, essential to our DP mission, and Global Security programs, with secondary benefits on our commercial CRADAs (we are not funding any CRADAs, but technology developed under this LDRD may become background intellectual property that results in funding of subsequent work by an existing CRADA partner). Our advances should allow us to catch-up with contemporary, undetectable adversaries, and build a base for the future. More broadly, it is a concrete project to rally interdisciplinary IS&T capabilities. There will be secondary impact on other sensing, situational awareness, and detection problems that can be represented as networks such as space events, biological networks, and semantic networks. Finally the data-intensive demands of this problem will lead to experience, insight, and tools for scalable data management and analysis for all domains from physics simulations to astronomical data analysis and bioinformatics.

Progress

We have developed a family of temporal graph models and are continuing to evolve and improve them. To model activity time-series for each edge in a graph, we have developed a two-state hidden Markov model that learns two different distributions of activity representing active and inactive (or high and low) levels of activity commonly seen in these edges. These models are then used to measure the likelihood of new events with respect to previous activity.   Fitting these models to data is computationally intensive.   For example, using our data-intensive computing framework, we modeled a month's worth of traffic on the LANL network (550,000 edges modeled). That computation required 1.5 CPU-years, but was completed in just over two days on a 256-core cluster.

To detect larger patterns of coincident anomalies, we have developed a detection approach that enumerates every instance of one or more graphlets (small subgraphs of a fixed shape) in the graph and computes a joint likelihood of the time-series data observed across that entire graphlet. By simple combinatorics, there are immense numbers of these graphlets in real-world graphs, but we have developed a hybrid parallel (both SMP and MPI) library for enumerating these graphlets and computing likelihood (or other arbitrary computation) on each.   Using the LANL network data set again, we enumerated and measured the anomalousness of 300 million graphlets in 5 seconds on a 48-core computer.   We have also scaled this anomalous graphlet detection work up to 10^{15} graphlets in less than 2 minutes of computation.

We have also worked also model the frequency at which graphlets occur in a given location in a graph in order to determine when anomalous structures exist. This work focused on graphlets that satisfy a certain structure in time such that the duration of one edge encompasses the duration of an adjoining edge.

We also classify temporal graphs. Specifically to detect if a program is malware or not, we use instruction trace graphs that describe the execution of computer programs. To classify these graphs, we transform them into a Markov model of the transition probabilities

between instruction families. We then use multiple graph kernels to provide distance metrics between pairs of Markov model graphs and use machine learning algorithms to build classifiers [1]. We have developed a similar approach for anomalous change detection that identifies when a program's execution changes more than it usually does [2].

Further, we have developed methods for detecting anomalous changes across graphs by examining the distributions of how those graphs change over time[6].

We have also evaluated how well peer-to-peer botnet communications graphs can be detected when sensor coverage limits visibility to subsets of the communications graph [5] and strategies that bot-herders could deploy to improve the resilience and robustness of peer-to-peer based botnet structures and possible countermeasures by the defender as a response [4].

We have expanded this work, by allowing bots to use spoofing packets to hide their identities [7]. The number of spoofing source IP addresses per bot is generated from high-variations distributions, so the sum over all observed bots converges slowly. Such behavior allows a bot-herder to obfuscate the size of a botnet. Figure 1 shows the effect of obfuscation.
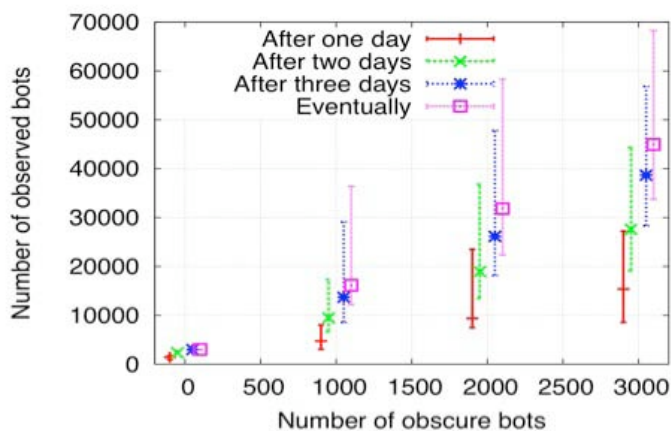
Figure 1. Effects of RatBot in obfuscating its size. The picture shows the number of observed bots by the adversary in different sample runs when we vary the number of bots that use spoofing packets to hide their identities.

As a final part of our focus on botnets, we have explored the idea of graph-based detection bots hidden in Twitter-like online social networks [8]. Our key idea is to look for the core of large graphs, which remain relatively stable over its evolution. Botnets are more likely to stay in the periphery of such large graphs. We developed efficient algorithms to find such a core of a large graph, after removing which the remaining graph has only small strongly connected components; thus only a small number of nodes and messages need to be monitored. We worked

on the Twitter dataset with more than 40 million nodes and 1.2 billion following relationships.

We have modeled how malware spread in online social networks is affected by the structure and activity patterns of social network users [3].

A novel approach to malware detection has been developed, based on the analysis of dynamic instruction traces from a large number of executable files. The base method can be trivially extended to an online procedure, provided the engineering hurdle of obtaining a sample of the instructions executed by a given process can be satisfactorily addressed. An execution trace collected from a running process is summarized by a state transition probability matrix, P, like that used to represent the probabilistic evolution of a Markov Chain. P is estimated by combining counts on all possible consecutive pairs of instructions with a prior model posing that the rows of P are independent Dirichlet vectors. Finally, a classification model is built from estimated P matrices for a large number of known malicious and known benign software samples using nonparametric logistic regression on the elements of P. The elastic net technique is used to perform logistic regression with careful selection of useful variables from among the many thousands of predictors represented by the elements of P. We illustrate the utility of the method on a sample of malware, and compare the results to other leading malware detection schemes (both signature and classification based). Figure 2 shows an illustration of how we classified executables.
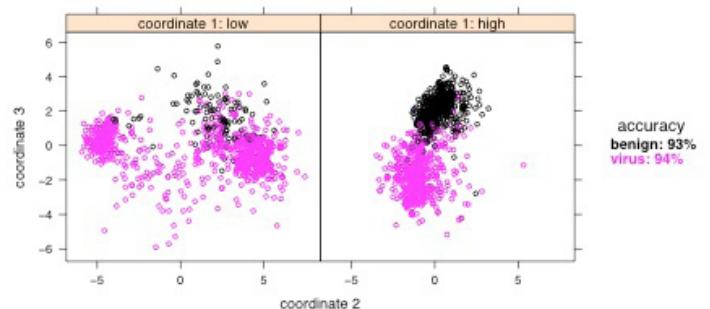
Figure 2. Over 2200 software executables are plotted in a three-coordinate projection formed from over 3000 predictor variables based on probability transitions matrices estimated separately for each executable. The three coordinates reliably separate malware and benign executables with high cross-validated accuracy.

We have spent substantial time pre-processing raw network events into higher-level data such as the graph of all e-mail communications at LANL. Email is of particular interest to us as it models the social network that exists at an institution such as LANL. We have analyzed the resulting temporal email graphs with respect to standard centrality measures, diameter, connections among and within groups, divisions and other organizational entities. We are

working towards a more systematic analysis, initial results that we have found is that administrative staff of upper management tend to have the highest centrality metrics, there are clear differences among divisions and group with respect to the destination set of their email traffic with some groups being more internally focused, others focused on a few divisions within LANL, and yet others focused even more towards external traffic.

Our graph-analytic approach has been used to analyze secure shell (ssh) connections as well with the goal of identifying long telescoping paths that indicate a potential attacker login into systems and using them as stepping stones. We used the notion of graphlets or motifs here as well, where we train an anomaly detection system on what graphlets are normal with the intent of flagging abnormal graphlets as they occur, the long telescoping path graphlet being just a single instance of such an anomaly [9]. Figure 3 shows an example of the ssh graph structure that we found.
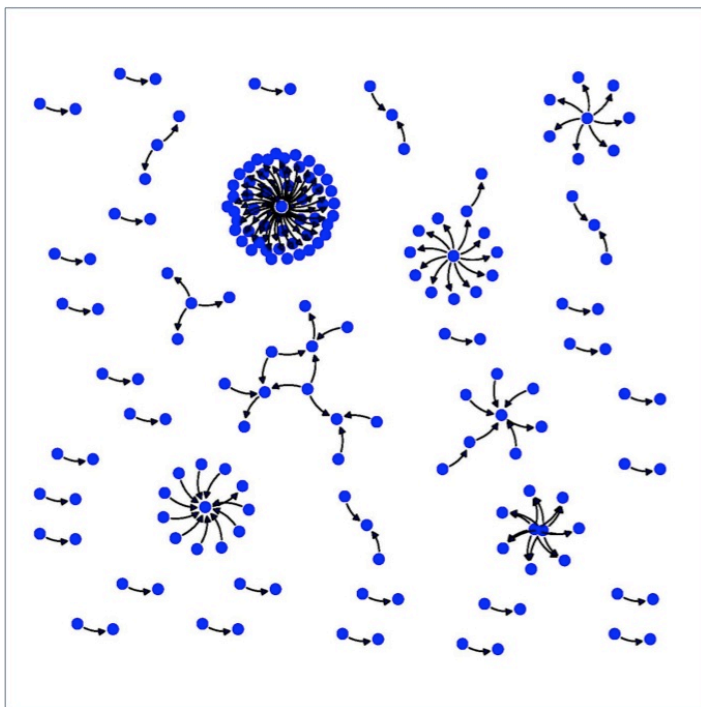
Figure 3. Example of SSH graphs. We see star-type graphs of both hosts that have many incoming SSH connections and also hosts that have many outgoing SSH connections. A larger connected graphlet component exists in the center of the picture

To enable this work, we have cultivated a repository of approximately 32TB of network event data we are using in this project as well daily snapshots of additional context information including the LANL phonebook and computer registration systems.

Future Work
We plan to continue the development of our framework

of treating cyber event data from multiple sensor types and locations as a large temporal graph. Recall that our program calls for extracting temporal and structural properties for the graph and partitions of the graph (temporal paths, protocols, etc.). We will consolidate our probabilistic models of sensor placement and bias to quantify the uncertainty inherent in the observed graphs. Using these properties, we will build sophisticated graph-based detection techniques leveraging graph theory, statistics, and machine learning. The resulting detectors will be designed for use online, on large networks with high data rates. Throughout all of this work – from data normalization and feature extraction through graph traversal and detection algorithms – we will employ map-reduce parallel computing to accelerate both the knowledge discovery process and online detection.

Conclusion
We will establish methods for constructing, analyzing, and modeling temporal graphs. We will make basic discoveries about how these graphs can be approximated with random models. Based on these discoveries, we will build new methods for applying detection algorithms to these graphs. The result will be a foundational, quantitative basis for detection and response-based cyber security.

References
1. Anderson, B., D. Quist, J. Neil, C. Storlie, and T. Lane. Graph-Based Malware Detection Using Dynamic Analysis. *Journal in Computer Virology.*

2. Anderson, B., D. Quist, and T. Lane. Detecting Code Injection Attacks in Internet Explorer. (Saarbruecken, 6-10 June 2011).

3. Yan, G., G. Chen, S. Eidenbenz, and N. Li. Malware propagation in online social networks: Nature, dynamics, and defense implications. 2011. p. 196.

4. Yan, G., D. Ha, and S. Eidenbenz. AntBot: Anti-pollution peer-to-peer botnets. 2011. *Computer Networks.* **55** (8): 1941.

5. Zeng, Yuanyuan, Guanhua Yan, S. Eidenbenz, and K. Shin. Measuring the Effectiveness of Infrastructure-level Detection of Large-scale Botnets. 2011. p. 1.

6. Arackaparambil, C., and G. Yan. Wiki-watchdog: Anomaly Detection in Wikipedia Through a Distributional Lens. (New York, 5-9 August, 2011).

7. Yan, null., and S.]. Chen. RatBot: anti-enumeration peer-to-peer botnets. 2010. *DOE.*

8. Yan, G.. Peri-Watchdog: Hunting for Hidden Botnets in the Periphery of Online Social Networks. 2011. *Los Alamos Unlimited Release.*

9. Djidjev, H., G. Sandine, C. Storlie, and S. Vander Wiel.

Graph Based Statistical Analysis of Network Traffic. (San Diego, C, 21-22 Aug. 2011).

10. Neil, J., C. Storlie, C. Hash, A. Brugh, and M. FIsk. Scan Statistics for the Online Idenfitication of Locally AnomalousSubgraphs. *Journal of the American Statistical Association.*

Publications

Anderson, B., D. Quist, J. Neil, C. Storlie, and T. Lane. Graph-Based Malware Detection Using Dynamic Analysis. *Journal in Computer Virology.*

Anderson, B., D. Quist, and T. Lane. Detecting Code Injection Attacks in Internet Explorer. To appear in *35th Annual IEEE International Computer Software and Applications Conference STPSA workshop, 2011.* (Saarbruecken, 6-10 June 2011).

Arackaparambil, C., and G. Yan. Wiki-watchdog: Anomaly Detection in Wikipedia Through a Distributional Lens. To appear in *Proceedings of IEEE/WIC/ACM Web Intelligence 2011.* (New York, 5-9 August, 2011).

Djidjev, H., G. Sandine, C. Storlie, and S. Vander Wiel. Graph Based Statistical Analysis of Network Traffic. To appear in *Ninth Workshop on Mining and Learning with Graphs.* (San Diego, C, 21-22 Aug. 2011).

Djidjev, H., and G. Sandine. Graph-Based Traffic Analysis for Network Intrusion Detection. 2011. *TSC Science Highlights, LA-UR 10-06320.*

Djidjev, H., and G. Sandine. Graph-Based Traffic Analysis for Network Intrusion Detection. To appear in *2010 Annual Computer Security Applications Conference (ACSAC).* (Orlando, F, 5-9 December 2010).

Jin, D., D. Nicol, and G. Yan. An Event Buffer Flooding Attack against DNP3-Controlled SCADA Systems. To appear in *Proceedings of the 2011 Winter Simulation Conference (WSC'11).* (Phoenix, AZ, 5-9 December, 2011).

Kakumanu, S., S. Eidenbenz, and R. Sivakumar. Lattice routing: A 4D routing scheme for multiradio multichannel ad hoc networks. 2011. *Ad Hoc Networks.* **9** (1): 95.

Neil, J., C. Storlie, C. Hash, A. Brugh, and M. FIsk. Scan Statistics for the Online Idenfitication of Locally AnomalousSubgraphs. *Journal of the American Statistical Association.*

Rahman, S., G. Yan, M. Faloutsos, H. Madhyashta, S. Eidenbenz, and M. Fisk. iDispatacher: A Unified Platform for Secure Planet-Scale Information Dissemination. 2011. *Los Alamos Unlimited Release LA-UR 11-02386.*

Yan, G.. Peri-Watchdog: Hunting for Hidden Botnets in the Periphery of Online Social Networks. 2011. *Los Alamos Unlimited Release.*

Yan, G., C. Arackaparambil, S. Bratus, and A. Caglayan. OnTuning the Knobs of Distribution-based Methods for Detecting VoIP Covert Channels. To appear in *Proceedings of Hawaii International Conference on System Sciences (HICSS-45).* (Hawaii, 4-9 January, 2011).

Yan, G., D. Ha, and S. Eidenbenz. AntBot: Anti-pollution peer-to-peer botnets. 2011. *Computer Networks.* **55** (8): 1941.

Yan, G., G. Chen, S. Eidenbenz, and N. Li. Malware propagation in online social networks: Nature, dynamics, and defense implications. 2011. In *6th International Symposium on Information, Computer and Communications Security, ASIACCS 2011 ; 20110322 - 20110324 ; Hong Kong, China.* , p. 196.

Yan, null., and S.]. Chen. RatBot: anti-enumeration peer-to-peer botnets. 2010. *DOE.*

Zeng, Yuanyuan, Guanhua Yan, S. Eidenbenz, and K. Shin. Measuring the Effectiveness of Infrastructure-level Detection of Large-scale Botnets. 2011. In *2011 IEEE Nineteenth IEEE International Workshop on Quality of Service (IWQoS 2011) ; 6-7 June 2011 ; San Jose, CA, USA.* , p. 1.

Correlations and Dynamics in Information Science

Robert E. Ecke
20110434DR

Introduction

National security increasingly depends on effective processing, transport, storage, and protection of information. For example, understanding and management of information systems in computer and communication networks, biological systems and social dynamics play a vital role in multiple national security challenges.

This project focuses on understanding the effects of 'correlations and dynamics' in information systems. We elucidate the effects of random influences (stochasticity), the consequences and prospects of coordinating the action of pairs or higher numbers of units or 'nodes', the dynamics of timing and coordinating signals, and the evolution and spread of information on static or dynamic networks as applied to diverse problems. This project supports and enhances the fundamental science of Information Science and Technology, an area of strategic interest to the Laboratory and a topic that is a Grand Challenge as well as a Pillar.

Benefit to National Security Missions

By underpinning the fundamental part of the 'S' (Science) in IS&T, the project helps the Laboratory fulfill its national security mission, growing the area of Information Science. This project substantially increases LANL's impact on IS&T research worldwide and helps with recruitment and retention. The science supports diverse applications relevant to the laboratory's mission including emergency management, epidemiology, materials modeling, synthetic vision, and energy distribution. The research simultaneously complements multiple efforts across the laboratory including cyber security, exa-scale computing, energy security through development of smart power grids, bio-security, and quantitative biology.

Progress

In the area of energy distribution, we developed an algorithm for determining the optimal placement and timing of battery exchange and charging stations (for plug-in hybrid electric vehicles – PHEV). This project produced a novel gradient descent algorithm for optimizing the placement of the stations that relied on continuous time optimization formulations. One of the more interesting aspects of the approach was the first-ever ability to model demand for PHEV charging as a function of the stations already built. In other words, we can model situations where technology availability increases technology adoption (i.e., the availability of stations increases the adoption of PHEVs). We developed a heuristic procedure for optimizing the placement and sizing of flexible energy storage in a grid that includes renewable energy sources, and studied a model of stochastic temporal fluctuations in a power grid. We have begun an effort to provide a quantitative characterization of energy systems across Latin America.

We studied the spread and evolution of viruses. We traced the spread and dynamics of Latvian HIV-1 epidemic using phylogenetic tools, finding an unexpected decrease in viral divergence due to the existence of a fast and slow rate of spread occurring simultaneously in this epidemic. We re-analyzed a previously described HIV-1 transmission chain in light of a phylogenetic model and found, contrary to previous thinking, that it might not be possible to extract a unique transmission history. This work has implications for court cases that rely on sequencing data to support transmission claims.

In the area of cybersecurity, we modeled the containment of malware on computer networks or rumors on social networks. We examined the possibility of partitioning a large network into small islands and monitoring the communication between the islands for malicious content. Both upper and lower bounds on the cost of the monitoring were established.

Game theoretic ideas were applied in multiple contexts. One example was resolving how to dynamically allocate tasks on an exascale machine. The most important issue is how to move tasks close to each other on the fly that require a lot of communication. We are testing preliminary ideas on a prototype architecture machine

that will be used for practical applications. We considered how to set compiler flags to optimize code performance in exascale using probability collective methods. We also started efforts on game theory related to general cybersecurity and to cyber-powergrid systems.

In the area of information processing, we applied a simple model describing the dynamics of neural activity in the primary visual cortex to show that certain low-level visual discrimination tasks involving "shape" and "saliency" could successfully be performed on very fast time scales. To achieve this, the model made use of long-range horizontal connections known to be present in the primary visual cortex. We estimated the parameters in a model of natural images, and found that hidden variables in the model form a sparse code that can be used to reconstruct the images. It is expected that the statistics of the estimated parameters will provide new alternative information on the statistical properties of natural images -- in much the same way that Fourier coefficients provide an alternative description of a time series.

We used our information science capabilities to improve materials modeling. In a major advance, we developed a new algorithm to simulate fermions coupled to a classical field. Our algorithm decreases the cost of a calculation from $O(N^3)$ to $O(N)$ (N is the number of lattice sites), enabling simulations of unprecedented system sizes, and revealing previously unknown quantum phases. We obtained coarse-grained dynamics of a quenched ferromagnet, generalizing conformal field theory results on a two-dimensional Ising model to higher dimensional, anisotropic systems.

We developed models of equitable allocation of humanitarian resources during a disaster and developed algorithms for optimizing these models. More formally, we made contributions in modeling a new variant of pickup and delivery optimization problems with an application to disaster relief (Equitable Pickup and Delivery Problem for Demand Response – EPDP-DR). The project produced results that demonstrated the difficulty in balancing equity and efficiency objectives and demonstrated that the problems can be solved tractably. The project also established the basic open questions with extending online vehicle routing to EPDP-DR and to pickup and delivery problems in general.

In general information science-related efforts, we analyzed and generalized the Belief Propagation (BP) approach to computing the permanent (a quantity much like the determinant, but harder to calculate) of a non-negative matrix. Known bounds and conjectures were verified in experiments, and some new theoretical relations, bounds and conjectures were proposed. We developed a simple greedy algorithm for learning the best planar Ising model to approximate an arbitrary collection of binary random variables (possibly from sample data), and applied the

algorithm to modeling voting. We analyzed the evolution of components in general random intersection graphs and obtained conditions for the existence and uniqueness of the giant component. By considering an auxiliary process that is stochastically equivalent but eliminates the structural dependencies of edges, we bounded the stopping time for a branching process. We considered various important problems in communications, e.g., decoding of Low-Density Parity-Check codes, detection in two-dimensional inter-symbol interference channels (magnetic and optical storage, cellular networks), etc., and modeled them as inference problems over graphs. Typically, optimal inference in these problems is NP-hard. We proposed detectors and decoders, based on linear programming, which have excellent performance as well as low computational complexity. The principle of spatial coupling was introduced in 2010 to explain the remarkable performance of convolutional Low-Density Parity-Check codes. In short, this principle provides a mathematical framework to explain the breakthrough performance of these codes, thus paving the way for a new paradigm for systematically designing capacity-achieving codes. We demonstrated that the principle of spatial coupling is very widely applicable to problems in multi-terminal communications and signal processing.

Future Work

The research of this project creates a broad backbone structure for information science by connecting disparate information science projects while forming a conduit for the exchange of information concepts across disciplines. On the short time scale, the inter-disciplinary studies of correlation and dynamics in information systems push the boundaries of the basic science of the IS&T area. The project is divided in three sub-projects: (i) sensing and processing of information, which includes bio-informatics and bio-inspired methods of speeding searches and fast processing of information, (ii) modeling and analysis of complex systems which focuses on applied mathematics analysis of tractable models and methods to make the models real-world relevant, allowing the description of epidemics and the development of fast, robust methods for real-time cyber security analysis, and (iii) inference and learning with stochastic information, which exploits statistical mechanics techniques to understand information science questions in the large systems limit. The methods used in this research come from different areas and the overall science package possesses a highly inter-disciplinary nature. The research will use insights from statistical mechanics, systems control theory, applied mathematics methods, and information science. The work will increase LANL's visibility in the general area of Information Science and Technology (IS&T) and we anticipate that the visibility will help with recruitment and retention. On the long time scale, through the synergy created by connecting the different areas of information problems, the project will contribute to the transfer of techniques and methods between different areas of

science and it will impact world-wide information science.

Conclusion

With this project, the Center for Nonlinear Studies (CNLS) targets fundamental science challenges that are central to long-term strategies for improving information management. The information systems targeted by the project are biological systems, bio-inspired systems (such as computer vision), energy-grid, and statistical mechanics systems. We expect that the project will contribute new basic insights and will transport methodologies and insights across traditional disciplinary boundaries.

Publications

Bradonjic, M., A. Gutfraind, and T. Novikoff. The neighbor aided network installation problems. *Discrete Applied Mathematics.*

Chandrasekaran, V., M. Chertkov, D. Gamarnik, D. Shah, and J. Shin. Counting Independent Sets Using the Bethe Approximation. 2011. *Siam Journal on Discrete Mathematics .* **25** (2): 1012.

Dvijotham, K., S. Backhaus, and M. Chertkov. Operations-based panning for placement and sizing of energy storage in a grid with a high penetration of renewables. *arXiv.* **1107.1382v2**.

Gutfraind, A.. Optimizing Network Topology for Cascade Resilience . To appear in *Handbook of Optimization in Complex Networks .* Edited by Thai, M. T., and P. M. Pardalos .

Gutfraind, A., A. Hagberg, D. Izraelevitz, and F. Pan. Interdiction of a Markovian Evader . 2011. In *Proceedings of the 12th INFORMS Computing Society Conference on OR, Computing, and Homeland Defense .* (Oregon, January 2011). , p. 3–15. INFORMS: INFORMS.

Johnson, J., P. Netrapalli, and M. Chertkov. Learning planar ising models. *arXiv.* **1101.3494**.

Johnson, M. P., and A. Gutfraind. Evader Interdiction and Collateral Damage . To appear in *Proceedings of the 7th International Symposium on Algorithms for Sensor Systems, Wireless Ad Hoc Networks and Autonomous Mobile Entities (ALGOSENSORS) .* (Saarbruecken, Germany, 8-9 Sep 2011).

Kudekar, S., J. Johnson, and M. Chertkov. Improved linear programming decoding using frustrated cycles. *arXiv.*

Kudekar, S., J. Johnson, and M. Chertkov. Linear programming based detectors for two-dimensional intersymbol interference channels. *arXiv.* **1105.5386**.

Kudekar, S., and N. Macris. Decay of Correlations for Sparse Graph Error Correcting Codes. 2011. *Siam Journal on Discrete Mathematics.* **25** (2): 956.

Loxley, P. N., L. M. Bettencourt, and G. T. Kenyon. Ultra-fast detection of salient contours through horizontal connections in the primary visual cortex. 2011. *Europhysics Letters.* **93**: 64001.

Loxley, P. N., and L. M. Bettencourt. Visually-salient contour detection using a V1 neural model with horizontal connections. *arXiv.* **1103.3131v1**.

Yedidia, A., and M. Chertkov. Computing the permanent with belief propagation. 2011. *ArXiv.* **1108.0065**: 1.

Zdeborova, L., and F. Krzakala. Quiet Planting in the Locked Constraint Satisfaction Problems. 2011. *Siam Journal on Discrete Mathematics.* **25** (2): 750.

Optimization Principles for Co-Design applied to Molecular Dynamics

Stephan J. Eidenbenz
20110710DR

Introduction

Our goal is to develop a framework for hardware-software codesign as a formally-posed optimization problem. While the optimization framework will be applicable to multiple problem domains, our target application is molecular dynamics (MD), an exemplar for the need for both weak (larger problems) and strong (faster time to solution) computational scaling, and archetypal of the obstacles thereof. We view codesign as search and selection from a vast space of hardware and software designs that map to performance metrics. The objective function that we aim to optimize contains, as main components, run time (or computational rate), problem size, simulated time duration, energy use, and hardware cost. The framework will manifest itself in the form of (i) optimization software addressing hardware and software design space enumeration, and performance prediction methods at multiple scales, (ii) documented best practice insights, and (iii) theorems on upper and lower bounds on theoretically achievable performance for some algorithmic and hardware architecture combinations. On the application side, our goal is to enable the atomistic simulation tools that can probe the physics of processes such as ductile spall failure under shock conditions, and the evolution of radiation damage. Achieving this requires two orders of magnitude increase in simulated time over current state-of-the art petascale computing, and cannot be realized without this codesign approach, as direct implementation on an exascale platform would not achieve it. These two problems are of great intrinsic interest to the lab, addressing the response of materials in extreme conditions and enabling the design of more durable and safe fission power plants, respectively.

Benefit to National Security Missions

Successful implementation of our optimization framework will provide the unique capability of codesigning hardware and software on a sound formal basis, and in a partially automated manner. It will enable effective implementation of physics simulations on future novel computer architectures, and provide a basis for more decisive influence on hardware design.

For our molecular dynamics application domain, we will identify hardware and algorithmic regimes that would enable study a wealth of poorly understood phenomena of critical importance to the lab mission, such as in nuclear weapons, energy systems, and armor, to name but a few.

Progress

The Accelerated Molecular Dynamics (AMD) methods, such as Temperature-Accelerated Dynamics (TAD) and Parallel Replica (ParRep) developed at LANL, as well as parallel molecular dynamics, have hit scalability walls. Performance boundaries on large-scale supercomputers are shown in Figure 1; linear extrapolation of the performance to an exa-scale supercomputer without fundamental changes in hardware and/or software will lead to only marginal improvements in terms of numbers of atoms and duration of time that can be simulated.

Our fundamental premise is that computational co-design can be posed as an optimization problem, and once so posed, an objective function can be maximized by the traditional iteration that we refer to as an optimization loop (see Figure 2):

- A model of a hardware-software solution pair is selected;

- A performance prediction model predicts performance in terms of computational rate (or time to completion), estimated energy usage and amortized hardware and software costs;

- After evaluating an objective function, the optimization strategy selects a new hardware software pair and we go back to step ii.

We have started to develop a hierarchy of hardware and software models as well as the performance prediction method at different levels of fidelity. The key idea is that the level of detail of modeling needs to make sense on

the hardware and software levels and its performance should be predicted by an adequate fidelity method. The different levels of details that we have defined on the software side are: i) Model/Equation/Algorithm; ii) Pseudo-Code; iii) Higher-language code (e.g., C code); and iv) Assembly language code. On the hardware side, specific levels we intend to address are i) Cluster; ii) Node-Interconnect-Filesystem; iii) Core-Memory-OS Level (to include caching hierarchies); and iv) Chip Logic level, which will include hardware design features such as pipelining. The performance prediction methods that we have identified are Mathematical Modeling, Discrete Event Simulation, and Emulation.
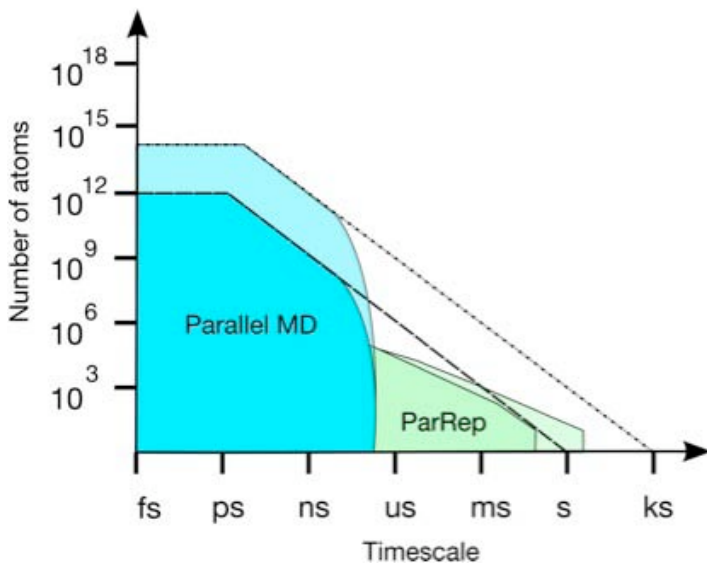
Figure 1. Scaling of Molecular Dynamics Codes: Strongly colored regions correspond to the accessible problem space on a current petascale computer (24 hours on Roadrunner) while paler regions are for an exascale machine. The dashed and dash-dotted lines correspond to the theoretical limit of a perfectly-scaling MD code, at the peta- and exascale, respectively. Note the capability hole at 106-109 atoms for micro- to milliseconds.
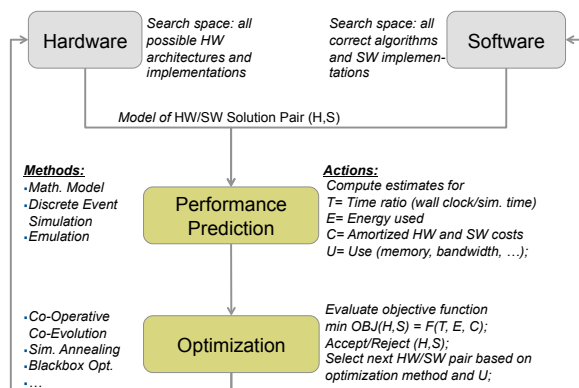
Figure 2. Optimization Loop in a Co-Design setting.

Different levels of fidelity are necessary to effectively search the vast span of hardware and software design spaces for our given molecular dynamics scaling problem: in our scheme we will identify promising designs in hardware and software at a high level and then drill down via higher-fidelity models all the way through emulation, chip level and assembly code, to predict performance.

We have structured our work along the tasks of performance prediction, semi-automated hardware space exploration, semi-automated software space exploration, optimization methods, and software framework integration. See our working document [1] for more details on these tasks and first results, which we describe here coarsely.

We have extended existing mathematical performance modeling results for the TAD method to include a model for a ParRep-TAD combination, which accounts for overhead. We are extending these models to account for details in the overhead computation (performance modeling task).

Leveraging earlier work on scalable discrete event simulation frameworks (namely the SimCore tool), we have implemented a simulation model of the TAD method, named TADSim [2], at essentially the Node-Interconnect-Filesystem level of detail on the hardware side and the Pseudo-Code level on the software side. In order to complete an optimization loop, we have used TADSim to predict the optimum temperature value that TAD should be run at for a specific material system. Results are illustrated in Figure 3—for this particular Al tetramer cluster system 400K gives the optimal real boost factor of 1.79e4. We view this as a first proof of principle for the optimization approach to codesign, albeit the software search space was limited to a single parameter and the hardware search space was fixed. Obviously a great deal more work remains to be done—this work represents the substance of the research for this project. Currently we are extending TADSim to include an explicit hardware model. Modeling ParRep at a similar level of detail is in its final stages, which is a prerequisite to actually building the ParRep/TAD-combination simulator, that we expect to test in the first half of FY12 (performance modeling, software space exploration, and optimization method tasks).

All molecular dynamics methods have the so-called force call at their core. The complexity of the force call usually dominates overall computation time. We have started to model force call code at the higher-language code level in our software module coupled with a Core-Memory-OS level of detail on the hardware side. We are using the same modeling principles as for TADSim and plan to combine TADSim with this force-call model—the initial force call model in TADSim is realistic but not detailed. This greater detail is needed for performance modeling on detailed hardware specifications.

We are using the QEMU emulation framework to build a performance prediction model at the near clock-cycle

accuracy. Our plan is to eventually build a seamlessly integrated optimization loop that iterates over different levels of model details (performance prediction and Software integration tasks).

We have started a collaboration with the Claremont Graduate University, POC Lukas Kroc, an expert in Artificial Intelligence and Machine Learning methods, to develop software and hardware exploration methods on relatively simple problems, such as optimum circuit design, which we plan to use as proof of principle for very low level hardware design exploration, and as building blocks for higher-level hardware designs.

Our project was presented in two posters in the LANL booth at the 2011 Supercomputing Conference [3].

Results (THigh = 400 K)	Predicted (1000 trials)	TAD Simulation (1 trial)
Raw Boost	3.70e+04	2.75e+04
Real Boost	1.79e+04	2.34e+04
TAD Low Temperature Time	6.36e-05 s	7.46e-05 s
MD Stop Time	1.44e-09 s	
Predicted Wall Clock Time	620 s	560 s
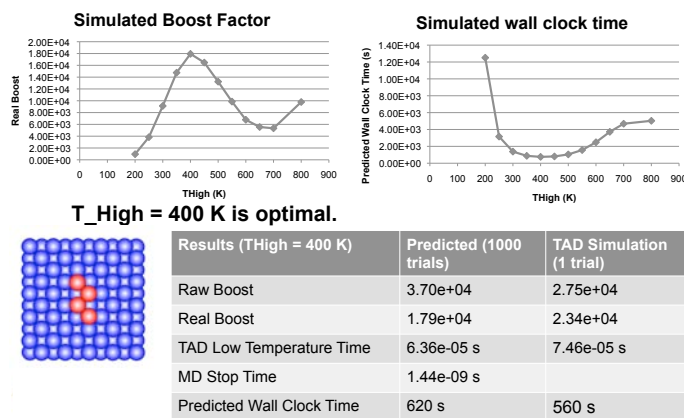
Figure 3. TADSim is a performance simulator of a Temperature-Accelerated Dynamics Simulation. TADSim allows us to quickly find an optimum value for simulation parameters, such as the temperature. Simulation run-time as predicted by TADSim and actual TAD run-time are correct to about 80%.

Future Work

Our semi-formal codesign optimization framework relies on (i) efficient enumeration methods for finding feasible hardware architectures and software designs; (ii) a multi-scale approach to performance prediction modeling, where we use cycle accurate virtual machine emulation, discrete event simulation, graph mapping, and constraint programming as different prediction methodologies; and (iii) optimization methods with fast identification of new hardware-software pairs to be tested, and acceptable convergence. Our future work is to broaden (scope of spaces), deepen (spanning of levels of abstraction), and refine capabilities for each of these elements. We define hardware and software designs in a hierarchical fashion. Enumeration of software designs is initially very domain specific; the longer-term goal is to relax this specificity. The enumeration of hardware architectures is done implicitly through parameter spaces and optimization search methods as well as (human, possibly machine-aided) design feasibility checking. Our performance prediction

methods model at different levels of detail, thus covering the trade-off space of accuracy vs. scalability in both time and size; performance prediction techniques we will employ include constraint mathematical programming, discrete event simulation, and virtual machine emulation. Optimization heuristics are necessary for the more detailed prediction methods of virtual machine emulation and discrete event simulation. Our framework allows for the adaptation of standard meta-heuristics such as simulated annealing, taboo search, gradient search, and genetic algorithms. The more coarse-grained prediction methods of graph mapping and constraint programming will optimize through graph algorithms and mathematical programming techniques.

Conclusion

A successful codesign optimization framework will fundamentally change the way scientific applications are constructed: HW/SW codesign fundamentals will become an essential part of software engineering. Our optimization framework will have manual and automated aspects, similar to compiler optimization techniques used in classical compilers for the automated aspects; it will achieve peak performance when the human designer allows the optimizer to test a large set of potential solutions in a high-throughput optimization loop.

References

1. Eidenbenz, S., A. Voter, K. Davis, S. Mniszewski, D. Perez, N. Santhi, S. Thulasidasan, H. Djidjev, L. Gurvits, and L. Kroc. Optimization Principles for Hardware/Software Co-Design with Applications in Molecular Dynamics. 2011. *Los Alamos National Laboratory Unlimited Release.*

2. Mniszewski, S.. TADSim: Discrete Event Simulation of Temperature Accelerated Dynamics Performance. 2011. *Los Alamos National Laboratory Unlimited Release Report.*

3. Optimization Principles for Hardware/Software Co-Design with Applications in Molecular Dynamics. (Seattle, WA, 12-18 Nov. 2011).

Publications

Optimization Principles for Hardware/Software Co-Design with Applications in Molecular Dynamics. To appear in *Poster at Supercomputing conference SC'11.* (Seattle, WA, 12-18 Nov. 2011).

Eidenbenz, S., A. Voter, K. Davis, S. Mniszewski, D. Perez, N. Santhi, S. Thulasidasan, H. Djidjev, L. Gurvits, and L. Kroc. Optimization Principles for Hardware/Software Co-Design with Applications in Molecular Dynamics. 2011. *Los Alamos National Laboratory Unlimited Release.*

Mniszewski, S.. TADSim: Discrete Event Simulation of

CoCoMANS: Computational Co-design for Multi-scale Applications in the Natural Sciences

Dana A. Knoll
20110737DR

Introduction

We will forge a qualitatively new predictive-science capability exploiting evolving high-performance computer architectures for multiple national-security-critical application areas—including materials, plasmas, and climate—by simultaneously evolving the four corners of science, methods, software, and hardware in an integrated computational co-design process. We will develop new "applications-based", self-consistent, two-way, scale-bridging methods that have broad applicability to the targeted science, will map well to emerging heterogeneous computing models (while concurrently guiding hardware and software to maturity), and provide the algorithmic acceleration necessary to probe new scientific challenges at unprecedented scales. Outcomes will 1) represent a paradigm shift in the pursuit of world-class science at LANL by bringing a wide spectrum of pertinent expertise in the computer and natural sciences in to play; 2) deliver a documented computational co-design knowledge-base, built upon an evolving software infrastructure; 3) foster broad, long-term research collaborations with appropriate hardware partners; and 4) deepen understanding of, and our experience-base with, consistent, two-way, scale-bridging algorithms.

Benefit to National Security Missions

The need for computational co-design and multiscale solution algorithms resides in almost every mission at LANL that involves computational science. Nowhere is the need greater than in the NNSA ASC program. We have carefully chosen two of our application areas, materials science and plasma physics, as these areas represent current and future multi-scale challenges to ASC. All three chosen application areas are relevant to the Office of Science mission. Most importantly, the research proposed here is a required investment to prepare for a LANL leadership role in the DoEExascale Initiative. Mission applications for computing at this scale are legion, and include nuclear weapons, fusion and fission energy, explosives and armor, and climate/energy effects.

Progress

The CoCoMANS project is a recent start, 7/2011. There has been limited progress to-date. Our research team is organized, we are executing on a number of fronts and we have a fairly well developed plan for FY-12. We will highlight progress in specific areas.

Compact-App-0: We have produced performance data for 1-D problem on advanced architectures. 2-D software is nearly complete.

Plasma Application: The initial definition of the plasma compact app goal is done and documentation is well underway. We have an initial prototype / mini-app plan defined.

Materials Application: The initial definition of the materials compact app is nearly complete. An initial prototype has been developed and is being tested. Documentation has started.

Work has progress on our experimental software framework, which will support, and document, our co-design process. We have also initiated some vendor / hardware collaboration and put the paperwork in place which will allow such collaborations to move forward.

Additionally, our general proposed co-design process and work on it thus far, has had a noticeable impact on the LANL ASC program office. They have clearly taken note of the COCOMANS directions, and the COCOMANS project is influencing the LANL ASC program planning for their own computational co-design activities.

Future Work

Our goal is to define, develop, and employ a computational co-design process, encompassing at one end, non-trivial computational physics problems, and at the other a range of current, emerging, and to some degree hypothetical, hardware architectures. This requires defining at a high level the co-design process we will follow, and in more detail, the methodology. The process broadly prescribes functional areas—domain science, numerical algorithms and solvers, computer

science, and hardware (processor and node-level architecture)—and the communication and feedback among them. The methodology distills our philosophy for this largely uncharted territory. The results and deliverables of this project fall into three main categories: a paradigm shift in multi-scale physics on emerging architectures, a knowledge base for computational co-design, and the development of a community—both internal and external—around LANL's approach to co-design.

Conclusion

The technical impact of this project will be a roadmap leading to a quantum leap forward in computational science for a variety of applications on modern architectures. No general scale-bridging algorithm of the type we propose has gone through a computational co-design activity. As a result of demonstrating a paradigm shift in specific application areas, we will define a computational co-design blue print for system-scale simulation with fine-scale physics fidelity for several applications. Furthermore, we will obtain a quantifiable understanding of the potential of various architectures to achieve such simulations resulting from our detailed interaction with vendors.

Synthetic Cognition Through Peta-Scale Models of the Primate Visual Cortex

Luis Bettencourt
20090006DR

Abstract

Our research program was dedicated to understanding and implementing the computational principles of the human brain as they apply to vision. To achieve these goals, we created synthetic cognition computational systems that emulate the functional architecture of the primate visual cortex. By using large-scale computational resources and exploring new hybrid chip architectures, such as GPUs, combined with our growing knowledge of the structure and function of biological neural systems, we investigated the limits of size and functional complexity necessary to generate the information processing capabilities of cortical circuits.

We achieved several scientific and technological breakthroughs. First, we have established the limitations of purely feed-forward models of visual cortex, in terms of their improvement in accuracy in object identification tasks with amount of visual experience. These limitations make it impractical to achieve human level performance with a practical amount of training. We the showed that lateral connections can help substantially improve performance by capturing and isolating global salient features of objects. Finally we developed a new theory and a new class of models that include feedback and lateral connections with feed-forward pathways as a probabilistic Bayesian network. We also began exploring the capabilities of these new models with excellent results overall, but more remains to be done.

The project has had tremendous impact in building a new community of researchers interested in neuroscience, image processing and their applications to technology and global security at Los Alamos. We have created a model of discussion and collaboration that transcended our project and is now part of interactions with the New Mexico Consortium and New Mexico universities. We stood up a number of new experimental capabilities in behavioral, cognitive and brain imaging that have already benefited other projects including applications for DARPA and in the realm of the Laboratory's global security mission.

Background and Research Objectives

Detection of familiar objects in natural images and video is an important problem than can enable many technologies from robotics to remote sensing. Vision is a common target for synthetic cognition and, not incidentally, the research area where neuro-mimetic approaches have been most successful so far. The best current machine vision systems, including scaled-down models of the visual cortex that lack spiking dynamics or synaptic feedback, achieve, at best, a 10% error rate on object detection tasks over many different object classes [1]. In contrast, under real life circumstances human performance is essentially perfect. The ultimate limit of new synthetic cognitive systems is to close this performance gap. While some tasks are easier for present algorithms, building a general purpose system that can learn and increase its performance with visual experience, instead of being fine tuned by hand for each task, remains perhaps the most important problem in the field. This was the central problem of our project.

To do this, we believe, it is necessary to create the opportunity for synthetic cognition systems to develop over time and incur a large amount of semi-supervised visual experience. The arrival new high performance computing allowed us to probe the limits of models, by bringing artificial computation to the scale of the human brain. Progress in hybrid computational architectures, such as GPUs, also allowed us gains in price and energy consumption that enable widespread experimentation with new models and algorithms.

The opportunity to re-create a functional model of the mammalian cortex, by bringing the necessary computational, theoretical and experimental resources to bear, has been the theme of several high profile workshops (including two extremely successful international conferences organized by out team, Grand Challenges in Neural Computation &). Groups in the US, Europe, China and Japan are gearing up to tackle this challenge.

, is creating open-source models of hierarchical temporal memory systems guided by the broad architecture of visual cortex. These models have not been vetted by peer review nor demonstrated performance on cognitive visual tasks comparable to human subjects. The European-led project (based at EPL Lausanne) represents the most impressive effort to model mammalian cortex, having just announced the first biologically faithful model of a rat's cortical column. It is unclear, however, how such detailed physiological models can be scaled up to the ~30K or more columns that constitute the human visual system; or if such detailed models are necessary to replicate the brain's functional performance. An alternative approach, the project at Stanford University seeks to develop special purpose hardware for implementing cortical circuits in electronic devices comparable in size and power consumption to biological systems. Compared to digital computers, such specialized hardware is very difficult to program and currently lacks any provision for synaptic plasticity.

Our research program consisted of 4 objectives: 1) Scaling up hierarchical feed-forward cortical networks, 2) Neuronal dynamics, learning, and lateral and feedback connectivity, 3) behavioral experiments and brain imaging, 4) high performance computational implementation in hybrid platforms.

Scientific Approach and Accomplishments

Our scientific approach from the outset relied on creating a working systems-level model of the primate visual cortex, benchmark it on object identification tasks, and add new functional elements that are useful at improving performance against these benchmarks. As such we maintained several lines of research in parallel, and integrated them when necessary. We describe them below.

Human performance on object detection tasks depends critically on exposure time. Given sufficient time to observe an image (> 250ms) adult human subjects achieve essentially perfect performance. However, in ultrafast *speed-of-sight* tasks (image exposure ~30ms), humans misidentify the presence of familiar objects in about 10% of trials, similar to the error rate of simplified feed forward cortical models [1]. The short exposure times were hypothesized at the time when we started this project, to exclude the use of lateral and feedback interactions, both within and between visual processing areas, thus effectively reducing the visual cortex to a feed-forward circuit. In this context our research investigated i) whether human subjects ability to identify objects in speed of sight tasks is consistent with feed-forward only mechanisms of cognition and ii) whether performance on speed of sight object identification tasks did indeed correlate with model performance in a much more extensive collection of tasks. The answer to both these questions was negative, making it necessary that we consider mechanisms of (local) feedback

that occurs faster than previously thought. We report the details below, after we describe visual identification tasks and new image datasets, developed by the project.

To define visual identification tasks we started by using standard image libraries for which performance benchmarks have been established for a variety of object detection algorithms. At the beginning of the project, *Caltech256* was the largest multi-category object recognition database available, with ~31,000 images covering 256 object categories. Test of performance for feed-forward models often use simplified versions of these and other datasets. As the project developed we found the need to build new much larger and better-defined (statistically) datasets. We developed a new amoeba generating algorithm, which is artificially rendered closed contours with clutter and controllable level of distortion, much larger natural image sets with object segmentation (partially obtained via flickr) and new rendered object sets, that allowed us to compare training on natural and rendered objects as well as issues of cross training. We have also explored new datasets such as imageNET and video, including annotated video collections built for DARPA challenges, see below.

Objective 1: Scaling up hierarchical feedforward cortical networks

The hypothesis that strictly feed-forward architectures suffice to match human performance in cognitive tasks—once scaled up to the size of the brain—has pervaded the history of Artificial Intelligence. With the advent of large-scale computation this hypothesis can finally be tested. Quantifying the extent of performance improvement achieved by scaling up network size and feature complexity was the first task of our project.

The human visual system is organized hierarchically into parallel processing streams. We built a model of the ventral stream of visual cortex according to this scheme and had it learn feature representations under both unsupervised video and image presentations and supervise smaller image sets, which train the uppermost system layers [2]. In particular we developed the ability of processing video in real time, and used in some cases many hours of video to assemble image representations at the various cortical layers. We then investigated the rise in object classification performance as the system is exposed to more and more visual imagery in a way that is analogous to development in vivo. We have found that the pure feedforward system learns very slowly in this mode, typically increasing its performance logarithmically with the number of image sin the training set and often saturating any improvements. Extrapolating these trends would require an exponentially large number of images for each object class, which we showed for similar objects (cat vs. dog for example) become impractical. We also spend much time understanding these slow trends in learning, which we attributed to the

identification pg low-level, non object specific features and the lack of sparseness inducing terms, meaning that representations of the image are not sufficient parsimonious to allow upper layers easy discrimination between object classes. The possible solution to these problems is found in models that introduce lateral and feedback connections as well as strong regularization of neural activity so that only the best representative features are passed on to upper layers.

Objective 2: Neuronal dynamics, learning, and lateral and feedback connectivity

Performance scaling limits of feed-forward hierarchical networks at the scale of the human visual cortex now provide baselines for performance improvement via the inclusion

of spiking dynamics and lateral and feedback connectivity.

In contrast to the non-dynamical units used in most feed forward models, the brain is made up of neurons with time dependent spiking dynamics. Spikes correspond to very short, essentially instantaneous pulses; their relative timing carries much of the information in different neural systems [3,8]. In addition, spike timing ultimately determines the strength of synaptic connections, and thus learning, in the brain. We built a petascale computational architecture, called Petavision, which allows us to create and solve large computational models of spiking neurons. During benchmarking tests of Roadrunner (Los Alamos petascale supercomputer) it achieved the world-record performance benchmark of 1.142 petaflots in June 2008. Unfortunately Roadrunner was never available to our team thereafter, as it was dedicated to its mission. Nevertheless we pursued several studies dedicated to learning the system's connectivity under time dependent learning rules and the role of synchronized oscillations across visual areas to achieve dynamical binding of memory related to object representations at different levels.

Much is known about feedback and lateral connectivity in the visual cortex. Feed-forward connections (e.g. V1 to V2), are always matched by strong feedback connections, (e.g. V2 to V1). We explored the computational role of horizontal connections in a diversity of studies that confirmed their importance in removing unessential elements in images that may clutter objects and possibly enabling ultra-fast object detection, consistent with the timescales observed in speed of sight experiments [3]. In [4] we used mean field models of neural dynamics to derive lateral interaction kernels that support smooth object continuation, and used them to demonstrate nearly perfect detection of objects with given boundary structures on time-scales of 10-20 ms. In another study [5] we explored more complex object and clutter datasets (amoebas and natural images) to learn these lateral connectivity kernels and again demonstrate that their use is consistent with human subject performance in speed of sight tasks. As a consequence of these results we developed new mathematical models and

algorithms for the de-cluttering of natural images and early identification of objects based on their topology.

The ultimate challenge for the project as a whole was to develop new mathematical models and their computational implementations that integrate the feed-forward architecture of visual cortex with lateral and feedback connections to deliver better performance and more general human like mechanisms of visual attention. The main difficulty of this task is that operation under top down connections is severely mathematically ill-posed.

To solve these problems we developed a new class of probabilistic graph models, which we dubbed deep generative networks. These models use reciprocal feed-forward and feed-back connections to predict incoming images given the internal state of the system (hence their name) and vice versa. As a result these models have imagination, i.e. they can build detailed images based on a few labels corresponding to classes of objects. They can also be used to remove clutter and reconstitute objects in given images.

Objective 3: Behavioral experiments and brain imaging

We stood up several key experimental capabilities at LANL and used them to perform an extensive number of experiments in visual object identification, and EEG brain imaging that helped us clarify the importance of non-feedforward mechanisms in early visual cognition.

Objective 4: High performance computational implementation in hybrid platforms.

We demonstrated that neural models are easily parallelized in hybrid supercomputing machines by establishing the early speed record for a scientific application in roadrunner (1.142 petaflops). We also developed our own CELL and GPU clusters (bambino and homunculus, housed at CNLS) and achieved speed of performance in video that matches or surpasses human abilities. These achievements established our leadership in visual synthetic cognition and have lead to a DARPA contract and a new LDRD DR dedicated to video processing [6].

Impact on National Missions

The project had significant impact in two areas of Laboratory scientific capabilities: Information Science and Technology and Cognitive and Neural Sciences. Synthetic Cognition has become one of the themes of the Information Science and Technology (IS&T) Center (John S. George, theme lead). Neuromimetic Computing had been the focus of LDRD ER and Engineering Reserve proposals and a DR Finalist proposal in the Computational Co-Design and IS&T category. Another DR project to explore the development of generative models applied to video data has been funded by the LDRD program (Steven Brumby, PI). We won a $1M seeding DARPA project and plan to compete for Phase 2 funding.

The project has also reinvigorated experimental capabilities in neurosciences at LANL. It has developed new expertise and infrastructure in cognitive and psychophysical investigation using behavioral techniques. These have been integrated with high density EEG and with high-resolution eye-tracking.   These methods will also be extended to other functional imaging technologies including ultralow field MRI and capacitance based EEG, which are the focus of other LDRD investments. The capabilities for advanced EEG, and eye-tracking will enable LANL investigators to participate in new initiatives at DARPA and elsewhere (e.g. the BioNav program) to develop noninvasive electro-neural interfaces for control of semiautonomous vehicles. Enhanced experimental capabilities will serve as a foundation for new programs from NIH, NSF and several DOD sponsors, as well as funding agencies with Global Security interests and applications [2,6].

The Synthetic Cognition project has lead to the coalescence of a community of shared interest consisting of over 25 researchers. In addition to many scientific staff members with long-term interests in this area, the project has supported a large number of postdoctoral fellows and students, several of whom are pursuing future employment opportunities with the Lab.

References

1.   Serre, T., A. Oliva, and T. Poggio. A feedforward architecture accounts for rapid categorization. 2007. *PROCEEDINGS OF THE NATIONAL ACADEMY OF SCIENCES OF THE UNITED STATES OF AMERICA.* **104** (15): 6424.

2.   Brumby, S. P., G. Kenyon, W. Landecker, C. Rasmussen, S. Swaminarayan, and L. Bettencourt. Large-scale Functional Models of Visual Cortex for Remote Sensing. 2009. In *2009 IEEE Applied Imagery Pattern Recognition Workshop (AIPR 2009) ; 14-16 Oct.* (2009 ; Washington, DC, USA). , p. 1.

3.   George, J. S., M. Ham, S. Barr, V. Gintautas, C. Rinaudo, A. Guthormsen, M. Anghel, P. Loxley, S. Brumby, L. Bettencourt, and G. Kenyon. Visual object recognition and masking in speed-of-sight tasks. 2010. In *40th Annual Meeting of the Society-for-Neuroscience ; November 13 -17, 2010 ; San Diego, CA, USA.* Vol. 40.

4.   Loxley, P. N., L. M. Bettencourt, and G. T. Kenyon. Ultrafast detection of salient contours through horizontal connections in the primary visual cortex. 2011. *EPL.* **93** (6): 64001.

5.   Gintautas, V., M. I. Ham, B. Kunsberg, S. Barr, S. P. Brumby, C. Rasmussen, J. S. George, I. Nemenman, L. M. A. Bettencourt, and G. T. Kenyon. Model Cortical Association Fields Account for the Time Course and Dependence on Target Complexity of Human Contour Perception. 2011. *PloS Computational Biology.* **7** (10): 1.

6.   Brumby, S.. Image fusion for remote sensing using fast, large-scale neuroscience models. 2011. In *Multisensor, Multisource Information Fusion: Architectures, Algorithms, and Applications 2011 ; 27-28 April 2011 ; Orlando, FL, USA.* Vol. 8064, p. 806402 (8 pp.).

Publications

Achler, T., D. C. Vural, and E. Amir. Counting objects with biologically inspired regulatory-feedback networks. 2009. In *2009 International Joint Conference on Neural Networks (IJCNN 2009 - Atlanta) ; 14-19 June 2009 ; Atlanta, GA, USA.* , p. 36.

Barr, S., V. Gintautas, J. L. Hammon, M. Ham, S. Brumby, G. T. Kenyon, and L. M. A. Bettencourt. Preliminary Results from the Comparison of Human Visual Performance to Biologically Inspired Computer Object Categorization. Presented at *Decade of the Mind.* (Albuquerque, 13-15 Jan 2009).

Bettencourt, L. M.. The Rules of Information Aggregation and Emergence of Collective Intelligent Behavior . 2009. *topics in Cognitive Scienc .* **1** (4): 598 .

Bettencourt, L. M., S. Brumby, J. George, M. I. Ham, and G. Kenyon. Receptive field properties in primate visual cortical hierarchy from large scale statistics of natural images. 2010. In *Neuroscience Meeting of Society-for-Neuroscience ; 2010, ; San Diego, CA, USA.* Vol. 40.

Bettencourt, L. M., S. Brumby, V. Gintautas, M. I. Ham, S. Barr, P. Loxley, K. Sanbonmatsu, S. Swaminayaran, J. George, G. Kenyon, and I. Nemenman. Image Categorization through Hierarchical Models of the Primate Visual System. Presented at *Neuroscience 09 .* (Chicago, 17-21 Oct 2009).

Brumby, S.. Image fusion for remote sensing using fast, large-scale neuroscience models. 2011. In *Multisensor, Multisource Information Fusion: Architectures, Algorithms, and Applications 2011 ; 27-28 April 2011 ; Orlando, FL, USA.* Vol. 8064, p. 806402 (8 pp.).

Brumby, S. P., G. Kenyon, W. Landecker, C. Rasmussen, S. Swaminarayan, and L. Bettencourt. Large-scale Functional Models of Visual Cortex for Remote Sensing. 2009. In *2009 IEEE Applied Imagery Pattern Recognition Workshop (AIPR 2009) ; 14-16 Oct.* (2009 ; Washington, DC, USA). , p. 1.

Brumby, S. P., G. Kenyon, W. Landecker, C. Rasmussen, S. Swaminarayan, and L. M. A. Bettencourt. Large-Scale

Functional Models of Visual Cortex for Remote Sensing. 2009. In *Applied Imagery Pattern Recognition (AIPR 2009): Visions: Human, Animal, and Machines.* (Washington DC, 13-15 Oct 2009). , p. 1. Washington: IEEE.

Brumby, S. P., K. L. Myers, and N. H. Pawley. Capturing Dynamics on Multiple Time Scales: A Multilevel Fusion Approach for Cluttered Electromagnetic Data. 2010. In *Multisensor, Multisource Information Fusion: Architectures, Algorithms, and Applications 2010 ; 7-8 April 2010 ; Orlando, FL, USA.* Vol. 7710, p. 771002 (8 pp.).

George, J. S.. Casting Light on Neural Function: A Subjective History. 2010. In *Imaging the Brain with Optical Methods* . Edited by Roe, A.. , p. 1. Heidelberg: Springer.

George, J. S., G. T. Kenyon, M. I. Ham, I. Nemenman, and L. M. Bettencourt. Modeling Consequences of Microscopic Eye Movements on Visual Spatial Perception. Presented at *Organization for Human Brain Mapping.* (San Francisco, 18-23 June 2009).

George, J. S., M. Ham, S. Barr, V. Gintautas, C. Rinaudo, A. Guthormsen, M. Anghel, P. Loxley, S. Brumby, L. Bettencourt, and G. Kenyon. Visual object recognition and masking in speed-of-sight tasks. 2010. In *40th Annual Meeting of the Society-for-Neuroscience ; November 13 -17, 2010 ; San Diego, CA, USA.* Vol. 40.

George, J. S., S. Barr, M. Ham, C. Renaudo, J. Hammond, V. Gintautas, S. Brumby, K. Sanbonmatsu, I. Nemenman, L. Bettencourt, and G. Kenyon. Not so Fast: Optimized Masks Increase Processing Time for Object Detection on Speed-of-Sight Tasks . Presented at *Neuroscience 09.* (Chicaho, 17-21 Oct 2009).

Gintautas, V., L. A. Bettencourt, and M. Ham. Identification of functional information subgraphs in cultured neural networks. 2009. *BMC NEUROSCIENCE.* **10** (1): O12.

Gintautas, V., M. I. Ham, B. Kunsberg, S. P. Brumby, C. Rasmussen, J. S. George, I. Nemenman, L. M. A. Bettencourt, and G. T. Kenyon. Model Cortical Association Fields Account for the Time Course and Dependence on Target Complexity of Human Contour Perception. 2011. *PLoS Computational Biology.* **7** (10): e1002162.

Ham, M., V. Gintautas, M. Rodriguez, R. Bennett, C. Santa. Maria, and L. A. Bettencourt. Density-dependence of functional development in spiking cortical networks grown in vitro. 2010. *Biological Cybernetics.* **102** (1): 71.

Ham, M., V. Gintautas, M. Rodriguez, R. Bennett, C. Santa. Maria, and L. A. Bettencourt. Density-dependence of functional development in spiking cortical networks grown in vitro. 2010. *Biological Cybernetics.* **102** (1): 71.

Henke, H., P. A. Robinson, P. M. Drysdale, and P. N. Loxley. Spatiotemporal dynamics of pattern formation in the primary visual cortex and hallucinations. 2009. *Biological Cybernetics.* **101** (1): 3.

Ji, Z., J. Weng, and IEEE. WWN-2: A Biologically Inspired Neural Network for Concurrent Visual Attention and Recognition. 2010. In *World Congress on Computational Intelligence (WCCI 2010) ; 2010 ; Barcelona, SPAIN.*

Ji, Z., M. Luciw, J. Weng, and S. Zeng. Incremental Online Object Learning in a Vehicular Radar-Vision Fusion Framework. 2011. *IEEE TRANSACTIONS ON INTELLIGENT TRANSPORTATION SYSTEMS.* **12** (2, SI): 402.

Kenyon, G. T.. Extreme Synergy:: Spatiotemporal Correlations Enable Rapid Image Reconstruction from Computer Generated Spike Trains . 2010. *Journal of Vision.* **10** (3): 1.

Loxley, P. N., L. M. Bettencourt, and G. T. Kenyon. Ultra-fast detection of salient contours through horizontal connections in the primary visual cortex. 2011. *EPL.* **93** (6): 64001.

Loxley, P. N., and P. A. Robinson. Soliton model of competitive neural dynamics during binocular rivalry. 2009. *Physical Review Letters.* **102** (25): 258701 (4 pp.).

Loxley, P. N., and P. A. Robinson. Soliton Model of Competitive Neural Dynamics during Binocular Rivalry. 2009. *PHYSICAL REVIEW LETTERS.* **102** (25): 258701.

Moody, D., S. Brumby, K. Myers, and N. Pawley. Classification of transient signals using sparse representations over adaptive dictionaries. 2011. In *Independent Component Analyses, Wavelets, Neural Networks, Biosystems, and Nanoengineering IX ; 20110427 - 20110429 ; Orlando, FL, United States.* Vol. 8058, p. var.pagings.

Rasmussen, C., G. Kenyon, and M. Sottile. Visual language recognition with a feed-forward network of spiking neurons. 2010. In *IADIS Int.* (Conf. Intelligent Systems and Agents 2010,ISA, IA). , p. 103.

RADIUS: Rapid Automated Decomposition of Images for Ubiquitous Sensing

Lakshman Prasad
20090104DR

Abstract

Images are the most tangible source of information, but also the hardest to analyze by computers due to their complexity and variability. Today's high-resolution sensors on satellite and airborne platforms deliver vast amounts of high-quality imagery that has stretched the capabilities of intelligence analysts to sift through them in a timely manner. Automating significant portions of image analysis by computers is therefore an imminent need.

The RADIUS (Rapid Automated Decomposition of Images for Ubiquitous Sensing) project has developed a novel methodology of transforming digital images represented by pixels into a hierarchy of polygons where each polygon corresponds to a feature in the image at a particular scale. This multiscale decomposition enables extraction of features and their spatial context, as well as facilitates detection of anomalies in images and changes between different images of the same scene. This has important applications to image-based Intelligence analysis, surveillance, and reconnaissance for National and Global Security missions and warfighter support. The project has resulted in publications, patents, software, and a funded follow-on project in the form of a cooperative research and development (CRADA) agreement with a leading defense contractor to analyze imagery from state-of-the-art sensors for defense applications.

Background and Research Objectives

The value of images in capturing, conveying, and digesting complex information about the world around us cannot be overstated. A testimony to this is their ubiquity in all walks of life. However, as the sophistication of image sensors, from the common household camera to space borne ones, have increased dramatically, we are inundated with imagery of ever-increasing resolution and size. In cases where such images may contain critically important information and are time-sensitive, such as intelligence, surveillance, reconnaissance applications, this is both a boon and a burden. For, while the images reveal greater detail and hence contain more information, they also confront the analyst with more pixels to pore over in order to distill information about the scene under scrutiny. Given the importance of imagery to national and global security missions, their timely analysis is vital. While it is hard to surpass the knowledge and skills of a trained human analyst in deciding what is important or valuable in an image, it is also hard to surpass computers at rapidly doing repetitive low-level tasks without fatigue. Thus, distilling the abundance of data by exploiting the correlations and redundancies in images using computers to provide fewer but higher-level bits of information to the analyst would greatly reduce the burden while still maintaining the semantic import of images that the human analyst is expert at assessing.

The primary goal of the RADIUS project has been to enable this by computer algorithms and software to represent images economically as an organized and interrelated set of features. Digital images are obtained as an array of pixels from cameras. A pixel, by itself, has no information about the uniformity of its neighborhood or whether it lies along a discontinuity (edge). Such information has to be obtained by analyzing other pixels in its neighborhood. The rectilinear array of such primitive elements is therefore neither a natural nor helpful representation scheme for images from the point of understanding them. Further, this representation is highly redundant: A region of constant color is represented by many identically colored pixels instead of, say, a single polygon. Thus a more informative and economical representation is desirable as this would facilitate analysis and also help expedite it due to fewer elements comprising it. To quote Max Wertheimer, the father of Gestalt psychology, I stand at the window and see a house, trees, sky. Theoretically I might say there were 327 brightnesses and nuances of color. Do I have "327"? No. I have sky, house, and trees. Much like the nuances of color, pixels are neither informative nor economical units of representation. They are but artifacts of image digitization by sensors.

Indeed, if we are to make computers help interpret images for us, we have to draw upon what we know of how we see the visual world around us. This act of *perception*, which delineates and makes apparent forms

in a visual scene, prior to and independent of the act of *recognition*, is a crucial first step in parsing complex visual information into semantic units. Computer Vision has addressed this problem as that of image segmentation—decomposing an image into cohesive regional units. Previous work by others in image segmentation has mostly centered on grouping pixels into regions based on spectral and textural similarity. The difficulty in estimating parameters for evaluating grouping criteria, coupled with the need to evaluate at each pixel, often results in erroneous decompositions and high processing times. Application-driven approaches, such as industrial vision for quality control, side step this problem by limiting the scope of segmentation to a specific class of distinctive objects imaged in controlled lighting and background settings. However, this is too restrictive to be of interest to the larger scientific goals of computer vision or to the wider applicability of its methods. Other methods, while not restricting the types of images or features, require specification of the number of segments or other parameters. Typically, the choice of these inputs is ad hoc as optimal settings for a particular image are not clear a priori. Furthermore, there is no single segmentation of an image that captures all possible features of interest. This is because objects and features occur at multiple scales and varying spectral prominences that determine their saliencies. Also, what is of interest in an image is quite often determined not only by the dominance of an object or feature but also what is sought in an image. This makes image segmentation an ill-posed problem. Taking these issues into consideration the main research objectives of the RADIUS project have been to address the challenges of image segmentation with a computational framework that provides

- data reduction by sparse representation of information through salient features,
- human-centric visual perception for robust feature extraction and tagging, and
- efficient processor-scalable software implementing our algorithms with wide applicability.

Scientific Approach and Accomplishments

To ensure data reduction for computational efficiency, we exploit redundancy in pixels of images by focusing on singularities (edges) rather than on regularities (regions between edges). Typically, the set of edge pixels in an image is much smaller than the total number of pixels. Edges are also perceptually relevant cues to image structure and content, and, being delineators of different surfaces, are also robust to changes in lighting and contrast, which are common variations between sensors, images, and ambient lighting. However, in practice, edges detected from an image are not complete or unambiguous in that they do not fully delineate objects by closed boundaries but, rather, are usually open curves partially delineating boundaries between features. Yet, humans presented with edges extracted from an image are able to discern shapes by solv-

ing a "join-the-dots" problem, relying on perceptual cues inherent in the spatial interactions of the edges. These cues, such as proximity, collinearity, continuity, and transversality, studied empirically by Gestalt psychologists, help organize the edges into boundaries of features and objects that form segments of the image. To mimic this human-centric visual perception in algorithms we use a proximity grid that links up edge pixels that are relatively closer to one another than other pixels in a special triangulation network known as a Delaunay triangulation. Indeed, Elder and Goldberg [*J. of Vision v2(4), 2002*] have argued that proximity is by far the strongest cue influencing perceptual organization of contours. The Delaunay triangulation of a point set is efficiently computed and yields a superset of all possible edge completions. However, only a very small fraction of these are perceptually meaningful. As a preamble to the project we had implemented edge-based perceptual criteria such as mentioned above as geometric filters that act on the triangulation to eliminate the perceptually irrelevant triangle edges and retaining only meaningful ones, resulting in a first-level segmentation of images into protofeatures that conform to image edges (Figure 1). At this stage, we have a fine-scale decomposition of an image into polygons, each of which serves as a "super-pixel", encompassing several similar pixels of the original digital image, while at the same time respecting the edges separating features of the image. Each of the polygons is attributed with a color or intensity that is the average of all pixels within it, its area, boundary structure, and neighboring polygons in a graph representation. This attribution enriches knowledge of the local characteristics of the image and individualizes each polygon with its own properties and neighborhood characteristics, providing a feature-adaptive representation of the image.
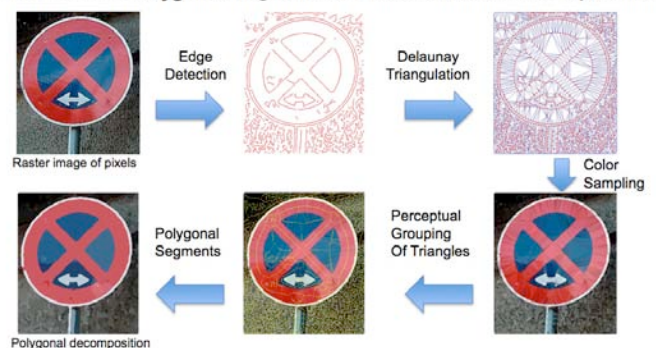
Figure 1. Synthesis of fine-scale polygons (super-pixels) from edge pixels using Delaunay triangulation.

In general, image features of interest are comprised of one or more of these fine-scale polygons. Since the polygons are faithful to detected image edges, they are ideal candidates for further grouping into successively larger polygons. The resulting polygons inherit their contours from their constituent polygons at the previous scale and therefore preserve fidelity to image edges. This, in essence, is the first guiding principle of the hierarchical

segmentation scheme developed in this project. The hierarchical segmentation of an image yields several levels of polygonal segmentations wherein each polygon at each level is obtained by grouping one or more polygons at the previous, finer, level. At each level the polygons inherit the area-weighted aggregate color or intensity of their constituent polygons, and an area that is the sum of the areas of its children polygons. New neighborhood relationships are computed and a measure of smoothness of the interface boundary segments between polygons is recorded. These attributes are represented as node and edge properties of a multi-tiered graph that is progressively built up as more levels in the hierarchy are added. The scientific challenge here is to decide at each level of the hierarchy which of the polygons should merge and which of them should not. From a perceptual standpoint it is desirable to preserve long, smooth edges as they likely constitute boundaries of features, merge similarly colored polygons as they are parts of the same surface, and progressively reduce the number of small size polygons as we extract larger-scale features, thus moving away from texture to structure. Because of spatial and spectral quantization of digital images, it is not practical to characterize size, smoothness or spectral proximity in absolute terms by means of strict criteria or thresholds. Indeed, in the process of synthesizing multiscale features, it is necessary to adaptively relax these criteria depending on the local and ensemble interactions of feature attributes if we are to discover complex features comprised of several smaller but differing features. At the same time, we would like to avoid the pitfall of other previous methods, which require input of parameters to determine grouping of features. We therefore compute the amount of energy in boundary interfaces of polygons (i.e., how "wiggly" they are), the spectral differences between neighboring polygons, the size distributions of polygons at each level and obtain statistical measures of similarity, normalcy and deviation based both on local neighborhood and global ensemble behaviors with respect to each spectral or structural attribute. These ecological statistics help establish adaptive thresholds that serve as parameters governing the merger of polygons at a given level to obtain the next coarser level of segmentation in the hierarchy. This adaptation of parameters to ecological statistics is perceptually motivated and is the second guiding principle of our hierarchical segmentation scheme. Our grouping criteria comprise both structural (contour smoothness, size) and spectral (color, intensity, textural variability) aspects of images wherein the criteria collaborate and compete with each other to effect segmentation. This multicriteria nonlinear filtering by explicitly modeling visual perceptual organization by means of image statistics and geometry is a novel departure of our method from previous methods that use global optimization or clustering techniques. Effectively, our approach seeks in spirit to minimize the two-term Mumford-Shah functional for image approximation by piecewise constant regions by perceptual filtering rather than functional optimization (Figure 2).

$$F(\tilde{I}, \Gamma) = \alpha \int_{\Omega - \Gamma} (\tilde{I} - I)^2 dxdy + \beta \int_{\Gamma} ds$$

$I:$ *digital image*

$\tilde{I}:$ *approximating polygonal image*

$\Gamma:$ *polygon contours*

$\Omega:$ *image region*

$\alpha, \beta:$ *level – dependent implicit parameters*

Figure 2. Version of the Mumford-Shah functional optimized by RADIUS hierarchical segmentation.

The hierarchy thus produced (Figure 3) allows features at different scales to emerge at different levels and be incorporated into larger features at coarser scales (Figure 2). Since each polygon is contained in a polygon at the next, coarser, level (if it exists), the hierarchy also provides spatial contextual information in terms of their relationship to other polygons. This is useful for automating image and scene understanding. The hierarchy may be represented as a multi-tiered graph, with each tier containing the polygon adjacency graph of the corresponding hierarchy level, and edges between consecutive tiers connecting a polygon with a constituent polygon at a previous level or a containing polygon at the next level. This provides a framework for efficient mining of the hierarchical segmentation for features, their contents, and their contexts.

RADIUS Hierarchical Segmentation: Example
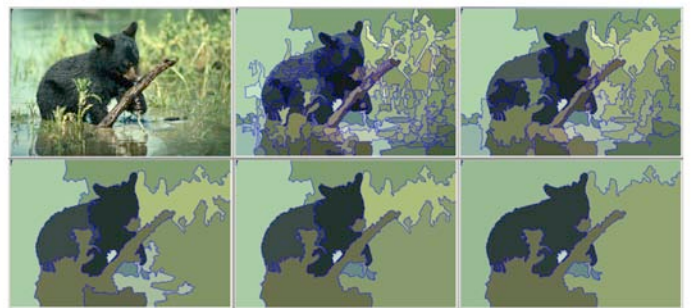
Emergence of fine to coarse features by successive polygon merging

Figure 3. Hierarchical segmentation on an image showing progressively coarser features.

We have developed a novel and highly efficient image segmentation scheme that is modeled after Gestalt principles of visual perception and allows the emergence of features at multiple scales in a hierarchical fashion. The efficiency of our segmentation is due to 1) the sparse prior of only edge pixels from which we reconstruct feature-based polygonal approximations, 2) use of Delaunay triangulation to relate edges which is of low computational complexity in space

and time, and 3) traversal of a multi-tiered graph comprised of planar graphs at each level for computing ecological statistics for iterative grouping. We have implemented the algorithm on a multi-core architecture and achieved rates of ~10 megapixels/sec; a rate commensurate with the data collection rates of DigitalGlobe Inc., a leading satellite imaging company. We have benchmarked our segmentation algorithm using the widely used Berkeley image segmentation dataset wherein 300 images representative of real world imagery are ground-truthed by human mark-up of segments. Using the probabilistic Rand index (PRI) score we achieve a rate of 0.82, with a maximum possible high of 0.87 that reflects the degree of mutual agreement among the different human mark-ups. This currently puts us at the top of segmentation algorithms in terms of performance. Thus we have met our objectives in terms of speed and quality of performance of our segmentation algorithm for it to viably assist in analyzing large amounts of imagery.

As another breakthrough, a benefit of our hierarchical segmentation scheme is the discovery of a method to simplify the machine-learning problem of finding outliers in a complex distribution. Traditionally, sophisticated techniques have been employed to learn a complex distribution characterizing an image and then finding outliers that correspond to anomalous pixels, or in the case of a pair of registered images of the same scene, changes that are interesting. The partitioning of an image into maximally homogeneous regions by our hierarchical segmentation results in multiple 'background' regions whose statistics are much simpler than that of the overall image. So finding fine-scale outlier polygons against these sub-backgrounds yields a much simpler and more robust approach to anomaly and change detection than conventional methods. Additionally, it provides a scale-space context for the anomalies and changes in imagery due the spatial localization to background polygons. This has resulted in an invention disclosure (CANT HIDE: Contextual ANomaly Tagging using a Hierarchical Image DEcomposition) and a follow-on project with a major defense contractor for use on imagery from their sensors. An example of change detection performed by this method is illustrated in Figure 4.

The project has resulted in several publications, a patent application, an invention disclosure, several software copyrights, a distinguished copyright award, multiple on-going negotiations on partnerships with industry, and a follow-on project in FY12 with an injection of funds of $ 450K for the first phase of a CRADA partnership.

Figure 4. Change detection using CANT HIDE method of multiple simpler backgrounds in the hierarchical segmentation.
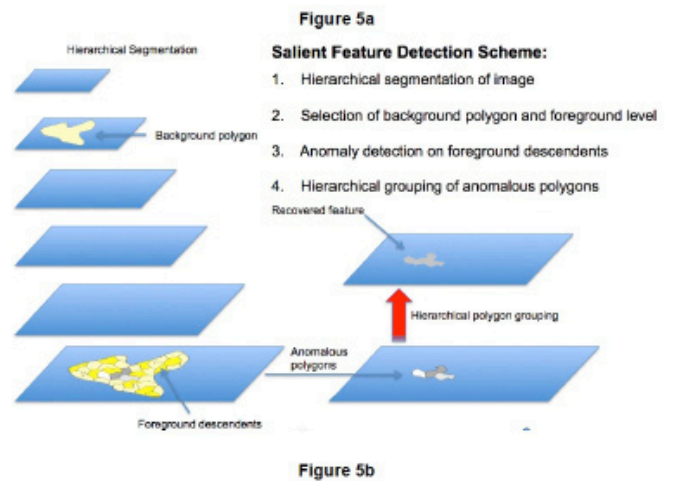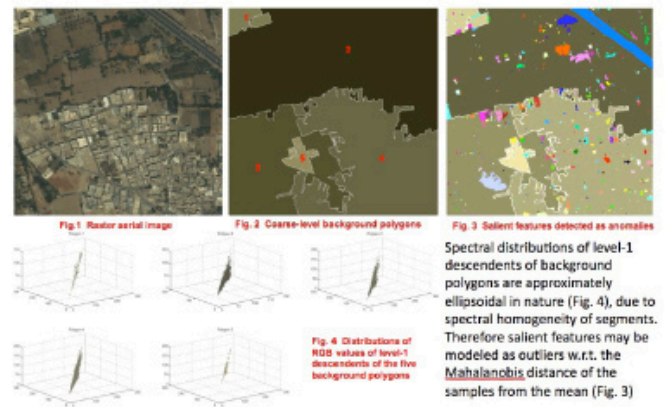
Figure 5. 5a. Backgrounds of coarse-level segmentation showing ellipsoidal distributions of the spectra of their finest level subpolygons 5b. Schematic diagram of the process of detecting and regrouping background specific anomalous polygons.

Figure 6. Application of CANT HIDE to broad area search and detection revealing tell-tale features of mining activity.

Impact on National Missions

This project addresses the DOE mission of Threat Reduction by developing a critical capability of timely and reliable information extraction from imagery for national security applications. Additionally it supports the DOE Office of Science mission by addressing the computational modeling and simulation of human visual perception for advancing information science and technology. The generality of the problem addressed, namely image feature extraction, also supports other mission applications including environmental monitoring for remediation and restoration and space and materials image data analysis.

Publications

Dillard, S., L. Prasad, and J. Grazzini. 6th International Symposium on Visual Computing. 2010. In *Region and edge-adaptive sampling and boundary completion for segmentation.* (Las Vegas, 29 Nov.-1 Dec. 2010). Vol. II, First Edition, p. 64. Berlin-Heidelberg: Springer.

Grazzini, J., S. Dillard, and L. Prasad. Simultaneous hierarchical segmentation & vectorization of satellite images through combined non-uniform anisotropic data sampling and triangulation. 2010. In *Image and Signal Processing for Remote Sensing XVI* . (Toulouse, France, 20-24 Sep. 2010). Vol. 7830, p. 78300F. On-line: SPIE Digital Library.

Grazzini, J., and L. Prasad. Amoeba-based superpixel partitioning of multispectral images into elementary, uniform, connected units. Presented at *IS&T/SPIE Electronic Imaging.* (San Francisco, 22-26 Jan. 2012).

Grazzini, J., and L. Prasad. Intermediate-level segmentation of color images through perception and geometry-based contour completions and shape cuts. Presented at *S&T/SPIE Electronic Imaging.* (San Francisco, 22-26 Jan 2012).

Grazzini, J., and P. Soille. Iterative ramp sharpening for

structure/signature-preserving simplification of images. 2010. In *20th International Conference on Pattern Recognition.* (Istanbul, Turkey, 23-26 Aug. 2010). , p. 4585. On-line: IEEE Computer Society.

Grszzini, J., S. Dillard, and P. Soille. Multichannel image regularization using anisotropic geodesic filtering. 2010. In *20th International Conference on Pattern Recognition.* (Istanbul, Turkey, 23-26 Aug. 2010). , p. 2664. On-line: IEEE Computer Society.

Matsekh, A., E. Rosten, A. Skhurikhin, and L. Prasad. Numerical aspects of spectral segmentation on polygonal grids. To appear in PARA 2010: State of the Art in Scientific and Parallel Computing.(Reykjavik, Iceland, 6-9 Jun. 2010). To appear in *Para 2010: Parallel and Scientific Computing Conference.* (Reykjavik, 6-9 June 2010).

Prasad, L.. Edge-based image reconstruction, hierarchical feature extraction, and analysis - A structural approach. Invited presentation at *SIAM IS Minisymposium on Inverse Problems and Image Analysis in Remote Sensing Science.* (Philadelphia, 20-22 May 2012).

Prasad, L., and J. Theiler. A structural framework for anomalous change detection and characterization. 2009. In *SPIE Defense and Security Symposium.* (Orlando, FL, April, 2009). , p. 7341. Bellingham, WA: SPIE.

Prasad, L., and S. Swaminarayan. A Framework for Perceptual Image Analysis. 2009. In *43rd Asilomar Conference on Signals, Systems, and Computers.* (Pacific Grove, CA, 1-4 Nov. 2009). Vol. CD-ROM, CD-ROM Edition, p. 867. Bryan, Texas, U.S.A.: IEEE.

Sankaranarayanan, K., and J. Davis. Learning directed, intention-driven activities using co-clustering. 2010. In *7th IEEE International Conference on Advanced Video and Signal-Based Surveillance.* (Boston, USA, 29 Aug.-1 Sep.2010). Vol. I, First Edition, p. 400. e-pub: IEEE.

Sankaranarayanan, K., and J. Davis. Attention-based target localization using multiple instance learning. 2010. In *6th International Symposium on Visual Computing.* (Las Vegas, Nevada, 29 Nov.-1Dec. 2010). Vol. I, First Edition, p. 381. Google e-book: Springer.

Sankaranarayanan, K., and J. Davis. Object association across PTZ cameras using logistic multiple instance learning. 2011. In *Computer Vision and Pattern Recognition.* (Colorado Springs, 20-25 June 2011). Vol. I, First Edition, p. 3433. Providence: IEEE.

Theiler, J., and L. Prasad. Overlapping image segmentation for context-dependent anomaly detection. 2011. In *SPIE Conference on Algorithms and Technologies for Multispectral, Hyperspectral, and Ultraspectral Imagery XVII* . (Orlando, 25 April 2011). Vol. 8048, First Edition, p. 804807. Bellingham: SPIE.

Yang, X., L. Prasad, and L. J. Latecki. Affinity Learning with Diffusion on Tensor Product Graph. To appear in *IEEE Transactions on Pattern Analysis and Machine Intelligence.*

A Novel Brownian-Poisson Algorithm for Modeling Ion Transport through Artificial Ion Channels

Cynthia J. Reichhardt
20100273ER

Introduction

Artificial nanochannels can be used to create highly sensitive single molecule detectors which are capable of detecting small quantities of biomolecules or infectious agents. These sensors would have longer life and operating characteristics better suited to field work than currently used biological nanochannels. Our project would permit the rapid optimization of nanochannels for devices intended to detect particular molecules, shortening the time required to create a working device.

Recent experimental advances have led to the fabrication of highly controlled artificial ion channels suitable for use in sensors and in a wide array of applications. The artificial channels are much more robust than channels produced by biological means, and their functionalization is more easily controlled since it does not require manipulation of a bacteria genome. A fundamental understanding of the interaction of hydrated ions with the artificial ion channels is still lacking and device development has proceeded purely through trial and error. In our project, we will develop a hybrid simulation tool capable of treating the discrete interactions of ions in the artificial channels. Our simulation can be used to rapidly test a series of nanochannel configurations, including different surface charge treatments, different channel opening angles, different ion charge species, and different functionalization of the channel mouth, for possible use in applications. The simulations can be performed more rapidly and with fewer resources than the equivalent experiments, and will permit the efficient identification of the most efficient operating regime of the artificial channel for a given device application. We will also explore new device applications beyond the most common area of biomolecule sensing, including ion channels for fuel cell applications and ion channel logic elements which could be used to control lab-on-a-chip devices.

Benefit to National Security Missions

Artificial nanochannels can be used to create highly sensitive single molecule detectors which are capable of detecting small quantities of biomolecules or infectious agents. These sensors would have longer life and operating characteristics better suited to field work than currently used biological nanochannels. Our project would permit the rapid optimization of nanochannels for devices intended to detect particular molecules, shortening the time required to create a working device.

Progress

During the past year, we have implemented and refined further components of our combined Brownian dynamics, Poisson solver, and analytic approach to modeling ion transport through artificial ion channels, and have carried out several studies on coupled channel interactions, funnel geometries, and charge ordering transitions which can be used to alter or control the flow of ions through the artificial channel. The Poisson solver uses an adaptive mesh technique and we have performed an adaptive mesh refinement study in order to optimize the generation of the meshes required by the Brownian dynamics simulations. By applying a discrete maximum principle we can avoid numerical instabilites in the adaptive mesh. Our further work with the funnel geometry has uncovered the occurrence of a clogging transition of the ions under certain conditions. This is of particular interest since a clogging transition was hypothesized to occur in the artificial ion channel experiments carried out at UC-Irvine. We are characterizing the clogging transition by studying its stochastic nature and the fragility of the clogged state against ac excitations, an issue that may have important implications for future ion channel applications. The clogged state is distinct from a jammed state both because of its spatial heterogeneity and also because it is possible to unclog the system by varying the driving protocol, whereas a jammed state remains jammed once it has formed. We have expanded the number of ion channel geometries under consideration and are exploring the influence of charge ordered states on the ion transport. Charge ordered states can arise when the effective interaction between the ions in the channel develop a short range attractive component in addition to the Coulomb repulsion. We

have explored the properties of the charge ordered states both analytically and in simulations, beginning with the equilibrium charge ordered states, where we delineated the regimes of stability for the different charge orderings and measured their sensitivity to thermal fluctuations. We also considered the effect of membrane disorder as well as the influence of an applied electric current on the charge ordered states, since each of these effects are relevant for devices. The nature of the ion flow varies from a low-noise, elastic state to a high-noise, plastic state depending on the type of charge ordering that is present. We find that it is possible to use the applied current to induce changes between different charge ordered states or to stabilize a charge ordered state that would not normally be stable at the given charge density in equilibrium. The ability to control the charge ordering as well as the resulting noise level of the ion flow using different current protocols could lead to device applications. We also studied the interactions between coupled channels of flowing ions and demonstrated that even in a clean system it is possible to induce drag effects between the channels, to couple or decouple the flowing channels, and even to generate a Brownian ratchet, where an asymmetric applied ac drive results in a net dc flow of the ions. When three channels are coupled, the nonequilibrium phase diagram becomes much richer and we find regimes of negative differential resistivity, where the ions in one channel can be induced to move in the direction opposite to the electric field. Each of these effects has potential applications and could be used in constructing lab-on-a-chip type logic circuits. We will further explore possible device applications in the coming year. We have written a series of papers detailing the results we have obtained up to this point in our project; many are now published, while some are in the revision or presubmission stages. We have also presented our results at national and international research conferences.

Future Work

We will develop a powerful new multi-scale simulation tool for the study of ion transport in artificial ion channels by combining a Brownian dynamics particle-based simulation of the ions, a Poisson solver for the electrostatic interactions with the nanopore walls, and a Poisson-Nernst-Planck analysis of the nonlinear response. Our simulation method will overcome the limitations of existing ion channel models which consider only short time scales and a small number of ions. This is crucial for future device applications based on ion channels made with artificial nanopores, where interactions between multiple ion species can produce ion transistors or diodes. Our approach is optimized for the rapidly developing area of artificial nanopore applications, ranging from new sensor technologies to novel microfluidic logic devices for use in lab-on-a-chip designs. We will test our simulation and analysis method by comparing the results to recent experimental work on nanopore diode devices. Our simulation toolkit will permit the detailed

analysis of experimental data and provide a predictive tool for determining parameter regimes where novel ion transport behavior should appear experimentally, including transport mechanisms for interacting ions and screening charge interactions with the channel walls or with elongated molecules such as DNA. After our toolkit has been thoroughly tested against the behavior of an isolated ion in a channel, we will apply it to studies of the dynamics of ion motion through channels, particularly in the poorly understood cases where multiple ions are present in the channel simultaneously and in channels close to the crossover size between discrete and continuum charge dynamics. This study is important not only for understanding ion transport through channels in the collective regime, but also for developing tailored nanochannels for devices such as biomolecule sorters or sensors.

Conclusion

We will develop a predictive simulation for artificial nanochannels that can be used for future device development. Artificial nanochannels show great promise for use as highly sensitive and robust sensors of biomolecules or infectious agents. Ion transistors and logic circuits made from nanochannels could be used to control advanced lab-on-a-chip circuitry or to perform highly efficient DNA sequencing. With the help of our predictive tool, completely new areas such as fuel cell applications of the nanochannels can be explored.

Publications

Bairnsfather, C., C. J. Reichhardt, and C. Reichhardt. The effect of pinning on drag in coupled one-dimensional channels of particles. 2011. *EPL.* **94** (1): 18001.

Lipnikov, K., G. Manzini, and D. Svyatskiy. Analysis of the monotonicity conditions in the mimetic finite difference method for elliptic problems. 2011. *Journal of Computational Physics.* **230**: 2620.

Martin, I., and C. Panagopoulos. Nernst effect and diamagnetic response in a stripe model of superconducting cuprates. 2010. *EPL.* **91**: 67001.

Reichhardt, C. J. O., C. Reichhardt, and A. R. Bishop. Anisotropic sliding dynamics, peak effect, and metastability in stripe systems. 2011. *Physical Review E.* **83**: 041501.

Reichhardt, C. J. O., and C. Reichhardt. Commensurability, jamming, and dynamics for vortices in funnel geometries. 2010. *Physical Review B (Condensed Matter and Materials Physics).* **81** (22): 224516 (14 pp.).

Reichhardt, C., C. Bairnsfather, and C. J. Olson Reichhardt. Positive and negative drag, dynamic phases, and commensurability in coupled one-dimensional

channels of particles with Yukawa interactions. 2011. *Physical Review E (Statistical, Nonlinear, and Soft Matter Physics).* **83** (6): 061404 (17 pp.).

Reichhardt, C., and C. J. O. Reichhardt. Jamming and diode effects for vortices in nanostructured superconductors. 2010. *Physica C.* **470**: 722.

Reichhardt, C., and C. J. Olson Reichhardt. Dynamical ordering and directional locking for particles moving over quasicrystalline substrates. 2011. *Physical Review Letters.* **106** (6): 060603.

Reichhardt, C., and C. J. Reichhardt. Switching and jamming transistor effect for vortex matter in honeycomb pinning arrays with ac drives. 2010. *PHYSICAL REVIEW B.* **81** (2): 024510.

Parallel Algorithms for Robust Phylogenetic Inference

Tanmoy Bhattacharya
20100395ER

Introduction

The historical relation of common descent has, since the time of Galton, fascinated statisticians attempting to analyze biological data. Constructing such histories, or `phylogenetic' trees, is an important branch of theoretical biology. Since these reconstructed histories are needed to properly account for the covariation in the data, phylogenetic inference forms an important core capability at the Laboratory. With the advent of petascale computing, however, traditional phylogenetic inference is undergoing a revolution. Instead of using algorithms that only estimate the most likely ancestral history, scientists are harnessing their newly acquired computational prowess to calculate the entire range of credible histories. The importance of quantifying the reconstruction uncertainty and propagating it to subsequent stages of analyses is only now coming to be realized. Soon, it will be a cornerstone capability, necessary for maintaining the leadership of the Laboratory in these sciences.

The problem, however, is that software has not kept pace with the hardware. Whereas dramatic computational speed-ups have occurred using modern architectures, software tools for sampling posteriors on spaces of trees have remained as minor enhancements of inherently serial algorithms. These algorithms are ill suited to the large data sets needed for the next generation of problems. Our project addresses the gap between software and hardware. It aims to provide new algorithms and implementations for carrying out large-scale phylogenetics on today's powerful parallel machines. We focus on the important special case in which the samples are drawn from a rapidly expanding population. As explained below, this is the case in which the benefits of having a large number of samples should be the greatest.

Benefit to National Security Missions

Phylogenetic analysis of evolutionary relationships has been a core Theoretical Biology competency at the Laboratory and lends itself to use in such diverse fields as unravelling host-pathogen interactions from population data, knowledge-based design of vaccine and therapeutics against rapidly evolving pathogens, and the attribution of pathogenic strains to precise origins. The next generation of problems in these fields will require substantially larger amounts of sequence data to be analyzed with known uncertainty margins. Our project directly targets this need and will develop the required algorithms as well as produce the documented implementation for the end-user.

Progress

Our project has two major goals: Design of new algorithms for analyzing the massive amounts of sequence data generated by the new sequencing methodologies; and development of a concrete, maintainable and parallelizable implementation of a phylogenetic inference algorithm. This year saw developments on both fronts.

On the algorithmic side, our work in the first year led to a new algorithm for estimating both the time of infection and the mutation rate from a single sample taken during the acute phase of infection. (Figure 1.) Patient samples during the acute phase are very rare, and the algorithm was validated primarily on synthetic data. When we evaluated the algorithm on real data, however, as we did this year, we found that the estimated mutation rates were implausibly high, and the time of infection too recent, in that it was inconsistent with known patient histories. We therefore decided to investigate the population genetics of these samples further.

In the course of this investigation, we realized that the essential difficulties in a phylogenetic analysis depend strongly on assumptions about population growth. The available literature is mostly concerned with the case that the population size remains constant, and the available algorithms are mostly designed for data satisfying this assumption. For us, however, the case of greatest interest is the case of exponential population growth, for two reasons. First, it is the relevant case for modeling the acute stage of HIV infection. Second, the benefit in having a large sample is much greater in the exponential case than in the constant case,

essentially because the total length of all the branches in the tree grows faster in the exponential case. That is, the exponential tree contains more information. For these reasons, we decided to focus this project exclusively on the special case of exponential growth.
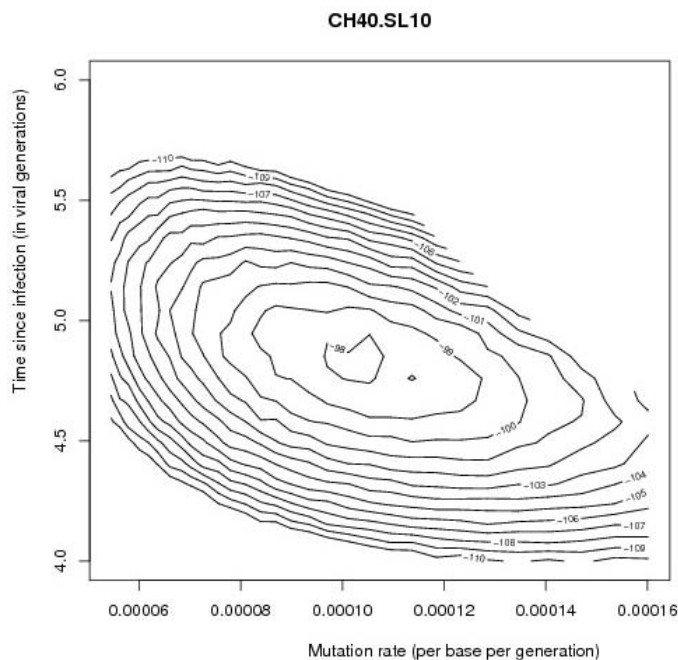
Figure 1. A contour plot of the log-likelihood, as calculated by our new importance-sampling algorithm, based on 4,047 HIV sequences from an epitope region of patient CH40 during acute infection.

In order to develop computational algorithms for the case of exponential growth, we have had to first develop the population genetics of exponential growth, and this undertaking has occupied most of the algorithmic effort in the present year. This work has been very successful, and has led to several new results. For example, we have developed a single-parameter model for the exponential coalescent, which smoothly interpolates between the constant population case and the exponential case. We have also developed new statistical methods for estimating goodness of fit in exponential models (Figure 2). Before publishing this work, however, we need to test the resulting algorithms, and show that they are robust under the many effects that arise in the generation of real data.

On the implementation side, in the first year we investigated the basic problem of parallelization and chose Haskell as our implementation language. We had developed techniques to obtain fine-grain parallelism for the evaluation needed at each bifurcation and to control the data movement. The problem that we still faced was how to split the graph of needed evaluations into pieces for parallel evaluation over nodes. Some graph-partitioning tools are available, like METIS and Chaco, but these are large and complex C++ codes. What we needed

for this work was something simple, standalone, fast, and purely functional. The algorithms used to study Branch Decomposition in operations research proved to be the most relevant. The rough idea is to transform a graph into a branch decomposition where edges become nodes, and can be subject to agglomerative clustering. Thus, different cuts in that clustering provide natural subsets of the graph.
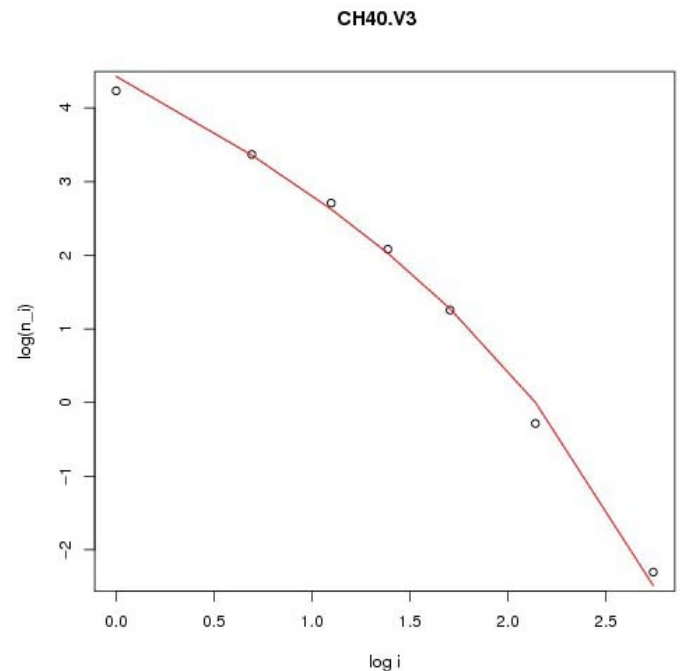
Figure 2. Log-log plot of n_i vs. i , where n_i is number of subsets of i identical sequences, in a sample of 3,354 sequences. Red line is theoretical curve. Analysis is used to assess goodness-of-fit.

What we finally chose to use was an adaptation of Voronoi diagrams to graphs. The idea is to contrast sets of nodes, where one node in a set is characteristic of the set and is called a Voronoi node. The selection criterion for members of a set is that the distance from its Voronoi node is no larger than the distance from those members to any other Voronoi node. To determine this, it is necessary to have shortest paths calculated between all nodes. The algorithm works for any measure of distance; for our implementation, we chose to use a fixed size for all branches of the tree.

The actual evaluation exploits the metaprogramming facilities in Haskell, which automatically pack and unpack various data types, such as transition matrices, alignment data, configuration data, and trees, for shipment over the network. These facilities automatically set up independent subtree evaluator programs, i.e., subtrees that can begin to be consumed (scored) by independent cluster nodes. We now have this part of the code working, and can evaluate the likelihood of a single tree by utilizing both a coarse-grain parallelism over subtrees, and a fine-grained parallelism at each bifurcation.

Future Work

In the first two years of this project, we have developed the Haskell kernels necessary for rapidly evaluating tree likelihoods, and the population genetics and importance sampling algorithms necessary for modeling rapidly expanding populations. In order to bring this work to fruition, however, significant additional work is required, which will be the focus of the third and final year of this project.

We consider first the implementation side. The kernel of any inference code is the likelihood evaluator, and this has been developed. In order to make inferences, however, we need a framework for moving around the space of trees and determining where the likelihood is greatest. To this end, we will wrap the likelihood code in a Markov Chain Monte Carlo (MCMC) superstructure, which will direct the evaluation of the likelihood on different trees. This work will involve coding the various local and global moves for reordering a tree, and choosing heuristic probabilities for the various moves that gives fast convergence.

On the algorithmic front, there remain a number of challenges in turning our theoretical results into robust and effective algorithms. In particular, we need to assess the robustness of these algorithms in the presence of realistic complications, such as recombination and sequencing errors. We will then apply these techniques to measure the *in vivo* mutation rates of HIV in three individuals with controlled systematics. In this way, we will connect our theoretical findings, as developed in the first two years, to the understanding of real data from patients with acute HIV infection.

Conclusion

This project will modernize the core capability of the laboratory for phylogenetic analysis by providing a well-documented Bayesian sampler that can be used on a wide variety of platforms, and which, in particular, will be capable of harnessing the power of the new and emerging massively parallel computer architectures acquired by the Laboratory. In addition, the novel importance sampling algorithms, which we have developed as part of this project, will be helpful in analyzing large datasets of viral sequences, which can now be readily obtained from acutely infected individuals. Our work has already paved the way to future research opportunities. Specifically, in recognition of the utility of our importance sampling algorithms in the development and evaluation of vaccines, we have been invited to participate in a grant application for studying vaccine efficacy.

Robust Unsupervised Operation Under Uncertainty Through Information Theoretic Optimization of Complex Systems.

Aric A. Hagberg
20100460ER

Introduction

The pace of technological advance in information science and technology is opening up immense new opportunities to accelerate scientific discovery. However, our increased ability to measure and observe complex natural and social systems also threatens to drown us in data. The fundamental question of finding the relevant information to solve a specific problem in a large and rich stream of information is the main objective of our research.

Successful new mathematical and computational methods must be able to extract information, without explicit human supervision from streaming data originating from distributed sensors in natural and social environments, from high throughput experiments in genetics, astronomy and high-energy physics. They will also guide sensors to actively pursue new pieces of information in large noisy environments that can help fulfill a task or answer a question.

Technically, we are developing and applying the principles of information theory, with techniques from inference and Bayesian statistics, to provide a systematic approach to multi-level (hierarchical) modeling of classes of complex systems. We expect that our methods will apply to inference of dynamical models and the discovery of structure in complex systems with unknown interaction structure. It will also generate predictions for the behavior of complex systems with quantified uncertainty, and new data assimilation schemes and unsupervised learning algorithms, guided by uncertainty reduction under constraints and operational goals.

 These methods will create new robust approaches to knowledge extraction from large (streaming) datasets of heterogeneous variables and the development of robust adaptive learning and control algorithms for application of strategic interest to LANL's Grand Challenges in information science and technology, ubiquitous sensing, complex systems and to DOE's missions of energy security, nuclear non-proliferation, and environmental stewardship.

Benefit to National Security Missions

Explosive progress in information technology is making possible vast increases in the amount of information that can be measured and retrieved from natural and engineered complex systems. However, the scientific underpinnings to make the most out of this information are still missing, severely handicapping LANL and DOE---specifically in missions of energy security, systems biology, nuclear nonproliferation, and environmental stewardship. Our project will create a mathematical framework for analysis and control of such complex natural and engineered systems.

Progress

This year the project has focused on the theory and design of optimal algorithms for collective search for stochastic (random) sources in space. We have also investigated the information-theoretical aspects of cohesive collective motion in models with and without informed individuals.

For cooperative searching we are exploring performance of searchers using parallel computational implementations of simple searcher agents. We use explicit models for agents searching for stationary, stochastic sources, along with our earlier developed theory, for classifying when multiple searchers provide the most (and least) benefit (Figure 1). By using high-speed simulations we are testing our theory for scaling of performance for many searchers across configuration space [1].

Similarly to cooperative searching we are deriving the interaction rules for cohesive collective motion [2] and decision-making in animal flocks using information-theoretic methods. We formulate flocking as a collective learning problem where the history of past observations about the environment (i.e. predator attacks, randomly located resources) is stored in the spatial arrangement of the group at time t. In our approach the histories (time series of past observations) are mapped onto the flock configuration as a result of the interactions of the individuals with the environment and among

themselves, but the individuals themselves have no explicit recollection of the past in order to make decisions about future actions, nor are they "learning" in the strict sense of the world. Rather, the relevant information about the environment is distributed in the configuration in the form of spatial and velocity correlations.
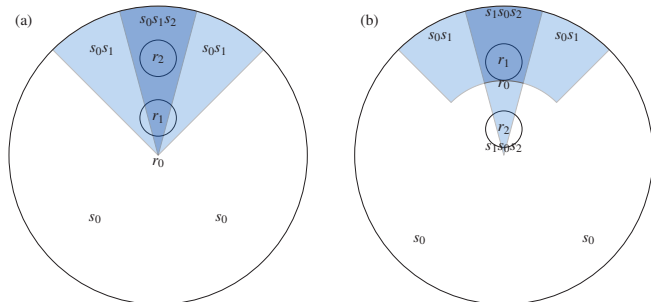
Figure 1. Configurations for synergy and redundancy for a simple 2d searcher model. The source position r0 is fixed in the center and the searchers are disks of radius d. At each time step the source emits two particles in in opposite directions with a random angle. Each possible emission axis passing through the source corresponds to one of six cases for source and searcher configurations.

Decisions about future actions are a function of a sample of the current state of the local configuration (and possibly some internal state) only. The decision mechanism does not have access to the full distribution of the configuration, but only to a finite sample; thus, the optimization problem for "distributed interactive learning" has to solve not only the decision mechanism given the sample of the configuration available to a focal individual, but also the sampling protocol itself (which is essentially a data assimilation problem).

This perspective has allowed us to formulate the problem of a principled approach to flocking as a variational problem in information theory by maximizing the joint information that the decision (or action) and the local sample have about future observations, constrained by an efficient mapping from histories to configurations and an efficient sampling protocol [3].

The framework of coarse-graining collective representation of agents was applied to the metabolic networks that regulate the synthesis of uptake proteins in marine microbes (autotrophs). The method maps cell-level processes (the internal nutrient concentration and the regulation of the synthesis of transporter proteins) and the local fluid environment surrounding a cell onto high-level metabolic functions of importance for global biogeochemical models, i.e. the nutrient uptake rate and the half saturation constant. For low to medium nutrient availability, our model predicts uptake and growth rates larger than the classic Michaelis-Menten (MM) formulation, while matching the classic MM results for

large nutrient concentration. These results have been known experimentally for several years, but a simple model had not been available until now. These results have important consequences for global coupled models of ocean circulation and biogeochemistry, which lack the regulatory mechanism and are known to underestimate phytoplankton abundances and growth rates in oligotrophic (nutrient-limited) regions of the ocean [4].

Future Work

We will develop a mathematical framework based on information theory for solving general optimization and prediction problems in the presence of uncertainty for complex natural and engineered systems of strategic importance to LANL and DOE missions.

Our main goals and tasks are:

Construct mathematical framework

Information theory provides a principled, general approach for designing objective functions that include fundamental properties of complex natural and engineered systems, such as stochastic heterogeneous variables, design constraints and quantitative performance goals.

Design algorithms for optimization and real time data assimilation

Information theoretic objective functions support seamless data assimilation in real time. e.g. via Bayesian schemes. We will develop methods and algorithms for systematic approximation of information quantities of many variables that locally minimize uncertainty at each time.

Target problems of strategic importance to LANL and DOE

- Discovering functional network structure in natural and engineered systems.

- Spatial coordinated search for stochastic sources (e.g. nuclear, pollutant) that can resist damage to parts of the system and interference in communications while automatically coordinating multiple (parallel) sensor/agents.

- Adaptive control of engineered systems through creation of a formalism and computational optimization methods so that a designer or engineer can specify rewards for the adaptive, unsupervised operation of complex engineered systems (e.g., distributed robots or infrastructure networks).

Conclusion

We will create a general class of methods - based on fundamental mathematics and computer science to identify where information is, and to solve general problems in complex systems. We will apply our formalism to network reconstruction (biology, infrastructure) for

identifying the most relevant bio-chemical processes in high level functions (metabolism, infection), and to assure quality of service of the electrical power grid or other infrastructure. The project will focus on fundamental concepts and specific applications where challenging data sets and experiments become available, including distributed sensor networks, robotics, and biological, social and technical network applications.

References

1. Bettencourt, L. M. A.. The Rules of Information Aggregation and Emergence of Collective Intelligent Behavior. 2010. *Topics in Cognitive Science.* (1): 598.

2. Gintautas, V., A. Hagberg, and L. M. A. Bettencourt. Synergy-based infotaxis motion of swarms. 2010. *Unpublished.*

3. Raghib, M., A. Hagberg, and L. M. A. Bettencourt. Information flow and decision making in swarms. 2011. *Working notes..*

4. Bonachela, J. A., M. Raghib, and S. A. Levin. Acclimation or starvation: A dynamic model of flexible phytoplankton uptake regulation. To appear in *Proceedings of the National Academy of Sciences..*

Publications

Bettencourt, L. M. A.. The Rules of Information Aggregation and Emergence of Collective Intelligent Behavior. 2010. *Topics in Cognitive Science.* (1): 598.

Bonachela, J. A., M. Raghib, and S. A. Levin. Acclimation or starvation: A dynamic model of flexible phytoplankton uptake regulation. To appear in *Proceedings of the National Academy of Sciences..*

Gintautas, V., A. Hagberg, and L. M. A. Bettencourt. Synergy-based infotaxis motion of swarms. 2010. *Unpublished.*

Gintautas, V., A. Hagberg, and L. M. A. Bettencourt. Cooperative searching for stochastic targets. 2010. *Journal of Intelligence Community Research and Development.* : 000.

Hagberg, A., J. Neil, G. Sandine, and S. Vander Wiel. Protocol Graph Anomaly Detection: Global graph invariants and graph metrics. 2010. *LA-UR 10-00756.*

Sandine, G., A. Hagberg, J. Neil, C. Storlie, and S. Vander Wiel. Relative entropy for anomaly detection in computer networks. 2010. *LA-UR 10-06099.*

Rare Category Detection

Donald R. Hush
20110126ER

Introduction
Perhaps the most difficult (and unsuccessfully treated) problem in data mining is the problem of extracting meaningful rare-event data from massive data sets when we don't know what is meaningful until we see it. It is obvious that a credible solution, whatever its form, must incorporate a human expert to determine what is meaningful and what is not. On the other hand it is impossible for human experts to directly examine even a small fraction of the data, thus creating what appears to be a fundamentally intractable problem. To confront this intractability we must make prior assumptions, and hope that they capture some relevant characteristics of meaningful data. The most common prior assumption, which is used in standard anomaly detection, has proved inadequate. For example, in astronomy approximately 0.1% of the objects in sky survey images correspond to standard anomalies, but only 1% of these anomalies (and only 0.001% of the full dataset) are "meaningful" in the sense that they correspond to potential new discoveries by the astronomer. The goal is to identify these "meaningful" anomalies as efficiently as possible. Similar examples are can be found in the areas of network monitoring and file system forensics for cybersecurity, and nuclear forensics, scenario extraction, and proliferation detection for national security. This project will develop theory, algorithms, and validation experiments for a new approach called rare category detection (RCD) that promises tremendous improvements in our ability to detect "meaningful" anomalies. RCD makes two obvious enhancements over standard anomaly detection: it makes a more realistic assumption about the statistical nature of meaningful data, and it exploits user interaction to establish ground truth and accelerate the process. Preliminary experiments suggest that RCD can improve the analyst's efficiency by at least an order of magnitude.

Benefit to National Security Missions
This project is directly linked to the core data analysis component of national security missions in cybersecurity and nonproliferation. It helps build a unique capability in machine learning that directly supports the future program development plans described by the LANL IS&T Center. Furthermore it will provide a new capability that can be used to leverage program development in several key areas including: file system forensics and network monitoring for cybersecurity (DOE/NSA/CIA), scenario extraction for WAMI (DoD), and threat detection for nonproliferation (DOE/NNSA).

Progress
Rare category detection (RCD) consists of two stages of operation. Stage 1 identifies the initial regions of interest in the data and stage 2 modifies/updates these regions after each user transaction. In this first year we have made progress on both stages. For stage 1 we have developed a new kind of anomaly detection where instead of locating data from sparsely populated regions (as in standard anomaly detection) we locate data from regions with high concentration (so they are meaningful) but low probability mass (so they are still rare). We have discovered that the key to doing this efficiently is to synthesize a background data set and then solve a 2-class pattern recognition problem that discriminates between the observed data and the background. The utility of this method depends on how we synthesize the background. Instead of adopting a conventional approach that would synthesize the background from scratch using an artificial model, we have begun the development and testing of methods that produce a background by applying a special mapping to the observed data. This has numerous advantages for implementation, performance, and robustness. We have also made significant progress on the development of 2-class pattern recognition problem algorithms for the discrimination task. This work has lead to publications [1,2,3].

Progress on stage 2 has revolved around the development of updating methods which are effective in cases where the ground truth provided by the user is both one-sided and limited. In particular the user is only required to make positive category identifications, i.e. he is not required to characterize data that is "not" in a category. We have begun the development,

implementation, and testing a special class of "hemi-supervised" methods for this type of problem. More specifically we have developed hemi-supervised methods that are effective for a wide range of situations that extend from cases where the data can be described by simple Gaussian probability distributions to cases where the data distribution is arbitrarily complex. A full documentation of this work is an ongoing task, but one of our methods has already been successfully applied in the medical field and is described in [4]. Furthermore, since the ground truth provided by the user is very limited we have begun to incorporate methods of "transfer learning" and "statistical relational learning" into our framework. Transfer learning is concerned with the storage of knowledge gained while solving one problem and then applying it to a different but related problem. This will allow us incorporate outside knowledge efficiently and effectively without burdening the user. Statistical relational learning is concerned with the discovery of relationships between different components of the data, and will be used to help us make connections between the small amount of ground truth data provided by the user and the other parts of the data.

We now describe some specific work on nearest neighbor classifiers that has been published in [2,3] and is is relevant to both stages 1 and 2. Nearest Neighbor classifiers define a family of pattern classifiers that are both simple to understand and implement. We developed a new empirical error minimizing algorithm for these classifiers that reduces the number of exemplars (and hence the memory storage required by Nearest Neighbor classifiers) and obtains competitive performance to the conventional K-Nearest Neighbor Classifiers which have significantly greater computational complexity. In addition, by directly minimizing error, our approach enables Nearest Neighbor Classifiers to be used for cost sensitive pattern recognition problems such as anomaly detection, rare category detection as well as hemi and semi-supervised learning problems.

Future Work

This project will develop theory, algorithms, and validation experiments for a new type of anomaly detection called rare category detection (RCD). Rare category detection is an emerging research area that promises tremendous improvements in user productivity over standard anomaly detection. It is based on the observation that data analysts are primarily interested in determining which rare categories are present and extracting a single prototype from each category as quickly a possible. This is fundamentally different from standard anomaly detection which attempts to identify all anomalies. Instead RCD aims to identify only "meaningful" anomalies, and only a few of them (ideally one from each rare category). A rigorous definition of "meaningful" anomalies is derived from a formal characterization of rare categories and explicit interactions with the user. Unlike standard anomaly detection, RCD is an interactive approach that

adapts to the user's responses. But unlike standard interactive learning methods RCD is focused on optimizing the user's productivity (as opposed to optimizing the data model). Our first research goal is to develop a theory for RCD that establishes fundamental limits on the realizable improvements in user productivity, and on the computational resources needed to approach these limits. Our second research goal is to develop interactive algorithms that scale to massive data sets and approach the performance limits established by the theory. Our third research goal is to develop validation methods for RCD based on a series of experiments tied to applications in remote sensing and cybersecurity.

Conclusion

This project will develop the theoretical foundations for a method that will replace standard anomaly detection as the default for the blind exploration of massive data sets by national security analysts. Furthermore it will develop computer algorithms that form the core of this new method, and will therefore be essential to the eventual integration into modern analysis tools. Finally, this project will prove the utility of this new method, and demonstrate how to integrate and apply it to specific applications by performing validation experiments for specific applications in cybersecurity and remote sensing.

References

1. Stearns, S. D., and D. R. Hush. Digital Signal Processing with Examples in MATLAB. 2011.

2. Zimmer, B. G., D. Hush, and R. Porter. Ordered Hypothesis Machines. 2011. *Journal of Mathematical Imaging and Vision.* : 1.

3. Porter, R., D. Hush, and B. G. Zimmer. Error Minimizing Algorithms for Nearest Neighbor Classifiers. 2010. In *Proceedings of the International Society for Optics and Photonics.* (San Francisco, January 23-28, 2010). , p. 1. New York: SPIE.

4. Zuluaga, M. A., D. Hush, E. J. F. Delgado Leyton, M. H. Hoyos, and M. Orkisz. Learning from Only Positive and Unlabeled Data to Detect Lesions in Coronary CT Images. To appear in *Proceedings of the International Conference on Medical Image Computing and Computer Assisted Intervention.* (Toronto, September 18-22, 2011).

Publications

Porter, R., D. Hush, and B. G. Zimmer. Error Minimizing Algorithms for Nearest Neighbor Classifiers. 2011. In *Proceedings of the International Society for Optics and Photonics.* (San Francisco, January 23-27, 2011). , p. 1. New York: SPIE.

Stearns, S. D., and D. R. Hush. Digital Signal Processing with Examples in MATLAB. 2011.

Zimmer, B. G., D. Hush, and R. Porter. Ordered Hypothesis Machines. 2011. *Journal of Mathematical Imaging and Vision.* : 1.

Zuluaga, M. A., D. Hush, E. J. F. Delgado Leyton, M. H. Hoyos, and M. Orkisz. Learning from Only Positive and Unlabeled Data to Detect Lesions in Coronary CT Images. To appear in *Proceedings of the International Conference on Medical Image Computing and Computer Assisted Intervention.* (Toronto, September 18-22, 2011).

Exact Renormalization Method for Frustrated Systems and Optimization

Cristian D. Batista
20110181ER

Introduction

We suggest a renormalization framework to study complex phenomena in interacting and frustrated systems, with additional applications in combinatorial optimization. Such phenomena are characterized by the competition and potential coexistence of various states of matter. Unveiling the organizing principles behind complex behavior in matter is a central problem in physics and other sciences. Our prime goal is to devise an exact and efficient computational method for understanding emergent behavior in physical systems with competing interactions. We will apply recent and advanced results in information theory, mathematics, and quantum many-body physics, to construct a scale-renormalization algorithm that is exact under certain assumptions. Next, we will use this algorithm to predict the low temperature physical properties of relevant models that remain unsolved. In addition, since combinatorial optimization problems can be reformulated in the physics language by associating a cost function with the energy of a physical system, we will use our method to solve spin glasses that encode the solution to these problems.

Benefit to National Security Missions

We are planning to develop a novel scientific approach that will create fundamentally new capabilities for bridging two LANL grand challenges: "Information, Science and Technology" (IS&T) and "Materials: Discovery Science to Strategic Applications"(MDSSA). The proposed re-search is a direct response to FY11 IS&T Grand Challenge priorities: development of methods for inference and prediction of large-scale complex systems and design of algorithms to efficiently ex-tract information from massive amounts of data. Our project is also a direct response to FY11 priorities of the Materials Grand Challenge and its three central themes: prediction and control, extreme environments, and emergent phenomena. Frustration is a challenging problem, identified in DOE's 'Directing Matter and Energy: Five Challenges for Science and the Imagination', that is ex-citing because of both, the scientific consequences of new states of matter and the technologically relevant multi-functional responses.

Progress

We developed a code that solves a family of XXZ spin Hamiltonians on a ladder by using the new algorithm that we described in our proposal. The algorithm is an exact renormalization method that allows us to obtain all the exact ground states of the Hamiltonian under consideration. In particular, our algorithm demonstrated to be very efficient for the problem under consideration: the memory requirements and CPU time scale with the square of the lattice size. This code is a proof of principle for the general algorithm that we proposed in this project in order to solve certain classes of highly frustrated models. It generates all the different ground states of the Hamiltonian under consideration for each system size between 3 and L. This numerical results played a crucial role in the determination of the anionic exact solutions that we describe below.

We are currently implementing the calculation of correlation functions that are relevant for identifying the order parameters associated to these solutions.

By running this new code we were able to identify the exact ground state degeneracy as a function of the system size. This information was crucial for guiding the analytical efforts that we describe below. The result of this combined approach (numerical plus analytical) is leading us to the potential discovery of a new state of matter that corresponds to a condensation of anyons. Anyons are particles that have fractional statistics, i.e., their statistics interpolates between bosons and fermions. Although anyons explain some aspects of the fractional Hall effect in two dimensions, they are not common in physics. In particular, there are very few one dimensional models that contain anyonic solutions. Our method allowed us to identify the first exact solution of a very simple spin Hamiltonian that corresponds to a condensate of anyons (generalization to fractional statistics of the Bose-Einstein condensate). Although the notion of fractional statistics has been discussed in different contexts, we are not aware of any exact solution of a spin model that corresponds to

an anyonic condensation. Therefore, we believe that our exact anionic solutions are the first example of anionic statistics in quantum magnets. We are currently computing the relevant correlation functions that are necessary for characterizing these new states of matter and we plan to submit a paper on the subject right after completing this final task.

We are also applying our algorithm to the computation of field-induced magnetization in a highly frustrated compound $Ca_3Co_2O_6$ that consists of a triangular lattice of ferromagnetic Co chains. The inter-chain coupling is antiferromagnetic leading to an enormous number of ground states. We are applying our algorithm to the generation of all the possible ground states and subsequent computation of the magnetization vs. field curve starting from each of them. The output of this calculation will be used to fit the experiments on the same compound that are currently being done at the National High Magnetic Field Laboratory of Los Alamos.
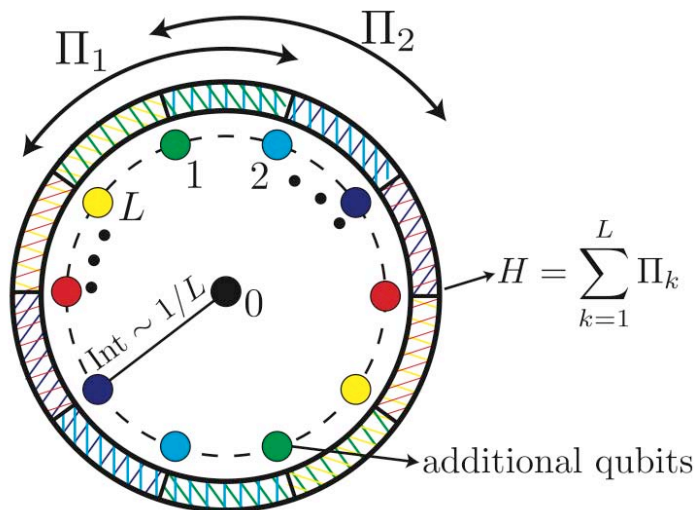
Figure 1. A physical representation of the Hamiltonian that amplifies the gap. Each additional spin 1,...,L has assigned a color and interacts with a particular term of the initial Hamiltonian and a centered spin.

In optimization, the ground state of the Hamiltonian encodes the solution to the problem. Fast algorithms to prepare such ground states are thus desired. Typically, the complexity of known algorithms for this problem depends strongly on the inverse of the spectral gaps to the next excited eigenstate; the smaller the gap, the larger the complexity. It is important then to devise other Hamiltonians that have the same ground states but a much larger spectral gap. These Hamiltonians can be used to solve the optimization problem more efficiently.

The family of Hamiltonians considered in the project satisfies certain interesting properties. One such property is that every ground state is also a ground state of local operators (projectors) that act trivially on it. We introduced

the so called "spectral gap amplification problem" (GAP) for this family and showed that a quadratic amplification of the gap is possible and optimal. This allows for new quantum speedups for optimization and for the preparation of a large class of relevant quantum states (projected entangled pairs or PEPS). Figure 1 gives a physical representation of the Hamiltonian that amplifies the gap. These results are now online (arXiv:1110.2494, LA-UR 11-05706) and will be submitted to SIAM J. on Comp.

Future Work

Frustrated systems give rise to rich and exotic phenomena that can lead to novel physical responses and functionalities. The variety of exotic states is due to the highly degenerate low-energy spectrum that results from the frustrated nature of the interactions. This property makes frustrated systems highly desirable for applications because small perturbations produce big changes in the response of the system . Frustrated systems are also at the root of Optimization: Certain instances of combinatorial optimization problems can be associated with frustrated systems whose ground states encode the solution to the problem.

We will develop a novel and exact computational renormalization approach that will overcome some of the problems of other well-established renormalization methods. We will use our new approach to solve several relevant models in an exact and efficient way. These include Heisenberg models that are important in quantum magnetism, highly frustrated quantum models currently studied in the Magnet Lab, and spin glasses with applications in optimization.

The main difficulty for studying interacting systems is the exponential increase of the number of states with the system size. Renormalization approaches avoid this problem by retaining only the state-variables that play a significant role in the low-temperature properties. We remark that computing ground-state properties of frustrated models cannot be done via convex optimization: The cost function to minimize has a complex landscape with multiple minima, each associated with the corresponding ground state. Our method goes beyond convex optimization, and allows for attacking combinatorial optimization problems where the cost function is non-convex.

Our renormalization method will allow us to: Connect seemingly unrelated physical phe-nomena; Identify the general symmetry principles behind complex phase diagrams; Unveil new states of matter; Obtain exact solutions with complex ordering.

Conclusion

One of the most important challenges in materials science is to discover states of matter with novel responses

and functionalities. The presence of strong competing interactions is the basic ingredient for achieving this goal. However, this characteristic also increases the complexity of these materials and challenges our ability of predicting their properties. We are proposing an algorithm for solving models that are relevant for describing such materials. We will implement codes that will allow us to solve these models under control and predict properties of a certain class of frustrated materials.

Publications

Somma, R. D., and S. Boixo. Spectral Gap Amplification. *SIAM Journal on Computing.*

Computational Modeling of Topo-Taxis: Directing the Motion of Bacteria and Cells with Microfabricated Topologies

Charles Reichhardt
20110189ER

Introduction

We will develop a novel computational toolkit which will be validated by experiments at Sandia to produce a comprehensive modeling capability for the directed motion of self-driven particles such as bacteria and cells in the presence of simple microfabricated substrate topologies. The experiments at Sandia are collaborative and complementary to this work and not directly supported by this project. The toolkit will incorporate novel rules for cell motion and particle-wall interactions. This model will be used to understand how to generate tailored directed motion of self-driven particles for the purpose of extracting useful work or to create novel devices, such as cell sorters that can discriminate bacteria or cell shape, size, motility, and species. Our toolkit is intended to provide a foundation for modeling in the field of "topo-taxis." It will facilitate the study of an entirely new branch of micro- and nanoscience which has numerous applications for laboratory missions including diagnostics, energy science, environmental science, biosciences, and new methods of self-assembly.

Benefit to National Security Missions

This project fits in extremely well with the overall security science mission of the laboratory. Possible applications in homeland defense include the detection and diagnostics of biological agents, creation of novel power and energy sources, and new devices for sorting certain microorganisms which may be useful as biofuels, as well as new types of microdevices. This work can also lead to novel devices of interest to DARPA, NIH, and BES at DOE. We will also develop university collaborations which can lead to UC-op funding.

Progress

We have developed a simulation model which incorporates collective interactions between self-propelled particles. The particles represent bacteria such as E. coli, and the collective interactions include flocking and wall following behavior, both of which have been observed in experiments on bacterial systems. We have carefully tested our simulation model and benchmarked it against experimental results obtained by the Princeton group; we are able to obtain quantitative agreement with experiment. Using our simulation model combined with theory, we have identified what we believe may be a key ingredient in determining whether directed motion of the bacteria can occur when a ratchet geometry is present. Specifically, the presence or absence of time-reversal symmetry breaking at interfaces appears to be crucial. For particles moving under standard Brownian motion, time-reversal symmetry is preserved and we find no evidence of rectification behavior. In contrast, when the particles move in a fixed direction for a specified time interval before reorienting, time-reversal symmetry is broken and rectification behavior becomes possible. We have tested the effects of different wall interaction rules as well as different wall geometries and find that the nature of the interaction with the wall can also determine whether rectification occurs. In experiment, changing the functionalization of the wall or selecting different bacterial species could be used to realize the different wall interaction rules we are considering. Applications of the rectification behavior include not only cell sorting and concentration, but also creation of bacterial nanomotors, a topic of current study. We have presented the results on creating directed motion with bacteria obtained so far in this project at several international venues including the University of Oslo and Universidad Autonoma de Madrid; researchers at these institutions are currently exploring related issues in self-driven particles in the context of biological or bacterial systems. We will also present the work in both paper and talk format at an SPIE annual meeting later this summer, as well as at a biological conference in Poland being co-organized by one of us. We have successfully recruited a top quality postdoc for the project, Jeff Drocco, who has just completed his degree at Princeton in biophysics. We have leveraged funding for the postdoctoral work through the Center for Nonlinear Studies (CNLS). We have performed preliminary studies of flocking interactions for the bacteria, and have found slow collective motion of a bacterial sludge along the container walls. Further flocking work is focused on more rapidly moving clusters of bacteria that will

interact collectively with the asymmetric ratchet potential. Theory suggests that reversal of the rectification effect in the presence of the collective interactions should be possible, and we are presently working to test this.

Future Work

The field of topo-taxis began with recent experiments demonstrating that simple microfabricated topologies can produce directed bacteria motion. The first model explaining this effect was developed by the PI and collaborators. The ability to produce directed motion of randomly moving self-driven particles makes it possible to create many new devices, such as bacteria-powered micro-gears, transport of objects by self-driven particles, cell sorting, and novel micro- and nano-devices. Recent experiments on self-driven particles with more complex interactions that produce swarming and crowding effects show that it is possible to produce powered microgears as well as regimes in which different species of self driven particles travel in opposite directions. Currently, there is no comprehensive modeling capability that provides an understanding of these effects, something required for the growth of the field. Topo-taxis could be applied in biology, energy science, environmental sciences, health, homeland defense, and micro- and nanoscience. We will develop a computational toolkit building on previous simulations of self-driven particles, particularly bacteria, that can address the effects of different rules of particle motion and different substrate topologies. The predictions from our simulations for different topologies and rules will be tested directly by the group of B. Kaehr at Sandia. We will also employ theoretical ideas from nonequilibrium statistical mechanics to develop a broader understanding of the rules and topologies that produce directed motion in this system.

Conclusion

We will produce a novel computational model for topo-taxis that will lead to an understanding of how different devices can be created from these systems. We will identify the optimum topologies for generating directed motion. These predictions and proposed devices will be compared to experiments performed at Sandia. We will develop a general theoretical framework for the general class of topologies that produce usable work or directed motion. Our computational toolkit will place Los Alamos as the leader in modeling of this rapidly growing area and will facilitate collaborations between LANL and external groups for funding and research.

Publications

Reichhardt, C. J. O., J. Drocco, T. Mai, M. B. Wan, and C. Reichhardt. Active matter on asymmetric substrates. 2011. *Proceedings of SPIE.* **8097**: 8970V.

Algorithmic Co-Design: Paradigms for Unstructured Problems on Accelerated Architectures

Sunil Thulasidasan
20110195ER

Introduction

In this project, we seek to develop algorithmic techniques to efficiently utilize the massive computing power afforded by today's stream processors for solving problems that lack obvious data parallelism. Such problems are often characterized by irregular memory accesses resulting from "pointer-chasing" and have traditionally been better suited for Central Processing Unit (CPU) architectures that are optimized for sequential and branch-heavy code.

The irregularity of these problems is a natural outcome of efficient representation of large and complex data that often utilize graph-based data structures. In fact, many important scientific problems can be intuitively formulated as graph-exploration and optimization problems. However, efficient graph representations, which are pointer-dense and unstructured, do not translate to efficient computations on graphics processors and many optimal graph algorithms do not lend themselves to easy parallelization.

Nevertheless, it is becoming increasingly clear that massive on-chip parallelism will continue to be the architectural trend in the foreseeable future. The potential performance benefits in extracting parallelism on unstructured problems are thus too compelling to ignore. Our main research goal in this proposal is to develop algorithmic techniques for efficiently implementing widely applicable graph algorithms on architectures with massive fine-grained parallelism. This will require a shift in algorithmic thinking; indeed, approaches that are theoretically non-optimal, but afford a greater degree of parallelism may actually be better suited to these architectures. We focus on graph-based problems in this proposal, but we believe the lessons learned will be applicable to other types of unstructured problems and will provide useful guidelines for designing compilers and run-time tools for heterogeneous platforms.

Benefit to National Security Missions

Advances in parallel graph clustering and community detection algorithms will find numerous uses for analyzing signaling path-ways and metabolic channels in biological networks (Grand Challenge: Complex Biological Systems), and network analysis in epidemiology (Bio-security Science). Community detection algorithms can also be readily applied to detecting and characterizing terrorist networks and channels (Grand Challenge: Sensing and Measurement for Global Security). Graph algorithms have also found numerous uses in LANL's efforts in infrastructure analysis (NISAC). The results of our effort can be used to vastly improve the scale and speed of current models and simulations.

LANL's efforts in data-intensive and exascale computing (Grand Challenge: IS&T) can directly leverage our work, since one of the major computational tasks in this domain will be inferring semantic relationships inside huge data sets that will necessarily involve massive amounts of unstructured computation.

Progress

Our new results on using Graphics Processing Unit (GPU) accelerated architectures [1] for graph exploration problems at the 4th ICST International Conference on Simulation Tools and Techniques (SimuTools 2011). We showed how path computations for real-world road network graphs can be accelerated using GPUs by exploiting structural properties of the graph. In particular, we show how the spatially constrained nature of the problem allows us to overcome memory limitations on the GPU. This has important practical implications for dealing with graph-based and other unstructured problems on streaming architectures such as the GPU, which while offering a great degree of parallelism, is also significantly constrained by memory limitations. GPUs have already been shown to significantly outperform CPUs in path computation problems for small graphs. Our results allow us to deploy GPUs for much larger graphs that arise in real world simulations.

SIMUTools 2011 is the premier International Conference on Simulation Tools and Techniques and focuses on all aspects of simulation modeling and analysis.

The aim of the conference is to bring academic and industry researchers together with practitioners from the simulation and user communities. The conference addresses current and future trends in broad simulation techniques, models and practices, and strives to foster interdisciplinary collaborative research in these areas.

In the paper, we show how path computations for real-world road network graphs can be speeded up using GPUs, in the context of a large scale transportation simulator. This is motivated by the following observations: (i) Routing is the most computationally intensive part of a large-scale transportation simulator, and thus, optimizations to routing that exploit any inherent structure and parallelism in the problem significantly improve application performance; (ii) near-optimal paths are often acceptable in lieu of the most optimal path, which motivates the use of heuristics in speeding up path computations; and finally (iii) paths from source to destination in real-world road network graphs are spatially constrained, implying that to solve the path problem, one needs to consider only a small subset of the routing graph. This has important practical implications for a GPU, which, while offering a great degree of parallelism, is also significantly constrained by memory limitations. GPUs have already been shown to significantly outperform CPUs in path computation problems for small graphs. The previous observations allow us to deploy GPUs for much larger graphs that arise in transportation simulations.

The techniques described in the paper are also applicable to other real-world graphs exhibiting similar structural properties, and many of these align directly with DOE missions. For example, advances in parallel graph algorithms will find numerous uses for analyzing signaling pathways and metabolic channels in simulations of biological networks

In addition, work is also currently underway to implement new parallel hierarchical routing and community detection algorithms on GPUs.

Hristo Djijdjev (Co-I) presented new results on fast queries on weighted polyhedral surfaces [2]. We designed an efficient algorithm and a data structure to answer approximate distance queries between points on a weighted planar surface. Using weights on surfaces makes it possible to model more accurately physical characteristics of the surface such as its type (e.g., sand, water, vegetation), steepness, hazards (e.g., radioactive contamination), or availability of obstacles. But it also makes the problem much more difficult compared to the problem for un-weighted (Euclidean) surfaces. It is believed that the general problem of finding shortest weighted paths in such surfaces cannot be solved exactly in finite time. Hence we design and analyze approximation algorithms for that problem with provable accuracy and much more efficient than the previous ones, reducing the dependence on n, the number of the triangles

in the triangulation representing the surface, from quadratic to nearly linear. The approach presented also offers significant potential for parallelism on streaming processors.

We are also conducting experiments on a new algorithm for shortest-path routing on approximately planar graphs that use matrix-algebra operations. Graphs represented in this manner offer much better potential for parallelism and structured memory accesses. Experiments on multi-core and GPU architectures are currently underway.

Future Work
Given the enormous sizes of the graphs we are planning to analyze (billions of edges) and the current processor speeds, the only option to achieving speeds allowing analysis in reasonable time is to make use of a high degree of parallelism. Towards this end, one of our research goals in this proposal is to devise efficient data structures that preserve some space efficiency but allow a greater degree of parallelism and a high intensity of local computations before a data exchange or synchronization is needed.

To overcome memory bottlenecks while dealing with large graphs, we plan to use contraction based methods which have been successfully used to devise efficient external memory algorithms for minimum spanning forests in undirected graphs. The idea is to compute a rooted tree (called a hierarchy tree) that provides a ``topological skeleton'' of the input graph G. On of our goals, therefore, is to design efficient GPU algorithms for computing hierarchy trees for G.

A general question that we plan to investigate is how can we devise an efficient GPU algorithm for a problem starting from its corresponding (parallel) PRAM (Parallel Random Access Machine) algorithm. If we could find a transformation that takes an existing PRAM algorithm and can decide which parts can be left unmodified, and which parts need to be modified and how, then we can leverage the existing literature on PRAM algorithms.

Conclusion
The following were our original goals in the proposal. Not only have we achieved all of our milestones for FY 11, we have also shown how our results can benefit specific applications (large scale transportation simulations).

FY11: Theoretical formulation and initial implementation of graph algorithms on accelerated architectures; design and engineering data structures for succinct representation of large graphs on streaming processors.

FY12: Investigation into memory and cache dynamics for graph-based problems; investigation into optimization techniques.

FY13: A comprehensive formulation of design principles for algorithms for graph-based problems

on heterogeneous and accelerated architectures, and applicability to other unstructured problems; software modules that were developed as part of this project and judged to be of obvious usefulness to the wider community will be packaged and released using an open-source license.

References

1. Thulasidasan, S.. Heuristic Acceleration of Routing in Transportation simulations using GPUs. To appear in *4th International Conference on Simulation Tools and Techniques 2011.* (Barcelona, Spain, 21-25 March 2011).

2. Djidjev, H., and C. Sommer. Approximate Distance Queries for Weighted Polyhedral Surfaces. To appear in *European Symposium on Algorithms.* (Saarbrucken, Germany, 5-9 Sep 2011).

Publications

Djidjev, H., and C. Sommer. Approximate Distance Queries for Weighted Polyhedral Surfaces. To appear in *European Symposium on Algorithms.* (Saarucken, Germany, 5-9 Sep 2011).

Thulasidasan, S.. Heuristic Acceleration of Routing in Transportation simulations using GPUs. To appear in *4th International Conference on Simulation Tools and Techniques.* (Barcelona, Spain, 21-5 March 2011).

Extreme Quantum Simulation: Co-Design from Desktop to Exa-Scale

Nicolas Bock
20110230ER

Introduction

Continued hardware and algorithm trends are transforming quantum simulation into an increasingly powerful technology that impacts chemistry, biology, and materials science with rigorous predictive and interpretive tools. However, these enabling trends have not kept pace with each other: On the one hand, conventional algorithms such as the so-called Big O algorithms (O(N)) for electronic structure are throttled by an O(N^3) computational cost with system size N, but are able to take full advantage of large parallel platforms through the use of standard software libraries. On the other hand, new O(N) algorithms exploit locality of quantum interactions to achieve a reduced complexity, but are irregular and do not lend themselves to Cartesian domains or standard libraries. Also, continued advances in O(N) algorithms are less well developed and coupled more tightly to architecture. Despite these challenges, the near exponential growth in computational power of the commodity GPU (graphics processing unit) trend and its massively parallel realization on platforms leading to the exa-scale, underscore the potential of O(N) algorithms across these computational scales. The goal of this project is to realize this potential through the co-design of next generation O(N) methods for the next generation hardware. Surprisingly, the same locality principles that lead to N-scaling and give rise to parallel irregularity also offer the solution for improved speed, resolution, and implementation onto increasingly heterogeneous platforms. Our goal is to further develop these locality principles to: (1) Achieve high performance, hardware oblivious methods across a wide range of memory hierarchies and platforms, from the desktop on towards the exa-scale. (2) Achieve greatly reduced cost prefactors for N-scaling methods, perhaps up to factors of 100x. (3) Overcome fundamental problems with the resolution of energy differences for very large calculations.

Benefit to National Security Missions

This research will deploy complimentary, LANL unique capabilities to establish a strategic thrust with broad Mission Relevance and a Program Development impact that is translational, providing coherence between basic research and engineering specifics. Narrowly, this work will directly support the developing SciDAC program Exascale for Energy, as well as DOE's Basic Research Needs: Catalysis for Energy, the BES grand challenge the ability to design and to implement new catalytic processes by design. More broadly, This project will develop basic capabilities with broad laboratory mission relevance, including DARPA's Quantum Effects in Biological Environments (QuBE), LANL's Matter-Radiation Interactions in Extremes (MaRIE). This project will also directly broadly impact the DOE and NNSA's push toward exascale computing, as well as BES and OBER missions in Energy and DHS Biothreat missions.

Progress

During the past year, we accomplished the following:

We implemented a proof of concept version of the Approximate Sparse Matrix-Matrix Multiply (SpAMM) based on Space Filling Curve (SFC) ordering of data storage and execution and demonstrated successfully that we can tightly bound the total multiplication error. In addition we showed that the computational complexity of this approach scales linearly with system size for larger realistic density matrices. This achievement is an important step in realizing our R&D goal (1) as it proves that we can utilize SFC technology to leverage locality, reduce total work by approximating to achieve linear scaling, while at the same time being able to bound the total error. This work was published (LA-UR 10-07458): M. Challacombe, N. Bock, "Fast Multiplication of Matrices with Decay", arXiv:1011.3534v1 (2010).

We implemented a serial high performance version of SpAMM, which achieves about 50% performance of GotoBLAS for dense matrices, but quickly outperforms GotoBLAS for larger matrices with increasing sparsity. We were able to achieve this result at a resolution of 4x4 matrix blocks. This result is another important step towards R&D goal (1) as it shows that a high performance SpAMM can be written without compromising any of the features shown in our proof of

concept code. This work was submitted for publication in SIAM Scientific Computing (LA-UR 11-06091): N. Bock, M. Challacombe, "An optimized implementation of the Sparse Approximate Matrix Multiply", submitted for publication (2011).

3) We implemented a prototype of a scalable version of SpAMM for shared and distributed memory architectures using task parallel programming models. We are in the process of implementing a high performance version of this prototype and expect completion very soon.

Future Work

Our R&D approach will involve multiple levels of co-design to achieve Extreme Quantum Simulation: (1) We will develop and reconcile two powerful space filling curve (SFC) heuristics, one in real space and one in the abstract convolution space. In each space, the SFC will be used to achieve a deterministic approach to domain decomposition and load balancing while maximizing spatial and temporal locality of data access. Co-design will be used to reconcile the work flow between these spaces, and to understand methods for achieving good average performance across a variety of modern architectures. (2) We will develop next generation linear scaling methods that not only exploit spatial locality of quantum interactions, but temporal locality as well, referring to the slow variation of matrices with respect to iteration or time step, rather than data access as in (1). By using the recently developed Density Matrix Perturbation Theory, we will reformulate O(N) electronic structure theory to work entirely with matrix differences, with two expected outcomes: First, because these matrix differences are hyper-sparse, we may be able to achieve large speedups, perhaps up to 100x. Second, working entirely with matrix differences will allow us to avoid the problem of energy precision that plagues large scale quantum simulation. How sparse and how much precision can only be determined by co-design in the context of simulation; what are the effects on energy conservation in large scale molecular dynamics? Monte Carlo? (3) Finally, we will explore co-design of elements (1) and (2) at the level of extreme quantum simulation, where spatial and temporal locality interact at the level of data access and quantum interaction. Does hyper-sparsity expose unforeseen overhead at scale? What about the granularity (blocking) trade-offs for GPU acceleration with hyper-sparse matrices?

Conclusion

The first milestone, a "scalable SpAMM", will be reached quickly. A major obstacle is to apply the convolution space SFC to sparse matrices, however, load balancing and data distribution can be done in a scalable fashion through trees. As we will draw on existent libraries for the block multiply to move onto the GPU we expect to reach our second milestone of a "parallel and GPU enhanced SpAMM" quickly as well.

InfoFusion: "Connecting the Dots" Using Cyberspace Information Models

Mary Linn M. Collins
20110746ER

Introduction

Making decisions by "connecting the dots" in real-time with incomplete information is an on-going challenge for many of LANL's sponsors and customers. Many partial solutions to the problem exist, from sensors that collect information to machine learning techniques for analyzing the information, once collected. Data and technologies cannot be exploited, however, unless analysts and operators know that they exist. This requires a comprehensive model of the available data and tools, yet typically analysts or operators do not have the experience or expertise to develop these models for themselves. This is a serious gap in current information systems. We propose to close this gap by developing techniques for tagging data with a cyberspace information model (C-SIM) that includes information about relevant data and tools. The result will be a prototype for a system of systems called InfoFusion that will provide users with the system overview they need in order to efficiently find, fuse, and exploit information.

Benefit to National Security Missions

The singular challenge facing many of LANL's sponsors and customers is that they have to "connect the dots" in real-time by detecting and connecting individual pieces of data that are scattered across multiple databases, repositories, and networks. Information scientists refer to this problem as "information exploitation" and it is arguably the key bottleneck in information systems. LANL's 2010 Information Science and Technology Strategic Plan calls information exploitation a "key capability for the Laboratory in the future..." [1] We are addressing this problem with techniques for socially constructing a system of systems called InfoFusion that will tag new information with a cyberspace information model (C-SIM) that provides the data, and the users, with information about how to efficiently find, analyze, and fuse related information in a form optimized for exploitation and "connecting the dots." In effect, InfoFusion will make data, systems, and users "smart" [2] and will facilitate information flow from data source to data use. Since InfoFusion addresses problems inherent in current information systems, it has the potential to

impact all of the Laboratory's national security missions.

Progress

InfoFusion received funding on July 25, 2011, thus the progress reported here represents three months of work. While our ultimate goal is to develop an advanced capability for our sponsors and customers, we began by conducting foundational research on two very different information exploitation problems: assessing LANL capabilities and global biosurveillance capabilities. To date we have (1) refined the general cyberspace information model (C-SIM) represented in Figure 1; (2) determined specific use cases in consultation with LANL subject matter experts in information science and technology, situation awareness, and biosurveillance; and (3) started to create C-SIMs for these use cases by hand-coding them based on subject matter expertise.
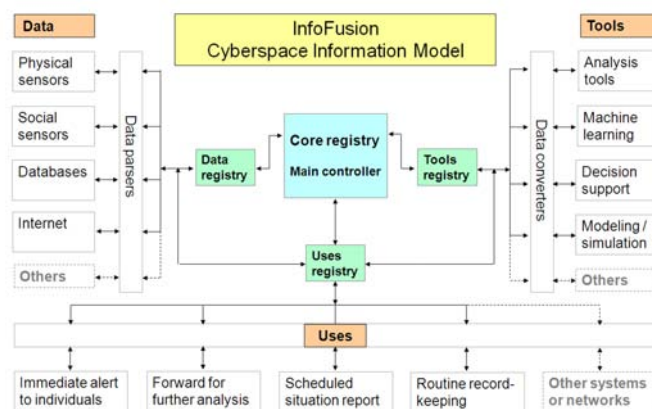
Figure 1. Cyberspace Information Model (C-SIM).

Specifically, we have refined C-SIMs so that they reference other kinds of models, such as domain models and threat models, which are independent of specific information systems but important in optimizing information flow through those systems [3]. For example, a simple domain space information model (D-SIM) for understanding research capabilities captures the fact that people work on projects, and projects result in products. Even if all of the DOE National Laboratories

use the same domain model when assessing their research capabilities their information systems are not the same, so their cyberspace information models (C-SIMs) will not be not the same. As illustrated in Figure 2, the domain model focuses on people, the projects they work on, and the products of those projects, whereas the cyberspace information model focuses on the specific data sources for data about people, projects, and products.
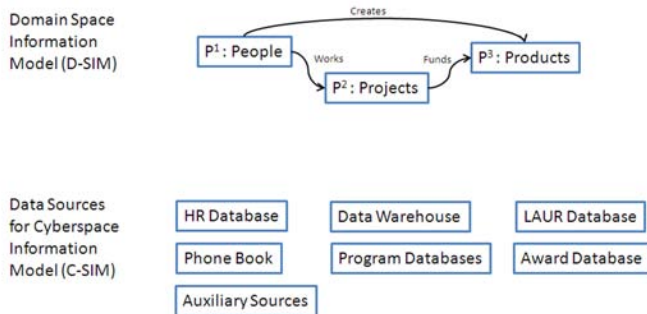
Figure 2. Domain Space Information Model (D-SIM) and Data Sources for C-SIM.

We are currently working on multiple models for InfoFusion: (1) a formal ontology for the general cyberspace information model (C-SIM) [4, 5]; (2) an instantiation of the general C-SIM ontology for specific use cases; (3) a domain space information model (D-SIM) that represents the general knowledge in the domain related to the use cases; (4) a problem space information model (P-SIM) or threat space information model (T-SIM) that represents the specific problem or threat related to the use cases; and (5) a user space information model (I-SIM) that represents a specific user's cognitive and interactive characteristics.

In the original C-SIM template these models would have been considered additional tools. Our current approach focuses on representing each model as a semantic graph and determining how to align the graphs to one another. [6, 7] In technical terms, we are conceptualizing the problem as a scalable graph theory problem. In practical terms, this allows us to consider the problem of how the models work together and to discover inconsistencies and gaps.

The most surprising result of analyzing models in this manner is that we have discovered gaps in the Laboratory's current technique for assessing capabilities. Using a C-SIM, alone, we would have mirrored existing practice, started with a use template (in this case, a Capability Review Self-Assessment Statistics Template), and worked backwards from that to identify the data sources and analysis tools relevant to that template. We interviewed two people who have extensive experience in collecting statistics for capability reviews and, while they approached the task differently, they did in fact rely on the same data sources (e.g. publication databases).

By including a domain model and problem model in addition to a C-SIM, we asked an additional set of questions – what does it mean to identify or define a capability and what problems does that solve – then worked backwards from those. The problem model (P-SIM) captures the fact that capability assessments are important in preparing the Laboratory to respond to sponsor and customer needs. As discussed above, the domain model (D-SIM) captures the fact that capabilities represent people, the projects they work on, and the products of those projects. Aligning these graphs with each other reveals that capability assessments need to include current, emerging, and future capabilities, as well as past capabilities. Aligning these graphs with the C-SIM for LANL Capability Assessments reveals a gap: the Capability Review Self-Assessment Statistics Template focuses on publications, patents, and other metrics that reflect past capabilities. Yet past capabilities may or may not reflect current or emerging capabilities. A current capability may exist in the form of a project two years or more before a publication results from the project. An emerging capability may exist in the form of a discussion group or proposal team several months or more before a project results from the proposal.

What data sources can we use to capture these capabilities? We believe that current capabilities can be assessed using the current fiscal year's charge codes and the work they represent, and emerging capabilities can be assessed using social network analysis, such as analysis of proposal co-authorship graphs and email traffic. Using charge codes instead of publication data to assess current capabilities has additional advantages. Charge codes map to the Laboratory's missions and organizations, whereas keywords associated with a journal publication may not. Many people at the Laboratory who charge their time to research projects do not publish papers because they provide research support: machinists, programmers, etc. Certainly the Laboratory's ability to propose and execute complex collaborative projects depends on this kind of research support. Thus by modeling more aspects of the information space and comparing the models by aligning the graphs, we are developing techniques for improving more aspects of information flow: not just speed, but comprehensiveness, relevance, and accuracy.

Models can be very complex and creating them can be very resource-intensive, as in the case of global biosurveillance. By developing a framework for aligning models, we hope to make it possible for government agencies to reference shared domain, problem, or threat models from their unique cyberspace information model. Thus the difficult work in developing a model for understanding a terrorist organization's capabilities or a pathogen's capabilities can be leveraged across multiple agencies, even though each agency has specific networks, data sources, analysis tools, and use templates related to its particular mission, tasks, and workflow.

Figure 3. Ideas for Design of InfoFusion Interface.

Future Work

We have much work to do in the next 11 months. First, we need to create models for a biosurveillance use case by hand-coding them based on subject matter expertise. Once we have hand-coded models for assessing LANL capabilities and global biosurveillance capabilities, we will focus on using machine learning techniques to validate and update the models. As illustrated in Figure 3, the machine learning techniques will consist of a software prototype that (a) indicates the data sources and tools used in the selected use cases; (b) allows users to modify the mapping between data sources, tools, and uses; and (c) analyzes the resulting patterns by applying inference methods from semi-supervised relational learning. Once we have a set of socially constructed C-SIMs, we will build prototype software agents for tagging data with C-SIMs for the LANL use cases and develop a plan for tagging data with C-SIMs for the biosurveillance use cases.

Conclusion

In this project, we propose to design, develop, and test three InfoFusion components: (1) cyberspace information models (C-SIMs) that provide a transparent view of the data and tools available to be exploited in a given time frame and for a given purpose; (2) software agents that tag new information, at the point of entry into the system, with an identifier indicating the appropriate C-SIM for a given purpose; and (3) machine learning techniques for automating the process of developing and improving C-SIMs based on users' interactions with the system. The goal is to use this socially constructed system of systems to make data "smart" and to optimize information flow from source to use.

References

1. Science that matters: integrating information, science and technology for prediction: strategic plan . 2010. *Los Alamos National Laboratory.*

2. Young, P.. DoD cyber operations. Presented at *DoD Enterprise Architecture Conference.* (Hampton, VA, April 11-15, 2011).

3. Thomas, C., P. Mehra, R. Brooks, and A. Sheth. Growing fields of interest - using an expand and reduce strategy for domain model extraction . 2008. In *International Conference on Web Intelligence and Intelligent Agent Technology* . (Sydney, 2008). , p. 496. Sydney: IEEE / WIC / ACM.

4. Suchanek, F., G. Kasneci, and G. Weikum. YAGO: a large ontology from Wikipedia and WordNet. 2008. *Web Semantics: Science, Services and Agents on the World Wide Web.* **6** (3): 203.

5. Protege ontology editor. *Stanford University.*

6. Bayati, M., M. Gerritsen, D. Gleich, A. Saberi, and Y. Wang. Algorithms for large, sparse network alignment problems. 2009. In *Ninth IEEE International Conference on Data Mining.* (Miami, 6-9 Dec. 2009). , p. 705. Miami: IEEE.

7. Eschenbacher, J., N. Zarvic, O. Thomas, and K. Thoben. Measuring and evaluating communication intensities in collaborative networks. 2010. In *Collaborative networks for a sustainable world.* Edited by Camarinha-Matos, L., X. Boucher, and H. Afsarmanesh. , p. 527. Boston: Springer.

Developing Adaptive High-Order Divergence-Free Methods for Magneto-Hydro-Dynamics Turbulence Simulations

Shengtai Li
20090210ER

Abstract

We have proposed a novel high-order numerical method for magneto-hydrodynamics (MHD) simulations. Our method is the first higher than second-order numerical method that can truly preserve the divergence-free property of the magnetic field. Using our method, we have developed a software package to simulate MHD flows. The software has been verified to achieve expected order of accuracy using problems with exact solution. This MHD code is fully parallelized and we have achieved 90% parallel efficiency on a number of super-computers.

We have used our MHD code to solve a number of MHD problems, which includes weakly turbulent MHD-wave interactions in plasmas with strong magnetic field to study the energy conversion and transfer between different MHD waves, magnetic field amplification by a supernova blast shock wave in a turbulent medium, and many high-resolution two-dimensional (2D) and three-dimensional (3D) MHD-turbulence simulations. Through the simulations, we have obtained a few scientific discoveries and results that will have great impact on understanding the compressible MHD turbulence and the role of magnetic field during the evolution of Universe.

Background and Research Objectives

Practically all the fluid flows that interest scientists and engineers are turbulent ones. Richard Feynman, the great Nobel Prize-winning physicist, called turbulence ``the most important unsolved problem of classical physics.'' The development of the modern supercomputer makes it possible for engineers and scientists to gain fleeting but valuable insights into turbulence.

The direct numerical simulations (DNS) of turbulence are required to accurately reproduce its evolution over a wide range of length and time scales. The compressibility of the flows adds more difficulties to the simulations because almost all of the compressible flows contain discontinuities such as shocks and contacts, which make many high-order numerical methods that work well for incompressible flows but cannot resolve the discontinuities ill-suited. On the other hand, the conventional second-order shock-capturing schemes are shown to be too dissipative for turbulence simulations. We have compared the numerical dissipation for methods with different orders of accuracy in [2]. It shows that the energy for the low-order method is quickly dissipated after a few periods whereas the high-order method preserves the energy very well for a long time.

For MHD flow, the additional challenge for a numerical method is to preserve the divergence-free condition of the magnetic field. The magnetic field loop example presented in [1] shows that an advected magnetic field loop becomes disintegrated quickly due to the divergence error, whereas divergence-free method preserves it very well. However, most of high-resolution shock-capturing (HRSC) schemes use second-order spatial averaging or interpolation to obtain the information required by the divergence-free method. This is why many higher than second order methods for hydrodynamic simulations become second-order methods when extended to the divergence-free MHD method.

The goal of this project is to develop an efficient and robust high-order methodology, which preserves the divergence-free conditions of the magnetic field for simulations of MHD flows. To achieve this goal, we have identified two major objectives: developing a new higher-order divergence-free method for the MHD flow and developing an adaptive method to improve the efficiency and robustness of the high-order method. To verify our method and apply it to MHD simulations, we have to develop a software package to implement the numerical method.

Scientific Approach and Accomplishments

The traditional numerical method for partial differential equations (PDE) uses only one computational grid to cover the physical domain. With this approach, it is difficult to achieve higher-order accuracy for the divergence-free magnetic field. The left plot of Figure 1 illustrates the difficulty: To advance the magnetic field B_x we need to calculate the electric field E at the cell corner, which is usually obtained via spatial averaging or interpolation from the four known fluxes at the cell faces. Because of

the spatial averaging, the electric field only has second-order accuracy even if the face fluxes are calculated with higher order accuracy.
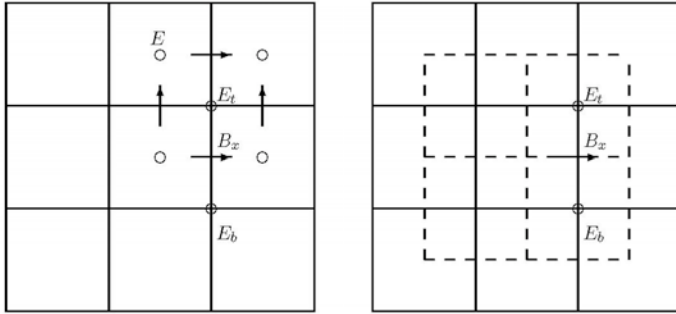
Figure 1. Illustration of the dual overlapping grid method for MHD flows. The dual grid (dashed-line in the right plot) provides a natural way to calculate electric field (E) at the corner with high-order accuracy without averaging from its connected faces (left).

We propose to use the dual overlap grid to by-pass the limitation of the current divergence-free methods. The right plot of Figure 1 illustrates the idea. We first have a primal grid (solid line). From the primal grid, we can construct a dual overlapping grid (dashed line) to cover the same domain. The dual grid provides a natural way to calculate the electric field at the corner with higher-order accuracy because it naturally resides at the center of the dual grid and hence no interpolation is required to obtain its value.

Using two overlapping grids, we need to advance two sets of solutions, one on each grid, simultaneously. It seems that the computational cost is doubled without any gain. However, we can construct the higher-order scheme using only the nearest neighbor cells from both the primal and dual grid. In [2], we have demonstrated that constructing a fourth-order scheme requires only one ghost cell in each grid using cells from both the primal and dual grid, but requires 3 ghost cells if only one grid is used. The reduced stencil is easy to implement and offers decreased communications costs for parallel computing.

We have constructed a 3rd order and a 4th order divergence-free methods, which are described in our papers [1] and [2] respectively. The order of accuracy of our method is verified using examples with exact solutions. Our numerical tests show that the computational cost of the fourth-order method is only double the cost of the third-order method for a grid of 64x64. However the accuracy of the fourth-order method on a grid of 64x64 is corresponding to that of 256x256 grid of the third-order method. Therefore to achieve the same accuracy, the fourth-order method is about 32 times more efficient than the third-order method. We have found that only the information provided from the face reconstructions is not enough for the four-order divergence-free reconstruction over the whole cell, which corrects a wrong assumption in the published literatures.

To resolve discontinuities (e.g., shock or contact) in the flow without artificial oscillations, we have extended the hierarchical reconstruction (HR) limiting process of Liu et al. [3] to our method. The HR uses only the nearest neighbor cells and is easy to parallelize for a supercomputer. Although the HR limiting reduces the overall accuracy (see results of [1] and [2]), the solution still converges with the expected order of accuracy for smooth problems. However, the HR process costs almost 40% of the CPU time if implemented everywhere. To improve the computational efficiency, we propose a discontinuity detector to flag those cells that require HR, and only perform limiting for those cells. We have found that the divergence-free method is crucial in achieving the expected order of accuracy and preserving the numerical stability for limited reconstruction (see the numerical results of [1] and [2]). This is because the limited reconstruction breaks the symmetry of a scheme and leads to drastic increase of the divergence-error of the magnetic field near those cells.

We have successfully extended our method from 2D to 3D (see [4]) and developed a new efficient time integration method for both 2D and 3D problems (see [5]). The traditional method to achieve higher-order accuracy in time is to use multi-stage Runge-Kutta (RK) method, which is also used in our paper [1] and [2]. Our new integration uses a different approach by representing the time derivatives locally with spatial derivatives via equation expansion. Using the higher-order spatial reconstruction as an initial condition, we can construct a local higher-order space-time polynomial via an iterative process. Unlike the RK method, which requires at least p times spatial reconstruction for a pth order method, the new time integration method requires only one spatial reconstruction in one time step. It not only reduces the computational cost, but also makes the solutions more accurate. We have proposed a new refinement strategy for the adaptive mesh refinement (AMR) of our dual overlapping grids and a new algorithm to achieve higher-order accuracy for AMR grid (see [6]).

We have developed a software package to implement our algorithm. To make our software package more efficient, robust and user-friendly, we reduce the number of ghost cells, which are used in communication between different processors in parallel computation, from 4 to 2. We optimize the data layout and store the data in cache as long as possible, which reduces the total CPU time to half. We also developed a parallel data input/output (I/O) algorithm for processors to read/write data independently without communication. This reduces the I/O time by a factor of 10. We have also developed an adaptive restarting mechanism for simulation to restart with a different number of processors.

Using our software package, we have performed a variety of simulations to study the MHD flows in an astrophysi-

cal system and MHD turbulence problems. In simulations of accretion disk problem, we find that the higher-order method is better in preserving the angular momentum than the low-order method for the accretion disk problem. The simulation results for the supernova blast shock show that the background weak magnetic field can be greatly amplified (see [7] and [8]) by shock-turbulence interaction and the Rayleigh-Taylor instability. However, we also find in our simulations that the magnetic field near the shock front has not reached a value comparable to the magnitude inferred from observation (Figure 2). This indicates other physics, such as the effect of cosmic rays, has to be considered to further understand the magnetic field amplification in supernova remnants. We have performed large-scale 2D, 2.5D, and 3D MHD decaying turbulence simulations. Our results show that we have achieved lower numerical dissipation and longer inertial range with our higher-order method than the low-order method (Figure 3). Therefore we have reproduced the published results with a lower resolution grid. To study the mode conversion during the turbulent nonlinear stage, we initialize the problem with a set of fast MHD wave. We find that due to the shock steepening and nonlinear wave interaction, the waves quickly become turbulent and the fast waves have been converted into the slow waves (see [9] and [10]). This is the first simulation result to confirm the theoretical result of [11]. In [10], we compare several publicly available astrophysics codes with our code. We find our method is the only one to produce a clean shock profile without any artificial numerical oscillations.

Magnetic field amplification factors
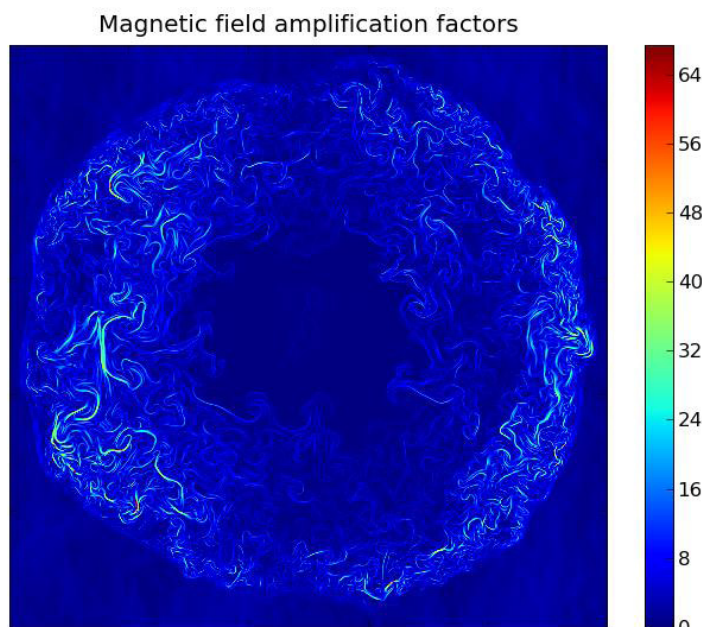
Figure 2. The initial magnetic field is greatly amplified by the shock-turbulence interaction and the Rayleigh-Taylor instability. The plot shows the amplification factor of the magnetic field after a strong supernova blast wave propagates through a background weak magnetic field.

We have also performed force-driven MHD turbulence simulations for both 2D and 3D problems. We found that the magnitude of the magnetic field can be amplified by a larger factor than published results. We have also performed simulations on an elongated box in solar wind applications to study the turbulent dynamics of the flux tube of solar wind. We have studied the scale decomposition and scale locality in compressible turbulence. We prove theoretically that inter-scale transfer of kinetic energy is dominated by local interactions (see paper [12] and [13]). We have performed large-scale 3D simulations and presented the first direct evidence that mean kinetic energy cascades conservatively beyond a transitional "conversion" scale range despite not being an invariant of the compressible flow dynamics (see Figure 4 and paper [14]). This is a fundamental result in compressible fluid dynamics and the astrophysical communities.
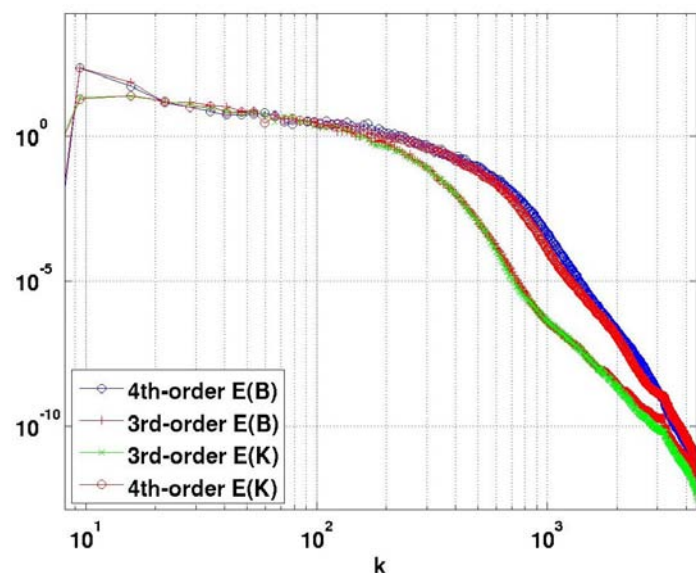
Figure 3. Kinetic energy and magnetic energy spectrum for MHD turbulence simulations. It shows the fourth-order method has longer inertial range (flat curve) than the third-order method.
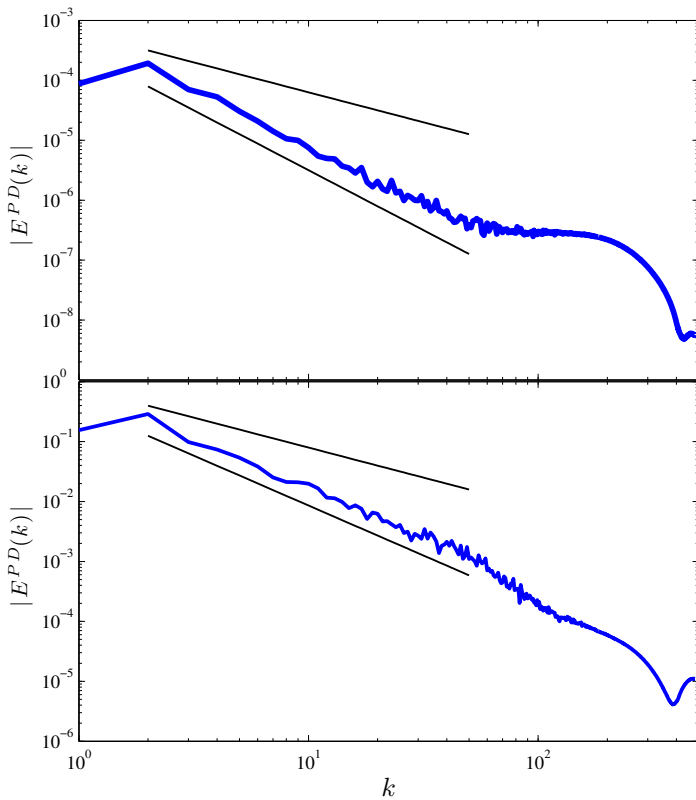
Figure 4. Magnitude of pressure dilatation cospectrum from compressible MHD turbulence simulations. Straight lines with slope of -1 and -5/3 are for reference and extend over the fitting region which gives a slope of 1.61. Theory in [12] predicts that if the slope is smaller than -1, the kinetic energy will cascade conservatively as incompressible fluid.

Impact on National Missions

The high-order numerical method and code we have developed addresses a critical need in current MHD flow simulations, especially the MHD turbulence simulations. Our research is perfectly aligned with the Lab's several grand challenges: beyond stand model, complex systems, boost physics, and information science and technology. It is also aligned well with the DOE mission of scientific discovery. We have seen immediate impact on computational astrophysics community. The compressible turbulence theory we have proposed and verified is applicable to other fluid simulations, such as climate and ocean modeling and atmosphere and weather forecast. The capability we have developed can be used in other plasma simulations: space weather forecast, corona mass ejection (CME), inertial confinement fusion (ICF), and magnetic confinement fusion (MCF) etc.

References

1. Li, S.. High order central scheme on overlapping cells for magneto-hydrodynamic flows with and without constrained transport method. 2008. *Journal of Computational Physics.* **227**: 7368.

2. Li, S.. A fourth-order divergence-free method for MHD flows. 2010. *Journal of Computational Physics.* **229**: 7893.

3. Liu, Y., C. W. Shu, E. Tadmor, and M. Zhang. Non-oscillatory hierarchical reconstruction for central and finite-volume schemes. 2007. *Communications on Computational Physics.* **2**: 933.

4. Li, S.. Higher-order divergence-free methods for three-dimensional MHD flows on overlapping grid. 2011. In *Numerical Modeling of Space Plasma Flows: ASTRONUM-2010.* (San Diego, CA, June 13-18). Vol. 444, 1 Edition, p. 242. San Francisco: ASP conference series.

5. Li, S.. Higher-order time integration with local Lax-Wendroff procedure for central scheme on overlapping grid. To appear in *Journal of Computational and Applied Mathematics.*

6. Li, S.. Higher-order adaptive mesh refinement on overlapping grid. *Journal of Computation Physics.*

7. Guo, F., S. Li, H. Li, J. Giacalone, and J. R. Jokipii. The magnetic field amplification downstream of supernova blast wave. Presented at *32nd International Cosmic Ray Conference .* (Beijing, Aug. 11-18, 2006).

8. Guo, F., S. Li, H. Li, J. Giacalone, J. Jokipii, and D. Li. On the magnetic fields amplification by a supernova blast shock wave in a turbulent Medium. *Astrophysics Journal.*

9. Buoni, M. J., H. Li, S. Li, and H. Aluie. A numerical study of two-dimensional compressible MHD wave turbulence in the low-beta plasmas. *Astrophysics Journal.*

10. Li, S.. Code Comparison for a MHD fast-wave propagation problem. To appear in *Numerical Modeling of Space Plasma Flows, ASTRONUM-2011.* (Valencia, Spain, June 13-17).

11. Chandran, B.. Weakly turbulent magnetohydrodynamic waves in compressible low-beta plasmas. 2008. *Physical Review Letters.* **101**: 235004.

12. Aluie, H., and G. L. Eyink. Scale locality of magnetohydrodynamic turbulence. 2010. *Physical Review Letters.* **104** (8): 09101.

13. Aluie, H.. Theoretical analysis of the energy flux in compressible MHD turbulence. 2011. *Physics Review Letters.* **106**: 174502.

14. Aluie, H., S. Li, and H. Li. The conservative cascade of kinetic energy in compressible Turbulence . To appear in *Astrophysics Journal.*

Publications

Aluie, H.. Theoretical analysis of the energy flux in compressible MHD turbulence. 2011. *Physics Review Letters.* **106**: 174502.

Aluie, H., S. Li, and H. Li. The conservative cascade of kinetic energy in compressible turbulence. To appear in *Astrophysics Journal Letters.*

Aluie, H., and G. L. Eyink. Scale locality of magneto-hydrodynamic turbulence. 2010. *Physical Review Letters.* **104** (8): 09101.

Collins, D. C., H. Xu, M. Norman, H. Li, and S. Li. Cosmological AMR MHD with ENZO. 2010. *Astrophysical Journal Supplement Series.* **151**: 308.

Li, S.. High-order central scheme on overlapping cells for magneto-hydrodynamic flows with and without constrained transport method. 2008. *Journal of Computational Physics.* **227**: 7368.

Li, S.. A fourth-order divergence-free method for MHD flows. 2010. *Journal of Computational Physics.* **229**: 7893.

Li, S.. Comparison of refinement criteria for structured adaptive mesh refinement. 2010. *Journal of Applied and Computational Mathematics.* **233**: 3139.

Li, S.. Higher order divergence-free methods for 3D MHD flows on overlapping grid. 2011. In *The ASP Conference Series on the 5th International Conference on Numerical Modeling of Space Plasma Flows.* (San Diego, 13-18 Jun. 2010). Vol. 444, p. 242. San Francisco: ASP Conference Series.

Li, S.. Code comparison on a MHD fast-wave propagation problem. To appear in *Numerical Modeling of Space Plasma Flows: ASTRONUM2011.* (Valencia, Spain, June 13-17).

Li, S.. High-order time integration with local Lax-Wendroff procedure for central scheme on overlapping grid. To appear in *Journal of Computational and Applied Mathematics.*

Li, S., and M. J. Buoni. High-order divergence-free method for MHD in three dimensions. 2009. *to be submitted.*

Svidzinski, V. A., H. Li, H. Rose, B. J. Albright, and K. J. Bowers. Particle in cell simulations of fast magneto-sonic wave turbulence in ion cyclotron frequency range. 2009. *Physics of Plasmas.* **16**: 122310.

Xu, H., H. Li, D. C. Collins, M. Norman, and S. Li. Evolution and distribution of magnetic fields from AGNs in galaxy clusters. I The effect of injection energy and redshift. 2010. *Astrophysical Journal.* **725**: 2152.

Xu, H., H. Li, D. Collins, S. Li, and M. Norman. Turbulence and dynamo in galaxy cluster media: implication on the origin of cluster magnetic fields. 2008. *Astrophysical Journal Letters.* : L14.

Xu, H., H. Li, D. Collins, S. Li, and M. Norman. Evolution and distribution of magnetic fields from active galactic nuclei in galaxy clusters. II. The effects of cluster size and dynamical state. 2011. *Astrophysical Journal.* **739**: 77.

Efficient Interdiction

Feng Pan
20090250ER

Abstract
Modern infrastructures, societies, and information are networked. A network is represented by nodes connected by edges which are interactions among nodes. A key question is what the vital components in a network are. This question is at the core of many applications in counterproliferation, cybersecurity, infrastructure protection. Network interdiction is a mathematical optimization approach to address this problem. Our objectives are to incorporate uncertainties into network interdiction models and develop efficient and scalable optimization models and algorithms for large scale networks.

In this project, we advanced network interdiction models for intercepting adversaries in transportation network by developing stochastic models and algorithms to capture the uncertainties associated with adversarial movements. In electric power grid, we developed new models to make a power grid resilient to large scale blackouts by placing sensors on critical locations and by configuring self-sustainable islands.

Background and Research Objectives
The goal of this research project was to develop efficient algorithms and models for the problem of network interdiction. In the interdiction mission an interdictor seeks to minimize the ability of an adversary to achieve high consequence activities. Conversely, the evader seeks to maximize the likelihood of success and impact of successful execution. Such a min-max problem can be posed mathematically in terms of graph analysis: the interdictor seeks to identify a set of vital arcs on an activity network whose removal minimizes the maximum reliable path from a source to a destination node, while the evader seeks to find and traverse the best unimpeded path. The activity graph may represent a transportation network, but more generally may correspond to resource allocation in an activity network. The interdictor and evader can be natural and physical processes too. For example, the propagation of instability in a power grid can be modeled as an evasion process, and sensors are placed to achieve the maximum probability of detecting such instability.

The interdiction problem has applications in many areas within threat reduction such as identifying key border control nodes, disrupting nuclear smuggling efforts or suicide bomber logistical support, and analysis of vulnerabilities in critical infrastructures. In fact, one may argue that threat reduction in toto, a major thrust within LANL, is essentially the problem of interdiction. In addition to our focus on efficient interdiction our project results may impact other research areas where combinatorial optimization problems appear such as resource allocation in operations research or coding theory in statistical physics.

Scientific Approach and Accomplishments
In the classical max-min interdiction model, an evader is assumed to travel on an optimal (shortest distance or least cost) path and an interdictor selects a fixed number of edges to thwart the evader's movement by increase the costs of these edges. The assumption of the evader's optimal behavior can be restrictive for certain scenarios. We developed the Markovian evader model to include the uncertainty of the evader's movements in a transportation network. In this model, instead of always following an optimal path, the evader moves on a guided random walk from the current location to the next in a probabilistic fashion according to the distance between the next location and the destination. Depending on the available information on the evader's movement, the guided random walk can converge to the deterministic case if the evader is known or can become complete a random walk if the least amount of information is available.

We explored two variants of the guided random walk interdiction model. In the nonreactive version, the evader is not aware of interdiction actions (or doesn't have enough time to respond to them) and does not change the probability of selecting a path in post-interdiction network. In the second version, a reactive evader adjusts the transition probability after an interdiction. Both problems were proven to be computationally hard (NP-complete). We developed efficient approximation algorithms based on the submodular property of the

nonreactive model. The performance of these algorithms is theoretically guaranteed to be within a constant factor of the optimal solution. The model with a reactive is much harder. In a large network, even evaluating the objective function becomes burdensome. We explored the relation between graph betweenness centrality and the evader's movements and developed polynomial time heuristic algorithms based on these centrality measures.

Quantifying the uncertainty of the evader's movements by itself has both practical and theoretical value. It is related to the stochastic shortest path problem receiving much attention recently. Unlike the deterministic version, there are variations of stochastic shortest path models that differ by the methods used to quantifying the uncertainties. The guided random walk considers localized uncertainty and is an adaptive way to traverse from an origin to a destination in which edge weights are random. Other research questions associated with stochastic shortest paths include determining the probability that a path, edge, or node is on a shortest path. This problem is known as #P-Complete (a counterpart of NP-Complete for counting problems). The existing methods for this problem are based on state space partition and Monte Carlo simulation. In our research on this problem, we discovered that there were correlations between the probability of a path, edge and node being optimal and certain graph centrality measures. We performed simulations on different types of networks and analyzed such correlations. Since the calculations of these graph centralities require only polynomial time, this discovery leads to scalable algorithms and enhanced Monte Carlo simulations for the stochastic shortest path problem.

We explored distributed heuristic algorithms for classical network interdiction models. To understand the performance of such algorithms, we started with a bipartite network interdiction model. This model is NP-Complete but with simpler graph structure that is important in the area of border security. We developed a message-passing algorithm based on a max-product algorithm for the bipartite network interdiction model. This message-algorithm has polynomial running time (efficient) and provides a solution comparable to the optimal solution. Due to the distributed naturel of such algorithms, it is challenging to develop theories related to the algorithm performance and convergence, an area of ongoing research.

Network interdiction is an effective method to identify vital components in a network and to partition a network. Modern power grids are interconnected. The connectivity may increase the reliability but also makes large scale cascading failure possible. One method to limit the scale of a cascading failure is to divide a power grid into self-sustainable islands. Traditionally, the power grid island problem was solved by heuristics. We developed a network optimization model which can form the optimal island configuration with load-generation balance within each island. Through this optimization model, we discovered optimal

islands are often not formed within geographical proximity, and forming a few islands in a power network is unlikely to result in load shedding. Phase angle is a measure for monitoring the stability of a power grid. A cut of a network is a set of lines connecting two non-overlapping regions of a network, and the phase angle across a cut can be an indicator of stability of the two regions. We developed a network optimization method to find an optimal cut where sensors can be placed and the instability is mostly likely to be detected. Our research in this area is a step toward to monitoring and "interdicting" large scale cascading failures

Our research resulted in about 20 publications related to combinatorial optimization, network modeling, and statistical analysis and was presented in numerous conferences. During this project we established collaborations with multiple universities. Three postdoctoral researchers working in this project are currently working at LANL, IBM, and Bell Labs. A graduate researcher recently received his Ph.D. degree. Based on our research in this project, we successfully developed two external research projects.

Impact on National Missions

The advances of network interdiction models made during this project will support multiple national security missions by providing basic science for threat reduction through modeling and decision support capabilities for interdiction related applications. Also the developed interdiction related models can be used for analyzing infrastructures vulnerability and for making them robust can be applied in counter-WMD missions. The progresses in network interdiction modes can be beneficial to relevant missions in DOE, DHS, and DoD.

Publications

Bradonjic, M., A. Hagberg, and F. Pan. Estimation of shortest paths in sensor network with random failures. To appear in *MilCom 2011*. (Baltimore, 7-10, 2011).

Cuellar, L., F. Pan, J. Roach, and K. J. Saeger. Distributional properties of stochastic shortest paths for smuggled nuclear material. 2011. In *International Multi-Conference on Complexity, Informatics and Cybernetics.* (Florida, 27-30 March. 2011). , p. . Orlando, Florida : iiis .

Dimitrov, N. B., D. P. Michalopoulos, D. P. Morton, M. V. Nehme, F. Pan, E. Popova, E. A. Schneider, and G. G. Thoreson. Network deployment of radiation detectors with physics-based detection probability calculations. 2009. *Annals of Operations Research.* : 1.

Fan, N., F. Pan, D. Izraelevitz, and P. M. Pardalos. Optimal Power Grid Islanding: A Mixed Integer Programming Approach. . *IEEE Transactions on Smart Grid.*

Fan, N., H. Xu, F. Pan, and P. M. Pardalos. Economic analysis of the N-k power grid contingency selection and evaluation by graph algorithms and interdiction Methods. To

appear in *Energy Systems.*

Fan, N., and F. Pan. Locating Phasor Measurements and Detecting Cutset Angles in Power Systems. 2011. In *IEEE Conference on Innovative Smart Grid Technologies*. (Anaheim, CA, January 17-19, 2011). , p. 1. : IEEE.

Gomez, V., H. J. Kappen, and M. Chertkov. Approximate inference on planar graphs using loop calculus and belief propagation. 2010. *Journal of Machine Learning Research.* **11**: 1273.

Gutfraind, A., A. Hagberg, D. Izraelevitz, and F. Pan. Interdiction of a Markovian Evader. 2011. In *Proceedings of the 12th INFORMS Computing Society Conference on OR, Computing, and Homeland Defense.* , p. 3. : .

Gutfraind, A., A. Hagberg, and F. Pan. Optimal interdiction of unreactive Markovian evaders. 2009. In *Lecture notes in computer science (CPAIOR 2009).* Edited by Hooker, J., and W. J. van Hoeve. , p. 102. Berlin / Heidelberg: Springer.

Hagberg, A.. Structure and dynamics of cybersecurity networks. Presented at *2009 Siam Annual Meeting.* (Denver, Co, 6 - 10 July 2009).

Kasiviswanathan, S. P., B. Zhao, B. Urgaonkar, and S. Vasudevan. Bandwidth provisioning in infrastructure-based wireless networks employing directional antennas. 2010. In *International Conference on Distributed Computing and Networking.* (India, 3-6 January, 2010). , p. 295. Berlin / Heidelberg: Springer.

Kasiviswanathan, S. P., and F. Pan. Matrix interdiction problem. 2010. In *Integration of AI and OR Techniques in Constraint Programming for Combinatorial Optimization Problems.* By Lodi, A., M. Milano, and P. Toth. , p. 219. Berlin / Heidelberg: Springer.

Pan, F., M. Bradonjic, and A. Hagberg. Interdicting shortest paths on random geometric graphs. Presented at *INFORMS Annual Meeting.* (San Diego, 11-14 October, 2009).

Pan, F., N. Santhi, and M. Chertkov. Message-passing algorithms for solving bipartite network interdiction. Presented at *2009 INFORMS Computing Society Conference.* (Chareston, SC, 11-13 Jan. 2009).

Pan, F., N. Santhi, and M. Chertkov. Network interdiction by securing edges. Invited presentation at *The 20th International Symposium of Mathematical Programming* . (Chicago, Illinois, 23 - 28 Aug. 2009).

Pan, F., and S. P. Kasiviswanathan. Placing directional antennas in infrastructure-based wireless networks. To appear in *MilCom 2011.* (Baltimore, 7-10, 2011).

Santhi, N., and F. Pan. A heuristic for restricted rank semi-definite programming with combinatorial applications. Presented at *The 20th International Symposium of Mathematical Programming.* (Chicago, Illinois, 23 - 28 Aug. 2009).

Santhi, N., and F. Pan. Detecting and mitigating abnormal events in large scale networks: Budget constrained placement. 2011. In *Hawaiian International Conference on System Science.* (Hawaii, 4-7 January, 2011). , p. 1. : IEEEE.

Sullivan, K. M., D. P. Morton, F. Pan, and J. C. Smith. Interdicting Stochastic Evasion Paths with Asymmetric Information on Bipartite Networks. *Naval Research Logistics.*

A Hybrid Transport-Diffusion Method for Radiation Hydrodynamics

Jeffery D. Densmore
20090420ER

Abstract

We have developed a hybrid transport-diffusion method for simulating thermal x-ray radiation transport as part of larger radiation-hydrodynamics calculations. This method combines Monte Carlo, which is inefficient when the photon mean-free path and mean-free time between collisions is small but is otherwise in accurate, with the diffusion approximation, which is valid in this same regime and computationally inexpensive. Specifically, our hybrid method employs the diffusion approximation where appropriate and resorts to Monte Carlo in the remainder of phase space. In this manner, our hybrid method is as accurate yet more efficient than using Monte Carlo only.

Radiation-hydrodynamics calculations are an important aspect of many of the DOE/NNSA missions involving massive scientific simulations, including astrophysics, inertial confinement fusion, and high energy density physics. We have implemented our work directly into production-level software, and thus our hybrid transport-diffusion method is available immediately for these types of calculations.

Background and Research Objectives

Radiation-hydrodynamics calculations model the nonlinear coupling between thermal x-ray transport and hydrodynamic motion. In addition to this multiphysics feature, these types of calculations are inherently multiscale; in some parts of phase space the photon mean-free path and mean-free time between collisions are much smaller than the length and time scales upon which the solution varies, while in other parts the mean-free path and mean-free time are of the same order as the characteristic length and time scales of the solution. We note that simulating radiation transport typically comprises the bulk of the computational effort in radiation-hydrodynamics calculations.

One technique for modeling radiation transport in radiation-hydrodynamics calculations is Monte Carlo [1]. This method has the desirable property that it is accurate for a wide range of values for the mean-free path and mean-free time. However, when the mean-free path and mean-free time are small, particles experience many collisions during their lifetimes. Thus, particle histories consist of an excessive number of steps and are time-consuming to process, which leads to a Monte Carlo simulation that is computationally inefficient.

An alternative to Monte Carlo is the diffusion approximation [2]. The resulting partial differential equation can be efficiently solved using, for example, standard deterministic techniques. Unfortunately, the diffusion approximation is only valid when the mean-free path and mean-free time are small. Outside of this regime, the diffusion approximation yields inaccurate solutions.

The prohibitive expense of Monte Carlo when the mean-free path and mean-free time are small in contrast with the accuracy of the diffusion approximation in this same situation suggests forming a hybrid method from these two techniques. Ideally, this hybrid transport-diffusion method would make use of the diffusion approximation where appropriate and resort to Monte Carlo in the remainder of phase space. Because Monte Carlo is not employed where the mean-free path and mean-free time are small, this hybrid method should be more efficient as compared to Monte Carlo only. In addition, because the diffusion approximation is only used where the mean-free path and mean-free time are small, this hybrid method should produce accurate solutions.

A hybrid transport-diffusion method of the type described above that is commonly used in radiation-hydrodynamics calculations is the Random Walk (RW) technique [3]. In RW, particles take steps over spheres centered about their current positions. The radius of the sphere is chosen such that the sphere lies entirely inside the particle's current spatial cell, and the step is governed by an analytic solution to the diffusion equation within the sphere. Each RW step from a sphere center to a sphere surface replaces several smaller Monte Carlo steps, which improves the efficiency of the simulation. To ensure the accuracy of the diffusion solution, the radius of the sphere is also required to be larger than a specified minimum as measured in mean-free paths. If

this minimum radius is not satisfied, the particle transports instead according to Monte Carlo. This property of RW causes Monte Carlo to be used to some extent even when the mean-free path is small, for example near cell edges. Thus, the efficiency gain of RW over Monte Carlo is not as great as one would hope.

A recently developed method for increasing the efficiency of Monte Carlo when the mean-free path and mean-free time are small that may have certain advantages over RW is Discrete Diffusion Monte Carlo (DDMC) [4,5]. In DDMC, particles take discrete steps between spatial cells according to a discretized diffusion equation. Each discrete step replaces many smaller Monte Carlo steps, which, as with RW, improves the efficiency of the simulation. However, a particle can travel to a new cell with each DDMC step, while a RW step is limited to within a cell. Furthermore, a particle transports according to DDMC exclusively when the mean-free path and mean-free time are small, whereas Monte Carlo is used somewhat with RW in this regime. Thus, DDMC should provide greater efficiency gains over Monte Carlo than RW. In practice, DDMC is combined with Monte Carlo when the mean-free path and mean-free time are not small to form a hybrid transport-diffusion method.

For this project, we have extended DDMC and the corresponding hybrid transport-diffusion method such that it can be applied to realistic radiation-hydrodynamics calculations. First, we have developed a generalization of DDMC that takes photon frequency dependence into account. In addition, we have adapted DDMC to the mesh types employed in the Jayenne Project [6], which provides production-level software for performing radiation-transport simulations as part of larger radiation-hydrodynamics calculations. Finally, we have implemented all of this research into Jayenne Project software.

Scientific Approach and Accomplishments

Previously developed DDMC methods have only considered grey (i.e., frequency-integrated) radiation transport. However, frequency dependence is an important aspect of thermal x-ray transport as material properties are typically strongly nonlinear functions of photon frequency. To account for frequency dependence, we have based our new DDMC technique on a frequency-integrated diffusion equation for frequencies below a certain threshold, while above this threshold we employ Monte Carlo [7,8]. This division is justified by the fact that mean-free path and mean-free time are typically increasing functions of frequency and thus the diffusion approximation is appropriate for sufficiently low frequencies. However, this approach does lead to the situation where, in a single spatial cell, both DDMC and Monte Carlo are employed. Thus, the diffusion equation is discretized to determine not only how particles travel between spatial cells, as in the grey case, but also when particles are above the frequency threshold and begin transporting according to Monte Carlo.

In order to implement our research into Jayenne Project software, we have developed specialized DDMC methods for the mesh types employed by this project. The first mesh type we considered was the Sphyramid mesh, which models one-dimensional spherical geometries with a three-dimensional Cartesian pyramid such that all cell faces are planar. The Cartesian coordinate system and planar surfaces of the Sphyramid mesh result in a much simpler Monte Carlo simulation than one performed in the original spherical coordinate system. Our development consisted of determining an appropriate discretization for this mesh type and extracting the probabilities of various events from the resulting discretized diffusion equation [9].

The other mesh type we examined was the RZWedge mesh. This mesh type models two-dimensional cylindrical geometries using a three-dimension Cartesian wedge in the same manner and for the same reason that the Sphyramid mesh is employed to model one-dimensional spherical geometries. The development of the corresponding DDMC method in this case is similar to that for the Sphyramid mesh [10], except that the RZWedge mesh also features local refinement such that a spatial cell may have more than one neighboring cell across each face. Local refinement is commonly used in Eulerian hydrodynamics calculations, for which, as part of larger radiation-hydrodynamics simulations, our hybrid transport-diffusion method is intended.

We have implemented the work described above into Jayenne Project software and used it to simulate a variety of radiation-transport problems. In nearly every case, our new hybrid transport-diffusion method yields order-of-magnitude efficiency gains over both using Monte Carlo only and RW. Furthermore, the solutions produced by our new hybrid method differ very little from those generated by using Monte Carlo only. We note that in many of these problems, RW, the hybrid technique employed in most radiation-transport software, yields little or no efficiency gain.

Impact on National Missions

This project supports the DOE/NNSA missions reliant upon massive scientific simulations where radiation-hydrodynamics are important, which include astrophysics, inertial confinement fusion, and high energy density physics. Because we have implemented our work directly into production-level software, our hybrid transport-diffusion method is immediately available for these types of calculations. Currently, our hybrid method is being used for simulations in support of the ASC program.

References

1. Fleck, J. A., and J. D. Cummings. An implicit Monte Carlo scheme for calculating time and frequency dependent nonlinear radiation transport. 1971. *Journal of Computational Physics.* **8**: 313.

2. Morel, J. E., E. W. Larsen, and M. K. Matzen. A synthetic acceleration scheme for radiative diffusion calculations. 1985. *Journal of Quantitative Spectroscopy and Radiative Transfer.* **34**: 243.

3. Fleck, J. A., and E. H. Canfield. A random walk procedure for improving the efficiency of the Implicit Monte Carlo method for nonlinear radiation transport. 1984. *Journal of Computational Physics.* **54**: 508.

4. Gentile, N. A.. Implicit Monte Carlo Diffusion - an acceleration method for Monte Carlo time dependent radiative transfer simulations. 2001. *Journal of Computational Physics.* **172**: 54.

5. Densmore, J. D., T. J. Urbatsch, T. M. Evans, and M. W. Buksas. A hybrid transport-diffusion method for Monte Carlo radiative-transfer simulations. 2007. *Journal of Computational Physics.* **222**: 485.

6. Urbatsch, T. J., and T. M. Evans. Milagro version 2 - an Implicit Monte Carlo code for thermal radiative transfer: capabilities development, and usage. 2006. *LA-14195-MS, Los Alamos National Laboratory.*

7. Densmore, J. D., and T. J. Urbatsch. Frequency-dependent Discrete Diffusion Monte Carlo. 2010. *CCS-2:10-20, Los Alamos National Laboratory.*

8. Densmore, J. D., K. G. Thompson, and T. J. Urbatsch. Discrete Diffusion Monte Carlo for frequency-dependent radiative transfer. n/a. In *International Conference on Mathematics and Computational Methods Applied to Nuclear Science and Engineering.* (Rio de Janeiro, Brazil, 8-12 May 2011). , p. n/a. n/a: n/a.

9. Densmore, J. D.. Discrete Diffusion Monte Carlo for the Sphyramid mesh. 2009. *CCS-2:09-04, Los Alamos National Laboratory.*

10. Densmore, J. D., and T. J. Urbatsch. Discrete Diffusion Monte Carlo for the RZWedge mesh. 2010. *CCS-2:10-01.*

Densmore, J. D., K. G. Thompson, and T. J. Urbatsch. Discrete Diffusion Monte Carlo for frequency-dependent radiative transfer. n/a. In *International Conference on Mathematics and Computational Methods Applied to Nuclear Science and Engineering.* (Rio de Janeiro, Brazil, 8-12 May 2011). , p. n/a. n/a: n/a.

Densmore, J. D., and T. J. Urbatsch. Discrete Diffusion Monte Carlo for the RZWedge mesh. 2010. *CCS-2:10-01, Los Alamos National Laboratory.*

Densmore, J. D., and T. J. Urbatsch. Frequency-dependent Discrete Diffusion Monte Carlo. 2010. *CCS-2:10-20, Los Alamos National Laboratory.*

Publications

Densmore, J. D.. Discrete Diffusion Monte Carlo for the Sphyramid mesh. 2009. *CCS-2:09-04, Los Alamos National Laboratory.*

Robust 3D Moving Mesh Adaptation Based on Monge-Kantorovich Optimization

John M. Finn
20090424ER

Abstract

This LDRD-ER has supported the development of methods of grid adaptation based on Monge-Kantorovich optimization (MKO). These methods are based on minimizing a norm of the distance from a previous grid (for example the grid at a previous time step) while equidistributing a monitor function based on an error estimate. We have developed the general method, using Jacobian-free Newton-Krylov (JFNK) methods with physics-based preconditioning. We have shown that the method is related to a different method, involving minimizing the mean distortion of the grid, its tendency to fold. We have developed alternate methods of solving the equations and investigated using more general norms to measure the motion relative to an earlier grid, and found that the original formulation is best, based on accuracy and computational efficiency. We have extended the theory to curved boundaries in 2D and to 3D. We have adapted a grid to the evolution of a passive scalar, comparing a sequential method (with grid adapted from the grid at the previous time step) and a direct method (adapted from the initial grid), and found the direct method to be superior. We have used this method to adapt a grid for a nonlinear magnetohydrodynamics code and shown that this can be done accurately and efficiently. We have investigated further the equidistribution principle supporting all these methods, and found that it is valid, but achieving slightly different objectives, for two classes of problems. We have shown how to develop a non-uniform grid particle-in-cell code for use in further adaptation studies.

Background and Research Objectives

The focus of this effort has been the development of grid adaptation methods based on Monge-Kantorovich optimization (MKO). This work stems from the need to pack the grid in a numerical computation of a partial differential equation where the error is highest, and allow the grid to be coarser in areas where a fine grid is not needed. The strict formulation of this concept leads to *equidistribution*, in which the cell volumes are inversely proportional to the monitor function, which is in turn computed from an error estimate. There has been a considerable amount of work in this general area, but the methods of adaptation to an error estimator have been ad-hoc and subject to problems. For example, in adaptive mesh refinement (AMR), the basic grid is rectangular, but is refined by adding more rectangular cells where needed, based on a monitor function specifying the numerical errors on the grid. Problems that arise include: (i) the grid is not smooth, but cells are adapted (cell dimension is halved) or not; (ii) cell orientation is not adapted, i.e. the cell boundaries are aligned as in the original grid.

Grid adaptation based on Monge-Kantorovich optimization was developed by the PI, the co-PI, and collaborators in the first paper published based on support by this LDRD-ER[1] . The work done to date has concentrated on structured grids, specifically grids on physical domains that can be obtained by mapping from a uniform grid on the unit square in the appropriate dimensions (interval, square, or cube.) In this paper, we therefore sought to create a map between a previous grid (for example the grid used on an earlier time step) and the present grid. This map is required to have two properties. First, it must minimize the mesh motion, the L_2 norm of the distance between the vertices of the mesh and the corresponding vertices of the earlier mesh. Second, the ratio of the grid volumes for the two grids are specified. That is, the Jacobian of the map between the grids is specified, thereby leading to equidistribution of the monitor function, related to the error estimate.

Scientific Approach and Accomplishments

In the early part of the period of this ER, we formulated the basic ideas of MKO, applied to grid adaptation minimizing the L_2 norm for distance between grid vertices in two dimensions (2D). This minimization leads to the Monge-Ampere (MA) equation, a well-known nonlinear partial differential equation. We developed numerical methods for solving this very nonlinear and very stiff system, based on Jacobian-free Newton-Krylov (JFNK) techniques, and showed that, because of the elliptic nature of the MA equation, the resulting grids are smooth, unlike the grids generated by AMR. A key to getting

these methods to work efficiently is the use of a good pre-conditioner. We used physics-based preconditioning, and obtained results with near-ideal scaling with the problem size. Other investigators had developed methods to solve the MA equation, but these methods proved to be very expensive in terms of computer time, and often quite inaccurate. In contrast, we showed that our JFNK methods are very efficient and accurate. This work was, however, restricted to a square physical domain.

We also formulated an optimization scheme based on minimizing the grid distortion, defined as the trace of the covariant metric tensor. This quantity measures the tendency of grid cells to distort. Very large distortion indicates the tendency of the grid to *fold*. We showed that, for certain boundary conditions on the grid mapping, the minimum distortion method and the L_2 method gave identical results. However, we found that the computational methods for solving the minimum distortion method were much less efficient than the L_2 method. The work on minimizing the L_2 norm (as well as the minimum distortion method) was reported in Ref. 1.

The main tasks to be accomplished, after the initial progress reported in Ref. 1, were: (i) determining whether norms other than L_2 might have more favorable properties; (ii) determining whether there were other, more efficient, numerical methods; (iii) formulating a way to solve the equations on more general physical domains, specifically domains in which there are non-convex areas on the boundary; (iv) extending the MKO methods to three dimensions (3D); (v) investigating and possibly extending the notion of equidistribution; and (vi) implementing MKO grid generation in a nonlinear code integrating nonlinear plasma physics phenomena, for example magnetohydrodynamic instability and nonlinear saturation, and showing this can be done accurately and efficiently.

In Ref. 2 we published work related to more general physical domains in 2D and to the unit cube in 3D. A new method was invented for specifying the boundary conditions for the grid with curved boundary, and it was shown to work as well as the methods of Ref. 1 for several challenging examples. The 3D problem in a cube was formulated and solved by JFNK methods. It was shown that the 3D Monge Ampere equation is more challenging because of cubic (rather than quadratic) nonlinearities. Nevertheless, for the example shown, it was shown to converge rapidly to an accurate solution of the grid equations. This work was presented as an invited talk at the 17th International Meshing Roundtable in Oct. 2009.

In Ref. 3 we studied the generalization from MKO based on the L_2 norm to MKO based on the L_p norm, for *p>1,* and to the smoothed L_1 norm, in order to determine whether MKO based on these norms might have better properties than those based on the L_2 norm. We compared the results for *p>1* to those for *p=2* (the L_2 norm) for several

examples, and in particular measured the mean distortion (defined above) for all the methods. We found that the optimal results were obtained for *p=2*, with somewhat worse results in the range *1.5<p<3*, and much worse results for *p* near unity. Also, we found that the numerical methods were less efficient for *p* other than *2* and very inefficient for *p* close to unity. Similarly, we found that the smoothed L_1 norm performed badly as e, the scale of the smoothing, was decreased toward zero, but gave results comparable to the L_2 results for larger e (as expected). Our conclusion, written up in Ref. 3, was that, among these norms, L_2 was the best from every point of view.

In Ref. 4 we investigated the 'fluid dynamic' approach to MKO, previously formulated for L_2. We generalized this formulation to arbitrary *p* and to the smoother L_1 norm. In this approach, the map from one grid to the next is considered to be the result of a continuous deformation in terms of a flow, with the density (the monitor function) propagated along the flow. We formulated the fluid dynamic approach for *p>1* and for the smoothed L_1 norm, and developed a numerical method based on this formulation. We found that this method worked best for *p=2* (and for large smoothing in the smoothed L_1 norm), both in the sense of computational efficiency and minimal distortion of the adapted grid. Our conclusion, documented in Ref. 4, was that this method was optimal in every way for *p=2*, and that the method for *p=2* was quite efficient, but less efficient than the method of Refs. 1 and 2.

In Ref. 5 we showed work indicating that the L_2 MKO methods could be coupled to the differential equations for a fluid quantity advected passively in time with large flow shear. We investigated two methods of adapting the grid. The first was the *sequential method*, in which the grid at the present time step was evolved from the grid at the previous time step. The second method was the *direct method*, in which the grid was evolved from the initial grid. It was considered that the sequential method could move to some degree with the fluid and therefore lead to the advantages – or the disadvantages – of a Lagrangian grid. For several examples, we showed that the sequential method has only the disadvantages of a Lagrangian grid, namely the tendency to develop severe distortion and eventually fold after some time. For every case studied, the direct method performed accurately and efficiently. We also showed that the grid behaved well over an arbitrarily large interval of time in 3D, with a passive scalar having shear in the aximuthal angle (q) and in the axial direction (*z*), a case developing much more challenging structure than the 3D example in Ref. 2.

The results of Ref. 5 showed much, but the physics model was the relatively simple case of advection of a passive scalar. We have begun a study of MKO grid adaptation to nonlinear magnetohydrodynamics (MHD). Specifically, we have developed a nonlinear MHD code with implicit time stepping using JFNK methods, coupled to a grid adaptation

scheme based on a monitor function related to the numerical error. This work, which was done in collaboration with Luis Chacon of ORNL, is essentially complete and a manuscript (Chacon, Delzanno, and Finn) is in preparation.

In the course of this work, issues related to the equidistribution principle have arisen. We have found some issues relating the form of the numerical errors in a scheme, for example of second order accuracy, to the relevant equidistribution principle derived. For the first class of difference algorithms, the second order error involves a positive definite form involving the grid spacings. In this case, the error can be minimized, and put into equidistribution form. For another class of algorithms, the second order error involves an indefinite error, and it is possible to set the second order error equal to zero, effectively obtaining a third order scheme, which can also be cast in the form of an equidistribution principle. (For higher order schemes, these two possibilities arise in the same manner.) This work is being completed and a manuscript is in preparation.

Another offshoot of this work is in the development of an adaptive grid particle-in-cell (PIC) code. PIC codes use particle methods to solve the kinetic equations of plasma physics and other areas. In the case of PIC, the formulation and development of a PIC code with nonuniform (and possibly non-orthogonal) grid contains many difficulties. The development of a non-uniform grid PIC code was the subject of the PhD dissertation of Chris Fichtl, a LANL GRA from the Department of Chemical and Nuclear Engineering at the University of New Mexico, and was partly supported by this LDRD-ER. The main challenges of this work involved integrating the particle equations of motion and solving for the electromagnetic fields on the logical domain for an arbitrary adapted grid. Chris graduated with his PhD in July 2010, and now holds a postdoctoral position in CCS-2 at LANL. A manuscript on this work is in preparation.

Impact on National Missions

The numerical simulation of nonlinear partial differential equations are of importance in many areas of National interest. These areas include the development of hydrodynamics codes for defense purposes and inertial confinement fusion (ICF). They also include magnetohydrodynamics codes for use in magnetic fusion and space plasma studies. In all of these areas, the efficiency afforded by an adaptive grid is essential, and the properties of our grid adaptation scheme, namely efficiency, accuracy and smoothness (stable to any tendency for grid folding) are essential. We have started working on finding support from NNSA or the DOE Office of Science to continue this promising work.

References

1. Chacon, L., G. L. Delzanno, and J. M. Finn. Robust, multidimensional mesh-motion based on Monge-Kantorovich equidistribution. 2011. *JOURNAL OF COMPUTATIONAL PHYSICS.* **230** (1): 87.

2. Delzanno, G. L., and J. Finn. The fluid dynamic approach to equidistribution methods for grid adaptation. 2011. *COMPUTER PHYSICS COMMUNICATIONS.* **182** (2): 330.

3. Delzanno, G. L., and J. M. Finn. GENERALIZED MONGE-KANTOROVICH OPTIMIZATION FOR GRID GENERATION AND ADAPTATION IN L-p. 2010. *SIAM JOURNAL ON SCIENTIFIC COMPUTING.* **32** (6): 3524.

4. Finn, J., C. L. Delzanno, and L. Chacon. Grid Generation and Adaptation by Monge-Kantorovich Optimization in Two and Three Dimensions. 2008. In *17th International Meshing Roundtable ; 20081012 - 20081015 ; Pittsburgh, PA.* , p. 551.

5. Delzanno, G. L., L. Chacon, J. M. Finn, Y. Chung, and G. Lapenta. An optimal robust equidistribution method for two-dimensional grid adaptation based on Monge-Kantorovich optimization. 2008. *JOURNAL OF COMPUTATIONAL PHYSICS.* **227** (23): 9841

Publications

Chacon, L., G. L. Delzanno, and J. M. Finn. Robust, multidimensional mesh-motion based on Monge-Kantorovich equidistribution. 2011. *JOURNAL OF COMPUTATIONAL PHYSICS.* **230** (1): 87.

Delzanno, G. L., L. Chacon, J. M. Finn, Y. Chung, and G. Lapenta. An optimal robust equidistribution method for two-dimensional grid generation based on Monge-Kantorovich optimization. 2009. *Journal of Computational Physics.* **227** (23): 9841.

Delzanno, G. L., and J. Finn. The fluid dynamic approach to equidistribution methods for grid adaptation. 2011. *COMPUTER PHYSICS COMMUNICATIONS.* **182** (2): 330.

Delzanno, G. L., and J. M. Finn. GENERALIZED MONGE-KANTOROVICH OPTIMIZATION FOR GRID GENERATION AND ADAPTATION IN L-p. 2010. *SIAM JOURNAL ON SCIENTIFIC COMPUTING.* **32** (6): 3524.

Finn, J. M., G. L. Delzanno, and L. Chacon. Grid generation and adaptation by Monge-Kantorovich optimization in two and three dimensions. 2009. In *Proceedings of the 17th international meshing roundtable.* Edited by Garimella, R. V. , p. 551. Berlin: Springer Verlag.

Compressive Sensing

Charles R. Farrar
20110462ER

Abstract

LANL's target detection, threat reduction, environmental monitoring, and situational awareness missions are requiring us to field sensors with finer temporal, spectral, and spatial resolution deployed over broader domains. This situation results in rapidly increasing volumes of data that must be stored and analyzed. Conventional data compression software cannot keep pace with these ever increasing demands on sensor system data storage capacity, processing and power. This situation is particularly acute for embedded "system on a chip" platforms that must operate with constrained memory, processing and power.

Compressive sensing aims to reduce this data volume as it is being collected. This approach does provide value, in terms of data compression, but the real value is that we can potentially get more "information" from a particular sensor whereas the current paradigm is to only obtain data from a sensor. With a well-designed compressive sensor, it is possible to collect fewer bits, and then (with well-designed algorithms) to reconstruct an accurate representation of the system being measured. It is also possible to embed some data interrogation procedures at the sensor node and implement these procedures on the compressed data. The work performed under this one-year LDRD feasibility study had the goal of developing and demonstrating such a capability with application to online mechanical damage detection in a structural system. A digital version of a compressed sensor was implemented on-board a microcontroller in an embedded sensor nodes. The sensor node was tested in a damage detection application using acceleration measurements. Currently the prototype compressed sensor is capable of collecting compressed coefficients from measurements and sending them to an off-board processor for reconstruction using l_1-norm minimization. A compressed version of the matched filter known as the *smashed filter*, has also been implemented on-board the sensor node, and its suitability for detecting structural damage will be summarized.

Background and Research Objectives

Compressed sensing has been a prolific research topic in computer science, signal processing and image processing over the last few years. Excellent tutorials covering the basics of compressed sensing can be found in [1], [2], and [3]. To summarize, a signal of interest, x, consisting of N discrete samples, can be represented by an orthonormal basis Ψ and "s," which is the representation of the signal in the Ψ domain. In compressed sensing we are interested in the case where x is compressible in some domain. That is, the number of significant non-zero elements of s is equal to K and $K << N$. K is known as the "sparsity" of the signal. A measurement matrix "Φ" is then introduced to produce compressed sensing representation of the original signal in terms of the coefficients y where Φ has $M<<N$ rows. An underdetermined system of linear equations must be solved to find the compressed representation of the signal (i.e. the y coefficients). One of the major breakthroughs of the compressed sensing community was the finding that by assuming $K<<N$, it is possible to recover x from y assuming the matrix Φ possesses the restricted isometry property and x is sparse [4]. The direct formulation of this problem is finding the vector s with minimal l_0 norm. Unfortunately l_0 norm minimization is numerically unstable. It has been shown though that the associated l_1 norm regularization problem [2][3] can be solved to recover the original signal from the compressed coefficients y.

In this work, our research objective has been to use the l_1 norm regularization approach described above to demonstrate that a signal x can be recovered from the compressed coefficients y. Furthermore, we want to show that anomaly detection can be performed in the compressed domain and can be implemented in an embedded sensor node where there are significant memory and computational constraints. In this case the anomaly detection consists of identifying changes in acceleration signals measured on a test structure that result from the introduction of simulated damage representative of a crack opening and closing or a loose connection rattling. A compression version of a matched filter referred to as

a *smashed filter* was implemented to perform the anomaly detection.

Scientific Approach and Accomplishments

In order to evaluate the applicability of compressed sensing for anomaly detection in an embedded sensing environment, a digital prototype of a compressed sensor node was built. The prototype consisted of an ATmega1281 microcontroller, an accelerometer, and the associated amplification and circuitry required to interface the analog-to-digital converter (ADC) of the microcontroller to the accelerometer. The accelerometer was then attached to the second floor of a representative 3-story structure as shown in Figure 1.
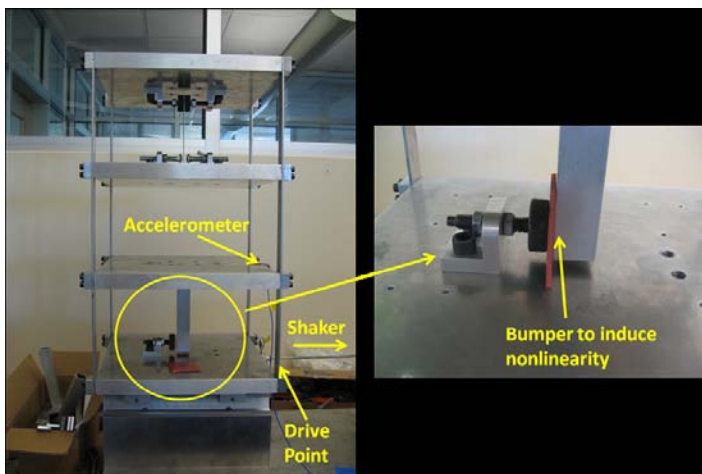
Figure 1. Three-story structure used to evaluate the compressed sensor node

The accelerometer was oriented to measure the transverse vibration of the 3-story structure. An electro-magnetic shaker attached to the base of the structure provided a source of excitation. The excitation to the structure was a sine wave with a frequency of 30.7 Hz, which corresponds to the first resonant frequency of this structure. In order to introduce damage into the structure, a rubber bumper was used to induce a nonlinear response when the relative transverse displacement between the second floor and the base would exceed a threshold value. The signal from the accelerometer was sampled by the ATmega1281 with a 10-bit ADC at a sampling rate of about 3000 Hz. In this work, 256-sample time series were collected by the Atmega1281 and subsequently converted into compressed measurements by the microcontroller. The elements of the measurement matrix Φ were chosen to be either ±1. The generation of the measurement matrix Φ was accomplished using a linear feedback shift register similar to that mentioned in [4]. The ±1 measurement matrix was selected in order to allow the generation of the compressed coefficients on-board the microcontroller using

integer arithmetic. The ATmega1281 was placed onboard an STK500 evaluation board. A base station laptop was then connected to the STK500 in order to facilitate the debugging of the compressed sensing algorithms, and to expedite the collection of compressed coefficients from the embedded sensor node. For the purpose of this experiment, the ATmega1281 would transmit both the compressed measurements as well as the original signal when it was queried for a measurement. By collecting both pieces of data the reconstructed signal derived from the compressed coefficients could be compared to the original signal in order to evaluate the performance of compressed sensing techniques.

The test structure was placed in a configuration so that it could assume either a simulated damaged state or an undamaged state. In the undamaged state, the output from the accelerometer should assume a sine wave with a frequency of 30.7 Hz that corresponds to the shaker excitation frequency. In the damaged state, the rubber bumper interacts with the structure and the frequency content of the resulting output from the structure is more widely distributed across the spectrum. Data were collected from the structure in both the damaged and undamaged states, and was subjected to the compressed sensing measurement process. The resulting compressed measurements were then cast into the l_1 norm regularization framework to attempt recovery of the original signal.

The l_1 norm regularization was implemented using the CVXMOD software [5]. 256 sample time series data were collected from the structure using the ATmega1281 and was transmitted to the base station laptop. The compressed coefficients were calculated using a standard Gaussian Φ matrix. The resulting compressed coefficients were subjected to the l_1 norm regularization. The l_1 norm regularization problem was solved using 32, 64, 100 and 120 compressed coefficients for both the damaged and undamaged cases. The basis in which the signal is sparse, Ψ, is taken to be the Fourier basis. These correspond to compression factors of 13%, 25%, 39%, and 47% respectively. The resulting reconstructions are shown in Figure 2 and Figure 3.
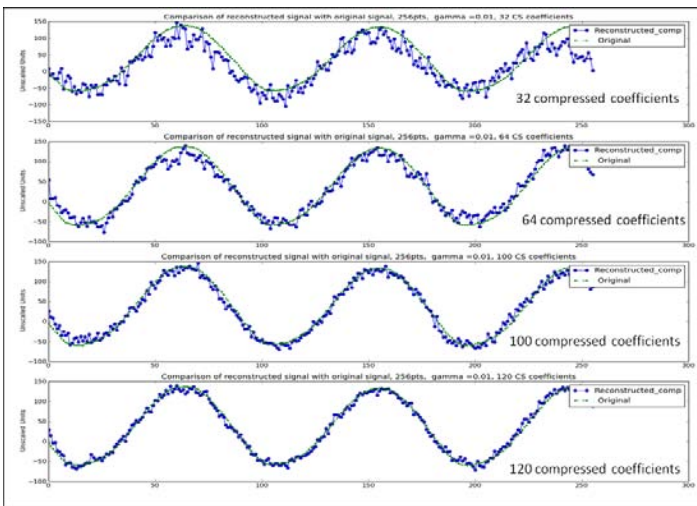
Figure 2. Undamaged case compressed sensing reconstruction of the original signal.
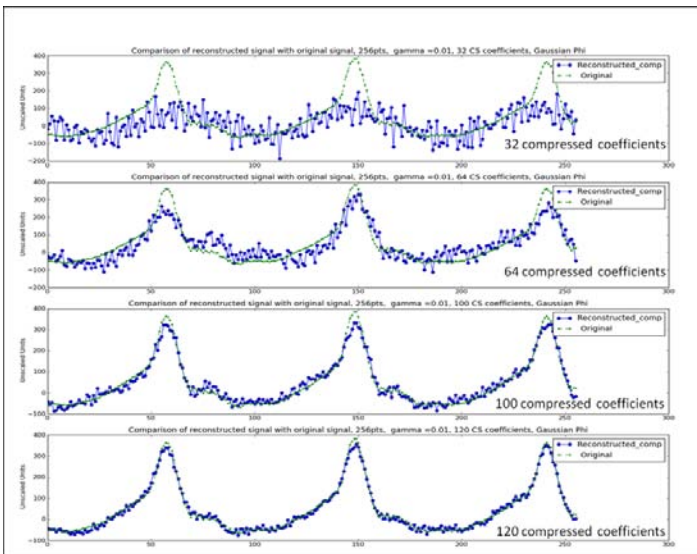
Figure 3. Damaged case compressed sensing reconstruction of the original signal.

It is interesting to note, that in both the undamaged and damaged cases, the signal reconstructions seem to basically become less distorted as additional coefficients are included in the l_1 norm regularization process. This phenomenon illustrates the democratic property possessed by compressed coefficients. Compressed coefficients are democratic in the sense that no particular compressed coefficient carries any more information than any other. If any compressed coefficient were to be lost, it could simply be replaced by another compressed coefficient. Alternatively, if the coefficient could not be replaced, the resulting reconstructed signal would be slightly distorted, but the main features of the signal would still be intact. The democratic nature of compressed coefficients can be exploited to produce measurement systems that degrade gracefully with minor failures and losses in communication.

For general anomaly detection and mechanical damage detection in particular, the main concern is the detection of the spurious phenomena and not necessarily the accurate reconstruction of the sensor signal. With this in mind it was decided to investigate techniques anomaly detection (presence of damage) while using a relatively small number of compressed coefficients. An extension of the matched filter to the compressed domain known as the "smashed filter" was investigated [6]. To summarize, the smashed filter is implemented in basically the same manner as the conventional matched filter. The main difference is that the smashed filters are generated by taking phase shifted versions of the signals of interest, and then subjecting them to the measurement process Φ.

For this work, training signals from both the damaged and undamaged states were collected. The damage case training signal was collected in such a manner that it featured a small mismatch with the operational damage case signals used to evaluate the performance of the smashed filter. By allowing a small mismatch between the training damage case and the operational damage case we can get an initial sense of the robustness of the smashed filter to small perturbations. This mismatch was achieved by perturbing the location of the rubber bumper. Once the smashed filters were generated, 100 experiments resulting in 128 compressed coefficients per experiment were collected from the structure in both the damaged and undamaged cases. Subsets of the 128 compressed coefficients were then used to evaluate the performance of the smashed filter for various numbers of compressed coefficients. To implement the smashed filter, the inner product of the compressed coefficients and the smashed filter vectors was calculated for each experiment. The smashed filter with the largest inner product was then selected and the experiment was classified as damaged or undamaged based on whether or not the corresponding smashed filter came from the damaged or undamaged case. Figures 4 and Figure 5 illustrate the results of applying the smashed filter to the experiments for the undamaged and damaged cases respectively. From these data we see that once at least 32 compressed coefficients are used to calculate smashed filters, the probability of misclassifications become very low. It is noteworthy that the number of compressed coefficients needed to achieve accurate classification with the smashed filter is only 1/8 the number of data points in the original time series measurement. Based on these results, the smashed filter has the potential to significantly reduce the number of measurements needed to perform the anomaly detection, or in this case classify whether or not a structure is damaged.
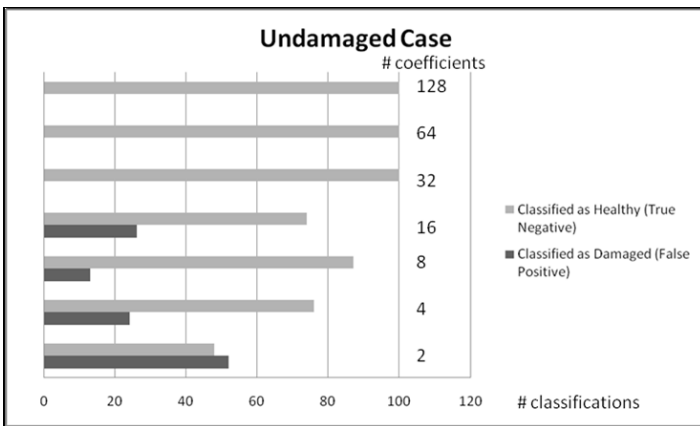
Figure 4. Smashed filter classification results for the undamaged case.
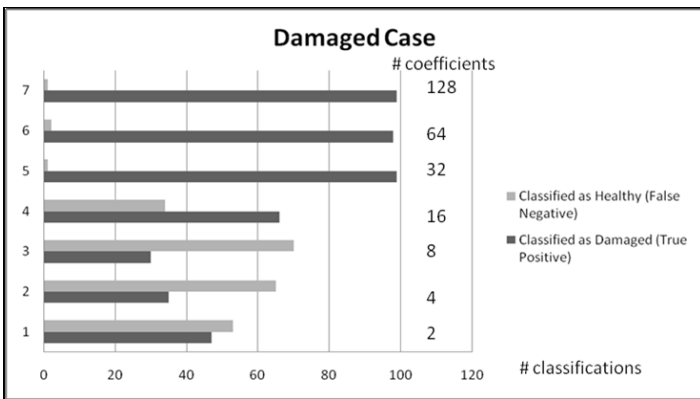
Figure 5. Smashed filter classification results for the damaged case.

Impact on National Missions

Because many of LANL's detection, tracking and classification problems are requiring us to field larger sensor networks with finer temporal, spectral, and spatial resolution, the potential to become overwhelmed with data, much of which is often not of interest, is a concern that must be dealt with. Applications include nonproliferation and global security, resilience of high-performance computing, global climate treaty verification, cyber security, damage detection in energy infrastructure, space situational awareness, weapons surveillance, accelerator beam diagnostics and nuclear forensics.

Conventional data compression software cannot keep pace with these ever increasing demands on sensor system data storage capacity, processing and power. This situation is particularly acute for embedded "system on a chip" platforms that must operate with constrained memory, processing and power. Furthermore, the analysis of these data is often decoupled from the compression process. In this study we were able to demonstrate the ability to compress measured time series data from an accelerometer and to perform anomaly detection in the compressed domain using a smashed filter, all on an embedded sensor node. Such coupling of data compression with data interrogation is key to increasing our ability to extract information from sensors in a more efficient manner and has the potential to change the way sensing and data interrogation are done for all of the application areas mentioned above. In the next year the compressed sensing and anomaly detection work reported herein will be applied to fatigue damage detection in wind turbine blades where extreme amounts of data are collected (millions of fatigue cycles), most of which is not if interest. Here the goal will be to find the rare event that indicated the onset of delamination in the blade using compressed sensing again directly coupled with anomaly detection algorithms.

References

1. Candes, E.. Compressive sampling. 2006. In *International Congress of Mathematics.* (Madrid, 22-30 Aug. 2006). Vol. III, p. 1433. Zurich: European Mathematical Society Publishing House .

2. Baraniuk, R.. Compressive sensing. 2007. *IEEE Signal Processing Magazine.* **24** (4): 118.

3. Candes, E., and M. Wakin. An introduction to compressive sampling. 2008. *IEEE Signal Processing Magazine.* **25** (2): 14.

4. Laska, J., S. Kirolos, Y. Massoud, R. Baraniuk, A. Gilbert, M. Iwen, and M. Strauss. Random sampling for analog-to-information conversion of wideband signals. 2006. In *IEEE Dallas Circuits and Systems Workshop.* (Dallas, 29-30 Oct 20062). , p. 119. Piscataway, NJ: Institute of Electrical and Electronics Engineers.

5. Mattingley, J., and S. Boyd. CVXMOD-Convex optimization software in python. 2008. *online documentation.*

6. Davenport, M., M. Duarte, M. Wakin, L. Laska, D. Takhar, K. Kelly, and R. Baraniuk. The smashed filter for compressive classification and target recognition. 2007. In *Computational Imaging V at SPIE Electronic Imaging.* (San Jose, Jan 2007). , p. 64980H. Bellingham, WA: SPIE.

Publications

Mascarenas, D., D. Hush, J. Theiler, and C. Farrar. The applicatio of compressed sensing to detecting damage in structures. 112. In *International Workshop on Structural Health Monitoring.* (Stanford, CA, 13-15 Sept 2011). Vol. I, p. 1013. Lancaster, PA: DEStech.

Exascale Sky (Cosmology)

Patrick S. Mccormick
20110530ER

Abstract
In this feasibility study we built a new integrated simulation and analysis capability for cosmological modeling aimed at next-generation GPU-accelerated supercomputers. As a multi-disciplinary collaboration, our effort represents a first-generation co-design effort that has resulted in a key proof-of-principle success. Co-design refers to the simultaneous optimization of hardware, software, and algorithms to solve the problems faced by large-scale modeling and simulation applications at the exascale, the next frontier in high performance computing (HPC). The Exascale Sky simulations target sky surveys such as the Large Synoptic Survey Telescope (LSST), the highest-ranked project in the just released DOE/NASA/NSF-sponsored Astro2010 Decadal Survey. These simulations cover very high dynamic range studies of structure formation, over cosmological volumes as large as can be observationally probed.

Background and Research Objectives
As supercomputing proceeds to the exascale, new technologies will be incorporated in a staged fashion. Large-scale GPU-accelerated systems are now among the fastest machines in the world; as heterogeneous systems they provide the most severe co-design challenge for the current HPC code base worldwide. Our co-design project, on a demanding and high-profile computational problem, has had a major technical impact, pointing the way to implementation of other applications and providing the initial evaluations of different hardware and software strategies for dealing with this next generation systems.

Co-design is the iterative process of developing the interacting components of a system together as a whole, rather than optimizing each component separately based on static interface requirements from the other components. Enlarging the design space yields greater opportunities for better, revolutionary solutions, but the design process becomes more complex, and the associated risks larger. Our philosophy has been to reduce co-design risk by limiting the process to subsets of components – "co-design blocks" – thus controlling the dimensionality of the design space. Our primary concern is the block that represents modeling at an intermediate, component, level where the focus is more on the architectural details, developing models for application processes which characterize the instruction mix and flow, functional unit utilization, full memory hierarchy, communication, I/O, power usage, etc. The primary purpose of the feasibility study was to alleviate certain key difficulties of hybrid programming – with the goal of a successful implementation and optimization of a large-scale cosmology simulation and analysis framework on a state of the art hybrid CPU/GPU cluster.

Scientific Approach and Accomplishments
A major bottleneck to scale the code to very large systems (with respect to the number of cores) has been solved by implementing a new pencil-decomposition for the FFT. With this accomplishment, we have shown scaling of the Poisson solver up to 40,000 nodes on ANL's BlueGene/P system (See Figure 1). This breakthrough will be critical as we push towards requesting an allocation on ORNL's upcoming Titan system (a GPU-system targeted at tens of petaflops). In addition, we have also completely rewritten the GPU portion of the code to plan prepare for Titan. Our most recent tests on small test clusters show that the code is performing extremely well. Given these results, we believe that we are one of the very groups who are actually ready to take advantage of Titan's architecture. This will enable us to carry out extremely large cosmological simulations in support of the major upcoming DES and LSST surveys.

Another new addition to the code was a demonstration at SC10 of the code running on a heterogeneous GPU-based system with fully integrated in situ, hardware-accelerated analysis and visualization operations. This capability will become increasingly important as we move into the exascale era of computing.
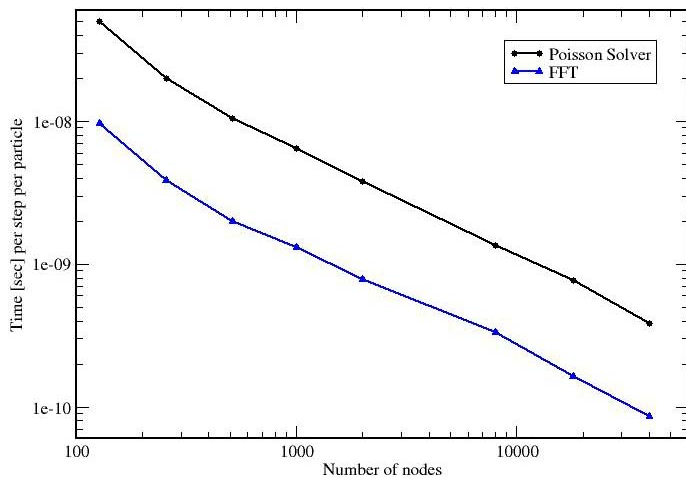
Figure 1. Scaling of the Poisson and FFT portions of the application on 40,000 nodes.

Impact on National Missions

The co-design approach, algorithms and broad design capabilities developed under this project have laid some groundwork to have an impact on LANL and DOE missions in computer science as well as computational physics. The unfortunate departure of the cosmology team from this project has likely impacted LANL's likely role as a key simulation partner for LSST and other sky survey projects sponsored by DOE HEP.

Let the Data Choose the Signatures

Rick Chartrand
20110627ER

Abstract

Our project considered methods for robust modeling of high-dimensional datasets. The basic idea is to decompose a matrix formed from the dataset into two components: one giving a low-dimensional model of most of the dataset, the other consisting of few, but possibly large, discrepancies from this model. Allowing these discrepancies allows the model to be much more robust, while the discrepancies themselves often constitute interesting signatures of the data.

We developed algorithms that compute this decomposition more faithfully than other approaches in the literature, by not requiring restrictive mathematical properties. One of these properties is that the dataset be well-described by a single, low-dimensional model; eliminating this requirement allows the dataset to be curved in space, which greatly increases the range of potential applications.

The methods we developed were tested in the context of surveillance video, and are thus applicable to several homeland security and nonproliferation needs. Analyzing text data with the goal of automatically determining authorship would be very useful to the intelligence community. Our short project made great strides at bringing our methods to external sponsors, and helped spawn a new LDRD-DR project on developing human-like ability to computationally understand the content of video scenes.

Background and Research Objectives

The progenitor of our approach is *compressive sensing* (CS), a recently-emerged subfield of applied mathematics which has developed powerful methods for information extraction [1]. With CS, high-dimensional signals and images can be reconstructed from very few measurements, far fewer than traditional sampling theory would predict. What makes this possible is the great redundancy inherent in high-dimensional data. Most real-world signals are *sparse*, meaning that they can be accurately described using much less information than is typically used to specify them (such as the pixel values in a high-resolution image).

A recent thrust within CS is matrix completion [2]. Given a large matrix with most of its entries missing, it is often possible to correctly fill in the missing entries, based on the assumption that the columns of the completed matrix span a low-dimensional space. A simple example is the "Netflix problem": given a collection of customers (matrix rows), each of which has given ratings (matrix entries) to a small subset of the available movies (matrix columns), try to predict each customer's ratings for all of the movies (i.e., fill in the matrix). What makes this possible is that the factors that go into customer opinions of movies are far fewer than the number of customers —the evaluation process is low-dimensional. The matrix completion process also yields a description of the opinion factors, giving signatures of the opinion data.

The starting point for our approach goes one step beyond matrix completion. Given a dataset (e.g., the frames of a video), we form a matrix having one column for each member of the dataset, whose rows are the values for that member (e.g., the pixel values of each frame). We can then decompose this matrix into the sum of two components. The first component will be a low-dimensional description of the matrix's columns; in linear algebra terms, it will have low rank. The other component will be as sparse as possible, such as by having mostly zero entries (though more general kinds of sparsity are possible). Such a low-rank + sparse decomposition accomplishes two things simultaneously. The low-rank portion provides us with the essence of the dataset, boiled down to its minimal description. The sparse portion gives us those parts of the data that do not conform to the model predicted by the rest of the data, serving to identify the anomalies that, for many applications, will be the part of the data that will be of greatest interest. We thus obtain two kinds of signatures at once: the minimal description of the dataset as a whole, and the characteristics that stick out from the rest of the dataset.

Computing the low-rank + sparse decomposition of a sizable matrix directly is a completely intractable prob-

lem, of the sort that all the world's computers working for trillions of years would not make a dent. However, in a manner analogous to some of the powerful theory of compressive sensing, it is possible in some cases to solve it indirectly, by solving instead a much easier proxy [3]. But by applying the same methodology as in the PI's pioneering CS work [4, 5] we will be able to solve a more faithful surrogate problem, and greatly expand the ability to compute low-rank + sparse decompositions. This will allow us to generate more accurate models of the data, while simultaneously reducing spurious anomalies.

As useful as the low-rank + sparse decomposition can be, we want to be able to construct more geometrically complex models. For example, low-rank models of image sets require careful alignment between corresponding objects in each image, because the translation of an object within an image does not correspond to a low-rank model. The most natural generalization is to *locally* low-rank, in which the behavior is low-rank within small neighborhoods, but not across the entire dataset. This allows representation of data that lies on a low-dimensional manifold (or surface). Such a generalization of our approach is one of our primary research goals, which will greatly expand the kinds of problems to which our tools will be applicable.

Scientific Approach and Accomplishments

The core of our approach is using models that are more faithful to what they are modeling. As a first example, most algorithms for enforcing sparsity use a model with the mathematical property known as *convexity*. On the one hand, this makes the computation easier: if one wants to find the highest point on the graph of a convex function, one can simply "head uphill," and there will be no "false summits" to prevent reaching the maximum value. On the other hand, a convex model gives a fairly coarse way of enforcing sparsity. Our models are *nonconvex*, allowing a more faithful expression of sparsity, while our computational implementation prevents the algorithm from being stuck in "false summits."

An example of what our approach can do with high-dimensional data is in Figure 1. We examine a video clip from a traffic camera on Lankershim Boulevard in North Hollywood. We convert the video into a matrix by taking each frame and putting the values of its pixels into a column. We then compute the low-rank + sparse decomposition of this matrix, and re-convert each component into a video. Figure 1 shows one frame from the videos. The sparse component video extracts the moving objects from the video: cars, a cyclist, and a pedestrian. The low-rank component contains the stationary background, including parked cars, and automatically fills in traffic lines that are occasionally occluded in the original video. We thus obtain a method for background removal, which in the context of surveillance would allow an operator (or processing software) to focus on only the moving objects. We obtain this outcome without any explicit modeling to this effect, using only

the geometry of the video frames as elements of a high-dimensional set to produce a low-dimensional description and a sparse set of salient features.

Figure 1. Left: one frame from a video sequence. Middle: corresponding frame from the low-rank component; all moving objects are absent, and road lines obscured by cars in the original frame have been filled in. Parked cars remain; an approach that simply identifies cars would be less useful. Right: the sparse component contains only the moving objects, including a cyclist and pedestrian on the sidewalk. The pedestrian is very difficult to notice in the original video, but is clear in the video sequence of the sparse component.

We also modified our original approach to better the handle the case of noisy data. We add a third component to the decomposition, one intended to contain only the noise. Our algorithm penalizes oscillation in the sparse component, which helps to prevent noise from being part of this component. Since noise would greatly increase the rank, the noise also does not end up in the low-rank component, resulting in most of the noise winding up in the third, residual component. Our penalty on oscillation is also nonconvex, since prior work [6] has shown that this is better able to preserve complex shapes.

A research article about the algorithms for this nonconvex approach to data decomposition, "Nonconvex Splitting for Regularized Low-Rank + Sparse Decomposition," has been submitted to IEEE Transactions on Signal Processing.

A deficiency in our approach is that it can only produce a low-dimensional model that is *linear*, that is, one that is geometrically "flat." A more realistic model would be one that says the data lie on a curved, low-dimensional surface (or *manifold*) within their high-dimensional space. As an example, in the case of surveillance video, a "flat" model is only appropriate if the camera is stationary. Camera motion has the effect of shifting coordinates within the high-dimensional space that each frame lies in, so that the frames lie on a curved path. Adapting our approach to be able to handle this case will make it suitable for many more applications.

To handle the more complex data geometry, we use a "windowed" approach, where the low-rank + sparse decomposition is computed separately over short segments of the data, effectively approximating the curved data geometry by one that is locally flat, but where the model changes over the course of the dataset. Although work is ongoing, we have preliminary results showing that this

can provide approximate decompositions that are faithful enough to be useful. As a test example, we created a synthetic copy of the traffic video with simulated camera motion. See Figure 2 for one frame from the results. The separation into moving and stationary objects is not as clean as in the case of a stationary camera, but it still isolates the moving objects well enough to accomplish the task of simplifying further analysis of the video.
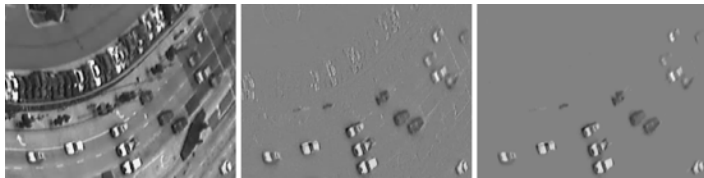
Figure 2. Left: one frame from a traffic video clip with a moving camera. Middle: the sparse component, using a single, low-dimensional model. The model has difficulty capturing the moving scene, resulting in portions of the background appearing in the sparse component. Right: sparse component using a local, low-dimensional model that varies over the course of the video. This gives a much cleaner separation of moving components from the background.

A research article about this approach, "Local Principal Component Pursuit for Nonlinear Datasets," has been submitted to the 2012 IEEE International Conference in Acoustics, Speech, and Signal Processing, the most prestigious signal processing conference.

As an example of an application of non-imagelike data, we considered text analysis for the purpose of author identification. One can distill a set of documents into a matrix by computing the frequency with which each word appears in the document. One obtains a "term-document matrix" (TDM) having one row per word that appears in any of the documents, and one column for each document. Previous work [7] has applied low-rank + sparse decomposition for topic identification, interpreting the words that appear in each column of the sparse component as "keywords" for the corresponding document. Our approach is to instead consider the low-rank component. Given a TDM for a set of documents with a given author, the low-rank component will give a robust model of the author's word usage, with effects of the choice of topic removed (as these appear in the sparse component). One can then take a column of a TDM corresponding to a document of unknown author, and determine which author's low-dimensional model it is closest to. Since the underlying model approach is completely geometric, the approach should work equally well for documents written in any language. Although our brief project came to a close before this approach could be properly tested, it has the potential to be useful in intelligence community applications.

Impact on National Missions

The methods developed in this project have the potential to have a substantial impact on several mission-related areas. The geometric nature of the modeling means the approach can be applied to any of many different application areas, without needing to re-customize the approach to each one. Topics most directly relevant to the applications considered in this project include all manners of surveillance, with relevance to homeland security and nonproliferation, and extracting "signatures" of authorship within text documents (though the approach could as well be applied to other forms of communication as well), with application to the intelligence community. Other possible applications include extracting novel signatures of material properties within experimental data, and other situations where scientific modeling may not capture all of the information contained within data, so that our data-driven approach has the potential to identify novel features.

The short duration of our project (less than half a year) did not allow for the beginning of new, external-funded projects, but the way has been paved for bringing our methods to external sponsors. Early results were part of a successful LDRD-DR proposal, "Hierarchical Sparse Models for Robust Analysis of Video Data," which will synthesize some of our modeling methods with hierarchical methods in machine learning, thereby maximally leveraging our algorithmic techniques in the attempt to computationally demonstrate human-like understanding of video scenes.

References

1. Candes, E. J., J. Romberg, and T. Tao. Robust uncertainty principles: exact signal reconstruction from highly incomplete frequency information. 2006. *IEEE Transactions on Information Theory.* **52**: 489.

2. Candes, E. J., and B. Recht. Exact matrix completion via convex optimization. 2009. *Foundations of Computational Mathematics.* **9**: 717.

3. Candes, E. J., X. Li, Y. Ma, and J. Wright. Robust principal component analysis?. 2011. *Journal of the ACM.* **58** (11): 37.

4. Chartrand, R.. Exact reconstructions of sparse signals via nonconvex minimization. 2007. *IEEE Signal Processing Letters.* **14**: 707.

5. Chartrand, R., and V. Staneva. Restricted isometry properties and nonconvex compressive sensing. 2008. *Inverse Problems.* **24** (035020): 1.

6. Chartrand, R.. Nonconvex regularization for shape preservation. 2007. In *IEEE International Conference on Image Processing.* (San Antonio , 16-19 Sep. 2007). Vol. I, p. 293. San Antonio : IEEE.

7. Min, K., Z. Zhang, J. Wright, and Y. Ma. Decomposing background topics from key-words by principal component pursuit. 2010. In *19th ACM International Conference on Information and Knowledge Management.* (Toronto, 26-30 Oct. 2010). , p. 269. Toronto: ACM.

Publications

Chartrand, R.. Nonconvex splitting for regularized low-rank + sparse decomposition. *IEEE Transactions on Signal Processing.*

Wohlberg, B., R. Chartrand, and J. Theiler. Local principal component pursuit for nonlinear datasets. Presented at *37th International Conference on Acoustics, Speech, and Signal Processing.* (Kyoto, 25-30 Mar. 2012).

Chinese Economic Output from Satellite Data

Petr Chylek
20110675ER

Abstract

We find that we can use satellite retrieved tropospheric columnar amount of NO_2 (nitrogen dioxide) to monitor Chinese economic activities as characterized by the GDP (Gross Domestic Product). Over the years 2004-2007 the average NO_2 amount over the Chinese industrial regions increased at the rate of about 8% per year. This is essentially identical to reported growth rate of Chinese economy (GDP). The rate of NO_2 increase over rural regions has been considerably slower, around 4.5% per year, indicating a slower pace of economic development of rural China. The NO_2 based estimate can be used to monitor economic growth over denied territory.

Background and Research Objectives

China is becoming an economic superpower, competing with the U.S. for global influence and markets. It is investing heavily in modernization of its army, space program, and energy production sector (both traditional fossil fuel based and the "green"). Since the economic expansion is necessarily connected to energy production, and traditional energy production to burning fossil fuels, we pose a question: Can we monitor the economic activities over China using satellite based instrumentation? In fossil-fuel-based economies the energy production is tied to the CO_2 and other gaseous emissions. The measurement of CO_2 columnar concentration from satellite is a difficult task which cannot be accomplished with the current on orbit satellite instrumentation. It would require a satellite instrument designed specifically for the task (small pixel size, pointing ability, specifically designed orbit for frequent repeat time). On the other hand, the fossil fuel co-emitted NO_2 can be retrieved using the current satellite instruments. Since fossil combustion technology evolves relatively slowly, within a limited span of time, the NO_2 emission is expected to correlate with intensity of fossil fuel based energy production.

China closely monitors the information it releases. The world, therefore, knows only what China wants them to know. Our goal was to show a general capability to esti-mate Chinese economic growth, map it in time by satellite measurements of NO_2, and compare with generally available economic growth data.

According to the World Bank data, China's economy has been growing at over 8% per year for the last 30 years. The Chinese GDP is now the second largest after the US. Over this time there has been unprecedented growth in energy production and consumption, infrastructure development, industrial activities, and resource exploitation.

As a part of this project we studied energy systems to demonstrate how rapidly China is developing its infrastructure and manufacturing capacity. China has added almost 100 GW of new capacity each year since 2004 (Figure 1), most of which is coal-fired.

In 2011 China is expected to surpass the US in installed capacity. The difference in quality of the US and Chinese systems is stark. Most of Chinese coal power plants built since 2005 have low NO_x burners, gas desulphurizing units, and other pollution controls. The gas turbines are latest technology units in combined cycle usage at about 57% efficiency.

Data on the location and details of about 100 GW of this coal-fired and 20 GW of CCGT has been collected as part of our effort and are available through the Internet using the tool GEO at www.globalenergyobservatory.org. The location of each coal and CCGT power plants was verified using Google Earth and is shown in Figure 2.

To enable this rapid growth, China has developed the complete manufacturing chain for all power generation systems and is now the largest manufacturer of thermal, hydro, CCGT, solar PV and wind turbine systems. Many international companies have set up joint venture with companies in China.
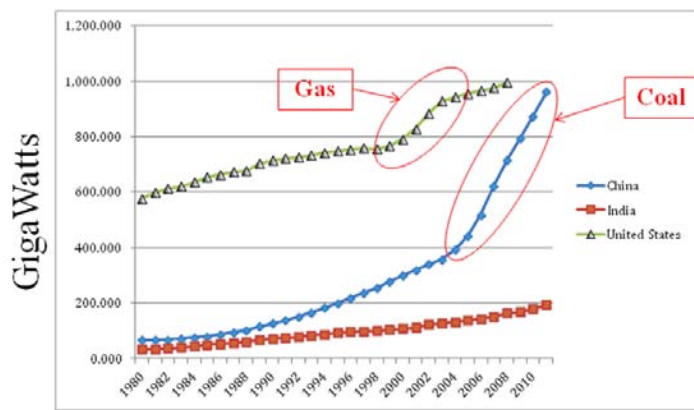
Figure 1. Comparison of the US, Chinese, and Indian electric power generation capacity over the last three decades (data are from http://www.world-nuclear.org/info/inf63.html).
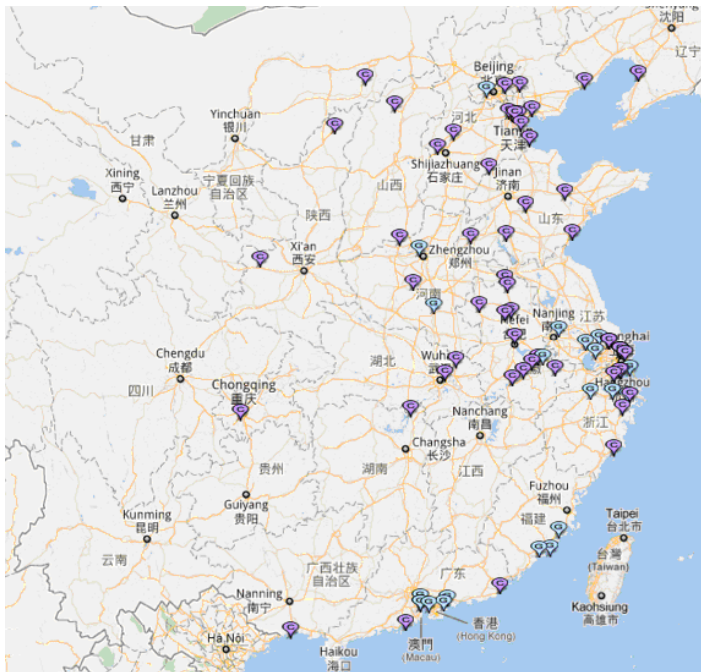
Figure 2. Location of over 100 GW of new coal-fired (C) and 20 GW gas (G) power plants installed mostly after 2004 and verified using Google Earth. Details are available at http://globalenergyobservatory.org.

Chinese industry has shown remarkable ability to absorb, adapt, and improve sophisticated technology and manufacturing processes in a very short period. In the case of gas turbines, China in 2004 set up an open competitive bid for about 40 units to be installed and operational by the end of 2007. All three major international manufacturers, GE, Siemens, and Mitsubishi set up joint ventures with Chinese companies and licensed their technology to bid for these contracts. GE paired up with Harbin, Mitsubishi with Dongfang, and Siemens with Shanghai. Initially, all the key components were imported but by the end of 2007 all

three Chinese companies were able to provide fully Chinese manufactured units at cheaper prices and now dominate the Chinese market.

A similar story has unfolded in the manufacture of wind turbines and solar PV cells and modules. In 2006, there was only one Chinese company in the top 15 (Goldwind) with 3% of the market share. By 2010 there were seven with a total market share of 38% and growing. Most international companies now have manufacturing units in China, and because of their cheaper costs, are being forced to close units in their home countries. The market share of Chinese PV cell and module manufacturers exceeded 40% in 2010 and increasing number of Western companies are finding it hard to compete and are either shifting their manufacturing to China or closing their operations.

In summary, China, by using its enormous domestic market and need for electric power generation, has become the largest manufacturer of all energy systems, from conventional thermal to solar to wind to nuclear. This LDRD supported project has tracked this growth by harvesting data from open sources on the internet and created a moderated and validated database. The geospatial location of this infrastructure has been verified using Google Earth.

Scientific Approach and Accomplishments

The combustion of fossil fuels leads to emission of carbon dioxide (CO_2) and few other co-emitted gases (e.g. carbon monoxide, nitrogen dioxide). We tried to connect energy production to CO_2 atmospheric column using satellite available data (GOSAT – Japanese hyperspectral satellite instrument designed specifically for CO_2 retrievals) and SCHIAMACHY (European satellite hyperspectral instrument). By performing an extensive radiative transfer modeling we found that the sensitivies of these instruments to changes of atmospheric CO_2 column are not sufficient to detect regional year to year changes, due to a high natural CO_2 background. Consequently we have shifted our investigation exclusively towards the NO_2.

The amount of NO_2 emitted is determined by the amount of energy produced and by technology of production. Since change in technology is a slow, time consuming process, it is reasonable to expect the technology to be fixed (unchanged) for a span of time of five to ten years. During this time span the NO_2 signal can be considered to be primarily a function of intensity of energy production. By monitoring NO_2 amount we expect to monitor growth of Chinese energy production and of the Chinese economic growth.

There are currently several satellite instruments capable of

NO$_2$ retrieval. The most accurate retrieval method is based on reflected solar radiances in the blue end of solar spectrum. Considering available options, we finally decided to use the data retrieved by the Ozone Monitoring Observatory on the NASA satellite.

We selected the Chinese industrial region bounded by 35-40°N and 115-120°E containing one of the most industrialized areas (including Beijing). We used the time span of data from Oct 1, 2004 to Oct 1, 2011. The annual averages of the NO$_2$ tropospheric column (in 10^{15} molecules per cm^2) are shown in Figure 3.
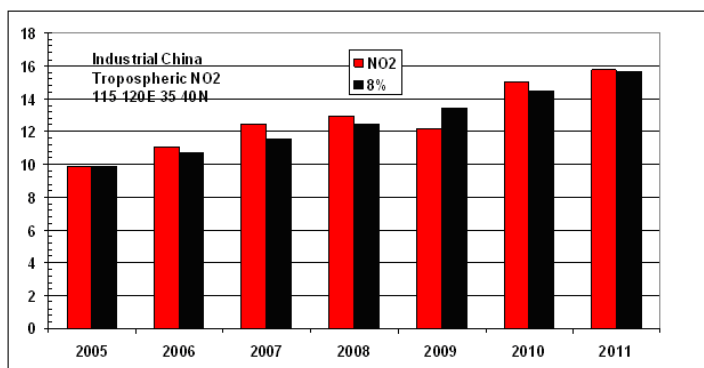
Figure 3. Satellite based retrieval of tropospheric columnar amount of NO$_2$ (in 10^15 molecules per cm^2) over an industrial region of China with 115-120 deg E and 35-40 deg N (red columns) compared to 8% annual growth (black columns). Average from Oct 1, 2004 to Oct 1, 2005 is plotted as 2005 value and similarly for other years.

The average observed annual NO$_2$ amount (red columns) over a considered seven year period is essentially identical with the reported Chinese economic growth of 8% per year (black columns). A decrease in the year 2009 (Oct 1 2008 to Oct 1, 2009) is very likely connected to the effort to clean the air for 2008 Beijing Olympic Games.

It is apparent that the average annual increase in the tropospheric NO$_2$ concentration over industrial region indicates very accurately the economic growth of the country. The next question we asked: Is the Chinese economy increasing at the same rate in the rural areas? Here we selected the same size area in the western China bounded by 35-40°N and 100-105°E. The tropospheric NO$_2$ amount is shown in Figure 4. The air is generally much cleaner than over the industrial east; the NO$_2$ concentrations are by about a factor of ten lower. The rate of annual increase is also significantly lower with an average growth of about 4.5% compared to the growth of 8% for the industrial region. It is interesting to note that the 2009 decrease is also observed in the rural region. It is not clear to us at this time if the effort to clean air for Olympics was applied to

the whole country or only to Beijing region. If only to the Beijing region, then the cause of 2009 NO$_2$ decrease has to have some other cause (change of technology or country-wide economic slowdown).

Figure 5 captures visually the expansion of industrialized region of China between the years of 2004 and 2010.
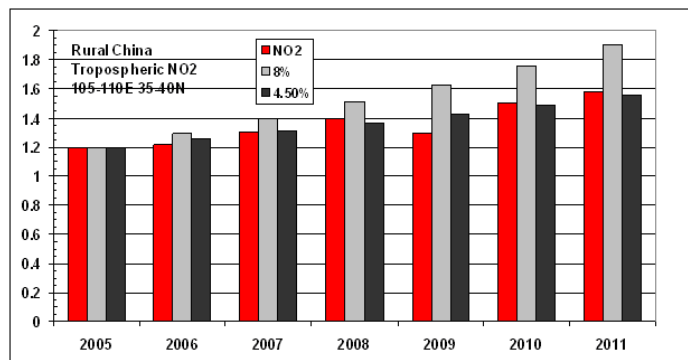
Figure 4. Satellite based retrieval of tropospheric columnar amount of NO^2 (in 10^15 molecules per cm^2) over a rural region of China with 105-110 deg E and 35-40 deg N (red columns) compared to 8% (gray columns) and 4.5% (black columns) annual growth. Average from Oct 1, 2004 to Oct 1, 2005 is plotted as 2005 and similarly for other years.
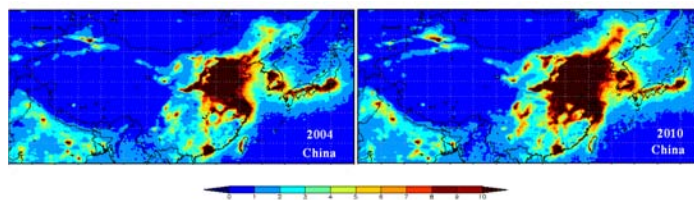
Figure 5. Columnar NO$_2$ over China, comparing Oct –Dec 2004 and Oct-Dec 2010.

Impact on National Missions

We have demonstrated that the rate of increase of the tropospheric column of the NO$_2$ is closely related to GNP growth of China. We found that different regions were growing at different rates, with lower rates of increase in rural regions. In general our data confirm our starting hypothesis: Satellite based NO$_2$ retrieval can serve as an indicator of economic growth of a region. It can serve to verify available reported economic data or to estimate the economic growth over denied territory.

Quantum Information Processing: Capabilities and Limitations

Robert E. Ecke
20090520PRD2

Introduction

The possibility of manipulating quantum states raises exciting possibilities for engineering and computer science. Because quantum systems are hard to simulate on conventional computers, computers utilizing quantum coherence should be intrinsically more powerful than their conventional counterparts. For example, exponentially faster quantum algorithms exist for factoring integers, for algebraic and optimization problems, and for simulating physical systems. Quantum mechanical noise is a challenging obstacle for experimental realizations of quantum computation. One promising idea to fight noise is error correction. The quantum capacity of a noisy process is the amount of quantum data that can be protected, in the limit of many transmissions affected by that noise; classical capacity is defined similarly. Determining these capacities from a description of the noise is an open problem. Another proposal to combat noise seeks to engineer exotic materials with topological order, as they are believed to have noise-resistant collective excitations that could be used to build a quantum computer. As a Richard P. Feynman Postdoctoral Fellow in Theory and Computing, Jon Yard's work in this project focuses on determining the quantum and classical capacities for practical noise models, while seeking better theoretical understanding of quantum capacity. He uses quantum information concepts he has developed, to better understand physical systems exhibiting topological order, and how they can be used to protect quantum information. He also analyzes the computational capabilities afforded by the existence of a quantum computer, and determines computational problems related to quantum mechanics and the characterization of entanglement that can be run on a conventional classical computer.

Benefit to National Security Missions

Understanding how quantum information processing can promote or jeopardize cybersecurity supports Threat Reduction. Quantum mechanics enables future-proof cryptographic protocols that can be backed by mathematically rigorous security claims, while using present-day technology. Quantum information helps understand properties of matter, such as superconductors and other exotic materials and phases, bearing on materials and device design for the Energy and Office of Science missions. Long-term leadership in cutting-edge computation supports all Laboratory missions.

Progress

With collaborators Graeme Smith (IBM) and John Smolin (IBM), Yard identified optical communication channels that have zero quantum capacity by themselves, but which nonetheless can have a nonzero capacity when used together. While such channels were shown to exist by Yard and Smith in their 2008 *Science* paper, this is the first known practical example that can be realized in a laboratory. This work resulted in a paper "Quantum communication with gaussian channels of zero quantum capacity," which was published in the journal *Nature Photonics*. It is expected that this will lead to other new results on the capacities of practical channels for transmitting secure and quantum information.

Yard has also been closely investigating quantum conditional information, which is an entropic quantity central to the connection between entanglement and topological order, while having equal importance in the study of quantum communication in general. Many quantities of interest in quantum information theory, such as channel capacities and measures of entanglement, are given as optimization problems involving quantum conditional information. With collaborators Matthias Christandl (ETH Zurich) and Fernando Brandão (Universitade de Minas Gerais, Brazil), Yard obtained a breakthrough result in the form of a new bound on quantum conditional information. In turn, this bound resolved several outstanding questions in quantum information theory and computation. Among these, it gave the first known characterization of approximate quantum Markov chains. It also led to the first known efficient classical algorithm for determining if a bipartite quantum state is entangled, while implying a similar algorithm for optimizing over the set of classically correlated quantum states. This work resulted

in two publications: "Faithful squashed entanglement," was published in *Communications in Mathematical Physics*, and "A quasipolynomial-time algorithm for the quantum separability problem," which was published in the *Proceedings of the ACM Symposium on the Theory of Computation* (STOC 2011).

Yard has also continued his research on entropic signatures of entanglement and topological order. Building on previous work, he has identified a class of model Hamiltonians - known as quantum double Hamiltonians - whose topologically ordered ground states lead to a direct connection between his previously discovered "state redistribution protocol" for quantum communication and a well-established entropic measure of topological order. Previously, the connection was only heuristic. He still is pursuing ways of making this connection applicable to a wider and more robust class of topologically ordered states.

Yard has also made recent progress on a conjecture of Renes et al. that, in each d-dimensional complex vector space, there exists a set of equiangular d^2 unit vectors. A proof of their existence in every dimension will have fundamental importance for the design of new quantum codes and algorithms, will provide new optimal methods for processing discrete-time radar signals, and will shed light on the relation between quantum mechanics in theoretical and in practical settings. Yard has discovered several unforeseen connections between this problem and other areas of mathematics and physics. These areas include classical 19th century mathematics such as elliptic curves, as well as a mathematical framework developed to study string theory and quantum systems at criticality, called conformal field theory. Some concrete results already obtained include a complete classification of the possible solutions in three dimensions, based on the intricate geometry of singular or "pinched" curves. He has found evidence that solutions to this problem can always be found over suitable number fields - so-called class fields of imaginary quadratic number fields. Through recent work by string theorists, this evidence leads to a natural conjecture that the sought-after solutions can be found using a quantum field theory of free bosons living on a torus, rather than the usual flat space-time. A novel aspect of this approach is to use the quantum fields as abstract representative for the states of a finite quantum system. This approach may lead to concrete realizations in quantum Hall systems.

Future Work

Work will continue towards determining the communication capacities of practical noise models, such as electromagnetic field modes affected by Gaussian noise. Work on the equiangular lines problem will continue as well. It is expected that the new light the approach to this problem sheds on the relation between quantum mechanics in finite and infinite dimensions

will give new techniques for analyzing the capacities and security of practical noise models. For instance, while the notion of Gaussian states is well-understood in infinite systems like the harmonic oscillator, a satisfactory counterpart in finite dimensions is in many ways still lacking. Future work will aim to identify such counterparts. Yard will also demonstrate relationships between an information-theoretic characterization of multipartite quantum correlations that he discovered, involving the quantum conditional mutual information, and entropic measures of topological order. Topological order appears in the quantum Hall effect and may play a role in other strongly interacting materials such as high-temperature superconductors, so there may be applications of his measure of multipartite correlations in these contexts. The mathematical approaches to relating finite and infinite-dimensional quantum mechanics that Yard has developed suggest other avenues towards relating conditional mutual information and topological order that are based on conformal field theory. These approaches will be investigated further. Yard will develop new algorithms for solving classically hard problems on a quantum computer. These include computing topological invariants, such as whether a knot can be untied without cutting, implementing Fourier transforms over new types of groups, and simulating physical systems.

Conclusion

Determining the quantum capacity of quantum channels will help in developing designs for reliable quantum computers and in improving quantum methods for secret key distribution. Yard's work on classical capacity will provide methods for achieving higher data rates in existing free-space and fiber optical networks. The algorithms he will design will help us understand whether and how one might design public-key cryptographic systems (e.g. for e-commerce, banking, and authenticated digital communication) resistant to quantum code-breaking. New algorithms, and theoretical concepts form quantum information, could help understand the properties of physical systems, for example, materials properties important in energy efficiency engineering. A fundamental issue that has arisen during this work is the need to expand upon and clarify the relation between quantum mechanics in finite dimensions, where theoretical protocols are devised, and quantum mechanics in infinite dimensions, which is the sort of physics imposed upon us by Nature. The natural course of this research points to some surprising applications of mathematical and physical tools to this end, despite their original motivations in string theory, condensed matter and number theory.

Publications

Brandao, F., M. Christandl, and J. Yard. Faithful Squashed Entanglement. 2011. *Communications in Mathematical Physics.* **306** (8): 805.

Brandao, F., M. Christandl, and J. Yard. A quasipolynomial-

time algorithm for the quantum separability problem. 2011. *Proceedings of the ACM Symposium on the Theory of Computation (STOC 2011).* : .

Smith, G., J. Smolin, and J. Yard. Quantum communication with Gaussian channels of zero quantum capacity. 2011. *Nature Photonics.* **5**: 624.

Yard, J., and I. Devetak. Optimal quantum source coding with quantum side information at the encoder and decoder. 2009. *IEEE Transactions on Information Theory.* **55** (11): 5339.

Quantum knowledge: A revolutionary approach to measurement

Bogdan F. Damski
20100619PRD2

Introduction

This is a theoretical physics project, which in its second year has begun to drive experimental collaboration. It begins with a recently-developed theory of agents, observation, and decision-making, which constructs an object that can interact with quantum systems in its environment to solve simple problems faster than can be done classically. This is a new way of observing and making decisions, centered around ``quantum knowledge''.

In the course of this project, this theory will be thoroughly explored and validated, including making testable predictions where possible. Furthermore, the theory of quantum knowledge will be applied to clarify and reconcile tensions and paradoxes within quantum theory, which have plagued it for nearly a century. The most ambitious goal of this theory is to resolve the tension between classical and quantum physics by showing that classical experience fits self-consistently within quantum theory.

In parallel, concrete applications of the theory will be developed. Potential applications arise in quantum metrology, quantum information theory, and quantum algorithms. The plan is to devise powerful techniques by modeling quantum devices as agents that gather and utilize information.

Finally, collaborations with experimental groups will test predictions made by the theory of quantum knowledge, and implement new algorithms and measurement techniques.

Benefit to National Security Missions

This project will support the missions of the Office of Science by enhancing our understanding of quantum theory, and our ability to probe and measure complex natural systems. It will also support the Homeland Security mission of the Laboratory by assisting the development of quantum computers, secure quantum communications, and improved precision sensing techniques.

Progress

In the past fiscal year, we have made several important – and useful – advances in the theory of quantum statistical inference that underlies quantum knowledge. We have also identified a new, simplified approach to demonstrating the difference between quantum and classical knowledge.

Matrix Product State Discrimination

In collaboration with Sarah Croke (Perimeter Institute), we designed a protocol using *coherent* measurements to discriminate optimally between several *matrix product* states (MPS) [1]. These finitely correlated lattice states are a hot topic in condensed matter physics, believed to accurately describe 1-D lattice systems' ground states. In an MPS, entanglement between lattice sites is limited but nontrivial, so key properties of laboratory-produced MPS can be hidden from local observations. Our algorithm is the most efficient possible way of probing and measuring these properties, and it promises dramatic accuracy improvements (over strictly classical techniques) using only a small quantum memory.

Gaussian designs: In collaboration with Peter Turner (U. Tokyo), we examined the quantum measurements that are available to extract information from *continuous variable* quantum systems (e.g., quantum light). Surprisingly, the entire class of measurements known as *2-designs*, which are known to be optimal for discrete systems, are unavailable for continuous systems. We nonetheless demonstrated measurements that are far more efficient than those currently used (coherent state POVMs) [2].

Paranoid Tomography: We completed the theoretical construction of an absolutely reliable protocol for assigning *confidence regions* in quantum tomography. Unlike prior tomographic protocols, which were limited to point estimators, our protocol can rigorously validate fault tolerant hardware. Furthermore, the paradigm of region estimators opens a new realm for coherent "quantum knowledge" protocols, suggesting the possibility of coherent region estimation as an

alternative to coherent decision-making. This work will be presented at the QIP 2012 conference (Montreal, 12/10-16/2011).

Quantum Agency

We developed a new, simple, and promising test to distinguish classical and quantum agency. Classical agents affect their world through a three-step process: (i) observe; (ii) process or think; (iii) act. These steps are distinct and definable even in quantum models. This means that interactions between an agent and an object are strictly limited to dynamical maps of a particular form, which we are currently studying

Adaptive Tomography

In collaboration with Chris Ferrie (U. Waterloo), we developed a protocol for *adaptive* quantum state tomography (preliminary work can be found in [3]). The protocol is quite simple, and easy to implement, and it yields a dramatic increase in accuracy over existing (static) tomography protocols. Static protocols have worst-case (over all possible true states) error that scales as $N^{-1/2}$, but our new protocol's inaccuracy scales as N^{-1} for *all* states (N is the number of measurements). Since fault tolerant quantum computing requires accuracies in the range of 10^{-5}, our protocol will reduce the number of measurements required to achieve this threshold by five orders of magnitude. We are currently collaborating with Aephraim Steinberg (U. Toronto) to test and implement our theory in photonic systems. At first glance, applying our adaptive protocol to many qubit systems *seems* to require the experimental capability to measure arbitrary – which is to say entangled – bases. Most experiments – including those of our experimental collaborator – can't make these measurements. So we have developed a remarkable and rather surprising method called *null space sampling* to achieve the same scaling with local measurements and feedforward.

Channel Coding

We have recently discovered that the ideas and insights that enabled *streaming entanglement concentration* (an early accomplishment of the Quantum Knowledge framework) can be applied to quantum and classical channel coding – i.e., error correction and communication over noisy channels. Our existing algorithm for concentration relies heavily on *randomness extraction* as a primitive notion. We are using the same principle (that information theoretic protocols can usually be reduced to a form of randomness extraction) to more simply understand *polar codes*, a recent (2008) and exciting invention based on the observation that certain circuits can *polarize* collections of identical communication channels, so that they separate into two collections of (i) almost perfectly noisy channels, and (ii) almost perfectly noiseless channels. We have applied our framework to show that the channel

polarizing circuits are in fact randomness extractors, which *compress* the noise. Using this insight, we believe we can develop more powerful decoders, and a much simpler and more elegant theory of polar codes. Furthermore, we expect that the specifically *quantum* aspects of the protocols underlying the Quantum Knowledge project will enable simple, elegant, efficient implementations of quantum polar codes.

Future Work

We will proceed on several fronts. First, we will further develop the theory of quantum agents and quantum knowledge, seeking in particular to understand:

- whether it is self-consistent,

- how much of the ``measurement problem'' can be resolved with it,

- what amount of decoherence is sufficient to make quantum agency unadaptive,

- how this theory relates to the many-worlds hypothesis, and

- what testable predictions can be made about the feasibility of quantum agents.

The second main thrust of this research is to use the theory to develop improved techniques for quantum metrology and estimation. The goal here is to surpass classical limits on sensitivity, while using very modest quantum resources. Candidate problems include quantum state estimation (a.k.a. tomography), state discrimination, and the detection of extraordinarily weak forces. Challenges include (i) discriminating complex states of many-body systems, and (ii) finding and measuring robustly quantum degrees of freedom outside of sheltered laboratory conditions.

We will also use ideas from quantum knowledge to inspire novel quantum algorithms and communication protocols. Protocols for coherent state discrimination and adaptive data compression (which achieve high efficiency on tiny quantum computers) are already being designed. Adaptive communication protocols show great promise. A variety of other computational problems may be addressed using the same intuitions.

Conclusion

The first goal of this project is improved understanding of quantum measurement. This will fill a longstanding gap in our most fundamental physical theory.

The second goal is improved quantum measurement technology. This will assist design of quantum computers; more broadly, it should have repercussions for a broad range of sensing applications, important to science, industry, and national security.

The third goal is development of new quantum information-processing protocols. This will enhance the utility of quantum computers (when they are built) and quantum communication devices (which already exist), as well as illuminating the fundamental limits of quantum information theory.

References

1. Blume-Kohout, R., S. Croke, and M. P. Zwolak. Perfect state discrimination with an O(1)-qubit quantum computer. 2011. *LA-UR 11-05457.*

2. Blume-Kohout, R., and P. S. Turner. The curious nonexistence of Gaussian 2-designs. *Journal of Mathematical Physics.*

3. Blume-Kohout, R., and C. S. Ferrie. Estimating the bias of a noisy coin. To appear in *MaxEnt 2011.* (Waterloo, ON, 10-15 July).

Publications

Blume-Kohout, R., S. Croke, and M. P. Zwolak. Perfect state discrimination with an O(1)-qubit quantum computer. 2011. *LA-UR 11-05457.*

Blume-Kohout, R., and C. S. Ferrie. Estimating the bias of a noisy coin. To appear in *MaxEnt 2011.* (Waterloo, ON, 10-15 July 2011).

Blume-Kohout, R., and P. S. Turner. The curious non-existence of Gaussian 2-designs. *Journal of Mathematical Physics.*

Multiscale Variational Approaches to Markov Random Fields

Michael Chertkov
20090516PRD1

Abstract

It is expected that by combining the multi-scale method with modern computational heuristics for graphical models, such as belief propagation and the variational approach, we can achieve improved performance (both better accuracy and faster convergence of distributed iterative algorithms) in those most challenging applications where current methods either fail or are inaccurate. This project goal was to build new tools for solving a wide range of challenging computational problems in science and engineering.

Methods and algorithms developed under the auspices of this project are relevant to a wide range of problems of interest to LANL that can be posed as one of inference or estimation in a graphical model. Consider reconstruction from a two-dimensional medium, like a network of sensors or compact computer disc. As the density of information increases, it becomes difficult to resolve individual bits, leading to inter-symbol interference. Then, the optimal inference strategy reduces to estimation of an intractable two-dimensional graphical models. This work has also contributed to the development of multi-scale approaches which are of a special importance for inference, optimization and learning problems involving long-range correlations and non-local measurements such as seismic or gravity inversion in geophysics, tomography, and radiography of all types. These methods may also prove relevant in monitoring non-equilibrium dynamical systems that exhibit interactions at multiple scales.

Background and Research Objectives

Graphical models, also known as Bayesian networks or Markov random fields, are statistical models for complex systems of random variables represented as a graph. The nodes of this graph correspond to random variables while its edges denote statistical interactions among those variables. Graphical models have now come to play a central role in many computational fields such as image restoration, computer vision, information theory, and statistical signal processing in oceanography and seismology and biological applications. However, optimal inference and estimation in these models is generally intractable for very large problems. This has driven research and development of principled yet tractable approaches to approximate inference for this rich class of models. These approaches typically involve a distributed message-passing algorithm that serves to propagate information throughout the graph. The performance of these method, however, often suffers in graphical models, which exhibit strong long-range correlations. Handling such situations is precisely the goal of multi-scale methods such as the renormalization group method of statistical physics or the multi-grid method for solving large-scale linear systems. It is the aim of this project to develop a new class of algorithms that combine modern advances in approximate inference and appropriate multi-scale algorithms inspired mainly by the renormalization group method of statistical physics. Our basic strategy is to first consider equivalent reformulation of the inference problem as a multi-scale model by defining an equivalent graphical model depended on an extended set of variables including new auxiliary variables that can be used to represent large-scale interactions of the model. Then, recently developed variational methods can be applied in this extended model where the new auxiliary variables provide additional degrees of freedom to obtain a more accurate solution.

Scientific Approach and Accomplishments

This project focused on combinatorial approaches to approximate inference in graphical models inspired by approaches in statistical physics. In June 2009, we presented the paper "Orbit-Product Representation and Correction of Gaussian Belief Propagation" at the International Conference of Machine Learning. This works build upon Jason's prior work in graduate school on walk-sums in Gaussian graphical models and on Michael Chertkov's prior work on loop series correction to belief propagation (BP) in discrete-variable graphical models. We developed an interpretation of inference in the Gaussian model (essentially computing a matrix determinant) as computing a weighted product over all orbits (closed walks) of the graph and demonstrate that BP captures a certain subset of these orbits. Using this interpretation,

we bound the error of BP and propose methods to compute corrections to BP.

In September 2009, we presented our work on Gaussian BP at the Physics of Algorithms Workshop (Jason was a co-organizer of this workshop). This presentation included extensions of our orbit-product framework to analyze Generalized Belief Propagation (GBP) [of Yedidia et al] in the context of Gaussian graphical models. The basic idea behind GBP is to use exact inference within small subgraphs together with message-passing between subgraphs to obtain a better approximation that captures small cycles of the graph. Our analysis confirms this intuition for Gaussian models, providing error-bounds dependent on the length of the shortest orbit omitted by GBP. However, we also show that the subgraphs used in GBP must be chosen properly to avoid over-counting orbits, which can destabilize the iterative algorithm or results in inaccurate estimates. We are currently preparing a conference paper on GBP, and plan a longer journal article combining both conference papers to be submitted in the fall.

In related work, we have developed an extension of these methods aimed at analysis of belief propagation in binary-variable graphical models. A key ingredient of this approach is a method of Kac and Ward that allows the partition function of the planar Ising model in statistical physics (a seemingly intractable sum over all states of the model) to be expressed simply as a determinant of a matrix which generates non-backtracking orbits of the graph. Using this construction, we have shown that it is possible to express the BP estimate of the partition function of the (non-planar) Ising model as a nonbacktracking orbit-product of the graph. Ultimately, we hope to use the representation to derive new results for the convergence and accuracy of BP in binary-variable graphical models, analogous to those we have already derived in the Gaussian model. A by-product of this work has been the invention of a new approach to approximate inference in graphical models. Whereas belief propagation may be seen as inference on the computation tree of the graph (the infinite tree cover of the graph), a more general approach is to construct iterative algorithms that can be interpreted as inference on other infinite planar covers of the graph. Similar as in GBP, this allows retaining many cycles of the graph so as to given a better approximation to the original graphical model. Inference in this planar cover may be implemented using a combination of message-passing ideas and Gaussian elimination to compute determinants of planar subgraphs of the non-planar graph.

Jason has also made contributions to an allied project, Optimization and Control of Smart Grids,adapting methods for learning sparse graphical models (part of his graduate work) to the problem of near-optimal design of power transmission networks. We pose the network design problem of selecting the network (both its graph structure and line conductances) to minimize a combination of the power er dissipation within the network and cost of resources needed to build the network. Building on work of Ghosh, Boyd and Saberi and of Candes and Boyd, we developed a principled optimization approach to solve this problem and have recently submitted the "A Majorization-Minimization Approach to Design of Power Transmission Networks" to the IEEE Conference of Decision and Control.

Impact on National Missions

This project will support the DOE mission in Office of Science by enhancing our understanding of Inference and Optimization Techniques. Our multiscale approach is relevant to long-range correlations and non-local measurements such as seismic or gravity inversion in geophysics, tomography, and radiography of all types, with several national security applications.

Publications

Johnson, J., D. Bickson, and D. Dalev. Fixing Convergence of Gaussian Belief Propagation. 2009. In *International Symposium on Information Theory (ISIT).* (Seoul, June 2009). , p. 1674. Piscataway, NJ, USA: atawa.

Johnson, J., V. Chernyak, and M. Chertkov. Orbit-Product Representation and Correction of Gaussian Belief Propagation. 2009. In *International Conference on Machine Learning (ICML).* (Montreal, June 2009). Vol. 38, p. 473. New York: ACM.

Johnson, J., and M. Chertkov. A Majorization-Minimization Approach to Design of Power Transmission Networks. 2010. In *49th IEEE Conference on Decision and Control.* (Atlanta, Georgia, , Dec. 2010). , p. 1. Atlanta: IEEE.

Netrapalli, P., J. Johnson, and M. Chertkov. Greedy Learning of Planar Ising Graphical Models. Presented at *Artificial Intelligence and Statistics (AISTATS 2011).* (Ft. Laudedale, Florida, Apr, 2011).

PHYSICS

New Generation Hydrodynamic Methods: from Art to Science (U)

Donald E. Burton
20100015DR

Introduction

Hydrodynamic simulations are central to the core missions of the National Laboratories. The DOE's Advanced Scientific Computing (ASC) program has developed simulation codes that have become successful tools, but because they are applied to increasingly challenging problems with higher expectations for accuracy, revision and improvements of the basic algorithms is badly needed. In fact, most of the simulation methods have a common origin dating back to the 1950s and constitute a common mode of failure for these new-generation codes across the DOE complex.

When applied to configurations that have been well studied, the errors associated with the current methods are acceptably small. However, when applied to some configurations, especially in 3D, these methods are known to produce unacceptable numerical errors that cannot be eliminated even by optimized meshing techniques. Demands on hydrodynamics simulators are increasing to the point where these errors can no longer be ignored, and it is necessary to turn to more advanced hydrodynamics methods.

For historical reasons, the term "hydrodynamics" encompasses the more commonly recognized branches of science known as computational fluid dynamics (CFD) and computational solid mechanics. To date, no perfect hydrodynamics method has been found. This research project proposes a new scheme that is in the family termed "cell-centered hydrodynamics" (CCH) and which appears to be highly promising. Preliminary theoretical analysis and a prototype implementation suggested the method to be superior to traditional methods for all test problems investigated. Whether it can be adapted for the full range of applications addressed by ASC codes remains to be determined.

Benefit to National Security Missions

As noted, hydrodynamic simulations are central to many missions of the NNSA and other agencies. In the past decade, the simulation tools have been acceptable for that mission. However, future demands on the simulation tools will require increased accuracy. Because of this, the errors in hydrodynamics simulation that were formerly acceptable will not be in the future. And this research intends to address that problem.

The project aims to develop the theory and numerical algorithms for this new hydrodynamics method, implement it in an established code framework, evaluate its performance relative to historical methods, and extend it as needed to address practical applications. The risk associated with developing a new hydrodynamics method is high. To successfully address the national security goal, the new method must not only offer substantial improvements over existing methods, it must be functionally equivalent. That is, it must have the same realm of physical applicability and support similar interfaces to related physics modules.

Progress

The project was reviewed by an external panel in March 2010 and was also reappraised in October 2011. The former reviewers concluded that the LDRD project "is highly relevant to the strategic directions of the laboratory. It has made substantial progress despite having been funded for only a few months, and is ahead of its planned schedule. The project team is first-rate and the technical work is of the highest quality." At the October 2011 reappraisal, reviewers rated the project Excellent to Outstanding in all four categories of quality, performance, relevance, and leadership.

The work divides into four areas: theory, implementation, verification, and publication.

Theory

Many areas of importance to practical applications have not been widely explored in the literature in a CCH context, including a full stress tensor formulation coupled to general solid models, unstructured polytopal grids, multi-dimensional formulation with curvilinear geometry, arbitrary Lagrange-Euler (ALE) with multi-material cells, and contact surfaces.

Since the above areas have not been well studied, considerable effort was expended this year on developing the mimetic foundations of the new CCH method. The term "mimetic" means that the numerical model should mimic all the properties of the physical system, including not only the usual conservation laws but also a number of ancillary relationships. In particular, we have shown that necessary conservation and ancillary relations are satisfied by CCH: the geometric conservation law is satisfied by corner fluxes; curl-divergence relations are satisfied; both the mechanical and viscous stress tensors are symmetric and preserve rotational equilibrium; the area weighted equations in axial geometry are conservative and preserve symmetry; rotational symmetry and adiabatic compression conditions can be satisfied.

Particular attention has been paid to entropy errors associated with walls as well as a limiting case of isentropic compression. We developed a new tensor dissipation model that corrects a long-standing error in the published literature and also offered an explanation and possible correction for a poorly understood numerical error termed "wall-heating."

Implementation

Considerable progress has been made on developing a code module suitable for large-scale simulations. We have written several prototype implementations in a relevant code framework (the ASC code FLAG) and are extending the latest to include essential capabilities for real-world applications as discussed above. To date, calculations have been done in one, two, and three dimensions, including several curvilinear geometries. Calculations involving elastic-plastic, strain-hardening solids have also been performed.

Verification

Verification of the code implementation involves applying it to problems with known solutions. Preliminary experience with the FLAG implementation suggests the new method is consistently superior to historical schemes. In particular we found improved robustness, accuracy, symmetry preservation, along with a reduction in mesh imprinting and entropy errors.

Publication

Preliminary results have been presented at several international forums: MultiMat09 (Pavia IT 2009), JOWOG-42 (Aldermaston 2009, Livermore 2010), NEDPC-09 (Livermore), NECDC-10 (Los Alamos 2010), SIAM (Reno 2011), and MultiMat11 (Arachon FR 2011).

Future Work
Future work in the coming year falls within the five areas mentioned in the previous section.

Theory: The team will continue to develop and extend current theory to encompass hydrodynamic and numerical capabilities required for a general-purpose hydrodynamics code. Specific tasks for the coming year include developing the theory for discontinuous slide/contact surfaces and also for arbitrary Lagrange-Euler (ALE) in which the mesh is adaptively modified during the calculation.

Implementation: Phased implementation in an established hydrocode framework will continue with focus on the aforementioned slide and ALE algorithms.

Testing and verification: As implemented capabilities become available, they will be tested against other codes and analytical solutions. Testing will be weighted toward assessing the method with regard to its ultimate applications.

Publication: Drafts of four journal articles have been prepared for submission in the near future. Participation at several conferences is planned.

Conclusion
The project team anticipates the effort will improve the ability of the national laboratories and other institutions to execute their core missions. This will result from significant improvements in the fidelity of hydrodynamic simulations. The effort will give rise to products on several levels. The theory, algorithms, and assessment of the method has been presented in open forums and will be published in peer-reviewed literature. There will be a prototype implementation suitable for large-scale simulations and compatible with ASC code requirements.

Publications
Burton, D. E.. New generation hydrodynamics methods. 2010. *Los Alamos National Laboratory report LA-UR-10-01398.*

Burton, D. E., T. C. Carney, N. R. Morgan, S. R. Runnels, and M. J. Shashkov. A cell-centered Lagrangian hydrodynamics method for multi-dimensional unstructured grids in curvilinear coordinates with solid constitutive models. Presented at *International Conference on Numerical Methods for Multi-Material Fluid Flows.* (Acachon FR, 5-9 Sep. 2011).

Burton, D. E., T. C. Carney, N. R. Morgan, S. R. Runnels, and M. J. Shashkov. Exploration of a cell-centered Lagrangian hydrodynamics method. Presented at *SIAM Conference on Computational Science & Engineering .* (Reno NV, 28 Feb. - 4 Mar. 2011).

Burton, D. E., T. C. Carney, N. R. Morgan, S. R. Runnels, and M. J. Shashkov. New generation hydrodynamics methods: from art to science. 2011. *Los Alamos National Laboratory Report LA-UR-11-05976.*

Burton, D. E., and M. J. Shashkov. Mimetic formulation

of cell-centered Lagrangian hydrodynamics. Invited presentation at *Numerical Methods for Multi-Material Fluids & Structures, LA-UR-09-05875.* (Pavia, Italy, 21-25 Sep. 2009).

Burton, D. E., and M. J. Shashkov. Mimetic formulation of cell-centered hydrodynamics (CCH), LA-UR-09-06533. Presented at *NEDPC 2009.* (Livermore, CA, 2-30 Oct. 2009).

Burton, D. E., and M. J. Shashkov. Mimetic formulation of cell-centered Lagrangian hydrodynamics (CCH), LA-UR-09-03454. Presented at *JOWOG 42 2009.* (Aldermaston, UK, 8-12 June 2009).

Burton, D., T. Carney, S. Runnels, and M. Shashkov. Exploration of a cell-centered Lagrangian hydrodynamics method, LA-UR-10-06548. Presented at *NECDC 2010.* (Los Alamos, NM, 18-22 Oct. 2010).

Morgan, N.. Numerical and physical dissipation in Lagrangian hydrodynamics. Presented at *International Conference on Numerical Methods for Multi-Material Fluid Flows.* (Arcachon FR, 5-9 Sep. 2011).

Runnels, S. R., and L. Gilman. Superposition and reconciliation based cell centered hydro method. 2011. *Los Alamos National Laboratory report LA-UR-06002.*

Runnels, S., and D. Burton. LANL cell-centered hydro research, LA-UR-10-04062. Presented at *JOWOG 42 2010.* (Livermore, CA, 21-24 Jun. 2010).

Cosmological Signatures of Physics Beyond the Standard Model: Petascale Cosmology Meets the Great Surveys

Michael S. Warren
20100023DR

Introduction

The unveiling of the secrets of the large-scale Universe by astronomical surveys has transformed cosmology, fundamental physics, and astrophysics. Dark energy and dark matter are at the focus of an intense global effort to understand the deep mysteries posed by their existence. Next-generation observations promise new discoveries and an unprecedented jump in our knowledge of the Universe. Along with these observations, computer simulations enable discovery. The only way to accurately model the evolution of dark matter in the Universe is through the use of advanced algorithms on massively parallel computers. In the words of the Astronomy and Astrophysics Decadal Survey, "Through computer modeling, we understand the deep implications of our very detailed observational data and formulate new theories to stimulate further observations." Our scientific aims are to use computer simulations to better understand the fundamental properties of the large-scale Universe. These questions at the frontier of science include:

- How do cosmic structures form and evolve?

- What are the connections between dark and luminous matter?

- What is dark matter?

- Why is the universe accelerating?

Cosmological simulations are the cornerstone of theoretical analysis of large-scale structure. During the next decade large astronomical observing projects such as the Large Synoptic Survey Telescope (LSST) in optical wavelengths and the Square Kilometer Array (SKA) in the radio spectrum will gather hundreds to thousands of petabytes of observational data. Advances in modeling must keep pace with observational advances if we are to understand the Universe, which led to these observations. To answer these questions, two newly developed capabilities, unique to our effort at Los Alamos, are very significant: (i) The Hashed Oct-tree (HOT) cosmology code, which has achieved remarkable performance on LANL institutional computing resources (Figure 1). This capability will establish new benchmarks for the state of the art in predicting cosmological statistics for large-scale structure surveys. (ii) A new statistical framework that melds precision predictions with observations, and removes the computational barrier to Monte Carlo analyses of cosmological data. This framework can combine datasets from different observations, detailed simulation predictions, and systematic and statistical error models. It will be essential for interpreting data, and for optimizing observational strategies.
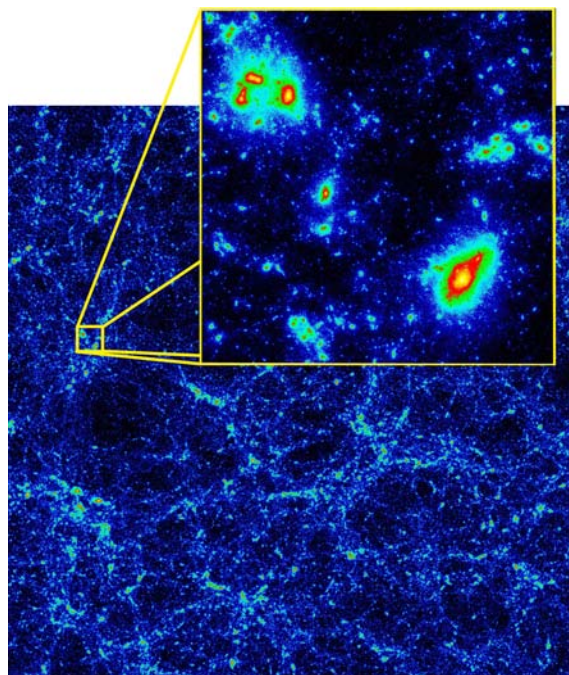
Figure 1. The logarithmically scaled density field of dark matter from an 8.6 billion particle simulation in a computational volume approximately 500 million light-years across (the densest galaxy halo regions are yellow, with the least dense areas in blue). The inset shows a 1/25 scale region at high resolution (12,000 light-years per pixel). The N-body simulation was performed by our highly optimized Hashed Oct-tree code on the LANL Conejo supercomputer, sustaining over 50% of the peak performance of the machine on 2048 CPU cores.

Benefit to National Security Missions

Our project targets questions about the nature of dark matter and dark energy, which is highly relevant to DOE/SC and NASA. A major component of our project involves innovative concepts for high-performance computing and another major component targets data-intensive computing, both very relevant to DOE/SC and DOE/ASCR. Our work on statistics applied to large datasets as well as code verification and validation builds capability for high-performance weapons program modeling.

Progress

Our project has made significant progress across a spectrum of theoretical and computational efforts. The Cosmic Emulator (CosmicEmu) was expanded to include the linear power spectrum for a given cosmology in addition to the nonlinear power spectrum. An additional improvement involved extending the range of wavelength over which the spectrum is produced [1]. Upcoming imaging surveys such as the Large Synoptic Survey Telescope will repeatedly scan large areas of sky and have the potential to yield million-supernova catalogs. Type Ia supernovae are excellent standard candles and will provide distance measures that suffice to detect mean pairwise velocities of their host galaxies. We showed that when combining these distance measures with photometric redshifts for either the supernovae or their host galaxies, the mean pairwise velocities of the host galaxies will provide a dark energy probe which is competitive with other widely discussed methods [2]. We studied a class of early dark energy (EDE) models, in which, unlike in standard dark energy models, a substantial amount of dark energy exists in the matter-dominated era. We self-consistently include dark energy perturbations, and show that these models may be successfully constrained using future observations of galaxy clusters, in particular the redshift abundance, and the Sunyaev-Zel'dovich (SZ) power spectrum [3]. The mass distribution of halos, as specified by the halo mass function, is a key input for several cosmological probes. The sizes of N-body simulations are now such that, for the most part, results need no longer be statistics-limited, but are still subject to various systematic uncertainties. We investigated some of the reasons for these differences. We conclude that fitting formulae based on a universal form for the mass function may have limited utility in high precision cosmological applications [4]. One way to help unravel the mystery of dark energy is to better characterize the redshift-dependence of the dark energy equation of state parameter, $w(z)$. To do this requires a robust and bias-free method for reconstructing $w(z)$ from data that does not rely on restrictive expansion schemes or assumed functional forms for $w(z)$. We presented a new nonparametric reconstruction method that solves for $w(z)$ as a statistical inverse problem, based on a Gaussian Process representation. This method reliably captures nontrivial behavior of $w(z)$ and provides controlled error bounds. [5]. We collaborated in a detailed comparison of fundamental dark matter halo properties retrieved by a substantial number of different halo finders. We further introduced a robust (and publicly available) suite of test scenarios that allows halo finder developers to compare the performance of their codes. All the halo finding codes tested could successfully recover the spatial location of our mock haloes. Via a resolution study we found that most of the finders could not reliably recover substructure containing fewer than 30-40 particles. However, also here the phase space finders excelled by resolving substructure down to 10-20 particles. By comparing the halo finders using a high resolution cosmological volume we found that they agree remarkably well on fundamental properties of astrophysical significance (e.g. mass, position, velocity, and peak of the rotation curve) [6]. The Hashed Oct-tree (HOT) cosmology code has been further optimized, and has demonstrated performance of over 50% of peak on 2048 processors of the Conejo system at LANL. This is a remarkable performance, as unoptimized codes often reach only a few percent of peak. Improvements in accuracy and efficiency have also been implemented [7]. As the mass of clusters is not directly measured in most cases, we must improve the observable-mass relations, and in particular to quantify the scatter these relations exhibit. For a sample of 4500 simulated clusters we experimented with different ways to classify clusters into different "types", based on their dynamical state. We selected fossil groups in simulations using merger trees to reconstruct their evolution [8]. We constructed weak lensing deflection maps by ray tracing through cosmological simulation density fields, as well as calibrating the Lyman-alpha forest using cross-correlation with the 21-cm radiation field [9]. Type Ia supernovae are standard candles and can be used to measure cosmic distances. Combined with their redshift information, large number of SNIa can be used to determine the bulk velocity of the universe. Such a dataset is obtainable from the future LSST SNIa survey, and can be used to determine the dark energy parameters. We show that combined with the standard luminosity distance test, SNIa derived velocity can help improve the measurements of dark energy parameters by a factor of 2 [10]. We completed a search for strongly lensed quasars with large separation of macro images in our light curve database based on image subtraction photometry of SDSS Stripe 82. Using our high signal to noise photometry based on the image subtraction technique, we computed the variability structure function in the g band for spectroscopically confirmed quasars in Stripe 82 (~7500 light curves). We clearly detected the presence of two power-law slopes in the structure function with a break at 43 days. We interpreted these results in the context of leading models of quasar variability. There is evidence that two separate variability mechanisms are operating: accretion disk instabilities short time scales (< 3 months) and starburst-related supernova explosions at long time scales [11].

Future Work

Cosmology is entering one of its most scientifically exciting phases. The last two decades have culminated in the celebrated Standard Model of cosmology. Yet, two pillars of the Standard Model, dark matter and dark energy -- together accounting for 95% of the mass-energy of the Universe -- remain its greatest mysteries. To venture beyond the current boundaries, cosmological survey capabilities are being spectacularly improved. Interpretation of future observations is impossible without a theory, modeling, and simulation effort fully as revolutionary as the new surveys. The fundamental parameters of the Universe are embedded in the statistical measures of galaxy positions and velocities, which hold the key to many cosmological questions. The most basic statistical measures of galaxy clustering are the power spectrum and the two-point correlation function. Our Discovery Science objectives will be enabled through the production of the world's highest-quality library of galaxy tracers (i.e. "mock catalogs"). Additionally, velocities are an underutilized statistic for understanding how cosmic structures form and evolve. We plan to use both pairwise velocity correlations and velocity dispersion statistics to illuminate the behavior of dark matter in a way that can be more easily related to the observed properties of luminous matter. The evolution of density fluctuations in dark matter at early times is a potentially major influence on the properties of galaxies today, and may provide clues to the fundamental nature of dark matter. An unresolved question is what is the smallest scale at which dark matter clusters? Answering this question requires careful consideration of the initial conditions of the dark matter in the Universe, as well as posing a severe computational challenge, since a small computational volume can not be considered in isolation from the rest of the Universe.

Conclusion

Observations indicate that the Universe consists of 70% of a mysterious dark energy and 25% of a yet unidentified dark matter. Understanding the physics of this dark sector is one the foremost challenges in all of physics. This project will make important contributions to further this understanding. We will provide the essential theoretical and modeling framework to interpret results from major upcoming observational missions. Only by performing complex simulations and modeling tasks will we be able to analyze the wealth of upcoming data and shed light on the physics of the dark Universe.

References

1. Lawrence, E.. Cosmic Emulators. 2011. *CosmicEmu v1.0.*

2. Bhattacharya, S., A. Kosowsky, J. A. Newman, and A. R. Zentner. Galaxy peculiar velocities from large-scale supernova surveys as a dark energy probe. 2011. *Physical Review D.* **83** (4): 043004.

3. Alam, U., Z. Lukic, and S. Bhattacharya. Galaxy Clusters as a Probe of Early dark Energy. 2011. *Astrophysical Journal.* **727** (2): 87 (8 pp.).

4. Bhattacharya, S., K. Heitmann, M. White, Z. Lukic, C. Wagner, and S. Habib. Mass Function Predictions Beyond ΛCDM. 2011. *Astrophysical Journal.* **732** (2): 122 (17 pp.).

5. Holsclaw, T., U. Alam, B. Sanso, H. Lee, K. Heitmann, S. Habib, and D. Higdon. Nonparametric reconstruction of the dark energy equation of state. 2010. *PHYSICAL REVIEW D.* **82** (10): 103502.

6. Knebe, A., S. Knollmann, S. Muldrew, F. Pearce, M. A. Aragon-Calvo, Y. Ascasibar, P. Behroozi, D. Ceverino, S. Colombi, J. Diemand, K. Dolag, B. Falck, P. Fasel, J. Gardner, S. Gottlober, C. Hsu, F. Iannuzzi, A. Klypin, Z. Lukic, M. Maciejewski, C. McBride, M. Neyrinck, S. Planelles, D. Potter, V. Quilis, Y. Rasera, J. Read, P. Ricker, F. Roy, V. Springel, J. Stadel, G. Stinson, P. M. Sutter, V. Turchaninov, D. Tweed, G. Yepes, and M. Zemp. Haloes gone MAD: The Halo-Finder Comparison Project. 2011. *MONTHLY NOTICES OF THE ROYAL ASTRONOMICAL SOCIETY.* **415** (3): 2293.

7. Warren, M. S.. Optimizing the inner loop of the gravitational force interaction on modern processors. 2010. *LA-UR-10-08134.*

8. Borozdin, K. N.. Properties of galaxy clusters in the hydrodynamical N-body simulations. 2011. *LA-UR-11-05565.*

9. Vallinotto, A.. Using CMB lensing to constrain the multiplicative bias of cosmic shear. 2011. *LA-UR-11-11572.*

10. Vallinotto, A.. The cross correlation between the 21-cm radiation and the CMB lensing field: a new cosmological signal. 2011. *LA-UR-11-10407.*

11. Wozniak, P. R., and A. Voevodkin. Structure function and variability mechanism of quasars from SDSS stripe 82. 2011. *LA-UR-11-00034.*

Publications

Ahrens, J., K. Heitmann, M. Petersen, J. Woodring, S. Williams, P. Fasel, C. Ahrens, C. H. Hsu, and B. Geveci. Verification of scientific simulations via hypothesis-driven comparative and quantitative visualization. 2010. *IEEE Computer Graphics and Applications.* **30** (6): 16.

Alam, U., Z. Lukic, and S. Bhattacharya. Galaxy Clusters as a Probe of Early dark Energy. 2011. *Astrophysical Journal.* **727** (2): 87 (8 pp.).

Bhattacharya, S., A. Kosowsky, J. A. Newman, and A. R.

Zentner. Galaxy peculiar velocities from large-scale supernova surveys as a dark energy probe. 2011. *Physical Review D.* **83** (4): 043004.

Bhattacharya, S., K. Heitmann, M. White, Z. Lukic, C. Wagner, and S. Habib. Mass Function Predictions Beyond ΛCDM. 2011. *Astrophysical Journal.* **732** (2): 122 (17 pp.).

Bhattacharya, S., L. D. Shaw, and D. Nagai. Measurement of ICM properties from the current cluster data. 2011. *LA-UR-11-00218.*

Borozdin, K. N.. Properties of galaxy clusters in the hydrodynamical N-body simulations. 2011. *LA-UR-11-05565.*

Borozdin, K., and Z. Lukic. Studying Dark Energy with eRosita. 2011. *LA-UR-11-11692.*

Higdon, D. M., E. Lawrence, K. Heitmann, and S. Habib. Bayesian approaches for combining computational model output and physical observations. 2011. *LA-UR-11-04315.*

Higdon, D., K. Heitmann, E. Lawrence, and S. Habib. Using the bayesian framework to combine simulations and physical observations for statistical inference. 2011. In *Large-scale inverse problems and quantification of uncertainty.* Edited by Biegler, L., G. Biros, O. Ghattas, M. Heinkenschloss, D. Keyes, B. Mallick, L. Tenorio, B. van Bloemen Waanders, K. Wilcox, and Y. Marzouk. , p. 87. West Sussex: Wiley.

Holsclaw, T., U. Alam, B. Sanso, H. Lee, K. Heitmann, S. Habib, and D. Higdon. Nonparametric dark energy reconstruction from supernova data. 2010. *Physical Review Letters.* **105** (24): 241302.

Holsclaw, T., U. Alam, B. Sanso, H. Lee, K. Heitmann, S. Habib, and D. Higdon. Nonparametric reconstruction of the dark energy equation of state. 2010. *PHYSICAL REVIEW D.* **82** (10): 103502.

Hsu, Chung-Hsing, J. P. Ahrens, and K. Heitmann. Verification of the Time Evolution of Cosmological Simulations via Hypothesis-Driven Comparative and Quantitative Visualization. 2010. In *2010 IEEE Pacific Visualization Symposium (PacificVis 2010) ; 2-5 March 2010 ; Taipei, Taiwan.* , p. 81.

Kaufman, C., D. Bingham, S. Habib, K. Heitmann, and J. Frieman. Efficient Emulators of Computer Experiments Using Compactly Supported Correlation Functions, With an Application to Cosmology. To appear in *The Annals of Applied Statistics.*

Knebe, A., S. Knollmann, S. Muldrew, F. Pearce, M. A. Aragon-Calvo, Y. Ascasibar, P. Behroozi, D. Ceverino, S. Colombi, J. Diemand, K. Dolag, B. Falck, P. Fasel, J. Gardner, S. Gottlober, C. Hsu, F. Iannuzzi, A. Klypin, Z. Lukic, M. Maciejewski, C. McBride, M. Neyrinck, S. Planelles, D. Potter, V. Quilis, Y. Rasera, J. Read, P. Ricker, F. Roy, V. Springel, J. Stadel, G. Stinson, P. M. Sutter, V. Turchaninov, D. Tweed, G. Yepes, and M. Zemp. Haloes gone MAD: The Halo-Finder Comparison Project. 2011. *MONTHLY NOTICES OF THE ROYAL ASTRONOMICAL SOCIETY.* **415** (3): 2293.

Lawrence, E.. Cosmic Emulators. 2011. *CosmicEmu v1.0.*

Lawrence, E., K. Heitmann, M. White, D. Higdon, C. Wagner, S. Habib, and B. Williams. The coyote universe. iii. simulation suite and precision emulator for the nonlinear matter power spectrum. 2010. *Astrophysical Journal.* **713** (2): 1322.

Pan, A. V., and U. Alam. Reconstructing dark energy: A comparison of different cosmological parameters. *Physical Review D.*

Pope, A., S. Habib, Z. Lukic, D. Daniel, P. Fasel, K. Heitmann, and N. Desai. The Accelerated Universe. 2010. *Computing in Science & Engineering.* **12** (4): 17.

Shandarin, S., S. Habib, and K. Heitmann. Origin of the cosmic network in Lambda CDM: Nature vs nurture. 2010. *PHYSICAL REVIEW D.* **81** (10): 103006.

Vallinotto, A.. Using CMB lensing to constrain the multiplicative bias of cosmic shear. 2011. *LA-UR-11-11572.*

Vallinotto, A.. The cross correlation between the 21-cm radiation and the CMB lensing field: a new cosmological signal. 2011. *LA-UR-11-10407.*

Warren, M. S.. Optimizing the inner loop of the gravitational force interaction on modern processors. 2010. *LA-UR-10-08134.*

White, M., A. Pope, J. Carlson, K. Heitmann, S. Habib, P. Fasel, D. Daniel, and Z. Lukic. Particle mesh simulations of the Lyα forest and the signature of baryon acoustic oscillations in the intergalactic medium. 2010. *Astrophysical Journal.* **713** (1): 383.

Woodring, J., J. Ahrens, J. Figg, J. Wendelberger, S. Habib, and K. Heitmann. In-situ Sampling of a Large-Scale Particle Simulation for Interactive Visualization and Analysis. 2011. *COMPUTER GRAPHICS FORUM.* **30** (3): 1151.

Woodring, J., J. Ahrens, J. Figg, J. Wendelberger, S. Habib, and K. Heitmann. In-situ Sampling of a Large-Scale Particle Simulation for Interactive Visualization and Analysis. 2011. *COMPUTER GRAPHICS FORUM.* **30** (3): 1151.

Woodring, J., K. Heitmann, J. Ahrens, P. Fasel, Chung-Hsing

Hsu, S. Habib, and A. Pope. Analyzing and Visualizing Cosmological Simulations with ParaView. 2011. *Astrophysical Journal Supplement Series.* **195** (1): 11 (12 pp.).

Woodring, J., K. Heitmann, J. Ahrens, P. Fasel, Chung-Hsing Hsu, S. Habib, and A. Pope. Analyzing and Visualizing Cosmological Simulations with ParaView. 2011. *Astrophysical Journal Supplement Series.* **195** (1): 11 (12 pp.).

Wozniak, P. R., and A. Voevodkin. Structure function and variability mechanism of quasars from SDSS stripe 82. 2011. *LA-UR-11-00034.*

Yang, H. -Y Karen., S. Bhattacharya, and P. M. Ricker. The Impact of Cluster Structure and Dynamical State on Scatter in the Sunyaev-zel'dovich Flux-mass Relation. 2010. *Astrophysical Journal.* **725** (1): 1124.

Information Science for Understanding Complex Quantum Matter

Malcolm G. Boshier
20100045DR

Introduction

The challenge motivating this project was famously articulated 25 years ago by Richard Feynman. He pointed out that simulating quantum many-body systems on a computer is exponentially difficult: just storing the state of a system with N parts requires an exponentially large memory. Exact simulation of large quantum systems on classical computers is thus impossible (e.g. Roadrunner might manage to do 42 spin-½ particles, but a future exaflop machine, 1000x faster than Roadrunner, could only increase this number to 52). Exponential complexity is the reason why a recent BES report discussing high-Tc superconductivity laments that "We do not even know whether the 2D Hubbard model has a stable superconducting ground state." Fundamental difficulties like these motivate our search for completely new ways to compute many-body quantum systems. Together, our capabilities in quantum information (QI) science and in quantum many-body physics can address this challenge. Feynman's visionary solution to the quantum complexity problem was effectively a restricted form of quantum computing: use a controllable quantum system with the same Hamiltonian as the system of interest to emulate its behavior. While easier than universal quantum computation, this quantum emulation is still technically extremely demanding because of the unavoidable coupling between a quantum system and its environment, which acts to destroy superposition through decoherence and to remove energy through dissipation. However, laboratory control over quantum systems, especially with QI techniques from ultracold atomic physics, is reaching a point where quantum emulation looks feasible. This unprecedented level of control opens up novel opportunities for probing complexity in quantum many-body systems. QI also inspires a second solution to the complexity issue: new algorithms to simulate (approximately, but efficiently) a large class of quantum systems on present day classical computers. Together, these QI-derived techniques could transform the simulation of quantum many-body systems.

Benefit to National Security Missions

The tools of quantum emulation and quantum-information-inspired algorithms developed in this project will provide powerful new ways compute the properties of complex quantum systems. This work is directly relevant to the missions of DOE/SC, in particular the Basic Understanding of Materials and, to a somewhat lesser extent, Fundamental Chemistry. The controllable quantum systems we will build for emulation may also have sensing applications ultimately useful to missions in DOE/NNSA, DOE/NN and the Intelligence Community.

Progress

Boshier, Ryu, and Blackburn continue to exploit our collaboration's newly demonstrated capability to create large toroidal Bose-Einstein condensates (BECs) and set them into quantized rotation [1]. Recent progress includes a rebuild of the optical part of the experiment to make the system more robust and to allow for higher resolution in both painting the trap and in imaging the result. We believe that we are now able to paint barriers which are thin enough to allow significant quantum-mechanical tunneling, which would enable us to create atom SQUIDs and even arrays of coupled quantum systems. The unique nature of the painted potential capability has naturally pushed the theoretical components of the project in the direction of more fully exploiting it.

Zurek and Das have investigated phase transition dynamics in toroidal BECs. A paper on this topic [2] has just been submitted. It studies behavior of the stochastic Gross-Pitaevskii equation during a phase transition and calculates expected winding numbers. The results confirm the predictions of the Kibble-Zurek mechanism. We have also studied influence of the imperfections in the experiment by considering a tilted torus (as a simple model of an imperfect torus potential with relevance to the experiment).

Timmermans anticipated quantum sensing applications with multi-spin component cold atoms and focused on BEC-phase separation, and on Superfluid Quantum

Interference (SQUID)-like toroidal BECs. With visitor Deborah Santamore, Timmermans developed the effective spin description of two-level atoms, mapping the many boson problem into spin systems [3]. They studied the control required for investigating scaling of the zero-temperature spin-domain formation transition. These studies revealed that the mean-field description breaks down near the transition that is a second-order transition at zero temperature. They found that long-range spin fluctuations dominate near the critical point whereas, for Rubidium atoms, the long-range density fluctuations will be suppressed [4]. With student Rudra Kafle, Timmermans found that the effective gauge induced by a position-dependent spin can tune the resolution of a gyroscope that is that is a toroidal BEC sensing rotation by observing a change in the winding number.

Mozyrsky, in collaboration with postdoc Solenov, studied dynamics of toroidal BECs with transverse size smaller than the coherence length. A BEC under such conditions can be considered 1-dimensional and, as a result, it exhibits a number of interested physical properties. In particular Mozyrsky considered a situation when such a BEC ring is rotating, which can be readily achieved in the experiment. For certain values of rotational frequencies, the ground state of such system turns out to be doubly degenerate. That is, the states with different persistent currents through the ring have equal energy. Mozyrsky and his collaborator considered several mechanisms that lead to the coherent transitions between such states as well as the means to control such transitions. Their study has included dynamics of BECs confined to ring-shaped trapping potentials containing Josephson junctions, as well as local scattering potentials [5-7].

Damski has studied dynamics of an ultracold atomic BCS superfluid driven by a gradual decrease of the pairing interaction [8]. We have used a cold fermion cloud as a quantum emulator of a conventional superconductor. Experimental realization of such driving in conventional superconductors would require a real-time change of either dopant concentration or lattice structure, which is essentially impossible. We found interesting dynamics of the Cooper pairs, which should stimulate future experiments on out-of-equilibrium fermionic gases. They also studied how non-equilibrium dynamics of an environment driven across the critical point affects decoherence rate of a qubit [9]. As an environment we have chosen a quantum Ising chain, while the qubit has been represented as a spin 1/2. We have found the exact solution for this problem, simplified it analytically and generalized our results to other universality classes (environments). This work demonstrated rich manifestations of decoherence induced by a dynamical phase transition in the environment. It also illustrates deep connections between non-equilibrium decoherence and the theory of topological defect creation in non-equilibrium phase transitions.

Dalvit and colleagues have studied effects of disorder in Bose-Einstein condensates induced by quantum vacuum effects. Disordered geometrical boundaries such as rough surfaces induce important modifications to the mode spectrum of the electromagnetic quantum vacuum. In analogy to Anderson localization of waves induced by a random potential, we showed that the Casimir-Polder interactions between a cold atomic sample and a rough surface produces localization phenomena [10]. These effects, which represent a macroscopic manifestation of disorder in quantum vacuum, should be observable with Bose-Einstein condensates expanding in proximity of rough surfaces. We have also studied the non-equilibrium dynamics of atom-dielectric interactions mediated by quantum field. We have given a first principles microphysics derivation of the non-equilibrium force between an atom and a bulk dielectric medium coupled to a reservoir. More recently, we have started to look into the problem of decoherence in atom-interferometry with atom-chips. The goal is to use methods of open quantum systems to control decoherence in atom-interferometry, which leads to dephasing of the atom beams in each interferometer arm. We are currently undertaking calculations, using open systems techniques, to assess the significance and effect of decoherence for atom beams travelling near metallic surfaces.

Future Work

Our primary goal is to make several significant advances in quantum emulation experiment and theory. A secondary goal is to enhance the state of the art in several important QI technologies.

LANL today possesses the two key ingredients for success in this plan: exquisite laboratory control over quantum systems with interesting Hamiltonians, and state of the art theory to devise clever strategies and targets for emulation. Our focus is now on building an emulator based on the QI technology of trapped Bose-Einstein condensates (BECs). This program harnesses original Los Alamos work both in theory and experiment which give LANL unique advantages in the race to build useful quantum emulators. LANL's theoretical expertise in decoherence, quantum computing, quantum phase transitions, and quantum many-body physics will both provide the crucial emulator and algorithmic theory and steer the project in exciting directions.

The classes of problems within reach of our techniques are large. We are considering systems governed by many-body Hamiltonians containing Ising/Heisenberg (spin-spin interactions) or Bose-Hubbard (tunneling and on-site interactions) terms. It should be possible to add interesting complexity and realism by controllably introducing frustration, disorder, decoherence, and dissipation to the systems. We will compute both static properties and dynamics, including those of quantum phase transitions (QPTs), with emphasis on scaling behavior and on what

QPT effects persist away from temperature T = 0.

Conclusion

This project is attempting to develop a range of new techniques to simulate large quantum systems. This is a task which is intractable on conventional computers because of the intrinsic complexity of quantum mechanics. This barrier to exact calculation is extremely important because it prevents us from modeling energy-relevant systems such as high-temperature superconductors from first principles, and so improving their performance. In this project we are using both experimental and theoretical tools derived from the field of quantum information processing to create new tools for simulating large quantum systems.

References

1. Boshier, M. G., C. Ryu, P. Blackburn, and K. Henderson. Bose-Einstein Condensates in Painted Potentials. (Atlanta, 13-17 June, 2011).

2. Das, A., J. Sabbatini, and W. H. Zurek. Winding up superfluid in a torus via Bose-Einstein condensation. *Nature Communications.*

3. Santamore, D. H., and E. Timmermans. Spin critical opalescence in zero-temperature Bose-Einstein condensates. *Europhysics Letters.*

4. Santamore, D. H., and E. Timmermans. Pseudospin and spin-spin interactions in ultracold alkali atoms. 2011. *NEW JOURNAL OF PHYSICS.* **13**: 023043.

5. Solenov, D., and D. Mozyrsky. Metastable states and macroscopic quantum tunneling in a cold-atom Josephson ring. 2010. *Physical Review Letters.* **104** (15): 150405.

6. Solenov, D., and D. Mozyrsky. Macroscopic two-state systems in trapped atomic condensates. 2010. *Physical Review A.* **82** (6): 061601.

7. Solenov, D., and D. Mozyrsky. Cold atom qubits. 2011. *Journal of Theoretical and Computational Nanotechnology.* **8**: 481.

8. Chien, C., and B. Damski. Dynamics of a quantum quench in an ultra-cold atomic BCS superfluid. 2010. *Physical Review A.* **82**: 063616.

9. Damski, B., H. T. Quan, and W. H. Zurek. Critical dynamics of decoherence. 2011. *Physical Review A.* **83** (6): 062104.

10. Moreno, G. A., R. Messina, D. A. R. Dalvit, A. Lambrecht, P. A. Maia Neto, and S. Reynaud. Disorder in quantum vacuum: Casimir-induced localization of matter waves. 2010. *Physical Review Letters.* **105**: 21040.

Publications

Behunin, R., and B. Hu. Nonequilibrium forces between atoms and dielectrics mediated by a quantum field. 2011. *Physical Review A - Atomic, Molecular, and Optical Physics.* **84** (1): 012902.

Boshier, M. G., C. Ryu, P. Blackburn, and K. Henderson. Bose-Einstein Condensates in Painted Potentials. Invited presentation at *DAMOP 2011 (42nd Annual Meeting of APS Division of Atomic, Molecular and Optical Physics).* (Atlanta, 13-17 June, 2011).

Chien, C., and B. Damski. Dynamics of a quantum quench in an ultra-cold atomic BCS superfluid. 2010. *Physical Review A.* **82**: 063616.

Cooper, F., C. Chien, B. Mihaila, J. Dawson, and E. Timmermans. Nonperturbative predictions for cold atom bose gases with tunable interactions. 2010. *Physical Review Letters.* **105** (24): 240402.

Damski, B., H. T. Quan, and W. H. Zurek. Critical dynamics of decoherence. 2011. *Physical Review A.* **83** (6): 062104.

Damski, B., and W. Zurek. Soliton creation during a Bose-Einstein condensation. 2010. *Physical Review Letters.* **104** (16): 160404.

Das, A., J. Sabbatini, and W. H. Zurek. Winding up superfluid in a torus via Bose-Einstein condensation. *Nature Communications.*

Intravaia, F., R. Behunin, P. W. Milonni, G. W. Ford, and R. F. O'Connell. Consistency of a causal theory of radiative reaction with the optical theorem. 2011. *Physical Review A - Atomic, Molecular, and Optical Physics.* **84** (3): 035801.

Moreno, G. A., R. Messina, D. A. R. Dalvit, A. Lambrecht, P. A. Maia Neto, and S. Reynaud. Disorder in quantum vacuum: Casimir-induced localization of matter waves. 2010. *Physical Review Letters.* **105**: 21040.

Santamore, D. H., and E. Timmermans. Pseudospin and spin-spin interactions in ultracold alkali atoms. 2011. *NEW JOURNAL OF PHYSICS.* **13**: 023043.

Santamore, D. H., and E. Timmermans. Spin critical opalescence in zero-temperature Bose-Einstein condensates. *Europhysics Letters.*

Santamore, D. H., and E. Timmermans. Multi-impurity polarons in a dilute Bose-Einstein condensate. To appear in *New Journal of Physics.*

Solenov, D., and D. Mozyrsky. Metastable states and macroscopic quantum tunneling in a cold-atom Josephson ring. 2010. *Physical Review Letters.* **104** (15): 150405.

Solenov, D., and D. Mozyrsky. Cold atom qubits. 2011. *Journal of Theoretical and Computational Nanotechnology.* **8**: 481.

Solenov, D., and D. Mozyrsky. Macroscopic two-state systems in trapped atomic condensates. 2010. *Physical Review A.* **82** (6): 061601.

Solenov, D., and D. Mozyrsky. Coherent phase slips in superconducting nanorings. *Physical Review Letters.*

CLEAN Detection & Identification of Dark Matter

Andrew Hime
20100063DR

Introduction

The direct detection and identification of dark matter presents one of the most compelling pursuits of modern science. LANL scientists co-invented a conceptually simple and novel approach to the direct detection of dark matter using, interchangeably, targets of liquid argon (LAr) and liquid neon (LNe) in a "single-phase" detector dubbed CLEAN (Cryogenic Low Energy Astrophysics with Noble liquids). This project focuses on a demonstration of the capabilities of this approach through the design, construction, assembly and commissioning of the MiniCLEAN detector. We combine this important and timely experimental opportunity with a theoretical program to establish the physical nature of dark matter through a comprehensive study of the experimental data available and within the broader framework of physics Beyond the Standard Model.

Benefit to National Security Missions

This project is synergistic with the DOE's Office of Science mission for discovery and innovation in basic research to understand the universe via the development of novel detector technologies and sophisticated modeling techniques and with the specific goal to directly detect and identify dark matter. These basic and fundamental techniques could revolutionize our view of the dark matter problem and also find application in missions relevant to national security such as non-proliferation.

Progress

Experimental Program

The MiniCLEAN detector is composed of three major elements, an Inner Vessel (IV) that contains the liquid cryogen, an array of 92 optical cassettes that are inserted into the IV and define the inner target region, and an Outer Vessel (OV) that provides secondary containment and the necessary thermal insulation of the inner cryostat. Progress on the fabrication of the IV and OV is shown in Figure 1. The entire detector will be shielded in a water tank with an active muon veto and operated 6800 feet underground in the Cube

Hall at SNOLAB (Figure 2). In addition to the progress made on these major components of the detector, we have completed an engineering design for the optical modules and are in the process of having prototypes fabricated for testing. A dedicated test stand has been constructed to test the mechanical, thermal and optical performance of these prototypes in LAr.
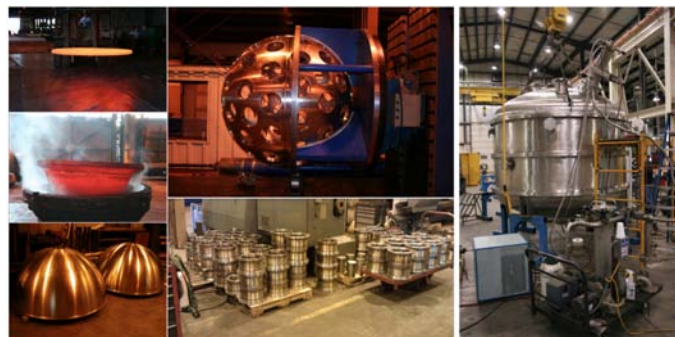
Figure 1. Shown in the three small photographs to the left are the early stages of forming the two hemispheres that make up the Inner Vessel (IV). The IV is being fabricated by Winchester Precision Technologies in Winchester, NH as an ASME Section VIII, Division-1 pressure vessel. The central-top picture shows a recent photograph of the IV with its 92 ports and the two hemispheres successfully welded together. A subset of the spools is shown at the bottom center. These spools will serve as the ports for the optical cassettes that will be bolted to the IV via conflat-seal. The Outer Vessel (OV) is shown at the far right and has been fabricated at PHPK Technologies in Columbus, OH. Also a code-stamped vessel, it is made up of four sections to allow transportation underground at SNOLAB. Both the IV (64 inches in diameter) and OV (104 inches in diameter and 106 inches high) are manufactured from low-radioactivity stainless steel and were designed by the engineering team at LANL.
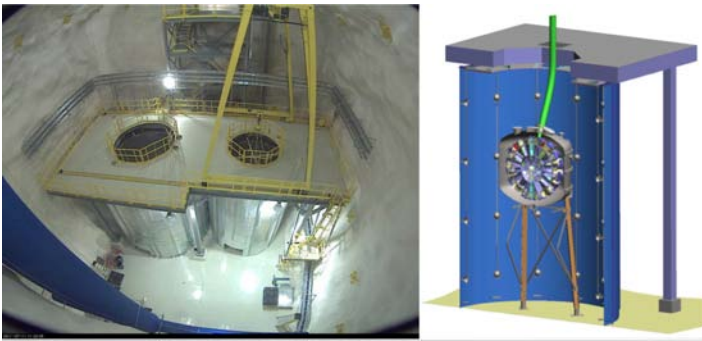
Figure 2. The SNOLAB Cube Hall (left) in July 2011 with the deck infrastructure and overhead 10-ton gantry crane installed. The water shield tanks for DEAP-3600 and MiniCLEAN have been constructed and are visible below the deck. The Cube Hall measures 50x50x60 feet and is presently operating as a Class-2000 clean room. The MiniCLEAN detector is shown conceptually on the right in its active water shield and supported by a stand that is being engineered to withstand seismic forces that might occur in the active nickel mine. The shield tank for MiniCLEAN is 18 feet in diameter and 25 feet high and equipped with a muon veto composed of 48 PMTs.

One of the great advantages of the MiniCLEAN design is that it is simple to model the detector's response to our backgrounds and the signals of interest. The optics of the detector are simulated within the particle propagation framework of GEANT4 with material properties extracted from the literature along with measurements we have made in the laboratory for specific detector elements such as the tetraphenyl butadiene (TPB) wavelength shifter, PMTs and acrylic to be used in the optical cassettes.

The progress that has been made in developing our simulation, benchmarked against data from our prototype detectors, has significantly increased our ability to accurately predict the performance of MiniCLEAN and thus its ultimate sensitivity in a direct search for WIMP dark matter. MiniCLEAN with LAr can establish sensitivity to the WIMP-nucleon cross-section at the 10^{-45} cm^2 level for the larger WIMP masses motivated by SUSY models. The result would be competitive with the liquid xenon programs of XENON-100 and LUX, and would very likely out-perform the next stage of the dual-phase LAr program (DarkSide).

We have met a major milestone with respect to a dominant radioactive background for dark matter experiments using LAr. ^{39}Ar is a beta emitter with endpoint energy of 565 keV and a half-life of 269 years. It is present in natural argon at ~8 parts in 10^{16}, yielding the intimidating rate of ~1 Bq/kg. A rejection factor of a few parts in 10^9 for low-energy electrons is required for MiniCLEAN in order to reach a background rate of < 1 event per year. Using the latest data from the DEAP-1 prototype experiment operating at SNOLAB, we have been able to demonstrate pulse-shape discrimination within about a factor of 3 of this goal when using a simple

statistic comparing the prompt (singlet) light to the total light integrated over the late (triplet) light tail. We have, however, developed a new method that makes direct use of the intrinsic nature of the scintillation time profile based on a log-liklihood statistic, indicating an order of magnitude improvement in comparison to the simple charge ratio method.

Theoretical Program

A major direction in the theoretical component of our project is in understanding the substructure of the dark matter in our galactic halo and how it impacts the direct detection searches. For this, we have performed extensive supercomputing simulations of galactic halos similar to our own. We have identified the high-energy dark matter particles and established that their phase-space distribution is highly inhomogeneous (Figure 3). This means that in a vast class of dark matter models, ranging from the low-mass WIMP to Inelastic Dark Matter, the often-used approximation of a uniform, isotropic, Maxwellian galactic halo fails.
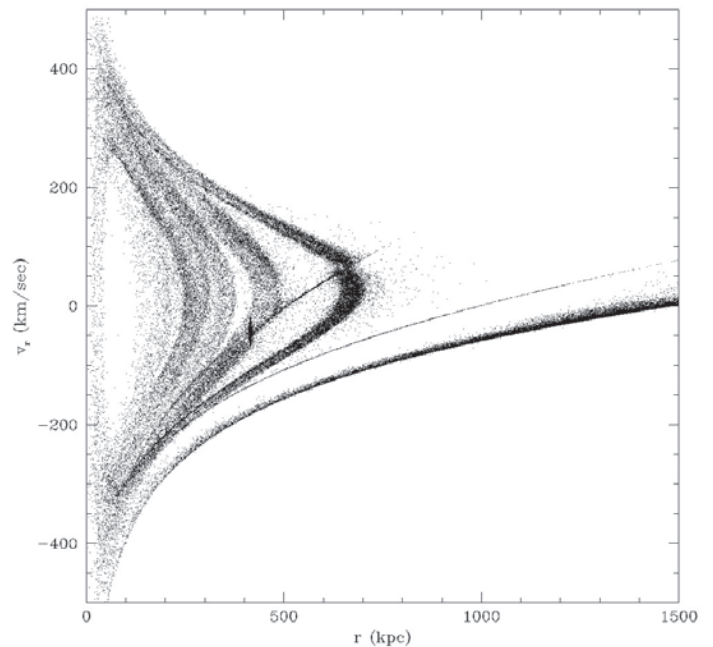
Figure 3. Snapshot from our supercomputer simulation of the evolution of a satellite dropped into the large parent halo. While the satellite has been disrupted, clear substructure in the phase space remains and would impact direct detection experiments. The dark matter flux at Earth might be more or less than the Galactic average.

We have also been investigating theories of dark matter that have a unified explanation for the cosmological abundances of baryons and dark matter. In "Asymmetric WIMP Dark Matter", a recently popular scenario for dark matter is generalized to a larger framework that includes

the more traditional WIMP paradigm. Bounds on this scenario can be set from the results of direct detection experiments.

In our paper "Pangenesis in a Baryon-Symmetric Universe: Dark and Visible Matter via the Affleck-Dine Mechanism," in collaboration with the University of Melbourne, we investigated models in which the baryon asymmetry can be exactly compensated by an asymmetry in dark matter. This could describe how the separation of baryonic and anti-baryonic number can originate in the vacuum, via the Affleck-Dine mechanism, due to spontaneous symmetry breaking and a second-order phase transition in the post-inflationary epoch.

We are also preparing a manuscript (LAUR-11-10573), wherein a new force mediates interactions between ordinary matter and dark matter. It is shown that in order to explain the observed abundances of dark matter and baryons, the dark matter must be significantly lighter than in the conventional WIMP scenario. The paper discusses a number of direct detection and collider constraints and demonstrates the viability of the scenario.

Future Work

Experimental Program

In FY12, focus for the MiniCLEAN experiment will be upon the completion of IV fabrication and testing of the prototype optical cassettes. The existing contract with Winchester Precision Technologies (WPT) includes complete fabrication of the IV and the 92 spools for mounting the optical cassettes into the IV. If FY12 funding for the project can be increased, we plan to finalize the design for the optical cassettes and fabricate the light guide assemblies in order to perform a "fry-fit". This dry-fit would reduce technical risk considerably and assure that the tight tolerances for this fit are met before the IV leaves the manufacturer.

Work will continue to refine our simulation and analysis program for MiniCLEAN with the aim of finalizing our background model and the ultimate scientific reach of the experiment. Based on the background goals of the experiment we will develop the assembly and commissioning plan necessary for reaching these goals and demonstrating the salient technical capabilities of our approach.

Theoretical Program

Following the work we have done in understanding the substructure of dark matter in the galactic halo, we performed high-resolution simulations of satellite halos dropped into the parent galactic halo. From this, we plan to extract the information on how much dark matter material is launched as a high-velocity stream.

We will continue our work on a merger-tree code. This

would allow us to combine the results from a single-halo disruption with the statistics of halo mergers, resulting in the prediction for the number and distribution of high-velocity streams. This ambitious program will be the first of its kind in the world.

We will investigate the nuclear effects that occur in direct detection experiments when dark matter particles scatter off of a nucleus. Characterizing these power law corrections is important in order to translate a measurement of a counting rate in an experiment with a specific target into a measurement of the short-distance scattering cross-section.

Conclusion

Significant progress has been made in the engineering and fabrication program for the MiniCLEAN experiment and we anticipate a major milestone in FY12 with the completion of the inner vessel and data from testing the prototype optical modules that will inform their final design. The maturity of our simulation and analysis program for the MiniCLEAN detector has allowed a quantitative projection of its capability and sensitivity in a dark matter search.

The theory program has provided great insight into our understanding of the distribution of dark matter within our galactic halo that indicates potential and significant departures from the standard assumptions of uniformity and isotropy. This, and investigations into non-standard models of the microscopic physics of the dark matter particles, could have profound implications in the interpretation of experiments searching for dark matter.

Publications

Bell, N. F., K. Petraki, I. M. Shoemaker, and R. R. Volkas. Pangenesis in a Baryon-Symmetric Universe: Dark and Visible Matter via the Affleck-Dine Mechanism. *Physical Review D.*

Gehman, V. M.. Fluorescence efficiency and visible re-emission spectrum of tetraphenyl butadiene films at extreme ultraviolet wavelengths. 2011. *Nuclear Instruments and Methods.* **A654**: 116.

Graesser, M. L., I. M. Shoemaker, and L. Vecchi. Asymmetric WIMP dark matter. 2011. *Journal of High Energy Physics.* **10**: 110.

Graesser, M. L., I. M. Shoemaker, and L. Vecchi. A dark force for baryons. *preprint arxiv:1107.2666.*

Hime, A.. The MiniCLEAN Dark Matter Experiment. 2011. In *DPF-2011 Conference.* (Providence, RI, 8-13, Aug. 2011). , p. 1. DPF Conference Proceedings: arXiv:1110:1005v1.

Shoemaker, I. M.. Indirect and direct detection of dark matter. Invited presentation at *Aspen Center for Physics.* (Aspen, CO, 6-12 Feb. 2011).

Probing Brain Dynamics by Ultra-Low Field Magnetic Resonance

Michelle A. Espy
20100097DR

Introduction

We seek to experimentally measure and understand, for the first time, the temporal and spatial dynamics of cognition in the human brain. Specifically, we are working to measure neural activity associated with visual cognition in ways that have not yet been demonstrated, combining high temporal and spatial resolution into a single measurement modality. We propose to achieve this by combining new neuroscience methods in ultra-low field (ULF) magnetic resonance imaging with existing neuroscience resources at LANL. Our research objective is to observe neural activity in the human brain with temporal (~ 2.5 ms) and spatial (< 5 mm) resolution capable of resolving the location and dynamics of visual cognition, and able to answer key hypotheses in neuroscience. Our technical approach is to initially employ multi-modality techniques to integrate data from conventional, separate measurements of MRI at high field and MEG. We will also develop new techniques for functional MRI measurements at ULF, and explore the feasibility of direct imaging of neural currents using ULF-MRI. We will employ simultaneous MEG and functional MRI at ULF to allow us to characterize the location and dynamics of the transient neural responses associated with visual cognition such as identification of a familiar object or face. In addition, we are exploring totally new methods enabled by ULF MRI, such as impedance tomography at low frequencies.

Benefit to National Security Missions

Understanding the Brain is an identified LANL Grand Challenge relevant to a number of NNSA/DOE, DOD/DARPA and Intel agency mission areas in surveillance and information processing for nonproliferation and national security. The basic technologies being developed are broadly applicable in energy, environment, biomedical and materials science in addition to the targeted breakthrough applications in basic and clinical neuroscience. For example, MRI has been proposed to track the movement of materials in nuclear facilities.

Progress

Recently it has become practical to perform MR at much lower field strengths compared to conventional MRI techniques. The so-called ultra-low field (ULF) regime, is compatible with simultaneous MEG. ULF MRI has unique advantages for measuring the direct interaction between magnetic fields arising from neural activity and the MRI signal, called direct neural-current imaging or DNI. DNI is considered the "holy grail" of functional neuroimaging because it would provide direct tomographic imaging of neural activity. ULF MRI also has intriguing prospects for functional MRI through the mapping of hemodynamic responses or metabolic activity. Combining MEG with functional data via fMRI or DNI may also allow for single pass analysis of functional dynamics combined with spatial localization. In order to achieve the scientific objectives of the project we proposed the following four technical aims:

1. Perform neuroscience experiments using existing resources in MEG and high field fMRI. Conduct visual recognition tasks and make separate MEG and fMRI measurements in the brain, to allow multimodality integration.

2. Develop the ability to perform fMRI at ULF. Extend our experimental capability beyond any presently available and show the feasibility of functional MRI based on blood flow, blood oxygenation, metabolic or tracer measurements at ULF.

3. Demonstrate direct neural current imaging at ULF. In principle, MRI allow direct detection of neuronal currents, which would allow tomographic reconstruction of neural activity. This is a high-risk objective, however success would revolutionize the field of human functional neuroimaging.

4. Resolve the sequence and location of visual cognition. Leverage and optimize our world-class capability in ULF-MRI to employ simultaneous MEG and fMRI or DNI to monitor neural activity during visual processing associated with behavioral tasks. This will allow us to determine the "when"

and "where" of visual cognition in single transient responses.

In support of Aim 1 we have developed the visual protocols for retinotopic mapping in separate magnetoencephalography (MEG) and functional magnetic resonance imaging (fMRI) studies, and the MEG protocol for frequency tagging. We have also developed amoeba recognition tasks for both MEG and fMRI similar to those used in the psychophysics experiments. Initial experiments have been conducted at the MIND institute in Albuquerque, using separate fMRI and MEG instrumentation. The analysis of these experiments has indicated that we are able to tag specific visual regions and pull out desired frequency responses associated with stimuli. This approach enables us to develop methods for single pass analysis and a foundation for comparison/integration with multi-modal methods developed at LANL. We have completed experimental protocols and analysis on two subjects (tasks 1-3), as outlined in the timeline for the project.

We have now made a definitive demonstration of Aim 2 in developing the protocol for fMRI at ultra-low fields (ULF). We have implemented a technique similar to traditional flow-based methods in fMRI (in particular the flow-sensitive alternating inversion recovery or FAIR technique), task 1. We have made modifications to account for the much shorter tissue relaxation times associated with ultra-low field MRI (about 10 times shorter than conventional approaches). The hardware design for execution of these experiments has been completed and tested, and now are demonstrated in a flow phantom. These data are shown in Figure 1. These results were recently presented at an international conference in the Netherlands (EUCAS 2011). The final ULF fMRI experiments are not scheduled until year 3 of the project, and we believe we remain on track. Upon recommendation of the 1st year external review committee, we have also pursued the higher payoff activity of ULF magnetic resonance electrical impedance tomography (ULF MREIT). There has been tremendous interest in recent work suggesting that impedance measurements may provide a new modality of functional neuroimaging, reflecting not only slow hemodynamic changes similar to functional MRI (fMRI), but fast changes in neural tissue impedance that are directly linked to polarization and depolarization of synchronous neuronal populations measured by EEG and MEG. Traditional MRI has been used to provide direct in situ measurement of local magnetic field perturbations produced by applied currents, which can be used to determine conductivity (MREIT).
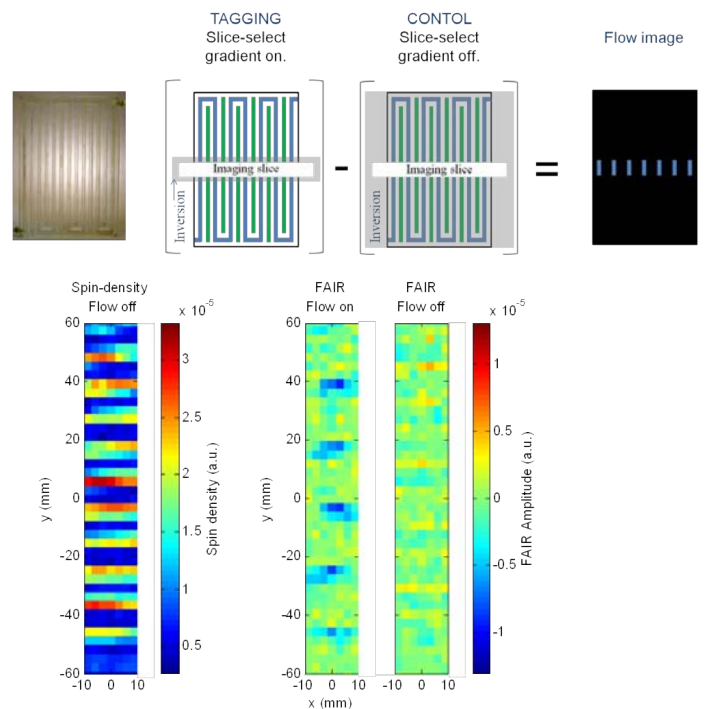
Figure 1. Upper row left to right: Picture of phantom. Schematic representation of a FAIR fMRI sequence. The phantom has chambers that flow (blue) and sections that do not flow (green). Lower left-to-right: Proton density of the center portion of the phantom showing all the water filled chambers. Note the phantom is rotated by 90 degrees from upper images. Right: FAIR sequence showing sensitivity only to parts of the phantom where water flowed.

However we have shown that MRI can be performed at much lower magnetic fields, in the ultra-low field (ULF) regime (1- 500 microTesla). ULF MRI offers important advantages including novel pulse sequences, flexible magnetic field configurations, compatibility with imaging methods such as MEG, and the ability to use resonance to probe interesting physiological processes at Larmor frequencies in the Hz-kHz (rather than MHz) range. The advantages of ULF MREIT also include the ability to measure all components of the applied magnetic field without object rotation Success could provide a way to reach clinically relevant MREIT which could in turn lead to better EEG/MEG, detection of cancer, stroke, and possibly even direct detection of neural function via electrical impedance changes. Preliminary experiments were completed in February 2011 and have resulted in an R01 application to NIH which received an excellent (although not yet fundable) priority score. Recently we improved the experimental hardware to make a new higher sensitivity demonstration using an adiabatic ramp-down approach. The adiabatic ramp down is critical to combined MEG/ULF MRI because it maintains the highest pre-polarization while reducing dead time and dB/dt. The results were presented at a recent international conference and a manuscript is in preparation. These activities have

contributed significantly to Aim 3 tasks 1-3.

The additional goals for Aim 2 are to implement an advanced imaging system complete with higher pre-polarization fields, and a dense sensor array. There has been significant R&D engineering and all of the coil sets are complete (Tasks 2 and 3) except the pre-polarization coil which is still under construction. Commissioning of the system with an alternate coil for pre-polarization is underway. Tasks 4 and 5 are scheduled to be completed by the second year of the project, but as mentioned, we believe our preliminary fMRI and ULF MREIT work with existing hardware will continue to make significant progress.

The final objective of the project (Aim 4) is to resolve the sequence and location of visual cognition using all progress from objectives 1-3 (in years 2-3 of the project). We believe our significant progress to-date positions us on track to make significant inroads to understanding the "when" and "where" of visual cognition in single transient responses.

Future Work

Our final year's efforts focus in three areas: 1) Commission the device and demonstrate simultaneous ULFMRI with voxel SNR > 10 and spatial resolution of 2x2x4 mm^3. 2) Demonstrate interleaved MEG and ULFMRI. The quality of the MEG should be sufficient to perform source localization to the ULFMRI image to within 1-2mm accuracy. 3) Implement protocols developed from Aim 1 to demonstrate use of retinotopic mapping to demonstrate novel source localization and a path to single-pass analysis of the MEG. 4) Improve and publish our demonstrations of both flow-based ULF fMRI and MREIT . 5) Conduct visual recognition protocol with the new instrument to demonstrate and validate our ability to localize the spatial-temporal locus of visual cognition.

Conclusion

In addition to providing important and unique new tools for human functional neuroimaging, the proposed work will provide new insight into how the brain processes information. Eventually this will enable us to harness the power of artificial intelligence, improve human-machine interfaces, or construct bio-mimetic sensors and networks approaching human performance. This LDRD project will position LANL to lead the world and serve the nation with a world-class capability in functional neuroscience, that can provide input to specific applications important for the Laboratory mission, and provide powerful new biomedical techniques for basic and clinical neuroscience and medical imaging. Several spin-off projects have already been identified, and one on evaluating ULF MRI as a method for assessing traumatic brain injury was recently funded by DoD. The method has also been recently commercially licensed, and development of a funds-in CRADA for the work is underway.

Publications

Magnelind, P. E., J. J. Gomez, A. N. Matlashov, T. Owens, J. H. Sandin, P. L. Volegov, and M. A. Espy. Co-Registration of Interleaved MEG and ULF MRI Using a 7 Channel Low-T$_c$ SQUID System. 2011. *IEEE Transactions on Applied Superconductivity.* **21** (3): 456.

Sandin, H. J., P. L. Volegov, M. A. Espy, A. N. Matlashov, I. M. Savukov, and L. J. Schultz. Noise Modeling From Conductive Shields Using Kirchhoff Equations. 2011. *IEEE Transactions on Applied Superconductivity.* **21** (3): 489.

Savukov, I., T. Karaulanov, A. Castro, P. Volegov, A. Matlashov, A. Urbatis, J. Gomez, and M. Espy. Non-cryogenic anatomical imaging in ultra-low field regime: Hand MRI demonstration. 2011. *Journal of Magnetic Resonance.* **211** (2): 101.

Volegov, P., M. Flynn, R. Kraus, P. Magnelind, A. Matlashov, P. Nath, T. Owens, H. Sandin, I. Savukov, L. Schultz, A. Urbaitis, V. Zotev, and M. Espy. Magnetic Resonance Relaxometry at Low and Ultra Low Fields. 2010. In *17th International Conference on Biomagnetism Advances in Biomagnetism - Biomag 2010 ; 28 March-1 April 2010 ; Dubrovnik, Croatia.* , p. 82.

Volegov, P., M. Flynn, R. Kraus, P. Magnelind, A. Matlashov, P. Nath, T. Owens, H. Sandin, I. Savukov, L. Schultz, A. Urbaitis, V. Zotev, and M. Espy. Magnetic Resonance Relaxometry at Low and Ultra Low Fields. 2010. In *39th Annual Clinical Aphasiology Conference ; 20090526 - 20090530 ; Keystone, CO.* Vol. 28, p. 82.

Zotev, V. S., T. Owens, A. N. Matlashov, I. M. Savukov, J. J. Gomez, and M. A. Espy. Microtesla MRI with dynamic nuclear polarization. 2010. *Journal of Magnetic Resonance.* **207** (1): 78.

Bridging Equilibrium and Non-equilibrium Statistical Physics

Robert E. Ecke
20100531DR

Introduction

The twentieth century saw unprecedented advances in our understanding of the properties of matter, culminating in the application of these ideas to produce the technology of the modern age from electronic devices to space age structural materials. This science was mostly based on thinking about materials near thermal and mechanical equilibrium with uniform or periodic atomic structure. In contrast, many of the scientific challenges of the twenty-first century involve behavior of greater complexity: competing interactions, geometric frustration, spatial and temporal intrinsic inhomogeneities, nano-scale structures and physics spanning many scales. We focus on a broad class of emerging problems that require new tools in non-equilibrium statistical physics, building on foundations in equilibrium statistical mechanics that will find applications in new material functionality, in predicting complex spatial dynamics, and in understanding novel states of matter. This work encompasses materials under extreme conditions involving elastic/plastic deformation, competing interactions, intrinsic inhomogeneity, frustration in condensed matter systems, scaling phenomena in disordered materials from glasses to granular matter, quantum chemistry applied to nano-scale materials, soft-matter materials and spatio-temporal properties of both ordinary and complex fluids.

Benefit to National Security Missions

Non-equilibrium processes are related to new materials functionality, to turbulence and mixing, and to structural properties of materials. The application of our theory, modeling and simulation approaches to non-equilibrium processes helps build fundamental science capability in areas related to Office of Science Programs in materials science, to climate modeling in DOE, to LANL efforts in MaRIE, and to interactions with NSF/DOE programs at NHMFL, at CINT, and at the Lujan Center.

Progress

Electronic transport

Our work on materials with electronic degrees of freedom includes semiconductors, polymers, and strongly correlated electron magnetic and superconducting materials. For semiconductor materials, we developed a model that treats various photo-excitation-induced processes in bulk and nano-structured semiconductors. We applied the model to analyze the efficiency of optical processes in bulk and nano-crystalline materials, thereby producing insight into critical processes needed for practical realization of a new generation of inexpensive, highly efficient solar cells. We also extended an efficient theoretical tool for molecular design (exciton scattering approach) to characterize molecular backbones using selected quantum chemical methods. We have applied this methodology to common organic semiconducting materials.

The structural and magnetic transitions of iron-based high-T_c superconductors occur simultaneously as a first-order transition in one doping group of the compounds whereas they are separate in another group with different doping. We explored the effects of dimensionality of the material and produced a model phase diagram using Monte Carlo simulations. The phase diagram provides an explanation of the experiments on the undoped compounds, suggesting that our model may help to understand the unconventional superconductivity in these materials. In related work, we investigated a two-impurity model using cluster dynamical mean field theory and elucidated the characteristic energy scales of heavy fermion materials and the relationship between superconductivity and magnetic fluctuations. In other electron transport materials, we interpreted the large thermoelectric effects in graphene, from an interplay of band structure, disorder and thermal activation. We also examined thermodynamic properties near generic quantum phase transitions and proposed that the accumulation of entropy can be employed to probe a quantum critical point.

Mechanical Properties of Materials

We actively explored the mechanical properties

of materials in different situations from idealized granular matter to complex metal and rock behavior. We investigated how stress is distributed in idealized 2D granular materials using an experimental setup to measure the force distribution of an ensemble of 2D granular materials and tested how force varied with depth for granular materials - behavior that determines failure thresholds for granular storage facilities, e.g., grain silos. We looked at mechanical properties of geophysical materials under shear. Our research elucidated how, in ductile rock, deformation occurs in a narrow shear band when driven by earthquake rupture, in agreement with observations. We developed a model for the deformation and failure of bulk metallic glasses, focusing on the temperature dependence of the dynamics of deformation below the glass transition temperature. This model captured basic temperature-dependence of stress drop and strain rate observed in stick-slip experiments.

We applied solid mechanics and dislocation dynamics modeling to examine the fundamental mechanisms of plasticity in small-scale face-centered cubic single crystals. We developed an analytical expression for the self-energy of dislocation loops in anisotropic crystals and applied our theory to the properties of nano-wires. We investigated the dislocation induced anomalous softening of solid helium and its implications for helium supersolidity.

We applied structural and thermodynamic analysis to DNA molecules. Thermal transport through DNA was shown to provide detailed insight into the nature of nonlinear vibrational dynamics of DNA, Figure 1. The possible usage of DNA molecule as a thermal switch device was proposed. We predicted the temperature dependence of the torsional response of DNA and compared to experiments.
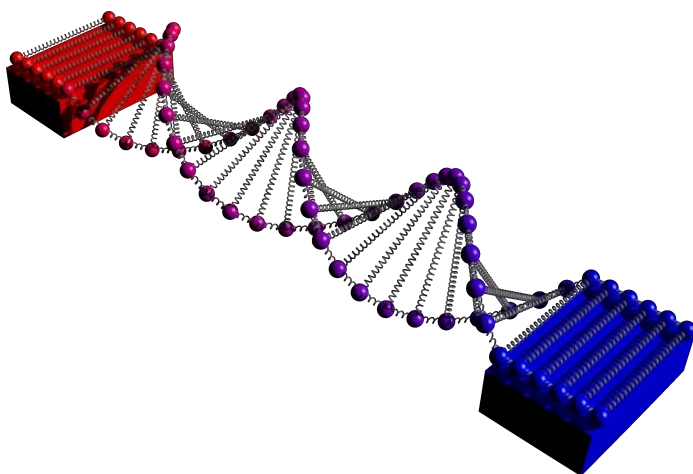
Figure 1. Schematic of DNA held between two heat reservoirs that probes its structures via an energy current.

Ordinary concrete, the most used building material, is the 3rd highest CO2 emitter, accounting for 5-8% of all man-made emissions; a compelling motive for developing alternative concretes. Our research advanced the nano-scale understanding of alternative cements, including geopolymer cement, by combining neutron and x-ray experimental data with atomistic and coarse-grained simulations. We developed a coarse-grained Monte Carlo computer simulation to accurately represent the formation of the nanostructure of geopolymeric materials depending on the type of precursor and activator used, thereby providing a predictive tool for geopolymer concrete mix design, Figure 2.

(a) S-activated: 0 iterations

(b) S-activated: 40,000 iterations

(c) S-activated: 400,000 iterations

(d) S-activated: 7,000,000 iterations
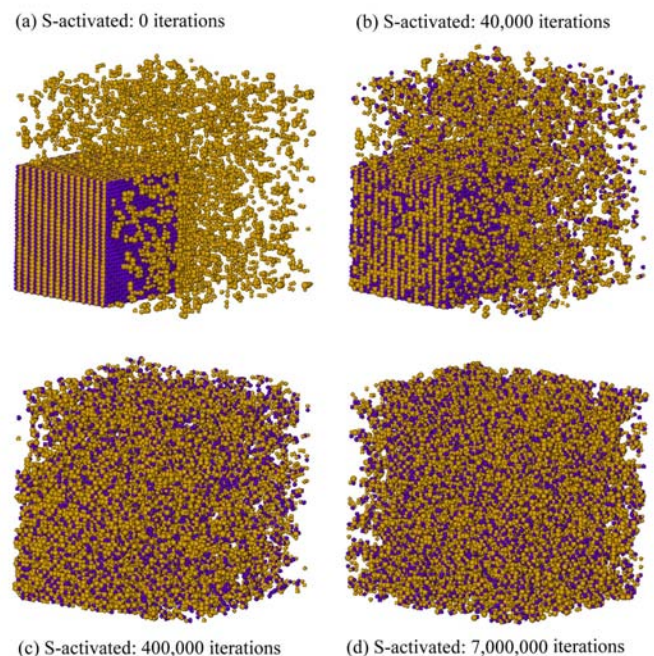
Figure 2. Progress of a coarse-grained Monte Carlo simulation of the formation of a geopolymer gel precipitating from a solid (metakaolin) in solution (sodium silicate).

Non-equilibrium steady-states may be related to equilibrium behavior using a temperature-like parameter called the "effective temperature". We measured an effective temperature from molecular dynamics simulations of crystalline and amorphous materials under ion irradiation that measures the structural disorder of the system. We developed a simple, physically motivated model that predicts the rate of decay and the final structure of the material.

Hydrodynamics

An important aspect of our work on non-equilibrium statistical physics is the flow of fluids in different contexts with varying combinations of compressibility, rotation, stratification, and magnetic field.   Magnetohydrodynamic (MHD) turbulence is important in nuclear fusion, space weather, and astrophysics. We developed a multi-scale analysis approach to understanding coupling of the flow

and the magnetic fields in such systems. Our efforts showed that interactions in MHD turbulence take place between scales of similar size and that the velocity and magnetic fields decouple at small scales. We demonstrated that the magnetic field at the largest scales has no role in the cascade dynamics in MHD turbulence, contrary to what is widely believed. Our results should have significant implications on devising reduced models of MHD turbulence. In related MHD studies, we considered spiral-galaxy magnetic fields that are dominantly large scale, consistent with dynamo theory in the core but not in the spiral arms. We developed a new theory that is consistent with numerical data and that reconciles turbulent dynamo theory and galactic observations.

Modern developments in incompressible turbulence rely on Kolmogorov's 1941 theory. No analogue exists for compressible flows; even to properly formulate the problem is ambiguous. We extended Kolmogorov's theory to flows with compressibility such as density variations, shock formation, and compression/rarefaction. We developed a framework to analyze highly compressible turbulence when viscosity is negligible. We proved that inter-scale transfer of kinetic energy in compressible turbulence is dominated by local interactions, precluding the commonly accepted transfer of kinetic energy from large to small scales via shocks. These results establish the fundamental basis for the study of compressible turbulence.

We developed an open-source software package for producing velocity fields from a series of images of passive tracers (e.g., particles in laboratory flows, clouds in planetary atmospheres). We used the code to study changes in Jupiter's mean zonal flow, leading to new understanding about its variability and about the dynamics of Jovian vortices, Figure 3. We demonstrated a period of rapid change as part of an approximately century-long Jovian climate cycle.

We developed a method for performing one-dimensional dust settling and three-dimensional simulations of dust-laden gas in the proto-planetary disks around newly formed stars. We showed that for disks of many solar masses dust can form a sufficiently dense cluster to collapse under its own gravity without exciting fluid instabilities.

We designed and implemented an immersed-boundary method for handling moving fluid/solid boundaries in geophysical fluid models (atmosphere or ocean). We developed an efficient algorithm for representing under-resolved rotation-induced boundary layers that include changes in stratification owing to phase changes at the interface.
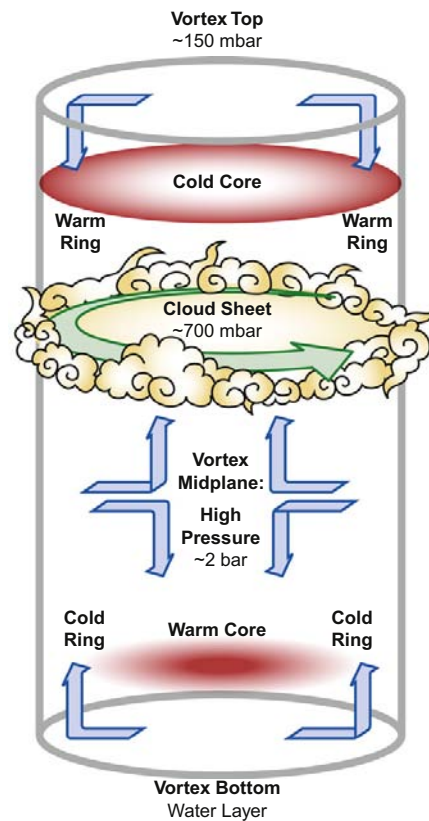
Figure 3. Schematic diagram of the vertical structure of Jupiter's vortices.

Future Work

Electronic transport: We will apply our new computational method to a wide array of problems in polymers and organic semiconductors. Our work on condensed matter systems will involve new computational approaches to fermionic systems with onsite disorder and will build collaborations with experimentalists in MPA Division.

Mechanical Properties of Materials: We propose to establish a link between microscopic and mesoscopic dislocation densities in order to understand heterogeneous nucleation in materials under extreme conditions. We will investigate concepts of irreversibility and continue work on effective temperature models of materials.

Hydrodynamics: We intend to capitalize on our formulation of compressible turbulence to explore a variety of problems involving shock physics. We will further develop our immersed-boundary method and apply it to problems in atmospheres and oceans.

Conclusion

This project exploits the capabilities of the Center for Nonlinear Studies to affect and guide interdisciplinary research. We use common threads of nonlinear physics, non-equilibrium physics, hydrodynamics and applied mathematics to impact strategic interests to the Laboratory including matter under extreme conditions

and nano-technology. Our work contributes fundamental insights and transfers concepts and techniques of quantum chemistry, non-equilibrium statistical mechanics, continuum mechanics, applied mathematics and many-body theory to meet new challenges in materials science, granular materials, nano-science, climate research, and strongly correlated electron systems.

Publications

Alberta, V. V., E. Badaeva, S. Kilina, M. Sykora, and S. Tretiak. The Frenkel exciton Hamiltonian for functionalized Ru(II)-bpy complexes. 2011. *Journal of Luminescence.* **131** (8): 1739.

Aluie, H.. Compressible Turbulence: The Cascade and its Locality. 2011. *Physical Review Letters.* **106** (17): 174502.

Aluie, H., and G. L. Eyink. Localness of energy cascade in hydrodynamic turbulence. II. Sharp spectral filter. 2009. *Physics of Fluids.* **21** (11): 115108.

Aluie, H., and G. L. Eyink. Scale Locality of Magnetohydrodynamic Turbulence. 2010. *Physical Review Letters.* **104** (8): 081101.

Asay-Davis, X. S., P. S. Marcus, M. H. Wong, and I. de Pater. Changes in Jupiter's zonal velocity between 1979 and 2008. 2011. *Icarus.* **211** (2): 1215.

Backhaus, S., K. Turitsyn, and R. E. Ecke. Convective Instability and Mass Transport of Diffusion Layers in a Hele-Shaw Geometry. 2011. *Physical Review Letters.* **106** (10): 104501.

Badaeva, E., V. V. Albert, S. Kilina, A. Koposov, M. Sykora, and S. Tretiak. Effect of deprotonation on absorption and emission spectra of Ru(II)-bpy complexes functionalized with carboxyl groups. 2010. *Physical Chemistry Chemical Physics.* **12** (31): 8902.

Bandi, M. M., T. Tallinen, and L. Mahadevan. SHOCK-DRIVEN JAMMING AND PERIODIC FRACTURE OF PARTICULATE RAFTS. 2011. *EUROPHYSICS LETTERS.* **96**: 36008.

Boffetta, G., and R. E. Ecke. Two dimensional turbulence. To appear in *Annual Reviews of Fluid Mechanics.*

Bouchet, F., S. Gupta, and D. Mukamel. Thermodynamics and dynamics of systems with long-range interactions. 2010. *Physica a-Statistical Mechanics and Its Applications.* **389** (20): 4389.

Bouchet, F., and H. Morita. Large time behavior and asymptotic stability of the 2D Euler and linearized Euler equations. 2010. *Physica D-Nonlinear Phenomena.* **239** (12): 948.

Bouchet, F., and M. Corvellec. Invariant measures of the 2D Euler and Vlasov equations. 2010. *Journal of Statistical Mechanics-Theory and Experiment.* **2010** (08): 08021.

Camassa, R., P. O. Rusas, A. Saxena, and R. Tiron. Fully nonlinear periodic internal waves in a two-fluid system of finite depth. 2010. *Journal of Fluid Mechanics.* **652**: 259.

Chernyak, V. Y., M. Chertkov, D. A. Goldberg, and K. Turitsyn. Non-Equilibrium Statistical Physics of Currents in Queuing Networks. 2010. *Journal of Statistical Physics.* **140** (5): 819.

Chernyak, V. Y., and N. A. Sinitsyn. Robust quantization of a molecular motor motion in a stochastic environment. 2009. *Journal of Chemical Physics.* **131** (18): 181101.

Chertkov, M., I. Kolokolov, and V. Lebedev. Universal velocity profile for coherent vortices in two-dimensional turbulence. 2010. *Physical Review E.* **81** (1): 015302.

Daub, E. G., D. R. Shelly, R. A. Guyer, and P. A. Johnson. Brittle and ductile friction and the physics of tectonic tremor. 2011. *Geophysical Research Letters.* **38**: L10301.

Daub, E. G., M. L. Manning, and J. M. Carlson. Pulse-like, crack-like, and supershear earthquake ruptures with shear strain localization. 2010. *Journal of Geophysical Research-Solid Earth.* **115**: B05311.

Daub, E. G., and J. M. Carlson. Stick-slip instabilities and shear strain localization in amorphous materials. 2009. *Physical Review E.* **80** (6): 066113.

Daub, E. G., and J. M. Carlson. Friction, Fracture and Earthquakes. 2010. *Annual Review of Condensed Matter Physics, Vol 1.* **1**: 397.

Eyink, G. L., and H. Aluie. Localness of energy cascade in hydrodynamic turbulence. I. Smooth coarse graining. 2009. *Physics of Fluids.* **21** (11): 115107.

Fredeman, D. J., P. H. Tobash, M. A. Torrez, J. D. Thompson, E. D. Bauer, F. Ronning, W. W. Tipton, S. P. Rudin, and R. G. Hennig. Computationally driven experimental discovery of the CeIr(4)In compound. 2011. *Physical Review B.* **83** (22): 224102.

Gao, X. L., J. M. Tao, G. Vignale, and I. V. Tokatly. Continuum mechanics for quantum many-body systems: Linear response regime. 2010. *Physical Review B.* **81** (19): 195106.

Goel, S., K. A. Velizhanin, A. Piryatinski, S. Tretiak, and S. A. Ivanov. DFT Study of Ligand Binding to Small Gold Clusters. 2010. *Journal of Physical Chemistry Letters.* **1** (6): 927.

Gottesman, D., and M. B. Hastings. Entanglement versus gap for one-dimensional spin systems. 2010. *New Journal of Physics.* **12**: 025002.

Grigorenko, I., and H. Rabitz. Optimal design strategies for electrostatic energy storage in quantum multiwell heterostructures. 2010. *Journal of Chemical Physics.* **133** (5): 054106.

Hauck, C. D., and R. B. Lowrie. Temporal Regularization of the P(N) Equations. 2009. *Multiscale Modeling & Simulation.* **7** (4): 1497.

Hermundstad, A. M., E. G. Daub, and J. M. Carlson. Energetics of strain localization in a model of seismic slip. 2010. *Journal of Geophysical Research-Solid Earth.* **115**: B06320.

Katan, C., M. Charlot, O. Mongin, C. Le Droumaguet, V. Jouikov, F. Terenziani, E. Badaeva, S. Tretiak, and M. Blanchard-Desce. Simultaneous Control of Emission Localization and Two-Photon Absorption Efficiency in Dissymmetrical Chromophores. 2010. *Journal of Physical Chemistry B.* **114** (9): 3152.

Kilina, S., S. Ivanov, and S. Tretiak. Effect of Surface Ligands on Optical and Electronic Spectra of Semiconductor Nanoclusters. 2009. *Journal of the American Chemical Society.* **131** (22): 7717.

Koposov, A. Y., T. Cardolaccia, V. Albert, E. Badaeva, S. Kilina, T. J. Meyer, S. Tretiak, and M. Sykora. Formation of Assemblies Comprising Ru-Polypyridine Complexes and CdSe Nanocrystals Studied by ATR-FTIR Spectroscopy and DFT Modeling. 2011. *Langmuir.* **27** (13): 8377.

Lammert, P. E., X. L. Ke, J. Li, C. Nisoli, D. M. Garand, V. H. Crespi, and P. Schiffer. Direct entropy determination and application to artificial spin ice. 2010. *Nature Physics.* **6** (10): 786.

Larkin, J., M. M. Bandi, A. Pumir, and W. I. Goldburg. Power-law distributions of particle concentration in free-surface flows. 2009. *Physical Review E.* **80** (6): 066301.

Larkin, J., W. Goldburg, and M. M. Bandi. Time evolution of a fractal distribution: Particle concentrations in free-surface turbulence. 2010. *Physica D-Nonlinear Phenomena.* **239** (14): 1264.

Lee, A. T., E. Chiang, X. Asay-Davis, and J. Barranco. Forming Planetesimals by Gravitational Instability. I. The Role of the Richardson Number in Triggering the Kelvin-Helmholtz Instability. 2010. *Astrophysical Journal.* **718** (2): 1367.

Lee, A. T., E. Chiang, X. Asay-Davis, and J. Barranco. Forming Planetesimals by Gravitational Instability. Ii. How Dust Settles to Its Marginally Stable State. 2010. *Astrophysical Journal.* **725** (2): 1938.

Li, H., C. Wu, S. V. Malinin, S. Tretiak, and V. Y. Chernyak. Excited States of Donor and Acceptor Substituted Conjugated Oligomers: A Perspective from the Exciton Scattering Approach. 2010. *Journal of Physical Chemistry Letters.* **1** (23): 3396.

Li, H., C. Wu, S. V. Malinin, S. Tretiak, and V. Y. Chernyak. Exciton Scattering on Symmetric Branching Centers in Conjugated Molecules. 2011. *Journal of Physical Chemistry B.* **115** (18): 5465.

Li, H., S. V. Malinin, S. Tretiak, and V. Y. Chernyak. Exciton scattering approach for branched conjugated molecules and complexes. IV. Transition dipoles and optical spectra. 2010. *Journal of Chemical Physics.* **132** (12): 124103.

Li, J., S. Zhang, J. Bartell, C. Nisoli, X. Ke, P. E. Lammert, V. H. Crespi, and P. Schiffer. Comparing frustrated and unfrustrated clusters of single-domain ferromagnetic islands. 2010. *Physical Review B.* **82** (13): 134407.

Liu, Y. M., and R. E. Ecke. Local temperature measurements in turbulent rotating Rayleigh-Benard convection. 2011. *Physical Review E.* **84** (1): 016311.

Mertens, F. G., N. R. Quintero, and A. R. Bishop. Nonlinear Schrodinger equation with spatiotemporal perturbations. 2010. *Physical Review E.* **81** (1): 016608.

Nelson, T., S. Fernandez-Alberti, V. Chernyak, A. E. Roitberg, and S. Tretiak. Nonadiabatic Excited-State Molecular Dynamics Modeling of Photoinduced Dynamics in Conjugated Molecules. 2011. *Journal of Physical Chemistry B.* **115** (18): 5402.

Nelson, T., S. Fernandez-Alberti, V. Chernyak, A. E. Roitberg, and S. Tretiak. NA-ESMD modeling of photoinduced dynamics in conjugated molecules. 2011. *Abstracts of Papers of the American Chemical Society.* **241**.

Nisoli, C., D. Abraham, T. Lookman, and A. Saxena. Thermally Induced Local Failures in Quasi-One-Dimensional Systems: Collapse in Carbon Nanotubes, Necking in Nanowires, and Opening of Bubbles in DNA. 2010. *Physical Review Letters.* **104** (2): 025503.

Nisoli, C., J. Li, X. L. Ke, D. Garand, P. Schiffer, and V. H. Crespi. Effective Temperature in an Interacting Vertex System: Theory and Experiment on Artificial Spin Ice. 2010. *Physical Review Letters.* **105** (4): 47205.

Nisoli, C., N. M. Gabor, P. E. Lammert, J. D. Maynard, and V. H. Crespi. Annealing a magnetic cactus into phyllotaxis. 2010. *Physical Review E.* **81** (4): 046107.

Nisoli, C., and A. R. Bishop. Thermomechanics of DNA:

Theory of Thermal Stability under Load. 2011. *Physical Review Letters.* **107** (6): 068102.

Pater, I. de, M. H. Wong, P. Marcus, S. Luszcz-Cook, M. Adamkovics, A. Conrad, X. Asay-Davis, and C. Go. Persistent rings in and around Jupiter's anticyclones - Observations and theory. 2010. *Icarus.* **210** (2): 742.

Perdew, J. P., and J. M. Tao. When does static correlation scale to the high-density limit as exchange does?. 2010. *Journal of Molecular Structure-Theochem.* **943** (1-3): 19.

Quintero, N. R., F. G. Mertens, and A. R. Bishop. Generalized traveling-wave method, variational approach, and modified conserved quantities for the perturbed nonlinear Schrodinger equation. 2010. *Physical Review E.* **82** (1): 016606.

Safarik, D. J., E. K. Salje, and J. C. Lashley. Spectral analysis of resonance ultrasonic spectroscopy: Kramers-Kronig analysis, Fano profiles, and the case of precursor softening in SnTe:Cr. 2010. *Applied Physics Letters.* **97** (11): 111907.

Salje, E. K.. On the dynamics of ferroelastic domain boundaries under thermal and elastic forcing. 2010. *Phase Transitions.* **83** (9): 657.

Salje, E. K., D. J. Safarik, K. A. Modic, J. E. Gubernatis, J. C. Cooley, R. D. Taylor, B. Mihaila, A. Saxena, T. Lookman, J. L. Smith, R. A. Fisher, M. Pasternak, C. P. Opeil, T. Siegrist, P. B. Littlewood, and J. C. Lashley. Tin telluride: A weakly co-elastic metal. 2010. *Physical Review B.* **82** (18): 184112.

Salje, E. K., X. Ding, Z. Zhao, T. Lookman, and A. Saxena. Thermally activated avalanches: Jamming and the progression of needle domains. 2011. *Physical Review B.* **83** (10): 104109.

Salje, E. K., and W. Schrang. Low amplitude, low frequency elastic measurements using Dynamic Mechanical Analyzer (DMA) spectroscopy. 2011. *Zeitschrift Fur Kristallographie.* **226** (1): 1.

Seidel, J., P. Maksymovych, Y. Batra, A. Katan, S. Y. Yang, Q. He, A. P. Baddorf, S. V. Kalinin, C. H. Yang, J. C. Yang, Y. H. Chu, E. K. Salje, H. Wormeester, M. Salmeron, and R. Ramesh. Domain Wall Conductivity in La-Doped BiFeO3. 2010. *Physical Review Letters.* **105** (19): 197603.

Tao, J. M., J. P. Perdew, and A. Ruzsinszky. Long-range van der Waals attraction and alkali-metal lattice constants. 2010. *Physical Review B.* **81** (23): 233102.

Tao, J. M., S. Tretiak, and J. X. Zhu. Prediction of excitation energies for conjugated polymers using time-dependent density functional theory. 2009. *Physical Review B.* **80** (23): 235110.

Tao, J. M., X. L. Gao, G. Vignale, and I. V. Tokatly. Linear Continuum Mechanics for Quantum Many-Body Systems. 2009. *Physical Review Letters.* **103** (8): 086401.

Tordesillas, A., Q. Lin, J. Zhang, R. P. Behringer, and J. Y. Shi. Structural stability and jamming of self-organized cluster conformations in dense granular materials. 2011. *Journal of the Mechanics and Physics of Solids.* **59** (2): 265.

Vasseur, R., T. Lookman, and S. R. Shenoy. Microstructure from ferroelastic transitions using strain pseudospin clock models in two and three dimensions: A local mean-field analysis. 2010. *Physical Review B.* **82** (9): 094118.

Vasseur, R., and T. Lookman. Effects of disorder in ferroelastics: A spin model for strain glass. 2010. *Physical Review B.* **81** (9): 094107.

Velizhanin, K. A.. Comment on "Impact Ionization and Auger Recombination Rates in Semiconductor Quantum Dots". 2010. *Journal of Physical Chemistry C.* **114** (39): 16859.

Velizhanin, K. A., C. C. Chien, Y. Dubi, and M. Zwolak. Driving denaturation: Nanoscale thermal transport as a probe of DNA melting. 2011. *Physical Review E.* **83** (5): 050609.

Velizhanin, K. A., M. Thoss, and H. B. Wang. Meir-Wingreen formula for heat transport in a spin-boson nanojunction model. 2010. *Journal of Chemical Physics.* **133** (8): 084503.

Velizhanin, K. A., and A. Efimov. Probing plasmons in graphene by resonance energy transfer. 2011. *Physical Review B.* **84** (8): 085401.

Vladimirova, N., and M. Chertkov. Self-similarity and universality in Rayleigh-Taylor, Boussinesq turbulence. 2009. *Physics of Fluids.* **21** (1): 015102.

Walker, D. M., A. Tordesillas, C. Thornton, R. P. Behringer, J. Zhang, and J. F. Peters. Percolating contact subnetworks on the edge of isostaticity. 2011. *Granular Matter.* **13** (3): 233.

White, C. E., J. L. Provis, T. Proffen, and J. S. J. van Deventer. MOLECULAR MECHANISMS RESPONSIBLE FOR THE STRUCTURAL CHANGES OCCURRING DURING GEOPOLYMERIZATION: MULTISCALE SIMULATION. To appear in *AICHE JOURNAL.*

Zhang, J., R. P. Behringer, and I. Goldhirsch. Coarse-Graining of a Physical Granular System. 2010. *Progress of Theoretical Physics Supplement.* **184**: 16.

Zhang, S., J. Li, J. Bartell, X. L. Ke, C. Nisoli, P. E. Lammert,
V. H. Crespi, and P. Schiffer. Ignoring Your Neighbors:
Moment Correlations Dominated by Indirect or Distant
Interactions in an Ordered Nanomagnet Array. 2011.
Physical Review Letters. **107** (11): 7401.

Zhu, J. Z., and M. Taylor. Intermittency and Thermalization
in Turbulence. 2010. *Chinese Physics Letters.* **27** (5):
054702.

Zhu, L. J., R. Ma, L. Sheng, M. Liu, and D. N. Sheng.
Universal Thermoelectric Effect of Dirac Fermions
in Graphene. 2010. *Physical Review Letters.* **104** (7):
076804.

Multi-Messenger Signals from Low-Mass Supernovae

Christopher L. Fryer
20110032DR

Introduction

Core-collapse supernovae have long been touted as nature's high-energy/high-density physics laboratories. The imploding stars reach densities in excess of nuclear (a few times 10^14g/cc) and energies in excess of 10 MeV. These "laboratories" are ideal probes of general relativity, nuclear and particle physics. But to use supernova observations to probe this physics, we must understand the supernova engine. Although the basic picture of the supernova engine is now confirmed by multiple diagnostics (of the progenitor stars prior to implosion, the neutrino signal of 1987A, and the emergence of the shock as it blows out of the star), the quantitative details of the convection-enhanced explosion mechanism needed to use supernovae as laboratories has thus far eluded scientists.

In this project, we have focused on a very specific supernova environment: the explosions of low-mass stars. The diagnostics of low-mass stars are ideal physics experiments: the explosions happen rapidly, minimizing the numerical uncertainties in calculations, the neutrino signal is not altered by extended convection or early-time fallback; these systems are likely to be fast-rotating and hence are ideal gravitational wave emitters; these systems are commonly believed to be the primary sites for r-process production; and over half of the nearby systems with pre-collapse progenitor observations fit into this class of supernovae. Many of these systems have been neglected primarily because the progenitors have been difficult to understand. Without progenitors, the supernova community has focused on more massive progenitors. But we now do have models of low-mass progenitors and we are in an ideal time to study these explosions.

Benefit to National Security Missions

The new algorithms, portable to heterogeneous machines, to simulate radiation-hydrodynamics will investigate new approaches in modeling basic computational physics issues relevant to the ASC program. The nuclear physics studies tie directly to thrusts within the nuclear physics division of DOE's office of science. In particular, the experimental nuclear physics program within this project, tied with nuclear theory, will develop new approaches and instruments usable by the facility for rare isotope beams. Nucleosynthetic yields and light-curves provide much needed data for NASA missions such as Swift and NUSTAR. Finally, the gravitational wave and neutrino diagnostics will drive development in both the instrumentation and observing for NSF-funded LIGO experiment and DUSEL. Both our modeling tools and our nuclear cross-section measurements build capability relevant to the weapons program.

Progress

The first year in this project has focused on developing the tools to allow us to calculate diagnostics for core-collapse supernovae. In addition, we have started to strengthen ties with observing programs so that our predictions are immediately coupled to the observational community.

The primary goal for our neutrino project has been to produce a Monte Carlo neutrino transport code including full differential scattering kernels and the most up-to-date neutrino cross-sections. We have developed a code to calculate these cross-sections and have implemented it into a stand-alone Monte Carlo code. This Monte-Carlo code is now being implemented into the core-collapse hydrodynamics package and this combined code will form the basis for the work in years two and three. As part of this effort, we have implemented the Shen equation of state (developed by post-doc Gang Shen in T-2) into the core-collapse code, allowing us to develop even more sophisticated neutrino opacity schemes. With the stand alone code, we have started a number of projects calculating detailed neutrino spectra to provide the neutrino observational community. We have also pursued issues in neutrino oscillations and have a number projects studying this physics.

Our primary goal for nucleosynthesis diagnostics is to develop new instrumentation capabilities to measure rates and implement these new rates into our

astrophysical nuclear networks. The network code has been ported to GPU architectures and is currently being tested. The experimental program has been focusing on purchasing the necessary equipment. We have developed a Monte Carlo simulation of the proposed detector array. We are presently testing the array against design parameters, including detector geometry and material in order to optimize the array. In addition, we are field testing the proposed detector components under vacuum and magnetic field to ensure they will perform adequately for the measurements. Lastly, we proposed a development run at Argonne for the new array. The proposal was accepted by the Argonne PAC and will be scheduled as the first pieces of the array are available.

The primary goal for our photon diagnostics was to create a broader simulation database of light-curves/spectra and tie more closely to the observational community. We have joined the NuSTAR collaboration and are working on gamma-ray signals from supernovae for this NASA satellite. We have also joined the NASA JANUS team. We are part of a 3-year Hubble Space Telescope proposal to observe compact remnant masses to test our theoretical predictions (awarded to us in June of this year). We also are part of 2 NASA theory proposals leveraging off of the work done in this DR. We continued our collaborations with DOE nuclear physics topical collaborations and have found synergistic collaborations within this effort.

Our code development in this project has led to algorithm development that can feed back into programs (campaigns, ASC) and scientists funded part-time in the above ground experiment community have leveraged of the the algorithm development in the DR to develop new diagnostic software for NIF experiments.

Finally, this project has led to over 20 papers published or submitted to physics/astrophysics journals (including 1 Nature paper) and we expect this rate of publication to increase in the next 2 years.

Future Work

The basic work behind this project can be broken into three primary parts:

1. Developing a detailed Monte Carlo neutrino, radiation-hydrodynamics, code to model the collapse of low mass stars. This detailed transport scheme is ideally suited to modeling full-physics collapse problems. We will develop new schemes for equations of state, neutrino interactions and opacities to integrate into this code. This will allow detailed studies of the explosion and the neutrino/gravitational wave signals from these collapses.

2. By combining detailed theoretical models for nuclear rates with full data analyses from experiment, we will develop a new set of nuclear reactions. Coupling these rates to our explosion calculations, we expect

a detailed set of yields from these supernovae. The experiment, and resulting nuclear theory program, will be directly beneficial for the Facility for Rare Isotope Beams (FRIB). The nucleosynthetic yields will be compared against galactic chemical evolution calculations (working with the Nucleosynthesis grid collaboration) and specific observations (e.g. NuSTAR satellite). We are already working closely with these missions.

3. In addition to these two efforts, we will use our existing supernova light-curve codes to model the photon emission from these explosions. This data will be prepared for such missions as the Large Synoptic Survey Telescope and the Swift satellite. We are already working closely with these missions.

Conclusion

We expect to produce full diagnostic predictions for these supernovae. These predictions will tie our understanding of nuclear and particle physics to a number of physics and astrophysics experiments: e.g. Laser Interferometer Gravitational-wave Observatory, Deep Underground Science and Engineering Laboratory, NASA Swift and NuSTAR satellites, supernova surveys such as the Large Synoptic Survey Telescope. The nuclear experimental and theoretical work will be directly applied to the goals of FRIB, both developing new instrument techniques and novel ways to take advantage of its data.

Publications

Belczynski, K., T. Bulik, C. L. Fryer, A. Ruiter, F. Valsecchi, J. S. Vink, and J. R. Hurley. On the maximum mass of stellar black holes. 2010. *Astrophysical Journal.* **714** (2): 1217.

Bennett, M. E., R. Hirschi, M. Pignatari, S. Diehl, C. Fryer, F. Herwig, A. Hungerford, G. Magkotsios, G. Rockefeller, F. Timmes, M. Wiescher, and P. Young. The effect of $^{12}C + ^{12}C$ rate uncertainties on s-process yields. 2010. In *Nuclear Physics in Astrophysics IV ; 8-12 June 2009 ; Frascati, Italy.* Vol. 202, 1 Edition, p. 012023 (4 pp.).

Fryer, C. L., A. J. Ruiter, K. Belczynski, P. J. Brown, F. Bufano, S. Diehl, C. J. Fontes, L. H. Frey, S. T. Holland, A. L. Hungerford, S. Immler, P. Mazzali, C. Meakin, P. A. Milne, C. Raskin, and F. X. Timmes. Spectra of type Ia Supernovae from Double Degenerate Mergers. 2010. *Astrophysical Journal.* **725** (1): 296.

Fryer, C. L., D. J. Whalen, and L. Frey. Modeling Emission from the First Explosions: Pitfalls and Problems. 2010. In *First Stars and Galaxies: Challenges for the next Decade ; 8-11 March 2010 ; Austin, TX, USA.* Vol. 1294, p. 70.

Fryer, C. L., and A. Heger. Forming massive black holes

through stellar collapse: Observational diagnostics. 2011. *Astronomische Nachrichten.* **332** (4): 408.

Herwig, F., M. Pignatari, P. R. Woodward, D. H. Porter, G. Rockefeller, C. L. Fryer, M. Bennett, and R. Hirschi. Convective-reactive Proton-^{12}C combustion IN Sakurai's object (V4334 Sagittarii) and implications for the evolution and yields from the first generations of stars. 2011. *Astrophysical Journal.* **727** (2): 89 (15 pp.).

Magkotsios, G., F. X. Timmes, A. L. Hungerford, C. L. Fryer, P. A. Young, and M. Wiescher. Trends in ^{44}Ti and ^{56}Ni from core-collapse supernovae. 2010. *Astrophysical Journal Supplement Series.* **191** (1): 66.

Raskin, C., E. Scannapieco, G. Rockefeller, C. Fryer, S. Diehl, and F. X. Timmes. Astrophysical Journal. 2010. *Astrophysical Journal.* **724** (1): 111.

Whalen, D. J., and C. Fryer. The Observational Signatures of Primordial Pair-instability Supernovae. 2010. In *Deciphering the Ancient Universe with Gamma-ray Bursts ; 19-23 April 2010 ; Terrsa, Kyoto, Japan.* Vol. 1279, p. 116.

Yuan, Qiang, Siming Liu, Zhonghui Fan, Xiaojun Bi, and C. Fryer. Modeling the multi-wavelength emission of the shell-type supernova remnant RX J1713.7-3946. 2011. *Astrophysical Journal.* **735** (2): 120 (9 pp.).

Probing New Interactions with Neutron Beta Decay

Mark F. Makela
20110043DR

Introduction

Outstanding questions about the observed Universe and the structure of fundamental forces strongly suggest the existence of new particles and interactions Beyond the Standard Model (BSM). These would be found at energies above the TeV range, or equivalently at distances smaller than 10^{-17} cm. The presence of such new physics can be probed by direct searches at high-energy particle colliders or by indirect searches through high-precision measurements of low-energy observables. This project aims to discover or strongly constrain new interactions Beyond the Standard Model (BSM) originating at the TeV scale or above by performing: The first ever measurement of neutrino momentum in polarized beta decay and a precision measurement of the decay electron energy spectrum. Simultaneously with the experimental effort, we will carry out a theoretical program to elucidate the implications for Standard Model (SM) extensions of b and B measurements at the 10-3 and 10-4 levels.

Benefit to National Security Missions

The DOE Office of Science funded Fundamental Symmetries program, which is a major component of the National Nuclear Physics program, will directly benefit from the experiments and theory proposed here. Also, a major recommendation of the LANL NPAC Strategic Plan is to "Make a concerted effort to plan, attract community support, market, and sell world-class, intermediate-scale National user facilities at LANL" and specifically "utilizing ultracold neutrons at full capacity". This project furthers this goal by developing world-class experiments and attracting world-class external collaborators. These collaborators will form the basis of a strong user group to support converting the LANL UCN source to a National UCN user facility that can support a broad range of future UCN experiments: precision neutron beta decay, neutron oscillations, quantum bound neutron states, and solid surface studies. We will stretch the bounds of detection technology, building a basis for contributions to nuclear nonproliferation and the weapons program.

Progress

In this first year, we have initiated a vigorous theoretical program aimed to understand the discovery potential of planned precision measurements of beta decay with ultracold neutrons. The theoretical program has several components, which we summarize below.

Within a model-independent effective theory approach, we have performed a detailed comparative study of the sensitivity of neutron decay, other low-energy precision measurements, as well as high energy collider experiments, to new scalar and tensor interactions. Our results show that measurements of b and B at an accuracy of 0.1% would provide the strongest limits on new tensor interactions (in combination with limit on the scalar interactions from nuclear beta decays). In Figure 1 we present the current constraints on the effective couplings for scalar and tensor interactions, from both low-energy and collider searches. In Figure 2, we show the projected limits assuming neutron measurements of b and B at 0.0.1% level, as well as future collider searches at the LHC, with higher energy and statistics. The effective new physics couplings are constrained already to be at 0.005 level or below, which probes scales of new physics well in the TeV region.

Robust extraction of bounds on new physics couplings in neutron decay requires knowledge of the nucleon scalar and tensor form factors gS and gT, so far assumed to be of order 1 based on quark model estimates. We have provided the first lattice QCD calculations of gS, finding gS = 0.8(4) and have re-analyzed previous lattice calculations of gT performing the appropriate chiral extrapolation, finding gT = 1.05(35).

Finally, we have explored the possibility that mediators of the new scalar interactions can be produced at high energy colliders such as the LHC. We have derived a general correlation between production cross-section at colliders and new physics signal in neutron decay, showing that observation of a scalar resonance in lepton production at hadron colliders implies a lower bound (guaranteed signal) in neutron decay non-standard signal. Moreover, within a simple two Higgs-doublet model we have illustrated the interplay of collider and low-energy measurements in the reconstruction of the underlying parameters.
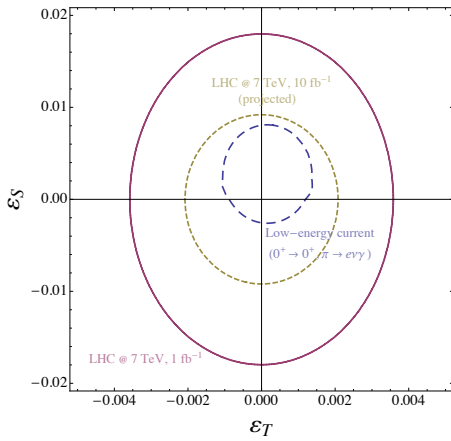
Figure 1. Currently, low-energy experiments provide constraints on scalar and tensor couplings that are stronger than the ones arising from the Large Hadron Collider (LHC), a ~$10B accelerator. The figure illustrates this point in detail, showing the 90% Confidence Level allowed regions for the scalar and tensor effective couplings (the allowed region is the one inside the various curves). The three curves correspond to constraints from: (i) current low-energy experiments including our own (blue, dashed) (ii) current results from the LHC searches at center-of-mass energy of 7 TeV; (iii) projected LHC searches with statistics increased by one order of magnitude (gold, dotted).
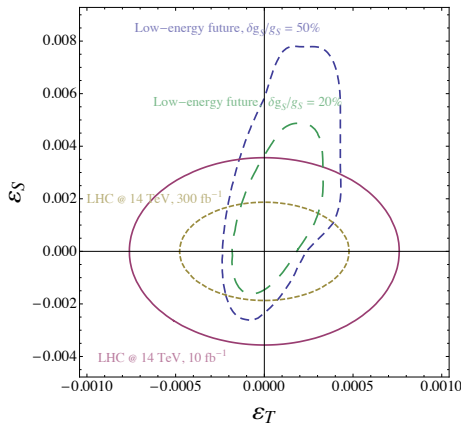
Figure 2. In coming years, the neutron experiments funded by this LDRD will compete with the Large Hadron Collider (a $10B accelerator) in providing the strongest constraints on the beyond-the-standard-model scalar and tensor couplings. Moreover, our theoretical modeling effort will provide the accuracy (~20%) needed to maximize the physics impact of ongoing measurements. The figure quantifies the above statements, showing the projected 90% Confidence Level allowed regions for the scalar and tensor effective couplings (the allowed region is the one inside the various curves). The various curves correspond to: (i) LHC searches at center-of-mass energy of 14 TeV for two different values of the accumulated statistics (solid,red and gold, dotted ellipses). (ii) Anticipated bounds from future low-energy experiments like ours (dashed green and blue curves). The latter two curves correspond to two different scenarios for the theoretical uncertainties on scalar and tensor matrix elements.

The theory progress has led to a paper, to be submitted for publication within the next month.

On the experimental side progress has been made on several fronts: UCNb has taken some data to test for systematics and a new detector is being built, we have seen 15-30 keV protons with the UCNB detector as well as low energy electrons, and are getting ready for run at the UCN source. Both efforts were presented to a NSAC review committee looking at the future of fundamental neutron physics experiments.

A first generation UCNb detector was tested on the UCN beam line at LANSCE. Several issues were identified. [6]He generated in the UCN source caused a short-lived background in the detector. This was eliminated by adding a thin polyethylene foil to the detector entrance. The deuterated scintillator purchased did not work up to our expectations; we are currently looking into procuring better scintillator and coating our own. Our first CaF2 scintillator box has arrived and is being fitted for the detector housing; this box should be ready to test in the early part of FY12. Data from the first run is still being analyzed to look for other problems and improve the design of the current detector.

The UCNb detector housing itself has undergone a significant redesign. This effort is focused to get better performance out of the PMTs and improve calibration.

for 42 degrees of freedom. The best fit sigma was 1.3 keV at 33 keV (the sigma was constrained to be proportional to sqrt(E) for each peak.)

Our UCNB large area silicon detector went through extensive offline testing and calibration this year. The system has achieved 3 keV resolution by cooling to 0 C. Cooling to 150K has further reduced this to 1.3 keV (Figure 3). To make this happen, we expended considerable effort to design the custom amplifiers and design a frontend FET that sits inside the vacuum and is also cooled. 15, 20, 25, 30 keV protons were observed at the TUNL accelerator, showing proof of principle for the detection of coincident betas and protons from UCN beta decay. The cooling system and high voltage standoffs will be integrated in FY12; after this the detector will be mounted at the LANSCE UCN source to detect UCN decay. An article is being drafted that documents the silicon detector design and data taken throughout FY 11.

Both UCNB and UCNb were presented to the NSCA review committee as possible future experiments that will need DOE funding. UCNB and UCNb were well received but we will have to wait for the report to understand our ranking for future funding.
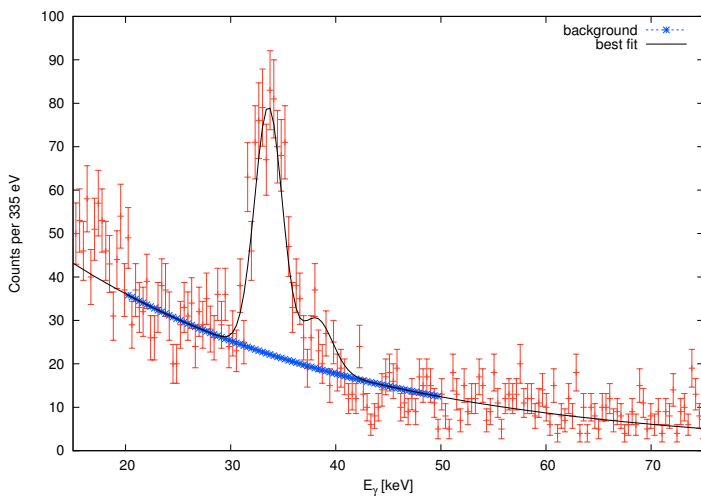
Figure 3. UCNB is first neutron beta decay experiment to measure both proton and beta decay particles with large area silicon detectors. Both dead layer and energy resolution need to be at the leading edge of large area silicon detector development to make this possible. We have partnered with Micron to develop the detectors needed for this experiment. Spectra from low energy sources, like 139 Ce spectrum shown, have been used to evaluate the detector's performance. The main peaks are x rays bunched together around 33 and 37 keV. The fit using Gaussian line shapes with the relative energies and amplitudes of x rays shows that we have a good understanding of the detectors response and that it is acceptable for the experiment.

Future Work

The purpose of this LDRD is to measure two neutron beta decay properties (the Fierz interference term b, that characterizes the energy spectrum of the electrons emitted in neutron decay, and the antineutrino momentum asymmetry relative to the neutron spin (called B)) which have maximal sensitivity to Physics Beyond the Standard Model (BSM) (of particle physics) and explore the theoretical implications of these measurements.

Measurements of b and B at the 10-3 level probe the existence of BSM scalar and tensor interactions generated by the exchange of particles with masses up to 10 TeV. Motivated by these considerations, we will perform the first ever measurement of b, with a sensitivity of 10^-3, and a measurement of B also at 10-3, representing a factor of five improvement over the most precise existing result. These two measurements will inaugurate a new class of precision neutron decay experiments, enabled by the unique features of the LANL UCN source. These benchmark experiments will allow us to quantify the systematics in B and b to perform a measurement at the 10^-4 level, for which we will develop and submit a proposal to DOE for external funding.

Future experimental work will focus on (FY 12):

- Improving the signal to noise in the UCNb detector system by using CaF2 Eu doped scintillator

- Observing p-e coincidences from UCN decay with the UCNB silicon detectors

- Constructing mounts for the stereo detector to measure "B"

- R&D running of a small scale UCNB (limited number of channels)

- Effort to promote the experiments to the n-decay community will start this spring

Future theoretical work will focus on:

- Improving the calculation of the hadronic matrix elements gS,gT with lattice QCD. In the next fiscal year we will focus on the calculation of the renormalization constants for the scalar and tensor operators

- Exploring in more detail the interplay of beta decays and collider searches in constraining physics beyond the Standard Model. Our first goal is to study models involving the so-called "leptoquarks" that arise in a number of Standard Model extension, from grand-unified models to supersymmetric models with R-parity violation

Conclusion

Our research will either discover or strongly constrain the existence of non-standard scalar and tensor charged-current interactions. Already with the precision of 10^-3 to be reached within the three years of LDRD funding, we will probe the existence of new particles (mediating the new forces) with masses in the multi-TeV range, possibly beyond the discovery reach of the Large Hadron Collider (LHC). Even if the new force mediators are discovered at the LHC, our proposed experiments will provide additional and unique information on the size of their couplings to light quarks and leptons.

Publications

Bhattacharya, T., V. Cirigliano, S. Cohen, A. Filipuzzi, M. Gonzalez-Alonso, M. Graesser, R. Gupta, and H. W. Lin. Probing novel scalar and tensor interactions form (ultra)cold neutrons to the LHC. 2011. *LANL Preprint LA-UR-11-1146, to be submitted for publication .*

Network-Centric Quantum Communications

Richard J. Hughes
20110046DR

Introduction

Creating new cyber security technologies is a National priority. Single-photon quantum communications (QC) has the potential to finally give defenders dominance over attackers in cyber space. QC has "future-proof" security rooted in laws of physics: today's quantum-secured communications cannot be compromised by unanticipated future technological advances. Today QC only exists in point-to-point instantiations that have limited ability to address the cyber security challenges of our increasingly networked world. Our foundational information science research project is developing a fundamentally new paradigm of network-centric quantum communications (NQC) that will leverage the network to bring QC-based security to user groups who may have no direct user-to-user QC connectivity. We will develop the theory, create the protocols, demonstrate them in hardware, and complete a system test that will attract future sponsors. NQC will be a scalable solution: with only QC links between each of N users and a trusted network node, quantum security would be brought to N^2 user pairs, and to multi-user groups. Central to NQC are four new QC primitives: quantum secure identification; multi-party quantum key distribution; quantum secret sharing; and quantum multiple access. These multi-party quantum protocols will provide the classical cryptographic services necessary for: encryption and authentication of data; secure identification; and access control. We will: devise practical, efficient NQC primitives, with precise security statements; establish how they can be composed into secure protocols; and experimentally implement them over optical fiber utilizing existing QC hardware and software. The results will establish protocol performance and provide the understanding of real-world impairments that we will use to analyze the ultimate limits to channel capacities, and to construct predictive NQC models. Using accepted information assurance methodologies we will design, perform and evaluate multi-node system trials of NQC that are representative of cyber security needs within a variety of network environments.

Benefit to National Security Missions

NQC will address long-duration/high-value security needs within many network environments, such as: certain DoD and DOE complexes; between government agencies in the Washington, DC area; financial networks; supervisory, control and data acquisition (SCADA) systems for critical infrastructure (power, water and SmartGrid) networks; and LANL's own network. NQC will extend security to constrained network environments. Examples include: IAEA treaty monitoring; within a US Embassy compound; or a military aircraft. NQC would enable a hand-held QC device to be used for identification, authentication, access control and secure telephone calls. NQC is extensible to other types of networks: an aircraft or satellite acting as a trusted node could establish ad hoc secure networks of ground, sea and air-based users on a continental or even a global scale. Cyberdefense of the NNSA complex itself is a likely application.

Progress

During the first year of the project we have made important experimental and theoretical progress towards the ultimate cyber security research objectives. We quickly established a first-generation experimental network-centric quantum communications (NQC) testbed, which is comprised of two client quantum communications (QC) (transmitter) nodes and one trusted authority (TA) server (receiver) node. The server node incorporates a novel method of single-photon detection at telecommunications wavelengths, enabling it to multiplex signals from multiple client nodes. The client nodes are each performing QC over independent optical fiber paths of up to 80km with the server, achieving sufficiently high signal-to-noise to permit first-generation NQC protocols to be implemented and evaluated. We have developed server software that is capable of supporting up to 100 clients nodes simultaneously, using a single PC, in current form. We have invented and implemented a first quantum secure identification (QSID) protocol between each client and the TA, in which the client convinces the TA that the client knows a secret password, but without revealing

any information about the password. From experimenting with this protocol we have gained important insights into how to set the QSID protocol parameters to provide strong security against online password cracking attacks. From the results of the QSID protocol we are able to derive a short, secret authentication key shared by a client and the TA, which they can use to initiate a quantum key distribution (QKD) session, resulting in multiple secret keys shared between client and TA. We have implemented a first multi-party key distribution protocol, which enables the two client nodes to establish a shared, secret session key, even though they have no direct client-to-client QC. This protocol is accomplished using the QKD keys shared by each client with the TA, together with non-secret ("quantum public key", QPK) information provided by the TA to each client. This research has resulted in two US Patent applications and one provisional US Patent application. We are investigating the security parameter that can be assigned to this client-to-client key and how it depends on the security parameter of each of the client-to-TA QKD sessions. This analysis is proceeding through an investigation of the min-entropy properties of the various keys involved. We have also invented a quantum digital signature protocol, which will enable the TA to function as a Certificate Authority for signing clients' quantum public keys, that can be incorporated into existing key management infrastructures. Additionally, this protocol enables a client to digitally sign a message to another client, even though they have no direct QC connectivity. An invention disclosure on this quantum digital signature has been made. With the addition of this new protocol we have within NQC a suite of primitives that together are capable of providing all of the cryptographic functionality required for a cryptosystem, with the highly attractive properties of forward security and immunity to attack by a future quantum computer [1]. The QPK invention also provides secure mechanisms for enrolling and revoking users. Jon Yard, in a joint paper "Quantum communication with Gaussian channels of zero quantum capacity" with Graeme Smith and John Smolin (IBM Watson), showed that physically realistic channels can have much larger communication capacities than previously thought [2]. We have set design requirements and are preparing to order the next generation of integrated photonics devices that will enable the client nodes to perform more advanced, higher security QC with the TA, such as "decoy state" coding, in a second-generation testbed. These new devices are required to permit a more rigorous and precise security statement for each of the NQC protocols than is possible with the present ones, and so enable the future stages of the project as described in the original proposal. We anticipate that the vendor will deliver these new devices in the second year of the NQC project.

Future Work

While QC is future-proof in principle, the security it provides in practice must be established and quantified in an integrated environment. We will: design practical, robust, secure NQC protocols; implement them in experiments to quantify their performance; design representative NQC network test scenarios; and evaluate their security in each threat environment using established information assurance methods. Both quantum information theoretic and classical cryptographic design principles will be used to create NQC protocols. We will leverage existing quantum communications hardware and software, suitably updated, to experimentally implement the NQC protocols, and to create representative test networks in a laboratory setting. Experimental tests will determine how the security of the NQC protocols depends on real-world issues such as transmission impairments and noise. Our team members' expertise in theoretical, experimental and engineering aspects of QC security will be applied to defining the threat environment for selected representative network scenarios, devising security test plans for them, and evaluating the results of experimental tests. Peer review and red-teaming will challenge our security hypotheses and help us look for the unexpected. Theoretical analyses of channel capacities will provide an understanding of how the NQC security paradigm will perform when scaled-up to real-world networks. Taken together, these results will constitute the knowledge base for quantifying the cyber security advantages that would result from applying NQC to a variety of future networks.

Conclusion

The experiments will be the first demonstration of an entirely new quantum-enabled cyber security concept that leverages the network environment to provide communications security even between nodes that lack direct quantum communications. This project will produce many prominently publishable results, furthering LANL's capability and leadership in this area, and will lead to a breakthrough technology for securing network communications. The research has considerable commercialization potential. Research performed during the first year of the NQC project has resulted in 12 invention disclosures, 2 US Patent applications, and 3 provisional US Patent applications. In March 2011 a commercialization opportunity for a portion of this Intellectual Property was presented at an Industry Workshop, which was attended by representatives of 10 major US corporations. LANL's Technology Transfer Division is now negotiating a CRADA with one of these companies. This project is well-aligned with the IS&T Grand Challenge, and the Lab's National Security mission.

References

1. Hughes, R. J., and J. E. Nordholt. Refining quantum cryptography. 2011. *Science.* **333**: 1584.

2. Smith, G., J. Smolin, and J. Yard. Quantum communication with Gaussian channels of zero quantum capacity. 2011. *Nature Photonics.* **5**: 624.

Publications

Hughes, R. J., and J. E. Nordholt. Refining quantum cryptography. 2011. *Science.* **333**: 1584.

Smith, G., J. Smolin, and J. Yard. Quantum communication with Gaussian channels of zero quantum capacity. 2011. *Nature Photonics.* **5**: 624.

Double Beta Decay

Steven R. Elliott
20090053DR

Abstract

Neutrinoless double beta decay can only exist if neutrinos are massive and are their own antiparticle. Experiments searching for this process represent the only practical technique to determine whether the neutrino is its own antiparticle. This question is critical for understanding how mass is incorporated into our models of the Universe and may also help us understand the preponderance of matter over antimatter. This LDRD investment allowed a great deal of R&D to show that a particular experimental design is feasible. As a result the project is now supported and underway.

Background and Research Objectives

The Standard Model (SM) has been very successful in describing the fundamental forces of nature for several decades. However, the preponderance of matter over anti-matter in the Universe, the origin of mass, and the unification of the forces are key aspects of the theory that are unanswered. The fundamental properties of the neutrino are critical to understanding these basic components of the SM. The answer to the question: "Is the neutrino its own anti-particle?", is needed to help uncover the reasons matter dominates over anti-matter in our Universe. If the neutrino is its own anti-particle, then a natural explanation for the matter/anti-matter asymmetry arises (leptogenesis). The answer is also critical for theories of the origin of mass. Another question: "What is the neutrino mass?", has implications for the large-scale structure of the Universe but also indicates the high energy scale at which the SM breaks down. A third question: "Is lepton number violated?", is a significant test of the SM in its own right as the model conserves the number of leptons (electrons and neutrinos) in any process. While as yet unobserved, models unifying the forces predict lepton number violation. Neutrinoless double-beta decay $(\beta\beta(0\nu))$ is the only practical experimental method for investigating the neutrino particle/anti-particle question. And if the neutrino is its own anti-particle, $\beta\beta(0\nu)$ will have the best sensitivity to neutrino mass of any laboratory technique. Finally, if $\beta\beta(0\nu)$ is observed, lepton number is not conserved. It is clear that $\beta\beta(0\nu)$ is a necessary component of any program searching for Beyond the Standard Model science. The results will change our view of the Universe [1, 2, 3].

If this lepton-number-violating, nuclear-decay process exists, one would observe a monoenergetic line originating from a material containing an isotope subject to this decay mode. One such isotope that would undergo this decay is ^{76}Ge. Germanium-diode detectors fabricated from material enriched in ^{76}Ge have established the best $\beta\beta(0\nu)$ half-life limits and the most restrictive constraints on the effective neutrino mass. Therefore, this material holds great promise for future advances in $\beta\beta(0\nu)$ experimental techniques. The technology has now reached the point that results from $\beta\beta(0\nu)$ projects will address the critical questions listed above.

The MAJORANA project [4] is a proposal by ~100 scientists from 15 institutions and 4 countries. LANL is one of the lead institutions of this collaboration and the PI of this proposal (Elliott) is the spokesperson of the MAJORANA experiment. The objective of the first experimental phase of MAJORANA is to build a 40-kg array of high-purity Ge, of which up to 30 kg will be enriched to 86% in ^{76}Ge, to search for neutrinoless double-beta decay. The array will be contained in 3 cryostats, one of which, the prototype cryostat, will incorporate P-type point-contact Ge detectors (PPC) fabricated from natural Ge.

Scientific Approach and Accomplishments

One significant result of this LDRD support was that significant research was done that led to the MAJORANA DEMONSTRATOR being funded. The DEMONSTRATOR will consist of 2 cryostats containing detectors that use Ge enriched in isotope 76. The LANL team established itself as a major contributor to the leadership of the MAJORANA collaboration. Elliott has been elected spokesperson for 3 consecutive 2-year terms. Elliott is the level 2 manager for host lab infrastructure (WBS 1.03), Rielage was the level 2 deputy for materials and assay (WBS 1.04), but has recently shifted to deputy for WBS 1.03. Boswell is the deputy level 2 manager for mechanical systems (WBS 1.09). Gehman has been the level 2 manager for commissioning (WBS 1.11), but Kidd will soon take over

that role.

Much of our experimental work has had to do with the design of the DEMONSTRATOR, particularly with respect to minimizing background in the detector. In addition, our theory component has also made progress. In the following sections, we describe specific contributions to these accomplishments.

Shield design

We have made substantial progress on the shield design (Figure 1) including the configurations of the passive Cu, Pb, and poly shielding and their support structures. We have also made progress on the veto system. We have designed the monolith transport systems and the assembly and shield tables. We have designed and ordered the air-bearing system that will transport the monolith. We have designed and are in the process of ordering the glove boxes. We have simulated the performance of the Veto system for the DEMONSTRATOR, establishing an expected efficiency and aiding with the mechanical design.
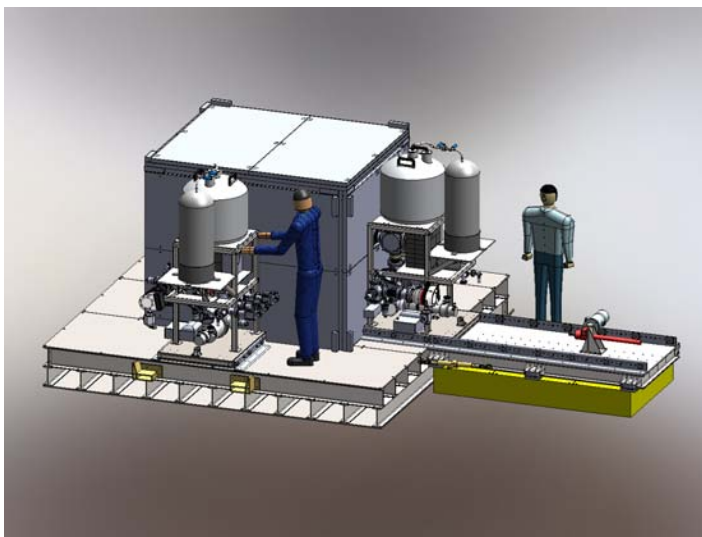
Figure 1. The DEMONSTRATOR shield design.

Calibration system

In past couple of years the MAJORANA calibration design has undergone significant development. The current configuration (Figure 2) envisions each monolith with a separate calibration track; a low-background source pathway of electro-formed Cu tubing spiraling around the outside of the cryostat. A line source of ^{228}Th will be remotely fed into the pathway, enabling the calibration of the entire cryostat with a single source. A detailed simulation study of the calibration setup has recently concluded; the study established the parameters of the calibration runs, evaluated any factors that might impact the successful calibration of the cryostats, and to determine the solid angle of the source.
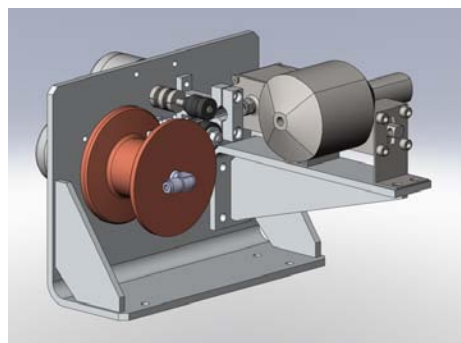
Figure 2. The drive system and storage reel for the calibration source.

Underground Lab Design Development

We worked with the architects and engineers of the Sanford Underground Laboratory (SUL) at Homestake to define the specifications of an underground laboratory that would suit the needs of the DEMONSTRATOR. The results of these efforts produced a lab design that is now being constructed at SUL.

Analysis and simulation

The LANL Weak Interactions Team (WIT) plays a key role in the development and testing of the analysis and simulations framework [5] for the MAJORANA experiment.

Canary cage

We have constructed a string test cryostat (nicknamed "The Canary Cage" and shown in Figure 3). The Canary Cage currently holds a string of four stainless steel detector blanks for thermal and mechanical tests to refine the design of the detector mounts and strings. In the past we have also deployed and operated detectors. We have already made several changes to the MAJORANA string design based on data from Canary Cage tests. These have included increasing the thermal conductivity of the string mounts, and realizing the need to eliminate threaded plastic nuts from the design.

Figure 3. A test string being deployed into the canary cage.

Detector R&D

The collaboration has selected p-type point-contact detectors [6]. We purchased and characterized four p-type, point-contact detectors from Ortec, a fifth from Princeton Gamma Tech and a sixth from PhD's to explore alternatives to the Canberra production BEGe detector design. The number of detectors that would be required to field a tonne-scale neutrinoless double-beta decay experiment would likely overwhelm the production capacity of single commercial vendor, so maintaining a relationship with multiple vendors and encouraging them to develop point-contact detector expertise is important to help lay groundwork for a tonne-scale project. We have studied the effects of systematic uncertainties associated with pulse shape analysis in Ge detectors [7].

We also purchased a detector for the study of alpha particles straggling through the thin dead layer of HPGe detectors. Even though the detectors in the MAJORANA DEMONSTRATOR are p-type and therefore have a large thick (0.5 – 1.0 mm) dead layer, there is a small region near the signal contact with a thin (few mm) dead layer. We purchased a commercial detector and modified the cryostat to allow us to scan a collimated, windowless alpha source (^{241}Am) at several angles across the front face of the detector. We then characterized the detector's response to these alpha particles, and estimated this potential background contribution to the continuum level in the double-beta decay region of interest. This work formed the foundation of the PhD thesis work for Rob Johnson (formerly a PhD student at the University of Washington).

Detector receipt and acceptance

We purchased all of the natural BEGe detectors that will go into the MAJORANA DEMONSTRATOR prototype module. These detectors underwent an extensive acceptance and characterization program. Each detector was checked to make sure that the manufacturer (Canberra) met all required performance specifications (energy resolution, leakage current, capacitance, and noise performance). A subset of these detectors also went through a full battery of characterization tests. The full characterization program also included sampling the dead volume of the detector with low-energy gamma sources scanned across the side of the detector and the collection of a large waveform data set to test the single and multi-site event tagging performance with pulse shape analysis. A paper summarizing the findings of our acceptance and characterization study is currently in preparation.

(n,n') Studies

Inelastic neutron scattering in detector and shielding materials is a significant problem in rare decay searches. The background requirements of these experiments are significantly lower than all previous measurements, and therefore rely heavily on simulations to estimate the contribu-

tions from backgrounds that were not considered before. One study with Pb [8], showed that many potentially very disruptive gamma-ray emissions were not being properly simulated because the nuclear physic data bases did not have values for excitation cross sections. See Figure 4 for an example spectrum.
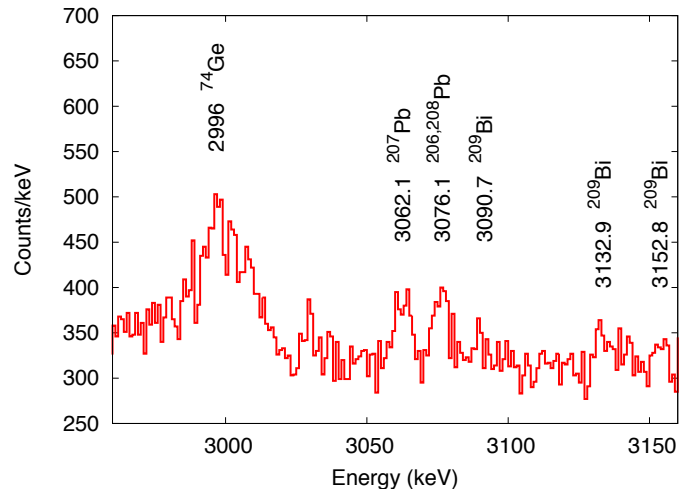
Figure 4. Spectrum from Pb(n,n') showing 3062-keV line that was not previously incorporated into the simulations because the cross section to excite that state was set to zero in ENDEF.

Recently we completed our analysis of (n,n _) on ^{nat}Cu. We extracted excitation functions for 46 states in ^{63,65}Cu, in addition to eight states in ^{62,64}Cu. These data will hopefully be added to the ENDF evaluation for Cu, filling in gaps of experimental data that until now were estimated only by theoretical models.

During FY11, we made measurements of Ar(n,n'g) at the GEANIE facility at LANSCE. The purpose was to better understand neutron-related backgrounds in Ar detectors and double beta decay experiments using Ar as a shield. The analysis of these data is ongoing and is part of a graduate student dissertation (Sean MacMullin from the University of North Carolina).

WIPP activities

We operate an underground R&D laboratory at WIPP for studies related to MAJORANA. At this laboratory, we operate a screening detector system that will provide data on materials for MAJORANA. We also performed some early underground electroforming experiments there.

This detector has been primarily used to radioassay material for MAJORANA including charcoal, high purity tin, and TIG welding rods. However, we have also used this detector to measure activity produced in enriched Ge by high-energy neutrons for studies on cosmogenic backgrounds. A paper [9] was published on this work providing a measurement of the cosmic-ray neutron production rate that was critically needed for background estimates. This important

result indicated that the production rate was twice that previously estimated. We performed measurements on Pb sheets that were exposed to a neutron beam at LANSCE with an energy spectrum similar to that of the cosmic-ray neutron spectrum. These activated sheets were counted at WIPP. The results show that Pb is activated by cosmic rays and the resulting activities may pose a threat to low-background experiments.

Activated detector studies

Cosmogenic isotopes are produced in Ge diodes while they are exposed to cosmic rays on the surface. Of those produced, $^{68}Ge/^{68}Ga$ and ^{60}Co are the most problematic because they decay with energies greater than the $0\nu\beta\beta$ Q value. Furthermore, the activation rates for ^{68}Ge available in the literature disagree by an order of magnitude. Reduction of these backgrounds (and many others) in MJD will be accomplished in part by applying pulse shape analysis (PSA) techniques that can distinguish single-site energy deposits (signal-like) from multiple-site depositions (background-like) in a single crystal.

In 2008, we irradiated a semi-coaxial, high-purity Ge (HPGe) detector with neutrons at LANSCE with two goals in mind: (1) to measure the activation rate of several cosmogenic isotopes, and (2) to experimentally verify the predicted efficacy of our pulse-shape analysis algorithms, which until recently was based only heuristic arguments. After irradiation, the detector was annealed and then operated in coincidence with two nearby radiation detectors in order to resolve the spectra of _+ decays inside the activated detector by externally tagging 511-keV annihilation gamma rays.

Theory

We have made progress in theoretical physics associated with the nuclear matrix element for double-beta decay and for the physics of neutrino oscillations and mass hierarchy more generally. In the physics of the nuclear matrix element, we have formed a collaboration with J. Engel of the University of North Carolina and R. B. Wiringa of Argonne National Laboratory. Recently there has been a recognition that relatively short-range correlations between the two protons that decay in double-beta decay are important for an adequate description of double beta decay.

We investigated the role of Jastrow short-range correlations in double-beta decay in a simple model that can be evaluated using Monte Carlo techniques. We find that various approaches to short-range correlations previously thought to yield different results can be, by including effects previously thought insignificant, reconciled to a large extent. These conclusions were published in Physical Review C [10]. We have also initiated other calculations in both light and heavy nuclei, and will propose calculations that will be proposed to the DOE through a SCIDAC call recently issued. This proposal will also include collaborations with other groups pursuing double beta decay.

We also investigated the extent to which the neutrino mass hierarchy may be observable through the effects of neutrino-neutrino scattering in supernovae neutrinos [11-16]. LANL researchers including Duan, Friedland and Carlson have pioneered this effort along with their collaborators. During the past few years we have developed the first full 3x3 neutrino flavor calculations including multi-energy and multi-angle effects. The calculations have shown that 'spectral swaps', or fast changes in neutrino and/or anti-neutrino flavor distributions as a function of energy, may tell us a lot about both the astrophysical environment and the fundamental neutrino physics including masses and mixing. We have investigated different astrophysical sites, including O-Ne-Mg supernovae where effects of inhomogeneous matter distributions are expected to be smaller. In many cases we have examined both normal and inverted mass hierarchy for the neutrinos.

Impact on National Missions
The work has developed science and technology underpinnings for new program areas. In particular, the path for impact on LANL programs are indicated by the Community support of this science as described by NRC committees and the DOE NP/HEP NuSAG review committee. The 2007 Nuclear Physics Long Range Plan strongly endorses research in this area. The DOE Office of Nuclear Physics has been very supportive and therefore the future funding potential is strong. The similarity in requirements means that the R&D for $0\nu\beta\beta$ will be applicable to certain environmental monitoring applications. Our team has already expanded our low-background and detector expertise capabilities into funding opportunities in homeland security.

References

1. Elliott, S. R., and P. Vogel. Double Beta Decay. 2002. *Annu. Rev. Nucl. Part. Sci. .* **52**: 115.

2. Elliott, S. R., and J. Engel. Double-Beta Decay. 2004. *J. Phys. G: Nucl. Part. Phys..* **30**: R183.

3. III, F. T. Avignone, S. R. Elliott, and J. Engel. Double Beta Decay, Majorana Neutrinos and Neutrino Mas. 2008. *Rev. Mod. Phys. .* **80**: 481.

4. others, V. E. Guiseppe and. The Majorana Experiment. 2010. *Nuclear Physics B (Proceedings Supplements).* **217**: 44.

5. others, M. Boswell and. MaGe - a Geant4-based Monte Carlo Application Framework for Low-background Germanium Experiments. 2011. *IEEE Trans. Nucl. Sci. .* **58**: 1212.

6. others, P. Finnerty and. Astroparticle Physics with a Customized Low-Background Broad Energy Germanium Detector. To appear in *Nucl. Instr. Meth. A Proceedings.*

7. Gehman, V. M.. Systematic Effects in Pulse Shape Analysis of HPGe Detector Signals for Neutrinoless Double-Beta Decay. 2010. *Nucl. Instr. Meth. A.* **615**: 83.

8. others, V. E. Guiseppe and. Neutron inelastic scattering and reactions in natural Pb as a background in neutrinoless double-beta decay experiments. 2009. *Phys. Rev. C.* **79**: 054604.

9. Engel, J.. Jastrow Correlations in Double-Beta Decay. 2011. *Phys. Rev C.* **83**: 034317.

10. Friedland, H. Duan and A.. Induced Suppression of Collective Neutrino Oscillations in Supernova. 2011. *Phys. Rev. Lett..* **106**: 091101.

11. Cherry, J. J., G. M. Fuller, J. Carlson, H. Duan, and Y. Qian. Analysis of Neutrino Flavor Evolution in the Neutronization Burst from an O-Ne-Mg Core-Collapse Supernovae. To appear in *Phys. Rev. d.*

12. Duan, H., A. Friedland, and G. McLaughlin. The influence of Collective Neutrino Oscillations on the Supernovae r-process. To appear in *J. Phys. G.*

13. Friedland, A.. Self-Refraction of Supernova Neutrinos: Mixed Spectra and 3-flavor Instabilities. 2010. *Phys. Rev. Lett..* **104**: 191102.

14. Cherry, J., G. M. Fuller, J. Carlson, H. Duan, and Y. Qian. Multi-Angle Simulation of Flavor Evolution in the Neutrino Neutronization Burst from an O-Ne-Mg Core-Collapse Supernova. 2010. *Phys. Rev. D.* **82**: 085025.

15. Duan, H., G. M. Fuller, and Y. Qian. Collective Neutrino Oscillations. *Ann. Rev. Nucl. Part. Sci..*

Publications

Boswell, M.. MaGe - a Geant4-based Monte Carlo Application Framework for Low-background Germanium Experiments. 2011. *IEEE Trans. Nucl. Sci..* **58**: 1212.

Cherry, J. F., G. M. Fuller, J. Carlson, H. Duan, and Y. Qian. Multi-Angle Simulation of Flavor Evolution in the Neutrino Neutronization Burst from an O-Ne-Mg Core-Collapse Supernova. 2010. *Phys. Rev. D.* **82**: 085025.

Cherry, J. J., G. M. Fuller, J. Carlson, H. Duan, and Y. Qian. Analysis of Neutrino Flavor Evolution in the Neutronization Burst from an O-Ne-Mg Core-Collapse Supernovae. *Phys. Rev. D.*

Duan, H., G. M. Fuller, and Y. Qian. Collective Neutrino Oscillations. *Ann. Rev. Nucl. and Part. Sci..*

Duan, H., and A. Friedland. Self-induced Suppression of Collective Neutrino Oscillations in Supernova. 2011. *Physical Review Letters.* **106**: 091101.

Elliott, S. R.. Double Beta Decay: Solid-State and Semiconductor Detectors. Presented at *Conference on the Intersections of Particle and Nuclear Physics.* (San Diego, CA, May 2009).

Elliott, S. R.. Toward a tonne-scale Ge experiment: the Majorana Demonstrator. Invited presentation at *Workshop on Germanium-Based Detectors and Technologies.* (Berkeley, CA, May 2010).

Elliott, S. R.. Experimental Overview of Neutrinoless Double Beta Decay. Invited presentation at *International Workshop on Double Beta Decay and Related Neutrino Measurements.* (Hawaii, October 2009).

Elliott, S. R.. Neutrinoless Double Beta Decay. Invited presentation at *238th American Chemical Society National Meeting.* (Washington DC, August 2009).

Elliott, S. R.. Double Beta Decay. To appear in *Rutherford Centennial.* (Manchester, UK, 8-12 Aug. 2011).

Elliott, S. R.. The Majorana Project. 2010. In *11th International Conference on Topics in Astroparticle and Underground Physics.* (Rome, IT, 1-5 July 2009). Vol. 203, p. 012057. Bristol: IOP.

Elliott, S. R., V. E. Guiseppe, R. A. Johnson, B. H. LaRoque, and S. G. Mashnik. Fast-Neutron Activation of Long-Lived Isotopes in Enriched Ge. 2010. *Physical Review C.* **82**: 054610.

Friedland, A.. Self-Refraction of Supernova Neutrinos: Mixed Spectra and 3-flavor Instabilities. 2010. *Physical Review Letters.* **104**: 191102.

Gehman, V. M., S. R. Elliott, and D. M. Mei. Systematic Effects in Pulse Shape Analysis of HPGe Detector Signals for Neutrinoless Double-Beta Decay. 2010. *Nuclear Instruments and Methods.* **615**: 83.

Guiseppe, V. E., M. Devlin, S. R. Elliott, N. Fotiades, A. Hime, R. O. Nelson, D. M. Mei, and D. V. Perepelitsa. Neutron inelastic scattering and reactions in natural Pb as a background in neutrinoless double-beta decay experiments. 2009. *Physics Review C.* **79**: 054604.

Mei, D. M., Z. B. Yin, and S. R. Elliott. Cosmogenic Production as a Background in Searching for Rare Physics Processes. 2009. *Astroparticle Physics.* **31**: 417420.

others, V. E. Guiseppe and. The production of 68Ge in Ge detectors due to fast neutrons. Presented at *April Meeting of the American Physical Society.* (Denver, CO, May 2009).

others, V. E. Guiseppe and. The MAJORANA Project. Presented at *Implications of Neutrino Flavor Oscillations.* (Santa Fe, NM, July 6-10, 2009).

Turbulence By Design

Malcolm J. Andrews
20090058DR

Abstract

This is the final report for the LDRD-DR #20090058 titled "Turbulence By Design". The purpose of the report is to provide an overview of the 3 year project, with a glimpse of the major results. The project itself has generated some 25 international journal publications, and over 60 conference presentations and publications, and also won the first LDRD Day in September 2010. For a detailed account of the technical details about results from the project the reader should refer to the extensive set of publications.

The LDRD Directed Research in this project focused on an investigation about the role of initial conditions and their development into turbulence. In the realm of fluid mechanics the transition from a well-defined initial condition to a turbulent flow is considered one of the hardest technical problems because of strong non-linear effects, and the difficulty obtaining repeatable experiments to study the problem.

At the outset it was not clear that memory of initial conditions was retained as the flow develops, and that if there was a methodology that would allow useful characterization of the transition to turbulence. We have definitively answered these concerns with a "yes", and in the process we have verified the fundamental hypothesis of the project: "Initially seeded small amplitude, long wavelength, perturbations can develop at late-time and be used to control turbulent transport and mixing effectiveness."

Our approach to the problem has centered on the development of buoyancy driven instabilities (Rayleigh-Taylor and Richtmyer-Meshkov) toward turbulent mixing. Our choice of these instabilities reflects our own areas of expertise, but also represents an active area of fundamental research whose results can transition to programmatic interests at Los Alamos, and can also guide the study of other unstable flows (e.g. shear driven Kelvin-Helmholz instabilities). Our results range from: a single parameter characterization of initial conditions that captures their late-time development, and provides a relatively simple guidance to setting initial conditions in turbulence; to a full-blown spectral model of the initial conditions that can handle complex initial spectra (e.g. banded spectra), and can not only be used to specify initial conditions, but also to predict the likely development and need for a complex specification of initial conditions or model coefficients in standard turbulence models. These two theoretical approaches have been supported by extensive sets of high fidelity experiments, integrated large eddy simulations, and direct numerical simulations, and it is this integrated nature of the project that has driven progress, discovery and success.

Background and Research Objectives

This report provides a glimpse of research performed under the LDRD-DR "Turbulence By Design." In this section we provide a brief overview of the project, then we provide a glimpse of the research performed by each co-PI. The report closes with a summary of the impact on National Missions.

Starting (initial) conditions (ICs) can influence the development of hydrodynamic turbulence and material mixing flows – a strategic problem in energy production and the environment. The central goal of this DR is to investigate the science of initial condition development in fluid mixing problems, and how it can be used to predict and design turbulent transport/material mixing - "Turbulence by Design" (TbD). This Directed Research (DR) couples a well-balanced set of world class LANL facilities and advanced diagnostics, with experts in theory and computation. By way of improved specification of initial conditions for mathematical models of turbulence we expect to improve fusion targets for net energy gain, understand early-late time astrophysical instabilities, gain a better understanding of climate and ocean flow dynamics, and improve energy production and use technologies.

Central Hypothesis: Initially seeded small amplitude, long wavelength, perturbations can develop at late-time and be used to control turbulent transport and mixing effectiveness.

Our overarching scientific goal is to explore, and make use of, large-structures embedded in the initial conditions – *memory of initial conditions is NOT lost*. Our practical goal is to describe birth to full development of turbulent mixing – so enabling prediction and design. After a second-year review we adjusted our goals to include the development of metrics to measure material mix development (i.e. where in the transition we might be, and/or what the consequences of various ICs might be on late-time development).

Scientific Approach and Accomplishments

Theory and Modeling

This part of the DR work has studied both the Rayleigh Taylor (RT) and the Richtmyer Meshkov (RM) shock AND reshock instability and transition to turbulence.

Research Highlight

Our main theoretical, and most useful, result is the development and validation of the "stochastic linear stability theory" (SLST) methodology in describing non-linear transition problems for problems starting from statistically quiescent conditions such as RT and RM. This will prove a long term tool in the study and understanding of the statistics of initial conditions and their effect on transition and subsequent turbulent states. Additionally the SLST serves as an important tool for the rational specification and design of initial conditions for moment models in a way that reflects the physical problem.

On the practical level this manifests itself as the simplest rigorous two length scale characterization of the interfacial morphology by that come from the analysis: an *rms* thickness and a zero crossing length scale. These objects can be thought of as the effective statistical thickness and the effective statistical "wavy-ness" of the interface that undergoes the RT or RM instability. The product of the two is the slope, in a statistical sense, of the interface and plays a crucial role in the evolution of the interface and the speed or even likely-hood (in the RM case) of the transition to turbulence. Previous to this analysis the effective thickness of the interface was taken as the initial length scale carried in a turbulence model for these interfacial instabilities.

Richtmyer-Meshkov Experiments

The biggest challenge we have faced to understand the impact of Richtmyer-Meshkov mixing on turbulence is that there have not been experiments of sufficient spatial and temporal resolution, that measure physical quantities such as density and velocity fields, while also characterizing initial conditions. We have applied advanced diagnostics at the gas shock tube in P-23 to better understand the impact of initial conditions on shock-driven mixing. This required modification of the test section of the shock tube to look at the late-time transition and evolution to turbulence of the flow field. Also, we have characterized the initial conditions of our experiments with higher spatial resolution

than any other previous experiments in the world. We worked closely with Grinstein and Gowardhan to understand the needs of the numerical modeling, and it has resulted in the best numerical simulations of the shocked gas curtain to date.

Research Highlight

For the first time, we have been able to experimentally differentiate the turbulent mixing of shocked flows with different initial conditions [1]. This required innovation in our experimental measurement techniques, how we characterize experimental initial conditions, and how we quantify mixing evolution.

In particular, simultaneous density and velocity field measurements have been made for three different sets of initial conditions, two single-mode and one multi-mode. Furthermore, we made the first experimental measurements in Richtmyer-Meshkov flows of the initial condition dependence of turbulent kinetic energy, turbulent Reynolds number, turbulent mass flux, and density self-correlation. In addition, we made the first three-dimensional characterization of the experimental initial conditions with sufficient resolution to provide a test problem for numerical simulation.

These experimental results quantitatively validate the underlying hypothesis of this LDRD research, namely that shock-driven turbulence retains memory of initial conditions.

As an example, we show in Figure 1 experiments that used reshock timing to vary the conditions upon which a reflected shock hits the evolving single-mode gas curtain. From these results we could observe turbulent transition in singly-shocked flows, and that led us to a more detailed parametric study of single- and multi-mode initial conditions, shocked once and allowed to evolve to late times. The density fields, shown in Figure 1 below, reveal differences in the mixing. More importantly, those differences have been quantified and related back to the different initial conditions, resulting in new information about the impact of initial conditions on transition and turbulence. Transition is clearly captured as the flow evolves from primarily large-scale mixing structures to the much smaller scales associated with turbulence.

ILES Simulations

We focused on shock driven turbulent mixing generated via the Richtmyer-Meshkov (RM) instability. Laboratory observations typically demonstrate the end outcome of complex non-linear 3D physical processes have many unexplained details and mechanisms. Carefully controlled computational experiments have a crucial role providing insights into the underlying flow dynamics. In this context, it is important to recognize the inherently intrusive nature of *observations* based on (numerical or laboratory) flow experiments [2]. The difficulties with the open problem of

predictability of material stirring and mixing by under-resolved multi-scale turbulent velocity fields in shock-driven turbulent flows are compounded with the inherent sensitivity of turbulent flows to initial conditions (ICs) [3]. Turbulent material mixing can be usefully characterized by the fluid physics involved: large-scale entrainment, stirring due to velocity gradient fluctuations; and, molecular diffusion. At moderately high Reynolds number, we are primarily concerned with the numerical simulation of the first two convectively-driven (interpenetration) mixing processes, which can be captured with sufficiently resolved implicit large eddy simulation (ILES) [4]. Our particular ILES strategy was based on using LANL's RAGE code [5].

We addressed effects of IC resolved spectral content [6,7] and initial interfacial morphology [8,9] on transitional and late-time planar shock-driven turbulent mixing, and extended our studies to the significantly more complex 3D shocked Gas Curtain (GC) P-23 experiments [10,11].
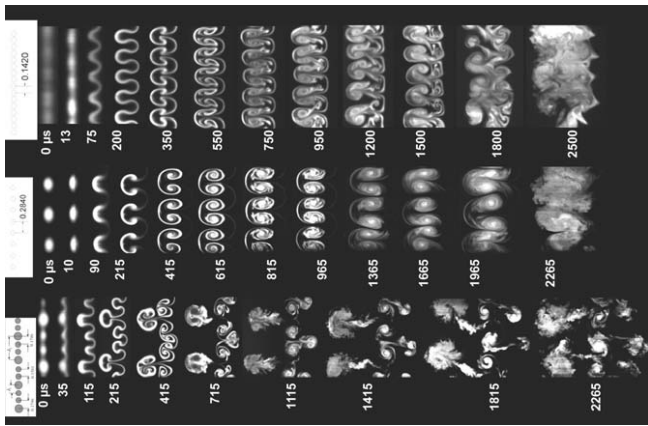
Figure 1. Time series of evolution of RM instability (Mach 1.2 incident shock from left to right) with single-mode short- and long-wavelength and multi-mode initial conditions. Times in microseconds.

Research Highlight
Our most significant result was achieved in our studies of the planar RM [2]. We demonstrated that a single IC parameter (η_o=_ _) characterizing the initial GC conditions (section section 2.2) can be usefully identified as relevant in determining whether the RM driven flow is in a linear ballistic regime (low η_o), or non-linear mode-coupling regimes (high η_o) – Figure 2. We have called this the *bipolar behaviour* of RM. Our findings present significant challenges for RM modelling and provide a significant basis to develop metrics for transition to turbulence. An important practical consequence is that *reshock* effects can be emulated at *first shock if* the initial *rms* material interface slope η_o is high enough [9].

DNS Computational "Experiments"

For this project, we have employed the CFDNS code [12], developed in the CCS-2 group at LANL over the last eight years by Livescu and collaborators. The code has been used on up to 150,000 processors on the LLNL BG/P Dawn and 50,000 processors on the ORNL Jaguar. The CFDNS kernel has also been successfully ported to Roadrunner (Cell SPE) with excellent performance. Computational allocations on these machines, as well as through Institutional Computing, were obtained during the course of the project.

We have used these allocations to perform the largest Direct Numerical Simulations of Rayleigh-Taylor instability to date for single-, two-, and multi-mode initial perturbations, in order to study the influence of initial conditions (ICs) on the instability growth and find ways of controlling the later development stages through appropriate choices of the initial conditions.
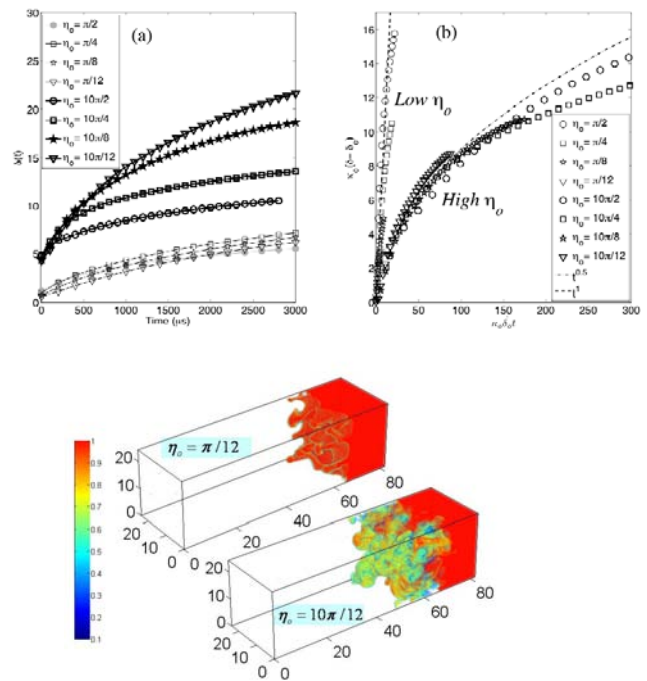
Figure 2. The bipolar RM behavior [8]. a) Mixedness width measures; (b) widths shifted and nondimensionalized; bottom: volume visualizations of mixing at time t = 3 ms (the air/SF6 interface is shocked at); ICs having spectral content, but significantly different thickness, can promote ballistic, or non-linear mode-coupling (high ηo) growth regimes, based on a single IC parameter.

Research highlight
We have found appropriate ICs for multi-mode RT which led to similar growth rates as in the experiments and also explained, for the first time, the new growth mechanisms associated with these ICs [13 - 16]. In addition, we have examined the mixing and turbulence characteristics in the RT mixing layer and showed that the mixing asymmetry found in our previous studies also occurs in RTI, and leads

to higher penetration distances of the pure heavy fluid in and explains the bubble-spike anomaly (higher velocities of the spike front compared to the bubble front and significant shape differences between the two sides – Figure 3 -, which was observed experimentally but never explained). None of the mixing metrics usually used by models can capture the asymmetry and thus new metrics have been proposed [13]. Moreover, 4) the small scale anisotropy discovered in our previous studies in other buoyancy driven flows was found to also occur in RTI, even close to the Boussinesq limit, so this may be a "universal" feature of buoyancy driven flows, in direct contradiction to one of Kolmogorov's postulates [17].
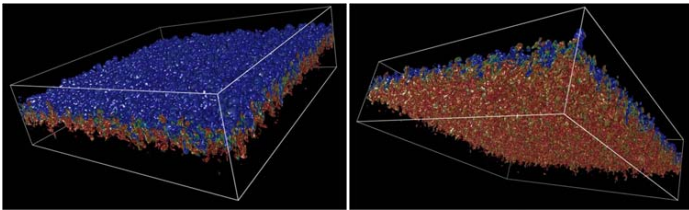
Figure 3. Three-dimensional view of the density field at early time seen from a) top and b) bottom, showing the influence of the mixing asymmetry within the RT mixing layer with the development of "bubbles" on the heavy fluid side and "spikes" on the light fluid side; from the largest instability simulation to date, at 4096^3. From Ref. [13].

A Spectral Model of Initial Condition Development
An engineering model for the initial development of Rayleigh-Taylor instability has been constructed as part of the LDRD-DR. The rationale for this effort is a physics-based description of the turbulence variables at the time the turbulence model will start, as opposed to a guess of these turbulence variables values.

Research Highlight
Experiments and simulations [18] have shown that the spectral composition of the initial perturbations that set off RTi have a major influence on the late development of the instability.

These results leaded us to choose a spectral-type approach for describing the dynamics of the fronts of the RTi mixing layer. Theories for interfacial dynamics of RTi are scarce and limited to RTi weakly linear development regime at best, because of the highly nonlinear character of the mixing layer front. We constructed our model for planar initial perturbation based on the state-of-the-art models available throughout literature. Comparable efforts have been made in the past [19] for 1D perturbations. Our requirements for the model were the following: (i) it handles modes interactions and generations; (ii) it produces a constant self-similar growth rate at late time. We use Haan's weakly nonlinear model [20] as it meets (i). We use Goncharov's model [21] for the prediction of a single mode perturbation front development. The Goncharov

model solution is used within Haan's model for the integration of our engineering model. As Haan's model prediction reaches its limit during the weakly nonlinear regime, we turn to a heuristic model [19] to describe the late time mode interaction.

The RTi mixing layer width is extracted from the amplitude spectrum computed by our model by looking for the dominant modes. As Figure 4 shows, our engineering model allows for tracking the mixing layer front dynamics to relatively late in time, and into the self-similar regime. We then have access to the size of the RTi mixing layer and its fronts' velocities.
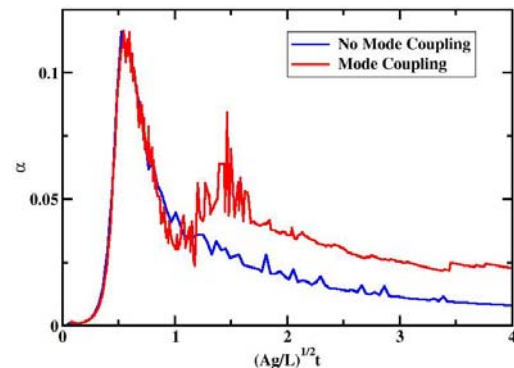
Figure 4. The modes generated by our model allow for a self-similar growth rate at late time. In comparison the simplified multimode model without mode interaction fail to reach a self similar growth rate.

Impact on National Missions
- A new understanding of "transitions" to turbulence, and how they can be controlled and employed for energy gain, production of materials, climate prediction, turbulence control, efficiency, science applications, and the core NNSA mission.

- Improve prediction of turbulence by demonstrating how initial conditions can be properly accounted and incorporated into mathematical models of turbulence.

- Demonstrate that commonly used under-resolved engineering simulations can correctly incorporate initial condition information.

- The possibility of "inverse" optimal design and "failure" analysis, i.e., by starting with a final condition determine the most likely initial conditions to give the final result.

References
1. Balasubramanian, S., K. P. Prestridge, G. C. Orlicz, and B. J. Balakumar. Experimental study of initial condition dependence on mixing in Richtmyer-Meshkov instabilities. Invited presentation at *International Workshop on the Physics of Compressible Turbulent Mixing.* (Mos-

cow, Russia, 11-17 July, 2010).

2. Gowardhan, A., J. Ray. Ristorcelli, and F. Grinstein. The bipolar behavior of the Richtmyer-Meshkov instability. 2011. *Physics of Fluids.* **23** (7): 071701.

3. Grinstein, F. F.. On integrating large eddy simulation and laboratory turbulent flow experiments. 2009. *Phil. Trans. R. Soc. A.* **367**: 2931.

4. George, W. K.. Recent advancements toward the understanding of turbulent boundary layers. 2006. *AIAA Journal.* **44**: 2435.

5. Grinstein, F. F., L. G. Margolin, and W. J. Rider. Implicit Large Eddy Simulation: Computing Turbulent Flow Dynamics. 2010. In *Implicit Large Eddy Simulation: Computing Turbulent Flow Dynamics.* By Grinstein, F. F., L. G. Margolin, and W. J. Rider. , p. 1. Cambridge: CUP.

6. Gittings, M., R. Weaver, M. Clover, T. Betlach, N. Byrne, R. Coker, E. Dendy, R. Hueckstaedt, K. New, W. R. Oakes, D. Ranta, and R. Stefan. The RAGE Radiation-Hydrodynamic Code. 2008. *Comput. Science & Discovery* . **1**: 015005.

7. Grinstein, F. F., A. A. Gowardhan, and A. J. Wachtor. On the Simulation of Shock-Driven Material Mixing in High Reynolds-Number Flows. 2010. *Phys. Scripta .* **T142**: 014066.

8. Dimonte, G., E. Frerking, and M. Schneider. Richtmyer-Meshkov intability in the turbulent regime. 1995. *Physics Review Letters.* **74**: 4855.

9. Jacobs, J. W., and J. M. Sheeley. Experimental study of incompressible Richtmyer–Meshkov instability. 1996. *Physics of Fluids.* **8**: 405.

10. Grinstein, F. F., A. A. Gowardhan, and A. J. Wachtor. On the Simulation of Shock-Driven Material Mixing in High Reynolds-Number Flows. 2011. *Physics of Fluids.* **23**: 034106.

11. Gowardhan, A. A., S. Balasubramanian, F. F. Grinstein, K. P. Prestridge, and J. R. Ristorcelli. Analysis of Computational and Laboratory Shocked Gas-Curtain Experiment. Presented at *6th AIAA Theoretical Fluid Mechanics Conference, .* (Honolulu, Hawaii, 27 - 30 June, 2011).

12. Gowardhan, A. A., and F. F. Grinstein. Numerical Simulation of Richtmyer-Meshkov Instabilities in Shocked Gas Curtains. To appear in *Journal of Turbulence.*

13. Wei, T., and D. Livescu. Pattern formation and initial conditions dependence in two-mode Rayleigh-Taylor instability. *Physica Scripta.*

14. Livescu, D., T. Wei, and M. R. Petersen . Direct Numerical Simulations of Rayleigh-Taylor instability. Presented at *ETC13.* (Warsaw, Poland, September 12-15, 2011).

15. Livescu, D., M. R. Petersen , and T. Wei. Turbulence and Mixing Characteristics in the Variable Density Rayleigh-Taylor Mixing Layer. Presented at *3rd International Conference Turbulent Mixing and Beyond.* (Trieste, Italy, 21 - 28 Aug., 2011).

16. Livescu, D., M. R. Petersen, and R. A. Gore. Turbulence and mixing characteristics in the variable-density Rayleigh-Taylor mixing layer. Invited presentation at *NEC-DEC-2010.* (. Los Alamos, NM, 18-22 Oct., 2010).

17. Petersen, M. R., D. Livescu, R. A. Gore , and K. Stalzberg-Zarling. High Atwood number Rayleigh-Taylor instability with gravity reversal. Invited presentation at *JOWOG 32MIX.* (Los Alamos, NM , 19-22 Apr., 2010).

18. Ramaprabhu, P., G. Dimonte, and M. J. Andrews. A numerical study on the influence of initial perturbations on the turbulent Rayleigh–Taylor instability. 2005. *J. Fluid Mech.* **436**: 285–319.

19. Banerjee, A., and M. J. Andrews. 3D Simulations to investigate initial conditions effects on the growth of Rayleigh-Taylor Mixing. 2009. *Int. J. Heat Transfer.* **doi:10.1016**: 1016.

20. Ofer, D., U. Alon, D. Shvarts, R. L . McCrory, and C. P. Verdon. Modal model for the nonlinear multimode Rayleigh-Taylor instability. 1996. *Phys. Plasma.* **3** (8): 100.

21. Haan, S. W.. Weakly nonlinear hydrodynamic instabilities in inertial fusion. 1991. *Phys. Fluids B.* **3** (8): 110.

Publications

Andrews, M. J.. LDRD-DR: Turbulence by design: 1st year review. 2009. *Poster given at the HED&P&F Capability Review, LANL, May 13, 2009. LA-UR 09-02673..*

Andrews, M. J.. Turbulence by design. 2009. *Poster, LDRD Day, Los Alamos National Laboratory, September 15, 2009. LA-UR # 09-05195. .*

Andrews, M. J.. LDRD-DR: Turbulence by design: 1st year review. Presented at *LDRD-DR 1st year review.* (Los Alamos National Laboratory, 13 May 2009).

Andrews, M. J., A. Duggleby, and Y. Doron. A PDF of molecular mix measurements in high Schmidt number Rayleigh-Taylor turbulence. Presented at *Turbulent Mixing and Beyond.* (Trieste, Italy, 27 July - 7 August, 2009).

Andrews, M. J., F. F. Grinstein, D. Livescu, and K. Prestridge. LDRD-DR: Turbulence by Design. 2009. *Poster presentation, at Boost Fest, Sandia National Laboratory, April 4, 2009. LA-UR 09-02673..*

Andrews, M. J., and B. Rollin. Incorporation of initial conditions in turbulence models for Rayleigh-Taylor instability driven mixing. Presented at *FEDSM2011/AJK2011.* (Hamamatsu, Japan, 24-28 July, 2011).

Bakosi, J., and J. R. Ristorcelli. Exploring the beta distribution in variable density turbulent mixing. 2010. *Journal of Turbulence.* **11** (37): 1.

Balakumar, B. J., G. Orlicz, J. R. Ristorcelli, S. Balasubramanian, K. P. Prestridge, and C. Tomkins. Turbulence in a Richtmyer-Meshkov Fluid Layer after Reshock: Velocity and Density Statistics. To appear in *Journal of Fluid Mechanics.*

Balasubramanian, S., B. J. Balakumar, G. Orlicz, C. Tomkins, and K. Prestridge. Initial conditions effects in shock-driven instabilities. 2009. In *APS Division of Fluid Dynamics Annual Meeting.* (Minneapolis, 22-24 Nov. 2009). Vol. 54, 19 Edition, p. 203. Minneapolis: American Physical Society .

Balasubramanian, S., G. C. Orlicz, K. P. Prestridge, and B. J. Balakumar. Experimental study of initial condition dependence on Richtmyer-Meshkov flows in the presence of reshock. *Physics of Fluids.*

Balasubramanian, S., G. C. Orlicz, K. Prestridge, B. J. Balakumar, G. R. Friedman, and C. D. Tomkins. Turbulence by Design: Richtmyer-Meshkov Experiments. Presented at *1st Annual Los Alamos Postdoc Research Day (LAPRD).* (Los Alamos, 16 June, 2010).

Balasubramanian, S., K. Prestridge, B. J. Balakumar, G. C. Orlicz, and C. D. Tomkins. Experimental study of initial condition dependence for turbulence design in shock-driven flows. Invited presentation at *12th International Workshops on the Physics of Compressible Turbulent Mixing (IWPCTM 12).* (Moscow, 12-17, July, 2010).

Balasubramanian, S., K. Prestridge, B. J. Balakumar, G. C. Orlicz, and G. R. Friedman. Influence of initial conditions on turbulence and mixing in Richtmyer-Meshkov flows in the presence of re-shock. Presented at *41st AIAA Fluid Dynamics Conference & Exhibit.* (Honolulu, Hawaii, 27-30 June, 2011).

Balasubramanian, S., K. Prestridge, B. J. Balakumar, and G. R. Friedman. Effect of multi-mode initial conditions in shock-driven flows. Presented at *63rd Annual Meeting of APS-DFD.* (Longbeach, CA, 22-24 Nov., 2010).

Banerjee, A., and M. J. Andrews. 3D Simulations to investigate initial condition effects on the growth of Rayleigh–Taylor mixing. 2009. *International Journal of Heat and Mass Transfer.* **52** (17): 3906.

Banesh, A., M. J. Andrews, and D. Ranjan. Effect of Shear on mixing in R-T mixing layers at low Atwood numbers.

Presented at *63rd Annual Meeting of APS-DFD.* (Long Beach, CA, 22-24 Nov., 2010).

Gowardhan, A. A., F. F. Grinstein, and A. J. Wachtor. Three Dimensional Simulations of Richtmyer-Meshkov Instabilities in Shock-Tube Experiments. 2010. In *AIAA ASM.* (Orlando, 4-7 Jan. 2010). Vol. Paper # 2010-1075, p. 1. AIAA: AIAA.

Gowardhan, A. A., F. F. Grinstein, and J. R. Ristorcelli. Planar Richtmyer-Meshkov Instabilities and Transition to Turbulence. Presented at *AIAA 2011-3039, Proc. 6th AIAA Theoretical Fluid Mechanics Conference.* (Honolulu, Hawaii, 27-30 June, 2011).

Gowardhan, A. A., F. G. Grinstein, and J. R. Ristorcelli. Planar Richtmyer-Meshkov Instabilities and Transition. To appear in *Proceedings of ETC13.* (Warsaw, Poland, September 12-15, 2011).

Gowardhan, A. A., J. R. Ristorcelli, and F. F. Grinstein. The Bipolar Behavior of the Richtmyer-Meshkov Instability. 2011. *Physics of Fluids 23 (Letters).* **23**: 071701.

Gowardhan, A. A., S. Balasubramanian, F. F. Grinstein, K. P. Prestridge, and J. R. Ristorcelli. Analysis of Computational and Laboratory Shocked Gas-Curtain Experiments. Presented at *AIAA 2011-3040, Proc. 6th AIAA Theoretical Fluid Mechanics Conference.* (Honolulu, Hawaii, 27 - 30 June, 2011).

Gowardhan, A. A., and F. F. Grinstein. Simulation of Material Mixing in Shocked Gas-Curtain Experiments. Presented at *63rd Annual Meeting of APS-DFD.* (Long Beach, CA, 22-24,Nov., 2010).

Gowardhan, A. A., and F. F. Grinstein. Numerical Simulation of Richtmyer-Meshkov Instabilities in Shocked Gas Curtains. *Journal of Turbulence.*

Gowardhan, A., and F. F. Grinstein. Simulation of Material Mixing in Shocked Gas-Curtain Experiments. 2009. In *APS Division of Fluid Dynamics Annual Meeting.* (Minneapolis, 22-24 Nov. 2009). Vol. 54, 19 Edition, p. 203. Minneapolis: APS.

Gowardhan, A., and F. F. Grinstein. Simulation of Material Mixing in Shocked Gas-Curtain Experiments. Presented at *WINNER, 1st Annual Los Alamos Postdoc Research Day (LAPRD).* (Los Alamos, 16 June, 2010).

Grinstein, F. F.. On integrating large eddy simulation and laboratory turbulent flow experiments. 2009. *Transactions of the Royal Society.* **A** (367): 2931.

Grinstein, F. F.. On Integrating LES and Laboratory Turbulent Flow Experiments. Presented at *Discussion Meeting on "Applied Large Eddy Simulation" of the Royal Society.* (London, 27-28 October 2008).

Grinstein, F. F.. Simulating vortex dynamics, transition, and turbulent mixing in high Reynolds-number flows. Presented at *Tutorial at "Turbulent Mixing and Beyond" Conference.* (Trieste, Italy, 5 August 2009).

Grinstein, F. F.. On credibility and convergence of hydro aspects of recent high resolution boost simulations (U). 2009. In *NEDPC.* (LLNL, 29-31 Oct. 2009). Vol. LA-CP-10-000163, p. 1. LLNL: LLNL.

Grinstein, F. F.. On the Simulation of Vortex Dynamics and Transition in High Reynolds-Number Inhomogeneous Flows. Invited presentation at *Invited Lecture, 1st Annual Workshop on "LES for Jet Flows".* (NASA GRC, Cleveland, OH, 2-3 June, 2010).

Grinstein, F. F.. Simulating Vortex Dynamics and Transition in High Reynolds-Number Flows. Invited presentation at *3rd International Conference on Jets, Wakes and Separated Flows.* (Cincinnati, 27-30 Sept., 2010).

Grinstein, F. F.. Simulating Vortex Dynamics and Transition in High Reynolds-Number Flows. 2010. *Phys. Scripta .* **T142**: 014013.

Grinstein, F. F.. Verification and Validation of CFD based Turbulent Flow Experiments. 2010. In *Encyclopedia of Aerospace Engineering, Volume 1 Fluid Dynamics and Aerothermal Dynamics, Computational Fluid Dynamics.* By Shyy, W., and R. Blockley. , p. 1. London: John Wiley & Sons.

Grinstein, F. F., A. A. Gowardhan, and A. J. Wachtor. Simulation of Shock-Driven High-Re Turbulent Mixing. Invited presentation at *IWPCTM12 Workshop.* (Moscow, 12-17 July, 2010).

Grinstein, F. F., A. Gowardhan, and A. J. Wachtor. On the Simulation of Shock-Driven Material Mixing in High Reynolds-Number Flows. 2010. *Phys. Scripta .* **T142**: 014066.

Grinstein, F. F., A. Gowardhan, and A. J. Wachtor. Simulations of Richtmyer-Meshkov Instabilities in Planar Shock-Tube Experiments. 2011. *Physics of Fluids,.* **23**: 034106.

Grinstein, F. F., A. Gowardhan, and A. Wachtor. On the Simulation of Shock-Driven Material Mixing in High Reynolds-Number Flows. 2009. In *APS Division of Fluid Dynamics Annual Meeting.* (Minneapolis, 22-24 Nov. 2009). Vol. 54, 19 Edition, p. 203. Minneapolis: APS.

Grinstein, F. F., M. J. Andrews, and B. Rollin. Progress on the LDRD-DR 'Turbulence by Design' (U) . Invited presentation at *NECDC-2010.* (Los Alamos, 18-22, 2010).

Grinstein, F. F., and A. A. Gowardhan. Effects of Initial Conditions on the Planar Richtmyer-Meshkov Instability. Presented at *63rd Annual Meeting of APS-DFD.* (Long Beach, CA, 22-24, Nov., 2010).

Grinstein, F. F., and A. Gowardhan. On the simulation of shock-driven material mixing in high Reynolds-number flows. Presented at *Turbulent Mixing and Beyond .* (Trieste, Italy, 6 August 2009).

Grinstein, F. F., and W. J. Rider. Turbulence: Monotone-Integrated and Implicit Large-Eddy Simulation. 2010. In *Scholarpedia Encyclopedia of Physics (Fluid dynamics), http://www.scholarpedia.org/article/Turbulence:_ Monotone-Integrated_and_Implicit_Large-Eddy_Simulation ..* Edited by Schilling, O.. , p. 1. www: www.

Livescu, D.. Direct Numerical Simulations of turbulence. Presented at *High energy Density Plasmas and Fluids Capability Review.* (Los Alamos National Laboratory, 13 May 2009).

Livescu, D., J. R. Ristorcelli, M. R. Petersen, and R. A. Gore. New phenomena in variable-density Rayleigh-Taylor Turbulence. 2010. *Phys. Scripta .* **T142**: 014015.

Livescu, D., J. R. Ristorcelli, and R. A. Gore. Mixing asymmetry in variable density turbulence. Presented at *62nd APS Dvision of Fluid Dynamics Annual Meeting.* (Minneapolis, MN, 24 November 2009).

Livescu, D., M. J. Petersen, S. Martin, and P. McCormick. Spikes and bubbles in turbulent mixing: High Atwood number Rayleigh-Taylor instability. 2009. *Poster to be presented at the 62nd APS/DFD annual meeting, Minneapolis, 2009..*

Livescu, D., M. R. Petersen, and R. A. Gore. Turbulence and mixing characteristics in the variable-density Rayleigh-Taylor mixing layer. Invited presentation at *NECDEC-2010.* (Los Alamos, 18-22 Oct., 2010).

Livescu, D., M. R. Petersen, and R. A. Gore. Turbulence characteristics in the variable-density Rayleigh-Taylor mixing layer. Presented at *63rd Annual Meeting of APS-DFD.* (Long Beach, 22-24 Nov., 2010).

Livescu, D., T. Wei, and M. R. Petersen. Direct Numerical Simulations of Rayleigh-Taylor instability. To appear in *Proceedings of ETC13, .* (Warsaw, Poland, September 12-15, 2011).

Livescu, D., and J. R. Ristorcelli. Mixing asymmetry in variable density turbulence. 2009. In *Advances in Turbulence XII.* Edited by Eckhardt, B.. Vol. 132, p. Not known. Berlin: Springer.

Petersen, M. R., D. Livescu, R. A. Gore, and K. Stalzberg-Zarling. High Atwood number Rayleigh-Taylor instability with gravity reversal. Presented at *JOWOG 32MIX.* (Los Alamos, 19-22 April, 2010).

Petersen, M. R., D. Livescu, and R. A. Gore. Direct numeri-

cal simulations of Rayleigh-Taylor instability with gravity reversal. Presented at *63rd Annual Meeting of APS-DFD.* (Long Beach, CA, 22-24 Nov., 2010).

Prestridge, K.. Richtmyer-Meshkov mixing and turbulence experiments. Invited presentation at *Invited seminar, Center for Turbulence Research, Stanford University.* (Stanford University, 4 May, 2010).

Prestridge, K.. Turbulent mixing in shocked variable-density flows. Invited presentation at *Invited seminar, Dept. of Mechanical Engineering, Arizona State University.* (Arizona, 4 May, 2010).

Prestridge, K. P., B. J. Balakumar, C. Tomkins, and S. Balasubramanian. Experiments for understanding shock-driven mixing and turbulence. Presented at *High Energy Density Plasmas and Fluids (HEDPF) Capability Review.* (Los Alamos National Laboratory, 13 May 2009).

Prestridge, K. P., B. J. Balakumar, G. Orlicz, C. Tomkins, C. Zoldi-Sood, and R. A. Gore. Understanding Turbulence in Richtmyer-Meshkov unstable flows. Presented at *NEDPC.* (Lawrence Livermore National Laboratory, 27 October, 2009).

Prestridge, K. P., B. J. Balakumar, G. Orlicz, and C. Tomkins. High resolution experimental measurements of Richtmyer-Meshkov turbulence in fluid layers after reshock. Presented at *APS Shock-Compression of Condensed Matter.* (Nashville, TN, 2 July 2009).

Prestridge, K. P., B. J. Balakumar, G. Orlicz, and C. Tomkins. Understanding experimental diagnostics and results for code and model validation. Presented at *Turbulent Mixing and Beyond.* (Trieste, Italy, 27 July 2009).

Reckinger, S. J., D. Livescu, and O. V. Vasilyev. Wavelet-Based Simulations of Rayleigh-Taylor Instability. Presented at *63rd Annual Meeting of APS-DFD.* (Long Beach, CA, 22-24 Nov., 2010).

Reckinger, S., D. Livescu, and O. Vasilyev. Compressibility effects on single mode Rayleigh-Taylor instability. 2009. *Poster given at Turbulent Mixing and Beyond Conference, Trieste, Italy, July 27, 2009..*

Ristorcelli, J. R., N. Hjelm, and T. Clark. LBM turbulence: multi-component turbulence without interface tracking. Invited presentation at *Symposium on Combustion and Turbulence.* (Cornell, Ithaca, NY, 3-4 Aug., 2010).

Ristorcelli, J. R., and D. Livescu. Correcting anisotropic gradient transport of k. 2010. *Flow Turb. Comb.* **85** (3-4): 443.

Ristorcelli, J. R., and N. Helm. Initial conditions for the turbulence moments at an unstable quiescent stochastic material interface. 2011. *Journal of Turbulence .* **11** (46): 1.

Ristorcelli, R. J.. Stochastic linear stability theory: obtaining statistics for moment closure models. Presented at *Turbulent Mixing Colloquium.* (Los Alamos National Laboratory, 1 July 2009).

Rollin, B., and M. J. Andrews. Progress Toward Specifying Initial Conditions for Variable Density Turbulence Models. 2009. In *APS Division of Fluid Dynamics Annual Meeting.* (Minneapolis, 22-24 Nov. 2009). Vol. 54, 19 Edition, p. 102. Minneapolis: APS.

Rollin, B., and M. J. Andrews. On the 'early-time' evolution of variables relevant to turbulence models for the Rayleigh-Taylor instability. Presented at *FEDSM2010.* (Montreal, Canada, 1-5, Aug., 2010).

Rollin, B., and M. J. Andrews. On Initial Conditions for Turbulent Rayleigh-Taylor Mixing. Presented at *63rd Annual Meeting of APS-DFD.* (Long Beach, CA, 22-24 Nov., 2010).

Rollin, B., and M. J. Andrews. A Mathematical Model of Rayleigh-Taylor and Richtmyer-Meshkov Instabilities for Viscoelastic fluids. 2011. *Phys. Rev. E..* **83**: 046317.

Wei, T., D. Livescu, and M. J. Andrews. The effects of initial conditions on single and two-mode Rayleigh-Taylor instability. Presented at *63rd Annual Meeting of APS-DFD.* (Long Beach, Ca, 22-24 Nov., 2010).

Wei, T., and D. Livescu. Initial conditions and Reynolds number dependence on single mode Rayleigh-Taylor instability. *Physics of Fluids*

New and Enhanced Capabilities in Quantum Information Processing

Robert E. Ecke
20090476DR

Abstract

Quantum mechanical entanglement underpins numerous modern advances in science and technology. It allows for the unbreakable transmission of information via quantum channels, the possibility of quantum computation where processes such as factoring can be done much faster than on a classical computer, the realization of quantum emulation in which important physics can be simulated with great efficiency, the possibility of new measurement devices with exceptional sensitivity, and the understanding of a wide range of many-body physics in condensed matter and atomic-molecular-optical systems from cold atoms and quantum phase transitions to superconductors and meta-materials. This project investigated a wide number of these areas with progress in both fundamental and applied areas with significant implications for technology development and mission relevance.

Background and Research Objectives

This project exploited new connections among several areas of quantum physics and information science to build new tools and technologies that support Laboratory missions. The specific areas of interest are macroscopic quantum systems such as Bose Einstein condensates (BEC) or strongly correlated electron systems, quantum phase transitions and nonlinear excitations in quantum systems, optical physics including Casimir physics, quantum information science, and the use of photon states for quantum communication.

When cooled to sufficiently low temperature, systems of interacting quantum particles can form a single coherent ground state consisting of many particles that manifests quantum behavior over macroscopic length scales. Prominent examples include superconductors and laser-cooled gas atoms that undergo Bose-Einstein condensation. The long-range quantum order in these states can be broken by various perturbations to give rise to defects in space, namely vortices. These vortices can often be described by nonlinear equations and form spatially-localized structures called solitons. Furthermore, the entanglement of quantum states gives rise to a new type of phase transition known as a quantum phase transition that occur at zero temperature [1].

The Casimir effect is another fascinating and useful manifestation of quantum interactions [2]. The basic idea is that the quantization of possible modes of interaction between parallel plates reduces the energy in the gap compared to the energy outside the plates, thereby causing a net attraction of the plates.   This is a tiny effect that is only felt for very small plate separation but which is both measurable and useful for nanoscale device technology. We describe research in which both the fundamental science and the applications have been addressed.

Information underpins much of the modern world from its manipulation by digital computers to its transmission by cellular telephones and smart devices. Information can also be encoded using powerful principles of quantum entanglement to produce novel computational devices and mechanisms to transmit information without the possibility of the information being compromised. The area of quantum information science and technology [3] is a critical mission-relevant area of research where innovative combinations of mathematics, physics and engineering come together in truly remarkable ways to create a unique technology. We have studied both mathematical concepts for quantum information transmission and developed new hardware for multi-photon quantum communication.

Scientific Approach and Accomplishments

Our work on quantum science has three main components: Macroscopic Quantum Systems, Casimir Physics, and Quantum Information and Communication. Our scientific approach is mainly theoretical and computational although we are both motivated by and collaborate with experimental groups. A portion of our effort was devoted to a proof-of-principle test of a new quantum communications technology.

Macroscopic quantum systems

This section includes quantum systems including Bose-

Einstein cold atom systems and novel materials where new quantum properties emerge, e.g., graphene. We also describe so-called quantum phase transitions [1] and defect formation in uniform quantum states, i.e., vortices, solitons, etc.

Graphene, graphite atoms in regular hexagonal arrays, has numerous fundamental and technological properties including very novel electronic band structure. We investigated the thermoelectric (conversion of heat to voltage) transport properties of single-layer and bi-layer graphene systems, and elucidated the effects of the impurity scattering, the magnetic field and the unique band structure in characteristic signatures of semiconductor materials. We also compared and explained the experimental results on a mobility-tuned graphene device. In a related system of a Kondo-lattice model on a triangular lattice, we discovered a thermodynamic phase transition into an exotic spin ordering with uniform chirality (handedness). The state exhibits a spontaneous quantum Hall effect with properties that depend on the strength of an applied external magnetic field.

We investigated the thermodynamic signature of several quantum critical systems, such as the entropy accumulation effect or the divergence of the Grueneisen ratio, which serve as a sensitive method to probe and classify quantum phase transitions. We studied these signatures in a specific material, $Sr_3Ru_2O_7$, to elucidate the nature of its quantum criticality. In other work on quantum criticality, we considered an inhomogeneous quantum phase transition across a multicritical point of a quantum spin chain. When a critical front propagates much faster than the maximal group velocity of quasiparticles, the transition is effectively homogeneous. The inhomogeneous transition, however, becomes adiabatic not below the maximal group velocity but at a lower threshold velocity, proportional to the inhomogeneity of the transition, where the excitations are suppressed exponentially.

Dark solitons are local excitations of a Bose condensate in which the local amplitude of the state becomes small, i.e., "dark", see Figure 1. These solitons are predicted to be stable in 1D trapping geometries and may play a role in the transport properties of a quantum fluid. Experimental studies look toward using these excitations to store or transport information. We conducted a theoretical study into the effect of thermal or quantum fluctuations on the stability of the solitons and showed how the soliton evolves when the fluid is not completely isolated from its environment. This constitutes a useful guide for experiments utilizing these unique excitations for applications.

The unprecedented control of quantum systems through the use of optical lattices (standing-wave patterns of laser beams) have allowed cold-atom simulations of strongly correlated lattice physics. For example, the Bose-Hubbard

Hamiltonian was quantitatively modeled with optical-lattice systems and the boson superfluid to Mott insulator phase transition was observed. We showed that an impurity added to the Mott insulator phase leads to a novel polaron (charged excitation with its polarization field) that exhibits correlated motion with an effective mass and a size that become large at a critical value of the impurity-boson interaction strength. We further predict that by combining control of optical lattice parameters, the inter-particle interactions, and the particle-species, cold atom experiments could realize a novel and controllable polaron in the Mott phase. In related fundamental research, we derived a theoretical description for dilute Bose gases. We demonstrated that this non-perturbative approach describes a large interval of coupling-constant values and yields a Bose-Einstein transition that is second order.
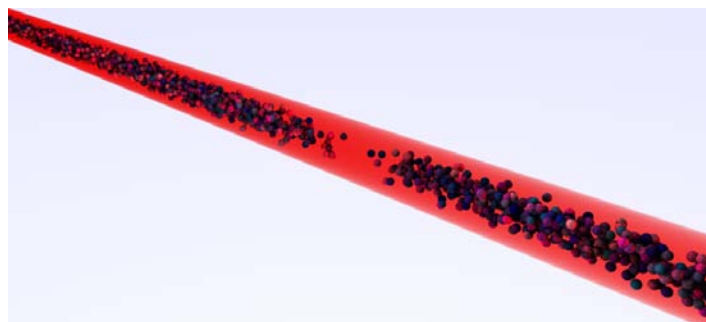
Figure 1. A dark soliton (localized state) in a 1D Bose condensate manifests as a notch of low density. This excitation is extremely stable against collapse, provided the atomic system is tightly confined in a quasi- 1D geometry.

Casimir Physics

The Casimir effect of the attraction of closely spaced objects is having a recognized impact on nano-scale devices and on the design and implementation of metamaterials [2]. Our approach is to consider both new idealized systems and to compute interactions for more complex and realistic micro- and nano-structures. There are opportunities to both characterize existing structures and to suggest new ones with novel functionality.

The Casimir effect is usually computed for flat plates or uniformly curved surfaces such as spheres. To explore the interactions of patterned surfaces that may arise in nano-scale structures, we calculated finite-temperature Casimir interactions between two periodically modulated surfaces by decomposing the electromagnetic field into the natural modes of the structures. The Casimir force gradient from an etched silicon grating was evaluated using this modal approach and compared to experiment for validation. In related research, we investigated properties of metamaterials – materials with periodic structures with spacing much less than the electromagnetic wavelength of interest that have great technological promise. In particular, we examined a recent prediction for the chirality dependence of the Casimir force in chiral metamaterials that are made

from materials with a right-left handedness asymmetry, i.e., that are intrinsically chiral. We computed the forces between exact microstructure rather than by assuming a homogeneous approximation. Although repulsion in the metamaterial regime is rigorously impossible, it is unknown whether a reduction in the attractive force can be achieved through suitable material engineering. We identified the effects of structural inhomogeneity, i.e., proximity forces and anisotropy and found that microstructure effects dominate the force for separations where chirality was predicted to have a strong influence. At separations where the homogeneous approximation is valid, the effects of chirality are less than 10^{-4} of the total force, making them virtually undetectable in experiments.

We also consider fundamental aspects of Casimir interactions. Electrostatic patch potentials give rise to forces between neutral conductors at distances in the micrometer range and must be accounted for in the analysis of Casimir force experiments. We developed a model for describing random potentials on metallic surfaces. In contrast to some previously published results, we discovered that patches provide a significant contribution to the measured signal, and may render the experimental data at distances below 1 micrometer compatible with theoretical predictions based on the Drude model – long a standard model for predicting electron transport in conducting materials.

Finally, we gave a first-principles microphysics derivation of the non-equilibrium forces between an atom, treated as a three-dimensional harmonic oscillator, and a bulk dielectric medium modeled as a continuous lattice of oscillators coupled to a reservoir. We assumed no direct interaction between the atom and the medium but there are mutual interactions transmitted by the electromagnetic field. By employing concepts and techniques of open quantum systems, we introduced coarse-graining of the physical variables—the medium, the quantum field, and the atom's internal degrees of freedom, in that order—to extract their averaged effects. The first tier of coarse-graining provided the averaged effect of the medium upon the field. The last tier of coarse-graining over the atom's internal degrees of freedom results in an equation of motion for the atom's center of mass from which we can derive the force on the atom. Our non-equilibrium formulation provides a dynamical description of the atom's motion.

Quantum Information and Communication

In quantum information and communication, we elucidated properties of quantum states involving the decoherence (loss of the ordering of the relative phases between different parts of the system) of quantum states interacting with an environment, investigated the adiabatic (no increase in entropy) evolution of quantum systems, showed how the unintuitive result that two zero-capacity quantum channels can have finite capacity is preserved in the presence of attenuation and noise, and demonstrated the feasibility of

multi-bit per photon quantum communication.

Quantum Darwinism provides an information-theoretic framework for the emergence of the objective, classical world from the underlying quantum system. The key to this emergence is the proliferation of redundant information throughout the environment where observers can then intercept it. We study this process for a purely decohering interaction when the environment is in a non-ideal (e.g., mixed) initial state. In the case of good decoherence, the mutual information between the system and an environment fragment is given solely by the environmental entropy increase. This demonstrates that the environment's capacity for recording the quantum state is directly related to its ability to increase its entropy. Environments that remain nearly invariant under the interaction with the quantum state therefore have a diminished ability to acquire information. Our results demonstrate that Quantum Darwinism is robust with respect to non-ideal initial states of the environment: the environment almost always acquires redundant information about the system but its rate of acquisition can be reduced.

We have investigated the evolution of a quantum system in the adiabatic limit of no change in the system entropy. This process may find application in implementing adiabatic quantum computation. There were, however, no effective methods for testing for the degree to which the evolution was adiabatic unless one had detailed information about the quantized energy states of the driven system. We proposed a simple method for checking this adiabatic property for an arbitrary quantum system. We also suggested a way to find efficient protocols that maximize the adiabatic measure for transitions where the beginning and ending states are known. This method should help to implement adiabatic quantum computation.

Capacity is the amount of information that can be transmitted over a communication channel. Error correcting codes enable reliable transmission of both classical and quantum information over noisy channels. In contrast to classical theory, however, quantum channels can manifest an unintuitive synergy where pairs of quantum channels, each with zero quantum capacity, can acquire positive quantum capacity when used together. We showed that this "superactivation" (going from nothing to something) occurs for realistic optical channels with attenuation and noise. This result paves the way for applications in real-world communication systems.

Squashed quantum entanglement is a measure for the entanglement of bipartite (two-party) quantum states. We determined that squashed entanglement is faithful, that is, it is strictly positive only if the state is entangled. The measure is based on quantum conditional mutual information and is given in terms of the optimal probability of distinguishing two bipartite quantum states, each shared by two parties, using any protocol formed by local quantum op-

erations and classical communication (LOCC) between the parties. This work is important in establishing multi-party quantum communication rather than the existing protocols that provide secret communication only between one party (a sender and receiver).

In the area of practical quantum communication, we successfully demonstrated the feasibility of multi-bit per photon quantum communication. To date all experimental quantum communication has been done in a one-dimensional sub-space or a two-dimensional Hilbert space, i.e., either optical phase or polarization providing only 1-bit per photon. There have been suggestions about how a larger Hilbert-space could be employed but the technique—time-bin encoding, required that the transmission rate be slowed so that no actual gain in bit rate was achieved. Our technique is completely new and allows the Hilbert-space to be expanded to thousands of dimensions without lowering the transmission rate, making it possible to produce ten or more secret bits per photon received. This makes practical longer distance QC without the use of repeaters and is far more efficient for secret-key production in demanding environments such as long-distance optical fiber or free-space atmospheric links. We have completed a classical-level demonstration of two-bit per photon QC. A further expansion of the Hilbert-space could simply be achieved with our existing hardware. With this demonstration we have sufficient results to file a patent application on the technique and to extend our results to the single-photon level.

Impact on National Missions

Quantum information and communication have great future promise in producing revolutionary computing paradigms and secure communication protocols. The latter is realized today at LANL with numerous potential improvements and advances. Our theory efforts coupled with the support of practical device development are accelerating that process. On a longer time horizon, macroscopic quantum systems from cold atoms to graphene will form the building blocks of new computation platforms and devices. Finally, work on Casimir physics couples nicely to development in CINT and MPA on novel functions of materials at the nanoscale including metamaterials with tunable optical properties.

References

1. Sachdev, S.. Quantum Phase Transitions. 2011.

2. Lecture Notes in Physics: Casimir Physics. 2011.

3. Information Science and Technology in a Quantum World. 2002. *LOS ALAMOS SCIENCE, NUMBER 27.*

Publications

Lecture Notes in Physics: Casimir Physics. 2011.

Behunin, R. O., F. Intravaia, D. Dalvit, P. A. Maia Neto, and

S. Reynaud. Modeling electrostatic patch effects in Casimir force measurements. 2011. *arXiv: Quantum Physics.* : .

Behunin, R. O., and B. L. Hu. Nonequilibrium forces between atoms and dielectrics mediated by a quantum field. 2011. *Physical Review A.* **84** (1): 012902.

Berman, G. P., A. R. Bishop, B. M. Chernobrod, A. A. Chumak, and V. N. Gorshkov. Suppression of scintillations and beam wandering in free space gigabit rate optical communication based on spectral encoding of a partially coherent beam. 2009. In *Photonics West.* (San Jose, 24-29 January). Vol. 7200, p. 72000H. Digital Library: The international Society for Optical Engineering.

Berman, G. P., B. M. Chernobrod, A. R. Bishop, and V. N. Gorshkov. Uncooled infrared and terahertz detectors based on micromechanical mirror as a radiation pressure sensor. 2009. In *Photonics West.* (San Jose, 24-29 January, 2009). Vol. 7204, p. 720403. Digital Library: The International Society for Optical Engineering.

Brandao, F., M. Christandl, and J. Yard. Faithful squashed entanglement. 2011. *Communications in Mathematical Physics.* **306**: 805.

Brandao, F., M. Christandl, and J. Yard. A quasipolynomial-time algorithm for the quantum separability problem. 2011. *Proceedings of the 43d ACM Symposium on Theory of Computing.* : 343.

Cooper, F., C. C. Chien, B. Mihaila, J. F. Dawson, and E. Timmermans. Nonperturbative predictions for cold atom bose gases with tunable interactions. 2010. *Phys Rev Lett.* **105**: 240402.

Damski, B., H. T. Quan, and W. H. Zurek. Critical dynamics of decoherence. 2011. *Physical Review A.* **83** (6): 062104.

Davids, P., F. Intravaia, F. Rosa, and D. Dalvit. Modal approach to Casimir Forces in periodic structures. 2010. *Phys Rev A.* **82**: 06211.

Dziarmaga, J., and M. Rams. Adiabatic dynamics of an inhomogeneous quantum phase transition: the case of a z>1 dynamical exponent. 2010. *New J. Phys..* **12**: 103002.

Intravaia, F., R. O. Behunin, P. W. Milonni, G. W. Ford, and R. F. O'Connell. Consistency of a causal theory of radiative reaction with the optical theorem. 2011. *Physical Review A.* **84** (3): 035801.

Kalas, R., D. Solenov, and E. Timmermans. Reentrant stability of BEC standing wave patterns. 2010. *Physical Review A.* **81** (05): 3620.

Kato, Y., I. Martin, and C. D. Batista. Stability of spontaneous quantum Hall state in the triangular Kondo lattice model. 2010. *Phys. Rev. Lett..* **105**: 266405.

Kato, Y., K. A. Al-Hassanieh, A. Feiguin, E. Timmermans, and C. D. Batista. Novel polaron state for single impurity in a bosonic Mott insulator. *Physical Review Letters.*

Law, K., A. Saxena, P. G. Kevrekidis, and A. R. Bishop. Stable structures with high topological charge in nonlinear photonic quasicrystals. 2010. *Phys Rev A.* **82**: 035802.

Liu, X., D. Wang, P. Wei, L. Zhu, and J. Shi. Magneto-thermoelectric transport properties in mobility tuned single-layer graphene. *Physical Review Letters.*

Ma, R., L. Zhu, L. Sheng, M. Liu, and D. N. Sheng. Thermo-electric and thermal transport in bilayer graphene systems. 2011. *Physical Review B.* **84** (7): 075240.

McCauley, A., R. Zhao, M. Reid, A. Rodriguez, J. Zhou, F. Rosa, J. Ioannopoulos, D. Dalvit, C. Soukoulis, and S. Johnson. Microstructure effects for Casimir forces in chiral metamaterials. 2010. *Phys Rev B.* **82**: 165108.

Merkli, M., G. P. Berman, F. Borgonovi, and K. Gebresellasie. Evolution of Entanglement of Two Qubits Interacting through Local and Collective Environments. 2011. *Quantum Information and Computation.* **11** (5): 390.

Merkli, M., G. P. Berman, and A. Redondo. Application of Resonance Perturbation Theory to Dynamics of Magnetization in Spin Systems Interacting with Local and Collective Bosonic Reservoirs. 2011. *Journal of Physics A: Mathematical and Theoretical.* **44** (30): 305306.

Nesterov, A. I., G. P. Berman, and A. R. Bishop. Non-Hermitian description of a superconducting phase qubit measurement. 2010. *International Journal of Quantum Information.* **8**: 895.

Quan, H. T., and W. H. Zurek. Testing quantum adiabicity with quench echo. 2010. *New Journal of Physics.* **12**: 093025.

Smith, G., J. Smolin, and J. Yard. Quantum communication with gaussian channels of zero capacity. 2011. *Nature Photonics.* **5** (Oct): 624.

Sykes, A.. Exact solutions to the four Goldstone modes around a dark soliton of the nonlinear Schrodinger equation. 2011. *Journal of Physics A.* **44**: 135206.

Wu, J., L. Zhu, and Q. Si. Entropy accumulation near quantum critical points: effects beyond hyperscaling. 2011. *Journal of Physics: Conference Series.* **273**: 012019.

Yard, J., and I. Devetak. Optimal quantum source coding with quantum side information at the encoder and decoder. 2009. *IEEE Transactions on Information Theory.* **55** (11): 5339.

Zwolak, M., H. T. Quan, and W. H. Zurek. Redundant imprinting of information in non-ideal environments: Objective reality via a noisy channel. 2010. *Phys Rev A.* **81**: 062110.

Revolutionary Science at the Intersection of Extreme and Transient Events, Natural Hazards, and National Security

Harald O. Dogliani
20090477DR

Abstract

The research overseen by the Institute of Geophysics and Planetary Physics addressed the following scientific issues: gamma-ray astronomy, using advanced theoretical concepts that describe observations; galaxy evolution; supernova simulations; cosmological structure formation; and the Earth's plasma environment. Other investigations included the physics responsible for fast versus slow earthquakes; hydrogeochemical and physical controls over volcanic eruptions; hydrogeochemical controls combined with fractures and porosity influences on carbon sequestration. The science of modeling, simulations, observations and measurements were advanced in an integrated manner to enhance the fidelity of forecasting of anthropogenic climate change and natural variability for societal assessments. Regional assessments spanned decades to centuries to epochs. New paleo-records were unearthed to discover past mega-droughts in the southwest US. The first realistic simulation of trends and variability in glacier and sub-glacial lakes were performed. It was discovered that the Arctic and Antarctic warming trends are out of phase; we and quantified the contributions of humans and natural variability to Arctic warming. We developed and applied methodology to interrogate the impact of tree mortality on the soil CO_2 emissions by respiration.

Background and Research Objectives

To keep Los Alamos researchers on the cutting edge of new scientific developments strong teaming relationships were encouraged. More than 40 external research institutions worldwide partnered with Los Alamos under IGPP. In addition to shared research, prospective new employees from the relevant graduate student programs were identified and encouraged to continue working with Los Alamos scientists, supplemented with active recruitment of the best and brightest.

Scientific Approach and Accomplishments

GeoScience

Seismic Triggering
Seismologists increasingly recognize that seismic shaking along faults can trigger earthquakes along adjacent faults, even hundreds of kilometers distant. We verified that triggering rate is positively correlated with seismic wave amplitude (Figure 1). To explain this effect we worked from the observation that faults are not simple planar disruptions of rocks; rather, they are zones filled with granular material--pulverized rocks and minerals--called "gouge." To better understand the rheology of fault gouge, we conducted experiments to measure volumetric changes in a variety of gouge-like materials with changing shear rates, such as might occur as faults propagate. We found that at higher velocities, especially in the presence of external acoustic vibrations, gouge becomes more fluid [5]. Effectively, fault gouge can, under appropriate conditions, lubricate faults. We inferred that this change in stiffness at higher shear rates results from collapse of stress-bearing "chains" of particles. Our work provides a mechanism for remote triggering of earthquakes and implies that risk may not depend solely on the closest faults.
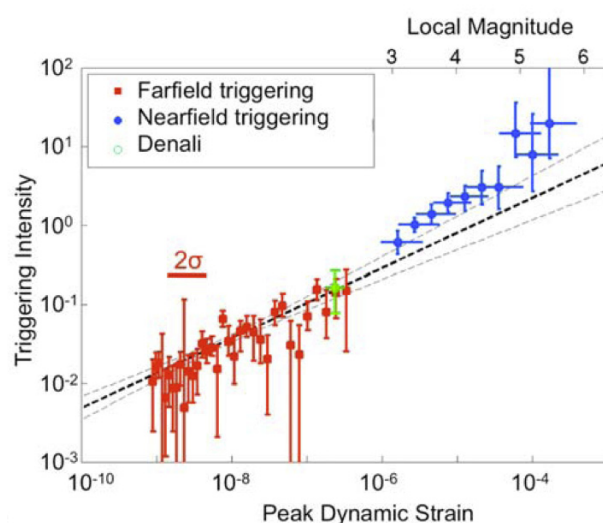
Figure 1. Observed triggering rate change as a function of the peak amplitude of ground motion in seismic waves. Triggering intensity is the inferred earthquake rate change normalized by the background rate (from Van der Elst and Brodsky, 2010).

Volcanic Venting

The behavior of volcanic plumes is largely determined by the jetting dynamics created where gas-charged magma issues into the atmosphere at the Earth's surface. Our simulations demonstrate that particulate size has a large effect on shock structures and eddy formation in the near-vent region of overpressured eruption columns. We also found that vent *shape* alone changes plume dynamics and may cause a transition between buoyancy and collapse. An increasing vent *angle* increases jet diameter and decreases jet velocity (Figure 2). Production of shock waves is dependent on vent shape and on the magnitude of decompression; the shape of the vent changes the acoustic signal produced by volcanic jets. Vent *pressure* controls crater formation and the entrainment and distribution of rock material from the walls of the conduit [3]. Our significant advances in modeling of explosive volcanic plumes will allow better hazards assessments.
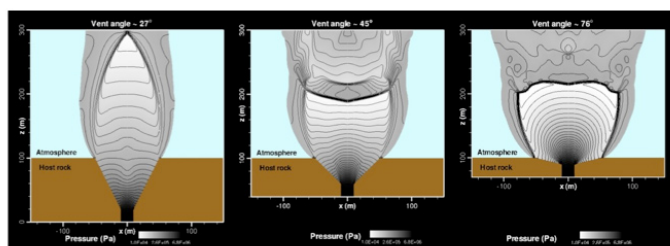
Figure 2. Pressure field as a function of vent angle.

Fluid Transport

Advanced numerical modeling permits the interrogation and evaluation of large-scale fluid-flow processes, especially important at sites that cannot be investigated in either the field or in laboratory settings. Examples include flow of contaminated groundwater through the shallow subsurface, and deep (thousands of feet below the surface) sites under consideration for carbon sequestration and repositories for nuclear waste. We developed robust new codes to predict the performance of engineered and natural systems by a) simulating reactive transport and b) estimating the uncertainty in our calculations. We considered many factors, including the fact that contaminants can be transported by any of several mechanisms (advection, diffusion, dispersion), each with its own governing equations; also that solutes can attach to rocks and minerals by sorption and/or reaction. Our results incorporate *continuous-time-random-walk* theory [4] in a particle tracking algorithm (known as *convolution-based-particle-tracking*). We verified our results against analytical solutions. A distinct advantage of our combined approach is that it allows modeling of non-Fickian transport at large scale sites with non-uniform properties (Fickian transport postulates that diffusion of a substance occurs from regions of high to low concentration and is proportional to concentration gradient). Our work expands the numerical tools that are available to researchers studying a variety of natural and engineered systems [1,2].

Global Climate

Southwest Megadroughts

IGPP-funded studies focused on the paleoclimate record of "megadroughts" in the southwestern United States. These studies took advantage of lake and bog sediments preserved in the Valles caldera of northern New Mexico (Figure 3). A nearly 200,000 yearlong mid-Pleistocene multi-proxy lake sediment record covers two glacial-interglacial cycles, including marine isotope stage (MIS) 11. MIS 11 is an important climate stage in that orbital parameters during this period were similar to those found today, such that MIS 11 is a good analog for natural climate variability. Maximum warming occurred early in MIS 11 with temperatures as high or higher than today. Warming was accompanied by centennial- to millennial-scale 'megadrought', leading to a significant decrease in productivity, including that of drought tolerant grasses [10]. Evidence for centennial- to millenial-scale mid-Holocene drought is seen in elemental, isotopic, pollen and charcoal records from a bog on the northern flank of the Valles Caldera [9]. Records such as these can be used to test the ability of climate models to capture the full range of natural climate variability occurring at the regional scale.
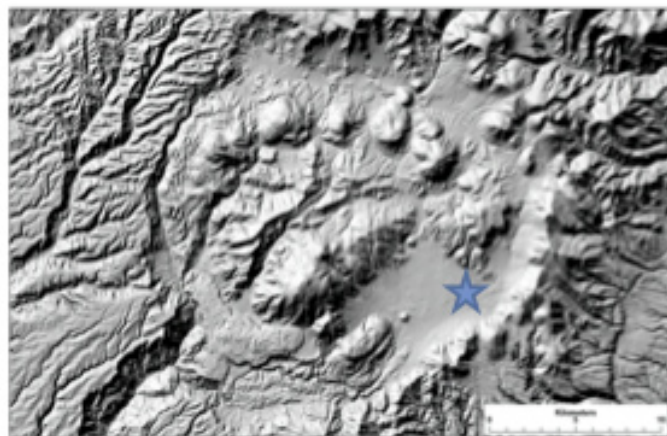
Figure 3. Mid-Pleistocene Paleoclimate Records from the Valles Caldera .

Greenland Surface Mass Balance

We carried out multiple decade-to-century scale simulations of the surface mass balance (SMB) of the Greenland ice sheet. In one study, Mernild et al. [12] (2011) simulated Greenland's SMB from 1960 to 2010 and compared results with available satellite observations (since 1979). After declining from 1960 to 1972, modeled melt extent increased by 13% between 1973 and 2010, with record melt simulated in 2010 (in agreement with observations). In another study, Mernild et al. [11] used output from a regional climate model to simulate Greenland's SMB from 1950 to 2080. The modeled mass balance became negative around 2040, when modeled mean surface temperatures are just 1.2°C higher than present-day values. If sustained for many centuries, a negative SMB would result in nearly total melting of the ice sheet.

Modeling Antarctic Subglacial Lakes

A simple model of filling and drainage of subglacial lakes beneath rapidly moving Antarctic ice streams was developed. Focusing on the MacAyeal Ice Stream in West Antarctica, Carter et al. [6] used the model to simulate lake evolution during the observing period of the Ice, Cloud and land Elevation Satellite (ICESat). Model volume change rates were consistent with changes inferred from ICESat laser altimetry. For this hydrologic system, nearly all meltwater passes through subglacial lakes, suggesting that these lakes play an essential role in ice stream dynamics.

Polar-Warming Contributions By Humans And Natural Variability

Understanding Arctic temperature variability is essential for assessing possible future melting of the Greenland ice sheet, Arctic sea ice and Arctic permafrost. Temperature trend reversals in 1940 and 1970 separate two Arctic warming periods (1910-1940 and 1970-2008) by a significant 1940-1970 cooling period. Analyzing temperature records of the Arctic meteorological stations we found that (a) the Arctic amplification varies on a multi-decadal time scale, (b) the Arctic warming from 1910-1940 proceeded at a significantly faster rate than the current 1970-2008 warming, and (c) the Arctic temperature changes are highly correlated with the Atlantic Multi-decadal Oscillation (AMO), suggesting that the Atlantic Ocean thermo haline circulation is linked to the Arctic temperature variability [8]. Understanding the phase relationship between climate changes in the Arctic and Antarctic regions is essential for our understanding of the dynamics of the Earth's climate system. We show that the 20th century de-trended Arctic and Antarctic temperatures vary in anti-phase seesaw pattern – when the Arctic warms the Antarctica cools and vice versa (Figure 4).
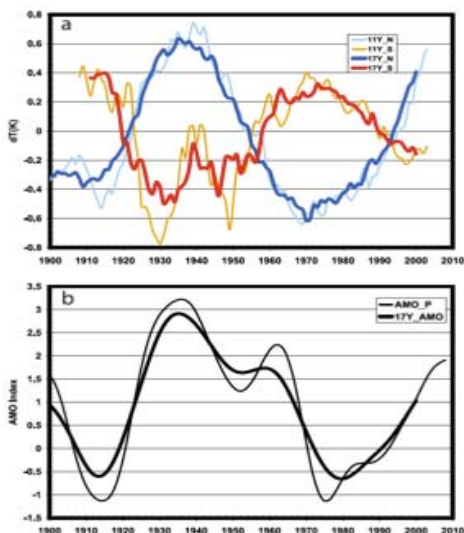
Figure 4. (a) De-trended Arctic (blue) and Antarctic (red) temperature time series smoothed by an 11 year running average (thin lines) or 17 year running average (thick lines) and (b) the AMO index (after Parker er al. 2007) annual values (thin lines) and 17 year running average (thick line).

This is the first time that a bi-polar seesaw pattern has been identified in the 20th century Arctic and Antarctic temperature records. The Arctic (Antarctic) de-trended temperatures are anti-correlated with the Atlantic Multi-decadal Oscillation (AMO) index suggesting the Atlantic Ocean as a possible link between the climate variability of the Arctic and Antarctic regions. Recent accelerated warming of the Arctic results from a positive reinforcement of the linear warming trend [7].

Tree Die-Off And Soil Carbon Cycle

We investigated the effects of tree mortality on the overall capacity of the soil to store and/or process carbon. As trees die, their root systems and the microbial and fungal communities that are associated with them are dramatically altered. Over two field seasons we monitored the carbon fluxes from two sites, one piñon-juniper site in which the piñon trees were girdled to create a mortality event and a similar site to serve as control. In the first season after tree death we observed that respiration under the recently dead piñon remained normal but that respiration in the open space between trees dropped significantly (Figure 5). Our hypothesis is that death of lateral root systems significantly reduces the supply of labile sugars to mycorrhizae and rhizosphere microbes, creating carbon limitation in the rhizosphere. We employed carbon isotopes to test this hypothesis and developed a new method for isotopic measurements that allows these analyses to be applied in the field in real time. We adapted continuous-flow cavity ring-down spectroscopy (CRDS) for batch analysis of $\delta^{13}C$ of CO_2
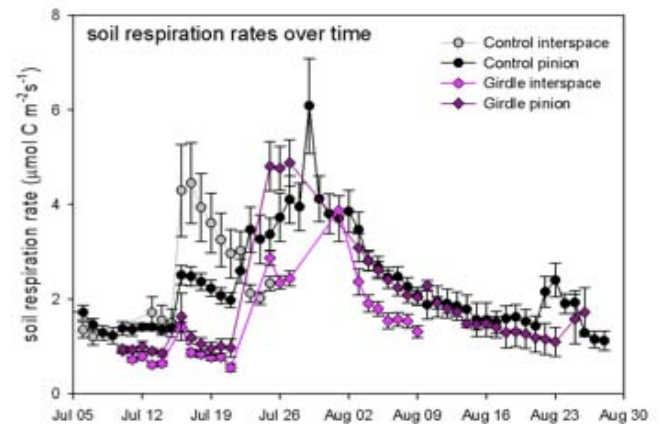
Figure 5. Soil respiration response to tree dieoff.

Space

The Space Science Focus area builds on Los Alamos's deep history of dominating many aspects of research into magnetospheres and solar wind, from instrument building to analyzing the resulting data.

Lightning Coupled to Ionosphere

Electromagnetic pulses (EMP) from lightning can affect the lower ionosphere. We used data from the Los Alamos

instruments on the GPS satellites to improve our ability to model changes in the electron density due to lightning. We found that reflected EMP time domain signals in the VLF and LF from 100's of km away can be used to probe the density structure of the D layer in the ionosphere. The observed spatial variations are apparently due to gravity waves from storms.

Ring Current Model
Ring currents in a magnetosphere can dominate the structure of the magnetosphere. The ring currents can couple to the upper atmosphere. We produced the first integrated ionospheric - magnetospheric model for ring currents. This is a first principle code that will help us understand, in particular, the importance of ionospheric oxygen and its role in coupling the upper atmosphere to the ring currents and the solar wind influence on the inner magnetosphere.

Saturnian Magnetosphere
We used a Los Alamos hybrid simulation code, combined with data from Los Alamos plasma spectrometer on the Cassini mission to Saturn, to study how the Saturnian magnetosphere is affected by water molecules from Saturn's moon, Enceladus. We found that there were no pickup ion waves observed near Titan and believe that the explanation is that the waves are swept downstream before they can grow in the vicinity of Titan.

Interplanetary Dust
We used data from Los Alamos's instruments on WIND, Stereo, and ACE along with other data from Venus Express to study the interaction between the solar wind and interplanetary dust. The dust can be accelerated by the solar wind to such speeds that are dangerous to both robotic and manned missions. We found an association between interplanetary magnetic field enhancements and dust. The dust can produce pressure gradients that couple with the magnetic field to produce currents that drive the dust to high speeds.

Astrophysics

IGPP has focused on topics in astrophysics, which are coupled to some of the biggest issues in science today. We combined theory, modeling, experimentation, and observations to key astrophysical objects such as gamma-ray bursts (GRBs) and supernove (SN), to understand how those objects can be used to study the Universe on the larger scales of galaxies and dark energy.

Gamma-ray Emissions
We used kinematic wave properties (including instabilities) to model relativistic plasmas with particle-in-cell simulations to understand the gamma-ray emissions as observed from the recently-launched Fermi satellite and the expanded Very Large Array (VLA) radio observations. Objects such as GRBs are characterized by jets that produce both gamma-ray and radio emission. For additional insight into those jets, we used laboratory-scale models of dynamos

that used liquid sodium as a surrogate for the astrophysical plasmas.

GRB Emission
When some supernovae are formed, they produce GRBs, which have jets that evolve into optical afterglows. We used Very Long Baseline Interferometry (VLBI) and the VLA to observe the expansion rate of such afterglows. These observations were fed back into a particle-in-cell code to model how the jets can produce the GRB emission.

Dark Energy
We used simulations of surveys such as the Sloane Digital Sky Survey to investigate how well future major missions such as and the Joint (DOE-NASA) Dark Energy Mission (JDEM) will be able to estimate the dark energy equation of state, a crucial component of understanding the overall evolution of the galaxies.

Galaxy Evolution
We completed the initial code for using improved chemical evolution (with radiation transport) in an adaptive mesh refinement code to understand the evolution of galaxies. This also predicted how best to use the upcoming James Webb satellite-based telescope. The initial results found that the Milky way has multiple kinematic and chemically distinct regions.

Impact on National Missions
The research significantly improves our understanding of the triggering of certain classes of earthquakes, volcanic plume dynamics, and subsurface fluid flow to allow society to mitigate catastrophic phenomena that threatens our Nation's populace. This leads to higher fidelity prediction of the onset of some natural geophysical events to determine evacuation routes, better preservation of property and protect critical natural resources and infrastructure.

Similarly, the global climate research leads to improved understanding of what may be a "natural" versus anthropogenic-induced climate change, ultimately leading to better informed national policy implementation to preserve a human-friendly climate. Aspects of the modeling work migrates to other agencies such NOAA, NCAR, and elements of DOE's Office of Science for application in large-scale climate studies, that also influence Congressional/Presidential policy.

The astrophysics and space science studies have direct bearing on understanding and better predicting a hostile space environment affecting satellite survivability.   Significant contributions were made in the quest to understand dark energy, dark matter and the evolution of the cosmos, directly impacting NASA, DOD, DOE, NSF and other federal agency programs.

References

1. Christensen, S., V. A. Zlotnik, and D. M. Tartakovsky. Optimal design of pumping tests in leaky aquifers for stream depletion analysis. 2009. *Journal Hydrology.* **375**: 554.

2. Christensen, S., V. Zlotnik, and D. Tartakovsky. On the use of analytical solutions to design pumping tests in leaky aquifers connected to a stream. 2010. *JOURNAL OF HYDROLOGY.* **381** (3-4): 341.

3. Ogden, D. E., K. H. Wohletz, G. A. Glatzmaier, and E. E. Brodsky. Numerical simulations of volcanic jets: importance of vent overpressure. 2008. *Journal of Geophysical Research-Part B-Solid Earth.* **113** (B2): B02204.

4. Srinivasan, G., D. M. Tartakovsky, M. Dentz, H. Viswanathan, B. Berkowitz, and B. A. Robinson. Random walk particle tracking simulations of non-Fickian transport in heterogeneous media. 2010. *Journal of Computational Physics.* **229** (11): 4304.

5. Elst, N. van der, and E. Brodsky. Connecting near-field and far-field earthquake triggering to dynamic strain. 2010. *JOURNAL OF GEOPHYSICAL RESEARCH-SOLID EARTH.* **115**: B07311.

6. Carter, S. P., H. A. Fricker, D. D. Blankenship, J. V. Johnson, W. H. Lipscomb, S. F. Price, and D. A. Young. Modeling five years of subglacial lake activity in the MacAyeal ice stream catchment through assimilation of IC-ESat laser altimetry. To appear in *Journal of Glaciology.*

7. Chylek, P., C. Folland, G. Lesins, and M. Dubey. Twentieth century bipolar seesaw of the Arctic and Antarctic surface air temperatures. 2010. *GEOPHYSICAL RESEARCH LETTERS.* **37**: L08703.

8. Chylek, P., C. Folland, G. Lesins, M. Dubey, and M. Wang. Arctic air temperature change amplification and the Atlantic Multidecadal Oscillation. 2009. *Geophysical Research Letters.* **36** (14): L14801.

9. Cisneros-Dozal, L., J. Heikoop, J. Fessenden, R. Scott. Anderson, P. Meyers, C. Allen, M. Hess, T. Larson, G. Perkins, and M. Rearick. A 15 000-year record of climate change in northern New Mexico, USA, inferred from isotopic and elemental contents of bog sediments. 2010. *Journal of Quaternary Science.* **25** (6): 171.

10. Fawcett, P., J. Werne, R. Scott. Anderson, J. Heikoop, E. Brown, M. Berke, S. Smith, F. Goff, L. Donohoo-Hurley, L. Cisneros-Dozal, S. Schouten, J. Sinninghe. Damste, Y. Huang, J. Toney, J. Fessenden, G. WoldeGabriel, V. Atudorei, J. Geissman, and C. Allen. Extended megadroughts in the southwestern United States during Pleistocene interglacials. 2011. *Nature (London).* **470** (7335): 518.

11. Mernild, S. H., G. E. Liston, C. A. Hiemstra, and J. H. Christensen. Greenland ice sheet surface mass-balance modeling in a 131-yr perspective, 1950-2080. 2010. *Journal of Hydrometeorology.* **11**: 25.

12. Mernild, S. H, T. Mote, and G. E. Liston. Greenland ice sheet surface melt extent and trends, 1960-2010. 2011. *Journal of Glaciology.* **57** (204): 621.

Publications

Burt, D. M., L. P. Knauth, K. H. Wohletz, and M. F. Sheridan. Surge deposit misidentification at Spor Mountain, Utah and elsewhere: A cautionary message for Mars. . 2008. *Volcanology and Geothermal Research.* : 755.

Carlson, J., M. White, and N. Padmanabhan. A critical look at cosmological perturbation theory techniques. 2008. *Astrophysical Journal.* : 479.

Chaudhuri, A., H. Rajaram, and H. Viswanathan. Alteration of fractures b precipitation/dissolution in gradient reaction environments: computational results and stochastic analysis. 2008. *Water Resources Research.* : 23.

Chaudhuri, A., H. Rajaram, and H. Viswanathan. Bouyant convection resulting from dissolution and pereability growth in vertical limestone fractures. 2009. *Geophysical Research Letters.* : 36.

Chaudhuri, A., H. Rajaram, and H. Viswanathan. Bouyant convection resulting from dissolution and pereability growth in vertical limestone fractures. 2009. *Geophysical Research .* : 36.

Chylek, P., C. Folland, G. Lesins, and M. Dubey. The 20th Century bipolar seesaw of the Arctic and Antarctic surface air temperatures. 2010. *Geophysical Journal.* : 1029.

Dentz, M., and D. M. Tartakovsk. Probability density functions for passive scalars dispersed in random velocity fields. 2011. *Geophysical Journal.* : 37.

Duan, H., G. Fuller, J. Carlson, and Y. Z. Qian. Flavor Evolution of the neutroni8zaiton neutrino burst from an O-Ne-Mg Core-Collapse Supernova. 2008. *Journal of Applied Physics.* : 100.

Duan, H., G. M. Fuller, and J. Carlson. Simulating nonlinear neutrino flavor evolution. 2008. *Computational Science and Discovery.* : Vol 1.

Elst, N. van der, and E. Brodsky. Connecting near-field and far-field earthquake triggering to dynamic strain. 2010. *JOURNAL OF GEOPHYSICAL RESEARCH-SOLID EARTH.* **115**: B07311.

Fawcett, P., J. Werne, R. Scott. Anderson, J. Heikoop, E. Brown, M. Berke, S. Smith, F. Goff, L. Donohoo-Hurley, L. Cisneros-Dozal, S. Schouten, J. Sinninghe. Damste,

Y. Huang, J. Toney, J. Fessenden, G. WoldeGabriel, V. Atudorei, J. Geissman, and C. Allen. Extended mega-droughts in the southwestern United States during Pleistocene interglacials. 2011. *NATURE.* **470** (7335): 518.

Haile-Selassie, Y., and G. WoldeGabriel. Introduction. 2009. In *Ardipithecus Kadabba: Late Miocene Evidence form the Middle Awash, Ethiopia.* Edited by WoldeGabriel, G., and Y. Haile-Selassie. , p. 1. Berkeley, CA: University of California Press.

Hariri, M. El, R. Abercrombie, A. A. Rowe, and J. do Nasci-mento. The role of fluids in trigerring earthquakes: Ob-servation from reservoir induced earthquakes in Brazil. 2010. *Geophysical Journal.* : 1566.

Hart, W. K., G. WoldeGabriel, Y. Haile-Selassie, and P. R. Renne. Volcanic record of the Adu-Asa Formation. 2009. In *Ardipithecus kababba: Late Miocene Evidence form the Middle Awash, Ethiopia.* Edited by Haile-Selassie, Y., and G. WoldeGabriel. , p. 63. Berkeley, CA: University of California Press.

Heitmann, K., M. White, C. Wagner, S. Habib, and D. Hig-don. The Coyote Universe I: Precision determination of the nonlinear matter power spectrum. 2009. *Astro-physical Journal.* : 50.

Heitmann, K., M. White, C. Wagner, S. Habib, and D. Hig-don. The coyote universe I: Precision determination of the nonlinear matter power spectrum. 2009. *Astro-physical Journal.* : 50.

Hill, T. W., M. F. Thomsen, M. G. Henderson, R. L. Tokar, A. J. Coates, H. J. McAndrews, G. R. Lewis, D. G. Mitchell, C. M. Jackson, C. T. Russell, M. K. Dougherty, F. J. Crary, and D. T. Young. Plasmoids in Saturn's magnetotail. 2008. *Journal of Geophysical Research.* : 113.

Hinz, E. A., J. F. Ferguson, L. Pellerin, and A. F. Ramenofsky. A geophysical investigation of subsurface structures and quaternary geology of San Marcos Pueblo, NM . 2008. *Archaeological Prospection.* : 247.

Huebner, W. F., L. N. Johnson, D. C. Boice, P. Bradley, S. Chocron, A. Ghosh, P. T. Giguere, R. Goldstein, J. A. Guzik, J. J. Keady, J. Mukherjee, W. Patrick, C. Plesko, J. D. Walker, and K. Wohletz. A comprehensive program for countermeasures against potentially hazardous ob-jects. . 2010. *Solar System Research.* **43**: 334.

Huebner, W. F., L. N. Johnson, D. C. Boice, P. Bradley, S. Chocron, A. Ghosh, P. T. Giguere, R. Goldstein, J. A. Guzik, J. J. Keady, J. Mukherjee, W. Patrick, C. Plesko, J. D. Walker, and K. Wohletz. A comprehensive program for countermeasures against potentially hazardous ob-jects (PHOs). 2009. *SOLAR SYSTEM RESEARCH.* **43** (4): 334.

Jiang, W., S. Liu, C. Fragile, C. Yu, and C. Fryer. Cascade and damping of Alfv' en-Cyclotron fluctuations: application to solar wind turbulence. 2009. *Astrophysical Journal.* **698**: 163.

Jiang, W., S. Liu, C. Fragile, C. Yu, and C. Fryer. Cascade and damping of Alfven-Cyclotron fluctuations: application to solar wind trubulence. 29. *Astrophysical Journal.* : 163.

Keeling, R., A. Manning, and M. Dubey. The atmospheric signature of carbon capture and storage. 2011. *PHILO-SOPHICAL TRANSACTIONS OF THE ROYAL SOCIETY A-MATHEMATICAL PHYSICAL AND ENGINEERING SCI-ENCES.* **369** (1943): 2113.

Lay, E., and X. Shao. High temporal and spatial-resolution detection of D-layer fluctuations by using time-domain lightning waveforms. 2011. *JOURNAL OF GEOPHYSICAL RESEARCH-SPACE PHYSICS.* **116**: A01317.

Maciera, M., C. A. Rowe, G. Beroza, and D. Anderson. Iden-tification of low-frequency earthquakes in non-volcanic tremor validated with the subspace detector method. 2010. *Geophysical Journal.* : 37.

Morgan, L. E., P. R. Renne, R. E. Taylor, and G. WoldeGabri-el. Archaeological age constraints from extrusion ages of obsidian: examples from the Middle Awash, Ethio-pia. 2009. *Quaternary Geochronology.* **4** (3): 193.

Ogden, D. E., K. H. Wohletz, G. A. Glatzmaier, and E. E. Brodsky. Numerical simulations of volcanic jets: Im-portance of vent overpressure. 2008. *Geophysical Re-search.* : 113.

Ogden, D. E., S. W. Kieffer, X. Lu, G. McFarquhar, and K. H. Wohletz. Fluid Dynamics of High Pressure Volcanic Eruptions. 2009. *Geophysical Research.* : 238.

Ogden, D. E., S. W. Kieffer, X. Lu, G. McFraquhar, and K. H. Wohletz. Fluid Dynamics of High Pressure Volanic Erup-tions. 2009. *Geophysical Journal.* : 238.

Renne, P. R., L. E. Morgan, G. WoldeGabriel, and W. K. Hart. Geochronology. 2009. In *Ardipithecus Kadabba: Late Miocene Evidence from the Middle Awash, Ethiopia.* Edited by Haile-Selassie, Y., and G. WoldeGabriel. , p. 93. Berkeley, CA: University of California Press.

Scollo, S., A. Folch, M. Coltelli, and V. J. Realmuto. Three-dimensional volcanic aeroProposed and numericall simulations. 2010. *J Geophys. Res.* : 115.

Srinivasan, G., D. M. Tartakovsky, M. Dentz, H. Viswana-than, B. Berkowitz, and B. A. Robinson. Random walk particle tracking simulations of non-Fickian transport in heterogeneous media. 2010. *JOURNAL OF COMPU-TATIONAL PHYSICS.* **229** (11): 4304.

Tague, C., and A. L. Dugger. Ecohydrology and Climate change in the Mountains of Western USA . 20. *Geography Compass.* : 1648.

Welling, D. T., V. K. Jordanova, S. G. Zaharia, A. Glocer, and G. Toth. The effects of dynamic ionospheric outflow on the ring current. 2011. *JOURNAL OF GEOPHYSICAL RESEARCH-SPACE PHYSICS.* **116**: A00J19.

White, T., B. Asfaw, Y. Beyene, Y. Haile-Selassie, C. Owen. Lovejoy, G. Suwa, and G. WoldeGabriel. Ardipithecus ramidus and the Paleobiology of Early Hominids. 2009. *Science (Washington D C).* **326** (5949): 75.

White, T., S. Ambrose, G. Suwa, and G. WoldeGabriel. Response to Comment on the Paleoenvironment of Ardipithecus ramidus. 2010. *SCIENCE.* **328** (5982).

Wohletz, K. H., D. Steedman, P. Giguere, and D. Zhang. PHO mitigation simulations using computational fluid and solid mechanics. 2008. *Los Alamos National Laboratory Report.* : 10.

WoldeGabriel, G., S. H. Ambrose, D. Barboni, R. Bonnefille, L. Bremond, B. Currie, D. DeGusta, W. K. Hart, A. M. Murray, P. R. Renne, M. C. Jolly-Saad, K. M. Stewart, and T. D. White. The Geological, Isotopic, Botanical, Invertebrate, and Lower Vertebrate Surroundings of Ardipithecus ramidus. 2009. *Science.* : 1126.

WoldeGabriel, G., W. K. Hart, P. R. Renne, Y. Haile-Selassie, and T. White. Stratigraphy of the Adu-Asa Formation, In. 2009. In *Late Miocene Evidence from the Middle Awash, Ethiopia.* By WoldeGabriel, G., and Y. Haile-Selassie. , p. 27. Berkeley, CA: University of California Press.

Zoglauer, A.. Application of neural networks to the identification of the compton interaction sequence in compton igagers. 2008. *IEEE.* : 701137.

A Transformational Fission Measurement and Simulation Capability

Morgan C. White
20110037DR

Abstract

Most nuclear reactions involve a projectile and target and produce only a small, fixed number of products. For example, capture might involve a neutron being absorbed by a hydrogen-1 nucleus to produce a gamma-ray and a hydrogen-2 recoil. The process of nuclear fission is unlike other reactions in that it produces a wide range of products, typically over one thousand different possibilities depending on the initial energy and isotope. While high-quality data exist for the fission-product yields at 0.025 eV (thermal) incident neutron energy on isotopes such as uranium-235, data at higher energies and for minor isotopes are scarce. The requirements on detectors and sources to efficiently and accurately measure such data are stringent. Although the basic detector components necessary are standard in particle physics, their use in this kind of nuclear data measurements is relatively novel and requires special considerations. One-year LDRD funding in FY11 has allowed us to examine these requirements and establish more confidence in a detector design capable of this feat. Additionally, the impact such data might have on fission theory and the use of fission data in various nuclear energy and security missions has been considered.

We desire accurate energy-dependent fission-fragment yields for two reasons. These data are the necessary inputs that will make possible the next generation of fission emission evaluations crucial to advanced simulation capabilities for nuclear weapons, reactors and other global security applications. They are also the key in the measurement process used to infer the number of fissions that have occurred in material of interest, e.g. a nuclear weapon or a reactor fuel rod. Improving our capability to measure, understand, and evaluate these data significantly advances our basic understanding of fission process and will answer crucial questions in the evaluation of nuclear weapons performance.

Background and Research Objectives

The term "fission" was first applied to the process by Frisch in 1938 and represents the initial insight from which fission theory derives. Hahn, Strassmann and

Meitner had performed experiments bombarding uranium with neutrons and using radiochemistry had isolated barium within the residual. Figure 1 shows the sequence of events as a neutron collides with uranium-235 and subsequently undergoes fission. When Meitner and Frisch conveyed their idea that the liquid-drop like nucleus could split in two, Bohr's response was "Oh, what idiots we have been that we haven't seen that before. Of course this is exactly as it must be." In their seminal paper, Bohr and Wheeler identify the nuclear shape as the primary degree of freedom defining the potential-energy surface and used a 1-D description as a function of nuclear elongation to define the fission barrier. These fundamental ideas underpin our concept of nuclear fission though our current fission models extend this description to the five dimensional shape shown in Figure 2.
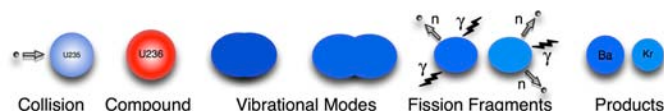
Figure 1. The 'fission' process as first conceived by Lise Meitner and Otto Frisch in December 1938.
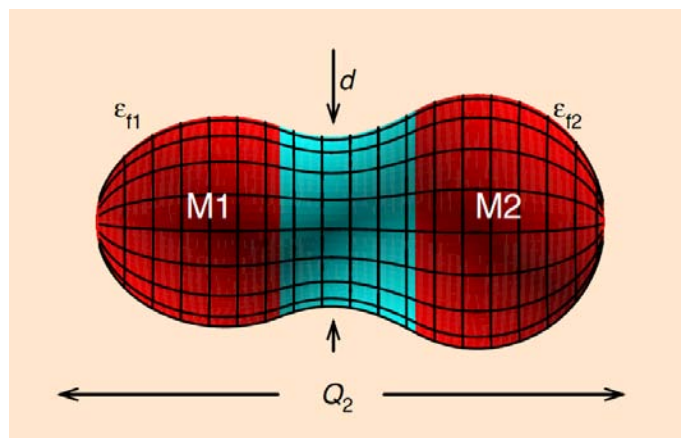
Figure 2. The five essential fission shape coordinates: elongation (Q_2), necking (d), mass asymmetry, and deformation of each fragment (eta).

Fission is considerably more complicated than most nuclear reactions and considerable confusion often arises from the nomenclature used to discuss it. There are several important time scales and events relevant to fission process. It takes on order of 1E-21 to 1E-17 seconds to go from neutron absorption to the peak of the fission barrier. Descent from the peak to scission is on order of 1E-21 to 1E-20 seconds and results in more than a thousand possible combinations of *primary fragments*. This breakup is statistical in nature and is dependent on the initial state, e.g. neutron-induced fission will be dependent on the incident neutron energy. Accelerated by Coulomb repulsion to their full kinetic energy in ~1E-19 seconds, the fragments reach velocities on order of 1 cm per ns. *Prompt* neutron and gamma emission occurs on timescales of 1E-17 to 1E-7 seconds resulting in the *independent yields* of *fission fragments*. *Delayed* beta, neutron and gamma emission occurs on timescales of milliseconds to days resulting in *cumulative yields* of *fission products*. Measurements are challenging but experimental data are necessary to validate the nuclear physics models that seek to describe these events.

The SPIDER detector seeks to measure energy-dependent neutron-induced independent fission-fragment yields with resolution on par with previous measurements using thermal neutron sources. This is a considerable challenge as higher energy sources are typically less intense than thermal sources. The fission cross section may be lower as well resulting in very low efficiency for detection. SPIDER seeks to find improvements to increase the sub-percent detection efficiency typically achieved in past experiments by more than an order of magnitude and couple this with the high-intensity neutron sources available at the LANL LANSCE Lujan (thermal and epi-thermal energies) and WNR (high-energy) facilities. This project has examined the requirements to build an instrument that should be able to measure with 2-5% accuracy or better the independent yield of 80-97% of the fission fragments over an incident neutron-energy range from 0.01 eV to 20 MeV for many actinides.

Scientific Approach and Accomplishments

This project was funded to help understand the feasibility of the SPIDER detector and assess its potential impact. The current section will document our understanding of the technical requirements for such a detector and the next will document the potential impact of the measurements. This document and a longer version of the technical requirements for the detector form the core of the accomplishments for this one-year feasibility study.

The time scale involved limits measurements of the fission process to either the fission fragments after prompt emission or the fission products after delayed emission. To study the energy dependence of this process using fission product measurements, one must have an intense mono-energetic source of neutrons. Such sources are rare and many of the typical measurements use critical assemblies with low energy-resolution fission spectra of differing hardness to approximate a mono-energetic source. The analysis process is time intensive to count each product, often involving significant radiochemical separations, and the best results have only accounted for ~90% of the total yield.

Measurements of the fission fragments are as close to the moment of fission as we can currently examine. The 2V, 2E method involves measuring the velocity and energy of both fragments emitted from a fission event. From the velocity and kinetic energy KE, we can infer the mass, and thus the atomic mass number A, of the fragment using energy equals one-half mass times velocity squared. The atomic number Z of the fragment can be inferred using Bragg spectroscopy based on the measurement of the variation in specific energy loss as the fragment interacts with the ionization chamber gas. The addition of the KE to Z and A in reporting the yields is significant as the nuclear models of the prompt emissions are most sensitive to this parameter.

This project initially focused on running simulations of prototype detector designs to estimate the technical requirements necessary. Through this process, we were able to estimate the expected measurement resolution for Z, A and KE and the overall detector efficiency for various designs based on previous experiments as reported in scientific journals. These calculations show that it is possible to reach a resolution from 0.75 to 1.6 for A equal to 85 to 160, respectively, given 150 ps timing in the velocity measurement. Current technology has advanced and 100 ps timing may now be possible. Simulations of the kinetic energy measurement for Bragg spectroscopy show a resolution of less than 1.5 for the Z of the light fragment. Unfortunately, the Z of the heavy fragment is difficult to distinguish and must be inferred from conservation of charge based on the light fragment measurement.

The fission fragments are emitted into 4π about the fission event. The velocity measurement requires a reasonable distance, 40-50 cm, to achieve good resolution. This implies a desire for detectors covering a 20-30 thousand square centimeter area. The best that can currently be done is to cover a few percent of this area. Similarly, the fissionable target material should have as much mass as possible to provide more fission events to observe. However, the fission fragments have a very short range in this target and must escape with most of their kinetic energy. This leads to very thin target designs with very low mass. Various design configurations for the target and detector layout have been examined. Given the Lujan neutron source characteristics, reasonable statistics can be collected for more than 99% of the thermal fission fragment yield for collection times of around a week. Given the WNR neutron source characteristics, reasonable statistics can be collected for more than 95% of the energy-dependent fragment yields for collection times on the order of three months. This experiment can be run 'parasitically', i.e. in parallel us-

ing unused beam neutrons, with other experiments allowing for easier scheduling of the necessary beam time.

Additional funds were provided late in the year to purchase and examine prototype timing detectors. Procurement difficulties delayed their arrival and prevented extensive testing but a mechanical examination of the systems helped refine many of the design requirements relating to the velocity measurement. An internal laboratory report has been produced documenting this work [LA-UR-11-05665].

Impact on National Missions

An understanding of the fission process is critical to the Laboratory's national security missions. One of the cornerstones in the annual assessment of the US nuclear weapons systems is the QMU process. Many of the reports contain a graph similar to Figure 3 in which our understanding of these issues is summarized. As a weapon ages, the expected primary yield goes down. At some point (Ypmin), it is no longer sufficient to ensure adequate secondary performance. The QMU process quantifies our uncertainties on the primary performance over time and shows the margin to Ypmin. This process derives from our understanding of a suite of baseline calculations. The fission yield is one of the principal metrics by which our calculations are benchmarked. The inferred fission yield of the weapon is directly proportional to these fundamental fission-product yields and shifts up or down with any changes. In the case that we can significantly reduce the fundamental uncertainties, as has recently happened, we can reduce our overall uncertainties thereby increasing margin (a shift from the outer to inner bands in our notional figure). Such gains must be validated through multiple means. The SPIDER detector seeks to make measurements of the fundamental data used in this process. There are few inputs in this process that have such dramatic, direct effect. The assessment of yield is an essential capability for all the nuclear weapons programs.
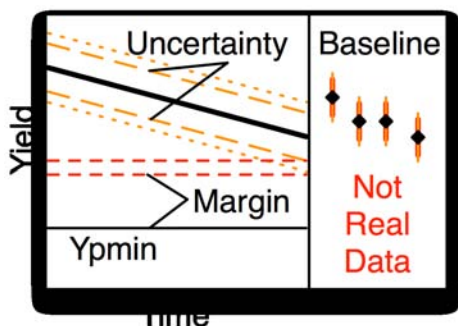
Figure 3. Notional weapons system QMU graph showing that baseline uncertainties are directly proportional to the fission-product yields. (U)

Similar to the impact on the nuclear weapons programs, the nuclear energy community is also dependent on these data. The assessment of burn-up in reactor fuel is an es-

sential metric in determining the life cycle of a fuel bundle. Like the assessment of yield, this is essentially a determination of the number of fissions that have occurred in the fuel and is directly proportional to the yield of key fission products. Critical experiments measuring the burn-up in prototypical fuel bundles have been used to establish the safety basis for many power reactors. An ability to better quantify the burn-up of the fuel would allow longer life cycles leading to potential savings in reactor fuel costs.

The national Non-Proliferation (NP) and Nuclear Counter-Terrorism (NCT) programs seek methods to identify and quantify Special Nuclear Material (SNM), e.g. material like plutonium that might be used in an Improvised Nuclear Device (IND). NP personnel examine processing facilities, nuclear reactors, and waste facilities with the goal to track SNM from its birth to its final disposition. NCT personnel examine border crossings and other key areas in order to interdict illicit transport of SNM. If found, they also seek to quantify the type of SNM and its potential danger. All of these missions rely heavily on the use of fission *signatures*, i.e. a set of neutron or photon emissions that are unique to a given SNM. At present, these signatures must be measured experimentally at a high cost in time and money. Given high-quality fission fragment yield data, we can predict many of these signatures thus greatly enhancing our abilities to perform these missions.

Modern nuclear fission theory remains a fitting process rather a predictive capability. Experimental data are required for each step of the process. Where they are not available, our confidence in these data is low. Unfortunately, this is the case for many materials of interest. High quality measurements of the fission fragment yields will lead to improved models of the fission barrier, and thus the fission cross section, as well as predictive capability for prompt and delayed neutron, gamma and beta emissions. Included within this framework, the correlations in emissions will greatly improve our ability to quantify the sources of uncertainty in our simulations. All of the nuclear related missions are dependent on these simulations and will greatly benefit from an advanced understanding of the fission process.

References

1. Tovesson, F. K., A. Laptev, H. J. Jorgenson, and M. C. White. A new instrument for fission fragment research at LANSCE -- Initial design study. 2011. *LANL Report LA-UR-11-05665.*

2. White, M. C., F. K. Tovesson, A. J. Sierk, T. A. Bredeweg, M. Jandel, P. Moller, J. P. Lestone, and R. O. Nelson. Advancing The Fundamental Understanding Of Fission - LANL LDRD Proposal 2012077DR. 2011. *LANL Report LA-UR-11-02772.*

Publications

Tovesson, F. K., A. Laptev, H. J. Jorgenson, and M. C. White.

A new instrument for fission fragment research at LANSCE - Initial design study. 2011. *LANL Report LA-UR-11-05665.*

Building the Astroinformatics Competency: Finding, Interrogating, and Understanding Cosmic Explosions (U)

W T. Vestrand
20110038DR

Abstract

We conducted a feasibility study with the goal of building new astroinformatics competencies and exploiting key elements of LANL's Thinking Telescopes/RAPTOR infrastructure to develop a new, modern, approach to Space Situational Awareness. This program successfully demonstrated the utility of wide-field persistent sky monitors that work in concert with robotic rapid response telescopes. We were able to build a Bayesian Belief Network for classifying explosive astrophysical transients. We also demonstrated the feasibility of using new non-volatile data storage technologies for the construction of rich context databases at remote observatory sites and machine learning techniques for monitoring telescope state-of-health.

Background and Research Objectives

A revolution in observational science is underway driven by new technologies: autonomous robotic sensors, distributed sensor networks, data intensive computing, and real-time knowledge extraction. Mastery of the new technology and its integration into practical systems is enabling previously impossible scientific discoveries and will be essential for modern National Security systems.

Our research objectives are to establish the feasibility some of the key aspects of our plan to build and operate a next-generation robotic telescope network for Space Situation Awareness (SSA) with important National Security applications. The feasibility study—which is a significantly de-scoped version of the original proposal—also aims to further build and to demonstrate LANL astroinformatics capability by taking the first steps toward up-grading the RAPTOR (*RAP*id *T*elescopes for *O*ptical *R*esponse) robotic telescope infrastructure (Figure 1) through the infusion of new data intensive supercomputing technology and structural health monitoring techniques.
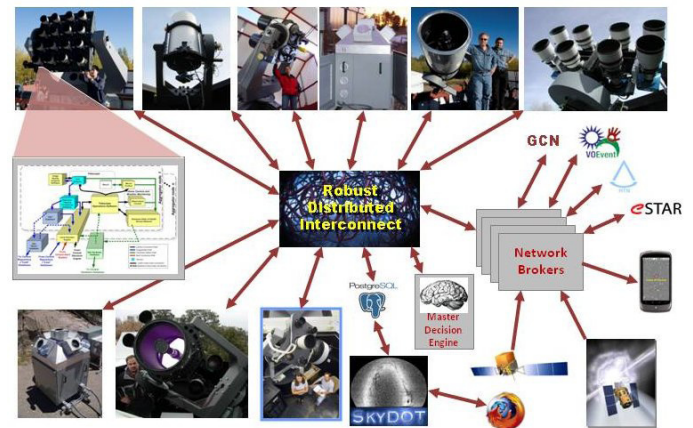
Figure 1. Depiction of the heterogeneous nature of Thinking Telescopes.

Scientific Approach and Accomplishments

A key goal of our feasibility study was the real world demonstration of a new approach to Space Situational Awareness employing ultra-wide field persistent sky monitors, real-time anomaly detection, and autonomous robotic follow-up telescopes. We successfully established the feasibility of new techniques to maintain custody of space objects using optical measurements which are irregularly spaced and sampled with varying precision. Further, we demonstrated an exciting new concept for detecting a class of anomalies of great importance. This new approach is generating significant interest across the National SSA community and has spawned three new sponsored projects.

An important component of our new approach is the presence of deep context information at distributed agile sensors. Emerging storage technologies based on Solid State Drives (SSD) and non-volatile Flash memories promise to replace Hard Disk Drives (HDD) as the primary storage medium for a range of data intensive and IO (input/output) intensive applications. We explored the design space for low-power deployable database platforms hosting large high-performance spatio-temporal databases based on SSD and Flash devices. For this pur-

pose we evaluated a Fusion-IO ioSAN device with 640 GB capacity and PCIe 8 high-performance inter-connect using end-to-end benchmarks. Our low-level device characterization using the fio IO benchmarking utility has shown that the ioSAN delivers sequential read/write IOPS (input/output operations per second) of 190,000/280,000 while sustaining sequential read/write bandwidths of 1.5/1.0 GB/s. More importantly, for data access patterns found in sky surveillance applications the device can sustain random read/write IOPS of 90,000/62,000. This is 3 orders of magnitude better than a commodity hard disk and demonstrates a tremendous potential of Flash-based storage for high-performance data intensive computing. We also considered two alternative solutions: 1) Vertex 3 SATA III devices from OCZ combined with LSI MegaRAID SAS 9261-8i controller, and 2) RAIDDrive RGS5 from SuperTalent with PCIe 8. While both alternatives outperform Fusion-IO in low-level testing, the latter technology has by far the most complete Linux. All three solutions are likely to be competitive in the near future.

Modern optical sky monitoring systems increasingly rely on high-level database management and sophisticated geometric querying. The RAPTOR/Thinking Telescopes software infrastructure for light curve tracking is a representative example. Our high-level benchmarks for this system were designed to verify what fraction of performance gains from Fusion-IO is actually utilized by the application. Using a PostgreSQL database and a standard test suite *pgbench* we obtained a factor of 15 improvements when comparing ioSAN to a single hard disk. The improvement in speed drops to a factor of 10 for the case of creating a large spatial index such as the Hierarchical Triangular Mesh (HTM) inside Postgres. However, tests with bulk inserts into large indexed tables result in only a modest performance gain around a factor of 2. The latter case is important for making the data searchable immediately after database ingest and minimizing the number of writes to the media ("write once, search immediately" functionality). The overall conclusion from this study is that the current database and middleware software (e.g. Linux file system and I/O subsystem layers) is unable to tap the performance potential of the new generation storage devices based on SSD and Flash technologies. Database management systems such as PostgreSQL provide complex buffer management designed to mask the latency of slow rotating disks. These systems are not required in emerging designs and actually inhibit the achievable performance when using SSDs. Another problem is obtaining sufficient levels of I/O concurrency in the database backend (~64 threads) required to reach the advertised device performance. Entirely new co-designed hardware/software architectures must be developed to overcome the legacy of disk-based storage systems. These results are in line with related studies presented at the 2011 Non-Volatile Memory Workshop (NVMW).

Our work on automated classification of explosive transients focused on the application of Bayesian Belief Net-

works (BBN). We developed a first generation classifier implementing a BBN. Upon submission of a new transient alert over the network the system cross-correlates the incoming information with existing data and external databases, filters out redundant measurements, builds historical context (light curve), assembles the feature vector, and feeds the available evidence to the network. This includes timing information and light curve statistics, simultaneous detections from high energy observatories (Swift, Fermi), progenitor information from catalogs of known explosive transient sources, and host galaxy information from SDSS. We also developed a web-based graphical user interface (GUI) that allows users to manually supply evidence to the network and quickly display posterior probabilities for class membership and all remaining nodes of the network. The network is configured using conditional probabilities and priors derived from published light curves and population studies. We maintain an SQL database of known variables and high energy sources (currently about a dozen catalogs) to aid the classification process. Currently the system can distinguish between optical GRB counterparts (Afterglows, Precursors, Prompt/Simultaneous), Active Galactic Nuclei (AGN), Cataclismic Variables (CV) and stellar flares (M dwarfs).

Robotic telescope systems, like all mechanical systems, are subject to wear and age related failure modes. Two of the most important mechanical failure modes are (1) faults in the telescope drive mechanism and (2) fatigue in the robotic mechanical structures. For telescopes deployed at remote sites on a global scale, it will be very expensive to perform on-site visual inspections to identify emerging faults. Therefore one of our key engineering goals was to explore the feasibility of deploying a cost-effective, autonomous, remotely monitored damage detection capability as part of a proactive approach to system diagnostics and maintenance.

We successful showed the feasibility of this remote monitoring approach by a deploying and operating miniature monitoring sensors on one of our autonomous fast slewing telescopes. Specifically we deployed a small array of accelerometers at various locations to measure vibrations in the mechanical structure during mount operation. These sensors were then used to characterize the vibrational properties during normal healthy conditions as well as a series of increasingly degraded or damaged mount conditions. Using these measurements we were able to construct and validate a damage classifier that can be deployed at remote telescopes as an autonomous fault warning system (see Figure 2). This approach enables the detection of damage at the earliest possible time and therefore helps mitigate the adverse effects on system level performance. This capability also allows current maintenance practices to evolve from scheduled visual inspections to a more cost-effective and autonomous condition-based approach that will reduce lifecycle costs and increase reliability of globally distributed telescope networks.
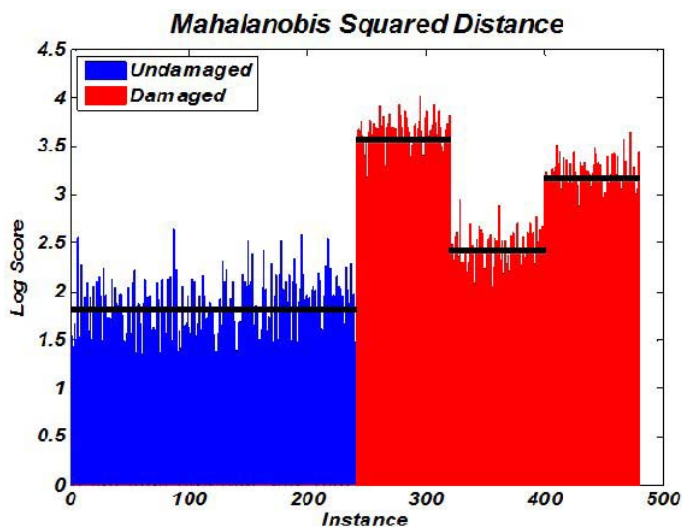
Figure 2. Depiction of automated system characterization, leading to fault detection. This figure shows accelerometer data taken when bad (red) and good (blue) mount drive parts are installed. The mahalanobis distance between families of accelerometer measurements allows characterization of good and bad system parts.

Impact on National Missions

This work has demonstrated the feasibility of an innovative new approach to Space Situational Awareness that employs autonomous networks of robotic sensors. Our work is receiving National attention and having a significant impact both because of its unprecedented capabilities and its cost effectiveness.

Publications

Panaitescu, A., and W. T. Vestrand. Optical afteglows of gamma-ray bursts: peaks, plateaus and possibilities. 211. *Monthly Notices of the Royal Astronomical Society.* **414** (4): 337.

al, S. Kozlowski et. SDWFS-MT-1: A Self-obscured Luminous Supernova at z ~= 0.2. 2010. *The Astrophysical Journal.* **722** (2): 124.

Development and Validation of an Advanced Turbulence Transport Model (U)

Michael J. Steinkamp
20110042DR

Abstract

Turbulent mixing in strongly compressible converging flows, with thermonuclear energy release, is an extremely challenging physical problem. This one-year project was focused on laying the ground work to achieving an understanding of the microscopic interplay between mix and burn in Inertial Confinement Fusion (ICF) capsules. We have explored the work of coupling a theoretical and computational investigation using LANL's state-of-the-art Besnard-Harlow-Rauenzahn (BHR-2) turbulence transport model in the Eulerian Application Project (EAP) code suite with an experimental program utilizing the extreme conditions (converging flow with thermonuclear (TN) burn) available at the National Ignition Facility (NIF). Our work focused on developing a new class of experimental data to advance our understanding of turbulence in these flows, including the first thermonuclear data to test LANL's computational modeling predictive capabilities.

Background and Research Objectives

We have explored the feasibility of designing and carrying out a set of well-defined turbulence mix experiments at the NIF. We have chosen NIF because at NIF we can vary the shock loading conditions and fabricate capsules with interfacial characteristics intended to influence the growth of instability and hydrodynamical mixing. We have explored the feasibility of diagnosing these experiments using a combination of neutron and x-ray imaging, and reaction history. We have targeted the NIF for the development of our experimental program due to the important role it will play in the future science of high energy density physics. This work also explores the feasibility of developing a strong theoretical and computational model necessary to complement future experiments.

Scientific Approach and Accomplishments

There were three distinct parts to this research effort: a subgrid computational modeling effort, an experimental program, and a theoretical developments to support the experimental diagnostics. All three coupled thrusts were necessary to support our research objectives.

Subgrid Computational Modeling

"Subgrid Models" are computational physics models that describe phenomena that occur at scales that are smaller than available grid resolution. For example, the dissipative fluid fluctuations of a high-Reynolds number turbulent flow may be at scales that are many times smaller than the finest available grid spacing. Likewise, the scales over which charged particle transport (CPT) phenomena occur can be much less than the grid spacing. In the case of turbulent flows, the fine-scale details of the dissipative fluctuations in the flow field are typically strongly driven by the large-scale, resolvable portions of the flow field. Thus the fine-scale details of dissipation may be ignored, and the loss of turbulent kinetic energy to viscous forces is treated by a "resolved-scale" dissipation model, as in the BHR model. However, for many lab-relevant physics issues, the subgrid scale phenomena may not be strongly driven by the resolved scale, but may are instead a driver to the resolved scales. For example, fine-scale, unresolved perturbations at a material interface may give rise to a fluid instability, e.g. Kelvin-Helmholtz, Rayleigh-Taylor or Richtmyer Meshkov, which in turn lead to resolved scale motions. Phenomena such as this can be described by subgrid scale models, and indeed was one of the initial motivations of the development of the BHR turbulence model. The BHR model described the initial, unresolved fluctuations at the material interface as a density fluctuation via an evolution equation for a density self-correlation variable, "b", and by a length-scale, described as a function of the initial turbulent kinetic energy, "K" and dissipation rate, "epsilon."

For example, the subgrid-scale dynamics of the flow field can have a dominating influence on chemical and nuclear reactions and particle transport. Currently, the subgrid modeling capability within Rage includes (1) the tracking of interfaces through computational cells via the Volume-Of-Fluids (VOF) approach, (2) the BHR model that permits a statistical description of the turbulence and permits a characterization of the turbulence to subgrid scales, (3) several multiple-temperature models that permit the characterization of the subgrid

thermodynamics by different temperatures for different materials or species. (The multiple temperature descriptions are currently under development.) However, there are still important subgrid-scale physical processes that are not represented accurately within Rage. For example, chemistry models and CPT algorithms are sensitive to the degree of homogeneity of the subgrid mixing, i.e. whether the mixing is at a molecular level, or is characterized by discrete particles or volumes of pure material, or perhaps characterized by a molecularly mixing zone separating two or more volumes of pure material. Models and methods that describe the state of subgrid mixing have been developed and implemented in other codes, notably the work of A. Scannapieco and colleagues. However, their approach assumes a simple subgrid configuration of the fluids and may not be suitable for, say, CPT where the details of the distribution of materials within the cell (i.e., particle or blob size, shape, and relative orientation) play a significant role.

Subgrid Modeling Goals

The ultimate goal for a subgrid-scale model would be a model that provides a subgrid realization of a cell, showing the distribution of particles or volumes of pure and molecularly mixed materials and their respective temperatures. For cases in which material strength plays a role, the pressures of the relevant materials within the cell would also be appropriate. Unfortunately, a precise picture of the subgrid state of the problem is not possible, thus the goal is to provide a "realization" of the subgrid state that is consistent with statistical estimates of the state of the subgrid-scale phenomena. This realization can be thought of as a "possible" (and we hope, "probable") subgrid state of the materials of use in determining reaction rates and in CPT algorithms. The development and implementation of such a model requires a great deal of research and investigation, although much has already been accomplished toward the goal, both within Rage and in other codes at LANL.

Subgrid Model Research Needs

An important requirement is an accurate subgrid description of the thermodynamic state of the material(s) within a cell. The current Equation of State formulations in Rage assume that the materials within a cell occupy their own discrete volumes, and are in temperature and pressure equilibrium. Grove, Masser, et al. have made significant progress in removing the temperature-equilibrium constraint in the Rage EOS. In addition, the pressure-equilibrium constraint is probably not a critical issue unless we are concerned with material strength issues. However, the lack of ability to treat a molecular mixture of fluids within a cell (at the subgrid scale as well as at the resolved scales) may be an important limitation in accurately describing the mixing and reaction rates of materials at the subgrid level. Thus a computational approach to treat a cell with regions of pure fluid as well as regions of molecularly mixed fluids

should be developed and implemented. (Note that this is not a trivial task due to the manner in which Rage treats tabular equations of state.)

The BHR model currently treats the evolution and transport of material mass-fractions as an advection by the mass-averaged velocity field and a turbulent diffusion, and neglects the detailed turbulent flux of materials in favor of the turbulent diffusion description. In order to accurately describe multi-material transport (more than two materials) between cells in mixing layer, the BHR model should be extended to provide a detailed description of the evolution of the turbulent material fluxes. Some work has been accomplished toward the development of such an approach, but much work remains to be done.

The BHR model is able to describe the early-time subgrid perturbations at material interfaces by exploiting the dimensional relationships between the turbulent kinetic energy and dissipation rate to determine the length-scale of the subgrid perturbations and the variable "b" to describe their amplitude. However, when the turbulence is well-developed (say, at late times) the length-scales described by BHR are now relevant to the resolved scales, note the subgrid phenomenon. However, the values of the turbulent kinetic energy and dissipation rate allow one to characterize a Kolmogorov inertial range (assuming that it exists for the problem at hand), which, in conjunction with the molecular properties of the materials, i.e., viscosities, and diffusivities, permit an estimate of the subgrid scales and rates at which mixing is occurring. This approach may be fruitful for subgrid modeling but has not yet been developed or exploited.

In order to fully characterize the subgrid material distributions, an estimate of the surface to volume ratio of the parcels of pure material at the subgrid scales is highly desirable. Such models have been developed for various multiphase flows, and should be examined and exploited, if possible, for use within the BHR/Rage framework. Note that the surface to volume ratio can play an important role in reaction rates.

In addition to the surface to volume ratio, the shape and orientation of the parcels within a zone plays a significant role in CPT. Methods to estimate subgrid orientations and distributions must be researched, and/or developed and implemented. Note that an obvious requirement for this task is the implementation of BHR3, i.e., BHR with a full Reynolds stress description, permitting a more detailed description of anisotropy of the turbulence.

A method of rapidly generating a "probable" realization of the subgrid material state, with parcels of materials whose size, distribution, temperatures and surface to volume ratios are "statistically consistent" with the modeling endeavors described in items 1 through 5 (above). Note that the level of statistical consistency may be only at the lowest level (i.e., the mean, rather than at higher

moments). Such details need to be worked out. We also note that methods for generating random fields that match given statistics are of interest to many different fields, from scene generation in the computer visualization field, to generation of phase-screens in the field of optics. The methods developed in these other areas may be exploited and adapted to produce an efficient and robust tool to generate artificial yet statistically accurate realizations of the subgrid material properties.

Experimental Diagnostics

The experimental portion of the turbulent mix DR effort accomplished two main goals during FY11. Early in the year the team, in collaboration with scientists from LLNL, successfully identified the presence of hohlraum gold on X-ray imaging snout pieces located 10 cm from ignition implosions. The gold was measured using X-ray fluorescence spectroscopy at LANL by the C-NR team.   The hydrodynamics of the target explosion require that activated target materials of interest for radiochemical assay will very likely be co-located with the hohlraum gold. Subsequent quantitative analysis by our LLNL collaborators and the Colorado School of Mines, using neutron activation techniques have shown that the amount of gold collected on these snout pieces is consistent with the geometric solid angle of the surface.   The detection of hohlraum gold on surfaces very near the target is an important milestone in the development of solid debris radiochemistry techniques at the NIF, and demonstrates that as at Omega, target debris collection is feasible, and that prompt radiochemical techniques are within the grasp of a focused development campaign.

In addition to NIF debris collection activities, the LANL team has designed and executed an experiment to determine the efficacy of noble gas collection using solid debris techniques. High-Z noble gases have low diffusive mobilities. If they are adequately implanted within the matrix of a "collector," will remain for periods of time long enough to allow a variety of assay techniques. We executed a day of experiments at the Omega laser at the Laboratory for Laser Energetics, University of Rochester, Rochester NY. Theses experiments were designed to implode shells filled with deuterium, tritium, and different concentrations of hi-Z materials, including Xe. The particular targets allow a variety of scientific studies to be carried out, including collection of target Xe and it's activated daughters.   Preliminary analysis of the collector foils showed the presences of the thermalization materials used to slow the target debris, indicating Omega debris collection techniques were working as expected.

Theory Supporting Experimental Diagnostics

One of the long-term needs for a turbulence and mix program at the National Ignition Facility is the ability to calculate charged-particle transport in plasmas involving mixed material. Such a mix program requires a computational tool capable of predicting expected nuclear physics signa-

tures for different mix scenarios. Many of the signatures that we have identified involve mix-induced changes in charged-particle transport. For this, we have been assessing the details of many of the incidental charged-particle reactions taking place in a NIF capsule. This includes developing a one-dimensional thermonuclear burn code that includes the non-equilibrium nuclear reactions of interest. We have also investigated Markovian charged-particle transport schemes. In general, we find that radiochemistry signatures for charged particle transport show sensitivity to both the degree and the chunkiness of the mix.

An important ingredient in these studies is an accurate model of charged particle stopping powers under NIF conditions. The most direct probe of stopping powers in this plasma regime are the knock-on deuterons and tritons and their interaction with the shell material. Transport of knock-on particles across the capsule results in a change in the shape and magnitude of the spectrum, a change that is determined by the form of the stopping power. We have derived a relationship between the energy spectrum of the knock-on charged-particle fluence at a given point in the capsule and the charged-particle stopping power. For regions in which the stopping power is homogeneous, i.e., regions of the capsule where the range of energetic charged-particles is short compared to the scale of variations in the temperature and density, we find that the relationship between the knock-on fluence and stopping can be expressed by Equation 1.

$$\frac{d\psi_{k.o.}}{dE}(E_f) = \frac{Q_0}{\left|dE/dx(E_f)\right|} \int\limits_{E_f}^{E_{0\max}} dE_0 q(E_0)$$

Equation 1. Our current model defining the relationship between the energy spectrum of the knock-on charged-particle fluence at a given point in the capsule and the charged-particle stopping power.

From Equation 1 it follows that determining the knock-on fluence $d\psi/dE$ in the capsule directly determines the stopping. Mix-induced changes in the electron temperature lead to corresponding changes in the shape of the triton flux, as shown in Figure 1. Detecting these changes is a central focus of our future mix studies via charged particle diagnostics at NIF.
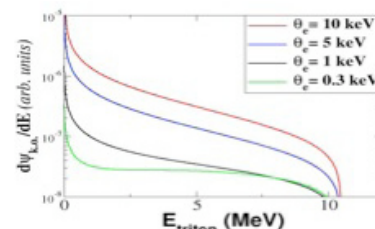
Figure 1. The stopping-induced shape of the knock-on triton spectrum for different electron temperatures.

Impact on National Missions

The impact of this year-long feasibility study is demonstration that the products of a full-term LDRD/DR research project will advance the state-of-the-art ICF modeling capabilities in LANL's Eulerian ASC code suite. Both this new computational capability and the new experimental mix diagnostics developed on NIF will directly address NNSA's goal of fostering a scientific program at NIF that is both of broad scientific interest.

Characterizing the Th-229 Isomer: A Nuclear Clock Candidate

Xinxin Zhao
20100184ER

Introduction

Atomic clocks are ubiquitous today in various research and technology areas including fundamental precision measurements, navigation (GPS) and defense applications. A 10-fold improvement in the accuracy of GPS satellite clocks, for instance, would substantially impact threat reduction and intelligence applications, especially for impulsive events where target and explosion sensing and localization are critical. In this project, we propose to study the underlying science for a new class of clock known as a nuclear clock.   This nuclear clock would be based on the energy difference between the ground and the lowest-lying isomeric nuclear level in Th-229. Compared to atomic clocks, a nuclear clock could be inherently more accurate and robust with respect to variations in its environment.   As such the development of an ultra-high precision clock would enable novel fundamental physics measurements at unprecedented accuracies and other important applications. Because no direct measurement of the Th-229 isomer has been made, our project is designed to directly measure the gamma de-excitation of the Th-229 isomer for the first time.

Benefit to National Security Missions

This project is the first step towards precisely measuring theTh-229 isomer transition and will lay the scientific foundation for developing a Th-229 based nuclear clock. The success of the project would have a transforming impact in many applications such as navigation, national defense and intelligence programs. Once its full precision potential is reached, this nuclear clock could be used in testing general relativity or in searching for physics beyond the Standard Model.

Progress

Due to the proprietary nature of this work, we provide only a summary of our research progress in this report. Although directly searching for the Th-229 isomer gamma-ray emission has proven to be very challenging, we have made great strides in this LDRD/ER project and are close to reaching a definitive conclusion.   Our final results are expected to determine whether Th-229m nuclei embedded in MgF2 decay through gamma-ray emission along with a measurement of the emission's lifetime and wavelength, if it exists.

Our direct search is complicated by several co-existing non-isomeric processes, including MgF2 scintillation fluorescence from the decay of impurities in the U samples we use and MgF2 phosphorescence after radiation exposure ("after-glow"). In addition, the anticipated small magnitude of the isomer signal together with shot-to-shot fluctuations in the measurements made the search and signal confirmation even more challenging. We have investigated these effects by making a series of systematic measurements, each of which unfortunately take a long time to complete due to the long lifetime of the phosphorescence and impurities. It turns out that quite a few parameters need to be checked in order to isolate the weak isomer gamma-ray emission (if present) from the parasitic non-isomeric background.

We have measured light emission in different wavelength regions (using Hamamatsu R8487, R8486 and R7639 PMTs with different spectral response ranges) after recoil ion implantation from either U-233, U-232 and Pu-239 sources. The three radioactive sources have enabled us to measure the phosphorescence effect unambiguously and extract a potential isomer signal from the non-isomeric processes.   The three PMTs will also enable us to reduce the gamma transition wavelength range once its existence is confirmed. Presently, we are working on reproducing the preliminary results we obtained from the measurements while also investigating new questions raised during our search.   Based on the measurements completed so far, we have some concern that our U-233 source is not pure enough. We are working with scientists at ORNL to acquire purer U-233 material.   With the purer U-233 material, effects from impurities would be negligible in our measurements. We also have a finalized draft of our first paper that necessitates only the concluding details from our remaining measurements.

In addition to the experiment described above, we are also designing a system to couple the Th-229m emission to a monochromator in an attempt to further resolve the

transition wavelength (if the isomer emission exists). One version of our design is complete and we have ordered various parts to set it up. Since the new system requires a different type of U-233 source plate from the ones used in the experiment described above, we designed a new electroplating cell and are in the process of testing it. We have also estimated the expected signal-to-noise ratio for the system.

Future Work

Once the observation is confirmed, we will setup the monochromator system and make optical spectroscopy measurements of the nuclear isomeric transition. The insight gained from our ongoing research will enable us to speed up the measurements and analysis in the new experiment. We expect to take the spectroscopy measurements in 3 nm resolution steps initially, and scan through the range over which we observe the ^{229m}Th decay signal. Further resolution should be straightforward to obtain. If successful, we will publish the work in a high profile journal and we expect exciting follow-on advances in optical and laser spectroscopy, quantum control of the ^{229m}Th nuclei, and in developing a ^{229}Th nuclear clock.

Conclusion

If successful, we will lay the foundation for a Th-229 nuclear clock with three advances: (1) search for the Th-229 isomer transition and to directly measure for the first time its energy and lifetime; (2) determine how often the isomer decay produces photon, and investigate chemical effects on this Th-229m "branching ratio"; (3) prepare Th-229 in a MgF2 crystal, a key component ("clock oscillator") for a nuclear clock.

A Plasma-Based Ultrafast THz Source

George Rodriguez
20100189ER

Introduction

Terahertz (THz) science and technology is one of the most intriguing and challenging research fields to emerge in the 21st Century. Terahertz radiation is loosely defined by the electromagnetic spectrum whose frequency range is between 0.1 to 30 THz (10^{12} cycles per second). Being situated between infrared light and microwave radiation, THz radiation is not well suited to the techniques commonly employed in these well-established neighboring bands. The terahertz region of the electromagnetic spectrum has proven to be one of the most elusive. High atmospheric absorption constrained early interest and funding for THz science. However, the past 10-15 years have seen a revolution in THz systems, as advanced materials and laser research provided new and higher-power sources. Terahertz science has now infused itself into important technological activities that range from fundamental investigations with applications in tomographic imaging, label-free genetic analysis, cellular level imaging, bio-chemical forensics, electro-optic metamaterials, plasmonic devices, manufacturing quality control inspection, security screening and perimeter defense in threat reduction, spectroscopic sensing, and THz-based ultra high-speed communications systems. Yet, despite this backdrop, there is a desperate need to fill a large peak power/energy void that plagues the THz community. For many applications, today's THz sources are still too weak. To overcome this limitation, this project's goal is to develop a new broadband pulsed femtosecond THz source with a large bandwidth (>30 THz) and microjoule-level pulse energies. This would represent a significant advance in the field of THz science. Our approach in this project is based on coherent THz generation from two-color ultrafast laser generated plasma filaments in gases. The project uses advanced laser-plasma physics models and experiments to develop an optimized source for increased output and wide tunability across the entire sub-millimeter and far-infrared electromagnetic spectral range.

Benefit to National Security Missions

Agency relevance: This THz source may be of interest for incorporation in THz-based electromagnetic sensing systems relevant to Intel, DOD, DHS, and Nonproliferation agencies. This includes THz methods for for trace or bulk detection technologies using specific spectral fingerprint analyses, chemical forensics, or non-destructive electro-magnetic imaging methodologies (including explosives detection). Other agencies such as NIH may be interested in applying this source to study THz-biofunction low energy interactions.

Mission relevance: Scientific discovery and innovation in basic understanding of materials and biology. The work would enable low-energy resonantly-tuned dynamics studies of high-temperature superconductors, actinides, biosystems, explosives chemistry, and other complex electronic materials that were previously not possible without such a THz source and where standard THz laser technology is lacking.

Progress

In FY11 second-year project activities included studies measuring the transverse mode spatial properties of the generated THz beam and understanding spectral response for development of a tunable source. Figure 1 is a photo our THz gas cell illustrating the THz generation mechanism. Briefly, a near-infrared femtosecond beam of ultrashort laser pulses (40 fs) is launched and focused into a gas cell filled with air or a noble gas such as argon. Before the focus position in the gas cell, a second color of laser light pulses (blue) is generated using a nonlinear optical frequency converting crystal called beta-barium borate (BBO). The colors (red and blue) converge to a focus in the gas cell to produce an ionization filamentation spark in the gas. It is the precise timing and phasing of the interaction of intense combined two-color laser optical pulse fields interacting in the gas ionization process that leads to the generation of coherent THz emission [1,2]. Quantum motion of the liberated electrons in the ionization filament under the action of the laser fields produces a quasi-DC transverse electron current that act as dipole-like radiators in the THz regime. A coherent superposition of these radiators along the length of the filament spark leads to a coherently generated THz beam with very large bandwidth across the far-infrared to infrared spectral range [1,2].
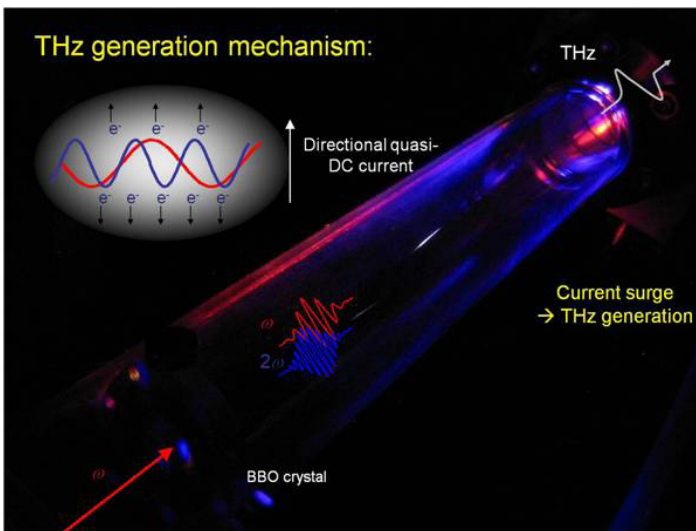
Figure 1. Photo of terahertz (THz) gas cell illustrating the THz generation mechanism. Briefly, a near-infrared (800 nm) femtosecond beam of ultrashort laser pulses (40 fs) is launched and focused into a gas cell filled with air or a noble gas such as argon. Before the focus position in the gas cell, a second color of laser light pulses (blue, 400 nm) is generated using the nonlinear optical frequency converting crystal called beta-barium borate (BBO). The two-colored (red and blue) laser beams come to a focus in the gas cell to produce an ionization filament spark in the gas. It is the precise timing and phasing of the interaction of intense combined two-color laser optical pulse fields interacting in the gas ionization process that leads to the generation of coherent THz emission [1,2].

In FY11, experimental results show that the THz beam emanates from the plasma filament region in a forward directed cone which appears as a ring-like structure along the beam's transverse spatial profile (Figure 2). The conical THz emission is attributed to beam interference effects within the two-color laser plasma filament, and this interpretation is now subject of study using sophisticated electromagnetic beam propagation models from project co-investigators in the Plasma Theory and Applications Group (X-XCP) in Applied Physics Division. Terahertz generation inside ionization filaments produced by self-focusing of high-intensity short laser pulses in a gas is a complex multi-dimensional nonlinear phenomenon. We are simulating these effects in 3-D using the electromagnetic pulse propagation code, PULSE. It models not only the laser-gas interaction and consequent plasma formation via the appropriate ionization mechanism, but also includes nonlinear optics physics models, such as Kerr self-focusing and self-phase modulation, group velocity dispersion, plasma defocusing and inverse Bremsstrahlung. Over the past year, we have modified the code to include the second harmonic of the laser field which gives rise to the THz signal through the beat frequency with the fundamental. In particular, we employ the principle of super-position that allows us to treat the two harmonically-related fields independently when they propagate through the gas and inhomogeneous plasma, while accounting for their combined effect on the ionization and THz transverse currents they generate. We have written a processing routine that calculates the resultant radiation field from the spatial and time dependent THz current that is generated by the co-propagating laser pulses in the filament. Our modeling investigation has revealed that the spatial distribution of the THz signal intensity possesses ring-like structures like those observed experimentally (Figure 3). We have developed a theory that can possibly explain such variations in the THz intensity profile. We stipulate that the change in the phase of the electro-magnetic radiation along the direction of the laser pulse propagation causes self-interference that is instrumental in producing these ring-like structures in the spatial profile of the signal at our simulated detection screen. We are currently testing our updated code and post-processing tools to compare our simulation results with the experiment. A journal publication manuscript describing these results is in preparation [3].
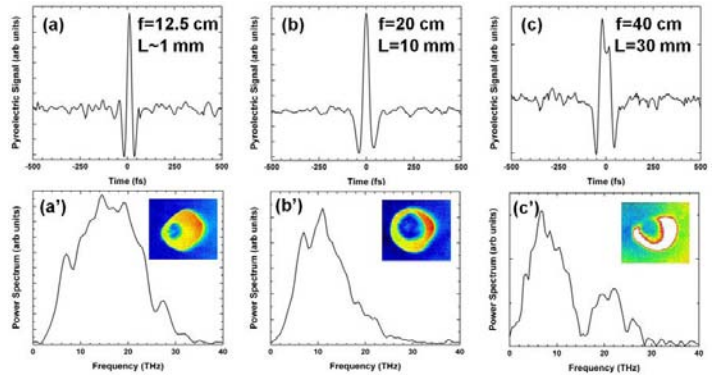
Figure 2. Plots and images of the THz temporal interferograms (a-c), power spectra (a'-c'), and transverse spatial mode patterns (insets to (a'-c')) for various focusing conditions in argon gas. The lens focal length is indicated by f, and the observed spark length is indicated by L. The shortest THz pulse and broadest emission spectrum is achieved with the tightest focusing lens (f=12.5 cm) that produces the shortest filament spark (L~1 mm). The longest THz pulse and narrowest spectrum is produced under the softest focusing condition (f=40 cm) with the longest filament spark, L=30 mm. In all cases, a complex ring-like structure is observed in images of the THz beam transverse mode spatial profiles.

In collaboration with the Center for Integrated Nanotechnologies User Program and Theoretical Division, application of powerful terahertz beams to in-vitro studies on biocelluar function is also reported. Molecular dynamics computer simulations indicate that the local electric field from THz radiation, if sufficiently large enough, may couple to the local breathing dynamics of DNA to induce gene response at specific activation sites upon transcription. Using our broadband powerful THz source for experiments, we confirmed that extended exposure of mammalian stem cells to this type of radiation does indeed induce gene specific response when exposed. Mouse stem cells un-

der multiple hour exposure experiments show that DNA-directed gene transcription is altered by inducing raised activity of certain protein coding genes and suppressing others. The response was gene specific as predicted by the computer simulations, but also irradiation dependent. Details of these results were published in the Public Library of Science One (PLoS One) online journal [4], and additional studies [5] were recently published in Biomedical Optics Express journal showing that the THz responses of the stem cells were non-thermal. It is hypothesized that stem cell DNA used in these studies are directly excited via THz driven coupling to natural breathing modes at specific transcription start sites along the DNA double helix structure. Further ultrafast time-resolved THz pump-probe studies are in progress to further our understanding of possible mechanisms. Nonetheless, this work demonstrates THz radiation as a potential tool for biocellular reprogramming applications.
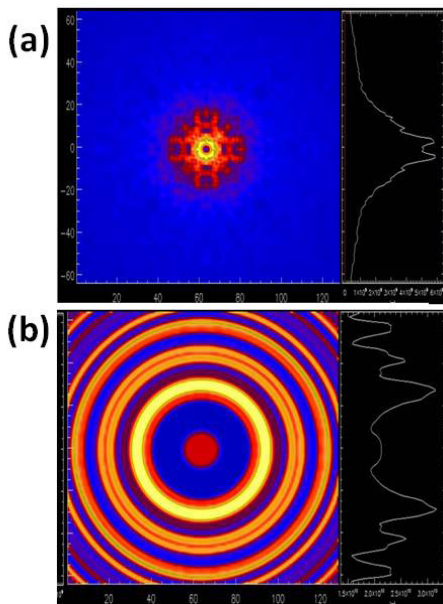
Figure 3. Computer simulation from 3D PULSE code of the THz beam transverse mode intensity pattern for (a) large area view and (b) zoomed in view. Comparative matching to experimentally measured patterns is work in progress.

Future Work

In FY12 we will demonstrate a high-energy, high-repetition rate, tunable THz source by introduction of tuning elements into the THz beam, or active control via spatio-temporal manipulation of the driving optical fields. Multi-dimensional simulations will be used for predicting THz radiation patterns and spectral content. Then, integration and characterization of the optimized high-energy THz system with tuning capability will be used to perform THz based pump-probe spectroscopic studies of materials. Application of this source to nonlinear THz material physics such as correlated electron materials THz spectroscopy or non-linear THz biology will be demonstrated.

Conclusion

The goal of this project is to experimentally and theoretically develop a plasma-based ultrashort pulse coherent terahertz (THz) source with peak pulse energy at the microjoule level and sufficient for THz induced changes in materials. A THz source of this kind with sufficient bandwidth and energy is still lacking. The THz source we are developing is based on ultrafast two-color laser generated plasma filaments in gases. Preliminary results by our group at LANL have been demonstrated, but the source is not yet optimized for peak power and tunability. It is expected that an optimal THz source technology for a myriad of applications in materials science dynamics, biology applications, active THz sensing and imaging, non-linear THz optics, THz electronics, forensics, and others.

References

1. Kim, K. Y., A. J. Taylor, J. H. Glownia, and G. Rodriguez. Coherent control of terahertz supercontinuum generation in ultrafast laser-gas interactions. 2008. *Nature Photonics.* **2** (10): 605.

2. Rodriguez, G., and G. L. Dakovski. Scaling behavior of ultrafast two-color terahertz generation in plasma gas targets: energy and pressure dependence. 2010. *Optics Express.* **18** (14): 15130.

3. Krasheninnikova, N. S., G. Rodriguez, and M. J. Schmitt. Simulation of Terahertz signal generation using PULSE. *Physics of Plasmas.*

4. Bock, J., Y. Fukuyo, S. Kang, M. Lisa. Phipps, L. Alexandrov, K. Rasmussen, A. Bishop, E. Rosen, J. Martinez, H. Chen, G. Rodriguez, B. Alexandrov, and A. Usheva. Mammalian Stem Cells Reprogramming in Response to Terahertz Radiation. 2010. *PLOS ONE.* **5** (12): e15806.

5. Alexandrov, B. S., K. O. Rasmussen, A. R. Bishop, A. Usheva, L. B. Alexandrov, S. Chong, Y. Dagon, L. G. Booshehri, C. H. Mielke, M. Lisa Phipps, J. S. Martinez, H. T. Chen, and G. Rodriguez. Non-thermal effects of terahertz radiation on gene expression in mouse stem cells. 2011. Biomedical Optics Express. **2** (9): 2679.

Publications

Alexandrov, B. S., K. O. Rasmussen, A. R. Bishop, A. Usheva, L. B. Alexandrov, S. Chong, Y. Dagon, L. G. Booshehri, C. H. Mielke, M. Lisa Phipps, J. S. Martinez, H. T. Chen, and G. Rodriguez. Non-thermal effects of terahertz radiation on gene expression in mouse stem cells. 2011. *Biomedical Optics Express.* **2** (9): 2679.

Alexandrov, B. S., K. O. Rasmussen, A. R. Bishop, L. B. Alexandrov, A. Usheva, E. D. Rosen, M. Lisa Phipps, J. S. Martinez, H. T. Chen, and G. Rodriguez. Gene specific response of mammalian stem cells to terahertz radiation. Presented at *Optical Terahertz Science and Technology 2011.* (Santa Barbara, CA, 13-17 Mar. 2011).

Bock, J., Y. Fukuyo, S. Kang, M. Lisa. Phipps, L. Alexandrov, K. Rasmussen, A. Bishop, E. Rosen, J. Martinez, H. Chen, G. Rodriguez, B. Alexandrov, and A. Usheva. Mammalian Stem Cells Reprogramming in Response to Terahertz Radiation. 2010. *PLOS ONE.* **5** (12): e15806.

Krasheninnikova, N. S., G. Rodriguez, and M. J. Schmitt. Simulation of Terahertz signal generation using PULSE. *Physics of Plasmas.*

Rodriguez, G.. Parametric studies of ultrafast two-color terahertz generation in gas plasma filaments. Invited presentation at *3rd International Symposium on Filamentation.* (Crete, Greece, 31 May - 5 Jun. 2010).

Rodriguez, G., N. Krasheninnikova, and M. J. Schmitt. Analytical and simulation study of laser-ionized plasma. Presented at *52nd Annual Meeting of the APS Division of Plasma Physics.* (Chicago, IL, USA, 8 2 Nov. 2010).

Rodriguez, G., and G. Dakovski. Scaling behavior of ultrafast two-color terahertz generation in plasma gas targets: energy and pressure dependence. 2010. *OPTICS EXPRESS.* **18** (14): 15130.

Rodriguez, G., and G. L. Dakovski. Parametric studies of two-color ultrafast terahertz generation in gas plasma filaments. Presented at *37th IEEE International Conference on Plasma Science.* (Norfolk, VA, USA, 20-24 Jun. 2010).

Hawking-Unruh Effect in Atomic Bose-Einstein Condensates

Emil Mottola
20100191ER

Introduction

The primary goal of this project is to test the hypothesis of a variant of the Hawking-Unruh effect, namely that an accelerated mirror will radiate with a thermal spectrum, predicted in relativistic field theories and black hole physics, in the concrete analog system of cold atomic Bose-Einstein condensates (BEC's). By carrying out detailed calculations for an accelerated "mirror" of sound waves in a BEC generated by a laser induced potential, we are studying the practical feasibility for detecting an analog of the Hawking-Unruh effect in a realistic laboratory experiment for the first time. The general scientific interest in black hole phenomena and Einstein's legacy guarantees that the results of our research will be a highly visible scientific accomplishment.

In this project, we focus on the most promising strategy for detection of the Hawking-Unruh radiation in a BEC. Our approach relies on the prediction of radiation produced by an accelerating laser "mirror" potential, i.e. the variant sometimes called the Davies-Fulling-Unruh effect. The key idea that distinguishes a BEC mirror environment from other analog Hawking proposals is that the acceleration of the laser mirror can be accurately controlled over a large dynamic range while this is not at all easy for the velocity gradient in a moving fluid. Since very large accelerations can be achieved with accurately controlled lasers focused on a BEC, it is possible to achieve temperatures as larger than the critical temperature of the BEC, and therefore detectable by current experiments. Thus, this extremely important prediction of fundamental physics may be measurable for the first time in the laboratory, and quite possibly in a cold atom BEC experiment at Los Alamos National Laboratory.

Benefit to National Security Missions

This is a basic research project, relevant to DOE OS programs in Particle Physics, Quantum Field Theory, Gravitation, Bose-Einstein Condensates, Many-Body and Statistical Physics. Verification of the Davies-Fulling-Hawking-Unruh effect in a BEC experiment would be a major achievement. If realized at Los Alamos, it would be a significant boost to the program in cold atoms at the Quantum Institute. The basic knowledge gained about BECs and detailed numerical codes could form the basis of a larger program in applications of cold atoms to fundamental gravitational physics. It will enhance the public image and scientific capabilities of the Laboratory by helping to attract future staff and help retain our excellent scientists and engineers, necessary for the laboratory's national security mission.

Progress

Over the last year we have made a great deal of progress in the practical testing of the Davies-Fulling-Hawking-Unruh effect in realistic laboratory Bose-Einstein condensates of cold gases.

The first problem we had to surmount is that an atomic BEC will respond to a laser disturbance in ways different from the quantum vacuum with an idealized perfectly reflecting potential "mirror," discussed in the literature. In particular, the BEC is a non-linear system and any laser disturbance will change the condensate number density itself, leading to unwanted time dependent effects from the point of view of the BEC as a model of the quantum vacuum. We have studied the response of the condensate to various stationary and moving external potentials, both analytically and numerically through the Gross-Pitaevskii eq. with the help of the code previously developed, and found a parameter regime of potential strength, V_{ext}, spatial width, σ, and time duration in which the disturbance of the background condensate density can be kept manageably small (of the order of 5% of the initial condensate). This is the appropriate range of parameters for experiment to explore which are relevant to the Davies-Fulling effect in BEC's. The potential, $V_{ext}[x(t)]$, moves along the orbit

$$\frac{\kappa}{c_s} x(t) = \kappa t + \frac{1}{2}\left(e^{-2\kappa t} - 1\right),$$

characterized by the unique parameter κ, **the rate of exponential approach to the speed of sound, c_s** . Since such an orbit can only be followed for a finite time in a real experiment, t must be finite, or equivalently, this orbit is

followed until a maximum speed, $v_{max} < c_s$, is attained. We have shown from the Gross-Pitaeveski Eq. that when V_{ext} varies slowly on the scale of the BEC coherence length the scaled deviation of the condensate density, $\delta n/n$, satisfies a linear wave equation for $\delta n/n \ll 1$, corresponding to the wave equation for a massless relativistic field in which the speed of light is replaced by the speed of sound c_s. The BEC chemical potential, μ, enters naturally is estimates of $\delta n/n$. Numerical solution of the equations in the thin width limit, $\kappa\sigma/c_s \ll 1$, for which analytical results are available[1] constrains V_{ext} in order to remain in the small deviation regime $\delta n/n \ll 1$.

Figure 1 shows our numerical results for the density deviation, scaled by the external potential in chemical potential units $(\delta n/n)/(V_{ext}/\mu)$ versus the scaled width, $\kappa\sigma/c_s$. Figure 2 shows the condensate density deviation in the neighborhood of the potential at the time of maximum velocity (where the deviation is largest). Since the laser "painting mirror" potential's amplitude can be less than μ, the small deviation regime is experimentally accessible and the unwanted time dependent effects of the condensate perturbations δn can be kept controllably small. This is vital if the quantum fluctuations about the condensate are to approximately satisfy the linear wave equation, as assumed in the Davies-Fulling effect.
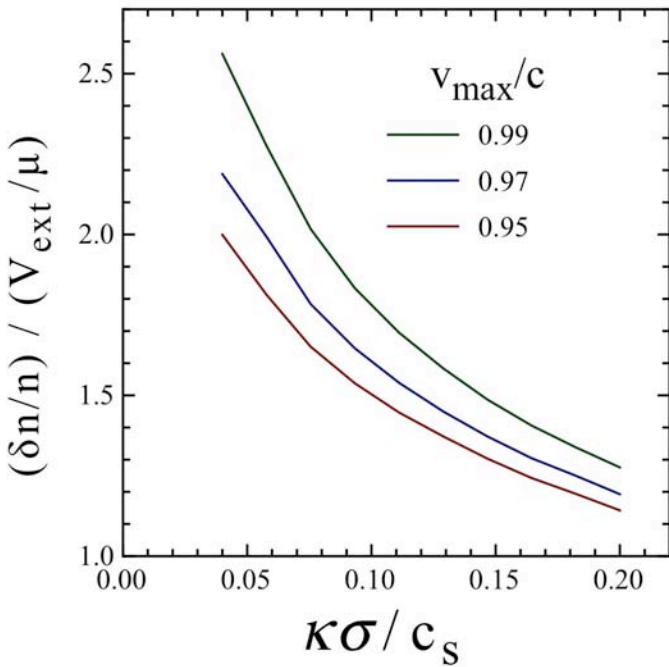
Figure 1. Shows our numerical results for the density deviation, scaled by the external potential in chemical potential units $(\delta n/n)/(V_{ext}/\mu)$ versus the scaled width $\kappa\sigma/c_s$.
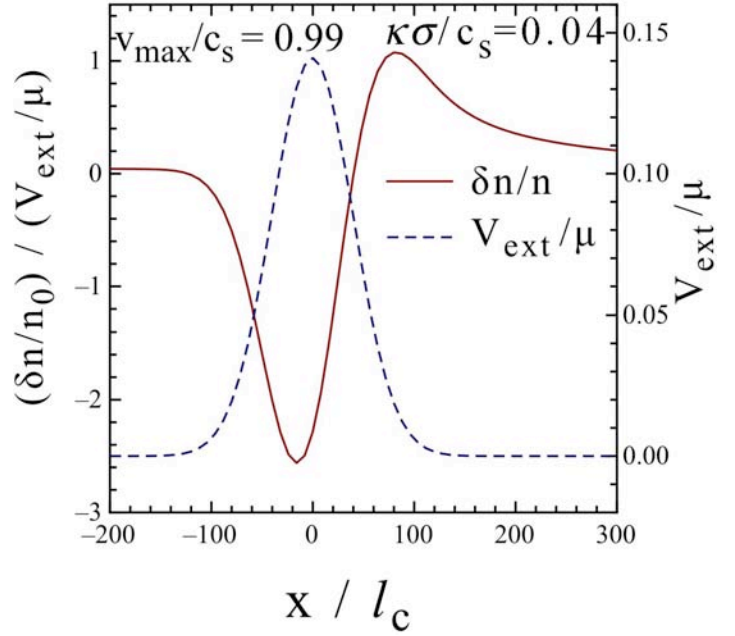
Next we have studied the case of finite mirror reflectivity, and determined that a laser can simulate the mirror within a BEC, provided its width and intensity are within certain quantitative limits, which are experimentally realizable. A code has been written to evaluate the energy flux per unit time and total energy deposited in the BEC by arbitrary accelerated motion of the laser "mirror" through it. We are currently comparing the output of this code with the analytic estimates [1] in various parameter regimes in order to evaluate the parameter dependences, which will make it easiest to identify the appearance and characteristics of the Davies-Fulling acoustical quanta in the BEC.

A new code for evaluation of the Green's function/condensate dynamics has been developed which preserves the fundamental invariants under arbitrary truncation of the modal expansion. In the framework of laser potentials of finite amplitude, width and temporal duration, this new code does rely on previous idealizations or calculations in certain limits, and is necessary for detailed comparison with experimental results. The code is currently being cross checked with previous results in their common domain of applicability, and is now being used to determine the sensitivity of the results to the precise boundary conditions and high frequency cut-off in the mirror's reflectivity.

Future Work

A paper with our detailed study of the Fulling-Davies effect in realistic BEC's is in preparation. We are consulting with M. Boshier about the optimal parameter ranges, with which we will present detailed results for the energy flux and total energy deposited. We expect to make precise quantitative predictions for existing experimental BEC setups at LANL and elsewhere.

We will study the drag and production of vortices at the

mirror edges and the contributions of the normal fluid component in the BEC, by including the nonlinear back-reaction effects of the phonon modes on the condensate, and investigate the effects of vorticity on the signal.

We continue our study of new theoretical approaches to many-body nonequilibrium dynamics in the BEC, which we have recently developed, and compare to BEC experiments.

Conclusion

We are investigating the Hawking-Unruh prediction under a wide variety of external conditions. This will lay the groundwork for the first possible experimental confirmation of the effect. Verification of the Davies-Fulling-Hawking-Unruh effect in a BEC experiment would be a major achievement. If realized at Los Alamos, it would be a significant boost to the program in cold atoms at the LANL Quantum Institute. In addition to enhancing the prestige of existing LANL program in this area, the basic knowledge gained about BECs could form the basis of a larger program in applications of cold atoms to fundamental gravitational physics.

References

1. Nicolaevici, N.. Quantum radiation from a partially reflecting moving mirror. 2001. *Classical and Quantum Gravity.* **18** (4): 619.

Publications

Mottola, E., and Z. Szep. Systematics of High Temperature Perturbation Theory: The Two-Loop Electron Self-Energy in QED. 2010. *Physical Review.* **D81**: 025014.

Cold Atoms in Quantum Periodic Potentials

Bogdan F. Damski
20100296ER

Introduction

This work is focused on studies of new solid state systems from the most basic, i.e., quantum level. This will advance our understanding of many-body quantum physics that provides a key insight into superconductors, superfluids, nano-scale devices, etc. Practical applications of the new systems and materials that we study include quantum processing and computing, advanced emulation of challenging condensed matter systems like superconductors, and sensing.

We will capitalize here on a revolutionary progress taking place in atomic and molecular physics. This progress is driven by efforts to study the most challenging quantum systems in easily controllable setups. It allows us to consider physical systems whose experimental studies were impossible a few years ago.

We will focus theoretically on many-body quantum systems exposed to quantum external fields.These fields can be in a superposition of various strengths and structures. They can be observed in cold ion, atom, electron and spin systems. In the cold ion systems, the quantized fields are emulated by laser-driven interactions between ions; in the cold atom systems, they come from quantized photon fields trapped between high-quality mirrors, etc.

As a result of interactions with quantum external fields, the systems that we consider have unique properties because atoms, ions, electrons and spins can exist in a simultaneous superposition of distinct quantum states (phases). We will develop a new theory of quantum phase transitions to account for this. We will investigate stability of these new phases and experimental prospects for their realization. We will advance current analytical techniques used for studies of quantum many-body systems (typically magnetic materials) and develop numerical approaches that can handle these problems efficiently.

Benefit to National Security Missions

This work will uncover properties of new physical systems whose potential applications may include quantum processing and computing, advanced emulation of chal-

lenging condensed matter systems like superconductors, and sensing. All of them are of interest to various federal agencies. On the technical level, this work contributes to the fundamental understanding of new materials through first principles quantum studies (bottom-up approach). This topic is also attracting attention of numerous sponsors including DOE.

Progress

We have focused on three goals over the last fiscal year.

First, we have studied quantum fidelity, which is defined as an overlap between two quantum ground states. Its understanding is crucial for characterization of all the properties of quantum systems being in a superposition of quantum phases, which is the goal of our ER. We have managed to formulate a scaling theory of quantum fidelity of thermodynamically large systems. Our results have been summarized in two papers. The first one has been published in Physical Review Letters [1], while the second one appeared in Physical Review A [2]. Both manuscripts contain significant new results that have already been appreciated in the community.

While the first paper formulates a general theory of quantum fidelity, the second manuscript is a very extensive contribution carefully verifying our theory in some spin chains as well as exploring the regimes of its applicability. We have found and explained different deviations from our "general result", which paves the way for reliable application of our theory to other systems (e.g., cold atoms placed in periodic potentials).

Second, we have been studying magnetization and correlation functions of the quantum Ising spin chain being prepared in the superposition of the paramagnetic and ferromagnetic phases. We have found novel effects resulting from the quantum nature of the effective magnetic field acting on the Ising spin chain (Figure 1). All our results here are given by the product of quantum fidelity (capturing leading-order finite size effects) and the prefactor whose properties weakly depend on the system size. We have focused on the latter, as the former was characterized in [1,2].
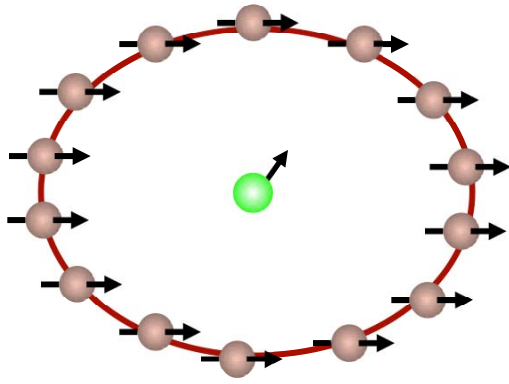
Figure 1. Illustration of the model system for studies of the influence of the quantized external field on a many-body system. Here, the Ising chain of spins, which can be either in the paramagnetic or the ferromagnetic phase, is interacting with the central spin. The coupling between the two systems can be shown to act like an effective quantized (magnetic) field due to (i) the preparation of the central spin in the quantum superposition of distinct spin states; (ii) proper engineering of the central spin-Ising chain coupling.

In particular, we have found that the quantized magnetic field acting on the Ising spin chain leads to (i) macroscopic modification of the system magnetization, an effect which is experimentally relevant; (ii) imprinting of the critical exponent and the location of the critical point of the Ising spin chain onto magnetization in the superposition state. We are currently preparing a manuscript summarizing this research.

Third, looking for experimentally-relevant applications of the concept of a quantum system exposed to the quantized external field, we have turned our attention to studies of the influence of the quantized (electric) Coulomb field of a proton on dynamics of an electron orbiting around it. We have formulated, for the first time, the Hamiltonian description of such a system allowing for , among other things, calculation of the influence of the quantum Coulomb field on energy levels of hydrogen-like atoms. This work, summarized in [3] and submitted to New Journal of Physics, has been completed in collaboration with Dr. Piotr Marecki from University of Duisburg-Essen, Germany. In particular, in this paper we have assigned for the first time energy to excitations of the Coulomb field of a charged particle like an electron or a proton. We have also proposed a quantum state of the Coulomb field of a stable charged particle such as an electron.

Next, we have developed a perturbative formalism for the calculation of the shift of energy levels of hydrogen-like atoms and started its analytical and numerical studies. This is ongoing research. We stress that the level shift that we are studying is directly measurable in precision spectroscopy experiments targeting hydrogen-like atoms (hydro-gen, muonic hydrogen, muonium, etc.).

Future Work

We will continue studies of quantum systems interacting with quantized external fields. These fields will result from either interactions with quantized (electromagnetic) photon fields or from interactions between two quantum systems (one of them emulating the source of the quantized field).

We will work out the mathematical description of these systems by proposing and solving experimentally-relevant models. We will develop a theory of quantum phase transitions that describes novel aspects of these systems such as simultaneous superpositions of distinct quantum phases. We will research experimental prospects for their observation and study equilibrium properties of these systems. As an immediate, experimentally-accessible, application of the ideas developed during this project, we will also study bound systems of charged particles in the quantized Coulomb field. Such a field exists in all atoms and we expect it to affect energy levels of hydrogen-like atoms most.

We will use various theoretical approaches to study the problem. For example, we will apply Bogolubov, variational and perturbative approaches to approximate the system's wave-function, as well as field theoretical techniques in the context of the quantized Coulomb field. We will compare our approximate analytical results to exact numerical simulations to quantify their accuracy.

Conclusion

We will study properties of new systems composed of matter coupled to quantum fields. Our work will characterize the unique properties of these novel systems, guiding future experimental work in this field. It shall advance understanding of many-body quantum physics (a key theory describing nano-scale systems) and contribute to development of high-impact practical devices for quantum processing and computing, advanced emulation of challenging condensed matter systems such as superconductors, and sensing.

References

1. Rams, M. M., and B. Damski. Quantum fidelity in the thermodynamic limit. 2011. *Physical Review Letters.* **106**: 055701.

2. Rams, M. M., and B. Damski. Scaling of ground-state fidelity in the thermodynamic limit: XY model and beyond. 2011. *Physical Review A.* **84**: 032324.

3. Damski, B., and P. Marecki. On the quantum Coulomb field. *New Journal of Physics (LA-UR 11-04745).*

Publications

Damski, B., and P. Marecki. On the quantum Coulomb field.

New Journal of Physics (LA-UR 11-04745).

Dziarmaga, J., and M. M. Rams. Adiabatic dynamics of an inhomogeneous quantum phase transition: the case of $z > 1$ dynamical exponent. 2010. *New Journal of Physics.* **12**: 103002.

Niederberger, A., M. M. Rams, J. Dziarmaga, F. M. Cucchietti, J. Wehr, and M. Lewenstein. Disorder-Induced Order in Quantum XY Chains. 2010. *Physical Review A.* **82**: 013630.

Rams, M. M., and B. Damski. Quantum fidelity in the thermodynamic limit. 2011. *Physical Review Letters.* **106**: 055701.

Rams, M. M., and B. Damski. Scaling of ground-state fidelity in the thermodynamic limit: XY model and beyond. 2011. *Physical Review A.* **84**: 032324.

BEC Waveguide Optics

Eddy M. Timmermans
20100302ER

Introduction

The cold atom Bose-Einstein condensates (BEC's), gas systems of atoms that have been laser-cooled to the lowest temperatures ever reached in a laboratory, simultaneously exhibit the characteristics of atom lasers and of superfluids.   As atom lasers, all atoms can be made to move in perfect lockstep coherence and the BEC acts as a single, giant quantum wave. The density of such systems can exhibit large contrast fringes (wiggles) when two waves intersect. This ability promises unprecedented atom optics applications for sensing rotations (gyroscopes), for sensing weak forces (metrology) and for imaging. As a superfluid system, an object can be dragged through the gas without causing drag or dissipation (heating). Another counter-intuitive property of superfluidity is exhibited by the Josephson junction that connects weakly connected superfluids: the sudden alteration of the relative energy of the fluids causes a back-and-forth current to set in instead of the classically expected flow from the most energetic region into the region of lower energy. Quantum mechanically, the weak connection and quantum nature can also greatly increase the uncertainty of the number of particles that find themselves on either side, which greatly increases the contrast of the interference fringes and, hence, the accuracy of optical sensing devices. In this project, we explore by means of theory and simulation the intriguing potential of BEC-physics for realizing novel atom optical applications by guiding the BEC-waves along well-defined directions. We also explore the prospect of exploiting many-body quantum physics and the unusual control knobs of cold atom technology to manipulate superfluid properties of the BEC to realize optical devices that reach the quantum limit of resolution.

Benefit to National Security Missions

The development of a practical, coherent atom optics is part of the quantum efforts, which fit in the charter of the information science grand challenge. The scientific goals satisfy calls in the broad agency announcements of DOE-BES, ASFR and ONR. The promise of metrology applications of unparalleled sensitivity may also find long-term applications in the threat-reduction part of the laboratory.

Progress

We have focused on the gauge tool in cold atom physics, the physics and possible uses of Bose-EInstein condensate (BEC)-impurity self-localization and composite particles in cold atom lattices, and of (possibly) confinement induced strong coupling physics in trapped and engineered cold atom systems.

Together with a summer student, Rudra Kafle, we have shown that the recently cold atom realized synthetic gauge can increase the rotation measurement sensitivity of a toroidal (ring) BEC gyroscope. The toroidal BEC is an analogue of the Superconducting Quantum Interference device (SQUID) and can measure a rotation or effective magnetic field by changing the winding number - the number of times the complex phase of the superfluid rotates by a full 2pi angle as the position is varied along the multiply connected geometry to return to the initial position. The winding number can be measured in a time of flight measurement by switching off the trap and imaging the falling atoms. What has not been fully appreciated is that the effective magnetic field itself can undergo its own quantization events (changing its own winding number) and that the system can take on vortex states in which the gauge and superfluid phases both have non-vanishing winding numbers.

In a collaboration with Fred Cooper, we have developed a new, non-perturbative description of boson gas systems that can describe strongly interacting and finite temperature boson gas systems without the usual problems associated with conserving and gapless approximations [1]. The formalism derived from the auxiliary field method of field theory yields a description that simultaneously satisfies the fundamental symmetries and yields collective modes with dispersions that vanish in the long wavelength limit even at finite temperature. Unlike previous descriptions, this formalism correctly predicts the Bose-Einstein condensation of interacting particles to be a second order transition and it correctly predicts the variation of the critical temperature with interaction at the lowest order (mean-field like level) of the calculation [2]. Intriguingly, the description does imply a temperature regime in which the boson system

does not have a condensate, but is superfluid, nonetheless [3]. This finding, which may be connected with the pseudo gap physics in fermion superfluids [4], merits follow-up as the BEC's may be realized in the strongly coupled regime in atomic traps that freeze out one direction by squeezing the atoms with strongly confining trapping frequency and possibly accessing the confinement induced resonances of the inter-particle interactions.

In a collaboration with a former Director's funded postdoc, Deborah Santamore, we have developed an effective spin-spin interaction description of the interaction of cold atoms trapped in two distinct hyperfine states [5]. We used this formalism to describe the zero-temperature phase separation transition of Bose-Einstein condensates [6]. We showed that the compressibility diverges at the transition, giving critical opalescence behavior. We determined the experimental conditions for observing this transition in a bulk-like environment. We found that for Rubidium-87, spin fluctuations exhibit the long-range fluctuations that characterize a critical point (here a critical line) whereas the density fluctuations are suppressed near the transition.

In another collaboration with Deborah, we have shown that the polaron-like strongly-coupled BEC-impurity self-localization can be generalized to N bosonic impurities [7]. The polaron self-localization sets in at a lower value of the impurity boson interaction and the impurity-extent can be substantially smaller than the coherence length of the surrounding BEC. We have shown that the N-impurity polarons are the nucleation droplets of the zero-temperature BEC phase separation transition, slightly away from the critical point so that the system can exhibit first order transition characteristics.

In a collaboration with Cristian Batista, we have shown that impurity-based self-localized polaron-like composite particles can also exist in bosonic lattice systems in the Mott-insulator phase. This finding may open up a new avenue for cold atom exploration of the composite particle scheme towards exotic superconductivity [8]. One set of theories describing the exotic and high temperature superconductors start from the assumption that the electron or hole that dopes the insulator/antiferromagnetic substrate forms a composite particle near the localization-delocalization transition and that these objects can then pair to give rise to the observed superconducting state. These theories are difficult to verify as calculations are extremely difficult in this regime and measurements are hard in the inaccessible experimental systems. While the bosonic cold atoms in an optical lattice or different from the heavy fermion systems, they do lend themselves to verifying a general theme that is important to exotic and high temperature superconductivity.

Future Work
The development of novel techniques to create and alter the external potential that traps and guides cold atom gas systems is opening up the prospect of realizing some of the long-promised advantages of atom optics and atom many-body physics. We will propose and explore cold atom realizations of quantum tunneling of composite particles – here Feshbach molecules – in optical lattices. We will study the interesting prospect of realizing an effective gauge potential. We will explore the use of narrow Feshbach resonances to realize effective interactions that have an effective range that is finite (i.e. comparable to or exceeding the average inter-particle distance), as opposed to the usual contact interaction limit of neutral cold atoms. We will further explore the mean-field description of phase separation dynamics in spin ½ Bose-Einstein condensate and we will show that the combination of magnetic fields and two-photon (Raman) transitions can demonstrate and test macroscopic quantum tunneling in an environment of unprecedented control.

Conclusion
Since its realization the BEC technology has been widely successful at demonstrating superfluid properties, but the development of a practical BEC-based atom optics has slowed to a trickle. We will show that guiding the BEC-wave along atom wave guides can overcome major hurdles and that manipulating the superfluid properties of the BEC can increase the accuracy of BEC-based sensors to reach the quantum limit. This project will guide the development of a waveguide BEC-optics, creating a mathematical description of the wave-dynamics and exploring the prospect for increasing the sensing accuracy even further by manipulating the superfluid properties.

References

1. Cooper, F., C. Chien, B. Mihaila, J. F. Dawson, and E. Timmermans. Nonperturbative Predictions for Cold Atom Bose Gases with Tunable Interactions. 2010. *Physical Review Letters.* **105**: 240402.

2. Mihaila, B., F. Cooper, J. F. Dawson, C. Chien, and E. Timmermans. Analytical Limits for Cold Atom Bose Gases with Tunable Interactions. 2010. *Physical Review A.* **84**: 023603.

3. Cooper, F., B. Mihaila, J. F. Dawson, C. Chien, and E. Timmermans. Auxiliary-field Approach to Dilute Bose Gases with Tunable Interactions. 2011. *Physical Review A.* **83**: 053622.

4. Mihaila, B., J. F. Dawson, F. Cooper, C. Chien, and E. Timmermans. Auxilliary Field Formalism for Dilute Fermionic Atom Gases with Tunable Interactions. 2011. *Physical Review A.* **83**: 05637.

5. Santamore, D. H., and E. Timmermans. Pseudospin and spin-spin interactions in ultracold alkali atoms. 2011. *New J. Phys..* **13**: 023043.

6.   Santamore, D. H., and E. Timmermans. Spin critical Opalescence in Zero-temperature Bose-Einstein Condensates. *European Physics Letters.*

7.   Santamore, D. H., and E. Timmermans. Multi-impurity Polarons in a dilute Bose-Einstein Condensate. To appear in *New Journal of Physics.*

8.   Kato, Y., K. A. Al-Hassanieh, A. E. Feiguin, E. Timmermans, and C. D. Batista. Novel Polaron State for Single Impurity in a Bosonic Mott Insulator. *Physical Review Letters.*

Publications

Cooper, F., B. Mihaila, J. F. Dawson, C. Chien, and E. Timmermans. Auxiliary-field Approach to Dilute Bose Gases with Tunable Interactions. 2011. *Physical Review A.* **83**: 053622.

Cooper, F., C. Chien, B. Mihaila, J. F. Dawson, and E. Timmermans. Nonperturbative Predictions for Cold Atom Bose Gases with Tunable Interactions. 2010. *Physical Review Letters.* **84105**: 240402.

Kato, Y., K. A. Al-Hassanieh, A. E. Feiguin, E. Timmermans, and C. D. Batista. Novel Polaron State for Single Impurity in a Bosonic Mott Insulator. *Physical Review Letters.*

Mihaila, B., F. Cooper, J. F. Dawson, C. Chien, and E. Timmermans. Analytical Limits for Cold Atom Bose Gases with Tunable Interactions. 2010. *Physical Review A.* **84**: 023603.

Mihaila, B., J. F. Dawson, F. Cooper, C. Chien, and E. Timmermans. Auxilliary Field Formalism for Dilute Fermionic Atom Gases with Tunable Interactions. 2011. *Physical Review A.* **83**: 05637.

Santamore, D. H., and E. Timmermans. Pseudospin and Spin-spin Interactions in ultracold Alkali Atoms. 2011. *New Journal of Physics.* **13**: 023043.

Santamore, D. H., and E. Timmermans. Spin critical Opalescence in Zero-temperature Bose-Einstein Condensates. *European Physics Letters.*

Santamore, D. H., and E. Timmermans. Multi-impurity Polarons in a dilute Bose-Einstein Condensate. To appear in *New Journal of Physics.*

Solenov, D., and D. Mozyrsky. Metastable states and macroscopic quantum tunneling in a cold atom Josephson ring. 2010. *Physical Review Letters.* **104**: 150405.

Digital Trigger for the High Altitude Water Cherenkov (HAWC) Observatory

Brenda L. Dingus
20100310ER

Introduction

This project will enable the highest energy observations of photons from distant astrophysical sources. These observations probe the fundamental physics of extreme gravitational and electromagnetic fields near black holes. The technique uses the novel detection of showers of particles in the atmosphere interacting with a large water detector located at 13,500' altitude in Mexico. A first generation version of this detector, called Milagro, was built at LANL. This project will result in a digital trigger for this High Altitude Water Cherenkov (HAWC) TeV gamma-ray observatory. The objective of this new trigger is threefold. 1) The new trigger will allow more information to be recorded about each gamma ray and therefore reduce the systematic uncertainties in flux measurements. 2) The new trigger will result in a lower energy threshold for the detector, by excluding non gamma-ray events through pattern recognition algorithms. 3) New triggers for exotic physics, such as magnetic monopoles or SUSY Q balls, will be possible with this more complex trigger. Therefore, this effort will enhance the success of the HAWC observatory and will maintain LANL's leadership in this forefront scientific field of high energy astrophysics.

Benefit to National Security Missions

High energy emission from astrophysical sources has been ranked by National Academy studies as forefront fundamental research. DoE Office of Science, NSF, and NASA support this research. In addition, this research will increase LANL's capabilities in forefront technologies of particle detection, computation, remote sensing, and digital electronics.

Progress

We have accomplished the following tasks:

1. Established that we can record 128 photomultiplier tube signals at a rate of ~38MB/sec. This rate was determined using a optical bridge reading a Time to Digital Converter (TDC). We have verified the proper recording of sub-nanosecond timing and investigated the signature of data loss that occur at higher rates. We have also identified methods that we will further investigate that can likely increase the rate to >60 MB/sec.

2. Developed a data acquisition system using this TDC to test at LANL up to 10 PMTs in a dark box with a fast laser pulse that is attenuated by optical filters of varying opacity. This test system has been used to calibrate over 200 PMTs over more than 5 orders of magnitude in light intensity. The analysis of this data has revealed important information about the PMTs and about the capabilities of the data acquisition system.

3. Determined the rate of single photoelectrons as recorded by our PMTs in a prototype detector that we helped install at Colorado State University, which is of the same size and geometry as the detectors that will be used in HAWC. The rate is ~20 KHz which would result in a data rate of 0.2 MB/sec/PMT which is therefore likely to be compatible with the findings of item 1.

4. Designed and installed a data acquisition system for the VAMOS (Verification And Measuring Observatory Subsystems) array of 7 water tanks which is located at the HAWC site. LANL helped with the construction of VAMOS as well, and we have now taken several weeks of data with VAMOS. The data acquisition system records hits for 36 PMTs at a total rate of 11 MB/sec.

5. Mined the VAMOS data set to understand the limitations and capabilities of the data acquisition system. For example, we have determined that nearly half of the signals recorded are due to afterpulsing of the PMTs. The number of afterpulses is correlated with the intensity of the first pulse and can be simply rejected in software by ignoring pulses for ~10 microseconds after a bright pulse.

6. Developed the capability to implement and test software triggers in simulated HAWC data. The simulations include air showers as well as random noise.

We have created a 1 sec sample that we have used to confirm trigger rates for different algorithms.

7. Implemented software trigger algorithms to show an increased efficiency for detecting lower energy gamma rays while not increasing the overall rate of events from the cosmic-ray background. For example, with the software trigger, the size of the PMT signals, and not just their times, can be used to identify events. This reduces the effect of the random noise, which tends to be smaller signals.

8. Submitted paper to refereed journal on HAWC sensitivity to gamma-ray bursts. The sensitivity depends greatly on the trigger condition. The paper includes the baseline trigger, which was in the original HAWC proposal to NSF and DOE, as well as a higher rate trigger that has been made possible by the data acquisition system developed with this LDRD.

9. Studied the sensitivity of HAWC when using the software trigger to detecting distant active galactic nuclei. Several of the known sources will be detectable in their quiescent state with flares detectable over very short time intervals.

10. Procured additional TDCs and bridges in order to do further testing of the timing synchronization between TDCs. HAWC will have 900 PMTs and the time difference between any 2 PMTs must be determined with sub-nanosecond accuracy.

Results of these tasks were presented by LANL scientists at the American Physical Society meeting in April 2011, the Origins of Ultra High Energy Cosmic Ray Workshop in Beijing in April 2011, the Guillermo Haro Workshop in Puebla Mexico in July 2011, the International Cosmic Ray Conference in Beijing in August 2011, and the TeV Particle Astrophysics meeting in Stockholm in August 2011.

Future Work

We will develop and install the data acquisition system and software trigger for the HAWC observatory. Milagro used a simple multiplicity trigger requiring a given number of photomultiplier tubes(PMTs)receive a signal within a 170 nanosecond time window. With HAWC, we have developed a data acquisition system, which can record all PMT signals at all times, so we can use software algorithms to define the trigger.   During the final year of this project, we will accomplish the following tasks.

1. Install the data acquisition system for HAWC. The first water tanks for HAWC will be installed in January and the counting house with electricity will be available at that time. Tanks will be constructed at the rate of 2/week until all 300 are constructed. The data acquisition system will be expanded as the number of PMTs installed increases. By the end of this project, we will have a tested and expandable system operating in HAWC.

2. Study VAMOS data to confirm the operation of the data acquisition system and to better simulate the PMT singles rates due to air showers, afterpulsing, random hits, single muons, and various electronics effects.

3. Develop trigger algorithms, which are efficient for finding air showers, but reject background. The data rate recorded from the full HAWC detector is anticipated to be ~500MB/sec, but the data rate of showers that we can save is only 20 MB/sec. These trigger algorithms are required to make this reduction in rate.

4. Use these algorithms on the VAMOS data to look for scientific results such as gamma-ray bursts.
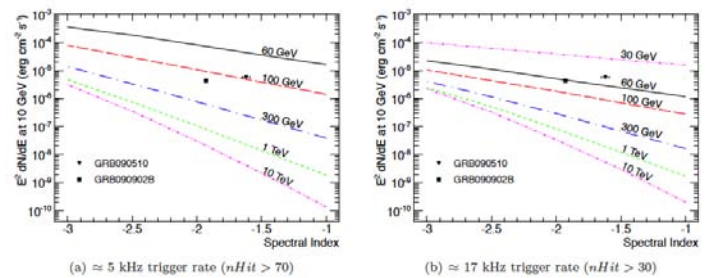
Figure 1. Sensitivity of HAWC to a gamma-ray burst as a function of the flux (y-axis) and the differential photon spectral index (x-axis) assuming the spectrum is sharply cut off at various energies as shown by different lines. (a) The trigger rate is 5 KHz which was the baseline before this LDRD project. (b) The trigger rate is 17 KHz which has now been demonstrated to be possible by this LDRD project.

Conclusion

Nature accelerates particles to energies over a million times higher than man made accelerators. This project will result in discovery of astrophysical accelerators and measure the high energy gamma-ray emission from these objects. The gamma rays are one of the most direct probes of the fundamental physics of extreme gravitational and electromagnetic fields and will increase our understanding of black holes and other astrophysical accelerators.

Publications

Abdo, A. A., et al., 2009. *NATURE.* **462** (7271): 331.

Abdo, A. A., et.al., 2009. *ASTROPHYSICAL JOURNAL LETTERS.* **706** (1): L138.

Abdo, A. A., et. al, 2009. *SCIENCE.* **323** (5922): 1688.

Abeysekara, A. U.. On the sensitivity of the HAWC observatory to gamma-ray bursts. *Astroparticle Physics.*

Ackermann, M., et.al., FERMI OBSERVATIONS OF GRB 090510: A SHORT-HARD GAMMA-RAY BURST WITH AN ADDITIONAL, HARD POWER-LAW COMPONENT FROM 10 keV TO GeV ENERGIES. 2010. *ASTROPHYSICAL JOURNAL.* **716** (2): 1178.

Gonzalez, M. M., M. Carrillo-Barragan, B. L. Dingus, Y. Kaneko, R. D. Preece, and M. S. Briggs. BROADBAND, TIME-DEPENDENT, SPECTROSCOPY OF THE BRIGHTEST BURSTS OBSERVED BY BATSE LAD AND EGRET TASC. 2009. *ASTRO-PHYSICAL JOURNAL.* **696** (2): 2155.

Pasquale, M. De, et.al., SWIFT AND FERMI OBSERVATIONS OF THE EARLY AFTERGLOW OF THE SHORT GAMMA-RAY BURST 090510. 2010. *ASTROPHYSICAL JOURNAL LETTERS.* **709** (2): L146.

Probing the Origin of Matter in the Universe

Vincenzo Cirigliano
20100394ER

Introduction

To a very good approximation, the laws of physics do not distinguish between matter and antimatter. Yet, the observed Universe is made up of matter and not antimatter. In order to produce the current asymmetry, in the primordial hot plasma one microsecond after the big bang there must have been a tiny imbalance of one part in a billion between matter and antimatter. As the Universe evolved and cooled down, most of the antimatter annihilated with matter, leaving the very small initial excess of matter to make up the observed stars and galaxies. Understanding how the observed imbalance has developed during cosmic evolution is one of the great open questions at the interface of cosmology, particle physics and nuclear physics.

A number of explicit mechanisms have been proposed to explain the origin of the matter-antimatter asymmetry. This project aims to address in a quantitative way theoretical predictions within the so-called weak scale baryogenesis scenario, in which the asymmetry develops at relatively late times in the cosmic evolution. Relatively late time means that the primordial plasma had temperatures comparable to the energy scale that can be reached in current laboratory experiments. Hence, the appeal of this scenario is that it can be tested through terrestrial experiments, that can either produce the particles responsible for the baryogenesis mechanism or feel their virtual quantum mechanical excitations.

Benefit to National Security Missions

Elucidating the origin of the matter-antimatter asymmetry is one of the priorities of the DOE Office of Science (for both Nuclear Physics and High Energy Physics). This is one of the questions at the heart of our basic understanding of matter and the universe around us and the laws that govern the universe. Our work addresses this priority and develops theoretical tools that can be potentially applied in other areas of interest to the Nuclear Physics Office of Science, such as nuclear and particle astrophysics.

Progress

Electroweak baryogenesis (EWBG) is an appealing mechanism to generate the matter-antimatter asymmetry in the early universe, at temperatures of the order of 100 GeV, corresponding to energy scales that can nowadays be probed in terrestrial experiments. EWBG has been shown not to work within the Standard Model (SM) of particle physics. EWBG in extensions of the Standard Model will betested quantitatively with upcoming nuclear and particle physics experiments, but only to the extent that theoretical computations are robust. Currently there exist orders-of-magnitude discrepancies between treatments of charge transport dynamics during EWBG performed by different groups, each relying on different sets of approximations.

In this past year, we have introduced a consistent power counting scheme (in ratios of length scales) for treating systematically the key ingredients of weak scale baryogenesis: CP-asymmetric flavor oscillations, collisions, and diffusion. Within the context of a simplified model of EWBG, we have derived the relevant transport equations using non-equilibrium field theory. Using numerical methods, we have solved the transport equations exactly without ansatz for the functional form of the density matrices (as far as we know this is the first full solution of quantum kinetic equations in a spatially non-homogeneous system). We have demonstrated the existence of a resonant enhancement in charge production when the flavor oscillation length is comparable to the wall thickness. The resonance is determined by the relative value of the diagonal mass parameters of the mixing particles in the underlying theory. We have determined how the width of the resonance depends on the parameters of the underlying SM extension, and have shown that the resonant enhancement is relevant in significant regions of the supersymmetric parameter space. This proves the relevance of our work for phenomenological studies.

Quite importantly for the advancement of the field, we have compared our results with the existing "state-of-the-art" treatment of EWBG by Konstandin, Prokopec, Schmidt, and Seco (KPSS) who previously identified the importance of flavor oscillations in EWBG. We conclude:

(i) the power counting of KPSS breaks down in the resonant regime, and (ii) this leads to substantial underestimation of the charge generated in the unbroken phase, and therefore of the final matter-antimatter asymmetry.

In a parallel effort within this project, Emil Mottola, in collaboration with B. Neufeld (T-2 Nucl. Phys. post-doc) is studying the next-to-leading order (NLO) corrections to the Hard Thermal Loop (HTL) electron self-energy in high temperature QED (quantum electro dynamics). Using the background field method, an effective action generating functional encapsulating the necessary higher order resummations (ladder sums in the vertex part beyond HTL's) has just been found, which we will test in finite temperature QED by checking against the detailed finite temperature fermion self-energy calculations, continued to real time.

Future Work
In the area of quantum transport equations including flavor degrees of freedom, work is in progress along two main directions:

- to extend the techniques developed so far to more realistic models of baryogenesis, involving mixing fermions (particles of spin 1/2);

- to find a set of diffusion equations (much simpler to solve than the full quantum transport equations) that captures the physics of CP violating flavor oscillations.

Both the above steps will be needed in order to predict the matter-antimatter asymmetry in realistic extensions of the SM.

In the area of quantum effective action and phase transition dynamics, we plan to extend the resummed effective action method to QCD, where we can compare it to other resummations of soft and collinear processes that have proposed in non-abelian gauge theories in certain special cases. Once in possession of the background field effective action, which generates and resums the most infrared and collinear divergent processes in the finite temperature fermion self-energy in QED, the same effective action in its Schwinger-Keldysh Closed Time Path form may be used in real time processes. The real time formulation of this effective action provides a variational principle for the non-equilibrium evolution of the mean fields in which gauge invariance is explicitly maintained. This will enable novel self-consistent studies of the dynamics of the electroweak phase transition, a crucial ingredient in electroweak baryogenesis.

Conclusion
This research addresses one of the deepest mysteries of science: what happened to the antimatter? The goal of the project is to validate or rule out one of the most appealing mechanisms for generating the matter-antimatter asymmetry of the Universe. Through this project, we have already made significant advances in the field, with two publications that are quickly gaining attention from the community. Moreover, this research supports experimental programs in which several federal funding agencies are currently heavily investing.

Publications
Cirigliano, V., C. Lee, M. Ramsey-Musolf, and S. Tulin. Flavored quantum Boltzmann equations. 2010. *Physical Review* . **D 81**: 103503.

Cirigliano, V., C. Lee, and S. Tulin. Resonant Flavor Oscillations in Electroweak Baryogenesis. 2011. *Physical Review D.* **84**: 056006.

Revolutionizing Short-Pulse Laser Generation using Stimulated Raman Scattering

Evan S. Dodd
20100413ER

Introduction

Stimulated Raman scattering (SRS) in laser-plasma interactions has typically been studied in order to avoid its detrimental effects on inertial confinement fusion (ICF). However, this physical process can be used to amplify short laser pulses without the expensive optical components used in the current state-of-the-art chirped pulse amplification (CPA) technique. Elimination of these components allows two revolutionary changes to be made to short-pulse amplification. First, intensity limits due to the CPA technique can be greatly exceeded in the laboratory setting. This technique can be applied to both existing lasers as an up-grade and to new laser systems built in the future. Second, the sensitivity of the gratings in CPA lasers prevents their use in environments where temperature and vibrations are present. In other words, this work will allow short-pulse lasers to move from laboratories and user facilities into real world settings.

Short-pulse lasers have been used in a number of applications, including: laser-plasma acceleration of ions and/or electrons; high-brightness short-pulse x-ray sources; and the fast-ignition concept for ICF. Any significant improvement in amplification technology will have direct relevance to a wide range of basic and applied research.

This project will apply numerical models that were developed at LANL for ICF to the problem of SRS amplification. Results from calculations using these models will be validated with data from experiments external to LANL.

Benefit to National Security Missions

The novel short-pulse laser amplifier resulting from this research is an enabling technology, and will have direct relevance to high-energy density physics experiments, fusion energy and charged particle beam acceleration. Accelerators are important components to basic research, and laser-based accelerators allow applications such as active interrogation of SNM (Special Nuclear Material).

Progress

Our initial proposal set a time-line and set of intermediate deliverables for each fiscal year, which would ensure successful completion of the overall project goals. However at the beginning of FY11, we modified these goals based on experimental results from FY10.

PIC modeling of SRS: At the beginning of the current fiscal year we purchased a license for the LSP particle-in-cell code from Voss Scientific, for two purposes. The first purpose is to verify the computational models developed for the saturation of SRS amplification, which we will test as a part of the project. The second purpose for purchasing this code is to model the plasma creation process in the experiments to be performed by our partner, Applied Energetics Inc. The ability to model these two different process using the same simulation was our motivation for the purchase.

Our post-doctoral researcher, Dr. Jun Ren, has begun using this code to model SRS amplification, and has made great progress this year. She has significantly advanced our physical understanding of the SRS amplification process through her high-resolution particle-in-cell (PIC) modeling. From this work, she has developed a novel theoretical design for an experimental demonstration that should reach a focused intensity of 1×10^{17} W/cm^2, and exceed any previous experiment. Her current results were presented at the Anomalous Absorption conference in June 2011, and are being written up for publication. This simulation work shows that electron trapping is present at the relevant experimental conditions. The simulations also show the same qualitative saturation and optimal plasma length that are found in experiment. This is important because for plasma length > 1.5 mm there is agreement between experimental results and theoretical predictions, but for longer lengths (~ 3.0 mm) the agreement is lost. This length scale has now been shown to occur in simulations when separate Langmuir waves in the pump pulse and amplified pulse overlap and have trapped electrons. This understanding is what allows the novel experimental design to be possible.

Experimental work

The contract with Applied Energetics was renewed and they have performed experimental work in FY11 based on an experimental plan that was developed jointly. The objective of the work was to observe stimulated Raman scattering in an electrical discharge capillary, and then perform SRS amplification experiment in the capillary plasma. The intent was to run through a series of tests to first find a Raman backscatter signal without seeding, because the experimental results form the first year showed no detectable SRS signal. The electrical discharge plasma spectrum was characterized using both an Echelle spectrometer and a high-resolution Chromex spectrometer, which was done since there was great uncertainty in the capillary-discharge plasma electron density. However, during the series of tests the Raman spectrum was still not observed; the two most likely reasons are severe plasma scattering effects and insufficient electrical plasma density. The first reason results from the electron density produced by the laser radiation being significantly larger than the electron density produced from the capillary discharge. The resulting spatial distribution of the electron density causes scattering of the pump laser radiation instead of guiding it without diffraction. Because of this scattering and because the SRS amplification process requires high density, attempts were made to increase the electron density of the capillary discharge. These attempts included: measuring the effects of Xe-gas pressure; changing the ionized gas to Argon (not significantly different); and measuring the effect of increased high voltage (now 20 kV) to the plasma generation.

0-d model development

A simple zero-dimensional model to estimate the electron plasma density created in a capillary discharge plasma system was created, for which the main objective was to give a first estimate to compare with the experimental measurement. The dynamics of plasma formation in a capillary discharge is a complicated problem that has typically been modeled using advanced time-dependent hydrodynamic simulation codes. The details of the discharge dynamics are complicated, but the principle mechanism of the discharge is simple. A high-voltage pulse is discharged through a gas confined by a glass capillary tube in an evacuated chamber. This plasma has a finite conductivity, and it is thus possible to model the discharge process as a RLC circuit model. And, because the plasma conductivity depends on the electron density, n_e, it is possible for a resistor, R, to mimic the plasma formation inside the channel. Numerical solutions of this model can estimate the electron plasma density, or total charge, in the channel, which agrees rather well with the experimental measurements. An analytic solution for the plasma resistance can then be fixed by measuring the discharge current and voltage in the experiment, and then from this solution it can be shown that several methods may be used to increase the plasma density, n_e. The most promising being that increasing the pressure will increase the probability of electron-impact ionization that creates plasma, and thus lead to higher n_e. It is also important to mention that several assumptions were used to develop the model. This is a lump circuit model and there is not spatial dependence. However, the total charge $Q = n_e \times$ volume should be a constant due to conservation of energy and a spatially dependent model should give a similar integrated result. It is a Maxwellian-equilibrium model, where the temperature of the plasma is assumed to be in the range of 2 to 5 eV and that the collision frequency is a relatively constant. It is also a slowly varying model and the rapid-time-varying of resistance due to plasma formation is ignored completely.

Future Work

Backscattered light from SRS can significantly affect capsule implosion and burn for ICF targets. Because of this fact, much effort has been applied to model the physics of SRS and its subsequent nonlinearities. This existing expertise has been, and will be, applied toward the development of the proposed novel amplification technique. The Lawrence Livermore National Laboratory code pF3d contains the physics needed to model SRS-based laser amplifiers. However, more importantly, LANL has recently developed a kinetic-based particle-trapping model and implemented it into pF3d for the nonlinear propagation of Langmuir waves that dominate the saturation of SRS. However, this model was developed to model saturation physics when a single Langmuir wave is involved in SRS. The recent work from this fiscal shows that two Langmuir waves undergoing trapping and subsequently interacting is the source of saturation in the SRS amplifier under study.

The kinetic saturation of SRS was assumed to dominate the short-pulse amplification process, and it has now been shown that it does. The LSP PIC code was obtained and used to verify this statement in the previous fiscal year, and will be tested using experiments in the coming fiscal year. The LANL model was developed from kinetic simulation (such as LSP) of the microscopic-scale plasma physics and implemented into the macroscopic-scale fluid and light-propagation code, pF3d. If the experiments confirm the LSP calculations then LANL is uniquely positioned to develop new models of kinetic saturation in SRS for use in optimizing the laser and plasma conditions for SRS-based amplification. Thus, at the conclusion of this project new funding can be sought out to design and field experiments, which further demonstrate the possibility of the amplification of laser pulses using SRS. It is a predictive capability that is our ultimate goal. LANL will be able to design new laser-based HED facilities to further its mission-oriented research with this capability, and engage in fundamental research at novel physical conditions.

Conclusion

The ultimate goal of this research is to demonstrate significant amplification (>25 times) over a long scale length plasma (> 1 mm). We will show that a newly developed

model for nonlinear SRS at ICF conditions is relevant to the development of this technology. In particular, we will show that our models: first, agree with measurements made by our external collaborators; and two, allow us to optimize the amplification process through calculation (i.e. increased amplification).

Surface Fitting for Thermodynamically Consistent Evaluation of Tabular Equations of State

John W. Grove
20100438ER

Introduction

An equation of state (EOS)is a thermodynamic description of the state of matter under a given set of physical conditions. This project produces algorithms and software for the construction of piecewise smooth representations of thermodynamic free energies for use in equation of state evaluation. The basic intent is to use tabular equation of state input for the construction of convexity constrained tensor product splines for the Helmholtz free energy. Evaluations of the EOS are based on evaluations of partial derivatives of the free energy. Equations of state are at the heart of most of science from nuclear detonations to material science.

We use surface fitting methods for tabular equations of state (EOS's) to address known problems with current evaluation and table development schemes. Our goal is to construct piecewise smooth free energies that reproduce the tabulated data in an optimal sense subject to the constraints of a physical equation of state, namely an appropriate convexity of the free energies.

Our approach is to develop smoothing tensor product B-spline approximations to the EOS data, in particular free energies derived from SESAME data, to produce optimal fits that are appropriately convexity/shape constrained. The developed algorithms and methods will be incorporated into the EOSPAC framework for use in the laboratory's production, research hydrodynamic codes, and EOS development codes. The resultant surface fit parameters are suitable for storage as part of the SESAME database to allow for exact reproducibility for verification and validation (V&V) purposes.

The approach consists of two parts, computing free energies from SESAME data, performing discrete Legendre transforms on the data to impose the proper discrete convexity, and constructing tensor produce spline fits to the data to produce a smooth globally defined free energy that can be differentiated to evaluate thermodynamic data. We apply sufficient but not necessary constraints on the spline coefficients to ensure that the spline surface itself is suitably convex.

Benefit to National Security Missions

The use of general equation of states in hydrodynamic simulations is central to almost all applications for which hydrodynamics is relevant. Our project is directed towards addressing the specific needs of hydrodynamic solvers for valid equation of state evaluations and production. By providing methods and tools that ensure consistent and stable EOS evaluations we will significantly enhance the ability of hydro codes to be used for predictive science. In particular we will ensure that numerical errors produced by thermodynamically inconsistent evaluations are not present in a computation and that the evaluations produce appropriate physically constrained results.

Progress

We have extended last year's work on surface fits for basic SESAME data, specifically tensor product spline surfaces for pressure and specific internal energy as functions of density and temperature, to produce a complete representation for the free energy. This is accomplished by using the pressure and energy surfaces as data for the partial differential equation that defines the free energy, i.e. $dF = -SdT - PdV = (F-e)dT/T - PdV$, where T is the temperature, V is the specific volume (the reciprocal of mass density), e is the specific internal energy, P is the pressure, S is the specific entropy, and F is the free energy. This equation is integrated by first solving for the free energy for a reference density rho0 using the equation $dF/dT = (F-e)/T$. The solution along this curve is then used as initial data to integrate the free energy along each isotherm using the equation $dF/dV = -P$, or equivalently $dF/drho = P/(rho*rho)$. The resulting surface is then processed by the beneath-and-beyond convexification algorithm to produce a function that is convex in specific volume and concave in temperature. Finally the tensor produce spline coefficients are modified to enforce full convexity of the free energy. A visualization of the reconstructed free energy is shown in Figure 1.
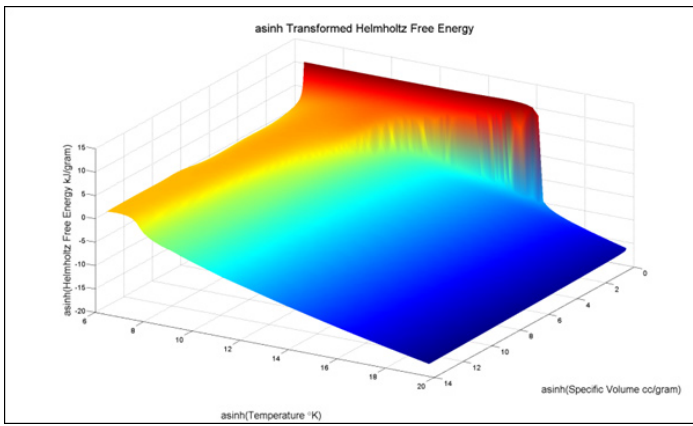
Figure 1. Reconstructed Free Energy from Legacy Sesame table.

In addition to the free energy we also provide reconstructions of the specific entropy. Entropy plays a key role in hydrodynamics solvers and the ability to evaluate the entropy from a Sesame table is an important extension of the utility of the tabular equation of state. As with the free energy we can integrate the entropy from the spline surfaces for the pressure and specific internal energy. Figure 2 shows a resulting surface.
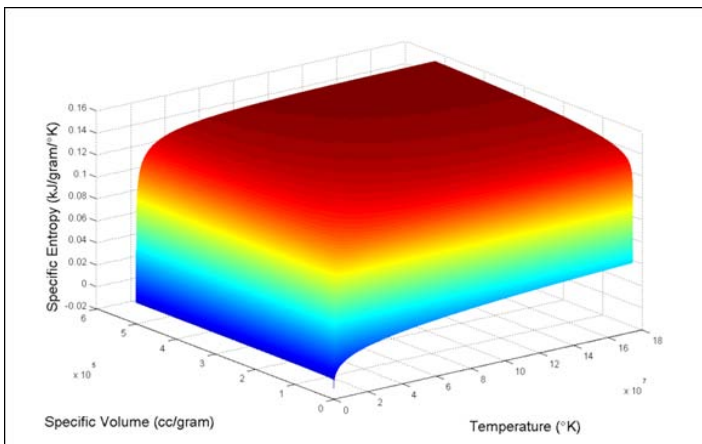
Figure 2. Reconstructed Specific Entropy.

A significant amount of effort has been devoted to improving the robustness of the surface fitting method for automatic generation of the tensor product spline surfaces. This is an area that is somewhat unique for our application since for geometric fitting of surfaces it is common that a significant amount of hand tuning guided by a human is done to produce optimal fits. In our case we wish the software to automatically fit the data with no human tuning. The basic tensor product smoothing spline method is based on constructing the spline knots and coefficients so as to minimize a weighted least squares residual for the data. In our case the automatic selection of weights is the key component of the process. The weights we use are based on performing an arc-hyperbolic sine transform on the data and then using weights based on the reciprocal of a discrete estimate of the data second derivative. This

choice is designed to smooth out numerical oscillations in the Sesame data.

Physical phase transitions in the data are also possible and the smoothing spline is designed to represent such curves as best as possible within the context of the tensor product spline representation. Generation of such curves is a two step process. First we fit the data isotherm by isotherm to pre-smooth the data. If it is detected that the isotherms contain van-der-waals loops a Maxwell construction is applied to the data as well. The pre-smoothed data are then used for the bi-variate spline reconstruction. Figure 3 shows P-V isotherms for water with the vaporization curves corresponding to the flat regions of the isotherms. For comparison these curves are overlaid over the original Sesame data. The spline fits show some differences from the original data and improving this fit is a topic for improvement.
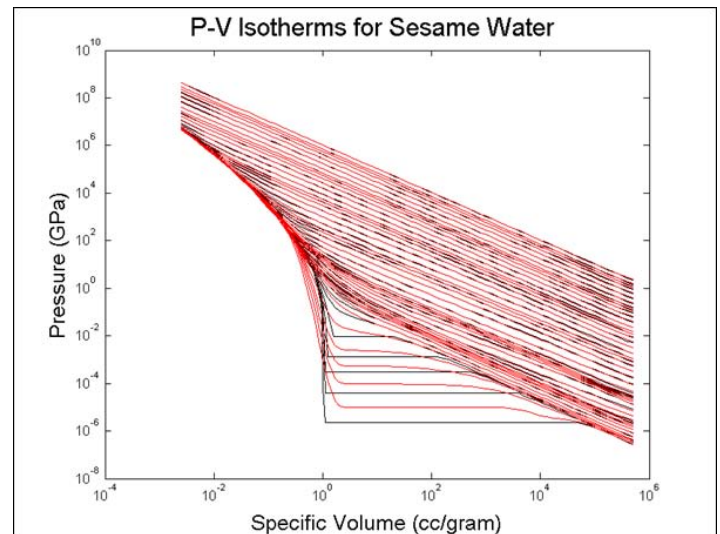
Figure 3. Reconstructed Specific Entropy

All of the basic fitting technology described above has been implemented within the AMCHTOOLS equation of state library that is to be incorporated into EOSPAC. As we advance towards full hydro implementation an important question is the cost of the individual EOS evaluations in a working hydro code. We measured the cost of each spline evaluation as compared to the cost of a similar EOS evaluation in EOSPAC and found that the spline method evaluation can be as much as ten times as long per evaluation as the simple bilinear interpolation used in EOSPAC. An analysis of the spline evaluation algorithm we are using shows that the bulk of this cost is due to the iterative method used to evaluate the B-spline basis functions which were reconstructed on the fly with each evaluation. This cost can be substantially reduced by pre-computing the polynomial coefficients for the basis functions in each knot interval. We have implemented this evaluation method as a multi-variate polynomial class. After the tensor product spline has been computed we evaluate the Taylor series for each knot rectangle and store these coefficients in the

polynomial class. The spline is then evaluated by using a fast bisection method to locate the knot rectangles containing the points to be evaluated and we then use a fast summation method to evaluation the polynomial. We have created extensive timing software into our EOS library and are in the process of evaluating the performance improvements achieved by this method.

Future Work

Our goals for this year are to complete the implementation of a thermodynamically consistent EOS module that can be used by production hydro codes. Specific tasks include:

- Continue work on improving the robustness of the automatic convexity constrained surface fits. We will seek to verify that all materials in the open Sesame database can be processed by this code.

- Material phase transitions are a key issue and we will seek improved methods that can reproduce vaporization and solid phase transitions as accurately as possible. Since the surface spline is constrained to be smooth, this work will necessarily require smoothing at the edges of the phase transition region, but we will seek to make these transitions as sharp as possible within the restrictions of the tensor product fit.

- Make the surface fitting technology available to EOS developers. Here the goal is to use this tool as a smoothing and consistency step prior to the release of new material tables. As an aspect of this work we also plan to include the spline knot sets and B-spline coefficients in the Sesame database. This will allow the hydro applications to directly use the Sesame data without having to pre-fit the data.

- Provide a robust polynomial class for the fast evaluation of the surface fit.

- Implement the evaluation class as part of EOSPAC. This will provide a quick vector into existing hydro code usage.

Conclusion

We have now developed the basic capability to construct tensor spline fits automatically for general Sesame data. This includes constructing a convex free energy that fits the data in some optimal sense. Our work for next year will focus on improving the robustness of the method for generic data and providing methods for the fast evaluation of this data. When incorporated within the EOSPAC software, these tools will provide a unique capability for the improved EOS treatment in application codes.

Publications

Grove, J. W.. So you want to use a "real" equation of state. 2011. *Unpublished Report.*

LES Modeling for Predictive Simulations of Material Mixing

Fernando Grinstein
20100441ER

Introduction

The mixing of initially separate materials in a turbulent flow by the small scales of turbulent motion is a critical element of many LANL programs including: 1) urban contaminant dispersal important for threat reduction, 2) the heat, mass, CO2, and salinity fluxes in ocean models needed for climate prediction, 3) plasma mixing during inertial confinement fusion, 4) combustion, 5) material processing, 6) nuclear weapons performance, and many other applications in engineering, geophysics, and astrophysics. Our broad research goal is to develop and validate a rational, first-principles theory and associated algorithm for simulation of material mixing by a turbulent velocity field. The precise physical problem we address is: the creation of a capability to calculate the (small) unresolved scales of material mixing generated by (small) unresolved scales of fluid motion. We will pursue this goal by accomplishing several separate goals in theory, computation, and analysis. The work aims at developing a new paradigm for mixing simulations and as a consequence has scope that includes, but far exceeds practical weapons applications. The expected impact is on, 1) extending recent new methodologies from turbulence to address material mixing issues, 2) providing a physical underpinning for this extension.

Benefit to National Security Missions

The mixing of initially separate materials in a turbulent flow by the small scales of turbulent motion is a critical and often poorly understood element of many LANL programs: 1) nuclear weapons performance and inertial confinement fusion, 2) urban contaminant dispersal in threat reduction, 3) combustion, 4) climate, and a host of other applications in engineering, geophysics, and astrophysics.

Progress

Relevant Proposed Schedule & Milestones. Year 1: Finite scale (FS) analysis of the flow and material fields are used to obtain FS equations. An equation of the small subgrid scales of the mixing field will be derived, based on extended self-similarity and renormalization ideas applied to a statistical moment equation. Years 1 & 2 :

Algorithm development and Flux-Corrected Transport code development will also be required to implement the algorithm and test it.

Finite scale theory is a transformation of the governing equations of fluid flow (Navier-Stokes equations) that accounts for the discrete nature of computer simulations. It represents a top-down philosophy that says the effects of the small eddies – those that cannot be resolved on the computational mesh -- are determined by the large resolved eddies. To test this idea, we employed a standard methodology from the field of turbulence modeling in a new and unconventional way. The methodology, termed Reynolds decomposition, is a technique to distinguish the mean and fluctuating parts of a fluid flow and to determine how these two parts interact. Whereas the usual application of this methodology is to solve the Navier-Stokes equations, we generalized the application to the finite scale Navier-Stokes (FSNS) equations that we have derived, and for comparison purposes to a generic form of the equations of large eddy simulation (LES) which represents a conventional approach to modeling turbulence. For the latter, we chose the classical Smagorinsky model.The comparison allows a critical assessment of the long term effects of the use of both FSNS and the Smagorinsky model in predicting the mixing of two materials due to turbulence. In general, we find that FSNS is more consistent with Navier-Stokes in predicting anisotropy (e.g., the dependence on the direction of velocity) and on including the effects of fluctuations in time as well as space. The analysis also produced some predictions of invariant quantities that can be tested numerically.

We have carried out the necessary code developments, testing, and validation of a forced, isotropic, compressible turbulent-mixing implicit in the large-eddy simulation (ILES) algorithm. The work has focused on simulating material mixing in a convergence study of increasing resolution, where the length scales of the mixing varies from being of the order of a cell size (coarse resolution) to where the mixing length scale is well-resolved by the mesh; results are compared with available direct numerical simulation reference data, as well as previously-

reported large eddy simulations. Effects of grid resolution and Mach number on the flow and scalar mixing were investigated. We demonstrated that ILES can capture the dominant aspects of the mixing transition namely, the scalar variance and energy-to-scalar time-scale ratio transients and asymptotic behaviors as function of effective Re determined by grid resolution.

We have also contributed to further addressing formalization of the perceived abilities of ILES in computing high Re (Reynolds number) flow, by developing a procedure to estimate a characteristic ILES Re number for ILES of transitional flow. This issue becomes particularly important when one considers typical time-dependent turbulent flows of LANL interest induced by Kelvin-Helmholtz, Rayleigh-Taylor and Richtmyer-Meshkov instabilities, and there is a need to accurately estimate the effective viscosity away from the small scales of the flow, where the numerically controlled dissipation takes place.

Future Work

Mixing is usefully characterized by the length scales of the fluid physics involved: 1) large-scale advection which brings relatively large regions of the fluids together, 2) an intermediate length scale associated with the convective stirring due to velocity gradient fluctuations, and, 3) a small scale interpenetration resulting from molecular diffusion. We are primarily concerned with numerical simulation of the first two processes as is appropriate to nonequilibrium transients in a mixing process with low volume fraction and low diffusivity of the heavier fluid. Our goal is the derivation of a convective stirring length scale concerned with characterizing the material mixing at length scales much smaller than the size of a computational cell. The proposed research can be conveniently organized in five steps. Steps 1 and 2 are primarily theoretical. Steps 3 and 5 are primarily computational. Step 4 is both.

1. Length scale of the sub-grid material field: a finite-scale equation (FSE) for the sub-grid length scales characterizing the mixing field is to be derived. Extended self-similarity and renormalization of statistical equation will be invoked.

2. Algorithm development: modified equation analysis is used to design an algorithm that matches the FSE derived from governing equations.

3. Direct numerical simulation (DNS) database creation: Very high resolution DNS and data analysis and averaging are conducted for the initial value problem of material mixing by a stationary forced turbulence.

4. Code development: implement and test the algorithm. We simulate material mixing in a convergence study of increasing resolution, where the length scales of the mixing varies from being much smaller than a cell (coarse resolution) to where the mixing length scale is well-resolved by the mesh. Initial conditions for the FSE consistent with those of the DNS will be designed.

5. Validation: ILES algorithms are used to compute averages of the DNS databases.

Conclusion

Our end product is to provide a prototype (tested) algorithm that can be used in the context of an ASC code and other LANL applications in which mix prediction is central. From the applied point of view our goal is to achieve high-resolution quality results on very low-resolution grids with a parameter free approach. In the bigger picture, our approach helps illustrate that better physics and rigorously derived finite scale algorithms provide a viable alternative to the "more cells and bigger computers" strategy for LANL applications.

References

1. Grinstein, F. F., A. A. Gowardhan, and A. J. Wachtor. Simulations of Richtmyer-Meshkov Instabilities in Planar Shock-Tube Experiments. 2011. *Physics of Fluids.* **23**: 034106.

2. Grinstein, F. F.. Verification and Validation of CFD based Turbulent Flow Experiments. 2010. In *Encyclopedia of Aerospace Engineering, Volume 1 Fluid Dynamics and Aerothermal Dynamics, Part 7 Computational Fluid Dynamics.* Edited by Shyy, W., and R. Blockley. Vol. 1, p.   . N. Y.: John Wiley & Sons.

3. Grinstein, F. F.. Simulating Vortex Dynamics and Transition in High Reynolds-Number Flows. 2010. *Physica Scripta.* **T142**: 014013.

4. Ristorcelli, J. R., L. G. Margolin, and F. F. Grinstein. Finite Scale Navier Stokes for Computations of a Turbulent Fluid. Part I: Passive Scalar Mixing. *Journal of Fluid Mechanics.*

5. Wachtor, A. J., F. F. Grinstein, and C. R. DeVore. Mixing in Implicit Large-Eddy Simulation of Statistically Stationary Compressible Isotropic Turbulence. *Physics of Fluids.*

6. Zhou, Y., F. F. Grinstein, and A. J. Wachtor. A Scheme For Estimating the Effective Numerical Viscosity in Implicit Large Eddy Simulation. *Journal of Turbulence.*

Publications

Grinstein, F. F.. Simulating vortex dynamics and transition in high Reynolds-number flows. 2010. *Physica Scripta (2010).* **T142**:   014013.

Grinstein, F. F.. Verification and validation of CFD based turbulent flow experiments. 2010. In *Encyclopedia of Aerospace Engineering, Volume 1, Fluid Dynamics and Aerothermal Dynamics, Computational Fluid Dynamics, Chapter eae049 ..* Edited by Shyy, W., and R. Blockley. Vol. 1, p.   . NY: Wiley.

Grinstein, F. F., A. A. Gowardhan, and A. J. Wachtor. Simula-

tions of Richtmyer-Meshkov Instabilities in Planar Shock-Tube Experiments. 2011. *Physics of Fluids.* **23**: 034106.

Ristorcelli, J. R., L. G. Margolin, and F. F. Grinstein. Finite Scale Navier Stokes for Computations of a Turbulent Fluid. Part I: Passive Scalar Mixing. *Journal of Fluid Mechanics.*

Wachtor, A. J., F. F. Grinstein, and C. R. DeVore. Mixing in Implicit Large-Eddy Simulation of Statistically Stationary Compressible Isotropic Turbulence. *Physics of Fluids.*

Zhou, Y., F. F. Grinstein, and A. J. Wachtor. A Scheme For Estimating the Effective Numerical Viscosity in Implicit Large Eddy Simulation. *Journal of Turbulence.*

Jet Probes of New Physics at RHIC and at the LHC

Ivan M. Vitev
20110098ER

Introduction

The overarching goal of this project is to develop modern theoretical and computational tools to identify and characterize new physics at the Relativistic Heavy Ion Collider (RHIC) [1] and at the Large Hadron Collider (LHC) [2]. To this end, we will advance the theory of jets - collimated showers of energetic subatomic particles [3] that are abundantly produced at these facilities when particle beams collide. RHIC and LHC explore a broad spectrum of exciting novel phenomena that range from the formation of the quark-gluon plasma (QGP) to the creation of new forms of matter that are believed to make up the fabric of our Universe. Understanding the Quantum Chromodynamics (QCD) theory of jet production and propagation in the vacuum and in matter having extremely high energy density is essential to elucidating both the unexpected properties of the QGP and the TeV-scale physics that is Beyond the Standard Model (BSM). We will identify experimental jet observables of new physics in proton-proton (p+p) and nucleus-nucleus (A+A) reactions and evaluate them using modern techniques, such as effective field theory. We will incorporate the theoretical advances in jet simulation packages and employ the resulting tools to interpret the anticipated copious data from RHIC and the LHC. We will establish the correct physics mechanisms of jet-plasma interactions and help eliminate the vast model dependence that currently hinders the precise determination of the plasma properties. We will identify search strategies for and/or place constraints on the Standard Model Higgs boson, as well as on models of supersymmetry, which predict massive new particles that decay into jets. The start-up of the LHC and the rapidly growing interest in jet physics make it timely for this project to have a significant impact.

Benefit to National Security Missions

This project supports the Laboratory Mission to enhance the nation's scientific capabilities, as defined by the DOE Office of Science. Within LANL, this project is well-aligned with the Beyond the Standard Model (BSM) Grand Challenge and responds directly to the LDRD Program Office call to "develop new theory to search for BSM physics" and to "further our understanding of quantum chromodynamics" at the Large Hadron Collider and the Relativistic Heavy Ion Collider. Within the scientific community at large, this project addresses top priorities established by the DOE and NSF Offices of HEP and NP in the 2008 High Energy Physics Advisory Panel P5 and the 2007 Nuclear Science Advisory Committee reports, respectively. Physics at the nuclear scale and below is an underlying capability for the weapons program.

Progress

During the first year of this exploratory research project there has been significant progress toward achieving its goals. One of the main tasks of the Large Hadron Collider (LHC) is to discover the Higgs boson and complete the Standard Model (SM) of particle physics. It turns out that if its mass is below O(135 GeV), then large statistics are required to discover the Higgs particle when conventional analyses are applied. New jet physics techniques to discover the Higgs boson, using less statistics and having different systematics, are therefore highly desired. Currently M. Graesser, along with LANL post-doc G. Ovanesyan and external collaborators J. Thaler and T. Chan (MIT) are investigating the potential of a new experimental observable to do just that. Specifically, we are investigating the so-called ``tau_N subjettiness", which was originally introduced to study boosted top quarks or boosted W bosons. The idea is to look for specific number of subjets in a big protojet and track back this number to a characteristic Higgs boson decay channel. We have made significant progress in investigating applications of tau_N for discovering a boosted SM Higgs boson in its decay mode to b-quark jets. The main new result of our work is that the tau_N method and previous analyses have comparable efficiencies for retaining the Higgs mass peak. We find however that the best discriminating observable is the ratio tau_2/tau_1, which provides higher efficiency than the previously used method, called the BDRS algorithm [4] (Figure 1).
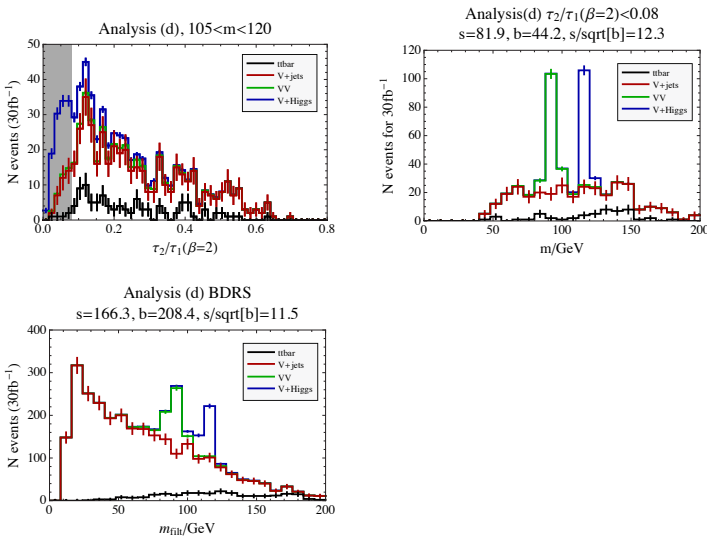
Figure 1. Top left plot represents N-subjettiness distribution shown for signal (blue) and various backgrounds. As one can easily see the signal is separated closer to zero in this plot as opposed to background that is further from zero. Thus, cutting on this observable value < 0.08 provides an excellent efficiency for Higgs boson discovery (top right plots) which exceeds the efficiency of the popular algorithm referred to as BDRS in the literature (bottom plot).

Another major component of the LHC program is to carry out ultra-high energy heavy ion reactions. Better understanding the physics of jets in these reactions requires the construction of a modern effective theory for jet propagation in matter. As a part of this project, I. Vitev and G. Ovanesyan constructed the Lagrangian for such theory, which we called Soft Collinear Effective Theory with Glauber gluons (SCET_G) [5]. We derived the Feynman rules for this Lagrangian for different types of scattering centers in the medium, with which an energetic jet may interact, and for different choices for the degrees of freedom of the gluons (the mediators of the strong force) that enter our calculations. We presented the first proof that the jet broadening and energy loss results do not depend on this artificial choice of "gauge." This fact, known as "gauge invariance", allows us to put calculations of jets in heavy ion reaction on firm theoretical footing. By virtue of SCET_G, we extended the evaluation of medium-induced radiation beyond the soft gluon approximation. We also showed how the process-dependent medium-induced radiative corrections factorize from the jet production cross section. Our paper "An effective theory for jet propagation in dense QCD matter: jet broadening and medium-induced bremsstrahlung" is published in JHEP [5]. We have given four invited talks on the subject at major conferences. In our second publication we apply this new effective theory SCET_G to calculate all the remaining quark and gluon splitting probabilities in the medium [6], for the first time without assumption that either of the splitted partons is soft. In Figure 2 one can see these full probabilities for all splittings and their comparison to the soft parton approximation.
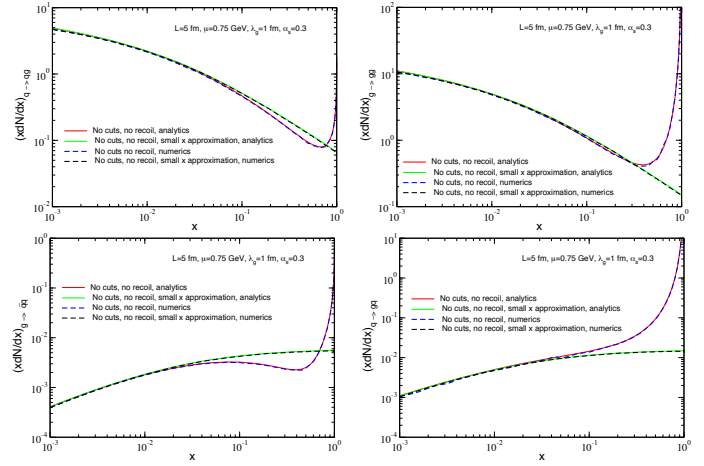
Figure 2. The splitting probabilities of partons in the medium are presented to accuracy beyond the soft parton emission approximation typically used in the literature. Calculation was done using effective theory SCETG.

In a third publication [7] I. Vitev and external collaborators B.W. Zhang and Y. He presented first results with high accuracy (known as next-to-leading order) for jet production in the recent LHC lead-lead run. Specifically, we focused on the suppression for the single and double inclusive jet cross sections in heavy ion collisions. Our analysis included not only final-state inelastic jet interactions in the quark-gluon plasma created in such collisions, but also initial-state cold nuclear matter effects and an estimate of the non-perturbative hadronization corrections. We demonstrated how an enhanced di-jet asymmetry in central Pb+Pb reactions at the LHC, recently measured by the ATLAS and CMS experiments, can be derived from these results. We showed quantitatively that a significant fraction of this enhancement may be related to the collisional interactions between the quarks and gluons in the jet and the strongly-interacting medium and pointed to a suite of measurements that can help build a consistent picture of parton shower modification in heavy ion collisions at the LHC. Figure 3 shows the comparison of the di-jet imbalance measured by ATLAS and CMS to our calculations. Our paper "Next-to-leading order analysis of inclusive jet and di-jet production in heavy ion reactions at the Large Hadron Collider" is submitted for publication to PLB. We have given one invited talk on the subject and published proceedings [8].
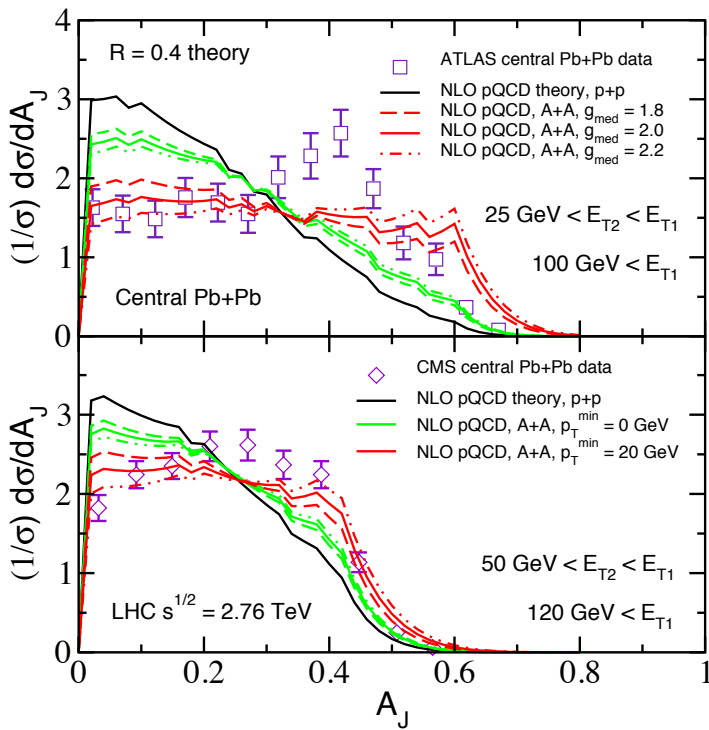
Figure 3. Predictions for the di-jet transverse energy assymetry AJ for radiative (green lines) and radiative + collisional energy losses for jets in the quark-gluon plasma arr compared to data from ATLAS and CMS.

Future Work

To achieve the theoretical goals of this project, we will employ the full power of modern field-theoretic approaches to evaluate both SM and BSM processes. A controlled expansion in the strength of the fundamental inter-particle interactions will be used to calculate for the first time, to the same high level of precision (next-to-leading order), the cross sections and shapes for jet processes in the vacuum and in the ambiance of a strongly interacting plasma. The application of effective field theory (EFT) will be facilitated by the presence of a well-established hierarchy of energy and/or mass scales in the physics processes upon which our research will concentrate. This is precisely the situation where EFTs excel in reducing theoretical uncertainties and in im-proving the computational accuracy. The complementarity of perturbative QCD and SCET approaches provides valuable alternatives to ensure that project milestones will be met. Our simulation effort will focus on developing flexible modular codes, designed to run on LANL open clusters. These computational tools will incorporate input from our new theoretical findings and from existing Monte Carlo event generators to provide the greatest flexibility in using jets as probes of new physics within the SM and beyond. In upcoming comparisons to experiment we will undertake a global analysis approach by incorporating all available RHIC and LHC data on jets, pertinent to the observables identified by this project as messengers of new physics. This will allow for unbiased model elimination and accurate constraints on the nature of the jet-plasma interactions, the properties of the QGP, and the characteristics of new particles.

Conclusion

This project will result in novel theoretical and computational tools to accurately describe jet observables in proton and nuclear reactions. We will develop strategies and methods to discern new QGP and BSM physics at RHIC and at the LHC using jets as probes. We will produce computations: i) for experimentally accessible jet channels where measurements can dramatically reduce the ambiguity in establishing the mechanisms of jet propagation and interaction in matter; ii) to increase the signal/background ratio for BSM discovery; and iii) theoretically validate jet substructure studies that are based on Monte Carlo simulations. We expect that this project will result in several high-impact refereed publications to disseminate these new results to the scientific community.

References

1. al, K. Adcox et. Formation of dense partonic matter in relativistic nucleus-nucleus collisions at RHIC: Experimental evaluation by the PHENIX collaboration. 2005. *Nuclear Physics A.* **757**: 184.

2. al, K. Aamodt et. Suppression of Charged Particle Production at Large Transverse Momentum in Central Pb-Pb Collisions at sqrt{s_{NN}} = 2.76 TeV [ALICE experiment]. 2011. *Physics Letters B.* **696**: 30.

3. Sterman, G., and S. Weinberg. Jets from Quantum Chromodynamics. 1977. *Physics Review Letters.* **39**: 1436.

4. Butterworth, J., A. Davison, M. Rubin, and G. Salam. Jet substructure as a new Higgs search channel at the LHC. 2008. *Physics Review Letters.* **100**: 242001.

5. Ovanesyan, G., and I. Vitev. An effective theory for jet propagation in dense QCD matter: jet broadening and medium-induced bremsstrahlung. . 2011. *Journal of high energy physics.* **2011** (6): 80.

6. Ovanesyan, G., and I. Vitev. Medium-induced parton splitting functions from Soft Collinear Effective Theory with Glauber gluons. *Physics Letters b.*

7. He, Y., I. Vitev, and B. Zhang. Next-to-leading order analysis of inclusive jet and di-jet production in heavy ion reactions at the Large Hadron Collider. *Physics letters b.*

8. Vitev, I.. NLO analysis of inclusive jet, tagged jet and di-jet production in Pb+Pb collisions at the LHC. To appear in *Journal of Physics G.*

Publications

He, Y., I. Vitev, and B. Zhang. Next-to-leading order analysis of inclusive jet and di-jet production in heavy ion reactions

at the Large Hadron Collider. *Physics letters b.*

Ovanesyan, G.. An effective theory for jet propagation in dense QCD matter: jet broadening, radiative energy loss and LHC phenomenology. 2011. *Poster for Quark Matter 2011, Annecy, France.*

Ovanesyan, G.. Effective theory approach to jet propagation in dense QCD matter. Invited presentation at *Boston jet physics workshop, Harvard University, Cambridge, January 2011.* (Cambridge, January 11-14. 2011).

Ovanesyan, G.. Effective theory description of jets in dense QCD matter. Invited presentation at *Winter Workshop on Nuclear Dynamics 2011.* (Winter Park, February 6-13).

Ovanesyan, G.. Effective theory approach to jet propagation in dense QCD matter. Invited presentation at *SCET workshop 2011.* (Pittsburg, 6-8 March, 2011).

Ovanesyan, G.. Effective theory for jets in medium. Invited presentation at *Department of particles and fields meeting.* (Providence, RI, 9-13 August, 2011).

Ovanesyan, G., and I. Vitev. An effective theory for jet propagation in dense QCD matter: jet broadening and medium-induced bremsstrahlung. . 2011. *Journal of high energy physics.* **2011** (6): 80.

Ovanesyan, G., and I. Vitev. Medium-induced parton splitting functions from Soft Collinear Effective Theory with Glauber gluons. *Physics Letters b.*

Vitev, I.. NLO analysis of inclusive jet, tagged jet and di-jet production in Pb+Pb collisions at the LHC. To appear in *Journal of Physics G.*

Daylight Imaging with Seismic Noise

Xiaoning Yang
20110108ER

Introduction

The main goal of this project is to derive the Earth's attenuation properties (how the Earth absorbs seismic energy) from seismic background noise. The technique is known as "daylight imaging," in analogy to the illumination of shaded areas by scattered daylight. The specific goals of the proposal are to 1) develop the theory and the methodology to obtain the Earth's attenuation properties from seismic noise cross-correlation (NCC) amplitudes; and 2) construct a tomographic attenuation image of the Earth using noise for the western United States. The proposed research addresses the fundamental problem of using seismic noise, which is traditionally considered to contain limited information, to improve our knowledge of the Earth. Using seismic noise to probe Earth's structure and property is an emerging science. Developing Earth attenuation property from noise is at the cutting edge of this new science. The successful execution of the project will enable us to use seismic noise as a new data source in Earth science research.

Benefit to National Security Missions

The research will create unique expertise at the Laboratory and enhance the Laboratory's capability to address some of its core missions including Ground-based Nuclear Detonation Detection under the mission of Nuclear Nonproliferation. Opportunities include NNSA/NA-22 sponsored nuclear nonproliferation R&D program, Broad Agency Announcement (BAA) projects sponsored by DOE/NNSA, DoD and Department of State, and BAA Service Calls by DoD/DTRA. The theoretical framework and methodology we develop also have applications in geological carbon sequestration under the mission of Energy Security.

Progress

The main tasks for FY11 were to collect continuous seismograms from the USArray required for the project, preprocess the data, and conduct research to develop the theory and method to accurately measure NCC amplitudes and to reduce seismic noise-field-intensity effect from measured amplitudes.

We have finished collecting required seismic data from the IRIS Data Center. The dataset contains continuous, long-period (one sample per second) seismograms from 805 USArray stations with two-years worth of data for each station. The dataset provides a complete coverage of the western US where USArray has been deployed. All collected data have been converted to Earth medium particle motions using the instrument response information from the IRIS Data Center. For each station, seismogram segments were merged to form a continuous signal trace to suit later analysis.

Accurate measurement of NCC amplitudes is critical for the reliable retrieval of attenuation information. The amplitude depends heavily on how the seismogram is processed and how NCC is calculated [1]. To develop a reliable data processing method, we selected multiple linear sub-arrays from among USArray stations with different lengths and directions. In addition, we searched the earthquake database that we hold here at LANL and selected earthquakes that are either in the vicinity of some of the USArray stations or lie along the extensions of the linear arrays. We collected waveforms from these earthquakes and measured surface-wave amplitudes. These earthquake amplitudes were used to benchmark the NCC data processing methods that we tested.

We processed the noise data from the linear arrays using two published methods [2] and a new method that we designed. The two published methods use either an amplitude-weighting scheme or an amplitude-clipping scheme to reduce the effect of earthquakes and other transient signals on calculated NCC. We designed a new data processing method that completely removes large transient signals from noise. In addition, the method accounts for the seasonal variation of noise strength. The new method uses a median-value technique to remove earthquakes and other transient signals. It corrects the noise amplitude for its seasonal variations using average values of the entire network. All data processing methods produce NCC amplitudes that generally decay with increasing distance – an indication of the attenuation of the Earth medium. Compared with earthquake data, however, NCC amplitudes measured with different

data-processing methods show different degrees of agreement. The new method that we designed yielded average amplitude decay that is most consistent with that from earthquakes. The other two methods, however, are less consistent.

Although NCC amplitudes calculated with the new data-processing method exhibit consistent average decay as that from earthquake data, individual linear arrays sometimes show amplitude decay patterns that are inconsistent with those from earthquakes. These differences may introduce bias in attenuation measurements and further refinement of the method is required. To address this issue, we first tested a technique called beam forming [3] to enhance the noise energy along the array direction before NCC calculation, thus minimizing the effect of the noise field in other directions. Test results show that the technique works well for linear arrays in certain directions, from which the main noise signal comes. For other directions, however, the technique is less effective.

Because the discrepancy between NCC amplitude decay and that from earthquakes for individual linear arrays is mainly due to the direction-dependence of the noise field intensity, we tested a modified NCC calculation method in order to reduce this effect. We first calculated NCC using the original noise signal. We then use the tail portion of the resulting NCC traces, which is called coda in seismology, as the signal to calculate another NCC. Doing double NCC maximizes the isotropic part of the noise field and reduces the effect of its directional variations [4]. Figure 1 is an example showing how the method improves the NCC amplitude behavior. Figure 1a plots the stations that constitute a linear array, along with an earthquake used for comparison. Figure 1b shows amplitudes from the earthquake and those from simple NCC of the original noise signal plotted against distance. It is clear that amplitudes from simple NCC do not follow those from the earthquake. We replaced the amplitudes from simple NCC with amplitudes from double NCC in Figure 1c. This time, the comparison is much better. The example illustrates that with double NCC method, we can make reliable amplitude measurements from noise. This establishes the foundation for our next-step research to develop the noise attenuation imaging technique.

In addition to research using the USArray noise data, we also conducted numerical simulations to test the hypothesis that attenuation, station amplification and noise-field intensity can be retrieved from NCC amplitudes even for an imperfectly diffuse noise field, which is the case for seismic data. In the simulation, we generated a synthetic noise field using sources with a skewed intensity distribution. Signals were recorded by a linear array inside the noise field and NCC was calculated between stations. The simulation shows that attenuation, station amplification and noise-field intensity can be retrieved if the noise field obeys the Radiative Transfer Theory, a known characteristic

of acoustic and elastic noise fields. The simulation result provides a theoretical confirmation that attenuation can be retrieved from seismic noise.

We will present our research results at the American Geophysical Union Fall Meeting later this year. The numerical-simulation result has been published in Comptes Rendus Geosciences [5]. We are preparing a second paper to document the research result using the USArray data.
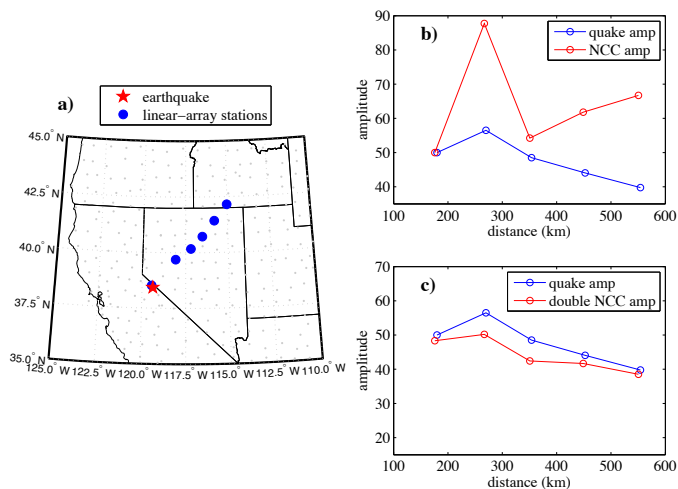
Figure 1. An example showing the amplitude behavior of NCC compared with that from an earthquake. a) Locations of stations for NCC calculation and the location of an earthquake for amplitude comparison. b) Comparison of amplitude behavior between simple NCC and the earthquake. c) Comparison of amplitude behavior between double NCC and the earthquake.

Future Work
We will further test and refine the double NCC method using more data. We will construct additional linear arrays and test different parameters in calculating double NCC to see their effects and to improve the method. In addition, we will develop a theoretical framework for the method.

Additional tasks for the remaining time period of this project include: a) Develop a new inversion formula to account for the directional and spatial dependence of the noise-field intensity for imaging; b) Derive an average attenuation model for the region from noise using a frequency-domain method and use it as the a priori constraint in the imaging; and c) Construct a two-dimensional tomographic attenuation model for the western U.S. using NCC amplitudes and a Bayesian tomographic imaging method; and d) Evaluate the attenuation model that we develop by comparing it with a well-accepted Lg (a seismic wave that travels in the crust) attenuation model and with the geology of the region.

Conclusion
We have finished collecting and preprocessing the complete USArray dataset for analysis. We also made signifi-

cant progress in developing a novel NCC method that yields reliable surface-wave amplitude measurements. In addition, we conducted numerical simulations to establish the theoretical basis for attenuation retrieval from noise. Some of the results have been published and some are being prepared for a paper. We will also present our results at professional meetings.

Through this project, we will develop new theory and methodology to derive Earth's attenuation property from seismic noise and construct a tomographic attenuation model for the western U.S. The project will allow us to use noise, which is ubiquitous, to study the Earth's interior. This is particularly important for regions where earthquakes are scarce. We will have a better understanding of how seismic noise propagates within the Earth and is affected by the Earth, which is a basic science problem. The effort will enrich our knowledge of the Earth system in which we live.

References

1. Larose, E., P. Roux, and M. Campillo. Reconstruction of Rayleigh-Lamb dispersion spectrum based on noise obtained from an air-jet forcing. 2007. *Journal of Acoustical Society of America.* **122**: 3437.

2. Bensen, G. D., M. H. Ritzwoller, M. P. Barmin, A. L. Levshin, F. Lin, M. P. Moschetti, N. M. Shapiro, and Y. Yang. Processing seismic ambient noise data to obtain reliable broad-band surface wave dispersion measurements. 2007. *Geophysical Journal International.* **169**: 1239.

3. Zhang, J., P. Gerstoft, and P. D. Bromirski. Pelagic and coastal sources of P-wave microseisms: Generation under tropical cyclones. 2010. *Geophysical Research Letters.* **37**: L15301.

4. Stehly, L., M. Campillo, B. Froment, and R. L. Weaver. Reconstructing Green's function by correlation of the coda of the correlation (C3) of ambient seismic noise. 2008. *Journal of Geophysical Research.* **113**: B11306.

5. Weaver, R. L.. On the amplitudes of correlations and the inference of attenuations, specific intensities and site factors from ambient noise. 2011. *Comptes Rendus Geosciences.* **343**: 615.

Publications

Weaver, R. L.. On the amplitudes of correlations and the inference of attenuations, specific intensities and site factors from ambient noise. 2011. *Comptes Rendus Geosciences.* **343**: 615.

Balanced and Unbalanced Turbulent Cascades

Balasubramanya T. Nadiga
20110150ER

Introduction

The climate system is forced at the large scales and the instability of the resulting large-scale flow gives rise to intermediate-scale eddies. The large-scale flow and the resultant eddies are both, however, in approximate geostrophic balance---a balance between pressure gradients and rotational effects. An important aspect of turbulence in the context of such balanced dynamics is an inverse cascade of energy. That is to say, energy moves from small scales to large scales. While this phenomenon is responsible for the formation of weather systems on earth and coherent structures such as the Great Red Spot on Jupiter, it leads to inconsistencies in our understanding of the energy cycle in such systems. In this setting, dissipation occurs only through bottom friction, recent estimates of which suggest their insufficiency in being able to establish equilibrium. Thus a fundamental conundrum of turbulent dynamics in the ocean, which we presently consider, is how the system equilibrates in the presence of continuous large scale forcing and an inverse cascade at the intermediate scales. (In contrast, in three-dimensional flows that we encounter on smaller scales, there is a forward cascade of energy, or energy moves from large scales to small scales. In this case, it is easy to imagine a continuation of such a process to smaller and smaller scales until it is dissipated by molecular viscosity.)

A possibility is that the large and intermediate scales cannot be analyzed in isolation, motivated by the notion that the turbulent nature of flow in the oceans entails continuous exchange of energy among all scales, ranging from the millimeter scale to the 1000km scale and results in a tight relationship between small-scale mixing and large-scale circulation. However, what is missing is an understanding of how the large and intermediate scales interact with the smaller scales since present day theories suggest that they do not. Stated in another way, how does balanced motion breakdown and result in a forward cascade of energy?

In this project, we will examine the role of stratification-dominated processes, frontal instabilities of the surface ocean including ageostrophic and other high frequency instabilities, processes that take place away from solid boundaries, in providing a way out of this dilemma by providing for a forward cascade of energy that is then dissipated by unbalanced three dimensional turbulence. We will do this using a combination of resolved simulations and analysis of cascades in a hierarchy of models.

Benefit to National Security Missions

DOE/SC Office of Biological and Environmental Research sponsors a large program in climate modeling at LANL and this program contributes key earth system components to one of the main US studies included in the Intergovernmental Panel on Climate Change (IPCC) assessments. Energy balance in such models is fundamental and ensuring that such balances are realistic will lead to enhancing their predictive capabilities. Furthermore this research will contribute to the goals of DOE/SC Advanced Scientific Computing Research. Other agencies such as NOAA have potential interest as well. The potential of this research project to contribute to improvements in ocean models is significant.

Progress

Scale analysis suggests that both large scale circulation and mesoscale eddies in the oceans are strongly influenced by earth's rotation. We call such flows under rotational-control balanced flows. The conundrum of oceanic turbulence is that while the bulk of kinetic energy is confined to such structures, dissipative mechanisms are least effective in them. However, as an analogy, consider the symmetry-breaking pitchfork bifurcation, e.g., the irregular (asymmetric) buckling of an empty but symmetric soda can under compression. Here systems with symmetry have corresponding symmetric solutions; but with the occurrence of a pitchfork bifurcation such solutions lose stability, leading to a spontaneous breakdown of symmetry. Similarly, we are exploring the possibility of spontaneous occurrence of structures that are weakly controlled by earth's rotation (we will call such structures unbalanced flows) in an ambient circulation that is strongly controlled by rotation (balanced flows). The dynamical consequences of the spontaneous occurrence of unbalanced structures are that they can allow for dissipation of energy that predominantly resides in the balanced

circulation. In the absence of such structures we would not be able to fully explain how energy in balanced flows is ultimately dissipated. In conventionally used ocean simulations; spatial resolutions are too coarse to study these questions.

In the first year of this project, we have made progress in three directions. First, we have considered the LANL Ocean General Circulation Model (OGCM) Parallel Ocean Program (POP), and setup configurations that use realistic stratification to study how the systems equilibrate. We are considering spontaneous breakdown of balance and excitation of inertial waves as the primary mechanisms leading to a forward cascade of energy and eventual dissipation. Stratification can be changed from that which corresponds to midlatitude oceans to the less-stratified higher latitude oceans. A highlight of this setup is the use of small-scale selective and low values of lateral friction to allow for a better representation of smaller scale processes. We are presently working on diagnostics designed to track explicitly the flow of energy in the system.

In the first of these studies, considering the Drake Passage region, a surprising, but preliminary finding is that some baroclinic instability events are associated with large dissipation of kinetic energy. A possible explanation is that such baroclinic instabilities are of the ageostrophic anticyclonic type; this instability has been suggested by McWilliams and co-workers [1-3] to play a role in effecting spontaneous breakdown of balance and a local forward cascade of energy. Figure 1 shows the near-surface temperature field as these instabilities develop in a high-resolution continuation of a circulation that had equilibrated at a lower resolution.
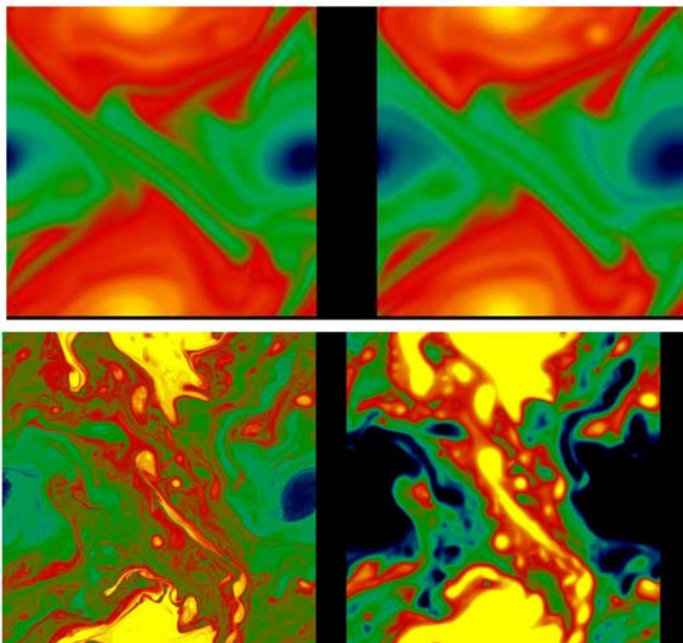
Figure 1. Temperature at 13m (left column) and 252m (right column) in the POP OGCM at 7.8km resolution (top row) and 977m resolution (bottom row). Temperature and salinity stratification correspond to that in the Antarctic

Circumpolar Current as obtained from Levitus. Forcing consists of a large-scale steady atmospheric windstress. The equilibrated circulation from the 7.8km run is used as initial conditions in the 977m run (not equilibrated yet.) The breakdown of the equilibrated run on increasing resolution is due to the resolution of a number of small-scale instabilities.

Next, to better understand balanced dynamics, we are investigating some of the regimes of balanced dynamics that have not been considered to date [3-5]. We find that in the most classical of settings of physical oceanography, steady wind forced ocean circulation in a basin, we find new regimes where alternating quasi-zonal stationary and propagating jets appear (Figure 2). It is only in the past 5-6 years that there has been observational evidence for such structures; the dynamics underlying these structures in an active area of research.
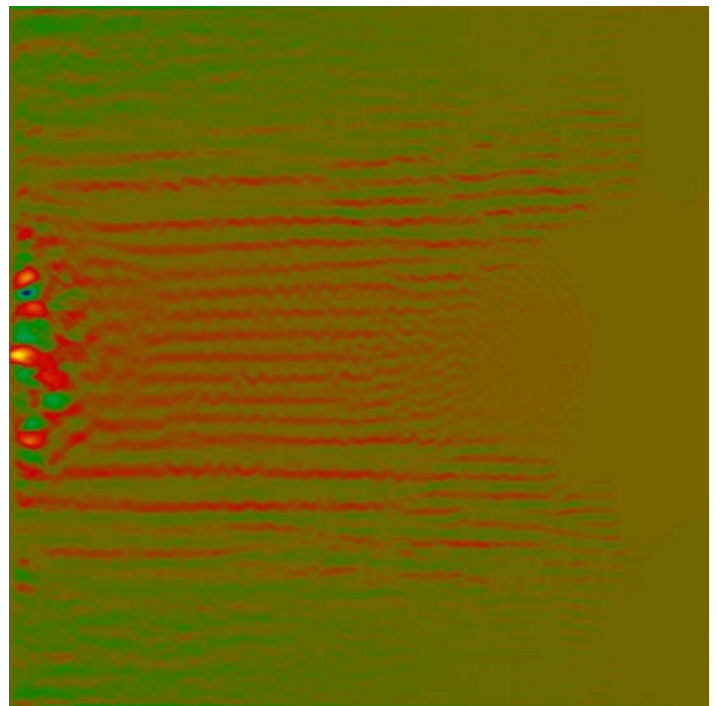
Figure 2. The east-west flow velocity in a 4000km x 4000km ocean basin is color-coded such that red-yellow indicated eastward flowing jets while black-blue indicate westward flowing jets. The forcing consists of a steady large-scale atmospheric forcing. The classical solution to this problem consists of a large-scale double-gyre circulation and mesoscale eddies. However, at the higher resolutions that we solve this problem, zonally-extended but meridionally confined, coherent, alternating zonal jets appear. There is recent satellite based observational evidence for the existence of these jets. Furthermore, we find that these jets can either be quasi-stationary or be of the north-south propagating kind, depending on the nonlinearity.

Finally, we are adapting the LANL-SANDIA Direct Numerical Solver to setup flows as encountered in the oceans. This

high fidelity model solves the incompressible-Boussinesq Navier-Stokes equations with variable density and unlike OGCMs is nonhydrostatic. While for the most part, the ocean is stably stratified and approximately hydrostatic, the top few hundred meters of the ocean is subject to gravitational instability (denser water overlying lighter water) due to interactions with the atmosphere and sun and is therefore nonhydrostatic. While this is a small fraction of the average 5km depth of the ocean, the importance of this upper region cannot be overemphasized: All interactions of the global ocean with the atmosphere are mediated through this region and all global ocean circulation can eventually be traced to these interactions. Because of computational costs, rather than resolve processes in this top layer, OGCMs approximate the effect of dynamics with parameterizations. Furthermore, the superior (exponential) accuracy of the spectral spatial discretization used in this solver compared to the low (second) order accuracy used in POP and other OGCMs will enable us to better capture the smaller scale processes that are more suseptible to dissipation.

The flowsolver presently can only handle triply-periodic boundary conditions and we are implementing a Chebyshev discretization in the vertical that will allow for a realistic representation of a typical ocean water column. Chebyshev-in-the-vertical naturally allows for high resolution at the top and bottom of the water column; the top is distinguished by its interactionss with the atmosphere that forces the global ocean circulation; the importance of the bottom derives from dissipation that occurs over small scale boundary layers due to bathymetric-interactions.

Future Work

When resolution is increased from state-of-the-art ocean circulation simulations by an order of magnitude, we find that circulations that were stable at the lower resolutions are destabilized. Characterization of these instabilities and their importance in opening up new pathways that lead to a cascade of energy to smaller scales is to be undertaken next. The high fidelity model of ocean circulation based on the incompressible-Boussinesq equations along with sophisticated numerics to adaptively resolve upper ocean and bottom ocean processes will be brought online and tested. The work on new regimes in the classical double-gyre wind-driven ocean circulation that display the recently observed quasi-zonal jets will be submitted to leading journals.

Conclusion

In the first year, we have developed diagnostics that clearly follow the transfer of energy across scales in a hierarchy of ocean circulation models that range from the quasi-geostrophic equations to the shallow water equations to the primitive equations. We have used these diagnostics to better explain the new regimes of the double-gyre circulation that we find (that displays recently-observed quasi-jet like features.) Next, we show that as resolution is increased from state-of-the-art ocean circulation studies by about an order of magnitude, numerous new instabilities develop. Characterization of these instabilities and their importance in opening up pathways that lead to a cascade of energy to smaller scales is to be undertaken next. Finally, we have written a 'Physics of Fluids' article related to improved parameterization of unrepresented subgrid dynamics in coarse resolution ocean models.

References
1. Molemaker, M. J., and J. C. McWILLIAMS. Local balance and cross-scale flux of available potential energy. 2010. *Journal of Fluid Mechanics.* **645**: 295.

2. Molemaker, M. Jeroen., J. McWilliams, and X. Capet. Balanced and unbalanced routes to dissipation in an equilibrated Eady flow. 2010. *JOURNAL OF FLUID MECHANICS.* **654**: 35.

3. McWilliams, J. C., M. J. Molemaker, and I. Yavneh. Ageostrophic, anticyclonic instability of a geostrophic, barotropic boundary current. 2004. *PHYSICS OF FLUIDS.* **16** (10): 3720.

4. Nadiga, B. T., and D. N. Straub. Alternating zonal jets and energy fluxes in barotropic wind-driven gyres. 2010. *OCEAN MODELLING.* **33** (3-4): 257.

5. Nadiga, B. T.. Flux of energy across scales in two oceanographic flows. 2011. (Montreal, 28-30 Sep. 2011). p. --. Montreal: Centre de Recherches Mathematiques.

6. Connaughton, C., B. Nadiga, S. Nazarenko, and B. Quinn. Modulational instability of Rossby and drift waves and generation of zonal jets. 2010. *Journal of Fluid Mechanics.* **654**: 207.

Publications
Connaughton, C., B. Nadiga, S. Nazarenko, and B. Quinn. Modulational instability of Rossby and drift waves and generation of zonal jets. 2010. *JOURNAL OF FLUID MECHANICS.* **654**: 207.

Nadiga, B. T.. Stochastic approaches for multiscale modelling in geosciences. 2011. In *European Geophysical Union, General Assembly 2011.* (Vienna, Austria, 3-8 Apr. 2011). Vol. 13, p. 13064. Munich: European Geophysical Union.

Nadiga, B. T.. Flux of energy across scales in two oceanographic flows. 2011. In *Balance, Boundaries, and Mixing in the Climate Problem.* (Montreal, 28-30 Sep. 2011). , p. --. Montreal: Centre de Recherches Mathematiques.

Nadiga, B. T., and D. N. Straub. Alternating zonal jets and energy fluxes in barotropic wind-driven gyres. 2010. *OCEAN MODELLING.* **33** (3-4): 257.

Nadiga, B. T., and F. Bouchet. When can we expect statistical mechanics to help predict large scale atmospheric and

oceanic features?. 2010. In *American Geophysical Union, Fall Meeting 2010.* (San Fransico, 13-17 Dec. 2010). , p. B1209+. Washington D.C.: American Geophysical Union.

Nadiga, B., and F. Bouchet. The equivalence of the Lagrangian-averaged Navier-Stokes-Œ± model and the rational large eddy simulation model in two dimensions. 2011. *Physics of Fluids.* **23** (9): 095105.

Time-Dependent Quantum Molecular Dynamic Simulations of Dense Plasmas Supporting Thomson X-ray Scattering Experiments

Jerome O. Daligault
20110228ER

Introduction

The understanding of strongly coupled quantum plasmas is an important challenge in modern physics. The new generation of X-ray light sources, such as the Linac Coherent Light Source at Stanford, holds the promise to profoundly advance our fundamental understanding of dense plasmas. X-ray scattering experiments will be performed with far greater spatial and energy resolution, and will provide access to measurements that have so far been impossible. As suggested by early experimental efforts, e.g. [2], the ability to model dynamical and non-equilibrium systems must be developed if we are to maximize the scientific impact of the wealth of data from those experiments. Indeed, in addition to the in-situ measurements, the coming experiments will make it possible to measure genuine dynamical properties of dense plasmas. Moreover, by their nature dense plasma experiments generally produce highly time-dependent (i.e. non-equilibrium) situations.

A main goal is to develop a new computational capability that solves the real-time dynamics of strongly interacting quantum electrons and classical ions in dense plasmas. This capability will make it possible to calculate truly dynamical and non-equilibrium properties that are so far inaccessible by state-of-the-art quantum molecular dynamics approaches. We will focus on one applicationthat demands time-dependent and non-equilibrium treatments and will shed much needed light on properties relevant to the coming X-ray scattering experiments. Simulations using first state-of-the-art classical molecular dynamics simulations and the newly developed simulation code will be performed and analyzed throughout the duration of the project to explore what dynamical information can be extracted from the frequency and wave-vector dependent X-ray scattering spectra.

Below, we describe the achievements of the ER-project for FY 2011.

Benefit to National Security Missions

The results of this effort will introduce a new and unique simulation capability in modeling extreme states of matter at LANL. The capability will allow significant scope for exploration of non-equilibrium conditions in dense plasmas and materials under extreme conditions (e,g, radiation damage, ion slowing-down, non-equilibrium phase transitions). By enhancing our basic science capabilities, this project will help LANL meet its current and future applied missions and challenges, including the science campaigns, Advanced Scientific Computing (ASC) and national High Energy Density Laboratory Plasma (HEDLP) programs. This exploratory research has strong ties to two LANL grand challenges, namely "Materials: Discovery Science to Strategic Applications" and "Nuclear Performance", and to the areas that will be explored in the future MaRie facility at LANL.

Progress

Development of the methodology and of the simulation code

Firstly, we derived the details of the equations and of the algorithms for their numerical solutions. The methodology proposed is based on a semi-quantal approximation of the Time-Dependent Density-Functional Theory (TDDFT) method that consist in the Newton's equations of motion for the ion dynamics coupled to Vlasov-like equation for the electron dynamics. Secondly, we designed the numerical algorithm. The different components were chosen in such a way that their implementation uses as much as possible the numerical tools used by the PI in a parallel molecular dynamics code for a previous project. The algorithm employs state-of-the-art particle-particle, particle-mesh algorithms (PPPM) in order to self-consistently combine high-resolution of close encounters (which are dealt with nearest neighbor techniques) and rapid, long-range force calculation (which are computed on a mesh with three-dimensional fast-Fourier transforms).

The main components of the code are now implemented. The code was written in Fortran 95 with Message Passing Interface (MPI) to make it fully parallel. After a fair amount of time spent debugging the code, we are presently testing and optimizing the various routines.

To that end, various diagnostics have been created and implemented, in particular methods to extract the electron entropy, density of states, occupation number and energy diffusion. We are also testing the performances of the algorithm as a function of the various purely numerical parameters (~ 10 parameters), including the number of numerical particles, the FFT mesh size and various parameters involved in the PPPM method. As illustrated in Figures 1 and 2, we are determining the domain of stability of the code as a function of the numerical parameters, where stability is measured by the time over which a simulation conserves energy, entropy and fermionic character. So far, all the tests have been performed on a simple model system, namely the jellium model, where ions are smeared out into a uniform neutralizing background. The results are very promising and we are getting ready to perform similar tests on more realistic models of dense plasmas including the ion dynamics explicitly. This part of the work has been done by the PI and by Dr Antonio Cadilhe, a Limited Term Visiting Staff Member (LTVSM) whom we hired in February 2011 to assist in the implementation and validation of the code. The results are presently being summarized into a publication that we hope to submit in the first semester of FY 2012.

(a)   (b)   (c)
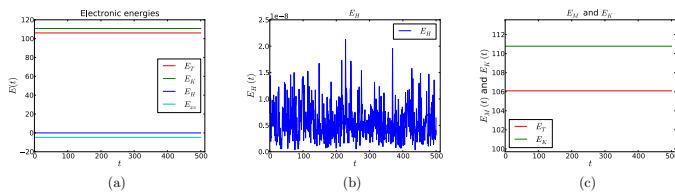
Figure 1. Test of the conservation of the electronic energy with time (in units of inverse plasma frequency) for a jellium plasma: Total energy (EM=EK+EH_Exc) , kinetic energy (EK), Hartree energy (EH and exchange correlation (Exc).
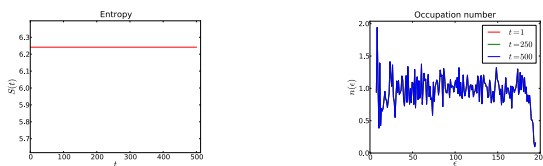
Figure 2. Test of the conservation of entropy conservation for a jeliium plasma. Left pannel: time dependence of the entropy. Right Pannel: Occupation number at different times.

In parallel, the PI has investigated with analytical theory how to include in the code the effect of quantum electronic fluctuation on the ionic dynamics, which are neglected in the present implementation. We believe that these fluctuations may be important in the overall non-equilibrium plasma dynamics. We have developed an expression for the electron-ion fluctuations and are in he process of evaluating it contribution to the ionic properties, i.e. the viscosity. These results will be important in other areas, e.g. in the study far-from-equilibrium phase transitions induced by radiation damage, where quantum fluctuations are usually neglected (Born-Oppenheimer approximation).

Advancing the modeling of X-ray Thomson scattering experiments

Following the proposed work outlined in the project, with PhD student James Mithen and the external co-PI GianlucaGregori from Oxford University, we have explored with classical molecular dynamics simulations and model the ion dynamics of dense single-component plasmas over a wide range of densities and temperatures. We obtained numerous new results (see below)that are important for maximizing the impact of the wealth of data from x-ray scattering experiments using 4th generation light sources and high power lasers. Two papers [1,2] were published and three manuscripts [3,4,5] have been submitted for publication. The work was presented at the Strongly Coupled Coulomb Systems (SCCS) 2011 conference, heldin Budapest (Hungary) in July 2011, and at the Strongly Coupled Ultra Cold and Quantum Plasmas conference inLisbon, held in Lisbon in September 2011.

X-ray Thomson scattering experiments will soon be able to fully resolve time dependent ion dynamics in dense plasmas. These ion dynamics are encoded in the wavevector(k) and frequency (w) dependent ion-ion structure factor, a.k.a. dynamic structure factor S(k,w) which is the Fourier transform in space and time of the density auto- correlation function. The ability to model S(k,w) must be developed if we are to maximize the scientific impact of the wealth of data from those experiments.In the past, a number of models for the ion-ion structure factor have been proposed thus far - but none seem to stand out and have been validated.

In [1], we addressed the question of the domain of applicability of the hydrodynamic description for plasmas at or near equilibrium as the level of many-body correlations in the system is varied.One ordinarily thinks of the hydrodynamic picture as applying only for wavenumbers k such that $kl_f \ll 1$ with l_f the mean free path and frequencies ω such that $w/w_c << 1$ with w_c the mean collision frequency.These conditions, derived and already rather qualitative for a system governed by uncorrelated binary collisions (e.g. a dilute gas), become even more indeterminate when many- body correlations are present (as is the case, for example, in a liquid) because the concepts of mean free path and mean collision time cease to have a clear physical meaning.Thus the applicability of the hydrodynamic description certainly depends strongly on the thermodynamic conditions - e.g. the density n and temperature T - as well as the strength and range of the particles' mutual interactions. We find the maximum wavenumber k_{max} at which the hydrodynamic description applies to be given by$k_{max} = 0.43 l_s$,where l_s is the electron screening length.In the extreme case of an OCP, l_s is infinite and, because of the long range Coulomb interactions, the system exhibits

the characteristic behavior of plasmas: density imbalances lead to high frequency plasma oscillations, rather than low frequency sound waves in a screened plasma.As a consequence, we found that the hydrodynamic description is never applicable in this limit.

In [2,3], we developed a model that works well at higher momentum transfer k (Figure 3) which is of even greater applicability to the experiments. It is based on an exact representation of S(k,w) in terms of a memory function m(k,w) that plays the role of a generalized wavevector and frequency-dependent viscosity. Using the Gaussian ansatz for m(k,w), we showed that this generalized model works remarkably well for all k values, i.e. the model describes both the conventional hydrodynamic limit at small k values and the large k behavior (when the ions behave as a collection of free particles), along with the entire intermediate dynamics between these two regimes.

In [4,5], we use the results obtained on [1,2] to explore what dynamical information can be extracted from the X-ray scattering spectra, in particular the viscosity and the dispersion relation of collective plasma modes.
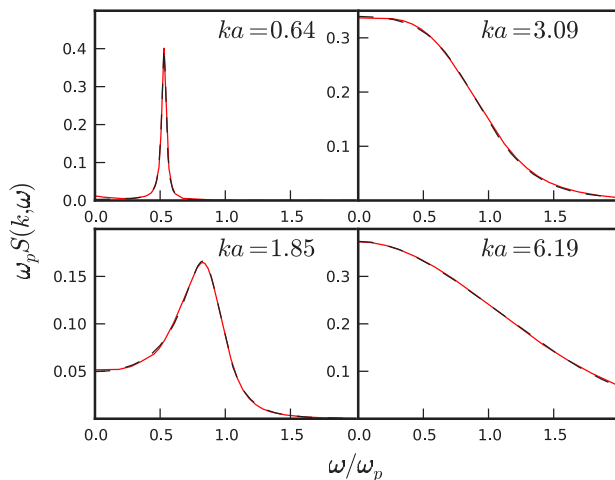
Figure 3. A simple generalization of the Navier- Stokes equations (dashed line) yields excellent agree- ment with the MD results for the dynamical structure factor S(k,w) for all reduced wavevectors k. Here w_p is the plasma frequency of the system.

Future Work

In FY 2012, we will pursue the validation of the code and of the semi-classical model. To this end, we will perform various simulations of three simple systems, namely

- the jellium model (where ions are smeared out into a uniform neutralizing background) to test the electron dynamics

- the jellium with a fixed impurity ion to test screening effects and electron-ion scattering

- a model of Aluminum plasmas with explicit treatment

of both quantal electrons and classical ions (the ultimate goal)

For each model, we will perform a systematic study of the code performance with the numerical parameters and adjust them to optimize the code performances, and check the conservation laws (e.g. energy, entropy, fermionic character). We will extract a number of physical quantities, e.g. the screening length, the electrical conductivity, the pair distribution functions... and compare them with known analytical results.

If all the tests are passed and the code is validated, we will apply it to physics problems inaccessible to existing simulation capabilities, namely (1) the calculation of the electron dynamic structure factor See(k,w) (this is relevant to many ongoing X-ray scattering experiments) and/or (2) the calculation of the electron-ion temperature relaxation rate in warm dense aluminum plasmas (this is especially relevant to ASC and Inertial Fusion Energy).

Conclusion

The progress made in the first year of this project isin accordance with the timetable outlined in the proposal. We have developed and implemented the time-dependent "semi-classical" molecular dynamics code by replacing the classical Newtonian electron dynamics of the current MD code by the Newtonian dynamics of the test-particles. Preliminary results are very encouraging. We have advanced the modeling of X-ray Thomson scattering in anticipation of the coming experiments.

References

1. Mithen, J., J. Daligault, and G. Gregori. Applicability of the hydrodynamic description of classical fluids. 2011. *Physical Review E.* **83**: 015401.

2. Mithen, J. P., J. Daligault, B. J. B. Crowley, and G. Gregori. Density fluctuations in the Yukawa one-component plasma: an accurate model for the dynamical structure factor. 2011. *Physical Review E.* **84**: 046401.

3. Mithen, J., J. Daligault, and G. Gregori. Comparative merits of the memory function and dynamic local field correction of the classical one-component plasma. *Physical Review E.*

4. Mithen, J. P., J. Daligault, and G. Gregori. Molecular Dynamics simulations for the viscosity of non-ideal plasmas. To appear in *Contributions to Plasma Physics.*

5. Mithen, J., J. Dalgault, and G. Gregori. Onset of negative dispersion in the one-component plasma. To appear in *Proceedings of the the Strongly Coupled Ultra Cold and Quantum Plasmas conference in Lisbon, held in Lisbon in September 2011.*

Publications

Mithen, J. P., G. Gregori, and J. Daligault. Comparative merits of the memory function and dynamic local field correction of the classical one-component plasma. *Physical Review E.*

Mithen, J. P., J. Daligault, B. J. B. Crowley , and G. Gregori. Density fluctuations in the Yukawa one-component plasma: an accurate model for the dynamical structure factor. 2011. *Physical Review E.* **84**: 046401.

Mithen, J. P., J. Daligault, and G. Gregori. Applicability of the hydrodynamic description of classical fluids. 2011. *Physical Review E.* **83**: 015401(R).

Mithen, J. P., J. Daligault, and G. Gregori. Molecular Dynamics simulations for the viscosity of non-ideal plasmas. To appear in *Contributions to Plasma Physics.*

Mithen, J. P., J. Daligault, and G. Gregori. Onset of negative dispersion in the one-component plasma. To appear in *Proceedings of the Strongly Coupled Ultra Cold and Quantum Plasmas conference in Lisbon, held in Lisbon in September 2011..*

Precision Measurement of Atomic Parity Violation in Trapped Yb+

Martin M. Schauer
20110258ER

Introduction

A single trapped ion provides a superior system for studying all aspects of atomic structure and numerous fundamental questions, but it has yet to be fully exploited for studying nuclear structure, the Weak interaction, or extensions to the Standard Model. Parity Violation (PNC) is particularly sensitive to the relatively weak signals due to the latter since all other known interactions conserve parity, and such effects have been measured in atoms.

Initial measurements of PNC effects with ~10% uncertainty can be done on Yb+ with existing systems at LANL and measurements with precision better than 1% can be made with straightforward modifications. We will use the existing systems and modifications to make such measurements of PNC in multiple isotopes of Yb+. Sensitivity will be increased and systematics improved by introducing a single mirror into the trap to create an optical standing wave, and the measurements will be repeated. Linewidth measurements made during these studies will determine whether a cleaner and more stable magnetic field environment is required for making higher precision measurements.

The highest precision measurements in Yb+ will also require a resonating cavity for the 436 nm laser to get higher electric field strength. This will require two mirrors in the trap vacuum chamber (a technology we have already proved is possible in our apparatus). We will introduce such a resonator into the vacuum system if we determine that we have exhausted the capability of our system with a single mirror/laser standing wave configuration. Ultimately, measurements will be made until the intrinsic sensitivity of the system is exhausted.

Benefit to National Security Missions

Our experimental efforts are centered on state-of-the-art techniques for optical and radio frequency (rf) spectroscopy. We have several ideas for measuring the characteristics of ejected material from shocked surfaces using the optics, laser, and trapping expertise and infrastructure we have developed in pursuit of ion PNC. The most developed of these is multi-wavelength, multi-angle Mie scattering to measure changes in ejecta particle sizes as a function of time or height above the free surface. We continue to look for ways to apply our atomic spectroscopy expertise to remote sensing of environmental contaminants, biological agents, and the byproducts of SNM enrichment, all in support of our threat reduction mission.

Progress

Although we are able to reliably load single ions of many of the stable isotopes of Yb into the trap (^{170}Yb, ^{171}Yb, ^{172}Yb, ^{174}Yb, and ^{176}Yb) we have chosen to concentrate our efforts of late on ^{171}Yb+. This allows us to study the hyperfine levels and develop microwave driving techniques that will serve us well throughout the remainder of the project.

We have conducted detailed studies of the lifetime of the $D_{3/2}$ (F=2) state in a single, trapped Ytterbium ion. Our preliminary result is statistics-limited at a few percent and is in agreement with published results to within the experimental uncertainty. A complete understanding of the systematic effects at play in the lifetime of this level is important in understanding the results of this project: interference between electric quadrupole and electric dipole transitions between this level and the $S_{1/2}$ ground state is the signature of parity violating interactions which this experiment will attempt to measure. We are writing a manuscript for submission to a peer-reviewed journal on these results.

We have developed the capability to measure microwave transitions between the different Zeeman-split hyperfine levels of the ground state. The aim of these measurements is to characterize the ambient magnetic field of the trap environment as well as any birefringence in the beam path of the lasers used to drive the various transitions. Fluctuations in the ambient magnetic field can cause shifts in the Zeeman components of the hyperfine levels masking the small splitting expected to arise from parity-violating interactions. Likewise, any birefringence in the optical path can change the polarization of the laser beams and thereby cause a shift of the

levels of interest. If such effects are present, but are stable and well characterized, their effects can be compensated, hence the importance of measuring and understanding them. This is absolutely essential to the success of this project.

Presently, our measurement of the $m_F=0 - m_F'=0$ transition yields a linewidth of 40 Hz, and we have measured the center frequency of this transition to ~0.6Hz. This corresponds to a fractional accuracy of $5*10^{-11}$. These transitions are "field insensitive," and our measurement is limited by the resolution of the microwave generator. The linewidths of the $\Delta m=\pm1$ transitions are ~7 kHz and are limited by magnetic field noise.

Measurements of the linear and quadratic Zeeman shifts, both of which we are able to detect, give us a very sensitive indicator of magnetic field noise. Monitoring of this noise indicates that it is discontinuous which is indicative of magnetic domain noise in the material of the vacuum system and trap support structures. This finding is consistent with the results of other research groups around the world involved in high precision atomic spectroscopy. To better understand the origin of this noise we have enlisted the support of the low-field NMR group under the direction of Michelle Espy to measure field fluctuations of candidate vacuum chambers and windows for the second generation trap. We will use this information to choose vacuum hardware and shielding configurations for this trap.

We have developed the capability of driving coherent $\Delta m=0$ transitions in the ground state hyperfine manifold (Figure 1). This is important in that it demonstrates that we have the control and stability to drive π- or $\pi/2$- pulses to prepare the ion in a particular state.

We have begun the initial design work of this trap. We have designed the mounting block that will hold trap electrodes, cavity mirrors, and laser beam access holes. We have done modeling of one and two layer mu-metal shield configurations to assess the impact of laser access holes on overall magnetic field shielding. Further work on this depends on results of noise measurements, both *in situ* and external measurements.

We are developing the 436 nm laser source that will be used to drive the S-D transition. Initially, we planned to use a commercial Ti:Sapph laser running at 871 nm that was already in our possession. Frequency-doubled light at 436 nm would then be produced by means of a nonlinear crystal in a resonant cavity. The cavity/crystal assembly was built here. We found this system not to be stable enough for our purposes due to the locking mechanism used in the 871 nm commercial laser. We have replaced the Ti:sapph laser with a home-built system based on an 871nm diode laser that is amplified in a tapered amplifier before doubling in the cavity mentioned previously. We are presently getting 150mW of light out of the tapered

amplifier and have coupled this light into the doubling cavity. This arrangement yields about 3mW of 436 nm light. We would like to increase this significantly, so we are adding a second tapered amplifier. This should provide more than 1 W of 871 nm light, which should produce up to 100 mW of 436 light

We have rewritten the data acquisition and control system to provide more flexibility in the laser pulse sequences that can be produced. Much work has been done to improve trap performance, specifically in eliminating electrical noise on the trap electrodes by use of better sources and more filtering. These improvements will significantly reduce uncertainties in the results.
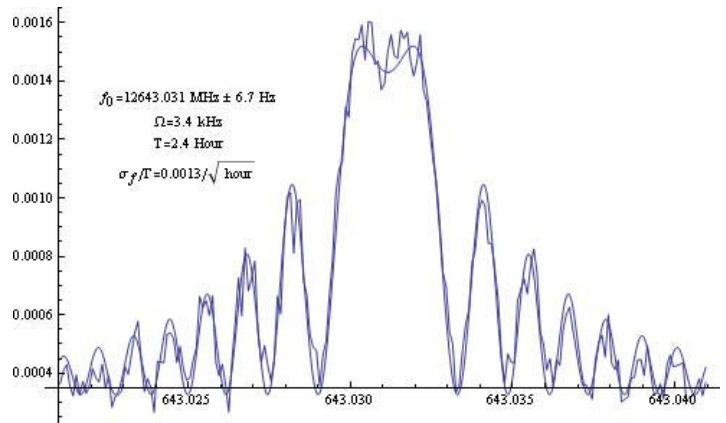
Figure 1. Fringes from driving coherent transitions between hyperfine levels of the ground state. Note that the excellent agreement of the fit provides a strong constraint on system parameters.

Future Work

Initial detection of PNC effects in a single ion can be done quickly and will be a significant achievement as it would demonstrate the utility of a fundamentally new method for studying atomic parity violation. 10% measurements can be made initially with a goal of approaching 0.1%.

To make the required measurements, circularly polarized laser light is used to drive the ion to an initial state with a well-defined spin, and an rf magnetic field is used to drive transitions between spin states. A transition is detected by using the laser beam as a probe to drive ions that have made a transition. Energy shifts are detected and measured through changes in the probability of this transition. This initial capability is the cornerstone of our experiment.

The ability to measure the alignment of the laser field polarization and the magnetic field in situ at the position of the ion is a top priority. The alignment of these fields must be accomplished to better than 1% for the best quality results. We have developed several ideas to carry out this task and the results will be both important and publishable.

Active control and shielding are required reduce initial rf

transition widths of ~10kHz to a few 100Hz. Implementation of active polarization and magnetic field control and installation of shielding will represent a major effort.

Further improvements in precision will require higher electric fields, a reduced quadrupole transition rate, and narrower spin transition linewidths. Increases of the electric field to generate higher signals could be done with a resonating cavity, or initially just a single in situ mirror. Each of these advanced tasked are major efforts and represent significant milestones for the experiment.

Conclusion

We expect to make measurements of the parity violating (PNC) effects in a single trapped atomic ytterbium ion to better than 10% accuracy. Our fundamental theories of Nature are incomplete and numerous additional theories have been proposed as solutions. Most of these additional theories with experimental predictions violate parity so that our results will provide sensitive tests of them. Our measurements will also be sensitive to the existence of previously undiscovered particles with masses up to 3 TeV; an energy similar to the current Large Hadron Collider but with better resolution, complimentary non-equivalent results and at far lower cost.

The Largest Cosmic Implosions: Formation of Supermassive Black Holes

Hui Li
20110300ER

Introduction

The past decade has witnessed the astonishing discovery that supermassive black holes (SMBHs) reside in the centers of nearly all galaxies [1,2]. An equally dramatic discovery is that QSOs (quasi-stellar objects, the most energetic objects in the Universe that are powered by accretion of matter onto SMBHs) exist at redshift z ~6.5, less than one billion years after the Big Bang [3,4]. To form SMBHs so early, the center of a galaxy must accumulate about 1065 baryons in a region the size of our solar system on a short timescale (≤ 109 yrs). This presents a direct challenge to the present paradigm of gravitational collapse. The physics of the SMBH formation now becomes a major mystery, given the important roles of SMBHs in cosmology, in cosmic re-ionization, and in shaping the subsequent cosmic structure formation. The primary objectives of this proposal are to investigate: a) How is the angular momentum of the matter transported so the collapse can occur? b) What are the physical processes in regulating the implosion and explosion of these objects? The proposed work is computationally intensive and it will build upon two unique strengths at LANL: 1) the 3-D cosmological magnetohydrodynamic (MHD) code ENZO+MHD developed jointly by University of California-San Diego and LANL; and 2) the 3-D radiation hydrodynamic code SNSPH that is developed at LANL. LANL has the unique advantage of being able to model the collapse of cosmological halos together with the central object's implosion and explosion. We expect that the planned work will take the SMBH research into a new realm and better position LANL for the up-coming revolution in astronomy to be initiated by the James Webb Space Telescope (JWST, 2014).

Benefit to National Security Missions

The work will address one of the most exciting and fundamental questions in modern astrophysics and cosmology, namely how the supermassive black holes (SMBHs) form at the centers of galaxies. The project will advance LANL's capabilities in: a) large-scale computational astrophysics by studying multi-dimensional gas collapse physics, b) cosmology by simulating the formation of SMBH from galaxy scale to black-hole scale, nuclear and particle physics by investigating the neutrino cooling signatures during the SMBH formation. Through making important contributions in this forefront scientific challenge, we will enhance LANL's scientific reputation and attract top scientists to the Laboratory.

Progress

We have been conducting research on three fronts:

- We have performed simulations of astrophysical disks that are undergoing instabilities driven by disk self-gravity. We found that the disks become turbulent and interestingly large-scale global spiral modes are also produced. We have been analyzing the rate of angular momentum transport driven by both the turbulence and the spiral waves. This helps us understand the dependence of mass accretion rate to the central region where the eventual black hole will form. We are also in the process of finishing up the development of a 3-D accretion disk code which will be used for investigating the star formation in such disks.

- We have developed a relativistic magnetohydrodynamic code that can be used to model the turbulence in disks near SMBHs. This code will help us to understand the accretion dynamics near the black hole in terms of determining the accretion rates and the black hole masses.

- We have modeled a suite of collapses of Hydrogen/Helium gas cloud assuming adiabatic collapse. More realistic stellar progenitor models were used for a range of star masses from 1000 to 1 million solar masses. Most of these stars undergo significant nuclear burning prior to collapse and the cores are more likely to collapse to form black holes without explosions of any kind (as predicted by members of this group). The first results of these calculations have been published, focusing on any observable diagnostics of the collapses of these stars (including the neutrino signal).

Future Work

Our future research will concentrate on two fronts, corresponding to the two main stages of the overall formation process: 1) Understanding the evolution of angular momentum during the gravitational collapse of matter from the proto-galactic halo down to the central disk (~pc) via cosmological ENZO hydrodynamics and magnetohydrodynamic (MHD) simulations. We have started the cosmological hydrodynamic simulation to study the collapse of a slow rotating cloud so that we can gain insights on how the collapse process will vary depending on the numerical resolution. We will elucidate the relative role between angular momentum transport and segregation. Furthermore, we will perform stand-alone thick disk simulations using our disk simulation codes to investigate in detail how the supersonic turbulence and shocks in disks can transport angular momentum. These studies will determine the input conditions for studying the central objects. 2) We will continue to study the formation of the central seed black hole, especially under the condition when the accretion rate is very high from the surrounding disk. We have begun to work with George Fuller (UCSD) to study the neutrino signal in detail if it is modified by neutrino oscillations. We have also begun to work with Dan Whalen to include the current understanding of the supernova engine into studies of low-mass black hole formation. By including this physics, it becomes even more certain that SMBHs cannot have been constructed from many 100-1000 solar mass black holes. The ultimate question from this stage is the final masses of the black hole that can serve as the "heavy seeds" for further growth.

Conclusion

Extensive simulations will take the study of SMBH formation into a new realm because of the accretion and explosion capabilities and the unique numerical tools LANL could provide. We expect to achieve quantitative understanding of how the central massive objects can form and whether such massive objects will eventually explode or form the seeds for the observed SMBHs. The possible detection by JWST as well as the possible accompanying signatures in neutrinos provides the necessary validation of our research.

Publications

Fryer, C. L., and A. Heger. Forming massive black holes through stellar collapse: Observational diagnostics. 2011. *Astronomische Nachrichten.* **332**: 408.

Li, S.. High-order time integration with local Lax-Wendroff procedure for central scheme on overlapping grid. To appear in *Journal of Computational and Applied Math.*

Li, S.. Code comparison on MHD wave propagation problems. To appear in *Numerical Modeling of Space Plasma Flows: ASTRONUM2011.* (Valencia, Spain, 13-17 June, 2011).

"Listening" to the Noise of a Single Electron Spin: Methods for Fast, Ultra-sensitive, Non-perturbative Noise Spectroscopy

Scott A. Crooker
20110306ER

Introduction

Not all noise in experimental measurements is unwelcome. Certain fundamental noise sources contain extremely valuable information about the system itself – a classic example being the inherent voltage fluctuations that exist across any resistor (Johnson noise), from which temperature can be determined. In magnetic systems, fundamental noise exists in the form of small, random spin fluctuations. For example, statistical fluctuations of N paramagnetic spins should generate "spin noise" of order $\sqrt{N}$, even in zero magnetic field. Crucially, the frequency spectra of these tiny fluctuations - if measurable - reveal the important dynamic properties of the spins (such as spin precession frequencies, decoherence times, and interparticle couplings), without ever having to excite, pump, or drive the spin ensemble away from thermal equilibrium. Such a noise-based approach to spin resonance is in marked contrast to conventional nuclear- or electron-spin resonance measurements, which necessarily perturb the spins. Nevertheless, this approach is guaranteed by the Fluctuation-Dissipation Theorem. Importantly, noise-based measurements become viable alternatives to conventional (dissipative) methods as the few-particle limit is approached ($N \rightarrow 1$), since noise signals fall only as $\sqrt{N}$ rather than as N. Our scientific goal is therefore to develop an ultra-sensitive magnetometer capable of "listening" to the tiny spin fluctuations of truly quantum-mechanical objects: single electron spins trapped in semiconductor quantum dots. New instrumentation for efficient digital signal processing based on configurable hardware (field programmable gate arrays (FPGAs)) are essential to this work. Preliminary studies of spin noise in various systems indicate that all aspects of this project are achievable in a 3-year timeframe.

Benefit to National Security Missions

This project builds Laboratory capabilities in the development of novel measurement methods that enable new scientific discovery at LANL. It is based on recent technological advancements that enable the use of FPGAs on the very large data storage and manipulation capabilities that have now become available. The project also depends on recent scientific discoveries in the field of spin noise spectroscopy and includes a theoretical underpinning with computation and modeling support. Our basic approach to noise spectroscopy goes well beyond the specific example of electron spin noise that will be investigated here and the advantages of noise spectroscopy as an experimental probe are very general. Demonstration of single spin noise spectroscopy measurements will generate worldwide attention and will form a robust platform for a nanoscale spintronics program at LANL. The team will work to develop a BES Materials Science funded lineup and to obtain DARPA funding for extending this work.

Progress

Since this project's inception in ~October 2010, we have first been able to hire key postdoctoral personnel (Dr. Yan Li from UC Riverside) in October 2010, and she has been working full-time on the spin noise project. (Note: owing to both her excellent performance while here at LANL, and also owing to her excellent research track record, she was very recently awarded Director's postdoctoral fellowship).

Over the past year, Dr. Li has made an essential breakthrough: she has taken a comprehensive set of data that clearly reveals an ultra-long spin coherence time of single holes that are localized in single semiconductor quantum dots. These long coherence times (well in excess of what has been published to date) were revealed via the application of longitudinal magnetic fields, a capability that she developed during her first months here at LANL. We now have a complete set of data as a function of temperature, field, laser probing conditions, and sample characteristics. An example of the latest data is shown in Figure 1, which shows the spin noise experiment (1a) and the very narrow noise peak that corresponds to hole spins with long spin lifetime (1b). Note further that these noise peaks follow a Lorentzian lineshape to a very high degree of precision (1c), which indicates exponentially-decaying spin relaxation dynamics. Moreover, we have found that these spin lifetimes increase dramatically upon application of small longi-

tudinal magnetic fields (Figure 2), which directly reveals the coupling of the hole spins to the bath of surrounding nuclear spins. Dr. Li is in the process of writing up these results that we (along with our collaborators in Germany) intend to submit to either Physical Review Letters or to Nature Physics.

Separately, our German collaborators are developing new semiconductor quantum dot samples with a low areal density that should facilitate our intended single-dot studies. Moreover, they are also working on quantum dots structures that include an electrostatic gate, so that we will be able to independently tune the background electron or hole concentration in these quantum dots.

On the theoretical front, we have also enlisted the involvement of Dr. Nikolai Sinitsyn (T-4), who has an established track record of work in the areas of spin decoherence. He and Dr. Bogdan Mihaila (a co-I) are developing models to put our data on a more solid theoretical footing.

And finally, we are working with our European collaborators to develop a theory of the large spin noise signals that we observe in semiconductor quantum dots. Part of this effort involved careful measurements of potassium atomic vapor (as an archetypical system with a homogeneously-broadened lineshape); these studies were conducted successfully in September 2011.
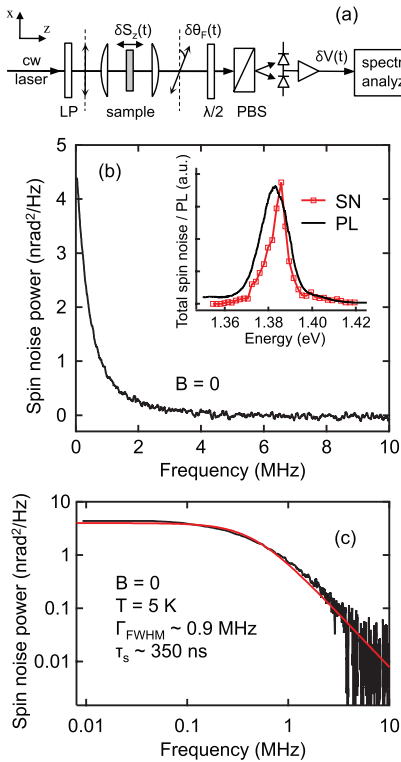
Figure 1. a) Schematic of the spin noise experiment. b) Frequency spectrum of the intrinsic spin fluctuations from hole spins in InGaAs quantum dots. The narrow (400 kHz half-width) peak indicates long (400 ns) spin relaxation times. c) the same noise, on a log-log scale. Data follow a Lorentzian lineshape.
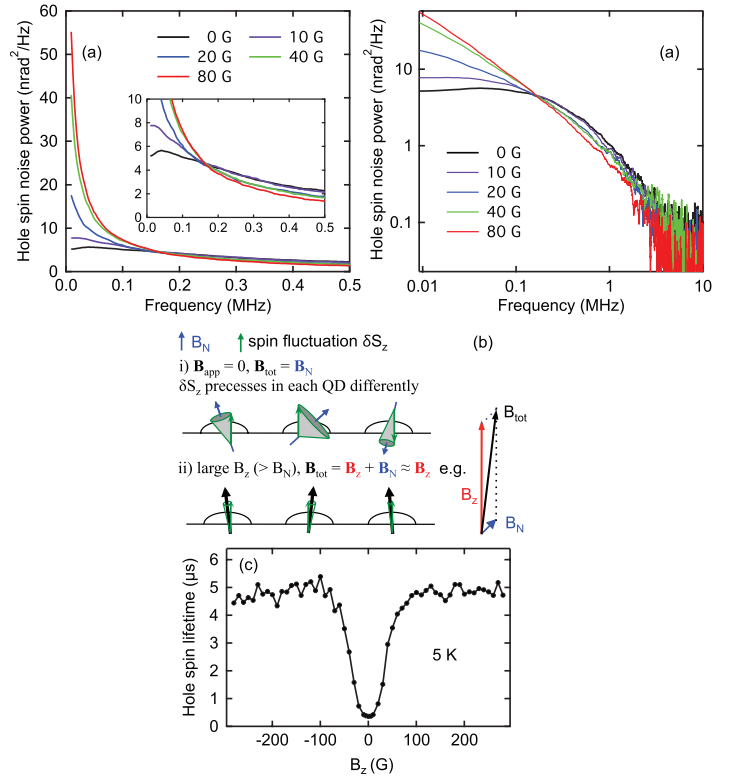
Figure 2. Hole spin noise spectra in the presence of small longitudinal magnetic fields. The noise peaks become much narrower, indicating that hole-nuclear coupling is suppressed, revealing extremely long hole spin lifetimes of order 5 microseconds. Data are also shown on a log-log plot. Bottom panel shows the spin lifetime as a function of longitudinal magnetic field.

Future Work

The key challenges for measuring single-electron spin noise are i) fabrication of semiconductor quantum dot containing single electrons, ii) construction of the high-res, low-T, scanning Fara-day rotation microscope to measure single dots, and iii) implementation of algorithms for real-time, ultra-efficient recovery of these tiny signals. These points are addressed as follows: i) Our overseas collaborators have been growing electron-doped InGaAs quantum dots for the past decade; what remains is to reduce the density of dots to ~10 dots/square micron (to facilitate spatial isolation) by changing growth temperatures. ii) The scanning FR microscope requires re-design and re-machining of our existing optical cryostat and spin noise apparatus, to permit the use of high-power optics. Nano-positioning of the dots will require commercial cryogenic piezoelectric xyz stages. iii) Development of our own suite of real-time digital signal processing algorithms will be accomplished using National Instruments' new FPGA hardware modules that are configurable within the standard LabView environment. Prototypes will be tested in software using stored data, then ported to FPGAs for ultra-sensitive, real-time applications. This new instrumentation will permit the first non-perturbative studies of single spins, revealing dynamic interactions with nuclei in the host crystal by recovering

2-, 3-, and 4-point correlations in the noise.

Conclusion

In the first year, we developed a single-dot scanning microscope (new optics, cryostat, piezoscanners) to measure optical transmission & Faraday rotation spectra from single quantum dots. We measured the 2-point noise correlations (power spectra) using FPGAs as $N->1$. This year we implemented ultra-efficient, real-time correlation algorithms (theory & experiment), including benchmarking algorithms in software using real (stored) data and programming on LabView FPGA hardware modules for real-time, ultra-sensitive detection. We expect to exploit single-spin noise for basic science and quantum measurement, specifically the study of electron-nuclear spin coupling via 3-, 4-pt correlations of noise in the final year of this work.

The Terahertz Quantum Hall Effect

Rohit P. Prasankumar
20110311ER

Introduction

Two-dimensional electron gases (2DEGs) in semiconductor heterostructures are a widely used platform for modern electronics. However, at very low temperatures (T<4 K) and high magnetic fields (B>>1 T), they evolve into a new frontier for quantum processes and a testing ground for novel theoretical predictions. This is arguably best exemplified by the quantum Hall effect (QHE), which has been the subject of intense research worldwide (and four Nobel Prizes) since its discovery in 1980. Despite the many publications devoted to elucidating different aspects of the static properties of the QHE, there remain several unanswered questions regarding the underlying physics of this unique phenomenon. Previous studies, although primarily limited to DC measurements, have not only led to a deeper understanding of the QHE, but have also created more general concepts that have impacted other areas of condensed matter physics as well as quantum field theory and metrology. In addition, researchers have recently predicted that the optical Hall conductivity will also have a plateau structure that persists even in the AC regime (at terahertz (THz) frequencies), which we refer to as the "Terahertz Quantum Hall Effect (THz-QHE)". Experimental characterization of the THz Hall conductivity could also conclusively resolve a host of anomalies regarding the existence of a quantum phase transition in quantum Hall systems. Therefore, we expect that bringing novel experimental techniques to bear on this important problem will have wide ranging implications across many areas of physics. The goal of this project is to use ultrafast THz spectroscopy to gain new insight into the quantum Hall effect by probing regimes inaccessible to conventional electrical measurement techniques.

Benefit to National Security Missions

Institutionally, the planned work addresses the Grand Challenge in Materials: Discovery Science to Strategic Applications, both in exploring the underlying mechanism of the quantum Hall effect and in developing new experimental techniques to probe complex materials. This coupling of forefront nanoscience and quantum physics is unique to the Center for Integrated Nano-technologies and meshes with similar efforts at Sandia National Laboratories, supporting the collaboration between LANL and SNL. The forefront science and capability development will attract high quality students, postdocs and collaborators to LANL.

Progress

In the first year of this project, our experimental efforts have focused on designing and building the novel setup required for measuring the THz-QHE. We spent a significant amount of time planning and designing this system, in which the major components are a femtosecond Ti:sapphire oscillator and a superconducting magnet. The superconducting magnet, which was custom designed to our specifications for these experiments by Oxford Instruments, was recently delivered (after a lead time of ~9 months), and we are currently scheduling the installation. We have also just hired a new postdoc, Stephane Boubanga Tombet, who is expected to arrive from Japan in November.

In parallel with the above described efforts, we have also collaborated with David Hilton's group at the University of Alabama-Birmingham (UAB) and Steve McGill at the NHMFL in Tallahassee to perform THz cyclotron resonance experiments on 2DEGs. Prashanth Upadhya visited the NHMFL and helped construct an ultrafast THz magnetospectrometer that is based on an Oxford Instruments split coil magnet (similar to the system we will build at the CINT Core Facility). This system allows the measurement of the conductivity tensor in a quantum confined semiconducting system at THz frequencies as a function of temperature (down to 0.4 K) and magnetic field (0 – 7 T). Experiments were then performed to test and study the behavior of the 2DEG sample that will be used for our THz QHE experiments at LANL. Under a perpendicular magnetic field, the density of states in 2DEGs clump into discrete Landau levels separated by the cyclotron energy (which is typically in the THz frequency range). Characterization of the cyclotron resonance in the time domain has revealed useful information on the carrier scattering dynamics and dephasing mechanisms in the high mobility samples that we tested. This under-

standing is essential for the experimental realization of the THz QHE. This collaboration has enabled us to be scientifically productive while waiting for different components of our setup to arrive, and a publication on our results is in preparation.

Our theoretical efforts have focused on identifying novel directions to pursue once our experimental setup is built. These efforts have resulted in several ideas that we are considering for future work. One of these is to study percolation clusters in quantum Hall systems, which are self-similar fractals. The conductivity, which can be measured with THz spectroscopy, is predicted to follow a power law scaling, with the power determined by percolation critical exponents (S. A. Trugman, *Phys. Rev. B* (1983)). Therefore, THz conductivity measurements could give insight on fractals in quantum Hall systems.

Another exciting direction is to use THz spectroscopy to study edge states of the QHE. These states should have a local cyclotron resonance that is systematically shifted to higher frequencies than the bulk states. By varying the external magnetic field and moving the THz beam spot closer to the sample edge, we should be able to observe this high frequency tail in the THz spectrum, which is an indicator of when the edge states are actively carrying current.

Future Work

After our new postdoc's arrival and the magnet installation, we expect to build our THz QHE setup at the CINT Core Facility and demonstrate our ability to measure the THz QHE in a two-dimensional electron gas under a variety of experimental conditions within the next year. Our initial focus will be on comprehensively characterizing the THz Hall conductivity in 2DEGs as a function of frequency, magnetic field, and temperature. We will then relate our results to existing scaling theories of the QHE, modifying these theories if necessary, which will potentially allow us to determine the mechanism for quantum phase transitions in the QHE. We will also measure the THz Hall conductivity in graphene, which will allow us to explore quantum Hall physics in a truly two-dimensional system that has not been as extensively characterized to date. Finally, if there is time remaining in the next year, we will then explore some of the theoretical directions outlined above, which will include THz spectroscopy of quantum Hall edge states and fractals in quantum Hall systems. We also expect to apply our ability to perform THz spectroscopy in a magnetic field to other systems, such as high-temperature superconductors and multiferroics.

Conclusion

The quantum Hall effect, observed in two-dimensional electron gases at very low temperatures and high magnetic fields, has fascinated physicists for nearly thirty years (resulting in four Nobel Prizes). In this project, we will use a novel non-contact optical technique, ultrafast terahertz spectroscopy, to gain new insight into the quantum Hall effect by probing regimes that are inaccessible to conventional electrical measurement techniques. This will allow us to explore theoretical predictions for the quantum Hall effect in the AC regime, shedding new light on one of the most exciting areas of condensed matter physics.

References

1. Trugman, S. A.. Localization, percolation, and the quantum Hall effect. 1983. *Physical Review B.* **27** (12): 7539.

A Compact, Brilliant, Coherent X-ray Source Based on a Dense Relativistic Electron Mirror

Bjorn M. Hegelich
20110341ER

Introduction

Opportunities for application of coherent, ultra-fast x-rays are severely limited by the sources developed to date. Free-electron-lasers provide coherent x-rays at one or two facilities worldwide but are so expensive that the instruments completely dominate the budgets of the scientific applications. Alternatively, university laboratory scale lasers can generate coherent x-rays via high harmonics from atomic scattering in gas but with insufficient yields for key single-shot applications. Here we report on 1st year progress of an LDRD ER award to investigate a new approach to coherently up-convert laser light to soft-x-ray energies. Of potentially revolutionary impact, the technique under study could produce single-shot yields rivaling those of conventional free-electron-lasers—but using only a table-top optical laser.

The scheme (Figure 1) is based in a well known approach to up-shift optical frequencies via relativistic Doppler shifting from energetic electrons. To date, the technique has been developed extensively in a regime in which the x-ray contributions from each electron sum linearly. In contrast, coherent scattering, in which the output goes with the *square* of the number of participating electrons, will occur if the electrons are bunched with a layer thickness less than that of the output x-ray wavelength. Remarkably, this bunch layer requirement can be achieved by using a fast rise intense laser pulse to rip an entire relativistic electron population from an ultra-thin foil target. A second, much thicker "reflector" foil positioned downstream then separates the light and electron thus leaving the electron sheet with purely forward momentum. This flying sheet of electrons will coherently up-shift head-on incident laser light.
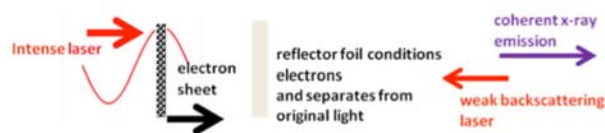
Figure 1. Schematic depiction of laser-based coherent x-ray generation by coherent Thomson backscatter from a relativistic electron mirror.

Benefit to National Security Missions

This project supports the LANL Materials Grand Challenge (GC) by developing a brilliant x-ray source to study the properties and structure of materials under extreme conditions of pressure and temperature in dynamic experiments. Investigating the transformational technologies within this proposal has the potential of fundamentally shaping the future signature facility (Matter and Radiation Interactions in Extremes (MaRIE)) and will establish leadership in advanced accelerator and light source technology.

Progress

In Year 1, we addressed issues fundamental to realization of this source. A simple technique has been identified to completely separate the optical phasing under the laser carrier envelope from the output electron sheet energy. Furthermore, the coherent scattering theory has been extended to account for a stronger backscattering light pulse. Regarding experimental science, an electron spectrometer has been designed to measure expected angular signatures of the accelerated electrons. We have explored the feasibility of plasma self-shuttering to create required ultra-fast rise times on the driving laser pulse. We have also identified an alternative regime in which multiple ultra-thin layers are pulled from a sufficiently thin foil and have identified a diagnostic technique to observe the phenomena.

Theory

Saturated yields at increased scattering laser strength

For generating more intense x-ray as sources, one can increase the strength of the scattering laser pulse. We have extended the theory of CTS into the relativistic regime [1,2]. Key conclusions are that (i) the nonlinear Doppler factor reduces due to the recoil caused by the relativistic light; and (ii) CTS reaches saturation (Figure 2a). The saturation effect arises because the radiating current approaches a transverse velocity of light speed. Furthermore, the number of optical cycles is found to be smaller than that in the scattering light at extremely high fields. We have termed this self-steepening; it oc-

curs due to sensitive dependence of CTS on RES thickness and the Doppler factor's strong dependence on laser amplitude.

Phase-independent relativistic electron mirror energy with circular polarization

We have found that our scheme does not need a phase-stabilized laser if using circularly polarized (CP) light [3]. This is a direct result of the single electron motion in the light field. For linearly polarized (LP) light, the motion contains a 2ω oscillation component, which is different for different CEP thus rendering the relativistic electron mirror (REM) sensitive to CEP. For CP light, no such oscillations occur and CEP plays no role. Thus CP pulse can generate phase-independent REM--a monumental relaxation of experimental requirements (Figure 2b)
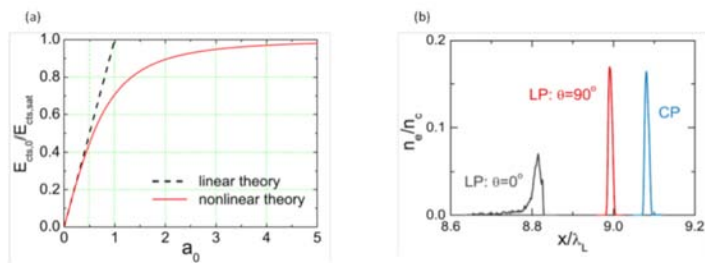
Figure 2. (a) Saturation of nonlinear scattering. a0 is the normalized electric field strength. (b) Relativistic electron mirror density profile snapshots as a function of polarization and carrier-phase relationship for linear polarization (black, linear polarization with phase =0 deg; red, linear polarization with phase of 90 deg.; and blue, circular polarization). There is no dependence of carrier phase for circular polarization.

Experiment and supporting simulation

Electron spectrometer for measurement of energy resolved divergence

Theory predicts that the use of a reflector foil will allow the electron to acquire the full momentum it experiences in the light field—entirely in the forward direction. We expect experimentally to observe a decrease in the electron divergence. For this measurement, we have designed an electron spectrometer as an adaptation of an ion wide angle spectrometer [4]. A bipolar magnetic field in a wedged yoke is used in combination with a thin but wide slit to measure angularly resolved spectra while preserving spectral resolution. The large acceptance angle and high solid angle captured by the spectrometer offers significantly improved quality of the data compared to standard pinhole spectrometers typically used.

Studies of pulse shaping for fast rise time via plasma self-shuttering

Generation of a relativistic electron mirror from thin solid

foil requires few optical cycle rise (~10 fs) with ultra-high, relativistic intensity ($I > 10^{20}$ W/cm^2). To satisfy this requirement we have examined the shuttering characteristics of self-induced transparency in plasma. In our ultra-thin targets this occurs due to a combination of relativistic mass increase of the electrons and plasma expansion (see concept illustrated in Figure 3a). We have extended previous measurements of pulse shortening to include measurement of the pulse shape for light both transmitted through, and reflected from, the thin foil target (two papers submitted to Nat. Phys.). Figure 3(b) shows that the *reflected* laser intensity (red solid line) drops within 50 fs when the plasma becomes transparent. However in Figure 3(c) the shape of the laser pulse we have measured *transmitted* through an initially opaque plasma slab shows a more gradual rise. Detailed simulations indicate this arises from strong transverse effects in the onset of transparency. The shortcomings in transmitted light quality might be able to be addressed with specialized laser focusing using custom and adaptive optics however such research exceeds the scope of the present ER. In addition to considering an alternative regime for electron mirror production on Trident (next section), we are also exploring off-site experiments at ultrashort pulse lasers. Options here are the Ti:Sa laser systems at MPQ (Munich, Germany), HZDR (Dresden, Germany) or GIST (Gwangju, Korea).
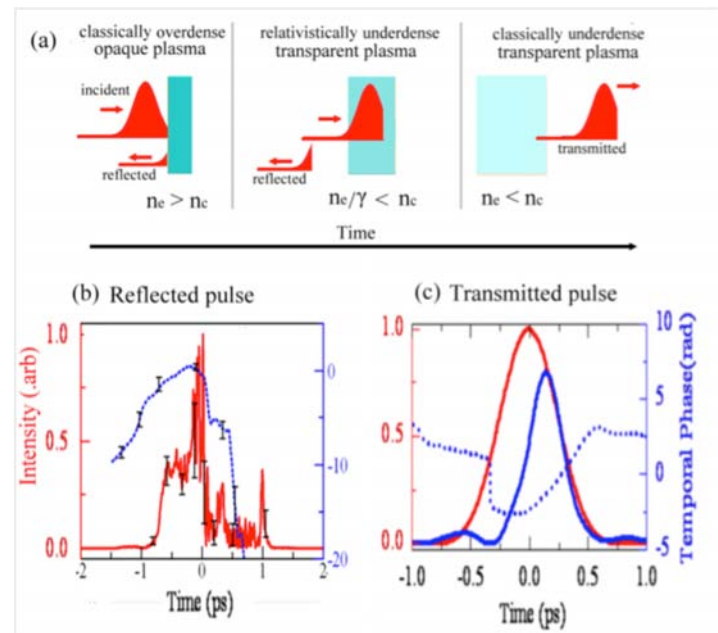
Figure 3. (a) shows the laser plasma interaction leading to transmitted laser pulse shaping via relativistic transparency. (b) Shows the laser pulse shape (red solid line) and its temporal pahse (blue dotted line) reflected from a 100 nm diamond foil. The reflected light intensity drops abruptly when the plasma becomes relativistically transparent. (c) Shows the incident laser pulse (red solid line) and the laser pulse transmitted through 10 nm DLC foil (blue solid line) and its temporal phase (blue dotted line). The sharp rise time in the transmitted laser pulse is degraded due to initial self-focusing and diffraction.

Multiple electron sheets

If the driving laser is not sufficiently fast and powerful to rip-out the entire electron population in a single cycle, fractions of the electrons will emerge every successive half-cycle of increasing laser strength. With nano-foil targets, these multiple electron bursts are produced--and emerge--from the target over ultra-short durations of the laser cycle. Multiple electron sheets can result for coherent light scattering, and the duration of each electron sheet (ξ) is predicted as ξ [as]~ (1000/(τ [fs])) where τ is the duration of the laser pulse [5]. According to this simple analytical theory, a longer pulse actually generates *shorter* electron micro-bunches (for our case of τ=500 fs, ξ=2 as!) with the tradeoff being decreasing charge.   Periodically micro-bunched electrons can be studied by looking at spectral signatures of the coherent transition radiation generated as they traverse an interface. Because of the periodic bunching, the transition radiation generated by each electron will sum coherently at twice the laser frequency (laser second harmonic). We have conducted initial experiments in which a "witness" foil provided such a radiation interface. The second harmonic signature was observed only for the nano-foil case. These measurements will be verified and expanded on this year.

Future Work

The emphasis in this second year will be on electron diagnosis. We will measure the electron spectrally resolved angular distribution to verify predicted change with reflector foil. We will conduct measurements of coherent optical transition radiation to look for multiple sheet formation, and simulations will explore this regime for conditions accessible in the experiments. If possible, experiments will be conducted using a 5fs, 50TW intense laser located at MPQ, (Garching) or on ~25fs, 0.3-1PW lasers at HZDR or GIST.

Conclusion

In our first year, our progress includes both experimental and theoretical advances towards realization of an ultra-thin, flying electron sheet for Doppler up-conversion of laser light. A polarization technique has been identified to control the electron sheet energy and theory has been extended to greater strengths of the scattering laser. On the experimental side, initial studies on the electrons using pinhole spectrometers have been performed and an improved imaging electron spectrometer has been designed to measure expected signatures in divergence; pulse shaping via plasma self-shuttering has been studied; and we have begun development of a technique to study formation of multiple electron mirrors, measuring coherent transition radiation. In the coming year we anticipate this ground-work will allow the strongest measurements to date of ultra-thin flying electron sheets from laser irradiated nano-foil targets.

References

1. Wu, H. C., J. Meyer-ter-Vehn, B. M. Hegelich, and J. C. Fernandez. Nonlinear coherent Thomson scattering from relativistic electron sheets as a means to produce isolated ultrabright attosecond x-ray pulses. 2011. *Physical Review Special Topics-Accelerators and Beams.* **14** (7).

2. Wu, H. C., J. Meyer-ter-Vehn, J. Fernandez, and B. M. Hegelich. Uniform Laser-Driven Relativistic Electron Layer for Coherent Thomson Scattering. 2010. *Physical Review Letters.* **104** (23).

3. Wu, H. C.. Phase-independent generation of relativistic electron sheets. 2011. *Applied Physics Letters.* **99** (2).

4. Jung, D., R. Hˆrlein, D. C. Gautier, S. Letzring, D. Kiefer, K. Allinger, B. J. Albright, R. Shah, S. Palaniyappan, L. Yin, J. C. Fern·ndez, D. Habs, and B. M. Hegelich. A novel high resolution ion wide angle spectrometer. 2011. *Review of Scientific Instruments.* **82** (4): 043301.

5. Bulanov, S. S., A. Maksimchuk, K. Krushelnick, K. I. Popov, V. Y. Bychenkov, and W. Rozmus. Ensemble of ultra-high intensity attosecond pulses from laser-plasma interaction. 2010. *Physics Letters A.* **374** (3): 476.

Publications

Habs, D., M. Hegelich, J. Schreiber, M. Gross, A. Henig, D. Kiefer, and D. Jung. Dense laser-driven electron sheets as relativistic mirrors for coherent production of brilliant X-ray and gamma-ray beams. 2008. *Applied Physics B: Lasers and Optics.* **93** (2-3): 349.

Jung, D., R. Hˆrlein, D. C. Gautier, S. Letzring, D. Kiefer, K. Allinger, B. J. Albright, R. Shah, S. Palaniyappan, L. Yin, J. C. Fern·ndez, D. Habs, and B. M. Hegelich. A novel high resolution ion wide angle spectrometer. 2011. *Review of Scientific Instruments.* **82** (4): 043301.

Kiefer, D., A. Henig, D. Jung, D. C. Gautier, K. A. Flippo, S. A. Gaillard, S. Letzring, R. P. Johnson, R. C. Shah, T. Shimada, J. C. Fernandez, V. K. Liechtenstein, J. Schreiber, B. M. Hegelich, and D. Habs. First observation of quasi-monoenergetic electron bunches driven out of ultra-thin diamond-like carbon (DLC) foils. 2009. *EUROPEAN PHYSICAL JOURNAL D.* **55** (2): 427.

Kiefer, D., A. Henig, D. Jung, D. Habs, B. M. Hegelich, J. C. Fernandez, K. A. Flippo, S. A. Gaillard, D. C. Gautier, R. P. Johnson, S. Letzring, R. C. Shah, and T. Shimada. Laser-driven electron breakout from ultra-thin targets. Presented at *IEEE Int. Conf. Plasma Science - Abstracts ICOPS 2009.*

Palaniyappan, S., R. C. Shah, R. Johnson, T. Shimada, D. C. Gautier, S. Letzring, D. Jung, R. Hoerlein, D. T. Offermann, J. C. Fernandez, and B. M. Hegelich. Pulse shape measurements using single shot-frequency resolved optical gating for high energy (80 J) short pulse (600 fs) laser. 2010. *Re-*

view of Scientific Instruments. **81** (10): 10E103.

Palaniyappan, S., R. Shah, H. Wu, C. Gautier, D. Jung, L. Yin, S. Letzring, B. Dromey, B. J. Albright, R. P. Johnson, T. Shimada, J. C. Fern\'andez, and B. M. Hegelich. High Resolution Dynamics of Ultra-fast Optical Switching in Relativistically Transparent Overdense Plasma. *Nat. Phys..* : {}.

Shah, R., S. Palaniyappan, H. Wu, C. Gautier, D. Jung, R. Horlein, D. Offermann, J. Ren, L. Yin, B. J. Albright, R. P. Johnson, T. Shimada, J. C. Fern\'andez, and B. M. Hegelich. Laser Pulse Shortening via Femtosecond Dynamics of Relativistic Transparency. *Nat. Phys..* : {}.

Wu, H. C.. Phase-independent generation of relativistic electron sheets. 2011. *Applied Physics Letters.* **99** (2).

Wu, H. C., J. Meyer-ter-Vehn, B. M. Hegelich, and J. C. Fernandez. Nonlinear coherent Thomson scattering from relativistic electron sheets as a means to produce isolated ultrabright attosecond x-ray pulses. 2011. *Physical Review Special Topics-Accelerators and Beams.* **14** (7).

Wu, H. C., J. Meyer-ter-Vehn, J. Fernandez, and B. M. Hegelich. Uniform Laser-Driven Relativistic Electron Layer for Coherent Thomson Scattering. 2010. *Physical Review Letters.* **104** (23).

Foundational Methods and Experiments in Ultracold Molecular Physics

Michael D. Di Rosa
20110356ER

Introduction

We are investigating a novel experimental approach for cooling and storing stable molecules at ultracold temperatures and high densities. Our method of cooling molecules involves lasers as established by us in 2004 [1], adopted recently by a pre-eminent research group in laser cooling, and featured in the Search & Discovery column of the January 2010 issue of Physics Today [2]. That column highlighted work at Yale University, where researchers combined both the type of (diatomic) molecule and the laser-induced transitions we had prescribed for cooling to "push" (actually deflect) a molecular beam by the photons of a laser beam [3]. Their observed photon force on molecules was an important if incomplete test of proving that the laser cooling of molecules was not impossible as supposed by the physics community prior to our paper and even afterwards. Once molecules were laser-cooled to temperatures below 1 millikelvin and collected, the column projected, there would be far-reaching consequences in the quantum and chemical sciences.

Molecules have not been laser cooled, however, let alone concentrated in the ultracold, dense ensembles needed for experiments. Our project aims to invent and supply the requisites of cooling, accumulation, and storage to the larger scientific community so that molecular physics may enter the same ultracold conditions that revolutionized atomic physics (read in particular the Nobel Lectures by William D. Phillips [4] and Steven Chu [5]).

Our two major experimental goals are the laser cooling of molecules in their lowest-energy internal state and the demonstration of an accumulator ring based on principles of high-energy physics and suitable for amassing high-density packets of (magnetic) molecules or atoms. The two achievements would each be noteworthy, laser cooling for its precedence and the accumulator as a new platform for experiments in ultracold physics and chemistry. In our research, these two elements will be integrated to allow for repeated, synchronous injections of laser-cooled molecules into the ring. A culminating experiment in molecular scattering will be compared with predictions for a first witness and test of ultracold molecular physics and theory.

Benefit to National Security Missions

The Laboratory recognizes that basic research stimulates ideas and programs for solving issues of national importance in nuclear weapons stewardship, homeland security, intelligence gathering, information analysis, and alternative energy. Our research similarly contains that intended essence of malleability toward Laboratory missions. Consider that reactive and condensed matter constitute a large share of the Laboratory's identity and goals (*e.g.*, the MaRIE (Matter and Radiation Interactions in Extremes) facility). Once we establish the means for accumulating ultracold atoms and molecules, we can adapt the new experimental platform and the alterable media it contains to research in the quantum mechanics of reactions, collective phenomena, and novel materials.

The overall benefit of our program to national security missions will come, if not directly, then by symbiosis. The development of this promising field is challenging and takes the combined expertise and resources such as the Laboratory possesses by virtue of its missions. Its later influence on Laboratory programs will then come naturally, by reciprocity, and by our firsthand practice in the basic research combined with our knowledge of national-security topics.

Progress

Our preparations for the experiments, in coordination with numerical simulations of the underlying physics, have been substantial this past fiscal year. Through our computer models, we have also solved the problem of how to inject magnetic particles (such as our atoms and molecules) into an accumulator ring, making more complete the analogy between our low-energy table-top experiment (~100 neV, meter) and the high-energy physics machines (~1 GeV, kilometers) with which we share general concepts and mathematics. We also hired two excellent postdoctoral researchers who will work full-time on the project. One started in June and the other in September.

Collimated beams of atoms and molecules are required for our research. For reasons outlined in our proposal, our molecule of choice is calcium monohydride (CaH). Our "toy" molecule is lithium (Li), a simple element with known properties we will use to diagnose the components of our accumulator before injecting into those devices the complexities of a molecule. Nearly all features of the beam machine we are building—from the source chamber that initiates an atomic or molecular beam with a laser pulse to various downstream chambers needed for manipulating and interrogating the beam—was designed to serve CaH and the diagnostic-molecule Li interchangeably.
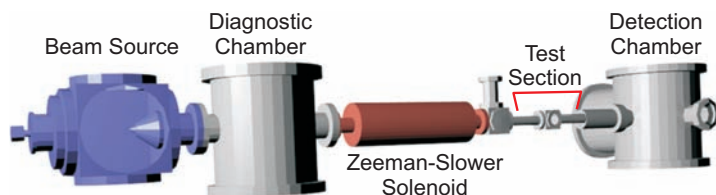
Figure 1. Diagram of our universal beam machine, nearing completion. Atomic and molecular beams, produced separately, originate in the Beam Source and proceed left to right for manipulation by our experiments.

Figure 1 diagrams the universal beam-machine that was designed in FY11 and is now nearly built. The flexible machine produces either atomic or molecular beams, allows laser-light access as needed for cooling and decelerating these beams, and accommodates proof-of-principle experiments. Whether atomic or molecular, the beam originates by a laser-ablation technique in the Beam Source chamber (see any number of chemical physics papers on the general method, which bears similarity to laser welding and drilling). The beam proceeds from left to right within chambers under vacuum, evacuated continuously by vacuum pumps. When the beam reaches the Diagnostic Chamber, it becomes the classic, pencil-like ray suitable for manipulation. Lasers (directed from right to left) propagate against the beam to both cool and slow the atoms or molecules. Our atomic beam of lithium is best cooled and slowed with the aid of a so-called Zeeman-slower solenoid, a device Bill Phillips describes in his Nobel Lecture [4]. Molecules are unresponsive to the Zeeman-slower technique and so will be cooled and slowed by the chirp-cooling method [6] with the Zeeman solenoid turned off. As part of our accomplishments last year, we specified, designed and either made or purchased the components needed for cooling and slowing both lithium (Li) and calcium monohydride (CaH). Prior to reaching the Test Section, Li and CaH, as the case may be, will be slowed to _30 m/s (_70 mph) and cooled to a moving-frame temperature of _300 _K (0.00054 °F above absolute zero). For comparison, air molecules in the ordinary office at 530 degrees Fahrenheit above absolute zero (i.e, 70 °F) move at 900 mph, on average.

Future Work
The summary list of work for FY 12 is: (1) Test, optimize,

and publish universal beam source, (2) Laser-cool CaH (resulting in a landmark publication), (3) Zeeman-slow Li in preparation for (4) Demonstrate injector concept (introduces high-energy-physics concepts to low-energy physics), (5) Design accumulator and begin construction, and (6) Define ultracold reactions / collisions for potential study in FY13. We elaborate below on the design and significance of the experiment surrounding No. 4.

Lenses and refractive elements for magnetic particles such as Li and CaH can be made out of magnets just as glass can be shaped to focus and disperse light, an analogy known since 1951. To date, however, we have not found experiments where one changes the magnetic quantum state—the identity—of an atom or molecule in transit through a magnetic lens or prism. Yet this is precisely what we must do, and can do according to our simulations, to create our injector. Our numerical modeling suggests the following conceptual test of an injector, which is readily accommodated by our beam machine.

Across the Test Section (labeled in Figure 1) we place a dipole magnet of 1 tesla peak field. LANSCE has loaned us the magnet, a generosity on their part that also speaks of the unique capacity of LANL for our type of interdisciplinary research. Showing the dipole magnet in place, Figure 2 illustrates the essence of our injector concept. Magnetic particles, represented by the blue ray, enter the field of the dipole in a particular quantum state (state 1). Left alone, they will exit the dipole magnet in the same state, with unchanged speed, and along a path parallel to the input trajectory. Within the center of the dipole field, however, the quantum state can be switched cleanly from 1 to 2 by illuminating the particles with a laser beam. When we turn on this state-switch laser, the particles exit in state 2 and with a trajectory and speed remarkably different from what the particles assume in state 1. One of our experiments in FY12 will test this expectation.

The injector concept, while it would be proved by a positive outcome of the experiment described above, would in practice be arranged with the arrows reversed for the blue and purple beams in Figure 2. A packet of particles in state 1 circulates around the accumulator and enters the dipole with every lap. State-2 particles are injected by their unique trajectory into the dipole when the circulating packet arrives. On application of a laser beam, the state-2 particles are switched to state-1 (but not vice versa), consequently increasing the number of state-1 particles in the circulating packet. Repeated, synchronous injections and state-switchings thus grow the number of atoms or molecules in the accumulator ring. Proton storage rings operate on a similar principle but with charged particles. Our adaptation and proof of these principles for magnetic particles will be, to our knowledge, a new result.
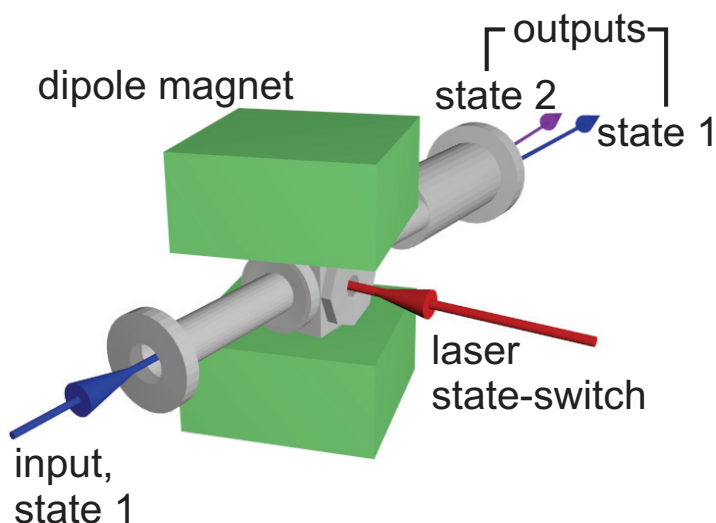
Figure 2. Illustration of the injector-concept test. A 1 tesla dipole magnet surrounds the Test Section (see Figure 1) and receives particles in a particular quantum state. When switched on, a laser optically-pumps the incoming state within the dipole field to a different state, which leaves the magnet in an independent trajectory. The actual injector would operate in the reverse direction, by merging initially unlike states of different trajectories into one packet.

Conclusion

Almost two decades of international activity in various techniques have yet to generate dense ensembles of molecules at the ideal starting point of less than 1 mK for further manipulation and study. Our project exploits the circumstances by which some molecules may be laser-cooled and then invents a means for accumulating and storing them at high densities. We are mindful of applications our research has in new types of sensors. More generally, however, the dense samples of ultracold molecules we seek to generate will give us and others a new view to the inner workings of chemistry and matter, for both discovery and exploitation.

References

1. Di Rosa, M. D.. Laser-cooling molecules. Concept, candidates, and supporting. 2004. *European Physical Journal D.* **31** (2): 395.

2. Miller, J.. Optical cycling paves the way for laser-cooled molecules. 2010. *Physics Today.* **63** (1): 9.

3. Shuman, E. S., J. F. Barry, D. R. Glenn, and D. DeMille. Radiative force from optical cycling on a diatomic molecule. 2009. *Physical Review Letters.* **103** (22): 223001 (4 pp.).

4. Phillips, W. D.. Laser cooling and trapping of neutral atoms. 2002. *Nobel Lectures, Physics 1996-2000.* : 199.

5. Chu, S.. The manipulation of neutral particles. 2002. *Nobel Lectures, Physics 1996-2000.* : 122.

6. Ertmer, W., R. Blatt, J. L. Hall, and M. Zhu. Laser manipulation of atomic beam velocities: demonstration of. 1985. *Physical Review Letters.* **54** (10): 996.

Understanding the Feedback of Active Galaxies in Galaxy Clusters

Hui Li
20090174ER

Abstract

Clusters of galaxies are the largest gravitationally bound objects in the Universe. However, there is a lack of understanding how the matter in the clusters is heated and cooled. In 2009, we proposed to perform the largest cosmological magnetohydrodynamic (MHD) simulation including the feedback of active galaxies in order to understand the dynamics of matter in the intracluster medium. With the support of this ER, we have been successful in completing this task and produced the first and most comprehensive picture on the origin and evolution of magnetic fields in the galaxy cluster, from their production by active galaxies to their amplification by the intracluster medium turbulence, and to their dissipation as heating of the cluster medium. These simulations were made possible by our unique cosmological MHD code (ENZO-MHD) that represents the state-of-the-art simulations in this field. These simulation results are being used to guide observing proposals on radio telescopes such as Extended Very Large Array (EVLA), as well as to estimate the content of cosmic rays in galaxy clusters observed by Fermi Gamma-ray Observatory.

Background and Research Objectives

Galaxy clusters, recognized as the largest gravitationally bound objects in the Universe, are used as key laboratories for several critical tests of the highly successful ΛCDM concordance cosmology model. A detailed understanding of the baryon dynamics in clusters, however, is still lacking. For example, the matter is observed to have a strong luminosity suggesting efficient cooling yet the matter stays hot over billions of years. This suggests that there is efficient heating to offset the cooling. We proposed to seek the physics underpinning for such an understanding and help to realize the potential of "precision cosmology." Our primary research objective was to investigate how the powerful astrophysical jets and lobes energized by active galaxies in the centers of galaxy clusters can heat the intra-cluster medium and prevent it from cooling catastrophically. We proposed that the energy from the active galaxies, especially the magnetic fields from these sources, will be spread out throughout the cluster medium. Furthermore, the mag-

netic fields can be further amplified by the intracluster medium turbulence. The sophisticated cosmological MHD code (ENZO-MHD), developed jointly between UCSD and LANL, will be the primary tool we utilize to study these highly nonlinear evolution processes.

Scientific Approach and Accomplishments

We have completed a suite of cosmological MHD simulations (> 50 simulation runs) using the Institutional Computing machines (Lobo, Coyote, Canejo and Mapache) to investigate the evolution of magnetic fields in clusters with different initial energy inputs from various active galaxies (AGNs). These runs are motivated by the variety of observed AGNs in galaxy clusters. Our most significant results include the following:

- A detailed characterization of multiple energy components in clusters. We found that, in a well relaxed cluster, the thermal energy is dominant, followed by the turbulent kinetic energy which is a factor of ~ 5 lower. The magnetic energy is about a factor of ~ 10 smaller than the thermal energy. This result provides critical information for modeling the energy contents of galaxy clusters as they are used for constraining the cosmological parameters.

- Based on simulations, we have derived the radial profiles for the thermal, turbulent, and magnetic energies. These profiles are needed in order to make detailed comparison with X-ray, Sunyaev-Zel'dovich effect and radio observations of clusters.

By varying the injected energy from AGNs, from 10^{57} ergs to 10^{60} ergs, we have shown that the MHD turbulence in the intra-cluster medium (ICM) is a robust environment for amplifying magnetic fields via a small-scale dynamo process that eventually produces cluster-wide magnetic energy that saturates at a fraction of the total turbulent energy. This robustness implies that nearly all clusters that had an AGN in the early formation history will be guaranteed to have magnetic fields. We further predict that the total magnetic energy in a cluster is proportional to its turbulent energy. Figure 1 shows the spatial distribution of magnetic fields in one galaxy cluster, based on our simulations.
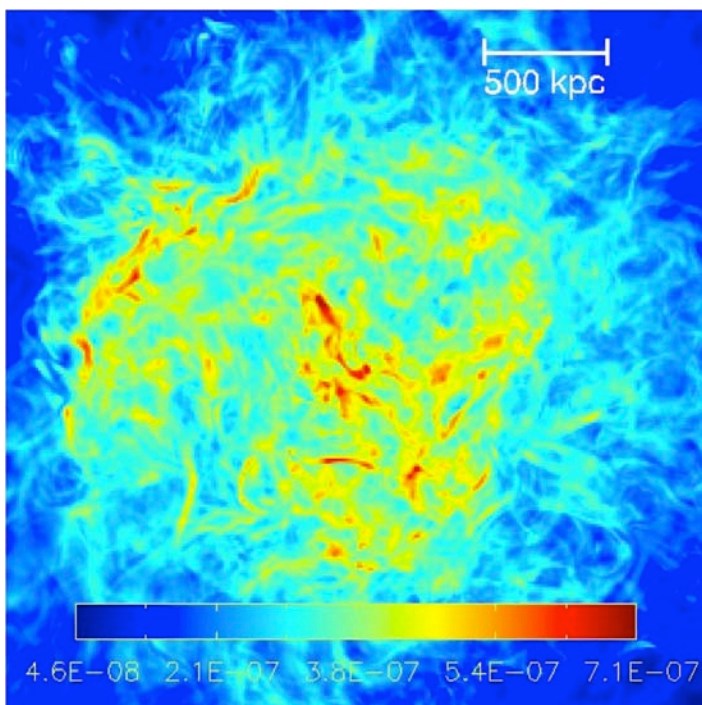
Figure 1. Distribution of magnetic field strengths in a turbulent galaxy cluster simulation. Strong filaments are embedded within the weaker turbulent field. The range of field strengths is similar to what is observed.

We have performed further detailed analysis to understand the microphysical processes that govern the saturation of the magnetic field amplification. The saturation is affected first by the energy density balance between the turbulence energy and magnetic energy at small scales. Because the turbulence driving is episodic, the magnetic saturation is at a sub-equipartition level. The magnetic field strength is a critical input parameter for modeling the nonthermal radiation (both gamma-rays and radio emissions) from clusters.

We have also formed new collaboration with scientists from University of New Mexico to use the Extended Very-Large-Array to observe several galaxy clusters so that we can make comparisons between our simulation results and the observations. The observing proposal has been accepted and observations were conducted in early 2011. The data is being reduced now.

Our results have generated much interest in the community, both for theorists and observers. New EVLA observations (both by us and other research teams) are being proposed and planned to test our results. In addition to a number of refereed publications, we have given numerous invited talks in international conferences, workshops and university department colloquia. We expect that there will be continued efforts in observing the predicted magnetic fields in galaxy cluster and quantifying their roles in galaxy clusters.

Impact on National Missions

This project supports the DOE mission in Office of Science by enhancing our understanding of the basic plasma processes that are operating in galaxy cluster turbulent medium. Furthermore, they provide important constraints on the energy contained in clusters, which can be utilized to help constrain the key cosmological parameters for Dark Matter and Dark Energy. Our effort has strengthened LANL's competencies in Basic Sciences, especially in large-scale computer modeling. In addition, the performed research addresses an important problem in modern astrophysics and cosmology. Clusters are being used as one of the important probes of fundamental cosmological parameters, and our simulation results have provided important inputs for modeling the X-ray, radio, gamma-ray and SZ effect observations (distortions in the spectrum of the cosmic microwave background caused by clusters). Detailed comparisons between the simulations and observations allow us to place constraints not only on our models but also on the cosmological parameters.

Publications

Collins, D., H. Xu, M. Norman, H. Li, and S. Li. Cosmological AMR MHD with Enzo. 2010. *Astrophysical Journal Supplements.* **186**: 308.

Guo, F., S. Li, H. Li, J. Giacalone, J. R. Jokipii, and D. Li. On the Magnetic Field Amplification by a Supernova Blast Shock Wave in a Turbulent Medium. *The Astrophysical Journal.*

Liu, W., H. Li, L. Yin, B. J. Albright, K. J. Bowers, and E. P. Liang. Particle energization in 3D magnetic reconnection of relativistic pair plasmas. 2011. *Physics of Plasmas.* **18** (5): 052105.

Pino, J., H. Li, and S. Mahajan. Relaxed states in relativistic multifluid plasmas. 2010. *Physics of Plasmas.* **17** (11): 112112.

Svidzinski, V. A., H. Li, H. Rose, B. J. Albright, and K. J. Bowers. Particle in cell simulations of fast magnetosonic wave turbulence in the ion cyclotron frequency range. 2009. *Physics of Plasmas.* **16**: 1310.

Xu, H., H. Li, D. Collins, S. Li, and M. Norman. Turbulence and Dynamo in Galaxy Cluster Medium: Implications on the Origin of Cluster magnetic fields. 2009. *Astrophysical Journal Letters.* **698**: L14.

Xu, H., H. Li, D. Collins, S. Li, and M. Norman. Evolution and Distribution of Magnetic Fields from AGNs in Galaxy Clusters. I. The Effect of Injection Energy and Redshift. 2010. *Astrophysical Journal.* **725** (2): 2152.

Xu, H., H. Li, D. Collins, S. Li, and M. Norman. Evolution and Distribution of Magnetic Fields from Active Galactic Nuclei in Galaxy Clusters. II. The Effects of Cluster Size and Dynamical State. 2011. *The Astrophysical Journal.* **739** (2): 77.

The First Characterization of Large Interstellar Dust

Rohan C. Loveland
20090176ER

Abstract

Micrometeoroids ablate when they encounter Earth's ionosphere, and are visible to radars as a result of the resulting plasma column. Various characteristics of these radar returns, such as signal-to-noise ratio (SNR), speed, direction, and deceleration, can be used to directly calculate flux density from the various sources, and to partially infer mass, density, composition, etc. In this effort, data from the ALTAIR high power large-aperture radar was used.

The two primary areas of this investigation involved direct analysis of the data, in order to study micrometeoroid sources through the construction of flux maps, mass inferences, etc., and plasma modeling and simulation to better understand the interactions of the micrometeoroids with the ionosphere. The pursuit of these investigations required the development of several algorithms allowing automated analysis of the data (e.g. ways of identifying the meteor "streaks"), and resulted in a novel method of refining range rate estimates in radar data.

The results of the effort show the ALTAIR characterization of micrometeoroid sources to be in good agreement with other studies (e.g. from the Jicamarca Radio Observatory), and further the general understanding of micrometeoroid induced plasmas in the ionosphere, as well as providing some inferences about masses, densities, and composition. No indisputable examples of interstellars were obtained; this may provide evidence that the generally accepted numbers of interstellars should be revised, or their absence may be due to the limitations of ALTAIR's sensitivity in the appropriate mass regime.

Background and Research Objectives

Earth is constantly impacted by micrometeoroids, coming from a variety of sources, ranging from cometary and inter-asteroidal collision debris, to interstellar dust. The micrometeoroids range in size from femto to micrograms, with typical speeds of 60 km/s. Several modalities exist to study these micrometeoroid populations, ranging from lunar microcraters to direct collection on spacecraft to optical observation to radars.

When a micrometeoroid penetrates Earth's atmosphere, it forms a high-density ionized plasma column immersed in the ionosphere between approximately 70 and 140 km altitude. High-power, large-aperture (HPLA) radars detect nonspecular trails when VHF or UHF radio waves reflect off structures in a turbulent meteor trail. These trails persist from a few milliseconds to many minutes and the return from these trails is referred to as nonspecular trails or range-spread trail echoes. In this effort, we present analysis of nonspecular trails detected with ALTAIR, which is an HPLA radar operating simultaneously at 160 MHz and 422 MHz on the Kwajalein Atoll.

The micrometeoroid induced plasmas occur relatively frequently (peak head echo detection rate of ~1/s) but are extremely diverse and have been difficult to define in a general sense. One particular type of plasma, referred to as the nonspecular trail, occurs when the micrometeoroid travels quasi-parallel to the radar beam with the radar beam lying quasi-perpendicular to the background magnetic field. Reflection is believed to occur from field aligned irregularities (FAIs) that form after the trail becomes unstable. While FAI scattering pertains to the majority of nonspecular trails that are short in duration, a subset of these trails, referred to as long-duration trails, still remains open to interpretation.

A number of micrometeoroid sources (e.g. North and South Apex) are known, but verification and refinement of estimates of source characteristics are desirable. In particular, significant uncertainty about the number of interstellars remains. Our solar system is traveling at 26 km/s through the Local Interstellar Cloud (LIC), which is a partially ionized cloud within 3 parsecs (pc, about 3 light years or 31 trillion kilometers) of the sun that is warmer and less dense than regions around it. Our limited un-

derstanding of the LIC has been gained through measurements of the spectral attenuation of star light, neutral atoms that flow to the inner Solar System, and interstellar dust (ISD), but is still largely unknown. ISDs are particularly difficult to measure due to their size and paucity; hence only a few sparse data sets exist. These data include in situ impact detections with space experiments, which have poorly determined velocity and mass measurements, and ground-based measurements of the plasma that is created when an ISD enters Earth's atmosphere (i.e. a "meteor'). An important subset of ISD is the large grains. Large grains are relatively unaffected by Lorentz forces in the interstellar medium, thus we can use large ISD to accurately determine their original provenance and allow direct measurement of debris generated during the disk formation stage of nearby stellar systems. Unfortunately, large ISD grains are typically invisible to most observational techniques because their contribution to the total cross section for extinction is low.

Specific research objectives included:

- better understanding of micrometeoroid sources through the construction of flux maps with source directionality,

- development of plasma models and simulations of micrometeoroid interaction with the ionosphere,

- inference of micrometeoroid characteristics such as mass, density, and composition.

Scientific Approach and Accomplishments

Approximately 4 Tb of ALTAIR radar data, containing approximately 100,000 micrometeoroid streaks, have been acquired and rendered usable through declassification. Pioneering techniques for declassifying large datasets through the LANL system were developed to deal with this; all 4 Tb of the raw data has now been declassified.

Data reduction tools for identifying micrometeoroid streaks have been developed, based on Delaunay triangulation and iterative closure. Tools for linking and filtering streaks based on signal-to-noise ratio (SNR), duration etc. have also been developed, as have automated scripts for applying these to multiple Terabytes of data. A novel method of calculating range rates using Doppler shifted phase has been developed, with aliasing removal made possible using differencing derived constraints. This was necessary due to quantization issues preventing a simple conversion of range to range rate using differencing.

We accordingly investigated three methods for evaluating range rates of micrometeoroids passing through the iono-

sphere, using linear frequency modulated (LFM) chirped pulse data from the ALTAIR radar. The first method is based on the simple calculation of range differences divided by interpulse intervals. The second method utilizes the dual-frequency capability of ALTAIR to solve for range rates based on the difference in the measured ranges due to range -Doppler coupling. The third method utilizes a simplified form of integer programming in order to unwrap the phase differences of the matched filter time response, with reliance on the rough approximation available from the first method to disambiguate the solution set. The results of the three methods, with error bounds, are given for a large set of micrometeoroid head echoes.

Algorithms for converting the radar monopulse information to 3-D trajectories have also been developed, as have density estimation methods based on the ballistic equation and a scattering model allowing conversion of the SNR to radar cross section.

Flux maps have been generated using the appropriate transformations to Heliocentric Earth Ecliptic (HEE) and Geocentric Solar Ecliptic (GSE) coordinate systems. These have been found to be in good agreement with other estimates from the meteor community. These provide an independent verification of observed known sporadic sources, including the North and South Apex, and the Anti-Helion source.

These methods have been applied to generate densities for ~15,000 streaks and two different methods have been used to estimate masses.

Work on modeling head echo polarization features in order to identify fragmentation has also been conducted, as has a computer model of the coupled processes of collisional heating, radiative cooling, evaporative cooling and ablation, and deceleration – for meteors composed of defined mixtures of mineral constituents.

We also present a case study analysis of a long duration, nonspecular trail and its associated head. The ALTAIR data are unique in that they are high resolution (with monopulse angles), dual frequency, and, most importantly, dual polarized, which allows for unprecedented insight into the scattering process from both heads and trails. First, we determine the velocity and mass of the parent micrometeoroid, which is a particle weighing more than a milligram and is one of the largest micrometeoroids ever detected by ALTAIR. Second, we determine the peak plasma density and polarization of the head echo and characterize the unique, yet strong returns in the opposite polarization, which may be due to multiple scattering centers within the range gate. Finally, we examine the polarization proper-

ties of the trail and discuss the first conclusive evidence of polarization flipping along the trail striations, which we believe corresponds to sharp gradients at the edges of the trail related to turbulent mixing of a dusty plasma that is elongating along the magnetic field. We look into a new idea, namely, the notion that some nonspecular echoes might correspond to a high Schmidt number, dusty plasma, as is found in and above noctilucent clouds. Our results show how polarized return can aid in scattering diagnostics and that single polarization radars must be used with caution for determining head and trail plasma densities given that some of the return can occur in the "unexpected" channel. A new analysis of a set of 32 UHF meteor radar traces recorded with the 422 MHz Advanced Research Project Agency Long-Range Tracking and Identification Radar facility in November 1998 was also conducted, with emphasis on the absolute velocity measurements and inferences that can be drawn from them regarding the micrometeoroid masses and mass densities. We find that the 3-D velocity versus altitude data can be fitted as quadratic functions of the path integrals of the atmospheric densities versus distance, and deceleration rates derived from those fits all show the expected behavior of increasing with decreasing altitude. We also describe a computer model of the coupled processes of collisional heating, radiative cooling, evaporative cooling and ablation, and deceleration for micrometeoroids composed of defined mixtures of mineral constituents. For each of the cases in the data set, we ran the model starting with the measured initial velocity and trajectory inclination and with various trial values of the quantity $m\rho_s^2$ (initial mass times mass density squared) and then compared the computed deceleration versus altitude curves versus the measured ones. In this way we arrived at the best fit values of the $m\rho_s^2$ for each of the measured traces. Then further, assuming various trial values of the density ρ_s, we compared the computed mass versus altitude curves with similar curves for the same set of micrometeoroids determined previously from the measured radar cross sections and an electrostatic scattering model. In this way we arrived at estimates of the best fit mass densities ρ_s for each of the cases.

We also investigated the aspect sensitivity of nonspecular trails and show that as the angle between the radar beam and the background magnetic field increases, the signal strength falls off 3 to 4 dB per degree at 160 MHz. For ALTAIR, this means that the aspect angle must be within approximately 12 degrees in order to detect nonspecular trails using the chosen waveforms. Second, we compare and contrast the micrometeoroids that form nonspecular trails and find that the micrometeoroid energy causes much of the variability in the nonspecular trail's signal-to-noise ratio (SNR) for a given aspect angle. In addition, we show two range-resolved fragmentation events that also affect the SNR. Finally, we determine the dependence of SNR on wavelength using two wavelengths and show that the maximum nonspecular trail SNR scales as approximately l_6, with a variation that depends upon altitude.

A model was also developed simulating the ablation of a small meteor (in the 10- microgram mass range, high velocity, large Knudsen number) and the associated expansion of its ablated vapors (which initially are moving at the meteor velocity), and their interaction with the opposing ambient air stream. An important result of this interaction is the collisional ionization of a fraction of the molecules, and associated formation of a plasma. The interaction of this plasma with the air stream results in its stretching out to large distances behind the meteor. We compute the spatial distribution of the meteor ablate molecules and the plasma. The spatial distribution of the plasma electrons determines the effective cross section for scattering of an incident radar beam.

Impact on National Missions
This project supported the missions of the Office of Science by enhancing our understanding of micrometeoroid dust and its impact on Earth's atmosphere. In addition, we enhanced our understanding of the hazards their potential impact poses to Earth orbiting satellites, including nuclear detection sensors, both by characterizing the flux of particles and also by conducting direct measurements of the effects of hypervelocity impacts on representative target plates in an accelerator sponsored by another customer.

Publications
Close, S., M. Kelley, L. Vertatschitch, P. Colestock, M. Oppenheim, and J. Yee. Polarization and scattering of a long duration meteor trail. 2011. *Journal of Geophysical Research - Radio Science.* **116**: 1.

Close, S., T. Hamlin, M. Oppenheim, L. Cox, and P. Colestock. Dependence of radar signal strength on frequency and aspect angle of nonspecular meteor trails. 2008. *Journal of Geophysical Research.* **113** (A06203): 1.

Loveland, R., A. Macdonell, S. Close, M. Oppenheim, and P. Colestock. Comparison of methods of determining meteoroid range rates from LFM chirped pulses. 2011. *Journal of Geophysical Research - Radio Science.* **46**: 1.

Zinn, J., S. Close, P. Colestock, A. Macdonell, and R. Loveland. Analysis of ALTAIR 1998 meteor radar data. 2011. *Journal of Geophysical Research - Space Physics.* **116**: 1.

Soild Helium-4: A Supersolid or Quantum Glass?

Matthias J. Graf
20090217ER

Abstract

The discovery of the putative supersolid state in solid Helium-4 in 2004 restarted an international race for new measurements and theories to prove or disprove the existence of such an exotic state of matter. This enigmatic state of matter is the crystalline analog of superfluidity and superconductivity. Essentially, the supersolid phase is the last remaining quantum phase that can exhibit persistent particle current of vacancies or interstitials with no dissipation, the analog to zero viscosity in a superfluid or zero resistance in a superconductor. Hence, the discovery and investigation of this phase is of fundamental importance to quantum physics and has created excitement far beyond the quantum solid and quantum fluid communities.

In this project, we explored the nature of the low-temperature phase in Helium-4, where the possible supersolid was reported by torsional oscillator measurements. The extremely low-temperature and high-pressure part of the Helium-4 phase diagram is the subject of our investigations. We investigated the consequences of disorder and contrasted a supersolid scenario with a possible quantum glass state in torsional oscillator, elastic shear modulus, specific heat, and dielectric susceptibility experiments.

Background and Research Objectives

This materials research topic is of general scientific interest as indicated by reports and articles in many high-impact and high-profile journals. There is a renewed and strong interest in fundamental science for filling in the complementary missing coherent quantum state of a solid - the last state that exhibits superflow. The discovery of this state will further validate our understanding of the role of quantum mechanics in condensed matter. So far, we have only proofs of the existence of quantum matter for the pairs of gas-supergas, fluid-superfluid, and conductor-superconductor. What is still missing is the enigmatic pair of the solid-supersolid quantum state.

The fundamental "ingredients" of superfluid behavior in a BEC (Bose-Einstein Condensate) are well known and have long been observed in liquid ^{4}He and other quantum liquids, as well as in tiny droplets of atomic gases in optical traps. The existence of a new state of supersolid matter was predicted in the late 1960s due to the presence of vacancies or insterstitials. So far, the nature of the observed low-temperature phase in solid ^{4}He, which exists above 25 bar and below 200 mK, is still disputed (Figure 1). Since the acclaimed discovery of such a state by Kim and Chan in 2004 [1] torsional oscillator (TO) experiments have been repeated by several other groups around the world, thereby confirming the undisputable existence of this phenomenon. This clearly indicates that there is a mechanical anomaly in the response of the TO, which shows a drop in the resonance period of order 10-100 ppm (parts-per-million), when crossing into this new phase (Figure 2). The ongoing dispute is not whether or not there is an anomaly – that is settled, but rather if it is of a supersolid or non-supersolid nature.
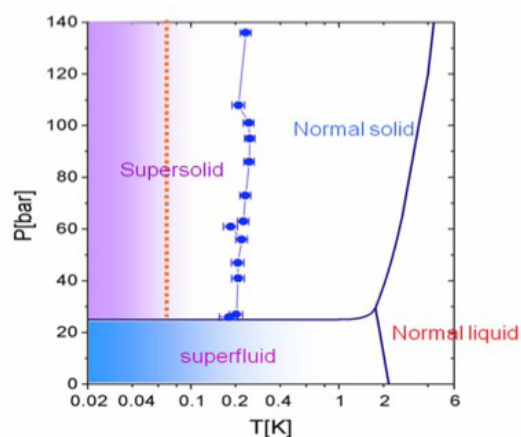
Figure 1. Pressure-temperature phase diagram of He-4 with the putative supersolid phase; symbols indicate the observed torsional oscillator anomaly; red dashed line is estimate for supersolid transition.
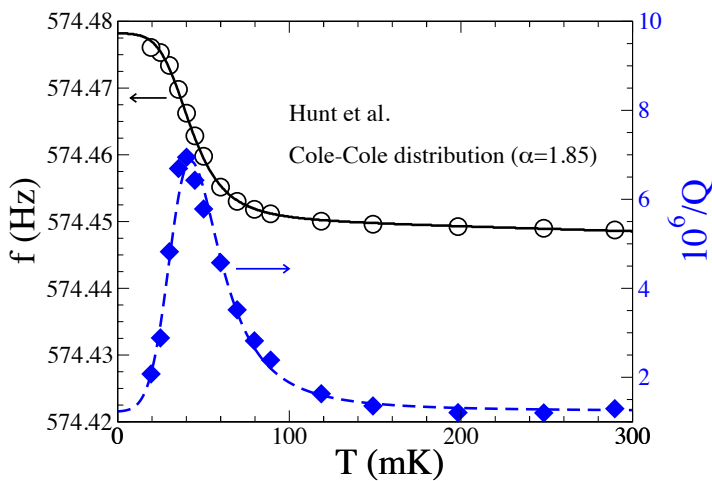
Figure 2. The resonant frequency (left axis) and dissipation (right axis) versus temperature of high-precision torsional oscillator. Our linear response model with a glassy backaction results in excellent agreement with experimental data by Hunt et al. and coworkers. We used a Cole-Cole distribution with exponent alpha=1.85 to describe the distribution of glassy relaxation times.

In a TO experiment a cylinder containing solid ^{4}He under pressure is externally driven back and forth measuring the resonance frequency of the combined container and solid ^{4}He system. This general technique was successfully used in the late 1960s to identify the superfluid density in liquid ^{4}He. The basic idea underlying the TO measurement is a test of the non-classical rotational inertia (NCRI) – the de-coupling of the superfluid component from the cell rotation under an applied torsional drive. As a consequence of a superfluid state, which no longer rotates with the "nor-mal" fluid, the effective moment of inertia decreases as the superfluid fraction increases, thus, resulting in a speed-ing up of the oscillator frequency or equivalently a drop in the TO resonance period when lowering temperature.

In this work we speculated that disorder in the form of dis-locations and defects appear to be crucial in producing this effect. This non-supersolid view is the conclusion one can draw from a growing list of experiments reporting anneal-ing, sample history, rapid cooling, and surface-to-volume dependences. In addition, the presence of tiny amounts of Helium-3 leads to a reduction of the signal, but at the same time shifts the onset temperature of the anomaly to higher values. The TO has been the pre-dominating technique to observe this low-temperature, high-pressure phase. However, the TO does not probe directly the su-perflow of the putative supersolid fraction (0.01-20%) of the sample, nor does it probe the crystalline quality of the sample grown under applied pressure.

The two central hypotheses of this research project have

been:

- The putative supersolid behavior in ^{4}He crystals is pos-sibly due to a glassy state.

- Defects or vacancies of the crystal are crucial for any supersolid or glassy behavior and one must first under-stand the dynamics of defects in order to assign any observed anomaly to a supersolid.

Scientific Approach and Accomplishments

Our theoretical work focused largely on the possible glassy state due to dislocations or two-level tunneling systems that might be responsible for the unusual behavior of solid Helium-4 at low temperatures. We developed a phenome-nological glass model to quantitatively account for general glass relaxation processes also known from conventional dielectric or structural glasses. An extension of our glassy scenario to more general distributions of relaxation times has led to better agreement with torsional oscillator ex-periments (Figure 2). Consequently, we were invited to present these results at the international conferences QFS 2009 at Northwestern University, Evanston, in August 2009 and at the Supersolid 2009 workshop in July 2009 at Banff, Canada.

Our hypothesis of a glassy component responsible for the anomalous behavior is also supported by new torsional oscillator measurements of our external collaborators headed by J. C. Davis at Cornell University and published in the journal of Science [2,3]. They found, using a new gen-eration of ultrahigh precision torsional oscillator that solid Helium-4 exhibits very long relaxation times (sometimes lasting up to days) in the period shift and damping. These results clearly point toward the presence of uncrystal-lized glassy components down to 10 mK. So far the lowest temperatures measured in this quantum solid. Their data analysis was strongly motivated by our theoretical predic-tions and subsequent interactions with his group lead to another joint work on the interplay of rotation, oscillation and shear in solid helium published in the journal of Sci-ence [3].

Additionally, we developed a theory of glassy and vis-coelastic dynamics of defects in solid Helium-4. We list de-tails of the model and theory developments in this project:

Thermodynamics

Pursuing our theory development, we found that glassy dynamics and glassy freeze-out allow us to address the anomalies observed in torsional oscillator, shear modulus, and pressure vs. temperature measurements. Developing a unified approach, we investigated the thermodynamic

signatures of either supersolidity or glassy response in specific heat measurements to address the question of the existence of a true phase transition in solid Helium-4 at low temperatures. Remarkably, this was still a hotly debated question after seven years of discovery. Our calculations indicated that the observed excess specific heat at low temperatures was more consistent with a crossover transition due to glassy relaxation processes of two-level tunneling systems than a Bose-Einstein condensation of vacancies. This calculation and data analysis further corroborated our proposed glassy interpretation of the observed anomaly [4].

Torsional oscillator

Our phenomenological theory for the glassy response in torsional oscillators covers a wide range of different distribution functions for glassy relaxors [5]. We demonstrated that the glass scenario accounts for many torsional oscillator experiments reported in the literature, Figures 2 and 3. We presented these findings at an invited talk at the international conference QFS (Quantum Fluids and Solids) and the Supersolid Workshop in 2009 and consequently published these results [5]. Based on this success, we developed a model with a glassy backaction for the coupled torsional oscillator experiment by Kojima's group at Rutgers. For the first time, a comprehensive interpretation of single and double torsional oscillators based on a linear response function analysis was possible [6]. We presented these results at the international workshops Supersolid 2010 in Paris and at Supersolid 2011 in New York City.
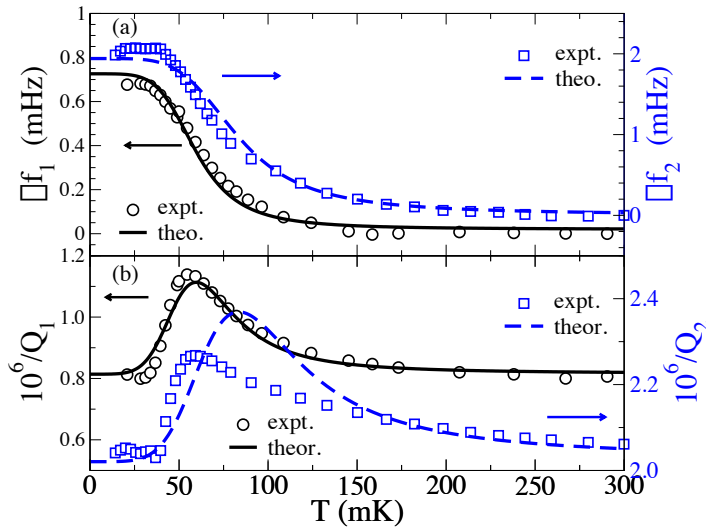
Figure 3. The resonant frequencies (top) and dissipation (bottom) of a coupled double torsional oscillator. Our linear response model with a glassy backaction results in excellent agreement with the experimental data by Aoki et al.

Shear modulus

Our most recent study of the anelastic response seen in shear modulus measurements was based on the glassy backaction onto the elastic deformation of a solid. The approach is similar in spirit to the linear response formulation of the torsion oscillator [7]. In this new work, we accounted for the frequency independence of the changes in the elastic modulus and the phase lag or dissipation as a function of temperature [8], Figure 4. Since a glass exhibits viscoelastic properties, we also developed a generalized Maxwell model comprised of elastic springs and dashpots to describe the anelastic shear modulus in terms of a viscoelastic theory [9]. In a related study, we investigated elastic deformations and their influence on a putative supersolid transition, which was submitted for publication by our long-term external collaborator Z. Nussinov at Washington University at Saint Louis [10].
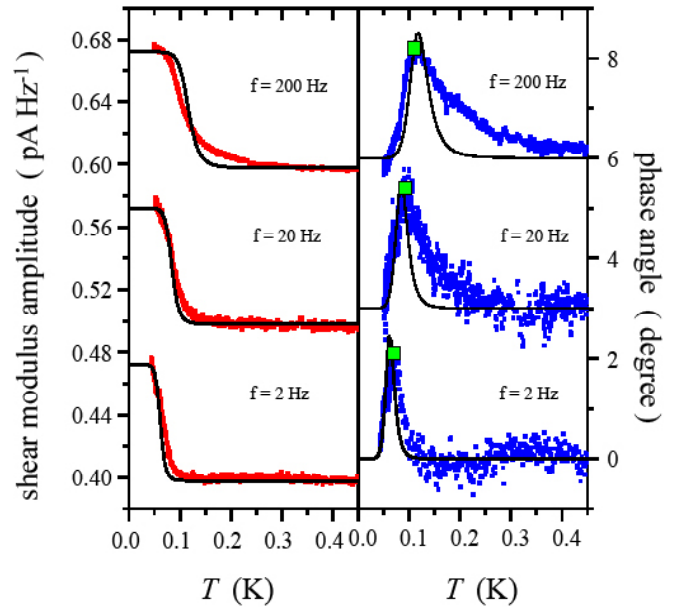
Figure 4. Experimental data and calculations of the shear modulus vs. temperature. The red and blue squares are the experimental data for the shear modulus amplitude and phase angle, respectively. The black lines are the results from our calculation. The green squares mark the dissipation peak location. For clarity the shear modulus amplitude and phase angle curves are shifted by 0.1 pA/Hz and 3 degree with respect to the 2 Hz data.

Dielectric function

After Sullivan's group at the University of Florida published in 2011 [11] results of an anomalous dielectric function behavior at low temperatures in solid Helium-4, we began developing a glassy dynamics model for the dielectric function. We proposed as the origin of the measured anomaly

an electro-elastic coupling mechanism also known as acousto-optical coupling. In our scenario, frozen-in local dilatory strains near crystal defects couple to the alternating electric field and cause a significant change in the dielectric function that cannot be explained by the conventional Clausius-Mossotti expression of dielectrics. Our model explained the observed anomaly in the dielectric function and furthermore we predicted a dissipation peak in the same temperature range. Measurement of the imaginary component of the dielectric function, that means the measurement of a dissipation peak, would validate our proposed mechanism of defect-induced strain fields coupling to the electric field [12]. This model also explains the lack of any signal in perfect crystals or crystals with low density of strain defects, since the magnitude of the coupling coefficient scales with the concentration of strain defects.

To summarize, we developed a theory for the torsional oscillator, shear modulus and dielectric function based on a glassy backaction, where all these experiments are showing anomalous behavior in the same low-temperature region. Finally, our study of the specific heat connected the glassy dynamics of our phenomenological models for various response functions with two-level systems necessary to explain the excess specific heat and linear-in-temperature heat coefficient in insulating Helium-4.

The outcome of our research strongly questions the discovery of the proposed supersolid state and provides an alternative interpretation, namely, that of a quantum glass or a solid whose dynamics is dominated by two-level systems or dislocation motion. We found that many of the observed anomalies in torsional oscillators, shear modulus, specific heat and dielectric function measurements can be explained in terms of glassy dynamics of crystalline defects acting onto the bulk of solid helium as described by a backaction term.

We expect that future materials science studies of the motion of dislocations gliding along slip systems or kinks moving along dislocation lines will provide the necessary explanation of many of the mechanical anomalies observed so far. It remains to be seen if quantum effects play any significant role in the motion of dislocations in the quantum solid Helium-4.

Impact on National Missions
This project answered to the missions of the Office of Science and LANL's Grand Challenge "Fundamental Understanding of Materials" by advancing the state-of-the-art of quantum state modeling in condensed matter physics at ultralow temperatures and high pressures, with ramifications to understanding the microscopic behavior of defect motion and dynamics in disordered solids.

A better understanding and theoretical description of supersolid or quantum glass behavior may lead to better experimental control and toward predictive capabilities for thermodynamic, mechanical and dielectric materials properties for a large class of materials exhibiting disorder.

This project supported the development and continuation of the modeling and theory capabilities for materials with defects and interfaces at the Laboratory.

References
1. Kim, E., and M. H. Chan. Probable observation of a supersolid helium phase. 2004. *Nature.* **427** (6971): 225.

2. Hunt, B., E. Pratt, V. Gadagkar, M. Yamashita, A. V. Balatsky, and J. C. Davis. Evidence for a superglass state in solid ^{4}He. 2009. *Science.* **324** (5927): 632.

3. Pratt, E. J., B. Hunt, V. Gadagkar, M. Yamashita, M. J. Graf, A. V. Balatsky, and J. C. Davis. Interplay of rotational, relaxational, and shear dynamics in solid He-4. 2011. *Science.* **332** (6031): 821.

4. Su, J., M. Graf, and A. Balatsky. A Glassy Contribution to the Heat Capacity of hcp He-4 Solids. 2010. *JOURNAL OF LOW TEMPERATURE PHYSICS.* **159** (3-4): 431.

5. Graf, M. J., Z. Nussinov, and A. V. Balatsky. The Glassy Response of Solid He-4 to Torsional Oscillations. 2010. *JOURNAL OF LOW TEMPERATURE PHYSICS.* **158** (3-4): 550.

6. Graf, M., J. Su, H. Dahal, I. Grigorenko, and Z. Nussinov. The glassy response of double torsion oscillators in solid ^{4}He. 2011. In *The glassy response of double torsion oscillators in solid ^{4}He.* Vol. 162, 5-6 Edition, p. 500.

7. Nussinov, Z., A. V. Balatsky, M. J. Graf, and S. A. Trugman. Origin of the decrease in the torsional-oscillator period of solid ^{4}He. 2007. *Physical Review B (Condensed Matter and Materials Physics).* **76** (1): 14530/1.

8. Su, J., M. Graf, and A. Balatsky. Glass anomaly in the shear modulus of solid He$_4$. 2010. *Physical Review Letters.* **105** (4): 045302.

9. Su, J., M. Graf, and A. Balatsky. Shear modulus in viscoelastic solid ^{4}He. 2011. In *Shear modulus in viscoelastic solid ^{4}He.* Vol. 162, 5-6 Edition, p. 433.

10. Arpornthip, T., A. V. Balatsky, M. J. Graf, and Z. Nussinov. The influence of elastic deformations on the supersolid transition. *Physical Review B.*

11. Su, J. J., M. J. Graf, and A. V. Balatsky. The role of glass dynamics in the anomaly of the dielectric function of solid helium. *New Journal of Physics.*

12. Yin, L., J. S. Xia, C. Huan, N. S. Sullivan, and M. H. Chan. Dielectric constant measurements of solid ⁴He. 2011. In *Dielectric constant measurements of solid ⁴He.* Vol. 162, 5-6 Edition, p. 407.

Publications

Arpornthip, T., A. V. Balatsky, M. J. Graf, and Z. Nussinov. The influence of elastic deformation on the supersolid transition. *Physical Revew B.*

Graf, M. J., A. V. Balatsky, Z. Nussinov, I. Grigorenko, and S. A. Trugman. Torsional oscillators and the entropy dilemma of putative supersolid He-4. 2009. *Journal of Physics: Conference Series.* **150** (3): 032025.

Graf, M. J., Z. Nussinov, and A. V. Balatsky. The Glassy Response of Solid He-4 to Torsional Oscillations. 2010. *JOURNAL OF LOW TEMPERATURE PHYSICS.* **158** (3-4): 550.

Graf, M., J. Su, H. Dahal, I. Grigorenko, and Z. Nussinov. The Glassy Response of Double Torsion Oscillators in Solid He-4. 2011. *JOURNAL OF LOW TEMPERATURE PHYSICS.* **162** (5-6): 500.

Hunt, B., E. Pratt, V. Gadagkar, M. Yamashita, A. V. Balatsky, and J. C. Davis. Evidence for a Superglass State in Solid He-4. 2009. *SCIENCE.* **324** (5927): 632.

Pratt, E. J., B. Hunt, V. Gadagkar, M. Yamashita, M. J. Graf, A. V. Balatsky, and J. C. Davis. Interplay of Rotational, Relaxational, and Shear Dynamics in Solid He-4. 2011. *SCIENCE.* **332** (6031): 821.

Su, J. J., M. J. Graf, and A. V. Balatsky. The role of glass dynamics in the anomaly of the dielectric function of solid helium. *New Journal of Physics.*

Su, J. J., M. J. Graf, and A. V. Balatsky. Shear modulus in viscoelastic solid helium-4. 2011. *Journal of Low Temperature Physics.* **162** (5-6): 433.

Su, J., M. Graf, and A. Balatsky. A glassy contribution to the heat capacity of hcp He-4 solids. 2010. *Journal of Low Temperature Physics.* **159** (3-4): 431.

Su, J., M. Graf, and A. Balatsky. Glass anomaly in the shear modulus of solid He-4. 2010. *Physical Review Letters.* **105** (4): 045302.

A Novel Millimeter-Wave Traveling-Wave Tube Based on an Omniguide Structure

Evgenya I. Simakov
20090265ER

Abstract

Millimeter (mm)-wave devices are proving to have many important applications from imaging to communication. Among the greatest impediments to exploiting this regime of the electromagnetic spectrum are the difficulties in building sources with sufficient power suitable for practical applications. This project's goal was to construct a novel mm-waves (100 GHz) amplifier that employs a cutting-edge concept of a traveling-wave tube (TWT) based on a dielectric photonic band gap (PBG) structure. A TWT is a vacuum electronics tube amplifier that delivers high microwave power, preferably, across a wide frequency band. Present state-of-the-art mm-wave TWT development has reached fundamental limitations in both frequency and bandwidth that can be overcome with the use of low-loss dielectric periodic electromagnetic structures (so called "PBG structure") instead of the sophisticated, especially from a fabrication point of view, metal structures which are used now. An extremely broadband TWT based on the PBG concept would enable new applications in mm-wave communications, radar receivers, radio astronomy, and remote mm-wave spectroscopy. The particular focus of this project was a cylindrically symmetric version of a PBG structure, called an "omniguide", attractive for a proof-of-principle demonstration. Omniguide TWT structures have great potential for generating high average power (up to 1 kW) with simultaneously large bandwidth (greater than 20 per cent) and linear dispersion [1]. In addition, being cheap to fabricate, omniguides enhance the commercial transferability of the W-band TWT technology. Because of new national security spectroscopy missions that would be enabled by this technology, this research directly addresses specific needs of the laboratory grand challenge "Detection of nuclear materials (Ubiquitous sensing)".

In the framework of this project we designed and built a 100 GHz dielectric PBG omniguide TWT amplifier and a 120 kV electron beamline for testing it. We confirmed the low loss and wide transmission band of the omniguide in simulations and measurements. We performed theoretical calculations of the omniguide TWT gain and of the optimum parameters of the electron beam. We completed mm-wave omniguide amplification experiments for frequencies from 91.5 to 101.5 GHz and demonstrated reproducible gain within the whole frequency range in microsecond pulses.

Background and Research Objectives

The emerging photonic band gap (PBG) technology has been recently successfully employed at LANL for construction of novel channel-drop filters, accelerator structures and a dielectric TWT prototype with estimated simultaneous high power capability and large bandwidth at around 94 GHz. Employing dielectric PBG structures (in particular, *omniguides*) for mm-wave power production enables a completely new generation of mm-wave sources [1]. The omniguide TWT (Figure 1 a, b) has a number of very important advantages over the conventional vane-loaded metallic devices. First, the simplicity of the design allows easy and cheap fabrication of the device with no novel and expensive manufacturing technologies (such as wire electro-discharge machining or even microfabrication) involved. Secondly, the bandwidth of the omniguide TWT is only limited by the width of the photonic band gap in the omniguide, which for the prototype was designed larger than 20 per cent. Third, the prototype's dispersion of the electromagnetic wave, which is slowed down by silica, matches very closely the dispersion of the electron beam which travels at about half of the speed of light (Figure 1 c). This ensures high interaction impedance over the whole bandwidth, and consequently, high output power. Adopting a PBG structure to TWT architecture was revolutionary. This is a real case of applying a new, cutting edge technology to real-world national security applications. Considering a standard figure of merit for TWTs being the maximum output power multiplied by the bandwidth, the novel omniguide TWT amplifier has a potential to perform 10 times better than former state-of-the-art traveling wave tubes at 100 GHz, with frequency scaling possible to 1 THz.
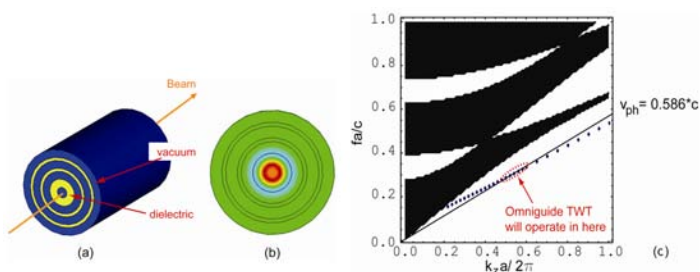
Figure 1. The schematic of an omniguide, the blue area is vacuum and the yellow area is dielectric (a); the longitudinal electric field magnitude in the E01-like mode of an omniguide (b); the eigenfrequency of the E01-like mode of a SiO2 omniguide plotted versus the longitudinal wave vector, the dependence is plotted with dots on top of the band gap diagram, white areas correspond to the bandgap regions, the solid line corresponds to the dispersion of the 120 keV electron beam (c).

The main objective was to test omniguide capabilities in a real gain experiment with a high-power electron beam. Several propositions had to find experimental proof before this PBG TWT concept could be considered feasible. One of them was the ability of the silica dielectric tube to transmit the beam, as electron deposition on the walls of the dielectric tube could cause charge accumulation leading to beam deflection and even to tube breaking under electrostatic forces. The value of power gain and amplification bandwidth needed experimental validation. Additionally there were some engineering problems to overcome in order to test the omniguide TWT experimentally, such as making the omniguide structure vacuum compatible, providing a proper coupling to the input solid state mm-wave source and output detectors with minimum reflection to prevent TWT from self-oscillations, and making it compatible with a 120 kV electron beamline [2-4].

Scientific Approach and Accomplishments

In its first year, the project has made significant progress in three areas. First, a significant level of effort was devoted to fabrication. Three new omniguide structures were fabricated in the machine shop and prepared for tests with the electron beam. Second, the pencil beam TWT test stand inherited from an old TWT experiment was brought back to service. We checked the proper operation of all the components, including the vacuum system, the high-voltage modulator, the electron gun, and steering and focusing magnets. Some new components had to be purchased to replace the old and problematic equipment. Next, the test stand was aligned first with a collimator and then with a dummy metallic structure to ensure the reliable electron beam transmission. The omniguide structure was installed on the test stand and ready for the first electron beam transmission and power generation tests. Third, we conducted theoretical computations of amplification gain in the omniguide taking into account the realistic electron beam spot size and energy dispersion. It was concluded that a 10 cm long struc-

ture was required to obtain 30 dB power gain. The bandwidth of the amplifier was found to be 10 per cent (90 to 100 GHz), which is better than in any currently existing mm-wave TWT [5-7].

The most significant outcome of the second year of the project was the first experimental demonstration of gain (power amplification in the presence of an electron beam) at 94 GHz in the omniguide tube [3,4]. This proved the physical concept of using a silica dielectric omniguide structure as a high frequency traveling wave tube amplifier.

We started the year with replacing the electron gun cathode on the test stand and incorporating some improvements into the electron gun itself to reduce arcing at high voltage. The beamline was realigned for two reasons. First, the electron beam helical trajectory induced by the new cathode had to be eliminated; and second, the beam diameter had to be reduced to the size small enough to pass through the omniguide tube. Significant efforts were also undertaken to improve the RF waveguide test stand for the gain measurement experiment. It included a repair of EIK input RF source for a high power gain test, and replacement of some of the waveguide components with new components with lower ohmic and reflection loss. A new omniguide tube was also manufactured and was 0.6 inches longer than the old tube (overall length of the new tube was 4.6 cm) and was supposed to provide higher gain (Figure 2). The new tube was tested for RF transmission with a network analyzer and performed according to the design (Figure 3).
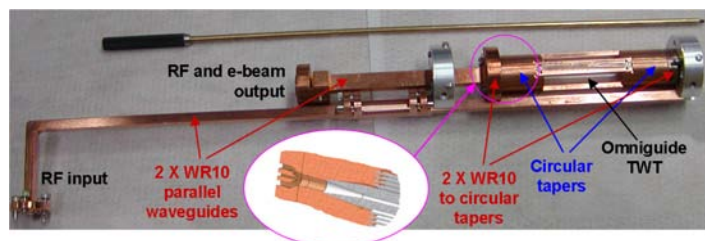
Figure 2. An assembled 46 mm long omniguide structure with the attached custom waveguide ports and adjustable aluminum mounts for the beamline. A part of the omniguide with a mode taper to a pair of WR10 waveguides is shown in the CAD section on top of the photograph.

The first gain experiment started in January 2010. The gain experiment produced three very important and promising results. First, the omniguide dielectric tube performed well with the electron beam and did not show any charge accumulation. The tube was inspected after many shots and we did not discover any damage of the silica tubes that could potentially affect the performance. Second, reproducible amplification of RF radiation at 94 GHz by the electron beam in the omniguide was demonstrated. Third, the value of the gain was consistent with theoretical calculations for the beam current and voltage achieved in the experiment.

It was discovered, however, that the present beamline did not produce an electron beam of sufficient quality. As a result, we were unable to pass the desired 2A of the electron beam through the omniguide at an optimum voltage. Thus, the observed gain varied between 1 and 3 dB, instead of the desired 10 dB. The problem was attributed to scraping of a high current 20 A electron beam to less than a 2 A electron beam for focusing to a small aperture of the omniguide tube. Scraping the high energy beam produced a plasma that deflected the rest of the beam in a random manner.
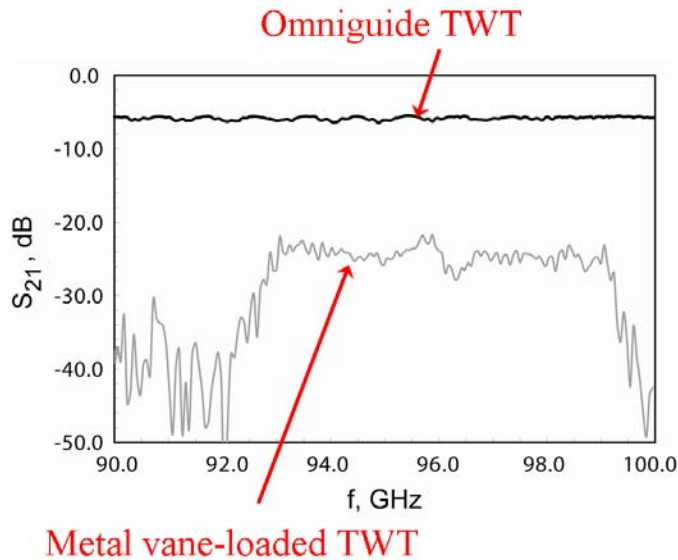
Figure 3. Measured transmission through the omniguide (black line) and through the LANL vane-loaded TWT structure (grey line) [5] for comaparison both with the same connection hardware. Small ripples on both curves are produced by the connection hardware. The vane-loaded structure has much smaller bandwidth (around 7 per cent). In case of the omniguide the main loss (about 6 dB) is in the connection hardware while vane-loaded structure has more than 20 dB loss itself.

To overcome the problem we were forced to switch to a new beamline, with a 2 A electron gun. The new beamline required some extensive modifications before it could be used for the omniguide experiment. First, we purchased most of the readily available necessary components. Second, we finished an extensive modification of a 2 A gun for ensuring high vacuum pumping speed. Third, we successfully integrated a 3.5 kG pulsed solenoid magnet used for the electron beam confinement with a DC power supply, and tested their operation. Finally, the new beamline with the installed electron gun passed the high vacuum tests. The new beamline is shown in Figure 4.

We started the third year with high-voltage conditioning of the new 2 A gun which was followed by a careful alignment of the 3.5 kG pulsed solenoid magnet to minimize any beam helix. In the end we could transmit as high as 1.6 A of the beam current at 125 kV through a special collima-

tor installed in front of the TWT, and a little smaller current at lower voltages. The pulse width of the transmitted current was the same as the width of the high voltage pulse applied to the gun (that is several microseconds) and the shape was very smooth with about 1 microsecond flat top.
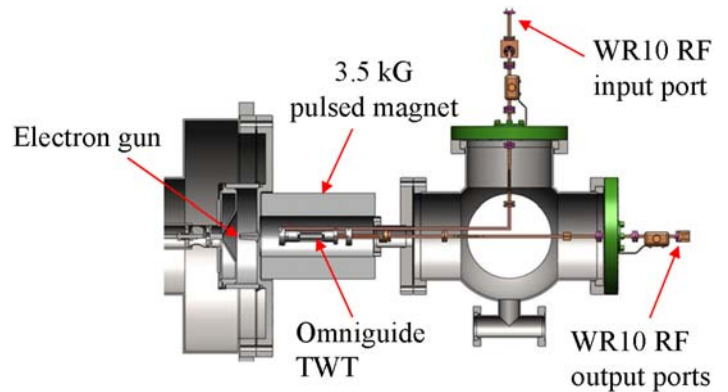
Figure 4. A new beamline consisting of a 2 A electron gun, single pulsed solenoid magnet and a microwave chamber with omniguide TWT inside of the magnet and input and output waveguides. Some elements in the CAD drawing are shown in section.

A solid state tunable frequency source was then purchased to drive the omniguide in a very wide frequency range. The source was capable of operation in between 91.5 to 101.5 GHz.

The omniguide TWT was finally installed on the beam line, and the gain experiment was performed. The experiment has been extremely successful and demonstrated millimeter-wave power generation in well reproduced pulses of about 1 us in duration at frequencies from 91.5 to 101.5 GHz (Figure 5) with about 3 dB to 4.5 dB gain. This gain translates into about 2.5 dB per centimeter of the structure length and was found to be in agreement with theoretical estimates if less than 1 A of the electron beam was transmitted through the omniguide. Indeed, although in the gain experiment we could not directly measure the transmitted current, the transmission of 1 A is reasonable. We also observed the effect of the millimeter-wave power attenuation in the omniguide when the speed of electrons (or voltage) was detuned from its optimum value. In Figure 5 this condition corresponds to the depths in the output power on both sides of the region of amplification, when the beam voltage is lower than the optimal voltage. However, for very low voltages, the electromagnetic wave and the beam do not interact, so there is neither gain, nor attenuation. Similar to year 2, in the course of the experiment the omniguide dielectric tube performed well with the electron beam and did not show any charge accumulation. This successfully concluded the project.
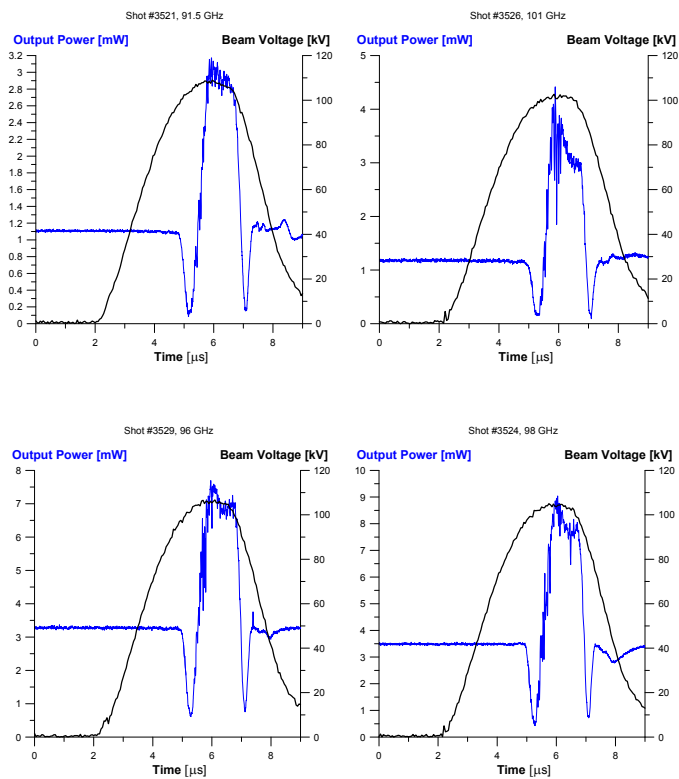
Figure 5. Measured amplification (attenuation) of mm-waves in the omniguide TWT amplifier caused by interaction with an electron beam passing through the structure. The input frequency tunable solid state mm-wave source works in a CW mode and the electron beam parameters change in time in accordance with the high voltage pulse applied to the electron gun. The plots show output mm-wave power from the omniguide for different input frequencies (91.5, 96, 98 and 101 GHz) within a 10% bandwidth and slightly different beam voltage pulses as functions of time. Up to 4.5 dB total mm-wave amplification is observed in the omniguide being 46 mm long resulting in 2.5 dB per centimeter gain. Estimated beam peak current is less than 1 A.

Impact on National Missions

This project demonstrated feasibility of a dielectric PBG TWT mm-wave amplifier concept and thus brought a new paradigm for developing high-power high-bandwidth mm-wave sources, impacting a broad range of applications including imaging, sensing, and communication. These technical areas are crucial for supporting threat reduction, nuclear material detection, and other missions important to DOE (NN), DHS (DNDO), DOD (DARPA) and other government agencies.

References

1.   Smirnova, E. I., B. E. Carlsten, and L. M. Earley. Design, fabrication, and low-power tests of a W-band omniguide traveling-wave tube structure. 2008. *IEEE Transactions on Plasma Science.* **36** (3): 763.

2.   Smirnova, E. I., L. M. Earley, W. B. Haynes, R. M. Ren-neke, and D. Yu. Shchegolkov. Omniguide traveling-wave tube structure testing with a 120 keV electron beam. (San Diego, CA, 31 May - 5 June, 2009).

3.   Shchegolkov, D., L. Earley, W. Brian. Haynes, R. Ren-neke, E. Smirnova, and N. Yampolsky. 20.2: Testing of the omniguide traveling-wave tube. 2010. p. 497.

4.   Shchegolkov, D., D. A. Dalmas, L. M. Earley, W. B. Haynes, R. M. Renneke, and E. I. Simakov. Progress on a 94 GHz omniguide traveling-wave tube experiment. Presented at *International Conference on Plasma Science.* (Chicago, 26-30 Jun. 2011).

5.   Carlsten, B. E., L. M. Earley, W. B. Haynes, F. L. Kraw-czyk, F. P. Romero, S. J. Russell, E. I. Smirnova, and Zhi-Fu Wang. Beam line design, beam alignment procedure, and initial results for. 2006. *IEEE Transactions on Plasma Science.* **34** (5): 2393.

6.   Theiss, A. J., C. J. Meadows, and R. B. True. Experimental investigation of a novel circuit for MM-wave TWTs. 2006. In *2006 IEEE International Vacuum Electronics Conference held jointly.* , p. 1.

7.   Millimeter wave tubes catalog. 2011. *Communications & Power Industries LLC (CPI).*

Publications

Shchegolkov, D. Y., D. A. Dalmas, L. M. Earley, W. B. Haynes, R. M. Renneke, and E. I. Simakov. Progress on a 94 GHz omniguide traveling-wave tube gain experiment. 2011. In *2011 IEEE 38th International Conference on Plasma Sciences (ICOPS) ; 26-30 June 2011 ; Chicago, IL, USA.* , p. 1.

Shchegolkov, D., L. Earley, W. Brian. Haynes, R. Renneke, E. Smirnova, and N. Yampolsky. 20.2: Testing of the omniguide traveling-wave tube. 2010. In *2010 IEEE International Vacuum Electronics Conference, IVEC 2010 ; 20100518 - 20100520 ; Monterey, CA, United States.* , p. 497.

Smirnova, E. I., L. M. Earley, W. B. Haynes, R. M. Renneke, and D. Y. Shchegolkov. Omniguide traveling-wave tube structure testing with a 120 KEV electron beam. 2009. In *2009 IEEE 36th International Conference on Plasma Science (ICOPS) ; 1-5 June 2009 ; San Diego, CA, USA.* , p. 1.

Development of a Muon to Electron Conversion Experiment at LANSCE/MaRIE: Search for Physics beyond the Standard Model

Takeyasu Ito
20090269ER

Abstract

The process of the neutrinoless conversion of a muon to an electron, if found, would unambiguously signify the existence of physics beyond the Standard Model, providing a new breakthrough in our understanding of the Universe. The original goal of the ER was to develop a concept of such an experiment that can be mounted at the LANSCE accelerator. Half way through the project, we decided to join the Mu2e effort at Fermi National Laboratory. As part of the Mu2e collaboration, our responsibility was to design the muon-stopping target. The muon-stopping target is the part of the experimental apparatus where the muons from the muon beam will be stopped and the sought-for process of muon-to-electron conversion could take place. The signal of the muon-electron conversion is a monoenergetic electron of 105 MeV emergin from the target. In this final FY of the ER funding, we made progress towards optimizing the target design by understanding the origin of the electron energy spread due to the muon-stopping target. We also finalized the conceptual engineering design of the muon stopping target and built a prototype in order to vet the design.

Background and Research Objectives

The ultimate goal of this research was to perform an experiment to search for a process in which a muon is converted to an electron in the field of an atomic nucleus without the emission of neutrinos. The muon is a particle that has very similar properties to those of the electron, except that the muon is much heavier than the electron. This process is highly suppressed in the Standard Model, a widely accepted theory that describes the ultimate constituents of matter and radiation, as we understand them. However, this theory is at best incomplete and the above-mentioned process is predicted by many extension of the Standard Model. Therefore, if found, this process would unambiguously signify the existence of physics beyond the Standard Model, providing a new breakthrough in our understanding of the Universe.

Physicists have been looking for muon-electron conver-sion for over 50 years. A new method, which was to increase the sensitivity by 3-4 orders of magnitude over the conventional method, was proposed by Lobashev [1]. The two new features of this new proposal were a use of pulsed proton beam and a use of solenoidal magnets to capture the pions and transport pions and muons. This became the basis for the proposed MELC experiment at Moscow Meson Facility and the MECO experiment at Brookhaven National Laboratory. Neither of these proposed experiments was realized.

The LANSCE accelerator at LANL is the best facility at which to perform such an experiment. The original goal of this ER project was to further develop the physics basis for the experiment to a point where it is possible for us to seek an external funding to construct the experiment. Issues studied on the ER project included:

Beam delivery and experimental siting

- Can the necessary amount of beam with the necessary beam structure be delivered to the mu-e experiment in a way that is consistent with other activities at LANSCE?

- Where can the mu-e experiment be sited?

Beam extinction

- Achieving a high extinction (the ratio of the accelerator current between beam-off vs beam-on, needs to be $\sim 10^{-9}$) is very important in order to suppress beam related background. We need to study the "base" extinction achievable just with the front-end chopper.

Expected sensitivity

Although we made progress in the first two areas in FY09, we decided to join the Mu2e collaboration in Fermi National Laboratory, our competitor, because it became clearer that the Mu2e project was likely to go ahead and had a higher chance of success in getting funded. Our responsibility in the Mu2e project includes:

- Conceptual design the muon-stopping target. The muon-stopping target is at the heart of the Mu2e experiment, where muons stop to form muonic atoms where the expected muon-electron conversion process would occur. In the current design, the muon-stopping target consists of a series of thin aluminum disks. A careful optimization of the design of the muon-stopping target is crucial in maximizing the overall sensitivity of the experiment. This involves maximizing the muon stopping while minimizing the energy loss of the outgoing signal electrons in the target material.

- Conceptual design of the muon stopping target monitor. The muon stopping in the target will be monitored by observing the muonic aluminum x rays using a germanium detector.

- Conceptual design of the proton absorber. The proton absorber slows down or absorbs the protons from the muon-stopping target due to muon capture in order to reduce the count rate at the tracking detector. The design needs to be properly optimized so that it effectively reduces the proton rate at the detector without affecting the energy of the signal electrons.

These tasks are in line with the expertise of the PI, who has an extensive experience in optimizing stopping target and detection of exotic atom x-ray measurements.

In this FY, out goal was to perform the tasks to finalize the conceptual design of the muon-stopping target, the muon-stopping target monitor, and the proton absorber, with an emphasis on optimizing the muon stopping target design. Our goal included constructing a prototype of the muon-stopping target to vet the preliminary engineering design.

Scientific Approach and Accomplishments
In order to maximize the sensitivity of the Mu2e experiment, the target needs to be optimized to meet the following two conditions:

1. Maximize the number of beam muons that stop in the target. In order to reach the targeted sensitivity, it is necessary to stop at least 40% of the muons transported through the muon transport beam line. (Note: in the background free condition, the sensitivity goes as 1/(stopped muons)).

2. Minimize the energy loss of the outgoing electrons and the resulting width in the energy distribution of the detected electrons. The sought-after muon-electron conversion events generate monoenergetic electrons of 105 MeV and are distinguished from other background processes only by the energy of the outgoing electrons. Therefore it is crucial to minimize the width of the energy distribution of the outgoing electrons by minimizing the energy loss (and energy loss straggling) due to going through the target material be minimized. In order to achieve the targeted sensitivity of the Mu2e experiment, the width of the distribution needs to be several 100 keV or smaller.

The design of the Mu2e experiment is based on that of the MECO experiment. We adopted the MECO stopping target design, which consists of 17 disks of pure aluminum each with a thickness of 0.2 mm, as our baseline. Our task was to validate the baseline design and hopely to improve its design and expected performance.

Meeting condition #1 above is rather trivial. We just have to make sure that there is enough thickness of the target material in the direction in which the muon beam propagates. On the other hand, for condition #2, there are several factors contributing to the width of the outgoing electrons. These include:

- Intrinsic energy loss straggling

- Variation in the path lengths through the target material (this depends on the electrons' angle and the number of times electrons pass through the target foils)

They, in turn, depend on geometrical factors such as the thickness of each disk and inter-disk spacing.

Rather than performing a computationally intense multi-dimensional optimization blindly, we focused our effort in understanding which factor impacts the width of the electron energy distribution in what way. Such information would allow us to optimize the stopping target design in an intelligent manner. We performed this study using a combination of Monte Carlo simulation and analytical calculation. We found that the contribution to the width of the electron energy distribution was dominated by the width of the distribution of the electrons' path length inside the target, which in turn, comes from the width of the distribution of the number of times electrons cross the target elements (note: the muon stopping target is in a solenoidal field and electrons follow spiral trajectories). The contribution to the width from the energy loss straggling is 50 keV. We then started full optimization of the target geometry. We set up the machinery necessary to perform the full optimization. However, we were not able to finish the full optimization before the end of the FY. We expect other people within the Mu2e collaboration will take over the task of optimizing the target design and complete the task.

Another important goal for this FY was to finalize the conceptual engineering design. The target disks need to be supported in a manner that does not interfere with the measurement; the target support needs to be made of materials that have a lower muon decay-in-orbit end point energy than the target material (aluminum). Also the mass of the target support needs to minimize to minimize muons stopping in the support structure and to minimize background generated by the support structure.

Our approach was to use thin Tungsten wires to support

the target disks. Tungsten is a high Z material and has sufficiently low end point energy of muon decay-in-orbit. The design we adopted uses 2-mil gold plated tungsten wire to support the target disks. Holes that are just large enough to thread the tungsten wire are punched on the target disks. The size of the holes is so small that the holes have no impact on the performance of the experiment. The other end of the wires is attached to a space frame, which has a large enough diameter, and therefore does not interfere with either beam muons or signal electrons.

We built a prototype based on this design in order to vet the design. By building the prototype, we learned how to handle thin aluminum disks and thin tungsten wires. We also identified several points on the design that can be improved. Through building the prototype, we gained valuable insights into the engineering aspect of the target design.

We plan to document both the details of the target design optimization and the details of the target design and the findings from the prototype building and share it with the rest of the Mu2e collaboration.

Impact on National Missions

This project will contribute to our basic understanding of forces and processes in the universe governed by the "Standard Model." It directly addresses issues in the LANL "Beyond the Standard Model" Grand Challenge and impacts basic understanding of physics that underlies nuclear weapons, a key DOE mission.

References

1. Dzhilkibaev, R. M., and V. M. Lobashev.   On the search for the muon to electron conversion process in a nucleus . 1. *Soviet Journal of Nuclear Physics.* **49** (2): 384.

Publications

Ito, T.. Possibility of a muon electron conversion experiment at LANSCE: search for physics beyond the standard model. Presented at *LANSCE users' group meeting.* (Santa Fe, NM, 30 Sep - 1 Oct, 2009).

McCrady, R. C., T. Ito, M. Cooper, and A. Saunders. Stripping of H-beams by residual gas in the linac at the Los Alamos Neutron Science Center. 2011. In *25th International Linear Accelerator Conference (LINAC10).* (Tsukuba, Japan, 12-17 September, 2010). , p. 908. http://www.jacow.org/: Joint Accelerator Conferences Website.

Unconventional Methods for Quantum-enhanced Metrology

Malcolm G. Boshier
20090284ER

Abstract
Precision measurement is crucial to many areas of national security and industrial technology, and basic science, for characterization and control of complex systems. The act of performing any physical experiment is, in fact, a measurement, and therefore metrological techniques are central to all we know about the world. There are obviously many practical applications as well; sensing of all types is rapidly becoming paramount for more complete knowledge of what is built, stored, or moved across borders, behind barriers, or underground. Reduction of the time or total energy in sensing can make the process harder for an adversary to detect. Hence reducing the resources required to make measurements to a given precision, or increasing the precision attainable with given resources, is a critical task for scientific, technological, and national security applications. Toward these ends, we are developing quantum-informational techniques and technologies that we expect will lead to new devices capable of measuring many physical quantities to what may be extraordinary precision while requiring significantly fewer resources than devices based on traditional measurement protocols. Specifically, we have built up experiments to demonstrate this new quantum enhanced metrology by measuring a force with a single trapped ion and by measuring the strength of the interaction between ultracold atoms using a form of interferometry. We have also considered the theoretical issues that must be addressed to make quantum metrology practical, and solved some of them. Finally, we have considered other applications of ultracold atoms as sensors, particularly of forces which become important on the nanoscale.

Background and Research Objectives
Optimizing the performance of measurement technologies is important for many sensing applications in areas such as national security, industry, and basic science. The fact that the fundamental limits to the sensitivity and efficiency of any sensor are ultimately determined by the laws of quantum mechanics has given rise to a new research field, quantum metrology, which tries to both understand these limits and to exploit them to make better sensors. It is now known that quantum sensing and quantum computing are closely connected, with the result that research in quantum information science is suggesting new techniques for making measurements which attain higher precision than the best conventional technologies while requiring fewer resources. In this project we are considering two experimental realizations of these ideas. First, single ions can be trapped in a vacuum by electromagnetic fields, and then used for quantum enhanced measurements of externally applied fields and forces of interest, surpassing the shot-noise "limit" to measurement. Second, a cold atomic gas (known as a Bose-Einstein condensate or BEC) can be employed as a kind of interferometer to measure small energy differences (the phenomenon is similar to how counting the colored fringes seen in a soap bubble tells us about the thickness of the film). We are investigating sensing applications of the BEC, and how interactions between the atoms in the ultracold atomic gas might enable interferometry with precision below the standard quantum limit. These experimental investigations are complemented by modeling and theoretical research. We have analyzed the expected performance of a nonlinear interferometer based on LANL's unique BEC technology, and we have considered the challenge of designing optimum measurement protocols, drawing on results from quantum information science theory and strengthening the connections between the two fields. Finally, in the course of this project it became clear that quantum systems such as BECs have additional advantages as sensors beyond quantum enhancement, such as reduced requirements for size-weight-power-cost, and application to probing forces on the nanoscale. We therefore invested some effort in exploring these new directions.

Scientific Approach and Accomplishments
The project has two experimental threads, one with trapped ions and the other with ultracold Bose-Einstein condensates (BECs), and two complementary theory threads, one focused on applying quantum information science to metrology and the other on considering applications of BEC to measuring forces on the nanoscale.

In the trapped ion thread we brought the laboratory to the point where everything is in place to implement the phase estimation algorithm which is one of the sub-standard quantum limit (SQL) measurement strategies we are pursuing, although a hardware failure in the last year of the project has prevented us from realizing this goal before the end of the project period. Through upgrades and enhancements in the laser systems, the imaging system, and the data acquisition and experiment control system, we are able to reliably prepare ions in the ground state of the trap potential with greater than 90% fidelity, and then control their subsequent evolution over times (a few milliseconds) which should be sufficient for demonstrating the principle. A novel transfer cavity system for stabilizing the frequencies of the four lasers required in the experiment has been an essential component of this part of the project [1]. We expect that workers in other areas of atomic and optical physics will find it to be a useful technology and so a paper is being prepared for publication. The performance of the system was demonstrated by using it to make a precise measurement of an isotope shift in strontium [2], the difference in the frequency of a given spectral line between two isotopes because of the different nuclear configuration.
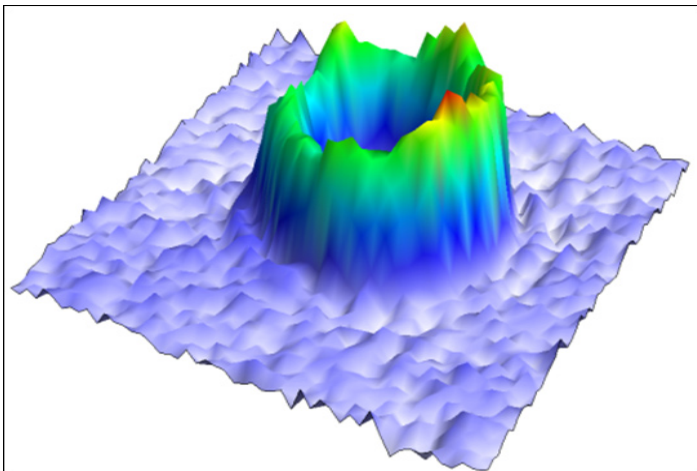
Figure 1. A toridal BEC created using the LANL painted potential technique. Image shows the density of the ultracold atoms arranged in a 50 micrometer diameter ring.

We simultaneously pursued a second experimental approach to sub-SQL metrology, namely a nonlinear interferometry scheme invented by Carl Caves' group at UNM [3]. This technique promises measurement precision which not only exceeds the SQL, but can also surpass the so-called Heisenberg limit where measurement uncertainty scales as $1/N$, with N being the number of resources involved in the measurement (in this case, the number of atoms in the BEC). The key requirement for implementing Caves' scheme is that the BEC not change size appreciably with the number of atoms N. We realized that the toroidal condensates (Figure 1) created with our painted potential technology [4] satisfy this requirement very well because the BEC is effectively frozen into the ground state of the

potential in the two radial coordinates, but completely free to move around the circumference of the torus. We have now performed extensive numerical simulations of Caves' interferometer scheme as it would be applied in our apparatus, and the results are extremely promising. Figure 2 shows that with a few thousand atoms in the BEC, a modest number for our system, the measurement sensitivity would increase with atom number N as $N^{1.25}$, a dramatic improvement over the $N^{1/2}$ scaling associated with the Standard Quantum Limit (shot noise). One initial cause for concern was that when the condensate is put into a superposition of two internal states (i.e. following the "beamsplitter" in the interferometer description of the process), the slightly different interaction strengths of each state with itself and with the other state would drive a complex evolution that would in turn decrease the spatial overlap and hence the fringe contrast. We now know from our simulations that this is not the case, and so we are now able to move forward with the experimental implementation.
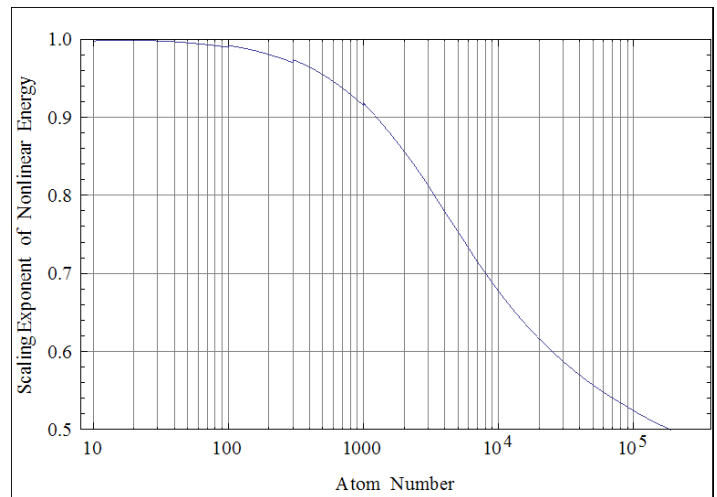
Figure 2. In a nonlinear interferometer the sensitivity increases with atom number N faster than the N to the 1/2 dependence associated with shot noise. This figure shows the simulated performance of an interferometer exploiting the nonlinear interaction of atoms in our toroidal BEC. From this graph showing the additional sensitivity beyond shot noise we see that an interferometer with 5000 atoms has an additional sensitivity enhancement of N to the 0.75, meaning that the interferometer total sensitivity scales as N to the 1.25.

One theory thread, in addition to supporting the two experiments, has also been considering the main goal in quantum metrology: the estimation of parameters at resolutions that are classically impossible. Methods for quantum metrology can be interpreted as quantum algorithms in the so-called quantum query model, where one is given a black-box that implements an unknown operation, and such operation encodes the parameter to be estimated (Figure 3). For example, the typical case in single parameter estimation is that where the black-box imple-

ments an unknown spin rotation around a given axis, and the magnitude of the rotation is the parameter that should be estimated. For this reason, it is important to study the costs of different quantum methods for black-box estimation. An important example is adiabatic quantum computing, where the goal is to estimate the black-box by performing continuous-time evolutions by interleaving the black-box with other, known, evolutions. Adiabatic quantum computing is important because it is equivalent to the standard model of quantum computation. Lower bounds on the cost of adiabatic-like quantum algorithms (in the query model) were unknown until we recently showed that general quantum processes that prepare a target state (eigenstate of a Hamiltonian) require a minimum time proportional to the ratio of the length of the eigenstate path to the gap. This result sets a lower bound on the cost of algorithms for black-box estimation and, in particular, it shows that adiabatic quantum methods could in principle estimate parameters with quadratically improved precisions over classical methods [5, 6]. In addition, we recently proposed and studied the so-called spectral gap amplification problem (GAP) that considers questions such as "what are the optimal quantum strategies to compute low-temperature parameters of quantum systems?". We showed that there exists a large family of systems for which quadratic gap amplification is possible. For this family, zero-temperature properties can be obtained with a quadratic enhancement in precision when compared to "classical" methods for the same goal. We plan to submit this work for publication in the near future.
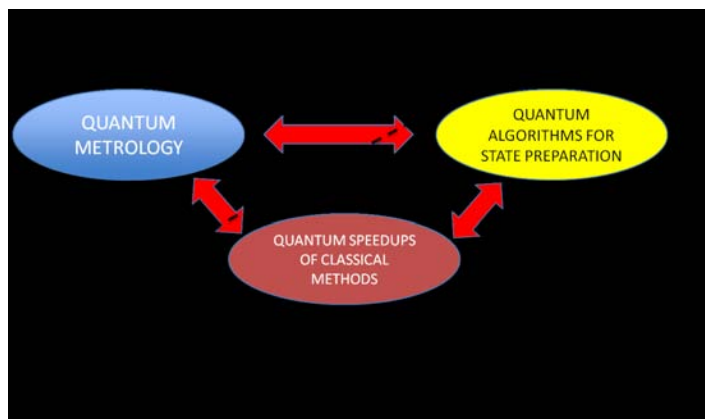
Figure 3. The problem of designing optimum protocols for quantum metrology has strong connections to the key quantum information processing challenges of efficient preparation of quantum states and of devising algorithms for quantum computers.

The second theory thread has been considering atom-surface interactions at the micron and sub-micron scales, generally known as Casimir-Polder (CP) forces. These interactions are due to quantum and thermal fluctuations of the electromagnetic field surrounding both the atom and the surface. They provide opportunities and challenges for quantum metrology in ion traps and atom-chips. For ex-

ample, engineered geometrical structures and/or material composition can tailor the magnitude and sign of near-field atom-surface interactions, with potential applications for trapping, transport, sensing, and metrology. On the other hand, the typically attractive nature of such forces can be deleterious for exactly the same purposes, so a trade-off between the advantages and disadvantages of Casimir-Polder interaction in quantum metrology is desired.

In this part of the project we have studied a variety of scenarios to measure, control, and manipulate atom-surface interactions at the micron and sub-micron scale. Our first work [7] dealt with the problem of probing dispersive atom-surface interactions, measuring via two-photon Bragg spectroscopy the dynamic structure factor of a Bose-Einstein condensate (BEC) above corrugated surfaces. This method takes advantage of the condensate coherence to reveal the spatial Fourier components of the lateral CP interaction force, which could be used for non-contact actuation on a BEC. In short, when a BEC is brought close to a corrugated material surface, its excitation spectrum is modified. For example, a quasi one-dimensional condensate develops first-order perturbation gaps in its energy spectrum. The Bogoliubov states of the condensate, which are significantly corrected, have wavenumber commensurable with the Fourier components of the Casimir-Polder potential, and this lateral force can be inferred from the modified spectrum. The latter can be read out using two-photon Bragg spectroscopy techniques, previously used in the literature to reveal the low-energy spectrum of BECs trapped in elongated potentials and optical lattices.

Another work [8] studied CP interactions between an atom and a dielectric grating. We developed an exact, first principles scattering approach to calculate the exact dispersive CP potential between a ground-state atom and a lamellar dielectric grating. The formalisms allows for arbitrary values of the grating amplitude and period, and of the atom-grating distance. We computed numerically the potential for a rubidium atom on top of a silicon grating and compared the results with the potential for a flat surface taken at the local atom-surface distance (proximity force approximation). Except for very short separation distances, the potential is nearly sinusoidal along the direction transverse to the grating's grooves. The scattering approach developed in this work may be readily adapted to consider more general two-dimensional periodic patterns, for instance the pillars structures employed in recent quantum reflection experiments and in measurements of plasmonically-tailored micropotentials for ultracold atoms.

Finally, we addressed the problem of driving quantized vortices with Casimir-Polder interactions. We proposed to use a rotating corrugated material plate to stir, through the CP interaction, quantized vortices in a harmonically trapped BEC [9]. The emergence of such vortices within the condensate cannot be explained with a computation of the CP potential based on the pairwise summation approach

or on the proximity force approximation. It thus appears as a genuine signature of non-trivial geometry effects on the electromagnetic vacuum fluctuations, which fully exploits the superfluid nature of the sample. We derived an exact non-perturbative theory of the CP potential for the BEC atoms in front of a rotating grating. Our numerical results for a rubidium condensate close to a silicon grating showed that the resulting quantum vacuum torque is strong enough to provide contactless transfer of angular momentum to the condensate and generate quantized vortices under realistic experimental conditions at separations distances around 3 microns.

Impact on National Missions

This project supported the DOE mission in Threat Reduction and the "Science of Signatures" Laboratory Pillar, by improving our understanding of how sensing can be enhanced beyond standard limits using quantum technology. In the course of this project we also realized that quantum systems have additional advantages over conventional sensing technologies, such as reduced values of size-weight-power-cost. This insight led us to organize a 2010 workshop that brought together staff from academia, industry, and government to discuss this aspect of quantum technology, and to interactions with sponsors in the IC. The project also enabled us to attract an outstanding postdoc working in quantum information theory who has now been converted to staff, strengthening our capability in that area and allowing him to contribute his expertise to other LANL science projects.

References

1. Lybarger, W. E., M. G. Boshier, and J. C. Chiaverini. Stabilizing frequencies of multiple lasers with a scanning transfer cavity. 2011. *Ph.D. thesis chapter. Will be made self-contained and submitted for publication..*

2. Lybarger, W. E., J. C. Berengut, and J. Chiaverini. Precision measurement of the 5 ^{2}S$_{1/2}$ - 4 ^{2}D$_{5/2}$ quadrupole transition isotope shift between ^{88}Sr$^+$ and ^{86}Sr$^+$. 2011. *Physical Review A (Atomic, Molecular, and Optical Physics).* **83** (5): 052509.

3. Boixo, S., A. Datta, M. J. Davis, A. Shaji, A. B. Tacla, and C. M. Caves. Quantum-limited metrology and Bose-Einstein condensates. 2009. *Physical Review A (Atomic, Molecular, and Optical Physics).* **80** (3): 032103 (16 pp.).

4. Henderson, K., C. Ryu, C. MacCormick, and M. G. Boshier. Experimental demonstration of painting arbitrary and dynamic potentials for Bose-Einstein condensates. 2009. *New Journal of Physics.* **11**: 043030.

5. Boixo, S., and R. D. Somma. Necessary condition for the quantum adiabatic approximation. 2010. *Physical Review A - Atomic, Molecular, and Optical Physics.* **81** (3): 032308.

6. Boixo, S., E. Knill, and R. D. Somma. Fast quantum algorithms for traversing paths of eigenstates. *Communications in Mathematical Physics.*

7. Moreno, G., D. R. Dalvit, and E. Calzetta. Bragg spectroscopy for measuring Casimir-Polder interactions with Bose-Einstein condensates above corrugated surfaces. 2010. *New Journal of Physics.* **12**: 033009.

8. Contreras-Reyes, A. M., R. Guérout, P. A. Maia Neto, D. A. R. Dalvit, A. Lambrecht, and S. Reynaud. Casimir-Polder interaction between an atom and a dielectric grating. 2010. *Physical Review A.* **82**: 052517.

9. Impens, F., A. M. Contreras-Reyes, P. A. Maia Neto, D. A. R. Dalvit, R. Guérout, A. Lambrecht, and S. Reynaud. Driving quantized vortices with quantum vacuum fluctuations. 2010. *Europhysics Letters.* **92**: 40010.

Publications

Boixo, S., E. Knill, and R. D. Somma. Fast quantum algorithms for traversing paths of eigenstates. *Communications in Mathematical Physics.*

Boixo, S., and R. D. Somma. Necessary condition for the quantum adiabatic approximation. 2010. *Physical Review A - Atomic, Molecular, and Optical Physics.* **81** (3): 032308.

Contreras-Reyes, A. M., R. Guérout, P. A. Maia Neto, D. A. R. Dalvit, A. Lambrecht, and S. Reynaud. Casimir-Polder interaction between an atom and a dielectric grating. 2010. *Physical Review A.* **82**: 052517.

Impens, F., A. M. Contreras-Reyes, P. A. Maia Neto, D. A. R. Dalvit, R. Guérout, A. Lambrecht, and S. Reynaud. Driving quantized vortices with quantum vacuum fluctuations. 2010. *Europhysics Letters.* **92**: 40010.

Lybarger, W. E., J. C. Berengut, and J. Chiaverini. Precision measurement of the 5 ^{2}S$_{1/2}$ - 4 ^{2}D$_{5/2}$ quadrupole transition isotope shift between ^{88}Sr$^+$ and ^{86}Sr$^+$. 2011. *Physical Review A (Atomic, Molecular, and Optical Physics).* **83** (5): 052509.

Lybarger, W. E., M. G. Boshier, and J. C. Chiaverini. Stabilizing frequencies of multiple lasers with a scanning transfer cavity. 2011. *Ph.D. thesis chapter. Will be made self-contained and submitted for publication..*

Lybarger, W. E., R. D. Somma, D. A. R. Dalvit, J. C. Chiaverini, and M. G. Boshier. Single-Ion Heisenberg-limited quantum phase sensors. Presented at *13th Annual Meeting of Southwest Quantum Information and Tech-*

nology Network. (Boulder, CO, 17-20 Feb. 2011).

Moreno, G., D. R. Dalvit, and E. Calzetta. Bragg spectros-
copy for measuring Casimir-Polder interactions with
Bose-Einstein condensates above corrugated surfaces.
2010. *New Journal of Physics.* **12**: 033009.

First Unambiguous Measurement of Jet Fragmentation and Energy Loss in the Quark Gluon Plasma

Andreas Klein
20090303ER

Abstract

During the evolution of the early universe, about one microsecond after the Big Bang, the universe consisted of mainly free quarks and gluons, commonly referred to as a quark-gluon plasma (QGP). This new form of matter, created under the most extreme of conditions, has since been reproduced in nuclear collisions at the Relativistic Heavy Ion Collider (RHIC) at the Brookhaven National Laboratory. Yet, after several years of research, its properties are still not understood quantitatively, largely due to the limitation of the observables available at RHIC energies. Leading hadrons from jets (collimated spray of hadrons) are the most widely used tool to measure QGP properties, such as energy density and temperature. Analyses of the suppressed production of these hadrons have provided the main evidence that the quark-gluon plasma has indeed been produced. However, this observable has severe inherent limitations. For example, these inclusive measurements do not allow for the determination of the initial jet energy and, consequently, the inferred jet energy loss is ambiguous. This results in a significant uncertainty in the extraction of QGP properties. We have been instrumental in analyzing the first Pb+Pb run at the Large Hadron Collider (LHC), specifically the first detection of Z^0 bosons. In addition, we have developed a hardware testing system for the Compact Muon Solnoid (CMS) pixel readout system. Finally, we have performed the first theoretical calculations of jet propagation and energy loss in the QGP formed at the LHC.

Background and Research Objectives

The qualitatively new experimental approach performed here is the measurement of jets tagged by Z^0s at the Large Hadron Collider. We have also concurrently developed the supporting perturbative many-body Quantum Chromo-dynamics (QCD) theory. The muon pair resulting from the Z^0 decay does not interact and escapes the collision undisturbed, while the opposite side jet probes the QGP through energy loss and scattering due to the strong nuclear force. The momentum of the muon pair is approximately equal on average to the original jet momentum, thus allowing for a direct measurement of the initial and final jet energies and an unambiguous identification of the jet's energy loss in the QGP. This breakthrough approach allows for the first time the reconstruction of the full jet fragmentation function and its effective in-medium modification. (Fragmentation functions describe the probability of a quark or gluon to produce a given momentum final state hadron.)

Since the LHC provides collision energies an order of magnitude above what is currently available at RHIC, we chose to carry out this work at the Compact Muon Solenoid experiment. At the LHC cross sections for jets are large enough that full jet reconstruction studies are possible for the first time. The physics results that will be obtained from our data will be the first direct measurement of in-medium jet fragmentation and will allow for a precise determination of the plasma properties in a new and unexplored energy regime corresponding to even earlier times in the evolution of our early universe.

Scientific Approach and Accomplishments

Theoretical accomplishments

On the theory side, we have concentrated on accurate calculations of Z^0 boson + jet production [1], which is the main proposed experimental channel to study the properties of the quark-gluon plasma in this LDRD project. Electroweak bosons, in conjunction with jets in high energy collider experiments, are one of the principle final-state channels that can be used to test the accuracy of perturbative QCD calculations and to assess the potential to uncover new physics through comparison between data and theory. We demonstrated conclusively that beyond the most naïve theoretical estimates, known as tree-level calculations, Z^0 boson measurements do not constrain the momentum of the jet with accuracy better than 25%. Sophisticated theoretical predictions, known

as next-to-leading order calculations [2,3,4], are necessary to make use of jet tagging in heavy ion collisions. An example of such a calculation in p+p reactions is shown by the black solid line in Figure 1. Dashed lines represent the first evaluation of modified jet production in association with a tagging Z^0 in central Pb+Pb collisions at the LHC. In Figure 1, the insert shows the ratio of the two cross sections that exhibits a predicted unique transition from suppression of jets at high transverse momenta to enhancement at low transverse momenta. When confronted by experimental data, our results will help confirm or refute the energy loss picture behind the particle and jet suppression phenomena in heavy ion reactions. Last but not least, we produced theoretical predictions for inclusive Z^0 production in Pb+Pb reactions at the LHC that have already been shown to be in excellent agreement with the new experimental data by the CMS collaboration [5].
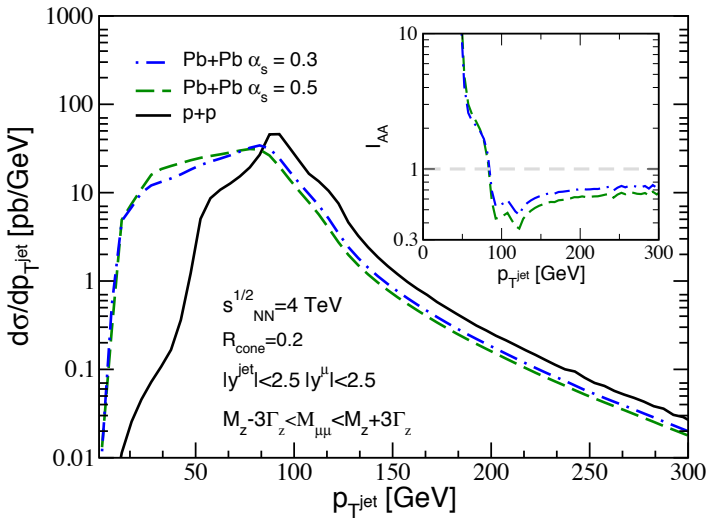
Figure 1. The NLO differential cross section per nucleon pair for jets of radius R = 0.2 tagged with a Z0 boson in p+p and central Pb+Pb reactions. The tagging Z0 is required to have 92.5 GeV < pT < 112.5 GeV. The ratio of the tagged QGP-modified cross section per nucleon pair to that in p+p, IAA, is shown in the inset.

We have made progress in understanding whether dynamical processes, such as quark and gluon radiative and collisional energy losses, particle dissociation in the QGP, or a possible universal modification to the hadronization process play a dominant role in attenuating the jet and particle production rates in the QGP. On the calculable example of heavy D and B mesons (elementary particles composed of a heavy-light quark-antiquark pair), we have demonstrated that universal finite-temperature effects are small [6]. These theoretical advances have helped place simulations of energy loss and collisional dissociation of heavy quarks and heavy mesons in the quark-gluon plasma on firmer theoretical ground. The result of our theoretical simulations for the suppression in the production rate of electrons that arise from the semi-leptonic decay of D and B mesons is shown in Figure 2 for two different collid-

ing systems: Cu+Cu (cyan band) and Au+Au (yellow band). There is good agreement between our results and the PHENIX and STAR experimental measurements [7,8], also shown in Figure 2.
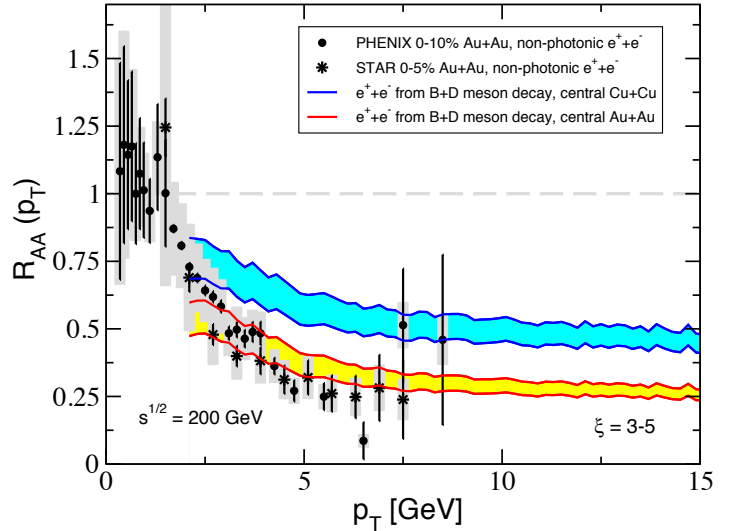
Figure 2. Nuclear modification for the single non-photonic electrons in central Au+Au and Cu+Cu collisions at RHIC. Is compared to theoretical predictions form a heavy meson dissociation model.

We are in the process of finishing two additional theory papers, funded in part by this LDRD project. With Dr. Bryon Neufeld, now a Director's Fellow at LANL, we are generalizing the first Z^0 + jet calculation in heavy ion collisions to make predictions for the asymmetry between the momentum distributions of the electroweak boson and the tagged jet when the jet traverses hot and dense nuclear matter. Since Z^0 measurements are free of soft hadronic background, in heavy ion collisions these asymmetries will shed light on the mechanisms of in-medium jet modification. With Dr. Rishi Sharma, now an external collaborator at TRIUMF, Canada, we are extending the formalism that described well the suppression of heavy D and B mesons in heavy ion collisions to closed heavy flavor, such as charmonia and bottomonia (elementary particles composed of heavy quark-antiquark pairs). We will make theoretical predictions for upcoming J/ψ and Υ measurements at RHIC and at the LHC. These two papers will be submitted for publication in the next several months.

Experimental Approach and Accomplishments
The innermost detector in the CMS system is the so called pixel detector, consisting of three layers of silicon pixels arranged in a barrel geometry around the interaction point together with two endcap disks on each side. This system is crucial for particle ID, reconstructing tracks and clusters as well as background reduction. The first barrel is located at a radius of 4.3 cm from the interaction point, which leads to a particle density as high as $4 \times 10^7\,cm^{-2}\,sec^{-1}$ at the full p+p design luminosity. While the Heavy Ion trigger rate is about a factor 10^4 lower than in the p+p case, the num-

ber of particles per trigger hitting the pixel system is much higher in Heavy Ion (HI) collisions, leading to large multiplicities. Once a level 1 trigger has been generated, an electronic module called the Front End Driver (FED) reads out the coordinates of every pixel together with the associated charge and forms event packets, which contain not only the raw information, but also event numbers and time stamps. This is achieved through a pipeline of three field programmable gate arrays (FPGA's) that ship the created information via a fast interface onto the data acquisition network. In case of either corruption of data or loss of synchronization with the trigger or backpressure due to large data volume, the FED will be reset or put on hold. This in term leads to dead time and subsequently to data loss.

Since the FED system was designed for p+p running and in the first run was tested only at low luminosity, it was not clear that the FEDs could handle the much higher multiplicities anticipated in Heavy Ion running. The first FED simulations for HI collisions, which we performed at LANL, indicated that the existing FED readout algorithm would fail in HI running at the design luminosity. We presented these results to the HI group and the pixel group, which is responsible for maintaining the hard and firmware of the whole pixel system. This, in turn, led the designers of the FED to develop new firmware that will alleviate some of the problems. While simulations can lead to a good overall understanding of the possible performance of the FEDs, only real running conditions can fully and reliably test such a system. However, achieving such a state requires HI beam interactions, which take place only 1 month per year, which precludes debugging the hardware with HI beam.

Recognizing this severe constraint, the LANL team has developed an electronic test system, which not only achieves the same conditions as running with HI beam, but furthermore allows us to predict the behavior of the FEDs under different scenarios. For instance, we can study the performance at higher luminosity than designed, higher repetition rates, different beams or different background environments. This unique contribution to the CMS community provides a fast and invaluable way to test new firmware, thus greatly reducing the risk of FED failure during beam time.

Our FED test system consists of two main components, a Xilinx ML605 FPGA development board, which is the controller of the whole setup, plus nine custom four-channel Spartan-3 FPGA cards developed in house at LANL. These 9 cards are directly connected to the input of an FED. The ML605 firmware consists of the filled beam bucket distribution of the LHC beam and a list of HI multiplicities in the pixel detector, as measured at CMS in November, 2010. In addition, the ML605 is also connected to all of the FED logic signals, which control the pixel data acquisition at CMS. The ML605 determines if a beam bucket is full or not, depending on the beam distribution and a random number. If it finds a full beam bucket, it then uses the

simulated HI cross section to determine if an event has occurred and if so, creates a trigger and a second random number. This information, together with the trigger bit and an event-counter, is passed to the Spartan-3 cards. As stated earlier, each card serves 4 channels of the FED, with nine cards providing a total of 36 channels. Each Spartan-3 card uses the random number to determine each channels multiplicity and constructs events in the same way as the real detector would have generated.

We have extensively tested our system and compared our results with the experimental measurements from the first run. We are currently testing the latest HI firmware upgrade from the Vienna group and have already indentified shortcomings, which are being addressed right now. We are negotiating with the high energy community at CMS to obtain support to extend the use of the system to p+p running, as well as maintaining it in the future. If CMS decides that a hardware upgrade of the FED FIFO system is required, LANL is now well positioned to lead this effort.

During the first Pb+Pb LHC run at the end of 2010, at a centre-of-mass energy per nucleon pair of $\sqrt{s_{NN}}$ = 2.76 TeV, Z^0 bosons were measured for the first time in heavy ion collisions. Our postdoctoral fellow Catherine Sylvestre, stationed at CERN, led the CMS dimuon analysis group of ~15 people group, leading to the publication of the results in Physical Review Letters [5]. The two years prior to data talking were dedicated to simulations [9,10], developing the analysis software and testing it in several mock data challenges. The muon offline reconstruction consists of first finding tracks in the muon detectors, which are then matched to tracks found in the silicon tracker using by an algorithm optimized for the heavy-ion environment. Our work enabled CMS to publish the Z^0 results in an extremely short time after the data were taken. Much of this work was done by Dr. Camelia Mironov, a Marie Curie Fellowship recipient and now an external collaborator in Ecole Polytechnique, France.

We reconstructed all dimuons with large transverse momentum from a triggered sample of 55 million events. The resulting dimuon mass spectrum [5] is shown in Figure 3. We observed 39 Z^0 candidates at the correct mass of 91 GeV/c^2. Their distribution is consistent with p+p data taken in CMS at 7 TeV (scaled down and displayed as the histogram in Figure 3). Studies show that the muon trigger, reconstruction and selection efficiencies are all well understood.

In the absence of in-medium modifications, the yield of perturbative processes such as Z^0 production should scale with the number of binary nucleon-nucleon collisions. The number of binary collisions in Pb+Pb has been computed using a Glauber calculation. The full circles in Figure 4 show the centrality dependence of the Z^0 yield in Pb+Pb scaled to p+p collisions, while the open square represents the measurement integrated over all centralities. The variable

used on the abscissa is the average number of participating nucleons (N_{part}) for the selected centrality intervals, computed in the same Glauber model. A large N_{part} is an indication of large overlap of the colliding nuclei. As seen in the figure, there is no observable centrality dependence of the binary-scaled Z^0 yields from Pb+PB. The normalized yields are in good agreement with our theoretical predictions (labeled Neufeld et al.) over the entire range of N_{part}.
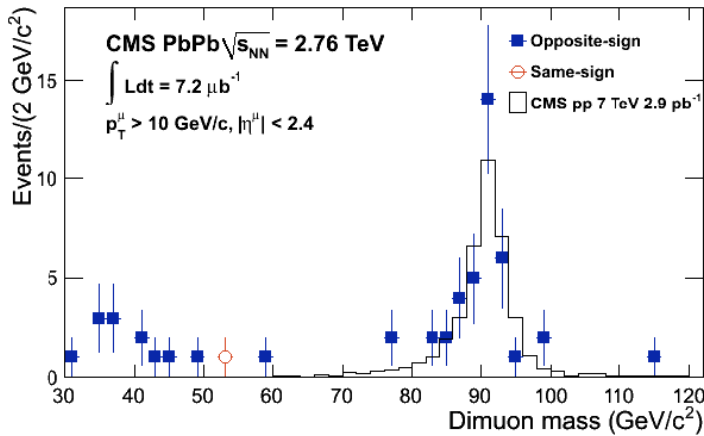
Figure 3. Dimuon invariant mass spectra. Full squares are opposite-sign dimuons, while the empty circle shows a unique like-sign dimuon candidate. The histogram shows the corresponding distribution measured in pp collisions at 7 TeV within 60–120 GeV, scaled to the 39 PbPb candidates.
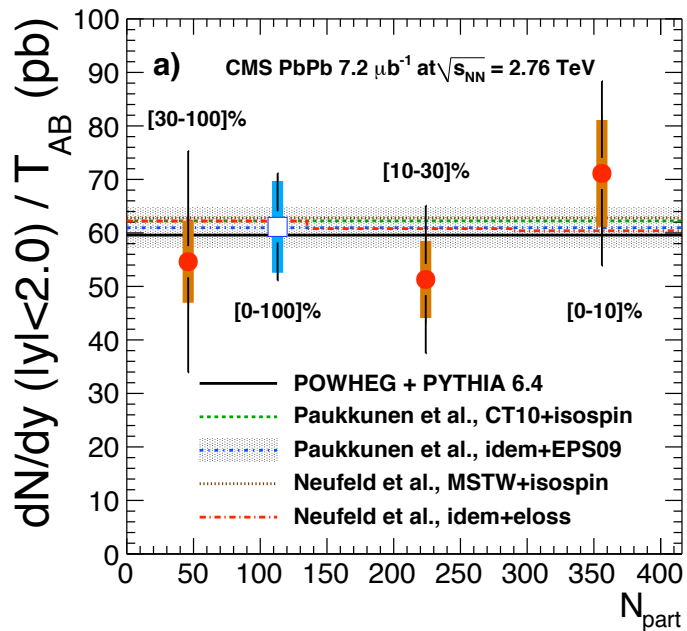
Figure 4. Centrality dependence of the Z0 boson production at the LHC is compared to theoretical predictions and shows absence of significant nuclear effects. LANL theory is included in this first CMS Z0 publication and labeled Neufeld et al.

Impact on National Missions

The theoretical and experimental tools that we developed to investigate and understand subatomic matter are specifically identified as strategic priorities of the Laboratory Directed Research and Development strategic investment plan. Exploration of extreme properties of matter is a cornerstone of the Department of Energy (DOE) nuclear science Long Range Plan and one of the Grand Challenges at Los Alamos - Beyond the Standard Model. The principal strength of this project has been the significant scientific impact on the nuclear physics community at large.

The experimental work we have performed is easily extendable to other systems which take large quantities of data in short time spans, like satellite detector systems, which are designed for particle measurements from nuclear explosions.

References

1. Neufeld, R. B., I. Vitev, and B. W. Zhang. The physics of Z0-tagged jets at the LHC. 2011. *Physical Review C.* **83**: 034902.

2. Vitev, I., and B. Zhang. Jet tomography of high-energy nucleus-nucleus collisions at next-to-leading order. 2010. *Physical Review Letters.* **104** (13): 132001.

3. Vitev, I.. A brief overview of fixed-order perturbative QCD calculations of jet production in heavy-ion collisions. 2011. *Progress in Theoretical Physics Suppliment* . **187**: 68.

4. Neufeld, R. B.. Tagged jets and jet reconstruction as a probe of the quark-gluon plasma. 2011. *Nuclear Physics A.* **855**: 428.

5. al., S. Chatrchyan et. Study of Z boson production in PbPb collisions at nucleon-nucleon centre of mass energy = 2.76 TeV. 2011. *Physical Review Letters.* **106**: 212301.

6. Sharma, R., I. Vitev, and B. W. Zhang. Light-cone wave function approach to open heavy flavor dynamics in QCD matter. 2009. *Physical Review C.* **80**: 034902.

7. al., A. Adare et. Energy loss and flow of heavy quarks in Au+Au collisions at s(NN)**(1/2) = 200-GeV. 2007. *Physical Review Letters.* **98**: 172301.

8. al., B. Abelev et. Transverse momentum and centrality dependence of high-pt non-photonic electron suppression in Au+Au collisions at sqrtsNN = 200 GeV. 2007. *Physical Review Letters.* **98**: 192301.

9. al., C. Mironov et. Dilepton-tagged jets in heavy-ion collisions at the LHC. 2011. *Journal of Physics G.* **38**: 065002.

10. al., G. Kunde et. Z0-tagged quark jets at the Large Hadron Collider. 2009. *European Journal of Physics C.* **61**: 785.

Publications

Neufeld, R. B.. Jets associated with Z⁰ boson production in heavy-ion collisions at the LHC. 2010. In *26th Winter Workshop on Nuclear Dynamics ; 2-9 Jan.* (2010 ; Ocho Rios, Jamaica). Vol. 230, 1 Edition, p. 012035 (6 pp.).

Neufeld, R. B.. Tagged jets and jet reconstruction as a probe of the quark-gluon plasma. 2011. *Nuclear Physics A.* **855**: 428.

Neufeld, R. B.. Tagged jets and jet reconstruction as a probe of QGP induced partonic energy loss. 2011. *International Journal of Modern Physics E.* **20**: 1605.

Neufeld, R. B., I. Vitev, and B. W. Zhang. The physics of Z0-tagged jets at the LHC. 2011. *Physical Review C.* **83**: 034902.

Sharma, R., I. Vitev, and B. W. Zhang. Light-cone wave function approach to open heavy flavor dynamics in QCD matter. 2009. *Physical Review C.* **80**: 034902.

Silvestre, C.. Quarkonia Measurements by the CMS Experiment in pp and PbPb Collisions. To appear in *Quark Matter.* (Annecy, 22-28 May 2011).

Vitev, I., S. Wicks, and B. W. Zhang. The theory and phenomenology of jets in nuclear collisions. 2009. *European Journal of Physics C.* **62**: 139.

Vitev, I., and B. Zhang. Jet tomography of high-energy nucleus-nucleus collisions at next-to-leading order. 2010. *Physical Review Letters.* **104** (13): 132001.

al., C. Mironov et. Dilepton-tagged jets in heavy-ion collisions at the LHC. 2011. *Journal of Physics G.* **38**: 065002.

al., G. Kunde et. Z0-tagged quark jets at the Large Hadron Collider. 2009. *European Journal of Physics C.* **61**: 785.

al., S. Chatrchyan et. Study of Z boson production in PbPb collisions at sqrt(sNN) 2.76 TeV. 2011. *Physical Review Letters.* **106**: 212301.

Breakthroughs in Magnetic Reconnection Enabled by Petaflop Scale Computing

Lin Yin
20090306ER

Abstract

Magnetic reconnection is an energy conversion process that occurs within very hot gases known as plasmas. The atoms in the plasma are ionized resulting in complex motions for electrons and ions, which are strongly influenced by the presence of magnetic fields. In many types of plasma, the magnetic fields can store a large amount of energy. Under certain circumstances, the process of magnetic reconnection causes a rapid conversion of energy stored within the magnetic fields into kinetic energy of the charged particles. This process is thought to play an important role in a range of applications including solar eruptions, the Earth's magnetosphere, magnetic fusion machines, and a wide variety of astrophysical problems. Despite a great deal of effort, scientists are still working to understand a range of basic questions regarding the physics of this process. Computer models have played a very important role in helping scientists understand the behavior of magnetic reconnection. However, until recently, these calculations were limited to two-dimensional models and employed many assumptions. The goal of this LDRD project was to study the physics of magnetic reconnection at the most basic level by exploiting the newest supercomputers. These new computers are massively parallel and challenging to utilize efficiently. To meet this challenge, this project utilized a LANL developed plasma simulation code called VPIC. Using up to 200,000 processors, the simulations performed for this project have revealed exciting new results regarding the three-dimensional evolution of magnetic reconnection and the acceleration of energetic particles. These new predictions are being tested against satellite observations of magnetic reconnection within the Earth's magnetosphere, a protective bubble of plasma surrounding our planet. The new capabilities developed during this project have resulted in follow-on funding from NASA's Heliospheric Theory Program. In addition, these new results are playing an important role in the final planning for the Magnetospheric Multiscale Mission – a constellation of four satellites that are being designed to study reconnection in the magnetosphere. This mission will launch in 2014 and the advanced simulation capabilities developed during this project are

expected to play an important role in understanding and interpreting these new observations.

Background and Research Objectives

In the study of magnetic reconnection, many of the scientific challenges arise from the large separation between the microscopic motion of the charged particles and the large problem sizes. High temperature plasmas are very good conductors of electricity. Normally this constrains the magnetic field lines to move together with the plasma motion. For magnetic reconnection to proceed, it is necessary to break this constraint within so-called diffusion regions. These diffusion regions are quite small in comparison to the larger problems of interest, but play a critical role in the evolution. Thus researchers are working to understand the basic physics of these regions, as well as the coupling to the larger problems of interest. Due to the complicated nonlinear physics, computer simulations have played an important role in the scientific progress. Most previous simulation studies have focused on simplified two-dimensional (2D) models. With increasing computer power, these 2D simulations have progressed to larger problems and have raised a number of new questions. In particular, recent 2D simulations have demonstrated that diffusion regions often develop very long current sheets. In the real world, these extended layers may be unstable and break-up through a variety of different plasma instabilities. However, the previous 2D simulations excluded this possibility. One of the main objectives of this project was to better understand how this process will occur In order to perform realistic 3D simulations, a factor of 1000 increase in computing power is needed beyond the previous 2D calculations. To meet this challenge, this project employed the plasma simulation code VPIC [1] that describes the process of magnetic reconnection at the most basic level. This is accomplished by decomposing the plasma into computational particles that interact with the electric and magnetic fields in the plasma. As illustrated in Figure 1, the new generation of peta-scale computers has allowed a large increase in the number of particles in these simulations. In the past year, the largest calculations for this project exceeded 3

trillion particles on the Jaguar machine at Oak Ridge. The unprecedented scale of these calculations has enabled many new scientific discoveries in this project as described below.

Figure 1. New petascale supercomputers have permitted a huge increase in the size of kinetic plasma simulations. Using the VPIC code, the largest simulations on the Jaguar machine now exceed ~3 trillion particles. These advances were crucial for the scientific discoveries in this project.

Background and Research Objectives

In the study of magnetic reconnection, many of the scientific challenges arise from the large separation between the microscopic motion of the charged particles and the large problem sizes. High temperature plasmas are very good conductors of electricity. Normally this constrains the magnetic field lines to move together with the plasma motion. For magnetic reconnection to proceed, it is necessary to break this constraint within so-called *diffusion regions*.   These diffusion regions are quite small in comparison to the larger problems of interest, but play a critical role in the evolution. Thus researchers are working to understand the basic physics of these regions, as well as the coupling to the larger problems of interest. Due to the complicated nonlinear physics, computer simulations have played an important role in the scientific progress. Most previous simulation studies have focused on simplified two-dimensional (2D) models. With increasing computer power, these 2D simulations have progressed to larger problems and have raised a number of new questions. In particular, recent 2D simulations have demonstrated that diffusion regions often develop very long current sheets. In the real world, these extended layers may be unstable and break-up through a variety of different plasma instabilities. However, the previous 2D simulations excluded this possibility. One of the main objectives of this project was to better understand how this process will occur In order to perform realistic 3D simulations, a factor of 1000 increase in computing power is needed beyond the previous 2D calculations.   To meet this challenge, this project employed the plasma simulation code VPIC [1] that describes the process of magnetic reconnection at the most basic

level.   This is accomplished by decomposing the plasma into computational particles that interact with the electric and magnetic fields in the plasma. As illustrated in Figure 1, the new generation of peta-scale computers has allowed a large increase in the number of particles in these simulations.   In the past year, the largest calculations for this project exceeded 3 trillion particles on the Jaguar machine at Oak Ridge. The unprecedented scale of these calculations has enabled many new scientific discoveries in this project as described below.

Scientific Approach and Accomplishments

Although the process of magnetic reconnection has many different applications, a primary focus for this project was parameter regimes relevant to the Earth's magnetosphere. As illustrated in Figure 2, this protective bubble partially shields our planet from the stream of high-energy particles coming from the Sun called the *solar wind.*   When this solar wind runs into the Earth, it creates an intense interaction region called the *magnetopause*. Magnetic reconnection can occur at the magnetopause and this allows plasma to enter the magnetosphere.   Over longer times, an extended tail-like structure can form in this bubble called the magnetotail.   Periodically, the magnetotail can become unstable to magnetic reconnection and produce energetic particles that cause auroral displays back on Earth.   Even with the largest available computers, it is not possible to model the entire system.   Instead, this project is focused on smaller regions where magnetic reconnection is known to occur.   At both the magnetopause and in the magnetotail, this happens in thin regions where the electrical charges in the plasma produce a current sheet. These currents cause the magnetic field to rapidly rotate across the layer, and ultimately this rotation is what drives magnetic reconnection.   The VPIC simulations in this project are setup with this type of initial condition and open boundary conditions are used to better mimic the large system [2]. Over the 3-year duration of this project, this basic research approach contributed to 16 publications and 12 invited talks.   Here we briefly highlight several of these new discoveries:

For configurations relevant to the Earth's magnetopause, we have demonstrated that magnetic reconnection occurs through a process that is intrinsically three-dimensional, and involves the formation rope-like structures called *flux ropes*. These results are described in a new paper [3] that recently appeared in *Nature Physics*, and was based on a series of calculations performed on Roadrunner at Los Alamos and the Kraken machine as Oak Ridge. The initial current layers quickly break-up into flux ropes as illustrated in Figure 3.   We have developed a new theory that describes the basic features of this process [3]. Over longer time scales, new current sheets form, which are much thinner than the original layer. These new current layers also break-up and form rope-like structures that can interact in complex ways as illustrated in Figure 4. This project has uncovered large differences in how this occurs

in real 3D applications in comparison to previous 2D models. As illustrated in Figure 4, the current layers break-up into oblique flux ropes in 3D, but this process is artificially suppressed in the previous 2D models. These new results imply that magnetic reconnection in large 3D systems proceeds through a turbulent scenario involving the continual formation and interaction of flux ropes. This complexity increases for larger systems as more flux ropes are permitted to grow. Our recent scaling study indicates that the average energy conversion rate may slow down due to this complexity, and we have demonstrated new features in the turbulent spectra as the flux ropes interact and the magnetic field becomes chaotic. This may have important implications for acceleration and transport of energetic particles. Many of these new predictions should be observable in existing and upcoming satellite missions. To test these ideas, we have begun a new collaboration with researchers at UC Berkeley in order to compare our results with satellite measurements.
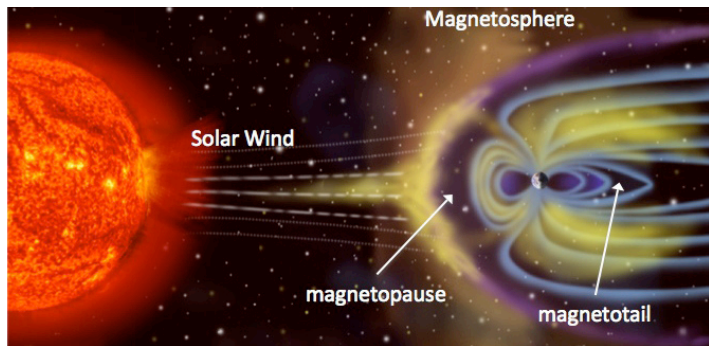
Figure 2. Charged particles stream outwards from the Sun to form the solar wind. These particles interact with the magnetic field of our planet to form the magnetosphere - a bubble of plasmas with an extended tail-like structure. The main locations for magnetic reconnection are at the magnetopause and within the magnetotail as shown in the figure.
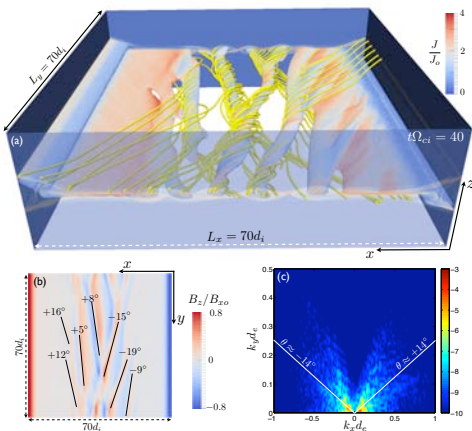
Figure 3. Three-dimensional VPIC simulation showing the formation of flux ropes within the initial current layer. The features of these ropes are well described by a new theory [3].
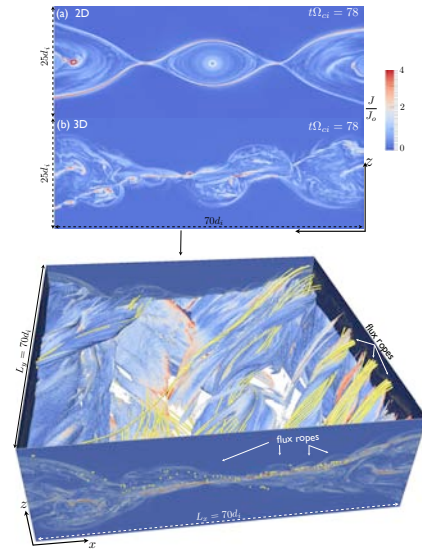
Figure 4. Over longer time scales, the VPIC simulation from Fig. 3 develops intense electron-scale current sheets as shown in the top panels. Within previous 2D simulations, these layers are stable while in 3D simulations these layers are violently unstable. As these current sheets break-up in 3D, they also form flux ropes as illustrated in bottom panel. For further details see Ref [3].

Another long-standing question in the study of magnetic reconnection is the influence of current driven instabilities. In high-temperature plasmas, ordinary electrical resistivity is very low which has important consequences for reconnection. However, researchers have hypothesized that certain types of plasma waves may be excited which can facilitate the exchange of momentum between ions and electrons and produce an effective electrical resistivity. If true, this type of resistivity would be extremely important for the dynamics of magnetic reconnection. In this project, our primary focus was a particular type of plasma instability that occurs in both space and laboratory experiments called *the lower-hybrid drift instability* (LHDI). We performed an extensive set of simulations relevant to both the magnetopause and laboratory plasmas with the goal of validating our results. As illustrated in Figure 5, these simulations have demonstrated that the lower-hybrid instability can generate resistivity under a certain range of conditions [4]. However, these conditions are more likely to occur in laboratory experiments [5] than in the magnetosphere. While there are still a few open questions, these results are the most definitive study to date on these long-standing questions. Working with space physicists at UC Berkeley, we have compared these predictions [5] with satellite data and the results confirm our conclusions.
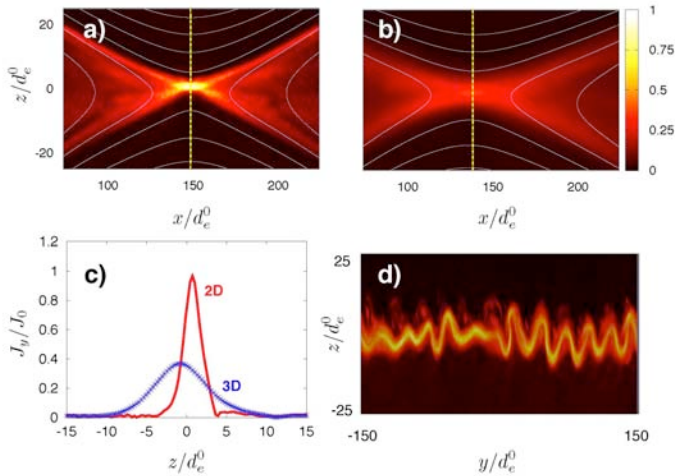
Figure 5. The three-dimensional evolution of the electron layers can produce a vigorous lower-hybrid instability that fundamentally alters the nature of the dissipation physics. The above panels compare the 2D evolution where the instability is suppressed with the 3D evolution where the instability can occur. See Ref. [4] for further details.

Impact on National Missions

This project supported the DOE mission in Nuclear Weapons by enhancing our understanding of high-temperature plasmas and exploiting the new generation of peta-scale supercomputers, including Roadrunner at Los Alamos, and Jaguar at Oak Ridge National Laboratory. The project supported the energy mission by advancing our understanding of magnetic reconnection, which is an important dynamical process in magnetic fusion machines. This research may indirectly benefit the nonproliferation mission since magnetic reconnection is also important in modeling the near-Earth space environment to better understand and mitigate the risks to satellites from extreme space weather events. The new simulation tools and theoretical expertise resulting from this project has attracted new external support from the NASA Heliophysics Theory Program (3 year $1.6M). This new follow-on project will examine detailed aspects of magnetic reconnection that occurs at the Earth's magnetopause, in support of ongoing and future NASA missions.

References

1. Bowers, K. J., B. J. Albright, L. Yin, W. Daughton, V. Roytershteyn, and B. Bergen. Advances in petascale kinetic plasma simulation with VPIC and Roadrunner. 2009. *Journal of Physics: Conference Series.* **180**: 012055.

2. Daughton, W., J. Scudder, and H. Karimabadi. Fully kinetic simulations of undriven magnetic reconnection with open boundary conditions. 2--6. *Physics of Plasmas.* **13**: 072101.

3. Daughton, W., V. Roytershteyn, H. Karimabadi, L. Yin, B. J. Albright, and K. J. Bowers. Role of Electron Physics in

the Development of Turbulent Magnetic Reconnection in Collisionless Plasmas. 2011. *Nature Physics.* **7**: 539.

4. Roytershteyn, V., W. Daughton, H. Karimabadi, and F. S. Mozer. Influence of the lower-hybrid drift instability on magnetic reconnection in asymmetric configurations. *Physical Review Letters.*

5. Roytershteyn, V., W. Daughton, L. Yin, B. J. Albright, K. J. Bowers, S. Dorfman, H. Ji, and M. Yamada. Driven Magnetic Reconnection near the Dreicer Limit. 2010. *Physics of Plasmas.* **17**: 055706.

Publications

Bowers, K. J., B. J. Albright, L. Yin, W. Daughton, V. Roytershteyn, B. Bergen, and T. J. T. Kwan. Advances in petascale kinetic plasma simulation with VPIC and Roadrunner. 2009. *Journal of Physics: Conference Series.* **180**: 012055.

Chen, L., W. Daughton, B. Lefebvre, and Roy B. Torbert. The inversion layer of electric fields and electron phase-space-hole structure during two-dimensional collisionless magnetic reconnection. 2011. *Physics of Plasmas.* **18**: 012904.

Daughton, W., V. Roytershteyn, H. Karimabadi, L. Yin, B. Albright, B. Bergen, and K. Bowers. Role of Electron Physics in the Development of Turbulent Magnetic Reconnection in Collisionless Plasmas. 2011. *Nature Physics.* **7**: 539.

Daughton, W., V. Roytershteyn, H. Karimabadi, L. Yin, B. Albright, and S. Gary. Secondary Island Formation in Collisional and Collisionless Kinetic Simulations of Magnetic Reconnection. 2011. *in AIP Conference on Modern Challenges in Nonlinear Plasma Physics.* **1320**: 44.

Daughton, W., and V. Roytershteyn. Emerging parameter space map of magnetic reconnection in collisional and kinetic regimes. 2011. *Space Science Reviews.* : DOI 10.1007/s11214.

Egedal, J., A. Le, P. L. Pritchett, and W. Daughton. Electron dynamics in asymmetric anti-parallel reconnection. To appear in *Physics of Plasmas.*

Egedal, J., A. Le, Y. Zhu, W. Daughton, M. Oieroset, T. Phan, R. Lin, and J. Eastwood. Cause of super-thermal electron heating during magnetotail reconnection. 2010. *Geophysical Research Letters.* **37**: L10102.

Egedal, J., N. Katz, L. Chen, B. Lefebvre, W. Daughton, and A. Fazakerley. Cluster observations of bi-directional beams caused by electron trapping during anti-parallel reconnection. 2009. *Journal Geophysical Research.* **115**: A03214.

Egedal, J., W. Daughton , and A. Le. Large-scale electron

acceleration by parallel electric fields during magnetic reconnection. *Nature Physics.*

Egedal, J., W. Daughton, J. F. Drake, N. Katz, and A. Le. Formation of a localized acceleration potential during magnetic reconnection with a guide field. 2009. *Physics of Plasmas.* **16**: 050701.

Ji, H., and W. Daughton. Phase diagram for magnetic reconnection in heliophysical, astrophysical and laboratory plasmas . To appear in *Physics of Plasmas.*

Karimabadi, H., J. Dorelli, V. Roytershteyn, W. Daughton, and L. Chacón. Flux pileup in collisionless magnetic reconnection: bursty interaction of large flux ropes. 2011. *Physical Review Letters .* **107**: 025002.

Karimabadi, H., V. Roytershteyn, C. Mouikis, L. Kistler, and W. Daughton. Flushing effect in reconnection: Effects of minority species of oxygen ions. 2011. *Planetary and Space Science.* **59**: 536.

Le, A., J. Egedal , and W. Daughton. Unmagnetized electron jets in reconnection with a guide field. *Physical Review Letters.*

Le, A., J. Egedal, W. Daughton, J. Drake, W. Fox, and N. Katz. Magnitude of the Hall fields during magnetic reconnection. 2010. *Geophysical Research Letters.* **37**: L03106.

Le, A., J. Egedal, W. Daughton, W. Fox, and N. Katz. Equations of State for Collisionless Guide-Field Reconnection. 2009. *Physical Review Letters.* **102**: 085001.

Ng, J., J. Egedal, A. Le, W. Daughton, and L. J. Chen. Kinetic structure of the electron diffusion region in anti-parallel magnetic reconnection. 2011. *Physical Review Letters.* **106**: 065002.

Oieroset, M., T. D. Phan, J. P. Eastwood, M. Fujimoto, W. Daughton, M. Shay, V. Angelopoulos, and F. S. Mozer. Direct evidence for a three-dimensional magnetic flux rope flanked by two active magnetic reconnection X-lines at the Earth's magnetopause. To appear in *Physical Review Letters.*

Quest, K., H. Karimabadi, and W. Daughton. Linear theory of anisotropy driven modes in a Harris neutral shee. 2010. *Physics of Plasmas.* **17**: 022107.

Royterhsteyn, V., W. Daughton, L. Yin, B. Albright, K. Bowers, S. Dorfman, Y. Ren, H. Ji, M. Yamada, and H. Karimabadi. Driven magnetic reconnection near the Dreicer limit. 2010. *Physics of Plasmas.* **17**: 055706.

Roytershteyn, V., W. Daughton, H. Karimabadi, and F. S. Mozer. Influence of the lower-hybrid drift instability on magnetic reconnection in asymmetric configurations. *Physical Review Letters.*

Scudder, J. D., R. D. Holdaway, W. Daughton, H. Karimabadi, and V. Roytershteyn. Resolved observations of the electron diffusion region during magnetic reconnection. To appear in *Physical Review Letters.*

Disentangling Quantum Entaglement

Wojciech H. Zurek
20090312ER

Abstract

Simulating quantum many-body systems efficiently is one of the major goals of modern science paving the way towards understanding of new states of matter. Understanding of quantum matter and its dynamics is also indispensable in developing technologies like quantum computers and quantum information gadgets. The possibility of efficient simulation of quantum systems on a classical computer is based on the fact that majority of classically observable states are "decohered" by an environment and require exponentially smaller amount of information for their accurate description as compared to the full quantum description. Basics of how to get rid of this enormous amount of redundant data to simulate those systems efficiently, lie in understanding how information about the state of a quantum system immersed in an environment is modified (decoherence), reproduced and propagated (Quantum Darwinism).

Here, we investigated these issues on the fundamental level. We introduced the concept of Quantum Darwinism [1] and studied its nature in the context of quantum spins (qubits for a quantum computer) in the presence of a decohered environment [2,3,4,5]. Our achievements include Shannon "channel capacity" understanding of the effect of environment. We found that decoherence indeed helps simplifying the computation of certain quantities. We have started the next steps to simplify calculations in realistic cases to make computer simulations easier. We also studied information dispersal by photon scattering [6] as well as an important information-theoretic result known as "no cloning theorem" [4].

Finally, we studied dynamics of driven spin systems, developing a scheme for determining how successful adiabatic quantum computation is [7]. We focused on the most challenging problem of adiabatic quantum computation: passage through a quantum critical point and the subsequent defect generation [8,9,10,11,12]. These studies are also of fundamental value as they have paved paths for future experiments on dynamics of quantum phase transitions.

Background and Research Objectives

Quantum systems are exponentially difficult to simulate on a classical computer: Storing an arbitrary state of just 42 spin-½ "qubits" would exhaust the memory of the "Roadrunner" (the most powerful LANL supercomputer). Quantum systems are also very difficult to control in the laboratory: Decoherence is present even when the system is only weakly interacting with its environment. This means that already modestly sized quantum systems are next to impossible to isolate. The broad research objective was to investigate the extent to which one can simulate many-body quantum systems.

We predicted that decoherence can simplify numerical simulations of quantum systems because it suppresses quantum entanglement and the latter is responsible for the exponential (in system size) computational expense of representing a quantum state on a classical computer. The focus was on exploring basic concepts of how information about a system can be extracted from its environment. This technique is known as either "environment as a witness" or "Quantum Darwinism". It is a natural extension of decoherence, which is one of the key themes of the project. It is motivated by very fundamental questions in quantum mechanics, and promises applications to quantum detection and several other problems in many-body quantum physics.

The problem with simulation of the quantum systems can be also approached from a different angle. Namely, one can use a well-controlled quantum system (a quantum computer) to emulate an otherwise inaccessible model of quantum physics (e.g. by using a cold atomic system one can try to emulate a Hubbard model that may be responsible for high-Tc superconductivity). This field of research is actively pursued nowadays. Its success depends on the ability to operate such a quantum computer adiabatically, which is demanding even without decoherence. We have performed several studies related to that problem studying relevant dynamics of many-body quantum systems. Its most challenging aspects appear whenever a quantum computer is driven across a quantum critical point (a quantum phase transition happens). Our goal was to relate the amount

of excitation created during a dynamical quantum phase transition to the rate at which the system is quenched. Naturally, the slower the quench proceeds, the smaller number of excitations is created. However, the longer the adiabatic quantum computation takes, the more decohered the quantum computer becomes. Therefore, it is crucial here to quantify the amount of excitation to be able to find an acceptable trade-off between the defect generation (spoiling quantum computation) and decoherence of a quantum computer. Our focus here was mainly on studies of dynamics of benchmarking systems like Bose-Einstein condensates and spin systems. Based on the outcome of this work, a general theory of defect (excitation) generation have been proposed.

Scientific Approach and Accomplishments

We have carried out studies of the propagation of quantum information throughout the environment in two distinct models: In a model that consists of multiple spins we have studied the effect of partially mixed environment on "Quantum Darwinism". We have concluded that while information gathering is more difficult in mixed environments, the same total information about the system can be obtained as long as the environment is not completely mixed. This observation (based on a combination of computer experiments and theoretical studies) was published in two papers [2,3]. Salient points include a Shannon "channel capacity" understanding of the effect of the mixed environment and an observation that decoherence makes it possible to simplify the computation of the information theoretic quantities that are needed to characterize "Quantum Darwinism".

We have also studied a very realistic and specific model of information dispersal by photon scattering [6]. The result is a huge redundancy (many orders of magnitude larger than redundancies obtained in the studies of more artificial models). This is an exciting development that appeared in Physical Review Letters. These results support "Quantum Darwinism" approach to the transition from quantum to classical [1].

Several studies have been devoted to the efficient numerical simulations of dynamics of systems undergoing a phase transition. This problem is highly relevant to the field of adiabatic quantum computation that targets exponential complexity of quantum systems. Our work on quantum many-body dynamics, using efficient algorithms, has lead also to important fundamental findings in the field of dynamics of phase transitions. Textbook accounts of second order phase transitions simplify what happens by treating them as equilibrium phenomena. This yields universality classes with telltale scaling behavior of the coherence length and relaxation time. Yet, near the critical point, relaxation time diverges to infinity. This "critical slowing down" implies that all second order transitions traversed at any finite rate are non-equilibrium. Topological defects –long-lived "fossils" of the ensuing symmetry breaking –

are predicted to emerge as a consequence.

We have proposed a method to experimentally evaluate adiabaticity of dynamical quantum phase transitions. Our approach was tested on the quantum Ising model [7]. The basic point is that as one drives the system back and forth at some arbitrary rate, the system remains in its instantaneous ground state only when such driving is sufficiently slow. Thus, if the system returns to the starting state after the "round trip", then it is very likely that the transition was, as a whole, adiabatic. Otherwise, for a part of the trip the rate of the transition was too high to allow for adiabaticity. This test of adiabaticity will be especially important in implementing adiabatic quantum computing as it allows one to test for adiabaticity without prior knowledge of the size of the energy gap (energy gaps are generally unknown in the proposed applications of adiabatic quantum computers).

We have also studied how non-equilibrium dynamics of an environment affects decoherence of a qubit [9]. As an environment we have chosen an Ising chain (a paradigmatic system for studies of quantum phase transitions), while the qubit was modeled as a spin-1/2. We have solved a theoretical model describing this system: an accurate analytical approximation has been worked out and numerically verified. We have found not only that decoherence of the qubit is greatly enhanced by the excitation of the environment, but also that there are interesting revivals of coherence in this system. A general scaling prediction for the dynamics of coherence in similar systems have been proposed. It generalizes our findings to a large class of systems.

We have also studied a novel type of dynamics of phase transitions by allowing the field driving the transition to be inhomogeneous in space. This work has been quickly recognized in the physics community. Two major results have been reported here [8,10]. First, the theory of how an atom cloud evolves during non-equilibrium cooling in a magnetic trap was developed [10]. This work predicts that finite-rate cooling shall lead to spontaneous creation of excitations called solitons (long-living density depression propagating without change of shape). This spectacular effect was recently experimentally observed. Second, we have considered how an inhomogeneous magnetic field affects phase boundary in a spin-1 Bose-Einstein condensate [8]. Our work supports the general hypothesis (formulated by Dorner & Zurek in 2008) that one of the critical exponents of the system can be deduced from the size of the interface between the two phases of the system exposed to the inhomogeneous field.

As a follow up to the above studies, we have researched how the cooling of atoms proceeds in a toroidal trap. In contrast to the former work where general scaling arguments have been proposed, we have studied in detail dynamics of the system using a very efficient numerical tech-

nique that we have mastered in the course of this project: a stochastic Gross-Pitaevskii equation. We have found that cooling can spontaneously generate topologically stable quantized circulation around the ring of the newborn condensate. Dispersion of the resulting winding numbers follows scaling predicted by the Kibble-Zurek mechanism (KZM). Density growth also exhibits scaling behavior predicted by KZM. Our results pave the way towards experimental determination of the critical exponents for the BEC transition: see [11] and Figure 1.
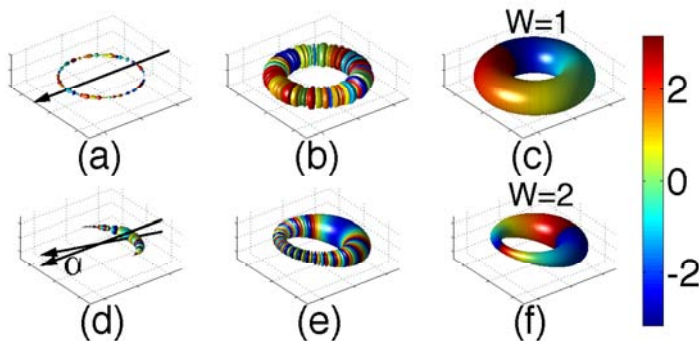
Figure 1. Growth of the Bose-Einstein condensate during a non-equilibrium cooling process (figure taken from [11]). Colors encode different phase regions. (a)-(c) dynamics in a symmetric ring. (d)-(f) dynamics in a ring that is tilted with respect to the gravitational field.

Finally, our investigations of the dynamics of many-body quantum systems has lead us to finding a new quantum phenomenon – Dynamical Quantum Freezing [12]. This effect shows up in many-body quantum systems subjected to coherent periodic driving. We found that, depending on the frequency and amplitude of periodic driving, the system can almost completely stop reacting to the perturbation that is imposed on it. This effect has no counterpart in classically driven systems. We have described it in great detail in the Ising spin chain, where the periodic driving is imposed through the modulation of the external magnetic field acting on the spins. We have studied dynamics of this model using efficient numerical techniques. The numerical results were then approximately analytically described.

Impact on National Missions

Our studies should allow us to investigate large class of many-body quantum systems of interest advancing nanoscience, condensed matter physics, and materials science. This will impact variety of fields in which the fundamental role of quantum phenomena is now being recognized by numerous sponsors including DOE.

References

1. Zurek, W. H.. Quantum Darwinism. 2009. *Nature Physics.* **5**: 181.

2. Zwolak, M., H. T. Quan, and W. H. Zurek. Redundant imprinting of information in nonideal environments: Objective reality via a noisy channel . 2010. *Physical Review A.* **81**: 062110.

3. Zwolak, M., H. T. Quan, and W. H. Zurek. Quantum Darwinism in a mixed environment . 2009. *Physical Review Letters.* **103**: 110402.

4. Wootters, W., and W. H. Zurek. The no-cloning theorem. 2009. *Physics Today.* **62(2)**: 76.

5. Zurek, W. H.. Entanglement Symmetry, Amplitudes, and Probabilities: Inverting Borns Rule. 2011. *Physical Review Letters.* **106**: 250402.

6. Riedel, J. C., and W. H. Zurek. Quantum darwinism in an everyday environment: Huge redundancy in scattered photons . 2010. *Physical Review Letters.* **105**: 020404.

7. Quan, H. T., and W. H. Zurek. Testing quantum adiabaticity with quench echo. 2010. *New Journal of Physics.* **12**: 093025.

8. Damski, B., and W. H. Zurek. Quantum phase transition in space in a ferromagnetic spin-1 Bose-Einstein condensate . 2009. *New Journal of Physics.* **11**: 063014.

9. Damski, B., H. T. Quan, and W. H. Zurek. Critical Dynamics of Decoherence. 2011. *Physical Review A.* **83**: 062104.

10. Zurek, W. H.. Causality in condensates: gray solitons as relics of BEC formation . 2009. *Physical Review Letters.* **102**: 105702.

11. Das, A., J. Sabbatini, and W. H. Zurek. Winding up superfluid in a torus via Bose Einstein condensation. *Physical Review Letters.*

12. Das, A.. Exotic Freezing of Response in Quantum Many-Body System. 2010. *Physical Review B.* **82**: 172402.

Publications

Damski, B., H. T. Quan, and W. H. Zurek. Critical dynamics of decoherence. 2011. *Physical Review A.* **83**: 062104.

Damski, B., and W. H. Zurek. Quantum phase transition in space in a ferromagnetic spin-1 Bose-Einstein condensate . 2009. *New Journal of Physics.* **11**: 063014.

Das, A.. Exotic Freezing of Response in Quantum Many-Body System. 2010. *Physical Review B.* **82**: 172402.

Das, A., J. Sabbatini, and W. H. Zurek. Winding up superfluid in a torus via Bose Einstein condensation. *Physical Review Letters.*

Quan, H. T., and W. H. Zurek. Testing quantum adiabaticity with quench echo. 2010. *New Journal of Physics.* **12**: 093025.

Riedel, J. C., and W. H. Zurek. Quantum darwinism in an everyday environment: Huge redundancy in scattered photons . 2010. *Physical Review Letters.* **105**: 020404.

Wootters, W. K., and W. H. Zurek. The no-cloning theorem. 2009. *Physics Today.* : 76.

Zurek, W. H.. Causality in Condensates: Gray Solitons as Relics of BEC Formation. 2009. *Physical Review Letters.* **102**: 105702.

Zurek, W. H.. Quantum Darwinism. 2009. *Nature Physics.* **5**: 181.

Zurek, W. H.. Entanglement Symmetry, Amplitudes, and Probabilities: Inverting Borns Rule. 2011. *Physical Review Letters.* **106**: 250402.

Zwolak, M., H. T. Quan, and W. H. Zurek. Quantum Darwinism in a mixed environment . 2009. *Physical Review Letters.* **103**: 110402.

Zwolak, M., H. T. Quan, and W. H. Zurek. Redundant imprinting of information in nonideal environments: Objective reality via a noisy channel . 2010. *Physical Review A.* **81**: 062110.

Backward Stimulated Raman and Brillouin Scattering of Laser in the Collisional Regime

Lin Yin
20090394ER

Abstract

The nonlinear dynamics of stimulated Raman scattering (SRS) and stimulated Brillouin scattering (SBS) in laser plasma interaction (LPI) is a problem of long standing interest in fundamental plasma science. Control of these instabilities is vital to the success of upcoming inertial confinement fusion (ICF) experiments at the National Ignition Facility (NIF).

New, yet fundamental, physics understanding regarding the instabilities' onset and saturation has been obtained through the use of highly resolved particle-in-cell (PIC) simulations. In particular, it is found that the essential physics governing nonlinear onset and saturation of SRS and SBS in the kinetic regime is a nonlinear process that involves the trapping and collisional de-trapping of particles in plasma waves and their subsequent effects on these waves.

The goal of this project was to extend our physics understanding of LPI to enable careful experimental validation of our LPI tools, which involves including the effects of collisions among plasma particles as well as understanding how collisions affect trapped particle physics. This work built upon unique LANL strengths: (1) modifications to our LANL VPIC (Vector Particle In Cell) code, presently one of the world's fastest plasma modeling codes, to enable it to run efficiently on the world's most powerful supercomputer, Roadrunner, and (2) implementation of binary collisions in VPIC, enabling the LPI modeling to transition from the collisionless to the collisional regime.

We validated the LPI physics by using small-scale Trident experiments to understand the nonlinear dynamics of a solitary laser speckle, the fundamental ``building block'' of an inertial fusion laser beam. VPIC on Roadrunner will enabled 3D simulations of hundreds of billions of computational particles and allowed accurate modeling of the key process of particle trapping in collisional plasma and allowed us to truly address the physics relevant to experimental setting.

Background and Research Objectives

In ICF experiments at the NIF, over a million Joules (MJ) of laser energy is focused into a gas-filled high-Z cylinder called hohlraum. The hohlraum walls absorb the laser energy and re-radiate the energy as x-rays, which are absorbed in a spherical capsule at the hohlraum center. This causes the capsule to compress, bringing the deuterium-tritium fuel to the high temperatures and pressures required to initiate thermonuclear fusion. As the laser propagates through the fill gas, SRS, the resonant amplification of electron density fluctuations by a laser, may arise, which scatters laser light out of the hohlraum, degrades capsule implosion symmetry, and pre-heats the fuel with hot electrons, making compression harder to achieve.

The primary research objective of this project was to improve dramatically our understanding and our ability to predict how nonlinear LPI behaves in laser-plasma media, such as those found in NIF inertial fusion experiments. Such an understanding would enable more successful experimental designs of inertial confinement fusion experiments that may, one day, pave the way to energy production from thermonuclear fusion, a grand challenge with enormous potential payoff for humanity. This project aimed to develop the world's first first-principles model of LPI in laser-driven hohlraums and we made tremendous progress toward that goal. Our work made heavy use of the Roadrunner petaflop supercomputer and the state-of-the-art VPIC kinetic plasma simulation code in order to conduct meaningful "Science at Scale" calculations that shed light on this important problem.

Scientific Approach and Accomplishments

Extensive VPIC simulations and analysis for this project have been conducted on the heterogeneous multi-core supercomputer Roadrunner at LANL and the Jaguar supercomputer at ORNL. Computer simulations of "stimulated scattering" of laser light in the trapping regime, where plasma waves and particles interact with one another in a profound way, have been performed in settings of single- and multiple laser "speckles," or localized "hot spots," i.e., regions of high laser intensity. Presently, High Energy Density Physics (HEDP) laser facilities

such as the LLNL NIF, the Univ. of Rochester Omega facility, and the LMJ facility in Bordeaux, France, use speckled laser beams in order to improve spatial homogeneity. Understanding LPI requires first understanding how individual speckles behave nonlinearly (no easy task!) and then understanding how speckles interact with one another.

A suite of VPIC simulations have been run to validate the physics using both LANL Trident short-pulse, signal speckle experiments in the strong laser intensity regime (peak intensity $> 10^{16}$ W/cm^2) and Raman amplification experiments on the LLNL Jupiter laser facility, where average laser intensity is lower ($\sim 10^{14}$ W/cm^2). The predicted nonlinear physics associated with electrons "trapped" in plasma waves has been observed in simulations of both experiments and *quantitative* agreement has been obtained. Surprisingly, "at scale" simulations of these large plasma volumes show for the first time that substantial electron trapping occurs and the effects of these trapped particles ultimately limit the amount of laser scattering, even at low average laser intensity. This surprising result has led to a sea change in our understanding of how LPI manifests and behaves at the "macroscale."

A key advance made possible by this project was the systematic study of the effects of binary particle collisions on the onset threshold intensity for stimulated Raman backscatter in lower temperature plasmas, such as those obtained in the LANL Trident experiments and the LLNL Jupiter experiments. One of the key results of this project was the demonstration that nonlinear trapping effects, which lead to the enhancement of backscatter, are indeed reduced by "collisional detrapping," resulting from both parallel (i.e., aligned along the direction of propagation of the plasma waves) and perpendicular (across the direction of plasma wave propagation) diffusion in velocity space. Furthermore, it has been shown that in these laboratory experiments, competition between particle trapping and collisional detrapping leads to a temporal delay in the onset of trapping enhanced SRS, and that this in turn leads to an increase in the onset laser intensity threshold for nonlinear SRS physics to manifest. Unraveling this picture was key to our being able to use these laboratory experiments to validate our models.

2D VPIC simulations of Trident short pulse experiments show the time-dependent nature of SRS backscatter. We found in this project that individual, sub-picosecond bursts of enhanced SRS backscatter occur at discrete wavelengths (frequencies) that have been shifted from their linear resonance values due to electron trapping. This frequency shifting explains the broad, time-integrated spectra seen in TRIDENT experiments. Our understanding of the effects of collisional detrapping and heating on the development of enhanced backscatter in the kinetic regime has been used to properly interpret results from LPI experiments at both LANL Trident and LLNL Jupiter laser facilities and it has provided us with redoubled confidence in the fidelity of our computational modeling of LPI.

A final chapter of this work centered on the importance of multi-speckle LPI. During this final phase, we applied our validated models, including the mm-scale plasma simulations of Jupiter experiments, to the problem of laser backscatter in NIF experiments, where the nonlinear trapping physics is present, but inter-particle collisions are unimportant. Because of the confidence gained in the early part of this project (as well as the development of critical diagnostics and wave launch boundary conditions) we were able to very quickly assess the LPI backscatter arising in these experiments and begin to unravel some of the difficulties arising in these experiments from LPI. We found that the very physics discovered during this project, namely the importance of nonlinear wave-particle trapping physics on LPI, is indeed responsible for the large levels of LPI found in present-day experiments.

As a consequence of this effort, which has gained much attention within the ICF community and the scientific community writ large (the PI has been invited to give a prestigious invited talk at the American Physical Society Division of Plasma Physics meeting this Fall), we are beginning to change the way in which the community thinks about LPI in ICF experiments. This work has had high visibility and was featured at the NNSA/LDRD Tri-Lab Symposium at the UC Washington Center in Washington DC on June 9, 2011; at the LANS Office independent Functional Management Review (FMR) of the Los Alamos LDRD Program on Aug. 16-19, 2011; and was presented at LDRD Day at Buffalo Thunder Resort in Pojoaque, New Mexico, on Sept. 13, 2011.

Impact on National Missions

Now that we have a validated, predictive modeling capability for LPI in collisional and collisionless plasma, we are poised to begin systematically study of the effects of coupling between and among laser speckles in "mesoscopic" laser-plasma media. This new work will focus on development, calibration, and testing of economical, reduced models of LPI backscatter that, we hope, will ultimately lend insight into how ICF experiments can be designed without the deleterious effects of LPI, while at the same time revealing the intricate, emergent physics governing LPI in nonlinear optical media, identified in a recent DOE ReNeW Report as being a "grand challenge" of high energy density laboratory physics. This work will involve extensive use of very large-scale kinetic simulations at a scale, which has never been attempted before, as well as careful validated against experimental results obtained from the LANL Trident experiments.

As a result of LDRD funding, we have validated our modeling in a range of parameter regimes and have gained confidence in our ability to model, and thus begin to explain, the governing physics of LPI in a host of settings. We have already begun to use this predictive modeling capability

to test hypotheses for mitigation of LPI backscatter on the NIF.

Publications

Bowers, K. J., B. J. Albright, B. Bergen, L. Yin, K. J. Barker, and D. J. Kerbyson. 0.374 Pflop/s Trillion-Particle Kinetic Modeling of Laser Plasma Interaction on Roadrunner. 2008. *Proceedings of the 2008 ACM/IEEE conference on Supercomputing, SC'08, Austin, Texas, IEEE Press, Piscataway, NJ, USA* . : 1.

Bowers, K. J., B. J. Albright, L. Yin, W. Daughton, V. Roytershteyn, B. Bergen, and T. Kwan. Advances in petascale kinetic plasma simulation with VPIC and Roadrunner. 2009. *Journal of Physics: Conference Series.* **180**: 012055.

Finnegan, S. M., L. Yin, J. L. Kline, B. J. Albright, and K. J. Bowers. Influence of binary Coulomb collisions on nonlinear stimulated Raman backscatter in the kinetic regime. 2011. *Physics of Plasmas.* **18**: 032707.

Kirkwood, R. K., Y. Ping, S. C. Wilks, N. Meezan, P. Michel, E. Williams, D. Clark, L. Suter, O. Landen, N. Fisch, E. O. Valeo, V. Malkin, D. Turnbull, S. Suckewer, J. Wurtele, T. L. Wang, S. F. Martins, C. Joshi, L. Yin, B. J. Albright, H. A. Rose, and K. J. Bowers . Observation of amplification of light by Langmuir waves and its saturation on the electron kinetic timescale. 2011. *Journal of Plasma Physics.* **77**: 521.

Kline, J. L., D. S. Montgomery, C. Rousseaux, S. D. Baton, V. Tassin, R. A. Hardin, K. A. Flippo, R. P. Johnson, T. Shimada, L. Yin, B. J. Albright, H. A. Rose, and F. Amiranoff. Investigation of stimulated Raman scattering using short-pulse diffraction limited Laser beam near the instability threshold. 2009. *Lasers and Particle Beams.* **27**: 185.

Transport in Magnetized Dense Plasmas for Magneto-Inertial Fusion

Xianzhu Tang
20090410ER

Abstract

Magneto-inertial fusion relies on a conventional inertial pusher, for example, imploding metal shells or merging plasma jets, to compress a magnetized plasma target to ignition temperature. The density is between that of a magnetic confinement fusion plasma and that of an inertially confined laser-fusion plasma. The transport physics of a target plasma in the magneto-inertial fusion regime was investigated in three distinct but related areas. The first is on the plasma behavior next to the metal pusher, where the magnetic field is nearly parallel to the metal surface. The crucial physics is on the metal shell electric potential due to excess ion charging, which is opposite to an un-magnetized plasma or a magnetized plasma with magnetic field intercepting the material surface at a large angle. The equilibrium structure of the electric field in the plasma near the wall, along with the magnetic field, determines the inward impurity ion transport due to plasma-material interaction. The second area is on the transport physics inside the target candidate of choice, the field reversed configuration (FRC). Unlike the conventional magnetic confinement plasma such as those in a tokamak, neither the electron nor the ion has integrable orbit even with perfect toroidal symmetry in the magnetic field. This is due to the large magnetic field strength variation along a magnetic field line in FRC, which violates the adiabatic invariance of the magnetic moment. We have carried out a systematic study of the loss versus confinement orbit for electrons and ions as a function of their velocity space distribution, and found large non-ambipolar particle transport. Hamiltonian analysis were performed to characterize the boundary between loss/confined orbits in the velocity space. This sets up a self-consistent evaluation of the large electric field, which enforces ambipolarity, and hence rotation of the FRC plasma target. The third area is specific to the plasma jet-based magnetic inertial fusion scheme where the inertial pusher is formed by merging plasma jets. This offers engineering control for optimizing the push radial profile in density and implosion speed. We discovered a new implosion regime, which is called bounce-free spherical implosion. Here bounce-free means that

upon stagnation, the hot spot target plasma does not bounce against the imploding pusher, so a longer dwell time can be achieved. A specific class of self-similar pusher solution is found to satisfy this requirement and has led to consideration by an experimental program at LANL.

Background and Research Objectives

To achieve controlled fusion for energy applications, one must reach the Lawson criteria for the plasma. The two standard approaches are to either reduce the transport loss by magnetic confinement in steady state or provide fast enough heating by inertial pusher for a pulsed thermonuclear burn. In magnetic confinement fusion, the density must be sufficiently low so collisional transport is small; this leads to a large system with large total energy content and concomitant increased cost. For inertial confinement fusion, the density must be very high to enable thermonuclear burn, and the rapid energy loss requires extremely high power for the inertial fusion to offset. This translates into expensive laser systems. The magneto-inertial fusion scheme aims to reduce the power requirement for the inertial pusher by using a magnetized target that has improved transport, while still achieving controlled burn in a small system by target compression on the order of ten in radius.

To maximize our impact on ongoing national experimental programs in magneto-inertial fusion, namely the LANL-AFRL experiment on solid-liner-based Magnetized Target Fusion experiment (PI: Tom Intrator and Glen Wurden) and LANL's Plasma-Jet Magneto-Inertial Fusion experiment (PI: Scott Hsu), we focus on the target of choice, the Field Reversed Configuration. Two FRC transport issues stood out as urgent and fundamental. The first is on the behavior of plasma near the imploding metal liner surface. The second is on the transport inside the core of the FRC, which was normally parameterized without a fundamental physics understanding. The importance of the near-wall region of the plasma is largely due to the inward impurity transport by sputtering at the liner surface. In a normal plasma of equal electron and ion temperature, the electron has a far greater thermal speed due to the much smaller mass compared with the

ions. So more electrons are initially lost to the wall surface, which is then charged negatively. Ambipolarity, or equal loss rates for ions and electrons, is established by the normal electric field pointing toward the wall surface inside the plasma. In other words, the electric field slows down the electrons while it speeds up the ions. A consequence is that should an impurity ion of the surface material type be produced, the electric field would impede the inward penetration of the impurity ion, which is positively charged. In the case of MIF, there is a strong magnetic field which is actually parallel to the metal liner surface, or nearly so. Both electrons and ions are magnetized, i.e. executing gyro-orbit, so their loss to the liner surface is by direct interception of the gyro-orbit with the liner surface. Now the ions, due to larger mass, have much wider gyro-orbit so more ions can reach the liner surface compared with the electrons. This results in a positively, as opposed to negatively, charged wall. The normal shielding effect by the sheath electric field of the impurity ions is absent. The first research objective was to establish the basic physics of the plasma sheath in a magnetized plasma with magnetic field parallel to the liner surface. We are specifically interested in the MIF regime where the plasma pressure to magnetic energy density is comparable.

A second transport issue concerns the core FRC particle transport. The idea of magnetic confinement rests on the behavior of the charged particle orbit, which is described, in general, by a three degrees-of-freedom Hamiltonian. It is well-known that any Hamiltonian system over one degree-of-freedom tends to produce a non-integrable or chaotic orbit, which translated into confinement terminology, is an unconfined or direct loss orbit. Magnetic confinement uses geometrical symmetry (in the toroidal direction for both tokomaks and FRCs) to reduce the particle Hamiltonian to two degrees-of-freedom. For tokamaks, a further reduction resides in the adiabatic invariant of the magnetic moment, which is the result of gyro-motion in a slowly varying magnetic field. The remaining one degree-of-freedom ensures that charged particle drift orbit in a tokamak is always integrable and hence confined in the absence of collision. FRC, on the other hand, has large field strength variation along the magnetic field line, due to the topological constraint of not having a toroidal magnetic field. The magnetic moment, consequently, is not an adiabatic invariant, so the particle motion is described by a two degrees-of-freedom Hamiltonian. Both ions and electrons have non-integrable or chaotic orbit, which lead to direct orbit loss. A key question is whether this loss is intrinsically ambipolar or not. If not, how does the electric field comes into play to ensure ambipolarity.

In addition to the two critical transport issues, there has been huge concern on the feasibility of the plasma jet magneto-inertial fusion scheme with regard to the dwell time of the compressed target. The issue is at what speed the target disassembles post-stagnation. A too short dwell time would cut burn time and hence burn rate. Parks from General Atomics has argued that the dissembling speed is on the order of implosion speed independent of the implosion liner profile. Interaction with LANL experimentalists and the external community has led us to address this in a more fundamental way, namely, what determines the target dissembling speed and how to use the liner profile to optimize the target dwell time. Our work in this area has led to a fundamental rethinking of how the PJMIF experiment should be pursued.

In summary, our ER project eventually had three focuses in its research objectives: (1) near-liner plasma sheath; (2) core FRC transport; (3) target dwell time optimization. The first and second are directly derived and refined from the original proposal. The third is a timely response to a critical need in the rapidly evolving, broader MIF research within the national program.

Scientific Approach and Accomplishments
Liner electric charging and near-liner-surface plasma behavior

To understand the electric charging of the liner surface and detailed plasma behavior near the surface of the imploding liner, we have performed both large-scale kinetic simulation using the VPIC code and analytical analysis of particle orbits and sheath structure. Specifically, a systematic investigation of the scaling of a one-dimensional plasma sheath with a magnetic field parallel to the wall was carried out using analytical theory and the particle-in-cell code VPIC. We established a model starting with a uniform Maxwellian distribution in three-dimensional velocity space, plasma consisting of collisionless electrons, and ions of the same temperature that interact with a perfectly absorbing wall. A much larger ion Larmor radius causes the wall to be charged positively, creating an electric field that tends to repel the ions and attract the electrons, which is the opposite of the conventional Bohm sheath. This manifests in the form of gyro-orbit modification by this spatially varying electric field, the degree of which is found to intricately depend on the relation between three parameters: electron and ion thermal Larmor radii and plasma Debye length. Furthermore, the study of the sheath width scaling through the analysis of the full width at half max of electric field, $x(E_h)$, elucidates three distinct types of behavior of $x(E_h)$, corresponding to three different regimes: ion theromal gyroradius less than Debye length, Debye length between ion and electron thermal gyro-radii, and Debye length shorter than electron thermal gyro-radius. In addition to the sheath width, the scaling of the wall potential, is established as a function of plasma temperature, the ion mass and charge.

The detailed equilibrium structure in the near-liner-surface plasma is further elucidated. Specifically, the analysis of the steady-state force balance of the entire plasma as well as its individual components illuminates the roles that the hydrodynamic, magnetic, and electric forces play. In

particular, when the ion thermal gyro-radius is less than the Debye length, the magnetic force balances the divergence of the pressure tensor. As the magnetic field is decreased, the electric force becomes prominent in areas where quasineutrality breaks, which can be a substantial part of the sheath. Its importance depends on the relation between three parameters, namely, electron and ion thermal Larmor radii and plasma Debye length. The relative importance of the electron and ion current in the magnetic or Lorentz force term can be understood through the analysis of the two-fluid force balance. It reveals that the current is carried primarily by the electrons. This is due to the direction of the electric field that helps confine the ions, but not the electrons, which are forced to carry a large current to be confined magnetically. In the regimes where the electric field is negligible, the ions also need the current for confinement, but in these cases the divergence of the ion pressure tensor is much smaller than that of the electrons. Consequently the ion current is also smaller. The study of the electron and ion flow parallel to the wall clarifies this picture even further. In the regime of strong magnetic field, the particle average velocity parallel to the wall is purely diamagnetic. However, since the ion number density is very low near the wall, they do not produce considerable contribution to the current. In the regime of ion gyroradius less than the Debye length, parallel flow consists of two parts: diamagnetic and ExB drifts. Since the direction of the former depends on the particle charge while the latter does not (at least to lowest order), the drifts for the electrons add, while for the ions they mostly cancel each other.

Further studies indicate that there are two kinds of instability in the near-liner-surface region of the plasma. The first is driven by a combination of temperature anisotropy (recall that temperature parallel to the magnetic field is hotter than temperature perpendicular to the magnetic field line because of loss to the wall) and density gradient. This gives rise to lower hybrid oscillation. The second is intrinsically a 2D (in space) effect, which is the Kelvin-Helmholtz instability driven by the large shear in the plasma flow parallel to the liner surface. We first establish that this instability is only triggered in the MIF regime where plasma thermal pressure is comparable to the magnetic energy density.

Research results under objective (1) have led to an invited talk in 2009 Annual Meeting of the Division of Plasma Physics of the American Physics Society, an invited paper in Physics of Plasmas (PHYSICS OF PLASMAS Volume: 17, Issue: 5, Article Number: 057103) and a regular paper in Physics of Plasmas (PHYSICS OF PLASMAS Volume: 17, Issue: 6, Article Number: 063508). The results on instabilities remain to be published.

Core FRC transport

Because of the absence of a toroidal magnetic field in an

FRC, there is order-unity magnetic field strength variation along a magnetic field. Both the electrons and ions, although magnetized, do not have the magnetic moment as an adiabatic invariant. The particle orbits are thus described by two degrees-of-freedom Hamiltonian, which in general produces both integrable and chaotic orbits. We have performed both numerical computation of the FRC charged particle orbit /loss rate and the analytical analysis of the confined versus loss orbit in the velocity space. Specifically, we have developed an orbit integration code for the FRC equilibrium magnetic field. For comparison purposes, both a high order (4th) Runge-Kutta scheme and a second order simplectic scheme are used. The larger time step and intrinsic conservation properties of the symplectic integrator were found to be extremely effective in dealing with the FRC particle orbit, particularly the electrons. Nonlinear analyses such as the Poincare plot were performed to understand the integrability of the orbit, and boundary between order and chaos. It was found that because of the energy constraint, not all chaotic orbits lead to direct orbit loss, and not all loss orbits are due to stochasticity. A clear boundary in the velocity space is established for confined versus lost particles. We also made the original discovery that the loss rate, in the absence of a ambipolar electric field, has an order unity difference for ions (high) and electrons (low). This implies that a large electric field must be established to ensure ambiploar transport. Equivalently, the ambipolar electric field, which is large, must induce large plasma rotation.

Our analytical analysis has confirmed the clear separation of the confined versus loss orbit in the velocity space. A manuscript is being finalized to publish this findings on the strong non-ambiploarity of the FRC electrons and ions in the absence of an ambipolar electric field. The more subtle issue of determining the ambipolar electric field motivates further development of a Poisson solver for the electric field. This is to be further pursued as a follow-up to the ER in the national program. A summary of our physics findings and the solution of the ambipolar electric field is to be presented at the 2011 Annual Meeting of the Division of Plasma Physics of the American Physics Society.

Dwell time and bounce-free hydrodynamic implosion

The MIF scheme, because of lower density compared with the conventional laser-driven inertial confinement scheme, does not rely on a thermonuclear burn wave. It is more accurately described as a batch burn which occurs volumetrically. The final burn rate thus crucially depends on the dwell time of the compressed target after stagnation. There has been a raging debate in the MIF community on how long this dwell time is, especially in the context of plasma-liner MIF. On one side, Paul Parks from General Atomics argued for a short dwell time, which comes from a bounce velocity of the assembled target the same as the implosion liner velocity. On the other side, Scott Hsu from LANL, and others have argued that the tapering effect of

a thick plasma liner can significantly slow down the target bounce speed, and hence prolong the dwell time and increase the burn fraction.

We have performed a fundamental study on what determines the dwell time or bounce of the compressed target post-stagnation. Specifically we found that the stagnation surface propogates outward as a shock with speed affected by the liner profile. It is through this shock that incoming thick liner materials convert their kinetic energy into thermal energy. There is a possibility, by tailoring the liner profile, one can achieve a scenario that the shocked liner maintains pressure balance with the compressed target so the compressed target never bounces. This demonstrates that the critical path to dwell time optimization is to shape the liner profile. Although complete bounce-free is practically difficult, this provides an experimentally accessible method for reducing the bounce and hence increasing the dwell time and burn fraction. We explicitly constructed a family of the self-similar spherical implosion flow solutions that maintains bounce-free for the post-stagnation target. This work is currently in review with the Physics of Plasmas. It was also an invited talk at the 2011 Anomalous Absorption Conference.

Impact on National Missions

Our work on the electric charging of the wall surface and the plasma structure near the wall surface for a magnetized plasma with magnetic field parallel to the wall is well received in the community, not only MIF but also the tokamak community. Experimentalists from Princeton Plasma Physics Laboratory and EPFL, Lausanne, Switzland, have contacted us for collaboration and input for their experimental campaigns.

The work on core FRC transport is new, and opens a critical path that could finally lead to an FRC transport theory and explain the long time puzzle of spontaneously generated FRC rotation.

The work on bounce-free hydrodynamic implosion settles a raging dispute on what determines the dwell time of MIF target and the clarifies the fundamental physics underlying the plasma liner optimization towards higher fusion burn fraction. This work was prominently featured in an invited talk in the 2011 ICOPS meeting and an invited paper in IEEE Transaction in Plasma Sciences.

This work strengthens Laboratory scientific capabilities in theory, computation, and modeling to understand the physis of high-energy density and plasmas that underpin our understanding of laboratory controlled fusion systems. It supports the DOE strategic themes of energy security and scientific discovery and innovation.

Publications

Hsu, S. C., T. Awe, A. Case, J. Cassibry, G. Kagan, M. Stanic, X. Z. Tang, D. Welch, and F. Witherspoon. Imploding plasma liners as a standoff driver for magneto-inertial fusion. *IEEE Trans. Plasma Science.*

Kagan, G., X. Z. Tang, S. C. Hsu, and T. Awe. Bounce-free spherical hydrodynamic implosion. To appear in *Physics of Plasmas.*

Krasheninnikova, N., X. Tang, and V. Roytershteyn. Scaling of the plasma sheath in a magnetic field parallel to the wall. 2010. *Physics of Plasmas.* **17** (5): 057103.

Krasheninnikova, N., and X. Tang. Equilibrium properties of the plasma sheath with a magnetic field parallel to the wall. 2010. *Physics of Plasmas.* **17** (6): 063508.

Novel Cone Targets for Efficient Energetic Ion Acceleration for Light Ion-Driven Fast Ignition Fusion

Kirk A. Flippo
20090466ER

Abstract

Intense particle beams are an important component for a host of applications, including fast ignition inertial confinement fusion, high energy density physics, creating and diagnosing warm dense matter, novel nuclear physics and laboratory astrophysics studies, active interrogation schemes, radioactive waste transmutation, and medical isotopes and cancer therapies. However, understanding the mechanisms that create these intense particle beams is in its infancy even after a decade of work, and yet it is so crucial for designing and optimizing systems based on this technology.

The goal of this project was to understand the fundamental physics of ion beams produced from some unique flat-top cone targets and to improve their performance. These cone-targets enhance the laser-to-ion conversion efficiency and the ion energies, to values that are able to realize Ion Fast Ignition (IFI) fusion energy using light ions, a concept recently championed by LANL. This project was aimed at understanding, specifically, the hot electron behavior in the targets, which affect how these ion beams are produced and determines their characteristics. Understanding and controlling these beams would not only make IFI fusion and energy independence closer to reality, but would also affect any other potential applications that would benefit from such beams like those listed above.

Background and Research Objectives

Laser-accelerated particle beams [1], and in particular ion beams [2,3,4,5], are of considerable interest for many applications in science and technology, such as the study of astrophysical phenomena [6], nuclear reactions and isotope production [7,8], ion fast ignition [9] inertial confinement fusion, the radiography of dense objects, transient electric and magnetic fields [10], and as an injector for accelerators [11]. They also have been proposed for use in medicine, for radiation oncology for proton or ion therapy [12]. For the latter application, techniques have been suggested to either use the entire spectral distribution of the proton beam [13], or to modify the proton spectrum to a quasi-monoenergetic narrow-band distribution [14]. However, the critical parameter remains being able to maximize the proton cutoff energy.

For an entire decade, using flat-foil targets, or any other target type or geometry, the highest recorded proton energy remained 58 MeV (Figure 1, green diamond), obtained 10 years ago on the Nova PW laser with 423 J of laser energy [22]. Though equaled at lower laser intensity (Figure 1, light purple square) on Trident [15], it had never been surpassed [16], despite some of the data being acquired with significantly higher laser energies, of up to 1000 J (Figure 1, purple triangle) [16] or intensity of up to 6E^{20} W/cm^2 [17].

In theory and simulations, new mechanisms have been proposed to significantly enhance the ion energy. They include the laser-piston regime [19,20], the break-out afterburner (BOA) mechanism [21,22] and the radiation pressure acceleration (RPA) mechanism [23,24]. All of these mechanisms, to be fully realized, have requirements which have, together, not yet been achieved in the laboratory: an ultra-high contrast (to be able to shoot targets thinner than 100 nm *without* any target disruption) and very high laser intensities, starting at ~1E^{21} W/cm^2; and RPA adds a third requirement, e.g. circular polarization. And for reasons pointed out below, these will not be realizable into the near future.

By concentrating and using the most understood and efficient laser-ion acceleration mechanism demonstrated to date, Target Normal Sheath Acceleration (TNSA) [25], one can use different targets geometries, other than flat foils, in order to achieve higher ion energies. Within this TNSA framework, where one usually assumes an isothermal [26] or adiabatic [27] expansion of the plasma into vacuum, increasing the electron temperature (while keeping the hot electron number constant) will increase the maximum ion energies. Target geometries proposed to do so include mass-limited or reduced-mass targets (RMTs) [28,29,30], stacked foils [31,32] and cone targets [33,34,35,36]. RMTs had recently been shown experimentally [30] to enhance the maximum proton energy due to re-circulating electrons, confined in a smaller tar-

get volume, so this approach was investigated as well.
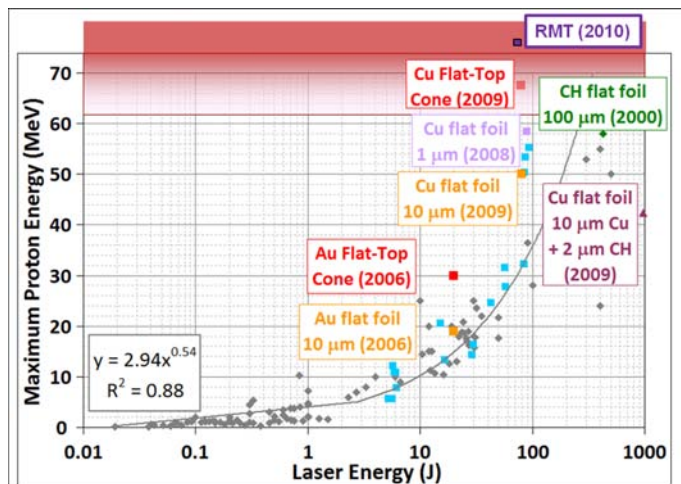
Figure 1. Maximum proton cutoff energy (MeV) as a function of laser energy (J) for all published laser systems, with laser intensities from 1E17 to 6E20 W/cm^2, energies from 19 mJ to 965 J, pulse durations from 30 fs to 10 ps, and reported contrasts from 1E-5 to <1E-9, for any type (metal and plastic) and thickness of flat-foil targets, but choosing, for each reported experiment, the highest proton energy (grey diamonds) [16, and references therein]; trend is for all diamonds; the purple triangle represents a shot from the Omega EP laser at 10 ps [16]; all squares are Trident data points; the light purple square represents a shot on a 1 μm Cu flat foil (using a laser contrast of <1E-7) [15], the red (orange) squares represent shots on Au and Cu Flat-Top Cone (flat foil) targets and the dark purple square is the RMT world record shot from 2010. The green diamond represents the 2000 Nova PW record [2]. The lower red line shows the beginning of the oncological therapeutic window at 62 MeV (depth of 30 mm) for eye cancer [18], which extends to >200 MeV (depth of 30 cm) for deeply-seated tumors [12].

Scientific Approach and Accomplishments

We have now completed a total or four experimental runs on the LANL Trident laser system, where we have shot a variety of flat-top cone targets (micro-grooves on the flat-top, various neck and top dimensions) to determine the TNSA sheath (accelerating field) and source size of the laser-accelerated ion beam as a function of energy, along with RMTs to study the laser-to-electron energy conversion and electron-to-ion energy transfer, and to use this information to model and enhance these characteristics.

In our studies we identified a new mechanism of laser light absorption named the Direct Laser Light Pressure Acceleration (DLLPA) of electrons [37], a process that we discovered via x-ray emission 2-D imaging and simulations in 2009. We deployed the most extensive suite of diagnostics to ever run at one time at the Trident facility to help us understand the laser-matter interaction. We built and fielded several new diagnostics: a high resolution ion en-

ergy analyzer, the Electron-Positron-Ion Correlating (EPIC) Spectrometer[38]; a flat crystal x-ray spectrometer; a 2 /3 omega probe beam line for looking at the target and sheath expansion via interferometry; a Raman backscatter diagnostics; a backscatter focal diagnostic; neutron diagnostics (bubble detectors); and two X-ray K-α imagers to look at orthogonal views of the target's X-ray emission to determine interaction of the laser with the cone walls.

With our suite of diagnostics and completed experiments we achieved record breaking energies in '09, which was the subject of a press release from the lab, and one of the selected press releases of the APS-Division of Plasma Physics (DPP) Conference in 2009. This led to the discovery of the above mentioned DLLPA mechanism, and a paper that has been on the AIP *Physics of Plasmas* 20 most down-loaded article list for 4 straight months (an unprecedented number in our experience), coming in at #13 for May, #12 for June, #11 for July) and #16 for August 2011 (numbers for Sept were not available as of this report). This new mechanism is having a large impact on the field (as judged just by the immediate interest and invited talks) and we should be able to boost ion energies even further. It will also be of special importance to the inertial confinement fusion community due to its implications for fast ignition fusion physics (electron and ion), as it may lead to electrons too energetic to be useful for electron fast ignition in a cone geometry. We broke the world record energy again (75 MeV) in 2010 using an RMT (Figure 1).

The new suite of diagnostics has also proven that as clean as the Trident laser pulse is, it is still not clean enough to support the new acceleration mechanisms like BOA, RPA et, as noted above, because of the ever present preplasma caused by the shoulder of the short-pulse beam as shown in Figure 2. This was discovered due to our need to understand the sheath, however we also measure the laser-interaction, and now we understand that it will take many years to produce a laser pulse of sufficient energy and contrast to realize those mechanisms.

We also produced over 8 billion neutrons on a single pulse (Figure 3) , which is to our knowledge the highest yield of neutrons from a short-pulse interaction (not involving kilojoules of compression lasers)[39].   This is a collaboration with the University of Illinois Urbana-Champaign to produce deuteron beams for our targets for Fast Ignition with deuterons [40,41,42], resulting in five publications on this topic so far.

This project involves nearly 30 scientists, of whom 9 are graduate students and 8 are Postdocs. We needed this large collaboration not only to leverage the LDRD funds, but also because this set of experiments was particularly resource intensive with the amount of diagnostics built and fielded. This arrangement fit us very well as we now have trained students in high-energy density physics with a suite of diagnostics and collaborators for the next round

of experiments and proposals. Overall the project resulted in 21 publications in print, with several more still pending (under review or in preparation).

Interest in these experiments continues to run high; the PI has presented 5 invited talks: the 7th International Conference on Inertial Fusion Sciences and Applications (Bordeaux, FRANCE), the 2010 US-Japan Workshop on Laser-Plasma Interactions (Chicago ,IL), the Antimatter Creation Using Intense Lasers Workshop (Berkeley, CA), The Advanced Accelerators Conference (Annapolis, MD), and the Anomalous Absorption Conference (Snowmass, CO). Two of our postdocs gave invited talks at the APS-DPP 2010, resulting in an invited paper on this subject in the journal *Physics of Plasmas* [37} that has garnered much attention. This work was also featured in an interview for educational videos on high tech jobs produced within a CRADA from the DOE distributed by Lincoln Interactive.
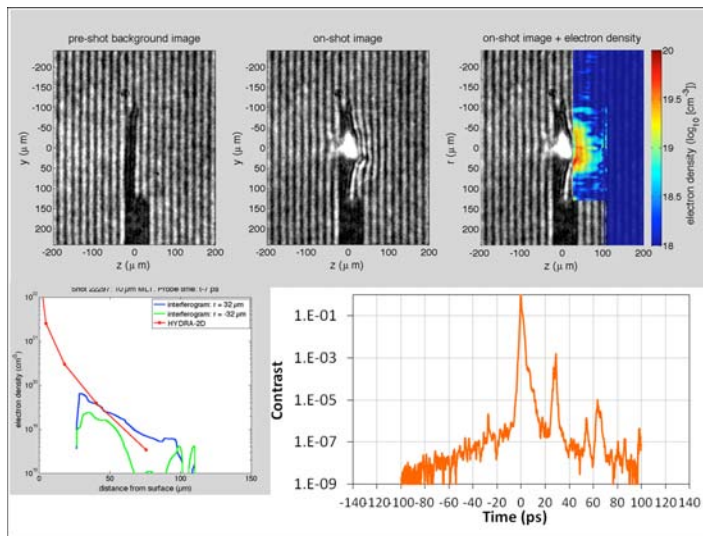
Figure 2. Upper panels show (from l - r) a target before the laser interacts and during the interaction, and the final panel is the reconstructed electron density profile, which is shown graphically in the bottom panel (left). The laser contrast is shown on the bottom panel (right), where the part responsible for producing the preplasma is the portion of the laser pulse from -100 ps to-10 ps.

Impact on National Missions

The project has yielded the world's record in proton energies for lasers in '09 (67.5 MeV), and again in '10 (75 MeV) and led to a new understanding and a new model of laser-electron absorption. We have also observed mono-energetic ion structures from the cone targets, and copious neutrons, which could open many new applications listed again below. This new mechanism (DLLPA) is having a large impact on the field (as judged just by the immediate interest and invited talks) due to the special importance to the inertial confinement fusion community and implications for fast ignition fusion physics (electron and ion), as it may lead to electron too energetic to be useful for electron fast ignition in a cone geometry.

In general this project has enhanced our understanding of laser-based ion acceleration relevant for ion Fast Ignition Fusion and by enabling future compact directed energetic particle and x-ray sources. Laser-based accelerator technology can now improve on the 75 MeV achieved by this project and impact applications like nuclear wastes transmutation, active interrogation of SNM, proton radiography and stockpile stewardship via warm dense matter studies - missions of interest to DOE, DHS, and other government agencies. This work also underpins the goal of producing compact ions sources for medical isotope production and hadron cancer therapy of interest to the DHHS/NIH and NNSA.
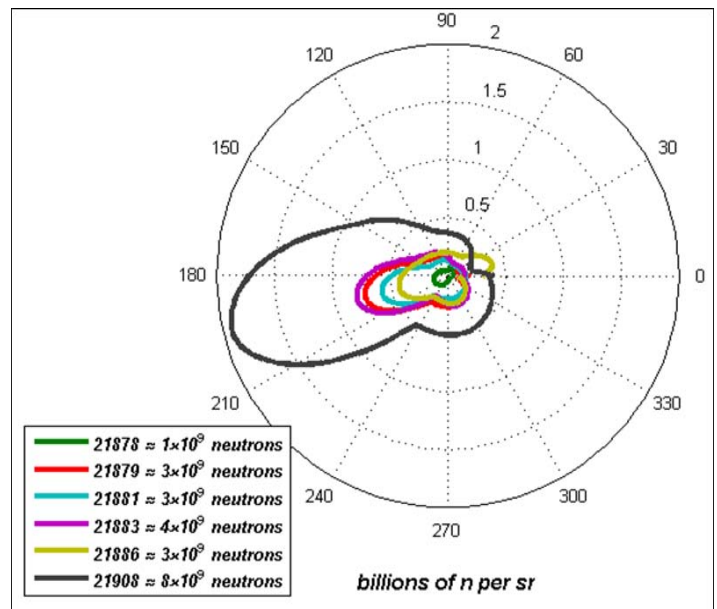
Figure 3. Multiple neutron yields from single shots on the Trident laser system using 10 micron Cu targets at 80 J and 650 fs at high contrast with up to 8 billion neutrons on a single shot.

References

1. Dunne, M.. Laser-driven particle accelerators. 2006. *SCIENCE.* **312** (5772): 374.

2. Snavely, R. A., M. H. Key, S. P. Hatchett, T. E. Cowan, M. Roth, T. W. Phillips, M. A. Stoyer, E. A. Henry, T. C. Sangster, M. S. Singh, S. C. Wilks, A. MacKinnon, A. Offenberger, D. M. Pennington, K. Yasuike, A. B. Langdon, B. F. Lasinski, J. Johnson, M. D. Perry, and E. M. Campbell. Intense high-energy proton beams from petawatt-laser irradiation of. 2000. *Physical Review Letters.* **85** (14): 2945.

3. Maksimchuk, A., S. Gu, K. Flippo, D. Umstadter, and V. Yu. Bychenkov. Forward Ion Acceleration in Thin Films Driven by a High-Intensity Laser. 2000.

4. Clark, E. L., K. Krushelnick, J. R. Davies, M. Zepf, M. Tatarakis, F. N. Beg, A. Machacek, P. A. Norreys, M. I. Santala, I. Watts, and A. E. Dangor. Measurements of

energetic proton transport through magnetized plasma from intense laser interactions with solids. 2000. *PHYSICAL REVIEW LETTERS.* **84** (4): 670.

5. Gaillard, S., N. Renard-LeGalloudec, T. E. Cowan, J. [Physics Department University of Nevada Reno. , and null. Laboratoire pour l'Utilisation des Lasers In. Comment on 'Measurements of Energetic Proton Transport through Magnetized Plasma from Intense Laser Interactions with Solids'. 2006. *Physical Review Letters.* **96** (24): 249201.

6. Remington, B., R. Paul. Drake, and D. Ryutov. Experimental astrophysics with high power lasers and Z pinches. 2006. *Reviews of Modern Physics.* **78** (3): 755.

7. Ledingham, K. W., P. McKenna, and R. P. Singhal. Applications for nuclear phenomena generated by ultra-intense lasers. 2003. *SCIENCE.* **300** (5622): 1107.

8. Nemoto, K., A. Maksimchuk, S. Banerjee, K. Flippo, G. Mourou, D. Umstadter, and V. Yu. Bychenkov. Laser-triggered ion acceleration and table top isotope production. 2001. *Applied Physics Letters.* **78** (5): 595.

9. Roth, M., T. E. Cowan, M. H. Key, S. P. Hatchett, C. Brown, W. Fountain, J. Johnson, D. M. Pennington, R. A. Snavely, S. C. Wilks, K. Yasuike, H. Ruhl, E. Pegoraro, S. V. Bulanov, E. M. Campbell, M. D. Perry, and H. Powell. Fast ignition by intense laser-accelerated proton beams. 2001. *Physical Review Letters.* **86** (3): 436.

10. Romagnani, L., J. Fuchs, M. Borghesi, P. Antici, P. Audebert, F. Ceccherini, T. Cowan, T. Grismayer, S. Kar, A. Macchi, P. Mora, G. Pretzler, A. Schiavi, T. Toncian, and O. Willi. Dynamics of electric fields driving the laser acceleration of. 2005. *Physical Review Letters.* **95** (19): 195001/1.

11. Cowan, T. E., J. Fuchs, H. Ruhl, A. Kemp, P. Audebert, M. Roth, R. Stephens, I. Barton, A. Blazevic, E. Brambrink, J. Cobble, J. Fernandez, J. C. Gauthier, M. Geissel, M. Hegelich, J. Kaae, S. Karsch, G. P. Le Sage, S. Letzring, M. Manclossi, S. Meyroneinc, A. Newkirk, H. Pepin, and N. Renard-LeGalloudec. Ultralow emittance, multi-MeV proton beams from a laser virtual-cathode plasma accelerator. 2004. *PHYSICAL REVIEW LETTERS.* **92** (20): 204801.

12. Linz, U., and J. Alonso. What will it take for laser driven proton accelerators to be applied to tumor therapy?. 2007. *Physical Review Special Topics-Accelerators and Beams.* **10** (9): 094801.

13. Schell, S., and J. J. Wilkens. Modifying proton fluence spectra to generate spread-out Bragg peaks with laser accelerated proton beams. 2009. *Physics in Medicine and Biology.* **54** (19): N459.

14. Fourkal, E., J. S. Li, W. Xiong, A. Nahum, and null. Ma. Intensity modulated radiation therapy using laser-accelerated protons: a Monte Carlo dosimetric study. 2003.

15. Gaillard, S. A., K. A. Flippo, M. E. Lowenstern, J. E. Mucino, J. M. Rassuchine, D. C. Gautier, J. Workman, T. E. Cowan, and IFSA. Proton acceleration from ultrahigh-intensity short-pulse laser-matter interactions with Cu micro-cone targets at an intrinsic similar to 10(-8) contrast. 2010. In *6th International Conference on Inertial Fusion Sciences and Applications ; 20090906 - 20090911 ; San Francisco, CA.* Vol. 244, p. 022034.

16. Flippo, K., T. Bartal, F. Beg, S. Chawla, J. Cobble, S. Gaillard, D. Hey, A. MacKinnon, A. MacPhee, P. Nilson, D. Offermann, S. L. Pape, and M. J. Schmitt. Omega EP, laser scalings and the 60 MeV barrier: First observations of ion acceleration performance in the 10 picosecond kilojoule short-pulse regime. 2010. In *6th International Conference on Inertial Fusion Sciences and Applications ; 20090906 - 20090911 ; San Francisco, CA, United States.* Vol. 244, PART 2 Edition, p. var.pagings.

17. Robson, L., P. T. Simpson, R. J. Clarke, K. W. Ledingham, F. Lindau, O. Lundh, T. McCanny, P. Mora, D. Neely, C. -G. Wahlstrom, M. Zepf, and P. McKenna. Scaling of proton acceleration driven by petawatt-laser-plasma interactions. 2007. *NATURE PHYSICS.* **3** (1): 58.

18. COSGROVE, V. P., A. C. ARO, S. GREEN, M. C. SCOTT, G. C. TAYLOR, D. E. BONNETT, and A. KACPEREK. STUDIES RELATING TO 62 MEV PROTON CANCER-THERAPY OF THE EYE. 1992. *RADIATION PROTECTION DOSIMETRY.* **44** (1-4): 405.

19. Esirkepov, T., M. Borghesi, S. V. Bulanov, G. Mourou, and T. Tajima. Highly efficient relativistic-ion generation in the laser-piston. 2004. *Physical Review Letters.* **92** (17): 175003/1.

20. Schlegel, T., N. Naumova, V. T. Tikhonchuk, C. Labaune, I. V. Sokolov, and G. Mourou. Relativistic laser piston model: ponderomotive ion acceleration in dense plasmas using ultraintense laser pulses. 2009. *Physics of Plasmas.* **16** (8): 083103 (16 pp.).

21. Robinson, A. P., M. Zepf, S. Kar, R. G. Evans, and C. Bellei. Radiation pressure acceleration of thin foils with circularly polarized laser pulses. 2008. *NEW JOURNAL OF PHYSICS.* **10**: 013021.

22. Macchi, A., S. Veghini, T. V. Liseykina, and F. Pegoraro. Radiation pressure acceleration of ultrathin foils. 2010. *New Journal of Physics.* **12** (4): 045013 (18 pp.).

23. Flippo, K., B. M. Hegelich, B. J. Albright, L. Yin, D. C. Gautier, S. Letzring, M. Schollmeier, J. Schreiber, R. Schulze, and J. C. Fernandez. Laser-driven ion accelera-

tors: spectral control, monoenergetic ions and new acceleration mechanisms. 2007. *Laser and Particle Beams.* **25** (1): 3.

24. Yin, L., D. Winske, W. Daughton, and K. J. Bowers. Kinetic Alfven waves and electron physics. I. Generation from ion-ion streaming. 2007. *Physics of Plasmas.* **14** (6): 062104.

25. Wilks, S. C., A. B. Langdon, T. E. Cowan, M. Roth, M. Singh, S. Hatchett, M. H. Key, D. Pennington, A. MacKinnon, and R. A. Snavely. Energetic proton generation in ultra-intense laser-solid. 2001. *Physics of Plasmas.* **8** (2): 542.

26. Mora, P.. Plasma expansion into a vacuum. 2003. *Physical Review Letters.* **90** (18): 185002/1.

27. Mora, P.. Thin-foil expansion into a vacuum. 2005. *Physical Review E (Statistical, Nonlinear, and Soft Matter Physics).* **72** (5): 56401.

28. Baton, S. D., M. Koenig, P. Guillou, B. Loupias, A. Benuzzi-Mounaix, J. Fuchs, C. Rousseaux, L. Gremillet, D. Batani, A. Morace, M. Nakatsutsumi, R. Kodama, and Y. Aglitskiy. Relativistic electron transport and confinement within charge-insulated, mass-limited targets. 2007. *High Energy Density Physics.* **3** (3-4): 358.

29. Perez, F., L. Gremillet, M. Koenig, S. D. Baton, P. Audebert, M. Chahid, C. Rousseaux, M. Drouin, E. Lefebvre, T. Vinci, J. Rassuchine, T. Cowan, S. A. Gaillard, K. A. Flippo, and R. Shepherd. Enhanced isochoric heating from fast electrons produced by high-contrast, relativistic-intensity laser pulses. 2010. *Physical Review Letters.* **104** (8): 085001.

30. Buffechoux, S., J. Psikal, M. Nakatsutsumi, L. Romagnani, A. Andreev, K. Zeil, M. Amin, P. Antici, T. Burris-Mog, A. Compant-La-Fontaine, E. D'HumieÃÄres, S. Fourmaux, S. Gaillard, F. Gobet, F. Hannachi, S. Kraft, A. Mancic, C. Plaisir, G. Sarri, M. Tarisien, T. Toncian, U. Schramm, M. Tampo, P. Audebert, O. Willi, T. E. Cowan, H. PeÃÅpin, V. Tikhonchuk, M. Borghesi, and J. Fuchs. Hot electrons transverse refluxing in ultraintense laser-solid interactions. 2010. *Physical Review Letters.* **105** (1): 015005.

31. Kluge, T., W. Enghardt, S. D. Kraft, U. Schramm, Y. Sentoku, K. Zeil, T. E. Cowan, R. Sauerbrey, and M. Bussmann. Efficient laser-ion acceleration from closely stacked ultrathin foils. 2010. *PHYSICAL REVIEW E.* **82** (1, 2): 016405.

32. Huang, C. -., B. J. Albright, L. Yin, H. -. Wu, K. J. Bowers, B. M. Hegelich, and J. C. Fernandez. Improving beam spectral and spatial quality by double-foil target in laser ion acceleration. 2011. *PHYSICAL REVIEW SPECIAL TOPICS-ACCELERATORS AND BEAMS.* **14** (3): 031301.

33. Kodama, R., Y. Sentoku, Z. L. Chen, G. R. Kumar, S. P. Hatchett, Y. Toyama, T. E. Cowan, R. R. Freeman, J. Fuchs, Y. Izawa, M. H. Key, Y. Kitagawa, K. Kondo, T. Matsuoka, H. Nakamura, M. Nakatsutsumi, P. A. Horreys, T. Norimatsu, R. A. Snavely, R. B. Stephens, M. Tampo, K. A. Tanaka, and T. Yabuuchi. Plasma devices to guide and collimate a high density of MeV electrons. 2004. *Nature.* **432** (7020): 1005.

34. Green, J. S., K. L. Lancaster, K. U. Akli, C. D. Gregory, F. N. Beg, S. N. Chen, D. Clark, R. R. Freeman, S. Hawkes, C. Hernandez-Gomez, H. Habara, R. Heathcote, D. S. Hey, K. Highbarger, M. H. Key, R. Kodama, K. Krushelnick, I. Musgrave, H. Nakamura, M. Nakatsutsumi, N. Patel, R. Stephens, M. Storm, M. Tampo, W. Theobald, L. Van Woerkom, R. L. Weber, M. S. Wei, N. C. Woolsey, and P. A. Norreys. Surface heating of wire plasmas using laser-irradiated cone geometries. 2007. *NATURE PHYSICS.* **3** (12): 853.

35. Nakamura, H., B. Chrisman, T. Tanimoto, M. Borghesi, K. Kondo, M. Nakatsutsumi, T. Norimatsu, M. Tampo, K. A. Tanaka, T. Yabuuchi, Y. Sentoku, and R. Kodama. Superthermal and efficient-heating modes in the interaction of a cone target with ultraintense laser light. 2009. *Physical Review Letters.* **102** (4): 045009 (4 pp.).

36. Sentoku, Y., K. Mima, H. Ruhl, Y. Toyama, R. Kodama, and T. E. Cowan. Laser light and hot electron micro focusing using a conical target. 2004. *Physics of Plasmas.* **11** (6): 3083.

37. Gaillard, S. A., T. Kluge, K. A. Flippo, M. Bussmann, B. Gall, T. Lockard, M. Geissel, D. T. Offermann, M. Schollmeier, Y. Sentoku, and T. E. Cowan. Increased laser-accelerated proton energies via direct laser-light-pressure acceleration of electrons in microcone targets. 2011. *PHYSICS OF PLASMAS.* **18** (5): 056710.

38. Offermann, D. T., K. A. Flippo, S. A. Gaillard, and J. C. Cobble. An Electron-Positron-Ion Correlating (EPIC) Spectrometer. *Review of Scientific Instruments.*

39. Yang, X., G. Miley, K. Flippo, S. Gaillard, D. Offermann, H. Hora, B. Gall, T. Burris-Mog, J. Rassuchine, C. Plechaty, and J. Ren. D-CLUSTER CONVERTER FOIL FOR LASER-ACCELERATED DEUTERON BEAMS: TOWARDS DEUTERON-BEAM-DRIVEN FAST IGNITION. 2011. In *19th Topical Meeting on the Technology of Fusion Energy (TOFE-19) ; 20111108 - 20111111 ; Las Vegas, NV.* Vol. 60, 2 Edition, p. 615.

40. Yang, X., G. Miley, K. Flippo, and H. Hora. Energy enhancement for deuteron beam fast ignition of a precompressed inertial confinement fusion target. 2011. *PHYSICS OF PLASMAS.* **18** (3): 032703.

41. Miley, G., X. Yang, H. Heinrich, K. Flippo, S. Gaillard, D. Offermann, D. Cort. Gautier, and IFSA. ADVANCES

IN PROPOSED D-CLUSTER INERTIAL CONFIMENT FUSION TARGET. 2010. In *6th International Conference on Inertial Fusion Sciences and Applications ; 20090906 - 20090911 ; San Francisco, CA.* Vol. 244, p. 032036.

Publications

Bartal, T., K. Flippo, S. A. Gaillard, D. T. Offermann, M. E. Foord, C. Bellei, P. K. Patel, M. H. Key, R. B. Stephens, H. S. McLean, L. C. Jarrott, and F. N. Beg. Proton Focusing Characteristics Relevant to Fast Ignition. To appear in *IEEE Transactions on Plasma Science .* **PP** (99): 1.

Bartal, T., M. E. Foord, C. Bellei, M. H. Key, K. A. Flippo, S. A. Gaillard, D. T. Offermann, P. K. Patal, L. C. Jarrott, D. P. Higginson, M. Roth, A. Otten, D. Krause, R. B. Stephens, and H. S. McLean. Focusing of short pulse high intensity laser accelerated proton beams. To appear in *Nature Physics.*

Cowan, T. E., U. Schramm, T. Burris-Mog, F. Fiedler, S. D. Kraft, K. Zeil, M. Baumann, M. Busmann, W. Enghardt, K. Flippo, S. Gaillard, K. Harres, T. Herrmannsdoerfer, F. Nurnberg, J. Pawelke, M. Roth, B. Schmidt, M. Sobiella, and R. Sauerbrey. Prospects For and Progress Towards Laser-Driven Particle Therapy Accelerators . 2010. In *14th Workshop on Advanced Accelerator Concepts.* (Annapolis, MD, 13-19 June 2010). , p. 721. College Park, MD: American Institute of Physics.

Flippo, K. A., E. d'Humieres, S. A. Gaillard, J. Rassuchine, D. C. Gautier, M. Schollmeier, F. Nurnberg, J. L. Kline, J. Adams, B. Albright, M. Bakeman, K. Harres, R. P. Johnson, G. Korgan, S. Letzring, S. Malekos, N. Renard-LeGalloudec, Y. Sentoku, T. Shimada, M. Roth, T. E. Cowan, J. C. Fernandez, and B. M. Hegelich. Increased efficiency of short-pulse laser-generated proton beams from novel flat-top cone targets. 2008. *Physics of Plasmas.* **15**: 056709.

Flippo, K. A., S. A. Gaillard, J. S. Cowan, D. C. Gautier, J. E. Mucino, and M. E. Lowenstern. Overcritical to Underdense Plasma in Under 1 Micron: 150 TW Laser-Thin-Target Interactions for Particle Acceleration. To appear in *IEEE Transactions on Plasma Science.* **PP** (99): 1.

Flippo, K., S. A. Gaillard, T. Kluge, and M. Bussmann. Advanced Laser Particle Accelerator Development at LANL: From Fast Ignition to Radiation Oncology. 2010. In *14th Workshop on Advanced Accelerator Concept.* (Annapolis, MD, 13-19 June, 2010). , p. 693. College Park, MD: American Institute of Physics.

Gaillard, S. A., K. A. Flippo, D. C. Gautier, J. L. Kline, J. Workman, F. Archuleta, R. Gonzales, T. Hurry, R. Johnson, S. Letzring, D. Montgomery, S. -M. Reid, T. Shimada, Y. Sentoku, T. E. Cowan, J. Rassuchine, M. Lowenstern, and E. Mucino. Proton, electron and K-alpha emission from micro-scale copper cone targets. 2009. In *2009 IEEE 36th International Conference on Plasma Science (ICOPS) ; 1-5 June 2009 ; San Diego, CA, USA.* , p. 1.

Gaillard, S. A., K. A. Flippo, M. E. Lowenstern, and J. E. Mucino. Proton acceleration from ultrahigh-intensity short-pulse laser-matter interactions with Cu micro-cone targets at an intrinsic ~10-8 contrast. 2010. *J. Phys.:Conf. Series.* **244**: 022034.

Gaillard, S. A., T. Kluge, K. A. Flippo, M. Bussmann, B. Gall, T. Lockard, M. Geissel, D. T. Offermann, M. Schollmeier, Y. Sentoku, and T. E. Cowan. Breaking the 60 MeV barrier, Direct Laser Light Pressure Acceleration (INVITED). 2011. *Phys. Plasmas.* **18**: 6710.

Kluge, T., M. Bussmann, S. A. Gaillard, K. Flippo, D. C. Gautier, B. Gall, B. Lockard, Y. Sentoku, K. Zeil, S. Kraft, U. Schramm, T. E. Cowan, and R. Sauerbrey. Wakefield Accelerated Electron Beams from Ultra-Thin Solid Foils. 2010. *2nd International Conference on Ultra-Intense Laser Interaction, AIP Conference Proceedings.* **1209**: 51.

Kluge, T., M. Bussmann, S. Gaillard, K. Zeil, S. Kraft, U. Schramm, T. Cowan, R. V. Sauerbrey, K. Flippo, null. Gautier, T. Lockard, null. Sentoku, M. Lowenstern, J. E. Mucino, and null. Gall. Low-divergent, energetic electron beams from ultra-thin foils. 2010. *Journal Name: Verhandlungen der Deutschen Physikalischen Gesellschaft.* (HANVER 2): Medium: X; Size: 1 pages.

Kluge, T., S. A. Gaillard, M. Bussmann, K. Flippo, T. Burriss-Mog, B. Gall, M. Geissel, S. D. Kraft, T. Lockard, J. Metzkes, D. T. Offermann, J. Rassuchine, U. Schramm, Y. Sentoku, K. Zeil, and T. E. Cowan. Theoretical Understanding of Enhanced Proton Energies from Laser-Cone Interactions. 2010. In *Advanced Accelerator Concepts: 14th Advanced Accelerator Concepts Workshop.* (Annapolis, 13-19 June, 2010). , p. 715. College Park, MD: AIP.

Miley, G. H., X. Yang, H. Heinrich , K. Flippo, S. Gaillard, D. Offermann, and D. C. Gautier. Advances in proposed D-Cluster Inertial Confinement Fusion Targets. 2010. *J. Phys.:Conf. Series.* **244**: 32036.

Miley, G. H., X. Yang, K. A. Flippo, and H. Hora. Fusion space propulsion using Fast-Ignition Inertial Confinement Fusion (FI-ICF) . 2011. In *Nuclear and Emerging Technologies for Space 2011, NETS-2011.* (Albuquerque, 2-7 Feb. 2011). , p. 726. La Grange Park, IL: American Nuclear Society.

Niemann, C., A. Bondarenko, C. Constantin, E. Everson, K. Flippo, S. Gaillard, R. Johnson, S. Letzring, D. Montgomery, L. Morton, D. Schaeffer, T. Shimada, and D. Winske. Collisionless shocks in a large magnetized laser-plasma-plume. To appear in *IEEE Transactions on Plasma Science .* **PP** (99): 1.

Nuernberg, F., M. Schollmeier, K. Harres, M. Roth, E. Brambrink, A. Blazevic, D. C. Carroll, P. McKenna, K. Flippo, D. C. Gautier, B. M. Hegelich, M. Geissel, O. Lundh, K. Markey, D. Neely, and J. Schreiber. Radiochromic film imaging spectroscopy of laser-accelerated proton beams. 2009. *Review of Scientific Instruments.* **80** (3): 03330.

Perez, F., L. Gremillet, M. Koenig, S. D. Baton, P. Audebert, M. Chahid, C. Rousseaux, M. Drouin, E. Lefebvre, T. Vinci, J. Rassuchine, T. Cowan, S. A. Gaillard, K. A. Flippo, and R. Shepherd. Enhanced Isochoric Heating from Fast Electrons Produced by High-Contrast, Relativistic-Intensity Laser Pulses. 2010. *PHYSICAL REVIEW LETTERS.* **104** (8): 085001.

Rassuchine, J., S. D. Baton, P. Guillou, M. Koenig, M. Chahid, F. Perez, J. Fuchs, P. Audebert, R. Kodama, M. Nakatsutsumi, N. Ozaki, D. Batani, A. Morace, R. Redaelli, L. Gremillet, C. Rousseaux, F. Dorchies, C. Fourment, J. J. Santos, J. Adams, G. Korgan, S. Malekos, S. B. Hansen, R. Shepherd, K. Flippo, S. Gaillard, Y. Sentoku, and T. E. Cowan. Enhanced hot-electron localization and heating in high-contrast ultraintense laser irradiation of microcone targets. 2009. *Physical Review E (Statistical, Nonlinear, and Soft Matter Physics).* **79** (3): 036408 (5 pp.).

Yang, X. L., G. H. Miley, K. A. Flippo, S. A. Gaillard, D. T. Offermann, H. Hora, B. B. Gall, T. Burris-Mog, J. Rassuchine, C. Plechaty, and J. Ren. D-Cluster Converter Foil For Laser-Accelerated Deuteron Beams: Towards Deuteron-Beam-Driven Fast Ignition. 2011. *. Fusion Science and Technology..* **60** (2): 615.

Yang, X., G. H. Miley, K. A. Flippo, and H. Hora. Energy enhancement for deuteron beam fast ignition of a precompressed inertial confinement fusion target. 2011. *Physics of Plasmas.* **18**: 032703.

Yang, X., G. H. Miley, K. A. Flippo, and H. Hora. Hot Sopt Heating by Laser-Accelerated Quasi-Maxwellian Deuteron Beam. To appear in *Laser and Particle Beams.*

General Relativity as a Probe of Cosmology

Daniel Holz
20090518ER

Abstract

We are in the midst of a revolution in astrophysics and cosmology. There has been an explosion of observational data, leading to a radical transformation in our understanding of our universe on the largest scales. The field of general relativity, with the advent of gravitational wave observatories, is also poised for major advances in the coming years. While the first direct detection of gravitational waves will be much celebrated, it is the ensuing astrophysical and cosmological observations that will have the greater scientific impact. Research in general relativity, and astrophysics and cosmology, is phenomenally vibrant and dynamic. The interplay of these fields offers particular promise, and it is here that we are focusing our work.

This project centered on gravitational waves and gravitational lensing: two uniquely powerful cosmological probes furnished by general relativity. The next generation of observational surveys can be expected to revolutionize the study of statistical lensing, and gravitational lensing is expected to become one of the most powerful probes of dark energy. In addition, as "first sound" for LIGO (and, hopefully, LISA) arrives, the birth of the age of gravitational-waves is imminent. We propose two complementary research directions, both of which can be expected to lead to elucidation of the nature of dark energy and dark matter.

Background and Research Objectives

One of the most dramatic discoveries of the last decade is that the expansion of the Universe appears to be accelerating. This has profound effects, not only on general relativity, astrophysics, and cosmology, but also on particle physics, and our attempts to find a fundamental theory of everything. There is a growing consensus that understanding the nature of the "dark energy" causing this cosmological acceleration could become one of the defining challenges to fundamental physics for the foreseeable future.

An important tool in current studies of the dark energy is the type Ia supernova: because it is an excellent standard candle (object of known intrinsic brightness), it can be used as a precise cosmological distance measure. Supernovae thus allow for direct observation of the cosmological luminosity distance-redshift relation, and hence the determination of the evolution history of the Universe. Future surveys are expected to measure thousands of Type Ia SNe, mapping the distance-redshift curve over a large span of redshift with good statistical significance.

There are a number of important caveats when considering Type Ia supernovae as standard candles. It is to be emphasized that, at this point, these events are phenomenological standard brightness indicators. The underlying theory is not yet well understood, and simulations are unlikely to provide modeling at the few percent level in the foreseeable future. Possible evolutionary trends may cause fatal systematic errors in dark energy measurements, and such effects are difficult to rule out in the absence of firm theoretical underpinnings. In addition, various astronomical issues (e.g., k-corrections, redening, gravitational lensing) may severely limit the utility of SNe in making precision measurements of the luminosity distance-redshift curve.

We have been actively developing a completely independent standard candle: the gravitational-wave driven inspiral of binary compact objects. These standard sirens are the gravitational- wave analogs of standard candles. The radiation emitted during the inspiral phase is well described using the post-Newtonian expansion of general relativity for the compact-object binary. Because these binary systems are relatively simple and well modeled, the gravitational waves they generate determine the source's luminosity distance with high accuracy.

This project has focused on developing and improving our understanding of standard sirens, and exploring their potential measurements of the Universe.

Scientific Approach and Accomplishments

In the first goal funded by this project, we explored the

capability of the Big Bang Observer, a post-LISA space-borne gravitational-wave observatory, to constrain cosmology. Improving our understanding of the dark energy responsible for the observed accelerating expansion of the Universe is one of the foremost challenges in physics. Our current theoretical models are exceedingly inadequate. In addition, given its extremely low energy density, there are no plausible scenarios for the direct detection of dark energy. Thus progress on this critical issue must be made through indirect observations. In this paper we show that the Big Bang Observer (BBO), a proposed space-based gravitational-wave (GW) mission designed primarily to search for inflation-generated stochastic GWs in the band 0.03Hz–3Hz, would also be an ultra-precise cosmology mission, measuring the Hubble constant H0 and the dark energy parameters w_0 and w_a far more accurately than other proposed dark energy missions. To observe an inflationary GW background, BBO would first have to detect and subtract out $\sim 3 \times 10^5$ merging compact-star binaries, out to a redshift z ~ 5. It is precisely this carefully measured "foreground" which would enable high-precision cosmology. BBO would determine the luminosity distance to each binary to ~ percent accuracy. In addition, BBO's angular resolution would be sufficient to uniquely identify the host galaxy for the majority of binaries; a coordinated optical/infrared observing campaign could obtain the redshifts. Combining the GW-derived distances and the electromagnetically-derived redshifts for such a large sample of objects, out to such high redshift, naturally leads to extraordinarily tight constraints on cosmological parameters. We emphasize that such "standard siren" measurements of cosmology avoid many of the systematic errors associated with other techniques: GWs offer a physics-based, absolute measurement of distance. In addition, we show that BBO would also serve as an exceptionally powerful gravitational lensing mission, and we briefly discuss other astronomical uses of BBO, including providing an early warning system for all short/hard gamma-ray bursts.

In a subsequent paper, we analyzed how the effects of gravitational lensing can be corrected for in the case of standard sirens. Gravitational wave sources are a promising cosmological standard candle because their intrinsic luminosities are determined by fundamental physics (and are insensitive to dust extinction). They are, however, affected by weak lensing magnification due to the gravitational lensing from structures along the line of sight. This lensing is a source of uncertainty in the distance determination, even in the limit of perfect standard candle measurements. It is commonly believed that the uncertainty in the distance to an ensemble of gravitational wave sources is limited by the standard deviation of the lensing magnification distribution divided by the square root of the number of sources. Here we show that by exploiting the non-Gaussian nature of the lensing magnification distribution, we can improve this distance determination, typically by a factor of 2–3; we provide a fitting formula for the effective distance accuracy as a function of redshift for sources where the lensing noise dominates.

In a third goal, we explored gamma-ray bursts as a potentially important standard siren source. Recent observations support the hypothesis that a large fraction of "short-hard" gamma-ray bursts (SHBs) are associated with the inspiral and merger of compact binaries. Since gravitational-wave (GW) measurements of well-localized inspiraling binaries can measure absolute source distances, simultaneous observation of a binary's GWs and SHB would allow us to directly and independently determine both the binary's luminosity distance and its redshift. Such a "standard siren" (the GW analog of a standard candle) would provide an excellent probe of the nearby (z < 0.3) universe's expansion, independent of the cosmological distance ladder, thereby complementing other standard candles. Previous work explored this idea using a simplified formalism to study measurement by advanced GW detector networks, incorporating a high signal-to-noise ratio limit to describe the probability distribution for measured parameters. In this paper, we eliminate this simplification, constructing distributions with a Markov Chain Monte Carlo technique. We assume that each SHB observation gives source sky position and time of coalescence, and we take non-spinning binary neutron star and black hole–neutron star coalescences as plausible SHB progenitors. We examine how well parameters (particularly distance) can be measured from GW observations of SHBs by a range of ground-based detector networks. We find that earlier estimates overstate how well distances can be measured, even at fairly large signal-to-noise ratio. The fundamental limitation to determining distance proves to be a degeneracy between distance and source inclination. Overcoming this limitation requires that we either break this degeneracy, or measure enough sources to broadly sample the inclination distribution.

In a related final project, we explored how well these gamma-ray burst sources could be localized on the sky. The inspirals and mergers of compact binaries are among the most promising events for ground-based gravitational- wave (GW) observatories. The detection of electromagnetic (EM) signals from these sources would provide complementary information to the GW signal. It is therefore important to determine the ability of GW detectors to localize compact binaries on the sky, so that they can be matched to their EM counterparts. We use Markov Chain Monte Carlo techniques to study sky localization using networks of ground-based interferometers. Using a coherent-network analysis, we find that the Laser Interferometer Gravitational Wave Observatory (LIGO)–Virgo network can localize 50% of their detected neutron star binaries to better than 50 sq deg with a 95% confidence interval. The addition of the Large Scale Cryogenic Gravitational Wave Telescope (LCGT) and LIGO-Australia improves this to 12 sq deg. Using a more conservative coincident detection threshold, we find that 50% of detected neutron star binaries are localized to 13 sq deg using the LIGO–Virgo network, and to 3 sq deg using the LIGO–Virgo–LCGT–

LIGO- Australia network. Our findings suggest that the coordination of GW observatories and EM facilities offers great promise.

Impact on National Missions

This project supports the DOE mission by directly addressing dark matter and dark energy, which form the heart of the unknowns in cosmology. These are a key element of the "Beyond the standard model" grand challenge at LANL. These topics are also essential of great interest to DOE Office of Science.

I have presented the results from this project at a number of institutions, including Colloquia at Harvard, Caltech, MIT, and Yale. These advertise the cutting-edge work being performed at LANL, and further our recruitment efforts.

Over the course of this project the PI has recruited two postdocs to come to LANL as Director's Fellows, to work on related projects. At least one of these fellows, if not both, are likely to remain at LANL and contribute directly to the programs.

References

1. Hirata, C. M., D. E. Holz, and C. Cutler. Reducing the weak lensing noise for the gravitational wave Hubble diagram using the non-Gaussianity of the magnification distribution. 2010. *Physical Review D.* **81** (12): 124046 (11 pp.).

2. Cutler, C., and D. E. Holz. Ultrahigh precision cosmology from gravitational waves. 2009. *Physical Review D.* **80** (10): 104009 (15 pp.).

3. Nissanke, S., D. E. Holz, S. A. Hughes, N. Dalal, and J. L. Sievers. Exploring short gamma-ray bursts as gravitational-wave standard sirens. 2010. *Astrophysical Journal.* **725** (1): 496.

4. Nissanke, S., J. Sievers, N. Dalal, and D. Holz. LOCALIZING COMPACT BINARY INSPIRALS ON THE SKY USING GROUND-BASED GRAVITATIONAL WAVE INTERFEROMETERS. 2011. *ASTROPHYSICAL JOURNAL.* **739** (2): 99.

Publications

Belczynski, K., M. Dominik, T. Bulik, R. O'Shaughnessy, C. Fryer, and D. E. Holz. The effect of metallicity on the detection prospects for gravitational waves. 2010. *Astrophysical Journal Letters.* **715** (2): L138.

Bloom, J., D. Holz, S. Hughes, and K. Menou. Coordinated Science in the Gravitational and Electromagnetic Skies. 2009. *Astro2010: The Astronomy and Astrophysics Decadal Survey, Science White Papers, no. 20.*

Cutler, C., and D. E. Holz. Ultrahigh precision cosmology from gravitational waves. 2009. *Physical Review D.* **80** (10): 104009 (15 pp.).

Hirata, C. M., D. E. Holz, and C. Cutler. Reducing the weak lensing noise for the gravitational wave Hubble diagram using the non-Gaussianity of the magnification distribution. 2010. *Physical Review D.* **81** (12): 124046 (11 pp.).

Nissanke, S., D. E. Holz, S. A. Hughes, N. Dalal, and J. L. Sievers. Exploring short gamma-ray bursts as gravitational-wave standard sirens. 2010. *Astrophysical Journal.* **725** (1): 496.

Nissanke, S., J. Sievers, N. Dalal, and D. Holz. LOCALIZING COMPACT BINARY INSPIRALS ON THE SKY USING GROUND-BASED GRAVITATIONAL WAVE INTERFEROMETERS. 2011. *ASTROPHYSICAL JOURNAL.* **739** (2): 99.

Analysis of Experimental Benchmarks (CFS)

Drew E. Kornreich
20110451ER

Abstract

We have performed a comprehensive exercise of modeling simple U-233 solutions to examine the difference between the recently produced ENDF/B-VII.0 cross sections and the historically used Hansen-Roach cross sections in their ability to accurately model the experimental benchmark systems. The results did not allow for an unequivocal determination that one cross-section set was better than the other for modeling U-233 solution systems. This work therefore provided a comprehensive set of analysis data to better display the problems with either or both of the cross-section sets. We have also updated a Los Alamos dose-modeling code to include the ability to modeling dose from operations with U-233 and the other important isotopes of uranium (U-232, U-235, and U-238).

Background and Research Objectives

Because of its multi-disciplinary nature, Los Alamos is uniquely positioned to support analysis of new technologies for future power production. As such, Los Alamos is also a key entity to integrate technical development and analysis of power systems with safety- and security-related issues such as nonproliferation. One such area of interest both domestically and internationally is future nuclear power production using a thorium/U-233 fuel cycle and associated Th-U-Pu fuels. The United States may be interested in such a fuel cycle because it contains attractive features for nonproliferation such as the ability to burn plutonium without generating new plutonium as occurs with mixed-oxide (MOX) fuel. The United States is also interested in monitoring activities related to a thorium fuel cycle as it is pursued internationally by states such as India because there are new proliferation concerns with the required breeding of U-233, which in a pure state could be attractive for proliferation. States like India are pursuing technologies related to this fuel cycle now, so it is very important that the United States keep abreast of these developments and drive them to internationally acceptable solutions; Los Alamos is clearly a key component for supporting the federal government to drive or affect policy related to thorium fuel cycles.

Los Alamos also maintains a diverse cadre of nuclear-materials processing experts as well as the nation's only multi-mission plutonium-processing plant in PF-4, where fuel development for advanced reactor systems could be performed. However, before being able to embark on missions that involve the use of plutonium in combination with thorium and/or U-233, several technical issues must be addressed; this proposal sought to analyze a key problem with handling U-233-bearing materials and sought to create a tool for simplified dose analysis wit hU-233 materials:

- There is a significant discrepancy in the calculated neutronic behavior of U-233 solution systems in the area of intermediate-density water mixtures using the currently accepted ENDF/B (Evaluated Nuclear Data File, Library B) cross sections versus the historical 16-group Hansen-Roach cross-section sets. Preliminary analyses seem to indicate that the 16-group Hansen-Roach cross sections better model relevant experimental systems than do the ENDF/B cross sections. This discrepancy will cause concern from safety oversight agencies for operations related to fuel reprocessing and may drive operations to be overly conservative for criticality safety and therefore more costly than required. This project sought to examine this issue further.

- Processing materials containing U-233 can be problematic because U-233 materials also contain small amounts of U-232, which has a radioactive decay chain to Pb-208 that results in 2.6-MeV gamma-ray emissions that are very difficult to shield. Los Alamos developed and maintains simplified dose-analysis tools for analyzing plutonium processing in gloveboxes; however, these tools do not contain relevant information for U-233 processing, nor do they have the ability to model such high-energy photon transport. This project sought to upgrade this modeling tool to allow it to calculate dose from U-233-bearing materials.

Scientific Approach and Accomplishments

We have performed a comprehensive exercise of modeling simple U-233 solutions to examine the difference

between the ENDF/B-VII.0 and Hansen-Roach cross sections in their ability to accurately model the experimental benchmark systems. The benchmarks used were derived from the International Handbook of Evaluated Criticality Safety Benchmark Experiments and consist of ten benchmark sets and analysis of about 150 individual experiments. The goal was to determine if the Hansen-Roach or ENDF/B-VII.0 cross sections better modeled the experimental benchmarks using both discrete-ordinates deterministic (Partisn) and Monte Carlo stochastic (MCNP5) transport codes.

The primary metric was to determine the effective multiplication (k, keff) of the various systems; a perfect model of a critical system would yield k = 1.0. For some summary data, we provide the average |k-1| values for each of the code/cross-section set variations in Figure 1. One of the "standout" results were that the Hansen-Roach cross sections resulted in remarkably small effective multiplication values for the Falstaff set of experiments (performed at Livermore in the 1950s and using relatively dense U-233 concentrations). The results of this simple bar chart indicate that the average absolute difference in the systems' effective multiplications from criticality is approximately 0.01 except for when the Hansen-Roach cross section analysis is included for the Falstaff data.

Figure 1. Average solution differences in keff from unity with and without Falstaff data.
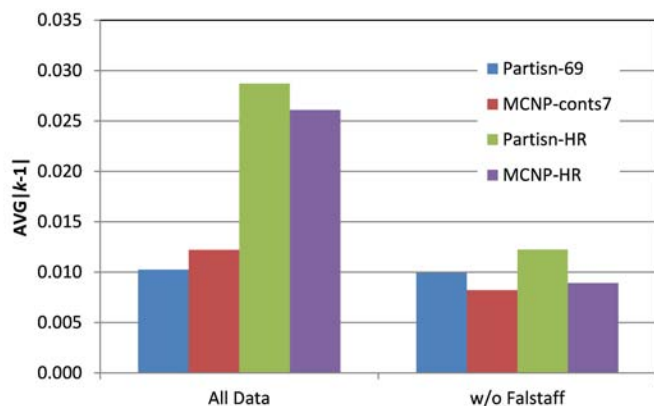
Several conclusions were drawn from the analysis:

- The Hansen-Roach cross sections do not model the Falstaff data well;

- If the Falstaff experiments are accurately described, the ENDF/B-VII.0 cross sections are better at modeling U-233 solutions;

- If the Falstaff data is discarded, we are unable to unequivocally state that there is a significant difference in the ability of the Hansen-Roach and ENDF/B-VII.0 cross sections to model U-233 solutions.

- The ENDF/B-VII.0 cross sections produce consistently larger effective multiplications than the Hansen-Roach cross sections; however, when the Falstaff data is

removed, the absolute difference in the effective multiplications from unity is about the same (the Hansen-Roach cross sections are below keff = 1 by about the same amount that the ENDF/B-VII.0 cross sections are above keff = 1).

Unfortunately, the results of this research do not provide a clear resolution on the best cross-section set to use for analysis of U-233 solution systems. The ENDF/B-VII.0 cross sections have a clear high bias on effective multiplication estimates, and Hansen-Roach cross sections yield a clear low bias on effective multiplication estimates. The benchmark evaluations used as the basis for the experimental data provided estimates of the benchmark keff, and in general, these are always very close to unity.

Because of the Falstaff data alone and absent any additional directed validation experiments, we would have to conclude that the ENDF/B-VII.0 cross sections model U-233 solutions better than Hansen-Roach cross sections. However, this conclusion is made with some reservations given the equivocal nature of the other results.

The updates to the dose modeling code (Pandemonium) to allow for analysis of U-233 operations in gloveboxes were completed. The previous version only included photon energies up to 1 MeV, which adequately accounted for all significant photon sources for plutonium isotopes and Am-241. U-233 operations generally include trace amounts of U-232, which has a decay chain to Pb-208, the last decay of which involves emission of a difficult-to-shield 2.6-MeV photon. The energy levels in Pandemonium were extended to 3.0 MeV according to the bin structure in the national standards for buildup factors and attenuation coefficients.

The photon source data for the three "main" uranium isotopes were included in the new version of Pandemonium. Plutonium source strengths were also updated. These source strengths were derived from calculations with the reactor burnup code ORIGEN-ARP. A set of test cases and sample problems were also derived to demonstrate proper operation of the code and its applicability to operations with U-233.

Impact on National Missions
This research indicates that more data gathering and associated experiments with U-233 are warranted if the United States has any potential of using U-233 materials, especially as related to a thorium-uranium fuel cycle. The work has produced tools (an updated simplified dose-modeling code) that allow for analysis of dose in glovebox operations with U-233 such that Los Alamos could examine the impact of working with such materials in a timely and cost-effective manner. U-233 is a key material for both domestic and international interest in both power reactor and nonproliferation arenas.

Searching for Low-Mass Dark Matter with the MAJORANA Low-Energy Physics Program

Victor M. Gehman
20110555ER

Abstract
Some of the most exciting prospects for physics beyond the Standard Model come from low-background, rare event searches. Two exciting parts of this effort are searches for: neutrinoless double-beta decay ($0\nu\beta\beta$, a rare nuclear decay forbidden by the Standard Model) and dark matter. In this LDRD, we endeavored to develop and characterize detectors for the MAJORANA experiment. MAJORANA's primary focus is double-beta decay, but the unique capability of the type of detectors chosen for the experiment allow for physics analysis of signals at very low energy (~0.5 - 5.0 keV) to look for the direct detection of dark matter. We completed the initial acceptance tests of a pair of detectors that we will use as an analysis test bed for the full MAJORANA DEMONSTRATOR array.

Background and Research Objectives
Most dark matter search experiments have an energy threshold between 5 and 10 keV (an order of magnitude higher than the DEMONSTRATOR). Because of its uncommonly low energy threshold, the DEMONSTRATOR will have an enhanced sensitivity to much lower mass dark matter particles compared to any other dark matter search. The CoGeNT experiment has pioneered this technique with a single detector and generated immense activity in the literature. The DEMONSTRATOR will dramatically expand this effort by deploying many more detectors with lower backgrounds. This proposal included acceptance and characterization work on a pair of R&D detectors to be used as an analysis test bed for the full demonstrator as well as the continued development of analysis tools (particularly those involved in background rejection through pulse shape analysis). These tools are for use not just by the Majorana collaboration but more generally for the broader community that uses HPGe detectors.

Scientific Approach and Accomplishments
Because of the short duration of this project, the primary accomplishments involved performing a suite of acceptance tests on the initial part of detectors bought as a test bed for the MAJORANA DEMONSTRATOR (the detectors themselves were bought using LDRD-DR funding related to the MAJORANA experiment). Both detectors performed admirably and will continue to be an integral part of the ongoing program in the P-23 Weak Interactions Team. Both detectors reported best fit energy resolution of less than 0.5 keV at 59.54 keV ([241]Am, most HPGe detectors are easily twice that value), and low energy thresholds comfortably below 1 keV. Typical HPGe detectors have thresholds between 5 and 10 keV. Furthermore, our detectors achieved this resolution and threshold with no vibrational isolation from the environment and no special effort to avoid ground loops or other electronic noise. This performance represents something of a "smoke test," meaning that significant improvements are likely as further noise reduction techniques are employed in the future. Additionally, a variety of analysis tools related to the handling of data from these detectors was developed under the purview of this proposal, and they are still in use in the Weak Interactions Team and elsewhere.

Impact on National Missions
In addition to the basic science goal of searching for dark matter, the work outlined in this proposal involved the detailed characterization of a pair of novel detectors with very low threshold, excellent resolution, and powerful PSA in a close-packed array. This apparatus will be excellent for environmental monitoring/nonproliferation applications. Understanding the response of these detectors will also inform the design of next generation counting facilities for DoE.

Physics

Synchrotron X-ray Laue Diffraction and Phase Contrast Imaging of Fe and Explosive Simulants under Shock Loading

Shengnian Luo
20110585ER

Abstract

X-ray imaging and diffraction are key diagnostic techniques for LANL's signature facility MaRIE (Matter-Radiation Interactions at Extremes) and promise significant advances in shock physics; development of such techniques is a necessary step toward MaRIE requiring dedicated research. We proposed to build shock loading capability with dynamic X-ray diagnostics at Advanced Photon Source (APS), and to investigate shock-induced phase transitions and deformation in Fe and explosive simulates. The work is an urgent step toward participation in Dynamic Compression Sector (DCS) on the roadmap to MaRIE, and relevant to MaRIE and several other proposed new and upgraded accelerator facilities; further technical development of this platform will enable momentous advances in shock physics. During the project period, we have built the gas gun launching capability, and designed and implemented 2D detectors for ultrafast Laue diffraction and phase contrast imaging (PCI).

Background and Research Objectives

Structural inhomogeneity in materials likely induces inhomogeneous shock response at different scales, and *in situ*, real-time, in-volume, dynamic measurements are essential capabilities for MaRIE and for solving many outstanding shock physics problems. The work will help establish a shock loading platform with dynamic X-ray diagnostics at synchrotrons for LANL, and demonstrate its feasibility and potential to deliver game-changing advances in shock physics.

The research goals are: (1) To establish LANL's capability of gas gun loading and dynamic X-ray Laue diffraction and phase contrast imaging techniques at APS, and perform experiments on Fe and engineered explosive simulants to investigate shock-induced phase transitions and deformation processes; (2) to obtain the knowledge, instrumentation (e.g., synchronization and detectors) and data processing techniques necessary for shock physics, and coherent photon diagnostics, and (3) to drive fast experimental and detection technology within the time-resolved community for scientific problems of importance to LANL's diverse missions.

Scientific Approach and Accomplishments

We proposed Laue diffraction and PCI experiments on selected materials under ambient conditions and shock loading (Figure 1), to help establish a synchrotron-based platform for dynamic experiments and to investigate phase transitions and deformation, with focus on Fe (phase change) and explosive simulants with engineered microstructure (deformation).
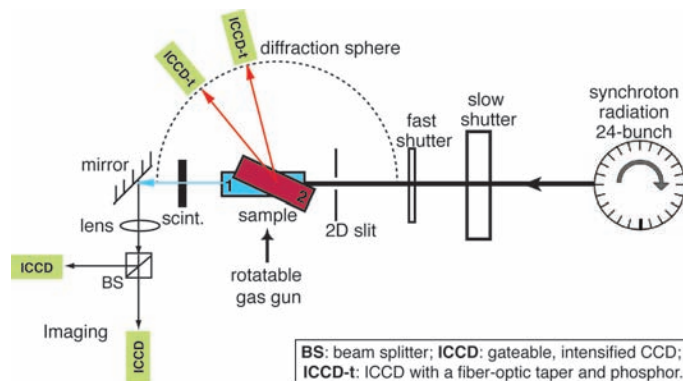
Figure 1. Schematic setup for gas gun experiments with dynamic x-ray diagnostics at APS. Sample geometry 1 and 2 are used for PCI and Laue diffraction, respectively, and the rotatable gas gun barrel is aligned normal to the target accordingly.

The gas gun loading system was fabricated and is ready now for on site experiments, although we were not able to install it at APS in July, 2011 due to the delay caused by the recent wildfire at Los Alamos. However, we performed tests on our detector schemes in static (non-shock) mode; the static testing results were extremely successful, and shock experiments can be done with the proposed diagnostics given these proof-of-principle experiments (Figure 2). A manuscript was submitted: Yeager, J.D., S.N. Luo, B.J. Jensen, K. Fezzaa, D.E. Hooks and D.S. Montgomery, High Speed X-Ray Phase Contrast Imaging for Analysis of Low-Z Composite Microstructure, *Composites Part A: Applied Science and Manufacturing*.
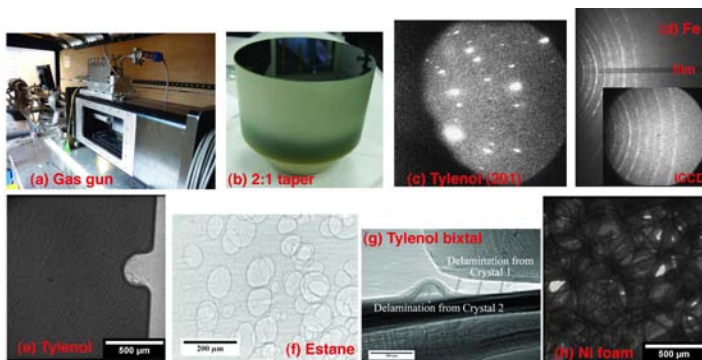
Figure 2. Dynamic loading device (a), fiber optic taper (b), and some representative results of synchrotron x-ray Laue diffraction (c-d) and phase contrast imaging (e-h) under static conditions.

Impact on National Missions

Materials for the Future is one of LANL's three pillars. *In situ*, dynamic measurements of multi-grain materials in relevant extremes that will transform the science of micro-structure, interfaces and defects critical to this vision. The proposed experiments are a necessary first step toward establishing MaRIE's diagnostic capabilities using photons and eventually coherent photons, and may bring upon transformational advances in shock physics and materials at dynamic extremes.

Coherence Effects in x-ray Diffraction Imaging

Quinn R. Marksteiner
20110603ER

Abstract

A major element of the proposed Matter-Radiation Interactions in Extremes (MaRIE) project is the inclusion of facilities for single-shot, *in-situ*, coherent x-ray diffraction imaging (CXDI) of dynamic processes. Such processes include the passage of shocks through polycrystalline metals, as well as other loading experiments involving material samples, and the proposed MaRIE facility seeks to reconstruct images of these processes as they occur from their x-ray diffraction patterns alone. However, the high photon energies required to penetrate a thick sample of dense matter occasion unique experimental difficulties requiring novel solutions. In this work, we address the effects of light source incoherence and Fresnel-regime geometries upon CXDI.

The high energies and photon fluxes called for by MaRIE require the use of an x-ray free electron laser (XFEL) operated in the SASE mode (self amplified stimulated emission), which implies a certain degree of incoherence in the characteristics of the beam [5]. However, until recently little has been known about what impact the imperfect coherence properties of a real-world XFEL source would have upon the effectiveness of CXDI. We have investigated this critical question by coupling an existing forward x-ray diffraction code -- which, given a hypothetical sample, light source, and experimental geometry, calculates the corresponding diffraction pattern – with the FEL simulation codes GENESIS [4]. The result was the development of capabilities to simulate the CXDI process using light source characteristics that capture the imperfections of a realistic XFEL source. Furthermore, this allowed a quantification of the degree to which realistic XFEL coherence properties affect the fidelity of CXDI.

A second difficulty which arises in hard x-ray imaging is the imposition of severe geometrical constraints on experimental design, which force any imaging to be performed in the so-called *Fresnel regime*, in which the relationship between the details of the sample and the characteristics of the diffraction pattern is not nearly as clear-cut as in the classical *far-field regime* which prevails at lower energies. CXDI has never before been experimentally demonstrated in the Fresnel regime, and in this work we explore both the experimental details inherent to Fresnel-regime CXDI, as well as the computational modifications required to make CXDI a robust tool in this novel experimental geometry. A thorough understanding of both of these problems is critical to the realization of the MaRIE project.

Background and Research Objectives

In the far-field regime of x-ray diffraction, in which there is a large separation between the sample and the detector, the diffraction pattern produced by illuminating a sample with a coherent, monochromatic source is closely related to the spatial Fourier transform of the sample. However, such a pattern preserves the magnitude, *but not the phase*, of the incident diffracted field. Due to this missing phase problem, a direct image of the sample cannot be immediately recovered via inverse Fourier transform (FT). In CXDI, one *oversamples* the diffraction pattern at an increased resolution, and this additional information allows the computational reconstruction of the missing phases – and hence an image of the sample – via a technique known as iterative phase retrieval (IPR). Two-dimensional IPR was first achieved experimentally in 1999 [1], and the more difficult three-dimensional version was accomplished in 2010 [2].

IPR results are achieved by iterating between real (sample) and Fourier (detector) space, serially imposing constraints in both the detector and sample planes. The rate of convergence and quality of the resulting sequence of reconstructed images depends strongly on, among other factors, the transverse and longitudinal (temporal) coherence of the light source. CXDI via IPR has been applied successfully using synchrotron light sources, in which the x-ray beam is tightly collimated and wavelength-filtered to achieve nearly-ideal coherence and monochromaticity. Nevertheless, this greatly reduces the flux of light incident on a sample. CXDI using a synchrotron can therefore take hours or days to probe a single sample with adequate resolution (10-50 nm), a time span which precludes the imaging of dynamic processes. Free electron lasers (FELs) yield orders of magnitude higher brilliance than synchrotrons, delivering more

power at the desired frequency and in the desired direction. It will therefore be possible to perform fast imaging with XFELs, and the creation of a dedicated experimental setup for CXDI at the Stanford Linac coherent light source (LCLS) XFEL is underway.

The most important parameter which characterizes the geometry of an x-ray diffraction experiment is the dimensionless Fresnel number $Fr = a^2 / p\, z$, where a is either the sample or x-ray spot size (whichever is smaller), p is the peak photon wavelength of the source, and z is the distance between the sample and the detector. The vast majority of the classical diffraction literature assumes the far-field regime, in which $Fr << 1$. In the Fresnel regime, however, in which Fr is of order 1, the simple Fourier relationship that exists at low Fresnel number is broken, rendering the process of IPR more involved. The possibility of performing IPR in the Fresnel regime was suggested and simulated in 2005 [3], but has not previously been demonstrated experimentally. In this work, we have modified and implemented the techniques in reference [3] to explore the methods and challenges of performing coherent x-ray diffraction imaging in the Fresnel regime.

Scientific Approach and Accomplishments

In modeling CXDI with a partially-incoherent XFEL light source, a critical first step is to efficiently quantify the characteristics of the electric field $E_i(x,y,z)$ in the incident beam. In general, a realistic source produces light which is not perfectly monochromatic, but which instead has intensity distributed over a range of spatial frequencies. This frequency spread accounts for the coherence, or lack thereof, in the longitudinal z direction. Thus the z dependence of $E_i(x,y,z)$ may be modeled as a simple Fourier sum over spatial frequencies. For each spatial frequency k_l it is most convenient to express the field variation in the transverse xy plane as a sum over so-called Hermite-Gaussian functions h_n. We have developed a code, which decomposed the output of the GENESIS FEL code into a sum of Hermite-Gaussian functions at each spatial frequency k_l. This facilitates the calculation of diffraction pattern, and can be used as a novel x-ray beam diagnostic to characterize x-ray outputs.Theoretical calculations suggest that the MaRIE XFEL will operate in a regime in which the transverse coherence of the beam is diminished. This effect, in particular, must be carefully simulated to determine its impact on CXDI at MaRIE and elsewhere. GENESIS is a type of software that simulates the progress of an ensemble of electrons through an XFEL undulator, as well as the characteristics of the beam of light they emit. Extensive simulations have been carried out using the FEL code GENESIS, over a variety of hard x-ray FEL parameters. The results of these simulations show the imperfect longitudinal and transverse coherence properties inherent in these types of hard x-ray sources. To gauge the effect of this limited incoherence on the fidelity of CXDI reconstruction, we have modified existing CXDI software to allow the calculation of diffraction patterns arising from a partially-incoherent source. An

example of this is shown in Figure 1.
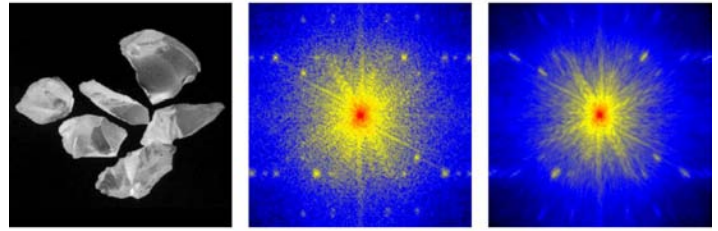
Figure 1. A test sample, along with the simulated diffraction patterns corresponding to narrow-spectrum (middle) and broad-spectrum (right) light sources. In both cases, the beam waist size was 50 microns and the peak photon energy was 50 keV. In the broad-spectrum case, the relative wavelength spread was approximately 5%.

For the Fresnel-regime CXDI (FR-CXDI) portion of the project, we analyzed the effects of CXDI in the Fresnel regime (small detector to sample distances), we created a code to model the Fresnel-regime diffraction, and have developed a robust code for reconstructing Fresnel-regime CXDI data. Additionally, we collaborated with the Kapteyn-Murnane group at the University of Colorado at Boulder and NIST by taking Fresnel-regime diffraction data from a high harmonic laser source. We are currently analyzing these results (Figures 2 and 3) and are preparing a paper for submission.
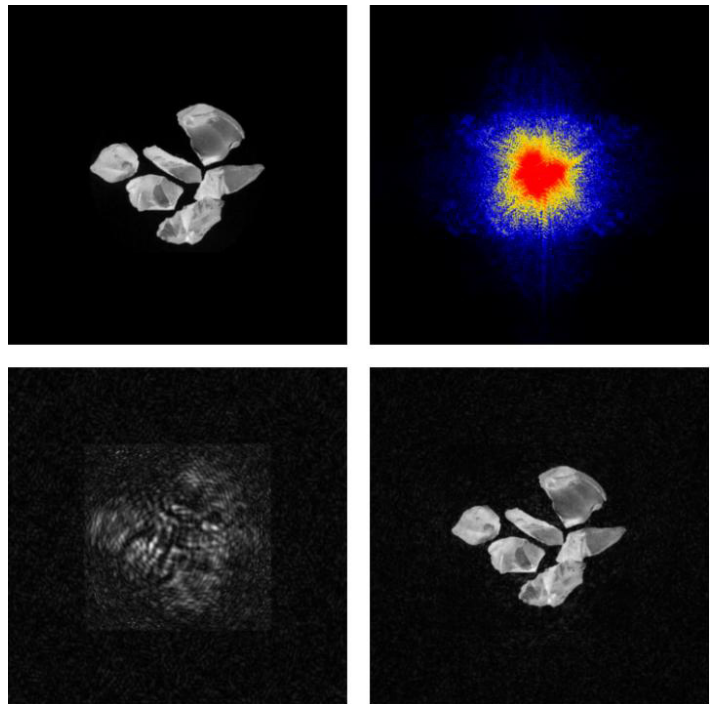
Figure 2. Simulated coherent x-ray diffraction imaging in the Fresnel regime, at Fresnel number 40. Top left: Test sample. Top Right: Calculated scattering pattern. Bottom: Sample image reconstruction after 2 (left) and 15 (right) iterations of phase retrieval.
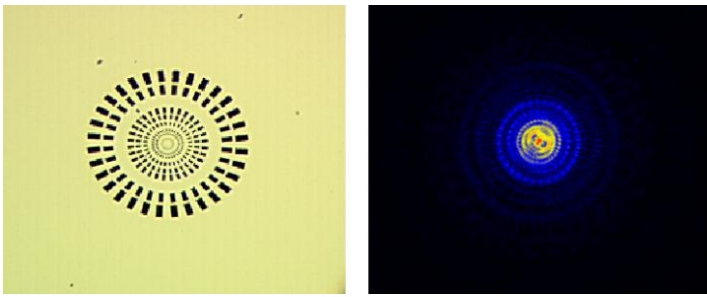
Figure 3. Sample (left) and diffraction pattern (right) images from a Fresnel-regime demonstration experiment. The sample is a spoke-shaped test pattern, and the experiment was performed at Fresnel number ~ 1.

Impact on National Missions

One of recurring themes in DOE urgent mission areas is the science of materials in extremes – both for the energy, national security, and basic science areas. LANL is aiming to fill this gap with the proposed MaRIE signature science facility (Matter-Radiation Interaction in Extremes). An important stated goal for MaRIE is the construction of facilities for 2D or 3D coherent x-ray imaging of dynamic processes in high-Z materials, for example in-situ imaging of a shock front passing through a polycrystal. This project is critically important for the stockpile stewardship mission and for basic science in extreme environments. However, the very ambitious goal of "freeze frame" imaging with x-rays at such high spatial resolutions (sub-100 nm) in such extreme environments requires revolutionary advances in source design, theoretical understanding, and experimental techniques.

This project provided a key advance by providing an interface between the FEL design and user communities, and will continue to be relevant to many FEL-based experiments on the cutting edge of imaging science. We collaborated with researchers involved in imaging science at other institutions. We will have established a leadership role in the field with our upcoming publications, and have bolstered the case for building the next large FEL light source at LANL. In order for the proposed MaRIE facility to be built, there remain a number of obstacles to be overcome, especially in FEL design and in the theory of hard x-ray imaging. This project provided not only quick answers to important questions in both of these areas but has set up a modeling capability that will continue to be beneficial to the MaRIE project as it evolves. This project has already helped the Laboratory focus its resources properly at this crucial early design stage. These advancements will also feed in to experiment design on existing and future light sources such as the LCLS, the European XFEL, and the SACLA Japanese XFEL.

References

1. Miao, Jianwei, P. Charalambous, J. Kirz, and D. Sayre. Extending the methodology of X-ray crystallography to allow imaging. 1999. *Nature.* **400** (6742): 342.

2. Raines, K. S., S. Salha, R. L. Sandberg, Huaidong Jiang, J. A. Rodriguez, B. P. Fahimian, H. C. Kapteyn, Jincheng Du, and Jianwei Miao. Three-dimensional structure determination from a single view. 2010. *Nature.* **463** (7278): 214.

3. Xiao, Xianghui, and Qun Shen. Wave propagation and phase retrieval in Fresnel diffraction by a. 2005. *Physical Review B (Condensed Matter and Materials Physics).* **72** (3): 33103.

4. Rieche, S.. Genesis 1.3: A fully 3D time-dependent FEL simulation code. 1999. *Nucl. Instrum. Methods Phys. Res. Sect. A.* **429**: 243.

5. Saldin, E., E. A. Schneidmiller, and M. V. Yurkev. Coherence properties of the radiation from x-ray free electron laser. 2008. *Optics Communications.* **281**: 5.

Publications

Barber, J., M. Seaberg, D. Adams, D. Gardner, H. Kapteyn, M. Murnane, and R. L. Sandberg. Fresnel-regime Coherent X-ray Diffraction Imaging. 2011. *to be submitted to Physical Review B* .

Barber, J., Q. Marksteiner, and R. Sandberg. Simulation of diffraction patterns produced by an imperfectly-coherent source . 2011. *To be submitted to Physical Review B.*

Marksteiner, Q., J. Barber, and R. Sandberg. Hermite Gaussian Decomposition of the X-ray Output from a Time Dependent FEL Code. 2011. *Will be submitted to PR ST-AB in the near future.*

Control of XFEL-Radiation Focusing through Electron-Beam Manipulation

Kip A. Bishofberger
20110605ER

Abstract

An X-ray Free-Electron Laser (XFEL) is a recently developed technology that utilizes an extremely small electron beam to generate a coherent, powerful stream of X-rays. These penetrating rays are capable of probing dense, complex objects with high resolution and fast time-scales. Due to the electron/photon interaction, however, the X-ray beam also has extremely small size and angular divergence; the beam needs to expand significantly for relevant experiments planned in future XFEL facilities, such as MaRIE (Matter and Radiation Interactions in Extremes), which is being pursued at LANL. The project developed a new method to control the divergence of the output XFEL radiation by adjusting the phase front of the microbunched electron beam, which is used to generate radiation inside the XFEL. Changing the phase fronts of the electron bunches would be mirrored by the generated X-ray radiation in XFEL; thus the X-ray divergence can be controlled. This technique introduced a noninvasive method for changing the radiation spot size in real time

The development of this technology significantly enhances the capabilities of MaRIE for addressing the technical needs of various users, particularly in the proposed Multi-Probe Diagnostic Hall (MPDH). Moreover, this technology holds promise for lowering the space and cost requirements for MaRIE, and is a superior option for future XFEL facilities. In the course of the work we studied the limits of the proposed technology and found to what extent the X-ray divergence can be increased without significant reduction in the output XFEL power.

Background and Research Objectives

Various experiments that are expected to be performed at the MaRIE MPDH facility require different spot sizes of the X-ray radiation. Studies of the grain boundary interface in materials will require the spot size of radiation of at least 100 microns. Other applications, such as biological, chemical, and physical studies may require higher intensity of radiation, but with smaller beam. While the total power of X-rays delivered by the XFEL is limited, the power density can be optimized by adjusting the transverse spot size. Therefore, developing technology for controlling the spot size of radiation will significantly increase capabilities of the XFEL and will enable a broader range of experiments using it. Adjusting the phase front of radiation through the electron beam introduces a noninvasive method for changing the radiation spot size in experiments in real time. This study will have a strong impact in FEL science revolutionizing the control over generated radiation.

Scientific Approach and Accomplishments

This project simulates an adjustable phase front of the electron bunches as they produce X-ray photons, thereby providing a more divergent X-ray beam. In this scheme the undulator would be split in two parts. The first undulator section provides the growth of the FEL mode, resulting in a microbunched electron beam. Any initial photons are eliminated at this point, where the electron bunches are put through the nonlinear optics section. The nonlinear section distorts the bunches so that the center of each bunch is slightly forward of the edges. This curved phase front in the electron microbunches is mirrored by the photons generated in the second undulator section. By having control over the strength of the nonlinear optics, we gain control over the X-ray beam spot size and power density.

At the conclusion of this project, we succeeded in simulations of each facet of our research objectives. Simulations of a MaRIE-like XFEL, utilizing curved phase-front beams, indeed generated a more divergent XFEL beam. While we hoped to increase the spot size by a factor of ten or more, the FEL mechanism limited the spot size expansion to a factor of three. This factor already reduces the final beam expansion drift (before the MPDH) by roughly 250 meters, a significant reduction on required footprint and cost. Simulations on the generation of these curved phase fronts were also successful; a straightforward beamline technique creates an adjustable curvature; hence, the spot size at the target is adjustable for different target requirements.

The accomplishments of this project are as follows:

- Successful simulations of the XFEL performance, using beam distributions from beamline codes.

- Analysis of X-ray divergence as a function of bunch curvature.

- Beamline simulations of curvature-inducing elements, and description of necessary elements for a physical design.

- Publication of results in multiple peer-reviewed proceedings, including beamline-manipulation techniques, XFEL simulations, and final results of divergence as a function of beam curvature.

In addition, the work has proved to be a foundation for future efforts in XFEL optimization and control. We are seeking direct funding for additional techniques to increase the XFEL spot size. Several ideas are already proposed, and we hope to pursue these options in the near future. This project allowed us to create the capability to analyze new techniques efficiently.

Impact on National Missions

The capability of changing the spot size of radiation in experiments is extremely important for XFEL science and the experimental goals of the MaRIE project. While Material Science studies require the radiation spot size to be on the order of a few hundred microns for resolving material grains, other experiments depend on higher intensities of radiation over much smaller beam sizes. Introducing this capability into MaRIE's design will enable a wide range of experiments to be performed.

Additionally, experiments requiring different spot sizes of radiation in quick succession can be performed if the optics design allows for microsecond-scale changes (achievable through pulsed-power technologies). This possible option is even more enticing to users requiring multiple scales of X-ray imaging. Developing tools for accurate tailoring electron beam conditions in FEL will make a strong impact on FEL science. Similar methods can be used for improving beam-radiation coupling in the wiggler which will increase the generated radiation power, reduce the wiggler length, and eventually further reduce the XFEL cost.

Achieving the Ultimate Spatial and Density Resolution of 800 MeV Proton Radiography

Alexander Saunders
20110632ER

Abstract

The proton radiography (pRad) facility at LANSCE (Los Alamos Neutron Sciences Center) has been used for over a decade to conduct mid-scale science experiments in support of the nuclear weapons stockpile steward-ship program. As we drive to the much smaller scale materials experiments proposed to be conducted at the Multi-Probe Diagnostic Hall of LANL's proposed MaRIE (Matter-Radiation Interactions in Extremes) Facility, we must improve the density and spatial resolution of the pRad system to its ultimate limits with 800 MeV protons. The goal of this project was to explore the fundamental resolution limits of 800 MeV pRad.

Background and Research Objectives

Multiple Coulomb scattering proton radiography (pRad) is a technology that was invented and developed at Los Alamos National Lab[1]. The facility at LANSCE has been used for over a decade to conduct mid-scale science ex-periments in support of the nuclear weapons stockpile stewardship program. In the future, much smaller scale experiments are expected to be conducted at the MPDH facility at MaRIE. To radiograph these experiments, pro-ton radiography must achieve finer resolution measure-ments than it has hitherto. The goal of this project was to start to investigate the factors affecting the ultimate resolution possible using 800 MeV protons from the LANSCE accelerator, which are expected to be used at MaRIE.

Proton radiography uses high energy protons to generate flash radiographs of objects. Since high energy protons do not range out in the objects of interest at LANSCE or MaRIE, essentially all of the incident protons emerge from the downstream side of the radiographic object, unlike in the case of attenuation radiography using X-rays, for example. Contrast is generated in proton ra-diographs by taking advantage of the multiple Coulomb scattering in the object (which causes each proton to emerge from the target at an angle distributed randomly around its incident angle) and a magnetic lens between the target and an image plane. The lens has the triple effect of focusing the protons to create a sharp image at

the image plane; acting as a filter for all background and non-desired energetic particles, so that only the desired protons reach the image plane; and eliminating from the image, via the use of a "Fourier plane" at the midpoint of the lens and a thick collimator, all protons that scat-tered through a sufficiently large angle. This last effect generates contrast in the image, since protons that pass through a thicker part of the object undergo more mul-tiple Coulomb scattering to a larger average angle, re-sulting in a smaller net transmission to the image plane through the collimator at the Fourier plane.

A schematic of the apparatus, including proton rays traced through the lens, is shown in Figure 1. The Fou-rier plane is shown in the middle of the lens. Ideally, protons are sorted at the Fourier plane by the angle through which they scattered in the target; protons that scattered through a larger angle should be farther from the center of the beam line as they cross the Fourier plane. However, this relationship only hold true if the proton beam incident on the target has the right cor-relation between position and angle, known as being "matched". The proton beam from the 800MeV LANSCE linac is tuned to form a double waist at the "diffuser" location indicated in Figure 1 where it is made to scat-ter through a tantalum foil of known thickness. This process, through multiple Coulomb scattering, creates a fan beam, which is then manipulated to a desired size at the object location using the quadrupoles QM6, 7 and 8. More importantly, it is also rotated in transverse phase space so that the proper matching condition is created. A properly matched beam has the second effect that the position-dependent part of the chromatic aberrations in the image is eliminated. Finally, the residual chromatic blur in the image is proportional to the average scatter-ing angle of the transmitted protons, so placing a smaller collimator at the Fourier plane should result in better spatial and density resolution at the image plane.

The original proposed goal of the project centered on measuring and understanding the main factors affecting the spatial and density resolution of pRad. Based on the above arguments, we began by studying in simulation the effect of different collimator sizes on the total resolu-

tion of the proton radiography system. Early in the project, however, we recognized that a second effect, never considered until now, might be important: the contribution of secondary radiation particles generated near the image plane[2]. Briefly, the proton radiography system includes an armored window just upstream of the image location. The purpose of this window is to contain any blast or debris from any high explosively-driven experiments conducted at the facility. As mentioned above, the magnetic lens filters out any background radiation from the incident beam or its interactions in the target; however, the beam's interactions in the armored window could generate background radiation which, being created downstream from the lens, could not be filtered. We thus added the goal of evaluating this previously unsuspected effect.
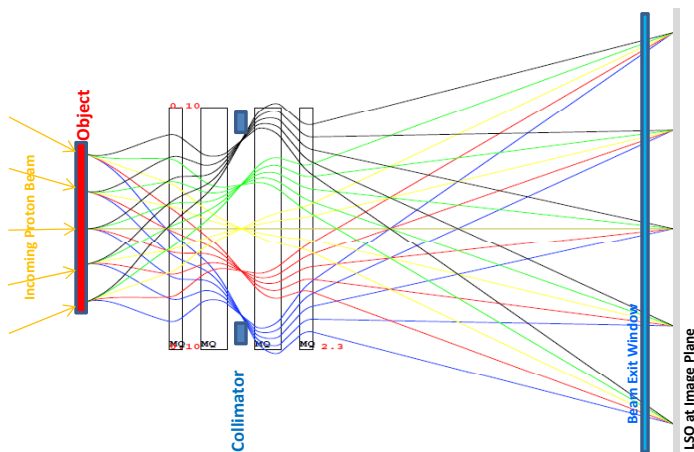
Figure 1. Schematic of the proton radiographic facility magnifier lens. The collimator location is shown at the center of the lens; the object on the left, and the image plane on the right. Each color ray represents a different angle of proton scattering.

Scientific Approach and Accomplishments

As described above, the project involved simulating and then measuring the major factors affecting the spatial and density resolution of proton radiography. The two main effects that we decided to study, based on the above discussion, were the size of the collimator and the generation of secondary particles in the armored window at the image plane. We started by performing a series of Monte Carlo simulations of each of these effects, while simultaneously designing and building a set of standard targets with which to measure the magnitude of the various effects.

The simulations were performed using a combination of particle tracking packages. The simulation tracked individual protons from the diffuser (shown in Figure 1) through the object, the lens, the collimator, and the entrance and exit windows to finally reach the image plane, in multiple stages. The incident beam location, size, emittance, and correlations were measured by the proton radiography team several years ago, and these parameters were used in the present simulations. The beam was tracked through

the object using the GEANT4 package, since it can handle the complicated interactions of protons with matter. Then, the protons were transported to the collimator location (the Fourier plane), through the first half of the lens, using the COSY magnetic transport package. This package does not incorporate the interaction of protons with matter, but can rapidly transport them through known magnetic fields. Those protons that arrived at the collimator location outside of the collimator opening physically interacted with its material (typically 5.08 cm of Tungsten); those that arrived inside its central opening passed right through. The physical interactions were again simulated using the GEANT4 package. After being transported using COSY through the second half of the lens and by GEANT4 through the armored exit window, the protons were tallied at the image plane. The whole process was repeated for different collimator opening sizes and different thicknesses of armored window.

Sample results of the simulations are shown in Figures 2 and 3. In Figure 2, the resolution of the simulated images is plotted as a function of the simulated collimator opening size. The resolutions are plotted separately for the x and y directions in the image, since these are not necessarily equal (and, as can be seen from the figure, were in fact not equal in the simulations. As can be observed, the simulations predict that the magnetic resolution should decrease linearly with collimator size, and with approximately the same dependence in the x and y directions, over the range from collimator cut angle of 10 mradians to 2.5 mradians. Based on the results of these simulations, we constructed a set of tungsten collimators with opening angles of 10, 7.5, 5, 2.5, and 1 mradian, to correspond with the entire range simulated and reach down to even smaller collimator size. We predicted that this effect should be measurable using the proton radiography apparatus at LANSCE, and determined to proceed with a set of such measurements.
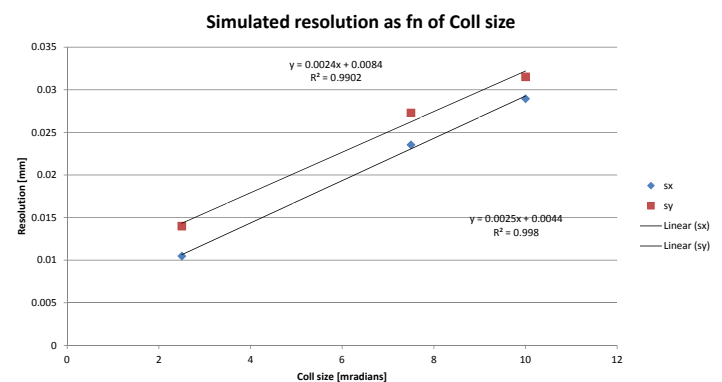
Figure 2. Simulated dependence of resolution on collimator size. The x and y directions are shown separately, since the lens is not necessarily symmetric. The dramatic relationship between resolution and collimator size can be seen.

In Figure 3, we show the simulations of the effect of sec-

ondary particle generation on the resolution of the proton radiography system. When a high energy proton passes through any material, it creates a spray of low energy background particles, including electrons, gamma rays, neutrons, and more rare charged particles, such as pions. Each of these particle species has a different generation probability, a different angular distribution, and a different probability of detection in the scintillator at the image plane that detects the proton beam. We performed some early simulations to roughly sort out the importance of the different species, as a result of folding the above factors together. A sample of the results is shown in the top row of Figure 3. On the left is the simulated proton beam in a small section of the image plane; on the right is the distribution, on the same spatial scale, of the secondary charged particles and gamma rays created by those protons passing through the armored window. These simulations led us to understand that the only secondary particles that could play an important role were the electrons and gamma rays; neutrons, protons, and other charged particles were either created too rarely, too widely spread, or too hard to detect to play a large role in the resolution. We therefore performed a more detailed set of simulations, focusing on the effects of electrons and gamma rays produced by the kind of thin window we would use in optimized pRad experiments, a 20 mil sheet of kapton.
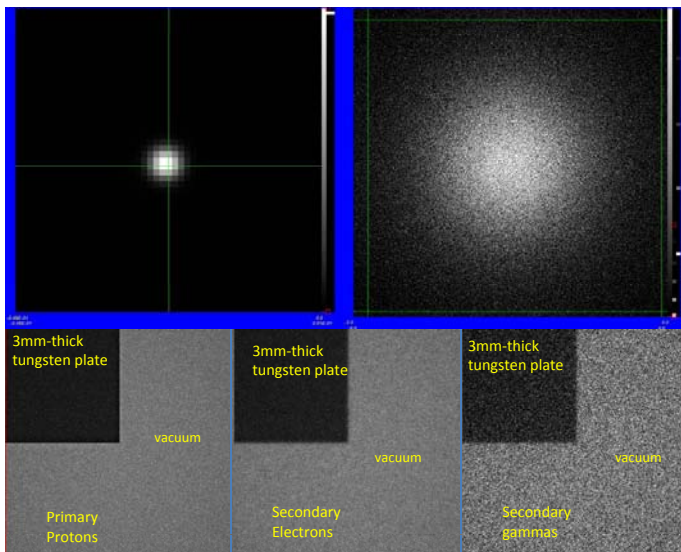
Figure 3. The simulated effect of secondary particle radiation on pRad resolution. The top row shows the distribution of protons and all secondary particles on the left and right, respectively; the bottom row shows a series of simulated raqdiographs of the corner of a tungsten plate. The left picture shows the proton distribution; the center the electrons; and the right side the gamma ray distribution.

A sample of the results is shown in the bottom half of Figure 3. Each of the panels shows the simulation of a radiograph of the edge of a 3 mm tungsten plate; the three panels show the distribution of the protons, the secondary electrons, and the secondary gamma rays respectively.

The relative blur of the sharp edge of the tungsten plate reveals that the secondary electrons and gamma rays are indeed much more blurred than the desired protons; however, the simulations also revealed that only 0.07% of the energy deposited in the scintillator comes from secondary gamma rays, while only 4% comes from secondary electrons. Thus, the simulations showed that the effect of gamma rays is totally negligible, while that of secondary electrons is small enough that it will be very hard to tease out from the other sources of blur in proton radiographs.

Based on the simulation results and our prior experience with the LANSCE proton radiography facility, we knew that the primary sources of blur in the proton images are magnetic blur, blur caused by the cameras and optical systems that record the proton images, and blur caused by the protons scattering and displacing in the thick objects. In the standard pRad experiment configuration, using our x3 magnifying lens built from permanent quadrupole magnets, and using typically explosively-driven objects, these three sources of blur are roughly evenly matched. The total resolution of the system in these conditions is about 150 _m. In order to separate out the three effects, we used only very thin objects in our resolution studies, and bought a new large format camera that mostly eliminated the camera blur. In order to investigate the effect of collimator size on the residual magnetic blur, we planned a set of experiments using the collimators mentioned above, extending from 10 mradian, which is the largest collimator size typically used for dynamic proton radiography experiments, down to 1 mradian, which is smaller than any collimator used for proton radiography up to now. Because our experimental beam time was strictly limited by LANSCE's and pRad's operating schedule, we also constructed a rapid collimator changer, which reduced the time required to switch between collimators from a few hours to a few minutes.

The first object that we used for these tests, designed to allow many spatial and density resolution measurements in a single experiment, is shown in Figure 4. The object consists of a 3 mm thick copper plate (thin enough that proton displacement in the object is a negligible source of blur), with 2 mm diameter cylindrical holes machined to different depths into its surface. The holes varied from a depth of 50 _m to a depth of 3 mm (all the way through the plate).

Some results of radiographs acquired using this object and two different collimators are shown in Figure 5. The top row shows the radiographs using the 7.5 mradian collimator, while the middle row shows the radiographs using the 1 mradian collimator. The left column shows the results of the resolution of the bare object, while the right column shows the resolution of the object sitting on another 2.73 mm thick copper plate. The bottom row shows our very preliminary extraction of the resolution of the system in each case. Unfortunately, our run was cut short after only

testing these two collimators by the failure of our magnifying lens. The general trend is clear, though, from this very early analysis (and visibly in the radiographs): the spatial resolution is substantially better in the case of the 1 mradian collimator than in the case of the 7.5 mradian collimator, although not as much better as was predicted by the simulations. The reason for the discrepancy between the simulations and experiments remains a matter for investigation, although we strongly suspect that the failing magnifying lens had a role to play here.
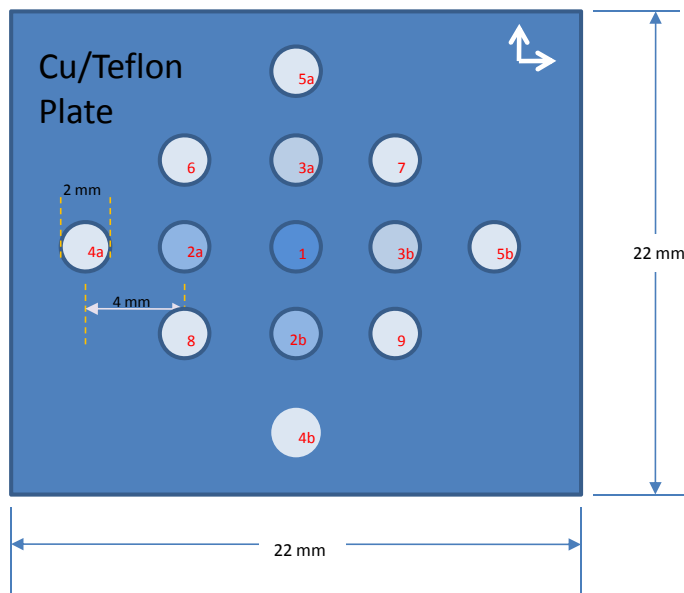
Figure 4. The first object used for our resolution studies. The object was machined form a 3 mm thick piece of copper plate.
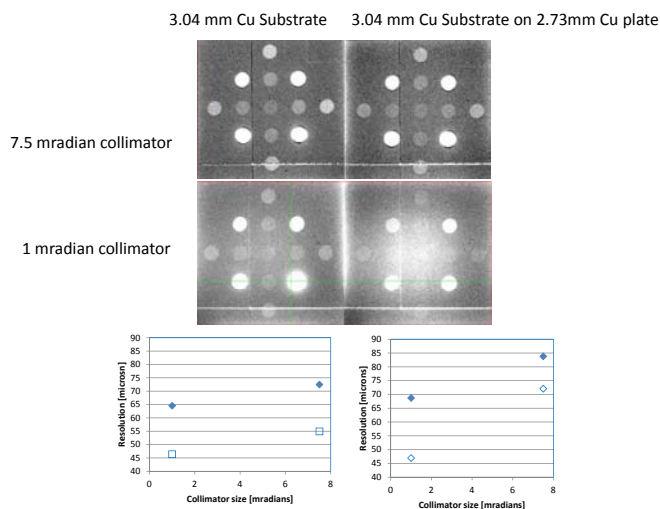
Figure 5. Preliminary radiographic results. The top row shows radiographs made with the 7.5 mradian collimator; the middle row, radiographs with the 1 mradian collimator; and the bottom row, plots of the extracted resolution functions. The left column shows results with the bare object; the right column, results with an additional 2.73 mm piece of copper plate blocking the beam.

In conclusion then, in this project we started and completed some very interesting studies into the sources of proton radiography resolution blur. Our simulations strongly indicate that secondary radiation generated in the exit window, although a potentially important factor for pRad blur, appears to be a small factor in our typical geometries. Our simulations suggested, and our experiments preliminarily confirmed, that smaller collimator sizes can lead to dramatically improved system resolution. The qualitative similarity but quantitative discrepancy between the simulations and experiments gives us hints into where to pursue our next studies: perhaps the beam is not properly steered on the upstream diffuser, or perhaps the collimator alignment is not optimized. Either one of these effects could account for the effects we are studying, and can be both simulated and measured in future studies.

Impact on National Missions
The results of this project will have a strong impact on the future of proton radiography at 800 MeV at LANSCE, which is closely tied both to the laboratory's weapons program mission and to the development of the future MaRIE facility. Because of this project, we now better understand the sources of blur in the resolution of the proton radiographs generated at the facility, which will help us define the best possible path forward to MaRIE and any future pRad facility. This will in turn ensure the best possible radiographic capabilities for any future flash radiographic facility, whether used for stockpile stewardship or material studies.

References
1. Mottershead, C. T., and J. D. Zumbro. Magnetic optics for proton radiography ; vol.2. 1998. In *Proceedings of the 1997 Particle Accelerator Conference ; 12-16 May 1997 ; Vancouver, BC, Canada.* , p. 1397.

2. Zumbro, J. D.. Private communication. 2011. *Private Communication.*

3. Agostinelli, S., J. Allison, K. Amako, J. Apostolakis, H. Araujo, P. Arce, M. Asai, D. Axen, S. Banerjee, G. Barrand, F. Behner, L. Bellagamba, J. Boudreau, L. Broglia, A. Brunengo, H. Burkhardt, S. Chauvie, J. Chuma, R. Chytracek, G. Cooperman, G. Cosmo, P. Degtyarenko, A. Dell'Acqua, G. Depaola, D. Dietrich, R. Enami, A. Feliciello, C. Ferguson, H. Fesefeldt, G. Folger, F. Foppiano, A. Forti, S. Garelli, S. Giani, R. Giannitrapani, D. Gibin, J. J. GoÃÅmez Cadenas, I. GonzaÃÅlez, G. Gracia Abril, G. Greeniaus, W. Greiner, V. Grichine, A. Grossheim, S. Guatelli, P. Gumplinger, R. Hamatsu, K. Hashimoto, H. Hasui, A. Heikkinen, A. Howard, V. Ivanchenko, A. Johnson, F. W. Jones, J. Kallenbach, N. Kanaya, M. Kawabata, Y. Kawabata, M. Kawaguti, S. Kelner, P. Kent, A. Kimura, T. Kodama, R. Kokoulin, M. Kossov, H. Kurashige, E. Lamanna, T. LampeÃÅn, V. Lara, V. Lefebure, F. Lei, M. Liendl, W. Lockman, F. Longo, S. Magni, M. Maire, E. Medernach, K. Minamimoto, P. Mora de Freitas, Y. Morita, K. Murakami, M. Nagamatu,

R. Nartallo, P. Nieminen, T. Nishimura, K. Ohtsubo, M. Okamura, S. O'Neale, Y. Oohata, K. Paech, J. Perl, A. Pfeiffer, M. G. Pia, F. Ranjard, A. Rybin, S. Sadilov, E. Di Salvo, G. Santin, T. Sasaki, N. Savvas, and et-al. GEANT4 - A simulation toolkit. 2003. *Nuclear Instruments and Methods in Physics Research, Section A: Accelerators, Spectrometers, Detectors and Associated Equipment.* **506** (3): 250.

How Trees Die: Signature Imaging to Unravel Carbon Starvation and Dehydration Dynamics in Vegetation During Drought

Michelle A. Espy
20110640ER

Abstract

We have observed, for the first time, that water content can be monitored non-invasively and un-obtrusively in intact trees via ultra-low field (ULF) magnetic resonance imaging (MRI). We have seen evidence of both changes in water content for day vs. night in an aspen tree, as well as the overall decline in water content as the tree is dying, as shown in Figure 1. The work, accomplished under a 6 month LDRD science of signatures reserve grant, represents a first in application of the ULF NMR method to the study of plant function and mortality, and to our knowledge the first such observations of water cycling in an intact plant by magnetic resonance methods. The work demonstrates that the combination of LANL's unique abilities in ULF MRI, with climate-driven vegetation mortality research can provide insight into basic questions of plant function and mortality. Our ultimate aim is to provide basic insights into questions such as how plants die, especially during drought. While the question of plant mortality is easy to conceptualize, it is difficult to study because of the spatial and temporal variation of processes over the plant. Understanding these mechanisms of mortality, especially the tipping points, will provide critical input to forecasts of future climate because presently models cannot forecast vegetation change and simulate the related climate effects. The work here represents a first step towards fieldable, non-invasive monitoring of changes in water content during tree mortality required to answer these fundamental questions.

Background and Research Objectives

The purpose of this project was to use the combination of LANL's unique abilities in ultra-low field (ULF) magnetic resonance imaging (MRI) and climate-driven vegetation mortality research to examine a basic question. How do plants die during drought?

This question is one of the largest uncertainties in determining how plants will succumb to changing climate, and impedes DOE and international forecasts of future climate because models cannot simulate vegetation change and related climate effects. While the question of plant mortality is easy to conceptualize, it is difficult to study because of the spatial and temporal variation of processes over the plant. We lack basic understanding about whether mortality is primarily due to carbon starvation, (exhaustion of carbohydrate reserves), hydraulic failure, (failure to maintain water transport and subsequent desiccation), or both, as we hypothesize.

Present techniques for studying plants are generally limited to invasive methods which cannot capture critical processes only available in vivo. DOE is actively pursuing tools from non-invasive medical imaging, such as MRI, for investigating problems in carbon sequestration and bioenergy. The instruments, however, have not been designed specifically for environmental applications and remain a laboratory R&D tool. We used LANL's world-leading capability in ULF MRI to develop a portable system to image signatures of water transport in a tree, in vivo.

The work here is a first step to developing a new research program with global implications for understanding the terrestrial carbon budget and climate change. It presents both a scientific and programmatic opportunity; there is a fundamental scientific question, LANL is presently leading the world in the required components to address it, and we have a critical time window to engage DOE for developing a research program.

Scientific Approach and Accomplishments

We observed *for the first time* that water content can be monitored non-invasively and un-obtrusively in intact trees via ultra-low field (ULF) nuclear magnetic resonance (NMR). We have demonstrated not only proof-of-concept (TRL 3) for portable sensing of water dynamics in trees, but also compelling science implications. The results indicate declining day/night variation in stem water content as the tree dehydrates (water is withheld) and dies (Figure 1). This is the first direct tree-level evidence of a primary tenet of the hydraulic failure hypothesis of progressive dehydration1. Thus, we are now positioned to realize enormous scientific gains in the near-term. The system is shown in Figure 2. Correlation of the NMR signal and water content of excised branches (Figure 3) yielded strong, positive, linear relationships

(avg r2=0.94, se=0.03, n=3); thus the data are the first-ever non-invasive test of dehydration during drought induced mortality. The downward oscillations indicate dehydration of the water transport conduits in the stem, and upward oscillations represent refilling of some of those conduits, directly consistent with the hydraulic failure hypothesis. These results demonstrate enormous promise of field portable ULF-NMR for monitoring (and understanding) how plants respond to climate variability. However, achieving our goal will require further intensive design and engineering of our NMR detection hardware.
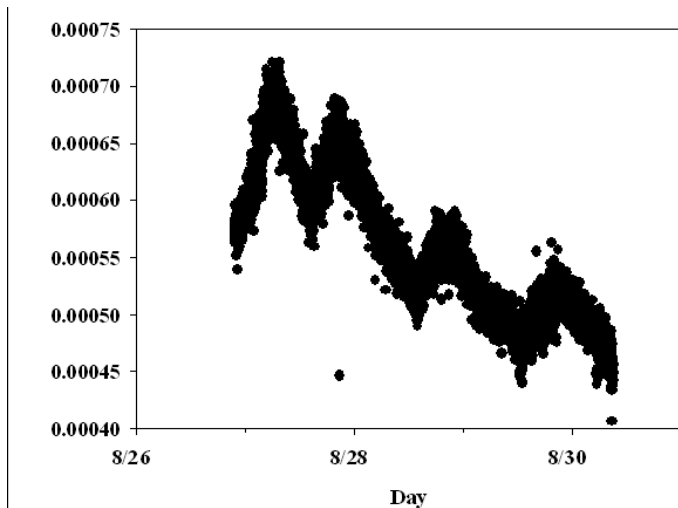
Figure 1. The ULF MRI signal of an aspen tree over four days during which irrigation water was withheld. The diel oscillation associated with variation in air temperature, and the declining trend as the plant exhausts its water supply, are both consistent with plant physiological theory. These are the first measurements of their kind using ULF MRI.

Figure 2. Top Row: Two photos of the tree in the ULF NMR system. The NMR system is located inside the silver magnetic shield. The photo at left was taken ~ 7 days before the photo at right, and significant decline in leaves is noted. Bottom Row: Left shows close up of leaves infected with parasite. Right shows close up of NMR system around tree trunk.
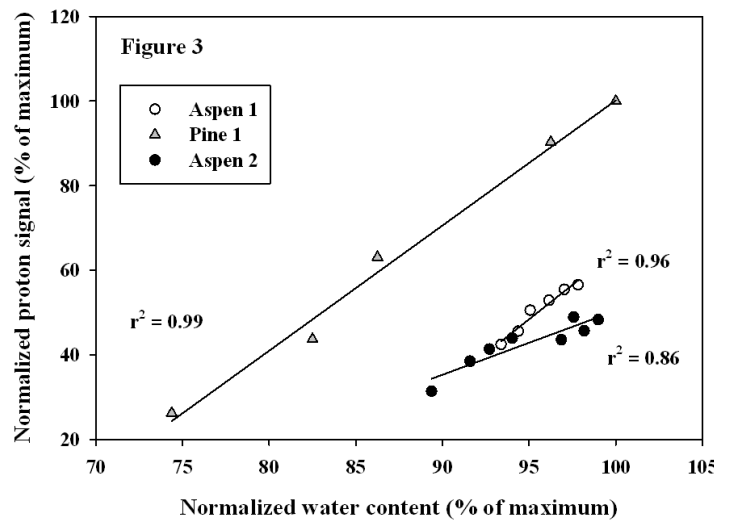
Figure 3. ULF NMR signal versus stem water content of excised, drying aspen and pine stems. We hypothesize variation in the relationships are driven by wood density and physics of proton exchange.

Impact on National Missions

We have demonstrated an in vivo signature measurement system of the movement of water through plants. Our approach will advance our existing capability and provide new tools for understanding fundamental plant biology, carbon sequestration, and bioenergy. Our research goals are directly in line with DOE OBER's mission to provide basic research and tools to address questions of carbon movement and climate change. Specifically, DOE OBER managers have ex-pressed strong interest in this project and are interacting with us as we develop this signature capability. They indicated that initial investment via LDRD is a critical consideration for them to further build this program. This SOS reserve funding will lead LANL to build a new multi-scale inter-disciplinary program focused on the DOE mission in climate change.

DOE OBER has specifically engaged the National Laboratories to build Science Focus Areas to address their mission in understanding climate impacts on bioenergy and terrestrial vegetation dynamics. Program managers from throughout the modeling, genomics, radiochemistry, and ecosystem programs within BER are actively interacting with the staff members on this project and are soliciting updates on future plans. This work would allow construction of a "Science Focus Area" within BER.

References

1. McDowell, N. G., W. Pockman, C. Allen, D. Breshears, N. Cobb, T. Kolb, J. Plout, J. Sperry, A. West, D. Williams, and E. Yepez. Mechanisms of plant survival and mortality during drought: why do some plants survive while others succumb? . 2008. *New Phytologist.* **178**: 719.

Signatures of Brain Functionality Detected using Direct Measurement of Blood Magnetic Susceptibility

Andrei N. Matlashov
20110670ER

Abstract

We have developed SQUID-based instruments for high resolution measurement of magnetic susceptibility of biological tissues and blood in the human body. The existing ultra-low field magnetic resonance imaging (ULF MRI) system was modified for magnetic susceptibility measurements at constant (DC) magnetic fields. The magnetizing coil that can generate 1 Gauss field was added together with current control electronics. An electrocardiogram amplifier was used to record heart beats as synchronization for signal averaging. Two SQUID systems were used for measurements – the seven-channel (original ULF MRI) system and a one-channel system with improved noise figure and more rigid gantry that decreased microphonic noise. Magnetic susceptibility plethysmography (MSPG) signals were recorded from human subject hearts with high signal to noise ratio (SNR), about 10. We tried to record MSPG signals from different areas of the brain but could not claim credible results. In spite of very low white noise level, 2 fT/sqrt(Hz), there were some resonant microphonic signals at 12-30 Hz range and also 1/f noise below 5 Hz caused by vibrating system parts in the presence of the 1 G magnetizing field. These signals masked MSPG signals from the brain although MSPG signal from the heart was recorded with good SNR. The designed system shows very high resolution in spite of vibrations and can be used for investigation of magnetic susceptibility of biological tissue *in vivo*. An alternating magnetizing field can be used in further experiments that will allow shifting the MSPG spectrum above the masking vibrations. The proposed method and instruments also can be used for detection of magnetic markers *in vivo* in different areas of the human body.

Background and Research Objectives

The purpose of this project was a proof of principle demonstration that, for the first time, directly recorded blood magnetic susceptibility signals can be measured and used as signatures of brain functionality similar to functional MRI. It is well known that changes in blood oxygenation and blood flow, collectively known as hemodynamics, are closely linked to neural activity, i.e. brain functionality. The functional MRI method is based on measurements of magnetic susceptibility of brain tissues with different oxygenation level. Modern medical MRI systems operate at 1.5 T or 3 T fields. We expect that magnetic susceptibility changes of brain tissues can be measured at much lower magnetization field in the range of 10^{-2} - 10^{-3} Tesla (1-10 Gauss). Such detected signals indicate parameters of the hemodynamics and can be used as signatures of the brain's functional activity.

Brain hemodynamics includes changes in blood oxygenation and blood flow. Blood oxygenation variations indicate local oxygen consumption rate by neural cells and the fMRI method allows detection of this slow (~1-5 sec) process with high spatial resolution. Blood flow changes have both slow and fast components. Slow blood flow changes indicate the need for oxygen and nutrition of the local cells and may provide information similar to oxygenation changes. Fast blood flow changes produced by heart beats that have 30-150 ms fronts, too fast to be detected by fMRI, but can be easily measurable using the MSPG method.

Traditional high field fMRI is based on physical phenomena associated with magnetic susceptibility difference of red blood cells in oxygenated (χ = - 0.749 ppm sgs) and deoxygenated state (χ = - 0.483 ppm sgs). Although this difference is small, only 0.27 ppm sgs, it produces a perturbation of the polarizing field that causes a measurable phase shift in NMR signal. Thereby tiny changes of magnetic susceptibility of brain tissue can be detected as a secondary effect of the NMR signal phase change. This magnetic field perturbation, however, is a primary low frequency effect that can be directly measured using a high resolution magnetometer that stays operational while immersed in a moderate ~10^{-3} T (10 G) external magnetization field.

Direct measurements of such magnetic field perturbations can be done with high temporal resolution that will allow detection of fast (~10 ms) mechanical tissue movements or volume changes caused, for instance, by heart beat pulsing. Heart beats generate hydrodynamic waves or pulses in the circulation system and produce local

volume changes especially in areas around main arteries and veins. Mechanical movement of tissues with different magnetic susceptibility can be detected as magnetic dipole signals when magnetized by an external uniform field.

We used LANL's world-leading capability in ULF MRI to develop SQUID-based instrumentation to image signatures of blood transport in the brain and other areas of a human body, *in vivo*.

Scientific Approach and Accomplishments

We observed MSPG signals from the human heart and recorded similar signals from different areas of the human brain. Our R&D approach included modification of existing an ULF MRI system for magnetic susceptibility measurement. We recorded MSPG signals from the heart synchronously with recording heart beats using an ECG amplifier while applying external magnetizing fields in two opposite orientations. We performed many experiments recording MSPG signals from the heart and different areas of the primary cortex of the brain. We used areas of the brain known for detection of somatosensory, auditory and visual evoked magnetic fields (EMF) with and without a magnetizing field.

We modified the ULF MRI system that consists of seven SQUID-based axial gradiometers, 37 mm diameter, placed inside a large fiberglass cryostat. The set of coils designed for MR imaging was replaced with a large Helmholtz coil that generates 1 Gauss magnetizing field in the vertical direction along the axis of the gradiometers. This sensor system has a magnetic field resolution of about 3 fT/√Hz. It was defined by Johnson noise from the thermal shield inside the fiberglass cryostat. The most difficult problem was associated with elimination of low-frequency noise caused by micro-vibrations of gradiometers in the presence of the 1 Gauss magnetizing field.

The second smaller size system was used to make a more rigid cryostat support system to decrease as much as possible the gradiometer micro-vibrations. This smaller system included only one-channel of the same size gradiometer. Its intrinsic noise was defined by Jonson noise of a gold-plated Mylar RFI shield at a level of about 1.2 fT/√Hz. An additional source of noise was a current noise in the magnetizing coils that led to total system noise during MSPG measurement of about 2 fT/√Hz. Noise associated with micro-vibrations was significantly lower but still about 5 times larger than the white noise in the frequency range 12 – 30 Hz. It significantly decreased the SNR in the case of the brain MSPG signal detection.

We were able to see the brain's spontaneous activity at different head areas without an external magnetizing field. But in presence of the magnetizing field, resonant and 1/f noise caused by micro-vibrations was too high and significantly masked possible signals that we expected to see at a level of about 0.2 pT peak-peak. We averaged

MSPG signals synchronously with the heart beats during about 2 minutes for each direction of the magnetizing field and once without the field as the signal reference. We recorded MSPG signals from the heart at levels about 2-3 pT peak-peak with noise of about 0.2 pT. This noise was still too large for brain MSPG signals detection. We estimate the SNR was about 1.

A substantial volume of signal processing algorithms and software was developed during our experiments. We were able to record MSPG signals from human heart with good SNR, nevertheless we also saw that ECG pulses are not very stable during 6 minutes trials that made the averaging process challenging. In further attempts we plan to increase the magnetizing field to at least 10 Gauss level and decrease micro-vibration noise down to 2 fT level. In addition, AC magnetizing measurements could be performed to eliminate noise associated with system vibration.

Impact on National Missions

In 2007 and 2010 the US Department of Defense released proposal calls toward development of MRI-based instruments for quick detection of brain internal bleeding (traumatic brain injuries) and brain functional state in extreme conditions of battlefield hospitals. Conventional MRI-based technology failed because of its complexity and cumbersome design but no other technologies have come forward to solve this problem. Brain magnetic susceptibility based technique might solve this problem or at least lead researchers to new directions for solving it.

We exploited a new signature of brain health and function, which will be the foundation for inexpensive and portable techniques and instrumentation for assessing human brain function. Magnetic susceptibility plethysmography (MSPG) applied to the human brain can lead to detection of signals related to brain hemodynamics, i.e. important signature of brain functionality. It can become a new research tool as well as a new medical diagnostic tool for extreme conditions such as emergency rooms or battlefield hospitals.

This research directly advances LANL's capabilities and addresses the Grand Challenge areas of Complex Biological Systems (new medical tools and understanding the brain) and Sensing and Measurement Science (via new non-invasive sensing methods).

Hyperspectral Intensity Correlation Interferometry

David C. Thompson
20110672ER

Abstract

Interferometric techniques have long been used to improve imaging resolution beyond what is possible with conventional imaging. Intensity Correlation Interferometry (ICI) has been an alternative to conventional Amplitude Interferometry (AI) since the 1950's, with many attractive features including much-reduced requirements on optics, only data rather than light being combined, and insensitivity to turbulence. But it has generally suffered from poor signal to noise ratio (SNR) performance in comparison to AI. Hyperspectral ICI (HICI) promises to overcome the SNR issue, increasing the SNR by dividing the light into many spectral channels, but it has never been experimentally demonstrated.

The key to enabling this technique is the use of picosecond time resolution photon counting imagers developed at LANL.   We proposed to make use of this technology to demonstrate HICI in the laboratory, to show that the technique works and to investigate its scaling properties so that performance in various applications can be projected.

We made substantial progress towards this experimental demonstration, but did not manage to complete the experiment during FY11. We discuss the work done under this project under task areas of theory, simulation and algorithms; the laboratory experiment; and analysis of data showing imaging of target.

Background and Research Objectives

Experimental verification of HICI would make the technique practical for many imaging applications. It would open up possibilities of diffraction-limited imaging through atmospheric turbulence, including imaging of distant objects through ground-level turbulence and simpler interferometers for astronomical applications. HICI systems appear possible both for sparse arrays suitable for ultra-high (nrad or better) angular resolution using just a few (~10) modest aperture (<1m) telescopes with baselines up to 100's of meters or more. HICI may also enable compact single aperture systems that are insensitive to atmospheric turbulence.

We proposed three main tasks for this effort. The theory, simulation and algorithms task included development of a model to describe the system SNR for a variety of system configurations; development of software for data acquisition and calculation of the correlations that are the experimental observable; and development of image processing algorithms operating on the data to produce a high quality image. The experimental task was to perform laboratory tests of a system based on two "NCam" cameras based on LANL's picosecond time resolution photon counting imaging technology and an incoherently illuminated target. This includes sensor calibration and time resolution characterization, confirmation of ps-level absolute timing and correlations for multiple wavelength channels, measurements of correlation SNR scaling with relevant parameters, and data collection for multiple baselines for image acquisition. The final task was use of analysis software developed in the first task to produce an image of the target.

Scientific Approach and Accomplishments

Theory: We developed an analytic model of Hyperspectral Intensity Correlation Interferometry, suitable for predicting the SNR under a broad range of conditions. The key parameter is the time-bandwidth product – the product of the sensor time resolution and the spectral resolution of the spectrometer used to spatially separate the many spectral channels that are independently observed to attain the high SNR in HICI. For example, in our laboratory experiment, we had a time resolution of ~140 ps and a spectral resolution of ~15 GHz giving a time-bandwidth product of 2.1. A time-bandwidth product of ~1 is the wave optics limit, reflecting the lack of independence of time and frequency measurements of a wave. As shown in Figure 1, our theory predicts increasing SNR as the time-bandwidth product decreases until the SNR gradually levels off as the product approaches and goes below unity.

Simulation: As a validation for simpler analytic models, as a means to test data analysis techniques, and for comparison with experimental data, we have developed a physically realistic numerical simulation of HICI. The

model simulates the incoherent nature of the target, with a randomly phased light emission at each of a 2D array of points and each of a large number of light frequencies. The simulation code propagates this light to a pair of spectrometers with NCam sensors, simulating the light intensity in each spectral channel of each spectrometer as functions of time. We have used this simulation code with parameters appropriate to the laboratory experiment. In Figure 2 we show the decrease in correlation of observed light intensities at different separations of the two spectrometers, for various positions of the first spectrometer. The random nature of the incoherent emission shows in the differences between the various curves, but they all follow approximately the same profile. This variation in correlation is what is used to reconstruct the intensity profile of the target to create an image. In Figure 2 we also plot the theoretically expected variation in correlation. The theoretical and simulated curves are similar, but there are some significant differences, which we have yet to explain.

Finally the code generates random photons with the rate of photons proportional to the light intensity at each point on the spectrometer and at each time. This final step of photon generation has not yet been fully validated. However it does generate data in the same format as the NCam sensors, as a list of detected photon events with the x-y position on the sensor and precise time of arrival for each photon. This enables testing data analysis techniques using the simulation results.
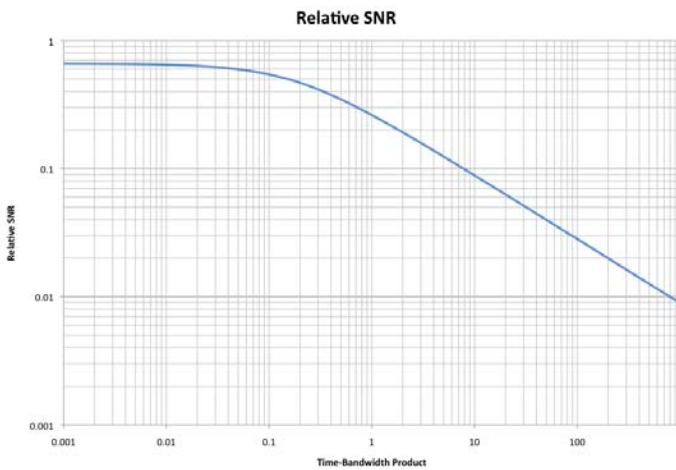
Figure 1. Normalized SNR as a function of the time-bandwidth product.
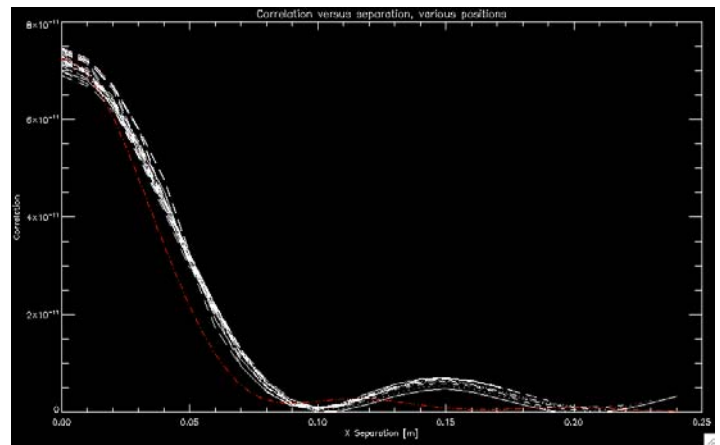
Figure 2. Simulated correlation between intensities, as a function of x separation for zero y separation.

Sensor time resolution characterization: Detector time resolution is a key driver of SNR and of system design for HICI. Therefore we spent considerable effort in improving and characterizing the timing performance of NCam, our high time resolution photon counting imaging system, and in investigating whether further improvements are possible. Our standard NCam system gave a time resolution of 140 ps FWHM, measured using a short (~10 ps) laser system and comparing the times measured by the sensor with the laser pulse times. The availability of high-speed multi-channel digitizers allows us to investigate an alternative approach to the analog electronics used in NCam. By directly digitizing the analog pulse outputs from the crossed delay lines of the NCam sensor tube (after preamplification), we can collect more information and have more flexibility in analyzing the data beyond the constraints of the NCam analog electronics. Using this technique we measured a time resolution of 87 ps FWHM. However the average throughput of the digitization system was much less than that of NCam, so we used NCam for the laboratory experiment.

Laboratory Experiment: At its simplest level, the laboratory experiment is shown schematically in Figure 3. A small incoherently illuminated target is collimated by a telescope. This places the target at infinity. At the output of the telescope a pair of spectrometers look at the same or different portions of the output aperture by means of a beamsplitter or mirrors. Each spectrometer disperses the light at its input onto an NCam sensor, so that light is dispersed along the horizontal direction.

The target consists of a pair of rectangular 50 μm X 100 μm pinholes separated by 150 μm. A LED fiber illuminator illuminates the target, with the fiber end placed as close as possible to the pinholes. The illuminator has a nominal output power of 5.1 mW from a 400 μm diameter NA 0.37 multimode fiber, with a peak wavelength of 530 nm. As a source, this should be quite ideal since the fiber output has high spectral brightness (2.9×10^6 W/m²-sr-μm) and is spa-

tially incoherent due to the very many, very small speckles in the multimode output (the average speckle "size" is ~0.7 μm).   This target should provide sufficient brightness to allow each NCam sensor to operate at about its maximum count rate of 10^6 detected photons per second. In turn, with a spectral resolution of 15 GHz and a time resolution of 140 ps, for a time-bandwidth product of 2.1, Figure 1 gives SNR = $0.2C_0$ and for a total spectrometer bandwidth of 3 THz and an observation time of 1s, we expect an SNR = 0.12. Since the SNR increases as the square root of the observation time, an integration of about 30 minutes would give an SNR of 5. This is practical, though longer than ideal.
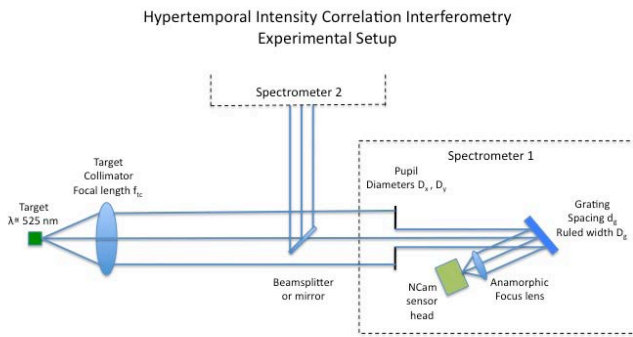
Figure 3. Schematic of experimental concept.

The spectrometers use a Volume Phase Holographic Grating (VPHG) as the dispersing element. VPHGs are transmission gratings featuring very high efficiency (~80%) over a fairly broad wavelength range and polarization insensitivity. Light dispersed by the grating is focused with a telephoto lens arrangement onto the 25 mm diameter NCam sensor, giving a total spectral range of 3 nm (or ~3 THz) within a 16 mm wide area of the sensor, and a spectral resolution of about 15 GHz, equivalent to 300 independent spectral channels.

It is critical that sufficient timing and spectral fiducials be provided to ensure that times and spectral channels can be properly matched between the two detectors to a small fraction of the temporal (~100 ps) and spectral (~10 GHz) resolutions. Therefore a ~50 kHz repetition rate train of short (10 ps pulse width) pulses from a mode-locked laser is inserted into the optical system. The power in this beam is adjusted so that only a small fraction of the detected photons at each NCam sensor come from this laser – less than $~10^4$ counts/s. Despite the less than complete sampling of these laser pulses, the frequency of this laser is sufficiently stable that times from the two detectors can be compared to <<100 ps. Another laser, a passively Q-switched micro-chip laser, also frequency doubled to 532 nm, is also inserted into the optical system. This laser has much longer (~10 ns) pulses and a much narrower spectral width suitable for tracking any drifts in the wavelength cali-

bration of the spectrometers. It should be noted that the short, regular pulses from the two lasers allow the laser photons to be definitively identified and removed from the data, eliminating all contamination of the LED light for ICI measurements.

An etalon can be inserted after the collimating telescope to provide a wavelength calibration scale for the spectrometers. This solid etalon, with fringes spaced by 60 GHz and a finesse of 6 (and therefore a 10 GHz fringe FWHM), can provide calibration of the spectrometers' wavelength scale to compensate for any nonlinearities. It also allows the resolution of the spectrometer to be measured.

Figure 4 shows the full experimental apparatus. All the parts of the experimental setup were laid out and individually tested. The alignment of the full experiment proved to be difficult and time-consuming, and was never completed. As a result, actual experimental data with both spectrometers and detectors aligned and collecting data at multiple pupil positions was never obtained. A re-evaluation of the alignment setup and procedures and improved alignment fixtures will be necessary as part of any completion of this experiment.
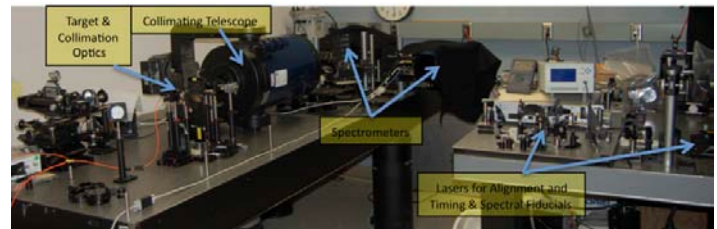
Figure 4. Photo of overall experimental setup.

Analysis of data to show imaging of target: This task was to use the analysis software developed in Task 1 to produce a target image. This task was not started, due to the lack of data from Task 2. However, we are confident that techniques developed in Task 1 would have sufficed to compare the experimental results (in the form of the variation of correlation with x and y separations) with the theoretically expected (and also simulated) results.

Full technical details of the results of this LDRD project can be found in the Technical Report, attached to this report.

Impact on National Missions

The Grand Challenge for Sensing and Measurement Science for Global Security explicitly calls out sensing and measurement science in support of national security in areas such as support for the warfighter, areas that HICI could significantly enhance. This work leverages previous LANL–developed technology and begins to develop a novel imaging capability with multiple applications in areas of growing national security interest and significant potential for the development of major programs. A successful

demonstration of HICI would help to grow the remote sensing and single photon imaging portfolios at LANL.

For terrestrial imaging, success here would be an important first step towards single pupil HICI, with many potential applications for imaging through turbulence both in the laboratory and for long range tactical imaging. It is likely that we would then be looking for further funding to pursue an experimental demonstration of this application.

Other applications in the field of quantum imaging such as time coincidence (or shadow) imaging could benefit from a successful demonstration since coincidence imaging experiments have been limited to relatively slow frame rate time resolution or high speed single-element detectors. It has also been suggested that ICI techniques may be used for detection of exo-planets, by detecting small periodic variations in the relative position of a star relative to nearby stars in the sky. There are a number of other astronomical applications: since only the photon timing data is combined, extremely long baselines are possible – even between satellites; it may be possible to measure the size and oblateness of much smaller stars or to resolve spectroscopic binaries. Spectral information from HICI may also provide important information about limb darkening.

References

1. Thompson, D. C., I. J. Owens, D. Palmer, and J. M. Cook. Hyperspectral Intensity Correlation Interferometry. 2011. *Technical Report on 20110672ER.*

Non-Invasive Imaging of Dense, Immobile Objects with Muon Tomography

Edward C. Milner
20110745ER

Abstract

In this LDRD project, we adapted and significantly extended the muon tomography technique to the task of non-invasively imaging very dense objects. Muon tomography (MT) creates an image of high-Z (Z is the nuclear charge) material (such as lead, tungsten, uranium, plutonium, etc.) by tracking cosmic ray muons before and after they pass through a volume. When muons collide with high-Z nuclei, they are deflected to larger scattering angles than in collisions with low-Z nuclei. The regions in which the largest-angle scattering events occur correspond to the location of high-Z material. Tracking information is used to establish the location of scattering vertices, and an "image" of the high-Z material is constructed from the pixels or voxels associated with high-scattering angle.

This work successfully demonstrated the feasibility of the technique, by producing images of a large volume of dense material (lead) concealed in an enclosure of thick concrete blocks (2.74 m on each side of the target) – analogous to uranium fuel inside the thick shielding of a reactor.

Background and Research Objectives

This LDRD project addressed and provided answers to the following crucial and new technical issues:

Is muon tomography (MT) a useful technique for creating images of very thick, high-Z objects (such as uranium) inside of very thick shielding?

We successfully demonstrated the detection and imaging of large masses of lead (Pb), concealed inside very thick (2.74 m) surrounding concrete using MT. Data plots below show the details. A thickness of Pb was chosen to be comparable to the thickness of uranium in a typical nuclear reactor. We therefore demonstrated the feasibility of using MT to non-invasively make an image of the fuel inside a nuclear reactor. This has not been done before, so the result is a significant extension of the technique.

For imaging the interior of thick objects, which is a better technique: muon radiography, or MT?

Muon radiography (MR) measures the density of thick objects by measuring relative rates of muons passing completely through the object. In contrast, MT creates an image by measuring scattering angle, not absorption.

Our Monte Carlo simulations suggest MT produces a superior image, compared to MR. Experimental data are still being analyzed to compare MT and MR.

For imaging thick objects inside thick shielding, will it be necessary to modify analysis and reconstruction algorithms?

A new algorithm was developed to analyze the MT data, discussed below.

A major failure of the Fukushima Daiichi (FD) nuclear plant occurred following the Great East Japan Earthquake and Tsunami, of March 11, 2011. It is likely the reactors cores sustained damage similar to that of the Three Mile Island (TMI) accident in 1979. In the TMI case, it took more than three years before a remote camera could be put into the reactor, and about 10 years before the total damage to the reactor could be assessed [1]. Understanding the nature of the damage and location of the fuel at TMI was crucial to making plans for remediating the site. The present work could be adapted to measuring the location and status of fuel at FD, but more quickly and effectively than by using cameras, since the technique is non-invasive.

The intensity of cosmic-ray muons at the surface of the earth is roughly $1/\text{min}/\text{cm}^2$, or approximately 1 Hz on the area of a human palm. As described in detail elsewhere [2] [3], cosmic-ray muons incident on the earth have a characteristic energy spectrum varying only by zenith-angle. The absolute scale of the energy spectrum is variable up to ~15% in time and also has altitude dependence, but otherwise is the same in any place in the world and at any time. Muons primarily interact electromagnetically (not via nuclear interactions), and

are ~200 times heavier than electrons (without conversion into photon), and therefore high-energy cosmic-ray muons can penetrate thick objects like volcanic mountains [4] [5] or Egyptian pyramids [6]. In previous work [7], we have demonstrated these muons can be used to image nuclear threats in relative short times by measuring their multiple scattering through modest shielding. High penetration ability of cosmic-ray muons is especially attractive for imaging objects of large size. In fact, this may be the only available technique for assessing damage at the Fukushima Daiichi reactors in relatively short time.

The MT method is unique in direct imaging of the nuclear fuel assembly in the present situation, and would allow assessing damage much sooner than this information was obtained for the Three Miles Island accident. The present work should be considered a first step in a possible series of cosmic-ray radiography measurements at Fukushima Daiichi nuclear plant, and could be the basis for a world-wide, large-scale application to help address nuclear safety issues. This work would also extend the MT technique into the realm of imaging large, dense objects inside very thick shielding – creating a generally useful technique independent of the present nuclear crisis.

Scientific Approach and Accomplishments

We adapted a previously developed research instrument for the experiment. This device is known as the "Muon mini-tracker" (MMT), and is shown and described in Figure 1. For the LDRD experiment, we disassembled the MMT and placed the top and bottom tracking units on opposite sides of the concrete shielding arrangement. In Figure 2, we show a drawing of the concrete, target and detector arrangement. Figure 3 is a photograph of the apparatus depicted in Figure 2. The standard MMT data acquisition system was used. Tracks were stored on disk for later analysis.

Four thick targets were studied in an accumulated period of 1769 hours of data collection. Table 1 (Figure 5) shows the targets, their masses, and the duration of data collection in hours. Images could be developed using as little as one week (168 hours) of data.

Data collection occurred between July 15, 2011 and September 27, 2011. Data analysis is reported here for the "80/40/20/0" target, which was an arrangement of lead bricks with four regions of lead with approximate thicknesses of 80 cm, 40 cm, 20 cm and 0 cm (no bricks). Data for the remaining targets is being analyzed.

Incoming and outgoing muon tracks were projected to the vertical mid-plane of the apparatus, which coincided with the mid-plane of the 80/40/20/0 target. For tracks passing within 20 cm of each other at this x-y mid-plane, the square of the difference of the track angles was plotted for each x-y "pixel" region. In Figure 4, we show a contour plot of scattering angle squared at the mid-plane. Next

to the plot is a photograph showing the target and the regions of 80-, 40-, and 20-cm thicknesses of lead. The regions are discernable in the reconstruction plot.

Preliminary Monte Carlo (GEANT4) models confirm this image. The models are still under development, and not reported here.
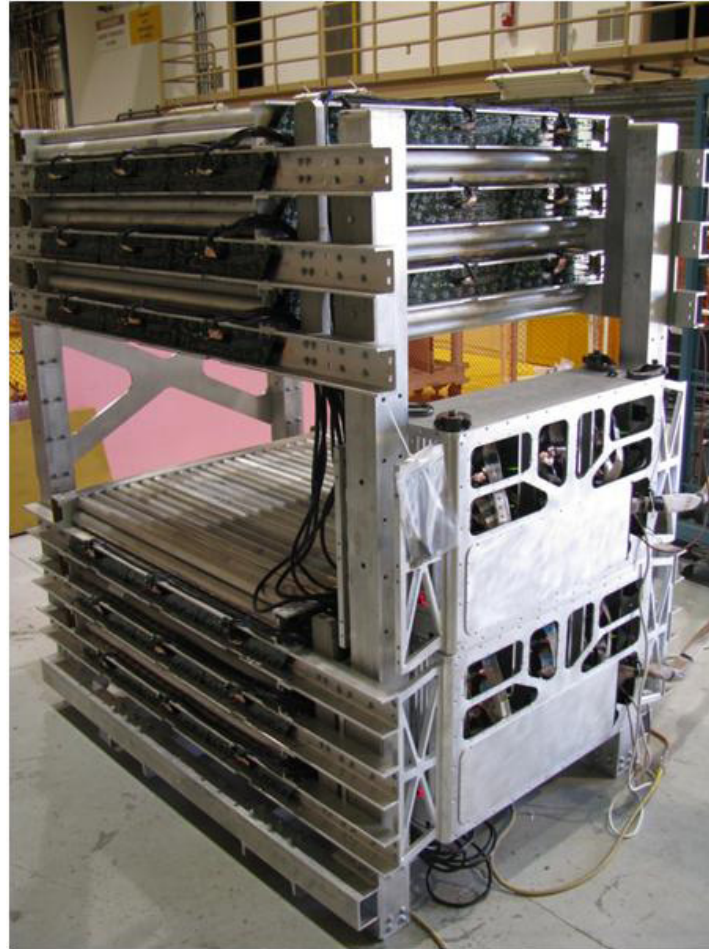
Figure 1. Photograph of the "muon mini-tracker" (MMT) built at Los Alamos for muon tomography appli-cations. There are 24 planes of four-feet long drift tubes to track muons in x- and y-directions. The top set of 12 detector planes is used to measure the direction of incoming muon tracks, and the bottom set of planes measures outgoing tracks. Objects to be imaged are placed in the gap between the upper and lower plane sets. Data acquisition electronics surround the detector edges.
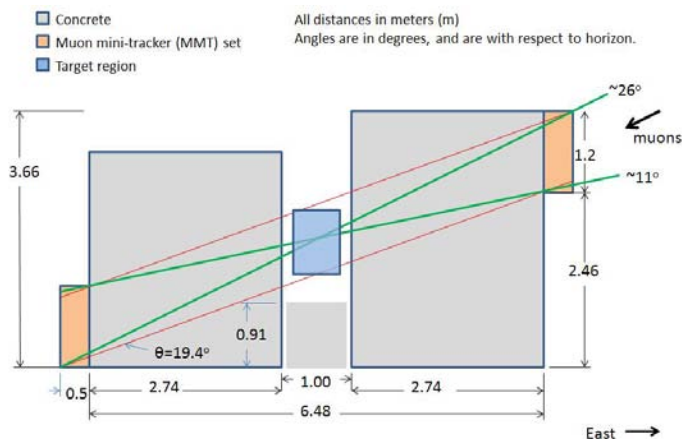
Figure 2. Elevation-view drawing of the experimental arrangement. Muons entered from the upper right and the apparatus had an acceptance of approximately 11 to 26 degrees above the horizon (64 to 89 degrees from Zenith). Their incoming direction was measured in the upper muon tracker set, then they traversed more than 2.74 m of concrete, various Pb targets, another mass of greater than 2.74 m of concrete, and their outgoing direction was measured by the lower tracker set.

Figure 3. Photograph of the experiment, looking East. Concrete blocks are prominently shown, and the lower MMT detector is in the foreground. The upper detector set is behind the higher concrete stack and not visible.

Figure 4. A contour plot (right) showing scattering angle squared at the mid-plane. Next to the plot (left) is a photograph showing the target and the regions of 80-, 40-, and 20-cm thicknesses of lead. The regions are discernable in the reconstruction plot.

Table 1:

Target Name	Mass (kg)	Duration (h)
Air (no concrete)	0	121.43
No target (concrete)	0	335.75
Conical Void	4094.83	497.73
80/40/20/0	2666.4	210.23
Pb Column	1523.66	292.63
PB + Fe Columns	2051.9	311.48

Table 1: Shows the targets, their masses, and the duration of data collection in hours. Images could be developed using as little as one week (168 hours) of data.

Impact on National Missions

In a study spanning 11 weeks, we collected data on a variety of thick targets surrounded by over 2.74 m of concrete. This study established the feasibility of imaging thick metal objects inside very thick shielding. This technique may be generally useful for detecting and imaging dense metal objects inside of thickly shielding objects, such as buildings, mountains, and nuclear reactors.

References

1. Broughton, J.M., P. Kuan, D.A. Petti, and E.L. Tolman. A scenario of the Three Mile Island Unit 2 accident. 1989. *Nuclear Technology.* **87**: 34.

2. Wada, T., A. Iyono, T. Katayama, S. Lan, T. Nakatsuka, K. Okei, M. Tokiwa, S. Tsuji, Y. Yamashita, and I. Yamamoto. Atmospheric muon measurements using the OKAYAMA telescope. 2006. *Nuclear Physics B, Proceedings Supplements.* **151**: 465.

3. Maeda, K.. Energy and zenith angle dependence of atmospheric muons. 1973. *Fortschritte der Physik.* **21**: 113.

4. Nagamine, . {Introductory Muon Science}. 2003.

5. ALVAREZ, LW, JA ANDERSON, ELBEDWE.F, J BURKHARD, A FAKHRY, A GIRGIS, A GONEID, F HASSAN, D IVERSON, G LYNCH, Z MILIGY, AH MOUSSA, MOHAMMED., and L YAZOLINO. SEARCH FOR HIDDEN CHAMBERS IN PYRAMIDS. 1970. *SCIENCE.* **167**: 832.

6. Morris, C.L., C.C. Alexander, J.D. Bacon, K.N. Borozdin, D.J. Clark, R. Chartrand, C.J. Espinoza, A.M. Fraser, M.C. Galassi, J.A. Green, J.S. Gonzales, J.J. Gomez, N.W. Hengartner, A.V. Klimenko, M.F. Makela, P. McGaughey, J.J. Medina, F.E. Pazuchanics, W.C. Priedhorsky, J.C. Ramsey, A. Saunders, R.C. Schirato, L.J. Schultz, M.J. Sossong, and G.S. Blanpied. Tomographic imaging with cosmic ray muons. 2008. *Science & Global Security.* **16**: 37.

7. Broughton, J.M., P. Kuan, D.A. Petti, and E.L. Tolman. A scenario of the Three Mile Island Unit 2 accident. 1989. *Nuclear Technology.* **87**: 34.

8. Wada, T., A. Iyono, T. Katayama, S. Lan, T. Nakatsuka, K. Okei, M. Tokiwa, S. Tsuji, Y. Yamashita, and I. Yamamoto. Atmospheric muon measurements using the OKAYAMA telescope. 2006. *Nuclear Physics B, Proceedings Supplements.* **151**: 465.

9. Maeda, K.. Energy and zenith angle dependence of atmospheric muons. 1973. *Fortschritte der Physik.* **21**: 113.

10. Nagamine, K., M. Iwasaki, K. Shimomura, and K. Ishida. Method of probing inner-structure of geophysical substance with the horizontal cosmic-ray muons and possible application to volcanic eruption prediction. 1995. *Nuclear Instruments & Methods in Physics Research, Section A (Accelerators, Spectrometers, Detectors and Associated Equipment).* **356**: 585.

11. Nagamine, . {Introductory Muon Science}. 2003.

12. ALVAREZ, LW, JA ANDERSON, ELBEDWE.F, J BURKHARD, A FAKHRY, A GIRGIS, A GONEID, F HASSAN, D IVERSON, G LYNCH, Z MILIGY, AH MOUSSA, MOHAMMED., and L YAZOLINO. SEARCH FOR HIDDEN CHAMBERS IN PYRAMIDS. 1970. *SCIENCE.* **167**: 832.

13. Morris, C.L., C.C. Alexander, J.D. Bacon, K.N. Borozdin, D.J. Clark, R. Chartrand, C.J. Espinoza, A.M. Fraser, M.C. Galassi, J.A. Green, J.S. Gonzales, J.J. Gomez, N.W. Hengartner, A.V. Klimenko, M.F. Makela, P. McGaughey, J.J. Medina, F.E. Pazuchanics, W.C. Priedhorsky, J.C. Ramsey, A. Saunders, R.C. Schirato, L.J. Schultz, M.J. Sossong, and G.S. Blanpied. Tomographic imaging with cosmic ray muons. 2008. *Science & Global Security.* **16**: 37.

Measurement of Transverse Single-Spin Asymmetries of Neutral Pion and Eta Meson Production in Polarized p+p Collisions Using the PHENIX Detector at RHIC

Melynda L. Brooks
20090498PRD2

Introduction
Dr. Aidala performs data analysis on data collected by the PHENIX detector at the Relativistic Heavy Ion Collider (RHIC) at Brookhaven National Laboratory for polarized proton-proton collisions. The purpose of her data analysis is to try to shed light on how the proton's spin - a fundamental property of the proton - is formed. It was originally thought that the three constituent quarks' spin (up, up and down) would completely determine the spin of the proton. However, data collected to date have shown that the constituent quarks can only account for approximately 20-30% of the proton's spin. The remaining portion is assumed to come from the sea of quarks and gluons which bind the quarks together, or from an intrinisic angular momentum carried by the proton. By colliding polarized protons on polarized protons and carefully measuring any asymmetry in particles produced, the contributions of the sea quarks and gluons can be extracted. Dr. Aidala has been looking at pion and eta production in the forward direction (near the direction of the colliding particles) and looking at asymmetries that are produced when the protons are polarized transversely with respect to the beam direction. These asymmetries can be related back to the quark and gluon contributions to the proton spin, and can also potentially be related back to the angular momentum. Since quark contributions have already been measured, the gluon contributions can then be extracted. With this new data, important new constraints are expected to be placed on the proton spin contributions. In addition to analysis work, Dr. Aidala has been making significant contributions to the construction of a silicon upgrade detector which will be added to the PHENIX detector to enhance the detector's ability to carry out heavy quark measurements.

Benefit to National Security Missions
This project will support the DOE missions of the Office of Science by enhancing our understanding of the origin of the proton's spin, and adding detector capabilities to the RHIC PHENIX detector, which will also gather data to study the Quark Gluon Plasma. The underlying detection science and technology builds capability for nuclear detection, e.g. for the nuclear nonproliferation mission.

Progress
Over the past year Christine has continued her focus on the nucleon structure program at PHENIX as well as the P-25 PHENIX team's efforts on the E906/SeaQuest experiment at Fermilab.

Several papers related to eta meson production on which Christine was working last year have now been published. She was a key contributor to a PHENIX paper on the eta meson cross section at midrapidity, the eta/pi0 production ratio, and the double-helicity asymmetry in eta production. The latter is sensitive to the gluon spin contribution to the spin of the proton. The eta cross section results in this PHENIX paper were used by Christine and four other authors to extract the fragmentation functions for eta production, previously unavailable in the published literature. The eta fragmentation function paper and the PHENIX eta paper were published simultaneously in Physical Review D. The availability of eta fragmentation functions allows a variety of theoretical calculations of eta production to be performed, including the transverse single-spin asymmetry in forward eta production, one of her continuing analysis focuses. This measurement provides sensitivity to quark and gluon dynamics inside transversely polarized protons. The transverse single-spin asymmetry in forward eta production was released as a PHENIX preliminary result at the Particles and Nuclei International Conference (PANIC) in Cambridge, Massachusetts in late July, for which Christine was on the Program Committee. The result was shown by University of California at Riverside graduate student David Kleinjan, with whom she has been working on this analysis. She has now started working with David on a measurement of the cross section for eta meson production in the same kinematic region covered by the released asymmetry measurement.

Another PHENIX paper to which Christine contributed significantly was on the transverse single-spin asymmetry in J/Psi meson production, sensitive specifically to gluon dynamics within transversely polarized protons. She was involved in this work with several other

LANL collaborators, who were key contributors to the data analysis. She took responsibility for developing the physics discussion in the paper, which has now been published in Physical Review D.

In 2006 PHENIX took a limited data set with polarized proton-proton collisions at a center-of-mass energy of 62.4 GeV, significantly below the energies of 200 and 500 GeV for proton collisions usually run at the Relativistic Heavy Ion Collider (RHIC). This energy is of interest because it falls in between the energy range of typical fixed-target experiments, where perturbative quantum chromodynamics (pQCD) calculations at next-to-leading order in the strong coupling fail to describe the data, and higher collider energies, where next-to-leading-order pQCD calculations describe the data successfully. Working closely with graduate student Amaresh Datta of the University of Massachusetts at Amherst, she has measured the cross section for charged hadron production at 62.4 GeV, which was released as preliminary and shown by Christine at the SPIN 2010 conference in Juelich, Germany in October 2010. She and Amaresh have also measured the double-helicity asymmetry of charged hadrons at this energy, extending the kinematic coverage of RHIC measurements sensitive to the gluon polarization in a longitudinally polarized proton. She is working with Amaresh on a PHENIX paper draft including both of these measurements from this intermediate-energy data set, the manuscript for which will be released next week to the collaboration for review.

In addition to her PHENIX data analysis and paper preparation work, Christine has continued supporting LANL's hardware responsibilities for PHENIX over the past year, working on assembly of the Forward Silicon Vertex Tracker, to be installed by the end of 2011, and providing six weeks of operations support for the Muon Tracker during the 2011 operations period.

The E906/SeaQuest experiment at Fermilab is expected to start taking commissioning data by the end of this year. Efforts so far have focused on building and preparing the detector for beam. Christine has made several trips to Fermilab over the past year to help build and instrument the Station 4 Tracker, for which LANL is responsible.

Future Work

Dr. Aidala will finalize her preliminary measurements of the transverse single-spin asymmetry of eta meson production in the RHIC PHENIX proton-proton data sets, via its decay to two photons. The asymmetry measurements extend previous work on the transverse spin structure of the proton and transverse-momentum-dependent distributions, which are sensitive to the intrinsic motion of quarks and gluons, and will provide essential data to continue fueling the rapid advance of the study of the origin of the proton's spin. She will also perform work to measure the cross section for eta production in proton-proton collisions, which will not only support her spin asymmetry studies but will

also serve as critical baseline measurements to compare to the deuteron-gold results in search for gluon saturation effects in heavy nuclei.

Conclusion

Dr. Aidala has made significant contributions to four new publications over the last year which provide new constraints on the origin of the proton's spin. The origin of the proton's spin is a basic scientific question which has yet to be understood based on data collected to date, and answering this will improve our understanding of one of the most fundamental building blocks of nature. Dr. Aidala's work on the silicon detector will help the detector construction to be completed and installed at BNL this summer.

Publications

Adare, A.. Measurement of neutral mesons in p+p collisions at √s = 200 GeV and scaling properties of hadron production. 2010. *Physical Review D.* **D83** (052004): 0.

Adare, A., and E. Tal. Double helicity dependence of jet properties from dihadrons in longitudinally polarized p+p collisions at sqrt(s) = 200 GeV. 2010. *Physical Review D.* **D81** (012002): 1.

Adare, A., and E. Tal. Transverse momentum dependence of η meson suppression in Au+Au collisions at √sNN = 200 GeV. 2010. *Physical Review C.* **82**: 011902.

Adare, A., and E. Tal. Measurement of transverse single-spin asymmetries for J/Ψ production in polarized p+p collisions at √s = 200 GeV. 2010. *Physical Review D.* **D82** (112008): 0.

Adare, A., and E. Tal. Cross section and double helicity asymmetry for eta mesons and their comparison to neutral pion production in proton-proton collisions at √s = 200 GeV. 2011. *Physical Review D.* **D83** (032001): 00.

Aidala, C. A., F. Ellinghaus, R. Sassot, J. P. Seele, and M. Stratmann. Global analysis of fragmentation functions for eta mesons. 2011. *Phys. Rev. D.* **D83** (034002): 0.

Exploring the Expanding Universe and the Nature of Dark Energy

Przemyslaw R. Wozniak
20090521PRD2

Introduction

In 1998, two independent teams measuring light from distant supernovae made an extraordinary discovery: the expansion of the Universe is accelerating. In the last 10 years, this discovery has been confirmed by completely different measurements of the large-scale distribution of galaxies in the Universe, of the cosmic microwave background radiation, and by measuring the abundance of clusters of galaxies in the Universe. The cause of the accelerating expansion is completely unknown, and understanding this cause is the major field of research in cosmology. The aim of the current project is to characterize the nature of dark energy with special emphasis on the dark energy equation of state. Currently, a cosmological constant is consistent with all measurements, but its size is in contradiction with the Standard Model of particle physics by ~100 orders of magnitude. In order to exclude a cosmological constant, the dark energy equation of state would have to be a dynamical quantity. In this project, three major research directions are investigated: (i) How can we extract a time variation in the dark energy equation of state from current and upcoming data in a model-independent way? (ii) What would be the observational signatures of an early dark energy scenario, which would point to different physics than a cosmological constant? (iii) How can we distinguish dark energy from a modification of gravity on the largest scales? The project makes use of sophisticated statistical methods, simulations, and publicly available data.

Benefit to National Security Missions

This project will support the DOE mission of the Office of Science and NASA which have made unraveling the secrets of dark energy one of their top priorities. In addition, as part of this project new statistical methods will be developed which will be important for our national security mission in general.

Progress

During FY 2011 postdoc Ujjaini Alam worked primarily on further development of statistical methods for analyzing cosmological observations with statisticians and cosmologists at LANL and UC Santa Cruz. They used a Gaussian Process Modeling formalism to analyze supernova Type Ia data and reconstruct the equation of state of dark energy. Their study found that the method is unbiased and able to accurately reconstruct both constant and variable equation of state dark energy models. In a paper published in Phys.Rev.Lett. 105:241302, 2010, the team showed that the current data are compatible with the cosmological constant model for dark energy. In another paper Phys.Rev.D 82:103502, 2010 they predicted that with data available from future surveys such as WFIRST, we can strongly constrain the true nature of dark energy as well as discriminate different physical models of dark energy. Further work was done on the non-parametric reconstruction of dark energy using diverse datasets and published in Phys.Rev.D 84:083501, 2011. In this paper Baryon Acoustic Oscillations and Cosmic Microwave Background data were used to deconstruct the degeneracy between different cosmological parameters. The main result is that using these diverse datasets results in a strong constraint on the equation of state of dark energy, Figure 1.
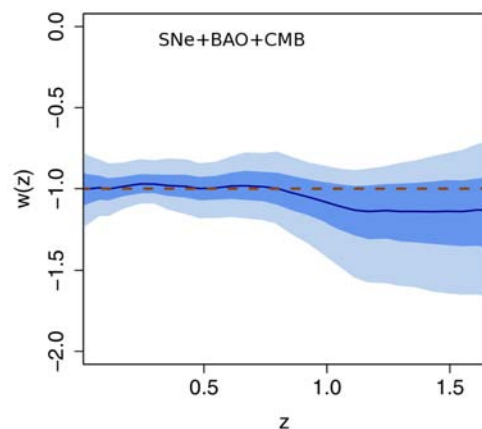
Figure 1. Constraints on the equation of state of dark energy w versus redshift z based on Supernovae, Baryon Acoustic Oscillations and Cosmic Microwave Background data. The dashed line shows the underlying theoretical model, the dark blue region shows the 68% confidence level, the light blue region shows the 95% confidence level, and the dark blue line shows the mean reconstructed history.
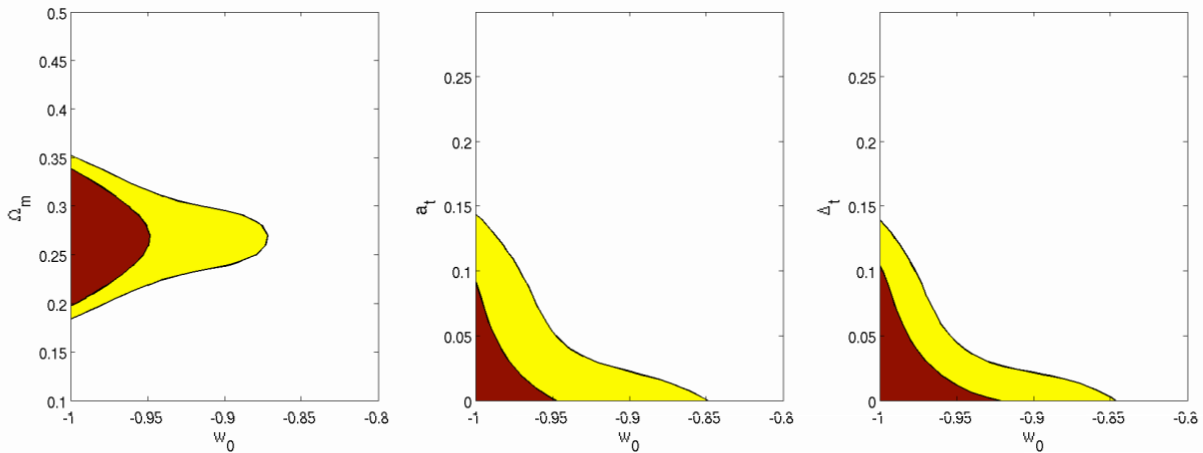
Figure 2. Predicted constraints on cosmological parameters from a full joined analysis of future large scale structure and CMB data. Contours are shown for 95% (red) and 68% (yellow) confidence levels. From left to right: 1) mean density of matter in the Universe, 2) scale factor at the time of transition between the present and the matter dominated equation of state, 3) width of transition in scale factor.

We expect to take this formalism further by using it to investigate different possible redshift distributions and controls of systematics for dark energy surveys in order to predict which configuration would yield the richest information on the nature of dark energy. In a separate project with other post-doctoral researchers at LANL, Ujjaini attempted to put constraints on a theoretical model of dark energy in which dark energy is non-negligible at early times. These early dark energy models are difficult to constrain using traditional background expansion observations such as supernova Type Ia, since at late times, they mimic the cosmological constant and therefore cannot be distinguished from it. In an Astrophys.J. paper 727:87,2011, we showed that using the perturbative history of the universe as encoded in large scale structure observations such as the Sunyaev-Zeldovich power spectrum, and galaxy halo mass function, we may differentiate these models from the cosmological constant up to redshifts of ~5 (Figure 2 shows the constraints on cosmological parameters from a full analysis of future large scale structure and CMB data). This result, in conjunction with future accurate observations of the CMB and supernovae, can rule out these models to a high degree of accuracy. This work is being further explored with Z. Lukic and K. Borodzin at LANL by consistently using dark energy perturbations in non-linear growth of structure simulations. Further work has been started on this with S. Bhattacharya and D. Nagai at the University of Chicago to extend the formalism to newly available SZ data. In March, 2011 Ujjaini visited and gave a seminar at the Institut de Recherche en Astrophysique et Planetologie, in Toulouse, France to facilitate collaborations with Alain Blanchard and Roser Pello, who are experts in the field of X-ray and optical observations of large galaxies. This team is now proceeding with a collaborative project to study modified gravity models of dark energy using X-ray observations, using data from e-Rosita and Chandra

XMMS. In August-September 2011 she visited the Institut d'Astrophysique in Paris, and the Institut de Recherche en Astrophysique et Planetologie, in Toulouse, France and gave seminars on this work. At that meeting Ujjaini also joined the theory working group of EUCLID survey, which will be studying the impact of the mission on our knowledge of dark energy.

Future Work

This project targets the characterization of dark energy. Currently, the accelerated expansion of the Universe can be explained by introducing a cosmological constant into Einstein's theory of general relativity. A cosmological constant has several theoretical problems: the origin is unclear and the prediction for such a term from the Standard Model of particle physics is ~100 orders of magnitudes different from what we observe. In order to disprove a cosmological constant, the first step is to find a time-dependence in the dark energy equation of state. The first major aim of this project is to develop a new way to constrain such a time dependence in a non-parametric way. This approach has to be applied to supernova measurements as well as large-scale structure probes. Currently, the dark energy equation of state is most commonly parametrized by a two-parameter fit which is too restrictive for gaining a deeper understanding of a possible deviation from a cosmological constant. The second major aim of the project concerns the investigation of early dark energy models and their imprints on current and future cosmological observations. The first step here is to characterize such imprints and to develop a strategy to disentangle them from other effects. Once a unique characteristic has been identified and maybe seen in observations, early dark energy models would replace the simple assumption of a cosmological constant. The third major part of this project concerns the question of how to distinguish a dark energy from modification of

general relativity on largest scales. If this turns out to be the reason for the accelerated expansion of the Universe, it would disprove the existence of a cosmological constant. Therefore, a major aim of our project is to find unique signatures in cosmological measurements that can distinguish these scenarios.

Conclusion

During this project a new non-parametric way for characterizing the dark energy equation of state will be developed, early dark energy models and their imprints on observations investigated, and modifications of general relativity on very large scales will be confronted with current observational data. This project will advance our understanding of the nature of dark energy, which makes up 70% of the content of the Universe and is one of the biggest puzzles in science today. Large billion dollar national and international programs are devoted to understanding the origin of dark energy.

Publications

Alam, U.. Constraining perturbative early dark energy with current observations. 2010. *Astrophysical Journal.* **714** (2): 1460.

Alam, U., Z. Lukic, and S. Bhattacharya. Galaxy clusters as a probe of early dark energy. 2011. *The Astrophysical Journal.* **727**: 87.

Holsclaw, T., U. Alam, B. Sanso, H. Lee, K. Heitmann, S. Habib, and D. Higdon. Nonparametric dark energy reconstructing from supernova data. 2010. *Physical Review Letter.* **105**: 241302.

Holsclaw, T., U. Alam, B. Sanso, H. Lee, K. Heitmann, S. Habib, and D. Higdon. Nonparametric reconstruction of the dark energy equation of state. 2010. *Physical Review D.* **82**: 103502.

Pan, A. V.. Reconstructing dark energy: A comparison of different cosmological parameters. 2011. *Physical Review D.* **84**: 083501.

Extra-Long-Range Energy Transfer in Hybrid Semiconductor-Metal Nanoassemblies

Victor I. Klimov
20100599PRD1

Introduction

In this project, we are studying the effect of surface plasmons (SPs) on dipole-dipole energy transfer (ET) in assemblies of semiconductor nanocrystals. Since SPs are characterized by a large oscillator strength and a significant spatial extent of the electric field, coupling to plasmons increases both the rate and the range of ET. In one example, we are studying directional transfer in quantum-dot bi-layers that are combined with metal nanoparticles. We will also investigate the regime of nonlinear transfer where SPs will be used to facilitate a simultaneous transition of excitons from two donor nanocrystals to a single acceptor quantum dot. We expect that this work will be the first unambiguous demonstration of SP-enhanced ET. The observation of robust long-range exciton migration would suggest the possibility of new strategies for light harvesting in photovoltaics, such as using multilayer ET cascades. Plasmon-enhanced ET in nanocrystals is also the first step towards realizing excitonic circuitry, where light may be used, e.g., to perform computations. These results will motivate the study of other more complex phenomena such as SP-assisted nonlinear ET, which could enable active elements of excitonic circuits.

Benefit to National Security Missions

The work conducted in this project is relevant to LANL and DOE interests in both world-class fundamental science and strategic applications. Successful implementation of new strategies for energy transport in hybrid semiconductor/metal assemblies can yield solar-energy-conversion technologies relevant to DOE and LANL missions in Energy Security. At the recent DOE workshop on Basic Research Needs for Solar Energy Utilization, it was recognized that while solar photovoltaics are an important clean energy source, the practical large-scale applications of solar cells would require new concepts and novel materials for solar energy conversion. A novel concept of hybrid semiconductor/metal nanostructures that is explored in this project can potentially help in the realization of such breakthrough technologies that combine low fabrication costs with high power conversion efficiencies.

Progress

The focus of our studies over the past year has been on the spectroscopic characterization of hybrid semiconductor-metal nanostructures. Using a base catalyzed hydrolytic procedure, we were able to prepare superstructures with independently tunable plasmon and excitonic components that may be located in any spectral region from the ultraviolet to the Mid-infrared. We make an accurate determination of the coupling between the plasmonic and the excitonic components of these materials through two-photon absorption spectroscopy. In samples where the plasmon position was optimally tuned to the wavelength of the incoming excitation, two-photon crosssections of these superstructures were determined to be almost 100 fold higher than the cross sections observed for bare QDs.

We also studied the possibility of driving two-photon nonlinearities in the low fluence regime. Two-photon absorption requires the concurrent incidence of two photons at the absorber. This stringent requirement implies that for most systems, two-photon absorption may only be observed when samples are illuminated by very short light pulses. A possible alternative is to utilize energy transfer to accomplish the same ends. In our proposed scheme, a low energy donor and a higher energy acceptor are held in close proximity. The assembly is irradiated with low energy photons that may only be absorbed by the donor and not by the acceptor. Nonlinear "uphill" transfer may occur after the arrival of a second photon in a previously excited assembly. Given its weak dependence on simultaneous photon arrival, nonlinear transfer may be readily distinguished from other nonlinearities by studying the process efficiency as a function of the pulse-length. For typical nonlinearities, the nonlinear signal falls linearly with increasing pulse length. In contrast, for nonlinear transfer, the signal is independent of the pulse length for pulses much shorter than the QD lifetime. This measurement enabled us to unambiguously detect the presence of nonlinear energy transfer. Our current measurements suggest that this process has an efficiency comparable to that of direct two photon absorption for picosecond pulses, while it is 10^3 times

more efficient than two-photon absorption for nanosecond long pulses.

In order to further boost the efficiency of this process, we also studied the properties of metal QD assemblies. It was observed that in an appropriately designed assembly, a metal plasmon may increase the rate of energy transfer between quantum dots to compete with biexciton decay. In this situation, excitons are rapidly funneled into the reddest members of the ensemble, akin to light harvesting architectures in plants.

Future Work

- Enhancing the rate of nonlinear transfer, study of its feasibility in light harvesting applications.

- Further spectroscopic studies of NC-metal hybrids: Multiexciton recombination, relaxation, emission etc.

- Development of active devices based on these concepts.

Conclusion

Our measurements have indicated that these structures exhibit clear signatures of nonlinear energy transfer in nanocrystal assemblies. This effect potentially allows a pathway for photovoltaics to harvest sub-bandgap photons, allowing for a route to increasing photovoltaic efficiency above the Shockley-Quiesser limit. Some of these results have been submitted to Nature Communications and others are being finalized for submission.

Publications

Li, L., A. Pandey, D. Werder, B. Khanal, J. Pietryga, and V. Klimov. Efficient synthesis of highly luminescent copper indium sulfide-based core/shell nanocrystals with surprisingly long-lived emission. 2011. *Journal of the American Chemical Society.* **133** (5): 1176.

Perfect Fluidity in Universal Quantum Systems

Joseph A. Carlson
20100606PRD2

Introduction

The ultimate goal of this project is to improve our ability to understand strongly correlated quantum systems. If successful, this project will significantly influence our understanding of physics in a variety of fields, including cold-atom physics, nuclear physics, and condensed matter. It may also lead to valuable insights to advance the prospects for quantum computation.

The project involves large-scale Monte Carlo simulations to evaluate the Feynman path Integrals that describe these systems. We are explicitly focusing on calculations of the dynamic properties, including spin response and viscosity. Several fundamental questions arise in studies of strongly-correlated quantum systems. For example, it has been conjectured that there is a fundamental lower bound on the ratio of viscosity to entropy in any system. Strongly-correlated matter such as cold atoms at unitarity (infinite scattering length) and QCD near the phase transition have the lowest measured values of viscosity over entropy.

While these properties are easy to compute in the weakly-interacting regime using perturbation theory, no clear picture has emerged in the strongly-interacting regime. We will develop advanced computational techniques to look at the linear response of strongly correlated matter, focusing especially on the viscosity of cold atomic gases. We will also calculate other types of linear response, including the RF spectroscopy recently measured in cold fermi atomic gases. These responses also give a picture of the dynamics of these intriguing systems. For example, the radio-frequency response is particularly sensitive to pairing and superfluidity, these systems have the highest known ratio of superfluid gap to Fermi energy and thus are quite different from traditional, or even High-TC, superfluids. If successful, this research could have a broad impact in atomic physics, nuclear physics, and QCD.

Dr. Drut has successfully completed his work on developing the methods for studying viscosity in ultracold atoms. He has used his code to calculate simpler quantities such as the static response. Work on the dynamic correlators, including viscosity, has begun.

Benefit to National Security Missions

This project is directly relevant to the Nuclear Physics office of the DOE Office of Science. Nuclei and cold atoms have some of the largest superfluid (pairing) gaps in all of nature. The ability to calculate dynamic properties of such systems would be very important to low energy nuclear physics (large nuclei, etc.) and also to experimental studies of the quark-gluon plasma at RHIC. Since nuclear physics is an essential component of weapons understanding, this work has long-term consequences for the weapons program. This work may also be relevant to quantum information and quantum computing over the longer term.

Progress

This past year was marked by considerable progress in the construction of computer codes for the calculation of the properties of strongly interacting many-particle quantum systems. The latter are realized in atomic table-top experiments in several laboratories around the world, as well as approximately in nuclei and in the crust of stars.

These codes are important for various reasons. In the first place, they are useful per se as a means to explore properties of many-particle quantum mechanics that are universal. In other words, these calculations allow us to understand multiple systems (from atoms to stars) at the same time, or more specifically, properties of quantum mechanics (which is more than 100 years old) that are still a puzzle. In addition, these codes are the starting point for their nuclear structure counterparts, the main difference being in the form of the interaction between the quantum particles. Finally, we expect these codes to provide accurate results that will become benchmarks for future nuclear structure calculations. Having this information is crucial in the road to understanding nuclei from first principles in a reliable fashion.

Apart from code development, and the adaptation of extant codes to run in LANL machines, we also created new versions that treat two-dimensional systems (currently

realized in various laboratories in the form of atomic "pancakes") as well as the zero-temperature case, both in two and three spatial dimensions. Since the high-temperature behavior of quantum systems is also of interest, especially in the determination of the real temperature of atomic clouds studied in the lab, we developed codes and formalism to perform calculations taking the high-temperature/low-density limit as a starting point.

Extensive testing was done throughout the year, some of which led to the first determination of the so-called "contact", which is a central quantity characterizing strongly interacting quantum gases. Our results where published in Physical Review Letters.

The nature of the computational methods we are using, namely Quantum Monte Carlo, has allowed us to create a database, such that new quantities can be computed without completely rerunning the calculation, which could take weeks each time. We have spent the last few months creating a thorough database, and we expect to make extensive use of it in the coming months and years, particularly toward studying the hydrodynamics of strongly interacting matter. It should be pointed out that this database could potentially be used by other groups.

In a separate line of research, we have continued our efforts to adapt state-of-the-art quantum chemistry methods, used to calculate the electronic structure of atoms and molecules, to treat the internal structure of nuclei. These methods, which go by the umbrella name of "orbital-based density functional theory", have had considerable success in linking electronic structure directly to the Coulomb interaction, in what we call an ab initio or first-principles manner. In a first step toward the nuclear case, we studied a hypothetical toy system made of a small number of neutrons (also known as neutron drops), testing two- and three-neutron forces, which are in many ways different from the Coulomb force between electrons. This first test was highly successful, and we concluded that the "orbital-based" route to nuclear structure is quite promising. Because the nuclear interaction is much richer than its chemical counterpart, further exploration is needed to push the boundaries of the method and make it fully functional for the nuclear case.

Apart from the actual research work outlined above, over 15 oral and poster presentations were given at various universities and national laboratories in the US and in Europe.

Future Work
Considerable progress has been achieved in calculating the static properties of the unitary Fermi gas and related systems, and in setting up the codes for the calculation of dynamic properties. Through a combination of advanced algorithms and improved computer implementations, the codes can now treat lattices of up to length 18 in each spatial direction and approximately 500 in the temporal direc-

tion. Calculations of static quantities are being completed; including the equation of state, the short-range physics embodied in the contact, and other quantities.

During the last year of this project, we intend to compute dynamic quantities including the spin response and the viscosity. This will be an extraordinarily challenging task, but it is of fundamental importance to many aspects of physics, including cold atom gases and the quark-gluon plasma explored at the RHIC facility at Brookhaven.

Conclusion
We are attempting to calculate dynamic properties of strongly-interacting quantum systems from first principles. We intend to calculate linear response, including the shear viscosity, of cold Fermi gases at unitarity. This is an extraordinary challenge, but if successful could build important new computational capabilities in nuclear, atomic, and high-energy physics.

Publications
Drut, J. E., R. J. Furnstahl, and L. Platter. Toward ab initio density functional theory for nuclei. 2010. *Progress in Particle and Nuclear Physics.* **64**: 120.

Drut, J. E., T. A. Lahde, and T. Ten. Momentum Distribution and Contact of the Unitary Fermi Gas. 2011. *Physical Review Letters.* **106**: 205302.

Drut, J. E., and L. Platter. Exact-exchange density functional theory for neutron drops. 2011. *Physical Review C.* **84**: 014318.

Wendt, K. A., J. E. Drut, and T. A. Lahde. Toward large-scale Hybrid Monte Carlo simulations of the Hubbard model on graphics processing units. 2011. *Computer Physics Communications.* **182**: 1651.

Search for CP and CPT Violation in the Neutrino Sector

William C. Louis III
20100607PRD2

Introduction

This project is designed to search for violations of some of the fundamental symmetries of nature. Such a discovery would be evidence for physics beyond the current, standard model. We are looking for CP and CPT violation in neutrinos, where C stands for charge conjugation, P for parity inversion, and T for time reversal. Such a violation would have an enormous impact on nuclear and particle physics because it could possibly explain the matter-antimatter asymmetry in the universe. After the Big Bang, the universe was presumably symmetric in terms of matter and antimatter. However, the universe we observe today consists almost entirely of matter. What has caused this matter-antimatter asymmetry? One possible explanation involves leptogenesis, where a lepton asymmetry in the early universe gets translated into a baryon (or matter) asymmetry. CP or CPT violation in the neutrino sector could then explain how the lepton asymmetry is generated. CP violation will be searched for by looking for a difference between electron-neutrino appearance and anti-electron-neutrino appearance in data from the SciBooNE, MiniBooNE, MicroBooNE, and IceCube experiments. CPT violation will be searched for by looking for a difference between muon-neutrino disappearance and anti-muon-neutrino disappearance.

Benefit to National Security Missions

This work addresses one of the major questions in nuclear, particle, astrophysics, and cosmology, which is the origin of the baryon asymmetry of the universe. A sensitive search for CP and CPT violation can be performed by looking for a difference between neutrino and antineutrino oscillations. Therefore, this work is of great benefit to the Department of Energy Office of Science.

Progress

During the past year, Warren Huelsnitz has successfully analyzed the MiniBooNE data for disappearing muon neutrinos and antineutrinos (numus and numubars). He is now working on an of the SciBooNE and MiniBooNE data. This will provide a much more sensitive test for numu and numubar disappearance and for CPT violation in the lepton sector. In addition, he is analyzing the IceCube atmospheric neutrino data for numu and/or numubar disappearance. At these high energies (~1 TeV), numubar disappearance into sterile neutrinos would be greatly enhanced by a well-known effect (MSW). Therefore, somewhat surprisingly, IceCube is quite sensitive to numubar disappearance at ~1 eV^2 and will be able to test for the existence of additional, sterile neutrinos. Results from these analyses are expected in the next 6-9 months.

Future Work

This project will search for evidence of CP and CPT violation in the neutrino sector, where C stands for charge conjugation, P for parity inversion, and T for time reversal, by using results from the SciBooNE, MiniBooNE, MicroBooNE, and IceCube experiments. SciBooNE is located at a distance of 100 meters from the Booster neutrino source at Fermilab, while MiniBooNE is located at a distance of 500 m. By comparing neutrino and antineutrino event rates in the two detectors, a sensitive search for CPT violation can be made. Therefore, our first goal was a search for CPT violation in the neutrino sector. The second goal is to analyze the atmospheric neutrino data from the IceCube experiment, which has sensitivity to neutrino oscillations at ~1eV^2. The third task is to help with the design and development of a new data acquisition system for the MicroBooNE experiment, which will determine whether the low-energy excess observed by MiniBooNE in neutrino mode is due to electron events or gamma events. If the excess is due to electron events, then this will open up the possibility of observing CP violation with the MiniBooNE experiment. Therefore, the third goal is to help design a data acquisition system for MicroBooNE.

Conclusion

This scientific effort will search for a difference between neutrino and antineutrino oscillations. Such a difference would be extremely important because it could possibly explain the reason why the universe we observe today consists almost entirely of matter and not antimatter, even though the universe presumably began with the Big Bang and with an equal amount of matter and antimatter. Therefore, this scientific effort may be able to provide an explanation for why we exist today.

Seeing the Invisible: Observational Signatures of Dark Matter

Alexander Friedland
20100608PRD2

Introduction

We see countless stars by naked eye and myriad of galaxies with powerful telescopes. However, we now have good evidence that the majority of the universe is actually made of an invisible substance called dark matter. Without the gravitational pull of dark matter, many stars would not stay in their orbits around galaxies. Many fewer galaxies would exist to harbor stars since galaxies are made from ordinary matter falling in regions of the Universe with high dark matter density. In addition, dark matter together with dark energy plays a key role in determining the fate of the Universe–whether it will keep expanding forever or eventually collapse back onto itself. Despite its importance, we know very little about the identity and properties of dark matter since it does not emit light. Resolving the mysteries of dark matter is one of the utmost challenges in fundamental physics.

A promising approach to detect dark matter is based on the fact that while dark matter particles do not emit ordinary light, they can still produce visible signatures through decaying or annihilating with other dark matter particles. Dr. Yuksel has been investigating the signatures of dark matter annihilation or decay products such as gamma rays, neutrinos, or anti-matter particles and make robust predictions for the experiments and observations. One major aim of his work is to incorporate his results into a broader picture of astrophysics, cosmology and physics beyond the Standard Model. Dr. Yuksel is a recognized world leader in this area. Among his many contributions is a seminal paper on pulsars as being the sources of the excess signal seen at Fermi and PAMELA experiments. His scientific leadership has been recognized by the LANL postdoc committee, which awarded him the Director's Postdoctoral Fellowship for this work.

Benefit to National Security Missions

One of the very high priorities of the DOE Office of Science (the High Energy Office) is detection and identification of dark matter. This requires understanding of the physical properties of dark matter such as its mass and self-annihilation cross-section into standard model particles and requires multi disciplinary studies. LANL has been involved in development of detectors for the direct detection of dark matter in underground experiments. Supercomputing simulations of dark matter performed at LANL have been recognized for two decades as world-leading. LANL has been making a considerable investment in the areas cosmic rays, particularly the Milagro experiment and the ongoing HAWC experiment. LANL also has a very strong program on simulations of magnetic fields in galaxy clusters and radio lobes of active galactic nuclei. The work of Dr. Yuksel outlined in this progress report and follow up projects on variety of open problems in particle astrophysics will strengthen all these areas and, importantly, will help to integrate them.

Progress

Dr. Yuksel has been pursuing studies of dark matter and neutrinos as outlined in his research proposal since the beginning of his employment at LANL. The primary goal of his research is to understand what dark matter is composed of and where it exists in the universe. Dr. Yuksel has presented part of his research in a poster entitled "The Centaurus A Ultrahigh-Energy Cosmic Ray Excess and The Local Intergalactic Magnetic Field" during 2011 LANL LDRD Day. He has also participated number of relevant workshops such as INFO 2011 in Santa Fe and Cosmic Ray Anisotropy Workshop in Madison. These workshops brought together experts from experimental and theoretical particle astrophysics and formed ideal venues to exchange ideas on how to utilize and expend capabilities of experiments such as IceCube, DeepCore, Fermi, Super-K, and KM3Net for the purpose to better scrutinize the theories of dark matter and cosmic rays. Motivated by the challenges and opportunities as identified in these workshops, Dr. Yuksel has been exploring new ideas towards understanding the identity and properties of dark matter and cosmic rays.

Dr. Yuksel has developed a transport code that can handle propagation of charged particles that could arise from either dark matter particles or astrophysical sources with very high accuracy in variety of magnetic

field configurations. This code has been adopted to study cosmic ray electron/positron and proton/nucleon fluxes inside our galaxy as well as extragalactic sources of Ultra-high-Energy Cosmic Rays (UHECRs).

Many dark matter candidates have been proposed, from axions to sterile neutrinos to weakly interacting massive particles spanning many orders of magnitude in particle mass. One may hope to reveal the identity of dark matter by direct detection in underground low background experiments, or through missing energy signals at particle accelerators. A promising alternative approach is based on the fact that dark matter could produce visible signatures through decaying or self-annihilating into photons or standard model particles. The corresponding signals depend on the concentration of dark matter, making precise knowledge of both dark matter distribution and associated astrophysical backgrounds essential. Dr. Yuksel has been investigating the signatures of dark matter annihilation or decay products such as gamma rays, neutrinos or anti-matter particles in order to make robust predictions for the experiments and observations. We are using the particle transport code to investigate and compare astrophysical and exotic (such as dark matter) sources of cosmic rays numerically since analytical prescriptions sometimes fail to correctly describe diffusion of particles (i.e., non relativistic analytical solution to diffusion equation could yield diffusion speed larger than the speed of light).

We also use the same transport code to investigate the implications of UHECR excess from Centarurus A in terms of intervening intergalactic magnetic fields during propagation, and charge, plausible production, acceleration and injection mechanism of the particles. The length of time that the origin of UHECRs has remained a mystery reflects the difficulty in definitively identifying their sources. The Pierre Auger Observatory has recently acquired data needed to achieve this showing a prominent excess of events in the vicinity of Centaurus A, a nearby active radio galaxy possessing well-studied giant radio lobes.

The major difficulty in tracing cosmic rays back to their sources is the uncertain nature of the magnetic fields permeating the intergalactic space in the vicinity of the Milky Way. Figure 1 shows a slice from the magnetic field configuration used in our study, which is obtained using a Kolmogorov turbulence spectrum on a cubic grid of size of 512^3. The deflections of UHECRs during propagation from their source to the observer depend on both any magnetic fields they encountered and their charge/momentum. Figure 2 illustrates stronger deflections experienced by low energy particles compared to high energy particles in a given magnetic field configuration.

In Figure 3, we compare the observed distribution of the extreme energy UHECR events with the expectations from UHECR propagation in a turbulent field. In order to understand the angular distribution of UHECR events from the

direction of Centaurus A, we first look for a range of magnetic field parameters for which a spread that averages 10 degree results for 60 EeV particles. We find that the overall angular distribution of UHECRs can be well reproduced only for certain ranges for the strength (B >10 nG) and the structure (coherence length < 1 Mpc) of the local intergalactic magnetic field.
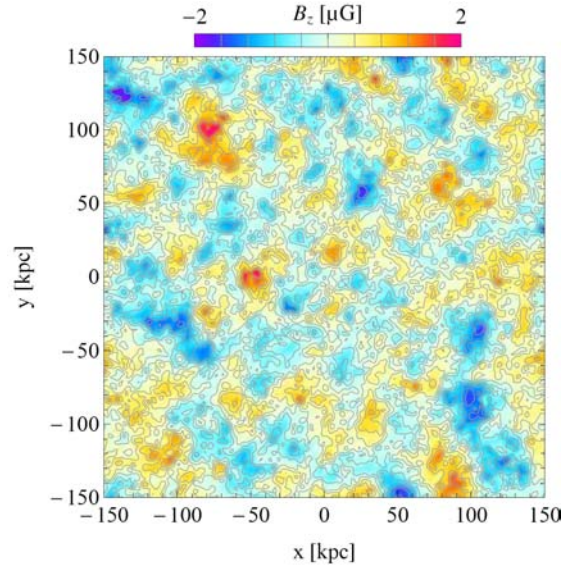
Figure 1. A slice from the magnetic field configuration used in our studies. Shown is the z component of the field in the x-y plane, obtained using a Kolmogorov turbulence spectrum within a cubic grid of size of 512^3.
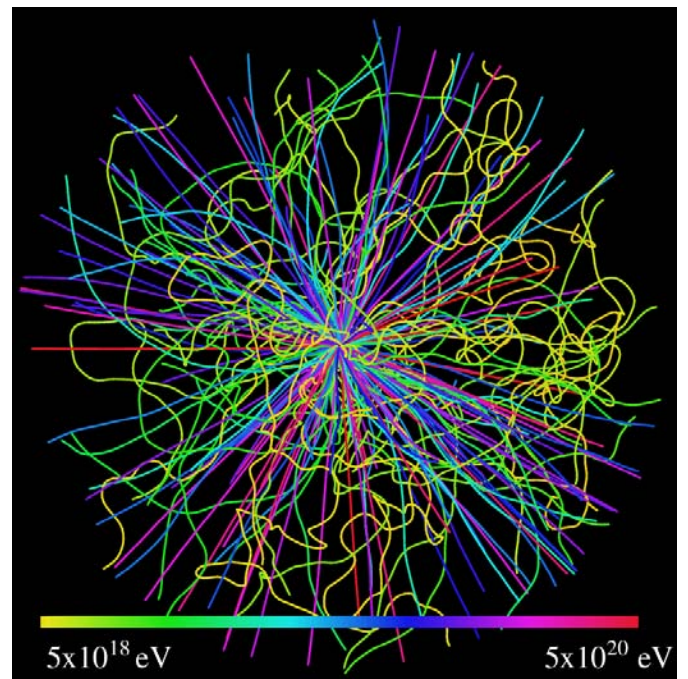
Figure 2. Trajectories of UHECRs (colored according to their energies) as they leave the source and propagate through the intergalactic magnetic field. Lower energy particles experience much stronger deflections compared to higher energy particles.
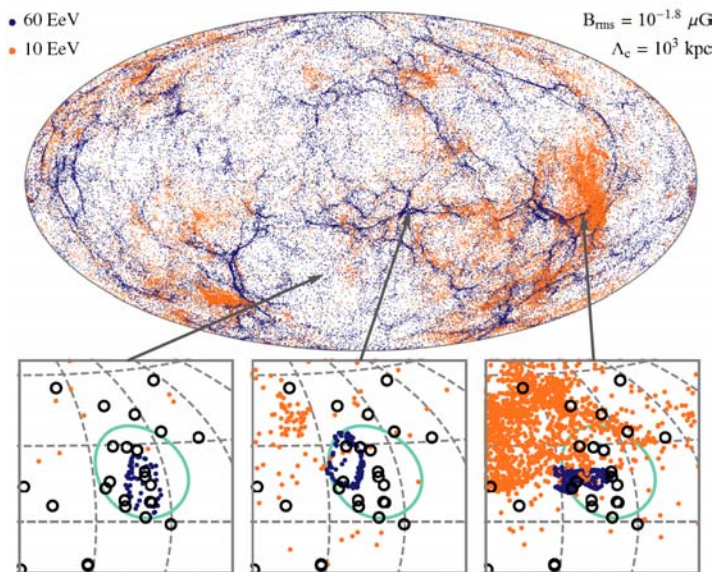
Figure 3. Top: Sky map of particles from the viewpoint of Centaurus A obtained using our model of magnetic field structure for populations of cosmic rays with two different energies (blue and orange dots). Bottom Panels: Three characteristic realizations of UHECR angular distributions arriving from Centaurus A, chosen from locations in the map above (as marked with arrows).

Future Work

It is timely to combine different parts of the dark matter puzzle, taking into account all new data and observations together with their astrophysical interpretations, in order to provide better guidance for relevant experimental and theoretical efforts. This has been the main guiding principle of the research outlined in this progress report. In the future, we hope to incorporate our conclusions into a broader picture of astrophysics, cosmology and physics beyond the Standard Model and help to integrate the results from the direct detection experiments, indirect detection experiments, and supercomputer simulations of dark matter.

Conclusion

Successful accomplishment of this proposed research will enable better discrimination of the candidate theories of dark matter, so that researchers could focus their efforts in more promising avenues. While this is a challenging task, it is also feasible as the quality and quantity of data is increasing at an unprecedented rate with new facilities now coming on-line, vastly improving past measurements and reaching never-before probed energy scales. For example Fermi and PAMELA space missions have brought a much greater clarity for the gamma ray and cosmic ray electron/positron observations.

Another aim of our research is understanding the origin of UHECR particles which are up to 10,000,000 times more energetic than what can be achieved in man made accelerators such as Large Hadron Collider (LHC), a particle accelerator located at the European Organization for Nuclear Research (Cern) laboratory in Geneva. Using our particle transport code we study how the local intergalactic fields could alter the distribution of UHECRs around their corresponding sources, which also yields important information about the strength and structure of the intervening magnetic fields.

Publications

Yuksel, H.. Ultrahigh-energy cosmic ray excess and the local intergalactic magnetic field. Invited presentation at *Implications of Neutrino Flavor Oscillations (INFO 11).* (Santa Fe, July 18 - 22, 2011).

Yuksel, H.. The Centaurus A Ultrahigh-Energy Cosmic Ray Excess and the Local Intergalactic Magnetic Field, LA-UR-11-10954. 2011. *LDRD poster session.*

Probing Fundamental Physics with Cosmological Surveys

Michael S. Warren
20100610PRD2

Introduction

The scientific community has reached consensus that the expansion of the universe is accelerating. A mysterious substance dubbed dark energy, thought to comprise about 70% of the total energy density in the universe, drives the acceleration. Over the next decade, the US and other countries will spend billions of dollars on cosmological surveys designed to address perhaps the greatest enigma in physics today: what is the dark energy? Due to the high volume of data, cosmological measurements will be so precise that the predominant uncertainty in addressing this question will be driven by systematic uncertainties stemming from our lack of knowledge in other areas of astrophysics. There are four science goals whose resolution will improve the ability to constrain dark energy:

1. Test for modifications of general relativity

2. Test for non-Gaussian initial conditions at the end of inflation and evidence of primordial gravitational waves, to constrain inflationary models that describe the rapid expansion of the universe just after the big bang

3. Examine more deeply the role of baryonic physics in the formation and shapes of cosmological structures, and what the ultimate fate of the baryons may be

4. Probe the evolution of galaxy morphology, metallicity, gas fraction and stellar mass; in short to develop a better understanding of the physics of galaxy formation

Benefit to National Security Missions

This work directly ties into the standard model for cosmology. It helps us elucidate the essential constituents of our Universe. In addition, the work entails data-intensive computing, with potentially important applications elsewhere.

Progress

Alexia has familiarized herself with the LANL computing system, and is beginning analysis of the large cosmo-logical datasets, which are being produced at LANL. In particular, she is exploring the importance of different halo finders (friends-of-friend and spherical overdensity) on properties of Sunyaev-Zelodovich maps. She has also submitted a paper (as lead author) regarding the physics of one-dimensional gravitating systems.

Future Work

Scientists must design new ways to leverage upcoming cosmological data to explore dark energy, general relativity, inflation, structure formation, and galaxy formation. One robust prediction of cosmological models yet to be constrained observationally is the filamentary cosmic web seen in simulations of structure formation. Filaments are interesting because they govern many aspects of hierarchical structure formation, and are key to understanding how baryons are deposited in galaxies and clusters. The nature of the filamentary structure is sensitive to the behavior of the dark energy. The degree of filamentary structure is also sensitive to the initial conditions at the end of inflation, and may contain evidence of modified gravity and non-Gaussianity. However, filaments are incredibly diffuse and have never been reliably detected with current technology. Upcoming surveys may well provide an opportunity to probe filamentary structure. Alexia will use N-body simulations to develop new cosmological observables and statistics that are sensitive to the same underlying physical processes as filamentary structure itself.

Another arena in Alexia's research is the level of small-scale substructure that exists in galaxies (and especially in the Milky Way). This is of relevance to galaxy formation because surviving substructure is sensitive to the initial distribution of sizes, shapes and orbits of objects accreting onto the galaxy. Substructure is also sensitive to the interplay between barons and dark matter. In hierarchical structure formation, small structures formed earliest when the universe was denser than it is today, therefore they ought to be the densest most bound objects (least affected by tidal stripping when falling into larger halos). On the other hand, the smallest sub-structures fell into the host much earlier than the larger

ones, which enhances the impact of stripping because they have undergone many more orbits, and also because there was less time to fully collapse before they were accreted. Alexia will work to resolve which effects dominate the small scale structure in dark matter halos, which is critical to rate predictions in dark matter detection experiments and helps constrain the influence of baryonic physics on structure formation.

Conclusion

What is the dark energy and dark matter? How are galaxies formed? Alexia will use simulations performed at LANL to address how upcoming surveys, with unprecedented amounts of cosmological data, can be used to investigate these fundamental questions. She will identify astrophysical observables to probe filamentary cosmological structure, as well as small-scale structure inside dark matter halos. These will help illuminate four areas of astrophysics that contribute to our uncertainty about the dark energy, and that are fascinating in their own right; (1) Gravity, (2) Inflation, (3) Baryons and (4) Galaxies. This work will provide observational tests to help bridge the theoretical gaps between cosmology, particle physics, string theory, relativity and astrophysics.

References

1. Schulz, A. E., W. Dehnen, G. Jungman, and S. Tremaine. One dimensional gravitating systems. *Monthly Notices of the Royal Astronomical Society.*

Physics of Cosmic Ray Shocks and the High Energy Universe

Hui Li
20100611PRD2

Introduction

Most matter in space and astrophysical systems (stars, galaxies, solar wind, etc.) are made of plasmas. These plasmas, together with magnetic fields, are often turbulent. The dynamic behavior of the turbulence is still a major mystery. This understanding fundamentally affects our interpretation of space and astrophysical observations and holds the key to many mysteries in space and astrophysical plasmas, such as the production and propagation of cosmic rays. We have developed some very innovative approaches in understanding how turbulence will transfer energy to different length scales and how they will scatter particles and energize them. These studies will provide the physics underpinning for understanding the electron and ion heating in the solar wind and cosmic rays in the interstellar medium.

Benefit to National Security Missions

This research addressed the fundamental question on how magnetohydrodynamic turbulence will behave in various space and astrophysical plasmas, including solar wind and interstellar medium. The tools developed from this study, in addition to the analytic results, will provide the physics underpinning for interpreting space and astrophysical observations. This will contribute the basic science capabilities at the Laboratory. It also provides the necessary physics basis for many problems associated with the Beyond the Standard Model Grand Challenge at LANL. Nuclear weapons themselves involve turbulent plasmas; we build capability for these problems. Understanding the space environment is important for supporting the satellites that are the basis for the nuclear non-proliferation mission.

Progress

Our progress in understanding cosmic ray acceleration and scattering begins with understanding basic underlying processes, i.e. MHD turbulence and scattering. In this respect last year we achieved significant progress in imbalanced MHD turbulence, verifying models with high-resolution numerical simulations.

The basic processes of scattering, i.e. scattering on mirrors and resonant scattering was studied in [1]. We found that resonant scattering on Alfvenic modes is negligible and is easily overcome by mirror scattering. On the other hand, fast mode scattering is supposed to be even more efficient. Our results are, on one hand insightful for understanding the basic properties of scattering, on the other hand, are directly applicable to situations when fast mode is significantly damped due to low collisionality.

We continue to work on acceleration in precursors. With respect to nonlinear small-scale dynamo we were able to measure the fundamental constant of a small-scale dynamo with greater precision and make a stronger claim on its universality. In the Alfvenic regime we were able to resolve the issue of dynamic alignment and measure the Kolmogorov constant of MHD turbulence, which is the first correct measurement of its kind [4]. Speaking of fast mode, which is the most efficient agent for passive scattering of cosmic rays, we developed a new method of mode decomposition based on structure functions, that is superior to previously known methods in that a) it does not rely on a global mean magnetic field for decomposition, b) is much superior to earlier published wavelet method in numerical efficiency that allowed us to analyze and use all the information from currently available highest-resolution simulations (1024^3 - 2048^3). There are ongoing efforts to implement our particle tracing that we used in our earlier simulations to fully relativistic MHD code, written by S.Li. This will allow us to test our previous assertions directly and also extend our study to relativistic turbulence which may be the cause of cosmic ray acceleration in gamma-ray bursts. During this project, our work has resulted in several publications and the results were presented in five invited talks at various conferences.

Dr. Beresnyak will be on leave of absence for one year, from June 1, 2011 to May 31, 2012. He has been awarded a Humboldt Research Fellowship in Germany during that time.

Future Work

To understand how magnetohydrodynamic (MHD)

turbulence evolve and affect the plasma dynamics, we will use large-scale numerical simulations combined with analytical studies to cover the scale separation between numerical simulations and realistic physical parameters (such as those in solar wind and the interstellar medium). Specifically, we will study the dynamic behavior of MHD turbulence both upstream and downstream of a shock that is modified by cosmic rays. In order to self-consistently address the problem of MHD flow coupled to the energetic particles, we will use the diffusion approximation for the particles and the corresponding small-scale MHD fluctuations will be calculated analytically on the basis of turbulent cascade. Supercomputing resources will be used to simulate such coupled systems.

Conclusion

We will use our newly developed MHD simulation tools, together with the analytic theory we have completed, to study how shocks in space and astrophysical plasmas can excite turbulence and, at the same time, being modified by the same turbulence. We expect to explore how much energy particles will gain through interactions with the MHD turbulence.

References

1. Beresnyak, A., H. Yan, and A. Lazarian. Numerical Study of Cosmic Ray Diffusion in Magnetohydrodynamic Turbulence. 2011. *Astrophysical Journal.* **728**: 60.

2. Beresnyak, A.. Spectral Slope and Kolmogorov Constant of MHD Turbulence. 2011. *Physical Review Letters.* **106**: 5001.

Publications

Beresnyak, A.. Spectral Slope and Kolmogorov Constant of MHD Turbulence. 2011. *Physical Review Letter.* **106**: 5001.

Beresnyak, A., H. Yan, and A. Lazarian. Numerical Study of Cosmic Ray Diffusion in Magnetohydrodynamic Turbulence. 2011. *Astrophysical Journal.* **728**: 60.

Beresnyak, A., and A. Lazarian. Scaling laws and diffuse locality of balanced and imbalanced magnetohydrodynamic turbulence. 2010. *Astrophysical Journal Letters.* **722** (1): L110.

Non-Condon and State Interaction Effects in Carbon Nanotubes

Stephen K. Doorn
20100629PRD3

Introduction

Our goal is to understand the interaction of carbon nanotubes and light. Recent results from the carbon nanotube effort at LANL suggest that molecular vibrations and electronic states are connected.   More technically, the transition moment dipole, which determines strength of electronic excitations, depends on the vibrational coordinate, indicating a breakdown in the fundamental Condon approximation for understanding spectroscopic quantum behavior. The approximation states that electronic excitations occur on a fast timescale relative to vibrational motion. This project aims to probe this violation of the Condon approximation using Raman spectroscopy. The goal is to probe the structural and energy dependence of this behavior. Ultimately, the aim is to understand the origins and consequences of this behavior for other photophysical behaviors in nanotubes. To do this requires access to high purity single-structure samples, which are only available at LANL.

Benefit to National Security Missions

Results of this project will have a direct bearing on developing optical and electronic properties of carbon nanotubes for photonic and energy harvesting applications and may also contribute to sensing and spectral tagging applications. As a result this work will have direct relevance to the mission of the DOE-BES funded Center for Integrated Nanotechnologies and the potential applications will be of interest to agencies including NIH, DOE, DHS, and DOD with potential impact on threat reduction amd renewable energy missions.

Progress

Since starting at LANL in October 2010, Hagen Telg has mainly worked on three aspects of this effort:

Determining the dependence of the LO and TO (two vibrational modes of the nanotube) phonon frequencies in nanotubes on the specific nanotube structure, interference and non-Condon effects in the Raman signal of carbon nanotubes, and the double-resonant Raman signal in nanotubes. The uniqueness in the field of nanotube research which all these investigations have in common is that the experiments were conducted on samples highly enriched in particular nanotube structures (or chiralities). Therefore we were able to observe spectral signatures of the particular nanotubes, which are masked, in typical samples of mixed chirality.

In our studies of the LO and TO modes (near 1590 cm^{-1} in frequency), we found their frequencies as well as intensities depend on diameter, chiral angle and nanotube family. The most significant result is the dependence of the TO frequency as a function of diameter, which shows a decrease proportional to $1/d^2$ (d: tube diameter). Therefore we could show how the TO frequency can be used to determine the diameter of nanotubes. By studying the deviations between experimental results and prediction from tight-binding approximations we can also provide insights on the restructuring of molecular orbitals that takes place in carbon nanotubes. These results were obtained on samples enriched in specific semiconducting nanotube structures. Recently available samples enriched in specific metallic nanotube structures have also allowed us to obtain the structural dependence of the TO mode for metallics. Two publications on these results (targeted for Physical Review B and ACS Nano) are in preparation. The manuscript on the semiconducting structures is nearly ready for submission to ACS Nano.

The second area of focus is on direct measurement of Raman non-Condon effects and Raman interference behaviors. Raman interference effects can occur when the separation between two optical transitions in a material is in the regime of the phonon energy and smaller. As a result of quantum interference between the two states, the Raman signal of the particular phonon mode is either enhanced or weakened. This effect depends on the sign of how optical excitations couple to phonons (exciton-phonon coupling). The effect also depends on the separation of the optical transitions. By fitting experimental results and simulating the interference effects we could prove for the first time the existence of interference in three types of nanotubes. Furthermore we could show that for the LO-phonon a sign-change in the exciton-phonon coupling elements is taking place

between different optical transitions. A publication on this work is in review at Physical Review Letters. We were also able to show that non-Condon effects must also be considered in evaluating the quantum interference impact. Evaluation of non-Condon effects has also now been done for the second, third, and fourth optical transitions for the LO mode, while studying them for the first optical transition and additional modes has recently begun and will be the subject of the continuing work on this project.

Hagen's third research focus has been on modeling the complex double resonant Raman process for the 2D mode (near 2600 cm^{-1} in frequency) and M mode (near 1750 cm^{-1}) in the nanotube Raman spectrum. Modeling is dependent on modification of a program that determines electronic and phonon density of states. Modification is now complete. Test runs of the program have been successful, but need to be applied on the different tube types and compared to experimental findings. We have also recently completed data acquisition focused on getting good intensities and frequencies for the M mode. We will use frequency as a function of structure to help identify the origins of this mode, which remains an open question in the field. Its excitation behavior in comparison to that of the LO and TO phonons will also help us address the physical origins of the non-Condon effects.

Future Work

The goal of this project is to reveal electronic and spectroscopic behaviors in carbon nanotubes (CNTs) that result from state interactions and a breakdown in the Condon approximation. This is generalized as resulting from a significant vibrational coordinate dependence appearing in the transition moment dipole. We seek to understand the origins and consequences of such behavior. The most direct probe of such behavior is Raman spectroscopy, which will be our primary tool in this investigation. Non-Condon effects are expected to appear as a strong asymmetry in the Raman response as excitation energy is varied. We expect non-Condon effects, like many other nanotube physical properties, to vary for different types of tubes. Therefore we will study various CNT chiralities, diameters, and metallicity. Furthermore we will probe different transitions of particular tubes to address state alternating behavior.

The coupling between a phonon (a vibrational mode) and an optical transition in the limit of breakdown of the Condon principle can lead to state-mixing. This phonon-mediated state-mixing enables the use of Raman to map out formally forbidden (dark) optical transitions. Therefore particular Raman modes will show an extra resonance at the energy of the dark transition. Here the Raman mode is either a well known or a new, formally forbidden mode, which becomes allowed in this process.

Quantum interference occurs in Raman when the resonance profiles of two transitions overlap. This results in a drastic enhancement or weakening of the Raman signal in this region. CNTs show a series of optical transitions whose separation decreases the higher the transition. However, only particular chiralities (tube structures) will meet the requirements and actually show interference. We will study resonance behavior of selected chiralities most likely to display such effects.

Future efforts in both the non-Condon and interference studies will be extended to include active perturbation of the behaviors. Our primary approach will be to apply strain to the nanotube samples. This will impact both the phonon mode behavior and transition energies. Both effects will impact the non-Condon and interference response. The result will be additional information that will aid in unraveling the origins of both behaviors.

Conclusion

We will reveal the nature and consequences of non-Condon and interference behaviors in carbon nanotubes. We will demonstrate the potential for quantum interference and mixing of electronic states. Such interference and state mixing will have a significant impact on potential applications of nanotubes in energy harvesting, photonics, electro-optics, and sensing.

Publications

Duque, J. G., H. Telg, H. Chen, A. K. Swan, A. P. Shreve, X. Tu, M. Zheng, and S. K. Doorn. Quantum interference between the third and fourth excitonic states in semiconducting carbon nanotubes. *Physical Review Letters.*

A New Regime of Carrier Multiplication Using Intraband Re-Excitation of Nanocrystals

Victor I. Klimov
20100632PRD4

Introduction

The solution to the global energy challenge requires revolutionary breakthroughs in areas such as the conversion of solar energy into electrical power. One such breakthrough is high-efficiency generation of multiple electron-hole pairs (excitons) from absorption of single photons, which is known as carrier multiplication (CM). In 2004, the LANL quantum-dot group discovered that PbSe nanocrystal quantum dots, in distinction from bulk semiconductors, undergo this process very efficiently for photons in the solar range (Schaller & Klimov, Phys. Rev. Lett. 92, 186601, 2004). Since then, efficient CM has also been in CdSe, PbS, PbTe, InAs, and Si nanocrystals. However, despite these unambiguous demonstrations of CM, detailed understanding of the CM mechanism in nanocrystals is still lacking. For example, it is still not clear why carrier multiplication, which is a low-efficiency process in bulk semiconductors, is enhanced in quantum-confined nanoparticles. In this project, we will conduct a set of experiments that aim at clarifying the mechanism for CM as well as the nature of competing processes. One specific goal is to distinguish between the contributions due to direct photogeneration mechanisms (e.g., "virtual exciton and biexciton" pathways) and impact-ionization scattering-like processes. Further, we will attempt to understand the roles of competing processes such as phonon emission and electron-hole energy transfer.

Benefit to National Security Missions

Several DOE reports have recognized that the solution to the global energy challenge will require scientific breakthroughs and truly revolutionary developments. One such breakthrough has been the discovery of carrier multiplication in semiconductor nanocrystals. This process has the potential to considerably increase the performance of solar cells through increased photocurrent. To take full advantage of this phenomenon, the carrier multiplication performance should approach the efficiency limit as defined by energy conservation. The studies conducted in this project will help one to understand both the mechanisms of carrier multiplication as well as the role of competing processes. This would represent an important step towards "ideal" carrier multiplication structures operating at the energy-conservation-defined limit. Deployable energy sources are a high priority for many agencies, including DoD.

Progress

Our research over the last year has focused on answering the primary question of this postdoctoral project: What are the dominant decay mechanisms that compete with carrier multiplication in semiconductor nanocrystals? Understanding the alternative decay pathways available to a hot electron is fundamentally important to improving carrier multiplication yields in nanocrystals and hence solar cell efficiencies. Our research has focused on studying the impact that both the material compound and material shape have on relative CM yields. Our previous study, which focused on the compound composition (PbSe and PbS), allowed us to confidently separate the dominant decay mechanism from the mechanism responsible for CM. Based on the success of our polaron model to describe the qualitative difference in the observed CM yields, we are confident that the dominant decay mechanism is phonon emission. Further, using the similarity of the PbX compounds and the polaron model we have predicted that PbTe should be a good candidate material for achieving higher CM yields. We have worked in an iterative process with our synthetic chemists to produce PbTe nanocrystals which are both highly stable and high quality. We have now measured the CM yields for a large number of PbTe samples over a variety of sizes and verified that the CM yields are indeed higher than either PbSe or PbS nanocrystals. We are now in the process of adapting our previous qualitative polaron model into a model which quantitatively predicts the CM yields based on bulk properties. If successful, this would prove to be the first ever predictive model to be applied to CM yields of nanocrystals. This work is in preparation for submission.

This work has made clear the importance of particular bulk properties for predicting CM yields in other nanomaterials. Due to the lack of CM yields in the literature for solar-relevant semiconductors, we have begun a

collaboration with researchers at the National Renewable Energy Laboratory to study in detail the bulk properties of materials we find particularly promising.

We have simultaneously been studying the effects of dimensionality on CM yields in nanomaterials. Again, through collaborative efforts with our synthetic chemists we now have access to high quality PbSe nanorods – an effectively one-dimensional material. By confining the excitons to a single dimension, it has been predicted that the Coulomb interaction will not be as effectively screened as is the case for quantum dots – an effectively zero dimensional material. It is predicted that this will enhance the rate of CM generation relative to the cooling rate as compared to quantum dots, increasing the CM yield. We have now studied a number of nanorod samples and have verified that the CM yields are indeed higher, by as much as 50% for some energy gaps. This work is also in preparation for submission.

Future Work

Our future studies will continue to study the relative mechanisms responsible for CM yields in nano and bulk semiconductors. In particular, we are interested in studying how an exciton decays just after excitation, as this is likely the most relevant time period for which CM can occur. Further, we have many ideas on how to increase this "time window" which is favorable for CM. For example, by coating PbSe samples with a material which has a much larger band-gap, the electron may become "stuck" in the higher band-gap material, effectively increasing the time a hot exciton stays in the "time window" for CM. Alternatively, it has been recently suggested that this same effect can be observed in a single compound by exciting the exciton above the "sigma point." We are in an ideal situation to test such a theory by working with extremely large PbSe nanocrystals, a material that our chemists have much experience with.

Conclusion

The research conducted in this project will answer important fundamental questions regarding the dominant relaxation processes in nanocrystals. By gaining knowledge of these decay mechanisms and by developing a predictive model for CM yields we will provide much needed direction for discovering new materials with higher CM yields. Further, these experiments will test the feasibility of enhancing CM efficiency via relatively simple changes in the chemical synthesis of nanoparticles by coating or changing the nanomaterials shape.

Shockwaves as Diagnostic of Strongly Coupled Plasmas

Ivan M. Vitev
20100634PRD4

Introduction

Strongly coupled and strongly interacting plasmas (SCPs) are a fascinating frontier of modern scientific research. SCPs are being studied on scales that range from the size of a gold nucleus to the crust of a neutron star; in some ways, they have more in common with liquids than the weakly coupled plasmas found in electric lamps, the ionosphere, and the Solar corona. A particularly exciting and relatively new area of SCP research is the study of the quark-gluon plasma (QGP). Preliminary results from the Relativistic Heavy Ion Collider (RHIC) indicate that the QGP formed in nucleus-nucleus collisions exhibits a viscosity over entropy density ratio (η/s) that approaches a value conjectured by string theory to represent the smallest viscosity in nature [1]. One of the characteristics of a SCP is strong collective behavior. This is especially true of the QGP created in heavy-ion collisions, where experimental indications of Mach cone shockwave formation induced by energetic particles have generated tremendous interest [2, 3]. It is a top science priority in the US and abroad to understand in the next few years the transport properties of SCPs, such as the viscosity, and the microscopic relationship between the stopping power of plasmas and the ability of a projectile to induce an observable Mach cone shockwave. It is also imperative to understand the properties of these systems in relation to the theoretical advances in describing the more-familiar electromagnetic plasmas.

Benefit to National Security Missions

This project supports Laboratory missions in Basic Science, Energy Security, and Nuclear Weapons. The quest to discover and quantify the properties of new states of matter, such as the quark-gluon plasma created at RHIC and the LHC, is central to the Beyond the Standard Model grand challenge. Advances on the properties of strongly coupled plasmas and materials in extreme conditions are an essential component of the Materials: Discovery Science to Strategic Applications and Nuclear Performance grand challenges. By enhancing its basic science capabilities, this project will help LANL meet its current and future applied missions and challenges. In addition, understanding the transport properties of strongly-coupled plasmas is one of the performance measures set forth by the DOE Office of Science to evaluate progress in Nuclear Theory in the next few years. The plasmas generated at NIF, the flagship facility of the NNSA program, fall in the strongly coupled regime.

Progress

During the past year there has been significant progress toward achieving the goals outlined in our proposal. Specifically, two fundamental building blocks in the investigation of shockwave formation in strongly coupled plasmas have been put into place.

The first of these achievements was recently published in Physical Review D83:065012, 2011, 'A Thermal Field Theory Derivation of the Source Term Induced by a Fast Parton from the Quark Energy Momentum Tensor' by R.B. Neufeld [4]. In this important work, the link between the energy-momentum tensor of a quantum system at finite temperature and the source term induced by a charged current was directly demonstrated. In particular, the source term induced by a charge distribution was derived directly from the underlying quantum theory of the system. The result can be generalized to many systems and paves the way for first principles investigation of shockwave formation for arbitrary current configurations, including phenomenological applications such as currents created through hard scattering or medium induced color charge evolution. One of the highlights of this work was that it extracted the sound excitation strength of a fast parton as a function of particle energy (Figure 1).

The work described above was presented as a talk at two conferences, including the 2010 Fall Meeting of the Division of Nuclear Physics in Santa Fe and the 2011 Winter Workshop on Nuclear Dynamics in Winter Park. The presentation at the Winter Workshop includes a contribution to the proceedings entitled 'A derivation of the source term induced by a fast parton from the quark energy-momentum tensor', by R.B. Neufeld [5].
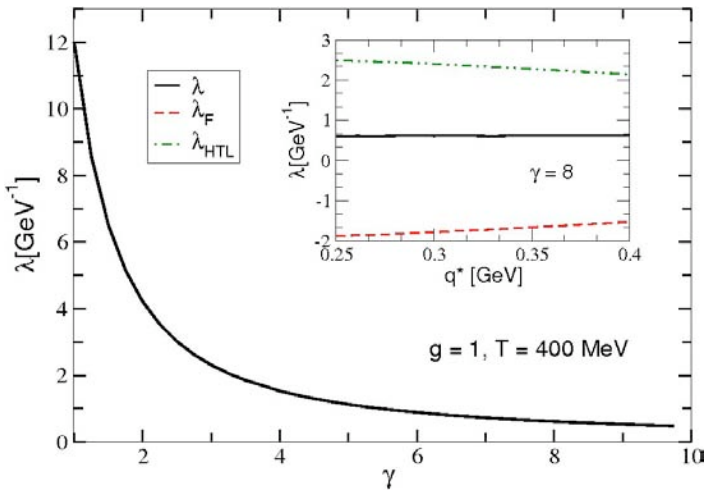
Figure 1. Sound excitation strength as a function of particle energy as calculated in reference 1.

The second fundamental building block we have put into place utilized the result of the first. Specifically, we calculated the source term of energy and momentum exchange between a parton shower and a thermalized quark gluon plasma. This work has also resulted in a journal submission to Physics Letters B, 'Parton showers as sources of energy-momentum deposition in the QGP and their implication for shockwave formation at RHIC and at the LHC', by R.B. Neufeld and Ivan Vitev [6]. This work is a more phenomenological application of the formalism described in the above two paragraphs. In heavy-ion collisions, energetic color charged particles evolve through medium induced interactions into a complicated color charged distribution constrained by the non-Abelian gauge symmetry of Quantum Chromodynamics. This evolving charge distribution is often referred to as a parton shower. The dynamics of parton showers are important in the description of full jet observables in heavy-ion collisions. The source term we have derived enables a unified description of the energy transfer from a parton shower to the underlying thermal medium, and the related issue of shockwave formation generated by parton showers.

Our calculation is unique in that we considered the quantum interference between the evolving components of a parton shower, a previously neglected contribution. We also considered the realistic large angle broadening associated with parton shower dynamics and the effect that has on well defined Mach cone formation. Our results suggest this large angle broadening has important implications for shockwave phenomenology. Specifically, multiple overlapping excitations in the plasma can wipe out the clear Mach cone signature (Figure 2). This work was recently presented as a poster at the 2011 Quark Matter Conference in Annecy, France and was also presented at the High PT Probes of High Density QCD Workshop in Paris, France and at the APS 2011 Meeting of the Division of Particles and Fields in Providence, Rhode Island.

The above result was recently incorporated in an important new phenomenological description of jet observables in heavy-ion collisions [7, 8]. The energy transfer rate calculated in [6] was applied to the modification of high-energy jet production in these collisions. It was found that the results of [6] are in qualitative agreement with what is necessary to reproduce experimental observation.
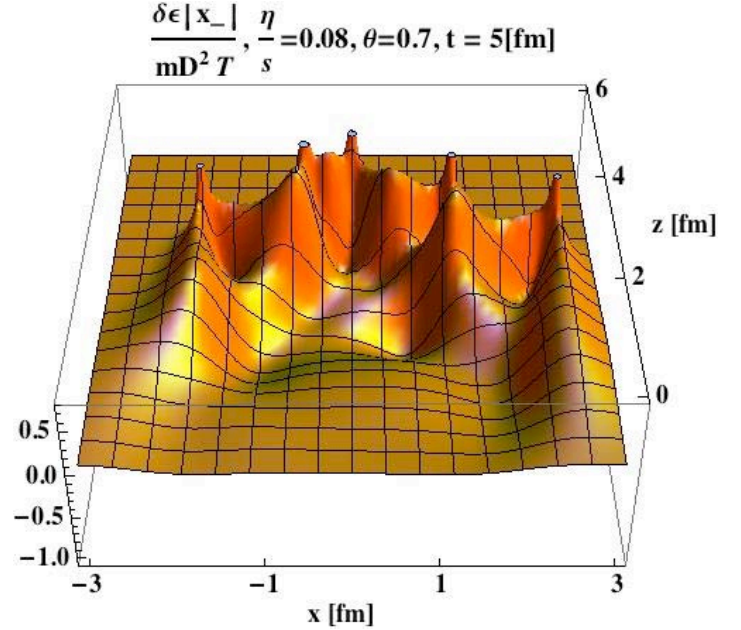
Figure 2. Mach cone shockwaves generated by a wide parton shower source. The multiple Mach cones combine with one another.

Future Work
In the coming year there are several exciting projects we hope to be able to undertake and complete. We are in the process of extending the formalism introduced in [5, 6] to include arbitrary angles of parton shower emission and explore areas beyond the hard thermal loop approximation. This will be a major advancement in our field and has direct experimental relevance. We will additionally consider projectiles created by hard scattering processes in the early moments of a heavy-ion collision. This particular scenario is relevant to heavy-ion phenomenology and has never been examined before.

Conclusion
We have made and continue to make much progress in the investigation of shockwaves as a diagnostic of strongly coupled plasmas. The evidence of our progress is amply illustrated in the preceding paragraphs. Our continued accomplishments will provide much-needed insight into the behavior and properties of strongly coupled plasmas. A quantitative relationship between plasma stopping power and shockwave excitation is of direct relevance to the nuclear and plasma physics communities. The analysis of Mach shocks in relativistic hydrodynamics will illuminate upcoming measurements at the flagship US nuclear physics

facility - the Relativistic Heavy Ion Collider. Our research is an important cog in helping to pin down the viscosity and speed of sound of the quark-gluon plasma.

References

1. Romatschke, P., and U. Romatschke. Viscosity Information from Relativistic Nuclear Collisions: How Perfect is the Fluid Observed at RHIC. 2007. *Physical Review Letters.* **99**: 172301.

2. STAR, B. I. Abelev. Indications of Conical Emission of Charged Hadrons at RHIC. 2009. *Physical Review Letters.* **102**: 052302.

3. Casalderrey-Solana, J., E. V. Shuryak, and D. Teaney. Conical flow induced by quenched QCD jets. 2005. *Journal of Physics Conference Series.* **27**: 22.

4. Neufeld, R. B.. Thermal field theory derivation of the source of term induced by a fast parton from the quark energy-momentum tensor. 2011. *Physical Review D.* **83**: 065012.

5. Neufeld, R. B.. A derivation of the source term induced by a fast parton from the quark energy-momentum tensor. 2011. (Winter Park, Colorado, 6-13 February 2011). Vol. 3161 Editionp. 012031. Winter Park: Journal of Physics Conference Series.

6. Neufeld, R. B., and I. Vitev. Parton showers as source of energy-momentum deposition in the QGP and their implication for shockwave formation at RHIC and the LHC. *Nuclear Physics A.*

7. He, Y., I. Vitev, and B. W. Zhang. Next-to-leading order analysis of inclusive jet and di-jet production in heavy ion reactions at the Large Hadron Collider. *Physics Letters B.*

8. Vitev, I.. NLO analysis of inclusive jet, tagged jet and di-jet production in Pb+Pb collisions at the LHC. To appear in *Journal of Physics G.*

Publications

He, Y., I. Vitev, and B. W. Zhang. Next-to-leading order analysis of inclusive jet and di-jet production in heavy ion reactions at the Large Hadron Collider. *Physics Letters B.*

Neufeld, R. B.. Thermal field theory derivation of the source of term induced by a fast parton from the quark energy-momentum tensor. 2011. *Physical Review D.* **83**: 065012.

Neufeld, R. B.. A derivation of the source term induced by a fast parton from the quark energy-momentum tensor. 2011. In *Winter Workshop on Nuclear Dynamics.* (Winter Park, Colorado, 6-13 February 2011). Vol. 316, 1 Edition, p. 012031. Winter Park: Journal of Physics Conference Series.

Neufeld, R. B., and I. Vitev. Parton showers as source of energy-momentum deposition in the QGP and their implication for shockwave formation at RHIC and the LHC. *Nuclear Physics A.*

Vitev, I.. NLO analysis of inclusive jet, tagged jet and di-jet production in Pb+Pb collisions at the LHC. To appear in *Journal of Physics G.*

Heavy quarks in Cold Nuclear Matter and in the Quark Gluon Plasma

Michael J. Leitch
20100635PRD4

Introduction

In this project we will measure the properties of a new state of matter that may have been absent from the Universe since a first few milliseconds after the Big Bang. To probe this hot dense state we use heavy quarks, with whimsical names like "charm", "bottom", and "top". These quarks are distinct from the up and down quarks of normal matter. This hot dense matter, called a Quark Gluon Plasma (QGP), is created in high-energy heavy-ion collisions at the Relativistic Heavy Ion Collider (RHIC) at Brookhaven National Laboratory. A new silicon vertex detector, developed under LANL leadership, will identify heavy quarks. These quarks travel only a short distance before decaying into muons. Although the distance is short, it can be measured by the new vertex detector, thereby detecting the ephemeral life of a heavy quark. Bound states of two heavy quarks will also be detectable. The quarks experience the effect of the QGP as they travel through it on the way to our detectors.

The new detector will be added to the existing PHENIX detector at RHIC in late 2011. The new detector will be commissioned early in 2012 when it sees its first colliding beams, and analysis for physics results will follow soon after. Collisions with various types of high-energy beams including gold nuclei, deuterons, and protons will deliver the data required to obtain a complete picture of the quark physics; and to extract properties of the QGP. Our data analysis will deliver scientific results that are not possible within the baseline project, which is focused on delivering and commissioning the instrument, not doing science.

Benefit to National Security Missions

We address the fundamental study of de-confined quark-gluon matter created in very high-energy heavy-ion collisions, which mimic the first few milliseconds of the universe. These studies are the primary goal of the forefront Relativistic Heavy Ion Collider facility which is the leading U.S. Nuclear Physics facility. We also address a U.S. Nuclear Science Advisory Committee (NSAC) Goal that deals with the structure of nuclei at a very small momentum scale where gluons in those nuclei become saturated and alter their structure compared with their normal structure in free protons.

Progress

Since Cesar da Silva began his Director's funded postdoc work with the heavy-ion group at LANL in November 2010, he has continued to establish himself as a leading international expert in the field of heavy-ion physics and has positioned himself to play a lead role in the new physics that will be enabled by the new LANL-led Forward Vertex Detector (FVTX).

He was nominated to represent the PHENIX collaboration and gave a major Plenary talk at the most important meeting in the field of high-energy heavy-ion collisions, the Quark Matter 2011 international conference, held in Annecy, France in May 2011. As a leading expert on heavy-quarks (charm and beauty) within PHENIX and in the world, he represented all results from the Relativistic Heavy Ion Collider (RHIC), including both those of PHENIX and of the other large experiment at RHIC (STAR) [1].

A milestone paper on production of heavy-quark bound states in high-energy proton-proton collisions, with a detailed description covering 25 pages, was written by Cesar for PHENIX, and has just been accepted for publication in Physical Review D [2]. This paper describes details of the production of these heavy-quark bound states as measured by PHENIX; much of the analysis having been done by Cesar himself in recent years. He is also leading the preparation of several other important papers for PHENIX in this area of physics.

The LANL group is leading the construction of the FVTX upgrade to the PHENIX detector at RHIC, and this new detector will be installed late in 2012. In order to prepare for new physics using muons with the FVTX, Cesar has begun work on analysis of existing forward muon data, including improving performance of the existing muon spectrometers that will detect muons in conjunction with the new FVTX, analysis of high-mass muon pairs, and simulations that provide direct preparation for using the new FVTX detector. His previous analysis

work before coming to LANL, involved measurements of similar heavy-quark signals, but with electrons instead of muons and using different detectors appropriate for these electron measurements. Now here at LANL, he has quickly picked up the expertise to lead analysis efforts with muons and is well positioned to lead the first analyses using the new FV TX – once it sees its first high-energy collisions at RHIC in 2012.

Future Work

Quarkonia (bound states of two charm or two beauty quarks) are identified in the PHENIX forward muon detectors as di-muon invariant mass peaks. At the same rapidities, D (charm) and B (beauty) meson yields are obtained from their decays to single muons, after subtracting contributions from light mesons (mostly Kaons and pions). LANL is working on the construction and installation of the forward vertex detector (FVTX), which consists of four silicon mini-strip detector layers in front of each of the two PHENIX muon detectors. These can measure the displacement between the creation point of the mesons and their decay point with a r-z distance resolution of 100 microns, and will be used to identify the D (B) mesons, which typically travel a distance of 100-300(460-500) microns before their decay. The hit information from tracks crossing the four FVTX stations can also improve the mass resolution of di-muons measured in the forward detectors and will allow separation of the J/ψ and ψ' mass peaks, two different charm pair bound states. The next year will be dedicated to simulations of the FVTX's predicted performance and in preparation for physics analyses. The first data using the FVTX will be taken for Copper+Gold collisions at 200 GeV in 2012. Cesar plans to play a major role in the monitoring and analysis of this data; as well as in the extraction of the D, B, J/psi and psi' yields. The magnitude of the suppression of their production due to the presence of the Quark Gluon Plasma will first be obtained by comparing yields in central (head-on) and peripheral (grazing) collisions. Later, complementary data from proton-proton and deuteron+Gold collisions will be obtained in order to arrive at final conclusions. Our data analysis will deliver scientific results that are not possible within the baseline project, which is focused on delivering and commissioning the instrument, not doing science.

Conclusion

Our measurements will elucidate the properties of a new state of matter, where quarks are no longer confined in nucleons, similar to the state of the Universe in the first few milliseconds after its creation. By contrasting these measurements with heavy quarks with earlier measurements of lighter particles such as pions and protons, the properties of this new state of matter can be determined - much like throwing a heavy rock in a river vs. throwing a small rock in a river, and observing how each is influenced by the flowing water.

References

1. Silva, C. da. Recent Heavy Flavor and Quarkonia Measurements by the PHENIX Experiment. To appear in *Proceedings for Quark Matter 2011.* (Annecy, France, May 22-28, 2011).

2. Adare, A., and e. al. Ground and excited charmonium state production in p+p collisions at sqrt(s)=200 GeV. *Phys. Rev. D and arXiv:1105.1966.*

Publications

Adare, , Afanasiev, S., Aidala, C., Ajitanand, N.N., Akiba, Y., and others. {Production of omega mesons in p+p, d+Au, Cu+Cu, and Au+Au collisions at sqrt(s_NN)=200 GeV}. 2011.

Adare, , Afanasiev, S., Aidala, C., Ajitanand, N.N., Akiba, Y., and others. {J/psi suppression at forward rapidity in Au+Au collisions at sqrt(s_NN)=200 GeV}. 2011.

Adare, , Afanasiev, S., Aidala, C., Ajitanand, N.N., Akiba, Y., and others. {Cold Nuclear Matter Effects on J/psi Yields as a Function of Rapidity and Nuclear Geometry in Deuteron-Gold Collisions at sqrt(s_NN) = 200 GeV}. 2010. *Phys.Rev.Lett..*

Adare, , and others. {Suppression of back-to-back hadron pairs at forward rapidity in d+Au Collisions at sqrt(s_NN)=200 GeV}. 2011.

Adare, , and others. {Observation of direct-photon collective flow in sqrt(s_NN)=200 GeV Au+Au collisions}. 2011.

Adare, , and others. {Measurements of Higher-Order Flow Harmonics in Au+Au Collisions at sqrt(s_NN) = 200 GeV}. 2011.

Adare, , and others. {Ground and excited charmonium state production in $p+p$ collisions at $\sqrt{s}=200$ GeV}. 2011.

Adare, , and others. {Heavy Quark Production in p+p and Energy Loss and Flow of Heavy Quarks in Au+Au Collisions at sqrt(s_NN)=200 GeV}. 2010.

Adare, , and others. {Suppression of away-side jet fragments with respect to the reaction plane in Au+Au collisions at sqrt(s_NN) = 200 GeV}. 2011. *Phys.Rev..* **C84**: 024904.

Adare, , and others. {Event Structure and Double Helicity Asymmetry in Jet Production from Polarized $p+p$ Collisions at $\sqrt{s} = 200$~GeV}. 2011. *Phys.Rev..* **D84**: 012006.

Adare, , and others. {Identified charged hadron production in $p+p$ collisions at $\sqrt{s}=200$ and 62.4 GeV}.

2011. *Phys.Rev..* **C83**: 064903.

Adare, , and others. {Azimuthal correlations of electrons from heavy-flavor decay with hadrons in p+p and Au+Au collisions at sqrt(s_NN)=200 GeV}. 2011. *Phys. Rev..* **C83**: 044912.

Adare, , and others. {Measurement of neutral mesons in p+p collisions at $\sqrt(s)$= 200 GeV and scaling properties of hadron production}. 2011. *Phys.Rev..* **D83**: 052004.

Adare, , and others. {Nuclear modification factors of phi mesons in d+Au, Cu+Cu and Au+Au collisions at sqrt(S_NN)=200 GeV}. 2011. *Phys.Rev..* **C83**: 024909.

Adare, , and others. {Cross Section and Parity Violating Spin Asymmetries of W+/- Boson Production in Polarized p+p Collisions at sqrt{s}=500 GeV}. 2011. *Phys.Rev. Lett..* **106**: 062001.

Adare, , and others. {Cross section and double helicity asymmetry for Eta mesons and their comparison to neutral pion production in p+p collisions at sqrt(s)=200 GeV}. 2011. *Phys.Rev..* **D83**: 032001.

Adare, , and others. {Measurement of Transverse Single-Spin Asymmetries for J/psi Production in Polarized p+p Collisions at sqrt(s) = 200 GeV}. 2010. *Phys.Rev..* **D82**: 112008.

Adare, , and others. {High pT direct photon and pi0 triggered azimuthal jet correlations and measurement of kT for isolated direct photons in p+p collisions at sqrt{s}=200 GeV}. 2010. *Phys.Rev..* **D82**: 072001.

Adare, , and others. {Azimuthal anisotropy of neutral pion production in Au+Au collisions at sqrt(s_NN) = 200 GeV: Path-length dependence of jet quenching and the role of initial geometry}. 2010. *Phys.Rev.Lett..* **105**: 142301.

Adare, , and others. {Elliptic and hexadecapole flow of charged hadrons in Au+Au collisions at sqrt(s_NN) = 200 GeV}. 2010. *Phys.Rev.Lett..* **105**: 062301.

Adare, , and others. {Transverse momentum dependence of meson suppression Eta suppression in Au+Au collisions at sqrt{sNN} = 200 GeV}. 2010. *Phys.Rev..* **C82**: 011902.

Adare, , and others. {Transverse momentum dependence of J/psi polarization at midrapidity in p+p collisions at sqrt(s) = 200-GeV}. 2010. *Phys.Rev..* **D82**: 012001.

Adare, , and others. {Trends in Yield and Azimuthal Shape Modification in Dihadron Correlations in Relativistic Heavy Ion Collisions}. 2010. *Phys.Rev.Lett..* **104**: 252301.

Adare, , and others. {Detailed measurement of the e+ e- pair continuum in p+p and Au+Au collisions at sqrt{sNN} = 200 GeV and implications for direct photon production}. 2010. *Phys.Rev..* **C81**: 034911.

Adare, , and others. {Enhanced production of direct photons in Au+Au collisions at sqrt(sNN)=200 GeV and implications for the initial temperature}. 2010. *Phys.Rev. Lett..* **104**: 132301.

Adare, , and others. {Double-Helicity Dependence of Jet Properties from Dihadrons in Longitudinally Polarized p+p Collisions at sqrt{s}=200 GeV}. 2010. *Phys.Rev..* **D81**: 012002.

Afanasiev, , and others. {Enhancement of the dielectron continuum in s(NN)**(1/2) = 200-geV Au+Au collisions}. 2007. *Phys.Rev.Lett..*

Silva, da, and others. {Recent Heavy Flavor and Quarkonia Measurements from the PHENIX Experiment}. 2011.

Silva, da, and others. {Decay Angular Distributions for the J/Psi Measured by PHENIX}. 2011.

The Formation and Evolution of Black Holes in the Universe

Christopher L. Fryer
20100636PRD4

Introduction

The formation of the first stars, and their subsequent evolution, is the first crucial step in the formation of galaxies and, eventually, life. At the end of their lives, these first stars are thought to collapse into the first black holes in the Universe. The subsequent evolution of these black holes plays a major role in galaxy formation. Understanding this process is one of the key goals of cosmology today, and we are on the cusp of major advances. While detailed observations of the cosmic microwave background have now elucidated the initial conditions for the formation of the first stars and black holes, in the next few years numerous new observational facilities, from the James Webb Space Telescope, operating in the infrared, to the Energetic X-ray Imaging Survey Telescope, will seek to capture the first images of these objects. This project will perform simulations of the formation of these first black holes, and their subsequent evolution. The development of black holes is a crucial unknown in our model for how galaxies form and evolve. The results of this project will have far-reaching impact, both in our models of galaxy formation, our models of star formation, and our models for sources for upcoming telescopes like LIGO.

Benefit to National Security Missions

This project will develop and utilize advanced radiation transport codes that are relevant to the simulation of thermonuclear explosions. This will have direct relevance to stockpile stewardship efforts at LANL.

Progress

Dr. Johnson has now just arrived and we have already begun the first project studying supermassive star formation. The first project focuses on studying the stellar mass formed in collapsing clouds. We are using cosmology calculations and determining whether radiative feedback can limit the mass of the star or whether stellar lifetime is the more constraining limit. Radiative feedback includes ionization effects and radiative momentum. Our preliminary results suggest that massive stars up to 100,000 solar masses can be formed in current clouds. If these pan out, we will input our accretion profiles into stellar evolution codes to evolve the stars produced in these clouds.

Future Work

Dr. Johnson will collaborate closely with Dr. Daniel Holz and Dr. Chris Fryer to carry out demanding, state-of-the-art cosmological radiation hydrodynamic simulations of the formation and accretion of gas onto massive black holes in the earliest galaxies, taking into special account the propagation of the high energy radiation generated in the accretion process. He will make use of the tremendous computing resources at Los Alamos National Laboratory, as has been done by Dr. Fryer for his recent simulations of the evolution of the earliest stars, which incidentally will help to inform this study.

An important outcome of the simulations will be the observational signatures of black hole accretion in the first galaxies, which can be used to constrain the properties of these black holes, such as their masses and growth rates; and of their host galaxies, such as their masses, chemical compositions, and cosmological environments. These signatures will be detected by upcoming observational facilities. The results will help to uncover the origins of the observed relations between black hole growth and the formation of their host galaxies, including our own galaxy which hosts its own massive black hole, as well as to shed light on the key processes shaping the formation of the first galaxies.

Conclusion

This project will help explain how black holes form and evolve in the Universe. Black holes play a critical role in the formation of the first stars and galaxies, and therefore underly many of the most important questions in modern astrophysics and cosmology. In short, if we want to understand why the night sky looks the way it does (full of stars and galaxies, of a certain characteristic shape and distribution), we need to understand when and where black holes form, and what happens to them.

Auger-Recombination-Free Nanocrystals by Rational Design of Confinement Potential

Victor I. Klimov
20110544PRD1

Introduction

This project focuses on investigations of the interplay between structural characteristics and photophysical properties of "designer" nanocrystals (NCs), built from a carefully engineered colloidal core and shell. The main aim of these studies is the development of new lasers based on NCs. NCs are particularly attractive for lasing applications due to their efficient and size-tunable emission. A significant impediment to applications of NCs in lasers is fast non-radiative Auger recombination, which carries away the energy that should go into the laser. Recent studies by LANL researchers have demonstrated that this undesirable Auger recombination is significantly reduced in so-called "giant" NCs (g-NCs), built from a small CdSe core overcoated with a thick CdS shell (Garcia-Santamaria et al., Nano Lett. 2009). Our conclusion was based on our observations of long biexciton lifetimes (>10 ns) as well as multicolor amplified spontaneous emission with record low excitation thresholds. The goal of this project is to understand why this good thing is happening – what are the reasons underlying the suppression of Auger decay in these NCs? We are conducting direct measurements of multiexciton dynamics in conjunction with studies of NC structure/composition via analytical spectroscopic methods, such as Raman scattering and fluorescence line narrowing. The insights gained from these studies will be used to design the structures in which Auger recombination is completely suppressed, which should allow us to greatly extend the optical gain lifetime and increase its magnitude. To demonstrate electrically pumped lasing, these NCs will be incorporated into electrical-injection structures using previous light-emitting-diode designs developed by LANL researchers (see, e.g., Achermann et al., Nature 2004).

Benefit to National Security Missions

The demonstration of steady state and electrically pumped lasing using nanocrystals has been a longstanding goal in the field of colloidal nanostructures and represents a critical milestone in the development of solution-based lasing technologies. The identification of compositional guidelines for nanocrystals with suppressed Auger is therefore expected to have a significant impact from the point of view of both fundamental and applied research. The spectrum of potential applications of "lasers made in a chemical beaker" is very broad and covers areas of integrated nano-optics, active plasmonics, telecommunication and lab-on-a-chip optical circuitry. All of these applications are relevant to the success of LANL and DOE missions in novel nanoengineered materials, energy efficiency, new sensing technologies, and solid-state lighting.

Progress

During the past year, the research activity in this project has revolved around the spectroscopic investigation of novel doped semiconductor nanocrystals where the intentional incorporation of copper atoms in the lattice allows for the achievement of new and highly controlled optical properties. Specifically, we have applied the core/shell motif, which has been the focus of previous investigations of undoped NCs, to doped systems, and synthesized for the first time copper doped core/shell ZnSe NCs overcoated with an increasingly thick CdSe shell. The use of core/shell architectures served two critical purposes: (1) It helped to retain the dopants in the core during the chemical synthesis and thus overcome the problem of "self purification", which represents one of the main limitations to the production of controlled doped nanocrystals; (2) further, it allowed for the extension of the range of spectral tunability into the near-infrared region through control of the spatial distribution of the electronic wave functions between the core and the shell regions. As a result, we obtained a new doped nanocrystal system with unprecedented emission tunability from near infrared (1.2 eV) to the blue (3.1 eV) and reduced losses from re-absorption due to a large Stokes shift (up to 0.7 eV). These properties make our copped doped nanocrystals very attractive for applications in light-emission and lasing technologies and especially for the realization of novel device concepts such as "*zero-threshold*" optical gain.

Further and possibly more importantly, this study demonstrated for the first time that copper ions incorporate as +2 ionic species in ZnSe, and therefore represent a

source of *permanent optically-active* holes. This result is particularly relevant as, at present, the applicability of NCs to real-world technologies is greatly limited by the difficulty of controlled introduction of permanent electrically and/or optically-active charges. The resolution of this problem would greatly benefit applications of NCs in areas such as photovoltaics and light-emitting diodes and could also enable new advanced device concepts such as "zero-threshold" optical gain.

Recently, several publications reported the development of a characteristic intra-gap Cu-related emission feature in copper-doped II-VI NCs. Several studies have also attempted to characterize the oxidation state of Cu upon incorporation into NCs. The results of these investigations, however, have been controversial as both +1 and +2 oxidation states have been ascribed to copper dopants. Distinguishing between these two possibilities is important for understanding the electronic, optical, and magnetic properties of Cu impurities. Specifically, the +1 state has a filled $3d^{10}$ shell and is not magnetic and cannot contribute to emission without first capturing an external hole. On the other hand, the +2 state has an unpaired electron in its $3d^9$ shell and is therefore paramagnetic and can be considered as a state with a *permanent* optically-active hole, which can participate in emission *without the injection of a hole*. Furthermore, if the Cu ions are preferentially in the +2 state, this implies that the Fermi level is below the Cu impurity *t*-level and hence is located near the valence-band edge, which is formally a signature of a *p*-type material.

Starting from this premise, we have used several spectroscopic techniques to investigate the nature of the copper impurities and unambiguously determine their oxidation state in our core/shell NCs. Specifically, we performed side-by-side spectroscopic measurements on undoped and copper doped NCs including continuous wave and time resolved photoluminescence measurements and circularly-polarized magneto-absorption experiments. All experiments yielded agreeing results which point to the +2 oxidation state. Circularly-polarized magneto-absorption measurements were performed in high magnetic fields up to 7 Tesla. In agreement with prior studies of nonmagnetic NCs, our undoped ZnSe/CdSe NCs exhibited a small Zeeman splitting of the 1S exciton. In contrast, copper-doped (but otherwise identical) NCs clearly revealed a markedly enhanced Zeeman splitting (~2.5 meV at B = 6 T), commensurate with an effective exciton *g*-factor of order 7. These results strongly suggested that the Cu dopants are incorporated as magnetically-active Cu^{2+} ions, in agreement with recent studies of EPR-active Cu^{2+} dopants in ZnSe nanocrystals. This further implied that the Fermi level in these NCs is located below the Cu impurity *t*-state and, hence, is within ~0.7 eV from the valence-band edge. Since E_g in our NCs is from ~2.0 to ~3.3 eV, this corresponds to the lower half of the forbidden gap, which is formally a signature of *p*-doping.

A conclusive proof that copper impurities incorporate indeed as +2 species was then obtained through photoluminescence measurements on doped NCs solutions in the presence of strong hole-withdrawing agents. In fact, as was mentioned earlier, an interesting feature expected for emission due to the Cu^{2+} centers is that it can be activated by injecting conduction-band electrons without the need for valence-band holes. The presence of a band-edge hole in the NC can, in fact, diminish the Cu-related PL as this hole will compete for the same conduction-band electron with a permanent hole associated with the Cu^{2+} impurity. These considerations suggested that one could attempt to shift the balance in favor of the Cu-related PL channel by *intentionally* introducing hole traps. To test this hypothesis, we treated NCs with dodecane thiols (DDT) that are known to act as hole-withdrawing species when attached to CdSe surfaces. In the case of undoped NCs, the treatment with thiols led to rapid quenching of emission, whereas the treatment of doped samples with DDT led to a gradual quenching of band-edge PL, accompanied by a complementary *growth* of the Cu-related PL. We also observed a dramatic change in *color*, which from green became orange due to increasing contribution from Cu PL. These observations are consistent with the model of the Cu^{2+} emission center where the permanent and photogenerated (transient) holes compete for the same conduction-band electron - when the transient hole is quickly removed from the NC the emission occurs solely through the Cu centers. In the case of the Cu^{1+} impurities, the Cu-related band would have been suppressed together with the band-edge emission. Therefore, the results of the thiol-titration experiments provided very strong evidence for the Cu^{2+} nature of the dopants in our structures. Interestingly the treatment with thiols also led to an overall increase of the PL quantum yield (from ~3.5% to ~6%), which suggested a possible strategy to design efficient copper-doped NC emitters through the use of hole-withdrawing organic ligands or inorganic capping. This work was published in Nano Letters.

Building on these results, in our future work in this project we will explore in detail the role of trapping on the optical properties of copper doped nanostructures and the effect of intentional insertion of hole-trapping agents on the recombination mechanisms and, ultimately, the emission efficiency.

Future Work

The field of doped colloidal nanocrystals is relatively young and is rapidly expanding. Our results on the ability of copper impurities to introduce permanent optically-active hole into NCs represent a crucial achievement in the field and will generate several studies both on the fundamental and the applicative aspects of this material system. Building upon the results we achieved so far, we will explore the role of trapping on the optical properties of copper doped NCs in order to identify the key factors that influence the

recombination mechanism and ultimately determine the emission efficiency. Detailed spectroscopic investigations will be conducted as a function of temperature, shell thickness, and type of organic passivation, both at ensemble and single dot levels. Exciton recombination mechanisms and the effect of surface treatments and passivation strategies will be investigated also by externally controlling the position of the Fermi level using an electrochemical approach. All these studies will allow us to develop a new strategy for controlling both the emission color and its efficiency via intentional introduction of surface hole traps in doped NCs. In this view, we will also further exploit the core/shell motif and synthesize new copper doped core/shell NCs in type II configuration, where the optically generated hole can be rapidly extracted from the copper-doped core to the undoped shell due to the large offset between the valence band energies of the respective semiconductors.

These studies will allow us to draw specific guidelines for the design of efficient doped NC emitters that we will apply to new concept devices such as monopolar light-emitting devices and low-threshold lasers. In this context, our research will include detailed characterization of the electrical properties of doped NCs.

Conclusion

We have a step-by-step approach to new doped nanocrystals for LEDs and laser applications:

1. Understanding of the role of trapping in the radiative recombination of impurity states in doped nanocrystals

2. Investigating the detail of the intragap states due to copper ions in the lattice

3. Development of strategic guidelines for the design and synthesis of efficient copper doped NCs

4. Fabrication and characterization of proof-of-concept light emitting devices and lasing structures based on this new type of material system.

Publications

Brovelli, S., R. D. Schaller, S. A. Crooker, Garci&acute, Y. Chen, R. Viswanatha, J. A. Hollingsworth, H. Htoon, and V. I. Klimov. Nano-engineered electron-hole exchange interaction controls exciton dynamics in core-shell semiconductor nanocrystals. 2011. *Nature Communications.* **2**: 280 (8 pp.).

GarciÃÅa-SantamariÃÅa, F., S. Brovelli, R. Viswanatha, J. Hollingsworth, H. Htoon, S. Crooker, and V. Klimov. Breakdown of volume scaling in auger recombination in CdSe/CdS heteronanocrystals: The role of the core-shell interface. 2011. *Nano Letters.* **11** (2): 687.

Universal Physics with Ultracold Atoms

Joseph A. Carlson
20110633PRD2

Introduction

This project outlines a theoretical research plan in cold atom physics. In cold atoms one can tune the interactions and thus mimic many different strongly-interacting Fermi systems. This research has important implications for many fields of physics including atomic physics, nuclear physics, astrophysics., and condensed matter. Cold atoms are also being used to study fundamental properties of quantum mechanics.

The Oppenheimer postdoc who will carry out this project will study new states of matter in cold atom systems, and bridge the fields of nuclear, particle, atomic, and condensed matter physics. A particular emphasis will be to study novel states of matter and their potential applications.

Benefit to National Security Missions

This work is particularly important to DOE/SC including nuclear physics and BES. The strongly-correlated fermi systems that will be studied are important in nuclear science, high-temperature superconductors and quantum computation.

Progress

Dr. Nishida arrived in early September, 2011. So far at Los Alamos, he has completed one paper in cold atom physics [1]. He is working on another describing high-energy scattering cold atom experiments [2]. This work connects the short-range physics (in particular the universal contact parameter) to possible observations of backward-angle scattering of high-energy incident atoms. This is closely related to similar work in electron and neutrino scattering, the latter of importance to the LANL experimental program in neutrino physics. We expect this task to be completed in the next few months.

Dr Nishida, in his relatively short time here, has initiated discussions and collaborations with others in T-2 and elsewhere in T-division.

Future Work

The research will be devoted toward finding new states of matter in strongly-correlated fermi systems.

The first goal is to further identify the characteristics of mixed-dimensional systems, where Dr. Nishida has been a leading authority. A critical aspect that will be addressed first is to make an accurate estimate of the critical temperature in such a system. This work will combine analytical and numerical methods that have been used in previous studies of simpler systems. The second goal is to enlarge the scope of present-day cold atom experiments to include the ability to study new systems including p-wave superfluids and trimer systems. The p-wave superfluids are potentially very important because it includes topological properties that can be of potential use in quantum computation. Another goal is to enable experimental investigations into states of three or four-particle condensates. These are intriguing because of the analogies in nuclear and particle physics, and the possibility of studying astrophysically relevant environments. In all cases few-body techniques will be used to investigate potential instabilities that could limit experimental approaches to these systems, and also to examine the expected properties of many-body systems once stability has been achieved.

Conclusion

This effort will produce new understanding of strongly-correlated fermionic matter and novel states in such systems. This work will have direct impact on nuclear physics, including the FRIB facility studying neutron-rich nuclei, in condensed matter, where analogues to high-Tc superconductors can be studied, and in quantum science generally.

References

1. Pietila, V., D. Pekker, Y. Nishida, and E. Demler. Pairing instabilities in quasi-two-dimensional Fermi gases. 2011. *Preprint on arxiv.org.*

2. Nishida, Y.. "Hard probes" of strongly-interacting atomic gases. *submitted, preprint at arxiv.org/ abs/1110.5926.*

Publications

Nishida, Y.. "Hard probes" of strongly-interacting atomic gases. *Physical Review B.*

Pietila, V., D. Pekker, Y. Nishida, and E. Demler. Pairing instabilities in quasi-two-dimensional Fermi gases. *Physical Review B.*

Quantum Simulations: From Superconductivity to Nanoscale Electronics

Bogdan F. Damski
20110711PRD2

Introduction

We are studying cold atom systems and their use as quantum simulators of superconductors and many-body effects in nanoscale transport. This is a competitive field with broad implications, e.g., in condensed matter physics, nanoscale science, and quantum information. Quantum simulation uses the highly controllable nature of one quantum system (here, a cold atom cloud) to create simplified analogs of complex materials and devices in order to gain direct theoretical and experimental insight into the underlying physical phenomenon. We will develop, theoretically, a scheme for emulation of various superconductors in cold atom setups to address problems inaccessible in traditional condensed matter settings. In particular, we will develop a unified theory of spectroscopic measurements on cold atom and superconducting systems in order to help understand the mechanisms of high-Tc superconductivity as revealed by cold-atom simulations. From here, more complex systems will be studied to understand quantum and non-equilibrium effects in nanoscale electronic systems, as well as to provide additional measurement techniques capable of probing the cold atom systems. This will help elucidate the role of interactions and dissipation in electronic transport – effects that are difficult to capture in traditional theoretical approaches to transport.

Our work will characterize promising methods for extracting information from cold atom systems that will help understand the underlying phenomena to high-Tc superconductivity. Superconducting materials have the potential to revolutionize power distribution, i.e., create more efficient means of distributing electricity that will be helpful in moving to green sources of energy among other things. Also, we will investigate nonequilibrium and inhomogeneous cold atom systems in order to understand quantum effects in electronic transport, which is crucial in designing functional nanoscale devices.

Benefit to National Security Missions

This work will bring better understanding of high-Tc superconductors: materials with zero electrical resistance. These materials have important applications like, e.g., they can eliminate virtually all the loss of energy that goes into resistive heating in the lines transmitting electricity. This research will also advance fundamental understanding of materials on the very quantum level and their dynamics. Both goals are becoming focus areas for numerous Federal agencies including DOE, for example for both applied and basic aspects of energy research.

Progress

We have made progress in three directions following our proposal. The first direction leads to a theoretical framework that unifies the description for superfluids and superconductors. Since both phenomena are consequences of a coherent macroscopic quantum state, we focus on a consistent description of the emergence of such coherence. An important advantage of our approach is that quantum coherence as well as fluctuations can be evaluated in a controlled fashion. One significant achievement of our theory is that it is the first theory to meet three stringent requirements for a satisfactory theory of interacting bosons, a criterion which has puzzled people for more than sixty years. The role of superfluidity and superconductivity is clearly explained in our theory as the dynamic response to disturbance of the coherent quantum state. Our theory not only captures experimental observations but also provides predictions for future investigations of superfluids and superconductors. For example, an additional excitation mode due to a broken internal symmetry by pairs of bosons could be a signature of a superfluid phase different from any current understanding. Our results are published in [1], [6], [7], and [8].

In the second direction, we have been studying the following important transport phenomena. The first is heat transport in nonlinear bosonic systems relevant to the most important biomolecule, DNA. We have shown in [3] that heat transport can be used to discriminate between proposed models for DNA denaturation. Second, we studied the dynamics of two clouds of fermions carrying different spins and colliding with each other. In the presence of strongly attractive interactions, our study shows that fermions tend to form correlated pairs and as a consequence, those paired fermions act as a barrier

for the diffusion of the two clouds. Our theory supports recent experiments on spin dynamics of ultra-cold atoms and is published in [5]. Third, we researched the possibility of inducing spatially -arying interactions using advanced techniques of optics [4]. Such inhomogeneous interactions may induce interesting patterns in ultra-cold atoms resembling the patterns observed in high-temperature superconductors. Fourth, we analyzed the differences in the dynamics of fermions and bosons when the system is suddenly set out of equilibrium. While the induced current of bosons oscillates and decays gradually, the current of fermions exhibit a quasi steady state. Moreover, the number fluctuations show clear signatures of which type of particles is the carrier of the current. We submitted our results for publication [10].

In the third direction we investigate signatures of pre-formed pairs of electrons in high-temperature superconductors. Those pre-formed pairs do not contribute to superconductivity and may account for the observed gaps in the non-superconducting state. We found that those pairs suppress the effective carrier density and this may be an explanation for the observed behavior of the low-frequency conductivity. Furthermore, by absorbing photons those pairs could dissociate into quasi-particles. We analyze the optical conductivity data and propose that the peak observed in the mid-infrared regime may be a signature of the dissociation of pairs because such process could shift the spectral weight. Our results are summarized in [2] and [9].

Future Work

We will continue to develop our general theory of super-fluids and superconductors. This theory will help build a theoretical description for spectroscopic measurements in cold-atom systems in order to investigate quantum simulations of high-temperature superconductors (HTSCs). These studies will set firm foundations for the cold-atom quantum simulation of high-Tc superconductors and shed light on its mechanisms. This is a promising direction because similar phases are observed in both systems and ultra-cold atoms have the advantage that interactions and trapping potentials are tunable. It remains a great challenge to explain why electrons form pairs as they do in conventional superconductors but show no superfluidity in some phases. Since electrons in HTSCs carry charges while ultra-cold atoms are neutral, not every measurement tool can be applied to both systems. By unifying the descriptions of superfluids and superconductors, we are on track to sort out common features that can be simulated using ultra-cold atoms.

As well, we will develop a theory of quantum transport that handles interactions, noises, geometries, and memory effects at the nanoscale, and propose well-controlled cold-atom experiments to test them. The goal is to build a unified description of transport phenomena. This work will help resolve key issues regarding, e.g., how many-body correlations relax into a set of non-interacting correlations away from the junction and how noise/dissipation induced by impurities or barriers – which can be engineered in cold-atom systems – affect the transport of electrons. A resolution of these issues will set the stage for a revolution in modeling transport properties of nanoscale devices, such as "memristors" and those based on strongly correlated materials. Furthermore, our theoretical work may help explore phenomena such as interaction-induced dynamics that could be formidable in conventional setups but is possible using advanced techniques of ultra-cold atoms.

Conclusion

Our results from quantum simulations will provide more insight into the parallels between cold atom and high-Tc superconducting systems, which is one of the greatest problems in physics. In addition to providing hints of the mechanism of superconductivity, our work may lead to the discovery of novel superconductors with even higher transition temperatures. Superconductivity is one of the most significant discoveries in the 20th century and has important applications in dissipationless power transmission and advanced medical instruments. Future progress in superconductors critically depends on a full understanding of their properties, which is a goal of our work. We have investigated several fundamental issues in quantum transport and tried to integrate their descriptions into a unified theory. This unified theory can help explore dynamics that may lead to new designs of nano devices. Those new nano devices could play a crucial role in next-generation electronics and atom-based sensors.

References

1. Cooper, F., C. C. Chien, B. Mihaila, J. F. Dawson, and E. Timmermans. Non-perturbative predictions for cold atom Bose gases with tunable interactions . 2010. *Physical Review Letters.* **105**: 240402.

2. Wulin, D., B. M. Fregoso, H. Guo, C. C. Chien, and K. Levin. Conductivity in Pseudogapped Superconductors: The Role of the Fermi Arcs . To appear in *Physical Review B.*

3. Velizhanin, K. A., C. C. Chien, Y. Dubi, and M. Zwolak. Driving denaturation: Nanoscale thermal transport as a probe of DNA melting . 2011. *Physical Review E.* **83**: 050906.

4. Chien, C. C.. Spatially varying interactions induced in atomic gases by optical Feshbach resonance. *Physics Letters A.*

5. Wulin, D., H. Guo, C. C. Chien, and K. Levin. Spin Transport in Cold Fermi gases: A Pseudogap Interpretation of Spin Diffusion Experiments at Unitarity. 2011. *Physical Review A.* **83**: 061601.

6. Cooper, F., B. Mihaila, J. F. Dawson, C. C. Chien, and E.

Timmermans. Auxiliary field approach to dilute Bose gases with tunable interactions. 2011. *Physical Review A.* **83**: 053622.

7. Mihaila, B., J. F. Dawson, F. Cooper, C. C. Chien, and E. Timmermans. Auxiliary field formalism for dilute fermionic atom gases with tunable interactions. 2011. *Physical Review A.* **83**: 053637.

8. Mihaila, B., F. Cooper, J. F. Dawson, C. C. Chien, and E. Timmermans. Analytical limits for cold-atom Bose gases with tunable interactions . 2011. *Physical Review A.* **84**: 023603.

9. Wulin, D., H. Guo, C. C. Chien, and K. Levin. A Pre-formed Pair Approach to Pseudogap Effects in the ab-Plane Optical Conductivity of the Cuprates. *Physical Review B.*

10. Chien, C. C., M. Zwolak, and M. Di Ventra. Bosonic and fermionic transport phenomena of ultra-cold atoms in 1D optical lattices . *Physical Review Letters.*

Publications

Chien, C. C.. Spatially varying interactions induced in atomic gases by optical Feshbach resonance . *Physics Letters A.*

Chien, C. C., M. Zwolak, and M. Di Ventra. Bosonic and fermionic transport phenomena of ultra-cold atoms in 1D optical lattices . *Physical Review Letters.*

Cooper, F., B. Mihaila, J. F. Dawson, C. C. Chien, and E. Timmermans. Auxiliary field approach to dilute Bose gases with tunable interactions . 2011. *Physical Review A.* **83**: 053622.

Cooper, F., C. C. Chien, B. Mihaila, J. F. Dawson, and E. Timmermans. Non-perturbative predictions for cold atom Bose gases with tunable interactions . 2011. *Physical Review Letters.* **105**: 240402.

Mihaila, B., F. Cooper, J. F. Dawson, C. C. Chien, and E. Timmermans. Analytical limits for cold-atom Bose gases with tunable interactions. 2011. *Physical Review A.* **84**: 023603.

Mihaila, B., J. F. Dawson, F. Cooper, C. C. Chien, and E. Timmermans. Auxiliary field formalism for dilute fermionic atom gases with tunable interactions. 2011. *Physical Review A.* **83**: 053637.

Velizhanin, K. A., C. C. Chien, Y. Dubi, and M. Zwolak. Driving denaturation: Nanoscale thermal transport as a probe of DNA melting. 2011. *Physical Review E.* **83**: 050906.

Wulin, D., B. M. Fregoso, H. Guo, C. C. Chien, and K. Levin. Conductivity in Pseudogapped Superconductors: The Role of the Fermi Arcs. To appear in *Physical Review B.*

Wulin, D., H. Guo, C. C. Chien, and K. Levin. Spin Transport in Cold Fermi gases: A Pseudogap Interpretation of Spin Diffusion Experiments at Unitarity . 2011. *Physical Review A.* **83**: 061601.

Wulin, D., H. Guo, C. C. Chien, and K. Levin. A Pre-formed Pair Approach to Pseudogap Effects in the ab-Plane Optical Conductivity of the Cuprates . *Physical Review B.*

A New Drift Shell Integration Technique for Inner Magnetospheric Space Weather Models

Josef Koller
20110735PRD2

Introduction

Abrupt solar activities can trigger geomagnetic storms and, consequently, the radiation environment in the Van Allen Belts can get severely enhanced. This enhanced energetic electron flux can damage satellites, instruments and be harmful to humans in space. Such geo-space disturbances are summarized under the term "space weather" [1]. The overarching goal of this project is to investigate the physical processes that are responsible for the dynamic variations in the radiation belts. We will develop a new model using a novel numerical approach that will remove a computational bottleneck for high-precision radiation belt models. This new tool will allow us to study decades of satellite data and reveal the underlying physical process responsible for the geomagnetic storm-time variations in the radiation belts.

Benefit to National Security Missions

This program will build a tool to calculate particle drift shells in the inner magnetosphere. The computational speed will be six orders of magnitudes faster than standard integration techniques. The tool will enable, for the first time, high precision space weather data assimilation and forecasting models, which are an important component to NOAA Space Weather Prediction Center and DoD Air Force Research Lab and Space Command. Understanding the space environment is critical to fielding the satellite systems that are needed to monitor nuclear nonproliferation. The underlying space physics builds capability to understand the effects of nuclear detonations in space, supporting stockpile stewardship.

Progress

In the first year of this project, Dr. Yiqun Yu used the physics-based ring current-atmosphere interaction model (RAM) [2] coupled with a self-consistent magnetic field code (SCB) [3, 4] to simulate seven different geomagnetic storm events with different activity levels by using different boundary conditions in the model (Figure 1). For the plasma boundary conditions, two kinds of boundary conditions were chosen: LANL geosynchronous measurements or Tsyganenko-Mukai plasma sheet empirical model. For the magnetic field boundary, Tsy-

ganenko 89 (T89) empirical model was utilized. For the convective electric field, two different models were used and compared against each other: the Weimer 2001 empirical model or Volland-Stern empirical model.
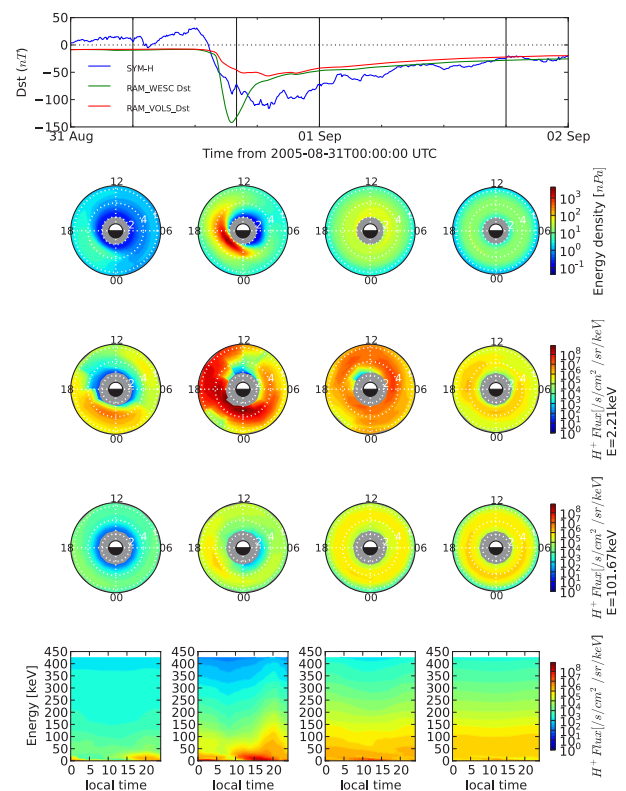
Figure 1. Simulation results for geomagnetic storm event August 31, 2005 with our coupled RAM-SCB model. We have tested this model with different boundary and electric fields. Top: The observed geomagnetic SYM-H index (blue) and the corresponding index calculated with our model for the following electric field models: Weimer (WESC) and Volland-Stern (VOLS). The rest of the rows represent simulation results using the Weimer electric field at four time snapshots providing energy density, proton flux at energy level of 2 keV, and above 100 keV. The bottom row shows energy - local time contour plot of proton flux at a distance of 4.0 Earth Radii.

After completing the simulation of these magnetic storm events, she carried out a study comparing the model output against in-situ satellite and ground-based magnetometer measurements. For the in-situ comparisons, she compared the following parameters: the magnetic field along the trajectory of satellites such as POLAR and Cluster, energy differential ion flux of (H+, O+, and He+) along these trajectories or at a certain location as a function of energy, and the electric field along the satellite trajectory (i.e., along Cluster/EDI). For the ground-based measurements, she compared the computed Dst/SYM-H index, which serves as a proxy of the energetic level of the ring current in the inner magnetosphere, with the observed index.

Dr. Yu also implemented the ONERA library to compute the L* parameter which contains the information of the magnetic flux enclosed by a particle's drift shell around the Earth. The L* calculation is based on tracing the magnetospheric magnetic field lines latitudinally as well as azimuthally. Hence, a magnetic field model of the magnetosphere is needed, such as the empirical models T89, T01storm, etc. as used in the ONERA library.

With the new physics-based inner magnetosphere model RAM-SCB, the magnetic field within the computational domain (r<6.5Re) is known and can be therefore utilized to calculate L*. Due to the irregular grid of this magnetic field, it is necessary to interpolate the magnetic field for specific location or onto the satellite trajectory. In order to have a better interpolation from the irregular grids, Dr. Yu adopted the natural neighbor interpolation method after creating the Delaunay triangulation mesh from the grids. She incorporated a package written in C, which is used to determine the Delaunay triangulation from three-dimensional irregular grids, into the ONERA library that is later used to compute the L* from the RAM-SCB magnetic field output. She has compared this interpolation method with other methods such as nearest neighbor interpolation, in terms of speed and accuracy during the above storm events. She has also successfully increased the computational speed of the L* calculation by parallelizing the computation using message passing interface (MPI).

Since this new model RAM-SCB only covers the domain within 6.5 Re, any satellite trajectory outside this domain cannot use the model to calculate the magnetic field, and L* is also undefined. In order to have continuous information (e.g., L* and magnetic field B) along the satellite trajectory, she filled the gap by combining the RAM-SCB model with the T89 empirical model, which is a global magnetic field.

Dr. Yu recently started to use a neural network training technique [5] to train the L* obtained from the physics-based RAM-SCB magnetic field output. The ultimate goal is to take advantage of the speed of the neural network to obtain the L* from the external solar wind conditions in microseconds, instead of slowly tracing the global magnetic field lines.

In summary, Dr. Yu has made tremendous progress towards the outlined goals in the project. She will soon have a neural network model ready for testing and converting radiation belt data into phase-space densities, which will advance current data assimilation calculations for the radiation belts and surpass the current fidelity of studying the physical processes in the radiation belts.

Future Work

In the second year of her project, Dr. Yu will complete the neural network training with RAM-SCB. Since the training data set has to be created with the traditional and slow numerical integration method, a lot of computing time is necessary. The codes are running almost independently and only minor supervision is necessary. Dr. Yu will use this time to finish and submit two refereed papers and write a third one.

She will use her novel approach towards answering the motivating science questions: (1) What is the relative contribution of radial transport, localized acceleration, and loss process that cause the storm-time dynamics of radiation belt electrons? (2) Do different types of solar wind events lead to different dynamics and acceleration processes in the radiation belt environment during different phases of the solar cycle? (3) Are the increased flux levels due to radial transport or a localized acceleration process and can they be linked to different solar wind driving conditions?

Dr. Yu will address these questions by using her new technique to compute the adiabatic coordinate L* six orders of magnitude faster than with the standard numerical field line tracing technique. This will allow her to place the radiation belt flux observations in the correct modeling coordinate system which is based on adiabatic invariants including L*. After converting a whole solar cycle worth of data into phase space densities, she will employ a data assimilation technique using an ensemble Kalman Filter [1] and create a highly accurate representation of the radiation belts for a whole solar cycle. This has never been attempted before since the long computing times for L* were so prohibitive. The newly created high-resolution map will, for the first time, allow a detailed study of the acceleration, loss and transport processes in the radiation belts.

Conclusion

In addition to developing a fundamental understanding of the physical processes responsible for the dynamics in the inner magnetosphere, this project will build a computationally efficient tool to solve pressing science questions regarding the highly energetic particle environment in near Earth space. The developed tool will be able to calculate particle drift shells in the inner magnetosphere several orders of magnitudes faster than standard integration techniques and remove a major computational bottleneck. This approach will, for the first time, allow a detailed study of the processes in the radiation belt covering a whole so-

lar cycle with high resolution. Together with a new global understanding of the radiation belts, this project will build the foundation for implementing the necessary physical processes into high precision space weather data assimilation and forecasting models.

References

1. Koller, J., Y. Chen, G. D. Reeves, R. H. Friedel, T. E. Cayton, and J. A. Vrugt. Identifying the radiation belt source region by data assimilation. 2007. *Journal of Geophysical Research-Part A-Space Physics.* **112** (6): 1.

2. Jordanova, V. K., Y. S. Miyoshi, S. Zaharia, M. F. Thomsen, G. D. Reeves, D. S. Evans, C. G. Mouikis, and J. F. Fennell. Kinetic simulations of ring current evolution during the Geospace Environment Modeling challenge events. 2006. *Journal of Geophysical Research-Part A-Space Physics.* : A11S10.

3. Zaharia, S., C. Z. Cheng, and K. Maezawa. 3-D force-balanced magnetospheric configurations. 2004. *ANNALES GEOPHYSICAE.* **22** (1): 251.

4. Zaharia, S.. Improved Euler potential method for three-dimensional magnetospheric equilibrium. 2008. *Journal of Geophysical Research - Part A - Space Physics.* **113** (A8): A08221 (7 pp.).

5. Koller, J., G. D. Reeves, and R. H. Friedel. LANL*V1.0: a radiation belt drift shell model suitable for real-time and reanalysis applications. 2009. *GEOSCIENTIFIC MODEL DEVELOPMENT.* **2** (2): 113.

Publications

Yu, Y., J. Koller, S. Zaharia, and V. Jordanova. L* Neural Network from Different Magnetospheric Field Models. *Space Weather.*

Yu, Y., V. Jordanova, S. Zaharia, J. Koller, J. Zhang, and L. Kistler. Validation Study of the Magnetically Self-Consistent Inner Magnetosphere Model RAMS-SCB. *Journal of Geophysical Research - Space Physics.*

Shortcuts to Adiabaticity in Quantum Devices

Wojciech H. Zurek
20110736PRD2

Introduction

The concept "Fast Good" pushed forward by the world-leading chef Ferran Adria might be a motto born in modern cuisine, but it actually applies to many areas of the day-to-day life. When it comes to technology there is certainly no doubt that shortening production processes pays great dividends, and the quest for faster and more powerful devices such as computers has been running for decades as dramatically illustrated by Moore's law.

But all quantum technologies crash with the Fast Good trend at a fundamental level. At a microscopic scale, higher performance of a quantum device comes generally at the price of slowing down its running time, as dictated by text-book theorems in quantum theory. The focus of this research project is to spur quantum technologies by changing this state of affairs and finding ways out to fulfill both sides of the Fast-Good dichotomy. It will deepen the current understanding of dynamical process, put forward new schemes in the state-of-the-art experimental control of quantum devices, and accelerate the development of new benchmarks in quantum metrology, simulation and computation.

Benefit to National Security Missions

This project will allow more powerful and better-controlled quantum systems. This has broad applications that cut across many areas of interest to DoE and LANL. This includes nanoscience, quantum sensitive measurement, information processing, and related areas. While this is admittedly long-term research, the measurement tools that may develop could impact any national security mission that depends on sensing technology.

Progress

There was not technical progress by the time of this writing, because the postdoctoral fellow was scheduled to join the Laboratory in September 2011.

Future Work

The project is aimed at developing a theoretical framework to engineer quantum quenches of an external parameter (field, frequency, temperature, etc.) that allow an ultrafast frictionless driving of a quantum system (trapped ions and ultracold atoms) in a controlled way, that is without inducing heating, undesirable excitations or other negative effects. Adiabatic theorems stand out as a main objection to such goal. However, systems exhibiting integrals of motion and self-similar dynamical laws are allowed to overcome adiabaticity requirements. For systems lacking these properties, the universal behavior in the neighborhood of a critical point can be exploited for the same goal. Three different types of systems will be considered:

1. Single quantum systems: trapped ions and atoms

2. Many-body systems such as Bose-Einstein condensates and strongly correlated quantum fluids

3. Quantum hybrid systems composed of subsystems of type 1 and/or 2.

A first task consists in providing a theoretical framework for shortcuts to adiabaticity. Goals include the identification of the necessary properties (such as symmetries or integrability) in experimentally relevant systems, the regime of validity /stability, and finding bounds to the speed of evolution.

A second task is to come out with robust experimental proposal to drive ultrafast operations in systems 1-3. The goal is to find the required trajectories of the control parameters in operations such as transport and expansion.

A third task consists in exploring the practical applications of such strategies. Goals are new probing techniques of quantum correlations, cooling schemes, and novel high-performance quantum engines. On the more applied side, this includes studying the impact of our ideason quantum technologies. As a goal, improvements of metrological standards follow from new transport strategies (higher feeding rate of interferometers); while in quantum simulation and computation they will be based on the controlled preparation and detection of many-body phases of matter.

Conclusion

Though quantum technologies such as atomic clocks have been benefiting society since the fifties, it is clear that they are playing an ever-increasing role. They have the potential to do better and completely outperform conventional electronics. The exploitation of quantum laws in metrology shows how the race for ever-better clocks have brought technological advances such as the GPS required for satellite navigation, ultimately transforming society in a global scale through new communication and business models. Other quantum technologies in a nascent stage might revolutionize the fields of simulation, computation and communication.

"Listening" to the Noise of a Single Electron Spin: Ultra-sensitive, Non-perturbative Spin Noise Spectroscopy

Scott A. Crooker
20110747PRD3

Introduction

Measurement of electron and nuclear spins forms the basis of modern magnetic resonance technologies such as NMR, MRI, and electron spin resonance. Driven by the desire and need for ever-increasing sensitivity and resolution (e.g., for MRI), the number of detected spins necessarily decreases. Ultimately we hope to reach the limit of *single* quantum-mechanical spins. At present, however, the direct magnetization measurement of a single spin is a tremendously difficult proposition, due to the extreme sensitivity required (conventional NMR or MRI lacks the sensitivity by about a factor of a trillion!).

Nonetheless, from viewpoints of both fundamental measurement and basic science, single-spin detection represents a truly landmark achievement in measurement science. Recent advances in optical detection and efficient digital signal processing, coupled with alternative measurement approaches based on passive spin noise detection (rather than conventional perturbative studies), suggest a viable route that forms the basis of this proposed work.

Benefit to National Security Missions

This project will build Laboratory capabilities in the development of novel measurement methods that enable new scientific discovery at LANL. It is based on recent technological advancements that enable the use of FPGAs and on the very large data storage and manipulation capabilities that have now become available. Our basic approach to noise spectroscopy goes well beyond the specific example of electron spin noise that will be investigated here. The advantages of noise spectroscopy as an experimental probe are very general. The project will advance new Laboratory capabilities that underpin a wide variety of Laboratory missions. Demonstration of single spin noise spectroscopy measurements will generate worldwide attention and will form a robust platform for nanoscale spintronics at LANL. The team will work with John Sarrao to support the BES Materials Science mission. Our work is also relevant to DoD, and we will work with DARPA to extend this work.

Progress

Yan has developed a working spin noise spectrometer that is currently taking data on hole spin fluctuations of holes in semiconductor quantum dots. She has re-equipped the apparatus to include the possibility of applying longitudinal magnetic fields, which have proven essential for revealing the coupling between holes spins and the surrounding bath of nuclear spins in these quantum dots. She is currently writing up her results for publication; Figures 1 and 2 show examples of the high quality data she has taken.
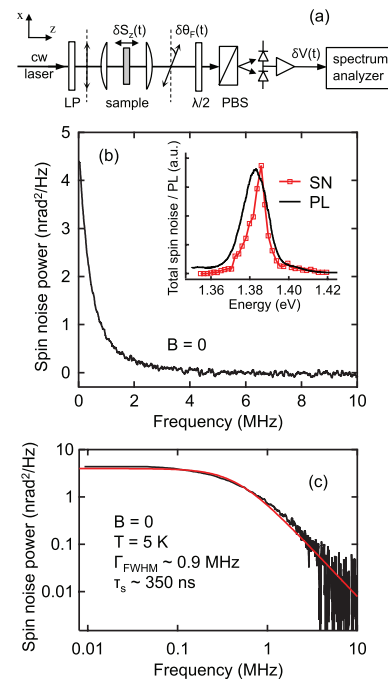
Figure 1. a) Experimental schematic of the optical spin noise magnetometer. b) Spin noise power from randomly fluctuating hole spins in semiconductor quantum dots. The narrow width indicates a long spin lifetime. c) this noise spectra follows a lorentzian lineshape to a very high degree of precision.
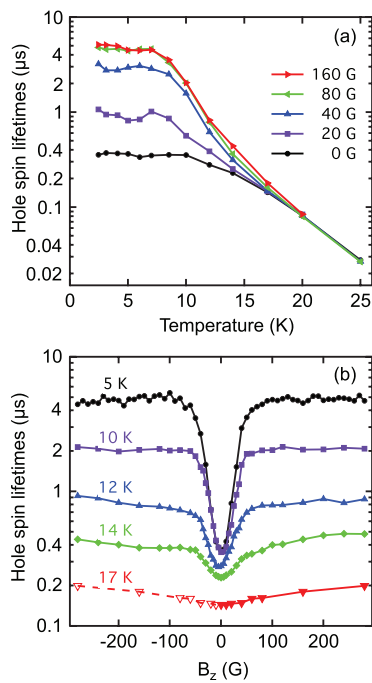
Figure 2. Plots show the measured spin lifetime (ie, the inverse width of the noise spectra) as a function of temperature fro different applied fields, and as a function of applied field at different temperatures.

Yan has also worked on measuring spin noise in atomic potassium vapors, in an effort to reveal how spin noise spectra behave in the presence of a homogeneously-broadened absorption resonance. This work is part of our spin noise collaboration w/ University of Dortmund.

Future Work

The overarching aim of this project is to develop a sensitive and ultra-efficient magnetometer based on the magneto-optical Faraday Effect, which is capable of measuring the tiny, random magnetization fluctuations of a single electron spin. Using this, we intend to measure the dynamics of truly quantum-mechanical objects, using a new and alternative approach to spin resonance measurement based on spin noise spectroscopy, which is in principle non-perturbative. These studies are directly relevant to the rapidly-expanding field of quantum measurement science.

To this end, we will:

- Isolate single electrons in single semiconductor quantum dots (grown by our collaborators using standard molecular-beam epitaxy), and address these dots individually with optical microscopy.

- Detect, or "listen", for the electron's spin fluctuations using our techniques for off-resonant (non-perturbative) Faraday rotation with narrowband, frequency-tunable lasers.

- Measure frequency spectra and higher-order correlation functions of these tiny noise signals using new

instrumentation for ultra-efficient, real-time digital signal processing that is based on field-programmable gate arrays, or FPGAs. (Originally developed for radio astronomy, our preliminary efforts to apply these new instruments to the tabletop lab environment already shows >1000x improvement over commercial RF spectrum analyzers!) Higher-order correlation measurements are expected to reveal new and important physics of spin interactions as N→1.

Conclusion

We expect to develop an ultra-sensitive magnetometer capable of "listening" to the tiny spin fluctuations of truly quantum-mechanical objects: single electron spins. New instrumentation for efficient digital signal processing based on configurable hardware (FPGAs, or "field-programmable gate arrays") are essential to this work. The proposal will advance new Laboratory capabilities that underpin a wide variety of Laboratory missions. Demonstration of single spin noise spectroscopy measurements will generate worldwide attention and will form a robust platform for nanoscale spintronics at LANL.

Determining the Origin of the Highest Energy Cosmic Rays with TeV Gamma-Ray Observations

Brenda L. Dingus
20110749PRD3

Introduction

Nature accelerates particles to energies millions of times higher than man-made accelerators. We do not know the type of astrophysical sources that accelerate these particles, and we do not know what physical mechanisms accelerate these particles. With this project, are making observations of gamma rays to determine if the gamma ray sources are also accelerating the highest energy particles. We will use the newest gamma-ray observatory, HAWC (High Altitude Water Cherenkov), to make these observations. LANL is leading the HAWC team, which is a consortium of universities in Mexico and USA.

Benefit to National Security Missions

This work is most closely tied to the High Energy Physics program of the DOE Office of Science. The HAWC observatory has been recognized by several National Academy studies as an important project and as making fundamental observations of the high energy Universe. HAWC is jointly funded by NSF and DOE.

Progress

Despite only having been working at LANL since mid July 2011, much progress has been made. Dr. Younk has designed a new technique for deploying the photo-multiplier tubes (PMTs) in the HAWC observatory that allows them to be installed after the water tanks have been filled with water. Thus the tasks of deploying 1200 PMTs, which must be done by physicists, are decoupled from the construction of the 300 water tanks, which is done by laborers. This decoupling reduces the number of trips to the site by physicists by allowing PMTs to be installed in large batches. It also gives much more flexibility to the construction schedule.

Dr. Younk has been heavily involved in the characterization of the PMTs that will be installed in HAWC. All the PMTs for HAWC are being tested at LANL prior to being sent to Mexico for installation. Dr. Younk is overseeing a graduate student who is doing the testing, and he is analyzing the data to determine the proper operating voltage for all 1200 PMTs. Since Dr. Younk has arrived over 200 PMTs have been tested.

Dr. Younk also continues to be active in the field of astroparticle physics. He has finished a single-author paper describing a statistical method to constrain the characteristic angular size of the brightest cosmic-ray sources observed above 57×10^{18} eV which was published in September 2011.

Future Work

Tasks to be accomplished:

- Assist in the commissioning of the HAWC observatory including calibrating the detector, designing event reconstruction algorithms, and developing analysis tools

- Search for flares from active galactic nuclei in the HAWC data

- Cross correlate these flares with observations at lower energies

- Describe the general attributes of these flares in a catalog

- Determine the variability of flares from active galactic nuclei to determine whether they are the sources of the highest energy cosmic rays

Conclusion

The unique observations of HAWC will characterize the total energy emitted by gamma-ray sources and investigate the time variability and energy spectra of these sources. These observations provide strong constraints on how the highest energy particles are accelerated and therefore, test our understanding of physics in the extreme environments of the astrophysical accelerators. The gamma ray emission is produced in the intense gravitational and electromagnetic field of black holes, which are extreme laboratories that cannot be replicated on Earth.

Publications

A method to constrain the characteristic angular size of the brightest cosmic-ray sources observed above 57 × 1018 eV. To appear in *Astrophysics and Space Sciences Transactions.*

Nonequilibrium Quantum Phase Transitions

Eli Ben-Naim
20080723PRD2

Abstract

This project constructed a theoretical framework of nonequilibrium Quantum Phase Transitions with two specific research areas, one on quantum drag and one on quantum synchronization. This research addressed an important science and technology need because such phase transitions involve significant quantum-level events that have a direct macroscopic effect and, as such, lend themselves to myriad applications in the rapidly expanding field of nanotechnology. This project also built an understanding of superfluidity that has the accuracy needed to turn the new dilute ultracold atom systems into applications such as atom lasers, precision clocks, and gyroscopes as well as prompt a review of our fundamental notions about areas of science related to superfluidity.

Background and Research Objectives

Nonequilibrium quantum phase transitions are poorly understood. The overall goal of the present project was to develop a firm theoretical foundation for quantum phase transitions. As applications of nanotechnological devices controlled by quantum behavior multiply and diversify, this understanding is increasingly important.

The primary subject of this project is quantum drag with the goal of new fundamental understanding of superfluidity. The phenomenon of superfluidity is well known for over half a century, yet it remains enigmatic in many respects. As the key to numerous applications, both current and future, such as atom lasers, precision clocks, and gyroscopes, it is of great importance that we move towards a more precise grasp of the physics underlying superfluidity.

The second topic of research was the development of an understanding of quantum synchronization, in which different regions of a material spontaneously lock into the same quantum phase. This research has strong implications for decoherence, the mechanism which connects the quantum and classical worlds, and hence, it help bridge the gap between the classical and quantum physics.

Scientific Approach and Accomplishments

We first elaborate on the accomplishments from the research into quantum drag. First, we succeeded in calculating the drag experienced by an impurity of any strength moving through a quasi one-dimensional BEC. We derived new analytical solutions of the equations governing these systems, which allowed us to calculate the drag solutions exactly. We showed, for the first time, that such a force exists in this geometry, and have also been able to calculate the force's dependence on velocity and impurity strength. These results are crucial for definitively demonstrating the presence of this effect in ultracold dilute atomic gases.

Second, considering a superfluid moving along a rough surface, as is the case in realistic experimental situations, we proposed a new explanation of the boundary effects. In particular, we made the case for a new hydrodynamic boundary condition, which has profound implications for the field of superfluidity, including a new theorized critical speed and the presence of normal fluid at any nonzero speed. The ramifications of this hydrodynamic boundary condition would be felt not only in experiments in superfluid helium but also those involving dilute Bose-Einstein condensates.

This research on the fundamental nature of superfluidity led us also to consider that of supersolidity (a theorized new phase of matter that combines attributes of both solids and superfluids). We determined that, in certain parameter regimes, impurity fields immersed in a Bose-Einstein condensate can spontaneously form a crystal that exhibits supersolid behavior as evidenced by nonclassical rotational inertia. Specifically, by using a combination of analytical and numerical methods, we were able to derive a functional form for the interaction between two impurity fields due to mediation by the surrounding condensate and apply this to a system of several impurity fields set in a three-dimensional condensate. Thus we showed that, in a simple system, one could create a solid composed of superfluid components (and that possesses supersolid characteristics).

One of the key outcomes of this project is that it has

laid the foundation not only for future experiments in superfluidity but also for further theoretical exploration of this phenomenon in other systems. Some of the results of this project provide the basis for numerous potentially fruitful lines of inquiry in superfluidity. For instance, we have fleshed out the phenomenon of Casimir drag to an extent that allows for numerical probing through the truncated Wigner approach (an approximation from quantum optics that has been applied with much success towards the simulation of quantum noise effects in BECs). We have also set up a framework in which to study the quantum drag behavior in fermionic systems; positive demonstration of this effect would constitute the first evidence of such a drag force existing in fermionic systems. Furthermore, our research results weigh in on the question of existence of a transverse acoustic force, the Iordanskii force, in superfluids and would contribute towards the resolution of this long-standing controversy.

Next, we have advanced our understanding of nonequilibrium quantum phase transitions through the quantum-synchronization approach. We extended previous results on linear reformulation of the canonical model of synchronization. Doing so allowed us to address, among other things, the issue of anomalous scaling that was found to occur in this new class of exactly solvable models. We succeeded in establishing a workable formalism that permits the application of spectral theory to our linear reformulation of Kuramoto synchronization, which in turn allowed us to generalize the reformulation to encompass much larger classes of coupled systems. Our results make it possible finally to be able to quantize the synchronization model using quantum optics techniques.

Impact on National Missions
This work supports LANL and the DE core capabilities in theoretical condensed matter physics, quantum science, nonlinear dynamics, and nanotechnology. This work supports the energy security mission as it leads to better fundamental understanding of superconductors, materials that have zero resistance. These materials' energy applications include efficient electric power transmission and power storage devices, and sensors for threat reduction.

Publications
Herrera, M., D. C. Roberts, and N. Gulbahce. Mapping the evolution of scientific ideas. 2010. *PLoS ONE.* **5** (5): e10355.

Pomeau, Y., and D. C. Roberts. On the hydrodynamic boundary condition for superfluid flow. 2008. *Phys. Rev. B.* **77**: 144508.

Rica, S., and D. C. Roberts. Induced interaction and crystallization of self-localized impurity fields in a Bose-Einstein condensate. 2009. *Physical Review A.* **80**: 013609.

Roberts, D. C.. Solving the Kuramoto model of a self-synchronizing, finite population of glob ally coupled oscillators. 2008. *Phys. Rev. E.* **77**: 03114.

Roberts, D. C.. When superfluids are a drag. 2009. *Contemporary Physics.* **50**: 453.

Roberts, D. C., and R. Teodorescu. A linear path toward synchronization: Anomalous scaling in a new class of exactly solvable Kuramoto models. 2008. *European Physical Journal.* **165**: 103.

Roberts, D. C., and R. Teodorescu. A linear path towards self-synchronization: Analysis of the fully locked transition of the Kuramoto model. 2008. In *First International Workshop on Nonlinear Dynamics and Synchronization INDS'08.* (Klagenfurt, Austria, 18-19 July, 2008). , p. 184. Germany: Shaker Verlag.

Roberts, D. C., and S. Rica. Impurity crystal in a Bose-Einstein condensate. 2009. *Physical Review Letters.* **102**: 025301.

Ruderfer, D. M., D. C. Roberts, E. O. Perlstein, S. L. Schreiber, and L. Kruglyak. Predicting individual drug response in a panel of 104 genotyped and expression-profiled yeast strains. . 2009. *PLoS ONE.* **4** (9): e6907.

Sykes, A. G., M. J. Davis, and D. C. Roberts. Drag force on an impurity below the superfluid critical velocity in a quasi-one-dimensional Bose-Einstein condensate. 2009. *Physical Review Letters.* **103**: 085302 .

Dissipation and Decoherence in Complex Many-Body Systems

Wojciech H. Zurek
20080728PRD2

Abstract

This project investigated several interrelated topics involving decoherence, dissipation, entanglement, and classical correlations in complex physical systems that have direct implications for many areas of physics, system modeling, and biological/single-molecule sensors. This work has focused on two areas in particular: (1) We have studied how a quantum mechanical system gets correlated with its environment, i.e., what parts of the environment correlate strongly with the system and how these parts of the environment influence systems behavior. These questions underlie many physical and technologically important issues, including how to understand and model decoherence in solid-state architectures for Quantum Computing and how one can construct efficient methods for simulating many-body quantum systems (such as strongly correlated systems in the presence of dissipation or electronic transport in nanoscale systems). As part of this focus, we have also developed a simulation technique for studying 100's-1000's of spins – the method scales polynomially in the system size as opposed to direct simulation, which scales exponentially. (2) We studied how several biophysical problems relating to DNA sequencing and ionic transport. For instance, we examined the effect of dephasing (the term for decoherence in the electronic transport community) on the ability to distinguish DNA bases via an electronic current. This work has been setting the theoretical foundations for electronic sensors for biomolecular systems.

Background and Research Objectives

Decoherence and dissipation are two processes that strongly influence physical behavior at the nanoscale and can dictate the operation of functional devices. For instance, quantum information processing requires quantum hardware for its implementation. Quantum computing would enable an enormous speedup in certain types of computation – the most outstanding current example is the exponential speedup in factoring large numbers, with which one could break some modern encryption techniques. What makes a quantum computer powerful, and correspondingly what makes quantum systems so hard to simulate classically, is the presence of a purely quantum mechanical correlation called entanglement. However, in order to successfully implement a quantum computation, one has to overcome decoherence and its resulting destruction of entanglement.

On the other side of the coin, though, it was recently realized (by looking at quantum systems from the point of view inspired by quantum information processing ideas) that a large and interesting category of quantum evolution can be simulated on a classical computer with resources that are only polynomial (rather than exponential) in the size of the system. In addition to applying these methods to simulate time-dependent evolution of quantum systems, we have also been trying to understand how decoherence/dissipation affect the efficiency of these techniques. The objectives of this work has been to (i) obtain a fundamental understanding of how quantum mechanical systems become entangled with their environment and (ii) develop efficient computational techniques to capture the influence of the environment on a system's behavior (with the long term goal of being able to simulate dissipation and decoherence in superconducting systems and also systems relevant to quantum computing).

This work has also tackled issues related to DNA sequencing and ionic transport. Core among them is a proposal to sequence DNA using nanopore-based electronic transport measurements. This is a novel single-molecule approach that has the potential to greatly reduce the time and cost of sequencing (and also, more generally, give a new approach to (bio)molecular detection). The successful implementation of this technique would have enormous implications for medicine and biology. We have investigated ionic transport in nanopores, as well as dephasing (decoherence) effects in electronic sensors. A longer-term project is on using the techniques above (on the influence of the environment) to simulate electronic transport in the presence of the strongly fluctuating environment of the type present in nanopore experiments.

Scientific Approach and Accomplishments

Simulating decoherence and information transfer – We have examined how information about a system is

distributed into its environment while undergoing decoherence. We demonstrated that noisy environments can effectively acquire and communicate certain classical information about the system, but at a reduced rate compared to "clean" environments. However, quantum information about coherence in the system is distributed globally into the environment, regardless of its noise level, and is therefore effectively lost. In addition to analytic techniques, we developed a simulation method that can handle symmetric qubit environments with a polynomial computational cost (and thus, we simulated 200 qubits, i.e., a state space of 2^{200}, which cannot be handled by direct diagonalization). We have a number of new developments that incorporate information-theoretic concepts (Quantum Chernoff Bounds; Data processing inequality; Fannes' and Fano's inequalities), and that promise to bring a universal understanding of information transfer during decoherence. A draft of this work is already completed. This work supports the LANL mission of gaining a fundamental understanding of materials and of complex natural systems. This work resulted in two articles, one in the prestigious journal Physical Review Letters and the other in Physical Review A, see Refs. [1,2].

Aspects of nanoscale electronic sensors – We have examined two issues in the behavior of nonequilibrium nanoscale systems: (i) The effect of noise on the ability to detect biomolecules with electronic sensors and (ii) how ionic transport occurs through nanopores. For (i), we investigated decoherence (also known as dephasing in this field) and inelastic scattering effects on rapid DNA sequencing using transverse electronic transport measurements and nanopores. We found that the efficient distinguishability of the bases is not influenced by white noise unless it is unrealistically strong, reaffirming that electronic transport might serve as a mechanism of rapid DNA sequencing. Our work has recently been confirmed experimentally, settling a long-standing debate concerning the feasibility of DNA base detection/sequencing with transport (see two articles in Nature Nanotechnology, Refs. [3,4]). For (ii), we studied how ions move from bulk into a nanopore to create an ionic current. This is process that occurs in natural (biological ion channels) as well as artificial systems (synthetic nanopores, e.g., made for sequencing and molecular detection). We showed that there should be a precipitous drop in ionic current when the radius of the nanopore is shrunk below the radius of the first hydration layer of the ions. This research will help the development of nanopore-based electronic sensors that will create new possibilities for ubiquitous sensors, and thus this work addresses the LANL mission of Threat Reduction. As well, such sensors open up new avenues for investigation into the complex interface between solids, liquids, and biomolecules, and increase our understanding of how materials behave at the nanoscale. The work resulted in four publications in prestigious journals (see Refs. [5-7] and a LabTalk article in J. Phys. Cond. Mat.).

Nonequilibrium thermal transport as a probe of biological processes – DNA denaturation has long been a subject of intense study due to its relationship to DNA transcription and its fundamental importance as a nonlinear, structural transition. Many aspects of this phenomenon, however, remain poorly understood. Existing models fit quite well with experimental results on the fraction of unbound base pairs versus temperature. Yet, these same models give incorrect results for other essential quantities, e.g., the predicted base pair fluctuation timescales - relevant to transcription - are orders of magnitude different from experimental ones. We demonstrated that nanoscale thermal transport can serve as a sensitive probe of the underlying microscopic mechanisms responsible for dynamics of DNA denaturation. Specifically, we showed that the heat transport properties of DNA are altered significantly and abruptly as it denatures, and this alteration encodes detailed information on the dynamics of thermal fluctuations and their interaction along the chain. This finding allows for the unambiguous discrimination between models of DNA denaturation. Measuring the thermal conductance will thus shed new light on the nonlinear physics of this important molecule. An article describing this work recently appeared as a Rapid Communications in Physical Review E, see Ref. [8].

Uncertainty relations and correlations in quantum systems – We developed a simple proof of the uncertainty principle with quantum side information, as in a recent Nature Physics article [9], invoking the monotonicity of the relative entropy. The Heisenberg uncertainty principle is the cornerstone of quantum mechanics. It is formulated in terms of variances of observables. However, one can equally well formulate these types of relations in terms of the entropy of the observables. The entropic uncertainty principle with quantum side information is the strongest uncertainly principle to date, and has applications from quantum cryptography to witnessing entanglement in quantum systems. Our proof shows that the entropic uncertainty principle can be viewed as a data-processing inequality, a special case of the notion that information cannot increase due to evolution in time. This leads to a systematic method for finding the minimum uncertainty states of various entropic uncertainty relations; interestingly such states are intimately connected with the reversibility of time evolution. This work (LAUR-11-10699) is under consideration at Physical Review Letters.

Impact on National Missions
This research is important in obtaining a fundamental understanding of the behavior of complex physical systems. In particular, it addresses how quantum systems evolve when in the presence of their environment, which is a situation that has to be accounted for in order to understand virtually any material or device. In addition to obtaining a theoretical understanding of this behavior, it also addresses how to construct efficient simulation techniques to tackle very complex physical systems where many interact-

ing components of a physical system are also interacting or being driven by their environment. More specific examples are given below under accomplishments.

The work in the biophysical arena is helping us comprehend how nanoscale devices detect molecules and physical processes. The successful fabrication and implementation of the sensors will revolutionize how we approach sensing at the nanoscale, e.g., in threat detection, and bring novel technologies into the medical/biological communities.

Further, this project supported the DOE mission in Scientific Discovery & Innovation and Energy Security by enhancing our understanding of nanoscale electronics, molecular detection, and using simulations for science-based prediction. It is important to other missions of the Laboratory as well, e.g., Homeland Security and Threat Reduction.

References

1. Zwolak, M., H. T. Quan, and W. Zurek. Quantum Darwinism in a Mixed Environment. 2009. *PHYSICAL REVIEW LETTERS.* **103** (11): 110402.

2. Zwolak, M., H. T. Quan, and W. H. Zurek. Redundant imprinting of information in nonideal environments: objective reality via a noisy channel. 2010. *Physical Review A (Atomic, Molecular, and Optical Physics).* **81** (6): 062110 (13 pp.).

3. Tsutsui, M., M. Taniguchi, K. Yokota, and T. Kawai. Identifying single nucleotides by tunnelling current. 2010. *Nature Nanotechnology.* **5** (4): 286.

4. Huang, S., J. He, S. Chang, P. Zhang, F. Liang, S. Li, M. Tuchband, A. Fuhrmann, R. Ros, and S. Lindsay. Identifying single bases in a DNA oligomer with electron tunnelling. 2010. *NATURE NANOTECHNOLOGY.* **5** (12): 868.

5. Zwolak, M., J. Lagerqvist, and M. Di Ventra. Quantized ionic conductance in nanopores. 2009. *Physical Review Letters.* **103** (12): 128102.

6. Krems, M., M. Zwolak, Y. Pershin, and M. Di Ventra. Effect of Noise on DNA Sequencing via Transverse Electronic Transport. 2009. *Biophysical Journal.* **97** (7): 1990.

7. Zwolak, M., J. Wilson, and M. Di Ventra. Dehydration and Ionic Conductance Quantization in Nanopores. 2010. *Journal of Physics: Condensed Matter.* **22** (45): 454126 (12 pp.).

8. Velizhanin, K., C. Chien, Y. Dubi, and M. Zwolak. Driving denaturation: Nanoscale thermal transport as a probe of DNA melting. 2011. *PHYSICAL REVIEW E.* **83** (5, 1): 050906.

9. Berta, M., M. Christandl, R. Colbeck, J. Renes, and R. Renner. The uncertainty principle in the presence of

quantum memory. 2010. *NATURE PHYSICS.* **6** (9): 659.

Publications

Krems, M., M. Zwolak, Y. V. Pershin, and M. Di Ventra. Effect of Noise on DNA Sequencing via Transverse Electronic Transport. 2009. *Biophysical Journal.* **97**: 1990.

Velizhanin, K., C. C. Chien, Y. Dubi, and M. Zwolak. Driving denaturation - Nanoscale thermal transport as a probe of DNA melting. 2011. *Physical Review E.* **83**: 050906.

Zwolak, M., H. T. Quan, and W. H. Zurek. Quantum Darwinism in a mixed environment. 2009. *Physical Review Letters.* **103**: 110402.

Zwolak, M., H. T. Quan, and W. H. Zurek. Redundant imprinting of information in nonideal environments: Objective reality via a noisy channel. 2010. *Physical Review A.* **81**: 062110.

Zwolak, M., J. Lagerqvist, and M. Di Ventra. Quantized ionic conductance in nanopores. 2009. *Physical Review Letters.* **103**: 128102.

Zwolak, M., J. Wilson, and M. Di Ventra. Dehydration and ionic conductance quantization in nanopores. 2010. *Journal of Physics: Condensed Matter.* **22**: 454126.

Zwolak, M., J. Wilson, and M. Di Ventra. Probing nanoscale physical processes with nanopores. 2010. *Journal of Physics: Condensed Matter.* : 1.

Unconventional Superconductivity in Heavy Fermion Materials

Cristian D. Batista
20090491PRD1

Abstract

We modeled different strongly correlated materials that exhibit unconventional physical properties and responses. This includes unconventional superconductivity (superconductivity from repulsive interactions), frustrated quantum magnets and frustrated metals. We found that strongly repulsive bare electron-electron interactions can lead to a robust effective attraction between quasi-particles that is a precondition for stabilizing a superconducting state. We also found novel magneto-electric effects of pure electronic origin that take place in Mott insulators, i.e., materials that have a very low conductivity at finite temperatures due to the strong Coulomb repulsion between their valence electrons. In particular, we demonstrated that these magneto-electric effects can only take place in geometrically frustrated materials. $Ba_3Mn_2O_8$ is one of these materials. By applying a combination of numerical and analytical techniques, we characterized the dynamical and static properties of this material in the presence of an applied magnetic field. For this purpose, we collaborated with our experimental group at NHMFL-LANL and with the group of Prof. Ian Fisher at Stanford University. The results of these fruitful collaborations explained a long list of dynamic and static properties that were measured as a function of field and temperature. In particular, we were able to fully characterize the experimental behavior near the field induced quantum critical point.

Background and Research Objectives

Some materials can conduct electricity without dissipating energy, i.e., with no energy losses in the form of heat. These materials are known as superconductors, and their unique properties lead to several technological applications. Unfortunately, most of the known materials that exhibit this property are superconductors only at low temperatures. The discovery nearly 20 years ago of high temperature superconductivity in complex copper oxide materials held great promise for revolutionizing electrical power transmission and storage. The promise of this discovery has not been realized fully, in part because we still do not understand how strongly interacting electrons can produce unconventional superconductivity.

One of the challenges for future technologies is to find materials that can superconduct at room temperature. To find guiding principles for designing such materials we need to understand the microscopic origin of superconductivity. This was the main purpose of this project. In particular, the project focused on f-electron materials that are at the center of the experimental effort of LANL (MPA-10 group). We studied the non-trivial interplay between magnetism and superconductivity in strongly correlated materials. One of the main goals was the derivation of guiding principles for optimizing the superconducting properties of unconventional superconductors. In addition, we derived effective low-energy models for these materials and unveiled some hidden connections between seemingly unrelated families of unconventional superconductors.

We focused on providing a basic understanding of the interacting electrons and how these electrons affect the utility of unconventional superconductors for energy applications. By means of the research that was performed under this project, we provided some guiding principles for finding superconducting materials with higher critical temperatures. In addition, we found novel states of matter that emerge in the neighborhood of the superconducting and magnetic phases out of the same electron-electron interactions that stabilize these phases. The discovery of these novel states of matter may also lead to novel technological applications.

Scientific Approach and Accomplishments

We have validated our low-energy effective theory by comparing the numerical results for the original Periodic Anderson Model and the low-energy effective Hamiltonian. The numerical technique that we used it the Density-Matrix Renormalization Group (DMRG) that is the state of the art method for solving correlated models in one-dimensional lattices. The impact of our work is reflected by the fact that it was immediately accepted for publication in the prestigious journal Physical Review Letters.

We have also demonstrated that a bare (Coulomb) repulsion between electrons described by a Periodic Anderson Model can lead to an effective attraction. The effective attraction is induced by the presence of antiferromagnetic correlations with long enough correlation length. This result is in correspondence with many experimental phase diagrams that show the presence of superconductivity in the neighborhood of an antiferromagnetic phase. An important result is that our pairing mechanism survives in dimension higher than one and is robust against the inclusion of the longer-range part of the Coulomb repulsion. The ultimate reason behind this property is that the attractive mechanism is produced by confinement of topological defects (solitons). Each hole (moving charge) carries a soliton (or domain wall for the antiferromagnetic ordering), and the antiferromagnetic interaction induces an attractive hole-hole potential that increases linearly in the distance between the holes. The results of this research were published in Physical Review B.

By starting from an inhomogeneous Hubbard model, we have demonstrated the existence of a d-wave superconducting phase. The model consists of Hubbard "molecules" or plaquettes that are connected by a weak hopping amplitude. The obtained quantum phase diagram includes a charge-density-wave and a d-wave superconducting phase. A remarkable conclusion of our work is that optimal superconductivity is obtained for optimal intra-plaquette kinetic energy frustration. This is an important association because it provides a guiding principle for maximizing the critical temperature of unconventional superconductors and understanding the role of frustration in this process. Our paper has been published in Physical Review Letters.

There are many other works that have been published under this project (see the list of publications). Most of these works are contributions to the general area of strongly correlated electrons. These ideas were derived along the process of working on the main subject of this project (magnetism and superconductivity). In particular, I would like to highlight the discovery of orbital electric currents in Mott insulators and the possibility of inducing orbital antiferromagnetism by the application of a uniform external magnetic field. These results were published in Physical Review Letters.

In addition to strongly correlated electronic material, mesoscopic structures such as quantum dots (QDs) are interesting from both fundamental and applied research points of view. QDs provide well-controlled and tunable systems for testing quantum many-body theories, and hold strong potential for applications particularly in quantum computing. We studied the transport properties of QDs connected in series in the Kondo regime, using DMRG and exact diagonalization techniques. The results were published in European Physics Journal. We also wrote an invited review paper on "Electron Transport in Strongly Correlated Nanostructures." The paper was published in Modern Physical

Letters B.

We also studied non-equilibrium and time-dependent phenomena in strongly-interacting electron systems. This became feasible in the past few years due to the development of techniques such as time-dependent density-matrix renormalization group (tDMRG). In particular, we investigated the real-time dynamics of an electron-hole pair in a one-dimensional Mott insulator. The results were published in Phys. Rev. Lett. (http://prl.aps.org/abstract/PRL/v100/i16/e166403), and Phys. Rev. B (http://prb.aps.org/abstract/PRB/v81/i12/e125113). In addition, using tDMRG, we istudied the non-equilibrium electron transport in a 1D Mott insulator coupled to two metallic leads. We obtained the current-voltage characteristics. We also studied the properties of the conducting state that results from applying a strong electric field in the insulator. The results were published in Physical Review Letters B.

Another interesting topic in strongly-correlated materials and quantum magnets is the Bose-Einstein condensation (BEC) of magnetic excitations (magnons). We worked closely with experimentalists both at and outside LANL. We used Quantum Monte Carlo (QMC) and analytical techniques. We reproduced the experimental magnetization curves of the spin-gapped compound DTN, and obtained the critical properties of the field-induced BEC. These results were published in Physical Review Letters. We also studied the frustrated spin-1-dimer compound $Ba_3Mn_2O_8$. The thermodynamic measurements revealed interesting asymmetry between the upper and lower critical fields for the quintuplet condensation. We explained this asymmetry in terms of the asymmetric boson mass renormalization due to quantum fluctuations. We published these results in Physical Review Letters. For the same compound, we studied the anisotropic phase diagram, the results were published in Physical Review Letters B. We are currently working on obtaining the magnon dispersion relation in the ordered phase using analytical techniques. The purpose of these calculations is to fit neutron scattering data obtained at the SNS at ORNL.

Impact on National Missions

Strong electronic correlations define every major problem at the forefront of condensed matter physics. Traditional electronic band structure calculations and minimal many-body models are inadequate to reproduce macroscopic electronic, metallurgical and crystallographic properties of strongly correlated materials and the rich spectrum of complex states found in them. These deficiencies have exposed critical gaps in our understanding of condensed matter that cannot be ignored. By providing an essential new understanding and interpretative frameworks for strongly correlated compounds, we have closed some of these gaps. The relevance of these achievements extends beyond the exciting challenges for condensed matter physics. Many of the Laboratory's special, materials-dependent mission needs depend critically on strong electronic corre-

lations, whether it is the equation of state and metallurgy of actinides, control of quantum excitations for new sensor technologies or emergent functionality in nano-structured materials. To ensure that its long-term core missions can be met, Los Alamos cannot afford to lose its leadership position in the synthesis, characterization and modeling of strongly correlated electron materials and phenomena. Substantial and internationally-recognized successes of team members in the study of strong correlations have come from close integration of experiment and theory, in a deliberate strategy built around a set of well-defined scientific problems. The challenge of discovering and understanding the physical manifestations of correlations and frustration and their implications for new states of matter has stretched limits of the Laboratory's experimental and predictive capabilities that underpin the science and technology needs of the Lab and addresses an exceptional problem of immediate interest to the international condensed matter community.

In summary, by exposing and understanding the role of strongly repulsive interactions in correlated materials we have underpinned our ability to predict the consequences of strong electronic correlations that are responsible for complex states of worldwide interest and that control solid state properties of mission-relevant materials.

Publications

Al-Hassanieh, K. A., C. A. Busser, and G. B. Martins. Electron transport in strongly correlated nanostructures. 2009. Modern Physics Letters B. 23 (18): 2193.

Al-Hassanieh, K. A., C. D. Batista, G. Ortiz, and L. N. Bulaevskii. Field-induced orbital antiferromagnetism in Mott insulators. 2009. Physical Review Letters. 103: 216402 .

Al-Hassanieh, K. A., C. D. Batista, P. Sengupta, and A. E. Feiguin. Robust pairing mechanism from repulsive interactions. 2009. Physical Review B. 80: 115116.

Al-Hassanieh, K. A., F. A. Reboredo, A. E. Feiguin, I. GonzaÃÅlez, and E. Dagotto. Excitons in the one-dimensional hubbard model: A real-time study. 2008. Physical Review Letters. 100 (16): 166403.

Hei, F. [Materials Science and Technology Division., null. Department of Physics and Astronomy, G. B. Martins, K. A. Al-Hassanieh, null. Department of Physics and Astronomy, A. E. Feiguin, E. [Materials Science and Technology Division. Dag, and null. Department of Physics and Astronomy. Finite-size scaling analysis of spin correlations and fluctuations of two quantum dots in a T-shape geometry. 2008. Physica. B, Condensed Matter. 403 (5-9): 1544.

Heidrich-Meisner, F. [., G. B. Martins, C. A. Busser, null. Al Hassanieh, A. E. Feiguin, G. [Universidad de Alicante]. Chiappe, E. V. Anda, and null. Dagotto. Transport through quantum dots: a combined DMRG and embedded-cluster approximation study. 2008. European Physical Journal - Applied Physics. 67: 527.

Heidrich-Meisner, F., G. B. Martins, C. A. Busser, K. A. Al-Hassanieh, A. E. Feiguin, G. Chiappe, E. V. Anda, and E. Dagotto. Transport through quantum dots: a combined DMRG and embedded-cluster approximation study. 2009. European Physical Journal B. 67 (4): 527.

Isaev, L., G. Ortiz, and C. D. Batista. Superconductivity in Strongly Repulsive Fermions: The Role of Kinetic-Energy Frustration   . 2010. Physical Review Letters. 105: 10.

Kohama, Y., A. V. Sologubenko, N. Dilley, V. S. Zapf, M. Jaime, J. Mydosh, A. Paduan-Filho, K. A. Al-Hassanieh, P. Sengupta, S. Gangadharaiah, A. L. Chernyshev, and C. D. Batista   . Thermodynamic and transport properties of NiCl2-4SC(NH2)2: Role of strong mass renormalization. To appear in Physical Review Letters.

Paduan-Filho, A., K. A. Al-Hassanieh, P. Sengupta, and M. Jaime. Critical Properties at the Field-Induced Bose-Einstein Condensation in NiCl2-4SC(NH2)2. 2009. Physical Review Letters. 102: 077204.

Paduan-Filho, A., K. A. Al-Hassanieh, P. Sengupta, and M. Jaime. Critical properties at the field-induced bose-einstein condensation in $NiCl_2$-4SC(NH_2)$_2$. 2009. Physical Review Letters. 102 (7): 077204 (4 pp.).

Samulon, E. C., K. A. Al-Hassanieh, Y. -J. Jo, M. C. Shapiro, L. Balicas, C. D. Batista, and I. R. Fisher. Anisotropic phase diagram of the frustrated spin dimer compound Ba3Mn2O8. 2010. PHYSICAL REVIEW B. 81 (10): 104421.

Samulon, E. C., Y. Kohama, R. D. McDonald, M. C. Shapiro, K. A. Al-Hassanieh, C. D. Batista, M. Jaime, and I. R. Fisher. Asymmetric Quintuplet Condensation in the Frustrated S=1 Spin Dimer Compound Ba3Mn2O8. 2009. Physical Review Letters. 103: 047202.

Silva, L. G. da, K. Al-Hassanieh, A. Feiguin, F. Reboredo, and E. Dagotto. Real-time dynamics of particle-hole excitations in Mott insulator-metal junctions. 2010. PHYSICAL REVIEW B. 81 (12): 125113.

Disorder in Frustrated Systems

Avadh B. Saxena
20090493PRD1

Abstract

During his two years tenure as Director's Fellow, Dr. Nisoli has conducted research on many different topics and has written 15 publications, 12 of which were published, while 3 are currently under submission. He has also given 12 talks at conferences and universities around the world. All his contributions were submitted to high profile journals, 5 to Phys. Rev. Letters, 1 to Nature Physics, the others to Phys. Rev. B, E and J. Phys: Cond. Matt. His research and results had a direct impact on many different fields: in frustrated metamaterials he has started a new field called "Artificial Spin Ice" which has been highlighted in Nature, Nature Materials, and other scientific journals; in the field of nonlinear physics and pattern formation he has revealed a number of new theoretical structures reminiscent of botany and nonlinear excitations in the physics of cylindrical systems, which was highlighted in Nature Materials and by the American Mathematical Society, as well as by many scientific websites and blogs; in the field of statistical mechanics of quasi-one-dimensional system he introduced a general framework to study instabilities and failure in such diverse objects as nanotubes, nanowires and DNA (his work received an honorable mention at the Leon Heller prize for theoretical Physics). He is currently extending his interests to biophysics and plasticity, and has recently submitted a Phys. Rev. Letter on the thermomechanics of DNA.

Background and Research Objectives

As a graduate student, before coming to Los Alamos, Dr. Nisoli, in collaboration with the group of P. Schiffer at Penn State, had introduced a new magnetic metamaterial (Artificial Spin Ice) which has now generated a new field of research (e.g. in Nature Physics alone, at least 4 papers have appeared on the subject in 2010). He had also worked on hard condensed matter of carbon nanostructures, especially their electromechanical properties. During the past two years he took these ideas further and applied to the stability of quasi-one-dimensional nanomaterials such as a nanowire in order to understand their potential applications.

Scientific Approach and Accomplishments

While a theorist, Dr. Nisoli has an holistic scientific approach to a problem, that includes analytical work, numerical work, and collaboration with experimentalists, engineers and biologists.

During his tenure as Director's Fellow Dr. Nisoli has worked on disorder of Artifical Spin Ice, an artificially frustrated metamaterial at the nanoscale, a novel material which he had introduced and which many different groups around the world are now developing. On this subject, he has authored and coauthored one Phys. Rev. Letter, two Phys. Reb B papers, a Nature Physics and was an invited speaker on a dedicated conference on this subject in UK. He has shown that the material, although athermal, can be described via an effective thermodynamics, and successfully predicted the experimental outcomes of rotational demagnetization. In a recent Nature Physics, in collaboration with P. Lammert (Penn State) he has shown how to quantify the information content encoded in these novel magnetic media. His work on Artificial Spin Ice was recognized at the postdoc research day by the Outstanding Poster Award, and featured many times as highlights in Nature and Nature materials.

His work on Dynamical Phyllotaxis (on this topic during his tenure he has published 1 Phys. Rev. Letter and 2 Phys. Rev. E papers), in which he has shown the emergence of botanical patterns in physical systems as well as novel sets of linear and topological excitations. This work was recognized when specific columns were devoted to it in Nature Materials and by the American Mathematical society.

He has established new collaborations with Prof. Douglas Abraham (Oxford), and with him he has worked on stability of Quasi-one-dimensional systems such as Carbon Nanotubes, DNA and nanowires. On the subject he has published two Phys. Rev. Letters. For one of these papers, in 2010 Dr. Nisoli was awarded honorable mention for the Leon Heller Prize in Theoretical Physics. He is submitting two more papers on the subject.

He has also recently started a new collaboration with

Alan Bishop on thermomechanics of DNA, and submitted a Phys. Rev. Letter on the subject.

Additionally, he has continued his research in hard condensed matter, and published a Phys. Rev. B on polarons in carbon nanotubes and a J. of Physics: Cond. Matt. on how to recognize presence and chirality of folds in grapheme via Raman spectroscopy. In the field of electromechanics of nanosctructures, he is currently working on piezoelectricity of boron nitride nanotubes.

While maintaining and developing his past collaborations, at LANL Dr. Nisoli has established new ones, with D. Abraham (Oxford University), Turab Lookman, Avadh Saxena (T4), and Alan Bishop (ADTSC), while at the same time interacting at various levels and to different degrees with many other researchers. He also has actively participated in the scientific aspects of CNLS, and in particular, as a member of the colloquium committee he has hosted more than ten speakers, many of which (Tom Witten, Dan Stein, Bob Behringer, Moses Chan, Giday WoldeGabriel, etc.) are internationally renowned.

Impact on National Missions

The various research topics impact LDRD as well as basic energy science program of DOE. In addition, the results benefit advanced materials, nanotechnology and related thrusts. Dr. Nisoli's work on carbon and boron nitride nanostructures is relevant to the realization of nano-actuators as well as novel functionalized nanomaterials. His work on magnetic frustration has applications in information encoding. His work on effective thermodynamics in dissipative systems has the potential to explain more complex materials and their plastic properties in extreme conditions away from equilibrium. His work on the statistical mechanics in quasi-one-dimensional systems has a broad impact from nanotechnology, to nanoelectronics, to biology of nucleic acids. Niloli's results on nonlinear physics, being scale independent and valid for a wide range of interactions, can predict patterns and dynamics in such diverse systems as ion beams, electronic crystals of dielectric nanotubes, bubbles in cylindrical foams, alpha-helices and more.

Publications

Gupta, A. K., C. Nisoli, P. Lammert, V. H. Crespi, and P. C. Eklund. Curvature-Induced D-Band Raman Scattering in Folded Graphene. 2010. *J. Phys.: Cond. Matt..* **22**: 334205.

Lammert, P. E., X. Ke, J. Li, and C. Nisoli. Direct Entropy Determination and Application to Articial Spin Ice. 2010. *Nature Phys. .* **6**: 786.

Li, J., S. Zhang, J. Bartell, C. Nisoli, X. Ke, and P. E. Lammert. Comparing Frustrated and Unfrustrated Clusters of Single-Domain Ferromagnetic Islands. 2010. *Phys. Rev. B.* **82**: 134407.

Li, J., X. Ke, S. Zhang, D. Garand, C. Nisoli, and P. Lammert. Comparing Artificial Frustrated Magnets by Tuning the Symmetry of Nanoscale Permalloy Arrays. 2010. *Phys. Rev. B.* **81**: 092406.

Nisoli, C.. Polarons Induced Deformations in Carbon Nanotubes. 2009. *Phys. Rev. B.* **80**: 113406.

Nisoli, C.. Spiraling Solitons. A Continuum Model for Dynamical Phyllotaxis and of Physical Systems. 2009. *Phys. Rev. E.* **80**: 0210.

Nisoli, C.. Static and Dynamical Phyllotaxis in a Magnetic Cactus. 2009. *Phys. Rev. Lett. .* **102**: 186103.

Nisoli, C., D. Abraham, T. Lookman, and A. Saxena. Thermally Induced Local Failures in Quasi-One-Dimensional Systems: Collapse in Carbon Nanotubes, Necking in Nanowires, and Opening of Bubbles in DNA. 2010. *Phys. Rev. Lett. .* **104**: 119902.

Nisoli, C., D. Abraham, T. Lookman, and A. Saxena. Thermal Stability of Strained Nanowires. 2009. *Phys. Rev. Lett. .* **102**: 245504.

Nisoli, C., J. Li, X. Ke, D. Garand, and P. Schiffer. Effective Temperature in an Interacting Vertex System: Theory and Experiment on Artificial Spin Ice. 2010. *Phys. Rev. Lett..* **105**: 047205.

Nisoli, C., N. M. Gabor, P. E. Lammert, J. D. Maynard, and V. H. Crespi. Annealing a Magnetic Cactus into Phyllotaxis. 2010. *Phys. Rev. E.* **81**: 0107.

Neutrino Physics and Its Applications

Joseph A. Carlson
20090522PRD2

Abstract

Core-collapse supernovae give off 90% of their energy in neutrinos. These neutrinos, if observed from a galactic supernovae, are a potential tremendous source of knowledge about both neutrinos and the supernovae in which they were created.   To understand potential supernovae neutrino signals we have to consider the flavor evolution of neutrinos, including both their scattering from the background and electron density and neutrino-neutrino scattering. The latter energy- and angular-dependent interactions must be solved as a very large system of coupled non-linear differential equations. The aim of this project was to determine what we can learn from future supernovae neutrino signals.

Background and Research Objectives

Neutrinos, a class of nearly massless, weakly interacting particles, are currently important subjects in nuclear, particle, and astrophysics. On the other hand, neutrinos play crucial roles in interesting astrophysical environments such as supernovae and the early universe, where they are copiously produced. For example, in supernovae neutrinos not only dominate the energetics but also influence how heavy elements are synthesized. On the other hand, because neutrinos interact only weakly with matter, they can easily escape the deep stellar interior of the sun or supernovae. Once detected, these extraterrestrial neutrinos can be used as unique probes to the physical conditions in the interior that can be difficult to measure directly. Recently Huaiyu Duan and collaborators have revealed a novel quantum phenomenon: dense neutrinos gases (such as supernovae and the early universe) can experience 'collective neutrino flavor transformation'. This is partly because neutrinos have non-zero masses. As a result, the energy spectra and the fluxes of neutrinos of different kinds or 'flavors' are modified in a collective manner. Because the neutrino reactions that occur in both astrophysical environments and terrestrial neutrino detectors are flavor dependent, this discovery can potentially be very important in accurate evaluation of the impact of neutrinos in these environments as well as in analyses of neutrino signals from these sources.

Scientific Approach and Accomplishments

This project involves large-scale computational and analytic approaches to understanding supernovae neutrinos. The large-scale simulations require the solution of several million coupled non-linear differential equations. Each equation describes the evolution of neutrinos with a specific energy at a specific angle from the surface of the proto-neutron star.   The calculation starts with assumed energy and angular distributions for the various types (flavors) of neutrinos and anti-neutrinos. The computation follows the paths of these neutrinos as they evolve from the proto-neutron star surface to larger and larger distances, tracing the evolving fluxes of different types of neutrinos as they move outwards. Terrestrial detectors can measure the signal at very large distances; the goal of this project is to predict what we may see in a future supernovae explosion and what it will teach us about supernovae and neutrinos. Of particular interest are the neutrino properties themselves, including their masses and mixing through weak interactions.

At the start of this project only simplified 2x2 flavor cases had been considered. In these calculations only the electron neutrino and an average 'heavy' neutrino were included. Though a significant advance over previous work, further research including all the known physics was required. During the year of this project, we performed the first full 3x3 simulations including all flavors of neutrinos and anti-neutrinos. This work has recently been published in Physical Review D. We have also begun to incorporate realistic supernovae simulation data into our calculations, using initial flux and electron density profiles from the groups at LANL and at ORNL.

Our calculations show that full multi-energy, multi-angle simulations are required for accurate studies of supernovae neutrinos. We specifically studied the neutronization burst of an oxygen-neon-magnesium supernovae where the initial neutrino spectra are comparatively well-understood. Previously, we had found 'spectral swaps', border energies where on one side the neutrino spectra are swapped from their original spectra. We find that the realistic simulations result in somewhat lower energies for the swaps, and that uncertainties in

neutrino mass and mixing parameters are still important in understanding future neutrino signals.

Figure 1 shows a color-coded conversion probability for electron neutrinos emitted from an oxygen-neon-magnesium supernovae. Dark Indicates near total conversion to another flavor, while light colors indicate no conversion. As is shown in Figure 1, neutrinos below 10 MeV are almost entirely converted, while those at higher energy are nearly unchanged.

We have also pursued analytic studies of these environments. With certain simplifying assumptions we can make credible predictions of parts of the simulations. A full analytic understanding of the problem is still lacking, however. Much work remains to be done to make credible predictions of future supernovae signals,;this work will be pursued by H. Duan and collaborators through the collaboration on neutrinos and dense matter physics lead by Sanjay Reddy of LANL and funded by the nuclear physics program of the DOE Office of Science.

Impact on National Missions

This work had direct impact upon our ability to accurately use the largest available supercomputers to solve highly oscillatory coupled non-linear equations. Advanced techniques using both the message passing interface (MPI) to parallelize the code and Open-MP to spread the effort across multiple cores have resulted in a very efficient computer program. Similar problems are important in many large-scale physics applications.

This work is also directly affecting the Deep Underground Science Laboratory, a project funded by the National Science Foundation and the US Department of Energy. The properties of neutrino detectors housed in this facility are now being decided upon. The type of neutrinos detectors employed are critical in determining what energies and types of neutrinos can be measured. The work on this project has made scientists realize the importance of being able to identify the energy-dependent fluxes of different types of neutrinos and anti-neutrinos.

Figure 1. Electron neutrino conversion probabilty as a function of energy and angle (left). Color coding for probabilities is indicated in the figure. The angle-integrated spectra are also plotted at 5000 km (right).

Publications

Cherry, J. F., G. M. Fuller, J. Carlson, Huaiyu Duan, and Yong-Zhong Qian. Multiangle simulation of flavor evolution in the neutronization neutrino burst from an O-Ne-Mg core-collapse supernova. 2010. *Physical Review D.* **82** (8): 085025 (10 pp.).

Cherry, J. F., G. M. Fuller, J. Carlson, Huaiyu Duan, and Yong-Zhong Qian. Multiangle simulation of flavor evolution in the neutronization neutrino burst from an O-Ne-Mg core-collapse supernova. 2010. *Physical Review D.* **82** (8): 085025 (10 pp.).

Duan, H.. A simple model for spectral swapping of supernova neutrinos. 2009. In *10th Conference on the Intersections of Particle and Nuclear Physics ; 20090526 - 20090531 ; San Diego, CA.* Vol. 1182, p. 36.

Duan, H., G. M. Fuller, and Y. -. Qian. Symmetries in collective neutrino oscillations. 2009. *JOURNAL OF PHYSICS G-NUCLEAR AND PARTICLE PHYSICS.* **36** (10): 105003.

Duan, H., and J. P. Kneller. Neutrino flavour transformation in supernovae. 2009. *JOURNAL OF PHYSICS G-NUCLEAR AND PARTICLE PHYSICS.* **36** (11): 113201.

Non-equilibrium Phenomena in Physics, Biology and Computer Science

Michael Chertkov
20090525PRD2

Abstract

The project aimed at improving our understanding of the processes responsible for unusual behavior of biological and synthetic systems on intra- and extra- cellular scales and suggested new ways of performing quantitative measurements. The numerical codes developed for simulation of membranes will later be integrated into large scale simulations. Understanding the statistical properties of noise in non-equilibrium systems achieved within the project should be useful for developing new micro-rheological experimental techniques. The irreversible modifications of MCMC algorithms developed could be incorporated into existing codes to accelerate simulations of proteins and macromolecules, biological and artificial networks, and other condensed and soft matter systems. Our efforts in analysis of non-equilibrium phenomena over networks, specifically power grids, will help to design efficient smart approaches to the network optimization and control.

Background and Research Objectives

In this project we studied non-equilibrium phenomena in physics, biology, computer science and power networks. We pursued research in four main directions. First, we worked on the dynamics of biological membranes, vesicles and cells. We developed a new spectral boundary integral code to simulate membrane dynamics that extends existing analytical models by including effects of membrane interaction with actin and cytoskeleton networks, membrane proteins and the environment. Armed with this code, we analyzed various intra-cellular biological processes, such as membrane nanotube formation, propulsion of active cells, viscoelastic mobility of blood and other complex biological fluids. Second, we studied statistics of pressure and stress fluctuations in complex fluids. The noisy part of measurements is usually considered to be an inevitable annoyance, but it actually contains valuable information which could be extracted and used in lieu of formal statistical modeling. We developed a data-driven modeling approach aimed at discovering which microscopic features can be inferred from the measurements. Third, we utilized methods of non-equilibrium statistical physics for build-ing better computer science algorithms. In particular, we also work on an accelerated Markov Chain algorithm via controlled violation of reversibility. Finally, we developed novel optimization and control schemes, based on ideas from statistical physics, to improve performance of power grids.

Scientific Approach and Accomplishments

New phenomena was discovered while studying the statistics of heat dissipation in single polymer dynamics. The probability distribution function does not have a large-deviation form, and is instead described by a universal exponential tail. (in collaboration with M. Vucelja, M. Chertkov)

The effect of membrane buckling was shown to explain the phase diagram of vesicle motion observed in experiments of Victor Steinberg. (in collaboration with S. Vergeles and V. Lebedev)

The large deviation function of currents and occupation numbers in Jackson queuing networks were shown to have a universal form. It was proven that the system is not ergodic, and the probability distribution function (PDF) of final occupation number is different from the PDF of average occupation number. The corresponding manuscript has been submitted to J. Stat. Phys. (in collaboration with D. Goldberg, M. Chertkov, V. Chernyak)

To control of losses and consumption in power grids, several decentralized control techniques based on smart inverters were proposed and analyzed. It was shown that these techniques achieve a very solid performance comparable to the control based on global optimization. One manuscript was submitted to IEEE PES conference, and was invited to the super-session on renewable generation. Another manuscript was submitted to IEEE SmartGridComm conference. (In collaboration with S. Backhaus, M. Chertkov, P. Sulc)

A novel computational method based on dynamic programming was proposed for assessing the risks of excessively high voltage drop in feeder lines with significant uncertainty in power generation/consumption. The man-

uscript was accepted for presentation at IEEE SIBIRCONN conference.

A scheduling technique for Plug-In-Hybrid-Electric-Vehicle charging was proposed and shown to achieve almost optimal performance. This technique allows significant reduction of fluctuations in consumption and reduces the risks of exceeding the maximal power consumption (in collaboration with S. Backhaus, M. Chertkov, N. Sinitsyn).

Impact on National Missions

This project had supported the DOE mission in Basic Science by enhancing our understanding of the dynamics of biological membranes, vesicles and cells, statistics of pressure and stress fluctuations in complex fluids and developing modeling approach aimed at discovering which microscopic features can be inferred from the experimental measurements. It also helped to advance DOE mission in Energy Security via developing new approaches to analysis, optimization and control of power grids.

Publications

Chernyak, V., M. Chertkov, D. Goldberg, and K. Turitsyn. Non-Equilibrium Statistical Physics of Currents in Queuing Networks. 2010. *JOURNAL OF STATISTICAL PHYSICS.* **140** (5): 819.

Turitsyn, K. S., Lipeng Lai, and W. W. Zhang. Asymmetric disconnection of an underwater air bubble: persistent neck vibrations evolve into a smooth contact. 2009. *Physical Review Letters.* **103** (12): 124501 (4 pp.).

Turitsyn, K., M. Chertkov, and M. Vucelja. Irreversible Monte Carlo algorithms for efficient sampling. 2011. *Physica D: Nonlinear Phenomena.* **240** (4-5): 410.

Turitsyn, K., N. Sinitsyn, S. Backhaus, and M. Chertkov. Robust Broadcast-Communication Control of Electric Vehicle Charging. 2010. In *2010 1st IEEE International Conference on Smart Grid Communications (SmartGridComm) ; 4-6 Oct.* (2010 ; Gaithersburg, MD, USA). , p. 203.

Turitsyn, K., P. Sulc, S. Backhaus, and M. Chertkov. Local Control of Reactive Power by Distributed Photovoltaic Generators. 2010. In *2010 1st IEEE International Conference on Smart Grid Communications (SmartGridComm) ; 4-6 Oct.* (2010 ; Gaithersburg, MD, USA). , p. 79.

Turitsyn, K., S&caron, S. Backhaus, and M. Chertkov. Distributed control of reactive power flow in a radial distribution circuit with high photovoltaic penetration. 2010. In *2010 IEEE Power & Energy Society General Meeting ; 25-29 July 2010 ; Minneapolis, MN, USA.* , p. 1.

Theoretical/Computational Research on Particle Acceleration by Intense Laser Pulse

Brian J. Albright
20090528PRD2

Abstract

Generation and acceleration of charged particles are of importance to many fields of activities, such as tumor treatment with proton/ion beams in medical physics, "fast ignition" of fuel capsule with electron/proton beams for inertial fusion energy, and radiation sources from electron beams for chemistry, biology and material science.

Conventional technologies to produce and accelerate charged particles are costly, however recently a class of novel particle sources and efficient acceleration methods has emerged following the development of high-power-lasers. When these lasers are tightly focused onto gas jets or solid targets, reaching ultrahigh-intensities of above 10^{18} W/cm^2, acceleration fields as high as 10s of Teravolts/m can be produced from the intense laser plasma interactions, surpassing those in conventional accelerators by six orders of magnitude. Electrons or ions in the targets can be accelerated promptly, forming beams with unprecedented low-emittance, short-duration, and high-brightness. At LANL, the Trident facility with its 250 TW, 500 fs laser beam is well suited for the study of laser-ion acceleration. A proposed Extreme Light Infrastructure in Europe as well as comparable intensity laser facilities envisioned as part of the LANL MaRIE facility would enable the laser matter interaction in ultra-relativistic regime (intensity I >10^{23} W/cm2), opening doors to energetic particles and radiation beams of femtosecond to attosecond duration.

We explored new concepts such as staging of ion acceleration with double foils to improve beam quality and develop a theoretical understanding of such processes, with the help of large scale Particle-In-Cell (PIC) computer simulations on Lobo, Coyote, and the open Roadrunner supercomputers at LANL, as well as the ORNL Jaguar supercomputer. The work involved close collaboration with the Trident short pulse experimental team from LANL P-24 in designing and interpreting experiments for laser ion acceleration.

Background and Research Objectives

One of the most active and important areas in plasma and high energy density science is the use of ultraintense (I > 1.4×10^{18} W/cm2) short-pulse (<ps) lasers to generate beams of energetic charged particles. These beams can be used in a host of settings, such as ion fast ignition inertial fusion energy, hadrontherapy of tumors, advanced xray sources, warm dense matter study, and active interrogation of special nuclear materials. Indeed, one of LANL's core strengths is the development of laser-generated ion beams using these lasers and our Trident User Facility is a world leading laser facility both in terms of laser contrast (by five orders of magnitude) and intensity of laser light on target. With new focusing optics on Trident, we anticipate a further fourfold increase in field intensity in the next two years.

The interaction between the intense laser and target plasma is highly dynamical and involves extreme nonlinearity and exotic relativistic plasma physics. In recent years, we have demonstrated at LANL a new regime of laser-matter interaction: the relativistically underdense (classically overdense) regime, where coupling between laser and plasma is dramatically enhanced. Understanding this novel regime requires high-fidelity kinetic modeling of relativistic plasma media and is well suited for first principle Particle-In-Cell (PIC) simulations, such as LANL's VPIC code. The PIC model of plasma represents the plasma as a collection of computational "macroparticles" whose motions mimic those of physical plasma electrons and ions. Co-evolving with the plasma is the self-consistent electromagnetic, obtained by evolving the discretized Maxwell equations for the electromagnetic fields. This description of the plasma dynamics is very accurate and captures all of the relevant collective length and time scales in the medium.

In the past decade, discovery in the field of laser ion acceleration has been driven by large-scale PIC simulations of the type we performed in this project. One such new mechanism, discovered on LANL supercomputers and that was further studied in this project, is the Break Out Afterburner (BOA), which involves use of a high-contrast laser pulse to produce a relativistically transparent, classically overcritical medium. In relativistic transparency, a plasma medium would be opaque to the laser except that the hot electrons, moving at speeds near the speed of light,

acquire substantially higher mass and thus cannot move quickly enough to short out the laser field. An exciting aspect of the BOA is that it leads to an order of magnitude increase in efficiency and peak particle energy over traditionally laser-ion accelerators. Moreover, it has the potential to generate ion beams, which are quasi-monoenergetic, a vital characteristic for many applications such as fast ignition inertial fusion.

Scientific Approach and Accomplishments

At the start of this work, the laser thin foil interaction was known to be a promising and unique source of ion beams. However, systematic studies were needed to explore how to control the ion beam quality and provide a viable path towards higher beam energy and efficiency. Ion fast ignition inertial fusion (supported by a DOE Office of Science project), in particular, poses stiff challenges: one must be able to transport the ion beam over a standoff distance of 2 cm between ion source and the D-T capsule (thus requiring very tight 10% energy spread) and at the same time collimate the beam so that it deposits in the DT fuel in a hot spot with radius of order of 20 microns. Moreover, to get there, the beam must propagate through low density coronal plasma.

The primary research objective of this project was to apply VPIC on LANL Institutional Computing resources to explore the idea of using composite, multi-foil targets for improvement of beam quality and collimation (Figure 1). This work involved running and analyzing a large number of 1D and 2D kinetic simulations in order to identify the key physics processes and to optimize the composition and thickness of the second target, as well as the distance of separation between the foils. This work was published in two high profile papers: one that was published in Physical Review Special Topics: Accelerators and Beams and the other, a conference paper published in Physics of Plasmas (the most cited plasma physics journal in the world) accompanying a prestigious invited talk that Dr. Huang presented at the 52nd Meeting of the American Physical Society Division of Plasma Physics held in Chicago.
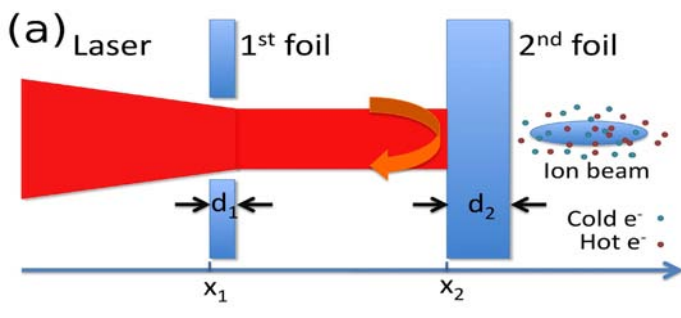

Figure 1. Schematic of the novel double-foil beam conditioning concept. The second foil serves to protect the laser-generated ion beam from late-time degradation through laser-plasma interaction, non-ideal ion phase space properties, and thermal expansion from hot electrons that co-move with the beam.

The work conducted during this project led not only to realization in a suite of Trident experiments, but also enhanced the applicability of these laser-generated ion beams for other potential applications. Multiple follow-on proposals to LANL LDRD, DOE OFES, and other WFO projects have been submitted as a result of this work (results pending). In these settings, PIC simulations have played a vital role in exploring and optimizing new acceleration concepts. In this project, the postdoc mastered running and analyzing VPIC simulations on some of the world's largest supercomputers and he has rapidly become a leader in the field of laser-ion acceleration. He reproduced, extended, and published new results on the BOA and developed a new wave-launch capability within VPIC as well as a suite of new diagnostics to analyze the simulations.

In this project, we made many major discoveries as a consequence of this project: we discovered that use of a second target foil placed behind the nm-scale BOA target, accomplishes three specific things: 1) it stops the laser, eliminating late-time laser-plasma interaction that degrades beam quality, as shown in Figure 2; 2) passage of an ion beam through the second foil exchanges hot co-moving electrons for cold target electrons, thereby slowing beam expansion (which occurs at the ion sound speed, which scales as the square root of the electron temperature), as shown in Figure 3; and 3) the production of a second electrostatic sheath at the rear of the second foil produces a "chirp" on the ion beam that counteracts the disadvantageous chirp the beam acquires as a result of the BOA mechanism. As a result of this work, we have learned how to maintain high beam quality at only a modest cost in mean beam energy, a substantial advancement toward the feasibility of using laser-ion accelerators for applications such as ion fast ignition inertial fusion.
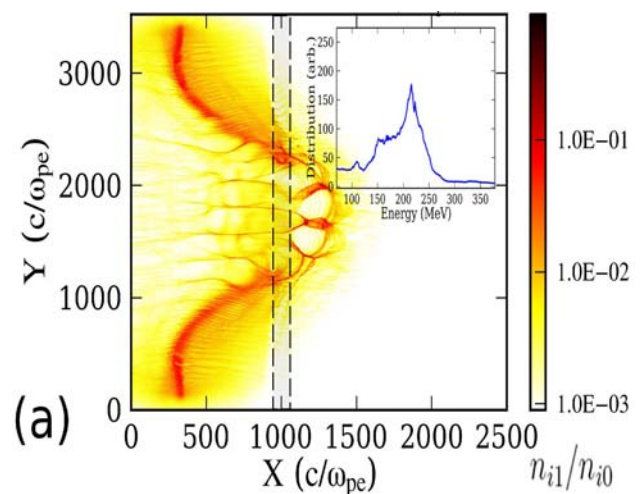

Figure 2. Ion beam density from two dimensional kinetic plasma simulation showing how placement of a second target foil (dashed lines) stops a laser beam from interacting with a propagating ion beam (color contours of ion density are shown). This technique preserves the quasi-monoenergetic ion energy distribution (inset).
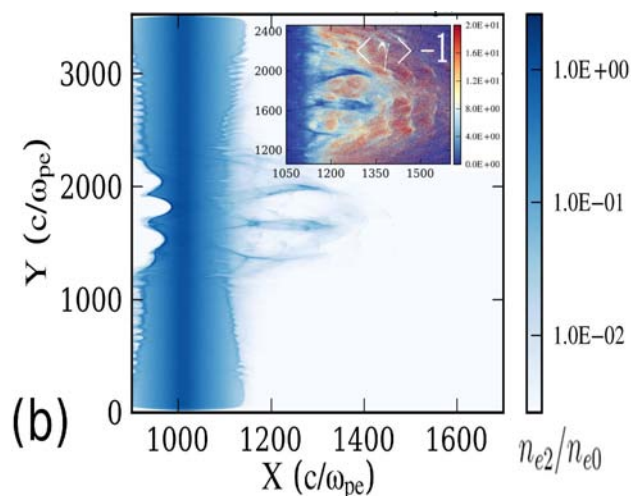
Figure 3. Contours of electron density and energy (inset), showing that regions of high electron density, corresponding to regions of high ion density (c.f. Figure 2) also have correspondingly low electron temperature. This feature of these laser-generated ion beams means that the ion beams will expand much more slowly, thus maintaining their high beam quality for longer than if a second target foil were not used.

In addition to the primary objective of this work (as represented in the postdoc's research proposal) he has also worked on various related side projects, including laser-acceleration of proton beams and the use of low-density aerogel targets and gas jets for ion beam collective acceleration and stopping, both of which have much potential applicability in laser-ion and conventional accelerator fields. He has also continued to work on positron and ion wakefield accelerators, which are related to (and complement) laser-ion accelerators and which enables him to remain a scientific leader in these fields. He visited the Max Planck Institute for Quantum Optics in Munich, Germany, for one month during Summer 2010 to collaborate on first-ever ion wakefield accelerator experiments. He spent two months being trained as an experimentalist and participated in an experimental campaign at Trident to try out some of his theoretical ideas (a rare opportunity for a theorist to be intimately involved in cutting-edge experiments). Finally, he began to apply his newfound experience with VPIC kinetic modeling toward the modeling of coherent synchrotron radiation, a novel approach to producing coherent xray sources presently supported by LDRD DR (PI: Carlsten). His work on this last project has contributed substantially to his likely conversion to technical staff at LANL.

As evidence of his prodigious accomplishments, Chengkun has presented papers and posters in several venues. He showed a poster at the Anomalous Absorption Conference in Snowmass, Colorado (the premier conference in the world for laser-plasma interaction), the European Physical Society Division of Plasma Physics meeting in Dublin, Ireland, the American Physical Society Division of Plasma Physics meeting in Atlanta, Georgia, an invited talk at the

American Physical Society Division of Plasma Physics meeting in Chicago, and he presented a poster on his work at the LANL Accelerators and Electromagnetic Radiation capability review.

Based on his work for this project, The postdoc authored or co-authored eight scientific papers in the past year, including a Physical Review Letter; he has one more paper in preparation based on his last Summer's research. An image he prepared appeared on the cover of *Symmetry* magazine, a popular journal focusing on advances in particle physics. The PI has spoken with individuals in the LANL Tech Transfer office about pursuing a patent on the concept developed as part of this research project.

Impact on National Missions

This project supported the DOE mission in Nuclear Weapons by enhancing our understanding of laser-particle sources related to boost in nuclear weapons and ICF physics; the work showed the efficacy of a novel technique for collimation and conditioning of laser-ion beams that will make these ion sources applicable to other missions of the Laboratory (e.g., Homeland Security) as well as enable various defense-related WFO projects for DTRA and DNDO.

Publications

Albright, B. J., L. Yin, B. M. Hegelich, K. J. Bowers, C. Huang, A. Henig, J. C. Fernandez, K. A. Flippo, S. A. Gaillard, T. J. T. Kwan, X. Q. Yan, T. Tajima, and D. Habs. Ultraintense laser interaction with nanoscale targets: a simple model for layer expansion and ion acceleration. 2010. *Journal of Physics: Conference Series.* **244** (4): 042022.

Gholizadeh, R., T. Katsouleas, P. Muggli, C. Huang, and W. Mori. Preservation of beam emittance in the presence of ion motion in future high-energy plasma-wakefield-based colliders. 2010. *Physical Review Letters.* **104** (15): 155001.

Hegelich, B. M., D. Jung, B. J. Albright, J. C. Fernández, D. C. Gautier, C. Huang, T. J. T. Kwan, S. Letzring, S. Palaniyappan, R. C. Shah, H. C. Wu, L. Yin, A. Henig, R. Hörlein, D. Kiefer, J. Schreiber, X. Q. Yan, T. Tajima, D. Habs, B. Dromey, and J. J. Honrubia. Experimental demonstration of key parameters for ion-based fast ignition. 2011. *Nuclear Fusion.* **51**: 52105.

Hogan, M. J., T. O. Raubenheimer, A. Seryi, P. Muggli, T. Katsouleas, C. Huang, W. Lu, W. An, K. A. Marsh, W. B. Mori, C. E. Clayton, and C. Joshi. Plasma wakefield acceleration experiments at FACET. 2010. *New Journal of Physics.* **12**: 085002.

Huang, C. K., B. J. Albright, L. Yin, H. C. Wu, K. J. Bowers, B. M. Hegelich, and J. C. Fernandez. Improving beam spectral and spatial quality by double-foil target in laser ion acceleration. 2011. *Physical Review Special Topics - Accelerators and Beams.* **14**: 1.

Huang, C. K., B. J. Albright, L. Yin, H. C. Wu, K. J. Bowers, B. M. Hegelich, and J. C. Fernandez. A double-foil target for improving beam quality in laser ion acceleration. 2011. *Physics of Plasmas.* **18**: 056707.

Lu, W., W. An, M. Zhou, C. Joshi, C. Huang, and W. Mori. The optimum plasma density for plasma wakefield excitation in the blowout regime. 2010. *New Journal of Physics.* **12**: 085002.

Muggli, P., I. Blumenfeld, C. E. Clayton, F. J. Decker, M. J. Hogan, C. Huang, R. Ischebeck, R. H. Iverson, C. Joshi, T. Katsouleas, N. Kirby, W. Lu, K. A. Marsh, W. B. Mori, E. Oz, R. H. Siemann, D. R. Walz, and M. Zhou. Energy gain scaling with plasma length and density in the plasma wakefield accelerator. 2010. *New Journal of Physics.* **12**: 045022.

Tuttle, K.. Crashing the size barrier. 2009. *Symmetry.* **6** (5): 1.

Single-Nanocrystal Photon-Correlation Studies of Carrier Multiplication

Victor I. Klimov
20090532PRD3

Abstract

Many nanomaterials with potential application in light emitting and light harvesting applications, such as lead-salt nanocrystals, emit light as photoluminescence (PL) in the near to mid-infrared (IR) range. Of particular interest, colloidal lead-salt (PbSe and PbS) nanomaterials have generated great interest as potential materials to boost photovoltaic efficiencies through carrier multiplication (CM).[1-2] The exact physical mechanism behind CM is debated in the literature in part due to the time consuming and difficult spectroscopic measurements required to accurately measure the CM process. Few low-noise single photon detectors exist for light above the silicon bandgap (> about 1 μm), and, until recently, those that did exist did not have sufficient time resolution. One of the most attractive systems under development for such applications is a superconducting nanowire single-photon detector (SNSPD). In this project, we developed and applied SNSPDs to study carrier multiplication (CM) in IR emitting nanomaterials. Of interest to next generation photovoltaics based on nanomaterials, we present CM efficiencies of PbSe nanocrystals and PbSe nanorods measured with an SSPD.

Background and Research Objectives

Colloidal semiconductor nanocrystals (or nanocrystal quantum dots – NQD) have been studied extensively over the last several years as a high quantum yield, tunable, low cost material for many light harvesting and light producing applications such as LEDs, detectors, lasers, and solar PV.[3] Perhaps the most impactful of all these potential applications would be as the active material in Generation-III (Gen-III) solar photovoltaics (PV), especially for NQD with narrow band gaps in the mid-infrared (IR) spectral range where most of the solar spectrum could be absorbed. Additionally, IR NQDs – such as PbSe and PbS – have demonstrated CM where one absorbed photon with two or more band gaps of energy can produce multiple electron hole pairs. Furthermore, it has been shown that CM in quantum dots is more efficient than in bulk.[1-2] If CM-based NQD solar cells can be realized they could increase the overall energy harvesting of PV past the thermodynamic limit of single junction silicon solar cells thus allowing low cost and high efficiency Gen-III solar cells to become a reality.[4]

One of the bottlenecks of realizing CM based solar cells is the accurate measurement of CM yields in nanomaterials. Accurate measurements of CM yields involve detailed and complicated measurements varying pump fluence and photon energy using spectroscopic techniques such as transient absorption (TA) or photoluminescence upconversion (UPL).[2] UPL in particular requires long scans (>10 hours) for lower fluence experiments in order to obtain an adequate signal-to-noise ratio (SNR) and determine accurate CM yields. However, measuring CM yields with UPL shows higher sensitivity than TA. Thus, accurately measuring the CM yields of a single nanomaterial sample at just two pump photon energies can take as long as a week. One reason for this difficulty is the lack of high quantum efficiency (QE), fast (ps resolution), low noise detectors in the mid-IR range, such as silicon avalanche photo diodes (APDs) for the visible range. This lack of fast IR detectors also prevents picosecond dynamical measurements using time correlated single photon counting (TCSPC) on single mid-IR nanomaterial studies, which have proven extremely powerful in visible emitting nanomaterials.

A relatively new technology for IR picosecond dynamics in the single photon regime are superconducting nanowire single photon detectors (SNSPD).[5,6] These systems were originally developed for quantum communications applications at telecom wavelengths (1.5 micron) where high detection efficiency, low noise, and low jitter/high temporal resolution are necessary. These detectors typically consist of a meandering thin nanowire (typically <10 nm thick by <100 nm wide) of niobium-nitride (NbN) that is cooled to below its superconducting critical temperature (T_c ~ 10K) and typically current biased to 95% of their superconducting critical current. The SNSPDs are usually patterned into a square (~10 micron by 10 μm) that is aligned with the core of a single mode optical fiber, and are thus fiber coupled into a cryo-stat and electrically read out (Figure 1a). When the meandering NbN nanowire absorbs a photon it produces a hot spot, which locally produces a resistive region and then a volt-

age spike (Figure 1b). The theoretical healing time of the resistive section is 30 ps. Detection efficiencies as high as 60% with very low dark count rate (10^{-3} Hz) and low timing jitter (~40 ps) have been reported making possible GHz count rates of single photons for IR spectroscopic studies (Figure 1c).
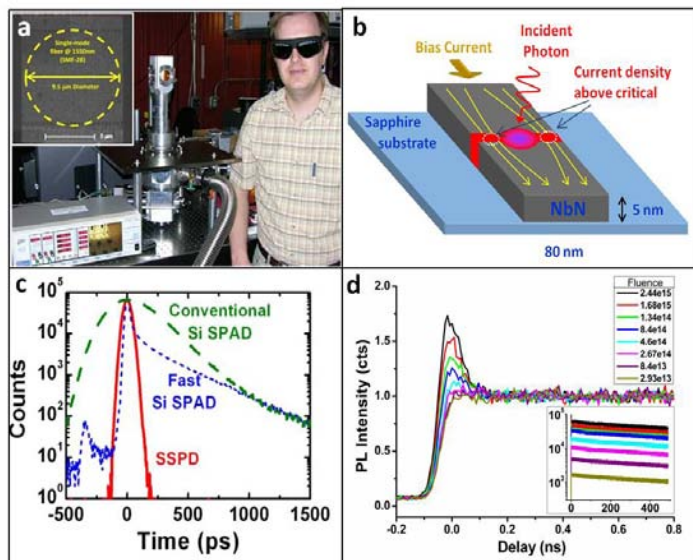

Figure 1. (a) Picture of LANL SNSPD system with Director's postdoc Sandberg (Inset) Electron microscope image of meandering NbN nanowire patterned to fill the core of a single mode optical fiber (yellow circle). (b) Principle of operation of an SNSP. (c) Measured instrument response functions of several single photon detectors showing the fast Gaussian response of the SSPD (from [6]). (d) Short time and long time (inset) PL dynamics of PbSe NQD at several 800 nm excitation fluences measured with the SNSPD system.

The goals of this project were to develop and demonstrate for the first time single nanomaterial spectroscopy (or micro-PL) in the IR range and to apply this technique to studying multi-exciton dynamics and CM. The main hurdle to obtaining this result was the lack of adequate detectors. Here, we report on how we overcame this hurdle by developing an SNSPD system that will allow single nanoparticle spectroscopy in the infra-red. After obtaining this system, we also realized its great strength in allowing the rapid screening of ensemble IR nanomaterials critical to the development of Gen-III solar PV. Thus, the bulk of the project to date has been devoted to developing the SNSPD capability at LANL and demonstrating its potential in ensemble CM measurements.

Scientific Approach and Accomplishments

The most important accomplishment during this project was developing the SNSPD time-resolved spectroscopic capability. The SNSPD system acquired at LANL was developed in collaboration with Dr. Sae Woo Nam's team in the Quantum Information and Terahertz Technology Group at the National Institute of Standards and Technology in Boulder, Colorado. This novel capability enabled a variety of first experiments that were not easily achievable before. We have studied the multi-exciton PL decays of PbSe NQD and nanorods at a variety of pump photon energies (1.55 eV, 3.1 eV, and 4.6 eV). We note that currently, studies at 4.6 eV pump photon energy are not possible with our UPL setup due to PL count rates and difficulty in generating the 3rd harmonic with the stretched out pulse needed for optimum photon counting. Additionally, since the SNSPD used had a 58.1 ps instrument response function, we develop a model to account for lost short time PL due to this response convolution (Figure 2). This PL model accurately models the fast Auger decay and long radiative decay of the PL signal (Figures 2a,b) and allowed us to correct the PL intensity (Figure 2c) in order to obtain accurate CM yields.
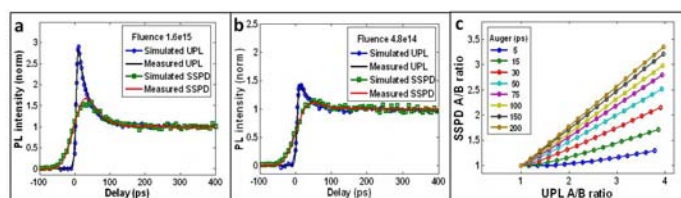

Figure 2. (a) and (b) comparison traces from UPL (blue dots) and SNSPD (green squares) showing the affect of the Gaussian IRF convolution. Also shown are two fits to the dynamic PL based on multi-exponential PL decay model with UPL model (black line) and SNSPD model (red line) with the same Auger time of 30 ps and same starting short time PL intensity. (c) Short time PL intensity (A/B ratio) correction curves generated by varying the A/B ratio for various Auger times using the PL decay model.

This SNSPD system allowed for 10-100 times higher count rates on low fluence data than with the UPL measurements, measurement of fast (~ 50 ps) and long lived (0.5 µs) dynamics simultaneous, and measurements of samples with broad PL and weak bleach that would be otherwise difficult or impossible with TA or UPL. This new capability enabled the measurement of a variety of materials and the accurate determination of their CM yield in about the same time it would take to measure a single sample with UPL. Therefore, we demonstrated that SNSPDs are a powerful rapid screening tool for IR nanomaterial CM yields and should be applicable to a variety of problems including time-resolved single IR nanoparticle studies (Sandberg *et al.* "Time-resolved multiexciton studies of nanomaterials with a superconductor nanowire single photon detector" *in preparation*).

As an example of the power of the SNSPD system to screening CM candidate materials, we studied the time resolved PL (Figure 3a,b) and measured the CM yields of novel PbSe nanorods synthesized by cation exchange. PbSe nanorods have been suggested as an attractive alternative to their spherical nanocrystal counterparts as they provide

a natural pathway for charge transport. Furthermore, it has been suggested that they may show higher CM efficiency due to proposed symmetry breaking and a lifting of the ground state degeneracy. The PbSe nanorods show bright photoluminescence with high quantum yield, and show modest improvements in carrier multiplication yields when compared to spherical PbSe nanocrystals. With the SNSPD, we were able to measure PL dynamics with *4.6 eV pump photon energy – something that was not possible with UPL or TA* (Figure 3b). As shown in Figure 4, the preliminary data shows a modest improvement (20-50%) in carrier multiplication efficiency compared to spherical PbSe nanocrystals (Sandberg *et al.* "Enhanced carrier multiplication efficiency of lead-salt nanorods studied with a superconducting nanowire single photon detector" *in preparation*).
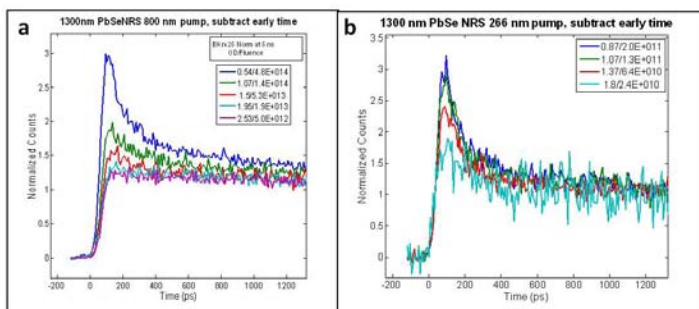

Figure 3. PL dynamics measurements of PbSe nanorods: (a) 800 nm pump PL traces through fluence measured with SNSPD; (b) 266 nm pump PL traces through fluence measured with SNSPD.
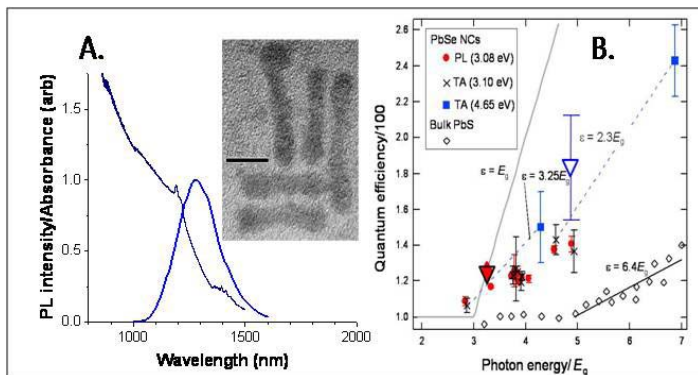

Figure 4. (a) Absorption (navy) and PL (blue) of PbSe nanorods with aspect ratio 3 (inset: TEM of nanorods - bar is 10 nm). (b) CM of PbSe nanorods measure with the SNSPD (triangles) compared to bulk (diamonds) and NQD (other symbols) in terms of efficiency per band gap of photon energy.

This new and unique capability will enable a whole series of novel studies in addition to providing critical rapid screening of potential IR nanomaterials for Gen-III photovoltaics. For example, we plan to use this system to study the dynamics in larger diameter/smaller band gap carbon nanotubes (CNT), energy transfer in novel narrow band gap nanocrystal/plasmonic hybrid particles, and multi-exciton dynamics in single IR nanoparticles. For this last application, traditional techniques for determining multi-exciton dynamics based on Auger recombination signals are difficult or impossible in many materials where there is no pronounced Auger recombination.

Impact on National Missions

The development of the SNSPD represents an entirely new and unique spectroscopic capability at LANL and has already enabled the study of a wide range of previously unexplored infrared nanomaterial ensembles. For example, as mentioned here, the SNSPD has enabled rapid screening of novel PbSe nanorods that have shown higher carrier-multiplication yields as compared to their spherical nanocrystal counterparts. Additionally, in the near future the SNSPD system will enable studies at the single nanoparticle level in the IR range, a first for nanomaterial spectroscopy. The studies carried out in this project are of high relevance to third generation photovoltaics and thus are in line with LANL's Materials and Renewable Energy Grand Challenges. We envision the SNSPD system to continue the rapid screening of IR nanomaterials for solar PV applications thus removing a major hurdle in applying nanomaterials to solar energy.

Moreover, this newly-developed capability will allow the study of radiation-matter interactions under extreme conditions on the single nanocrystal level: extremely high photon densities can be attained by using amplified femtosecond lasers in our setup and in turn, these lasers can generate extremely high carrier densities in a single nanocrystal. Thus, the development of this new experimental capability is in line with the mission of LANL's MaRIE program. This new capability allows us to obtain fundamental scientific information on how single- and multiple charge carriers are created by the absorption of a single photon in an infrared nanocrystal. These types of processes are in line with LANL's Grand Challenges in the Materials for Clean Energy category, "Electricity generation and efficiency through the use of nano-structured materials."

References

1. Schaller, R. D., and V. I. Klimov. High Efficiency Carrier Multiplication in PbSe Nanocrystals: Implications for Solar Energy Conversion. 2004. *Physical Review Letters.* **92** (18): 186601.

2. McGuire, J. A., J. Joo, J. M. Pietryga, R. D. Schaller, and V. I. Klimov. New Aspects of Carrier Multiplication in Semiconductor Nanocrystals. 2008. *Accounts of Chemical Research.* **41** (12): 1810.

3. Klimov, Victor I.. Detailed-balance power conversion limits of nanocrystal-quantum-dot solar cells in the presence of carrier multiplication. 2006. *Applied Physics Letters.* **89** (12): 123118.

4. Klimov, V. I.. Nanocrystal Quantum Dots. 2010.

5. Gol'tsman, G., O. Minaeva, A. Korneev, M. Tarkhov, I. Rubtsova, A. Divochiy, I. Milostnaya, G. Chulkova, N. Kaurova, and B. Voronov. Middle-infrared to visible-light ultrafast superconducting single-photon detectors. 2007. *IEEE TRANSACTIONS ON APPLIED SUPER-CONDUCTIVITY ASC.* **17** (2): 246.

6. Stevens, Martin J., Robert H. Hadfield, Robert E. Schwall, . , Richard P. Mirin, and James A. Gupta. Fast lifetime measurements of infrared emitters using a low-jitter superconducting single-photon detector. 2006. *Applied Physics Letters.* **89** (3): 031109.

Publications

Sandberg, R. L.. Carrier Multiplication Studies of Lead-Salt Nanorods with a Superconducting Nanowire Single Photon Detector. Invited presentation at *Department of Physics & Astronomy Colloquium, University of Denver.* (Denver, Colorado, 10 Nov. 2010).

Sandberg, R. L., L. A. Padhila, J. J. Stewart, W. K. Bae, M. M. Qazilbash, B. P. Khanal, R. D. Schaller, J. M. Pietryga, M. J. Stevens, B. Baek, S. W. Nam, and V. I. Klimov. Enhanced Carrier Multiplication Efficiency of Lead-Salt Nanorods Studied with a Superconducting Nanowire Single Photon Detector. To appear in *To be submitted to Nano Letters.*

Sandberg, R. L., M. M. Qazilbash, B. P. Khanal, R. D. Schaller, J. M. Pietryga, M. J. Stevens, B. Baek, S. W. Nam, and V. I. Klimov. Carrier Multiplication Studies of Lead-Salt Nanorods with a Superconducting Nanowire Single Photon Detector . Presented at *Materials Research Society (MRS) Fall 2010 Meeting.* (Boston, Massachusettes, 29 Nov. 2010).

Sandberg, R. L., M. M. Qazilbash, R. D. Schaller, J. M. Pietryga, M. J. Stevens, B. Baek, S. W. Nam, and V. I. Klimov. Time-Resolved Multiexciton Studies of Nanomaterials with a Superconductor Nanowire Single Photon Detector. To appear in *To be submitted to ACS Nano.*

Correlation in Ultracold and Ultrafast Systems

Lee A. Collins
20090533PRD3

Abstract

The ability to examine basic material systems at the time scale of their most fundamental motions opens broad prospects for both deeper understanding and the development of new materials and new probes that can have a broad impact in a variety of areas. We have developed large-scale, highly-sophisticated computational tools to explore two representative systems: ultracold dipolar gases and ultrafast interactions of radiation with atoms.

Background and Research Objectives

The project has two parts: one treats very fast processes and the other very cold gases. The first part follows the reaction of an atom or molecule to a very short pulse of light produced by a laser. As technology has advanced, lasers have been engineered to produce shorter and shorter pulses that now reach lengths on the order of the time scale that an electron moves within an atom. This interval is an attosecond, which is about the time light takes to cross an atom. Long pulses interact weakly with atoms since the electrons have ample time to relax to the slow changes in the light field. However, for the attosecond case, since the pulse and electron interact on the same time scale, the effects on the atom can be dramatic. Even at the level of quantum mechanics, which governs the behavior of microscopic particles, we can still in certain cases, view an electron as orbiting the central nucleus of an atom, much like a planet around the Sun. Since the laser pulse is shorter than the period of the electron, we can take a snapshot at a particular point within its orbit, in much the same way as a strobe light "freezes" motion. By probing at different times, we can construct a series of frames or a movie of the motion of the electron around its path. This particular sequence in which one laser pulse places the electron in a given orbit while a second laser pulse snaps a picture at a later time is refer to as a pump-probe experiment and occupies our main study into the effects of light on matter. We can also use this device to control the process itself by readjusting the state of the system at a particular time. Since electrons form the glue that binds atoms, and molecules, and solids together, an understanding of their behavior at such a basic level can lead to the development of new materials, the real-time control of atomic processes, and the detailed imaging complex systems.

In the second part, we studied a strange state of matter called the Bose-Einstein Condensate (BEC), which for a gas exists just one billionth of a degree above absolute zero, the lowest temperature possible at which all motion ceases. The temperature is so cold that all the atoms move together, and the BEC acts as a unified object with very different properties than a usual gas. For example, disturbances in the medium flow without friction and once set in motion will continue to travel undisturbed for as long as the BEC is stable. This effect is know as superfluidity and exists in many materials under a variety of conditions. In addition, the medium supports certain stable structures such as vortices, much like little whirlpools but with special properties due to their quantum nature. Crossed laser beams have been used to form optical lattices, which trap various parts of the BEC. By adjusting the trap depth, various situations can be studied in analogy to solid-state materials. One great advantage of the gaseous BECs is their dilute nature allows them to be imaged and easily manipulated so that their properties can be determined in great detail. The first BECs used simple atoms with very short-range interactions. However, new experiments have begun to study BECs consisting of atoms and molecules with more complicated longer-range interactions. We have focused our studies on a particular set with dipoles moments. In a simple analogy, these dipoles can be viewed as bar magnets influencing each other at a distance through their fields. This longer-range aspect complicates the description in that all parts of the BEC can now interact with each other. A basic understanding of these systems can have important applications to such areas as high-precision measurements and even quantum computing.

Scientific Approach and Accomplishments

We have examined the basic interactions of attosecond pulses with atoms in order to determine the effects of correlation and the ability to manipulate various excitation paths by employing large-scale, highly-parallel simulation methods for solving the time-dependent

Schrodinger equation to determine the evolution of the electrons. This in turn permits manipulating the mechanisms in order to tune the outcome. The understanding at such a fundamental level will greatly elucidate these effects in more complicated systems. Our techniques employ the finite-element discrete variable representation (FEDVR), which has shown linear scaling out to thousands of processors. Our first demonstration has focused on the two-electron Helium atom to understand the attosecond interaction and its effects on photoionization by multiple photons.

This demonstration involves providing theoretical support for a set of basic pump-probe experiments that first excite Helium into correlated states and then ionize these states to determine their basic characteristics. Since the pulses are on the scale of the interaction, these experiments provide new insights into basic quantum mechanical processes not attained by long-pulse lasers. This work is in collaboration with the Technical University of Vienna and the Institute for Theoretical Atomic and Molecular Physics at Harvard. A series of calculations on Helium has recently been completed on which a paper will soon appear. In this case, the pump laser populates several coupled doubly-excited states. The superposition of these states produces a wave packet that moves around the system. A probe laser at various delay times examines the packet throughout its journey between weak and strong mixings of the states and thus provides a real-time map the basic electronic motion that can directly be compared to experiments. This project serves as a first step to treating simple molecules in which additional pathways such as rotation, vibration, and dissociation open.

For the ultracold BEC investigation, we have developed large-scale quantum mechanical scattering programs to follow the interactions of ultracold polar molecules and techniques for solving the two-dimension nonlinear equation to treat quantum many-body problems in condensed systems. We focused on understanding the effects of long-range interactions on the basic condensate properties and how these might be manipulated to design simple quantum algorithms as a basis for computing**.** Additionally the ultracold dipolar gases present a highly controlled and clean means to study the collective behavior at a fundamental level.

The dipolar condensate project has resulted in two publications, one in Physical Review Letters (PRL) and the other in Physical Review A (PRA) as well as a PRL in preparation. The research has focused on several important aspects of these systems. The first contribution concerns the basic stability of molecular condensates. We and a collaborator at Harvard determined, for the first time, the rates of three-body processes for dipolar particles, which provides an important guide to the experimental realization and lifetimes of these objects. The second contribution, reported in a sole-author PRA, also concerns scattering effects but

this time confined to two dimensions. The calculations determine the consequence of this restriction and its signature in the collision process. Once again, the research was the first of its kind and is vital to current experimental efforts that also are investigating dipolar gases in reduced dimensions. A third contribution focuses more on the condensate as a whole and investigates many-body effects such as superfluidity. The research shows that an obstacle moving in the dipolar gas will generate distinct effects depending on which way it moves in the gas. This anisotropic response offers an important means to understand collective quantum behavior at a fundamental level. This work will be presented in seminars at CNLS and T-1 at LANL, and at an invited seminar at UNM's Center for Quantum Information and Control.

Impact on National Missions

Fast pulse interactions with materials from atoms to solids allow us to probe and control basic quantum processes in order to improve our understanding of basic materials, to better design new materials, and to change reaction rates in chemical processes. In addition, these fast probes provide new imaging techniques for complex systems. Ultracold systems can provide precision measurement devices such as interferometers and gyroscopes, which significantly exceed current optical capabilities. Dipolar condensates also have applications to the construction of quantum devices, which might be the key to high performance computing.

Publications

Ticknor, C.. Quasi-two-dimensional dipolar scattering. 2010. *Physical Review A.* **81**: 042708.

Ticknor, C., and R. M. Wilson. Asymptotic superfluidity in dipolar BECs. To appear in *Physical Review Letters.*

Ticknor, C., and S. T. Rittenhouse. Three-body recombination in ultracold dipoles to weakly bound dimers. 2010. *Physical Review Letters.* **105**: 01201.

Cold-Atom-Based Theory and Quantum Simulations for Many-body Physics

Bogdan F. Damski
20090536PRD3

Abstract
We studied quantum simulations of complex many-body systems such as high-Tc superconductors and nanoscale electronic devices by using controllable ultra-cold atomic systems. Our work provides insight into different phases of superconductors. We developed a unified theory of transport properties in high-Tc superconductors and ultra-cold atomic systems. In contrast to previous work, our theory is consistent with important conservation laws. By generalizing our theories, we investigated dynamics of superfluids, which is important in understanding the analogous problems in superconductors. Moreover, we have been developing simulation tools for quantum transport at the nanoscale and our results will lead to new design of nano devices, which will play a crucial role in next-generation electronics. This project has lead to four published articles (including one Physical Review Letter) and will benefit future research in many-body systems.

Background and Research Objectives
We studied cold atomic systems and their applications as quantum simulators of both superconductors and many-body effects in nanoscale transport. This is a competitive field with broad implications, e.g., in condensed matter physics, nanoscale science, and quantum information. Quantum simulations use the highly controllable nature of one quantum system (here, a cold atom cloud) to create simplified analogs of complex materials and devices in order to gain direct theoretical and experimental insight into the underlying physical phenomena. We developed a theoretical scheme for emulation of various properties of superconductors in cold atom setups to address challenging problems inaccessible in traditional condensed matter settings.

In particular, we developed a unified theory of different phases of cold atom systems that incorporates many analogous features of high-Tc superconductors. Furthermore, we have theoretically studied interesting properties of these phases and the response of the system to external perturbations (e.g., time dependent magnetic fields). From here, more complex systems can be ana-lyzed. Our theories help understand quantum and non-equilibrium effects in nanoscale electronic systems, as well as provide novel measurement techniques capable of probing engineered cold atomic systems. Our studies help elucidate the role of electron-electron interactions and dissipation in electronic transport – effects that are difficult to capture in traditional theoretical approaches to transport.

Our work explored a promising method for cold atom emulation of superconductors that will help explain the underlying mechanism involved. Moreover, our investigations into nonequilibrium and inhomogeneous cold atomic systems help understand quantum effects in electronic transport, which is crucial in designing functional nanoscale devices. The advantages of simulating electronic transport using ultra-cold atomic systems come from the powerful tunability of their interaction strength and confining geometry (dimensionality). This allows us to analyze the dominant effects in nanoscale transport phenomena.

Scientific Approach and Accomplishments
The project started with studies of the ground state properties of ultra-cold atoms with tunable interactions. We found that with weakly repulsive interactions cold atoms could simulate a very important paradigm in condensed matter physics called the Fermi liquid. A detailed study of Fermi liquids helps us understand how atoms can form unconventional superfluids as the interaction varies. This has been widely studied in Helium-3; A. J. Leggett won a Nobel prize for his work on the subject. We generalized his theory so that it can be applied to ultra-cold atoms. There were only limited studies on Fermi liquid properties of ultra-cold atoms so we systematically evaluated the parameters needed for characterizing a Fermi liquid and addressed how those parameters can be extracted experimentally. The results are summarized in Ref. [1].

Subsequent studies of how a cloud of ultra-cold atoms responds to density or spin disturbance were performed. Past work on this subject usually ignores the important contribution from the collective excitations of the super-

fluid. As a consequence the essential conservation laws of mass and spin are not respected. We developed a consistent theory that is shown to satisfy the required conservation laws. Based on our findings, we have suggested future improvement of experimental techniques that can better resolve the emergence of superfluidity. The results have been published [2].

The theoretical framework of this work has been further generalized to obtain transport coefficients such as viscosity and conductivity. There has been growing interest in the viscosity of quantum fluids such as atomic superfluids or quark-gluon plasma in high-energy physics. The conductivity of high-Tc superconductors is also of great interest because it deviates significantly from metallic behavior. We found that our unified description can explain these puzzling phenomena in atomic gases and superconductors. Our work resulted in an invited review paper that is in press [3].

In addition, we have studied how cold-atom superfluids can simulate nonequilibrium dynamics of conventional superconductors that would be virtually impossible in conventional condensed matter setups. We have studied the dynamics of a superfluid approaching a quantum critical point by numerically simulating its equations of motion. We have analyzed the scaling behavior of nonequilibrium quantities and found that quantum criticality imprints nonequilibrium length and energy scales on the coherence length and the order parameter, respectively. Furthermore, to account for real experimental situations, we studied finite-temperature effects and searched for parameters where signatures of quantum criticality can still be observed. We published a paper summarizing these results [4].

Finally, we have studied quantum transport of ultra-cold atoms in periodic potentials made of laser beams. We followed a simulation technique that can monitor the full quantum dynamics of the system and developed a theory of nanoscale quantum transport in one-dimensional geometries. The obtained results are currently being prepared for a publication.

Impact on National Missions

This work brings better understanding of high-Tc superconductors: materials with zero electrical resistance. These materials have important applications like, e.g., they can eliminate virtually all the loss of energy that goes into resistive heating in the lines transmitting electricity. Thus our research will support the development of energy-saving materials. This research will also advance fundamental understanding of materials on the very quantum level. Both goals are becoming focus areas for numerous sponsors including DOE as they touch both applied and basic aspects of energy research.

References

1. Chien, C. C., and K. Levin. Fermi liquid theory of ultra-cold trapped Fermi gases: Implications for pseudogap physics and other strongly correlated phases. 2010. *Physical Review A.* **82**: 013603.

2. Guo, H., C. C. Chien, and K. Levin. Establishing the presence of coherence in atomic Fermi superfluids: Spin-flip and spin-preserving Bragg scattering at finite temperatures . 2010. *Physical Review Letters.* **105**: 120401.

3. Guo, H., D. Wulin, C. C. Chien, and K. Levin. Perfect fluids and bad metals: Transport analogies between ultra-cold Fermi gases and high Tc superconductors. To appear in *New Journal of Physics.*

4. Chien, C. C., and B. Damski. Dynamics of a quantum quench in an ultra-cold atomic BCS superfluid . 2010. *Physical Review A.* **82**: 063616.

Publications

Chien, C. C., and B. Damski. Dynamics of a quantum quench in an ultra-cold atomic BCS superfluid . 2010. *Physical Review A.* **82**: 063616.

Chien, C. C., and K. Levin. Fermi liquid theory of ultra-cold trapped Fermi gases: Implications for pseudogap physics and other strongly correlated phases. 2010. *Physical Review A.* **82**: 013603.

Guo, H., C. C. Chien, and K. Levin. Establishing the presence of coherence in atomic Fermi superfluids: Spin-flip and spin-preserving Bragg scattering at finite temperatures. 2010. *Physics Review Letters.* **105**: 120401.

Guo, H., D. Wulin, C. C. Chien, and K. Levin. Perfect fluids and bad metals: Transport analogies between ultra-cold Fermi gases and high Tc superconductors . To appear in *New Journal of Physics.*

Tracing Fluctuations in the Universe

Katrin Heitmann
20100605PRD2

Abstract

Cosmology is the study of the history and dynamics of the universe itself. Gravitational attraction causes tiny over-dense fluctuations in the smooth, hot, and dense early universe to grow and become the host environments for galaxies and galaxy clusters as the universe expands and cools. The statistics of these fluctuations are our key source of observational information in cosmology, both through the temperature anisotropies in the Cosmic Microwave Background and in the large-scale structure of the universe today. Questions about conditions in the early universe, the nature and distribution of dark matter and dark energy, and the overall geometry of the universe can only be answered through grand observations of the cosmos. Years of telescope time have been spent conducting surveys that have measured the angular positions and redshifts (a proxy for distance in an expanding universe) of millions of galaxies over a significant fraction of the observable universe. Surveys in progress and being planned will probe even more volume. We can use the statistical distribution of galaxies to answer fundamental questions in cosmology provided we understand the details of how galaxies in redshift space trace the underlying matter fluctuations.

With the completion of the Sloan Digital Sky Survey we have reached a point where our ability to learn about cosmology from galaxy surveys is limited more by the quality of our theoretical models than by our data. Analytic models based on perturbation theory fail to adequately describe the effects of gravitational clustering in highly over-dense environments where galaxies reside, so we cannot use them to study the details of how galaxies trace fluctuations. The dramatic increases in speed and dynamic range that are possible with new simulation capabilities developed at Los Alamos give us the capability to run the ``super'' simulations that will be necessary to study the detailed environments of galaxies embedded in the immense volumes that are needed for cosmological studies. Speed is crucial as we will need to run simulations for a variety of models to look for cosmological dependence. Even with fast simulations we will need to be judicious in choosing

which models to run, and we will use the sophisticated statistical methods to design our experiment. We will use these simulations to develop models for how galaxies trace fluctuations in redshift space based on numerical studies. Developing accurate models in redshift space is key, as this puts the theory into the same space as observations.

Background and Research Objectives

The project will lead to (i) improved, world-leading simulation capabilities to follow structure formation in the Universe, (ii) sophisticated models which will allow us to connect the distribution of galaxies to the underlying matter in the Universe at very good accuracy, (iii) new cosmological constraints by comparing different cosmological models to observations, (iv) the development of important new capabilities to analyze future cosmological surveys.

Scientific Approach and Accomplishments

The principal investigator of this project left the laboratory. More information about the project is available from the Los Alamos LDRD Program Office.

Publications

Habib, S., A. Pope, Lukic&acute, D. Daniel, P. Fasel, N. Desai, K. Heitmann, Chung-Hsing Hsu, L. Ankeny, G. Mark, S. Bhattacharya, and J. Ahrens. Hybrid peta-computing meets cosmology: the Roadrunner Universe project. 2009. *Journal of Physics: Conference Series.* **180** (1): 012019 (10 pp.).

Percival, W., B. Reid, D. Eisenstein, N. Bahcall, T. Budavari, J. Frieman, M. Fukugita, J. Gunn, Z. Ivezic, G. Knapp, R. Kron, J. Loveday, R. Lupton, T. McKay, A. Meiksin, R. Nichol, A. Pope, D. Schlegel, D. Schneider, D. Spergel, C. Stoughton, M. Strauss, A. Szalay, M. Tegmark, M. Vogeley, D. Weinberg, D. York, and I. Zehavi. Baryon acoustic oscillations in the Sloan Digital Sky Survey Data Release 7 galaxy sample. 2010. *MONTHLY NOTICES OF THE ROYAL ASTRONOMICAL SOCIETY.* **401** (4): 2148.

Pope, A., S. Habib, Z. Lukic, D. Daniel, P. Fasel, K. Heitmann, and N. Desai. The Accelerated Universe. 2010. *Computing in Science & Engineering.* **12** (4): 17.

Reid, B., W. Percival, D. Eisenstein, L. Verde, D. Spergel, R. Skibba, N. Bahcall, T. Budavari, J. Frieman, M. Fukugita, J. Richard. Gott, J. Gunn, Z. Ivezic, G. Knapp, R. Kron, R. Lupton, T. McKay, A. Meiksin, R. Nichol, A. Pope, D. Schlegel, D. Schneider, C. Stoughton, M. Strauss, A. Szalay, M. Tegmark, M. Vogeley, D. Weinberg, D. York, and I. Zehavi. Cosmological constraints from the clustering of the Sloan Digital Sky Survey DR7 luminous red galaxies. 2010. *MONTHLY NOTICES OF THE ROYAL ASTRONOMICAL SOCIETY.* **404** (1): 60.

White, M., A. Pope, J. Carlson, K. Heitmann, S. Habib, P. Fasel, D. Daniel, and Z. Lukic. Particle mesh simulations of the Lyα forest and the signature of baryon acoustic oscillations in the intergalactic medium. 2010. *Astrophysical Journal.* **713** (1): 383.

Woodring, J., K. Heitmann, J. Ahrens, P. Fasel, C. Hsu, S. Habib, and A. Pope. ANALYZING AND VISUALIZING COSMOLOGICAL SIMULATIONS WITH ParaView. 2011. *ASTROPHYSICAL JOURNAL SUPPLEMENT SERIES.* **195** (1): 11.

Woodring, J., K. Heitmann, J. Ahrens, P. Fasel, Chung-Hsing Hsu, S. Habib, and A. Pope. Analyzing and Visualizing Cosmological Simulations with ParaView. 2011. *Astrophysical Journal Supplement Series.* **195** (1): 11 (12 pp.).

Probing Dark Energy and Modified Gravity via Interactions with Normal Matter

Patrick S. Mccormick
20100609PRD2

Abstract

Just a decade ago, the startling discovery was made that the expansion of the Universe is accelerating. The equations of General Relativity admit such an accelerating solution if we include among the contents of the universe a negative-pressure substance known as dark energy. If we assume, in the spirit of Feynman, that any interaction not forbidden is mandatory, then we must consider couplings between dark energy and known, Standard Model particles. However, the "fifth forces" that would arise from such interactions have not been seen. A more careful study of these couplings and their interplay with dark energy self interactions reveals the existence of the "chameleon effect," by which the mass of a dark energy particle depends on the density of known particles.

This project work concerns the phenomenology of chameleon dark energy, and its close cousin modified gravity, from submillimeter to cosmological scales. Remarkably, laboratory experiments are powerful probes of dark energy couplings to matter and photons. The GammeV–CHASE experiment at Fermilab will search for photon-coupled chameleon dark energy through an effect known as "afterglow." A photon passing through a magnetic field may oscillate into a chameleon particle, which in turn may be trapped inside a container if its energy inside the container is less than its mass in the container walls. Such chameleon particles will gradually oscillate back into photons, emitting an afterglow of photons once the light source has been turned off. As part of this project, the results of GammeV–CHASE will be analyzed and interpreted, particularly as it applies to chameleon dark energy. In addition, work will be carried out to investigate early universe physics constraints on chameleon dark energy, for example, by investigating big bang nucleosynthesis. Another avenue will be the production of light, weakly coupled particles in stars and supernovae, as well as their propagation through the universe. The aim would be to extend previous work to the understanding of chameleons, whose stellar production may be suppressed by large masses, and whose oscillations may be enhancedby fluctuations in the matter density.

Background and Research Objectives

The acceleration of the Universe requires either a negative-pressure substance known as dark energy or a new theory of gravity acting on cosmological scales. From the point of view of particle physics, there is no reason why couplings between dark energy and known, Standard Model particles should not exist. However, the "fifth forces" that would arise from such interactions have not been seen. A more careful study of these couplings and their interplay with dark energy self interactions reveals the existence of the "chameleon effect," by which the mass of a dark energy particle depends on the density of known particles.

This project work concerns the phenomenology of chameleon dark energy and modified gravity, from submillimeter to cosmological scales. It will cover analysis and interpretation of laboratory experiments investigating dark energy couplings to matter and photons (the GammeV–CHASE experiment at Fermilab). In addition, work will be carried out to investigate early universe physics constraints on chameleon dark energy by investigating big bang nucleosynthesis. Another avenue will be the production of light, weakly coupled particles in stars and supernovae, as well as their propagation through the universe. The aim would be to extend previous work to the understanding of chameleons, whose stellar production may be suppressed by large masses, and whose oscillations may be enhanced by fluctuations in the matter density.

Scientific Approach and Accomplishments

The principal investigator of this project left the laboratory. More information about the project is available from the Los Alamos LDRD Program Office.

Publications

Steffen, J. H., A. Upadhye, A. Baumbaugh, A. S. Chou, P. O. Mazur, R. Tomlin, A. Weltman, and W. Wester. Laboratory constraints on chameleon dark energy and power-law fields. 2010. *Physical Review Letters.* **105** (26): 261803.

TECHNOLOGY

Nanoscale Superconductivity for Single Photon Detection

Michael W. Rabin
20100006DR

Introduction

Photon detection lies at the heart of numerous applications in national security and fundamental science. Space surveillance, nuclear threat detection, quantum science, and biomolecular imaging all have a compelling need for broadband, high efficiency, low noise, and fast single photon detectors. Conventional technologies fall short in at least one of these areas, forcing application-specific compromises. A new class of detector, the superconducting nanowire single photon detector (SNSPD), has the potential to revolutionize the field of single photon detection through a combination of unsurpassed performance in all critical parameters (scalability, broadband efficiency, dark count rate, speed). Current development of these detectors is limited by materials difficulties that affect yield and performance, making it impossible to study the underlying physics and determine the fundamental limits of detector operation. At LANL, we have key advantages: two complementary thin-film growth techniques (Energetic Neutral Atom Beam Lithography & Epitaxy, or ENABLE,3 and Polymer Assisted Deposition, or PAD) and our ability to integrate expertise over a wide range of fields. This approach will transform the SNSPD field from one based on empirical device designs (i.e. irreproducible recipes) to a quantitative, systematic discovery of device physics (predictive science with control).

Benefit to National Security Missions

In the long term, we anticipate the development of large-format SNSPD-based cameras that will have extraordinary applicability in areas that include:

- Surveillance and reconnaissance in support of nuclear, biological, chemical, and environmental treaty verification.

- All-sky search for small, dark, unknown space objects (space situational awareness or SSA).

- Determining reaction history at picosecond time resolution in thermonuclear burn or ignition experiments (e.g. ICF at OMEGA or NIF).

- Remote chemical identification of trace-level efflu-ents using hyperspectral imaging for nonproliferation (nuclear, biological, chemical).

- Ultrafast single photon detector with gigahertz repeat rate for applications in fundamental quantum optical sciences.

Progress

We have grown a series of ENABLE (energetic neutral atom beam lithography/epitaxy) and PAD (polymer assisted deposition) NbN films ranging from 4-50 nm thickness. We discovered a strong dependence of film properties on growth conditions and are exploring how to better control film properties through control of growth conditions. We performed extensive characterization of our PAD and ENABLE grown films to correlate growth conditions with micro-structural and physical properties. Using HRTEM (high-resolution transmission electron microscopy, as illustrated in Figure 1), we characterized the morphology of films. Using XRD (x-ray diffraction) we confirmed the crystalline structure of NbN films. Using SIMS (Secondary Ion Mass Spectrometry) we identified atom specific compositions of films.

Over the last year, our ENABLE grown films were far superior compared to PAD grown films with respect to film quality, materials properties, and reproducibility. The PAD technique was able to produce superconducting films, but they were generally not dense at the thickness ranges relevant for SNSPDs and related devices (below 20 nm). The PAD films instead had a network or sometime island structure. Films with network structure with characteristic size scale of a few hundred nanometers to micrometers are not consistent with our need for dense, uniform films. This requirement is driven by the need for repeatability in making micro and nano devices with consistent performance. Therefore, we decided to discontinue the PAD synthesis and growth effort by shifting full emphasis on high quality ENABLE films that rival the best in the literature. Using the ENABLE technique we now consistently grow 4-15 nm epitaxial NbN films that are dense, crystalline, highly ordered, with or without capping layers, and with superconducting transition temperatures as high as 14 K. We now operate with a large

selectable set of options in the ENABLE lab for growth. These options include substrate choice (c-, a-, r-, or m-plane sapphire, <111> or <100> silicon, or MgO), growth temperature (300-1000 degrees C), buffers materials under the NbN layer (AlN, GaN, SiN) and capping layers to prevent oxidation of the NbN (AlN, GaN).
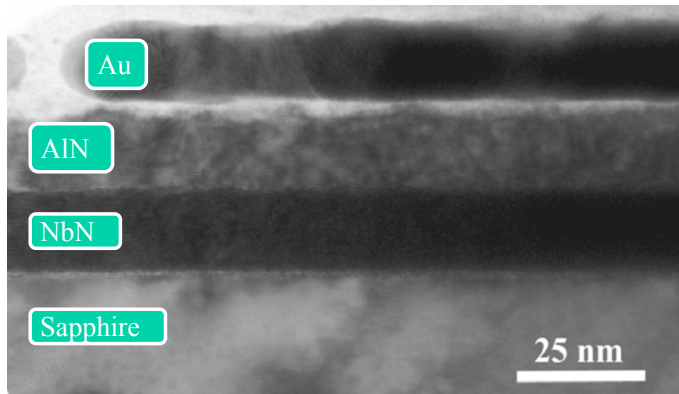

Figure 1. High resolution transmission electron micrograph (HRTEM) showing cross sectional view of an ENABLE-grown NbN film. Scale bar at 25 nm. Lowest layer is the sapphire substrate, followed by the superconducting NbN with thickness ~15 and similar thickness AlN capping layer. (The Au layer is part of the HRTEM preparation process).

In the next step, the best thin films have been successfully micro and nano patterned for testing. Micro and nano patterning of devices has required substantial process development. The result is a variety of micro- and nanoscale devices as shown in Figure 2. These devices fall into four major categories: SNSPD sensors, devices to test vortex-crossing-based theories, structures to test materials parameters (e.g. superconducting transition temperature, critical current, etc.), and diagnostic devices specifically to assess the influence of micro or nanopatterning steps on performance. Considerable effort goes into the design phase prior to micro and nano fabrication to decide which devices we will make, how many of each kind, and with what range of varied parameters. The tools used for making all these devices are photolithographic patterning, electron beam lithographic patterning, dry (plasma) etching, and metal deposition. Significantly, we have produced both micro and nanoscale devices with little or no change in material parameters from those of unpatterned ENABLE-grown 5-15 nm NbN, as illustrated in Figure 3. This includes devices that are ~100 nm wide and ~50 mm long.

At the same time, we used resistivity measurements with and without magnetic field to determine the superconducting transition temperature of dozens of films. In the meantime, we continued with setting up a cryogenic optical measurement station (probe station) for future testing of devices. First test showed that we get similar results to PPMS measurement stations but with the additional optical fiber. Also, in collaboration with NIST at Boulder, we packaged a single-photon detector, which has been tested

at LANL for performance. Preliminary results are encouraging. New results on NbTiN films and structures are promising, but revealed problems with capping of films that complicates micro patterning.
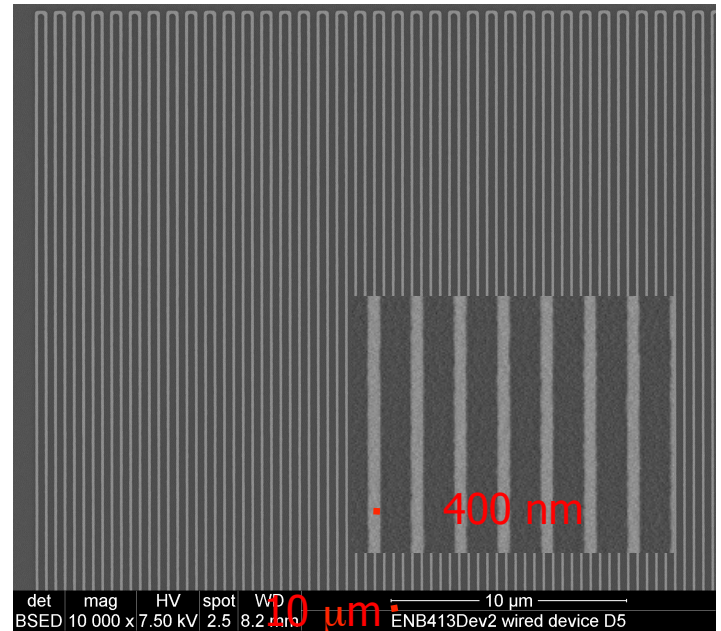
Figure 2. Very long NbN nanowire. ENABLE-grown NbN is patterned by electron beam lithography and plasma etching into this ~130 nm wide nanowire. Inset shows 400 nm center-to-center spacing of the serpentine nanowire. Main panel shows very large region of high uniformity coverage. Total length of this nanowire is ~50 mm.
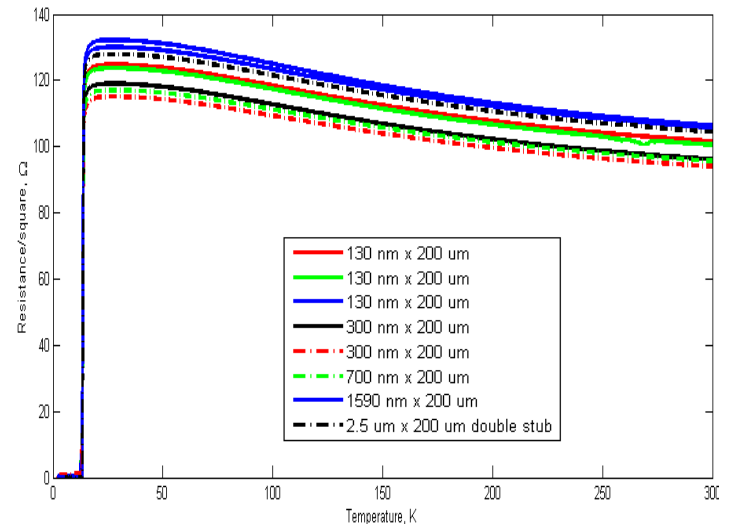
Figure 3. Sheet resistance (in units of ohms per square) versus temperature (in degrees Kelvin) for wide range of nano and micro devices. Device widths range from 130 nm to 2500 nm. The conclusion here is that the above transition sheet resistance and superconducting transition temperature are not affected by the processes used to make micro and nano devices. There is also tight clustering above the transition indicative of growth and process consistency.

In parallel, we developed a theory based on order parameter fluctuations to account for excess dissipation due to vortex crossings in superconducting films with thickness on the order of the coherence length, and width much narrower than the magnetic Pearl length in thin films. We found that for technologically relevant thin and narrow films or strips with width much larger than the coherence length, the dominant process is a vortex crossing the strip from one edge to the other, perpendicular to the bias current, resulting in detectable voltage pulses. We derived the rate of vortex crossings using the Langevin and Fokker-Planck equations for vortex motion (published in Phys. Rev. B 83 (2011) 144526).

We started experiments to test the theory and provide important feedback on further theory developments for the heat released by a single photon interacting with superconducting film. We considered counts in photon detectors caused by (a) incident photons whose energy is sufficient to create a normal-state belt across the whole width of the superconducting strip (pure photon counts), (b) thermally induced vortex crossings without photons (dark counts), and (c) by photons with energy insufficient to create the normal-state belt across whole strip width but assists the next vortex crossing by providing parts of the energy necessary to create normal-state belt across the strip (vortex-crossing-assisted photon counts). We have also recently used measurements in the flux-flow regime of microdevices to extract superconducting materials parameters including the vortex viscosity (Bardeen-Stephen) and quasiparticle relaxation time.

Future Work
The ENABLE technique provides us with an exceptional opportunity to develop a theoretical framework that can be validated by controlled experimental studies. Films will be characterized using several diagnostics resources, and the results will be used to predictably grow films with specific physical properties. In parallel, a theoretical model will be developed for predicting the relationships between material characteristics (crystallinity, grain size, dynamic response) and basic superconducting properties. Film characterization results and device performance will be used to test theoretical models. In this manner, theory and experiment will be coupled to utilize predictive science, rather than trial and error, to optimize detector design and performance. To allow the controlled design of materials and SNSPD devices, we must understand the relevant physical regimes and parameters for nanowires, the origin of dark counts, and the electrothermal runaway processes and dissipation of thermal energy. ENABLE can be used to controllably grow extremely high-quality epitaxial, highly crystalline thin films at low temperatures. ENABLE utilizes a collimated beam of neutral reactive nitrogen atoms with kinetic energies of a few electron volts to activate surface chemical reactions. Patterned SNSPD devices will be tested electrically and optically between room temperature and 2 K. Electrical characterization will include measurements of Ic(T), kinetic inductance, high frequency properties, and noise power spectral density.

Conclusion
We will construct a prototype array of SNSPDs, an important step toward our ultimate goal of moving SNSPDs from a single or few pixel technology with limited efficiency to a high-efficiency single photon imaging array. We will establish the scientific foundation in nanoscale superconductivity (theory, materials & device physics) necessary to develop SNSPDs into a technology that will deliver a broadband, high-efficiency, high-speed, low-noise single photon camera.

References
1. Bulaevskii, L. N., M. J. Graf, C. D. Batista, and V. G. Kogan. Vortex-induced dissipation in narrow current-biased thin-film superconducting strips. 2011. *PHYSICAL REVIEW B.* **83** (14): 144526.

Publications
Bulaevskii, L. N., M. J. Graf, C. D. Batista, and V. G. Kogan. Vortex-induced dissipation in narrow current-biased thin-film superconducting strips. 2011. *PHYSICAL REVIEW B.* **83** (14): 144526.

Bulaevskii, L. N., M. J. Graf, and V. G. Kogan. Vortex-assisted photon counts and their magnetic field dependence in single-photon detectors. *Physical Review B.*

Luo, H., H. Wang, G. Zou, E. Bauer, T. M. McCleskey, A. K. Burrell, and Q. X. Jia. A Review of Epitaxial Metal-Nitride Films by Polymer-Assisted Deposition. 2010. *Trans. Electrical & Electronic Mater..* **11**: 54.

Intelligent Wind Turbines

Curtt N. Ammerman
20100040DR

Introduction

Ours is a multi-disciplinary wind turbine project that will develop predictive models, advanced sensing technologies, novel data interrogation techniques, active performance control, and reliability-based decision-making algorithms. We will then merge these advances to provide a revolutionary capability to develop future generations of wind turbines with increased energy conversion efficiencies and dramatically reduced lifecycle costs. We will develop i) multi-physics modeling capabilities to assess and control the effect of coupled aerodynamic and structural conditions on power output and blade health; ii) sensing technologies to measure wind turbine response on multiple time- and length-scales for state awareness, control, and damage detection; and iii) active turbine and blade control to improve efficiency and compensate for structural damage. These components will be coupled with novel data interrogation and uncertainty quantification techniques to produce the hardware and software tools necessary to realize a system state awareness, control, and predictive capability for wind turbines. Our team is unique in that we can combine these complimentary tasks into a single coordinated effort that will significantly impact the current practice of harvesting wind energy and position LANL to bring innovative technology to this rapidly growing alternative energy area.

Benefit to National Security Missions

DOE proposes to meet 20% of the nation's energy needs with wind power by the year 2030. Although wind turbines have a design lifespan of 20 years, they typically fail 2.6 times per year during their first 10 years. The industry is struggling to understand these premature failures and predict and manage the growth of defects. We will transform current engineering practice by advancing and integrating innovative techniques to understand, identify, and manage wind power systems. The same advances in engineering practice will improve the Lab's ability to deliver systems solutions for a wide range of missions. For example, distributed sensor systems could have application to monitoring components and systems in the nuclear weapons complex.

Progress

We have made significant progress this past year in several areas, including turbine blade sensing, model validation, and modeling and simulation.

In the area of turbine blade sensing, we have developed a unique, dual-use technique for piezoelectric sensors. The sensors can detect and locate structural damage using high frequency structural excitation/sensing, and are also used to monitor low-frequency response, which enables estimates of the effect of damage on the system level performance. A new low-cost sensor node was also developed this past year that can excite and measure responses up to 100 kHz, perform intensive local computing for turbine monitoring, and survive field deployment. This sensor node is currently being tested with special consideration given to power consumption and operational effects. Some of the important parameters in the sensing system, such as monitoring of sensor functionality and embedding of data processing algorithms directly into the sensor node, are currently being implemented. A full-scale fatigue test of a CX-100 wind turbine blade is underway in collaboration with researchers from the National Renewable Energy Laboratory (NREL). More than a hundred sensors are installed on the surface of the blade, including piezoelectric transducers, accelerometers, microphones, acoustic emission sensors, fiber optic sensors, and strain gauges (Figure 1). The blade will be fatigue-tested to failure and the sensing system will monitor damage and associated changes in the blade.

In the area of model validation, large-format particle image velocimetry (LF-PIV) measurements were successfully performed using an 11-megapixel camera, extending the field of view to 1m x 3m with a resolution greater than 1mm/pixel. These measurements, along with design rules governing LF-PIV performance, were compiled into a peer-reviewed AIAA conference paper. Another conference paper summarizing the recent progress in LANL's wind turbine program is under preparation and will be presented in an invited session at the 41st AIAA fluid dynamics conference and exhibit. New measurements of the flow around scaled model

wind turbines were performed at the New Mexico State University (NMSU) wind tunnel by modifying the tunnel to remove boundary layer contamination. The turbine was located near the converging inlet section and PIV data were obtained under 0, 10 and 20 degree yawed, laminar inflow conditions. These data were complemented by direct thrust and torque measurements using a 6-axis load cell. Different stepper motor and controller systems were tested at LANL for the active grid system, which will be installed in the NMSU wind tunnel. System integration for the measurement of wind data simultaneously from five sonic anemometers was completed. Three-component velocity spectra in the near-wall region of the atmospheric boundary layer was obtained from the anemometers to validate operation. The anemometers are now ready to be mounted on the inflow and wake towers of the LANL wind turbine field station. Design and construction of the wind turbine and sensor towers at the LANL field station has been completed (Figure 2). Experiments at the LANL field station will take place in FY12.

Figure 1. LANL's 9m-Long, CX-100 Wind Turbine Blade Mounted at NREL's Fatigue Test Facility.

In the area of modeling and simulation, the NREL TurbSim turbulent wind simulator software package, which was integrated last year with our WindBlade wind turbine/wind plant simulation code, has been tested and applied to a variety of simulations. Topics currently under investigation include an exploratory study of the interaction between ambient and turbine-induced turbulence in the vicinity of multiple turbines. We are also investigating turbine wake meandering by applying a cyclic boundary condition to the computational domain to simulate an infinitely long wind farm. We have also incorporated a pitch/yaw control module within the WindBlade code. Yaw control is essential for simulations involving complex topography since flow direction is heavily influenced by local ground conditions (Figure 3). Among the most important capabilities we have

developed to date is the ability to extract transient aerodynamic loads along the length of the rotating turbine blades within WindBlade. Enabling this load extraction capability is crucial for the addition of fluid-structure-interaction (FSI) modeling. The FSI modeling effort is currently being developed and will incorporate the ability to simulate turbine blades as highly accurate, non-linear geometrically-exact beam models.

Figure 2. Wind Turbine and Sensor Towers at LANL's Newly Constructed Wind Turbine Field Station.
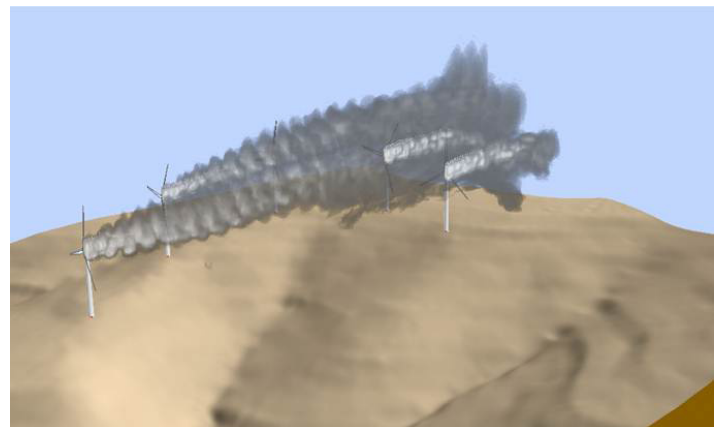

Figure 3. WindBlade Simulation of Five, 126-meter-diameter Wind Turbines on Terrain Near Las-Vegas, NM (Vegetation Removed for Clarity).

Future Work

In the coming year, our project will culminate in a full-scale flight test on a 20-meter-diameter turbine at Sandia National Lab's (SNL) Bushland, Texas test facility. For this

test, we will fabricate a custom-built, 9m turbine blade integrated with our SHM sensing node hardware. This test will provide proof-of-concept for our SHM sensing nodes, in both a pristine and damaged-blade environment. With the completion of LANL's wind turbine field station, we will conduct an experimental campaign to obtain high-quality, aerodynamic validation data. We will begin taking large-format PIV measurements of airflow both upstream and downstream of this turbine. We will also be implementing the first-ever rotating PIV measurement techniques to visualize the flow around the rotating turbine blade. These measurements will provide researchers with unprecedented insights into the nature of the airflow around an operating wind turbine. Also this year, we will implement our newly developed aeroelastic blade modeling capability within WindBlade. This fluid-structure interaction capability will enable the unprecedented ability to extract real-time dynamic loads on wind turbines operating in the wake of upstream turbines.

Conclusion

The expected deliverables for this effort include a validated wind turbine and wind plant simulation tool capable of modeling true wind loading (with realistic terrain, vegetation, and upstream turbines), blade and hub loading, damaged and undamaged rotors, and various control schemes. We will also develop self-powered structural health monitoring hardware nodes capable of being deployed on wind turbines that will enable damage detection and prognosis and will provide damage mitigating control. This project will result in increased wind turbine reliability and efficiency enabling DOE to meet their goal of reducing wind power operation and maintenance costs by 40 percent.

Publications

Ahrens, J., K. Keitmann, M. Petersen, J. Woodring, S. Williams, P. Fasel, C. Ahrens, C. H. Hsu, and B. Geveci. Verifying scientific simulations via comparative and quantitative visualization. 2010. *IEEE Computer Graphics and Applications.* **30** (6): 16.

Balakumar, B. J., R. C. Alarcon, J. T. Hoffman, and S. Pol. Detailed flow-field measurements around a small wind turbine, and an array of small turbines, designed using blade element momentum theory. Presented at *ASME/JSME/KSME Joint Fluids Engineering Conference.* (Hamamatsu, Japan, 24-29 Jul. 2011).

Bazilevs, Y., M. C. Hsu, I. Akkerman, S. Wright, K. Takizawa, B. Henicke, T. Spielmanand, and T. E. Tezduyar. 3D simulation of wind turbine rotors at full scale. Part I: Geometry modeling and aerodynamics. 2011. *International Journal of Numerical Methods in Fluids.* **65** (1-3): 207.

Bazilevs, Y., M. C. Hsu, J. Kiendl, R. Wuechner, and K. U. Bletzinger. 3D simulation of wind turbine rotors at full scale. Part II: Fluid-structure interaction. 2011. *International Journal of Numerical Methods in Fluids.* **65** (1-3): 236.

Bazilevs, Y., M. Hsu, J. Kiendl, and D. Benson. A computational procedure for pre-bending of wind turbine blades. 2011. *International Journal for Numerical Methods in Engineering.* : Published Online.

Buren, K. Van, M. Mollineaux, and F. Hemez. Simulating the dynamics of wind turbine blades: Part II, model validation and uncertainty quantification. To appear in *52nd AIAA/ASME/ASCE/AHS/ASC Structures, Structural Dynamics, and Materials Conference and 13th AIAA Non-Deterministic Approaches Conference.* (Denver, 4-7 Apr. 2011).

Carlson, C. P., S. Schlichting, S. Ouellette, K. M. Farinholt, and G. Park. Energy harvesting to power sensing hardware onboard a wind turbine blade. Presented at *Proceedings of IMAC-XXVIII, A Conference & Exposition on Structural Dynamics.* (Jacksonville, FL, 1-4 Feb. 2010).

Claytor, T. N., C. N. Ammerman, G. Park, K. M. Farinholt, C. R. Farrar, and M. K. Aterbury. Structural damage identification in wind turbine blades using piezoelectric active sensing with ultrasonic validation. Presented at *Proceedings of The American Society of Nondestructive Testing 19th Annual Research Symposium and Spring Conference.* (Williamsburg, VA, 22-26 Mar. 2010).

Farrar, C., K. Worden, and G. Park. Complexity: a new axiom for structural health monitoring?. Presented at *Proceedings of the 5th European Workshop on Structural Health Monitoring .* (Sorrento, Italy, 29 Jun.-2 Jul. 2010).

Figueiredo, E., G. Park, K. Farinholt, and C. Farrar. Use of time-domain predictive models for piezoelectric active-sensing in structural health monitoring applications. *ASME Journal of Vibration and Acoustics.*

Haynes, C., N. Konchuba, K. M. Farinholt, and G. Park. Estimation and modeling of force transmission in wind turbines. Presented at *Proceedings of IMAC-XXVIII, A Conference & Exposition on Structural Dynamics.* (Jacksonville, FL, 1-4 Feb. 2010).

Hsu, M. C., I. Akkerman, and Y. Bazilevs. High-performance computing of wind turbine aerodynamics using isogeometric analysis. 2011. *Computers and Fluids.* **49** (1): 93.

Hsu, M. C., Y. Bazilevs, I. Akkerman, and J. Kiendl. Fluid-structure interaction modeling of wind turbine rotors at full scale. Presented at *4th Southern California Symposium on Flow Physics.* (Irvine, CA, 17 Apr. 2010).

Hsu, M. C., Y. Bazilevs, and I. Akkerman. Isogeometric fluid-structure interaction analysis for wind energy applications. Presented at *UCSD Jacobs School of Engineering*

29th Annual Research Exposition. (Irvine, CA, 15 Apr. 2010).

Hsu, M. C., and Y. Bazilevs. Computational fluid-structure interaction: from wind turbines to cerebral aneurysms. Presented at *22nd International Conference on Parallel Computational Fluid Dynamics.* (Kaohsiung, Taiwan, 17-21 May 2010).

Hsu, M., I. Akkerman, and Y. Bazilevs. High-performance computing of wind turbine aerodynamics using isogeometric analysis. 2011. *Computers and Fluids.* **49** (1): 93.

Hush, null., null. Porter, and null. Ruggiero. Density-based similarity measures for content based search. 2009. *DOE.*

Mollineaux, M., K. Van Buren, and F. Hemez. Simulating the dynamics of wind turbine blades: Part I, model development and verification. To appear in *52nd AIAA/ASME/ASCE/AHS/ASC Structures, Structural Dynamics, and Materials Conference and 13th AIAA Non-Deterministic Approaches Conference.* (Denver, 4-7 Apr. 2011).

Park, G., E. F. Figurido, K. M. Farinholt, and C. R. Farrar. Time series analysis of piezoelectric active-sensing for SHM applications. Presented at *Proceedings of the 17th SPIE Conference on Smart Structures and Nondestructive Evaluation.* (San Diego, CA, 7-11 Mar. 2010).

Park, G., K. M. Farinholt, and C. R. Farrar. SHM of wind turbine blades using piezoelectric active-sensors. Presented at *Proceedings of 5th European Structural Health Monitoring Conference.* (Sorento, Naples-Italy, 29 Jun.-2 Jul. 2010).

Schlichting, A., S. Oullette, C. Carlson, K. M. Farinholt, G. Park, and C. R. Farrar. Multi-source energy harvester to power sensing hardware on rotating structures. Presented at *Proceedings of 17th SPIE Conference on Smart Structures and Nondestructive Evaluation.* (San Diego, CA, 7-11 Mar. 2010).

Sobin, A., A. Light-Marquez, K. M. Farinholt, and G. Park. Structural damage identification in wind turbine blades using piezoelectric active-sensing. Presented at *Proceedings of IMAC-XXVIII, A Conference & Exposition on Structural Dynamics.* (Jacksonville, FL, 1-4 Feb. 2010).

Steinwart, I., D. Hush, and C. Scovel. Training SVMs without offset. 2011. *Journal of Machine Learning Research.* **12**: 141.

Takizawa, K., B. Henicke, D. Montes, T. Tezduyar, M. Hsu, and Y. Bazilevs. Numerical-performance studies for the stabilized space-time computation of wind-turbine rotor aerodynamics. 2011. *Computational Mechanics.* : Published Online.

Takizawa, K., B. Henicke, T. Tezduyar, M. Hsu, and Y. Bazilevs. Stabilized space-time computation of wind-turbine rotor aerodynamics. 2011. *COMPUTATIONAL MECHANICS.* **48** (3, SI): 333.

Taylor, S. G., K. M. Farinholt, G. Park, M. D. Todd, and C. R. Farrar. Application of a wireless sensor node to health monitoring of an operation wind turbine blade. Presented at *Proceedings of IMAC-XXVIII, A Conference & Exposition on Structural Dynamics.* (Jacksonville, FL, 1-4 Feb. 2010).

Theiler, J., and D. Hush. Statistics for characterizing data on the periphery. Presented at *IEEE International Geoscience & Remote Sensing Symposium.* (Honolulu, HI, 25-30 Jul. 2010).

Harnessing Nonlinearity for Transformative Metamaterial Technology

Houtong Chen
20110027DR

Introduction

The transistor is a device that uses nonlinearity to perform its functions. Harnessing nonlinearity with transistors heralded groundbreaking electronic technologies such as radar, wireless communications, and computers. Revolutions like this are rare, but another has surfaced in recent years: metamaterials. Metamaterials are composite materials with special electromagnetic properties. They can be designed to perform functions that natural materials cannot. They do this by providing a new level of control over electromagnetic waves. As such, scientists have predicted that metamaterials will provide radically improved electromagnetic devices, such as light-weight optics, ultra-efficient antennas, and cloaking devices. But it has been found that this control comes at a cost: metamaterials suffer high loss and dispersion (frequency dependent behavior), their main weaknesses. These have stubbornly prevented metamaterials from realizing their potential in modern technology. Our project seeks to combine the benefits of metamaterials, in terms of wave control, with the benefits of nonlinearity, which provides numerous properties that can be used to address metamaterial loss and dispersion. Though this approach is highly complex and still very immature, the combination is widely seen as the next major step forward in metamaterial research. We will develop nonlinear metamaterials both experimentally and theoretically, providing a solid foundation for creating real-world devices that exhibit the substantial advantages of nonlinear metamaterials. We will also develop two signature devices that demonstrate these advantages.

Benefit to National Security Missions

As electromagnetic devices (telephones, cameras, etc.) become smaller and more powerful, we become more productive at less cost. The same principle applies to technologies in LANL mission areas including threat reduction, treaty monitoring, intelligence gathering, nonproliferation, basic science, and others. All such missions benefit from devices that offer smaller size/weight, greater efficiency, lower cost, higher sensitivity or dynamic range, etc. Nonlinear metamaterials offer these advantages. Most immediately, nonlinear metamaterials will improve LANL's Global Security missions in counter-terrorism and warfighter support, and space situational awareness. Here they can support mobile, covert, or space-based platforms, where energy efficiency, size, and weight are critical challenges. Given the ubiquity of EM devices, these same benefits may apply almost universally to other LANL missions. An understanding of NL-MM would also support LANL missions in emergent phenomena and materials science, particularly MaRIE priorities such as building deliberate material functionality, nano-to-bulk synthesis, and detector technologies.

Progress

During the first year of the project, we have made much progress in this DR project, both experimentally and theoretically.

Experiments

Nonlinear effects have been experimentally investigated in gain-loaded metamaterial elements operating in the gigahertz (GHz) frequency range, which has provided insight into the design and operation of similar elements at terahertz (THz) frequencies. Metamaterial elements, such as split-ring resonators (SRRs), were fashioned from copper cladded printed circuit (PC) board stock. The nonlinear element that provides gain was a commercially available gallium arsenide (GaAs) tunnel diode with a 12 GHz bandwidth. The nonlinear tunnel diodes were loaded to the gaps of the SRRs, which were designed in order to take advantage of the harmonic generation and self-oscillation. The SRRs provide the feedback required to initiate self-oscillation and act as the antenna element for receiving and emitting radiation into free space. We investigated a series of harmonic and broadband designs with the following achievements [1]: 1) Using a single active SRR with a resonance at 1 GHz parasitically coupled to a passive SRR with a resonance at 2 GHz; 2) Demonstrated self-oscillation in the active SRRs, i.e. radiating electromagnetic waves in the microwave frequency regime, which can be frequency shifted through gain tuning, frequency pulling and external frequency locking to an external driving field; 3) Observed heterodyning

in the active SRRs when biased below the self-oscillation threshold; 4) Demonstrated resonance tuning in active SRRs through externally applied microwave at a different frequency; 5) Observed conversion of the incident electromagnetic wave energy into DC electricity, with a much higher efficiency than reported in literature.

Additional efforts have been the hybridization of resonant tunneling diode (RTD) with metamaterials towards the generation of THz radiation. The semiconducting epilayers for the RTD were simulated by employing a self-consistent device simulator. With the obtained parameters, we are collaborating with Prof. Josh Zide of University of Delaware and Prof. Arthur Gossard of UCSB to grow the epilayers using a molecular beam epitaxy (MBE) system. At the same time, we have developed a unique fabrication technology utilizing microscopic air-bridge structures to incorporate resonant tunneling diodes from epitaxial semiconductors into metamaterial structures for ~100 GHz or THz operation.

As for our second experimental goal of enhancing the sensitivity of electro-optic (EO) modulation, we have developed two capabilities during the first year. These are: 1) high-precision sample fabrication technique using laser machining, and 2) setting up sensitive EO detection system which can synchronize the phase between optical pulses and continuous wave (CW) microwave radiation. SRR structures have been designed through a series of numerical simulations to maximally concentrate field within the gaps of SRRs, which has been fabricated on (110) zinc telluride (ZnTe) nonlinear crystal substrate. In parallel with traditional electrical SRRs we have studied coupled SRRs in which the unit cell is comprised of two closely spaced resonators. A scaled version of such coupled system was fabricated and measured at THz frequencies [2]. The result shows that the separation between individual SRRs and the relative positioning of their split gaps play a significant role in manipulation of field strengths and field orientations in the crystal plane. We also optimized the fabrication techniques using a laser cutter in a variety of substrates within sub-micron precision. The first microwave meta-atom (single SRR) was fabricated on a ZnTe substrate with a minimum feature size of 0.5 mm using a thick copper tape. We are currently performing microwave measurements to obtain the resonance behavior of this sample. Our high sensitive EO detection system is comprised of a ZnTe crystal, which modulates the optical beam polarization state via nonlinear mixing of quasi-DC component (microwave or THz radiation). For the demonstration of our detection scheme, we fabricated two parallel copper electrodes 1 mm apart through which we applied a 10V peak-to-peak 2 GHz microwave signal. The relative phase between the microwave signal and optical laser pulses has been precisely controlled using a microwave phase shifter. We have successfully detected an EO modulation signal revealing phase dependent periodic nature.

Additionally, we are interested in obtaining nonlinear metamaterial response when complex oxides materials are incorporated into the metamaterial structures. Temperature and optical tunable metamaterial resonances [3,4] have been observed in high-temperature superconducting metamaterials [5,6] and when using ferroelectric strontium titanates as the substrate [7], where we also achieved reasonable understanding of the underlying resonance tuning mechanism [5]. Finally, we have investigated the feasibility of enhanced nonlinear response employing perfect metamaterial absorbers [8-10]. We have demonstrated broadband metamaterial absorbers in the THz frequency range, which will be further developed in the microwave and optical frequency regimes for experimental nonlinear investigation.

Theory:

Our theory work has focused on three threads: 1) the development of the fundamental equations for a modal analysis to describe metamaterials, 2) the modeling of split-ring resonators and tunnel diodes as lumped circuits, and 3) enhancing nonlinear response by employing perfect metamaterial absorbers.

We have developed a rigorous eigenmode analysis to study linear electromagnetic properties of metamaterials [11]. Our method is valid for arbitrary metamaterial geometries, and includes effects of dispersion, dissipation, and the presence of substrate materials on top of which metamaterials are fabricated. Eigenmodes and eigenfrequencies are computed using a finite-difference time-domain (FDTD) method, in which random source currents are located close to the metamaterial structure, and the evolution of the polarization currents inside the metamaterial are numerically computed. From the frequency-spectrum of such polarization currents we derive the eigenmodes and eigenfrequencies of the structure under study. We have checked that our FDTD approach predicts the same eigenmode structure as other less general approaches, including those of commercial codes.

We have then extended our modal approach, valid for linear systems, to the case of weak nonlinear metamaterials. In this case we showed that the nonlinear response of the metamaterial can be totally described by the linear eigenmodes. We applied our theory to one specific example: second-harmonic spectroscopy of metallic metamaterials, in which the nonlinearity arises from the intrinsic electronic structure. We found that in order to enhance the nonlinear response one must optimize not only the resonant frequency, but also the modal pattern.

A second theoretical model was successfully constructed to reproduce the experimental results obtained from individual nonlinear cells that were illuminated by a microwave source [12]. The model was based on a nonlinear circuit that was coupled to an external oscillator. The results showed frequency mixing, amplitude-dependent fre-

quency locking, and banded chaos, all qualitatively similar to the experimental observations. A one-dimensional array model was also constructed which showed the possible existence of dissipative solitons on an array of such cells.

Additionally, we have performed theoretical investigations for possibly enhanced nonlinear response when employing metamaterial perfect absorbers [13]. We found that metamaterial perfect absorbers have been established on a wrong foundation. We demonstrated that the impedance matching of metamaterial absorbers to free space does not involve the assumed magnetic response. In contrast, we found that a Fabry-Perot-like resonance is responsible for the observed high absorption. This interference model suggests that the incident light is trapped in the thin metamaterial layer with a much longer lifetime and enhanced field strength, which are of great significance for nonlinear response.

Future Work

Our technical approach for the future work has two main goals: to further establish the 1) theoretical and 2) experimental foundations of nonlinear metamaterials.

Theoretically, we will carry out the following tasks: 1) We will further develop the eigenmode analysis approach to three-dimensional by FDTD approach, for both linear and nonlinear response of metamaterials. The linear response will be compared to commercial codes, while the nonlinear response will rely on the experimental validation. 2) We will also extend the nonlinear circuit based model to two-dimensional arrays. Work is being carried out to include inherent propagation delays by an S-parameter approach, a method that has been developed for linear metamaterial arrays. Expectations are that domain formation and phase changes will be observed in a manner very similar that observed in certain other strongly polarizable and permeable materials. 3) We will further investigate the possibility of enhanced nonlinearity in perfect metamaterial absorbers through the FDTD approach. We will use dielectric material with nonlinear response as the spacer material in metamaterial absorbers, and numerically investigate power dependent resonance, harmonic generations, and polarization control and conversion.

Experimentally, we will perform the following: 1) We will scale down the successfully demonstrated simple microwave active metamaterial elements to operate at THz frequencies. Fabrication of the hybridized RTD-based metamaterials will commence after the semiconducting epilayers are grown for the resonant tunneling diodes. 2) The impact of lead lines in active SRRs, an unavoidable structural requirement for many active metamaterial designs, will be investigated in order to create arrays of active oscillators with controllable resonance behaviors. Initial observations of bistability in parasitically coupled elements will be further examined for potential device applications. 3) For the EO modulation, we would like to replace the

parallel electrodes with our meta-atom resonator, which would optimize the microwave field concentration and thereby would enhance the EO effect. 4) We will experimentally demonstrate microwave and optical metamaterial perfect absorbers, and test their nonlinear response. We also will experimentally demonstrate the complete polarization conversion in metamaterial absorbers with coupled resonators, which is of significant relevance to our project though it is a linear response.

Conclusion

Our main technical contribution will be a comprehensive theoretical and experimental foundation for creating revolutionary electromagnetic technology using nonlinear metamaterials. During the past year we have made significant progress bother theoretically and experimentally. We have been successful in developing theoretical tools for predictive design of nonlinear metamaterial-based devices, crucial to advance metamaterials beyond scientific novelties. Additional theoretical development in metamaterial perfect absorbers provides new opportunity in expanding our research scope. We have achieved significant advances in experimental investigation of two signature applications, 1) an electromagnetic emitter and mixer and 2) an EO modulator, towards electromagnetic devices by using nonlinear metamaterials. Furthermore, we have clearly identified the future work during the following two years. We expect that this project will be fruitful, and this work will have broad implications in all electromagnetic technologies especially where compact size, power efficiency, and improved performance are critical.

References

1. O'Hara, J. F., M. T. Reiten, P. Colestock, L. Earley, and A. Taylor. Tunnel-diode loaded split-ring resonators as a foundation for nonlinear metamaterials. 2011. In *Proceedings of SPIE.* (San Diego, 21-25 August 2011). Vol. 8093, p. 809304. Bellingham: SPIE.

2. Chowdhury, D. R., R. Singh, M. Reiten, J. Zhou, A. J. Taylor, and J. F. O'Hara. Tailored resonator coupling for modifying the terahertz metamaterial response. 2011. *Optics Express.* **19** (11): 10679.

3. Chen, H. T., A. K. Azad, J. F. O'Hara, R. Singh, J. Zhou, M. T. Reiten, D. Chowdbury, Q. Jia, S. A. Trugman, and A. J. Taylor. Active terahertz metamaterials. To appear in *36th International Conference on Infrared, Millimeter and Terahertz Waves (IRMMW-2011).* (Houston, 2-7 October 2011).

4. Chen, H. T., J. F. O'Hara, A. K. Azad, and A. J. Taylor. Manipulation of terahertz radiation using metamaterials. 2011. *Laser & Photonics Reviews.* **5** (4): 513.

5. Chen, H. T., H. Yang, R. Singh, J. F. O'Hara, A. K. Azad, S. A. Trugman, Q. X. Jia, and A. J. Taylor. Tuning the resonance in high-temperature superconducting terahertz

metamaterials. 2010. *Physical Review Letters.* **105** (24): 247402.

6. Singh, R., J. Xiong, A, K. Azad, H. Yang, S. A. Trugman, Q. X. Jia, A. J. Taylor, and H. T. Chen. Ultrafast dynamics of high-temperature superconducting terahertz metamaterials . *Nature Communications.*

7. Singh, R., A. K. Azad, Q. X. Jia, A. J. Taylor, and H. T. Chen. Thermal tunability in terahertz metamaterials fabricated on strontium titanate single-crystal substrates. 2011. *Optics Letters.* **36** (7): 1230.

8. Huang, L., D. R. Chowdhury, S. Ramani, M. T. Reiten, S. N. Luo, A. J. Taylor, and H. T. Chen. Experimental demonstration of terahertz metamaterial absorbers with a broad and flat high absorption band. To appear in *Optics Letters.*

9. Chowdhury, D. R., R. Singh, M. Reiten, H. T. Chen, A. J. Taylor, J. F. O'Hara, and A. K. Azad. A broadband planar terahertz metamaterial with nested structure. 2011. *Optics Express.* **19** (17): 15817.

10. Shchegolkov, D. Y., N. A. Moody, E. Simakov, A. Azad, and J. F. O'Hara. Controlling terahertz waves with meta-materials and photonic bandgap structures. 2011. In *2011 IEEE 12th Annual Wireless and Microwave Technology Conference (WAMICON).* (Clearwater Beach, 18-19 April 2011). , p. 5872861. Washington: IEEE.

11. Zeng, Y., D. A. R. Dalvit, J. O'Hara, and S. A. Trugman. Modal analysis for metamaterials. *Physical Review B.*

12. Colestock, P. L., M. Reiten, and J. O'Hara. Modeling of nonlinear metamaterials. 2011. In *Proceedings of SPIE.* (San Diego, 21-25 August 2011). Vol. 8093, p. 809327. Bellingham: SPIE.

13. Chen, H. T.. A theory of metamaterial perfect absorbers. *Physical Review Letters.*

Publications

Chen, H. T.. A theory of metamaterial perfect absorbers. *Physical Review Letters.*

Chen, H. T., A. K. Azad, J. F. O'Hara, R. Singh, J. Zhou, M. T. Reiten, D. Chowdbury, Q. X. Jia, S. A. Trugman, and A. J. Taylor. Active terahertz metamaterials. To appear in *Conference Proceeding of IRMMW-2011.*

Chen, H. T., H. Yang, R. Singh, J. F. O'Hara, A. K. Azad, S. A. Trugman, Q. X. Jia, and A. J. Taylor. Tuning the resonance in high-temperature superconducting terahertz metamaterials. 2011. *Physical Review Letters.* **105** (24): 247402.

Chen, H. T., J. F. O'Hara, A. K. Azad, and A. J. Taylor. Manipulation of terahertz radiation using metamaterials. 2011. *Laser & Photonics Reviews.* **5** (4): 513.

Chowdhury, D. Roy, R. Singh, M. Reiten, H. T. Chen, A. J. Taylor, J. F. O'Hara, and A. K. Azad. A broadband planar terahertz metamaterial with nested structure. 2011. *Optics Express.* **19** (17): 15817.

Chowdhury, D. Roy, R. Singh, M. Reiten, J. Zhou, A. J. Taylor, and J. F. O'Hara. Tailored resonator coupling for modifying the terahertz metamaterial response. 2011. *Optics Express.* **19** (11): 10679.

Colestock, P. L., M. Reiten, and J. O'Hara. Modeling of nonlinear metamaterials. 2011. *Proceedings of SPIE.* **8093**: 809327.

Huang, L., D. Roy Chowdhury, S. Ramani, M. T. Reiten, S. N. Luo, A. J. Taylor, and H. T. Chen. Experimental demonstration of terahertz metamaterial absorbers with a broad and flat high absorption band. To appear in *Optics Letters.*

O'Hara, J. F., M. T. Reiten, P. Colestock, L. Earley, and A. Taylor. Tunnel-diode loaded split-ring resonators as a foundation for nonlinear metamaterials. 2011. *Proceedings of SPIE.* **8093**: 809304.

Shchegolkov, D. Y., N. A. Moody, E. I. Simakov, A. Azad, and J. F. O'Hara. Controlling terahertz waves with meta-materials and photonic bandgap structures. 2011. *Proceeding of Wireless and Microwave Technology Conference (WAMICON), 2011.* : 5872861.

Singh, R., A. K. Azad, Q. X. Jia, A. J. Taylor, and H. T. Chen. Thermal tunability in terahertz metamaterials fabricated on strontium titanate single-crystal substrates. 2011. *Optics Letters.* **36** (7): 1230.

Singh, R., J. Xiong, A. K. Azad, H. Yang, S. A. Trugman, Q. X. Jia, A. J. Taylor, and H. T. Chen. Ultrafast dynamics of high-temperature superconducting terahertz metamaterials. *Nature Communications.*

Zeng, Y., D. A. R. Dalvit, J. O'Hara, and S. A. Trugman. Modal analysis for metamaterials. *Physical Review B.*

Exploiting Hamiltonian Properties of Beams to Revolutionize X-Ray Free-Electron Laser Architectures

Bruce E. Carlsten
20110067DR

Introduction

Recent theoretical work has identified a revolutionary approach to achieving ultra-high brightness electron beams, based on the theoretical nature of electron beam dynamics. This approach can potentially increase electron beam brightness by orders of magnitude, which can, for example, lead to two or three orders of magnitude increases in photon yield in next generation light sources. Since next generation light sources are billion-dollar class facilities and few will be built, these kinds of increases are very important and will lead to significant increases in the amount of discovery science that will be able to be performed on these devices. Additionally, new insights into seeding the light source by microbunching the electron beam will lead to the narrowest possible X-ray bandwidth

Benefit to National Security Missions

Current technology is not sufficient to address MaRIE mission needs, particularly in generating sufficient 50-keV photon flux for dynamic studies of transient material behavior at grain boundaries, which is important to stockpile stewardship. The results of this project can potentially lead to two or three orders of magnitude increases in photon flux, thereby closing this critical technology gap in instruments to probe materials in extreme conditions (relevant to the weapons program). Additionally, this technology will enable new Global Security missions supporting the warfighter. It will lead to smaller and less expensive free-electron laser architectures at weaponizable photon energies, as well as significant improvements in other methods of producing coherent radiation for applications that include directed energy attacks, long-range tracking and imaging radar, spectroscopy, and secure communications.

Progress

Significant theoretical and numerical progress in many key areas of advanced X-ray free-electron laser (XFEL) science and technology has already been accomplished. Work is all directed towards increasing the performance of future XFELs operating with ultra-hard X-rays from 42 keV to 50 keV, particularly by increasing the flux of

X-rays and narrowing the X-ray bandwidth, all while decreasing the length (and cost) of the XFEL.

Emittance Partitioning

Beam emittance is the most useful metric to describe the electron beam quality. Emittance is the area in phase space (both transverse and longitudinal), and is equivalent to the beam size times the relative energy spread in that dimension. Thus a lower emittance beam has a lower energy spread in the dimension of interest, and practically can be maintained at a smaller size for a longer time. This leads to better overlap with the X-ray beam in an FEL, leading to better energy conversion from the electron beam to the X-ray beam and better transverse coherency. An electron beam's initial phase space is typically roughly equipartitioned in all three dimensions when it is formed at a cathode, but, due to the relativistic cooling of an accelerated beam, an XFEL can tolerate about three orders of magnitude larger emittance in the longitudinal dimension relative to the transverse dimensions.

This remarkable fact motivates us to consider how to control the initial emittance partitioning so that phase-space area that would otherwise end up in the transverse dimensions is transferred to the longitudinal dimension. Using preliminary work as a foundation, our understanding of manipulating the phase-space partitioning of electron beams has greatly matured. We understand the underlying principles, called eigen-emittances, and based on that, have identified four promising configurations to lower beam transverse emittances by an order of magnitude each. One is shown schematically in Figure 1, where two correlations are varied. When the correlations vanish the three eigen-emittances (one for each dimension) are nearly equal, but two are tiny at the expense of growth in the third when the correlations are properly adjusted. Alternatively, a two-stage architecture was identified that appears to be easily implemented. The majority of the needed work on emittance partitioning was completed in FY11 to establish the fundamental theoretical understanding of the technique and to identify promising implementation candidates. Most of the

eigen-emittance effort in FY12 will be to down-select to the most favorable single implementation and to design a proof-of-concept experiment for FY13.
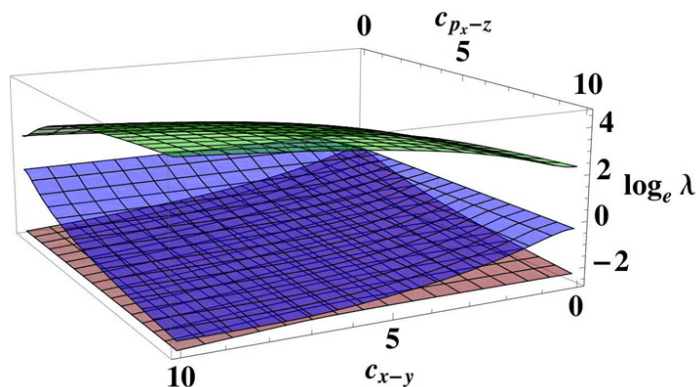

Figure 1. This figure shows the three beam eigen-emittances as a function of two different correlations that are imposed on the beam when it is formed, specifically here correlations between horizontal and vertical positions and horizontal velocity and axial position. When the correlations vanish, the beam emittances are roughly equipartitioned between the three dimensions. However, a large asymmetry in the eigen-emittances forms when the correlations become large, which can be exploited to make beams with extraordinarily low transverse emittances.

Microbunching the Electron Beam for Seeding

Seeding XFELs is an emerging field and is a major international thrust. Electron-beam based seeding techniques are based on microbunching the electron beam at the X-ray wavelength before the XFEL undulator (which is called pre-microbunching. Previous work has identified high-gain harmonic generation (HGHG) and echo-enhanced harmonic generation (EEHG) as leading microbunching candidates. We have identified a new scheme using an emittance exchanger (EEX), and believe that an optimized seeding configuration will include several sections, with initial seeding starting anywhere from 250 nm to 1 nm with an external laser, and with possible multiple EEX, HGHG, and EEGH harmonic cascades. The metric for comparison of possible schemes is phase and amplitude noise at the final microbunched harmonic at the hard X-ray wavelength, which is then injected into the XFEL undulator. This noise is the convolutions of the initial laser noise with the noises induced by all the elements of the different schemes, which include the transform limited bandwidth of the electron's cooperation length and gain bandwidth of the HGHG stages. To help define this metric, we successfully developed a new formalism for describing the bandwidth, which mirrors the framework to describe the beam rms properties. An example of this formalism is shown in Figure 2, for the energy and longitudinal wavenumbers resulting from a simple harmonic energy deviation of a beam with an initial energy spread. The bulk of the FY12 work on this project will be to evaluate this metric for various seeding

configurations to quantify the level of bandwidth narrowing for each individual configuration, and to use that result to identify the most promising seeding architecture.
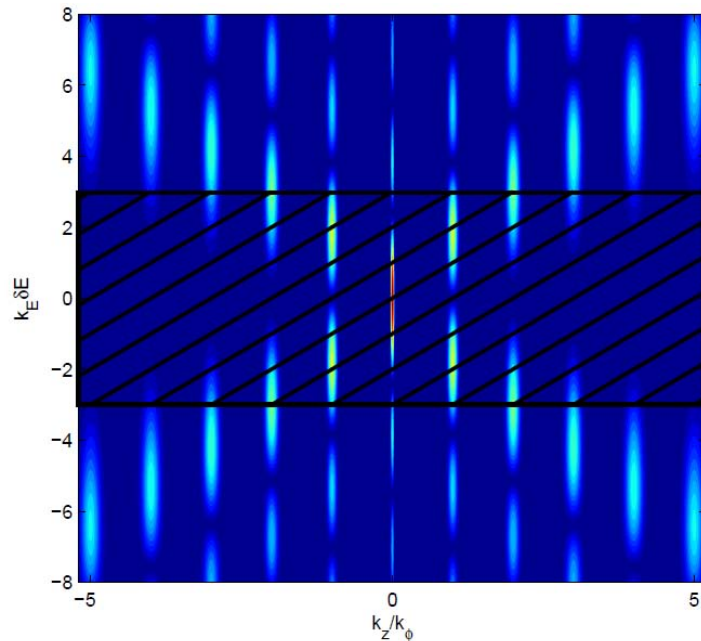

Figure 2. This plot shows the distribution of a beam in modulation space after the beam has been given a periodic energy modulation from interaction with a laser (which is typically used for seeding an XFEL). Here the horizontal axis is the Fourier transform of the longitudinal coordinate and the vertical axis is the Fourier transform of the energy. The dashed area shows the bandwidth of the beam due to its intrinsic energy spread - modulation outside this area is suppressed. This type of plot provides a visual tool to estimate XFEL bandwidth from harmonic generation schemes.

Emittance Exchanger

Levering work at FNAL, we have developed a new family of electron beam optics based on the EEX architecture, including a novel type of bunch compressor and a novel source of beam microbunching (both by employing a physical mask with slits and by modulating the electron beam's energy with laser interaction in a preceding undulator as with an EEHG). These new EEX applications can be used in a variety of microbunching schemes, with the noise contribution a function of the relative linearity of the optics themselves.

Coherent Synchrotron Radiation

Coherent synchrotron radiation (CSR) is produced when an electron bunch is compressed in magnetic elements. CSR interacts with the beam and can increase the transverse beam emittance and can degrade any microbunching imposed on the beam. The bunch charges, emittance, and compressed bunch lengths considered in this project for XFELs represent a new, untested regime, and CSR needs to be evaluated. Significant work has begun on large-scale

simulations of coherent synchrotron radiation (CSR), at Los Alamos and by both our LBNL and our Fermilab/Northern Illinois University collaborators. This brute force technique exactly solves the fields on the bunch using the Lienard-Wiechert fields at a single time primarily for evaluating the ability of different approaches to capture the essential physics (a single time step takes about 20 minutes using 40,000 processors on the DOE NERSC computer cluster). Results are shown in Figure 3 for various bunch sizes at 100 MeV and 1 GeV. The noise on the fields for a 1-GeV electron bunch is due to coherent emission at scales comparable to the electron spacing itself, which appears to lead to increase in the CSR field strength by multiple orders of magnitude for a mircobunched beam. Several papers on the numerical model and its results are in preparation and an evaluation of the degradation of beam quality will be conducted in FY12. This degradation will likely impact the bandwidth noise evaluation for different seeding architectures.
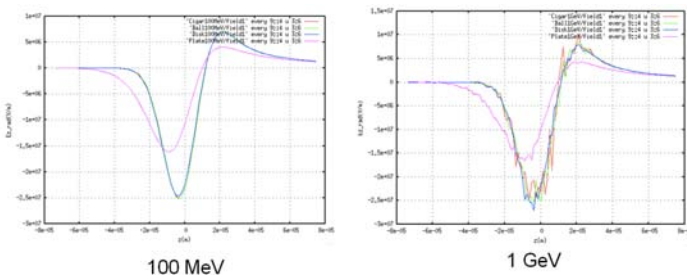

100 MeV   1 GeV

Figure 3. The coherent synchrotron radiation (CSR) field is plotted along a 10-micron long bunch, for different transverse sizes (cigar: 1-micron radius, ball: 10-micron radius, disk: 100-micron radius, plate: 0.5-mm radius), all for a 1-m bend radius, for both 100-MeV and 1-GeV beam energies. This plot shows two important results. First, the CSR field is well approximated by a 1-D representation (represented by the cigar case) up to transverse sizes of 100 microns. Second, the interparticle spacing leads to noise at the higher beam energy, which also leads to greatly enhanced fields for microbunched beams.

Incoherent Synchrotron Radiation

Using the novel bandwidth formalism we developed, we are also able to quantify the effect of incoherent synchrotron radiation (ISR) on the beam. In this regime, quantum fluctuations in ISR lead to a minor energy spread. However that induced energy spread leads to a smearing of axial position in magnetic elements, which limits the maximum bend angle a microbunch can pass through before the structure is lost. We found that the extinguishing factor of a microbunch harmonic scales exponentially as the harmonic wavelength squared, the beam energy to the fifth power and the bend angle to the seventh power. Because of these severe scalings, an Angstrom-level wavelength will be eliminated with bend angles greater than about ½ degree at beam energies of 20 GeV.

Future Work
The FY11 work has established the foundation for optimizing future XFEL designs. We have identified the core beam physics issues and developed a framework for comparing harmonic generation schemes in terms of quantifying the decrease in the X-ray bandwidth. The thrust of the FY12 work will be to extend our new theoretical and numerical tools (especially for CSR) and integrate them to accurately predict the bandwidth for various seeding configurations using a novel rms bandwidth formalism. A second thrust area is to identify the optimum emittance partitioning scheme and to define a proof-of-principle demonstration experiment to be performed in FY13 either at LANL or at FNAL.

Conclusion
Next generation light sources, used for cutting-edge materials, chemistry, and biological research, will be billion-dollar class facilities, mostly funded by DOE's Office of Science. This research will have the potential to increase the productivity of these types of facilities by two to three orders of magnitude, resulting in a significant potential increase in the rate of discovery science. This advance is enabled by unique properties of high-brightness electron beams and requires an integrated engineering analysis to determine how much of the potential of this new concept can be achieved with real, not idealized, components.

Publications
Carlsten, B. E., K. A. Bishofberger, L. D. Duffy, C. E. Heath, Q. R. Marksteiner, D. C. Nguyen, R. D. Ryne, S. J. Russell, E. I. Simakov, and N. A. Yampolsky. New X-ray free-electron laser architecture for generating high fluxes of longitudinally coherent 50 keV photons. 2011. *Journal of Modern Optics.* **58** (16): 1374.

Carlsten, B. E., K. A. Bishofberger, L. D. Duffy, S. J. Russell, R. D. Ryne, N. A. Yampolsky, and A. J. Dragt. Arbitrary emittance partitioning between any two dimensions for electron beams. 2011. *Physical Review Special Topics - Accelerators and Beams.* **14**: 050706.

Carlsten, B. E., K. A. Bishofberger, S. J. Russell, and N. A. Yampolsky. Using an emittance exchanger as a bunch compressor. 2011. *Physical Review Special Topics - Accelerators and Beams.* **14**: 084403.

Carlsten, B. E., M. Ben-Naim, K. A. Bishofberger, L. D. Duffy, M. Holloway, Q. R. Marksteiner, R. McCrady, and N. A. Yampolsky. Two-stage generation of beam correlations in electron beams to establish low transverse beam emittances. To appear in *Physical Review Special Topics - Accelerators and Beams.*

Duffy, L. D., K. A. Bishofberger, B. E. Carlsten, A. Dragt, Q. R. Marksteiner, S. J. Russell, R. D. Ryne, and N. A. Yampolsky. Exploring minimal scenarios to produce transversely bright electron beams using the eigen-emittance concept. 2011. *Nuclear Instruments and Methods in Physics Research A.* **654**: 52.

Yampolsky, N., B. Carlsten, K. Bishofberger, S. Russell, R. Ryne, and A. Dragt. Controlling electron-beam emittance partitioning for future X-ray light sources. To appear in *Physical Review Letters.*

A Metamaterial-Inspired Approach to RF Energy Harvesting

Md A. Azad
20100241ER

Introduction

Metamaterials are composite media that exhibit unique properties, such as negative refractive index, in response to electromagnetic waves, including visible and near-infrared light, microwaves and frequencies in between. Metamaterials are typically composed of split-ring resonators that, by virtue of their ability to store electric and magnetic energy, impart unusual properties to the materials. But split-ring resonators can also be viewed as small antennas, with properties not found in traditional antennas. For example, recent work has shown that split-ring resonator antennas can be made to operate efficiently even when their size is less than 1/100th of the electromagnetic wavelength. We intend to design and build these split-ring resonator (or metamaterial-inspired) antennas for the purpose of low-power electromagnetic energy harvesting. Traditional antennas are typically too large or inefficient for such a task. But metamaterial antennas offer a new and unobtrusive approach that could provide power to small electric devices that operate in embedded or inaccessible environments, where maintenance is impossible or undesirable. Examples include bio-sensors embedded in living organisms, covert communication or data exfiltration devices, and monitoring sensors buried in structural members (e.g. bridge pylons). This work leverages the fact that we are often immersed in electromagnetic energy, from radio antennas, for example, that is predominately wasted. Further, in support of compact wireless devices such as cell phones, technologists have developed a class of very low power electronic devices that can operate on the amount of power harvested by a small metamaterial antenna. These circumstances provide a unique opportunity to diversify our methods of efficiently utilizing free energy with cutting-edge metamaterial-inspired technology. It is difficult to improve upon several decades of antenna research, but metamaterial concepts provide an optimistic path forward that will also have a large impact on future compact wireless device design.

Benefit to National Security Missions

This project will diversify our capabilities in energy usage and production by creating methods of utilizing now wasted ambient electromagnetic energy. This specifically impacts the mission of renewable energy. This project will also create a method to remotely provide power to embedded, buried, or inaccessible electronics, thus enabling new modes of covert communications and sensing, data exfiltration, surveillance, and remote sensing and monitoring. As such it is relevant to missions of DOE, DOD, DHS, and intel agencies. We are continually working with LANL program managers and Tech Transfer to protect our results and seek external funding. Finally, the work expands on our fundamental understanding of engineered electromagnetic materials, related to the basic understanding of materials.

Progress

Our progress, at the end of second year, has covered following areas: general study of metamaterial design suitable for an antenna towards RF energy harvesting, understanding the design of electrically small antennas using metamaterial concept, and application of these antennas for microwave energy harvesting.

In the second year, our primary focus was to understand the basics of electrically small antenna. A series of electromagnetic simulations were carried out to design split-ring-resonator (SRR) based antenna, a building block of metamaterials, which has a physical size smaller than a resonating dipole antenna. We found the natural resonance mode of an individual SRR can be modified through magnetic/electric interaction that arises from the nearest neighbor. To increase the interaction between SRRs the unit cell is designed using two coupled resonators. The resonance frequency of this coupled resonator system can be modified by adjusting the separation between resonators in both the vertical and horizontal directions. Using electromagnetic simulations and subsequent experiments we investigated these effects for scaled version metamaterials at terahertz frequencies that should be directly relevant to microwave applications. These studies reveal that the resonance frequency can be reduced significantly through the interaction between resonating elements. For example, we have fabricated and measured closely spaced bilayer SRRs. Our measurement shows that the

resonance frequency of this bilayer metamaterial is greatly reduced by tuning the separation between layers and their relative orientations. The combined resonant frequency could be reduced significantly compared to lowest possible resonant frequency obtained in an individual SRR as shown in Figure 1. This result has been published in Applied Physics Letter [1]. We also investigated capacitive and inductive interaction of planer metamaterial where the unit cell was comprised of a pair of laterally coupled SRRs. The resonance of this planer coupled system can be tuned in frequency through the relative positioning of the gaps as well as offsetting the gap position in the opposite direction from their symmetry point. The experimental results were verified through electromagnetic simulation which also demonstrates the critical points within the unit cell where electromagnetic field concentration is maximized. Finding such points might be important for diode placement for efficient RF to DC conversion. This result has been published in Optics Express [2].
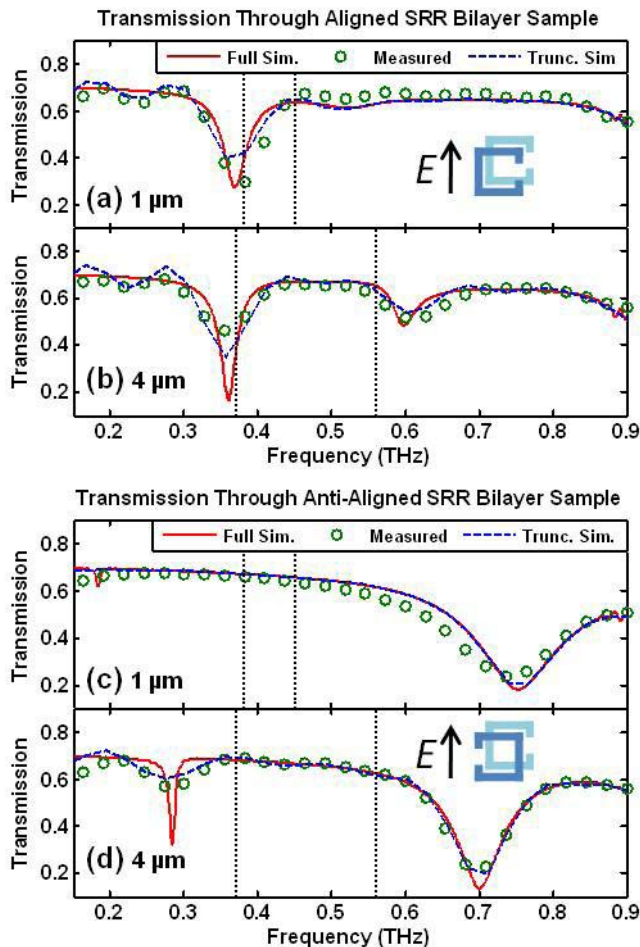

Figure 1. Transmission curves of bilayer metamaterial as a function of frequency for the full simulation (solid), measurement (circles), and truncated time domain simulation (dashed) for aligned SRRs at a separation thickness d = 1 μm (a) and d = 4 μm (b) and for anti-aligned SRRs at d = 1 μm (c) and d = 4 μm (d).

One of the major disadvantages of metamaterials is their narrow band operation which limits their application only for a particular frequency bandwidth. Once fabricated, the resonance frequency cannot be changed dynamically. This means, if a resonator is designed for 1 GHz frequency it will be active only for that frequency. This will make the energy harvesting device inefficient in the multi-frequency environment because of its inability to interact frequency other than its resonance frequency. We initially proposed a tunable Metamaterials which can be tuned dynamically to be resonant within a certain frequency band. However, every dynamical frequency tuning process demonstrated so far requires some sort of external stimulus. The external stimulus comes at the expense of energy in the form of electrical, magnetic, or optical which is detrimental to the primary goal of energy harvesting. To mitigate the requirement of dynamical frequency tuning, we have studied possibilities of broadband metamaterials to extend the frequency range of their operations. We have designed, fabricated, and characterized broadband planar metamaterials with nested structure. We demonstrate the broadening of fundamental resonance in metamaterials by successive insertion of inner metal rings inside the original unit cell of a split ring resonator, forming an interconnected nested structure. With the subsequent addition of each inner ring, the fundamental resonance mode shows gradual broadening and a blue shift. For a total of four rings in the structure the resonance linewidth is enhanced by a factor of four as shown in Figure 2. Even though the experimental demonstration was carried out using terahertz frequencies the result would be directly applicable for designing a broadband RF energy harvesting antenna. This result has produced a journal publication in Optics Express [3].
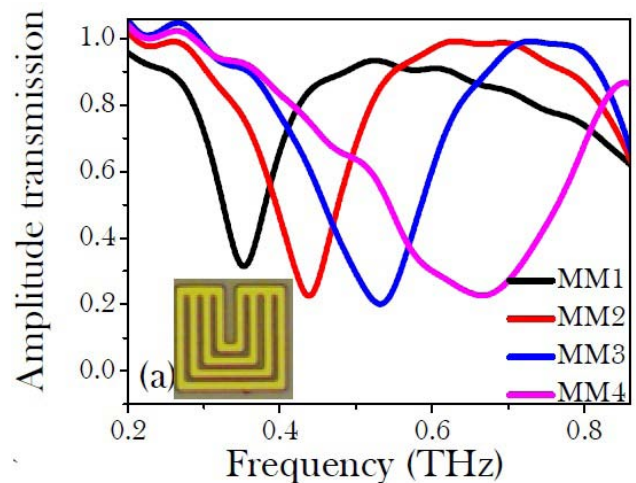

Figure 2. Measured transmission through the nested metamaterial samples. The linewidth of the resonance increases with every successive inner ring. The inset shows the SRR with four inner rings.

We also fabricated our initial SRR based RF energy harvesting antenna loaded with a diode. The antenna is capable of RF energy harvesting from an incident RF radiation field.

The size of the antenna is about ten times smaller compared to the RF radiation wavelength. The harvested DC power was larger than a similar size dipole antenna. It is worth mentioning here that small antennas are normally not impedance matched to the external circuit such as a coaxial cable which prevents optimal power transfer. To enhance the DC power and reduce the physical size of the antenna we developed a new bilayer based RF antenna. We are currently investigating two aspects of bilayer antennae. First, interconnected bilayers where both layers are loaded with diodes and they are connected in series. We have observed a fourfold enhancement of the harvested energy compared to a single layer SRR antenna. The harvested energy seems to be sensitive to the separation between layers. Also the physical size of the antenna is eighteen times smaller than the RF radiation. Our preliminary results indicate that this bilayer antenna can generate DC power when it is excited with either the electric field or magnetic field, or both, of the RF radiation. Second, we also initiated the investigation of electrically small antennas (ESA). In this case, the active layer of the antenna is directly connected to the coaxial feed-line and a second layer is parasitically coupled to the active layer through magnetic induction. The design employs split ring resonators loaded with lumped capacitors. The operating wavelength can be tuned by simultaneously adjusting the separation between layers and individual capacitance of each layer. Our initial measurement shows that the reflection from such bilayer antenna is very small, means that the antenna is inherently impedance matched to the feed line. This might be open up a new avenue to design ultra compact RF antennae for wireless application.

Finally, we fabricated anenergy harvesting panel made of 3x3 elements loaded with diodes for energy harvesting as shown in Figure 3. We have noticed the interconnect bus line dramatically changes and complicates the resonance mode. We obtained a good RF to DC conversion efficiency; however, at this point it is not clear how metamaterials resonances are being renormalized because of the interconnected bus line; this requires further investigation.
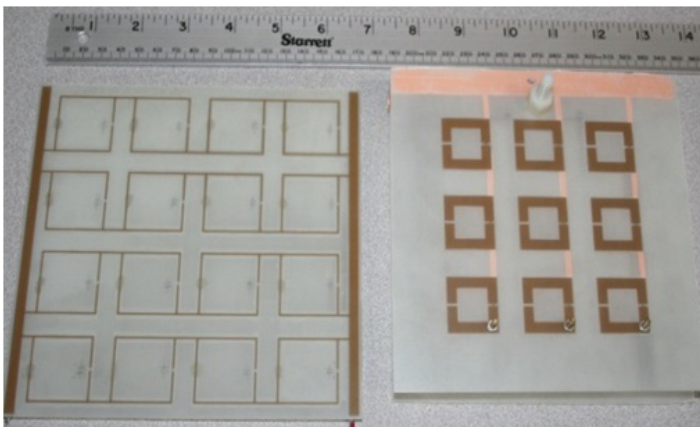

Figure 3. Fabricated RF energy harvesting antenna panels.

Future Work

With the motivation of improving wireless communication devices, the past decade has witnessed rapid progress in improving the efficiency of electronics. Indeed, many electronic devices operate so efficiently that we can envision new ways of powering them with otherwise wasted energy sources. One approach is radio frequency energy harvesting (RFEH). In this scheme, electromagnetic energy in the ambient environment, for example from radio or television broadcasts, is collected by efficient antennas and funneled into the electronic device. To make this scheme practical, antennas must be maximally efficient and much smaller than the electromagnetic wavelength. Metamaterial principles provide a method of making antennas with highly efficient operation and smaller sizes than traditional antenna technology. Critically, metamaterial-inspired antennas permit control over both magnetic and electric antenna resonant responses, thus allowing the antenna to be impedance matched to the incoming waves and the electronic circuit and preventing energy reflection from the circuit. The resonant response further enhances harvesting by creating a known power-funneling effect around the antenna. Our goal is to design metamaterial-inspired antennas that collect as much RF energy in as small a package as possible, in an effort to provide a new way to wirelessly power embedded, covert, or otherwise inaccessible electronic devices. Our most immediate future work is to understand the role of an interconnected bus line in a panel environment and their effect on energy harvesting. We will reinvestigate our single element bilayer diode loaded RF antenna again to verify diligently the effect of bus lines and connections by using two elements, and three elements that will help designing an arrayed antenna panel. At this work progresses, we intend to compare the performance of our RF energy harvesting panel to the current state-of-the-art. In parallel, we will investigate bilayer, electrically small antenna. Our plan is to fabricate a series of antennas whose physical dimension will be varied from ten to sixty times smaller than the RF radiation wavelength while maintaining ultra low reflection losses. These antennae will be studied experimentally and numerically to obtain the radiation efficiencies, radiation pattern, and bandwidths.

Conclusion

We have demonstrated metamaterials-inspired antennae that harvest radio frequency energy. However, the optimization of energy harvesting is a real challenge that includes efficiency of the antenna, compactness of the antenna, and more importantly arranging the antennas in a panel. The concepts of shrinking antenna size and increasing resonance linewidth have been verified through numerical simulation and scaled version measurements that are important from the design point of view. Also, our unoptimized panel shows good RF to DC conversion. This will be a promising route to recycle wasted radio frequency energy. In addition, our approach of making electrically small antenna should improve wireless technologies such as more compact wireless devices or covert sensors.

References

1. Reiten, M. T., D. Roy Chowdhury, J. Zhou, A. J. Taylor, John F. O'Hara, and Abul. K. Azad. Resonance tuning behavior in closely spaced inhomogeneous bilayer metamaterials. 2011. *Applied Physics Letter.* **98**: 131105.

2. Chowdhury, D. R., R. Singh, M. T. Reiten, J. Zhou, A. J. Taylor, and John F. O'Hara. Tailored resonator coupling for modifying the terahertz metamaterial response. 2011. *Optics Express.* **19**: 1079.

3. Chowdhury, D. R., R. Singh, M. Reiten, H. T. Chen, A. J. Taylor, and J. F. O'Hara. A broadband planar terahertz metamaterial with nested structure. 2011. *Optics Express.* **19** (17): 15817.

Publications

Chen, H., J. O'Hara, A. Azad, and A. Taylor. Manipulation of terahertz radiation using metamaterials. 2011. *Laser and Photonics Reviews.* **5** (4): 513.

Chowdhury, D. R., R. Singh, M. Reiten, Hou-Tong Chen, A. Taylor, J. O'Hara, and A. Azad. A broadband planar terahertz metamaterial with nested structure. 2011. *Optics Express.* **19** (17): 15817.

Chowdhury, D. R., R. Singh, M. Reiten, J. Zhou, A. Taylor, and J. O,ÄôHara. Tailored resonator coupling for modifying the terahertz metamaterial response. 2011. *OPTICS EXPRESS.* **19** (11): 10679.

Reiten, M. T., A. K. Azad, D. R. Chowdhury, A. J. Taylor, and J. F. OaHara. Multilayer terahertz metamaterials: Interactions between layers within the deep-subwavelength limit. 2010. In *2010 35th International Conference on Infrared, Millimeter, and Terahertz Waves (IRMMW-THz 2010) ; 5-10 Sept.* (2010 ; Rome, Italy). , p. 1.

Reiten, M. T., D. Roy Chowdhury, J. Zhou, A. J. Taylor, J. F. O'hara, and A. K. Azad. Resonance tuning behavior in closely spaced inhomogeneous bilayer metamaterials. 2011. *Applied Physics Letters.* **98** (13): 131105.

Ultra High Quality Electron Source for Next Generation Vacuum Electronic Devices

Nathan A. Moody
20100262ER

Introduction

There are many application-specific free state electron devices ranging from small x-ray generators to very large, high power sheet electron beam generators used in materials processing and food irradiation. Free state electrons must necessarily be created and transported in a vacuum and the majority of these devices only require moderate quality electron beams, where all electrons do not necessarily have the same velocity and trajectories. However, advanced applications in high-energy accelerators, next generation light x-ray light sources and high-resolution imaging tools such as scanning electron microscopes require very high quality electron beams. The broad set of all these devices producing free state electrons are commonly categorized as vacuum electronics [1].

The technology base for the emission surfaces in these devices, where electrons transition from a conducted state in a solid, to the free state in a vacuum, has not appreciably changed for several decades. As the requirements for higher power, higher beam quality, and very short pulse electron bunches increases, the limitation of present technologies becomes pronounced. Our approach, using semiconducting diamond with a unique carbon nanotube (CNT)/platinum (Pt)/ultrananocrystalline diamond (UNCD) electrical contact-device interface, may significantly improve electron source technology by addressing a fundamental limitation shared by many high current electron emission schemes. The special design of the atomic scale interfaces between the CNT's, Pt, UNCD enhance the highly probabilistic quantum mechanical processes that will likely increase charge transfer into the diamond by several orders of magnitude. This design approach will allow the fabrication of electron sources from low current millimeter dimensions to ultra-high current, high duty factor devices with large area emission. Additionally the form factor can vary from round flat, to round concave surface electrostatic lensing emitters as well as high aspect ratio rectangular emitters for sheet electron beam production. An illustration of one possible cathode configuration is shown in Figure 1.
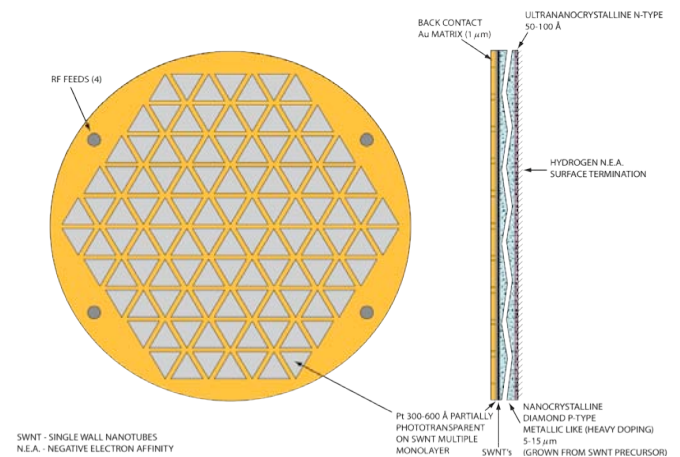

Figure 1. Typical device configuration.

Benefit to National Security Missions

The important mission of stand-off detection of nuclear and non-nuclear materials requires smaller, more powerful, and higher frequency sources of GHz and THz radiation for remote interrogation than are currently available. From the physics point of view, vacuum electronics (VE) is the technology of choice for building such high power sources and next generation light sources (e.g. free electron lasers), currently limited by weaknesses associated with creating the requisite electron beam. Our ultra-high quality electron source can directly address this vulnerability and enable VE-based source development to continue.

Progress

Accomplishments for year two have been focused on the development and process improvements for the platinum (Pt)/carbon nanotube (CNT) matrix discussed in the year one report. At that time we had envisioned the Pt/CNT matrix would be fabricated by using a Pt physical vapor deposition (PVD), or a foil melt process combined with surfactant free metallic carbon nanotubes treated with a single atomic interfacial layer of titanium for uniform grading of the materials surface work function. Variations in technique and the refinement of process parameters yielded some successes but were all deemed

inadequate for reproducible device production. Considerable effort has been expended to find suitable materials science methods to develop the novel combination of a noble metal and single walled carbon nanotubes [2]. The final achievement of this goal will have a dramatic and lasting impact on the field of vacuum electronics as well as the high power semiconductor industry.

Over the past few years the production of high quality metallic single walled nanotubes has matured to the point where very high purity >98% metallic nanotubes are available in quantity from commercial sources. Due to recent developments in process control commercial entities are able to produce high purity metallic, very high-density carbon nanotube films. The availability of these films along with a mixed gas phase platinum/reactant process being developed at LANL is a strong indication that a completely homogeneous Pt/CNT interface is possible without perturbing the ballistic electron transport characteristics of the CNT's at the Pt/CNT/UNCD interface. In recent years a variation on the chemical vapor deposition (CVD) technique, atomic layer deposition (ALD) has been developed. The advantage of this process is the excellent control of conformal coating of the individual CNT's. In this process an organometallic precursor gas is introduced into the reactor and a monolayer is allowed to adsorb and infiltrate the CNT film surface. The excess precursor gas is then removed and a second species is introduced which reacts with the adsorbed monolayer forming the desired solid phase. The process is self-limiting and can be repeated building up the coating one monolayer at a time. Mass transport occurs during the initial charging cycle and reaction occurs during the second cycle, eliminating issues associated with coupled mass transport/reaction. This is an ideal approach for fabricating nanocomposites. The very fine pores require a strong or complete separation of mass transport and reaction to achieve a fully infiltrated structure. Highly reproducible Pt/CNT substrates with large surface areas will be able to be produced using the method described (Figure 2).

Fabrication of the first generation of Pt/CNT substrates is now in the start up phase. All apparatus, gas phase and solid materials are in hand. At this time the control system software is being implemented for the mass flow devices and temperature control of the reaction chamber. A commercial source for the diamond growth has been identified and contacted to verify the suitability of capabilities and gain concurrence for the establishment of a non disclosure agreement. Following this, the Pt/CNT substrates will then be sent to the commercial diamond film production facility for growth of ultra-high purity ultra nanocrystalline diamond (UNCD) boron doped and undoped films. Diamond coatings of various thicknesses are possible, ranging in diamond crystallite size from 3-5 nanometers to .5 microns, depending on electron emitter application (photoemission, photo-stimulated field emission etc.). The creation of this condensed matter composite will likely result in quantum

states where potential barriers at the Pt/CNT and CNT/UNCD transitions will be extremely small. In addition, considering the CNT's electrical conductivity is >100 times that of copper, along with the high carrier mobility of diamond, it is anticipated that the emission current density of these devices will be in the multi-kilo amperes per square centimeter range rather than the originally targeted hundred of amperes per square centimeter range.
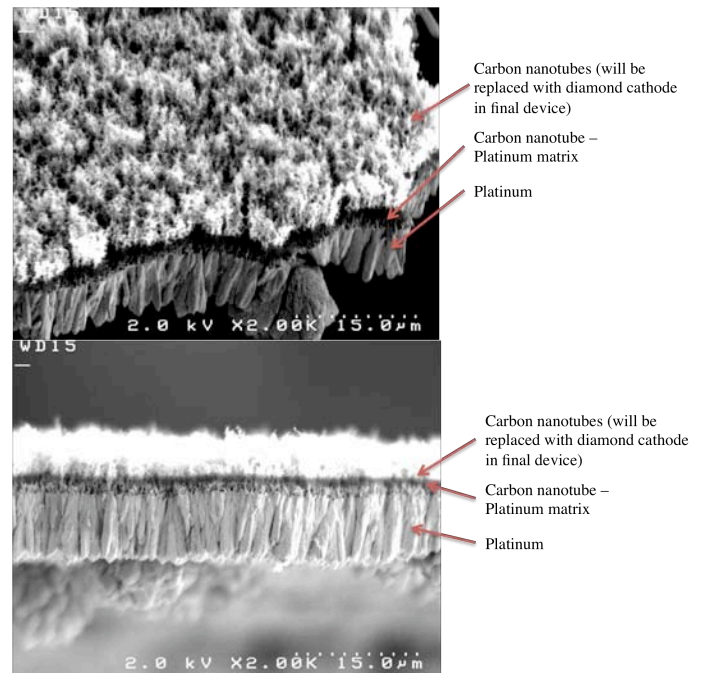

Figure 2. Platinum/nanotube matrix.

Future Work

In all very high power semi-conductor, solid state, or condensed matter electronic devices the most critical limiting factor is the back electrical contact, and in switching devices it is the back contact as well as the switching junction. Since our device does not require internal gating or switching, our greatest challenge is the back contact. This is the single critical point for destructive heating. Fortunately, the back contact is at the device surface and is bounded by highly thermally conductive diamond greatly, facilitating the ability to dissipate extreme heat leading to sudden thermal runaway and device destruction. As we all are aware, the past decade has brought many new discoveries in materials science; most notable are the various new forms or allotropes of carbon, one being carbon nanotubes, now well characterized. The standard back contact approach is to create an oxide free metal to semi-conductor interface using a multiplicity of exotic techniques. In these devices there is always a potential barrier of some height. Our approach is to use CNT's to enhance the probabilistic quantum mechanical processes by having a three dimensional interface with materials that will have an intrinsically low potential barrier. This is achieved by creating a component atomic structure approaching the atomic scale (CNT's are several tens of Bohr radii). The CNT platinum

interface was chosen because the interface between platinum and CNT's form a thin carbide layer through catalysis, when the platinum/CNT matrix is heated to ~500°C. The carbide layer has a work function nearly perfectly bridging that of platinum and carbon. Also, the packing density of the CNT's, at 3-5 nanometers diameter, forms a homogeneous interface layer suitable for nucleation and growth of the diamond emission structure. Initial investigations have also just begun to consider using a unique mechanism, employing technology developed by Vanderbilt University for the implementation of bremstrauhllung backplane illumination as a prompt cathode gating mechanism. Our goal for the future is to thoroughly test and characterize devices based on these combined technologies. These data will provide the benchmarked basis for the development of theoretical codes to define, mechanistically, properties and provide the basis for reproducible device production for many future configurations.

Conclusion

Our research goal is to transition our novel diamond field emitter concept into a versatile, robust electron source whose form factor and emission characteristics can be tailored to any number of specific applications. We will fabricate prototype polycrystalline diamond films and demonstrate their revolutionary and robust capacity to serve as an ultra-high quality, high current, high duty factor electron source for almost any vacuum electronic device, including high-frequency (>100 GHz) microwave tubes and advanced accelerator applications which are likely to continue to be the core technologies for many defense related missions.

References

1. Granatstein, V. L., R. K. Parker, and C. M. Armstrong. Vacuum electronics at the dawn of the twenty-first century. 1999. *Proceedings of the IEEE.* **87** (5): 702.

2. Matsuda, Y., W. Deng, and W. A. Goddard. Contact resistance properties between nanotubes and various metals from quantum mechanics. 2007. *Journal of Physical Chemistry C.* **111**: 11113.

Solid State Neutron Detector

Rico E. Del Sesto
20100389ER

Introduction

This project details the development of a completely new class of solid state neutron detectors based upon scintillator materials recently discovered at Los Alamos National Laboratory. The traditional neutron absorber used to detect neutrons is ^{3}He, a material that is becoming difficult to obtain throughout the world. Furthermore, the detector system will not employ high-pressure gas or toxic materials and as such will have few limitations on transport. The scintillator comprises a completely new composition. We believe these new scintillators will provide neutron detectors with performance comparable to existing ^{3}He without the cost or difficulties associated with compressed gas. As a result of reduction in cost of over 80% and increased portability of the detector system, more detector systems can readily be deployed. These detectors will also be light, thin, tolerant of extremes temperature and vibration, low in power demand and insensitive to radiation other than neutrons.

Benefit to National Security Missions

Neutron detectors are critical for missions from nuclear physics to nonproliferation and forensics. Conventional neutron detectors typically include devices that operate as ionization chambers or proportional counters. The ^{3}He proportional counters are currently the most widely used thermal neutron detectors for nonproliferation-related activities. Besides the clear problems that the limited supply of ^{3}He is causing, these counters also suffer to some extent from transportation-related disadvantages including the perceived dangers of high pressure gas containment. This device will replace ^{3}He detectors with a cheaper and safer alternative.

Progress

We have scaled up the synthesis of inverse opals and currently prepare these materials based upon SiO_2 up to the 10 gram scale, which have pore sizes on the order of 350 nm. The inverse opals have been fully characterized using surface area analysis, X-Ray diffraction and photo-luminescence. These materials we also used as the standards in the gamma spectroscopy work.

The inner walls of the inverse opals have been coated with a number of materials to provide luminescence. This includes metals (Zr, Hf), metal oxides (Zr, Hf, Ln/rare earths, Zn), and metal vanadates. The PAD technique works well for producing films that are fairly uniform in coating, ranging from 50-200nm. XAFS (X-ray Absorption Fine Structure) experiments show that the composition of the films at the surface and in the inner walls of external pores is also fairly uniform. These material also exhibit broad ranges of photoluminesence, ranging from short lifetime (5ns) almost-white light from Hf coated materials, to multicolored emission from Zn/Eu:YVO4 coating that emit broad spectrum light. These latter materials are of interest for solid state lighting applications. These materials were filled with an aqueous solution of ^{6}Li and exposed to x-ray, gamma, and neutron irradiation. While the x-ray excitation resulted in weak luminescence, gamma and neutron radiation exhibit no response. This is likely a result of the aqueous component that may interfere with the charge transfer processes of scintillation. We will be developing these materials in organic solvents in the future containing lithium or boron, which is used in polymeric and organic scintillators for neutron detection.

Similar materials have also been synthesized, utilizing smaller-pored metal organic framework and zeolite materials, with pore sizes on the order of 5-10nm. These materials allow for immobilization of standard scintillator dyes, such as PPO (poly(phenylene) oxides and p-terphenyl, in the pores with increase light output efficiency due to their isolated nature. Both types of materials are being placed in solutions containing high Li-6 and B-10 loaded solutions with pathlengths of 1mm or less. The hybrid solutions are currently being examined for the response to neutron and gamma radiation, to determine their effectiveness at detection and also discrimination, the latter being a significant requirement for new neutron detectors and He-3 replacement.

Future Work

Future work will entail the assessment of different hole

sizes and the effect the optical band gap change has on emission. We will assess if the rare earth doped inverse opals have any effect on the emission from the zirconium or hafnium coated inverse opals. We will also determine if a barrier coating on the zirconium or hafnium is advantageous in the ability to index match the fill solution.

Project Milestones

- Prepare and characterize photonic crystal scintillators with lifetimes < 20 ns and quantum efficiencies (lifetime vs λ etc).

- Fill photonic crystal scintillators, zeolites, and metal organic frameworks with boron or lithium material that provides an index match and thereby a transparent scintillator.

- Determine neutron capture and gamma exclusion efficiencies of new neutron phosphor.

- Assemble a device consisting of a neutron detector 0.5 mm x 1 cm x 1 cm.

Conclusion

The success of the proposal will be the production of a working prototype solid state neutron detector, which has efficiencies and gamma exclusion properties comparable to the 3He detectors. This will reduce the dependency on ^{3}He which is a scare material and therefore enable wide spread deployment of neutron detectors at ports of entry.

Publications

Li, A., N. Smith, M. P. Hehlen, E. A. McKigney, and R. Gardner. Light yield measurement method for milled nanosize inorganic crystals. To appear in *Applied Radiation and Isotopes.*

Li, A., N. Smith, M. P. Hehlen, V. M. Montoya, J. M. Cook, E. A. McKigney, and R. Gardner. Light yield measurements of milled BaFCl:Eu inorganic crystals. 2011. *Proceedings of the SPIE.* **8144**: 814404.

Exploration of Megawatt Heat Pipe Reactor Concepts

Patrick R. Mcclure
20110141ER

Introduction

Heat pipes move heat (thermal power) between two bodies with little temperature change from hot to cold. This makes them an ideal means to extract thermal power from a nuclear reactor. Heat pipes are especially appropriate for robust, reliable, remotely controlled reactors. To date most proposed heat pipe reactors have capacities of less than 1 MW. The design of larger heat pipe reactors that can operate at power levels of wide spread public interest is unchartered. We are exploring the possibility of building heat-pipe-cooled reactors with capacities greater than 1 MW. Such reactors would be suitable for future emission-free energy generation. With proper safeguards such reactors can be readily and securely used by cities, states, or in developing countries.

Benefit to National Security Missions

DOE-NE has established a program for innovative reactor design. One aspect of this program is support for compact modular reactors reflecting a trend toward small reactors and reactors that embody bold approaches. Novel small reactor designs can significantly improve performance, safety, and reliability, and improve the economics and security of reactor production and operation. This project supports transformational concepts in small modular nuclear reactors. The results of the project would be relevant to missions in DOE-NE, NASA and the DOD. DARPA is currently developing a small mobile reactor project for which a 5 MW electric heat pipe reactor would be ideal.

Progress

Work on a megawatt-sized heat pipe reactor began with the development of a base-line design. The goal of this base-line design was to use the most conventional materials, approaches and components that can achieve or closely achieve a megawatt-scale heat pipe reactor. After a baseline design was developed, variations to the design were postulated and tested analytically to determine their suitability for scaling up the power of the reactor. Variations to the design could include any parameter, such as types of reactor material, heat pipe working fluid, reactor fuel, core geometry, or number of heat pipes. Variations in parameters were required to result in a design that remained within the practical and accepted design limits for a reactor. An example of a design limit is the ASME limits for stress in the monolithic reactor block following a transient reactor condition such as a failed heat pipe.

The conditions under which a design was evaluated were: 1) normal operating conditions for 5 years of operation and 2) a design basis accident considered typical for a heat pipe reactor. For a heat pipe reactor the design basis accident is called "Cascade Failure." Cascade Failure is the loss of a single or multiple heat pipes causing the failure of surrounding heat pipes in a cascade (like dominoes falling in a line). If a sufficient number of heat pipes fail the situation could lead to inadequate cooling of the reactor core. To achieve success the heat pipe reactor design is required to withstand the failure of two adjacent heat pipes at the worst-case location (highest power fuel pin).

The baseline design is a 5 MW thermal, fast spectrum reactor with cross section shown schematically in Figure 1. This baseline reactor consists of a solid stainless steel monolithic block core (a steel block with fuel and heat pipes in holes in the block), potassium working fluid heat pipes with stainless steel sleeves and wicks, and 19.75% enriched uranium oxide fuel pellets in a helium filled fuel holes in the stain-less steel monolithic block. The baseline design has 2112 fuel pins (or holes) and 1224 heat pipes. To keep the design manufacture-able, the core was divided into six "pie-shaped" segments that are mechanically and thermally isolated but communicate neutronically. This geometric change kept the number of heat pipes to approximately 200 per pie shaped segment, a number that is considered practical to manufacture by experts in machining and welding. The reactor is controlled neutronically by 12 control drums in the outside reflector and central shutdown rod is used to provide redundant safety margin. The reactor has an aluminum oxide reflector. When the reactor is paired with a carbon dioxide Brayton cycle power conversion

system, the baseline design produces approximately 1 to 2 MW of electric power.
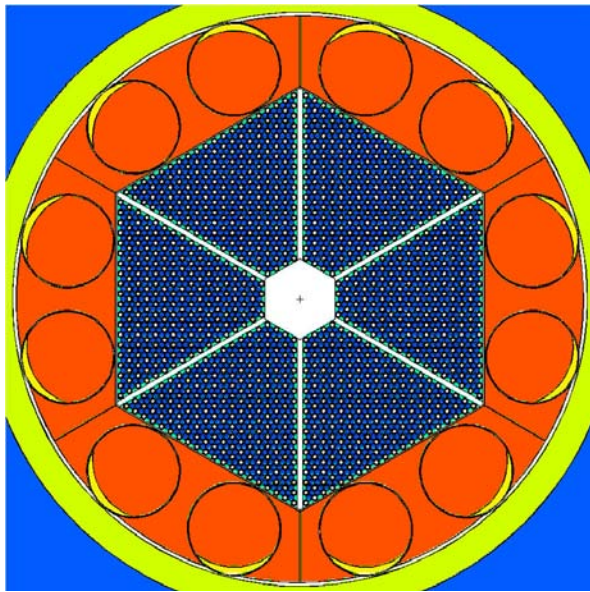

Figure 1. Schematic of Reactor Core.

Neutronic, mechanical and thermal calculations were done for both operating and accident conditions for the baseline design. The baseline reactor concept met the acceptance criteria for a practical design (could be manufactured) and met acceptable design limits. The accident calculation of most interest is the multiple failed heat pipes in a geometric pattern (three adjacent failures) that could lead to "Cascade Failure." This analysis is shown in Figure 2 for a failed heat pipe. The baseline reactor design was shown to survive this situation by either 1) not exceeding heat pipe design limits or 2) not exceeding ASME design limits for thermal stress.
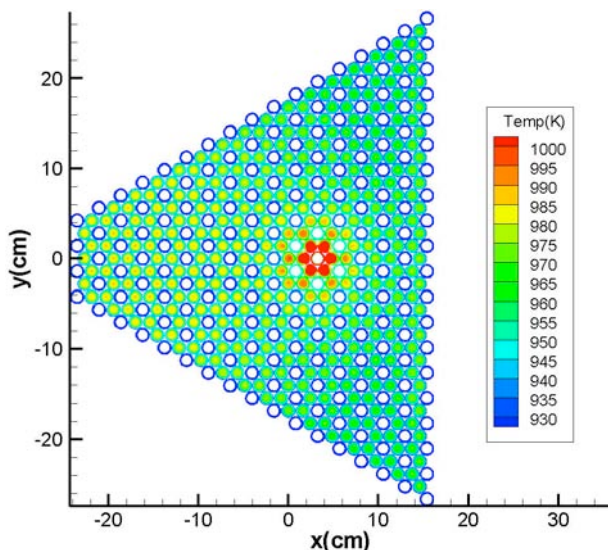

Figure 2. Schematic of a Failed Heat Pipe.

The second variation on the baseline design followed the path outlined above, namely to vary core materials, heat pipe working fluid and fuel composition. These changes included:

1. Replacing the 316 stainless steel with a molybdenum alloy, TZM (Mo (~99%), Ti (~0.5%), Zr (~0.08%) and some C) that has better thermal and mechanical properties at high temperature than stainless steel;

2. Replacing the potassium working fluid in the heat pipe with a sodium working fluid that allows for higher temperatures and improved axial power density per heat pipe; and

3. Replacing the Uranium Oxide fuel pellets with Uranium Nitride pellets to improve the fuel heat transfer and centerline fuel temperatures.

This second variation allowed for a design with a thermal power of 15 MW, (a potential electrical output of 3 to 6 MW electric.) This design, like the baseline, was demonstrated to meet the acceptance criteria set for operational and accident conditions and as such is also a viable concept. It is identical in configuration to the baseline design shown in Figure 1, but has a slightly larger geometry.

The third variation that has been postulated for increasing the thermal power of the design is to increase the thermal throughput of the heat pipes (increasing axial power density.) The mechanisms to achieve greater thermal throughput is the idea of a "double ended" heat pipe. The double ended heat pipe increases the axial power density of a heat pipe cooled nuclear reactor by placing the fuelled region at the center of the heat pipe array rather than at one end. This idea is shown schematically in Figure 3. The linear heat rates of the fuel in baseline stainless steel reactor design and in TZM variation to the baseline are much lower than has been historically used in fast reactors. So increases in the axial power density of the heat pipe will allow for higher core thermal powers without pushing limits on the core and fuel.
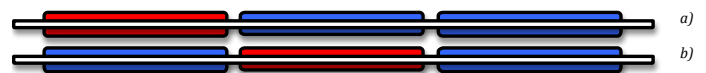
Figure 3. Illustration of a Double Ended Heat Pipe.

Analytical models have demonstrated that, if successful, the double-ended heat pipe will allow a significant increase in the thermal power of the core. The predicted axial power density from a conventional heat pipe with power applied at one end to that of a heat pipe compared with power applied in the middle shows the middle heated pipe has an axial heat flux over twice an end-heated configuration.

A fourth planned variation to baseline reactor design is to replace the solid block core with a liquid core (not a moving or pumped liquid by a stagnant liquid). A liquid core could eliminate one predominant design limit for heat pipe reactors, namely the impact of a failed heat pipe on system performance, reliability and safety. Previous heat pipe reactors have attempted to avoid this problem by either 1) using a modular, decoupled design and operating at very low powers or 2) fabricating a complex, expensive core block that is limited by thermal-structural issues. A liquid-metal bath will increase efficiency by allowing enhanced heat transfer from fuel pins to heat pipes, in particular in the event of failed heat pipes. The bath will also increase affordability by removing the most challenging design and fabrication feature (the core block) from the only other viable high-power heat pipe concept. Finally, the bath should improve safety by minimizing the possibility of cascading failures and allowing more safety margin to be designed into the system. This could alleviate one of the prime constraints on the design, thermally induced stress limits in the solid block. The liquid core would not have these constraints but still allow for a redistribution of heat to other heat pipes in the event of a failed heat pipe.

Future Work

Variations in design parameters will continue as the project moves forward. An experiment of the double-ended heat pipe to demonstrate its capability is planned for the end of FY2012 as the research effort moves into its final year. The current goal is to see if a 100 MW or higher heat pipe reactor is feasible.

Conclusion

This work is examining megawatt sized heat-pipe reactors. There are many potential benefits derived from a heat-pipe reactor if they can be scaled. First, a heat-pipe-cooled reactor could be safer than other reactor concepts. A heat-pipe reactor is the only reactor concept in existence that does not rely on a single circulating fluid to cool the core. Instead, a heat pipe cooled reactor uses hundreds of heat pipes to remove heat from the reactor. Second, a heat-pipe reactor should be reliable given its nearly solid-state construction.

Full-Frame Programmable Spectral Imagers Based on Micro-Mirror Arrays

Steven P. Love
20110267ER

Introduction

This project seeks to develop a powerful new class of programmable spectral imagers based on rapidly-addressable micro-mirror arrays. In the instruments, the micro-mirror array (MMA) and associated optics act as a rapidly-reconfigurable multi-band spectral filter wherein any combination of dozens or hundreds of spectral bands can be selected and used to form a chemical-specific image. In essence, the MMA performs hyperspectral image (HSI) processing directly in the optical hardware, rather than in post-processing. The proposed technology represents a major advance over earlier MMA-based spectral imager concepts (and traditional HSI instruments as well) in the following crucial respect: Previous concepts, based on classical optics (standard lenses, mirrors, etc.), inevitably suffered from a large spatial variation across the image of the selected wavelengths. This necessitated a time-consuming spatial scan to form the image, negating the speed advantages that are the major attraction of a programmable filter. In contrast, the technology proposed here incorporates micro-fabricated non-classical optical elements, permitting the wavelengths selected by the MMA to be the same throughout the image. With this full-frame capability, the selected spectral bands can now be programmed and reprogrammed, over the entire image, on millisecond timescales, allowing sophisticated background-suppressing matched filters to be implemented at real-time video rates. This new capability opens up potential applications ranging from rapid broad-area search for proliferation telltales (with the time required to scan a given area reduced 2-3 orders of magnitude over traditional hyperspectral imagers), real-time medical imaging, spectral monitoring of rapid transients, spectrum-based tracking of vehicles and individuals, and (when coupled with the appropriate ultra-fast detector) ultra-fast spectral imaging on ns timescales.

Benefit to National Security Missions

This new technology, by offering a 2- to 3-order-of-magnitude speed improvement over standard hyperspectral instrumentation, directly addresses the long-standing need for a broad-area search capability for the laboratory's DOE proliferation detection remote sensing mission. The elimination of traditional HSI's slow scanning also enables a range of more general military and national security missions, such as spectrally-based tracking of vehicles and real-time imaging of chemical agent plumes. Coupling with LANL developed high-speed imaging capabilities (e.g. the RULLI/ASPIRE program) would add an as yet unexplored spectral dimension to these technologies. These capabilities open up exciting new scientific missions as well, including ultra-fast spectral imaging of shock waves and explosions, planetary mineral and gas reconnaissance, spectral imaging for volcano monitoring, real-time medical imaging, and many others.

Progress

The primary goal in this first year of the project has been to assemble a working prototype of the key optical components, in order to unambiguously demonstrate that the very unconventional basic optical concept will indeed work as envisioned. This goal was achieved, with a working prototype showing full-frame spectral selectability, with negligible wavelength variation across the frame, demonstrated in April 2011. This prototype, working in the visible spectral region, relies on a liquid crystal device (LCD)-based pixilated spatial light modulator, rather than a micro-mirror array (MMA). For work in this spectral region, the LCD offers some advantages over the MMA, including a straight-through transmissive optical path that considerably simplifies the optical design (very useful for rapid prototyping and testing the innovative non-classical components), and continuous gray-scale selection of the spectral components rather than binary 1 or 0 transmission (valuable for implementing rigorous adaptive matched filters for materials of interest). A schematic of the original prototype is shown in Figure 1. The prototype, now in its second iteration with 2x improved spectral resolution, was implemented using a color CCD camera, which allows easy visualization of the resulting spectral mix as the spectral function programmed onto the LCD array is varied (i.e. one can create an endless variety of colors, uniform across the image, intuitively demonstrating that this is a true

2D programmable filter.) This prototype performs as envisioned, allowing continuous viewing of the spectrally-manipulated 2D image at real-time video rates, with speed limited only by readout rate of the CCD, and with the spectral bands changeable essentially instantaneously via software control. Currently, all lenses are inexpensive, off-the-shelf components, which allows rapid turnaround as new insights drive revisions to the prototype design. The performance of this prototype, devoid of spectral shifts with image position, together with an illustration of the strong spectral shifts encountered prior to this work, is shown in Figure 2.
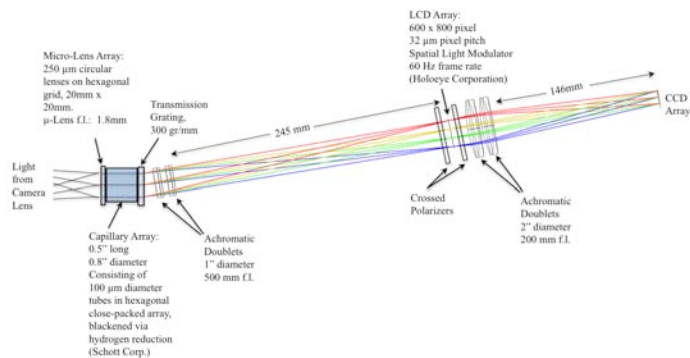

Figure 1. The first prototype LCD-based full-frame programmable spectral imager. This schematic of our first working prototype was included in the patent application filed with the U.S. Patent Office on September 30, 2011. Light from the scene is imaged in front of the micro-lens array, which collimates the light from each image point individually. A blackened capillary array (an array of micro-tubes) rejects off-axis light, further improving the collimation of the light from each image location. This collimated light impinges on a transmission grating, which spectrally disperses it. The dispersed spectrum is imaged onto the spectral-selection array, in this case a liquid crystal array between crossed polarizers, and chosen wavelengths are switched on or off. The spectrally manipulated light is re-formed into a full two-dimensional image at the detector.

As expected, this prototyping phase has elucidated how the difficult-to-model unconventional optical components interact and behave in the real world. For instance, the off-axis rejection component, originally envisioned as a probably optional "micro-louver" assembly, has been found to be essential to proper function of the spectral imager. In the actual implementation, a commercially available 2D array of blackened glass tubes, rather than micro-louvers, was found to be an excellent choice for this component. Experimenting with off-the-shelf versions of these arrays reveals that ultimate spectral resolution depends strongly on the length and aspect ratio of the tubes, and that considerable improvement can be expected from a custom-designed array. On the other hand, the diffuser or fiber bundle on the input side, originally envisioned in the proposal as being important for overall throughput,

has been found to be largely unnecessary.

With a working prototype now in hand, a patent application for these innovations was filed with the U.S. Patent Office on September 30, 2011.
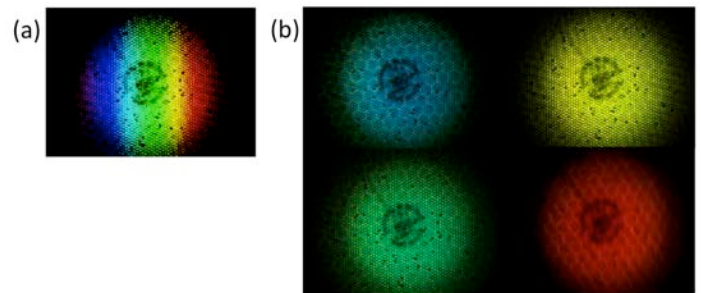

Figure 2. Achieving a full-frame programmable spectral imager, and comparison to earlier non-full-frame versions. (a) Simulated color image of a light bulb from our early, pre-LDRD, non-full-frame prototype, showing how a single narrow wavelength band programmed on the spectral selection array (MMA or LCD) is shifted with image position. (b) Actual color images from the new prototype programmable spectral imager illustrated in Figure 1. In each image, the LCD array is programmed for a single spectral band, corresponding to a visible color. Note that the color is the same throughout each image, demonstrating the lack of any significant spectral shift with image position.

Future Work
In the coming fiscal year, work will be focused in the following directions: (1) Continued iterations of the prototype design, aimed primarily at improving spectral resolution, varying in particular the micro-tube and micro-lens arrays, together with the grating dispersion. (2) Creating a more optimal optical design, using custom rather than off-the-shelf lenses, that will optimize overall image quality, spectral resolution, and throughput. This will be done once the issues with the non-classical components are well understood. (3) Integrating the CCD and LCD control systems in order to implement synchronized spectral selection and image readout, necessary for the more sophisticated matched filter applications envisioned for this project. (4) Implementing a micro-mirror version of the instrument, a necessary step in order to expand beyond the visible spectral region. A custom micro-mirror array, with a sapphire window covering the 0.25 – 5.5 micron spectral region, coupled with an up-to-date high-speed programmable interface was specified and purchased, and it was delivered at the end of FY11. This will pave the way for mid-infrared versions of the instrument.

Implementing the micro-mirror array versions will involve considerably more complex optical designs than the LCD version, because, unlike the transmissive LCD device, the reflective micro-mirror array involves re-imaging the micro-mirror plane as an intermediate optical object that is not perpendicular to the axis of propagation (the micro-mirror

reflections occur at an angle of 24 degrees to the device plane when illuminated at normal incidence). That this difficult optical design problem can be solved and good image quality achieved was demonstrated in an earlier visible-region, non-full-frame prototype, constructed prior to the current project. The design concepts developed in that exercise will be extended to the UV and infrared, and optimized for the spectral ranges and spectral resolutions of greatest interest.

Conclusion

Hyperspectral imaging (HSI) in which each pixel contains a high-resolution spectrum, has proven indispensible for remote detection and quantification of chemicals, in applications ranging from proliferation detection to medical imaging. But HSI as currently implemented is inherently slow, requiring several seconds per image. Monitoring faster phenomena required sacrificing either spectral specificity (e.g., camera with a simple filter) or spatial information (e.g., non-imaging spectrometers). The MMA-based technology being developed here aims at an optimal compromise: providing the spectral specificity of HSI, with hundreds of reconfigurable chemical-specific spectral bands, while offering the instantaneous 2D imaging capability of a simple filter. With a working prototype now produced, and hardware for extending the spectral range and speed now in hand, we are ready to proceed to more sophisticated and capable implementations, and application demonstrations.

Publications

Love, S. P., T. C. Hale, and P. Chylek. Advanced Instrumentation for Hyperspectral Imaging. Invited presentation at *LDRD Day 2011.* (Santa Fe, NM, Sept. 13, 2011).

Novel Broadband Tera Hertz Sources for Remote Sensing, Security and Spectroscopic Applications

John Singleton
20110320ER

Introduction

The goal of this project is to design, simulate, construct and test a completely new source of broadband THz radiation. This source employs polarization currents that both accelerate and travel faster than the speed of light. These faster-than-light, or superluminal, disturbances have been demonstrated in experiments at LANL (carried out under LDRD 20080085DR "Construction and use of superluminal emission technology demonstrators with applications in radar, astrophysics and secure communications") and elsewhere [1]. Similar superluminal mechanisms are also thought to be responsible for the radiation from pulsars [1,2]. Whereas the LDRD-DR project focused on communications and radar uses of superluminal sources, the current work is motivated by the need for reliable, robust THz sources for a wide variety of applications in homeland security, threat detection and basic science, as identified by DOE-NSF-NIH working groups and others. The proposed THz source uses LANL expertise in metamaterials and electronics to emulate the emission of pulsars [2]. It consists of a pair of coils, driven at a frequency of around 2.5 GHz by a few tens of Watts of power to produce a rotating dipole field. This magnetic field will rotate at superluminal speeds through a surrounding dielectric, simulating the plasma atmosphere of the pulsar. To ensure that the bulk of the emission occurs in the useful THz region, the dielectric will be a metamaterial designed in-house to exhibit a resonant dielectric constant at a particular frequency. The possible use of such sources as turn-key systems will be examined, and any intellectual property protected. Following the procedures applied in the preceding LDRD-DR project, the results will be discussed with industrial partners through LANL Technology Transfer with a view to licensing the technology.

Benefit to National Security Missions

One of LANL's aims is to "strengthen the core Laboratory capabilities in engineering to enable developing practical implementations... of "discovery" successes realized in... LDRD". Superluminal emission is such a discovery, and by studying one such approach to THz emission, the current will apply basic science discovery to solve real-world problems. Broadband THz sources will have a wide range of applications in remote sensing (e.g. detection of concealed controlled substances or explosives), non-intrusive medical applications and homeland security; all are relevant to the core mission of LANL to be the leading laboratory for National Security Science. The project will also develop and maintain LANL's expertise in metamaterials and simulation. Through LANL Technology Transfer, the PI has contacts with local industries and investors to spin out applications from superluminal work; thus, any intellectual property will positively impact job-creation in New Mexico.

Progress

The primary objective of the first year of this project was to design, model and fabricate the coil system that provides the rotating magnetic field for the THz source. This has been carried out successfully, and the coil system is being tested in experiments. A picture of the completed coilset is shown in Figure 1.
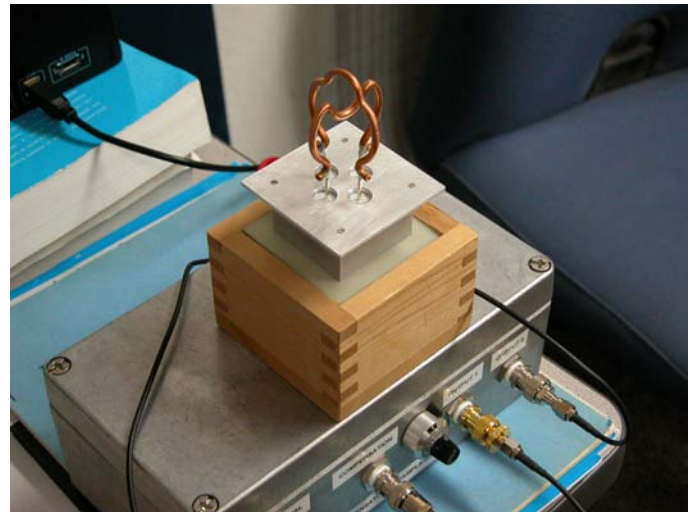

Figure 1. The completed coil system (impedance matching, loads, shielding and coils) for generating magnetic fields that rotate faster than the speed of light. It operates at 2.5 GHz and is small enough to fit in a coffee cup. This is an excellent precedent for the final source to be compact, as desired in the original proposal.

Magnetic fields that rotate at very high frequencies have both military and fundamental science applications [3]. However, the rotation in such equipment is achieved using waveguides and resonant cavities; by contrast, the current application requires the field to rotate superluminally (faster than light) in a metamaterial that is unconfined, so that the induced THz radiation can escape. Consequently, the project uses a completely new approach based on two orthogonal coils driven by GHz alternating currents. Though this approach sounds simple, very extensive electromagnetic modeling and engineering work was necessary to achieve an optimized design that is both compact and matched to typical 50 Ohm electronics. At GHz frequencies, the coil parameters (impedance and radiation resistance) are very sensitive to the exact dimensions and geometry of the coils. The situation is complicated by the tendency of the coils to behave resonantly, so that the time-averaged current is no longer uniform around the conductor, distorting the rotating field. In addition, inductive coupling between the coils and the need to water-cool them for eventual high-power operation further complicates the design. In the end, the pivotal breakthrough was the provision of a resistive load, behind the coils, that suppresses the tendency of the system to function as a resonant antenna, and yet allows the maximum amount of power to be coupled into the region where the field is produced.

The completed coil system (impedance matching, loads, shielding and coils) operates at 2.5 GHz and is small enough to fit in a coffee cup (Figure 1). This is an excellent precedent for the final source to be compact, as desired in the original proposal.

The THz emission in the final source is caused by a rotating, superluminal polarization current induced by the rotating magnetic field. In parallel with the development of the rotating coil system, experiments were carried out using an electrostatically-excited, rotating, superluminal polarization current, to test theories about focusing in the time domain (temporal focusing) that are an essential part of the THz production mechanism. The experiments were successful [4,5], demonstrating once again that the radiation from superluminal polarization currents is completely unlike the emissions from conventional antennas; in particular, the resulting beams become narrower with increasing distance due to the temporal focusing (Figure 2). As a consequence of these tests, the communications company Commscope has negotiated a CRADA with LANL Tech. Transfer to carry out a demonstration experiment to assess whether superluminal sources could be applicable to telecommunications backhaul. After further measurements, a scheme based on a linearly-accelerated polarization current was chosen for the technology demonstration, which is due to be carried out in early November 2011 (Figure 3). To this end, two patents on parts of the key technology are also being filed [5,6].
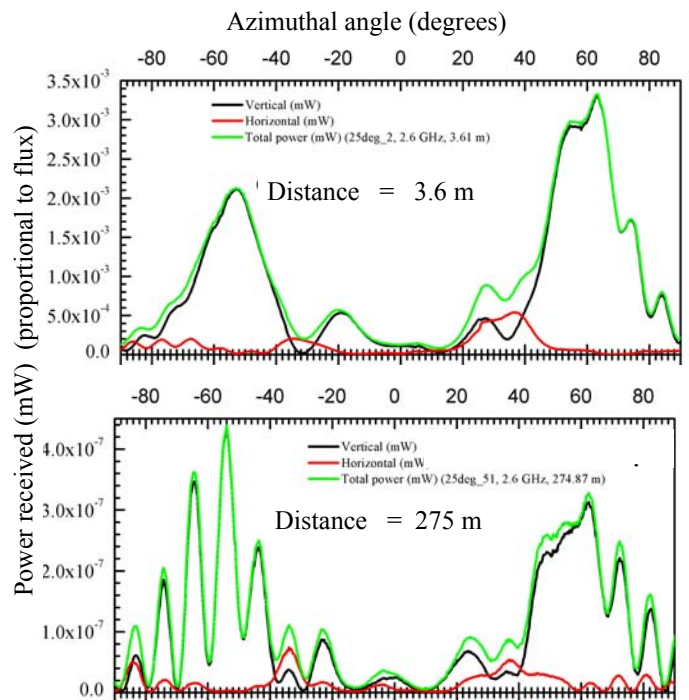

Figure 2. Radiofrequency power emitted by a rotating, superluminal polarization current as a function of orientation of the source. The experiments were carried out on ranges at Kirtland Air Force Base. Horizontally-polarized power is shown in red, vertically-polarized power in black, and the total power in green. Data for distances of 3.6 m (upper) and 275 m (lower) from the source are shown. Focusing in the time domain (temporal focusing) results in the development of very sharp features in the power distribution at larger distances (lower figure). These are far narrower than conventional diffraction limits, suggesting applications in directed energy and radar.
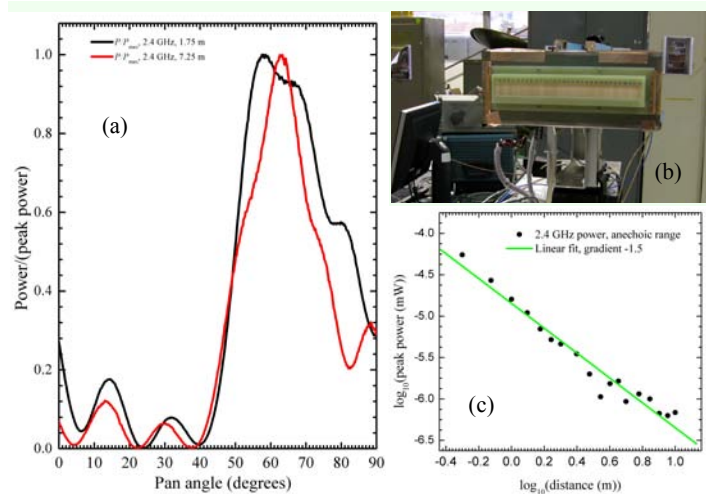

Figure 3. Power (normalized to the peak (maximum) value) emitted as a function of orientation (a) for the linear superluminal antenna shown in (b). This accelerates a faster-than-light polarization current. As in Figure 2, temporal focusing results in sharpening of the peak in power as the

distance increases (a). This results in a maximum power than falls off with increasing distance at a slower rate than for a conventonal antenna (c); the signal for a conventional antenna would have a gradient of -2. This particular geometry of superluminal antenna has been selected for telecommunications trials financed by a CRADA with the company CommScope.

The modeling of the superluminal THz source also has spin-off applications in astrophysics; similar techniques predict the emissions from pulsars and gamma-ray bursts [1,2]. As shown in the attached publication list, these results have been reported in six papers at two AAS conferences, and are being prepared for publication.

Finally, preliminary studies of the metamaterials to be used with the source in the second year of the project are underway.

Future Work

The THz region of the electromagnetic spectrum from 0.3 to 20 THz is a frontier area for research in physics, chemistry, biology and medicine [7]. THz radiation is also proposed for security and remote sensing applications; e.g., a "quick and dirty" THz spectrum can detect illegal pharmaceuticals and explosives concealed about a person's body. However, this region corresponds to the "THz gap" between sources such as klystrons and Gunn diodes (frequencies < ~200 GHz), and LEDs and semiconductor diode lasers (frequencies > ~10 THz) [7]. Accelerator–based sources are being built as THz user facilities, and there are commercial THz spectrometers employing femtosecond laser technology. However, the former are large, whilst the latter are expensive and too fragile to deploy widely in the field. By developing a robust, economical source, we allow THz spectroscopy to reach its potential in a range of applications.

Our source uses a magnetic field that rotates through a metamaterial designed to show resonant behavior at a particular frequency. The moving field displaces ions in the metamaterial, leading to a moving, electrically-polarized region, i.e. a polarization current. For a rotation frequency of 2.5 GHz, the current will move through the metamaterial faster than the speed of light for radii greater than about an inch. From both theoretical models and experiments [1,2], we know that this centripetally-accelerated, superluminal polarization current acts as the electromagnetic equivalent of the sonic boom produced when an aircraft accelerates through the speed of sound; intense bursts of focused, higher frequency radiation are emitted, the dominant frequencies being defined by the metamaterial's resonances.

The tasks are (i) to build the coil set and electronics producing the rotating magnetic field (completed); (ii) to test and optimize composite metamaterials made using a recently-developed powder in resin technique (commenc-

ing); and (iii) to fully characterize the performance of the source through experiment and numerical modeling (under way).

Conclusion

We expect to design, construct, test and assess the feasibility of a new broadband THz source based on rotating superluminal polarization currents for spectroscopic and security applications. The novel electronics to control the source will be optimized, and various metamaterials will be screened to give the best possible emission in the THz region. The possible use of such sources as turn-key systems will be examined, and any intellectual property protected. Following the procedures applied in the preceding LDRD-DR project, the results will be discussed with industrial partners with a view to licensing the technology.

References

1. Ardavan, H., A. Ardavan, J. Singleton, J. Fasel, and A. Schmidt. Inadequacies in the conventional treatment of the radiation field of moving sources. 2009. *Journal of Mathematical Physics.* **50**: 103510.

2. Singleton, J., P. Sengupta, and J. Middleditch. A Maximum-Likelihood Analysis of Observational Data on Fluxes and Distances of Radio Pulsars: Evidence for Violation of the Inverse-Square Law . To appear in *Physical Review Letters.*

3. Simpson, J. E., and M. Kamarchi. Microwave lamp with rotating field. 1992. *United States Patent.* : 5227698.

4. Singleton, J., A. Schmidt, Z. Wang, and Q. R. Marksteiner. Non-dispersing radiofrequency wavepackets generated by a rotating superluminal polarization current . 2011. *Preprint for submission to Journal of Applied Physics.*

5. Singleton, J., F. Krawczyk, Z. Wang, and L. Earley. Superluminal antenna. *US Patent.*

6. Ardavan, H., A. Ardavan, and J. Singleton. Generating a nondiffracting radiation beam by means of a polarization current with a superluminally moving distribution pattern. *US Patent.*

7. Baragwanath, A. J., G. P. Swift, D. Dai, A. J. Gallant, and J. M. Chamberlain. Silicon based microfluidic cell for terahertz frequencies. 2010. *Journal of Applied Physics.* **108** (1): 013102 (8 pp.).

Publications

Singleton, J., A. Schmidt, Z. Wang, Q. Marksteiner, H. Ardavan, and J. Middleditch. Comparisons between Ground-based, Artificial Pulsars and Data from the Parkes Multibeam Survey. 2011. In *AAS 217th Meeting, Seattle, Washington.* (Seattle, Jan. 2011). Vol. 43, p. 2. Washington: Bulletin of the American Astronomical Society.

Pyroelectric Heat Engines: Highly Efficient, Environmentally Friendly Cooling

Markus P. Hehlen
20110425ER

Introduction

We intend to develop a new class of solid-state heat engines that would be more efficient and environmentally benign than conventional vapor-compression devices. These heat engines, which are based on thin films of pyroelectric polymers, perform all the functions of conventional thermoelectrics, but are not constrained by the competition between thermal and electrical conductivity that has hampered the development of high-efficiency Peltier devices. The flexible, low-weight and durable thin-film format of these pyroelectric heat engines (PHE) opens many new opportunities for thermal management. PHE is composed of a layer of pyroelectric material sandwiched between two thin-film heat switches. The thin-film heat switches are an essential, new technology and are a major focus of this project. The thermal-conductivity contrasts K of the switch (the ratio of the thermal conductivities in the open and closed states) sets the overall efficiency of the PHE. Values of $K>60$ enable PHEs to outperform conventional vapor compression devices.

Cooling and thermal management are important for high-power computing, satellite performance, national energy consumption, and controlling global warming. Air conditioning and refrigeration account for more than 20% of the Nation's electrical power consumption. Optimizing and tuning traditional thermal technologies is not adequate to address the current needs of these important applications. Our proposed thin-film pyroelectric heat engines are a potentially disruptive approach that can increase the efficiency of cooling while lowering the cost and removing hazardous chemicals.

Benefit to National Security Missions

The successful execution of this project will position LANL to grow substantial programs in pyroelectric heat engines. We will work to obtain programmatic funding from the DOE and other federal agencies and to collaborate with industry to develop and commercialize this technology. DOE's Office of Energy Efficiency and Renewable Energy has shown interest in PHE with the ultimate goal of improving energy efficiency in residences.

To assist our interactions with industry, LANL and the University of New Mexico (UNM) previously have jointly filed two US patents on thin-film switches and thin-film heat engines. This project ties in with the LANL Grand Challenges in Energy and Earth Systems and Ubiquitous Sensing.

Progress

A PHE consists of a pyroelectric layer sandwiched between two thin heat switches. The basic device concept is depicted in Figure 1. The highest technical risk and the most innovative element of our project are the thin-film heat switches that control the heat flow between the hot side and the cold side. They are based on electrohydrodynamic (EHD) flow in dielectric fluids. Applying an electric field to a thin dielectric fluid film induces convective flows that transport heat more efficiently than thermal diffusion alone, thereby allowing for a switching of the thermal conductivity. The goal is to gain a fundamental understanding of the EHD processes and to maximize the thermal-conductivity contrast of an actual thin-film heat switch. FY11 work therefore focused on identifying device geometries suited for inducing EHD flow on the micro-scale, and demonstrating electric-field-induced switching of the thermal conductivity. We have successfully achieved both of these goals. This constitutes a major breakthrough as it is the first experimental demonstration of thermal switching in a thin-film device.

Our initial approach to inducing EHD flows was to inject charge from sharp conductive tips into a dielectric fluid which then gets dragged towards the opposite electrode in the electric field. This well-known charge-injection phenomenon occurs in dielectric fluids at high fields above several MV/cm [1]. The first step was to explore this effect in a simple, single-tip geometry. Sharp tungsten tips were fabricated by etching wire in concentrated KOH under AC current, which produced radii of curvature <1000 nm. A single tip was then immersed into a dielectric fluid (such as 3M Novec HFE 7100) in a clear cuvette and precisely positioned close to a planar copper counter electrode, enabling electric fields of up to 15-20 MV/cm at the tungsten tip. Current-voltage curves, charge-injection thresholds, and fluid motions were

measured. The fluid motion was visualized by suspending micrometer-sized beads (latex or silica) in the fluid, illuminating them, and imaging their motion with a high-speed camera. In these experiments we observed an unexpected onset of fluid motion at electric fields that were several orders of magnitude lower than published charge-injection thresholds [2]. We discovered that in some dielectric fluids, vigorous fluid motion occurs between two nominally planar electrodes at fields as low as a few kV/cm. Similar observations have previously been reported in the literature under the broad term of "EDH conduction pumping" [3, 4]; but the underlying mechanism remain poorly understood.
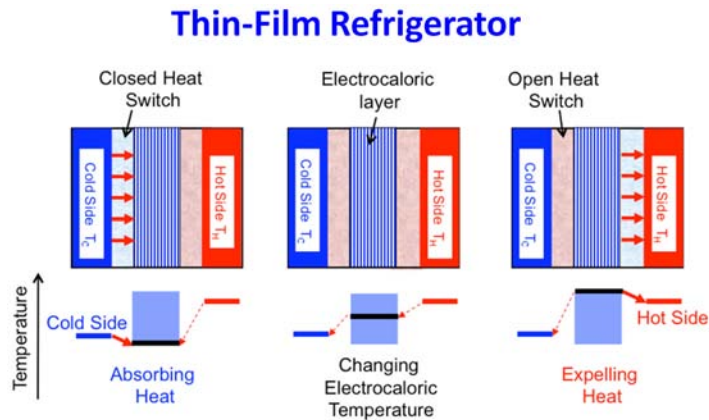

Figure 1. Schematic of a single stage PHE cooler. The top panels show the device when the electrocaloric layer is absorbing heat from the cold side, when it is changing temperature, and when it is expelling heat to the hot side. The bottom panels show the temperature of the layers of the device and the heat flows. The solid arrows show the ideal heat flows and the dashed show unwanted heat leakages.

The study of such EHD flows at low (few kV/cm) electric fields was the focus of the second part of FY11. A microfluidic test cell was designed and constructed, and it allowed the simultaneous measurement of thermal, electrical, and fluid-dynamic properties of thin-film heat switches. A cross-sectional view of the test cell is shown in Figure 2 (left). It consisted of a heated aluminum fluid cup in which a thin-film heat switch could be assembled and tested. The first devices consisted of a substrate 1 inch by 1 inch in size, a silicone gasket with defined thickness (e.g. 0.5 mm), and a copper top cover, which sandwiched the dielectric fluid in the well-defined gap. Thermocouples at the top of the substrate and cover enabled the measurement of the temperature gradient across the device. A thermal or high-speed camera was used to observe the device from above. Two types of devices were designed and fabricated (Figure 3): a conductive silicon substrate containing an array of plasma-etched sharp tips (anode) with the copper top cover being the cathode; and a circuit board containing interdigitated anode and cathode stripes with an electrically passive top cover. We observed thermal switching in both device geometries. Figure 2 (right) presents an example of such a measurement for the etched silicon sample: The top

two traces are the substrate (hot) and cover (cold) temperatures as a function of time going through a sequence of electric field OFF and electric field ON (8 kV/cm). The bottom (dotted) trace is the respective temperature difference. It shows that the thermal gradient across the device of ~1.7 degC (no field) is reduced to ~0.7 degC upon applying the electric field, corresponding to a thermal-conductivity contrast K=2.4. This is direct evidence for electrically-induced convective heat transport in the fluid and is the major accomplishment of the first project year. This result constitutes the first-ever observation of thermal switching in a thin-film device. While the thermal-conductivity contrasts of K=2.4 achieved in this first device is less than our ultimate goal of K>60, we are confident that significant improvements are possible in FY12. Parameters that will be optimized include the type of substrate, type of dielectric fluid, the cover material, and the fluid layer thickness. The fact that we can observe thermal switching from a device with simple patterned electrodes is particularly exciting. It may enable thin-film heat switches that can be fabricated in large area at low cost, and that could be flexible and even transparent.
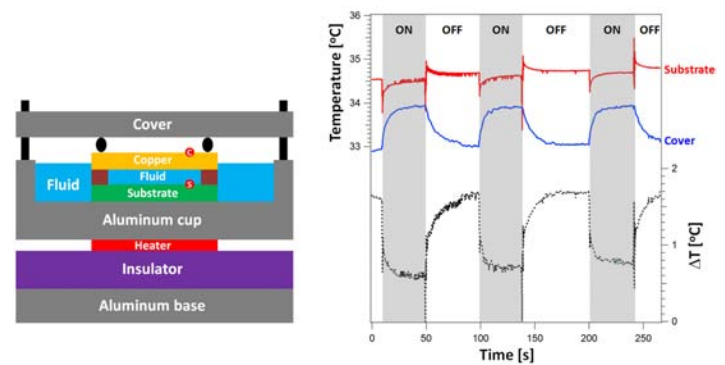

Figure 2. LEFT: Cross sectional view of the microfluidic test cell. A heater creates a temperature gradient across the dielectric fluid layer. The temperature difference is measured by thermocouples at the top of the substrate (S) and copper cover (C) as the high voltage to the device is turned on and off. RIGHT: Heat switching using an etched silicon substrate, a 500-micron thick dielectric fluid film (HFE 7100), and an 8 kV/cm electric field. The upper two traces show the substrate (red) and copper cover (blue) temperature, and the respective temperature difference is shown below (dotted black). A field-induced thermal-conductivity contrast of K=2.4 was achieved in this first experiment.

We conducted additional experiments aimed at elucidating the fundamental mechanism of EHD flow at low field. First, a trace-metal analysis of several commercial dielectric fluids was carried out to address the possibility of dissolved metal ions causing fluid flow under an electric field. The fluids were found to be very pure, having total metal-ion concentrations of ~50 ppb, thus ruling out this mechanism. Second, Raman spectroscopy of the fluids as a function of electric field was performed to probe any field-induced chemical changes such as dissociation. No change in the

Raman spectra was observed upon applying fields up to ~20 kV/cm, indicating that the fluid is chemically stable under such electric fields. Electron paramagnetic resonance (EPR) spectroscopy is currently underway to find evidence for field-induced electron-transfer processes.

Project staff also mentored a Los Alamos High School student and a UC Davis undergraduate student to work on dielectric fluid characterization during the summer months. We also continued our collaboration with Prof. Kevin Malloy (University of New Mexico) and Dr. Richard Epstein (ThermoDynamic Films, LLC) by conducting regular project meetings at the Santa Fe Complex. These collaborators are currently developing the pyroelectric polymer films that will be needed to construct a thin-film heat engine in FY13. Finally, a new collaboration was initiated with Dr. Miad Yazdani (United Technologies Research Center) who is an expert in EHD computational fluid dynamics and who has provided his COMSOL code as the basis for upcoming device modeling tasks.
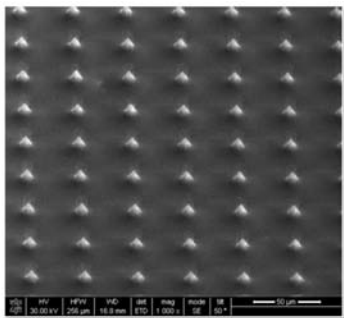
Array of tips in silicon fabricated by SF_6/O_2 plasma etch
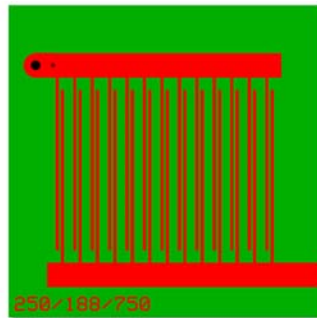
Interdigitated anode/cathode pairs on 1"×1" FR4 circuit board

Figure 3. Samples used for low-field thermal switching experiments (see Figure 2): LEFT: Scanning electron micrograph of array of sharp tips (tip radius of curvature ~700 nm) fabricated by SF_6/O_2 plasma etch into silicon; RIGHT: Layout of interdigitated anode/cathode stripes fabricated on a standard FR4 circuit board.

Future Work

Our research and development has two major goals: modeling, fabricating, and characterizing electrohydrodynamic (EHD) heat switches; and integrating the heat switches with pyroelectric layers to demonstrate a proof-of-concept (POC) pyroelectric heat engine (PHE). The work in FY12 will focus on maximizing the thermal-conductivity contrast of the thin-film heat switches by optimizing the device architecture. This will include fundamental studies of the origins of EHD flow at low fields, computational fluid dynamics to explore the device parameter space, and design, construction, and testing of thin-film heat switches to optimize performance. The collaboration with UNM and ThermoDynamic Films, LLC will continue, and first pyroelectric polymers will be tested in anticipation of a full device integration into a thin-film heat engine in FY13.

Conclusion

We have met the major FY11 project milestone by demonstrating electric-field induced switching of the thermal conductivity for the first time ever. This result was achieved at unexpectedly low electric fields and with simple device structures, providing exciting prospects for creating manufacturable thin-film heat switches in the future. Based on this accomplishment we are on track to explore and optimize the performance of the thin-film heat switches in FY12.

References

1. Castellanos, A.. Coulomb-driven convection in electro-hydrodynamics. 1991. *IEEE Transactions on Electrical Insulation.* **26** (6): 1201.

2. Vazquez, P. A., A. T. Perez, A. Castellanos, and P. Atten. Dynamics of electrohydrodynamic laminar plumes: Scaling analysis and integral model. 2000. *Physics of Fluids.* **12** (11): 2809.

3. Pearson, M., and J. Seyed-Yagoobi. Advances in electrohydrodynamic conduction pumping. 2009. *IEEE Transactions on Dielectrics and Electrical Insulation.* **16** (2): 424.

4. Yazdani, M., and J. Seyed-Yagoobi. Electrically induced dielectric liquid film flow based on electric conduction phenomenon. 2009. *IEEE Transactions on Dielectrics and Electrical Insulation.* **16** (3): 768.

Development of an Interface-Dislocation Dynamics Model to Incorporate the Physics of Interfaces in Predicting the Macroscopic Mechanical Properties of Nanoscale Composites

Jian Wang
20110573ER

Introduction

Experimental measurements at LANL show that metallic nanolayered composites have over two orders of magnitude higher strength than bulk single crystal metals while still preserving high deformability. Atomistic modeling seem to explain this high strength, showing that interfaces are strong traps for single defects. However, currently, there are no models available to predict macroscopic properties (such as strength, work hardening rate, ductility, etc) of nanocomposites; hence, there is a gap between experiments and atomistic models that probe the defect-interface interactions. We propose to develop the first of its kind interface-dislocation dynamics (Interface-DD) model that captures the dynamics of defect ensembles at interfaces at higher length scale. This program pioneers the first Interface-DD model to incorporate the defect-interface interactions with macroscopic mechanical properties, and will fill the gap of materials modeling between atomic-scale model and macro-scale model. The developed model can be validated with existing experimental measurements, and in the future will be applied to predict and control mechanical behavior of nanomaterials in extreme conditions. The development of this Interface-DD model will provide a way to tailor the macroscopic properties of nanolayered composites to make the strongest and most damage tolerant metals known to humankind, with strengths within a factor of two or higher of the theoretical limit. Without such a predictive model to guide materials design, further developments in the properties of nanocomposites can only come from Edisonian approaches.

Benefit to National Security Missions

This project addresses two themes of our Materials Grand Challenge: Defects & Interfaces and Extreme environments. This LDRD project will develop a new modeling tool that is of great significance to programmatic work at LANL, such as the materials science underlying stockpile stewardship and a number of DoD missions, as well as energy applications e.g. turbines. The capabilities to be developed are relevant to DOE/BES objectives as well.

Progress

We advance a concept of "interface strengthening" in designing ultra-high strength, damage-tolerant nanocomposites. Interfaces become crucial in determining the properties of nanoscale materials due to the change of deformation mechanisms from phase-dominated to interface-dominated as length-scale is reduced from micro- to nanoscales. To succeed in this effort, the key challenges are: understanding the role of interface structures and properties during deformation and developing a design principle for high strength composites through control of interfaces.

The breakthroughs achieved in this project will be realized through the development of an interface-DD model to link atomic-scale interface structures and properties with macroscopic material deformation. The development of interface-DD model mainly relies on the understanding of dislocation processes both in the bulk and at the interfaces. Here we summarize the key accomplishments corresponding to the tasks defined in this project.

Task 1: Develop reaction rules of defects interactions at interfaces using atomistic simulations

These rules are necessary in developing interface-DD model, and were not systematically studied at interfaces yet. To do so, we first study the motion of dislocations (lattice and interfacial) at interfaces. Three motion mechanisms are glide, climb, and cross-slip.

We have developed a rule used in the DD-interface code by which we can account for the weak interface shear accompanying with the slip transmission for a single dislocation across the interface [1-4].

Task 2: Develop interface structure description using topological model coupled with atomistic simulations

Interface roles that were not incorporated in existing models are ascribed to the lack of interface model. The interface governs the motion, storage, reassembly (recovery and nucleation), and emission of dislocations. The interface structure includes the atomic arrangement and

the basic geometric features (orientation relationship and interface plane).

We have been developing a geometrical classification scheme by which we can classify the interface into four types [5]. Corresponding to each type of interface, we are analyzing the intrinsic defects, interface shear response, and the influence of interface structure on the interface-dislocation interactions [1, 3, 4].

Task 3: Develop Green's function (GF) for forces calculation

The current DD models do not have stress calculation for defects in anisotropic, multiple interface nanocomposites. GF theory shows the promising in solving stress/strain fields of a defect in anisotropic bi-materials that could be applied to a curved dislocation in multilayered composites.

We have been developing a GF solution for dislocations in anisotropic, multiple interface nanocomposites, and have applied the solution to calculate (1) Elastic fields of dislocation loops in three-dimensional anisotropic bimaterials [6] and (2) predict the critical thickness of the shell in defect-free core-shell nanowires [7].

Task 4:Develop an interface-DD code through implementing reaction rules, interface models, and GF for force calculation into existing DD codes

Currently, we are implementing the rule of slip transmission across a weak interface and twin boundaries.

Future Work
The breakthroughs achieved in this project will be realized through the development of an interface-DD model to link atomic-scale interface structures and properties with macroscopic material deformation. This model incorporates the role of interfaces in storage, recovery, nucleation, and emission of dislocations in interfaces, unlike existing models. The development of interface-DD model mainly relies on the understanding of dislocation processes both in the bulk and at the interfaces. The proposed work builds upon the PI's experience in using atomistic modeling and dislocation theory to understand defect physics at interfaces.

Task 1: Develop reaction rules of defects interactions at interfaces using atomistic simulations.

Task 2: Develop interface structure description using topological model coupled with atomistic simulations.

Task 3:Develop Green's function for forces calculation.

Task 4:Develop an interface-DD code through implementing reaction rules, interface models, and GF for force calculation into existing DD codes.

Conclusion
Through this project, we will develop the first Interface-DD code that can be used in predicting mechanical response of nanocomposites with the interface physics. Moreover, we also provide insight in describing interface structures and properties and building the reaction rules of defect-interface interactions, which can be applied to other continuum scale models, as well as developing a Green function solution for dislocations in multi-phase composites.

References
1. Zhang, R. F., J. Wang, and I. J. Beyerlein. Influence of interface structure on nucleation of lattice dislocations at fcc/bcc interfaces. *Physical Review B* .

2. Chu, H. J., J. Wang, and I. J. Beyerlein. Reactions of a coplanar glide dislocation dipole at high velocity: annihilation, pass-by or twinning? . *Physical Review Letters* .

3. Wang, J.. A Multi-scale Perspective of Interfaces-dominated Mechanical Behavior. 2011. *JOM.* **63** (9): 57.

4. Zhang, R. F., J. Wang, and I. J. Beyerlein. Dislocation Nucleation Mechanisms from fcc/bcc Incoherent Interfaces. 2011. *Scripta Materialia.* **65**: 1022.

5. Wang, J.. Atomistic modeling of dislocation-interface interactions. 2011. In *Advances in HeterogeneousMaterial Mechanics* . Edited by Fan, J., and J. Zhang. , p. 88. China: DEStech Publications, Inc.

6. Chu, H. J., J. Wang, and X. Han. Elastic fields for dislocation loops in three-dimensional anisotropic bimaterials. To appear in *Journal of the Mechanics and Physics of Solids.*

7. Chu, H. J., J. Wang, C. Zhu, and I. J. Beyerlein. Self-energy of elliptical dislocation loops in anisotropic crystals and its application for defect-free core/shell nanowires. 2011. *Acta Materialia* . **59**: 7114.

Publications
Chu, H., J. Wang, I. Beyerlein, and C. Zhu. Self-energy of elliptical dislocation loops in anisotropic crystals and its application for defect-free core/shell nanowires. 2011. *Acta Materialia* . **59**: 7114.

Wang, J.. A Multi-scale Perspective of Interfaces-dominated Mechanical Behavior. 2011. *JOM.* **63** (9): 57.

Wang, J.. Atomistic Modeling of Dislocation-Interface Interactions. 2011. In *Advances in HeterogeneousMaterial Mechanics 2011.* (ShanHai, May, 2011). , p. 91. ShanHai: DEStech Publications, Inc.

Zhang, R., J. Wang, I. Beyerlein, and T. Germann. Dislocation Nucleation Mechanisms from fcc/bcc Incoherent Interfaces. 11. *Scripta Materialia* . **65** (11): 1022.

Efficient and Selective Photon Detection

Michael D. Di Rosa
20090189ER

Abstract

The eavesdropper at a party strains to hear the quietest conversation in the room for a snippet of information. In applications of light detection, it is similarly the fainter signals within the glare of sun and streetlights that are the more interesting. But how does one isolate the signal of interest from the din? Our snoop might excuse himself to an adjacent room, knowing the wall will preferentially transmit the baritone voice he is keen on hearing. Indeed, the wall serves as an acoustic filter, but it also mutes the baritone's voice to unintelligibility. In the technology of light detection, we find a similar compromise between spectral selectivity and signal sensitivity. Techniques that narrow the spectral window of light transmission ordinarily reduce the sensitivity of the overall filtered-detector system, sometimes so drastically that the system cannot see the intended weak light.

In this LDRD program, we attempted to break from this customary tradeoff in light detection. We appealed to a class of phenomena in which lasers manipulate media in such a way that its atoms act synchronously—quantum-coherently—to unusual effect. For example, quantum coherence can be used to convert a medium from opaque to transparent at the switch of a laser. The same type of coherence can also be adapted to a new type of photon detector, an amplifier where entrant faint light triggers a beam-like avalanche of similar photons. Not a laser, theory indicates the amplifier is reasonably low in noise and has a spectral selectivity of 1 part in ten million (equivalent to an inch-wide strip along a 100-mile stretch) but is otherwise blind. The promise of such an amplifier is that it will allow researchers in biology and remote sensing, among others, to detect signals of extremely faint light with surgical spectral precision.

Background and Research Objectives

We want to demonstrate the technology for an optical detector that sits apart from the common compromise between sensitivity and spectral selectivity. In terms of these parameters, we survey in Figure 1 the performance of common and specialized optical and near-infrared detectors as reported in either the literature or manufactur-

ers' data sheets. Sensitivity (vertical axis) is reported by the maximum quantum efficiency (q.e.), and selectivity is cast as spectral resolution, __, of the device in energy units of cm^{-1}. A scale of wavelength resolution, __, is also provided.
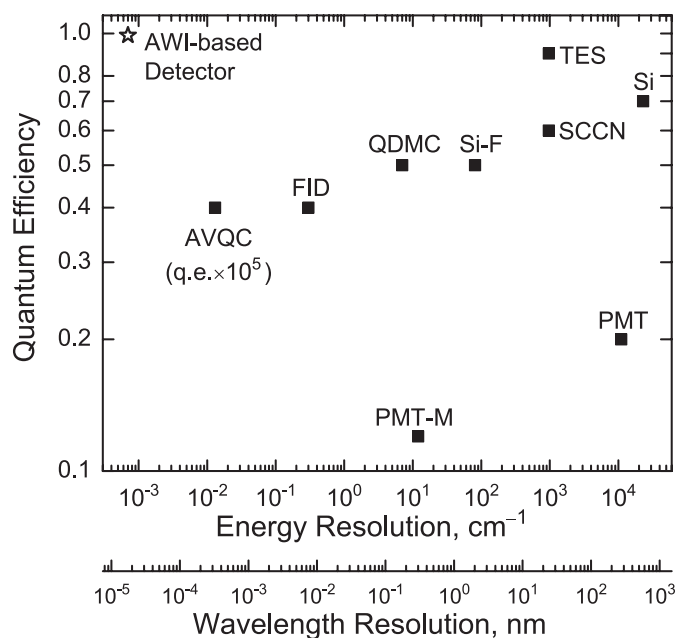

Figure 1. Survey of common and specialized photodetectors in terms of resolution and quantum efficiency. Point AWI pertains to the proposed detector. Other labels refer to detector systems described in the text.

The tradeoff between sensitivity and selectivity is most evident in the use of passive spectral filtering. The ordinary silicon PIN photodiode, with point labeled Si in Figure 1, has a maximum q.e. of 0.7 at 700 nm and a broad bandpass of __ _ 700 nm. High-quality, commercially available transmission filters placed in front of the photodiode can narrow this bandpass to 4 nm but at a loss (~30%) in overall q.e., as seen by comparing point Si to Si-F. A general purpose photomultiplier tube (PMT) that covers the visible to the ultraviolet can detect lower light levels than a Si PIN diode can but at a further drop in q.e. (to about 0.2). A PMT fronted by a monochromator (PMT-

M) makes for a detection system of narrow and tunable resolution of __ ∏ 0.3 nm but with an overall q.e. reduced by 40%, from 0.2 to 0.08.

A variety of cryogenic bolometers offer remarkably low noise, very high single-photon quantum efficiencies, and often a coarse degree of photon-energy resolution. Transition-edge sensors (TES), for example, can detect single photons with nearly 90% efficiency [1] and can distinguish photons differing in energy by about 0.12 eV [2] (equivalent to __ = 24 nm at 500 nm). New single-photon detectors based on a Russian design [3] that use superconducting niobium nanowire (SCNN) have appeared domestically [4, 5]. They offer very fast detection rates of infrared photons at a q.e. of 60% [4] but presently cannot resolve either photon number or energy (we arbitrarily assign the SCCN detector the same energy resolution as the TES bolometer).

Media conditioned by lasers have achieved very narrow-band detection but with varying results in q.e. The atomic vapor quantum counter (AVQC) showed promise for low-noise, narrow-band detection of discrete IR wavelengths but mustered quantum efficiencies of only 4×10^{-6} [6]. Other active schemes that turned to atomic vapors include the fast atomic line filter/field ionization detector (FID) [7] and the resonant ionization detector [8]. Both required one or more tunable pulsed lasers of moderate pulse energies, performed similarly in ___and q.e. (0.3 cm^{-1} and 0.4), and offered minimum detections of 10^4_10^7 photons per pulse. Recent results with quantum dots placed in microcavities (QDMC) have shown that specialty passive detectors can also produce sharp bandpasses (__ = 7 cm^{-1}) with little degradation in q.e. (at 0.5) [9].

In the landscape presented by Figure 1, our detector concept sits apart in performance from others as a combination of the high q.e. and single-photon detection capacity of TES detectors with the narrow bandpass of AVQC detectors. This rare concurrence is brought about by our use of coherent processes that along with producing the overt characteristics of q.e. and __ also suppress noise. The calculated performance of our model system is charted by point AWI in Figure 1. Though particular to our archetypal system, its expected q.e. _ 1 and __ = 7×10^{-4} cm^{-1} are unprecedented figures, individually and combined, among photodetectors.

The acronym AWI stands for Amplification without Inversion and is due a brief explanation. In regular lasers, light is amplified through a condition known as population inversion, a non-equilibrium state akin to keeping the heavy end of a see-saw raised above the light end. A coherently-manipulated medium, however, allows amplification without the expenditure of energy needed to generate and sustain a population inversion. Mainly, AWI is theorized as a means of generating continuous-wave coherent light from the extreme ultraviolet into the x-ray region [10]. Our plan is to research what appears to be the overlooked and special capacity of AWI as a photon and faint-light detector; the

idea grew from our research in the quantum nondemolition detection of photons [11].

Figure 2 summarizes our objective pictorially. The light to be amplified, termed the signal in Figure 2a, traverses a medium prepared for AWI. A drive laser establishes the quantum-coherence that causes AWI-type amplification of the signal. We chose the medium of mercury vapor because, among other technical advantages, it allows for a signal and drive light that are considerably different in color (blue and green, respectively) and therefore easily separated by a filter. Light from a simple mercury germicidal lamp "pumps" the mercury vapor within the cell into the atomic populations conducive to AWI. Figure 2b shows our calculated expectation for AWI by way of the absorption cross section the medium presents to signal light. Positive values for the absorption cross section indicate a complete extinction of signal light by the ~1-cm-long cell. However, signal light within a well-defined and narrow band of frequency (centered about zero detuning in Figure 2b) remarkably happens on a negative absorption cross section, or gain. Renowned theorist Girish Agarwal recognized that these signature spikes of gain of AWI are quite unlike those of lasers and ought to display considerably less noise in amplification [12]. Our culminating goal was thus to demonstrate and characterize the narrow gain of AWI under circumstances, such as widely different signal and drive wavelengths, useful for applications.
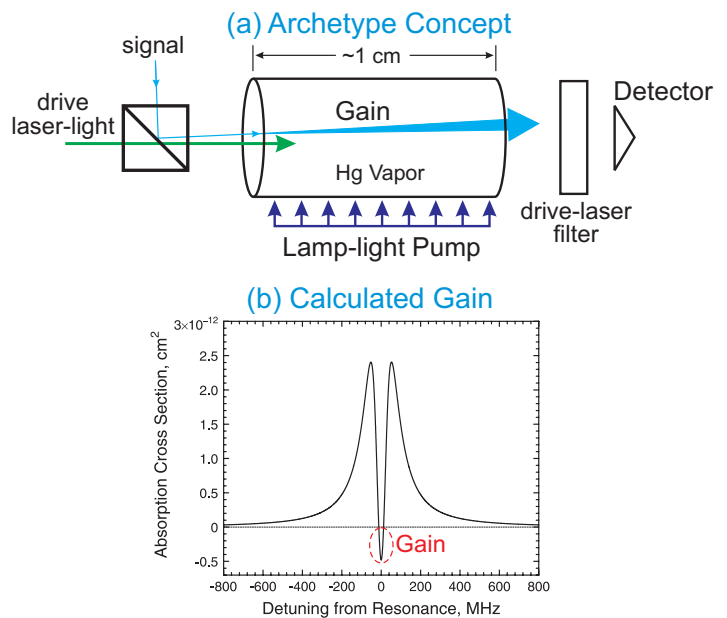
Figure 2. Simple diagram and calculated expectations for our AWI archetype composed from transitions in atomic mercury. (a) Signal light incident on the cell is amplified by AWI on simultaneous, collinear application of the drive laser. Uncommon for AWI research, the drive light (at 546.1 nm) differs greatly in wavelength from the signal light (404.7 nm) for easy rejection by a filter prior to a detector, an important consideration for our intended application. (b) The absorption cross section of the coherently-driven medium turns negative for the signal beam in a narrow region, indicating AWI gain.

Scientific Approach and Accomplishments

AWI makes use of discrete, quantum-mechanical transitions in a medium. Because the use of AWI to detect faint light is conceptually new, we turn to a simple and controllable system of transitions in atomic mercury (Hg). One advantage of using Hg is that we can draw on its vast history in photophysics experiments. Another, as a detail, is that Hg naturally consists of a reasonable abundance of even and odd isotopes with which to experiment. Overall, the spectroscopy of Hg is well known. The drive and signal light of Figure 2 excite precise transitions of atomic mercury (Hg), at 404.7 nm and 546.1 nm, respectively.

Despite its many desirable traits for our research, Hg posed a technical challenge. The atomic states within Hg we needed to manipulate are not occupied at room temperature. Secondly, we had to identify with high precision (*cf*. Figure 2b) the transitions of different isotopes. A spectroscopic study at hair-splitting (1 MHz) resolution of mercury's upper-state transitions was no easy undertaking, we knew, but was prerequisite for knowing and setting the frequencies composing the AWI effect.

It turns out that the needed states are most easily populated by placing Hg vapor in a plasma discharge not unlike those used in household fluorescent lamps. But a plasma discharge is ordinarily a noisy environment, liable to degrade the precision of a spectral measurement. This risk of enlisting a plasma, however, was eventually overcome. Displeased with commercial offerings, we built our own quiet and stable plasma discharge for mercury spectroscopy. We then developed a spectroscopic technique that cuts underneath the collisional noise in the plasma and allows us to observe in fine detail the very component transitions in AWI. Figure 3 shows the progressively better resolution—from the blue trace, to the red, to the black—of the separate transitions composing the "green line" (at 546.1 nm) of mercury as the technique is optimized. Similar spectra were obtained for the blue line, at 404.7 nm. The detail and high level of signal at which we measure these transitions is unseen in the literature for this type of simple mercury discharge. A publication on the discharge design and the spectroscopic technique is being prepared [13]. While the elementary research in laser spectroscopy benefited the AWI program, it might also find use in analytical chemistry, where distinguishing one or more isotopes from others is often paramount. The technique can also be adapted to measurements of the velocity of atoms, ions, and their isotopes, as might be important in research topics of flowing or diffusive plasmas.

By our excursion into high-resolution spectroscopy, we could also lock the drive-laser frequency on a particular transition. We were then ready to measure spectra such as shown in Figure 2b, where the drive-laser frequency is held fixed while the frequency of the probe light (which we obtained from a second laser) is varied to look for features indicative of quantum coherence. The easiest demonstration

of quantum-coherent phenomenon at our disposal was not AWI but the related effect of electromagnetically-induced transparency, or EIT. The experimental arrangement looked much as diagrammed in Figure 2a. A vapor cell containing mercury vapor was optically pumped (with a lamp) in a way that caused the signal beam to suffer absorption on transit. With simultaneous application of the drive beam, signal-beam absorption would still maintain except for, theoretically, a narrow region of complete transparency, the hallmark of EIT. Shown in Figure 4, our measured EIT spectrum for the signal beam is almost the ideal expectation. Few EIT spectra in the literature attain, as we did, nearly perfect transparency when the drive beam is applied. Fewer spectra are seen for the circumstance of disparate wavelengths such as we used. Ordinarily, the signal and drive wavelengths differ by less 0.1%. In our case, the ratio of drive-to-signal wavelengths was 1.35. Our EIT spectrum was an encouraging step toward attaining AWI.
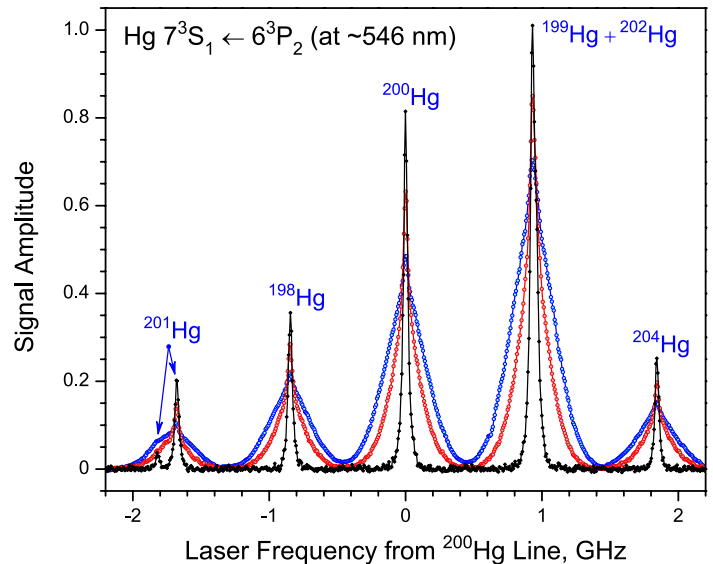

Figure 3. Progression in measurement resolution of the "green line" of atomic mercury to the absolute Doppler-free limit, represented by the black diamonds and trace. All measurements were obtained from a simple, homebuilt dc-discharge plasma of natural Hg in argon. The isotopic identities of the transitions are labeled.

Figure 5 contrasts the absorption spectrum of the probe beam obtained on a later day with that measured under conditions conducive to AWI. The experimental layout of Figure 2a pertains again, though now the optical-pumping light from the lamp could be switched from conditions causing only absorption to that inducing AWI. When the absorption-only case is established, we obtain the blue trace of Figure 5, a spectrum consistent with the blue (absorption) spectrum of Figure 4 measured earlier. Under conditions we believe should induce AWI, the spectrum changes to the red trace (vertically scaled by the right axis).

We cannot yet proclaim evidence of AWI, however. The AWI experiments, conducted in the last days of the pro-

gram, left it unclear whether the positive AWI signals as seen in Figure 5 indicated gain. Given the potential applications for this special light amplifier, along with the fundamental aside and unmet challenge of using AWI as intended for frequency-upconversion [10], we hope to return to this unsettled matter in the near future.
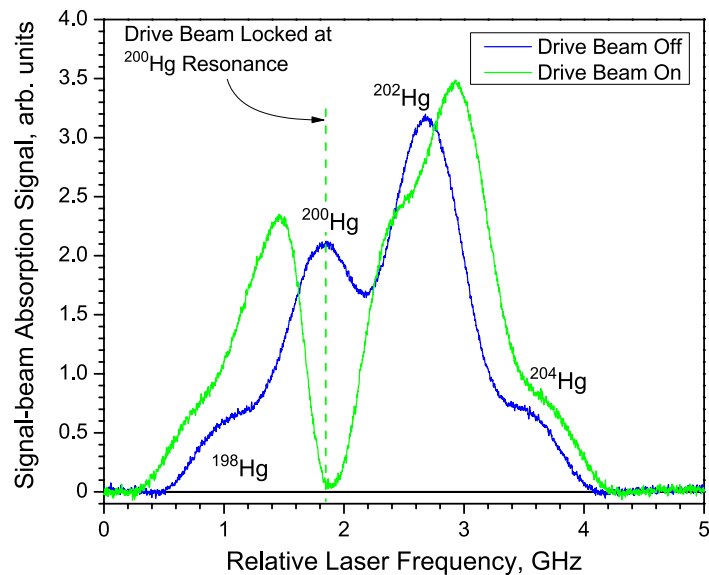

Figure 4. Demonstration of electromagnetically-induced transparency within the absorption spectrum of the signal beam (~404.7 nm). Only in the presence of the drive beam (~546.1 nm) does the signal-beam spectrum switch from absorption to nearly complete transparency. Isotopic transitions are labeled. Isotopic transitions are labeled. EIT was arranged for the transition of Hg-200.
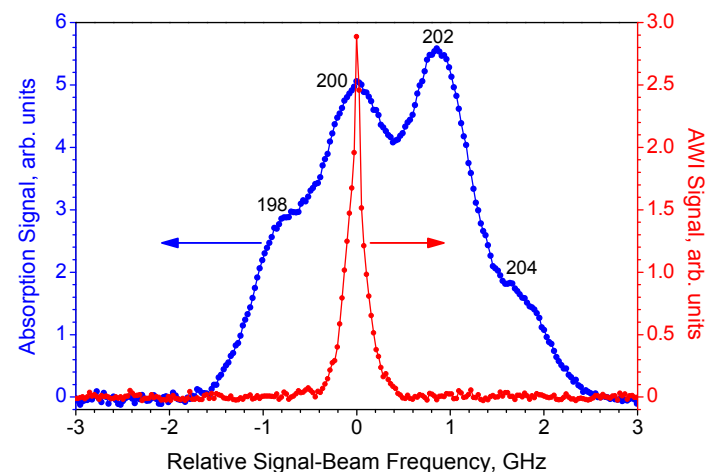

Figure 5. Signal-beam spectra obtained for cases without and with optical pumping conducive to AWI, shown respectively by the blue and red traces. Isotopic transitions are labeled, and AWI was arranged for the transition of Hg-200. The blue trace (left vertical scale) shows the ordinary absorption spectrum for comparison with the red trace (right vertical scale) measured under conditions thought to generate AWI. It is presently unclear whether AWI gain was observed.

Impact on National Missions
Research on light detection, especially of faint signals and single photons, has numerous applications including detecting chemical/biological agents, low-light imaging, and weapons activities. A new weak-light detection method is consistent with many missions including threat reduction, human health, and basic science of interest to DOE, DHS, and other government agencies. Other applications pertain in the field of absolutely-secure quantum communication and quantum-information processing.

References
1. Rosenberg, D., A. E. Lita, A. J. Miller, and Sae Woo Nam. Noise-free high-efficiency photon-number-resolving detectors. 2005. *Physical Review A (Atomic, Molecular, and Optical Physics).* **71** (6): 61803.

2. Kozorezov, A. G., J. K. Wigmore, D. Martin, P. Verhoeve, and A. Peacock. Resolution limitation in superconducting transition edge photon. 2006. *Applied Physics Letters.* **89** (22): 223510.

3. Gol'tsman, G. N., O. Okunev, G. Chulkova, A. Lipatov, A. Semenov, K. Smirnov, B. Voronov, A. Dzardanov, C. Williams, and R. Sobolewski. Picosecond superconducting single-photon optical detector. 2001. *Applied Physics Letters.* **79** (6): 705.

4. Kerman, A. J., E. A. Dauler, W. E. Keicher, J. K. Yang, K. K. Berggren, G. Gol'tsman, and B. Voronov. Kinetic-inductance-limited reset time of superconducting nanowire. 2006. *Applied Physics Letters.* **88** (11): 111116.

5. Annunziata, A. J., A. Frydman, M. O. Reese, L. Frunzio, M. Rooks, and D. E. Prober. Superconducting niobium nanowire single photon detectors. 2006. In *Advanced Photon Counting Techniques ; 1 Oct.* (2006 ; Boston, MA, USA). Vol. 6372, p. 63720V.

6. Gelbwachs, J. A., C. F. Klein, and J. E. Wessel. Infrared detection by an atomic vapor quantum counter. 1978. In *1977 IEEE/OSA Conference on Laser Engineering and Applications.* Vol. QE-14, 2 Edition, p. 77.

7. Bloom, S. H., E. Korevaar, M. Rivers, and C. S. Liu. Fast atomic line filter/field ionization detector. 1990. *Optics Letters.* **15** (5): 294.

8. Petrucci, G. A., R. G. Badini, and J. D. Winefordner. Photon detection based on pulsed laser-enhanced ionization and photoionization of magnesium vapour: Experimental characterization. 1992. *Journal of Analytical Atomic Spectrometry.* **7** (3): 481.

9. Deppe, D. G., A. Kudari, D. L. Huffaker, H. Deng, Q. Deng, and J. C. Campbell. Mode coupling in a narrow spectral bandwidth quantum-dot. 1998. *IEEE Photonics Technology Letters.* **10** (2): 252.

10. Mompart, J., and R. Corbalan. Lasing without inversion. 2000. *Journal of Optics B-Quantum and Semiclassical Optics.* **2** (3): R7.

11. Rosa, M. D. Di. Quantum nondemolition detection of photons (invited). Invited presentation at *Eighth Annual Southwest Quantum Information Technology (SQuInT) Workshop.* (Albuquerque, NM, 17-19 Feb. 2006).

12. Agarwal, G. S.. Inhibition of spontaneous emission noise in lasers without. 1991. *Physical Review Letters.* **67** (8): 980.

13. Mertes, K. M., and M. D. Di Rosa. Simple dc discharge and measurement techniques for Doppler-free spectroscopy of excited-state transitions. 2011. *Review of Scientific Instruments (in preparation).*

Publications

Bradshaw, D., Z. Shi, R. Boyd, and P. Milonni. Electromagnetic momenta and forces in dispersive dielectric media. 2010. *Optics Communications.* **283** (5): 650.

Bradshaw, D., and M. Di Rosa. Vacuum field energy and spontaneous emission in anomalously dispersive cavities. 2011. *Physical Review A - Atomic, Molecular, and Optical Physics.* **83** (5): 053816.

Mertes, K. M., and M. D. Di Rosa. Efficient and selective photon detection using amplification without inversion. Presented at *2009 American Physical Society March Meeting.* (Pittsburgh, PA, 16-20 March 2009).

Mertes, K. M., and M. D. Di Rosa. Building an efficient and selective photon detector using amplification without inversion. Presented at *March Meeting of the American Physical Society.* (Portland, Oregon, 15-19 March 2010).

Mertes, K. M., and M. D. Di Rosa. Simple dc discharge and measurement techniques for Doppler-free spectroscopy of excited-state transitions. 2011. *Review of Scientific Instruments (in preparation).*

Compact Solid State Tunable THz Source

Nathan A. Moody
20090321ER

Abstract

THz lies between the IR/optical and microwave regimes that have formed the cornerstones of most active and passive remote sensing and communications technologies to date. A survey of the spectrum shows that the THz band is dramatically underutilized, prompting the NSF (2004) to indentify THz as a frontier research area because of its potential for discovery science and transformative applications. THz offers strengths which overlap both optical and RF: quasi-optical diffraction limited focusing that enables high resolution imaging with penetrating capability (for such applications as viewing through walls, packaging, and clothes) and beam-like propagation (for applications such as tactical high-bandwidth communications). Importantly, most chemical explosives and their precursors have absorption signatures in the THz band, due to rotational and intramolecular degrees of freedom. This motivates using THz as a robust chemical sensor in a number of versatile configurations (including ones cwhich tend to ameliorate the issue of atmospheric attenuation). Recent experimental and theoretical studies have shown that Intrinsic Josephson Junctions (IJJs), micron-scale structures made of high temperature superconductors, can be made to directly generate and strongly interact with THz signals. A Josephson junction consists of two superconductors separated by a thin insulating layer; an applied DC voltage causes it to oscillate and emit coherent electromagnetic radiation, with frequency proportional to applied voltage. Our work in this project extends the state-of-the art in IJJ-based THz generation by producing a novel device design which enables frequency tunability while addressing the limitations of thermal management and device fabrication.

Background and Research Objectives

The motivation for this project has been the so-called "THz gap," referring to the portion of the electromagnetic spectrum from approximately 0.5 to 10 THz in which there are essentially no practical sources of radiation [1]. This same spectral region, because of its unique propagation characteristics and interaction with matter, corresponds to some of the most exciting applications to date for national security [1-5]. The well established emission techniques for the neighboring microwave and optical regions of the spectrum have proven ineffective for the THz band, despite over a decade of intense effort. The frequency of alternating currents in semiconductors is limited from above by finite electron velocities, while that of conventional lasers is limited from below by non-zero thermal energies which prevent the small electronic transition required for lasing at THz wavelengths. This general lack of THz sources, in particular tunable narrow-band sources, motivated the work in this project to take advantage of the Josephson junction interaction, which *is particularly suited to operate in the THz band*, as it naturally converts a dc voltage into millimeter wave radiation (1 mV corresponds to 0.483 THz) via the Josephson effect [6].

Vacuum electronic devices, such as backward wave oscillators (BWOs), provide milliwatts of tunable power up to about several hundred GHz at high efficiency, but are not practical for portable applications due to their large size (and their need for a high-voltage supply and an external magnetic field). Despite their potential for high power, the same is true of all devices based on modulation of a high energy electron beam: their essential component is a large electron beam accelerator which cannot be made portable or lightweight with today's accelerator technologies. Quantum cascade lasers (QCL) have recently emerged as a new THz source, but these require complicated fabrication of quantum wells, lack tunability, and suffer from high power consumption, short lifetime (several hundred hours), and very low efficiency. Harmonic THz generation using microwave sources is a commercially available technology, but again limited tunability and low efficiency remains a problem because of the losses associated with harmonic up-conversion. Finally, parametric generation is a common optical-based method of launching weak THz signals: two laser beams with slightly different wavelengths beat together in a nonlinear medium such as $MgO:LiNbO_3$. The beat wave can be outcoupled using a silicon prism, but power is limited (μWs) and the system cannot be made portable or robust [1]. In light of these limitations, Intrinsic Josephson junctions (IJJs) are a compelling alternative because our

work in this project has provided a technological pathway to significantly improve upon the deficiencies listed above.

Investigation of Josephson Junctions as high frequency RF sources began as early as 1994, with the fabrication of an array that successfully functioned in the super-radiation regime at GHz frequencies [7]. The total output power was 10µW and was delivered to a load instead of emitted into free space and detected as radiation. The state-of-the-art in using superconductive materials to generate RF uses what are called artificial Josephson junctions [8], as opposed to the *intrinsic* type we are proposing, and consequently suffers from disadvantages which have prevented development of practical THz components. The first problem is that the small energy gap associated with most conventional superconductors limits the upper operating frequency to just a few hundreds of GHz and the large junction dimensions require that they be spaced far (at least one wavelength) apart. Such an arrangement not only requires tedious fabrication but limits the strength of the interaction because only a small number (~100) could ever be made to synchronize. The second problem associated with artificial Josephson junctions is that the insulating layer, artificially grown amorphous material, is not identical from one junction to the next, leading to slight variations in their electrical properties. This likely complicates the process of synchronization and therefore limits the total power of the array.

Our approach advances the state-of-the-art by taking advantage of the *intrinsic* Josephson junction that forms between adjacent layers of certain superconducting materials due to their specific crystal structure [9]. This scheme allows many such junctions, up to 50,000, to fit into the space of one THz radiation wavelength, and the junctions are geometrically identical because the crystal structure of each layer is dictated by the atomic dimensions of the one beneath it. We are essentially letting nature help us overcome what has always been an insurmountable fabrication issue. The intrinsic junction arrangement is crucial because it dramatically enhances the THz interaction over a large spectrum from 0.3 to ~10 THz, enabling a technology path toward practical devices. For example, as a source the IJJs enable the junctions to interact with one another such that their output is in phase with output power, proportional to the number of junctions squared, approaching milliwatt levels with an anticipated efficiency of ~30%.

The present state-of-the-art involves the use of IJJs in what is termed a "mesa structure," as designed by a group in Argonne and shown in Figure 1 [10]. This is so far the only configuration of a junction stack that has produced THz radiation and it does so by coupling the individual junctions through a cavity resonance that is set up in the device itself [11]. This was an excellent proof-of-principle demonstration which motivates further research, including the tunable structures in our project, but progression beyond this initial demonstration has stagnated within the last four years [12]. There are several problems with the mesa-type devices that prevent them from scaling beyond their present demonstrations. The first problem is thermal management, referring to how one manages the heat generated within the junction stack. In the mesa geometry, the conduction of heat from within the sample to the substrate occurs along the crystal axis with the worst thermal conductivity. Secondly, because the mechanism for synchronizing the individual junctions depends upon a cavity field within the device (i.e., a resonant cavity whose physical dimensions fix the resonant frequency), it is inherently a fixed-frequency source. Thirdly, mesa structures have difficulty scaling to higher frequency, as is required to achieve true operation in the THz band, because current fabrication techniques produce mesas with slightly slanted walls degrading the quality factor of the effective cavity. This, in turn, reduces the coupling effect which provides the synchronization, especially at higher frequencies. Most importantly, the largest limitation to the conventional mesa design (i.e., Figure 1) is the fact that they must remain very small in height, about 1 micron. This limits the number of junctions in the mesa and therefore also strictly limits the power to several microwatts [13]. These fundamental problems, namely a lack of frequency tunability as well as the inability to scale to higher frequencies and powers, have motivated the direction of research in this project.
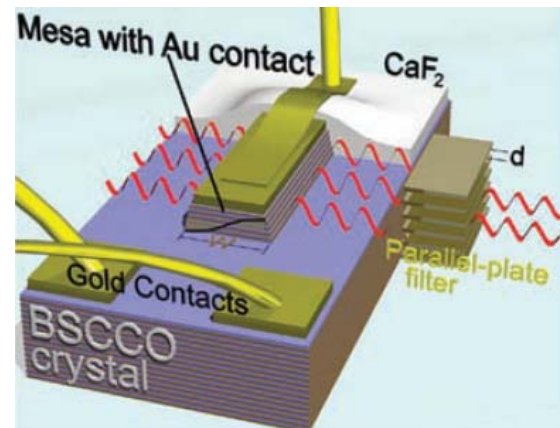

Figure 1. Circa 2007 state of the art (Argonne National Laboratory) mesa structure in BSCCO utilizing cavity resonance for synchronization of intrinsic Josephson junctions.

The research objectives in this three-year project have been to develop a new device design which does not require cavity resonances to achieve junction synchronization, identify and develop the fabrication tools required to work with the chosen material, and develop methods for validating the emission of THz radiation and characterizing performance. These objectives are slightly different than those originally stated in the proposal. We first attempted to push the limits of readily available conventional techniques, such as photolithography and focused ion beam milling, with the hope of rapid prototyping. However, we found these techniques, when applied to the required etch depths in this project, led to inferior results. Therefore,

the priority in years 2-3 shifted toward completion of a suite of fabrication techniques which enable construction of near-perfect IJJ devices starting from high purity single crystals. We are pleased to report the development of new techniques which together yield a start-to-finish technology pathway for our proposed devices. Prior to the end of the project, we demonstrated the feasibility of these techniques and began device fabrication in earnest.

Scientific Approach and Accomplishments

Understanding the fundamental IJJ oscillation was our starting point in this research program, occupying the entire first year of work. We selected the superconducting material $Bi_2Sr_2CaCu_2O_8$ (known as BSCCO) because it uniquely manifests intrinsic Josephson effects and LANL has proven experience in its fabrication [14]. Since our structures are small with a moderate anticipated heat load, they can be cooled using compact, lightweight (<250g) commercial cryo-cooler modules. Analytical models were developed during the first year which enabled an idealized device design and which led to important studies of dc-to-rf efficiency [15], stability of synchronized oscillations [16], and calculated linewidth of radiation [17]. These important studies, which led to eventual publications, led us to develop a realistic design which recognizes and accommodates the limitations of device fabrication. This second year of work led to a patent application on the idealized source design and defined the scope of work for the 3rd year, which became development of the specialized fabrication techniques required to transition the device design to real single crystals of BSCCO while addressing issues such as heat load and preservation of crystalline purity. This source design also led to a best-paper award at the 2010 DOE Tri-Lab LDRD Symposium in Washington, DC. It is shown diagrammatically with dimensions in Figure 2.
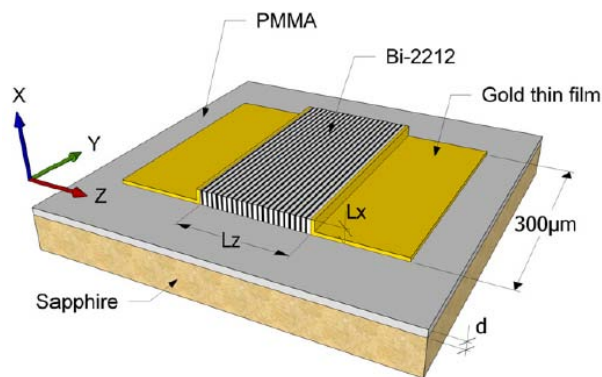

Figure 2. Idealized tunable (planar) Intrinsic Josephson junction source made of Bismuth based high temperature superconducting film (known as Bi2212 or BSCCO) attached to sapphire substrate with organic adhesive, poly(methyl methacrylate) or PMMA.

The final year of the project focused on development of a practical device design which preserves the essential features of the idealized structure (Figure 2) used in the analytical modeling effort but also accounts for constraints in device fabrication and thermal management. Fabrication techniques were also systematically developed to arrive at such a structure starting from bulk single crystal. This represented an ambitious body of work to be accomplished within the final year, but we have indeed completed these last crucial steps, as discussed below.

The large (up to 50,000) number of IJJs required defines the minimum necessary thickness (along c-axis) of the BSCCO crystal – tens or even hundreds of microns. Such thicknesses are routine for single crystals but are yet not achievable with the thin layer technology. The other (*a*- and *b*-) dimensions of the designed source structure are about the same size or larger. Consequently, to define the active (emitting) area of the one has to be able to process (remove) large volumes of the bulk. This precludes the use of conventional fabrication techniques, as discussed above. We instead developed a novel multi-stage technological procedure. First, the BSCCO crystal, as shown in Figure 3, is cut into blocks sized ~1 mm x 300 µm x 100 µm by precision wire saw. Low resistance Au contact pads are deposited onto the (unglued) sample after pre-etching which removes surface contamination/oxidation. The sample then can be annealed in oxygen atmosphere for reduced contact resistance.
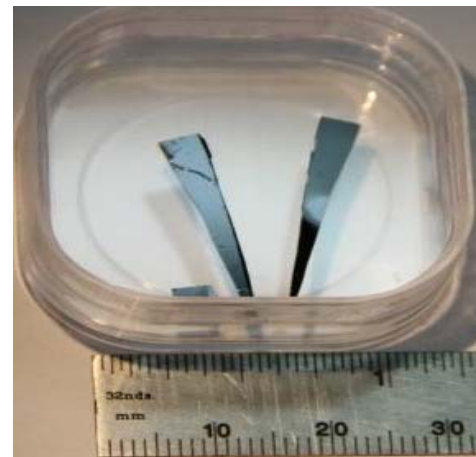
Figure 3. Large single crystals of BSCCO; reflective surfaces indicates high quality.

The desired geometry is obtained by a series of etches in a broad ion beam (10 kEV Ar @ 250 uA current with ~1 mm beam diameter). The complex geometry, shown in Figure 4, requires a multiplicity of masks which must be thick (comparable to or thicker than the sample itself) and precisely aligned with the sample. For the bottom trench, a slot in the substrate is cut by precision wire saw. For the top trenches, commercially available slot-type TEM grids are used, as well as single- or double-blade fixtures designed specifically for the broad ion beam. The blade's sharpened surface is nearly vertical and results in almost

perfect vertical sidewall of the etched sample, as shown in Figure 5. Both types of masks are suspended over the sample in a specialized fixture that allows precise alignment by set-screws. Although expected efficiency of the device is very high, the vast majority of power in the device is dissipated as heat within the sample [18]. Therefore, after the required geometry of BSCCO crystal is defined by etching, a heat sink made of single crystal with high thermal conductivity (e.g. MgO) can be glued directly to the sidewall of the active (emitting) area. The smooth sidewall, as shown in Figure 5, allows the use of very thin glue layer, minimizing the effect of poor heat transfer in organic glues. Another advantage of the design is that the heat transfer from the bulk of the crystal's active volume (hottest point) proceeds via *ab*-planes rather than in *c*-axis direction, resulting in an order of magnitude increase in thermal conductivity. Especially for the thin (5-10 μm) tunable-type structures, this approach to cooling is particularly effective.
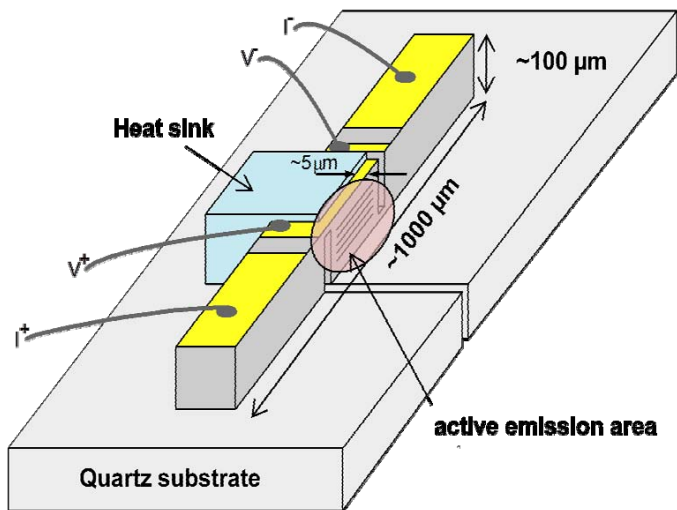

Figure 4. Schematic of practical IJJ source design, based on zig zag geometry, including integrated heat sink and gold contact pads.

Within a matter of months, we expect to measure THz radiation power and characterize frequency tunability of these new devices (using a small amount of short-term follow-on funds from Office of Naval Research). Our prototype devices are a result of approximately 50 fabrication cycles which were closely examined using scanning electron microscopy throughout the process to monitor quality and make adjustments to the broad ion beam etch process. The demonstration of these devices will occur by the end of CY11 in an optical cryostat that has been coupled to a sensitive THz bolometer. The design and fabrication of our frequency tunable THz source was filed for patent application (#12-421073) and was given a publishing number (0062423-A1) in March, 2011. We strongly anticipate that the intellectual property and eventual performance data from this project will result in a compelling capability at

the Laboratory for attracting larger follow-on programs in THz science and science of signatures as well as potential licensing of key technologies.
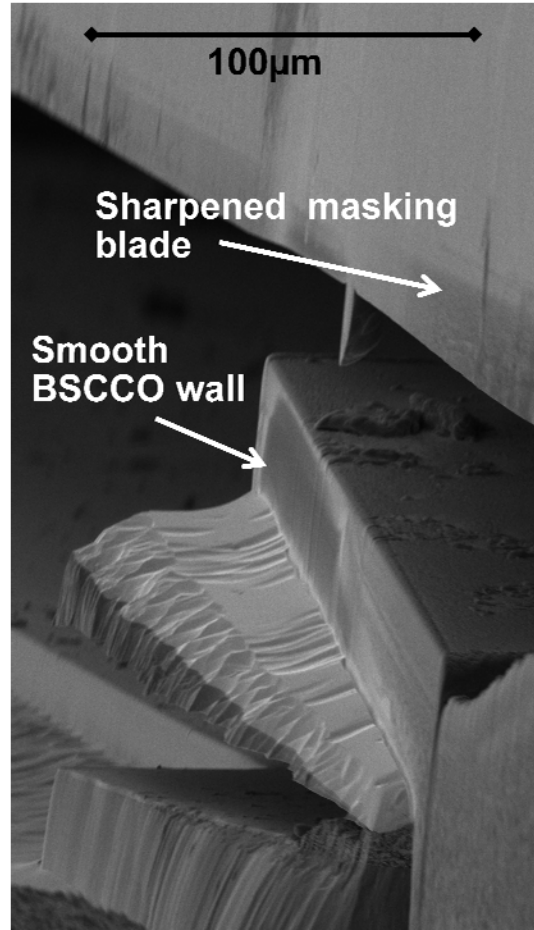
Figure 5. SEM micrograph illustrating the sharp masking blade for the broad ion beam and the resulting smooth sidewall of a deep cut in BSCCO.

Impact on National Missions
This project impacts a broad range of missions centered on imaging, sensing, and high-speed tactical communications. Enhancing our understanding of THz radiation particularly suited to spectroscopy applications for detection of chemical, nuclear, and biological threats, supporting threat reduction and other missions, is particularly critical to DOE, DOD, DHS, and other government agencies.

References
1. Tonouchi, M.. Cutting-edge terahertz technology. 2007. *Nat. Photon.*. **1** (2): 97.

2. Federici, J., B. Schulkin, F. Huang, D. Gary, R. Barat, F. Oliveira, and D. Zimdars. THz imaging and sensing for security applications, explosives, weapons and drugs . 2005. *Semicond. Sci. Technol.*. **20** (7): S266.

3. Moore, D.. Recent Advances in Trace Explosives Detection Instrumentation. 2007. *Intl. Journ. Sens. and*

Imag.. **8** (1): 9.

4. Rosker, M.. Opportunities for the Application of Terahertz Technologies in Defense. Marc. *SURA Applications Symposium.*

5. Sherwin, M. A., P. H. Bucksbaum, C. A. Schmuttenmaer, J. Allen, S. Biedron, L. Carr, M. Chamberlain, T. Crowe, F. DeLucia, Q. Hu, B. Jones, B. Noordham, T. Norris, J. Orenstein, K. Unterrainer, L. Van der Meer, I. Wilke, G. Williams, X. C. Zhang, A. Cheville, A. Markelz, B. Parks, P. Plancken, J. Shan, B. Austin, D. Basov, D. Citrin, W. Grundfest, T. Heinz, J. Kono, D. Mittleman, P. Siegel, T. Taylor, B. Jones, A. Markelz, M. Martin, K. Nelson, T. Smith, G. Williams, M. Allen, R. Averitt, L. Brunel, T. Heilweil, J. Heyman, P. Jepsen, R. Kaind, W. Leemans, L. Mihaly, C. Rangan, H. Tom, V. Wallace, and D. Zimdars. DOE-NSF-NIH Workshop on Opportunities in THz Science, February 12-14, 2004. 2004.

6. Josephson, B. D.. Possible new effects in superconductive tunnelling. 1962. *Phys. Lett..* **1** (7): 251.

7. Han, S., B. Bi, W. Zhang, and J. E. Lukens. Demonstration of Josephson effect submillimeter wave sources with increased power. 1994. *Appl. Phys. Lett..* **64** (11): 1424.

8. Barbara, P., A. B. Cawthorne, S. V. Shitov, and C. J. Lobb. Stimulated Emission and Amplification in Josephson Junction Arrays. 1999. *Phys. Rev. Lett..* **82** (9): 1963.

9. Kleiner, R., and P. Müller. Intrinsic Josephson effects in high-temperature superconductors. 1994. *Phys. Rev. B.* **49** (2): 1327.

10. Ozyuzer, L., A. E. Koshelev, C. Kurter, N. Gopalsami, Q. Li, M. Tachiki, K. Kadowaki, T. Yamamoto, H. Minami, H. Yamaguchi, T. Tachiki, K. E. Gray, W. K. Kwok, and U. Welp. Emission of Coherent THz Radiation from Superconductors. 2007. *Science.* **318** (5854): 1291.

11. Wang, H., and . . Coherent Tetrahertz Emission of Intrinsic Josephson Junction Stacks in the Hot Spot Regime. 2010. *Physical Review Letters.* **105** (5): 057002.

12. Benseman, T. M., A. E. Koshelev, K. E. Gray, W. K. Kwok, U. Welp, K. Kadowaki, M. Tachiki, and T. Yamamoto. Tunable terahertz emission from Bi2Sr2CaCu2O8+d. 2011. *Physical Review B.* **84** (6): 064523.

13. Kadowaki, K., H. Yamaguchi, K. Kawamata, T. Yamamoto, H. Minami, I. Kakeya, U. Welp, L. Ozyuzer, A. Koshelev, C. Kurter, K. E. Gray, and W. K. Kwok. Direct observation of tetrahertz electromagnetic waves emitted from intrinsic Josephson junctions in single crystalline Bi2Sr2CaCu2O8+d. 2008. *Physica C: Superconductivity.* **468** (7-10): 634.

14. Jia, Q. X., S. R. Foltyn, P. N. Arendt, and J. F. Smith. High-temperature superconducting thick films with enhanced supercurrent carrying capability. 2002. *Appl. Phys. Lett..* **80** (9): 1601.

15. Moody, Nathan A., Lev N. Boulaevskii, and . . Optimized THz emission from intrinsic Josephson junctions. 2011. In *Proc. SPIE.* (Orlando). Vol. Proc. SPIE 8023, 1 Edition, p. 80230J.

16. Martin, I., Gabor B. Halasz, L. N. Bulaevskii, and A. E. Koshelev. Shunt-capacitor-assisted synchronization of oscillations in intrinsic Josephson junctions stack. 2010. *Journal of Applied Physics.* **108** (3): 033908.

17. Bulaevskii, L. N., I. Martin, and G. B. Halasz. Intrinsic lineshape of Josephson radiation from layered superconductors. 2011. *Physical Review B.* **84** (1): 014516.

18. Kurter, C., K. E. Gray, J. F. Zasadzinski, L. Ozyuzer, A. E. Koshelev, L. Qing'an, T. Yamamoto, K. Kadowaki, W. K. Kwok, M. Tachiki, and U. Welp. Thermal Management in Large Bi2212 Mesas Used for Terahertz Sources. 2009. *Applied Superconductivity, IEEE Transactions on.* **19** (3): 428.

Publications

Bulaevskii, L. N., A. E. Koshelev, and M. Tachiki. Shapiro steps and stimulated radiation of electromagnetic waves due to Josephson oscillations in layered superconductors. 2008. *Physical Review B (Condensed Matter and Materials Physics).* **78** (22): 224519.

Bulaevskii, L. N., A. E. Koshelev, and M. Tachiki. Shapiro steps and stimulated radiation of electromagnetic waves due to Josephson oscillations in layered superconductors. 2008. *Physical Review B (Condensed Matter and Materials Physics).* **78** (22): 224519.

Bulaevskii, L. N., I. Martin, and G. B. Halasz. Intrinsic lineshape of Josephson radiation from layered superconductors. 2011. *Physical Review B.* **84** (1): 014516.

Bulaevskii, L. N., and A. E. Koshelev. Stabilization of synchronized oscillations and radiation line width of intrinsic Josephson junctions. Invited presentation at *The 7th International Symposium on Intrinsic Josephson Effects and Plasma Oscillations in High T-c Superconductors (PLASMA 2010).* (Hiosaki, Japan, 29 April - 2 May, 2010).

Koshelev, A. E., and L. N. Bulaevskii. Resonant electromagnetic emission from intrinsic Josephson-junction stacks with laterally modulated Josephson critical current. 2008. *Physical Review B (Condensed Matter and Materials Physics).* **77** (1): 014530.

Martin, I., Gabor B. Halasz, L. N. Bulaevskii, and A. E. Koshelev. Shunt-capacitor-assisted synchronization of os-

cillations in intrinsic Josephson junctions stack. 2010. *Journal of Applied Physics.* **108** (3): 033908.

Moody, Nathan A., and Lev N. Boulaevskii. Optimized THz emission from intrinsic Josephson junctions. 2011. In *Society of Photo-optical Instrumentation Engineers.* (Orlando, 25-27 April 2011). Vol. 8023, 1 Edition, p. 80230J. Orlando, FL: SPIE.

Yurgens, A., and L. N. Bulaevskii. Temperature distribution in a stack of intrinsic Josephson junctions with their CuO-plane electrodes oriented perpendicular to supporting substrate. 2011. *Superconductor Science and Technology.* **24** (1): 015003.

Hyperspectral Satellite Instrument for Environmental Treaty Verification

Steven P. Love
20110456ER

Abstract
A satellite-based greenhouse gas monitoring system will likely need to be developed in the near future in order to address the verification requirements for upcoming climate treaties. This project addresses the question of what type of instrument would best serve this purpose. In a combined atmospheric radiative transfer simulation and instrument performance modeling study, issues of spectral band selection, mitigation of interference by other atmospheric gases, and the trade-off between spectral resolution, signal-to-noise ratio, and ultimate retrieval accuracy are quantitatively compared for the two major types of hyperspectral imager — dispersive spectrometers and Fourier transform spectrometers.

Background and Research Objectives
In coming years, an international treaty to limit and regulate greenhouse gas emissions will likely be agreed upon. But any treaty can be effective only if it can be verified. A satellite-based system for monitoring CO_2, other greenhouse gases (GHGs), and co-emitted source-attribution signature gases (e.g. CO, SO_2, NO_x) appears the most workable solution. Existing satellite instruments, however, are grossly inadequate for treaty verification, with even the newest generation, such as Japan's GOSAT and NASA's OCO / OCO-2 (Orbiting Carbon Observatory), being narrowly designed for specific scientific missions and ill-suited to treaty verification. Their coarse spatial resolution (~10x10 km^2 and ~1.6 x 1.6 km^2 for GOSAT and OCO, respectively) precludes detailed, sensitive observation of the highly localized sources (e.g. power plants) responsible for a major fraction of a typical nation's carbon emissions. High spatial resolution hyperspectral imagery, on scales of meters or tens of meters, would enable close-ups of localized sources at the point of emission, where gas concentrations are many times higher than downwind, alleviating the daunting problem of the large and variable natural background that plagues dilute low-spatial-resolution measurements. It would also allow co-emitted signature gases to be accurately characterized for individual power plants, eventually enabling nation-level assays of power plant emission profiles and subsequent long-range track-ing and attribution. Given these advantages, a high spatial resolution hyperspectral imager will likely emerge as a key component of any GHG treaty verification system.

Despite shortcomings, existing instruments do exemplify two very different instrumental strategies, either of which might be adapted to treaty verification: OCO's narrow-band, high-resolution dispersive spectrometers aim at high-accuracy CO_2 retrievals in daylight, and nothing else. GOSAT, with its wide spectral coverage Fourier transform spectrometer (FTS), aims at a broad survey of many gases, and has thermal IR nighttime capability, but sacrifices sensitivity for generality.

What form should a treaty verification instrument take: OCO-like dispersive spectrometers, or a GOSAT-like Fourier transform spectrometer? Which instrument type will provide the greatest sensitivity to GHGs and source-attribution trace gases? What sensitivity levels are possible with the current state of the art in infrared detectors, and what are the fundamental physical limits? This small one-year, 0.3 FTE study aimed to answer these questions, and leave us with a highly capable set of modeling tools for exploring detailed variations on these instrument design questions in the future.

Scientific Approach and Accomplishments
This study proceeded in two parts. First, we model the radiative transfer problem, following the light from the surface, through the atmosphere, to the satellite, to predict how a change in gas amount manifests as a change in spectral radiance at the satellite. Next, we model the instrument itself, taking into account its available observing time, its mode of operation, and detailed parameters of its detectors and optics.

A brief examination of CO_2 retrieval illustrates the sorts of things learned from our radiative transfer modeling. Early on, we determined that the best spectral region for CO_2 quantification is the near-infrared. Two prominent near-infrared CO_2 vibrational-rotational bands lie in this region, centered near 2.06 μm and 1.6 μm, the 2.06 μm band having the stronger absorption. Because atmospheric aerosols interfere with CO_2 retrieval, and aerosol

scattering varies inversely with wavelength, the longer-wavelength 2.06 µm band is better suited to CO_2 retrieval.

Perhaps the most important interference, however, comes from water vapor, as illustrated in Figure 1, which compares modeled satellite-level radiance in the 2.06 µm band with high-resolution observations. The numerous line shape distortions seen here are caused by interfering water vapor lines. Only the two central lines in Figure 1 are essentially undisturbed by water vapor. Water vapor interference is usually handled by fitting observed radiances with calculated model radiances, varying the amount of CO_2 and H_2O until acceptable agreement is reached. An alternative approach – preferred for a simple one-task instrument – is to select for retrieval only those lines unaffected by water vapor. About ten CO_2 lines in the 2.06 µm band are virtually unaffected by H_2O; one is visible in Figure 1, near 4864.8 cm^{-1}. Although at line-center this line is almost 100% absorbing and therefore unsuitable for CO_2 retrieval with a high spectral resolution instrument, at its shoulders it is quite sensitive to CO_2 amount. Which location offers the highest sensitivity? This depends on the spectral resolution of the instrument. At high resolution (0.1 cm^{-1}) the region between the lines is sensitive to CO_2 (Figure 2a), while the center of the line, being almost completely absorbed, is insensitive (Figure 2b). At lower spectral resolution of 1 cm^{-1} (Figure 2, c and d) both the between-line and at the line-center regions are sensitive to CO_2 amount, with line-center radiance changing by about 6% with the CO_2 changing from 370 to 405 ppmv, while the between-line radiance changes by about 4.5%. Thus most sensitive retrieval can be achieved at the center of absorbing line with a theoretical sensitivity of about 0.17% per 1 ppmv of CO_2. Such considerations feed into the choice of instrument resolution and spectral coverage.

To understand the instrument modeling part of the problem, let us begin by considering ultimate limits. At the most fundamental level, any spectral instrument's sensitivity is limited by the nature of light itself. Light is composed of discrete packets of energy, known as photons, and these arrive not in a precisely timed stream, like machine gun bullets, but randomly, more like raindrops. For a given an average brightness, the exact number of photons arriving in a given time interval fluctuates randomly, by an amount whose average equals the square root of the total number of photons in that time interval. These statistical fluctuations make light intrinsically noisy, and proportionally noisier as it gets dimmer. This "photon shot noise" sets the fundamental limit on the signal-to-noise performance of any optical system. In real instruments, noise from the detector and associated electronics can further degrade the performance; these contributions must be modeled as well.
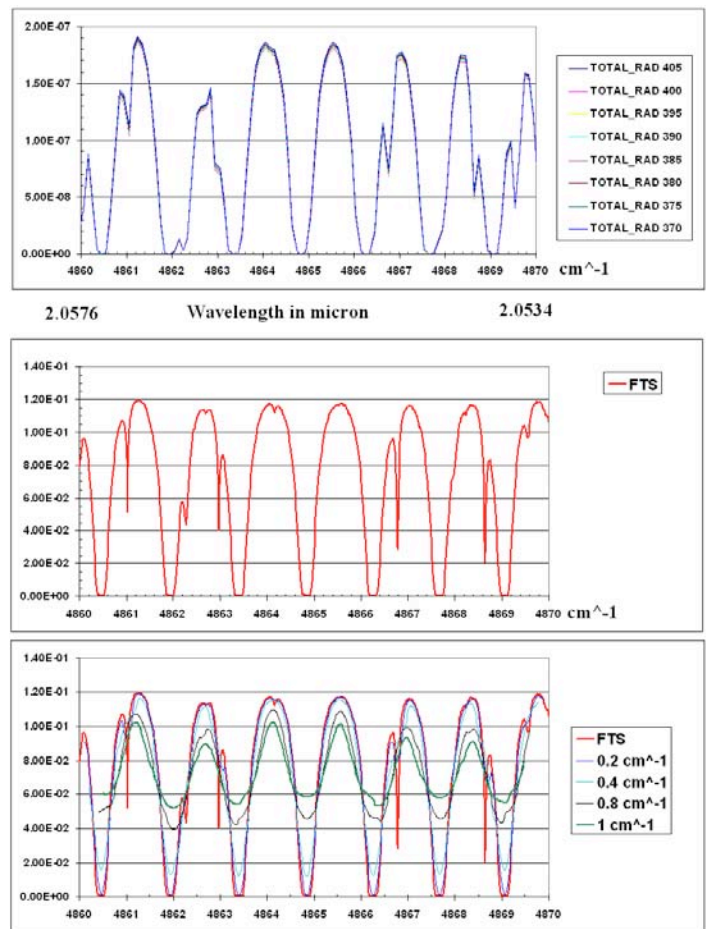

Figure 1. Satellite-level radiances (in relative units), (a) for different columnar CO_2 concentration (from 370 to 405 ppmv) in the 4860-4870 cm-1 range, calculated using the MODTRAN radiative transfer program at spectral resolution of 0.1 cm-1; (b) spectral radiances observed by the LANL-owned high spectral resolution (0.02 m-1) FTS instrument located at the Four Corners, NM, site; and (c) the FTS spectral radiances averaged over an indicated spectral width windows. (Throughout this report, we often follow the spectroscopists' convention of expressing spectral position and resolution in terms of wavenumber, the reciprocal of wavelength, in units of cm-1, rather than in terms of wavelength.)

In this study, we consider the two most well established and proven types of spectral imager. These instrument types use radically different strategies for obtaining spectral information, and make use of the available time and photon flux in very different ways. The first is the familiar dispersive spectrometer, which uses a prism or diffraction grating to separate light into its component wavelengths and spread them spatially across a detector array. One dimension of the 2-dimensional detector array is devoted to spectral information, with a full row of pixels devoted to recording the spectrum of a single spatial pixel in the scene, so that the instrument can only image a single line of the scene at a time. The full 2D spatial image is built up by sweeping this line across the scene using the motion of
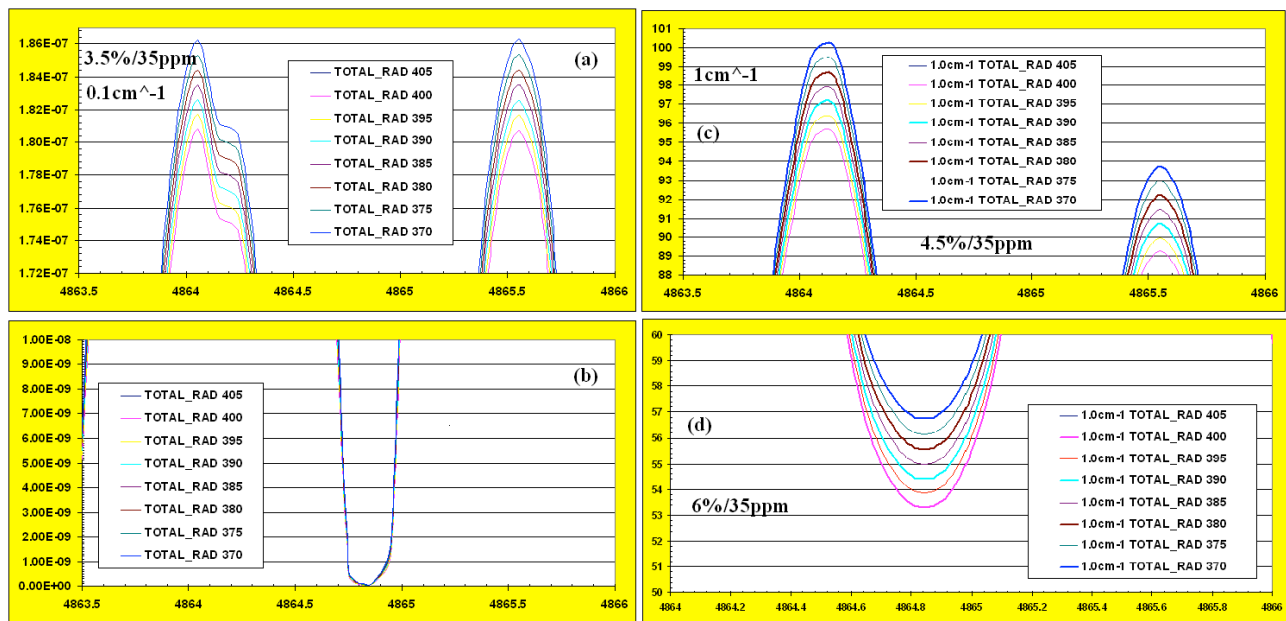
Figure 2. Satellite-level radiances (in relative units) for CO_2 columnar amounts from 370 to 405 ppmv, calculated using the MODTRAN radiative transfer code for the case of mid-latitude summer atmosphere. The sensitivity (defined here as a percentage change of a maximum radiance corresponding to 35ppmv change in CO_2 amount) varies between 3.5% and 6% per 35 ppmv depending on the position of measurement (at the center of the line or between lines), and on the spectral resolution of the instrument.

the satellite platform. This is known as push-broom imaging. The second instrument type is the Fourier transform spectrometer (FTS). The FTS uses a partially reflecting, partially transmitting mirror, a "beam splitter," to send light down two possible paths, including one whose length can be varied by a movable mirror. Mirrors at the ends of each path send the light back to the beam splitter, which recombines the light from the two paths and sends them to the detector array. Because light has a wave nature, these two components interfere with each other: If the wave crests from one path land on the troughs from the other path, the two waves cancel each other and the detector sees darkness (destructive interference). If crests land on crests and troughs on troughs, the two waves reinforce each other and the detector sees light of doubled brightness (constructive interference). Depending on the position of the moving mirror, a given wavelength will experience either constructive or destructive interference, making its signal go up and down as the mirror is moved. The mirror performs a carefully monitored scan, and each pixel records the resulting interference pattern. A mathematical analysis of the interference pattern, a Fourier transform, is then used to calculate the spectrum. The greater the distance the moving mirror scans, the finer the spectral resolution.

Two major differences between the instrument types are immediately apparent. First, because the FTS sends all the light within the spectral region of interest to the detector at once, whereas the dispersive spectrometer breaks it up into narrow spectral bins, the FTS presents much more light to the detector, typically hundreds to thousands of

times more. This means that any noise from the detector or electronics is much less an issue for the FTS. Secondly, the dispersive spectrometer uses all its available observation time simply to stare and integrate each spectral band, whereas the FTS must use its time to perform the mirror scan. To achieve finer spectral resolution in a dispersive spectrometer, it must be redesigned with greater dispersion and more pixels. However, once this is done, every pixel again gets to use the full observation time to integrate the incoming light. In contrast, finer resolution in an FTS is achieved simply by scanning the mirror further, but this must be done within the same available observation time, so that finer resolution means faster scans and less time devoted to each data point in the interference pattern. The end result is that, in the dispersive spectrometer, the signal-to-noise ratio (SNR), all else being equal, increases as the square root of the width of the spectral bins as resolution is made coarser, whereas in the FTS, SNR increases linearly with spectral bin width.

There is always a tradeoff between spectral resolution and SNR. Finding the optimal spectral resolution that optimizes sensitivity to gases for each instrument type is one key question answered in this study. If the resolution is coarse, gas absorption lines appear broad and shallow. As resolution is improved, they appear narrower and deeper, providing a larger signal, until the instrument can fully resolve the true line shape. However, finer resolution always leads to lower SNR. The optimum strategy is quite different for the two instrument types, as illustrated in Figure 3. In the FTS, noise increases so rapidly with improving reso-

lution that it is actually better to use as coarse a resolution as will still allow features of interest to be separated from interfering features. The dispersive instrument's noise increases more slowly, and it is advantageous to make the resolution as fine as technologically feasible.
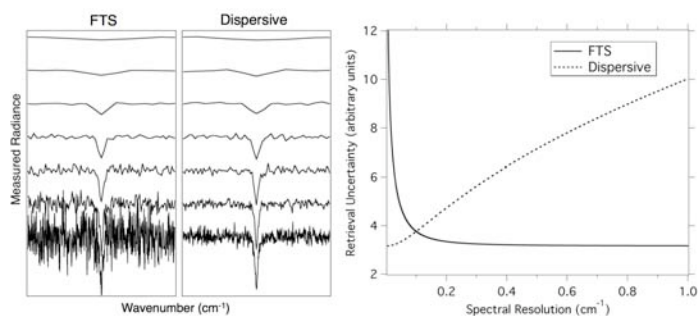

Figure 3. Optimizing spectral resolution to maximize gas quantification accuracy, for Fourier transform (FTS) and dispersive instrument types. Left: Simulated spectra from FTS and dispersive instruments, showing how an isolated gas absorption line appears at various levels of spectral resolution. The true line width here is 0.1 cm-1; this true width together with the instrument spectral resolution determines the apparent line width Spectral resolutions modeled here are, from top to bottom, 2, 1, 0.5, 0.2, 0.1, 0.05, and 0.02 cm-1. In both instruments, noise increases as resolution is improved, but it does so more rapidly in the FTS. Right: Uncertainty in retrieving gas concentration from spectral data, as a function of spectral resolution, for the FTS and dispersive instrument types. The optimal resolution for a dispersive spectrometer is as fine as technologically feasible; for the FTS the optimum is as coarse as other considerations (separating out interfering species, etc.) will allow.

A more detailed and realistic comparison between the FTS and dispersive strategies is shown in Figure 4. Here we use NASA's Orbiting Carbon Observatory (OCO) instrument and its detector arrays as a well-characterized benchmark for dispersive spectrometer performance and the state of the art in near-infrared detector arrays. To perform as direct an "apples-to-apples" comparison as possible, in modeling the competing FTS systems, we matched OCO's spectral resolution, spatial pixel footprints, and observation time (and assumed a satellite could be configured to track the target in the appropriate way to accomplish this), and based our detector model on published OCO and detector performance parameters [1-4]. We also tested our model by predicting OCO's performance based on these measured parameters, and achieved very good agreement with OCO's measured performance.

The results shown in Figure 4 illustrate another of the fundamental differences between the two instrument types: Whereas a dispersive spectrometer measures each spectral band independently, without interference from other spectral regions, the FTS mixes all collected light together at the detector and analyzes it collectively. The

consequence is that, in the FTS, photon shot noise from all spectral regions allowed to reach the detector adds to the noise in every spectral channel. It is very important, therefore, that the FTS collects only light that is of interest; other spectral regions should be discarded using optical filters. For this reason, we model three different versions of the FTS, with varying degrees of optical filtering. The simplest version uses a single band-pass optical filter that admits the entire region spanning the three gas bands of interest — the oxygen A-band, which is used as a reference, and the strong and weak CO_2 near-IR bands. The second FTS variation modeled uses a filter having three very narrow transmission bands that admit just the three gas bands (this filter might be very difficult to manufacture in practice), placed in front of a single detector array. The third version assumes three independent detector arrays, each with its own narrow-band optical filter corresponding to one of the gas bands.
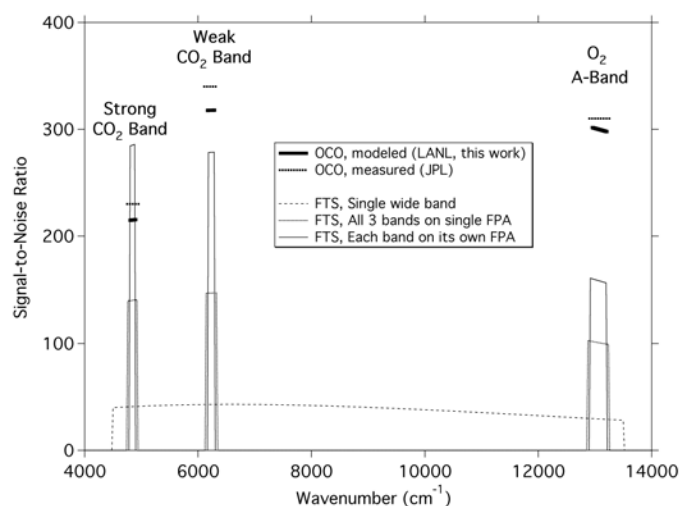

Figure 4. Performance comparison between NASA's Orbiting Carbon Observatory (OCO) instrument, and a hypothetical FTS instrument having identical spatial sampling and detector characteristics. OCO consists of three narrow-band, high-spectral-resolution dispersive spectrometers operating in the near infrared region, one for each gas band of interest: the strong and weak CO_2 bands, and the oxygen A-band. Three versions of the FTS are modeled here, having different optical band-pass filters placed in front of the detector(s): One covering the entire spectral region of interest, spanning all three CO_2 and O_2 bands, in a single broad band; a second having a single detector array with an optical filter having three narrow transmission bands centered on the three gas bands; and a third having three independent detector arrays, each with its own narrow-band optical filter. Photon shot noise from spectral regions between the primary gas bands seriously degrades the SNR of the single-band FTS, whereas the restricted-band versions show progressively better performance, though still not matching the dispersive. Note that our model, using published detector and optical parameters for OCO_2 agrees well with the performance measured by the OCO team [1-4].

Figure 4 shows that even this most extreme and diffi-cult- to-realize version of the FTS barely approaches the performance of the much simpler OCO. Indeed, we find in virtually every case examined, high-spectral-resolution per-formance of an FTS falls short of a dispersive instrument. At OCO-level spectral resolution (~0.25 cm^{-1}), a dispersive strategy is the clear choice. The FTS becomes competitive, and eventually out-performs dispersive designs, as the spectral resolution requirement is relaxed. At the coarse resolution indicated as quite useable by our radiative transfer modeling, an FTS is a viable option. Regardless of spectral resolution and noise performance, however, high spatial resolution imaging using an FTS requires much more stringent pointing and tracking by the satellite, and is generally technologically much more demanding, higher risk, and more expensive. Simplicity of construction, align-ment, and operation, combined with superior noise perfor-mance in most circumstances, overall favors the dispersive strategy.

Impact on National Missions

With climate change emerging as a major national security issue, the laboratory's long tradition of treaty verification in the nuclear realm expands quite logically into this new arena. New initiatives such as the greenhouse gas informa-tion system (GHGIS) are laying the groundwork for this new role; the present study lays another important piece of this foundation. GHG monitoring for treaty verification requires unprecedented sensitivity and accuracy. Quantitative understanding of the performance of various instrument options, as provided by this study, is crucial to defining a workable system. This work answers long-standing theo-retical questions regarding the interplay between spectral resolution and retrieval accuracy for different instrument types, challenges some long-held assumptions, and posi-tions LANL to proceed toward informed proposals for fu-ture satellite systems.

References

1. Crisp, D.. Measuring CO2 from space: The NASA Orbit-ing Carbon Observatory-2. 2010. In *61st International Astronautical Congress.* (Prague, CZ, 2010). Vol. IAC-10-D9.2.8, p. 1. Prague: International Astronautical Federation.

2. Day, J., C. O'Dell, R. Pollock, C. Bruegge, D. Rider, D. Crisp, and C. Miller. Preflight Spectral Calibration of the Orbiting Carbon Observatory. 2011. *IEEE TRANSAC-TIONS ON GEOSCIENCE AND REMOTE SENSING.* **49** (7): 2793.

3. O'Dell, C., J. Day, R. Pollock, C. Bruegge, D. O,ÄôBrien, R. Castano, I. Tkatcheva, C. Miller, and D. Crisp. Pre-flight Radiometric Calibration of the Orbiting Carbon Observatory. 2011. *IEEE TRANSACTIONS ON GEOSCI-ENCE AND REMOTE SENSING.* **49** (6, 2): 2438.

4. Pollock, R., R. Haring, J. Holden, D. Johnson, A. Kapi-tanoff, D. Mohlman, C. Phillips, D. Randall, D. Rech-steiner, J. Rivera, J. Rodriguez, M. Schwochert, and B. Sutin. The Orbiting Carbon Observatory Instrument: Performance of the OCO Instrument and Plans for the OCO-2 Instrument. 2010. In *Conference on Sensors, Systems, and Next-Generation Satellites XIV ; 20100920 - 20100923 ; Toulouse, FRANCE.* Vol. 7826, p. 78260W.

Study of Small Thorium Heavy-Water Reactor Systems

Holly R. Trellue
20110523ER

Abstract
This paper describes research devoted to developing a systems model for a new reactor concept, the Salt-cooled Modular Innovative Thorium HEavy water-moderated Reactor System (SMITHERS). SMITHERS addresses the goals of evolving deployment needs, increasing overall fuel burnup, reducing proliferation risk, and providing high-efficiency power generation. The reactor is modular and thus scalable from a few to 100s of MW_t. The concept further burns used fuel from Light Water nuclear Reactors (LWRs) without aqueous separations, reducing costs and proliferation pathways relative to current reprocessing plants. The additional burning of LWR fuel reduces proliferation risk by drawing down global inventories of plutonium (Pu) from used fuel in a way that does not isolate weapons-useable material and that increases the amount of power produced per ton of mined uranium (U). Finally, improved fuel utilization through the potential use of thorium (Th) provides cost benefits by pursuing higher neutron economy and enabling operation at higher efficiencies. Neutron economy is increased by using the thermal neutron energies associated with large quantities of heavy water moderation and thorium for innovative reactor control and constant long-term power generation (i.e. sustainability). Current reactor designs strive to make the most of every neutron but still "waste" neutrons through capture reactions in poison material such as soluble boron and control rods, especially at the beginning of an irradiation when many absorbers are required. SMITHERS can employ innovative reactivity control techniques to maximize neutron economy [1]. The proposed reactor also generates high temperature coolant discharge in the form of liquid salt without coolant pressurization for external process heat applications such as oil extraction. Salt offers significant improvement over existing coolants such as light and heavy water, which require pressurization to operate at high temperatures, reducing the cost and complexity of reactor operation. As part of developing a system model for SMITHERS, the time-dependent irradiation simulation capability at LANL was enhanced to represent a HWR with more fidelity, and material options for SMITHERS were explored. By full implementation of
SMITHERS and thorium in the fuel cycle, the amount of plutonium generated per reactor can be reduced by approximately an order of magnitude.

Background and Research Objectives
Non-aqueous fuel reprocessing techniques such as voloxidation or pyroprocessing support the Department of Energy's Modified Open Fuel Cycle in further destroying used fuel that is discharged from current reactors [2]. Used fuel comprises ~2wt% fissile content (U and Pu) and a significant amount of fission products, minor actinides, and other absorbing materials, preventing LWRs from burning it further without separations. However, such fuel can be burned in reactors using heavy water moderation. Heavy Water Reactors (HWRs) have been used for many years in Canada and other countries. The most popular type of HWR is probably the Canada Deuterium Uranium (CANDU) Pressurized Heavy Water Reactor, which is both moderated and cooled using heavy water. HWRs operate with lower average neutron energies (thermalization) than LWRs, where fission cross sections of fissile isotopes are larger. Thus, uranium does not have to be enriched to achieve criticality in a HWR, and the actinides from used fuel can be burned directly in one.

More recently, other countries, such as China, are burning used fuel processed using non-aqueous separations techniques in HWRs. Both Japan and India have developed advanced HWR concepts, the Advanced Thermal Reactor FUGEN, and the Advanced Heavy Water Reactor (AHWR) respectively [3, 4]. These reactors use a heavy water moderator but contain unique fuel clusters cooled by light water. Japan implemented the first uranium-plutonium mixed oxide (MOX) fuel in the FUGEN reactor, and India is proposing the use of thorium in their AHWR. Nonetheless, the use of liquid salt as a coolant instead of light or heavy water is unique to SMITHERS because it can produce high temperature discharge for auxiliary applications without the pressurization requirements of other reactors. SMITHERS is also multi-purpose in that it not only destroys fissile material from used fuel, but it can also irradiate thorium, which is highly abundant

in the earth. Thorium is beneficial because it produces U-233, which is neutron-efficient at very thermal energies, as is evident by the number of neutrons emitted per capture [5]. Further, studies for LWRs have shown that $ThPuO_2$ irradiated to high burnups can reduce the materials attractiveness Figure of Merit (FOM) for plutonium by a factor of two, which is a benefit in decreasing proliferation risk [6].

Most nuclear design work in the world has been performed for Light Water Reactors, and the design methods that have been developed are in large part specific to these reactors. However, Monte Carlo design tools such as MCNP/X for neutron transport and *Monteburns* for burnup that are developed by LANL are capable of modeling any type of nuclear system because they provide continuous energy cross sections and fluxes to simulate large numbers of particle interactions in a specific geometry [7, 8]. These tools were enhanced in this research for HWR simulation.

The main objective of this research was to develop a reactor concept capable of destroying used fuel through the Modified Open Fuel Cycle and/or to generate less plutonium per MW_t of power produced than currently achievable. Such a design was accomplished by performing both calculational and materials studies applicable to the final concept.

Scientific Approach and Accomplishments

Approach

Changes to the nuclear fuel cycle required for SMITHERS could be as simple as adding a HWR to the back end of the current LWR nuclear fuel cycle, or they could become as complex as implementing thorium in both LWRs and HWRs (Figure 1). The fuel material combinations examined in this research included:

- Case 1: Destruction of used fuel in a heavy water-moderated, liquid salt-cooled system following solely the voloxidation separations technique.

- Case 2: Irradiation of used fuel in one part of the HWR; Th and Pu in other parts.

- Case 3: Separation and re-irradiation of uranium and Pa-233 from the HWR itself.

- Case 4: Implementation of a Th fuel cycle in both Light Water Reactors (LWRs) and HWRs with U recycle for significant plutonium reduction.

These case options were studied after a sufficient methodology was established and preliminary materials research was explored.
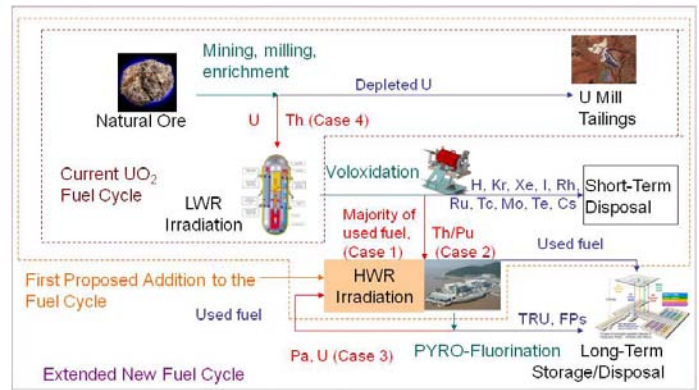

Figure 1. Proposed Changes to the Nuclear Fuel Cycle for SMITHERS.

Accomplishments

Accomplishments achieved during this research supported the tasks set forth in the LDRD Reserve project are as follows [1].

Improved Refueling Simulation

A new refueling capability to simulate HWR operation (on-line refueling) was developed using a Perl script to create detailed *Monteburns* input files for burnup calculations. Continuous on-line refueling refers to the removal and replacement of fuel bundles at frequent intervals while operating, and each of these horizontal bundle zones had to be modeled separately to represent accurate neutron transport. Several example cases were executed and showed the benefit of using on-line refueling to extend lifetime and burnup of the system (Figure 2). Such a capability required enhancement of *Monteburns* to handle an increased number of individual burnup material regions, and the resulting methodology can be applied to multiple reactor applications in the future.
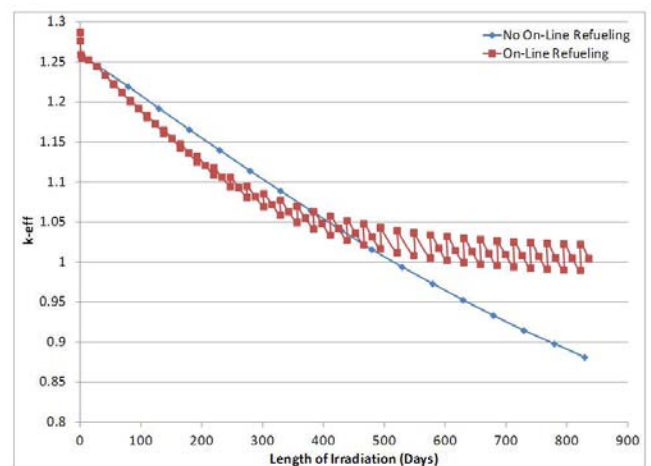

Figure 2. Increase in Lifetime (i.e. Days When k-eff >1) With New Online Refueling Capability.

Validated Methods/Data

A benchmark for the AHWR calculation was performed using *Monteburns* and showed less than 6% relative error for isotopic concentrations in comparable burnups with published results from a different code. The benchmark verified the ability of our computational tools to model a heavy water-moderated system.

Compared Fuel Material Compositions

Reactivity (a measure of the number of neutrons produced per neutrons destroyed) behaviors for different feed streams were analyzed (used fuel, Th/Pu, Th/LEU, etc.). As will be described in the next section, multiple feed streams can be irradiated in SMITHERS, but the extent of burnup depended on the feed stream that entered the reactor and how it was managed.

Calculated Self-Sustainability Conditions for Thorium in an HWR

Many designs were explored to determine how or if a self-sustaining reactivity condition could be achieved with thorium fuel containing a small amount of fissile material initially to produce neutrons. A self-sustaining condition would exist if approximately the same amount of fissile material existed throughout the length of irradiation (i.e., the same quantity of fissile material was both generated and destroyed). Although isotopic combinations with a majority of the fuel being thorium (and typically the other portion being a small amount of plutonium) were determined to be self-sustaining, a reactor comprising only that fuel never maintained criticality (k_{eff} = 1.0), which is required for reactor operation.

Explored New Coolant Type

Liquid salt was preliminarily evaluated both as a coolant and as a molten salt fuel and appears feasible for use in SMITHERS. However, implementation of the separate loops containing salt (coolant) and heavy water (moderator) still need to be studied along with interaction of the salt with cladding.

Results and Conclusions from Case Studies

Calculations showed that approximately five 150 MW_t SMITHERS would be required to further destroy some fissile content in used fuel discharged every 12-18 months from a LWR. In addition, Figure 3 indicated that plutonium production could be reduced by ten times and uranium mining requirements decreased by three times if Case 4 were fully implemented with U and Pa recycle, which is a significant improvement over the current nuclear fuel cycle (Case 1 without additional HWR irradiation).

In the base design for SMITHERS using Case 2 materials, roughly half of the core was loaded with used fuel oxide and half with thorium oxide containing 1.2w% weapons-grade plutonium with the cluster and core geometries given in Figure 4. Every six to twelve months, the used fuel was replaced with "fresh" used fuel feed (the "seed"), but the thorium/plutonium fuel remained because the goal was to continuously breed ^{233}U from thorium (the "blanket"). After the weapons-grade plutonium in the thorium fuel was burned out during the first fuel cycles, the thorium/plutonium fuel reached a self-sustaining condition. However, the burnup of the used fuel was relatively low because it had to be refueled frequently (i.e. every six months) to keep the reactor critical. The reason that used fuel was required was that although the Th/Pu reached a self-sustainable condition, it did not provide enough reactivity by itself for power production. Thus, if used fuel destruction was the primary goal of SMITHERS, then the fuel should have consisted solely of used fuel. However, to maximize neutron economy, the dually-loaded case showed that thorium fuel was self-sustaining in the SMITHERS reactor for ten or more years and destroyed weapons-grade plutonium and used fuel in the process.

To provide additional reactivity and/or to extend the lifetime of the HWR, it would be beneficial after each cycle to reuse the U-233 and Pa-233, which decays into U-233 following the irradiation of thorium, from the HWR itself (Case 3). However, recycling these isotopes would require

Requirements	Mined U (T/GWe-yr)	Disposal (T/GWe-yr)	Amount of ^{239}Pu Generated /kgU (cannot be obtained if initial Pu exists)	% Initial Pu Destroyed	% Fissile Content of Ending Pu
Current UO$_2$ Fuel in LWR	200	24	7.92	-	70.8
U/Pu Mixed Oxide Fuel in LWR	175	22	-	-39%	52.9
Thorium/LEU in LWR	180	24	2.45	-	70.9
Case 1 (used fuel from LWR further irradiated in HWR)	140	18	3.29	-	41.9
Case 2 (used fuel in 1/2 HWR; Th/Pu in other half)	70	18	-	(up to ~93%)	-
Case 4 (Th fuel cycle in both LWRs and HWRs)	70	8	0.91	-	43.5

Figure 3. Impact of SMITHERS on Mass of Uranium Mined and Plutonium Produced.

additional separations and re-fabrication processes. In addition to the design using used fuel from 4.2w% enriched uranium oxide in PWRs, a design with used fuel from PWRs fueled with LEU/Th oxide (20% 19.9wt% enriched uranium, 80% thorium) was also analyzed (Case 4 without recycle). The reactivity swings for this design were smaller than those for the 4.2w% enriched uranium case as shown in Figure 5. About four times less [239]Pu was produced when thorium-based fuels were irradiated in a PWR instead of UO_2 used fuel. Additionally, with a Th/LEU fuel cycle in both LWRs and HWRs, the amount of [239]Pu generated was almost an order of magnitude below that currently discharged in once-through fuel cycles. Thus, implementation of SMITHERS would provide a significant reduction in plutonium for future used fuel inventories.

Figure 5 shows the reactivity swings obtained per cycle when various fuels were used and replaced about every 18 months. With solely used fuel, the system did not stay critical over ten years using 18-month cycles, so yearly or more frequent reloading was required. Alternatively, a feed stream was created containing a combination of voloxidized-Th/LEU used fuel from a LWR and [233]Pa and U obtained from previous SMITHERS runs to provide additional reactivity (a fully-implemented Case 4). This feed stream had a high reactivity and could thus sustain cycle lengths longer than 18 months but required additional separations and re-fabrication of the SMITHERS used fuel itself.

In conclusion, SMITHERS would enhance the nuclear fuel cycle by providing additional power from existing used fuel or by decreasing overall plutonium production from nuclear reactors by an order of magnitude!
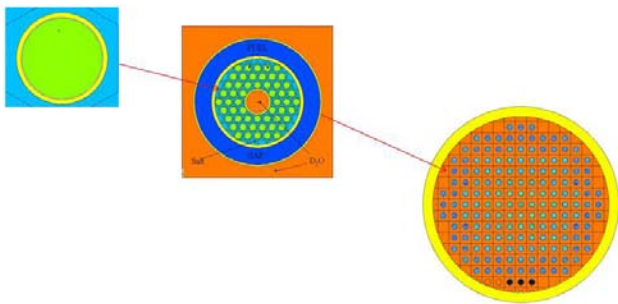

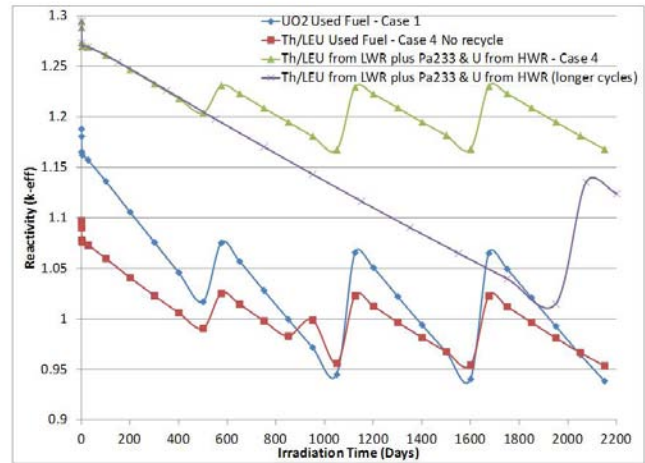Figure 4. Cross-Sectional Geometry of SMITHERS.

Figure 5. Reactivity Changes from Various Feed Materials for SMITHERS.

Impact on National Missions

We have designed a new reactor concept (SMITHERS) with multiple benefits. The reactor is modular such that it can produce power regardless of what size it is. SMITHERS can be used for lower power applications such as at a military base or on a larger-scale (the base design was 150 MW$_t$). The reactor also produces high temperature steam for auxiliary applications without requiring pressurization of the coolant. Finally, the reactor can either further irradiate used fuel or use thorium fuel with weapons- or reactor-grade plutonium as initial fissile content. Thus, it can help destroy some portion of fissile material in our radioactive waste and reduce demand for uranium and/or enrichment facilities.

To understand evolving nuclear technology worldwide and to develop a technique to destroy our used fuel efficiently, the United States would benefit from examining heavy water systems in more detail. Los Alamos National Laboratory has a unique opportunity to show its expertise in small reactor design by providing a concept that is economic yet solves one of the nation's nuclear waste problems. A majority of codes used for nuclear system analyses worldwide rely upon multi-group cross sections for a particular reactor design, mainly Light Water Reactors with low-enriched uranium oxide fuel. LANL is uniquely qualified to create nuclear data and accurately model any type of nuclear system and fuel type, then perform transport and burnup calculations to determine system performance and discharge isotopics. This research has increased the fidelity of such simulations for upcoming reactor designs. In addition, the ability to model similar reactors being built in other countries is beneficial for nonproliferation analyses.

References

1. Trellue, H. R., D. V. Rao, R. J. Kapernick, J. Zhang, J. D. Galloway, W. J. Sames, D. I. Poston, and D. E. Kornreich. Salt-cooled modular innovative thorium heavy water-moderated reactor system. 2011. *Los Alamos National Laboratory report LA-UR 11-05667.*

2. Spencer, B. B., G. D. Del Cul, E. C. Bradley, R. T. Jubin, T. D. Hylton, and E. D. Collins. Design, fabrication, and testing of a laboratory-scale voloxidation system for removal of tritium and other volatile fission products from used nuclear fuel. 2008. In *Transactions of the American Nuclear Society and Embedded Topical Meetings Isotopes for Medicine and Industry and Nuclear Fuels and Structural Materials for the Next Generation Nuclear Reactors (NFSM) ; 8-12 June 2008 ; Anaheim, CA, USA.* Vol. 98, p. 103.

3. Kannan, U., N. P. Pushpam, A. Kumar, S. Ganesan, P. D. Krishnani, R. Srivenkatesan, and R. K. Sinha. Physics design aspects of thorium fueled advanced heavy water reactor (AHWR). 2009. In *American Nuclear Society - 4th Topical Meeting on Advances in Nuclear Fuel Management 2009, ANFM IV ; 20090412 - 20090415 ; Hilton Head Island, SC, United States.* Vol. 2, p. 943.

4. Ohtani, T., T. IIjima, and Y. Shiratori. Analysis of Mixed Oxide Fuel Loaded Cores in the Heavy Water Reactor FUGEN. 2003. *Journal of Nuclear Science and Technology.* **40** (11): 959.

5. Chadwick, M. B., P. Oblozinsky, M. Herman, N. M. Greene, R. D. McKnight, D. L. Smith, P. G. Young, R. E. MacFarlane, G. M. Hale, R. C. Haight, S. Frankle, A. C. Kahler, T. Kawano, R. C. Little, D. G. Madland, P. Moller, R. Mosteller, P. Page, P. Talou, H. Trellue, M. White, W. B. Wilson, R. Arcilla, C. L. Dunford, S. F. Mughabghab, B. Pritychenko, D. Rochman, A. A. Sonzogni, C. Lubitz, T. H. Trumbull, J. Weinman, D. Brown, D. E. Cullen, D. Heinrichs, D. McNabb, H. Derrien, M. Dunn, N. M. Larson, L. C. Leal, A. D. Carlson, R. C. Block, B. Briggs, E. Cheng, H. Huria, K. Kozier, A. Courcelle, V. Pronyaev, and S. der Marck. ENDF/B-VII.0: Next Generation Evaluated Nuclear Data Library for Nuclear Science and Technology. 2006. *USDOE.*

6. Trellue, H., C. Bathke, and P. Sadasivan. Neutronics and material attractiveness for PWR thorium systems using monte carlo techniques. 2011. *Progress in Nuclear Energy.* **53** (6): 698.

7. Waters, L., G. McKinney, J. Durkee, M. Fensin, J. Hendricks, M. James, R. Johns, and D. [Los Alamos National Laboratory. Pelowitz. The MCNPX Monte Carlo Radiation Transport Code. 2007. *AIP Conference Proceedings.* **896** (1): 81.

8. Trellue, Holly R.. Development of Monteburns: A Code That Links MCNP and ORIGEN2 in an Automated Fashion for Burnup Calculations. 1998. *USDOE Office of Defense Programs (DP).*

Publications

Trellue, H. R., D. V. Rao, R. J. Kapernick, J. Zhang, J. D. Galloway, W. J. Sames, D. I. Poston, and D. E. Kornreich. Salt-cooled modular innovative thorium heavy water-moderated reactor system. 2011. *Los Alamos National Laboratory report LA-UR 11-05667.*

Trellue, H. R., D. V. Rao, R. J. Kapernick, and J. Zhang. Small integral thorium heavy water reactor system. 2011. In *2011 American Nuclear Society Annual Meeting Transactions.* (Hollywood, Florida, 26-30 Jun. 2011). Vol. 104, p. 927. La Grange Park, IL: American Nuclear Society.

Superconducting Overhead Power Lines

Stephen P. Ashworth
20110713ER

Abstract

LANL electric power comes along two 114kV power lines, before 2020 LANL will require a third line which will need a 100 ft right of way some 15 miles long, cleared of trees, running towards Santa Fe. We have examined the application of high temperature superconductors in overhead transmission to upgrade an existing 15 mile long, 100MW line to carry 200MW of power using the same poles and right of way.

This study has shown that there are no obvious technical barriers to retrofitting the existing Buckman-Los Alamos 114kV power line with high temperature superconductor (HTS) to achieve a 100% increase in power transmission capability to 200MVA. This upgrade would assure adequate power to LANL for at least the next two decades. Although some construction would be needed on the LANL site for the cooling system, there would be no significant construction along the route of the power line as the existing support structures (mainly wooden H frames) would be re-used.

As no off-site construction is required, the permitting delay for this upgrade is minimal and, given the go-ahead, construction could probably start within a year and be completed within 12 months after that. In contrast the delay to obtain permits for a new line can be in the range 5 – 15 years. The HTS solution might avoid CO_2 emissions of 50,000 – 100,000 tons initially and a further 3,000 – 10,000 tons per year of operation. This is from a single, 15 mile power line. The nationwide potential for avoided CO_2 emission is significant.

These savings come at a financial cost though; the HTS ac solution is expensive ($40m - $70m depending on assumptions) compared to a new, conventional power line (probably in the range $25m - $45m at LANL). However, if the existing power lines become unable to support the load growth at LANL before the permitting process for a new line is completed, the extra cost might not be a deciding factor. Development of, and a mass market for, HTS technologies could be expected to reduce the cost of this line to perhaps $30m, comparable to the new conventional cable costs.

Background and Research Objectives

This study is the first attempt to design an HTS overhead power line *system*. It is based on a topical case at LANL where there is a need within the next few years to implement an upgrade to the power supply. LANL electric power comes along two 114kV power lines; before 2020 LANL will require a third line which will need a 100 ft right of way some 15 miles long, cleared of trees, running towards Santa Fe. We have examined the application of HTS overhead transmission to upgrade one of the existing 114kV lines to carry 200MW of power using the same poles and right of way.

Electricity transmission using high temperature superconductivity (HTS) could allow significantly more renewable energy onto the power grid. LANL is a world leader in this technology and has supported DoE in developing HTS *underground* cables. The greatest national impact though would come from HTS suspended *overhead* transmission where large amounts of power could be transmitted at lower voltages. At the present time, the only suspended HTS conductor in the world is a 100 ft experimental section at LANL, first energized two years ago and still under test and development

Nationwide, the growth of renewable generation on the electricity grid is limited by transmission capacity. HTS overhead technology would allow the transmission of large amounts of power (up to 1GW) at voltages < 200kV instead of > 500kV. A 114kV transmission line can be supported on simple wooden poles 50 ft high in a 100 ft corridor, while 500kV require steel towers nearly 150 ft high, dwarfing the surrounding features, in a cleared corridor up to 250 ft wide. There is usually significant opposition to building new transmission lines, often based on the visual impact of high voltage towers. A delay of 7 – 10 years for permitting a new line is often quoted within the industry, this hides the fact that most proposed lines *never* obtain permits. For example, the proposal by T. Boone Pickens to site 1000 wind turbines in west Texas was shelved because of lack of transmission, this wind power could have avoided the emission of 10,000,000 tons of CO_2 emissions *each year.* Using the LANL 114kV

line as a case study allows us to develop the underpinning technologies to speed up the connection of renewable generation into the US power grid.

When a new power line is planned for an area there is often considerable local opposition. The reasons for the opposition are both known and real: the visual impact perhaps, and unknown, the electromagnetic fields from the line. Due in part to the response to this opposition there is a cumbersome permitting process for power lines often taking over 5 years. The objective of this study was to demonstrate the possibility of new HTS power lines with very significantly reduced visual impact and to evaluate the upgrade of existing lines to very much higher capacity than possible with non-HTS technology, completely avoiding the problems of siting new power lines.

Scientific Approach and Accomplishments

This is a conceptual study where the various novel elements of a HTS power line are considered. This is the first time an overhead superconducting power line has been examined as a total system and as a solution to a particular problem. The line conductor is a novel design and significant effort was put into determining and minimizing the energy losses of the conductor, which are central to the engineering and economic feasibility of the system. A new cooling scheme for HTS cables, developed under DoE funding at LANL, is modeled for use in the system and is optimized for the line length, energy losses, changes in elevation and efficiency.

This study has shown that there are no obvious technical barriers to retrofitting the existing Buckman-Los Alamos 114kV power line with high temperature superconductor (HTS) to achieve a 100% increase in power transmission capability to 200MVA. This upgrade would assure adequate power to LANL for at least the next two decades. Whilst some construction would be needed on the LANL site for the cooling system, there would be no significant construction along the route of the power line as the existing support structures (mainly wooden H frames) would be re-used. The HTS line has been designed to place lower forces on the structures compared to the conventional line and also to be capable of the span lengths, including the extreme span at the Rio Grande crossing.

The energy losses of the HTS conductor are central to the feasibility of this line. We have developed a 2D finite element model to estimate the losses and optimize the conductor design. This has allowed us to achieve direct energy losses of < 0.3W/m in conductor carrying over 1000A at full load. The total energy losses of the 15 mile, 200MVA system are estimated to be equivalent to 0.5 – 1.0MW depending on the efficiency of liquid nitrogen production, this is significantly less than the conventional solution which might be expected to lose over 3MW at full load.

This loss figure does not, however, tell the full story. The cooling system for this cable is designed to use liquid nitrogen (LN). This nitrogen would be produced off-site and transported by tanker to storage tanks at the head of the cable. The cable will use some 7500 gallons / day of LN (LANL already receives deliveries by tanker of 15,000 gallons per day). The cost of LN production is very largely the cost of the power to run the system: the raw material (nitrogen gas) is 'free'. A LN production plant will almost always operate during off-peak electricity consumption periods, when the electricity is cheapest. In New Mexico we can expect the off-peak electricity to be largely wind generated. Consequently, the power to cool the cable could be largely derived from non-emitting sources. In contrast the power lost from the conventional solution is always taken off the cable as the power is transmitted; at peak load times it is peak (i.e. highly polluting) power being wasted as heat.

As no off-site construction is required the permitting delay for this upgrade is minimal and, given the go-ahead, construction could probably start within a year and be completed within 12 months after that. In contrast the delay to obtain permits for a new line can be in the range 5 – 15 years. If a 5 year delay occurs the HTS solution might avoid CO_2 emissions of 50,000 – 100,000 tons, and once installed might avoid 3,000 – 10,000 tons per year of further emissions. This is from a single, 15 mile power line. The nationwide potential for avoided CO_2 emission is obviously significant.

These savings come at a financial cost. The HTS ac solution is expensive ($40m - $70m depending on assumptions) compared to a new, conventional power line (probably in the range $25m - $45m at LANL). However, if the existing power lines become unable to support the load growth at LANL before the permitting process for a new line is completed the extra cost might not be a deciding factor. There are cheaper HTS solutions based on dc transmission. AC-DC conversion is expensive but reduces the number of conductors, much reducing the cost of the HTS system. Ironically for this study, we have identified that the most cost effective upgrade to 200MVA might be by using the existing conductors as a three wire, monopole dc system. Such a system could probably be in place and operating with 24 months, is modular (ie there is a phased upgrade path) and resilient (can always fall back to ac operation).

Conventional overhead power conductor is an established technology. We cannot expect significant cost decreases to occur. HTS conductor is a developing technology and does not yet have a mass market. We have used a 'high' cost of $250 /kA.m in our calculations, which is the low volume price today. As an indication we have also performed calculations at $100/kA.m to reflect possible process improvements. If HTS conductor becomes a mass produced material with good yields we can expect the price to drop to $50 / kA.m. Similarly the price for cryostat could drop to $50/m (we assumed $200/m). In this case the HTS solution would

fall to about $30 m, comparable to the new conventional cable costs.

Impact on National Missions

Energy security not only entails finding new, domestic sources for energy but also delivering that energy to the user. People are attracted to the idea of renewable sources for electricity, but are reluctant to allow the connection of those sources to the grid by power lines '*in their backyard*'. This study has shown the potential for a low environmental impact transmission system. By retrofitting existing power lines and doubling their capacity we can avoid the need for new lines in many cases and get the renewably sourced energy to the user. If a new line *is* necessary, HTS technology allows it to be much less intrusive and hopefully more acceptable. This directly supports the energy security mission.

Low-Temperature Thermal Storage: A Renewable Carbon Neutral Technology

Stephen J. Obrey
20110728ER

Abstract

Environmental temperature control is a critical factor in maintaining a productive and healthy workplace. It is well-known that office worker productivity is maximized at temperatures in the range of 68-72°F. Currently, more than 30% of the electricity produced in the United States is directly tied to temperature control in buildings primarily accomplished using energy intensive refrigerated air-conditioning. The goal of this project was to develop and demonstrate a low-temperature thermal storage system for facility cooling applications. This system is specifically designed to utilize natural temperature swings to provide a thermal energy sink for formation of the thermal storage media. This method not only shifts the major parasitic power demands by operating during off-hours but is also designed to potentially eliminate the majority electrical energy costs associated with refrigerated air-conditioning. In this project we have identified suitable thermal storage media, designed and fabricated a bench-scale unit and demonstrated the ability to reversible capture and release thermal energy from ambient air. Our engineering analysis has shown that our system consumes nearly 40% less energy than a conventional vapor compression system during the cooling season with operating costs reduced by 60%. Our estimates show that, like most alternative energy solutions, the capital investment for the installation of the thermal storage system will be larger than traditional vapor compressor AC units. A modest increase in initial capital outlay is not unexpected. It is counter-balanced by system simplicity as well as long-term monthly savings in system operation.

Background and Research Objectives

Environmental temperature control is a critical factor in maintaining a productive and healthy workplace. It is well known that office worker productivity is maximized at temperatures in the range of 68-72°F. Computing facilities, such as supercomputer data centers, typically require even cooler temperatures. LANL's petaflop computer, Roadrunner, consumes some 2.35 MW of electrical energy. To the facility engineer, Roadrunner can be viewed as a giant resistor converting 2.35 MW of electrical energy directly into low-grade heat, which must be continuously removed from the facility. Presently that is accomplished using energy intensive refrigerated air-conditioning. Recent discussions of a 10-15 MW exaflop computing capability, combined with the DOE mandates to freeze carbon dioxide footprint and energy consumption levels at 2008 levels, present additional challenges for high-performance facilities operation. The purpose of this work is to provide a practical means of meeting these new operational constraints without significantly increasing the site's carbon footprint.

The goal of this project was to develop and demonstrate a low-temperature thermal storage system for facility cooling applications. This technology is particularly well-suited for Los Alamos as it takes full advantage of the temperate climate and low overnight temperatures that can serve as the operating energy sink, Figure 1. The proposed approach includes identifying appropriate thermochemical energy sinks, identification of the thermodynamic properties (i.e. phase boundaries), and the physical properties of thermal storage media. These thermodynamic and physical properties form a basis for engineering analysis to assess performance of an integrated system and air-to-liquid heat exchanger requirements. Finally, a small bench-scale test bed was assembled and the ability to utilize the cool night air to form the thermal storage material was demonstrated. This work identifies the key technical issues and provides system design recommendations required to advance to a larger demonstration.

Scientific Approach and Accomplishments

Several thermal storage media were down-selected in this program including hydrated metal salts, organic phase change materials, and aqueous phase change materials based on the semi-clathrate compounds. Preliminary down-selection criteria included material costs, industrial-scale availability, phase change temperature, susceptibility to other environmental factors such as extreme heat or cold, and the influence of impurities. The optimal thermal storage temperature was selected to provide an intermediate operating temperature between

the daily average nighttimes low and the nominal average building temperature. After down-selection of the most suitable thermal storage media, physical properties including density, viscosity, specific heat capacity, viscosity, and thermal conductivity were measured to provide the input data required for a preliminary engineering analysis.
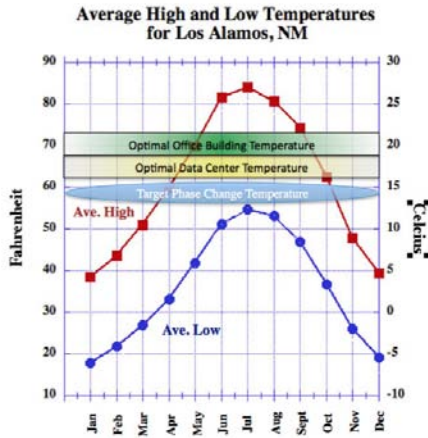

Figure 1. A plot of the average high and low temperatures for Los Alamos, NM with overlays describing the temperature ranges for Data Centers and Office buildings as well as the targets for thermal storage material.

Two practical thermal energy storage system configurations were considered using the down-selected thermal storage media. Since, after the phase transition during cooling, the thermal storage media remains a pumpable slurry, the thermal storage media can be used directly as a heat transfer fluid. In such a system, the thermal storage media would be pumped from a storage tank, through an air-to-liquid heat exchanger and back to the storage tank. During nighttime pumping and heat exchange with outdoor air, the thermal storage media would be continuously generated, and the concentration of solid in the storage tank would increase over time. An alternative system can be envisioned, where the thermal storage media is kept in a storage tank as a secondary refrigerant, and water or a water/ethylene glycol mixture is used as a primary refrigerant for heat exchange with the ambient air or the air-conditioned space. This system would resemble a conventional ice-storage system. However, because the melting temperature can be tuned to a much higher temperature than melting water, one can avoid using vapor compression refrigeration for nighttime phase change (i.e. freezing). As such, the low temperature thermal storage system only requires a water pump, an air-to-water heat exchanger, and a storage tank equipped with tubes that facilitate heat exchange with the semi-clathrate slurry. Through some preliminary calculations, we found that the system configuration employing water as a primary refrigerant and semi-clathrate as a storage medium requires much lower energy consumption and smaller heat exchanger sizes. A system capable of providing 4 tons of air conditioning capacity to a typical US home with water as the primary refrigerant was

modeled and compared to a conventional vapor compression refrigeration cycle. A demonstration system was constructed and completed in July, Figure 2. There were major delays related to the institutionally required pressure safety review, which took over two months to complete. As a result, the initially scheduled operating time, data collection, and system optimization work had to be adjusted.

Figure 2. Thermal Storage Unit in a fully instrumented test module that demonstrates on a "bench-scale" the ability to utilize ambient air as a heat sink to reversibly capture and release thermal energy. Preliminary engineering analysis shows that the Thermal Storage Unit operates at a SEER rating of greater than 40.

Technological Assessment

Our thermal model was used to show that the low temperature thermal energy storage system can be scaled to provide air-handling for a typical residential home that might be conventionally equipped with a 4 ton electrical compressor driven air-conditioner. Our system calculations show that a home equipped with a properly sized thermal storage system consumes nearly 40% less energy than a conventional vapor compression system during the cooling season with operating costs reduced by 60%. A thermal storage system would require only simple commercial off-the-shelf refrigeration equipment (heat exchangers and pumps). For comparison purposes, a typical vapor compression refrigerator with an ENERGY STAR rating operates with a coefficient of performance (COP) of 3.6, which corresponds to a Seasonal Energy Efficiency Ratio(SEER) rating of 14. Our thermal storage system operates with a SEER rating of greater than 40. This is not unexpected and a high COP for the thermal energy storage system is to be expected, since only a liquid pump and an air-handling fan need to be run during operation. Our calculations show that there is a very high correlation between the system SEER rating and the temperature difference between the thermal storage media and the ambient air temperature. It is important to keep in mind that the stated SEER rating is not a static number and is highly dependent on the temperature differential between the ambient air and the temperature at which the thermal storage system captures and releases thermal energy. The simulated system uses a very small 3°C temperature differential. In cases where this temperature difference is smaller, the system SEER rating drops but in cases where this temperature differential is greater than 3°C, SEER ratings higher than 40 are expected. A fair comparison between traditional vapor compression

air conditioning (AC) and the system developed herein is the kWh of electricity consumed and operating costs. We find that the vapor compression system uses 77% more energy, which at 2010 electrical prices costs 150% more than the thermal storage system.

Although the energy consumption and operating cost of the thermal energy storage system are considerably lower than a conventional vapor compression refrigerator, the thermal energy storage system does require purchase of a storage tank and a large heat exchanger. More specific cost comparisons are difficult at this stage of development. Our estimates show that, like most alternative energy solutions, the capital investment for the installation of the thermal storage system will be larger than traditional vapor compressor AC units. A modest increase in initial capital outlay is not unexpected. It is counter-balanced by system simplicity (that will require very little maintenance), as well as, long-term monthly savings in system operation. Furthermore, all projections are that future energy costs are hedging toward significant increases hence the offset between capital and operating costs shifts more favorably toward the installation of thermal storage systems.

Impact on National Missions

This technology demonstration is a first generation example-of thermal storage technology to store energy in a thermal reservoir for later reuse in building HVAC system. Beyond initial applications that lower the overall power demand and subsequent costs to the end user, these thermal storage system can serve a major role in shifting peak load power to off-peak power production. Currently, more than 30% of the electricity produced in the United States is directly tied to temperature control in buildings, which provides immediate applications. Also, systems to shift the electricity expenditure directly from peak power demand to off-peak times can alleviate grid strain, extend the longevity of our current fossil-fuel power production fleet, and open opportunities for the installation of renewable power on a grid-scale. Advances in this area also demonstrate the ability of LANL to capture and advance basic scientific results into field-able technology platforms in a short time frame.

Innovative Concepts for Highly-Efficient, On-Site Cogeneration

Mahlon S. Wilson
20110732ER

Abstract

LANL projects significant growth in electric power demand, and due to limited transmission line capacity, lacks the ability to import more power from offsite. LANL's projected peak power requirements in 2014 will increase 25%-50% over current peak usage. The increase in demand will need to be met with either a massive investment in electric transmission line expansion, with consequent permitting uncertainties, or by on-site generation. Phosphoric acid fuel cell (PAFC) systems have the potential to provide highly efficient and low-emission generation of heat and power using natural gas. PAFCs lead, among fuel cell types, in installed capacity, despite their modest performance. Overcoming their technological weaknesses (such as those identified in a recent DOE workshop [1]) would significantly improve the marketability of PAFCs as alternatives to conventional power production alternatives, which tend to have significantly higher emission profiles and relatively poor transient responses. Solving these technological issues also provides a compelling solution to LANL's future energy needs. A recent LANL study to evaluate the potential of PAFCs for on-site combined heat and power (CHP) applications illuminated issues that the commercially available units face when operating at high altitude. This project investigates innovative solutions to overcoming the recognized PAFC weaknesses as well as the high-altitude "de-rating" problem. Success of this project holds the promise of a major breakthrough for implementation of clean energy technologies here and elsewhere.

The key concept in this proposal is to combine the existing technology of commercial PAFCs with innovative concepts utilizing unique nanocrystalline ionic conductive materials. The research focuses on developing "drop-in" catalyst layer and separator technologies that allow the continued use of the majority of components in an existing commercial product, but will revolutionize the overall performance, durability, and cost effectiveness. In the novel catalyst layer, ionic access to the fuel cell catalyst is provided by the nanocrystalline ionic conductor (NIC), instead of the phosphoric acid used in a conventional

PAFC. This overcomes the PAFC performance and durability weaknesses otherwise encountered with phosphoric-acid-saturated catalyst layers. In the case of the separator, the conventional inert silicon carbide matrix is replaced by these same ionically conductive materials, which serves to significantly increase overall conductivity of the separator. The development of the innovative components utilizes LANL's experience in the synthesis of high-quality and nanoscale materials and LANL expertise in fuel cell electrode development.

Background and Research Objectives

PAFCs have been in commercial use for decades, primarily because of their suitability in systems that are fueled by natural gas. Over 260 UTC Power PAFC systems, such as the one portrayed in Figure 1, have been installed in nineteen countries with a combined 8.7 million hours of operation and 1.4 billion kWh of electricity generation (as of 2010). However, the lack of technology advancement from a cost and performance perspective has significantly limited the use of this clean energy technology.

Figure 1. A 400 kW natural gas Purecell® PAFC power module (UTC).

The primary weaknesses of current PAFC technology are low catalyst activity, poor catalyst durability, electrolyte loss, and high cell resistances. In the first case, the kinetics of the oxygen reduction reaction (ORR) with PAFC catalysts are quite poor compared to other fuel cell technologies such as polymer electrolyte membrane fuel cells (PEMFCs). In PAFCs, phosphate ions from the liquid electrolyte strongly adsorb onto the surface of the

catalyst, thereby inhibiting reactant catalysis. In contrast, the catalytic sites remain accessible in "solid" electrolyte systems such as PEMFCs and solid oxide fuel cells (SOFCs), and catalyst activities are thus much higher in these technologies.

Poor catalyst durability is also a consequence of the aggressive phosphoric acid electrolyte. Since PAFCs operate at ~ 200°C and the liquid electrolyte envelopes the nanoscale Pt catalyst particles, a substantial amount of Pt particle dissolution, growth, and agglomeration occurs. In comparison, activity losses are minimal in SOFCs despite the much higher operating temperatures since the catalysts cannot dissolve in the "dry" solid oxide electrolytes.

Phosphoric acid loss is due to the small but finite vapor pressure of the acid at the high PAFC operating temperatures (4.5×10^{-7} atm at 175°C). Thus, acid is slowly removed in the effluent air and fuel streams. This loss becomes a factor over the years and is a potential cause of system failures due to corrosion of downstream components and electrolyte maldistribution within the cells. Reducing electrolyte loss would substantially improve reliability and decrease mitigation and maintenance costs.

Cell resistances of PEMFCs are typically less than 0.1 Wcm^2, one of the key reasons that the technology is capable of high power densities, and hence the leading candidate for transportation applications. In contrast, the cell resistances in PAFCs are around three times higher. Although the intrinsic ionic conductivity of phosphoric acid is quite high, it is necessary to imbibe the acid into a microporous cell separator matrix that serves as the physical barrier between the electrodes. Clearly, large matrix pores, high pore volumes, and thin layers improve ionic conductivity, but a competing requirement is the need to form a hermetic seal between the fuel and oxidant gasses supplied to the respective opposing electrodes. Consequently, small pores with high bubble-points are necessitated, even though the low pore volume and increased tortuosity result in unfavorably high cell resistances.

Despite all the difficulties described above, PAFCs have assumed the lead in utility-scale fuel cell technologies because there is a "gap" region in effective electrolytes between the <100°C PEMFCs and the >800°C SOFCs (PEMFCs only operate well on pure hydrogen and SOFCs are prohibitively expensive and fragile due to their ceramic construction – the other competing liquid electrolyte technology, molten carbonate fuel cells, has far more significant difficulties than PAFCs). Attempts to develop solid ionic conductors to fill this temperature gap include oxoacids and their salts that exhibit anhydrous protonic conduction [2]. However, most of these oxoacids had very low conductivities until the discovery of $CsHSO_4$ in 1982 with a conductivity of 10^{-3}-10^{-2} S/cm above 141°C [3]. Although the use of a $CsHSO_4$ electrolyte in a fuel cell was demonstrated, this material is water-soluble and is easily reduced under hydrogen conditions [4]. More recently, the phosphates (CsH_2PO_4) have been used as electrolytes and show good stability up to 250°C in humid conditions [5]. However the conductivities of these materials are still orders of magnitude too low and require aggressive humidification of the reactants.

Recently, an overseas research team developed an innovative nanocrystalline ionic conductor (NIC) that demonstrated excellent protonic conductivities (up to 10^{-1} S/cm) at 80-300°C. Further, the materials were stable and highly conductive in the anhydrous state. The research team assembled a small fuel cell and demonstrated very promising results, close to that of PAFCs, even though the electrolyte was a very thick (0.35 mm) pressed pellet of NIC. Correspondingly, the cell resistance was particularly high; an electrolyte thickness closer to that used for other technologies (e.g., 25-50 µm for PEMFCs and SOFCs) would be expected to provide significantly greater performance. Unfortunately, attempts to form thin NIC membranes have been disappointing. It is very difficult to form thin, robust, and crack-free films of the material.

Our approach is to synergistically combine the two ionically conductive materials, the liquid phosphoric acid and the nanocrystalline conductor, in fuel cell configurations that maximize the benefits of the two materials and minimize their deficiencies.

Scientific Approach and Accomplishments

The key concept in this project was to combine the PAFC and NIC technologies to provide an overall superior fuel cell system. The basic approach is to use NIC material in the catalyst layers and matrix separator, with phosphoric acid (phos-acid) preferentially imbibed in only the latter. The assembly is intended to be a drop–in replacement for the core materials in a conventional PAFC stack to minimize development and engineering costs.

The use of the phos-acid imbibed NIC matrix separator overcomes the difficulties with forming a highly conductive, leak-free, and robust NIC separator. Combining the highly conductive imbibed phosphoric acid with an intrinsically conductive NIC matrix significantly increases cell conductivity. The use of NICs in the catalyst layers helps overcome the three electrode weaknesses discussed above. To help improve the poor kinetics with PAFCs, the use of the "dry" ionic conductor within the catalyst layers decreases the amount of phosphate inhibition of the catalyst surface. Ideally, catalyst activity could approach that projected for non-adsorbing electrolytes at high-temperatures, about ~ 100 mV/cell.

Likewise, overcoming the poor catalyst durability due to attack by phos-acid is also mitigated by the use of the "dry" ionic conductor within the catalyst layer. PAFC catalyst particles are quite stable up to 300°C if dry, and dissolution/growth proceeds rapidly when immersed in phos-acid.

Minimizing the phosphoric acid content of the catalyst layers by relying primarily on NICs for ionic conductivity helps maintain catalyst particle dispersion and improve cell durability.

In a conventional PAFC, the phosphoric acid is ideally distributed in a manner that maximizes the interfacial area between the acid, catalyst, and reactants. By default, this maximizes the exposed surface area of the phosphoric acid and hence susceptibility to volatilization. Unfortunately, the loss of phosphoric acid from within the cells limits the long-term durability of PAFCs. The use of NICs into the catalyst layers for conduction decreases the exposed phosphoric acid surface area and provides an additional diffusion barrier to loss of phosphoric acid.

Synthesizing NIC materials with high ionic conductivities are not without difficulties. It became necessary in this project to continue the investigation into producing NIC materials that simultaneously provide the desired properties of high crystallinity, small particle size, and ideal stoichiometric levels. Despite achieving the desired bulk composition and crystallite properties, difficulties arise with any of these synthesis techniques in reproducibly obtaining the high conductivities attained by the original research team. The primary reason is that the ionic conduction in NICs is most likely through grain boundary pathways where ionic transport is highly sensitive to composition.
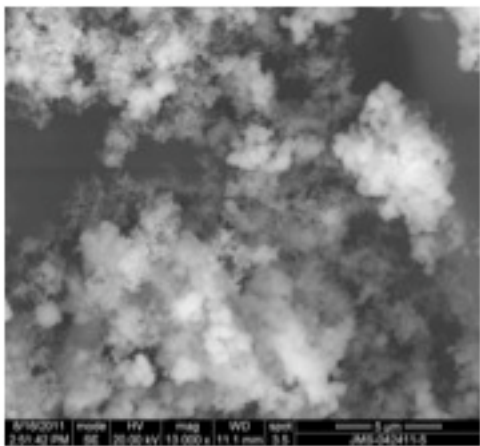

Figure 2. Scanning electron micrograph of an 85% crystalline NIC sample with 20 nm crystallites prepared at LANL.

High synthesis temperatures are required to crystallize these materials to provide an insoluble and stable scaffold. The crystallinities achieved range from primarily amorphous at 600°C to practically 100% crystalline at 950°C. Ultimately, we developed highly crystalline NIC particles with crystal sizes that are less than 25 nm in diameter, as compared to the roughly 500 nm crystallites obtained with the original process. A micrograph of one such sample is shown in Figure 2. The smaller crystallites should provide a higher density of proton conductive surfaces, and hence higher bulk ionic conductivities, all else being equal. In practice, the bulk conductivity becomes ever more de-

pendent upon inter-particle ionic transport, the number of interfaces, and the ability to closely pack the particles. Optimizing conductivity is consequently an area under investigation.

The immersion of the NICs in phosphoric acid eliminates difficulties with inter-particle ionic transport and conductivity, consequently progress is more easily achieved in developing NIC-based cell separators. In conventional PAFCs, the typical separator consists of a 100 micron thick matrix of silicon carbide (SiC) powder with several percent PTFE (polytetrafluoroethylene, or "Teflon") binder that is imbibed with the phosphoric acid electrolyte. The inert SiC/PTFE matrix provides a structural element that can withstand a 200°C acidic environment, and the phosphoric acid provides ionic conductivity. In order to maximize the bubble pressure and durability of the separator in commercial PAFCs, the SiC particle size and shape are optimized and the layer is compacted to increase densification. While the separator conductivities are correspondingly rather low (~0.035 S/cm), as shown in Figure 3, PAFCs with such separators can operate for 10 years without loss of physical integrity or the hermetic seal. PAFC test cells were fabricated here at LANL using home-made SiC/PTFE separators to provide baselines for comparison with subsequent separator improvements. Two somewhat different SiC/PTFE formulations, designated as "SiC-A" and "SiC-B" are also compared in Figure 3. Conductivities are somewhat higher than the commercial standard, but these home-made separators are not as durable or gas-tight as the commercial versions.
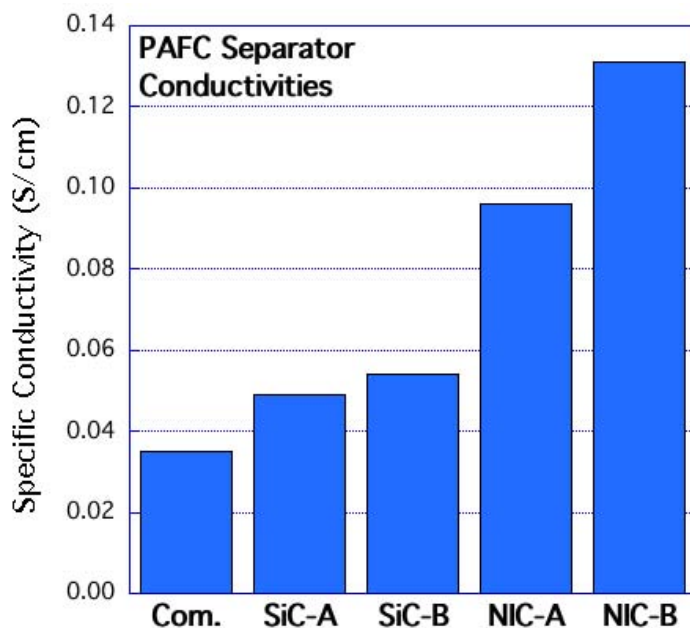

Figure 3. Comparison of separator ionic conductivities at 200°C for a typical commercial SiC-PTFE matrix, two slightly different LANL-made SiC-PTFE matrices, and two additional LANL NIC-PTFE matrices.

Replacing the SiC in the matrix with NIC powder improves separator conductivity markedly. Shown in Figure 3 are

two samples, "NIC-A" and "NIC-B". Sample "A" uses NIC fully heat-treated to 100% crystallinity with an average crystal size of 55 nm, and "B" is 85% crystalline with 25 nm crystallites. The introduction of the NIC powder clearly improves conductivity compared to the SiC, with "B" more than doubling even the better of the two home-made SiC separators. The greater than 0.1 S/cm conductivity is at least the equal of the membranes used in PEMFCs, a significant increase for PAFCs. The higher conductivity of the "B" sample compared to the "A" possibly reflects the slightly lower degree of crystallinity, which appears to provide a higher proportion of the proton conductive phase. Likewise, the somewhat smaller crystallite size may also be beneficial by increasing the volume fraction of the proton conductive phase.

Doubling the separator conductivity essentially halves the PAFC cell resistance. In fuel cell operation, a significant amount of energy previously lost to resistive heating then becomes available to either increase the amount of electrical power produced by the cell or to further increase the efficiency of the fuel cell. This change alone is expected to improve the power output of commercial PAFC systems by several percent, with no change in natural gas fuel input or emissions. And, if the more significant catalyst layer improvements under investigation are realized, the benefit of doubling the separator conductivity is further compounded.

Impact on National Missions

Not only does LANL have an Energy Security Goal reflecting national priorities, but LANL itself has pressing additional energy needs in the near future. Typical LANL and Los Alamos County daily power requirements are on the order of 100 MW, with LANL peak demand (estimated) of approximately 84 MW in 2010. LANL's projected peak power requirements in 2014 will be on the order of 125-150 MW. However, the transmission lines into LA County are limited to about 110 MW [6]. Installation of additional transmission capacity is difficult due to cost, regulatory, and right-of-way issues. Additional generation capacity is then needed locally, which would ideally provide combined heat and power (CHP). PAFCs nominally provide highly efficient heat and power, but performance is negatively affected by LANL's high altitude. Even so, current PAFC commercial offerings promise very high capacity factors and attractive fuel costs, as well as significant reduction of both greenhouse gas emissions and criteria pollutants when compared with other natural-gas fueled technologies. But capital cost and maintenance costs, compounded by the ten-year life of existing systems, remains a barrier to widespread use. Realizing a portion of the improvements in PAFC technology explored by this LDRD project has the potential to off-set the performance de-rating. Achieving all possible gains can provide a truly compelling increase in power density and durability, and hence decreased cost, especially at lower altitudes where the benefits are even greater, and most markets are located.

References

1. Remick, R. J., D. Wheeler, and P. Singh. MCFC and PAFC R&D workshop summary report. 2010. *Office of Energy Efficiency & Renewable Energy, United States Department of Energy.*

2. Kreur, K. D.. Proton Conductivity: Materials and Applications. 1996. *Chemistry of Materials.* **8** (3): 610.

3. Baranov, A. I., L. A. Shuvalov, and N. M. Shchagina. Superion Conductivity and Phase-Transitions in CsHSO4 and CsHSeO4 Crystals . 82. *JEPT Letters.* **36** (11): 459.

4. Haile, S. M., D. A. Boysen, C. R. Chisholm, and R. B. Merle. Solid acids as fuel cell electrolytes. 2001. *Nature.* **410** (6831): 910.

5. Boysen, D. A., T. Uda, C. R. I. Chisholm, and S. M. Haile. High-performance solid acid fuel cells through humidity stabilization. 200. *Science.* **303** (5654): 8.

6. Jones, W. H., and J. E. Arrowsmith. Renewable energy feasibility study LA-UR 08-07230. 2008. *Los Alamos National Laboratory - Los Alamos County.*

Control/Path Planning Strategies for Nonholonomic, High-Speed, Autonomous Unmanned Ground Vehicles

Charles R. Farrar
20100594PRD1

Introduction

Mobile sensor nodes have proven to provide considerable utility for collecting data for any number of missions. They can be used to collect data from an environment, manipulate an environment as deemed necessary, and even provide energy to sensor nodes when their power supply diminishes. A major goal of the mobile sensor node community is the development of techniques to allow the widespread deployment of unattended mobile sensor nodes in unstructured, dynamic environments, with a minimum of human intervention during deployment and operation. In order to make this vision a reality, a number of challenges must be overcome. Examples include the development of high-reliability power sources that can be replenished by the mobile sensor node during its operation, health monitoring systems to provide information concerning the current physical state of the mobile sensor node, and systems to help the mobile sensor node ensure its own self-preservation in the face of adversarial agents in its environment. This work is concerned with an unsolved problem: how to select control policies to help mobile sensor nodes ensure their own self-preservation in the face of adversarial agents. These adversaries, whether people or machines, can pose a variety of threats to mobile sensor nodes, including tampering with the physical structure of the sensor node, tampering with the data placed on the sensor node, adding malicious software/hardware to the sensor node, and stealing/damaging the sensor node. It is important to note that the threat to mobile sensor nodes posed by adversarial agents is quite asymmetrical. The sensors onboard a mobile sensor node can be seriously disrupted simply by throwing a blanket over the mobile node or spray painting its cameras. Addressing these asymmetrical threats is a key challenge that must be overcome in order to enable the widespread use of unattended, ground-based mobile sensor nodes.

Discussions with Los Alamos National Laboratory staff with experience operating in adversarial environments has shown that one of the most effective techniques for avoiding tampering by unfriendly agents is to operate in as unpredictable a manner as possible. Conventional control policies for mobile sensor nodes that minimize time or energy consumption may be relatively simple for an intelligent adversary to anticipate. By observing the actions of the mobile sensor node, the adversary would be able to construct a model of the mobile sensor node's control policy, and then proceed to devise a strategy to take advantage of that policy. If, however the mobile sensor node employs paths that exhibit an element of randomness, it will be much more difficult for an adversary to be able to devise a control policy model to exploit the mobile sensor node. Generating random control policies is a relatively simple task, but generating random control policies that accomplish various objectives while taking into account hazards in the environment is somewhat more difficult. It is also very common for adversarial environments to exhibit large amounts of uncertainty in the state estimate. Given a high amount of uncertainty, it may be the case that it is preferable to select a control policy that is robust to uncertainty at the cost of performance. This work will make use of info-gap theory to analyze the tradeoffs between robustness and performance for a set of randomly generated paths for a mobile sensor node operating in an uncertain, adversarial environment.

In addition, we are researching a vibration cancellation system to enable unattended High Purity Germanium (HPGe) sensor nodes for nuclear spectroscopy. HPGes are currently used for nuclear detection and discrimination. One major drawback of germanium detectors is that, in order to produce spectroscopic data, they must be cooled to cryogenic temperatures. Typically HPGe detectors are cooled using dewars filled with liquid nitrogen (LN2). Unfortunately this solution requires that the dewar be periodically refilled with LN2, which may not be practical for unattended long-term monitoring applications. One promising alternative to LN2 cooling is the use of piston-driven cryocoolers. These cryocoolers can achieve LN2 temperatures with the only requirement being a source of electrical power and adequate heat dissipation. Unfortunately the vibrations transmitted by the cryocooler piston to the HPGe detector induce microphonic noise in the HPGe crystal. The mi-

crophonic noise reduces the resolution of spectroscopic measurements making them less useful for nuclear physics measurements. Our techniques will reduce that noise and improve performance.

Benefit to National Security Missions

The development of control policies to facilitate mobile sensor node operation in adversarial environments, will be a significant step forward towards deploying unattended, long-term, low-cost mobile sensor networks for Intelligence, Surveillance, and Reconnaissance (ISR) missions. The need for this technology was emphasized in the 2009 Unmanned Systems Integrated Roadmap:

"The key technologies that enable UGVs include complex world modeling, ground based hazard detection (e.g., mines, explosives), lane detection/road following, anti-tamper/self protection, highly dexterous manipulation, collaborative teaming in urban environments, etc. Of particular note among ground systems is the requirement for anti-tampering. In no other environment is an unmanned system more vulnerable to human tampering than when on the ground. It is imperative for the success of UGV operation that it be invested with the ability to deter humans from interfering with its activities, as well as from tampering with or damaging it via close physical contact."

Furthermore, this work begins to fill in the gap for the basic research needed to enable the development of mobile stealth/clandestine sensor nodes. The recent solicitation from the U.S. Air Force, "Special Ops Transport challenge (RFI-PKD-FY11-001)" is a good example of the need for mobile platforms that can quickly move materials and personnel, while maintaining low auditory and visual observability across an adversarial environment. The basic research effort being undertaken in this LDRD effort will provide the fundamental theory and technology needed to begin to undertake these future challenges.

Our nuclear sensor work will have broad applications to national security. It will be directly applicable to the development of unattended, long-term, remote nuclear detection sensor nodes for non-proliferation and treaty verification applications.

Progress

FY11 has been a very productive year for our research. The postdoc achieved some initial experimental success on his project to implement a control policy for car-like mobile sensor node that can both execute and avoid the precision immobilization technique (PIT maneuver). This work was presented at the SPIE Defense Security and Sensing conference 2011 [1]. Following this initial success, the postdoc then began work on a random-path generator to help car-like, ground-based mobile sensor nodes avoid theft and tampering. The goal of this effort was to help mobile sensor nodes (Figure 1) make use of random paths

to complete their objectives in an unpredictable fashion that complicates attempts by adversarial agents to exploit them. This work makes use of info-gap decision theory to select random paths that ensure a required minimum level of performance in the face of a given level of uncertainty (Figure 2). This work was implemented both in simulation and in field experiments. The results of this effort were presented that the SPIE Security and Defense Conference [2].
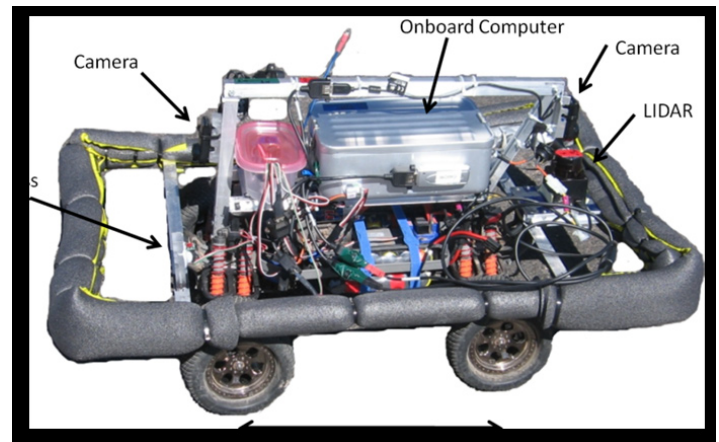

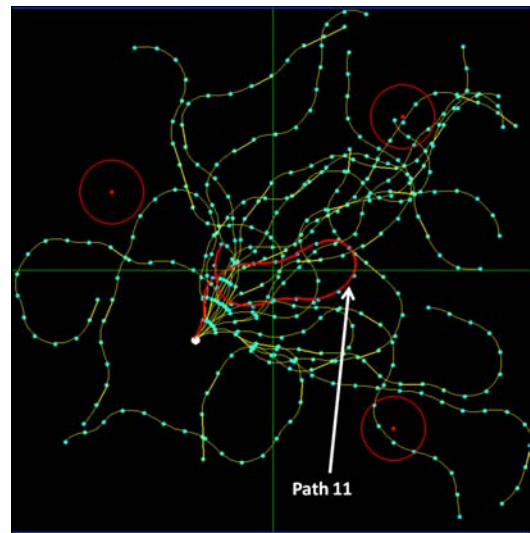Figure 1. Experimental car-like mobile sensor node.

Figure 2. Selecting randomly generated paths using info-gap decision theory analysis.

The postdoc also spent significant time during the summer of FY11 working on the piston-driven cryocooler vibration cancellation project [3]. He designed and managed the fabrication of a cryostat to interface the cryocooler to a germanium detector as shown in Figure 3. He assembled the control electronics and power supplies needed to power the germanium detector. Initial software libraries were written to implement an adaptive least-mean-squares (LMS) vibration canceller onboard an embedded comput-

ing platform. A high vacuum pump was procured to pump down the cryostat. Lastly, the postdoc managed the development of software to monitor and control the cryocooler temperature. At this time, the hardware is in place to perform initial vibration cancellation experiments with the cryocooler hardware. Work has also begun on the embedded software to cancel cryocooler vibrations.

Figure 3. Cryocooler and germanium detector mechanical assembly.

Future Work

As the postdoc's Director's funded research comes to an end, he is currently working on performing some final refinements to the software used to generate admissible paths for car-like, ground based mobile sensor nodes and evaluate the performance of these paths in the face of uncertainty.

The postdoc is also planning to continue the work on the vibration cancellation system for the piston-driven cryocooler. The underlying hardware and sensors are in place to begin evaluating the performance of candidate adaptive control policies for vibration cancellation. The goal is to write the software to implement the proposed LMS adaptive control policy and evaluate its performance.

At this point enough results have been collected to begin writing journal articles on the work the postdoc has completed during his postdoc research. Efforts to write and submit journal articles are underway and will be a main focus of the remaining time that he will be supported as a Director's funded postdoctoral fellowship.

Conclusion

The end state of this work will be field-tested mobile sensor node (MSN) path planning software capable of high speed operation while adapting to unforeseen environmental stimuli. The development of high-speed control and path planning strategies for MSNs has the potential to revolutionize the next generation of safe, high-performance, adaptive, self-sufficient, MSNs. The path planning strategies will also be applicable to extraterrestrial MSNs (e.g. Mars rovers).

The expected end product of the HPGe detector vibration damping project will be an embedded controller that can adaptively reduce the vibrations in a piston-driven cryocooler for unattended nuclear material monitoring applications (e.g. treaty verification/nonproliferation).

References
1. Mascarenas, D., C. Stull, and C. Farrar. Escape and evade control policies for ensuring the physical security of nonholonomic, ground-based, unattended mobile sensor nodes. 2011. In *Conference on Unattended Ground, Sea, and Air Sensor Technologies and Applications XIII ; 20110428 - 20110429 ; Orlando, FL.* Vol. 8046, p. 80460G.

2. Mascarenas, D., C. Stull, and C. Farrar. Towards the development of tamper-resistant, ground-based mobile sensor nodes. To appear in *SPIE Security and Defense.* (Prague, 19 - 22 Sept. 2011).

3. Johnson, W., R. Long, M. Nelson, and D. Mascarenas. Embedded active vibration vancellation of a piston-driven cryocooler for nuclear spectroscopy applications. To appear in *IMAC a Structural Dynamics Conference.* (Jacksonville, FL, 30 Jan. - 2 Feb. 2012).

Publications

Johnson, W., R. Long, M. Nelson, and D. Mascarenas. Embedded active vibration cancellation of a piston-driven cryocooler for nuclear spectroscopy applications. To appear in *IMAC a Structural Dynamics Conference.* (Jacksonville, FL, 30 Jan. - 2 Feb. 2012).

Macknelly, D., J. Mullins, H. Wiest, D. Mascarenas, and G. Park. Dynamic characterization of satellite components through non-invasive methods. 2011. In *29th IMAC, a Conference on Structural Dynamics, 2011 ; 20110131 - 20110203 ; Jacksonville, FL, United States.* Vol. 1, p. 321.

Mascarenas, D., C. Stull, and C. Farrar. Escape and evade control policies for ensuring the physical security of nonholonomic, ground-based, unattended mobile sensor nodes. 2011. In *Conference on Unattended Ground, Sea, and Air Sensor Technologies and Applications XIII ; 20110428 - 20110429 ; Orlando, FL.* Vol. 8046, p. 80460G.

Mascarenas, D., C. Stull, and C. Farrar. Escape and evade control policies for ensuring the physical security of nonholonomic, ground-based, unattended mobile sensor nodes. 2011. In *Unattended Ground, Sea, and Air Sensor Technologies and Applications XIII ; 28-29 April 2011 ; Orlando, FL, USA.* Vol. 8046, p. 80460G (12 pp.).

Mascarenas, D., C. Stull, and C. Farrar. Towards the development of tamper-resistant, ground-based mobile sensor nodes. To appear in *SPIE Security and Defense.* (Prague, 19-22 Sept. 2011).

Mascarenas, D., D. Macknelly, J. Mullins, H. Wiest, G. Park, and C. Farrar. Characterization of Satellite Assembly for Responsive Space Applications. 2011. In *Conference on Health Monitoring of Structural and Biological Systems 2011 ; 20110307 - 20110310 ; San Diego, CA.* Vol. 7984, p. 79842I.

Development of an Acoustic Exotic Metamaterial Slab Using the Acoustic Radiation Force and Micro-streaming of High-order Bessel Helicoidal Beams

Dipen N. Sinha
20100595PRD1

Introduction

Periodic structures made of objects many orders of magnitude larger than atomic length scales have been shown to manipulate various waves e.g., elastic, electromagnetic, etc. The waves can be deflected, reflected, refracted or stopped depending on their wavelength and the periodicity within the structure. This important characteristic of periodicity has given rise to a new class of materials that are artificially made and have unusual properties, such as negative refractive index, which are not found in naturally occurring materials. Materials that exhibit such negative properties are called metamaterials (acoustic or optical) and open up possibilities for creation of new devices that may allow for sub-wavelength imaging or focusing, energy harvesting, cloaking or directional propagation and other novel devices with important national security implications. Optical metamaterials have been studied extensively over the past two decades but very little work has been done on acoustic metamaterials. Acoustic metamaterials have been demonstrated only for low frequency (<100 kHz) waves using handmade or machined mechanical structures. However, this approach is totally impractical for automated production of such materials with 1-500 micron periodicity needed for many practical applications. We have developed an acoustic technique that fills this major technology gap by providing a technical approach [1] that can use any kind of materials (metal, plastic, insulator, semiconductor, nanoparticles, nanowires, biological material, etc.), is inexpensive (~$1000), fast (< 5 minutes), bench-top and provides frequency tunable 3D periodic structures. It can become a general purpose 3D material fabrication tool with wide scale applications in many fields that LANL can pioneer and can contribute to national security.

Benefit to National Security Missions

A successful completion of this project will introduce the necessary engineering knowledge to build a completely new capability at LANL to engineer novel materials for sensing devices and energy harvesting specifically, and 3D periodic patterned structures generally, for widespread engineering use. Acoustic metamaterials represent an important class of these types of periodic structures. This type of innovative engineering will form the basis of a platform technology that encompasses a wide range of applications (e.g., threat detections, innovative fabrication and manufacturing, energy harvesting, etc.) and this will serve the laboratory's national security missions well into the future.

The results of this research will be most relevant to agencies, such as DOD and DOC (in the area of non-nuclear forensics), in terms of having a very low cost and easily manufacturable means of creating ultrasonic superlenses with sub-wavelength resolution and highly directional sound source among other applications.

Progress

Task 1. Creation of periodic patterns of nanoparticles in a host curing fluid

We, F. G. Mitri (postdoctoral fellow) and I, have synthesized a 3D periodic composite material using acoustic radiation force acting on nanoparticles in a liquid suspension inside a resonator cavity [1]. This resonator consisted of a container (12x12x45 mm^3, wall thickness of 1 mm) and had two ultrasonic transducers (~ 1MHz) attached to it on the outside surface on opposite sides to set up standing waves inside the liquid-filled cavity. Using dilute epoxy (5 Minute$^\lozenge$ Epoxy) as the host fluid for 5 nm-diameter diamond nanoparticle suspension we were able to solidify the periodic structure for characterization as the epoxy set. The experimental set up is illustrated in Figure 1. The particular beauty of this technique is that acoustic radiation force does not discriminate and can apply force on any material, thus making the technique universal in terms of material types that can be manipulated. The acoustic radiation force magnitude needed to organize particles depends on the density and compressibility of both the solid particles and the host fluid (can even be molten metal). Depending on these values, particles can be forced to collect either at standing wave nodes or antinodes of the resonator cavity and thus alternating patterns of particles can be produced. When

the particles get very close to each other, a new attractive force takes over (Bjerknes force) that causes the particles to aggregate together creating well-defined structures. For creating acoustic metamaterials the periodic arrays may be formed using either gas-filled microspheres, or polymer-coated metals spheres to serves as local mechanical resonators in certain frequency regions. In other words, the metamaterials consist of a 3D periodic array where each element is a resonator that can vibrate at certain frequencies in unison and this produces the unusual properties in such artificial materials.
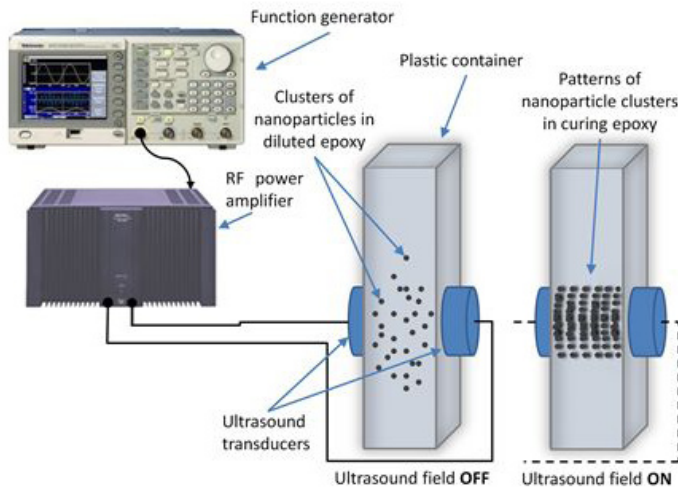

Figure 1. Experimental setup.

Task 2. Characterization of the nano-particle based composite material with micro-computed X-ray tomography (microXCT)

With microXCT, it is possible to verify the quality of the patterns periodicity in addition to other micro-structural features. To accomplish this task, the specimen was scanned using a microXCT system (Xradia, Micro-XCT-400, CA, USA). Its X-ray tube has an energy ranging from 20-90 keV, and the achievable resolution of the detector using the 2X, 4X, 10X and 20X magnification lenses are ~10 micron, ~5 micron, ~2.5 micron and 1.5 micron, respectively. In X-ray computed tomography, first, a set of individual radiographs (X-ray projections indicative of integrated X-ray absorption) is collected from a sample from all different viewing directions. Then, via the mathematical technique of tomographic reconstruction, the data set of radiographic images from different view angles is used to reconstruct the internal structure of the sample.

Figure 2a shows the 3D rendering of a tomographic section using the 2X detector lens, in which all the patterned planes (i.e. 12 parallel planes) of diamond nanoparticle clusters are clearly visible. Figures 2b-2d show the 3D ren-

dered images of volumetric tomographic sections of the assembled periodic composite structure obtained at higher resolutions using the 4X-, 10X- and 20X-lenses, respectively. As the detector resolution increases from ~10 micron (using the 2X lens) to 1.5 micron (using the 20X lens), the field-of-view (FOV) decreases as shown in the figures. The spacing of arranged particles, which corresponds to half the wavelength of 1 MHz ultrasound waves in ethanol-diluted epoxy, is 800 micron. Moreover, an average thickness of each plane of nanoparticle clusters may be estimated, which is found to be about 215 micron. It should be pointed out that these are the first such measurements anywhere on an acoustically created 3D periodic composite structure using nanoparticles. Previously, only surface photographs could be taken and it was not possible to see the internal structure. This is only a first step and with microXCT system with higher resolution, detailed morphology of such structures can be obtained that can help us understand this technique better.
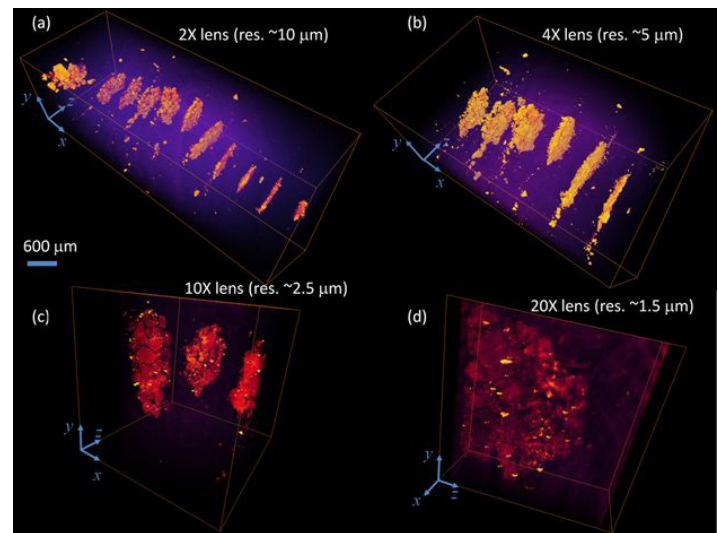

Figure 2. 3D Renderings of the diamond nanoparticle-based metamaterial.

Task 3. Creation and use of high-order Bessel beams (ultrasonic)

So far, we have only demonstrated how a periodic structure can be obtained using the acoustic radiation force in a resonator cavity. This works well for creating an object that is only a few cm in dimension and structures with low packing fraction (ratio of solid particles and host material). To create structures with very high packing fraction of suspended particles that may be needed for various practical applications, one needs to consider the scattering effect of these particles, which may weaken and disturb (diffract) the sound field pattern inside the resonator cavity. To overcome this limitation, we focused on the study of Bessel beams. A Bessel beam is a field of electromagnetic

or acoustic radiation whose amplitude is described by a Bessel function of the first kind. A true Bessel beam is non-diffractive. This means that as it propagates, it does not diffract and spread out; this is in contrast to the usual behavior of light (or sound), which spreads out after being focused down to a small spot. One of the most prized attributes of Bessel beams is the fact that the central core of the beam can be blocked, without interrupting the beam. Bessel beams are self-healing, meaning that the beam can be partially obstructed at one point, but will reform at a point further down thebeam axis. Approximations of such beams have been demonstrated for both light and sound. We have studied theoretically various higher order acoustic Bessel beams and their advantages. Analytical solutions up to the fourth-order level of approximation were derived. Figure 3 shows the results of such calculations where lateral magnitude and phase profiles of the beam compared and this is shown in. The results showed that the beam's width reduces and becomes narrower, the side-lobes decrease in magnitude, and the hollow region diameter (or null in magnitude) increases as the order of nonlinearity increases. Furthermore, the nonlinearity of the medium preserves the non-diffracting feature of the beam's harmonics. This indicates that indeed ultrasonic Bessel beams can be used to create large 3D periodic composite structures and metamaterials.
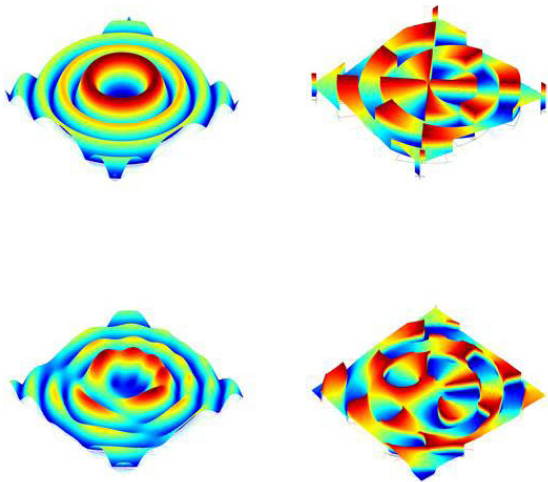

Figure 3. Theoretical magnitude and phase profiles.

Future Work
The proposed research consists of the following remaining tasks and research goals.

Task 4. Creation and use of high-order Bessel helicoidal beams (HOBHB)

The typical Gaussian beams will be replaced by higher order Bessel beams to study the improvement that can be gained from these types of beams as these are diffraction free beams.

Task 5. Exploration of applications of these exotic microstructures

The final objective of this project is to explore how these exotic materials can be used in applications such as creating novel sensors.

Conclusion
The anticipated results of this project will be a laboratory proof-of-concept to demonstrate the feasibility of producing a stable Acoustic Exotic Material (AEM) microstructure. The successful completion of this research will certainly lead to factual advancements in the field of AEMs research with potential for a wide range of applications. Only our own imagination may limit the wide range of applications of this proposed research spanning basically all areas of applied sciences (Physics, Materials Science, Chemistry, Biology, Geology…). Diverse commercial applications can be developed and patents can be filed based on the proposed technology.

References
1. Mitri, F. G., F. H. Garzon, and D. N. Sinha. Characterization of acoustically engineered polymer nanocomposite metamaterials using x-ray microcomputed tomography. 20. *Review of Scientific Instruments.* **82** (3): 034903.

Publications
Mitri, F. G.. Acoustic scattering of a high-order Bessel beam of fractional type a incident upon a rigid immovable sphere. 2010. *Journal of the Acoustical Society of America.* **128,** (4): 2314.

Mitri, F. G.. Linear axial scattering of an acoustical high-order Bessel trigonometric beam by compressible soft fluid spheres. 2011. *JOURNAL OF APPLIED PHYSICS* . **109** (1): 014916.

Mitri, F. G.. Arbitrary scattering of an electromagnetic zero-order Bessel beam by a dielectric sphere. 2011. *OPTICS LETTERS* . **36** (5): 766.

Mitri, F. G.. Vector wave analysis of an electromagnetic high-order Bessel vortex beam of fractional type alpha. 2011. *OPTICS LETTERS.* **36** (5): 606.

Mitri, F. G.. Axial time-averaged acoustic radiation force on a cylinder in a nonviscous fluid revisited . 2011. *Ultrasonics.* **551**: 645.

Mitri, F. G.. Potential-Well Model in Acoustic Tweezers-Comment. 20. *IEEE TRANSACTIONS ON ULTRASONICS FERROELECTRICS AND FREQUENCY CONTROL* . **58** (3): 662.

Mitri, F. G.. Arbitrary acoustic scattering of a high-order Bessel vortex beam by a sphere. Presented at *161st*

Meeting of the Acoustical Society of America. (Seattle, 23-27 May, 2011).

Mitri, F. G., F. H. Garzon, and D. N. Sinha. Characterization of acoustically engineered polymer nanocomposite metamaterials using x-ray microcomputed tomography. 2011. *Review of Scientific Instruments.* **82** (3): 034903.

Mitri, F. G., and D. N. Sinha. Metamaterial Synthesis using the Acoustic Radiation Force and Characterization with X-ray micro-computed tomography. Presented at *161st Meeting of the Acoustical Society of America.* (Seattle, 23-27 May, 2011).

Mitri, F. G., and Z. E. A. Fellah. Instantaneous axial force of a high-order Bessel vortex beam of acoustic waves incident upon a rigid movable sphere. 2011. *Ultrasonics.* **651**: 719.

Optimization of Heterogeneous Sensing Systems for Risk-Minimized Decision Making

Charles R. Farrar
20110575PRD1

Introduction

Making optimal decisions with respect to real-world events requires effective and robust sensing systems. These systems are always limited in scope, and need to spend their resources as effectively as possible to deliver the most important data. Sensing systems are limited by their operating costs, their burden on the processes the observe, and their cost, weight, and power. Common approaches to sensor optimization are of limited use for data-driven decision making. Such approaches do not take into consideration the relative value of each observation or the costs associated with the sensing system design, and they do not offer straightforward support for variable design sizes (i.e. number of design parameters) or systems involving multiple sensor types or data types, i.e., heterogeneous sensing systems. Our research will develop a Bayesian experimental design framework that addresses these shortcomings in sensor design. Successful completion of this project will yield a general sensor system design methodology that is applicable to all sensing applications.

Benefit to National Security Missions

The proposed work focuses on developing optimal sensing systems based on minimizing a Bayes Risk term. This approach is applicable to any sensing system where there is a finite sensor budget and the tradeoff between various sensor design parameters (e.g. type, number, location) must be addressed. As such, almost all DOE technology areas will benefit from this research and the results will be applicable to sensing activities associated with many different government agencies. By using data from various mission activities in the development of this optimization process, Eric will necessarily interact with various programs at LANL that can subsequently fund the application of his technology to their systems once his Director's funded postdoctoral fellowship has been completed.

Progress

The Post doc, Eric Flynn, did not arrive until August, 29th, 2011. Progress to date has primarily focused on background literature reviews regarding sensing systems be-ing employed on high performance computers (HPC). In addition, Eric has met with HPC scientists and engineers regarding HPC sensing issues.

Eric presented a paper on phase-array, guided-wave damage detection [1] at The International Workshop on Structural Health Monitoring that was held at Stanford University. This paper was selected for the best paper award at the workshop.

Future Work

The objective of the proposed research is to develop and apply an experimental design framework for the optimization of heterogeneous sensing systems. The framework will be built around the minimization of the total risk over the lifetime of the sensing system, which is a function of system performance, costs of decision errors, the cost and maintenance of the sensing system itself, and the probabilities of the relevant events. Design parameters include, but are not limited to, sensor selection (including simultaneous use of multiple sensor types), sensor counts, sensor placement, sensor interrogation equipment, and measurement scheduling.

While a strong theoretical foundation will be important, the proposed work is intended to be application-centric. This additionally entails the significant tasks of decision cost analysis, model development, and model approximation. Internal applications of interest include High Performance Computing Resilience: Optimal placement of physical sensors, such as those that measure temperature, humidity, and voltage, and virtual sensors which reside in software and sample communication, data, errors, and hardware status information, and International Emissions Treaty Verification: Selection and placement of ground based chemical sensors and selection of measurement points and measurement types for air and space-based sensing systems. Each application will require evaluating the sets of decision costs and costs associated with instrumentation, constructing models of the measured process and the sensing system, deriving optimal decisions rules, calculating and approximating the decision rules performance as a function of the sensing system design parameters, and designing tailored,

efficient search algorithms for finding optimal or near-optimal design solutions. Propagating decision statistics in the context of optimization searches will require a mix of analytical approximation and efficient numerical simulation (such as Markov chain Monte Carlo methods). Variable design sizes will necessitate the construction of unique metaheuristics for efficiently searching the design spaces.

Conclusion

The result of this proposed research will be the development and validation of a Bayesian experimental design framework for sensor systems that allows optimization of heterogeneous sensing systems and associated decision making processes. This framework will provided a scientific approach to sensor system design allowing finite sensing resources to produce the maximum amount of information for a given application. Better sensing will provide benefit for all Los Alamos missions.

References

1. Flynn, E., M. Todd, S. Kessler, and C. Dunn. Identifying scatter targets in 2D space using in situ phased-arrays for guided wave structural health monitoring. 2011. In *International Workshop on Structural Health Monitoring.* (Palo Alto, CA, 13-15 Sept. 2011). , p. 200. Lancaster, PA: DEStech.

Publications

Flynn, E., M. Todd, S. Kessler, and C. Dunn. Identiying scatter targets in 2D space using in situ phased-arrays for guided wave structural health monitoring. 2011. In *International Workshop on Structural Health Monitoring.* (Palo Alto, CA , 13-15 Sept. 2011). , p. 200. Lancaster, PA: DEStech.

Chiral Metamaterials for Terahertz Frequencies

John F. O'Hara
20080796PRD4

Abstract

Electromagnetic radiation influences nearly every aspect of our lives, from cell phone communication to simple photography. Photography leverages centuries of technology development in focusing, image recording, and of course materials (i.e. glass). Today, scientists are studying "metamaterials" to radically advance such technologies. Metamaterials are engineered materials that exhibit properties not found in nature. Imagine a material that could change color on demand. The military implications would be enormous. Metamaterials enable such behavior. Our project was to use metamaterials for two purposes. First, we showed that metamaterials can fill a technology vacuum in the terahertz frequency range. Terahertz (THz) waves, electromagnetic (EM) waves whose frequency lies between microwaves and the infrared, are notoriously difficult to control. Second, we quantified the effectiveness of a new design strategy for negative index metamaterials. Negative index metamaterials have drawn much interest in their ability to improve imaging technologies.

Our main success in this project was to create chiral THz materials that can be actively controlled. Normal chiral materials rotate the polarization of a wave. Ours does this much more strongly and without altering any other aspect of its polarization qualities! In addition, we showed that this metamaterial behavior can be turned on or off dynamically. This difficult combination of qualities was never before demonstrated. We were also successful in determining limitations of chiral metamaterials. We showed how chirality affected absorption in negative index metamaterials. And with collaborators, we also helped determine the role chirality might play in tuning the Casimir force. All of this has positively impacted the LANL mission by creating new metamaterial capabilities, and helped foster external funding.

Background and Research Objectives

Terahertz science has been pursued since 1990 in an effort to make THz waves practical. Still, devices suitable for controlling THz waves are not yet adequate. One area of development that has remained unusually weak is polarization control. Control over polarization is important in many technologies such as wireless communications and global positioning systems. Before THz technology can become practical, the basic devices for controlling THz waves must be developed, including devices for controlling THz wave polarization. The first objective of this project was to create a new metamaterial that enables us to control the polarization of THz waves.

Metamaterials research has led to many new EM technology ideas. One idea was the notion of negative index materials (NIMs). Negative index materials are not naturally occurring; they must be engineered. With respect to our project, the novelty of NIMs is that they enable "super-resolution" imaging. All imaging schemes are limited in resolution to the wavelength of the EM waves used. For example, millimeter resolution is possible by imaging with EM waves of millimeter wavelength. Nanometer resolution is possible with ultraviolet or x-rays. With NIMs, it is theoretically possible to achieve unlimited resolution at any wavelength. Real NIMs, however, are highly absorbing. In other words, you might make a super-resolution lens out of NIMs, but it is nearly opaque! When we began this work, chiral metamaterials were seen as a new approach that enables negative index (and thus super-resolution), but with much lower absorption. That defined our second research objective: determine whether NIMs with very low absorption could be created using the chiral metamaterial approach.

Our objectives met with great success. We were able to design a THz metamaterial that not only featured tuned chirality, but this chirality was about 10,000 times stronger than in natural materials. Even more important, the chirality could be actively turned on and off. In addition, this metamaterial featured negative refractive index, enabling us to quantify absorption.

Scientific Approach and Accomplishments

Our approach to this work was partially described in the previous section. In more detail, we aimed to create a chiral THz metamaterial. Chirality is a rather vague description and can mean different things. Chirality, like color, is a property of a material. But chirality can mean

that a material is "optically active" or "dichroic". Optical activity means that the material rotates the polarization plane of an EM wave passing through it. Dichroism means that a wave of one polarization is more highly absorbed than another polarization. Technical details are not necessary to understand the importance. For example, optical activity is critical to the understanding of molecular biology and analytical chemistry. In addition, optical activity is the basis of numerous display technologies, such as LCD computer monitors. Control over optical activity in the THz frequency range may prove particularly useful in biomedical imaging and sensing applications. Our approach was therefore to create a chiral THz metamaterial that could tune optical activity. Dichroism generally represents increased absorption, which we wanted to avoid. Therefore, we aimed for metamaterial designs that featured zero dichroism.

Optical activity originates from the molecular structure of a chiral material. The double-helix DNA molecule is a good example. These molecules are shaped such that the wave must rotate or twist in one direction as it propagates through the material. This is similar to a corkscrew moving through a cork. Like natural materials, chiral metamaterials are designed at the "molecular" level. Our task was to create a metamaterial molecule that twisted the THz wave as it passed through. When these molecules are packed tightly together they form the metamaterial as a whole. The molecule in our metamaterial is a bi-layer structure comprised of two resonators (Figure 1). The top and bottom resonators work together to force the wave to twist as it passes through the array of molecules.
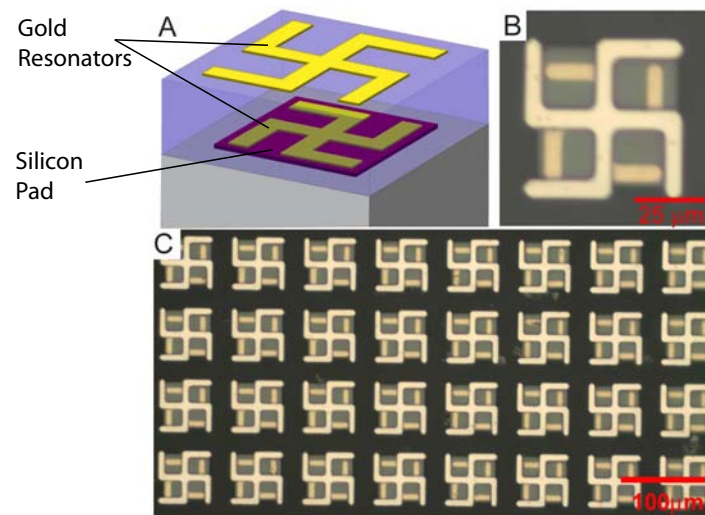

Figure 1. Tunable chiral THz metamaterial. Panel A shows the design of the metamaterial "molecule". Two gold resonators are separated by a dielectric spacer. Under the bottom resonator is a silicon pad that enables active control of chirality. Panel B shows a picture of one actual molecule taken through a microscope. The silicon pad under the lower resonator is light gray in the picture. Panel C is a picture of part of the array of molecules, which comprises the chiral metamaterial as a whole.

Our design process was constrained by several factors. First, we had to establish a design that twisted the wave. Second, we had to ensure that the wave passed through the metamaterial without any modifications except the twist. Third, we wanted the wave to experience little absorption. This combination was very difficult to achieve. Our design process started with an asymmetric molecule. That is, the top and bottom resonators shown in Figure 1 are oriented oppositely; one is clockwise and the other is counter-clockwise oriented. This combination forces the wave to twist. However, resonators are functional only at particular frequencies. When operated at these "resonant frequencies" resonators exhibit high absorption. Through EM simulations and iterative design we were finally able to create a metamaterial that operated slightly off-resonance. In this way we reduced absorption and maintained the twisting behavior we desired. Numerous design iterations were required to arrive at this point.

Our next task was to modify our design so that it was controllable. Typically, metamaterials have a certain response that is tuned by the size and shape of the resonators. Once fabricated, these metamaterials have a fixed response. It may be a novel response that cannot be obtained in natural materials, but it is fixed nonetheless. Our group at LANL has pioneered metamaterial designs that feature dynamic responses. In our modified designs, an electrical or optical (laser) signal is applied to the metamaterial. This signal changes the behavior of the individual resonators and thereby alters the overall metamaterial response. We were able to add this feature to our chiral THz metamaterial by placing a small silicon pad underneath the lower resonator (Figure 1). In normal operation the metamaterial twists the wave by 12 degrees. When we illuminate the silicon pad with laser light it turns off the lower resonator. This also disables the chirality so the metamaterial can no longer twist the wave. Using the laser, we can actively control how much twist the wave experiences. These design modifications were done using semiconductor analysis and EM simulation tools.

Having reached several suitable designs, we fabricated our metamaterials. Fabrication was performed at the Center for Integrated Nanotechnologies cleanroom in Albuquerque, NM. This was a multi-layer fabrication. Each layer of the metamaterial was consecutively patterned using conventional photolithographic techniques.

We then used our THz characterization labs to measure the metamaterials. We found that our measured results were very consistent with our simulations. Our originally designed THz chiral metamaterial featured optical activity, low absorption, and affected nothing but the polarization rotation (or twist). The twist was found to be 12 degrees, yet the metamaterial was only about 1/18th of a wavelength thick. This corresponded to chirality about 10,000 times stronger than in natural materials such as quartz. We fabricated and measured three other metamaterials

that had even greater chirality. The strongest could twist the EM wave about 45 degrees. However, these stronger metamaterials also produced distortions of the wave, which was an undesirable trade-off.

Next we demonstrated that our metamaterials were dynamic. By illuminating the metamaterial with an infrared laser we could switch the chirality on and off. This was the first demonstration of an engineered material that could actively control the twist of a passing THz wave. It represents an enormous step forward in THz technology (in terms of polarization control). But this technology is generally important to all EM technologies, across the spectrum. Our designs are scalable, meaning this approach should work well at almost any frequency.

Finally, we analyzed our results to see how chirality could affect absorption in NIMs. Mathematical inversion techniques are available to extract "effective parameters" of metamaterials. One example of an effective parameter is refractive index. We performed these extractions and found that we had indeed achieved negative index. Though already demonstrated, this was still a useful result in our work because it allowed us to quantify absorption in a NIM. This was one of our original goals. We found that chirality was not a route to low absorption NIMs, despite earlier conjectures in the community. More importantly, however, we demonstrated something that had never been done. Our metamaterial was dynamic; it had switchable chirality. As such it also had the ability to switch from negative to positive index, on demand! All of these interesting results were prepared into a paper, which has been submitted to Nature Photonics [1] and is currently under review. Many of our results have already been published [2] or presented at various conferences [3-8] as invited works.

One project that has spawned from our original work is the study of how chiral metamaterials might reverse the Casimir force. This is a weak nuisance force that causes nano-machines to stick together. Its reversal would be highly important for future nano-mechanical devices. We are collaborating with Iowa State University to study this phenomenon further. This also supports an external project of more general scope studying the Casimir force and its relation to all types of metamaterial.

Impact on National Missions

This project positively impacted both Laboratory and national missions. First, it enhances our fundamental understanding of engineered materials. As such, it has built LANL's capability to understand the limitations and applications of metamaterials. This is most relevant in the THz frequency region, where natural materials have proven less than ideal. This capability is important for other efforts also. We were funded ($975k) with the LANL Theoretical division to study how metamaterials might tune the Casimir force. Our chiral metamaterials work is going to

add value to this project. The work has generally drawn the interest of several government agencies including DOD, DOE, and DHS, who are interested in technologies supporting ubiquitous sensing and threat reduction. We continue to pursue external opportunities based on the results of this project. Lastly, this project helped propel our group to worldwide metamaterial leadership in dynamic and THz metamaterials. This has opened the door to fruitful collaborations and commercialization opportunities, which we have pursued through patent applications.

References

1. Zhou, J., D. Roy Chowdhury, R. Zhao, A. K. Azad, H. Chen, C. M. Soukoulis, A. J. Taylor, and J. F. O'Hara. Active terahertz chiral metamaterial with tunable optical activity. *Nature Photonics.*

2. Zhao, R., J. Zhou, T. Koschny, E. N. Economou, and C. M. Soukoulis. Repulsive casimir force in chiral metamaterials. 2009. *Physical Review Letters.* **103** (10): 103602.

3. Zhou, J., B. Wang, E. Plum, T. Koschny, V. Fedotov, H. Chen, A. Taylor, J. O'Hara, N. Zheludev, and C. Soukoulis. Chiral metamaterials with negative refractive index. Presented at *International Workshop on Electromagnetic Metamaterials, III.* (Los Alamos, New Mexico, 18-19 May, 2009).

4. O'Hara, J., J. Zhou, A. Taylor, D. Dalvit, F. da Rosa, P. Milonni, I. Brener, and P. Davids. Metamaterial design considerations for Casimir force control. Invited presentation at *New Frontiers in Casimir Force Control.* (Santa Fe, New Mexico, 26-28 Sep. 2009).

5. Zhao, R., J. Zhou, T. Koschny, E. Economou, and C. Soukoulis. Repulsive Casimir force in chiral metamaterials. Presented at *New Frontiers in Casimir Force Control.* (Santa Fe, New Mexico, 26-28 Sep. 2009).

6. Zhou, Jiangfeng, Rongkuo Zhao, C. M. Soukoulis, A. J. Taylor, and J. O'Hara. Chiral THz metamaterial with tunable optical activity. 2010. In *2010 Conference on Lasers and Electro-Optics (CLEO) ; 16-21 May 2010 ; San Jose, CA, USA.* , p. 1.

7. O'Hara, J. F., J. Zhou, D. Roy Chowdhury, M. T. Reiten, A. K. Azad, H. Chen, L. Earley, A. J. Taylor, C. Soukoulis, R. Zhao, T. Koschny, A. Gossard, and H. Lu. Nonlinear metamaterial investigations from RF to terahertz... and more. Invited presentation at *International Workshop on Electromagnetic Metamaterials, IV.* (Santa Ana Pueblo, New Mexico, 11-12 Aug. 2010).

8. Zhou, J., R. Zhao, C. Soukoulis, A. J. Taylor, and J. F. O'Hara. Chiral THz metamaterial with optical activity. To appear in *Metamaterials 2010: Fourth International Congress on Advanced Electromagnetic Materials in Microwaves and Optics.* (Karlsruhe, Germany, 13-16 Sep. 2010).

Publications

O'Hara, J., J. Zhou, A. Taylor, D. Dalvit, F. da Rosa, P. Milonni, I. Brener, and P. Davids. Metamaterial design considerations for Casimir force control. Invited presentation at *New Frontiers in Casimir Force Control.* (Santa Fe, New Mexico, 26-28 Sep. 2009).

O'Hara, J., J. Zhou, D. Roy Chowdhury, M. T. Reiten, A. K. Azad, H. Chen, L. Earley, A. J. Taylor, C. Soukoulis, R. Zhao, T. Koschny, A. Gossard, and H. Lu. Nonlinear metamaterial investigations from RF to terahertz... and more. Invited presentation at *International Workshop on Electromagnetic Metamaterials, IV.* (Santa Ana Pueblo, New Mexico, 11-12 Aug. 2010).

Zhao, R., J. Zhou, T. Koschny, E. Economou, and C. Soukoulis. Repulsive Casimir force in chiral metamaterials. Presented at *New Frontiers in Casimir Force Control.* (Santa Fe, New Mexico, 26-28 Sep. 2009).

Zhao, R., J. Zhou, T. Koschny, E. N. Economou, and C. M. Soukoulis. Repulsive Casimir Force in Chiral Metamaterials. 2009. *Physical Review Letters.* **103**: 103602.

Zhou, J., B. Wang, E. Plum, T. Koschny, V. Fedotov, H. T. Chen, A. J. Taylor, J. F. O'Hara, N. Zheludev, and C. Soukoulis. Chiral Metamaterials with Negative Refractive Index. Presented at *International Workshop on Electromagnetic Metamaterials III: Toward Real World Applications.* (Los Alamos, NM, 18-19 May, 2009).

Zhou, J., D. Roy Chowdhury, R. Zhao, A. K. Azad, H. Chen, C. M. Soukoulis, A. J. Taylor, and J. F. O'Hara. Active terahertz chiral metamaterial with tunable optical activity. *Nature Photonics.*

Zhou, J., R. Zhao, C. Soukoulis, A. J. Taylor, and J. F. O'Hara. Chiral THz metamaterial with optical activity. To appear in *Metamaterials 2010: Fourth International Congress on Advanced Electromagnetic Materials in Microwaves and Optics.* (Karlsruhe, Germany, 13-16 Sep. 2010).

Zhou, Jiangfeng, Rongkuo Zhao, C. M. Soukoulis, A. J. Taylor, and J. O'Hara. Chiral THz metamaterial with tunable optical activity. 2010. In *2010 Conference on Lasers and Electro-Optics (CLEO) ; 16-21 May 2010 ; San Jose, CA, USA.* , p. 1.